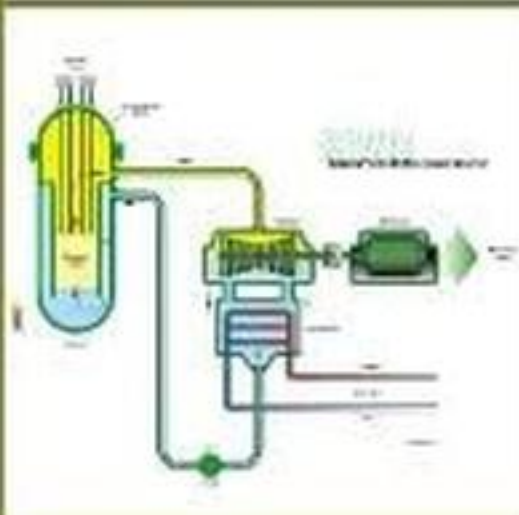
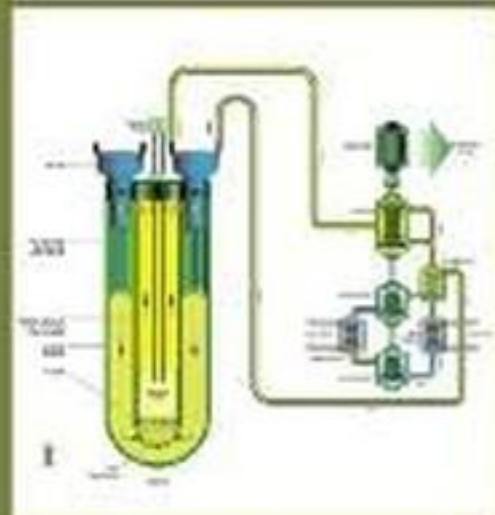
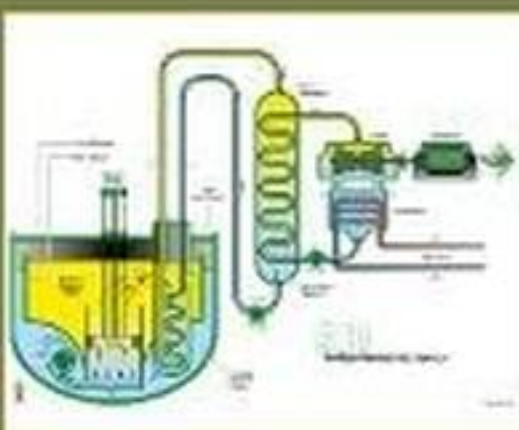
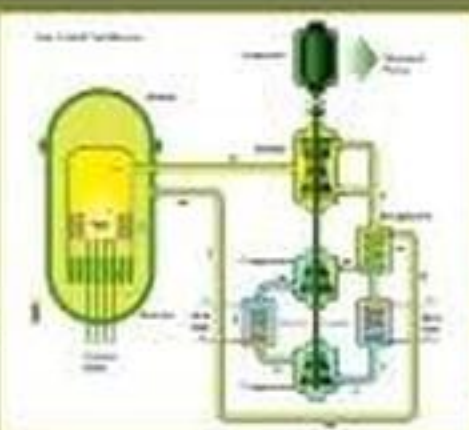
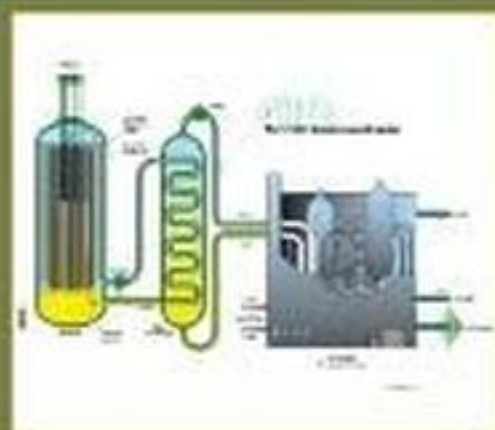


WOODHEAD PUBLISHING SERIES IN ENERGY



HANDBOOK OF GENERATION IV NUCLEAR REACTORS

SECOND EDITION

Edited by
DR. IGOR PIORO



Handbook of
Generation IV
Nuclear Reactors

Woodhead Publishing Series in Energy

Handbook of Generation IV Nuclear Reactors

A Guidebook

Second Edition

Edited by

IGOR L. PIORO

*Faculty of Energy Systems and Nuclear Science, University of Ontario Institute of Technology,
Oshawa, ON, Canada*



ELSEVIER

WP

WOODHEAD
PUBLISHING

An imprint of Elsevier

Woodhead Publishing is an imprint of Elsevier
50 Hampshire Street, 5th Floor, Cambridge, MA 02139, United States
The Boulevard, Langford Lane, Kidlington, OX5 1GB, United Kingdom

Copyright © 2023 Elsevier Ltd. All rights reserved.

No part of this publication may be reproduced or transmitted in any form or by any means, electronic or mechanical, including photocopying, recording, or any information storage and retrieval system, without permission in writing from the publisher. Details on how to seek permission, further information about the Publisher's permissions policies and our arrangements with organizations such as the Copyright Clearance Center and the Copyright Licensing Agency, can be found at our website: www.elsevier.com/permissions.

This book and the individual contributions contained in it are protected under copyright by the Publisher (other than as may be noted herein).

Notices

Knowledge and best practice in this field are constantly changing. As new research and experience broaden our understanding, changes in research methods, professional practices, or medical treatment may become necessary.

Practitioners and researchers must always rely on their own experience and knowledge in evaluating and using any information, methods, compounds, or experiments described herein. In using such information or methods they should be mindful of their own safety and the safety of others, including parties for whom they have a professional responsibility.

To the fullest extent of the law, neither the Publisher nor the authors, contributors, or editors, assume any liability for any injury and/or damage to persons or property as a matter of products liability, negligence or otherwise, or from any use or operation of any methods, products, instructions, or ideas contained in the material herein.

ISBN: 978-0-12-820588-4 (print)

ISBN: 978-0-12-822653-7 (online)

For information on all Woodhead publications
visit our website at <https://www.elsevier.com/books-and-journals>

Publisher: Joe Hayton

Editorial Project Manager: Tim Eslava

Production Project Manager: Erragounta Saibabu Rao

Cover Designer: Matthew Lambert

Typeset by STRAIVE, India



Contributors

- Michel Allibert** LPSC/IN2P3/CNRS—Grenoble Alpes University—Grenoble Institute of Technology, Grenoble, France
- Fatih Aydogan** Jacksonville University, Jacksonville, FL, United States
- Janos Bodi** Paul Scherrer Institut, Villigen, Switzerland
- Shridhar K. Chande** Atomic Energy Regulatory Board, Mumbai, India
- Perumal Chellapandi** BHAVINI, Kalpakkam, India
- Lin Chen** Institute of Engineering Thermophysics, Chinese Academy of Sciences & University of CAS, Beijing, People's Republic of China
- Yoshitaka Chikazawa** Japan Atomic Energy Agency (JAEA), Ibaraki, Japan
- Luciano Cinotti** Newcleo Ltd, London, United Kingdom
- Michel Claessens** European Commission and Free University of Brussels, Brussels, Belgium
- Gerald Clark** United Kingdom
- Dahvien Dean** Department of Nuclear Engineering, Texas A&M University, College Station, TX, United States
- Sylvie Delpech** IJC Lab/IN2P3/CNRS, Orsay, France
- Nikita Dort-Goltz** Faculty of Energy Systems and Nuclear Science, University of Ontario Institute of Technology, Oshawa, ON, Canada
- Alexey Dragunov** Faculty of Energy Systems and Nuclear Science, University of Ontario Institute of Technology, Oshawa, ON, Canada
- Romney B. Duffey** Idaho Falls, ID, United States
- Indravadan Dulara** BARC, Mumbai, India
- Rami S. El-Emam** Faculty of Engineering and Applied Science, Ontario Tech University, Oshawa, ON, Canada
- Seyun Eom** Canadian Nuclear Safety Commission, Ottawa, ON, Canada
- Natalia M. Fialko** Institute of Engineering Thermal Physics, National Academy of Sciences of Ukraine, Kyiv, Ukraine
- Kamiel S. Gabriel** Faculty of Engineering and Applied Science, Ontario Tech University, Oshawa, ON, Canada
- Arnold A. Gad-Briggs** EGB Engineering UK LTD, Southwell, United Kingdom
- Delphine Gerardin** LPSC/IN2P3/CNRS—Grenoble Alpes University—Grenoble Institute of Technology, Grenoble, France
- Enrico Girardi** EDF Lab Paris-Saclay, Palaiseau, France
- Filip Grochowina** EGB Engineering UK LTD, Southwell, United Kingdom
- Joel Guidez** CEA, CEN SACLAY, Gif-sur-Yvette, France
- Dohee Hahn** Korea Atomic Energy Research Institute, Daejeon, Republic of Korea
- Daniel Heuer** LPSC/IN2P3/CNRS—Grenoble Alpes University—Grenoble Institute of Technology, Grenoble, France
- Mohammad Hosseiny** Faculty of Energy Systems and Nuclear Science, University of Ontario Institute of Technology, Oshawa, ON, Canada

- Dan Hughes** Hughes and Associates, Perth, NY, United States
- Brian Ikeda** Faculty of Energy Systems and Nuclear Science, University of Ontario Institute of Technology, Oshawa, ON, Canada
- Hideki Kamide** Japan Atomic Energy Agency (JAEA), Ibaraki, Japan
- Pavel L. Kirillov** State Scientific Centre of the Russian Federation—Institute of Physics and Power Engineering (IPPE) named after A.I. Leipunsky, Obninsk, Russia
- Ken Kirkhope** Canadian Nuclear Safety Commission, Ottawa, ON, Canada
- Natalia P. Kozioura** AETC Inc., Toronto, ON, Canada
- Shigenobu Kubo** Japan Atomic Energy Agency (JAEA), Ibaraki, Japan
- Axel Laureau** IN2P3/CNRS - IMT Atlantique, Nantes, France
- Laurence K.H. Leung** Canadian Nuclear Laboratories, Chalk River, ON, Canada
- Mohammed Mahdi** Faculty of Energy Systems and Nuclear Science, University of Ontario Institute of Technology, Oshawa, ON, Canada
- Jennifer McKellar** Faculty of Energy Systems and Nuclear Science, University of Ontario Institute of Technology, Oshawa, ON, Canada
- Elsa Merle** LPSC/IN2P3/CNRS—Grenoble Alpes University—Grenoble Institute of Technology, Grenoble, France
- Konstantin Mikityuk** Paul Scherrer Institut, Villigen, Switzerland
- Sarah J. Mokry** Faculty of Energy Systems and Nuclear Science, University of Ontario Institute of Technology, Oshawa, ON, Canada
- Theoklis Nikolaidis** Gas Turbine Engineering Group, Cranfield University, Cranfield, United Kingdom
- Thambiayah Nitheanandan** Canadian Nuclear Safety Commission, Ottawa, ON, Canada
- Hiroyuki Ohshima** Japan Atomic Energy Agency (JAEA), Ibaraki, Japan
- Emmanuel O. Osigwe** EGB Engineering UK LTD, Southwell, United Kingdom
- Wargha Peiman** Faculty of Energy Systems and Nuclear Science, University of Ontario Institute of Technology, Oshawa, ON, Canada
- Pericles Pilidis** Gas Turbine Engineering Group, Cranfield University, Cranfield, United Kingdom
- Igor L. Pioro** Faculty of Energy Systems and Nuclear Science, University of Ontario Institute of Technology, Oshawa, ON, Canada
- Roman M. Pioro** Faculty of Physics, Lomonosov Moscow State University, Moscow, Russia
- Evgen N. Piśmennyi** National Technical University of Ukraine “Igor Sikorsky Kiev Polytechnic Institute”, Kyiv, Ukraine
- Roman Popov** Faculty of Energy Systems and Nuclear Science, University of Ontario Institute of Technology, Oshawa, ON, Canada
- Victor G. Razumovskiy** National Technical University of Ukraine “Igor Sikorsky Kiev Polytechnic Institute”, Kyiv, Ukraine
- Jovica Riznic** Canadian Nuclear Safety Commission, Ottawa, ON, Canada
- Gilles H. Rodriguez** Technical Director of the Generation IV International Forum, France
- Eugene Saltanov** Faculty of Energy Systems and Nuclear Science, University of Ontario Institute of Technology, Oshawa, ON, Canada
- Suresh Sampath** Gas Turbine Engineering Group, Cranfield University, Cranfield, United Kingdom
- Thomas Schulenberg** Karlsruhe Institute of Technology, Karlsruhe, Germany
- Ratan K. Sinha** Department of Atomic Energy, Mumbai, India
- Anton D. Smirnov** National Research Nuclear University MEPhI (Moscow Engineering Physics Institute), Moscow, Russia

- Craig F. Smith** Naval Postgraduate School, Monterey, CA, United States
- Gopala I. Srinivasan** IGCAR, Kalpakkam, India
- Joao Amaral Teixeira** Gas Turbine Engineering Group, Cranfield University, Cranfield, United Kingdom
- Georgy V. Tikhomirov** National Research Nuclear University MEPhI (Moscow Engineering Physics Institute), Moscow, Russia
- Mark Tsai** Faculty of Energy Systems and Nuclear Science, University of Ontario Institute of Technology, Oshawa, ON, Canada
- Pavel Tsvetkov** Department of Nuclear Engineering, Texas A&M University, College Station, TX, United States
- Georges Van Goethem** Former Principal Scientific Officer at the European Commission, DG Research and Innovation, Dir. Energy, Unit Euratom—Fission, Brussels, Belgium
- Pallippattu K. Vijayan** BARC, Mumbai, India
- Hanqing Xie** Faculty of Energy Systems and Nuclear Science, University of Ontario Institute of Technology, Oshawa, ON, Canada
- Xing L. Yan** Japan Atomic Energy Agency, Oarai-Machi, Ibaraki-ken, Japan
- Calin Zamfirescu** Durham College, Oshawa, ON, Canada
- Dalin Zhang** Xi'an Jiaotong University, Xi'an, People's Republic of China
- Constantin O. Zvorykin** National Technical University of Ukraine “Igor Sikorsky Kiev Polytechnic Institute”, Kyiv, Ukraine

Foreword

Dear Readers:

Handbook of Generation IV Nuclear Reactors, Second Edition has been written by recognized nuclear-energy system experts from around the world. The need for this new edition is based on the success of the first edition, published in 2016 and, until now, the only book in the world dedicated solely to Generation IV nuclear-power reactors and related topics. Of course, within the last 6 years, many new developments in nuclear power and engineering have taken place, especially in relation to Generation IV nuclear-power reactors. Thus a major purpose of this edition is to summarize the latest achievements, developments, and trends within these areas.

Currently, 443 nuclear-power reactors^a generate about 10.4% of electricity worldwide. Global demand is and will be growing for this essential and reliable energy source, almost free from greenhouse gases (if the whole nuclear cycle is considered, i.e., from extraction of uranium ore to demolition of old Nuclear Power Plants (NPPs)). Interest in the use of nuclear energy for electricity generation has led to nuclear reactors being currently built in 33 countries, and 3 countries without reactors are currently working on adding new builds.

The safe and efficient operation of the current fleet of nuclear-power reactors is essential, as is their life extension for global sustainability and human well-being. This current generation of reactors/NPPs, most being light- and heavy-water cooled, has served and is serving the world well. The remaining challenges include advances in thermal efficiency, managing rare-event safety, fuel-cycle enhancements, improved economic competitiveness, ensuring that nuclear-weapon-proliferation concerns are addressed, and managing radioactive waste with full public and political participation. These topics are indeed the Generation-IV goals and encompass so-called reactor systems. These needed technical developments are set against the global backdrop of concerns and issues over climate change, economic growth, sustainable and renewable energy use, optimal resource development, political stability, international security, and environmental conservation.

The future, therefore, also lies in the development of the next generation of nuclear-energy systems: Generation-IV nuclear-power reactors and other advanced-reactor concepts/designs, which offer potential solutions to many of these problems, including advances in the use of risk-informed decision making and safety regulations. New reactor/NPP designs, including small-modular-reactors (SMRs), and regulations will incorporate the latest developments and understanding in this important engineering/scientific discipline.

Therefore, to place the latest developments in context and elaborate on the global technical and social issues, this new second edition of the *Handbook* contains the following sections:

1. Introduction, in which all industrial methods of electricity generation worldwide are listed, including nonrenewable and renewable sources, with the emphasis on nuclear energy and its role in future electricity generation.
2. Part I, which is completely dedicated to six Generation-IV concepts: (1) Very high-temperature-reactor (VHTR); (2) Gas-cooled Fast Reactor (GFR) or just High Temperature Reactor (HTR); (3) Sodium-cooled Fast Reactor (SFR); (4) Lead-cooled Fast Reactor (LFR); (5) Molten Salt Reactor (MSR); and (6) SuperCritical Water-cooled Reactor (SCWR); and which begins with official information from the Generation IV International Forum (GIF).

^a Refers to reactors connected to electrical grids. This number includes 33 reactors left in Japan of which only 6 Pressurized Water Reactors (PWRs) are currently in operation as of November 3, 2022; however, more reactors are planned to be put into operation soon.

3. Part II, which is a summary of Generation-IV activities in the following countries: (1) United States; (2) European Union; (3) Japan; (4) South Korea; (5) China; and (6) India. (For developments in Russia, please refer to Chapter 12 of the first edition and also the latest developments presented in various chapters and Appendix A1 of this new edition.)
4. Part III, which is dedicated to related topics for Generation-IV reactors, including: Safety and risk assessment of advanced reactors; Nonproliferation for advanced reactors—political and social aspects; Thermal aspects of conventional and alternative fuels; Hydrogen production pathways for Generation-IV reactor technologies; Systems of advanced Small Modular Reactors (SMRs); Alternative power cycles for selected Generation-IV reactors; and Regulatory and licensing challenges with Generation-IV nuclear-energy systems.
5. Part IV, which is dedicated to nuclear-power technologies beyond Generation-IV concepts, i.e., the ITER fusion energy megaproject, the way to fusion energy.
6. Technical Appendices, which provide readers with additional information and data on current nuclear-power reactors and NPPs; thermophysical properties of reactor coolants; thermophysical properties of fluids at subcritical and critical/supercritical pressures; heat transfer and pressure drop in forced convection to fluids at supercritical pressures; world experience in nuclear steam reheat; and other topics.

In general, it should be noted that the first edition of *Handbook of Generation IV Nuclear Reactors* is also still quite a valuable source of previous years statistics, older designs of nuclear-power reactors and NPPs, and other important subjects.

Our editorial and author team contains top international experts in the corresponding nuclear-engineering areas from the following countries: 1. Belgium (2); 2. Canada (20); 3. China (2); 4. France (9); 5. Germany (2); 6. India (5); 7. Japan (5); 8. Russia (4); 9. South Korea (1); 10. Ukraine (6); 11. Switzerland (2); 12. United Kingdom (9); and 13. United States (5) (72 experts in total). Members of the editorial team are from academia, industry including nuclear vendors and NPPs, international organizations, government and research agencies, and scientific establishments.

We welcome you to the *Handbook of Generation IV Nuclear Reactors, Second Edition*, and we are looking forward to seeing your comments, suggestions, and criticisms to improve our future editions. Also, please enjoy reading the chapters and Appendices that follow.

This new edition of a unique international *Handbook* combines the history of development, research, industrial-operating experience, new designs, systems and safety analysis, and applications of nuclear energy, and includes many other related topics that help change the world and our lives for the better! It is recommended for a wide range of specialists within the areas of nuclear engineering, power engineering, mechanical engineering, environmental studies, and for undergraduate and graduate students of the corresponding faculties/departments as a textbook.

SUPPLEMENTARY DATA

Please find the supplementary appendices at the companion site: <https://www.elsevier.com/books-and-journals/book-companion/9780128205884>



Igor L. Pioro^b, Ph.D., Dr. Tech. Sc., P.Eng. (Ont.), Fellow ASME, CSME & EIC

Foreign Fellow of National Academy of Sciences of Ukraine

Professor, Editor-in-Chief of ASME Journal of Nuclear Engineering and Radiation Science

Department of Energy and Nuclear Engineering, Faculty of Engineering and Applied Science

Ontario Tech University (University of Ontario Institute of Technology); Oshawa, Ontario, Canada



**Romney B. Duffey^c, BSc., PhD., FASME, member INEA, ANS, SRE
Scientist and Author**

Idaho Falls, Idaho, United States

^b <https://engineering.ontariotechu.ca/people/ene/dr-igor-pioro.php> and <https://asmedigitalcollection.asme.org/nuclearengineering/article/8/1/010304/1122288>

^c <https://asmedigitalcollection.asme.org/nuclearengineering/article/8/3/030201/1140193>

Preface

The inspiration for creating a forum for international collaboration on advanced reactor research came out of a meeting in Washington, DC, in 2000. The nine founding members of the Generation IV International Forum (GIF) carefully set about establishing system performance goals, identifying six major development tracks from more than 100 competing concepts using a screening methodology along with four goal areas (sustainability, economics, safety and reliability, and proliferation resistance and physical protection), 15 criteria, and 24 metrics. Chartered in 2001, GIF formally began collaborative research in 2006 after a legal framework, a technology road map, and detailed initial project plans were completed.

The 2015 United Nations Climate Change Conference (COP21) helped highlight the essential role of nuclear energy in climate-friendly electricity production. The International Energy Agency (IEA) estimated that current global use of nuclear energy avoids 1.7 Gt of CO₂ emissions annually at that time. Going forward, in order for nuclear energy to meet its potential in abating climate change, new plants will employ advanced technology. Notably, the next generation of nuclear power systems will produce electricity at competitive prices and heat for industry use, e.g., hydrogen production, process heat, and seawater desalination, while assuring a concerned public that the issues of safety, waste management, proliferation resistance, and resource optimization have been satisfactorily addressed.

These concerns are the very issues that guide Generation IV research and development. When successfully deployed, the robust safety of Generation IV systems will assuage public anxiety and assure protection of capital investment. Coupled with an advanced fuel cycle, Generation IV reactors will reduce the volume of nuclear waste and improve uranium resource utilization by two orders of magnitude, without increasing proliferation risk.

This *Handbook of Generation IV Nuclear Reactors* is organized along the lines of the six systems originally selected by GIF in 2002 (and reaffirmed in 2022). It summarizes the collective progress made under the GIF banner as well as the status of development in countries with substantial advanced reactor and fuel cycle research and development programs. Both are important. The bulk of the global funding and effort goes into national programs, which ultimately produce costly prototypes and demonstrations that will lead to the commercialization of these systems. On the other hand, GIF fosters collaboration in the earlier stages of research and technology development by arranging joint projects and sharing key research facilities. GIF also takes the lead on developing criteria and guidelines for Generation IV designs and supports regulatory bodies in developing rational strategies for licensing advanced reactors. Collaboration with private sectors is also the current concern for early deployments of Generation IV systems.

GIF welcomes Elsevier's publication of this *Handbook of Generation IV Nuclear Reactors*, which is a significant addition to the growing body of literature on advanced nuclear power systems. A convenient overview of all Generation IV systems, it will meet the information needs of those who seek a basic familiarization as well as those who want a solid basis for further study. GIF congratulates the editor and Elsevier for undertaking this ambitious project.

Generation IV International Forum (GIF)

1

Introduction

1.1

Current status of electricity generation in the world

Igor L. Pioro^a, Romney B. Duffey^b, Pavel L. Kirillov^{c,*}, Lin Chen^d,
Constantin O. Zvorykin^e, Mark Tsai^a, and Hanqing Xie^a

^aFaculty of Energy Systems and Nuclear Science, University of Ontario Institute of Technology,
Oshawa, ON, Canada ^bIdaho Falls, ID, United States ^cState Scientific Centre of the Russian
Federation—Institute of Physics and Power Engineering (IPPE) named after A.I. Leipunsky, Obninsk,
Russia ^dInstitute of Engineering Thermophysics, Chinese Academy of Sciences & University of CAS,
Beijing, People’s Republic of China ^eNational Technical University of Ukraine “Igor Sikorsky Kiev
Polytechnic Institute”, Kyiv, Ukraine

Nomenclature

P Pressure, MPa

T Temperature, °C

Greek letters

η Thermal efficiency, %

Subscripts

cr critical

el electrical

f force

gr gross

in inlet

out outlet

sat saturation

* Professor P.L. Kirillov has participated in preparation of this Chapter, unfortunately, he has passed away on October 10, 2021 (for details, see <https://asmedigitalcollection.asme.org/nuclearengineering/issue/8/2>).

Abbreviations

AC	Alternative Current
BWR	Boiling Water Reactor
CANDU	CANada Deuterium Uranium
CAR	Central African Republic
CCGT	Combined Cycle Gas Turbine
CCUS	Carbon Capture, Utilization and Storage
CPV	Concentrated PhotoVoltaic
DOE	Department Of Energy (USA)
EEC	Electrical Energy Consumption
EI	Education Index
EI	Electricity
EPR	European Power Reactor
EU	European Union
HDI	Human Development Index
hp	horse power
IEA	International Energy Agency
II	Income Index
LCOE	Levelized Cost Of Energy
LED	Light Emitting Diode
LEI	Life Expectancy Index
LNG	Liquefied Natural Gas
Ltd	Limited
LTO	Long-Term Operation
LWR	Light-Water Reactor
M	Million or Mega
MHI	Mitsubishi Heavy Industries
NASA	National Aeronautics and Space Administration (USA)
NEA	Nuclear Energy Agency
NOAA	National Oceanic and Atmospheric Administration
NPP	Nuclear Power Plant
NY	New York
O&M	Operation & Maintenance
OECD	Organization for Economic Co-operation and Development
OPG	Ontario Power Generation (Canada)
PHES	Pumped Hydro-electric Energy Storage
PHWR	Pressurized Heavy-Water Reactor
PSH	Pumped-Storage Hydro-electricity
PSHEPP	Pumped-Storage Hydro-Electric Power Plant
PV	PhotoVoltaic
PWR	Pressurized Water Reactor
Q	Quarter
REG	Recovered Energy Generation
Rep.	Republic
S.	South
SAR	Syrian Arabic Republic
SCR	Selective Catalytic Reduction
SFR	Sodium Fast Reactor
SMR	Small Modular Reactor
UAE	United Arab Emirates
UK	United Kingdom
US	United States
USA	United States of America
USSR	Union of Soviet Socialists Republics
VVER	Water-Water Power Reactor (in Russian abbreviation)

1.1.1 Electricity generation in the world

This chapter is a logical continuation of our previous publications on this topic (Pioro et al., 2016, 2020, 2022; Pioro and Duffey, 2015, 2019; Pioro, 2012).

It is well known that electricity generation and consumption are the key factors for advances in industry, agriculture, technology, and the standard of living (see Table 1.1.1, Figure 1.1.1, and Appendix A8, Tables A8.1.1–A8.1.3). Also, a strong power industry with diverse energy sources is very important for a country's independence.

Table 1.1.1 lists selected countries in all four categories of Human Development Index (HDI), i.e., (1) very high HDI (65 countries); (2) high HDI (54 countries); (3) medium HDI (36 countries); and (4) low HDI (33

Table 1.1.1. Population (<https://www.worldometers.info/world-population/population-by-country/>), Electrical Energy Consumption (EEC) (https://en.wikipedia.org/wiki/List_of_countries_by_electricity_consumption), and Human Development Index (HDI) (<http://hdr.undp.org/en/content/latest-human-development-index-ranking>) in the world and selected countries (for exact details on years, see original sources)

HDI ^a Rank (2019)	Country	HDI ^a (2019)	EEC ^b (2018–2019)		Population in millions (2019)
			W/Capita	GWh	
Very high HDI (65 countries)					
1	Norway	0.957	2648	124,130	5.35
2	Switzerland	0.955	750	56,350	8.57
4	Iceland	0.949	5898	18,680	0.36
6	Germany	0.947	719	524,270	83.20
7	Sweden	0.945	1462	131,800	10.29
8	Australia	0.944	1084	241,020	25.36
13	United Kingdom (UK)	0.932	513	300,520	66.80
16	Canada	0.929	1706	549,260	37.53
17	United States of America (USA)	0.926	1387	3,989,570	328.20
19	Japan	0.919	816	902,840	126.86
23	South Korea	0.916	1163	527,040	51.71
26	France	0.901	765	449,420	66.98
31	United Arab Emirates (UAE)	0.890	1395	119,460	9.77
40	Saudi Arabia	0.854	1073	322,370	33.41
52	Russia	0.824	763	965,160	146.70
64	Kuwait	0.806	1607	59,280	4.21

Continued

Table 1.1.1. Population (<https://www.worldometers.info/world-population/population-by-country/>), Electrical Energy Consumption (EEC) (https://en.wikipedia.org/wiki/List_of_countries_by_electricity_consumption), and Human Development Index (HDI) (<http://hdr.undp.org/en/content/latest-human-development-index-ranking>) in the world and selected countries (for exact details on years, see original sources)—cont'd

HDI Rank (2019)	Country	HDI (2019)	EEC (2018–2019)		Population in millions (2019)
			W/Capita	GWh	
High HDI (54 countries)					
74	Ukraine	0.779	331	128,810	44.39
84	Brazil	0.765	323	597	210.00
85	China	0.761	527	7,225,500	1427.65
99	<i>World</i>	<i>0.737</i>	<i>350</i>	<i>23,398,000</i>	<i>7800.00</i>
Medium HDI (36 countries)					
131	India	0.645	107	1,547,000	1384.66
Low HDI (33 countries)					
160	Rwanda	0.543	7	760	12.63
175	Guinea-Bissau	0.480	2	40	1.92
180	Eritrea	0.459	14	410	3.21
182	Sierra Leone	0.452	4	240	7.81
185	Burundi	0.433	3	340	11.53
185	South Sudan	0.433	5	530	11.06
187	Chad	0.398	2	210	15.95
188	Central African Rep. (CAR)	0.397	3	140	4.75
189	Niger	0.394	8	1590	22.31

^a HDI—Human Development Index by United Nations (UN); HDI is a comparative measure of **life expectancy**, **literacy**, **education** and **standards of living** for **countries** worldwide. HDI is calculated by the following formula: $HDI = \sqrt[3]{LEI \times EI \times II}$, where LEI—Life Expectancy Index, EI—Education Index, and II—Income Index. It is used to distinguish whether the country is a **developed**, a **developing** or **an underdeveloped country**, and also to measure the impact of economic policies on quality of life. Countries fall into four broad human-development categories: (1) very high, 65 countries; (2) high, 53; (3) medium, 36; and (4) low, 33 (Wikipedia, 2019).

$$^b \text{EEC, } \frac{W}{\text{Capita}} = \frac{\left(\text{EEC, } \frac{\text{TWh}}{\text{year}} \right) \times \frac{10^{12}}{365 \text{ days} \times 24 \text{ h}}}{(\text{Population, Millions}) \times 10^6}$$

Data for all countries in the world are listed in Appendix A8, Tables A8.1.1–A8.1.3. In bold—highest values for countries; world data—in italic.

countries), in total, 188 countries of the world plus average data for the whole world. Together with HDI, **Table 1.1.1.** contains data on Electrical Energy Consumption (EEC) in W/Capita and in GWh, and Population in millions. The corresponding formulas for HDI and EEC are provided right below **Table 1.1.1.** It should be noted that such data are usually related to 2 to 3 years prior to the current year.

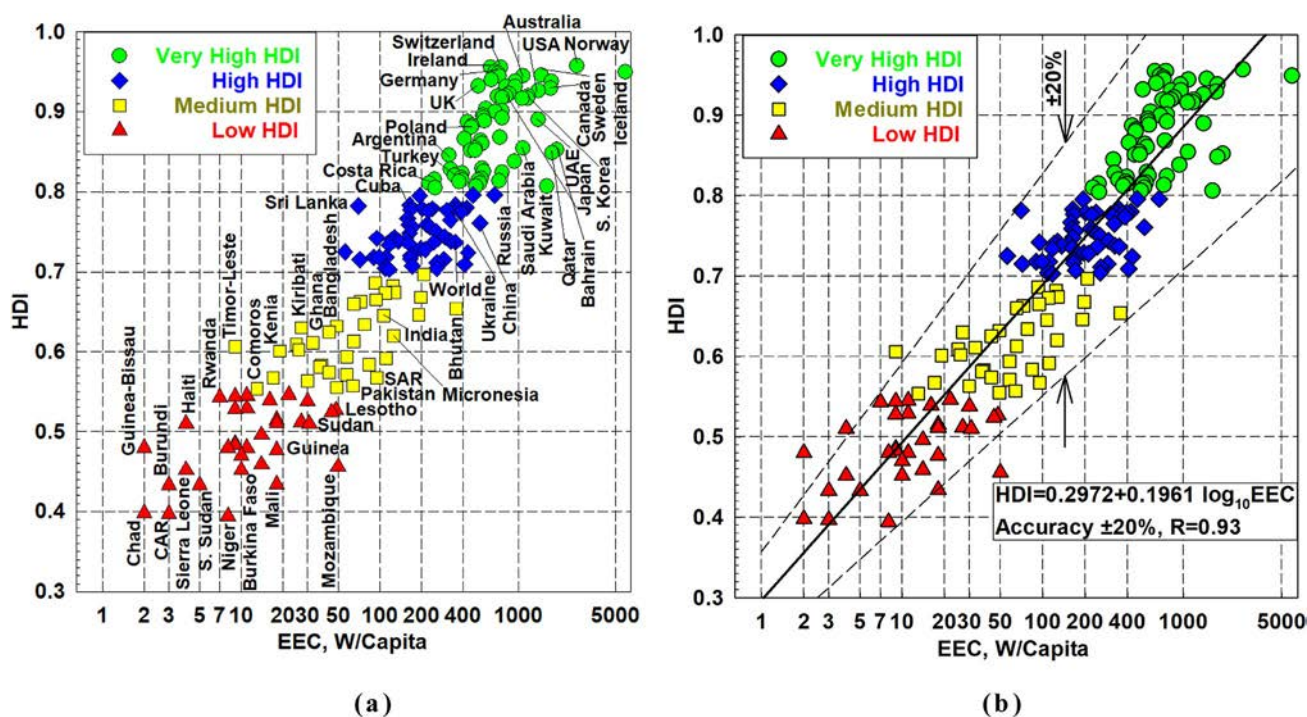


Figure 1.1.1. Electrical-Energy Consumption (EEC) (W/Capita) vs Human Development Index (HDI) for all countries of the world (based on data from Appendix A8, Table A8.1.1.): (a) graph with selected countries shown and (b) HDI correlation (in general, the HDI correlation might be an exponential rise to maximum (1), but based on the current data it is a straight line in regular–logarithmic coordinates)

In Appendix A8.1, Tables A8.1.1–A8.1.3 list HDI, EEC, and Population data for all countries in the world and the world average. To emphasize their importance, Table A8.1.1 is ranked based on decreasing HDI values; Table A8.1.2 based on decreasing EEC (TWh) values; and Table A8.1.3 based on decreasing EEC (W/Capita) values.

It was found that HDI has strong dependence on EEC (W/Capita) (see Figure 1.1.1). In Figure 1.1.1: HDI has a linear scale, and EEC is a logarithmic with base 10. In Figure 1.1.1b: The corresponding correlation is provided, which fits all data with the uncertainty of $\pm 20\%$. Based on this correlation it is clear that to be in the group of countries with: (a) very high HDI the minimum HDI value should be ~ 400 W/Capita (however, in reality, we have the range of 227–5900 W/Capita); (b) for high HDI should be ~ 100 W/Capita (actual range is 56–674 W/Capita); (c) for medium HDI should be ~ 20 W/Capita (actual range is 9–207 W/Capita); and (d) for low HDI the actual range is 2–50 W/Capita.

More or less everybody knows the standards or level of living we have within very high HDI 65 countries. To understand what 2 W per person means in a country, we can make a comparison that this power equals approximately only one mini or small LED (Light Emitting Diode) bulb, implying that there is absolutely no possibility for modern education, agriculture, industry, and level of living conditions! Of course, while government buildings; embassies; wealthy people; diamond, gold, and platinum mines; property owners; etc. have electricity, but, actually, the rest of the population is living without it! And vast majority of Low HDI countries are located in Africa (see Table A8.1.1), but “energy poverty” also occurs among minority populations, refugees, and resource-deprived communities in many countries and regions of social disparity.

In support of our statements above, Figure 1.1.2 shows a composite image of a global view of our planet Earth at night, which was compiled from over 400 satellite images (Image Credit: NASA/NOAA). In general, more lights at night means higher EEC values (W/Capita) and corresponding to that higher HDI values. However, we have to take into consideration also the density of population (see Table 1.1.2) and its

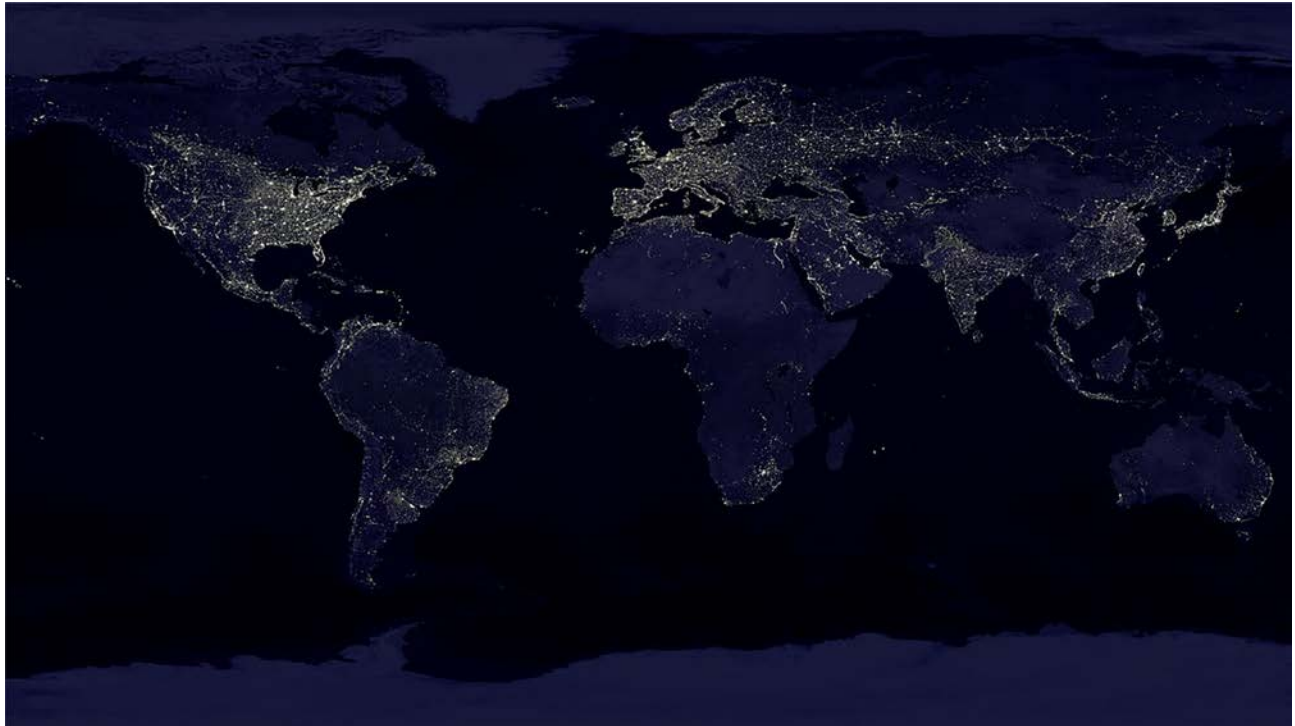


Figure 1.1.2. This composite image shows a global view of Earth at night, which was compiled from over 400 satellite images. (For selected general data on world population, see Table 1.1.2 and for detailed data by countries of the world—see Appendix A8, Table A8.1.1.) *Image Credit: NASA/NOAA. Last Updated: Aug. 4, 2017. Editor: NASA Content Administrator: https://www.nasa.gov/topics/earth/earthday/gall_earth_night.html*

Table 1.1.2. World population and other related data

No.	Region	Population (urban, %) Millions	% of world population %	Area Million km ²	Population density People/ km ²	Median age Years
0	World	7890 (56%)	100	148.940	52	31
1	Africa	1378 (44%)	16.7	29.648	45	20
2	America Latin + Caribbean	661 (83%)	8.4	20.139	32	31
3	America Northern	372 (83%)	4.7	18.652	20	39
4	Asia	4687 (51%)	59.8	31.033	150	32
5	Europe	748 (75%)	9.8	22.135	34	43
6	Oceania (Australia, New Zealand, etc.)	43 (68%)	0.5	8.486	5	33

(Based on data from August 30, 2021) by regions (<https://www.worldometers.info/population/>).

non-homogeneous distribution inside a country. As an example, Canada despite being an “industrially developed” country with high EEC and HDI values (1706 W/Capita and Rank 16), has the vast majority of population concentrated along the busy trading boarder with the Unites States. Therefore, the Canadian North is dark in this figure. In the same way, Australia is one of the top countries in the world by HDI value (Rank 8 and 1084 W/Capita); however, the vast majority of population is located on the East coast of the continent. Therefore, all the central part of this huge island continent is completely dark! At the opposite extreme, the continent of Africa consists of many countries within a population of about 1378 million people (~16.7% of the world), but only in a limited number of regions and cities we can see lights mainly located in the coastal areas of this continent. The rest of the continent with many people living there is almost completely without electricity and the transport, facilities, and industrial development that it enables.

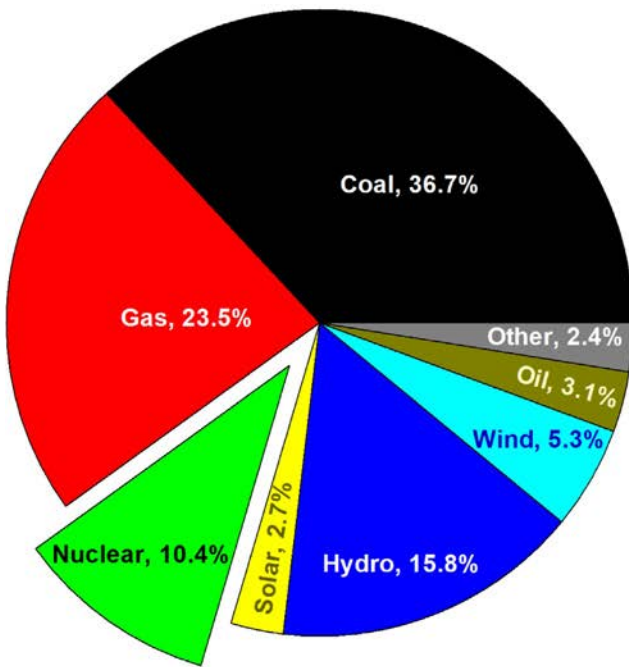
In general, electricity (see [Figure 1.1.3](#)) can be mainly generated from: (1) non-renewable energy sources such as coal, natural gas, oil, and nuclear; and (2) renewable energy sources such as hydro, biomass, wind, geothermal, solar, and marine power.

Today, the main sources for global electrical-energy generation (see [Figure 1.1.3a](#)) are: (1) Thermal power—primarily using coal (36.7%) and secondarily using natural gas (23.5%); (2) “Large” hydroelectric power plants (15.8%); and (3) Nuclear power (10.4%). The last 13.6% of the electrical energy is generated using oil (3.1%), and the remainder (10.5%)—from intermittent wind (5.3%), solar (2.7%), and from biomass, geothermal, and marine energy (2.5%). Main sources for electrical-energy generation in selected countries are also shown in [Figures 1.1.3b–y](#).

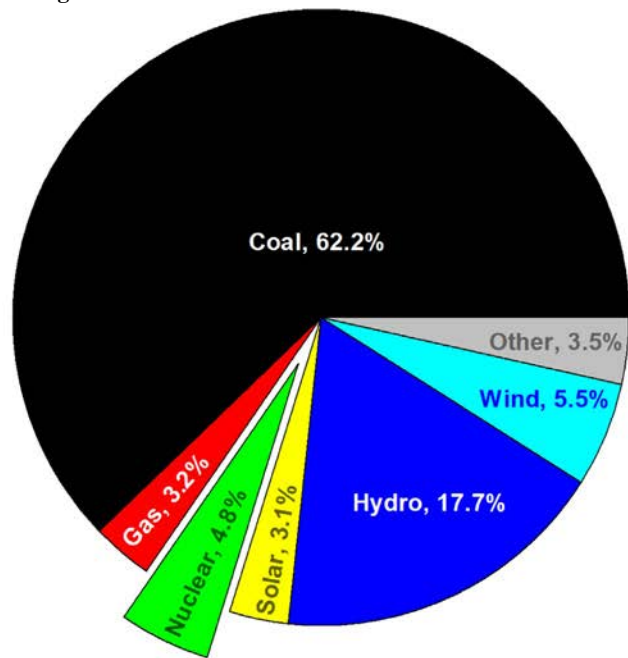
[Figures 1.1.3b–v](#) show sector diagrams for the largest countries by population in the world located by the decreasing population. [Figures 1.1.3w–y](#) show sector diagrams of countries with quite unusual combination of electrical-energy sources. In addition to [Figures 1.1.3a–y](#) with the sector diagrams, [Table 1.1.3](#) lists electricity generation in the world and selected countries by source (data on the world and 13 countries with the largest installed capacities of nuclear-power reactors).

Analysis of the data shown in these sector diagrams (see [Figure 1.1.3](#)) shows that the world (~37%) ([Figure 1.1.3a](#)) and, especially, countries with the largest population, i.e., China (~62%) ([Figure 1.1.3b](#)), and India (~71%) ([Figure 1.1.3c](#)), as well as Indonesia (~59%) ([Figure 1.1.3e](#)), Turkey ([Figure 1.1.3j](#)), Germany (~30%) ([Figure 1.1.3l](#)), South Korea (~40%) (see [Figure 1.1.3p](#)), and Poland (~74%) ([Figure 1.1.3t](#)) rely heavily on coal for electricity generation! The USA (~37%) ([Figure 1.1.3d](#)), Russia (~46%) ([Figure 1.1.3g](#)), Mexico (~60%) ([Figure 1.1.3h](#)), Japan (~34%) ([Figure 1.1.3i](#)), Iran (~73%) ([Figure 1.1.3k](#)), UK (~41%) (see [Figure 1.1.3m](#)), Italy (~49%) ([Figure 1.1.3o](#)), Spain (~31%) ([Figure 1.1.3q](#)), Saudi Arabia (~58%) ([Figure 1.1.3v](#)), and UAE (~98%) ([Figure 1.1.3x](#)) use mainly natural gas or Liquefied Natural Gas (LNG) (Japan) for electricity generation, which is better than to use coal, but still for now we cannot avoid emission of carbon dioxide. On opposite, France (~70%) ([Figure 1.1.3n](#)), Ukraine (~55%) ([Figure 1.1.3s](#)), and Sweden (~40%) ([Figure 1.1.3w](#)) heavily rely on nuclear power, which is, in general, the lowest emitter of carbon dioxide compared to all other electricity-generating sources including renewables (for details, see [Section 1.1.2](#) of this chapter). Brazil (~64%) ([Figure 1.1.3f](#)), Canada (~58%) ([Figure 1.1.3u](#)), and Iceland (~71%) heavily rely on hydro electricity generation due to their unique geographical location. Four European countries: Germany (~20%) ([Figure 1.1.3l](#)), UK (~20%) ([Figure 1.1.3m](#)), Spain (~20%) ([Figure 1.1.3q](#)), and Italy (~16%) ([Figure 1.1.3o](#)) quite substantially rely of wind power. Solar energy is quite popular in Japan (~7%) ([Figure 1.1.3i](#)), in Germany (~8%) ([Figure 1.1.3l](#)), in Italy (~8%) ([Figure 1.1.3o](#)), and in Spain (~6%) ([Figure 1.1.3q](#)). It is interesting to note that among all these countries shown in [Figure 1.1.3](#), Iceland is the leader in using geothermal energy for electricity generation (~29%) ([Figure 1.1.3y](#)). In addition, Iceland is the only one country from all mentioned above, actually, ~100% rely on renewable energy sources such as hydro (71%) and geothermal (29%)! And again, this is only due to absolutely unique location with rivers, many volcanoes and very active geothermal sources. That is why Iceland is the world leader in the EEC value (~5900 W/Capita and HDI Rank 4), which

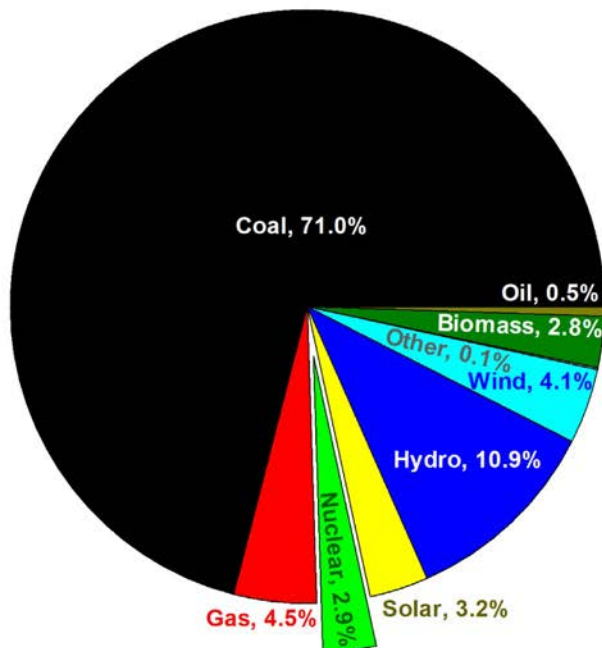
(a) World: Population 7,871 millions; EEC 350 W/Capita; and HDI Rank 99.



(b) China: Population 1,439 millions; EEC 527 W/Capita; and HDI Rank 85; 13.1% of world coal reserves and 2.7% - of gas.



(c) India: Population 1,380 millions; EEC 107 W/Capita; and HDI Rank 131; 9.5% of world coal reserves.



(d) USA: Population 331 millions; EEC 1,387 W/Capita; and HDI Rank 17; 22.3% of world coal reserves and 7.6% - of gas.

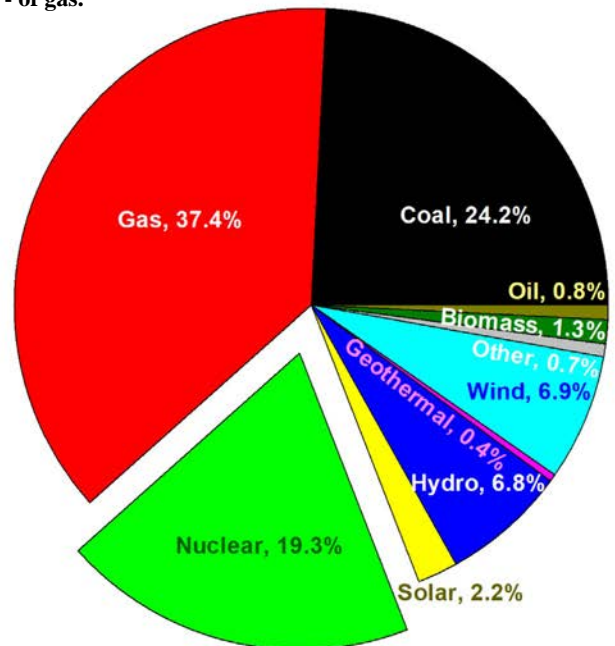
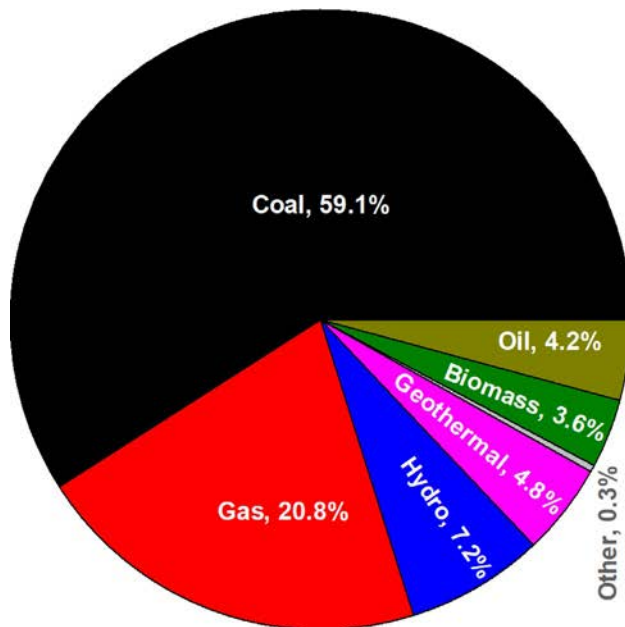


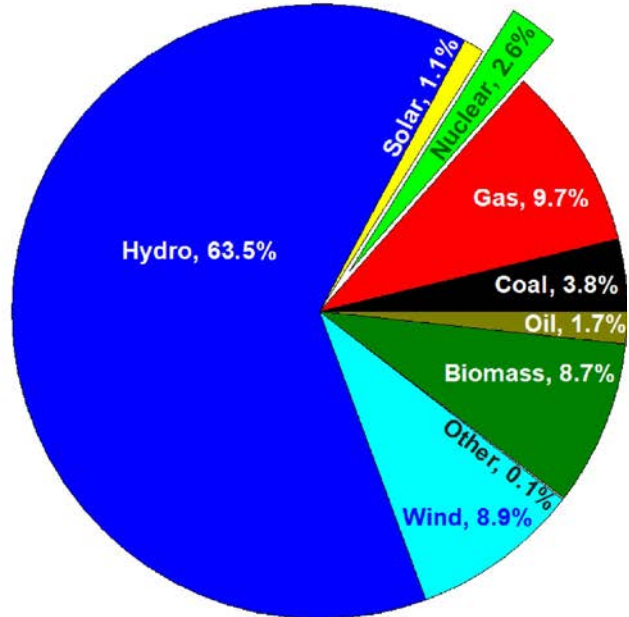
Figure 1.1.3. Electricity generation by source in the world and selected countries (data on the world and 23 countries are located by decreasing population). Population from <https://www.worldometers.info/world-population/population-by-country/> (June 2021); EEC from https://en.wikipedia.org/wiki/List_of_countries_by_electricity_consumption (2018–2019); HDI from <http://hdr.undp.org/en/content/latest-human-development-index-ranking> (2019); and the rest of the data (2019) are from: <https://www.iea.org/data-and-statistics/data-browser/?country=WORLD&fuel=Energy%20supply&indicator=TPESbySource>. (a) World: Population 7871 million; EEC 350 W/Capita; and HDI Rank 99. (b) China: Population 1439 million; EEC 527 W/Capita; and HDI Rank 85; 13.1% of world coal reserves and 2.7% of gas. (c) India: Population 1380 million; EEC 107 W/Capita; and HDI Rank 131; 9.5% of world coal reserves. (d) USA: Population 331 million; EEC 1387 W/Capita; and HDI Rank 17; 22.3% of world coal reserves and 7.6% of gas.

(Continued)

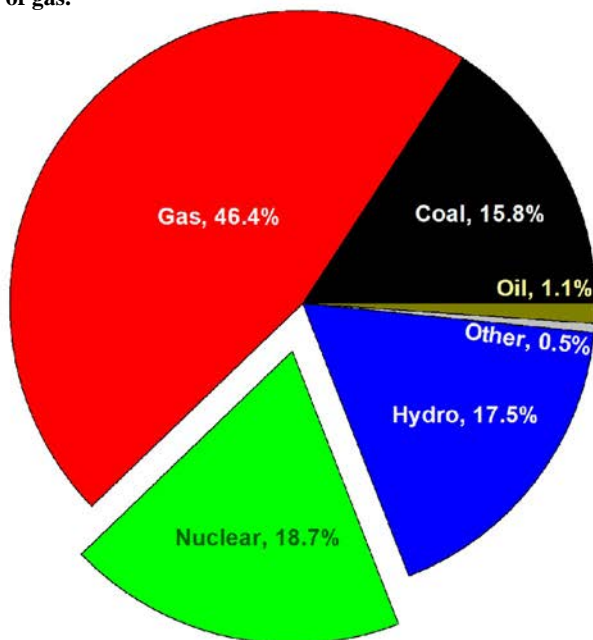
(e) Indonesia: Population 274 millions; EEC 111 W/Capita, and HDI Rank 107; 2.2% of world coal reserves.



(f) Brazil: Population 213 millions; EEC 323 W/Capita; and HDI Rank 84; 0.6% of world coal reserves.



(g) Russia: Population 146 millions; 763 W/Capita; and HDI Rank 52; 15.5% of world coal reserves and 23.4% - of gas.



(h) Mexico: Population 129 millions; 240 W/Capita; and HDI Rank 74.

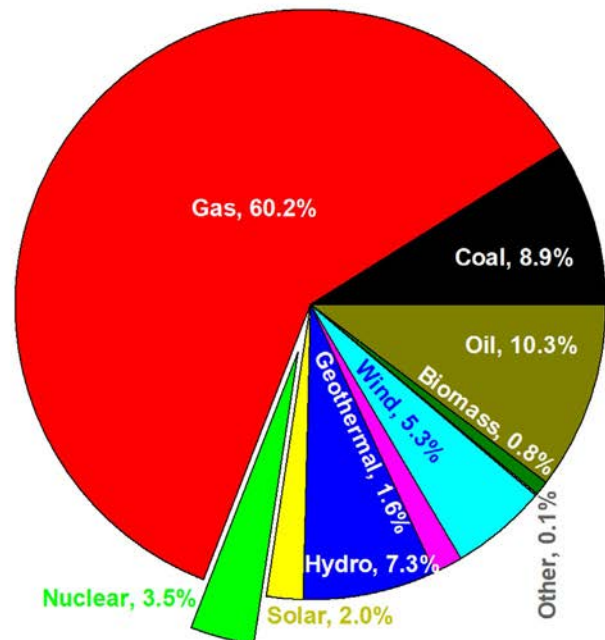
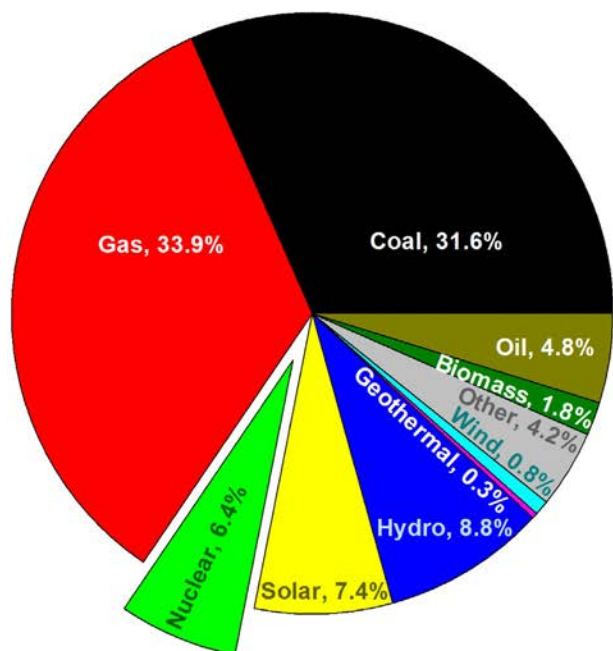


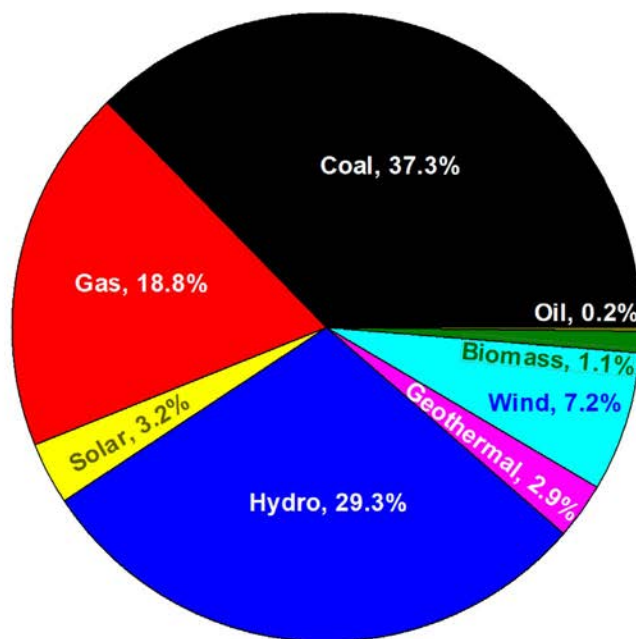
Figure 1.1.3, Cont'd (e) Indonesia: Population 274 million; EEC 111 W/Capita, and HDI Rank 107; 2.2% of world coal reserves. (f) Brazil: Population 213 million; EEC 323 W/Capita; and HDI Rank 84; 0.6% of world coal reserves. (g) Russia: Population 146 million; 763 W/Capita; and HDI Rank 52; 15.5% of world coal reserves and 23.4% of gas. (h) Mexico: Population 129 million; 240 W/Capita; and HDI Rank 74.

(Continued)

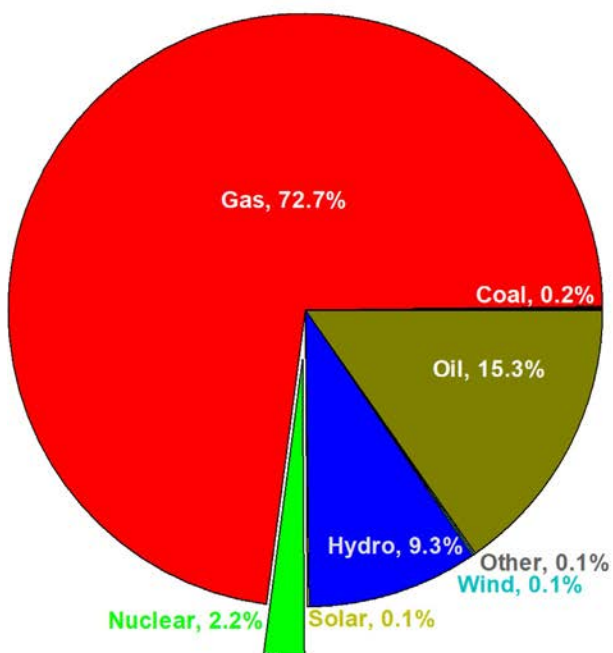
(i) Japan: Population 126 millions; 816 W/Capita; and HDI Rank 19.



(j) Turkey: Population 84 millions; 344 W/Capita; and HDI Rank 54; 1.1% of world coal reserves.



(k) Iran: Population 84 millions; EEC 350 W/Capita; and HDI Rank 70; 16.5% of world gas reserves.



(l) Germany: Population 84 millions; 719 W/Capita; and HDI Rank 6; 3.5% of world coal reserves.

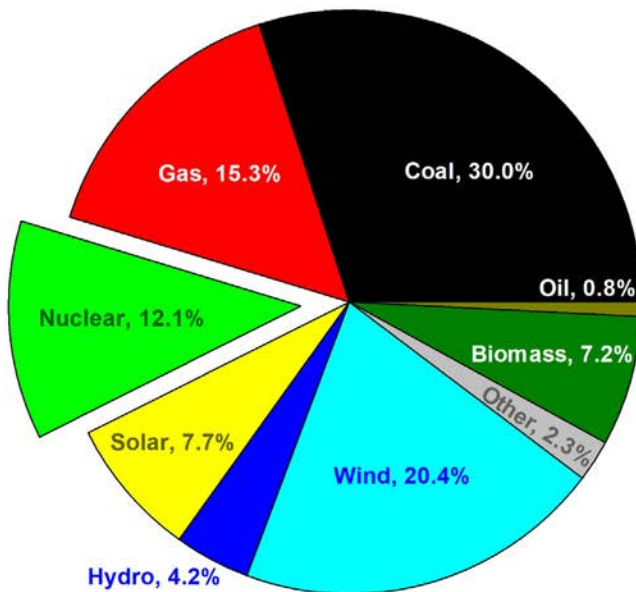
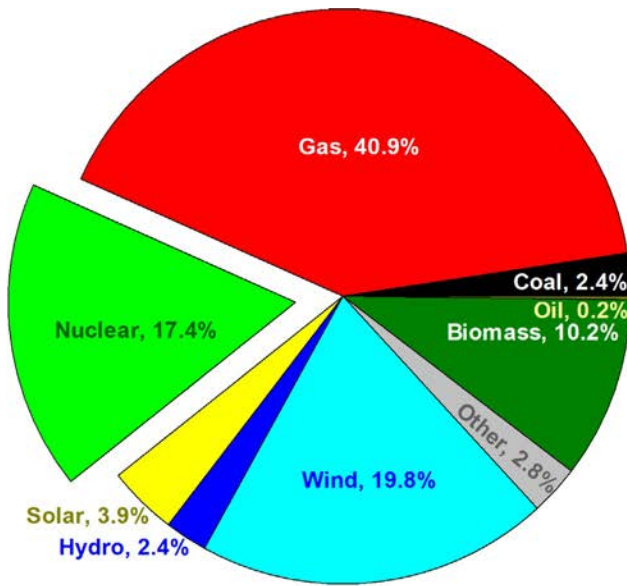


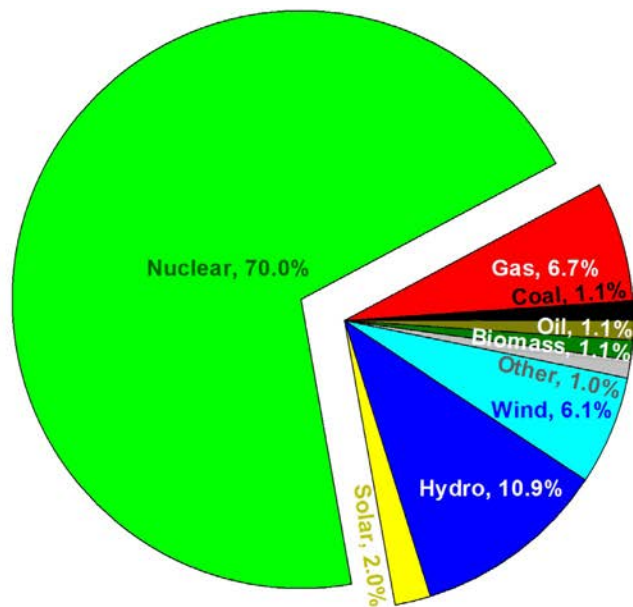
Figure 1.1.3, Cont'd (i) Japan: Population 126 million; 816W/Capita; and HDI Rank 19. (j) Turkey: Population 84 million; 344 W/Capita; and HDI Rank 54; 1.1% of world coal reserves. (k) Iran: Population 84 million; EEC 350 W/Capita; and HDI Rank 70; 16.5% of world gas reserves. (l) Germany: Population 84 million; 719 W/Capita; and HDI Rank 6; 3.5% of world coal reserves.

(Continued)

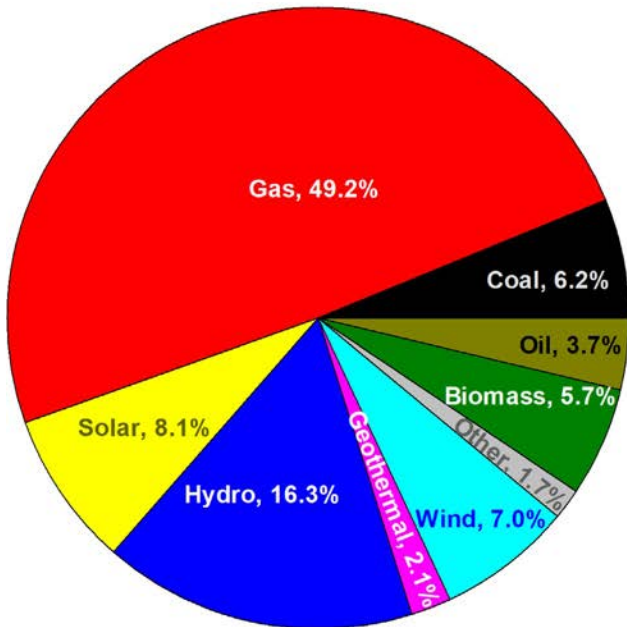
(m) UK: Population 68 millions; 513 W/Capita; and HDI Rank 13.



(n) France: Population 65 millions; 765 W/Capita; and HDI Rank 26.



(o) Italy: Population 60 millions; 562 W/Capita; and HDI Rank 29.



(p) S. Korea: Population 51 millions; 1163 W/Capita; and HDI Rank 23.

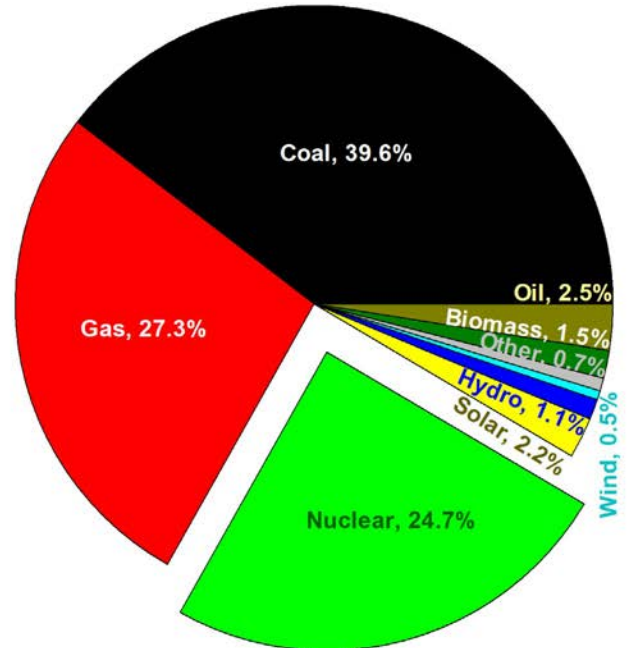
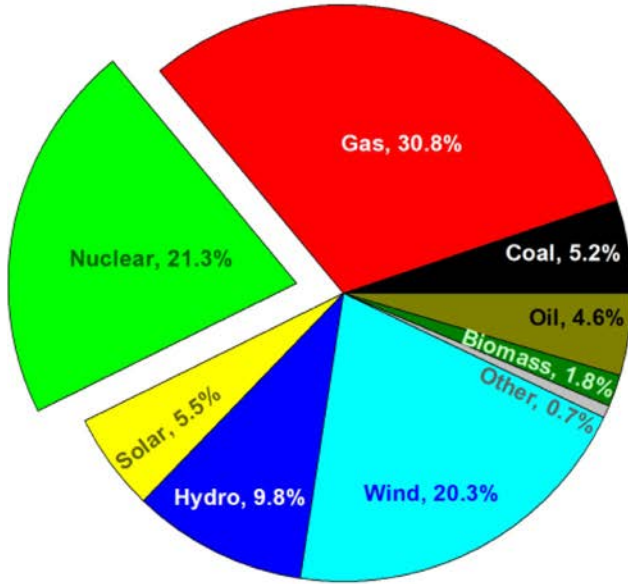


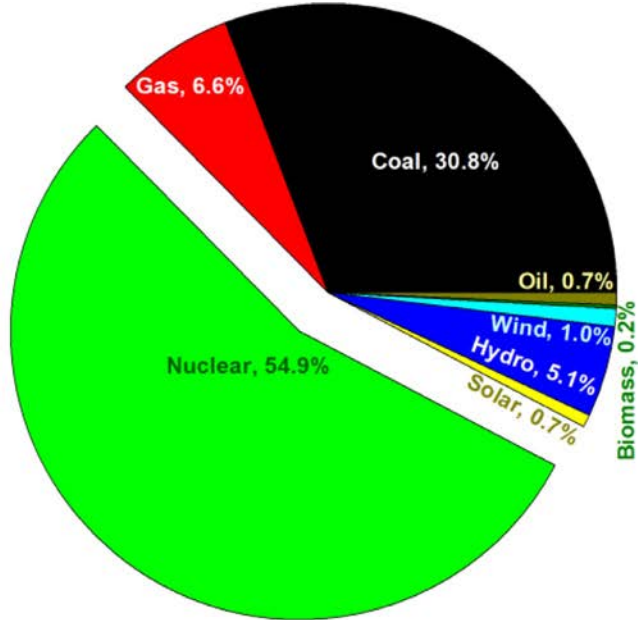
Figure 1.1.3, Cont'd (m) UK: Population 68 million; 513 W/Capita; and HDI Rank 13. (n) France: Population 65 million; 765 W/Capita; and HDI Rank 26. (o) Italy: Population 60 million; 562 W/Capita; and HDI Rank 29. (p) S. Korea: Population 51 million; 1163 W/Capita; and HDI Rank 23.

(Continued)

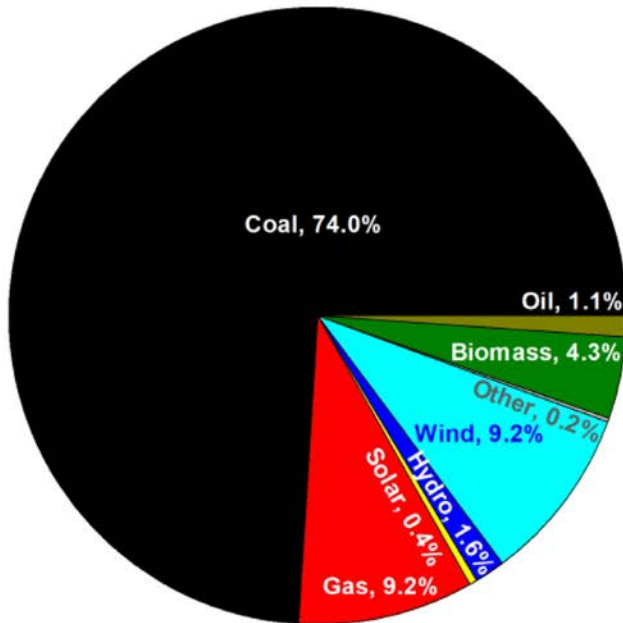
(q) Spain: Population 47 millions; 585 W/Capita; and HDI Rank 25.



(s) Ukraine: Population 44 millions; 331 W/Capita; and HDI Rank 74; 3.3% of world coal reserves.



(t) Poland: Population 38 millions; 458 W/Capita; and HDI Rank 35; 2.5% of world coal reserves.



(u) Canada: Population 38 millions; EEC 1706 W/Capita; and HDI Rank 16; 0.6% of world coal reserves and 1.0% of gas.

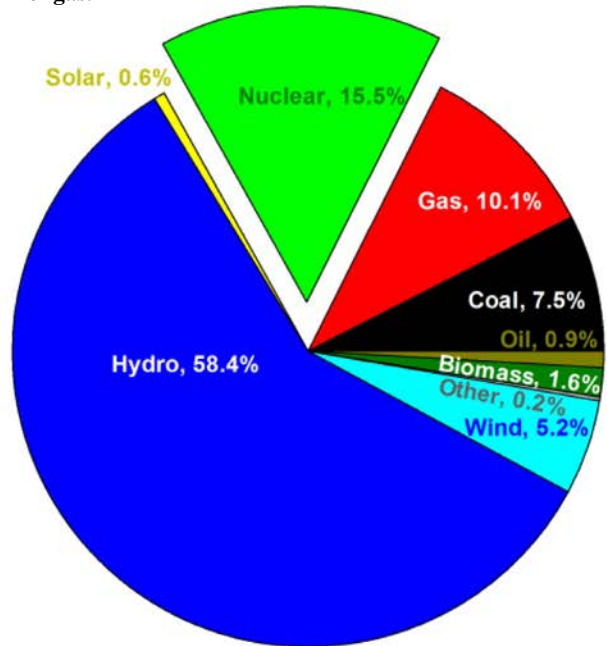
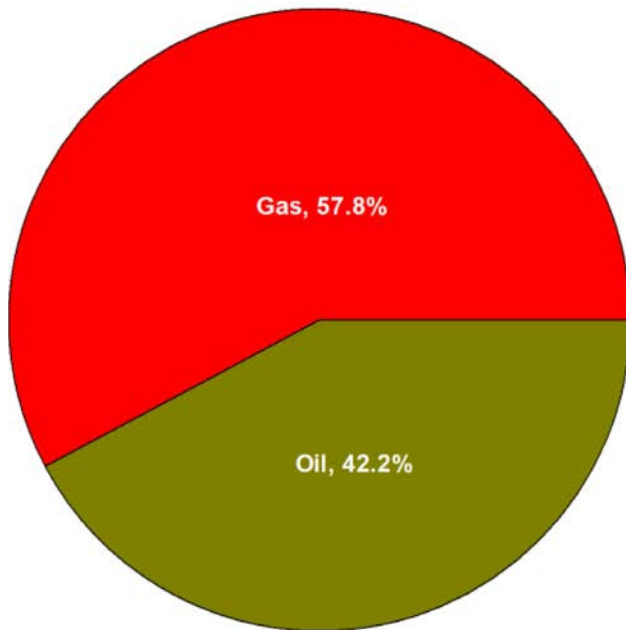


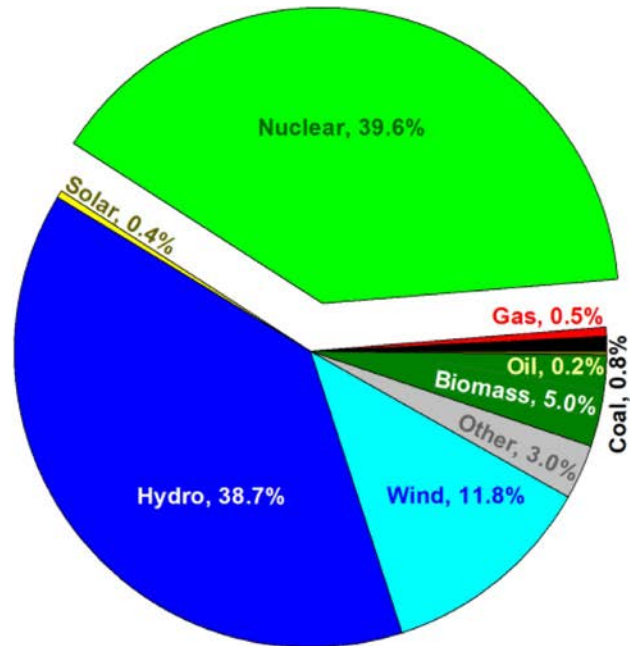
Figure 1.1.3, Cont'd (q) Spain: Population 47 million; 585 W/Capita; and HDI Rank 25. (s) Ukraine: Population 44 million; 331 W/Capita; and HDI Rank 74; 3.3% of world coal reserves. (t) Poland: Population 38 million; 458 W/Capita; and HDI Rank 35; 2.5% of world coal reserves. (u) Canada: Population 38 million; EEC 1706 W/Capita; and HDI Rank 16; 0.6% of world coal reserves and 1.0% of gas.

(Continued)

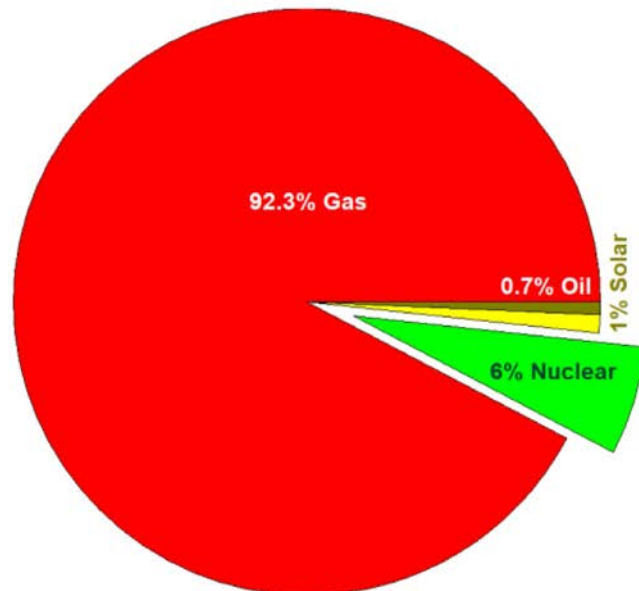
(v) Saudi Arabia: Population 35 millions; EEC 1073 W/Capita; and HDI Rank 40; 4.5% of world gas reserves.



(w) Sweden: Population 10 millions; EEC 1462 W/Capita; and HDI Rank 7.



(x) UAE: Population 10 millions; EEC 1395 W/Capita; and HDI Rank 31; 3.0% of world gas reserves.



(y) Iceland: Population 0.34 millions; EEC 5898 W/Capita; and HDI Rank 4.

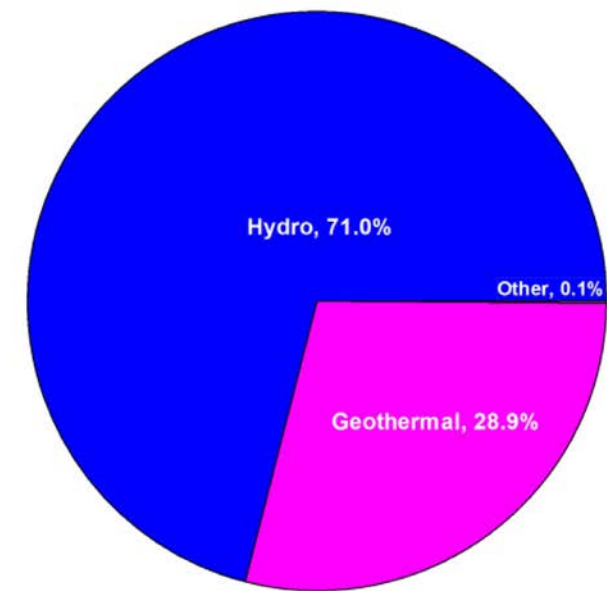


Figure 1.1.3, Cont'd (v) Saudi Arabia: Population 35 million; EEC 1073 W/Capita; and HDI Rank 40; 4.5% of world gas reserves. (w) Sweden: Population 10 million; EEC 1462 W/Capita; and HDI Rank 7. (x) UAE: Population 10 million; EEC 1395 W/Capita; and HDI Rank 31; 3.0% of world gas reserves. (y) Iceland: Population 0.34 million; EEC 5898 W/Capita; and HDI Rank 4

Table 1.1.3. Electricity generation in the world and selected countries by source (data on the world and 13 countries with largest installed capacities of nuclear-power reactors are located by decreasing population) (in bold—highest values for countries; in *Italic*—lowest values) (data from 2018 to 2019)

No	Country	World	China	India	USA	Russia	Japan	Germany	UK	France	S. Korea	Spain	Ukraine	Canada	Sweden
–		0	1	2	3	4	5	6	7	8	9	10	11	12	13
–		Population, EEC, and HDI per country													
1	Population, M	7871	1439	1380	331	146	126	84	68	65	51	47	44	38	<i>10</i>
2	EEC TWh/year	23,398	7226	1547	3990	965	903	524	301	449	527	242	<i>129</i>	549	132
3	W/Capita	350	<i>527</i>	<i>107</i>	1387	763	816	719	513	765	1163	585	331	1706	1462
4	HDI Total	0.737	0.761	<i>0.645</i>	0.926	0.824	0.919	0.947	0.932	0.901	0.916	0.904	0.779	0.929	0.945
5	Rank	99	85	<i>131</i>	17	52	19	6	13	26	23	25	74	16	7
–	El.-Gen. Sources	Non-renewable													
1	Coal	36.7	62.2	71.0	24.2	15.8	31.6	29.3	2.4	<i>1.1</i>	39.6	5.2	30.8	7.5	0.8
2	Gas	23.5	3.2	4.5	37.4	46.4	33.9	10.5	40.9	6.7	27.3	30.8	6.6	10.1	<i>0.5</i>
3	Nuclear	10.4	4.8	2.9	19.3	18.7	6.4	13.7	17.3	70.0	24.7	21.3	54.9	15.5	39.6
4	Oil	3.1	–	0.5	0.8	1.1	4.8	–	0.3	1.1	2.4	4.6	0.8	0.9	0.2
–	–	Renewable													
1	Hydro	15.8	17.7	10.9	6.8	17.5	8.8	3.8	2.4	10.9	<i>1.1</i>	9.8	5.1	58.4	38.7
2	Wind	5.3	5.5	4.1	6.9	–	0.8	24.5	19.8	6.1	0.5	20.3	1.0	5.2	11.8
3	Solar	2.7	3.1	3.2	2.2	–	7.4	9.1	3.9	2.0	2.2	5.5	0.7	0.6	0.4
4	Geothermal	2.5	–	–	0.4	–	0.3	–	–	–	–	–	–	–	–
5	Biomass	–	–	2.8	1.3	–	1.8	8.6	10.2	1.1	1.5	1.8	0.1	1.6	5.0
–	–	Other													
1	Other	–	3.5	0.1	0.7	0.5	4.2	0.5	2.8	1.0	0.7	0.7	–	0.2	3.0

Population from <https://www.worldometers.info/world-population/population-by-country/> (June 2021); EEC from https://en.wikipedia.org/wiki/List_of_countries_by_electricity_consumption (2018–2019); HDI from <http://hdr.undp.org/en/content/latest-human-development-index-ranking> (2019); and the rest of the data (2019) are from: <https://www.iea.org/data-and-statistics/data-browser/?country=WORLD&fuel=Energy%20supply&indicator=TPESbySource>.

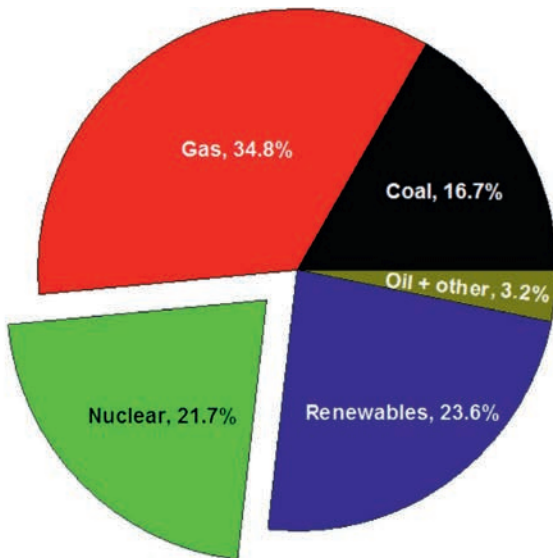
is way above the closest competitor—Norway with EEC value of ~ 2650 W/Capita and HDI Rank 1 (see [Tables 1.1.1](#) and [A8.13](#)). And in the case of Norway, which also has a unique location, due to that heavily rely on hydro power (92%)!

A selected comparison of the data presented in [Figure 1.1.3](#) with those data presented in our previous publication—Handbook (Edition 1) ([Pioro, 2016](#)) ([Figure 1.1.2](#)) (data on population from 2015; electrical-energy generation and EEC—from 2012 to 2014; and HDI from 2014) shows that:

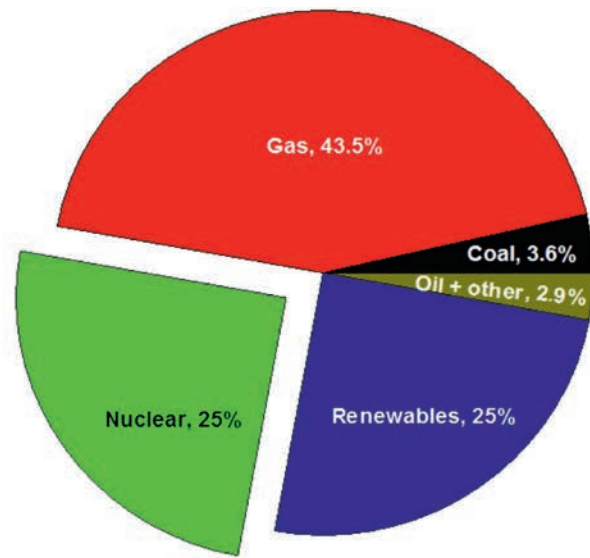
1. World usage of coal and oil for electricity generation has slightly decreased, i.e., coal from 39.9% to 36.7% (\downarrow by 3.2%) and oil from 4.2% to 3.1% (\downarrow by 1.1%), respectively, on opposite usage of gas, wind and solar energy has slightly increased by 1% to 3%, which are in general good trends (see [Figure 1.1.3a](#) and [Figure 1.2a](#) in [Pioro \(2016\)](#)). However, it is definitely not enough to prevent quite fast climate change! In addition, and unfortunately, usage of nuclear and hydro power has decreased by 0.8% and 1.4%, respectively, which is a detrimental trend.
2. China has significantly decreased usage of coal for electricity generation from 80% to 62% and increased usage of hydro power from 15% to $\sim 18\%$, gas from 1% to $\sim 3\%$, nuclear from 2% to $\sim 5\%$, wind from $\sim 0\%$ to 5.5%, and solar from $\sim 0\%$ to $\sim 3\%$, which is a very good trend, i.e., decreasing usage of “dirty” coal for electricity generation ([Figure 1.1.3b](#) and [Figure 1.2b](#) in [Pioro \(2016\)](#)).
3. India has just slightly decreased usage of coal for electricity generation from 72% to 71% within last years; at the time, usage of gas is also decreased from 11% to 4.5%, nuclear from 3.2% to 2.9%, and hydro power from 12.2% to 10.9%, which is a detrimental trend. However, usage of wind energy increased from $\sim 0\%$ to 4.1%, and solar from $\sim 0\%$ to 3.2%, which is a good trend ([Figure 1.1.3c](#) and [Figure 1.2c](#) in [Pioro \(2016\)](#)).
4. United States have decreased usage of coal quite visibly, i.e., from $\sim 39\%$ to $\sim 24\%$; increased usage of gas from $\sim 28\%$ to $\sim 37\%$; and nuclear, hydro power, and other renewables are approximately on the same level, i.e., $\sim 19\%$; $\sim 7\%$, and $\sim 7\%$, respectively, which is a good trend ([Figure 1.1.3d](#) and [Figure 1.2d](#) in [Pioro \(2016\)](#)).
5. Brazil: As it was mentioned above, this country heavily relies on hydro power, and this is understandable, because it has the largest river in the world by water flow. Amazon river is located in Brazil plus a number of other large rivers. However, possibly due to climate change hydro electricity generation has decreased quite substantially from $\sim 77\%$ to 64%! To compensate these losses, mainly usage of gas, biomass, and wind has increased ([Figure 1.1.3f](#)) and [Figure 1.2i](#) in [Pioro \(2016\)](#)).
6. Russia has not significantly changed their usage of gas, nuclear, hydro, and coal within last years ([Figure 1.1.3g](#) and [Figure 1.2g](#) in [Pioro \(2016\)](#)).
7. Germany has decreased quite substantially usage of coal for electricity generation from $\sim 47\%$ to 30%; but, at the same time, the usage of nuclear power was also decreased from $\sim 16\%$ to 12% (as per December of 2021) ([Figure 1.1.3l](#) and [Figure 1.2e](#) in [Pioro \(2016\)](#)). However, in January of 2022, 3 of 6 large nuclear-power reactors have been shut down forever, and the decision was made to shut down the rest of 3 reactors before the end of 2022! Due to this it is understandable why Germany is desperate for much more natural-gas supply than before, because they must cover lost nuclear capacities and decrease the use of “dirty” coal! Also, it should be admitted that Germany has impressive portfolio and experience in using renewables for electricity generation. As such, Germany generates electricity from wind resources (20.4%), from solar (7.7%), from biomass (7.2%), and from hydro (4.2%), i.e., in total $\sim 40\%$!
8. The United Kingdom (UK) has decreased very significantly their usage of coal for electricity generation from 34% to 2.4%, and, instead, more electricity is generated from gas (increased from $\sim 27\%$ to $\sim 41\%$), from wind (increased from $\sim 4\%$ to $\sim 20\%$), and the use of solar and hydro power is also slightly increased ([Figure 1.1.3m](#) and [Figure 1.2f](#) in [Pioro \(2016\)](#)). However, in January of 2017, quite

unusual events have happened, which affected significantly the electricity generation from various sources (Figure 1.1.4d). At that time, the UK grid faced a “perfect storm,” which coincide with a shutdown of a number of Nuclear Power Plants (NPPs) in France, nuclear trips in the UK, and a broken interconnector with France (UK also imports electrical energy from French NPPs). On the top of that, on January 16th of 2017, wind has diminished for the whole week. These special and unexpected conditions could definitely lead to a complete blackout. However, gas- and coal-fired power plants have saved the grid (usage of gas for electricity generation has increased by $\sim 11\%$ and

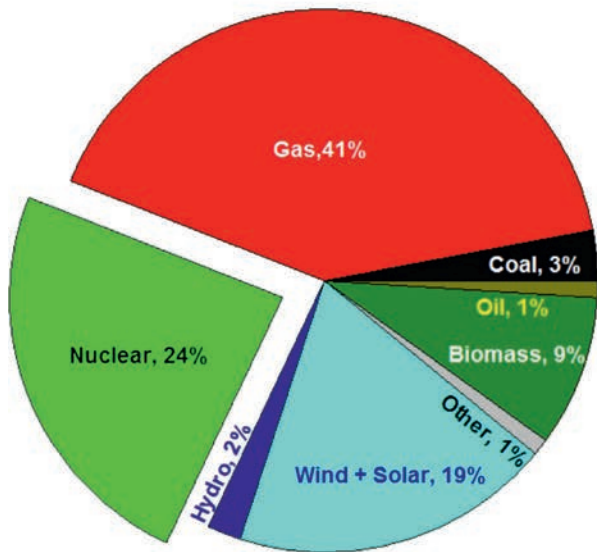
(a) Q3 2015



(b) Q3 2016



(c) Q3 2017 (30% renewables: wind + solar 19%)



(d) Jan. 16-22, 2017 (11% renewables: wind + solar 4%)

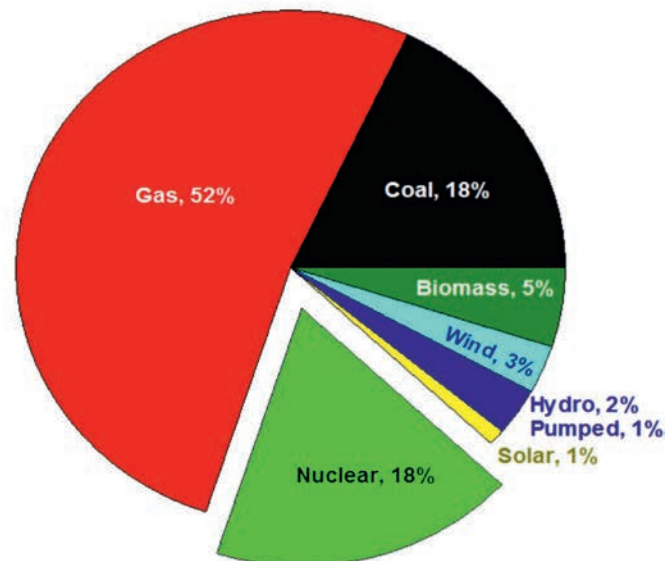


Figure 1.1.4. Changes in electricity generation in UK by source within Q3 2015–2017 including 1 week of 2017, when almost no winds across the UK. (a) Q3 2015, (b) Q3 2016, (c) Q3 2017 (30% renewables: wind + solar 19%), (d) January 16–22, 2017 (11% renewables: wind + solar 4%). Based on data from: <http://euanmearns.com/uk-grid-january-2017-and-the-perfect-storm/>; <https://www.ofgem.gov.uk/data-portal/electricity-generation-mix-quarter-and-fuel-source-gb>; <https://utilityweek.co.uk/low-carbon-generation-supplies-half-britains-power/>

of coal by ~15%). This is the very good (actually, very bad) example what might happen if unreliable renewable sources such wind and solar have large share in the electrical grid (in the particular case up to 30%)

9. France has not significantly changed their usage of various sources for electricity generation (Figure 1.1.3n and Figure 1.2l in Piore (2016)) over the same period, they are still No. 1 country in the world for generating electricity mainly at NPPs (~70% of the total generation).
10. Now several words about Middle East countries (see below), which moved recently to top EEC (W/Capita) values (for full details, see Table A8.1.3, also, see Figure 1.1.1a), but still have a room for HDI ranks improvements:

Country	EEC (2018–2019) W/Capita	HDI (2019) Rank	Year average temperature, °C
Bahrain	1908	42	28
Qatar	1747	45	29
Kuwait	1607	64	27
UAE	1395	31	27
Saudi Arabia	1073	40	29

These countries are very rich with oil and gas reserves (see Tables A8.2.3 and A8.2.5), and to be efficient in oil and gas extraction and transportation they need to have modern power industry. However, the main sources for electricity generation are gas and oil (Figures 1.1.3v and x). Also, these countries are located in a very hot climate (see data above). Therefore, to work and to live in comfortable conditions you need quite sophisticated air-conditioning systems. On the top, nowadays, these countries became world resorts, therefore, they need even more air-conditioning. Nevertheless, the UAE is the first among these countries, which put into operation three large nuclear-power reactors in 2021–2022 and finalizing construction of 1 more to be put into operation in 2024.

Table 1.1.4 lists data on CO₂ emissions in the world & selected countries from coal- and gas-fired thermal power plants, which are the most significant emitters of carbon dioxide in power industry. Analysis of the data for coal electricity generation shows that China generates ~31% of the world coal-based electricity; the US - ~17%; and India ~7%. Therefore, only these three countries cover ~55% of the world coal-based electricity generation. If we add another two countries: Russia and Japan, a share of these five countries will reach ~63% of the world coal-based electricity generation. If we assume that firing coal produces ~800 g of CO₂/kWh of electricity (see Figure 1.1.5), we can estimate that China share of the CO₂ emissions, from coal-fired power plants can be ~52% of the world coal-based emissions, and if we add the USA and India to that, we can reach about 76%. All five countries shown in this Table can be responsible for 81% of world share. In the same way, if we look at the data for gas-fired CO₂ emissions (~400 g of CO₂/kWh), the USA is responsible for 27% of the world gas-fired emission of CO₂. All five countries listed in Table 1.1.4 can be responsible for ~46% of the world share! Therefore, China and the USA should do everything possible to get rid primarily of coal-fired electricity generation and secondary of gas-fired one!

Question No. 1 is that if China and the USA as well as other large countries can replace coal and gas with other less CO₂-emitting sources for electricity generation? Theoretically yes, but practically, each country always tries to use their own reserves of fossil fuels. As such, data below provide explanations why these countries rely quite significantly on coal-based electricity generation (for data on other countries with largest coal reserves, see Table A8.2.1, and for coal consumption—Table A8.2.2).

Country	Coal reserves (million tonnes)	World percentage (%)	% of coal used for electricity generation*
USA	254,197	22.3	24.2
Russia	176,771	15.5	15.8
China	149,818	13.1	62.2
India	107,727	9.5	71.0
Germany	39,802	3.5	30.0
Ukraine	37,892	3.3	30.8
Poland	28,451	2.5	74.0
Indonesia	24,910	2.2	59.1
Turkey	12,515	1.1	37.3

For completeness, countries with the largest oil reserves and consumption are listed in Tables A8.2.5 and A8.2.6.

In the same way, if we look on the countries with the largest natural-gas reserves (see Table A8.2.3; and consumption A8.2.4), we will understand, why these countries rely quite significantly on gas-fired power plants.

Country	Volume of natural gas reserves (km³)	World percentage (%)	% of gas used for electricity generation
Russia	47,805	23.4	46.4
Iran	33,721	16.5	72.7
Qatar	24,072	11.8	–
USA	15,484	7.6	37.4
Saudi Arabia	9,200	4.5	57.8
UAE	6,091	3.0	98.3

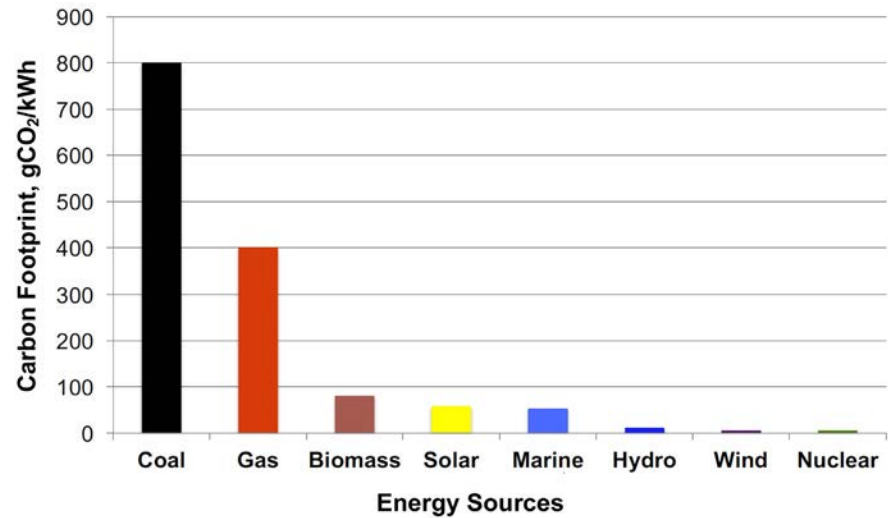
It should be mentioned that, currently, China is No. 1 country in the world for construction and putting into operation of nuclear-power reactors/plants on their soil. However, in spite of all these quite substantial achievements, China has about 52 of 56 large nuclear-power reactors connected to grid as of today, which generate about 5% of the total electricity in the country. Therefore, based on simple mathematics: 10% of electricity generation—100 reactors; 20%—200 reactors; 40%—400 reactors, and currently in the world we have about 443 reactors connected to grid!

Table 1.1.4. Electrical Energy Consumption (EEC) in the world and selected countries (HDI Rank—from 2019; EEC and other data—2018–2019; population in millions from June 2021)

No.	Country	Population in millions		EEC (2018–2019)				Coal		Gas			Hydro	Nuclear	Wind	Solar	Biomass	Other	
		June 2021		TWh	Country World, %	%	TWh	CO ₂ , Mt	Country World, %	%	TWh	CO ₂ , Mt	Country World, %	%	%	%	%	%	%
	World	7871		23,398	100	37	8587	6870	100	24	5499	2199	100	15.8	10.4	5.3	2.7	–	5.6
1	China	1439		7226	31	62	4494	3595	52	3	231	93	4	17.7	4.8	5.5	3.1	–	3.5
2	USA	331		3990	17	24	966	772	11	37	1492	597	27	6.8	19.3	6.9	2.2	1.3	1.9
3	India	1380		1547	7	71	1098	879	13	5	70	28	1	10.9	2.9	4.1	3.2	2.8	0.6
–	<i>Sum of 1–3</i>	<i>3150</i>		<i>12,763</i>	<i>55</i>	–	6558	5246	<i>76</i>	–	1793	718	<i>33</i>	–	–	–	–	–	–
4	Russia	146		965	4	16	153	122	2	46	448	179	8	17.5	18.7	–	–	–	1.6
5	Japan	126		903	4	32	285	228	3	34	306	122	6	8.8	6.4	0.8	7.4	1.8	9.3
–	<i>Sum of 1–5</i>	<i>3422</i>		<i>14,631</i>	<i>63</i>	–	6996	5596	81	–	2547	1019	<i>46</i>	–	–	–	–	–	–

Sources for all data are the same as in Table. M—means Million. Carbon footprint used: (a) for coal—800 g of CO₂ per 1 kWh and (b) for gas—400 g of CO₂ per 1 kWh.

Figure 1.1.5. Carbon footprint of various energy sources. *Courtesy of Dr. J. Roberts, University of Manchester, UK: <http://research.briefings.files.parliament.uk/documents/POST-PN-268/POST-PN-268.pdf>*



1.1.2 Largest power plants of the world, industrial electricity-generating sources, and their pros and cons

1.1.2.1 Largest power plants of the world

Next step in our overview of the power industry of the world will be to present the most significant achievements of the mankind within this area. As such, [Table 1.1.5](#) lists the largest in the world power plants and their classification by installed capacities. It was decided to list power plants with installed capacities of $\sim 6000 \text{ MW}_{\text{el}}$ and up.

Analysis of the data in [Table 1.1.5](#) shows that 12 from 22 largest power plants in the world are hydro-electric power plants. And within these 12 hydro plants, Three Gorges Dam power plant (China) is the largest power plant in the world with 22,500- MW_{el} installed capacity (see [Figures 1.1.16b and 1.1.16c](#))! It should be admitted that China has eight largest power plants of the world: five hydro-power plants, one wind-power plant (see [Figure 1.1.21](#)), one coal-fired power plant, and one NPP. No doubt that these plants are great achievements of Chinese people.

In terms of hydro-power plants, there should be very unique geographical locations, i.e., large rivers (large flow rates) and a possibility to have a high hydrostatic pressure (difference in heights between upper lake (water reservoir) and lower lake (water-discharged level)). Due to this super- and very-large hydro-power plants have been built in Brazil, China, Paraguay, Russia, USA, and Venezuela. All these countries have large rivers and unique locations, where large artificial lakes can be created upstream of dams.

In terms of wind-power plants, it should be also very special geographical locations, i.e., with year around strong winds from 22 to 90 km/h and away from populated areas.

Within the very-large power plants (range of installed capacities ($5000 < 10,000 \text{ MW}_{\text{el}}$)), there are several largest in the world thermal power plants: gas-fired—Jebel Ali (power & water desalination) (UAE), and coal-fired—Tuoketuo (China) and Taean and Dangjin (South Korea).

Several NPPs are also included into this category of very-large power plants: Kashiwazaki-Kariwa (Japan) (unfortunately, after the Fukushima Daiichi NPP severe accident in March of 2011, it is not yet in service), Bruce (Canada), Yangjiang (China), Hanul and Hanbit (S. Korea).

Discussion on capacity factors of various power plants (see [Table 1.1.5](#), 6th column) is provided later in this Section.

Table 1.1.5. Top 22 largest^a power plants of the world^b (Wikipedia, 2022)

No	Plant	Country	Capacity MW _{el net}	Ave. annual generation TWh _{year}	Capacity factor %	Plant type
– Ultra-large power plants by installed capacity ($\geq 20,000$ MW _{el})						
1	Three Gorges Dam (Figure 1.1.16b)	China	22,500	111.8 ₂₀₂₀	57	Hydro
– Super-large power plants by installed capacity (10,000–<20,000 MW _{el})						
2	Baihetan	China	16,000	62.4 _{average}	45	Hydro
3	Itaipu Dam	Brazil/ Paraguay	14,000	76.4 ₂₀₂₀	62	Hydro
4	Gansu (Figure 1.1.21)	China	14,000	49.3 ₂₀₂₀	40	Wind
5	Xiluodu	China	13,860	57.1 _{average}	47	Hydro
6	Belo Monte	Brazil	11,233	39.5 _{expected}	40	Hydro
7	Guri Dam	Venezuela	10,235	47.0 _{average}	52	Hydro
– Very-large power plants by installed capacity (5000–<10,000 MW _{el})						
8	Jebel Ali (power and water desalination)	UAE	8695	–	–	Natural Gas
9	Tucuruí Dam	Brazil	8370	21.4 _{average}	29	Hydro
10	Kashiwazaki-Kariwa (not in service)	Japan	7965	(60.3 ₁₉₉₉)	(86)	Nuclear
11	Xiangjiaba	China	7750	30.7 _{average}	45	Hydro
12	Grand Coulee Dam	USA	6809	20.2 _{average}	34	Hydro
13	Tuoketuo	China	6720	33.3	57	Coal
14	Longtan Dam	China	6426	18.7 _{estimated}	34	Hydro
15	Sayano-Shushenskaya	Russia	6400	23.5 _{average}	42	Hydro
16	Bruce (Figure 1.1.15)	Canada	6288	49.0 ₂₀₁₇	87	Nuclear
17	Tae'an	S. Korea	6100	–	–	Coal
18	Dangjin	S. Korea	6040	–	–	Coal
19	Krasnoyarsk Dam	Russia	6000	18.4 _{average}	35	Hydro
20	Yangjiang	China	6000	48.0 _{average}	90	Nuclear
21	Hanul	S. Korea	5924	48.2	93	Nuclear
22	Hanbit	S. Korea	5924	47.6	92	Nuclear

^a It should be mentioned that the data listed in the table might be correct within a certain time frame, because there is a possibility that new largest in the world power plant(s) will be put into operation or new units will be added to the existing plant(s), or, on opposite, current largest power plant(s) can be temporary out of service, e.g., the Kashiwazaki-Kariwa NPP, or even to be in the shut-down state for some unit(s) or entirely.

^b There are, at least, three known proposals for possible future largest power plants in the world: (1) Penzhin Tidal Power Plant Project in Russia with the maximum installed capacity of 87,000 MW_{el}; (2) mega-dam hydro-power plant with the maximum installed capacity of 60,000 MW_{el} on the Yarlung Tsangpo river in the Tibetan Autonomous Region (TAR) (construction and operation will be done by China); and (3) Grand Inga Dam in Democratic Republic of Congo with the maximum installed capacity of 39,000 MW_{el}.

1.1.2.2 Industrial electricity-generating sources

The largest operating power plants of the world by energy source together with the current maximum installed capacities are listed in [Table 1.1.6](#). Analysis of the data in [Table 1.1.6](#) shows that, in general, we have the following energy sources for industrial electricity generation:

A. Non-renewable:

1. Fossil-fuel-fired thermal power plants (for averaged heating values of fossil fuels and combustible gases, see [Table A8.2.7](#)):

Fuels—natural gas, coal, fuel oil, oil shale, peat, and diesel.

Combustible gases as a by-product of metallurgical (blast-furnace gas) or other technological processes, but primary fuels for production of these gases are usually fossil fuels.

2. Mined resources (for averaged heating values of nuclear fuels, see [Table A8.2.7](#))

Nuclear fuels (for general information on nuclear fuels, see [Appendix A8.3](#)).

About NPPs, which operate with nuclear fuels: Current NPPs are equipped with thermal-spectrum nuclear-power reactors (vast majority, i.e., 440 from 443 (99.3%)) or with fast-spectrum reactors (only 3 from 443 (0.7%)), however, which do not operate as breeder reactors. Therefore, modern nuclear reactors are considered as a non-renewable-energy source. Hopefully, when fast-spectrum-reactor technologies will become more mature and can operate in the breeding mode, i.e., produce new nuclear fuel, nuclear energy can be moved into the category of renewable sources.

B. Renewable:

1. Hydro;
2. Wind;
3. Biomass;
4. Solar;
5. Geothermal;
6. Tidal; and
7. Wave.

The sun is the major source for hydro, wind, solar, and wave power, and, partially, for production of bio-fuel, which coming from plants (so-called, energy crops) and from agricultural, commercial, domestic, and/or industrial wastes (if these wastes have a biological origin). Therefore, any changes or interruptions in sun energy reaching the Earth, i.e., decreased sun activity, increased cloudiness due to climate change, ash clouds due to increased volcanoes activity or eruption of a super-volcano, can affect all five renewable-energy sources, such as hydro, wind, solar, wave power, and even production of biofuel.

Geothermal energy is based on the heat produced deep in the Earth's core (about 2900 km below the Earth's crust with temperatures of about 5000°C). This heat is constantly generated by the decay of radioactive isotopes, such as potassium-40 (K) and thorium-232 (Th), i.e., has a nuclear origin. And finally, tidal energy is due to the combined gravitational effects of the moon (the main contributor), the sun, and by the rotation of the Earth.

It should be noted that the following two parameters are important characteristics of any power plant: (1) overall (gross) or net efficiency¹ of a plant (see [Table 1.1.7](#)); and (2) capacity factor² of a plant (see [Tables 1.1.5 and 1.1.8](#)).

¹ Gross efficiency of a unit during a given period of time is the ratio of the gross electrical energy generated by a unit to the energy consumed during the same period by the same unit. The difference between gross and net efficiencies is internal needs for electrical energy of a power plant, which might be not so small (5% or even more).

² The net capacity factor of a power plant is the ratio of the actual output of a power plant over a period of time (usually, during a year) and its potential output if it had operated at full nameplate capacity the entire time. To calculate the capacity factor, the total amount of energy a plant produced during a period of time should be divided by the amount of energy the plant would have produced at the full capacity. Capacity factors vary significantly depending on the type of a plant.

Table 1.1.6. Top largest operating power plants of the world by energy source (see explanations to Table 1.1.5) (Wikipedia, 2021)

Rank	Plant	Country	Capacity MW _{el net}	Plant type/Energy source
Ultra-large power plants by installed capacity ($\geq 20,000$ MW_{el})				
1	Three Gorges Dam (Figure 1.1.16b)	China	22,500	Hydroelectric (dam)
Super-large power plants by installed capacity (10,000–<20,000 MW_{el})				
2	Baihetan	China	16,000	Hydroelectric (run-of-the-river)
3	Gansu (Figure 1.1.21)	China	14,000	Wind (onshore)
Very-large power plants by installed capacity (5000–<10,000 MW_{el})				
4	Jebel Ali	UAE	8695	Natural Gas
5	Tuocketuo	China	6720	Coal
6	Bruce NPP (Figure 1.1.15)	Canada	6288	Nuclear
7	Shoaiba	S. Arabia	5600	Fuel Oil
Large power plants by installed capacity (700–<5000 MW_{el})				
8	Bath County	USA	3003	Hydroelectric (pump storage ^a)
9	Drax	UK	2595	Biomass
10	Bhadla	India	2245	Solar (PV)
11	Eesti (Figure 1.1.12)	Estonia	1615	Oil Shale
12	Geysers	USA	1517	Geothermal
13	Shatura ^b	Russia	1500	Peat
14	Hornseal 1	UK	1218	Wind (off-shore)
Medium power plants by installed capacity (300–<700 MW_{el})				
15	IPP3 ^b	Jordan	573	Internal combustion engines
16	Ouarzazate	Morocco	510	Solar (concentrated solar)
17	Sihwa Lake	S. Korea	254	Tidal
Small power plants by installed capacity (10–<300 MW_{el})				
18	Vasavi Basin Bridge	India	200	Diesel
19	Golmud 2	China	60	Concentrated PhotoVoltaic (CPV)
Mini power plants by installed capacity (1–<10 MW_{el})^c				
20	Veyo	USA (Yuta)	9	Recovered energy ^d
21	Sotenäs	Sweden	3	Marine (wave)

^a Pumped-Storage Hydro-electricity (PSH) or Pumped Hydro-electric Energy Storage (PHES) is a type of hydro-electric power plant used by electric grids for load balancing.

^b Some thermal power plants use multifuel options, for example, Shatura power plant (Russia): peat—11.5%, natural gas—78%, fuel oil—6.8% and coal—3.7%.

^c Power plants with installed capacities <1 MW_{el} should be called micro power plants.

^d It is very difficult or just impossible to find the largest recovered-energy power plant(s) in the world, therefore, just for reference purposes, one of the ORMAT recovered-energy power plants is shown here. Usually, their installed capacities can be within 2 to 9 MW_{el} (<https://www.ormat.com/en/renewables/reg/view/?ContentID=231>).

Table 1.1.7. Typical ranges of thermal efficiencies (gross) (η_{gr}) of modern thermal and nuclear power plants^a

No	Power plant	η_{gr} (up to)
1	Combined-cycle power plant (combination of Brayton gas-turbine cycle (fuel—natural gas or Liquefied Natural Gas (LNG); combustion-products parameters at gas-turbine inlet: $P_{in} \approx 2.5$ MPa, $T_{in} \approx 1650^\circ\text{C}$) and Rankine steam-turbine cycle (steam parameters at turbine inlet: $P_{in} \approx 12.5$ MPa ($T_{sat} = 327.8^\circ\text{C}$), $T_{in} \approx 620^\circ\text{C}$ ($T_{cr} = 374^\circ\text{C}$))	62%
2	Supercritical-pressure coal-fired power plant (Rankine-cycle steam inlet turbine parameters: $P_{in} \approx 23.5\text{--}38$ MPa ($P_{cr} = 22.064$ MPa), $T_{in} \approx 540\text{--}625^\circ\text{C}$ ($T_{cr} = 374^\circ\text{C}$); and $P_{reheat} \approx 4\text{--}6$ MPa ($T_{sat} = 250.4\text{--}275.6^\circ\text{C}$), $T_{reheat} \approx 540\text{--}625^\circ\text{C}$)	55%
3	Internal-combustion-engine generators (Diesel cycle and Otto cycle with natural gas as fuel)	50%
4	Subcritical-pressure coal-fired power plant (older plants; Rankine-cycle steam: $P_{in} = 17$ MPa ($T_{sat} = 352.3^\circ\text{C}$), $T_{in} = 540^\circ\text{C}$ ($T_{cr} = 374^\circ\text{C}$); and $P_{reheat} \approx 3\text{--}5$ MPa ($T_{sat} = 233.9\text{--}263.9^\circ\text{C}$), $T_{reheat} = 540^\circ\text{C}$)	43%
5	Advanced-Gas-cooled-Reactor (AGR) NPP (reactor coolant CO_2 : $P = 4$ MPa, $T = 290\text{--}650^\circ\text{C}$; and steam: $P_{in} = 17$ MPa ($T_{sat} = 352.3^\circ\text{C}$) & $T_{in} = 560^\circ\text{C}$ ($T_{cr} = 374^\circ\text{C}$); and $P_{reheat} \approx 4$ MPa ($T_{sat} = 250.4^\circ\text{C}$), $T_{reheat} = 560^\circ\text{C}$)	42%
6	Gas-Cooled Reactor (GCR) (High Temperature Reactor – Pebble-bed Module (HTR-PM)) NPP (Generation-IV) (reactor coolant - helium: $P = 7$ MPa, $T = 250\text{--}750^\circ\text{C}$; and Rankine-cycle steam: $P_{in} = 14.2$ MPa ($T_{sat} = 337.8^\circ\text{C}$), $T_{in} = 556^\circ\text{C}$ ($T_{cr} = 374^\circ\text{C}$); and $P_{reheat} \approx 3.5$ MPa ($T_{sat} = 242.6^\circ\text{C}$), $T_{reheat} = 560^\circ\text{C}$). (For details, see Figures A1.88–A1.91).	42%
7	Sodium-cooled-Fast-Reactor (SFR) NPP (reactor coolant: $P = 0.1$ MPa, $T = 377\text{--}550^\circ\text{C}$; and steam: $P_{in} = 14.2$ MPa ($T_{sat} = 337.8^\circ\text{C}$), $T_{in} = 505^\circ\text{C}$ ($T_{cr} = 374^\circ\text{C}$); and $P_{reheat} \approx 2.5$ MPa ($T_{sat} = 224^\circ\text{C}$), $T_{reheat} = 505^\circ\text{C}$)	40%
8	Pressurized-Water-Reactor (PWR) NPP (reactor coolant: $P = 15.5$ MPa ($T_{sat} = 344.8^\circ\text{C}$), $T_{out} = 327^\circ\text{C}$; steam: $P_{in} = 7.8$ MPa, $T_{in} = T_{sat} = 293.3^\circ\text{C}$; and $P_{reheat} \approx 2$ MPa ($T_{sat} = 212.4^\circ\text{C}$), $T_{reheat} \approx 265^\circ\text{C}$)	38%
9	Boiling-Water-Reactor (BWR) NPP (Generation-III+) (reactor coolant: $P = 7.2$ MPa, $T_{out} = T_{sat} = 287.7^\circ\text{C}$; steam: $P = 7.2$ MPa, $T_{in} = T_{sat} = 287.7^\circ\text{C}$ and $P_{reheat} \approx 1.7$ MPa ($T_{sat} = 204.3^\circ\text{C}$), $T_{reheat} \approx 258^\circ\text{C}$)	34%
10	Pressurized-Heavy-Water-Reactor (PHWR) NPP (reactor coolant: $P_{in} = 11$ MPa/ $P_{out} = 9.9$ MPa ($T_{sat} = 310.3^\circ\text{C}$) & $T = 260\text{--}310^\circ\text{C}$; steam: $P_{in} = 4.7$ MPa, $T_{in} = T_{sat} = 260.1^\circ\text{C}$; and $P_{reheat} \approx 1.2$ MPa ($T_{sat} = 188^\circ\text{C}$), $T_{reheat} \approx 240^\circ\text{C}$)	32%
11	PWR Small-Modular-Reactor (SMR) NPP (KLT-40S, Russia) (reactor coolant: $P = 12.7$ MPa ($T_{sat} = 329^\circ\text{C}$), $T = 280\text{--}316^\circ\text{C}$; steam: $P_{in} = 3.72$ MPa ($T_{sat} = 246.1^\circ\text{C}$), $T_{in} = 290^\circ\text{C}$; no secondary-steam reheat)	26%

^a Thermal efficiency for any type of nuclear/thermal power plant primary depends on: (1) type of power cycle (combined, Brayton gas-turbine, Rankine steam (vapor)-turbine), etc.; (2) working-fluid parameters at the turbine inlet (T_{in} and P_{in}), (3) existence of steam (vapor) reheat for Rankine cycle; and (4) type of working fluid (for Brayton cycle: combustion products, helium, nitrogen, mixture of helium-nitrogen, etc.; for Rankine cycle: usually steam, but can be carbon dioxide, etc.). Therefore, based on this Table, thermal efficiencies of other thermal power plants (geothermal, solar thermal, any other types of fuel, etc.) can be estimated, if the abovementioned types of power cycles, their arrangements, working fluids and their parameters are known.

Table 1.1.8. Average (typical) capacity factors of various power plants

No.	Power plant type	Location	Year	Capacity factor, %
1	Nuclear	USA	2019	93.5
		Romanian CANDU reactors	2017	93
		Canadian CANDU reactors	Lifetime average	87
		China	2019	86
		Russia	2019	85
		World	2017	81
		France	2019	77
		UK	2015	75
		Indian PHWRs	2015–2017	69
2	Geothermal	USA	2017	76
3	Bioenergy	USA	2017	51–71
4	Combined-cycle	USA	2017	55
5	Coal-fired	USA	2017	54
6	Hydroelectric	USA	2017	45
		World (average)	–	~45
		World (range)^a	–	10–99
7	Wind	USA	2017	34
		World	2011–2013	20–40
8	Concentrated-solar thermal	USA California	2017	22
		Spain (molten salt with storage)	2014	63
9	PhotoVoltaic (PV) solar	USA	2017	27
		UK	2015	12
10	Concentrated solar photovoltaic	Spain	–	12
11	Wave	UK	2015	3

^a Capacity factors depend significantly on a design, size, and location (water availability) of a hydro-electric power plant. Small plants built on large rivers will always have enough water to operate at full capacity. Source: Wikipedia.

Typical ranges of thermal efficiencies (gross) (η_{gr}) of modern thermal and nuclear power plants are listed in [Table 1.1.7](#). Analysis of these data shows that combined-cycle power plants (combination of Brayton gas-turbine cycle (fuel—natural gas, LNG, or any other clean combustible gases) and Rankine cycle (for details on both cycles, see Appendix A1)) are the leaders in thermal efficiency (up to 62%) compared to those of any other thermal and nuclear power plants. Thermal efficiency of 62% means that 62% of the total energy introduced inside a power cycle from combustion of gaseous fuel is transferred into useful energy, mainly/usually electrical one, and 38% of the total energy is lost into environment near a power plant. Also, it should be stated here that thermal efficiency is the driving force for all advances in thermal and, nowadays, nuclear power plants! Of course, in all these advances in thermal and nuclear power plants safety of a plant and its operation cannot be compromised! In reality, the safety is enhanced with appearance of new modern advanced thermal and nuclear power plants.

Analysis of the data in [Tables 1.1.5 and 1.1.8](#) shows that capacity factors of different power plants vary very significantly, i.e., from 3% for wave-energy plants to almost 100% for NPPs. It should be noted that capacity factors can be of different nature: (1) artificially induced (mainly, non-renewable-energy power plants); and (2) induced by Mother Nature (mainly, all renewable-energy power plants with the exception of biofuel and geothermal power plants).

The capacity factor is a very important parameter, but, unfortunately, not so well-known to general public. For our opinion, this is because non-renewable-energy power plants eventually can operate for long time at 100% capacity factors, but, on opposite, renewable-energy power plants usually on average have significantly lower capacity factors than 100%. And this is the nature of things. Due to this governments in many countries worldwide, when promoting intermittent and unreliable wind- and solar-power plants, don't want to emphasize these lower capacity factors.

What means artificially induced capacity factors: Almost any electrical grid has variable consumption of electricity during a day, i.e., usually less energy consumption at night and more during daytime. Also, if an electrical grid contains variable electricity-generating renewable-power plants, mainly, wind and solar, other power plants in a grid must compensate this variable generation of electricity. Therefore, it is very common that thermal power plants and, in some cases, large hydro-power plants will compensate all these energy variations within a grid, because, especially, thermal power plants are independent of Mother Nature and many of them are fast-response power plants. Due to this, thermal power plants usually put into the worst operating conditions with significantly variable electricity generation, and due to that have on average artificially induced lower capacity factors (see [Table 1.1.8](#)) compared to that of NPPs.

Of course, some solar thermal-power plants are equipped with thermal-energy-storage systems, and due to that can operate almost 24/7 (i.e., 24 h per 7 days of a week), at least, during a summer, or any other renewable-energy power plants can be equipped with electrical-storage systems. However, any conversion of energy decreases efficiency/thermal efficiency plus this option requires additional equipment, which is not so cheap, i.e., electricity cost will be increased.

Also, it should be noted that almost all renewable-energy power plants, even the largest in the world hydro- and wind-power plants (see [Table 1.1.5](#)), have capacity factors lower than those of thermal and nuclear power plants.

In general, the following ideal/ultimate requirements for electrical-energy sources can be deduced:

1. Concentrated in terms of energy density per unit or area covered with power plant (including artificial-lake area or volume of water for hydro plants).
2. Large installed capacity possible.
3. High-capacity factors achievable for long-term operation.
4. High efficiency/thermal efficiency.
5. Reliable and safe.

6. Long-term operational.
7. Minimized environmental impacts.
8. Independent of Mother Nature including location.
9. Maneuverable/fast response in terms of power variability (load following) to meet fluctuating and daily-demand cycles.
10. Low capital and operational costs. And
11. Low Levelized Cost Of Energy (LCOE).

1.1.2.3 Pros and cons of various electricity-generating sources

This Subsection is dedicated to comparison of various electricity-generating sources in terms of their advantages/disadvantages or pros/cons.

Carbon footprints of various energy sources are shown in [Figure 1.1.5](#) and listed in [Table 1.1.9](#), which based on two different literature sources. Comparison of data from these two sources shows that both data are quite close to each other. Analysis of these data shows that coal-fired power plants have the highest emissions of CO₂ compared to any other energy sources. Natural-gas-fired power plants have approximately twice less emissions of CO₂ than coal-fired ones. Renewables sources and NPPs have significantly lower emissions of CO₂ compared to fossil-fired power plants. As a matter of fact, nuclear power has one of the smallest values of carbon-dioxide footprint.

Table 1.1.9. Carbon-dioxide emissions from various energy sources

No.	Energy sources	gCO ₂ equivalent/ kWh
1	Coal	820
2	Biomass cofiring ^a	740
3	Natural gas	490 ^a
4	Biomass	230 ^a
5	Solar PV—utility	48
6	Solar PV—roof ^a	41
7	Geothermal ^a	38
8	Solar—concentrated ^a	27
9	Hydro-power	24
10	Wind offshore ^a	12
11	Nuclear	12
12	Wind onshore	11 ^a

^a New data or different data compared to those in [Figure 1.1.5](#).

Based on data from Intergovernmental Panel on Climate Change (IPCC) and <https://world-nuclear.org/information-library/energy-and-the-environment/carbon-dioxide-emissions-from-electricity.aspx>.

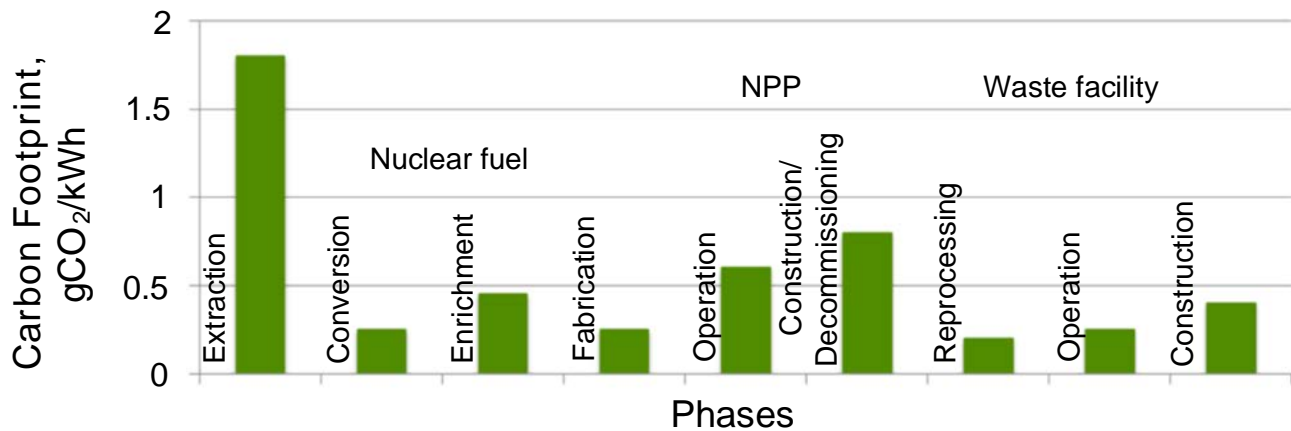


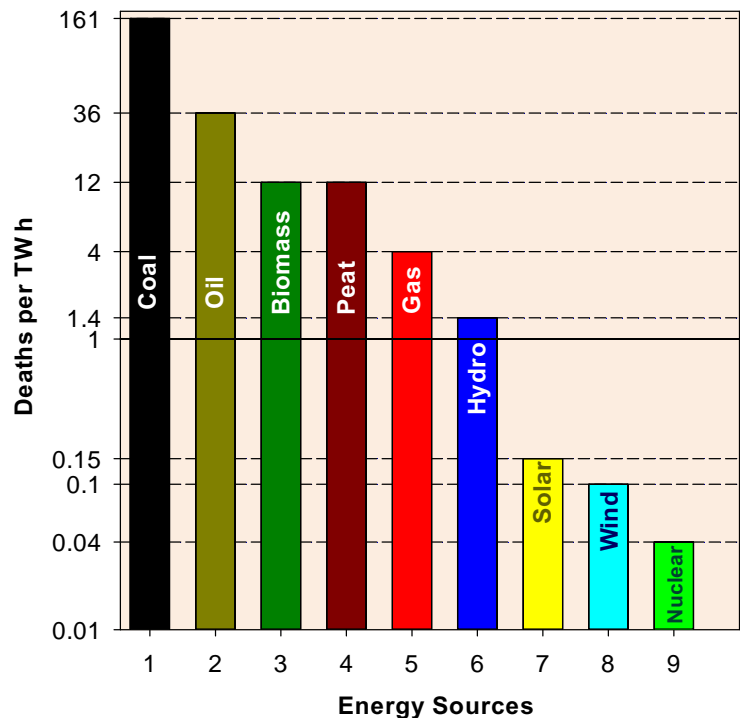
Figure 1.1.6. Carbon footprint of Nuclear Power Plant (NPP) various phases. *Courtesy of Dr. J. Roberts, University of Manchester, UK; based on data from British Energy for Torness AGR NPP*

It should be noted that when we compare CO₂ emissions from all these energy sources, we consider full cycle, i.e., production of fuel and/or materials used in construction and operation of power plants, their construction and operation, demolition, etc. (for details, see Figure 1.1.6, which is related to NPPs).

Another comparison of nine energy sources (eight previous ones plus oil) is shown in Figure 1.1.7. This comparison is related to Deaths/TWh, and, also, includes full cycle. Coal has the highest value, and this is mainly due to dangerous conditions in many coal mines around the world, i.e., eruption of combustible gases, fires, flooding, etc. Solar, wind, and nuclear have the minimum values of this very sad parameter.

In addition to data in Figure 1.1.7, Table 1.1.10 lists casualties due to various accidents in power and chemical industries, transportation, and from firearms (based on data from Wikipedia (2021)). Analysis

Figure 1.1.7. Deaths per TWh for various energy sources. *Based on data from <https://www.nextbigfuture.com/2011/03/deaths-per-twh-by-energy-source.html>*



of the data in this Table shows that the most dangerous in our life, of course, if we are not soldiers participating in any war conflict(s), is a driving a car (see Item 8). Approximately 1.3 million people died every year in car accidents around the world, and, in addition, between 20 and 50 million people suffer non-fatal injuries, with many incurring a disability as a result of their injury.

However, in spite of all these huge numbers of casualties every year, no one is proposing to return back to horses, because we, as the mankind, have reached very significant progress in all aspects of our lives, and we cannot go back to significantly lower level of our civilization! Of course, we must take all possible actions to decrease significantly, eventually, to eliminate completely these terrible numbers of casualties and injuries for our everyday life.

Table 1.1.10. Casualties due to various accidents in power and chemical industries, transportation, and from firearms (in (...))—population in millions, June 2021)

No.	Accidents/causes of death	Year	Region	No of deaths
1	Fukushima Daiichi NPP accident (deaths due to earthquake, not radiation)	2011	Japan (127)	Few workers
2	Chernobyl NPP accident	1986 ^a	Ukraine (44)	56
		1986–now ^b		>4000
3	Kyshtym radiation-release accident (Chelyabinsk region)	1957 ^c	Russia (146)	>>200
4	Sayano-Shushenskaya hydro-plant accident (6000 MW _{el})	2009	Russia (146)	75
5	Banqiao Dam ^d	1975	China (1439)	>26,000
6	Vajont Dam	1963	Italy (60)	~2000
7	Bhopal Union Carbide India Ltd. Accident: Immediate deaths (official data)/By Government of Madhya Pradesh	1984	India (1380)	2259/3787
	Other estimations (since the disaster)			8000
	No. of people exposed to methyl isocyanate gas and other chemicals			500,000
8	Car accidents ^e (in (...) population in millions)	Annually	World (7871)	~1,350,000
		2019	USA (331)	36,120
			EU (445)	22,800
9	Shipwreck accidents	2019	World (7871)	3174
10	Railway accidents	2019	EU (445)	802
			USA (331)	862
			India (1380)	~24,000

Continued

Table 1.1.10. Casualties due to various accidents in power and chemical industries, transportation, and from firearms (in (...))—population in millions, June 2021—cont'd

No.	Accidents/causes of death	Year	Region	No of deaths
11	Air accidents ^f	2020 (9 accidents) 2016 (16 accidents) 2014 1972 11.09.2001	World (7871) NY USA	137 303 ~990 3344 >4500
12	Firearms casualties (~70% suicides and ~30% homicides)	2019	USA (331)	38,300

^a Fifty-six direct deaths (47 NPP and emergency workers and 9 children with thyroid cancer), i.e., deaths due to the explosion and initial radiation release.

^b Deaths from cancer, heart disease, birth defects (in victims' children) and other causes, which may result from exposure to radiation. Various sources provide significantly different estimations starting from 30,000 to 60,000 casualties and up to 200,000 and even up to 985,000 casualties. However, these deaths may also result from other causes not related to the accident, for example, pollution from non-nuclear sources—industry, transportation, etc. In general, accurate estimation of all deaths related to the Chernobyl NPP accident is impossible.

^c It is impossible to estimate accurately all casualties. Other sources estimate casualties from cancer within 30 years after the accident up to 8000.

^d Also, 145,000 died during subsequent epidemics and famine. Other sources estimate casualties as high as 230,000. About 11 million residents were affected.

^e In addition to car fatalities, between 20 and 50 million people suffer non-fatal injuries, with many incurring a disability as a result of their injury. **Therefore, driving a car is a quite dangerous mode of travel!**

^f In 2000, commercial air carriers transported about 1.1 billion people on 18 million flights, while suffering only 20 fatal accidents. **Therefore, air transportation remains among the safest mode of travel.**

Source: Wikipedia, 2021.

In terms of other modes of transportation, all of them, unfortunately, have casualties annually, but on significantly lower level compared to that of car accidents (see Items 9–10). Accounting that commercial air carriers transport approximately more than 1 billion people on tens of million flights, while suffering only 9 fatal accidents with 137 casualties in 2020. Therefore, air transportation remains among the safest modes of travel.

In chemical industry, one of the most severe accidents within last 40 years is the Bhopal Union Carbide India Ltd. Accident (1984, India) (see Item 7) in which thousands of people were killed and hundreds of people were exposed to methyl isocyanate gas and other chemicals.

Accidents with dams and hydro-power plants (Items 4–6): The most severe accident by the number of casualties was happened with Binqiao Dam (China) in 1975 (see Item 5).

Accidents related to nuclear/nuclear-power industry (Items 1–3): Chernobyl NPP severe accident (1986, Ukraine) is the most severe one in the world nuclear-power industry by short- and long-term consequences (see Item 2). And, unfortunately, the exact number of casualties will be never known due to very significant difficulties in estimation of the actual cause of death with time, i.e., if the particular death is related to consequences of this accident or not. It can be thousands or even tens of thousands of deaths up till now. However, it should be admitted that this is the only one such scale accident in nuclear-power industry from appearance of first nuclear-power reactors in the mid of 1950s.

The most recent severe accident at the Fukushima Daiichi NPP (2011, Japan) (see Item 1) costs tens of billions of dollars, but only several casualties were reported (deaths due to earthquake, but not radiation).

Table 1.1.11. Approximate volumes of wastes per 1000-MW_{el} power per year for nuclear and coal-fired power plants

Nuclear power plant	Coal-fired power plant
Fuel	
25 t of UO ₂	2.6 million t of coal (5 × 1400 t trains a day)
Wastes	
35 t High Level Wastes (HLW)	6,500,000 t of CO ₂
310 t Intermediate Level Wastes (ILW)	900 t of SO ₂
460 t Low Level Wastes (LLW)	4500 t of NO _x
	320,000 t of ash
	400 t of toxic heavy metals

Courtesy of Dr. J. Roberts, University of Manchester, UK.

However, impact of these two severe nuclear accidents is huge and can be seen even now. A number of countries have stopped construction of nuclear-power reactors, and some of them have decided to shut-down part or all reactors connected to grid.

Table 1.1.11 lists approximate volumes of wastes per 1000-MW_{el} power per year for nuclear and coal-fired power plants. Analysis of these data shows that coal-fired power plants create huge amount of various wastes compared to NPPs. However, we don't want to say that even small amount of radioactive wastes from nuclear-power industry is OK to have. We must definitely get rid of them. Currently, just small amount of these wastes is reprocessed, and a larger amount is stored, but with the appearance of next generation or Generation-IV fast-spectrum reactors, which can operate as breeders, we can solve much of this problem through better handling and destruction of these wastes in these reactors. Also, the ultimate storage of high-level radioactive wastes should be their vitrification and putting them inside deep underground facilities (Pioro et al., 2001) (Table 1.1.12).

Comparison of selected parameters of various type's power plants are presented in Tables 1.1.13a and 1.1.13b. Table 1.1.13a lists selected parameters including energy density of various type power plants. And Table 1.1.13b lists selected parameters of generic NPP and onshore wind farm (power plant). Analysis of the data in these tables shows clearly that nuclear power has a number of advantages compared to that of renewable-energy sources, and No. 1 parameter is higher energy density. And, the reliability is also higher.

Figure 1.1.8 shows a comparison of more or less all non-renewable and renewable energy sources based on Levelized Cost Of Energy (LCOE). Analysis of the data in this figure shows that the lowest LCOE value (below 50) is for nuclear (Long-Term Operation (LTO)); slightly higher LCOE values (~50) are for onshore wind; next higher level (around 75) are gas (Combined Cycle Gas Turbine (CCGT)), nuclear, solar PhotoVoltaic (PV) (utility scale), and both hydro (reservoir (artificial lake) and run-of-the-river types); close to 100 value of LCOE are lignite, coal, offshore wind, geothermal, and gas (CCGT plus CCUS—Carbon Capture, Utilization and Storage); within 100 to 125 are solar thermal, biomass, and coal (CCUS); and the highest LCOE value is for solar (PV residential).

More detailed information on various energy sources including their advantages/disadvantages or pros and cons is provided in the next Sections 1.1.3–1.1.5.

Table 1.1.12. Percent of various wastes in total amount

No	Wastes	% in total amount
1	Mining and quarrying	27.30
2	Agriculture	20.13
3	Demolition and construction	18.51
4	Industrial	12.73
5	Dredged spoils	7.64
6	Household	6.94
7	Commercial	6.48
8	Sewage sludge	0.23
9	Radioactive	0.04

Courtesy of Dr. J. Roberts, University of Manchester, UK; partially based on data from: <https://publications.parliament.uk/pa/cm200405/cmselect/cmenvfru/130/130we13.htm>.

Table 1.1.13a. Comparison of selected parameters including energy density of various type power plants

No.	Power plant	Installed capacity MW _{el net}	Plant area km ²	Energy density kW/m ²	Capacity factor %	Energy density kW/m ²
–	–					
1	Bruce NPP	6288	9.3	0.68	87	0.59
2	Three Gorges Dam	22,500	1084 ^a	0.021	57	0.012
3	Roscoe wind	781	400	0.002	34	0.0007
4	Ivanpah Solar (thermal)	377	16	0.02	31	0.007
			2.4 ^b	0.16		0.05
5	Gemasolar (thermal)	20	1.95	0.01	75	0.008
			0.3 ^b	0.07		0.05

^a Artificial lake area.

^b Total reflecting area.

1.1.3 Non-renewable-energy power plants

1.1.3.1 Thermal

In this Section only fossil-fuel-fired thermal power plants are considered. These plants have a quite large share of electricity generation in the world (36.7% coal +23.5% gas +3.1% oil = 63.3%; Figure 1.1.3a) and many countries worldwide (for details, see Figure 1.1.3).

Table 1.1.13b. Comparison of selected nuclear-power-plant parameters to those of onshore wind farm

Parameters	NPP	Onshore wind farm
Carbon saved	86/100	90/100
Energy density	75/100	10/100
Reliability	90/100	20/100

Courtesy of Dr. J. Roberts, University of Manchester, UK.

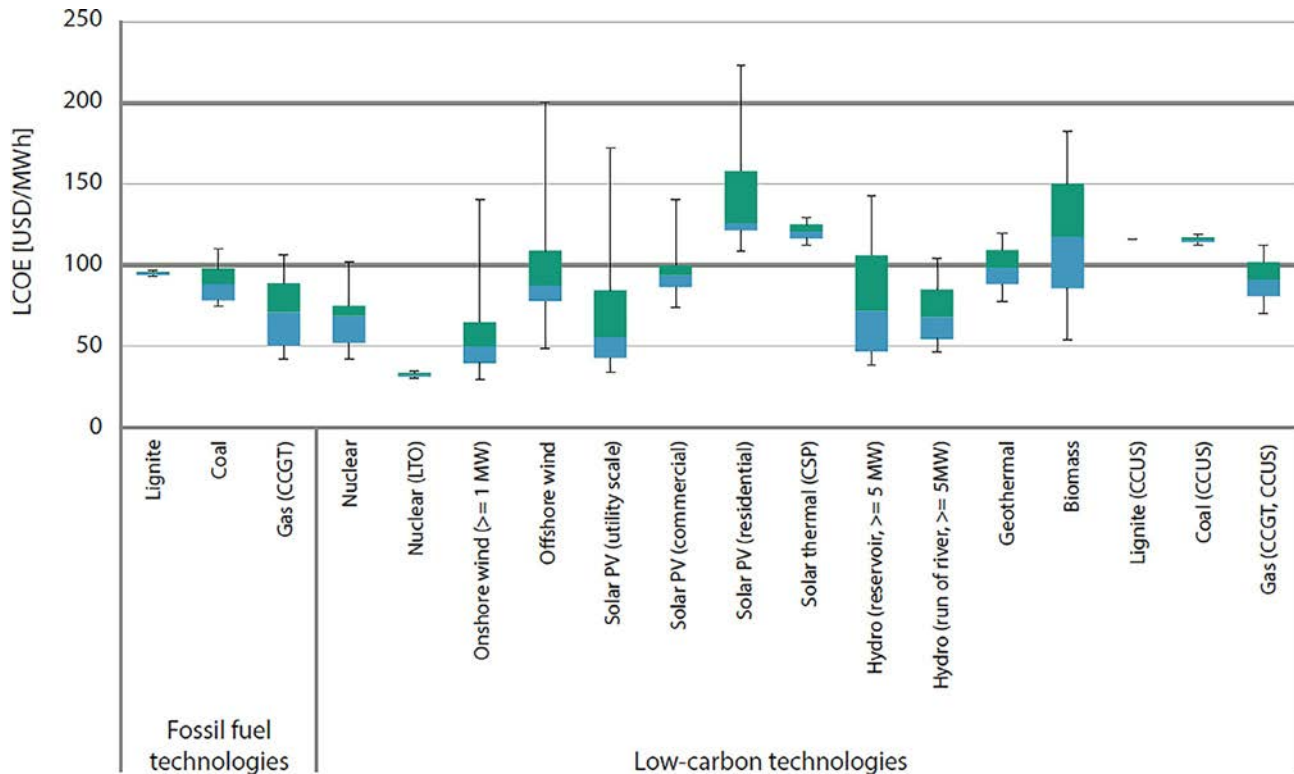


Figure 1.1.8. Levelized Cost Of Energy (LCOE) by technology. Note: values at 7% discount rate. *Box plots* indicate maximum, median, and minimum values. *Boxes* indicate central 50% of values, i.e., second and third quartile. *USD*—US Dollar; *CCGT*—Combined-Cycle Gas Turbine; *LTO*—Long-Term Operation; *PV*—PhotoVoltaic; *CSP*—Concentrated Solar Power; *CCUS*—Carbon Capture, Utilization and Storage. *Courtesy and copyright by IEA, NEA, and OECD (<https://www.iea.org/reports/projected-costs-of-generating-electricity-2020>)*

1.1.3.1.1 Coal-fired thermal power plants

In the world the largest group of thermal power plants use coal as the fuel. These plants are based on the Rankine steam-turbine cycle with single secondary steam reheat (double steam reheat is possible, but quite seldom used), which can be with supercritical-pressure parameters of water (see Table 1.1.7 Item 2) at the outlet of a “steam” generator/inlet into a high-pressure turbine (newer plants see Figure 1.1.9); the supercritical-pressure Rankine cycle was introduced into the power industry at the end of 1950s (Pioro and Duffey, 2007) or at subcritical-pressure parameters of water/steam (see Table 1.1.7 Item 4). Major



Figure 1.1.9. Aerial view of 5550-MW_{el} Taichung coal-fired power plant (Taiwan)—one of the largest in the world. The plant equipped with 550 MW_{el} × 10 coal-fired steam-generators-turbines + 70 MW_{el} × 4 gas-fired steam generators-turbines and is one of the world’s largest emitters of carbon dioxide with over 40 million tons per year. (For more details on supercritical-pressure coal-fired thermal power plants (layout, power cycle, diagram, etc.)—see Appendix A1.) *Photo taken from: https://zh.wikipedia.org/wiki/File:Taichung_Fire_Power_Plant.jpg, author/username Altus. Source: Wikipedia*

advantage of supercritical-pressure power plants is high thermal efficiency (up to 55%) compared to that of subcritical-pressure plants (up to 43%) (see Table 1.1.7).

Advantages/disadvantages or pros/cons of coal-fired power plants are:

1. Concentrated in terms of energy density per unit.
2. Very large installed capacity possible currently up to 6720 MW_{el} (see Table 1.1.5 Item 13).
3. High-capacity factors achievable for long-time operation (however, they are used to compensate variable consumption of electricity plus variable generation of electricity with renewable-energy power plants, therefore, on average their artificially induced capacity factors can be around 55%).
4. High thermal efficiency (supercritical-pressure plants can reach 55%, which is the second highest value in power industry).
5. Reliable and, eventually, safe. However, coal is a fuel, i.e., fires possible, and coal dust can explode at certain conditions.
6. Long-term operational.
7. *Worst polluters in power industry: largest CO₂ emissions compared to that of any other energy sources (see Figures 1.1.5, 1.1.9, and Table 1.1.9), combustion products contain NO_x; SO₂, which creates acid rains as the result of reaction with water vapor; and natural radioactivity from coal, therefore, these plants equipped with very high stacks (see Figure 1.1.9); twice less heating values compared to that of natural gas (see Table A8.2.7); burning of coal creates a lot of ash and mountains of slag (see Table 1.1.11), which is going into dumps damaging environment; highest death rates compared to that of any other energy sources (see Figure 1.1.7).*

8. More or *less* independent of Mother Nature. However, steam at the outlet of a low-pressure turbine has to be condensed with outside cooling water (natural source, i.e., river, lake, sea, ocean) or with cooling towers (air-cooling). *Plants have to be built in locations to which large volumes of coal (millions of tons) can be supplied continuously year around, e.g., to be built near coal mines, open pit mines, cost line of seas and oceans, or to be delivered by heavy trains and/or large ships.*
9. Maneuverable/fast response in terms of power variability.
10. Relatively low capital cost, but *relatively high operational costs due to a large amount of coal required.* (As a joke, but, please remember that in every joke there is a true part: If coal-fired power plant is not in operation, it saves a lot of money on fuel!)
11. LCOE within the medium range compared to that of other energy sources (see [Figure 1.1.8](#)).

Modern approaches to address listed above selected deficiencies of coal-fired power plants:

7. In general, there is a number of approaches to decrease CO₂ emissions or even to eliminate them (see [Figure 1.1.10a](#)). For our opinion, an industrial method is the geological sequestration of carbon-dioxide emissions. However, this method will require the use of compressors, which in turn requires use of electricity for their operation. As the result, internal needs of a plant will go up, amount of net electricity will go down for the invariable gross output and price for electricity will go up (for details, see [Figure 1.1.8](#) right three items on X-scale: Lignite (CCUS), Coal (CCUS), and Gas (CCGT, CCUS))! Also, [Figure 1.1.10b](#) shows the Selective Catalytic Reduction (SCR) (DeNO_x) system,

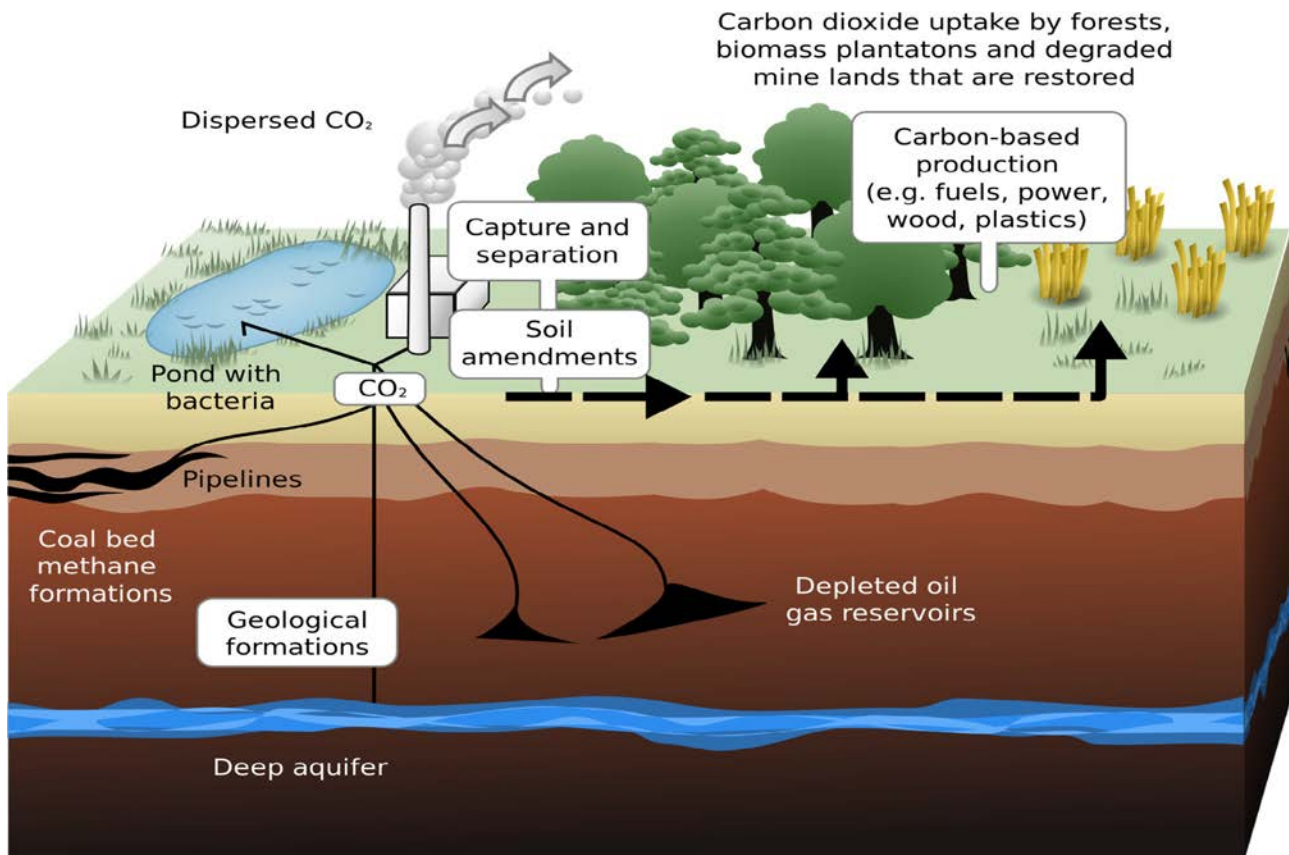


Figure 1.1.10a. Possible solutions for carbon-dioxide capture and storage: Schematic showing terrestrial and geological sequestration of carbon-dioxide emissions from coal-fired power plant. *Rendering by L. Hardin and J. Payne; http://www.ornl.gov/info/ornlreview/v33_2_00/research.htm*



Figure 1.1.10b. Photo of thermal-power-plant Selective Catalytic Reduction (SCR) (DeNO_x) system with capacity of 746,000 nm³/h of exhaust gases. The SCR system helps to reduce NO_x and CO emissions up to 96%. The DeNox system is based on the following reaction: $4\text{NO} + 4\text{NH}_3 + \text{O}_2 \rightarrow 4\text{N}_2 + 6\text{H}_2\text{O}$. *Courtesy and copyright of MHI*

which helps to reduce NO_x and CO emissions up to 96%. In terms of slag: It should be fully reprocessed into building materials (Pioro and Pioro, 2003).

8. To be more independent from Mother Nature—large cooling towers (usually, direct-contact heat exchangers) (see Figure 1.1.10c) is an option, but, usually, it is more expensive option than just using natural source of water (in general, a cooling-water supply from rivers and lakes is less expensive than to use salty waters from seas and oceans (high rates of corrosion, requires usage of expensive stainless-steels piping)). Also, it should be mentioned that water vapor is also green-house gas, which contributes to Earth overheating, therefore, using of “dry” cooling towers (no direct contact between atmospheric air and cooling water, i.e., transmural-type heat exchangers) might be better, but more expensive another option for cooling steam condensers.

1.1.3.1.2 Gas-fired thermal power plants

Gas-fired thermal power plants usually use natural gas or LNG, also, some other clean gases can be used, e.g., combustible gases as a by-product of metallurgical (blast-furnace gas) or other technological processes. These plants are usually based on the combined cycle, i.e., combination of high-temperature Brayton gas-turbine cycle and lower-temperature subcritical-pressure Rankine steam-turbine cycle with single secondary steam reheat (see Table 1.1.7 Item 1 and Figure 1.1.11). Major advantage of these plants is the highest thermal efficiency (up to 62.5%) in power industry (see Table 1.1.7).



Figure 1.1.10c. Cooling towers. Courtesy of Rosatom: <https://www.flickr.com/photos/rosatom/47368931231/in/album-72157672133127091/>



Figure 1.1.11. One of the largest in the world 5040-MW_{el} Futtsu natural-gas-fired combined-cycle power plant (Japan). The plant consists of five generating units: $1520 \text{ MW}_{el} \times 1 + 1000 \text{ MW}_{el} \times 2 + 507 \text{ MW}_{el} \times 2$, and uses Liquefied Natural Gas (LNG). (For more details on combined-cycle gas-fired thermal power plants (layout, power cycle, T - s diagram, etc.)—see Appendix A1.) Photo taken from Wikimedia Commons, author Mr. Hayata. Source: Wikipedia

Advantages/*disadvantages* or pros/*cons* of gas-fired power plants are:

1. Concentrated in terms of energy density per unit.
2. Very large installed capacity possible currently up to 8695 MW_{el} (see [Table 1.1.5](#) Item 8).
3. High-capacity factors achievable for long-time operation (however, they are used to compensate variable consumption of electricity plus variable generation of electricity with renewable-energy power plants, therefore, on average their artificially induced capacity factors can be around 55%).
4. Highest thermal efficiency (up to 62.5%) in power industry.
5. Reliable and, eventually, safe. *However, gas is a fuel, i.e., fires and explosions possible at certain conditions.*
6. Long-term operational.
7. More environmentally friendly compared to that of coal-fired power plants (see [Figures 1.1.5, 1.1.10a, 1.1.10b, 1.1.10c](#) and [Table 1.1.9](#)), *combustion products also contain CO₂ and NO_x*; one of the highest heating values among fossil fuels (see [Table A8.2.7](#)); no ash or slag as that at coal-fired power plants; medium death rates compared to other energy sources (see [Figure 1.1.7](#)).
8. More or *less* independent of Mother Nature. However, steam at the outlet of a low-pressure turbine has to be condensed with outside cooling water (natural source, i.e., river, lake, sea, ocean) or with cooling towers (air-cooling). *Plants have to be built in locations to which large volumes of gas (millions of m³) can be supplied continuously year around, e.g., to be built near cost line of seas and oceans to be delivered by large ships or can be efficiently and relatively inexpensively delivered through gas pipelines, which can be thousands of kilometers.*
9. Maneuverable/fast response in terms of power variability.
10. Relatively low capital cost, but *relatively high operational costs due to a large amount of gas required.* (This item is eventually almost the same as that for coal-fired power plants.)
11. LCOE below the medium range compared to that of other energy sources (see [Figure 1.1.8](#)).

Modern approaches to address listed above selected deficiencies of coal-fired power plants:

7. In general, in terms of emissions of CO₂ and NO_x, please refer to approaches discussed in Item 7 for coal-fired power plants.
8. For details, see Item 8 for coal-fired power plants.

1.1.3.1.3 Oil-shale-fired thermal power plants

Quite seldom used thermal power plants, mainly in countries with natural reserves of oil shale, e.g., Estonia (see [Figure 1.1.12](#)); 80% of oil shale used globally is extracted in Estonia. Eventually, everything what is related to coal-fired power plants can be applied and for oil-shale-fired ones. Specifics are: the maximum known installed capacity (up to 1615 MW_{el}) is significantly less than that for gas- and coal-fired power plants (see [Table 1.1.6](#) Item 11); oil shale as a fuel is even worse than coal, i.e., the lowest one heating value among fossil fuels and quite high content of incombustible substances (Estonian oil shale is 33% organic, 41% inorganic carbonate, and 26% sand/clay composite (Source: Wikipedia, 2022)), which might require to use gas burners to sustain combustion of oil shale; possibly only subcritical-pressure Rankine cycle is used.

1.1.3.1.4 Peat-fired thermal power plants

Information is quite similar to what we have on coal/oil-shale power plants. Peat has heating values within the same range as those for oil shale (see [Table A8.2.7](#)). However, burning peat releases more CO₂ than coal. Peat is the result of generations of partially and decayed organic matter, and, eventually, peat is the first step in coal formation. To transform fully into coal, the substance must be buried under sediment at the depth of 4 to 10 km (Source: www.engineerlive.com/content/peat-energy-source).



Figure 1.1.12. Photo of the largest in the world 1615-MW_{e1} Eesti oil-shale-fired power plant (Estonia). The plant equipped with 14 steam generators connected to $\sim 230 \text{ MW}_{e1} \times 7$ turbines. In 2003, the Unit 8 was reconstructed to use the Circulated Fluidized-Bed Combustion (CFBC) technology, which is more efficient and environmental-friendly (lower SO₂ and CO₂ emissions) compared to the previous technology. Plant has two 251.5-m tall chimneys, which are the tallest chimneys in Estonia. In 2007, the Eesti plant together with the second largest in the world 765-MW_{e1} Balti oil-shale-fired power plant (so-called, Narva plants) generated about 95% of total power production in Estonia. The oil shale burnt at Narva plants produces about 46% of ash, which is about 4.5 million tons of ash per year. *Photo taken from Wikimedia Commons, author A. Simonov. Source: Wikipedia*

1.1.3.1.5 Mazut/heavy-oil-fired power plants

Mazut and heavy oil are liquid fuels with heating values close to that of natural gas, used mainly in countries rich with oil reserves. Mazut and heavy oil can contain sulfur, therefore, combustion products will have SO₂ and as the result of this acid rains are also possible. Combustion products of these liquid fuels are not so clean as those from the natural-gas combustion, therefore, usually, only Rankine steam-turbine power cycle is used. The rest of the information is quite similar to what we have on gas-fired power plants.

1.1.3.1.6 Internal-combustion engines power plants

Number 1 will be the Diesel cycle, and one of the largest in the world diesel-engine generators is shown in Figure 1.1.13. Also, large, medium, and small diesel engines are used for a ship/submarine propulsion and power. Number 2 will be smaller by the installed capacity Otto-cycle natural-gas-engine power-generating unit (see Figure 1.1.14). These types of thermal power plants are quite seldom, but smaller diesel- and gas-engines electrical generators are commonly used as emergency power units at many power plants including NPPs (see Table 1.1.14). Specifics of these internal combustion engines compared to those used in ground transportation, i.e., car, trucks, trains, are quite large installed capacities and higher thermal efficiencies up to 50% (see Table 1.1.7, Item 3).

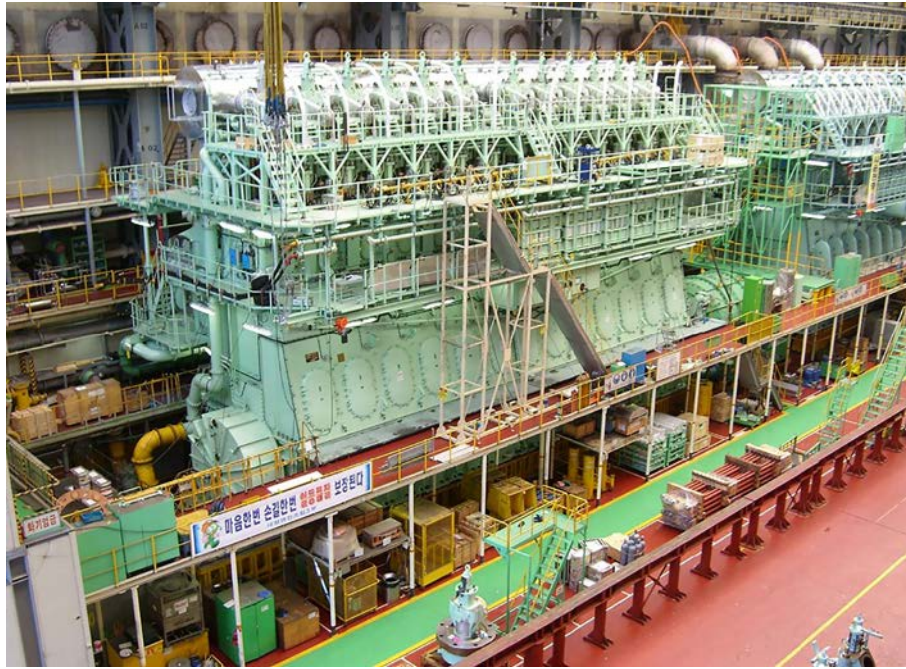


Figure 1.1.13. Photo of 50-MW_{el} (~68,000 hp) Hyundai diesel engine—one the largest in the world, installed at 200-MW_{el} (50 MW_{el} × 4 engines) GMR, Vasavi Basin Bridge Diesel-Generator Plant (Chennai (formerly Madras) India). Eventually, modern diesel engines for ship's propulsion and/or generation can have installed capacities up to 80 MW_{el} (~109,000 hp) (www.hyundaicorp.com). Courtesy of www.worldmaritimenews.com



Figure 1.1.14. The largest in the world 18-cylinder Otto-cycle natural-gas-engine (18V50SG) power-generating unit with output of up to 18.3 MW_{el} (~25,000 hp), 50 Hz and 500 rpm. The natural gas fueled, lean-burn, medium-speed engine is a reliable, high-efficiency and low-pollution power source for flexible base load, intermediate peaking and combined-cycle power plants. Efficiency—48.6%. Dimensions in m: length—18.8; width—5.33; height—6.34; bore—500 mm; and weight—360 t. Engine is 4-stroke spark-ignition with a prechamber. Courtesy of WÄRTSILÄ, Finland

Table 1.1.14. List of emergency diesel-generator packages at selected nuclear power plants (Alstom Power/Man Diesel SA Worldwide References) (Shown here just for reference purposes.)

Country	Customer	Power plant	Reactor type	Commission year	Engine type	No. of engines	Unit power (kW)
Africa S.	ESKOM	KOEBERG 1+2	PWR	1985	18 PA6 V 280	5	4400
China	CNPE	TAINWAN 5+6	PWR	2014	18 PA 6B	5	6100
China	CNPEC	TAISHAN 1+2	EPR	2013	14 PC 2.6B	8	9100
China	NPQJVC	QINSHAN 3-1+2	CANDU	2003	16 PC2.5 V 400	4	8200
Finland	AREVA NP	OLKILUOTO 3	EPR	2011	18 PA 6B	4	6300
France	EDF	FLAMANVILLE 3	EPR	2012	12 PC 2.6B	4	7255
India	Atomstroyexport	KUDANKULAM 1+2	VVER	2010	18 PA 6B	10	6300
India	Larsen & Toubro	TARAPUR	PHWR	2005	9 PA 6 L	8	2700
Korea S.	KEPCO	WOLSONG 3+4	CANDU	1999	16 PC2.5 V 400	4	6000
Korea S.	KEPCO	ULCHIN	PWR	1999	16 PC2.5 V 400	5	7000
Korea S.	KHNP	SHIN-KOI 3+4	PWR	2013	14 PC 2.6B	5	8000
Pakistan	CZEC	CHASMA 2	PWR	2008	12 PA 6B	2	3400
Romania	SNN	CERNAVODA 2	CANDU	2005	16 PC2.5 V 400	2	6700
Russia	A-AEM	LENINGRAD II UNIT 1	VVER	2014	16V32	5	6300
Taiwan	TPC	LUNGMEN	BWR	2011	16 PC2.5 V 400	6	7500

1.1.3.1.7 Recovered energy generation

In general, electrical energy can be also produced from waste energy such as high-temperature flue gases from various technological processes. For example, Ormat Technologies Inc. (<http://www.ormat.com/recovered-energy>) is a pioneer in Recovered Energy Generation (REG) power plants for a wide range of industrial applications. Ormat REG power plants capture unused waste heat from industrial processes and converts it into electricity that can be sold to the grid or used on-site, without any additional fuel consumption and with zero emissions. Ormat has developed specialized solutions for energy recovery systems on gas-pipeline compressor stations, oil and gas refineries, cement factories, paper mills, incinerators, chemical plants, glass plants, and metal refineries.

Ormat REG power plants provide an uninterruptible power supply that enables customers to meet critical-power demand during blackouts and grid outages. It also enables them to reduce power consumption during peak electricity demand hours, reducing price premiums for peak electricity demand. These power plants

have usually capacities from hundreds kilowatts to several megawatts, which depends significantly on the amount of waste heat and its temperature.

1.1.3.2 Nuclear

This Handbook is eventually dedicated to modern and future nuclear-power reactors and plants. Therefore, in this Subsection we will present information on NPPs in a very concise form. [Table 1.1.5](#) lists five NPPs with the installed capacities ranging from 5924 to 7965 MW_{el}, which are the largest in the world so far. However, the largest in the world the Kashiwazaki-Kariwa NPP (Japan) is not in service yet after the Fukushima Daiichi NPP severe accident in March of 2011. Therefore, in [Table 1.1.6](#) the Bruce NPP (Canada) is only shown as the largest operating power plant (see [Figure 1.1.15](#)). Of course, it should be mentioned that three other NPPs (see [Table 1.1.5](#): one in China—Item 20; and two in South Korea—Items 21 and 22) are very close to the Bruce NPP by the installed capacities, therefore, any time one of these plants can the largest operating one. Of course, when the Kashiwazaki Kariva NPP will restart its operation, it will be not easy to overcome its installed capacity.



Figure 1.1.15. Aerial view of the largest operating NPP in the world—6384-MW_{el} Bruce NPP. (The Douglas Point NPP was Canada’s first full-scale NPP and the second CANDU reactor. Its success was the major milestone for Canada to enter into the global nuclear-power scene. Construction began on Feb. 1, 1960 and the decommission date: May 4, 1984.) (For more details on all current nuclear-power reactors and plants (layouts, power cycles, diagrams, etc.)—see Appendix A1.) *Courtesy of Bruce NPP: www.brucepower.com*

Advantages/*disadvantages* or pros/*cons* of NPPs are:

1. Concentrated in terms of energy density per unit as well as area (see [Tables 1.1.13a and 1.1.13b](#)).
2. Very large installed capacity possible currently up to 8000 MW_{el} (see [Table 1.1.5](#) Item 10).
3. High-capacity factors achievable for long-time operation (about 80%–90% and up 100% for new plants) (see [Table 1.1.8](#) Item 1).
4. *Thermal efficiencies are lower up to two times compared to that of combined-cycle power plants* (see [Table 1.1.7](#)).
5. Reliable and, eventually, safe. However, *three severe accidents have been happened within last 43 years: (1) Three Mile Island NPP (March 1979, USA); (2) Chernobyl NPP (April 1986, USSR (Ukraine)); and (3) Fukushima Daiichi NPP (March 2011, Japan)*. Nevertheless, lessons from these severe accidents have been learned and the required safety enhancements have been incorporated in new reactors designs (for details, see [Chapter 1.2](#) and Appendix A1).
6. Long-term operational (for details, see [Chapter 1.2](#)).
7. The least emitters of CO₂ through the whole life cycle (see [Figure 1.1.5](#) and [Table 1.1.9](#)), *negligible emissions of radioactive gases*, minimum amount of nuclear fuel within the range of 100 to 150t for a couple of years is required, heating value of nuclear fuel is the highest one compared to that of top fossil fuels (can be from 50 to 560 times higher) (see [Table A8.2.7](#)); minimum percent of wastes in total wastes (~0.04%) (see [Table 1.1.12](#)); minimum death rates per TWh compared to that of any other energy sources (see [Figure 1.1.7](#)).
8. More or *less* independent of Mother Nature. However, steam at the outlet of a low-pressure turbine has to be condensed with outside cooling water (natural source, i.e., river, lake, sea, ocean) or with cooling towers (air-cooling) (see [Figure 1.1.10c](#)). Plants can be built almost anywhere, just cooling conditions for turbine condensers have to be satisfied.
9. *Current reactors are not so maneuverable and not fast response ones in terms of power variability*. However, oncoming Small Modular Reactors will be more flexible with power variations.
10. *High capital cost*, but low operational costs due to a small amount of nuclear fuel required for operation during a year. Therefore, NPPs should operate 24/7 with full installed capacity, and this is the only one economical and safe mode of operation for NPPs!
11. LCOE is the lowest one for Long-Term Operation (LTO) (see [Figure 1.1.8](#)).

Modern approaches to address listed above selected deficiencies of NPPs:

4. Current NPPs equipped with subcritical-pressure water-cooled reactors have reached their maximum values of thermal efficiencies (up to 38%, see [Table 1.1.7](#) Item 7). Therefore, next generation or Generation-IV reactors are being designed. These new reactors will be high-temperature reactors cooled with helium, molten metals and/or salts, and supercritical water (for general overview, see [Chapter 2](#)), which allow to increase thermal efficiencies to the level of those of modern thermal power plants (see [Table 2.3](#)).
7. Radioactive wastes should be reprocessed as much as possible, and the rest should be properly stored for tens, hundreds and even more years as required. Next generation or Generation-IV fast-spectrum reactors, which can work as breeders, will help to solve problems with destruction of radioactive wastes. Also, the ultimate storage of high-level radioactive wastes should be their vitrification and putting them inside deep underground facilities ([Pioro et al., 2001](#)).
8. For details, see Item 8 for coaled-fired power plants.

1.1.4 Renewable-energy power plants

1.1.4.1 Hydro

In general, hydro-power plants can be of three types:

1. Plants built on rivers with artificial lakes created upstream of dams—vast majority of the hydro plants (see [Figures 1.1.16a, 1.1.16b and 1.1.17](#)); can be ultra- and superlarge in terms of installed capacities (see [Table 1.1.5](#) Items 1–3, 5–7).

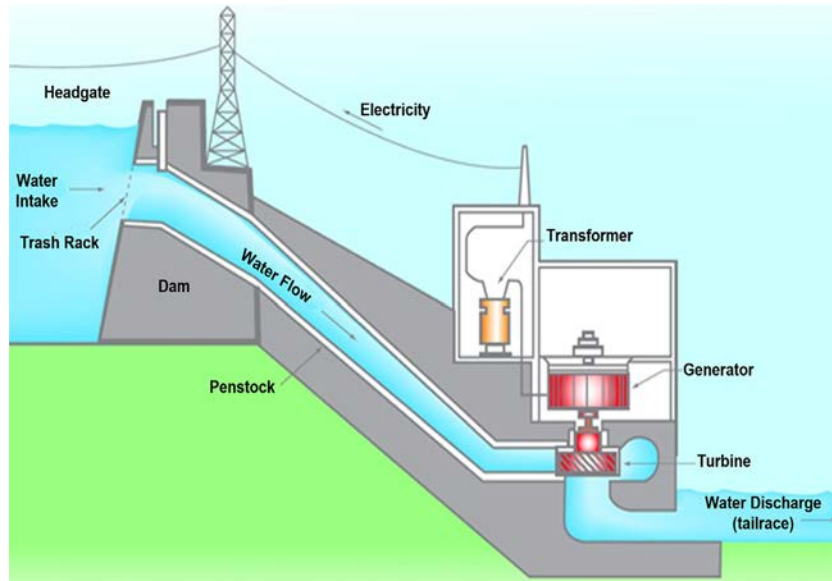


Figure 1.1.16a. Layout of conventional hydroelectric power plant with dam and artificial lake upstream. *Courtesy of Ontario Power Generation (OPG), Canada: www.opg.com*



Figure 1.1.16b. Largest in the world by installed capacity (22,500-MW_{el}) hydroelectric power plant (700 MW_{el} × 30 + 2 × 50 MW_{el} Francis turbines (see [Figure 1.1.16c](#))) (Yangtze River, China). The project costs \$32 billion USD (built within 1992–2012) (\$ 10 billion USD were used for relocation of people). Height of the gravity dam is 181 m, length—2.335 km, top width—40 m, base width—115 m, flow rate—116,000 m³/s, artificial lake capacity—39.3 km³, surface area—1045 km², length—600 km, maximum width—1.1 km, normal elevation—175 m, hydraulic head—80.6–113 m. *Courtesy of Chinese National Committee on Large Dams. Source: Wikipedia*



Figure 1.1.16c. Francis-turbine runner (Yangtze River, China). The Francis turbine is a type of water turbine developed by James B. Francis in 1848 in Lowell, Massachusetts. It is a high-efficiency (90% and beyond) inward-flow reaction turbine that combines radial and axial flow concepts. Francis turbines are the most common water turbine in use today. These turbines are primarily used for electrical-power generation and operate within the head range of 10 to 650 m and the power-output range of 10 to 750 MW_{el}. In general, mini-hydro installations may be with even lower output power. Runner diameter can be between 1 and 10 m, and the speed range of turbine—from 83 to 1000 rpm. Large- and medium-size Francis turbines are most often arranged with a vertical shaft. However, small-size turbines have usually a horizontal shaft. *Courtesy of Chinese National Committee on Large Dams. Source: Wikipedia*



Figure 1.1.17. Photo of the highest in the world 3000-MW_{el} Nurek dam (300 m, Tajikistan). The plant equipped with $335 \text{ MW}_{el} \times 9 = 3015 \text{ MW}_{el}$ Francis turbines. *Photo taken from Wikimedia Commons, author I. Rustamov. Source: Wikipedia*

2. Run-of-the-river in which an artificial lake upstream the dam is not able to store large amounts of water (see Figure 1.1.19), usually have significantly smaller installed capacities within several thousands of MW_{el}, however, the Baihetan hydro plant (see Table 1.1.6 Item 2 (China)) can be up to 16,000 MW_{el}. And,
3. Pumped-Storage Hydro-electricity (PSH) or Pumped Hydro-Electric Energy Storage (PHES), is a type of hydro-electric power plant used by electric grids for load balancing (see Figure 1.1.20 and Table 1.1.6 Item 8).

1.1.4.1.1 Conventional hydro-power plants

Figure 1.1.16a shows a layout of conventional hydroelectric power plant with dam and artificial lake upstream. The vast majority of hydro-power plants are of this type worldwide. Installed capacities are within a very wide range from 22,500 MW_{el} (see Figure 1.1.16b) and to just several kW_{el}. The installed capacity of a hydro plant depends primarily on a river, where it was constructed, i.e., river flow rate, size and depth (i.e., hydrostatic pressure) of an artificial lake. Therefore, locations of such hydro plants are quite unique places on our planet, especially, for ultra-, super-, and very-large power plants (see Table 1.1.5 and Figures 1.1.17 and 1.1.18). Usually, hydro plants built on plains have less installed capacities compared to those built in hilly/mountain areas, because on plains large artificial lake will cover significantly larger area.

Advantages/*disadvantages* or pros/*cons* of hydro-power plants are:

1. Here we have a dilemma in terms of: If hydro plants are concentrated source of energy or not! The answer is that everything depends on how we estimate area of a plant, i.e., (based on the largest in the world Three Gorges Dam hydro plant, see Table 1.1.5 and Figure 1.1.16b) if we take into consideration only dam length (2.4 km) and knowing that this plant has installed capacity of 22,500 MW_{el}, it will be ultra-high density per dam length. Just for comparison with NPP, this installed capacity means ~22 nuclear-power reactors with 1000-MW_{el} capacity each within 2.4 km! However, if we consider the area of the artificial lake, which is 1084 km², the Bruce NPP energy density (0.68 kW/m²) will be in 32 times higher than for that of this hydro plant (is 0.021 kW/m²) and if account average capacity factors it will be even much more difference (see Table 1.1.13a)!
2. Very large or the largest in the world installed capacities are possible, currently, up to 22,500 MW_{el}.
3. High-capacity factors achievable only for small installed-capacity hydro plants with large artificial lakes. Based on the world average (see Table 1.1.8), *the capacity factor is about 45%, and it is the Mother Nature controls capacity factors*. In general, capacity factors depend significantly on a design, size, and location (water availability) of a hydro-electric power plant. Small plants built on large rivers will always have enough water to operate at full capacity year-round.
4. Usually, it is quite efficient plants.
5. Reliable and safe—in general, yes. However, *in a dry season (if it's possible, with climate change it is started to be more often possible) electricity generation can be decreased significantly or even seized. Any dam is a potential danger, usually, for people living downstream of the dam, if the dam collapses or equipment fails*. And, unfortunately, we have such accidents around the world (see Figure 1.1.7 and Table 1.1.10 Items 4–6).
6. Long-term operational.
7. Hydro power is one of the most environmentally-friendly renewable-energy source (see Figure 1.1.5 and Table 1.1.9 Item 9). However, *artificial lakes cover quite significant areas of land, which in many cases can be used for agriculture, for forestry, for recreational purposes, and for other more useful applications, especially, on plains*. In mountains, a land is usually unused by humans, and artificial lakes can be with smaller surface areas, but quite deep (see Figure 1.1.17), which is better for large installed-capacities hydro plants. Nevertheless, *higher dams—more danger from their collapsing. Moreover, deep mountain artificial lakes can be a source to trigger earthquakes due to an extra pressure of water on the surface below (300 m of water = 30 kg_f/cm² = 300 t_f/m² = 300 Mt_f/km²)*.
8. *Very dependable on Mother Nature through climate and location*.
9. Maneuverable/fast response in terms of power variability.
10. *High capital cost*, but relatively low operational costs (see Figure 1.1.8). And
11. Levelized Cost Of Energy (LCOE) is within from low to medium range (see Figure 1.1.8).

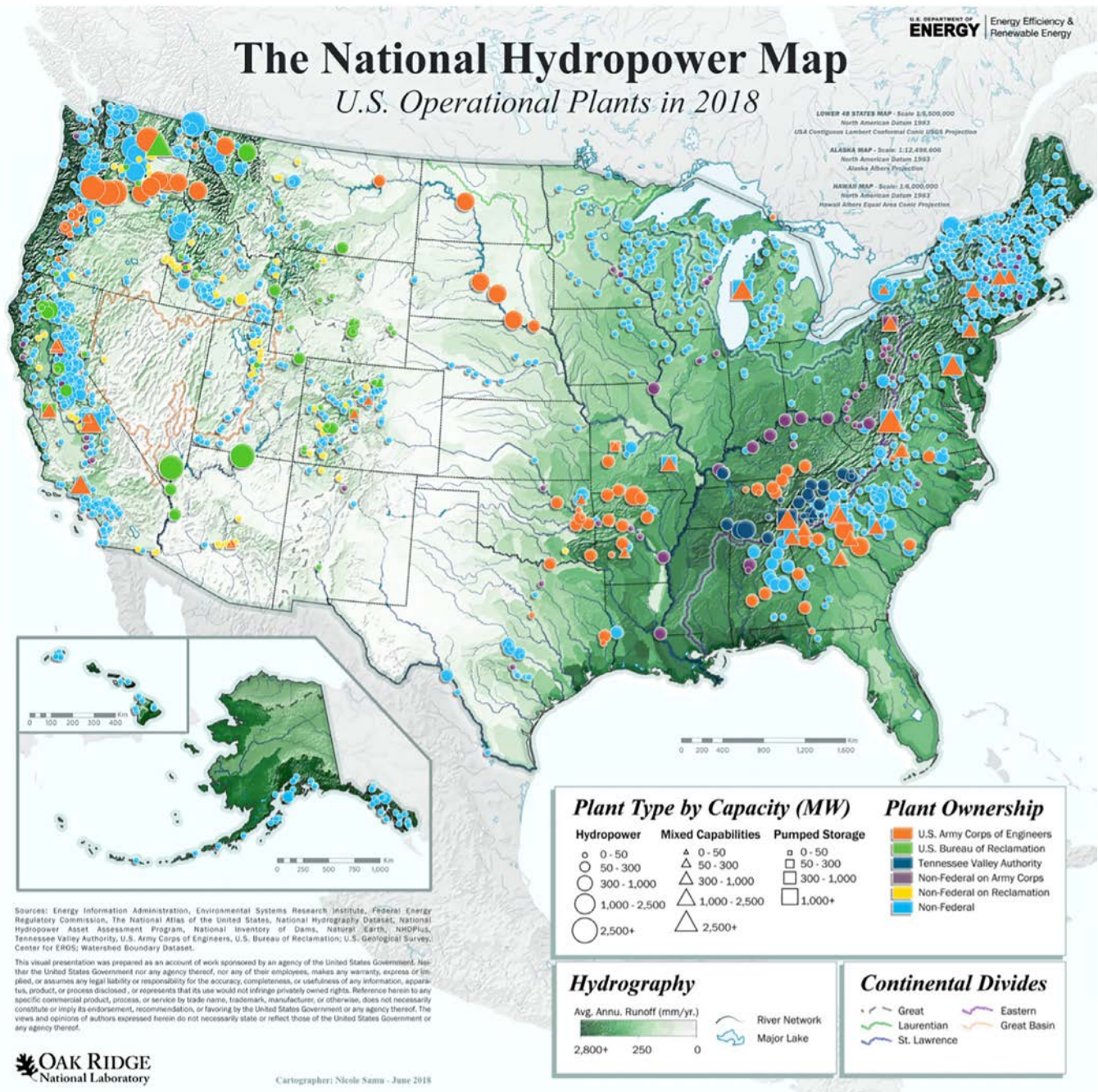


Figure 1.1.18. The USA national hydropower map. Courtesy of DOE USA: https://www.energy.gov/sites/default/files/2018/06/f53/national_hydropower_map_2018.pdf

1.1.4.1.2 Run-of-the-river hydro-power plants

These hydro plants are less common, because it is even more difficult to find such locations, where there is no need to have a large artificial lake upstream of a dam (see Figure 1.1.19). Due to this their installed capacities are usually lower than those of conventional hydro plants (see Table 1.1.6 Item 8). In general, more or less all advantages/disadvantages or pros/cons are quite similar to those of conventional hydro-power plants.



Figure 1.1.19. Aerial view of 2620-MW_{el} run-of-the-river (i.e., an artificial lake upstream the dam is not able to store large amounts of water) Chief Joseph hydroelectric power plant—one of largest in the world (Bridgeport, WA, USA). The plant equipped with 27 Francis turbines ~ 100 MW_{el} each. Height of the gravity dam is 72 m, length—1.817 km, top width—7 m, base width—50 m, flow rate—6030 m³/s, artificial lake capacity—0.636 km³, surface area—34 km², length—82 km. *Photo taken from Wikimedia Commons, original photo by U.S. Army Corps of Engineers. Source: Wikipedia*

1.1.4.1.3 Pumped-Storage Hydro-Electric Power Plant (PSHEPP)

These hydro plants can be also named as Pumped-Storage Hydro-electricity (PSH) or Pumped Hydro-electric Energy Storage (PHES). Layout of a PSHEPP is shown in Figure 1.1.20. These plants have two modes of operation: (1) during peak hours, usually during a day, they operate as a conventional hydro plant and supply electricity into a grid and (2) during off-peak hours, usually, at night, they pump up water from lower lake into the upper lake to be ready for operation next day. During a year PSHEPPs have negative balance of electrical power, i.e., less electricity generation, more energy taken from the electrical grid for their operation. Such plants quite often operate in the grids with NPPs using cheaper energy from NPPs during night hours and supplying energy during rush hours helping for NPPs to operate in the most economical and efficient way, i.e., at 100% installed capacity. Relatively small number of such hydro plants have been built in the world. And, of course, their locations are even more unique compared to those of two other types' hydro plants.

1.1.4.2 Wind

Wind power plants are separated into two types: (1) on-shore or in-land and (2) off-shore, which are located in shallow waters of lakes, seas, and oceans.

1.1.4.2.1 On-shore wind farms (power plants)

Figure 1.1.21 shows the world's largest 14,000-MW_{el} wind power plant (Gansu, China) (see also, Tables 1.1.5 and 1.1.6). In addition, Figures 1.1.22a and 1.1.22b show some details of a wind turbine and its foundation, and Figure 1.1.23—one of the largest in US onshore wind-turbine power plant (Roscoe, Texas, USA). In general, a number of different types' of wind turbines are being developed, but those commonly used are shown in Figures 1.1.21, 1.1.22a, and 1.1.23. It seems that although, we have winds almost

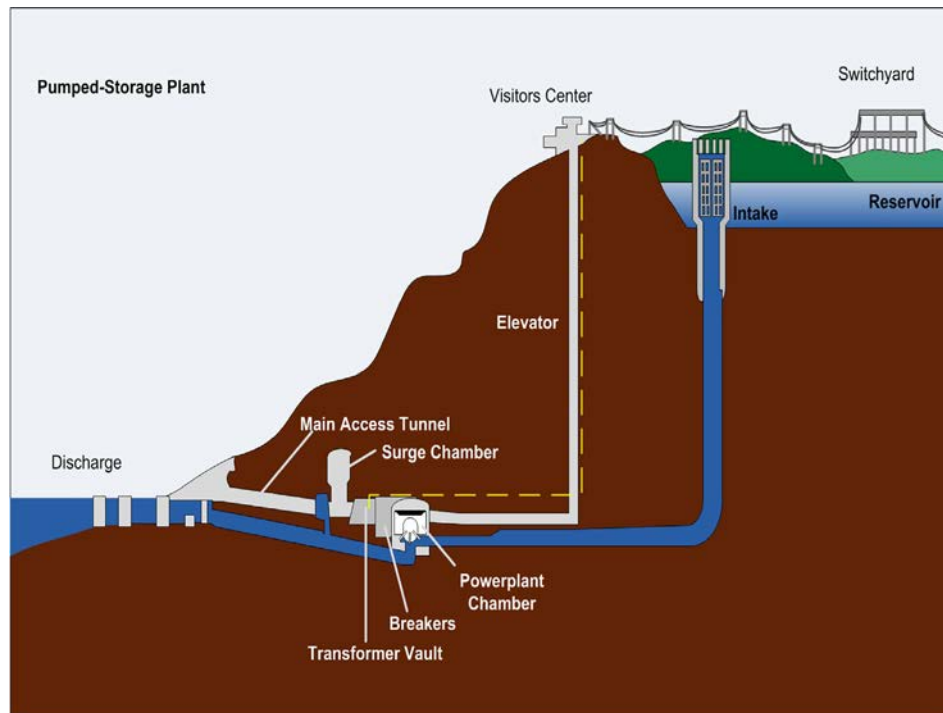


Figure 1.1.20. Layout of Pumped-Storage Hydro-Electric Power Plant (PSHEPP). *This image is work of US Tennessee Valley Authority employee: http://en.wikiversity.org/wiki/Power_Generation-hydro_Power (no copyright has been claimed)*



Figure 1.1.21. The world's largest 14,000-MW_{e1} wind power plant (Gansu, China) (https://en.wikipedia.org/wiki/Gansu_Wind_Farm). The total project investment is RMB 120 billion (~\$18.6 billion USD). In 2010, the installed wind power capacity in Jiuquan was mainly 200 MW_{e1} wind farm. The wind farm included 134 wind turbines with a single capacity of 1.5 MW_{e1}, 11 in each row, 12 rows in total with a row spacing of 900 m at intervals of 300 m. The first 3800-MW_{e1} phase includes 18 set of 200-MW_{e1} wind farms and two sets of 100-MW_{e1} wind farms. The second 8000-MW_{e1} phase includes 40 sets of 200-MW_{e1} wind farms. *Photo by Popolon: https://commons.wikimedia.org/wiki/File:Guazhou.champs_%C3%A9oliennes.jpg*



Figure 1.1.22a. Kochubeevskaya Wind Power Plant (Russia). Eighty-four wind turbines by NowaWind (each 2.5MW_{el} installed capacity), total 210MW_{el} , area 2km^2 , energy density $\sim 105\text{W}/\text{m}^2$ ($105\text{MW}_{\text{el}}/\text{km}^2$), wind turbine height 150m with rotor, turbine blade 50m and mass 8.6t, tower mass 200t, generator mass 52t, and total mass 320t (<http://novawind.ru/production/our-projects/kochubeyevskaya-wind-farm/>). Courtesy of Rosatom: <https://www.flickr.com/photos/rosatom/50173012221/in/album-72157713699988403/>



Figure 1.1.22b. Each wind turbine requires relatively large and heavy concrete foundation to withstand possible high winds and requires road access for servicing. Courtesy of Rosatom: <https://www.flickr.com/photos/rosatom/50173267572/in/album-72157713699988403/>



Figure 1.1.23. 781-MW_{el} onshore Roscoe wind-turbine power plant (Texas, USA)—one of the largest in US. Plant equipped with 627 turbines: 406 MHI 1-MW_{el}; 55 Siemens 2.3-MW_{el} and 166 GE 1.5-MW_{el}. The project cost more than 1 billion dollars, and provides enough power for more than 250,000 average Texan homes and covers a land area of nearly 400 km², which is several times the size of Manhattan, New York, NY, USA. In general, wind power is suitable for harvesting when an average air velocity is at least 6 m/s (21.6 km/h) (It should be noted that the latest and the largest in the world wind turbine by Alstom (6-MW_{el net} wind turbine for the Haliade Offshore Platform has a rotor with the diameter of 150 m and tower 100-m high) can operate within the following range: from 3 m/s (10.8 km/h) and up to 25 m/s (90 km/h) (<http://www.alstom.com/power/renewables/wind/turbines/>)) (see also wind-speed distribution over the US in Figures 1.1.24a and 1.1.24b). *Wikimedia Commons, photo by author/username: Fredlyfish4*

everywhere, in spite of that, the vast majority of wind turbines can operate within the following range of wind speeds from 6 m/s (21.6 km/h) to 25 m/s (90 km/h). Therefore, if we look at the map of the wind-speed distribution over the US (Figures 1.1.24a and 1.1.24b), we can see that large inland areas of the US have average wind speeds below 6 m/s (all the following colors: dark green, green, light green, yellow, and light brown), i.e., not really suitable to harvest wind power on industrial scale, while the US coastal areas are more suited for harvesting the wind power.

Advantages/disadvantages or pros/cons of wind power plants are:

1. Based on the data listed in Tables 1.1.13a and 1.1.13b, it can be concluded that on average *wind has an energy density significantly lower even than that for hydro*, as this is the nature of things.
2. However, using large areas covered with many turbines, wind power plants can be within super-large power-plants range (see Tables 1.1.5 and 1.1.6). Currently, the largest in the world wind power plant is Gansu (China) (see Figure 1.1.21) with installed capacities up to 14,000 MW_{el}. Modern wind turbines have installed capacities usually within the range of 1 to 2.5 MW_{el}.
3. In general, *high-capacity factors are not possible due to natural wind variability*, as such, on average the capacity factor in the US is about 34%, and in the world, it is about 20% to 40% (see Table 1.1.8). In general, as it is for other renewable sources, *capacity factors depend significantly on a location, climate, time-of-day, and weather*. Small wind farms built within areas with relatively high and consistent winds (coastal areas, in mountains, etc.) might have enough power to operate at full capacity year-round.
4. *As the result, Load Factor and overall generating Efficiency are not very high*, so back-up generation for low wind days is required.

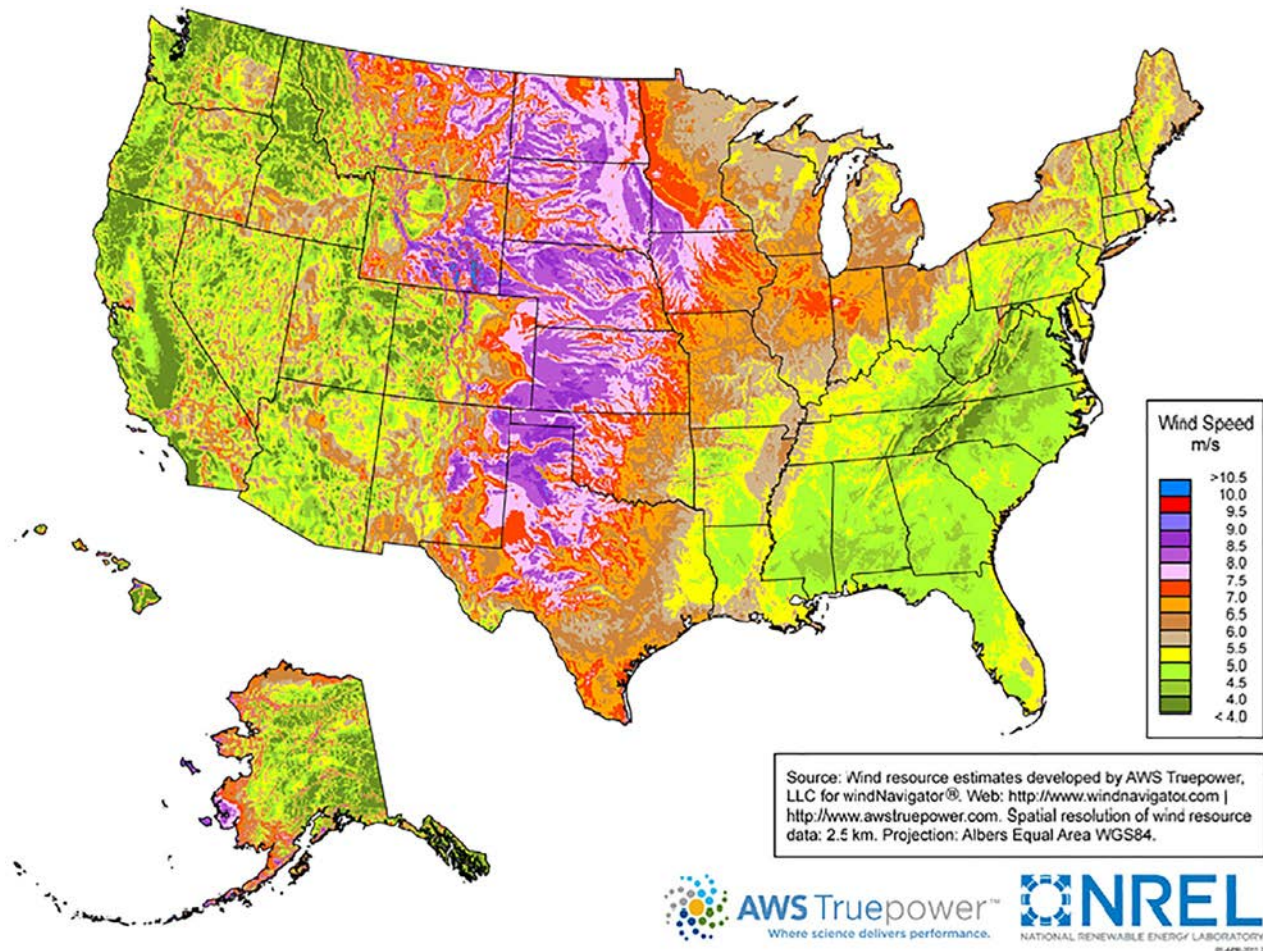


Figure 1.1.24a. Map of wind-speed distribution over the US. Shown here just for reference purposes and as an example, winds with average speed of 6 m/s and above (*brown, red and purple colors*) exist inland only over the central part of the US from North to South. However, average wind speeds along the US shores of Great Lakes, Atlantic and Pacific oceans, and Gulf of Mexico are usually higher than 6 m/s at the height of 90m from the sea level. *Courtesy of DOE, USA*

5. *Potentially unreliable and have ecological impacts* (for details, see [Figure 1.1.25](#)). For people, these plants in general are safe (see [Figure 1.1.7](#)). Usually, wind farms are built in remote areas, because at certain conditions ultrasound can be generated with turbine rotors, which can be unpleasant for humans. Moreover, in addition to direct collisions, due to high turbulence created with rotating blades bird and bats wings can be damaged, and they will die.
6. Long-term operational is possible with effective maintenance and replacement strategies.
7. Wind power plants have the lowest CO₂ emissions as those from NPPs, if the whole cycle is considered (see [Figure 1.1.5](#) and [Table 1.1.9](#) Item 12).
8. *See Item 3.*
9. *Cannot be maneuverable and fast response in terms of power variability.*
10. Low capital and operational costs, especially, with subsidies and preferential supply contracts. And
11. Lower Levelized Cost Of Energy (LCOE) for the on-shore wind farms is quite low compared to that for many other power plants, but for the off-shore plants will be above the medium level (see [Figure 1.1.8](#)).

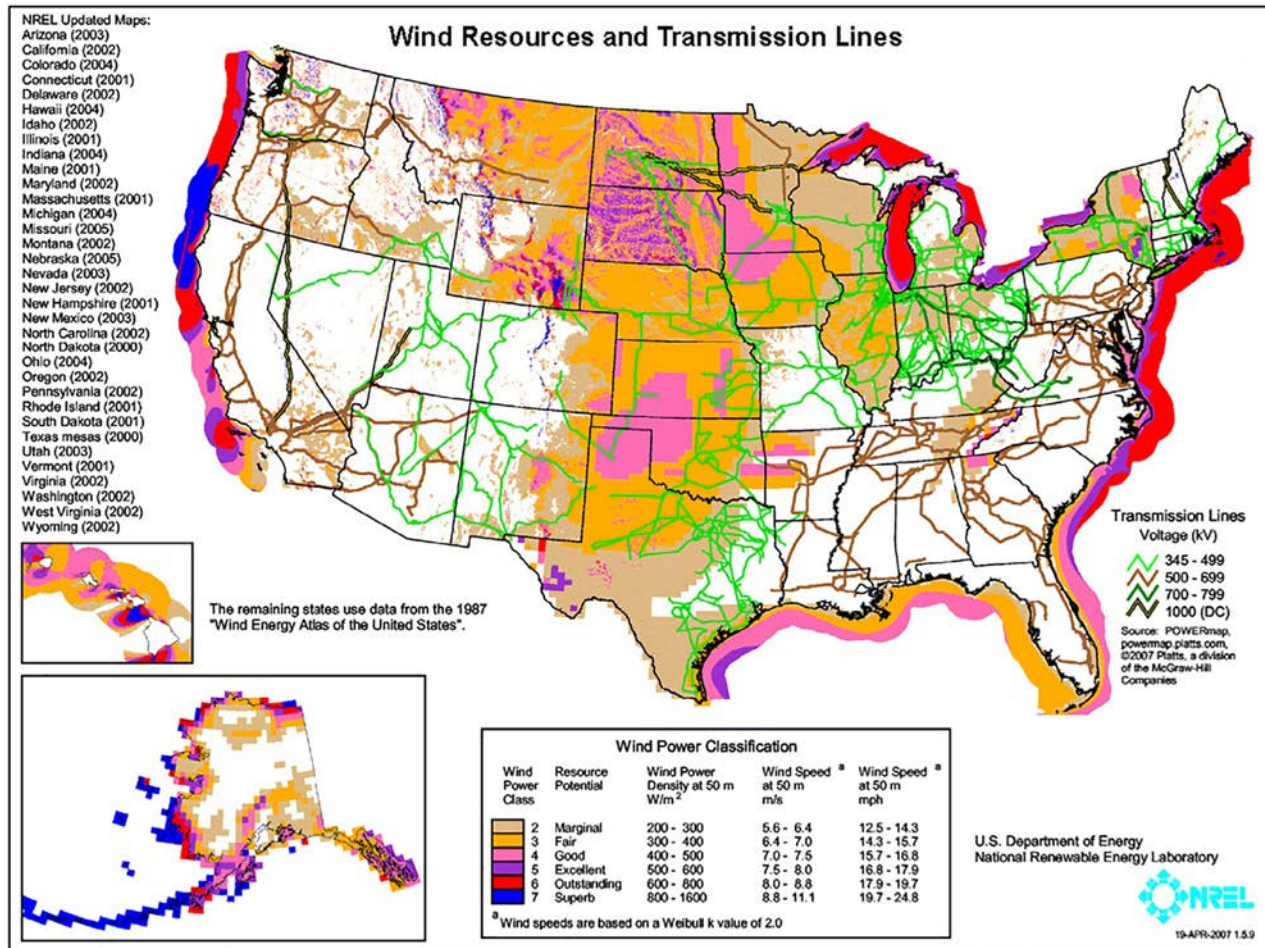


Figure 1.1.24b. Map of wind-speed distribution over the US (including coastal areas) with major transmission power lines (voltage ranges are show in legend) for electricity distribution (Shown here for reference purposes and as an example). *Courtesy of DOE, USA, <https://i.pinimg.com/originals/df/ac/c6/dfacc6ecb1e0fc32890473d5343e8c4f.jpg>*

1.1.4.2.2 Off-shore wind farms (power plants)

Figure 1.1.26a shows the aerial view of 207-MW_{el} off-shore Nysted (Rødsand) wind-turbine power plant (Denmark); Figure 1.1.26b is a photo of the off-shore wind park (Horns Rev. II, Denmark) with a ship for installation of off-shore turbines; and Figure 1.1.26c—an off-shore Nysted (Rødsand-1, Denmark) wind turbine with basic dimensions. In general, off-shore wind plants have on average significantly smaller installed capacities (see Table 1.1.6 Item 14), but wind turbines can be significantly larger than those installed in-land (see Figure 1.1.26c and Table 1.1.15).

Advantages/disadvantages or pros/cons of these wind plants are more or less the same as for those installed in-land. Specifics can be stronger winds near coastal lines, and large turbines with installed capacity 6 MW_{el} and up can harvest wind at the minimum speed of 3 m/s (10.8 km/h).

1.1.4.3 Solar

Solar power plants can be of several types: (1) concentrated-solar thermal power plant with a tower and sun-tracking heliostats (see Figures 1.1.27a and 1.1.28a); (2) concentrated-solar thermal power plant with parabolic mirrors (see Figures 1.1.29–1.1.32); (3) flat-panel PhotoVoltaic (PV) power plant (see

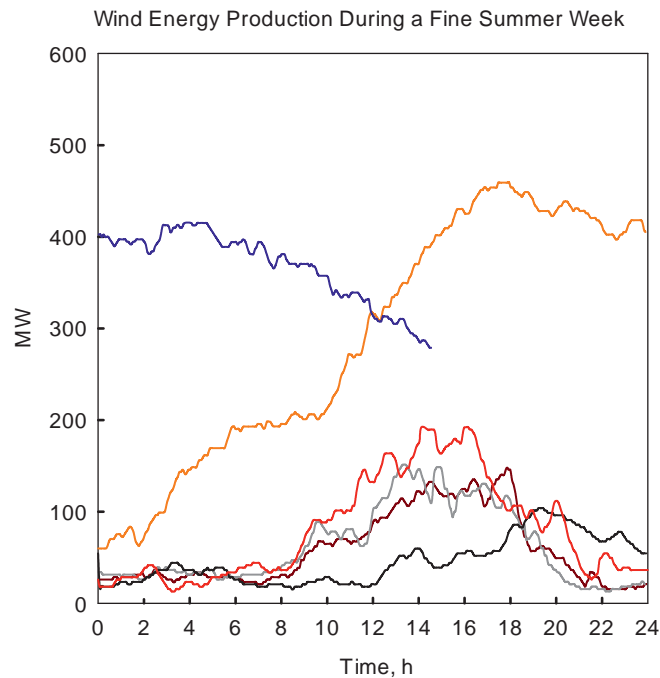


Figure 1.1.25. Power generated by 650-MW_{el} wind power plant in the Western Part of Denmark. Shown a summer week (6 days, see various color profiles) of wind-power generation. Power profiles show significant impact of the sun on operation of wind plant per day and week. *Based on data from www.wiki.windpower.org/index.php/variations_in_energy*

Figure 1.1.33); and (4) concentrated PV solar-power plant (see Figures 1.1.34 and 1.1.35). Figures 1.1.27b and 1.1.36 show maps of concentrating solar-power resources and PV solar resources over the US, respectively. These maps show clearly that to have higher solar-energy flux, we have to move south and into dry areas (deserts).

1.1.4.3.1 Concentrated-solar thermal power plant with a tower and sun-tracking heliostats

Figure 1.1.27a shows one of the largest in the world concentrated-solar thermal power plant—the Ivanpah Solar Electric Generating System (Mojave Desert, California, USA), where the extremely bright lights at the focal points on the towers can be seen from great distances. This plant has three towers with heat exchangers and corresponding to that three fields of heliostats around them. The plant uses subcritical-pressure Rankine steam-turbine cycle for the power conversion of solar energy into electricity with the working fluid being water/steam, heated in heat exchangers installed inside each tower and undergoing boiling process and steam reheating. Gross thermal efficiency of the plant is $\sim 29\%$, which is almost 2 times lower than that of the top supercritical-pressure coal-fired power plants and 1.5 times lower than that of subcritical-pressure coal-fired power plants (see Table 1.1.7), it is understandable, because of lower steam parameters at the turbine inlet and, possibly, no secondary-steam reheat. The significant disadvantage of using single-loop Rankine cycle is that this plant cannot operate at night and forced to use electricity from a grid (steam cannot be stored for night operation), so the capacity factor is not very high $\sim 31\%$.

Figure 1.1.28a shows similar thermal solar plant as above, but this plant has double loop arrangement, with molten salt as the working fluid in the primary loop, and is equipped with molten-salt heat-storage system.

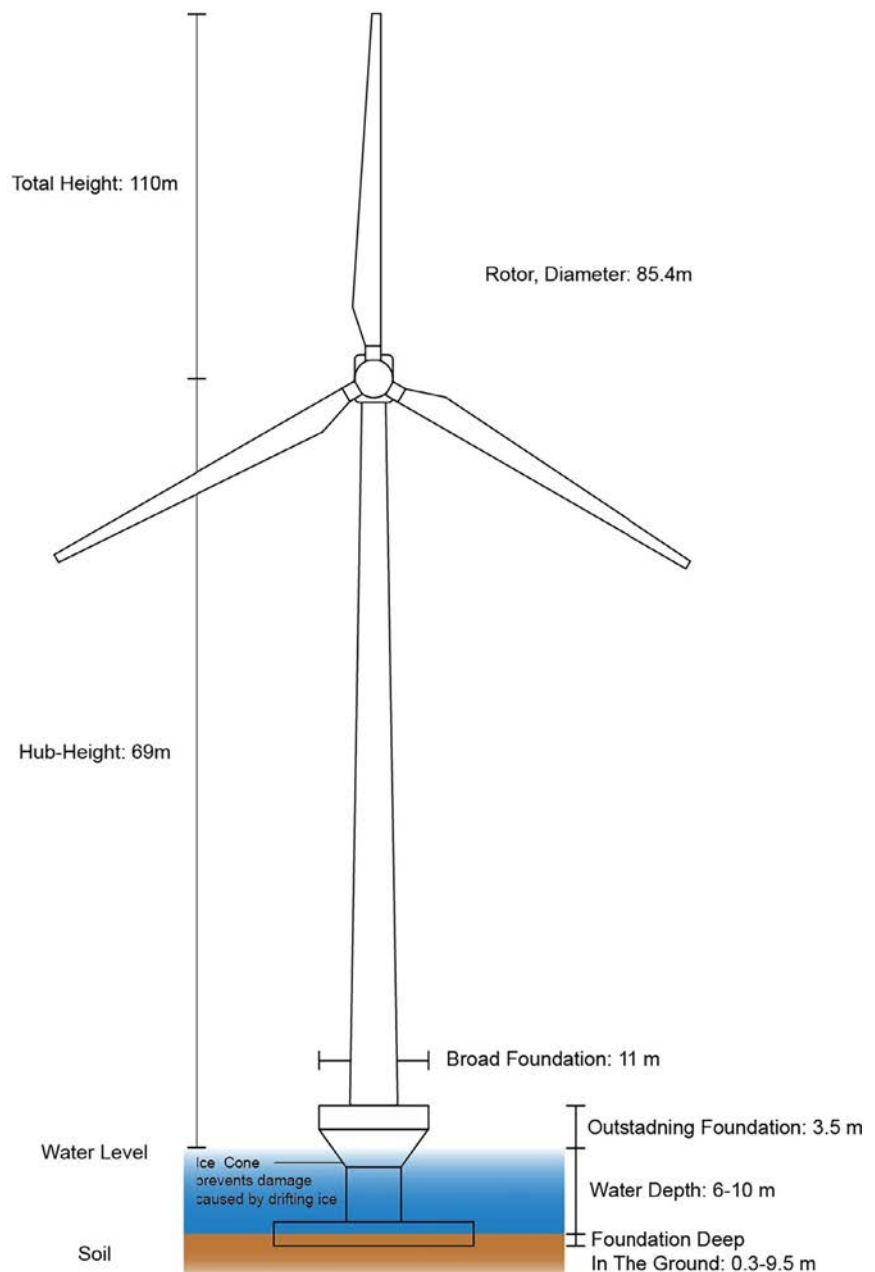


Figure 1.1.26a. Aerial view of 207-MW_{el} off-shore Nysted (Rødsand) wind-turbine power plant (Denmark). The plant equipped with ~ 90 turbines 2.3-MW_{el} each. The power plant provides enough power for more than 246,000 average Danish homes. *Photo taken from Wikimedia Commons, author Plenz: https://en.wikipedia.org/wiki/Nysted_Wind_Farm#/media/File:Windpark_Nysted.jpg. Source: Wikipedia*



Figure 1.1.26b. Photo of off-shore wind park (power plant), Horns Rev. II (Denmark). The facility, located in the North Sea, has the maximum output of about 210 MW_{el} (91×2.3 MW_{el} Siemens wind turbines), enough to meet the electricity needs of approximately 200,000 households. In general, as of today, offshore wind power plants are, at least, 2.5–3 times smaller by installed capacity than onshore wind power plants, but offshore wind turbines can be significantly larger by power and by a rotor diameter compared to that of onshore turbines (see [Figure 1.1.26c](#)). *Siemens press photo; copyright Siemens AG, Munich/Berlin, Germany*

Figure 1.1.26c. Off-shore Nysted (Rødsand-1) wind turbine (Denmark). New wind turbines: (1) Alstom 6-MW_{el net} wind turbine for Haliade Off-shore Platform: Rotor diameter—150-m and tower 100-m high; in operation (<http://www.alstom.com/power/renewables/wind/turbines/>) (see also, Table 1.1.15). (2) MHI Vestas Off-shore Wind: 10-MW_{el}, rotor diameter—164 m; 3 blades—each 80-m long and 35 t weight; swept area 21,124 m²; nacelle (gondola with power equipment on tower)—20 m long, 8-m wide and 8-m high, weight 390 t; hub height 105 m; tip height 187 m; can be delivered in 2021. And (3) Siemens Gamesa (SG 10.0–193 DD): 10-MW_{el}, rotor diameter—193 m; three blades—each 94-m long; swept area 29,300 m²



Secondary loop is water-steam subcritical-pressure Rankine power cycle. This plant can operate at night or/ and on cloudy days using stored energy in the molten salt, but, within winter time, a couple of hours of operation might not be covered with stored energy (see Figure 1.1.28b,c). Due to this the overall capacity factor is very high (on average 63%–75%) compared to that of other types' solar plants, but, this plant has quite low thermal efficiency (about 19%) even lower than that of the Ivanpah previous one.

Figures 1.1.29–1.1.32 show slightly different concentrated-solar thermal power plant, which equipped with parabolic mirrors: Figure 1.1.29—aerial view of Solar Energy Generating Systems (SEGS)

Table 1.1.15. Basic parameters of Alstom 6-MW_{el net} wind turbine (<http://www.alstom.com/power/renewables/wind/turbines/>)

Parameters	Operating data
Wind turbine class	I-B IEC ^a -61,400–1/IEC-61400-3
Rated power	6.0 MW _{el} (net after transformer)
Cut-in wind speed	3 m/s (10.8 km/h)
Cut-out wind speed (10 min average)	25 m/s (90 km/h)
Grid frequency	50/60 Hz
<i>ROTOR</i>	
Rotor diameter	150 m
Blade length	73.5 m
Rotor swept area	17,860 m ²
Rotor speed range	4–11.5 rpm
Tip speed	90.8 m/s (324 km/h)
<i>GENERATOR</i>	
Type	Direct drive permanent magnet
Rated voltage	900 V per phase
Number of phases	3 × 3
Protection class	IPPss
<i>CONVERTER</i>	
Type	Back-to-back 3-phase AC/AC
Output voltage	900 V
<i>TOWER</i>	
Type	Tubular steel
Hub height	100 m (or site-specific)
Standard color	RAL 7035
<i>POWER-CONTROL SYSTEM</i>	
Type	Variable speed and independent pitch control by blade
<i>ENVIRONMENTAL SPECIFICATIONS</i>	
Normal air temperature range	–10 to +40°C
Extreme air temperature range	–30 to +50°C
Lighting protection	Class I acc. IEC 62305-1

^a IEC—International Electrotechnical Commission.



Figure 1.1.27a. Aerial view of one of the world's largest concentrated-solar thermal power plant—the Ivanpah Solar Electric Generating System, Mojave Desert, California, USA situated in a remote and largely uninhabited area, but close to a US interstate highway from near Los Angeles to Las Vegas, Nevada (visible crossing the top of picture). Installed capacities: Gross—392 MW_{e1} and net—377 MW_{e1}; capacity factor 31%; planned annual generation ~1040 GWh; site area 16 km² (4000 acres); deploys 173,500 sun-tracking heliostats, each has two mirrors (reflecting-surface area is $7.02 \times 2 = 14.04 \text{ m}^2$; total reflecting area is 2.4 km^2). The intercepted average solar heat flux is about 0.31 kW/m^2 , but taking into consideration reflection, transmission, radiation, and absorption losses, becomes about 0.17 kW/m^2 (efficiency is ~55%). The heliostat mirrors focusing sunlight on receivers located on solar-power towers (~140-m height), which generate steam to drive single-casing reheat turbines (~130 MW (174,000 hp)) with a gross thermal efficiency of the plant ~29%. The plant is equipped with air-cooled condensers. The project cost is \$2.2 billion US, and the electricity generated can serve more than 140,000 homes in California during the peak hours of the day, while reducing carbon dioxide (CO₂) emissions by more than 400,000 tons per year. Negative impact: (a) birds killed by instantaneous burning and due to crashing into mirrors (150 birds were killed in 1 month); (b) cannot operate at night, since, there is no thermal-storage system. Accidents/Incidents: Quite unusual accident has happened at the Ivanpah Solar Electric Generating System in May of 2016 (<https://www.powernmag.com/fire-is-latest-hurdle-for-ivanpah-concentrating-solar-power-plant/>). Based on the article by A. Larson and according to the San Bernardino County (CA) Fire Department (SBCFD) the following information was reported: The Ivanpah Unit 3 fire “was caused by the heliostats (mirrors) being locked in place in preparation for a maintenance activity (maintenance mode), causing the solar flux to briefly move over a portion of the boiler tower. The mirrors were unlocked and moved to remove the solar flux from the tower. The damage to Unit 3 was primarily limited to the aluminum covering of the insulation around pipes, as well as wiring and some valves.” *Photo by Craig Butz. Source: Wikipedia*

(California, USA); **Figure 1.1.30**—General layout of a typical Concentrated Solar Power Plant (CSPP); **Figure 1.1.31**—close view of parabolic mirrors; and **Figure 1.1.32**—a photo of molten-salt heating element consisted of stainless-steel pipe inside glass tube and vacuumed annular gap between them for decreased heat losses to be used in parabolic-trough solar thermal power plants.

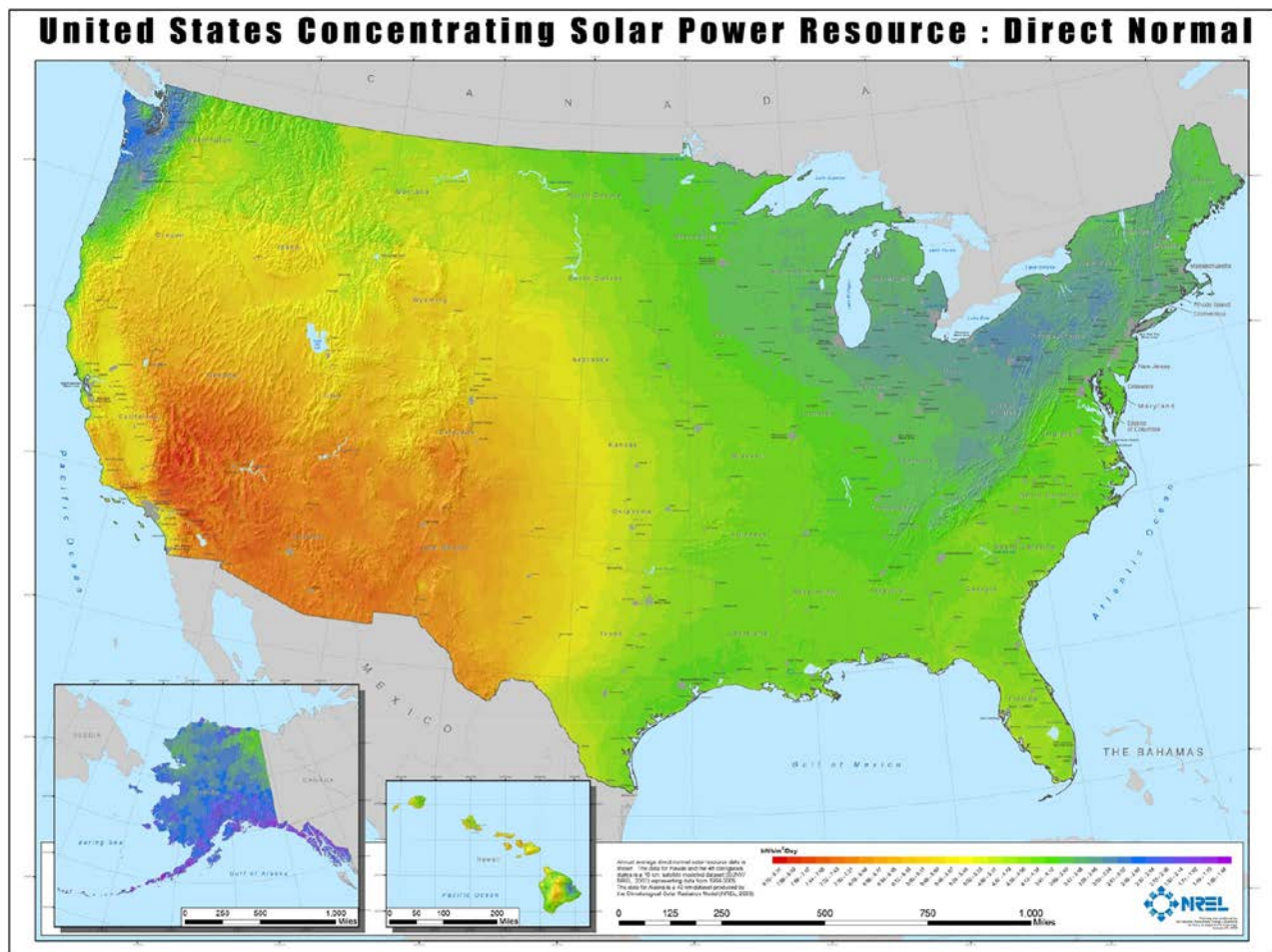


Figure 1.1.27b. Map of concentrating solar-power resources over the US: Direct normal (shown here just for reference purposes and as an example). In general, the amount of solar radiation that reaches any one spot on the Earth's surface varies according to: (1) Geographic location; (2) Time of day; (3) Season; (4) Local landscape, and (5) Local weather. *Courtesy of DOE, USA*

1.1.4.3.2 Flat-panel PV and concentrated PV solar-power plants

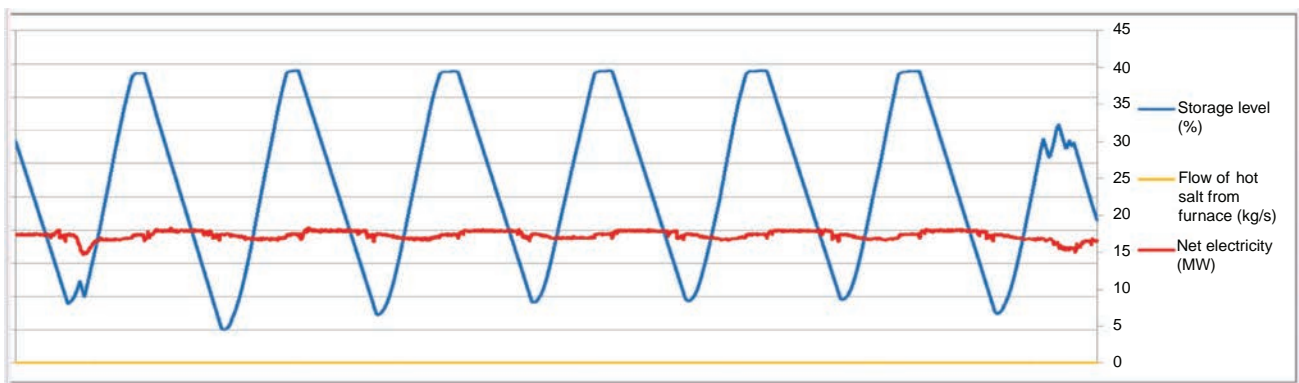
Flat-panel PV solar-power plant is shown in Figure 1.1.33a; and PV panels installed on a house and a roof of a parking lot are shown in Figure 1.1.33b and c, respectively. New concentrated PV panels, which are currently developed, are shown in Figures 1.1.34 and 1.1.35. PV panels allow to transfer solar energy directly into electrical current, the basic idea to eliminate the extra energy conversion step, which in general decreasing energy efficiency, and to simplify layout of solar power plant (Figure 1.1.36).

Advantages/disadvantages or pros/cons of solar power plants are:

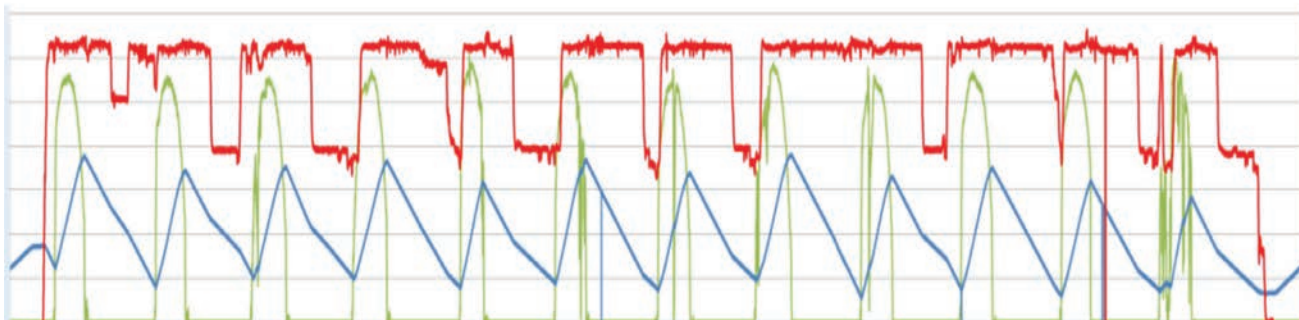
1. Based on the data listed in Table 1.1.13a, it can be concluded that *solar power plants have quite low energy density lower than that for hydro, so require large land areas, which should not displace other beneficial uses.*
2. By using very large areas covered with many PV panels, heliostats or parabolic mirrors, or concentrated PV panels, solar power plants can be within the ranges of large, medium, and small power-plants, respectively (see Table 1.1.6 Items 10, 16, 19). Currently, the largest in the world solar plants are: solar PV plant in Bhadla (India) with installed capacities up to 2245 MW_{el}; solar (concentrated)—up to 510 MW_{el}; and concentrated PV—up to 60 MW_{el}.



Figure 1.1.28a. Aerial view of the first of such kind Gemasolar—19.9-MW_{el} concentrated solar-power plant with 140-m high tower and molten-salt heat-storage system (Seville, Spain). The plant consists of 2650 heliostats (each 120 m² and total reflective area 304,750 m²), covers 1.95 km² (195 ha) and produces 110 GWh annually, which equals to 30,000 t/year carbon-dioxide emission savings. This energy is enough to supply 25,000 average Spanish homes, with the storage system allowing the power plant to produce electricity for 15 h without sunlight (at night or on cloudy days). Capacity factor is 63%. Solar-receiver thermal power is 120 MW_{th}, and plant thermal efficiency is about 19%. Molten salt is heated in the solar receiver from 260°C to 565°C by concentrated sun light reflected from all solar-tracking heliostats, and transfers heat in steam generator to water as working fluid in subcritical-pressure Rankine-steam-power cycle. *Source: Wikipedia. Courtesy of SENER/TORRESOL ENERGY*



(b) Summer operation



(c) Winter operation (for description of profiles, see Figure (b))

Figure 1.1.28b,c. Operation of Gemasolar concentrated solar-power plant (Seville, Spain): (b) Summer operation. During summer time, days are long. Hot molten-salt tank reaches upper limit in the middle of the afternoon, forcing plant to reduce collection of energy in receiver; and (c) in winter time, days are shorter and at the end of the day, tank is not full. *Courtesy of SENER/TORRESOL ENERGY*



Figure 1.1.29. Aerial view showing portions of Solar Energy Generating Systems (SEGS), California, USA. SEGS is the largest solar-energy power plant in the world consisting of nine concentrated-solar-thermal plants with $354 \text{ MW}_{\text{el}}$ installed capacity. (See annual average direct normal solar-resource-data distribution over the US in Figure 1.1.27b.) The average gross solar output of SEGS is about $75 \text{ MW}_{\text{el}}$ (capacity factor is $\sim 21\%$), and at night, turbines can be powered by combustion of natural gas. NextEra claims that the SEGS power 232,500 homes and decrease pollution by 3800 t/year (if the electricity had been provided by combustion of oil). The SEGS have 936,384 mirrors, which cover more than 6.5 km^2 . If the parabolic mirrors are lined up, would extend over 370 km. In 2002, one of the 30-MW_{el} Kramer Junction sites required 90 million dollars to construct, and its O&M costs are about 3 million dollars per year, which result in an initial generating cost of 4.6 ¢/kWh , but, with a considered lifetime of 20 years, the O&M and investments interest and depreciation triples the price, to approximately 14 ¢/kWh . *Wikimedia Commons: Photo by A. Radecki. Source: Wikipedia.*

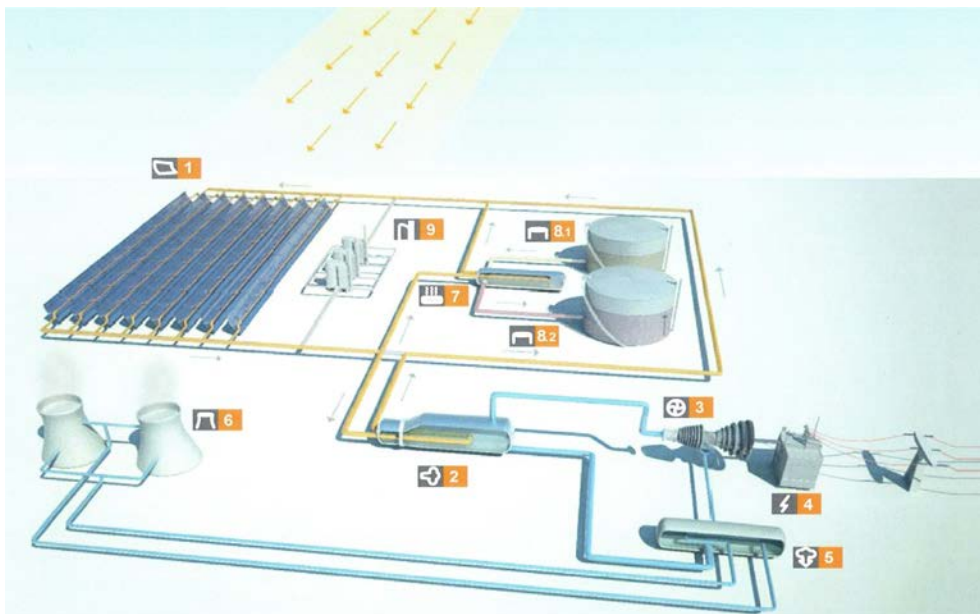


Figure 1.1.30. General layout of typical Concentrated Solar Power Plant (CSPP): 1—SENERtrough[®] collectors; 2—steam-generator system; 3—steam turbine with electrical generator; 4—electrical transformer; 5—condenser; 6—cooling towers; 7—heat exchanger; 8—thermal-storage system; and 9—Heat Transfer Fluid (HTF) boiler. *Based on Valle 1 and 2 CSPP built in the province of Cadiz, Spain by SENER/TORRESOL ENERGY. Courtesy of SENER/TORRESOL ENERGY.*



Figure 1.1.31. The parabolic mirrors are shaped like a half-pipe, where the sun shines onto the glass panels, which are 94% reflective, unlike a typical mirror, which is only 70% reflective, and the mirrors automatically track the sun throughout the day. The greatest source of mirror breakage is wind, with 3000 mirrors typically replaced each year, so operators can turn mirrors to protect them during intense wind storms. An automated washing mechanism is used to clean periodically parabolic-reflective panels. The reflected sunlight is directed to a central tube filled with synthetic oil, which heats to over 400°C (750°F). The light focused at the central tube is 71 to 80 times more intense than the ordinary sunlight. The synthetic oil transfers its heat to water, which boils and drives the Rankine-cycle steam turbine for generating electricity, the oil being used (instead of water) to keep the pressure within manageable parameters. Accidents/incidents: In February 1999, a 900,000-US-gallon (3400 m³) Therminol storage tank exploded at the SEGS II (Daggett) solar power plant, sending flames and smoke into the sky. Authorities were trying to keep flames away from two adjacent containers that held sulfuric acid and sodium hydroxide. The immediate area of 0.5 mile² (1.3 km²) was evacuated. *Courtesy of SENER/TORRESOL ENERGY. Source: Wikipedia*



Figure 1.1.32. Photo of molten-salt heating element consisted of stainless-steel pipe inside glass tube and vacuumed annular gap between them for decreased heat losses to be used in parabolic-trough solar thermal power plants (so-called, High-Performance Solar Thermal Power (HPSThP) project). *Siemens press photo; copyright Siemens AG, Munich/Berlin, Germany*



(a) Photo of a typical flat-panel photovoltaic power plant (19-MW_{el}) located near Thüngen, Bavaria, Germany (Wikimedia Commons: Photo by OhWeh).



(b) photovoltaic panels installed on roof of house.



(c) photovoltaic panels installed on roof of parking lot.

Figure 1.1.33. “Improper” (a) and “proper” (b) and (c) installation of photovoltaic panels: (a) Photo of a typical flat-panel photovoltaic power plant (19-MW_{el}) located near Thüngen, Bavaria, Germany; (b) Photovoltaic panels installed on roof of house; and (c) Photovoltaic panels installed on roof of parking lot. (a) *Wikimedia Commons: Photo by OhWeh*. Photos (b) and (c) by I. Pioro, Bavaria, Germany

3. In general, *high-capacity factors are not possible due to daily cycles*, so, on average the capacity factor in the US for concentrated solar is 22% and for PV about 27%, in Spain for concentrated solar with molten-salt storage about 63% and for concentrated PV only 12%; in UK for PV also 12% (see [Table 1.1.8](#)). In general, as it is for other renewable sources, *capacity factors depend significantly on a location, climate, and weather in addition to the inevitable day/night variation*.
4. *Efficiency is not very high due to natural cycles and variability, including cloud cover, summer/winter seasons*, so desert-like and hot climates are best, which usually means added transmission costs.
5. *Unreliable, especially, PV plants* (for details, see [Figure 1.1.37](#)), but for people these plants in general are safe (see [Figure 1.1.7](#)). However, ecological impacts beyond large-land-use areas include *concentrated-solar thermal power plants with towers and heliostats setting birds on fire, when they get into very intensive reflected light from heliostats* (working fluid temperature inside heat exchanger in the



Figure 1.1.34. Photo of 1.2-MW_{el} concentrated PhotoVoltaic (PV) solar-power plant (Spain). The plant has 154 two-axis tracking units, consisting of 36 PV modules each, which cover area of 295,000 m² with a total PV-surface area of 5913 m². Plant generates 2.1 GWh annually. Conversion efficiency is 12%. *Wikimedia Commons, author/username: afloresm*



Figure 1.1.35. Photo of a test system consisting of 40 High Concentrating PhotoVoltaic (HCPV) modules with about 34% efficiency. This test system is a joint effort of Semprius (Durham, North Carolina, USA) and Siemens in collaboration with the Spanish Institute of Concentration Photovoltaic Systems (ISFOC) and the University of Madrid. Leading modules' manufacturers of conventional PV technologies achieved the maximum module efficiency of about 20% with mono-crystalline PV modules and about 16% with polycrystalline technology. *Siemens press photo; copyright Siemens AG, Munich/Berlin, Germany*

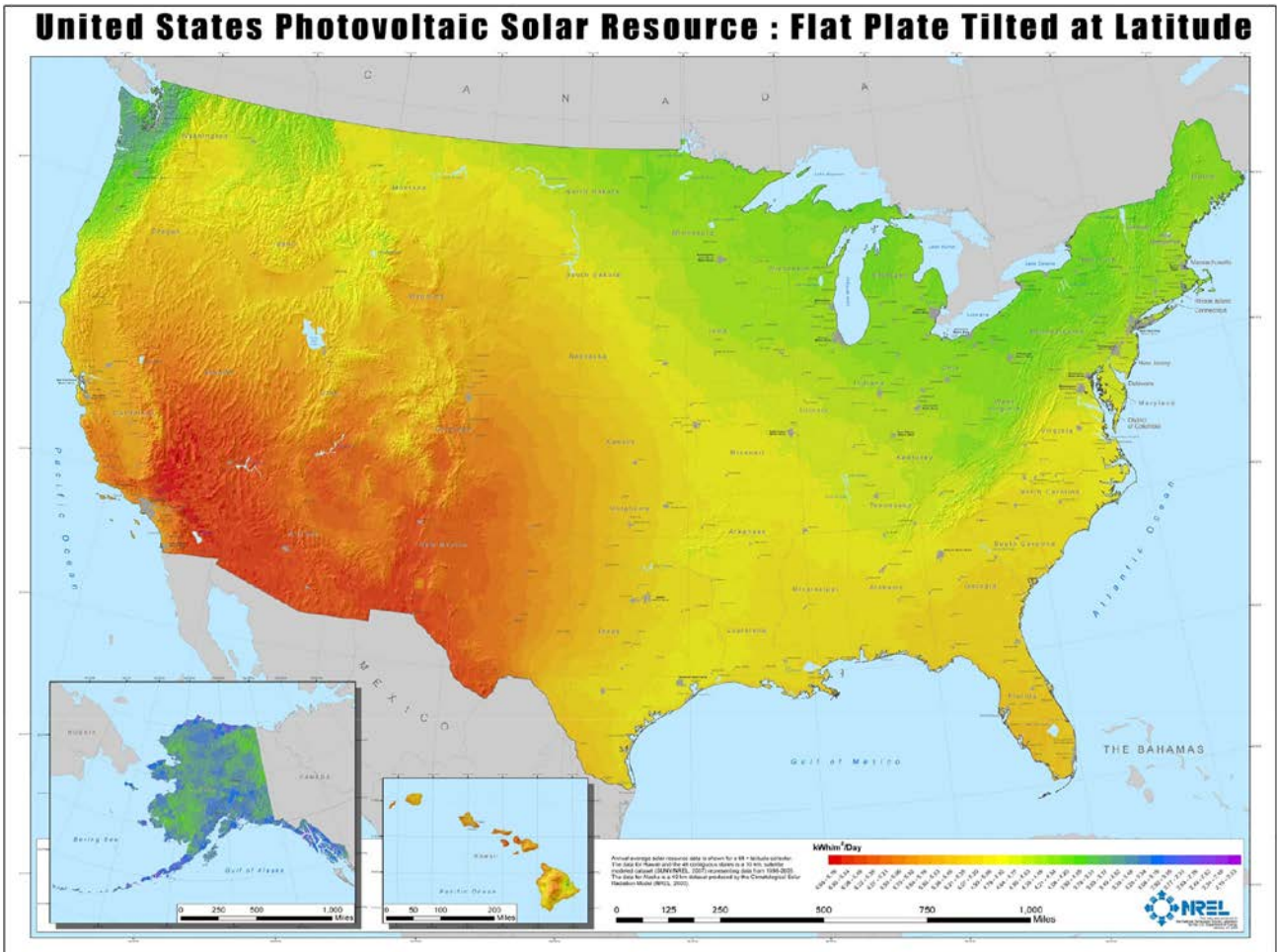


Figure 1.1.36. Map of photovoltaic solar resources over the US: Flat plate tilted at latitude (shown here just for reference purposes and as an example). In general, the amount of solar radiation that reaches any one spot on the Earth’s surface varies according to: (1) geographic location; (2) time of day; (3) season; (4) local landscape and (5) local weather. *Courtesy of DOE, USA*

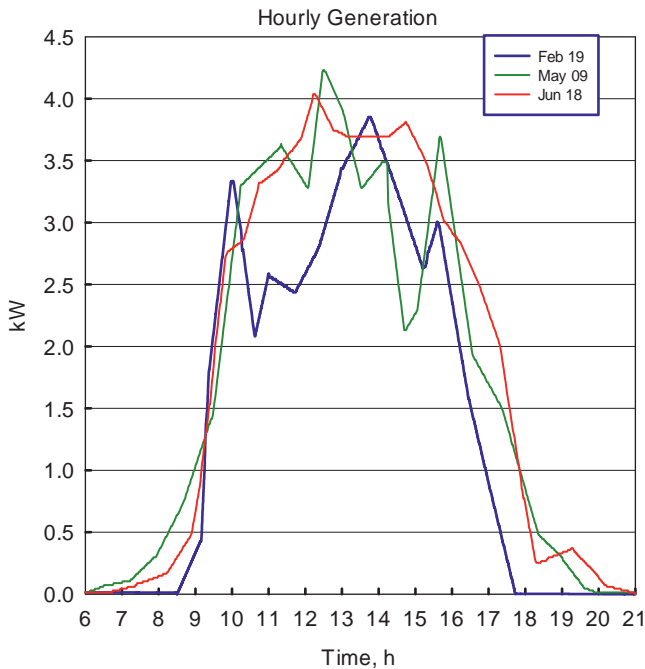


Figure 1.1.37. Power generated by photovoltaic system in New York State (USA): Shown three mostly sunny days: February 19th; May 9th, and June 18th. *Based on data from www.burningcutlery.com/solar*

tower can reach 565°C). Also, water birds can hit heliostats and damage themselves, assuming that this is a water surface.

6. Long-term operational is possible with adequate maintenance, replacement, and repair strategies.
7. Solar power plants have quite low CO_2 emissions close to that of wind and NPPs, if the whole cycle is considered (see [Figure 1.1.5](#) and [Table 1.1.9](#) Item 8).
8. *Very dependable on Mother Nature through location, climate, and weather.*
9. *Cannot be maneuverable and fast response in terms of power variability*, so requires back up generation (e.g., CCGTs), which increases costs.
10. Not very high capital and operational costs. And
11. Levelized Cost Of Energy (LCOE) for the solar power plants is the highest one in power industry (see [Figure 1.1.8](#)).

1.1.4.4 Geothermal

1.1.4.4.1 Geothermal plants

As it was mentioned before, geothermal energy is based on the heat produced deep in the Earth's core (about 2900 km below the Earth's crust with temperatures of about 5000°C). Therefore, this heat is considered as renewable source of energy. [Figure 1.1.38](#) shows aerial view of the Hellisheiði geothermal power plant, which supplies electricity and heat to nearby settlements, and [Figure 1.1.39](#)—map of geothermal resources of the US. Geothermal plants as other renewable energy sources can be built only in special locations, where very hot layers of the Earth crust are quite close to the surface (see [Figure 1.1.39](#)). [Table 1.1.16](#) lists selected countries with geothermal power plants.

In general, geothermal plants can be of three basic types (see [Figure 1.1.40](#)): (1) dry-steam plants; (2) flash-steam type; and (3) binary-cycle type. Usually, these plants are of smaller installed capacities compared to those of fossil-fuel-fired thermal power plants (see [Table 1.1.16](#)). The Ormat company (<http://www.ormat.com/geothermal-power>) gave us permission to show their more detailed layouts of various types geothermal power plants together with photos of these plants put into operation around the world. As such, [Figure 1.1.41a](#) shows Ormat air-cooled binary geothermal power plant and [Figure 1.1.41b](#)—photo of the same type plant in Nevada (USA); [Figure 1.1.42a](#)—Ormat air-cooled



Figure 1.1.38. Aerial view of 303-MW_{el} and 133-MW_{th} Hellisheiði geothermal power plant (45 MW_{el} × 6 units + 33 MW_{el} unit) (Iceland). *Photo taken from Wikimedia Commons, original photo from www.thinkgeoenergy.com. Source: Wikipedia*

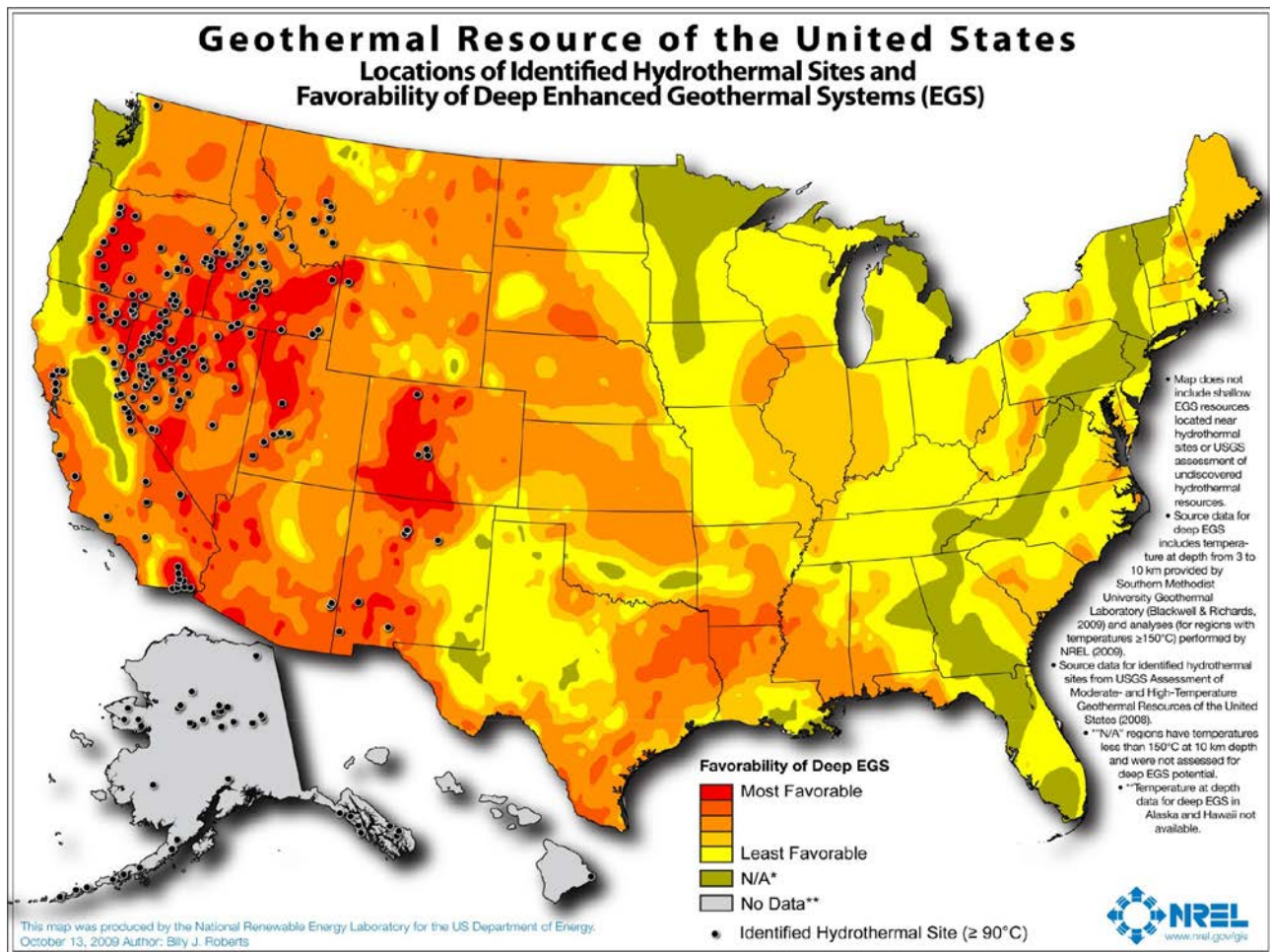


Figure 1.1.39. Map of geothermal resources of the US (shown here just for reference purposes and as an example). *Courtesy of DOE, USA*

Table 1.1.16. List of selected countries with geothermal power plants

No.	Country	Capacity (MW_{el}), 2010	% of national production
1	United States	3086	0.3
2	Philippines	1904	27
3	Indonesia	1197	4
4	Mexico	958	3
5	Italy	843	1.5
6	New Zealand	628	10
7	Iceland	575	30
8	Japan	536	0.1
9	Iran	250	—

Continued

Table 1.1.16. List of selected countries with geothermal power plant—cont'd

No.	Country	Capacity (MW _{el}), 2010	% of national production
10	El Salvador	204	25
11	Kenya	167	11
12	Costa Rica	166	14
13	Nicaragua	88	10
14	Russia	82	—
15	Turkey	82	—
16	Papua-New Guinea	56	—
17	Guatemala	52	—
18	Portugal	29	—
19	China	24	—
20	France	16	—
21	Ethiopia	7.3	—
22	Germany	6.6	—
23	Austria	1.4	—
24	Australia	1.1	—
25	Thailand	0.3	—
—	Total	10,960	—

Source: Wikipedia.

geothermal combined-cycle power plant and [Figure 1.1.42b](#)—photo of the same type plant in Puna, Hawaii (USA); and [Figure 1.1.43a](#)—Ormat air-cooled integrated geothermal combined-cycle power plant and [Figure 1.1.43b](#)—photo of the same type plant in New Zealand.

Geothermal power plants are equipped with subcritical-pressure Rankine steam-turbine cycle. Their steam parameters at the turbine inlet are usually lower than those in fossil-fuel-fired power plants and very significantly depend on the temperature of a heat source.

1.1.4.5 Tidal

1.1.4.5.1 Tidal plants

Tidal plants are eventually hydro plants, because working fluid is sea or ocean water. Not too many of them operate around the world, because to have a relatively reasonable installed capacity absolutely unique places have to be found in which tides are very high. [Figure 1.1.44a](#) shows a photo of 240-MW_{el} Rance tidal power plant in France, and [Figure 1.1.44b](#)—a schematic of the tidal plant dam and turbine. It should be noted that at the highest tide and the lowest one, there is no water movement within short time, therefore, these plants have a cyclic operation. [Table 1.1.17](#) lists selected tidal power plants of the world. Installed capacities of these plants are quite low due to the nature of things.

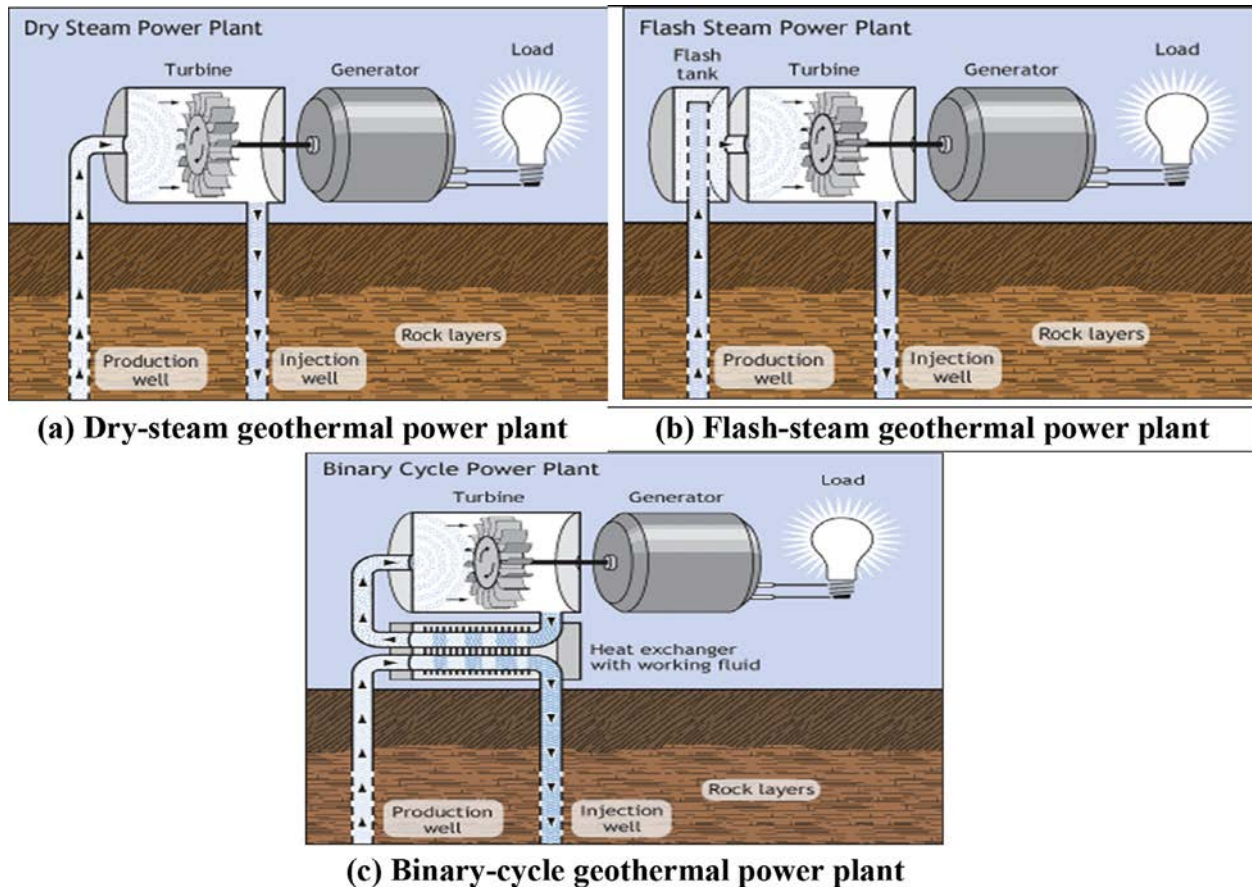


Figure 1.1.40. Three basic types of geothermal plants: (a) Dry-steam geothermal power plant, (b) flash-steam geothermal power plant, and (c) binary-cycle geothermal power plant. *Courtesy of DOE USA: www1.eere.energy.gov/geothermal/images/drysteam.gif*

1.1.4.6 Wave

1.1.4.6.1 Wave power plants

Wave power plants are the smallest group of renewable-energy power plants with the smallest installed capacities and capacity factors. Figures 1.1.45 and 1.1.46 show photos of such plants in two different locations and from different angles; and Figure 1.1.47—schematic of wave-energy converter. Table 1.1.18 lists wave power plants of the world. It is very difficult to believe that these types of plants will be used widely, because of their characteristics/parameters discussed above.

1.1.5 Actual examples of operating power grid with non-renewable and renewable sources

The Province of Ontario (Canada) uses non-renewable and renewable energy sources to generate electricity for decades. In this Section two examples of electrical-grid operation during: (1) 2012–2013, which included coal-fired power plants and (2) 2019, when coal-fired power plants have been eliminated; are presented and discussed.

Figure 1.1.48 shows sector diagrams of installed capacity (a) and electricity generation (b) by energy source in the Province of Ontario (Canada) during 2012, when population was about 13.4 million people.

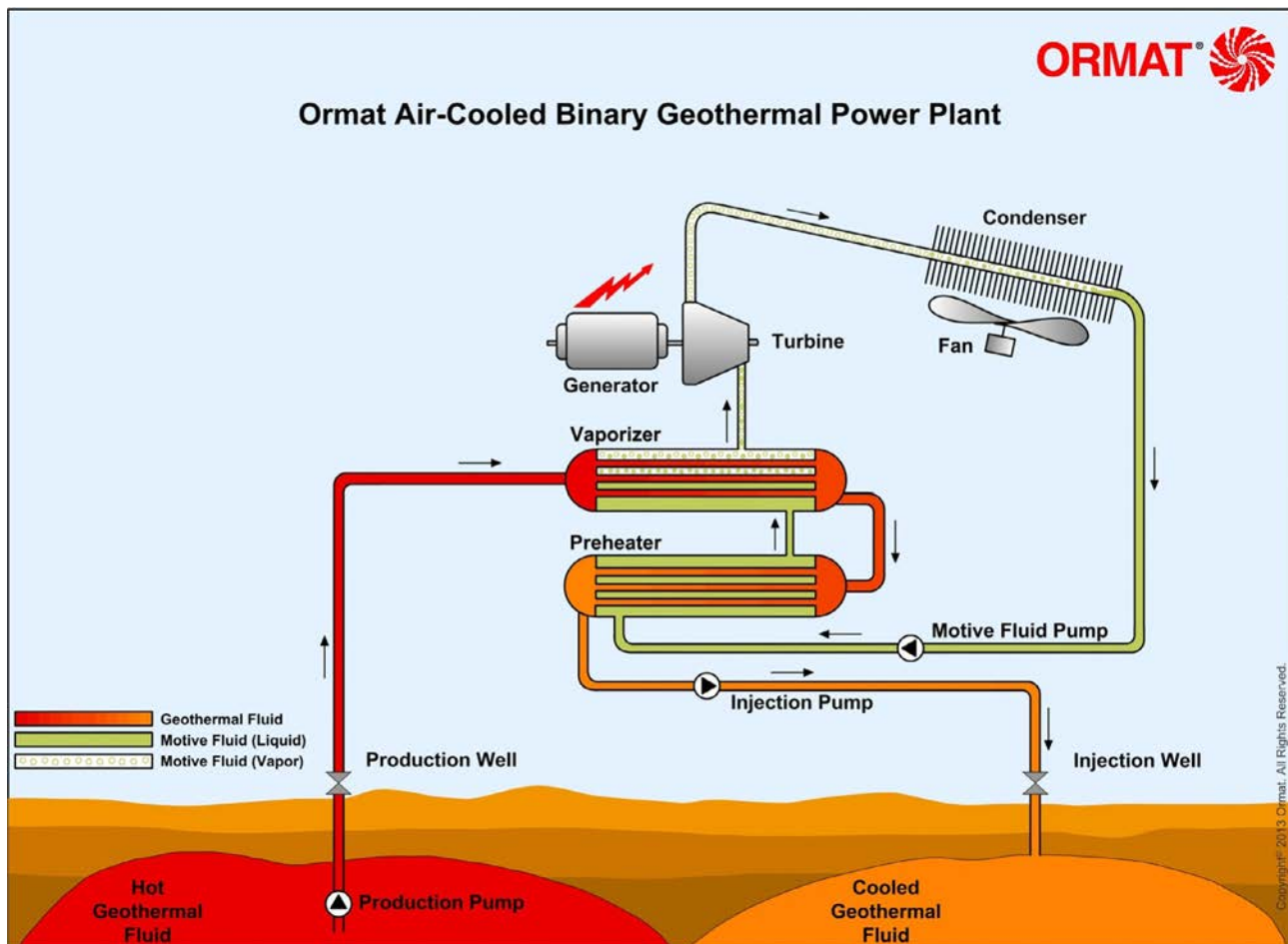


Figure 1.1.41a. Ormat air-cooled binary geothermal power plant. *Courtesy of ORMAT, USA: <http://www.ormat.com/geothermal-power>*

Figure 1.1.41b. Photo of Ormat air-cooled binary geothermal power plant (20 MW_{el})—Galena I, Nevada, US. *Courtesy of ORMAT, USA: <http://www.ormat.com/geothermal-power>*



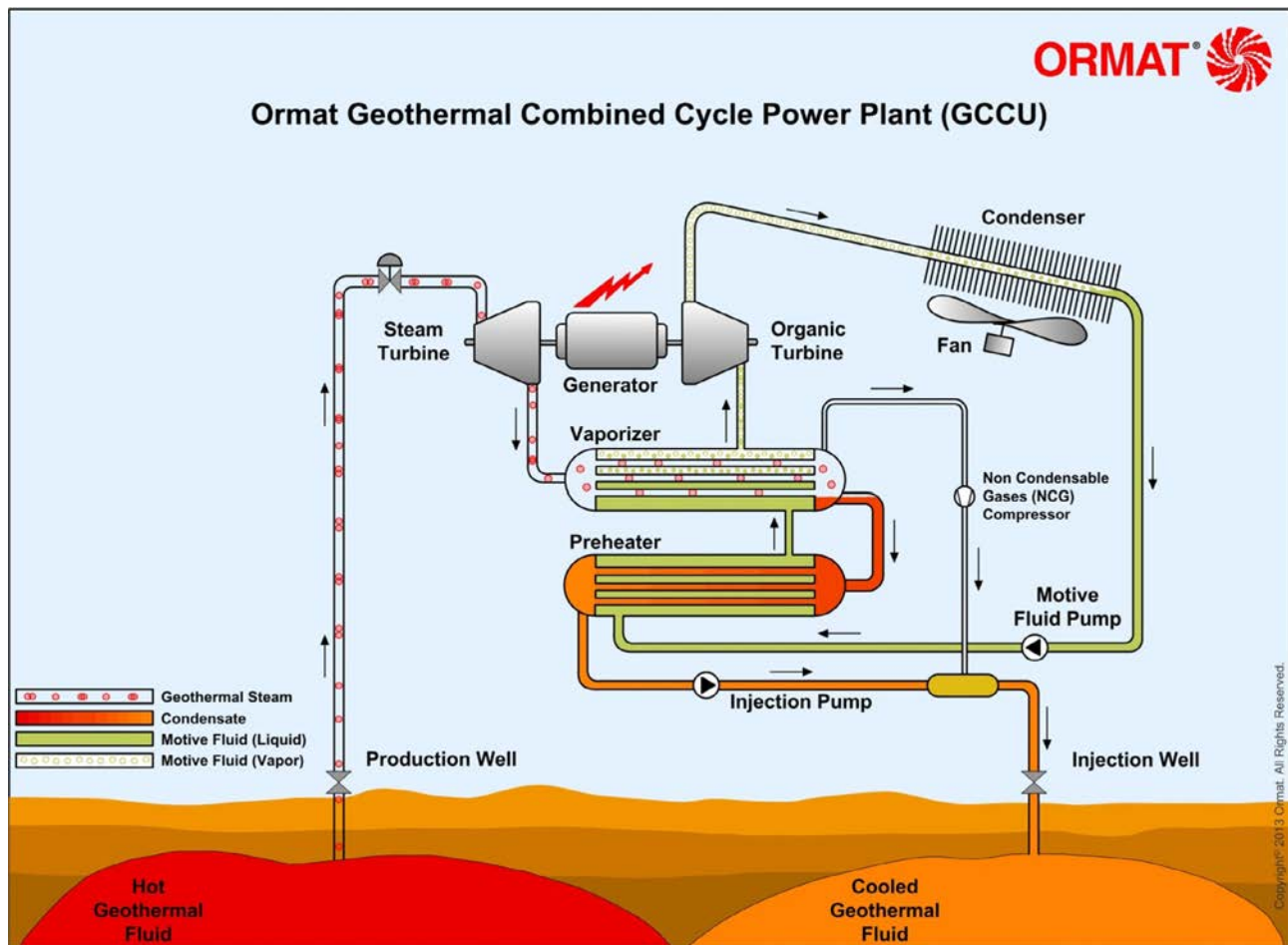
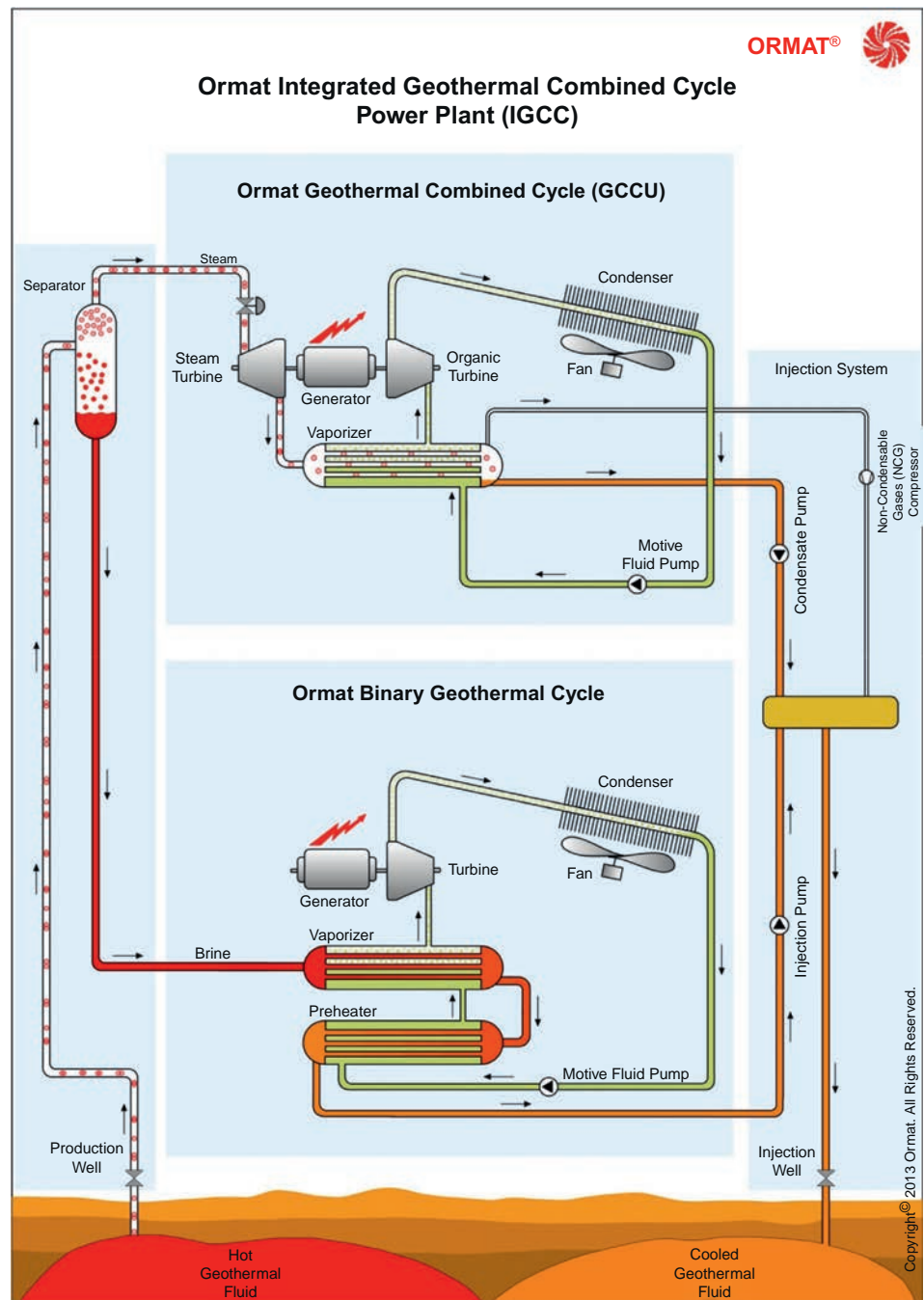


Figure 1.1.42a. Ormat air-cooled geothermal combined-cycle power plant. *Courtesy of ORMAT, USA:* <http://www.ormat.com/geothermal-power>



Figure 1.1.42b. Photo of Ormat air-cooled geothermal combined-cycle power plant (30 MW_{el})—Puna, Hawaii, US. *Courtesy of ORMAT, USA:* <http://www.ormat.com/geothermal-power>

Figure 1.1.43a. Ormat air-cooled integrated geothermal combined-cycle power plant. Courtesy of ORMAT, USA: <http://www.ormat.com/geothermal-power>



Analysis of Figure 1.1.48a shows that in Ontario the major installed capacities in 2012 were nuclear (31%), gas (24%), hydro (21%), coal (7%), and renewables (mainly wind) (7%). However, electricity (see Figure 1.1.48b) was mainly generated with nuclear (56%), hydro (22%), natural gas (10%), renewables (wind 3%, solar 1%, and bioenergy 1%), and coal (2%). The basic idea behind such electricity generation with various sources is to generate electricity mainly with energy sources, which have the lowest emissions of CO₂, and to use natural gas and “dirty” coal at the minimum possible level.

Figure 1.1.49a shows power generated by various energy sources in Ontario (Canada) on June 19, 2012 (a peak power on hot and humid summer day, when major air-conditioning was required) and corresponding to that Figure 1.1.49b shows capacity factors of various energy sources. Analysis of Figure 1.1.49 shows that



Figure 1.1.43b. Photo of Ormat air-cooled integrated geothermal combined-cycle power plant (60MW_{el})—Mokai I, New Zealand. *Courtesy of ORMAT, USA: <http://www.ormat.com/geothermal-power>*



Figure 1.1.44a. Photo of $240\text{-MW}_{\text{el}}$ Rance tidal power plant ($10\text{MW}_{\text{el}} \times 24$ units)—one of the largest in the world (France). The plant supplies on average 96MW with a capacity factor of 40% , providing an annual output of $\sim 600\text{GWh}$. The barrage is 750-m long. The plant portion of the dam is 332.5-m long. The tidal basin measures 22.5km^2 . *Photo taken from Wikimedia Commons, author/username Dani 7C3*

electricity that day from midnight till 3 o'clock in the morning was mainly generated with nuclear, hydro, gas, wind, "other," and coal (on the minimum possible level). After 3 o'clock in the morning, wind power fell due to Mother Nature, but electricity consumption started to rise. Therefore, "fast-response" gas-fired power plants and later, hydro and coal-fired power plants plus "other" power plants started to increase electricity generation to compensate for both decreasing in wind power and increasing demand for electricity. After 6 o'clock in the evening, energy consumption slightly dropped in the province, and at the same time, wind

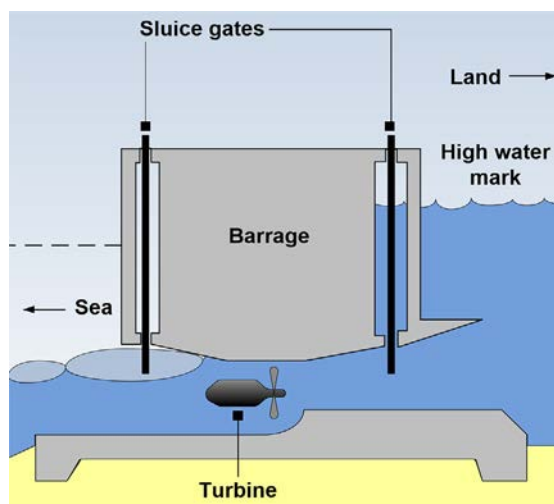


Figure 1.1.44b. Schematic of tidal-power-plant dam with hydro turbine and gates. *Based on Figure from Strathclyde University/Energy Authority of New South Wales*

Table 1.1.17. List of selected tidal power plants of the world (https://en.wikipedia.org/wiki/List_of_tidal_power_stations)

Rank	Power plant/station	Capacity (MW _{el})	Country	Starting year
1	Sihwa Lake Tidal Power Station	254	S. Korea	2011
2	Rance Tidal Power Station	240	France	1966
3	MeyGen	6	UK	2017
4	Jiangxia Tidal Power Station	3.2	China	1980
5	Kislaya Guba Tidal Power Station	1.7	Russia	1968
6	Uldolmok Tidal Power Station	1.5	S. Korea	2009
7	Eastern Scheldt Barrier Tidal Power Plant	1.3	Netherlands	2015
8	Bluemull Sound Tidal Stream Array	0.3	UK	2016
In total		508	–	–
Under construction				
1	Pempa'q In-Stream Tidal Energy Project	1.3 (planned up to 9)	Canada	2021
Proposed				
1	Penzhinskaya Tidal Power Plant	87,100	Russia	–
2	Mezenskaya Tidal Power Plant	24,000	Russia	–
3	Severn Barrage	8640	UK	–

Continued

Table 1.1.17. List of selected tidal power plants of the world (https://en.wikipedia.org/wiki/List_of_tidal_power_stations—cont'd

Rank	Power plant/station	Capacity (MW _{el})	Country	Starting year
4	Tugurskaya Tidal Power Plant	3640	Russia	–
5	Incheon Tidal Power Station	818 or 1320	S. Korea	–
6	Garorim Bay Tidal Power Station	520	S. Korea	–
7	Tidal Lagoon Swansea Bay	320	UK	–
7	Alderney Tidal Plant	300	UK	–
8	Gulf of Kutch Project	50	India	–
9	Skerries Tidal Stream Array	10.5	UK	–



Figure 1.1.45. Photo of the first in the world 2.25-MW_{el} Aguçadoura wave power plant (Portugal). Pelamis machine is made up of connected sections, which flex and bend relative to one another as waves run along the structure. This motion is resisted by hydraulic rams, which pump high-pressure oil through hydraulic motors, which in turn drive electrical generators. Three machines within three 120-m long cylinders, each rated at a peak output of 750 kW_{el}, have been installed. The total peak power of 2.25 MW_{el} enough to cover electrical needs of more than 1500 Portuguese homes. However, the average output from a Pelamis machine depends on the wave resource in a particular area. According to information on the Pelamis website, it appears that the average power output for a Pelamis wave machine is about 150 kW. *Photo taken from Wikimedia Commons, author/username P123. Source: Wikipedia*

power started to be increased by Mother Nature. Therefore, gas-fired, hydro, and “other” power plants decreased energy generation accordingly (“other” plants dropped power quite abruptly, but their contribution to the total energy generation is quite small). After 9 o’clock in the evening, energy consumption dropped even more. Therefore, coal-fired power plants with the most CO₂ and other emissions decreased abruptly their electricity generation followed by gas-fired and hydro-power plants. It should be admitted that NPPs operated almost invariable during the whole day. Figure 1.1.49b shows, correspondingly to variations of power (see Figure 1.1.49a), very significant variations of all energy-sources capacity factors with the exception of nuclear-power one, which was very close to 100%.

Currently, the Province of Ontario (Canada) has completely eliminated coal-fired power plants from the electrical grid. Some of them were closed, others—converted to natural gas. Figure 1.1.50a shows installed capacity and Figure 1.1.50b—electricity generation by energy source in the Province of Ontario (Canada) in



Figure 1.1.46. Photo of the Pelamis Wave-Energy Converter on site at the European Marine Energy Test Centre (EMEC), Orkney, Scotland, 2007. This converter was rated at 750kW and was the world's first off-shore wave-power machine to generate electricity into a grid system. The prototype is 120-m long and 3.5 m in diameter. It consisted of four tube sections linked by three, shorter, power-conversion modules. *Photo taken from Wikimedia Commons, author/username P123. Source: Wikipedia*

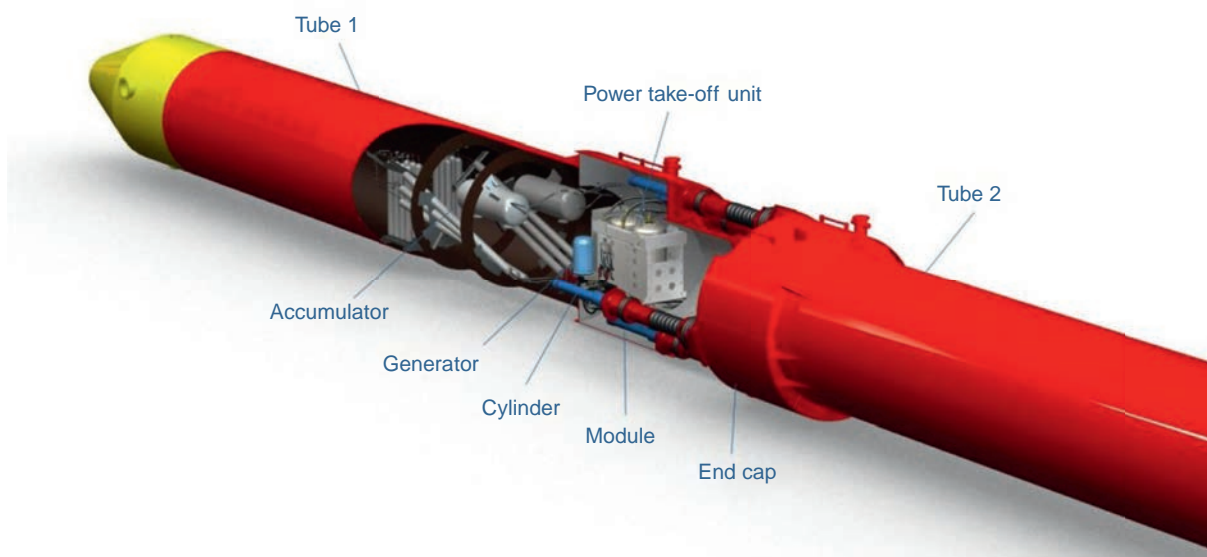


Figure 1.1.47. Schematic of Prototype 2 Pelamis Wave-Energy Converter. *Courtesy of Pelamis Wave Power.*

2019. Analysis of [Figure 1.1.50a](#) shows that in Ontario major installed capacities in 2019 were nuclear (32%), gas (26%), hydro (23%), and renewables: wind (12%), solar (6%), and biofuel (1%). However, electricity (see [Figure 1.1.50b](#)) was mainly generated with nuclear (61%), hydro (25%), natural gas (6%), and renewables (mainly wind) (8%).

[Figure 1.1.51](#) shows power generated by various energy sources in Ontario (Canada) (a) and their capacity factors (b) for 1 day in winter (a_1, b_1); spring (a_2, b_2), summer (a_3, b_3), and fall (a_4, b_4). It was decided to pick up for the analysis electrical-power generation during hot summer day of July 17, 2019. Analysis of [Figure 1.1.51a₃](#) shows that electricity that day from midnight till 4 o'clock in the morning was mainly

Table 1.1.18. Wave power plants/stations (https://en.wikipedia.org/wiki/List_of_wave_power_stations)

Rank	Station	Capacity (MW _e)	Country	Type	Starting year
1	Sotenäs Wave Power Station	3	Sweden	Point absorber	2015
2	Orkney Wave Power Station	2.4	UK	Oscillating wave surge converter	?
3	Aguçadoura Wave Farm	2.25	Portugal	Surface-following attenuator	2008
4	Islay Limpet	0.5	UK	Oscillating water column	2000
5	Pico Wave Power Plant	0.4	Portugal	Oscillating water column	2010
6	Ada Foah Wave Farm	0.4	Ghana	Point absorber	2016
7	Mutriku Breakwater Wave Plant	0.3	Spain	Oscillating water column	2009
8	SDE Sea Waves Power Plant	0.04	Israel	Oscillating wave surge converter	2009
9	BOLT Lifesaver	0.03	USA	Point absorber	2016
10	Azura	0.02	USA	Point absorber	2015
11	SINN Power wave energy converter	0.02	Greece	Point absorber	2015
In total		9.36	–	–	–

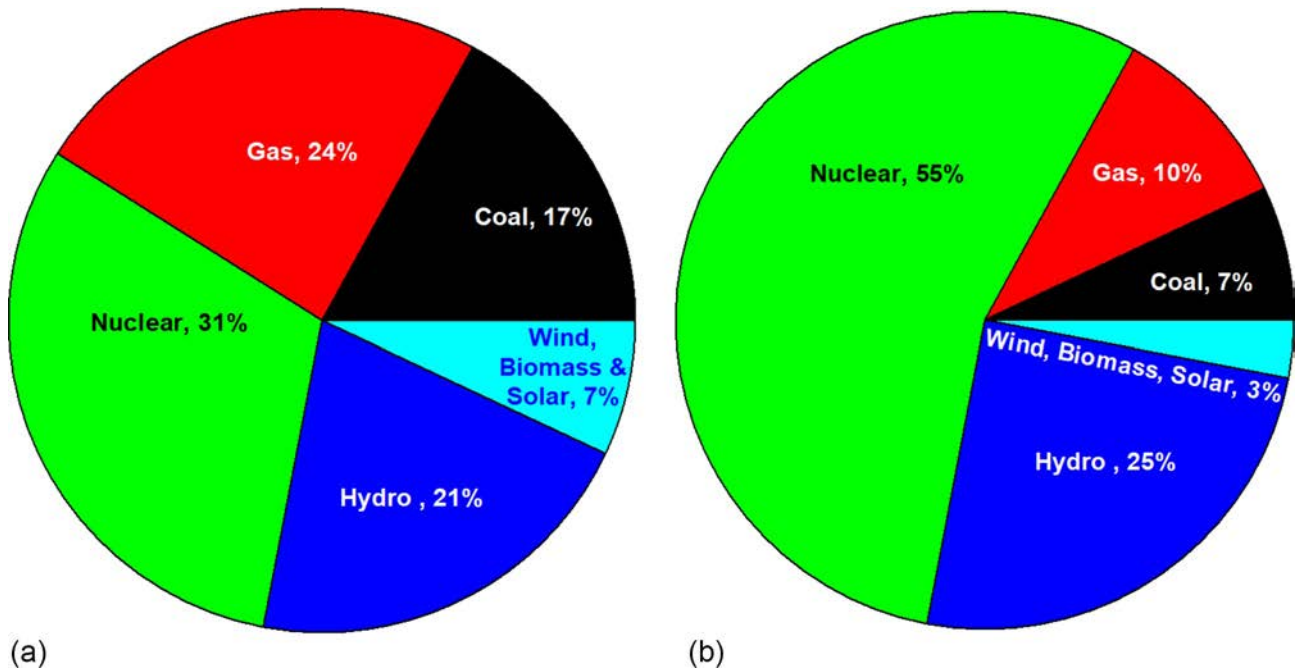


Figure 1.1.48. Sector diagrams of installed capacity and electricity generation by energy source: Province of Ontario (Canada), year 2012 (population 13.4 million). (a) Installed capacity by energy source, (b) electricity generation by energy source. Based on data from Ontario Power Authority: <http://www.powerauthority.on.ca> and Ontario's Long-Term Energy Plan

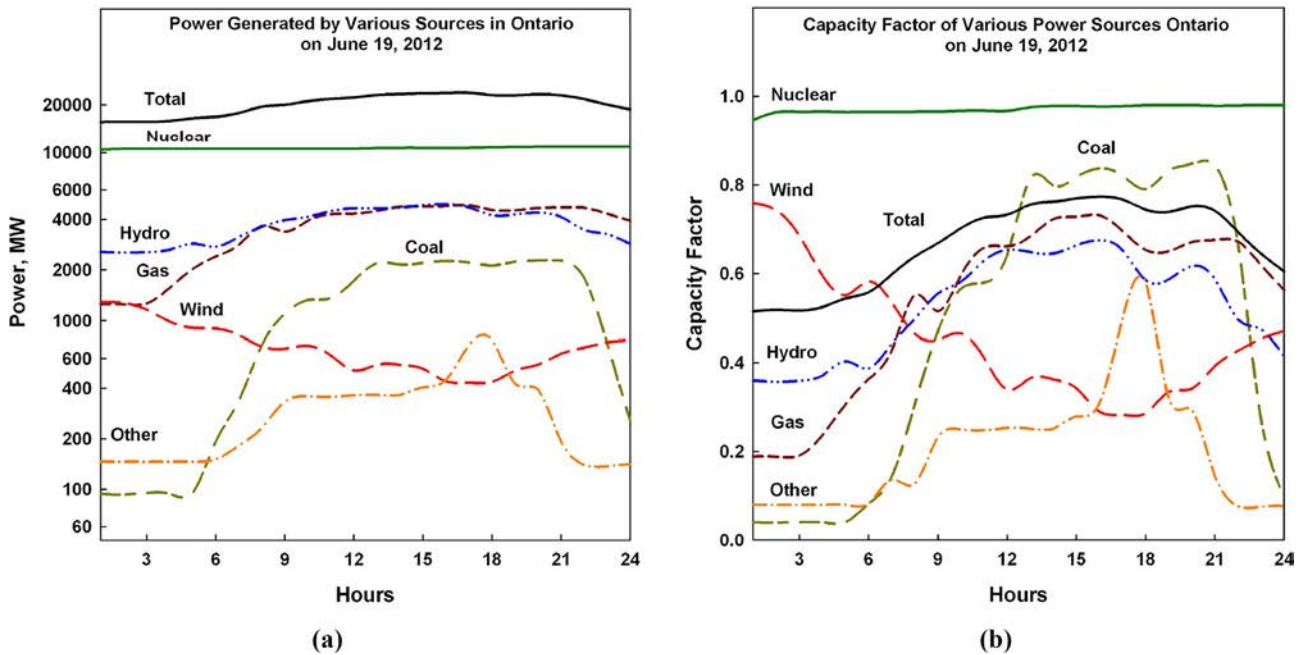


Figure 1.1.49. Power generated (a) and capacity factors (b) of various energy sources in Ontario (Canada) on June 19, 2012. Weather data ($\sim 39^{\circ}\text{C}$, high humidity) is related to Toronto with suburbs (population 6.66 million, so-called: Greater Toronto area)—capital of Ontario and the largest city in Canada. Three NPPs equipped with 18 CANDU reactors, including the largest operating one—Bruce NPP, are located nearby. (Shown here just for reference purposes.) Based on data from <http://ieso.ca/imoweb/marketdata/genEnergy.asp>

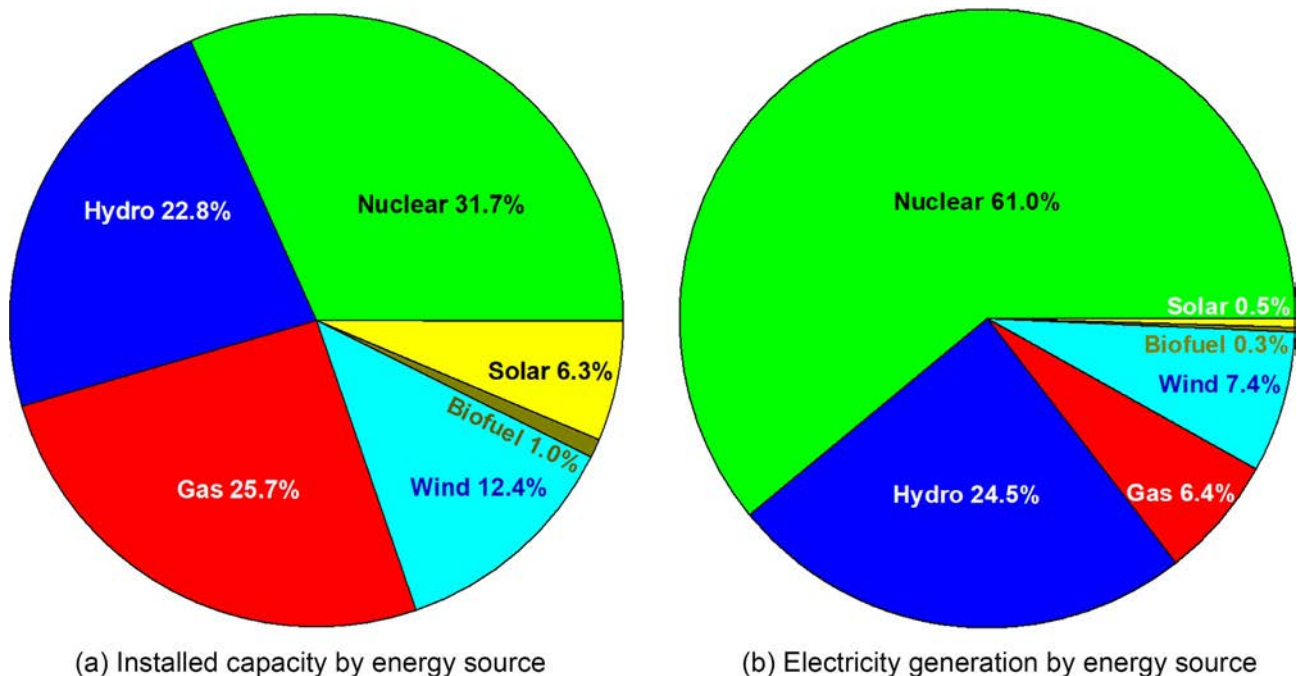


Figure 1.1.50. Sector diagrams of installed capacity and electricity generation by energy source: Province of Ontario (Canada), 2019 (population 14.6 million). (a) Installed capacity by energy source. (b) Electricity generation by energy source. Based on data from Ontario Power Authority: <http://www.powerauthority.on.ca> and Ontario's Long-Term Energy Plan

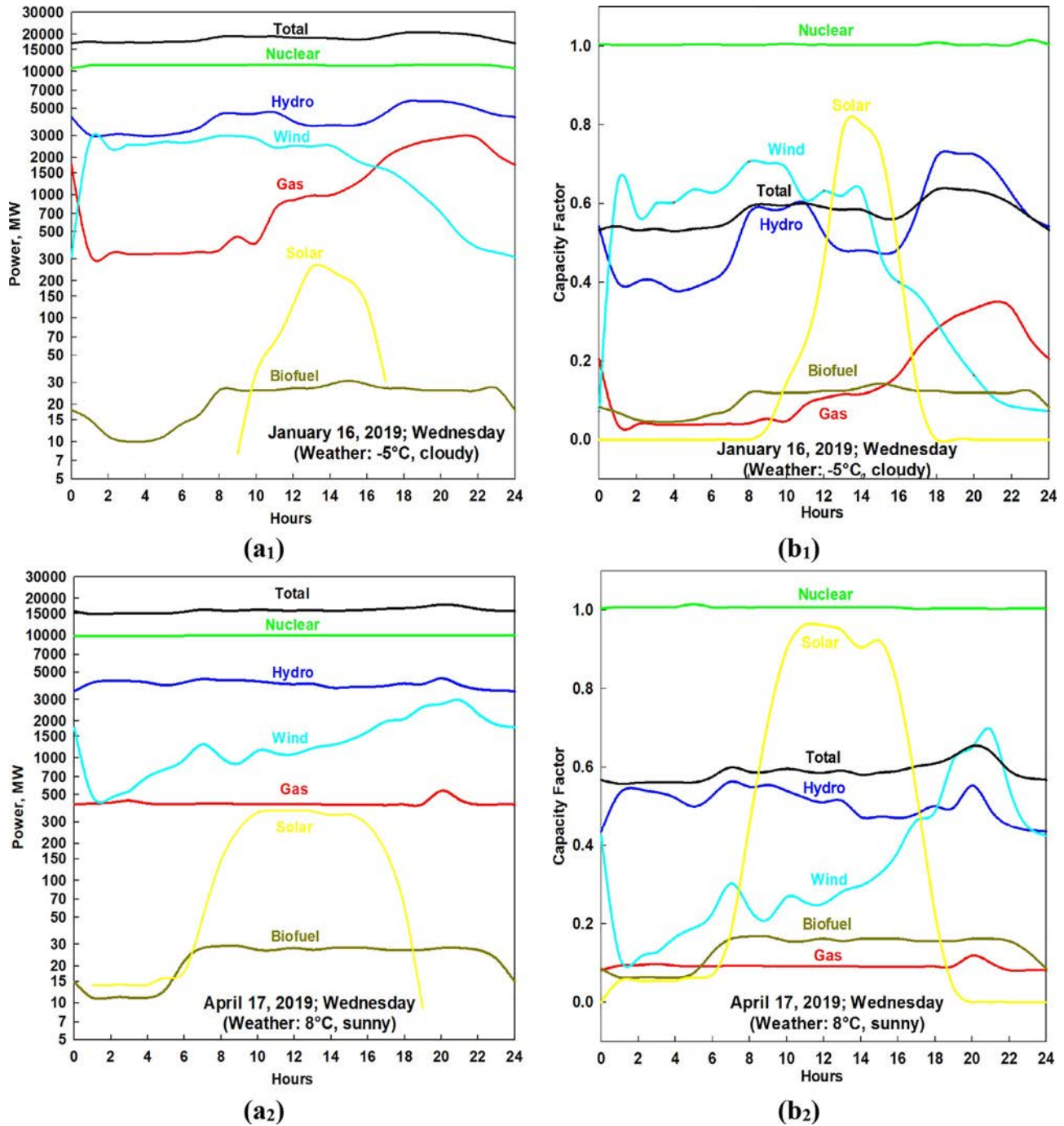
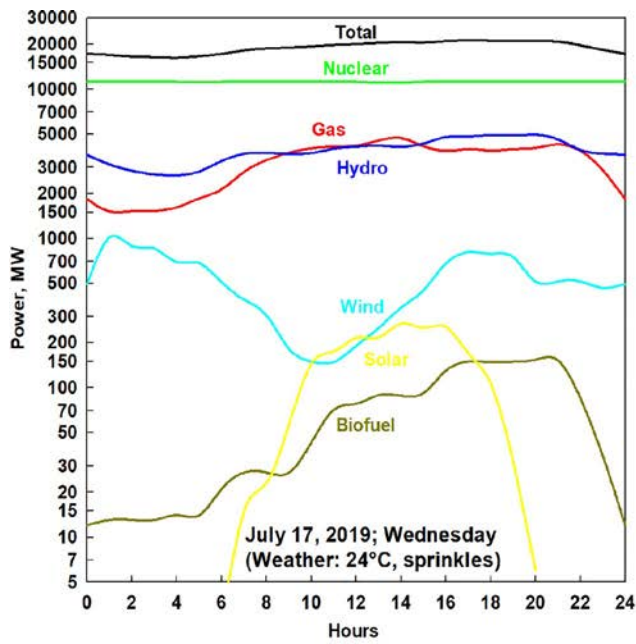
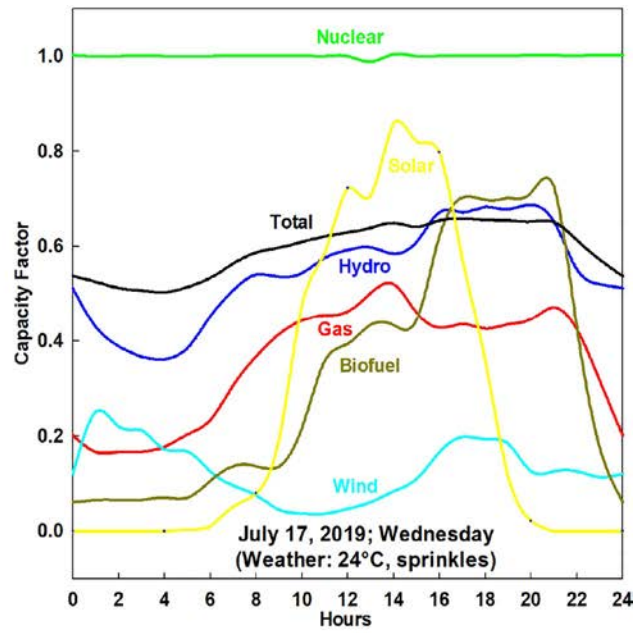


Figure 1.1.51. Power generated (a) and capacity factors (b) of various energy sources in Ontario (Canada) (population ~14.6 million people, year 2019) in Winter₁; Spring₂; Summer₃; and Fall₄; working day (Wednesday) of 2019. Weather data is related to Toronto with suburbs (population 6.14 million, so-called: Greater Toronto area)—capital of Ontario and the largest city in Canada.

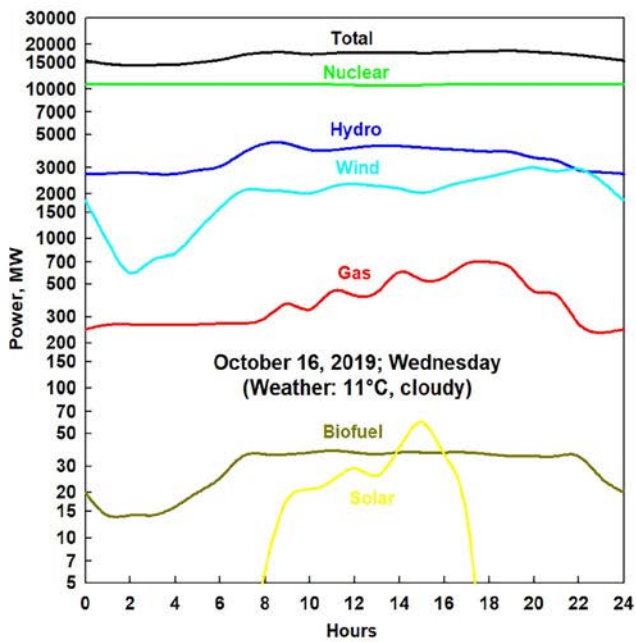
(Continued)



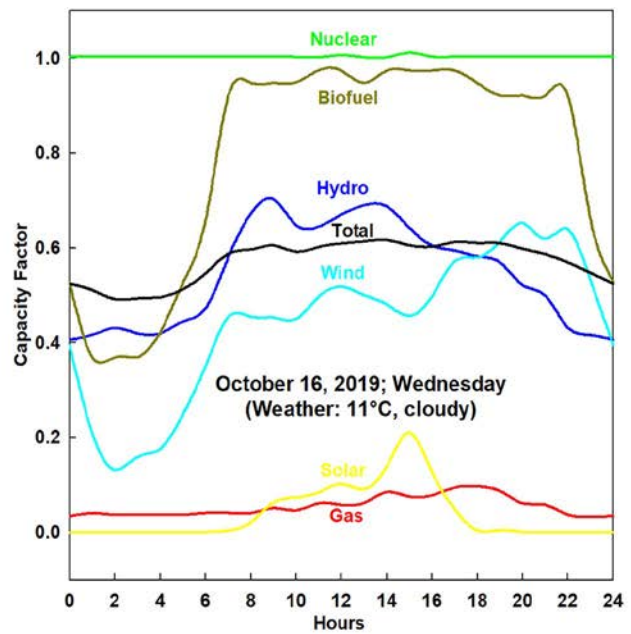
(a3)



(b3)



(a4)



(b4)

Figure 1.1.51, Cont'd Three NPPs equipped with 18 CANDU reactors, including the largest operating one—Bruce NPP, are located nearby. (Shown here just for reference purposes.) Based on data from <http://ieso.ca/Power-Data/Data-Directory>.

generated with nuclear, hydro, gas, wind, and biofuel. After 4 o'clock, hydro, gas, and biofuel power plants started to increase electricity generation. However, wind power plants started to decrease electricity generation due to Mother Nature after 1 o'clock at night. Around 6 o'clock in the morning, solar power plants started to generate electricity. Also, after 5 o'clock in the morning the electricity consumption in the province started to grow, which was mainly compensated with hydro, gas, biofuel, and after 6 o'clock with solar power plants. After 10 o'clock in the morning, wind power started to be increased by Mother Nature. Due to this gas-fired power plants decreased slightly their power. After 4 o'clock in the afternoon, solar generation started to drop very fast, and due to that, hydro plants increased slightly their power. After 10 o'clock in the evening, energy consumption in the province started to decrease, due to that biofuel, gas, and hydro plants decreased their generation of electricity. It should be admitted that NPPs operated almost invariable during the whole day. Figure 1.1.51_{b₃} shows, correspondingly to the variations of power (see Figure 1.1.51_{a₃}), very significant variations of all energy-sources capacity factors with the exception of nuclear-power one, which was around 100%. All other Figure 1.1.51_{a₁,b₁;a₂,b₂;a₄,b₄} show quite similar results.

These examples show clearly that any grid that includes NPPs and/or renewable-energy sources must also include “fast-response” power plants such as gas- and coal-fired and/or large hydro-power plants. This is due not only to diurnal and seasonal peaking of demand, but also the diurnal and seasonal variability of supply. Thus, for any given market, the generating mix and the demand cycles must be matched 24/7/365, independent of what sources are used, and this requires flexible control and an appropriate mix of base-load and peaking plants.

Also, it should be noted here that having a large percent of variable power sources mainly such as wind and solar, and other, i.e., which generating capacity depends on Mother Nature, an electrical grid can collapse due to significant and unpredicted power instabilities! In addition, the following detrimental factors are usually not considered during estimation of variable power-sources costs: (1) costs of fast-response power plants with service crews on site 24/7 as a back-up power and (2) faster amortization/wear of equipment of fast-response plants.

1.1.6 Conclusions

1. It is well known that electrical-power generation is the key factor for advances in industry, agriculture, technology, and the economic and social level of living. Also, a strong power industry with diverse energy sources is very important for any country's independence.
2. The Human Development Index (HDI) is the official United Nations (UN) parameter, which generally represents level of living, is calculated, so all 188 countries in the world fall into 4 categories: (1) very high HDI (65 countries); (2) high HDI (54 countries); (3) medium HDI (36 countries); and (4) low HDI (33 countries), with a range from 0.957 for Norway (Rank #1) to 0.394 for Niger (Rank #188). The HDI actually depends significantly on Electrical Energy Consumption (EEC) in W/Capita: $HDI = 0.2972 + 0.1961 \log_{10} EEC$; with an uncertainty of $\pm 20\%$ for 188 countries, while ranging from Iceland's 5898 W/Capita (HDI Rank #4) to Guinea-Bissau (HDI Rank #175) and Chad (HDI Rank # 187) at 2 W/Capita, representing a “dead-end” to advances in industry, agriculture, technology, education, and level of living.
3. Major sources for electrical-energy generation in the world are: (1) thermal—primary coal (36.7%) and secondary natural gas (23.5%); (2) “large” hydro (15.8%); and (3) nuclear (10.4%). The remaining 13.6% of the electrical energy is generated using oil (3.1%) and renewable sources: intermittent wind (5.3%) and solar (2.7%), and from geothermal, biomass, and marine (2.5%).

4. Unfortunately, the world and large countries rely heavily on fossil-fuels electricity generation: World—coal $\sim 37\%$ and gas $\sim 24\%$ (in total $\sim 61\%$); China—coal $\sim 62\%$; India—coal $\sim 71\%$; USA—coal $\sim 24\%$ and gas $\sim 37\%$ (in total $\sim 61\%$); Russia—coal $\sim 16\%$ and gas $\sim 46\%$ (in total $\sim 62\%$), and Japan—coal $\sim 32\%$ and gas $\sim 34\%$ (in total 64%), which means very significant emissions of CO_2 into atmosphere. These five countries generate $\sim 63\%$ of the world's electricity and are responsible for 81% of CO_2 emissions due to coal electricity generation and 46% due to gas of the total world's CO_2 emissions.
5. Renewable energy sources such as wind and solar have a visible impact just in some countries, especially, where governments provide incentives with electricity prices guaranteed by legislation and power-purchase contracts. However, as well known, these apparently attractive renewable-energy sources (wind and solar) are not reliable as full-time energy sources for industrial-power generation, requiring the electrical grid to have “fast-response” or back-up power plants such as gas-(coal-) fired and/or large hydro-power plants.
6. Analysis of the modern energy sources for electricity generation shows that we have two major groups of sources: (1) Non-renewable: Fossil-fuel-fired thermal power plants (fuels—natural gas, coal, fuel oil, oil shale, peat, and diesel; and combustible gases as a by-product of metallurgical (blast-furnace gas) and other industries); and Nuclear Power Plants (NPPs), which use mined resources—nuclear fuels (uranium dioxide); and (2) Renewable: Hydro, wind, biomass, solar, geothermal, tidal, and wave.
7. The sun is the major source for hydro, wind, solar, and wave power, and, partially, for production of biofuel, which coming from plants (so-called, energy crops) and from wastes of a biological origin. Therefore, any changes or interruptions in sun energy reaching the Earth, i.e., decreased sun activity, increased cloudiness due to climate change, ash clouds due to increased volcanoes activity or eruption of a super-volcano, can affect all five renewable-energy sources, such as hydro, wind, solar, wave power, and even production of biofuel.
8. It is particularly noted that the following two parameters are important characteristics of any power plant: (1) Overall (gross) or net efficiency of the electricity-conversion cycle, and (2) Capacity factor reflecting the fraction of time actually producing the nameplate power. Analysis of the thermal efficiencies shows that combined-cycle power plants (combination of Brayton gas-turbine cycle and Rankine steam-turbine cycle) are the highest (up to 62%) compared to those of any other thermal and nuclear power plants. Also, thermal efficiency is the driving force for all advances in thermal and, nowadays, nuclear power plants! Analysis of capacity factors shows very significantly variations for different types of power plants, i.e., from 3% for wave-energy plants to over 90% for NPPs. It should be noted that capacity factors can be of different nature: (1) artificially induced (mainly, non-renewable-energy power plants); and (2) induced by Mother Nature (mainly, all renewable-energy power plants with the exception of biofuel and geothermal power plants). Due to this thermal and nuclear power plants can operate for long time with high capacity factors up to 100% , when many renewable-energy sources usually have lower capacity factors, i.e., hydro—world average $\sim 45\%$ and wind—world average 20% to 40% .
9. In general, the following ideal/ultimate requirements for electrical-energy sources can be deduced: (1) concentrated in terms of energy density per unit or area covered with power plant (including artificial-lake area or volume of water for hydro plants); (2) large installed capacity possible; (3) high-capacity factors achievable for long-time operation; (4) high efficiency/thermal efficiency; (5) reliable and safe; (6) long-term operational; (7) minimized environmentally impacts including location; (8) independent of Mother Nature including location; (9) maneuverable/fast response in terms of power variability (load following) to meet fluctuating and daily-demand cycles; (10) low capital and operational costs; and (11) Low Levelized Cost Of Energy (LCOE).
10. In spite of advances in coal-fired thermal power-plants design and operation worldwide they are still considered as not particularly environmentally friendly due to producing gaseous carbon-dioxide,

NO_x, SO₂ and other emissions as a result of combustion process, plus significant tailings of slag and ash. Coal electricity generation has the highest CO₂ emissions per kWh and death rates per TWh in power industry. Combined-cycle thermal power plants with natural-gas fuel are considered as relatively clean fossil-fuel-fired plants compared to coal and oil power plants and are dominating new capacity additions, because of lower gas production costs, especially, when using “fracking” technology, but still emit carbon dioxide and NO_x due to the combustion process.

11. The major advantages and challenges of nuclear power are well known, including cheap reliable base-load power, high capacity factors, small amount of nuclear fuel is required compare to that for coal- and gas-fired power plants, lowest CO₂ emissions, and minor environmental impact. But these factors are offset today by the challenges of competitive disadvantage with natural gas, the occurrence of three severe nuclear accidents (Fukushima, Chernobyl, and Three Mile Island), which caused significant social disruption and the high capital costs.
12. Major disadvantages of many renewable energy sources, i.e., hydro, wind, solar, etc., are low energy density, therefore, large areas should be covered with artificial lakes, wind turbines, solar panels or heliostat mirrors to obtain large installed capacities of these plants, significant dependence on location, climate and weather conditions. Also, wind and solar power plants are unreliable and not maneuverable plants. Actual operation of an electrical grid in the Province of Ontario (Canada) during all four seasons showed clearly that any grid that includes NPPs and/or renewable-energy sources must also include “fast-response” power plants such as gas- and coal-fired and/or large hydro-power plants. This is due not only to diurnal and seasonal peaking of demand, but also the diurnal and seasonal variability of supply. Thus, for any given market, the generating mix and the demand cycles must be matched 24/7/365, independent of what sources are used, and this requires flexible control and an appropriate mix of base-load and peaking plants.
13. Finally, it is noted here that having a large percent of variable power sources mainly such as wind and solar, which generating capacity depends on natural fluctuations, an electrical grid can collapse due to significant and unpredicted power instabilities or adverse weather conditions! In addition, the following factors are usually not considered during estimation of variable power-sources costs: (1) costs of back-up fast-response power plants with service crews on site 24/7 and (2) shorter lifetimes with faster amortization/wear of equipment of fast-response plants.

Acknowledgments

The authors would like to express their great appreciation to companies (MHI (Japan), Rosatom (Russia), Hyundai (S. Korea), WÄRTSILÄ (Finland), Bruce Power (Canada), OPG (Canada), Siemens (Germany), Alstom (France), SENER/TORRESOL ENERGY (Spain), SEGs (USA), ORMAT (USA), Pelamis Wave Power (Portugal), etc.), government departments and committees (Chinese National Committee on Large Dams, U.S. Army Corps of Engineers, US Tennessee Valley Authority, DOE (USA)), laboratories (ORNL (USA), NREL (USA), Energy Authority of New South Wales (Australia), Ontario Power Authority (Canada)), agencies (NASA), international agencies (IEA, NEA, OECD), and universities (Strathclyde University (Australia)) for providing very valuable information, figures, and photos. Also, information provided by unidentified authors of Wikipedia-website articles and photos provided by a number of authors from the Wikimedia-Commons website are greatly appreciated.

References

- Pioro, I., 2012. Nuclear power as a basis for future electricity production in the world, chapter #10. In: Mesquita, A.Z., Rezende, H.C. (Eds.), *Current research in nuclear reactor Technology in Brazil and Worldwide*. INTECH, Rijeka, Croatia, pp. 211–250. Free download from <http://www.intechopen.com/books/current-research-in-nuclear-reactor-technology-in-brazil-and-worldwide/nuclear-power-as-a-basis-for-future-electricity-production-in-the-world-generation-iii-and-iv-reacto>.
- Pioro, I.L. (Ed.), 2016. *Handbook of Generation IV Nuclear Reactors*. Elsevier – Woodhead Publishing (WP), Duxford, UK. 940 p. Free download of content https://www.gen-4.org/gif/jcms/c_9373/publications.

- Pioro, I.L., Duffey, R.B., 2007. Heat Transfer and Hydraulic Resistance at Supercritical Pressures in Power Engineering Applications. ASME Press, New York, NY, USA, p. 334.
- Pioro, I., Duffey, R., 2015. Nuclear power as a basis for future electricity generation. ASME J. Nuclear Eng. Radiat. Sci. 1 (1), 19. Free download from <http://nuclearengineering.asmedigitalcollection.asme.org/article.aspx?articleID = 2085849>.
- Pioro, I., Duffey, R., 2019. Current status of electricity generation in the world and future of nuclear-power industry, pp. 67-114, chapter 3. In: Letcher, T. (Ed.), Managing Global Warming, an Interface of Technology and Human Issues. Elsevier – Academic Press, London, UK, p. 804.
- Pioro, L.S., Pioro, I.L., 2003. Wasteless combined aggregate—coal-fired steam-generator/melting-converter. Int. J. Waste Manag 23 (4), 333–337.
- Pioro, L.S., Sadvoskiy, B.F., Pioro, I.L., 2001. Research and development of high efficiency one-stage melting converter-bunker method for solidification of radioactive wastes into glass. Nucl. Eng. Des. 205 (1–2), 133–144.
- Pioro, I.L., Duffey, R., Kirillov, P.L., Panchal, R., 2016. Chapter 1. Introduction: a survey of the status of electricity generation in the world, pp. 1-34. In: Pioro, I.L. (Ed.), Handbook of Generation IV Nuclear Reactors. Elsevier – Woodhead Publishing (WP), Duxford, UK, p. 940.
- Pioro, I., Duffey, R.B., Kirillov, P.L., Dort-Goltz, N., 2020. Current status of reactors deployment and small modular reactors development in the world. ASME J. Nuclear Eng. Radiat. Sci. 6 (4), 24. Free download from <https://asmedigitalcollection.asme.org/nuclearengineering/article/6/4/044001/1085654/Current-Status-of-Reactors-Deployment-and-Small>.
- Pioro, I., Duffey, R.B., Pioro, R., 2022. Overview of current status of nuclear-power industry of the world. In: Boucau, J. (Ed.), Fundamental Issues Critical to the Success of Nuclear projects. Elsevier – Woodhead Publishing (WP), Duxford, UK, p. 392.

Further reading

- Pioro, I., Duffey, R.B., Kirillov, P.L., Pioro, R., Zvorykin, A., Machrafi, R., 2019. Current status and future developments in nuclear-power industry of the world. ASME J. Nuclear Eng. Radiat. Sci. 5 (2), 27. Free download from <https://asmedigitalcollection.asme.org/nuclearengineering/article/doi/10.1115/1.4042194/725884/Current-Status-and-Future-Developments-in-Nuclear>.

1.2

Current status and future trends in the world nuclear-power industry

Igor L. Pioro^a, Romney B. Duffey^b, Pavel L. Kirillov^{c,}, Natalia M. Fialko^d,
and Roman M. Pioro^e*

^aFaculty of Energy Systems and Nuclear Science, University of Ontario Institute of Technology,
Oshawa, ON, Canada ^bIdaho Falls, ID, United States ^cState Scientific Centre of the Russian
Federation—Institute of Physics and Power Engineering (IPPE) named after A.I. Leipunsky, Obninsk,
Russia ^dInstitute of Engineering Thermal Physics, National Academy of Sciences of Ukraine, Kyiv,
Ukraine ^eFaculty of Physics, Lomonosov Moscow State University, Moscow, Russia

Nomenclature

P Pressure, MPa
T Temperature, °C

Subscripts

el electrical
in inlet
max maximum
min minimum
out outlet

Abbreviations

ABB	ASEA/Brown Boveri (Sweden Switzerland)
ABWR	Advanced Boiling Water Reactor
ACPR	Advanced Chinese Pressurized-water Reactor
AECL	Atomic Energy of Canada Limited
AEP	AtomEnergoProekt (Russia)
AGR	Advanced Gas-cooled Reactor
ANS	American Nuclear Society
APR	Advanced Pressurized-water Reactor (S. Korea)
ARIS	Advanced Reactors Information System (IAEA)
ASE	AtomStroyExport (Russia)
Ave	Average
Ba.	Bavaria
BN	Fast Sodium (reactor) (Быстрый Натриевый (in Russian abbreviations)) (Russia)
BWR	Boiling Water Reactor
CANDU	CANada Deuterium Uranium (reactor) (Registered Trademark of AECL, used under license by Candu Energy Inc., Member of SNC-Lavalin Nuclear Group)
CGNPC	China General Nuclear Power Group
CNNC	China National Nuclear Corporation

* Professor P.L. Kirillov has participated in preparation of this chapter; unfortunately, he has passed away on October 10, 2021 (for details, see <https://asmedigitalcollection.asme.org/nuclearengineering/issue/8/2>).

CNP	China Nuclear Power
DAI	Department of Atomic Energy (India)
EGP	Power Heterogeneous Loop (reactor) (Энергетический Гетерогенный Петлевой (реактор с 6-ю петлями циркуляции теплоносителя) (in Russian abbreviations))
EPR	European Pressurized-water Reactor (original acronym, later changed to Evolutionary Power Reactor) (France)
GCR	Gas-Cooled Reactor
GE	General Electric (USA)
HPR	Hualong Pressurized-water Reactor (so-called, Hualong One design)
HTC	Heat Transfer Coefficient
HTR	High-Temperature Reactor
IAEA	International Atomic Energy Agency
KEPCO	Korea Electric Power COrporation
KLТ	Container-carrier cargo-Lighter Transport (reactor) (Контейнеровоз Лихтеровоз Транспортный (реактор) (in Russian abbreviations)) (Russia)
КОPEC	КОrea Power Engineering Company
KWU	KraftWerk Union (Germany)
LGR	Light-water-cooled Graphite-moderated Reactor
LMFBR	Liquid-Metal Fast-Breeder Reactor
LWR	Light Water-cooled Reactor
MOX	Mixed OXide (fuel)
MTM	Ministry of Heavy Machine Building (in Russian abbreviations) (Russia)
NNC	National Nuclear Corporation (UK)
NPP	Nuclear Power Plant
OKBM	Experimental Design Bureau of Mechanical-engineering (Опытно-Конструкторское Бюро Машиностроения (in Russian abbreviations))
PBMR	Pebble-Bed Modular Reactor
PCh	Pressure Channel (reactor)
PHWR	Pressurized Heavy-Water Reactor
PM	Ppebble-bed Module
PV	Pressure Vessel
PWR	Pressurized Water Reactor
RBMK	Reactor of Large Capacity Channel type (Реактор Большой Мощности Канальный (in Russian abbreviations) (Russia)
R&D	Research and Development
Rep.	Republic
RITM-200M	Reactor Integral Type Modular 200 MW _{el} Modernized (Реактор Интегрального Типа Модульный мощностью 200 МВт Модернизационный (in Russian abbreviations) (Russia)
RPV	Reactor Pressure Vessel
S.	South
SFR	Sodium-cooled Fast Reactor
SMR	Small Modular Reactor, also, Small and Medium size Reactor
SS	Stainless Steel
Th.	Thermal
U.	University
UAE	United Arab Emirates
UK	United Kingdom
USA	United States of America
USSR	Union of Soviet Socialist Republics
V	Vessel
Vert.	Vertical
VVER	Water-Water Power Reactor (Водо-Водяной Энергетический Реактор (in Russian abbreviations) (Russia)

Nuclear power without used-fuel reprocessing and recycling is often considered to be a non-renewable energy source like the mined fossil fuels, such as coal, oil, and natural gas. Moreover, the resources of naturally occurring fissile fuels (uranium and thorium) are limited in extent, and geographically concentrated in regions of relatively lower population (see Appendix A8.3). However, nuclear resources can be used for significantly longer time than some fossil fuels, and in some cases almost indefinitely, if recycling of unused or low burn-up uranium fuel, thoria-fuel resources, and fast-neutron-spectrum reactors that literally can “breed” plutonium are used.

Current statistics on all world nuclear-power reactors connected to electrical grids are listed in Tables 1.2.1, 1.2.2, and 1.2.5–1.2.9 and shown in Figures 1.2.1–1.2.5. Statistical data from previous years are shown in Piore et al. (2019, 2020, 2021, 2022); Piore and Duffey (2015), and Handbook (2016). In general, the primary sources for statistics on all nuclear-power reactors of the world are: (1) Magazine Nuclear News by the American Nuclear Society (ANS)—<https://www.ans.org/pubs/magazines/nn/>, March issue annually; (2) Power Reactor Information System (PRIS) by the International Atomic Energy Agency (IAEA)—<https://pris.iaea.org/pris/> (Advanced Reactors Information System (ARIS) by the IAEA—<https://aris.iaea.org/>); (3) database by the World Nuclear Association (WNA)—<http://www.world-nuclear.org/>; and (4) for latest events, World Nuclear News (WNN) by the WNA—wnn@world-nuclear-news.org.

Table 1.2.1. Number of nuclear-power reactors connected to electrical grids and forthcoming as per September 2022 and before the Japan earthquake and tsunami disaster (March 2011) (Nuclear News (ANS), 2011, 2022; <http://www.world-nuclear.org/>; <https://pris.iaea.org/pris/>; and wnn@world-nuclear-news.org). (For graphical representation of the current data, see Figure 1.2.1) (Technical parameters of various reactors’ types are listed in Tables 1.2.3 and 1.2.4, and in details are shown in Appendix A1).

No.	Reactor type (% of total reactors/average installed capacity)	No. of units		Installed capacity, GW_{el}		Forthcoming units	
		As of Sep. 2022	Before March 2011	As of Sep. 2022	Before March 2011	No. of units	GW_{el}
1	Pressurized Water Reactors (PWRs) (largest group of nuclear reactors in the world—69%/955 MW_{el})	309 ↑	268	297 ↑	248	34 + 29? ^a	38+31?
2	Boiling Water Reactors (BWRs) or Advanced BWRs (2nd largest group of reactors in the world—14%/1030 MW_{el})	61 ↓	92	63 ↓	84	2?	2.7?
3	Pressurized Heavy Water Reactors (PHWRs) (3rd largest group of reactors in the world—11%/500 MW_{el} ; mainly CANDU-reactor type)	48 ↓	50	24 ↓	25	4 + 7?	2.5 + 4.6?

Continued

Table 1.2.1. Number of nuclear-power reactors connected to electrical grids and forthcoming as per September 2022 and before the Japan earthquake and tsunami disaster (March 2011) (Nuclear News (ANS), 2011, 2022; <http://www.world-nuclear.org/>; <https://pris.iaea.org/pris/>; and wnn@world-nuclear-news.org). (For graphical representation of the current data, see Figure 1.2.1) (Technical parameters of various reactors' types are listed in Tables 1.2.3 and 1.2.4, and in details are shown in Appendix A1)—cont'd

No.	Reactor type (% of total reactors/average installed capacity)	No. of units		Installed capacity, GW _{el}		Forthcoming units	
		As of Sep. 2022	Before March 2011	As of Sep. 2022	Before March 2011	No. of units	GW _{el}
4	Advanced Gas-cooled Reactors (AGRs) (UK, 13 reactors); (all these CO ₂ -cooled reactors will be shut down in the nearest future and will not be built again) (2.9%/555 MW _{el})	9 ↓	18	5.2 ↓	9	0	0
5	Gas-Cooled Reactors ^b (GCRs) (China) (0.5%/100 MW _{el})	2 ↑	-	0.2 ↑	-	-	-
6	Light-water, Graphite-moderated Reactors (LGRs) (Russia, 8 RBMKs and 3 EGPs; these pressure-channel boiling-water-cooled reactors will be shut down in the nearest future and will not be built again) (2.5%/675 MW _{el})	11 ↓	15	7.4 ↓	10	0	0
7	Liquid-Metal Fast-Breeder Reactors (LMFBRs) (Russia, SFRs—BN-600 and BN-800) (0.7%/465 MW _{el})	3 ↑	1	1.4 ↑	0.6	2 + 1?	1.1 + 0.6?
In total		443 ↓	444	398 ↑	377	40 + 39?	42 + 39?

^a ? means “Commercial start date—indefinite.”

^b Helium-cooled reactors—High-Temperature Reactor Pebble-bed Module (HTR-PM) (China) (Generation-IV concept).

Data in Table include 33 reactors in Japan from which only 6 PWRs were in commercial operation in November of 2022 (<https://www.fepec.or.jp/theme/re-operation/>).

Arrows mean decrease or increase in a number of reactors.

The largest group of nuclear-power reactors by type is Pressurized Water Reactors (PWRs) (309 from 443 reactors or 70% of the total number), and quite a significant number of PWRs are planned to be built (about 34 (+29?)) (for details, see Table 1.2.1). The second largest group of reactors is Boiling Water Reactors (BWRs)/Advanced BWRs (ABWRs) (61 (57/4) reactors or 14% of the total number). The third group is Pressurized Heavy-Water Reactors (PHWRs) (48 reactors or 11%). Considering the number of forthcoming

Table 1.2.2. Average, maximum and minimum installed capacities of nuclear-power reactors of the world of various types (values rounded to nearest 0 or 5) (based on data from Nuclear News (2022); <http://www.world-nuclear.org/>; <https://pris.iaea.org/pris/>; and wnn@world-nuclear-news.org)

Type of reactor	PWRs	BWRs	PHWRs	AGRs (CO ₂ -cooled)	GCRs (He-cooled)	LGRs	LMFBRs (SFRs)
Parameter	Installed capacities, MW_{el}						
Average	960	1030	510	575	100	675	470
Maximum	1,660	1435	880	620	100	925	820
Minimum	30	150	90	480	100	10	20

reactors, the number of BWRs/ABWRs and PHWRs will decrease globally within next 20–25 years. The fourth group is relatively old carbon-dioxide-cooled Advanced Gas-cooled Reactors (AGRs) (9 reactors or 2%), which will be shut down in the nearest future and will not be built again. The fifth group is the newest helium-cooled Gas-Cooled Reactors (GCRs) (only 2 for now or 0.5%), which actually represent one concept of Generation-IV reactors (Very High Temperature Reactor (VHTR))—High-Temperature Reactor Pebble-bed Module (HTR-PM). The sixth group is also relatively old Light-water, Graphite-moderated Reactors (LGRs) (11% or 2.5%). One of these reactors, RBMK-1000, has exploded at the Chernobyl NPP in April of 1986, and due to that all these reactors will be shut down in the nearest future and will not be built again. The seventh group is Liquid-Metal Fast-Breeder Reactors (LMFBRs), currently, we have 3 of them and they are Sodium-cooled Fast Reactors (SFRs) (3 or 0.7%). Eventually, SFRs are also one of the Generation-IV concept. SFRs are unique fast-spectrum reactors, which considered as future of nuclear power, but, currently, they don't operate as breeder reactors.

Figure 1.2.1 shows the data from Table 1.2.1 in the form of sector diagrams for a number of reactors by type (a) and by installed capacities (b) (subscript 1 represents data from September 2022, and 2 represents planned reactors and their capacities).

Table 1.2.2 lists average, maximum, and minimum installed capacities of nuclear-power reactors of the world of various types (values were rounded to nearest 0 or 5). Analysis of the data in Table 1.2.2 shows that the largest reactor by installed capacity is 1660-MW_{el} PWR (EPR, Generation-III⁺, Areva design, France) (two EPRs are in operation in China and 1 in Finland, and more are under construction in several countries), and the smallest one is a 10-MW_{el} LGR (EGP, former USSR design) (three EGPs are still in operation in Russia (Bilibino NPP), but all of them will be shut down in several years).

Tables 1.2.3 and 1.2.4 list basic parameters of various nuclear-power reactors and thermal efficiencies of the corresponding Nuclear-Power Plants (NPPs), respectively (for more information on basic parameters of advanced reactors, see <https://aris.iaea.org/sites/Characteristics.html>). Analysis of the data in Table 1.2.3 shows that Light Water-cooled Reactors (LWRs) (PWRs (309) and BWRs (61)) is the largest group of all reactors (370 from 443 or 84%); therefore, light water is the most used reactor coolant and moderator. Heavy water as the reactor coolant and moderator, which used in PHWRs, is on the second place by a number of applications (48 from 443 or 11%). Carbon dioxide as the reactor coolant is used only in AGRs (9 from 443 or 2%). Liquid sodium is used in SFRs (3 from 443 or 0.7%). And the smallest group of reactors is GCRs in which helium is use as the reactor coolant (2 from 443 or 0.5%). It should be mentioned that from the thermodynamic point of view helium is supercritical fluid (helium parameters inside GCRs are: pressure 7.0 MPa and temperature 250–750°C, when critical parameters are: 0.22832 MPa and –267.9547°C (NIST

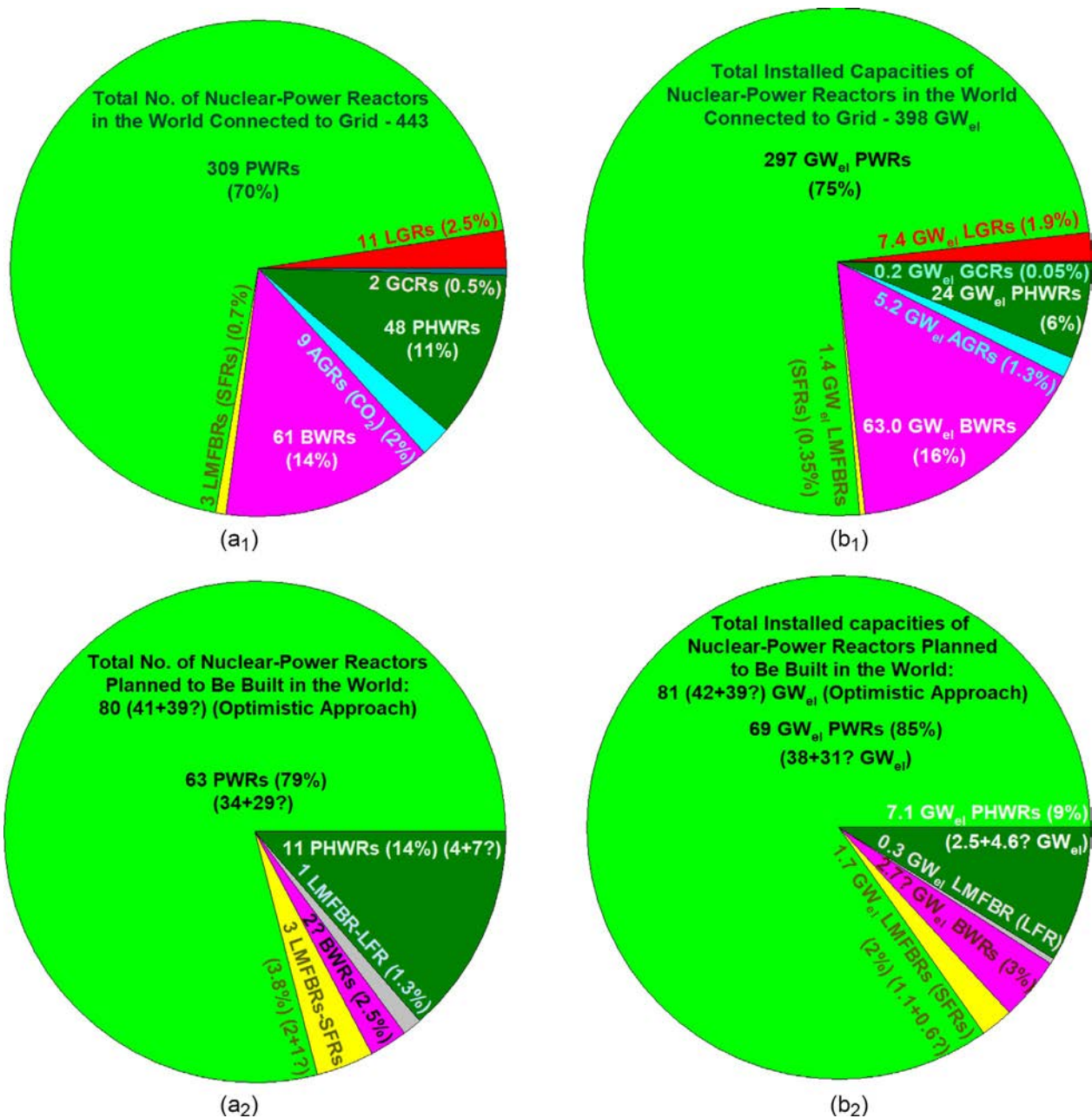


Figure 1.2.1. Nuclear-power reactors of the world (based on data from Table 1.2.1: (a) connected to grid—(a₁) number of reactors by type and (a₂) installed capacities by reactors' types; and (b) planned to be built (optimistic approach, i.e., including those under ?)—(b₁) number of reactors by types and (b₂) installed capacities by reactors' types.

REFPROP, 2018)). However, helium behavior at the reactor's operating conditions is similar to that of compressed gas. In terms of moderators only three substances are used: (1) Light water (LWRs, i.e., 370 or 84%); (2) Heavy water (PHWRs, 49 or 11%); and (3) Graphite (AGRs, LGRs, and GCRs, 5.9%). Due to this, 440 reactors (LWRs, LGRs, AGRs, and GCRs are of thermal spectrum (99.3%) and only 3 reactors (SFRs) of fast spectrum (0.7%). By design: PWRs, BWRs, AGRs, and GCRs are Reactor-Pressure-Vessel (RPV) type (381 or 86%); PWRs, BWRs, and GCRs-RPVs made of steel and AGRs-RPV made of concrete. SFRs are vessel reactors, because above the pool of liquid sodium is about atmospheric pressure. PHWRs and LGRs are pressure-channel-type reactors (59 or 13%).

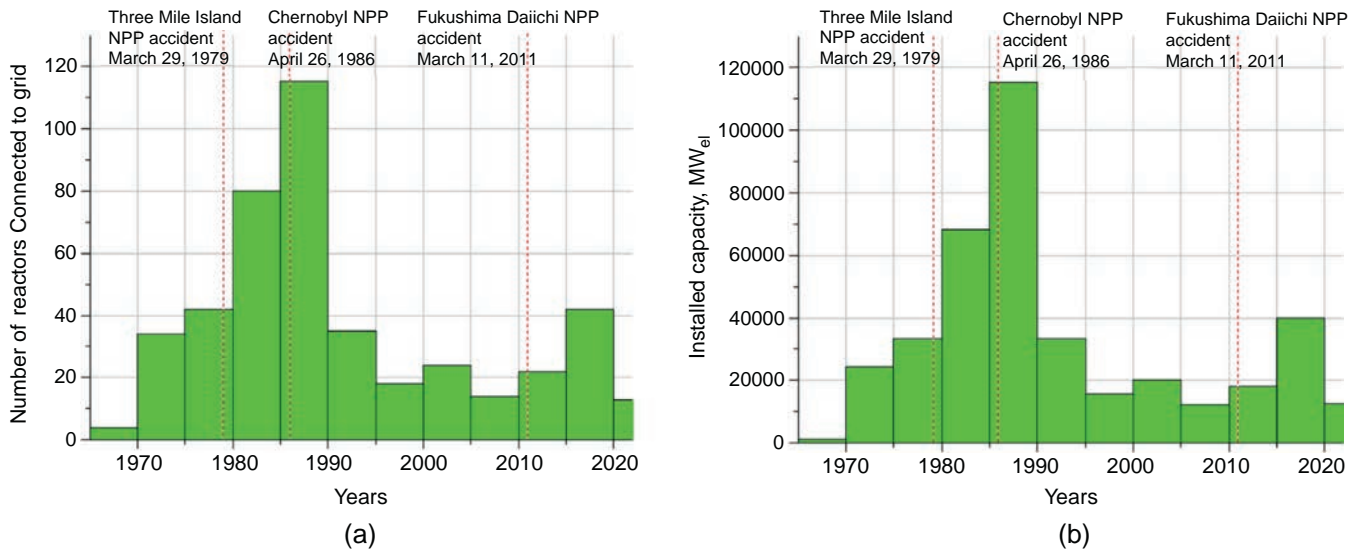


Figure 1.2.2. Number of nuclear-power reactors in the world connected to grid (as per January, 2022) vs. years of their commercial operation (a) and their installed capacities (b) (based on data from Nuclear News (2022); <http://www.world-nuclear.org/>; and <https://pris.iaea.org/pris/>) (for previous data, see Piro et al. (2019) and Handbook (2016)). Four reactors (India $2 \times 150\text{MW}_{eI}$; Switzerland $1 \times 365\text{MW}_{eI}$; and USA $1 \times 613\text{MW}_{eI}$ and $1 \times 650\text{MW}_{eI}$) have been put into operation in 1969, i.e., they operate for more than 50 years. It is clear from this diagram that the Chernobyl NPP severe accident has tremendous negative impact on nuclear-power industry, which is lasting for decades, and, currently, we have additional negative impact of the Fukushima Daiichi NPP severe accident.

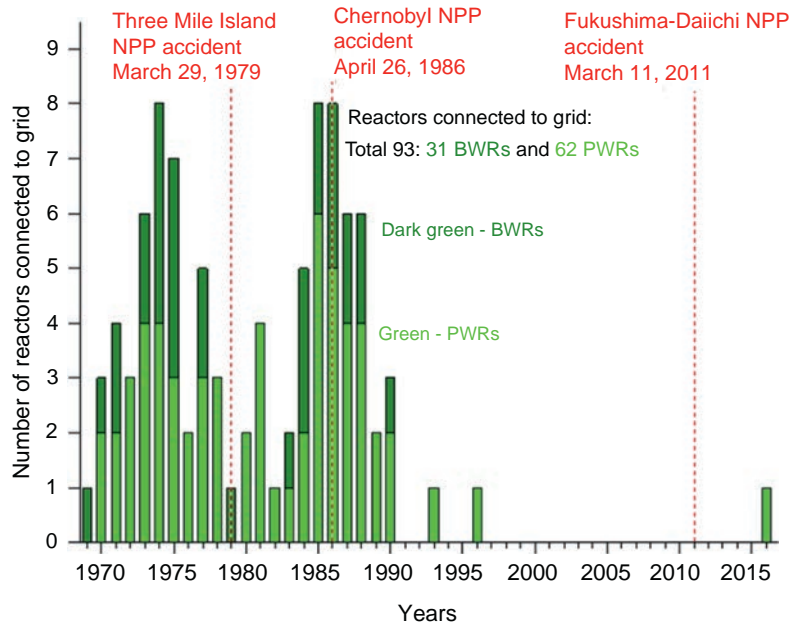


Figure 1.2.3. Number of nuclear-power reactors in the United States connected to electrical grid (as per January, 2022) vs. years of their commercial operation (based on data from Nuclear News (2022); <http://www.world-nuclear.org/>; and <https://pris.iaea.org/pris/>).

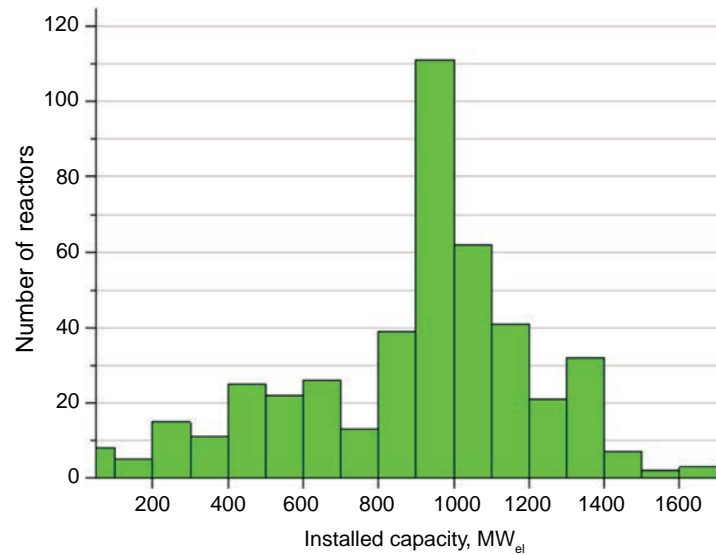


Figure 1.2.4. Number of nuclear-power reactors in the world by installed capacity as per January, 2022 (based on data from Nuclear News (2022); <http://www.world-nuclear.org/>; and <https://pris.iaea.org/pris/>). For better understanding of this figure, the largest number of reactors have installed capacities within the range of 900–999 MW_{el}. Generation-III⁺ reactors, usually, have installed capacities from 1100 and up to 1660 MW_{el} (exception is SMRs).

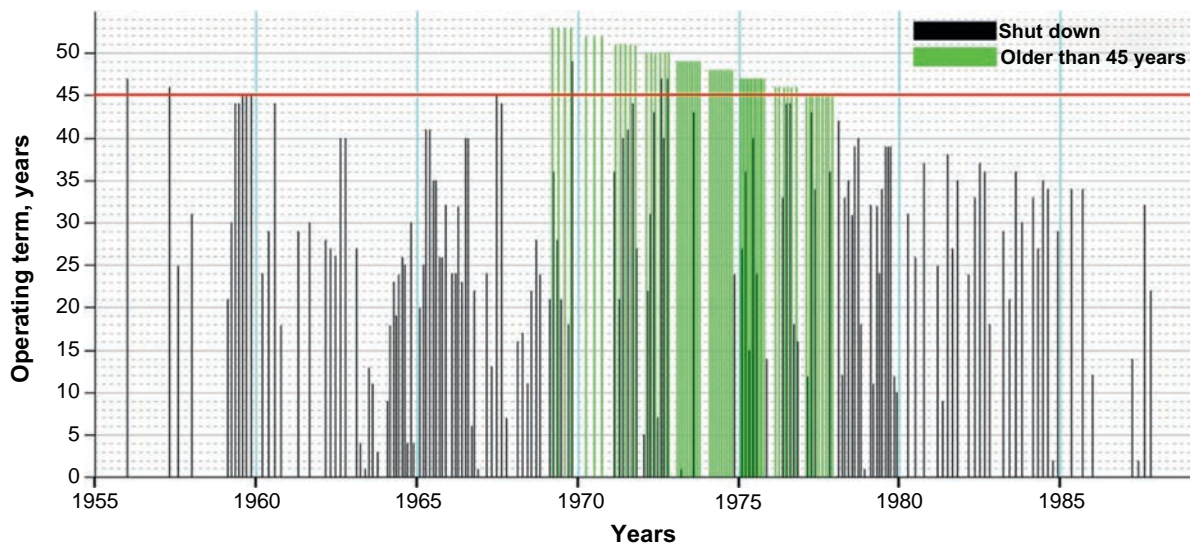


Figure 1.2.5. Operating terms of all nuclear-power reactors built in the world. The figure shows clearly that the vast majority of reactors have been shut down before 45 years of operation. However, four reactors (India—BWRs: 2 × 150 MW_{el}; Switzerland—PWR: 1 × 365 MW_{el}; and USA—BWR: 1 × 620 MW_{el}) have been put into operation in 1969, i.e., they operate for more than 50 years.

Table 1.2.3. Basic parameters of all current reactors' types (based on data from Handbook (2016) and <http://www.world-nuclear.org/>) (for details, also see Appendix A1)

No.	Reactor type	Fuel bundle orientation	Sheath (cladding) material ²	Neutron spectrum	Reactor		Reactor coolant		Refueling	Fuel ⁵	Fuel enrichment (%)	HTC ⁶ (kW/m ² K)	
					Coolant	Moderator	<i>P</i> (MPa)	<i>T</i> (°C)					
1	PWR	RPV	Vert.	Zr	Th.	H ₂ O		15–16.2	295 → 330	Batch	UO ₂	3–5	~30
	SMR KLT-40S	RPV	Vert.	Zr	Th.	H ₂ O		12.7	280 → 316	Batch	UO ₂	18.6	–
2	BWR	RPV	Vert.	Zr	Th.	H ₂ O		7.2	287.7	Batch	UO ₂	~2	~60
3	PHWR (CANDU)	PCh	Hor.	Zr	Th.	D ₂ O	D ₂ O ³	11 → 10	260 → 310	On-line	UO ₂	0.7	~50
4	AGR	RPV ¹	Vert.	SS	Th.	CO ₂	C	~4	290 → 650	Batch ⁴	UO ₂	2.5–3.5	~2–5
5	GCR ⁷ (HTR PM)	RPV	– ⁸	– ⁸	Th.	He	C	7.0	250 → 750	–	UO ₂	8.5	–
6	LGR (RBMK)	PCh	Vert.	Zr	Th.	H ₂ O	C	6.9	284.9	On-line	UO ₂	2–2.4	~60
7	LMFBR (SFR: BN-800)	V	Vert.	SS	Fast	Na	–	~0.1	354 → 547	Batch	MOX	17/20/24	55–85

¹Concrete RPV. ²Zr—Zirconium alloys; SS—Stainless Steel. ³CANDU-reactor moderator has $P = \sim 0.1$ MPa at the top of calandria vessel and $T = \sim 70^\circ\text{C}$. ⁴AGRs were designed to be refueled on-line. However, it was found that during refueling at full power fuel assemblies can vibrate, due to that the on-line refueling was suspended from 1988 till the mid-1990s. Nowadays, only refueling at a part load or in shut-down state is now undertaken in AGRs. ⁵Commonly used fuel. ⁶Heat Transfer Coefficients (HTCs) are approximate values, shown just for reference purposes. ⁷Design parameters. ⁸Spherical fuel with diameter of 6 cm.

Table 1.2.4. Basic parameters of all current reactors' types power cycles (based on data from Handbook (2016) and <http://www.world-nuclear.org/>) (for more details, see Handbook (2016) and Appendix A1 in this edition)

No.	Reactor type	Cycle ¹	No. of loops	Rankine-cycle parameters						Thermal efficiencies (gross) (%)
				Primary steam			Secondary-steam reheat			
				P_{in} (MPa) ^a	T_{in} (°C)	Steam	P_{in} (MPa)	T_{in} (°C)	Steam	
1	PWR	Indirect	2	7.72	292.5	Saturated	2	265	Overheated	Up to 38
	SMR KLT-40S	Indirect	2	3.72	290	Overheated		N/A		Up to 26
2	BWR	Direct	1	7.2	287.7	Saturated	1.7	258	Overheated	Up to 34
3	PHWR (CANDU)	Indirect	2	4.7	260.1	Saturated	~1.2	240	Overheated	Up to 34
4	AGR	Indirect	2	17	560	Superheated	4	560	Superheated	Up to 42
5	GCR ³ (HTR PM)	Indirect	2	14.1	566	Superheated	3.5 ⁴	560 ⁴	Overheated	40
6	LGR (RBMK)	Direct	1	6.9	284.9	Saturated	~0.3	~263	Overheated	Up to 33
7	LMFBR (SFR: BN-800)	Indirect	3 ²	14.2	505	Superheated	2.5	505	Superheated	Up to 40

¹All current reactors connected to Rankine steam cycle (light-water working fluid). ²BN-800 has 3 loops: (1) liquid sodium circulating inside reactor; (2) intermediate loop with liquid sodium; and (3) water-steam in Rankine cycle. ³Design parameters. ⁴Estimated parameters.

Analysis of the data in Table 1.2.4 shows that all current nuclear-power reactors are connected to a subcritical-pressure Rankine steam-turbine cycle. Rankine power cycle for all LWRs (exception is PWRs-KLT-40s Small Modular Reactors (SMRs)), PHWRs, and LGRs has saturated primary steam at the high-pressure turbine inlet and slightly overheated secondary steam, and due to that have relatively low thermal efficiencies up to 38% compared to those of supercritical-pressure coal-fired (up to 55%) and gas-fired combine-cycle (up to 62.5%) power plants. PWRs-KLT-40s SMRs are the first SMRs in the world (connected to grid in December of 2019) have overheated steam at the high-pressure turbine inlet, but no reheat of secondary steam. Due to this the thermal efficiency of this floating NPP (two reactors installed on a barge) is the lowest one compared to those of other NPPs equipped with PWRs, and PHWRs/LGRs, i.e., only 26%. The highest thermal efficiencies in the nuclear-power industry within the range of 40%–42% have NPPs equipped with AGRs, GCRs, and SFRs in which carbon dioxide, helium, and liquid sodium, respectively, are used as high-temperature reactor coolants. These NPPs have subcritical-pressure Rankine cycle with primary and secondary steam superheat up to 560°C for AGRs and GCRs and up to 505°C for SFRs and higher steam pressures compared to those for LWRs and PHWRs, i.e., about 17 MPa for AGRs and about 14 MPa for GCRs and SFRs.

Table 1.2.5 lists a number of nuclear-power reactors connected to grid by selected nations (13 nations with the largest number of nuclear-power reactors/their installed capacities ranked by installed capacities; other data on these nations are listed in Table 1.1.3 (Chapter 1.1)). Analysis of the data in Table 1.2.5 shows that real nuclear “renaissance” is in China (43 reactors have been built and put into operation within past 11 years),

Table 1.2.5. Number of nuclear-power reactors connected to electrical grids by nation (13 nations ranked by nuclear-reactor installed capacities) as per September 2022 (based on data from Nuclear News (2022); <http://www.world-nuclear.org/>; <https://pris.iaea.org/pris/>; and wnn@world-nuclear-news.org) and before the Japan earthquake and tsunami disaster (based on data from Nuclear News (2011)). (Data for all countries with nuclear-power reactors are listed in Table 1.2.6)

No.	Nation	No. of units (PWRs/ BWRs/Other types)		Installed capacity, GW _{el}			Changes in number of reactors from March 2011	% of electricity generated by nuclear (2019)
		As of Sep. 2022	Before March 2011	As of Sep. 2022	Before March 2011	Before March 2011		
1	USA	92 (61/31)	104	96	103	↓ by 12 reactors	19.3	
2	France	56 (56/–)	58	61	63	↓ by 2 reactors	70.0	
3	China	56 (51/–/1 ² /2 ³ /2 ⁵)	13	52	10	↑ by 43 reactors	4.8	
4	Russia	37 (24/–/11 ¹ /2 ²)	32	28	23	↑ by 5 reactors	18.7	
5	Japan ^a	33 (16/17)	54	32	47	↓ by 21 reactors	6.4	
6	S. Korea	26 (23/–/3 ³)	20	26	18	↑ by 6 reactors	24.7	
7	Canada	19 (–/–/19 ³)	22	14	15	↓ by 3 reactors	15.5	
8	Ukraine	15 (15/–)	15	13	13	No changes	54.9	
9	UK	10 (1/–/9 ⁴)	19	6	10	↓ by 9 reactors	17.4	
10	Spain	7 (6/1)	8	7	8	↓ by 1 reactor	21.3	
11	India	23 (2/2/19 ³)	19	7	4	↑ by 4 reactors	2.9	
12	Sweden	6 (2/4)	10	7	9	↓ by 4 reactors	39.6	
13	Belgium	7 (7)	7	6	6	No changes	52	
In total		387 (264/55/11 ¹ /3 ² /43 ³ /9 ⁴ /2 ⁵)	391	355	343	↓ by 4 reactors, but installed capacity ↑ by 12 GW _{el}	-	

^a Data in table include 33 reactors in Japan from which only 5 PWRs were in commercial operation in September of 2022 and 1 PWR—in coordinated operation (<https://www.fepec.or.jp/theme/re-operation/>).

Explanations to Table 1.2.5:

Arrows mean decrease ↓ or increase ↑ in a number of reactors.

¹No. of LGRs; ²LMFBRs; ³PHWRs; ⁴AGR; and ⁵GCRs (He cooled).

in Russia (addition of 5 reactors), in South Korea (addition of 6 reactors), and in India (addition of 4 reactors). Meanwhile, the most significant drop in a number of reactors is in Japan (21 reactors were shut down and only 5 PWRs of 33 were in commercial operation in September of 2022 and 1 PWR—in coordinated operation (<https://www.fepc.or.jp/theme/re-operation/>)), in the United States (12 reactors), in UK (9 reactors), in Canada (3 reactors), and in Sweden (4 reactors). In addition, Canada and Sweden have no plans to build new reactors. It should be noted that, in spite of outstanding achievements in nuclear-power industry, especially, in China, and, partially, in India, electricity share by nuclear power is very small in these countries (see Table 1.1.3 in Chapter 1.1), i.e., in China only 4.8% and in India 2.7%.

Table 1.2.6 lists a number of nuclear-power reactors connected to grids or to be connected to grids in reasonable time by all countries in the world. Analysis of the data in Table 1.2.6 shows that, currently, 33 countries in the world have operating nuclear-power reactors (within these countries: 18 plan to build new

Table 1.2.6. Number of nuclear-power reactors connected to electrical grids and forthcoming units as per September 2022 (based on data from Nuclear News (2022); <http://www.world-nuclear.org/>; <https://pris.iaea.org/pris/>; and wnn@world-nuclear-news.org) (countries planning to build new reactors are in bold)

No.	Nation	# Units (type)	Net MW _{el}	# Units	Net MW _{el}	Type
(connected to grid)			(forthcoming)			
1	Argentina	3 (PHWRs)	1641	1? ¹	25?	PWR
2	Armenia	1 (PWR)	415	0	0	–
3	Bangladesh	–	–	2	2160	PWR
4	Belarus	1 (PWR)	1110	1	1110	PWR
5	Belgium	7 (PWRs)	5942	0	0	–
6	Brazil	2 (PWRs)	1889	1?	1340?	PWR
7	Bulgaria	2 (PWRs)	2006	0	0	–
8	Canada	19 (PHWRs)	13,554	0	0	–
9	China	56 (51 PWRs; 2 PHWRs, 2 GCRs², 1 LMFBR (SFR))	2 51,850	8 + 9? 1 + 1?	8800 + 13,843? 600 + 600?	PWR LMFBR
10	Czech Rep.	6 (PWRs)	3932	0	0	–
11	Egypt	–	–	4?	4776?	PWR
12	Finland	5 (3 PWRs; 2 BWRs)	4394	0	–	–
13	France	56 (PWRs)	61,370	1	1600	PWR
14	Germany	3 (3 PWRs)	4055	0	0	–
15	Hungary	4 (PWRs)	1902	2?	2400?	PWR
16	India	23 (19 PHWRs; 2 BWRs; 2 PWRs)	2 6885	4 + 5? 2 + 2? 1	2520 + 3150? 1834 + 1834? 470	PHWR PWR LFMBR
17	Iran	1 (PWR)	915	2	1889	PWR

Continued

Table 1.2.6. Number of nuclear-power reactors connected to electrical grids and forthcoming units as per September 2022 (based on data from Nuclear News (2022); <http://www.world-nuclear.org/>; <https://pris.iaea.org/pris/>; and wnn@world-nuclear-news.org) (countries planning to build new reactors are in bold—cont’d

No.	Nation	# Units (type)	Net MW _{el}	# Units	Net MW _{el}	Type
(connected to grid)			(forthcoming)			
18	Japan ³	33 (16 PWRs; 13 BWRs; 4 ABWRs)	31,679	2?	2653?	ABWR
19	Mexico	2 (BWRs)	1552	0	0	—
20	Netherlands	1 (PWR)	482	0	0	—
21	Pakistan	6 (6 PWRs)	3256	1?	1000?	PWR
22	Romania	2 (PHWRs)	1300	2?	1440?	PHWR
23	Russia	37 (24 PWRs; 11 LGRs; 2 LMFBRs)	27,653	6 + 3? 1	5965 + 3393? 300	PWR 4 FR
24	Slovakia	4 (PWRs)	1848	2?	880?	PWR
25	Slovenia	1 (PWR)	688	0	0	—
26	S. Africa	2 (PWRs)	1860	0	0	—
27	S. Korea	26 (23 PWRs; 3 PHWRs)	25,816	2	2680	PWR
28	Spain	7 (6 PWRs; 1 BWR)	7121	0	0	—
29	Sweden	6 (2 PWRs; 4 BWRs)	6884	0	0	—
30	Switzerland	4 (3 PWRs; 1 BWR)	2960	0	0	—
31	Taiwan	3 (2 PWRs; 1 BWRs)	2859			
32	Turkey	—	—	4	4456	PWR
33	Ukraine	15 (PWRs)	13,107	2?	2135?	PWR
34	UAE	3 (PWRs)	4035	1	1345	PWR
35	UK	10 (1 PWR; 9 AGRs)	6378	2	3260	PWR
36	USA	92 (61 PWRs; 31 BWRs)	96,452	2	2200	PWR
In total		443 (309 PWRs; 61 BWRs; 48 PHWRs; 9 AGRs; 11 LGRs; 3 LMFBRs; 2 GCRs)	397,810	41 + 39?	42,099 + 38,589?	-

Summary: 33 countries have operating nuclear-power reactors; **18 countries from these 33 and 3 countries without nuclear-power build nuclear-power reactors (in bold)**. In addition, 30 countries are considering, planning, or starting nuclear-power programs, and about 20 countries have expressed their interest in nuclear power. However, 15 countries with NPPs don’t plan to build nuclear-power reactors.

Explanations to Table 1.2.6:

¹? means “Commercial start date – indefinite” (Nuclear News, 2022).

²GCR is a helium-cooled reactor—High-Temperature Reactor Pebble-bed Module (HTR-PM) (China).

³As of September 2022, only 5 PWRs were in commercial operation in January of 2022 and 1 PWR—in coordinated operation (<https://www.fepec.or.jp/theme/re-operation/>).

reactors, and 15 don't plan to build new reactors) and 3 countries without nuclear-power reactors (Bangladesh, Egypt, and Turkey) are working toward introducing nuclear energy on their soils.

Figure 1.2.2a shows a number of nuclear-power reactors in the world connected to grids (as per September, 2022) vs. years of their commercial operation and their installed capacities (Figure 1.2.2b). And Figure 1.2.3 shows a number of nuclear-power reactors in the United States connected to grid (as per January 2022) vs. years of their commercial operation.

Analysis of the data in Figure 1.2.2 shows that the Chernobyl NPP severe accident (April 26, 1986), which had happened with the RBMK-1000—LGR (former USSR design), has forced Ukraine to shut down this NPP, and Russia—to cancel any further R&D and construction of new LGRs. In the same way, a small number of BWRs/ABWRs planned to be built is due to the Fukushima-Daiichi NPP severe accident, which had happened with older design BWRs in March of 2011. However, it should be mentioned that all nuclear vendors, of course, including BWRs and ABWRs, have updated their designs with additional features/systems to enhance safety based on lessons learned from all nuclear accidents.

In the case of the United States (see Figure 1.2.3), their nuclear industry was hit quite hard with the Three Mile Island NPP severe accident and right after that with the Chernobyl NPP severe accident, which, eventually, decreased a number of reactors built and connected to grid to only six per last 25 years.

Therefore, the history of nuclear-power industry shows that nuclear accidents, especially, severe ones, can override any advantages of various reactors' types, and significantly affect future builds of certain types of reactors, e.g., LGRs and BWRs, or even all types of reactors. **We have to remember that one more severe accident somewhere in the world can and does adversely affect the whole nuclear-power industry and broader societal acceptance. Due to this, we must continuously to enhance safety of all nuclear-power reactors.**

It should be mentioned that globally current successes in nuclear-power industry are far away from previous “glorious” days, when ~80 and ~120 reactors have been built and connected to grids within 1980–84 and 1985–89, respectively (see Figure 1.2.2). Just within 5 years, i.e., from 2015 to 2019, about 40,000 MW_{el} of new installed capacities have been added, which match approximately the same amount added within 1975–79 (see Figure 1.2.2b).

Figure 1.2.4 shows a number of nuclear-power reactors in the world by installed capacity as per January, 2022. Analysis of the data in this figure shows that the largest group of reactors is within the range of installed capacities from 900 MW_{el} and up to 999 MW_{el}. However, oncoming reactors of Generation-III⁺, usually, have higher installed capacities compared to those of Generation-III reactors, i.e., within the range of 1100 MW_{el} and up to 1660 MW_{el} (the exception is SMRs).

Table 1.2.7 lists the smallest and the largest nuclear-power reactors of the world, and Table 1.2.8 nuclear-power reactors, which operate 45+ years (also, see Figure 1.2.5). Based on the data from Table 1.2.8 and Figure 1.2.5, it can be assumed that for future trends in nuclear-power industry of the world, 45 years can be taken as an average operational term for current reactors. Of course, for many modern Generation-III⁺ reactors, usually, 60-year operational term is promised. Moreover, some countries consider extensions of operational terms for current Generation-III reactors up to 60 and even more years, e.g., four PWRs and two BWRs in the United States have granted permission to operate for 80 years!

Table 1.2.9 lists latest years, when various types of reactors have been built and connected to electrical grids. The latest AGR (carbon-dioxide-cooled) in UK was connected to grid in 1989, i.e., no new AGRs have been built for the last 33 years, and the latest LGR in Russia was connected to grid in 1990, i.e., no new LGRs have been built for the last 32 years. And, as it was mentioned before, these reactors/NPPs will be never built again.

Figure 1.2.6 shows impact of the major/severe NPPs accidents within the last 50 years on new builds. Analysis of the data in this figure shows that we might face a very significant drop (up to 3 times) in a number of operating nuclear-power reactors somewhere between 2030 and 2040 (see Figure 1.2.6); if we assume that the current operating term of reactors is on average 45 years, and the rate of building and putting into

Table 1.2.7. The smallest and the largest nuclear-power reactors of the world (based on data from Nuclear News (ANS), <http://www.world-nuclear.org/>; <https://pris.iaea.org/pris/>; and wnn@world-nuclear-news.org)

Name	No. of units	Net MW_{el}	Reactor		Commercial start	Reactor supplier	Country	Company
			Type	Model				
<50 MW_{el}								
Bilibino	3	11	LGR	EGP-6	1974–77	MTM	Russia, Bilibino, Chukotka	Rosenergoatom
CIAE	1	20	SFR	CEFR	2011	OKBM Afrikantov	China, near Beijing	CIAE
Akademik Lomonosov	2	35	PWR SMR	KLT-40S	2019	OKBM Afrikantov	Russia, Port Pevek, Chukotka	Rosenergoatom
50 – 99 MW_{el}								
Rajasthan	1	90	PHWR	CANDU	1973	AECL/DAE	India, Kota, Rajasthan	Nuclear Power Corp. of India
1400 – 1499 MW_{el}								
Oskarshamn	1	1400	BWR	BWR 75	1985	ABB-Atom	Sweden, Oskarshamn, Kalmar	OKG Aktiebolag
Shin-Kori	1	1416	PWR	APR-1400	2016	Doosan	S. Korea, Ulju-gun, Ulsan	KOPEC, Hyundai, SK
Isar	1	1410	PWR	Konvoi	1988	KWU	Germany, Essenbach, Ba.	E.ON Kernkraft GmbH
Civaux	2	1495	PWR	N4	2002	Framatome	France, Civaux, Vienne	Electricité de France (EDF)
≥1500 MW_{el}								
Chooz	2	1500	PWR	N4	2000	Framatome	France, Chooz, Ardennes	Electricité de France (EDF)
Olkiluoto	1	1600	PWR	EPR	2022	Framatome	Finland	
Taishan	2	1660	PWR	EPR	2018	Areva	China	

operation new reactors is ~ 20 reactors ($\sim 20,000 MW_{el}$ installed capacities) per 5 years (as it was within 2010–14, see Figure 1.2.2). If we base our predictions on statistical data within 2015–19, when ~ 40 reactors ($\sim 40,000 MW_{el}$ installed capacities, see Figure 1.2.2) were built and connected to grid, we can see the better trend represented by lower posts. Even with higher rates of new nuclear-capacities additions, i.e., ~ 60 reactors ($\sim 60,000 MW_{el}$ installed capacities) or even ~ 80 reactors ($\sim 80,000 MW_{el}$ installed capacities) per 5 years (as it was within 1980–84, see Figure 1.2.2), we will still have a tangible decrease in a number of operating reactors. If this forecast(s) is correct, the nuclear-power industry will face

Table 1.2.8. List of nuclear-power reactors, which operate 45+ years (data from March, 2022) (Nuclear News (2022); <http://www.world-nuclear.org/>). In total: 62 reactors or 14% of all reactors in the world (also, see Figure 1.2.5)

Country	Installed capacity, MW _{el}	Reactor type	Commercial start, year	No. of years in operation
Argentina	340	PHWR	1974	48
Belgium	2 × 445; 962	PWR	1975	47
Canada	515; 515; 2 × 760	PHWR	1971; 1973; 1977	51; 49; 45
Finland	507	PWR	1977	45
India	2 × 150; 90	BWR; PHWR	1969; 1973	53; 49
Japan	780; 780	PWR	1974; 1976	48; 46
Netherlands	482	PWR	1973	49
Pakistan	90	PHWR	1972	50
Russia	385; 2 × 411; 3 × 11	PWR	1972; 1973/1975; 1975/1976/1977	50; 49/47; 47/46/45
Switzerland	2 × 365	PWR	1969/1972	53/50
UK	480/490; 495	AGR	1976; 1977	46; 45
USA	620	BWR	1969	53
	925/576/615	BWR/PWR/PWR	1970	52
	811/920/671	PWR/BWR/BWR	1971	51
	874/615/844	PWR	1972	50
	874/847/937/840/550	PWR/PWR/BWR/PWR/PWR	1973	49
	848/859/836/2 × 1322/815/550/1255	PWR/PWR/PWR/BWR/BWR/PWR/BWR	1974	48
	1084/884/932/907/842/885/1255	PWR/PWR/BWR/PWR/BWR/BWR/BWR	1975	47
	963	PWR	1976	46
	938/881/1169/854/1255	BWR/PWR/PWR/PWR/BWR	1977	45

very difficult times ahead. Conservative projections for selected countries in terms of a number of reactors, which might be shut down within future years, are shown in [Figures 1.2.7 and 1.2.8](#).

It should be once more emphasized that, in general, current problems in the world nuclear-power industry are: significant delays in putting into operation new, mainly, Generation-III⁺ reactors, indecision of governments in terms of support of nuclear-based electricity generation; and radioactive-waste management and safe storage.

Table 1.2.9. Latest years when various types of reactors have been built and connected to grid (based on data from Nuclear News (2022); <http://www.world-nuclear.org/>; <https://pris.iaea.org/pris/>; and wnn@world-nuclear-news.org) (reactors built before 1992, i.e., more than 30 years old, are in bold)

No.	Type of reactor	Model	Reactor supplier	Country	Installed capacity, MW _{el}	Year	Reactor age, years
1	PWR	VVER-1200	ASE	Belorus'	1110	2020	2
		HPR-1000	CNNC	China	1000	2021	1
		ACPR-1000			1000	2021	1
		CNP-1000			1000	2021	1
		EPR	Areva	Finland	1600	2022	0.5
		VVER-1200	AEP	Russia	11066	2021	1
		KLT-40S SMR	OKBM		32	2019	3
		APR-1400	KEPCO	UAE	1345	2022	0
2	BWR	ABWR	Hitachi	Japan	1108	2006	16
3	PHWR	PHWR-700	Owner	India	630	2021	1
4	AGR	AGR	NNC	UK	605	1989	33
5	GCR	HTR PBMR	Tsinghua U.	China	100	2022	0.5
6	LGR	RBMK-1000	MTM	Russia	925	1990	32
7	LMFBR	BN-800	OKBM	Russia	820	2016	6

Table 1.2.10 lists current activities in various countries worldwide on new nuclear-power-reactors build. Analysis of the data in Table 1.2.10 clearly shows that Russia and China are the front runners in new nuclear builds in their countries and abroad, largely because both governments provide significant political and long-term support with various funds for nuclear-power R&D and for their government-controlled nuclear vendors, as, also, do South Korea and France, especially, to build NPPs abroad plus credits and other incentives for foreign buyers to introduce nuclear power.

Last years were very important for the nuclear-power industry of the world. Russia put into operation a number of Generation-III⁺ VVERs (PWR—VVER-1200) and the SFR—BN-800 reactor in 2016 and continues to lead the SFR technologies in the world (Pioro et al., 2019; Handbook, 2016).

China put into operation many reactors/NPPs including the largest in the world Generation-III⁺ PWR-EPR (Areva design) with amazing installed capacity of 1660MW_{el}. In addition, several AP1000 reactors

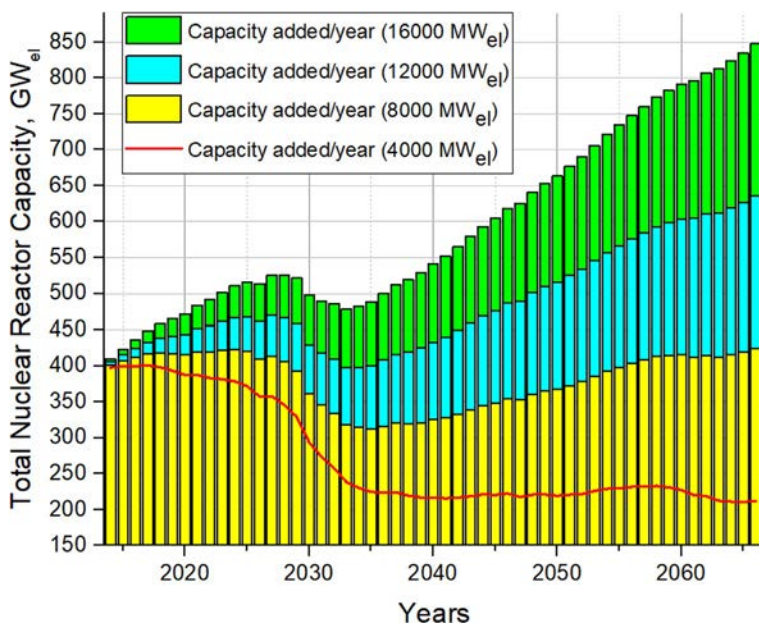


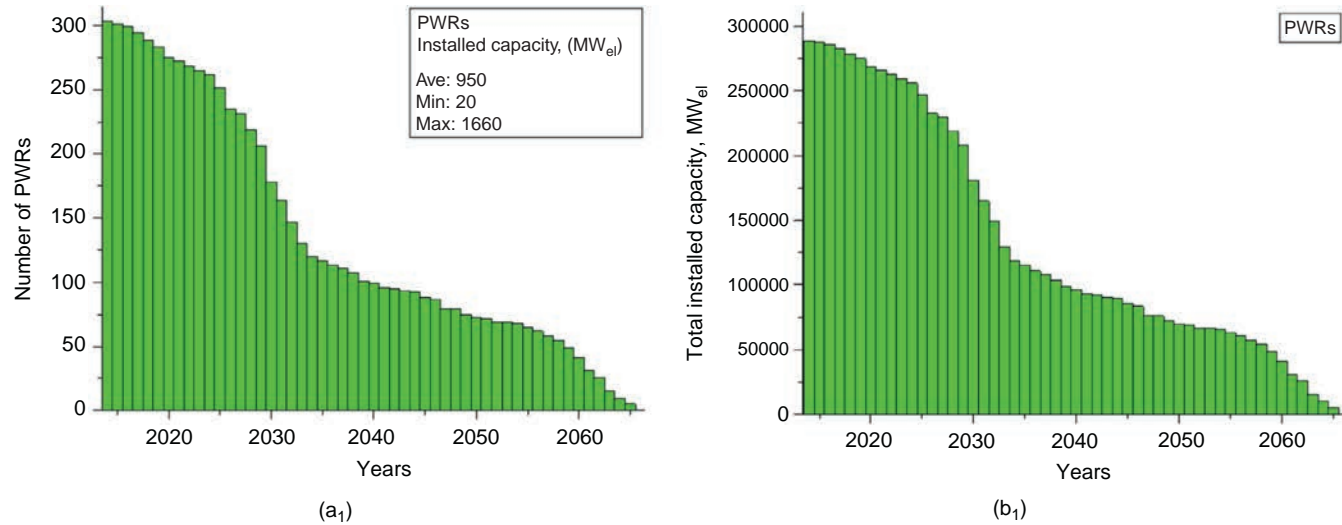
Figure 1.2.6. Possible scenarios of nuclear-power development in the world (based on 45-year operational term; all current reactors older than 45 years are taken from consideration; January, 2022): solid-line curve is based on data from 2010 to 2014; lower-posts profile—2015–19, and highest-posts profile—1980–84 (for details, see Figure 1.2.2).

(Westinghouse design) (Friedman, 2019), also, a Generation-III⁺ design, were put into operation in China first time in the world (Nuclear News, 2022). In general, Generation-III⁺ water-cooled reactors/NPPs have enhanced safety due to passive-safety systems (Friedman, 2019) and can reach slightly higher thermal efficiencies up to 36%–37% (38%) compared to those of Generation-III water-cooled reactors/NPPs (the exception is SMRs) (see Table 1.2.4). Also, China put into operation the Hualong One PWR or HPR-1000—a domestically developed Generation-III reactor design, and put into operation the first in the world GCR—a helium-cooled reactor: High-Temperature Reactor Pebble-bed Module (HTR-PM) in 2022 and plan to put two SFRs—China Fast Reactors (CFR-600) within next several years.

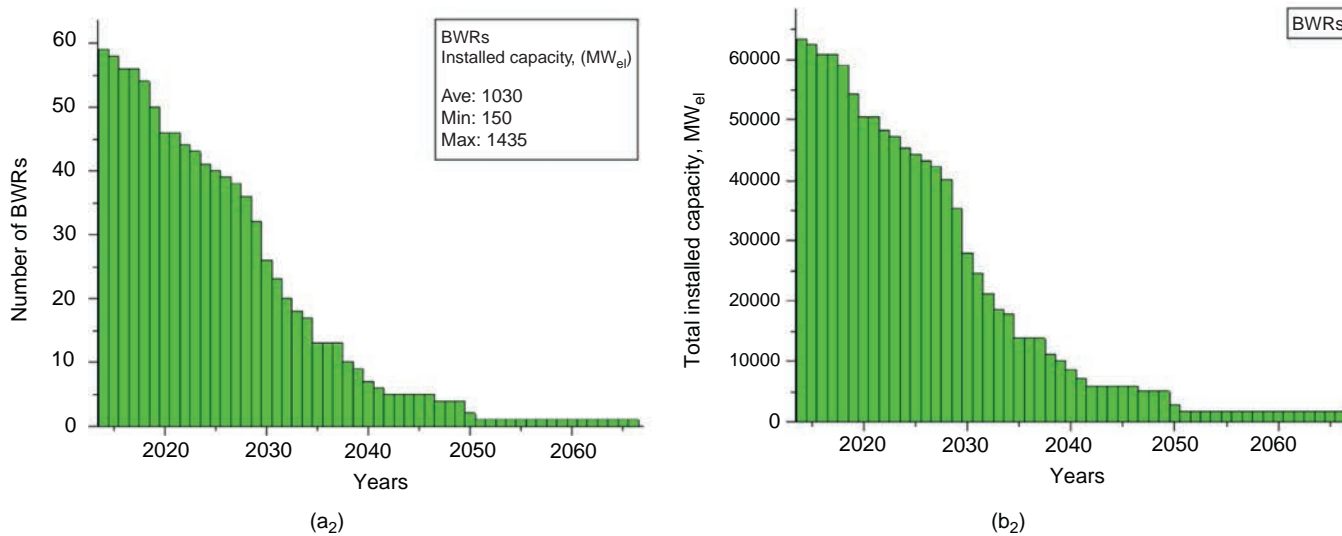
South Korea put into operation several their Generation-III⁺ APR-1400 (Doosan design) on their soil, three APR-1400 (KEPCO) in the UAE, and plans to put four more these reactors into operation soon: 3 inside country and 1 in the UAE (Nuclear News, 2022).

India put into operation their latest domestically developed design of PHWR—PHWR-700 in January of 2021.

Current trend in new builds is to build Generation-III⁺ reactors, mainly PWRs. Another trend, which just has appeared, is to build SMRs with installed capacities up to 300 MW_e for applications in remote areas, small electrical grids, military facilities, and as floating NPPs; and first two SMRs are 35-MW_e PWRs installed on a floating barge, so-called, Floating Nuclear Thermal-Power Plant (FNThPP) by the name of Academician Lomonosov (Russia) (for details, see Tables 1.2.3 and 1.2.4, and Piro et al. (2020, 2019)). Also, in 2021, Rosatom has started work on a site of the future SMR NPP, which is planned to be built in Yakutia. The SMR will be a RITM-200M (Generation-III⁺) ship-based reactor (<https://www.neimagazine.com/news/newsrosatom-to-being-work-on-land-based-smr-8436408>).



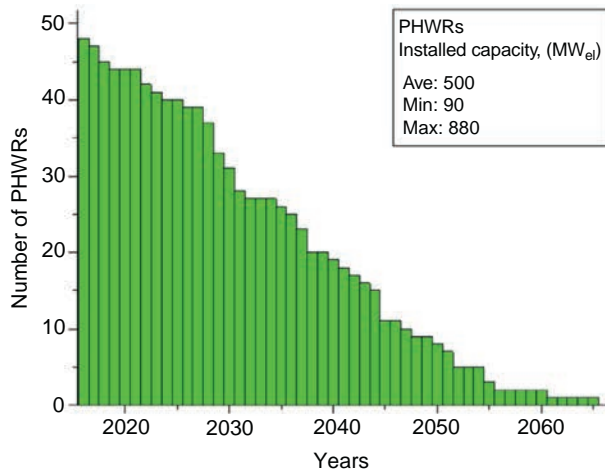
For PWRs – this is very conservative estimation, because, currently, this type of reactors is the most build in the world.



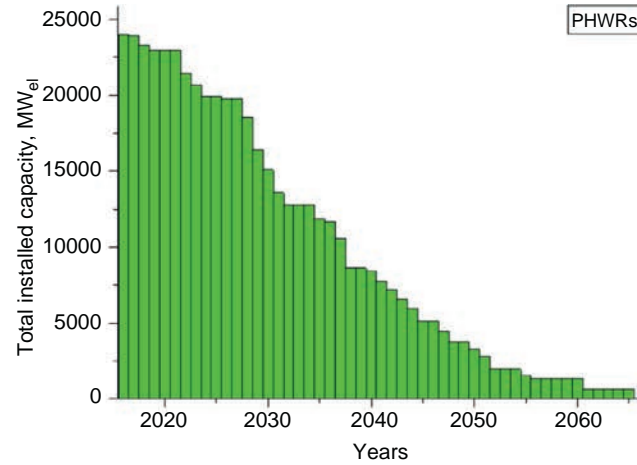
For BWRs – this is optimistic estimation, because, currently, there are no new builds of this type reactors in the world.

Figure 1.2.7. Possible scenarios for future of nuclear-power reactors of various types, if no additional reactors are built, based on 45 years in service of current reactors: (a) number of reactors and

(Continued)

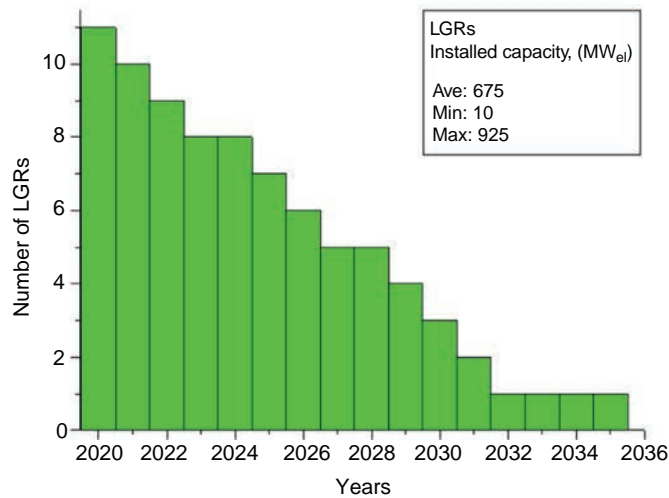


(a₃)

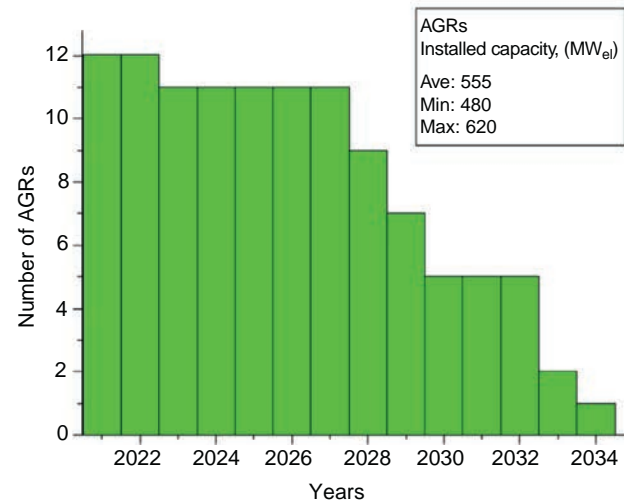


(b₃)

For PHWRs - this is very close to be conservative estimation, because, currently, there is few new builds of this type reactors in the world.



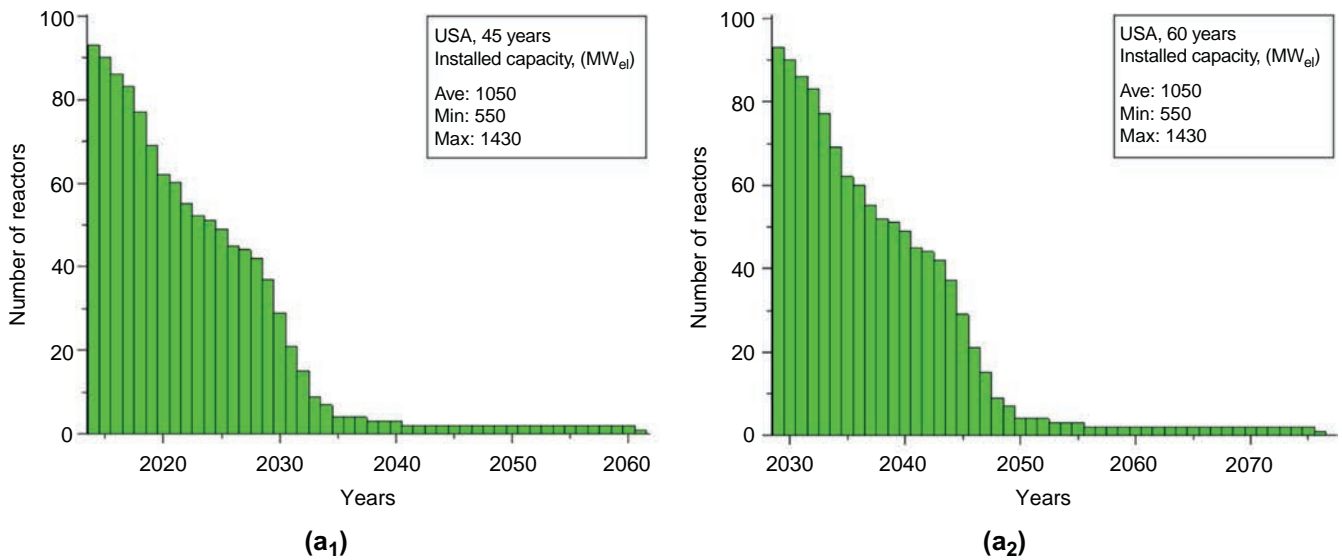
(a₄)



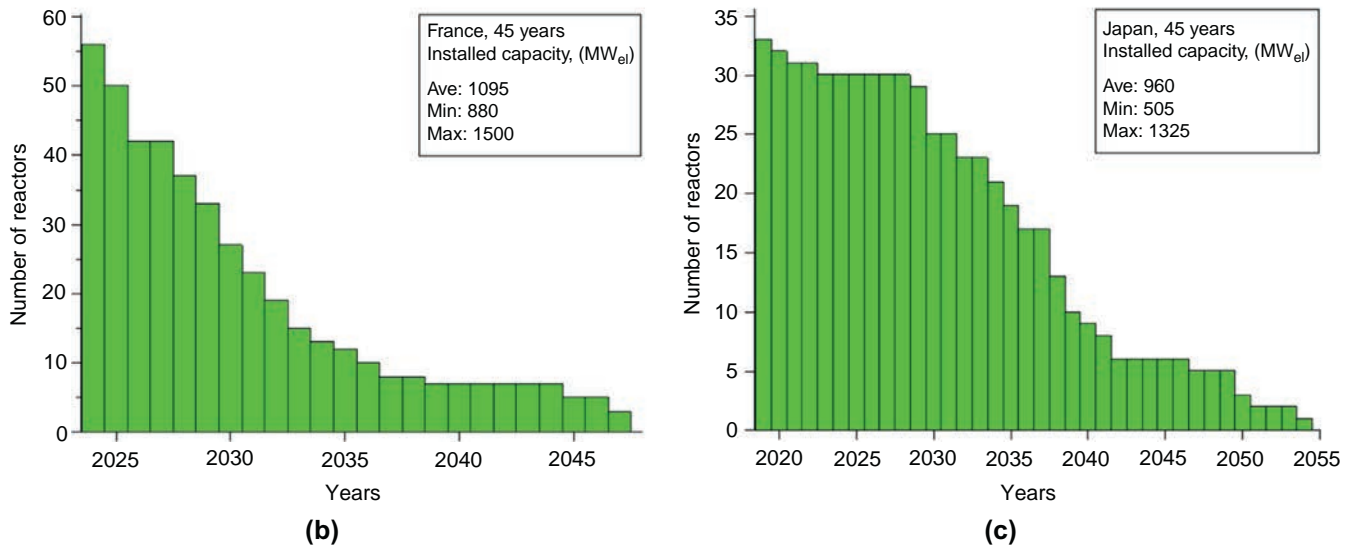
(a₅)

These are very optimistic estimations, because Russian government (for LGRs) and UK government (for AGRs) have decided not to proceed with these types or reactors anymore. Therefore, even if a few of them is left, their operation will be very expensive, and they can be shut down ahead of time.

Figure 1.2.7, Cont'd (b) installed capacities.



Current status of nuclear power in USA: 93 reactors are connected to grid; the latest reactor was connected to grid in 2016; number of reactors decreasing every year (~1 per year); 2 AP-1000 reactors should be connected to grid in 2021 and 2022? 4 PWRs and 2 BWRs built at the beginning of 1970s were permitted to operate for 80 years.



In France: 56 reactors; two latest reactors were connected to grid in 2002; 2 reactors were shut down within last 10 years; 1EPR is under construction?

In Japan: 33 reactor conncted to grid left after the fukushima Daiichi NPP serve accident; the latest reactor was connected to grid in 2009; 2 ABWR were planned to be built? Number of operating reactors vary from year to year from 2 to 9.

Figure 1.2.8. Conservative scenarios for future of nuclear power in the United States (a), France (b), and Japan (c), if no additional reactors are built, based on 45 years in service of current reactors.

Table 1.2.10. Current activities worldwide on new nuclear-power-reactors build (based on data from Nuclear News (2022) and updated up to September of 2022)

No.	Country/nuclear supplier	Countries, which are looking forward for new builds (no. of possible units)
1	Russia/Rosatom (outside Russia—ASE (Atom StroyExport) is the Russian Federation’s nuclear-power equipment and service exporter. It is a fully-owned subsidiary of Rosatom. Nuclear-power activities are financially supported by the Russian government)	Russia (6 + 3? ¹), Bangladesh (2), Belarus (1), China (4), Egypt (4?), Hungary (2?), India (2 + 2?), Iran (2), and Turkey (4) In total: 21 + 11? = 32
2	China/Various vendors (Nuclear-power activities are supported by the Chinese government)	China (5 + 13? ¹), Pakistan (1?), Romania ² (2? CANDU reactors) In total: 5 + 16? = 21
3	S. Korea/Doosan and KEPCO	S. Korea (2) and UAE (2) In total: 4
4	India/Various vendors	India (4 + 5? PHWRs) In total: 9
5	France/Framatome	France (1), and UK (2) In total: 3
6	USA/GE and Westinghouse	USA (2) and Ukraine (1?), In total: 2 + 1? = 3
7	Czech Rep./Skoda	Slovakia (2), Ukraine (1?) In total: 2 + 1? = 3
8	Japan/Toshiba + Hitachi	Japan (2?) In total: 2?
9	Canada/AECL (Candu Energy, Inc.) together with CGNPC (China)	Romania ² (2? CANDU reactors) In total: 2?
10	Germany/KWU (KraftWerk Union AG)	Brazil (1?) In total: 1?
11	Argentina/CNEA (Comisión Nacional de Energía Atómica)	Argentina (1?) In total: 1?

¹? means “Commercial start date – indefinite” (Nuclear News, 2022).

²Two CANDU reactors in Romania for the Cernavoda NPP are a joint venture proposal from China and Canada.

1.2.1 Conclusions

1. Currently, i.e., as of September 2022, 33 countries have operating nuclear-power reactors, and 3 countries without nuclear power build nuclear-power reactors. In addition, 30 countries are considering, planning, or starting nuclear-power programs, and about 20 countries have expressed their interest in nuclear power. However, 15 countries with NPPs don’t plan to build new nuclear-power reactors.

2. In September of 2022, 443 nuclear-power reactors were connected to electrical grids around the world, which is less by 1 reactor compared to that before the Fukushima NPP severe accident in March of 2011 (however, the total installed capacity increased by 21 GW_{el}). This number includes 309 PWR_S, 61 BWRs, 48 PHWRs, 9 AGRs (CO₂-cooled), 11 LGRs, 3 LMFBRS (SFRs), and 2 GCRs (He-cooled). Considering the number of forthcoming reactors, the number of BWRs/ABWRs and PHWRs will decrease within next 20–25 years. Furthermore, within next 10–15 years or so, all AGRs (carbon-dioxide-cooled) and LGRs will be shut down forever.
3. Also, it should be stated that the history of the nuclear-power industry shows that nuclear accidents, especially, severe ones, can override any advantages of various reactors' types, and significantly affect future builds of certain types of reactors, e.g., LGRs, BWRs, or even all types of reactors.
4. Today, based on a summary of various parameters including all pros and cons, PWRs are considered as the most “popular” reactors, which are being built around the world. However, tomorrow and in the future the next generation or Generation-IV reactors/NPPs offering improved performance are planned to be eventually built (currently, two prototypes of these reactors are in operation—3 SFRs (2 larger ones in Russia and 1 small in China) and 2 GCRs (in China)).
5. In general, the major advantages of nuclear power are: (1) concentrated and reliable source of almost infinite energy, which is more or less independent of weather conditions; (2) high capacity factors are achievable, often in excess of 90% with long operating cycles, making units suitable for continuous base-load operation; (3) essentially negligible operating emissions of carbon dioxide and relatively small amount of wastes generated compared to alternate fossil-fuel thermal power plants plus the nuclear has the lowest death rate per TWh compared to that for other energy sources; and (4) relatively small amount of fuel required compared to that of fossil-fuel thermal power plants. As the result, nuclear power is considered as the most viable source for electricity generation within next 50–100 years. However, nuclear power must operate and compete in energy markets based on relative costs and strategic advantages of the available fuels and energy types.
6. In spite of all current advances in nuclear power, NPPs have the following deficiencies: (1) generate radioactive wastes; (2) have relatively low thermal efficiencies, especially, NPPs equipped with water-cooled reactors (up to 1.6 times lower than that for modern advanced thermal power plants); (3) risk of radiation release during severe accidents; and (4) production of nuclear fuel is not an environment-friendly process. Therefore, all these deficiencies should be addressed in next generation—Generation-IV reactors and NPPs.

References

- Friedman, B.N., 2019. The AP1000 plant and the China Project Commissioning success. *ASME J. Nucl. Eng. Radiat. Sci.* 5 (1). 3 pp.
- NIST REFPROP, 2018. In: Lemmon, E.W., Bell, I.H., Huber, M.L., McLinden, M.O. (Eds.), *Reference Fluid Thermodynamic and Transport Properties*, NIST Standard Reference Database 23, Ver. 10.0. National Institute of Standards and Technology, USA.
- Nuclear News, 2011. Reference Special Section, March, Publication of American Nuclear Society (ANS), March, pp. 45–78.
- Nuclear News, 2022. 23rd Annual Nuclear News Reference Section, March, Publication of American Nuclear Society (ANS), March, pp. 41–69.
- Pioro, I., Duffey, R., 2015. Nuclear power as a basis for future electricity generation. *ASME J. Nucl. Eng. Radiat. Sci.* 1 (1). 19 pp. Free download fro <http://nuclearengineering.asmedigitalcollection.asme.org/article.aspx?articleID=2085849>.
- Pioro, I., Duffey, R.B., Kirillov, P.L., Dort-Goltz, N., 2020. Current status of reactors deployment and small modular reactors development in the world. *ASME J. Nucl. Eng. Radiat. Sci.* 6 (4). 24 pp. Free download fro <https://asmedigitalcollection.asme.org/nuclearengineering/article/6/4/044001/1085654/Current-Status-of-Reactors-Deployment-and-Small>.
- Pioro, I., Duffey, R.B., Kirillov, P.L., Pioro, R., 2021. Pros and Cons of commercial reactor designs, section 2: Chapter. Part 2. Current status and future trends in the world nuclear-power industry and technical considerations of nuclear-power reactors. In: Greenspan, E. (Ed.), *Encyclopedia of Nuclear Energy*, first ed. Elsevier, UK, pp. 288–303. 3656 pp.

- Pioro, I., Duffey, R.B., Kirillov, P.L., Pioro, R., Zvorykin, A., Machrafi, R., 2019. Current status and future developments in nuclear-power industry of the world. *ASME J. Nucl. Eng. Radiat. Sci.* 5 (2). 27 pp. Free download from <https://asmedigitalcollection.asme.org/nuclearengineering/article/doi/10.1115/1.4042194/725884/Current-Status-and-Future-Developments-in-Nuclear>.
- Pioro, I., Duffey, R.B., Pioro, R., 2022. Overview of current status of nuclear-power industry of the world, Chapter 2. In: Boucau, J. (Ed.), *Fundamental Issues Critical to the Success of Nuclear Projects*. Elsevier—Woodhead Publishing (WP), Duxford, UK. 392 pp.
- Pioro, I.L. (Ed.), 2016. *Handbook of Generation IV Nuclear Reactors*. Elsevier—Woodhead Publishing (WP), Duxford, UK. 940 pp. Free download of content: https://www.gen-4.org/gif/jcms/c_9373/publications.

Further reading

- Duffey, R.B., Pioro, I., Pioro, R., 2021. World Energy Production and the contribution of PHWRs, Chapter 1. Introduction. In: Riznic, J. (Ed.), *Pressurized Heavy Water Reactors: CANDU*. vol. 7. Elsevier, UK, pp. 1–44. 546 pp.

Generation IV International Forum (GIF)

Igor L. Pioro^a and Gilles H. Rodriguez^b

^aFaculty of Energy Systems and Nuclear Science, University of Ontario Institute of Technology, Oshawa, ON, Canada ^bTechnical Director of the Generation IV International Forum, France

Nomenclature

P Pressure (MPa)
T Temperature (°C)

Subscripts

cr critical
el electrical
in inlet
out outlet
sat saturation
th thermal

Abbreviations

AMME-TF Advanced Material & Manufacturing Engineering Task Force
AMR Advanced Modular Reactor
ANTARES Areva's New Technology and Advanced gas-cooled Reactor for Energy Supply (France)
AR Advanced Reactor
AVR Arbeitsgemeinschaft VersuchsReaktor (GmbH) (Germany)
BARC Bhabha Atomic Research Centre (India)
BN Fast Sodium (reactor) (БН—Быстрый Натриевый (in Russian abbreviations) (Russia))
BREST-OD Fast Reactor with Inherent safety Lead Coolant—Experimental Demonstration (БРЕСТ-ОД—Быстрый Реактор Естественной безопасности со Свинцовым Теплоносителем—Опытно-Демонстрационный or Быстрый Реактор Естественной безопасности—Опытно-Демонстрационный (in Russian abbreviations) (Russia))
BWR Boiling Water Reactor
CHP Combined Heat and Power
DOE Department Of Energy (USA)
ELFR European Lead-cooled Fast Reactor (EU)
EMWG Economics Modelling Working Group
EPRI Energy Power Research Institute (USA)
ETWG Education & Training Working Group
EU European Union
FHR Fluoride-salt-cooled High-temperature Reactor
FMSR Fast Molten Salt Reactor
GENIV GENeration IV
GFR Gas-cooled Fast Reactor

GIF	Generation IV International Forum
GTHT300	Gas Turbine High-Temperature Reactor 300MW _{e1} (Japan)
GT-MHR	Gas Turbine-Modular Helium Reactor (Russia/USA)
HM	Heavy Metal
HTGR	High-Temperature Gas-cooled Reactor
HTR	High-Temperature Reactor
HTR-PM	High-Temperature Reactor Pebble-bed Module (China)
HTTR	High-Temperature Test Reactor (Japan)
IAEA	International Atomic Energy Agency
IMSBR	Indian Molten Salt Breeder Reactor
IMSR	Integral Molten Salt Reactor (Canada)
INPRO	INternational PROject on Innovative Nuclear Reactors and Fuel Cycles
KI	Kurchatov Institute (Russia)
LBE	Lead-Bismuth-Eutectic
LEU	Low Enriched Uranium
LFR	Lead-cooled Fast Reactor
LFTR	Liquid-Fluoride Thorium Reactor
LWR	Light Water Reactor
MCFR	Molten Chloride Fast Reactor (USA)
MCSFR	Molten Chloride Salt Fast Reactor (Canada/USA)
MF	Metallic Fuel
MOSART	MOlten Salt Actinide Recycler and Transmuter reactor (Russia)
MoU	Memorandum of Understanding
MOX	Mixed OXide (fuel)
MSR	Molten Salt Reactor
NGNP	Next-Generation Nuclear Plant (USA)
NEaNH TF	NonElectrical applications of Nuclear Heat Task Force
NHDD	Nuclear Hydrogen Development and Demonstration project (South Korea)
NPP	Nuclear Power Plant
OECD	Organization for Economic Co-operation and Development
PBMR	Pebble-Bed Modular Reactor (South Africa)
PRPPWG	Proliferation Resistance and Physical Protection Working Group
PWR	Pressurized Water Reactor
R&D	Research and Development
RDTF	R&D infrastructure Task Force
RSWG	Risk and Safety Working Group
SC	SuperCritical
SCF	SuperCritical Fluid
SCP	SuperCritical Pressure
SCW	SuperCritical Water
SCWR	SuperCritical Water-cooled Reactor
SDC-TF	Safety Design Criteria Task Force
SFR	Sodium Fast Reactor
SIAP	Senior Industrial Advisory Panel
SINAP	Shanghai INstitute of Applied Physics (Chinese Academy of Sciences)
SMR	Small Modular Reactor
SSR-W	Stable Salt Reactor—Wasteburner
SSTAR	Small Sealed Transportable Autonomous Reactor (USA)
THTR	Thorium High-Temperature nuclear Reactor (Germany)
TMSR-LF	Thorium Molten Salt Reactor-Liquid Fuel (China)
TRISO	TRi-structural ISOTropic
TRU	TRansUranium (burners)
UK	United Kingdom
U.S. (or US)	United States (of America)
VHTR	Very-High-Temperature Reactor

VNIIM High-Technology Scientific-Research Institute for Inorganic Materials (Высокотехнологический Научно-Исследовательский Институт Неорганических Материалов имени Академика А.А. Бочвара (in Russian abbreviations)) (Russia)

This chapter consists of materials and figures taken directly from the Generation IV International Forum (GIF) website: www.gen-4.org/gif/jcms/c_9260/public (accessed June 8, 2022). GIF, with its six Generation-IV (Gen-IV) nuclear-reactor concepts, is not the only world forum/program/project on the next generation of nuclear-power reactors or Advanced Reactors (ARs). It is important, however, to underline that for more than two decades, the GIF has been a unique international organization ensuring the overall coherency of these six innovative-system designs, as well as some studies on essential cross-cutting subjects such as safety, techno-economics, proliferation resistance, and physical protection, education, and training (Figure 2.1).

In parallel, the International Atomic Energy Agency (IAEA) in Vienna (Austria) established in 2000 “The International PROject on innovative nuclear reactors and fuel cycles (INPRO)” (www.iaea.org/INPRO/about.html) “to help ensure that nuclear energy is available to contribute to meeting the energy needs of the 21st century in a sustainable manner. It is a mechanism for INPRO Members to collaborate on topics of joint interest. The results of INPRO’s activities are being made available to all IAEA Member States.” The major driving force behind these activities relates to “concerns over energy resource availability, climate change, and energy security [which] suggest[s] an important role for nuclear power in supplying energy in the 21st century.” Many countries worldwide have also implemented national programs in support of next-generation nuclear reactors or ARs.

However, for the purposes of this Handbook, the focus will be on the six GIF Gen-IV nuclear-reactor concepts alone (see below). Also, Advanced Small Modular Reactors (ASMRs or AMRs is more often used) (see Chapter 20 of this Handbook) can be considered under the class of ARs or next-generation reactors. In addition, it should be noted that various nuclear-engineering companies worldwide are researching or developing other, next-generation nuclear-reactor concepts or ARs. The IAEA is in fact regularly updating its compendium of Small Modular Reactors (SMRs) and AMRs.

The GIF website, and more specifically the GIF annual reports, propose a relevant and complementary list of GIF publications available to the public, all of which are dedicated to GIF nuclear-power systems and to cross-cutting topics as well. It is recommended, therefore, that interested parties consult regularly these publications, as well as the GIF website and GIF Newsletter for more details and for regular updates.

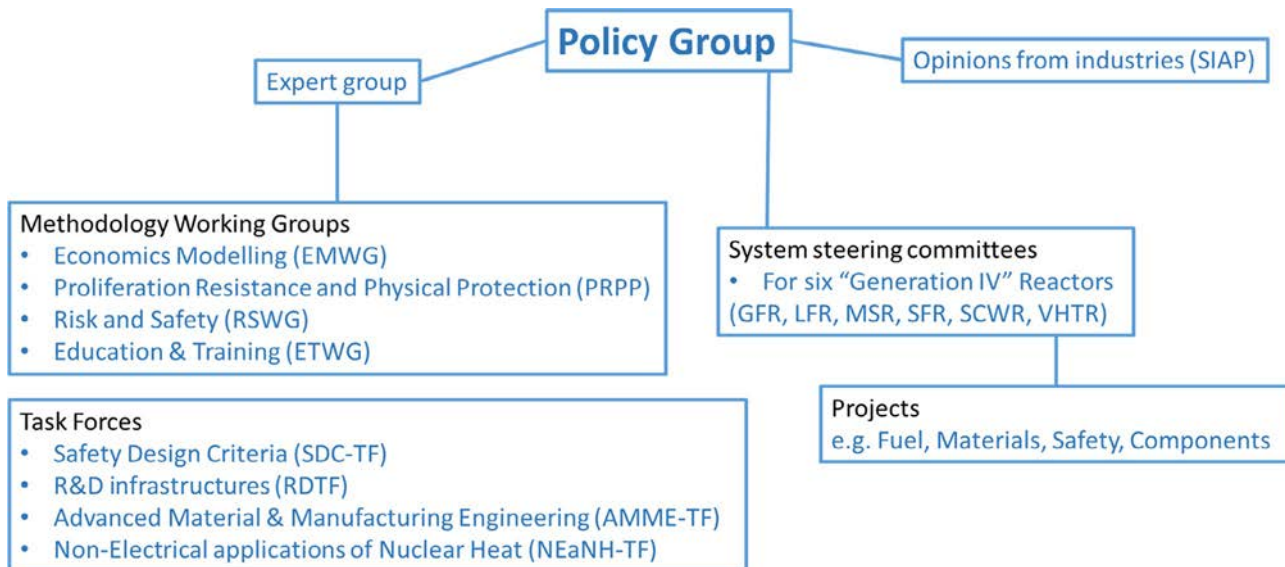


Figure 2.1. Status of the GIF Organization (as of June 2021). *Source: GIF.*

2.1 Origins of GIF

GIF meetings have begun in January of 2000, when the US Department Of Energy’s (DOE) Office of Nuclear Energy, Science, and Technology convened a group of senior governmental representatives from the original nine GIF member countries to begin discussions on international collaboration in the development of Gen-IV nuclear-energy systems.

This group, subsequently named the GIF Policy Group (PG), also, decided to form a group of senior technical experts to explore areas of mutual interest and make recommendations regarding both research and development areas, as well as processes by which collaboration could be conducted and assessed. This senior Technical Experts Group first met in April of 2000.

The founding document of the GIF—a framework for international cooperation in research and development for the next generation of nuclear-energy systems—is set out in the GIF Charter, first signed in July of 2001 by Argentina, Brazil, Canada, France, Japan, the Republic of Korea, South Africa, the United Kingdom (UK), and the United States (US). The Charter has since been signed by Switzerland (2002), Euratom (2003), and the most recently by the People’s Republic of China and the Russian Federation in November of 2006. Australia joined GIF in December of 2017, and the United Kingdom became an “active member” by ratifying the Framework Agreement on October of 2019 (before that date, UK R&D teams were involved in GIF projects through Euratom).

In 2020, the GIF decided to completely renew its different interfaces through a revamp of the entire GIF website, structuring it toward recent and actualized GIF news and easier access to GIF public material (e.g., documents, publications, white papers) for industry. A new GIF logo was also designed at the end of 2020, with GIF entering its third decade of existence (Figure 2.2).

2.2 Gen-IV goals

Eight technology goals have been defined for Gen-IV systems in four broad areas: sustainability, economics, safety and reliability, and proliferation resistance and physical protection. These ambitious goals are shared by a large number of countries as they aim at responding to the economic, environmental and social requirements of the 21st century. They establish a framework and identify concrete targets for GIF R&D efforts. The four objectives defined by the Gen-IV Forum are considered by the Forum to be more than just objectives; they are the GIF values. In fact, in its 20 years of existence, with the GIF now entering its third decade, and despite significant evolutions in the global energy context, GIF has never moved toward redefining the conditions required for a reactor to be considered the fourth generation: again, these conditions are sustainability, economics, safety and reliability, proliferation resistance, and physical protection.



Figure 2.2. The new GIF logo representing all involved countries, and the three terms representing the GIF motto: Expertise/Collaboration/Excellence: (countries from left to right)—(1) Argentina; (2) Australia; (3) Brazil; (4) Canada; (5) China; (6) Euratom; (7) France; (8) Japan; (9) Republic of Korea; (10) Russia; (11) South Africa; (12) Switzerland; (13) UK; and (14) USA. *Source: GIF.*

Goals for Gen-IV nuclear-energy systems

Sustainability-1	Gen-IV nuclear-energy systems will provide sustainable energy generation that meets clean air objectives and provides long-term availability of systems, as well as the effective use of fuel for worldwide energy production
Sustainability-2	Gen-IV nuclear-energy systems will minimize and manage their nuclear waste and considerably reduce the long-term stewardship burden, thereby, improving protection of public health and the environment
Economics-1	Gen-IV nuclear-energy systems will have a clear life-cycle-cost advantage over other energy sources
Economics-2	Gen-IV nuclear-energy systems will have a level of financial risk comparable to other energy projects
Safety and reliability-1	Gen-IV nuclear-energy-systems' operations will excel in safety and reliability
Safety and reliability-2	Gen-IV nuclear energy systems will have a very low likelihood and degree of reactor-core damage
Safety and reliability-3	Gen-IV nuclear-energy systems will eliminate the need for off-site emergency response
Proliferation resistance and physical protection	Gen-IV nuclear-energy systems will increase assurance that they are very unattractive and the least desirable route for diversion or theft of weapons-usable materials, and provide increased physical protection against acts of terrorism

Given the context and the design that has been established, these objectives could at times seem contradictory, and strict adherence to such objectives difficult. The Gen-IV Forum thus requires that each of the proposed designs can, at least, self-evaluate in terms of these four criteria. Such an analysis should then enable the emergence of R&D strategies aimed at improving the level of respect for those criteria that are currently the least well respected. These goals guide the cooperative R&D efforts undertaken by GIF members. The challenges raised by GIF goals are intended to stimulate innovative R&D that covers all of the technological aspects related to the design and implementation of reactors, energy-conversion systems, fuel-cycle facilities, and beyond, for example, the mechanistic understanding of Gen-IV systems that results from fostering innovation on enabling processes or approaches (e.g., digital transformation, advanced manufacturing, design codes, and methodologies).

In addition, the increasing share of renewables in the electricity grid is having an impact on the deployment of Gen-IV energy systems. The intensifying development of variable renewable electricity sources has meant that Gen-IV systems will need to be more flexible compared to current reactors for their deployment in low-carbon energy systems. The concept of flexibility is defined by the Electric Power Research Institute (EPRI) as three-fold for Gen-IV reactors—namely operational, product, and deployment flexibility. Advanced Gen-IV reactors differ significantly from Generation III Pressurized Water Reactors (PWRs) with their use of different fuels and coolants, and operation at higher temperatures. These differences make them suitable for applications beyond electricity production, including industrial heat, heat storage, or massive hydrogen production.

Flexibility is not included in the current goals for the development of Gen-IV systems. However, considering the importance of flexibility for the deployment of Gen-IV systems in future energy markets, all Gen-IV systems should ensure that flexibility aspects are part of their R&D program. More than a goal, flexibility could be considered a key asset of Gen-IV systems.

In light of the ambitious nature of the goals involved, international cooperation is essential for timely progress in the development of Gen-IV systems. This cooperation would make it possible to pursue multiple systems and technical options concurrently and to avoid any premature down selection due to a lack of adequate resources at the national level. Working together with the different countries involved is also an asset in terms of providing shared views, white papers, guidelines, shared safety design requirements and guidelines. These international documents could ultimately become referenced documents in all of the respective countries. In this way, it would lead to the dissemination of a general “Gen-IV culture” and best practices.

2.3 Selection of Gen-IV systems













For more than two decades, GIF has led international collaborative efforts to develop next-generation nuclear-energy systems that can help meet the world’s future energy needs. Gen-IV designs aim to use fuel more efficiently, reduce waste production, be economically competitive, and meet stringent standards of safety and proliferation resistance.

With these goals in mind, some 100 experts evaluated 130 reactor concepts before GIF selected six reactor technologies for further research and development. These concepts include the: Gas-cooled Fast Reactor (GFR), Lead-cooled Fast Reactor (LFR), Molten Salt Reactor (MSR), SuperCritical Water-cooled Reactor (SCWR), Sodium-cooled Fast Reactor (SFR), and Very-High-Temperature Reactor (VHTR).

The latest information on the status of GIF system arrangements and memoranda of understanding is shown in [Figure 2.3](#), and the system development timelines defined in the original Technology Roadmap (2002) and in the 2014 Technology Roadmap Update are shown in [Figure 2.4](#).

The goals adopted by GIF provided the basis for identifying and selecting six nuclear-energy systems for further development. The selected systems rely on a variety of reactor, energy-conversion, and fuel-cycle

Figure 2.3. Status of the GIF-system arrangements and memoranda of understanding (as of June, 2022) Upper row (countries from left to right)—(1) Australia; (2) Canada; (3) China; (4) France; (5) Japan; (6) Republic of Korea; (7) Russia; (8) S. Africa; (9) Switzerland; (10) USA; (11) UK; and (12) Euratom. *Source: GIF.*

												
SFR			•	•	•	•	•			•	•	•
VHTR	•	•	•	•	•	•			•	•	•	•
LFR			•		•	•	•			•		•
SCWR		•	•		•		•					•
GFR				•	•							•
MSR	•	•		•			•		•	•		•

• : signatory of System Arrangement
• : signatory of Project Arrangement • : signatory of MoU

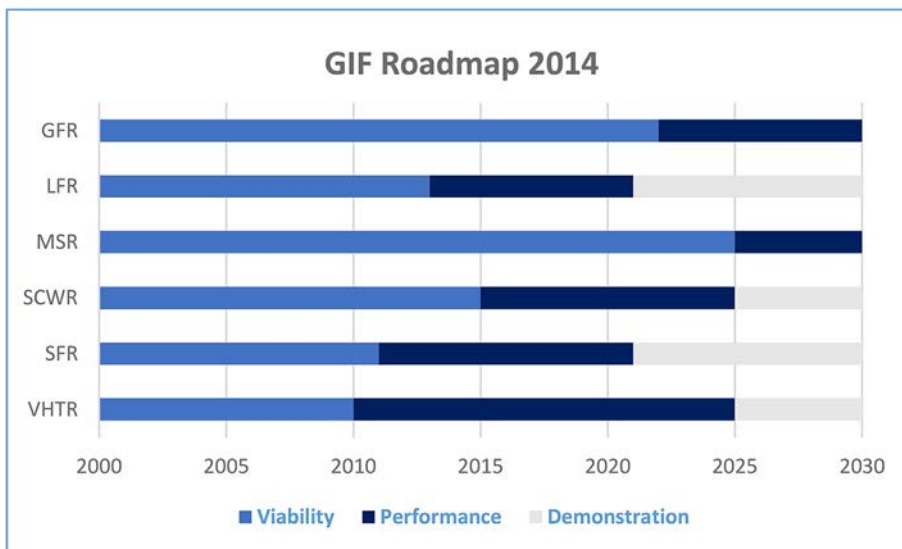
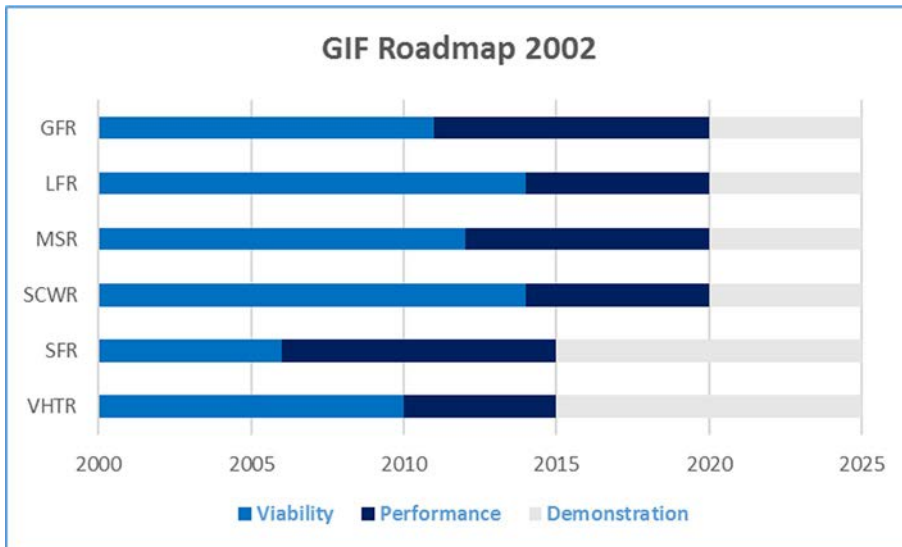


Figure 2.4. System development timelines as defined in the original Technology Roadmap (2002) and in the 2014 Technology Roadmap update. *Source: GIF.*

technologies. Their designs feature thermal- and fast-neutron spectra, and closed and open fuel cycles, as well as a wide range of reactor sizes from very small to very large. Depending on their respective degrees of technical maturity, the Gen-IV systems are expected to become available for commercial introduction in the period from 2030 and beyond. The path from current nuclear systems to Gen-IV systems is described in the 2014 roadmap update mentioned above. The 2002 report, entitled *A Technology Roadmap for Generation IV Nuclear Energy Systems*, is currently being updated; along with the *GIF R&D Outlook for Generation IV Nuclear Energy Systems: 2018 Update* and its executive summary “Preparing the Future Through Innovative Nuclear Technology: Outlook for Generation IV Technologies.”

All Gen-IV systems aim at performance improvement, new applications for nuclear energy, and/or more sustainable approaches to the management of nuclear materials. High-temperature systems offer the possibility of efficient process-heat applications and hydrogen production. Enhanced sustainability is achieved primarily through the adoption of a closed fuel cycle, including the reprocessing and recycling of plutonium, uranium, and minor actinides in fast reactors, and, also, through high thermal efficiency. This approach provides a significant reduction in waste generation and uranium-resource requirements. [Table 2.1](#) summarizes the main characteristics of the six Gen-IV systems.

Table 2.1. EPRI attributes of advanced reactor flexibility and benefits

Attribute	Subattribute	Benefits
Operational flexibility	Maneuverability	Load following
	Compatibility with hybrid energy systems and poly-generation	Economic operation with increasing penetration of intermittent generation, alternative missions
	Diversified fuel use	Economics and security of the fuel supply
	Island operation	System resiliency, remote power, micro-grid, emergency-power applications
Deployment flexibility	Scalability	Ability to deploy at scale needed
	Siting	Ability to deploy where needed
	Constructability	Ability to deploy on schedule and on budget
Product flexibility	Electricity	Reliable, dispatchable power supply
	Process heat	Reliable, dispatchable process-heat supply
	Radioisotopes	Unique or high demand isotope supply

Source: EPRI.

It should be noted that the six nuclear-reactor concepts on the GIF website are listed in the alphabetical order (see Figure 2.4), with other referencing sequences being used elsewhere. For Table 2.2, it was decided to list the six Gen-IV concepts according to the type of reactor coolant, meaning that the first two reactors (i.e., VHTR and GFR) are helium-cooled; the next two concepts (i.e., SFR and LFR) are liquid-metal-cooled; the following concept (i.e., MSR) is molten-salt-cooled; and the last concept (i.e., SCWR) is supercritical-water-cooled.

Table 2.2. Overview of Gen-IV systems

No.	System	Neutron spectrum	Coolant	Outlet T ($^{\circ}\text{C}$)	Fuel cycle	Size (MW_{el})
1	VHTR	Thermal	Helium	900–1000	Open	250-300
2	GFR	Fast	Helium	850	Closed	1200
3	SFR	Fast	Sodium	500-550	Closed	50-150 300-1500 600-1500
4	LFR	Fast	Lead	480-570	Closed	20-18 300-1200 600-1000
5	MSR	Thermal/Fast	Chloride or fluoride salts	700-800	Closed	300-1000
6	SCWR	Thermal/Fast	Water	510-625	Open/closed	300-700 1000-1500

Source: GIF

2.4 Six Gen-IV nuclear-energy systems

This section provides a short description of the six GIF systems. Each of these systems will be described more extensively in the following chapters.

1. VHTR: High-Temperature Gas-cooled Reactors (HTGRs or simply HTRs) are helium-cooled graphite-moderated nuclear-fission reactors utilizing fully ceramic fuel (see Figure 2.5). They are characterized by inherent safety features, excellent fission-product retention in the fuel, and high-temperature operation suitable for the delivery of industrial process heat, and, in particular, hydrogen production. Typical reactor-coolant outlet temperatures range between 750°C and 850°C, thus enabling power-conversion efficiencies up to 48%. The VHTR is understood to be a longer-term evolution of the HTR, targeting even higher efficiency and more versatile use by further increasing the helium outlet temperature to 950°C or even higher, up to 1000°C. Such high temperatures will require the use of new structural materials.

These reactors can be built with power outputs that are typical for SMRs. They are primarily dedicated to the cogeneration of electricity and process heat (Combined Heat and Power (CHP)), for example, in the case of hydrogen production. The initial driver for VHTR development in GIF was thermo-chemical hydrogen production, with the sulfur-iodine cycle requiring a core outlet temperature of $\sim 950^\circ\text{C}$. Further market

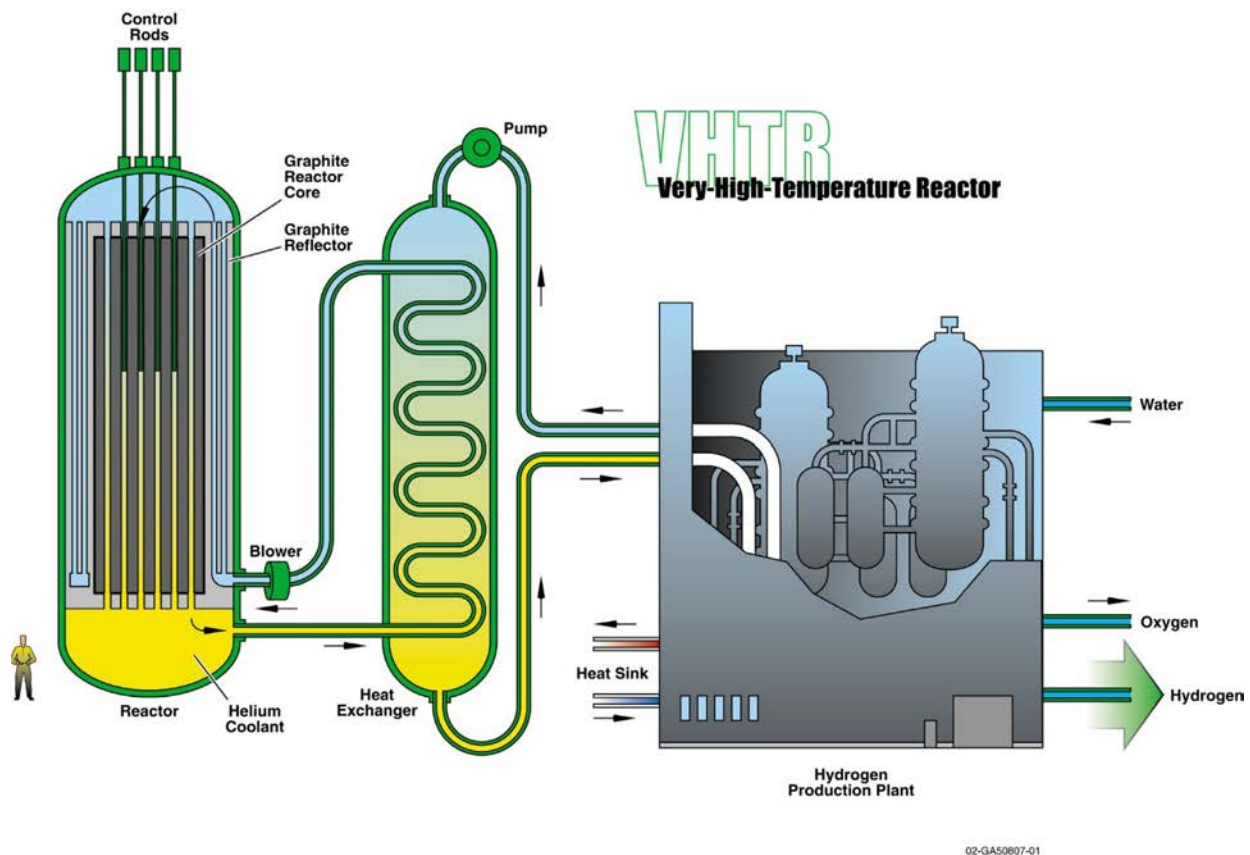


Figure 2.5. Very-High-Temperature Reactor (VHTR): Helium-gas-cooled, graphite-moderated, thermal-neutron-spectrum reactor with core outlet temperatures between 900°C and 1000°C (shown with hydrogen cogeneration). *Source: GIF.*

research across the GIF signatories has shown that there is also a very large near-term market for process steam of $\sim 550^{\circ}\text{C}$, achievable with lower temperature HTR designs. Therefore, R&D in GIF has shifted to cover both the lower- and higher-temperature concepts of this reactor type. Owing to the significant amount of past experience accumulated in the area of HTRs in several countries, the deployment of HTR systems is already considered feasible.

The potential for cogeneration of heat and power makes HTRs and VHTRs attractive heat sources for large industrial complexes such as chemical plants to substitute large amounts of process heat at different temperatures, which are today produced with fossil fuels. Depending on the coolant-outlet temperature, such reactors can be deployed to produce hydrogen from heat and water by using thermo-chemical, electro-chemical, or hybrid processes with a considerable reduction in CO_2 emissions. Typical HTR coolant-outlet temperatures range from below 750°C to 850°C , thus enabling power-conversion efficiencies of up to 48% in “pure” power generation and much higher in CHP mode.

HTRs and VHTRs can be operated with a once-through Low-Enriched-Uranium (LEU) ($<20\% \text{ }^{235}\text{U}$) fuel cycle and with a closed fuel cycle (improved sustainability). Quite early, this reactor type was identified as particularly suitable for the Th-U fuel cycle, while potential symbiotic fuel cycles with other reactor types (e.g., light-water and fast reactors) are also an option.

The operational temperatures of HTRs and VHTRs can be adapted to specific end-user needs. Thermal reactor power is limited by the requirement for fully passive heat removal in accidental conditions. Owing to different core pressure drops, which govern the capacity for passive heat removal, this translates to $<250 \text{ MW}_{\text{th}}$ for pebble-bed reactors and $<625 \text{ MW}_{\text{th}}$ for hexagonal-block-type reactors. The actual reactor power can be flexibly adapted to local requirements, e.g., the electricity/heat ratio of an industrial site. The power density is low, and the thermal inertia of the core is high, thus granting walk-away safety in accidental conditions. The potential for high-fuel burn-up (150-200 GWd/tHM, where HM stands for Heavy Metal), high efficiency, high market potential, low operational and maintenance costs, as well as modular construction, constitute advantages favoring commercial deployment.

This basic technology has been established in former HTGR plants, starting with the OECD Dragon Project, which led to the development of coated-particle fuel and demonstrated the safety features of HTRs, including through a final core heat-up experiment. Later, the United States Peach Bottom and Fort Saint-Vrain plants were built, as well as the German AVR and THTR prototypes, which produced high quality steam up to 550°C . After resolving some initial complications, the technology has now advanced through near- and medium-term projects led by several plant vendors and national laboratories, such as HTR-PM (China), PBMR (South Africa), GTHTR-300C (Japan), ANTADES (France), NHDD (Korea), GT-MHR (Russia and US), and NGNP (US). Experimental reactors such as the HTTR (Japan, $30 \text{ MW}_{\text{th}}$) and HTR-10 (China, $10 \text{ MW}_{\text{th}}$) support technology development including CHP, hydrogen production and other nuclear-heat applications.

A VHTR can be designed with either a pebble-bed or a prismatic-block core. Despite these differences, however, all VHTR concepts show extensive commonalities, which would enable a joint R&D approach. The standard fuel is based on UO_2 TRistructural ISotropic (TRISO) coated particles (UO_2 kernel, buffer/iPyC/SiC/oPyC coatings) embedded in a graphite matrix, which is then formed either into pebbles (tennis-ball-size spheres) or into compacts (thumb-size rodlets). This fuel form exhibits a demonstrated, long-term temperature tolerance of 1600°C in accidental situations. Such a safety performance may be further enhanced, for example through the use of a Uranium Oxycarbide (UCO) fuel kernel, a ZrC coating instead of Silicon Carbide (SiC), or the replacement of the graphite-matrix material with SiC. The fuel cycle will first be a once-through, very high burn-up, LEU fuel cycle. Solutions to adequately manage the fuel cycle back end are under investigation, and the potential operation with a closed fuel cycle will be prepared by specific head-end processes to enable the use of existing reprocessing techniques. Power-conversion options include indirect Rankine cycles, or direct or indirect Brayton

cycles (for details, see [Chapter 21](#)). Near-term concepts will be developed using existing materials, whereas more advanced concepts will require the development, qualification and coding of new materials, and manufacturing methods.

High-core outlet temperatures enable high efficiencies for power conversion and hydrogen production, as well as high steam qualities (superheated or supercritical). Hydrogen-production methods include high-temperature electrolysis, thermo-chemical cycles, or steam-methane reforming. The transfer of heat to a user facility over a distance of several kilometers can be achieved with steam, gases, certain molten salts, or with liquid metals. The use of nuclear CHP with high-temperature reactors has considerable potential for the reduction of fossil-fuel use and of noxious emissions, which is the prime motivation for the signatories of the VHTR system. The expanded use of nuclear energy for powering industrial processes and for large-scale bulk hydrogen is a strong motivation for VHTR development and enables the integration of nuclear with renewable energies in hybrid-energy systems.

2. GFR: The GFR (see [Figure 2.6](#)) is a high-temperature helium-cooled fast-spectrum reactor with a closed fuel cycle. The core outlet temperature will be in the order of 850°C . The GFR combines the advantages of fast-spectrum systems for the long-term sustainability of uranium resources and waste minimization (through multiple fuel reprocessing and the fission of long-lived actinides), with those of high-temperature systems

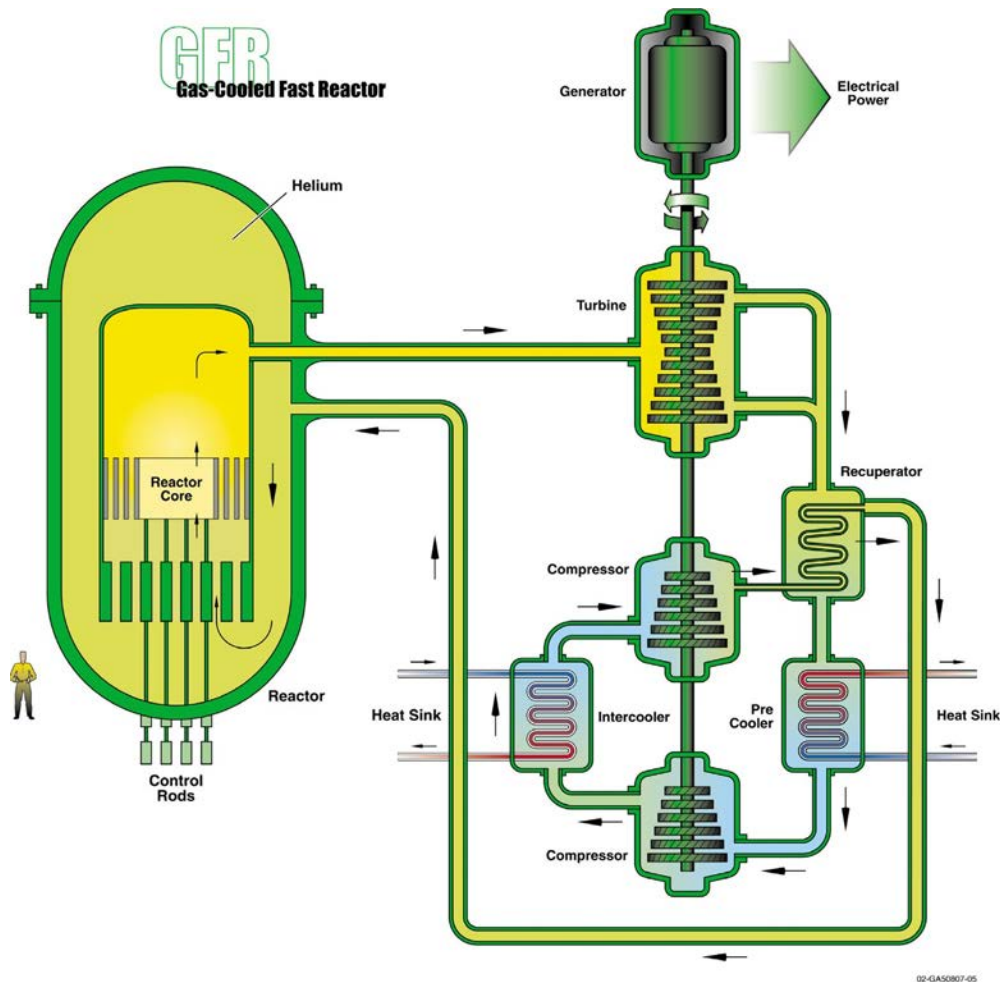


Figure 2.6. Gas-cooled Fast Reactor (GFR): Helium-gas-cooled, fast-neutron-spectrum reactor with closed fuel cycle and outlet temperature of about 850°C (shown with direct gas-turbine Brayton power cycle). *Source: GIF.*

(e.g., high thermal-cycle efficiency and industrial use of generated heat and/or hydrogen production). It requires the development of robust refractory fuel elements and an appropriate safety architecture. The use of dense fuel such as carbide or nitride provides good performance regarding plutonium breeding and minor-actinide burning.

The GFR uses the same fuel-recycling processes as the SFR and the same reactor technology as the VHTR. Its development approach is, therefore, to rely, in so far as it is feasible, on technologies developed for the VHTR in terms of structures, materials, components, and the power-conversion system. Nevertheless, it does call for specific R&D beyond current and foreseen work on the VHTR system, mainly on core design and the safety approach.

The reference concept for the GFR is a 2400-MW_{th} plant having a breakeven core, and operating with a core outlet temperature of 850°C that would enable an indirect, combined gas-steam cycle to be driven via three intermediate heat exchangers. The high-core outlet temperature places onerous demands on the capability of the fuel to operate continuously with the high-power density necessary for “good” neutron economics in a fast-reactor core. The core is made up of an assembly of hexagonal fuel elements, each consisting of ceramic-clad, mixed-carbide-fueled pins contained within a ceramic hextube. The favored material for the pin clad and hextubes is for the moment Silicon-Carbide fiber reinforced Silicon Carbide (SiCf/SiC). The entire primary circuit, with its three loops, is contained within a secondary pressure boundary, the guard containment. The heat produced is converted into electricity in the indirect combined cycle, with three gas turbines and one steam turbine. Cycle efficiency is approximately 48%. A heat exchanger transfers the heat from the primary helium coolant to a secondary gas cycle containing a helium-nitrogen mixture, which in turn drives a closed-cycle gas turbine. The waste heat from the gas-turbine exhaust is used to raise steam in a steam generator, which is then used to drive a steam turbine. Such a combined cycle is common practice in natural gas-fired power plants, and so it represents an established technology, with the only difference in the case of the GFR being the use of a closed-cycle gas turbine (for details, see [Chapter 21](#)).

3. SFR: The SFR (see [Figure 2.7](#)) uses liquid sodium as the reactor coolant. It features a closed fuel cycle for fuel breeding and/or actinide management. The two, primary fuel-recycle-technology options are advanced aqueous and pyrometallurgical processing. A variety of fuel options are being considered for the SFR, with Mixed OXide (MOX) preferred for advanced aqueous recycle and mixed metal alloy preferred for pyrometallurgical processing. Owing to the significant amount of past experience accumulated with SFRs in several countries, the deployment of SFR systems is already feasible.

Using liquid sodium as the reactor coolant, allowing high power density with low coolant volume fraction and operation at low pressure. While the oxygen-free environment prevents corrosion, sodium reacts chemically with air and water and requires a sealed coolant system.

Plant-size options under consideration range from small—50–300-MW_{el} modular reactors to larger plants of up to 1500-MW_{el}. The outlet temperature is 500°C–550°C for these options, which allows for the use of materials developed and proven in prior fast-reactor programs.

The SFR closed fuel cycle enables regeneration of fissile fuel and facilitates management of minor actinides. However, this requires that recycle fuels be developed and qualified for use. Important safety features of this Gen-IV system include a long thermal-response time, a reasonable margin to coolant boiling, a primary system that operates near atmospheric pressure, and an intermediate sodium system between the radioactive sodium in the primary system and the power-conversion system. Water/steam (Rankine cycle), supercritical carbon-dioxide (see [Figure 21.1.7](#)) or nitrogen (Brayton cycle) can be considered as working fluids for the power-conversion system to achieve high performance in terms of thermal efficiency, safety, and reliability. With innovations to reduce capital cost, the SFR is aiming to be economically competitive in future electricity markets. In addition, the fast-neutron spectrum greatly extends the uranium resources compared to thermal reactors. The SFR is considered to be the nearest-term deployable system for actinide management.

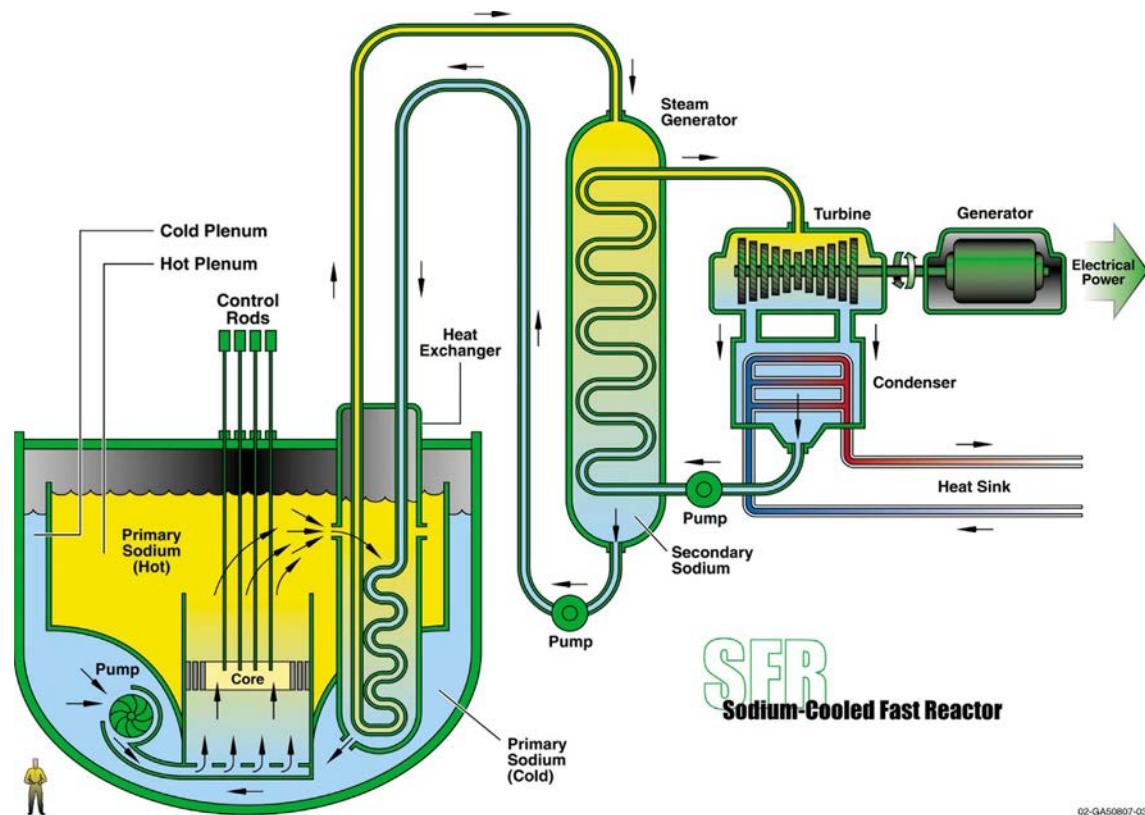


Figure 2.7. Sodium-cooled Fast Reactor (SFR): Molten-sodium-cooled, fast-neutron-spectrum reactor with closed fuel cycle and outlet temperatures within 500°C-550°C (a pool-type reactor is shown with an indirect steam-turbine Rankine power cycle). *Source: GIF.*

Much of the basic technology of the SFR has been established in former fast-reactor programs, and is being confirmed by the Phenix end-of-life tests in France and the lifetime extension of the BN-600 and the BN-800 operation in Russia. New programs involving the SFR technology include the Chinese Experimental Fast Reactor (CEFR), which was connected to the grid in July 2011, and India's Prototype Fast Breeder Reactor (PFBR).

The SFR is an attractive energy source for nations that would like to make the best use of limited nuclear-fuel resources and manage nuclear waste by closing the fuel cycle.

Fast reactors hold a unique role in the actinide-management mission, because they operate with high energy neutrons that are more effective at fissioning actinides. The main characteristics of the SFR for the actinide management mission are:

- consumption of transuranics in a closed fuel cycle, which thus reduces the radiotoxicity and heat load, and facilitates waste disposal and geologic isolation; and
- enhanced utilization of uranium resources through efficient management of fissile materials and multirecycle.

The high level of safety achieved through inherent and passive means also allows for the accommodation of transients and bounding events with significant safety margins.

The reactor unit can be arranged in a pool layout or in a compact loop layout. Three options are being considered:

- a large size (600–1500 MW_{el}) loop-type reactor with mixed uranium-plutonium oxide fuel and potentially minor actinides, supported by a fuel cycle based upon advanced aqueous processing at a central location serving a number of reactors;
- an intermediate-to-large size (300–1500 MW_{el}) pool-type reactor with oxide or metal fuel; and
- a small size (50–150 MW_{el}) modular-type reactor with uranium-plutonium-minor-actinide-zirconium metal-alloy fuel, supported by a fuel cycle based on pyrometallurgical processing in facilities integrated with the reactor.

4. LFR: The LFR (see [Figure 2.8](#)) is characterized by a fast-neutron spectrum, a closed fuel cycle with full actinide recycling, a possible location in central or regional fuel-cycle facilities, and high-temperature operation at low pressure. The coolant may be either lead (preferred option), or Lead-Bismuth Eutectic (LBE). The LFR may be operated as a breeder or as a burner of actinides from spent fuel, and it may use inert-matrix fuel or act as a burner/breeder using thorium matrices. Two reactor-size options are being considered: a small 10-100- MW_{el} transportable system with a very long core life, and a medium 300-600- MW_{el} system. In the long term, a large system of 1200 MW_{el} may be envisaged. The LFR system may be deployable by 2025, with Russia already having started to build the first LFR—the BREST-300-OD in Seversk (Tomsk district).

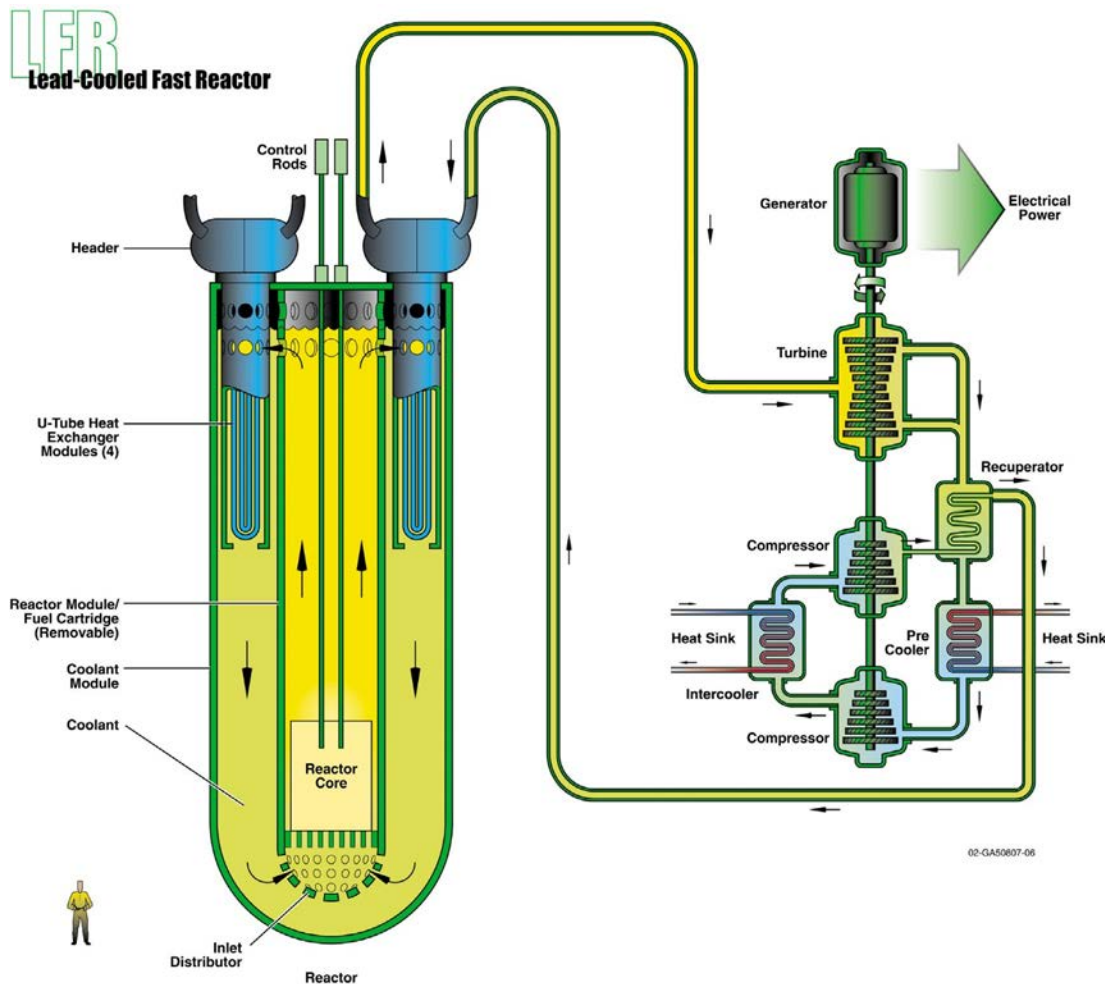


Figure 2.8. Lead-cooled Fast Reactor (LFR): Molten-lead-cooled, fast-neutron-spectrum reactor with closed fuel cycle and outlet temperatures within 500°C-550°C (shown with indirect Brayton power cycle).

Source: GIF.

Lead and LBE are chemically inert liquids with very good thermophysical properties. The LFR would have multiple applications, including the production of electricity, hydrogen, and process heat. The LFR concepts include three reference systems: (1) a large system rated at 600 MW_{e1} (ELFR EU), intended for central-station power generation; (2) a 300-MW_{e1} system of intermediate size (BREST-OD-300, Russia); and (3) a small transportable system of 10-100 MW_{e1} in size (SSTAR, US) that features a very long core life.

The LFR has excellent materials-management capabilities, since it operates in the fast-neutron spectrum and uses a closed fuel cycle for efficient conversion of fertile uranium. It can also be used as a burner to consume actinides from spent LWR fuel and as a burner/breeder with thorium matrices. An important feature of the LFR is the enhanced safety that results from the choice of molten lead as a chemically inert and low-pressure coolant. In terms of sustainability, lead is abundant and, hence, available, even in the case of the deployment of a large number of reactors. More importantly, as with other fast systems, fuel sustainability is greatly enhanced by the conversion capabilities of the LFR fuel cycle. Because they incorporate a liquid coolant with a very high margin to boiling and benign interaction with air or water, LFR concepts offer substantial potential in terms of safety, design simplification, proliferation resistance, and the resulting economic performance. An important factor is the potential for benign end state to severe accidents.

The LFR has developmental needs in the areas of fuels, materials performance, and corrosion control. During the coming years, progress is expected in relation to materials, system design, and operating parameters. Significant test and demonstration activities are underway and planned during this time frame.

5. MSR: MSR concepts (see Figure 2.9) have been studied since the early 1950s, but with only one test reactor having operated at the Oak Ridge National Laboratory (ORNL, United States) in the 1960s.

For the past 15 years, there has been a renewal of interest in this reactor technology, in particular, for its acknowledged inherent reactor safety and its flexibility. MSRs use molten salts as fuel and/or coolant. When

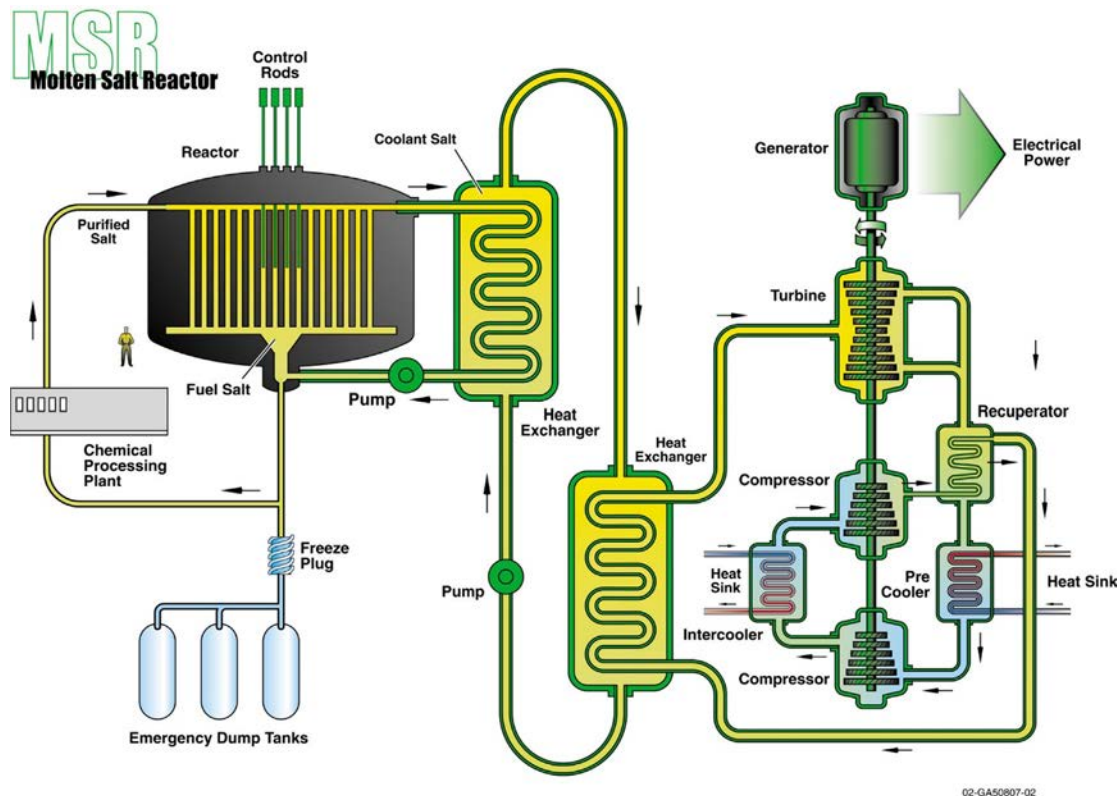


Figure 2.9. Molten Salt Reactor (MSR): Molten-salt-cooled reactor with outlet temperatures within 700°C-800°C (shown with indirect Brayton power cycle). Source: GIF.

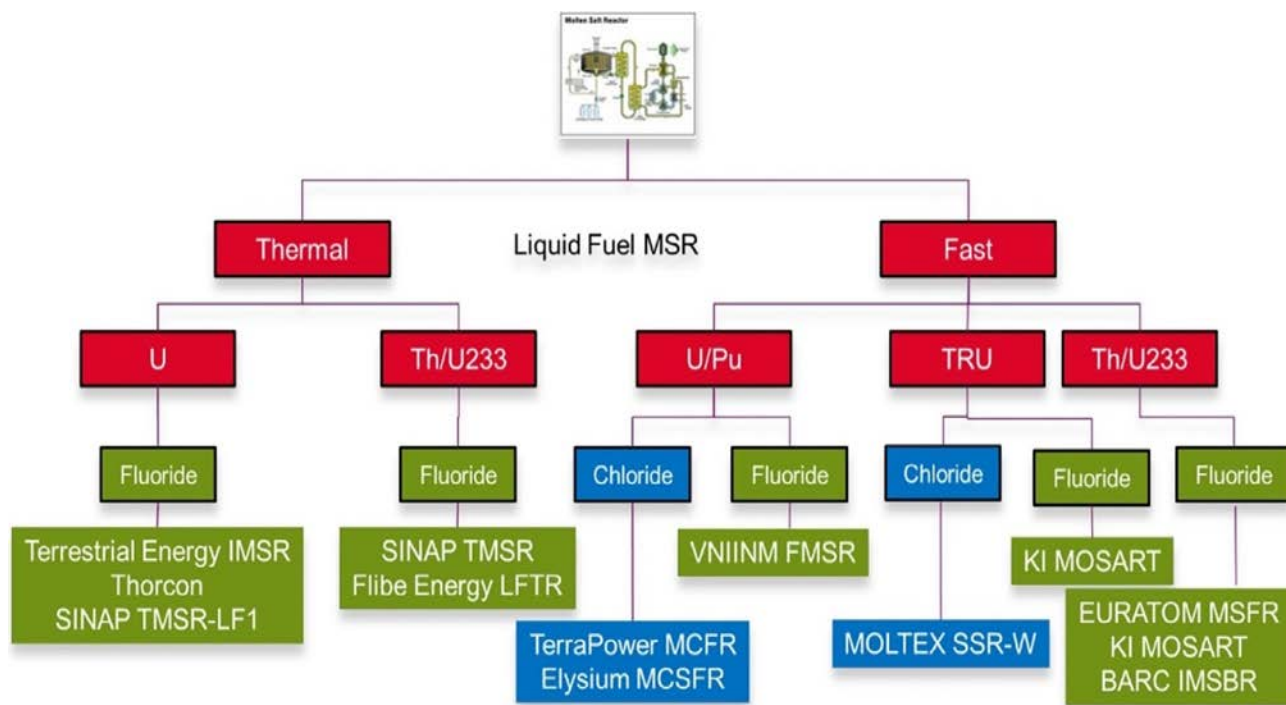


Figure 2.10. The most studied MSR concepts, with key players (Research & Technology Organizations or vendors). *Source: GIF.*

a fluoride salt is the coolant alone, the concept is called a Fluoride-salt-cooled High-temperature Reactor (FHR). Today, most, if not all, the studied concepts in GIF MSRs use liquid fuel. The MSR is a concept and not a technology. Indeed, the MSR generic name covers thermal and fast reactors, operated with a U/Pu or a Th/²³³U fuel cycle, or as TRans-Uranium (TRU) burners, with a fluoride or a fluoride-carrier salt. An illustration of the most studied concepts is provided in [Figure 2.10](#).

Depending on the fuel cycle, MSRs can reuse fissile and fertile materials from LWRs. They can also use uranium, or burn plutonium or minor actinides. They have an increased power-conversion efficiency (the fission directly occurs in the carrier salt, which transfers its heat to the coolant salt in the heat exchangers). MSRs are operated at low pressure, slightly above atmospheric pressure. They can be deployed as large power reactors or as SMRs. Their deployment is today limited by technological challenges, such as high temperatures, structural materials, and corrosion.

The common objective of MSR projects is to propose a conceptual design with the best system configuration—resulting from physical, chemical, and materials studies—for the reactor core, the reprocessing unit and waste conditioning. Mastery of the technically challenging MSR technology will require concerted, long-term international R&D efforts, namely:

- the study of salt chemical and thermo-dynamic properties;
- for the system design, the development of advanced neutronic and thermal-hydraulic coupling models;
- the study of materials compatibility with molten salt;
- progress in salt Redox control technologies to master corrosion of the primary fuel circuit and other components;
- the development of efficient techniques for the extraction of gaseous fission products from the coolant through He bubbling;
- for salt reprocessing, the growth of reductive extraction tests (actinide-lanthanide separation); and
- the development of a safety approach dedicated to liquid-fueled reactors.

More generally, there has been a significant renewal of interest in the use of liquid salt as a coolant for nuclear and non-nuclear applications. These salts could facilitate heat transfer for nuclear-hydrogen-production concepts, concentrated-solar electricity generation, oil refineries, and shale-oil processing facilities, among other applications.

6. SCWR: SCWRs (see Figure 2.11) are a class of high-temperature, high-pressure water-cooled reactors operating with a direct energy-conversion cycle and above the thermo-dynamic critical point of water (374°C and 22.1 MPa). The higher thermo-dynamic efficiency and plant simplification opportunities afforded by the high temperature, single-phase coolant translate into improved economics. A wide variety of options are currently being considered: both thermal-neutron and fast-neutron spectra are envisaged; both pressure-vessel and pressure-tube configurations are also being considered, and thus light water or heavy water can be used as a moderator. The operation of a $30\text{--}150\text{-MW}_{\text{el}}$ technology demonstration reactor is being targeted for the mid-2020s.

Unlike current water-cooled reactors, the coolant used in SCWRs will experience a significantly higher enthalpy rise in the core, which reduces the core mass flow for a given thermal power and increases the core outlet enthalpy to supercritical conditions. For both pressure-vessel and pressure-tube designs, a once-through steam cycle has been envisaged, omitting any coolant recirculation inside the reactor. As in the case of the Boiling Water Reactor (BWR), the supercritical “steam” will be supplied directly to the high-pressure “steam” turbine, and the feed water from the steam cycle will be supplied back to the core. SCWR concepts thus combine the design and operation experiences gained from hundreds of water-cooled reactors with those experiences from hundreds of fossil-fired power plants operated with SuperCritical Water (SCW). In contrast

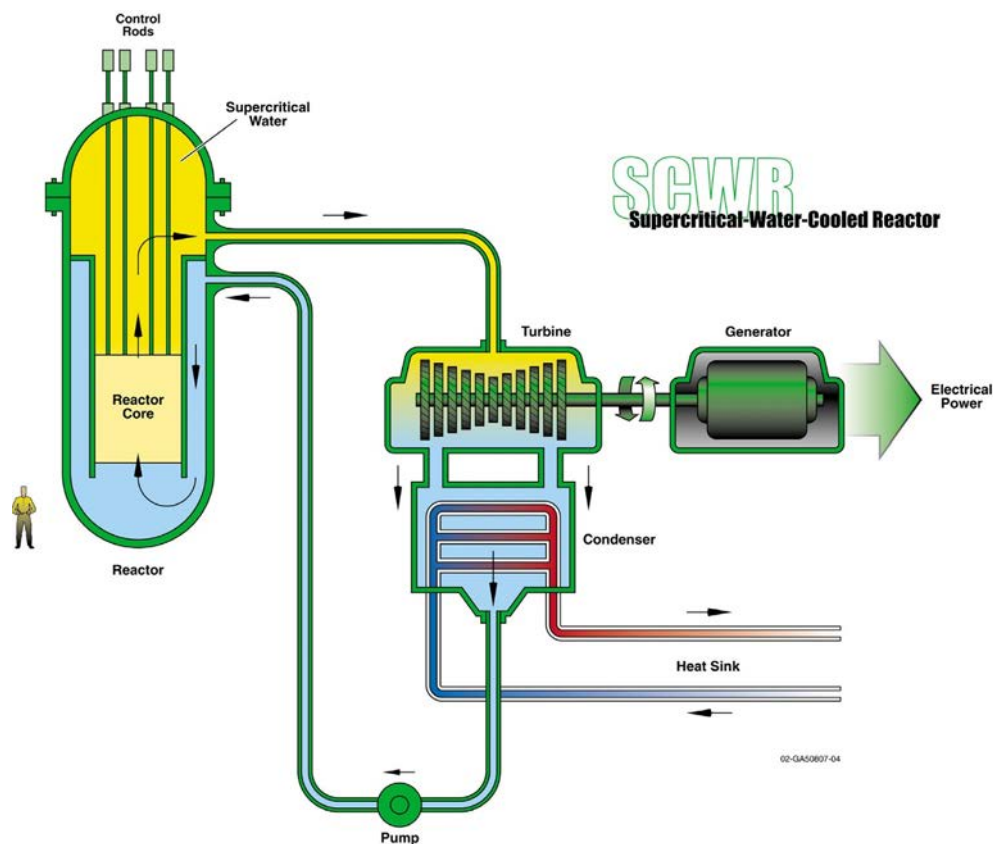


Figure 2.11. SuperCritical Water-cooled Reactor (SCWR): Supercritical water-cooled, thermal-neutron-spectrum reactor with outlet temperatures within $510^{\circ}\text{C}\text{--}625^{\circ}\text{C}$ (shown with direct steam-turbine Rankine power cycle). *Source: GIF.*

to some of the other Gen-IV nuclear systems, the SCWR can be developed incrementally based on current water-cooled reactors.

In general, SCWR designs have unique features that offer many advantages compared to state-of-the-art water-cooled reactors. The main advantage of the SCWR is improved economics, because of the high thermodynamic efficiency and the potential for plant simplification. Improvements in the areas of safety, sustainability, and proliferation resistance, as well as physical protection are also possible and are being pursued by considering several design options that use thermal and fast spectra, including the use of advanced fuel cycles. However, there are several technological challenges associated with the development of the SCWR, particularly, the need to validate transient heat-transfer models (to describe the depressurization from supercritical to subcritical conditions), qualification of materials (namely advanced steels for cladding) and demonstration of the passive-safety systems.

2.5 Methodology working groups, task forces, cross-cutting items and the Senior Industrial Advisory Panel

In parallel to the work on the six aforementioned systems—although in close relationship with them—GIF has developed several methodology working groups and task forces to deal with cross-cutting items. The task forces are tasked with specific actions to be taken under consideration for a limited period (usually two to three years). GIF members (i.e., Expert Group and PG) then evaluate with the task force members, if the conclusions provided will lead to the closure of the task force, its extension for a new period with new goals, or its evolution to a perennial working group with annual and long-term objectives.

There are four working groups:

- The Economics Modelling Working Group (EMWG) was established in 2003 to provide a methodology for the assessment of Gen-IV systems against two economic related goals: (1) to have a life-cycle cost advantage over other energy sources (i.e., to have a lower levelized unit cost of energy) and (2) to have a level of financial risk comparable to other energy projects (i.e., to have a similar total investment cost at the time of commercial operation).
- The Proliferation Resistance and Physical Protection Working Group (PRPP WG) was established to develop, implement and foster the use of an evaluation methodology so as to assess Gen-IV nuclear energy systems with respect to the GIF PR&PP goal, whereby: “*Generation IV nuclear-energy systems will increase the assurance that they are a very unattractive and the least desirable route for diversion or theft of weapons-usable materials, and provide increased physical protection against acts of terrorism.*” The methodology provides designers and policymakers with a technology-neutral framework and a formal comprehensive approach to evaluate, through measures and metrics, the PR&PP characteristics of advanced nuclear systems. As such, the application of the evaluation methodology offers opportunities to improve the PR&PP robustness of system concepts throughout their development cycle.
- The Risk and Safety Working Group (RSWG) has been an active methodology working group since 2005, with a mission to establish a harmonized approach to, and provide assessment tools for, the risk and safety of Gen-IV systems. RSWG membership currently includes representatives from Canada, China, the European Union, France, Japan, Korea, Russia, South Africa, the United Kingdom and the United States as a forum of AR designers and regulators. The International Atomic Energy Agency (IAEA) also participates as an observer.
- The Education and Training Working Group (ETWG) started as a task force in November 2015 and was elevated to a working group in 2020. It serves as a platform to enhance open Education and Training (E&T), as well as communication and networking of people and organizations in support of the

Gen-IV International Forum. Objectives of the working group focus on promoting E&T by developing the webinar series dedicated to Gen-IV systems and related cross-cutting topics, advertising these at the international level, and creating and maintaining a modern social-media platform to exchange information and ideas on GIF R&D topics, as well as on related GIF E&T activities.

And four task force groups have thus far been created.

- The Advanced Manufacturing and Material Engineering Task Force (AMME TF): Innovation in the nuclear-supply chain, particularly, in the areas of advanced manufacturing and materials engineering, is necessary if AR technologies are to be delivered on time and within budget. However, nuclear-design codes typically dictate that only qualified materials and processes can be used. Getting new materials or new manufacturing processes qualified can, therefore, be a long and difficult process. Furthermore, current developments in advanced manufacturing are occurring much faster than the ability of most to introduce new materials and methods into design codes, potentially stifling innovation and hampering deployment. Such issues need to be addressed if ARs, integrating innovative materials, and components, are to be brought to the market in reasonable time frames. The AMME TF was, therefore, formed in order to better characterize and address these issues.
- The R&D infrastructure Task Force (RDITF) identifies essential R&D experimental facilities needed for the development, demonstration, and qualification of Gen-IV components and systems, including activities to meet safety and security objectives. To this end, the task force prepared relevant presentations and papers, and engaged with the private sector, as was the case at a dedicated workshop in 2020. In the second phase, the task force promoted the use of experimental facilities for collaborative R&D activities among GIF partners. This 2-year task force completed its work and was disbanded in 2021.
- The GIF PG created the Safety Design Criteria Task Force (SDC-TF) in 2011 to establish an international safety design standard. GIF has promoted the development of Safety Design Criteria (SDC) and safety design Guidelines (SDGs) for each of the GIF systems, and the first mission of this task force was to develop the SDC for SFRs. The task force developed an SFR SDC report in 2012 and then launched its Phase 2 activities for quantifying and qualifying the key aspects of the SFR SDC to demonstrate the advantages of Gen-IV SFRs. After several versions and additions, the latest and definitive versions of the SFR-SDC report and of the SFR-SDG report are now available on the GIF website. Having completed its missions, the task force joined the Risk and Safety Working Group in 2020 so as to contribute to the drafting of the SDC and SDGs for other GIF systems.
- Nuclear-energy production has the potential to play a major role in today's context, where the reduction of CO₂ emissions and of fossil-fuel use, as well as improvements in energy-supply security, are being pursued by governments. Regarding the reduction of CO₂ emissions, substantial efforts are being undertaken to decarbonize the electricity-generation sector, and nuclear energy is key to meeting this objective. On the other hand, decarbonation of electricity production will not be sufficient to meet CO₂-emission-reduction targets. The non-electric industry and transport could, however, offer significant potential for further emission reduction through the direct use of nuclear heat and/or via the key energy vector of hydrogen production. AR technologies, especially, their SMR versions, may be suitable to address environmental and economic challenges with their potential to be integrated into energy mixes with high shares of renewables. The GIF Non-Electrical application of Nuclear Heat Task Force (NEaNH TF) is tasked with reviewing these systems in view of assessing: (1) technology readiness levels and timeliness; (2) adaptability to peculiar geographical conditions; (3) CO₂ emission reduction potential cost/benefits (\$/t CO₂ saved); and (4) economic boundary conditions needed to make such systems viable. This task force was created in 2021 for a first set of 24 months.

Last, the Senior Industrial Advisory Panel (SIAP) is directly advising the GIF PG. Its role is to understand cost drivers, opportunities and constraints related to the market environment with the objective of identifying the most appropriate advice in terms of GIF activities, in collaboration with the System Steering Committee (SSC) chairs, task forces and working groups, and with the guidance of the members of the GIF PG. All SIAP members are from nuclear related industries. They are providing industrial insights for GIF activities and strengthening their collaboration with the GIF Economic Modelling Working Group (EMWG) so as to assess cost reduction and safety improvement opportunities arising from new design methodologies for Gen-IV concepts.

2.6 Summary

In summary, [Table 2.3](#) lists estimated ranges of thermal efficiencies (gross) of Gen-IV nuclear-reactor concepts for reference purposes ([Pioro, 2020](#); [Pioro et al., 2017](#)).

Table 2.3. Estimated ranges of thermal efficiencies (gross) of Generation-IV reactor concepts (Gen-IV concepts are listed according to thermal efficiency decreases) (shown here for reference purposes)

No	Nuclear reactors	Gross eff. (%)
1	Very-High-Temperature Reactor (VHTR) (reactor coolant—helium (SCF): $P = 7$ MPa and $T_{in}/T_{out} = 640/1000^{\circ}\text{C}$; primary power cycle ^a —direct SCP Brayton helium-gas-turbine cycle; possible back-up—indirect Brayton ^b , Rankine ^c or combined cycles ^d)	≥ 55
2	Gas-cooled Fast Reactor (GFR) or High-Temperature Reactor (HTR) (reactor coolant—helium (SCF): $P = 9$ MPa and $T_{in}/T_{out} = 490/850^{\circ}\text{C}$; primary power cycle ^a —direct SCP Brayton helium-gas-turbine cycle; possible back-up—indirect SCP Brayton ^b , Rankine ^c or combined cycles ^d)	≥ 50
3	SuperCritical Water-cooled Reactor (SCWR) (one of the Canadian concepts; reactor coolant—SC light water: $P = 25$ MPa and $T_{in}/T_{out} = 350/625^{\circ}\text{C}$ ($T_{cr} = 374^{\circ}\text{C}$); direct cycle; SCP Rankine cycle with high-temperature secondary steam superheat: $T_{out} = 625^{\circ}\text{C}$; possible back-up—indirect SCP Rankine “steam”-turbine cycle with high-temperature secondary steam superheat)	45–50
4	Molten Salt Reactor (MSR) (reactor coolant—sodium-fluoride or chloride salts with dissolved uranium fuel: $T_{in}/T_{out} = 700/800^{\circ}\text{C}$; primary power cycle—indirect SCP CO ₂ Brayton gas-turbine cycle; possible back-up—indirect Rankine steam-turbine cycle)	~ 50
5	Lead-cooled Fast Reactor (LFR) (Russian design BREST-OD-300: reactor coolant—liquid lead: $P \approx 0.1$ MPa and $T_{in}/T_{out} = 420/540^{\circ}\text{C}$; primary power cycle—indirect subcritical-pressure Rankine steam cycle: $P_{in} \approx 17$ MPa ($P_{cr} = 22.064$ MPa) and $T_{in}/T_{out} = 340/505^{\circ}\text{C}$ ($T_{cr} = 374^{\circ}\text{C}$); high-temperature secondary steam superheat); (in one of the previous designs of BREST-300 NPP primary power cycle was indirect	~ 41 –43

Continued

Table 2.3. Estimated ranges of thermal efficiencies (gross) of Generation-IV reactor concepts (Gen-IV concepts are listed according to thermal efficiency decreases) (shown here for reference purposes—cont'd)

No	Nuclear reactors	Gross eff. (%)
	SCP Rankine “steam”-turbine cycle: $P_{in} \approx 24.5$ MPa ($P_{cr} = 22.064$ MPa) and $T_{in}/T_{out} = 340/520^\circ\text{C}$ ($T_{cr} = 374^\circ\text{C}$); also, note that power-conversion cycle in a different LFR design than that of other countries is based on SCP CO ₂ Brayton gas-turbine cycle)	
6	Sodium-cooled Fast Reactor (SFR) (Russian design BN-600: reactor coolant—liquid sodium (primary circuit): $P \approx 0.1$ MPa and $T_{in}/T_{out} = 380/550^\circ\text{C}$; liquid sodium (secondary circuit): $T_{in}/T_{out} = 320/520^\circ\text{C}$; primary power cycle—indirect Rankine steam-turbine cycle: $P_{in} \approx 14.2$ MPa ($T_{sat} \approx 337^\circ\text{C}$) and $T_{in\ max} = 505^\circ\text{C}$ ($T_{cr} = 374^\circ\text{C}$); secondary-steam superheat: $P \approx 2.45$ MPa and $T_{in}/T_{out} = 246/505^\circ\text{C}$; possible back-up in some other countries—indirect SCP CO ₂ Brayton gas-turbine cycle)	~40

- ^a It should be noted that the originally proposed direct SCP Brayton helium-gas-turbine cycle has started to experience some technical difficulties, including the ingress of helium into gas-turbine bearings, which limits continuous long-term operation.
- ^b The indirect Brayton cycle might include, as the working fluid, SCP N₂, SCP CO₂ or a mixture of SCP N₂ (80%) and He (20%).
- ^c The indirect Rankine cycle is proposed, at least, for the High-Temperature gas-cooled Reactor (HTR) Pebble-bed Module (PM) built in China.
- ^d Combined cycles might include, as the primary one, the Brayton cycle with working fluids such as SCP He, SCP N₂, SCP CO₂ or a mixture of SCP N₂ (80%) and He (20%); and as the secondary one, the Rankine cycle with subcritical-pressure steam or SCP CO₂; or the SCP CO₂ Brayton cycle.

Acknowledgments

The authors would like to express their great appreciation to all System Steering Committee chairs, task-force and working-group leaders for the materials used in this chapter, as well as Dr. P. Guiberteau, Ms. S. Anglade-Constantin, and Ms. J. Griffiths for their contributions.

References

- Pioro, I.L., 2020. In: Pioro, I. (Ed.), *Supercritical-Fluids Thermophysical Properties and Heat Transfer in Power-Engineering Applications*, Chapter 1 in *Advanced Supercritical Fluids Technologies*. IntechOpen Ltd., London, pp. 1–42. <http://mts.intechopen.com/articles/show/title/supercritical-fluids-thermophysical-properties-and-heat-transfer-in-power-engineering-applications>.

Further reading

- EPRI, 2016. *Program on Technology Innovation: Interim Progress on Two White Papers Supporting Advanced Reactor Commercialization—Expanding the Concept of Flexibility and Exploring the Historical Role of Public-Private Partnerships*. Electric Power Research Institute (EPRI). Report No. 3002008046.
- EPRI, 2017. *Program on Technology Innovation: Expanding the Concept of Flexibility for Advanced Reactors: Refined Criteria, a Proposed Technology Readiness Scale and Time-Dependent Technical Information Availability*. Electric Power Research Institute (EPRI). Revision 13, Report No. 3002010479.
- GIF, 2019a. *GIF R&D Outlook for Generation IV Nuclear Energy Systems: 2018 Update*. Generation IV International Forum (GIF), Paris. www.gen-4.org/gif/jcms/c_108744/gif-r-d-outlook-for-generation-iv-nuclear-energy-systems-2018-update.
- GIF, 2019b. *Preparing the Future through Innovative Nuclear Technology*. GIF, Paris. www.gen-4.org/gif/jcms/c_104633/preparing-the-future-through-innovative-nuclear-technology-web.
- GIF, 2020a. *2018 GIF Symposium Proceedings*. GIF, Paris. www.gen-4.org/gif/jcms/c_117863/2018-gif-symposium-proceedings.

- GIF, 2020b. GIF 2019 Annual Report. GIF, Paris. www.gen-4.org/gif/jcms/c_119034/gif-2019-annual-report.
- GIF, 2021. GIF 2020 Annual Report. GIF, Paris. www.gen-4.org/gif/jcms/c_177757/gif-annual-report-2020.
- IAEA, 2022. Advances in Small Modular Reactor Technology Developments. A Supplement to: IAEA Advanced Reactors Information System (ARIS), IAEA 2022 Edition. IAEA, Vienna, 424 pages: https://aris.iaea.org/Publications/SMR_Booklet_2022.pdf.
- Sadhankar, R., 2019. Position Paper on Flexibility of GENIV Systems. Economic Modelling Working Group. Gen-IV Document.

Very High Temperature Reactor

Xing L. Yan

Japan Atomic Energy Agency, Oarai-Machi, Ibaraki-ken, Japan

Nomenclature

AREVA	French nuclear plant vendor company
ATWS	Anticipated Transient Without Scram
AVR	Arbeitsgemeinschaft VersuchsReaktor, an HTGR test reactor in FZJ
bb1	One oil barrel ($\approx 159\text{L}$)
BISO	Bi-ISotropic
CITATION	Diffusion computer code
CV	Control Valve
DRI	Direct Reduction Iron
EED	Electro-ElectroDialysis
EFPD	Effective Full Power Day
FEPC	Federation of Electric Power Companies of Japan
FSV	Fort St. Vrain, an HTGR prototype power station in the United States
GTHTTR300	Gas Turbine High Temperature Reactor 300 MW _{el} in Japan
GTHTTR300C	Gas Turbine High Temperature Reactor 300 MW _{el} Cogeneration in Japan
HTR-10	High Temperature test Reactor 10 MW _{th} in Tsinghua University's INET
HTR-PM	High Temperature gas-cooled Reactor Power Module, China
HTTR	High Temperature engineering Test Reactor, 30 MW _{th} test reactor in JAEA
IHM	Initial Heavy Metal
INL	Idaho National Laboratory (USA)
IPyC	Inner layer of (high-density) Pyrolytic Carbon
IS	Iodine-Sulfur cycle hydrogen production process
IV	Inventory flow Valve
JAEA	Japan Atomic Energy Agency
LOCA	Loss Of Coolant Accident
MHI	Mitsubishi Heavy Industries of Japan
MIGD	Million Imperial Gallon per Day
MMBtu	Metric Million British thermal unit (1 MMBtu = 1.054615 GJ)
MWD	MegaWatt Day
MW_{el}	MegaWatt electric
MW_{th}	MegaWatt thermal
NGNP	Next-Generation Nuclear Plant project in the United States
Nm³	Normal cubic meter
NSSS	Nuclear Steam Supply System
NuH₂	Nuclear Hydrogen and process heat demonstration reactor in Korea
OECD	Organization for Economic Co-operation and Development, Paris, France
OEM	Original Equipment Manufacturer
OPyC	Outer layer of (high-density) Pyrolytic Carbon

RCR	Reactivity Control Rod
SAS	Small Absorber Sphere
SC	Steam Cycle or Rankine cycle
SiC	Silicon Carbide
THTR-300	Thorium High Temperature Reactor 300 MW _{el} built in Germany
TRISO	TRI-ISOTropic coating of fuel particle
TRU	TRansUranium
TWOTRAN	Name of computer code
UCO	Uranium Oxide/Uranium Carbide
UO₂	Uranium dioxide
VHTR	Very-High Temperature gas-cooled Reactor
WTI	West Texas Intermediate (oil benchmark)
YSZ	Yttria-Stabilized Zirconia
ZrC	Zirconium Carbide

3.1 Development history and current status









Development of High Temperature Gas-cooled Reactor (HTGR), also known as Very-High Temperature gas-cooled Reactor (VHTR) for its Generation-IV designs, has continued for over half a century. Several reactors have been built or being constructed. These are identified in [Table 3.1](#). Still others are being developed at various stages, including Xe-100 (80 MW_{el} high temperature reactor-pebble-bed module) (in the United States, multipurpose GTHTR300C (gas turbine high temperature reactor 300 MW_{el} cogeneration) in Japan, NuH₂ for nuclear hydrogen and process heat in Korea, an experimental power reactor in Indonesia, and others.

Dragon, the first reactor built, pioneered the use of TRI-ISOTropic (TRISO)-coated particle fuel, still the standard fuel form today. The AVR (Arbeitsgemeinschaft VersuchsReaktor) tested additional fuel designs and accumulated extensive performance data. The prototypical FSV (Fort St. Vrain) validated the prismatic core physics design with high burnup (90 GWd/t) on thorium fuel and demonstrated steam turbine power generation at 39% thermal efficiency and easy load following. Yet the component failures, such as with the primary coolant circulator, forced excess outage and undermined its economics. The THTR-300 (thorium high temperature reactor 300) of a pebble bed core design encountered technical problems after only a brief period of operation, and their scrutiny led to protracted shutdown. The FSV and THTR-300 were prematurely decommissioned largely as business decision.

Asia then became home to the latest builds. The High Temperature engineering Test Reactor (HTTR) in Japan and the High Temperature test Reactor (HTR-10) in China were constructed and started up around the turn of the millennium. Both remain operational today. The 30-MW_{th} HTTR demonstrated operation of 950°C reactor outlet coolant and export of 863°C process heat. Such high temperature capability would raise reactor thermal efficiency and support advanced applications as reported by the plant design of GTHTR300 by Japan Atomic Energy Agency (JAEA) ([Sato et al., 2014](#); [Yan et al., 2014](#)). The Generation-IV system employs a 600-MW_{th} prismatic-core reactor with outlet coolant temperature of 950°C to power a gas turbine for electricity generation and a thermochemical process for hydrogen production, yielding thermal efficiency of 50% or higher. JAEA has also been developing a design variant GTHTR300C with ability to co-cogenerate one or more products of hydrogen, process heat and desalination ([Yan et al., 2005](#)). Mitsubishi Heavy Industries (MHI) of Japan has been further investigating the feasibility of such design variant for cogeneration of power and large-scale hydrogen production to enable decarbonized steelmaking ([MHI, 2019](#)).

Based on the experience of HTR-10 and extensive engineering development of the reactor components, China is constructing the world's first prototype modular reactor plant HTR-PM in the northeastern Shandong province ([Fu et al., 2014](#)). Although not a VHTR by coolant temperature, the power plant, which

Table 3.1. High temperature gas-cooled reactors built worldwide

	Test HTGRs				Prototype HTGRs			
								
	Dragon	AVR	HTTR	HTR-10	Peach bottom	FSV	THTR-300	HTR-PM
Country	United Kingdom (OECD)	Germany	Japan	China	United States	United States	Germany	China
Period of operation	1963–1976	1967–1988	1998–Present	2000–Present	1967–1974	1976–1989	1986–1989	2021 - present
Reactor core type	Tube	Pebble bed	Prismatic	Pebble bed	Tube	Prismatic	Pebble bed	Pebble bed
Thermal power (MW _{th})	21.5	46	30	10	115	842	750	2 × 250
Coolant outlet temperature (°C)	750	950	950	700	725	775	750	750
Coolant pressure (MPa)	2	1.1	4.0	3.0	2.25	4.8	3.9	7.0
Electrical output (MW _{el})	–	13	–	2.5	40	330	300	211
Process heat output (MW _{th})	–	–	10	–	–	–	–	–
Process heat temperature (°C)	–	–	863	–	–	–	–	–
Core power density (W/cm ³)	14	2.6	2.5	2	8.3	6.3	6.0	3.2
Fuel design	UO ₂ TRISO	(Th/U, U)O ₂ ,C ₂ BISO	UO ₂ TRISO	UO ₂ TRISO	ThC ₂ BISO	(Th/U, Th) C ₂ TRISO	(Th/U)O ₂ BISO	UO ₂ TRISO

BISO, BI-ISOTropic coating of fuel particle.

features twin-unit ($2 \times 250 \text{ MW}_{\text{th}}$) pebble-bed core modular reactors operating at 750°C coolant temperatures and connecting to a common $110\text{-MW}_{\text{el}}$ steam turbine, shares some of the design approaches of VHTR, including passive safety features and high temperature heat application potential.

The construction began in December 2012. Cold functional tests to verify the primary system and equipment under pressure higher than the design pressure were carried out on October 19 and November 3, 2020. This was followed by a series of hot functional tests to verify the primary systems at the operation temperatures from January 2021. The nuclear fuel loading started the day after the National Nuclear Safety Administration, the national nuclear regulator, issued the operating license to the HTR-PM on August 20, 2021. In September 2021, the first reactor achieved criticality, followed by the 2nd unit in November the same year, the first reactor connected to the grid to begin generating power in December 2021.

The current plan calls for construction of further 18 HTR-PM units on the same site. In the meantime, the feasibility to uprate the plant, which sees one $650\text{-MW}_{\text{el}}$ turbine driven by six reactor units ($6 \times 250 \text{ MW}_{\text{th}}$) is being investigated for deployment elsewhere in China.

In 2001, the GIF endorsed six nuclear system concepts, which will deliver affordable energy products while satisfactorily addressing the issues of nuclear safety, waste, and proliferation (Petti, 2014). Recognizing the VHTR to be nearest term deployable and exceptionally suitable, not only for electricity generation, but also for hydrogen production and other industrial applications, the US Department Of Energy (DOE) has placed the Generation-IV priority on the VHTR. The Energy Policy Act of 2005 formally established the Next-Generation Nuclear Plant (NGNP) as a DOE project to demonstrate commercial high-efficiency generation of electricity and hydrogen (The US Energy Policy Act of 2005, 2005). At present, the Advanced Gas Reactor (AGR) fuel development and qualification program at the US Idaho National Laboratory is qualifying Uranium Oxide/uranium Carbide (UCO) TRISO fuel (Petti, 2014). The NGNP Industry Alliance, a consortium of HTGR designers, utility plant owner/operators, suppliers, and end users, had been promoting the reactor commercialization and industrial applications in a NGNP project (INL, 2011). In 2012, the Alliance selected AREVA's prismatic SC-HTGR (Steam Cycle-HTGR) of $625 \text{ MW}_{\text{th}}$ that provides steam and electricity cogeneration as its primary choice of reactor design for prototype implementation in the mid-2020s (Shahrokhi et al., 2014). Although the NGNP project was terminated without plant construction, the reactor plant vendor Framatome, a member of the NGNP Project, continues to promote the HTGR design (Delrue et al., 2018).

The US Department of Energy's Advanced Reactor Demonstration Program provided the US company X-energy with an initial funding of US\$80 million in 2021 to demonstrate a $320\text{-MW}_{\text{el}}$ plant within the next 7 years (US DOE, 2021). Each plant consists of 4 units of Xe-100 pebble-bed core modular reactor with coolant temperature of 750°C and using TRISO UCO particle fuel. The plan to develop the demonstration plant includes completion of the plant basic design in 2021 and completion of the commercial scale TRISO-X fuel fabrication facility construction by the mid-2020s.

3.2 Technology overview

3.2.1 Reactor design types

The two primary types of core design are prismatic and pebble bed. Both are in use today. They employ the same particle fuel, but differ in the method of packaging the fuel particles and subsequently loading the fuel in the core. Figure 3.1 compares the design approaches of the pebble bed HTR-10 (Wu et al., 2002) and the prismatic HTTR (Saito et al., 1994).

The spherical fuel particle measuring about 1 mm in diameter consists of an inner nuclear kernel coated in successive layers of carbon and ceramics. Thousands of the particles are packed in graphite matrix into a spherical pebble of roughly tennis ball size or a cylindrical compact about the size of man's thumb.

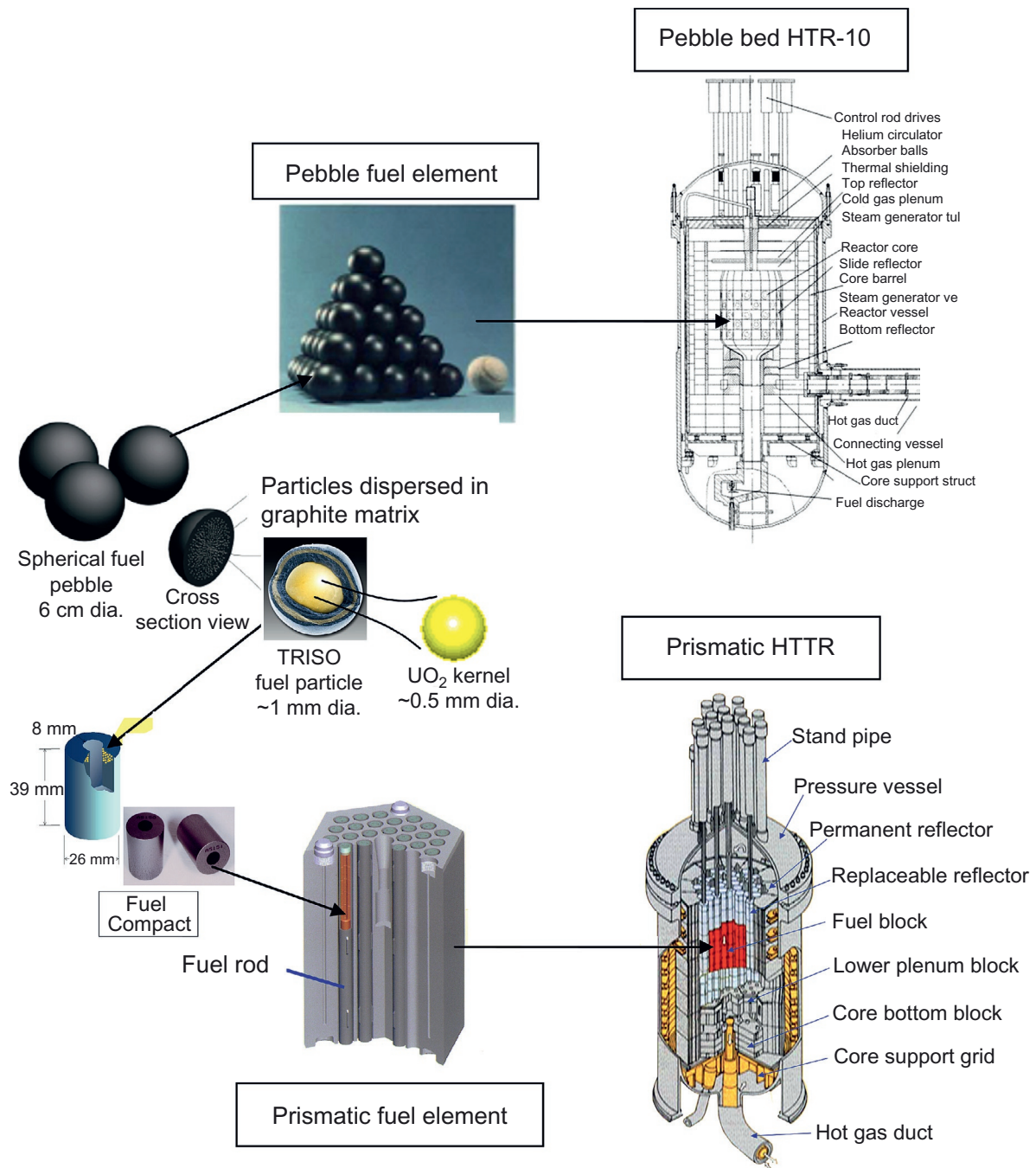


Figure 3.1. Pebble bed reactor design and prismatic reactor design

A pebble bed core contains a large number of fuel pebbles (for example, 27,000 in the HTR-10 core), and the helium coolant flows in the void volume formed in the pile of the pebbles. On the other hand, a prismatic core contains many hexagonal graphite blocks (150 in the HTTR core) in which the fuel compacts are embedded and the helium coolant flows in the channels provided in the block. Both cores are surrounded by graphite reflector and enclosed in steel pressure vessel. Reactivity Control Rods (RCRs) are inserted from above the Reactor Pressure Vessel (RPV).

3.2.2 Design features

3.2.2.1 Safety

Constructed entirely of highly heat resistant materials, the HTGR fuel and core structure maintain their integrity at extreme temperatures. Most reactor designs set the fuel temperature limit to 1600°C based on proof of fuel performance data. The reactor temperature is then capped under it by a combination of inherent design choices made. Starting with the choice of low power density and of the large quantity of graphite materials used in the core, it limits the extent and rate of reactor temperature excursion in an accident. This is aided by the further choice of negative temperature coefficient of reactivity in the core, which would shut the reactor down upon any occurrence of abnormal rise in temperature. Decay heat is then removed from the core by thermal conduction. Finally, helium is the choice of reactor coolant. Remaining in single phase as well as being neutronically transparent and chemically inert, use of helium would mitigate the consequences such as radioactive coolant release or hydrogen generation in the case of a loss of coolant accident. Together, these inherent design features prevent core melt and significant radioactivity release in any licensing basis events. Such safety performance has been demonstrated in the Anticipated Transient Without Scram (ATWS) tests carried out on the HTR-10 (Hu et al., 2004) and HTTR (Takamatsu et al., 2014).

3.2.2.2 Fuel cycle

HTGR offers various options of fuel cycle. Typically, low-enriched (<20%) uranium is used as is in the HTTR and HTR-10, both of which select fuel form of Uranium diOxide (UO₂). An alternative form of Uranium OxyCarbide (UOC) is currently under development and qualification (Petti, 2014).

Thorium is attractive regionally or in longer term, since the world reserve of thorium is more abundant than that of uranium. Although not fissile, Th-232 is fertile and breeds fissile U-233 by absorbing neutrons produced, for example, by fission of initial U-235. Various forms of thorium fuel have been operated in the reactors (see Table 3.1).

More fuel options exist but require development (Greneche, 2003; Kuijper et al., 2006). The fuel cycles that can effectively destruct weapons-grade plutonium and transmute minor actinides while engaging in energy production have been studied (Oak Ridge National Laboratory, 2008; Fukaya et al., 2014). The particle fuel has demonstrated up to 700 GWd/t burnup, an important asset in the plutonium and TRansUranium (TRU) fuel cycles, since the high burnup provides deep burn and thus reduces the quantity and cost of reprocessing (Richards et al., 2008). Since 2015 Japan has launched a study of PuO₂-YSZ (Yttria-Stabilized Zirconia) fuel and core design with a burnup limit of 500 GWd/t with the aim to validate clean burning of plutonium in HTGR (Goto et al., 2015).

Spent fuel may be directly disposed or recycled. In the case of direct disposal, separation and reduction of waste streams could be made prior to disposal. Separated graphite blocks may be treated and reused. Separated fission products and actinides can be confined in stable matrices such as glasses. In the case of recycling, mechanical separation of spent fuel compacts from bulk graphite block, pulsed currents to free the fuel particles from the compact, and subsequent removal of ceramic coating layers by high temperature oxidation or by carbochlorination to access spent kernels of the particle have been studied (Masson et al., 2006).

The fuel is proliferation resistant. Not only does the TRISO structure make it difficult to illicitly access the isotopes of spent fuel kernel, but also the high burnup target in commercial systems will leave little and poor isotopes in spent fuel such that it would require diversion of large material quantities to pose a nuclear risk.

3.2.2.3 Multipurpose

Figure 3.2 identifies a number of applications that fall in the supply temperature range of the VHTR. Power generation can be performed by steam turbine with efficiency at about 40% or by gas turbine at about 50%. Industrial heat applications have been extensively studied, including thermochemical hydrogen production, reforming of fossil fuels and biomass, steelmaking, desalination, and district heating. The VHTR is well posed for cogeneration. As an example, a 600-MW_{th} reactor could simultaneously produce 200 MW_{el} electricity

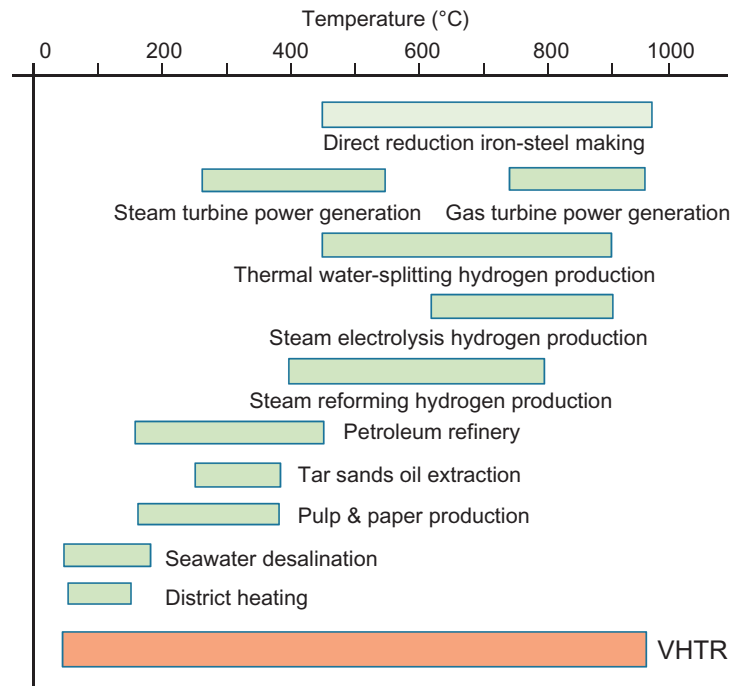


Figure 3.2. Temperature range of VHTR and heat demand of industries

using gas turbine, 66 t/day hydrogen from thermochemical decomposition of water, and 40,000 t/day potable water from desalination. The utilization of the reactor thermal power would reach 85% through cogeneration.

3.3 Detailed technical description

3.3.1 Fuel design

TRISO-coated particle is the standard fuel used today. As shown in Figure 3.3, the innermost of the particle is a low-enriched fuel kernel of usually UO_2 and sometimes UOC . The kernel is coated by a buffer layer of porous carbon and then by the successive TRISO layers, including the Inner layer of high-density Pyrolytic Carbon (IPyC), the Silicon Carbide (SiC) layer, and the Outer layer of high-density Pyrolytic Carbon (OPyC).

The buffer layer acts a container for the fission product gases and the CO gas resulting from fuel burnup. The IPyC layer protects the kernel during the manufacture coating of the outer SiC layer and also provides a gas barrier for the inner buffer. The SiC layer, being the hardest of the structural layers, acts as both a pressure

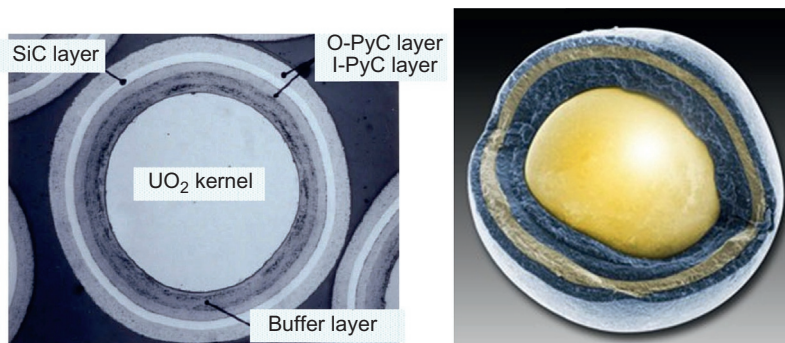


Figure 3.3. TRISO-coated fuel particle

container for the gases generated in the kernel and a material barrier for the metallic fission products. The OPyC provides a protective cushion for the SiC layer during the binding and pressing of the particles into the cylindrical compact or spherical pebble.

A compact, as used in the HTTR, contains about 13,000 particles of 0.92-mm diameter. The particles are dispersed in the graphite matrix in a packing fraction of about 30%. Each compact includes about 14 g of heavy metal. [Table 3.2](#) lists further details of the fuel design for the HTTR and also for the GTHTR300.

A pebble as used in the HTR-10 contains about 12,000 particles. The fuel zone is a ball of binding graphite matrix in a particle packing fraction of about 10%. The fuel zone measured in a diameter of 50 mm is wrapped by a fuel-free layer of graphite with a thickness of 5 mm, resulting in an overall diameter of 60 mm for the pebble. The heavy metal loading of each pebble is around 7 g.

The high level of safety performance provided by the VHTR requires a high level of fabrication quality for the fuel. This is judged with the failure rates of the TRISO ceramic layers in manufacture. An acceptance criterion for the HTTR fuel, for example, is through-coating defect in 1.5 per 10,000 particles, or 0.015% as fabricated. The operation of the HTTR first loading of fuel has proved that the actual fraction of fabrication defect is about two orders of magnitude less than the specification.

The technology of TRISO particle fuel has been established for the UO₂ kernel type at commercial production scale in Germany, China, and Japan and for the UOC kernel type at pilot production scale in the United States. France, Korea, and South Africa have pursued fuel technology development programs including fuel manufacturing and irradiation tests.

Advanced fuel designs are proposed in the United States and Japan. One such design replaces the SiC layer with Zirconium Carbide (ZrC), which increases heat resistance by about 200°C over the limit of the SiC layer ([Goto et al., 2015](#)). Another design adds a thin layer of ZrC over the buffer layer. This layer acts as a reactive oxygen getter to remove the oxygen gas freed in fission and thus mitigates the gas pressure buildup associated with high burnup.

3.3.2 Fuel burnup

Fuel burnup in the VHTR is explained using the example of core physics design calculation for uranium and plutonium fuels as follows.

3.3.2.1 Uranium fuel

[Table 3.3](#) includes the core design parameters and burnup calculation conditions for the 600-MW_{th} reactor of the GTHTR300 ([Nakata et al., 2003](#)). The calculation procedure considers effective averaged six-group macroscopic cross sections in each of the burnup regions of the core. A one-dimensional lattice burnup cell calculation code, DELIGHT, is used to generate the group constants of fuel blocks, reflector blocks, etc. A transport code, TWOTRAN-2 ([Lathrop and Brinkley, 1973](#)), is used to generate details of flux distributions in the regions containing the control rods, where the neutron flux may vary suddenly. With these six-group macroscopic cross sections, a spatial power distribution is calculated by CITATION, a diffusion code ([Fowler et al., 1971](#)), for a 3-D one-sixth core model. The calculated spatial power distribution is used as an input to calculate the next burnup step.

From the core analysis, it becomes clear that the excess reactivity has to be compensated by the burnable poisons until the middle of an operation cycle so that the design target of a 2-year refueling cycle (730 days) is achievable. A half core of fuel blocks is exchanged with fresh fuel every 2 years. As seen in [Table 3.3](#), the residual uranium enrichment is reduced to 4.42% below the design target of 5% from the initial uranium enrichment of 14%.

Table 3.2. Fuel design specification

	Burnable poison pin diameter (mm)	
	HTTR	GTHTR300
Burnup up limit (GWd/t)	33	150
<i>FUEL ROD</i>		
Rod structure	Graphite sleeved	Graphite cladde
Length (mm)	546	1050
Diameter (mm)	34	26
<i>FUEL COMPACT</i>		
Length (mm)	39	83
Inner diameter ID/outer diameter OD (mm)	10/26	9/24
Cladding thickness (mm)	–	1
Particle packing fraction (vol%)	30–35	21–29
<i>COATED FUEL PARTICLE</i>		
Coating type	TRISO	TRISO
Diameter (μm)	920	1010
<i>FUEL KERNEL</i>		
Material	UO ₂	UO ₂
Enrichment (wt% average)		14
Diameter (μm)	600	550
Density (g/cm^3)	10.80	10.80
<i>BUFFER LAYER</i>		
Thickness (μm)	60	140
Density (g/cm^3)	1.15	1.15
<i>IPYC LAYER</i>		
Thickness (μm)	30	25
Density (g/cm^3)	1.85	1.85
<i>SIC LAYER</i>		
Thickness (μm)	25	40
Density (g/cm^3)	3.20	3.20
<i>OPYC LAYER</i>		
Thickness (μm)	45	25
Density (g/cm^3)	1.85	1.85

Table 3.3. Result of uranium fuel burnup calculation for a 600-MW_{th} VHTR

Item	Unit	Value	
Reactor power	MW _{th}	600	
<i>CORE CROSS-SECTION</i>			
Number of fuel blocks		90	
Inner graphite blocks		73	
Outer graphite blocks		48	
Core height	m	8.4	
Fuel blocks in core height		8	
<i>FUEL BLOCK</i>			
Height/across flat	mm	1050/410	
Number of fuel rods		57	
Fuel rod diameter	mm	26	
Coolant channel diameter	mm	39	
Number of burnable poison rods		3	
Average core power density	W/cm ³	5.4	
Fuel cycle length	EFPD	1460	
Refueling batches (w/axial shuffling)		2	
Fuel enrichment	%	14	
Average fuel burnup	GWd/t	120	
Fuel design		UO ₂	
Full-core initial heavy metal	kg	7090	wt% of initial heavy metal
U-235		993	14.0
U-238		6097	86.0
Full-core discharged heavy metal	kg		
Uranium		5839	82.4
U-235		258	3.6
U-236		0	0.0
U-238		5581	78.7
Plutonium		155	2.2
Pu-239		72	1.0

Continued

Table 3.3 Result of uranium fuel burnup calculation for a 600-MW_{th} VHT—
cont'd

Item	Unit	Value
Pu-240		27 0.4
Pu-241		37 0.5
Pu-242		19 0.3
Residual uranium enrichment	%	4.42
Fissile plutonium isotope rate	%	70.2
Natural uranium requirement	kg/(GW _{el} * day)	467.0
Natural uranium utility rate	%	0.57

3.3.2.2 Plutonium fuel

Table 3.4 details the fuel burnup calculation conditions for a proposed plutonium fuel cycle concept for the GTHTR300 core. The proposal by JAEA, called the Clean Burn concept (Fukaya et al., 2014; Goto et al., 2015), is intended to consume the plutonium recovered from reprocessing Japan's commercial Light Water Reactor (LWR) spent fuel while relying on fuel design features that enhances proliferation resistance. The concept requires modification to the above-described uranium core design. A major change is that more fuel columns are added in the inner reflector region, increasing the total number of the fuel columns in the core to 144 from 90.

Table 3.4. Result of plutonium fuel burnup calculation for a 600-MW_{th} VHTR

Item	Unit	Value
Reactor power	MW _{th}	600
<i>CORE CROSS SECTION</i>		
Number of fuel blocks		144
Inner graphite blocks		48
Outer graphite blocks		19
Core height	m	8.4
Fuel blocks in core height		8
<i>FUEL BLOCK</i>		
Height/across flat	mm	1050/410
Number of fuel rods		57
Fuel rod diameter	mm	26
Coolant channel diameter	mm	39

Continued

Table 3.4 Result of plutonium fuel burnup calculation for a 600-MW_{th} VHT—cont'd

Item	Unit	Value	
Number of burnable poison rods		3	
Average core power density	W/cm ³	5.4	
Fuel cycle length	EFPD	1000	
Refueling batches (with axial shuffling)		4	
Fuel enrichment	%	58.6	
Average fuel burnup	GWd/t	500	
Fuel design		PuO ₂ -YSZ	
Full-core Initial Heavy Metal (IHM)	kg	1200	
		Fresh fuel	Spent fuel
²³⁷ Np	wt% IHM	4.6	2.4
²³⁸ Pu	wt% IHM	1.3	7.4
²³⁹ Pu	wt% IHM	51.0	2.8
²⁴⁰ Pu	wt% IHM	20.8	9.1
²⁴¹ Pu	wt% IHM	7.6	9.1
²⁴² Pu	wt% IHM	4.9	10.6
²⁴¹ Am	wt% IHM	8.2	1.2
²⁴² Am	wt% IHM	0.0	0.0
²⁴³ Am	wt% IHM	1.5	2.9
²⁴² Cm	wt% IHM	0.0	0.7
²⁴³ Cm	wt% IHM	0.0	0.1
²⁴⁴ Cm	wt% IHM	13.2	1.8
²⁴⁵ Cm	wt% IHM	4.4	0.1
Fissile nuclides	wt% IHM	58.6	12.0
Neptunium (Np) and precursor	wt% IHM	20.4	12.8

To limit the plutonium enrichment in fresh fuel to the allowable level in Japan, the Clean Burn concept employs PuO₂ in an inert YSZ microsphere kernel. It avoids mixing with uranium so that no additional plutonium is generated during a fuel burnup cycle. As shown in Table 3.4, about 95% of initial plutonium-239 is consumed during 250 EFPD (Effective Full Power Day). In order to target the fuel burnup of 500 GWd/t, the traditional SiC TRISO fuel architecture is modified by coating a thin (about 10 μm) layer of ZrC over the PuO₂-YSZ kernel. The ZrC layer acts as oxygen getter to remove oxygen gas freed from the kernel burnup and is the key to permitting the targeted level of burnup. Presently, JAEA (Japan Atomic Energy Agency), in cooperation with its technical partners, is validating the fuel design by test fabrication (Goto et al., 2015).

3.3.3 Reactor design

3.3.3.1 Prismatic core reactor design

Figure 3.4 depicts the HTTR reactor design (Saito et al., 1994; Fujimoto et al., 2004). The cylindrical core consists of columns of removable hexagonal graphite blocks. Thirty of the columns are fuel columns stacked in five blocks high. Dowels are used to align fuel blocks in a column. There are a total of 150 fuel blocks of varying uranium enrichments as identified in the table included in the figure. The other columns in the core are control rod guide columns provided for insertion of RCRs and release of reserved core shutdown system. The permanent graphite reflector blocks embrace a ring of replaceable side reflector blocks that surround the central core. The control rods containing Boron Carbide (B_4C) are moved in and out of the core from atop of the RPV. The control rods are used for adjustment and shutdown of core power in addition to compensating for reactivity due to changes in core temperature, fuel burnup, and concentration of fission products such as ^{149}Sm and ^{135}Xe with large neutron absorption cross sections. The reserved core shutdown system is provided as backup for reactor shutdown with the releasing of B_4C pellets into the channels bored in the control rod blocks. The entire core is affixed by the lateral restraint mechanism from the outer side of the permanent reflector to the inner wall of the RPV. The RPV is made of low alloy steel of 2.25 Cr-1 Mo and sized to 5.5 m in diameter and 13.2 m in height.

Unlike test reactors such as the HTTR, larger commercial-scale reactor design tends to select annular, instead of cylindrical, active core configuration, mainly to minimize fuel temperature in the event of passive core conduction cooldown. This design choice is highlighted by the GTHTR300 reactor design shown in Figure 3.5 (Nakata et al., 2003). The commercial reactor is designed using the code system and design procedure that have been validated by the HTTR operation.

The annular core of the GTHTR300 reactor consists of 90 fuel columns with each column stacked of 8 hexagonal fuel blocks high and is capped at top and bottom with reflector blocks. The active core is surrounded by inner and outer side graphite reflector columns, some of which also serve as control rod guide

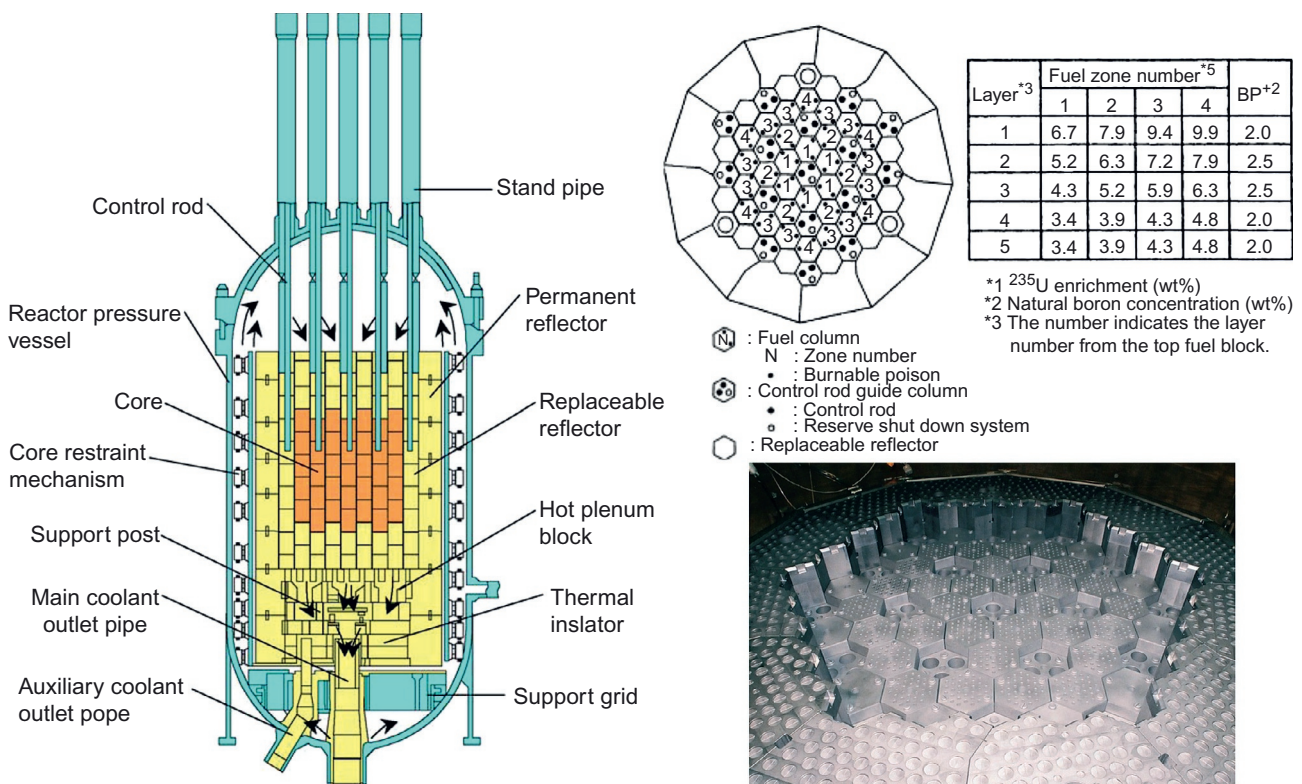


Figure 3.4. The HTTR test reactor design (photo is the top view of the reactor core)

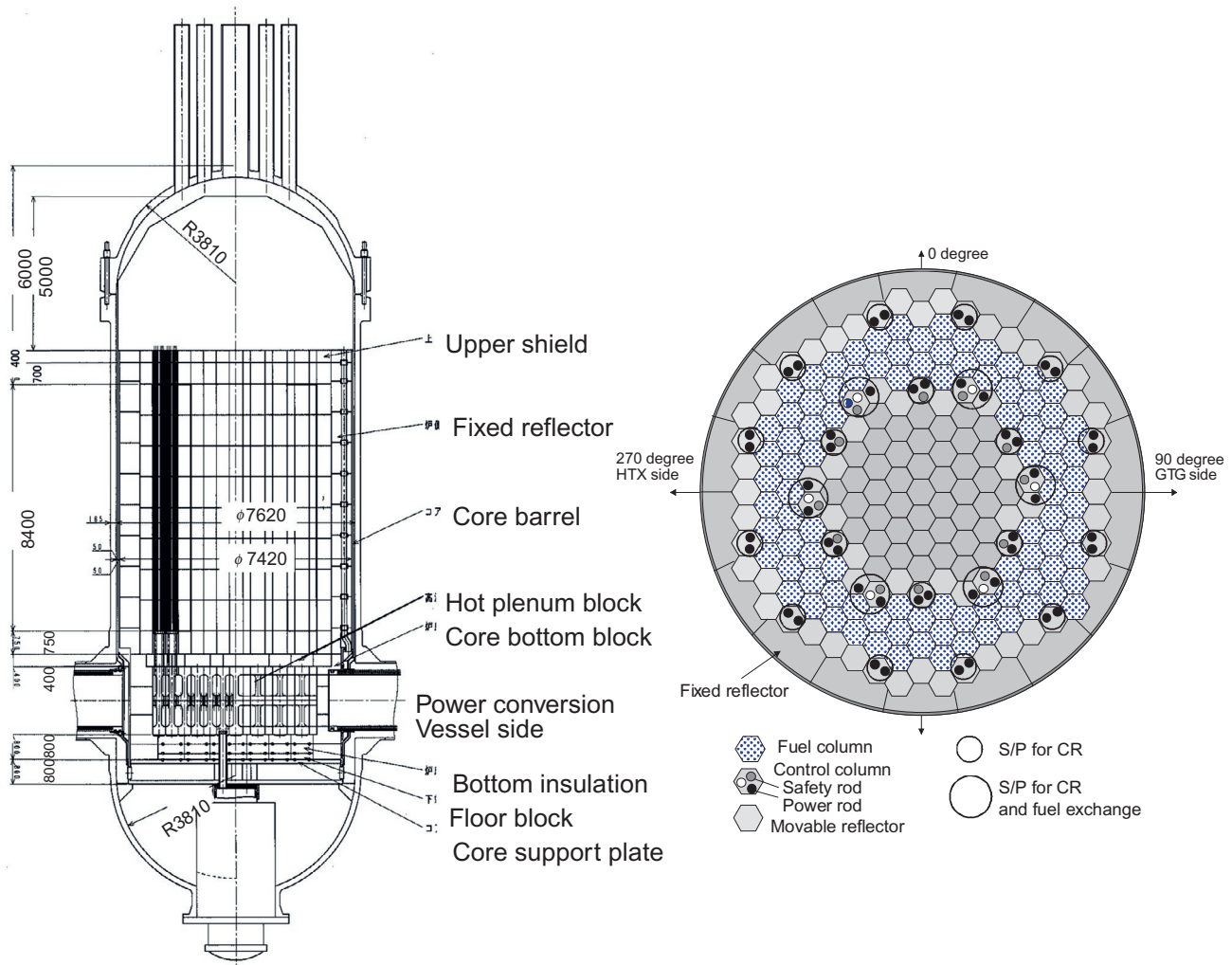


Figure 3.5. GTHTR300's prismatic core reactor design

columns. The core is enclosed by a steel core barrel, which is in turn housed in the steel RPV. The coolant enters the reactor via the inner pipe of the horizontal coaxial duct on the left of the vessel and travels upward in the flow channels embedded in the outer side reflector, turns in the top plenum of the core, then flows downward into the active core and then exits into the bottom plenum of the core, and finally exits through the inner pipe of the horizontal coaxial duct on the right of the RPV.

Table 3.5 compares the design parameters for the HTTR test reactor and GTHTR300 commercial reactor. The table includes three sets of commercial design parameters. The two sets pertain to the core outlet temperature of 850°C, while the third set pertains to 950°C. The main difference is the number of enrichments used. In the baseline design with uniform enrichment for the whole core, the resulting peak operating fuel temperature is higher than the other sets with multiple enrichment count. In general, the number of enrichments placed in the core may be varied and optimized to minimize power peaking and thus peak fuel temperature throughout a core burnup period. The refueling interval is shortened to 1.5 years in the case of the 950°C core design from the 2 years in the 850°C core designs.

3.3.3.2 Pebble bed core reactor design

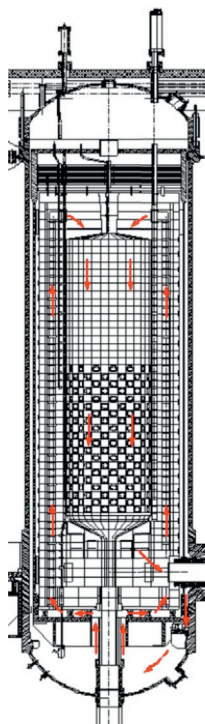
Rated at relatively small thermal power of 250 MW_{th} per reactor unit, the HTR-PM still allows for the use of a cylindrical pebble bed core (see Figure 3.6). The active core is 3 m in diameter and 11 m in height and

Table 3.5. Reactor design specification

		HTTR	GTHTR300
Reactor rating	MW _{th}	30	600
Coolant inlet temperature (°C)	°C	395	587, 587, 594
Coolant outlet temperature (°C)	°C	850, 950	850, 850, 950
Coolant pressure (MPa)	MPa	4	7.0, 7.0, 5.1
Coolant (helium) flow rate (kg/s)	kg/s	12.7/10.4	439, 439, 322
Fuel type		TRISO U ₂ O	TRISO U ₂ O
Refueling interval (days)	day	660	730, 730, 548
		Full core	Half core
Number of fuel blocks (columns × stacks)		150 (30 × 5)	720 (90 × 8)
Core height (m)	m	2.9	8.4
Effective core inner/outer diameter	m	0/2.3	3.7/5.6
Average power density (W/cm ³)	W/cm ³	2.5	5.4
Average burnup (GWd/t)	GWd/t	22	120
Maximum burnup	GWd/t	33	155
Fuel block height/across flat (mm)	Mm	550/360	1050/410
Fuel rods per block		33	57
Fuel rod diameter (cm)	Mm	34	26
Core enrichment count		12	1/8/7
Average enrichment (%)	wt%	6	14.0, 14.3, 14.5
Burnable poison count		2	1, 6, 5
Burnable poison pin diameter (mm)			4.8, 4.8, 3.6
Max fuel temperature (nominal) (°C)		1350	1150, 1108, 1244
Max fuel temperature (loss of coolant accident) (°C)		–	1562, 1546, 1535

contains a loose pile of approximately 420,000 spherical fuel pebbles. The core geometry is maintained by side graphite reflectors and carbon bricks. The pebbles are continuously recirculated downward through the core for more than a dozen times using a pneumatic fuel transport line, until reaching the design burnup of 100 GWd/t. The spent fuel pebble is discharged through the core bottom center tube and transported into the spent fuel storage tank.

Figure 3.6. HTR-PM's pebble bed core reactor design and technical parameters



Parameter	Unit	Value
Reactor total thermal power	MW _t	2 × 250
Rated electrical power	MW _e	210
Average core power density	MW/m ³	3.22
Electrical efficiency	%	42
Primary helium pressure	MPa	7
He temperature at reactor inlet/outlet	°C	250/750
Helium flow rate	kg/s	96
Heavy metal loading per fuel element	g	7
Enrichment of fresh fuel element	%	8.5
Active core diameter	m	3
Equivalent active core height	m	11
Diameter of the RPV	m	~6.0
Number of fuel elements in a module		420,000
Number of fuel cricle in the core		15
Average burnup	GWd/tU	90
Main steam pressure	MPa	13.9
Main steam temperature	°C	571
Main feedwater temperature	°C	205
Feedwater flow rate for a module SG	kg/s	98

Two reactivity control systems are provided in the side reflector. One consists of 8 RCRs that are inserted to regulate the core reactivity for power modulation and to shut down the reactor in hot condition, and the other consists of 22 small absorber sphere shutdown units used to provide backup shutdown and to maintain cold shutdown. Besides, 30 gas boreholes are provided in the outer area of the side reflector as coolant flow channels. The core support structure consists of a steel core barrel, steel bottom supporting structure, and top thermal shield. It supports the ceramic structure of the pebble bed core by transferring various loads to the RPV. During operation, the annular area between the RPV and the core barrel is filled with cold helium to guarantee the temperature of pressure vessel not exceeding the limitation.

3.3.4 Reactor safety

Figure 3.7 highlights the safety approaches taken generally by the VHTR, which relies on three inherent design features:

- (1) The ceramic-coated fuel particle, which maintains the integrity of containment for fission products under a design temperature limit of 1600°C;
- (2) The helium coolant that is chemically inert and thus absent of explosive gas generation or phase change; and
- (3) The graphite structured and moderated core, having characteristics of negative reactivity coefficient, low power density, and high thermal conductivity.

Owing to these features, the VHTR reactor core, whether it is prismatic or pebble bed geometry, may be removed of decay heat by thermal conduction through the graphite core to the RPV and further, in the case of GTHTR300 design, by heat radiation to a naturally circulated vessel cooling system. As shown by the simulation result in the lower right side of Figure 3.7, such decay heat removal process is capable of keeping the fuel from exceeding its design temperature limit for a period of days, or months, if necessary, without reliance on any equipment or operator action, even in such severe accidents as loss of coolant or station blackout.

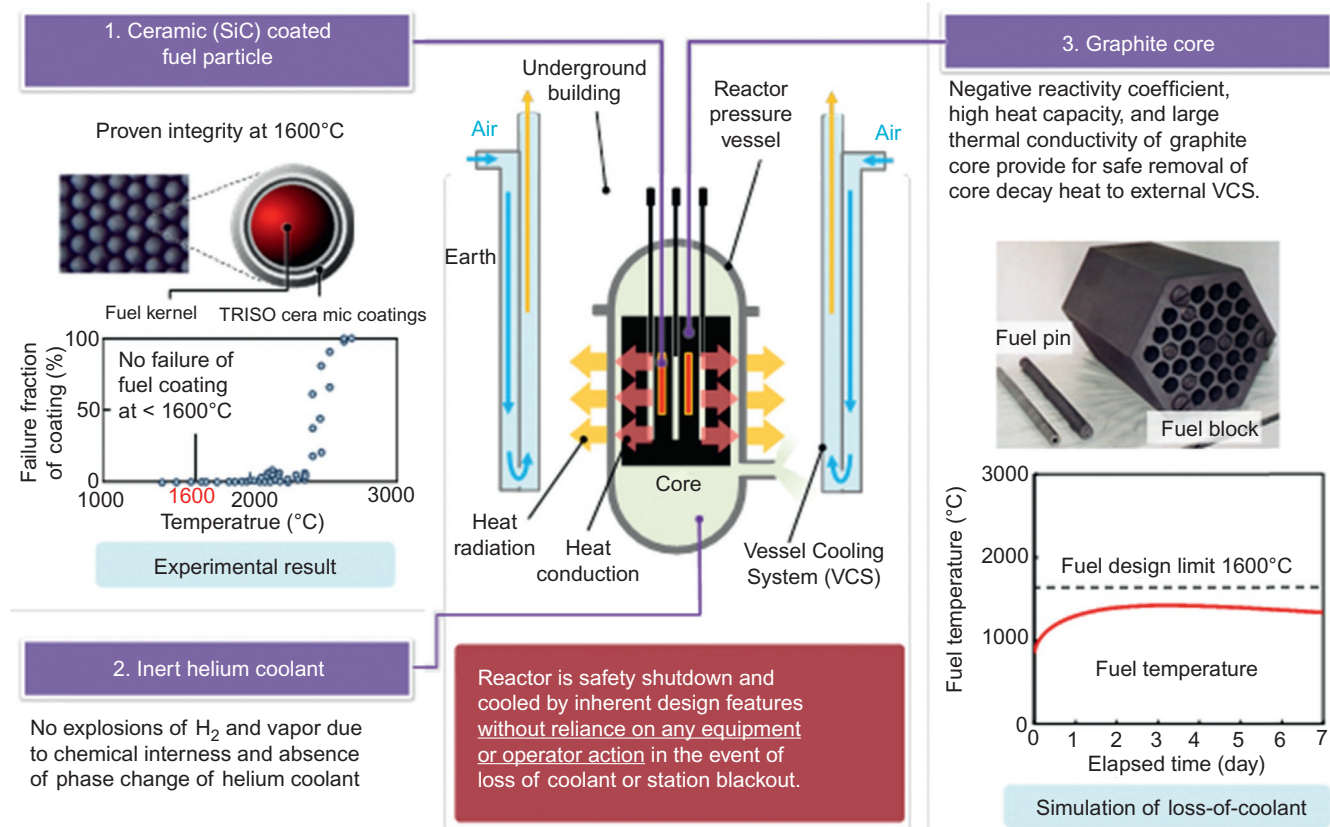


Figure 3.7. Inherent safety features of VHTR

In the case of HTR-PM, which features a steam generator in the primary loop, the water ingress into the reactor core in case of a rupture of one or more steam generator tubes is one of the most severe accidents (Zheng et al., 2010). The HTR-PM is designed to minimize insertion of water-ingress-induced positive reactivity by limiting the heavy-metal loading of the fuel element to 7 g. In addition, the steam generator is arranged below the level of the reactor core and equipped with an emergency steam blowdown system in order to minimize the amount of the water ingress. The analysis for the selected design basis accident of either a single tube rupture or a large break of the steam outlet tube header plate indicate the HTR-PM is able to keep the fuel temperature, the primary loop pressure and the graphite corrosion within the allowable design values (Wang et al., 2014).

3.3.5 Plant design

GTHT300 is a multipurpose, inherently safe, and site flexible Small Modular Reactor (SMR) that JAEA is developing for commercialization. As shown in Figure 3.8, the reactor system combines an HTGR with helium gas turbine to generate power while circulating the reactor coolant. The system consists of three pressure vessel units housing the reactor core, gas turbine, and heat exchangers, respectively. The multivessel system facilitates modular construction and independent maintenance access to functionally oriented equipment and systems in the vessel units. The reactor system is placed below grade in the reactor building.

While the reactor technologies have been demonstrated with the successful construction and continual operation of JAEA's 30 MW_{th} and 950°C test reactor HTTR, the key technologies required for the GTHT300's balance of plant system have been developed through out-of-pile tests. The technologies developed include the helium gas turbine compressor at one-third of the full scale, 200-MW_{e1}-class gas turbine and generator magnetic bearings, and full-scale compact heat exchanger module. In addition, subscale

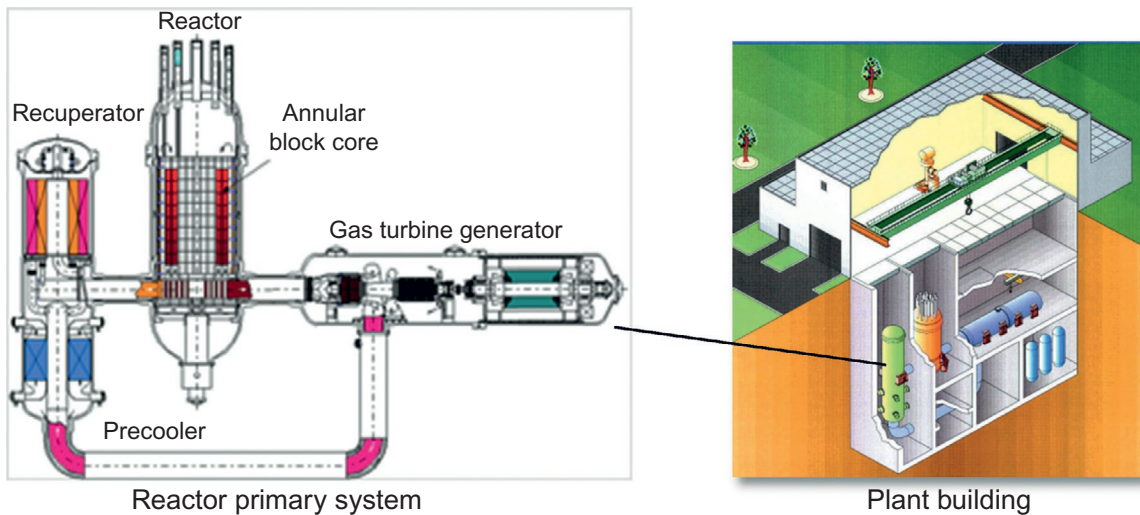


Figure 3.8. GTHTR300 plant design (600-MW_{th} reactor)

tests for high temperature helium/helium intermediate heat exchanger and isolation valve required for the reactor heat cogeneration applications have also been conducted (Nishihara et al., 2018).

The HTR-PM shown in Figure 3.9 contains two parallel trains of Nuclear Steam Supply System (NSSS) of identical design, each consisting of a 250-MW_{th} pebble bed reactor and a steam generator. The two NSSS systems have independent primary loops but share auxiliary facilities, such as fuel handling system and helium purification system. The two trains jointly supply superheated steam to a common steam turbine power generator rated at 210 MW_{el}.

3.3.6 Plant operations

3.3.6.1 Startup, rated operation, and shutdown

This sequence of reactor power operation is explained using a high temperature (950°C) rise-to-power test carried out on the HTTR (Fujikawa et al., 2004). The reactor power control device consists of control systems for the core power and for core outlet coolant temperature. These control systems are cascade connected; the latter control system ranks higher to give demand to the reactor power control system. The signals from each channel of the power range monitoring system are transferred to three controllers using microprocessors. In the event of a deviation between the process value and set value, a pair of control rods is inserted or

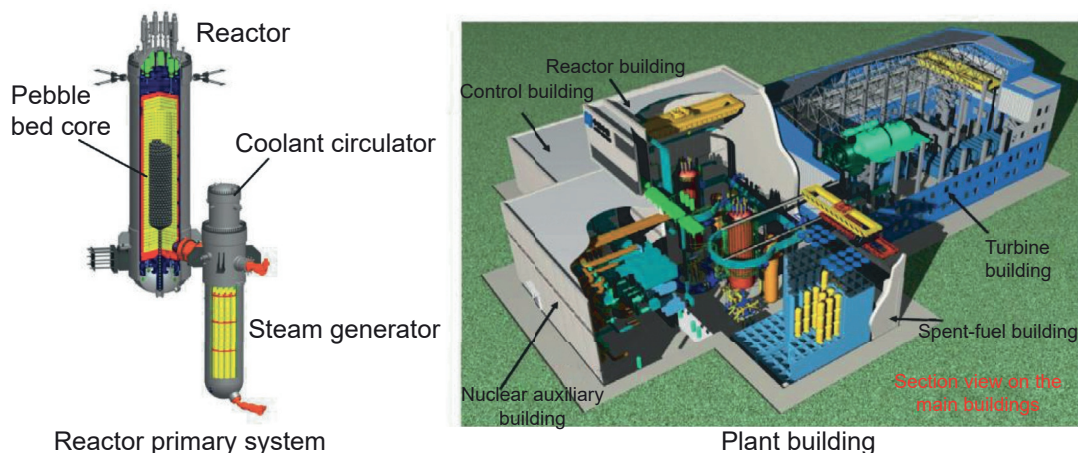


Figure 3.9. HTR-PM plant design (2 × 250 MW_{th} reactors)

withdrawn at the speed from 1 to 10 mm/s, according to the deviation. The relative position of the 13 pairs of control rods, except for 3 pairs of control rods used only for a scram, are controlled within 20 mm of one another by the control rod pattern interlock to prevent any abnormal power distribution. The plant control device controls plant parameters such as the coolant temperature of the reactor inlet, flow rate of the primary coolant, pressure of the primary coolant, and differential pressure between the primary cooling system and pressurized water-cooling system. The schematic diagram of the plant control system is shown in Figure 3.10. The reactor power, the reactor inlet coolant temperature, and the primary coolant flow rate are controlled to constant values by each control system. The reactor outlet coolant temperature is adjustable by the control system of the primary coolant flow rate.

Figure 3.11 are measurements of the sequence of startup, rated operation, and shutdown of the HTTR operating test, which began on March 31, 2004. The reactor power was increased in steps with monitoring all of the parameters, i.e., thermal parameters and coolant impurities. To minimize thermal stress in high temperature components, the temperature was raised within the rate of 35°C/h when the outlet coolant temperature is less than below 650°C and 15°C/h when the coolant temperature is above 650°C. The reactor power was kept at 50% (15 MW_{th}), 67% (20 MW_{th}), and 100% (30 MW_{th}), each step for more than 2 days in a steady temperature condition in order to measure the power coefficients of the reactivity. The reactor power was also kept at 82%, at which the reactor outlet coolant temperature is slightly below 800°C, in order to remove the chemical impurity in the coolant by helium purification system. The calibration of the neutron instrumentation system with the reactor thermal power was performed at the 97% power level.

The reactor outlet coolant temperature of 950°C was achieved on April 19, 2004, during the single loaded operation mode. During the parallel loaded operation mode, the reactor outlet coolant temperature reached

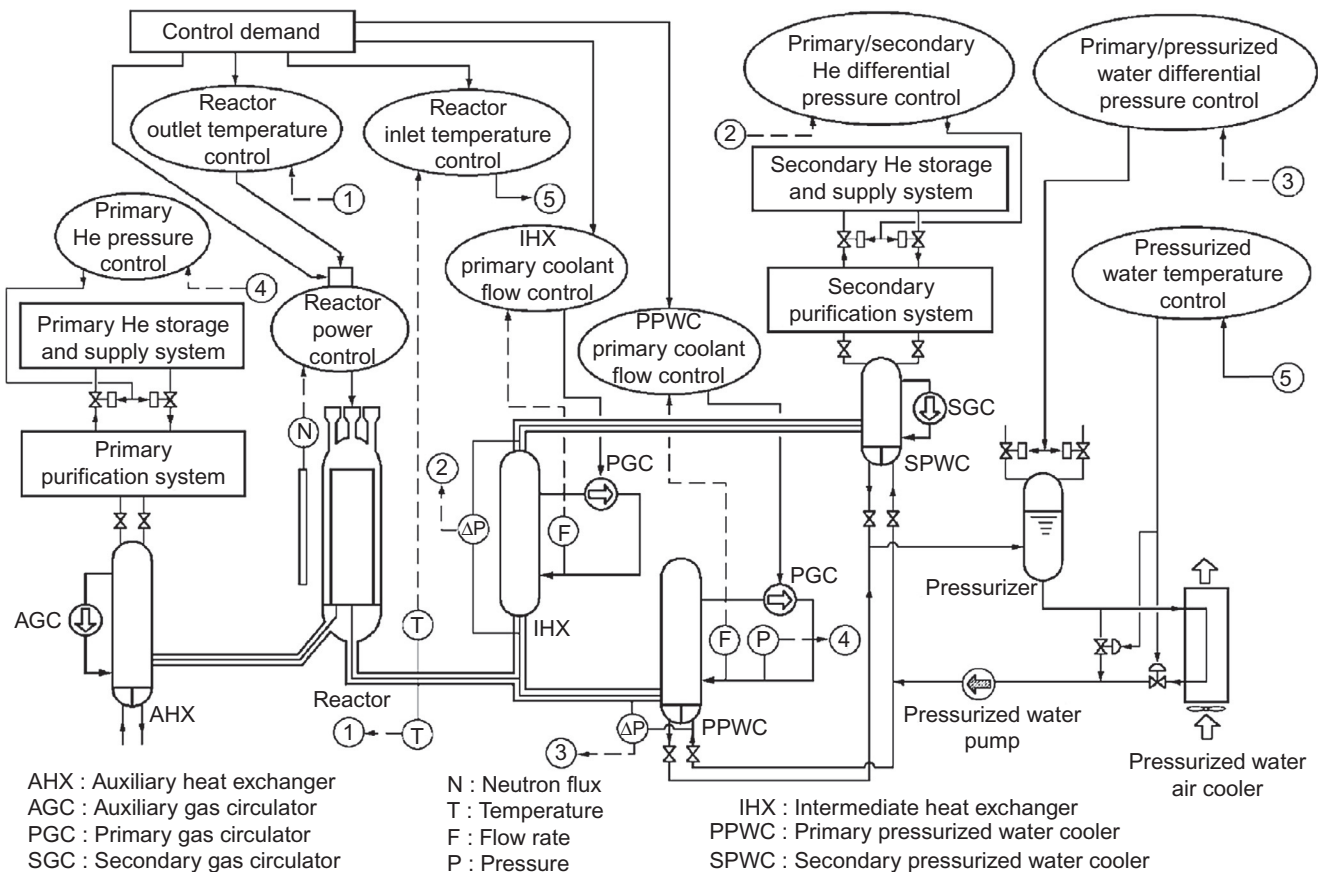


Figure 3.10. The HTTR reactor control system

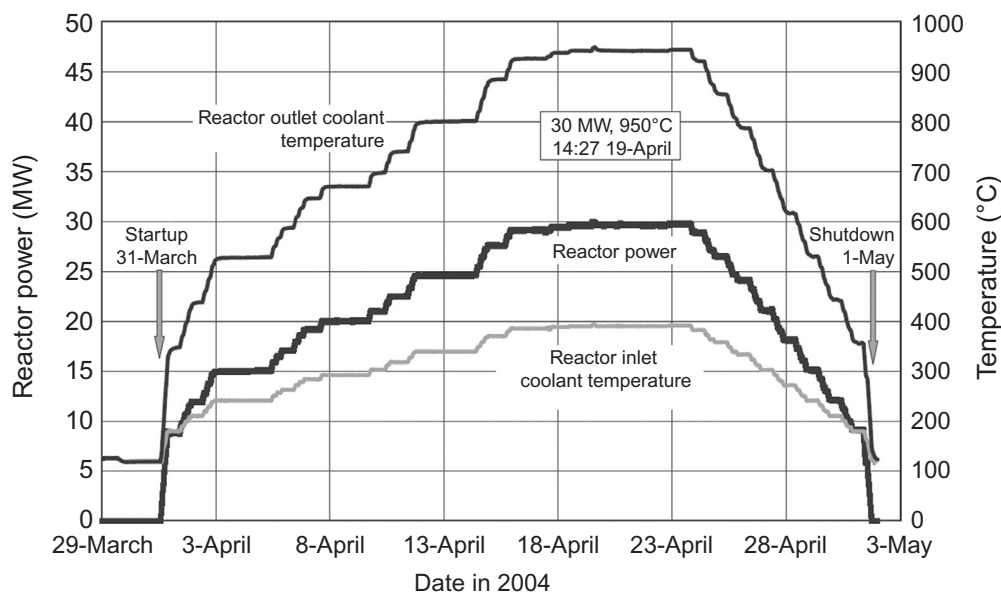


Figure 3.11. Measured HTTR operation sequence: startup, rated operation, and shutdown

941°C, and the secondary helium temperature at the Intermediate Heat eXchanger (IHx) outlet reached 859°C on June 24, 2004. The difference of the reactor outlet coolant temperature from the design value of 950°C was caused by a permitted margin for error of the flow rate indicators of the primary cooling system. The temperature deficiency implied that the flow rate in the parallel loaded operation mode was about 1% higher than that of the single loaded mode.

3.3.6.2 Dynamic operation

Dynamic simulation was done on the GTHTR300C plant. Figure 3.12 illustrates the plant process and associated control system. The GTHTR300C consists of a 600-MW_{th} HTGR with outlet coolant temperature of 950°C, an IHx to supply 900°C process heat to a thermal plant to produce hydrogen or other industrial products, and a direct-cycle recuperated gas turbine to generate power while circulating reactor coolant (Kunitomi et al., 2007). Section 3.4.2.1 details an example of this system to coproduce electricity and hydrogen.

The overall approach to dynamic operation integrates the following four load control strategies (Yan et al., 2012a):

- (1) Control of turbine speed, S_d , through flow bypass valve CV1.
- (2) Control of recuperator low-pressure side inlet temperature, T_x , through flow bypass valve CV2.
- (3) Control of turbine inlet temperature, T_t , by flow bypass valve CV3.
- (4) Control of turbine inlet temperature and pressure, T_t and P_t , by bypass valve CV4, and inventory flow valves IV1 and IV2.

The first two strategies are used to control rapid transients, such as a sudden loss of electric generator load. They are effective to protect the gas turbine from excess overspeed and prevent thermal shock in the recuperator.

The third strategy is used to automate heat rate to follow slow or fast changes of heat load in the IHx perturbed from the thermal production plant. As the IHx primary exit flow temperature rises or falls in response to a change in the IHx secondary heat load, the flow valve CV3 opens or closes to introduce more or less of cold flow to upstream of the turbine from the compressor discharge to the turbine inlet so as to keep the turbine inlet temperature constant. The overall control strategy aims to continue normal power generation, unaffected by any heat load change in the IHx.

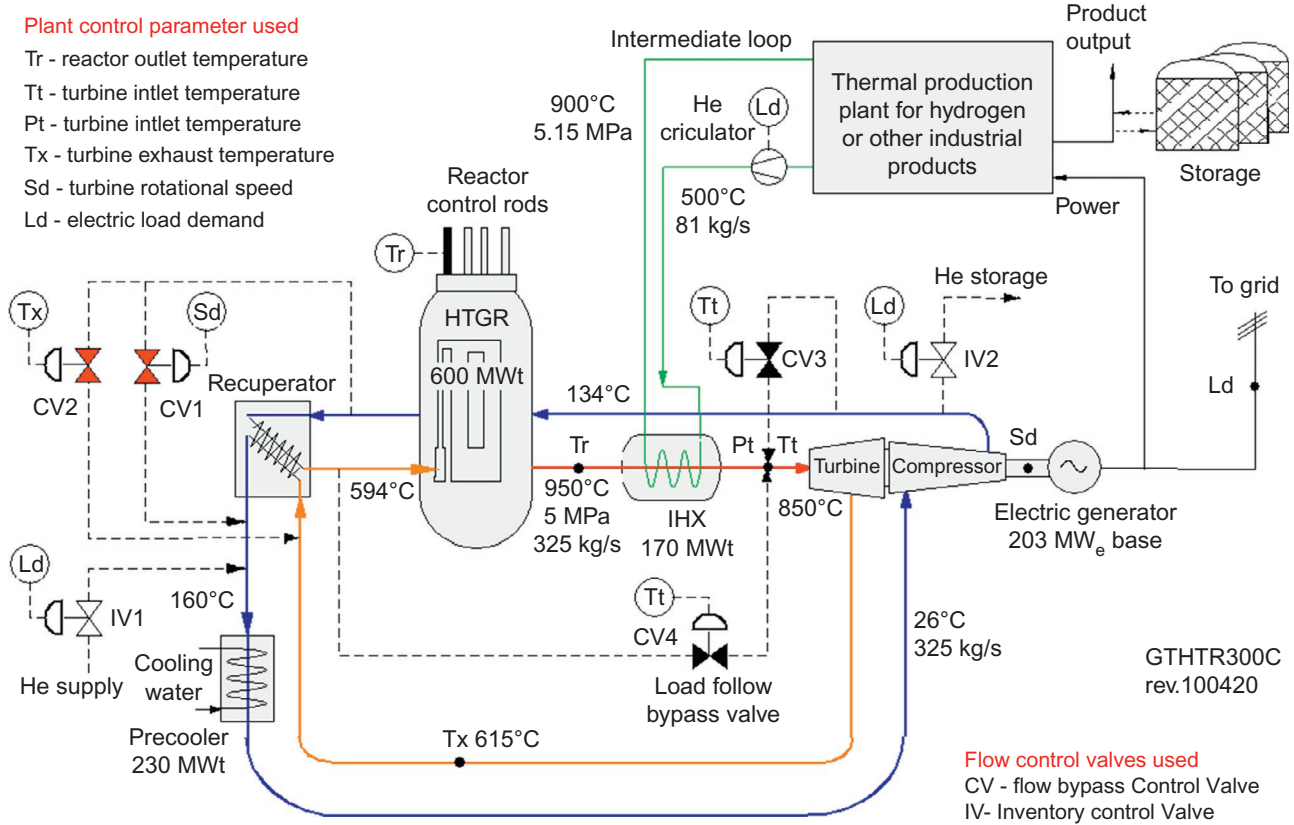


Figure 3.12. Control system for a 600 MW_{th} power and heat cogenerating VHTR

The fourth control strategy is applied to automate cogeneration load follow. The conditions to be met include: (1) constant reactor temperature to avoid thermal stress in high temperature structure; (2) constant reactor thermal power to yield base load economics; and (3) constant power generation efficiency over a broad range of load follow. The ability to follow variable power and heat loads is simulated with the results given in Figure 3.13. The simulation examines the plant response to an electric demand increase of 5% of the

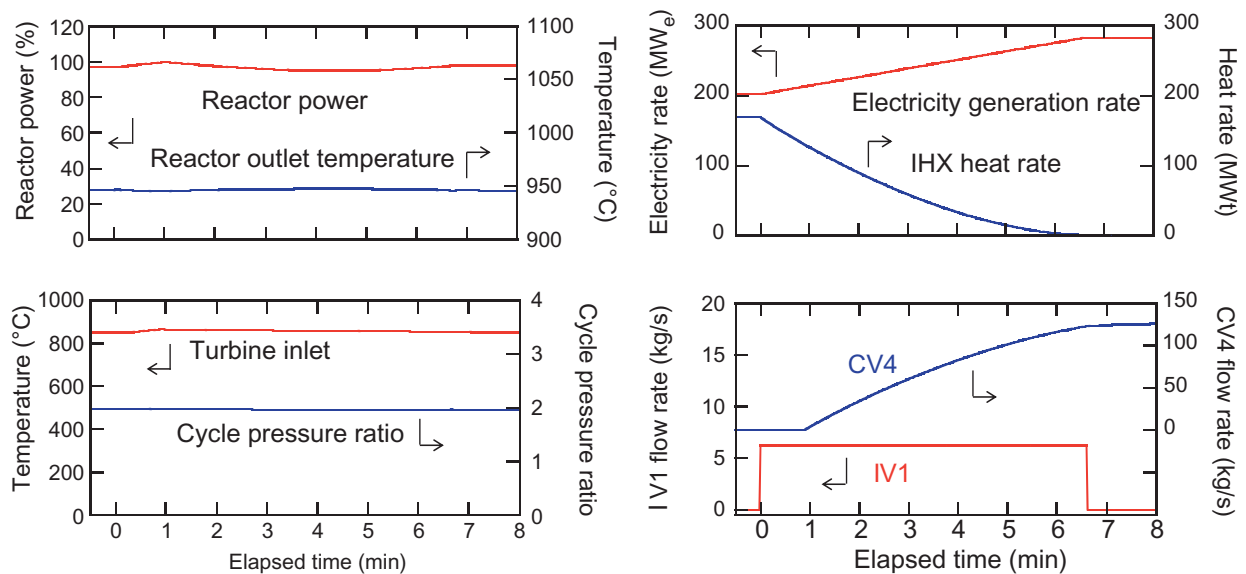


Figure 3.13. Simulation of VHTR cogeneration load follow to +5%/min electric load increase

base rate per minute with corresponding reduction of the heat rate, which is the maximum requirement for cogeneration load follow. The reactor remains at 100% power at all times. Starting from the base cogeneration rates, turbine power generation is raised to follow the electric load demand increase by increasing the primary coolant inventory through the inventory control valve IV1. The IHX heat rate to the thermal production plant is lowered by lowering the intermediate loop flow circulation rate with the variable speed gas circulator. As the primary exit temperature of the IHX begins to rise, the valve CV4 is opened by active or prescheduled control to follow load demand to direct cold flow from compressor discharge to mix with the hot exit gas of the IHX primary side. The goal of applying flow bypass via CV4 to maintain turbine inlet temperature near the rated 850°C is achieved, as shown in [Figure 3.13](#). The power sent out to external grid increases to 276 MW_{el} from 178 MW_{el} in as little as 7 min. The pressure in the reactor and at turbine inlet increases to 7 MPa from 5 MPa. To return to the base cogeneration rates, the control is reversed by reducing primary coolant inventory through another inventory control valve IV2 and simultaneously by closing the bypass valve VC4.

One attractive feature of the above-described control scheme is that the reactor operates at full power with little changes in the core and fuel temperatures, despite the rapid and wide-ranging load following. Under this condition, the control rod position is essentially unchanged. The core coolant temperatures are not changed. Neither is the core coolant flow rate. The rise in coolant pressure has large effect on the core and fuel temperatures. The heat transfer conditions in the core remain in the well-developed turbulent flow regime in the entire load range of interest.

Another merit of the control scheme is that the operating points of the gas turbine, including turbine inlet temperature and pressure ratio, are unchanged as shown in [Figure 3.13](#) such that aerodynamic performance of both turbine and compressor remains at their optimum design conditions. This allows for constant power generation efficiency of 46% over the entire load following range.

3.4 Applications and economics

Proven at coolant temperature of 950°C, the highest among the Generation-IV reactors, the VHTR enables not only high-efficiency electric power generation, but also broad cogeneration and industrial heat applications.

3.4.1 Power generation

A nuclear system supply steam may be used to power a steam turbine to produce electricity. This is done in HTR-PM. At reactor outlet temperature of 750°C, the plant generating efficiency is 42% at generator terminal and 40% net at busbar. Other detail of design parameters include the Rankine cycle main steam conditions are provided in [Table 3.6 \(International Atomic Energy Agency, 2020\)](#).

More advanced performance features are possible with the VHTR to power a gas turbine. [Figure 3.14](#) shows the direct gas turbine cycle of Japan's GTHTR300 design. The cycle attains thermal efficiency in the range of 46%–51%, corresponding to the range of reactor outlet temperatures of 850–950°C ([Yan et al., 2003](#); [Sato et al., 2014](#)). Further, the plant simplification is achieved due to eliminating essentially all water and steam systems from the plant. Dry cooling also becomes economically feasible because the rejection of the waste heat from the gas turbine cycle occurs from around 200°C, creating a large temperature difference from ambient air. As a result, the dry cooling tower size required per unit of power generation is comparable to the wet cooling towers used in nuclear plants today. The economical dry cooling would permit inland and remote reactor siting even without a large source of cooling water.

Table 3.6. HTR-PM design parameters

Reactor thermal power	$2 \times 250 \text{ MW}_{\text{th}}$
Electricity generation	$210 \text{ MW}_{\text{el}}$
Fuel element	Spherical pebble in 6 cm diameter
Number of fuel elements in core	420,000
Heavy metal loading per fuel element	7 g
Fuel enrichment	8.5% uranium
Fuel burnup	90 GWd/tU
Reactor cylindrical core height/diameter	11 m, 3 m
Reactor core average power density	3.22 MW/m^3
Reactor core inlet/outlet temperature	$250^\circ\text{C}/750^\circ\text{C}$
Reactor coolant circulation rate	96 kg/s
Reactor coolant pressure	7 MPa
Main steam supply temperature and pressure	$571^\circ\text{C}/13.9 \text{ MPa}$
Steam generator feed water temperature	205°C

3.4.2 Cogeneration

Cogeneration may improve the plant economics because systems and operations are shared between multiple production activities or because overall thermal efficiency is usually increased from when power is produced alone.

3.4.2.1 Hydrogen cogeneration

Hydrogen may be efficiently produced in the system illustrated earlier in Figure 3.12, where nuclear heat is transferred from the primary side coolant in the IHX and then transported in a closed heat transport loop to the thermal hydrogen production plant (Yan et al., 2005). The process parameters in Figure 3.15 indicates that the IHX transfers $170 \text{ MW}_{\text{th}}$ of the total $600 \text{ MW}_{\text{th}}$ reactor thermal power to the hydrogen process. The balance of the reactor thermal power is used by the gas turbine to generate $203 \text{ MW}_{\text{el}}$ electricity.

While many hydrogen processes have been proposed, the most studied include the copper-chlorine cycle in the process temperature range of $200\text{--}600^\circ\text{C}$ (Orhan et al., 2012), the Iodine-Sulfur (IS) process of $450\text{--}850^\circ\text{C}$ (Kasahara et al., 2014), and the hybrid sulfur cycle of $600\text{--}850^\circ\text{C}$ (Gorensek and Summers, 2011).

Figure 3.15 illustrates the principle of the IS process. The energy and material balance correspond to the heat rate of $175 \text{ MW}_{\text{th}}$, of which $170 \text{ MW}_{\text{th}}$ is supplied in the IHX, and 5 MW_{th} is input from the helium circulator heating in the secondary loop that connects the reactor and the hydrogen plant. The electricity consumption is $25.4 \text{ MW}_{\text{el}}$, accounting for the process electric utilities for helium gas circulator, process fluid pumps, and the Electro-ElectroDialysis (EED) to concentrate the Hydrogen Iodide (HI) flow stream.

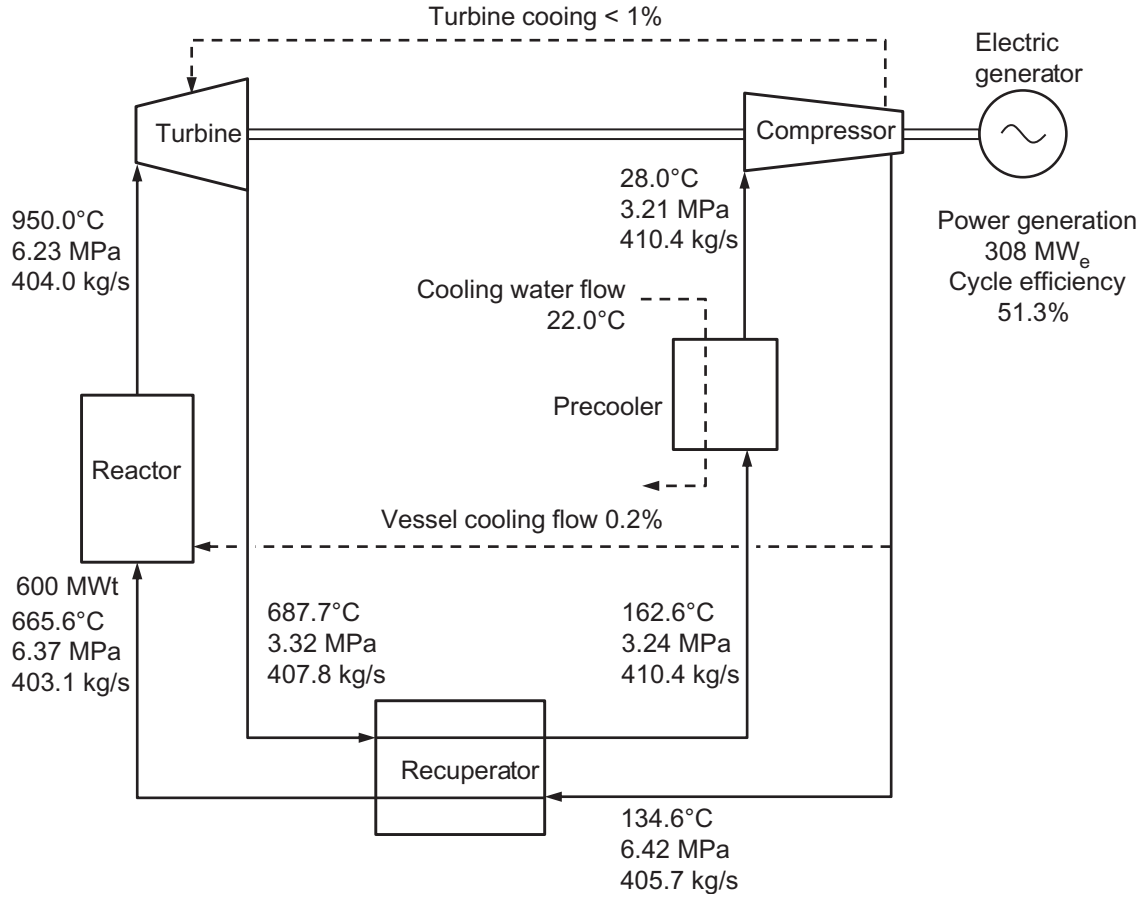


Figure 3.14. A gas turbine power generation cycle based on VHTR

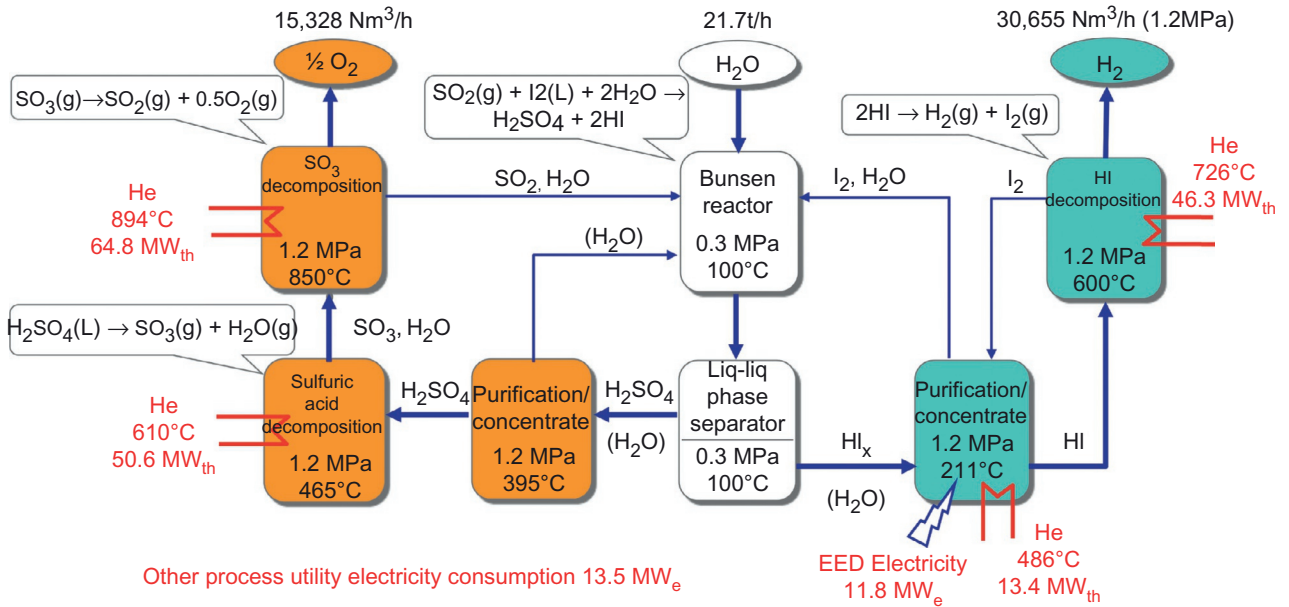


Figure 3.15. Thermochemical iodine sulfur process for hydrogen production

Accordingly, the thermal efficiency of the IS process plant is estimated to be 48.6% Higher Heating Value (HHV) as detailed below.

$$\begin{aligned} \text{IS process thermal efficiency} &= \frac{\text{H}_2 \text{ production rate} \times \text{HHV} (\text{H}_2)}{\text{net heat consumed} + \frac{\text{net electricity consumed}}{\text{power generation efficiency}}} \\ &= \frac{\frac{30,655 \text{ Nm}^3/\text{h}}{3600 \text{ s}} \times 12.76 \text{ MJ/Nm}^3}{170 \text{ MW}_{\text{th}} + \frac{25.4 \text{ MW}_e}{47.3}} = 48.6 \end{aligned}$$

A key factor that contributes to the high process efficiency is use of the innovative cobalt-reactive HI decomposing process developed by Japan's Toshiba Corporation. The test of the process has yielded nearly 100% HI decomposition rate in one pass through the Co and HI reaction. Another factor is that electricity used by the hydrogen plant is most efficiently cogenerated in-house by the nuclear reactor power plant. The thermal efficiency is 47.3% for power generation.

3.4.2.2 Desalination cogeneration

Figure 3.16 shows a desalination cogeneration process designed for efficient recovery of the waste heat from a VHTR. Table 3.7 summarizes the design parameters of the process. A MultiStage Flash (MSF) system is connected to the reactor plant cycle via a closed intermediate loop that transports the waste heat from the reactor to the desalination plant while acting as a barrier to prevent accidental material exchange between the two plants. To efficiently recover the waste heat, the MSF increments the thermal load of the multistage heat recovery section in a number of steps as opposed to keeping it constant in the traditional MSF process (Yan et al., 2013). As the number of steps increases, more waste heat becomes recoverable, while the top brine temperature, a sensitive MSF process parameter, is also increased. Both lead to increased water yield. Operating with a similar number of stages, the present MSF process is shown to produce 45% more water than the traditional process operating over the same temperature range. Connected to a 600-MW_{th} VHTR gas turbine power plant, the desalination yield is 54,552 m³/day without penalizing to the power generation. The overall utilization of the nuclear reactor thermal power is increased to 83% from 47% in power generation alone.

3.4.3 Industrial application

The heat supply from the VHTR covers the temperature range of heat demands in many industries, some of which, such as large-scale hydrogen production and desalination, are described earlier, and the others that

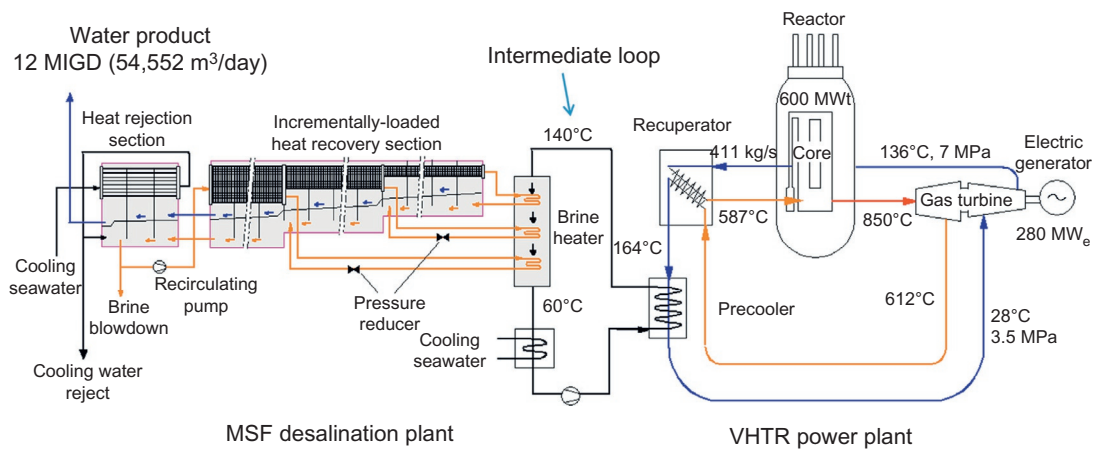


Figure 3.16. VHTR desalination cogeneration process

Table 3.7. Desalination cogeneration performance

Reactor thermal power	600 MW _{th}
Reactor outlet temperature	850°C
Power generation rate	280 MW _{el}
Seawater desalination rate	12 MIGD (54,552 m ³ /day)
Effective thermal input to desalination	220 MW _{th}
Heat supply (hot water) temperature	140°C
Hot water return temperature	60°C
Top brine temperature	112°C
Design seawater temperature	25°C
Seawater temperature rise at heat rejection	10°C
Design seawater salinity	45,000 ppm
Recycle brine concentration	62,000 ppm

HRJ, Heat Rejection section.

have been frequently studied include oil extraction, coal gasification, oil refinery and petrochemical, and steelmaking. The inherent safety of the VHTR makes the industrial heat applications economically attractive, as it permits siting proximity to the industry customers, in particular to high temperature heat users so as to minimize the cost and loss of heat transmission.

Figure 3.17 shows a system that ties a direct reduction steelmaking plant to a VHTR (Yan et al., 2012b). The latter supplies the former all energy and feedstock with the exception of iron ore. The process takes on a multidisciplinary approach: the reactor plant employs a VHTR with 950°C outlet temperature to produce electricity and heat. The steelmaking plant employs conventional furnaces but substitutes hydrogen and oxygen for hydrocarbons as reactant and fuel. Water decomposition through an experimentally demonstrated thermochemical process manufactures the feedstock gases required. Through essential safety features, particular a fully passive nuclear safety, the design achieves physical proximity and yet operational independence of the two plants to facilitate interplant energy transmission. The calculated energy and material balance given in Figure 3.17 yields slightly over 1000 t of annual steel output per 1 MW_{th} of reactor thermal power and is essentially free of CO₂ emission.

3.4.4 Economics

3.4.4.1 Cost of electricity generation

A summary of the cost evaluation for the GTHTTR300 power plant is given. Details can be found elsewhere (Takei et al., 2006). For the purpose of cost estimation, the plant construction assumes the following:

- Nth-of-a-kind plant that allows for learning effects
- replacement of LWR on existing site
- modular method of construction
- equipment shipped to exclusive port on site
- reactor building and structures similar to the HTTRs

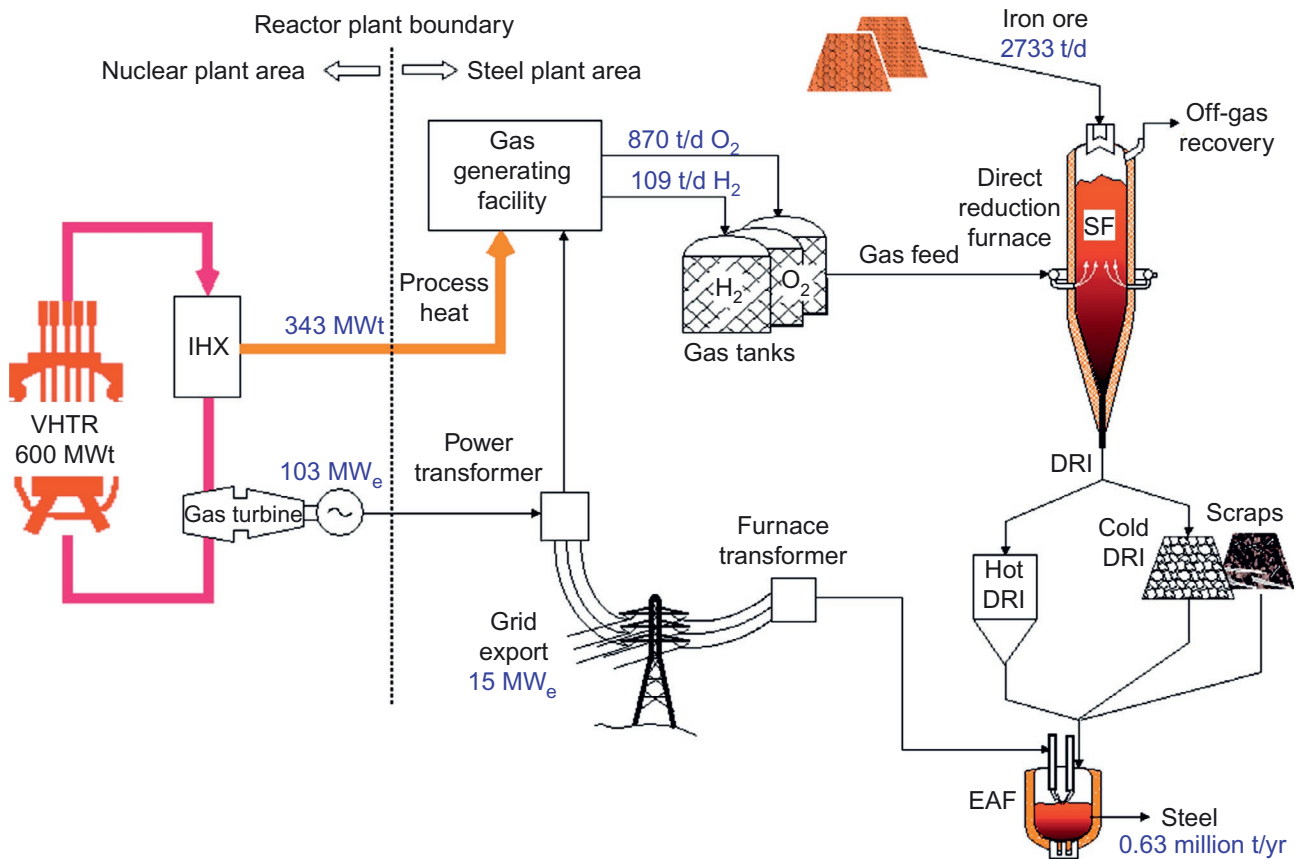


Figure 3.17. Energy and material balance of a VHTR-based steelmaking process

- seismic design conditions same as that of the HTTR
- cost accounts for design, fabrication of facilities, plant construction, and commission operations
- plant siting in Japan

The capital cost estimation assumes a plant life of 40 years. The depreciation period is 20 years. Thereafter, the book value of the plant is assumed to be 5% constant for the remainder of the plant life. The financial parameters assumed are 3% discount rate, 3% interest rate, and 1.4% property tax.

Capital cost

Figure 3.18 shows the capital cost of the plant that includes four reactor units ($4 \times 274 \text{ MW}_{\text{el}}$) comparing with the LWR. The cost for the reference LWR of $1180 \text{ MW}_{\text{el}}$ was estimated by Federation of Electric Power Companies (FEPC) of Japan. The cost of decommissioning GTHTR300 is higher because the number of systems and structures, such as pressure vessels and primary biological shielding, that become radioactive in operation and must be disposed of during decommission, are bulkier in the GTHTR300. However, the total capital cost of GTHTR300 ($1.31 \text{ US}\$/\text{kWh}$) is about 25% lower than the LWR ($1.77 \text{ US}\$/\text{kWh}$) because of the greater power generating efficiency of GTHTR300.

Operating cost

Figure 3.19 shows the operating cost in comparison with the LWR. The operating cost of the GTHTR300 ($0.92 \text{ US}\$/\text{kWh}$) is about 35% lower than the LWR ($1.42 \text{ US}\$/\text{kWh}$) since the plant generating efficiency is higher and because the maintenance cost is lower, owing to less number and material of systems to be regularly serviced.

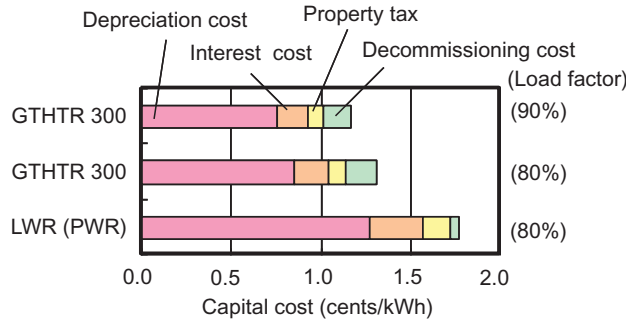


Figure 3.18. Capital cost

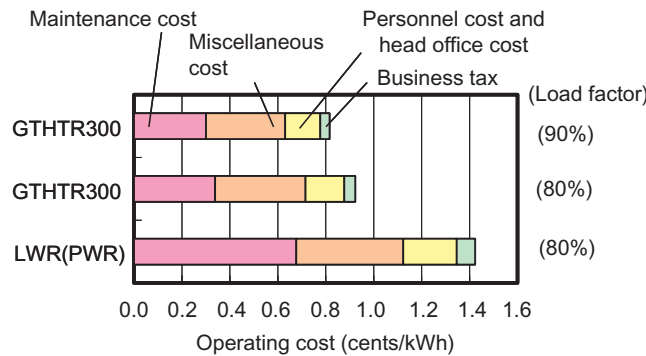


Figure 3.19. Operating cost

Fuel cost

Figure 3.20 shows the fuel cycle cost comparing with the LWR. The overall fuel cycle cost of GTHTR300 (1.22 US¢/kWh) is comparable to that of the LWR (1.23 US¢/kWh). In the front-end process, the higher enrichment and the fabrication of coated fuel particles make the cost of enrichment, conversion, and fabrication higher in the GTHTR300. In the back-end process, although unit costs in almost all processes of the GTHTR300 are higher, the back-end cost of the GTHTR300 is lower than the LWR because the material quantity of spent fuel is less as a result of higher burnup and because of the greater plant efficiency.

Power generation cost

Figure 3.21 shows the power generation cost by summing up the above capital, operation, and fuel cycle costs. The power generation cost is 3.2 US¢/kWh at the load factor of 90% and increases to 3.45 US¢/kWh at

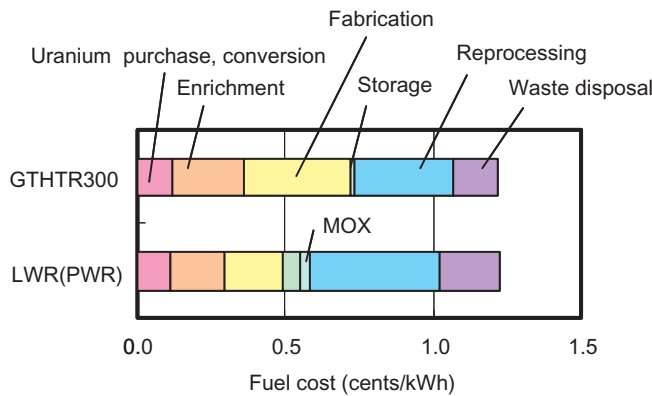


Figure 3.20. Fuel cost

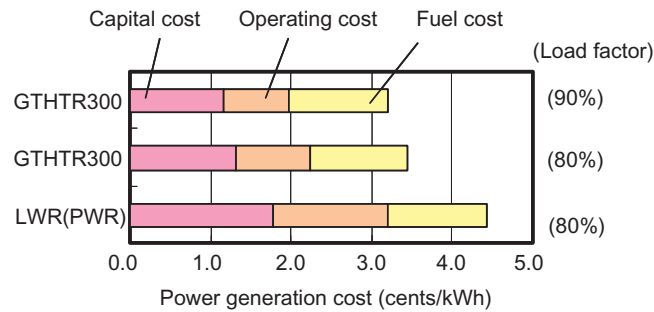


Figure 3.21. Power generation cost

a reduced factor reduced of 80%. The GTHTTR300 offers a 20% cost advantage over the 4.42 US¢/kWh of LWR estimated by FEPC.

3.4.4.2 Cost of hydrogen production

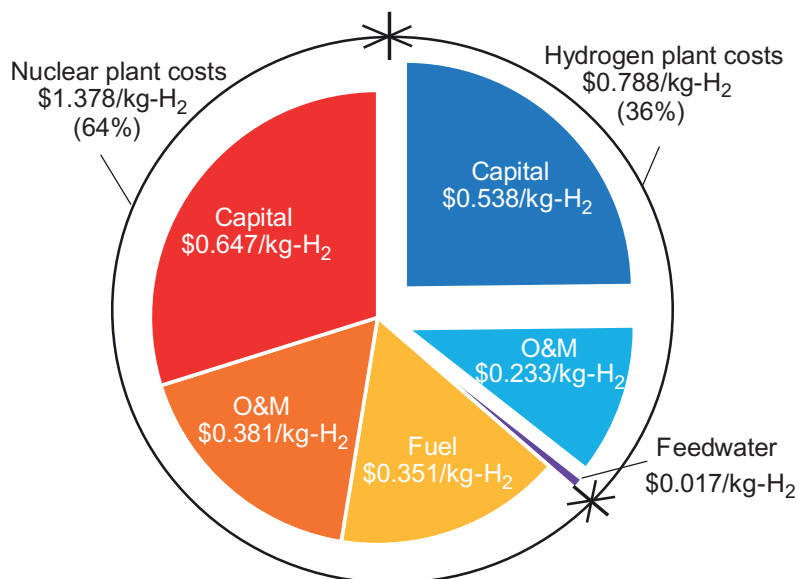
Table 3.8 summarizes the estimated cost of the GTHTTR300 for cogenerating hydrogen with a colocated IS process water-splitting thermochemical plant. The estimation of the plant design, referred as GTHTTR300C + IS below, assumes a load factor of 90% for both the reactor and hydrogen plants. The capital cost of hydrogen plant covers equipment cost, site construction cost, and indirect cost. Nuclear heat is assumed to be cogenerated in the 600-MW_{th} reactor plant, 170 MW_{th} of which is supplied via IHX to the hydrogen plant facility, while the balance is used to generate power in the reactor plant. The utilities include the feed water to IS process, 25.4 MW_{el} electricity that is supplied in house by the nuclear reactor plant at a cost of 3.2 ¢/kWh (see Section 3.4.4.1 for detail) and consumed to power the EED, the process pumps, the helium circulator of the heat transport loop, and catalysts and chemicals used in the IS process. Return on investment is 8%. Note that the value difference in the two columns of the table results from whether a credit is taken from the sale of by-product oxygen.

Final hydrogen production cost is US \$2.169/kg-H₂, of which 64% is the cost of nuclear heat and electricity supplied in house by the colocated GTHTTR300C. The cost distributors are identified in Figure 3.22.

Table 3.8. Hydrogen production cost by GTHTTR300C

H ₂ production rate (H ₂ production efficiency)		30,655 Nm ³ /h (48.8%)	30,655 Nm ³ /h (48.8%)
H ₂ plant life	Year	15	15
H ₂ plant capital	\$/kg-H ₂	0.657	0.657
Nuclear heat	\$/kg-H ₂	0.965	0.965
Nuclear electricity	\$/kg-H ₂	0.294	0.294
H ₂ plant utilities	\$/kg-H ₂	0.091	0.091
By-product (O ₂) credit	\$/kg-H ₂	0	-0.278
Return on investment (8%)	\$/kg-H ₂	0.161	0.161
Total production cost	\$/kg-H ₂	2.169	1.891
	¢/Nm ³	19.5	17.0

Figure 3.22. Cost share of hydrogen production by GTHTR300C + IS



3.4.4.3 Cost of desalination cogeneration

Table 3.9 compares the estimated costs of potable water production through seawater desalination cogeneration with conventional and VHTR power plants (Sato et al., 2014). The conventional plant is based on a modern Gas Turbine Combined Cycle (GTCC) power plant at 55% power generation efficiency. The VHTR cogeneration system is that described in Section 3.4.2.2. The costs were evaluated by an Original Equipment Manufacturer (OEM) vendor active in the Middle East desalination plant construction. The vendor carried out the plant equipment design and evaluated the required operation and maintenance. The cost estimation was then developed based on the vendor construction and operation know-how of comparable-scale MSF plants.

Table 3.9. Fossil-fired and VHTR seawater desalination cogeneration cost estimates

Plant ->	GTCC (Gas Turbine Combined Cycle)		VHTR desalination cogeneration
	Oil-fired	Natural gas-fired	
Capital (\$/m ³)	0.29	0.29	0.39
<i>ENERGY (\$/M³)</i>			
Heat	1.65	0.67	0.04
Electricity	0.13	0.13	0.09
<i>OPERATION (\$/M³)</i>			
Consumables	0.02	0.02	0.02
O&M	0.03	0.03	0.03
Water cost (\$/m ³)	2.13	1.14	0.57

O&M, Operation and Maintenance.

The prices of oil and natural gas are referred to the World Bank Commodity Prices Date (also known as Pink Data). The 10-year average (July 2004–July 2014) crude oil prices of the three primary benchmarks (Brent, Dubai, and West Texas intermediate) fall in the narrow range of 79.8–84.1 US \$/bbl. During the same 10-year period, the average natural gas benchmark prices (the United States, Europe, and Japan) are in the range of 5.6–11.1 US \$/MMBtu. For this study, the lower values of the above ranges for oil and gas are used to calculate the heat costs of the conventional plant.

The estimated water cost with the VHTR desalination cogeneration is US \$0.57/m³ comparing to US \$2.13/m³ for the oil-fired plant and US \$1.14/m³ in the case of the gas-fired plant. Despite the higher capital cost of the VHTR desalination plant, the considerable energy cost saving by cogeneration using the VHTR power generation waste heat provides 50% or more water cost advantage comparing the fossil-fired Gas-Turbine Combined Cycle (GTCC) options widely practiced for desalination cogeneration today.

3.5 Summary

VHTR technology is well advanced through the decades of international research, development, and commercialization efforts. Several reactors have been built. Two test reactors remain operational in China and Japan. Still others are being developed.

Pebble bed and prismatic reactor are the two major design variants. Both are in use today. In either case, the basic fuel construction is the TRISO-coated particle fuel. Uranium, thorium, and plutonium fuel cycle options have been investigated and some have been operated in the reactors. Spent fuel may be direct disposed or recycled. The unique construction and high burnup potential of the TRISO fuel enhances proliferation resistance.

The VHTR safety relies mostly on passive and inherent design features. The choice of low core power density limits the decay heat generation rate to the extent that can be safely removed by thermal conduction only. The choice of the core negative reactivity coefficient provides reactor shutdown in case of accidental rise in core temperature. Helium coolant used is chemically inert and thus absent of explosive gas generation or phase change. The robust design and proven fabrication quality of the TRISO fuel prevents significant release of fission products in any licensing events.

The VHTR coolant temperature (950°C) is the highest among the Generation-IV reactors. This enables not only for efficient power generation by either steam or gas turbine, but also for high temperature heat application and attractive cogeneration. The VHTR-based hydrogen production, steelmaking, and seawater desalination have been found cost competitive.

The world first modular prototype plant, HTR-PM, consisting of two reactor units of 250 MW_{th} each at 750°C reactor outlet temperature, is being built in China. The operation is expected in 2017. The quest in the current development for the 950°C GTHTR300 reactor in Japan and for the systems in the United States, Korea, and other countries is to demonstrate the technologies of advanced fuels, power conversion, and heat applications that can satisfactorily address the set of Generation-IV objectives for safety, economics, waste management, and proliferation resistance.

References

- Delrue, J., Shahrokhi, F., Lommers, L., 2018. The Framatome SC-HTGR heat transport system, HTR 2018-7068. In: Proceedings of the HTR 2018, Warsaw, Poland, October 8–10.
- Fowler, T.B., Vondy, D.R., Cunningham, G.W., 1971. Nuclear Reactor Core Analysis Code: CITATION. ORNL-TM-2496 (Rev.2), Technical Report. Oak Ridge National Lab, Tenn., United States.
- Fu, J., Jiang, Y., Cheng, H., Cheng, W., 2014. Overview and progress of high temperature reactor pebble-bed module demonstration project (HTR-PM), HTR2014-11125. In: Proceedings of the HTR 2014, Weihai, China, October 27–31.

- Fujikawa, S., Hayashi, H., Nakazawa, T., Kawasaki, K., Iyoku, T., Nakagawa, S., Sakaba, N., 2004. Achievement of reactor-outlet coolant temperature of 950°C in HTTR. *J. Nucl. Sci. Technol.* 41 (12), 1245–1254.
- Fujimoto, N., Nojiri, N., Ando, H., Yamashita, K., 2004. Nuclear design. *Nucl. Eng. Des.* 233, 23–36.
- Fukaya, Y., Goto, M., Ohashi, H., Tachibana, Y., Kunitomi, K., Chiba, S., 2014. Proposal of a plutonium burner system based on HTGR with high proliferation resistance. *J. Nucl. Sci. Technol.* 51 (6), 818–831.
- Gorensek, M., Summers, W., 2011. The hybrid cycle. In: Yan, X., Hino, R. (Eds.), *Nuclear hydrogen production handbook*. CRC Press, Florida, USA.
- Goto, M., Ueta, S., Tachibana, Y., Inaba, Y., Aihara, J., Fukaya, Y., Kunitomi, K., Demachi, K., Okamoto, K., Nakano, M., Tsuji, M., Ohashi, K., Honda, M., Takahashi, M., Saiki, Y., Hayato, K., Kitagawa, K., 2015. Conceptual study of a plutonium burner high temperature gas-cooled reactor with high nuclear proliferation resistance. In: *Proceedings of Global 2015*, September 20–24, 2015, Paris, France. Paper 5426.
- Greeneche, D., 2003. HTR fuel cycles: a comprehensive outlook of past experience and an analysis of future options. In: *Proceedings of the ICAPP 2003*, Córdoba, Spain, May 4–7.
- Hu, S., Wang, R., Gao, Z., 2004. Safety demonstration tests on HTR-10. In: *Proceedings of the HTR 2004*, Beijing, China, September 22–24. Paper HTR2004-H06.
- INL, 2011. NGNP Project 2011 Status and Path Forward, INL/EXT-11-23907, December 2011.
- International Atomic Energy Agency, 2020. *Advances in Small Modular Reactor Technology Developments*, A Supplement to IAEA Advanced Reactors Information System (ARIS) 2020 Edition. pp. 137–140.
- Kasahara, S., Tanaka, N., Noguchi, H., Iwatsuki, J., Takegami, H., Yan, X., Kubo, S., 2014. JAEA's R&D on the thermochemical hydrogen production process. In: *Proceedings of the HTR 2014*, Weihai, China, October 27–31. Paper HTR2014-21233.
- Kuijper, J., Raepsaet, X., de Haas, J., von Lensa, W., Ohlig, U., Ruetten, H., Brockmann, H., Damian, F., Dolci, F., Bernnat, W., Oppe, J., Kloosterman, J., Cerullo, N., Lomonaco, G., Negrini, A., Magill, J., Seiler, R., 2006. HTGR reactor physics and fuel cycle studies. *Nucl. Eng. Des.* 236, 615–634.
- Kunitomi, K., Yan, X., Nishihara, T., Sakaba, N., Mouri, T., 2007. JAEA's VHTR for hydrogen and electricity cogeneration: GTHTR300C. *Nucl. Eng. Technol.* 39 (1), 9–20.
- Lathrop, K., Brinkley, F., 1973. TWOTRAN-II: An Interfaced Exportable Version of the TWOTRAN Code for Two Dimensional Transport. LA-484-MS.
- Masson, M., Grandjean, S., Lacquement, J., Bourg, S., Delauzun, J.-M., Lacombe, J., 2006. Block-type HTGR spent fuel processing: CEA investigation program and initial results. *Nucl. Eng. Des.* 236, 516–525.
- Mitsubishi Heavy Industries, Japan, 2019. MHI's experiences & contributions in HTGR development in Japan. In: *Side Event of 63rd IAEA General Conference*, IAEA, Vienna, Austria, September 18, 2019.
- Nakata, T., Katanishi, S., Takada, S., Yan, X., Kunitomi, K., 2003. Nuclear, thermal and hydraulic design for gas turbine high temperature reactor (GTHTR300). *AESJ Trans.* 2 (4), 478–489.
- Nishihara, T., Yan, X., Tachibana, Y., Shibata, T., et al., 2018. Excellent Feature of Japanese HTGR Technologies, JAEA-Technology 2018-004. Japan Atomic Energy Agency.
- Oak Ridge National Laboratory, November 2008. Deep Burn: Development of Transuranic Fuel for High-Temperature Helium-Cooled Reactors. ORNL/TM-2008/205.
- Orhan, M., Dincer, I., Rosen, M., 2012. Design and simulation of a UOIT copper–chlorine cycle for hydrogen production. *Int. J. Energy Res.* 37 (10), 1160–1174.
- Petti, D., 2014. Implications of results from the advanced gas reactor fuel development and qualification program on licensing of modular HTGRs. In: *Proceedings of the HTR 2014*, Weihai, China, October 27–31. Paper HTR2014-31252.
- Richards, M., Venner, F., Shimakawa, S., 2008. VHTR deep burn applications. In: *16th Pacific Basin Nuclear Conference (16PBNB)*, Aomori, Japan, October 13–18. Paper ID P16P1238.
- Saito, S., Tanaka, T., Sudo, Y., Baba, O., Shindo, M., 1994. Design of High Temperature Engineering Test Reactor (HTTR). *JAERI* 1332.
- Sato, H., Yan, X.L., Tachibana, Y., Kunitomi, K., 2014. GTHTR300—a nuclear power plant design with 50% generating efficiency. *Nucl. Eng. Des.* 275, 190–196.
- Shahrokhi, F., Lommers, L., Mayer III, J., Southworth, F., 2014. US HTGR deployment challenges and strategies. In: *Proceedings of the HTR 2014*, Weihai, China, October 27–31. Paper HTR2014-11309.
- Takamatsu, K., Yan, X., Nakagawa, S., Sakaba, N., Kunitomi, K., 2014. Spontaneous stabilization of HTGRs without reactor scram and core cooling—safety demonstration tests using the HTTR: loss of reactivity control and core cooling. *Nucl. Eng. Des.* 271, 379–387.
- Takei, M., Kosugiyama, S., Mouri, T., Katanishi, S., Kunitomi, K., 2006. Economical evaluation on gas turbine high temperature reactor 300 (GTHTR300). *Trans AESJ* 5 (2), 109–117.
- The US Energy Policy Act of 2005, August 5, 2005.

- US Department of Energy, 2021 <https://www.energy.gov/ne/articles/x-energy-developing-pebble-bed-reactor-they-say-cant-melt-down> (Accessed 05.09.2021).
- Wang, Y., Zheng, Y., Li, F., Shi, L., 2014. Analysis on blow-down transient in water ingress accident of high temperature gas-cooled reactor. *Nucl. Eng. Des.* 271, 404–410.
- Wu, Z., Lin, D., Zhong, D., 2002. The design features of the HTR-10. *Nucl. Eng. Des.* 218, 25–32.
- Yan, X., Kunitomi, K., Nakada, T., Shiozawa, S., 2003. GTHTTR300 design and development. *Nucl. Eng. Des.* 222, 247–262.
- Yan, X., Kunitomi, K., Hino, R., Shiozawa, S., 2005. GTHTTR300 design variants for production of electricity, hydrogen or both. In: *Proc. 3rd of OECD/NEA Information Exchange Meeting on Nuclear Production of Hydrogen, Oarai, Japan.*
- Yan, X., Kasahara, S., Tachibana, Y., Kunitomi, K., 2012a. Study of a nuclear energy supplied steelmaking system for near-term application. *Energy* 39, 154–165.
- Yan, X., Sato, H., Tachibana, Y., Kunitomi, K., Hino, R., 2012b. Evaluation of high temperature gas reactor for demanding cogeneration load follow. *J. Nucl. Sci. Technol.* 49 (1), 121–131.
- Yan, X., Noguchi, H., Sato, H., Tachibana, Y., Kunitomi, K., Hino, R., 2013. Study of an incrementally loaded multistage flash desalination system for optimum use of sensible waste heat from nuclear power plant. *Int. J. Energy Res.* 37, 1811–1820.
- Yan, X., Sato, H., Kamiji, Y., Imai, Y., Terada, A., Tachibana, Y., Kunitomi, K., 2014. GTHTTR300 cost reduction through design upgrade and cogeneration. In: *Proceedings of the HTR 2014, Weihai, China, October 27–31. Paper HTR2014-21436.*
- Zheng, Y., Shi, L., Wang, Y., 2010. Water-ingress analysis for the 200MWe pebble-bed modular high temperature gas-cooled reactor. *Nucl. Eng. Des.* 240, 3095–3107.

4

Gas-cooled Fast Reactors (GFRs)

Pavel Tsvetkov

Department of Nuclear Engineering, Texas A&M University, College Station, TX, United States

Nomenclature

ABR	Advanced Burner Reactor
GFR	Gas-cooled Fast Reactor
HTR	High-Temperature Reactor
LFR	Lead-cooled Fast Reactor
LMFR	Liquid Metal Fast Reactor
LOCA	Loss-Of-Coolant Accident
R&D	Research and Development
SFR	Sodium-cooled Fast Reactor
VHTR	Very-High-Temperature Reactor

4.1 Rationale and generational R&D bridge

The history of gas-cooled fast reactors dates back to the dawn of nuclear era. It needs to be noted that the gas-cooled fast reactor technology is being pursued to this day and remains to be of contemporary interest in many countries worldwide ([Gas-cooled Fast Reactors, 1972](#); [Fast Spectrum Reactors, 2012](#)).

The biggest potential advantage of GFRs is in their expected technological range of applications—from electricity to process heat to waste minimization. Both breeders and burners were of initial interest taking advantage of the very nature of this concept to offer a fast spectrum system that can be tailored to desired conversion ratios. The reactors using air, helium, carbon dioxide, and dissociating gasses as coolants have been explored ([Fast Spectrum Reactors, 2012](#)). General Atomics in the United States originated the initial conceptual effort. The interests in the design expanded globally after that including Germany, France, and Russia. Soviet Union explored N_2O_4 as a coolant ([Gas-cooled Fast Reactors, 1972](#); [Fast Spectrum Reactors, 2012](#)).

The unique robustness of the technology is unmatched in the engineering domain of nuclear reactors. There are thermal reactor and fast reactors with various coolants but none of them offers the option to fit in all anticipated deployment domains supporting the complete range of energy system applications in the way GFRs integrate into the overall sustainable energy system portfolio: electricity, process heat applications, high level waste incineration through conversion and transmutation pathways, new fuel breeding, and deployment scenarios within uranium-plutonium and thorium fuel cycles ([Fast Spectrum Reactors, 2012](#)). Efficient deployment options are feasible for GFRs in contemporary open fuel cycles as well as in more forward-looking closed fuel cycles.

Despite of the great promise of GFRs, so far these systems have not been deployed and operated. No true GFR concept has ever been brought to operation. The marketed promise of GFRs does not come without

complicating factors. For GFRs to fully realize their potential and become technically feasible, enabling engineering solutions are needed to bring the GFR technology to life and assure its commercial success ([Fast Spectrum Reactors, 2012](#); [A Roadmap, 2002](#)). While there are no scientific challenges in bringing GFRs to reality, there are numerous engineering challenges that require solutions before any GFR concept has a chance for its deployment. The main obstacles are reactor vessel and primary system materials, in-vessel structural materials, fast reactor fuel forms suitable for GFR environments, and safety characteristics of GFR configurations. Advances in manufacturing technologies and emergence of novel materials gradually resolve these issues bringing GFRs closer to becoming a reality.

The major perceived economic advantages of GFRs are in their promise to operate at high power densities and with no intermediate loops. The He-cooled GFRs have an advantage of using chemically and neurotically inert single-phase gas although characterized by its extreme mobility and resulting challenges to contain. It has to be noted that challenges of using helium are being addressed and resolved not only in the GFR programs but also in the HTR programs ([Fast Spectrum Reactors, 2012](#); [Weaver, 2005](#)).

These enabling solutions include materials, fuel, control, instrumentation and other design features assuring reliability and safety in extreme operational conditions of GFRs over projected operational lifetimes. The significant challenges of needed enabling technologies resulted in global GFR R&D efforts to deliver on the GFR promise. Significant results have been achieved so far contributing to the expectation of GFRs to become deployable and commercially viable sometime in the future ([Technology Roadmap Update, 2014](#)).

The achieved progress in the development, deployment, and operation of high-temperature Helium-cooled Thermal Reactors (HTRs) brings GFRs closer to the time when they will be able to cross from being promising “paper reactors” to the world of real systems. Some of the needed enabling solutions have already been proposed in the feasibility programs for GFRs ([Fast Spectrum Reactors, 2012](#)).

However, it has also been concluded over the years that further work would be required to advance the GFR technology to the level of prototypes demonstrating its performance characteristics and commercial viability. The key research areas of contemporary GFR R&D efforts include reactor design, fuel, fuel cycles, structural materials, system optimization and, most importantly, safety ([Technology Roadmap Update, 2014](#)).

Developments related to GFRs based on the Generation-I era accomplishments advanced the conceptual premise while further Generation-II–III advancements and subsequent evolving operation and safety considerations allowed to refine the GFR concept as well as contributed some of the vital enabling technologies. The Generation-IV GFR is the culmination of decades of preceding R&D efforts with an expectation of its potential deployment and commercialization by 2030 ([A Roadmap, 2002](#); [Technology Roadmap Update, 2014](#)).

The Generation-IV GFR concept is being developed with the following objectives in mind meeting the Generation-IV reactor criteria: economic competitiveness, enhanced safety and reliability, minimal radioactive waste generation, and proliferation resistance. Safety considerations are of the utmost priority for Generation-IV GFRs.

The GFR cores are inherently characterized by higher core neutron leakage than liquid metals leading to increased fissile loadings that challenge both safety and proliferation resistance characteristics. Higher fissile loadings and harder spectra in GFRs further reduce the fuel Doppler coefficient relative to other fast reactors. Required pressures of GFR systems are around 7 MPa for He-cooled configurations and around 20 MPa for supercritical CO₂-cooled configurations.

High system pressures are needed to compensate for low heat capacity of He and to achieve high thermal efficiency for CO₂, respectively. Highly-pressurized systems require special design provisions to mitigate the potential for and consequences of rapid depressurization scenarios. Generation-IV GFRs have provisions for heat removal from the core in accident scenarios as well as in planned maintenance processes.

At reduced pressures in these systems, natural circulation may not be sufficient for adequate heat removal. This leads to the use of ceramic high-temperature materials in Generation-IV designs to further substantiate the licensing case for GFRs ([Fast Spectrum Reactors, 2012](#); [Weaver, 2005](#)).

The GFR concept is beyond the contemporary nuclear power technologies. The 2002 technology roadmap qualified GFRs based on their potential robust operational domain. The analysis and recommendations have been deeply rooted in the 2000s-era nuclear renaissance expectations.

The updated 2014 roadmap accounts for subsequent accomplishments of over 10-year R&Ds as well as relates to the Fukushima Daiichi accident lessons and contemporary economics of the 2010s. Because needed enabling technologies need to mature to the level of commercial deployment, the GFRs are no longer expected to reach the demonstration phase within the roadmap projected time range ([Technology Roadmap Update, 2014](#)).

As already above-indicated, decades of technology development efforts for GFRs serve as a foundation for deployment expectations assuming vital enabling technologies mature in the coming decades of R&D efforts. Generation-IV GFRs are expected to be the result of international collaborative efforts bringing novel technologies to energy markets and customizing them according to local conditions.

It is expected that global interests in GFRs will ultimately lead to growing practical operational experiences and deployments consequently contributing to establishing and developing the GFR safety case needed for reactor successful licensing and eventual commercialization ([Choi et al., 2006](#)). The objectives are for GFRs to be sustainable, safe, reliable, economically competitive, and proliferation resistant and secure ([Fast Spectrum Reactors, 2012](#); [Weaver, 2005](#)).

4.2 Gas-cooled Fast Reactor technology

Historical GFR concepts as well as the Generation-IV GFR represent an alternative to Liquid-Metal-cooled Fast Reactors (LMFRs). The use of gases leads to a harder neutron spectrum compare to the fast reactor cores of SFRs and LFRs using sodium and lead, respectively ([Fast Spectrum Reactors, 2012](#)).

Harder spectra in GFRs allow for a broad range of fast spectrum system applications ranging from historical breeder cores to Advanced Burner Reactors (ABRs). High breeding ratios, shorter doubling times and high-power densities are characteristic design features of historical gas-cooled fast breeder reactors ([Fast Spectrum Reactors, 2012](#); [Weaver, 2005](#)).

The burner version of GFRs yields higher transmutation efficiencies in waste management application scenarios. Unlike LMFRs operating at near atmospheric pressures, GFRs require significant in-core pressurization thus complicating reactor dynamics in transient scenarios during normal and off-normal situations as well as adding procedures to reactor maintenance schedules compare to LMFRs ([Gas-cooled Fast Reactors, 1972](#); [Fast Spectrum Reactors, 2012](#)).

The Generation-IV GFR design is identified in Generation IV International Forum documents as the reactor concept with significant sustainability expectations. This assertion is based on the reduced core volume and the reactor ability to minimize its own spent fuel inventory as well as to manage uranium resources and actinide waste streams in various future closed fuel cycle scenarios ([Technology Roadmap Update, 2014](#)).

Utilization of gases in GFRs leads to R&D efforts to create power units with GFRs using direct cycle balance of plant configurations based on Brayton cycle options. Gas coolants can be pumped directly through the turbine without the need for an intermediate loop ([Fast Spectrum Reactors, 2012](#)). Expected elevated in-core temperatures result in high energy conversion efficiencies of power units with GFRs in Brayton cycles and potential heat utilization for process heat applications. Furthermore, utilization of high efficiency Brayton cycles minimizes environmental impact of GFRs ([Weaver, 2005](#)).

The historical GFR concepts include designs of smaller 300-MW_{e1}-rated units and 1000-MW_{e1} units. Generation-IV power units with GFRs assume 600 MW_{th} and 2400 MW_{th}. Lower power unit ratings enable modularity and load-follow operation modes as well as facilitate synergies with VHTRs. Higher power unit ratings facilitate neutron economy with consequent reductions of core fuel inventories, are more compatible

with base-load operation modes ([Fast Spectrum Reactors, 2012](#)). The reference Generation-IV GFR is a 2400-MW_{th} configuration consisting of a reactor core unit in a steel pressure vessel. Metal clad fuel elements with oxide or carbide fuels are traditionally considered for GFRs. In recent years, GFRs evolved to adopt ceramic-clad, mixed-carbide-fuelled elements within hexagonal closed-packed lattices pushing all undesirable moderating materials out to the extent engineering design allows; thus, assuring very hard fast neutron energy in-core spectral conditions. The current, most promising viable material choices for in-core structures of GFRs are silicon carbide-based fiber composites ([Fast Spectrum Reactors, 2012](#); [Technology Roadmap Update, 2014](#); [Meyer, et al., 2006](#)).

Table 4.1 summarizes fuel and core configuration options that are being explored for Generation-IV GFRs ([Fast Spectrum Reactors, 2012](#); [Meyer et al., 2006](#); [Ryu and Sekimoto, 2000](#); [Ryu, et al., 2000](#); [Dumaz, et al., 2007](#)). Notably, the core concepts developed for GFRs follow both prismatic block/hexagonal lattice path as well as pebble bed core path ([Weaver, 2005](#); [Ryu, et al., 2000](#)). The high outlet temperatures of GFRs eliminate considerations of steel-based alloys as cladding materials. Ceramic materials and refractory metals are the most feasible in-core materials for GFRs ([Fast Spectrum Reactors, 2012](#)). Silicon carbide composite materials are the potential cladding choices for future GFRs assuming sufficient performance characteristics can be achieved for in-core applications ([Fast Spectrum Reactors, 2012](#)).

The use of helium in Generation-IV GFRs stems from decades of R&D efforts for HTRs ([Fast Spectrum Reactors, 2012](#); [Mahdi, et al., 2018](#)). The projected thermal efficiencies for Generation-IV GFRs can reach 45% to 50% depending on a thermodynamic cycle. The original Generation-IV GFR concept was based on a direct 48% efficient Brayton gas-turbine cycle. The direct cycle evolved into an indirect configuration due to helium ingress effects on gas-turbine bearings. The indirect cycles consider the use of He-N₂ mixtures (20% He and 80% N₂) ([Mahdi, et al., 2018](#)). The attainable efficiencies in those cycles approach 45%.

Alternative gases are also explored including air, steam, and Carbon dioxide (CO₂). Air poses activation and corrosion concerns but is much easier to resupply in LOCA scenarios ([Mahdi et al., 2018](#)). Helium and supercritical CO₂ received the most significant attention as potential coolants for GFRs. For the desired high thermal efficiencies, the use of supercritical CO₂ allows for lower outlet temperatures compare to helium cooled designs while still operating very efficiently ([Fast Spectrum Reactors, 2012](#)). Because thermal decomposition of CO₂ is accelerated starting 700°C, the oxidation/corrosion rates increase significantly beyond those temperatures providing further performance limits for maximum operating temperatures in supercritical CO₂ cooled GFR systems not to exceed 600°C ([Fast Spectrum Reactors, 2012](#); [Weaver, 2005](#)).

Steam introduces cladding compatibility challenges, potential for positive coolant reactivity effects and reduced conversion rates. Carbon dioxide leads to higher pressure drops and associated forces across components, increased acoustic loadings, as well as economic penalties due to increased primary coolant

Table 4.1. In-core design options for Generation-IV GFRs

Fuel	Fuel element	Core configuration
Dispersion fuels	Coated compacts	Hexagonal lattices with stacks of compacts
– Cylinders	Coated plates	Plate-geometry configurations
– Hexagons		Prismatic block arrays
– Spheres		
– Arbitrary geometry		
Microparticle, HTR-type, fuels	Microparticles	Particulate beds
	Spherical pebbles	Pebble beds
– Single size particles	Compacts with coated microparticles	Hexagonal configurations
– Multisize particles		Prismatic block array configurations

pumping requirements. The challenges of CO₂ are potentially off-set by its heat removal and energy conversion advantages (Fast Spectrum Reactors, 2012; Advanced Reactor Concepts, 2012).

The GFR safety case is complicated by the recognized challenges of passive heat removal during accident scenarios, fuel reliability, and in-core materials under extreme conditions of high temperature and fast neutron fields (Technology Roadmap Update, 2014; Advanced Reactor concepts, 2012). It is recognized that although fully passively safe GFRs are possible at lower power densities, the economic competitiveness is challenging for those designs. This can be address through the use of guard (or secondary) vessels for GFRs.

Economics of closed fuel cycles with GFRs as well as other reactor options is not expected to be immediately commercially viable. Closed fuel cycles will be economical at the end of the 21st century or early in the 22nd century assuming conditions of limited fuel resources (Fast Spectrum Reactors, 2012; Technology Roadmap Update, 2014; Weaver, 2005). Implementation of advanced closed uranium-plutonium fuel cycles and thorium fuel cycles with added actinide burning capabilities along with achieving either burning or breeding ratios of choice have been shown to be viable design pathways for future GFRs (Kumar, et al., 2014; Choi, et al., 2006). Table 4.2 provides some representative reference GFR design characteristics (Choi, et al., 2006).

Furthermore, hybrid systems combining advantages of GFRs with advantages of other energy sources as well as integrating power and process heat applications may potentially make the economic case for a Generation-IV GFR more competitive and bring the deployment of these systems closer to reality as it allows fuller realization of their performance potential. Yet, deployment of prototype systems to demonstrate both performance characteristics including reliability and economics is of paramount importance for viability of GFRs. Construction of a GFR prototype would address the limited experience challenge that has impeding GFRs.

4.3 Evolution of Generation-IV GFRs into small modular reactor and micro reactors

In recent years, relatively new, highly deployable types of nuclear reactors are gaining increasing attention—small modular reactors and micro reactors, as the most promising near-term candidates. These are smaller units with thermal power generation capabilities under 30 MW_{th} (10MW_{el}) for micro reactors and under 1000MW_{th} (300MW_{el}) for small modular reactors (Advanced Nuclear Directory, 2021).

Several dozens of small modular reactors and micro reactors are under active development in the United States targeting their deployment in the next decade. These systems are expected to be highly deployable and commercially competitive. In particular, micro reactors are going to be factory-fabricated, highly transportable, and highly adaptable to deployment domains ranging from terrestrial urban environments and

Table 4.2. Representative Generation-IV GFR design characteristics

Design parameter	Value	Design parameter	Value
Thermal power	600 MW _{th}	Number of fuel assemblies	142
Fuel	(U,Pu)C	Number of control assemblies	6
In-core structural material	SiC	Number of radial reflector blocks	180
Reflector material	Zr ₃ Si ₂	Active core height	170 cm
Absorber material	B ₄ C (90% ¹⁰ B)	Active fuel height	34 cm
Inlet-core temperature	395°C	Fuel temperature	1227°C
Core pressure	7 MPa	In-core structural material temperature	665°C

Table 4.3. Generation-IV GFR-based small modular reactors and microreactors

Reactor	Vendor
50 MW _{el} Fast Modular Reactor (FMR)	General Atomics
265 MW _{el} Energy Multiplier Module (EM2)	
1–3 MW _{el} NuGen engine	NuGen

emergency response areas to space power and propulsion. Several of emerging small modular reactors and micro reactor concepts can be considered as Generation-IV GFRs. [Table 4.3](#) provides the list of GFR-based small modular reactors and micro reactors and their developers ([Advanced Nuclear Directory, 2021](#)).

4.4 Conclusions

The Generation-IV GFR is the robust nuclear reactor design offering a broad range of potential applications—from electricity to process heat to waste minimization. The objectives are for GFRs to be sustainable, safe, reliable, economically competitive, and proliferation resistant and secure. Decades of technology development efforts for GFRs serve as a foundation for deployment expectations assuming vital enabling technologies mature in the coming decades of R&D efforts.

References

- Anon., 2002. A Roadmap to Deploy New Nuclear Power Plants in the United States by 2010. Volumes I and II, Nuclear Energy Research Advisory Committee, Subcommittee on Generation IV Technology Planning, U.S. DOE Office of Nuclear Energy, Science and Technology.
- Advanced Nuclear Directory, 2021. Gateway for Accelerated Innovation in Nuclear. Idaho National Laboratory.
- Advanced Reactor Concepts, 2012. Technical Review Panel Report, Evaluation and Identification of Future R&D on Eight Advanced Reactor Concepts, December 2012. U.S. DOE Office of Nuclear Energy.
- Choi, H., Rimpault, G., Bosq, J., 2006. A physics study of a 600-MW(thermal) gas-cooled fast reactor. Nucl. Sci. Eng. 152, 204–218. American Nuclear Society.
- Dumaz, P., All’egre, P., Bassi, C., Cadiou, T., Conti, A., Garnier, J., Malo, J., Tosello, A., 2007. Gas-cooled fast reactors—status of CEA preliminary design studies. Nucl. Eng. Des. 237, 1618–1627. Elsevier.
- Gas-Cooled Fast Reactors, 1972. Proceeding of IAEA Study Group Meeting Sponsored by the USSR State Committee on the Utilization of Atomic Energy, Institute of Nuclear Energy, Minsk, July 24-28, 1972, IAEA-154. International Atomic Energy Agency.
- Kumar, A., Chirayath, S., Tsvetkov, P., 2014. Analysis of a sustainable gas-cooled fast breeder reactor concept. Ann. Nucl. Energy 69, 252–259. Elsevier.
- Mahdi, M., Popov, R., Piro, I., 2018. Research on thermal efficiencies of various power cycles for GFRs and VHTRs. In: Proceedings of 2018 26th International Conference on Nuclear Engineering, July 22–26, 2018, London, England. American Society of Mechanical Engineers.
- Meyer, M., Fielding, R., Gan, J., 2006. Fuel Development for Gas-Cooled Fast Reactors, INL/CON-06-11085. Idaho National Laboratory.
- Anon., 2014. Technology Roadmap Update for Generation IV Nuclear Energy Systems. GENIV International Forum, January 2014, OECD Nuclear Energy Agency for the Generation IV International Forum.
- Ryu, K., Sekimoto, H., 2000. A possibility of highly efficient uranium utilization with a pebble bed fast reactor. Ann. Nucl. Energy 27, 1139–1145.
- Waltar, A., Todd, D., Tsvetkov, P. (Eds.), 2012. Fast Spectrum Reactors. Springer, ISBN: 978-1-4419-9572-8.
- Weaver, K., 2005. Interim Status Report on the Design of the gas-Cooled Fast Reactor (GFR), Gen IV Nuclear Energy Systems, INEEL/EXT-05-02662. Idaho National Laboratory.

Sodium-cooled Fast Reactors (SFRs)

Hiroyuki Ohshima and Shigenobu Kubo
Japan Atomic Energy Agency (JAEA), Ibaraki, Japan

Nomenclature

Subscripts

el electrical

th thermal

Acronyms and abbreviations

AESJ	Atomic Energy Society of Japan
ASME	American Society of Mechanical Engineers
ASTRID	Advanced Sodium Technological Reactor for Industrial Demonstration (France)
BN-350	Fast Sodium (reactor)-350 MW _{el} (БН-350—Быстрый Натриевый (in Russian abbreviations) (Russia))
BOR-60	Fast Experimental Reactor-60 MW _{th} (БОР-60—Быстрый Опытный Реактор (in Russian abbreviations) (Russia))
BR-5	Fast Reactor-5 MW _{th} (БР-5—Быстрый Реактор (in Russian abbreviations) (Russia))
CABRI	Pool-type research reactor operated by CEA (France)
CCFR	China Commercial Fast Reactor (China)
CEA	Commissariat à l'Énergie Atomique et aux Énergies Alternatives (France)
CEFR	China Experimental Fast Reactor (China)
CFR-600	China Fast Reactor-600 MW _{th} (China)
CFV	Coeur 'a Faible Vidange
CRBR	Clinch River Breeder Reactor (US)
DFR	Dounreay Fast Reactor (UK)
EBR-I	Experimental Breeder Reactor I (US)
EBR-II	Experimental Breeder Reactor II (US)
ESFR	European Sodium-cooled Fast Reactor
FBTR	Fast Breeder Test Reactor (India)
FFTF	Fast Flux Test Facility (US)
FP	Fission Product
Gen-IV	Generation IV
GIF	Generation IV International Forum
IAEA	International Atomic Energy Agency
IHX	Intermediate Heat Exchanger
INPRO	International Project on Innovative Nuclear Reactors and Fuel Cycles (IAEA)
JAEA	Japan Atomic Energy Agency (Japan)
JNC	Japan Nuclear Cycle development institute (predecessor of JAEA) (Japan)
JSFR	Japan Sodium-cooled Fast Reactor (Japan)
JSME	Japan Society of Mechanical Engineers
KNK-II	Compact sodium-cooled nuclear reactor (Germany)
LWR	Light Water Reactor

MA	Minor Actinide
NEA	Nuclear Energy Agency (OECD)
ODS	Oxide-Dispersion-Strengthened
OECD	Organization for Economic Co-operation and Development
PFBR	Prototype Fast Breeder Reactor (India)
PFR	Prototype Fast Reactor (UK)
PGSFR	Prototype Gen-IV Sodium-cooled Fast Reactor (Korea)
PRISM	Power Reactor Innovative Small Module (US)
R&D	Research and Development
RCC-MRx	Design and Construction Rules for Mechanical Components in high-temperature structures, experimental reactors and fusion reactors (France)
RSWG	Risk & Safety Working Group (GIF)
SDC	Safety Design Criteria
SDG	Safety Design Guideline
SEFOR	Southwest Experimental Fast Oxide Reactor (US)
SFR	Sodium-cooled Fast Reactor
SNR-300	Kalkar sodium-cooled fast breeder reactor prototype-300 MW _{el} (Germany)
SSC	Structure, System, and Component
SSR	Specific Safety Requirements (IAEA)
TREAT	Transient Reactor Test Facility (US)
TWR-P	Traveling Wave Reactor-Prototype (US)
UK	United Kingdom
US	United States
USDOE	United States Department Of Energy

5.1 Introduction

Since the beginning of the peaceful use of nuclear energy, Sodium-cooled Fast Reactors (SFRs) have a long history of their Research and Development (R&D), led by the United States, Russia (the former Soviet Union), the United Kingdom, and France, followed by Japan and Germany. The focus was to utilize uranium resources by using plutonium, which is generated by the transmutation of ^{238}U during the operation of a reactor. After testing various materials for the coolant, sodium was selected. SFR development has slowed since the late 1980s, presumably because of the commercially successful Light-Water Reactors (LWRs) and the fact that uranium resource depletion was under the surface. Moving into the 21st century, new energy demands arise in developing countries such as China and India, whereas global warming due to the use of fossil fuels and the growing disposal problem of radioactive wastes from LWR spent fuel became major issues. Thus, SFR R&D has been in the limelight again to realize their commercialization, mainly in the United States, Russia, France, the Republic of Korea, Japan, China, and India. The performance for the fuel breeding and power generation is confirmed, and the improvements are identified through the operation experiences of the current and past SFRs. The R&D is turning into a new phase for the demonstration of reactor design, construction, and operation.

5.2 Development history

Since the early days of nuclear energy development, R&D for realizing the fast reactor and the thermal reactor were conducted in parallel. In fact, in 1951, the very first nuclear reactor, Experimental Breeder Reactor-I (EBR-I) in the United States, produced electricity. As for the fast reactor coolant, after some trial works, it was recognized that sodium would be the most suitable coolant among various coolant materials

such as mercury and sodium-potassium alloy. In the 1960s and 1970s, several experimental SFRs were built and operated successfully in the United States (Fermi-1, EBR-II, the Fast Flux Test Facility (FFTF)), the former Soviet Union (Fast Reactor-5 MW_{th} (BR-5)/Fast Reactor-10 MW_{th} (BR-10), Fast Experimental Reactor-60 MW_{th} (BOR-60)), the United Kingdom (Dounreay Fast Reactor (DFR)), France (Rapsodie), Germany (Compact sodium-cooled nuclear reactor-II (KNK-II)), and Japan (Joyo) (Aoto et al., 2014; Cacuci, 2010).

Reflecting the valuable knowledge and experiences gained through the operation of these experimental reactors, the design and construction of prototype or demonstration SFR have started in some countries, such as the former Soviet Union (Fast Sodium (reactor)-350 MW_{el} (BN-350), Fast Sodium (reactor)-600 MW_{el} (BN-600)), the United Kingdom (Prototype Fast Reactor (PFR)), France (Phenix, Super-Phenix), and Japan (Monju) (Aoto et al., 2014; Cacuci, 2010). Through the design, construction, and operation of these SFRs, a great deal of engineering knowledge was accumulated on SFR technology, including plutonium fuel performance, fissile material breeding, operation and maintenance, fuel handling for refueling, the related nuclear fuel cycle process, and the safety features. Concerning the safety features, incident control such as sodium coolant leakage was also attained (International Atomic Energy Agency (IAEA), 1998, 2007). It was recognized that the SFR would be a feasible nuclear technology in the near future.

However, the demand-and-supply balance of the uranium resources did not become as serious as it had been foreseen in the days of introduction of thermal reactors such as LWRs. As a result, many LWRs have been used all over the world to date. On the other hand, SFR development, where the sodium coolant technology and the plutonium technology are deeply involved, had slowed down or completely shut in some countries because of the economical aspect in the short term or the enhancement of the nuclear non-proliferation policy.

After entering the 2000s, nuclear energy caught people's attention again for its capacity of supplying sustainable energy without giving harmful effects to the environment such as global warming. In France, Russia, India, China, the Republic of Korea, and Japan, each country made a development plan for the realization of the next-generation SFR technology, which has economic competitiveness in parallel with further enhanced built-in safety features.

In Russia, although they have faced the slow-down phase in the past, such as a postponement of the construction of BN-800 reactor, they are now attaining excellent capacity factor in the BN-600 reactor, have completed the construction of the BN-800 reactor, and achieved the first criticality in 2014. Since its start-up in 1980, BN-600 has been stably operated for more than 40 years. During this long period, the average load factor is about 75%. Only the long-time outage was that for large maintenance work for a half-year in 1988. After 2014, the load factor has been kept around 85%–88%. The current operation permission is up to 2025, which will be extended up to 2040. Fast Sodium (reactor)-800 MW_{el} (BN-800) achieved 100% power in 2016 and 68% load factor in 2019. It was reported that 160 Mix-Oxide (MOX) fuel assemblies were loaded in February 2021, aiming at transforming the full MOX core in 2022. The Fast Sodium (reactor)-1200 MW_{el} (BN-1200) design has been in progress as the next-generation reactor (Aoto et al., 2014; Shepelev, 2017). In China, an experimental fast reactor has been connected to the grid in 2011 and reached 100% power in 2014 as the result of vigorous R&D as a response to the foreseen large increase in the domestic energy demand. Then a prototype reactor, China Fast Reactor 600 (CFR-600), is planning to be built by 2023, and the following commercial reactor, CCFR, is planned (Huang, 2021). India is also about to start a Prototype Fast Breeder Reactor (PFBR) operation via an experimental reactor, the fast breeder test reactor, foreseeing future construction of the next SFRs (Chellapandi, 2015). France has proceeded a Generation-IV (Gen-IV) SFR prototype project called Advanced Sodium Technological Reactor for Industrial Demonstration (ASTRID) (Rouault et al., 2015; Varaine et al., 2017). According to the update of the multiannual energy plan, the ASTRID project was terminated by the end of 2019, and the R&D program for the development of SFR and associated fuel cycle is continued (Devictor and Abonneau, 2019). The Republic of Korea and Japan proceed in their design of the Prototype Gen-IV Sodium-cooled Fast Reactor (PGSFR) and the Japan Sodium-cooled Fast Reactor

(JSFR), respectively (Yoo et al., 2017; Hayafune et al., 2017a). The conceptual design of the European Sodium-cooled Fast Reactor (ESFR) has been continued in Euratom (Tsige-Tamirat et al., 2019). The United States is continuing a modular SFR development, whereas 4S (Tsuboi et al., 2004), Power Reactor Innovative Small Module (PRISM) (Triplett et al., 2012), and Traveling Wave Reactor-Prototype (TWR-P) (Hejzlar et al., 2013) are being developed in the industry. Natrum is also being developed as a part of advanced reactor demonstration program in the United States. This SFR features a molten salt energy storage system for integrating with renewable energies. Versatile Test Reactor under development in the United States is also an SFR, which will serve the capability for testing and qualification of advanced fuels and materials for various types of reactors. Several countries such as the US, Canada, the UK, and Japan are implementing their national program to support the industry for developing advanced reactor design, including SFRs (Bell, 2017).

In addition to each country's domestic development project, some international frameworks of bilateral and multilateral cooperation, such as the Generation IV International Forum (GIF) (GIF, 2019a), were established by countries conducting fast reactor technology development. Utilizing these international frameworks, each country is promoting the SFR development project while balancing international competition and international cooperation (Hayafune et al., 2017b; Vasile et al., 2017). In the GIF, the member states and international organizations have recognized the importance of having an international safety design standard or Safety Design Criteria (SDC). The task force to develop the GIF, SFR SDC started the work in 2011 and completed the SDC report in 2013. Nowadays, Safety Design Guidelines (SDGs) are developed to support the practical application of the SDC in the design process for safety improvement (IAEA, 2021).

5.3 System characteristics

5.3.1 Design features with sodium properties

Sodium properties are shown in Table 5.1 (Sodium Technology Education Committee, 2005; Japan Nuclear Cycle development institute (JNC), 1986). Sodium is used as a liquid metal coolant for the fast spectrum reactor. It has a rather high atomic mass number and good neutronic features. Its neutron cross section is small enough to make a critical system with a fast neutron spectrum. For uranium-plutonium (U-Pu) fuel, breeding can be obtained only with a fast neutron spectrum. Using sodium as coolant, the neutron spectrum is

Table 5.1. Sodium and light water properties

Item	Sodium	Light water
Mass number of natural isotopes	23	H:1, O:16
Absorption cross section to thermal neutron (0.025 eV)	0.53 b	0.66 b
Total cross section to thermal neutron (0.025 eV)	3.9 b	104 b
Melting point	97.82°C	0°C
Boiling point (at atmospheric pressure)	881.4°C	100°C
Density (liquid) (kg/m ³)	856 (400°C)	770 (277°C, 15 MPa)
	820 (550°C)	660 (327°C, 15 MPa)
Thermal conductivity (liquid) (W/mK)	72.2 (400°C)	0.5 (327°C, 15 MPa)

hard enough to provide breeding performance with U-Pu fuel. A major radioactive isotope generated by neutron capture is ^{24}Na with a half-life of 15 h. Another radioactive isotope is ^{22}Na with a half-life of 2.58 years. Gamma rays from those isotopes have to be taken care of for maintenance.

From the viewpoint of heat transfer, sodium has attractive features such as a relatively high boiling point (881°C) and high thermal conductivity. Thanks to these features, the reactor core can be designed with high power density without pressurization. For the power generation, high-temperature dry steam (superheated steam) can be provided from sodium-heated steam generators with an operation temperature of approximately 500°C, and a high-performance steam turbine system similar to the one used in subcritical-pressure fossil power plant with the dry steam. From a safety point of view, the coolant inventory necessary to submerge the core can be maintained without pressurization in operating and under accidental conditions because of the high boiling point. The natural circulation capability is excellent because of the high thermal conductivity, high system temperature, and large temperature difference between the core inlet and outlet coolant. Several experimental and prototype reactors succeeded in demonstrating the full natural circulation capability of decay heat removal (Lucoff et al., 1992; Tenchine et al., 2012). Compatibility with structural materials is excellent under the deoxidization condition. Corrosion and surface changes of structural materials can be controlled during the plant lifetime by controlling and monitoring concentration of impurities such as hydrogen and oxygen. On the other hand, chemical features are active. Liquid sodium in the air burns spontaneously in certain conditions and reacts with water, producing hydrogen and heat. Measures for sodium fire and sodium-water reaction should be taken into account in the system design. In maintenance operation, the sodium temperature is maintained at approximately 200°C, which is much higher than the melting point of 98°C. Because of the high-temperature conditions, chemical reactivity, and liquid-metal opacity, maintenance on SFRs requires further development of inspection and repair technologies.

5.3.2 Core configurations

Schematic views of the typical core configurations for SFRs are shown in Figure 5.1. The core consists of core fuel, control rods, blanket fuel, and shields. In general, the core fuel is a mixture of plutonium and depleted uranium. The blanket fuel is depleted uranium. The chemical forms of the fuel element, close to its final stage of development, are oxide and metal (U-Pu-Zr alloy). Nitride fuel is also available. The neutron absorber used in control rods is Boron Carbide (B_4C).

In the core fuel region, fissile nuclides such as ^{239}Pu and ^{241}Pu undergo fission to produce energy and excess neutrons. At the same time, in the core and blanket fuel regions, fertile nuclides such as ^{238}U and ^{240}Pu contribute to the fissile nuclides breeding by efficiently capturing excess neutrons. Compared with LWRs, the burn-up reactivity change is rather small because of the conversion of fertile nuclides to fissile ones in the core fuel region, which results in the high fuel burn-up and long operation cycle length, and less reactivity control requirement.

A homogeneous core is shown in Figure 5.1a. The core fuel region is surrounded by axial and radial blanket fuels so that the leaking neutrons from the core fuel region can be captured efficiently by the blanket fuels. The core fuel region consists of a few (two in most cases) types of fuel with different plutonium enrichments. The outer core fuel has higher plutonium enrichment than that of inner core fuel to flatten the radial power distribution.

A heterogeneous core configuration uses fertile blanket fuels in the core fuel region. There are two types of core design: the axial heterogeneous core and the radial heterogeneous core, as shown in Figure 5.1b, c, respectively. The neutron leakage from the core fuel region to the internal blanket fuel region is enhanced in these core configurations, which yield higher breeding ratios and reduced sodium void reactivity compared with those of the homogeneous core, but it requires higher fissile fuel inventories.

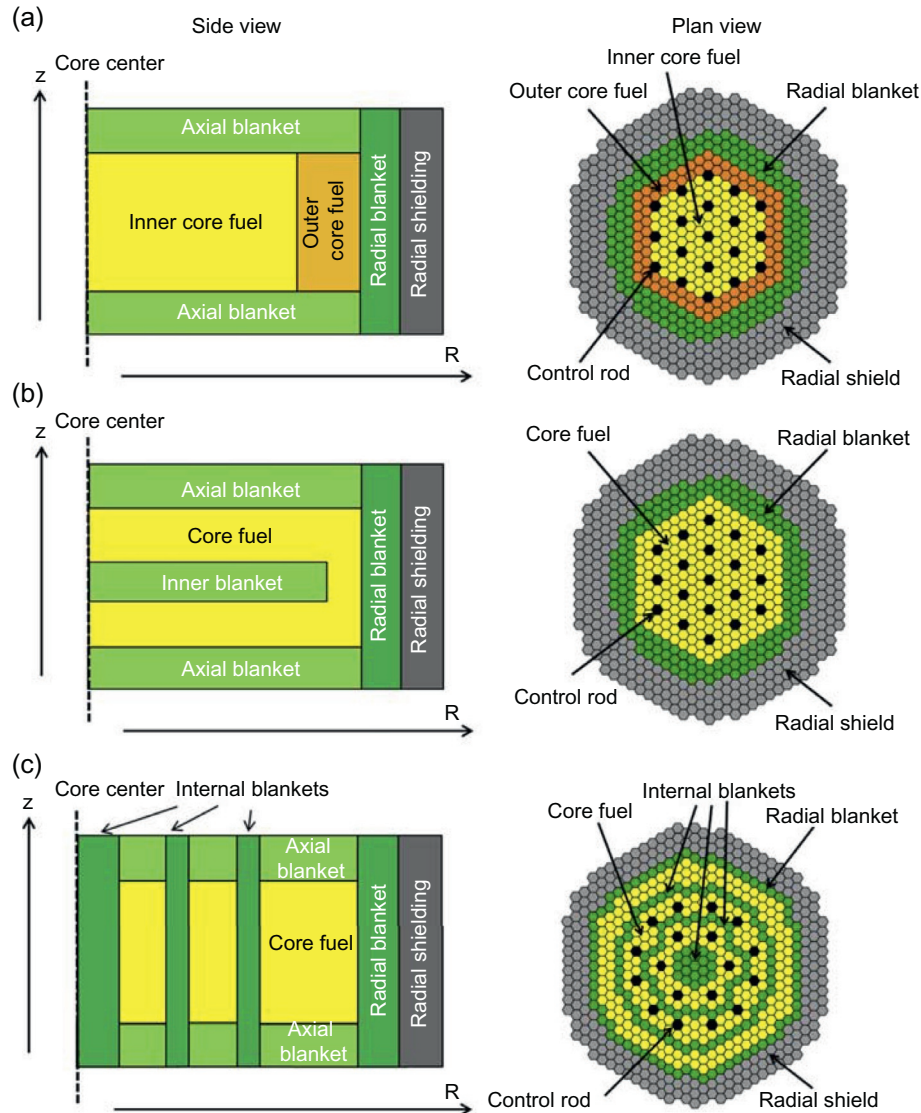


Figure 5.1. Typical homogeneous and heterogeneous SFR core configurations: (a) homogeneous core, (b) axial heterogeneous core, and (c) radial heterogeneous core. *All rights reserved by JAEA*

Figure 5.2 shows a typical core fuel element (also called a fuel pin) and fuel assembly (also called a fuel subassembly). The core fuel element contains the core fuel, upper and lower axial blanket fuels, and a space called the fission gas plenum within a cladding tube. Then they are assembled as a fuel element bundle. The fuel assembly contains the fuel element bundle in a hexagonal assembly duct called a wrapper tube.

The cladding and wrapper tubes are made of high-strength stainless steel that can endure high-temperature and fast-neutron irradiation conditions.

The fuel elements are separated by a spiral wrapping wire (alternatively, grid spacers can be used). The sodium coolant flows through the spaces between the fuel elements. The fuel elements are placed in a tight triangular lattice arrangement to maximize the fuel volume fraction for core neutron performances and to minimize the core size for the plant capital cost reduction.

In recent SFR developments, some advanced ideas have been introduced to core conceptual designs. From an economic point of view, Japan and France proposed a large homogeneous core concept with a high internal conversion rate (Mizuno et al., 2005; Buiron et al., 2007). Large-diameter fuel elements were used to

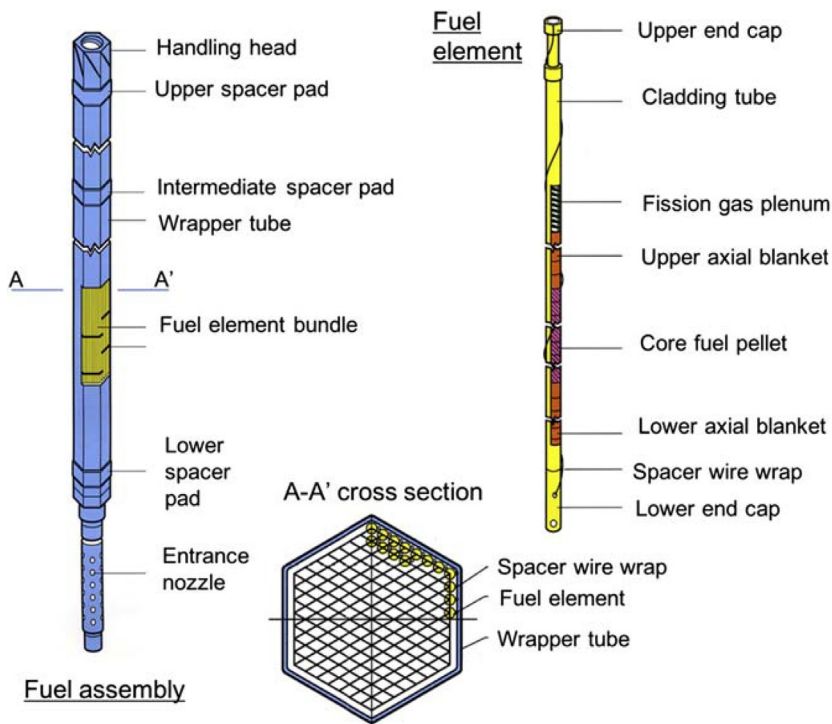


Figure 5.2. Typical SFR core fuel element and fuel assembly. *All rights reserved by JAEA*

increase the internal conversion ratio, which provided a high total fuel burn-up (including core and blanket fuel), a long operation period, and a sufficient breeding ratio with a small amount of blanket.

To enhance safety, France made a decision to adopt an innovative core concept with low sodium void reactivity, called *Coeur 'a Faible Vidange* (CFV) (Sciora et al., 2011). The CFV is an axially heterogeneous core with a stepwise core height and a sodium plenum. This configuration exhibits the multiplier effect on the significant reduction of sodium void reactivity coefficients. The concept of an upper sodium plenum had been originally proposed by Russia in the 1980s and introduced in BN-800.

Because of the rich neutron economics, the SFR core has a large design flexibility. Depending on the requirements of place and time, the core can be designed not only as a breeder but also as a burner. In typical burner-core designs (Languille et al., 1995; Yang et al., 2007), the blanket fuels are eliminated, and the plutonium enrichment is increased to reduce the internal conversion ratio by means of, for instance, reducing the core height (pancaking the core shape), introducing diluent material, and so on.

5.3.3 Plant system

An overview of a typical SFR system is shown in Figures 5.3 and 5.4. The core is accommodated in the reactor vessel. The reactor vessel is generally composed of a vessel and a plug because of its low-pressure conditions. Sodium generally has a liquid level in the vessel and is covered by inert gas. Sodium-contained components of the SFR, including the reactor vessel, are designed as thin-walled structures because the major load comes from the thermal stress due to transient temperature change under elevated temperature. Although its internal pressure is not a critical load factor, the seismic load can be critical in the design of the components depending on the site condition. A seismic isolation system is useful for SFRs to reduce the seismic load on the sodium-containing components. Most plants adopt guard or safety vessels outside of reactor vessels that can maintain the sodium level in case of a primary sodium leak. The plug is required to have functions of thermal insulation and shielding against high operation temperature and high neutron flux.

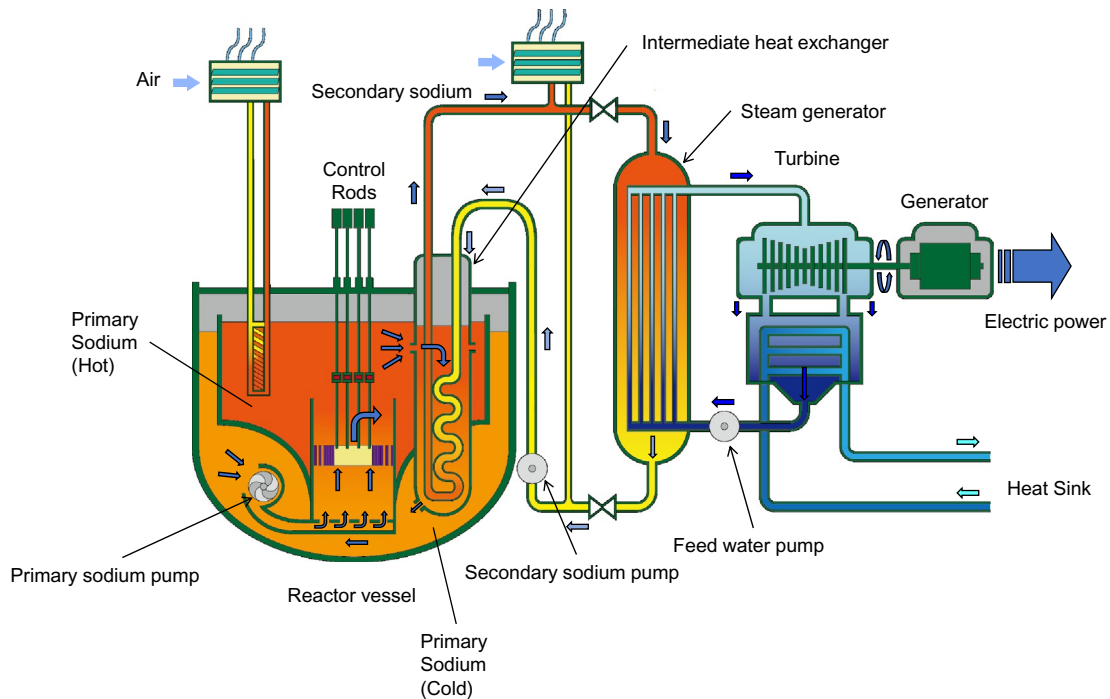
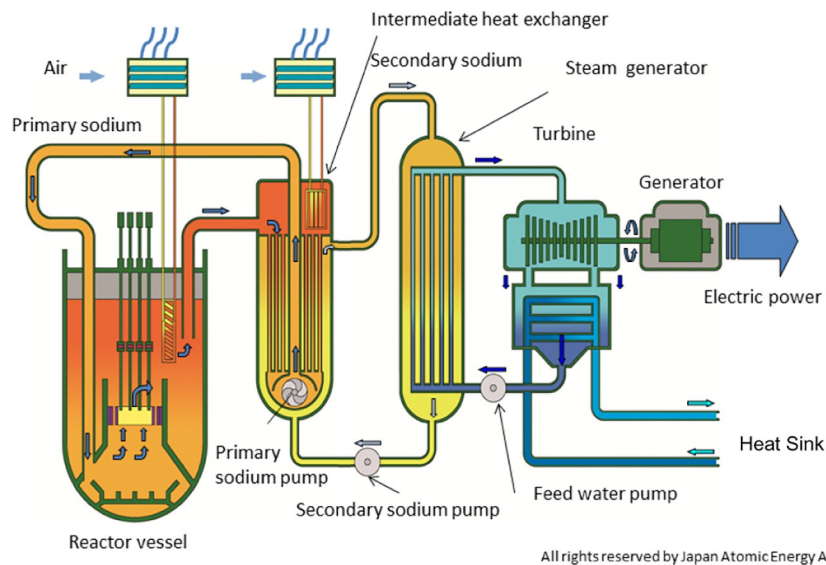


Figure 5.3. SFR system (pool type). *All right reserved by JAEA*



All rights reserved by Japan Atomic Energy Agency

Figure 5.4. SFR system (loop type). *All rights reserved by JAEA*

On the plug, an upper core structure is installed and provides control rod driver line guides and support for core instrumentations. The control rods are inserted from above the core by gravity or other acceleration devices. Because of the chemical reactivity of sodium, fuel handling is generally operated under the plug with special fuel handling machines and rotating plugs. That fuel handling under the plug affects the diameter and height of the reactor vessel.

For the cooling system, there are the primary sodium cooling systems, secondary sodium cooling systems, and steam-water cooling systems. Because SFRs generally use steam turbines for energy conversion, system design has to take care of sodium-water reaction at sodium-heated steam generators. To protect the core from

the effects of the sodium-water reaction, an SFR generally has intermediate cooling systems (secondary cooling systems).

Major components in the primary cooling system are primary pumps and Intermediate Heat Exchangers (IHXs). Primary pumps have redundancy, and mechanical pumps are generally selected. A few experimental reactors selected a single mechanical pump or electromagnetic pumps for the primary system. IHXs transport heat generated in the core from the primary sodium to the secondary one. The shell and tube type with straight tubes is generally used. Supporting the primary cooling system, a primary sodium purification system, a sodium charge-drain system and a cover gas system are required.

A major role of the secondary cooling system is to create dry steam at the sodium-heated steam generators. Because the secondary sodium temperature can be designed at approximately 500°C, the steam conditions can be similar to those of the subcritical-pressure fossil power plants, and the thermal efficiency is approximately 40%. For the sodium-heated steam generator, several designs were tested as mockups or in the existing reactors (Chikazawa et al., 2008). Recent designs generally select straight or helical coil tube types based on previous studies. Water is in the tube side, and sodium is in the shell side, generally considering pressure conditions and material coexistence. In some designs, steam generators are divided into an evaporator, superheater, and reheater or an evaporator and superheater. Recent designs tendency is an integral type. In some designs, double or triple tubes are selected to prevent or mitigate the sodium-water reaction. For the secondary pump, mechanical pumps were generally selected in the past reactors. Only a few experimental reactors selected electromagnetic pumps. Supporting the secondary cooling system, a secondary sodium purification system, a sodium charge-drain system and a cover gas system are required. Those systems are independent from those of primary systems because the sodium in the primary system is radioactive.

Decay heat could be removed by the steam generators or by installing independent systems cooled by the air. Because of the lower system pressure, an emergency core cooling system such as a coolant injection system required in LWRs is not required. Furthermore, in the case of air-cooling systems, because of the sodium features, several experimental and prototype reactors succeeded in demonstrating the full natural circulation capability of decay heat removal.

Because of the chemical reactivity of sodium, the fuel-handling system is completely different from that of LWRs. The refueling at the reactor vessel is generally operated under the plug. For the ex-vessel handling system, various types of systems were tested in the past reactors (Chikazawa et al., 2009). For spent fuel transportation, decay heat has to be removed during transportation. Inert gas cooling or sodium pot transportation is generally selected. For the spent fuel storage, in-vessel and/or ex-vessel sodium storages are selected. Spent fuels are washed to remove active sodium and transferred to the secondary non-sodium storage or other facilities such as test facilities after being stored under sodium.

Maintenance and repair under high-temperature sodium conditions of approximately 200°C have been taken into account in the plant design. Under sodium viewer or volumetric testing devices in sodium conditions have been proposed and are still under development. Access routes for such testing devices shall be provided in the plant design. Because of the high melting point, sodium heating is required to prevent sodium freeze.

5.3.4 Loop type and pool type

SFRs could be categorized into two types: loop and pool types (Figures 5.3 and 5.4). In the loop types, major components in the primary systems are connected by piping. Existing reactors have nozzles on the reactor vessels for the piping. Some advanced designs eliminate nozzles adopting piping through the plug. The pool-type system accommodates major primary components inside of the reactor vessel. Primary pumps and IHXs are located on the reactor vessel plug, and hot and cold sodium are separated by reactor

Table 5.2. Pool- and loop-type reactors in the world

Countries	Pool	Loop
United States	EBR-II	EBR-I, Fermi, SEFOR, CRBR ^a , FFTF
United Kingdom	PFR	DFR
France	Phenix, Super-Phenix	Rapsodie
Germany		KNK-II, SNR-300 ^b
Russia	BN-600, BN-800	BOR-60, BN-350
India	PFBR	FBTR
China	CEFR	
Japan		Joyo, Monju

^a Terminated during construction.

^b Terminated before operation.

CEFR, China Experimental Fast Reactor; CRBR, Clinch River Breeder Reactor; DFR, Dounreay Fast Reactor; EBR, Experimental Breeder Reactor; FFTF, Fast Flux Test Facility; FBTR, Fast Breeder Test Reactor; SEFOR, Southwest Experimental Fast Oxide Reactor.

vessel inner structures. Advantages of the loop type are a compact reactor vessel/structure that can be fabricated in the factory and has better seismic resistance. On the other hand, those of the pool type are large thermal inertia and primary sodium contained by a simple vessel. In recent comparative studies (United States Department Of Energy (USDOE) and GIF, 2002; Chikazawa et al., 2011; Francois et al., 2008; Devictor et al., 2013), both concepts are technologically feasible and meet design goals. Adopting innovative cost-reduction technologies, the loop type shows slightly lower construction costs. Table 5.2 shows past and existing pool- and loop-type reactors in the world. Many experimental and prototype reactors chose the loop type. From the viewpoint of operational experiences in the prototype class, BN-350 had operational experiences, and Monju is the only existing reactor as the loop prototype because the Clinch River Breeder Reactor (CRBR) and Kalkar sodium-cooled fast breeder reactor prototype-300MW_{el} (SNR-300) were terminated before operation. For the pool type, PFR, Phenix, and BN-600 accumulated operational experiences. BN-600 is still in operation, and BN-800 has started operation. As the next-generation reactors, PRISM, ASTRID, BN-1200, and PGSFR have selected the pool type. JSFR has adopted the loop type, reducing construction costs with innovative technologies (Kamide et al., 2015).

5.3.5 Consistency with fuel cycle system (fuel cycle technology)

Fuel cycle studies showed that SFRs could contribute to worldwide sustainable development with the assurance of stable energy sources and consideration of environmental destruction issues. Currently operating LWRs with low-enriched uranium containing 3%–5% of ²³⁵U utilize only less than 2% of the natural uranium energy potential. Depending on the available resources and prices of natural uranium, the nuclear energy utilization of only ²³⁵U has a possibility to face the limitations in approximately 100 years. However, the nuclear fuel recycling with SFRs can produce more than 50 times energy as compared to that of LWRs from the same quantity of natural uranium. This means that SFRs potentially extend the uranium resources by several thousands of years. Moreover, the SFR technology is essential not only as an energy supply but also

as the prevention of greenhouse gas emission; thus, it will be one of the important future energy sources available for long-term global development. Many studies discussed the timing for the deployment of the commercial SFR and the transition strategies from LWRs to SFRs ([Organization for Economic Co-operation and Development/Nuclear Energy Agency \(OECD/NEA\), 2017](#); [IAEA, 2018](#)). LWRs have already converted (and will convert) some ^{238}U to plutonium in their operation. There already exists enough ^{238}U as depleted uranium from the uranium enrichment process. Therefore, the introduction of SFRs seems consistent with the current LWR system in terms of the nuclear material supply. The breeding ratio necessary for SFRs is estimated as 1.0–1.2 and more depending on the deployment scenarios.

Another benefit for the SFR fuel cycle system is the reduction of the environmental burden by recycling all actinide nuclides and partitioning selected Fission Products (FPs). The spent fuel contains Minor Actinides (MAs) (i.e., neptunium, americium, curium, etc.) as well as uranium and plutonium. In the conventional nuclear fuel cycle, those MAs and FPs are disposed in a deep geological repository as high-level radioactive wastes. Because of the long-lived radioactive MAs such as ^{241}Am (half-life: 433 years) and ^{237}Np (half-life: 2.1 million years), it takes several hundred thousand years to reduce the radiotoxicity of high-level radioactive waste to the level of natural uranium. Therefore, the partitioning and transmutation approach has been studied in several SFR developing countries. SFRs are excellent in their neutronic characteristics for the capability of using MAs as the nuclear energy resources and the resulting MA minimization in the closed fuel cycle. The recycling of plutonium and MAs make great contributions to the reduction of radiotoxicity in the waste: studies showed that it could shorten the duration to bring it into the natural uranium level down to only a few hundred years. Moreover, the high-level waste volume and necessary repository area can be reduced by removing not only the heat source nuclides such as ^{241}Am but also some influential FPs on the strength of vitrified wastes.

Note that the radiotoxicity reduction strongly depends on the nuclide losses during reprocessing. The following high-level development target is pursued in most of the development projects ([Sato et al., 2005](#); [Commissariat à l'énergie atomique et aux Énergies Alternatives \(CEA\), 2012](#)): the reprocessing losses of plutonium and MAs are less than 0.1%.

The high decay heat and radioactivity of MA-bearing fuel have a large influence on the fuel fabrication, transportation, and handling, which gives many development challenges to the fuel cycle system.

5.4 Safety issues

5.4.1 Safety design criteria and safety design guidelines

For LWRs, the IAEA established comprehensive and systematic safety standards that consist of safety fundamentals ([IAEA, 2006](#)), requirements ([IAEA, 2016](#)), and guides ([IAEA, 2019a, b, 2020](#)). The GIF has developed safety principles for the next-generation nuclear energy systems that are safety goals under the GIF technology roadmap ([GIF, 2014](#)) and the basis for the safety approach ([Risk and Safety Working Group \(RSWG\)-GIF, 2008](#)). These documents correspond to the upper level of the IAEA safety standards, whereas there were no documents corresponding to safety requirements and guides for Gen-IV reactors on the basis of international consensus.

SFRs are one of the most promising reactors and are expected to enter the demonstration phase sometime after 2020 ([GIF, 2014](#)). Gen-IV SFR prototype/demonstration reactors are progressing into the conceptual design stage for future licensing applications. It was therefore indispensable to establish internationally harmonized safety design requirements/criteria for the realization of enhanced safety designs common to different SFR systems. With this background, the development of SDC for SFRs, corresponding to the IAEA Specific Safety Requirements (*SSR*)-2/1, was initiated in 2011. The objective of this SDC is to provide reference criteria of the safety approach, mainly focusing on specific criteria to the fast spectrum reactor and the sodium coolant.

The Fukushima Daiichi nuclear power plant accident has emphasized the importance of designing nuclear systems with a higher level of safety than existing reactors. Lessons learned from the accident have been reflected in the SDC, in particular indicating the need for reliable decay heat removal over long periods as well as the necessity of enhancing design measures against external hazards. Taking SFR characteristics into account, the SDC was introduced to enhance safety measures against severe accidents by utilizing inherent and passive safety features. SFR safety experts developed the SDC report (Phase 1) in May 2013, and this report was referred to as the basic document for discussions between the GIF and the IAEA/The International Project on Innovative Nuclear Reactors and Fuel Cycles (INPRO) in terms of developing the international safety standardization (Nakai, 2015). Since then, external reviews of this report have been performed by regulatory authorities of the GIF-SFR member countries and the IAEA, etc. (Okano et al., 2014). The SDC report was revised based on the feedback and the revision of IAEA SSR-2/1 (GIF, 2017).

During the development, the GIF-SDC developers suggested to establish more detailed guidelines, which correspond to the IAEA safety guides, to support practical application of the SDC and to discuss further specific items, such as practically eliminated accident conditions. Since May 2013, the GIF-SFR members have been developing SDGs (Nakai, 2014). In the early stage of SDG development, the SDG on safety approach and design conditions are developed to be used as a supplementary technical document for SDC clarification in 2015 (GIF, 2019b). In the latter stage, the SDG on the key Structures, System, and Components (SSCs) will be developed by around 2019, which provides recommendations in considering the design of SSCs important to safety and supports the practical application of the SDC and the SDG on Safety Approach to the design of safety-related SSCs. The SDG on SSC covers SFR specific points related to three fundamental systems: (1) reactor core system, (2) coolant system, and (3) containment system. These recommendations on the specific SSCs are developed to clarify the safety requirements for the Gen-IV SFR systems (Kubo et al., 2018).

5.4.2 Safety characteristics and safety design

Each country has also been making efforts on the design study and also on R&D of SFR systems to enhance the safety depending on the safety characteristics and to satisfy the high safety demands required by the SDC.

5.4.2.1 Reactor shutdown

A SFR is operated under a critical condition with fast neutrons using liquid sodium as the reactor coolant, allowing high power density. Positive reactivity insertion might happen, because of fuel compaction in the degraded core, because the core is usually not designed in the most critical configuration. Although the sodium void reactivity depends on the core size and design, it is generally positive at the center of the core in a large-sized core. Active shutdown systems are provided in the existing SFR designs with diversity so that core damage caused by a design basis accident can be prevented. To further improve the safety of SFRs, a passive shutdown mechanism or inherent negative reactivity feedback or their combination is considered as one of the core damage prevention measures even under active shutdown system failure. The effect of the inherent reactivity feedback for the mitigation of power increase has been demonstrated in EBR-II and Rapsodie (Lucoff et al., 1992; Kriventsev et al., 2017), and its related R&D is undertaken for reactor application. As for the metal fuel core, R&D is underway to investigate the inherent reactivity characteristics with negative reactivity effects due to thermal expansions of control rod drive lines and fuel assemblies (Chang et al., 2011; Tae-Ho, 2015). For example, core designs with an upper sodium plenum and heterogeneous configuration are currently being developed for an intermediate to a large-sized reactor with an oxide or nitride fuel core so as to make an effective coolant temperature reactivity-coefficient negative or zero (Verrier et al., 2013; Chebeskov, 1996; Puthiyavinayagam et al., 2017; Venard et al., 2017; Belov et al., 2017). Passive reactor shutdown systems that utilize a Curie-point magnetic alloy (Nakanishi et al., 2010; Saito et al.,

2017), thermal expansion, and hydraulic force change (Alexandrov et al., 1996; Dufour, 2015) for automatic de-latching/insertion of control rods under loss of flow, and that increase neutron leakage by gas expansion under a flow reduction condition in pipes filled with gas, are under development (Triplett et al., 2012).

5.4.2.2 Decay heat removal

The large temperature margin to sodium boiling (the boiling point is 880°C, the melting point is 98°C at atmospheric pressure) enables reactor operation in a wide range without pressurization of the reactor coolant systems. The high thermal conductivity of sodium provides heat removal from the core with high power density. Because an SFR is operated at low pressure, a sodium leakage accident does not lead to loss of coolant due to flashing. Therefore, it enables to maintain the coolant level for reactor cooling by providing back-up structures that can retain leaked sodium. Moreover, decay heat removal can be achieved by its natural circulation capability to an ultimate heat sink (atmosphere) utilizing the high heat transport capability and temperature difference between the core inlet and outlet coolant. These safety features had been adopted into the design since its experimental stage, then Joyo (Sawada et al., 1990) and Phenix (Guidez, 2013) have demonstrated the natural circulation capability. In addition, a SFR with the primary and secondary systems (sodium) together with the tertiary system (water/steam) allows various combinations of diversified systems because of its flexibility in items such as types of heat exchangers and the installation locations. For practical elimination of accident situations that result in core damage from a complete loss of decay heat removal function, a cooling system design is pursued to maintain its function against extreme internal and external hazards using an appropriate combination of redundancy and/or diversity of systems and the natural circulation function (Kubo and Shimakawa, 2015; Tae-Ho, 2015; Dufour, 2015; Triplett et al., 2012).

5.4.2.3 Design measure against sodium chemical reactions

Typical influences of accidental sodium chemical reactions in SFRs are possible interruption of safety functions such as decay heat removal due to leaked sodium combustion in air and possible damage to the secondary sodium cooling system, especially, on the boundary between the primary and the secondary sodium cooling system in IHX, because of the sodium–water reaction induced by heat transfer tube failure in a steam generator.

Numerous sodium-combustion experiments have been conducted to understand the consequences and phenomenology, and analysis tools have been developed in various countries (Cherdron, 1996; Malet, 1996; Olivier et al., 2007, 2008; Yamaguchi et al., 2001; Ohno et al., 2012; Sathiah and Roelofs, 2014; Chikazawa et al., 2014; Lebel and Girault, 2017; Aoyagi et al., 2017; Vinogradov et al., 2017). Sodium leak events experienced in the plant operation gave feedbacks on the design, manufacturing, and operation. For the prevention of sodium leaks, a simple design with less branching or fewer connection pipes should be pursued. Early detection of leaks and mitigation of sodium combustion are important. For the mitigation, a guard vessel and a guard pipe are feasible to suppress leakage and combustion (Yamano et al., 2012). Sodium components and pipes are installed in the room, which is filled with an inert gas such as nitrogen, and steel liner is also provided for another design measures to mitigate sodium chemical reactions to prevent leaked sodium from contacting the floor or wall concrete.

Design measures have been developed based on the operational experiences of past and current SFRs and the relevant R&D. When a water leak happens at a steam generator, a corrosive sodium-water product jet is generated in the shell side and attacks other tubes. Because the sodium-water reaction accompanies hydrogen and heat generation, it also causes pressure elevation. Prevention and mitigation of sodium-water reaction are important in the sodium-heated steam generator design. For the steam generator leak protection, systems of leak detection, steam blow down, and pressure relief are installed. Rupture disks located in the sodium side of the steam generator passively burst by pressure increase due to the sodium-water reaction. The rupture disks are connected with the sodium–water reaction product treatment system. Because

steam generators become larger in size as the plant power increases (Vasyaev et al., 2015), higher sensitivity for the detection systems and quicker response for the mitigation systems will be required for the future SFRs (Hune et al., 2015). Analysis tools for the sodium–water reaction, which can simulate complicated coupling of thermal hydraulics, chemical reaction, and structural response, have been developed (Takata et al., 2009). A double-walled tube is a possible measure for prevention and mitigation of the sodium-water reaction (Enuma et al., 2015). A gas turbine system is considered for elimination of the sodium-water reaction (Cachon et al., 2012).

5.4.2.4 Containment measures

By means of the above-mentioned design measures, core damage can be prevented even under plant conditions beyond the design basis accidents. However, consequences of core damage are evaluated, and design measures are provided from the viewpoint of defense-in-depth. Typical initiating events that might result in core damage situations are unprotected transients for SFRs (Walter et al., 2012). In a loss of flow type unprotected transient, the reactivity effect comes from coolant boiling characterized by the power change at the beginning, the so-called “initiating phase.” The degree of the power increase depends on the core reactivity characteristics, including coolant void reactivity. Although the coolant void reactivity is positive, there are competitive negative reactivity effects such as Doppler, axial expansion of intact fuel, and failed fuel dispersion. Thus, prompt criticality can be prevented. It is reported that the limit value for oxide fuel cores is approximately \$6 to prevent prompt criticality (Suzuki et al., 2014). Such kinds of evaluations are made by analysis tools based on the experimental data related to fuel pin failure and failed fuel behavior obtained in the safety research reactors such as Pool-type research reactor operated by CEA (CABRI) and Transient Reactor Test Facility (TREAT) (Nonaka and Sato, 1992; Kayser and Papin, 1998; Bauer et al., 1990; Weber, 1988; Kang et al., 2017). The subsequent accident phase is called the “transition phase,” in which core damage progression depends on the extent of core damage in the initiating phase, net reactivity, power, and cooling conditions. In case of insufficient cooling, degraded core materials greatly increase their mobility as core melt escalates due to wrapper tube failure and molten materials such as fuel and steel. According to analyses for oxide fuel cores, severe recriticality might happen because of mobile fuel compaction under certain conditions (Kondo et al., 1992; Maschek and Asprey, 1983; Maschek et al., 1992; Yamano et al., 2008; Bachrata et al., 2015). The core expansion due to massive fuel vaporization, causing significant pressure load on the reactor vessel and reactor roof via the surrounding liquid sodium, might happen when the recriticality event is so severe. Therefore, prevention of such excess energy release due to recriticality and maintaining reactor and cover gas boundary function are important. As a design measure to prevent severe recriticality under core degradation, core designs with steel duct structures for molten fuel discharge are developed (Suzuki et al., 2014; Bertrand et al., 2017; Serre et al., 2017). On the other hand, the structural response of the reactor vessel and reactor roof to the core expansion has been studied using scale models (Chellapandi et al., 2013; Nakamura et al., 2004). A numerical analysis code was also developed for the assessment of mechanical energy and structural response (Onoda et al., 2017). Sodium inside of the reactor vessel is useful to cool the degraded core. Because sodium has the retention capability of radioactive materials in the core, it is desirable to submerge the core even in the case of core damage. Design measures to achieve in-vessel retention have been developed (Suzuki et al., 2014; Bertrand et al., 2017; Serre et al., 2017; Osipov et al., 2013).

5.5 Future trends and key challenges

Technology and experience have been accumulated from actual reactor plant design, construction, and operation throughout the long development history of SFRs, and now it has reached the technical maturity

to move toward the demonstration phase to realize the sustainable energy supply system. R&D is moving on to the important aspects in realizing closed fuel cycle as a sustainable energy supply system; excel in safety and reliability, economic competitiveness, minimizing radioactive waste and radiotoxicity, and proliferation resistance and physical protection.

The basic safety design technology has been established through the history of the design, construction, and operation of SFRs, and the next step is to adopt new design features for reactor shutdown/cooling utilizing inherent characteristics or a passive mechanism. The design with a combination of conventional active safety features and inherent characteristics or passive mechanisms is pursued so that the core degradation is extremely unlikely to occur even though the design extension conditions and the design basis accidents are taken into account. Furthermore, the mitigation measures against core degradation are investigated, and evaluation and design measures are studied to achieve in-vessel retention and cooling of the degraded core material by taking advantage of the sodium physical properties and the low system pressure. The following R&D activities are held in GIF ([GIF, 2014](#)).

Inherent safety features:

- Safety principles (reactivity feedback, core design goals, balanced safety approach),
- Passive or self-actuated shutdown system,
- Decay heat removal options (short- and long-term),
- Reactor transient behavior and testing experience, and
- Severe accident prevention.

Severe accident mitigation:

- Experiments on fuel melting behavior,
- Specialized fuel assembly design for severe accident behavior (e.g., sacrificial inner duct), and
- Core catcher options.

Safety analysis tools:

- Validation and uncertainty quantification,
- Severe accident modeling, and
- Probabilistic safety assessment techniques.

Lessons learned from the Fukushima Daiichi nuclear power plant accident ([Atomic Energy Society of Japan \(AESJ\), 2015](#)) should be reflected so that sufficient countermeasures are provided for a severe external event or possible multiple events and possible subsequent events such as long-term loss of external power. Seismic isolation is effective in enhancing the structural design margin against earthquakes; for instance, a combination of laminated rubber bearings and hydraulic dampers are developed as a seismic isolation system for the reactor building. Natural convection is a possible effective measure for decay heat removal against the long-term loss of external power. Electrical equipment important to safety should be protected against floods or tsunamis to avoid failure as in an LWR. In addition, the area where the sodium-containing facility is installed also needs countermeasures against flooding. Key issues in GIF are as follows ([GIF, 2014](#)):

- Robust and highly reliable systems for adequate cooling of safety-relevant components and structures,
- Geometric stability of the SFR core in case of a strong earthquake and assurance of reliable performance of the control rods,
- Seismic-resistant design of the spent fuel pools and fuel-handling devices,
- Integrity of the primary circuit and its cooling,
- Design features aimed at the risk aversion of the flooding of the reactor building, and
- Effective options for dealing with severe accidents.

Major factors for the improvement of economic competitiveness are capital cost, capacity factor, and fuel cost. One approach is to reduce construction cost-per-unit power generation (i.e., increasing plant output while simplifying and making compact structures, systems, and components (Kotake et al., 2010)). Extension of the plant lifetime (e.g., to 60 years) is also effective in reducing the capital cost. Hence, manufacturing technology for the large components and their functional demonstration, adoption of new material such as Mod.9Cr-1Mo steel, and advanced codes and standards on the design and construction have considerable attention. On the other hand, small modular reactors have another cost reduction potential through R&D cost and manufacturing cost reductions by mass production (Triplett et al., 2012; Kim, 2017). Longer operation cycle length and shorter maintenance period are desirable to achieve a higher capacity factor. Because the longer operation cycle length means the higher burn-up, fuel cost reduction is also achievable. More than 2 years of continuous operation is possible for SFRs by making the core designed with a higher conversion ratio for its driver fuels. Because the cooling system of SFRs is kept under a deoxidization atmosphere, stress corrosion cracking is not a concern. However, technology development for inspection and repair is important because the cooling system is filled with high-temperature opaque chemically active liquid sodium (Aizawa et al., 2017; Baque et al., 2017). Shortened refueling time and reliability improvement are important for the fuel-handling systems because of their remote operation under sodium (Dechelette et al., 2017). Appropriate consideration is required in handling MA-bearing fuel for slow decay heat attenuation of spent fuel and heat generation of new fuel.

Conventional SFR power conversion is made by a steam turbine system connected to the secondary sodium cooling system. Water leaks in the heat transfer tube of the steam generator often became a decreasing capacity factor (Guidez, 2013). Hence, gas turbine power conversion systems using supercritical carbon dioxide or nitrogen (Plancq et al., 2017) and steam generators using double-walled tubes are studied. In these fields, the following R&D are in progress in GIF (GIF, 2014):

- Reduced duration of fuel loading outage through the improvement of fuel-handling systems,
- Increased fuel burn-up and cycle length,
- Improved instrumentation for detection and localization of sodium leaks,
- Improved in-service inspection and repair capabilities, which play a key role in SFR operation (due to the opaqueness and elevated temperature of the sodium coolant), through advanced instrumentation (ultrasonic techniques, robotics),
- Extended plant lifetime to 60 years, comparable to current Generation-III/III+ reactors, through:
- Development and qualification of materials with enhanced resistance to aging degradation and
- Development of improved inspection and diagnostic capabilities for verifying fitness of materials and structures for continued service,
- Codes and standards such as the Design and Construction Rules for Mechanical Components in high-temperature structures, experimental reactors and fusion reactors (RCC-MRx) code in Europe or the new American Society of Mechanical Engineers (ASME) Section III, Division 5, and the series of JSME Nuclear Power Generation Codes for fast reactors in Japan, which provides design and construction rules for mechanical components such as vessel, piping, and support structures (core excluded).

One of the important roles of SFRs is to contribute to minimizing radioactive waste and radiotoxicity in addition to the effective utilization of uranium resources by the establishment of a closed fuel cycle. R&D has been performed for MA-bearing fuel manufacturing, irradiation, and handling. In addition, cladding tube material such as Oxide Dispersion Strengthened (ODS) steel (Kaito et al., 2013; Logé et al., 2013; Ohtsuka et al., 2018) has been developed aiming for high burn-up of more than 150 GWd/t. There has been R&D related to SFR core design with MA-bearing fuel in which an effective loading method of MA is investigated taking into account the influence on the fuel property and core nuclear characteristics (e.g., homogeneous loading to driver fuel and loading to the blanket fuel).

References

- AESJ, 2015. The Fukushima Daiichi nuclear accident final report of the AESJ Investigation Committee. Springer, <https://doi.org/10.1007/978-4-431-55160-7>.
- Aizawa, K., Chikazawa, Y., Ara, K., Yui, M., Uemoto, Y., Kurokawa, M., Hiramatsu, T., 2017. Development of under Sodium Viewer for Next Generation Sodium-Cooled Fast Reactor, FR'17, Paper CN245-267.
- Alexandrov, Y.K., Rogov, V.A., Shabalin, A.S., 1996. Main features of the BN-800 passive shutdown rods. In: Absorber Materials, Control Rods and Designs of Shutdown Systems for Advanced Liquid Metal Fast Reactors Proceedings of a Technical Committee Meeting Held in Obninsk, Russian Federation, 3–7 July 1995, IAEA TECDOC 884. IAEA, Vienna, pp. 107–112.
- Aoto, K., Dufour, P., Hongyi, Y., Glats, J.P., Kim, Y.I., Ashurko, Y., Hill, R., Uto, N., 2014. A summary of sodium-cooled fast reactor development. *Prog. Nucl. Energy* 77, 247–265.
- Aoyagi, M., Uchibori, A., Kikuchi, S., Takata, T., Ohno, S., Ohshima, H., 2017. Identification of Important Phenomena under Sodium Fire Accidents Based on PIRT Process, FR'17, Paper CN245-93.
- Bachrata, A., Bertrand, F., Lemasson, D., 2015. Unprotected loss of flow simulation on ASTRID CFV-V3 reactor core. In: Proceedings of ICAPP 2015, May 03-06, 2015-Nice (France) Paper 15356.
- Baque, F., Giraud, M., Gresset, L., Marlier, R., Jouan de Kervénoaël, T., Riwan, A., Vulliez, K., Augem, J.M., 2017. Main R&D Objectives and Results for Under-Sodium Inspection Carriers—Example of the ASTRID Matting Exceptional Inspection carrier, FR'17, Paper CN245-417.
- Bauer, T.H., Wright, A.E., Robinson, W.R., Holland, J.W., Rhodes, E.A., 1990. Behavior of modern metallic fuel in TREAT transient overpower tests. *Nucl. Technol.* 92, 325. <https://doi.org/10.13182/NT92-325>.
- Bell, H., 2017. Overview of U.S. Fast Reactor Technology Development Programme, FR'17, Paper CN245-357.
- Belov, S., Vasiliev, B.A., Farakshin, M.R., Kiselev, A.V., Klinov, D.A., Gulevich, A.V., Eliseev, V.A., Malyshev, I.V., 2017. Specific Features of BN-1200 Core in Case of Use of Nitride or MOX Fuel, FR'17, Paper CN245-408.
- Bertrand, F., Marie, N., Bachrata, A., Brun-Magaud, V., Droin, J.B., Manchon, X., Herbreteau, K., Farges, B., Carlucc, B., Pomerouly, S., Lemasson, D., 2017. Status of Severe Accident Studies at the End of the Conceptual Design: Feedback on Mitigation Features, FR'17, Paper CN245-410.
- Buiron, L., Dufour, P., Rimpault, G., Prulhiere, G., Thevenot, C., Tommasi, J., Varaine, F., Zaetta, A., 2007. Innovative core design for generation IV sodium-cooled fast reactors. In: Proceedings of ICAPP 2007, May 13–18, 2007, Nice, France.
- Cachon, L., Biscarrat, C., Morin, F., Haubensack, D., Rigal, E., Moro, I., Baque, F., Madeleine, S., Rodriguez, G., Laffont, G., 2012. Innovative power conversion system for the French SFR prototype, ASTRID. In: Proceedings of ICAPP'12, Chicago, USA, June 24–28, 2012, Paper 12300.
- Cacuci, D.G. (Ed.), 2010. Handbook of Nuclear Engineering. vol. 4. Springer. <https://www.springer.com/gp/book/9780387981307>.
- CEA, 2012. Rapport sur la gestion durable des matières nucléaires. In: Séparation-transmutation des éléments radioactifs 'a vie longue. vol. 2, p. 24. <http://portail.cea.fr/multimedia/Documents/publications/rapports/rapport-gestion-durable-matieres-nucleaires/Tome%202.pdf>.
- Chang, W.P., Kwon, Y.M., Jeong, H.Y., Suk, S.D., Lee, Y.B., 2011. Inherent safety analysis of the KALIMER under a LOFA with a reduced primary pump halving time. *Nucl. Engineering Technology* 43 (1). <https://doi.org/10.5516/NET.2011.43.1.063>.
- Chebesskov, A.N., 1996. Evaluation of sodium void reactivity on the BN-800 fast reactor design. In: *Physor. 2*, p. C-49. https://inis.iaea.org/search/search.aspx?orig_q=RN:28021892.
- Chellapandi, P., Srinivasan, G.S., Chetal, S.C., 2013. Primary containment capacity of prototype fast breeder reactor against core disruptive accident loadings. *Nucl. Eng. Des.* 256, 178–187. <https://doi.org/10.1016/j.nucengdes.2012.12.014>.
- Chellapandi, P., 2015. Status of PFBR. In: 5th Joint IAEA-GIF TM/WS on Safety of SFR, IAEA, Vienna, June 23–24, 2015. https://inis.iaea.org/search/search.aspx?orig_q=RN:49059897.
- Cherdron, W., 1996. Review of the sodium fire experiments including sodium-concrete-reactions and summary of the results. In: IAEA/IWGFR Technical Committee Meeting on Evaluation of Radioactive Materials Release and Sodium Fires in Fast Reactors. O-arai, Ibaraki, Japan, November 11–14, 1996, IWGFR/92, pp. 39–48. https://inis.iaea.org/search/search.aspx?orig_q=RN:31044822.
- Chikazawa, Y., Famer, M., Grandy, C., 2008. Technology gap analysis on sodium-heated steam generators supporting advanced burner reactor development. *Nucl. Technol.* 164, 410–432. <https://doi.org/10.13182/NT08-A4035>.
- Chikazawa, Y., Famer, M., Grandy, C., 2009. Technology gap analysis on sodium-cooled reactor fuel-handling system supporting advanced burner reactor development. *Nucl. Technol.* 165, 270–292. <https://inis.iaea.org/search/searchsinglerecord.aspx?recordsFor=SingleRecord&RN=41090449>.
- Chikazawa, Y., Kotake, S., Sawada, S., 2011. Comparison of advanced fast reactor pool and loop configurations from the viewpoint of construction cost. *Nucl. Eng. Des.* 241, 378–385. <https://doi.org/10.1016/j.nucengdes.2010.10.008>.

- Chikazawa, Y., Katoh, A., Yamamoto, T., Kubo, S., Iwasaki, M., Hara, H., Shimakawa, Y., Sakaba, H., 2014. Performance evaluation on secondary sodium fire measures in JSFR. In: Proceedings of ICAPP 2014, April 6–9, 2014, Paper 14106, Charlotte, USA, pp. 523–530.
- Dechelette, F., Courcier, C., Him, J., Lorcet, H., Vulliez, K., 2017. ASTRID Fuel Handling Route for the Basic Design, FR'17, Paper CN245-395.
- Devictor, N., Chikazawa, Y., Saez, M., Rodriguez, G., Hayafune, H., 2013. R&D in support of ASTRID and JSFR: cross-analysis and identification of possible areas of cooperation. Nucl. Technol. 182 (2), 170–186. <https://doi.org/10.13182/NT13-A16429>.
- Devictor, N., Abonneau, E., 2019. Gen IV programs at CEA. In: Proceedings of ICAPP2019, Juan les pins, France, No. 502, May 2019.
- Dufour, P., 2015. Status of the ASTRID project. In: 5th Joint IAEA-GIF TM/WS on Safety of SFR, IAEA, Vienna, June 23–24, 2015. https://inis.iaea.org/search/search.aspx?orig_q=RN:49059889.
- Enuma, Y., Kawasaki, N., Orita, J., Eto, M., Miyagawa, T., 2015. JSFR design progress related to development of safety design criteria for generation IV sodium-cooled fast reactors (3). Progress of component design. In: 23rd International Conference on Nuclear Engineering, Paper 1492, May 17–21, 2015, Chiba, Japan. <https://inis.iaea.org/search/searchsinglerecord.aspx?recordsFor=SingleRecord&RN=48051357>.
- Francois, G., Serpantie, J.P., Sauvage, J.F., Lo Pinto, P., Saez, M., 2008. Sodium fast reactor concepts. In: Proceedings of ICAPP'08, Paper 8096, Anaheim, CA, USA. <https://inis.iaea.org/search/searchsinglerecord.aspx?recordsFor=SingleRecord&RN=42094797>.
- Generation IV International Forum, 2014. Technology Roadmap Update for Generation IV Nuclear Energy Systems. GIF-002-00. OECD Nuclear Energy Agency, Paris. <https://www.gen-4.org/gif/upload/docs/application/pdf/2014-03/gif-tru2014.pdf>.
- Generation IV International Forum, 2017. Safety Design Criteria for Generation IV Sodium-Cooled Fast Reactor System (Rev. 1). OECD Nuclear Energy Agency, Paris. https://www.gen-4.org/gif/jcms/c_176130/lfr-sdc-report-rev-1-march-2021.
- Generation IV International Forum, 2019a. Annual report 2019. OECD Nuclear Energy Agency, Paris. https://www.gen-4.org/gif/jcms/c_119025/gif-2019-annual-report.
- Generation IV International Forum, 2019b. Safety Design Guidelines on Safety Approach and Design Conditions for Generation IV Sodium-Cooled Fast Reactor Systems (Rev.1). OECD Nuclear Energy Agency, Paris. https://www.gen-4.org/gif/jcms/c_116489/gif-safety-approach-sdg-august-2019.
- Guidez, J., 2013. Phenix the Experience Feedback. EDP Sciences., ISBN: 979-10-92041-04-0.
- Hayafune, H., Chikazawa, Y., Kamide, H., Iwasaki, M., Shoji, T., 2017a. Advanced Sodium-Cooled Fast Reactor Development Regarding GIF Safety Design Criteria, FR'17, Paper CN245-158. https://inis.iaea.org/collection/NCLCollectionStore/_Public/49/085/49085659.pdf?r=1.
- Hayafune, H., Glatz, J., Yang, H., Ruggieri, J., Kime, Y., Ashurko, Y., Hill, R., 2017b. Current Status of GIF Collaborations on Sodium-Cooled Fast Reactor System, FR'17, Paper CN245-156. https://inis.iaea.org/collection/NCLCollectionStore/_Public/49/085/49085660.pdf?r=1.
- Hejzlar, P., Petroski, R., Cheatham, J., Touran, N., Cohen, M., Truong, B., Latta, R., Werner, M., Burke, T., Tandy, J., Garrett, M., Johnson, B., Ellis, T., McWhirter, J., Odedra, A., Schweiger, P., Adkisson, D., Gilleland, J., 2013. Terrapower, LLC traveling wave reactor development program overview. Nucl. Eng. Technol. 45 (6), 731–744.
- Huang, D., 2021. Status and prospects of China sodium-cooled fast reactor. In: 9th Joint IAEA-GIF TM/WS on Safety of LMFRs, March 30–April 1, 2021.
- Hune, A.W., Gerber, A., Pirus, J.P., Soucille, L., Beauchamp, F., Rodriguez, G., 2015. ASTRID SFR prototype steam generator design evolution related to safety and cost issues. In: Proceedings of ICAPP 2015, May 03–06, 2015-Nice (France) Paper 15236. <https://inis.iaea.org/search/searchsinglerecord.aspx?recordsFor=SingleRecord&RN=49004853>.
- IAEA, 1998. Unusual Occurrences During LMFR Operation. IAEA-TECDOC-1180. https://www-pub.iaea.org/MTCD/Publications/PDF/te_1180_prn.pdf.
- IAEA, 2006. Fundamental Safety Principles. Safety Fundamentals No. SF-1. International Atomic Energy Agency, Vienna. https://www-pub.iaea.org/MTCD/publications/PDF/Pub1273_web.pdf.
- IAEA, 2007. Liquid Metal Cooled Reactors: Experience in Design and Operation. IAEA-TECDOC-1569. https://www-pub.iaea.org/MTCD/Publications/PDF/te_1569_web.pdf.
- IAEA, 2016. Safety of Nuclear Power Plants: Design. Specific safety Requirements No. SSR2/1 (Rev1). International Atomic Energy Agency, Vienna. <https://www-pub.iaea.org/MTCD/publications/PDF/Pub1715web-46541668.pdf>.
- IAEA, 2018. Enhancing Benefits of Nuclear Energy Technology Innovation through Cooperation among Countries: Final Report of the INPRO Collaborative Project SYNERGIES. IAEA Nuclear Energy Series NF-T-4.9. <https://www.iaea.org/publications/12200/enhancing-benefits-of-nuclear-energy-technology-innovation-through-cooperation-among-countries-final-report-of-the-inpro-collaborative-project-synergies>.
- IAEA, 2019a. Design of the Reactor Core for Nuclear Power Plants Specific Safety Guide. SSG-52. International Atomic Energy Agency, Vienna. https://www-pub.iaea.org/MTCD/Publications/PDF/PUB1859_web.pdf.

- IAEA, 2019b. Design of the Reactor Containment and Associated Systems for Nuclear Power Plants Specific Safety Guide. SSG-53. International Atomic Energy Agency, Vienna. https://www-pub.iaea.org/MTCD/publications/PDF/P1856_web.pdf.
- IAEA, 2020. Design of the Reactor Coolant System and Associated Systems in Nuclear Power Plants, Specific Safety Guide. SSG-56. International Atomic Energy Agency, Vienna. https://www-pub.iaea.org/MTCD/Publications/PDF/PUB1878_web.pdf.
- IAEA, 2021. Ninth joint IAEA-GIF technical meeting/workshop on safety of liquid metal fast reactors information sheet. In: 9th Joint IAEA-GIF TM/WS on Safety of LMFRs, March 30–April 1, 2021. https://www.iaea.org/sites/default/files/20/01/evt1701718_information_sheet.pdf.
- JSME, 1986. JSME Data Book: Heat Transfer, fourth ed. Japan Society of Mechanical Engineering.
- Kaito, T., Ohtsuka, S., Yano, Y., Tanno, T., Yamashita, S., Ogawa, R., Tanaka, K., 2013. Irradiation Performance of Oxide Dispersion Strengthened (ODS) Ferritic Steel Claddings for Fast Reactor Fuels. FR'13, Paper CN-199-252. https://inis.iaea.org/search/search.aspx?orig_q=RN:46091127.
- Kamide H., Ando M., Ito T., 2015. JSFR design progress related to development of safety design criteria for generation IV sodium-cooled fast reactors (1). Overview. In: 23rd International Conference on Nuclear Engineering, Paper 1666, May 17–21, 2015, Chiba, Japan.
- Kang, S., Tentner, A., Karahan, A., 2017. Advances in the Development of the SAS4A Code Metallic Fuel Models for the Analysis of PGSFR Postulated Severe Accidents, FR'17, Paper CN245-56.
- Kaysner, G., Papin, J., 1998. The reactivity risk in fast reactors and the related international experimental programmes CABRI and SCARABEE. Prog. Nucl. Energy 32, 631–638. <https://www.sciencedirect.com/science/article/pii/S014919709700067X>.
- Kim, Y., 2017. Feasibility and Challenges for Self-Sustainable Long-Life SMR without Refuelling, FR'17, Paper CN245-566.
- Kondo, S., Tobita, Y., Morita, K., Shirakawa, N., 1992. Simmer-III: an advanced computer program for LMFBR severe accident. In: ANP'92, Tokyo, Japan (1992) October 25–29, No 40-5. <https://inis.iaea.org/search/searchsinglerecord.aspx?recordsFor=SingleRecord&RN=25006719>.
- Kotake, S., Sakamoto, Y., Mihara, T., Kubo, S., Uto, N., Kamishima, Y., Aoto, K., Toda, M., 2010. Development of advanced loop-type fast reactor in Japan. Nucl. Technol. 170, 133–147.
- Kriventsev, V., Briggs, L., Monti, S., Hu, W., Sui, D., Su, G., Maas, L., Vezzoni, B., Sarathy, U.P., Del Nevo, A., Petrucci, A., Zanino, R., Ohira, H., Van Rooijen, W.F.G., Morita, K., Choi, C., Shin, A., Stempniewicz, M., Rtischev, N., Mikityuk, K., Truong, B., 2017. Benchmark Analyses of EBR-II Shutdown Heat Removal Tests, FR'17, Paper CN245-4.
- Kubo, S., Shimakawa, Y., 2015. JSFR design progress related to development of safety design criteria for generation IV sodium-cooled fast reactors (2). Progress of safety design. In: 23rd International Conference on Nuclear Engineering, Paper 1748, May 17–21, 2015, Chiba, Japan.
- Kubo, S., Nakai, R., Sofu, T., 2018. Development of Safety Design Guidelines on Structures, Systems and Components for Generation IV Sodium-Cooled Fast Reactor Systems, GIF Symposium—Paris (France)—16–17 October 2018.
- Languille, A., Gamier, J.C., Lo Pinto, P., Na, B.C., Verrier, D., Deplaix, J., Allan, P., Newton, T., Sunderland, R.E., Kiefhaber, E., Maschek, W., Struwe, D., 1995. CAPRA core studies the oxide reference option. In: Proceedings of Global 1995, September 11–14, 1995, Versailles, France. https://inis.iaea.org/search/search.aspx?orig_q=RN:29062152.
- Lebel, L., Girault, N., 2017. Learning from 1970 and 1980-Era Sodium Fire Experiments, FR'17, Paper CN245-326.
- Logé, R.E., Toualbi, L., Vanegas-Marques, E., de Carlan, Y., Mocellin, K., 2013. Optimization of the Fabrication Route of Ferritic/Martensitic ODS Cladding Tubes: Metallurgical Approach and Pilgering Numerical Modeling. FR'13, Paper CN-199-380.
- Lucoff, D.M., Walter, A.E., Sackett, J.I., Salvatores, M., Aizawa, K., 1992. Experimental and design experience with passive safety features of liquid metal reactors. In: Proceedings of ANP'92, Tokyo, Japan.
- Malet, J.C., 1996. Ignition and combustion of sodium-fire consequences-extinguishment and prevention. In: IAEA/IWGFR Technical Committee Meeting on Evaluation of Radioactive Materials Release and Sodium Fires in Fast Reactors, O-arai, Ibaraki, Japan, November 11-14, 1996, IWGFR/92, pp. 13–37. https://inis.iaea.org/collection/NCLCollectionStore/_Public/31/044/31044821.pdf?r=1.
- Maschek, W., Asprey, M.W., 1983. Simmer-II recriticality analyses for a homogeneous core of the 300-Mwe class. Nucl. Technol. 63, 330. <https://www.tandfonline.com/doi/abs/10.13182/NT83-A33291>.
- Maschek, W., Munz, C.D., Meyer, L., 1992. Investigation of sloshing motions in pools related to recriticalities in liquid-metal fast breeder reactor core meltdown accidents. Nucl. Technol. 98, 27.
- Mizuno, T., Ogawa, T., Naganuma, M., Aida, T., 2005. Advanced oxide fuel core design study for SFR in the “feasibility study” in Japan. In: Proceedings of Global 2005, October 9–13, 2005, Tsukuba, Japan.
- Nakai, R., 2014. GIF-SDC phase 2 activity status of the safety design guideline (SDG) development. In: 4th GIF-IAEA Workshop on Safety of SFR, Vienna, June 10–11. https://inis.iaea.org/search/search.aspx?orig_q=RN:49059914.
- Nakai, R., 2015. RSWG and SFR SDC TF progress update. In: 9th GIF-IAEA/INPRO Interface Meeting, Vienna, March 4–5. https://inis.iaea.org/collection/NCLCollectionStore/_Public/49/097/49097763.pdf?r=1.
- Nakamura, T., Kaguchi, H., Ikarimoto, I., Kamishima, Y., Koyama, K., Kubo, S., Kotake, S., 2004. Evaluation method for structural integrity assessment in core disruptive accident of fast reactor. Nucl. Eng. Des. 227, 97–123.

- Nakanishi, S., Hosoya, T., Kubo, S., Kotake, S., Takamatsu, M., Aoyama, T., Ikarimoto, I., Kato, J., Shimakawa, Y., Harada, K., 2010. Development of passive shutdown system for SFR. *Nucl. Technol.* 170, 181–188.
- Nonaka, N., Sato, I., 1992. Improvement of evaluation method for initiating-phase energetics based on CABRI-1 in-pile experiments. *Nucl. Technol.* 98, 54–69.
- Ohno, S., Ohshima, H., Tajima, Y., Ohki, H., 2012. Development of PIRT and assessment matrix for Verification and validation of sodium fire analysis codes. *J. Power Energy Syst.* 6 (2), 241–254. https://www.jstage.jst.go.jp/article/jpes/6/2/6_241/_pdf/-char/ja.
- OECD/NEA, 2017. The Effects of the Uncertainty of Input Parameters on Nuclear Fuel Cycle Scenario Studies, Nuclear Science NEA/NSC/R(2016)4. https://www.oecd-nea.org/jcms/pl_19754/the-effects-of-the-uncertainty-of-input-parameters-on-nuclear-fuel-cycle-scenario-studies?details=true.
- Ohtsuka, S., Tanno, T., Oka, H., Yano, Y., Tachi, Y., Kaito, T., Hashidate, R., Kato, S., Furukawa, T., Ito, C., Yoshitake, T., 2018. Development of ODS tempered martensitic steel for high burn up fuel cladding tube of SFR. In: GIF Symposium—Paris (France)—16–17 October 2018.
- Okano, Y., Nakai, R., Kubo, S., 2014. International reviews on safety design criteria and development of safety design guidelines for generation-IV sodium-cooled fast reactors. In: The Ninth Korea-Japan Symposium on Nuclear Thermal Hydraulics and Safety (NTHAS9), Buyeo, Korea, November 16–19, Keynote Lecture 1.
- Olivier, T.J., Blanchat, T.K., Dion, J.A., Hewson, J.C., Nowlen, S.P., Radel, R.F., 2008. Metal Fire Implications for Advanced Reactors. Part 2. PIRT results. SANDIA Report Sand 2008-6855.
- Olivier, T.J., Radel, R.F., Nowlen, S.P., Blanchat, T.K., Hewson, J.C., 2007. Metal Fire Implications for Advanced Reactors. Part 1. Literature Review. SANDIA REPORT SAND 2007-6332. https://digital.library.unt.edu/ark:/67531/metadc901843/m2/1/high_res_d/946583.pdf.
- Onoda, Y., Matsuba, K., Tobita, Y., Suzuki, T., 2017. Preliminary analysis of the post-disassembly expansion phase and structural response under unprotected loss of flow accident in prototype sodium cooled fast reactor. *Mech. Eng. J.* 4 (3). No. 16-00597.
- Osipov, S.L., Rogozhkin, S.A., Sobolev, V.A., Shepeleva, S.F., Kozhaev, A.A., Mavrin, M.S., Ryabov, A.A., 2013. Analytical and Experimental Study for Validation of the Device to confine BN Reactor Melted Fuel FR'13, Paper CN-199-374. https://inis.iaea.org/search/search.aspx?orig_q=RN:46090984.
- Plancq, D., Cachon, L., Remy, A., Quenaut, J., Gama, P., Dirat, J., Raquin, L., Levoir, B., 2017. Progress in the ASTRID gas Power Conversion System Development, FR'17, Paper CN245-285.
- Puthiyavinayagam, P., Devan, K., Aithal, S.R., Athmalingam, S., Vijayashree, R., Raghupathy, S., Velusamy, K., Theivarajan, N., Usha, S., Bhaduri, A.K., 2017. Advanced Design Features of MOX Fuelled Future Indian SFRs, FR'17, Paper CN245-300.
- Rouault, J., Abonneau, E., Settimo, D., Hamy, J.M., Hayafune, H., Gefflot, R., Benard, R.P., Mandement, O., Chauveau, T., Lambert, G., Audouin, P., Mochida, H., Iitsuka, T., Fukuie, M., Molyneux, J., Mazel, J.L., ASTRID, 2015. The SFR GENIV technology demonstrator project: where are we, where do we stand for? In: Proceedings of ICAPP 2015 May 03–06, 2015-Nice (France), Paper 15439.
- Risk and Safety Working Group of the Generation IV International Forum, 2008. Basis for the Safety Approach for Design & Assessment of Generation IV Nuclear Systems, Revision 1. Gif/RSWG/2007/002. OECD Nuclear Energy Agency, Paris. https://www.gen-4.org/gif/jcms/c_66624/basis-for-the-safety-approach-for-design-assessment-of-generation-iv-nuclear-systems-revision-1-2008?details=true.
- Saito, H., Yamada, Y., Oyama, K., Matsunga, S., Yamano, H., Kubo, S., 2017. Safety evaluation of self actuated shutdown system for Gen-IV SFR. In: The 2017 International Congress on Advances in Nuclear Power Plants (ICAPP 2017), Fukui and Kyoto, Japan (April 24–28, 2017) ICAPP2017-17439.
- Sathiah, P., Roelofs, F., 2014. Numerical modeling of sodium fire. Part I. Spray combustion. *Nucl. Eng. Des.* 278, 723–738. <https://www.sciencedirect.com/science/article/pii/S0029549313007309?via%3Dihub>.
- Sato, K., Koma, Y., Nakabayashi, H., Yano, K., Amamoto, I., Kitajima, S., Kobayashi, T., Higuchi, T., Nakanishi, S., Yoshiuji, T., 2005. Conceptual design study and evaluation of advanced reprocessing plants in the feasibility study on commercialized FR cycle systems in Japan. In: Proceedings of GLOBAL 2005 Tsukuba, Japan, Oct 9-13, 2005, Paper No. 502. https://inis.iaea.org/search/search.aspx?orig_q=RN:37082385.
- Sawada, M., Arikawa, H., Mizoo, N., 1990. Experiment and analysis on natural convection characteristics in the experimental fast reactor Joyo. *Nucl. Eng. Des.* 120, 341–347. <https://www.sciencedirect.com/science/article/pii/002954939090385B>.
- Sciora, P., Blanchet, D., Buiron, L., Fontaine, B., Vanier, M., Varaine, F., Venard, C., Massara, S., Scholer, A.C., Verrier, D.P., 2011. Low void effect core design applied on 2400 MWth SFR reactor. In: Proceedings of ICAPP 2011, May 2–6, 2011, Nice, France. https://www.researchgate.net/publication/299533268_Low_void_effect_core_design_applied_on_2400_MWth_SFR_reactor.

- Serre, F., Bertrand, F., Bachrata, A., Marie, N., Kubo, S., Kamiyama, K., Carlucci, B., Farges, B., Koyama, K., 2017. France-Japan Collaboration on the severe accident studies for ASTRID: outcomes and future work program. In: Proceedings of ICAPP 2017, April 24–28, 2017—Fukui & Kyoto, Japan. <https://inis.iaea.org/search/searchsinglerecord.aspx?recordsFor=SingleRecord&RN=49024800>.
- Shepelev, S., 2017. Development of the New Generation Power Unit with the BN-1200 Reactor, FR'17, Paper CN245-402. Sodium Technology Education Committee, September 2005. Sodium Technology Handbook. JNC TN9410 2005-001. <https://inis.iaea.org/search/searchsinglerecord.aspx?recordsFor=SingleRecord&RN=36108944>.
- Suzuki, T., Kamiyama, K., Yamano, H., Kubo, S., Tobita, Y., Nakai, R., Koyama, K., 2014. A scenario of core disruptive accident for Japan Sodium-cooled Fast Reactor to achieve in-vessel retention. J. Nucl. Sci. Technol. <https://www.tandfonline.com/doi/full/10.1080/00223131.2013.877405>.
- Tae-Ho, L., 2015. Fundamental approach to safety design of prototype Gen-IV SFR. In: 5th Joint IAEA-GIF TM/WS on Safety of SFR, IAEA, Vienna, June 23–24, 2015. https://inis.iaea.org/collection/NCLCollectionStore/_Public/49/059/49059892.pdf?r=1.
- Takata, T., Yamaguchi, A., Uchibori, A., Ohshima, H., 2009. Computational methodology of sodium-water reaction phenomenon in steam generator of sodium-cooled fast reactor. J. Nucl. Sci. Technol. 46, 613–623. <https://www.tandfonline.com/doi/abs/10.1080/18811248.2007.9711568>.
- Tenchine, D., Piella, D., Gauthé, P., Vasile, A., 2012. Natural convection test in Phenix reactor and associated CATHARE calculation. Nucl. Eng. Des. 253, 23–31. <https://www.sciencedirect.com/science/article/pii/S0029549312004244>.
- Triplett, B.S., Loewen, E.P., Dooies, B.J., 2012. PRISM: a competitive small modular sodium-cooled reactor. Nucl. Technol. 178, 186–200. <https://www.tandfonline.com/doi/abs/10.13182/NT178-186>.
- Tsige-Tamirat, H., Vasile, A., Mikityuk, K., Guidez, J., 2019. Update on safety considerations for ESFR. In: 8th Joint IAEA-GIF TM/WS on Safety of LMFBRs, IAEA, Vienna, March 20–22. https://inis.iaea.org/collection/NCLCollectionStore/_Public/50/041/50041676.pdf.
- Tsuboi, Y., Matsumiya, H., Hasegawa, K., Kasuga, S., Sakashita, Y., Handa, N., Ueda, N., Greci, T., 2004. Development of the 4S and related technologies (1). Plant system overview and current status. In: ICAPP9. Tokyo, 2009-05. ANS, 2009, Paper 9214. https://inis.iaea.org/search/search.aspx?orig_q=RN:43084195.
- U.S. DOE Nuclear Energy Research Advisory Committee and the Generation IV International Forum, 2002. A Technology Roadmap for Generation IV Nuclear Energy Systems. GIF-002-00. OECD Nuclear Energy Agency, Paris. https://www.gen-4.org/gif/jcms/c_40473/a-technology-roadmap-for-generation-iv-nuclear-energy-systems.
- Varaine, F., Rodriguez, G., Settimo, D., Hamy, J., Romdhane, S., Benard, R., Remy, A., Hayafune, H., Chauveau, T., Helle, J.P., Gautier, V., Mochida, H., Lambert, G., Iitsuka, T., Fukuie, M., Lefrançois, M., Maze, J., 2017. ASTRID Project, from Conceptual to Basic Design: Progress status, FR'17, Paper CN245-413. <https://hal.archives-ouvertes.fr/hal-02419661>.
- Vasile, A., Ren, L., Fanning, T., Tsige-Tamirat, H., Yamano, H., Kang, S.-H., Ashurko, I., 2017. Recent Activities of the Safety and Operation Project of the Sodium-Cooled Fast Reactor in the Generation IV International Forum, FR'17, Paper CN245-133.
- Vasyaev, A.V., Shepelev, S.F., Bylov, I.A., Poplavskiy, V.M., Ashurko, I.M., 2015. Provision of safety design criteria for generation-IV sodium-cooled fast reactor system implementation in BN-1200 reactor design. In: 5th Joint IAEA-GIF TM/WS on Safety of SFR, IAEA, Vienna, June 23–24, 2015. <https://www.iaea.org/sites/default/files/18/10/622-i3-tm-50169-bylov.pdf>.
- Venard, C., Coquelet-Pascal, C., Conti, A., Gentet, D., Lamagnère, P., Lavastre, R., Gauthé, P., Bernardin, B., Beck, T., Lorenzo, D., Scholer, A., Perrin, B., Verrier, D., 2017. The ASTRID core at the End of the Conceptual Design Phase, FR'17, paper CN245-288. <https://hal.archives-ouvertes.fr/hal-02419651/document>.
- Verrier, D., Scholer, A.C., Chhor, M., 2013. A New Design Option for Achieving Zero Void Effect in Large SFR Cores. FR'13, Paper CN-199-347. https://inis.iaea.org/search/search.aspx?orig_q=RN:46091018.
- Vinogradov, A., Kamaev, A., Drobishev, V., Kochetkov, N., Pakhomov, A., Martianova, G., 2017. Numerical—Experimental Research in Justification of Fire (Sodium) Safety of Sodium Cooled Fast Reactors, FR'17, Paper CN245-102. https://inis.iaea.org/search/search.aspx?orig_q=RN:51002851.
- Walter, A.E., Todd, D.R., Tsvetkov, P.V., 2012. Fast Spectrum Reactors. Springer.
- Weber, D.P., 1988. The SAS4A LMFBR Accident Analysis Code System. ANL/RAS 83-38.
- Yamaguchi, A., Takata, T., Okano, Y., 2001. Numerical methodology to evaluate fast reactor sodium combustion. Nucl. Technol. 136, 315–330. <https://www.tandfonline.com/doi/abs/10.13182/NT01-A3248>.
- Yamano, H., Fujita, S., Tobita, Y., Sato, I., Niwa, H., 2008. Development of a three-dimensional CDA analysis code: SIMMER-IV and its first application to reactor case. Nucl. Eng. Des. 238 (1), 66–73. <https://www.sciencedirect.com/science/article/pii/S0029549307003640>.

- Yamano, H., Kubo, S., Shimakawa, Y., Fujita, K., Suzuki, T., Kurisaka, K., 2012. Safety design and evaluation in a large-scale Japan sodium-cooled fast reactor. *Sci. Technol. Nucl. Install.* 2012, 614973. 14 pp. <https://www.hindawi.com/journals/stni/2012/614973/>.
- Yang, W.S., Kim, T.K., Grandy, C., 2007. A metal fuel core concept for 1000 MWt advanced burner reactor. In: *Proceedings of Global 2007*, September 9–13, 2007, Boise, Idaho, US. <https://www.osti.gov/biblio/20979520-metal-fuel-core-concept-mwt-advanced-burner-reactor>.
- Yoo, J., Kim, J., Lee, C., Joo, H., 2017. Status of sodium cooled fast reactor development program in Korea, FR'17, paper CN245-460. https://inis.iaea.org/search/search.aspx?orig_q=RN:49085729.

6

Lead-cooled Fast Reactors (LFRs)

Craig F. Smith^{a,*} and Luciano Cinotti^b^aNaval Postgraduate School, Monterey, CA, United States ^bNewcleo Ltd, London, United Kingdom

Nomenclature

2-D	Two Dimensional
AEP	AtomEnergoproekt Moscow (Russia)
ALFRED	Advanced Lead Fast Reactor European Demonstrator
Am	Americium
BELLA	A computer code written specifically for the purpose of safety-informed design of lead-cooled fast reactors
BREST	Bystry REaktor so Svintsovym Teplonositelem in Russian or “Fast Reactor with Lead Coolant”
CAS	Chinese Academy of Sciences
CLEAR	China LEAd-based Reactor
Cm	Curium
CPS	Control and Protection System
CRDM	Control Rod Drive Mechanism
DC	Dip Cooler
DHR	Decay Heat Removal
DHX	Decay Heat eXchanger
dpa	displacements per atom
DRC	Direct Reactor Cooling
DU	Depleted Uranium
ECCS	Emergency Core Cooling System
el	electrical
ELFR	European Lead Fast Reactor
ELSY	European Lead Cooled System
ESNII	European Sustainable Nuclear Industrial Initiative
FA	Fuel Assembly
FGC	Functionally Graded Composite
FP	Fission Product
GIF	Generation IV International Forum
HM	Heavy Metal
IC	Isolation Condenser
IPPE	The Institute of Physics and Power Engineering (Obninsk, Russia)
LBE	The eutectic mixture of lead and bismuth (Lead-Bismuth Eutectic)
LEADER	Lead-cooled European Demonstrator Reactor
LFR-AS-200	Lead-cooled Fast Reactor-Amphora Shaped-200 MW _{el}
LIPOSO	<i>Llaison-POMpe-SOmmier</i> : French for the hydraulic connection between the pump and the core supporting grid
LOCA	Loss Of Coolant Accident

* Participating in personal capacity.

MA	Minor Actinide
MCP	Main Coolant Pump
MWd/kg-HM	MegaWatt days per kilogram of Heavy Metal
MW_{el}	MegaWatts electrical
MW_{th}	MegaWatts thermal
MYRRHA	Multipurpose hYbrid Research Reactor for High-tech Applications
N	Nitrogen or Nitride
Np	Neptunium
NU	Natural Uranium
OECD-NEA	Organization for Economic Cooperation and Development-Nuclear Energy Agency
PBWFR	Pb-Bi-cooled direct Contact boiling Water Fast Reactor
PP	Primary Pump
pSSC	provisional System Steering Committee
Pu	Plutonium
RMB	Reactor MonoBlock
RVACS	Reactor Vessel Air Cooling System
SCK-CEN	The Belgian nuclear research center located in Mol, Belgium. The acronym comes from the Dutch: Studiecentrum voor Kernenergie; and the French: Centre d'Etude de l'énergie nucléaire
SEALER	SwEdish Advanced LEad Reactor
SG	Steam Generator
SGTR	Steam Generator Tube Rupture
SNETP	Sustainable Nuclear Energy Technology Platform
SNU	Seoul National University
SS	Stainless Steel
SSTAR	Small Secure Transportable Autonomous Reactor
STSG	Spiral Tube Steam Generator
SVBR	Svintsovo-Vismutovyi Bystryi Reaktor in Russian, or “Lead-Bismuth Fast Reactor”
th	thermal
TRU	TRansUranic
U	Uranium
URANUS	Ubiquitous, Robust, Accident-forgiving, Non-proliferating and Ultra-lasting Sustainer
WG-LBE	Working Group on Lead-Bismuth Eutectic
WPFC	Working Party on scientific issues of the Fuel Cycle
y	years

6.1 Overview and motivation for lead-cooled fast reactor systems

Lead-cooled Fast Reactors (LFRs) are fast spectrum reactors cooled by molten lead (or lead-based alloys) operating at high temperatures and at near atmospheric pressure, conditions enabled because of the very high boiling point of lead (i.e., 1737°C) and its low vapor pressure (i.e., 2.9×10^{-5} Pa at 400°C). The coolant is either pure lead or an alloy of lead, most commonly the eutectic mixture of lead and bismuth, also known as LBE. The predominant coolant considered in the Generation-IV reference LFR systems is pure lead; however, other systems cooled by LBE are also under consideration and are included in this chapter as appropriate. It is noted that there are many similarities and some differences between lead and lead alloys as reactor coolants, and a brief discussion of some of the important differences is presented. The LFR reactor core is characterized by a fast neutron spectrum, owing to the scattering properties of lead that allow the sustainment of high neutron energy and relatively low parasitic absorption of neutrons.

Lead coolants are relatively inert from a chemical perspective and possess several attractive properties that enable a high degree of inherent safety and simplification of design:

- There are no rapid chemical reactions between the lead coolants and either water or air.
- The high boiling point of lead allows reactor operation at near atmospheric pressure and eliminates the risk of core voiding due to coolant boiling.
- The high heat capacity of lead provides significant thermal inertia in the event of a loss of heat sink.
- Lead shields gamma radiation and tends to retain iodine, cesium, and other Fission Products (FPs) at temperatures up to 600°C, thereby reducing the source term in case of release of FPs from the fuel.
- The low neutron moderation of lead allows greater spacing between fuel pins, leading to low core pressure loss and reduced risk of flow blockage.
- The simple coolant flow path and low core pressure loss as well as the thermodynamic properties of lead allow a high level of natural circulation cooling in the primary system for Decay Heat Removal (DHR).

Starting in the late 1950s, LBE-cooled reactors were designed and built in the Soviet Union for the purpose of submarine propulsion. Eight such submarines were built and operated along with two on-shore reactors. The reactor power of these systems included two levels, with thermal outputs of 73 and 155 MW. From the early 1960s until decommissioning of the final submarine in 1995, a total of 15 reactor cores were operated, providing an estimated 80 reactor years of operating experience. While significant differences exist between these reactors and currently considered Generation-IV LFR systems, this operational experience provided a strong base for understanding the technology and identifying solutions to the technical challenges to be overcome to exploit the significant advantages summarized above.

As early as 1989, new concepts for land-based reactors cooled by lead and lead-based alloys were under consideration in Russia. Since 2000, and stimulated in part by the Generation IV International Forum (GIF) program, several additional new initiatives were being developed by organizations in many different locations around the globe.

In Russia, two initiatives have been pursued. One of these is known as the SVBR (*Svintsovo-Vismutovyi Bystryi Reaktor* or “Lead-Bismuth Fast Reactor”) (Zrodnikov et al., 2009). The SVBR-100 is generally considered a follow-on technology to the prior submarine propulsion technology, and is a small reactor cooled by LBE. Although in 2018 Russian state budget support for SVBR-100 was eliminated, development of the SVBR has since been continued and activities such as site selection for a first-of-a-kind unit have proceeded.

The second major initiative, known as the BREST (*Bystryi Reaktor so Svintsovym Teplonositelem* or “Fast Reactor with Lead Coolant”) (Dragunov et al., 2012), is a demonstration reactor cooled by pure lead and detailed further in this chapter as one of the reference LFR reactor systems in the GIF program (GIF-LFR-pSSC, 2014). With its construction currently underway, the BREST-OD-300 is now scheduled to be the first Generation-IV LFR reactor to begin operation. The power level of 300 MW_{el} is the minimal possible power for the reactors of the BREST type. After BREST-OD-300 commissioning, subsequent designs of BREST reactors can be anticipated with power ratings from 300 to 1200 MW_{el}.

In Europe, the European Sustainable Nuclear Industrial Initiative (ESNII) (SNETP Secretariat, 2010) selected the LFR as a technology of interest. Thus, the ELSY (European Lead-cooled SYstem) project was initiated in 2006 to define the main options of an LFR of industrial size with a power of 1500 MW_{th} and 600 MW_{el} (Cinotti et al., 2008). This was followed in 2010 by the LEADER project (European Advanced Lead-cooled Reactor Demonstration) (De Bruyn et al., 2013); both ELSY and LEADER were projects funded by the European Commission (EC/Euratom). The LEADER project continued the study of an industrial-sized reactor under the name ELFR (European Lead Fast Reactor) and also initiated the concept of a demonstration LFR of power 100 MW_{el} called ALFRED (Advanced Lead Fast Reactor European Demonstrator) (Frogheri et al., 2013) that is under consideration for construction in Romania. The ELFR system is detailed further in this chapter as one of the reference LFR reactor systems in the GIF program (GIF-LFR-pSSC, 2014). Finally, in Belgium, SCK-CEN intends to build an Accelerator Driven System (ADS) demonstrator, called MYRRHA (Multi-purpose hYbrid Research Reactor for High-tech Applications) (De Bruyn et al., 2007), coupling a particle accelerator with a reactor. MYRRHA would use LBE as a

coolant and as a neutron source of spallation activated by a proton beam. The reactor is expected to be capable of functioning in either a subcritical or critical mode.

Several additional design studies have been or are being carried out in a number of other countries including the United States, South Korea, Japan, China, and Sweden. It should be noted in particular, that the US design of a small LFR known as SSTAR (Small Secure Transportable Autonomous Reactor) (Sienicki et al., 2006; Smith et al., 2008) is a legacy preliminary design and is included as the reference design of a small LFR in the GIF program (GIF-LFR-pSSC, 2014). At the same time, new concepts under current development in the United States as well as these other countries are summarized in Section 6.6. In particular, over the past 10 years, a significant new development initiative has been conducted by China. The China LEAd-based Reactor (CLEAR) (Wu et al., 2013) is the reference reactor for China's Lead-based Fast Reactor Development Plan.

6.2 Basic design choices

6.2.1 Lead versus LBE

Pure lead and the Lead-Bismuth Eutectic (LBE) alloy (consisting of 44.5% lead and 55.5% bismuth) are the principal potential coolants for LFR systems. Table 6.1 shows some key properties of LBE and lead with sodium also included for reference and comparison. Further details on the properties of lead coolants can be found in OECD-NEA (2015). The shared property that both LBE and lead are essentially inert in terms of interaction with air or water is the noteworthy advantage that LFRs have in comparison with the other principal liquid metal-cooled reactor, the Sodium-cooled Fast Reactor (SFR). This basic property has significant implications for design simplification, safety performance, and the associated economic performance of such systems in comparison with SFRs and other Generation-IV systems.

When comparing lead to LBE, it should be noted that the LBE coolant has the advantage of a lower melting point (125°C) in contrast with the 327°C of pure lead. For this reason, LBE was used in early lead-cooled reactors (i.e., the reactors used for propulsion of the Soviet/Russian alpha-class submarines as well as their land-based counterparts) and in research facilities investigating the use of heavy liquid metals as reactor coolants. The lower melting point of LBE (and the resulting operational advantages) made this a logical choice for such early applications and is also the chosen coolant for several more modern reactor designs (e.g., the SVBR-100 design previously mentioned, the Chinese CLEAR-I system, and several others). Additionally, LBE as a coolant has been proposed for several ADS reactor systems (e.g., MYRRHA) designed for the purpose of transmuting long-lived radionuclides from spent nuclear fuel.

While LBE continues to be considered for some future LFR concepts, reactors cooled by pure lead have become the primary focus of the GIF set of reference systems, and this approach appears to represent the most promising future direction due to conspicuous advantages in comparing these options.

The use of LBE as a coolant has some important drawbacks (in comparison to the choice of pure lead) that are appropriate to note. First, as a raw material, LBE (due to the bismuth content) is more expensive, and there

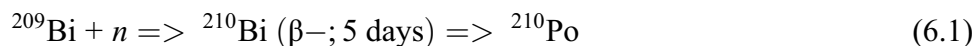
Table 6.1. Comparative properties of liquid metal coolants (as reported by Todreas et al. 2004)

Coolant	Melting point (°C)	Boiling point (°C)	Chemical reactivity (w/air and water)
Lead-bismuth (Pb-Bi)	125	1670	Essentially inert
Lead (Pb)	327	1737	Essentially inert
Sodium (Na)	98	883	Highly reactive

is even some doubt that the availability of bismuth could be sufficient in the event of developing a large fleet of LBE-cooled LFRs.

Second, it is noted that LBE is somewhat more corrosive than lead (when comparing the corrosion potential of the two coolants at the same temperature), and LBE has a lower thermal conductivity: 14.3 W/mK for LBE versus 17.7 W/mK for lead, at a temperature of 500°C (OECD-NEA, 2015).

The greatest drawback of the LBE is, however, its relatively large production of polonium-210 (^{210}Po), which is generated primarily by neutron capture of bismuth-209 (^{209}Bi) as follows:



^{210}Po decays with a half-life of 138.4 days into ^{206}Pb by an α emission of 5.3 MeV. Therefore, it represents a potent heat load within the coolant as well as being a dangerous and radiotoxic material in the event of its leakage or release.

The polonium production in an LBE-cooled reactor is so high that in the 80 MW_{th}, LBE-cooled ADS developed in the 5th Framework Program of Euratom, the polonium inventory within the primary coolant circuit was evaluated to be 2 kg at equilibrium. This amount of polonium generates a decay heat in the primary system that, 5 days after a reactor shutdown, would equal the decay heat power of the fuel itself (Cinotti et al., 2011).

Pure lead is not completely exempt from polonium formation because pure lead coolant contains impurities including Bi ($\sim 10^{-3}\%$). This and the small additional contribution of polonium from activation processes starting with ^{208}Pb represent the main contribution to the appearance of ^{210}Po in the lead coolant of an LFR. However, the level of polonium production in the pure lead coolant does not present major difficulties for such LFRs and is several orders of magnitude lower than that of a comparably sized LBE-cooled reactor.

Since the rate of polonium production in pure lead is much lower than in the case of LBE, it has a negligible effect in terms of decay heat power. In fact, the polonium inventory at equilibrium in the primary system of a 1500 MW_{th}, pure lead-cooled reactor (i.e., ELSY) has been calculated to be less than 1 g after 40 years of irradiation (Cinotti et al., 2011).

The low moderating capability^a and low neutron absorption of lead not only enable the operation of a fast reactor with an energy spectrum that is harder than other fast reactor types, but also permit core designs in which the fuel pin lattice has a large spacing, thereby increasing the coolant volume fraction without a significant reactivity penalty. Increasing the coolant volume fraction increases the hydraulic diameter for coolant flow through the core with a corresponding reduction of the core frictional loss. As a result of the neutronic and transport properties of lead, natural circulation is effective and can remove up to 100% of the core power, depending on reactor design, and can be relied upon for passive shutdown heat removal.

6.2.2 Design choices for reactors with lead as the coolant

The favorable properties of the lead coolant and nitride fuel (a feature of some advanced LFR designs), combined with high-temperature structural materials, can extend the reactor coolant outlet temperature up to the 750–800°C range in the long term (GIF, 2002, 2014), but this will require the development of new structural materials. For that reason, most of the present LFR projects limit the mean core outlet temperature to about 550°C, which is the same core outlet temperature typically found in SFRs. In the EC/Euratom projects, the core outlet temperature is further reduced to 480°C for easier resolution of the issue of corrosion in lead, a phenomenon that depends strongly on temperature.

^a It should be noted that, although the energy loss due to elastic scattering in lead or LBE is significantly smaller than in sodium, the energy loss from inelastic scattering is greater, and this partially offsets the comparative advantage of lead or LBE in maintaining fast neutron energies.

On the other hand, it is well known that the thermal efficiency of the Rankine cycle depends more on the core inlet temperature (which is linked to the steam pressure) than on the core outlet temperature (primarily affecting only the level of steam superheating), so that the efficiency of LFRs operating in the outlet range of 480–550°C can be projected to remain at a high level.

In fact, considering also that an intermediate circuit is not needed for the LFR [since, due to the coolant's relative chemical inertness, there is no need to isolate the primary coolant from the Steam Generator (SG) circuit], and that as a result, there is no degradation of the thermal cycle from such an intermediate circuit, a net efficiency of over 40% is reached for each of the GIF reference reactor systems (see Table 6.2), despite the moderate values of the core outlet temperatures. The parameters shown in this table are representative of modern designs serving as reference designs in the LFR System Research Plan of the GIF (GIF-LFR-pSSC, 2014). Note that the use of CO₂ as a secondary coolant has been proposed in one of the Generation-IV reference designs, and that it also reflects a net efficiency level well above 40%.

6.2.3 Primary system concepts: Evolution and challenges

Although LBE-cooled reactors were initially designed and operated for the propulsion of a limited number of Soviet/Russian submarines, this design experience cannot be fully extrapolated to the full range of LFR concepts, since these reactors were small, operated at low capacity factor, and featured an epithermal (as opposed to fast) neutron energy spectrum (GIF, 2002, 2014).

Meanwhile, the designs of LFRs have profited, perhaps to an even greater degree, from the large experience in the design, construction, and operation of the SFR. It is not surprising, therefore, that several of the early LFR projects were heavily based on solutions typical of SFRs.

6.2.3.1 Early conceptual designs derived from sodium-cooled fast reactor concepts

Early LFR concepts initially considered both pool-type and loop-type primary coolant systems; however, more recent designs have focused on pool-type primary systems, mainly to avoid the seismic issues associated with lead-filled piping.

Owing to the low chemical reactivity of lead with water, in contrast with sodium in the SFR, current LFR projects generally dispense with the intermediate loop between the primary system and the steam-water loop

Table 6.2. Selected design parameters of Generation-IV reference LFR concepts

Parameter	ELFR	BREST-OD-300	SSTAR
Core power (MW _{th})	1500	700	45
Electrical power (MW _{el})	600	300	20
Primary system type	Pool	Pool-loop hybrid	Pool
Core inlet temperature (°C)	400	420	420
Core outlet temperature (°C)	480	540	564
Secondary cycle	Superheated steam	Superheated steam	Supercritical CO ₂
Net efficiency (%)	42	43.5	44
Turbine inlet pressure (bar)	180	170	200
Feed temperature (°C)	335	340	420
Turbine inlet temperature (°C)	450	505	550

or other power conversion equipment. In fact, LFR primary system designs, especially in the past, have been very similar to those normally adopted for the SFR, but with the replacement of the intermediate heat exchanger with the SG or, in the case of SSTAR, with a lead-CO₂ heat exchanger. The opening up of the fuel pin lattice, however, while providing major benefits in terms of reduced flow resistance and enhanced potential for natural circulation cooling, also results in the reduction of the core power density and would therefore require a larger core diameter than that of an SFR of the same nominal power.

In addition, to avoid excessive corrosion and erosion by flowing lead, the speed of lead has been cautiously limited by design to values much lower (less than 2–3 m/s in most of the channels) than the flow speed of sodium in SFRs (typically 5–7 m/s). Since the heat capacity per unit volume of lead is only about 40% higher than the volumetric heat capacity of sodium, it follows that the volume of an LFR based on typical SFR solutions would be much larger than the primary system of the SFR of the same nominal power.

If, in addition, the density of lead is taken into account (it is higher than the density of sodium by more than a factor of 10), it is evident that the mass of lead of an LFR would be very large and could even become prohibitive for the seismic design of the primary system of the reactor unless a design approach different from that of an SFR is utilized.

6.2.3.2 Primary system development and evolution

Gradual improvements in the understanding of the properties of lead have resulted in LFR design evolution and diversification (deviation) from SFR concepts to exploit the unique characteristics of lead as a coolant. Considering that much of the intense design effort for modern LFR systems has taken place only during the last 20 years, it is not surprising that there are multiple approaches being considered by designers for selection from among many options.

As an example, consider the ELSY project, which is a predecessor to the ELFR concept. ELSY represented a milestone in the quest for innovative solutions, and this quest has continued as designers have explored additional improvements to be embodied in subsequent designs.

The adoption of the pool-type reactor configuration and, more importantly, the incorporation (within the reactor vessel) of a new-design, short-height SG with integrated mechanical pump, represents an important set of innovations leading to achievement of the design goal of enhanced system compactness (see [Figure 6.1](#)).

The anticipated primary system pressure loss of this LFR is about 1.5 bar; thus, a free level difference between the cold and the hot collector of only about 1.5 m is sufficient to feed the core.

Thus, it is noted that in ELSY, as well as the subsequent EC/Euratom projects (ELFR and ALFRED), an unconventional solution has been adopted, namely the installation of the Primary Pumps (PPs) in the hot collector.

While the European design efforts leading to the ELSY/ELFR/ALFRED series of LFR concepts were being conducted, parallel efforts were being pursued to develop an array of innovative designs. Projects in Russia, Japan, S. Korea, Sweden, the United States, and China concurrently pursued a variety of different concepts with considerable innovation and creativity with respect to primary system design as well as the entire reactor systems.

The Russian BREST-OD-300/1200 concepts (discussed further in [Section 6.6](#)) feature a multizone concrete reactor vessel with the reactor core in the central zone, and reactor coolant pumps and SGs in separate zones to which the lead coolant flows through interconnecting channels.

The SSTAR concept (also discussed further in [Section 6.6](#)) relies on natural convection for coolant flow during operational as well and shutdown conditions. It also features an in-vessel lead-to-CO₂ heat exchanger to enable power conversion by a supercritical carbon dioxide Brayton-cycle system.

In summary, the system designs of the GIF reference reactors (as well as a multitude of other design concepts in various stages of development) provide a range of different approaches to primary system design appropriate for LFR reactor systems.

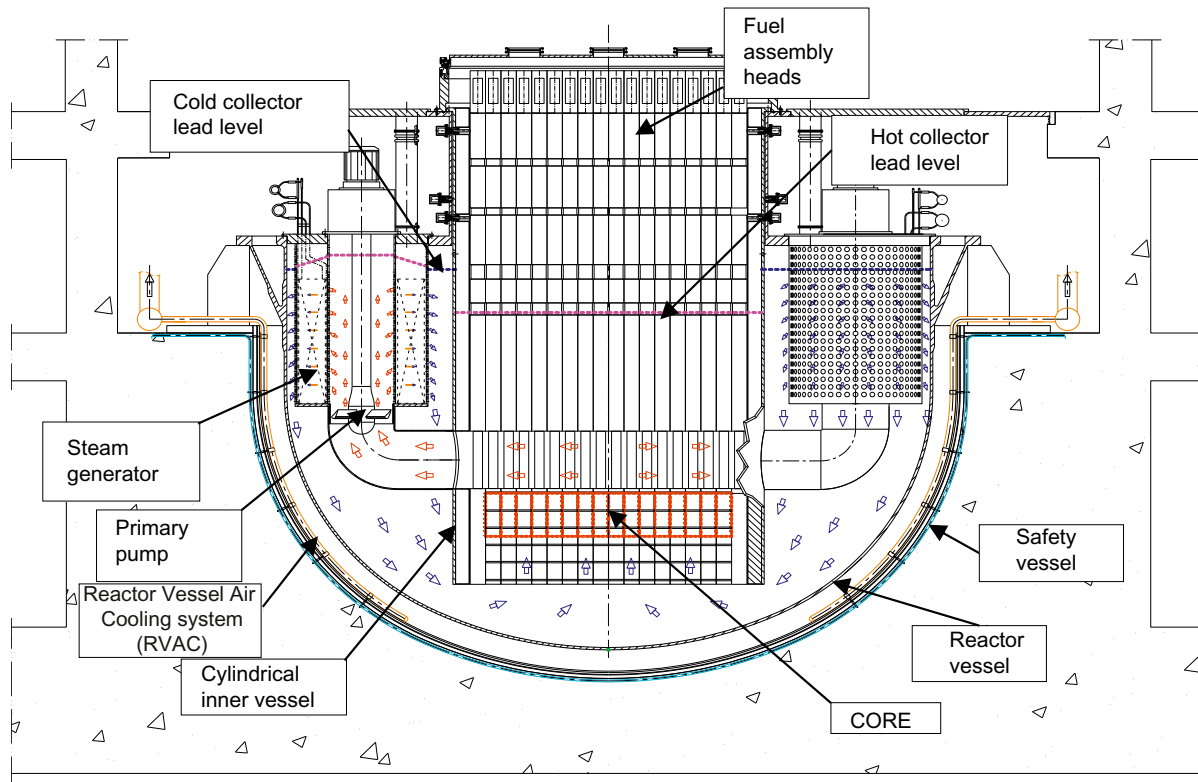


Figure 6.1. Primary system configuration of ELSY. Credit: Dr. Alessandro Alemberti, Ansaldo Nucleare

6.3 Safety principles

The fundamental safety functions (control of reactivity, core cooling, and confinement of radioactive material) are achieved and enhanced for the LFR by exploiting the favorable characteristics of the lead coolant.

For reactor shutdown, LFR designs are equipped with redundant and diversified control rod systems. Peculiar to the LFR is the high buoyancy of lead, which facilitates rod insertion from the bottom of the core (which would be more difficult from above, requiring active means or the use of ballast materials).

The high thermal inertia and negative reactivity feedback of lead systems offer, in general, large grace times for corrective operator action, even in case of an unprotected transient during which small positive reactivity feedbacks are counterbalanced by the strong negative core radial expansion feedback, which limits the reactor power.

For shutdown heat removal and in some cases operational heat removal, LFR designs are generally characterized by the existence of strong natural circulation characteristics, and the provision of passive, redundant, and diverse DHR systems. The final heat sink can be stored or otherwise available water (as in the case of ELFR), atmospheric air (as in the case of BREST or SSTAR), or potentially both for a higher degree of diversification.

For confinement of radioactive material, a pool-type LFR with a guard vessel would not suffer loss of primary coolant, even in the event of failure of the reactor vessel. The core would remain covered and, by design provision, natural circulation flow paths would be maintained.

No hydrogen generation that can damage the containment system is expected in an LFR because of the relative chemical inertness of the coolant.

The containment system design pressure is not affected by the primary system and can be limited by optimizing the water inventory in the secondary system in the designs that utilize steam cycle power conversion.

The tendency of lead to retain bulk FPs, thereby reducing the source term to containment, limits the potential for release of radionuclides and may reduce the requirements for emergency planning zones and emergency evacuation plans.

The Fukushima accident has reinforced the awareness, already well appreciated by designers, of the importance of DHR systems and of the necessity that they continue to operate, even following loss of station service power.

In the LFR designs, three different DHR approaches have been considered and incorporated into LFR reactor designs:

- Reactor Vessel Air Cooling System (RVACS).
- Direct Reactor Cooling (DRC) through Dip Coolers (DCs).
- Heat removal through the water/steam main loops.

RVACS is a reliable system, but its use can be considered only for small-size reactors, since in such systems, the vessel outer surface is relatively large in comparison with the reactor power.

DRC solutions can operate in a natural circulation mode and, new design solutions have been conceptualized, which are not only passively operated, but also passively actuated. This is possible because in an LFR, there is a margin of more than 200–300°C between the temperature of the cold collector of the reactor and the temperature that represents a safety limit; hence thermal expansion of materials, or gas expansion, can be used to initiate the operation of DHR systems.

Typical solutions include a dip cooler with water/steam at the secondary side connected to an external condenser that uses either water or air as the heat sink.

The main water-steam loops (secondary system) provide the normal route for non-safety-related DHR, but the interest in their use with safety function may be limited for the following three reasons:

- The secondary system of a reactor with a superheated steam cycle is a system with relatively low reliability;
- Unlike the Pressurized Water Reactor (PWR), the secondary system of the LFR does not offer much in terms of heat capacity; and
- In the LFR, the most efficient means to mitigate the consequences of the Steam Generator Tube Rupture (SGTR) accident is the prompt, simultaneous depressurization of all secondary loops and isolation of the in-vessel SGs. Any safety-related DHR function bound with the SGs would require, instead, discrimination and isolation of the ruptured SG only, an action to be carried out preferably in a very short time (of the order of a few seconds), and this is risky if the discrimination is not fully reliable.

The SG, when functionally unavailable for heat removal, becomes a portion of the hot leg of the primary loop. A short SG helps provide a minimum difference in the lead coolant level between the SG outlet and the active core mid-plane sufficient for adequate natural circulation, without requiring an excessive increase in the overall height of the reactor vessel.

The main topics of ongoing and near future research, as far as safety is concerned, are related to experimental activities for the demonstration of LFR safety system functionality and performance. Although safety system capabilities have been assessed through numerical simulations and separate effects tests have been performed, it is expected that licensing authorities will require integral testing at appropriate scale to assess the behavior of the systems to be licensed. Other experimental testing is also necessary to confirm other attributes of LFRs, such as the expected tendency for fuel dispersion instead of consolidation in case of cladding failure.

The elimination of the intermediate cooling system (in comparison to other reactor types, such as the SFR) and the installation of high-pressure SG equipment inside the reactor vessel operating at ambient pressure are features that require a rigorous approach focused to the achievement of three main objectives:

- low failure probability of the pressure boundary of the SG;
- low water/steam release in case of rupture of one or more tubes of the SG;
- low impact of any SG release of water/steam from the SG with respect to:
 - pressurization of the primary boundary;
 - mechanical loadings on the internals, core included; and
 - steam entrainment into the core.

Among other safety-related investigatory efforts, specific activities are currently planned or ongoing for SGTR tests at small scale with extension to larger scale in the future.

6.4 Fuel technology and fuel cycles for the lead-cooled fast reactor

6.4.1 Fuel assembly characteristics

The fuels anticipated for modern LFR concepts are generally in the form of annular pellets of (U, Pu)O₂ as in the Euratom concepts or (U, Pu, MA^b)N in the Russian and US concepts BREST and SSTAR.

Fuel pellets are stacked inside fuel rods (rod outside diameter of ~10 mm) of stainless steel (e.g., 15–15 Ti stabilized) to form a fuel column of typical height of 0.6–1 m. The typical length of a fuel rod is at least twice the active length in order to include a lower gas plenum and an upper gas plenum with a spring to compact the fuel pellets.

Fuel rods (typically 100–300 in number) are arranged as a bundle to form the Fuel Assembly (FA), with a hexagonal or square cross section, which can either be open or have a flow duct (wrapper) of lateral containment of the bundle.

The solution with the wrapper has the advantage of enabling varying pressure losses through the various FA in order to control the radial distribution of core temperature, but it is disadvantageous from the neutronic viewpoint in addition to requiring greater quantities of steel and lead in the core region.

The upper head of the FA is appropriately shaped for its connection with the gripping mechanism of the handling machine. The handling machine can be designed to operate either in lead (as in BREST) or in gas (as in ELFR) to avoid the difficulties of qualification of mechanisms operated in lead.

By extending the FA with a stem that is well above the lead coolant surface level, it is possible to use a handling machine that operates exclusively in gas. This solution has also other advantages including the fact that the mass of the FA that emerges from the lead can compensate for the excess buoyancy of the immersed portion, and that the FA does not need to be connected to a lower support grid to prevent its vertical motion. Moreover, the extended FA stem can house the core instrumentation eliminating the need for the above-core structure typical of other liquid metal-cooled reactors (i.e., the SFR).

The power density, the operating temperature, the neutron flux, and the transients of the fuel of an LFR are similar to those of an SFR so that the experience gained by the large investments made for SFR fuels can be used for the LFR.

6.4.2 Fuel cycle for the lead-cooled fast reactor

The LFR is compatible with a closed fuel cycle or an open fuel cycle. Fast reactors have been conceived for either fuel cycle scenario, and LFRs can be Plutonium (Pu) breeders, Pu burners, or reactors with equilibrium

^b In the nuclear fuel context, MA refers to Minor Actinides.

fuel composition and long core life. In the present scenario characterized by a general surplus of Pu and uncertainty on nuclear power development, the designers of LFRs have devoted relatively little attention to the potential roles of LFR as a Pu breeder or burner, and the main attention has been devoted to the role of reactors with equilibrium fuel composition. This is the case for ELFR, BREST, and SSTAR, as well as other concepts under consideration. Microreactor concepts under consideration (e.g., CLEAR-M10 or Hydromine LFR-TL-5) will likely take alternative approaches such as High Assay-Low Enriched Uranium (HALEU) fuel.

An adiabatic core (Artioli et al., 2010) is a fuel cycle strategy able to convert an input feed of either Natural or Depleted Uranium (NU or DU, respectively) into energy, with FP and actinide reprocessing losses as the only output stream. This allows the full closure of the fuel cycle within the reactor (thus the term adiabatic, because of its having no “significant” exchange with the environment) with the concentrations of uranium and transuranics remaining at equilibrium in the core, as shown in Table 6.3, which depicts the results of an analysis carried out for the ELSY reactor.

The use of the LFR in an open cycle, loaded with enriched Uranium (U), would require competitiveness with present Light Water Reactors (LWRs), and the authors are not aware of any systematic studies, but only of promising preliminary evaluations related to the potential cost reductions made possible by recent conceptual projects.

An additional consideration exemplified in designs such as SSTAR is the ability to achieve very long core life in LFRs that operate with a conversion ratio at or slightly above one. This approach yields minimum burnup swing and thus enables long core life in such systems.

6.5 Summary of advantages and key challenges of the lead-cooled fast reactor

6.5.1 Advantages of the lead-cooled fast reactor

Lead is unique among the coolants available for nuclear reactor systems for a number of reasons. As a dense liquid, it has excellent cooling properties, while its nuclear properties (i.e., its low tendency to absorb neutrons or to slow them down) enable it to maintain a hard neutron energy spectrum, resulting in flexibility in fuel management and coolant flow design. These characteristics facilitate improved resource utilization, longer core life, effective burning of Minor Actinides (MA), and open fuel pin spacing, important features in achieving sustainability, proliferation resistance, fuel cycle economics, and enhanced passive safety by enabling fuel cooling by natural circulation.

Lead has the very high boiling temperature of 1737°C. Consequently, the problem of coolant boiling is, for all practical purposes, eliminated. The high margin to boiling leads to important safety advantages including design simplification and improved economic performance.

Table 6.3. Fuel composition at equilibrium for an adiabatic ELSY (derived from Artioli et al. (2010))

Element	Composition (mass %)
Uranium	81.94
Plutonium	17.18
Neptunium	0.08
Americium	0.64
Curium	0.16

As a coolant operating at atmospheric pressure, the Loss Of Coolant Accident (LOCA) is virtually eliminated by use of an appropriately designed guard vessel. This not only is a safety advantage, but also offers additional potential for plant simplification and improved economic performance, since the complex process of simultaneous management of temperature, pressure, and coolant level (as is seen in water-cooled reactors) is not necessary. One of the most significant advantages of lead as a coolant is its low chemical activity. In comparison with other coolants, especially sodium and water, lead presents a relatively benign coolant material that does not support chemical interactions that can lead to energy release in the event of accident conditions. Further, the tendency of lead to retain FPs and other materials that might be released from fuel in the event of an accident is another important advantage. The elimination of the need for an intermediate coolant system to isolate the primary coolant from the water and steam of the energy conversion system represents a significant advantage and potential for plant simplification and improved economic performance.

Following the Fukushima-Daiichi reactor accidents, it is important to consider future reactor technologies in light of the potential for severe accident conditions. The LFR can demonstrate superior features to avoid the consequences of such severe accidents. First, one of the primary issues was the common-mode loss of on-site diesel generators (caused by the tsunami) during an extended blackout condition (caused by the earthquake). An LFR would not need to rely on such backup power and would be resilient in the face of blackout conditions because of passively operated DHR enabled by the natural circulation capabilities of the lead coolant.

Second, the loss of primary coolant at the Fukushima-Daiichi reactors resulted from the use of pressurized water coolant. An LFR with guard vessel would not suffer a loss of primary coolant, even in the event of a failure of the reactor vessel.

The steam-cladding interactions at the Fukushima-Daiichi reactors resulted in the liberation of hydrogen and associated explosions. With the relative chemical inertness of lead as a coolant, no hydrogen generation would be enabled.

6.5.2 Key challenges of the lead-cooled fast reactor

As for all Generation-IV advanced reactor technologies, there are technology challenges associated with development of the LFR. These challenges include those related to the high melting point of lead, its opacity, the coolant mass as a result of its high density, and the potential for corrosion/erosion when the coolant is in contact with structural steels.

The high melting temperature of lead (327°C) requires that the primary coolant system be maintained at temperatures to prevent the solidification of the lead coolant or at least to maintain a recirculation at the core level to allow its cooling. The use of a pool-type configuration and appropriate primary system design can provide a safe and effective resolution to this issue.

The opacity of lead, in combination with its high melting temperature, presents challenges related to inspection and monitoring of reactor in-core components as well as fuel handling. This issue can also be addressed by appropriate and specific design features; for example, innovative core configurations with FAs extended above the lead-free level, as implemented in the recent European projects, would serve to alleviate this issue.

The high density and corresponding high mass of lead as a coolant result in the need for careful consideration of structural design to prevent seismic impacts to the reactor system. Innovative primary systems configurations with short reactor vessels and the introduction of seismic isolation are options to address such issues.

Possibly the most difficult challenges result from the tendency of lead at high temperatures to be corrosive when in contact with structural steels. This tendency, which is accelerated at higher temperatures, will require careful material selection, coolant chemistry control and component and system monitoring during plant operations.

Pending the development of materials resistant to lead corrosion at higher temperature, surface treatment, and small quantities of additional elements in the structural matrix and oxygen control are necessary to protect materials immersed in lead from corrosion and also to protect against the formation of solids in the lead coolant from oxidation processes. In the design configurations developed to date, limitations on coolant outlet temperatures serve to reduce the potential impact of this issue.

Some research priorities currently receiving attention include: (i) material qualification in a lead or LBE environment, including under conditions of irradiation; (ii) the development of design codes and standards tailored to LFR needs; (iii) fission and activation product retention in lead at higher temperatures; and (iv) severe accident phenomenology.

Each of these areas of challenge is a topic of ongoing research; it is likely they can be addressed by effective research, design, and engineering. Further discussion of developments to address corrosion/erosion follows.

Considerable past research has been conducted on the topics of oxygen control and protective coatings to control the potential for corrosive damage to in-vessel materials (OECD-NEA, 2015). One of the new strategies to address high-temperature corrosion issues in lead is the use of ceramic coatings. Specifically, some oxide coatings are basically insoluble in heavy liquid metals and would enable corrosion protection at low and high temperatures. However, the structural integrity of the coating substrate system must be guaranteed at all times. Therefore, coatings are not only required to be corrosion resistant, but they must also withstand a harsh environment in which the combination of high temperature and radiation damage can affect the materials in question.

It is well known that molten lead and LBE can attack conventional structural steels, such as AISI 316L and 15-15Ti, at temperatures in excess of 500°C, thus limiting the operating temperature of the reactor in the near term and requiring the development of new materials in the longer term to enable higher temperature operations.

Since martensitic steels have the potential for Liquid Metal Embrittlement (LME) between 300°C and 450°C, they have been avoided by several designers. For other steels, in order to enable near-term development (i.e., before more advanced corrosion-resistant materials can be qualified), operating temperatures below 450°C have been selected to avoid corrosion while still delivering thermal energy at a temperature range enabling acceptable power conversion efficiency. At such temperature ranges (300–450°C), materials already qualified for SFRs (i.e., the alloy 316LN) can be used for the reactor vessel and internals, and the alloy 15-15Ti for fuel cladding. To operate at higher temperatures, considerable work is being conducted to develop materials qualified for such conditions. The use of austenitic stainless steels and ceramic coatings for this purpose are examples of these efforts.

In recent years, Alumina-Forming Austenitic (AFA) stainless steels have gained interest following successful work carried out by Oak Ridge National Laboratory (ORNL) in the United States. AFA alloys have shown great creep resistance in the temperature range of 600–900°C and excellent corrosion resistance in dry and humid air. The creep strength and corrosion resistance (i.e., the ability to form Al₂O₃ scales) have been attributed to the Nb content of the alloys. Formation of nanosized Nb carbides throughout the matrix leads to a significant increase in creep resistance, and simultaneously improved corrosion resistance (Ejenstam et al., 2015).

Another interesting strategy to address high-temperature corrosion in Gen-IV LFRs is the use of ceramic coatings for steel (fuel cladding) substrates. This is because most oxides (e.g., Al₂O₃, SiO₂, Cr₂O₃, Y₂O₃) are practically insoluble in heavy liquid metals and are relatively more thermodynamically stable than PbO and Fe-based oxides at all temperatures (Schroer and Konys, 2007). Therefore, an oxide coating would mitigate liquid metal corrosion effects at both low and high temperatures. However, the structural integrity of the coating-substrate system must also be guaranteed at all times. Therefore, coatings are not only required to be corrosion-resistant, but they must also withstand a harsh service environment, where the combination of high temperatures and radiation damage ultimately results in the development of stresses/strains and the

possible mobilization and concentration of radiation-induced defects (i.e., voids) at performance-defining interfaces, such as the coating/substrate interface.

Since 2013, amorphous/nanocrystalline Al_2O_3 coatings deposited by Pulsed Laser Deposition (PLD) have been demonstrated at the Italian Institute of Technology (IIT) as a viable option to protect both ferritic/martensitic (i.e., T91 and EUROFER) and austenitic (i.e., AISI 316L and 15-15Ti) steels from dissolution corrosion attack by lead, LBE and Pb-Li (García Ferré et al., 2013a, b; Iadicicco et al., 2018, 2019; Hernández et al., 2019). This process deposits a fully dense oxide thin film (thickness on the order of a micrometer) with high adhesion at room temperature, hence avoiding microstructural changes and property degradation of the underlying steel components. Being a line-of-sight, vacuum deposition technique, it is best suited for simple, critical components such as, for example, fuel cladding. The as-deposited coatings are amorphous and fully dense and exhibit an excellent combination of metal-like mechanical properties and ceramic hardness, together with strong interfacial bonding and resistance to wear. Recent in-situ TEM experiments showed how this material exhibit unique elastoplastic response under both tensile and compressive tests at room temperature. A clear onset of plastic deformation (as high as 7% in tension and 100% in compression) has been observed and a yield stress as high as 4 GPa (tensile and compressive) has been measured (Frankberg et al., 2019). Moreover, testing results have provided confirmation of the merits of alumina coatings including performance under thermal cycling conditions, resistance to damage from heavy-ion irradiation (García Ferré et al., 2018) (an indication of potential resistance to damage under neutron irradiation) and low permeability to hydrogen (suggesting its use for tritium confinement within fuel cladding). As a result, the interest in alumina coatings for use in LFRs is increasing.

6.6 Overview of Generation-IV lead-cooled fast reactor designs

6.6.1 Reference Generation IV systems

The GIF LFR provisional System Steering Committee, which was organized in 2005, identified as reference designs the large central station design (ELSY) and the small modular system (SSTAR). In 2011, the committee was reformulated, and the new committee changed the European reference system from ELSY to the European Lead-Cooled Fast Reactor (ELFR) and added an intermediate-size LFR (i.e., the BREST-OD-300) as a new thrust and reference reactor system, while the SSTAR legacy system was retained as the reference small LFR. The typical design parameters of these GIF-LFR reference systems were previously summarized in Table 6.2 and are described further in the following subsections.

Early designs of LFRs were heavily influenced by earlier efforts to develop the SFR; however, over time, new solutions have been developed, recognizing the unique characteristics of the coolant. The reference GIF systems, in particular, introduce several innovations such as the following:

- the BREST reactor's use of a concrete outer vessel
- the SSTAR reliance on natural circulation cooling for operational heat removal
- the ELSY/ELFR use of compact, extended stem FAs

6.6.1.1 The European Lead-cooled Fast Reactor (ELFR)

The ELFR is a design resulting from the update and modification of the earlier ELSY reactor concept. Figure 6.2 provides an overview sketch of the primary system configuration of the ELFR reactor.

The overall primary system is contained inside a reactor vessel of stainless steel and is shaped as a cylindrical vessel with a dished bottom head. A safety vessel, anchored to the reactor pit, collects and contains lead in the event of reactor vessel leakage. The reactor vessel is a thin shell structure, the design of which is largely governed by seismic loadings and those potentially associated with lead sloshing.

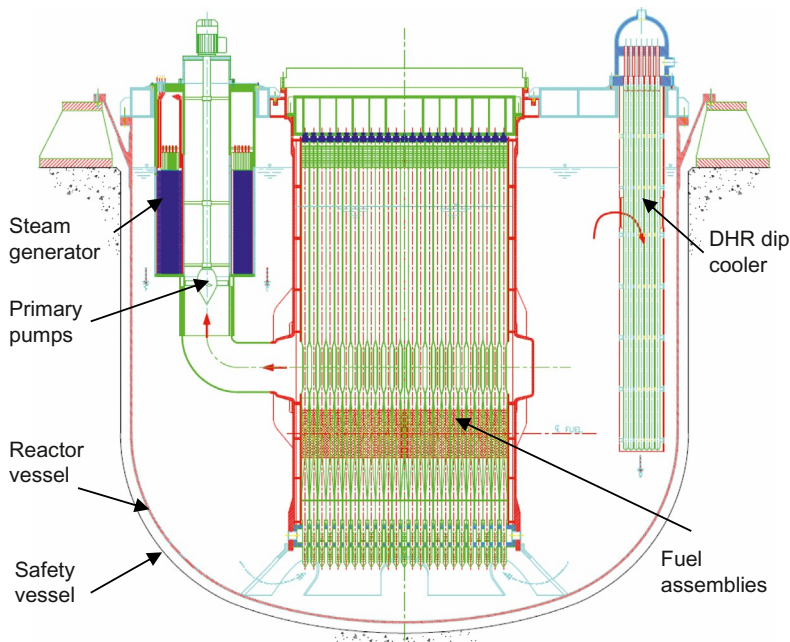


Figure 6.2. Primary system configuration of ELFR. Credit: Dr. Alessandro Alember, Ansaldo Nucleare

Within the vessel are eight removable SG-PP assemblies, arranged symmetrically around the core close to the wall of the reactor vessel.

Under normal, steady state operation, the lead-free level inside the inner shell of the SG is higher than the free level in the cold collector (outside the SG), which is higher than the free level in the inner vessel. The three equilibrium levels are the result of the hydraulic head provided by the PP, the different lead density in the legs of the primary circuit and the friction in the circuit. Thus, lead circulation is driven both by the hydraulic head provided by the PP and the natural draft. Lead enters the core at 400°C, where it is heated up to an average of 480°C. At the core outlet, it flows outward entering the suction ports of the eight PPs and then upward into the annular space between the pump shafts and the inner shells of the SGs. It flows then across the perforated inner shell and the tube bundles of the SGs, where lead is cooled to 400°C and finally down to the core inlet, thereby closing the circuit.

Inside the reactor vessel, the cold collector is located in the annular space between the reactor vessel and the cylindrical inner vessel.

Two different and independent (physically separated) DHRs are provided for the ELFR. Each DHR system includes:

- DHR1: four Isolation Condenser Systems (ICs) connected to four SGs.
- DHR2: four ICs connected to four DCs.

The core design has demonstrated that it is possible to provide an *adiabatic* reactor concept with equilibrium fuel so that the fuel composition remains the same between two successive loadings, ensuring the full recycling of all the actinides, with either NU or DU as the only input and FPs as output. The equilibrium fuel composition is shown in [Table 6.4](#).

The FA is characterized by a wide pitch-to-diameter ratio favoring the establishment of natural circulation at sustainable thermal regimes during unprotected loss of flow accidents ([Table 6.5](#)).

6.6.1.2 The BREST-OD-300 reactor

The BREST-OD-300 reactor (and its companion larger system design, the BREST-1200) is a system developed by the Russian organization NIKIET in association with a number of other organizations with the goal of realizing a “naturally safe” LFR concept.

Table 6.4. Composition of the ELFR equilibrium fuel^a
(derived from [Artioli et al. \(2010\)](#))

Element	Composition (mass %)
Uranium	80.56
Plutonium	18.15
Neptunium	0.11
Americium	1.02
Curium	0.16

^a In comparing the equilibrium fuel compositions of ELSY ([Table 6.3](#)) and ELFR ([Table 6.4](#)), the differences arise mainly from the effect of different burnups of the two systems (78 MWd/kg HM for ELSY, 52.4 MWd/kg HM for ELFR).

Table 6.5. ELFR main parameters

ELFR design options	
Electrical power, MW_{el}	600
Primary coolant	Pure lead
Primary system	Pool type, compact
Primary coolant circulation	Forced; DHR in natural circulation is possible
Core inlet temperature, °C	400
Steam generator inlet temperature, °C	480
Secondary coolant cycle	Water-superheated steam
Feed-water temperature, °C	335
Steam pressure, MPa	18
Secondary system efficiency, %	~43
Reactor vessel	Austenitic SS, hung
Safety vessel	Anchored to reactor pit
Inner vessel (core barrel)	Cylindrical
Steam generators	Integrated in the reactor vessel and removable. Preferred option: spiral tubes
Primary pumps	Mechanical pumps in the hot collector, removable
Fuel assembly	Closed (with wrapper), hexagonal
Fuel type	MOX
Maximum discharged burnup, MWd/kg of heavy metal	100

Continued

Table 6.5. ELFR main parameter—cont'd

ELFR design options	
Electrical power, MW_{el}	600
Refueling interval, y	2
Fuel residence time, y	5
Fuel clad material	T91, coated
Maximum clad neutron damage, dpa	100
Maximum clad temperature in normal operations, °C	550
Maximum core pressure drop, MPa	0.1
Control/shutdown system	Two diverse and redundant systems: pneumatic inserted absorber rods (with backup tungsten ballast) from the top; buoyancy absorber rods from the bottom
Refueling system	No in-vessel fuel handling machine
DHR systems	Two diverse and redundant systems (actively actuated, passively operated):
Seismic damping devices	2-D isolators below reactor building

Its objectives include the elimination of severe accidents, including those related to power excursions, cooling loss, loss of external and backup power, or multiple common cause threats. It features the ability to be self-sustaining in an equilibrium operating mode and is unique in its provision for a complete fuel pyro-processing capability colocated with the reactor.

The BREST-OD-300 is a pilot technology demonstration reactor being developed as a prototype of future commercial reactors of the BREST family, such as the larger BREST-1200. Table 6.6 provides a summary of key parameters for both the BREST-OD-300 and BREST-1200 concepts. It should be noted that the BREST-OD-300 is currently under construction having received a construction license on February 10, 2021.

The BREST-OD-300 is a reactor of pool-type design. It incorporates, within the pool, the reactor core with reflectors and control rods, the lead coolant circulation circuit with SGs and pumps, equipment for fuel reloading and management, and safety and auxiliary systems. These reactor systems and items of equipment are included in a steel-lined, thermally insulated concrete vault.

BREST has a widely spaced fuel lattice with a large coolant flow area. This results in low-pressure losses, enabling natural circulation of the primary lead coolant for DHR. It does not utilize U blankets, but instead takes account of the reflecting properties of lead to improve power distribution and provide negative void and density coefficients. By design, it is not suitable for the production of weapons-grade Pu. The BREST DHR systems feature passive and very long-term residual heat removal directly from the primary coolant by natural circulation of air through air-cooled heat exchangers with the heated air vented to the atmosphere.

The fuel type planned for the first core of the BREST reactor is DU mixed with Pu and MA in the nitride form. The composition corresponds to that resulting from spent fuel from PWRs following reprocessing and a ~20-year cooling period.

The properties of lead allow for the operation with such fuel as an equilibrium composition. This mode of operation features full sustainment of the fissile nuclides in the core (the core breeding ratio is ~1) with

Table 6.6. Technical parameters of BREST-OD-300 and BREST-1200

Characteristic	BREST-OD-300	BREST-1200
Thermal Power, MW _{th}	700	2800
Electric Power, MW _{el}	300	1200
Core diameter, mm	2650	4755
Core height, mm	1100	1100
Fuel rod diameters, mm	9.7–10.5	9.1–9.7
Fuel rod pitch, mm	13.0	13.0
Core fuel	(U+Pu)N	(U+Pu+MA)N
Core charge (U+Pu+MA)N, t	19	64
Charge of (Pu+MA)/(²³⁹ Pu+ ²⁴¹ Pu), t	2.5/1.8	8.56/6.06
Fuel lifetime, y	5	5–6
Refueling interval, y	1	1
Maximum fuel burnup % h.a.	9.0	10.2
Total margin of reactivity % $\Delta K/K$	0.24	0.35
Lead inlet/outlet temperature, °C	420/535	420/540
Maximum fuel cladding temperature, °C	650	650
Maximum lead velocity, m/s	1.9	1.7
Water-Steam temperature at steam generator inlet/outlet, °C	340/505	340/520
Pressure at steam generator outlet, MPa	17	24.5
Net efficiency of power unit, %	43.5	43
Design service life, y	30	60

irradiated fuel reprocessing in a closed fuel cycle. Reprocessing is limited to the removal of FPs without separating Pu and MA from the mix (U-Pu-MA). One of the unique characteristics of the BREST reactor is that a fuel fabrication/reprocessing plant is colocated with the reactor. This eliminates in principle any issues or concerns due to spent nuclear fuel transportation.

Figure 6.3 is a sketch of the BREST-OD-300 reactor.

6.6.1.3 The Small Secure Transportable Autonomous Reactor (SSTAR)

SSTAR is the legacy design of a reactor originally intended for deployment to countries with developing economies and infrastructures, or to sites with remote locations requiring standalone power supply. Though not currently under active development, the SSTAR design has been retained as the GIF reference design for a small modular LFR system.

The SSTAR development focused on the concept of a small transportable reactor system for international deployment, especially to remote locations or those disconnected from well-developed electricity distribution systems. SSTAR has the following features: (1) a reactor core that is designed for no refueling or whole-

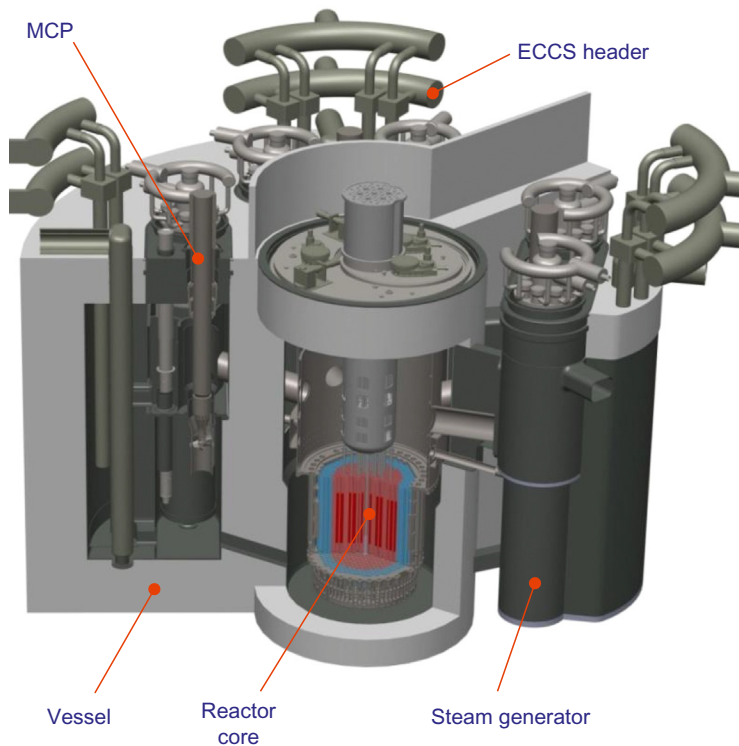


Figure 6.3. Sketch of the BREST-OD-300 reactor system. Credit: Dr. Andrei Moiseev, NIKIET

core replacement to eliminate the need (and ability for) on-site refueling; (2) transportability: the entire core and reactor vessel would be delivered by ship or overland transport; (3) a very long-life core design: 15- to 30-year core life is the target; (4) the capability for autonomous load following with simple integrated controls allowing minimal operator intervention and enabling minimized maintenance; and (5) local and remote monitorability to permit rapid detection/response to operational perturbations. These features permit installation and operation in places with minimal industrial infrastructures. Additionally, they provide a facility characterized by a very small operational (and security) footprint.

Key characteristics of the SSTAR system are summarized in Table 6.7 and illustrated in Figure 6.4. They include the following: coolant circulation is by natural convection for both operational and shutdown heat

Table 6.7. Technical parameters of SSTAR

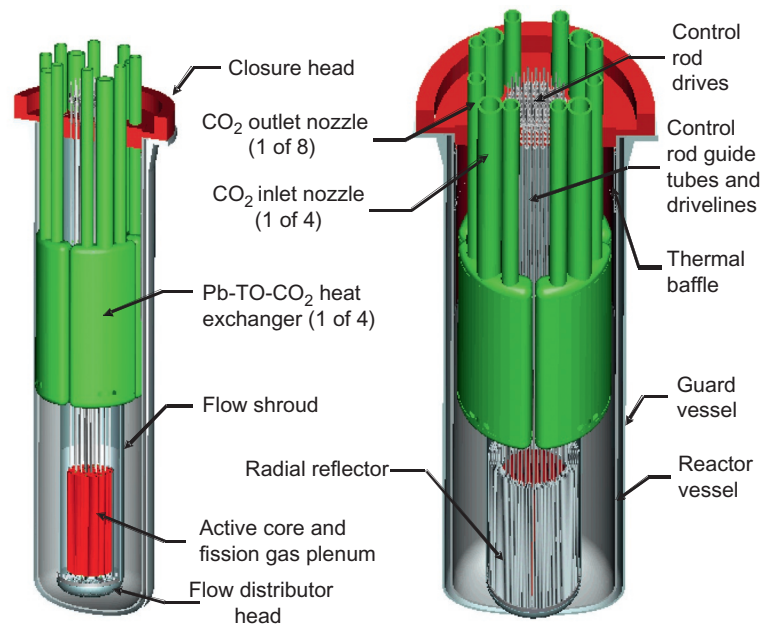
SSTAR parameters, features and performance	
Coolant	Lead
Coolant circulation	Natural convection
Power conversion	Supercritical CO ₂ , Brayton cycle
Fuel	TRU nitride using nitrogen enriched in ¹⁵ N
Enrichment, %	5 radial zones; 1.7/3.5/17.2/19.0/20.7
Core lifetime, y	30
Core inlet/outlet temperatures, °C	420/567
Coolant flow rate, kg/s	2107

Continued

Table 6.7. Technical parameters of SSTAR—cont'd

SSTAR parameters, features and performance	
Coolant	Lead
Power density, W/cm ³	42
Average (peak) discharge burnup, MWd/kg HM	81 (131)
Burnup reactivity swing, \$	<1
Peak fuel temperature, °C	841
Cladding	Silicon-enhanced ferritic/martensitic SS bonded to fuel pellets by lead
Peak cladding temperature, °C	650
Fuel/coolant volume fractions	0.45/0.35
Core lifetime, y	15–30
Fuel pin diameter, cm	2.50
Fuel pin triangular pitch-to-diameter ratio	1.185
Active core dimensions height/diameter, m	0.976/1.22

Figure 6.4. Sketch of SSTAR. *Credit: Dr. James Sienicki, Argonne National Laboratory*



removal; there are no reactor coolant pumps. The system uses a supercritical CO₂ power conversion system providing for improved efficiency and a small footprint. The core is designed for an ultra-long core life and the vessel is sealed and designed for complete cassette-core replacement when refueling is required; this confers a high degree of proliferation resistance.

6.6.2 Additional Generation IV systems under study or development, and new directions

In addition to the Generation-IV reference systems described above, there are several other system design activities that are being pursued. Additional new ideas are reflected in the many designs that are being actively developed. A sample of these is presented in the following sections. Though this selection of additional systems is not exhaustive, it is representative of the diversity of approaches being considered to exploit the favorable potential of the LFR. It is also noted that, in contrast to the GIF reference designs, some of these additional systems rely on LBE as the coolant. The selection includes systems that have been or are being considered in Europe, the United States, Korea, China, Japan, and Sweden.

6.6.2.1 *The Advanced Lead-cooled Fast Reactor European Demonstrator (ALFRED)*

ALFRED, the Advanced Lead-cooled Fast Reactor European Demonstrator, is conceived as a reactor designed with the specific purpose of testing and qualifying innovative components and procedures to be used in the following step to a commercial ELFR reactor (Grasso, 2018). It offers a representative operational environment, but also constitutes an early realization of a LFR-SMR (Frignani et al., 2017 and Frignani et al., 2019).

Safety has been integrated into the design from the beginning, leading to a robust baseline configuration of ALFRED (Frogheri et al., 2013). In particular, the passive nature of the safety systems has been demonstrated to ensure no external radioactivity release will occur even in severe conditions, alleviating the need of off-site or emergency AC electrical power supply (Bubelis et al., 2013; Bandini et al., 2013). For this reason, the ALFRED design has been also used as a reference reactor in a recent white paper on safety issued by the Risk and Safety Working Group of the Generation IV International Forum (Alemberti et al., 2015).

The fundamental criteria and design features of the ALFRED reference configuration include: (i) a pool type configuration for a compact and robust design, to avoid out-of-vessel primary coolant recirculation; (ii) a reactor vessel surrounded by an additional safety boundary, to ensure DHR flow-path in case of any unexpected vessel failure; (iii) a layout of the core and internals to promote natural circulation, maximizing the grace time in case of loss of flow; (iv) Hexagonal wrapped FA, extended above the lead free level to simplify fuel handling; (v) MOX hollow fuel pellets, to mitigate maximum fuel temperature and reach the target peak burn-up; (vi) two redundant safety shutdown systems, based on diverse actuation principles; (vii) -once-through Steam Generators (SG), without an intermediate circuit, to improve economic competitiveness; (viii) axial flow pumps, located in at the core outlet, to minimize the shaft length and simplify the pool flow-path configuration; and (ix) two diverse, redundant and fully passive DHR systems, based on water/steam as the cooling medium, able to ensure a minimum grace time of 72 h.

The ALFRED configuration is shown in Figure 6.5, and some selected parameters are shown in Table 6.8. The main characteristics of the design include: a power level of $300 \text{ MW}_{\text{th}}/125 \text{ MW}_{\text{el}}$; a secondary side characterized by once through SGs at 180 bar and temperatures of 335°C (inlet) and 450°C (outlet); and a primary side outlet temperature of 520°C .

6.6.2.2 *Westinghouse LFR*

The Westinghouse Lead Fast Reactor (LFR), under development by Westinghouse Electric Company, LLC, USA., is a medium-output, modular plant harnessing a lead-cooled, fast spectrum core operating at high temperature in a pool configuration reactor, and coupled with an air-cooled Supercritical CO_2 (sCO_2) Balance of Plant (BoP) system. With the ultimate goal to be competitive even in the most challenging global markets, the Westinghouse LFR has baseload electricity production and load leveling as the primary design focus.

Figure 6.5. Sketch of the ALFRED reactor system. Credit: Dr. Alessandro Alemberti, Ansaldo Nucleare and the FALCON Consortium

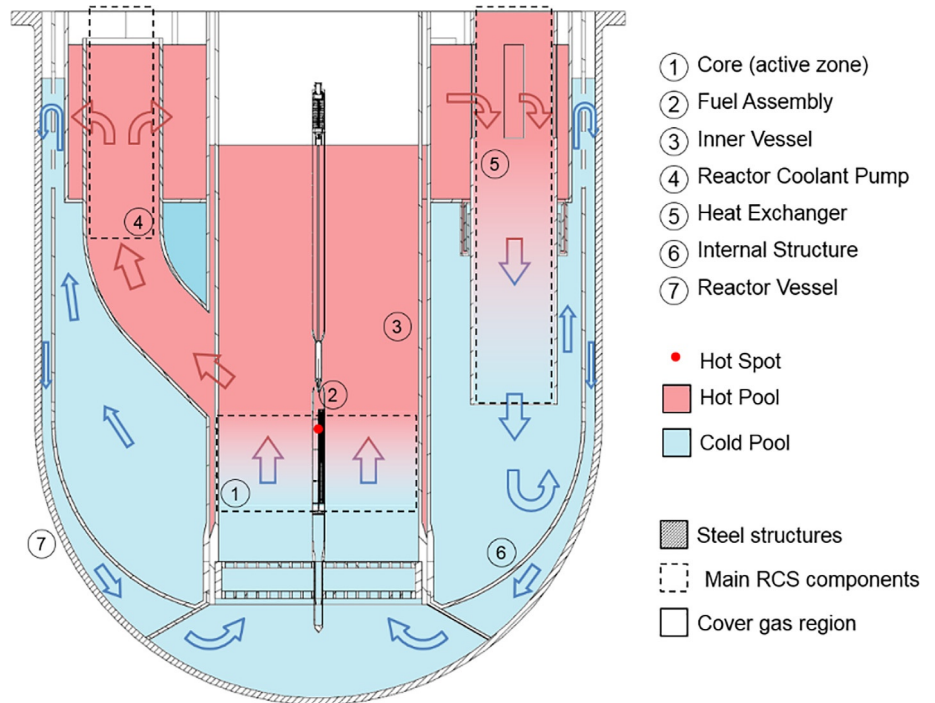


Table 6.8. Summary parameters of ALFRED (condensed and updated from Alemberti and Mansani, 2015)

Characteristic	Value
Core power (MW_{th}/MW_{el})	300/125
Core inlet/outlet T ($^{\circ}C$)	400/520
Net efficiency (%)	42
Feed temperature ($^{\circ}C$)	335
Turbine inlet T ($^{\circ}C$)	450

Specifically, integrated thermal energy storage using low-cost materials, coupled to existing BoP equipment, allows for non-reactor-based load following to complement non-dispatchable energy forms while maximizing energy production. These capabilities could allow for the increased use of renewable technologies, making nuclear power and renewables complementary.

Being air-cooled and with high turbine outlet temperatures, the proposed sCO_2 power cycle allows for a greatly-expanded variety of plant siting options and applications, including combined heat and electricity in captive markets. The plant's output, selected based on economic considerations, is sufficiently small to integrate into lower-capacity grids while also being substantial enough to be used in standard baseload plant applications. Figure 6.6 provides a schematic of the primary system, and Table 6.9 summarizes some of its key parameters. Additional information on the Westinghouse LFR can be found in Ferroni et al. (2019), Franceschini et al. (2018), Liao and Utley (2019), Stansbury et al. (2018) and, together with other new SMR concepts, in IAEA (2018).

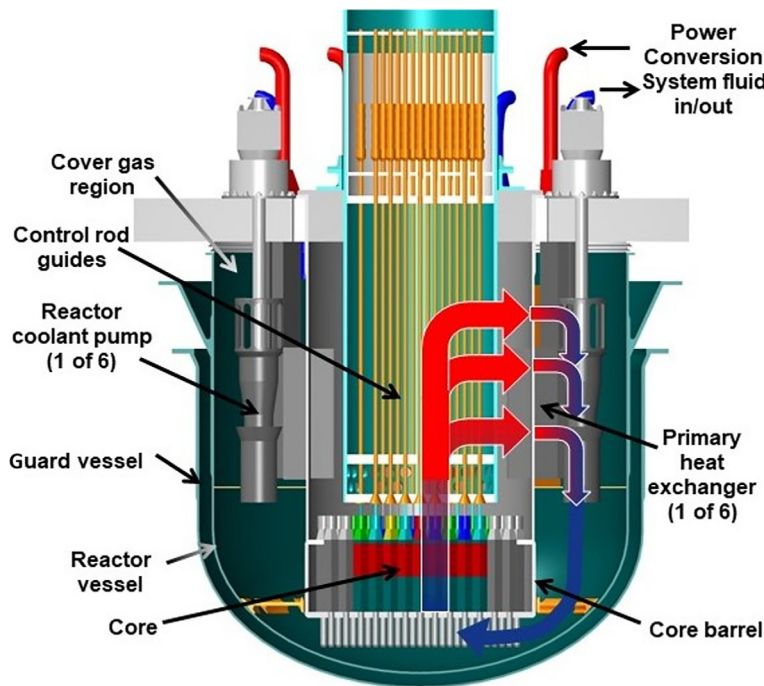


Figure 6.6. Schematic of the Westinghouse LFR. Credit: Dr. Fausto Franceschini, Westinghouse Electric Company

Table 6.9. Selected technical parameters of the Westinghouse LFR

Selected technical parameters	
Reactor type	Pool-type, liquid-metal-cooled fast reactor
Primary coolant	Pb
Secondary coolant	Supercritical CO ₂
Core inlet/exit temperatures	~400/650°C
Thermal power output, MW(th)	950
Electric power output, MW _{el}	>450 (Net)
Fuel type	Oxide (UO ₂ or MOX), with provision for transition to advanced, high-density fuel
Fuel enrichment (%)	≤19.75%
Fuel burnup (GWd/ton)	≥100
Fuel cycle (months)	≥24
Reactor vessel height/diameter (m)	Approx. 9.5/8.5
Load following capability	Thermal energy storage system with constant core thermal power output between 65% and 125% of full power

6.6.2.3 Newcleo LFR-AS-200

The LFR-AS-200 concept (AS stands for Amphora-Shaped, referring to the shape of the inner vessel, and 200 represents the electrical power in MW_{el}) is an innovative small reactor cooled by molten lead initially developed by Hydromine Nuclear Energy S.à.r.l., Luxembourg) now a part of Newcleo Ltd, London – UK, which continues its development. Figure 6.7 presents a sketch and rendering of the LFR-AS-200. The innovations introduced in this concept are intended to fully exploit the favorable properties of lead as a coolant and thereby enhance the potential for future commercial deployment by achieving plant simplification, compactness and passive safety; many of its features are quite distinct from previous LFR designs.

The innovations result in the achievement of a very compact reactor: the absence of intermediate loops, the primary system specific volume of less than $1 \text{ m}^3/\text{MW}_{\text{el}}$ and the compact reactor building are key factors for competitive kWh cost.

The LFR-AS-200 is an integral pool-type fast reactor with all the primary components installed inside the Reactor Vessel (RV). The main primary components are six innovative Spiral-Tube Steam Generators (STSGs), six Mechanical Pumps (MPs), flag-type control rods and three + three dip coolers belonging to two diversified, passive, redundant DHR systems.

Thanks to the properties of lead, intermediate loops are not required with several special precautions intended to deterministically eliminate any risk of important primary system pressurization: among them are water and steam collectors that are located outside the RV and short in-vessel Spiral-Tube Steam Generators (STSGs) partially raised above the lead-free level of the cold collector. The FAs extend with a stem above the lead-free level eliminating the necessity of an in-vessel refueling machine. Refueling is performed under visual control and sealed conditions by means of two rotating plugs and an ex-vessel refueling machine.

A summary of key parameters of the LFR-AS-200 is provided in Table 6.10.

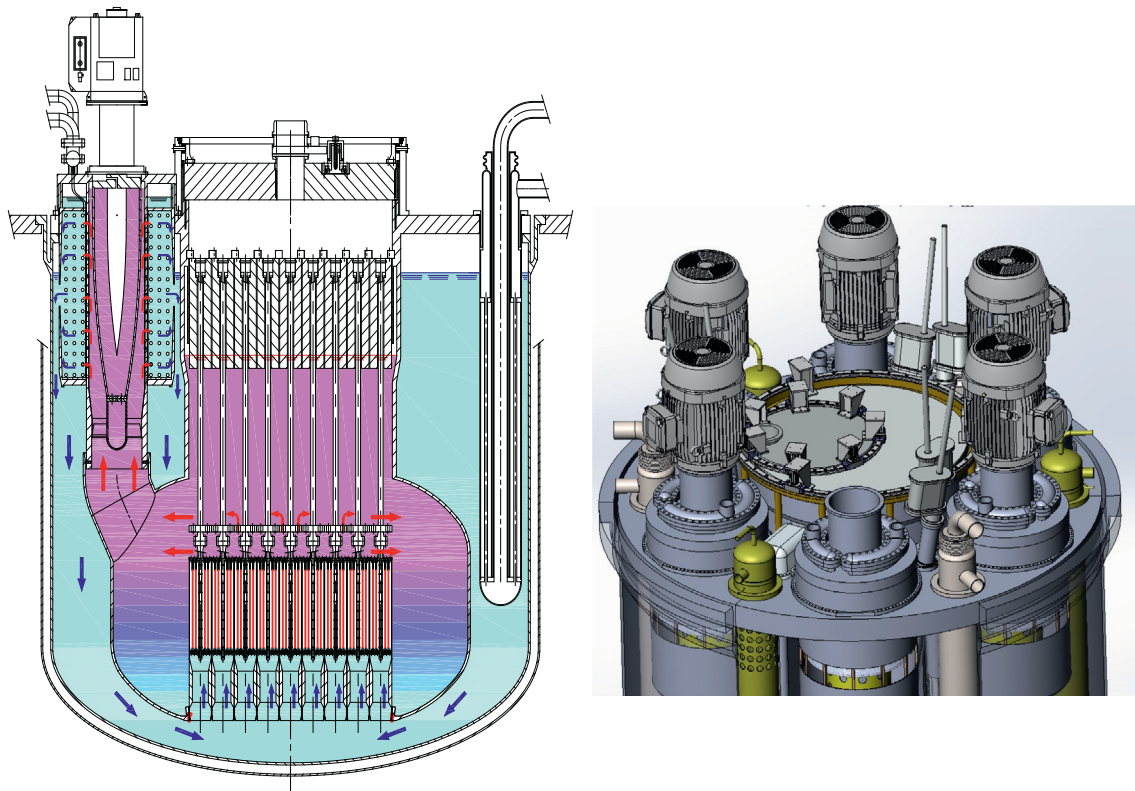


Figure 6.7. Sketch and rendering of the Newcleo LFR-AS-200. Credit: Dr. Luciano Cinotti, Newcleo Ltd

Table 6.10. Selected operating parameters of the LFR-AS-200

Parameter	Value	Parameter	Value
Power (MW_{th}/MW_{el})	480/200	Number of FAs	61
Core inlet/outlet temperature ($^{\circ}C$)	420/530	Core active height (cm)	85
Primary side pressure loss (bar)	1.3	Type of fuel	MOX
Turbine inlet pressure (bar)	180	Mass of fuel (t)	12.8
Feed water /steam temperature ($^{\circ}C$)	340/500	Breeding ratio	0.9
Reactor vessel height/diameter (m)	6.2/6		

6.6.2.4 LFR-TL-X

The LFR-TL-X is a series of LFR very Small Modular Reactors (vSMRs). In the designation, TL stands for Transportable Long-lived reactor, and X (= 5, 10, or 20) is the electrical power in MW_{el} . It is a joint concept proposal initially proposed by Hydromine Nuclear Energy and ENEA (the Italian National Committee for Research and Development of Nuclear and Alternative Energy). The objective of this conceptual design is to implement the simplifications embodied in the LFR-AS-200 in a family of very small reactors with a similar level of compactness and simplification.

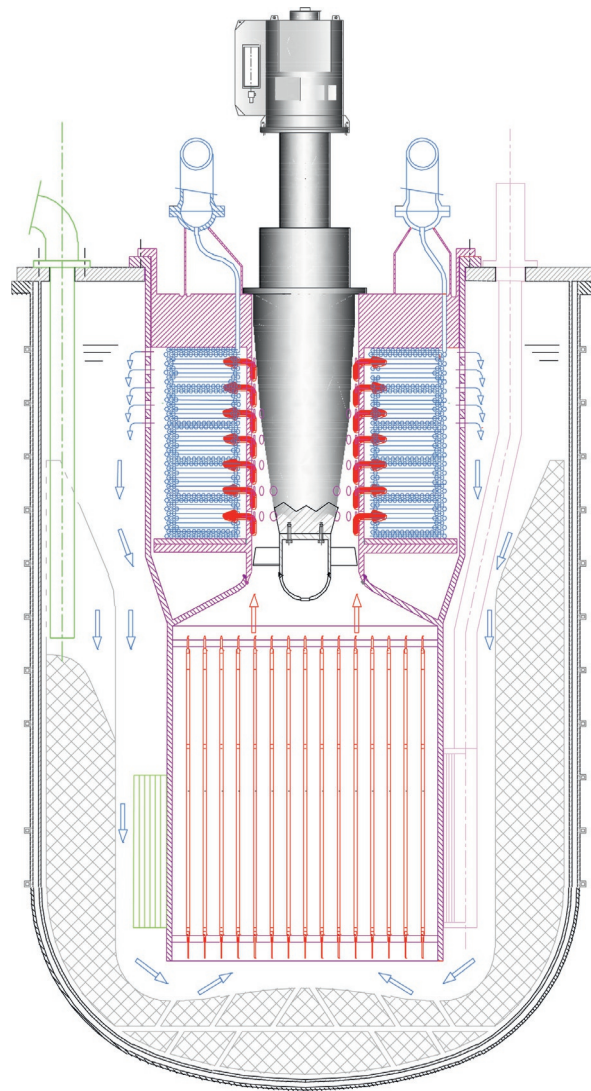
An important cost parameter to be considered when designing a vSMR is the plant cost per unit power ($\$/W$). While, within limits, it is possible to reduce reactor size while reducing power, the plant $\$/W$ ratio is likely to become prohibitively high. This is due to the fact that many costs, including such things as the cost of the fuel handling machines, buildings and facilities for storage of the fresh and spent FAs and regulatory activities are relatively independent of the reactor power, and hence the $\$/W$ ratio increases as the reactor size declines.

An approach to overcome such cost issues while also addressing the issue of proliferation is to design vSMRs capable to be transported as a new reactor and then again as a system at the end of its design life, complete with the reactor core, from and to centralized facilities for initial manufacture, and end-of-life recycling, refurbishment and maintenance of main components. For this design approach to become viable, the vSMR must be provided with a long-life core and be capable of transport in an upright position, in order to maintain its mechanical and thermal-hydraulic configuration while traveling.

The lead-cooled vSMRs derived from the LFR-AS-200 can be designed to comply with both features of long-life core and transportability in an upright position. Long-life cores are possible owing to the high breeding capability of the fast reactor; transportability is facilitated by the compact reactor assembly, in particular to the short overall height, resulting from the very compact pump-Spiral-Tube Steam-Generator (pump-STSG) assembly previously conceived for the LFR-AS-200. Figure 6.8 presents a Schematic of the LFR-TL-X series.

No on-site refueling being required, it is possible to install a single pump-STSG assembly center-line above the core. This is the main characteristic of the LFR-TL-X reactors, which allows the balancing of the unfavorable scale effect with respect to the LFR-AS-200 against the very favorable effect of a highly compact primary system of about $1\text{ m}^3/MW_{el}$, also an important feature of the LFR-AS-200.

The development of the Hydromine transportable vSMR thereby exploits and further reveals the flexibility of the LFR, so that, rather than a single reference configuration, several options are enabled, which



Scheme of LFR-TL-5, LFR-TL-10, LFR-TL-20

Figure 6.8. Schematic of the LFR-TL-X series. *Credit: Mr. Peter Briger, CEO Hydromine Nuclear Energy*

incorporate certain differences regarding the fuel type, the power level and the thermal cycle. In particular, although currently considered designs range in power from 5 to 20 MW_{el}, the maximum power of such a reactor could be up to about 60 MW_{el}.

A summary of selected parameters of the LFR-TL-X family of vSMRs is provided in [Table 6.11](#).

6.6.2.5 The South Korean URANUS-40 system

Over the past 20 years, Seoul National University has considered the development of innovative reactor systems based on LBE cooling along with advanced fuel recycle ([Choi et al., 2011](#)). A noteworthy current result of these efforts is the small modular LBE-cooled reactor designated as the Ubiquitous, Robust, Accident-forgiving, Non-proliferating, and Ultra-lasting Sustainer (URANUS-40). This system has a nominal electric power rating of 40 MW_{el} (100 MW_{th}), a power level selected for use as a distributed power source for production of electricity, heat supply, and desalination. It is a pool-type fast reactor with a heterogeneous

Table 6.11. Selected operating parameters of the LFR-TL-X

Parameter	Value
Coolant	Lead
Thermal/electrical capacity, MW(th)/MW(e)	15/5; 30/10; 60/20
Core inlet/exit temperatures (°C)	360/420
Fuel enrichment (%)	19.75
Fuel cycle (months)	≥100
Design life (years)	30
RPV height/diameter (m)	From about 3.5/2 for 5 MW _{el} to about 4.5/2.5 for 20 MW _{el}
Main reactivity control mechanism	Ex-core, reversed-flag type, rotating staff moves absorbers closer to or away from the core

hexagonal core, fueled by low-enriched uranium dioxide fuels. The primary cooling system relies on natural circulation. The system features a 3-D seismic base isolation system underneath the entire reactor building. The system also features a capsulized core design and a very long refueling period (25 y).

[Table 6.12](#) presents a summary of the parameters of the URANUS-40 system, and [Figure 6.9](#) is a sketch of the concept.

Table 6.12. URANUS-40 selected parameters

Design parameter	Value or characteristic
Core power rating	40 MW _{el} (110 MW _{th})
Refueling interval	20 years (with 2-year inspection interval)
Primary coolant	LBE (move to pure lead coolant when advanced cladding materials available)
Primary cooling mode	Natural circulation
Core inlet/outlet temperature	305°C/441°C
Secondary coolant	Subcooled water/superheated steam
Mode of operation	Autonomous Load Following
Fuel	Low-enriched uranium UO ₂
Cladding	FGC of T91 and Si-containing ferritic steel (with advance FGC of HT-9 and Al-containing ferritic steel)
Seismic design	3-D base isolations of entire nuclear steam supply systems

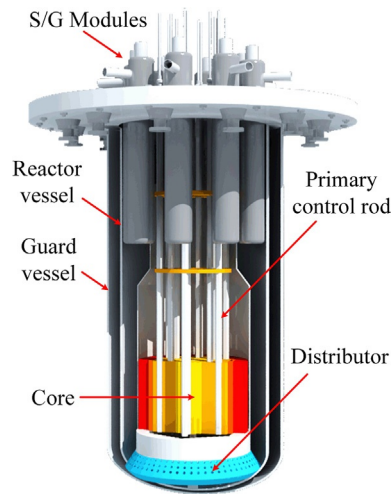


Figure 6.9. Sketch of the URANUS-40 system. Credit: Prof. (Emeritus) Il Soon Hwang, Seoul National University

6.6.2.6 The Chinese CLEAR-I reactor

In 2011, the Chinese Academy of Sciences launched a project to develop ADS and LFR technology, and the CLEAR family of systems was selected as the reference for both the ADS and the LFR. CLEAR consists of three stages: a 10 MW_{th} lead-based research reactor (CLEAR-I), a 100 MW_{th} lead-based engineering demonstration reactor (CLEAR-II), and a 1000 MW_{th} lead-based commercial prototype reactor (CLEAR-III) (Wu et al., 2013).

The conceptual design of CLEAR-I was completed in 2013, and engineering design is underway. CLEAR-I has a subcritical and critical dual-mode operation. Key components of CLEAR-I, including the control rod drive mechanism, refueling system, FA, and a simulator for principle verification, have been fabricated and tested. Table 6.13 and Figure 6.10 provide a summary of the key parameters and a sketch of CLEAR-I.

Table 6.13. CLEAR-I key parameters

Selected key parameters of CLEAR-I	
Parameter	Value
Thermal power	10 MW
Primary coolant	LBE
Fuel material	UO ₂ (19.75%)
k_{eff} in subcritical mode	0.973
Primary system	Pool type, compact
Primary circulation	Forced
Core inlet/outlet temperature	300°C/385°C
Secondary coolant	Pressurized liquid water
Heat sink	Air cooler
Reactor height/diameter (mm)	6800/4680

Continued

Table 6.13. CLEAR-I key parameter—cont'd

Selected key parameters of CLEAR-I	
Parameter	Value
Primary coolant inventory (t)	600
Heat exchangers	4 units, shell and tube heat exchanger, double-walled bayonet tube, removable
Main vessel height	6300 mm
Main vessel diameter	4650 mm
Primary pumps	2 units, mechanical pumps in the cold pool, removable

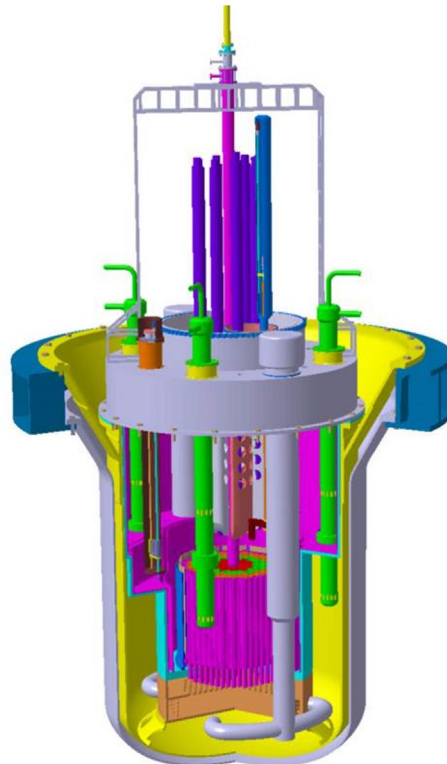


Figure 6.10. Sketch of the CLEAR-I reactor. Credit: Dr. Tao Zhou, FDS, China Academy of Sciences

6.6.2.7 The Pb-Bi-cooled direct contact boiling Water Fast Reactor (PBWFR)

The Pb-Bi-cooled direct contact boiling Water Fast Reactor (PBWFR) is a design concept of a small-size innovative direct contact (LBE-water) LFR being developed by [Takahashi et al. \(2008a, b\)](#) at the Tokyo Institute of Technology. In this concept, steam is generated by direct contact between feed water and the primary LBE coolant in the upper core plenum, and is transported through the LBE coolant as a result of the buoyancy of the steam bubbles.

The idea of a direct contact system was earlier identified by [Buongiorno et al. \(1999, 2001\)](#) as a more compact and economical LFR than those featuring conventional forced circulation. In the PBWFR, primary pumps and SGs are eliminated. The conceptual design for the PBWFR features a long-life core with a core breeding ratio higher than unity for efficient U utilization, high proliferation resistance because of reduced

risk from refueling, small size for portability, modularity and low capital investment, a negative void reactivity for safety enhancement, and reliance on steam lift and direct contact steam generation.

Table 6.14 provides a summary of selected key parameters of the PBWFR, and Figure 6.11 is a sketch of the reactor system.

Table 6.14. Parameters of the PBWFR

Selected parameters of the PBWFR	
Power (thermal/electric) (MW)	450/150
Thermal efficiency (%)	33
Core inlet/outlet temperature (°C)	310/460
Core pressure drop (MPa)	0.04
Maximum cladding temperature (°C)	619
LBE flow rate (t/h)	73,970
Steam temperature (°C)	296
Steam flow rate (t/h)	863
Steam pressure (MPa)	7
Feed water temperature (°C)	220
Refueling interval (y)	10
Refueling	One batch refueling
Candidate materials for cladding and structural equipment	Aluminum-iron alloy-coated high chromium steels, high chromium steels with aluminum and silicon addition, ceramics (SiC, etc.) and refractory metals

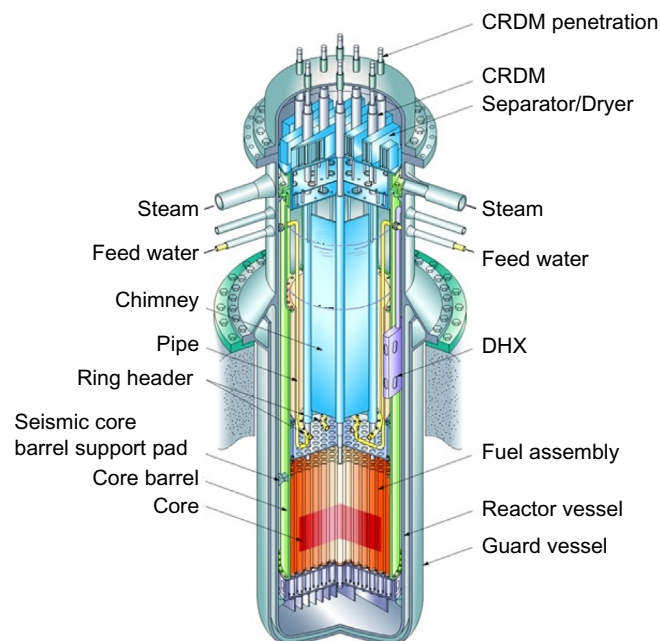


Figure 6.11. Sketch of the PBWFR. Credit: Prof. (Emeritus) Minoru Takahashi, Tokyo Institute of Technology

6.6.2.8 The SVBR-100

The SVBR project is the reactor system most closely aligned with the previous generation of Soviet/Russian lead-bismuth cooled reactors used for submarine propulsion. As such, the SVBR design efforts draw more directly than other systems from the operational experience from that military application.

The SVBR-100 reactor (Zrodnikov et al., 2009; Toshinsky et al., 2013) is intended to be a prototype system under design by a consortium of Russian organizations including OKB Hidropress, the Institute of Physics and Power Engineering, and Atomenergoproekt Moscow.

The SVBR-100 is intended for use in remote, isolated, or coastal locations, or for dedicated industrial applications. It could be used to provide a variety of outputs, including electricity, process heat, or desalination, depending on actual system configuration.

At the present time, project documentation has been developed by ATOMPROEKT JSC under the scope of Resolution No. 87 of the Government of the Russian Federation. A siting license has been issued and agreements are in place for development of this project in the city of Dimitrovgrad, in the eastern Ulyanovsk oblast of western Russia.

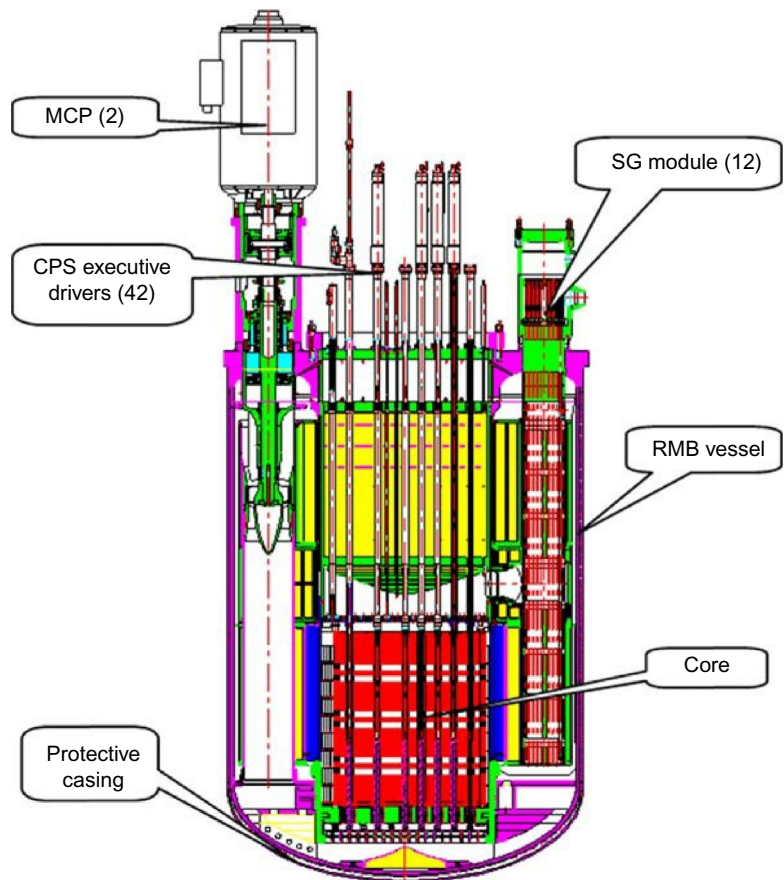
Table 6.15 provides a summary of selected parameters for the SVBR-100, and Figure 6.12 is a sketch of the reactor.

Table 6.15. Selected parameters of the SVBR-100

SVBR-100 power plant parameters	
Reactor thermal output, MW_{th}	280
Electric power output, MW _{el}	100
Primary coolant temperature: inlet/outlet, °C	335/477
Steam production rate	580 t/h at pressure 6.7 MPa, and temperature 278°C
Average core power density, kW/dm ³	160
Fuel: type	UO ₂
Uranium loading, kg	~9200
Average U-235 enrichment, %	~16.7
Core lifetime, full power hours	50,000
Time interval between refueling, years	~6–7
Reactor module dimensions	4.4/12.4 m (diameter/height)

Figure 6.12. Sketch of the SVBR-100.

Credit: Prof. Georgi Toshinsky, IPPE



6.6.2.9 Swedish Advanced Lead Reactor (SEALER)

SEALER is a small lead-cooled nuclear battery-type reactor designed by the Swedish company LeadCold Reactors for commercial power production in off-grid applications. The dimensions of the primary system are indicated in Figure 6.13, and were established to enable transport of the vessel by cargo aircraft to destinations in the Canadian arctic. Using 2.4 tons of 19.9% enriched UO_2 fuel, the life of the core is 27 full power years when operating at 8 MW_{th} (up to 3 MW_{el}). Nineteen FAs (each with 91 pins) are located in the center of the core, surrounded by 12 reactivity control elements and 6 shutdown elements. Heat is removed by forced circulation of the lead coolant, using 8 pumps. Operating at a total mass flow of 1300 kg/s , the ΔT over the core is 40°C , keeping the average coolant temperature at the outlet below 430°C and the maximum cladding temperature below 450°C . One compact SG is connected to each of the pumps, using a new spiral tube design.

The anticipated fuel cladding tube material is a 15-15Ti steel, surface alloyed with Fe-10Cr-4Al-Zr. This choice is intended to ensure negligible swelling at the peak cladding dose of 60 dpa, while providing sufficient corrosion resistance.

Transient simulations of SEALER have been carried out using the SAS4A/SASSYS-1 codes as well as BELLA, a code written specifically for the purpose of safety-informed design of LFRs. Analysis shows SEALER to withstand unprotected withdrawal of a single control rod, loss of forced flow and loss of heat sink, thanks to its low power density, the capability of natural convection for DHR, and reliance on thermal radiation from the vessel as the ultimate heat sink.

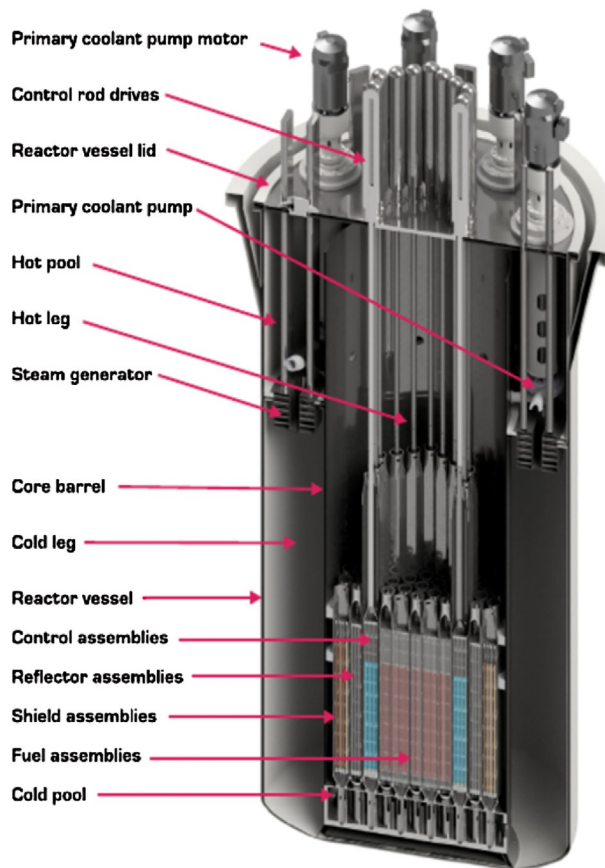


Figure 6.13. Sketch of the SEALER reactor. *Credit: Dr. Janne Wallenius, CEO, LeadCold Reactors Inc*

In the case of a full core melt, the fraction of iodine and cesium released from the lead and the primary system is sufficiently small that radiological exposure to the public remains below Canadian regulatory limits at a distance of 100m from the reactor. Hence, there is no need for evacuation or sheltering under licensing requirements for reactors sited in Arctic communities.

6.7 Sources of further information

There are four especially important international sources of information on the development of LFR that can be considered in expanding the information in this chapter.

- A survey of lead coolant technology has been carried out by a working group under the auspices of the Working Party on Scientific Issues of the Fuel Cycle of the Organization for Economic Cooperation and Development-Nuclear Energy Agency. Created in 2002, this Working Group on Lead-Bismuth Eutectic (WG-LBE) coordinates and guides LBE research in participating organizations while promoting closer and broader-based collaboration. The aim of the group is to develop a set of requirements and standards as well consistent methodology for experimentation, data collection, and data analyses. Due to increasing interest in the lead-cooled reactor option in GIF, the WG-LBE also decided to include data and technology aspects of both LBE and lead. The results have been published in (OECD-NEA, 2015) the 2015 “Handbook on LBE Alloy and Lead Properties, Materials compatibility, Thermal-hydraulics and Technologies.” The publication of a revised edition of the handbook is foreseen.

- Surveys of information and coordination of international efforts on all Generation-IV systems, including the LFR systems, is an important function of GIF. The Generation-IV Technology Roadmap was issued in 2002 and updated in 2014 (GIF, 2002, 2014) with several annual reports published in the interim between the main documents. The roadmap provides a foundation for formulating national and international program plans on which the GIF countries may collaborate to advance Generation-IV systems.
- These above documents, as well as additional information on Generation-IV systems, may be accessed through the Generation-IV website at www.gen-4.org.
- Additional information on safety requirements and safety progress of specific designs, as well as comprehensive topical reviews, can be obtained from the International Atomic Energy Agency (IAEA). IAEA (2013) is an example of such a reference source, and additional information can be found at the IAEA website, www.iaea.org.
- Additional information on selected topics can be found at Grasso et al. (2013, 2019) and Kim et al. (2019).

Acknowledgments

The preparation of this chapter has benefited from the input of many individuals for which the authors are thankful. Included among these are the following:

Alessandro Alemberti, Ansaldo Nucleare.

Paolo Ferroni, Westinghouse Electric Company.

Fabio Di Fonzo, Istituto Italiano di Tecnologia, (IIT).

Fausto Franceschini, Westinghouse Electric Company.

Boris Paladino, Istituto Italiano di Tecnologia, (IIT).

Giacomo Grasso, Agenzia Nazionale per le nuove tecnologie, l'energia e lo sviluppo economico sostenibile (ENEA).

Il-Soon Hwang, Seoul National University (Emeritus).

Konstantza Lambrinou, SCK-CEN.

Andrei Moiseev, NIKIET.

Cory A. Stansbury, Westinghouse Electric Company.

Minoru Takahashi, Tokyo Institute of Technology (Emeritus).

Kamil Tucek, European Union Joint Research Center, Petten.

Janne Wallenius, Lead Cold Reactors (Blykalla Reaktor).

Tao Zhou, FDS, China Academy of Sciences.

References

- Alemberti, A., Mansani, L., 2015. *The Advanced Lead Fast Reactor European Demonstrator (ALFRED)*. NURETH-15, Pisa, Italy.
- Alemberti, A., Froggeri, M., Hermsmeyer, S., Ammirabile, L., Smirnov, V., Takahashi, M., Smith, C., Wu, Y., Hwang, I., 2015. *Lead-cooled Fast Reactor Risk and Safety Assessment White Paper*. GIF 2015. Available from https://www.gen-4.org/gif/jcms/c_9373/publications.
- Artoli, C., Grasso, G., Petrovich, C., 2010. A new paradigm for core design aimed at the sustainability of nuclear energy: the solution of the extended equilibrium state. *Ann. Nucl. Energy* 37, 915–922.
- Bandini, G., Bubelis, E., Schikorr, M., Stempnievicz, M., Lazaro Chueca, A., Tucek, K., Kudinov, P., Kööp, K., Jeltsov, M., Mansani, L., 2013. Safety analysis results of representative DEC accidental transients for the ALFRED reactor. In: *International Conference on Fast Reactors and Related Fuel Cycles (FR13)*. Vienna, Austria.
- Bubelis, E., Schikorr, M., Mansani, L., Bandini, G., Mikityuk, K., Zhang, Y., Geffraye, G., 2013. *Safety Analysis Results of DBC Transients Performed for the ALFRED Reactor*. IAEA FR13, Paris, France.
- Buongiorno, J., Todreas, N., Kazimi, M., Czerwinski, K., 2001. *Conceptual Design of a Lead-Bismuth Cooled Fast Reactor with In-vessel Direct-Contact Steam Generation*. MIT-ANP-TR-079. Massachusetts Institute of Technology.
- Buongiorno, J., Todreas, N., Kazimi, M., Driscoll, M., Hejzlar, P., 1999. Key features of an integrated lead-Bi-cooled reactor based on water/liquid metal direct heat transfer. *Trans. Am. Nucl. Soc.* 81, 360–361.
- Choi, S., Hwang, I.S., Cho, J.H., Shim, C.B., 2011. URANUS: Korean Lead-Bismuth cooled small modular fast reactor activities. Paper No. SMR2011-6650. In: *ASME 2011 Small Modular Reactors Symposium*. Washington, DC, USA, pp. 107–112.

- Cinotti, L., Locatelli, G., Ait Abderrahim, H., Monti, S., Benamati, G., Tucek, K., Struwe, D., Orden, A., Corsini, G., Le Carpentier, D., 2008. The ELSY project. Paper 377. In: Proceedings of the International Conference on the Physics of Reactors (PHYSOR). Interlaken, Switzerland.
- Cinotti, L., Smith, C., Sekimoto, H., Mansani, L., Reale, M., Sienicki, J., 2011. Lead-cooled system design and challenges in the frame of Generation IV International Forum. Proceedings of the international DEMETRA workshop on development and assessment of structural materials and heavy liquid metal technologies for transmutation systems. *J. Nucl. Mater.* 415 (3), 245–253.
- De Bruyn, D., Alemberti, A., Mansani, L., Grasso, G., Bandini, G., Artioli, C., Bubelis, E., Mueller, G., Wallenius, J., Orden, A., 2013. Main achievements of the FP7-LEADER collaborative project of the European Commission regarding the design of a lead-cooled fast reactor. In: Proceedings of ICAPP 2013. Jeju Island, Korea.
- De Bruyn, D., Maes, D., Mansani, L., Giraud, B., 2007. From MYRRHA to XT-ADS: the design evolution of an experimental ADS system. In: Proceedings of the 8th International Topical Meeting on Nuclear Applications and Utilization of Accelerators (AccApp'07). Pocatello, Idaho.
- Dragunov, Y., Lemekhov, V., Smirnov, V., Chernetsov, N., 2012. Technical solutions and development stages for the BREST-OD-300 reactor unit. *At. Energy* 113 (1), 70.
- Ejenstam, J., Thuvander, M., Olsson, P., Rave, F., 2015. Microstructural stability of Fe-Cr-Al alloys at 450–550°C. *J. Nucl. Mater.* 457, 291–297.
- Ferroni, P., Stansbury, C., Liao, J., Levinsky, A., Franceschini, F., 2019. The Westinghouse lead fast reactor program. In: International Nuclear Fuel Cycle Conference (GLOBAL). Seattle, WA, USA, September 22–26, 2019.
- Franceschini, F., Grasso, G., Ferroni, P., 2018. Advanced fuel cost performance assessment for the Westinghouse LFR. In: International Congress on Advances in Nuclear Power Plants (ICAPP). Charlotte, NC, USA, April 8–11, 2018.
- Frankberg, E.J., Kalikka, J., García Ferré, F., Joly-Pottuz, L., Salminen, T., Hintikka, J., Hokka, M., Koneti, S., Douillard, T., Le Saint, B., Kreiml, P., Cordill, M.J., Epicier, T., Stauffer, D., Vanazzi, M., Roiban, L., Akola, J., Di Fonzo, F., Levänen, E., Masenelli-Varlot, K., 2019. Highly ductile amorphous oxide at room temperature and high strain rate. *Science* 366, 864–869.
- Frignani, M., Alemberti, A., Villabruna, G., Adinolfi, R., Tarantino, M., Grasso, G., Pizzuto, A., Turcu, I., Valeca, S., 2017. ALFRED: a Strategic Vision for LFR Deployment. *Trans. Am. Nucl. Soc.* 117, 1468–1471. Washington, D.C.
- Frignani, M., Alemberti, A., Tarantino, M., Grasso, G., 2019. ALFRED staged approach. In: ICAPP 2019. France, Juan-les-pins, May 12–15, 2019.
- Frogheri, M., Alemberti, A., Mansani, L., 2013. The lead fast reactor: demonstrator (ALFRED) and ELFR design. In: IAEA-International Conference on Fast Reactors and Related Fuel Cycles: Safe Technologies and Sustainable Scenarios (FR13). Paris, France.
- García Ferré, F., Bertarelli, E., Chiodoni, A., Carnelli, D., Gastaldi, D., Vena, P., Beghi, M.G., Di Fonzo, F., 2013b. The mechanical properties of a nanocrystalline $\text{Al}_2\text{O}_3/\text{a-Al}_2\text{O}_3$ composite coating measured by nanoindentation and Brillouin spectroscopy. *Acta Mater.* 61, 2662–2670.
- García Ferré, F., Mairov, A., Vanazzi, M., Serruys, Y., Lepître, F., Beck, L., Van Brutzel, L., Chartier, A., Beghi, M.G., Sridharan, K., Di Fonzo, F., 2018. Extreme ion irradiation of oxide nanoceramics: Influence of the irradiation spectrum. *Acta Mater.* 143, 156–165.
- García Ferré, F., Ormellese, M., Di Fonzo, F., Beghi, M., 2013a. Advanced Al_2O_3 coatings for high temperature operation of steels in heavy liquid metals: a preliminary study. *Corros. Sci.* 77, 375–378.
- Generation IV International Forum (GIF), 2002. Technology Roadmap for Generation IV Nuclear Energy Systems. GIF-002-00. <https://www.gen-4.org/gif/upload/docs/application/pdf/2013-09/genivroadmap2002.pdf>.
- Generation IV International Forum (GIF), 2014. Technology Roadmap Update for Generation IV Nuclear Energy System. <https://www.gen-4.org/gif/upload/docs/application/pdf/2014-03/gif-tru2014.pdf>.
- Generation IV International Forum LFR provisional System Steering Committee (GIF-LFR-pSSC), 2014. Generation IV Nuclear Energy Systems System Research Plan for the Lead-Cooled Fast Reactor. Draft.
- Grasso, G., 2018. ALFRED on the Licensing Path. EUROSAFE News. November 2018 (ENEA).
- Grasso, G., Doederlein, C., Tucek, K., Mikityuk, K., Manni, F., Gugiu, D., 2013. A core design approach aimed at the sustainability and intrinsic safety of the European Lead-cooled Fast Reactor. In: Proceedings of Fast Reactors and Related Fuel Cycles: Safe Technologies and Sustainable Scenarios (FR13). Paris, France, March 4–7.
- Grasso, G., Levinsky, A., Franceschini, F., Ferroni, P., 2019. A MOX-fuel core configuration for the Westinghouse lead fast reactor. In: International Congress on Advances in Nuclear Power Plants (ICAPP). Juan-les-pins. France, May 12–15.
- Hernández, T., Sánchez, F., Di Fonzo, F., Vanazzi, M., Panizo, M., González-Arrabal, R., 2019. Corrosion protective action of different coatings for the helium cooled pebble bed breeder concept. *J. Nucl. Mater.* 516, 160–168.
- Iadicco, D., Bassini, S., Vanazzi, M., Muñoz, P., Moroño, A., Hernandez, T., García-Cortés, I., Sánchez, F.J., Utili, M., García, F.F., Di Fonzo, F., 2018. Efficient hydrogen and deuterium permeation reduction in Al_2O_3 coatings with enhanced radiation tolerance and corrosion resistance. *Nucl. Fusion* 58, 126007.

- Iadicicco, D., Vanazzi, M., García Ferré, F., Paladino, B., Bassini, S., Utili, M., Di Fonzo, F., 2019. Multifunctional nanoceramic coatings for future generation nuclear systems. *Fusion Eng. Des.* 146, 1628–1632.
- International Atomic Energy Agency (IAEA), 2013. Status of Innovative Fast Reactor Designs and Concepts. Supplement to the IAEA Advanced Reactors Information System (ARIS). <http://aris.iaea.org>.
- International Atomic Energy Agency (IAEA), 2018. Advances in Small Modular Reactor Technology Developments, A Supplement to: IAEA Advanced Reactors Information System (ARIS), 2018 Edition. https://aris.iaea.org/Publications/SMR-Book_2018.
- Kim, T., Stauff, N., Stansbury, C., Levinsky, A., Franceschini, F., 2019. Long core life design options for the Westinghouse LFR. In: *International Nuclear Fuel Cycle Conference (GLOBAL)*. Seattle, WA, USA, September 22–26.
- Liao, J., Utley, D., 2019. Study on reactor vessel air cooling for the westinghouse lead fast reactor. *Nucl. Technol.* 2019. <https://doi.org/10.1080/00295450.2019.1599614>.
- Organization for Economic Co-operation and Development—Nuclear Energy Agency (OECD-NEA), 2015. Handbook on Lead-Bismuth Eutectic Alloy and Lead Properties, Materials Compatibility, Thermal-Hydraulics and Technologies, 2015 Edition. NEA No. 7268, 954 pp.
- Schroer, C., Konys, J., 2007. *Physical Chemistry of Corrosion and Oxygen Control in Liquid Lead and Lead-Bismuth Eutectic*. 47 pp., ISSN: 0947-8620.
- Sienicki, J., Moisseytsev, A., Yang, W., Wade, D., Nikiforova, A., Hanania, P., Ryu, H., Kulesza, K., Kim, S., Halsey, W., Smith, C., Brown, N., Greenspan, E., de Caro, M., Li, N., Hosemann, P., Zhang, J., Yu, H., 2006. Status Report on the Small Secure Transportable Autonomous Reactor (SSTAR)/Lead-Cooled Fast Reactor (LFR) and Supporting Research and Development. Argonne National Laboratory Report ANL-GenIV-089., <https://doi.org/10.2172/932940>. September 29.
- Smith, C., Halsey, W., Brown, N., Sienicki, J., Moisseytsev, A., Wade, D., 2008. SSTAR: the US lead-cooled fast reactor (LFR). *J. Nucl. Mater.* 376 (3), 255–259.
- Stansbury, C., Smith, M., Ferroni, P., Harkness, A., 2018. Westinghouse lead fast reactor development: safety and economics can coexist. In: *International Congress on Advances in Nuclear Power Plants (ICAPP)*. Charlotte, NC, USA, April 8–11.
- Sustainable Nuclear Energy Technology Platform (SNETP) Secretariat, 2010. ESNII: The European Sustainable Nuclear Industrial Initiative: Demonstration Programme for Fast Neutron Reactors, Concept Paper. <http://www.snetp.eu/wp-content/uploads/2014/05/esnii-folder-a4.pdf>.
- Takahashi, M., Uchida, S., Kasahara, Y., 2008a. Design study on reactor structure of Pb-Bi-cooled direct contact boiling water fast reactor (PBWFR). *Prog. Nucl. Energy* 50, 197–205.
- Takahashi, M., Uchida, S., Yamada, Y., Koyama, K., 2008b. Safety design of Pb-Bi-cooled direct contact boiling water fast reactor (PBWFR). *Prog. Nucl. Energy* 50, 269–275.
- Todreas, N., MacDonald, P., Buongiorno, J., Loewen, E., 2004. Medium-power lead alloy reactors: missions for this reactor technology. *Nucl. Technol.* 147 (3), 305.
- Toshinsky, G., Komlev, O., Tormyshev, I., Petrochenko, V., 2013. Effect of potential energy stored in reactor facility coolant on NPP safety and economic parameters. *World J. Nucl. Sci. Technol.* 3 (2), 59–64. www.scirp.org/journal/wjnst.
- Wu, Y., Yunqing, B., Song, Y., Huang, Q., Chen, H., Song, G., Hu, L., Jiang, J., 2013. Overview of lead based reactor design and R&D status in China. In: *Proceedings of the International Conference on Fast Reactors and Related Fuel Cycles: Safe Technologies and Sustainable Scenarios (FR-13)*. Paper INV-417. Paris, France.
- Zrodnikov, A., Toshinsky, G., Komlev, O., Stepanov, V., Klimov, N., Kudryavtseva, A., Petrochenko, V., 2009. SVBR-100 module-type reactor of the IV generation for regional power industry. In: *International Conference on Fast Reactors and Related Fuel Cycles: Challenges and Opportunities*. IAEA-CN-176-FR09P1132 (Kyoto, Japan).

Homogeneous Molten Salt Reactors (MSRs): The Molten Salt Fast Reactor (MSFR) concept

*Michel Allibert^a, Sylvie Delpech^c, Delphine Gerardin^a, Daniel Heuer^a,
Axel Laureau^b, and Elsa Merle^a*

^aLPSC/IN2P3/CNRS—Grenoble Alpes University—Grenoble Institute of Technology, Grenoble, France ^bIN2P3/CNRS - IMT Atlantique, Nantes, France ^cIJC Lab/IN2P3/CNRS, Orsay, France

Nomenclature

Abbreviations and acronyms

ACSEPT	Actinide reCycling by SEparation and Transmutation
ADS	Accelerator-Driven System
ALISIA	Assessment of LIquid Salt for Innovative Applications
CANDU	CANada Deuterium Uranium nuclear reactor
CFD	Computational Fluid Dynamics
CNRS	Centre National de la Recherche Scientifique, France
EdF	Electricité de France
EPFY	Equivalent Full Power Years
EPR	Evolutionary Power Reactor
EVOL	Evaluation and Viability Of Liquid fuel fast reactor
FFFER	Forced Fluoride Flow for Experimental Research
FFMEA	Functional Failure Mode and Effects Analysis
FP	Fission Product
FP7	7th European Framework Program
GFR	Gas-cooled Fast Reactor
GIF	Generation IV International Forum
HRE	Homogeneous Reactor Experiment
IN2P3	Institut National de Physique Nucléaire et de Physique des Particules, CNRS, France
IRSN	Institut de Recherche sur la Sureté Nucléaire, France
ISAM	Integrated Safety Assessment Methodology
LOCA	Loss Of Coolant Accident
LoD	Lines of Defense
LOF	Loss Of Flow
LOH	Loss Of Heat sink
LOLF	Loss Of Liquid Fuel
LPSC	Laboratoire de Physique Subatomique et Cosmologie, France
LWR	Light Water Reactor
MA	Minor Actinides
MARS	Minor Actinide Recycling in molten Salt
MC	Monte Carlo

MLD	Master Logic Diagram
MOSART	MOlten Salt Actinide Recycler and Transmuter
MOST	European Project, review of MOlten Salt Technology
MOX	Mixed OXide (oxide fuel pellet containing Pu and U) for spent fuel recycling
MSBR	Molten Salt Breeder Reactor
MSFR	Molten Salt Fast Reactor
MSR	Molten Salt Reactor
MSRE	Molten Salt Reactor Experiment
ORNL	Oak Ridge National Laboratory, USA
OVC	OVer Cooling
PIE	Postulated Initiating Event
Pu+MA MoX	Pu & Minor Actinides Mixed OXide fuel
Pu-MOX	Pu-contained in Mixed OXide fuel
Pu-UOX	Pu-contained in Uranium OXide fuel
PWR	Pressurized Water Reactor
PYROSMANI	PYROchemical processes Study for Minor ActiNides recycling in molten chlorides and fluorides
RAA	Reactivity Anomaly Accident
SACSESS	Safety of ACTinide SEparation proceSSes
SAMOFAR	Safety Assessment of MOlten salt FAsT Reactor
SAMOSAFER	Severe Accident MOdeling and Safety Assessment for Fluid-fuel Energy Reactors
SFR	Sodium-cooled Fast Reactor
SMART-MSFR	Safety of Minor Actinides Recycling and Transmuting in Molten Salt Fast Reactor
S-MSFR	Small modular Molten Salt Fast Reactor
SSC	System Steering Committee
TFM	Transient Fission Matrix
Th-Pu MOX	Th & Pu-containing Mixed OXide fuel
TLOP	Total Loss Of Power
TOP	Transient Over-Power
TRU	TRansUranic element
UOX	Uranium OXide (oxide fuel pellet containing U enriched between 3 and 5% of ²³⁵ U)
US DOE	United States Department Of Energy

Symbols

C_p	Heat capacity in J/kg K
GW_e	Electrical power, GW
GW_{th}	Thermal power, GW
MW_{th}	Thermal power, MW
$\beta_{eff.}$	Effective delayed neutron fraction
λ	Thermal conductivity in W/m K
μ	Dynamic viscosity in Pas
ν	Kinematic viscosity in m ² /s
ρ	Density in kg/cm ³

7.1 Introduction

MSRs are a family of liquid-fueled fission reactor concepts using a fluid molten salt mixture as fuel. In most of the MSR concepts studied today, the fuel is circulating and also acts as coolant. Such liquid-fueled reactors, also called homogeneous reactors, benefit from some potential advantages over solid-fueled systems, among which:

- the possibility of fuel composition (fertile/fissile) adjustment and fuel reprocessing without shutting down the reactor;

- the possibility of overcoming the difficulties of solid fuel fabrication/refabrication with large amounts of TRansUranic (TRU) elements;
- the potential for better resource utilization by achieving high fuel burn-ups (with transuranic elements remaining in the liquid fuel to undergo fission or transmutation to a fissile element).

A circulating liquid fuel playing also the role of the coolant presents some more advantages, such as:

- heat production directly in the fuel, which is also the coolant (no heat transfer delay);
- fuel homogeneity (no loading plan required);
- rapid, passive, fuel geometry reconfiguration via gravitational draining.

This type of reactor is at a conceptual level, mainly based on numerical modeling. However, very significant experimental studies were carried out at Oak Ridge National Laboratory (ORNL), in the 1950s and 1960s, providing an experimental basis for their feasibility. In 1958, a water-based liquid fuel was used in a 5 MW_{th} Homogeneous Reactor Experiment called HRE-2, demonstrating the intrinsic stability of homogeneous reactors. Later on, the Molten Salt Reactor Experiment (MSRE) (ORNL-TM-728, 1965; Haubenreich and Engel, 1970), with a liquid fluoride-based fuel at 650°C and a graphite moderated neutron spectrum, operated for 4 years, from 1966 to 1969, without trouble. It demonstrated the possibility of circulating a liquid fluoride mixture without corrosion problems. This was achieved by using nickel-based alloy (Hastelloy N) and oxidation control of the fuel by use of the U₃+/U₄+ buffer. However, this 8 MW_{th} thermal reactor only tested fissile isotopes (²³³U, ²³⁵U, Pu) and not fertile ones such as ²³⁸U or Th due to the capture cross sections which are large with thermal neutrons. Nevertheless, a continuous physical processing of the fuel was successfully tested, consisting in contacting the fuel with a neutral gas to extract gaseous Fission Products (FPs) such as Kr and Xe before they decay into Rb and Cs (poisons for thermal neutrons). Unexpectedly, this processing also removed most of the metallic FPs. Although successful, these tests did not lead to the construction of the Molten Salt Breeder Reactor (MSBR) (Bettis and Robertson, 1970; Whatley et al., 1970) studied in details by ORNL, partly, because its thermal spectrum requires intensive chemical processing for FP removal as well as Pa extraction (related to proliferation issues due to the possible ²³³Pa decay in pure ²³³U in such conditions) to avoid neutron captures leading to minor actinides. These drawbacks are eliminated by using a fast spectrum.

Within the MSR System Steering Committee (SSC) of the Generation-IV International Forum (GIF/MSR), two fast spectrum homogeneous MSR concepts are being studied (Serp et al., 2014), both based on a liquid circulating fuel: The Molten Salt Fast Reactor (MSFR) concept initially developed at CNRS, France and the MOLten Salt Actinide Recycler and Transmuter (MOSART) concept under development in the Russian Federation. Simulation studies and conceptual design activities are on-going in order to verify that fast spectrum MSR systems satisfy the goals of Generation-IV reactors in terms of sustainability (closed fuel cycle, breeder system), non-proliferation (integrated fuel cycle, multirecycling of actinides), safety (no reactivity reserve, strongly negative feedback coefficient), and waste management (actinide burning capabilities). Compared with solid-fueled reactors, fast MSR systems have lower fissile inventories, no radiation damage constraints on attainable fuel burn-up, no reactivity reserve, strongly negative reactivity coefficients, no requirement to fabricate and handle solid fuel, and a homogeneous isotopic fuel composition in the reactor.

Here, we will focus on the MSFR concept but some elements pertaining to the MOSART concept will be provided. Regarding the MSFR, presented hereafter, its design is not fixed yet but all important issues have been considered since the beginning: nuclear effectiveness, safety, proliferation resistance, in order to reach a design that does not encounter a major obstacle at any level of development. This is why, after the presentation of the physics and chemistry aspects, of safety analysis and of deployment scenarios are discussed. Finally, a path for future research is presented.

7.2 The MSFR concept

Conceptual design activities are currently underway so as to ascertain whether MSFR systems can satisfy the goals of Generation-IV reactors in terms of sustainability, non-proliferation (integrated fuel cycle, multi-recycling of actinides), resource saving (closed fuel cycle, no uranium enrichment), safety (no reactivity reserve, strongly negative feedback coefficient) and waste management. The calculation results presented in this paper were obtained for a reactor configuration called “reference MSFR” studied in the frame of the EVOL (Evaluation and Viability Of Liquid fuel fast reactor systems, 2009–2013), SAMOFAR (Safety Assessment of MOlten salt FAst Reactor, 2015–2019) and SAMOSAFER (Severe Accident MOdeling and Safety Assessment for Fluid-fuel Energy Reactors, 2019–2023) Euratom projects of respectively the Framework Program 7 (Brovchenko et al., 2014a; Dulla et al., 2014) and the Horizon2020 Program (Gerardin et al., 2017). These design calculations have to be seen as a basis for interdisciplinary studies and not some plans to build a reactor directly.

The reference MSFR was the first version of the MSFR studied since more than 10 years (see Figure 7.1), it is a large power reactor based on a Lithium Fluoride (LiF) molten salt and optimized as breeder in the Thorium fuel. Some alternative versions of the MSFR are now studied as breeder in the U/Pu fuel cycle or as actinide burner. Some of these new versions correspond to small modular reactors (Small-MSFR or S-MSFR) and are based on a chloride (NaCl) molten salt. All these MSFR versions (the reference and the alternative ones) use a fast neutron spectrum.

7.2.1 Core and system description

The reference MSFR is a 3-GW_{th} reactor with a total fuel salt volume of 18 m³, operated at a max fuel salt temperature of 750°C (Mathieu et al., 2009; Merle-Lucotte et al., 2012; Brovchenko et al., 2019). The system includes three circuits: the fuel circuit, the intermediate circuit and the power conversion circuit. The fuel circuit, defined as the circuit containing the fuel salt during power generation, includes the core cavity, the inlet and outlet pipes, a gas injection system, salt-bubble separators, pumps and fuel heat exchangers.

As shown in the sketch of Figure 7.1, the fuel salt flows from the bottom to the top of the core cavity (note the absence of in core solid matter). In preliminary designs developed in relation to calculations, the core of the MSFR is a single compact cylinder (2.25 m high per 2.25 m diameter), where the nuclear reactions occur within the liquid fluoride salt acting both as fuel and as coolant. Recently, thermal-hydraulic studies performed in the frame of the EVOL project have shown that a torus shaped core (see Figure 7.1) improves thermal flow (Laureau et al., 2013; Rouch et al., 2014).

The properties of the fuel salt used in these simulations are summarized in Table 7.1. The fuel salt considered in the simulations is a molten binary fluoride salt with 77.5 mol% of lithium fluoride; the other

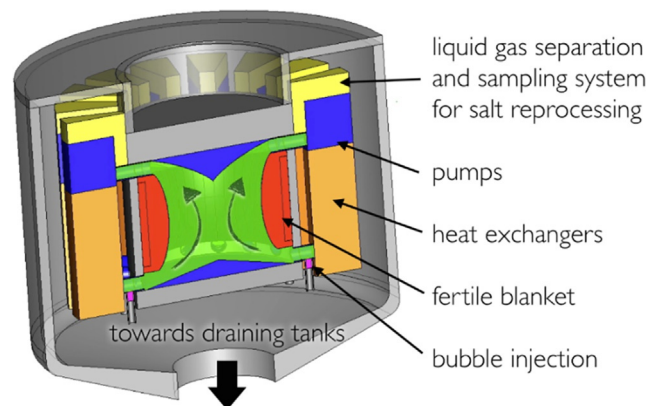


Figure 7.1. Schematic representation of the reference MSFR fuel circuit

Table 7.1. Physicochemical properties of the fuel salt and of the intermediate fluid, measured for the salt 78% mol LiF–22 mol% ThF₄ (Ignatiev et al., 2012)

	Formula	Value (at 700°C)	Validity Range (°C)
Density ρ (kg/m ³)	4094–0.882 (T _(K) –1008)	4125	[617–847]
Kinematic viscosity ν (m ² /s)	$5.54 \times 10^{-8} \exp(3689/T_{(K)})$	2.46×10^{-6}	[625–847]
Dynamic viscosity μ (Pa s)	ρ (g/cm ³) $5.54 \times 10^{-5} \exp(3689/T_{(K)})$	10.1×10^{-3}	[625–847]
Thermal conductivity λ (W/m K)	$0.928 + 8.397 \times 10^{-5} * T_{(K)}$	1.0097	[618–847]
Heat capacity C_p (J/kg K)	$-1.111 + 0.00278 \cdot 10^3 T_{(K)}$	1594	[595–634] ^a

^a The formulas have been extrapolated up to 700°C.

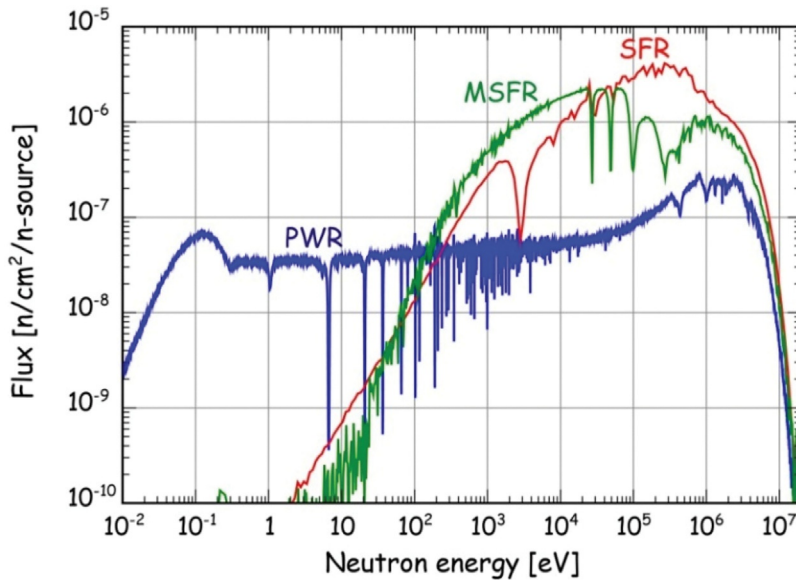


Figure 7.2. Calculated neutron spectrum of the reference MSFR (green curve). For comparison, a typical Sodium-cooled Fast neutron Reactor spectrum (SFR, in red) and a typical PWR thermal spectrum (in blue) are shown

22.5 mol% are a mix of heavy nuclei fluorides. This proportion, maintained throughout the reactor evolution, leads to a fast neutron spectrum in the core as shown in Figure 7.2. This MSFR system thus combines the generic assets of fast neutron reactors (extended resource utilization, waste minimization) and those associated to a liquid-fueled reactor.

Both contributions to the feedback coefficient: density coefficient (or void, related to the salt thermal expansion) and Doppler coefficient are largely negative, leading to a total feedback coefficient of -5 pcm/K. This is a significant advantage for both the operation and the safety of the reactor as discussed below. The characteristics of the reference MSFR configuration are summarized in Table 7.2.

In the fuel circuit, after exiting the core, the fuel salt is fed into 16 groups of pumps and heat exchangers located around the core. The salt traveling time through the whole fuel circuit is 3–4 s (Brovchenko et al., 2012; Gerardin et al., 2017). The total fuel salt volume is distributed half in the core and half in the external portion of the fuel circuit.

Table 7.2. Characteristics of the reference MSFR

Thermal/electric power	3000 MW _{th} /1300 MW _{el}
Fuel salt temperature rise in the core (K)	100
Fuel molten salt—initial composition	LiF-ThF ₄ -(²³³ U or ^{enr} U)F ₄ or LiF-ThF ₄ -(Pu-MA)F ₃ with 77.5 mol% LiF
Fuel salt melting point (°C)	565
Mean fuel salt temperature (°C)	700
Fuel salt density (g/cm ³)	4.1
Fuel salt dilation coefficient (g/cm ³ K)	8.82 × 10 ⁻⁴
Fertile blanket salt—initial composition (mol%)	LiF-ThF ₄ (77.5%–22.5%)
Breeding ratio (steady-state)	1.1
Total feedback coefficient (pcm/K)	-5
Core dimensions (m)	Radius: 1.1275 Height: 2.255
Fuel salt volume (m ³)	18
Total fuel salt cycle in the fuel circuit	3.9 s

The external core structures and the fuel heat exchangers are protected by thick reflectors made of nickel-based alloys, which are designed to absorb more than 99% of the escaping neutron flux. These reflectors are themselves surrounded by a 20 cm thick layer of B₄C, which provides protection from the remaining neutrons. The radial reflector includes a fertile blanket (50 cm thick—red area in [Figure 7.1](#)) to increase the breeding ratio. This blanket is filled with a LiF-based fertile salt with initially 22.5 mol% ²³²ThF₄. Due to the neutron inelastic scattering on Fluorine nuclei (see [Figure 7.2](#)), the MSFR spectrum is a bit less fast than that of solid-fueled fast reactors. This fact, combined to the absence of solid material in the core, results in reduced irradiation damages of the materials surrounding the core.

The fuel circuit is connected to a salt draining system which can be used for a planned shut down or in case of any incident/accident resulting in an excessive temperature being reached in the core. In such situations, the fuel salt geometry can be passively reconfigured by gravity driven draining of the fuel salt into tanks located under the reactor and where a passive cooling and adequate reactivity margin can be implemented.

The MSFR, as a liquid-fueled reactor, calls for a new definition of its operating procedures ([Heuer et al., 2017](#)). The negative feedback coefficient provides intrinsic reactor stability. The reactor may be driven by the heat extracted, allowing a very promising flexibility for grid load-following for example. Unlike with solid-fueled reactors, the negative feedback coefficient acts very rapidly since the heat is produced directly in the coolant, the fuel salt itself being cooled in the heat exchangers.

7.2.2 Transient calculations

The definition and assessment of MSFR operation procedures requires dedicated tools to simulate the reactor's behavior and assess its flexibility during normal (e.g., load-following or start-up) or incidental

(e.g., pump failure or overcooling) transients. The reactor modelization requires specific treatments to take into account the phenomena associated to the liquid fuel circulation. Two kinds of approaches have been developed: a multiphysics code (TFM-OF) coupling CFD thermalhydraulics and neutronics for precise calculations of the core behavior during normal and abnormal transients, and a power plant simulator containing simplified modeling of the neutronics and the thermalhydraulics of the core but representative of the core behavior while allowing real-time calculations and including models for the whole circuits from the core to the turbine.

Concerning the first approach, classical calculation codes can't be employed directly because of the characteristics of the core cavity's geometry (turbulent flow...), and because of the precursor motion. The latter and the MSFR thermal feedback effects imply a strong coupling between the neutronics and the thermalhydraulics during reactor transient calculations. Dedicated tools are thus currently being developed and validated that take into account all these specifics of the reactor physics of circulating-fuel systems confronted to thermal feedbacks on the neutronics.

The use of a CFD code allows the calculation of the 3D velocity and temperature distributions. The latter, along with the density distribution, has a significant impact on the neutronic behavior through the induced variations in the neutron macroscopic cross-sections. Recent studies highlighted the large impact of CFD modeling hypotheses on the MSFR analysis and the need to adopt accurate turbulence models and realistic three-dimensional geometries (Rouch et al., 2014; Brovchenko et al., 2014a; Dulla et al., 2014; Laureau et al., 2013). In this view, the OpenFOAM multiphysics toolkit allowed an efficient simulation of steady-state and transient cases on detailed, full core, 3D geometries (Jasak et al., 2007).

As mentioned, the effective delayed neutron fraction (β_{eff}) represents an important reactor kinetics parameter. In circulating-fuel systems, because of the delayed neutron precursors drift, the β_{eff} calculation requires special techniques (Aufiero et al., 2014). The coupled neutronics/CFD simulations represent a necessary step for the accurate calculation of the effective delayed neutron fraction in the MSFR. The simulation tools also have to take into account all the specifics of the reactor physics of circulating-fuel systems confronted to thermal feedbacks on the neutronics.

The Transient Fission Matrix (TFM) approach (Laureau, 2015; Laureau et al., 2017a, b, c, d, e) has been developed specifically as a neutronic model able to take into account the precursor motion associated phenomena and to perform coupled transient calculations with an accuracy close to that of Monte Carlo calculations for the neutronics while incurring a low computational cost. This approach is based on a precalculation of the neutronic reactor response through time prior to the transient calculation. The results of the SERPENT Monte Carlo code (Leppänen, 2013) calculations are condensed in fission matrices, keeping the time information. These fission matrices are interpolated to take into account local Doppler and density thermal feedback effects due to temperature variations in the system. With this approach, an estimation of the neutron flux variation for any temperature and precursor distribution in the reactor can be obtained very quickly.

The results obtained with this method applied to an instantaneous load following transient are shown in Figure 7.3 and 7.4 (Laureau, 2015; Laureau et al., 2017a). The initial condition corresponds to a critical reactor with 1.5 GW_{th} power. At the beginning of the simulation, the temperature of the intermediate circuit is reduced to increase the power extracted up to 3 GW_{th}. After 1 s, the feedback effect stops the increase of the neutron population, and the reactivity progressively returns to its initial value with a time constant corresponding to the balancing of the delayed neutron precursor population. An oscillation corresponding to the circulating time of the fuel salt can be observed. This application case highlights the good behavior of the reactor to load following transients.

The TFM neutronic approach has been successfully adapted and used for transient calculations of other types of reactors as PWRs (Laureau, 2015), sodium fast reactor (Laureau et al., 2017b; Laureau et al., c; Laureau et al., d; Laureau et al., e) and research reactors (Blaise et al., 2019).

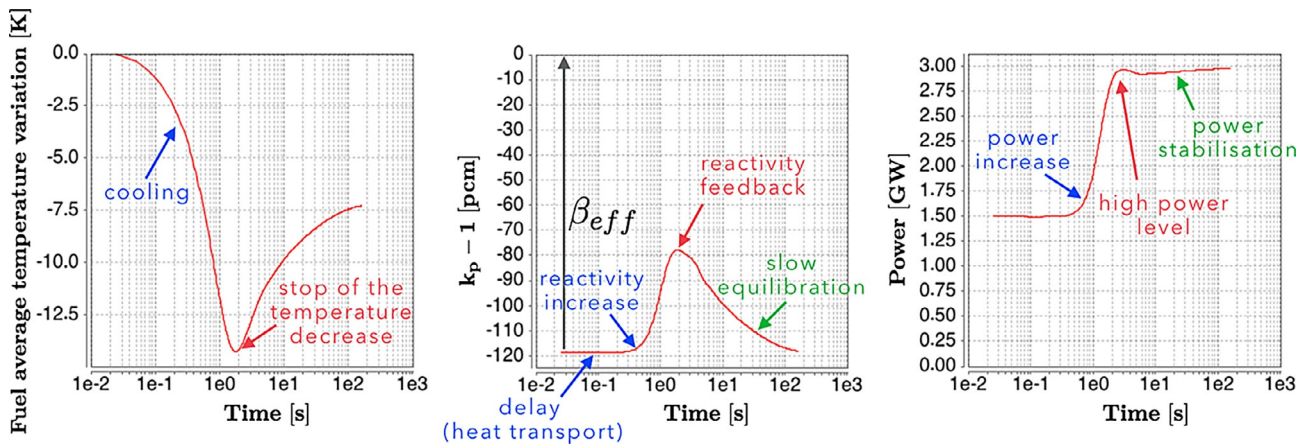


Figure 7.3. Instantaneous load-following transient of the MSFR from an extracted power of 1.5 to 3 GW_{th} computed with the TFM-OpenFoam coupled code (Laureau, 2015; Laureau et al., 2017a)

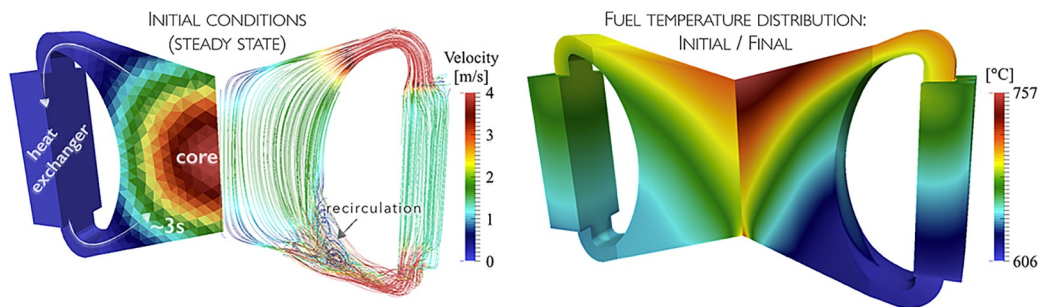


Figure 7.4. Distribution of power, velocity and temperature in the MSFR (Laureau, 2015)

Concerning the second approach developed, a power plant simulator of the MSFR is currently being developed thanks to a cooperation between CNRS/LPSC and the CORYS company, world leader of dynamic simulators for energy, transport and oil industries (Laureau et al., 2020).

7.3 Fuel salt chemistry and material issues

7.3.1 Overview of the processing schemes

The fuel salt undergoes two types of treatment: on-line neutral gas bubbling in the core and delayed mini-batch on-site reprocessing (Delpéch et al., 2009), see Figure 7.5. These salt treatments aim at removing most of the FPs without stopping the reactor and thus securing a rather small fissile inventory outside the core compared to present day LWRs. The reprocessing rate itself is assumed equivalent to the present LWR rate, although it could be possible to reprocess the fuel salt every 10 years but to the detriment of economical yield.

The other is a semicontinuous salt reprocessing at a rate of some tens (10–40) liters per day, in order to limit the lanthanide and Zr concentration in the fuel salt. The salt sample is returned to the reactor after purification and after addition of ^{233}U and Th as needed to adjust the fuel composition and the redox potential of the salt by controlling the U^{4+} to U^{3+} ratio.

These two processes are aimed at keeping the liquid fuel salt in an efficient physical and chemical state for long time periods (decades). The gas bubbling has two objectives: removing metallic particles by capillarity (floating) and extracting gaseous FP before their decay in the salt. The pyrochemical salt batch reprocessing avoids the accumulation in the fuel salt of large quantities of lanthanides and zirconium that could be

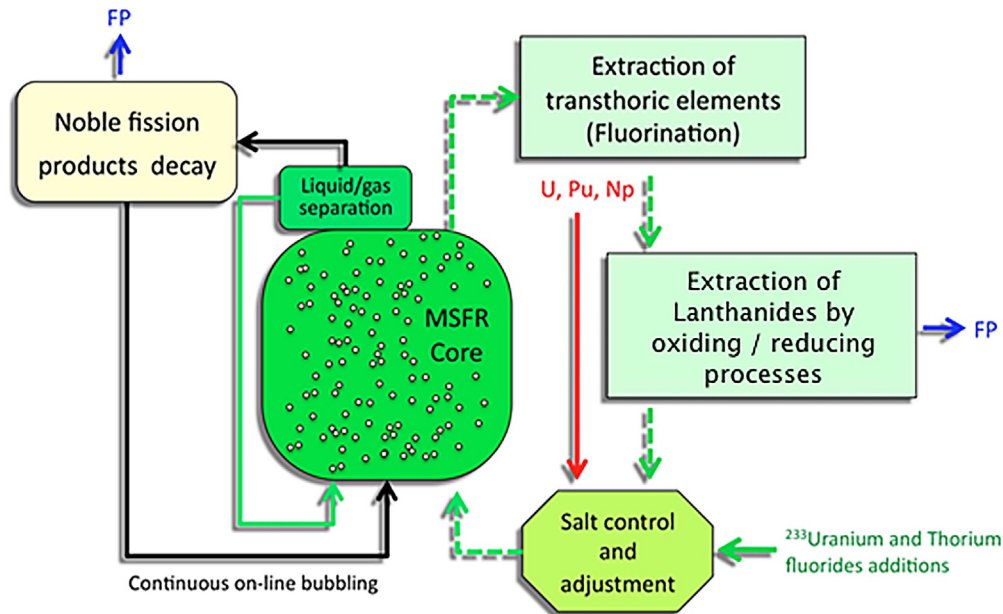


Figure 7.5. Schematic representation of the fuel salt treatment with two loops. On the left is the on-line treatment with gas bubbling in the core to extract noble gases and metallic particles (Fission Products). On the right is the mini-batch on-site reprocessing with two objectives: removing FP (Zr, Ln) and adjusting the fuel content in fissile and fertile isotopes

detrimental to several properties such as Pu solubility or salt volatility. Conversely to the thermal Molten Salt Reactor (MSR), none of these processes are vital to the fast reactor operation. If they were interrupted for months or years the MSFR would not stop but would have a poorer breeding ratio and could suffer from partial clogging of the heat exchangers, leading to poorer efficiency.

The impact of the batch pyro processing rate is shown in Figure 7.6. Note that with the reactor configuration used for the calculation, the core is under-breeder. The addition of a fertile blanket secures breeding, up to a reprocessing time of the total fuel salt volume as large as 4000 days.

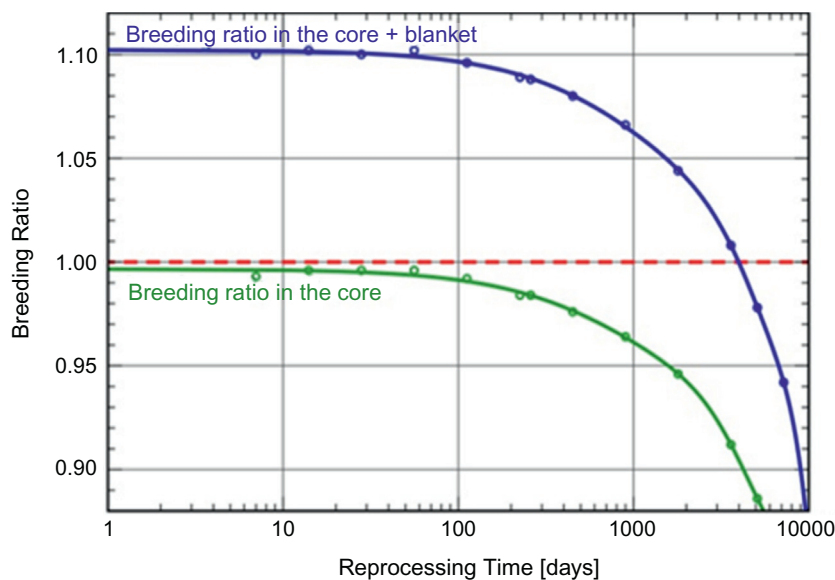


Figure 7.6. Influence of the batch reprocessing rate on the breeding ratio in the core and in the whole MSFR system (core + fertile blanket)

7.3.2 Impact of the salt composition on the corrosion of the structural materials

Material corrosion in molten salt nuclear reactors results from the evolution of the salt composition during operation: production of HF by an uncontrolled purification process or by hydrolysis reactions, production of corrosive FPs, mass transfer in thermal gradients and increase of the redox potential due to fission reaction. Ni-based alloys have been recognized the most suitable materials for their mechanical and chemical resistance up to about 700°C in the presence of fluoride salts. Hastelloy N (Ni-based alloys containing mainly Ni, Cr, and Mo) has been developed by ORNL in the 1960s. Graphite presents an excellent compatibility with molten fluorides but cannot be used for structural applications submitted to a neutron flux. Silicon carbide has a good irradiation and very high temperature resistance but its corrosion resistance has to be studied carefully. However assembling SiC parts is not usual technology and its long term chemical behavior has not yet been tested in molten fluorides.

The historical tests carried out at ORNL have shown that a chemical potential control of the salt was necessary to prevent two types of corrosion: Cr oxidation and intergranular corrosion by Te (a FP). This was achieved by using a chemical buffer based on the U^{4+}/U^{3+} couple. The proper U^{4+}/U^{3+} concentration ratio was obtained by contacting the salt with metallic Be from time to time to keep this ratio in a suitable range (60–20 for instance). The change of chemical potential of the fuel salt is intrinsic to the fission of fissile elements present in the fuel at valence IV, because the resulting FPs have a mean valence close to III. Therefore, the salt becomes more oxidizing as fissions occur; an initial chemical potential control of the salt is necessary but not sufficient to prevent corrosion. It has been shown that chromium contained in Ni-based alloys (such as Hastelloy N) is necessary to the mechanical properties of Ni-based alloys and not only to their chemical resistance to oxidation in air. However, chromium being the most readily oxidizable element of the alloy, its concentration should be limited to about 6 to 8 wt% to keep the corrosion rate at an acceptable level.

Prior to the use of the U^{4+}/U^{3+} chemical buffer a salt purification is required for the initial salt preparation or when recycling the actinides after lanthanide extraction. H_2O and HF are the most oxidizing compounds present as impurities in solid fluorides and in the molten salt. High oxidation state, H_2O and dissolved oxides can be eliminated by using gaseous H_2/HF mixtures but some HF may remain dissolved in the salt. Care should be taken to limit this dissolved amount. For a salt without Be ions the introduction of U(III) can be achieved by direct addition or by chemical reduction using Th or U metal added anyway, to compensate neutron captures.

7.4 MSFR fuel cycle scenarios

To produce power, a fission nuclear reactor requires fissile material. Generation 2 or 3 reactors (PWR, CANDU, EPR, ...) being under-breeder systems, i.e., using more fissile material than they produce, need to be regularly refueled with fissile material all along their operation time. On the contrary, breeder Generation-4 reactors (SFR, MSFR, GFR, ...) require only one (or two in the case of solid fuel reactors) initial fissile material load. They then produce at least the fissile material they need to be operated during their entire lifespan. MSRs require only one fissile load since no fuel refabrication is necessary and the fuel salt composition is controlled on-line without stopping reactor operation whereas 2 loads are necessary for solid-fueled reactors with one fissile load inside the reactor and the other in the reprocessing/fuel manufacturing process.

According to our simulations results, the Thorium based reference MSFR can be started with a variety of initial fissile loads as discussed below (Heuer et al., 2014; Merle-Lucotte et al., 2009a, b):

- With $^{235}U^*$ enriched uranium, the only natural fissile material available on earth is ^{235}U (0.72% of natural uranium). Enriched uranium can be used directly as initial fissile material to start MSFRs, with an enrichment ratio less than 20% due to proliferation resistance issues.

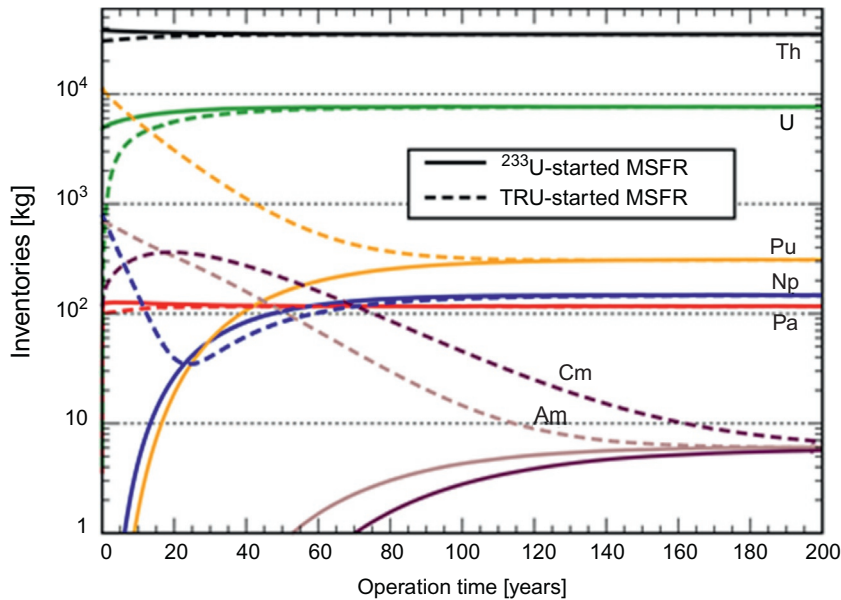


Figure 7.7. Time evolution up to equilibrium of the heavy nuclei inventory for the ^{233}U -started MSFR (solid lines) and for the TRU-started MSFR (dashed lines)—operation time is given in Equivalent Full Power Years (EFPY)

- With ^{233}U directly as initial fissile material, assuming that this ^{233}U can be produced in fertile blankets of other reactors (SFR...) or by irradiating ^{232}Th in an Accelerator-Driven System (ADS) for example. Once an initial park of MSFRs based on the Th- ^{233}U cycle is launched, ^{233}U will also be produced in breeder MSFR reactors, allowing the deployment of such ^{233}U -started MSFRs in a second phase even if no ^{233}U is produced elsewhere.
- With the plutonium produced in current PWRs or in future EPRs or, even better, the mix of TRU produced by these Generation-II–III reactors as initial fissile load.
- With a combination of the previous starting modes. For example, ^{233}U may be produced by using special devices containing Thorium and Pu-MOX in current PWRs or in future EPRs.
- Figure 7.7 presents two examples of fuel composition evolutions for a “3 GW_{th} reference MSFR” reactor started with ^{233}U or TRU. An optimized fuel salt initially composed of LiF-ThF₄-enriched UF₄-(TRU)F₃ with uranium enriched at 13% in ^{235}U and a TRU proportion of 3% (see Figure 7.8), has been selected in the frame of the EVOL project taking into consideration the neutronics, chemistry and material issues.

Given the absence of naturally available ^{233}U , a standing question is whether a park of MSFRs can be deployed whether at the French national, the European or the worldwide scales. In this section, we illustrate the flexibility of the concept in terms of deployment and end-of-game capacities of the MSFR at the French national scale.

The deployment scenarios of a park of nuclear reactors also led to an estimation of the amount of heavy nuclei produced by such a deployment. We aim at evaluating the complexity of the management of these heavy nuclei stockpiles, as well as their radio-toxicity. The French scenario, displayed in Figure 7.9, assumes that the natural uranium resources available are large enough to require Generation-IV reactors in 2070 only. The deployment scenario starts with the historical French nuclear deployment based on light water reactors (PWRs followed by EPRs). By 2040, some Generation-III reactors are fueled with Pu-UOX in a Thorium matrix both to reduce minor actinide production and to prepare the launching of the Thorium fuel cycle in MSFRs. The park of these Generation-III reactors is then progressively replaced with MSFRs started with this Th-Pu MOX fuel from the last Generation-III reactors. The deployment is finally completed with MSFRs started with a mix of ^{233}U produced in the existing MSFRs and the remaining stockpiles of Pu-UOX and Pu-MOX irradiated in the light water reactors.

Figure 7.8. Time evolution up to equilibrium of the heavy nuclei inventory for the optimized MSFR configuration started with enriched Uranium and TRU elements. Operation time is given in Equivalent Full Power Years (EFPY)

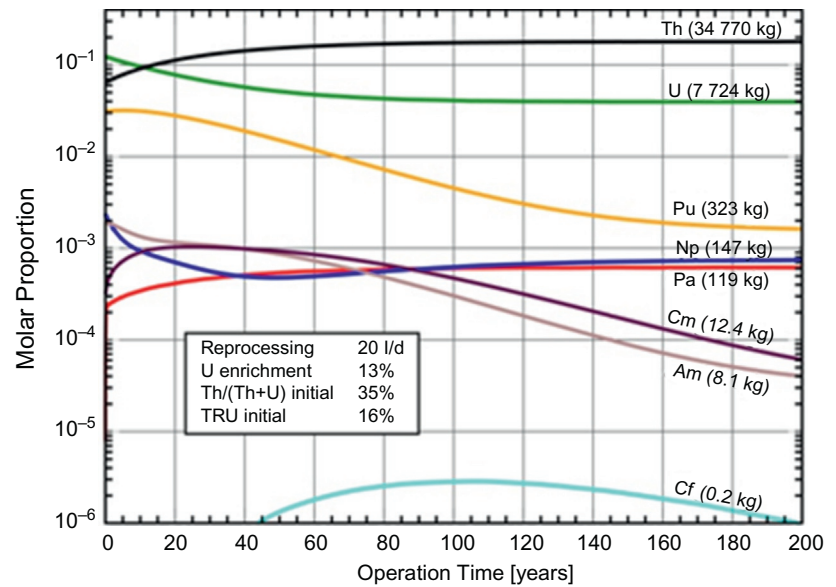
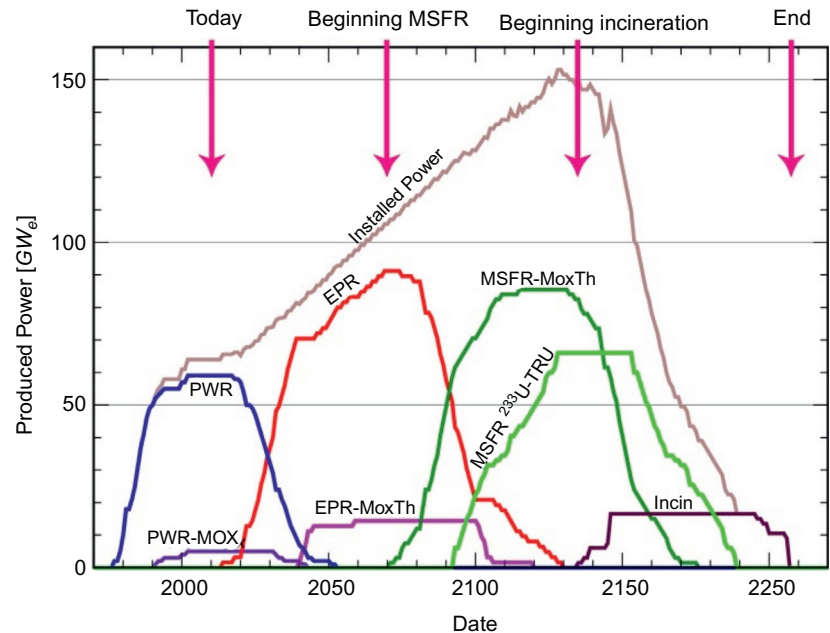


Figure 7.9. French nuclear power deployment exercise based on PWRs, EPRs, and MSFRs



Assuming that, at any time in the future, here in the first half of the 22nd century, France resolves to disperse from the production of fission based nuclear energy, the scenario ends with the introduction of burners with a view to optimizing the end-of-game and further reducing the final TRU inventories after MSFR shut-down. Note that the end-of-game situation would not be different if it occurred after hundreds of years of operation; it depends only on the installed power.

The evolution of the radioactive element stockpiles other than the FPs during the scenario is shown in Figure 7.10. The final stockpiles that will have to be managed as the scenario ends are the following:

- Depleted uranium at 0.1%: 803,700 tons
- Uranium from reprocessing (minimized by the scenario management): 3250 tons
- Irradiated thorium: 5100 tons

- Irradiated UOX fuel (minimized by the scenario management) represented in Figure 7.10 by its Pu content (labeled “Pu-UOX”): 5 tons of Pu standing for 450 tons of irradiated UOX fuel
- Irradiated MOX fuel (minimized by the scenario management) represented in Figure 7.10 by its Pu content (labeled “Pu+MA MOX”): 0.76 tons standing for 12.4 tons of irradiated MOX fuel
- Minor actinides separated from the Pu when the latter is used as MOX fuel in light water reactors, and vitrified (labeled “MA from UOX”): 612 tons
- Final burner inventories: 106 tons.

The evolution of the radiotoxicity corresponding to the final radioactive stockpiles of this scenario including the FPs is displayed in Figure 7.11, where it appears that the short-term radiotoxicity (a few dozen years) is dominated by the FP while the long-term radiotoxicity (10^3 – 10^6 years) is mainly due to the vitrified minor actinides produced in light water reactors and not reused in MOX fuel.

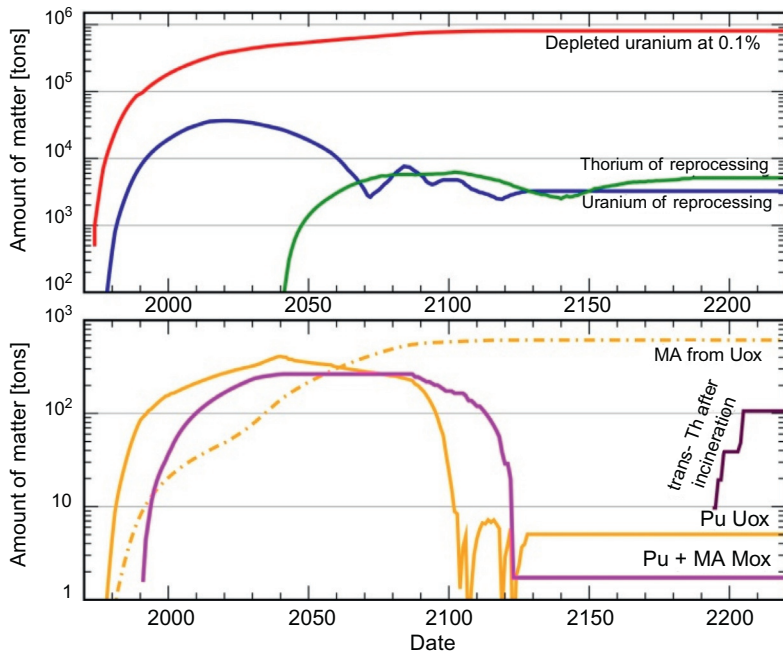


Figure 7.10. Evolution of the actinide stockpiles during the scenario considered

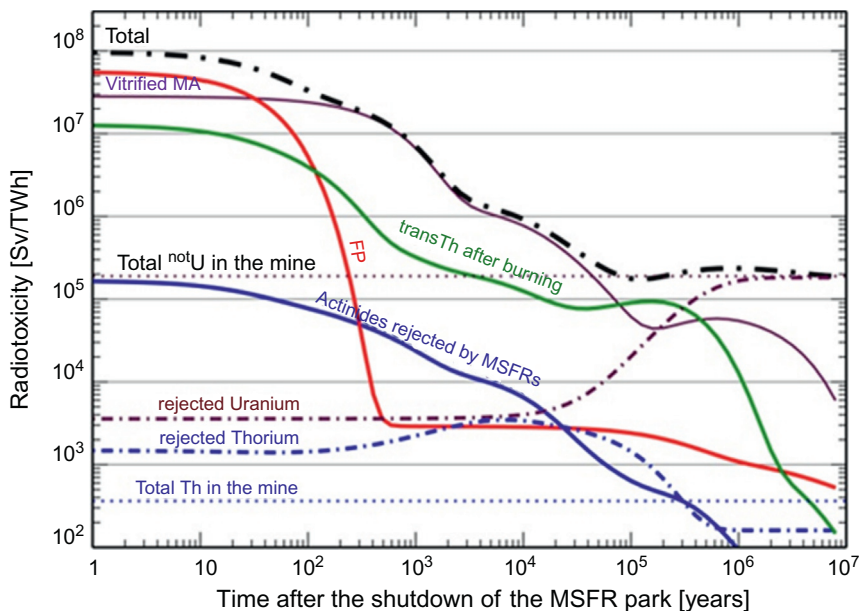


Figure 7.11. Time evolution of the various contributions to the radiotoxicity of the final radioactive stockpiles

7.5 Safety methodology and risk analysis

In the frame of the SAMOFAR and EVOL Euratom projects, this latter being in collaboration with Russian research organizations cooperating in the ROSATOM project MARS (Minor Actinides Recycling in molten Salt) (Ignatiev et al., 2012), design and safety studies of the MSFR system have been led (Beils et al., 2019; Gerardin et al., 2019; Uggenti et al., 2017; Brovchenko et al., 2014b; Gerardin, 2018).

A MSR has some specific safety features; notably, the fuel salt geometry can be modified quickly and passively by draining to subcritical tanks. It is possible to design the system with a maximum of passive devices to cool the fuel in all circumstances and for long time periods without human intervention. Moreover, the MSFR reactor stability is enhanced by its largely negative feedback coefficients. Some of these features are discussed below but not all safety provisions are detailed.

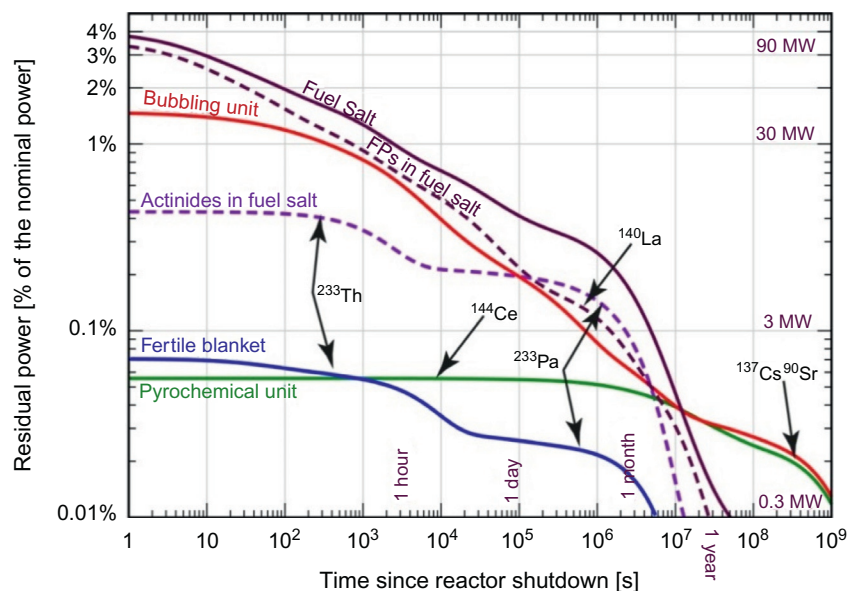
7.5.1 Liquid-fuel reactor specificities and decay heat removal

The unique characteristics of a liquid-fueled reactor strongly impact its design and safety analyses. For example:

- The application of the defense-in-depth principles and the definition of multiple barriers (such as clad, primary circuit and reactor building in LWRs) are no longer applicable.
- The quality, diversity and mutual independence of the MSFR reactivity control mechanisms have to be demonstrated, especially to verify that no additional system is needed to ensure this safety function (no control or shutdown rods or burnable poisons...).
- New safety criteria to evaluate reactor response during normal, incidental and accidental conditions are needed since the structural materials and the temperature and pressure ranges are different from current operated reactors, and the MSFR fuel is in liquid state—which is not an acceptable situation for the LWR fuel. This also affects the definition of the reference severe accident that cannot be the melting of the core.
- In the evaluation of severe accident scenarios with leakage to the environment, any interactions between the fuel salt and groundwater should be investigated in detail and the source term be determined.
- The risk posed by the residual decay heat and the radioactive inventory in the reprocessing unit must also be evaluated.

The decay heat generation is represented versus time in Figure 7.12. The MSFR design implies that FPs are present in two different places when the reactor is stopped. Some are in the liquid fuel salt and some in the gas

Figure 7.12. Residual heat in the different radioactive fluids of the MSFR, after the total fission shutdown of the reactor previously in steady-state (Brovchenko et al., 2012, 2013)



processing unit. About one-third of the heat is produced in the gas processing unit and two-third in the liquid fuel. The power of both heat sources decreases rapidly (by a factor 10 in about 1 day) from the value at shut down, which depends on the history of power generation. The total amount of power at shut down is about 5% of the nominal power. This value is lower compared to solid fuel reactors because FPs are continuously removed in this concept.

In case of cooling problems, the fuel salt and the fluid containing FPs (salt or metal) of the gas processing unit can be drained simply by gravity into the emergency subcritical draining tank where the decay heat extraction will be passively done during short to long periods by a gas circulation in natural convection (Gerardin et al., 2017; Gerardin, 2018).

7.5.2 Safety approach

A novel methodology for the design and safety evaluations of the MSFR is needed. Nevertheless, it would be desirable that the MSFR methodology rely on current accepted safety principles such as the principle of defense-in-depth, the use of multiple barriers and these three basic safety functions: reactivity control, fuel cooling and radioactive product confinement. In addition, due to the limited amount of operation experience and some of its novel features, any new methodology shall be robust and comprehensive, and integrate both deterministic and probabilistic approaches.

In the frame of the SAMOFAR project, the development of the safety approach has been driven by IRSN with the support of Framatome, CNRS, and POLITO. The objective of this work was to define a risk assessment methodology which could be applied from the earliest stages of design to licensing, operation and decommissioning. This methodology had to take into account the Generation-IV safety requirements, the international safety standards, the available return of experience and the peculiarities of this kind of reactor with the help of available risk analysis tools, with the idea to achieve a safety which is “built-in” and not “added-on” providing with a detailed understanding of safety related design vulnerabilities, and resulting contributions to risk. As such, new safety provisions or design improvements as well as R&D needs could be identified, developed, and implemented relatively early. The MSFR technology being at its first stages of design will benefit from such an approach. The methodology is based on the Integrated Safety Assessment Methodology (ISAM) developed in the framework of the GIF. ISAM is best thought of as a tool kit of useful analysis tools for Gen IV systems. Some of these tools are primarily qualitative, others quantitative. Some are primarily probabilistic, others deterministic. Some focus on high-level issues such as systemic response to various phenomena, others focus on more detailed issues. This diversity helps to provide a robust guidance based on a good understanding of risk and safety issues.

The ISAM tools have been reviewed, completed and adapted, when needed, to better reflect the European standards/rules, the available return of experience on MSRs and to better fit the scope of the SAMOFAR project. In addition, the usual risk analysis methods have been reviewed and their integration within the ISAM framework studied (see Figure 7.13). This adapted method has then been declined to be applied to the MSFR technology. A focus has also placed on the safety-related subjects to be examined as a priority at the basic design stage and on the depth of their analysis.

7.5.3 Safety evaluation

A preliminary list of accident initiators has resulted from the analysis performed during the EVOL European project. This first step of a safety evaluation has been completed during the SAMOFAR project with the application of the safety analysis methodology described in the previous section and the related recommendations on the MSFR for the normal conditions of power production. The identification of the accident initiators has been performed using both bottom-up and top-down approaches. The Functional Failure Mode

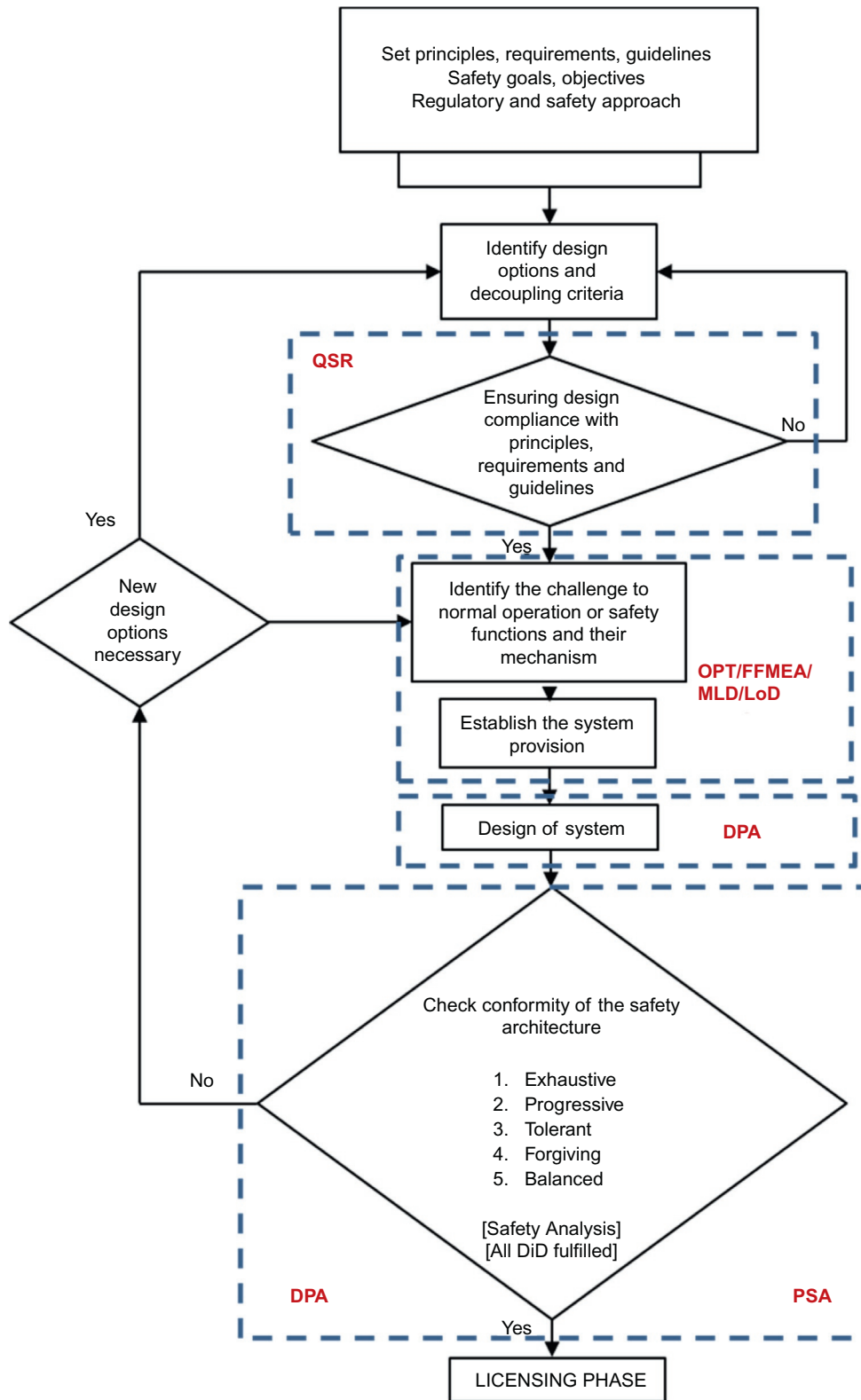


Figure 7.13. Flowchart of the MSFR design/safety assessment and relevance of the different tools

and Effects Analysis (FFMEA), bottom-up approach, has been performed by CIRTEN/POLITO and CNRS/LPSC and the Master Logical Diagram (MLD), top-down approach, has been performed by CNRS/LPSC and Framatome for the plant state corresponding to the power production of the MSFR. This has led to the identification of the Postulated Initiating Events (PIEs) of the MSFR (Gerardin et al., 2019; Ugenti et al., 2017). The families of events identified for the MSFR are currently:

- Reactivity insertion
- Loss of fuel flow
- Increase of heat extraction/over-cooling
- Decrease of heat extraction
- Loss of fuel circuit tightness
- Loss of fuel composition/chemistry control
- Fuel circuit structures over-heating
- Loss of cooling of other systems containing radioactive materials
- Loss of containment of radioactive materials in other systems
- Mechanical degradation of the fuel circuit
- Loss of pressure control in fuel circuit
- Conversion circuit leak
- Loss of electric power supply

This list will be updated with the progress of the MSFR safety analysis if other phenomena are identified. Then, event categories are defined with associated occurrence frequency ranges as presented in Figure 7.14. Some scenarios or phenomena have been classified as “limiting events,” even if no specific cause of the scenario/phenomenon have yet been identified, because they constitute bounding cases or specific risks for the concept. The objective is to drive the analysis toward the consideration of all phenomena of potential interest (for example fuel salt freezing scenario, postulated prompt critical power excursion...).

This methodology can be iteratively applied, following the design development; similarly, the lists of the PIEs will evolve with the detail of the design and the investigation of the physical phenomena governing the behavior of the system, through deterministic analyses.

Finally the method of the Lines of Defense (LoD) has been applied for the MSFR during nominal power production (Beils et al., 2019). The main objective of the LoD method is to ensure that every accidental evolution of the reactor state is always prevented by a minimum set of homogenous (in number and quality) safety provisions—called LoD—before a given situation may arise. It allows the designer to determine

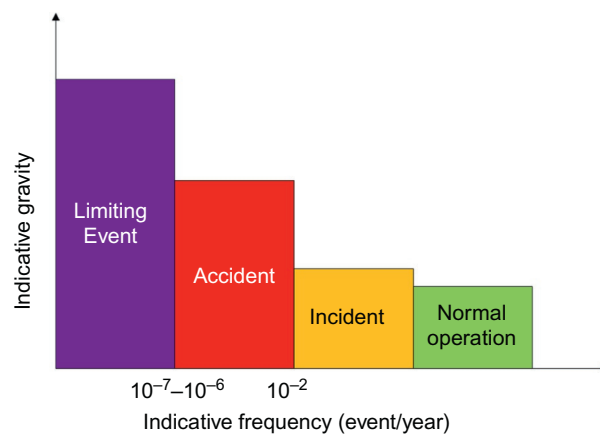


Figure 7.14. Categories of initiating events

whether sufficient safety provisions are put in place between initiating events and a given accidental situation, and contributes to justify the acceptable safety level of the plant in the licensing process. A very first step of the method is to identify and characterize the situations for which prevention is researched. Then, the events that may lead to the situation considered (so-called initiating events) must be identified. The definition of the severe accident is key in the usual application of the LoD method. Cliff edge effects studies allowing to precisely define severe accident for the MSFR are still on-going. Considering the barriers envisaged, a situation with potential for large and early radiological releases in the environment would require at least the failure of the two first barriers (the fuel circuit/core containment structures and the reactor vessel). The general objective retained is thus to prevent the situation of failure of the two first barriers, with a potential for large radiological releases in the environment, through at least two strong and one medium LoD. More precisely, the following rules have been proposed for a preliminary allocation of the LoD:

- Sequences or situations which could significantly impair the reactor availability or which could lead to limited radiological releases should at least be prevented by one medium line of defense.
- Sequences or situations which could significantly impair the reactor investment (or which could lead to significant radiological releases (with no need for off-site confinement measures) should at least be prevented by one strong line of defense.
- Sequences or situations which could threaten safety (with the loss of one of the three safety function or the occurrence of a severe accident situation if any is identified for the MSFR), with potentially important radiological releases should at least be prevented by two strong and one medium LoD.

An example of the LoD analysis of the Loss of Pressure Control event for the MSFR is given in Figure 7.15.

These studies have also been used to provide a list of design key-points that are relevant for safety and should be further documented such as the type of pumps used for the fuel circulation, the definition of the

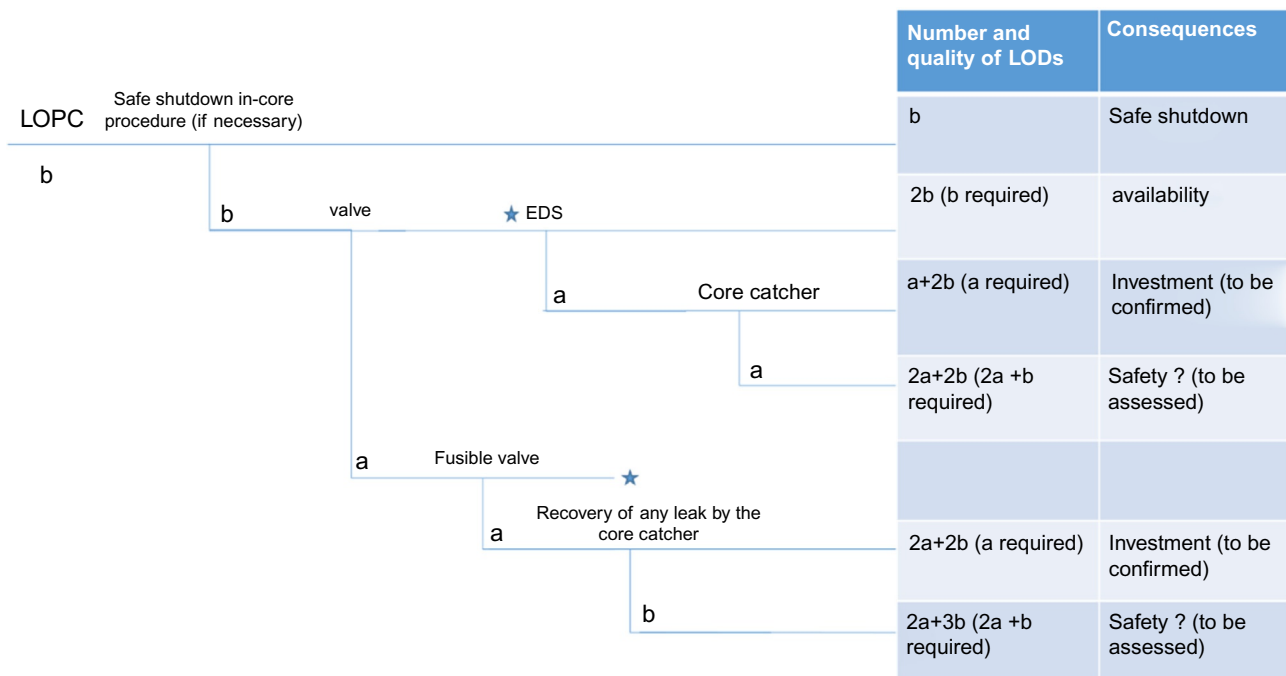


Figure 7.15. Line of defense analysis of the Loss of Pressure Control event for the MSFR

decay heat removal system or the components of the FP removal systems. It has also highlighted the need to further define the operation and accidental procedures. For instance, the cases in which the emergency draining system, the routine draining system or in-core shutdown are used should be defined.

Finally, several proposals for the confinement barriers of the MSFR have been discussed within the SAMOFAR project (see Figure 7.16) and the version presented in Figure 7.17 has been selected.

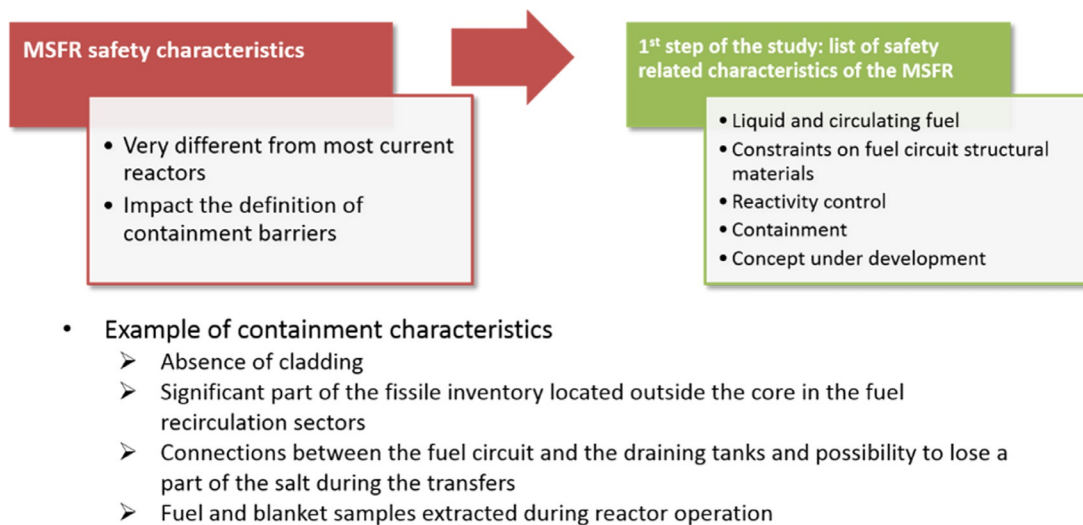


Figure 7.16. Confinement barrier definition for the MSFR system

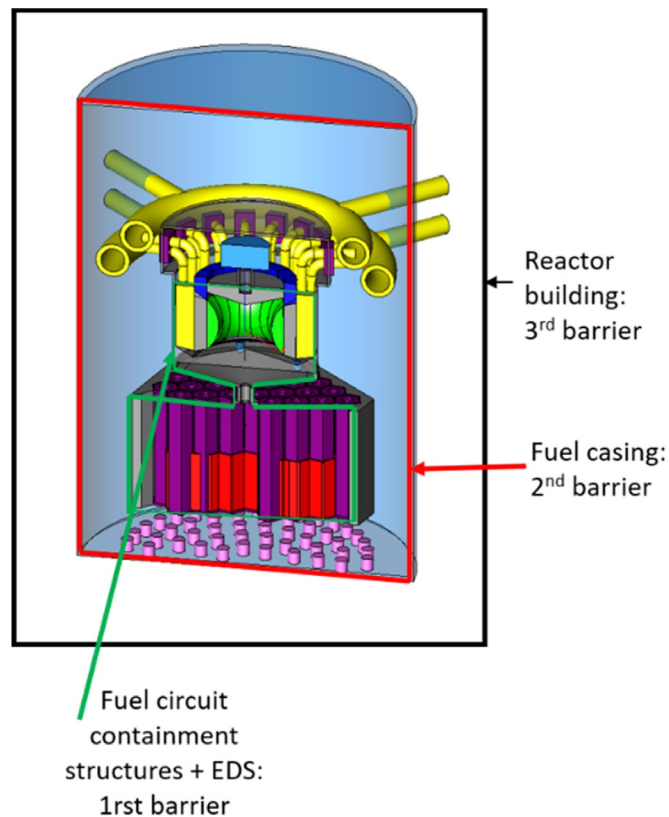


Figure 7.17. Definition of the MSFR confinement barriers after the SAMOFAR project (Gerardin, 2018)

7.5.4 Conclusions and recommendations of the MSFR safety evaluation

Thanks to the risk analysis performed up to now, coupled to multiphysics calculations as described above, the safety advantages identified for the MSFR concept are the followings:

- With the liquid fuel and a fast neutron spectrum, a negative temperature feedback coefficient is obtained, whose action is immediate (around some tens microseconds for the Doppler effect and around the millisecond for the density effect that corresponds to the extraction of fuel salt from the core) in the event of a salt temperature variation. This ensures an intrinsic safety with respect to reactivity accidents.
- The liquid fuel unloading (called draining) from the core zone is easier and faster compared to the unloading of a solid fuel; this allows to maintain subcritical the salt and to cool the fuel in a dedicated fuel tank if necessary.
- The fuel circuit is not pressurized and the fluoride salt is not likely to cause violent exothermic chemical reactions when it is in contact with the materials of the plant. Lithium fluoride does not react violently with air; it does not represent a fire hazard. It should not react violently with water either.
- Fission gases (and possibly some non-volatile and non-soluble FPs) are released from the fuel during operation, reducing the radiological salt inventory, in particular that of the gaseous FPs which are the most likely to be released in case of accident with a solid fuel. The FPs that remain within the salt, in particular cesium, are not significantly released in the event of an accident.
- The absence of fuel structures in the core such as cladding and subassemblies removes any risk of fuel compaction, a major risk of reactivity insertion in a fast neutron reactor with solid fuel.
- The intrinsic temperature feedback effect could eliminate the need of a control rod system for adjusting the operating conditions. Moreover, the amount of fissile matters dissolved in the critical zone of the fuel circuit is just necessary to maintain a critical state. For a breeder reactor as the reference MSFR, fertile matters are periodically injected in the core without needing to shut down the reactor. This allows to intrinsically reduce the risk of accidental reactivity insertion.

The other output of these risk analysis and multiphysics calculations is the identification of the following safety related challenges/R&D studies needed for the MSFR concept, some of them being studied in the SAMOSAFER European project (2019–2023):

- The safety analyses led until now must proceed more in depth to make sure the identification of risks is exhaustive. Some major achievements have been performed in that respect when it comes to identification of initiating events on the reactor during power production. This risk identification exercise should be further continued, trying notably to consider all initial states/operation modes (start-up, shutdown phases etc,...) and all the facilities, including the fuel treatment units.
- Noted that, as the fuel is in the liquid state, there is no accident similar to the severe accident of core meltdown as on solid fuel reactors, where the impact of such an accident on the safety functions is an important aspect for the reactor design and R&D. The definition and the studies of the severe accidents to be considered are in progress and must be continued, including a focus on the reactor behavior in case of a postulated prompt-critical jump that will be studied during the SAMOSAFER European project.
- The prevention of corrosion of the structures in contact with the salt, especially the reactor vessel, must be shown to be sufficient. Suitable measures of surveillance are to be developed.
- The absence of risk of severe chemical reactions between the salt and the other materials employed is to be confirmed, especially the absence of risk of producing some hydrogen by the dissociation of water. Also, the consequences of a contact between salt and water need to be assessed, in particular the risk of steam explosion.

- The risk of precipitation and concentration of fissile matters in the salt, as well as more generally speaking the criticality risk of the salt which is not in the reactor zone, are to be further examined.
- FPs extracted from the fuel circuit during operation are stored in particular in the salt treatment unit. The associated risks (i.e., presence of a radiological source term, production of residual power, criticality risk) must be analyzed in detail.
- The monitoring of the reactor and the salt treatment unit, the features for in-service inspection and repair or replacement of equipment in contact with the salt, must be defined. It should be possible to monitor the envelopes containing the salt from the outside.
- The current report presents significant progresses as regard the definition of confinement barriers for fuel salts and FPs. Next steps could include the definition of their performances required by considering normal and accident conditions.

Just to remind that this risk assessment process for an advanced nuclear plant is proposed to be iterative rather than serial: as the design matures and more design details become available, the set of accident initiators will be updated and broadened to gradually address other plant systems and operational states. At the same time, the selected events are studied through deterministic analyses in order to define more accurate event sequences.

7.6 Concept viability: Issues and demonstration steps

7.6.1 Identified limits

Although the MSFR is still at the preconception design stage, several limiting factors can be identified in the development of the concept.

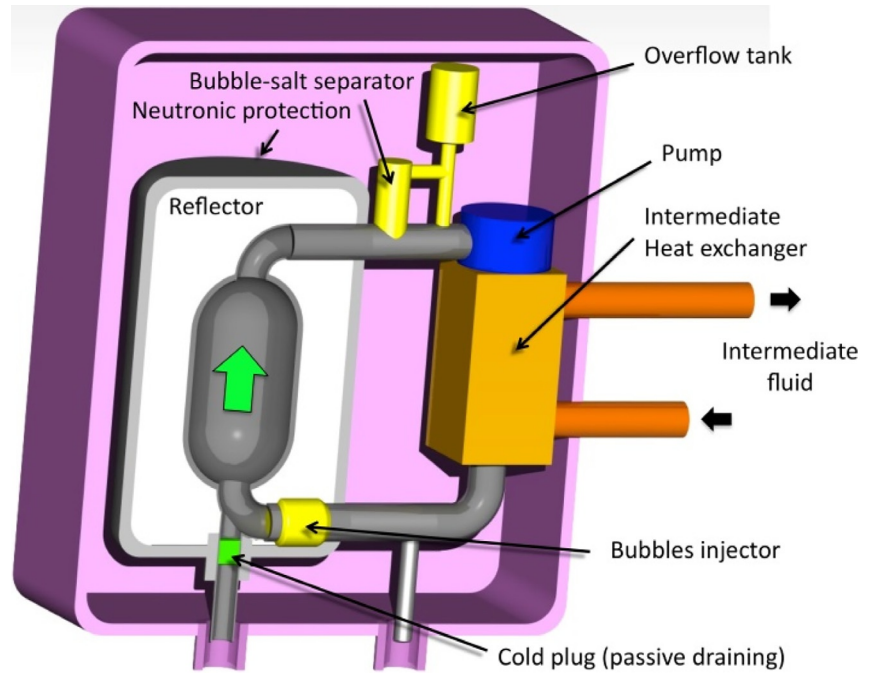
The first, obvious, issue is materials resistance to high temperatures under irradiation, if the reactor is to be operated with a reasonably high-power density. A first temperature limit is given by the fuel salt melting point (565°C) to which a safety margin should be added to avoid local solidification (50°C for instance). To this, add 100°C–150°C for in core temperature heating corresponding to a salt circulation period of 3–4 s, so as to satisfy heat transfer dynamics in the heat exchangers without incurring an excessive pressure drop within these. This leads to a temperature of about 750°C at the core outlet to the gas-salt separation device and the pump (hot leg). Those devices may be maintained at 700°C by cooling, i.e., the same temperature as the heat exchanger plates during the heat transfer, the intermediate coolant salt being at about 650°C. It seems that there are today alloys that can withstand such temperatures for a long time but this could be a limit, unless the material is replaced regularly as is done with solid fuel cladding.

The second issue arises in the attempt to limit the per GW fissile inventory. This implies restricting as much as possible the proportion of fuel salt out of the core, in the tubing, pumps and heat exchangers. One of the main constraints on the design of the MSFR fuel circuit is the ability to evacuate the heat generated while restraining the fuel salt volume mobilized for that task. It seems technically challenging to reduce this “useless” amount of salt to less than 50% of the total load and 30% appears as a limit.

The third issue is a question more than it is a real limit: the safety evaluation. Indeed, as discussed above, today’s safety evaluation techniques apply to solid fuel water reactors but are partly irrelevant for liquid fuel reactors. A new way of tackling the problem should find a consensus before any national safety authority can approve of a liquid fuel reactor design and this will take time and resources.

From the parametric studies that were carried out on the MSFR, the concept does not exhibit any major stumbling blocks and the various limits can all be circumvented by reducing the power density.

Figure 7.18. Sketch of a liquid fuel single loop reactor for demonstration purposes or modular conception. The fuel volume (1.8 m^3) is reduced by a factor 10 from the 3 GW_{th} reactor and the power (200 MW_{th}) by a factor 15 to use the same intermediate heat exchanger



7.6.2 Demonstration steps

It is possible to design a low power demonstration reactor in which to test all the features expected for a full size “Reference MSFR” with a single fuel loop, as shown in Figure 7.18. Its fissile inventory lies in the range of 400–500 kg of ^{233}U (if started with ^{233}U but starting with $^{\text{enriched}}\text{U}$ mixed or not with Pu will be more feasible) for a zero power version and up to 670 kg for a 200 MW_{th} version.

The size of the reactor liquid fuel loop is not a limit as shown by the calculation of a single loop 200 MW reactor instead of a 16 loop 3 GW_{th} reactor. The low power demonstration version (Merle-Lucotte et al., 2013) is sketched in Figure 7.18 could be replaced by a breeder version if the reflectors were replaced by a blanket. The size of this fuel loop assembly is about 2.5 m in diameter and 3 m high (core: 1.1 m diameter and 1.1 m high). The power is limited by the intermediate exchanger size, which is assumed to be the same as that of the 3 GW_{th} reactor.

Before reaching this advanced level, it will be necessary to bring evidences of safety for all experiments involving nuclear materials, under the supervision of nuclear safety agencies. To get the clearance of these authorities the reliability and safety of the technical solutions involved should be demonstrated before on pieces of equipment operating with non-nuclear materials (simulant salts or chemicals). Therefore, the following simplified scheme is foreseen:

- basic data determination and assessment (It is the present stage up to about 2020);
- technical devices testing on non-nuclear simulants up to the full scale;
- chemical separation tests on nuclear materials at small laboratory scale and by remote handling;
- development of numerical simulation tools validated on experimental equipment using circulating simulant salts at high temperature.

Obviously, all the stages mentioned above will overlap in time, not only for practical reasons but because all the aspects of the design should be kept in mind and documented during the whole development procedure.

7.6.3 Other R&D activities on molten salt systems

Various MSR concepts (see <https://aris.iaea.org/sites/MSR.html>) are studied around the world by academic teams and by start-ups mainly located in USA, Canada and England. MSR development worldwide is still at a conceptual design stage, with most investigations around these concepts based today on numerical modeling, with the notable exception of the People's Republic of China, where a large project to develop a thorium MSR prototype started some years ago at SINAP with a demonstrator under construction in the Gansu province.

The Russian Federation also announced in Nuclear Engineering International in November 2019 a new project to build an MSR burner demonstrator. Recent MSR developments in the Russian Federation are focused on the 1000 MW_{el} Molten-Salt Actinide Recycler and Transmuter (MOSART). The primary specifications for a MOSART core were to provide the fissile concentration and fuel salt geometry such that about 2.4 GW_{th} nuclear heat would be released at conditions affording efficient transmutation & recycling of TRUs from MOX PWR spent fuel (Ignatiev et al., 2012). The MOSART reference core with no graphite moderator is a cylinder 3.4 m in diameter and 3.6 m high. The fuel salt inlet and outlet pipe diameters are fixed at 1 m. Radial, bottom, and top reflectors are attached to the reactor vessel. This leaves a ring filled with fuel salt surrounding the core to cool reflector and reactor vessel. The molten salt flow rate is 10,000 kg/s. In nominal conditions, the fuel salt enters the core at 600°C and transports 2.4 GW_{th} to the secondary salt in the primary heat exchanger. The fluoride fuel salt mixture is circulated through the reactor core by four pumps operating in parallel. Other pumps circulate the salt through the heat exchangers and return it to a common plenum at the bottom of the reactor vessel. In the reference MOSART design, the out of core salt volume is 18 m³. The MOSART concept is being studied in different configurations which consider different core dimensions and different compositions of the fuel salt and/or salt blanket that allow for different modes of utilization. A detailed description of MOSART can be found in Afonichkin et al. (2014).

7.7 Conclusion and perspectives

The MSFR concept has been recognized as a long-term alternative to solid-fueled fast neutron reactors because of attractive features that remain to be confirmed.

It is characterized by:

- Liquid fuels of fluoride or chloride molten salts with various compositions (solvent, fertile, and fissile) allowing operation as breeder or burner with many different possible fertile and fissile compositions.
- A fast neutron spectrum.
- A homogeneous fuel composition thanks to fast fuel circulation (in-core turbulence and multiple heat exchanger channels). This homogeneity allows continuous fuel monitoring.
- A continuous extraction of volatile or metallic FPs via neutral gas bubbling.
- The possibility of quasi continuous light chemical fuel processing (rate comparable to LWR solid fuel but on a daily basis) without stopping the reactor.

These characteristics result in a reactor with a high safety potential due to:

- Negative temperature feedback reactivity coefficients (Doppler and density) leading to high thermal stability in operation and in all perturbing circumstances.
- Homogeneous liquid state allowing passive draining of the core fuel into passively cooled geometrically non-critical tanks.
- Absence of significant reactivity reserve because of the quasi continuous adjustment of the fuel composition.
- No pressurization required due to the absence of any volatile fluid susceptible to be contaminated by fuel leaks.

The international MSFR collaboration is presently focused on technology-independent safety issues, considering that only a high safety level may convince safety agencies to authorize the development of such a new reactor concept. Since 2001, calculations and experimental research were conducted in Europe in national programs (CNRS-France, KI-Russia) and in a European network supported by Euratom and Rosatom (MOST, ALISIA, ACSEPT/PYROSMANI, EVOL/MOSART, SAMOFAR/SMART-MSFR,...). This collaboration is presently continuing with the SAMOSAFER European project (2019–2023) where industrial partners (Framatome, Orano, EDF), CEA, and the French technical safety organization (IRSN) will be actively involved. This project, mainly centered on the “reference MSFR,” i.e., the breeder version in the Th/U fuel cycle with a fluoride salt, is devoted to the continuation of the safety studies and demonstration related to the operation of the system. Alternative versions of the MSFR are now under study as breeder in the U/Pu fuel cycle or as actinide burner, based on a chloride (NaCl) molten salt. Some of these new versions correspond to small modular reactors (Small-MSFR or S-MSFR).

Since the beginning, the common philosophy of the MSFR community was to give priority to knowledge over technology assuming that a long time will be devoted to assess the safety of technological solutions, i.e., assuming that safety is the primary concern for public acceptance of new nuclear reactors. The resulting roadmap for future developments is presently concerned with all the chemical and physical knowledge that help to assess the MSFR characteristics and design, including basic data measurements and multiphysics simulation tools. A second step will be the development of technological means, using simulant salts instead of real fuel, in order to demonstrate, at the proper scale, the validity of the proposed technology and to validate fluid flow and heat transfer models. The third step is the zero power demonstration small reactors, with the objectives of checking the neutronic properties (eliminating data uncertainties) and testing the start-up and shut-down processes. Some design developments have been done during the SAMOFAR project mainly focused on the decay heat removal function in the core and in the emergency draining system, together with a functional scheme of the intermediate circuit. Then, it will be possible to test a small power reactor with two new tests: the heat transfer with internal heat source and the FP extraction (continuous and quasi-continuous). This means that the pyroprocessing of the fuel by remote handling should be studied and tested in parallel to the first three steps, as well as the safety and proliferation issues. Indeed, the option of studying all the aspects of the concept was taken from the beginning to render the safety constraints inherent to the design and not have them added after. This implies using new approaches in agreement with the GIF community for safety and proliferation resistance. All these steps are mandatory to develop the technical and scientific background and knowledge for further practical demonstrations of the flexibility and viability of MSRs on a reactor scale. Such R&D activities are being conducted in the world, particularly by a European network supported by EURATOM and ROSATOM to confirm the validity of the theoretical advantages of this concept and to assess the potential advantages of fast spectrum MSRs.

Acknowledgments

The authors wish to thank the PACEN (Programme sur l’Aval du Cycle et l’Energie Nucléaire) and NEEDS (Nucléaire: Energie, Environnement, Déchets, Société) French interdisciplinary programs, the IN2P3 department of the National Centre for Scientific Research (CNRS), Grenoble Institute of Technology and Grenoble Alpes University, and the European programs EVOL (Evaluation and Viability Of Liquid fuel fast reactor system) of FP7, and SAMOFAR and SAMOSAFER of Horizon2020 for their support. We are also very thankful to Elizabeth Huffer for her help during the translation of this paper and to our colleagues from the MSR communities, in France (with a special thanks to Stéphane Beils, Bernard Carluéc, and Alain Gerber from Framatome and Frédéric Bertrand from CEA), in Europe and in the frame of the MSR-SSC of the Gen4 International Forum for all the very interesting discussions and exchanges.

References

- Afonichkin, V., Bovet, A., Gnidoi, I., Khokhlov, V., Lizin, A., Merzlyakov, A., Osipenko, A., Sannikov, I., Shishkin, V., Subbotin, V., Surenkov, A., Toropov, A., Uglov, V., Zagnitko, A., 2014. Molten salt actinide recycler and transforming system without and with Th-U support: fuel cycle flexibility and key materials properties. *Ann. Nucl. Energy* 64, 408–420.

- Aufiero, M., Brovchenko, M., Cammi, A., Clifford, I., Geoffroy, O., Heuer, D., Laureau, A., Losa, M., Luzzi, L., Merle-Lucotte, E., Ricotti, M., Rouch, H., 2014. Calculating the effective delayed neutron fraction in the molten salt fast reactor: analytical, deterministic and Monte Carlo approaches. *Ann. Nucl. Energy* 65, 78–90.
- Beils, S., Gerardin, D., Uggenti, A.C., Carpignano, A., Dulla, S., Merle, E., Heuer, D., Allibert, M., 2019. Application of the lines of defence method to the molten salt fast reactor in the framework of the SAMOFAR project. *EPJ Nucl. Sci. Technol.* 5, 18. <https://doi.org/10.1051/epjn/2019031>.
- Bettis, E.S., Robertson, R.C., 1970. The design and performance features of a single-fluid molten salt breeder reactor. *Nucl. Appl. Technol.* 8, 190–207.
- Blaise, P., Laureau, A., Ros, P., Leconte, P., Routsonis, K., 2019. Transient fission matrix approach for assessing complex kinetics behavior in the ZEPHYR ZPR coupled core configurations. *Ann. Nucl. Energy* 128, 390–397.
- Brovchenko, M., Heuer, D., Huffer, E., Merle-Lucotte, E., Allibert, M., Feynberg, O., Ghetta, V., Ignatiev, V., Kloosterman, J.L., Lathouwers, D., Laureau, A., Rineiski, A., Rouch, H., Rubiolo, P., Rui, L., Wang, S., 2014b. Safety Approach of a Fast Liquid Fuel System, Work-Package WP2, Deliverable D2.5, EVOL (Evaluation and Viability of Liquid fuel fast reactor system) European FP7 project, Contract number: 249696.
- Brovchenko, M., Heuer, D., Merle-Lucotte, E., Allibert, M., Capellan, N., Ghetta, V., Laureau, A., 2012. Preliminary safety calculations to improve the design of molten salt fast reactor. In: *Proceedings of the International Conference PHYSOR 2012 Advances in Reactor Physics Linking Research, Industry, and Education*, Knoxville, Tennessee, USA.
- Brovchenko, M., Kloosterman, J.L., Luzzi, L., Merle, E., Heuer, D., Laureau, A., Feynberg, O., Ignatiev, V., Aufiero, M., Cammi, A., Fiorina, C., Alcaro, F., Dulla, S., Ravetto, P., Frima, L., Lathouwers, D., Merk, B., 2019. Neutronic benchmark of the molten salt fast reactor in the frame of the EVOL and MARS collaborative projects. *EPJ Nucl. Sci. Technol.* 5. <https://doi.org/10.1051/epjn/2018052>.
- Brovchenko, M., Heuer, D., Merle-Lucotte, E., Allibert, M., Ghetta, V., Laureau, A., Rubiolo, P., 2013. Design-related studies for the preliminary safety assessment of the molten salt fast reactor. *Nucl. Sci. Eng.* 175, 329–339.
- Brovchenko, M., Merle-Lucotte, E., Rouch, H., Alcaro, F., Allibert, M., Aufiero, M., Cammi, A., Dulla, S., Feynberg, O., Frima, L., Geoffroy, O., Ghetta, V., Heuer, D., Ignatiev, V., Kloosterman, J.L., Lathouwers, D., Laureau, A., Luzzi, L., Merk, B., Ravetto, P., Rineiski, A., Rubiolo, P., Rui, L., Szieberth, M., Wang, S., Yamaji, B., 2014a. Optimization of the pre-conceptual design of the MSFR, Work-Package WP2, Deliverable D2.2, EVOL (Evaluation and Viability of Liquid fuel fast reactor system) European FP7project, Contract number: 249696.
- Delpesch, S., Merle-Lucotte, E., Heuer, D., et al., 2009. Reactor physics and reprocessing scheme for innovative molten salt reactor system. *J. Fluor. Chem.* 130 (1), 11–17.
- Dulla, S., Krepel, J., Rouch, H., Aufiero, M., Fiorina, C., Geoffroy, O., Hombourger, B., Laureau, A., Merle-Lucotte, E., Mikityuk, K., Pautz, A., Ravetto, P., Rubiolo, P., 2014. Sensitivity studies of the salt flux in the optimized design of the MSFR, Deliverable D2.3, EVOL (evaluation and viability of liquid fuel fast reactor system) European FP7 project, Contract Number: 249696.
- Gerardin, D., Uggenti, A.C., Beils, S., Carpignano, A., Dulla, S., Merle, E., Heuer, D., Laureau, A., Allibert, M., 2019. Identification of the postulated initiating events with MLD and FFMEA for the molten salt fast reactor. *Nucl. Eng. Technol.* <https://doi.org/10.1016/j.net.2019.01.009>.
- Gerardin, D., 2018. Développement d’outils numériques et réalisation d’études pour le pilotage et la sûreté du réacteur à sels fondus MSFR. Ph.D. thesis, Grenoble Alpes University, France.
- Gerardin, D., Allibert, M., Heuer, D., Laureau, A., Merle-Lucotte, E., Seuvre, C., 2017. Design evolutions of the molten salt fast reactor. In: *Proceedings of the International Conference on Fast Reactors and Related Fuel Cycles: Next Generation Nuclear Systems for Sustainable Development (FR17)*, Yekaterinburg, Russian Federation.
- Haubenreich, P.N., Engel, J.R., 1970. Experience with the molten salt reactor experiment. *Nucl. Appl. Technol.* 8, 107–117.
- Heuer, D., Laureau, A., Merle-Lucotte, E., Allibert, M., Gerardin, D., 2017. A starting procedure for the MSFR: approach to criticality and incident analysis. In: *Proceedings of the ICAPP’2017 International Conference*, Kyoto, Japan.
- Heuer, D., Merle-Lucotte, E., Allibert, M., Brovchenko, M., Ghetta, V., Rubiolo, P., 2014. Towards the thorium fuel cycle with molten salt fast reactors. *Ann. Nucl. Energy* 64, 421–429.
- Ignatiev, V., Afonichkin, V., Feynberg, O., Merzlyakov, A., Surenkov, A., Subbotin, V., et al., 2012. Molten salt reactor: new possibilities, problems and solutions. *At. Energy* 112 (3), 157.
- Jasak, H., Jemcov, A., Tukovic, Z., 2007. Openfoam: a c++ library for complex physics simulations. In: *Proceedings of the International Workshop on Coupled Methods in Numerical Dynamics*. vol. 1000, pp. 1–20.
- Laureau, A., Rosier, E., Merle, E., Beils, S., Bruneau, O., Blanchon, J.C., Gathmann, R., Heuer, D., Passelaigue, F., Vaiana, F., Zanini, A., 2020. The LiCore power plant simulator of the molten salt fast reactor. In: *Accepted at the ‘PHYSOR 2020: Transition to a Scalable Nuclear Future’ International Conference*, Cambridge, United Kingdom.
- Laureau, A., Heuer, D., Merle-Lucotte, E., Rubiolo, P., Allibert, M., Aufiero, M., 2017a. Transient coupled calculations of the molten salt fast reactor using the transient fission matrix approach. *Nucl. Eng. Des.* 316, 112–124.

- Laureau, A., Buiron, L., Fontaine, B., 2017b. Local correlated sampling Monte Carlo calculations in the TFM neutronics approach for spatial and point kinetics applications. *EPJ Nucl. Sci. Technol.* 3, 16.
- Laureau, A., Buiron, L., Fontaine, B., 2017c. Towards spatial kinetics in a low void effect sodium fast reactor: core analysis and validation of the TFM neutronic approach. *EPJ Nucl. Sci. Technol.* 3, 17.
- Laureau, A., Buiron, L., Fontaine, B., 2017d. Fission matrix interpolation for the TFM approach based on a local correlated sampling technique for fast spectrum heterogeneous reactors. In: *Proceedings of the International Conference in Mathematics and Computational Methods (M&C)*, Jeju, Korea.
- Laureau, A., Lederer, Y., Krakovich, A., Buiron, L., Fontaine, B., 2017e. Transient coupled neutronics-thermohydraulics study of ULOF accidents in sodium fast reactors using spatial kinetics: comparison of the TFM Monte Carlo and SN approaches. In: *Proceedings of the ICAPP'2017 International Conference*, Kyoto, Japan.
- Laureau, A., 2015. Développement de modèles neutroniques pour le couplage thermohydraulique du MSFR et le calcul de paramètres cinétiques effectifs. Ph.D. thesis, Grenoble Alpes University, France.
- Laureau, A., Rubiolo, P., Heuer, D., Merle-Lucotte, E., Brovchenko, M., 2013. Coupled Neutronics and thermal-hydraulics numerical simulations of the molten salt fast reactor (MSFR). In: *Joint International Conference on Supercomputing in Nuclear Applications and Monte Carlo 2013*. Paris, France.
- Leppänen, J., 2013. *Serpent—A Continuous-Energy Monte Carlo Reactor Physics Burnup Calculation Code, User's Manual*. VTT Technical Research Centre of Finland.
- Mathieu, L., Heuer, D., Merle-Lucotte, E., et al., 2009. Possible configurations for the thorium molten salt reactor and advantages of the fast non-moderated version. *Nucl. Sci. Eng.* 161, 78–89.
- Merle-Lucotte, E., Heuer, D., Allibert, M., Doligez, X., Ghetta, V., 2009a. Minimizing the fissile inventory of the molten salt fast reactor. In: *Proceedings of the Advances in Nuclear Fuel Management IV (ANFM 2009)*. Hilton Head Island, USA.
- Merle-Lucotte, E., Heuer, D., Allibert, M., Doligez, X., Ghetta, V., 2009b. Optimizing the burning efficiency and the deployment capacities of the molten salt fast reactor. In: *Proceedings of the International Conference Global 2009—The Nuclear Fuel Cycle: Sustainable Options & Industrial Perspectives*, Paper 9149. Paris, France.
- Merle-Lucotte, E., Heuer, D., Allibert, M., Brovchenko, M., Ghetta, V., Laureau, A., 2012. Preliminary design assessments of the molten salt fast reactor, Paper A0053. In: *Proceedings of the European Nuclear Conference ENC2012*. Manchester, UK.
- Merle-Lucotte, E., Heuer, D., Allibert, M., Brovchenko, M., Ghetta, V., Laureau, A., Rubiolo, P., 2013. Recommendations for a demonstrator of molten salt fast reactor. In: *Proceedings of the International Conference on Fast Reactors and Related Fuel Cycles: Safe Technologies and Sustainable Scenarios (FR13)*. Paris, France.
- ORNL-TM-728, 1965. *MSRE Design and Operations Report—Part I: Description of Reactor Design*, Technical Report ORNL-TM-728. Oak-Ridge National Laboratory.
- Rouch, H., Geoffroy, O., Rubiolo, P., Laureau, A., Brovchenko, B., Heuer, D., Merle-Lucotte, E., 2014. Preliminary thermal-hydraulic core design of the molten salt fast reactor (MSFR). *Ann. Nucl. Energy* 64, 449–456.
- Serp, J., Allibert, M., Beneš, O., Delpéch, S., Feynberg, O., Ghetta, V., Heuer, D., Holcomb, D., Ignatiev, V., Kloosterman, J.L., Luzzi, L., Merle-Lucotte, E., Uhlřr, J., Yoshioka, R., Zhimin, D., 2014. The molten salt reactor (MSR) in generation IV: overview and perspectives. *Prog. Nucl. Energy* 77, 1–12.
- Ugenti, A.C., Gerardin, D., Carpignano, A., Dulla, S., Merle, E., Heuer, D., Laureau, A., Allibert, M., 2017. Preliminary functional safety assessment for molten salt fast reactors in the framework of the SAMOFAR project. In: *Proceedings of the 2017 International Topical Meeting on Probabilistic Safety Assessment and Analysis (PSA 2017)*. Pittsburg, USA.
- Whatley, M.E., McNeese, L.E., Carter, W.L., Ferris, L.M., Nicholson, E.L., 1970. Engineering development of the MSBR fuel recycle. *Nuclear Applications and Technology* 8, 170–178.

Sources for further information

Bibliography web sources

- Anon. <http://lpsc.in2p3.fr/gpr/gpr/publis-rsfE.htm>.
- Anon. https://www.gen-4.org/gif/jcms/c_9260/public.
- Anon. <http://www.ornl.gov/info/reports/>.

Further reading

- Boussier, H., Delpech, S., Ghetta, V., Heuer, D., Holcomb, D.E., Ignatiev, V., Merle-Lucotte, E., Serp, J., 2012. The molten salt reactor in generation IV: overview and perspectives. In: Proceedings of the Generation4 International Forum Symposium, San Diego, USA.
- Briggs, R.B., Swartout, J.A., 1955. Aqueous homogeneous power reactors. In: Proceedings of the International Conference on the Peaceful Uses of Atomic Energy, Held in Geneva, 8–20 August. vol. III, p. 496.
- Brovchenko, M., 2013. Etudes préliminaires de sûreté du réacteur à sels fondus MSFR (Ph.D. thesis). Grenoble Institute of Technology, France (in French).
- Degtyarev, A., Myasnikov, A., Ponomarev, L., 2015. Molten salt fast reactor with U—Pu fuel cycle. *Prog. Nucl. Energy* 82, 33–36.
- Engel, J., Bauman, H., Dearing, J., Grimes, W., McCoy, H., 1979. Development Status and Potential Program Development of Proliferation Resistant Molten Salt Reactors. USAEC Report ORNL/TM-6415, Oak Ridge, USA.
- GIF (Generation IV International Forum), 2008. Annual Report 2008. pp. 36–41. http://www.gen-4.org/PDFs/GIF_2008_Annual_Report.pdf.
- GIF (Generation IV International Forum), 2009. Annual Report 2009. pp. 52–58. <http://www.gen-4.org/PDFs/GIF-2009-Annual-Report.pdf>.
- Ignatiev, I., Feynberg, O., Gnidoi, I., Merzlyakov, A., Surenkov, A., Uglov, V., Zagnitko, A., Subbotin, V., Sannikov, I., Toropov, A., Afonichkin, V., Bovet, A., Khokhlov, V., Shishkin, V., Kormilitsyn, M., Lizin, A., Osipenko, A., 2014. Molten salt actinide recycler & transforming system without and with Th-U support: fuel cycle flexibility and key material properties. *Ann. Nucl. Energy* 64, 408–420.
- Laureau, A., Aufiero, M., Rubiolo, P., Merle-Lucotte, E., Heuer, D., 2015a. Coupled neutronics and thermal-hydraulics transient calculations based on a fission matrix approach: application to the molten salt fast reactor. In: Proceedings of the Joint International Conference on Mathematics and Computation (M&C), Supercomputing in Nuclear Applications (SNA) and the Monte Carlo (MC) Method. Nashville, USA.
- Laureau, A., Aufiero, M., Rubiolo, P., Merle-Lucotte, E., Heuer, D., 2015b. Transient fission matrix: kinetic calculation and kinetic parameters β_{eff} and Λ_{eff} calculation. *Ann. Nucl. Energy* 85, 1035–1044.
- Lizin, A.A., Tomilin, S.V., Gnevashov, O.E., Gazizov, R.K., Osipenko, A.G., Kormilitsyn, M.V., Ponomarev, L.I., 2013. Solubility UF₄ and ThF₄ in molten salt LiF-NaF-KF. *At. Energy* 115 (1), 22–25.
- Merle-Lucotte, E., Heuer, D., Allibert, M., Brovchenko, M., Capellan, N., Ghetta, V., 2011. Launching the thorium cycle with molten salt fast reactor. In: Proceedings of ICAPP 2011, Nice, France, May, Paper 11190.
- US DOE Nuclear Energy Research Advisory Committee and the Generation IV International Forum, 2002. A Technology Roadmap for Generation IV Nuclear Energy Systems, GIF-002-0.
- Wang, S., Rineiski, A., Li, R., Brovchenko, M., Merle-Lucotte, E., Heuer, D., Laureau, A., Rouch, H., Aufiero, M., Cammi, A., Fiorina, C., Guerrieri, C., Losa, M., Luzzi, L., Ricotti, M.E., Kloosterman, J.-L., Lathouwers, D., van der Linden, E., Merk, B., Rohde, U., 2014. Safety Analysis: Transient Calculations, EVOL (Evaluation and Viability of Liquid Fuel Fast Reactor System) European FP7 Project, Contract number: 249696.

SuperCritical Water-cooled Reactors (SCWRs)

Thomas Schulenberg^a and Laurence K.H. Leung^{b,}*

^aKarlsruhe Institute of Technology, Karlsruhe, Germany ^bCanadian Nuclear Laboratories, Chalk River, ON, Canada

Acronyms

ADS	Automatic Depressurization System
BWR	Boiling Water Reactor
CANDU	CANada Deuterium Uranium
CEP	Condensate Extraction Pump
DA	DeAerator
FP	Feed-water Pump
FWP	Feed-Water Pump
HP	High Pressure
HPLWR	High-Performance Light Water Reactor
HP-PH	High-Pressure PreHeaters
HPT	High-Pressure Turbine
IAEA	International Atomic Energy Agency
IASCC	Irradiation-Assisted Stress Corrosion Cracking
IC	Isolation Condenser
IP	Intermediate Pressure
IPT	Intermediate-Pressure Turbine
LEU	Low Enriched Uranium
LOCA	Loss-Of-Coolant Accident
LP	Low Pressure
LP-PH	Low-Pressure PreHeater
LPT	Low-Pressure Turbine
LWR	Light Water Reactor
MOX	Mixed OXide
MSR	Moisture Separator Reheater
PHWR	Pressurized Heavy Water Reactor
PMCS	Passive Moderator Cooling System
Pu	Plutonium
PUREX	Plutonium Uranium Redox EXtraction
PWR	Pressurized Water Reactor
SCC	Stress Corrosion Cracking
SCWR	SuperCritical Water-cooled Reactor
Th	Thorium
ZrH	Zirconium Hydride

* Retiree.

Nomenclature

- D* Density, kg/m³
H Specific enthalpy, J/kg
T Temperature, °C or K
P Pressure, Pa
W Mass flow rate, kg/s

8.1 Introduction

Pressurized Water Reactors (PWRs) and Boiling Water Reactors (BWRs) are the most successful nuclear reactors during the last 40 years. More than 300 PWRs have been built up to now, of which the latest ones exceed a net electric power output of 1600 MW_{el} and a net efficiency of 36%. With more than 100 units built, the BWR is almost as successful, although power and efficiency levels are somewhat lower. Both reactor types use a saturated steam cycle of approximately 7–8 MPa live steam pressure, corresponding with a boiling temperature of 286–295°C. However, these live steam conditions are still almost the same as those used in the 1960s. Improvements in cycle efficiency attributed primarily to the design of steam turbine blades. The situation is similar with heavy water moderated pressure-tube reactors, of which more than 60 have been built up to now. On the other hand, fossil-fired power plants have increased their efficiencies significantly since the 1960s. Steam has been superheated, and live steam temperatures and pressures have been increased stepwise to 600°C and 30 MPa, respectively. Since around 1990, all new coal-fired power plants have been using supercritical steam conditions, reaching more than 46% net efficiency today. Consequently, the application of such steam-cycle technologies to the well-proven design of water-cooled nuclear reactors could offer a huge potential for further improvements.

A SuperCritical Water-cooled Reactor (SCWR) is cooled with light water at supercritical pressure (i.e., beyond 22.1 MPa) in a once-through steam cycle. It may be moderated with light water or heavy water. Feed-water of the steam cycle is heated-up inside the reactor core to superheated steam, without any coolant recirculation, and the steam is supplied directly to a steam turbine. The general advantages of SCWRs, compared with conventional water-cooled reactors, are a higher steam enthalpy at the turbine inlet, which increases efficiency, reduces fuel costs, and reduces the steam mass flow rate needed for a target turbine power. This lower steam mass flow rate reduces the turbine size and the size of condensers, pumps, preheaters, tanks, and pipes and thus the costs of the overall steam cycle. Because the capital costs of nuclear power plants are usually higher than their fuel costs, this latter advantage has even a higher impact on electricity production costs than efficiency. Even more cost advantages are expected from plant simplifications such as eliminating steam separators or primary pumps in the case of a once-through steam cycle at supercritical pressure. Another advantage of using supercritical water in a nuclear reactor is that a boiling crisis is physically excluded, which adds a new safety feature to the design.

8.2 Types of supercritical water-cooled reactor concepts and main system parameters

A general sketch of the SCWR steam-cycle concept is shown in [Figure 8.1](#) to illustrate the once-through design principle. Feed-water is heated up to 280–350°C by steam turbine extractions using several Low-Pressure PreHeaters (LP-PH) and High-Pressure PreHeaters (HP-PH). The Feed-water Pumps (FPs) supply the feed-water to the reactor at a pressure of approximately 25 MPa. The reactor may be designed with a pressure vessel or with multiple pressure tubes, but it does not require any recirculation pumps in any case. In addition to the Condensate Extraction Pumps (CEPs) of the condensers, the only pumps driving the steam cycle are the feed-water pumps. The reactor produces superheated steam at a pressure of 24–25 MPa and at a

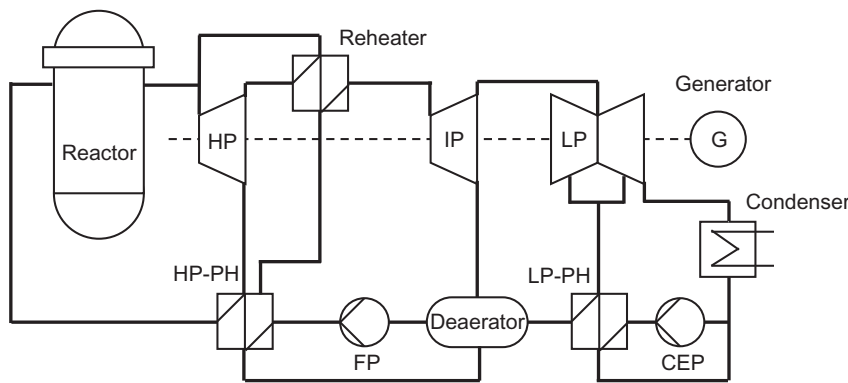


Figure 8.1. Simplified supercritical water-cooled reactor design principle with a once-through steam cycle

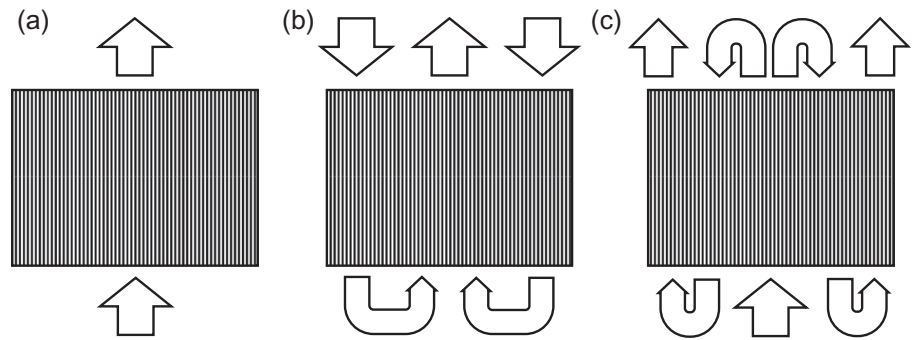
temperature of 500°C or more, depending on material limitations. The superheated steam is supplied directly to the High-Pressure (HP) turbine. The steam is reheated by some extracted steam and supplied to the Intermediate-Pressure (IP) and Low-Pressure (LP) turbines.

A reactor core, which is cooled with SuperCritical Water (SCW), can be designed with a thermal or a fast neutron spectrum, in general. The option of a thermal spectrum requires additional water as a moderator because of the low density of superheated steam, which can be provided in water rods inside fuel assemblies or in gaps between assembly boxes. Examples can be seen in the latest boiling water reactor design or in the SCWR concepts by [Oka et al. \(2010\)](#). If these gaps and water rods are omitted, the neutron spectrum will become fast, which simplifies the design and increases the core power density. However, a general safety concern of the fast core option is the reactivity increase if the core should be voided under accidental conditions. Such a reactivity increase must definitely be avoided by suitable core design, for which the addition of some solid moderator, an increased neutron leakage, and a heterogeneous arrangement of seed and blanket assemblies are common measures. [Oka et al. \(2010\)](#) presented examples of their fast reactor concept.

The enthalpy increase from the inlet to the outlet of the reactor exceeds those of conventional nuclear reactors by more than a factor of eight. The higher enthalpy increase of the coolant would not matter if it were uniform in the entire core. However, this can never be fully achieved. Fuel composition and distribution, water density distribution, size and distribution of subchannels, neutron leakage and reflector effects, burn-up effects, effects of control rod positioning, or effects due to the use of burnable poisons will influence the radial power profile of the core. Variations of fluid properties, uncertainties of the neutron physical modeling, heat transfer uncertainties, uncertainties in thermal-hydraulic modeling, scattering of the inlet temperature distribution, manufacturing tolerances, deformations during operation, or measurement uncertainties will cause a statistical scatter of the enthalpy increase. Finally, some small but allowable transients might be caused by controls of power, coolant mass flow, and core exit temperature and pressure. [Schulenberg and Starflinger \(2012\)](#) estimated that a total hot channel factor of 2 should be multiplied with the average enthalpy increase, as a first guess, to yield the maximum increase in local enthalpy under worst-case conditions. An analog problem is also known from the boiler design of fossil-fired power plants. It has been solved there by splitting the total enthalpy rise into an evaporator and two successive superheaters and by homogeneously mixing the coolant between each of these components.

Different core design concepts have been proposed to apply this technology to the SCWR ([International Atomic Energy Agency, 2014](#)). Starting from a single heat-up process of conventional nuclear reactors, as sketched in [Figure 8.2a](#), the peak coolant temperatures inside of the reactor core can be reduced by a two-step process with a downward flow of coolant in the outer core region, followed by coolant mixing underneath the core and a second heat-up in the inner core region ([Figure 8.2b](#)). For example, such technology has been applied by [Oka et al. \(2010\)](#) for their SCWR concept. Even better coolant mixing is enabled with a

Figure 8.2. Different SCWR core design options with multiple heat-up steps. (a) Single-pass design, (b) two-pass design, and (c) three-pass design



three-pass core (Figure 8.2c), with the evaporator as the first heat-up step in the inner core region, surrounded by a first superheater with downward flow and a second superheater with upward flow. The coolant is mixed between each step to eliminate hot streaks. This concept has been adopted for the High-Performance Light Water Reactor (HPLWR) and will be described in more detail in the next section. The higher the number of heat-up steps, the lower will be the peak coolant temperature at an envisaged average core outlet temperature, and thus the less stringent the material requirements, but the higher will be the complexity of core design.

8.3 Example of a pressure vessel concept

The High-Performance Light Water Reactor (HPLWR) is a pressure vessel-type SCWR with a thermal neutron spectrum, which was worked out by a European consortium in 2006–2010. [Schulenberg and Starflinger \(2012\)](#) summarize the design features and the analyses of the conceptual design phase. The reactor is designed for a thermal power of 2300 MW, resulting in a net electric power of 1000 MW and a net efficiency of 43.5% of the steam cycle. With a target coolant outlet temperature of 500°C, the superheated steam is thermally insulated from the reactor pressure vessel, keeping it below 350°C, as shown in Figure 8.3. The core design applies the three-pass design concept (Figure 8.2c), and mixing plena are foreseen above and underneath the core to maintain the peak coolant temperature below 600°C. Control rods are inserted from top as in a PWR, aligned by the control rod guide tubes in the upper half of the reactor pressure vessel. The fuel assemblies of the reactor core are standing on the thick core support plate of the core barrel, which is suspended in the reactor flange. The steam plenum, including its mixing plenum in the inner region, can be removed after extraction of the hot steam pipes for yearly fuel shuffling and replacement. Feed-water enters the reactor pressure vessel through four backflow limiters to minimize loss of coolant in case a break of a feed-water line. Half of the supplied feed-water is purging the upper half of the reactor pressure vessel, serving afterward as moderator water inside of water rods of the fuel assemblies and inside gaps between assembly boxes. After cooling the radial core reflector, this water is mixed with the remaining feed-water in the lower mixing plenum underneath the core. The mass flow split is adjusted by orifices of the lower mixing plenum.

The reactor has a total height of 14.29 m and an inner diameter of 4.46 m. The wall thickness of the cylindrical shell is 0.45 m and the spherical bottom shell has a thickness of 0.30 m. Similar to a PWR, the vessel material is 20MnMoNi55, but the hotter steam outlet must be made, for example, from P91 steel to withstand the superheated steam temperature of 500°C. The reactor internals are made from stainless steel.

The steam cycle is designed with three LP preheaters, condensing steam that is extracted from the LP turbines, and with four HP preheaters, condensing steam from the HP and IP turbines. The reheat pressure is 4.25 MPa, achieving a reheat temperature of 442°C. The design pressure of the deaerator is 0.55 MPa.

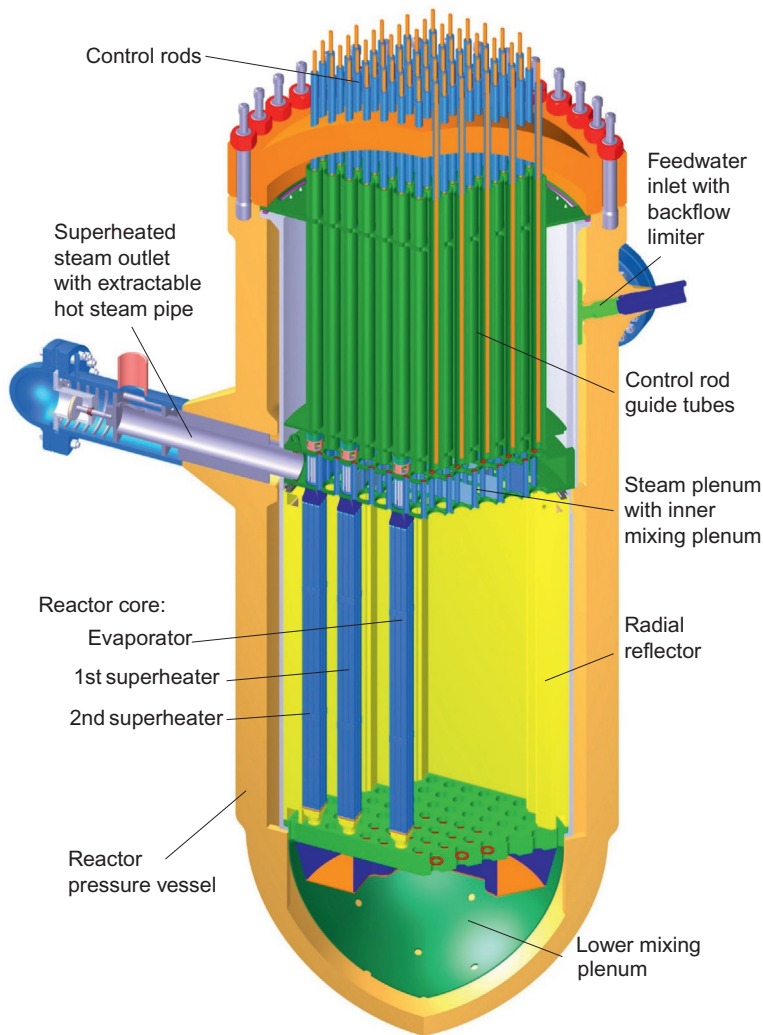


Figure 8.3. Pressure-vessel design of the High-Performance Light Water Reactor (HPLWR) with a three-pass core (Schulenberg and Starflinger, 2012)

Four parallel feed-water pumps are foreseen, of which three are needed to provide the mass flow of 1179 kg/s at full power and the fourth one is kept on hot standby.

8.4 Example of a pressure tube concept

The Canadian SCWR concept is a pressure-tube type of concept. It adopts the direct cycle, which includes a 2540 MW_{th} core that receives feed-water at 315°C and 1176 kg/s and generates supercritical steam at 625°C and 25 MPa. The cycle includes steam reheat using a Moisture Separator Reheater (MSR) between the IP turbine and LP turbine. The MSR separates the moisture from the steam and reheats the steam to ensure an acceptable moisture level at the outlet of the LP turbine. Four LP condensate heaters are included in the cycle as well as a deaerator and four HP feed-water heaters. The gross electrical output is calculated as 1255 MW_{el}, giving a gross thermal efficiency of 49.4%. A schematic diagram of the direct cycle is shown in Figure 8.4 (Zhou, 2009).

The Canadian SCWR core concept is illustrated in Figure 8.5. It consists of a pressurized inlet plenum, an LP calandria vessel that contains heavy water moderator, and 336 fuel channels that are attached to a common outlet header. A counter-flow fuel channel is adopted to position the inlet and outlet piping above the reactor

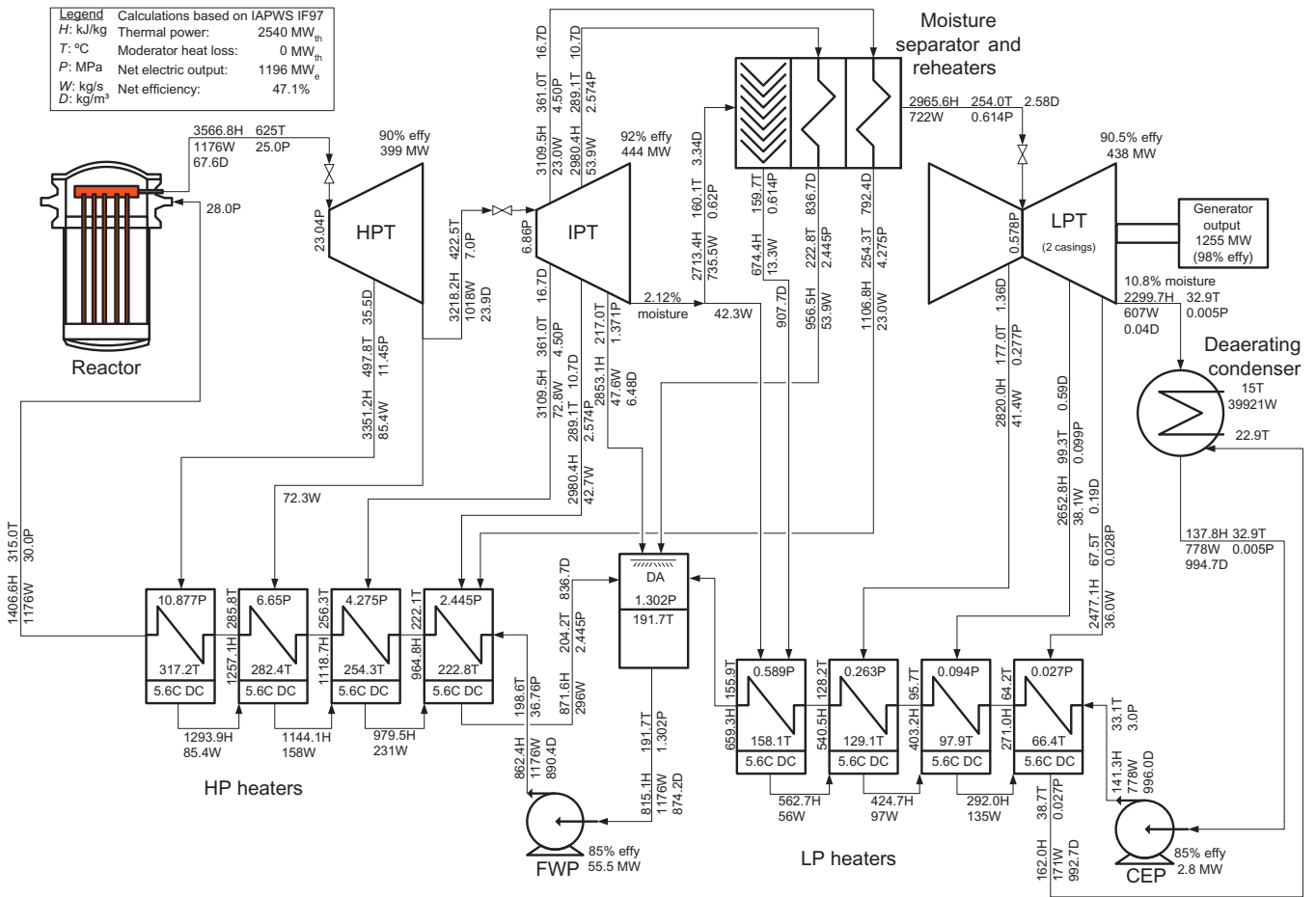


Figure 8.4. Schematic of direct steam cycle with a Moisture Separator Reheater (MSR) in a SuperCritical Water-cooled Reactor (SCWR) plant. *HPT*, High-Pressure Turbine; *IPT*, Intermediate-Pressure Turbine; *LPT*, Low-Pressure Turbine; *CEP*, Condensate Extraction Pump; *LP*, Low Pressure; *HP*, High Pressure; *FWP*, Feed-Water Pump

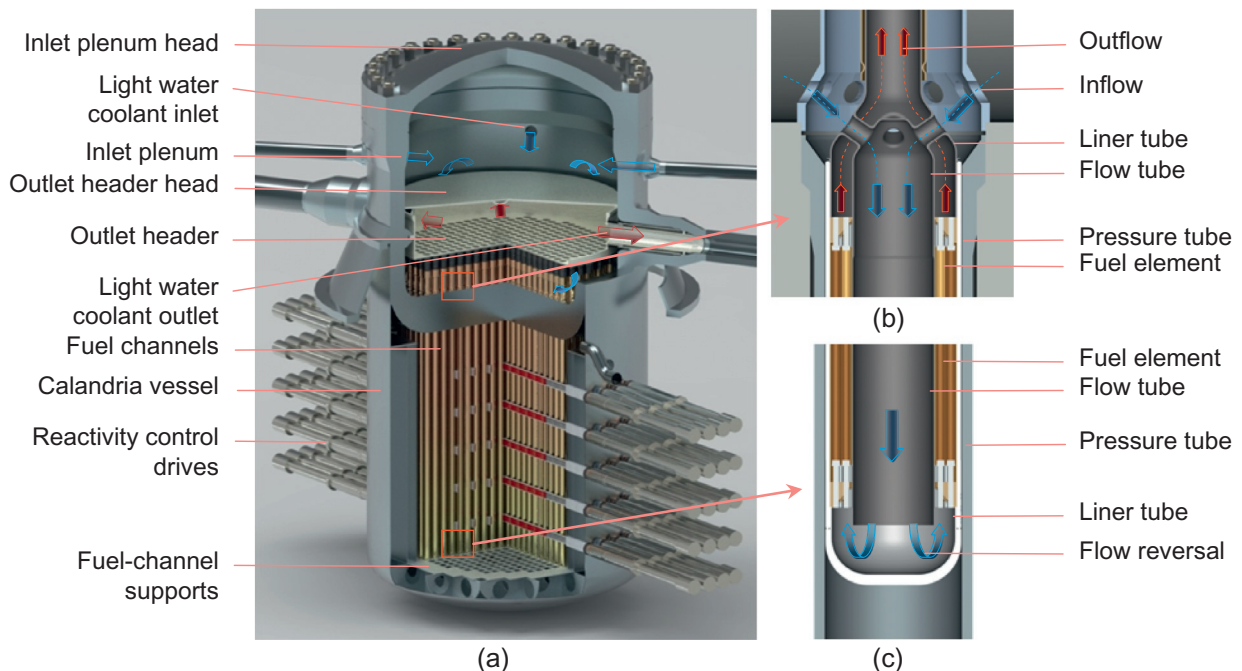


Figure 8.5. Canadian SuperCritical Water-cooled Reactor (SCWR) core concept. (a) Reactor core, (b) cross-over piece, and (c) bottom of fuel channel

core so that a complete break of either an inlet pipe or an outlet pipe will not result in an immediate loss of coolant at the reactor core. A nonfuel central flow channel is located at the center of the fuel channel to increase neutron moderation close to the inner fuel rings. This feature results in reasonably uniform radial power distributions across the fuel channel as well as a desirable negative coolant void reactivity throughout the burn-up cycle.

The coolant flows into the inlet plenum, around the outside of the outlet header (blue arrows in Figure 8.5), and then enters the pressure tube extension through a series of slots, into the fuel assembly through a cross-over piece (top right figure), down through a flow tube in the center of the fuel assembly, back up through the fuel elements (bottom right figure), and then out through the outlet header.

Although the inlet plenum is a pressure vessel, none of the components are subject to high neutron fields; consequently, irradiation damage is not a major concern. A pressure-vessel steel containing approximately 3–4 wt% nickel, SA 508 grade 4N, has been selected because the operating temperature inside of the inlet plenum is only approximately 315°C. To further inhibit corrosion, the interior surfaces of the vessel could be overlaid with 308 or 309 stainless steel weld materials. The material selected for the outlet header and head is Alloy 800H, which is an Fe-Ni-Cr alloy that demonstrates excellent high-temperature properties such as strength, toughness, and corrosion resistance. Because of the low differential in pressure from inlet to outlet conditions, no large forces or stresses are generated; consequently, the design requirements are relatively light. The header is supported by brackets placed on a plane running through the outlet penetrations of the inlet plenum wall, ensuring that movement due to differential thermal expansion between the plenum and header is purely in the radial direction. The outlet sleeves are decoupled from the inlet plenum wall by means of a flexible thermal isolation sleeve as shown in Figure 8.6.

The fuel channel consists of the pressure tube extending into the moderator and an extension connecting the pressure tube to the outlet header. All internals of the pressure tube are part of the fuel assembly. The pressure tube has an open end and a closed end (i.e., a test-tube shape). It is inserted into one of the openings of the tubesheet of the inlet plenum with a seal weld between the HP inlet plenum and LP calandria. A pressure-tube extension is connected to the pressure tube at the top of the tubesheet and incorporates several openings near the interface with the pressure tube to allow coolant entering into the fuel channel and subsequently to the fuel assembly. These openings act as orifices to control the amount of coolant flowing into each channel and to suppress instability. The size of these openings is determined through matching the channel power output to provide an outlet coolant temperature as close to 625°C as possible. The outlet of the pressure-tube extension is attached to a corrugated bellows expansion joint, which in turn is welded to the bottom plate of the outlet header (see Figure 8.7). The bellows expansion joint facilitates differential

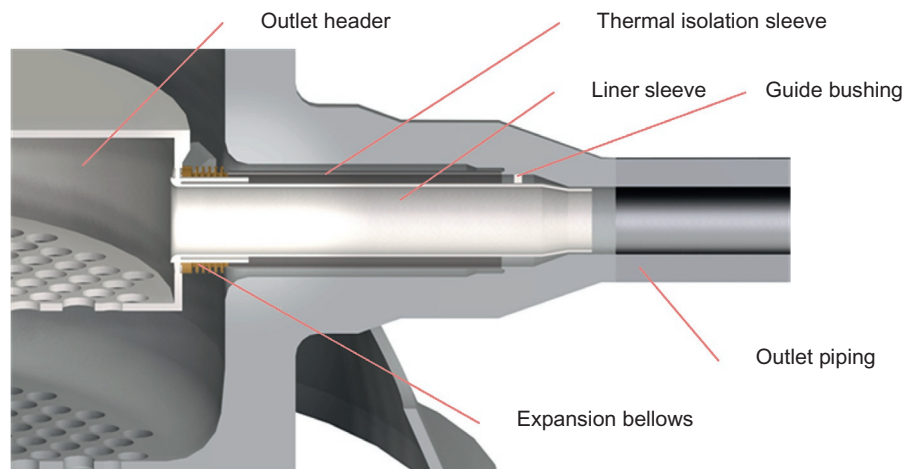
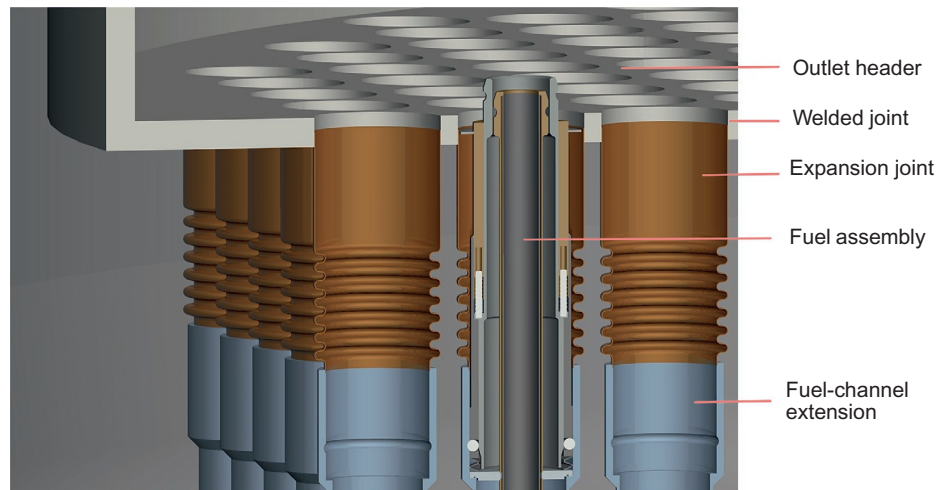


Figure 8.6. Cutaway view of outlet sleeves

Figure 8.7. Fuel-channel connection to the outlet header



movement between the outlet header and the channel. This connection configuration would allow single-channel replacement, if required.

The calandria vessel is an LP vessel that contains the heavy water moderator, fuel channels, reactivity control mechanisms, and emergency shut-down devices. Internal structures include lateral supports for the fuel channels, reactivity control mechanism guides, and flow channels ensuring circulation of the moderator. Heavy water at low pressures and low temperatures is chosen for the moderator because of its low neutron absorption compared with light water. Additional moderator surrounding the core is included, acting as a neutron reflector and shielding. The tubesheet of the inlet plenum is located 0.75 m above the core, protecting the plenum material from radiation damage. The reactivity control mechanisms located at the sides of the core are shielded, at a minimum, with a similar volume of moderator and with an increasing amount at the reactor centerline due to the curvature of the calandria vessel. The moderator operates at subcooled temperatures using a pumped recirculation system, but in case of a station blackout, core decay heat is passively removed through the use of a flashing-driven natural circulation loop. Inlet and outlet nozzles for these systems are located above the core, ensuring that the calandria will not drain due to a pipe break.

8.5 Fuel cycle technology

The pressure-vessel type of SCWR may use UO_2 in a once-through fuel cycle, with an enrichment of 5%–7%, or Mixed OXide (MOX) fuel if plutonium should be recycled in a closed fuel cycle. In the case of a thermal neutron spectrum, the use of MOX fuel is optional as in a conventional PWR or BWR. As the higher temperatures of the SCWR require stainless steel fuel claddings instead of Zircaloy claddings, however, the enrichment is typically 2% points higher than for conventional water-cooled reactors to compensate for the additional neutron absorption of nickel. Therefore, the use of MOX fuel might be more economical to recycle the residual discharge fuel.

The reference fuel for the pressure-tube type of SCWR is a mix of thorium and plutonium, which is extracted from the spent Light Water Reactor (LWR) fuel. On average, the weight percentage of plutonium is 13% in the fuel (Wojtazek, 2015). With the high neutron economy of the heavy water moderator, other fuel mixes can also be accommodated. Studies have demonstrated the feasibility of using Low Enriched Uranium (LEU) of 7% (Yetisir et al., 2012); a mix of LEU at 7.5% with Th; a mix of transuranics at 21 wt% with Th (Winkel et al., 2013); or a mix of Pu at 8%, Th, and ^{233}U (at 2 wt%) extracted from the SCWR fuel (Magill et al., 2011).

In the case of a fast neutron spectrum, MOX fuel has been proposed by Oka et al. (2010) with an average concentration of fissile plutonium of approximately 20%. Such fuel can be produced from recycling spent fuel of LWRs with the Plutonium Uranium Redox EXtraction (PUREX) process, a mature fuel cycle technology.

8.6 Fuel-assembly concept

Beyond 390°C, the coolant density is less than 200 kg/m³, hardly enough to produce a thermal neutron spectrum. Therefore, a moderator is needed for a thermal neutron spectrum, either as feed-water running through moderator boxes inside of the fuel assemblies and in gaps between assembly boxes or as separate heavy water in case of a pressure tube concept. In any case, the mass of structural material inside of the reactor core should be minimized to limit neutron absorption.

8.6.1 High-Performance Light Water Reactor (HPLWR) fuel-assembly concept

In case of the HPLWR (Section 8.3), the fuel assemblies are designed with 40 fuel pins each and a single moderator box in their center to enable a small wall thickness of moderator and assembly boxes, as shown in Figure 8.8. To ease handling during maintenance, Schulenberg and Starflinger (2012) recommended grouping nine assemblies to a cluster with common head and foot pieces as shown in Figure 8.9. The fuel rods have an outer diameter of 8 mm and a wall thickness of 0.5 mm, arranged with a pitch-to-diameter ratio of 1.18. A wire of 1.44 mm thickness is wrapped around each fuel rod to serve as a spacer and as an effective mixing device. The assembly box and moderator box are designed as a sandwich construction with a thermal insulation between two stainless steel sheets to minimize heat-up of the moderator water. Control rods, filled with boron carbide, are running inside five of the nine inner moderator boxes of a cluster. The fuel assembly has a heated length of 4.2 m. A fission gas plenum of 0.5 m length on top of the fuel pellets helps in minimizing the pressure increase during burn-up. The headpiece of the assembly cluster has windows for steam release to the steam plenum, which need to be sealed with C-rings against moderator water ingress into the steam.

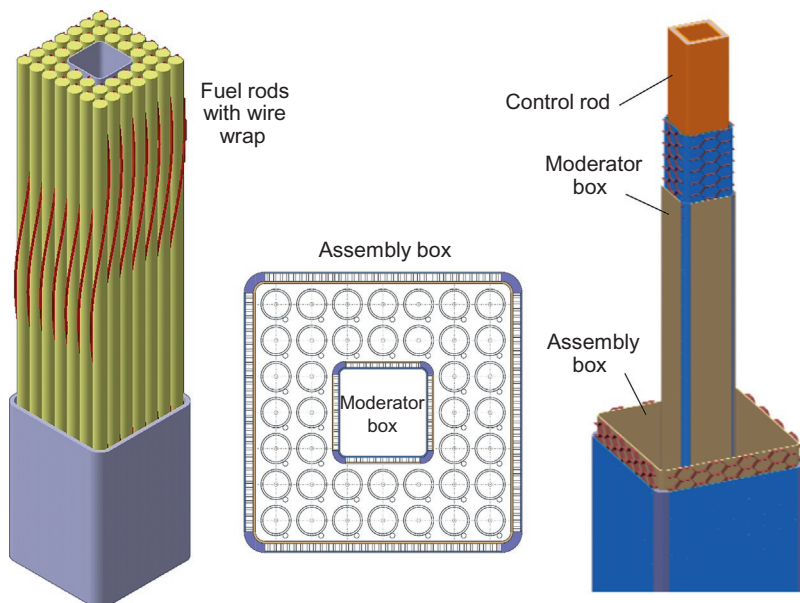
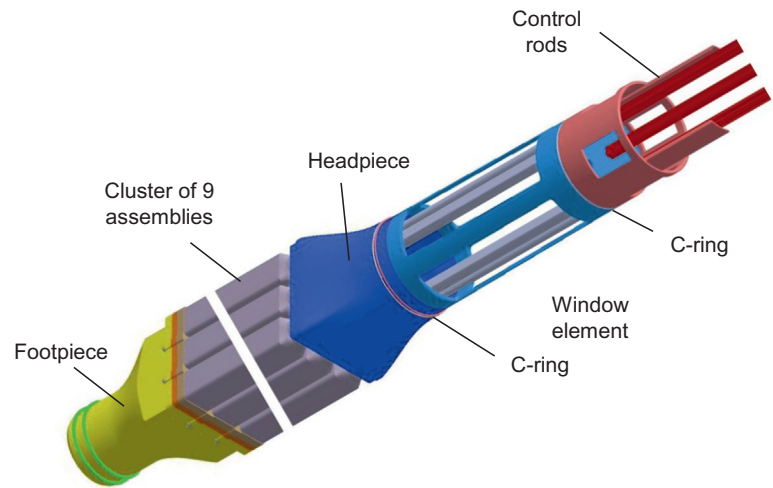


Figure 8.8. Fuel-assembly concept of the High-Performance Light Water Reactor (HPLWR) (Schulenberg and Starflinger, 2012)

Figure 8.9. High-Performance Light Water Reactor (HPLWR) assembly cluster design with head and foot piece; control rods are running inside five of the nine moderator boxes, inserted from the top (Schulenberg and Starflinger, 2012)



For a thermal power of 2300 MW, 52 of these clusters form the evaporator of the reactor core with an upward flow of coolant. They are surrounded by another 52 clusters with downward flow, serving as the first superheater. Fifty-two clusters at the core periphery, where the core power density is low enough to keep the cladding surface temperature below 650°C, provide the second superheater. The average core power density of the HPLWR is 57 MW/m³, comparable with the power density of a BWR, and the evaporator has a power density of approximately 100 MW/m³, comparable with a PWR.

Once a year, the reactor is opened to shuffle assembly clusters, mainly from the evaporator to the first superheater and from there to the second superheater, and to replace the new assembly cluster in the evaporator. The excess reactivity of the reactor core at the beginning of each burn-up cycle is compensated with gadolinia pellets mixed with fuel pellets in four fuel rods per assembly. Boric acid, as used in a PWR to compensate for excess reactivity, may not be used for burn-up compensation because its solubility in supercritical water changes drastically when the coolant passes the pseudo-critical line (384°C at 25 MPa). Instead, injection of boric acid is used only as a second shut-down mechanism in emergency cases.

8.6.2 Fast reactor fuel-assembly concept

The fuel-assembly design looks simpler for a reactor core with fast neutron spectrum. Oka et al. (2010) proposed using hexagonal fuel assemblies as seed assemblies with approximately 25% fissile plutonium, depending on the core size, mixed with blanket assemblies with pure ²³⁸U in a heterogeneous arrangement. The coolant flow is upward or downward, depending on the headpiece, which may be designed with or without windows to the steam plenum above the core. According to Figure 8.2, the concept may be categorized as a two-pass design with a flexible flow path. Control rod fingers are running inside thimble tubes as in a PWR, as shown in Figure 8.10. The stainless steel cladding of the fuel rod is designed with an outer diameter of 7 mm and a pitch of 8.12 mm. This tight hexagonal arrangement enables a high average core power density of 158 MW/m³. For a core with 1650-MW thermal power, we would need 126 seed assemblies and 73 blanket assemblies at an active core height of 3 m.

A general problem of such fast reactor concept is an increase of the core reactivity with decreasing coolant density if the neutron spectrum is too fast. The problem may be overcome and the local void reactivity can be kept negative throughout the entire burn-up cycle by adding a solid moderator, in this case Zirconium Hydride (ZrH) and stainless steel around the blanket assemblies, which increases the neutron leakage and softens the spectrum. The concept is sketched in Figure 8.10. However, as a drawback of this concept, the reactor is consuming more plutonium than breeding, which is not ideal for a sustainable nuclear energy concept.

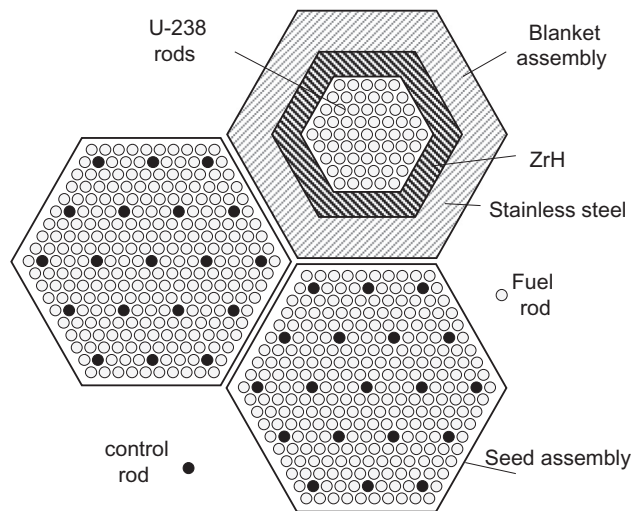


Figure 8.10. Fuel-assembly design for a reactor core with fast neutron spectrum (Oka et al., 2010)

8.6.3 Canadian SCWR fuel-assembly concept

The fuel for the Canadian SCWR concept is similar to existing power reactor fuel in that a ceramic pellet produces heat, which is transferred through the metallic cladding to the primary coolant. Significant differences between the Canadian SCWR concept and existing power reactor fuels, which have been considered, are the normal operating conditions and accident conditions of higher temperature and pressure. These additional considerations (combined with corrosion concerns) necessitate the rejection of zirconium-based alloys as fuel cladding candidates.

The fuel assembly consists of the fuel elements, central flow tube, encapsulated insulator, upper and lower fuel element supports, inlet/outlet flow exchanger, and outlet flow tube. The arrangement is illustrated in Figure 8.11. Inlet coolant enters the fuel assembly from the inlet plenum and initially flows through the periphery of the fuel assembly. Above the fuel elements and upper fuel element support, a flow exchanger transfers the inlet coolant to the central flow tube. The same flow exchanger transfers the outlet coolant from the periphery of the fuel assembly to the outlet flow tube where it proceeds to the outlet header. Inlet coolant flows down the central flow tube to the bottom of the fuel assembly. The coolant reverses direction at the bottom of the fuel assembly and flows up the periphery of the fuel assembly over the fuel elements to the flow exchanger-outlet flow tube. The fuel bundle concept consists of 64 fuel elements with 32 fuel elements in each ring (see Figure 8.12 for the cross-sectional view). The outer diameter of fuel elements is 9.5 mm in the inner ring and is 10 mm in the outer ring. Each fuel element is 6.5 m long housing the fuel pellets, an inner filler tube in the plenum area to prevent collapse under external pressure, and a spring to hold the pellets in place but allow for pellet expansion. The active length of the fuel element is 5 m. Each end of the fuel element is closed with an end plug, which is welded to the cladding tube.

Spacings between fuel elements, between inner-ring elements and the central flow tube, and between outer-ring elements and the inner insulator liner are maintained by wires arranged in a spiral wrap around every fuel element. In addition to maintaining spacings, these wires minimize vibration of each element and enhance heat transfer from the cladding to the coolant. The effectiveness of wire-wrapped spacers on heat transfer enhancement has been demonstrated through experiments using tubes, annuli, and bundles. One of the concerns of using wrapped-wire spacers is fretting on the fuel cladding. In view of the relatively low channel flow, fretting is not anticipated to be an issue. Nevertheless, a confirmatory experiment may be needed.

Figure 8.11. Cross-section views of the supercritical water-cooled reactor fuel-assembly concept

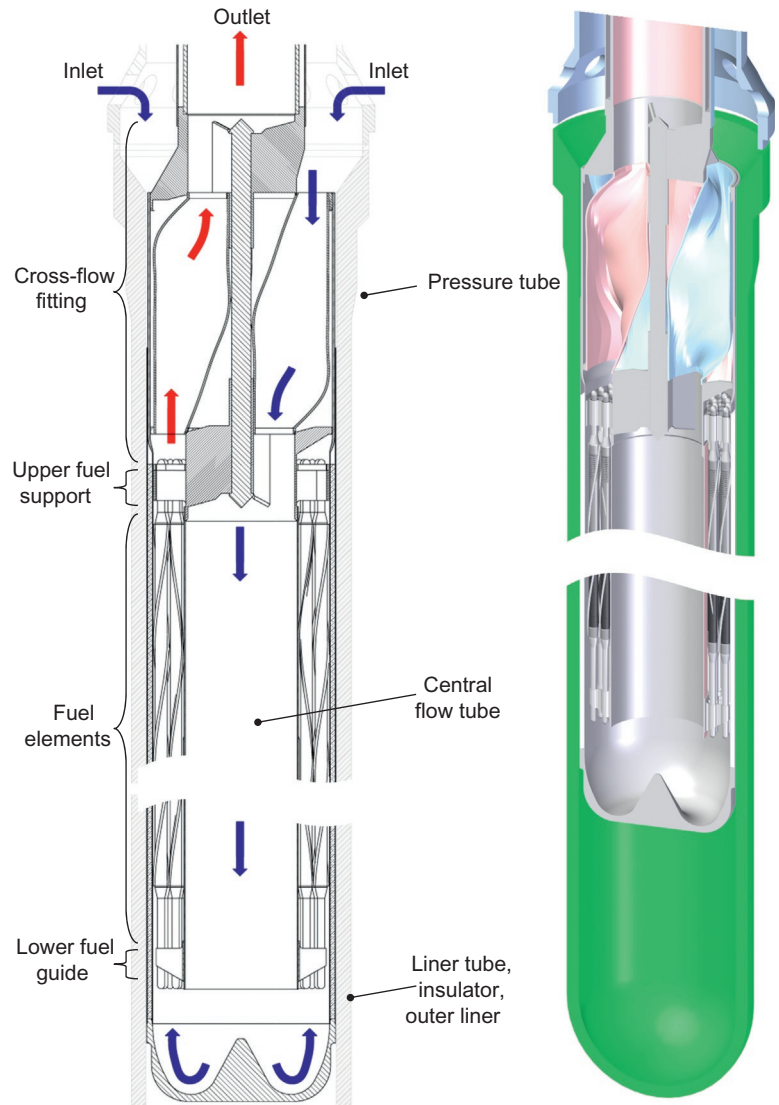


Figure 8.12. Cross-sectional view of the 64-element fuel bundle concept inside of the pressure tube

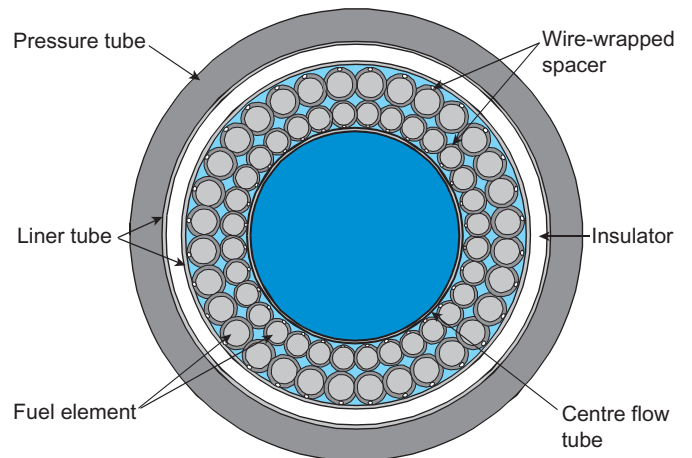


Table 8.1. Scorecard for fuel cladding material candidates

Material	Property							
	Corrosion	Oxide thickness	SCC (un-irradiated)	IASCC	Creep	Void swelling	Ductility (4% elongation)	Strength
800H	Green	Green	Yellow	Yellow	Green	Green	Gray	Green
310S	Green	Yellow	Yellow	Gray	Green	Green	Gray	Green
625	Green	Green	Yellow	Yellow	Green	Green	Gray	Green
347	Green	Yellow	Yellow	Yellow	Green	Yellow	Gray	Green
214	Green	Green	Gray	Gray	Green	Gray	Gray	Green

Green, available data suggest that this alloy meets the performance criteria under all conditions expected in the core; *yellow*, some (or all) available data suggest that this alloy may not meet the performance criteria under some conditions expected in the core; *gray*, there are insufficient data to make even an informed decision as to the behavior in a Canadian SCWR core concept

A key feature of the Canadian SCWR fuel concept is the adoption of the proven “collapsible cladding” concept utilized in CANDU^a fuel. This feature is especially suited to the Canadian SCWR concept because of the high temperature and pressure experienced under normal operating conditions. The choice of a collapsible cladding requires that the cladding material has sufficient ductility in the beginning of the fuel cycle to deform onto the fuel pellets. This relaxes the requirements on the creep strength and yield strength relative to a free-standing fuel cladding increasing the number of materials that can be viable for use. Five candidates of fuel cladding materials were assessed for their suitability based on various material properties (Table 8.1). Alloy 800H and Alloy 625 have been considered as prime candidates, whereas Stainless Steel 214 is excluded because of missing information on several properties.

Another feature of the current Canadian SCWR fuel element concept is the adoption of a colloidal-graphite coating of the internal surface of the cladding (Wood et al., 1980). The graphite coating of standard CANDU PHWR fuel cladding has been proven to provide additional margin to (internal) stress-corrosion cracking. Although the mechanism of this protection is not clearly understood, the most popular theories involve either the graphite acting as a “getter” for volatile corrosive fission products or because it provides a physical barrier between the fuel pellet and the cladding, protecting the cladding from fission fragment damage. In both cases, the graphite coating should provide the same protection for the Canadian SCWR fuel cladding as it does for the CANDU fuel cladding.

In keeping with the collapsible cladding concept, the Canadian SCWR fuel concept will utilize the standard CANDU-type pellet configuration. Pellets will be high-density, double-dished, and chamfered. High-density pellets negate problems associated with in-reactor sintering (shrinkage); double dishes negate the problems associated with axial expansion stresses due to radial variations in pellet thermal expansion; and the chamfers avoid problems with pellet-end chipping, ease pellet loading, and ensure that pellet axial expansion is transferred via the (cooler) periphery of the fuel (at the union of the chamfer and the dish). The standard practice of pellet centerless grinding would be used to achieve very tight tolerances on pellet diameter.

The insulator consists of a series of identical plates formed on a radius. The plates are produced such that they cover 50 cm of vertical and 120 degrees of circumferential coverage around the fuel bundle. The plates have beveled edges such that they overlap at intersections vertically and circumferentially (see Figure 8.13). The use of the plate concept is necessary for plate fabrication and fuel performance considerations. From a fabrication perspective, for sintered ceramic materials, the tolerances achievable are a function of the size of the part. Therefore, very large/long parts cannot be fabricated to the tolerances required. From a performance perspective the plate concept allows for the following:

^a CANDU[®]—CANada Deuterium Uranium (a registered trademark of Atomic Energy of Canada Limited).

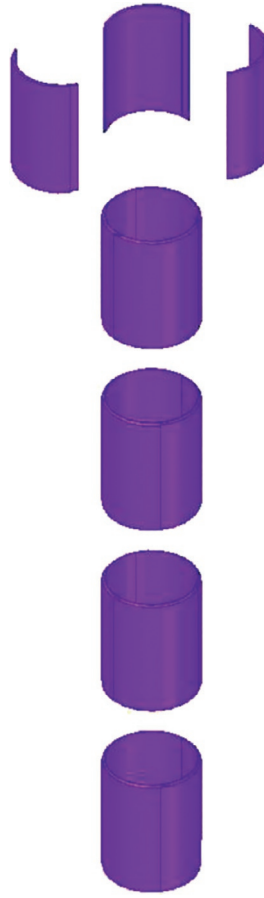


Figure 8.13. Segmented insulator concept

- the ability to minimize gaps between insulator and inner and outer liner tubes, and
- accommodating differences in thermal expansion (axial and radial) between the inner and outer liners.

The beveled edges give the plates some (limited) ability to slide past each other. This allows consideration of techniques such as heat shrinking the outer liner and/or cryoexpanding the inner liner to minimize gaps between the insulator and the liners. Because of temperature differences between the inner and outer liners at normal operating conditions and accident scenarios, differences in thermal expansion are anticipated. The plate concept allows the insulator to accommodate the thermal expansion differences while minimizing insulator gaps due to cracking.

The insulator material is yttria-stabilized zirconia, and the ceramic insulator is cladded by the inner and outer liner tubes. The insulator-liner tube assembly is attached to the fuel assembly, rather than the pressure tube, and is replaced after three fuel cycles. The insulator size and geometry are determined by the requirement that the fuel-channel concept incorporates the ability to maintain core components below melting temperature even under accident scenarios that require long-term passive cooling.

8.7 Safety system concept

Defense-in-depth is one of the important principles in all safety concepts of current reactors and it shall consequently also be applied for the SCWR. Accordingly, the safe operation of the power plant shall be ensured by the following measures:

Normal operation shall be safeguarded by the operating systems. Moreover, the power plant shall be based on

- conservative design with high reliability and availability and
- proven technology and quality assurance.

Operational occurrences of seldom events ($<10^{-2}$ /year) shall be controlled and limited by

- surveillance and diagnostics and
- inherent safety and nuclear stability.

Design basis accidents with a probability of $<10^{-5}$ /year shall be controlled by safety systems, which include

- redundancy and train separation,
- protection against internal and external hazards,
- qualification against accident conditions,
- automation, and
- autarchy of the safety systems.

Multiple failure scenarios (e.g., station blackout, total loss of feed-water, and loss of coolant accidents) and severe external events (e.g., military or large commercial airplane crash) are included in the design extension scenarios, which shall be protected by

- diversified systems and
- design against external event loads.

If severe accidents should still occur, then the SCWR needs to be protected by

- mitigative features and
- prevention of energetic consequences that could lead to large early containment failure (e.g., steam explosion, direct containment heating, and global hydrogen detonation).

8.7.1 Safety system in a pressure vessel-type supercritical water-cooled reactor concept

For a pressure vessel design of the SCWR, there are several common safety system requirements that can be taken directly from PWR or BWR designs without significant modifications. These are

- the reactor shut-down system by control rods or by a boron injection system as a second, divers shut-down system,
- containment isolation by active and passive containment isolation valves in each line penetrating the containment to close the third barrier in case of an accident,
- steam pressure limitation by pressure relief valves,
- automatic depressurization of the steam lines into a pool inside of the containment through spargers to close the coolant loop inside of the containment in case of containment isolation,
- a coolant injection system to refill coolant into the pressure vessel after intended or accidental coolant release into the containment,
- a pressure suppression pool to limit the pressure inside of the containment in case of steam release inside of the containment, and
- a residual heat removal system for long-term cooling of the containment.

An example of a containment with such safety systems is the compact HPLWR containment shown in [Figure 8.14](#) with 20 m inner diameter and 23.5 m inner height ([Schulenberg and Starflinger, 2012](#)). The cylindrical containment from prestressed concrete is designed for an internal pressure of 0.5 MPa. It contains the reactor pressure vessel, an annular pressure suppression pool with 900 m³ of water and 500 m³ of nitrogen, four upper pools with a total water volume of 1121 m³, and a drywell gas volume of 2131 m³. Four feed-water lines with check valves and four steam lines with containment isolation valves, each inside and outside

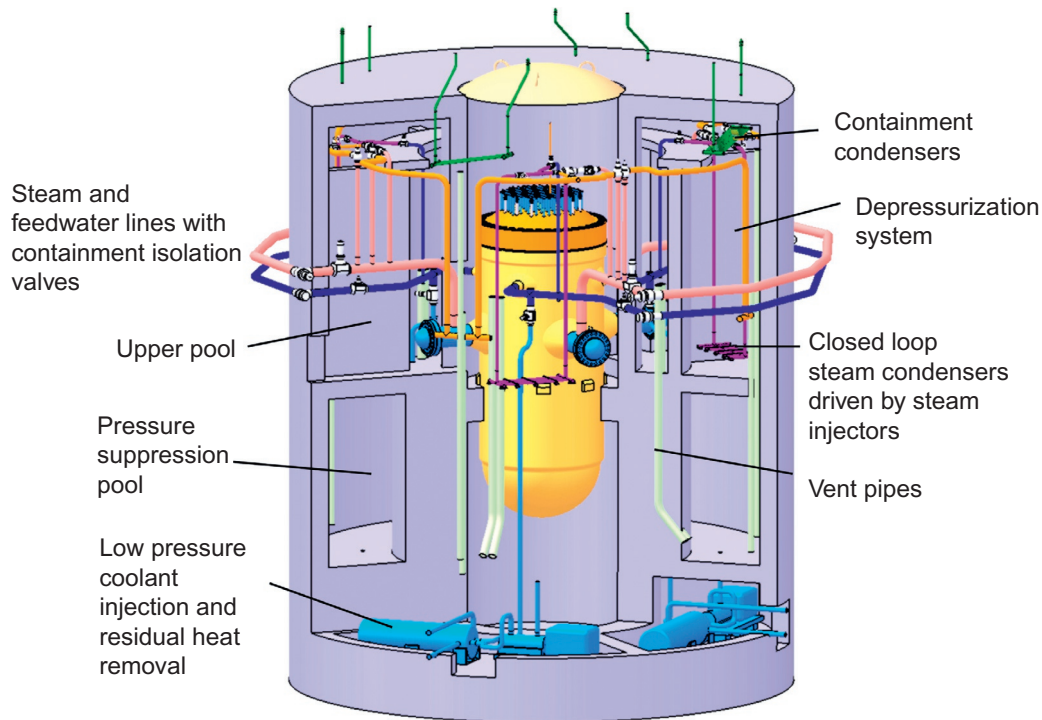


Figure 8.14. Containment of the HPLWR with safety systems (Schulenberg and Starflinger, 2012)

of the containment, connect the reactor with the steam cycle. These valves are designed with a stroke time of 3 s, closing both actively and passively. Four Automatic Depressurization Systems (ADSs), each equipped with two safety relief valves and two depressurization valves, open a flow cross section of 110 cm^2 each to eight spargers in the upper pools.

Underneath the pressure suppression pool, four redundant and separated LP coolant injection pumps, with an outlet pressure of at least 6 MPa and a maximum flow rate of 180 kg/s each, supply coolant from the pressure suppression pool via a heat exchanger for residual heat removal and via a check valve to the feed-water line. Overflow pipes from the upper pools to the pressure suppression pool close the coolant loop inside of the containment. Sixteen vent tubes for pressure suppression in the containment connect the drywell with the pressure suppression pool.

Four emergency condensers are connected with the four steam lines and with the four feed-water lines hanging from the top in the upper pools. For example, flow through these condensers is driven by a steam injector. In addition, there are four containment condensers mounted at the ceiling of the drywell, which are connected on their secondary side to pools above the containment. Their secondary side is permanently open so that steam in the containment can condense as soon as the saturation temperature in the pools has been reached and the containment pressure is starting to increase, in the unlikely case that the heat sink of the residual heat removal system is not available. Open connecting pipes from the ceiling to the pressure suppression pools enable a discharge of hydrogen from the drywell. In turn, the pressure suppression pool can be vented to the stack through aerosol and iodine filters.

Outside the containment, a boron poisoning system on top of the containment with a tank of about 10 m^3 of B-10 with a concentration of 20%–25% is connected with the feed-water lines by two lines including pumps. It serves as the second, redundant shut-down system.

8.7.2 Safety system in the Canadian SCWR concept

The safety approach adopted for the Canadian SCWR concept follows those of advanced reactors in that multiple levels of independent and diverse safety systems are used as defense-in-depth, and passive safety

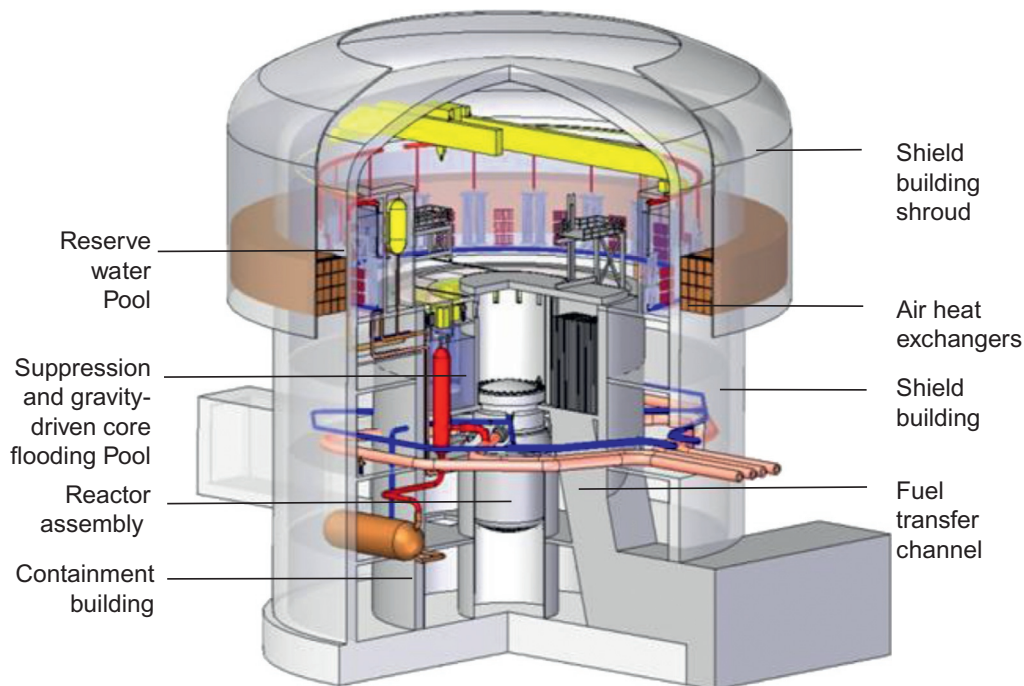


Figure 8.15. Safety system inside of the reactor building of the pressure tube-type SuperCritical Water-cooled Reactor (SCWR) concept

systems are adopted for increased reliability. One of the major development goals of the Canadian SCWR concept is to enhance safety such that the risk of core damage and release of radioactive materials to the environment is significantly reduced. The unique features of the pressure-tube-based concept allow for an optimal balance of passive safety features on the moderator systems for emergency heat removal (e.g., a prolonged station blackout event) and a combination of active and passive safety systems in the main cooling system. The primary system components are selected to provide multiple and redundant decay heat removal paths; these defense-in-depth concepts considerably reduce plant risk over existing reactors. In addition, there is a transformative improvement in core damage risk by including a further passive decay heat removal pathway for emergencies. This capability is possible through a combination of a natural circulation-driven moderator cooling system, the fuel-assembly concept, fuel-channel concept, and direct radiation heat transfer from the fuel to the insulator liner. The safety concept adopted for the Canadian SCWR concept is described by Novog et al. (2012), and a detailed design description of the safety systems is given by Yetisir et al. (2014) and Gaudet et al. (2014). Figure 8.15 illustrates the safety system inside of the reactor building.

8.7.2.1 Containment pool

The primary function of the containment pool is to provide a volume of water into which steam flows from the ADS so that large-scale Loss-Of-Coolant Accidents (LOCAs) can be suppressed. In addition, the containment pool provides a gravity-driven water flow to the reactor inlet plenum to replace inventory lost during an LOCA and subsequent decay heat boil-off. This pool consists of an annular-shaped tank and is located in the containment building above the reactor. It is divided into two sections to reflect the bilateral symmetry of the reactor and safety systems, with each half functioning independently of the other.

Located above the liquid level within the pool is the containment steam condenser gallery, which houses containment steam condenser heat exchangers and passive autocatalytic recombiner units. Physically, the condenser gallery is an annular-shaped, enclosed area, with a series of openings located on the outer wall. This outer wall forms a separation between the steam tunnel and condenser gallery. Located within these openings are the containment steam condenser heat exchangers, placed to allow condensed steam to drain

directly within the condenser gallery. The condenser gallery floor is equipped with a series of drains equipped with suppression nozzles, discharging into the containment pool below the liquid level.

This layout permits the containment steam condensers and containment pool to act in unison to condense steam accumulating in the steam tunnel because of a LOCA event. In a high steam-flow regime found in a large-scale LOCA, the steam condensers will be overwhelmed, allowing steam to flow past these condensers and be injected and suppressed within the containment pool via the drains. A low steam-flow regime will result in the direct condensing of the steam by the heat exchangers, with the condensate draining into the containment pool.

The volume above the liquid level of the containment pool can be considered as a wetwell. In a high steam-flow regime from the steam tunnel to containment pool, air and gases may be entrained and deposited in the wetwell above the surface of the containment pool. To prevent the pressure in this area from rising excessively, a series of rupture panels are located above the containment pool water line, separating the drywell space from the wetwell. These panels allow gases and entrained air to escape to the larger drywell space should the wetwell volume be insufficient.

The secondary side of the containment steam heat exchangers are connected to the reserve water pool, with circulation established through gravity-driven flow. With this, heat from an LOCA event will be deposited into the reserve water pool through the containment steam condensers.

8.7.2.2 Automatic depressurization system

The ADS consists of several valves through which the reactor can be rapidly depressurized. It also provides overpressure protection to the reactor and outlet piping. The valve banks are located in the containment building steam tunnel, with the discharge flow suppressed into the containment pool.

8.7.2.3 Gravity-driven core flooding system

The gravity-driven core flooding system consists of a pipe connecting the containment pool to the reactor cold leg coolant piping. A check valve permits the reactor to operate at its operating pressure, yet it allows water to flow into the reactor from the containment pool under accident conditions.

To ensure long-term decay heat removal in the event of a piping breach within the containment building steam tunnel, the volume of the containment pool exceeds that of the steam tunnel. Because of the seal between the reactor and steam tunnel floor, coolant will accumulate within the steam tunnel, with steam condensed and returned to the containment pool. With the steam tunnel filled with water from the containment pool, a sufficient level will remain in the containment pool to cover both the suppression nozzles and the gravity-driven core flooding system inlet pipe. This feature eliminates the need for an active pumping system and other related components (e.g., sump strainers).

8.7.2.4 Isolation condensers

The primary function of the Isolation Condensers (ICs) is to passively remove sensible and core decay heat from the reactor, preventing reactor overpressure, and to serve as a long-term cooling system under station blackout conditions. The IC heat exchangers connect with the reactor coolant piping and remove heat from the reactor by depositing this into the reserve water pool.

The IC system is divided into two independent trains, with each train consisting of a piping loop running from the reactor outlet, to heat exchangers located in the reserve water pool, and returning to the reactor inlet. The system is pressurized and on hot standby under normal reactor operations. A connection valve is located on the system's low point near the reactor inlet and is closed under normal reactor operations. The closed valve disrupts the flow through the system to minimize heat loss.

The IC relies on the difference of densities between the IC hot leg and cold leg fluid to initiate and maintain a gravity-driven circulation. Under station blackout conditions, the reactor can be depressurized and cooled by first closing the main steam and feed-water isolation valves, followed by opening the IC connection valve.

The liquid column normally trapped by the connection valve is allowed to flow into the reactor inlet. As this drains into the reactor, the IC heat exchanger tubing will be exposed to steam from the reactor outlet, allowing heat transfer to the reserve water pool. Further steam produced by the reactor due to the decay heat will sustain the circulation.

Although two independent trains of ICs are considered as the reference configuration for the Canadian SCWR concept, the required capacity of the ICs varies as the reactor is cooled to prevent unnecessarily rapid cooling rates. The current two-train configuration may not allow plant operators to adequately control the cool-down rate and would require further subdivision into four independent trains, with one train attached to each of the reactor outlets. Details on the configuration will be established in future design phases.

8.7.2.5 Reserve water pool

The primary function of the reserve water pool is to serve as a buffer between the passive safety systems and the ultimate heat sink. The large mass of water available in the pool allows heat to be absorbed and subsequently removed by the atmospheric air heat exchangers or by evaporation.

The pool is located in the upper section of the shield building and occupies an annular space against the building's outer wall. It is divided into two sections, each section housing one train of ICs and the passive moderator cooling system. All heat exchange areas of the ICs and the passive moderator heat exchangers are located in the lower half of the pool. The pool enclosure is equipped with a filtered vent to the atmosphere to permit the release of water vapor. Pool levels can be remotely maintained by means of a fill line connected to an external emergency supply such as lake water or a water truck.

8.7.2.6 Atmospheric air heat exchangers

The primary function of the atmospheric air heat exchangers is to reject heat from the reserve water pool to the atmosphere. Although not considered as a safety system, the heat exchangers serve to extend the period of time in which the reserve water pool can function as a heat sink before intervention under a high core decay heat regime. At a lower core decay heat regime, the atmospheric air heat exchangers can reject the entire heat load, extending indefinitely the point of intervention.

The atmospheric air heat exchangers consist of a series of plate-type heat exchangers located on the periphery of the shield building. These exchangers are enclosed in a shroud, which forms a chimney to further increase gravity-driven air flow. To minimize the number of penetrations into the shield building, the heat exchangers are grouped and connected to common hot leg and cold leg headers. Valves are located on both the hot leg and cold leg headers and are closed under normal reactor operating conditions to prevent freezing in cold climates.

Under accident conditions, with the valves opened, water is drawn from the upper surface of the pool, allowed to cool in the heat exchanger, and returned to the bottom of the pool by means of a gravity-driven convection current. Likewise, cooler air is drawn through the heat exchangers from the bottom of the shroud, with the heated air escaping at the top of the shroud.

8.7.2.7 Passive moderator cooling system

The Passive Moderator Cooling System (PMCS) serves as an additional barrier to core damage. In an accident scenario, decay heat generated in the fuel within the fuel channel is transferred through radiation from the cladding to the inner liner of the insulator, flows through the channel insulator and pressure tube, and is deposited into the moderator. The PMCS uses a flashing-driven natural circulation loop to remove heat from the moderator, and it deposits the heat into the reserve water pool.

The PMCS is divided into two independent trains, with each train consisting of a piping loop running from the reactor calandria to heat exchangers located in the reserve water pool and returning to the calandria. The system is totally passive and is functional during normal reactor operation. A head tank, located above the heat exchangers, maintains a constant pressure within the system.

8.8 Dynamics and control

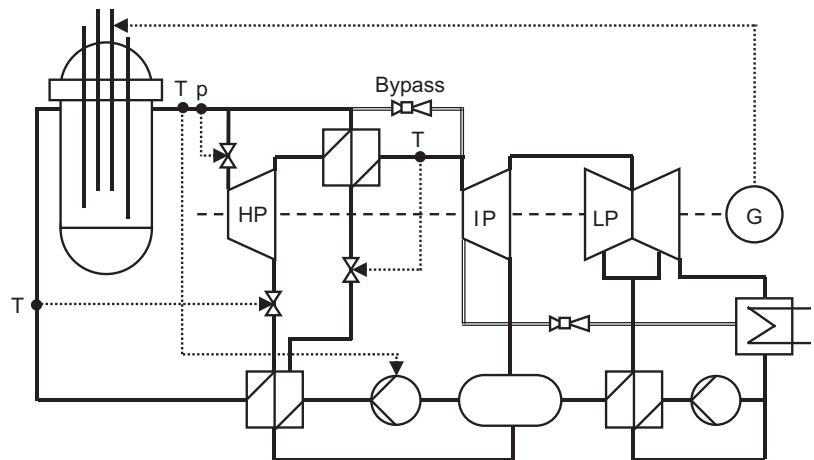
Because the SCWR has a once-through steam cycle, in which steam from the core outlet is directly supplied to the HP turbines, it has many similarities with BWRs. On a closer look, however, there is a basic difference in the coolant flow path inside the reactor that causes a difference of the steam-cycle control. In a BWR, the feed-water pump controls the liquid level in the reactor pressure vessel and the steam pressure is controlled by the turbine governor valve. The core power is either controlled by the control rods or by the speed of the recirculation pumps. The SCWR concepts do not include any recirculation loop. The feed-water pump can control either the steam temperature at the core outlet, if the core power is controlled by the control rods, or it can control the core power if the steam outlet temperature is controlled by the control rods. Again, the steam pressure is controlled by the turbine governor valve in both cases.

An example of control loops for operation in the load range is sketched in Figure 8.16. Here the speed of the feed-water pump is controlled by the temperature of the superheated steam at turbine inlet, the mass flow of the HP steam extractions is controlled by the feed-water temperature, the reheat temperature is controlling the steam mass flow of the reheater, and the pressure at the reactor outlet is controlling the turbine governor valve. The thermal power of the reactor, and thus with some delay in the generator power, is controlled by the control rods of the reactor core.

A supercritical fossil-fired power plant with a once-through steam cycle is usually operated with a sliding pressure: the turbine governor valve is kept open in the upper load range and the boiler outlet temperature is kept constant such that the boiler outlet pressure increases proportionally with the steam mass flow and thus with load. Consequently, the boiler is operated at subcritical pressure below approximately 80%–90% load. However, such control is not permitted for the SCWR because dryout or even film boiling of the coolant at the fuel rods would overheat and damage the cladding (Schulenberg and Raqué, 2014). Instead, the SCWR is operated at constant supercritical pressure in the entire load range.

The best thermal efficiency at part load can be achieved at maximum core outlet temperature. A constant temperature implies that the coolant mass flow increases proportionally with load. However, because the reactor core requires a minimal coolant mass flow, in particular for downward flow regions of the two-pass or three-pass concept (Figure 8.2), the reactor must be operated with a colder core outlet temperature in the lower load range. Once the core outlet temperature and thus the turbine inlet temperature becomes so small that condensation and droplet erosion must be expected in the HP turbine, the steam has to bypass the turbine. Likewise, the reheat temperature is colder in the lower load range because it cannot exceed the core outlet temperature, and the steam also has to bypass the IP and LP turbines.

Figure 8.16. Control loops to operate the supercritical water-cooled reactor in the load range. *HP*, High Pressure; *IP*, Intermediate Pressure; *LP*, Low Pressure; *G*, Generator



Oka et al. (2010) discussed the plant dynamics using such a control system. They concluded that stable operation of the thermal reactor as well as of the fast core option are achievable by tuning the controllers.

8.9 Start-up

Starting from cold conditions, the first reactor power will be needed to warm up the steam cycle. Oka et al. (2010) suggested either to start with a constant supercritical pressure by depressurizing some coolant into a flash tank or to start with a sliding, subcritical pressure by separating water and steam from the reactor core in external cyclone separators. In either case, the separated liquid is taken to preheat the feed-water and the remaining steam is warming up the turbines. Because dryout will be unavoidable in the reactor core during subcritical operation, the maximum cladding surface temperature of the fuel rods needs to be checked to avoid damage.

Schulenberg and Starflinger (2012) reported about a constant pressure start-up and shut-down system for the three-pass core design of the HPLWR, trying to keep the feed-water temperature constant to minimize thermal stresses of the reactor pressure vessel. This concept also includes a warm-up procedure for the deaerator during start-up from cold conditions. A battery of cyclone separators is foreseen outside of the containment to produce some steam from depressurized hot coolant of the reactor.

8.9.1 Start-up system in a pressure tube-type supercritical water-cooled reactor concept

The key requirement for the start-up system is to maintain adequate flow through the core to protect the fuel from overheating during start-up. As the reactor is brought from low-pressure and low-temperature conditions to operating conditions, two-phase flow can occur within the core, giving rise to the possibility of dryout. The reduced heat transfer occurring under dryout conditions can lead to fuel overheating. For this reason, the maximum allowable cladding surface temperature is set as a criterion and is determined by the cladding material.

An additional concern during reactor start-up is the steam quality to the HP turbine. To avoid turbine blade damage, the moisture content in the saturated steam at subcritical temperatures is normally limited to less than 0.1%. In addition, the enthalpy of the core outlet coolant must be high enough to provide the required turbine inlet steam enthalpy.

The modified sliding pressure start-up as proposed by Yi et al. (2005) can be adapted to the proposed operating conditions in the Canadian SCWR concept. To provide a starting point for future analysis of critical performance characteristics (e.g., fuel cladding temperatures and thermal-hydraulic and neutron stabilities), reference operating conditions (e.g., flow rates, reactor power levels, and mechanical equipment configurations) have been selected.

The recirculation flow rate chosen is to match a suggestion for the SCWR by Yi et al. (2005), namely 25% of full power flow, with reactor power levels and warm-up times chosen to limit temperature gradients within the pressure boundary as the reactor comes to operating temperature. The maximum feed-water temperature is adjusted to 350°C to reflect the proposed Canadian SCWR operating conditions. All start-up components are rated for a maximum operating temperature of 450°C, reducing the overall weight of the construction because of greater mechanical strength at lower metal temperatures. Finally, make-up feed-water flow during turbine warm-up is to be supplied by the feed-water system because the Canadian SCWR concept does not have a reactor core isolation cooling system.

In addition to the feed-water and inlet and outlet piping normally found in a reactor, the start-up system consists of a steam drum, a heat exchanger, and circulating pump, as shown in Figure 8.17. The function of the steam drum is to provide a liquid level at which pressure equilibrium can be established based on the

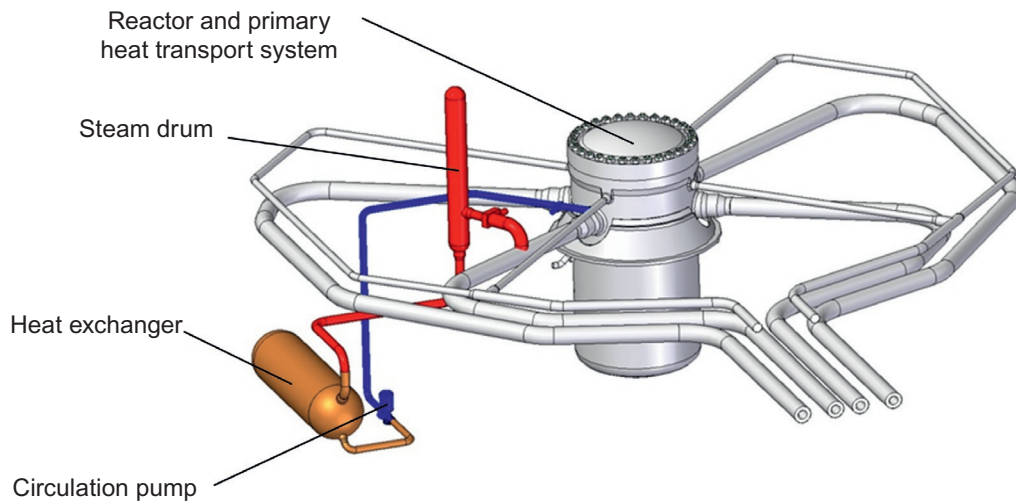


Figure 8.17. Component layout of the start-up system concept

temperature of the water. Because no steam is allowed to escape the system, the system pressure is at the saturation temperature of the liquid. The function of the heat exchanger is to limit the coolant temperature being returned to the reactor to 350°C , and it is utilized in the start-up sequence only after the outlet temperature exceeds this limit. To limit the thermal gradient stresses within this heat exchanger and to reduce the capacity requirement, the maximum operating temperature of the start-up components will be limited to 450°C , beyond which line switching will occur and the start-up system stopped.

To avoid additional penetrations to the reactor inlet plenum, the start-up system piping is connected to one of the four heat transport piping connections to the reactor. The connection point is within the containment building, between the reactor and main steam isolation valves and the feed-water isolation valves. The start-up system can be isolated from the reactor by means of valves located on the start-up system piping at the connection points.

A recirculation pump shall provide a constant mass flow to the reactor, regardless of the instantaneous fluid density. The pump is to be equipped with a variable-speed drive motor to maintain the desired mass flow rate throughout the start-up cycle. The pump is to be located in proximity to the heat exchanger within the shield building.

8.10 Stability

A stability problem that is well known from BWRs is the occurrence of density wave oscillations. It is caused by the large density change of the boiling coolant in the core, in particular if the local coolant pressure loss increases with decreasing mass flow. The coolant density ratio in the SCWR changes by more than a factor of eight in the core, which is even higher than in a BWR (International Atomic Energy Agency, 2014).

Stability analyses of the coolant flow through the three-pass core of the HPLWR have been studied by Ortega Gomez (2008). As with BWRs, he showed that the most effective measure to avoid density wave oscillations in the core is the installation of orifices at the inlet of fuel assemblies. These orifices need to be customized for a hot fuel assembly.

In the case of a BWR, the operation point of the average heated fuel assembly should correspond to a decay ratio less than 0.5 for a single-channel density wave oscillation, and a decay ratio less than 0.25 should correspond to the coupled thermal-hydraulic/neutronic density wave oscillation. Furthermore, the whole operation range, also including hot fuel assemblies, should be in the linear stable region of the stability map.

Ortega Gomez (2008) showed that the average and even the hot fuel assemblies of the HPLWR superheaters fulfill the stability criteria for all three types of density wave oscillations without applying any orifice.

However, the average fuel assemblies of the evaporator have a decay ratio larger than 0.25 at normal operation parameters for the in-phase and out-of-phase density wave oscillation. Furthermore, hot fuel assemblies of the evaporator would operate in the linear unstable region. Thus, although the fuel assemblies of the superheaters do not need additional inlet flow restriction, all fuel assemblies of the evaporator stage must be equipped with inlet orifices.

Although the first superheater is stable with respect to density wave oscillations, even without orifices, we have to expect flow reversal in some fuel assemblies of the first superheater of a three-pass core at low mass flow rates because of an unstable stratification of the downward flow. The mass flow control of the reactor is usually such that flow reversal is excluded, as discussed in [Section 8.8](#). However, low mass flow rates are unavoidable during some sequences when the reactor is opened and the core is disassembled or during accident scenarios. [Schulenberg and Starflinger \(2012\)](#) reported about flow analyses for such scenarios, concluding that flow reversal will not be a concern for the core as long as enough margin is kept from the cladding temperature limits.

Another stability issue, which has been reported by [Schulenberg and Starflinger \(2012\)](#), is the xenon oscillation of the core power, such as those known from conventional LWRs. [Reiss et al. \(2009\)](#) studied these oscillations for a simplified HPLWR core geometry. The diameter of the core of the HPLWR is approximately 3.5 m, whereas the active height is 4.2 m. These dimensions are in the range of LWRs where xenon oscillations cannot be excluded. On the other hand, because of the large density drop of water after crossing the pseudo-critical point, the migration length of the neutrons, which is an important parameter for the stability of the reactor against xenon oscillations, is larger than in current LWRs. The preliminary results of [Reiss et al. \(2009\)](#) indicated that the HPLWR will be unstable against xenon oscillations. Nevertheless, its stable operation can be ensured with proper control equipment (e.g., partly inserted control rods), which is already well established and will be similar to today's large reactors. At the beginning of the burn-up cycle of the HPLWR, some of the control rods are inserted to compensate for excess reactivity, which makes them suitable, in addition to power control, for xenon oscillation control. At the end of the cycle, some of the control rods will still be inserted because of power control and safety considerations; therefore, they could also prevent large oscillations. On the other hand, partly inserted control rods could be useful not only for controlling xenon oscillations but also to fine tune the power distribution during normal operation.

8.11 Advantages and disadvantages of supercritical water-cooled reactor concepts

Differences in system configurations would lead to specific advantages and disadvantages between pressure vessel and pressure-tube types of SCWR concept. Rather than focusing on each system, the following general advantages of SCWR concepts are foreseen:

- The SCWR concepts are evolutions of the current fleet of nuclear reactors (either LWR or PHWR) combining the nuclear reactor with the balance of plant of the fossil-fired power plant. Once constructed, the SCWRs can be easily adopted into the existing systems of utilities because most utilities operate nuclear and fossil-fired power plants.
- System configurations of the SCWR concept are simpler than existing reactors; hence they can provide economic advantage.
- The SCWR concept is a water-cooled reactor, which has the distinct advantages of safeguard and proliferation resistance.
- With the introduction of a passive safety system, the safety characteristics of the SCWR concepts are as good as or better than existing reactors.
- All SCWR concepts have higher thermal efficiency than the current fleet of nuclear reactors; hence they would reduce the fuel utilization and waste stream, improving the sustainability.

The following disadvantages may be associated with the SCWR concepts:

- The high coolant temperature has led to high cladding temperature, which requires the use of stainless steels or nickel-based alloys as fuel cladding materials. Because of the high neutron absorption of these materials, the fuel burn-up is reduced or the fuel enrichment is increased. In addition, the refueling frequency is increased compared with the current fleet of nuclear reactors.
- All current SCWR concepts adopt the direct cycle to simplify the system configuration. Although the direct cycle is also being used in the BWR, the single-phase steam flow in the SCWR would transport the radioactive materials from the core to the HP turbine (the presence of liquid phase in the BWR minimizes the transfer because the radioactive materials remain in the liquid whereas the steam is directed to the turbine). This could hamper maintenance and inspection of the turbine and increase dosage to staff. Introducing the indirect cycle would alleviate the issue, but it would escalate the capital cost of the plant.
- The fuel assemblies of current SCWR concepts contain more parasitic materials than those of existing reactors, increasing the waste stream.

8.12 Key challenges

The basic idea for development of the SCWR is to use the long-term experience of PWRs and BWRs on one hand and the experience with supercritical fossil-fired power plants on the other hand, to derive an innovative plant concept with a minimum of research needs. Obviously, the reactor core of such a power plant will be new then, and the core outlet temperatures as well as the enthalpy increase of coolant in the core will exceed by far the current experience. However, all other components of the SCWR power plant, including the steam-cycle components and the containment with its safety systems, are not considered to cause any major challenge because the latest fossil-fired power plants are operated even with a life steam temperature of 600°C at pressures above 30 MPa.

A key challenge for core design is a cladding material for elevated temperatures above 600°C. Zircaloy is certainly not applicable at these temperatures. Ferritic-martensitic boiler steels used for supercritical fossil-fired power plants are hardly applicable because the small wall thickness of fuel claddings of approximately 0.5 mm would not provide enough corrosion margin. Austenitic stainless steels with more than 20% Cr are still among the most promising candidates; however, they have compromises in creep resistance. Nickel-based alloys can tolerate even higher temperatures in the supercritical water environment, but the high nickel concentration will cause helium embrittlement and stress-corrosion cracking under neutron irradiation. As an alternative option, the use of coatings has been considered recently such that a corrosion-resistant coating is applied on a creep-resistant substrate. [Guzonas and Novotny \(2014\)](#) summarized the latest status of SCWR material research.

Another key issue is the prediction of cladding surface temperatures at bulk temperature close to the pseudo-critical point. The strong change of almost all coolant properties with temperature may cause a deterioration of heat transfer and associated hot spots, which can hardly be predicted with current computational fluid dynamics ([Pioro and Duffey, 2007](#)). A recent blind benchmark exercise on heat transfer in an electrically heated rod bundle in supercritical water, summarized by [Rohde et al. \(2015\)](#), confirmed that we are still far from reliable predictions.

8.13 Fuel qualification test

A European consortium coordinated by the Research Center Rez in the Czech Republic has worked out an in-pile test of a small-scale fuel assembly with four fuel rods of 8-mm outer diameter inside a loop with

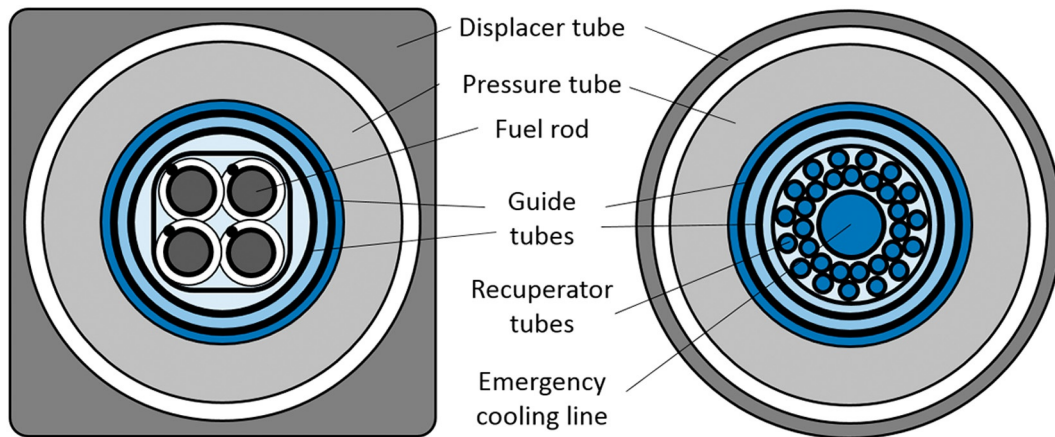


Figure 8.18. Cross sections of the pressure tube for the fuel qualification test; left: heated test section, right: recuperator section

supercritical water, as reported by [Ruzickova et al. \(2014\)](#). The fuel rods contain UO_2 fuel, enriched to almost 20%, to provide a total rod power of more than 60 kW over an active length of 60 cm. A cross section of this pressure tube is shown in [Figure 8.18](#). The bottom part of the pressure tube ([Figure 8.18](#), left) contains the heated test section, where four fuel rods with a wire wrap are housed in an assembly box like in the HPLWR. Two concentric guide tubes around this assembly provide a coolant flow along the inside of the pressure tube, keeping its temperature below a limit of 400°C, and through a recuperator above the heated section ([Figure 8.18](#), right). The coolant is thus preheated to 364°C at the inlet of the heated section, which is close to the pseudo-critical temperature of 384°C at 25 MPa. From the test section outlet, the coolant exchanges heat inside the recuperator tubes and it is finally cooled down to 300°C in a U-tube cooler in the top part of the pressure tube. With a peak heat flux of 1500 kW/m² at a mass flux of 1380 kg/m²s, the design conditions in the heated section are close to the envisaged peak conditions in the HPLWR evaporator. The pressure tube is thermally insulated from the reactor pool by an aluminum displacer tube and by an air gap between both parts.

A hermetically sealed recirculation pump in a separate room next to the reactor hall is driving the required coolant flow of 0.25 kg/s at 300°C through the supercritical pressure loop, using a feed line and a return line inside a shielded duct to the reactor. This separate room contains also the secondary cooling loop, safety systems and residual heat removal systems. An independent third coolant line is an emergency cooling line which may feed the central emergency tube shown in [Figure 8.18](#) in case of a loss of coolant. It ends on top of the heated section and thus may cool the test section, if needed, with a reverse flow.

An out-of-pile prequalification test of this arrangement has been performed in the SWAMUP test facility at Shanghai Jiao Tong University. Results have been reported by [Li et al. \(2017\)](#). The fuel rods were scaled up by a factor of 1.25 to an outer diameter of 10 mm to ease the installation of thermocouples inside. They were heated by DC power with an inside heater coil. Most interesting to mention were the transient tests, during which the pressure changed from supercritical to subcritical pressure and back. These tests were run only at a moderate heat flux up to 650 kW/m². As expected already from experience with supercritical fossil fired power plants, the two-phase flow at subcritical pressure was temporarily running into a boiling crisis at near critical pressure, which was quite different with decreasing than with increasing pressure. The transient temperature peaks could exceed the steady-state temperatures at supercritical pressure by far. A direct conclusion from these tests is that a sliding pressure operation, with a high heat flux at subcritical pressure, cannot be allowed in an SCWR.

Meanwhile, the in-pile tests, which were planned to be performed in the Czech Republic, had to be given up as the research reactor LVR-15 in Rez cannot be licensed for these tests.

References

- Gaudet, M., Yetisir, M., Haque, Z., 2014. Physical aspects of the Canadian generation IV supercritical water-cooled pressure tube reactor plant design. In: Proc. 2014 Canada–China Conference on Advanced Reactor Development (CCCARD-2014), Niagara Falls, Ontario, Canada, April 27–30.
- Guzonas, D., Novotny, R., 2014. Supercritical water-cooled reactor materials—summary of research and open issues. *Prog. Nucl. Energy* 77, 361–372.
- International Atomic Energy Agency, September 2014. Heat Transfer Behaviour and Thermohydraulics Code Testing for Supercritical Water Cooled Reactors (SCWRs). IAEA-TECDOC-1746, Vienna, Austria. 496 pp. Free download from <http://www-pub.iaea.org/books/IAEABooks/10731/Heat-Transfer-Behaviour-and-Thermohydraulics-Code-Testing-for-Supercritical-Water-Cooled-Reactors-SCWRs>.
- Li, H.B., Hu, Z.X., Zhao, M., Gu, H.Y., Lu, D.H., 2017. Experimental investigation on transient heat transfer in 2x2 bundle during depressurization from supercritical pressure. *Ann. Nucl. Energy* 109, 237–248.
- Magill, M., Pencer, J., Pratt, R., Young, W., Edwards, G.W.R., Hyland, B., 2011. Thorium fuel cycles in the CANDU supercritical water reactor. In: Proc. 5th Int. Sym. SCWR (ISSCWR-5), Vancouver, British Columbia, Canada, March 13–16, 2011.
- Novog, D., McGee, G., Rhodes, D., Yetisir, M., 2012. Safety concepts and systems of the Canadian SCWR. In: Proc. 3rd China–Canada Joint Workshop on Supercritical Water-Cooled Reactors (CCSC-2012), Xi'an, Shaanxi, China.
- Oka, Y., Koshizuka, S., Ishiwatari, Y., Yamaji, A., 2010. *Super Light Water Reactors and Super Fast Reactors*. Springer. ISBN: 978-1-4419-6034-4.
- Ortega Gomez, T., 2008. Stability Analysis of the High Performance Light Water Reactor. University of Karlsruhe. FZKA 7432 (Dissertation).
- Pirotto, I.L., Duffey, R.B., 2007. *Heat Transfer and Hydraulic Resistance at Supercritical Pressures in Power Engineering Applications*. ASME Press, New York, NY, USA.
- Reiss, T., Fehér, S., Czifus, S., 2009. Calculation of xenon-oscillations in the HPLWR. In: Proc. ICAPP 09, Tokyo, Japan, May 10–14 Paper 9067.
- Rohde, M., Peeters, J.W.R., Pucciarelli, A., Kiss, A., Rao, Y.F., Onder, E.N., Mühlbauer, P., Batta, A., Hartig, M., Chatoorgoon, V., Thiele, R., Chang, D., Tavoularis, S., Novog, D., McClure, D., Gradecka, M., Takase, K., 2015. A blind, numerical benchmark study on supercritical water heat transfer experiments in a 7-rod bundle. In: The 7th International Symposium on Supercritical Water-Cooled Reactors ISSCWR-7, March 15–18 Paper 2044, Helsinki, Finland.
- Ruzickova, M., Schulenberg, T., Visser, D.C., Novotny, R., Kiss, A., Maraczy, C., Toivonen, A., 2014. Overview and progress in the European project: “supercritical water reactor—fuel qualification test”. *Prog. Nucl. Energy* 77, 381–389.
- Schulenberg, T., Raqué, M., 2014. Transient heat transfer during depressurization from supercritical pressure. *Int. J. Heat Mass Transf.* 79, 233–240.
- Schulenberg, T., Starflinger, J., 2012. *High Performance Light Water Reactor, Design and Analyses*. KIT Scientific Publishing. ISBN 978-3-86644-817-9.
- Winkel, S., Sullivan, J., Hyland, B., Pencer, J., Colton, A., Jones, S., Sullivan, K., 2013. Discussing spent nuclear fuel in high-school classrooms: addressing public fears through early education. In: Proc. Global 2013, Salt Lake City, Utah, September 29–October 3, 2013.
- Wojtazek, D., 2015. Future nuclear power generation in Canada: transition to thorium fuelled SCWRs. In: Proc. 7th International Conference on Modeling and Simulation in Nuclear Science and Engineering (7ICMSNSE), Ottawa, October 18–21, 2015.
- Wood, J.C., Surette, B.A., Aitchison, I., Clendening, W.R., 1980. Pellet cladding interaction evaluation of lubrication by graphite. *J. Nucl. Mater.* 88 (1), 81–94.
- Yetisir, M., Pencer, J., McDonald, M., Gaudet, M., Licht, J., Duffey, R., 2012. The Supersafe© reactor: a small modular pressure tube SCWR. *AECL Nucl. Rev.* 1 (2), 13–18.
- Yetisir, M., Gaudet, M., Rhodes, D., Guzonas, D., Hamilton, H., Haque, Z., Pencer, J., Sartipi, A., 2014. Reactor core and plant design of the Canadian supercritical water-cooled reactor. In: Proc. 2014 Canada–China Conference on Advanced Reactor Development (CCCARD-2014), Niagara Falls, Ontario, Canada, April 27–30, 2014.
- Yi, T.T., Ishiwatari, Y., Liu, J., Koshizuka, S., Oka, Y., 2005. Thermal and stability considerations of super LWR during sliding pressure startup. *J. Nucl. Sci. Technol.* 42 (6), 537–548.
- Zhou, T., 2009. Super-critical water-cooled reactor (SCWR) steam cycle design options. AECL Report, 195-01290-ASD-001.

Generation IV: United States

Pavel Tsvetkov

Department of Nuclear Engineering, Texas A&M University, College Station, TX, United States

Nomenclature

ABR	Advanced Burner Reactor
ABWR	Advanced Boiling Water Reactor
AHTR	Advanced High-Temperature Reactor
ALWR	Advanced Light Water Reactor
ANRE	Agency for Natural Resources and Energy, Japan
ARC	Advanced Reactor Concepts
BWR	Boiling Water Reactor
CAEA	China Atomic Energy Authority, People's Republic of China
CANDU	CANada Deuterium Uranium reactor
CEA	Commissariat à l'Énergie Atomique et aux énergies alternatives, France
DOE NE	DOE Office of Nuclear Energy
DOE	Department of Energy
ESBWR	Economical Simplified Boiling Water Reactor
FHR	Fluoride-cooled High-temperature Reactor
GE	General Electric
GFR	Gas-cooled Fast Reactor
GIF	Generation-IV International Forum
GT-MHR	Gas Turbine Modular Helium-cooled Reactor
HTR	High-Temperature Reactor
IRIS	International Reactor Innovative and Secure
JAEA	Japan Atomic Energy Agency, Japan
JRC	European Commission's Joint Research Centre, Euratom
LFR	Lead-cooled Fast Reactor
LMFR	Liquid Metal Fast Reactor
LOCA	Loss-Of-Coolant Accident
LWR	Light Water Reactor
MOST	Ministry of Science and Technology, People's Republic of China
MSIP	Ministry of Science, ICT and Future Planning Technology, Republic of Korea
MSR	Molten Salt Reactor
NGNP	Next-Generation Nuclear Plant
NNSA	The National Nuclear Security Administration
NRC	Nuclear Regulatory Commission
NRCan	Department of Natural Resources, Canada
NRF	National Research Foundation, Republic of Korea
NTDG	Near-Term Deployment Group
PBMR	Pebble Bed Modular Reactor

PSI	Paul Scherrer Institute, Switzerland
PWR	Pressurized Water Reactor
RFI	Request For Information
Rosatom	State Atomic Energy Corporation, Russian Federation
SCWR	SuperCritical Water Reactor
SFR	Sodium-cooled Fast Reactor
SMR	Small Modular Reactor
SWR1000	SiedeWasser Reactor-1000
TRP	Technical Review Panel
VHTR	Very-High-Temperature Reactor
WF	Working Fluid

9.1 Generation-IV program evolution in the United States

Nuclear power industry is a relatively young industrial enterprise that continues to evolve following both global macroeconomic energy trends and domestic developments in countries with nuclear energy use interests. James Chadwick discovered neutrons in the 1930s of the last century. By doing so, he kicked off the quest for utilizing neutron-induced fissions as an energy source in a broad range of applications.

The first critical nuclear reactor went operational on December 2, 1942, in Chicago. Since then, three generations of nuclear reactors can be distinctively identified with the fourth generation emerging at the onset of the 21st century energy technology developments ([DOE Office of Nuclear Energy](#); [Weaver, 2005](#)). These four consecutive generations of nuclear energy systems have significant historical impact on nuclear power industry efforts to innovate itself while remaining commercially viable and competitive in the US domestic energy markets and globally ([Office of Nuclear Energy, 2001](#)):

- Generation I (1950–1970)—experimental and prototype reactors: the first power reactors generation was introduced during the period 1950–1970 and included early prototype reactors such as Shippingport, Dresden, and Fermi I in the United States.
- Generation II (1970–1990)—large, central-station nuclear power reactors: the second generation included commercial power reactors built during the period 1970–1990 such as the Light Water-cooled Reactors (LWRs) with enriched uranium including the Pressurized Water Reactor (PWR) and the Boiling Water Reactor (BWR). In the United States, it includes constructed 104 nuclear power plants. There were several leading US-based Generation-II reactor vendors in the early nuclear energy years. Only two of them have ultimately been successful to grow into multinational corporations and to diversify and sustain their relevance into the 21st century. These two companies are Westinghouse and General Electric.
- Generation III and III+ (1990–2030)—evolutionary designs: the third generation started being deployed in the 1990s and is composed of the Advanced Light Water Reactors (ALWRs) including the Advanced Boiling Water Reactor (ABWR) and the System 80+. These were primarily built in East Asia to meet that region's expanding electricity needs. New designs that are being deployed include the Westinghouse Advanced Passive AP1000 and the General Eclectic ESBWR. These are considered as evolutionary designs offering improved safety and economics, taking these technologies beyond Generation-II advancements.
- Generation IV (2030 and beyond)—next-generation novel designs: while the current second- and third-generation nuclear power plant designs provide an economically, technically, and publicly acceptable electricity sources in many markets, further advances in nuclear energy system design technologies can broaden the opportunities for the use of nuclear energy. The fourth generation of nuclear reactors is expected to start being deployed by 2030. The Generation-IV reactors are designed with the following

objectives in mind: economic competitiveness, enhanced safety and reliability, minimal radioactive waste generation, and proliferation resistance.

While gaining power operation experience in nuclear engineering ever since 1942 through Generation-I–III+ systems and including emerging Generation-IV systems, it was quickly established through early industrial efforts that nuclear reactions offer not only uniquely dense power sources but also a potential for a sustainable power to meet energy demands far beyond the reaches of fossil fuels including electricity and process heat applications from district heating to potable water production to large scale industrial uses. The nuclear energy sustainability and security over fossil fuel alternatives together with its potential for minimized environmental impact are the unique nuclear industry traits to be carried forward by Generation-IV reactors.

Retrospectively, following the end of World War II, efforts to develop and deploy nuclear power plants began worldwide. So far, the majority of operating and currently underconstruction power plants are with Light Water Reactors (LWRs). Pressurized Water Reactors (PWRs) lead the industry, while Boiling Water Reactors (BWRs) are not far behind. This technological reality of Generation-I–III+ systems dates back to early decisions related to naval propulsion applications of nuclear energy as well as water economics characteristics as the cheap and universally abundant reactor coolant (Weaver, 2005).

The LWR technology is well understood, matured, and optimized for traditional and novel applications. A lot of work has been done around the world to improve the existing reactor designs (Weaver, 2005; Yang, 2014). Safety demands of LWRs led to elaborate and extensive engineered safety features in Generation-II–III+ reactors. The key historical technology limitations of LWRs are: (1) significant system complexity emanating from naval origins and affecting both performance and reliability, (2) limited operating temperatures subsequently restricting attainable balance of plant energy conversion efficiencies, and (3) safety characteristics of LWR cores limiting core internals survivability in accident scenarios with accident-impeded or without built-in engineered safety features, especially in Loss-Of-Coolant Accidents (LOCA).

Although existing designs, which are denoted as Generation II and III, provide a reliable, economical, and publicly acceptable supply of electricity in many markets, further advances in nuclear energy system design can broaden the opportunities for the use of nuclear energy. Other coolant types have been explored resulting in nuclear power plants with heavy water reactors, gas reactors, and liquid metal reactors. Recognizing the advantages of non-light-water systems, it is also apparent that light water early deployment and its economics determined its leading use in contemporary nuclear reactors. The large base of experience with the current nuclear plants has been used to guide development efforts of the new Generation-IV designs to contemporary readiness-for-deployment levels. Common goals are simplification, larger margins to limit system challenges, longer grace periods for response to emergency situations, high availability, competitive economics, and compliance with internationally recognized safety objectives (Dean and Ludington, 2018; Bistline and James, 2018).

Table 9.1 summarizes the contemporary reactor technologies of accepted use and relevance to Generation-IV systems and beyond (Yang, 2014; U.S. DOE Office of Nuclear Energy, U.S. Department of Energy, 2012). Typical LWR design traits like primary coolant doubling as a moderator, need for pressurization in PWRs to avoid bulk boiling, and enriched fuels to compensate for parasitic absorption are noted recognizing their impact in the global nuclear technology evolution. Moving from LWRs to HTRs and eventually to LMFRs progressively leads to lower pressures but potentially higher fissile content needs. Developments of HTRs and LMFRs are founded on decades of R&D efforts in the United States and other countries since the 1950s alongside development and successful commercialization of LWRs. Historically, the design development efforts have been driven by several major objectives, all of which target addressing and resolving above-noted technology limitations of LWRs: (1) system design simplification trends, (2) implementation of modularity principles, (3) higher operating temperatures and (4) (inherent) safety features. Combined, these

Table 9.1. Contemporary nuclear power technologies

Reactor	Fuel	Core coolant, MPa	Core moderator	Turbine WF	No. of loops	Applications
LWR—PWR ^a	UO ₂ , 3%–5% ²³⁵ U	H ₂ O, 16	H ₂ O 16 MPa	H ₂ O steam	2	Electricity, desalination
LWR—BWR ^b	UO ₂ , 3%–5% ²³⁵ U	H ₂ O, 7	H ₂ O 7 MPa	H ₂ O steam	1	Electricity, desalination
CANDU ^c	Natural uranium	D ₂ O, 9	D ₂ O 9 MPa	H ₂ O steam	2	Electricity
HTR ^d	UCO, 8%–15% ²³⁵ U	He, 6	Graphite	H ₂ O steam He	2 1	Electricity, process heat, waste management
LMFR ^e	UO ₂ , UO ₂ -PuO ₂ , (U, Pu)O ₂ , UC, 10%–20% fissile	Na, NaK, 0.5	None	H ₂ O steam	3	Electricity, process heat, waste management

^a LWR—PWR—Light Water Reactor—Pressurized Water Reactor.

^b LWR—BWR—Light Water Reactor—Boiling Water Reactor.

^c CANDU—CANadian Deuterium Uranium reactor.

^d HTR—High-Temperature Reactor.

^e LMFR—Liquid Metal Fast Reactor.

developments enhance performance characteristics facilitating competitiveness against other energy technologies. The development trends based on these objectives matured in the 1970s and continue to present days (Weaver, 2005; Krahn and Croff, 2017). Enabling developments in materials and energy conversion technologies facilitate design efforts toward next generations of nuclear reactors. As nuclear engineering technologies mature, energy use efficiencies continuously increase. These studies allow to benefit from the extensive operational experience of LWRs and to adopt new technologies (Bistline and James, 2018).

The US Department Of Energy (DOE) has been working with the nuclear industry to establish a technical and regulatory foundation for the next generation of nuclear plants (DOE Office of Nuclear Energy; Office of Nuclear Energy, 2001; U.S. DOE Nuclear Energy Research Advisory Committee and the Generation IV International Forum, U.S. Department of Energy, 2002). The DOE Generation-IV Initiative began in the early 2000s to facilitate developing technologies that achieve safety, performance, waste reduction, and proliferation resistance while serving as an energy option that is economically competitive and ready for deployment by 2030 (OECD Nuclear Energy Agency, 2002, 2005). The licensing process is being developed jointly with the US Nuclear Regulatory Commission (NRC), while proliferation resistance and physical protection are being developed and evaluated following the guidelines produced by the National Nuclear Security Administration (NNSA) (Nuclear Regulatory Commission, 2017; U.S. Nuclear Regulatory Commission, 2012). The initial technology roadmap was completed in 2002 for the program and subsequently updated in 2014 (U.S. DOE Nuclear Energy Research Advisory Committee and the Generation IV International Forum, U.S. Department of Energy, 2002; GEN IV International Forum, 2014). The original roadmap was focused on selection methodology details and kick-off of R&Ds for recommended most promising systems. The analysis and recommendations have been deeply rooted in the 2000s-era nuclear renaissance expectations. The updated 2014 roadmap provides an overview of the original 2002 document, adds evaluations of subsequent accomplishments of over 10-year R&Ds as well as provides analyses of Generation-IV systems accounting for the Fukushima Daiichi accident lessons and contemporary economics of the 2010s. Both documents discuss projected developments in the United States and globally (DOE Office of Nuclear Energy, 2005; Committee on Review of DOE Nuclear Energy Research and Development Program et al., 2007).

The Generation-IV International Forum (GIF) was established in 2000 with its charter formalized in 2001 (OECD Nuclear Energy Agency, 2002). The original membership consisted of representatives from nine countries stemming from their participation in the US DOE-led intergovernmental group discussing international collaboration opportunities in nuclear energy technologies, later named as the GIF Policy Group. The nine founding members, signatories to the original GIF Charter of 2001, are Argentina, Brazil, Canada, France, Japan, the Republic of Korea, the Republic of South Africa, the United Kingdom, and the United States. Switzerland, Euratom, the People's Republic of China, and the Russian Federation signed the GIF Charter in 2002, 2003, and 2006, respectively, bringing the GIF membership to 13 countries.

The US DOE initiated the international program and remains playing the leading role in the GIF efforts while Argentina, Brazil, and the United Kingdom are non-active members. The extended GIF Charter was signed by representatives from all 13 countries in 2011 reaffirming national interests in collaborative efforts toward Generation-IV systems (OECD Nuclear Energy Agency, 2005, 2011). In 2015, the GIF Framework Agreement was extended for another 10 years facilitating continued collaborative efforts. The current list of implementing agents includes NRCan (Canada), Euratom, CEA (France), ANRE and JAEA (Japan), CAEA and MOST (China), MSIP and NRF (Korea), South Africa, Rosatom (Russia), PSI (Switzerland), and DOE (United States) (OECD Nuclear Energy Agency for the Generation IV International Forum, 2014).

The Generation-IV nuclear energy systems comprise nuclear reactor technologies that could be deployed by mid-21 century and present significant advancements in economics, safety and reliability, and sustainability over currently operating reactors. Described in the initial roadmap are six system concepts chosen by the United States Department of Energy's Nuclear Energy Research Advisory Committee and the Generation-IV International Forum to be investigated (OECD Nuclear Energy Agency for the Generation IV International Forum, 2009):

- Gas-cooled Fast Reactor (GFR);
- Very-High-Temperature Reactor (VHTR);
- SuperCritical-Water-cooled Reactor (SCWR);
- Sodium-cooled Fast Reactor (SFR);
- Lead-cooled Fast Reactor (LFR);
- Molten Salt Reactor (MSR).

The Generation-IV International Forum nations trust that development of these six concepts leads to a range of long-term benefits in the United States and worldwide. The US DOE supports domestic nuclear energy community interests in exploring and developing SFRs and VHTRs via signing formal GIF System Arrangement Documents for these designs (GEN IV International Forum, 2014). In addition, the US nuclear energy community participates in collaborative efforts toward developing various concepts of LFRs and MSRs (Committee on Review of DOE Nuclear Energy Research and Development Program et al., 2007; U.S. DOE Office of Nuclear Energy, U.S. Department of Energy, 2012). The basis enabling technologies to achieving high-performance characteristics are also accounted and supported by the forum member's national R&D programs. These developments include novel system concepts and energy architectures, new materials, designs for on-line maintenance and technological solutions needed to shorten outages.

Many related current efforts, such as improvements in man-machine interfaces using computers and information visualization systems, operator licensing program tools including simulator training, which have been applied at current plants, will ultimately contribute to high performance of future nuclear power plants (Dean and Ludington, 2018). Particularly, taking advantage of these technological advances, the new designs also assume plant lifetimes beyond 60 years (Weaver, 2005). Table 9.2 summarizes principal design characteristics thought-after and represented by the identified six Generation-IV design concepts (U.S. DOE Nuclear Energy Research Advisory Committee and the Generation IV International Forum, U.S. Department of Energy, 2002; OECD Nuclear Energy Agency for the Generation IV International Forum, 2009; GEN IV International Forum,

Table 9.2. Generation-IV nuclear power technologies

Reactor	Neutron spectrum	Core coolant	Max. achievable temperature, °C	Envisioned fuel cycle	Power rating (MW _e)	Applications
LWR—SCWR ^a	Thermal/fast	H ₂ O	510–625	Open/closed	300–1500	Electricity, process heat
HTR—VHTR ^b	Thermal	He	650–1000	Open/closed	250–300	Electricity, H ₂ , process heat, waste management
LMFR—SFR ^c	Fast	Na	550	Closed	30–2000	Electricity, process heat, waste management
LMFR—GFR ^d	Fast	He	850	Closed	1200	Electricity, H ₂ , process heat, waste management
LMFR—LFR ^e	Fast	Pb	800	Closed	20–1000	Electricity, H ₂ , process heat, waste management
MSR ^f	Thermal/Fast	Fluoride salts Chloride Salts	700–800	Closed	1000	Electricity, H ₂ , process heat, waste management

^a SCWR—SuperCritical Water Reactor.

^b VHTR—Very-High-Temperature Reactor.

^c SFR—Sodium-cooled Fast Reactor.

^d GFR—Gas Fast Reactor.

^e LFR—Lead-cooled Fast Reactor.

^f MSR—Molten Salt Reactor.

2014). Notably, only one of these systems uses light water as a coolant to achieve its performance characteristics while being potentially either thermal or fast spectrum system.

As already above-indicated, decades of technology development efforts for some of these systems serve as a foundation for early commercial deployment perspectives, within next decade or so, assuming viable marketing-consumer cases can be established on a competitive basis against alternative energy technologies targeting 2030–2100 (Bistline and James, 2018). International collaborations within the GIF framework are expected to facilitate early marketing and deployment opportunities.

Generation-IV advanced reactors are expected to be the result of international collaborative efforts bringing novel technologies to energy markets and customizing them according to local conditions. The universal objectives are for these systems to be sustainable, safe, reliable, economically competitive, and proliferation resistant and secure (Yang, 2014).

9.2 Energy market in the United States and Generation-IV systems

Nuclear power has had a substantial role in the supply of electricity in the United States for over three decades reaching contributions of nearly 20% of the domestic electricity generation (DOE Office of Nuclear Energy; Yang, 2014). There are several types of nuclear driven power units meeting a range of applied needs and forming an overall domestic nuclear energy system market.

In addition to the nuclear power plant reactors, there are several hundreds of pressurized water reactors for naval propulsion and hundreds of research and special purpose reactors of various types. The domestic energy demand projections within the major industrial sectors, including electricity and other energy products, coupled with environmental and sustainability considerations suggest an increasing role for nuclear energy by the end of this century (DOE Office of Nuclear Energy; U.S. DOE Nuclear Energy Research

Advisory Committee and the Generation IV International Forum, U.S. Department of Energy, 2002; GEN IV International Forum, 2014; OECD Nuclear Energy Agency for the Generation IV International Forum, 2009).

To take full advantage of fission energy, the need for greater energy efficiency is becoming an increasingly important component in development efforts toward sustainable energy resources. Cogeneration systems, producing heat and electricity, offer a solution for optimization of nuclear energy usage and increased energy security.

Nuclear power plants represent a viable energy source for cogeneration options. Currently operating nuclear power plants discard thermal energy into a heat sink at temperatures of about 280°C. Heat at these temperatures is suitable for desalination plants and various other process heat applications. Future Very-High-Temperature Reactors (VHTR) offer much higher temperatures and energy conversion efficiencies that would allow electricity generation, potable water production, and hydrogen production in a single multipurpose cogeneration system. The coupling of a nuclear energy system with a cogeneration facility creates unique challenges as well as unique opportunities for competitive performance characteristics (GEN IV International Forum, 2014).

The nuclear energy source determines the maximum energy production rate for all of the coupled energy systems driven by the reactor. Following traditional Generation-II–III+ operation strategies, a continuous operation mode might be implemented as a preferable mode for next-generation nuclear reactors as well. Assuming the continuous operation scenarios, the interface between the various product streams will need to be dynamically managed in such a way that reactor availability to the energy grid (the key continuous operation trait) is not challenged. If electricity generation is primary and chemical processing is secondary, then the “product shifting” protocol must be responsive to the needs of the electrical grid. High demand periods could force the chemical plants into standby mode, whereas low demand periods could see increased chemical production. If chemical processing is primary and electricity generation is secondary, electricity would only be sold as a commodity when demand and availability coincide. These protocols could be combined dynamically to meet grid fluctuations in a novel on-demand operation mode while reactors would be left to operate as desired from the reactor side—in base load or load following modes. The direct-cycle high efficiency Generation-IV VHTRs have a unique potential to offer both high-temperature process heat as well as electricity in an operation scenario with very-high-energy conversion efficiencies of modern Brayton cycles. The direct cycle nature of the plants allows for a load following mode with dynamic responses to energy grid fluctuations (Massachusetts Institute of Technology, 2011). Close-relatives to gas-cooled VHTRs, fluoride-salt-cooled high-temperature reactors serve as viable competitive alternatives to gas-cooled technologies with unique safety and operational characteristics. In particular, fluoride-salt-cooled high-temperature reactors carry native integration advantages for power and process heat applications (Forsberg et al., 2011).

As there are existing market penetration challenges for any novel energy technology, Generation-IV reactors will have significant uncertainties in their ability to capture sizable energy market shares (Krahn and Croff, 2017). There are significant impediments, which may prevent rapid or even accelerated deployment of near-term construction-ready Generation-IV systems. Natural gas price fluctuations and localized economics conditions in the highly-decentralized US energy market lead to shutdowns of existing Generation-II LWR-based plants purely based on economic considerations. The domestic energy economics creates adverse conditions for any new commercial nuclear deployments and has the potential to significantly slow down or even completely stop deployment efforts of novel nuclear technologies. Historical absence of significant observable focus on nuclear energy technologies in domestic energy policy considerations and predominantly decentralized market-driven energy grid architectures in the United States have already contributed to slower novel nuclear energy systems deployments and increasing numbers of Generation-II LWR-based plants to be decommissioned. The utility companies and high-energy-demand industries are naturally

reluctant to become early adopters of emerging novel energy systems despite of the actual technical characteristics and advantages resorting to well-known energy solutions as long as alternatives to nuclear remain available to meet energy needs.

This domestic situation is very challenging but reversible. Advancing the recognition of nuclear energy as a clean sustainable energy source within a comprehensive environmentally responsible energy portfolio and properly sizing nuclear units to match energy grid structures and demands are expected to change the situation and lead to favorable conditions for expanding nuclear market shares if those measures receive both federal and state support (Nordhaus et al., 2013).

Introduction of Generation-IV systems to the US energy markets is naturally expected to be slower and more sporadic compare to developments observed in other countries, Russia and China to be the most significant examples (Weaver, 2005; Krahn and Croff, 2017; Nordhaus et al., 2013). Generation-IV technologies are being advanced in those countries with significant federal support driven by anticipated energy needs, climate and environmental considerations, anticipated resource shortages and expected resulting economic demand for nuclear energy in the long term.

Domestic US energy markets are driven by near term phenomena and nuclear technologies are not expected to see rapid market penetrations under existing conditions until nuclear energy is broadly recognized as a clean sustainable energy source and incentivized at all levels and accepted by local utility companies. About 54 GW_{el} of the domestic US nuclear capacity is in regulated markets while 45 GW_{el} is in deregulated markets driven by short-term competitive power sales.

Early adoptions of Generation-IV technologies, including those originating in the United States, will likely occur with federal support and in friendly local communities. It is also conceivable to imagine early successful commercial deployments abroad, in Canada, for example, and then Generation-IV designs will be returning to the United States in a longer term as market conditions and licensing support deployments evolve to become more favorable to nuclear systems (Idaho National Laboratory, 2021; U.S. NRC, 2007, 2021).

Emerging environmental standards and regulations are beginning to recognize the role of nuclear power as a clean energy source (GEN IV International Forum, 2014; Yang, 2014; Massachusetts Institute of Technology, 2011). These changes will ultimately facilitate deployments of Generation-IV reactors as sustainable environmentally responsible energy sources that are clean and immune to environmental changes because of uses of non-light-water-based power cycles. It is expected that efficient electricity generation, process heat production and waste management capabilities will be the key features of Generation-IV reactors offering opportunities and advantages for successful energy market penetrations accounting for decentralized and centralized market conditions (DOE Office of Nuclear Energy; Nordhaus et al., 2013).

9.3 Electrical grid integration of Generation-IV nuclear energy systems in the United States

The US energy system is very complex. It is actually represented by not a single electrical grid, but a complex architecture of state and local grids, which are loosely interconnected to meet energy needs of its customers, both in electricity demands and in process heat applications (DOE Office of Nuclear Energy; Nordhaus et al., 2013; Massachusetts Institute of Technology, 2011).

The average capacity factors of US nuclear power plants have increased from about 60% attainable in the 1960s and 1970s to over 90% attainable in the 2000s. Reliability levels of base load contributions to the domestic electrical grid have been steadily increasing over the same period as demonstrated through substantial reductions in operating and maintenance expenses as well as reductions in personnel radiation exposure levels at the Generation-II through Generation-III nuclear power plants (Nordhaus et al., 2013; Massachusetts Institute of Technology, 2011).

While nuclear power plants, Generation II and Generation III, have been operating more and more efficiently in recent years, reliably contributing base load capacity, the US electrical grid has been getting more and more dated requiring significant upgrades in its infrastructure. The challenges are further complicated by existing uncertainties in planning, predictions of future energy needs, forms and infrastructure demand forecasts, from integration of renewable sources to electrical vehicles to environmentally responsible sustainable energy ecosystems to simply managing large power consumers and individual households. A range of new technologies, from smart meters to smart grids to smart houses, is already available and expected to become available in the near future to replace aging systems and meet the energy needs by offering dynamic architectures supporting adaptable “smart” energy solutions for all customers (Araujo, 2014; Massachusetts Institute of Technology, 2011).

Emerging novel power units with Generation-IV reactors must be adaptable to energy grid architectures in their ability to meet load demands faster than traditional Generation-II and III power plants characterized by slow ramp rates, meeting the competitor’s challenges of load changes on minutes-hours scales (Nordhaus et al., 2013; Idaho National Laboratory, 2014).

Fortunately, direct cycle power units with Generation-IV reactors and so-called hybrid systems combining advanced reactors and renewable energy sources offer desired dynamic capabilities to meet load requests on-demand, operating either in a traditional load-following mode or dynamically (Idaho National Laboratory, 2014). Emerging heat storage technologies, originating from solar power industries, allow for base-load operating plant configurations with Generation-IV reactors to meet market demands while remaining in base-load mode and with high degree of integration to renewable sources (Forsberg et al., 2019).

Hybrid systems integrate nuclear reactors, renewable sources, energy storage/recovery buffer systems and dynamic interfaces with electrical grids (Idaho National Laboratory, 2014; Forsberg et al., 2019). Significant flexibilities in potential architectures are available and are being explored for applications in Generation-IV technology deployment scenarios (GEN IV International Forum, 2014; Idaho National Laboratory, 2014). Flexible power ratings of Generation-IV reactors, as shown in Table 9.2, facilitate grid integration capabilities of these systems (Nordhaus et al., 2013; Idaho National Laboratory, 2014).

9.4 Industry and utilities interests in Generation-IV nuclear energy systems in the United States

The US domestic nuclear industry is in the process of transforming itself toward a much more consolidated modern enterprise (Bistline and James, 2018). The changes are driven by deregulation and economics considerations. In 1991, 101 individual utilities had ownership interests in operating nuclear power plants. In 1999, the number reduced to 87 dominated by the top 12 owning 54% of the capacity. Today, the top 10 utility companies own in excess of 70% of the total domestic nuclear capacity. These changes amount to a significant consolidation of technological resources and operational expertise.

The domestic consolidated nuclear enterprise is founded on Generation-II technologies supporting LWRs. There is a systemic effort driven by reactor vendors, General Electric, Westinghouse, and emerging new vendors, to commercialize and deploy Generation-III and III+ LWRs and Generation-IV reactors abroad and then bring them back and introduce into the domestic energy markets.

While the current domestic nuclear fleet consists of Generation-II and Generation-III LWRs with efforts currently in progress to deploy Generation-III+ LWRs, reactor vendors, plant operators and utility companies do express their interest in novel nuclear technologies ranging from light-water-based small modular reactors to advanced reactors using gas, salts and liquid metals. They do recognize the need for further R&D and express their expectation for federal programs targeting novel technologies (Bistline and James, 2018).

Table 9.3. Commercial development interests in Generation-IV technologies

Reactor	Reference reactor	Project	Lab	Illustrative industry examples
HTR—VHTR	GT-MHR	NGNP	INL	General Atomics, BWXT, HolosGen, NuGen, Radiant, USNC, XEnergy
LMFR—SFR, LFR	PRISM	Reactor R&D	ANL, INL	General Electric, TerraPower Westinghouse, CBCG, Niowave
MSR	MSR AHTR ^a	MSR FHR ^b	ORNL ORNL	TerraPower, Elysium, Flibe, Micronuclear, Terrestrial Kairos

^a AHTR—Advanced High-Temperature Reactor.

^b FHR—Fluoride-cooled High-temperature Reactor.

Table 9.3 summarizes illustrative domestic commercial interests in Generation-IV reactors (DOE Office of Nuclear Energy; GEN IV International Forum, 2014; Yang, 2014; Nordhaus et al., 2013; U.S. DOE Office of Nuclear Energy, U.S. Department of Energy, 2012; Gateway for Accelerated Innovation in Nuclear, 2021). Financial interests of utility companies in advanced reactors beyond Generation III+ are only sporadic and need strong marketing campaigns and federal-level support to secure actual buy-ins.

The domestic fast reactors are envisioned to be capable to serve as Advanced Burners (ABR) in waste management scenarios or as breed-and-burn sustainable systems (Nordhaus, 2013). The domestic VHTR is being marketed as a system that is suitable for process heat applications. The molten salt reactors are being developed as liquid fuel systems or as reactors cooled with fluoride salt (Forsberg et al., 2011). Over the years, each advanced reactor concept attracted federal and industrial interests facilitating further R&D activities.

The commercial viability cases are expected to be realized for VHTRs by 2050 accounting for growing needs for high temperatures and potable water and then for fast reactors by 2100 accounting for waste management and sustainability demands. The MSR deployment scenarios as FHRs have similarities to VHTRs in the near term (Forsberg et al., 2011). The longer-term goal is to deploy a liquid-fuel system that is expected to have advantages beyond conventional fast reactors with solid fuels (Nordhaus, 2013). While system-level domestic R&D efforts are focused on VHTRs, SFRs and MSRs, the materials R&D support all six Generation-IV concepts (Yang, 2014; Nordhaus, 2013).

9.5 Evolution of Generation-IV nuclear energy systems into small modular reactors and micro reactors

In recent years, relatively new, highly deployable types of nuclear reactors are gaining increasing attention—small modular reactors and micro reactors, as the most promising near-term candidates. These are smaller units with thermal power generation capabilities under 30 MW_{th} (10 MW_{el}) for micro reactors and under 1000 MW_{th} (300 MW_{el}) for small modular reactors (Gateway for Accelerated Innovation in Nuclear, 2021).

Several dozens of small modular reactors and micro reactors are under active development in the United States targeting their deployment in the next decade. These systems are expected to be highly deployable and commercially competitive.

In particular, micro reactors are going to be factory-fabricated, highly transportable, and highly adaptable to deployment domains ranging from terrestrial urban environments and emergency response areas to space power and propulsion. Emerging small modular reactors and micro reactor concepts are considered as

Generation-IV reactors. [Table 9.3](#) provides examples of emerging commercial vendors ([Gateway for Accelerated Innovation in Nuclear, 2021](#)).

9.6 Deployment perspectives for Generation-IV systems in the United States and deployment schedule

Domestic nuclear power plant owners have been applying to NRC for their license extensions since the 1990s and many got approvals to operate for additional 10 to 20 years or more beyond their original plant lifetimes. This trend extends LWRs and naturally expands the deployment need window for Generation-IV units. Construction of new units with LWRs will further extend the need for Generation-IV units. However, the clearly emerging opposing trend is also present. Some of the domestic utilities are supportive of novel Generation-IV systems and related R&D but do consider and may decommission nuclear power plants with Generation-II LWRs due to economic considerations ([Weaver, 2005](#)).

In the early 2000s, the US Department Of Energy (DOE) engaged the nuclear industry in a joint effort to establish a technical and regulatory foundation for the next generation of nuclear plants. The DOE Generation-IV (Gen IV) Program produced a 30-year roadmap of R&D efforts toward advanced nuclear power plant and fuel cycle options ([Office of Nuclear Energy, 2001](#); [U.S. DOE Nuclear Energy Research Advisory Committee and the Generation IV International Forum, U.S. Department of Energy, 2002](#); [GEN IV International Forum, 2014](#); [OECD Nuclear Energy Agency for the Generation IV International Forum, 2009](#)). The roadmap underwent several revisions and has been most recently updated in 2014 to include and address new technical issues and modifications, to reevaluate the original six concepts vs any potentially emerged new concepts meeting Generation-IV criteria, to incorporate the Fukushima Daiichi accident lessons for Generation-IV systems, as well as to include the 10-year technology demonstration horizon needs ([U.S. DOE Nuclear Energy Research Advisory Committee and the Generation IV International Forum, U.S. Department of Energy, 2002](#); [GEN IV International Forum, 2014](#); [OECD Nuclear Energy Agency for the Generation IV International Forum, 2009](#); [DOE Office of Nuclear Energy, 2005](#); [U.S. DOE Office of Nuclear Energy, U.S. Department of Energy, 2012](#)).

To complement Gen IV, DOE also organized a Near-Term Deployment Group (NTDG) to examine prospects for the deployment of new nuclear plants in the United States and to identify obstacles to deployment and actions for resolution. The group commenced its work in February 2001 and evaluated a wide spectrum of factors that could affect prospects for near term deployment of new nuclear plants. The readiness and technical suitability of various new plant designs were assessed considering these designs as candidates for near term deployment as Generation III+.

In recent years, the DOE advanced reactor programs have been evaluated to make assure the R&D efforts are in line with existing and expected licensing processes ([Office of Nuclear Regulatory Research, U.S. Nuclear Regulatory Commission, 2003](#); [U.S. Nuclear Regulatory Commission, 2012](#); [Committee on Review of DOE Nuclear Energy Research and Development Program et al., 2007](#); [Idaho National Laboratory, 2021](#)). The established DOE NE Technical Review Panel (TRP) gathered input from the nuclear industry and conducted evaluations of the eight reactor concepts ranging from Generation-III+ LWRs to Generation-IV systems—General Atomics Energy Multiplier Module (GFR), Gen4 Energy Reactor Concept (Pb-Bi fast reactor), Westinghouse Thorium-fueled Advanced Recycling Fast Reactor for Transuranics Minimization (SFR), Westinghouse Thorium-fueled Reduced Moderation BWR for Transuranic Minimization, Flibe Energy—Liquid Fluoride Thorium Reactor (MSR), Hybrid Nuclear Advanced Reactor Concept, GE-Hitachi Nuclear Energy PRISM and Advanced Recycling Center (SFR), and Toshiba 4S Reactor (SFR) ([U.S. DOE Office of Nuclear Energy, U.S. Department of Energy, 2012](#)). The reactor concepts ranged from SMRs to large power reactors. The TRP objective was to establish federal prioritization horizons based on the established state-of-the-art and industry interests.

Through DOE, in April 2001, the NTDG issued a Request For Information (RFI) seeking input from the nuclear industry and the public on nuclear plant designs that could be deployed in the near term. The eight reactor design candidates were identified by international reactor suppliers in response to the RFI as near term deployable in the United States: advanced Boiling Water Reactors (BWRs), Pressurized Water Reactors (PWRs) and High-Temperature gas-cooled Reactors (HTRs) ([U.S. DOE Nuclear Energy Research Advisory Committee and the Generation IV International Forum, U.S. Department of Energy, 2002](#); [GEN IV International Forum, 2014](#)).

Table 9.3 provides illustrations of Generation-IV reactor types, reference reactor designs and related emerging commercial vendors pursuing commercial deployment projects as well as engaged national laboratories. Effective industry-national laboratories partnerships have been formed to accelerate R&D in support of Generation-IV systems.

As early development success examples, two of the six original Generation-IV systems, ESKOM PBMR and General Atomics GT-MHR came close to meet Generation-IV reactor classification requirements early although being conceived and developed in the 1980s and 1990s. The PBMR system, as developed in South Africa, is no longer planned for construction. Domestic commercial vendors emerged in the United States and are actively developing these gas-cooled technologies ([Gateway for Accelerated Innovation in Nuclear, 2021](#)) such as:

- Prismatic-core HTR—BWXT, General Atomics, HolosGen, Hybrid Power, NuGen, Radiant, USNC;
- Pebble-bed core HTR—X-Energy.

China has been and is currently operating pebble bed reactor prototypes that may impact perspectives for this concept deployment in the United States. Japan has been operating its High-Temperature Test Reactor (HTTR), prismatic core HTR, since the late 1990s. Prior to 2010, the GT-MHR evolved into the Next-Generation Nuclear Plant (NGNP) developed up to the conceptual design level by INL.

While prospects of deploying fast reactors in the US energy markets have challenges, the domestic R&D efforts continue and the relevant technology prototypes are in operation and under construction in China, India and Russia (Nordhaus, 2013; [U.S. DOE Office of Nuclear Energy, U.S. Department of Energy, 2012](#)). TerraPower jointly with General Electric is developing its sodium-cooled fast reactor, while Westinghouse is pursuing lead-cooled fast reactor technology options ([Gateway for Accelerated Innovation in Nuclear, 2021](#)). Several emerging new commercial vendors are pursuing sodium-cooled and lead-cooled fast reactor configurations ([Gateway for Accelerated Innovation in Nuclear, 2021](#)).

There are numerous commercial vendors pursuing molten-salt-reactor technologies targeting both thermal and fast spectrum systems ([Gateway for Accelerated Innovation in Nuclear, 2021](#)). Advancements in MSR-related R&D have been dramatically accelerating deployment schedules for MSRs. The contemporary MSRs are founded on the successfully-run Molten Salt Reactor Experiment at ORNL.

The original NTDG assessed each candidate design including the design-specific gaps to near term deployment, based on information provided by the respondents. From these evaluations, the NTDG formed judgments regarding each candidate's potential for near-term deployment ([U.S. DOE Office of Nuclear Energy, U.S. Department of Energy, 2012](#)). The 2014 updated roadmap reevaluates the recommended six Generation-IV systems and extends demonstration expectation horizons to 2030 vs original 2025.

The 2014 roadmap update also incorporates the lessons learnt from the Fukushima Daiichi accident. It has been recognized that non-water coolants of Generation-IV systems offer advantages over LWRs but require further evaluations. The impact of higher operating temperatures and power densities in Generation-IV systems need to be assessed from the point of view of reliable heat removal options under extreme natural and man-made accident conditions ([GEN IV International Forum, 2014](#)). The Generation-IV systems designed for process heat applications assume collocation or integration of power, fuel cycle and process heat facilities. Accident responses of such configurations need to be evaluated.

The overall system development timelines are revised for all six systems to reflect both up-to-date accomplishments and changes in priorities ([GEN IV International Forum, 2014](#)). The updated roadmap and recent Generation-IV International Forum reports recognize that Generation-IV systems are likely to be deployed globally first and then introduced into the US energy markets ([GEN IV International Forum, 2014](#); [Generation IV International Forum, 2014](#)).

In 2020–2021, all domestic efforts to develop and deploy Generation-IV nuclear reactors have been accelerated through the US Department of Energy Advanced Reactors Development Program. This federal program is designed to assist domestic vendors through three cost-shared pathways:

- Advanced reactor demonstrations, which are expected to result in a fully functional advanced nuclear reactor within 7 years of the award.
- Risk reduction for future demonstrations, which will support up to five additional teams resolving technical, operational, and regulatory challenges to prepare for future demonstration opportunities.
- Advanced reactor concepts 2020, which will support innovative and diverse designs with potential to commercialize in the mid-2030s.

The program leverages the National Reactor Innovation Center at the Idaho National Laboratory to test and demonstrate advanced reactor technologies.

The US Department of Energy selected Terra Power and X-energy to develop and build two advanced nuclear reactors following the advanced reactor demonstration pathway. The reactors are to be operational within 7 years of the project start. TerraPower together with GE-Hitachi will be developing and demonstrating a sodium-cooled fast reactor, Natrium reactor, coupled to thermal energy storage. X-energy will be developing and demonstrating a commercial four-unit nuclear power plant based on X-energy Xe-100 pebble bed reactor design. This 7-year effort toward advanced reactor demonstrations sets the near-term domestic deployment schedule for two of the six Generation-IV reactors. Through the other two pathways, the US Department of Energy supports developments toward other advanced reactors by boosting their technology readiness levels.

9.7 Conclusions

Nuclear power plants emit no greenhouse gases and offer an opportunity to develop into a sustainable energy solution. This is of global importance for the US energy industry to meet international climate management commitments. Generation-IV reactors are of significant design development interest to the US nuclear engineering community for their superior design characteristics vs LWRs. The US Nuclear Regulatory Commission and domestic energy markets are getting ready to handle licensing requests and novel system economics and operation of advanced nuclear reactors ([Idaho National Laboratory, 2021](#); [U.S. NRC, 2007, 2021](#)). It is recognized by the domestic nuclear industry that early Generation-IV deployments will require additional financial support and it is being offered from the US DOE Office of Nuclear Energy. Development efforts and energy economics are expected to converge after 2030 and yield favorable domestic conditions for Generation-IV reactors. At that time, it is expected to see global deployments of Generation-IV systems supporting domestic licensing and marketing efforts.

References

- Araujo, K., 2014. The emerging field of energy transitions: progress, challenges, and opportunities. *Energy Res. Soc. Sci.*, 112–121. Elsevier.
- Bistline, J., James, R., 2018. “Exploring the role of advanced nuclear in future energy markets”, EPRI final report 3002011803, March 2018. Electric Power Research Institute.
- Committee on Review of DOE Nuclear Energy Research and Development Program, Board on Energy and Environmental Systems, Division on Engineering and Physical Sciences, National Research Council, 2007. Review of DOE Nuclear Energy

- Research and Development Program. Committee on Review of DOE Nuclear Energy Research and Development Program, Board on Energy and Environmental Systems, Division on Engineering and Physical Sciences, National Research Council of the National Academies, The National Academies Press, Washington, DC.
- Dean, A., Ludington, A., 2018. Program on technology innovation: owner-operator requirements guide (ORG) for advanced reactors, EPRI final report 3002011802, March 2018. Electric Power Research Institute.
- DOE Office of Nuclear Energy, 2005. Generation IV Nuclear Energy Systems Ten-Year Program Plan, Generation IV Nuclear Energy Systems, Fiscal Year 2005 Report. Office of Advanced Nuclear Research, U.S. DOE Office of Nuclear Energy, Science and Technology, U.S. Department of Energy.
- DOE Office of Nuclear Energy, September 2003. The U.S. Generation IV Implementation Strategy, 2003. U.S. DOE, Office of Nuclear Energy, Science and Technology, U.S. Department of Energy.
- Forsberg, C., Hu, L., Peterson, P., Allen, T., 2011. Fluoride-Salt-Cooled High Temperature Reactors for Power and Process Heat. U.S. DOE Integrated Research Project, U.S. Department of Energy.
- Forsberg, C., Sabharwall, P., Gougar, H., 2019. Heat storage coupled to generation IV reactors for variable electricity from base-load reactors, workshop proceedings: changing markets, technology, nuclear-renewables integration and synergisms with solar thermal power systems, INL report, September 2019, INL/EXT-19-54909. Idaho National Laboratory.
- Gateway for Accelerated Innovation in Nuclear, 2021. Advanced Nuclear Directory. Idaho National Laboratory.
- GEN IV International Forum, 2014. Technology Roadmap Update for Generation IV Nuclear Energy Systems. OECD Nuclear Energy Agency for the Generation IV International Forum. January 2014.
- Generation IV International Forum, 2014. Gen IV International Forum, Annual Report 2014. OECD Nuclear Energy Agency for the Generation IV International Forum.
- Idaho National Laboratory, 2014. Report on integrated nuclear-renewable energy systems development. Idaho National Laboratory. INL Report, INL/MIS-14-32387.
- Idaho National Laboratory, 2021. Regulatory Research Planning for Microreactor Development. Idaho National Laboratory. INL Report INL/EXT-21-61847.
- Krahn, S., Croff, A., 2017. Program on technology innovation: expanding the concept of flexibility for advanced reactors: refined criteria, an proposed technology readiness scale, and time-dependent technical information availability, EPRI final report 3002010479, November 2017. Electric Power Research Institute.
- Massachusetts Institute of Technology, 2011. Study on The Future of the Electric Grid, An Interdisciplinary MIT Study. Massachusetts Institute of Technology. ISBN 978-0-9828008-6-7.
- Nordhaus, T., Lovering, J., Shellenberer, M., 2013. How to Make Nuclear Cheap. Breakthrough Institute.
- Nuclear Regulatory Commission, 2017. A Regulatory Review Roadmap for Non-Light Water Reactors. Nuclear Regulatory Commission. NRC ML17312B567, December 2017.
- OECD Nuclear Energy Agency, 2002. Charter of the Generation IV International Forum. OECD Nuclear Energy Agency.
- OECD Nuclear Energy Agency, 2005. Framework Agreement for International Collaboration on Research and Development of Generation IV Nuclear Energy Systems. OECD Nuclear Energy Agency.
- OECD Nuclear Energy Agency, 2011. Extended Charter of the Generation IV International Forum. OECD Nuclear Energy Agency.
- OECD Nuclear Energy Agency for the Generation IV International Forum, 2009. GIF R&D Outlook for Generation IV Nuclear Energy Systems. OECD Nuclear Energy Agency for the Generation IV International Forum.
- OECD Nuclear Energy Agency for the Generation IV International Forum, 2014. Generation IV Program Implementing Agents List. OECD Nuclear Energy Agency for the Generation IV International Forum.
- Office of Nuclear Energy, 2001. A Roadmap to Deploy New Nuclear Power Plants in the United States by 2010. vols. I and II Nuclear Energy Research Advisory Committee, Subcommittee on Generation IV Technology Planning, U.S. DOE Office of Nuclear Energy, Science and Technology.
- Office of Nuclear Regulatory Research, U.S. Nuclear Regulatory Commission, 2003. Proposed Plan for Advanced Reactor Research. Office of Nuclear Regulatory Research, U.S. Nuclear Regulatory Commission.
- U.S. DOE Nuclear Energy Research Advisory Committee and the Generation IV International Forum, U.S. Department of Energy, 2002. A Technology Roadmap for Generation IV Nuclear Energy Systems. U.S. DOE Nuclear Energy Research Advisory Committee and the Generation IV International Forum, U.S. Department of Energy.
- U.S. DOE Office of Nuclear Energy, U.S. Department of Energy, 2012. Advanced Reactor Concepts, Technical Review Panel Report, Evaluation and Identification of Future R&D on Eight Advanced Reactor Concepts, December 2012. U.S. DOE Office of Nuclear Energy, U.S. Department of Energy.
- U.S. NRC, 2007. Feasibility Study for a Risk-Informed and Performance-Based Regulatory Structure for Future Plant Licensing. vol. 1 U.S. Nuclear Regulatory Commission. Main Report, NUREG-1860.

- U.S. NRC, 2021. White Paper on Micro-Reactors Licensing Strategies. U.S. Nuclear Regulatory Commission. White Paper, ADAMS Accession ML21235A418.
- U.S. Nuclear Regulatory Commission, August 2012. Report to Congress: Advanced Reactor Licensing, 2012, U.S. NRC. U.S. Nuclear Regulatory Commission.
- Weaver, K., 2005. Future nuclear energy systems: generation IV. In: 50th Annual Meeting of the Health Physics Society, July 11, 2005, Spokane, Washington, USA.
- Yang, W.S., 2014. Advances in Reactor Concepts: Generation IV Reactors, Research Workshop on Future Opportunities in Nuclear Power, October 16–17, 2014. Purdue University.

Further reading

- Generation IV International Forum, 2016. Gen IV International Forum, Annual Report 2016. OECD Nuclear Energy Agency for the Generation IV International Forum.

10

Generation IV: European Union

Breakthrough technologies to improve sustainability,
safety & reliability, socio-economics and proliferation resistance

Georges Van Goethem

Former Principal Scientific Officer at the European Commission, DG Research and Innovation, Dir.
Energy, Unit Euratom—Fission, Brussels, Belgium

Nomenclature—Acronyms and abbreviations

ALFRED	Advanced Lead Fast Reactor European Demonstrator (project)
ALLEGRO	Gas Cooled Fast Reactor demonstrator (project)
ASTRID	Advanced Sodium Technological Reactor for Industrial Demonstration
BOOT	Build-Own-Operate-Transfer
CAPEX	CAPital EXpenditures
DG	Directorate General (33 departments in the European Commission/EC/)
E&T	Education & Training
EFSI	European Fund for Strategic Investments
EGE	European Group on Ethics in Science and New Technologies
EMWG	Economics Modeling Working Group (GIF methodology)
ENEN	European Nuclear Education Network
ENSREG	European Nuclear Safety Regulators Group
ESNII	European Sustainable Nuclear Energy Industrial Initiative
EIT	European Institute of Innovation and Technology
ETIP	European Technology and Innovation Platforms (stakeholder groups)
EU	European Union (27 member states)
EUR	European Utility Requirements
Euro	European currency (1 Euro = 1.11 US Dollar, average over year 2020)
FISA	series of Euratom conferences on RTD and JRC results in Fission SAFETY
GIF	Generation-IV International Forum
INPRO	IAEA INTERNATIONAL PROJECT on Innovative Nuclear Reactors and Fuel Cycles
ISAM	Integrated Safety Assessment Methodology (GIF)
JHR	Jules Horowitz Reactor (CEA Cadarache, south-eastern France)
JRC	Joint Research Centre (“science for policy,” EC Directorate General)
KSC(A)	Knowledge, Skill and Competences (Attitudes)
LERF	Large Early Release Frequency
LUEC	Levelized Unit Energy Costs
MA	Minor Actinides (e.g., neptunium (Np), americium (Am), curium (Cm))

MEUR	Million Euros (see Euro value 2020 above)
MS	Member State
MYRRHA	Multipurpose Hybrid Research Reactor for High-technology Applications (accelerator-driven system under construction at SCK-CEN, Mol, Belgium)
NC2I	Nuclear Cogeneration Industrial Initiative (part of SNETP)
NGEU	Next Generation EU fund 2020
NGO	Non-Governmental Organization
NPP	Nuclear Power Plant
NPT	Treaty on the Non-proliferation of Nuclear Weapons (IAEA 1970)
NRG	Nuclear Research and Consultancy Group (Petten, the Netherlands)
NUGENIA	NUclear GENeration-II & -III Association (part of SNETP)
PALLAS	Research reactor (thermal neutrons) under construction in Petten (NL)
PIRT	Phenomena Identification and Ranking Table
PR&PP	Proliferation Resistance and Physical Protection group (GIF methodology)
RATEN-ICN	Regiei Autonome Tehnologii pentru Energia Nucleară—Institutul de Cercetari Nucleare—Pitesti (national nuclear institute of Romania)
R&D	Research and Development
RD&DD	Research-Development & Demonstration-Deployment
RSWG	Risk and Safety Working Group (GIF methodology)
RTD	Research and Technological Development (one of the DGs in the EC)
3S	Safety, Security and Safeguards (nexus—3 disciplines related to nuclear)
SCK-CEN	StudieCentrum voor Kernenergie—Centre d'Étude de l'énergie Nucléaire (nuclear research center, Mol, Belgium)
SDG	Sustainable Development Goals—17 in total—UN 2030 Agenda (2015)
SET Plan	“Strategic Energy Technology” Plan (EU, 2008)
SMR	Small and Medium nuclear power Reactors (also called “Modular”)
SNF	Spent Nuclear Fuel
SNETP	Sustainable Nuclear Energy Technology Platform (ETP)
SRA	Strategic Research Agenda
STC	Scientific and Technical Committee (Euratom Treaty—Articles 4, 7 and 8)
TMI	Three Mile Island
TSO	Technical Safety Organization (usually associated with nuclear regulator)

*Se défier du ton d'assurance qu'il est si facile de prendre et si dangereux d'écouter.
Beware of the tone of assurance that is so easy to take and so dangerous to listen to.*

*Charles Coquebert de Montbret, scholar and state clerk, professor of mining statistics at the École des mines, Paris, 1755–1831
(Journal des mines n°1, Vendémiaire An III—i.e.: September 1794—<http://Annales.org>).*

10.1 Introduction: “EU Energy Union” (2015) and “EU Green Deal” (2020)—Going climate neutral by 2050—Euratom contribution

10.1.1 Total of 106 nuclear power reactors in the EU (= 26% of gross electricity production)

The European Union (EU)^a covers a total land area of over 4.23 million km² and has a combined population of approximately 450 million inhabitants as of June 2021 (27 Member States/MS/—reminder: The United Kingdom withdrew on January 31, 2020).

^a “Fact Sheets on the European Union” (European Parliament)—designed to provide non-specialists with a straightforward overview of the EU’s policies—<https://www.europarl.europa.eu/factsheets/en/home>.

In the EU, nuclear fission falls under the Euratom Treaty (“European Atomic Energy Community,” signed in 1957 in Rome)^b which is one of the founding Treaties of the EU.

Nuclear is a major contributor already today as a low-carbon technology in the EU’s strategy to reduce its fossil fuel dependency and to fulfill its 2020/2030/2050/COP21 energy and climate policy objectives.

The EU is a major player in the world of nuclear fission. As of 2020, a total of 106 units are operable in 13 of the 27 of the EU Member States, that is: Belgium (7 units), Bulgaria (2), the Czech Republic (6), Germany (6), Spain (7), France (56), Hungary (4), the Netherlands (1), Romania (2), Slovenia (1), Slovakia (4), Finland (4) and Sweden (6). The 106 nuclear power reactors (104 GWe net, 15,300 tons uranium required yearly) account for over one-quarter of the electricity generated in the whole of the EU. Over half of the EU’s nuclear electricity is produced in only one country—France (61 GWe net). Moreover, the European nuclear industry sustains more than 1.1 million jobs in the EU and generates more than 100 billion euros per year in GDP, according to a 2019 study by Deloitte.

At the end of 2019, above EU countries represented a gross nuclear electricity generation of 732 TWh (i.e., 26% of gross electricity production in the EU). Five among those countries (Bulgaria, the Czech Republic, Finland, Hungary, and Slovakia) operate 18 Russian-designed VVER reactors with a total electricity output of 80 TWh, which corresponds to approximately 11% of nuclear electricity generation in the EU.

As of June 2021, it should be noted that 4 reactors are under construction in the EU (1 in Finland/EPR—1600 MW_{el} at Olkiluoto/, 1 in France/EPR—1650 MW_{el} at Flamanville/and 2 in Slovakia/two V-213+ of 471 MW_{el} each, at Mochovce 3 and 4/), while 13 reactors are planned (6 in Poland, 2 in Hungary, 2 in the Czech Republic, 2 in Romania and 1 in Finland—16 GWe gross capacity in total) and a further 8 reactors have been proposed.

World-wide, around 10% of the world’s electricity is generated by about 440 nuclear power reactors operating in 32 countries plus Taiwan, with a combined electrical capacity of about 400 GWe. In 2019, nuclear plants supplied 2657 TWh of electricity, up from 2563 TWh in 2018. As of June 2021, about 50 power reactors are being constructed in 16 countries (notably China, India, Russia and the United Arab Emirates) with a combined capacity of 57 GWe, equivalent to approximately 15% of existing capacity. About 100 power reactors with a total gross capacity of about 110 GWe are on order or planned, and over 300 more are proposed. Most reactors currently planned are in Asia, with fast-growing economies and rapidly-rising electricity demand. It should be noted that Russia and China have taken the lead in offering Nuclear Power Plants (NPPs) to emerging countries (approximately 30 in total), usually through state-owned nuclear companies with finance and fuel services.

10.1.1.1 District heating and industrial heat applications world-wide

It is worth discussing non-electric applications of nuclear fission in the world. Russia, several East European countries, Switzerland and Sweden have all had nuclear-fuelled district heating schemes. Heat from NPPs has also been sent to industrial sites in several countries. In 2019, 71 nuclear power reactors in 11 countries utilized 2146 GWh (gigawatt-hours) of electrical equivalent heat to support non-electric applications of nuclear energy such as for district heating, process heat supply (including chemicals refinement and hydrogen production) or seawater desalination purposes. As NPPs supplied 2657 TWh of electricity world-wide in 2019, non-electric applications represent only 0.8‰. About 88% of that heat was supplied by 57

^b “Consolidated version of the Treaty establishing the European Atomic Energy Community (Euratom)” OJ C 327, 26.10.2012: <https://eur-lex.europa.eu/legal-content/EN/TXT/?uri=CELEX:12012A/TXT>—see also “50 years of the Euratom Treaty—Communication from the Commission to the Council and the European Parliament” COM/2007/0124/, 20 March 2007—(EU Monitor’s view on how to improve future action)—https://www.eumonitor.eu/9353000/1/j4nvhdhcs8bljza_j9vvik7m1c3gyxp/vikqhl1ogox3.

reactors in Europe and 12% by 14 reactors in Asia. Further, 10 reactors supported seawater desalination (using 48 GWh), 56 reactors supported district heating (1871 GWh) and 32 reactors supported industrial heat applications (1248 GWh). Source: IAEA and WNA.

NB—In Europe, the low carbon hydrogen production through electrolysis using nuclear power could be the most economical way to achieve the hydrogen productivity levels foreseen by the EU Hydrogen strategy (as part of the EU Green Deal 2020).

10.1.1.2 Good health and well-being (SDG 3-2030 Agenda, United Nations/UN/2015)

The 17 Sustainable Development Goals (SDGs) are integrated and indivisible and balance the three dimensions of sustainable development: the economic, social and environmental. The use of nuclear technology in medicine (SDG 3) has become one of the most widespread uses of nuclear energy in the non-electric sector.^c Nuclear techniques play an important role in diagnosing and treating various health conditions, in particular non-communicable diseases. Reminder—The fission of Uranium-235 (U-235) produces a spectrum of fission products including Molybdenum-99/Mo-99/(as well as I-131 and Xe-133). More than 80% of all nuclear medicine Single Photon Emission Computerized Tomography (SPECT) scans used each year to detect diseases like cancer and cardiovascular diseases require Technetium-99m (Tc-99m)—the most widely used radioisotope in radiopharmaceuticals. Tc-99m is the decay product of Mo-99, which is mainly generated in research reactors (usually using proliferation-sensitive “highly enriched uranium”/HEU/).

10.1.2 EU’s ambition to become the world’s 1st major economy to go climate neutral by 2050

Euratom is not isolated in the EU policies. Nuclear fission is part of the European energy mix,^d together with the two other primary energy sources: renewable and fossil.

Remember Article 194 of the Lisbon Treaty^e (signed in 2007, entered into force in 2009):

“Union policy on energy shall aim, in a spirit of solidarity . . . : .. Such measures shall not affect a Member State’s right to determine the conditions for exploiting its energy resources, its choice between different energy sources and the general structure of its energy supply.”

The EU energy and climate strategy during the coming decades is defined in the “EU Energy Roadmap 2050” (issued in 2011) which originally proposed several scenarios toward a low-carbon economy, based on a balance between sustainable development, security of supply and industrial competitiveness. Two messages are important for the nuclear fission sector at horizon 2050. Firstly, one of the “decarbonization scenarios” is based on a 20% share of electricity generation by nuclear fission, which represents an equivalent operating capacity of 127 GWe, to be compared to today’s total nuclear generation of 104 GWe. Secondly, the general conclusion for all “decarbonization scenarios” (still valid today) is that electricity will play a much greater role than now (almost doubling its share in final energy demand, from 21% today to 40% in 2050).

^c IAEA website—17 Sustainable Development Goals (SDGs) set out in the UN 2030 Agenda—nuclear development in areas such as: energy, human health, food production, water management and environmental protection—<https://www.iaea.org/about/overview/sustainable-development-goals>.

^d EC DG (Directorate General) ENERGY programmes related to Nuclear safety; Radioactive waste and spent fuel; Radiation protection; Decommissioning of nuclear facilities; Safeguards to avoid misuse; Security (non-proliferation and physical protection): <http://ec.europa.eu/energy/en/topics/nuclear-energy>.

^e Treaty of Lisbon amending the Treaty on European Union and the Treaty establishing the European Community—<https://eur-lex.europa.eu/legal-content/EN/TXT/?uri=CELEX%3A12007L%2FTXT> (in general, summaries of EU Legislation: <http://eur-lex.europa.eu/browse/summaries.html>).

The “EU Energy Union Package” (2015): secure, sustainable, competitive and affordable energy.

In February 2015, EC President Jean-Claude Juncker (in office during 2014–2019) presented the overall EU energy strategy in the “Energy Union Package,”^f aiming at building an energy union that gives EU consumers—households and businesses—secure, sustainable, competitive, and affordable energy.

The above Energy Union Package is based on five closely related and mutually reinforcing objectives:

- *Security, solidarity and trust*—diversifying Europe’s sources of energy and ensuring energy security through solidarity and cooperation between EU countries.
- *A fully integrated internal energy market*—enabling the free flow of energy through the EU through adequate infrastructure and without technical or regulatory barriers.
- *Energy efficiency*—improved energy efficiency will reduce dependence on energy imports, lower emissions, and drive jobs and growth
(NB: in the EU in 2019, the dependency rate was equal to 61%, which means that more than half of the EU’s energy needs were met by net imports).
- *Climate action, decarbonizing the economy*—the EU is committed to the 2015 Paris Agreement (NB: draft in December 2015 and formal entry into force on November 4, 2016) and to retaining its leadership in the area of renewable energy.
- *Research, innovation and competitiveness*—supporting breakthroughs in low-carbon and clean energy technologies by prioritizing research and innovation to drive the energy transition and improve competitiveness.

Here are two excerpts related to nuclear fission in the above 2015 Energy Union Package:

- *putting the EU at the forefront of ... all innovative energy technologies ..., including ... the world’s safest nuclear generation, is central to the aim of turning the Energy Union into a motor for growth, jobs and competitiveness.*
- *The EU must ensure that ... it maintains technological leadership in the nuclear domain, including through ITER, so as not to increase energy and technology dependence.*

An important preliminary step in the European Energy policy was made on January 13, 2015, when the EU adopted the “European Fund for Strategic Investments” (EFSI),^g which is at the very heart of the 315 billion euros Investment Offensive of EC president J C Juncker. The EFSI was the central pillar of the Investment Plan for Europe in the mid-2010s. EFSI aimed originally to tackle the lack of confidence and investment which resulted from the economic and financial crisis, and to make use of liquidity held by financial institutions, corporations and individuals at a time when public resources were scarce. The EFSI was mobilizing public and private investments in the real economy in areas including infrastructure, energy efficiency and renewable energy, research and innovation, environment, agriculture, digital technology, education, health and social projects. To reach these goals, the Commission works together with the European Investment Bank (EIB), which is also used to help small businesses to start up and to grow.

A few years later (in 2018), the European Commission presented an updated strategic vision showing how it could lead the way to climate neutrality by investing in realistic technological solutions, empowering citizens, and aligning action in key areas such as industrial policy, finance, or research—while ensuring

^f ENERGY UNION PACKAGE/Communication from the EC to the European Parliament, The Council, the European Economic and Social Committee, the Committee of the Regions and the European Investment Bank (COM(2015) 80, Brussels, 25.2.2015) “A Framework Strategy for a Resilient Energy Union with a Forward-Looking Climate Change Policy”—<http://www.consilium.europa.eu/en/policies/energy-union/>.

^g EC priority—Investment Plan—https://ec.europa.eu/info/strategy/priorities-2019-2024/economy-works-people/jobs-growth-and-investment/investment-plan-europe/european-fund-strategic-investments-efsi_en.

social fairness for an equitable transition. This was the subject of the EC Communication “*A Clean Planet for all*” which stated, in particular, that “*renewable energies together with a nuclear power share of ca. 15%, (...) will be the backbone of a carbon-free European power system*” in 2050.^h

Moreover, as far as nuclear is concerned, the following messages could be derived from the above 2018 EC Communication “*A Clean Planet for all*”:

- nuclear will remain an important component in the EU 2050 energy mix,
- the capacity of nuclear in 2050 could be between 99 and 121 GWe, and
- in the baseline, hydrogen use develops mainly for transport, industry (e.g. fertilizers) and power generation.

NB: According to Foratom (the Brussels-based trade association for the nuclear energy industry in Europe), in the longer run with 15% nuclear generation foreseen in 2050, most of the existing fleet will have to be renewed.

The 2020 (fifth) report on the State of the Energy Union COM (2020)950ⁱ is the first such report since the adoption of the European Green Deal (European Parliament, January 15, 2020, discussed further down). It looks at the energy union’s contribution to Europe’s long-term climate goals. It highlights how the “Next Generation EU” recovery plan can support EU countries through a number of flagship funding programs, especially through energy-related investments and reforms.

Here is an excerpt of this 2020 report on the Energy Union, related to nuclear fission:

On nuclear safety and security, the EU has a comprehensive framework that covers the full nuclear life cycle, including the safe and responsible management of spent fuel and radioactive waste. The Commission has continued to carefully monitor the implementation of this framework in Member States. The EU has also continued to promote high levels of nuclear safety outside the EU, particularly in neighboring countries that operate or plan to build NPPs. This includes support in conducting stress tests and follow up to promote proper and transparent implementation of recommendations.

The EU Green Deal (2020): toward a European climate-neutral economy by 2050.

On December 1, 2019, Ms. Ursula von der Leyen, the current President of the European Commission (in office until the 2024 elections), took office with a new program focused on six main priorities: (1) a European Green Deal; (2) an economy that works for people; (3) a Europe fit for the digital age; (4) a protection of the European way of life; (5) a stronger Europe in the world; and (6) a new push for European democracy.

On December 11, 2019, The EC issued a communication that sets out the European Green Deal^j for the European Union and its citizens, toward a European climate-neutral economy by 2050, aimed at mobilizing at least 1 trillion euros of public/private investment over the course of 10 years to achieve net zero greenhouse gas emissions for EU countries as a whole. Several initiatives have been launched by the EC in the frame of the implementation of this EU Green Deal. The most important initiative is the EC’s proposal to cut greenhouse gas emissions by at least 55% below 1990 levels by 2030. This is a substantial increase compared to the existing target, upward from the previous target by at least 40%. It is in line with the 2015 Paris Agreement objective to keep the global temperature increase to well below 2°C, and pursue efforts to keep it to 1.5°C.

^h “A Clean Planet for all—A EU strategic long-term vision for a prosperous, modern, competitive and climate neutral economy” COM (2018) 773—https://ec.europa.eu/clima/policies/strategies/2050_en and “EC Staff Working Document supporting in-depth analysis” (393 pages)—Brussels, 28/11/2018—https://ec.europa.eu/clima/sites/clima/files/docs/pages/com_2018_733_analysis_in_support_en_0.pdf.

ⁱ “Fifth report on the state of the energy union”, including the national energy and climate plans, EC, 14 Oct 2020—https://ec.europa.eu/energy/topics/energy-strategy/energy-union/fifth-report-state-energy-union_en.

^j EU climate action and the EU Green Deal—https://ec.europa.eu/clima/policies/eu-climate-action_en.

10.1.3 Energy transition toward climate neutrality: EU's support for "green" technologies

Next Generation EU fund 2020 (NGEU): what are sustainable "green" economic activities?

The Next Generation EU (NGEU) fund is a European Union recovery package to support the Member States after the COVID-19 pandemic, thereby preparing a better future for European next generation. Initiated by EC President Ursula von der Leyen and agreed to by the EU Council on July 21, 2020, the fund is worth 750 billion euros (in fact, 360 billion euros in loans and 390 billion euros in grants). The NGEU breaks away from the austerity policy adopted after the 2008 financial crisis as the EU's main response to economic crises. The NGEU fund will be tied to the regular 2021–2027 budget of the EU's 2027 Multiannual Financial Framework (MFF) which amounts to 1074.3 billion euros. Hence, the comprehensive NGEU and MFF packages are projected to reach 1824.3 billion euros.

The EU has launched the above COVID-19 recovery plan for several objectives. The primary objective is to help its Member States to repair the immediate economic and social damages caused by the coronavirus pandemic.

Secondly, alongside tackling the economic and social impacts of the pandemic, the plan has other objectives. It also aims to assist the green transition, digital transformation, smart, sustainable, and inclusive growth and jobs, social and territorial cohesion, health and resilience, policies for the next generation, including education and skills.

The third objective of the NGEU is modernizing the EU infrastructure. Therefore, more than 50% of support for the plan will be spent on modernization. Such as: research and innovation, via Horizon Europe; fair climate and digital transitions, via the Just Transition Fund and the Digital Europe Programme; preparedness, recovery and resilience, via the Recovery and Resilience Facility; and a new health program, EU4Health.

EU green Taxonomy: technical assessment of nuclear energy with respect to the "Do No Significant Harm" (DNSH) criteria.

The European Commission intends to strongly link the above recovery plan NGEU to the need to fight climate change with the objective of reducing greenhouse gas emissions. The NGEU approach is in line with the objectives of the 2020 EU Green Deal, the flagship initiative to address the climate emergency that seeks to make of the EU the global leader on climate change and achieve carbon neutrality by 2050. For example, there is a general agreement on the cross-cutting lifecycle emissions threshold of 100 g CO₂ equivalent/kWh. Moreover, an overall climate target of 30% will apply to the total amount of expenditure from the MFF and NGEU in compliance with the 2015 Paris climate accord.

In this context, the EU Council and Parliament adopted in June 2020 a regulation (EU-2020/852—the so-called "EU green Taxonomy") that establishes the general framework for determining whether an economic activity qualifies as environmentally sustainable. The purpose is to define the degree to which an investment may be environmentally sustainable. The regulation empowers the Commission to establish, for each of the environmental objectives laid down in that regulation, the technical screening criteria for determining the conditions under which specific economic activities qualify as contributing substantially to that objective and ensuring that those economic activities Do Not cause Significant Harm (DNSH) to any of the other environmental objectives.

The EU green Taxonomy is a green classification system that translates the EU's climate and environmental objectives into criteria for specific economic activities for investment purposes. This EU green Taxonomy is the world's first-ever "green list" classification system for sustainable economic activities. As a result of this taxonomy, there is no risk of greenwashing: the industrial and economic activities are classified according to their ecological impact and investments are directed toward projects that are recognized as "sustainable" through the recognition of a "green label."

All technologies, with the exception of power generation activities using solid fossil fuels, have been assessed based on life cycle considerations, as well as in accordance with the additional requirements that

apply to so-called transition activities. Appropriate technical screening criteria have been developed including to avoid “significant harm” (including with regard to the disposal of waste). The separate classification of energy technologies (which all together in the EU account for about 22% of direct greenhouse gas/GHG/emissions), deserving of the green label and therefore of being financed by the NGEU, is the subject of heated debate, especially when it comes to natural gas and nuclear energy (as well as agricultural activities).

As part of the political compromise reached, neither natural gas, nor nuclear energy were explicitly included or excluded from the first list (the so-called first Delegated Act). The Commission stated in April 2021, that it will issue by the end of 2021 a complementary Delegated Act covering nuclear energy “subject to and consistent with the results” of a review process that is underway in accordance with above Taxonomy Regulation.

A key milestone in that process was a nearly 400-page report issued in March 2021 by the Joint Research Centre (JRC), called JRC Report on DNSH.^k JRC is the EU’s technical in-house science and knowledge body. This report concludes that nuclear energy “Does No Significant Harm” (DNSH) to the environment. Indeed, the subject JRC report states:

“there is no science-based evidence that nuclear energy does more harm to human health or to the environment than other electricity production technologies already included in the EU Taxonomy as activities supporting climate change mitigation.”

With regard to nuclear waste specifically, the JRC revealed a broad scientific consensus that the EU’s current disposal strategy, which places high-level, long-lived radioactive waste inside deep geologic formations, is considered an appropriately safe means of isolating radioactive waste from the biosphere in the long-term. The JRC report drew comparisons to the sequestration of carbon dioxide in carbon capture and sequestration technology, when discussing long-term disposal of radwaste in geological facilities.

Many organizations welcomed the publication of this DNSH report by JRC which provides a technical basis for the political debate to move forward on climate change mitigation solutions. *This may be a sign that science (and not politics) is finally driving the EU Taxonomy.* This landmark JRC report is under review by two other expert groups, the Euratom Article 31 experts’ group and the Scientific Committee on Health, Environmental and Emerging Risks (SCHEER), both composed of radiation protection and public health experts. The review is targeted for completion by the end of 2021.

10.2 EURATOM: Research & training; safety of nuclear installations; health and safety (radiation protection); safeguards; radwaste management

10.2.1 EURATOM—Brief history (21st century challenges) and links with IAEA and OECD/NEA

The Treaty establishing the European Atomic Energy Community (the Euratom Treaty) was signed in 1957 by the six founding States of the European Union (Belgium, France, Germany, Italy, Luxembourg and the Netherlands) who joined together to form Euratom. The Euratom Treaty is dedicated to peaceful and sustainable applications of nuclear fission.

Originally, in the mid-1950s, the Euratom Treaty proposed NPPs as part of the solution to the energy crisis in Western Europe. It should be noted that, already at that time, security of energy supply was a concern. Remember the oil crisis in 1956 due to the closure of the Suez Canal. Moreover, in the fossil energy sector (in particular, in coal mines), severe accidents with many casualties were also a concern: remember still in 1956, the major mining disaster in Marcinelle, Belgium, with a total of 262 miners killed (a.o. Italian, Moroccan, Spanish, Polish, Greek and Turkish victims).

^k “Technical assessment of nuclear energy with respect to the ‘do no significant harm’ criteria of Regulation (EU) 2020/852 (‘Taxonomy Regulation’), EC JRC report 124,193, Petten, 29 March 2021 https://ec.europa.eu/info/sites/default/files/business_economy_euro/banking_and_finance/documents/210329-jrc-report-nuclear-energy-assessment_en.pdf.

Before the European integration was finalized, there had been the Founding Treaties: the Treaty of Paris in 1951 ECSC (European Coal and Steel Community) and the two Treaties of Rome in 1957—EEC (European Economic Community) and Euratom (European Atomic Energy Community). In 1967 they were all merged to become later the European Union. While the first two ended, Euratom is left unchanged and only was added as a protocol to the new EU Treaty (Lisbon Treaty 2009).

The Euratom Treaty had originally set highly ambitious objectives, including the “speedy establishment and growth of nuclear industries.” In other words: the Treaty was developed at the end of the 1950s to foster nuclear energy with governmental funds. However, at the beginning of the 21st century, owing to the complex and sensitive nature of the nuclear sector, which touches on social acceptance in some Member States and on vital interests (defense and national independence), those ambitions had to be scaled back. Remember: *Nuclear energy is the energy that generates most emotion per MWh produced!*

Other important objectives of the Euratom Treaty are the promotion of research and dissemination of knowledge (training); safety of nuclear installations; health and safety (in particular, radiation protection in connection with ionizing radiation); safeguards (security); as well as radioactive waste management. As far as security of energy supply is concerned, the Euratom Treaty is also aiming at (1) ensuring that all users in the Community receive a regular and equitable supply of ores and nuclear fuels and (2) exercising the Community’s right of ownership with respect to special fissile materials.

The Euratom Community works in synergy with its own institutional laboratories (i.e., the Joint Research Centre/JRC/) and with national programs in the EU Member States dedicated to applications of nuclear fission and ionizing radiation. Equally important is international collaboration outside the EU frontiers, in industrialized countries or in emerging countries using, considering, planning or starting nuclear power programs.

Euratom policies of course are closely related to the two most important international organizations dedicated to nuclear fission and radiation protection:

- (1) the UN/IAEA (International Atomic Energy Agency, created in 1957, headquarters in Vienna—173 member states world-wide) and
- (2) the OECD/NEA (Organization for Economic Co-operation and Development/Nuclear Energy Agency, created in 1972, headquarters in Paris—34 member states from Europe, North America and the Asia-Pacific region).

Of particular importance in the Euratom safeguards policy is to share the objective of IAEA: to deter the spread of nuclear weapons by the early detection of the misuse of nuclear material or technology. In this context it is worth recalling that the European Union (in particular, Euratom) has the power to establish legally-binding acts (Euratom Directives) with regard to the safety of nuclear facilities as well as radiation protection and security and safeguards. IAEA may only make non-binding recommendations in its Nuclear Security Reports, while the EU may impose direct sanctions on nuclear operators whenever they have been violating the nuclear safeguards framework. Similarly, the OECD/NEA helps to establish the global framework of guidance, standards and best practices through non-binding recommendations in their domain of competence.

World-wide, besides supply of energy for an ever-growing world population, a number of other challenges in the energy domain are emerging, especially the issue of sustainability in connection with the UN Sustainable Development Goal no 7 (SDG-7) which calls for “affordable, reliable, sustainable and modern energy for all” by 2030.

More generally, energy is an enabler to foster economic development and to perform many actions required for overall development of societies. SDG-7 specifically is aiming at:

- (1) decarbonizing the global economy (connected to protecting the environment)
- (2) providing easy access to energy for all (connected to global population growth)
- (3) ensuring a stable supply of affordable energy for industry and households (connected to improving economy and increasing everyone’s standard of living).

The focus on sustainability in Euratom programs goes together with a better governance structure in the decision-making process. Also important is public information and engagement in energy policy issues, notably in connection with nuclear decision making.

Euratom research, innovation, and education programs are well aware of the importance of good governance. As a consequence, the major stakeholder groups of nuclear fission and radiation protection are brought together within the “Sustainable Nuclear Energy Technology Platform” (SNETP) which is one of the so-called “European Technology and Innovation Platforms” (ETIPs) and within the “European Energy Research Alliance” (EERA) which is a key player in the European Union’s “Strategic Energy Technology” (SET) Plan and the Clean Energy Transition (more information further down).

The major stakeholder groups concerned with nuclear energy in the EU are:

- research organizations (e.g., from public and private sectors)
- systems suppliers (e.g., nuclear vendors, engineering companies)
- energy providers (e.g., electrical utilities and associated fuel cycle industry)
- Technical Safety Organizations (TSO) associated with nuclear regulatory authorities
- academia and higher education and training institutions dedicated to nuclear
- civil society (e.g., policy makers & opinion leaders), NGOs, citizens’ associations.

The above stakeholder groups are instrumental, in particular, in the design of the Euratom research and innovation programs (the current one 2021–2025 is discussed below). They encourage, in particular, the scientific community to participate in collaborative projects wherever appropriate. It is clear that, in this collaboration, the participating TSOs adhere strictly to their prescribed roles, powers and independence as a support to the national regulators in decision making. Moreover, non-EU research organizations are welcome to join Euratom projects provided that their scientific contribution brings clear added value to the project and that they pay the full costs of their participation.

It should be noted that in the EU, socioeconomics is at the heart of many policies. In this context, it is no wonder that the EU Council at their meeting of June 28, 2011, requested that the EC “*organise a symposium in 2013 on the benefits and limitations of nuclear fission for a low carbon economy. The symposium will be prepared by an interdisciplinary study involving, inter alia, experts from the fields of energy, economics and social sciences.*” As a consequence, a “*2012 Interdisciplinary Study*” was launched in April 2012, composed of two parts (scientific-technological and sociopolitical) and published on the occasion of and presented at the 2013 “Symposium on the benefits and limitations of nuclear fission for a low carbon economy” (Brussels, February 26–27, 2013).¹

An *Ethics study* covering all primary energy sources was also conducted in this context and was published in the proceedings of the above 2013 Symposium as well as in a separate EC/EGE document. The title of the *Ethics study* is “*Ethical framework for assessing research, production, and use of Energy.*” It was issued on January 16, 2013, and referred to as “Ethics Opinion no. 27.” This *Ethics study* advocates a fair balance between four criteria in the light of *social, environmental and economic* concerns.^m The four criteria of the *Ethics study* are: (1) *access*

¹ 2012 Study—coorganized by European Commission and European Economic and Social Committee (EESC)—https://www.eesc.europa.eu/sites/default/files/resources/docs/nucf_p_wip14_17june13.pdf and synthesis report available in the Publications Office of the EU (194 pages—free of charge)—<https://op.europa.eu/en/publication-detail/-/publication/e92b20be-9163-4aee-b469-87828b10c0f1>.

^m “*Ethical framework for assessing research, production, and use of Energy*”, Brussels, 16 January 2013—EC/EGE study—<https://publications.europa.eu/en/publication-detail/-/publication/44f7f1fa-eb0c-44e7-9a75-45377d5abd73/language-en>—Note on EC/EGE. The *European Group on Ethics in science and new technologies* (EGE) was asked by EC President Mr. José Manuel Durão Barroso (in office from 2004 to 2014) on 19 December 2011 to contribute to the debate on a sustainable energy mix in Europe by studying the impact of research into different energy sources on human well-being.

to energy as a human right; (2) security of EU energy supply; (3) sustainability/environmental responsibility; (4) safety, imminent, indirect and long term. The authors also insist on more science-based support for EU energy policy. For example, one of the key messages reads: “*Proper impact assessment methodologies to compare the security and safety of the energy mix technologies are necessary.*”

10.2.2 EURATOM legal framework—The most stringent safety requirements in the world

The EU became the first major regional actor with a legally binding regulatory framework for nuclear safety following implementation of the Euratom Directives on safety (2014), waste management (2011) and basic safety standards (2013). As a consequence, today, all 27 EU Member States meet equally high standards of safety, radiation protection, safeguards and security.

Not surprisingly, the above statements from the “Energy Union Package” (2015) regarding nuclear safety and EU technological leadership in the nuclear domain were at the heart of the three important Euratom Directives discussed below.

Particularly important are the lessons drawn from the three severe accidents that happened: during the last five decades: Three Mile Island/TMI/1979 in the United States (INES scale 5); Chernobyl 1986 in the former Soviet Union (INES 7); Fukushima 2011 in Japan (INES 7).

NB: INES is the “International Nuclear and Radiological Event Scale,” introduced by IAEA and OECD/NEA in 1990 as a tool for promptly communicating the safety significance of reported nuclear and radiological incidents and accidents (7 levels).

In short, the following lessonsⁿ were drawn in the nuclear energy sector world-wide:

- TMI 1979: need for more robust safety assessment methods (deterministic versus probabilistic approaches) and importance of human failures
- Chernobyl 1986: implementation of safety culture and development of laws and regulations related to safety and health at work (IAEA and Euratom)
- Fukushima 2011: design against Beyond Design Basis (BDB) accidents (design extension) and independence of national regulatory authorities (to be required by law).

Particularly important is the *revised 2014 Euratom Safety Directive*^o which introduces the following legally binding requirements for the safety of nuclear installations:

- a high-level “Nuclear Safety Objective for Nuclear Installations” avoiding radioactive releases (including *the practical elimination of accident situations with core melt which would lead to large early releases*)—*the most stringent safety goal in the world*
- instigation of topical peer reviews by competent regulatory authorities every 6 years (focusing on safety issues)
- an obligation to ensure transparency of regulatory decisions and operating practices, as well as an obligation to foster public participation in the decision-making process

ⁿ “Root Causes and Impacts of Severe Accidents at Large Nuclear Power Plants,” Lars Högberg, *Ambio* (courtesy of Springer), 2013 April; 42(3), 267–284—National Center for Biotechnology Information, U.S. National Library of Medicine—<https://www.ncbi.nlm.nih.gov/pmc/articles/PMC3606704/>.

^o Council Directive 2014/87/Euratom of 8 July 2014 *amending Directive 2009/71/EURATOM establishing a Community framework for the nuclear safety of nuclear installations*—(L 219/42 OJ of the EU 25.7.2014)—EU-Euratom nuclear safety legislation—https://ec.europa.eu/energy/topics/nuclear-energy/nuclear-safety_en (in EC DG ENERGY website) including subject Euratom Safety Directive—<https://eur-lex.europa.eu/legal-content/EN/TXT/?uri=celex:32014L0087>.

- definition of strong and effective benchmark criteria and requirements to guarantee the effective independence of national regulators in decision-making, own appropriate budget allocations and autonomy in implementation
- establishment of a strong safety culture (*a number of indicators are also provided*)
- an obligation to obtain, maintain and further develop expertise and skills in nuclear safety, in particular, via a special effort vis-à-vis education and training.

The latter requirement actually reads as follows: “*Member States shall ensure that the national framework require all parties to make arrangements for education and training for their staff (...).*”

Equally important in this context are the legally binding standards regarding the health of workers and of the general public in the 2013 Euratom “*Basic Safety Standards*” (BSS) Directive^P (incorporating lessons learnt from the Fukushima accident), which provides:

- better protection of workers and of the public, also taking into account economic and societal factors, as well as of patients (e.g., radio-diagnosis and radio-therapy)
- emergency preparedness and response (“Emergency exposure situations”)—*in the EU Member States there are variations in the levels of dose at which specified actions are required (evacuation, sheltering, iodate tablets, etc.)*
- an obligation to ensure transparency (communication with external parties).

Worth noting is that the above BSS Directive includes social, legal and ethical aspects in addition to purely technical considerations. As a way of comparison, in the US approach to safety objectives until recently, the emphasis was placed on mortality and direct monetary costs of in- or off-site consequences, i.e.: Cost Benefit Analysis aspects were key (e.g., taking into account the monetary value of human life, at up to several million US \$ following, for example, calculations by the US Environmental Protection Agency).

Finally, the legally binding standards regarding radioactive waste management at EU level are described in Council Directive 2011/70/Euratom of July 19, 2011, establishing a Community framework for the responsible and safe management of spent fuel and radioactive waste.

They are mostly based on the IAEA Safety Standards and propose the following general principles:

- ultimate responsibility lies with the Member State
- embrace passive safety features for long term management
- the generator of the waste to bear the cost
- export under only very strict conditions.

This Euratom waste directive also contains requirements regarding education and training.

Extended lessons were drawn world-wide from the Fukushima 2011 accident, in particular in the EU, which organized “stress tests”^Q in all European nuclear installations (i.e., 131 NPP units in 2011). This was a request from the European Council on March 24/25, 2011 (thus very shortly after the accident). These “stress tests” were defined by the EC as *targeted reassessments of the safety margins of nuclear power plants* and were developed by the *European Nuclear Safety Regulators’ Group* (ENSREG). The “stress-tests,”

^P “Council Directive 2013/59/Euratom of 5 December 2013 laying down Basic Safety Standards (BSS) for protection against the dangers arising from exposure to ionizing radiation”—EU-Euratom radiation protection legislation (EC DG ENERGY website): https://ec.europa.eu/energy/overview-eu-radiation-protection-legislation_en including subject Euratom BSS Directive—<https://ec.europa.eu/energy/sites/ener/files/documents/CELEX-32013L0059-EN-TXT.pdf>.

^Q EC Communication COM(2012) 571, dated 4 October 2012—“*EC Communication on the comprehensive risk and safety assessments (‘stress tests’) of nuclear power plants in the EU and related activities*”—<https://eur-lex.europa.eu/legal-content/EN/ALL/?uri=CELEX%3A52012DC0571> and follow-up implementation actions—<https://ec.europa.eu/energy/en/topics/nuclear-energy/nuclear-safety>.

based on a deterministic approach (postulated conditions), examined the European NPPs resilience against events like extreme earthquake or flooding, and the response in case of partial or total loss of the ultimate heat sink and/or loss of electrical power supply.

WENRA which is the Western European Nuclear Regulators' Association (a European network of chief regulators of EU countries with NPPs, created in 1999), played a key role in the formulation of these stress tests. Moreover, WENRA updated its so-called 2014 reference levels, thereby increasing its requirements, especially on the topics of design extension and natural hazards (e.g., defense-in-depth approach for new NPPs), which have been integrated in many national nuclear regulations. It should be noted that many non-EU countries also conducted comprehensive nuclear risk and safety assessments based on the EU "stress test" model. These include Switzerland and Ukraine (both of which fully participated in the EU "stress tests"), Armenia, Turkey, the Russian Federation, Taiwan, Japan, South Korea, South Africa and Brazil.

In conclusion (EC, April 26, 2012), "*the stress tests have demonstrated that nuclear safety is an area where cross-border cooperation and action at EU level bring tangible benefits. Significant safety improvements have been identified in all participating countries. The total cost of the upgrades is estimated at some Euro 25 billion, averaging about Euro 190 million per reactor.*" The conclusion indeed was that the level of robustness of the NPPs under investigation was sufficient but, for many plants, safety reinforcements have been defined or recommended to face the likelihood of BDB events.

These reinforcements include (see e.g., results of stress tests in Belgium, 2020 report^f):

- protective measures against external hazards (earthquake, flooding, fire, extreme weather conditions or phenomena, oil spills, industrial accident, explosion, etc.),
- additional emergency equipment, such as pumps and generators, to support all reactors at a given site simultaneously following a natural disaster (BDB events),
- protective structures (reinforced local crisis centers, secondary control room, hardened stationary equipment, protective building for mobile equipment, ...),
- severe accident management provisions, in particular for hydrogen management and containment venting (in particular, emergency filtered venting systems),
- install enhanced equipment for monitoring water levels in spent fuel pools,
- new "extended PSA" methodologies considering, for all reactors and spent fuel storages on a nuclear site, contributions to risk originating from single and correlated external hazards of the beyond design type,
- new organizational arrangements (procedures for multiunit accidents, external intervention teams able to secure a damaged site).

As far as risk and acceptance is concerned, it is worth mentioning the discussion in the mid-2010s about "advanced" Resilience Engineering vs. "classical" Safety Management. Remember, in simple words: the goal of resilience engineering is to increase the number of things that go right rather than to reduce the number of things that go wrong, noting that the latter will be a consequence of the former. Safety cannot be seen independently of the core process (or business) of the system, hence the emphasis on the ability to function under "both expected and unexpected conditions" rather than just to avoid failures.^s Search for causes is replaced with understanding of how the system failed in its performance.

^f "National final report on the stress tests of nuclear power plants," Brussels, Belgium, 1 Sept 2020, Federal Agency for Nuclear Control (FANC) and Bel V (TSO)—<https://afcn.fgov.be/fr/system/files/best-2020.pdf>.

^s "The Fukushima disaster-systemic failures as the lack of resilience" by Hollnagel, Erik, University of Odense (Denmark)) and Fujita, Yushi (Technova Incorporation, Tokyo (Japan)), in Nuclear Engineering and Technology, Volume 45, Issue 1, February 2013—<https://doi.org/10.5516/NET.03.2011.078>.

10.2.3 EURATOM—Science, technology and innovation (several ambitious Framework Programmes since 1994)

Science, Technology and Innovation (STI) as well as education and training are at the heart of the Euratom Treaty. Article 4.1 indeed explicitly mentions **research** and **training** as a twofold objective:

*“The EC is in charge of promoting and facilitating nuclear research activities in the MS and to complement them through a Community **Research and Training** programme.”*

Nuclear STI in general contributes to social well-being, economic prosperity and environmental sustainability by improving nuclear safety, radiation protection, security and waste management. Euratom research and training programs indeed are funding international projects focusing on safety improvements in Generation II (e.g., related to long-term operation) and in Generation III (e.g., related to severe accident management). Large efforts are also dedicated to Generation-IV developments aimed at efficient resource utilization and waste minimization. The implementation of geological disposal for spent fuel and high-level radioactive waste is also addressed. As regards radiation protection research, the emphasis is on better quantification of risks at low dose (in particular, in the domain of radio-diagnosis and radio-therapy) and how these vary between individuals.

More generally, the Euratom Research and Training program (fission and fusion) has the following specific objectives since the very beginning:

- improve and support nuclear safety, security, safeguards, radiation protection, safe spent fuel and radioactive waste management and decommissioning, including the safe and secure use of nuclear power and of non-power applications of ionizing radiation
- maintain and further develop expertise and competence in the nuclear field within the community
- foster the development of fusion energy as a potential future energy source for electricity production and contribute to the implementation of the fusion roadmap
- support the policy of the EU and its Member States on continuous improvements in the “3S” domain, i.e., Safety, Security, and Safeguards.

Since 1994, more than 1000 research projects under the “indirect actions” in nuclear fission, safety, radioactive waste management and radiation protection have been funded within various EU Framework Programmes (FP), namely:

170 million euros in the Fourth (FP-4/1994–1998); 191 million euros in the Fifth (FP-5/1998–2002); 209 million euros in the Sixth (FP-6/2002–2006); 287 million euros in the Seventh (FP-7/2007–2013).

The program after FP-7 was called Horizon 2020/FP-8/(duration 2014–2020) with a Euratom funding of 355 million euros under the “indirect actions,” aligned with the three priorities of Horizon 2020: excellent science, industrial leadership, societal challenges. Euratom funding under Horizon 2020 was approximately 92%, whereas it was 54% under FP-7—the complement was provided by the contracting parties as usual.

As far as the current “Horizon Europe” framework program for research and innovation (/FP-9/duration 2021–2027) is concerned, a global budget of 95.5 billion euros was agreed by the EU leaders, including new knowledge and innovative solutions across all scientific disciplines to overcome our societal, ecological and economic challenges (in particular, how to satisfy constantly increasing energy needs while fighting climate change is particularly crucial?). This EU budget is complemented by 1.38 billion euros for Euratom research and training over 5 years (2021–2025) and 5.61 billion euros for the ITER project (“International Thermo-nuclear Experimental Reactor,” CEA Cadarache, south-eastern France) over 7 years (2021–2027) through a dedicated EC Decision—all amounts are in 2020 prices. The text of the Euratom research and training

program 2021–2025 in nuclear fission, safety and radiation protection under “Horizon Europe,” as well as the ITER text, was adopted on May 12, 2021.[†]

Mariya Gabriel, Commissioner for Innovation, Research, Culture, Education and Youth, said:

“The newly adopted Euratom Programme will complement Horizon Europe. It will support research and innovation in areas such as cancer treatment and diagnostics, nuclear safety and fusion.

Thanks to Euratom, Europe will maintain world leadership in fusion, nuclear safety, radiation protection, waste management and decommissioning, safeguards and security with the highest level of standards.”

The objectives of the current Framework program for Euratom research and training (2021–2025) remain the same as those for the precedent framework program, i.e.: to improve and support nuclear safety, security, safeguards, radiological protection, safe spent fuel and radioactive waste management and decommissioning; maintain and further develop expertise and competence in the nuclear field; develop fusion energy; and support the policy of the EU and its member states in these domains.

The EU added a new objective on the safe and secure use of non-power applications of ionizing radiation. In this regard, the medical field is the most prominent and Euratom is supporting the European’s Beating Cancer Plan (cf. ionizing radiation used for diagnostics and therapy). There is also much potential in the application of nuclear science (in particular, ionizing radiation) to fields like industry (e.g., nucleonic gauges and on-stream analyzers), agriculture, environment as well as security and space.

Moreover, special efforts are being dedicated to the development of a common culture for nuclear safety and radiation protection at EU level, based on the highest achievable standards (in particular, regarding a sense of responsibility and a questioning attitude of all staff members in nuclear installations and in nuclear medicine centers). Finally, increasing attention is dedicated to threats and counter efforts in CBRNE-Cyber fields (that is: chemical, biological, radiological, nuclear, explosives and cyber risks), thereby raising awareness and education enforcing a CBRNE-Cyber security culture.

The current Euratom Programme (2021–2025) uses the same instruments and rules for participation as Horizon Europe. The breakdown of the 1.38 billion euros budget for Euratom research and training during the period 2021–2025 is as follows:

- euro 266 million for indirect actions in fission safety and radiation protection
- euro 532 million for direct actions undertaken by the EC’s Joint Research Centre
- euro 583 million for indirect actions in fusion research and development.

In line with the Euratom Treaty, the Program will run for 5 years, from 2021 to 2025, to be extended in 2025 by 2 years in order to be aligned with the EU’s long-term budget (Multiannual Financial Framework 2021–2027).

Finally, the Program puts emphasis on Europe’s nuclear expertise and competences through mobility, education and training (cf. Marie Skłodowska-Curie Actions) as well as dissemination and technology transfer. Moreover, special attention is dedicated to access to research infrastructures, especially those of JRC. This will allow Europe to maintain world leadership in nuclear safety, radiation protection and waste management.

The Euratom **Research and Training** programme[‡] consists of indirect and direct actions.

[†] “EU adopts Euratom Research and Training Programme,” EU NEWS—12 May 2021, Brussels, Belgium—https://ec.europa.eu/info/news/eu-adopts-euratom-research-and-training-programme-2021-may-12_en.

[‡] “Horizon Europe—Euratom Research and Training Programme” containing also Euratom Factsheets—https://ec.europa.eu/info/research-and-innovation/funding/funding-opportunities/funding-programmes-and-open-calls/horizon-europe/euratom-research-and-training-programme_en.

- (1) Indirect actions are research activities undertaken by multipartner consortia who respond to specific Euratom competitive calls-for-proposals, focusing on 2 areas
- nuclear fission, safety, waste management and radiation protection
 - nuclear fusion research and development (*not discussed in this article*).

Indirect actions are cofunded by the Euratom budget and are carried out by private and public R&D (Research and Development) organizations in the EU Member States, in the form of collaborative projects initiated and monitored by EC DG RTD (Directorate General *Research and Innovation*), Brussels.^v Overall supervision of these projects is left to Euratom staff working with EC DG RTD to ensure that the actions are implemented properly in compliance with the contracts signed. Euratom projects under indirect actions usually involve up to 10 research organizations and have a duration of up to 4 years.

Specific objectives of the indirect actions encompass:

- supporting the safety of nuclear systems;
- contributing to the development of safe, longer-term solutions for the management of ultimate nuclear waste, including final geological disposal as well as partitioning and transmutation;
- supporting radiation protection and the development of medical applications of radiation, including, inter alia, the secure and safe supply and use of radioisotopes;
- promoting innovation and industrial competitiveness;
- ensuring the availability and use of research infrastructures of pan-European relevance;
- supporting the development and sustainability of nuclear expertise and excellence in the Union.

- (2) Direct actions are funded and carried out by the Commission's Joint Research Centre (JRC)^w which is the EC's science and knowledge service (see above mentioned Euratom Article 4.1 about research and training). They complement the research conducted at national level in the fields of nuclear safety, security, safeguards and non-proliferation. JRC also plays a central role in nuclear training and knowledge management and open access of its nuclear research facilities to EU scientists and also abroad. The institutional laboratories of the Joint Research Centre are spread over five EU countries and consist of six institutes:

(1) Growth and Innovation (Seville, Spain); (2) Energy, Transport and Climate (Petten, the Netherlands); (3) Sustainable Resources (Ispra, Italy); (4) Space, Security and Migration (Ispra); (5) Health, Consumers and Reference Materials (Geel, Belgium); and (6) Nuclear Safety and Security (Karlsruhe, Germany).

Specific objectives of the direct actions are very close to indirect actions and encompass:

- improving nuclear safety, including: nuclear reactor and fuel safety, waste management, including final geological disposal as well as partitioning and transmutation; decommissioning, and emergency preparedness;
- improving nuclear security, including: nuclear safeguards, non-proliferation, combating illicit trafficking, and nuclear forensics;
- increasing excellence in the nuclear science base for standardization;
- fostering knowledge management, education and training;
- and supporting the policy of the Union on nuclear safety and security.

^v All funding information and details on how to apply are provided in the Funding and Tenders portal: <https://ec.europa.eu/info/funding-tenders/opportunities/portal/screen/opportunities/topic-search>.

^w EC DG JRC—the European Commission's in-house science service (science hub): <https://ec.europa.eu/jrc/>.

10.2.4 EURATOM—Dissemination of knowledge—“European Nuclear Education Network”

Education and training are particularly important in the Euratom history. Remember Article 2.1 of the Euratom Treaty 1957: “*In order to perform its task, the Community shall, as provided in this Treaty: (a) promote research and ensure the dissemination of technical information; (b) ...*” It is therefore not surprising that all European universities that teach nuclear fission have decided to join their efforts in the “European Nuclear Education Network” (ENEN). This is an international non-profit organization, created in 2003 (AISBL established under the Belgian law).^x As of June 2021, ENEN has 62 full members (from the EU Member states), 7 international members and 10 partners (mostly international organizations). The main purpose of ENEN is the preservation and further development of expertise in the nuclear field via higher education and training in Europe.

This objective is realized through the cooperation of organizations involved in the application and teaching of nuclear science and ionizing radiation, including universities, research organizations, regulatory bodies and industry. ENEN has established close collaborations with major national nuclear E&T operators in Europe such as:

- The French “Institut National des Sciences et Technologies Nucléaires” (CEA-INSTN, Paris), with its own Nuclear Engineering Master level (or specialization) degree and a catalogue of more than 200 vocational training courses (22,000 teaching hours per year; 1100 students, including 320 apprentices/30% foreign students/)—top-level training courses in French or English upon client request.
- The Belgian “SCK-CEN Academy for Nuclear Science and Technology” with the “Belgian Nuclear higher Education Network” (BNEN), a master-after-master academic program organized through a consortium of six Belgian universities and SCK-CEN (BNEN served as a role model for the foundation of ENEN in 2003).

Moreover, the *Euratom Fission Training Schemes* (EFTS) should be mentioned, aimed at structuring Higher University Education Master of Science (MSc) training and career development. These schemes are funded through Euratom indirect actions, focusing on lifelong learning and borderless mobility: they are based on mutual recognition of learning outcomes across various countries. The concept of “learning outcomes” related to Knowledge (= understanding), Skills (= how to do) and Competences (= how to be)/altogether KSC/is at the heart of the EFTS. This approach is aligned with the EU policy in education and culture, i.e., the “Bologna 1999” process for mutual recognition of academic grades (Erasmus) and the “Copenhagen 2002” process for continuous professional development (ECVET) across the EU Member States. *NB: Erasmus is the world’s most successful student mobility program. Since it began in 1987–1988, the Erasmus programme has provided over three million European students with the opportunity to go abroad and study at a higher education institution or train in a company.*

It is no surprise that the format adopted by the IAEA training programs is based on a concept very close to the above KSC approach. Following the IAEA definition (Safety Standard Series, 2001),^y

^x “European Nuclear Education Network” (ENEN)—<https://enen.eu/> + list of ENEN courses and Nuclear Masters Programs delivered by Members of ENEN—<https://enen.eu/index.php/about-enen/nuclear-masters/> + Euratom overview article (2005–2015) by Georges Van Goethem, 30 Sept. 2015—“Euratom Research, Innovation and Education: stakeholder needs, common vision, implementation instruments,” EC DG RTD, Dir Energy—Euratom—<https://enen.eu/index.php/publications/e-c-paper-by-georges-van-goethem/>.

^y “*Building competence in radiation protection and the safe use of radiation sources*” (jointly sponsored by IAEA, ILO, PAHO, WHO), IAEA 2001—<https://www.iaea.org/resources/safety-standards/search>.

competence means the ability to apply knowledge, skills and attitudes so as to perform a job in an effective and efficient manner and to an established standard.

Of particular interest regarding education and training in innovative nuclear technologies are the two following initiatives:

- a highly successful European Master in Innovation in Nuclear Energy (EMINE) promoted by EIT KIC InnoEnergy which is one of the “Knowledge Innovation Communities” (KIC) of the “European Institute of Innovation and Technology” (EIT), involving major industrial partners, such as: EDF-Framatome (FR), ENDESA (ES) and VATTENFALL (SE), CEA (FR) and universities KTH (SE), University of Catalonia (UPC, ES), INP (Grenoble, FR) and Paris-Saclay (FR)

NB there are 8 EIT’s Knowledge and Innovation Communities (partnerships that bring together businesses, research centres and universities in the EU):

EIT Climate-KIC; EIT Digital; EIT Food; EIT Health; EIT InnoEnergy; EIT Manufacturing; EIT Raw Materials; and EIT Urban Mobility. For example, InnoEnergy invested EUR 560 million into more than 480 products.

- a 5-day “INSTN Course on Generation IV Nuclear Reactor Systems for the future”^z coorganized in November 2020 by CEA-INSTN (Paris) and ENEN.

Many of above Euratom E&T actions are closely associated with the series of Generation-IV webinars^{aa} that were launched in September 2016 and are currently offered once a month. A total of 54 webinars have been presented as of June 2021 (one-hour on-line lecture on one GIF system or cross cutting topic from top level experts with Q&A session).

10.3 Generation-IV: Breakthrough developments in sustainability, safety and performance through multilateral collaboration (GIF, IAEA-INPRO)

10.3.1 Generation-IV International Forum (GIF): USA, Canada, France, Japan, South Africa, South Korea, Switzerland, Euratom, China, Russia, and Australia

10.3.1.1 Innovation in nuclear fission from Generation I to IV (Euratom contribution)

Several generations of nuclear fission reactors are commonly distinguished (Generation-I, -II, -III and -IV).

- Generation-I reactors were developed in the 1950–1960s, and none are still running today. Gen-I refers to the prototype and power reactors that launched civil nuclear power, running on natural uranium. This kind of reactor typically ran at power levels that were “proof-of-concept” from 50 to 500 MW_{el} (e.g., the graphite-moderated reactors, such as the gas-cooled Magnox/UK/and UNGG/FR/).
- Generation-II refers to a class of commercial reactors designed to be economical and reliable, using enriched uranium. Gen-II systems began operation in the late 1960s and comprise the bulk of the world’s 400+ commercial Pressurized Water Reactors (PWR) and Boiling Water Reactors (BWR). They are derived from US designs originally developed for naval use. However, they have also

^z European GEN-IV course—targeted skills: (1) Acquire a general view of GIF objectives and organization; (2) Explain the rationale for the development of GEN-IV; (3) Describe the main characteristics of each system, and formulate their design, performance and safety characteristics. (4) Discuss the technical challenges ahead—https://enen.eu/index.php/2020/09/04/instn_geniv_course/.

^{aa} GIF webinars can be viewed at: https://www.gen-4.org/gif/jcms/c_82831/webinars—the webinars have been converted to YouTube Video: <https://www.youtube.com/channel/UCEHOQ63gD01fSKbCIY9XvSQ>.

produced a legacy of significant quantities of used fuel, they require relatively large electric grids, and present social acceptance challenges in some countries.

As far as safety is concerned, the basic concept is Defense-in-Depth (DiD—INSAG 10 report—IAEA, Vienna 1996) which aims to prevent and mitigate accidents during the entire life of nuclear facilities. The key of DiD is the creation of multiple independent and redundant layers of defense. This means that the safety and security systems in place should be able to compensate for potential human and mechanical failures so that no single layer, no matter how robust, is exclusively relied upon. DiD includes the use of stringent access controls, physical barriers, redundant and diverse key safety functions (in particular, 1—control of reactivity, 2—cooling of fuel elements, and 3—activity retention), and effective emergency response measures. These reactors use traditional active safety features involving electrical or mechanical operations that are initiated automatically or which can be initiated by the operators of the nuclear reactors. DiD is a safety approach whose effectiveness must be periodically evaluated, tested, and improved upon should new concerns or challenges arise.

- Generation-III nuclear reactors are essentially Gen-II reactors with evolutionary, state-of-the-art design improvements. They have a standardized design for each type to expedite licensing, reduce capital cost and reduce construction time. Gen-III designs have advanced safety features and set worldwide standards for the *Safety, Security and Safeguards* concept (“3S”). Improvements in Gen-III reactor technology aim to achieve longer operational life for NPPs (typically up to 60 years of operation) and fuel burn-up (also known as fuel utilization) rates of 60 GWd/tHM or more—thus reducing fuel consumption and waste production

– NB: GWd/tHM means gigawatt-days/metric ton of heavy metal (U or Pu).

There are a number of evolutionary improvements in the areas of safety systems (notably those related to severe accident management), fuel technology, thermal efficiency and digital instrumentation & control. The advancements of DiD to GEN-III reactors primarily address *the practical elimination of accident situations with core melt* which would lead to large early releases. Perhaps the most significant advantage of Gen-III systems over Gen-II designs is the incorporation in some of these of passive safety features that do not require active controls or operator intervention, but which rely instead on gravity or natural convection to mitigate the impact of abnormal events. As a consequence, the so-called “grace” period becomes quite substantial, so that—in some designs—following shutdown, the plant requires no active intervention for 72 h.

- Generation-IV reactor systems are breakthrough developments, some of which still require considerable research and development efforts. Conceptually, Gen-IV reactors have all of the features of Gen-III units, as well as the ability, when operating at high temperature, to support combined heat and power/CHP/ generation (e.g., aiming at producing economical and decarbonized H₂ through thermal energy off-taking). In addition, these designs, when using a fast neutron spectrum, include full actinide recycling and on-site fuel-cycle facilities based on advanced aqueous, pyro-metallurgical, or other dry-processing options. Gen-IV options include a range of power ratings, including “batteries” of 100 MW_{el}, modular systems rated around 300 MW_{el}, and large plants of up to 2000 MW_{el}. As far as DiD is concerned (i.e., the basis of the safety philosophy of NPPs), the Gen-IV reactors as innovative design concepts take up the cause of
 - excelling in safety and reliability
 - having a very low likelihood and degree of reactor core damage
 - eliminating the “technical” need for offsite emergency response.

In this context, it is worth recalling the IAEA definition of advanced nuclear plant designs:

- “evolutionary” (Generation-III/III+): these designs emphasize improvements based on proven technology and experience. No prototype is needed for their industrial deployment. From a safety point of view, the two aims of “evolutionary” reactors are a further reduction in core damage frequency (e.g., through increased

use of passive safety, wherever justified) and a limitation of off-site consequences in the event of a severe accident (e.g., by strengthening the containment function). Examples of GEN III are APR-1400/KHNP in South Korea. Examples of GEN III+ are: EPR/EDF-Framatome in France/; AP-1000/Westinghouse-Toshiba in the United States/; and VVER-1200/OKB Gidropress under Rosatom in Russia.

- “visionary” or “revolutionary” (Generation-IV): these designs emphasize the use of new or entirely revisited features, particularly with regard to efficient resource utilization and waste minimization as well as enhanced safety. Prototypes will be needed for industrial deployment. The main aim of these reactors is to integrate all *Generation-IV International Forum* (GIF) goals in the design (“built in,” rather than “added” features) and, in particular, to develop a “robust” safety architecture whereby to demonstrate the “practical elimination” of severe accidents.

In 1999 a group of nine countries, led by the U.S. Department of Energy (DOE), launched an international project to select a series of nuclear systems of a “revolutionary” type that would deploy industrially before 2045. The countries involved at the beginning were (in alphabetical order): Argentina, Brazil, Canada, France, Japan, South Africa, the Republic of South Korea and the United Kingdom, and the United States. These all signed the GIF Charter in 2001, thereby creating GIF. In 2002, Switzerland too became a forum member. The Charter was originally for a duration of 10 years, but in 2011 the signatories unanimously prolonged this duration indefinitely.

The *European Atomic Energy Community* (Euratom), which represents the EU Member States, signed the Charter on July 30, 2003, by a decision of the EC pursuant to Article 101(3) of the previously-mentioned Euratom Treaty. The EU Council approved the accession of Euratom to the GIF Framework Agreement in its Decision no. 14929/05, Brussels, December 2, 2005. This accession was notified in EU Commission Decision (2006)7 of January 12, 2006. On May 11, 2006, Euratom formally acceded and thus became a Party to the GIF Framework Agreement. As far as practical implementation in the EU is concerned, Article 2 of the latter EU Commission Decision states the following:

“The Joint Research Centre is confirmed in its role as coordinator of the Community participation in GIF and thus will represent Euratom as its own “Implementing Agent” in accordance with Article III.2 of the Framework Agreement.”

Accession to GIF brings with it certain obligations, including cofunding of the Nuclear Energy Agency (OECD/NEA)’s GIF technical secretariat activities. OECD/NEA is indeed the official Depository of the GIF Framework Agreement. As a consequence, OECD/NEA is in charge of coordinating the international GIF R&D programme through various dedicated committees (see GIF website).

After establishing the GIF Roadmap 2002, the GIF members expressed a strong will to establish an international legal framework.^{ab} An important step at this point was the signature of the *Framework Agreement for International Collaboration on Research and Development of Generation-IV Nuclear Energy Systems* (in short, the GIF Framework Agreement or FA)—the original version of this FA was open for signature on February 28, 2005. On February 26, 2015, the GIF Framework Agreement was extended for another 10 years, thereby paving the way for continued collaboration among participating countries. It is in fact an intergovernmental agreement, comparable from a legal point of view to the ITER agreement which was officially signed in Paris on November 21, 2006, by Ministers from the seven ITER countries concerned (including Euratom which represents the EU).

As far as fusion is concerned, remember that China, the European Union, India, Japan, South Korea, Russia and the United States are engaged in a 35-year collaboration to build and operate the ITER experimental device, and together bring fusion to the point where a demonstration fusion reactor can be designed. During

^{ab} GIF website (hosted at OECD/NEA, Paris) containing Newsletters; 2018 GIF Symposium Proceedings; Technology Roadmap; R&D Outlook Publications; as well as Annual Reports up to 2020. Information about the Generation IV International Forum in: https://www.gen-4.org/gif/jcms/c_9260/public and about technology (systems and goals) in: https://www.gen-4.org/gif/jcms/c_59461/generation-iv-systems.

the construction phase of the project, EU has responsibility for approximately 45% of construction costs, whereas China, India, Japan, South Korea, Russia, and the United States will contribute approximately 9% each. The lion's share (90%) of contributions will be delivered "in-kind."

Russia and China joined GIF in 2006. Australia joined the Forum in 2016. As a result, GIF has had 11 active members since 2016, i.e., members who have signed the Charter and signed, ratified or acceded to the above GIF Framework Agreement and are effectively contributing to GIF work. The 11 active members of GIF are: the United States, Canada, France, Japan, South Africa, the Republic of South Korea Switzerland and Euratom, as well as the People's Republic of China, the Russian Federation and Australia.

The main goal of GIF is to foster world-wide a multilateral collaborative effort involving the next generation of nuclear reactor systems (comprising power reactor and fuel cycle) by setting high-level goals and providing guidance regarding the viability and performance capabilities of the selected reactor systems.

GEN-IV concepts indeed feature extended capabilities beyond those of light water reactors and complement existing and evolutionary Gen III/III+ reactors—to be deployed up to the end of the century—by providing additional options and applications such as:

- optimization of resource utilization;
- multirecycling of fissile materials/used fuel and reduction the footprint of geological repositories for High-Level Waste (HLW);
- low-carbon heat supply for cogeneration and high-temperature industrial applications (e.g., process steam, synthetic fuels, hydrogen production);
- enhanced integration of nuclear and other low-carbon sources.

Six innovative nuclear reactor systems were selected in 2002 after evaluation of more than 100 different designs by over 100 experts from a dozen countries world-wide, namely:

- Sodium-cooled Fast Reactors (SFR)
- Lead-cooled Fast Reactors (LFR)—or Lead-Bismuth Eutectic cooled
- Gas-cooled Fast Reactors (GFR)
- Very-High-Temperature Reactors (VHTR), with thermal neutron spectrum
- Molten Salt Reactors (MSR), with fast or thermal neutron spectrum
- SuperCritical Water Reactors (SCWR), with fast or thermal neutron spectrum.

Out of the six GIF systems, three are fast neutron reactors and thus have a closed fuel cycle to maximize the resource base and minimize HLWs to be sent to a repository (which makes them "sustainable"). They utilize fast neutrons, generating power from plutonium while making more of the same from the U-238 isotope. Reminder: fast neutrons are more efficient in transmuting non-fissionable U-238 to fissionable Pu-239. The Sodium-, Lead- and Gas (helium)-cooled Fast Reactors (SFR, LFR, and GFR) are designed to burn plutonium and minor actinides. The actinides are separated from the spent fuel and returned to the fission reactors. One may consider fuel cycle closure also in two other reactor systems: the Molten Salt Fast Reactor (MSFR) and the SuperCritical Water-cooled Reactor (SCWR) which both can be built as fast reactor systems with full actinide recycle.

The bulk of the GIF international R&D effort is on power sizes ranging from 1000 to 1500 MW_{el}. All the above systems operate at higher temperatures than the Generation-II and III reactors currently in operation—this is a 21st century industry requirement. The new systems range from a SuperCritical-Water-cooled Reactor (SCWR, the only one cooled by water), which operates above 500°C, to a helium-cooled Very-High-Temperature gas Reactor (VHTR), which has an operating temperature of up to 1000°C—compared with less than 330°C for today's light water reactors. In particular, four GIF systems are designed to generate electricity and also to operate at sufficiently high temperatures, e.g., to produce hydrogen by thermochemical water cracking (without CO₂). Namely: the Very-High-Temperature Reactor (VHTR—max

coolant temperature 1000°C), the Gas- and Lead-cooled Fast Reactors (GFR, LFR—max 550°C), and the Molten Salt Reactor (MSR—max 1000°C).

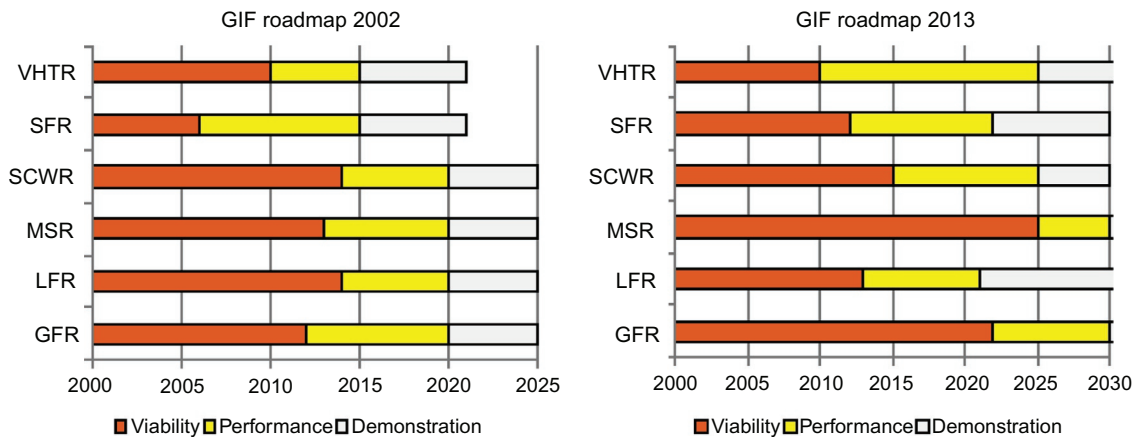
GEN IV systems take into account, in particular, lessons learnt from the Fukushima Daiichi accident (March 2011) by reinforcing the defense-in-depth approach against external events and promoting the robustness of safety demonstration, as it is reported in the GIF website and in the GIF Annual Reports^{ac} as well as in other articles of this handbook.

10.3.1.2 GIF Technology Roadmap (viability, performance, demonstration)—toward industrial deployment by 2045

The 2002 GIF Technology Roadmap^{ad} defines three phases for each GIF system:

- viability phase: basic concepts for reactor technologies, fuel cycle and energy conversion processes, established through testing on an appropriate scale under relevant conditions, with all potential obstacles identified and resolved, at least in theory; very preliminary cost analysis—conceptual design/ 5–15 years needed
- performance phase: assessment of the entire system, sufficient for procurement specifications for construction of a demonstration plant; validation of waste management strategy; materials capabilities are optimized under prototypical conditions; detailed cost evaluation—preliminary design/ 5–15 years needed
- demonstration phase: demonstration of safety features through large scale testing; environmental impact assessment; safeguards and physical protection strategy for the system; application meetings with regulatory agency; detailed design—in view of the engineering design for the industrial phase/at least 15 years needed.

According to the updated *2013 GIF Roadmap*, the most advanced GIF systems are as follows: SFR and LFR (performance phase due to finish in the early 2020s), followed by VHTR and SCWR (2025) and GFR and MSR (after 2030)—see Figure below.



^{ac} GIF Annual Report (in particular, 2020)—https://www.gen-4.org/gif/jcms/c_44720/annual-reports.

^{ad} Technology Roadmap for Generation IV Nuclear Energy Systems, issued by OECD/NEA for the GIF—www.gen-4.org/gif/jcms/c_40473/a-technology-roadmap-for-generation-iv-nuclear-energysystems

* GIF Roadmap 2002/"A Technology Roadmap for Generation-IV Nuclear Energy Systems" (Dec. 2002): <https://www.gen-4.org/gif/upload/docs/application/pdf/2013-09/genivroadmap2002.pdf>.

* GIF Roadmap 2013/"Technology Roadmap Update for Generation-IV Nuclear Energy Systems—<https://www.gen-4.org/gif/upload/docs/application/pdf/2014-03/gif-tru2014.pdf>.

10.3.2 GIF Roadmaps 2002 and 2013—viability, performance and demonstration phases

It should be noted that only the above phases 1 (viability) and 2 (performance) are covered by the GIF collaboration agreements. In other words, the multilateral collaborative effort covers the following design phases:

- viability—preconceptual and conceptual design: a “Viability Report” is produced, involving mainly fundamental research institutions (mainly public funding)
- performance—preliminary design: a “Performance Report” is produced, involving mainly applied research organizations and industrial experts (public and private funding).

The implementation of phase 3 (demonstration) is left to specific arrangements among GIF members, because it is considered too close to commercial exploitation. At the time being, half of the GIF systems are well advanced in their performance phases (preliminary design) whereas the other half are still in the viability phase (preconceptual design).

The general strategy of the GIF member countries is to continue to build Generation-III reactors between now and 2045 when the first commercial Generation-IV reactors will be built, i.e., when the demonstration phase has been implemented. Expenditure so far is in line with the initial estimate of approximately USD 6 billion relating to all six systems over 20 years—about 80% of the cost being met at the onset by the United States, Japan, and France.

10.3.3 IAEA programme INPRO (International Project on Innovative Nuclear Reactors and Fuel Cycles)

In millennium year 2000, the IAEA in Vienna launched an important initiative: the INPRO programme (*International Project on Innovative Nuclear Reactors and Fuel Cycles*).^{ae} Its aim was to foster availability of nuclear energy, thereby contributing to the energy needs of the 21st century in a sustainable manner. This project was proposed at the *United Nations Millennium Summit* and confirmed by the UN General Assembly in 2001. To achieve this, INPRO brings together nuclear technology users (as opposed to developers who are the main target in GIF) to consider international and national actions to promote innovation in nuclear reactors, fuel cycles and institutional approaches.

As of June 2021, INPRO’s membership consists of 42 Members (41 IAEA Member States, plus the European Commission represented by Euratom), namely:

Algeria, Argentina, Armenia, Bangladesh, Belarus, Belgium, Brazil, Bulgaria, Canada, Chile, China, Czech Republic, Egypt, France, Germany, India, Indonesia, Israel, Italy, Japan, Jordan, Kazakhstan, Kenya, Republic of Korea, Malaysia, Mexico, Morocco, Netherlands, Pakistan, Poland, Romania, Russian Federation, Slovakia, South Africa, Spain, Switzerland, Thailand, Turkey, Ukraine, United States of America, Vietnam and the EU. Several other countries participate at a working level or as observers in meetings.

In the early 2000s, INPRO produced a methodology to assess the sustainability of *Innovative Nuclear energy Systems* (INS). In 2005, INPRO was requested to provide guidance in using the proposed methodology in the form of an INPRO assessment manual. The resulting INPRO manual^{af} comprises an overview volume (no 1), and eight additional volumes covering the areas of economics (Volume 2), infrastructure

^{ae} IAEA—INPRO collaborative platform—“International Project on Innovative Nuclear Reactors and Fuel Cycles”—“Enhancing Global Nuclear Energy Sustainability”, 2012—<https://www.iaea.org/services/key-programmes/international-project-on-innovative-nuclear-reactors-and-fuel-cycles-inpro>.

^{af} INPRO manual (128 pages)—http://www-pub.iaea.org/MTCD/publications/PDF/TE_1575_web.pdf.

(Volume 3), waste management (Volume 4), proliferation resistance (Volume 5), physical protection (Volume 6), environment (Volume 7), safety of reactors (Volume 8), and safety of nuclear fuel cycle facilities (Volume 9).

In summary, INPRO focuses on the needs of the “end-users” of innovative systems (i.e., focus on the demand side), including in emerging countries, while GIF is more concerned with the “suppliers” mostly concerned with innovative Research—Development & Demonstration—Deployment/RD&DD/(i.e., international collaboration of the GIF type involving industrialized countries). As a result of the GIF and INPRO programs, a framework exists world-wide for all stakeholders interested in research and innovation in nuclear fission. The aim is to solve not only scientific and technological but also political, socio-economic and environmental challenges related to nuclear fission systems.

10.3.4 GIF interaction with industry: The “Senior Industrial Advisory Panel” (SIAP)

Of particular importance in the GIF governance is the feedback provided by SIAP. It is composed of executives from the nuclear industries. It was established in 2003 to provide recommendations on long-term strategic issues, including regulatory, commercial and technical aspects. In particular, the SIAP provides guidance on investor-risk reduction and incorporating the associated challenges in system design at an early stage of development.

The SIAP agreed on three main attributes necessary for Gen IV to compete in the “market”:

- to be economic,
- to be publicly accepted,
- and to be able to be integrated in the energy mix.

For example, the SIAP was asked to advise the GIF on the following:

- how to ensure the supply chain for Gen-IV systems, including identification of gaps in the supply of non-Light-Water-Reactor (LWR) components (e.g., emphasis on availability of materials and industrial practices as well as international standards)
- how to enhance knowledge management in advanced reactor R&D, given the history of knowledge management in the LWR industry (e.g., emphasis on capture of expert knowledge in a manner that “survives” changes in personnel).

According to the SIAP, the time perspective is a *readiness for commercial fleet deployment by around 2045* (for the first systems). Industry is expecting to have viable and performing “options” available in this time frame. Timely R&D and further industrial-type demonstration phases should make this possible.

GIF decided recently to improve their communication of results not only to industry but also to citizens, policy makers and regulators (e.g., through education and training initiatives including the above-mentioned 54 webinars, newsletters and visual branding).

10.3.5 GIF interaction with regulators: NRC (USA), IRSN (FR) and MDEP (OECD/NEA)

Looking to the future, GIF expects to continue its work on safety and regulatory frameworks. Engagement with regulators and Technical Support Organizations (TSOs) will also continue, and the regulators are expected to begin providing guidance to Gen IV system developers on regulatory requirements in the not-too-distant future. Two recent initiatives should be mentioned: (1) the development of system specific Safety Design Criteria (SDC) and Guidelines, e.g., in association with NRC and (2) an increased interaction in the frame of the OECD/NEA Working Group on Safety of Advanced Reactors (WGSAR). Continuing this dialogue with the regulators will benefit not only GIF system developers, but also the regulators and their TSOs.

It is worth recalling that the US Nuclear Regulatory Commission (NRC) issued in 2018 a draft “Regulatory Guide/RG/on the General Design Criteria for non-water-cooled reactors.”^{ag} In this report NRC proposes guidance on how the General Design Criteria (GDC) in Appendix A, “General Design Criteria for Nuclear Power Plants,” of Title 10 of the Code of Federal Regulations (10 CFR) Part 50, “Domestic Licensing of Production and Utilization Facilities,” may be adapted for non-light-water reactor designs. Appendix A of this RG is quite general and covers Advanced Reactor Design Criteria related to the following six types of non-light-water reactor: SFR, LFR, GFR, VHTR, fluoride high-temperature reactors, and MSR.

An interesting study by the French Technical Safety Organization IRSN (*Institut de Radioprotection et de Sûreté Nucléaire*) should also be mentioned: “*An overview of the safety potential of Generation-IV Nuclear Energy Systems*,”^{ah} December 2014. The IRSN carried out a review of all six Generation-IV systems from the point of view of safety and radiation protection. Their conclusion reads:

“It should be borne in mind that any industrial deployment of a Generation-IV reactor system in France will be linked to its advantages, not only regarding reactor fleet operation and safety, but also in terms of the coherence and performance of the associated fuel cycle. This concerns all aspects relating to safety, radiation protection, material management and efforts made to minimise the quantities of radioactive waste generated, without overlooking the overall economic competitiveness of the nuclear system. Ultimately, the choice of system must be made as part of an integrated approach, based on studies that cover multiple criteria and all the aspects mentioned above.”

Finally, it is worth mentioning that a number of national regulatory authorities world-wide agreed to develop innovative approaches to leveraging the resources and knowledge accumulated during their assessment of Generation-III reactor designs. As a result, the *Multinational Design Evaluation Programme* (MDEP) was established in 2006—the technical secretariat is within the OECD/NEA.^{ai} The nuclear regulatory authorities of 15 countries participate in the multinational initiative MDEP, which includes 5 design-specific working groups dedicated to Generation-III reactors: EPR (1600 MW_e, EU), AP-1000 (USA), APR-1400 (South-Korea), VVER-1200 (Russia), and HPR-1000 (China).

MDEP’s main objectives can be defined as follows:

- to enhance multilateral cooperation within existing regulatory frameworks
- to encourage multinational convergence of codes, standards and safety goals
- to implement MDEP products in order to facilitate the licensing of new reactors, including those being developed by the Generation IV International Forum.

Particular attention is devoted in MDEP to “common regulatory practices and regulations that enhance safety,” e.g., in the areas of design basis accidents and emergency core cooling system performance, severe accident requirements, digital *Instrumentation & Control* (I&C). There are also three issue-specific working groups: the Vendor Inspection Co-operation Working Group (VICWG); the Codes and Standards Working Group (CSWG); the Digital Instrumentation and Controls Working Group (DICWG).

^{ag} NRC Regulatory Guide 1.232 Rev.0, April 2018—<https://www.nrc.gov/docs/ML1732/ML17325A611.pdf>.

^{ah} IRSN 2014 Report “*Review of Generation-IV Nuclear Energy Systems*” https://www.irsn.fr/EN/newsroom/News/Documents/IRSN_Report-GenIV_04-2015.pdf.

^{ai} *Multinational Design Evaluation Program* (OECD/NEA)—<https://www.oecd-nea.org/mdep/index.html>

As of June 2021, the MDEP members include national regulators from 15 countries world-wide: Argentina (ARN), Canada (CNSC); People’s Republic of China (NNSA); Finland (STUK); France (ASN); Hungary (OAH); India (AERB); Japan (NRA); Republic of Korea (NSSC); Russian Federation (Rostechnadzor); Republic of South Africa (NNR); Turkey (NDK); United Arab Emirates (FANR); United Kingdom (ONR); United States of America (NRC). IAEA also participates in some activities.

10.4 Eight high-level goals for generation-IV nuclear energy systems and associated world-wide GIF R&D collaborative effort

In order to prepare the first Generation-IV Technology Roadmap (2002), it was necessary to establish goals for these innovative nuclear energy systems. The goals had three purposes:

- they served as the basis for developing criteria to assess and compare the systems in the technology roadmap
- they were challenging and stimulated the search for innovative nuclear energy systems (both fuel cycles and reactor technologies)
- they also served to guide the R&D on Generation-IV systems as collaborative efforts got underway.

Broad R&D areas were defined in connection with the four GIF objectives (details about major achievements and current outlook in synthesis document “GIF R&D Outlook”^{aj}):

1. sustainability (in particular, optimal utilization of natural resources and waste minimization) including decarbonization of the economy and security of supply
2. safety and reliability (through design, technology, regulation and culture)
3. economics (industrial competitiveness, integration in low-carbon energy mix) together with social aspects (in particular, easy access to affordable energy for all)
4. Proliferation resistance and physical protection (aligned with the non-proliferation treaty, IAEA 1970)

Eight high-level “*Goals for Generation-IV Nuclear Energy Systems*” were announced in the original GIF Charter of 2001 pertaining to the four above GIF objectives (sustainability; safety; economics; proliferation resistance and physical protection). These challenges are key concerns of the public with regard to “nuclear.” Gen IV systems need to demonstrate real progress in those areas. It may become more of a communication issue (related to social acceptance) than a technical issue, but it deserves a lot of attention.

10.4.1 Sustainability (efficient resource utilization and minimization of radioactive waste)

Two GIF high-level goals (nos. 1 and 2) are defined in connection with *Sustainability*:

- Generate energy sustainably and promote long-term availability of nuclear fuel
- Minimize radioactive waste and reduce the long-term stewardship burden.

Consensus was reached, in particular, on the following items:

- the needs of improved waste management, minimal environmental impact, effective fuel utilization (e.g., by converting non-fissile U-238 to new fissile fuel)
- development of new energy products that can expand nuclear energy’s benefits beyond electrical generation.

More generally, this GIF goal of sustainability aims at guaranteeing a very low full-lifecycle environmental footprint (CO₂, SO_x, NO_x, water and land usage and pollution) during normal functioning of the system (plant and associated fuel cycle). For example, by minimizing land impacts, cooling requirements (water reliance) and waste generation during operation and decommissioning.

Part of GIF R&D efforts are concentrated on the back-end of the nuclear fuel cycle, that is: reduce the amount and lifetime of the ultimate high-level radioactive waste, e.g., by developing, demonstrating and

^{aj} GIF R&D Outlook for Generation IV Nuclear Energy Systems: 2018 Update”, 2019—https://www.gen-4.org/gif/upload/docs/application/pdf/2019-06/7411_gif_r_and_d_outlook_update_web.pdf.

quantifying improvements in HLW management and by addressing the potential for partitioning and transmutation of transuranic elements. Diverse routes to be investigated include multirecycling in a fleet of fast neutron reactors, or with dedicated transuranic burners.

Like all industries, the generation of electricity produces waste. Whatever fuel is used (fossil or nuclear), this waste must be managed in ways which safeguard human health and minimize the environmental impact. Unlike other industrial toxic wastes, however the principal hazard associated with HLW (i.e., radioactivity) diminishes with time.

GIF high-level Goal no. 1 above, “*Generate energy sustainably and promote long-term availability of nuclear fuel*” leads to considering plutonium (in particular, Pu-239) as fuel for fast neutron spectrum reactors (i.e., plutonium is a valuable asset—not a liability).

In this type of reactor, a chain reaction takes place in which the neutrons are not thermalized (there is no moderator) but instead produce fission at relatively high energies (in the order of 1.0 MeV). With uranium fuel, Pu-239 is produced by the capture of neutrons in U-238. As a result of this physical process (based on breeding of fissile Pu-239 fuel from non-fissionable but fertile U-238), fissile material is produced and consumed in the reactor before the fuel is removed, supplementing the original U-235 in the fresh fuel. To avoid thermalization of the neutrons, fast breeder reactors use coolants with a high mass number to reduce moderation, such as liquid metals (e.g., sodium Na-23 or lead Pb or eutectic lead-bismuth Pb-Bi). The fuel of fast breeder reactors consists of pellets of mixed Pu and U oxides (MOX): PuO₂ (about 20%) and UO₂ (about 80%). Uranium depleted in U-235 (residue from earlier enrichment) is commonly used in fast reactors—non-conventional (usually more expensive) uranium ores could also be used.

An alternate breeding cycle is based on Thorium (Th); this implies conversion of fertile Th-232 to fissile U-233 which is being investigated in some countries (e.g., India, Canada). We should remember that Th is about three times more abundant than U in the earth’s crust. Basic development work has been conducted in Germany, India, Canada, Japan, China, Netherlands, Belgium, Norway, Russia, Brazil, the United Kingdom, and the United States.

According to the GIF strategy, fast neutron reactors can also be used to consume unwanted Pu (rather than to produce Pu as a fuel) and to destroy other heavy elements in weapon stockpiles or radioactive waste: in this case they act as burners instead of breeders.

GIF high-level Goal no. 2 above, “*Minimise radioactive waste and reduce the long-term stewardship burden*” implies consideration of recycling, i.e., minimizing the volume, heat and toxicity of ultimate radioactive waste while separating and conserving everything that is potentially recyclable (namely U and Pu).

As regards Generation-II and -III, recycling U and Pu is rather exceptional. Worldwide, only 44 nuclear reactors have used Mixed Oxide fuel since 1972 (*NB: MOX consists of about 7%–11% Pu mixed with depleted U*), including 22 in France, 10 in Germany, 5 in Japan, 3 in Switzerland, 2 in Belgium, 1 in the Netherlands and 1 in the United States.

Recycling (or reprocessing) of civilian fuel in view of MOX fuel fabrication is performed in only a few countries (current reprocessing capacity is about 2000 tons per year):

- in Europe—LWR fuel at the Cap de la Hague site/CEA-Orano/in France
NB: operations at the Sellafield reprocessing site THORP in the United Kingdom ended in 2018
- in the Russian Federation—LWR fuel at the Ozersk site (Mayak Chemical Combine), situated in the province of Chelyabinsk in the southern Ural Mountains
- in Japan—LWR fuel at the long-delayed reprocessing plant at Rokkasho—Pu-U coextraction technology—Japan Nuclear Fuel Ltd. (scheduled in 2022).

A reminder about natural U and composition of Spent Nuclear Fuel (SNF) may be necessary.^{ak} The core of a standard LWR of 1000 MW_{el} contains about 72 tons of Low-Enriched U (LEU)—the SNF usually contains 94% U-238. In a yearly operating cycle (refueling annually with one third replaced, i.e., 24 tons of LEU per year), the SNF contains about 23 tons of U (including 240 kg U-235), 240 kg Pu-239 and about 1 ton of fission products and trans-uranium elements other than Pu. There are about 36 kg minor actinides (neptunium/Np/, americium/Am/, and curium/Cm/, equivalent to 0.15% of total SNF). Despite their relatively small mass in SNF, transuranic elements such as Pu, Np, Am, and Cm, are the primary contributors to long term radiotoxicity and long-term heat generation in SNF.

According to the GIF strategy, partitioning and transmutation techniques are fostered in GEN-IV to further improve the desired recycling process. Application of these techniques to Pu and other heavy radionuclides, such as the minor actinides Np, Am and Cm, aims at reducing the volume, heat and toxicity of ultimate radioactive waste for disposal. Much of the calculated long-term waste hazard actually comes from a limited set of minor actinides (about 0.15% of the SNF, as explained above), with half-lives ranging from tens to millions of years such as Cm-244 and Np-237, respectively. Exposure of these radionuclides to high neutron fluxes can transmute them into much less hazardous nuclides. In such cases, chemical separations are necessary to allow partitioning of selected groups of radio-nuclides into different waste streams.

Generation-IV reactor systems of the fast neutron spectrum type include high level waste destruction as an integral part of the fuel cycle, rather than as a separate process. In a still more ambitious project such as the international fission research reactor project MYRRHA (an accelerator-driven system/ADS/, discussed below), the main purpose is to demonstrate that it is technically feasible to process the most radiotoxic elements (neptunium, americium, and curium) by transmutation. The fission of these long-lived elements into products that are radiotoxic for a considerably shorter period of time ensures further reduction of the quantity and life span of the waste. As a consequence, fast neutron reactors do not obviate the need for deep geological repositories but the required storage time is drastically reduced, from hundreds of thousands of years to a few hundred.

Concluding this Section on sustainability, GEN-IV systems of the fast neutron type will manage to enhance fuel utilization (by recycling U and Pu), while minimizing the volume, heat and toxicity of ultimate radioactive waste (by partitioning and transmutation). As a consequence, in GEN-IV systems, SNF is not waste but could become a source of power for the future, since the current NPPs burn only a very small amount of the U resource.

In other words, a very large amount of energy is still to be found in what has erroneously come to be known as “waste.” In fact, up to 96% (U-238, U-235, and Pu) could be recycled in Generation-IV reactor systems with a fast neutron spectrum. Thus, Pu is not a liability but a “valuable asset.” There will be adequate fuel once the U-238 resource can be optimally exploited, i.e., when fast neutron spectrum reactors of the Generation-IV type with actinide burning capacities come into service.

10.4.2 Safety (maximum safety performance through design, technology, regulation and culture) & Reliability

Three GIF high-level Goals (nos. 3, 4 and 5) are defined in connection with *Safety*:

- Excel in safety and reliability

^{ak} “The Nuclear Fuel Cycle—Material balance for the annual operation of a 1000 MW_{el} NPP,” World Nuclear Association—including “Material balance in the nuclear fuel cycle” (Fuel removed from a reactor, after it has reached the end of its useful life, can be reprocessed so that most is recycled for new fuel)—<http://www.world-nuclear.org/info/Nuclear-Fuel-Cycle/Introduction/Nuclear-Fuel-Cycle-Overview/>.

- Have a very low likelihood and degree of reactor core damage
- Eliminate the need for offsite emergency response.

Consensus was reached, in particular, on the following items:

- simplified designs that are safe and further reduce the potential for severe accidents and minimize their consequences, thereby enhancing public confidence in nuclear
- systematic consideration of human performance as a major contributor to plant availability, reliability, inspectability, and maintainability.

More generally, this GIF goal of safety aims at excluding severe accident/core melt or ensure no off-site radioactive release in case of severe accident/core melt, through reactor concept-dependent prevention measures, e.g., low power density fuel, Accident-Tolerant Fuel (ATF) and systems, high core thermal inertia, resistance to black out, smaller power ratings (Small and Medium Reactors—also called “Modular”—SMRs), etc. and through mitigation measures, e.g., in-vessel/ex-vessel corium cooling, in-containment management, etc.

Gen IV systems need to demonstrate real progress in safety. In addition, the “residual nuclear accident risk” needs to be put into perspective in comparison to other accident risks in the energy domain.

GIF high-level Goal no. 3 above, “*Excel in safety and reliability*” refers, for example, to the need to provide robust safety cases describing safety practices. In fact, there is a good convergence of safety practices in the Member States, notably in the following domains:

- defense in depth and integrity of the successive barriers between radioactive products and the environment (including active and passive safety systems)
- radiological consequences of postulated accidents (see above 2013 Euratom BSS Directive)
- deterministic analysis based on the identification of postulated or design basis accidents
- Probabilistic Safety Analysis (PSA) based on the evaluation of the overall risk from the plant, including severe accidents analysis and management (e.g., mitigation measures for high-consequence low-frequency events)
- ALARA (*As Low As Reasonably Achievable*) policy to reduce doses affecting personnel and the public.

GIF high-level Goal no. 4 above, “*Have a very low likelihood and degree of reactor core damage*” requires a reminder of the Reactor Safety Study WASH-1400^{al} in the United States which was in 1975 among the first to examine the phenomenology of severe accidents. They used methodologies developed by the US Department of Defense (DoD) and the National Aeronautics and Space Administration (NASA) such as event trees and fault trees. They were then able to compare the likelihood of nuclear and non-nuclear accidents (man-caused events as well as natural events) having similar consequences (expressed in terms of fatalities and property damage in US Dollars). The main risk issues in NPPs of the LWR type were identified in the WASH-1400 report, namely: molten corium behavior, fission product release and hydrogen combustion. The total risk is the expected loss: it is the sum of the products of the consequences multiplied by their probabilities. A number of containment failure modes or challenges were identified as follows: 1. Overpressure; 2. Dynamic pressure (shock waves); 3. Internal missiles; 4. External missiles (not applicable to core melt accidents); 5. Melt-through; and 6. Bypass. As a consequence of WASH-1400 and of the introduction of PSA after the TMI accident in

^{al} N.C. Rasmussen, “Reactor Safety Study: An assessment of accident risk in US commercial nuclear power plants”, AEC Report, WASH-1400-MR (NUREG-75/014), United States NRC, Washington, DC, October 1975—http://www.iaea.org/inis/collection/NCLCollectionStore/_Public/35/053/35053391.pdf.

1979, a number of regulatory authorities world-wide introduced nuclear safety objectives of the probabilistic type.

Of particular interest are the probabilistic safety criteria proposed by IAEA: *Core Damage Frequency* (CDF) and *Large Early Release Frequency* (LERF—a large release is typically 100 TBq Cs-137) calculated in Level 1 and Level 2 PSA, respectively. In 75-INSAG-3 (IAEA 1988, Basic Safety Principles for NPPs), the following safety goals of a quantitative probabilistic type are proposed: the LERF value should be 10 times smaller than the CDF value. For existing NPPs, a safety target of $<10E-4$ /reactor-year was proposed as the likelihood of CDF. Accident management and mitigation measures should reduce the probability of large off-site releases (requiring short term off-site response) to $<10E-5$ /reactor-year. Implementation at future plants should lead to safety improvements by a further factor of 10 for all events (75-INSAG-3 Rev. 1, INSAG-12, IAEA 1999). The threshold value $<10E-6$ /reactor-year for unacceptable consequences is already required for existing NPPs in many OECD countries. For radiological definition of off-site release limits during normal operation and incidents, and for off-site release targets for accidents, other internationally recognized standards are usually taken, such as the specific IAEA recommendations and/or the above Euratom Basic Safety Standards (“BSS”).

GIF high-level Goal no. 5 above, “Eliminate the need for offsite emergency response” is embedded in the revised 2014 Euratom Safety Directive. It is also at the heart of the *European Utility Requirement* (EUR)^{am} organization. The EUR initiative was launched in December 1991 by several European utilities interested in Generation-III reactors. The main objective of EUR was to produce a common set of utility requirements (so-called “EUR standards”), endorsed by major European utilities for the next generation of LWRs. Seven GEN-III reactors were considered, some of which with passive safety features, namely: EP-1000—European Passive LWR (based on AP-600, Westinghouse-Ansaldo); EPR—Evolutionary Pressurized Reactor (EDF-Framatome); BWR90/90+—Evolutionary Boiling Water Reactor (ABB Atom); ABWR—Advanced Boiling Water Reactor (GE-Hitachi); SWR 1000—Boiling Water Reactor (Siemens); AP-1000—Advanced Passive PWR (Westinghouse); and VVER-1200—PWR (OKB Hidropress).

As far as safety requirements are concerned, the EUR organization dedicated special attention to severe accident management. Situations and phenomena which could lead to early failure of the containment system and subsequent uncontrolled large releases of fission products into the environment should be *practically eliminated by design*. For example, for EPR, the main safety objectives are to *further reduce the core melt probability and, in the hypothetical case of a severe core melt accident, to improve the containment of fission products by excluding in a “deterministic” way any major off-site damage*, i.e., by design, to “practically eliminate” accident situations and phenomena that could lead to large early releases.

To better understand the safety challenge, an integral assessment approach is needed. This is provided by the GIF via their *Risk and Safety Working Group* (RSWG). This group produced a methodology called the “*Integrated Safety Assessment Methodology*” (ISAM—GIF/RSWG)^{an} for use throughout the Gen-IV technology development cycle. ISAM allows evaluation of a particular Gen-IV concept relative to various

^{am} “European Utility Requirement” (EUR): <https://www.europeanutilityrequirements.eu/Welcome.aspx>. Started by five partners in 1991, the EUR Organization nowadays brings together 13 Utilities which represent the major European electricity producers.: CEZ—EDF—EDF Energy—ENERGOATOM—Fortum—GDF SUEZ/Tractebel Engineering (now Engie)—GEN energija (Slovenia)—IBERDROLA—Paks II (Hungary)—NRG (Netherlands)—ROSENERGOATOM—TVO—VGB Power Tech (Germany).

^{an} “Guidance Document for Integrated Safety Assessment Methodology (ISAM)—(GDI): EC JRC report prepared for GIF Risk and Safety Working Group,” JRC 2014—(“science for policy” report no 92779)—<https://ec.europa.eu/jrc/en/publication/euro-scientific-and-technical-research-reports/guidance-document-integrated-safety-assessment-methodology-isam-gdi-ec-jrc-report-prepared>.

potentially applicable safety metrics or “figures of merit.” ISAM is particularly efficient for assessing active versus passive safety components and systems.

The ISAM is a tool that can be used throughout, from concept development to design and to licensing. It combines probabilistic and deterministic perspectives. It improves understanding of safety related design vulnerabilities and the contribution to risk. It also helps identify areas for additional research and data collection. The ISAM consists of five steps: (1) Qualitative Safety Features Review; (2) Phenomena Identification and Ranking Table; (3) Objective Provision Tree; (4) Deterministic and Phenomenological Analyses; (5) Probabilistic Safety Analysis.

As far as practical applications of the ISAM are concerned, it is worth mentioning two trial applications to a realistic advanced reactor development effort: one for a Japanese Sodium Fast Reactor (JSFR) concept, and one for a French Sodium Fast Reactor concept.

Other applications of the ISAM were conducted in Euratom RTD projects such as:

- LEADER (“*Lead-cooled European Advanced DEMonstration Reactor*”/2010–2013), coordinated by Ansaldo in Italy, connected to the ALFRED design
- EVOL (“*Evaluation and Viability Of Liquid fuel fast reactor systems*”/2010–2013), associated with the Rosatom MARS project (“*Minor Actinides Recycling in molten Salt*”), connected to Th-U MSFR (Molten Salt Fast Reactor)
- SARGEN-IV (“*Proposal for a harmonized European methodology for the safety assessment of innovative reactors with fast neutron spectrum planned to be built in Europe*”/2012–2013), coordinated by IRSN in France.

Moreover, considerable effort has been dedicated to cross-cutting issues in Generation-IV reactors, such as major safety issues. For example, the above-mentioned Euratom project SARGEN-IV identified phenomena and issues able to affect the safety of more than one Generation-IV concept, i.e.:

- for the coolant: sensitivity to impurities, coolant activity, retention of fission products, toxicity, opacity,
- for the structural materials: corrosion, erosion, irradiation behavior, aging effects,
- management of the three safety functions (reactivity control, decay heat removal, containment),
- passive safety systems, including capability to cool the core by natural circulation,
- considerations relating to the Fukushima-Daiichi events (extreme flooding, extreme earthquakes, total loss of electricity supply, accident management),
- categorization of initiating events organized by challenges: challenge to clad integrity, challenge to reactor boundary, containment challenge,
- advanced modeling simulation (advanced computational techniques for multiphysics, multiscale, and multiphase problems where the time and length scales of the individual processes involved often differ by orders of magnitude),
- specific issues in relation to fast reactors: sensitivity to blockage, power density, core compaction, reactivity void effects, handling hazards, failure of core supporting structures.

To conclude this Section on safety and to answer the question “*how safe is safe enough?*,” attention is drawn to *managerial and human factors* and, in particular, to their impact on safety performance. This concern is at the heart of the development of a common *nuclear safety culture* in nuclear fission installations, and, in particular after the Chernobyl accident, in NPPs and in the fuel cycle industry. In medical, industrial and scientific applications of ionizing radiation, the focus is on *radiation protection safety culture*.

10.4.3 Economics (competitiveness w.r.t. other energy sources) and social aspects (e.g., public engagement in decision making)

Two high-level GIF goals (nos. 6 and 7) are defined in connection with *Economics*:

- Have a life cycle cost advantage over other energy sources
- Have a level of financial risk comparable to other energy projects.

Consensus was reached, in particular, on the following items:

- accommodation of future nuclear energy systems to the worldwide transition from regulated to deregulated energy markets (including integration in smart grids)
- anticipate needs for a broader range of energy products beyond electricity (including smaller units), such as process heat, district heating, potable water and hydrogen.

More generally, this GIF goal of economics aims at reducing the costs of investment (overnight capital cost), reducing and mastering the duration of construction (financing cost), optimizing the costs of licensing, Operation and Maintenance (O&M), the fuel cycle and waste management, as well as optimizing the decommissioning costs as early as at the design stage in order to be competitive in the market with other sources of energy. It should be noted, however, that the unknowns and uncertainties in electricity (and possible future energy) market design and operation make it difficult to go beyond the pure cost dimension. The maximum therefore has to be done to reduce all elements of Gen IV costs, including the cost of licensing in each country.

More generally, to assess socioeconomics, the collaboration of experts is needed, in particular those with skills in finance and accounting, in the hard sciences (e.g., energy, environment, new technologies, life sciences), as well as the soft sciences (e.g., sociology, psychology, risk perception). This issue is particularly complex due to various technological and socioeconomic uncertainties and because of the long-time horizon involved (remember: “A successful nuclear power programme requires broad political and popular support and a national commitment of at least 100 years,” IAEA 2018).

GIF high-level Goal no. 6 above, “*Have a life cycle cost advantage over other energy sources*” means in fact minimizing *Levelized Unit Energy Costs* (LUEC): this favors large units with economies of scale. The LUEC methodology is an economic assessment of the cost of building and operating a power-generating asset over its lifetime (usually several decades) divided by the total power output of the asset over that lifetime; typically, the unit of LUEC is euro/MWh or US\$/MWh. In this accounting system, no benefit is drawn from the avoided CO₂ emissions.

A good understanding of nuclear economics is provided, in particular, by an authoritative cost study conducted by OECD/NEA in 2019.⁴⁰ This study assesses the costs of alternative low-carbon electricity systems capable of achieving strict carbon emission reductions consistent with the fifth report of the “Intergovernmental Panel on Climate Change” in 2014 (UN IPCC—195 members) and with the aims of the 2015 Paris Agreement (COP-21). It analyses several deep decarbonization scenarios designed to reach the same stringent carbon emission target but characterized by different shares of the variable renewable technologies, hydroelectric power and nuclear energy.

The conclusion of the study reads: “*Nevertheless, this study shows how nuclear power still remains the economically optimal choice to satisfy stringent carbon constraints despite the economic challenges it faces during the changeover between different reactor generations. The reason for nuclear power’s cost advantage is not in its plant-level costs. Instead, it resides in its overall costs to the electricity system. Variable renewables have reduced quite impressively their plant-level costs, but their overall costs to the system are not*

⁴⁰ “The Costs of Decarbonization: System Costs with High Shares of Nuclear and Renewables,” OECD NEA, June 2019 (W. D’haeseleer et al.)—<https://www.oecd-nea.org/ndd/pubs/2019/7299-system-costs.pdf>.

accounted for as their output is clustered in a limited number of high-level hours. All of these factors will come to play in the ultimate choices of each country.”

Realistic cost estimates for electricity production are provided by the nuclear market. For example, in Turkey, the discussion with Rosatom in 2015 focused on a 15-year fixed price *Power Purchase Agreement* (PPA) within a *Build-Own-Operate-Transfer* (BOOT) scheme: the weighted average cost is USD 123.5 per MWh (i.e., 111 euro in 2015 prices) and the quantity of electricity is fixed. In the United Kingdom, in 2015, EDF has been offered an investment contract for Hinkley Point C (i.e., the first construction of a nuclear plant in the United Kingdom after 1995, when the last one constructed, Sizewell B, had begun operating) with a “strike price” for its electricity output of GBP 92.50 (i.e., 132 euro in 2015 prices) per MWh which will be adjusted (linked to inflation) during the construction period and over the subsequent 35 years tariff period; this “strike price” for electricity from Hinkley Point C is roughly twice the wholesale price of power in 2020.

GIF high-level Goal no. 7 above, “*Have a level of financial risk comparable to other energy projects*” means minimizing Capital-at-Risk (i.e., investment before commercial operation): this Goal rewards smaller units that require less capital. Capital investment costs should be seen in the context of total social costs (= private + external costs) and the nuclear sector should be compared to the renewable and fossil energy sectors.

Private and external costs (i.e., the total social costs) can be described as follows:

- Private costs: (i) capital investment cost (60%–85%); (ii) O&M cost (10%–25%); (iii) Fuel-cycle cost (7%–15%) including natural uranium (c.5%)
- External Costs: (i) Radioactive emissions; (ii) Long-term waste disposal (often already internalized); (iii) Accidents—liability; (iv) Proliferation; (v) Avoided CO₂ emissions; (vi) System effects (in particular, on electrical grid stability).

NPPs are expensive to build but relatively cheap to run. In many countries, nuclear energy is competitive with fossil fuels as a means of electricity generation. External costs, such as waste disposal and decommissioning costs, are usually fully included in the operating costs. If the societal, health and environmental costs of fossil fuels are taken into account, the competitiveness of nuclear power is enhanced. A large part of the external costs is indeed included in the price of nuclear electricity production. Some external costs, however, are difficult to estimate, such as insurance to cover nuclear accident damage (e.g., what reasonable measures should be implemented? what is the causal link between an accident and disease occurring many years after the event?).

The uncertainty is greater when it comes to estimating the “*Capital Expenditures*” (CAPEX) for new build reactors, be it Generation-III or -IV. Construction costs have been estimated by scaling from known cost distributions and adaptation by expert judgment. Besides scaling to power level, other considerations may lead to increases or decreases in certain accounts with respect to the accounts of the reference design, such as: the reactor vessel and other reactor plant equipment; space requirements; containment size; application of passive safety systems; need for an intermediate circuit; complex fuel handling in all GIF systems; use of complex fluids or gases as coolants (e.g., chemically highly reactive sodium in SFR); use of Rankine vs. Brayton cycle.

The *Economics Modeling Working Group* (EMWG)^{ap} of GIF prepared “*Cost Estimating Guidelines for Generation-IV Nuclear Energy Systems*” (GIF/EMWG) for economic optimization during the viability and performance phases of the Generation-IV projects. This Group has upgraded existing nuclear-economic

^{ap} Economic Modeling Working Group, also focusing on the deployment of Gen-IV systems in future low-carbon energy markets, including flexibility requirements for integration in grids with significant renewable resources—https://www.gen-4.org/gif/jcms/c_40407/economic-modelling-working-group-emwg and 2013 GIF EMWG “*Cost Estimating Guidelines for Generation-IV Nuclear Energy Systems*”—https://www.gen-4.org/gif/jcms/c_40408/cost-estimating-guidelines-for-generation-iv-nuclear-energy-systems.

submodels, and developed new ones where needed, addressing each of the following five economic areas: Capital and Production Cost Models, Nuclear Fuel Cycle Model, Optimal Scale Model, and Energy Products Model. These five models have been brought together in an *Integrated Nuclear Energy Economic Model* (INEEM).

The GIF Cost Estimating tool G4-Econs has been applied to provide an overall economic assessment and to assess the plant design characteristics of future nuclear reactors and their associated fuel cycles. All six GEN-IV designs have been investigated and compared to a reference GEN-III design. Fuel cycle costs were divided into front-end and back-end costs. When estimating costs for GEN-IV reactor fuel cycles, non-conventional fuels (e.g., MOX, nitride ceramics, carbides, and metallic fuels) should be taken into account.

Evaluating the wider aspects of competitiveness in a full-cost approach, in comparison with the cost of Renewable Energy Sources (RES) and other low-carbon dispatchable sources and taking into account CCS/U (carbon capture and storage/usage) and large-scale storage, would be useful. It would require making necessary assumptions linked to the evolution of the market design and operation, which have, in particular, an impact on the system costs. In addition, applications beyond pure electricity production have to be considered, such as district heating and industrial heat applications.

Moreover, it is important to ensure that Gen IV nuclear systems are sufficiently flexible, at minimal cost, to be integrated in electricity systems with increasing shares of variable/intermittent RES, using diverse possible options: load following, remote control, modularity (SMRs), cogeneration and hybrid systems. A highly flexible hybrid electricity system with 50% variable (or intermittent, non-dispatchable) RES might be considered as challenging but realistic.

To conclude this Section on socioeconomics, one should stress the following question: *How to improve public information and engagement in energy policy issues, notably in connection with nuclear decision making?* Breakthrough technologies in the nuclear sector are under development world-wide: they are under discussion not only among scientists and engineers but also by national regulators and civil society (see *Science based policies and legislation* in Topic 8 of above “2012 Interdisciplinary Study”).

10.4.4 Proliferation resistance and physical protection (Non-Proliferation Treaty, IAEA 1970)

One GIF high-level Goal (no. 8), the last one in the general GIF strategy, is defined in connection with “*Proliferation resistance and physical protection*”:

- 8. Be a very unattractive route for diversion or theft of weapon-usable materials, and provide increased physical protection against acts of terrorism.

Consensus was reached, in particular, on the following items:

- further improvement of the safeguards in all nuclear material inventories involved in enrichment, conversion, fabrication, power production, recycling, waste disposal
- design of advanced systems from the start with improved physical protection against acts of terrorism, thereby increasing public confidence in nuclear facilities.

Remember the “Atoms for Peace” conference (speech delivered by U.S. President Dwight D. Eisenhower to the UN General Assembly in New York City on December 8, 1953). This event created the ideological background for the creation of the IAEA and the “Treaty on the Non-Proliferation of Nuclear Weapons” (NPT). The NPT is an international treaty whose objective is (1) to prevent the spread of nuclear weapons and weapons technology, (2) to promote cooperation in the peaceful uses of nuclear energy, and (3) to further the goal of achieving nuclear disarmament and general and complete disarmament. Opened for signature in

1968, the NPT entered into force in 1970. The Treaty defines nuclear-weapon states as those that have built and tested a nuclear explosive device before January 1, 1967: these are the United States, Russia, the United Kingdom, France, and China. As of today, 191 states have adhered to the NPT (NB: 5 states are non-parties).

The fear of so-called “rogue nations” acquiring nuclear weapons, or terrorist organizations carrying out malevolent actions by misuse of nuclear materials, clearly remains intense. As a consequence, a great number of political and technological experts are working on reducing the risk of dissemination and proliferation of nuclear weapons. It should be recalled, however, that during the Cold War, the objective risk of proliferation was high, with more than 20 countries attempting to develop nuclear weapons, nine of which eventually did so. In contrast, since the end of the Cold War, less than a handful of countries have attempted proliferation and only one—North Korea—has succeeded.^{aq}

The long-term safe, secure and sustainable use of nuclear energy must be ensured by a consistent approach to the “3S” nexus, namely: safety (implementation of appropriate and commensurate common principles, rules and standards); security (prevention, detection and response), as well as international acceptance and mutual trust (transparency); and safeguards (verification, reporting and non-proliferation commitments such as export controls). This can only be achieved based on sound scientific evidence, reliable nuclear measurements and appropriate control tools, as well as on public involvement, which at the same time can only be guaranteed if competence and technology leadership are maintained world-wide (research, education, training and knowledge management).

In this context, it is worth recalling the JRC activities in the field of “3S.” Their focus is in four areas: effective and efficient safeguards (through research in, e.g., nuclear material measurements, containment and surveillance, process monitoring and on-site laboratories); verification of absence of undeclared activities (through, e.g., trace and particle analysis, and development of in-field tools); nuclear non-proliferation (through, e.g., export control, trade analysis, and studies); and combating illicit trafficking (through, e.g., equipment development and validation, nuclear forensics, preparedness plans).

Some experts claim that recycling plutonium in the form of MOX fuel helps to combat nuclear proliferation by “burning” it in the reactor, while other experts claim that handling and storing plutonium should be prohibited, due to the risk of diversion by terrorists.

The ambitions of Generation-IV in this domain focus on two breakthrough technologies:

- (1) new reprocessing (partitioning) techniques where U and Pu are no longer separated, as is the case in the traditional PUREX process, and
- (2) new fuel fabrication techniques for fast neutron flux reactor (transmutation) systems aiming to use (fertile) U-238 to breed (fissionable) Pu-239, while burning the minor actinides Np, Am and Cm (thereby preventing the use of the isotopes Np-237 and Am-241, Am-242m, and Am-243 in a nuclear explosive).

The *Proliferation Resistance and Physical Protection (PR&PP)* Working Group of GIF issued a document: “*Evaluation methodology for PR&PP of Generation-IV nuclear energy systems.*”^{ar} For a proposed design, the methodology defines a set of challenges, analyses system response to these challenges, and assesses outcomes. Uncertainty of results is recognized and incorporated into the evaluation. The results are intended for three types of users: system designers, policy makers, and external stakeholders.

The PR&PP methodology can be applied to the entire fuel cycle or to portions of a design. It was developed, demonstrated, and illustrated by use of a hypothetical “Example Sodium Fast Reactor” (ESFR), by members of the PR&PP WG. The ESFR case study was the first opportunity to test the full methodology

^{aq} “*Nothing to Fear but Fear Itself? Nuclear Proliferation and Preventive War,*” by Debs and Monteiro, Pol. Science, Yale Univ, 2010—<http://www.nunomonteiro.org/wp-content/uploads/DebsMonteiro2010.pdf>.

^{ar} GIF—“*Evaluation Methodology for Proliferation Resistance and Physical Protection of Generation IV Nuclear Energy Systems—Rev 6*”—GIF PR&PP-WG 2011—https://www.gen-4.org/gif/jcms/c_9365/prpp.

on a complete system, and many insights were gained from the process. Others, in national programs, have adapted the PR&PP methodology to their specific needs and interests, such as:

- in the United States, where the methodology has been used to evaluate alternative spent fuel separations technologies
- in Belgium, where the PR&PP methodology was used in the analysis of the MYRRHA accelerator-driven system (fast spectrum Pb-Bi irradiation facility).

To conclude this section on proliferation resistance, one could expand the discussion toward cyber-terrorism, e.g., an attack causing serious damage to a critical infrastructure. Until the 2010s, only hackers targeting industrial systems have been involved in cyber-terrorism actions. In the nuclear sector, however, there are strong defenses. In principle, a cyber-attack cannot prevent critical systems in a nuclear energy facility from performing their safety functions (i.e., reactivity control, decay heat removal, containment), NPPs are designed to shut down safely, if necessary, even if there is a breach of cyber-security. They are also designed to automatically disconnect from the power grid if there is a disturbance caused by a cyber-attack. Nevertheless, other types of cyber-attacks could destroy, for example, vulnerable physical components of the electricity grid.

10.5 Euratom research and training actions in innovative reactor systems and EU “Sustainable Nuclear Energy Technology Platform”

10.5.1 EURATOM actions that are considered as contributing to the six GIF reactor systems

While the fast reactor systems of Generation-IV type produce substantially more energy (up to 50 times) from the original uranium than conventional reactors, they are expensive to build and still need to demonstrate that they can offer, in particular, a significantly improved level of safety compared with Generation-III reactors. As a consequence, additional R&D is necessary in areas, such as: instrumentation & control; human machine interface; reactor physics and thermal-hydraulics; risk management; operation and maintenance. Further research is required, in particular regarding the behavior of these systems under severe accident conditions. Each Generation-IV system requires challenging R&D common to all systems, whereas others are system-specific. The list of Generation-IV crosscut items in the domain of safety comprises, for example, system optimization and safety assessment methodology; emergency planning methods; a licensing and regulatory framework; radionuclide transport and dose assessment; human factors (see above mentioned “GIF R&D Outlook for Generation IV Nuclear Energy Systems” 2019).

Detailed information on Euratom research in Generations II, III, and IV is available in the proceedings of the 2019 conference FISA and EURADWASTE.^{as} This conference was coorganized by the EC with the Ministry of Research and Innovation of Romania and the Institute for Nuclear Research (RATEN ICN) under the auspices of the Romanian Presidency of the Council of the European Union in 2019. The event took place on June 4–7, 2019, in Pitesti, Romania. A lot of information is also available in the previous FISA-2013 conference in Safety of Reactor Systems (Vilnius, Lithuania, October, 14–17, 2013).

^{as} FISA 2019 and EURADWASTE’19 (ninth) EU conference—<http://fisa-euradwaste2019.nuclear.ro/> and proceedings in Publications Office of the EU <https://op.europa.eu/en/publication-detail/-/publication/9cfc43f8-cbc7-11ea-adf7-01aa75ed71a1/language-en/format-PDF/source-140481060>.

The aim of FISA-2019 was to present progress and key achievements of the most relevant Euratom projects—both indirect actions^{at} and direct actions^{au}—carried out since 2013.

Focusing on GEN-IV, an extensive investigation over the 10-year period 2010–2020, going through all the existing Euratom Fission Projects of FP5, FP6, FP7 and Horizon 2020 (RTD indirect and JRC direct actions), produced the following list of Euratom actions that are considered as contributing to the six GIF systems. These Euratom actions are cross-cutting: safety of NPPs, fuel developments, thermal hydraulics, materials research, numerical simulation and design activities, partitioning and transmutation, as well as support to infrastructures, education, training and knowledge management, international cooperation. It is worth mentioning that many of these Euratom projects were conducted in the wake of the above-mentioned EU “stress tests” (i.e., 131 reactor units in 2011) and produced results that are applicable to current GEN-II and -III as well as to GEN-IV.

Some RTD indirect actions in the Generation-IV domain during the 10-year period 2010–2020 were “concept oriented” such as: *CP-ESFR (2009–2013)* Collaborative Project on European Sodium Fast Reactor; *LEADER (2010–2013)* Lead-cooled European Advanced Demonstration Reactor; *HELMINET (2010–2012)* Heavy liquid metal network; *GOFASTR (2010–2013)* European Gas Cooled Fast Reactor; *VINCO (2015–2018)* Visegrad Initiative for Nuclear Cooperation (Advanced GFR Safety Allegro); *ESNII+ (2013–2017)* Preparing ESNII for HORIZON 2020; *EVOL (2010–2013)* Evaluation and Viability of Liquid Fuel Fast Reactor System; *SAMOFAR (2015–2019)* A Paradigm Shift in Reactor Safety with the MSFR; *MYRTE (2015–2019)* MYRRHA Research and Transmutation Endeavor; and *ESFR-SMART (2017–2021)* European Sodium Fast Reactor Safety Measures Assessment and Research Tools.

Other RTD indirect actions addressed cross-cutting research and innovation areas such as:

GETMAT (2008–2013) Gen-IV and Transmutation MATerials; *MATTER (2011–2014)* MATerials TEsting and Rules; *MATISSE (2013–2017)* Materials’ Innovations for a Safe and Sustainable nuclear in Europe; *FAIRFUELS (2009–2015)* FABrication, Irradiation and Reprocessing of FUELS and targets for transmutation; *F BRIDGE (2008–2012)* Basic Research for Innovative Fuels Design for GEN IV systems; *THINS (2010–2015)* Thermal-hydraulics of Innovative Nuclear Systems; *SEARCH (2011–2015)* Safe ExploitAtion Related CHEmistry for HLM reactors; *SESAME (2015–2019)* Thermal hydraulics Simulations and Experiments for the Safety Assessment of METal cooled reactors; *SACSESS (2013–2016)* Safety of ACTinide Separation processes; *GENIORS (2017–2021)* GEN IV Integrated Oxide fuels recycling strategies (FC Partitioning); *CINCH-II (2013–2016)* Cooperation in education and training In Nuclear Chemistry; *ASGARD (2012–2016)* Advanced fuels for Generation-IV reActors: Reprocessing and Dissolution; *TALISMAN (2013–2016)* Transnational Access to Large Infrastructure for a Safe Management of ActiNide; *ARCAS (2010–2013)* ADS and fast Reactor CompARison Study in support of Strategic Research Agenda of SNETP; *JASMIN (2012–2016)* Joint Advanced Severe accidents Modeling and Integration for Na-cooled fast neutron reactors; and *SARGEN-IV (2012–2013)* Toward a harmonized European methodology for the safety assessment of innovative reactors with fast neutron spectrum planned to be built in Europe.

Here are a series of more recent Horizon 2020 indirect actions related to Generation-IV:

PASCAL (LFR—Advanced HLM—ALFRED—MYRRHA); *SafeG* (GFR—Advanced Safety—Allegro); *GEMINI+* (Advanced HTR—Cogeneration); *ECC—SMART* (SCWR—Advanced SMR safety features); *SAMOSAFER* (MSR—Advanced Molten Salt); *PUMMA* (FC Fuel Pu management); *INSPIRE* (FC—

^{at} Summary of indirect actions (RTD) in “Euratom Research and Training in 2019: challenges, achievements and future perspectives,” by Roger Garbil, Christophe Davies, Daniela Diaconu, in EPJ Nuclear Sci. Technol. 6, E2 (2020)—<https://epjn.epj.org/articles/epjn/abs/2020/01/epjn190056/epjn190056.html>.

^{au} Summary of direct actions (JRC) in “JRC Euratom Research and Training Programme—2014–2020,” by Said Abousahl, Andrea Bucalossi, Victor Esteban Gran, Manuel Martin Ramos, EPJ Nuclear Sci. Technol. 6, 45 (2020)—<https://epjn.epj.org/articles/epjn/abs/2020/01/epjn190067/epjn190067.html>.

MOX fuel licensing); *PATRICIA* (FC—P&T MYRRHA); *MEET-(&A) CINCH* (FC—E&T RadioChemistry); *GEMMA* (Advanced Materials); *M4F* (Fu/Fi materials); *McSAFER* (Advanced Modeling SMR).

Under the current Euratom Research and Training Programme (2021–2025), the selected projects for 2019–2020 covering Generations II, III and IV amounted to a budget of 140 million euros. Five projects on advanced systems are funded on topics such as: fuel cycle Pu management, safety of Gas Fast Reactors, partitioning and transmutation, safety of SCWR SMR, and the high-performance computing safety evaluation of SMRs.

The main JRC direct actions in the Generation-IV domain during the 10-year period 2010–2020 under consideration are the following:

- *ANFC*—Alternative Nuclear Fuel Cycles (e.g., development of aqueous and pyrochemical processes for the separation of long-lived radionuclides and the conversion into shorter-lived or stable ones by irradiation in dedicated reactors)
- *ND-MINWASTE*—Nuclear data for radioactive waste management and safety of new reactor developments (e.g., contribution to the Joint Evaluated Fission and Fusion nuclear data file—JEFF–, and Evaluated Nuclear Data File, ENDF/B-VII).
- *FANGS*—Feasibility Assessment of Next Generation nuclear energy Systems (e.g., feasibility and performance investigations regarding fast reactor/transmutation fuel and high-temperature reactor fuel, for which several successful irradiation tests in the High Flux Reactor (HFR) Petten, the Netherlands, were performed)
- *MATTINO*—MATERials performance assessmentT for safety and Innovative Nuclear reactOrs (e.g., thermo-mechanical properties, corrosion resistance, and irradiation and environmental safety performance assessment of structural materials; input to material design codes and standards)
- *NURAM*—Nuclear Reactor Accident Analysis and Modeling (e.g., in the area of severe accident management)
- *SNF*—Safety of Nuclear Fuels and Fuel cycles (e.g., conventional and advanced fuels including minor actinide containing fuels, going from the traditional postirradiation techniques providing information on microstructure and fission gas release to advanced techniques providing fundamental data on the thermo-physical and thermomechanical properties of nuclear fuel)
- *CAPTURE*—Knowledge and Competence Management, Training and Education in Reactor design and Operation (e.g., evaluation of human resources trends in the energy sector; harmonization and standardization of nuclear skills recognition within the EU; open database taxonomy of commonly recognized nuclear skills and competences, implementation of the ECVET system in the nuclear energy sector)

NB: ECVET = European Credit System for Vocational Education and Training.

It is worth recalling that JRC owns nuclear research installations in four sites in the EU, some of them focusing on specific aspects of Generation-IV: JRC-Geel in Belgium, JRC-Karlsruhe in Germany, JRC-Petten in the Netherlands and JRC-Ispra in Italy:

- JRC-Geel research infrastructure mainly focuses on nuclear data, radioactivity metrology, and nuclear reference materials. It is one of the few laboratories in the world which is capable of producing the required accuracy for neutron data needed for the safety assessments of present-day and innovative nuclear energy systems.
- JRC-Karlsruhe mainly focuses on properties of irradiated and non-irradiated nuclear materials, as well as on research in fuel, fuel cycle, radioactive waste, security and safeguards. Their materials research laboratories contain unique, mostly home-built experimental installations dedicated to the study of thermodynamic and thermo-physical properties of actinides and nuclear materials.

- JRC-Petten hosts and operates laboratories for the assessment of materials and components performance under thermo-mechanical loading, corrosion, and neutron irradiation. Their Structural Materials Performance Assessment (SMPA) laboratories are used for the mechanical performance characterization, life assessment and qualification of materials for present and next generation nuclear systems.
- JRC-Ispra carries out research in safeguards and security. Their Advanced Safeguards, Measurement, Monitoring and Modeling Laboratory (AS3ML) is used for testing and developing innovative integrated solutions for the implementation of safeguards in the different types of nuclear installations.

Also, worth mentioning are the three direct actions conducted by JRC as major projects in the domain of Gen-IV: (1) The Safety of Advanced Nuclear Systems and Innovative Fuel cycles (SEAT-GEN-IV), (2) System Analysis of Emerging Technologies (SAITEC), and (3) Waste from Innovative fuel (WAIF). The topics covered are focusing on SFR, LFR, VHTR and MSR, such as: reactor safety of Gen-IV reactor designs, including modular reactors (severe accident modeling), materials R&D, safety of fuel, conditioning matrices for waste from innovative fuels, and safeguards. Activities in support of the GIF PR&PP-WG are carried out in the MEDAKNOW project (Methods, Data analysis and Knowledge management for Nuclear Non-proliferation, Safeguards & Security).

Moreover, the Euratom RTD action “Research Infrastructures—Material Testing Reactors” includes two actions on the Jules Horowitz Reactor (JHR, CEA Cadarache) that will allow for innovative fuel and material testing:

- access rights for Euratom researchers (6% JHR irradiation time, 6 million euros from Euratom, leading today to about 40 million euros in collaborative projects);
- the JHR operation plan 2040 in the context of the optimized use of research reactors to plan European specific irradiations (2.6 million euros from Euratom).

Also worth mentioning is the adoption of the Supplementary Programme for HFR Petten, supported by about 30 million euros from the governments of the Netherlands and France.

As far as innovative materials and fuels are concerned, a number of promising technologies to further improve safety are being tested in national and Euratom laboratories, in particular, in the context of the “Joint Programme on Nuclear Materials” (JPNM) under the “European Energy Research Alliance” (EERA).^{av} As a result, development of innovative materials and fuels benefits from advancements of EERA JPNM for fission and fusion.

Regarding above JPNM, it is worth mentioning that cross-thematic activities with non-Euratom programs are quite successful. For example, many technologies and innovative approaches for fabrication, repair and joining (including surface modification of materials) are currently available in non-nuclear industries, but are not yet addressed in nuclear codes and standards or endorsed by regulatory bodies. Here is the list of Standards Development Organizations recognized by above MDEP of OECD/NEA: ASME (USA), AFCEN (France), CSA (Canada), JSME (Japan), KEA (Korea), and NIKIET (designated in Russia).

Regarding nuclear safety improvements, the development of Accident-Tolerant Fuel (ATF) and materials is of particular interest. Fuel and fuel elements in Gen-IV reactor systems will need to ensure that high burnups are reached, including the possibility of burning minor actinides. Fuels and materials will be exposed to high levels of temperature and irradiation, with some in contact with potentially aggressive

^{av} European Energy Research Alliance—more than 250 organizations from 30 countries—<https://www.eera-set.eu/> and Joint Programme on Nuclear Materials—<http://www.eera-jpnm.eu/>. The EERA-JPNM has currently 50 between full (18) and associate (32) members. Members are research centres, universities, umbrella organizations and industries. Altogether they represent 17 European countries.

non-aqueous coolants, targeting 60 years of reactor operation. As a consequence, ATFs are being developed, as a means of preventing the release of fission products. Surface modification on ATF cladding materials can result in significant enhancement on both oxidation resistance and cooling performances, which are essential to ensure the integrity of fuel claddings (under normal operations and accident conditions). For example, the Euratom project II TROVATORE, 2017–2022 (30 beneficiaries across 3 continents, 5 million euros) focuses on innovative ATF cladding material concepts such as SiC/SiC composite clads, MAX phase-coated ceramic materials and Oxide-Dispersed-Strengthened (ODS) FeCrAl alloy clads.

Additionally, the entire nuclear fuel cycle is studied. Innovative strategies and technologies, from front-end to back-end of the fuel cycle, including waste streams and HLW management (in particular, partitioning and transmutation), should help to meet the sustainable goals of minimization of waste and better use of natural resources.

A number of Euratom research and innovation projects are also devoted to cross-cutting nuclear data activities to the level needed by simulation codes to fulfill present requirements for the safe and sustainable operation as well as development of future reactors. Close collaboration exists between Euratom research programs and the Nuclear Data bank of OECD/NEA and IAEA (70 years of nuclear research, including about 2000 computer codes), which are the main repositories of data and standards for nuclear energy applications, thereby providing open access to the scientific community.

The Euratom technical contribution to the GIF systems consists not only of above-mentioned Euratom DG RTD indirect actions and JRC direct actions, but also of direct contributions from the EU Member States.

During this reporting period 2010–2020, EU Member States have indeed invested through their national research programs in several GIF systems. France estimated its investment on Generation-IV R&D at 102 MEUR on a yearly basis. Belgium and Italy have been investing mainly in Lead-bismuth and Lead systems. SCK-CEN (Belgium) has also obtained a grant from its government for MYRRHA R&D (Pb-Bi LFR and ADS—*NB: the Belgian federal government decided to invest 558 million euros during the 2019–2036 period*). Italy has dedicated a 30 MEUR to LFR ALFRED reactor systems. Romania has also allocated around 6 MEUR for the innovative systems with a focus on LFR during the 10-year reporting period. Germany has allocated 3–4 MEUR for each of the 3 fast reactors technologies and VHTR. Finland has invested 0.5–1 MEUR for each of the 3 fast reactors, VHTR and SCWR. The Czech Republic has focused on SCWR (3 MEUR) and LFR (1 MEUR). The Netherlands invested in VHTR, SCWR, MSR and LFR with budgets of 0.4–0.8 MEUR each. Hungary focused on SCWR systems (0.6 MEUR) and on GFR (0.3 MEUR—ALLEGRO reactor system). Poland has invested 1.5 MEUR in the HTRPL project on VHTR. Spain has supported VHTR (0.5 MEUR), SFR (0.1 MEUR) and LFR (0.1 MEUR) R&D activities. Sweden has focused on SFR (0.3 MEUR) and LFR (0.2 MEUR).

10.5.2 European Sustainable Nuclear Fission Industrial Initiative (ESNII) and Nuclear Cogeneration Industrial Initiative (NC2I)

As a consequence of Euratom accession to the GIF Framework Agreement in 2005, the EU is committed to international cooperation in Generation-IV development. This commitment has been entrusted to SNETP, the “Sustainable Nuclear Energy Technology Platform” (over 110 members).^{aw} SNETP was set up in 2007 under

^{aw} List of *European Industrial Initiatives* of interest to research, innovation and education in reactor safety

* SNETP = “Sustainable Nuclear Energy Technology Platform”—<http://www.snetp.eu/>.

- NUGENIA = *NUclear GENeration-II & III Association*—<http://www.nugenia.org/>

- ESNII = *European Sustainable Nuclear energy Industrial Initiative*—<http://www.snetp.eu/esnii/>

- NC2I = *Nuclear Cogeneration Industrial Initiative*—<http://www.snetp.eu/nc2i/>

the auspices of the European Commission: It is composed of three pillars (NUGENIA, ESNII, and NC2I). Of particular interest for Generation-IV are pillar no 2, the “European Sustainable Nuclear Fission Industrial Initiative” (ESNII)—somehow equivalent to the above SIAP—and pillar no 3, the “Nuclear Cogeneration Industrial Initiative” (NC2I). More precisely, ESNII focuses on the Fast Neutron Reactor systems that are considered as key for the deployment of sustainable nuclear fission energy, whereas nuclear fission applications beyond electricity production are favored in NC2I. As a consequence, EU/Euratom contributions cover all six GIF Systems.

The three pillars of SNETP do cover all generations of NPPs and the most important applications of nuclear fission while being aligned with the EU policy for a more competitive resource-efficient economy (including circular economy):

1. *NUclear Generation-II & -III Association/NUGENIA*/dedicated to Gen-II (e.g., long-term operation issues) and Gen-III (e.g., severe accident management)
2. *European Sustainable Nuclear energy Industrial Initiative/ESNII*/dedicated to Gen-IV systems of fast neutron type and associated fuel cycle facilities
3. *Nuclear Cogeneration Industrial Initiative/NC2I*/dedicated to combined heat and power/CHP/generation.

The role of SNETP should be stressed in the context of the ambitious 2008 EU Strategic Energy Technology/SET/Plan (“Making the European energy system more sustainable and secure”), which has identified 10 actions for research and innovation at EU level: action no 10 is “nuclear safety.” SNETP has evolved to form a “European Technology & Innovation Platform” and became an international non-profit legal association in 2019. It is now in the process of updating its Strategic Research and Innovation Agenda.

Originally, ESNII was a Task Force, comprising research organizations and industrial partners, addressing the need for demonstration of Generation-IV Fast Neutron Reactor technologies, together with the supporting research infrastructures, fuel facilities and R&D work. The focus was thus on Euratom and national actions aiming at improving sustainability (i.e., efficient resource utilization and minimization of volume, heat and radio-toxicity of waste) and safety & reliability, as well as proliferation resistance.

According to ESNII, the three types of fast reactors (using as coolant, respectively, sodium/SFR/, lead/LFR/or gas/GFR/) have a comparable potential for making efficient use of uranium and minimizing the production of high-level radioactive waste. When it comes to priorities, the experience accumulated in the EU in sodium technology gives this option a strong starting position. As an alternative to sodium, however, the lead and gas fast reactors also offer a number of interesting features. Lead, for example, is chosen as a coolant for being high-boiling, radiation-resistant, low-activated and at atmospheric pressure.

As a consequence, the different Generation-IV systems were prioritized as follows:

- (1) the sodium-cooled fast neutron reactor technology (ASTRID-like SFR prototype sodium cooled fast reactor) as the reference solution;
- (2) two alternatives (“ex aequo”): the lead-cooled fast reactor ALFRED supported by the lead-bismuth irradiation facility MYRRHA as a first alternative; the gas-cooled fast reactor ALLEGRO as a second alternative.

As far as ASTRID (*Advanced Sodium Technological Reactor for Industrial Demonstration*) is concerned, it should be noted, however, that on August 30, 2019, the CEA confirmed the abandonment of their plans to build this prototype fast neutron reactor. This French Gen-IV prototype is no longer “programmed in the short or medium term.” Work on the sodium technology, however, is expected to be continued, but the construction of a potential demonstrator of this technology will be postponed until the second half of the 21st century. Education and training activities will be continued, in particular, in collaboration with the ESML (“Ecole du

Sodium et des Métaux Liquides”) and the EC (“Ecole des Combustibles”), both located at CEA Cadarache in France. Though some research may be continued in fast neutron technologies in France, many experts fear that it will not be enough to maintain industrial expertise in developing new reactor systems.

Besides the three above priorities of ESNII, the MSFR is considered as a very attractive long-term option. Two other fast neutron Generation-IV technologies are also of interest for Euratom: the European Sodium Fast Reactor (ESFR) and the Swedish Advanced Lead Reactor (SEALER).

As a conclusion of this subsection, through Euratom and national research effort coordinated by ESNII and NC2I, the EU supports R&D activities in all innovative reactor systems proposed by GIF. The Euratom obligations within the GIF Framework Agreement are thus covered (see comprehensive description in JRC 2017 report^{ax}).

Moreover, it should be stressed that, in the EU, public participation in the decision-making process is crucial in the development of energy policies, notably in the domain of nuclear fission (see *revised 2014 Euratom Safety Directive* and *2013 Euratom BSS Directive*). Worth noting in this context is the interest of an increasing number of citizens’ associations for getting reliable information (facts and figures) regarding nuclear fission, including Generation-IV. For this purpose, a European association was created in February 2019: weCARE^{ay} (“Clean Affordable Reliable Energy for Societal Sustainability”). This is an Alliance pooling existing NGO type organizations that share and foster common objectives that can be best summarized using one of their mottos: “*Restore the facts; Change the tone; Refocus the debate on the contributions of nuclear energy, rather than on nuclear itself.*”

10.6 Experimental research reactors in the EU and small modular reactors

10.6.1 Experimental research reactors (training, materials testing, isotope production)

As far as experimental research reactors in the world are concerned, the situation has recently evolved, with the shutdown of several Material Testing Reactors (MTRs):

- the Osiris reactor (radioisotope productions, 70 MW_{th}) in CEA, France in 2015
- the Japan Material Test Reactor (Japan Atomic Energy Agency, 50 MW_{th}) in 2017
- the Halden BWR in Norway (heavy water, 25 MW_{th}) in 2018.

A quick look at some major remaining MTRs in operation today indicates that several of these are quite old: ATR (USA, 1967), MIR and SM3 (Russia, 1967 and 1961 resp.), BR2 (Belgium, 1962), HFR (the Netherlands, 1961), while LVR-15 (Czech Republic, 1995) and the TRIGA in Pitesti (Romania, 1980) are younger. The probability of final shutdown in the next 10–20 years of facilities built in the 1960s appears very high. To cope with this situation, only a limited number of projects of new MTRs are under construction.

Moreover, high performance research reactors have to overcome the challenging conversion from highly enriched to low enriched uranium fuels, to fulfill a worldwide non-proliferation effort.

^{ax} “Euratom Contribution to the Generation IV International Forum Systems in the period 2005–2014 and future outlook”—<http://publications.jrc.ec.europa.eu/repository/bitstream/JRC104056/kjna28391enn.pdf>.

^{ay} The European weCARE Alliance groups together 10 members and 2 associates as of June 2021—it is listed in the EU Transparency Register under no 473723535459-78—<https://www.wecareeu.org>

* 10 Member Organizations: 100 TWh (Belgium); Ekomodernist Finland, European Association for Energy Security (Slovak Republic); Institute for Sustainable Energy Poland; Jihocesti Tatkove (Czech Republic); Patrimoine Nucléaire et Climat (France); Sauvons Le Climat (France); Stichting Energietransitie & Kernenergie (the Netherlands); Terraprxaxis (United Kingdom); 18for0 (Ireland);

* Two Associated Organizations: European Physical Society (international); Les Voix du Nucléaire (FR).

Major experimental facilities are needed to support Generation-IV systems (SFR, LFR, GFR, VHTR, MSR and SCWR).^{az} This enables progress to be made in the three above-mentioned phases of the GIF roadmap (viability, performance, demonstration), depending on the Technological Readiness Level (TRL) of each GIF reactor system.

In line with the priority assigned to fast neutron spectrum reactors, ESNII is supporting the design and construction of four demonstrators related to Generation IV in the EU, namely:

1. The ASTRID-like SFR demonstration reactor with sodium coolant, to be built in France in the second half of the century as a project led by French government/CEA/(using originally a national loan of EUR 650 million) in association with a number of industrial national and international partners. ASTRID was originally designed to pursue R&D on sodium fast reactors and demonstrate the feasibility of transmutation of minor actinides. ASTRID's main technical choices (basic design phase) were originally: 1500MW_{th} to 600MW_{el} pool type reactor; with an intermediate sodium circuit; CFV core (low sodium void worth); oxide fuel UO₂-PuO₂; preliminary strategy for severe accidents (internal core catcher); diversified decay heat removal systems; fuel handling in gas; internal storage; conical inner vessel ("redan") adopted; open design option: energy conversion system (classical Rankine water-steam cycle or Brayton gas cycle). It should be recalled, however, that CEA confirmed in August 2019 the abandonment of their plans to build ASTRID but work on the sodium technology is expected to be continued.
2. The MYRRHA fast spectrum irradiation facility^{ba} in a research reactor with lead-bismuth coolant, open to international collaboration ("*Multipurpose hYbrid Research Reactor for High-technology Applications*", 50–100MW_{th}). MYRRHA is led by and hosted at SCK-CEN Mol, Belgium: its aim is to replace the high thermal neutron flux research reactor BR2. It has featured in the roadmap of the "*European Strategy Forum on Research Infrastructures*" /ESFRI/since 2010.

The focus is on minor actinide burning (i.e., radioactive waste minimization) via an Accelerator Driven System (ADS) using a subcritical fast neutron spectrum core. With the subcritical concentration of fission material, the nuclear reaction is sustained by the particle accelerator only. Turning off the proton beam results in an immediate and safe halt of the nuclear reactions.

The MYRRHA facility which is a Material and Fuel Testing Reactor, consists of four major components:

- the Linear Accelerator (linac injector)—the 4-mA proton beam is injected into the reactor, generating a flux of fast neutrons through spallation
- the Lead-Bismuth Eutectic (LBE) cooled fast reactor will utilize U-235 and U-238 as well as MOX fuel; and may contain up to 30% of long-lived minor actinides, such as Np, Am and Cm (thereby reducing the waste burden)
- the Proton Target Facility (aimed at the production of radioisotopes and research into several fields)
- the Fusion Target Station (high constant fast flux level and large irradiation volume of 3000 cm³, thereby meeting the irradiation conditions required for fusion materials).

MYRRHA will be implemented in three phases (2026; 2033; 2036). On September 7, 2018, the Belgian Federal Government decided to have the MYRRHA project built on the SCK-CEN site in Mol. Based on a total budget of 1.6 billion euros, the federal government decided to invest 558 million euros

^{az} "GIF R&D Infrastructure Task Force" (GIF RDTF—final report—96 pages—January 2021)—https://www.gen-4.org/gif/upload/docs/application/pdf/2021-02/gif-rdtf_final_report_jan2021.pdf.

^{ba} MYRRHA—Less (toxic) nuclear waste (testing of Partitioning & Transmutation); Production of medical radio-isotopes; New reactor concepts; Fundamental research—<https://www.sckcen.be/en/projects/myrrha>.

during the 2019–2036 period in phase 1 of MYRRHA including the construction of the MYRRHA accelerator up to 100 MeV and its proton target facilities as well as in the preparatory phases of design & R&D for extending the accelerator up to 600 MeV. The reactor is scheduled to be commissioned in 2036.

3. ALFRED demonstrator with lead coolant (*Advanced Lead Fast Reactor European Demonstrator*),^{bb} project to be hosted in the Nuclear Research Institute (ICN), Pitești, Romania, in collaboration with the FALCON consortium “Fostering ALFRED Construction.” The partners are Romania’s Nuclear Research Institute (RATEN-ICN) as well as Ansaldo Nucleare and Italy’s National Agency ENEA. ALFRED is expected to produce 125 MW_{el}; its design should as far as possible be based on available technology, in order to speed up the construction time; it will use structural materials compatible with the corrosive lead used as coolant (selected candidate: AISI 316LN, 15–15/Ti). Decay Heat Removal Systems will be based on passive technology to reach the expected high safety level (low primary system pressure drops to enhance natural circulation).
4. ALLEGRO (not an acronym), a *Gas Cooled Fast Reactor demonstrator* with helium coolant,^{bc} resulting from regional collaboration in the V4G4 Centre of Excellence (*Vișegrad 4* countries for *Gen-IV* reactors) composed of Hungary’s Academy of Sciences Centre for Energy Research (MTA EK); the Czech Republic’s ÚJV Rež; the Slovak engineering company VUJE Trnava; and Poland’s National Centre for Nuclear Research (NCBJ Swierk). The project started in 2009 as a close collaboration with French CEA which provided a good technical base for further development by V4G4. Short-term priorities in the development are as follows: improve level of safety using passive systems (where possible); design UOX-based driver core while maintaining interesting power density & irradiation characteristics. The short-term priorities in R&D are: coolability in protected transients using natural convection (core outlet $T < 530^{\circ}\text{C}$); feasibility of guard vessel for elevated pressure; optimization of Decay Heat Removal systems (valves, heat exchangers, pressure drop, etc.); turbomachinery in secondary circuit; potentially alternative cladding material for the driver core.

An important achievement in the context of thermal neutron spectrum facilities under construction in the European Union is the *Jules Horowitz Reactor* (JHR).^{bd} This is a research reactor (100 MW_{th}, pool-type, JHR school added in 2019) under construction at CEA Cadarache. The JHR construction was recommended by ESFRI as a replacement for the EU’s existing MTRs, which were all built in the 1960s, and which are expected to reach the end of their service lives in the 2020s. The JHR is funded and steered by an international consortium bringing together the following partners: CEA (France), EdF-Framatome (France), TechnicAtome (France), SCK-CEN (Belgium), ÚJV (Czech Republic), CIEMAT (Spain), Studsvik (Sweden), DAE (India), IAEC (Israel), NNL (United Kingdom), and the European Commission (Euratom) and its JRC (EU) as observer. The European Commission has secured 6% of the guaranteed access to irradiation capacity. It makes the EC the larger non-French contributor to the JHR, seven bilateral foreign

^{bb} ALFRED—“Research and Innovation in Romania,” European Research Area and Innovation Committee, 21 March 2019—https://era.gv.at/public/documents/3781/3_Research_and_Innovation_in_Romania.pdf and LFR related GIF webinars no 10 in 2017 by US Naval Graduate School and no 23 in 2018 by Ansaldo.

^{bc} “The ALLEGRO experimental gas (helium) cooled fast reactor project,” GIF webinar no 27 (20 March 2019) by ÚJV ŘEŽ—https://www.gen-4.org/gif/upload/docs/application/pdf/201903/geniv_template-dr_ladislav_belovsky_final_3-20-19.pdf and GFR related GIF webinar no 6 in 2017 by CEA.

^{bd} “SUPPORTING INFRASTRUCTURES AND RESEARCH REACTORS: STATUS, NEEDS AND INTERNATIONAL COOPERATION, with emphasis on JHR” by CEA France at FISA-2019 conference (Pitești, Romania, 4–7 June 2019)—<http://fisa-euradwaste2019.nuclear.ro/wp-content/uploads/2019/07/Jean-Yves-BLANC-presentation.pdf> and CEA JHR website <http://www-rjh.cea.fr/news.html>.

partners having taken 2% each and India 3%. When operating at full capacity, the JHR will produce, in the reflector surrounding the core area, a thermal neutron flux to study current and innovative nuclear fuels. In-core experiments will address typically material experiments with high fast flux capability up to 5.5×10^{14} n/cm²/s fast neutron flux with energy larger than 1 MeV. By the end of 2023, the new cost assessment of the JHR and the project plan have to be completed, but first criticality is not expected before the end of this decade.

As far as plans for construction of thermal neutron research reactors in the EU are concerned, the *PALLAS* reactor project should be mentioned. It is aimed at taking over from the 50-year-old HFR in Petten, the Netherlands, dedicated to medical isotope production and other applications of ionizing irradiation.^{be} The Pallas design and construction contract was awarded in January 2018 by the “Foundation Preparation PALLAS Reactor” to a consortium led by the Argentinean company Invap (Argentine National Atomic Energy, Bariloche). The Pallas reactor is to be of the “tank-in-pool” type, with a thermal power of around 55 MW_{th}. Basic design is completed, construction will begin in 2022. In 2025, a four-year transition period is planned to finish construction and commissioning of the reactor and transfer of all irradiation programs from the HFR to the PALLAS reactor. The lifetime of the new reactor is expected to be at least 40 years. *NB: Invap has a broad experience in the construction and operation of research reactors and has been exporting its technology to Peru, Algeria, Egypt, Australia and Brazil.*

As far as the Nuclear Cogeneration Industrial Initiative (NC2I) is concerned, it should be recalled that, in Europe, about 89 GW_{th}, i.e., 50% of the process heat market is found in the temperature range up to 550°C (today mainly in the chemical industry, in the future possibly in steelmaking, hydrogen production, etc.). NC2I thus strives to provide a non-electricity nuclear contribution to the decarbonization of industrial energy. NC2I gives highest priority to HTR. The Polish government has shown interest in developing HTR technology for heat supply to its industry (reference: 2017 policy document), because:

- it is the most mature technology (750 reactor-years of operational experience), capable of industrial deployment before 2050
- it can fully address, without further development, the needs of a large class of processes receiving heat or steam as a reactant from steam networks (typically around 550°C), as is the case in the chemical and petrochemical industries
- it has the potential to address, in the longer-term, other types of applications which are not connected at present to steam networks, in particular bulk hydrogen production and other applications at temperatures higher than 550°C.

Commonalities between fusion and Generation-IV fission reactors are also worth discussing. Because of the extreme conditions characteristic of these systems, several safety concerns and materials issues are relevant to both of them. A number of Euratom fast neutron experimental facilities and R&D projects are investigating shared solutions. We should remember that (1) the main wastes in fusion are activated structural materials (tritiated waste management is a common concern), and that (2) the main safety issue for fusion is represented by tritium management in terms of the need to reduce inventory and avoid release (tritium, as an isotope of hydrogen, is easily absorbed in any material).

^{be} “The Foundation Preparation Pallas-reactor”—<https://www.pallasreactor.com/en/pallas-organisation/> and “Green light for Pallas reactor”, NEI, 17 March 2020—<https://www.neimagazine.com/news/newsgreen-light-for-pallas-reactor-7830460> (NB—The costs for the new reactor are estimated at 700 million euros).

10.6.2 SMR technology is a great opportunity for the nuclear industry and could lead to a nuclear renaissance

A special mention is needed regarding Small and Medium nuclear power Reactors (also called “Modular”—in short SMR) that are awaiting licensing and industrial deployment. The IAEA defines “small” as under 300 MW_{el}, and “medium” as up to about 700 MW_{el}.^{bf} SMRs (both evolutionary and innovative) are characterized by components and systems that can be shop fabricated and then transported as modules to the sites for installation as demand arises. Generally, SMRs are expected to have greater simplicity of design, and to benefit from economies of series production, largely in factories, with short construction times and reduced siting costs. As a result, capital costs are reduced and electric power (and/or heat in the case of cogeneration plants) is provided away from large grid systems.

As of 2020, there are about 50 SMR designs and concepts globally. Most of them are in various developmental stages and some are claimed as being near-term deployable. One SMR (PWR, thermal neutron spectrum, cogeneration of heat and power) began commercial operation in May 2020: it is the world’s only floating NPP, the Akademik Lomonosov (KLT-40S), in the Russian Arctic region—the power capacity is 70 MW, the heat capacity is up to 60 MW - another joint product is freshwater made from seawater. Another thermal neutron SMR worth mentioning is Argentina’s CAREM reactor (integrated PWR): it will generate 25 MW (construction start date 2015 - first criticality date N/A), adjacent to the Atucha I Nuclear Power Plant.

SMRs are also expected to have lower core damage frequencies and longer postaccident coping (so-called “grace”) periods, due to a high level of passive or inherent safety. They are usually more resistant to natural phenomena and have potentially smaller emergency preparedness zones than currently licensed reactors. Implementation of DiD in SMRs is relatively simpler than in large power reactors, that is: the use of stringent access controls, physical barriers, redundant and diverse key safety functions (in particular, 1—control of reactivity, 2—cooling of fuel elements, and 3—activity retention), and effective emergency response measures. Here are some objectives set by the SMR developers: having full understanding of cost–benefit (the first requirement); simplifying operations (e.g., by reducing reliance on human actions); harmonizing safety and security; considering remotely operated defense systems; having as much containment as possible; building the nuclear island below ground; ensuring online refueling; developing new (international) transport regulations if the SMR (e.g., floating NPP) is transported; apply integrated security and safety cost-benefit analysis to ensure affordability.

Within GIF, there is revival of interest in SMRs for generating process heat and/or electricity (combined heat and power or CHP), mainly in view of applications such as: (1) replacing aging fossil (in particular coal-fired) power plants; (2) integrating hybrid nuclear/renewables energy systems; (3) providing cogeneration for developing countries with small electricity grids, underdeveloped infrastructure and/or limited financial resources; (4) operating in remote settlements (off grid areas) or industrial facilities with insufficient cooling capacity for large NPPs; (5) technology process applications (e.g., water desalination, petro-chemistry, hydrogen production and others).

In addition, flexibility in electricity generation from nuclear can be enhanced by the development of SMRs. In recent years, with large new nuclear projects advancing slowly, as well as an increased presence of variable (intermittent, non-dispatchable) sources in the energy mix and progressive decentralization of the grid, opportunities in smaller scale nuclear power reactors have again become subject to analysis. In SMR design, attention is paid in particular to the capacity of the reactor to respond rapidly to changes in the

^{bf} “Advances in small modular reactor technology developments” IAEA, Sept 2020—This IAEA report covers land based and marine based water-cooled reactors, high temperature gas cooled reactors, liquid metal (sodium and lead), gas-cooled fast neutron spectrum reactors, molten salt reactors, and the recent micro modular reactors (up to 10 MW_{el})—https://aris.iaea.org/Publications/SMR_Book_2020.pdf and IAEA website “small modular reactors”—<https://www.iaea.org/topics/small-modular-reactors>.

required power output. It should be noted, however, that a switch from traditional base-load operations to load-following operations leads to increased temperature and pressure cycling, which may lead to a new type of material degradation (e.g., thermal fatigue).

A few SMRs of power under $300 \text{ MW}_{\text{el}}$ are considered among the GIF systems and are under construction in the world, notably in the areas of (V)HTR and LFR:

1 (V)HTR (High-Temperature Reactor-Pebble-bed Modules/HTR-PM or HTR-200/) designed for commercial power generation, under construction in China:

It is the world's first modular high-temperature helium gas-cooled reactor demonstration plant (composed of two modules of $250 \text{ MW}_{\text{th}}$, jointly driving a steam turbine generating $200 \text{ MW}_{\text{el}}$)—it has been installed at the Shidaowan plant, near the city of Rongcheng in Shandong Province. Design is by the *Institute of Nuclear Energy Tsinghua University* (INET) and development is by *China Nuclear Engineering Corporation* (CNEC) and Huaneng. Construction began at the end of 2012. Main component installation started with the first reactor pressure vessel in March 2016. The project completed cold tests and began hot testing in January 2021. Reactor 1 of the demonstration HTR-PM has been connected to the grid in December 2021, the partners in the consortium building the plant have announced. A further 18 such HTR-PM units are proposed for the Shidaowan site ($2000 \text{ MW}_{\text{el}}$ in total).

2 LFR (pool type) planned in the EU (Belgium), in Russia and in the United States

2.1 in the European Union, the above MYRRHA facility under construction at SCK-CEN Mol Belgium: fast spectrum irradiation, accelerator driven system of $50\text{--}100 \text{ MW}_{\text{th}}$, focusing on minor actinide burning (commissioning planned by 2036).

2.2 in the Russian Federation, a system of intermediate size (lead-cooled fast reactor BREST-300-OD of $700 \text{ MW}_{\text{th}}/300 \text{ MW}_{\text{el}}$) with high density U-Pu nitride fuel. The license for construction in Seversk (near Tomsk) has been issued by Russian regulator Rostechнадзор in February 2021. According to the planned timeline, the BREST-OD-300 reactor should start first of a kind engineering demonstration in 2026.

2.3 another challenging Russian design is the Lead-Bismuth Fast Reactor SVBR-100 of $280 \text{ MW}_{\text{th}}/100 \text{ MW}_{\text{el}}$, with a wide variety of fuels (refueling interval of 8 years). This multipurpose prototype reactor is under construction by OJSC OKB Gidropress at the Research Institute for Atomic Reactors/NIAR/in Dimitrovgrad. Last project milestone (planned): serial production and supply of packaged equipment in 2032.

2.4 in the United States, a small size transportable system (“Small, sealed, transportable, autonomous reactor”/SSTAR/: $45 \text{ MW}_{\text{th}}/20 \text{ MW}_{\text{el}}$) with a very long core life (30 years). This lead-cooled nuclear reactor, primarily developed by the Lawrence Livermore National Laboratory, was meant for use in developing countries (which would use the reactor for several decades and then return the entire unit to the manufacturing country).

3 Also worth mentioning amongst the SMRS of Generation IV type is the small modular SFR /SMFR/ planned in the United States. It is a small size ($50\text{--}150 \text{ MW}_{\text{el}}$) reactor with the following features: uranium-plutonium-minor-actinide zirconium metal alloy fuel; fuel cycle based on pyro-metallurgical processing in facilities integrated with the reactor.

N.B.: Historical reminder regarding the “European Fast Reactor” project (1984–1993).

The bases for the “European Fast Reactor” (EFR) cooperation were laid in 1984 when the governments of Belgium, France, Germany, Italy and the United Kingdom signed a memorandum of understanding to harmonize their fast reactor development programs and achieve more efficient pooling of their experiences and

resources.^{bg} Utilities, design companies and R&D organizations were involved during a decade. The main funding was originally provided by national programs and by utilities from the five EU countries concerned.

Three subsequent specific agreements were signed shortly after 1984:

- the “*R&D Agreement*,” relating to research and development, which was signed by European R&D organizations
- the “*Industrial Agreement*,” relating to cooperation in design, construction and marketing, which was signed by European design and construction companies
- the “*Intellectual Property Agreement*,” setting out the terms and conditions controlling the use of existing and future know-how information at the disposal of the European partners.

More than 1000 specialists worked efficiently together, even though they were located in 20 or so offices and laboratories spread across Europe, and although they belonged to several companies with diverse backgrounds, terms of reference and management structures. The EFR approach was very similar to the above-mentioned three phases of the Generation-IV deployment strategy (viability—performance—demonstration).

One of the main activities of R&D management was to identify current research needs and avoid duplication (or even triplication) of efforts in existing research programs (related to Phenix, SPX-1 and -2 in France; KNK-2, SNR-300 and SNR-2 in Germany, PFR and CDFR in the United Kingdom). For this purpose, EFR created a number of Working Groups called “AGT”: AGT is a German-French acronym Arbeits-Gruppe—Groupe de Travail.

Here is the list of AGT Working Groups (each of them comprising tens of different tasks):

AGT1 Fuel Elements and Core Materials; AGT2A Sodium Chemistry; AGT2B Instrumentation; AGT3 Core Physics; AGT4 Safety Research; AGT5 Thermal Hydraulics and Core Mechanics; AGT6 Reactor Vessel, Handling, and Auxiliaries; AGT7 Thermal Transfer Systems and Components; AGT8 Reactor Operation; AGT9A Plant Structural Materials; and AGT9B Structural Integrity.

The end of the EFR Project came almost unnoticed after the Concept Validation Phase, which expired at the end of 1993 (step 2 out of 3). Firstly, the governments, especially in the United Kingdom and in Germany, withdrew from financing the Research and Development Programme. Then the European utilities (European Fast Reactor Utilities Group/EFRUG/) stopped financing the design companies. It is nevertheless considered that the EFR collaboration was a very successful example of how an advanced technological development can be handled across nations, thereby sharing costs and reaping the benefits of international skills and expertise.

10.7 Conclusion: The Euratom research and training program—Maintaining EU leadership in nuclear fission developments

Thanks to Euratom, the European Union will maintain world leadership in nuclear safety, radiation protection, radioactive waste management and decommissioning as well as in non-proliferation (safeguards and security) with the highest level of safety standards. Moreover, fission technologies will be transmitted to coming generations within the framework of a responsible strategy (science for policy).

^{bg} EFR—merge the on-going efforts for the national commercial projects (SuperPheniX-2 or SPX-2 in France, SNR-2 in Germany and CDFR in the United Kingdom) into a single European project (originally 3 step plan)—http://www.iaea.org/inis/collection/NCLCollectionStore/_Public/25/028/25028985.pdf “*The Story of the European Fast Reactor Cooperation*,” Dr. Willy Marth, Kernforschungszentrum Karlsruhe KfK 5255, Dezember 1993—<http://bibliothek.fzk.de/zb/kfk-berichte/KFK5255.pdf>.

Sustainability comes as an additional challenge in our 21-st century, with requirements such as recycling of fissile and fertile nuclear materials, which are satisfied by GEN-IV reactors of the fast neutron type.

The Euratom research and training programme in nuclear fission naturally contributes to the achievement of the main objectives of the EU’s energy and climate policy, namely:

- the EU Energy Union Package (2015) aligned with the ambitious 2008 EU SET Plan: toward secure, sustainable, competitive and affordable energy systems
- the EU Green Deal (2020): toward a European climate-neutral economy by 2050.

Regardless of the EU Member States decisions on continuing, phasing out or embarking in new build NPPs, nuclear energy will continue for the next decades to be part of the energy mix in the EU and also world-wide, especially in a low-carbon economy. Efficient research, innovation and training under Euratom framework programs are crucial to help achieve the above EU objectives (in particular, regarding the EU Green Deal 2020), which will also help reduce energy and technology dependence at EU level.

In this article, the last two decades of Euratom research, innovation and development in reactor systems and associated fuel manufacturing facilities regarding Generation II, III, and IV are taken into consideration, focusing on safety and sustainability. Small and Medium Reactors (SMRs) also require a lot of attention: this technology is a great opportunity for the nuclear industry and could lead to a nuclear renaissance. A number of scientific-technological and sociopolitical challenges are discussed in connection with the three phases of Generation-IV deployment (viability—performance—demonstration).

The “Technology Roadmap” for the six GIF systems (updated in 2013) and the main Euratom achievements are presented in connection with the GIF objectives:

1. sustainability (in particular, optimal utilization of natural resources and waste minimization) including decarbonization of the economy and security of supply
2. safety and reliability (through design, technology, regulation and culture)
3. economics (industrial competitiveness, integration in low-carbon energy mix) together with social aspects (in particular, easy access to affordable energy for all)
4. proliferation resistance and physical protection (aligned with the non-proliferation treaty, IAEA 1970).

As a consequence of Euratom accession to the GIF Framework Agreement in 2005, the EU is committed to international cooperation in Generation-IV development. This commitment has been entrusted to the “European Sustainable Nuclear Fission Industrial Initiative” (ESNII) and to the “Nuclear Cogeneration Industrial Initiative” (NC2I). It has been shown that ESNII focuses on the Fast Neutron Reactor systems that are considered as key for the deployment of sustainable nuclear fission energy, that is: Sodium-cooled Fast Reactors (SFR); Lead-cooled Fast Reactors (LFR); Gas-cooled Fast Reactors (GFR); Molten Salt Reactors (MSR); and SuperCritical Water Reactors (SCWR). A fast neutron reactor deployment would extract far greater energy per ton of uranium than is obtained from other reactors (gain factor of up to 50 as compared to LWR fleet). On the other hand, NC2I focuses on nuclear fission applications beyond electricity production—in particular, process heat supply (including chemicals refinement and hydrogen production). NC2I is concentrated on the Very-High-Temperature Reactors (VHTR), with thermal neutron spectrum. As a consequence, EU/Euratom contributions cover all six GIF reactor systems.

As regards the criterion of competitiveness, considerable effort is being put by both the research community and the industrial organizations concerned, into reducing the costs of installed capacity (euro/kWe) and of power generation (euro/MWh). Also worth noting is the challenge of integrating nuclear fission in a

low-carbon energy mix: this is actually the main change compared to the start of GIF in 2000 when the question was focused on Gen IV versus Gen III, while still assuming reactors would operate in baseload.

As far as the future of Euratom research and training programs is concerned, it should be noted that the Scientific and Technical Committee/STC/(Euratom Treaty—Article 7) put the following questions to the Euratom community (i.e., a challenge for the EU):

- what should be the immediate research priorities to be considered at EU level?
- what are the key assumptions underpinning the development of these priorities?
- what is the output and impact that could be foreseen if the development of these priorities is successful?
- which are the bottlenecks, risks and uncertainties, and how could these be addressed?
- which science and technology gaps and potential game changers need to be taken into account?
- what are the perspectives for cross-thematic activities of Euratom research with other areas under Horizon Europe 2021–2027?
- what are the perspectives for supporting horizontal activities, notably international cooperation, education and training, social sciences and humanities?

Restoring the nuclear industry’s lead in technology development is critical in the EU if it is to regain its attractiveness as a sector to work in. Transmission of knowledge, skills and competences to coming generations is at the heart of Euratom programs (see Euratom Treaty, 1957). The central role of the “European Nuclear Education Network” (ENEN) in this regard has been illustrated. Results were presented of the close cooperation of organizations involved in the application and teaching of nuclear science and ionizing radiation, including universities, research organizations, industry and regulatory bodies.

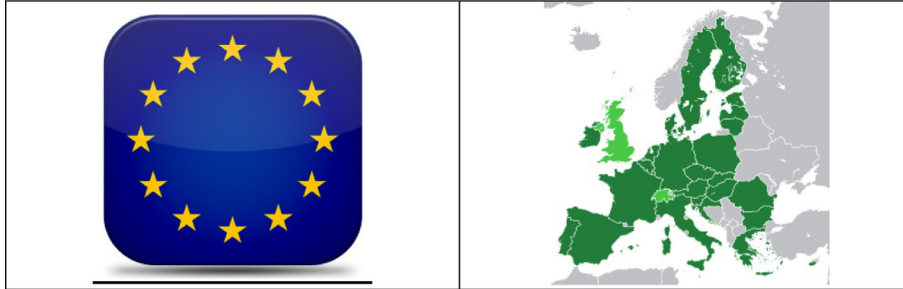
EU research and innovation programs (in particular in the nuclear fission sector) are conducted in the context of a new governance structure, based on greater openness, participation, accountability, effectiveness and coherence. In the Euratom R&D programs, participation of all stakeholders, for example, through SNETP (“Sustainable Nuclear Energy Technology Platform”) helps to build the climate of confidence that is needed to continuously improve applications of nuclear fission science and technology, notably through the development of sustainable Generation-IV reactor systems.

More generally, effective interaction is maintained in the Euratom nuclear fission community thanks to the participation of all stakeholders concerned, i.e.:

- research organizations (e.g., public and private sectors)
- systems suppliers (e.g., nuclear vendors, engineering companies)
- energy providers (e.g., electrical utilities and associated fuel cycle industry)
- Technical Safety Organizations (TSO) associated with nuclear regulatory authorities
- academia and higher education and training institutions dedicated to nuclear
- civil society (e.g., policy makers & opinion leaders), NGOs, citizens’ associations).

In conclusion, a new way of “developing/teaching science” is emerging in the EU, closer to end-user needs of the 21st century (in particular, society and industry). A strong scientific foundation is being established to support decision making in regulatory and/or industrial organizations, based on confirmed facts and research findings stemming from “Best Available Science.” For example, proper impact assessment methodologies are being developed in the EU energy policy decision process to compare the pros and cons of the primary energy sources (renewables, fossil and nuclear) in terms of sustainable development, security of supply and industrial competitiveness.

As a result of this “science for policy” approach, science is no longer confined to the laboratories: it is discussed in the public arena. A clear signal is sent to the young generations to undertake scientific studies in the field of energy—in particular, nuclear—which will contribute to optimize the energy mix in accordance with the expectations of the 21st century (toward secure, sustainable, competitive and affordable energy systems).



ESFR SMART: A European Sodium Fast Reactor concept including the European feedback experience and the new safety commitments following Fukushima accident

Joel Guidez^a, Janos Bodi^b, Konstantin Mikityuk^b, and Enrico Girardi^c
^aCEA, CEN SACLAY, Gif-sur-Yvette, France ^bPaul Scherrer Institut, Villigen, Switzerland
^cEDF Lab Paris-Saclay, Palaiseau, France

Nomenclature

ACS	Above Core Structure
ASTRID	Advanced Sodium Technological Reactor for Industrial Demonstration
BN-800	Russian sodium fast reactor 800MW _{el}
CP-ESFR	Collaborative Program—European Sodium Fast Reactor
DHR	Decay Heat Removal
DHRS	Decay Heat Removal System
DLCM	Direct Lift Charge Machine
EFR	European Fast Reactor
ESFR	European Sodium Fast Reactor
FACM	Fixed Arm Charge Machine
GEN IV	Generation IV
GIF	Generation IV International Forum
IHX	Intermediate Heat eXchanger
I&C	Instrumentation and Control
ISIR	In Service Inspection and Repair
KNK 2	German SFR prototype
LMTD	Logarithmic Mean Temperature Difference
PP	Primary Pump
PFBR	Prototype Fast Breeder Reactor (India)
PFR	Prototype Fast Reactor (UK)
PGSFR	Prototype G Sodium Fast Reactor (Korea)
Phenix	French fast reactor 250MW _{el}
PWR	Pressurized Water Reactor
R&D	Research and Development
SFR	Sodium Fast Reactor
SG	Steam Generator
SMART	Safety Measures Assessment and Research Tools
Superphenix	French fast reactor 1200MW _{el}
UK	United Kingdom

11.1 The ESRF-SMART project

In 1988, while the European Superphenix reactor was in operation, a new European (Sodium) Fast Reactor (EFR) project, with a slightly higher power of 1500 MW_{el}, was launched in collaboration between Italy, Germany, and the United Kingdom. This project was stopped by the shutdown of Superphenix reactor (see [Figure 11.1](#)) and was closed by a final file summarizing all the options selected ([EFR associates, 1998](#)). On this basis, a project called CP ESRF (Collaborative Project on European SFR) was initiated a few years later to “groom” EFR options and integrate the new technical developments ([Fiorini and Vasile, 2011](#)). It is on this new basis that a project called ESRF-SMART (Safety Measures Assessment and Research Tools) started at the end of 2017 mainly with the objective of integrating the new safety rules resulting primarily from the Fukushima accident ([Mikityuk et al., 2017](#)).

The ESRF-SMART project is what in the Anglo-Saxon world is called a “working horse” or a “concept car.” Its role is to introduce, outside any constructive planning, new ideas for the future, which can be valuable guides for R&D. Unlike in an “industrial” project, which initially had a construction schedule, one can introduce innovative ideas, even if their lower technological-readiness level would require development and time. For these new ideas, research and first calculations are performed to check their general feasibility and the absence of major impossibilities. The project is not designed to necessarily create solutions, which can be readily used by a committed industrialist, requiring validation after numerous additional files submitted to the Nuclear Safety Authority (ASN), but as was earlier mentioned, rather narrow down further R&D directions to the most feasible and promising concepts in the future.

In this sense, one of the main goals of the project was to select, implement, and assess new safety measures for a commercial-size SFR in Europe.

11.2 Sodium fast reactors history in Europe

On the basis of the SFR promises, France, Germany, and the United Kingdom (UK) embarked on the construction of SFRs in the 1970s: The “Phénix” SFR in France, the Prototype Fast Reactor (PFR) in the United



Figure 11.1. View of Superphenix reactor in 1987 ([Guidez and Prele, 2017](#))

Kingdom, and an SFR called KNK2, in Germany. The gradual withdrawal of nuclear power in Germany and England in the 1980s led to the termination of fast-reactor development programs in these countries.

Only France, backed by the success of its reprocessing activities, continued along this path with the construction of the Superphénix reactor (1200 MW_{el}) (see [Figure 11.1](#)). This was already a European reactor with strong participation from Italy (30%) and a Germany/Netherlands consortium (around 5%). As it was subject to strong opposition from environmentalist groups and a lack of political support, the reactor was shut down in 1996 for purely political reasons, after a year of successful steady operation. During the 10 years of operation, Superphénix spent more than a third of these 10 years, able to operate, but shutdown only waiting for administrative authorizations ([Guidez and Prêlé, 2017](#)).

A new project on a smaller SFR of 600 MW_{el}, called ASTRID (Advanced Sodium Technological Reactor for Industrial Demonstration), was recently launched in France. The studies have enabled new advances in this field, in particular, in the design of the reactor core. Sadly, the project was stopped in 2019, and, currently, no large- or medium-size commercial SFR project is planned today in France or in Europe before the end of this century.

Given the huge potential advantages of these reactors, and their active development in countries as Russia and China, the question naturally arises, why we do not see this type of reactor emerging in Europe today, with all the experience accumulated during the past years.

There are several reasons for this:

- There are some technical difficulties specific to the SFR. Several experimental reactors (such as the PFR in the United Kingdom) had technical difficulties, which led to their premature shutdown.
- The public opinion is generally negative in relation to plutonium in the United States, which, due to political reasons, led to the abolition of fuel reprocessing, where the plutonium is separated from the used fuel. Unavailable reprocessing leads to the lack of plutonium, which, eventually, ends the fast-reactors development. Therefore, the SFR development has been stopped in the United States, even if some research-reactor projects remain in 2021.
- Only countries with reprocessing plants remained interested in this technology. In 2020, outside France, we find, mainly, Russia and Japan with reprocessing plants in operation or close to commissioning, what is crucial to close the fuel cycle of the reactor.
- Uranium prospecting, from the 1960s onward, led to significant discoveries of many high-rate mines. This drove the price of uranium to a historical low point. Further prospecting has almost stopped and some mines were even closed. Correspondingly, this motivation for fast reactors has temporarily disappeared.
- There is an additional cost. By design, an SFR is more expensive than a PWR, which is more compact and without secondary circuits. The additional costs are estimated to be between 30% and 40%. On top of this, additional costs have to be added, inherent in the prototype reactors with which the knowledge is not accumulated by mass production.
- Reprocessing and fuel fabrication are feasible, but complex. The specific global fuel cycle requires significant investments.
- It exists, at least in France, a strong opposition of environmentalists. This type of reactor, claiming to be able to operate without uranium mines and to produce our energy for thousands of years, based on the available nuclear wastes, has been a real red flag for environmentalists seeking to exit from nuclear power. Their opposition is today anticipated to be strong and constant.
- Under these conditions political support collapses and, in particular, in France, Superphénix was shut down after elections, as a pledge of a political coalition with environmentalists.
- It is difficult to defend long-term investments in a world, which rather demands short-term returns on these investments.

In conclusion, the fast-reactor technology has ecological interests, but its development requires significant long-term investments, hardly compatible with economic models of rapid profitability. In addition,

the environmentalists, who could have been the defenders of the concept, carried out, at least in France, a bitter fight against Superphénix. This opposition remains strong today and has led to a lack of support from recent French politicians. This explains why in the short term, a solution that could potentially solve humanity's energy problems, in particular with regard to climate change, uranium supply and waste management, is currently at a standstill. Under these conditions, Europe needs to maintain, with projects like ESFR-SMART, competence and overview on what could be an SFR in the future. This view is supported by the fact that the pressure to solve climate change fosters the reintroduction of efforts to implement new nuclear technology into the energy generation mix, thus the political interest can potentially change in the future.

11.3 Safety improvement: Objectives and methodology

Since the previous CP ESFR project, the safety groups of the Generation IV International Forum (GIF) have published new documents. In particular, a "task force" dedicated to SFRs proposed a set of rules to be applied for these reactors (GIF, 2017). At international level, the Fukushima accident in 2011 led to the issuance of new rules for all reactors (WENRA, 2013). These rules, not applied in the CP ESFR project, have been applied to the ESFR-SMART project.

All the analyses and modifications proposed in ESFR-SMART are based on simplifications of the systems rather than adding new systems to the design, which is an important guarantee of safety. In general, safety authorities around the world tend to favor intrinsic and passive safety (IAEA, 2020). Many passive arrangements have, therefore, been introduced in ESFR SMART design to exploit the remarkable potentials of SFRs in this field with a fluid at low pressure with good natural-convection capacities.

In addition, the so-called practical elimination method was used to make by design, impossible to happen, the unacceptable incidents, identified today for SFRs. More generally, significant feedback exists on the operation of the SFRs and on accidents that have occurred (Guidez and Prêle, 2017; Guidez, 2014; IAEA, 2012; Baldev et al., 2017). The ESFR SMART design takes into account this feedback and valuable experience to both prevent such accidents or even make them impossible and to minimize their consequences.

Design was guided by the following objectives:

- Simplification of structures to enhance safety and improve manufacturing conditions for cost reduction and quality increase.
- Introduction of passive measures.
- Long duration (at least several days) before any external intervention needed.
- Improvement of In-Service Inspection and Repair (ISIR) possibilities.
- Reduction of risks related to sodium fires and to the water/sodium reaction.
- Possibility to use the handling building for twin reactors (in order to reduce costs, the layout of the buildings is made so that the handling building can serve two reactors).

The evaluation of the reactor design compliance with new safety rules provided the following recommendations:

- The loss of the DHR function should be by design practically eliminated on a basis of deterministic and probabilistic demonstration. This demonstration is managed by the use of diverse and redundant active systems in the pit (DHRS-3), by the possibility to use each secondary loop in active or passive way (DHRS-2) and by six independent passive systems (DHRS-1) operating with the IHX, even if the secondary loop is drained. The DHR function must be maintained in case of sodium leakages of the main reactor vessel.

- Passivity: additional passive systems are introduced such as: passive control rods operated without needing Instrumentation and Control (I&C) and electrical supply; natural-convection capabilities of the primary and secondary system and of DHR1 and DHR2 systems; thermal pumps able to passively assure some flow rate or increased possibilities of operation in natural-convection regime.
- Sodium fires. Design measures are taken to avoid any primary sodium leak above the roof even in case of severe accident with mechanical-energy release. These measures aim at allowing a simplification of the design and avoiding any dome or polar table in the primary containment. Measures are also taken to quickly detect and mitigate any secondary sodium leaks.
- Prompt criticality risks: situations of large and rapid reactivity insertion likely to lead to prompt criticality must be practically eliminated. This notably concerns the risk of core compaction, which must be practically eliminated by a robust design and the possibility to monitor the core geometry in operation. Gas entrainment must be prevented by a careful design of structures, notably to minimize volumes of gas-retention zones in the primary circuit.
- Mitigation of whole core meltdown: primary circuit must be mechanically robust, with a massive roof and a pit able to withstand any sodium leakage. Decay-heat-removal systems as well as core catcher must not be sensitive to mechanical-energy release (if any).
- Sodium/water reaction: secondary-loop and steam-generator designs must be demonstrated robust against the largest possible sodium/water reaction. The largest possible reaction must be intrinsically limited and demonstrated acceptable. The choice of small modular steam generators should facilitate this demonstration.
- External hazards: new rules on external hazards are applied.

11.4 Some examples of safety improvement approach in the ESRF SMART

11.4.1 Reactivity control

11.4.1.1 *New core concept with reduced sodium void effect*

It is proposed to adopt a core with a globally zero or slightly positive sodium void effect, which contributes to reduce the consequences, in terms of potential mechanical-energy releases, of the severe accident (Rineiski et al., 2021).

11.4.1.2 *Passive-control rods*

Passive-control rods are proposed as self-actuated reactivity-control devices for the core. The absorber insertion into the reactor is thus passively obtained, i.e., without any use of I&C, when some criteria on physical parameters are met, e.g., low primary-sodium flow rate or high primary sodium temperature (Rineiski et al., 2021).

11.4.1.3 *Ultra-sonic measurements for knowledge of the core geometry*

As in the reactors already in operation, the pads at the subassemblies come into contact, when the power grows and, therefore, the temperature increases. This prevents any significant compaction of the core and any reactivity increase during operation. Nevertheless, these measures are efficient if the pads are really in contact during the plant operation. In the fast-reactor feedback experience, we have already seen on some subassemblies under irradiation swelling or bending effects that can induce some disturbance in the core geometry. So, in order to practically eliminate any significant core-compaction possibility, several measures are prescribed in ESRF-SMART to ensure that the pads are in contact. To do so, some ultrasonic measurements at the core periphery would make it possible to monitor its global geometry during operations and to verify the absence of significant changes of this geometry during the cycle.

11.4.1.4 *Practically eliminated situations*

More generally, preventive measures are to be taken for the others practically eliminated situations related to the core-reactivity control, which includes:

- Significant gas amount passing through the core.
- Sudden core-support deterioration.
- Loading/unloading errors likely to make critical the core during handling operations.

11.4.2 Containment

11.4.2.1 *Reactor pit taking over the functions of the safety vessel*

- The CP ESRF safety vessel function was to contain the sodium in the event of the main vessel leakage, while maintaining in it a level of sodium sufficient to allow the sodium inlet into the Intermediate Heat eXchanger (IHX) and keeping a sodium circulation cooling the core. To recover this function by the reactor pit (hence, suppressing the safety vessel), it is necessary to overlay the reactor pit with a metal-sheet liner so as to withstand the reception of a possible sodium leak and to bring it closer to the main vessel so that the volume between vessel and pit remains identical to the volume between the two vessels. The replacement of the safety vessel by a liner with a DHR system attached gives following anticipated advantages:
 - The increase of the decay-heat-removal capabilities through the reactor pit.
 - The simplification of the safety demonstration with respect to the question related to the double leak of the main and safety vessels.
 - A fault-tolerant structure well adapted to the mitigation functions.
 - A main vessel in-service inspection that remains possible, as the main vessel remains accessible from the reactor pit, by the top of the space between vessel and liner.

A special arrangement of the reactor pit is necessary in order to be able to operate in normal conditions, to support an accidental sodium leak of the primary vessel and to be able to cope with severe-accident mitigation.

It is proposed for ESRF-SMART a “mixed” steel-concrete structure for the reactor pit (see [Figure 11.2](#)). A metallic liner is disposed in front of the safety vessel as support of an oil-cooling system. A material chemically compatible with sodium is provided between this “mixed structure” and the liner. This material has to be and must protect the “mixed structure” even in case of leak of sodium through the inner-sheet liner. This liner has no mechanical connection with the roof and, therefore, has more freedom for thermal expansion. Two reactor-pit cooling systems are used. The first system is attached to the liner and very efficient in normal operation for residual-power removal. The second system is installed in the mixed steel-concrete structure and should be able alone to maintain the concrete temperature under 70 °C, even in severe-accident mitigation case.

A description can be found in [Guidez et al. \(2018\)](#) and detailed description with thermal calculations of this pit organization is available in [Guidez et al. \(2019\)](#).

11.4.2.2 *In-vessel core catcher*

The mitigation of a severe accident with whole core meltdown will be achieved by means of a corium receiver, also called core catcher, located at the bottom of the vessel, under the core support structures called also a strongback (see [Figure 11.3](#)).

Transfer tubes, coming from the core, emerge above the core catcher to channel the molten corium. The use of molybdenum, as for BN-800 ([Sedakov et al., 2017](#)) characterized by a high fusion temperature, is proposed for avoiding melting of the core-catcher structure. The hafnium-type poisons can be used as regards avoidance of any potential recriticality. The core catcher is designed for the whole core meltdown.

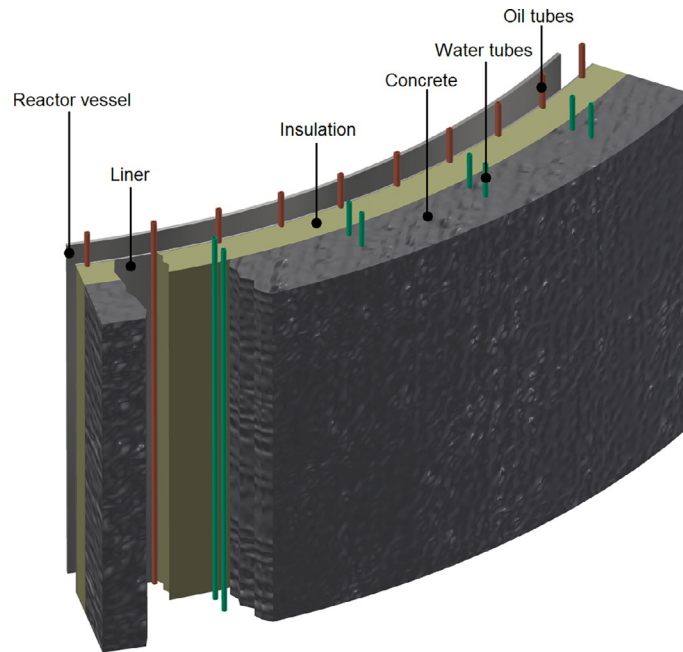


Figure 11.2. Details of reactor pit with Reactor Vessel (RV), Gas Gap (GG), Metallic Liner (ML); Sacrificial Material (SM), Concrete (C), and Decay-Heat-Removal System (DHR3) in oil attached to liner and in water inside concrete

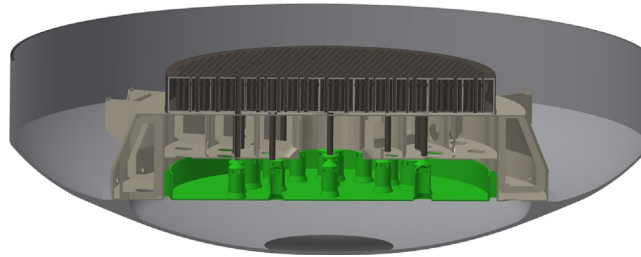


Figure 11.3. View of core-catcher position inside primary vessel: vessel bottom (1), strongback (2), corium-discharge tube (3), diagrid (4) and core catcher (5)

Pre calculation of the core catcher has been provided (Guidez et al., 2020a) with calculation of the residual power of the melted core, and cooling of this core catcher by natural convection of the sodium around it.

Figures 11.4 and 11.5 explain the concept with conical chimneys under the transfer tubes.

11.4.2.3 Massive metallic roof

Superphénix experience feedback (Guidez and Prêle, 2017) leads to recommend that the roof is hot at its bottom part, to minimize the sodium-aerosol deposits. Moreover, in order to contribute to the practical elimination of any large water ingress into the primary circuit, it is recommended to avoid water as roof coolant. This last recommendation will be a key point for demonstrating the practical elimination of huge entry of water into the primary circuit. The EFR massive metallic roof is, therefore, taken over, which presents many other advantages such as neutron shielding and mechanical resistance. Its thickness will be defined by the industrial-manufacturing contingencies, but should be about 80 cm. In the upper part, a heat insulator will eventually be installed so as to limit the heat flux to be evacuated during nominal conditions by air flow in forced convection or even natural convection.

- For rotating plugs: independently of the possible inflatable seals, the leak tightness with eutectic seals, which are liquefied during the handling phases so as to enable the rotation, is recommended. Conversely, when operating the reactor, these seals are solidified, and the design retained should be such that there is no leakage possibility in the case of a severe accident with mechanical-energy release. These systems were used successfully on Phenix and Superphénix reactors with a good feedback experience (Guidez, 2014; Guidez and Prêle, 2017; IAEA, 2012).
- Consistently with this strategy, to improve the primary-sodium confinement in the main vessel, it is also proposed to consider:
 - an integrated primary cold trap, likewise at Superphénix, so as to limit the amount of primary sodium outside the vessel;
 - a sufficiently low argon pressure in the cover gas to avoid any accidental sodium-fountain effect of a plunging pipe.

11.4.3 Decay-heat removal

The secondary circuits are the nominal power-removal circuits. Their use for DHR in case of all primary pumps trip is very useful since that allows creating, in the IHX, a cold column essential for the establishment of a good natural convection in the primary circuit. The secondary-circuit design will be optimized so as to enable a good heat removal by air in natural convection, that is to say, in the “Fukushima” situation, when both the cooling water and any alternating-current-power supply have been lost. For this purpose, several measures are taken:

- A secondary-loop design enabling an easy establishment of natural convection will be adopted. The sodium leaks, inherent to a mechanical pump in operation, are recovered by gravity in the pump-body-free level toward the storage tank as on Superphénix. The sodium purification is made at this level and the purified sodium comes back to the main circuit.
- The CP ESFR design for Steam Generators (SGs), with six modules per loop will be kept. We will take advantage of the large exchange surface, related to the SG modular design, to have opportunities for cooling these modules by air in natural or forced convection (through hatch openings, likewise at the Phénix reactor). This will be the heat sink for the secondary loop. We will call this system DHRS-2 (Decay Heat Removal System).
- Finally, it is foreseen to add one or more thermal pumps in the secondary circuits. Thermal pumps are passive electromagnetic pumps using thermoelectricity provided by the difference in temperatures and with no need of external electricity supply (see Figure 11.6). They provide a flow rate also in nominal conditions, and contribute to avoid stratification in the secondary loops, in case of loss of the forced convection.

In addition to these secondary DHRS loops, there will be in the pit two independent cooling circuits: One in the reactor pit with oil, installed on the liner and one with water inside the concrete, capable to maintain the entire pit at temperatures below 70°C. Suppressing the safety vessel will make these devices disposed in the liner much more efficient, with the goal to assure a large part of the Decay Heat Removal (DHR). We will call this system DHRS-3 (see thermal calculations of DHRS-3 in Guidez et al. (2020b)).

To further reinforce the practical elimination of loss of DHR function, we add cooling circuits by sodium/air heat exchangers connected to the IHXs piping. These circuits, that we will call DHRS-1 (primary decay heat removal system) have the following advantages compared to independent systems located in the primary circuit (formerly used in the CP ESFR design):

- No additional roof penetrations are required (gain on the main vessel diameter).
- The cold column is maintained in the IHX, which is the guarantee of a good natural convection in the primary circuit.

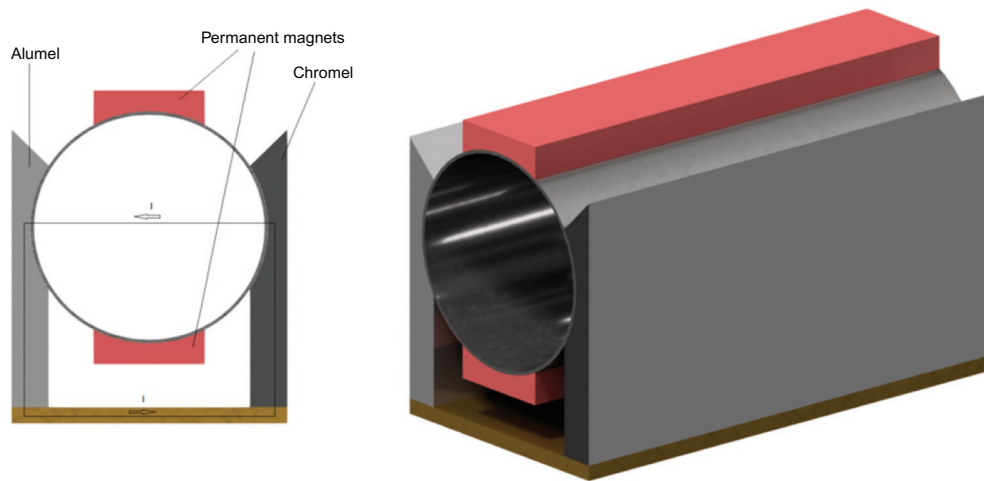


Figure 11.6. ESRF-SMART thermal-pump concept for secondary circuit: alumel (1), chromel (2), and permanent magnet (3)

- These systems are less sensitive to mechanical damage in case of severe accident, because they operate out of the vessel.
- These systems operate in natural convection both for air and sodium.

This circuit DHRS-1 is still available even, when the secondary loop is drained. It operates in natural convection, but the addition of a thermal pump can further increase its capabilities and help for the starting of the operation.

Indeed, in case of draining of the secondary circuit, the secondary sodium in the IHX would be near atmospheric pressure. It is then necessary to place the Na-air HX below ~ 12 m (it is the sodium height corresponding to 0.1 MPa of atmospheric pressure) up the upper point of the IHX, to avoid any cavitation (Figure 11.7).

Thermal calculations of the three DHRS have been provided: for DHRS-3 in Guidez et al. (2020a) and for DHRS-1 and -2 in Guidez et al. (2020b). For the calculation of DHRS-2 operation in natural convection, the code Cathare was used to determine the efficiency of the cooling by natural convection of air in the casings (Bittan et al., 2020 and Bittan et al., 2021).

11.4.4 Sodium fire

As the provisions to prevent any leakage of primary sodium have already been outlined, for the risks related to a secondary-sodium leakage, it should be noted that releases are mainly a chemical risk considering that no or very little radioactivity is present in the secondary-sodium circuit. Special dispositions are provided for easy detection and mitigation and are explained in the chapter on secondary loops.

11.4.5 Sodium/water reaction

Rather conventional devices enable to efficiently and quickly control this risk. Modular steam generators are retained, considering the possibility to quickly detect sodium/water reaction, followed by the depressurization/isolation and draining of the faulty module. The choice of modular SG allows also minimizing the theoretical-envelope accidents. In case of water/sodium reaction, the objectives are to limit consequences on the plant operations such that operation can continue with remaining modules, after faulty-module isolation. Mitigation means against risk of sodium/water/air reaction are taken in account by related casing sizing.

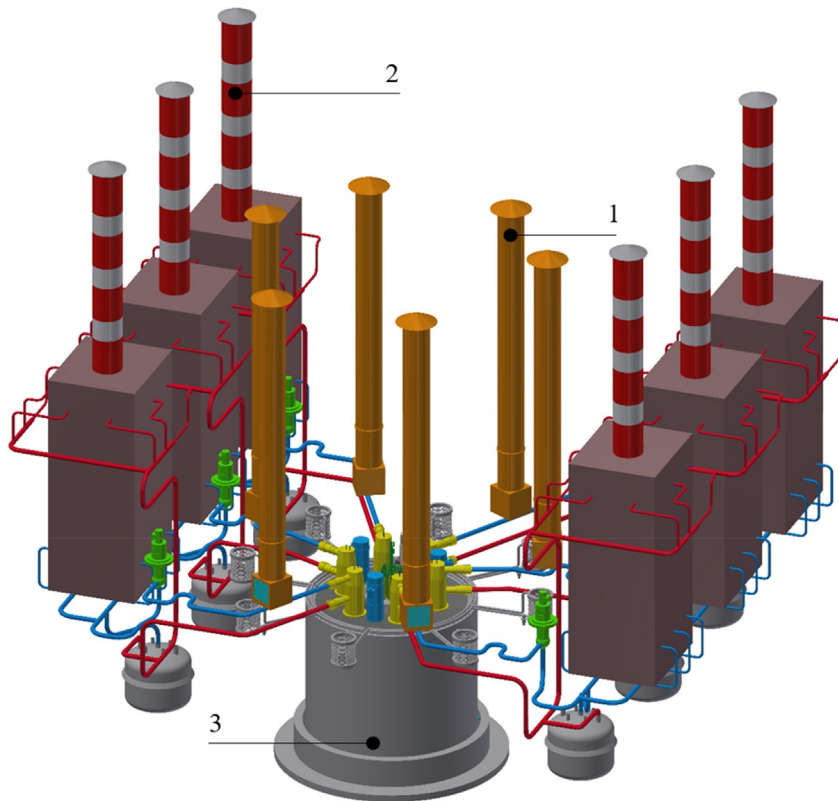


Figure 11.7. ESFR-SMART main view of reactor with three DHRS

11.4.6 Severe-accident mitigation

A more robust design than CP ESFR is researched for severe-accident mitigation studies, with the following objectives:

- A core catcher is provided at the bottom of the vessel, designed for the whole core meltdown.
- Mitigation devices inside the core (corium-discharge tubes) are intended to channel the molten fuel to the core catcher.
- The recriticality of the molten core should be prevented by using dedicated material such as hafnium inside this core catcher.
- The reactor pit should accept sodium leakage and, with its upper thick metal roof, should form a solid, tight and that-can-be-cooled containment system.
- The cooling of the primary circuit structure is achieved by DHRS systems even in case of severe accident.

11.4.7 Dosimetry and releases

It is known that, during SFR normal operations, the radiological releases are almost zero for gas. The releases of primary argon, which could be done in normal operation, are sufficiently delayed for reducing their radioactivity. The only liquid-radioactive release is the liquid used to wash fuel subassemblies or for washing and decontamination of components (EFR Associates, 1998; Guidez and Prêlé, 2017). In terms of the personnel dosimetry, this reactor design leads to a dosimetry much lower than on PWRs (Guidez and Saturnin, 2017).

Indeed, for PWRs the work sites bringing the highest doses, either do not exist on SFRs or exist, but lead to very little doses, due to the fact that the primary circuit is entirely contained in a vessel, and that the secondary

circuits are not active. It is for example the case of the reactor-vessel opening operation (which do not exist on SFRs), or the removal and installation of thermal insulation (a frequent operation on SFRs, but with negligible radiological doses).

Other elements also explain this difference in dosimetry. So, it may be mentioned, not exhaustively:

- In SFRs, primary sodium-purification-cartridge handling and processing are conducted under biological protections.
- On SFRs, primary components are decontaminated prior to the maintenance operations they have to undergo.
- It is also reminded that SFR secondary circuits are not radioactive.

This benefit will be kept for ESRF-SMART.

11.4.8 Simplicity and human factor

Starting from the CP ESRF design, our approach has consisted in proposing the simplest possible reactor, while keeping the necessary lines-of-defense. It is expected that this simplicity should contribute to the whole reactor safety, by making it easier to operate. Compared to CP ESRF, the following simplifications are proposed:

- dome (or polar table) suppression;
- safety-vessel functions taken over by the reactor pit;
- primary sodium containment improvement;
- natural-convection cooling enhancement in the secondary side; and
- optimized and simplified DHRS dedicated circuits.

Passive and redundant systems, which are independent of I&C or of the operators' action, will enable the reactor-reactivity control and its cooling by natural convection, even in the most severe cases of simultaneous loss of cooling water and power supply. With all those improvements, the new design is then more forgiving; both with respect to the reactivity control, as well as at the intervention time required from the operator (enhanced grace period).

11.5 Description of ESRF SMART primary system including these new options

11.5.1 General-plant characteristics

The 1500-MW_{e1} reactor is of pool type and based on several key-design options aiming at a high level of safety, robustness, and manufacturability of all components, including:

- A massive metallic reactor roof (~80 cm thickness), limiting heat fluxes, providing good dosimetry behavior, and able to withstand any accidental situation. This design was already proposed for the EFR (EFR Associates, 1998). In normal operation, the roof is hot in the lower part (to avoid any sodium deposition) and actively or passively cooled by air in the upper part.
- A diagrid with two primary sodium inlets for each pump.
- An inner vessel with a conical part (redan) with 25° slope.
- An internal-core catcher of high capacity located under the diagrid and strongback.
- A safety liner on the reactor pit surface able to withstand any sodium leak and to mitigate any accidental situation.
- An inner storage of spent fuel near the core.

Other components are based on classical designs:

- An Above Core Structure (ACS) to guide control rods, support instrumentation, and to reduce the high sodium velocity at core outlet.
- Two eccentric rotating plugs to take any of the fuel assemblies by means of a Direct Lift Charge Machine (DLCM) and a Fixed Arm Charge Machine (FACM).
- Six IHXs.
- Three Primary Pumps (PPs).
- A Decay Heat Removal System (DHRS-3) integrated in the reactor pit.

The general view of the primary system is shown in [Figure 11.8](#).

Main parameters of the ESFR-SMART plant are given in [Table 11.1](#). The following considerations were taken into account, when selecting the main temperature parameters of the plant:

1. Core inlet and outlet temperatures (395–545°C): this choice provides a substantial Logarithmic Mean Temperature Difference (LMTD) for the IHX. The core-temperature increase of 150°C is a compromise between plant capital cost, thermal loading considerations, material behavior and pumping-power requirements.
2. Secondary sodium temperature at steam generator inlet (530°C): this is a compromise between acceptable material properties and minimization of surface area requirements. Moreover, this temperature seems a reasonable upper limit for the secondary hot leg temperature.
3. Secondary-sodium temperature at steam-generator outlet (345°C): this choice provides acceptable temperature differences and limits the temperature difference between sodium and water on the lower tubular plate of the SGs. And
4. Steam temperature (528°C): this choice is connected to the creep properties of the steam tube and tube-plate materials of the steam generator.

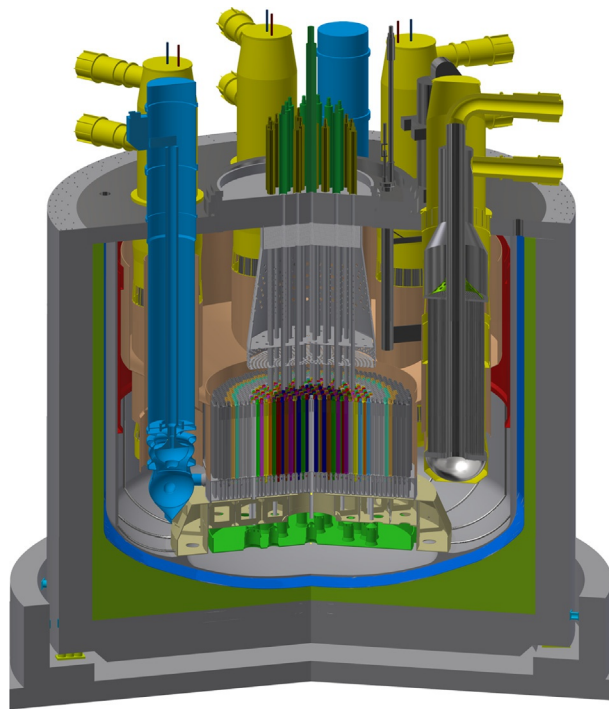


Figure 11.8. View of ESFR-SMART primary system

Table 11.1. Main parameters of the plant

Parameters	Values
Thermal power (MW_{th})	3600
Net electrical power (MW_{el})	1500
Global efficiency (%)	42
Plant lifetime (years)	60
Availability target (%)	90
Mass of sodium in main vessel, t	2350
Total pressure losses in primary system, MPa	0.45
Cover gas above primary sodium-free level	Argon
Pressure of cover gas, MPa	0.115
Core	
Core inlet/outlet temperatures, °C	395/545
Type of fuel	(U,Pu)O ₂
Fuel Enrichment, %	17.99
Core global geometry	Cylindrical, 3 layers of reflectors
Core Support	Strongback resting on primary vessel bottom
Core mass, t	~430
Core outside diameter, m	~8
Core flow rate, kg/s	18,705
Core bypass flow rate, kg/s	831
Sodium supply	Pump connection to diagrid
Diagrid and core support materials	316L(N)
Diagrid mass, t	~70
Sodium leak in diagrid for cooling systems, kg/s	830
Core pressure drop (including inlet and outlet), MPa	0.38
Core support pressure drop (diagrid), MPa	0.07
IHX	
Number of IHXs	6
Power of one IHX, MW	600
Type	Tubular, counterflow

Continued

Table 11.1. Main parameters of the plant—cont'd

Parameters	Values
Material	Stainless steel
Pressure loss (primary), MPa	0.025
Working fluids, primary/ secondary	Sodium/sodium
Mass of one IHX, t	127
Primary sodium temperature at IHX inlet/outlet, °C	545/395
Secondary sodium temperature at IHX inlet/outlet, °C	530/345
Primary pumps	
Number of primary pumps	3
Type	Mechanical, radial admittance, axial exhaust, antireverse-flow diode
Mass of one pump with motor, t	~164
Location	In reactor vessel
Nominal rotational speed, rot/min	450
Net positive suction head, available, m	13
Pressure head, MPa	0.45
Nominal flow rate, kg/s	6512
Halving Time (LOSSP), s	~10
Min Time from 100% to 25% of nominal speed, s	30
Secondary loops	
Number of secondary loops	6
Composition	1 IHX, 6 SGs, 1 secondary pump, 1 thermal pump, 1 purification system, 2 draining systems
Nominal flow rate per loop, kg/s	2541
Length of pipes with \emptyset 0.850/ \emptyset 0.350 m per loop, m	~193/~30
Mass of secondary sodium per loop, t	~254
<i>Steam generator</i>	
Number of steam generators per secondary loop	6
Type	Modular, tubular, counterflow
Mass of one SG, t	~50

Continued

Table 11.1. Main parameters of the plant—cont'd

Parameters	Values
Material	9Cr-1Mo modified
Working fluids, secondary/ tertiary	Sodium/water
Power of one SG, MW	100
Water inlet/steam outlet temperature, °C	240/528
Steam pressure, MPa	18.5
Steam flow rate per secondary loop, kg/s	287
Vessels and structures	
Main vessel height/diameter, m	17.185/17.56
Main vessel material	Stainless steel 316 L(N)
Main vessel mass, t	~900
Main vessel cooling	With cold sodium taken from diagrid, immersed weir
Main vessel cooling mass, t	~80
Cold/hot sodium separation	Inner vessel with conical part (redan)
Redan mass, t	~200
Safety liner mass, t	~284
Reactor roof type	Massive, hot in the lower part and cooled by air in upper part
Reactor roof material	Stainless steel 16MND5
Reactor roof mass, t	~1300
Total mass supported by reactor roof, t	~7300
Above core structure type	Conical
Above core structure mass, t	~550
Decay heat removal system-1	
Number of DHRS-1 loops	6
Material	Stainless steel
Mass of one loop, t	~20
Fuel handling	
Fuel handling mechanism	2 rotating plugs (1 eccentric) in reactor roof
Mass of each rotating plug, t	~200
Spent fuel extraction from reactor	Gas flask
Spent fuel transfer	With in-reactor fuel handling station
Intermediate storage	External storage in water pool

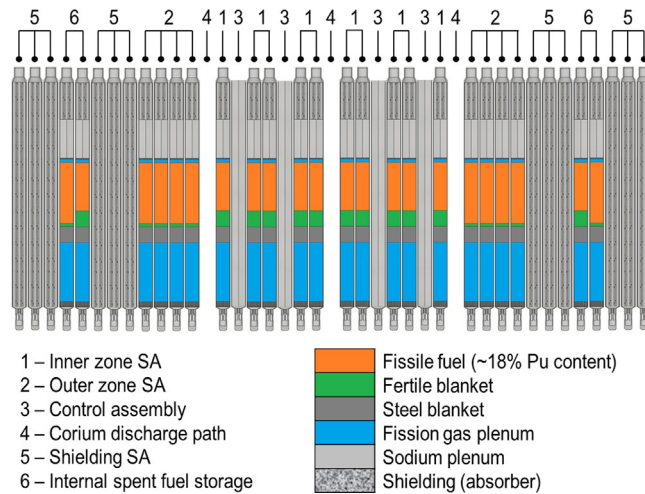


Figure 11.9. Core-axial map

11.5.2 Core

Compared to the core defined in the CP ESMR project, the following major modifications are done in the axial layout of the core in order to reduce reactivity effects in case of sodium boiling under hypothetical accident conditions: (a) a large sodium plenum topped by absorber is introduced above the core, (b) the inner/outer core heights are reduced by 25/5 cm, and (c) a lower fertile blanket is introduced below the fuel, with a steel blanket below. The Pu content is the same in the inner- and outer-core zones. The full specification of the new core can be found in [Rinieski et al. \(2021\)](#) and a view of the core is given in [Figure 11.9](#).

The measurement of the core dimensions with ultrasound sensors is expected to be achievable and should be studied taking into account uncertainty measurements during the reactor lifetime. Devices of this kind had been installed at the Phenix after the observation of some negative-reactivity trips, so as to monitor the core geometry.

Concerning the maturity of the passive-control rods, several types of passive-control rods are being studied or even tested ([Rinieski et al., 2021](#)). For example, the Curie-point rods triggering on a temperature level seem feasible and are currently being tested. Other types (differential thermal expansions, etc.) do also exist. Passive hydraulic-control rods were already installed in the BN-800 reactor in Russia ([Sedakov et al., 2017](#)).

11.5.3 Main vessel

The main vessel has a diameter of 17.56 m, and a height of 17.19 m. Compared to EFR (16 m high), it is taller, because the sodium level is 1-m higher mainly to increase the IHX heat-exchange length. The main vessel is fabricated of austenitic steel (316LN) and hanged to the civil work by means of a forged piece. The upper cylindrical part is cooled by a small sodium flow taken from the cold plenum below the diagrid. An immersed weir limits the risk of gas entrainment and ensures creep and fatigue resistance of the main vessel over 60 years.

11.5.4 Inner vessel

The inner vessel is an asymmetrical shell-fabricated structure, comprising:

- A conical part (redan).
- A cylindrical inner-vessel upper skirt.
- A cylindrical-core barrel welded on the strongback.
- A minimum set of nine penetrations in the conical skirt: six for IHXs and three for primary pumps.

The inner vessel separates the hot pool, which contains the core subassemblies and the IHX inlets from the cold pool, where the IHX outlets and the primary pumps inlets are located. It provides a leak-tight barrier between the hot and cold pools and provides geometric and hydraulic guide to the pump inlets. It serves together with other internal structures for distribution of the primary sodium flow inside the main vessel.

A conical skirt (redan) is proposed in place of the oval skirt of EFR to simplify manufacturing. The core barrel is welded on the strongback (and not on the diagrid). As a result, the conical skirt is less sensitive to buckling by plastic ruin. It also decreases the surface subjected to the difference in pressure between collectors and provides a natural protection of the diagrid against hot shocks at the exit of the IHX.

The upper part of the inner vessel is subject to high thermo-mechanical constraints at the free surface (sodium at 545°C, argon at 400°C), leading to minimization of the wall thickness in that region to lower thermal fatigue. On the other hand, it must also sustain high mechanical and fluid loads during an earthquake, and its thickness must be large enough to ensure its stability.

11.5.5 Reactor roof

A massive steel reactor roof is proposed, following design and feasibility studies of EFR. It has several advantages over the conventional fabricated box structure filled with concrete of the Superphénix:

- No water inside the roof.
- Good dosimetry protection.
- Low heat flux by conduction.
- No sodium deposit in the hot lower part. And
- Very good mechanical behavior even in the worse accidental cases.

The roof is 0.8m thick, made of the same steel grade as a PWR vessel and fabricated in sectors using narrow gap welding. All welded joints can be controlled. Component penetrations are machined to reduce tolerances, limiting heat transfer from the gas cover (compared to conventional designs with concrete). Access to the top surface of the roof could be made possible by extra sheets of insulation material, but in case of loss of power supply, natural cooling has to be optimized to maintain an acceptable roof temperature. The roof lies on the mixed concrete/metallic structure of the reactor pit that also supports the main vessel weight. Access to circumferential welded joints is made possible by a series of regularly spaced holes.

The rotating plugs are also solid and made of stainless steel, making a consistent design for the whole reactor roof regarding heat-transfer constraints. Since eutectic seal reduces its volume when frozen, the plugs are lowered for normal reactor operation, so that the thermocouples, which monitor the core can be set closer to the subassembly heads to provide a more representative measurement during power operation.

A mechanical seal is insuring the roof-leak tightness at component penetrations (IHX, primary pump) and a supplementary ring around these components is welded to assure total leak tightness during reactor operation, even in the most severe accidental cases. With the same objective, a frozen eutectic seal ensures the tightness of the rotating plugs during reactor operation (as it was done in the Phenix and Superphénix).

Concerning the degree of maturity, this type of a roof, perfectly meets all requirements. The industrial feasibility of great-height welds could, however, require the reduction of the thickness. It is then possible to add, in multi layers, heat insulation and several metallic thickness.

11.5.6 Reactor pit

The reactor pit is a concrete/metallic structure supporting the roof. The safety vessel between the pit and main vessel is proposed to be suppressed. A metallic liner is covering a structural insulation between the main vessel and the concrete/metallic structure (Figure 11.10).

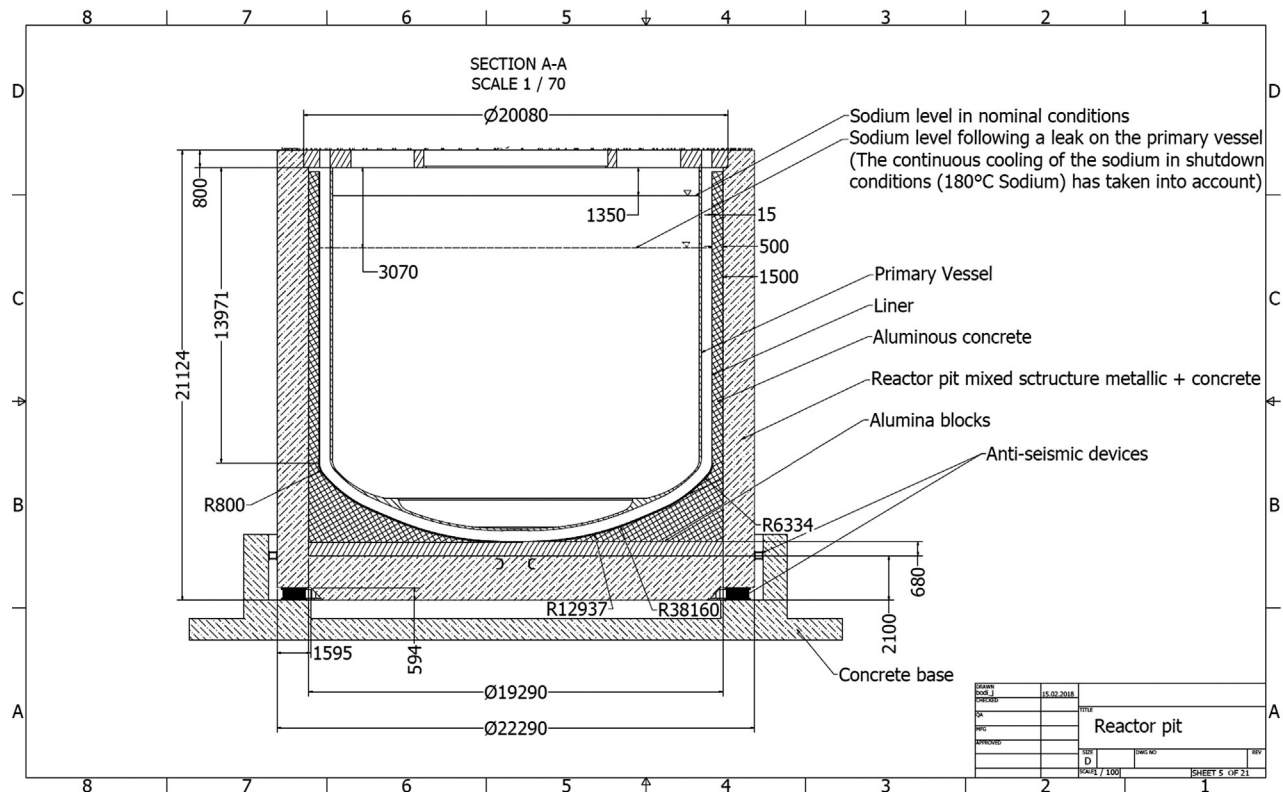


Figure 11.10. ESRF SMART pit drawings

In the unlikely event of a leakage of the main vessel, hot sodium would flow in the pit. The liner should prevent contact between hot sodium and insulation and provide improved thermal exchange for cooling. The insulation is chosen to be chemically compatible with sodium. The volume available for the sodium between the liner and the main vessel is calculated to maintain the sodium circulation between the heat exchangers and the core.

11.5.7 DHRS-3

The concrete/metallic structure of the reactor pit is cooled during normal operation by the pit cooling system. Two independent active cooling systems are proposed in the reactor pit (we use the acronyms DHRS-3 for the combination of these two systems):

- The oil cooling system (DHRS-3.1) is installed in the gap between the insulation and the reactor vessel or inside the insulation as shown in Figure 11.4. The oil system is in direct view of the main vessel and, therefore, more efficient without the screen of a safety vessel. The oil under forced convection can remove the heat transferred by radiation from the reactor vessel at high temperature. Conversely, to water, oil is able to operate at high temperature.
- The water-cooling system (DHRS-3.2) for the concrete cooling is installed in the concrete/metallic structure and aims at maintaining the concrete temperature under 70°C in all situations, even if the oil system is lost.

Both oil and water circuits work during normal operation and have to provide the concrete temperature below 70°C. After the reactor shutdown, the oil system alone has to be able to remove all the decay heat generated in the reactor, after a certain time delay (3 days). In case of the reactor vessel leak and loss of the oil system, the water system should be able to remove all the decay heat generated in the reactor.

All these measures make the pit able to withstand in a long-term mitigation situation.

11.5.8 Primary sodium confinement

A number of measures have been taken to assure the primary sodium confinement:

- Tightness measures already described.
- A reactor pit able to withstand sodium leakage.
- No circulation of primary sodium out of the vessel. The purification circuits are components integrated in the vessel (as in the Superphenix).
- Low pressure of cover gas (argon), to avoid any “geyser effect.”
- A massive roof to withstand any accidental case with large margins. And
- Slight overpressure in the secondary loops to avoid any primary sodium leaks inside the secondary loop.

All these measures aim at avoiding any consequent overpressure due to a primary sodium fire and thus avoiding dome or polar table that are very large components (about 15 m high), quite expensive and making the handling operations difficult for the reactor operator. It is a major simplification of the design, and so a safety improvement.

11.5.9 Core support structure and connection to pump

The core support structure, including strongback and diagrid, has to be designed to enable the practical elimination of their brutal ruin.

The lower part of the reactor vessel is shown in [Figure 11.3](#). The core and neutron shielding are supported by a diagrid, which is resting on the strongback. The strongback is laid on the main vessel bottom and transfers the total core and diagrid weight.

The diagrid is a stainless-steel cylindrical structure of 8 m in diameter containing a large number of vertical circular shroud tubes into which the core subassemblies are inserted. These shroud tubes provide the positioning and support for the subassemblies and allow the sodium feed from the diagrid through holes. The detailed flow arrangements are such that the hydraulic forces acting on the subassemblies serve to hold them down in the diagrid.

The diagrid structure is entirely welded. The absence of bolts removes any risk of loose parts inside the primary circuit. The diagrid structure needs high stability (thermal and mechanical) to avoid changes in core geometry. The pumps are connected to the diagrid, by two tubes, like in the Superphénix.

The strongback is a stainless-steel box-type structure comprising two circular plates linked by welded webs. It is resting on the vessel bottom, supports the diagrid and allows the feeding of cold sodium to the primary-vessel cooling system.

Thirty-one discharge tubes are also coming from the core and crossing diagrid and strongback to arrive above the core catcher. These tubes are closed and filled with sodium in normal operation. Their function is, in case of severe accident with core melting, to give a natural way to escape for the corium to the core catcher ([Figure 11.4](#)).

11.5.10 Core catcher

The mitigation of a severe accident with whole core meltdown will be achieved by means of a corium receiver, also called core catcher, located at the bottom of the vessel, under the core support plate called also a strongback (see [Figure 11.3](#)). The target is to design the core catcher for the whole core fissile inventory. Corium-transfer tubes, coming from the core, emerge above the core catcher so as to channel the molten corium. Stacks are designed under these tubes to allow a good dispersion of the corium inside this core catcher (see [Figs. 11.4 and 11.5](#)). The use, as in the Russian reactor BN-800 ([Sedakov et al., 2017](#)) of molybdenum, characterized by a high melting temperature, avoids melting of the core-catcher structure.

The use of hafnium-type poisons inside the discharge tubes is possible to increase the margin to recriticality. General design of the strongback structures is made to improve the natural convection of the sodium around the core catcher (see calculations in [Guidez et al., 2020b](#)).

11.5.11 Primary pump

The primary pumps are mechanical pumps for which there are good feedback on experience and reliability ([Guidez, 2014](#); [Guidez and Prêlé, 2017](#)). The selection of three primary sodium pumps is consistent with the compact primary circuit layout incorporating six IHX, which enables the vessel size to be minimized. These three pumps are utilized in the primary circuit, located on a common pitch-circle diameter and forming a parallel circuit with the same pump head and the same flow. The design includes the following main features, which are similar to the Superphénix pumps:

- Single mixed flow impeller.
- Top inlet entry flow to the impeller.
- Subcritical hollow drive-shaft, designed to get the first critical whirling speed above the maximum operating speed with a comfortable margin. And
- Synchronous motor to allow easy operation of the pump over the whole range of required speeds (with specific regulations).

The primary pump comprises a cylindrical casing, vertical shaft machine inserted into the primary circuit via a penetration in the reactor roof, on which it is mounted. The upper part of the pump is firmly connected (to avoid displacement during seismic events) and even welded to avoid any sodium leakage during any accidental event. To allow radial displacement between the upper part that remains cold and the lower part at hot sodium temperature, the lower part of the pump can bend to accommodate differential thermal expansion. The impeller is mounted on the drive shaft. The advantages and disadvantages to implement a flywheel in order to extend the rundown time have to be assessed. The shaft is supported at the top end by a magnetic axial thrust bearing and a radial bearing. A hydrostatic sodium radial bearing is located at the bottom of the shaft above the impeller.

11.5.12 Intermediate heat exchanger

A simple straight-tube design is proposed for the IHX. This is a counter-flow heat exchanger with the secondary sodium flowing downward through a central duct before turning upward in the bottom header and flowing vertically inside the heat-exchanger tubes, where the primary sodium flowing downward on the shell side heats it. Rated unit power and thermal cycle are in accordance with the specified performance ($600 \text{ MW}_{\text{th}}$). This design is a proven version used in all SFRs worldwide, taking into account the Phenix and Superphénix experience feedback and the need for an efficient mixer in the secondary sodium outlet recovery box after heating.

The IHX unit is connected physically and functionally to both the primary and secondary-sodium circuits and as such must be designed to withstand the specified maximum secondary-circuit pressure coming from the steam-generator-unit design-based accident (about 5.5 MPa on the IHX in case of a sodium/water reaction resulting from the failure of all the tubes of a modular SG).

The IHX has a valve on the primary sodium side allowing the inlet window to be closed and the secondary circuit and steam plant to be isolated from the primary circuit. That allows the reactor to be operated with one or two IHX isolated. The IHX is firmly connected on the roof (to avoid seismic displacements) and even welded to avoid any sodium leakage. So, a seal between the IHX and the inner vessel must accommodate thermal expansions between the components and the conical part of the inner vessel (redan). A gas seal is not

recommended to avoid any risk of gas entrainment into the core, and a dedicated oscillating mechanical seal is considered.

The IHX must have a tube in the upper part to extract the hot secondary sodium for the DHRS-1 and a tube for the cold secondary sodium returning in the central part of the IHX. To take in account these new measures introduced in ESRF-SMART, the IHX diameter was increased by 10% in comparison to the EFR IHX.

11.5.13 Decay-heat removal concept

While in the CP ESRF design there were dedicated DHRS in the primary circuit, in the ESRF SMART design there are no dedicated DHRS in the primary circuit either in the cold pool or in the hot pool. Indeed, the best way to have a good natural-convection level through the core is to always remove heat from IHX and, therefore, maintain in the IHX the cold column of the primary sodium. Following this concept, the heat-removal possibilities of the secondary loops are used to the maximum extent possible, including the cases, when the secondary sodium operates in natural convection, and when the feedwater supply is lost. If the secondary loops are completely lost and drained, special systems (DHRS-1) maintain the cold column of the primary sodium in the IHX, which allows a good core cooling.

Another advantage of the proposed measures is reduction of the number of the sodium circuits (each circuit should have his draining and purification systems). In the proposed design, there are only the secondary sodium circuits that are used for both DHRS-1 and DHRS-2. It simplifies the work of operators. The only decay heat removal system in the reactor itself is the DHRS-3, located inside the reactor pit. This system is more efficient than in the Superphénix, due to suppression of the safety vessel and the direct view of the primary vessel by the oil-cooling system (DHRS-3.1), without the screen of the safety vessel. A second system with water (DHRS-3.2) is mainly used for mitigation situations.

In summary, the DHRS operation is as follows:

- If feed water is available, one secondary circuit is enough to remove decay heat from the core at acceptable temperatures.
- If feed water is lost, the opening of the windows in the SG modules creates the passive heat sink by natural convection of the atmospheric air (DHRS-2).
- If all the AC power supplies are lost, the taken measures ensure good natural convection, including of the secondary sodium assisted by a thermal pump (Guidez et al., 2020a, b; Bittan et al., 2021).
- The studies have been done so as to prevent as much as possible all the common modes, which can lead to a simultaneous loss of all six loops. If secondary loops are nevertheless drained, DHRS-1 connected to the IHX enables to remove alone, decay heat in a passive way by natural convection of the atmospheric air and natural convection of the secondary sodium assisted by a thermal pump.
- Furthermore, redundant circuits diversified and secured at the reactor pit (DHRS-3) enable another cooling of the primary set, including in the mitigation cases. This system is able after several days to assure alone the decay heat removal.

11.5.14 Polar table or dome

Neither polar table nor dome is considered in the ESRF-SMART design. Specific measures have been taken to avoid leakage of sodium in the primary building and so any over pressure due to a sodium fire. All these measures aim at allowing, even in case of a severe accident, to avoid any severe sodium fire and so any severe overpressure in the reactor building.

11.6 Description of ESRF SMART secondary loops

11.6.1 General description of ESRF SMART secondary loop

The secondary system transfers the heat from the IHXs to the steam generator units during nominal operation and during operational decay-heat removal via the tertiary water/steam system after reactor shutdown. It represents a non-radioactive barrier between the radioactive primary-sodium system and the non-radioactive tertiary water/steam system.

Each of the six loops has one intermediate IHX, one secondary pump, and one steam-generator unit with six modules. Each of the loops has also one DHRS-1 able to keep heat removal from IHX even if the main secondary loop and one purification circuit are drained. A quick draining system allows draining the sodium of the loop to the storage tank dedicated to this loop (see Figure 11.11).

The sodium flow rate in each loop is $10,800 \text{ m}^3/\text{h}$ (2541 kg/s) and the power removed by each of the steam generators is $100 \text{ MW}_{\text{th}}$.

Note that there is a permanent flow of sodium in the loop for purification and monitoring. The sodium leaks at the secondary pump (hydrostatic bearing and impeller labyrinths, either a few percentages of the flow) and is collected passively by gravity and sent to the storage tank. There a lift pump returns this flow

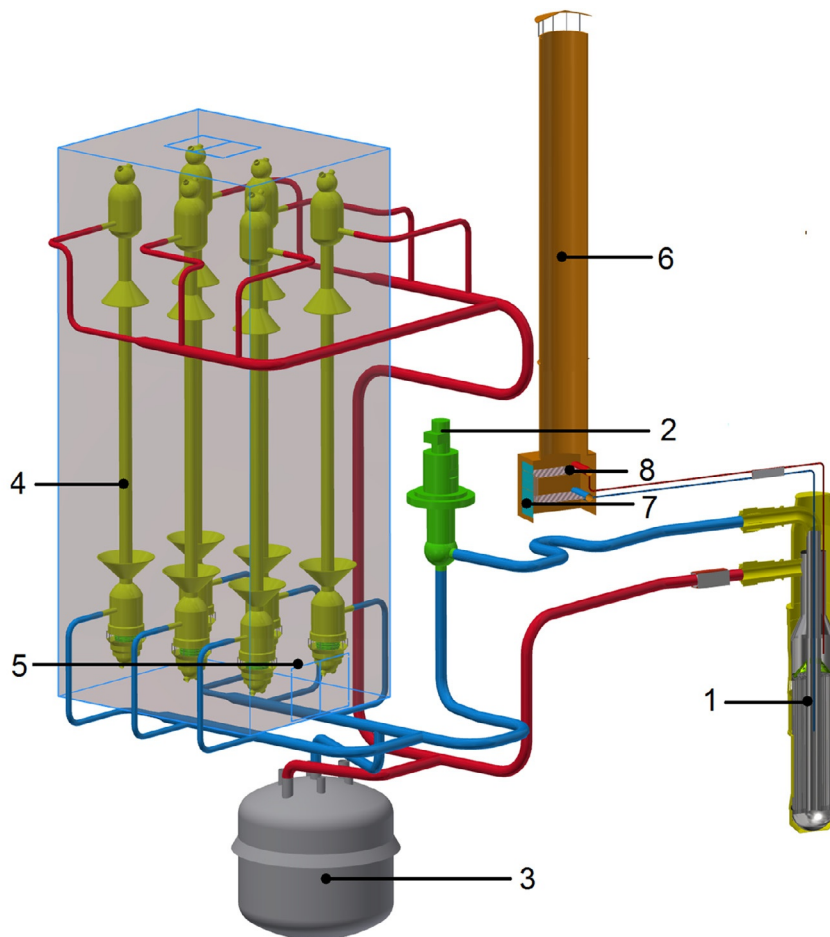


Figure 11.11. General view of ESRF-SMART secondary loop with initial option of flexible pipes between components

- | | |
|---------------------------------|---|
| 1 - Intermediate heat exchanger | 5 - Decay Heat Removal System (DHRS-2) |
| 2 - Secondary pump | 6 - Air stack of DHRS-1 |
| 3 - Sodium storage tank | 7 - Openings of air circulation |
| 4 - Steam generator modules | 8 - Sodium-air heat exchanger of DHRS-1 |

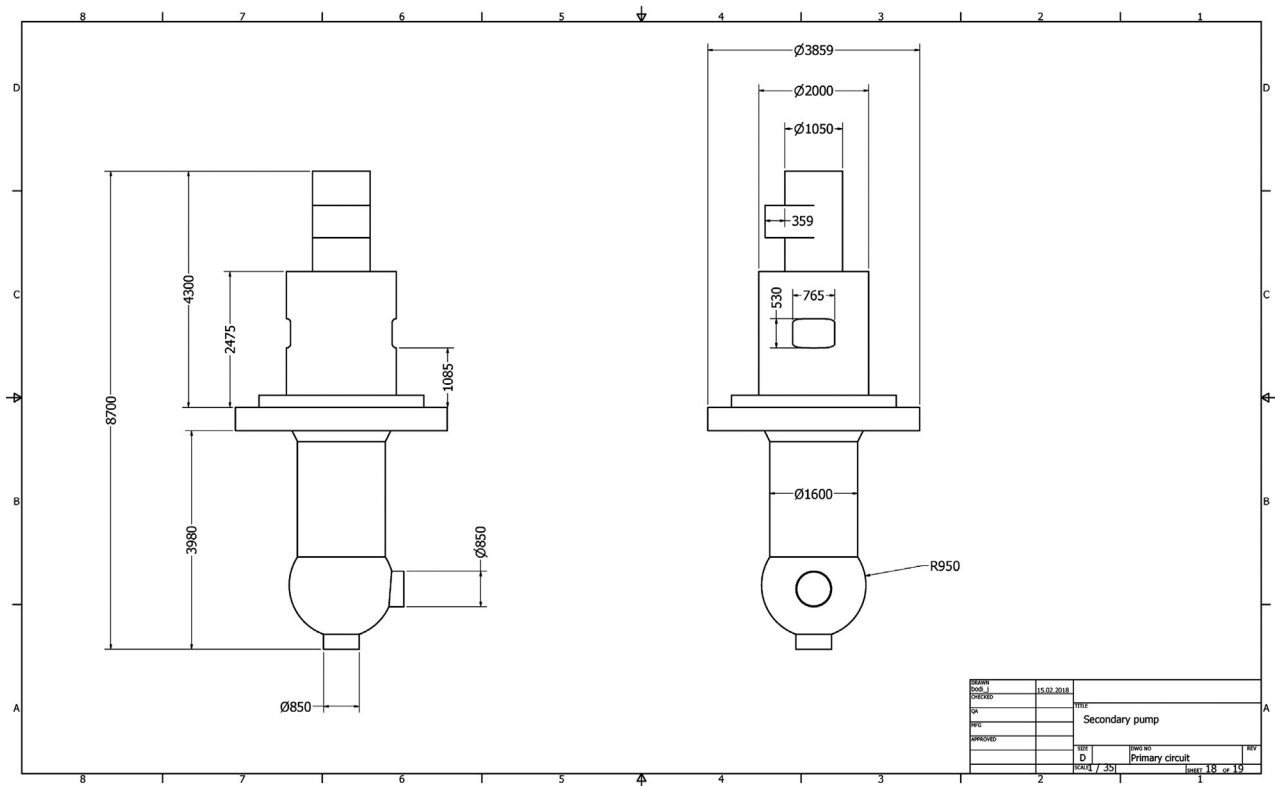


Figure 11.12. View of mechanical secondary pump

through a purification circuit to the loop. The permanent circulation of sodium is passively ensured in the DHRS-1, which, therefore, does not require any sodium monitoring or purification circuit.

11.6.2 Secondary pump

The operational experience of the secondary pumps shows high reliability of these components and only a few problems in operation (Guidez, 2014; Guidez and Prêle, 2017). Tests of high power electromagnetic pumps were carried out in the frame of the ASTRID project in France in 2017–18 to try to appreciate the advantages/disadvantages of these systems in regards to usual mechanical pumps. As of today, there are not yet clear advantages demonstrated in the cost, sizing, or reliability of these new systems. At the ESFR SMART level, therefore, the EFR size mechanical pumps were kept.

The dimensions of the secondary pump are given in Figure 11.12. One potential issue with mechanical pumps is the sodium leakage in operation with the hydrostatic bearing and with the impeller seals. These leakages arrive to the cylindrical casing of this pump with a free surface of sodium. At this level, the leaked sodium is passively (by gravity) drained to the storage tank through a pipe. Similarly, to the Superphénix, this sodium, after purification, is sent back by the purification circuit to the secondary circuit. Even, when the pump is stopped, a little leakage always exists due to the difference of the levels of the pump free surface (at low point) and the steam-generator free surface. Therefore, a small electromagnetic pump of the purification system has to be always in operation to avoid unexpected draining of the loop, when the secondary loop is stopped. The possibility of using batteries as the power supply for this pump will be analyzed to ensure mechanical-pump-leakage recuperation even in the case, when all the AC power supplies are lost.

Table 11.2. Main geometric parameters of the steam generator

Parameters	Value
Number of heat exchange tubes	364
External diameter/wall thickness of the exchange tube (mm)	15.6/2.5
Active/total length of the tube (m)	26.4/26.8
Outer shell diameter/wall thickness at the level of tubes (mm)	750/28
Outer shell diameter/wall thickness at the level of collectors (mm)	1900/40
Diameter of inlet, outlet and discharge pipes (mm)	350
Tube material (chosen because of low thermal expansion coefficient)	9Cr-1Mo
Total length of SG (m)	29.1

11.6.3 Steam generator

As for the steam generators, the modular, straight-tube option was kept, which was the EFR initial option also. This type of module is used in the Indian PFBR (Baldev et al., 2017) and Russian BN-800 reactors; furthermore, it is selected in several projects such as Korean and Chinese fast-reactor projects.

This modular option is preferred over the concept of the helical steam generator, selected and used for the Superphenix, due to several advantages in terms of industrial manufacturing, maintenance (possibility of periodically replacing a module), and safety files (better detection and mitigation of accidents with sodium/water reactions). Moreover, having six modules on a loop makes it possible to increase the available heat-exchange surface and, therefore, to create a possibility of removing the decay heat by simple natural convection of the atmospheric air around the walls of these modules.

The main geometric characteristics of a 100-MW_{th} module are given in Table 11.2.

The global view of the steam-generator module is shown in Figure 11.13. The six modules are hosted in a casing with the possibility to open their windows and, with the help of a dedicated chimney, establish an appropriate level of natural convection of the atmospheric air. Sodium and water circuits are separated inside the casing, nevertheless, adequate prevention and mitigation of chemical releases in the environment in case of sodium leak should be further studied. Besides, the casing should be able to support an airplane crash, to avoid fires from mixed air, water, and sodium.

For the choice of steam-generator type, the first calculations show that a printed plate-type steam generator could enable water vaporization to be achieved with a height of only around 1.5 m (in comparison to the 28 m of EFR module). This type of steam generator could allow a very important gain in terms of building volumes and costs. That could be a promising concept to study and to develop in the near future.

11.6.4 DHRS-1 system

To ensure the highest safety in case of the unavailability of the main heat-removal route through the secondary sodium loop, a special decay-heat removal system, DHRS-1, is implemented at each of the six IHXs (see Figure 11.14). The DHRS-1 loop operates in parallel to the secondary loop using the hot secondary sodium extracted from the IHX as the working medium. The heat is rejected to the environment using a sodium/air heat exchanger located at the bottom of the air stack, which is situated outside of the reactor

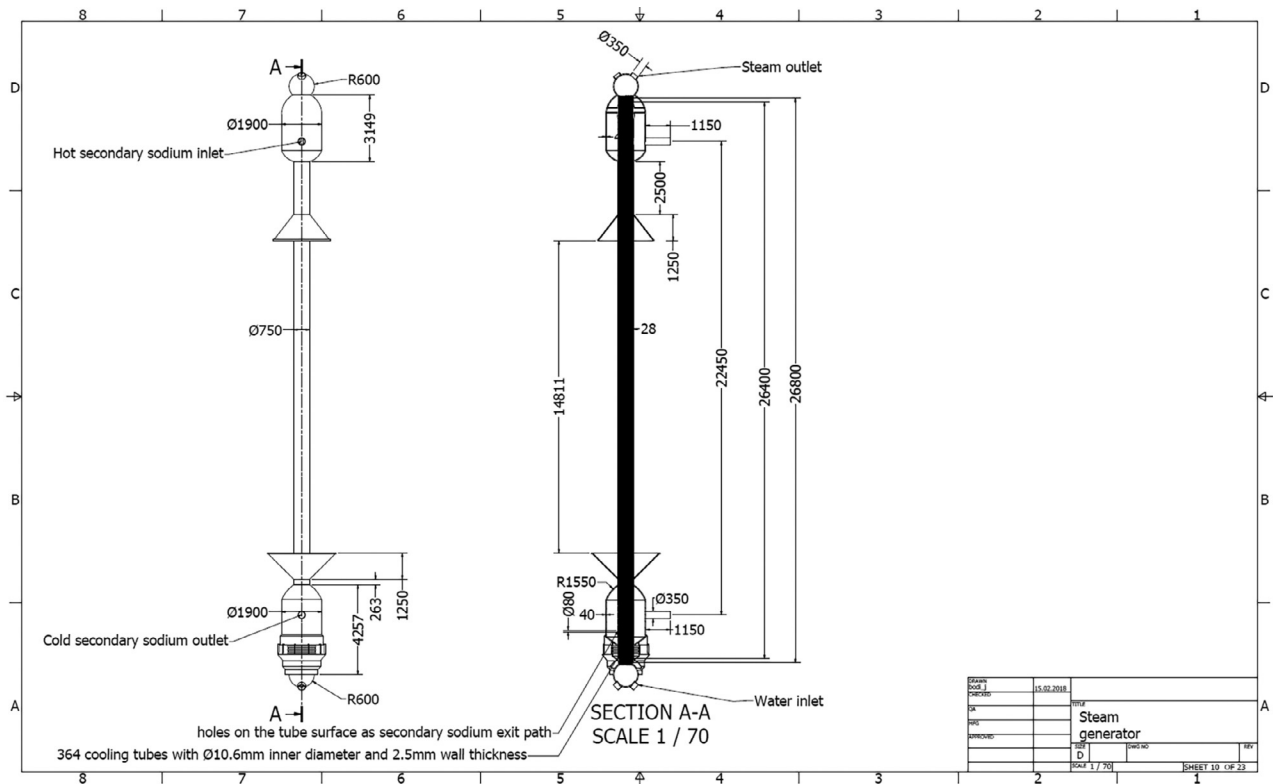


Figure 11.13. View of steam-generator module

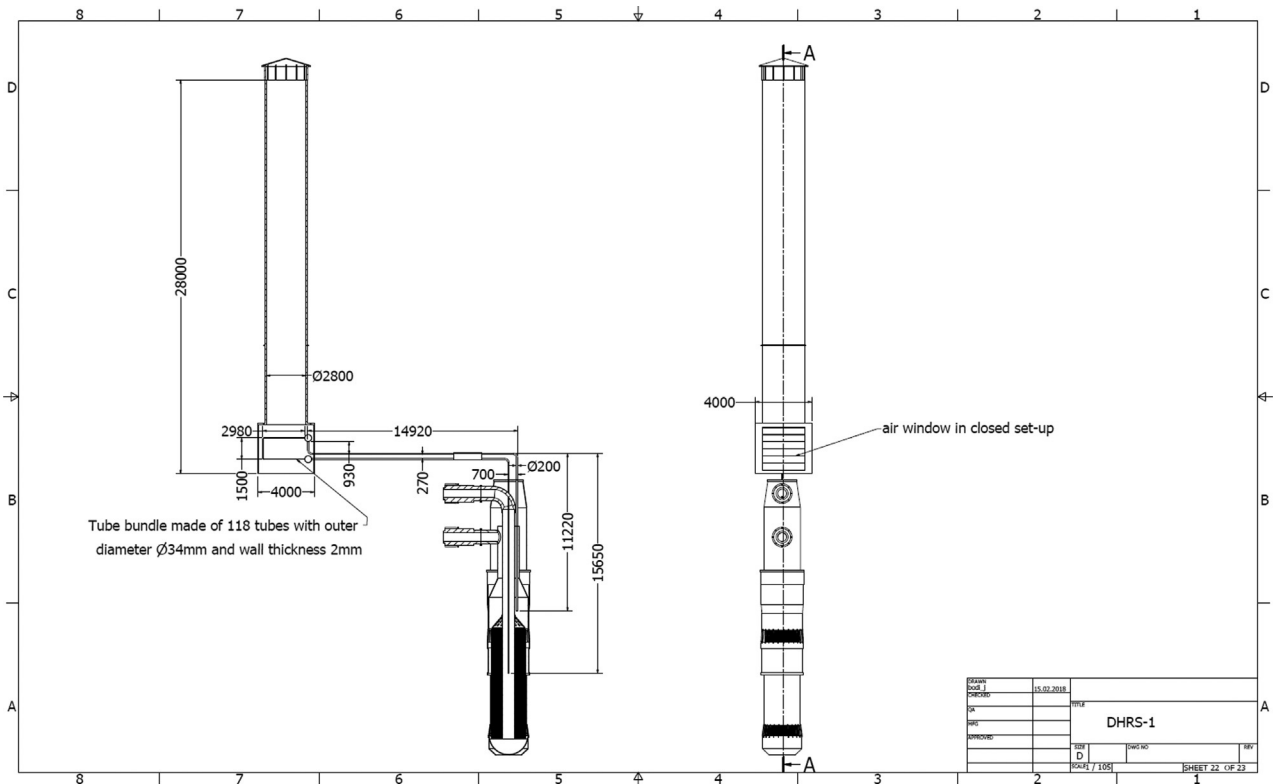


Figure 11.14. View of DHRS-1 system attached to its heat exchanger

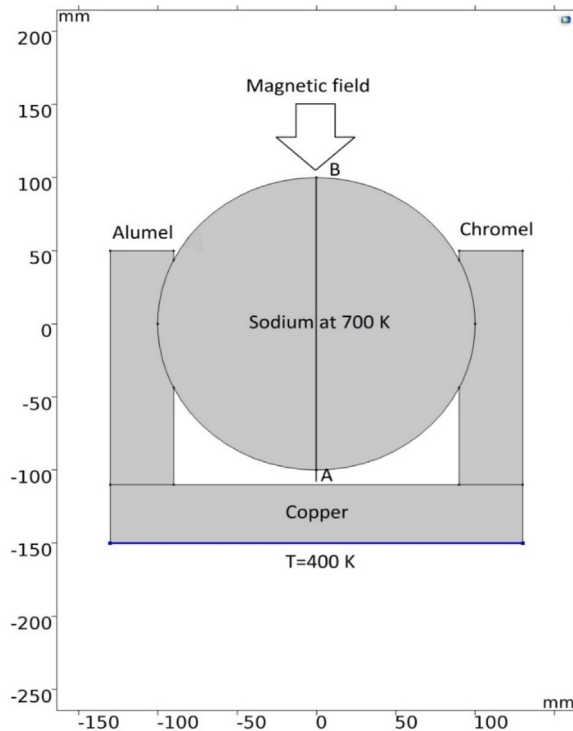


Figure 11.15. Principle of thermal pump

building. The cold secondary sodium comes back to the IHX cold sodium entry. Such a scheme promotes cooling of the primary sodium in the IHX and, therefore, enhances the primary-sodium natural convection through the core and IHX. This operation is mainly passive, where the operator has only to open the window of the air circuit and the heat removal starts from the already established sodium circulation (enhanced by the thermal pumps) within the DHRS-1 loop.

To increase the passivity of the system, a thermal pump of 200-mm diameter can be installed on the hot line. The thermal pump is a passive electromagnetic pump, which uses thermoelectricity generated by the difference in temperatures (hot sodium and atmospheric air). This pump does not need an external electricity supply and provides a supplementary flow rate. The concept of the thermal pump is illustrated in Figure 11.15, where a magnetic field is created by permanent magnets. An electric current is produced by the attached thermo-elements, being exposed to a temperature gradient. The resultant magnetic field and electric current initiate a pressure increase and a flow rate in the liquid-metal coolant.

The aforementioned component needs further R&D, i.e., a test in a sodium loop. In case this R&D is not performed to validate the concept, a small electromagnetic pump with a secured power supply could replace this component.

11.6.5 Piping

To limit the sodium velocity to about 5 m/s in normal operation, the proposed diameters of the secondary pipes are \varnothing 850 mm for the main lines and \varnothing 350 mm for the steam-generator main lines.

Two options are possible for these pipes:

The first option is to have pipes relatively long and flexible, to be able to accommodate thermal expansion. It has been the option of almost all existing plants and particularly for the Phenix and Superphenix. In this case, the main pipes have a wall thickness of 12.5 mm and a length of about 220 m, including elbows to accommodate thermal expansion and discharge lines for sodium draining at the hot and cold legs. As for the steam-generator lines, there is a wall thickness of 15 mm and a length of about 30 m, including elbows

to accommodate thermal expansion and discharge lines for sodium draining at the lower part of each steam generator. The lengths of the lines depend on the chosen material and its thermal expansion coefficient. The resulting volume of the secondary sodium in each of the six loops is about 250 m³, including 90 m³ in SGs, 27 m³ in IHX, 7 m³ in the secondary pump, and about 116 m³ inside the piping.

Indeed, the feedback from these flexible pipes shows some problems. On the Superphenix the sodium pipes had lyres to resume the dilations between cold and operational states. However, the heavy weight of these pipes requires supports in which the pipes would necessarily need to slide. However, antiseismic standards require pipes firmly maintained during an earthquake. This led to the definition of rather complex systems on the Superphenix that did not work well. After each transient, the pipe was found in abnormal positions (see below [Guidez and Prêle, 2017](#), p. 135):

“The long length of the relatively flexible pipes led to numerous support devices (self-locking devices) allowing their expansion, while blocking them in the event of an earthquake. Many of these numerous devices (2400!) and the non-linearity of their behavior made their monitoring and maintenance very cumbersome. Indeed, these devices in bad state could induce blockages of pipes, which would cause significant mechanical stresses.”

Another component that worked poorly was the thermal insulation on these flexible pipes. This led to difficulties in detecting leaks, risks of corrosion by undetected leaks, and numerous false alarms that were very difficult to verify ([Guidez, 2014](#); [Guidez and Prêle, 2017](#)).

Based on this negative feedback in terms of investment (significant extra) and safety (risk of rupture of the piping blocked in their support), ESRF SMART proposes a second option with straight and rigid piping, where thermal expansion is taken up by bellows. Fixed and non-sliding supports play their support role in normal operation and in case of an earthquake. Between these fixed points, the pipes are straight. A bellow is installed in the middle of this right part, which supports the dilatation effect. A choice of material other than 316L, for example 9 Cr, would also significantly reduce this dilatation. It should be noted that the Russians on the BN-1200 project chose this bellows option for their design.

The benefits are as follows:

- Cost reduction due to the decrease of the pipe lengths, quantities of secondary sodium, volumes of the storage tanks, etc.
- Simpler, cheaper, and more efficient pipe supports resulting in safety gain and ease to manage in exploitation.
- Ability to use removable insulation including a gap between this and the sodium pipe, which makes the installation easier on these straight parts and improves the sodium-leak detection, decreasing the number of false alarms, which results in improved safety for the reactor operation.
- Improvement of the circuit’s natural-convection circulation due to the shorter lines.
- Reduction of the distance between fixed points and thus the dimensions and cost of secondary building.
- In addition, the mechanical dimensioning of the pipes is simpler in contrast to the flexible option, which required a small thickness for the pipes and numerous welds for the elbows and expansion lyres. With straight piping, it is possible to minimize the number of welds and take the desired thickness for the pipes.

In practical terms, on the drawings, straight pipes are used to join the fixed points that are the components: heat exchangers, steam generators, pumps, DHRS-1. In this case, using reduced lengths for the secondary circuits, the implementation of a circular secondary building arrangement is proposed around the primary vessel. This disposition allows also to have the same chimney for the casing and the DHRS-1.

The aforementioned disposition of the secondary loop is presented in [Figure 11.16](#).

The initial flexible loop had a length of 195 m of 850-mm diameter tubing (or 220 m, if we count the piping toward the sodium-draining tank) and around 150 m of 350-mm diameter piping. In contrast, with the new design, it was reduced to 67 m of 850-mm diameter tubing (or around 88.5 m, if the piping toward the sodium-draining tank is counted) and around 12 m of 350-mm diameter tubing. Based on the above lengths,

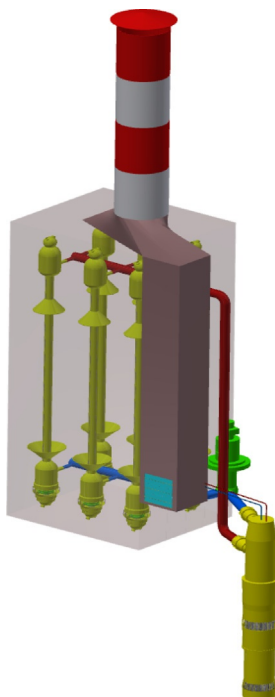


Figure 11.16. View of compact secondary loop with shared chimney for casing and DHRS-1

the available sodium volume in the piping only (so not taking into account the steam generators, IHX, and secondary pump) for one secondary circuit for the original case is around 116 m^3 , whereas, for the simplified circuit this number is around 37 m^3 . In this sense, the reduction in sodium volume is 79 m^3 .

11.7 Safety analysis of the secondary loop

In terms of safety, three points are mainly to be optimized in these secondary circuits:

Firstly, secondary circuits have the role of evacuating the power of the reactor, and in case of a shutdown, it actively participates in the evacuation of the residual power. The use of these circuits has been favored for residual-power removal as it is the loop normally used by the operator for this purpose in all operating circumstances. Therefore, we tried to design a loop capable of removing this power by natural convection, passive way, and with a minimum of necessary interventions of operators.

Secondly, the operation experience of the SFRs shows that sodium leaks mainly take place at the level of the secondary circuits. For example, in the Phenix (Guidez, 2014) the 31 leaks of sodium were on the secondary loops and auxiliary systems. Note also, that for the ESFR SMART specific measures have been taken to avoid any leakage of primary sodium. These possible leaks of non-active secondary sodium are more of a security than a safety concern. That being said, proposals have been made to both minimize the risk of sodium leaks and increase the possibilities of rapid detection and mitigation.

Thirdly, sodium/water interaction is a problem to be tackled at the steam generator level. So, the steam-generator type has been chosen aiming to improve the speed of detection and to minimize the consequences. It also shows that corresponding provisions are to be taken at the level of the casings containing the modules.

All these points have been taken into account in the ESFR SMART design essentially based on the existing feedback experience on the SFR secondary circuits, but also on published results of studies on previous projects as the ASTRID in France, BN-1200 in Russia, or PGSFR in Korea.

- Decay-heat removal

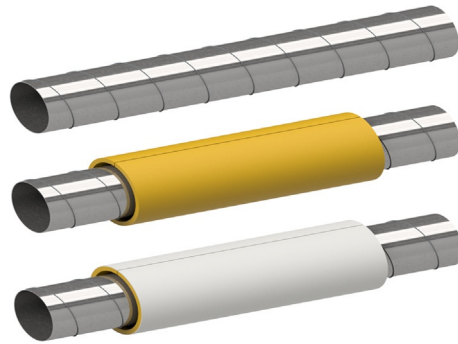


Figure 11.17. View of straight tube with its external and removable insulation

The secondary circuit was predimensioned to be able to evacuate this residual power, even after the loss of the water circuits, only by natural convection of the air around the modules of steam generators. However, this presizing revealed that natural convection in the circuits was not sufficient and that an operation of the secondary pumps at reduced speed (100 rpm) was necessary, at least, at the start of the event, to increase the heat removal from the circuit (Bittan et al., 2020).

In case of unavailability of the secondary loop and even if this loop is drained, the DHRS-1 can provide 100% of the decay-heat removal function, completely passively in natural convection of the air and sodium (Guidez et al., 2020a, b; Bittan et al., 2021).

The whole system allows being consistent with the new GEN-IV safety rules following Fukushima accident.

– Sodium leaks and fires

The option of straight lines without elbows allows the use of protection against leakage by a double wall piping, shown in Figure 11.17. This installation would be difficult on large flexible pipes with large movements. The external wall is covered from underneath with insulation, followed by a gap and the sodium pipe. This external wall can be easily opened to allow interventions, for example, in case of an alarm.

Classical sodium-fire detections are fitted on the sodium pipe to detect any leak from it. These detections are particularly installed around the bellows and in the lower part of the circuit. Therefore, sodium-leak detection is possible before any chemical interaction of the sodium with the insulation. Complementary detections can be added between the pipe and the removable insulation, such as sodium-smoke detection in the partitioned interior zone. This set of provisions allows quick detection and good containment of any sodium leak inside this double wall.

– Sodium/water reaction

Conventional devices enable to efficiently control the risk of water/sodium reaction by detection of hydrogen in the sodium at the outlet of each steam-generator module. The modularity of the steam generators makes it easier to quickly detect a sodium/water reaction, isolate and drain the failed module. It allows also to minimize the theoretical envelope accidents. Even with a hypothetical rupture of all the tubes in a module, the accident can be managed in terms of overpressure and mitigation. In the case of water/sodium reaction, the consequences for the plant operations are limited and the operation can continue with the remaining modules, after isolation of the defective module. Mitigation measures against the risk of sodium–water–air reaction also have to be taken into account in the building concept. In particular, “water area” and “sodium area” in the secondary system buildings should be strictly separated to avoid any interaction. The casing is sized to resist any external aggression.

11.8 General layout of the plant

The secondary circuits disposition with short and straight tubes allows a circular disposition of the secondary circuits around the primary block.

It carries an important benefit on the final sizing of the secondary building including all the related pipes and components, as shown in [Figure 11.18](#).

This new circular disposition allows a significant improvement of the general layout, in comparison with initial design with flexible pipes as shown in [Figures. 11.19](#) and [11.20](#).

We arrive in [Figure 11.21](#), at this final design of the plant with the chimneys common to steam generators casings and DHR1 systems. On the right, we have the turbine building and on the left the handling building with his own chimney.

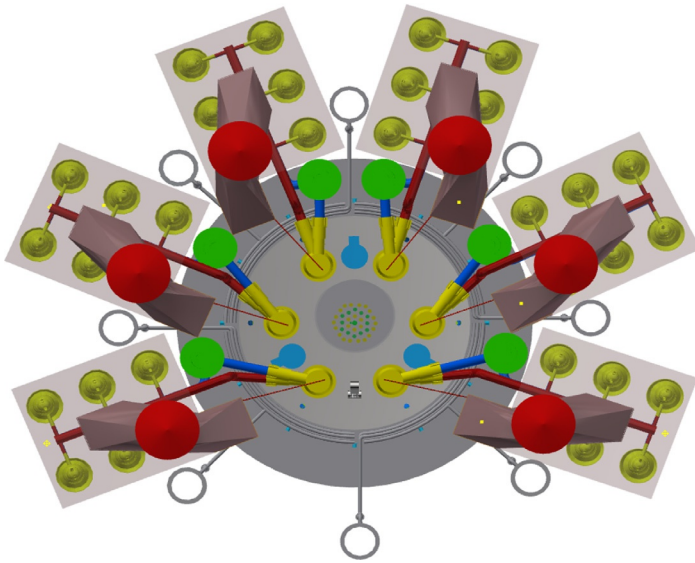


Figure 11.18. Circular disposition of secondary loops around primary vessel

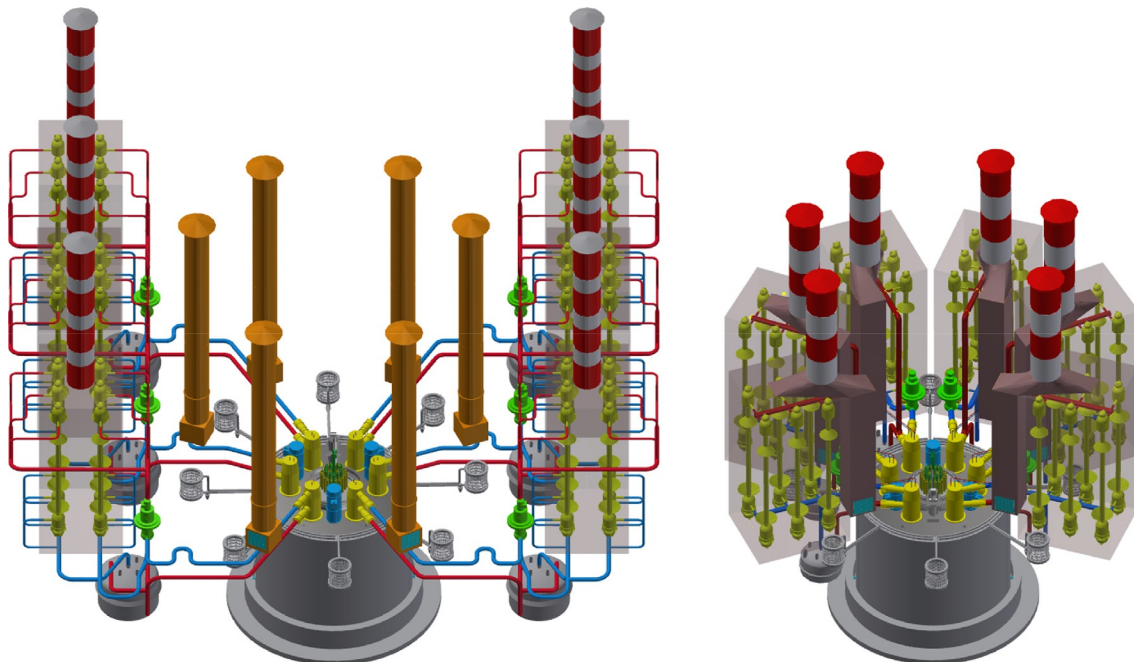


Figure 11.19. Original plant layout (left) vs new circular layout (right) in general view of plant

Figure 11.20. Comparison of initial layout and new circular disposition

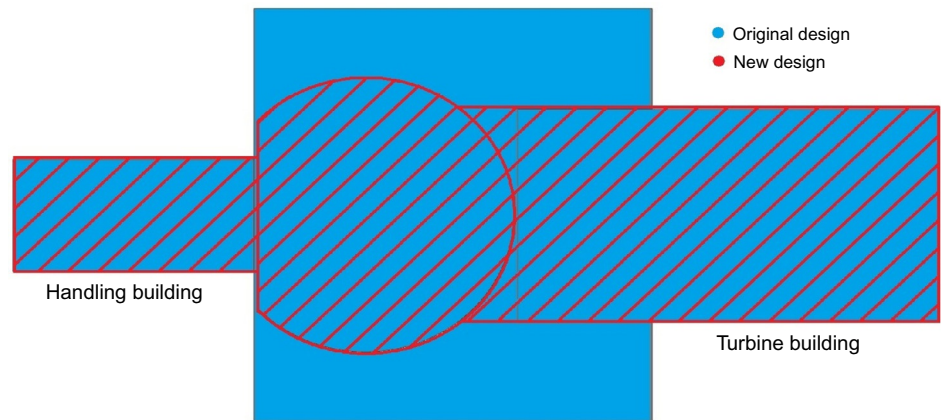
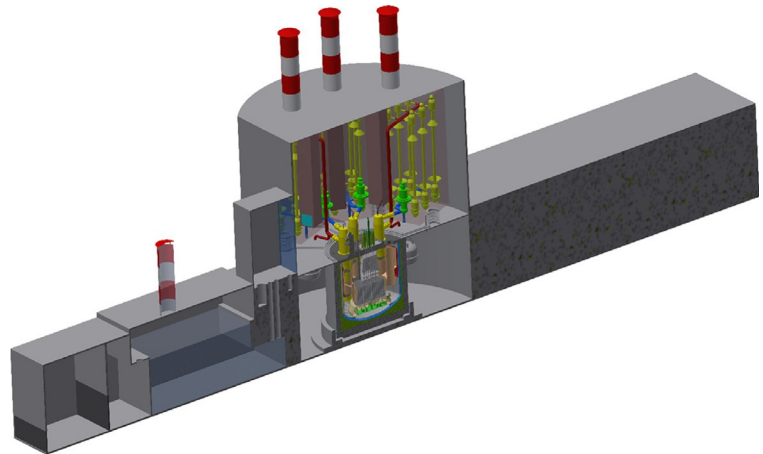


Figure 11.21. View of final layout with circular disposition and with common chimneys between casing and DHRS-1



11.9 Handling systems

11.9.1 Spent-fuel handling

Refueling takes place during scheduled reactor shutdowns, which occur annually. Spent-fuel subassemblies are removed from the core and placed in the inner spent-fuel storage at the periphery of the core. Other irradiated-core components, such as reflector or absorber subassemblies, can be removed from the reactor vessel without using this inner storage. Fuel subassemblies, which have been retained in the inner spent fuel storage for 3 years and, therefore, have a low decay-heat power ($<10\text{ kW}$) are transferred from the inner spent-fuel storage to the secondary fuel-handling facilities.

During reactor operation, special instrumentation systems are continuously used to detect the failed fuel and once detected to locate the failed subassembly in the core. This failed subassembly is removed from the core during an exceptional shutdown and placed in a special position in the inner storage, while fresh fuel subassembly is loaded in the core. After reduction of the decay-heat power to the level compatible with the secondary fuel-handling system, the failed subassembly is removed from the reactor the same way as the other spent-fuel subassemblies.

The in-vessel fuel-handling system (Figure 11.22) provides access to any core position by means of two eccentric rotating plugs (large and small) in the reactor roof, a Direct Lift-Charge Machine (DLCM) and a Fixed Arm Charge Machine (FACM). At operational position of the plugs (as shown in Figure 11.22), the DLCM is positioned at the center of the above core structure. During refueling by rotation of the small and large rotating plugs the DLCM can be positioned above any subassembly from the inner handling zone of

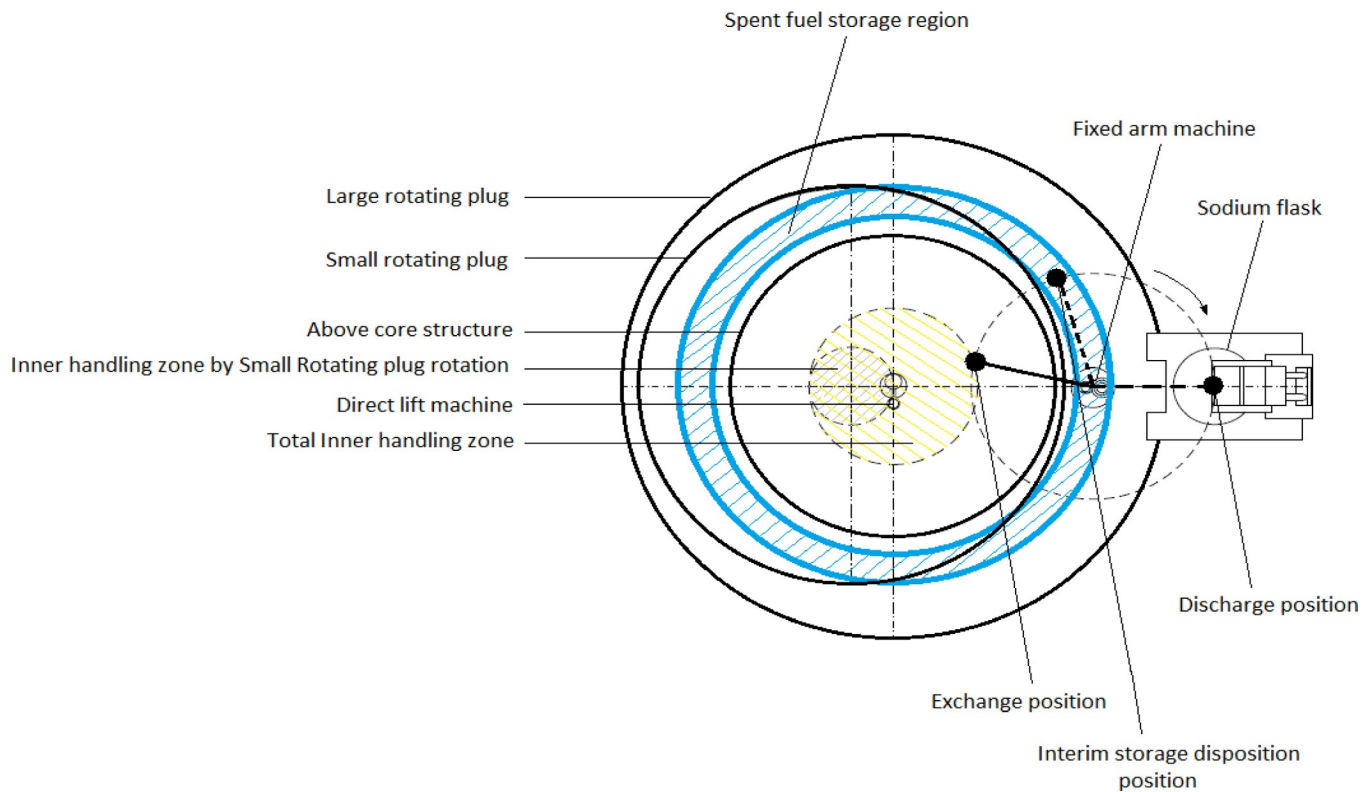


Figure 11.22. In-vessel fuel-handling system

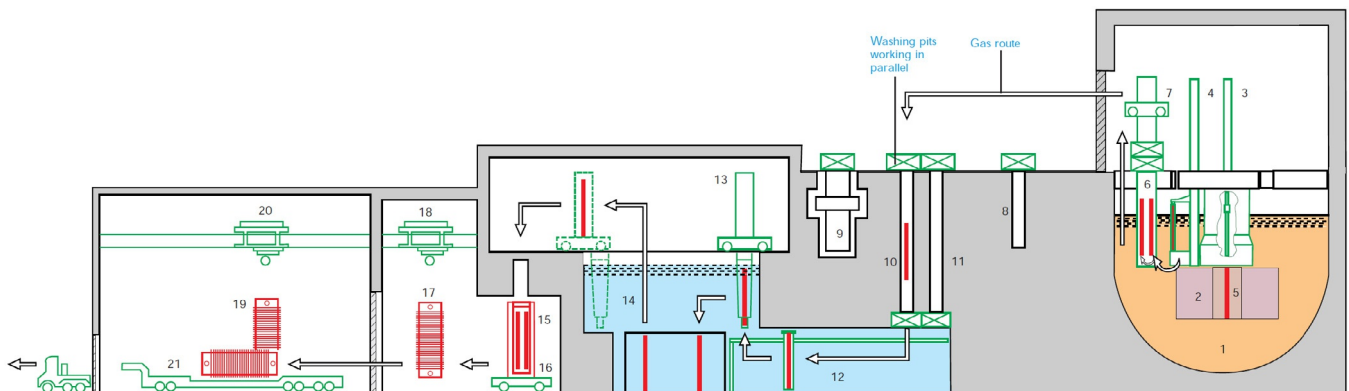


Figure 11.23. Fuel-handling principle in ESRF SMART

the core shown by shaded circle. The subassembly from the inner handling zone can be lifted and moved to the exchange position also shown in [Figure 11.22](#) from where it can be taken by the FACM and positioned in the inner spent fuel storage. The FACM is located outside the above core structure and by rotation of the large rotating plug can be positioned above any subassembly of the outer handling zone of the core, take this subassembly and move it to the inner spent fuel storage.

The interface with the secondary fuel handling system (see [Figure 11.23](#)) is provided by a two-position rotor suspended from the reactor roof. A fresh-fuel subassembly is deposited in the external position of the rotor from the fuel-handling cask, while a spent assembly is deposited in the internal position by the FACM. After a half turn of the rotor, the fresh-fuel subassembly is taken by the FACM, and the spent fuel subassembly is lifted into the fuel-handling cask. The cask encloses the subassembly in an inert-gas atmosphere and incorporates biological shielding. The spent-fuel subassembly is transported in the fuel-handling cask, along the fuel-transfer corridor direct to one of two washing pits in the fuel-handling area, where the

subassemblies are cleaned. An encapsulation facility is also provided for failed subassemblies. After washing, the spent-fuel and breeder assemblies are unloaded through a valve at the lower end of the washing pit, directly into the water-transfer corridor through which they are transferred to the spent-fuel storage pond. In the case of encapsulation, the subassembly, in its canister, is transferred to a dedicated storage position or to a special transport cask. Absorber assemblies are loaded directly into casks after washing and transported to the reprocessing plant.

After four-year storage, the decay heat has reduced to about 2 kW, the intact subassemblies are loaded bare into transport casks. These casks leave the fuel-handling building via an air lock to an on-site or off-site dry fuel storage for long-term storage. Alternatively, they can be transferred to the reprocessing plant.

11.9.2 Fresh-fuel handling

Fresh-fuel subassemblies enter the fuel-handling building via the transport-cask air lock and are inspected and stored in the fresh-fuel dry storage. They are transferred from the fresh-fuel storage via the fresh-fuel transfer pit into the fuel-handling cask and then into the reactor vessel, as described above (see [Figure 11.23](#)).

11.9.3 Handling of components

In case of necessity, in service inspection, repair or replacement, it is possible to extract the large components that are the IHXs or primary pumps. The height of the primary building allows performing these operations.

Facilities for washing, decontamination and maintenance of reactor components are located in the maintenance building, which is separated from the reactor building. Components can be serviced and repaired after washing and decontamination. Activated and contaminated components are transferred from the reactor building to the maintenance building within shielded transport casks by means of a special-purpose transport system. Within the reactor building, the active-component handling system provides the means of removing and replacing both active and inactive reactor components.

The handling system comprises a series of casks sized to accommodate the different components to be handled. In the Superphenix, a large cask was used for transportation of the large components and an adapted small cask for small components or materials, such as cold traps, instrumentation, etc. ([Guidez and Prêle, 2017](#)). The cask encloses the component in an inert atmosphere and incorporates appropriate biological shielding. The casks are transported by the high-integrity overhead crane in the crane hall. They are raised to a fixed height, and a redundant retention feature is engaged, which is directly attached to the bridge of the crane. All operations above the reactor are carried out at this fixed height with the redundant retention feature engaged.

11.10 Conclusions on safety improvements

The general principle of the studies was to increase the safety in operation, by increasing the simplicity of the design, avoiding adding new systems and by using at maximal level the possibilities given by the sodium in terms of natural convection and of passivity. So, we can here resume the improvements in terms of passivity, simplicity, easy operation, and severe accident mitigation.

In terms of passivity:

- The void reactivity effect is very low, to reduce drastically any mechanical-energy release, in case of accidental sodium boiling. That was obtained by many various dispositions, with diameter of pins increased, with a plenum above the fuel assemblies, with mixing of fertile and fissile parts in the core, etc.

- Passive-control rods able to stop the plant without control order, but only on the abnormal variation of a physical parameter as temperature or flow rate.
- Better design to allow easy natural convection of sodium in the secondary loop, even without water supply and without power supply.
- Possibility of power extraction without water supply, only by natural air convection, in the casing containing the six modules of steam generator.
- A passive decay-heat removal system on each loop able to maintain a cold leg in the heat exchanger by passive way with air, even if the secondary loop is drained.
- Thermal pumps, passive, able to maintain permanent flow rates in the secondary loops and in the DHRS-1, even without any power supply.

In terms of simplifications:

- Suppression of the safety vessel.
- No dome or polar table.
- No DHRS systems inside the primary vessel.
- Minimization of the number of sodium circuits.
- Very simple massive roof.
- Reduction of more than 50% of pipe length and of general reactor lay out, with the use of straight pipes in secondary loops.

In terms of operation:

- New measures against sodium leaks and better protection of the building with strong separation of water- and sodium-circulation areas.
- Better concept to avoid any primary-sodium leakage.
- Better access for handling operations (no polar table).
- Quick water/sodium reaction detection and good protection against consequences based on choice of modular steam generator.
- Dispositions to avoid by design any consequent gas entrainment in the core.
- Reactor very forgiving with a high inertial capacity and possibility to wait a long time without operator actions.
- Minimization of the number of sodium circuits to operate and survey.

In terms of severe-accident mitigation:

- Discharge tubes inside the core to stream the corium to the core catcher in mitigation situation (see [Figure 11.24](#)).
- Low potential for mechanical-energy release with a new core concept.
- In case of severe accident, large mechanical margins with the massive reactor roof and with the reactor pit able to withstand sodium leaks. That allows to assure no radioactive release at short and long term.
- Ability to cool the primary vessel during long duration after the severe accident with three independent systems, each one being sufficient alone.
- A dedicated core catcher able to receive the whole core materials, with materials protecting the core catcher against ablation by corium, with efficient natural convection cooling and without any recriticality potential.

The proposed set of the modifications compared to the EFR and CP ESFR design, aims at consistency with the main lines of safety evolutions for Generation-IV SFRs since the Fukushima accident.

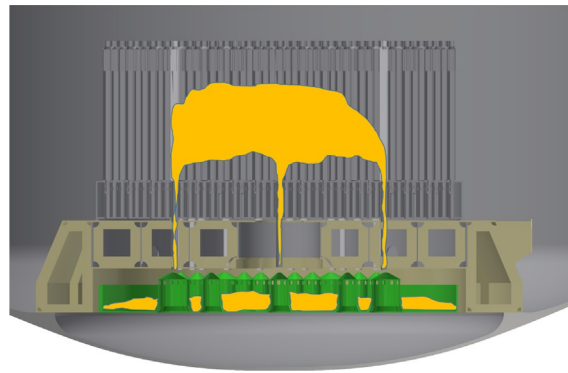


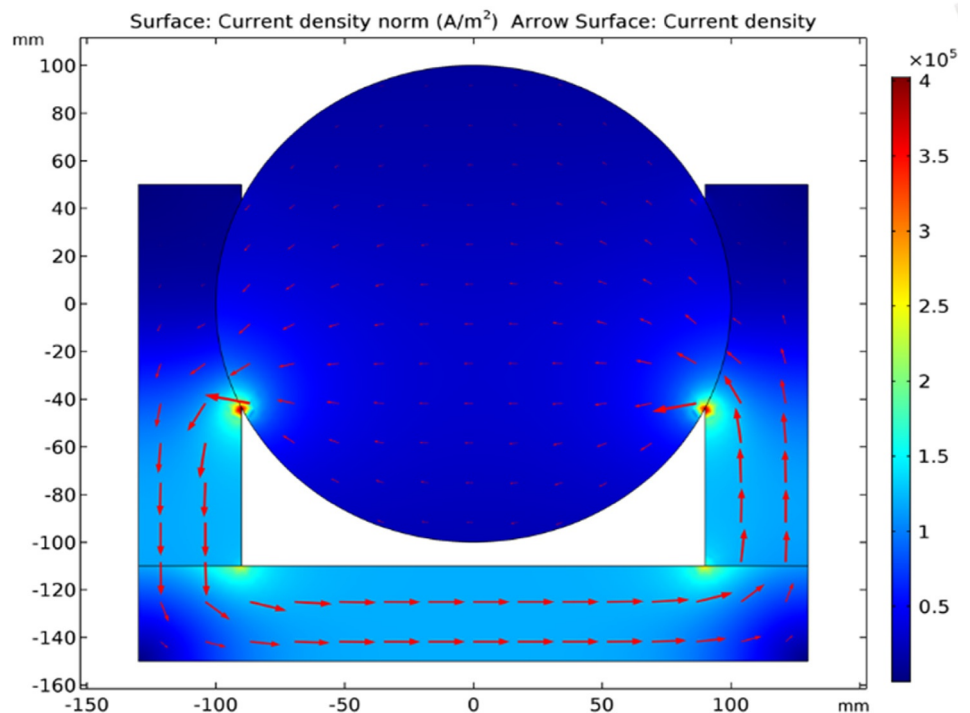
Figure 11.24. “Artistic view” of preferential ways for melted core

11.11 R&D needs for the ESRF SMART options

For the main options of ESRF SMART design, the entire reactor has been drawn on plans and precalculated. In particular, calculations were made to provide a preliminary assessment and to verify the large lines of feasibility of these options:

- The pit organization was presented in [Guidez et al. \(2020b\)](#), with thermal calculations in nominal and accidental situations. The thermal possibilities of the DHR-3 system were also calculated.
- The thermal calculation of the three DHR systems was made. For the DHRS-2, CATHARE calculations were necessary to calculate the natural convection and the cooling by air in the steam-generators casings. These calculations show the compliance of the three DHR systems with the new GEN-IV safety rules ([Bittan et al., 2020](#)).
- For the core catcher, calculations were provided of the core melting, of the residual power, and of the ability of the core catcher to evacuate by natural convection of sodium around it this power ([Guidez et al., 2020b](#)).
- Some calculations were provided on the thermal pumps (see [Figure 11.25](#)) for presizing of DHRS-1.

Figure 11.25. Computed current density in DHRS-1 thermal pump (A/m^2)



However, and if one day, Europe wanted to build a reactor on these bases, some points remain still to be developed. They require few R&D and would relate mainly to the following points.

– **Industrial confirmation of the proposed organization for the reactor pit.**

The organization proposed is based on developments already made for EFR, as test of a dedicated concrete without reaction with sodium. The global organization of the pit should be validated.

– **Industrial validation of the manufacturing method of the EFR-type thick slab.**

Thick slab needs thick welds. This type of operation has already been manufactured. But the global organization of the slab fabrication, with a part in factory, and final welding on site, has to be managed by the industrial.

– **Qualification of low-expansion materials and large-diameter bellows for the secondary circuit.**

Further R&D is necessary for the bellows of diameter 850 mm in terms of dilatation capacity and operating lifetime. However, the use of bellows on sodium loops is not unprecedented.

These bellows exist on many sodium valves especially in the Phenix and Superphenix, and inside the Phenix heat exchangers.

A bellow of large diameter (approximately 800 mm) was installed in the Superphenix (Figure 11.26) on the internal part of the hot collector of the intermediate heat exchangers to take up the differential expansions with the external part. This device had several expansion waves and a thickness of 8 mm. It has undergone a cycling test with a large number of cycles for validation.

On the ESRF SMART steam-generator module, a bellow of large diameter (750 mm) is designed to allow relative dilatation between the external wall of the steam generator, and its internal bundle.

This R&D consists, based on the dimensions of the circuit, of specifying the specifications requested for these bellows in terms of resumption of expansion. Then it is necessary to build some in industry and make them execute a large number of cycles in a furnace to qualify them. This is what was done to qualify the Superphenix bellows.



Figure 11.26. View of bellow tested on Superphenix heat exchanger (EFR Associates, 1998)

Another aspect of R&D is to study and qualify for the pipes, new materials with lower expansion coefficients. Some are already available, but need qualification in this new utilization.

– R&D on thermal pumps

Thermal pumps are not new and were already used on the Siloe reactor to ensure the flow in the test loops. However, and although some preliminary calculations were performed on the thermal pump of the DHRS-1, a full-scale test on a sodium loop would be necessary for final validation and industrial demonstration of the results.

11.12 Conclusion

Thanks to the ESFR-SMART project, precalculations and a set of new safety measures are already available for the design of an SFR, meeting the new reinforced post-Fukushima safety criteria. This reactor brings about significant simplifications, incorporating feedback from previous European reactors and projects. These simplifications bring safety improvements, cost savings and ease of operation.

This project makes it possible to have a database available for the future for a European development of these reactors, which could potentially solve the energy problems of humanity, but are today without any short-term project in Europe.

Acknowledgment

The work has been prepared within EU Project ESFR-SMART, which has received funding from the EURATOM Research and Training Programme 2014–18 under the Grant Agreement No. 754501.

References

- Baldev, R., Chellapandi, P., Vasudeva Rao, P.R., 2017. *Sodium Fast Reactors with Closed Fuel Cycle*. November 15, CRC Press, ISBN: 9781138893047, p. 720.
- Bittan, J., Boré, C., Guidez, J., 2020. Preliminary assessment of decay heat removal systems in the ESFR-SMART design: the role of natural air convection around steam generator outer shells in accidental conditions. In: *Proceedings of the International Youth Nuclear Congress (IYNC)*, March 8–12, Sydney, Australia, p. 10.
- Bittan, J., Boré, C., Guidez, J., 2021. Preliminary assessment of decay heat removal systems in the ESFR-SMART design: the role of natural air convection around steam generator outer shells in accidental conditions. submitted to *ASME J. Nucl. Eng. Radiat. Sci.* NERS-20-1079.
- EFR Associates, 1998. *European Fast Reactor: Outcome of Design Studies*.
- Fiorini, G.L., Vasile, A., 2011. European Commission—7th framework programme. The collaborative project on European sodium fast reactor (CP ESFR). *Nucl. Eng. Des.* 241 (9), 3461–3469. <https://doi.org/10.1016/j.nucengdes.2011.01.052>.
- Guidez, J., 2014. *Phénix Experience Feedback*. Edition EDP Sciences, p. 300. EAN13: 9791092041057.
- Guidez, J., Prêle, G., 2017. *Superphenix. Technical and Scientific Achievements*. Edition Springer, ISBN: 978-94-6239-245-8, p. 342.
- Guidez, J., Saturnin, A., 2017. Evolution of the collective radiation dose of nuclear reactors from the 2nd through to the 3rd generation and generation-IV sodium-cooled fast reactors. In: *Proceedings of the International Conference on Fast Reactors and Related Fuel Cycles: Next Generation Nuclear Systems for Sustainable, Development (FR17)*, Yekaterinburg, Russia, 26–29 June, IAEA-CN245–016, p. 12.
- Guidez, J., Bodi, J., Mikityuk, K., Rineiski, A., Girardi, E., 2018. New safety measures proposed for European sodium fast reactor in horizon-2020 ESFR-SMART project. In: *Proceedings of the GIF Symposium*, Paris, France, October 16–17, p. 14.
- Guidez, J., Gerschenfeld, A., Girardi, E., Mikityuk, K., Bodi, J., Grah, A., 2019. European sodium fast reactor: innovative design of reactor pit aiming at suppression of safety vessel. In: *Proceedings of the International Congress on Advances in Nuclear Power Plants (ICAPP 19)*, Juan-les-Pins, France, May 12–15, p. 10.

- Guidez, J., Gerschenfeld, A., Bodi, J., Mikityuk, K., Alvarez Velarde, F., Romojaro, P., Diaz-Chiron, U., 2020a. ESFR SMART project conceptual design of in vessel core catcher. In: Proceedings of the PHYSOR 2020, Cambridge; United Kingdom 29 March 2 April 2020, p. 9.
- Guidez, J., Gerschenfeld, A., Mikityuk, K., Bodi, J., Girardi, E., Bittan, J., Bore, C., Grah, A., 2020b. Innovative decay heat removal systems in European sodium fast reactor. In: Proceedings of the International Congress on Advances in Nuclear Power Plants (ICAPP2020, 15–19 March, Abu Dhabi, Paper 20106, p. 10.
- IAEA Nuclear Energy Series No. NR-T-1.16, 2020. Passive Shutdown Systems for Fast Neutron Reactors. Vienna, Austria. Free download from https://www-pub.iaea.org/MTCD/Publications/PDF/P1863E_web.pdf.
- IAEA-TECDOC-1691, 2012. Status of Fast Reactor Research and Technology Development. IAEA TECDOC Series, p. 846. Vienna, Austria. Free download from https://www-pub.iaea.org/MTCD/Publications/PDF/TE_1691_CD/PDF/IAEA-TECDOC-1691.pdf.
- Mikityuk, K., Girardi, E., Krepel, J., Bubelis, E., Fridman, E., Rineiski, A., Girault, N., Payot, F., Buligins, L., Gerbeth, G., Chauvin, N., Latge, C., Garnier, J.C., 2017. ESFR-SMART: new horizon-2020 project on SFR safety. In: Proceedings of the International Conference on Fast Reactors and Related Fuel Cycles: Next Generation Nuclear Systems for Sustainable, Development (FR17), Yekaterinburg, Russia, 26–29 June, IAEA-CN245–450, p. 17.
- Rineiski, A., Mériot, C., Marchetti, M., Krepel, J., Coquelet-Pascal, C., Tsige-Tamirat, H., Alvarez-Velarde, F., Girardi, E., Mikityuk, K., 2021. New ESFR-SMART core safety measures and their preliminary assessment. submitted to ASME J. Nucl. Eng. Radiat. Sci., 26.
- Sedakov, V.Y., Lyubimov, M.A., Shkarin, V.I., Shokhonov, V.P., 2017. Manufacture, installation and adjustment of BN-800 RP Equipment. In: Proceedings of International Conference on Fast Reactors and Related Fuel Cycles: Next Generation Nuclear Systems for Sustainable, Development (FR17), Yekaterinburg, Russia, 26–29 June, IAEA-CN245–425, p. 10.
- The Generation IV International Forum: The Safety Design Criteria Task Force (SDC-TF), 2017. Safety Design Criteria for Generation IV Sodium-Cooled Fast Reactor System (Rev. 1). SDC-TF/2017/02, p. 91. Free download from https://www.gen-4.org/gif/upload/docs/application/pdf/2018-06/gif_sdc_report_rev1-sept30-2017_afteregpg20171024a.pdf.
- WENRA, 2013. Safety of New NPP Designs, WENRA/RHWG Report., p. 52. Free download from http://www.wenra.org/media/filer_public/2013/08/23/rhwg_safety_of_new_npp_designs.pdf.

Generation-IV Sodium-cooled Fast Reactor (SFR) concepts in Japan

Hideki Kamide, Hiroyuki Ohshima, Shigenobu Kubo, and Yoshitaka Chikazawa
Japan Atomic Energy Agency (JAEA), Ibaraki, Japan

Nomenclature

Non-dimensional number

Re Reynolds number

Subscripts

el electrical

th thermal

Acronyms and abbreviations

AC	Alternating Current
AM	Accident Management
ASME	American Society of Mechanical Engineers
ASTM	American Society for Testing and Materials
ASTRID	Advanced Sodium Technological Reactor for Industrial Demonstration (France)
ATWS	Anticipated Transient Without Scram
CABRI	Pool-type research reactor operated by CEA (France)
CCWS	Components Cooling Water System
CFD	Computational Fluid Dynamics
CL	Cold Leg
CT	Cold Trap
CV	Containment Vessel
DBA	Design Basis Accident
DBE	Design Basis Event
DEC	Design Extension Condition
DEG	Double-Ended Guillotine
DHRS	Decay Heat Removal System
DHX	Direct Heat eXchanger
DiD	Defense-in-Depth
DP	Dip Plate
DRACS	Direct Reactor Auxiliary Cooling System
EVST	Ex-Vessel Storage Tank
FaCT	Fast reactor Cycle Technology development (Japan)

FAIDUS	Fuel Assembly with an Inner DUct Structure
FHM	Fuel Handling Machine
FHS	Fuel Handling System
FS	Feasibility Study on commercialized fast reactor cycle systems (Japan)
FSL	reFueling Sodium Level
GIF	Generation IV International Forum
GTG	Gas Turbine Generator
GTHTR 300	Gas Turbine High-Temperature Reactor 300 MW _{el} (Japan)
GV	Guard Vessel
HL	Hot Leg
IHX	Intermediate Heat eXchanger
ISIR	In-Service Inspection and Repair
IVR	In-Vessel Retention
JAEA	Japan Atomic Energy Agency
JSFR	Japan Sodium-cooled Fast Reactor
JSME	Japan Society of Mechanical Engineers
LEAP	Leak Enlargement And Propagation
LES	Large Eddy Simulation
LOF	Loss Of Flow
LOHRS	Loss Of Heat Removal System
LOHS	Loss Of Heat Sink
LORL	Loss Of Reactor Level
LWR	Light Water Reactor
MOX	Mixed OXide Fuel
NIS	Neutron Instrumentation System
NSL	Normal Sodium Level
NSSS	Nuclear Steam Supply System
ODS	Oxide-Dispersion-Strengthened
PFR	Prototype Fast Reactor (UK)
PRACS	Primary Reactor Auxiliary Cooling System
R&D	Research and Development
RD	Roof Deck
RP	Rotating Plug
RSS	Reactor Shut-down System
RV	Reactor Vessel
SA	SubAssembly
SASS	Self-Actuated Shutdown System
SC	Steel plate reinforced Concrete
SCCV	Steel plate-reinforced Concrete Containment Vessel
SDC	Safety Design Criteria
SDG	Safety Design Guideline
SFR	Sodium-cooled Fast Reactor
SG	Steam Generator
SIMMER	Sn, Implicit, Multiphase, Multicomponent, Eulerian, Recriticality
STAR-CD	General-purpose CFD code
SWACS	Sodium-Water reaction Analysis Code System
TEPCO	Tokyo Electric Power COmpany
TOP	Transient Over Power
TREAT	Transient Reactor Test facility (US)
TRU	TRansUranium
UIS	Upper Internal Structure
UK	United Kingdom
USDOE	United States Department Of Energy
VHTR	Very-High-Temperature Reactor

12.1 Introduction

With respect to advanced reactor designs, Japan has put most of its resources and efforts into the development of Sodium-cooled Fast Reactors (SFRs), which consist of a key element of the closed nuclear fuel recycling system along with spent fuel reprocessing technology. Japan's efforts for SFR development go back to the 1970s when the experimental reactor JOYO was designed and constructed with a thermal capacity of 75 MW_{th} and a loop-type system. JOYO reached its first criticality in 1978 (Maeda et al., 2005) and uprated to 140 MW_{th} in 2003 to upgrade the irradiation test capacity of the reactor. Then design and construction of the prototype power reactor named MONJU began in the 1980s, also with a loop-type system. MONJU was first taken critical in April 1994 and generated electricity for the first time in August 1995 (Kondo et al., 2013). A study related to safety requirements expected for MONJU as a prototype fast breeder reactor was made after the Tokyo Electric Power Company's (TEPCO's) Fukushima Daiichi nuclear power plants accident in 2011. In 2016, the Japanese government made a decision on SFRs development due to large uncertainty on the cost estimation for MONJU restart. MONJU will not restart as a nuclear reactor and will make the transition to decommissioning. Research and Development (R&D) on SFRs and nuclear fuel cycles is continued and promoted for future commercialization. Although the term of MONJU power operation was limited, a lot of knowledge and experiences have been obtained from various kinds of R&D, the design/fabrication/construction, trouble shootings, and their repair work. These achievements are assembled and organized for the future SFRs.

With a purpose of probing a commercially feasible fast reactor system, a feasibility study on commercialized Fast reactor cycle Systems (FS) was initiated in 1999 (Aizawa, 2001). In the FS, survey studies were made to identify the most promising concept among various systems such as SFRs, gas-cooled fast reactors, heavy metal-cooled fast reactors (lead-cooled fast reactors and lead-bismuth cooled fast reactors), and water-cooled fast reactors with various fuel types such as oxide, nitride, and metal fuels. The FS concluded to select an advanced loop-type SFR with mixed oxide fuel named Japan Sodium-cooled Fast Reactor (JSFR) (Kotake et al., 2005).

On the basis of the conclusion of the FS as well as check and review by relevant government bodies, a project named the Fast reactor Cycle Technology development (FaCT) project was launched in 2006 by the Japan Atomic Energy Agency (JAEA) under cooperation with the Ministry of Education, Culture, Sports, Science and Technology of Japan; the Ministry of Economy, Trade and Industry of Japan; electric utilities; and vendors as an advanced stage toward commercialization of fast reactor cycle technology by 2050. In the FaCT project, both a conceptual design study of JSFR with several key innovative technologies adopted and R&D on these innovative technologies were conducted. The development targets related to sustainable energy production, radioactive waste reduction, safety equal to the future Light Water Reactor (LWR), and economic competitiveness against other future energy sources were presented by the Japan Atomic Energy Commission, which is consistent with the goals of Generation IV International Forum (GIF) (US DOE and GIF, 2002).

In 2010, at the end of Phase I of the FaCT project, technical assessments on the achievement of the development targets and feasibility of the innovative technologies were made. The purpose of this assessment was to evaluate the degree of achievement at that time in the midterm stage until 2015, to affirm the validity of the direction of R&D, and to identify technical challenges toward future R&D. As a result of the assessments, it was revealed that the development targets were mostly achieved, and some challenges that may indicate the direction of future R&D were identified (Chikazawa et al., 2015).

The finalization of the FaCT Phase I and initiation of FaCT Phase II, which is the demonstration phase of the innovative technologies, were suspended because of the sociopolitical situation changes after the Great East Japan Earthquake of March 11, 2011. Since 2011, to contribute to the development of the Safety Design Criteria (SDC), which include the lessons learned from the TEPCO's Fukushima Daiichi nuclear power plants accident, in the framework of GIF, the design study is focusing on the design measures against severe

external events such as earthquakes and tsunamis. At the same time, the design study is going into detail and paying much attention to the maintenance and repair to make its feasibility more certain.

During 2014–19, JAEA and Japanese industry participated to the French-Japanese collaboration on the Advanced Sodium Technological Reactor for Industrial Demonstration (ASTRID) program and R&D in support of SFRs. In the field of design, the Japanese team contributed the conceptual and basic design of important systems and components of ASTRID, such as active decay heat removal system, Curie point electromagnet for diversified control rods, seismic isolation system, and the above core structure. This collaboration also covered R&D on severe accidents, fuel technology, sodium technology, In-Service Inspection and Repair (ISI&R), and instrumentation (Varaine, 2018).

A conceptual design study of a 1500 MW_{th} (650 MW_{el}) class pool-type SFR, which addresses Japan's specific siting conditions such as earthquakes and SDC and Safety Design Guidelines (SDGs) for Generation-IV SFRs, was conducted by applying design technology obtained from the design of JSFR (Kubo, 2020).

According to the strategic roadmap decided as the national nuclear energy policy in 2018, which specifies the development work of fast reactor for approximately 10 years, various fast reactor technologies including SFRs are pursued by promoting the development of private sectors for future nuclear innovation while maintaining and expanding the technical foundation for fast reactors in JAEA, which consists of a database of scientific expertise, consolidation of research facilities, common technical platform, and technological development for improving safety and economy.

Japan also participates in the other reactor systems in GIF. Especially Japan proposes Gas Turbine High-Temperature Reactor 300 MW_{el} (GTHTR 300) as one of Very-High-Temperature Reactor (VHTR) reference concepts, and related R&Ds are undergoing (GIF, 2020).

This chapter focuses on the design features of JSFR and the accompanying key innovative technologies. The conformity of JSFR design to the SDC by GIF and reflections on lessons learned from the TEPCO Fukushima Daiichi accident are also discussed.

12.2 JSFR design and its key innovative technologies

12.2.1 General design features of JSFR

The very basic target of JSFR development is to achieve sustainable energy supply by SFRs by reducing radioactive waste, achieving safety equal to that of future LWRs, and realizing economic competitiveness against other future energy sources.

With this target in mind, a plant design concept was established for JSFR. It is a loop-type plant with a two-loop heat transport system. Designs for a commercial version with 1500 MW_{el} and a demonstration version with 750 MW_{el} are pursued in the design study. A bird's eye view of the Nuclear Stream Supply System in Figure 12.1, and the major design specifications are summarized in Table 12.1 for the demonstration version design (Sakai et al., 2010).

JSFR utilizes the advantage of “economy of scale” by setting the electricity output of 1500 MW_{el}, and it has economic competitiveness that benefits from advanced design, such as simplified and compact structure of the reactor, integration of the Intermediate Heat Exchanger (IHX) and the primary circulation pump, shortened piping layout, and reduction of loop number. Furthermore, a special effort has been made to meet the safety requirements, which include enhancement of passive safety capabilities and the In-Vessel Retention (IVR) of the degraded core under a core disruptive accident.

These measures are expected to be more realistic by introducing some innovative technologies such as Mod.9Cr-1Mo steel with high strength and low thermal expansion at high temperature, advanced elevated

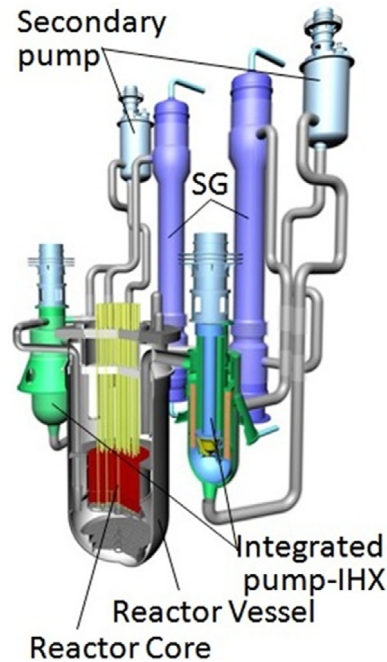


Figure 12.1. Bird's eye view of NSSS of JSFR. *IHX*, Intermediate Heat Exchanger; *SG*, Steam Generator

temperature structural design standards, two-dimensional seismic isolation, and a recriticality free core as well as by taking into account the desirable characteristics of sodium coolant such as operability in a low-pressure system and excellent heat transfer characteristics.

The guard pipes are provided for primary and secondary cooling systems, and those annular spaces would be filled with inert gas. There are no penetrations in the primary cooling system, and there is only one penetration for the sodium drain line in the secondary cooling system. The penetration would be covered by the guard pipes of a double boundary system. As for the Steam Generator (SG), a double-walled straight tube type has been adopted for both safety and investment protection. Periodical inspections on both inner and outer tubes are required to keep reliable sodium-water boundaries. The double-walled tube SG aims at preventing occurrence of any sodium-water reactions during the plant life time and preventing tube failure propagation in case water leaks.

A schematic of the reactor and cooling system is shown in [Figure 12.2](#). Two Primary Reactor Auxiliary Cooling Systems (PRACs) and one Direct Reactor Auxiliary Cooling System (DRACS) have been applied as a Decay Heat Removal System (DHRS) suitable for the two-loop cooling system and the adopted type of SG. These systems are passive type by natural circulation.

To enhance the passive decay heat removal capability by natural circulation, the pressure drop of the core has been limited below 0.2 MPa at a full power condition, and the difference of elevation between the core and heat exchangers has been enlarged, such as 38.7 m between the core and air cooler of PRACs and 37.9 m between the core and the air cooler of DRACS. The in-service inspection and repair capabilities are improved to confirm the integrity of internal structures, including core support structure and coolant boundaries.

[Figure 12.3a](#) shows a vertical sectional view, and [Figure 12.3b](#) shows the top of the reactor block. At the near center of the Reactor Vessel (RV), a roof structure called a Roof Deck (RD) is installed. The center part of the RD is a Rotating Plug (RP), and outside the plug is a fixed deck. At this fixed deck, there are Hot Legs (HLs), cold legs, a direct heat exchanger, an auxiliary core cooling system, sodium level meters, in-vessel

Table 12.1. Major design specifications of demonstration Japan sodium-cooled fast reactor

Electricity output	750 MW _{el}
Thermal output	1765 MW _{th}
Number of loops	2
Primary sodium temperature	550/395°C
flow rate	1.62 × 10 ⁷ kg/h per loop
Secondary sodium temperature	520/335°C
flow rate	1.35 × 10 ⁷ kg/h per loop
Main steam temperature	497°C
pressure	19.2 MPa
Feed water temperature	240°C
flow rate	1.44 × 10 ⁶ kg/h
Plant efficiency	~ 42%
Fuel type	TRU-MOX
Burn up (average) for core fuel	~150 GWd/ton
Breeding ratio	Breakeven (1.03), 1.1, 1.2
Cycle length	26 months or less, four batches
Structural materials reactor block	316 FR
heat transport system	Mod. 9Cr-1Mo steel

TRU-MOX, TransUranium contained Mixed Oxide fuel

neutron instrumentation systems, and Cold Traps (CTs). The height of the upper plenum is 9.3 m, including the cover gas region. In the plant operation, Normal Sodium Level (NSL) is 1.6 m below the bottom of the RD, and during the reFueling Sodium Level (FSL) is 3.1 m below the bottom of the RD. Dip Plates (DPs) are hung from the RP, and the vertical level of the DPs is slightly below the FSL. The diameter of the RV is 11.98 m, including the sodium dam, the width of which is 0.2 m. The dam is a bottom-closed cylindrical wall, and the highest level of the dam is slightly above the NSL. The bottom of the dam is in the middle plenum, which is under negligible creep conditions (Hayafune et al., 2017).

For the safety design (Kotake et al., 2009; Kubo et al., 2011), JSFR adopts the Defense-in-Depth (DiD) principle according to the SDC for SFRs by the GIF. The plant states in SDC are normal operation, anticipated operational occurrences, Design-Basis Accidents (DBAs), and Design Extension Conditions (DECs). The deterministic approach is adopted considering DBAs to specify safety functions such as a Reactor Shut-down System (RSS) and a DHRS for prevention of core damage. JSFR installs several design measures

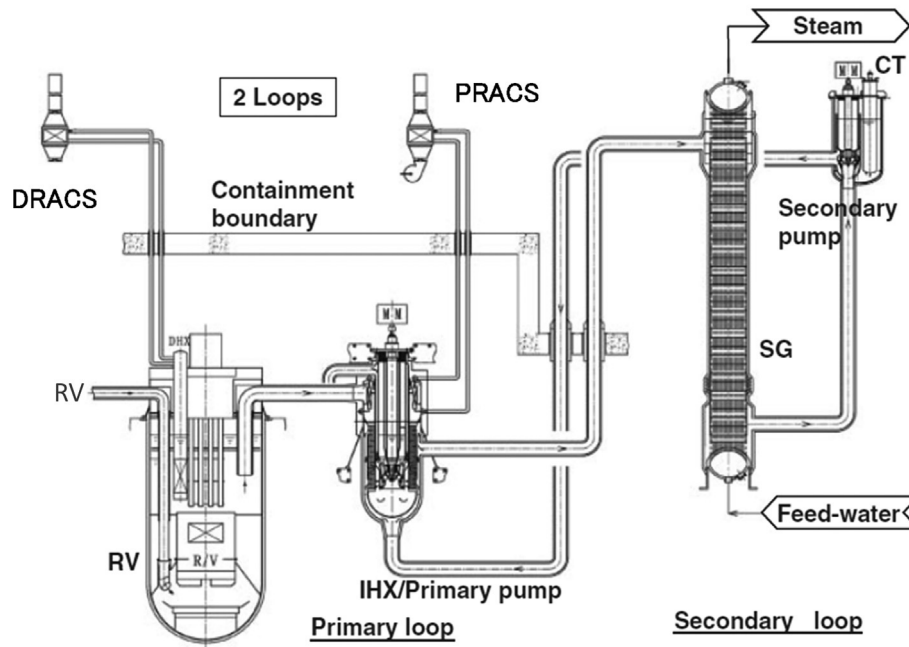


Figure 12.2. Japan sodium-cooled fast reactor and cooling system. *CT*, Cold Trap; *DRACS*, Direct Reactor Auxiliary Cooling System; *IHX*, Intermediate Heat Exchanger; *PRACS*, Primary Reactor Auxiliary Cooling System; *RV*, Reactor Vessel; *SG*, Steam Generator

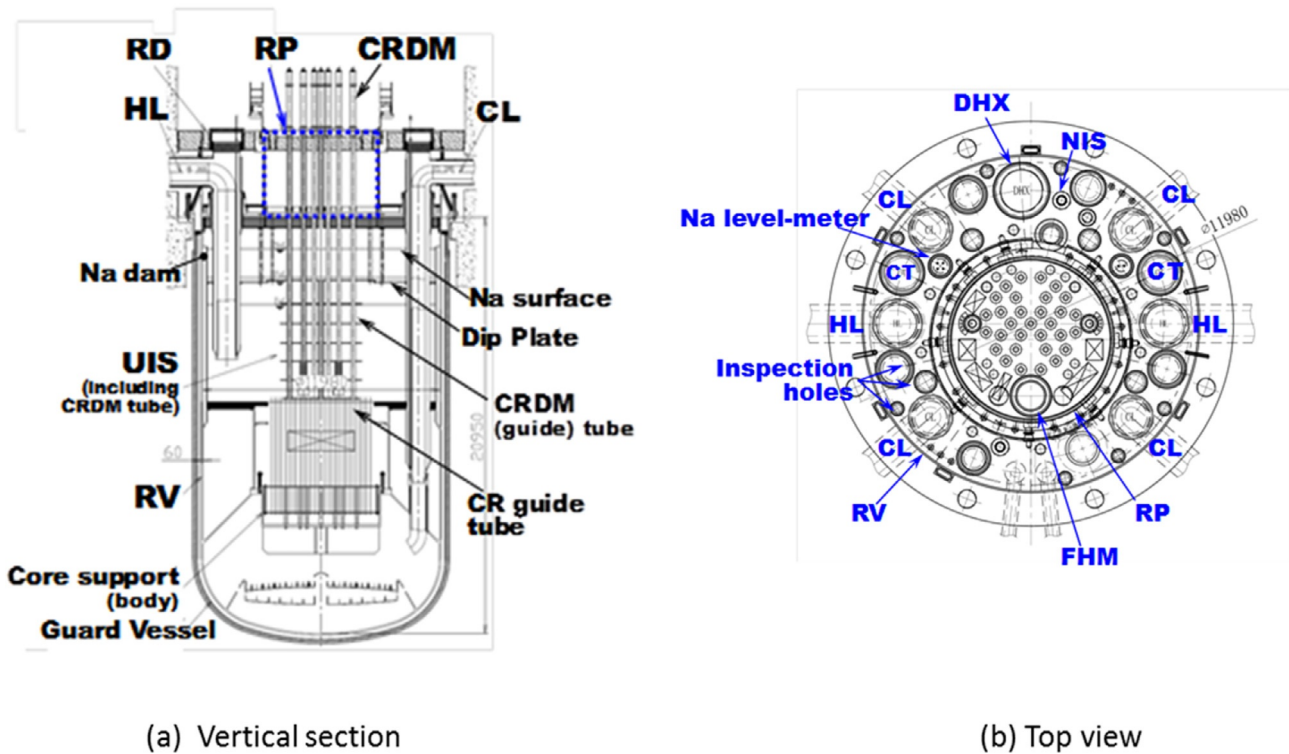


Figure 12.3. Reactor vessel (a) vertical section and (b) horizontal section at the top. *RD*, Roof Deck; *CL*, Cold Leg; *CR*, Control Rod; *CRDM*, Control Rod Drive Mechanism; *DHX*, Direct Heat Exchanger; *FHM*, Fuel Handling Machine; *HL*, Hot Leg; *NIS*, Neutron Instrumentation System; *RP*, Rotating Plug; *RV*, Reactor Vessel

against severe accidents, explicitly taking into account those accidents as DEC. In addition to the DiD principle, JSFR also adopts a risk-informed approach that plays a role in considerations on the proportion or balance of different levels of DiD.

Securing reactor shutdown, two independent RSSs (i.e., primary and backup RSSs) are installed. Each RSS is initiated by independent/diversified signals from the reactor protection system. The fourth level of DiD considers design measures against DEC. In this level, including prevention and mitigation of severe accidents, the RSS provides passive shut-down capability by means of a Self-Actuated Shut-down System (SASS). Performances of the SASS had already been confirmed through the transient experiments in a sodium loop, and reliability testing has been achieved by installing a SASS mock-up into JOYO (Takamatsu et al., 2007).

The recriticality free core concept is adopted in JSFR and has great importance to ensure the IVR against whole-core accidents. Energetics due to exceeding the prompt criticality in the initiating phase must be prevented by means of restriction of the sodium void worth and the core height (Sato et al., 2011). The possibility of molten fuel compaction must be prevented by enhancing the fuel discharge from the core, adopting Fuel Assembly with Inner DUct Structure (FAIDUS).

For measures against sodium leak, all sodium and cover gas boundaries are double structured. The RV and the Guard Vessel (GV) are simple structures with piping penetration on the roof deck without nozzles on the vessel wall. In addition, the piping system is also simplified, eliminating branch piping as possible. With those design measures, the possibility of Loss of Reactor Level (LORL) was evaluated to be less than the target value (Kurisaka, 2006).

The DHRS consists of a combination of one loop of DRACS and two loops of the PRACS. The heat exchanger of DRACS is dipped in the upper plenum within the RV. The heat exchanger of each PRACS is located in the primary-side upper plenum of an IHX. All of these systems can be operated based on a fully passive feature with natural circulation, which requires no active components such as pumps (Yamano et al., 2010).

Because JSFR adopts fully natural-circulation DHRS, JSFR is free from heavy electric load and quick activation of the emergency electric supply. JSFR is then capable of using a self-air-cooling Gas Turbine Generator (GTG) independent from the Components Cooling Water System (CCWS) (Hishida et al., 2007). In fact, JSFR CCWS is non-safety grade because of the natural convection DHRS and self-air-cooling GTG. This configuration reinforces defense against external hazards. In the case of external hazards such as tsunamis, the CCWS could be damaged, as seen in the Fukushima Daiichi accident, because the heat sink of CCWS depends on seawater.

For seismic design, JSFR adopts an advanced seismic isolation system for SFR that mitigates the horizontal seismic force by thicker laminated rubber bearings with a longer period and the improvement of damping performance by adopting oil dampers (Okamura et al., 2011).

A compact plant component layout is achieved by adopting an L-shaped HL piping, a combined IHX/pump component, a once-through type SG, and other technologies, which leads to a cost reduction through fewer plant materials.

Because SFR is a high-temperature reactor operated at creep temperature range, the selection of structural materials is very crucial. In the JSFR design, an austenitic stainless steel 316FR is used for the RV and its internal structures. 316FR is a material developed in Japan for fast breeder reactors. The chemical composition of the conventional 316 stainless steel was modified to improve creep resistance; the carbon content was lowered, and nitrogen and phosphorous were added (Asayama et al., 2013; Onizawa et al., 2013a,b; Japan Society of Mechanical Engineers (JSME), 2012). Mod.9Cr-1Mo steel is used for the primary and secondary heat transport systems, expecting its high strength at elevated temperatures and low thermal expansion. Mod.9Cr-1Mo steel is basically the same material as the American Society for Testing and Materials

(ASTM)/American Society of Mechanical Engineers (ASME) Grade 91 steel (Asayama et al., 2013; Onizawa et al., 2013a, 2013b; JSME, 2012).

12.2.2 Key innovative technologies in the Japan sodium-cooled fast reactor design

JSFR achieves the FaCT development targets and the Generation-IV reactor goals by adopting the following key technologies:

1. high burn-up core with Oxide-Dispersion-Strengthened (ODS) steel cladding material,
2. safety enhancement with SASS and recriticality free core,
3. compact reactor system adopting a hot vessel and in-vessel fuel handling with a combination of an Upper Internal Structure (UIS) with a slit and advanced Fuel Handling Machine (FHM),
4. two-loop cooling system with large-diameter piping made of Mod.9Cr-1Mo steel,
5. integrated IHX/pump component,
6. reliable SG with a double-walled straight tube,
7. natural-circulation DHRS,
8. simplified Fuel Handling System (FHS),
9. Steel plate reinforced Concrete (SC) Containment Vessel (CV), and
10. advanced seismic isolation system.

The technical feasibility of these technologies has been confirmed by various experimental tests and numerical computations that will be discussed hereafter.

12.2.2.1 High burn-up core

One of the important targets in the core design is to achieve a high core average burn-up up to approximately 150 GWd/ton. The most important key technology to achieve this target is advanced cladding that can stand with the target discharge burn-up of 150 GWd/ton, and the ODS steel cladding has the potential to meet this requirement. Two ODS steel claddings have been developed: a 9Cr-ODS and a 12Cr-ODS.

Fast reactor core materials, including the fuel cladding tube, suffer severe radiation damage by high-dose fast neutron irradiation at high temperatures. Thus irradiation resistance (i.e., swelling resistance and resistance to mechanical property degradation under irradiation) and high-temperature strength are indispensable for fast reactor core materials. Conventional alloys for a fast reactor cladding tube are modified type 316 stainless steels, which have substantial industrial backgrounds, adequate strength at high temperature, and improved swelling resistance by microstructure optimization (Ukai, 1998; Akasaka et al., 2001). However, high-dose neutron irradiation exceeding approximately 100 dpa leads to the onset of swelling in this type of alloy, thus increasing the risk of flow channel obstruction in the fuel assembly. JAEA has been developing ODS ferritic steel for the long-life fuel cladding tube that can be used in the high burn-up and high-temperature irradiation environment: average discharge burn-up to 150 GWd/ton, peak neutron dose to 250 dpa, and maximum temperature to 973 K (Shimakawa et al., 2002; Kaito et al., 2007). ODS steels have matrices highly resistant to irradiation-induced swelling (i.e., tempered martensitic matrix and fully ferritic matrix). Nanosized oxide particle dispersion in the matrix improves the high-temperature creep strength for a long duration. Therefore, ODS steels have a good combination of swelling resistance and creep strength.

JAEA has been developing two types of ODS steels: ODS-tempered martensitic steel (9Cr, 11Cr) and ODS recrystallized ferritic steel (12Cr). In JAEA, the ODS-tempered martensitic steels are ranked as the primary candidate material because of their superior irradiation resistance and manufacturability. JAEA derived neutron irradiation data of 9Cr, 12Cr-ODS steel cladding tubes using JOYO (Kaito et al., 2009;

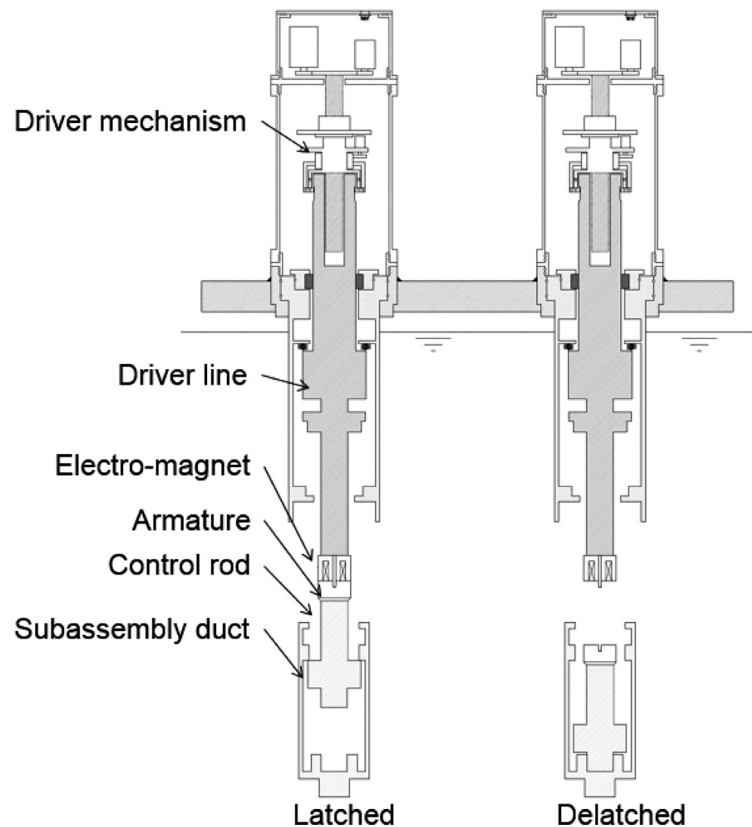
Yano et al., 2011). Postirradiation examination revealed adequate irradiation resistance of the ODS steels (i.e., very small degradation of mechanical strength and ductility by neutron irradiation). ODS steels are fabricated by a powder metallurgy process, which does not necessarily have plenty of industrial background. Therefore, the fabrication technology development of the ODS steel cladding tube is an important task. JAEA has already completed the development of laboratory-scale fabrication technology, including tube manufacturing, welding, and inspection technology (Kaito et al., 2007; Uehira et al., 1999).

12.2.2.2 Safety enhancement

For reactor shutdown, two independent RSSs (primary and backup) are installed. In addition to the two independent systems, an additional passive shut-down system using a Curie point-type SASS is adopted. The SASS, which is schematically illustrated in Figure 12.4, is a device that provides passive shut-down capability in the case of Anticipate Transient Without Scram (ATWS) such as Loss of Flow (LOF) type, Transient Over Power (TOP) type, and Loss of Heat Sink (LOHS) type. When the coolant temperature increases in ATWS, the SASS passively detaches control rods using the nature of ferromagnets that lose their magnetic property around their Curie points. The Curie point of the temperature-sensing alloy can be controlled by using the 30Ni-31Co-Fe alloy. The other part of the magnetic route is composed of soft magnetic iron. A spacer between the electromagnet part and the armature part is made from Inconel not to affect the magnetic force of the SASS.

Several out-of-pile mock-up experiments have been conducted to demonstrate performances on holding force, response time, thermal endurance test under sodium, and measures against particle accumulation on the magnetic surface. The transient response tests with simulated ATWS conditions confirmed the time constant of the armature. In addition to the out-of-pile tests, in-pile mock-up and material experiments were

Figure 12.4. Structure and mechanism of the self-actuated shut-down system



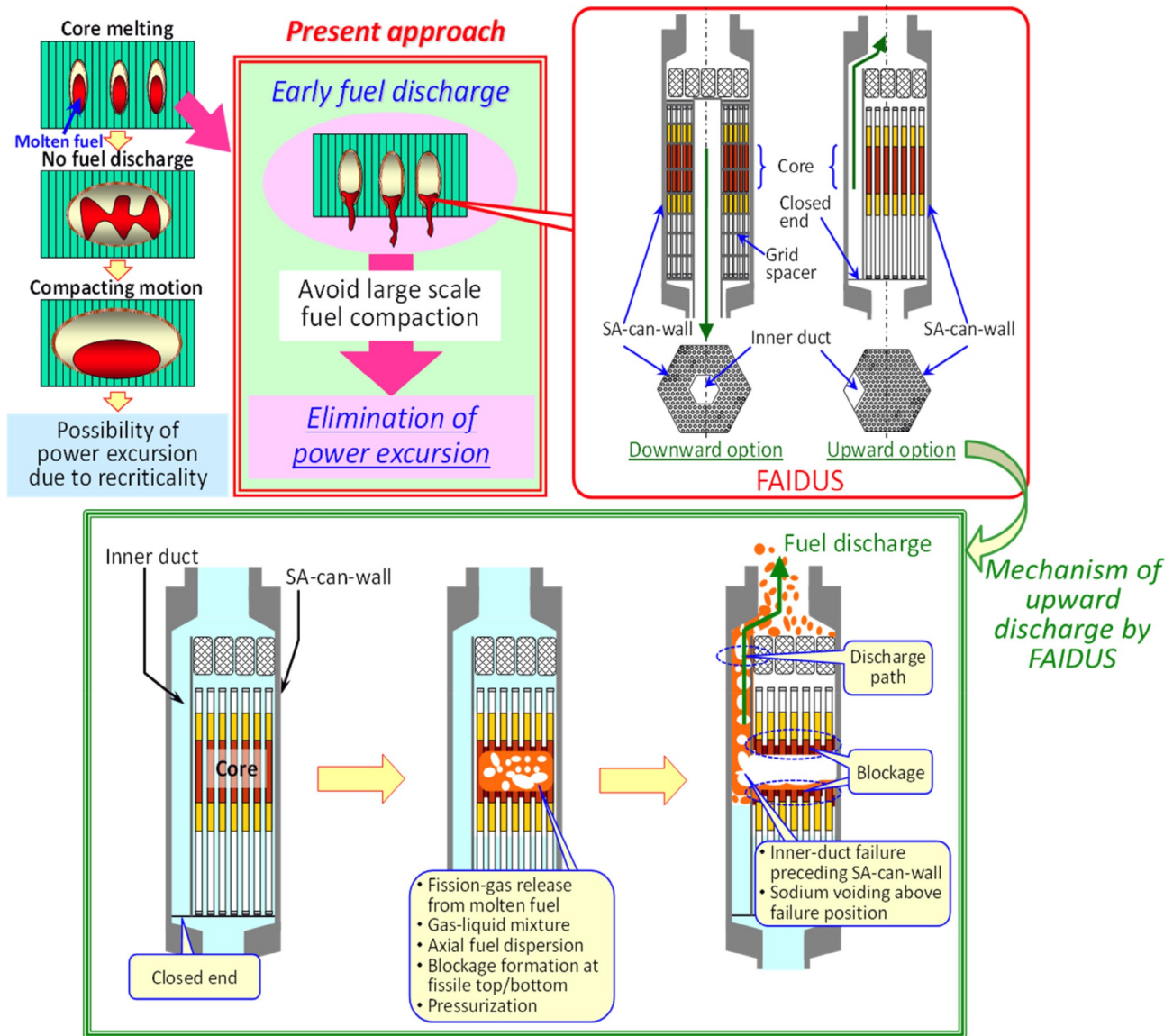


Figure 12.5. Concept of early fuel discharge and molten-fuel discharge by FAIDUS. *SA*, SubAssembly

conducted in JOYO (Nakanishi et al., 2010; Fujita et al., 2011). The control rod holding stability under the actual reactor-operational environment was successfully confirmed.

In the present approach for JSFR to mitigate a core disruptive accident, the core design and fuel characteristics are intended to eliminate the possibility of prompt criticality leading to energetic core expansion. In addition, the fuel assembly, FAIDUS, is introduced as a design measure for realizing early fuel discharge before the formation of a large-scale molten pool, which has recriticality potential because of large-scale fuel compaction (Niwa et al., 2007).

The concept of early fuel discharge and two design options for FAIDUS are shown in Figure 12.5. Because the downward option involves difficulties in fabrication using a grid-type spacer, the feasibility of the upward option driven by the pressurization of the disrupted core has been investigated by utilizing the phenomenological evidence obtained through well-designed experiments.

The EAGLE project, which includes out-of-pile and in-pile tests, was planned for this purpose and has been successfully conducted in the impulse graphite reactor of Kazakhstan. It was confirmed by the wall failure, fuel discharge, and integral demonstration tests of the EAGLE project that the inner-duct failure would precede subassembly-can wall failure and that pressure-driven molten fuel discharge is possible (Konishi et al., 2007; Sato et al., 2011), and it was also confirmed by the Pool-type research reactor operated by CEA (CABRI) program (Sato et al., 2004; Onoda et al., 2011) and Prototype Fast Reactor (PFR) experiments of the Transient Reactor Test Facility (TREAT) program (Rothman et al., 1979; Bauer et al., 1986) that a sufficient driving force, i.e., pressure build-up in the molten core, for upward discharge would be obtained. In addition to this experimental knowledge, the behavior of fuel discharge through the inner duct was evaluated by parametric analyses using the Sn, Implicit, Multiphase, Multicomponent, Eulerian, Recriticality (SIMMER) code (Kondo et al., 1992; Tobita et al., 2006), taking into account the uncertainty of wall deformation and/or failure. The effectiveness of FAIDUS as a design measure, which can eliminate the recriticality leading to a power excursion, was confirmed through the experimental investigation and parametric analyses as previously described.

12.2.2.3 Compact reactor system

The JSFR design uses a compact RV because of a simple vessel wall structure without a cooling system (hot vessel) and a compact in-vessel FHS with a combination of a slit UIS and an advanced FHM (see Figures 12.3b and 12.11). In Japan, hot vessels without a reactor cooling system have successfully accumulated operating experience in JOYO (Hara et al., 1976) and MONJU (Yokota et al., 1991). The JSFR vessel protection is further simplified from JOYO and MONJU without an ex-vessel overflow system; JOYO and MONJU have ex-vessel overflow systems to maintain steady sodium level during start-up operation to reduce transient thermal stresses.

As an important part of the design study on SFRs, thermal-hydraulic issues in the RV are carefully addressed. At the core outlet region, temperature fluctuation due to the mixing of hot and cold flows from the core is inevitable, and the potential risk of thermal fatigue is concerned. For the accurate simulation of the mixing phenomena, the key is the precise modeling of the large-scale eddy structures. Therefore, the Large Eddy Simulation (LES) modeling is demanded (Tanaka and Miyake, 2015). Several experiments (e.g., the triple jet experiment) are conducted to validate the developed simulation code (Kobayashi et al., 2015; Tanaka et al., 2016). Another concern is the vibration of structural components, especially HL piping, in the hot pool. The LES and model experiments are performed to investigate the vibration characteristics (i.e., the amplitude and the frequency) (Ono et al., 2011; Tanaka and Ohshima, 2012). At the free surface, a free surface vortex may cause gas entrainment, which should be suppressed to avoid a positive void reactivity effect in the core. Two types of evaluation methods for gas entrainment are proposed. One is the practical evaluation method, composed of a vortex model (Burgers vortex model) with rather coarse mesh Computational Fluid Dynamics (CFD) (Sakai et al., 2008; Ito et al., 2010). The other is a high-precision simulation method based on an interface-tracking approach, which is shown in Figure 12.6 (Ito et al., 2013). Several simple experiments and a large-scale water test are conducted to investigate the onset mechanism of gas entrainment and to obtain the validation data of the evaluation methods (Kimura et al., 2008; Ezure et al., 2008).

There is another thermal-hydraulics issue induced by a vortex (i.e., the vortex cavitations) at the HL inlet. A simple vortex experiment and scaled tests are conducted to investigate (e.g., the influence of the fluid property), and the obtained data are analyzed to establish a mechanistic evaluation method for the onset condition of the vortex cavitations (Ezure et al., 2013). After the scram, the primary flow rate decreases, and hot sodium remains in the upper part of the upper plenum region, whereas cold sodium comes from the core into the lower part (i.e., the thermal stratification occurs). Since the large temperature gradient at the hot/cold interface may impact the integrity of structural objects (e.g., the RV), numerical simulations of some basic tests are performed with various simulation models to establish appropriate simulation conditions (e.g., the

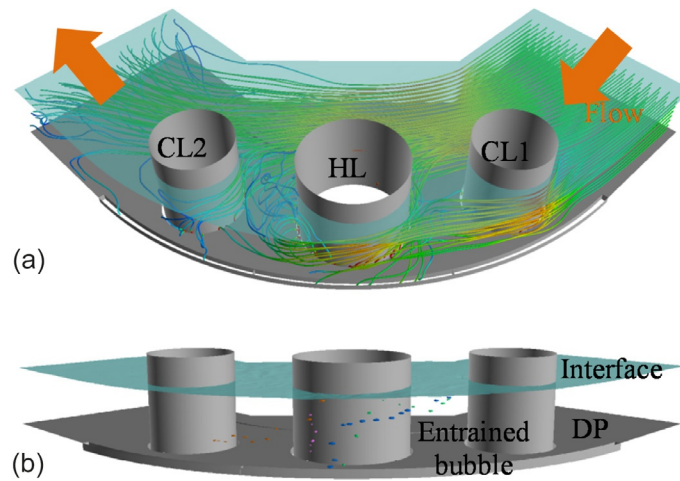


Figure 12.6. Simulation result of gas entrainment in large-scale test: (a) stream line around HL and C/L and (b) trajectory of entrained bubble. *CL*, Cold Leg; *DP*, Dipped Plate; *HL*, Hot Leg

turbulence model) (Ohno et al., 2011). In addition, natural-circulation decay heat removal after the scram is considered as one of the most important safety characteristics of SFRs. The potential upper limit of the core fuel cladding temperature is evaluated with numerical simulation codes to confirm the feasibility of natural-circulation decay heat removal (Watanabe et al., 2015). The sodium fire and sodium-water reaction are specific accidental phenomena in SFRs. Several simulation codes (e.g., the mechanistic sodium-water reaction simulation code) are developed to establish the evaluation system of those phenomena (Yamaguchi et al., 2001; Uchibori and Ohshima, 2015).

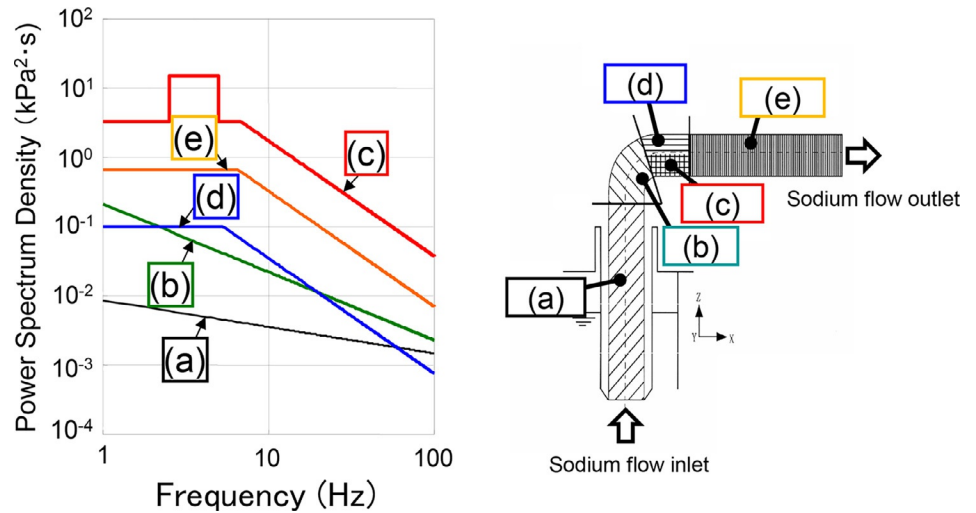
12.2.2.4 Two-loop cooling system

The two-loop cooling system contributes to a simple cooling system and a compact component arrangement. An L-shaped pipe for the primary HL piping also enables a compact component arrangement. Because major issues (e.g., decay heat removal, LOF accident, and hydraulics) were clarified and evaluated in a previous study (Yamano et al., 2010), the basic feasibility of the two-loop cooling system has already been confirmed. Recent results on decay heat removal are described later in this chapter. As for Design Basis Events (DBEs), the pump seizure accident has appeared to be the most severe event, and the transient analysis taking into account the latest design has shown that the two-loop cooling system meets safety criteria (Okubo et al., 2011).

This primary cooling system increases the primary coolant flow rate per loop. As a result, a large-diameter piping system with high coolant velocity is required. That high coolant velocity may result in a flow-induced vibration issue. In the JSFR primary piping system, the number of elbows is reduced by adopting high-chromium steel with low thermal expansion characteristics. JSFR has only one L-shaped elbow for the HL piping system between the RV and IHX. The curvature radius of the L-shaped elbow is equivalent to the piping diameter to configure the compact system design. On the basis of those features in the JSFR cooling system design, the flow dynamics in the piping were investigated, particularly focusing on the flow separation behavior that would be a major source of pressure fluctuations in the piping.

Hydraulics in the large-diameter piping have been revealed by one-third scale HL pipe water experiments with an acrylic pipe for visualization and a stainless-steel pipe for vibration data accumulation (Yamano et al., 2009, 2010). The experiment extended the pressure loss coefficient data against Reynolds number (Re) up to $Re = 8 \times 10^5$. The results showed that the pressure loss coefficient saturates and there is no Re dependency with $Re > 3 \times 10^5$, showing that the real scale with $Re = 3.7 \times 10^6$ could be extrapolated from the one-third scale experimental data.

Figure 12.7. Power spectrum densities for HL piping design



Detailed vibration data were also accumulated from the water experiment with the stainless-steel pipe. With the accumulated data, conservative design power spectrum density for stress analysis on random vibration has been defined as is shown in Figure 12.7. Random vibration in the HL piping has been analyzed, and the maximum stress is evaluated to be lower than the criteria of high cycle fatigue stress. The LES simulation and model experiments were performed in order to investigate the eddy behavior of flow-induced vibration, i.e., the amplitude and the frequency (Ohno et al., 2011; Tanaka and Ohshima, 2012).

12.2.2.5 Integrated intermediate heat exchanger/pump component

The integrated IHX/pump component is one of the JSFR key technologies to achieve a compact primary cooling system. As is illustrated in Figure 12.8, it includes a primary pump, IHX tube bundles, and PRACS heat exchange tubes. Major issues of this component are prevention of gas entrainment from the sodium free

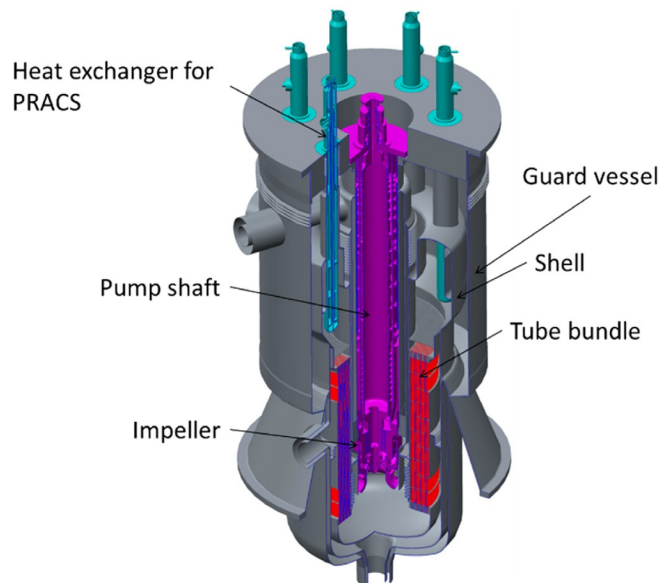


Figure 12.8. Integrated intermediate heat exchanger/pump component. PRACS, Primary Reactor Auxiliary Cooling System

surface, sodium level control, pump shaft stability, tube wear due to vibration, temperature distribution control, and fabrication capability.

Technical feasibility of these issues is examined by various tests using a full-scale mock-up and a one-fourth scale mock-up (Hayafune et al., 2006; Handa et al., 2009). For example, the one-fourth scale mock-up experiments have revealed basic mechanisms of vibration transmission and tube wear. An evaluation method on tube wear has been proposed (Handa et al., 2009) showing that tube wear can be accommodated by the tube thickness margin. In another recent study, several additional experiments, such as a partial tube bundle model vibration test and a full-scale tube bundle water experiment, have been conducted to validate and verify the proposed evaluation method.

Because the JSFR pump shaft is long (~ 15 m) in height, a damper is installed at the lower bearing to increase rotation stability. A full-scale mock-up of the lower pump shaft bearing with a damper has been manufactured, and water tests at 80°C with the same viscosity condition of sodium have been conducted, accumulating data of shaft holding force and damping performance.

12.2.2.6 *Reliable steam generator*

The JSFR design adopts a double-wall, straight-tube reliable SG for safety and investment protection. Periodical inspections on inner and outer tubes are required to maintain reliable sodium-water boundaries. Development targets of SG tube inspection devices are detection of 10% thickness defect for inner tubes and 20% for outer tubes. The JSFR double-wall tube SG can eliminate tube failure propagation as DBEs taking into account the previously mentioned inspection capabilities. The prevention of tube failure propagation has been confirmed covering the following double-boundary failure modes:

- Common mode failure: Inner and outer tube failure due to a common cause.
- Dependent double failure: Inner tube failure caused by outer tube failure or outer tube failure caused by inner tube failure.
- Independent double failures: Inner and outer tube failure coincidentally happen at the same tube.
- Tube-to-tube sheet weld failure: Leak at tube-to-tube sheet weld.

For each of these failure categories, detailed assessments were made, and it was shown that there is no failure propagation in the range of DBEs. Although the large leak is eliminated in the DBE, a Double-Ended Guillotine (DEG) rupture of one double-wall tube is assumed as the maximum Leak rate for a bounding event to confirm a certain design margin. SG tube failure propagation analyses using the Leak Enlargement And Propagation (LEAP) code (Tanabe et al., 1982; Hamada and Tanabe, 1992) have been conducted with an initial leak rate from a small one DEG or DBE with hydrogen monitoring failure. The results show that the maximum tube failure propagation is within the range of five DEG, and the spike pressure on the primary-secondary and secondary sodium boundaries due to this range of sodium-water reaction has been evaluated using the Sodium-Water Reaction Analysis Code System (SWACS) code (Ono and Kurihara, 2005) and found to be in the design limits (Figure 12.9).

Several simulation codes, e.g., the mechanistic sodium-water reaction simulation code, are developed to establish the evaluation system of those phenomena (Yamaguchi et al., 2001; Uchibori and Ohshima, 2015).

12.2.2.7 *Natural-circulation decay heat removal system*

The JSFR design adopts fully natural convection to achieve reliable decay heat removal. All of the sodium boundaries, including air cooler tubes, are double walled, providing sodium leak monitoring and inspection access. Several safety analyses in various operating conditions in categories II and IV (e.g., loss of off-site power for category II and one PRACS sodium leak combined with loss of off-site power and one dumper failure of the other PRACS for category IV) have been conducted confirming the performance of the JSFR DHRS system. Decay heat removal with only the DRACS has also been evaluated using a three-dimensional

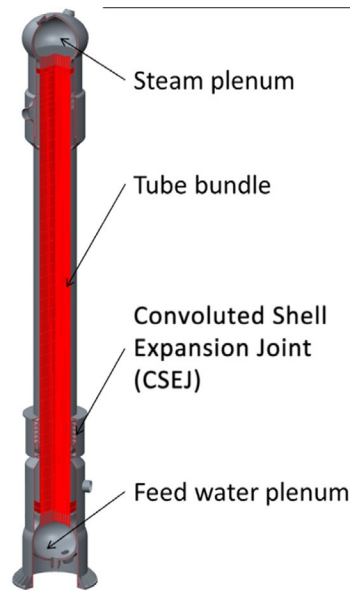
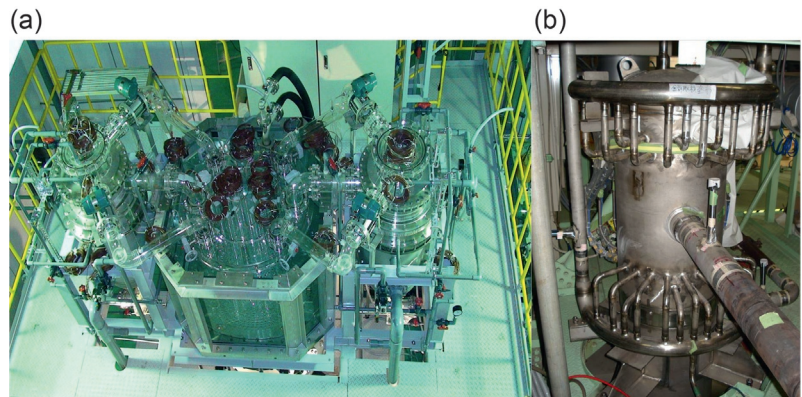


Figure 12.9. Steam generator with double-walled straight heat transfer tubes

Figure 12.10. The decay heat removal system test apparatus: (a) one-tenth scale water test apparatus and (b) sodium test apparatus



analysis code assuming the failure of PRACS in loop A during loop B maintenance with sodium drain (PRACS in loop B is unavailable during maintenance). The results show that the peak temperature is lower than 700°C, meeting the criteria with decay heat 7h after the reactor trip.

The potential upper limit of the core fuel cladding temperature is evaluated with numerical simulation codes to confirm the feasibility of natural circulation decay heat removal (Watanabe et al., 2015).

For verification and validation of design and evaluation tools, a one-tenth scale water test on the whole DHRS system and a sodium test on the PRACS heat exchanger with 1/8 scale piping diameter have been conducted, as shown in Figure 12.10. A one-dimensional flow network analysis code and a three-dimensional analysis model using STAR-CD have been compared with those experimental data showing that they are in good agreement (Ohyama et al., 2009; Kamide et al., 2010).

12.2.2.8 Simplified fuel handling system

The JSFR design has adopted a simple FHS with advanced technologies. The JSFR in-vessel FHS consists of a combination of a UIS with a slit and a pantograph-type FHM (Figure 12.11) to dramatically reduce the RV diameter. The FHM is removed from the RV during power operation. From the RV to the Ex-Vessel Storage Tank (EVST), a spent subassembly, which is accommodated by a sodium pot, is transported by

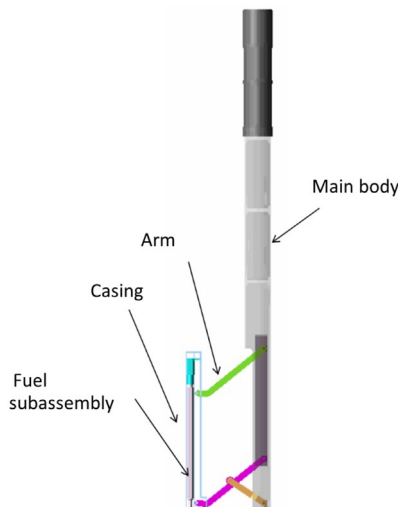


Figure 12.11. Pantograph-type fuel handling machine

an ex-vessel transfer machine in a similar manner as in MONJU. A two-position sodium pot has been installed for the transportation of subassemblies from the RV to the EVST to reduce the refueling time and thereby increase plant availability. Active cooling is not necessary during the transportation from the RV to the EVST because of the heat capacity of the sodium pot. The sodium pot cooling system is activated only when the transportation has a malfunction or becomes stuck. The sodium pot cooling system consists of a combination of direct cooling with argon gas blow and indirect cooling with thermal emission. The EVST has a sufficient capacity for full-core evacuation to enhance the plant's In-Service Inspection and Repair (ISIR) capability (Chikazawa et al., 2011).

12.2.2.9 Steel plate-reinforced concrete containment vessel

The CV of the JSFR design is made of SC. The structure of SC, as shown in Figure 12.12, consists of two steel plates facing each other and concrete filled in between. One of the advantages of the SC structure is that its steel parts can be fabricated in a factory with shorter a construction period compared with on-site construction, which leads to a reduction of the plant construction period and cost (Hara et al., 2009).

Experiments were performed, including shear strength tests of SC beams to obtain data for evaluating containment response in case of sodium fire. Two types of reinforcement specimens: tie bars and partitioning

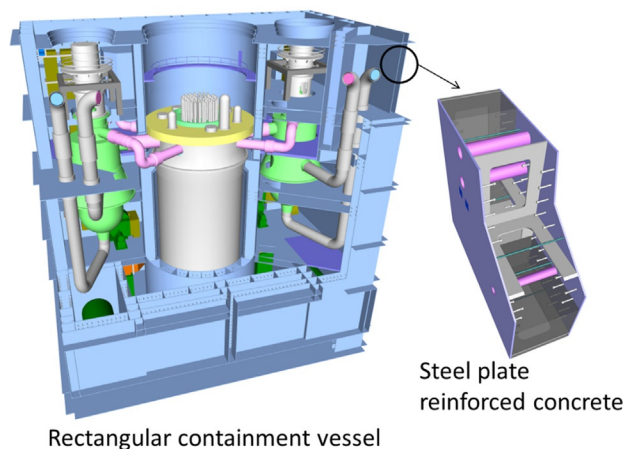


Figure 12.12. Steel plate-reinforced concrete containment structure

plates. In both types of specimens, temperature and amount of reinforcement material were the main parameters of the tests. The results for the tie bar type realized the degree of reduction tendency of shear strength as temperature increased. As a result of a series of experiments, sufficient data to estimate behavior under high temperatures were acquired, and methods to estimate the support and the boundary function of the Steel plate-reinforced Concrete Containment Vessel (SCCV) were developed (Katoh et al., 2011).

12.2.2.10 Advanced seismic isolation system

SFR components tend to be designed as thin-walled structures because their thermal stress due to elevated temperature is much higher, and their internal pressure is much lower than that of an LWR. Thin-walled structures are relatively vulnerable to severe earthquakes. The design seismic loading was greatly increased over the previous seismic condition because of the Niigata-ken Chuetsu-oki earthquake in 2007 (Nuclear Safety Commission of Japan, 2006). Hence, the demonstration reactor of JSFR must adopt an advanced seismic isolation system, which is a practicable modification of previous technologies because the earthquake force that affects the primary components must be mitigated more than that of the previous seismic isolation system.

The advanced seismic isolation system for SFRs adopts laminated rubber bearings, which are thicker than those of the previous design, as well as oil dampers. As a result of the examination, the specification of the advanced seismic isolation system for SFRs is that the natural frequency in the horizontal direction is 0.29 Hz, and in the vertical direction, it is 8.0 Hz (Okamura et al., 2011).

12.3 Update of the Japan sodium-cooled fast reactor design with lessons learned from the Fukushima Daiichi accident

After the accident at Fukushima Daiichi, the safety of nuclear power plants has been strongly recognized to be a common issue worldwide. Therefore, enhancing nuclear safety, taking into account the lessons learned from the accident, has the highest and the most urgent priority. For the development of next-generation SFRs, global standards for safety criteria were expected to be established in an international framework in consideration of the lessons learned from the accident. For the international safety criteria, activities on developing SDC for SFRs were undertaken, and SDC created by a GIF task force were approved by the GIF policy group in May 2013 (Nakai et al., 2012).

It is recognized that there are three major points of lessons learned from the accident (Japanese Government, 2011). The first point is the enhancement of systems that may be needed to decrease the likelihood of a severe accident due to extreme external hazards. Namely, robustness should be enhanced in power supplies [direct current and Alternating Current (AC), if needed to power an active safety system], cooling functions (core, CV, and spent fuel pools), and the heat transportation system, including the final heat sink. The second point is the enhancement of response measures against severe accidents. The means should be provided to prevent severe mechanical loads on CVs, and the instrumentation should be prepared to identify the status of the reactor core and the CV. The third point is the reinforcement of safety infrastructure by ensuring the independence and diversity of safety systems. These points are incorporated into SDC, taking the characteristics of SFRs into account (Kamide et al., 2015).

Although numerous types of events, including internal and external ones, can be considered as initiators of the accident conditions, those events can be grouped into two major types of events from the viewpoints of plant responses and consequences: ATWS type and Loss of Heat Removal System (LOHRS) type.

To contribute to the development of SDC by providing the technical solutions to be required for the higher safety level as a next-generation reactor, a series of design studies for JSFR has been conducted. As a first step, the effectiveness of the current design measures of JSFR against severe plant conditions was evaluated.

Then design modifications have been investigated for the ATWS and LOHRS type events. Such design study has also been conducted for the fuel storage systems.

From the viewpoint of toughness against external events, JSFR had already improved safety features as a next-generation reactor in a preconceptual design version in 2010 (Chikazawa et al., 2015). The JSFR toughness against earthquakes and tsunamis was evaluated based on the 2010 design version. Seismic analyses showed that JSFR had a sufficient design margin for shut-down capability and integrity of major components against severe seismic conditions enveloping the Fukushima Daiichi accident conditions. In a tsunami, the sea-water pumps for the CCWS could be totally damaged because they are located at sea level; thus, the CCWS could fail because of the tsunami because it depends on seawater as the final heat sink. In the JSFR design, safety components including DHRS and emergency power supply are independent from the CCWS because of full natural convection DHRS and air-cooling GTG. Even in station blackout, decay heat could be removed by natural convection DHRS. An analysis showed that the time margin was more than 10 days to LOHS because of sodium freezing in case of the damper operation failure in the air coolers. That time margin is sufficient for implementing recovery actions by operators. However, additional design improvements still have the potential to reduce core damage frequency because of LOHS.

In ATWS type events, in-balance of power and cooling might cause core damage within a shorter time period. A passive shut-down mechanism can prevent core damage even under such conditions. In addition, mitigation of core damage is considered in design because of the shorter time period to reach core damage and the potential mechanical energy release, which might appear in the core damage situations. JSFR adopts SASS incorporated into the two independent, active shutdown systems for the prevention of core damage. To achieve IVR, FAIDUS and an in-vessel core catcher are introduced in the core and RV design.

LOHRS includes LOHS and LORL. For LOHRS, SFR has superior characteristics because of sodium coolant features such as low pressure and high natural convection capability. Utilizing those superior characteristics of sodium, the JSFR already equipped the reliable DHRS with natural convection, which does not depend on emergency AC power. The additional measures against LOHRS are summarized in Table 12.2.

For LOHS, manual control of the air cooler damper during 10 days was investigated. Transient analyses showed that the air cooler dampers were capable of being controlled manually by adopting a simple operation

Table 12.2. Measures against loss of heat removal system type events

Category A	Event	Measures
LORL type	Simultaneous failure of RV and GV	Design measures and evaluation to prevent simultaneous failure of RV and GV
	Double failure in a piping system	Cooling by DRACS with low sodium level in case of double boundary failure in a piping system
LOHS type	Loss of PRACS and DRACS	AM on design base DHRS (DRACS and PRACS)
		– Manual operation of air cooler – Back-up power supply for air cooler control
		Alternative cooling system independent of design base DHRS (DRACS and PRACS)

AM, Accident Management; DHRS, Decay Heat Removal System; DRACS, Direct Reactor Auxiliary Cooling System; GV, Guard Vessel; LOHS, Loss of Heat Sink; LORL, Loss of Reactor Level; PRACS, Primary Reactor Auxiliary Cooling System; RV, Reactor Vessel.

procedure with a sufficient operation time (Chikazawa et al., 2015). Core damage frequency due to LOHS was evaluated to be lower than 10^{-8} /reactor-year, taking into account accident management (Chikazawa et al., 2012). Although the JSFR DHRS configuration in the 2010 version has sufficient reliability, the installation of additional DHRS with independence and diversity from the DBA DHRS could improve toughness against LOHS. As a countermeasure against an LORL type event, double failure of the RV and GV is prevented by securing a margin to earthquake-resistant performance and reliability of the RV and GV. Furthermore, the function of the DRACS is extended to maintain the heat removal capability even in case of low sodium level when siphon break occurs by multiple leakages on the primary cooling circuit. It is important that RV melt-through due to LOHRS type events can be practically eliminated by those design measures in Table 12.2 to achieve core cooling without significant core damage.

12.4 Concluding remarks

The design concept of JSFR, Japan's Generation-IV reactor, was reviewed. It is a loop type and is characterized, in terms of safety, by a self-actuated (passive) RSS, a recriticality free core design, and a natural-circulation DHRS. It is also characterized, from the viewpoint of economy, as a two-loop heat transport system, integrated IHX/pump component, and others.

Ten key innovative technologies were identified, and R&D was conducted to confirm the feasibilities of these technologies. These 10 key innovative technologies—high burn-up core, safety enhancement, a compact RV, a two-loop cooling system using high-chromium steel, an integrated IHX/pump component, a reliable SG, natural-circulation DHRS, a simplified FHS, a CV made of concrete that is reinforced with steel plates, and advanced seismic isolation systems—were evaluated to be suitable for implementation to the demonstration JSFR plant. The JSFR design with those key technologies has the potential to meet the targets of the FaCT project and Generation-IV reactors.

To contribute to the development of the SDC of the GIF by providing the technical solutions to be required for the higher safety level as a next-generation reactor and to reflect on the lessons learned from the Fukushima Daiichi accident to further enhance the safety of the plant against severe external events, a series of design studies for JSFR was conducted. As the first step, the effectiveness of the current design measures of JSFR against severe plant conditions was evaluated. Then, design modifications were also investigated for the ATWS and LOHRS type events. Such design study has also been conducted for the fuel storage systems.

References

- Aizawa, K., 2001. R&D for fast reactor fuel cycle technologies in JNC. In: Proceedings of GLOBAL 2001, Paris, France, September 9–13, 2001. https://inis.iaea.org/collection/NCLCollectionStore/_Public/33/034/33034355.pdf.
- Akasaka, N., Yamagata, I., Ukai, S., 2001. Effect of irradiation environment of fast reactor's fuel elements on void swelling in P, Ti-modified 316 stainless steel. In: Effects of Radiation on Materials: 20th International Symposium, ASTM STP 1405, pp. 443–456.
- Asayama, T., Dozaki, K., Otani, T., Inatomi, T., Ando, M., 2013. Development of 2012 edition of JSME code for design and construction of fast reactors (1) overview. In: Proceedings of the ASME 2013 Pressure Vessels and Piping Conference PVP2013, PVP2013–98061, July 14–18, 2013, Paris, France. <https://asmedigitalcollection.asme.org/PVP/proceedings-abstract/PVP2013/55645/V01BT01A046/283135>.
- Bauer, T., Morman, J.A., Hill, D.J., Devolpi, A., Goldman, A.J., Cooper, A.A., Davies, A.L., 1986. Postfailure material movement in the PFR/TREAT experiments. In: Proceedings of International Meeting on Fast Reactor Safety and Related Physics, 1986 May 12–16; Guernsey (UK), p. 1647. <https://inis.iaea.org/search/searchsinglerecord.aspx?recordsFor=SingleRecord&RN=19002299>.
- Chikazawa, Y., Katoh, A., Obata, H., Nishiyama, N., Uzawa, N., Tozawa, K., Chishiro, R., 2011. Conceptual design study for the demonstration reactor of JSFR (6) fuel handling system design. In: Proceedings of 19th International Conference on

- Nuclear Engineering (ICONE19), Osaka, Japan, October 24–25, 2011. https://inis.iaea.org/search/search.aspx?orig_q=RN:44115395.
- Chikazawa, Y., Aoto, K., Hayafune, H., Kotake, S., Ohno, Y., Ito, T., Toda, M., 2012. Evaluation of JSFR key technologies. *Nucl. Technol.* 179, 360–373. <https://www.tandfonline.com/doi/abs/10.13182/NT179-360>.
- Chikazawa, Y., Katoh, A., Hayafune, H., Shimakawa, Y., Kamishima, Y., 2015. Severe external hazard on hypothetical JSFR in 2010. *Nucl. Technol.* 192, 111–124. <https://www.tandfonline.com/doi/abs/10.13182/NT14-151>.
- Ezure, T., Kimura, N., Hayashi, K., Kamide, H., 2008. Transient behavior of gas entrainment caused by surface vortex. *Heat Transfer Eng.* 29 (8), 659–666. <https://www.tandfonline.com/doi/abs/10.1080/01457630801980574>.
- Ezure, T., Ito, K., Kimura, N., Onojima, T., Kamide, H., Kameyama, Y., 2013. Effects of fluid viscosity on occurrence behavior of vortex cavitation-vortex structures and occurrence condition. In: *Proceedings of NURETH-15, Pisa, Italy, May 12–17, 2013*.
- Fujita, K., Yamano, H., Kubo, S., Etoh, M., Yamada, Y., Toyoshi, A., 2011. Development of a self-actuated shutdown system for large-scale JSFR. In: *Proceedings of 19th International Conference on Nuclear Engineering (ICONE19), Osaka, Japan, October 24–25, 2011*. https://inis.iaea.org/search/search.aspx?orig_q=RN:46084120.
- Generation IV International Forum, 2020. Annual Report 2019. OECD Nuclear Energy Agency, Paris. https://www.gen-4.org/gif/jcms/c_119034/gif-2019-annual-report.
- Hamada, H., Tanabe, H., 1992. A Study of the Selection of Rational Design Basis Leak. PNC TN9410 92-097. Power Reactor and Nuclear Fuel Development Corp. (in Japanese).
- Handa, T., Oda, Y., Ono, Y., Miyagawa, K., Matsumoto, I., Shimoji, K., Ide, A., Ishikawa, H., Hayafune, H., 2009. Research and development for the integrated IHX/pump. In: *Proceedings of International Conf. Fast Reactors and Related Fuel Cycles (FR09), Kyoto, Japan, December 7–11, 2009*. https://inis.iaea.org/search/search.aspx?orig_q=RN:43118961.
- Hara, T., Kosugi, H., Abe, S., 1976. JOYO construction and preoperational test experience. In: *Proceedings of International Conference on Advanced Nuclear Energy Systems, Pittsburgh, Pennsylvania, March 14–17, 1976*. American Society of Mechanical Engineers.
- Hara, H., Hosoya, T., Negishi, K., Kotake, S., Suzuki, I., 2009. Japan conceptual design study of JSFR (4) reactor building layout. In: *Proceedings of International Conference on Fast Reactors and Related Fuel Cycles (FR09), Kyoto, Japan, December 7-11, 2009*.
- Hayafune, H., Konomura, M., Morita, H., Usui, Y., Sawa, N., Tsujita, Y., 2006. Development of the integrated IHX/pump component 1/4-scale vibration testing. In: *Presented at 14th International Conf. Nuclear Engineering (ICONE14), Miami, Florida, July 17–20, 2006*. ICONE14-89745, pp. 271–278. <https://asmedigitalcollection.asme.org/ICONE/proceedings-abstract/ICONE14/42444/271/313821>.
- Hayafune, H., Chikazawa, Y., Kamide, H., Iwasaki, M., Takashi, S., 2017. Advanced Sodium-Cooled Fast Reactor Development Regarding GIF Safety Design Criteria, FR'17, paper IAEA-CN245–158. https://inis.iaea.org/search/search.aspx?orig_q=RN:49085659.
- Hishida, M., Kubo, S., Konomura, M., Toda, M., 2007. Progress on the plant design concept of sodium-cooled fast reactor. *J. Nucl. Sci. Technol.* 44 (3), 303–308. <https://www.tandfonline.com/doi/abs/10.1080/18811248.2007.9711286>.
- Ito, K., Sakai, T., Eguchi, Y., Monji, H., Ohshima, H., Uchibori, A., Yongze, X.U., 2010. Improvement of gas entrainment evaluation method introduction of surface tension effect. *J. Nucl. Sci. Technol.* 47 (9), 771–778. <https://www.tandfonline.com/doi/abs/10.1080/18811248.2010.9711653>.
- Ito, K., Kunugi, T., Ohshima, H., Kawamura, T., 2013. A volume-conservative PLIC algorithm on three-dimensional fully unstructured meshes. *Comput. Fluids* 88, 250–261. <https://www.sciencedirect.com/science/article/abs/pii/S0045793013003617>.
- Japanese Government, 2011. Report of Japanese Government to the IAEA Ministerial Conference on Nuclear Safety, “The Accident at TEPCO’s Fukushima Nuclear Power Stations”. https://japan.kantei.go.jp/kan/topics/201106/iaea_houkokusho_e.html.
- JSME, 2012. Codes for Nuclear Power Generation Facilities Rules for Design and Construction for Nuclear Power Plants, Section II: Fast Reactor Standards (2012). JSME S NC2-2012. (in Japanese).
- Kaito, T., Otsuka, S., Inoue, M., 2007. Progress in the R&D project on oxide dispersion strengthened and precipitation hardened ferritic steels for sodium cooled fast breeder reactor fuels. In: *GLOBAL 2007, September 9–13, 2007, Boise, Idaho, USA*.
- Kaito, T., Ohtsuka, S., Inoue, M., Asayama, T., Uwaba, T., Mizuta, S., Ukai, S., Furukawa, T., Ito, C., Kagota, E., Kitamura, R., Aoyama, T., Inoue, T., 2009. In-pile creep rupture properties of ODS ferritic steel claddings. *J. Nucl. Mater.* 386-388, 294–298. <https://www.sciencedirect.com/science/article/pii/S0022311508008635>.
- Kamide, H., Kobayashi, J., Ono, A., Kimura, N., Miyakoshi, H., Watanabe, O., 2010. Sodium experiments on decay heat removal systems of Japan sodium cooled fast reactor start-up transient of decay heat removal system. In: *Presented at Seventh Korea-Japan Symp. Nuclear Thermal Hydraulics and Safety, Chuncheon, Korea, November 14-17, 2010*.
- Kamide, H., Ando, M., Ito, T., 2015. JSFR design progress related to development of safety design criteria for generation IV sodium-cooled fast reactors (1) overview. In: *Proceedings of 23rd International Conference on Nuclear Engineering*

- (ICONE-23), May 17–21, 2015, Chiba, Japan. https://www.jstage.jst.go.jp/article/jsmeicone/2015.23/0/2015.23__ICONE23-1_331/_article.
- Katoh, A., Negishi, K., Akiyama, Y., Hara, H., 2011. Experimental investigations of steel plate reinforced concrete bearing wall for fast reactor containment vessel. In: Proceedings of 19th International Conference Nuclear Engineering (ICONE19), Osaka, Japan, October 24–25, 2011.
- Kimura, N., Ezure, T., Tobita, A., Kamide, H., 2008. Experimental study on gas entrainment at free surface in reactor vessel of a compact sodium-cooled fast reactor. *J. Nucl. Sci. Technol.* 45 (10), 1053–1062. <https://www.tandfonline.com/doi/abs/10.1080/18811248.2008.9711892>.
- Kobayashi, J., Ezure, T., Kamide, H., Ohyama, K., Watanabe, O., 2015. Water experiments on thermal striping in reactor vessel of Japan sodium-cooled fast reactor countermeasures for significant temperature fluctuation generation. In: Proceedings of ICONE 23, May 17–21, Chiba, Japan, 2015. <https://inis.iaea.org/search/searchsinglerecord.aspx?recordsFor=SingleRecord&RN=48047708>.
- Kondo, S., Tobita, Y., Morita, K., Shirakawa, N., 1992. An advanced computer program for LMFBR severe accident analysis. In: Proceedings of ANP'92; 1992 Oct 25–29; Tokyo (Japan). IV, pp. 40.5-1–40.5-11. https://inis.iaea.org/search/search.aspx?orig_q=RN:25006719.
- Kondo, S., Deshimaru, T., Konomura, M., 2013. Recent progress and status of Monju. In: Proceedings of International Conference on Fast Reactors and Related Fuel Cycles; Safe Technologies and Sustainable Scenarios (FR-13) (USB Flash Drive), March. 6 pp. https://inis.iaea.org/search/search.aspx?orig_q=RN:46087733.
- Konishi, K., Toyooka, J., Kamiyama, K., Sato, I., Kubo, S., Kotake, S., Koyama, K., Vurim, A.D., Gaidachuk, V.A., Pakhnits, A.-V., Vassiliev, Y.S., 2007. The results of a wall failure in-pile experiment under the EAGLE project. *Nucl. Eng. Des.* 237 (22), 2165–2174. <https://www.sciencedirect.com/science/article/pii/S0029549307002324>.
- Kotake, S., Sakamoto, Y., Ando, M., Tanaka, T., 2005. Feasibility study on commercialized fast reactor cycle systems current status of the FR system design. In: Proceedings of GLOBAL 2005, Tsukuba, Japan, October 9–13, 2005. <https://inis.iaea.org/search/searchsinglerecord.aspx?recordsFor=SingleRecord&RN=37054233>.
- Kotake, S., Uto, N., Aoto, K., Kubo, S., 2009. Safety design features for JSFR-passive safety and CDA mitigation. In: Proceedings of Annual Meeting on Nuclear Technology, Dresden, Germany.
- Kubo, S., Yoshio, S., Hidemasa, Y., Shoji, K., 2011. Safety design requirements for safety systems and components of JSFR. *J. Nucl. Sci. Technol.* 48 (4), 547–555. <https://www.tandfonline.com/doi/abs/10.1080/18811248.2011.9711732>.
- Kubo, S., Chikazawa, Y., Ohshima, H., Uchita, M., Miyagawa, T., Eto, M., Suzuno, T., Matoba, I., Endo, J., Watanabe, O., Higurashi, K., 2020. A conceptual design study of pool-type sodium-cooled fast reactor with enhanced anti-seismic capability. *Mech. Eng. J.* 7 (3). https://www.jstage.jst.go.jp/article/mej/advpub/0/advpub_19-00489/_pdf/_char/ja.
- Kurisaka, K., 2006. Probabilistic safety assessment of Japanese sodium-cooled fast reactor in conceptual design stage. In: Proceedings of Pacific Basin Nuclear Conference (PBNC-15), pp. 225–231.
- Maeda, Y., Aoyama, T., Odo, T., Nakai, S., Suzuki, S., 2005. Distinguished achievements of a quarter-century operation and a promising project named MK-III in Joyo. *Nucl. Technol.* 150 (1), 16–36. <https://www.tandfonline.com/doi/abs/10.13182/NT05-A3602>.
- Nakai, R., Okano, Y., Kubo, S., 2012. Development of safety design criteria for the generation-IV sodium-cooled fast reactor. In: Keynote Lecture at NTHAS8: The Eighth Japan-Korea Symposium on Nuclear Thermal Hydraulics and Safety, Beppu, Japan, December 9–12. https://inis.iaea.org/search/search.aspx?orig_q=RN:46004717.
- Nakanishi, S., Hosoya, T., Kubo, S., Kotake, S., Takamatsu, M., Aoyama, T., Ikarimoto, I., Kato, J., Shimakawa, Y., Harada, K., 2010. Development of passive shutdown system for SFR. *Nucl. Technol.* 170, 181–188. <https://www.tandfonline.com/doi/abs/10.13182/NT10-A9456>.
- Niwa, H., Tobita, Y., Kubo, S., Sato, I., 2007. Safety implications of the EAGLE experimental results for the FaCT project. In: Proceedings of International Conference on Nuclear Power of Republic Kazakhstan, September 3–5, 2007, Kurchatov, Kazakhstan.
- Nuclear Safety Commission of Japan, 2006. Regulatory Guide for Reviewing Seismic Design of Nuclear Power Reactor Facilities. NSCRG: L-DS-I.02.
- Ohno, S., Ohki, H., Sugahara, A., Ohshima, H., 2011. Validation of a computational simulation method for evaluating thermal stratification in the reactor vessel upper plenum of fast reactors. *J. Nucl. Sci. Technol.* 48 (2), 205–214.
- Ohyama, K., Watanabe, O., Eguchi, Y., Koga, T., Kamide, H., Ohshima, H., 2009. Decay heat removal system by natural circulation for JSFR. In: Proceedings of International Conf. Fast Reactors and Related Fuel Cycles (FR09), Kyoto, Japan, December 7–11, 2009. https://inis.iaea.org/search/search.aspx?orig_q=RN:43118975.
- Okamura, S., Kamishima, Y., Negishi, K., Sakamoto, Y., Kitamura, S., Kotake, S., 2011. Seismic isolation design for JSFR. *J. Nucl. Sci. Technol.* 48 (4), 688–692. <https://www.tandfonline.com/doi/abs/10.1080/18811248.2011.9711750>.

- Okubo, T., Oki, S., Ogura, M., Okubo, Y., Kotake, S., 2011. Conceptual design for a large-scale Japan sodium-cooled fast reactor (3) core design in JSFR. In: Presented at International Congress on Advances in Nuclear Power Plants (ICAPP'11), Nice, France, May 2–5, 2011. https://inis.iaea.org/search/search.aspx?orig_q=RN:44092831.
- Onizawa, T., Nagae, Y., Takaya, S., Asayama, T., 2013a. Development of 2012 edition of JSME code for design and construction of fast reactors (2) Development of the material strength standard of 316FR stainless steel. In: Proceedings of the ASME 2013 Pressure Vessels and Piping Conference PVP2013, PVP2013–97608, July 14–18, 2013, Paris, France. <https://asmedigitalcollection.asme.org/PVP/proceedings-abstract/PVP2013/55645/V01BT01A034/283129>.
- Onizawa, T., Nagae, Y., Takaya, S., Asayama, T., 2013b. Development of 2012 edition of JSME code for design and construction of fast reactors (3) Development of the material strength standard of modified 9Cr-1Mo steel. In: Proceedings of the ASME 2013 Pressure Vessels and Piping Conference PVP2013, PVP2013–97611, July 14–18, 2013, Paris, France.
- Ono, I., Kurihara, A., 2005. Quasi-Steady Pressure Analysis in Intermediate Water Leak Rate with swac-13 Module in SWACS Code. JNC TN9400 2005-047. Japan Nuclear Cycle Development Institute (in Japanese) <https://jopss.jaea.go.jp/pdfdata/JNC-TN9400-2005-047.pdf>.
- Ono, A., Kimura, N., Kamide, H., Tobita, A., 2011. Influence of elbow curvature on flow structure at elbow outlet under high Reynolds number condition. Nucl. Eng. Des. 241 (11), 4409–4419. <https://www.sciencedirect.com/science/article/pii/S0029549310006205>.
- Onoda, Y., Fukano, Y., Sato, I., Marquie, C., Duc, B., 2011. Three-pin cluster CABRI tests simulating the unprotected loss-of-flow accident in sodium-cooled fast reactors. J. Nucl. Sci. Technol. 48 (2), 188–204. <https://www.tandfonline.com/doi/abs/10.1080/18811248.2011.9711693>.
- Rothman, A.B., Simms, R., McNary, O., Stanford, G.S., Marsh, G.E., 1979. TREAT experiments with irradiated fuel simulating hypothetical loss-of-flow accidents in large LMFRs. In: Proceedings of International Meeting on Fast Reactor Safety Technology, 1979 August 19–23, Seattle, USA, p. 924. https://inis.iaea.org/search/search.aspx?orig_q=RN:12627148.
- Sakai, T., Eguchi, Y., Monji, H., Iwasaki, T., Ito, K., Ohshima, H., 2008. Proposal of design criteria for gas entrainment from vortex dimples based on a computational fluid dynamics method. Heat Transfer Eng. 29 (8), 731–739.
- Sakai, T., Kotake, S., Aoto, K., Ito, T., Kamishima, Y., Ohshima, J., 2010. Conceptual design study toward the demonstration reactor of JSFR. In: Proceedings of International Congress on Advances in Nuclear Power Plants (ICAPP '10), San Diego, USA, June 13–17, 2010. <https://asmedigitalcollection.asme.org/ICONE/proceedings-abstract/ICONE18/49347/333/347755>.
- Sato, I., Lemoine, F., Struwe, D., 2004. Transient fuel behavior and failure condition in the CABRI-2 experiments. Nucl. Technol. 145 (1), 115–137. https://inis.iaea.org/Search/search.aspx?orig_q=RN:38013454.
- Sato, I., Tobita, Y., Konishi, K., Kamiyama, K., Toyooka, J., Nakai, R., Kubo, S., Kotake, S., Koyama, K., Vassiliev, Y., Vurim, A., Zuev, V., Kolodeshnikov, A., 2011. Safety strategy of JSFR eliminating severe recriticality events and establishing in-vessel retention in the core disruptive accident. J. Nucl. Sci. Technol. 48 (4), 556–566. <https://www.tandfonline.com/doi/abs/10.1080/18811248.2011.9711733>.
- Shimakawa, Y., Kasai, S., Konomura, M., Toda, M., 2002. An innovative concept of a sodium-cooled reactor to pursue high economic competitiveness. Nucl. Technol. 140, 1–17.
- Takamatsu, M., Sekine, T., Aoyama, T., Uchida, M., Kotake, S., 2007. Demonstration of control rod holding stability of the self-actuated shutdown system in Joyo for enhancement of fast reactor inherent safety. J. Nucl. Sci. Technol. 44 (3). <https://www.tandfonline.com/doi/abs/10.1080/18811248.2007.9711316>.
- Tanabe, H., Miyake, O., Daigo, Y., Sato, M., 1982. Analysis Code for Failure Propagation of Steam Generator Tube-LEAPII. PNCTN952 82–04. Power Reactor and Nuclear Fuel Development Corp (in Japanese).
- Tanaka, M., Miyake, Y., 2015. Numerical simulation of thermal striping phenomena in a T-junction piping system for fundamental validation and uncertainty quantification by GCI estimation. Mech. Eng. J. 2 (5). Paper no. 15-00134 https://www.jstage.jst.go.jp/article/mej/2/5/2_15-00134/_article/-char/en.
- Tanaka, M., Ohshima, H., 2012. Numerical investigation on large scale eddy structure in unsteady pipe elbow flow at high Reynolds number conditions with large eddy simulation approach. J. Power Energy Syst. 6 (2), 210–228. https://www.jstage.jst.go.jp/article/jpes/6/2/6_210/_article.
- Tanaka, M., Ohno, S., Ohshima, H., 2016. Development of V2UP (V&V plus uncertainty quantification and prediction) procedure for high cycle thermal fatigue in fast reactor framework for V&V and numerical prediction. Nucl. Eng. Des. 299 (2016), 174–183. <https://www.sciencedirect.com/science/article/pii/S0029549315002800?via%3Dihub>.
- Tobita, Y., Kondo, S., Yamano, H., Morita, K., Maschek, W., Coste, P., Cadiou, T., 2006. The development of SIMMER-III, an advanced computer program for LMFR safety analysis and its application to sodium experiments. Nucl. Technol. 153 (3), 245–255. <https://kyushu-u.pure.elsevier.com/ja/publications/the-development-of-simmer-iii-an-advanced-computer-program-for-lm>.

- Uchibori, A., Ohshima, H., 2015. Development of a mechanistic evaluation method for wastage environment under sodium-water reaction accident. In: Proceedings of NURETH-16, Chicago, Illinois, August 30–September 4, 2015. <http://glc.ans.org/nureth-16/data/papers/13542.pdf>.
- Uehira, A., Ukai, S., Mizuno, T., 1999. Evaluation of Swelling and Irradiation Creep Properties of High Strength Ferritic/Martensitic Steel (PNC-fms). JNC report no. TN9400 99-022. Japan Nuclear Cycle Development Institute, Ibaraki, Japan (in Japanese) <https://jopss.jaea.go.jp/pdfdata/JNC-TN9400-99-022.pdf>.
- Ukai, S., 1998. Irradiation Performance of FBR Monju-Type Fuel with Modified Type 316 Stainless Steel at High Burn-up. *American Nuclear Society Transactions*, p. 115.
- US DOE and GIF, 2002. A Technology Roadmap for Generation IV Nuclear Energy Systems. GIF-002-00. https://www.gen-4.org/gif/jcms/c_40473/a-technology-roadmap-for-generation-iv-nuclear-energy-systems.
- Varaine, F., Rodriguez, G., Hamy, J.M., Kubo, S., Iitsuka, T., Mochida, H., 2018. The significant Collaboration of Japan and France on the design of ASTRID sodium fast reactor since 2014. In: Proceedings of the GIF Symposium, Paris, France. <https://core.ac.uk/download/pdf/237325048.pdf>.
- Watanabe, O., Oyama, K., Endo, J., Doda, N., Ono, A., Kamide, H., Murakami, T., Eguchi, Y., 2015. Development of evaluation methodology for natural circulation decay heat removal system in a sodium cooled fast reactor. *J. Nucl. Sci. Technol.* 52 (9), 1102–1121. <https://www.tandfonline.com/doi/full/10.1080/00223131.2014.994049>.
- Yamaguchi, A., Takata, T., Okano, Y., 2001. Numerical methodology to evaluate fast reactor sodium combustion. *Nucl. Technol.* 136 (3), 315–330. <https://www.tandfonline.com/doi/abs/10.13182/NT01-A3248>.
- Yamano, H., Tanaka, M., Kimura, N., Ohshima, H., Kamide, H., Watanabe, O., 2009. Unsteady hydraulic characteristics in large-diameter piping with elbow for JSFR (1) current status of flow-induced vibration evaluation methodology development for the JSFR piping. In: Proceedings of 13th International Topical Meeting Nuclear Reactor Thermal Hydraulics (NURETH-13), Kanazawa, Japan, September 27–October 2, 2009. https://inis.iaea.org/search/search.aspx?orig_q=RN:43036677.
- Yamano, H., Kubo, S., Kurisaka, K., Shimakawa, Y., Sago, H., 2010. Technological feasibility of two-loop cooling system in JSFR. *Nucl. Technol.* 170, 159–169. <https://www.tandfonline.com/doi/abs/10.13182/NT09-6>.
- Yano, Y., Ogawa, R., Yamashita, S., Ohtsuka, S., Kaito, T., Akasaka, N., Inoue, M., Yoshitake, T., Tanaka, K., 2011. Effects of neutron irradiation on tensile properties of oxide dispersion strengthened (ODS) steel claddings. *J. Nucl. Mater.* 419, 305–309. <https://www.sciencedirect.com/science/article/pii/S0022311511004740>.
- Yokota, Y., Okada, K., Onuki, K., Otsubo, T., 1991. Design and construction of the reactor structure of the prototype fast breeder reactor Monju. In: Proceedings of International Conference on Fast Reactors and Related Fuel Cycles, Kyoto, Japan, October 28–November 1, 1991. https://inis.iaea.org/search/search.aspx?orig_q=RN:24042663.

Generation-IV concepts in Korea

Dohee Hahn

Korea Atomic Energy Research Institute, Daejeon, Republic of Korea

Acronyms

ADHRs	Active DHRs
AHX	natural-draft sodium-to-Air Heat eXchanger
AMBIDEXTER-NEC	Advanced Molten-salt Break-even Inherently-safe Dual-function EXcellentTly-Ecological Reactor Nuclear Energy Complex
BOEC	Beginning Of Equilibrium Cycle
DHRS	Decay Heat Removal System
DHX	Decay Heat eXchanger
ENHS	Encapsulated Nuclear Heat Source
EOEC	End Of Equilibrium Cycle
FHX	Forced-draft sodium-to-air Heat eXchanger
IHTS	Intermediate Heat Transport System
KAEC	Korea Atomic Energy Commission
KAERI	Korea Atomic Energy Research Institute
KAERI-DySCo	Korea Atomic Energy Research Institute-Dynamic Simulation Code
KALIMER	Korea Advance LIquid METal Reactor
KIST	Korea Institute of Science and Technology
LACANES	Lead Alloy-Cooled Advanced Energy Systems
LBE	Lead–Bismuth Eutectic
LMR	Liquid Metal-cooled Reactor
MSIP	Ministry of Science, ICT and Future Planning
NHDD	Nuclear Hydrogen Development and Demonstration
NUTRECK	NUclear TRansmutation Energy research Center of Korea
ORNL	Oak Ridge National Laboratory
PCS	Power Conversion System
PDHRs	Passive DHRs
PDRc	Proliferation-resistant core without a blanket, and a Decay heat Removal Circuit
PHTS	Primary Heat Transport System
PRIDE	PyRoprocess Integrated inactive DEMonstration facility
pSSC	provisional Systems Steering Committee
RVACS	Reactor Vessel Air Cooling System
SFRA	SFR development Agency
STELLA	Sodium Test Loop for Safety Simulation and Assessment
TRU	TRansUranic elements
VHTR	Very-High-Temperature gas-cooled Reactor
YSZ	Yttria-Stabilized Zirconia

13.1 Current status of nuclear power in Korea

Nuclear power generation is not an option but a necessity for energy security in Korea, which is poor in natural energy resources. Nuclear energy has played a major role as the main source of power generation in Korea for the past 40 years. Korea currently operates 24 reactors, which account for 22% of its total electricity generation capacity. Prior to the Fukushima nuclear accident in Japan, the direction of nuclear power technology focused on improving the economic efficiency without exceeding the safety regulation level. However, with increased public interest in the safety of nuclear power plants, the development of technology to improve the safety rather than the economic feasibility of nuclear power plants has recently become more important.

Recognizing that nuclear safety is a top priority, Korea will continue to utilize nuclear energy as a practical solution to address issues such as rising energy demand and climate change. Under the 2nd National Energy Basic Plan, the portion of nuclear power in the total energy mix will be 29% by 2035. According to the plan, 11 nuclear power plants will be built by 2024 with the start of commercial operation of Shin Kori units 3 and 4 slated for 2015 and 2016, respectively.

Korea's Science, ICT and Future Planning Minister and the President of King Abdullah City for Atomic and Renewable Energy signed a Memorandum of Understanding (MoU) aimed at establishing SMART partnership for joint development and commercialization of SMART in March 2015. Under the MoU, the two countries are set to conduct a 3-year preproject engineering project to review the feasibility of constructing at least two SMART plants in Saudi Arabia. The agreement is expected to provide opportunities for Korea to commercialize, for the first time in the world, the indigenously designed SMART by constructing it in Saudi Arabia if Saudi Arabia decides to build additional reactors after a preliminary review. It is expected to help Korea exploit the global small-and medium-sized reactor market if the two countries are to cooperate on the commercialization and export of the SMART reactor to third countries.

Korea has been developing a Prototype Generation-IV (Gen-IV) Sodium-cooled Fast Reactor (PGSFR) design according to the national long-term plan for the development of future nuclear energy systems. A specific safety analysis report of the PGSFR will be submitted to the regulatory authority in 2017 for its design approval by 2020. As a preliminary step before a formal safety evaluation, the Korea Atomic Energy Research Institute (KAERI) is going to submit a preliminary safety information document to the regulatory authority by the end of 2015 for an independent and authorized peer review on the safety of the PGSFR. For the successful development of the PGSFR design, Korea has been actively engaged in international collaborative research activities. As part of this effort, Korea has been actively participating in collaborative Research and Development (R&D) activities of the Gen-IV International Forum (GIF). Large experimental facilities have been constructed to conduct various experiments to validate thermal-hydraulic phenomena and a large sodium loop, called Sodium Test Loop for Safety Simulation and Assessment (STELLA)-1, for the test of key Decay Heat Removal System (DHRS) components, started its operation in 2014. Design work started in early 2015 for STELLA-2, which is an integral test loop for a simulation of the thermal-hydraulic characteristics of the PGSFR primary and intermediate heat transport systems.

A Very-High-Temperature Reactor (VHTR) is primarily dedicated to the generation of hydrogen, which has been dubbed as the fuel of the future and an alternative energy source to replace fossil fuels. Hydrogen production using a VHTR in conjunction with thermochemical water splitting does not emit greenhouse gases, unlike the conventional natural gas steam methane reforming. Therefore, hydrogen production using a VHTR is a clean and efficient method to reduce dependence on fossil fuel in Korea. KAERI has been developing a VHTR and nuclear hydrogen key technologies since 2006, targeting the demonstration of nuclear hydrogen by 2030.

VHTR R&D consists of two major projects: the key technology development project of nuclear hydrogen and the Nuclear Hydrogen Development and Demonstration (NHDD) project. The key technology development project focuses on the development and validation of key and challenging technologies required for the realization of a nuclear hydrogen system. The key technologies, which are the basis of Gen-IV VHTR R&D

collaboration, are mainly focused on the development of computational tools, high-temperature experimental technology, a high-temperature material data-base, TRi-ISOTropic (TRISO) fuel fabrication, and the hydrogen production process. The NHDD project is aimed at the design, construction, and demonstration of a nuclear hydrogen system using a VHTR. Preparation for the NHDD project began by launching an alliance for nuclear hydrogen, which consists of nine nuclear industry companies or institutes and five end users in 2009. To enhance international collaboration, a MoU with NGNP industrial alliance was signed in 2013.

13.2 Plans for advanced nuclear reactors in Korea

13.2.1 Sodium-cooled fast reactor

Although the energy supply in Korea has been ensured by nuclear power, the continuous increase of the nuclear power plants has caused a spent fuel storage problem. Therefore, a technical alternative to solve the spent fuel management is necessary to technically support the decision making process for spent fuel management.

It has been recognized nationwide that a fast reactor system is one of the most promising nuclear options for electricity generation with an efficient utilization of Uranium (U) resources and a reduction of the radioactive wastes from nuclear power plants. In response to this recognition, Sodium-cooled Fast Reactor (SFR) technology development efforts in Korea commenced in June 1992 with the Korea Atomic Energy Commission's approval of a national mid- and long-term nuclear R&D program. At the early stages of its development, the research efforts focused on the basic R&D of core neutronics, thermal hydraulics, and sodium technology, with the aim to enhance the basic liquid metal-cooled reactor technology capabilities.

The basic R&D efforts made in the early development stage had been extended to develop the conceptual designs of KALIMER (Korea Advanced LIquid METal Reactor)-150 (150 MW_{eI}) (Hahn et al., 2002) and -600 (600 MW_{eI}) (Hahn et al., 2007), and the basic key technologies over the past 10 years since 1997 under the revised nuclear R&D program. According to the Nuclear Technology Roadmap established in 2005, an SFR was chosen as one of the most promising future types of reactors, which could be deployable by 2030.

The KALIMER-600 features a proliferation-resistant core without a blanket, and a decay heat removal circuit using natural sodium circulation cooling for a large power system. In addition, a shortened Intermediate Heat Transport System (IHTS) piping and a seismic isolation are incorporated into the KALIMER-600 design. The KALIMER-600 conceptual design, which evolved on the basis of the KALIMER-150 (150 MW_{eI}) design, was selected as one of promising Gen-IV SFR candidates. R&D efforts have been made on the development of advanced design concepts including a supercritical CO₂ Brayton cycle energy conversion system, design methodologies, computational tools, and sodium technology.

The development of the SFR technology in Korea entered a new phase from 2007 with Korea's participation in the Gen-IV SFR collaboration project. An advanced SFR design concept that can better meet the Gen-IV technology goals had developed until 2011. R&D efforts were conducted to develop the conceptual design of the advanced SFR, focusing on the core and reactor systems, and a development of the advanced SFR technologies necessary for its commercialization and basic key technologies. To develop these advanced technologies, R&D was conducted to improve the economics, safety assurance, and metal fuel performance of an SFR in the areas of safety, fuels and materials, reactor systems, and the balance of plant. To provide a consistent direction to long-term R&D activities, the Korea Atomic Energy Commission (KAEC) authorized a long-term development plan in December 2008 for future nuclear reactor systems, which include SFR, pyroprocess, and Very-High-Temperature gas-cooled Reactor (VHTR). KAEC authorized the modification of the plan in November 2011, reflecting the maturity of technology achieved hitherto and the budget condition (Kim et al., 2013a,b). The modified plan includes a design development of the prototype SFR by 2017, its design approval and construction by 2020 and 2028, respectively, as shown

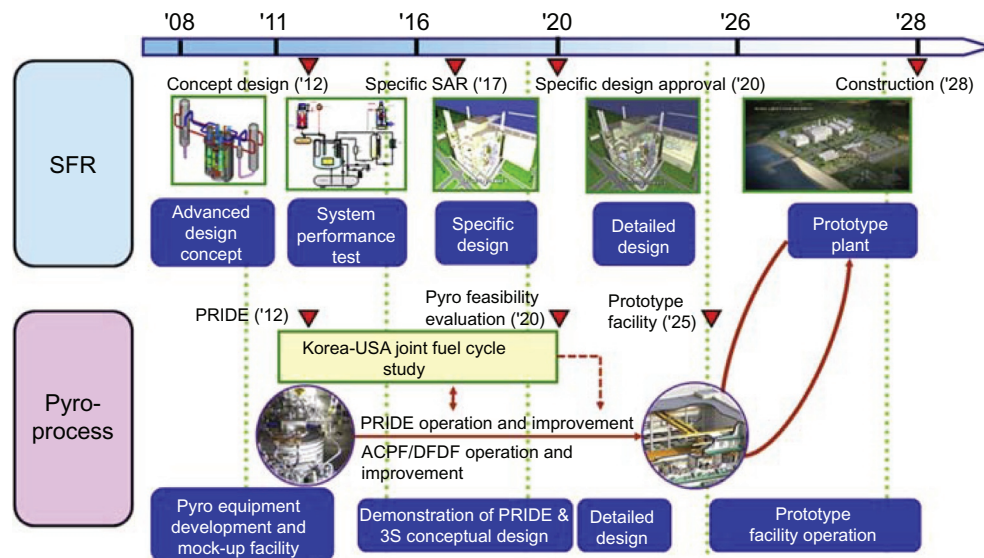


Figure 13.1. SFR pyroprocess development plan. *PRIDE*, PyRoprocessing Integrated inactive DEMonstration facility; *ACPF*, Advanced spent fuel Conditioning Process Facility; *DFDF*, Dupic Fuel Development Facility; *3S*, Safety, Security, Safeguards (Kim et al., 2013a)

in Figure 13.1. This long-term plan has been implementing through nuclear R&D programs of the National Research Foundation, with funds from the Ministry of Science, ICT and Future Planning. The SFR Development Agency was organized in May 2012 to secure the budget and efficiently manage the SFR Development Project. According to the plan, KAERI, the main body responsible for the fast reactor development in Korea, is developing a design of the prototype SFR. The prototype SFR development will be extended to the commercialization phase with its initialization in around 2050.

For the development of pyroprocess, KAERI constructed the Pyroprocess Integrated Inactive Demonstration Facility, which is a mock-up facility for pyroprocessing. After engineering-scale demonstration by 2020, the Korea Advanced Pyroprocess Facility, being a prototype facility, will be constructed by 2025.

The metal fuel for the prototype SFR is being developed in accordance with the SFR and pyroprocess development plan. Fuel fabrication technology will be developed by 2018, and a U–Zirconium (Zr) fuel manufacturing facility will be constructed by 2024. U–Zr fuel will be used as a starting fuel for initial core, and U–TRU–Zr fuel will replace U–Zr fuel after verification of its in-pile performance.

13.2.2 Very-High-Temperature gas-cooled Reactor (VHTR)

A Very-High-Temperature gas-cooled Reactor (VHTR) is an inherently safe reactor that can produce heat of 750–950°C. By virtue of its high-temperature heat, a VHTR can be used in high-temperature process heat applications, including hydrogen production and high-efficiency electricity generation. The most effective application of a VHTR is the massive hydrogen production in support of the hydrogen economy.

The rapid climate changes and heavy energy reliance on imported fossil fuels have motivated the Korean government to set up a long-term vision for transition to the hydrogen economy in 2005. One of the big challenges is how to produce massive hydrogen in a clean, safe, and economic way. Among the various hydrogen production methods, massive, safe and economic production of hydrogen by water splitting using a VHTR can provide a successful path to the hydrogen economy. Particularly in Korea, where the use of land is limited, the “nuclear” hydrogen is deemed a practical solution, due to its high energy density.

Another merit of the nuclear hydrogen is that it is a sustainable and technology-led energy unaffected by the unrest of fossil fuel. Current hydrogen demand is mainly from oil refinery and chemical industries. Hydrogen is mostly produced by steam reforming using fossil fuel heat, which emits a large amount of greenhouse gases. Today in Korea, more than 1 Mtons/year of hydrogen is produced and consumed in oil refinery industries. In 2040, it was projected on a hydrogen roadmap that 25% of the total hydrogen demand will be supplied by the “nuclear” hydrogen, which is around 3 Mtons/year, even without considering the hydrogen iron ore reduction.

In order to prepare for the upcoming hydrogen economy, the nuclear hydrogen key technologies development project was launched at KAERI in 2006 as a national program of the Ministry of Education, Science and Technology (Chang et al., 2007). KAERI has taken a leading role in the project and the development of VHTR technologies. The Korea Institute of Energy Research (KIER) and the Korea Institute of Science and Technology (KIST) are leading the development of the SI (Sulfur–Iodine) thermochemical hydrogen production technology. The KAEC officially approved the nuclear hydrogen program in 2008, the amendment of which was made in 2011. The final goal of the program is to demonstrate and commercialize the nuclear hydrogen by 2030.

The nuclear hydrogen program consists of two major projects: the nuclear hydrogen key technologies development project and the NHDD project. Figure 13.2 illustrates the plan of the nuclear hydrogen program.

The key technologies development project focuses on the development and validation of key and challenging technologies required for the realization of the nuclear hydrogen system. The key technologies selected are the design codes, high-temperature helium experiment, high-temperature material database, TRISO fuel, and thermochemical hydrogen production. This project has been carried out in phase with both the NHDD project and the GIF projects, and will continue until 2016.

The NHDD project is aimed at the design and construction of a nuclear hydrogen demonstration system for demonstration of massive hydrogen production and system safety. A VHTR systems concept study has been performed for 3 years since 2011. The main objectives of this study are to develop the VHTR systems concept for nuclear process heat and electricity supply to industrial complexes, for the massive nuclear hydrogen

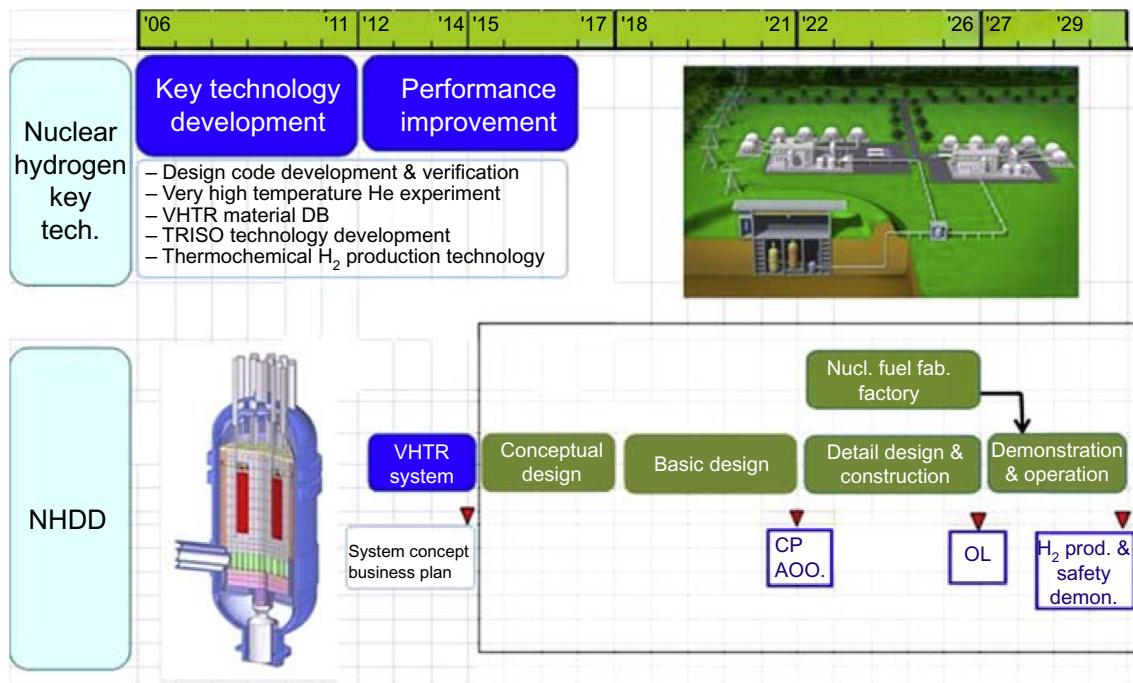


Figure 13.2. Nuclear hydrogen project plan in Korea

production required to enter into a future clean hydrogen economy, and to establish the demonstration project plan of VHTR systems for subsequent commercialization.

As part of the VHTR system concept study, (1) the plant design and functional requirements for both commercial-scale nuclear process heat and nuclear hydrogen systems are developed; (2) the design concepts, layout, and operating parameters of reactor and plant systems are optimized; (3) the design concepts of key high-temperature components and materials are investigated and assessed for manufacturing and procurement purposes; and (4) the design concepts of underground reactor building, radioactive waste management, and radiation protection are evaluated. In parallel, the design analysis systems of reactor and plant systems are constructed and applied for a performance analysis, and the system concept of a demonstration plant is developed and suggested.

As part of the demonstration project plan, commercial-scale plant concepts of both nuclear process heat and nuclear hydrogen systems were first selected reflecting the market needs and opinions of potential customers and vendors, and an economic feasibility study was carried out. Based on the above, the project structure and strategy of the demonstration project and subsequent commercialization project were established together with the relevant business model.

The project plan includes not only the project structure, schedule, budget, and project strategies to secure project financing, government support, site, and licensing, but also the technology development and validation plan required in the process of licensing of the demonstration plant. A stepwise demonstration using a single reactor system was adopted to reduce the technology and business risks, as shown in Figure 13.3. The reactor technology is demonstrated first at the core outlet temperature of 750°C based on mature technologies. The demonstration of reactor technology will be finished in 10 years. The hydrogen production technology will be developed through international collaboration in parallel with the basic and detailed design of the reactor technology demonstration. The construction of a hydrogen production system will be finished before the demonstration of the reactor technology, which will be followed by the reactor system modification and integration. After that, the demonstration of nuclear hydrogen production will be completed in 2 years.

According to the government suggestion, VHTR systems point design started in 2015 instead of the conceptual design of the demonstration plant. The purpose of the point design is to generate design data of the stepwise and integrated demonstration plant. The data will be used not only for the conceptual design, but also for a feasibility assessment of the demonstration project. KAERI will apply for prefeasibility approval to

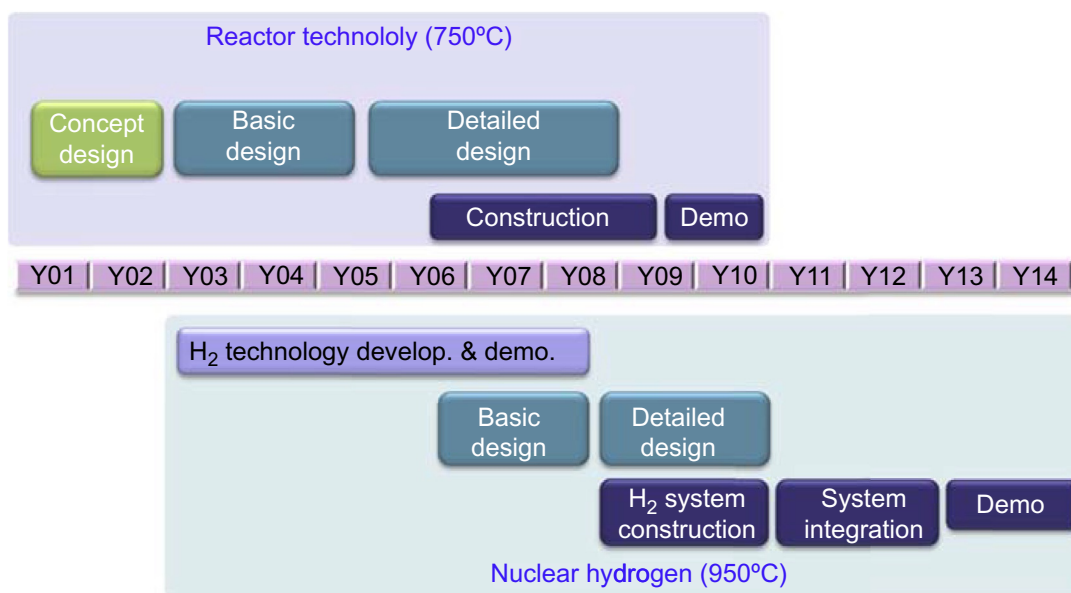


Figure 13.3. The stepwise demonstration plan of NHDD

the government based on the point design results to be given support from the government. Regardless of launching the demonstration project, the GIF studies will continue because the Korean government signed an extension of the GIF framework agreement for another 10 years until 2026.

13.3 Current research and development on Generation-IV reactor in Korea

13.3.1 Sodium-cooled Fast Reactor (SFR)

13.3.1.1 Development of a 150 MW_{el} prototype Sodium-cooled Fast Reactor (SFR)

Top-tier design requirements

Based upon the experiences gained during the development of the conceptual designs for KALIMER-150 and KALIMER-600, the design of an SFR prototype plant has been carried out since 2012. The objectives of the prototype SFR (Kim et al., 2013a,b) are to test and demonstrate the performance of TRansUranics (TRU)-containing metal fuel required for a commercial SFR, and to demonstrate the TRU transmutation capability of a burner reactor as a part of an advanced fuel cycle system. The primary mission of the prototype SFR is to demonstrate the transmutation of TRU recovered from the Pressurized Water Reactor (PWR) spent fuel, and hence the benefits of the integral recycling of all actinides (U and TRU) in a closed fuel cycle to nuclear waste management.

Based on the objectives above, the top-tier design requirements for the prototype SFR and related design parameters that were extensively discussed are given in Table 13.1. The lessons learned from fast reactor programs and the operating experience of fast reactors worldwide, particularly for metal fueled reactors, as well as the experience gained during the development of conceptual designs of KALIMER and advanced SFR design concepts and the trade-off studies, have been incorporated in the top-tier design requirements to the extent possible.

Core design

A candidate reactor core uses a single enrichment fuel with a U–10% Zr binary metal alloy form initially and will be changed to an enrichment split core to flatten the power distribution when TRU fuel will be adopted. To accept two different types fuel in the same core dimension, the initial U core was designed with TRU core transition capability (Kim et al., 2013a,b).

Figure 13.4 shows the layout of the U-fueled core. As shown in the figure, the core consists of two regions of fuel. Table 13.2 shows a summary of the core performance analysis results, obtained with the equilibrium cycle analysis. The Beginning Of Equilibrium Cycle (BOEC) to end of equilibrium cycle depletions was modeled with a burnup chain having descriptions for all of the U–Plutonium (Pu)–MA isotopes. A zone reload without fuel shuffling was developed for the equilibrium cycle, wherein one-fourth of the inner core fuels and one-fifth of the outer core fuels were refueled at each outage.

All reactivity coefficients for U core have negative values, which means this core design holds inherent safety characteristics. In particular, the sodium void effect also shows a negative value, which is a different tendency in a typical SFR because of plutonium-free core. For the diversity of a shutdown system, two types of control assemblies are arranged to secure sufficient shutdown margin.

Fuel design

Cladding failure or damage during the steady state and transient conditions must be evaluated by appropriate predictive codes. To prevent a metallic fuel rod failure in a fast reactor, it is required to evaluate the design limits such as (1) cladding integrity including cladding strain and CDF (cumulative damage fraction); and (2) fuel melting.

TABLE 13.1. Top-tier design requirements for the prototype SFR

General design requirements	Plant size	• 150 MW _{el} (~400 MW _{th})
	Plant design lifetime	• 60 years
	Seismic design	• Design basis earthquakes (SSE: 0.3 g) • Safety structures and equipments on a horizontal seismic isolation
	Fuel type	• Initial core: U-Zr metal • Reference core: U-TRU-Zr metal
Safety and investment protection	Accident resistance	• Design simplification in all aspects of design, construction, operation, and maintenance. Complexity of the plant design has been one of the main sources of high capital cost and threat to the safety of nuclear plants • A large thermal capacity of the primary system in a pool-type reactor
	Core damage prevention	• CDF < 10 ⁻⁶ /reactor-year • A diversified core shutdown mechanism • A highly reliable and diversified decay heat removal (2 active systems and 2 passive systems) • Capable of accommodating unprotected ATWS events without any operator's action
	Accident mitigation	• A large radioactivity release frequency < 10 ⁻⁷ /reactor-year • Core protection limits should not be exceeded for at least 7 days without any operator's action for design basis events
Plant performance and economy	Plant availability	• An annual average plant availability ≥ 75%
	Refueling interval	≥ 6 months
	Load rejection capability	• Capable of accommodating 100% off-site load rejection without a reactor trip
	Operation, maintenance, and serviceability	• Major equipments affecting the plant lifetime shall be replaceable • An occupational radiation exposure < 1 man-Sv/year
	Construction cost	Competitive with that of similar types of fast reactors in future
Main components	Intermediate heat exchanger	An immersed cylindrical type
	Internal structure	Cooling facility in reactor vessel against core melting
	Primary pump	An immersed mechanical pump
	Power conversion system	• Reference: superheated steam Rankine cycle • Alternative: S-CO ₂ Brayton cycle

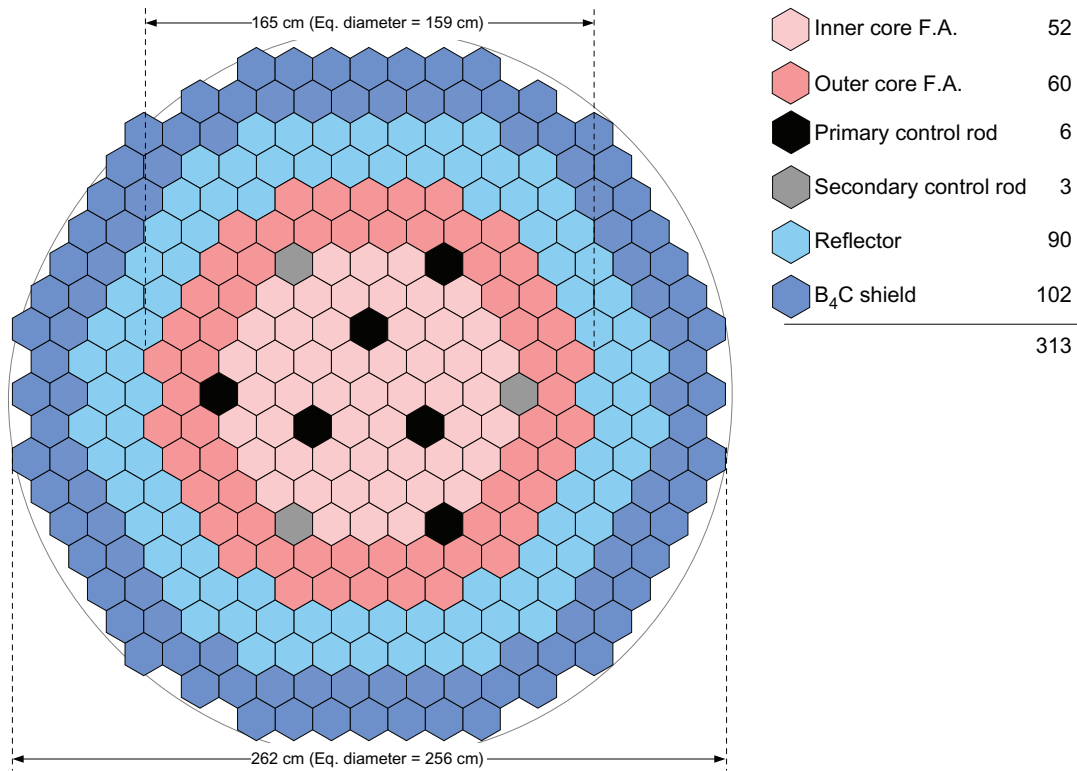
Figure 13.4. Layout of U core (150 MW_{el})

TABLE 13.2 U-Zr core design and performance parameters

Design/performance parameters		Design/performance parameters	
EFPD/No. of Batch (IC/OC) (day/#)	290/4/5	Burnup (avg./peak) (MWd/kg)	66.4/107.1
No. of fuel assembly (IC/OC)	52/60	Burnup reactivity swing (pcm)	2297
Fuel pin diameter (cm)	0.74	Fast neutron flux ($\times 10^{15}$ n/cm ² s)	1.43
P/D ratio	1.14	Peak fast N. fluence ($\times 10^{23}$ n/cm ²)	2.93
Active core height (cm)	90.0	Ave. linear power density (W/cm)	163.4
Lower shield height	90.0	Peak linear power density (W/cm)	338.7
Fission gas plenum height (cm)	125.0	Ave. power density (W/cm ³)	218.4
Enrichment (wt%)	19.50	Peak power density (W/cm ³)	452.6
Heavy metal loading (Mt)	7.33	Bundle pressure drop (MPa)	0.423
Charge HM mass (t/year)	1.68	Max. flow rate (kg/s)	25.5

Fuel melting temperature limits of 955°C and 1200°C are used for U–TRU–Zr and U–Zr fuel, respectively. It was estimated that the metallic fuel had a sufficient margin to the melting temperature.

The cladding integrity including cladding strain limit, swelling limit, and CDF limit for metal fuel were evaluated by the LIFE-METAL code. In particular, CDF and cladding strain limits were estimated for the candidates for cladding material, HT9 and FC92. These limits depend on plenum-to-fuel ratio, cladding thickness/temperature, and burnup. A sensitivity analysis to evaluate these limits was carried out for the target coolant outlet temperature of 545°C. Design parameters such as maximum cladding temperature, plenum length, and cladding thickness were established to satisfy the design limits.

Fluid system design

The heat transport system is composed of a Primary Heat Transport System (PHTS), an IHTS, and a Power Conversion System (PCS). The heat transport system has features such as pool-type PHTS, two IHTS loops, and a superheated steam Rankine cycle PCS, as shown in [Figure 13.5](#).

The PHTS consists of two PHTS pumps, four Intermediate Heat eXchangers (IHx), and reactor structures. The PHTS pump is a centrifugal-type mechanical pump. The IHx is counter flow shell and tube types with a vertical orientation inside the reactor vessel where the PHTS sodium flows through the shell side and IHTS sodium flows through the tube side.

The IHTS consists of two IHTS pumps, two single-wall straight tube type steam generators, two expansion tanks, and pipings. The IHTS pump is an electromagnetic type and is located in each cold leg of the two IHTS loops. Each steam generator has a thermal capacity of 197 MW_{th} and is installed in each IHTS loop. The steam temperature and pressure at 100% normal operating condition are 503°C and 16.7 MPa, respectively.

As one of the safety design features, the DHRS is composed of two Passive DHRSs (PDHRSs) and two Active DHRSs (ADHRSs). It was designed to have the sufficient capacity to remove the decay heat in all design basis events by incorporating the principles of redundancy and independency. The PDHRS is a safety-grade passive system, which comprises two independent loops with a Decay Heat Exchanger (DHX) and a natural-draft sodium-to-Air Heat eXchanger (AHX). The ADHRS is a safety-grade active system, which is comprised of two independent loops with a DHX, a Forced-draft sodium-to-air Heat eXchanger (FHX), an electromagnetic pump, and an FHX blower for each loop. The ADHRS can also be operated in natural convection mode against a loss of power supply with ~50% of its designed heat removal capacity. The heat transferred to the DHRS can be finally dissipated into the atmosphere through AHXs and FHXs by the natural convection mechanism of sodium and air only.

Mechanical structure design

The reactor structures, system, and components were designed as shown in [Figure 13.6](#). In this design, the reactor vessel size is determined to be 8.7 m in diameter, 1 and 5.4 m in height. The main design features are that the reactor internals are very simple, and the reactor support structure is a skirt-type structure supporting the reactor head and the reactor vessel jointed with bolts. The core support structure is a simple skirt-type structure, partly welded between keys and lugs forged with the vessel bottom head. The IHTS piping layout is established in a way to minimize the nozzle loads through the weight and seismic load analyses. The total IHTS piping length is significantly reduced using Gr91 material. The main advantage of Gr91 for IHTS piping and heat exchangers material is to avoid the dissimilar weld joints at any NSSS location.

13.3.1.2 Research and development activities

Large-scale sodium thermal–hydraulic test program

A large-scale sodium thermal–hydraulic test program called STELLA ([Eoh et al., 2013](#)) is being progressed by KAERI. As the first step of the program, the sodium component test loop called STELLA-1 has been completed, which is used for demonstrating thermal–hydraulic performance of major components,

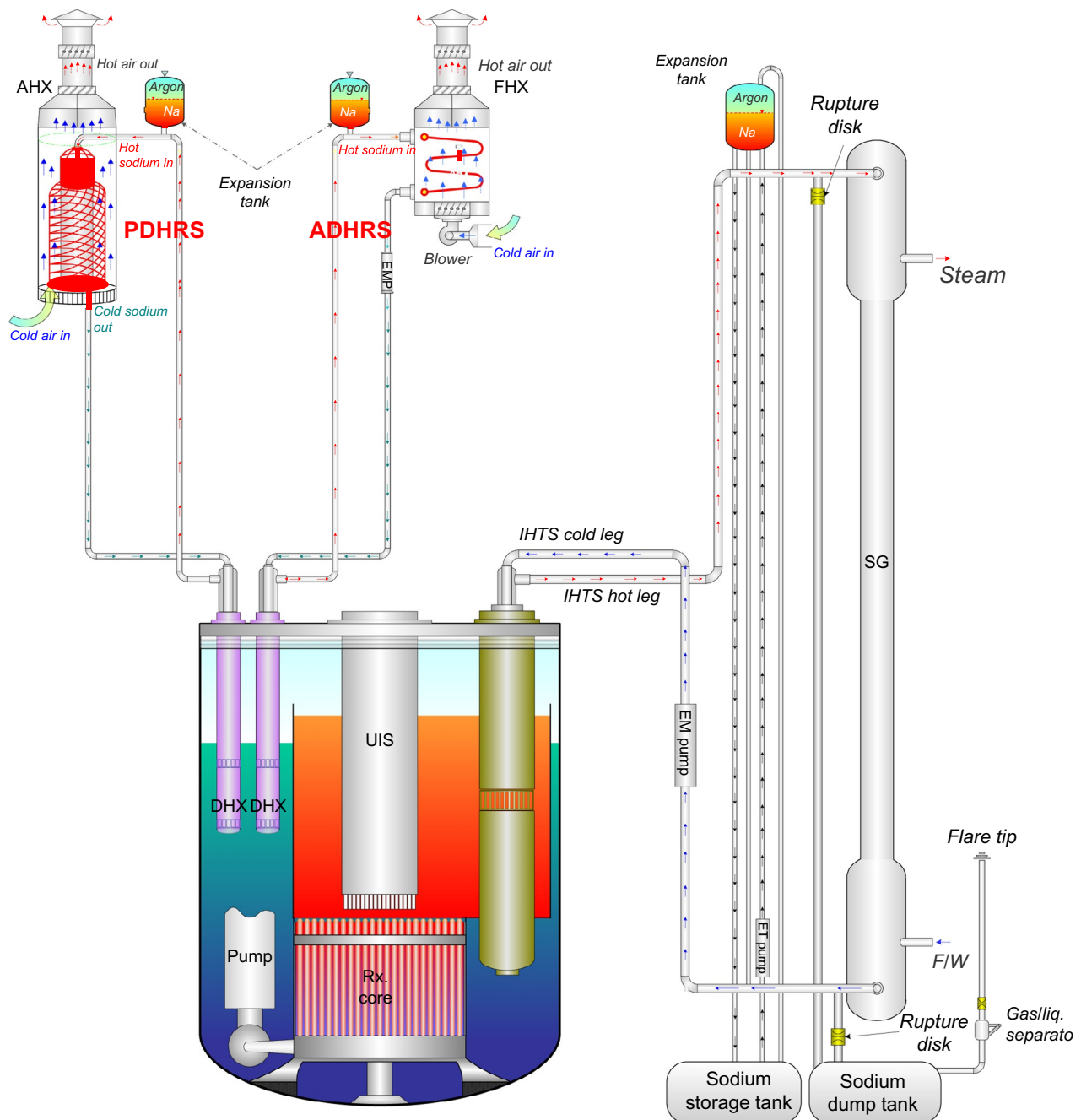


Figure 13.5. Configuration of fluid system

such as heat exchangers and a mechanical sodium pump, and their design code V&V. The second step of an integral effect test loop called STELLA-2 will be constructed to demonstrate the plant safety and support the design approval for the prototype SFR. Starting with the conceptual design of the prototype SFR, the basic and detailed design of the test facility reflecting the prototype design concept will be performed on the basis of the design requirements subject to the prototype reactor. According to the program schedule, the facility was planned to be installed by the end of 2018 and the main experiments including the start-up tests to be commenced in 2019, as shown in Figure 13.7. The STELLA program finally aims at an integral effect test to support specific design approval for the prototype reactor.

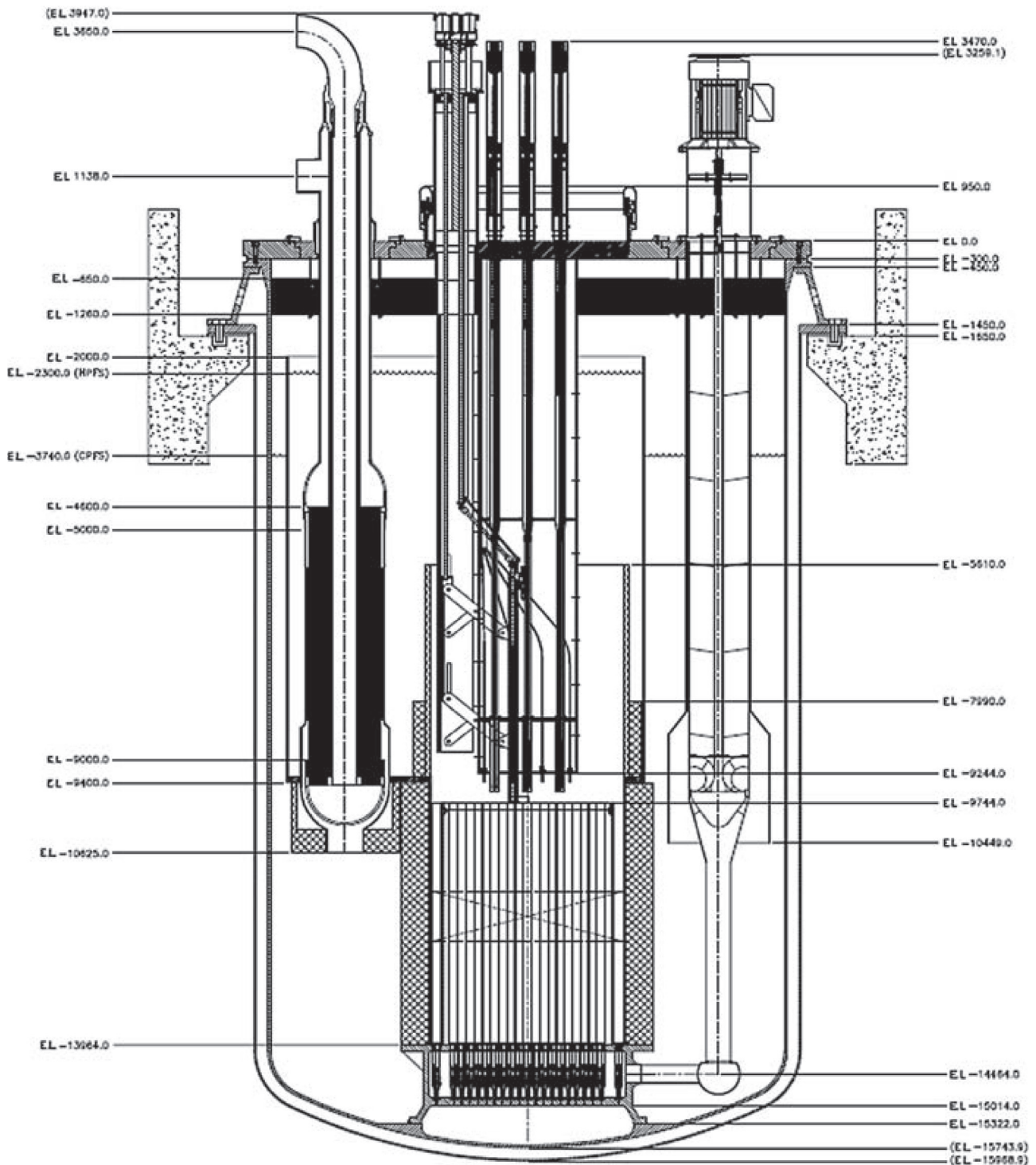


Figure 13.6. PHTS arrangement (front view)

Metal fuel development

Fuel slugs have been fabricated by modified injection casting and particulate fuel in KAERI to prevent the evaporation of volatile elements such as Americium (Am) (Lee et al., 2013). The U-10wt%Zr-5wt%Mn fuel slug containing a volatile surrogate element such as Manganese (Mn) was soundly cast by an improved injection casting method to prevent the evaporation of volatile elements such as Am, where the volatile U alloy is

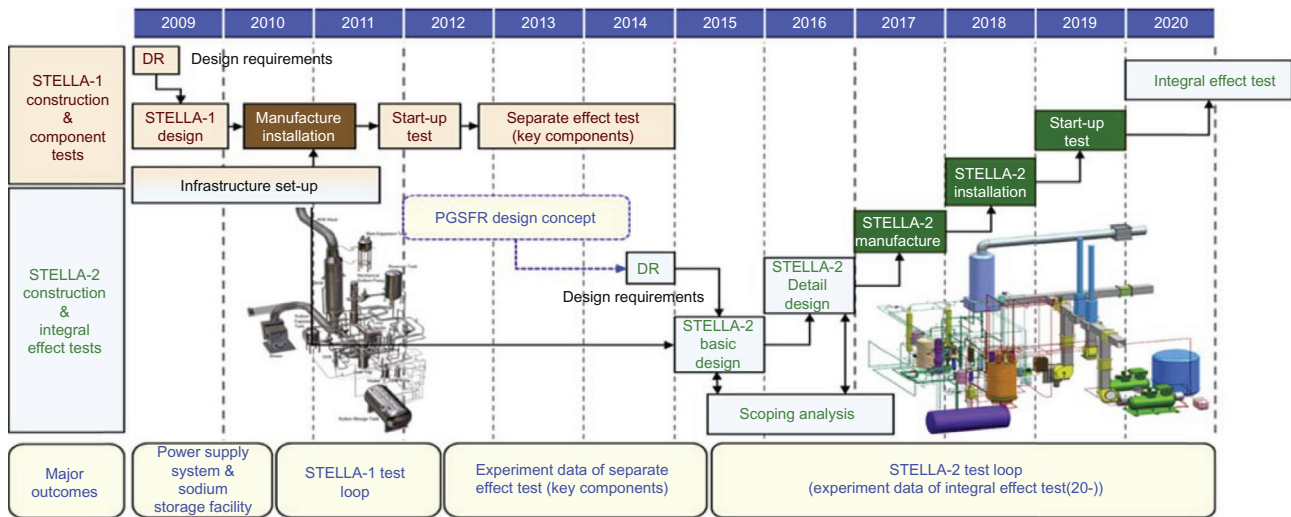


Figure 13.7. Overall schedule of the STELLA program (Eoh et al., 2013)



Figure 13.8. U-10wt%Zr-5wt%Mn fuel slug, fabricated by improved casting method

melted under an inert atmosphere. The general appearance of the slug was smooth, and the diameter and length were 5.4 mm and about 250 mm, respectively, as shown in Figure 13.8. The gamma-ray radiography of the as-cast surrogate slug was performed to detect internal defects such as cracks and pores. The mass fraction of the fuel loss relative to the charge amount after fabrication of U-10wt%Zr-5wt%Mn was low, up to 0.1%. It was seen that the losses of these volatile elements such as Am can be effectively controlled to below the detectable levels using modest argon overpressures.

For particulate fuel fabrication, it is an atomization technology considered as an alternative fabrication method of fuel slugs. Spherical U-10wt%Zr alloy particles were fabricated by centrifugal atomization at about 1500°C. Green compacts of atomized U-10wt%Zr powder were fabricated with quartz compaction dies. The compacts of U-Zr powder were sintered, ranging from 1000°C to 1100°C under a vacuum. The bonding of particles was not active in U-Zr powder pellets, mainly because of their limited interdiffusion at the sintering temperature. In addition, the use of sodium bond in the metal fuel cladding can be eliminated, owing to porous particulate fuel such that the handling of spent fuel containing radioactive sodium can be simplified.

HT9 and FC92 cladding tubes were fabricated in 2013. The ingots were melted by a vacuum induction melting process. The ingots were refined through the electro-slag remelting process. The mother tubes were fabricated by hot forging and hot extrusion. The cladding tubes were fabricated by a pilgering and drawing process. Intermediate heat treatment was carried out after cold working. The intermediate cladding tubes were normalized at 1050°C for 6 min and tempered at 800°C for 8 min. After the final cold working, the cladding tubes were normalized at 1038°C for 6 min and tempered at 760°C for 60 min. The dimensions of cladding tube, as shown in Figure 13.9, were 7.4 mm in outer diameter, 0.5 mm in thickness, and 3000 mm in length. The mechanical tests such as creep, burst, and tensile test have been performed (Kim et al., 2013c), and irradiation tests of the cladding tubes in BOR-60 started in 2014. The irradiation test will be finished in 2019, and the PIE will be done in 2020.



Figure 13.9. FC92 cladding tubes

Reactor physics experiment

To validate the neutronic characteristics of SFRs, KAERI has been collaborating with the Institute for Physics and Power Engineering (IPPE) in Russia. Three critical assemblies were already constructed in BFS-1 and BFS-2 facilities, called as BFS-73-1, -75-1, and -76-1A. The first two critical assemblies represent the early phase of KALIMER-150 core design during the late 1990s. Recently, two more critical experiments, BFS-76-1A and BFS-109-2A, were conducted at IPPE. The BFS-76-1A critical experiment, constructed in 2010, is a mock-up experiment for the TRU burner core, which is characterized by a blanket-free concept, low conversion ratio, high burnup reactivity swing, and the consequent deep insertion of a primary control rod at BOEC. The BFS-109-2A critical experiment, constructed at 2012, is a mock-up experiment for the metallic U-Zr fueled core with various control rod positions. Another mock-up experiment for the initial U core of the prototype SFR, BFS-84-1, is ongoing in 2015. The BFS-84-1 is planned to measure key safety-related reactivity parameters such as sodium void reactivity, fuel axial expansion reactivity, and core radial expansion reactivity.

13.3.2 Very-high-temperature reactor

13.3.2.1 Design and analysis codes

KAERI has been developing computer code systems for graphite-moderated, helium-cooled VHTR. Figure 13.10 shows the overall code system for VHTR licensing developed at KAERI.

KAERI has been developing a two-step neutronics analysis code system for VHTR core design (Jeong et al., 2013), in which the DeCART code (Cho et al., 2013) is used for generation of few-group cross sections together with the equivalent parameters. The CAPP code (Lee et al., 2012a,b) is used for the analysis of core physics parameters of VHTR using the few-group parameters generated by DeCART. The sensitivity and uncertainty analysis code, MUSAD (Han et al., 2015), is being developed for an uncertainty analysis of the few-group parameters generated by DeCART and eventually the uncertainty of the core physics parameters evaluated by the CAPP code. Figure 13.11 shows the two-step neutronics analysis code system for the VHTR developed at KAERI.

The GAMMA+ code (Lim, 2014) has been developed by KAERI for system and safety analysis of VHTR. The code has the capabilities for multidimensional analyses of the fluid flow and heat conduction as well as the chemical reactions related to the air or steam ingress event in a multicomponent mixture system. As a

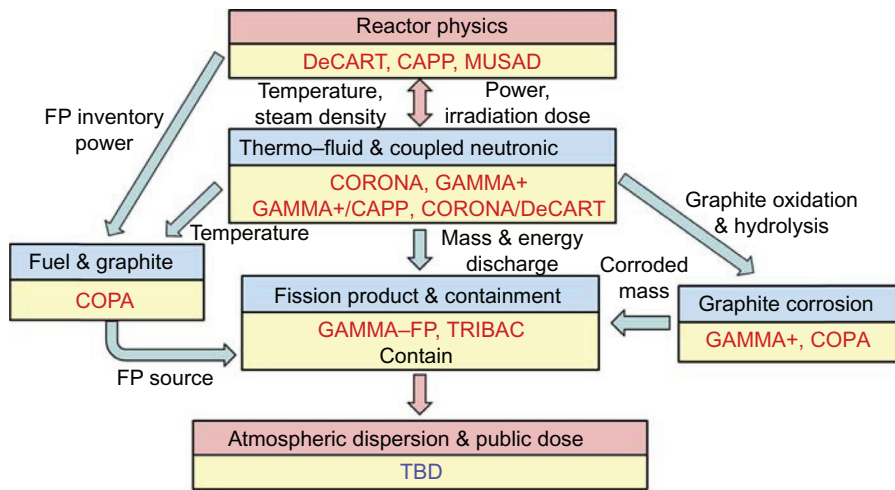


Figure 13.10. Overall code system for VHTR licensing developed at KAERI

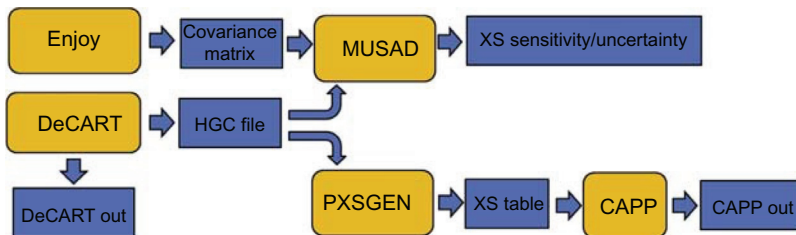


Figure 13.11. KAERI two-step neutronics analysis code system for VHTR

system thermo-fluid and network simulation code, GAMMA+ includes a non-equilibrium porous media model for pebble-bed and prismatic reactor core, thermal radiation model, point reactor kinetics, and special component models such as pump, circulator, gas turbine, valves, and more.

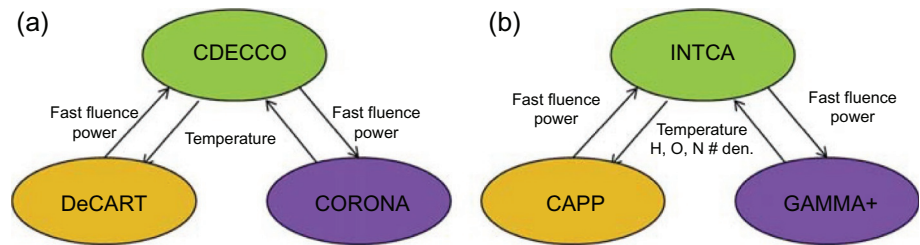
KAERI has been developing the CORONA code (Tak et al., 2014) for a core thermo-fluid analysis of a prismatic VHTR. The CORONA code is targeted for a whole core thermo-fluid analysis of a prismatic VHTR with fast computation and reasonable accuracy. The computational efficiency was achieved by combining the 3-D solid heat conduction with a one-dimensional fluid flow network and adopting a block-wise parallel computation.

For a high fidelity core multiphysics analysis, KAERI has been developing a coupled code system using DeCART and CORONA (Lee et al., 2012a,b). DeCART transfers the power density and the fast neutron fluence to CORONA. On the other hand, CORONA transfers the temperature to DeCART. A separate computer code named CDECCO was developed for communication between DeCART and CORONA. No mapping is required in this coupled code system because the two codes use the same structure of the computational grids.

A neutronics/thermo-fluid coupled analysis code system is being developed by coupling the CAPP code and the GAMMA+ code (Tak et al., 2015). A server program called INTCA is utilized for the coupling of the two codes. The INTCA code not only controls the calculation procedure of the two client codes, but also performs the mapping between the variables of the two codes for coupling. Figure 13.12 shows the neutronics/thermo-fluid coupled analysis code systems developed at KAERI.

KAERI has developed a tritium transport code, TRIBAC (Yoo et al., 2010), for the analysis of tritium behavior in a VHTR system under normal operating conditions. It can calculate the tritium distribution within the reactor system and the leakage of tritium. A fission product transport analysis code, GAMMA-FP (Yoon

Figure 13.12. Neutronics/thermo-fluid coupled analysis code systems: (a) DeCART/CORONA System and (b) CAPP/GAMMA+ System



et al., 2013), has been developed as well for coupled analysis with GAMMA+ code. The GAMMA-FP has the capabilities of transport analyses of gaseous and aerosol FP species during postulated accident transients.

A seismic analysis code is being developed to assure the structural integrity under seismic loads. The multibody dynamic analysis of multicolumned stacks of graphite blocks was implemented in the code (Kang et al., 2011). The procedure for the thermal stress analysis of graphite fuel blocks was established using ABAQUS, a commercial FEM code, with thermal and neutron-induced material property changes of graphite (Kang et al., 2012).

13.3.2.2 TRISO fuel technology

Since 2006, KAERI has made significant progress and the manufacturing process for the TRISO-coated particle fuel has been established at the lab scale. The TRISO fuel R&D activities that have been carried out at KAERI include the development of the kernel fabrication and the TRISO coating technologies, the overcoating, and the compaction technologies of the coated fuel particles using graphite powder.

Figure 13.13 shows a part of the lab-scale equipment for kernel fabrication. KAERI uses gel supported precipitation technology for the fabrication of spherical UO_2 kernels (Brambilla et al., 1970). The process parameters used to make up the broth solution and droplets have been studied extensively. Heating curves for the UO_2 kernel during the calcination and sintering processes were determined in the lab-scale experiments. Figure 13.14 shows the kernel products in successive steps obtained from the kernel fabrication process at KAERI.

KAERI uses the Fluidized Bed Chemical Vapor Deposition (FB-CVD) technology for TRISO coating (Kim et al., 2009a). Figure 13.15 shows the arrangement of the FB-CVD furnace with the gas supply and off-gas system. Continuous coating techniques for SiC TRISO layers have been developed, and the optimization of the coating procedure has been completed at the 20 to 30 g/batch scale. Figure 13.16 shows KAERI's pilot SiC TRISO-coated fuel particle.

R&D for advanced TRISO fuel technologies such as the UCO kernel fabrication and the ZrC coating has been carried out. As for the UCO kernel fabrication, a process for the carbon dissolution was established, and well-shaped discrete ADU liquid droplets were obtained using an external gelation method (Jeong et al., 2007). Currently, a new kiln-type heating furnace has been built for the heat treatment experiment of

Figure 13.13. Kernel fabrication system



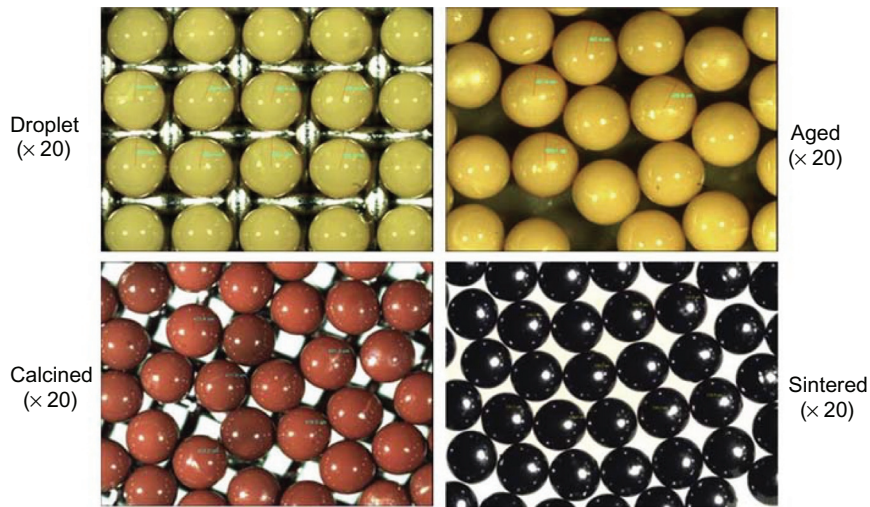


Figure 13.14. Intermediate and final products of kernel fabrication process



Figure 13.15. TRISO coating system



Figure 13.16. KAERI's pilot TRISO fuel particles and a microscopic image

the UCO kernel. KAERI's advanced pilot fuels with UCO kernels and ZrC coating layers will be produced by 2016.

In parallel, KAERI is developing a fuel performance analysis code called COPA, which estimates the thermal and mechanical behavior of a coated fuel particle, a pebble, and a fuel block and the fission product migration through a coated particle and a fuel element as well as the failure fractions of coated particles under irradiation and heating tests (IAEA, 2012). COPA has been improved to treat the behavior of the advanced fuel under irradiation and heating. A consistent calculation system has been built, which can be used to estimate the gas pressure and species in the coated fuel particle under irradiation. A software verification and validation report for COPA will be issued in 2016.

An irradiation test of KAERI's pilot TRISO particle fuel was started on October 5, 2013, and completed on March 31, 2014 (Kim et al., 2014). The average power of the fuel was evaluated to be 610 W, and the average burnup was calculated to be about 37,000 MWd/MTU. Non-destructive PIEs of the test fuel were completed, and the destructive tests are currently being carried out at KAERI's irradiated material examination facility. Simulated heat-up test equipment to perform a simulated heating test in a laboratory is under construction. It is expected to provide fundamental data for the construction of the actual heat-up test equipment for use in a hot cell.

13.3.2.3 High-temperature materials

High-temperature materials are one of the main issues for a demonstration of the VHTR, which needs to maintain the safety at very high temperatures of above 950°C to produce hydrogen with a high efficiency. The main purposes of the VHTR material R&Ds were (1) material screening/selection and qualification; (2) codifications of the relevant high-temperature structural design rules to the very-high-temperature region and to support the licensing of a system design; (3) material characterizations and a database establishment; (4) alloy modifications and developments; and (5) Gen-IV VHTR materials collaborations and contributions. Since 2006, the material R&Ds have been being performed for graphite, alloy 617, modified 9Cr-1Mo steel, and a ceramic composite at KAERI (Park et al., 2008; Kim et al., 2009b).

Experimental data for the mechanical and physical properties of the selected graphite candidates (IG-110, IG-430, NBG-18, and NBG-25) were produced. In addition, the fracture and oxidation behaviors were estimated. To understand the radiation effects in nuclear-grade graphite, an atomistic structural change in IG-110 irradiated with 3 MeV H⁺ and gamma-irradiation effects were characterized (Kim et al., 2009b; Hong et al., 2012; Corwin et al., 2008).

Creep data for alloy 617 and weldment by gas tungsten arc welding were obtained from the creep tests in air and He environments conducted in temperature ranges of 800–950°C, and creep crack growth data have also been produced. Long-term creep tests of alloy 617 weldment were conducting at 850°C for more than 13,000 h. In parallel, a constitutional equation to predict a fatigue life with strain ranges was developed for alloy 617. The creep tests for alloy 800 HT Base Metal (BM) and Weld Metal (WM) are also being conducted in the ranges of 800–900°C. Mechanical properties of modified 9Cr-1Mo steel welded by SMAW were measured. To evaluate the degradation behavior by thermal aging, the weldment of modified 9Cr-1Mo steel was heat-treated, and the impact and tensile test were then performed (Kim et al., 2009b; Hong et al., 2012; Corwin et al., 2008; Carre et al., 2010).

Future projects are considering the use of ceramic composites where radiation doses, environmental challenges, or temperatures (up to or beyond 1000°C) will exceed the capabilities of the metallic materials (Corwin et al., 2008). However, widespread property data, standardization of the characterization methods and the development of design codes of ceramic composites are required for in-core structural components. The baseline thermal and mechanical properties of some nuclear-grade C/C composites were measured. The oxidation behaviors of composites in air and He with controlled minor impurities and irradiation effects using Si ions were also evaluated (Kim et al., 2009b; Hong et al., 2012; Corwin et al., 2008; Carre et al., 2010).

KAERI has contributed to all working groups of Gen-IV VHTR material collaboration: graphite, metal and design method, and ceramic and composite. By the end of 2014, 37 technical reports have been uploaded into the Gen-IV materials handbook. In addition, creep test records (45 data) of alloy 617 and tensile test results for the BM, WM, and weld joint of alloy 617 (32 ea) were uploaded into the Gen-IV materials handbook ([Generation IV International Forum annual report, 2013](#)).

13.3.2.4 Hydrogen production

Development of the SI cycle has been pursued by several countries within the framework of the GIF for hydrogen production with the next generation of nuclear reactors. Due to its higher temperature requirements in comparison with other thermochemical cycles, the SI cycle is particularly well matched with the VHTR.

A Korean research network consisting of KAERI, KIER, and KIST is developing an integrated 50 NL·H₂/h scale demonstration of the SI cycle through the GIF collaboration.

Past studies have focused on not only the process evaluation using a commercial computer code, but also the screening test of the component structural materials. Experiments to develop the catalysts for sulfur trioxide and hydrogen iodide decompositions were carried out successfully, and their manufacturing technologies were established. The experimental feasibility test of a 3.5 NL·H₂/h-scale SI test facility under atmospheric operation conditions has been performed in early 2008. As a result, we secured the continuous operation hydrogen production data for 6h.

Few studies have examined the integration of reactions and interaction between processes. Individual unit operations have been developed, built, and tested in combination with the subsequent intermediate processes.

The computer code, KAERI–Dynamic Simulation Code (KAERI–DySCo), was developed to analyze the dynamic behavior of the VHTReSI process coupling system. KAERI–DySCo was also verified using the code-to-code benchmark calculation through the international GIF collaboration, and steady state values calculated by the commercial computer code “ASPEN.” [Figure 13.17](#) shows the main window of the KAERI–DySCo simulation code.

In addition, the KAERI-DySCo simulation code has been used for the dynamic startup simulations of a sulfuric acid distillation column, H₂O₂ distillation column, and its thermal decomposers, which are the main

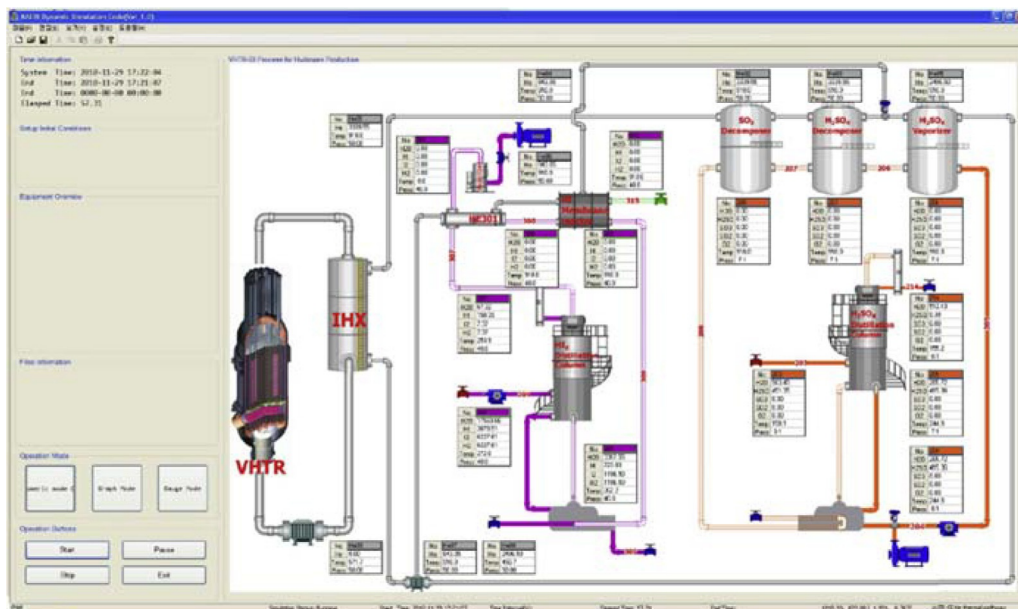


Figure 13.17. The KAERI-DySCo code main window



Figure 13.18. 50 NL·H₂/h-scale SI test facilities

components of an SI integrated test facility with a hydrogen production rate of 50 NL·H₂/h. Figure 13.18 shows 50NL·H₂/h-scale SI test facilities built at KIER, which is under modification for improvements in its operational efficiency.

Recent advances in the thermochemical SI cycle have been reported (Bae et al., 2015; Jung et al., 2015; Lee et al., 2014). An integrated operation test of more than 8 h was successfully conducted to demonstrate the promising potential of the pressurized operation for hydrogen production in 2014.

Further research is underway to reconfirm the hydrogen productivity of the 50 NL·H₂/h SI test facilities for an extended operation time. On the other hand, the domestic research partners, KIER and KIST, are also investigating the scale-up technologies of SI process components to obtain the equipment design information. The goal is to establish an engineering database to design a pilot scale SI process coupled to the secondary helium loop of the VHTR.

13.3.3 Lead fast reactor

The Republic of Korea (ROK) nuclear power program has been rapidly developing since the 1970s. Spent nuclear fuel management has been one of major obstacles in maintaining the public support for the Korean nuclear power program. Therefore, the minimization of high-level waste has been the principal goal of Lead Fast Reactor (LFR) and related R&D in ROK. LFR R&D in ROK has been led by the Seoul National University (SNU), Seoul, since the 1990s, as shown in Figure 13.19. The program has been consisted of LFR design, partitioning, and experimental benchmark and software development for design and safety analysis without discontinuity during the past two decades.

In 1996, LFR R&D was begun in ROK by a small group of researchers at SNU with the goal of developing a fast neutron based waste transmutation system, designated as PEACER with the financial support of then the Ministry of Science and Technology (Hwang et al., 2000). Medium-size transmutation reactors with electric power rating of 550 and 300 MW_{el}, respectively, were designed with loop-type system cooled by Lead–Bismuth Eutectic (LBE). An integral closed fuel cycle was conceptualized with collocated pyrochemical partitioning and fuel recycling facilities. TRU transmutation rates of PEACER were estimated to be 2.0 for TRansUranic elements (TRU) and about 6 for Tc-99 and I-129. For proliferation resistance, an international control of the PEACER Park was proposed, as depicted in Figure 13.20.

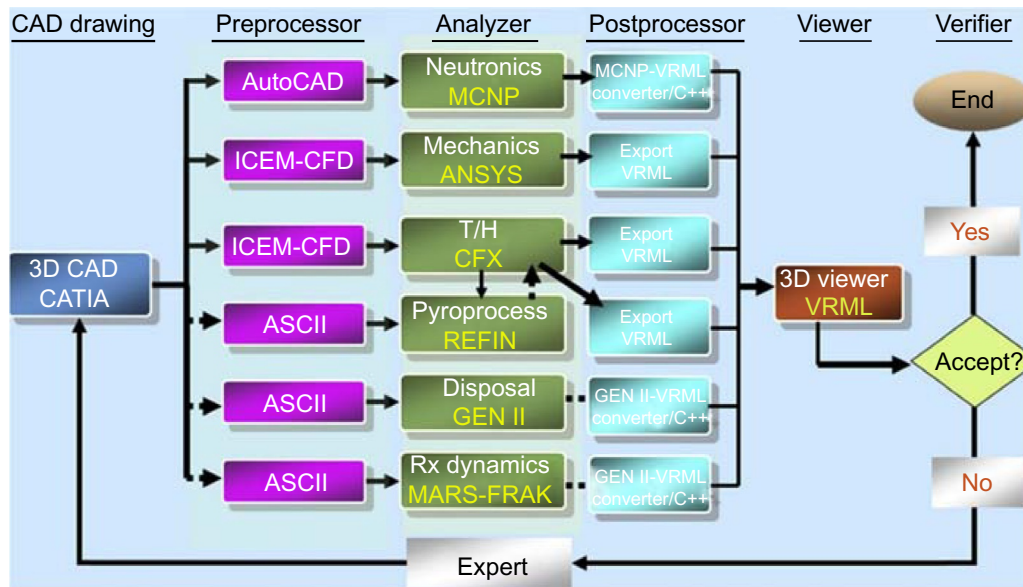


Figure 13.21. LFR design code system of SNU-NUTRECK

that later became Handbook on LBE and Lead from OECD/NEA, as summarized in Figure 13.21. Materials R&D was made to determine optimal concentrations of oxygen in LBE coolant, by using Yttria-Stabilized Zirconia (YSZ)-based membranes. Reliable oxygen sensors were developed by using metal ceramic joining technology for YSZ-tube and Type 316 stainless steel with Bi/Bi₂O₃ reference.

SNU's first international collaboration project on LFR R&D was conducted under I-NERI program for developing the conceptual design of Encapsulated Nuclear Heat Source (ENHS) (Greenspan, 2003). The ENHS design of full natural circulation of LBE was then selected as Gen-IV LFR reference design. The natural circulation concept was further developed at SNU-NUTRECK as a pool-type small modular transmutation reactor, designated as PASCAR, in order to meet objectives for cradle-to-grave approach of Global Nuclear Energy Partnership (Choi et al., 2011). SNU also has collaborated with Los Alamos National Laboratory on corrosion testing of materials in LBE.

In 2005, a large-scale LBE test loop, HELIOS, has been commissioned at SNUNUTRECK. HELIOS is a thermal-hydraulic scale-down facility for PEACER-300, with the thermal power ratio of 5000:1 and the height ratio of 1:1, as shown in Figure 13.22. HELIOS was world's tallest LBE test loop at the time with 12m height, containing 2 Mt of LBE. The elevation difference between the heat exchanger and the mock-up core region is about 8m, providing the same driving force for natural circulation of PEACER-300. The OECD/NEA thermal-hydraulic benchmark program, designated as Lead Alloy Cooled Advanced Energy Systems, is carried out on the isothermal forced circulation and non-isothermal natural circulation with the experimental database produced using HELIOS. OECD/NEA technical report was published from the forced circulation study where the final summary is under the progress for the natural circulation. The natural circulation capability required for normal operation as well as safety of PASCAR was demonstrated by long-term HELIOS tests (Cho et al., 2011; OECD/NEA, 2012).

In 2008, the design of a pool-type transportable small modular reactor, designated as URANUS, using enriched UO₂ fuels with a 20-year-life, has been developed for underground deployment with a 3-D seismic isolation system and the reactor vessel air cooling system, as shown in Figure 13.23. The safety of the URANUS design in various accident scenarios was verified by a system analysis code, MARS-LBE (KAERI, 2004). 3-D seismic isolation was shown to increase the safe shutdown earthquake acceleration drastically. Corrosion mechanisms of stainless steels have been investigated by testing in LBE and subsequent examinations to find that Chromium (Cr)-iron (Fe) oxide spinel layers grow with appreciable

Accident-tolerant natural circulation design



Parameter	Value
Core	60 kW
Power	Electric (4EA)
Height	~12 m
LBE	2 ton
LBE natural flow rate	~4 kg/s
LBE natural flow speed	~30 cm/s
Maximum DT	100°C
Temperature range	200–500°C
Secondary	Oil (dowtherm RP)

*HELIOS data are used in OECD-NEA benchmark (LACANES)

Figure 13.22. Integral LBE test loop HELIOS and its design features

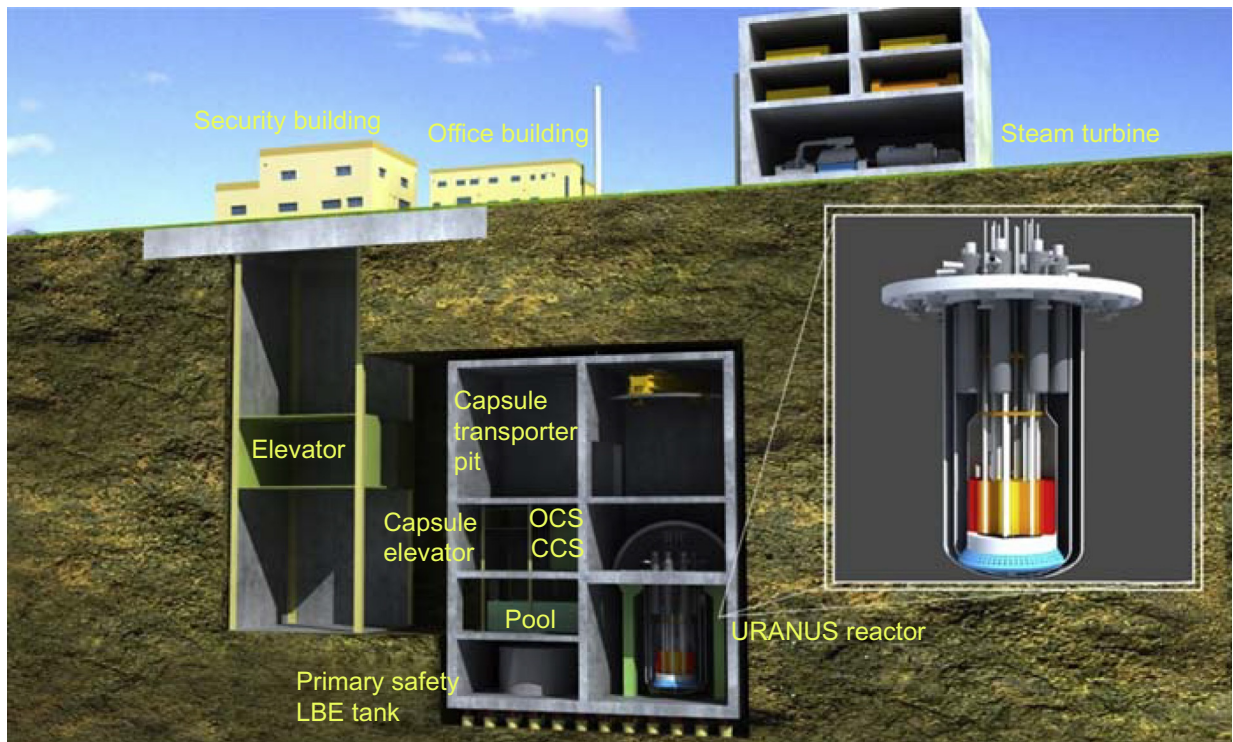


Figure 13.23. Concept of URANUS deployed underground for security enhancement

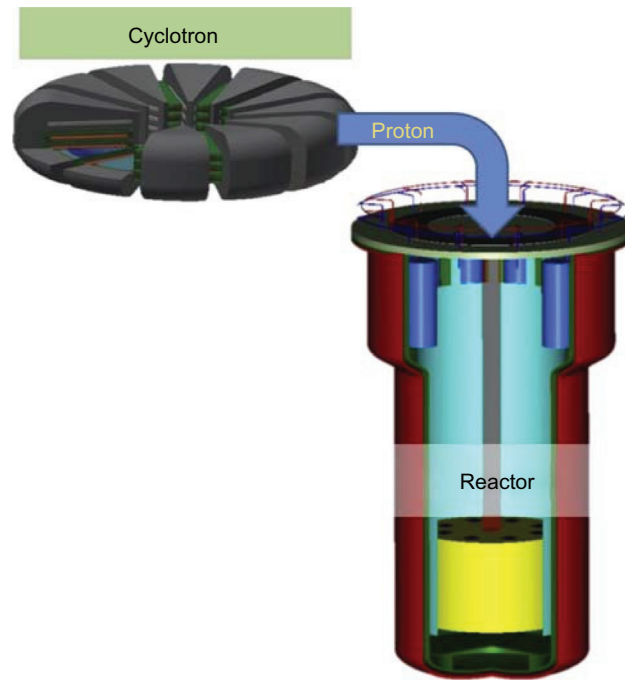


Figure 13.24. Concept of thorium-based accelerator driven system, TORIA

leaching of Cr, resulting in a Cr-depleted region near metal oxide interfaces. Aluminum (Al) or Silicon (Si) can greatly enhance the oxide passivity and retard leaching of metal substrate. Development of corrosion-resistant materials led to a new series of Al-containing ferritic stainless steels, which display innovative corrosion resistance in LBE, opening the way to explore the 20-year-long life core for URANUS. In order to further enhance the cost-competitiveness of URANUS, the load follow capability is fully embedded in control system designs so that its early units can enter peak-load market and can operate in symbiosis with renewable energy sources (Shin et al., 2015).

A thorium-based Accelerator Driven System (ADS) for TRU transmutation has been conceptually designed, as shown in Figure 13.24. The development of pyrochemical partitioning technology for the transmutation technology R&D at SNU-NUTRECK has been aimed at the decontamination of all final waste streams into low-level waste and intermediate-level waste so that the geological repositories after several hundred years can be adequately safe, secure, and proliferation-resistant. The goal has been shown to be viable by a new flow sheet designated as PyroGreen (Jung et al., 2012). In parallel, KAERI has been developing pyrochemical partitioning technology designed for collocated sodium fast reactors, with the goal of 99.9% recovery of TRU. The high-level waste stream can be decontaminated by PyroGreen to yield TRU-rich fuels that can be burnt by thorium-based ADS, designated as TORIA. In its conceptual design, compact proton cyclotrons with moderate energy and beam current is coupled to LBE-cooled target in TORIA that will burn all residual TRUs from entire Korea nuclear power fleet with economic viability.

Currently, LFR R&D in ROK is focused on the further development of computer codes and corrosion-resistant materials as well as the safety design criteria. System design codes for URANUS have been focused on neutronic models and safety analysis codes. It is planned that the developed codes will be verified by independent experts. Thermomechanical processing of corrosion-resistant materials developed for long-life core will be explored to achieve desirable combination of proven mechanical properties in fast neutron environment and innovative corrosion resistance. The ROK LFR R&D community has been participating in the GIF LFR provisional Systems Steering Committee as an observer. It is planned that the safety design criteria for URANUS will be derived from the international collaboration.

13.3.4 Molten Salt Reactor (MSR)

The beginning of Molten Salt Reactor (MSR) research in Korea dates back to 1998. A basic concept of an MSR that burns the DUPIC fuel was first developed in Ajou University. More studies on MSR, including a recent fluoride-salt-cooled high-temperature reactor, are under progress in UNIST (Ulsan National Institute of Science and Technology) and other institutes. Described below is a summary of the progress so far and future research plans of the MSR research in Korea.

Ajou University developed AMBIDEXTER-NEC (Advanced Molten-salt Breakeven Inherently-safe Dual-function EXcellenTly-Ecological Reactor Nuclear Energy Complex). The objective of the reactor is to burn DUPIC fuel, minimize minor actinides production, and of course, generate electric power. To achieve the objectives, the AMBIDEXTER reactor core consists of two parts, a blanket and a seed. The blanket consists of only molten salt fuel ($\text{LiF-BeF}_2\text{-(Th,U,Pu)F}_4$), and the seed consists of the molten salt fuel and graphite moderator channel. The blanket area has very hard neutron spectrum, almost looks like fast reactor neutron spectrum, and the seed area has a soft neutron spectrum almost looks like PWR. Therefore, AMBIDEXTER can achieve low conversion ratio, about 0.298, i.e., it is a burner reactor. The code developed to analyze AMBIDEXTER is called AMBIKIN2D. The code system consists of HELIOS, AMDEC, and AMBIKIN2D.

In the area of neutronic analysis of the MSR core, UNIST is developing a code system for reactor core neutronic analysis of the MSBR, which was designed by Oak Ridge National Laboratory in the 1970s. To obtain equilibrium composition of MSR, three kinds of the equilibrium composition search methods are investigated by the nuclear reactor core analysis computer code system, which is based on MCNP6 Monte-Carlo code. The 680-cm diameter by 610-cm-high reactor vessel contains molten salt core and graphite material for neutron moderation and reflection. The fuel zone is divided into two zones of different fuel to graphite ratios. The Zone-1 has low fuel-to-graphite ratio, and most of fission reaction occurs; the Zone 2 has high fuel-to-graphite ratio, and most of breeding occurs. The first method uses the representative single unit cell for both zones. Single unit cell is set by volume-wise fuel and moderator weighting. The second method uses the representative unit cells for each zone, which are set by maintaining fuel-to-moderator ratio for each zone. The third one models directly the MSR whole core. The code system was set up with the MCNP6 Monte-Carlo code, its depletion module CINDER90, and the Python script language. The Python script is required for implementing the batch-wise reprocessing and refueling. The MSBR continuously adds fertile material and removes fission products and actinides. The core removes all volatile gases and noble metals every 20 s and separates ^{233}Pa from molten salt fuel every 3 days, allowing it to decay to ^{233}U . Other fission products have specific removal rates. After 3 days, depletion calculation is performed, and new inputs are created by using reprocessed materials. If the material compositions reach an equilibrium state, the equilibrium compositions of each method could be found. Twelve thousand days, 9000 days, and 7000 days are required to reach equilibrium states by using the single-cell model, two-cell model, and whole core model through depletion calculation. In the process of calculating the equilibrium fuel compositions, various parameters like multiplication factor, breeding ratio, and number density can be obtained to analyze the MSBR. The MSBR whole core analysis is performed at the initial and equilibrium core conditions for various reactor design parameters such as normalized neutron flux distribution, temperature coefficients, rod worth, and power distributions. The neutronics core characteristics were analyzed using a four-factor formula applied to the single-cell model, two-cell model, and the two zones of the whole core separately. UNIST has a plan to improve the code system to achieve higher accuracy and shorter calculation time and to design a new conceptual MSR core using the developed code system.

In the molten salt chemistry area, we are setting up a long-term experiment system to conduct the corrosion tests of structural materials under high-temperature molten salt environment, and this system will be used to measure redox potential in associated test conditions. Several techniques have been adopted to obtain fundamental properties such as chronoamperometry, cyclic voltammetry, AC impedance method, and laser

spectroscopy. We have also conducted a 3-D multiphysics computational analysis using parallel computing technique for multistep electrochemical processes in molten salt environment. In addition, it is required to investigate a way to safely store discharged solid spent fuel with extremely high burnup and to environmentally friendly dispose of the spent fuel. Regarding this issue, we will first investigate thermal, material, and radiological characteristics of spent nuclear fuel.

The salt used in an MSR is very noxious material, and its operating temperature is very high (710–560°C). So, simulant material, like heat transfer oils, is used at relatively low temperature in the preliminary study for safety. The interesting similarity has been found and reported first by University of California Berkeley (UC Berkeley) (Bickel et al., 2014). Thus, for understanding of high Prandtl number molten salt as a heat transfer medium, a fundamental molten salt study has been performed using similarity technology with the simulant oils, which have a lower working temperature range. Based on UC Berkeley's previous works, using scaling law, a research will be performed with simulant oil at reduced scale with different characteristics of natural circulation condition. Also, two rectangular MSR test loops were designed for the similarity experiment with scale-down parameters. They will be used to verify the heat transfer ability of working fluid in coolant loop. Preliminary experiment for low power was conducted preferentially. Additionally, for both liquid and vapor phases, thermophysical properties of simulant oils, which are candidates of simulant, were generated and implemented into thermal–hydraulic code, which helps investigation of thermal behavior analysis with experimental data. Ultimately, our main purpose is the development of dimensionless heat transfer correlation of high Prandtl number molten salt through similarity technology application with scaled experiments and simulation of thermal–hydraulic code. Furthermore, the outcomes of the follow-up study will be used for the benchmark in terms of collaborations with UC Berkeley.

Appendix: Paper list related to PEACER (including P-demo and Pyroprocess), PASCAR, URANUS, and other SNU-NUTRECK activities

Year accepted/ submitted	No.	First author	Journal/conference	Title
2000	001	Il Soon Hwang	Progress in Nuclear Energy	The concept of Proliferation-resistant, Environment-friendly, Accident-tolerant, Continual and Economical Reactor (PEACER)
2005	002	Seung Ho Jeong	ICAPP 2005	Overview and status of HELIOS
	003	Seung Hee Chang	Global 2005	Development of LBE loop (HELIOS) for advanced materials studies
	004	Judong Bae	Global 2005	Development of an electrochemical–hydrodynamic model for electrorefining process
	005	Hyong Won Lee	ICAPP 2005	Solver-interfaced virtual reality approach for life-cycle management of nuclear energy systems

Continued

—cont'd

Year accepted/ submitted	No.	First author	Journal/conference	Title
2006	006	Won Chang Nam	Nuclear Engineering and Design	Fuel design study and optimization for PEACER development
2007	007	Jae-Yong Lim	Progress in Nuclear Energy	A new LFR design concept for effective TRU transmutation
	008	Jungmin Kang	Progress in Nuclear Energy	Proliferation resistance of PEACER system
	009	Sung Il Kim	Progress in Nuclear Energy	Requirement of decontamination factor for near-surface disposal of PEACER wastes
	010	Jun Lim	ANS 2007	Corrosion experiments in large-scale LBE loop: HELIOS
2008	011	Jun Lim	ICAPP 2007	Progresses in the operation of Large scale LBE loop: HELIOS
	012	Il Soon Hwang	HLMC 2008	Passive safety characteristics of demo version of PEACER
	013	Il Soon Hwang	KNS 2008	PASCAR-DEMO – a small Modular reactor for PEACER demonstration
	014	Il Soon Hwang	ICAPP 2008	Development of transportable capsule version of PEACER design
	015	Il Soon Hwang	Actinide and fission product Partitioning and transmutation	Development of PASCAR (Proliferation- resistant, Accident-tolerant, Self- sustainable, Capsular, Assured Reactor) design and safety analysis
	016	Jun Lim	HLMC-2008	Corrosion behaviors of commercial FeCrAl alloys in liquid lead–bismuth eutectic environments
	017	Jun Lim	ICAPP 2008	Corrosion test of Cr- and Al- containing alloys in static LBE at 550 °C
2009	018	Sungyeol Choi	Global 2009	P-DEMO for demonstration of PEACER concept
	019	Jun Lim	Journal of Nuclear Materials	Corrosion behaviors of FeCrAl alloys in liquid lead–bismuth eutectic environments
	020	Kwang Rak Kim	Global 2009	Computational multiphysics analysis of a molten-salt electrolytic process for a nuclear waste treatment
	021	Hyo on nam	Global 2009	All the spent nuclear wastes to low and intermediate level wastes: PyroGreen

Continued

—cont'd

Year accepted/ submitted	No.	First author	Journal/conference	Title
2010	022	Jun Lim	Journal of Nuclear Materials	A Study of early corrosion behaviors of FeCrAl alloys in liquid lead–bismuth eutectic environments
2011	023	Sungyeol Choi	Nuclear Engineering and Design	PASCAR: Long burning small modular reactor based on natural circulation
	024	Sungyeol Choi	ASME 2011 SMR Symposium	URANUS: Korean lead-bismuth cooled small modular fast reactor activities
2012	025	V. Shankar Rao	Annals of Nuclear Energy	Analysis of 316L stainless steel pipe of lead–bismuth eutectic cooled thermo-hydraulic loop
	026	V. Shankar Rao	Corrosion Science	Characterization of oxide scales grown on 216L stainless steels in liquid lead–bismuth eutectic
2013	027	Jun Lim	Journal of Nuclear Materials	Design of alumina forming FeCrAl steels for lead or lead–bismuth cooled fast reactors
	028	Jae Hyun Cho	HLMC-2013	Design optimization of small modular reactors with natural circulation of lead–bismuth coolant
	029	Seung Gi Lee	HLMC-2013	Corrosion of T91, HT9, and stainless steel 316L in static cell of liquid lead–bismuth eutectic at 600 °C
2014	030	Jae Hyun Cho	ICONE22	Power maximization of fully passive lead–bismuth eutectic cooled small modular reactor
2015	031	Yong-Hoon Shin	Progress in Nuclear Energy	Advanced passive design of small modular reactor cooled by heavy liquid metal natural circulation
	032	Jae Hyun Cho	Nuclear Engineering and Design	Power maximization method for land-transportable fully passive lead–bismuth cooled small modular reactor systems

References

- Bae, K.-K., et al., 2015. Development of Key Technologies for Nuclear Hydrogen/Development of SI Hydrogen Production Process. Report # 2012M2A8A2025688. Korea Institute of Energy Research.
- Bickel, J.E., et al., 2014. Design, Fabrication and Startup Testing in the Compact Integral Effects Test (CIET 1.0) Facility in Support of Fluoride-Salt-Cooled, High-temperature Reactor Technology. University of California, Berkeley.

- Brambilla, G., et al., 1970. The SNAM process for the production of ceramic nuclear fuel microspheres. In: Symposium on Sol-Gel Processes and Reactor Fuel Cycles. Gatlinburg, Tennessee, May 4–7, pp. 191–209.
- Carre, F., et al., 2010. Update of the French R&D strategy on gas-cooled reactors. Nucl. Eng. Des. 240, 2401–2408.
- Chang, J., et al., 2007. A study of a nuclear hydrogen production demonstration plant. Nucl. Eng. Technol. 39 (2), 111–122.
- Cho, J.H., et al., 2011. Benchmarking of thermal hydraulic loop models for lead-alloy cooled advanced nuclear energy system (LACANES), phase-I: isothermal steady state forced convection. J. Nucl. Mater. 415 (3), 404–414.
- Cho, J.Y., et al., 2013. DeCART2D User's Manual. KAERI/TR-5116/2013. KAERI.
- Choi, S., et al., 2011. PASCAR: long burning small modular reactor based on natural circulation. Nucl. Eng. Des. 241 (5), 1486–1499.
- Eoh, J.H., et al., 2013. Design features of a large-scale sodium thermal-hydraulic test facility: STELLA. In: Internal Conference on Fast Reactors and Related Fuel Cycles (FR13), Paris, France.
- Generation IV, 2013. International Forum Annual Report 2013. OECD/NEA for the Generation IV International Forum.
- Greenspan, E., The ENHS Project Team, 2003. STAR: The Secure Transportable Autonomous Reactor System Encapsulated Fission Heat Source (the ENHS Reactor) Final Report, NERI Program Grant Number DE-FG03-99SF21889. Department of Nuclear Engineering, University of California.
- Hahn, D., et al., 2002. KALIMER Conceptual Design Report. KAERI/TR-2204/2002. Korea Atomic Energy Research Institute, Daejeon, Korea.
- Hahn, D., et al., 2007. KALIMER-600 Conceptual Design Report. KAERI/TR-3381/2007. Korea Atomic Energy Research Institute, Daejeon, Korea.
- Han, T.Y., et al., 2015. Verification of a sensitivity and uncertainty analysis code based on GPT using MHTGR-350 benchmark. In: Proceedings of ICAPP 2015, France, May 3–6.
- Hong, S.D., et al., 2012. Development of Essential Technology for VHTR. KAERI/RR-3425/2011.
- Hwang, I.S., et al., 2000. The concept of proliferation-resistant, environment-friendly, accident-tolerant, continual and economical reactor (PEACER). Prog. Nucl. Energy 37 (1–4), 217–222.
- IAEA, 2012. Advances in High Temperature Gas Cooled Reactor Fuel Technology. IAEA-TECDOC-1674. IAEA.
- Jeong, K.C., et al., 2007. ADU compound particle preparation for HTGR nuclear fuel in Korea. J. Ind. Eng. Chem. 13, 744–750.
- Jeong, C.J., et al., 2013. Preliminary verification calculation of DeCART/CAPP system by HTTR core analysis. In: Transactions of Korean Nuclear Soc. Autumn Meeting, Gyeongju, Korea, October 24–25.
- Jung, H.S., et al., 2012. Environmental assessment of advanced partitioning, transmutation, and disposal based on long-term risk-informed regulation: PyroGreen. Prog. Nucl. Energy 58, 27–38.
- Jung, K.-D., et al., 2015. Development of Key Technologies for Nuclear Hydrogen/Sulfuric Acid Decomposition Process for SI Cycle. Report # xxxxx. Korea Institute of Science and Technology.
- KAERI, 2004. MARS Code Manual Volume I – Code Structure, System Models, and Solution Methods. KAERI/TR-2812/2004, Daejeon, Korea.
- Kang, J.-H., et al., 2011. Development of core seismic analysis model of VHTR. In: Transactions of the Korean Nuclear Society Autumn Meeting, Gyeongju, Korea, October 26–28.
- Kang, J.-H., et al., 2012. Thermo-mechanical analysis of the prismatic fuel assembly of VHTR in normal operational condition. Ann. Nucl. Energy 44 (5), 76–86.
- Kim, W.J., et al., 2009a. Effect of coating temperature on properties of the SiC layer in TRISO-coated particles. J. Nucl. Mater. 392, 213–218.
- Kim, Y.W., et al., 2009b. Development of Essential Technology for VHTR. KAERI/RR-2992/2008.
- Kim, Y.I., et al., 2013a. Status of SFR development in Korea. In: Internal Conference on Fast Reactors and Related Fuel Cycles (FR13). Paris, France.
- Kim, Y.I., et al., 2013b. Conceptual Design Report of SFR Prototype Reactor of 150MW_{e1} Capacity. KAERI/TR-4978/2013. Korea Atomic Energy Research Institute, Daejeon, Korea.
- Kim, S.H., et al., 2013c. Fabrication and evaluation of SFR cladding tubes. In: International Conference on Fast Reactors and Related Fuel Cycles (FR13), Paris, France.
- Kim, B.G., et al., 2014. Irradiation testing of TRISO-coated particle fuel in Korea. In: Proceedings of the HTR 2014, Weihai, China, October 27–31.
- Lee, H.C., et al., 2012a. Development of HELIOS/CAPP Code System for the Analysis of Block Type VHTR Cores. PHYSOR 2012, Knoxville, Tennessee, USA. (April 15–20).
- Lee, H.C., et al., 2012b. Advanced Multi-Physics Simulation Capability for Very High Temperature Reactor. KAERI/RR-3295/2010. KAERI.
- Lee, C.B., et al., 2013. Status of SFR metal fuel development. In: International Conference on Fast Reactors and Related Fuel Cycles (FR13), Paris, France.

- Lee, Y.-W., et al., 2014. Microstructural modification and porosity evolution during carbonization of fuel element compact for HTGR. *Nucl. Eng. Des.* 271, 244–249.
- Lim, H.S., December 2014. General Analyzer for Multi-component and Multi-dimensional Transient Application (GAMMA +1.0) volume II: Theory Manual. KAERI/TR-5728/2014.
- OECD/NEA, The LACANES Taskforce, 2012. Benchmarking of Thermal-Hydraulic Loop Models for Lead-Alloy Cooled Advanced Nuclear Energy Systems – Phase I: Isothermal Forced Convection Case, 17. NEA/NSC/WPFC/DOC., p. 2012.
- Park, J.Y., et al., 2008. Development of materials for a high temperature gas cooled reactor in Korea. In: *Proceedings of HTR2008*, HTR 2008e58149, September 28–October 1, Washington DC, USA.
- Shin, Y.H., et al., 2015. Advanced passive design of small modular reactor cooled by heavy liquid metal natural circulation. *Prog. Nucl. Energy* 83, 433–442.
- Tak, N.I., et al., 2014. Development of a core thermo-fluid analysis code for prismatic gas cooled reactors. *Nucl. Eng. Technol.* 46 (5), 641–654.
- Tak, N.I., et al., 2015. Steady-state core temperature prediction based on GAMMA+/CAPP coupling. In: *Transactions of the Korean Nuclear Society Spring Meeting*, Jeju, Korea, May 7-8.
- Yoo, J.S., Tak, N.I., Lim, H.S., 2010. Development of Tritium Behavior Analysis Code for Very High Temperature Gas-Cooled Reactor. KAERI/TR-4096/2010.
- Yoon, C., Yoo, J.S., Lim, H.S., 2013. Preliminary Theory Manual for GAMMA-fp (Fission Product Module of the Transient Gas Multicomponent Mixture Analysis). KAERI/TR-4933/2013. KAERI.

Further reading

- Corwin, W.R., ORNL, et al., 2008. Generation IV Reactors Integrated Materials Technology Program Plan: Focus on Very High Temperature Reactor Materials. ORNL/TM-2008/129.
- Lee, K.-Y., et al., 2015. Development of Key Technologies for Nuclear Hydrogen/Development of Interface Technology for Nuclear Hydrogen Production System. KAERI/RR-3923/2014. Korea Atomic Energy Research Institute.

Generation-IV concepts: China

Dalin Zhang

Xi'an Jiaotong University, Xi'an, People's Republic of China

Nomenclature

Abbreviations and acronyms

863 Program	National High Technology Research and Development Program of China
973 Program	National Key Basic Research Program of China
ACC	ACCumulators
ADS	Accelerator-Driven Subcritical system/Automatic Depressurization System
ASME	American Society of Mechanical Engineers
BCC	Body Center Cubic
CAP	China Advance Pressurized water reactor
CAS	Chinese Academy of Sciences
CCFR-B	China Commercial Fast Reactor-Breeding
CCFR-T	China Commercial Fast Reactor-Transmutation
CDFR	China Demonstration Fast Reactor
CEDM	Control Element Drive Motor
CEFR	Chinese Experimental Fast Reactor
CHNG	China HuaNeng Group
CIAE	Chinese Institute of Atomic Energy
CLEAR	China LEad-Alloy-cooled Reactor
CLEAR-0	A zero-power fast spectrum experimental facility
CLEAR-I	10-MW _{th} lead-bismuth cooled research reactor
CLEAR-II	100-MW _{th} lead-alloy-cooled experimental reactor
CLEAR-III	1000-MW _{th} lead-alloy-cooled demonstration reactor
CNEC	China Nuclear Engineering and Construction
CRDM	Control Rod Drive Mechanism
CSR1000	1000-MW _{el} Chinese SCWR
DBA	Design Basis Accident
DHX	Decay Heat eXchanger
DPA	Displacement Per Atom
FA	Fuel Assembly
FCC	Face Center Cubic
FCD	First Concrete Date
FHR	Fluoride-salt-cooled High-temperature Reactor
FMS	Free-Machining Steel
FREDO-CSR1000	FREquency DOrain analysis of CSR1000
FSAC	FHR Safety Analysis Code

FuSTAR	Fluoride-Salt-cooled high-Temperature Advanced Reactor
GDCS	Gravity Driven Cooling Systems
HDPV	Hot gas Duct Pressure Vessel
HTGR	High-Temperature Gas-cooled Reactor
HTR	High-Temperature Reactor
HTR-10	10-MW _{th} prototype pebble-bed High-Temperature Reactor of China
HTR-PM	High-Temperature Reactor Pebble-bed Modular
IAEA	International Atomic Energy Agency
ICS	Isolation Cooling Systems
IHX	Intermediate Heat eXchanger
INET	Institute of Nuclear Energy Technology
LBE	Lead-Bismuth Eutectic
LESMOR	LEad Small MODular Reactor
LFR	Lead-cooled Fast Reactor
LOCA	Loss Of Coolant Accident
LOOP	Loss Of Offsite Power
MAs	Minor Actinides
MAC	Multiple-channel Analysis Code
MCNP	Monte Carlo code for Neutron and Photon transport
MLD	Master Logic Diagram
MOSART	MOLten Salt Actinide Recycler and Transmuter
MOX	Mixed OXide
MSR	Molten Salt Reactor
MSRE	Molten Salt Reactor Experiment
NPIC	Nuclear Power Institute of China
NPP	Nuclear Power Plant
NSFC	Natural Science Foundation of China
ORNL	Oak Ridge National Laboratory
OTTO	Once-Through-Then-Out
PB-FHR	Pebble-Bed FHR
PRHR	Passive Residual Heat Removal
PyC	Pyrolytic Carbon
R&D	Research and Development
RFQ	Radio Frequency Quadrupole
RVACS	Reactor Vessel Air Cooling System
SA	SubAssembly
SBO-ATWS	Station BlackOut Anticipated Transient Without Scram
SCALE	Standardized Computer Analyses for Licensing Evaluation
SCO₂	Supercritical Carbon dioxide
SCWR	Super Critical Water-cooled Reactor
SCWR-M	Mixed spectrum SCWR
SFR	Sodium-cooled Fast Reactor
SG	Steam Generator
SGPV	Steam Generator Pressure Vessel
SINAP	Shanghai Institute of Applied Physics
SJTU	Shanghai JiaoTong University
SLCS	Standby Liquid Control System
TIMDO-CSR1000	TIMe DOrain analysis of CSR1000
TMSR	Thorium Molten Salt Reactor
TMSR-LF	Liquid-Fueled TMSR
TMSR-SF	Solid-Fuel TMSR
TRISO	TRI-ISOtropic

TRU	TRansUranic element
UCB	University of California-Berkeley
ULOF	Unprotected Loss Of Flow
ULOHS	Unprotected Loss Of Heat Sink
UOC	Unprotected OverCooling accident
UTOP	Unprotected Transient OverPower
VHTR	Very-High-Temperature gas-cooled Reactor
WNA	World Nuclear Association
XJTU	Xi'an JiaoTong University

14.1 Current status of nuclear power in China

The development of nuclear power in China has occurred in three stages as shown in Figure 14.1. The first stage was the starting stage represented by the Qinshan and Daya Bay Nuclear Power Plants (NPPs) and their building and operation. With the economic development of China, and the encouraging policy issued, such as “energy technology revolution and innovation action plan (2016–2030),” the construction of nuclear power entered the stage of accelerated development. Before 2008, the government had planned to increase nuclear generating capacity to 40 GW_{el} by 2020, with a further 18 GW_{el} of nuclear capacity being under construction. Furthermore, projections for nuclear power then increased to 70–80 GW_{el} by 2020, 200 GW_{el} by 2030, and 400–500 GW_{el} by 2050. However, after the Fukushima Daiichi NPP severe accident and consequent pause in approvals of new plants, the target adopted by the China State Council in October 2012 became 58 GW_{el} by 2020, with 30 GW_{el} under construction (WNA, 2005). National policy has moved from “moderate development” of nuclear power to “positive development” in 2004 and in 2012 to “steady development with safety.”

As of June 2021, China (mainland) has 51 nuclear power reactors in operation, which contribute 4.89% of the total electricity production according to the International Atomic Energy Agency (IAEA). Thirteen reactors are under construction; this is 25% of all reactors under construction in the world. Additional reactors are also planned, including some of the world’s most advanced reactors, to provide more than a 3-fold increase in nuclear capacity. More than 20 NPPs are about to be approved and start construction. After the Fukushima accident, the impetus for increasing the nuclear power share in China is still increasing, mainly due to four primary reasons: (1) strong energy demand for the fast growth of the domestic economy, (2) air pollution from coal-fired power plants, (3) acute fluctuation of the regular energy price creating risk for investors, and (4) increasingly intensified constraints from other energy environments and resources. The Chinese government began to learn lessons from the Fukushima accident, and nuclear safety receives more attention for the development of nuclear power. In the third stage, the advanced reactors will be developed using

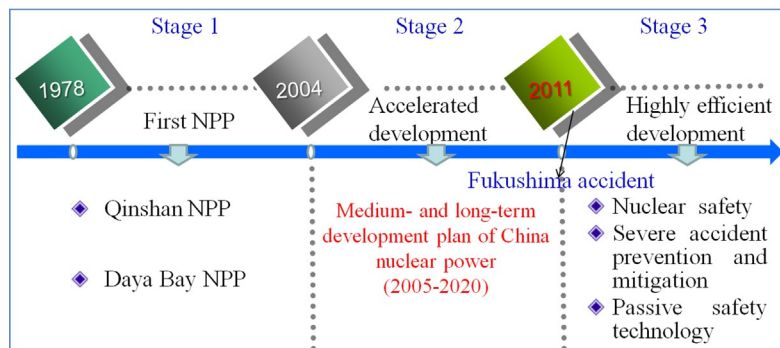


Figure 14.1. Three stages of China nuclear power development

evolutionary technologies, such as passive-safety technologies, and severe accident preventions and mitigations to ensure nuclear-power safety. Therefore, China is becoming largely self-sufficient in reactor design and construction, as well as other aspects of the fuel cycle, by not only making full use of Western mature technologies, but also adapting and improving them. On the basis of this, China would like to go global with exporting nuclear technologies, including heavy components in the supply chain.

14.2 Plans for advanced nuclear reactors in China

China sponsors a series of programs to research, develop, and demonstrate advanced reactors, including both the Generation-III reactors for commercial purposes and Generation-IV reactors for nuclear sustainable development. A white paper on energy policy released by the State Council in October 2012 pointed out that China will invest more in nuclear-power technological innovations, promoting application of advanced technology, improving the equipment level, and attaching great importance to personnel training. In addition, the State Council published the Energy Development Strategy Action Plan 2014–2020 in November 2014, which aims to cut China's reliance on coal and promote the use of clean energy, confirming the 2012 target of 58 GW_e nuclear in 2020 with an additional 30 GW_e under construction. The plan calls for the “timely launch” of new nuclear-power projects on the east coast and for feasibility studies for the construction of inland plants. It also says that efforts should be focused on promoting the use of large Pressurized Water Reactors (PWRs) (including the CAP1400 and Huanlong-I designs), High-Temperature Reactors (HTRs), and fast reactors. From this plan, it is seen that advanced PWRs will be the mainstream in Chinese nuclear-power development, but they are not the sole reactor type.

Two Generation-IV reactor concepts, HTR and Sodium-cooled Fast Reactor (SFR), are considered the most promising reactors for sustainable nuclear development in China. In February of 2006, the State Council announced that the small HTR was the second of two high-priority National Major Science and Technology projects for the next 15 years; this aims at exploring co-generation options in the near term and producing hydrogen in the long term. The small HTR Pebble-bed Modular (HTR-PM) is now under construction at Shidaowan, Shandong province. On the basis of the successful operation of the China Experimental Fast Reactor (CEFR), the design and relative research of the demonstrative China Fast Reactor 600 (CFR-600) are now intensively performed, and it has been under construction at Xiapu, Fujian province since 2017.

In addition to HTR and SFR, the other Generation-IV concepts are also supported by different government agencies. The SuperCritical Water-cooled Reactor (SCWR) was supported under the National Key Basic Research Program of China (973 project) by the China Ministry of Science. The studies of Molten Salt Reactors (MSRs) and Lead-cooled Fast reactors (LFRs) are performed in the framework of the Chinese Academy of Sciences (CAS) pilot projects. In the following section, the current Research and Development (R&D) on Generation-IV reactors in China will be briefly introduced.

14.3 Current research and development on Generation-IV reactors in China

14.3.1 SFR research and development

SFR development in China can be generally divided into two main phases by CEFR construction, which can be divided into four subphases: (1) basic technology research phase (before 1986), (2) application technology research phase (1987–1993), (3) engineering application research phase (1994–2010), and (4) large-scale commercial SFR R&D phase (2010–2030). In the following section, China SFR R&D will be introduced in two parts: (1) research before CEFR construction and (2) China SFR development strategy.

14.3.1.1 Research before CEFR construction

In the late 1960s, China began SFR research activities. The initial studies focused on neutronics, thermal-hydraulics, sodium technology, material, sodium equipment and instruments, and small sodium facilities. Later on, approximately 12 experimental setups and one sodium loop were constructed, among which a 50-kg ^{235}U zero-power neutron setup reached criticality in June 1970 (Rouault et al., 2010).

In 1986, SFR-technology development was involved in the first National High Technology Research and Development Program (863 Program) of China, which started the application technology research stage aiming at the construction of the 65-MW_{th} (20 MW_{el}) CEFR. Institutes, universities, and companies such as the China Institute of Atomic Energy (CIAE), Xi'an JiaoTong University (XJTU), etc. were organized to work on the reactor design, fuel and materials, sodium technology, and safety research. Until 1993, there were in total more than 20 experimental setups and sodium loops in China. The experimental validation phase focused on sodium-loop technology. Two sodium loops were imported from Italy and one sodium loop was established at XJTU. The conceptual design of CEFR was completed in 1997, and in order to validate CEFR design, a zero-power simulation experiment was carried out in cooperation with Russia.

14.3.1.2 China SFR development strategy

The SFR development strategy in China involves three steps: the CEFR with a power of 20 MW_{el}, the China Demonstration Fast Reactor (CDFR) with a power larger than 600 MW_{el}, and the post-CDFR commercial breeding or transmutation reactor with a power of 1000 MW_{el} (Xu, 2009).

CEFR

China's first fast reactor CEFR was constructed by CIAE in cooperation with the Beijing Institute of Nuclear Engineering. During the design of CEFR, approximately 50 tests for design verifications were conducted to confirm the performance and obtain the operation experiences.

The CEFR site excavation was started in October 1998, and it achieved criticality for the first time in July 2011. On July 21 of 2011, the reactor was successfully connected to the grid. CEFR is an experimental SFR with a power of 65 MW_{th}, and the designed fuel is PuO₂-UO₂. In the first loading, UO₂ was used as the fuel with cladding, and the reactor-block structure material was made of Cr-Ni austenitic stainless steel. The reactor is a pool type with two main pumps, and there are two loops in the intermediate circuit. The superheated steam in the two loops in the third circuit (water-steam) combined together before entering the turbine.

As shown in Figure 14.2, the core of CEFR is composed of 81 fuel assemblies, three safety assemblies, three compensation assemblies, and two regulation assemblies (Xu, 2008). There are 336 steel shielding assemblies, 230 boron fuel assemblies, and 56 spent fuel assemblies primary storage locations. Each fuel

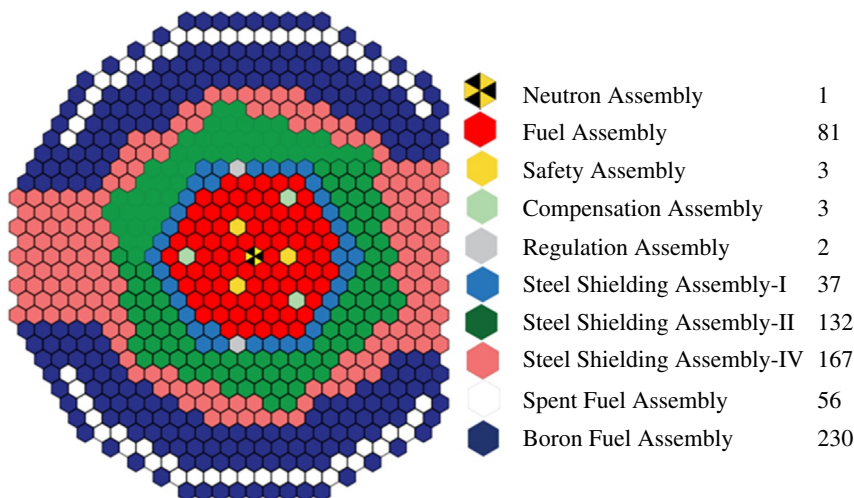


Figure 14.2. CEFR core layout. Reproduced from Xu (2008)

assembly has 61 triangular arranged rods, which are located in a radial direction with a wire wrap. Hexagonal tubes are used to connect with the assembly operating head at the top and the assembly pin at the bottom. The pins are inserted into the pressure header, which has upper and lower grids. On the one hand, the header can locate the core axially, and on the other hand, it can guide the primary sodium into the core.

The control and safety assemblies have the same structure, and the reactor is controlled or shut down by their movement in the tubes. There are two separate reactor shutdown systems, both of which can quickly shut down the reactor. The compensation and regulation assemblies form the first shutdown system, whereas the safety assemblies form the other shutdown system.

The CEFR block is shown in Figure 14.3 (Xu, 2008). It is mainly composed of a reactor cover, a sodium pool, and internal structures. The reactor cover is an approximately 2-m-thick steel-concrete structure that acts as the reactor upper shielding and provides support for the plug, main pumps, Intermediate Heat eXchangers (IHXs), Decay Heat eXchangers (DHXs), and the circuits and pipes of various auxiliary systems. The driving mechanisms of control and safety, the fuel manipulator, and various measurement instruments are all fixed on the small plugs of the plug system.

The sodium pools are mainly composed of a main vessel and guard vessel, with a temperature and pressure measurement instrument on the wall and a sodium-leak detector in the gap of the vessels. The main vessel acting as the boundary of the primary circuit is a very important item of safety equipment. The internal structures involve the inner pool used to separate the hot and cold pools, the reactor core and its pressure header, and supports and shieldings.

The primary circuit of the CEFR in the sodium pool has two primary sodium pumps, which drives the 360°C cold sodium from the cold pool into the core and cools it. The average core-outlet temperature can be as high as 530°C. Via the hot pool, the hot sodium flows into four IHXs, where the heat is transferred to the intermediate circuit through the tube wall of the IHX. The intermediate circuit has two loops, and each has an intermediate pump, a Steam Generator (SG) composed of an evaporator and a super heater, and two IHXs connected to the primary circuit. In the third water-steam system, the 480°C superheated steam at 14 MPa

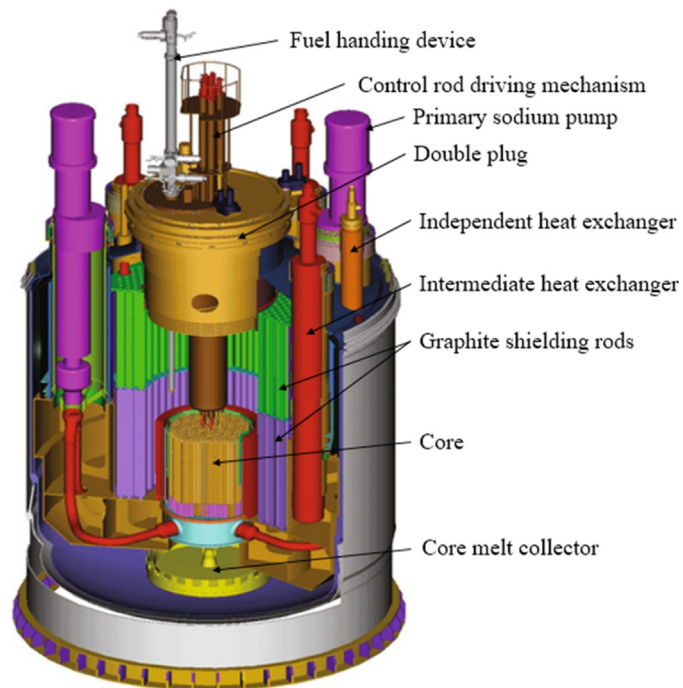


Figure 14.3. CEFR block. *Reproduced from Xu (2008)*

from two SGs is guided into the turbine to generate electricity, and condensed water returns to the evaporator through the high-pressure heater and deaerator. The heat from the condensers is transferred to the atmosphere by cooling water. The heat transport system is shown in Figure 14.4 (Xu, 2008).

The decay heat removal system also consists of two separate loops, and each has an independent heat exchanger, an air heat exchanger, and pipes (Xu, 1995). Totally relying on natural convection and natural circulation, the residual heat under accidental conditions is removed.

CDFR

CDFR is a pool-type SFR with a preliminary designed thermal power of 2100 MW and an electrical power of 800 MW (Yang et al., 2007). Mixed OXide (MOX) is used as the fuel, and sodium is the main coolant. The reactor is a three-loop, three-circuit design, and there is only one set of steam turbine generators. In 2017, the demonstrative China Fast Reactor 600 (CFR-600) was started to be constructed in Xiapu, Fujian province, under the cooperation of the China National Nuclear Corporation (CNNC), the Fujian Investment and Development Group, and the Xiapu state-owned assets investment management company with the investigation ratio of 51:40:9. Figure 14.5 shows the preliminary core layout of CFR-600 (Yue, 2016).

The heat-transport flowchart of CDFR is shown in Figure 14.6 (Wang, 2021). The main heat-transport system includes three circuits. The primary circuit is pool-type and consists of three loops, each of which has a primary pump and two IHXs. These components together with the pipes of the primary circuit, grid header, core, and sodium pool constitute the primary sodium-circulation system. The intermediate circuit also comprises three loops, and each loop has an intermediate pump, a SG group composed of 10 modules (each module has an evaporator and a superheater), a sodium-buffer tank, two IHXs located in the main vessel, a sodium distributor, and connection pipes. The water-steam circuit is composed of three parallel SG groups and a turbine generator. Each of the SG group receives water from a water pump, and generated superheated steam from the SG groups is collected in the main steam pipe to supply the turbine.

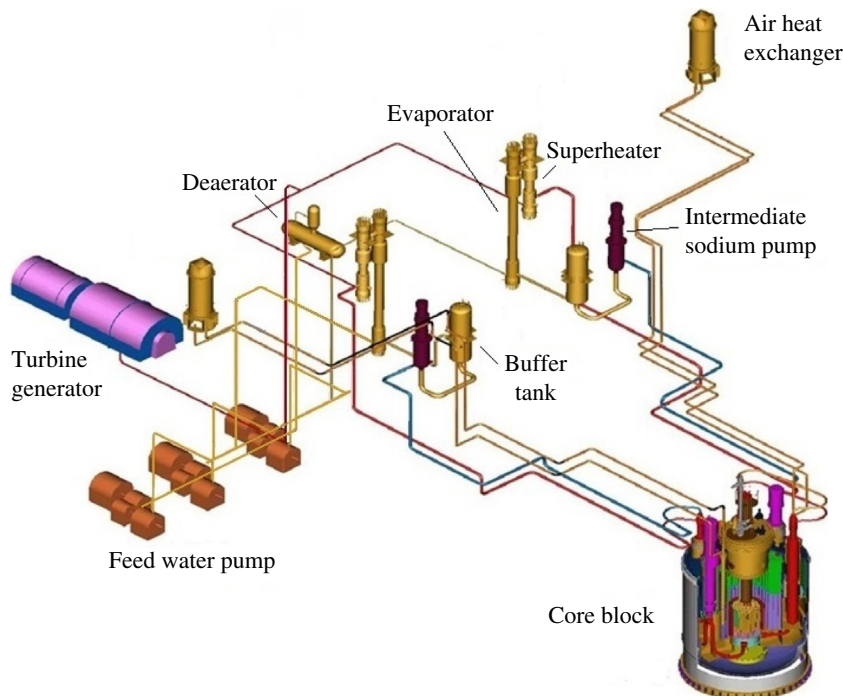


Figure 14.4. The heat-transport system of CEFR. Reproduced from Xu (2008)

Figure 14.5. Core layout of the CDFR.
 Reproduced from Yue (2016)

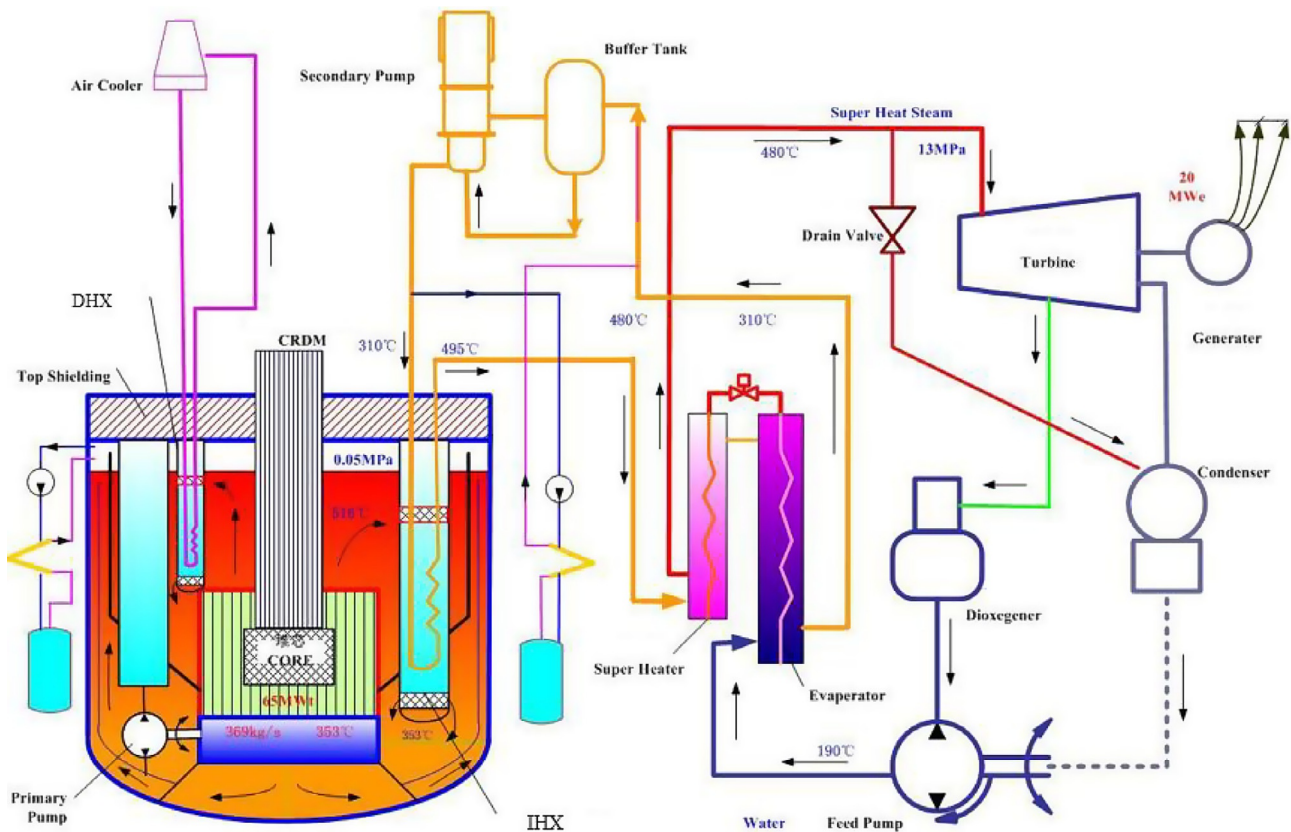
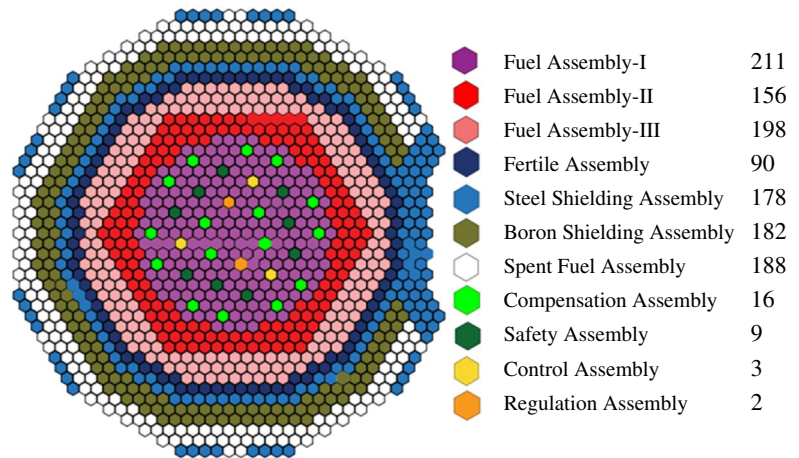


Figure 14.6. The heat transport flowchart of the CDFR. Reproduced from Wang (2021)

The main technical features of the CDFR are proposed as follows (Yang et al., 2007):

1. The primary circuit operates under atmospheric pressure.
2. The primary circuit is a pool-type, and the reactor vessel has a large heat-storage capacity, which guarantees that operators have sufficient time to analyze accident conditions and take necessary mitigation steps under relevant transition and accident conditions.
3. The core-temperature design has a large boiling margin.

4. Fluid floating passive-shut-down system is used as an emergency shutdown method, which should ensure that the reactor can shut down before exceeding the core-temperature limit and a 200°C margin to boiling (883°C).
5. The heat can be removed from the main transport system and the special air-cooling system connected with three loops of the intermediate circuit. The air-cooling system can ensure that the residual heat is removed by natural circulation under station-blackout accident.
6. A special core-melting collecting unit is designed to prevent corium from contacting with the reactor-vessel bottom under beyond-design accident of core collapse.
7. The core top shield is used as an additional barrier for radiation.
8. Passive liquid-seal device is used to prevent the reactor vessel from overpressure.
9. The passive siphon-destruction device is used to prevent excessive loss of sodium, when the primary-circuit auxiliary system leaks.
10. The radioactive inclusive system composed of a sealing workshop and several radioactive inclusive cells is designed to guarantee the radiation emission under the national nuclear-safety limit.
11. Performability is improved with the use of digital instruments and control-system design and simplification of the main control room and instrument-detection system.

Post-CDFR

After CDFR, there are two possibilities (Xu, 2009). CDFR can be deployed in a manner of a modular, one-site multireactor breeding nuclear reactor, called the China Commercial Fast Reactor-Breeding mode (CCFR-B), which will increase the nuclear-power capacity in China. The other one is that if the experience with Minor Actinide (MA) isolation techniques and transmutation of MAs and long-lived fission products in a fast reactor is enough, whereas the automatic depressurization system technology is not mature, CDFR can be deployed in a manner of a one-site multireactor transmutation nuclear reactor, called the China Commercial Fast Reactor-Transmutation mode (CCFR-T). Thus, the first strategy for China SFR development is to build the CDFR and deploy it in a manner of a one-site multireactor, such as five to six commercial fast reactors with a power of 800–900 MW_{el} by approximately 2030. The second strategy is to increase the nuclear-power capacity to 240 GW_{el} by approximately 2050 by developing the high-breeding fast reactors. The third strategy is to replace much fossil fuel with nuclear power in 2050–2100 to drastically reduce the carbon-dioxide emissions.

14.3.2 Very-high-temperature reactor research and development

In China, the Very-High-Temperature Reactor (VHTR) concept has another name, the High-Temperature Gas-cooled Reactor (HTGR), which has been developed since the 1970s. On the basis of the intensive research, a 10-MW_{th} prototype pebble-bed HTR (HTR-10) has been built at Tsinghua University, and a demonstration HTR-PM is under construction.

14.3.2.1 Early development of the HTGR program in China

In China, the research and development program for HTGR began in the mid-1970s, when the target for constructing a 100-MW_{th} thorium thermal breeder was set. The conceptual design of a pebble-bed HTGR with a core blanket of two zones was proposed and accomplished. This conceptual design was characterized with (1) the compactness due to high specific power, (2) a high breeding ratio (almost approaching unity in such a small reactor), and (3) operating ability (inherently stable, online refueling property, etc.).

During the China sixth 5-year plan (1981–1985), the State Science and Technology Committee financially supported the research for the basic technology of HTGR. The main goal was to complete the design of a HTR Module (HTR-Module); research its safety features; and develop computer codes for reactor physics, thermo-hydraulics, and safety analyses. The conceptual designs of HTR-Module-334, an HTR-Module with

a thermal power of 334 MW and fuel multipass mode, as well as HTR-OTTO-200, an HTR-Module with 200 MW of thermal output and a Once-Through-Then-Out (OTTO) mode, were completed (Zhong and Gao, 1985).

In 1986, China 863 Program was launched and the HTGR research and development program was involved in the energy field of this 863 Program. From 1986 to 1990, eight research topics for fundamental technologies were defined and put in place (Zhao et al., 2001). These eight topics were as follows:

1. A conceptual design and development of computer codes for reactor physics, thermo-hydraulics, and the safety analyses;
2. Development of fuel-element manufacturing;
3. The reprocessing of the thorium-uranium fuel cycle;
4. The ceramic reactor design together with a stress analysis;
5. Development of the helium technology;
6. Design of pressure vessels;
7. Development of a fuel-handling system; and
8. Development of materials.

In addition, many experimental facilities were set up and the theoretical calculations for the HTR-OTTO-200 were completed. The intention was to begin building a real HTGR reactor after accomplishing the eight research topics mentioned here.

14.3.2.2 HTR-10 test module project

The Institute of Nuclear Energy Technology (INET) of Tsinghua University performed the conceptual design of the 10-MW_{th} HTGR test module (HTR-10) in 1990 (Steinwarz and Xu, 1990), and 2 years later the construction of HTR-10 was approved by the State Council. Supported by the China 863 Program, the construction of the HTR-10 was commenced in 1995. It reached first criticality in December of 2000 and full-power operation in January of 2003.

The design, construction, and operation of the HTR-10 were important steps toward the commercialization of the modular HTGR in China, which may indeed influence HTGR future development.

Conceptual design and objectives of HTR-10

Figure 14.7 shows the schematic diagram of the HTR-10 system. During the conceptual design of the HTR-10, the following critical issues were particularly considered (Sun and Xu, 2000):

1. A pebble-bed reactor was chosen rather than a block reactor, which has been researched for almost 20 years.
2. The 10 MW of thermal power would be suitable for both the initial investment, supported by the 863 Program, and the transition from the HTR-10 to a prototype HTR-Module.
3. To smooth the transition from the HTR-10 to the prototype HTR-Module without performing repetitive research work in the future, the HTR-10 should fundamentally represent the basic features used in the HTR-Module (e.g., the multiloading mode, control rods at the reflector sides, confinement, etc.).
4. The HTR-10 was adopted to generate electricity, although its power rate might be limited. The advantages of using HTR-10 to generate electricity were to save operating costs and to present a “real power plant” instead of an experimental reactor. The HTR-10 operation success would be crucial in obtaining approval from the Chinese government for the HTR-Module construction to meet the future energy needs of China.
5. During the HTGR conceptual design, its applications and safety-related experiments were taken into account. These applications and safety-related issues included the investigation of the possibility of nuclear processing-heat applications and a test of the mass fuel elements at the temperature of 1600°C.

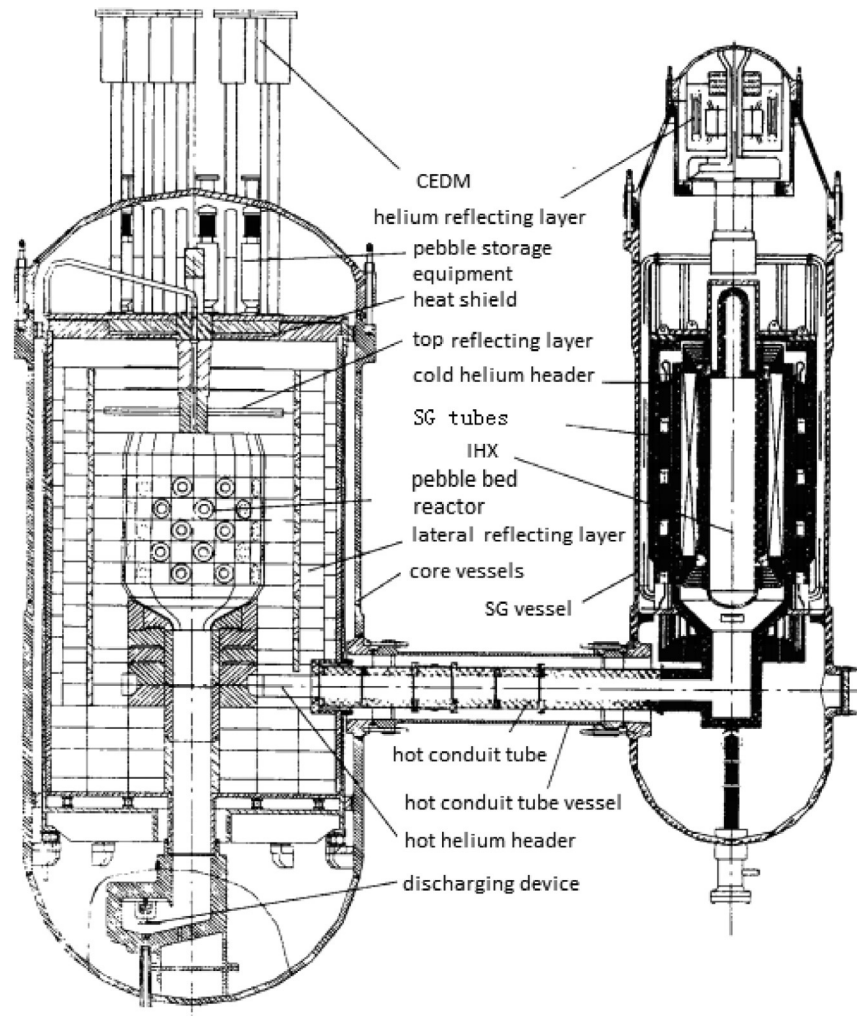


Figure 14.7. Schematic diagram of the HTR-10 system

HTR-10 engineering experiments

During the HTR-10 operation, a series of engineering experiments for the test and development of the eight HTR-10 key technologies was performed on HTR-10 in INET (Xu et al., 1997). Those engineering experiments included the following:

1. The performance test of the hot-gas duct;
2. The measurement test of the temperature-mixture degree at the core bottom;
3. The two-phase-flow instability test for the once-through SG;
4. The performance test for the pebble-fuel handling system;
5. The performance test of the control-rod driving mechanism;
6. The validation and verification tests for the full-digital reactor-protection systems;
7. The measurement test of the neutron-absorption cross section in the reflector graphite; and
8. The performance test for the helium circulator.

The main objective of these engineering experiments was to validate the design characteristics and performance of the reactor components and systems and to obtain information on the design and operating experiences of the HTR-10.

Experiences learned by constructing HTR-10

Much knowledge and experience were obtained from the HTR-10 design, construction, and operation. These knowledge and experience can well guide the design of the large prototype plants, such as the HTR-Module. Most importantly, the advantages of the HTR-Module became much clearer as a result of the HTR-10 construction. It is more obvious that the HTR-Module is inherently safe and capable of achieving economic competitiveness. The primary experiences learned from the HTR-10 construction are summarized as follows:

1. It is possible to build the HTR-Module in a short period. Approximately 5 years were spent in the construction of the HTR-10 from the First Concrete Date (FCD) to achieving criticality. The construction period could be shortened for the HTR-Module in the future. Design delays considerably lengthened the HTR-10 construction period. In fact, the installation of all reactor components and systems only needed approximately 1 year, and the civil-engineering work also required only approximately 1 year. In addition, it is also possible to complete the installation of reactor components and systems in a short period, because they are simple in the HTR-10. The adoption of the full-digital reactor-protection and control system can also shorten the period of precommissioning.
2. The components and systems of the HTR-Module are simple and can be produced in a modular way. There are only two slightly complex systems from the point view of the system arrangement and the number and requirement of system components, which are the pebble-fuel handling system and the helium-purification system. Other systems are very conventional and are easy to install.
3. The classification of all components and systems should be reconsidered, because the classification for the HTR-10 during the initial design stage mainly referred to Light-Water-Reactor (LWR) classifications. This is really not very proper. For example, the safety function of the helium circulator for the HTR-10 is not the same as that of the primary pump for an LWR.
4. To promote the HTGR development throughout the world, intensive international cooperation is necessary. International support speeded the construction of the HTR-10. If China didn't have international support, particularly, from German institutes and companies, then it would have been impossible for HTR-10 to reach criticality in the year 2000. It should be pointed out that the HTGR development level is not the same as the development of the other reactors. The prospect of the HTGR development would be uncertain if its development could not be performed with international cooperation.

14.3.2.3 HTR-PM project

The overall HTR-PM project

On the basis of the success of the HTR-10, the China State Council declared in 2006 that the small HTR was the second of two high-priority National Major Science and Technology projects for the next 15 years. It aimed to explore co-generation options in the near term and producing hydrogen in the long term. The first two 250-MW_{th} HTR-PMs with twin 105-MW_{el} reactors driving a single 210-MW_{el} steam turbine was approved (Zhang and Yu, 2002; Xu and Zuo, 2002) to be installed at Shidaowan in Weihai city of Shandong province. The reactor core is 11 m in height, and the steam will be at 566°C. The engineering of the key components, structures, and systems is based on China's own capabilities, although they include completely new technical features. It is envisaged that the thermal efficiency of 40%, localization of 75%, and 50-month construction period for the first unit can be realized. The construction of the HTR-PM started at the beginning of 2014, which was delayed after the Fukushima accident. Construction of the reactor building is now ongoing and is expected to be critical in 2021.

In the organization category, the China HuaNeng Group (CHNG) is the lead organization to build the demonstration Shidaowan HTR-PM with the China Nuclear Engineering and Construction (CNEC) group and the INET of Tsinghua University, which is the China HTGR R&D leader. Chineryg Company, a joint

venture of Tsinghua University and CNEC, is the main contractor for the nuclear island. CNEC and Tsinghua University signed the agreement on HTR industrialization cooperation in 2003, and a further agreement on commercialization of the HTR was agreed between the two parties in March of 2014. CNEC is responsible for China HTR technical implementation and is becoming the main investor of HTR commercial promotion at home and abroad.

Design of HTR-PM

HTR-PM uses helium as coolant and graphite as moderator as well as structural material. A single-zone core design was adopted, in which the spherical fuel elements are placed. The cylindrical active reactor core has an outer diameter of 3.0 m and effective height of 11.0 m. The effective core volume is 77.8 m³. In the equilibrium core, the reactor core contains 420,000 fuel elements.

The reflectors include top, side, and bottom graphite reflectors. Graphite reflectors are made from graphite blocks, which are constructed layer by layer. In the circumferential direction, every layer of graphite reflectors consists of 30 graphite blocks. Inside of the side graphite reflector blocks, the corresponding numbers of channels are designed for reactor shutdown systems and for helium flow. The bottom reflector takes a cone shape at the upper surface to facilitate the pebble flow. Inside of the bottom reflector, channels are designed for the flow of hot helium. The hot helium chamber is designed in the bottom reflector area, where hot helium of different outlet temperatures is mixed and then directed to the hot-gas duct in which the hot helium flows to the SG. In the center of the bottom reflector is the fuel-discharge tube.

The primary helium coolant works at the pressure of 7.0 MPa. The mass flow rate is 96 kg/s. Helium coolant enters the reactor in the bottom area inside of the pressure vessel with an inlet temperature of 250°C. Helium coolant flows upward in the side reflector channels to the top reflector level, where it reverses the flow direction and flows into the pebble bed in a downward flow pattern. Bypass flows are introduced into the fuel-discharge tubes to cool the fuel elements there and into the control-rod channels for control-rod cooling. Helium is heated up in the active reactor core and then is mixed to the average outlet temperature of 750°C and then flows to the SG.

The reactor core and the SG are housed in two steel pressure vessels that are connected by a connecting vessel. Inside of the connecting vessel, the hot-gas duct is designed. All of the pressure-retaining components, which comprise the primary pressure boundary, are in touch with the cold helium of the reactor inlet temperature. The primary pressure boundary consists of the Reactor Pressure Vessel (RPV), the SG Pressure Vessel (SGPV), and the Hot-gas Duct Pressure Vessel (HDPV), which are all housed in a concrete shielding cavity as shown in [Figure 14.8](#).

[Table 14.1](#) lists some key-design parameters of the HTR-PM. Its nominal thermal power is 500 MW_{th}, and the generator power output is 210 MW_{el}. The reactor active zone has a height of 11 m and an outside diameter of 3 m. Every spherical fuel element contains 7 g of heavy metal with an enrichment of nearly 8.5%. The overall height of the RPV is 25 m, and the inner diameter of the vessel is 5.7 m. The reactor is designed for 40 years of operational life with a load factor of 85%.

14.3.3 SCWR research and development

In China, the experiences and the technologies developed in the design, manufacture, construction, and operation of NPPs are mainly concentrated on water-cooled reactors. In addition, from a technological point of view, an SCWR is a combination of the water-cooled-reactor technology and the supercritical fossil-fired power-generation technology. Thus, the development of SCWRs is considered as a smooth extension of the existing nuclear-power generation in China. In 2007, a National Key Basic Research Program of China (973 Program) on SCWR was initiated by the China Ministry of Science. Since then, several universities, industrial companies, and academic institutions in China successively contribute to the SCWR-associated-

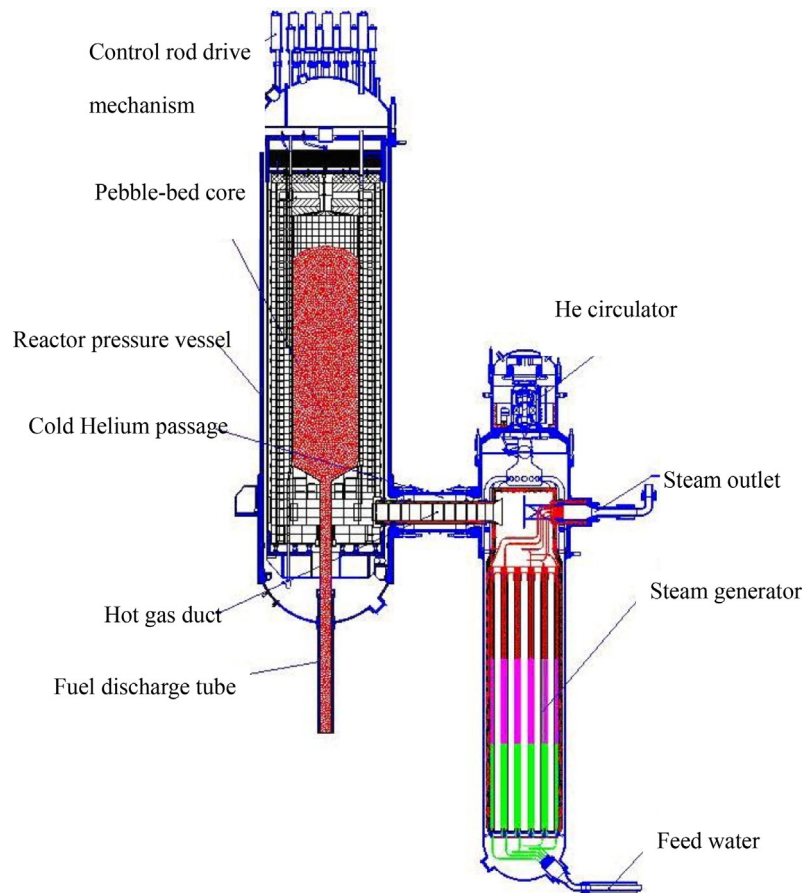


Figure 14.8. The primary loop of the HTR-PM

research activities based on which two conceptual designs have been proposed: (1) the Mixed spectrum SCWR (SCWR-M) by Shanghai JiaoTong University (SJTU) and (2) the 1000-MW_{el} China SCWR (CSR1000) by the Nuclear Power Institute of China (NPIC). In the following section, these two SCWR concepts are introduced.

14.3.3.1 SCWR-M conceptual design

The SCWR-M concept (Cheng et al., 2008) was proposed in the SCWR 973 project, which was led by SJTU and performed under the cooperation of eight institutes, universities, and industrial companies. SCWR-M is a mixed spectrum core consisting of a thermal spectrum zone (the outer zone) and a fast spectrum zone (the inner zone), as shown in Figure 14.9. According to the latest design, there are a total of 284 Fuel Assemblies (FAs) in the SCWR-M core, 164 of which are in the thermal zone. As schematically shown in Figure 14.9, the water from the core inlet firstly flows downward through both coolant channels and moderator channels of the thermal zone, mixing in the lower plenum, and then it flows upward through the fast zone. The main design parameters of a SCWR-M are listed in Table 14.2.

Comparing with the PWR rods and assemblies, the rod design and assembly arrangement of SCWRs are obviously optimized (Yang et al., 2012). The assemblies in the thermal and fast zones have different structures. As illustrated in Figure 14.10, it can be seen that additional moderator channels exist in the thermal FA to provide enough moderation. For simplification, the co-current flow mode is adopted between the coolant channels and the moderator channels in the thermal zone. The optimization work (Liu and Cheng, 2010) suggests that 20% of water flow from the inlet flows through moderation channels serving as moderator,

Table 14.1. HTR-PM main design parameters

Category	Design parameters	Unit	Design value
General plant data	Reactor thermal power	MW _{th}	500
	Power plant output	MW _{el}	210
	Plant design life	Year	40
	Primary coolant material	–	Helium
	Expected load factor	%	85
	Moderator material	–	Graphite
	Thermodynamic cycle	–	Rankine
Reactor core	Active core height	m	11
	Fuel column height	m	11
	Average fuel power density	kW/kgU	85.7
	Fuel material	–	UO ₂
	Fuel element type	–	Spherical
Primary coolant system	Mass flow rate	kg/s	96
	Operating pressure	MPa	7
	Core inlet temperature	°C	250
	Core outlet temperature	°C	750
Power conversion system	Working medium	–	Steam
	Mass flow rate	kg/s	99.4
	SG outlet pressure	MPa	14.1
	SG outlet temperature	°C	570
Fuel element	Enrichment	%	8.5
	Diameter of kernel	mm	0.5
	Diameter of sphere	mm	60
	Diameter of fuel zone	mm	50

and the rest serves as coolant through the coolant channels. To achieve a sufficiently large negative-void reactivity coefficient and increase the conversion ratio, 11 layers of seed and blanket regions are introduced.

Along with proposal of its core and assembly design, R&D activities have been extended to safety design and analysis. Some important features of SCWR-M under loss of flow accident were investigated (Xu et al., 2011; Zhu et al., 2012), and a reverse flow was observed and confirmed with the pressure keeping over the critical point in these analyses. The safety system for SCWR-M (Liu et al., 2013a, b) is derived from the passive design of AP1000 (Schulz, 2006) and the Economic Simplified Boiling Water Reactor (ESBWR) (Hinds and Maslak, 2006). It contains the isolation cooling systems, Gravity-Driven Cooling Systems (GDCS), ACCumulators (ACCs), Automatic Depressurization System (ADS), and standby liquid control system as schematically shown in Figure 14.11. On the basis of the modified system code Analysis of

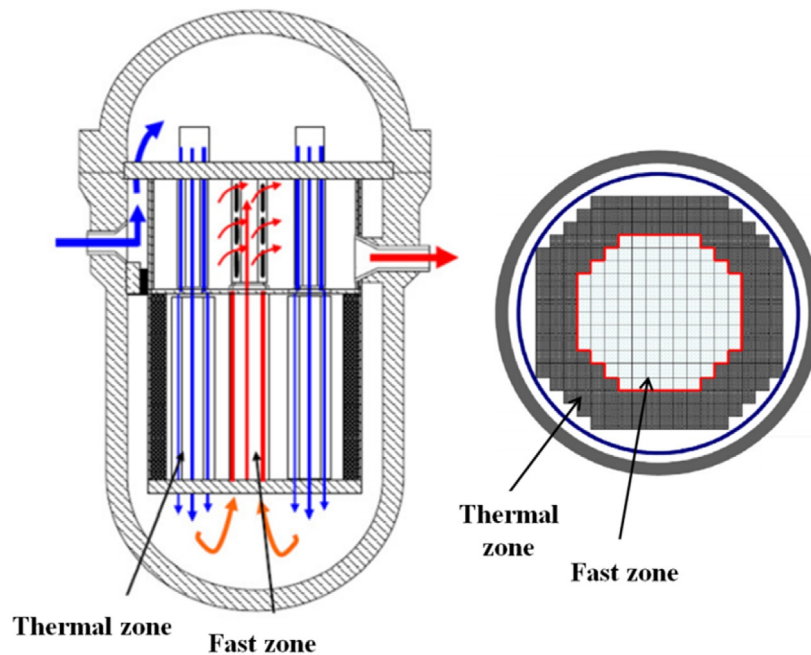


Figure 14.9. Schematic diagram of the SCWR-M core

Table 14.2. Main design parameters of the SCWR-M

Parameters	Units	Thermal zone	Fast zone	Entire core
Thermal power	MW	2460	1100	3560
Inlet temperature	°C	280	400	280
Outlet temperature	°C	400	510	510
Active height	m	4.0	2.0	–
Fuel assembly box size	mm	173.2	173.2	–
Number of fuel assemblies	–	180	100	280
Number of fuel pins	–	180	289	–
Fuel pin diameter	mm	8.0	8.0	–
Pitch-to-pitch ratio	–	1.20	1.27	–
Average linear power	W/cm	190	190	–
Power density	MW/m ³	114	92	102
Relative moderation capacity	–	1.53	0.15	–
Equivalent outer diameter	–	3.3	2.0	3.3
Mass flux	kg/(m ² s)	922	1145	–
Maximum fluid velocity	m/s	5.5	13.1	–
Pressure drop	kPa	25.0	98.0	123.0
Maximum coolant temperature	°C	550.5	526.9	550.5
Maximum cladding temperature	°C	610.4	616.7	616.7
Fuel	–	UO ₂ or MOX	MOX	–
Enrichment	–	5%–6%	~20%	–

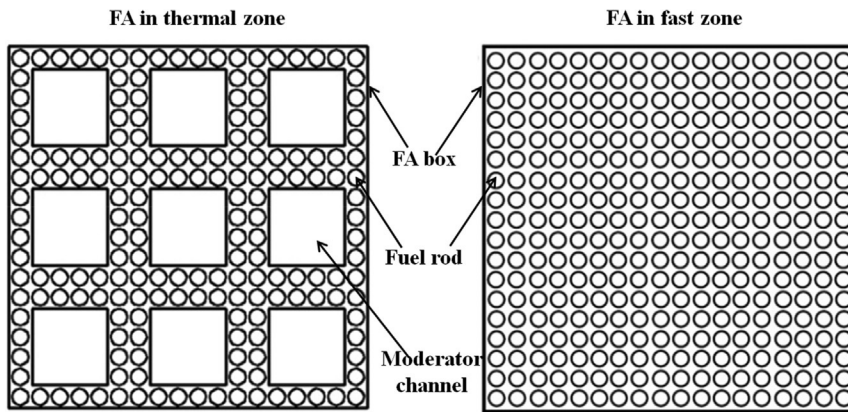


Figure 14.10. FA structure in the thermal and fast zones of the SCWR-M

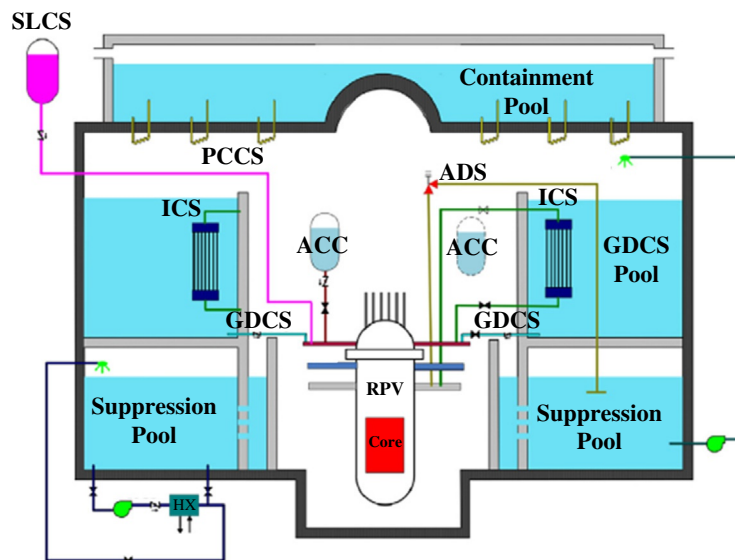


Figure 14.11. The SCWR-M safety system. ICS, Isolation Cooling System; GDCS, Gravity-Driven Cooling System; ACC, ACCumulators; ADS, Automatic Depressurization System; PCCS, Passive Core Cooling System; SLCS, Standby Liquid Control System

Thermal-Hydraulics of Leaks and Transients-SuperCritical water (ATHLET-SC), Loss Of Coolant Accident (LOCA) analysis is performed (Liu et al., 2013a, b).

14.3.3.2 The CSR1000 concept design

CSR1000, the 1000-MW_{e1} China SCWR design concept is proposed by NPIC with China's independent intellectual property (Li et al., 2013; Xia et al., 2013; Zhang et al., 2013). The Phase I R&D activities on key technologies for CSR1000 began in 2010 and finished in 2013. The main objectives of Phase I are R&D on concept design, experiment, and material research for SCWRs. Its follow-up activities are ongoing. The main design parameters of CRS1000 are listed in Table 14.3.

The CSR1000 is designed to be a thermal spectrum reactor based on the existing technologies of PWRs, SCWRs, and Advanced Boiling Water Reactors (ABWR). As schematically shown in Figure 14.12, the FA in the CSR1000 core is divided into two zones, the inner zone with 57 FA clusters and the outer zone with 120 FA clusters. Entering the core from cold legs, water partially flows upward to the upper plenum, with the rest

Table 14.3. The main technical parameters of CSR1000

Design parameters	Units	Value
Pressure	MPa	25.0
Electric power	MW	1000
Thermal power	MW	2300
Thermal efficiency	%	43.5
Core height	m	4.2
Number of fuel assemblies	–	177
Fuel rod diameter	mm	9.5
Pitch-to-diameter ratio	–	1.105
Flow rate	kg/s	1190.0
Fuel	–	UO ₂
Cladding	–	Alloy 310S
Enrichment	%	4.3 (Conner); 5.7 (Other)

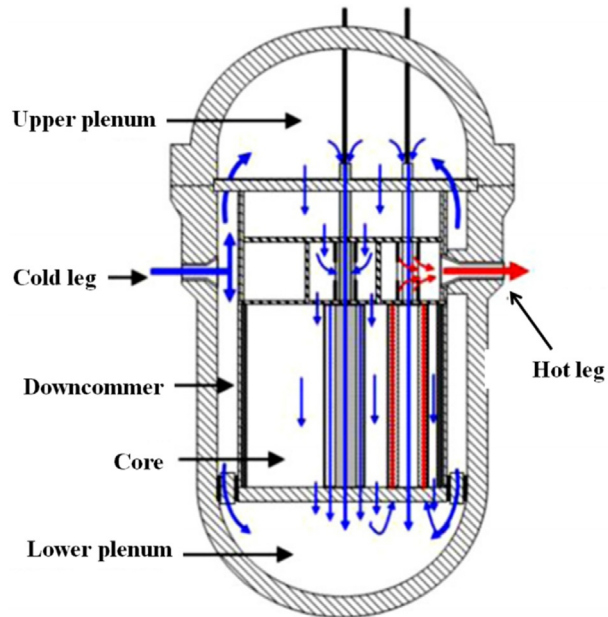


Figure 14.12. Scheme of the CSR1000 core

flowing downward through the down comer to the lower plenum. The water in the upper plenum divides into three parts and flows downward: (1) coolant through the outer zone coolant channels, (2) moderator through the outer zone moderator channels, and (3) moderator through the inner zone moderator channels. All of the water mixes in the lower plenum and then flows through the coolant channels of the inner zone.

As mentioned, there are a total 177 FA clusters in the core. The FA clusters in both the outer zone and inner zone are in the same structure design. To simplify the structural design and obtain more uniform moderation, the CSR1000 typical FA cluster is composed of four sub-FAs, each of which is a 9×9 fuel rod configuration

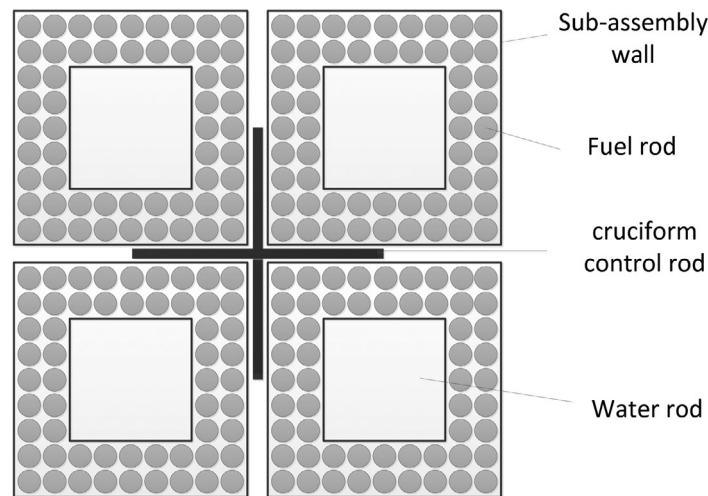


Figure 14.13. Cross section of the CSR1000 FA

with one square water channel in the center, as shown in Figure 14.13. The rods in a sub-FA are surrounded by an assembly wall, which is made of ZrO_2 for thermal insulation covering with two 310S layers. In addition, a cruciform control rod is adopted in each FA cluster.

To hold more fissile gas with a shorter gas plenum at the ends of the fuel rod, and to decrease the highest temperature of fuel pellets as much as possible, annular fuel pellets are adopted. The outside diameter of the rod is 8.19 mm, whereas the diameter of the inner gaseous space is 1.5 mm. 310S is selected as the cladding material and other structure material.

According to public literature, some preliminary fundamental analyses have been performed on the CSR1000 concept. With a homemade code named FREDO-CSR1000 (FREquency DOmain analysis of CSR1000) and TIMDO-CSR1000 (TIME DOmain analysis of CSR1000), the analysis of flow instability for CSR1000 both in the average channel and the hot channel within rated power and flow has been performed (Tian et al., 2012). The calculation results indicated that the decay ratio of the first flow path monotonically varies with power and flow. However, the decay ratio of the second flow path ascends firstly and then descends, the trend of which is fluctuant because of the simultaneous influence of a multitude of variables. Furthermore, it is found that the location where the flow instability happened is directly determined by the point at which the pseudocritical temperature is reached.

Subchannel analysis models have been investigated for CSR1000 FA by using the experimental data available and the Computational Fluid Dynamics (CFD) code (Du et al., 2013). The analysis results are used to improve a subchannel code. The steady-state subchannel analysis is conducted on the CSR1000 FA to obtain the temperature distribution of coolant and cladding, and pressure drop in the FA. The results show that smaller pitch will flatten the profile of the coolant temperature and reduce maximum cladding surface temperatures, but it increases the pressure drop in the assembly.

Large-break accident analysis for CSR1000 was performed using the Advanced PROcess Simulation software (APROS) code to clarify its characteristics and to evaluate the capability of its safety system (Dang et al., 2013). At the cold-leg large-break accident, the maximum cladding temperature is lower than the criterion 1260°C by approximately 340°C , which appears during the blow-down phase.

14.3.4 MSR research and development

In January 2011, the CAS launched a pilot project of the Thorium Molten Salt Reactor (TMSR) nuclear energy system aiming at developing solid- and liquid-fuel MSRs. The Shanghai Institute of Applied Physics

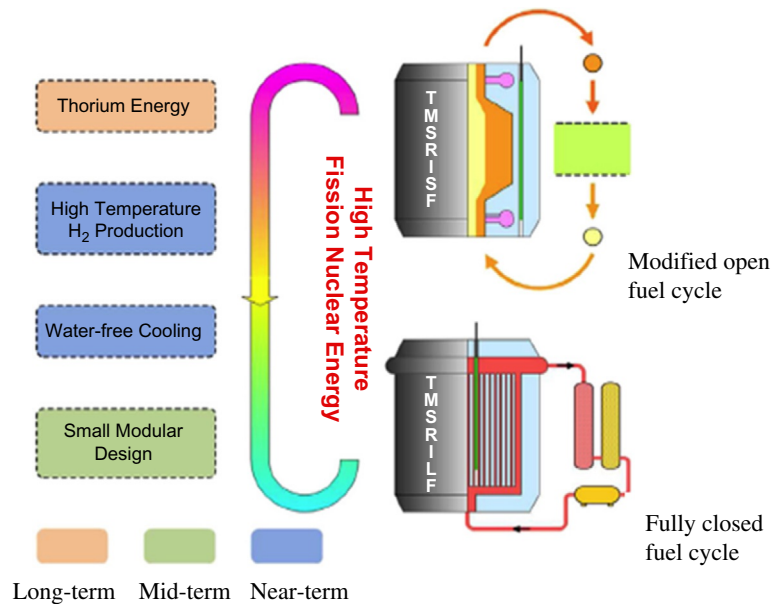


Figure 14.14. Strategy of China TMSR research and development. TMSR-SF, Solid-Fueled Thorium Molten Salt Reactor; TMSR-LF, Liquid-Fueled Thorium Molten Salt Reactor

(SINAP) is in charge of this project, which strives for realizing effective thorium utilization and hydrogen production by nuclear energy within 20–30 years. The near-term goals of the TMSR project are to build two test reactors: a Solid-Fueled TMSR (TMSR-SF) and a Liquid-Fuel TMSR (TMSR-LF). Figure 14.14 presents the strategy of the China TMSR R&D. In addition, the project also includes the development of a pyro-process complex (Serp et al., 2014). The nominal power of the first solid-fuel test reactor was initially designed with power of 2 MW_{th} , and it was increased to $10 \text{ MW}_{\text{th}}$ in 2013. The solid-fuel 10-MW_{th} test reactor will be constructed as the initial step with the expectation of a larger $100\text{-MW}_{\text{th}}$ Fluoride-salt-cooled High-temperature Reactor (FHR) shortly thereafter. This reactor designated as TMSR-SF will be a Pebble-Bed FHR (PB-FHR) concept developed by the University of California-Berkeley (UCB), which may be the first FHR ever built in the world (Forsberg et al., 2014).

Before launching the CAS TMSR project, XJTU was financially supported by Natural Science Foundation of China (NSFC) to perform the fundamental research on the neutronics, thermal-hydraulic modeling, and safety analysis of MSR. In November 2020, XJTU was supported by the National Key Research and Development Program of China to perform the conceptual design of an integral inherently safe Fluoride-Salt-cooled high-Temperature Advanced Reactor (FuSTAR).

In this section the fundamental research of MSRs under the framework of the pilot TMSR project and NSFC projects are firstly summarized, then the conceptual design of FuSTAR will be introduced briefly.

14.3.4.1 Thermal-hydraulic modeling and safety analysis

Several types of thermal-hydraulic models from simple to complex were developed to calculate the temperature and flow distributions in the MSR core. A one-dimensional single-phase flow model was proposed to simulate the flow and heat transfer of the fuel salt in the graphite-moderated channel-type MSR. The axial and radial power factors necessary for the thermal-hydraulic calculation were calculated by the DRAGON code (Zhang et al., 2008). A two-dimensional thermal-hydraulic model was developed to calculate the flow and heat transfer in the core, coupled with the two-group neutron diffusion equation to obtain the flux distribution (Qian et al., 2010). The steady thermal-hydraulic characteristics were also

analyzed by a three-dimensional coupled neutronics/thermal-hydraulic analysis code (Zhou et al., 2014). The CFD is often adopted to simulate the multidimensional porous media flow for pebble-bed MSR. By using simplified Body Center Cubic (BCC) and Face Center Cubic (FCC) models, pore scale thermal-hydraulic characteristics of pebble-bed advanced high-temperature reactor (FHR type) proposed by UCB were also investigated, in which the temperature distribution, pressure drop, and local mean Nusselt number were calculated (Song et al., 2014). Similar studies were also performed for the TMSR-SF and the 2-MW PB-FHR (Wang et al., 2014a, 2015).

Initial events analysis is necessary to be performed before the reactor safety analysis and the Probabilistic Safety Assessment (PSA). Referring to the initial events of the LWRs, HTRs, and SFRs, the initial event lists of the TMSR-SF, containing 37 initial events, were determined and grouped into six types using the Master Logic Diagram (MLD) (Mei et al., 2014). Table 14.4 lists the initial events and their grouping of the TMSR-SF. Through the PSA analysis of the Loss Of Offsite Power (LOOP) using the PSA process risk spectrum, the accident sequences of the radioactive material release to the core and its frequency were obtained (Mei et al., 2013).

Many efforts have also been focused on the safety analysis of MSRs. A safety analysis code was developed by establishing a kinetic model to consider the flow effects of the fuel salt coupled with a simplified heat

Table 14.4. Initial events lists and their grouping of the TMSR-SF

No.	Accident types	Initial events
1	Reactivity accidents	A control rod out of control under the condition of subcritical or low-power operation A control rod out of control under the condition of power operation Control rod operation in error Accident critical in the process of charge
2	Core heat removal increase accidents	Secondary circuit flow increase Secondary circuit temperature lower
3	Core heat removal decrease accidents	Primary circuit main pump stuck shaft Primary circuit main pump trip Secondary circuit circulating pump trip Secondary circuit circulating pump stuck shaft Fuel assembly entrance jam Loss of off-site power Loss of the inside and outside AC power at the same time (loss of non-emergency AC power) Intermediate heat exchanger leakage Secondary circuit air heat exchanger fault Air cooling tower ventilation doors get stuck Air heat exchanger of the cabin failure

Continued

Table 14.4 Initial events lists and their grouping of the TMSR-S—cont'd

No.	Accident types	Initial events
4	Pipeline crevasse and equipment leakage accidents	Primary circuit pipeline small crevasse Secondary circuit pipeline small crevasse Primary container leakage Main heat exchanger tube rupture Fuel sphere breakage Isolation valve abnormal open Molten salt pipe rupture out of containment Connecting pipe between containment and the first isolation valve crevasse Primary circuit molten salt purification system pipeline leakage Radioactive waste gas disposal system leakage or breakage Radioactive liquid waste disposal system leakage or breakage
5	Anticipated Transients Without Scram (ATWS)	Loss of off-site power without scram Control rods miss out without scram
6	Disasters (internal and external)	Earthquake Fire Flooding Strong wind Explosion Tsunami Plane crash

AC, ALternating Current.

transfer model in the core. The safety characteristics of the MOlten Salt Actinide Recycler and Transmuter (MOSART) were investigated by simulating three types of basic transient accidents including the Unprotected Loss Of Flow (ULOF), Unprotected OverCooling accident (UOC), and Unprotected Transient OverPower (UTOP) (Zhang et al., 2009a). The results indicate that the conceptual design was an inherently safe one. The ULOF and the combination of ULOF and Unprotected Loss Of Heat Sink (ULOHS) were studied on the MOSART by supplementing a heat sink model (Guo et al., 2013b). Using the conceptual design of the TMSR-LF as the reference case, a pump stop accident was simulated at nominal power of 2 MW_{th} by the Cinsf1D code (Wei et al., 2014). In addition, the reactivity-initiated transients of the TMSR-LF without thorium fuel, including the step reactivity initiated event, ramp reactivity initiated event, UOC, and ULOF, were analyzed as well as those of the reactor with thorium fuel (Cai, 2013).

The safety analysis of the TMSR-SF has also drawn much attention. Three types of transient conditions including ULOF, UOC, and UTOP were examined on the TMSR-SF by an FHR safety analysis code named the FHR Safety Analysis Code (FSAC) (Xiao et al., 2014). The Station BLackout Anticipated Transient

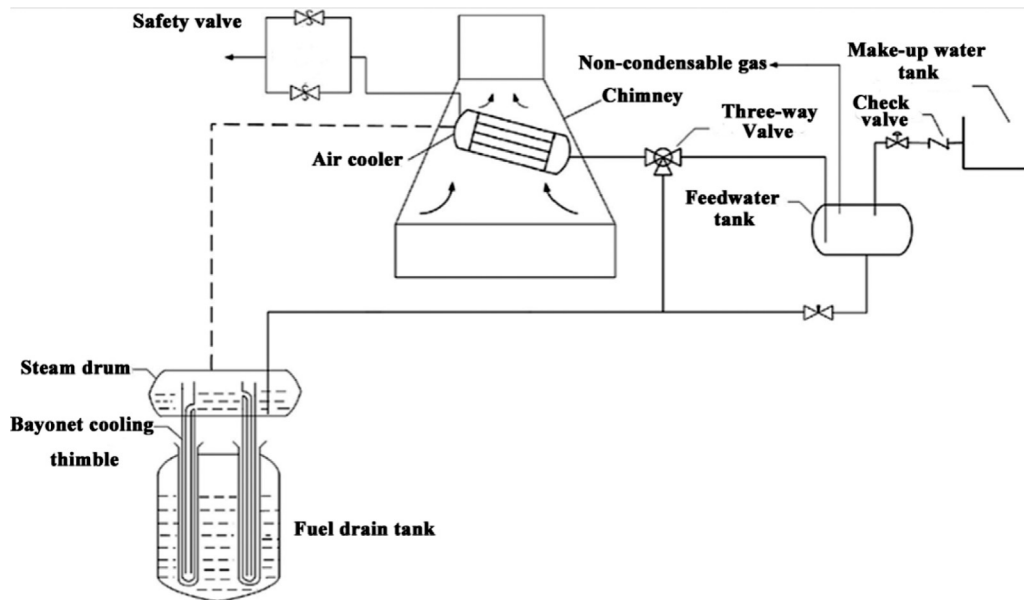


Figure 14.15. Schematic diagram of the PRHR system

Without Scram (SBO-ATWS) accident was analyzed by the modified RELAP5/MOD 4.0 code with the responses of the Passive Residual Heat Removal (PRHR) system (Jiao et al., 2015).

Several types of PRHR system have been proposed to enhance the inherent safety of the MSR. On the basis of the residual heat removal system for the Molten Salt Reactor Experiment (MSRE) developed by Oak Ridge National Laboratory (ORNL), a conceptual design with passive characteristics was completed using natural air cooling rather than the forced water circulation to cool the condenser (Figure 14.15). The passive heat removal system is composed of three natural-circulation loops, including (1) the two-phase natural circulation in the bayonet cooling thimble transferring the decay heat to the second loop, (2) the two-phase natural circulation between the air cooler and the steam drum, and (3) the open loop where steam in the air cooler was condensed by the circulation of air in the chimney (Sun et al., 2014). A more detailed design was put forward with the L-type fin tube chosen as the heat exchanger tube of the air cooler (Zhao et al., 2015). Thermal-hydraulic characteristics of this type of PRHR system were investigated (Cai et al., 2014; Sun et al., 2014; Zhao et al., 2015).

Using heat pipes might help to improve the heat dissipation performance of the PRHR system of MSRs. Two types of conceptual designs of PRHRs, using high-temperature sodium heat pipes and sodium-potassium alloy ones, respectively, were proposed as shown in Figures 14.16 and 14.17. Transient analysis results indicate that the high-temperature sodium heat pipe had a successful startup and could rapidly remove the residual heat of fuel salt in the MSR accidents (Wang et al., 2013a,b,c).

14.3.4.2 Neutronic modeling

Neutronic characteristics of MSRs have been explored in the literature. Flow effects were considered when calculating the effective multiplication factor and fast neutron, thermal neutron, and delayed neutron precursor distribution of the liquid-fuel MSR based on the multigroup neutron diffusion equation and delayed neutron precursor conversation equation (Zhang et al., 2009b; Cheng and Dai, 2014; Zhou et al., 2014). Spatial kinetic models were developed for better neutronic analysis of the MSRs (Zhang et al., 2015; Zhuang et al., 2014).

Neutron absorption of the poisons such as ^{135}Xe and ^{85}Kr has an important impact on the reactor reactivity. The calculation method of the source terms for the MSRE with online removal of radioactive gases was

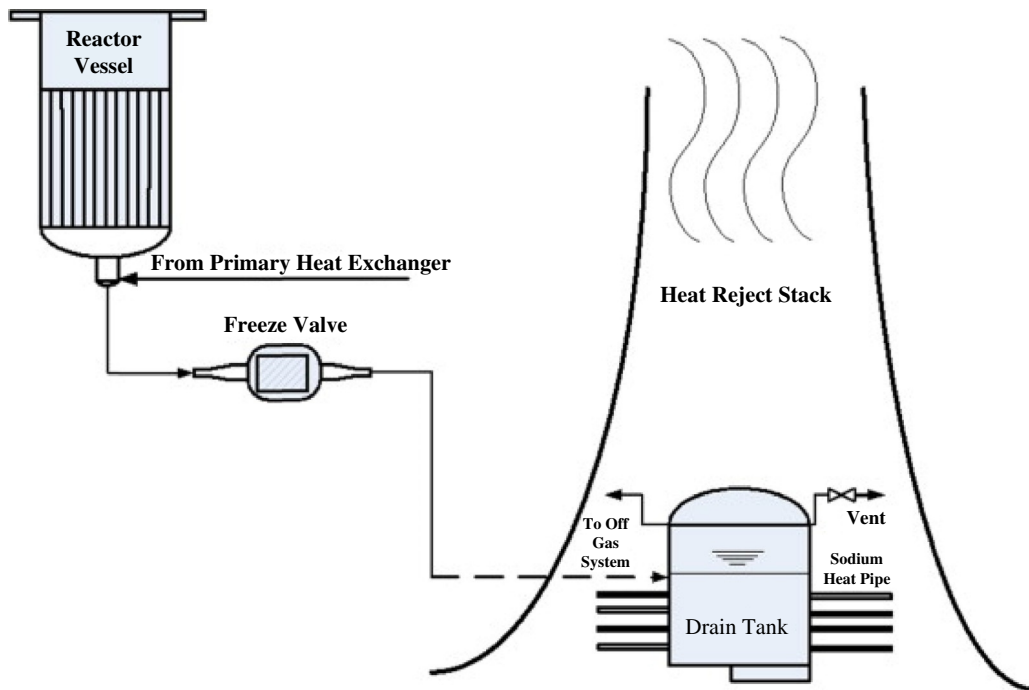


Figure 14.16. Schematic diagram of the new-concept MSR PRHR system using the sodium heat pipe

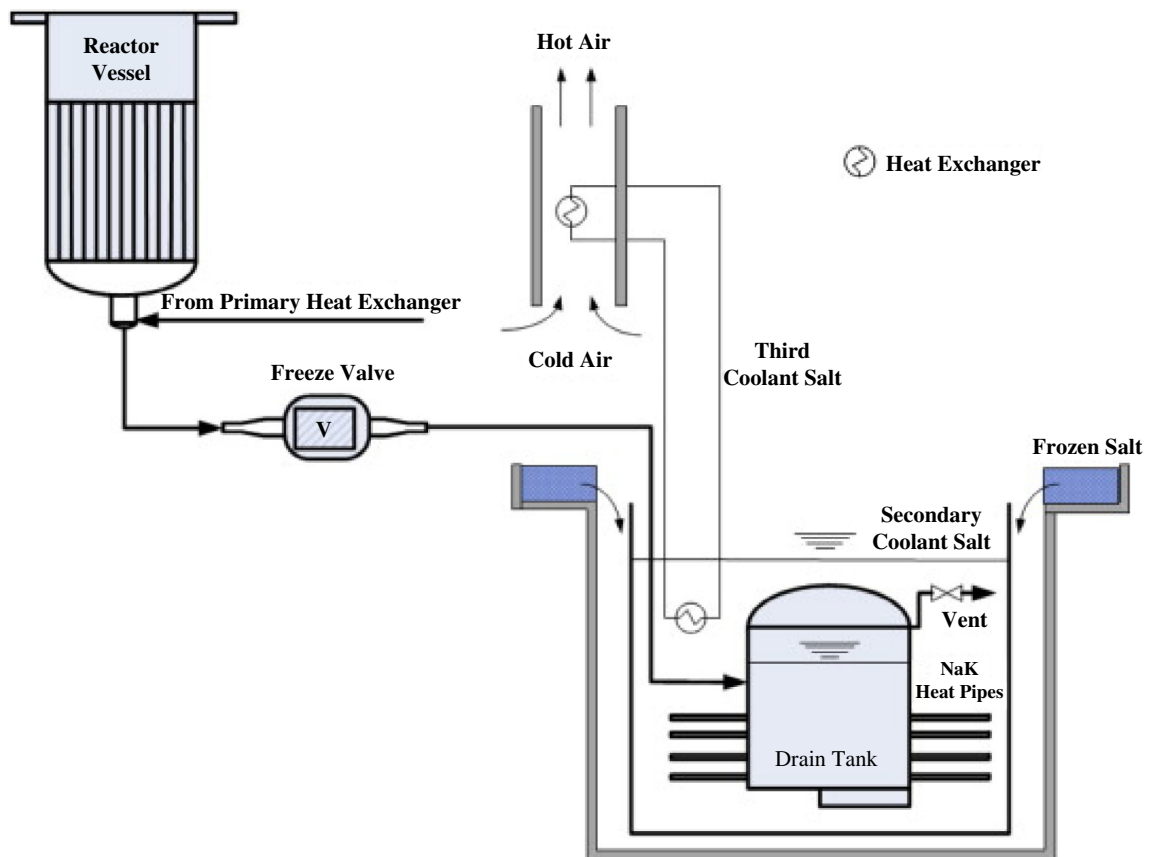


Figure 14.17. Schematic diagram of the new-concept MSR PRHR system using the sodium-potassium heat pipe

developed to analyze the radioactivity of fission products and the tritium products (Zhang et al., 2014b). ORIGEN2 was applied to study the variation of the xenon and krypton fission gases varying with neutron spectrum and flux in TRI-ISOTropic (TRISO) fuel particles (Yin, 2014).

Reactor physical characteristics have also drawn much attention. The control rod worth, including the differential worth and integral worth, were calculated by the Monte Carlo code for Neutron and Photon transport (MCNP) for the 2 MW TMSR-SF (Zhou and Liu, 2013). The measurement of the neutron energy spectrum was also theoretically and experimentally studied (Zhou, 2013). Parametric study of the thorium-uranium conversion rate was conducted to optimize the core structure for the improvement of the economics of the TMSR using the Standardized Computer Analyses for Licensing Evaluation (SCALE) code (Cai, 2013).

14.3.4.3 Thermo-hydraulics and neutronics coupling analysis

It can be noted that much work has been done on coupling thermo-hydraulics and neutronics analysis for the liquid-fuel MSR. Neutronic models based on the multigroup diffusion theory while considering the flow effects of the liquid fuel were proposed to couple the flow and heat transfer models in performing the steady and transient analysis of the MSR (Cai, 2013; Guo et al., 2013a; Wei et al., 2014; Zhang et al., 2009a; Zhou et al., 2014). The delayed neutron precursor movement including its turbulence also was especially considered in these analyses (Cheng and Dai, 2014; Zhang et al., 2009b). COUPLE (a time-space-dependent coupled neutronics and thermal-hydraulic code), was developed on the basis of the previous work (Zhang et al., 2014a). In addition, the general MCNP is coupled with a Multiple-channel Analysis Code (MAC) by a linking code to perform parametric studies of the MSRE (Guo et al., 2013a, c). The traditional safety analysis code CATHARE (Code for Analysis of Thermal-Hydraulics during an Accident of Reactor and safety Evaluation) was also modified to perform the study of a single channel in the MSR core (Peng et al., 2013).

14.3.4.4 Molten salt test loops

Several experimental loops have been constructed at SINAP, including the HTS molten salt test loop (Figure 14.18), the FLiNaK molten high-temperature salt test loop (Figure 14.19), and the nitrate natural circulation loop. The FLiNaK test loop was constructed to study the heat transfer and corrosion between the FLiNaK molten salt and fuel pebbles. Hastelloy C 276 alloy was adopted to fabricate the pipe in the loop. The FLiNaK molten salt test loop operates within the temperature range of 550–700°C, whereas the heat power is approximately 200 kW (Zou et al., 2013). The high-temperature molten salt test loop and the nitrate natural circulation loop operate with the liquid nitrate (Han et al., 2013).

14.3.4.5 Material and salts research

An experimental device was constructed by SINAP for measuring the density and liquidus temperature of molten fluorides typically used in the TMSR project. A candidate molten salt coolant, FLiNaK (LiF-NaF-KF:46.5-11.5-42 mol%) was investigated (Cheng et al., 2013).

The immersion corrosion of ZrC-SiC-based ceramics was performed in molten fluoride salt FLiNaK, with the goal of assessing their capability with candidate materials in molten fluoride preparation, thermal storage, and transfer application. Results show that the ZrC-SiC composites represented better corrosion resistance than the single content of ZrC or SiC. With an increase in the SiC content, the corrosion resistance could be improved (Wang, 2013; Wang et al., 2014b). Another type of candidate high-temperature material, MAX (Mn+1AXn) phase materials, was also investigated for corrosion resistance in molten fluoride salts at the temperature of approximately 850°C, approximately the operating temperature of the MSR (Li et al., 2014). Alloys including the China Hastelloy-N alloy were also examined for performance in the high-temperature FLiNaK molten salt. It can be found that temperature and the existence of water in the molten salt had significant impact on the corrosion (Liu et al., 2015).

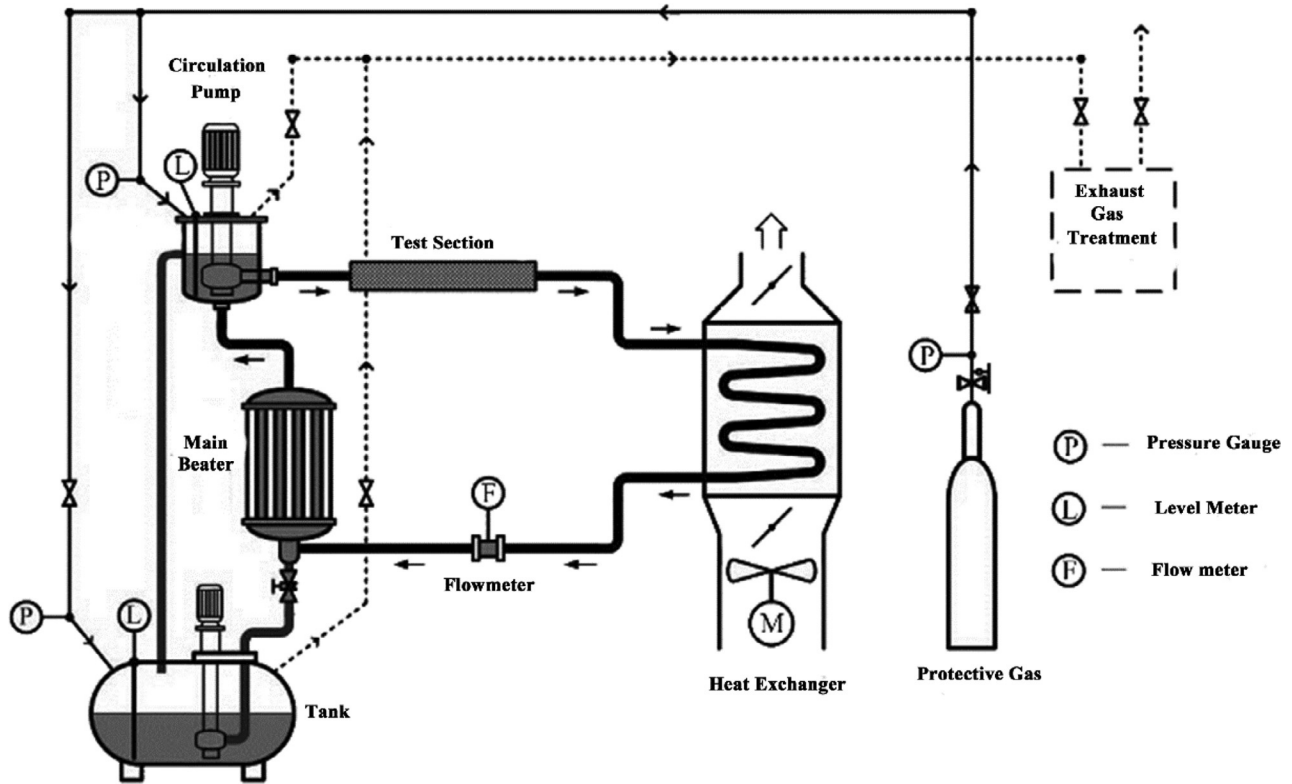


Figure 14.18. Schematic diagram of the high-temperature molten salt test loop

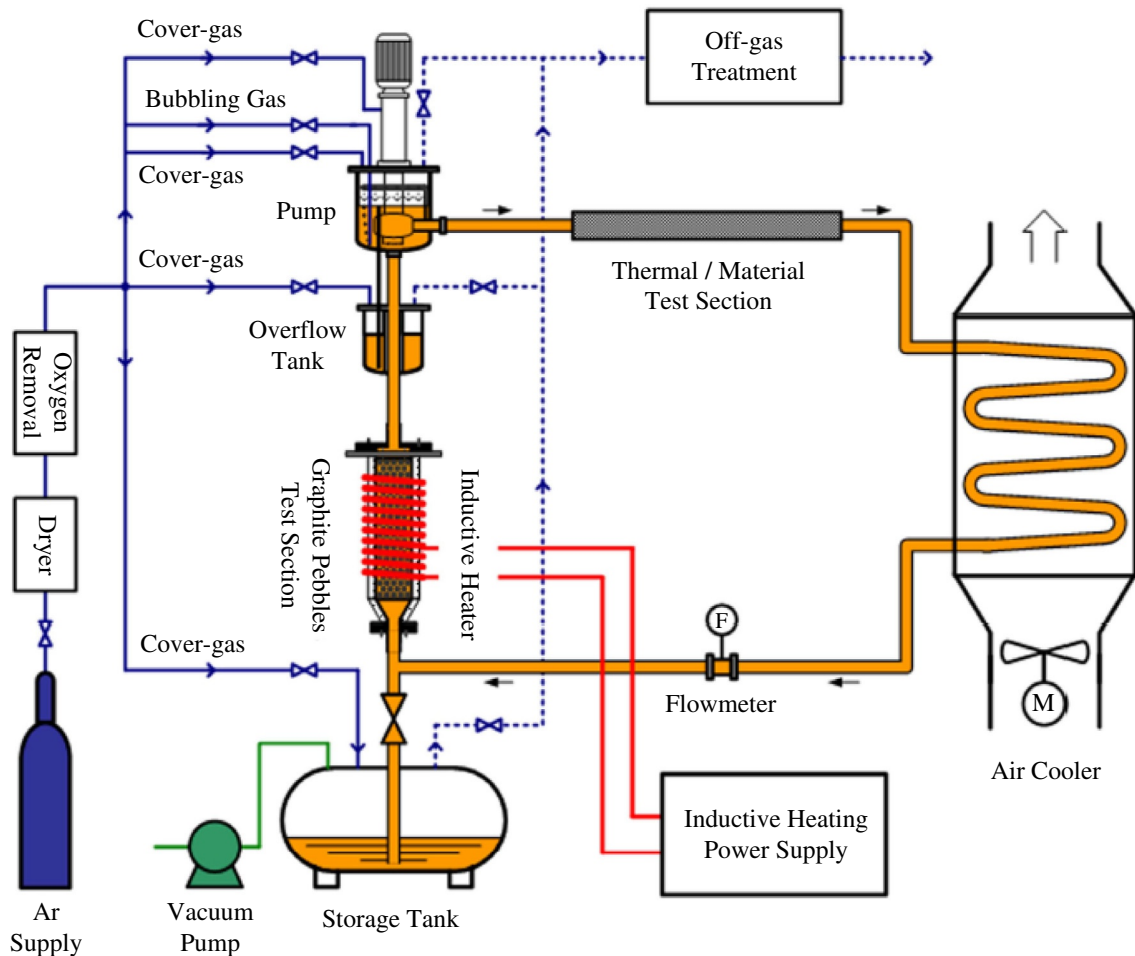


Figure 14.19. Schematic diagram of FLiNaK molten salt high-temperature testing loop

The irradiation resistance of the structural materials used in the MSRs are of great importance. The Pyrolytic Carbon (PyC) coating adopted in the TRISO fuel particles was studied in the ion irradiation and static FLiNaK molten salt experiments. The results showed that irradiation defects might increase the fluorination of PyC coating in FLiNaK salt (Feng, 2014). As a candidate structural material for MSRs, the 316 austenitic stainless steel (316SS) was investigated in a high-temperature environment with Xe ion irradiation. The temperature effect of Xe ion irradiation on the 316SS was obvious (Huang et al., 2014).

The permeation behaviors of tritium in the candidate structural materials of the TMSR was studied because the tritium can easily diffuse through the structural materials at high temperatures and go into the atmosphere. The permeation process of tritium at the temperature of 400–700°C was simulated using hydrogen and deuterium with the method of gas-driven permeation. The experimental results of the permeation are similar in Hastelloy-N and GH3535 (Pi et al., 2015). Furthermore, the solubility and diffusivity of tritium in molten salts was evaluated in a two-chamber permeability apparatus separated by a nickel plate (Zeng et al., 2014). In addition to the experiments, the Displacement Per Atom (DPA) rates for the MSRE core can and vessel were calculated and analyzed by the MCNP5, providing guidance for the MSR design and parameter selection (Liu et al., 2013a, b).

14.3.4.6 Conceptual design of FuSTAR

FuSTAR uses helical cruciform fuel elements, hexagonal component design, and the entire core is arranged in a hexagonal grid. The TRISO particles dispersed in the graphite matrix, all of which form the fuel pellet. The cladding material is the carbon-carbon composite material, which has the advantages of high strength and corrosion resistance. The TRISO coated particles have a high melting point, and the cracked carbon coating layer can effectively contain the fission gas, avoid obvious swelling of the fuel element, and has a small temperature gradient and good neutron economy. The coolant uses FLiBe molten salt with a ^7Li enrichment of 99.99%, which can realize the reactor's high-temperature and low-pressure operation. The designed thermal power of FuSTAR is 125 MW.

FuSTAR adopts a modular design and is divided into four main modules: reactor body, intermediate heat exchange loop, power conversion system, and passive heat removal system. Among them, the reactor body adopts an integrated design, including reactor primary-loop equipment, with atmospheric primary loop FLiBe molten salt as the pressure boundary. The core coolant inlet temperature is 650°C, and the outlet temperature is greater than 700°C. According to application requirements, FuSTAR can operate in comprehensive utilization mode and compact high-power mode (shown in Figure 14.20).

The comprehensive utilization mode includes reactor body, intermediate heat exchange loop, and power conversion system. In the reactor body, the main pump drives the liquid molten salt FLiBe to cool the reactor core, and the intermediate heat exchange loop is driven by the molten salt pump to drive the normal pressure FLiNaK molten salt as the heat transfer working medium, which outputs heat from the molten salt main heat exchanger and collects it in the molten salt pool. As a heat storage device, the molten salt pool can provide high-temperature process heat for the comprehensive application of combined heat, power and steam, and hydrogen production from thermal energy. The immersed compact molten salt/carbon dioxide heat exchanger is installed in the molten salt pool to transmit heat to the power circulation system. This mode can realize energy storage and full utilization based on the molten salt pool.

The compact high-power mode only includes the reactor body and power conversion loop. The reactor body uses the main pump to drive the primary coolant FLiBe to cool the reactor core. A compact molten salt/carbon dioxide main heat exchanger is installed in the reactor body to directly transmit heat to the power circulation loop. This mode can ensure as little heat dissipation as possible to meet high-power demand.

When the reactor is operating normally, the heat in the reactor is discharged from the secondary loop. In the case of reactor shutdown or accident conditions, the core heat is mainly carried out by the passive heat removal system. The main equipment of the passive heat removal system includes 3 DHXs located in

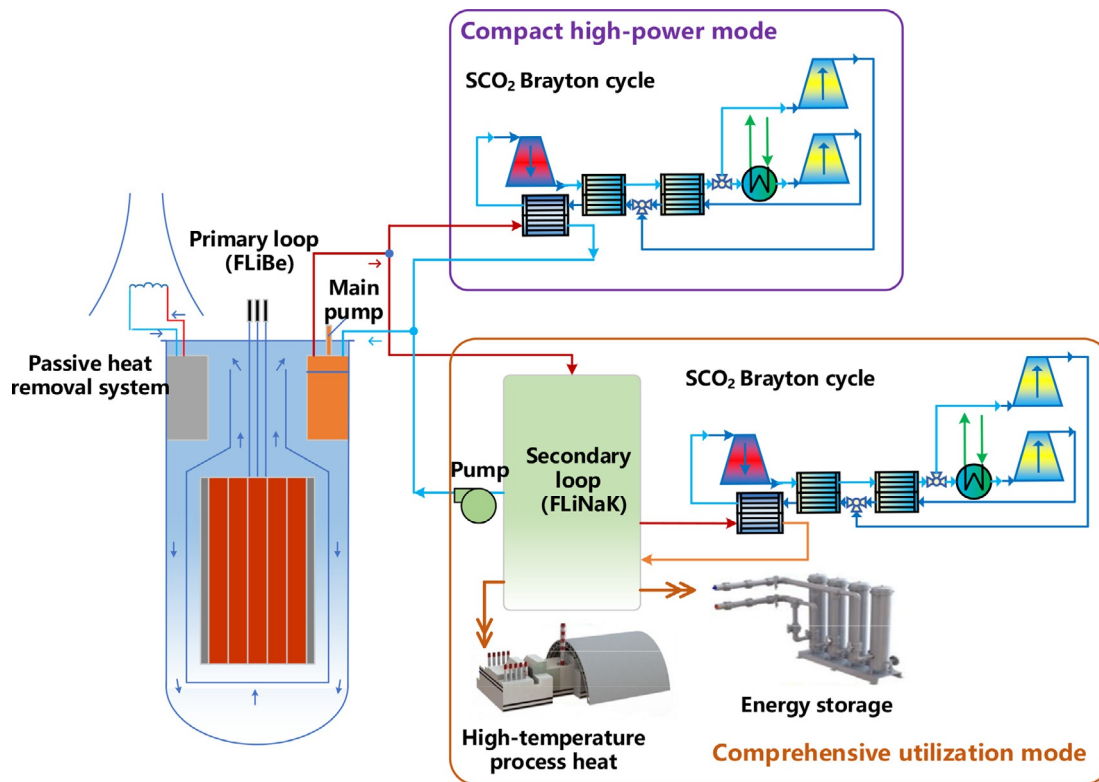


Figure 14.20. Schematic diagram and operation mode of FuSTAR

the pressure vessel, molten salt/air heat exchangers located in the air-cooling tower outside the pressure vessel, and connected pipes. The three constitute a natural circulation loop. The heat of the coolant is transferred to the FLiNaK loop of the passive heat removal system through the DHX in the vessel and is transported to the molten salt/air heat exchanger in the cooling tower by natural circulation, and finally transferred to the atmosphere.

The Brayton power cycle system has advantages of compact structure and flexible control, which can be given priority as a power conversion system for small fluoride salt reactors. Supercritical Carbon dioxide (SCO₂) has good nuclear and chemical stability, high density, and good heat transport characteristics. The size of a carbon dioxide turbine of the same power scale is much smaller than that of a conventional Rankine cycle power generation steam turbine. Combined with the requirements of compact structure and flexible control of a small fluoride salt reactor, FuSTAR adopts an S SCO₂ Brayton cycle. In terms of cycle configuration, studies have shown that for small-scale systems, the cold end layout of split recompression can better balance the control characteristics and thermal efficiency, thus the SCO₂ recompression power cycle configuration is selected as the basic design.

14.3.5 LFR research and development

There is no special project on LFR research in China, which is only a constituent part of the CAS Accelerator-Driven Subcritical (ADS) system project. CAS launched this ADS system project in 2011 as another pilot project parallel with the TMSR project and planned to construct the demonstration ADS system until the 2030s. The China LEad-Alloy-cooled Reactor (CLEAR) is proposed as the reference reactor in the ADS system. CAS plans to develop the lead-based reactors through three phases (Wu et al., 2014): (1) a 10-MW_{th} Lead-Bismuth Eutectic (LBE)-cooled research reactor (CLEAR-I) to be built in the 2010s, (2) a 100-MW_{th} lead-alloy-cooled experimental reactor (CLEAR-II) to be built in the 2020s, and (3) a 1000-MW_{th} lead-alloy-cooled

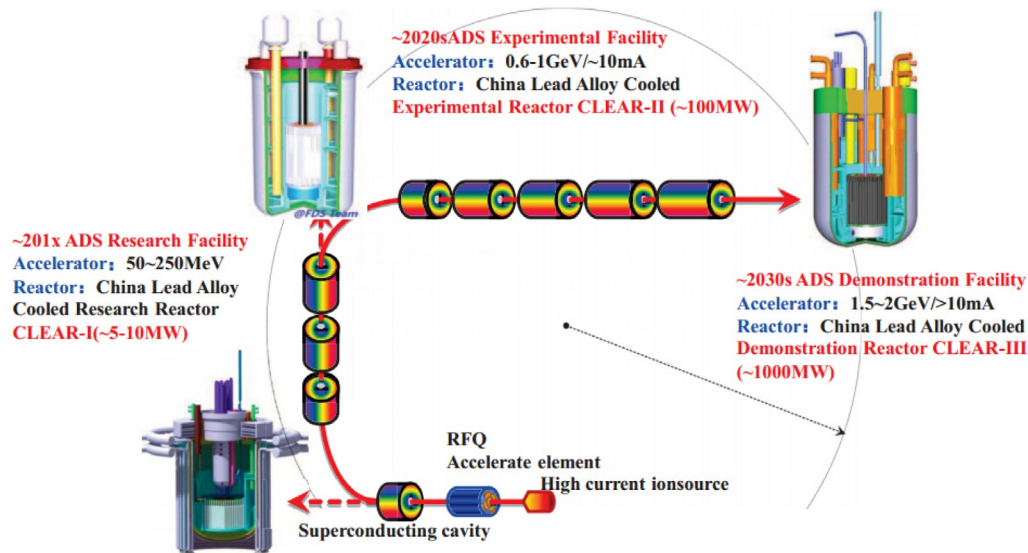


Figure 14.21. CLEAR series reactor development plan in the ADS system project. RFQ, Radio Frequency Quadrupole

demonstration reactor (CLEAR-III) to be built in the 2030s. As a pretesting facility, a lead-alloy-cooled zero-power reactor (CLEAR-0) is required to obtain the neutronics data for the CLEAR series reactor. However, lead-alloy material as a coolant for a reactor has some challenges that are required to be considered in the fields of neutronics, thermal hydraulics, material compatibility, physical chemistry, safety characteristics, etc. To achieve these goals, several heavy liquid metal experimental facilities have been built to investigate the critical characteristics and key technologies of lead-alloy-cooled reactors, such as material issues, thermo-hydraulics, etc. Figure 14.21 shows the CLEAR series reactor development plan map of China along with the ADS system project. On the other hand, XJTU proposed a 300 MW_{th} LESMOR concept for electricity generation in remote areas (Wei et al., 2019). LESMOR is the abbreviation of LEad-based Small Modular Reactor; meanwhile, it adopts the design philosophy of “LESS is MORE,” which aims to achieve more function, more flexibility and more sustainability with less volume, less power and fewer requirements for maintenance. Currently, XJTU conducted a series of neutronic/thermal-hydraulic analysis and finished preliminary core design of LESMOR.

14.3.5.1 CLEAR-0

To validate the nuclear design codes and databases used in the CLEAR design, to develop the nuclear measuring methods and instruments, and to support CLEAR licensing application, it is necessary to perform the zero-power neutronics experiments. Therefore, CLEAR-0, a zero-power fast spectrum experimental facility, was firstly designed to meet this requirement. The conceptual design of CLEAR-0 was finished in 2013. Under its conceptual design, the facility main structure sits in the reactor pit, above which there is a removable biological shield. The cores designed in CLEAR-0 comprise a lattice of standard SubAssemblies (SAs). By changing the simulation materials loaded in standard SAs, CLEAR-0 can simulate various cores. Meanwhile, two reactor trip systems based on a different mechanism are designed to ensure CLEAR-0 safety. CLEAR-0 has two operation modes: one is the critical mode for fast reactor validation and the other one is the subcritical operation mode driven by the accelerator neutron source for ADS validation.

14.3.5.2 Clear-I

CLEAR-I was designed to validate the lead-alloy-cooled research reactor and ADS system coupling operation technology. Figure 14.22 presents the overall view structure design of the CLEAR-I reactor. There are

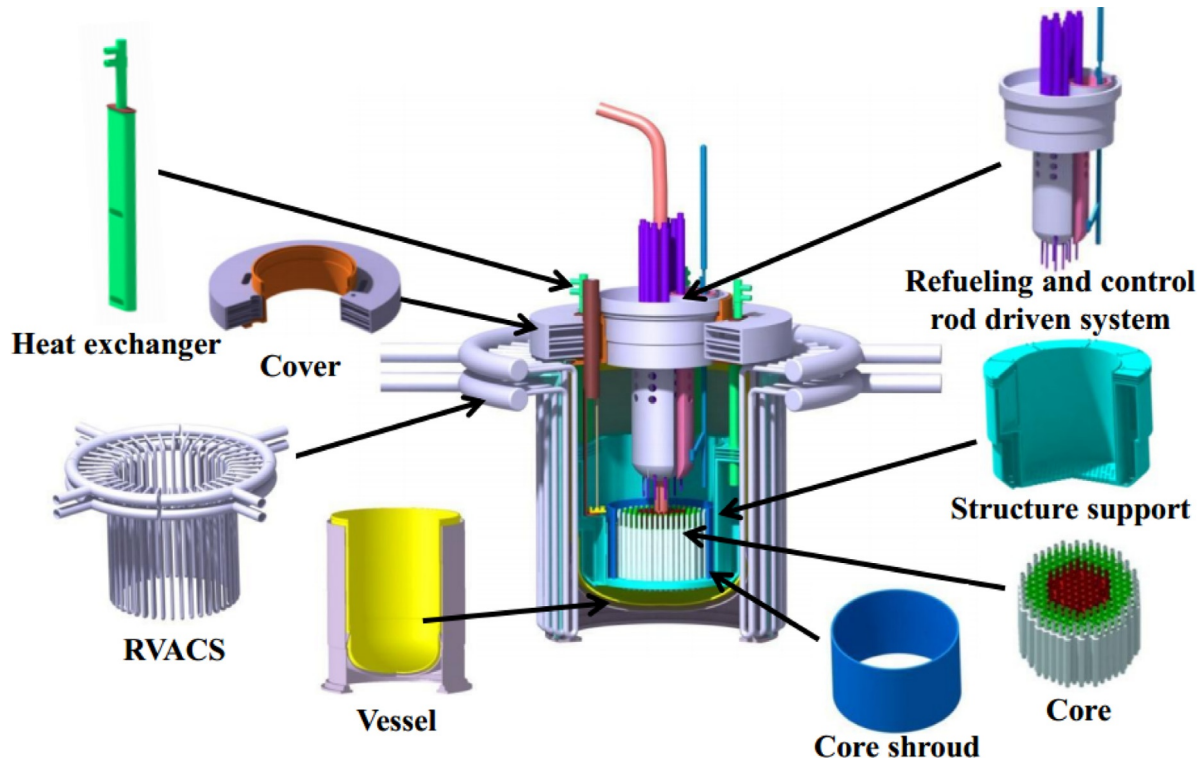


Figure 14.22. Overall view structure design for CLEAR-I. RVACS, Reactor Vessel Air Cooling System

six design principles in CLEAR-I: (1) mature fuel and material technology, (2) passive heat removal system and inherent safety design, (3) pool-type reactor vessel for continuous technology, (4) remote-handling refueling system for flexible experimentation, (5) critical/subcritical dual-mode operation capability, and (6) advanced fuel test capability. CLEAR-I will be operated in critical/subcritical modes. The subcritical operation mode reactor is named CLEAR-IA and is driven by a spallation neutron source created by the proton accelerator. The critical operation mode reactor is named CLEAR-IB. The objective of CLEAR-IA research is to test the ADS integration technology. The CLEAR-IA can be changed to CLEAR-IB by replacing the target of the spallation neutron source to some FAs. The objective of CLEAR-IB research is to validate the thermo-hydraulics, neutronics, and safety characteristics of a lead-alloy-cooled fast reactor and to test the fuel and material technologies. In addition to dual-mode operation, CLEAR-I has another unique characteristic, inherent safety, which is realized primarily in two ways:

1. Negative reactivity feedback: The negative reactivity coefficient of fuel temperature and negative coolant reactivity feedback are achieved through proper neutronics design and passive safety system design.
2. Two independent water-cooled secondary cooling systems are designed: Air is used as the final heat sink by water/air heat exchangers. CLEAR-I incorporates a reactor vessel air cooling system to remove the decay heat in case the normal heat removal path is unavailable.

In the reference parametric design of CLEAR-I, the pool-type configuration is selected. The thermal power is 10 MW and no electric power is generated. LBE is chosen as the primary coolant and UO_2 with 9.75% ^{235}U enrichment is adopted as the first loading fuel. Hexagonal-wrapped FAs are used in the hexagonal lattice core, in which the cladding material is 15-15Ti steel whereas the structure material is SS316L. To satisfy the experiment flexibility requirements, the primary cooling system is driven by a mechanical pump. Large-diameter pins are designed to achieve a higher fuel volume fraction, but lower core pressure drop. [Table 14.5](#) lists the main design parameters for the CLEAR-I reactor.

Table 14.5. Main design parameters of CLEAR-I

Parameter	Unit	Value
Thermal power	MW	10
Primary coolant	–	Lead-bismuth eutectic
Fission fuel	–	UO ₂ (19.75% enrichment)
Driven force	–	Natural circulation
Subcritical mode k_{eff}	–	0.98
Primary coolant inventory	t	~700
Reactor core inlet/outlet temperature	°C	260/390
Circulation height	m	2
Secondary coolant	–	Water
Secondary coolant pressure	MPa	4
Secondary coolant temperature	°C	215/230
Primary heat exchanger	–	4 (two independent loops)
Main vessel height	–	6300
Main vessel diameter	mm	4650

14.3.5.3 Clear-II

For the second stage of the China ADS system program, an experimental facility will be built to test the platform for the ADS system integration and materials experiment. It is also used as a high neutron flux test reactor for demonstration of ADS system and fusion reactor materials. Therefore, a 100-MW_{th} lead-cooled or LBE-cooled experimental reactor named CLEAR-II will be built coupled with a proton accelerator of approximately 600–1000 MeV/10 mA and a spallation target. On the basis of CLEAR-II success, the high-power ADS system design, construction, and operation technology may be preliminarily obtained. To increase the reactor neutron flux and power density, the nuclear fuel will use high-enriched MOX fuel; FAs can partially be replaced by MA SAs to test the nuclear waste transmutation mechanism. CLEAR-II also can be used as a high neutron flux reactor to perform material irradiation experimental study.

14.3.5.4 Clear-III

In the third stage of the China ADS program, CLEAR-III is a lead-alloy-cooled demonstration reactor that aims to demonstrate the technology of nuclear waste transmutation capability of the commercial ADS system. For the CLEAR-III reference scenario, an accelerator-driven lead-alloy-cooled subcritical reactor for transmutation of long-lived high-level nuclear wastes is developed based on the neutronics, thermo-hydraulics, materials, and mechanics analysis. The lead and LBE are still considered as the potential coolant for CLEAR-III to investigate the highly efficient power generation and waste transmutation. A linear accelerator produces the proton beam of 1.5 GeV/10 mA and the proton impinges on the windowless LBE target in the CLEAR-III central region. The CLEAR-III system is rated at 1000 MW of thermal power. Currently, one fuel type considered for CLEAR-III is the transuranic element TRU-Zr dispersion fuel, in which TRU-Zr particles are dispersed in a Zr matrix. The advanced ferritic/martensitic steel is selected as the fuel cladding and other structure materials because of its good performance under the highly corrosive and radioactive environment.

14.3.5.5 LESMOR

LESMOR is a 300-MW_{th} modular LFR proposed by XJTU, which can be fabricated in the factory and transported through vehicles or ships to a fixed location to solve the power supply problems in remote and isolate areas. At the initial stage, the preliminary core scheme of LESMOR has been brought forward after a series of detailed neutronic and thermal hydraulic analysis. Figure 14.23 shows the scheme diagram of the LESMOR core. Currently, (Th, Pu)N fuel is considered as a candidate of the fuel type. The purpose is to consume the spent-plutonium and make full use of the abundant thorium resources to meet the requirements of sustainability. However, the cost and the complex manufacturing process of this new advanced fuel need to be further investigated. Same with CLEAR series, the ASME codified T91 FMS is chosen as the cladding and structure materials. The fuel assembly adopts open square lattice with 11 × 11 bundles and has a large pitch-to-diameter ratio of 1.4 to decrease the flow resistance and enhance the natural circulation capability. Table 14.6 presents the main parameters of the core.

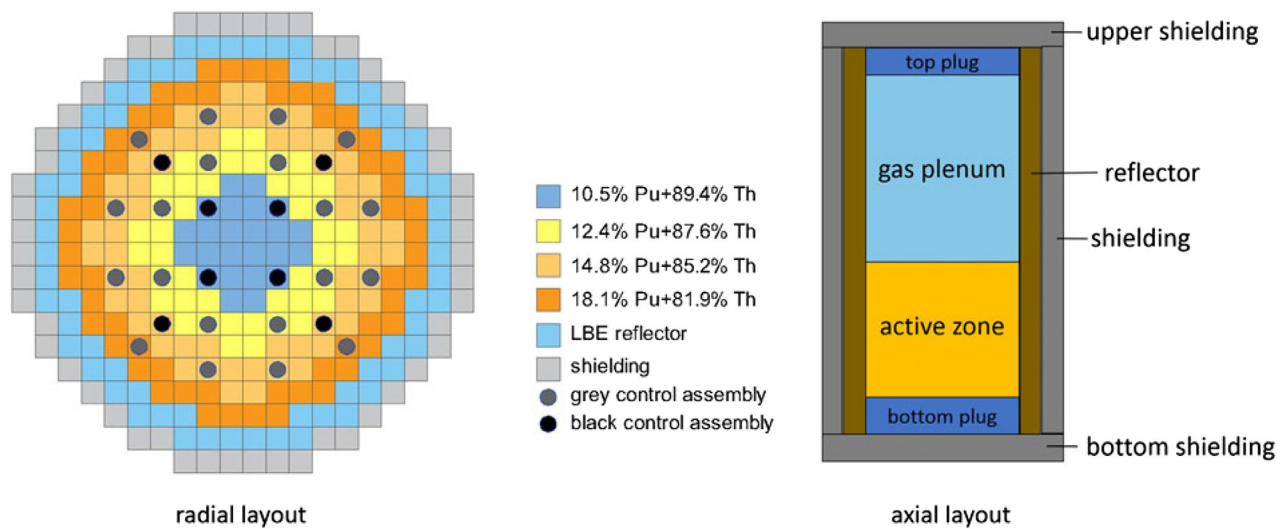


Figure 14.23. Core configuration of LESMOR

Table 14.6. Main parameters of LESMOR core

Parameter	Unit	Value
Thermal power	MW	300
Primary coolant	–	Lead-bismuth eutectic
Fission fuel	–	(Th, Pu)N
Driven force	–	Natural circulation
Reactor core inlet/outlet temperature	°C	300/420
Active height	m	2.5
Core total height	m	6.5
Pitch-to-diameter ratio	–	1.4
Core diameter	m	3.2
Core mass flow rate	kg/s	17,400

References

- Cai, B., Wang, J., Sun, L., Zhang, N., Yan, C., 2014. Experimental study and numerical optimization on a vane-type separator for bubble separation in TMSR. *Prog. Nucl. Energy* 74, 1–13. Available from: <https://www.sciencedirect.com/science/article/pii/S0149197014000353>.
- Cai, J., 2013. *The Preliminary Analysis on Reactivity Initiated Transient of Molten Salt Reactor*. Shanghai Institute of Applied Physics, CAS. The University of Chinese Academy of Sciences.
- Cheng, J., Zhang, P., An, X., Wang, K., Zuo, Y., Yan, H., Li, H., 2013. A device for measuring the density and liquidus temperature of molten fluorides for heat transfer and storage. *Chin. Phys. Lett.* 30 (12). Paper #126501.
- Cheng, M., Dai, Z., 2014. Turbulent transport effect of delayed neutron precursor in molten salt fast reactor. *At. Energy Sci. Technol.* 48, 131–137.
- Cheng, X., Liu, X.J., Yang, Y.H., 2008. A mixed core for supercritical water-cooled reactors. *Nucl. Eng. Technol.* 40 (2), 117–126. Available from: http://ocean.kisti.re.kr/download/volume/nuclear/OJRHBJ/2008/v40n2/OJRHBJ_2008_v40n2_117.pdf.
- Dang, G., Huang, D., Lu, J., Gao, Y.X., Shan, J.Q., 2013. Large-break accident analysis of supercritical water-cooled reactor CSR1000 using APROS code. *Nucl. Power Eng.* 34 (1), 72–82. Available from: http://en.cnki.com.cn/Article_en/CJFDTotal-HDLG201301016.htm.
- Du, D., Xiao, Z., Yan, X., Zeng, X.K., Huang, Y.P., 2013. Subchannel analysis of SCWR CSR1000 assembly. *Nucl. Power Eng.* 34 (1), 40–44. Available from: http://en.cnki.com.cn/Article_en/CJFDTotal-HDLG201301008.htm.
- Feng, S., 2014. *Studies on Irradiation Damage and Molten Salt Penetration in Pyrolytic Carbon Coating on Nuclear Graphite*. Shanghai Institute of Applied Physics. The University of Chinese Academy of Sciences.
- Forsberg, C., Hu, L., Richard, J., Romatoski, R., Forget, B., Stempien, J., Ballinger, R., Sun, K., 2014. Fluoride-Salt-Cooled High-Temperature Test Reactor (FHTR): Goals, Options, Ownership, Requirements, Design, Licensing, and Support Facilities. Massachusetts Institute of Technology. Report Number: MIT-ANP-TR-154. Available from: <https://web.mit.edu/nse/pdf/researchstaff/forsberg/FHR%20Test%20Reactor%20ANP-154%20MIT.pdf>.
- Guo, Z., Wang, C., Zhang, D., Chaudri, K.S., Tian, W., Su, G., Qiu, S., 2013a. The effects of core zoning on optimization of design analysis of molten salt reactor. *Nucl. Eng. Des.* 265, 967–977. Available from: <https://www.sciencedirect.com/science/article/pii/S002954931300544X>.
- Guo, Z., Zhang, D., Xiao, Y., Tian, W., Su, G., Qiu, S., 2013b. Simulations of unprotected loss of heat sink and combination of events accidents for a molten salt reactor. *Ann. Nucl. Energy* 53, 309–319. Available from: <https://www.sciencedirect.com/science/article/pii/S0306454912003593>.
- Guo, Z., Zhou, J., Zhang, D., Chaudri, K.S., Tian, W., Su, G.H., Qiu, S., 2013c. Coupled neutronics/thermal-hydraulics for analysis of molten salt reactor. *Nucl. Eng. Des.* 258, 144–156. Available from: <https://www.sciencedirect.com/science/article/pii/S0029549313000290>.
- Han, L., Chen, Y., Zhou, D., Yin, C., Zhang, F., 2013. Design of the distributed control system for HTS molten salt test loop. *Nucl. Tech.* 36 (9). Paper #090603. Available from: <https://d.wanfangdata.com.cn/periodical/hjs201309013>.
- Hinds, D., Maslak, C., 2006. Next-generation nuclear energy: the ESBWR. *Nucl. News* 4 (9), 35–40.
- Huang, H., Li, J., Liu, R., Chen, H., Yan, L., 2014. Temperature effect of Xe ion irradiation to 316 austenitic stainless steel. *Acta Metall. Sin.* 50 (10), 1189–1194. Available from: http://en.cnki.com.cn/Article_en/CJFDTOTAL-JSXB201410005.htm.
- Jiao, X., Wang, K., He, Z., Chen, K., 2015. Core safety discussion under station blackout ATWS accident of solid fuel molten salt reactor. *Nucl. Tech.* 38 (2). Paper #020604. Available from: http://en.cnki.com.cn/Article_en/CJFDTOTAL-HJSU201502013.htm.
- Li, L., Yu, G., Zhou, X., 2014. Corrosion behavior of Ti_3SiC_2 and Ti_3AlC_2 with LiF-NaF-KF molten salt. *Nucl. Tech.* 37 (6). Paper #060602. Available from: http://en.cnki.com.cn/Article_en/CJFDTOTAL-HJSU201406016.htm.
- Liu, K., Xu, L., Liu, Z., Long, S., 2015. Impact of temperature on the molten salt corrosion of Hastelloy-N alloys. *Nucl. Tech.* 38 (2). Paper #020602. Available from: http://en.cnki.com.cn/Article_en/CJFDTOTAL-HJSU201502011.htm.
- Li, X., Li, Q., Xia, B., Li, M., Liu, L., 2013. Overview on overall design of CSR1000. *Nucl. Power Eng.* 34 (1), 5–8. Available from: http://en.cnki.com.cn/Article_en/CJFDTotal-HDLG201301001.htm.
- Liu, X.J., Cheng, X., 2010. Coupled thermal-hydraulics and neutron-physics analysis of SCWR with mixed spectrum core. *Prog. Nucl. Energy* 52 (7), 640–647.
- Liu, X.J., Fu, S.W., Xu, Z.H., Yang, Y.H., Cheng, X., 2013a. LOCA analysis of SCWR-M with passive safety system. *Nucl. Eng. Des.* 259, 187–197. Available from: <https://www.sciencedirect.com/science/article/pii/S0029549313001490>.
- Liu, Y., Mei, L., Cai, X., 2013b. Physics research for molten salt reactor with different core boundaries. *Nucl. Tech.* 36 (3). Paper #030601. Available from: http://en.cnki.com.cn/Article_en/CJFDTOTAL-HJSU201303014.htm.
- Mei, M., Shao, S., Zuo, J., Yu, Z., Chen, K., 2013. Probability safety assessment of LOOP accident to molten salt reactor. *Nucl. Tech.* 36 (12). Paper #120604. Available from: http://en.cnki.com.cn/Article_en/CJFDTOTAL-HJSU201312010.htm.

- Mei, M., Shiwei, S., He, Z., Chen, K., 2014. Research on initial event analysis for solid thorium molten salt reactor probabilistic safety assessment. Nucl. Tech. 37 (9). Paper #090601. Available from: http://en.cnki.com.cn/Article_en/CJFDTotal-HJSU201409009.htm.
- Peng, C., Yan, X., Peng, J., Zeng, X., Huang, Y., Xiao, Z., 2013. CATHARE simulation on coupled neutronics/thermal-hydraulics of molten salt reactor (MSR). Nucl. Power Eng. 34 (4), 16–19. Available from: http://en.cnki.com.cn/Article_en/CJFDTotal-HDLG201304004.htm.
- Pi, L., Liu, W., Zhang, D., Qian, Y., Wang, G.H., Zeng, Y.S., 2015. Estimation of permeability of tritium in structural materials of molten salt reactor based on hydrogen isotope. Nucl. Tech. 38 (3). Paper #030602. Available from: http://en.cnki.com.cn/Article_en/CJFDTOTAL-HJSU201503014.htm.
- Qian, L., Qiu, S., Zhang, D., Su, G.H., Tian, W., 2010. Numerical research on natural convection in molten salt reactor with non-uniformly distributed volumetric heat generation. Nucl. Eng. Des. 240 (4), 796–806. Available from: <https://www.sciencedirect.com/science/article/pii/S0029549309005640>.
- Rouault, J., Chellapandi, P., Raj, B., Dufour, P., Latge, C., Paret, P., Rodriguez, P.H., Gautier, G.M., Fiorini, G.L., Pelletier, M., Gosset, D., Bourganel, S., Mignot, G., Varaine, F., Valentin, B., Masoni, P., Martin, P., Queval, J.C., Broc, D., Devictor, N., 2010. Sodium fast reactor design: fuels, neutronics, thermal-hydraulics, structural mechanics and safety. In: Handbook of Nuclear Engineering. Springer, US, pp. 2321–2710.
- Schulz, T.L., 2006. Westinghouse AP1000 advanced passive plant. Nucl. Eng. Des. 236 (14–16), 1547–1557. Available from: <https://www.sciencedirect.com/science/article/pii/S0029549306003190>.
- Serp, J., Allibert, M., Beneš, O., Delpech, S., Feynberg, O., Ghetta, V., Heuer, D., Holcomb, D., Ignatiev, V., Kloosterman, J.L., 2014. The molten salt reactor (MSR) in generation IV: overview and perspectives. Prog. Nucl. Energy 77, 308–319. Available from: <https://www.sciencedirect.com/science/article/pii/S0149197014000456>.
- Song, S., Cai, X., Liu, Y., Wei, Q., Guo, W., 2014. Pore scale thermal hydraulics investigations of molten salt cooled pebble bed high temperature reactor with BCC and FCC configurations. Sci. Technol. Nucl. Install. 2014. Paper #589895, 16 pp. Available from: <https://downloads.hindawi.com/journals/stni/2014/589895.pdf>.
- Steinwarz, W., Xu, Y.H., 1990. Status of design of the HTR test module China. Nucl. Eng. Des. 121 (2), 317–324. Available from: <https://www.sciencedirect.com/science/article/abs/pii/002954939090117G>.
- Sun, L., Yan, C., Fa, D., Wang, N., 2014. Conceptual design and analysis of a passive residual heat removal system for a 10MW molten salt reactor experiment. Prog. Nucl. Energy 70, 149–158. Available from: <https://www.sciencedirect.com/science/article/pii/S0149197013001923>.
- Sun, Y.L., Xu, Y.H., 2000. Licensing of the HTR-10 test reactor. In: Workshop on ‘Safety and Licensing Aspects of Modular High Temperature Gas Reactors’ Aix-en-Provence, France.
- Tian, X., Tian, W., Zhu, D., Qiu, S., Su, G., Xia, B., 2012. Flow instability analysis of supercritical water-cooled reactor CSR1000 based on frequency domain. Ann. Nucl. Energy 49, 70–80. Available from: <https://www.sciencedirect.com/science/article/pii/S0306454912002368>.
- Wang, C., Guo, Z., Zhang, D., Qiu, S., Tian, W., Wu, Y., Su, G.H., 2013b. Transient behavior of the sodium–potassium alloy heat pipe in passive residual heat removal system of molten salt reactor. Prog. Nucl. Energy 68, 142–152. Available from: <https://www.sciencedirect.com/science/article/pii/S0149197013001261>.
- Wang, C., Zhang, D., Qiu, S., Tian, W., Wu, Y., Su, G.H., 2013c. Study on the characteristics of the sodium heat pipe in passive residual heat removal system of molten salt reactor. Nucl. Eng. Des. 265, 691–700. Available from: <https://www.sciencedirect.com/science/article/pii/S002954931300530X>.
- Wang, C., Xiao, Y., Zhou, J., Zhang, D., Qiu, S., Su, G., Cai, X., Wang, N., Guo, W., 2014b. Computational fluid dynamics analysis of a fluoride salt-cooled pebble-bed test reactor. Nucl. Sci. Eng. 178, 86–102.
- Wang, Y., Huang, S., Tang, Z., Xie, L., Yin, H., Zhao, S., 2014a. Corrosion behavior of ceramics immersed in LiF-NaF-KF molten salt. New Chem. Mater. 42 (3), 111–117. Available from: http://en.cnki.com.cn/Article_en/CJFDTOTAL-HGXC201403038.htm.
- Wang, G., Li, W., Li, N., Han, S., 2015. Thermal-hydraulic simulation for pebble-bed fluoride salt-cooled high temperature reactor core. At. Energy Sci. Technol. 49 (4), 629–633. Available from: http://en.cnki.com.cn/Article_en/CJFDTotal-YZJS201504009.htm.
- Wang, H., Cai, X., Mei, L., Chen, J., Guo, W., Jiang, D., 2013a. Impact on breeding rate of different molten salt reactor core structures. Nucl. Tech. 36 (9). Paper #090601. Available from: http://en.cnki.com.cn/Article_en/CJFDTotal-HJSU201309011.htm.
- Wang, X., 2021. Numerical Research on Three-Dimensional Thermal Hydraulic Characteristics in Once-Through Steam Generator of the Sodium Cooled Fast Reactor (Ph.D. thesis). Xi'an: Xi'an Jiaotong University (in Chinese).
- Wang, Y., 2013. Corrosion Behavior of Novel Ceramics Immersion in FLiNaK Molten Salt. Xiangtan University.

- Wei, Q., Mei, L., Zhai, Z., Wei, G., Chen, J., Cai, X., 2014. Preliminary study on safety characteristics of molten salt reactor. *At. Energy Sci. Technol.* 48 (12), 2280–2286. Available from: http://en.cnki.com.cn/Article_en/CJFDTOTAL-YZJS201412018.htm.
- Wei, S., Sun, H., Wang, C., Chen, R., Tian, W., Qiu, S., Su, G.H., 2019. Neutronic/thermal-hydraulic design features of an improved lead-bismuth cooled small modular fast reactor. *Int. J. Energy Res.* 43 (8), 1–12. Available from: <https://onlinelibrary.wiley.com/doi/10.1002/er.4541>.
- WNA, 2005. <http://www.world-nuclear.org/>.
- Wu, Y., Bai, Y., Song, Y., Huang, Q., Jiang, J., 2014. Design and R&D progress of China lead-based reactor. In: *Proceedings of the 22nd International Conference on Nuclear Engineering*, July 7–11, 2014, Prague, Czech Republic. Paper No. 31136.
- Xia, B., Yang, P., Wang, L., Ma, Y., Li, Q., Li, X., Liu, J., 2013. Core preliminary conceptual design of supercritical water-cooled reactor CSR1000. *Nucl. Power Eng.* 34 (1), 9–14. Available from: http://en.cnki.com.cn/Article_en/CJFDTOTAL-HDLG201301002.htm.
- Xiao, Y., Hu, L., Qiu, S., Zhang, D., Su, G., Tian, W., 2014. Development of a thermal-hydraulic analysis code and transient analysis for a FHTR. In: *22nd International Conference on Nuclear Engineering*. American Society of Mechanical Engineers. V005T016A005.
- Xu, M., 2009. Fast reactor and sustainable nuclear energy development in China. *China Nucl. Power* 2 (2), 106–110. Available from: http://en.cnki.com.cn/Article_en/CJFDTOTAL-ZGHD200902006.htm.
- Xu, M., 2008. The status and prospects of fast reactor technology development in China. *China Eng. Sci.* 10 (1), 70–76. Available from: http://en.cnki.com.cn/Article_en/CJFDTOTAL-GCKX200801010.htm.
- Xu, M., 1995. China experimental fast reactor. *High Technol. Lett.* 09, 53–59. Available from: <http://www.cnki.com.cn/Article/CJFDTOTAL-YNXB500.079.htm>.
- Xu, Y.H., Liu, J.G., Yao, M.S., Zhou, H.Z., Ju, H.M., 1997. High temperature engineering research facilities and experiments in China. In: *NEA Workshop on High Temperature Engineering Research Facilities and Experiments*. Petten, The Netherlands.
- Xu, Y.H., Zuo, K.F., 2002. Overview of the 10 MW high temperature gas cooled reactor—test module project. *Nucl. Eng. Des.* 218 (1–3), 13–23. Available from: <https://www.sciencedirect.com/science/article/pii/S0029549302001814>.
- Xu, Z.H., Hou, D., Fu, S.W., Yang, Y.H., Cheng, X., 2011. Loss of flow accident and its mitigation measures for nuclear systems with SCWR-M. *Ann. Nucl. Energy* 38 (12), 2634–2644. Available from: <https://www.sciencedirect.com/science/article/pii/S0306454911003495>.
- Yang, H., Zhou, P., Yu, H., 2007. Preliminary consideration of overall technical scheme for China demonstration fast reactor. In: *Annual Report of China Institute of Atomic Energy*, pp. 3–5.
- Yang, T., Liu, X.J., Cheng, X., 2012. Optimization of multilayer fuel assemblies for supercritical water-cooled reactors with mixed neutron spectrum. *Nucl. Eng. Des.* 249, 159–165. Available from: <https://www.sciencedirect.com/science/article/pii/S0029549311005607>.
- Yin, W., 2014. *Production of Radionuclide and Safety Analysis of TRISO Coated Fuel Particles*. Shanghai Institute of Applied Physics Chinese Academy of Sciences.
- Yue, N., 2016. *Research on Transient Thermal-Hydraulic Characteristics and Safety Analysis for Pool-Type Sodium-Cooled Fast Reactor* (Ph.D. thesis). Xi'an Jiaotong University, Xi'an (in Chinese).
- Zeng, Y., Wu, S., Qian, Y., Wang, G., Du, L., Liu, W., Xia, Z.-H., 2014. Apparatus for determining permeability of hydrogen isotopes in molten-salt. *Nucl. Sci. Tech.* 25. Paper #040602. Available from: <http://www.cnki.com.cn/Article/CJFDTOTAL-HKXJ201404015.htm>.
- Zhang, D., Qiu, S., Liu, C., Su, G.H., 2008. Steady thermal hydraulic analysis for a molten salt reactor. *Nucl. Sci. Tech.* 19 (3), 187–192. Available from: <http://www.cnki.com.cn/Article/CJFDTOTAL-HKXJ200803014.htm>.
- Zhang, D., Qiu, S., Su, G.H., 2009a. Development of a safety analysis code for molten salt reactors. *Nucl. Eng. Des.* 239 (12), 2778–2785. Available from: <https://www.sciencedirect.com/science/article/pii/S0029549309004191>.
- Zhang, D., Rineiski, A., Qiu, S., 2009b. Comparison of modeling options for delayed neutron precursor movement in a molten salt reactor. *ANS annual meeting 2009*, June 14–18, 2009, Atlanta, USA. *Trans. Am. Nucl. Soc.* 100, 639–640.
- Zhang, D., Rineiski, A., Wang, C., Guo, Z., Xiao, Y., Qiu, S., 2015. Development of a kinetic model for safety studies of liquid-fuel reactors. *Prog. Nucl. Energy* 81, 104–112. Available from: <https://www.sciencedirect.com/science/article/pii/S0149197015000153>.
- Zhang, D., Zhai, Z., Rineiski, A., Guo, Z., Wang, C., Xiao, Y., Qiu, S., 2014b. COUPLE, a time-dependent coupled neutronics and thermal-hydraulics code, and its application to MSFR. In: *22nd International Conference on Nuclear Engineering*. American Society of Mechanical Engineers. Paper# V003T005A019.
- Zhang, Z., Xia, X., Zhu, X., Cai, J., 2014a. Source terms calculation for the MSRE with on-line removing radioactive gases. *Nucl. Tech.* 37 (2). Paper #020603. Available from: http://en.cnki.com.cn/Article_en/CJFDTOTAL-HJSU201402012.htm.

- Zhang, H., Luo, Y., Li, X., Fan, H., Liu, X., Zhou, Y., 2013. Research on overall structure design of CSR1000. Nucl. Power Eng. 3-4 (1), 52–56. Available from: http://en.cnki.com.cn/Article_en/CJFDTOTAL-HDLG201301010.htm.
- Zhang, Z.Y., Yu, S.Y., 2002. Future HTGR developments in China after the criticality of the HTR-10. Nucl. Eng. Des. 218 (1–3), 249–257. Available from: <https://www.sciencedirect.com/science/article/pii/S0029549302002042>.
- Zhao, H., Yan, C., Sun, L., Zhao, K., Fa, D., 2015. Design of a natural draft air-cooled condenser and its heat transfer characteristics in the passive residual heat removal system for 10 MW molten salt reactor experiment. Appl. Therm. Eng. 76, 423–434. Available from: <https://www.sciencedirect.com/science/article/pii/S1359431114010849>.
- Zhao, R.K., Yuan, K.Q., Shu, T.W., 2001. Project Progress in the Energy Field. Atomic Energy Press, pp. 121–206 (in Chinese).
- Zhong, D.X., Gao, Z.Y., 1985. Study on Modular High Temperature Gas-Cooled Reactor and its Application for Heavy Oil Recovery 1985.11 INET Report. (in Chinese).
- Zhou, J., Zhang, D., Qiu, S., Su, G., Tian, W., Wu, Y., 2014. Three-dimensional code development for steady state analysis of liquid-fuel molten salt reactor. At. Energy Sci. Technol. 48 (8), 1369–1374. Available from: http://en.cnki.com.cn/Article_en/CJFDTOTAL-YZJS201408005.htm.
- Zhou, X., 2013. A Study on Measurement of Neutron Energy Spectrum for Thorium Molten Salt Reactor. Shanghai Institute of Applied Physics. The University of Chinese Academy of Sciences. Available from: <http://cdmd.cnki.com.cn/article/cdmd-80014-1014042681.htm>.
- Zhou, X., Liu, G., 2013. Study of control rod worth in the TMSR. Nucl. Sci. Tech. 24. Paper #010601. Available from: http://en.cnki.com.cn/Article_en/CJFDTotal-HKXJ201301010.htm.
- Zhu, D.H., Zhao, H., Tian, W.X., Su, Y.L., Chaudri, K.S., Su, G.H., Qiu, S.Z., 2012. Development of TACOS code for loss of flow accident analysis of SCWR with mixed spectrum core. Prog. Nucl. Energy 54 (1), 150–161. Available from: <https://www.sciencedirect.com/science/article/pii/S014919701100151X>.
- Zhuang, K., Cao, L., Zheng, Y., Wu, H., 2014. Studies on the molten salt reactor: code development and neutronics analysis of MSRE-type design. J. Nucl. Sci. Technol. 52 (2), 251–263. Available from: <https://www.tandfonline.com/doi/full/10.1080/00223131.2014.944240>.
- Zou, X., Dai, Z., Tang, Z., 2013. Numerical simulation of induction heating in FLiNaK molten salt high temperature testing loop. Nucl. Tech. 36 (7). Paper #070601. Available from: http://en.cnki.com.cn/Article_en/CJFDTOTAL-HJSU201307015.htm.

Generation-IV concepts: India

*Ratan K. Sinha^a, Perumal Chellapandi^b, Gopala I. Srinivasan^c,
Indravadan Dulera^d, Pallippattu K. Vijayan^d, and Shridhar K. Chande^e*

^aDepartment of Atomic Energy, Mumbai, India ^bBHAVINI, Kalpakkam, India ^cIGCAR, Kalpakkam, India ^dBARC, Mumbai, India ^eAtomic Energy Regulatory Board, Mumbai, India

Nomenclature

AHWR	Advanced Heavy Water Reactor
AMD	Atomic Minerals Directorate
ATWS	Anticipated Transient Without Scram
BARC	Bhabha Atomic Research Center
BCRs	Burn-up Compensation Rods
CDA	Core Disruptive Accident
CHTR	Compact High-Temperature Reactor
CSRDM	Control and Safety Rods in their Drive Mechanisms
DAE	Department of Atomic Energy
DBA	Design-Basis Accident
DBE	Design-Basis Events
DC	Dump Condenser
DEC	Design Extension Condition
DHR	Decay Heat Removal
DSRDM	Diverse Shutdown Rod Drive Mechanisms
ECCS	Emergency Core Cooling System
FBR	Fast Breeder Reactor
GDWP	Gravity Driven Water Pool
HTR	High-Temperature Reactor
IGCAR	Indira Gandhi Center for Atomic Research
IHTR	Innovative High-Temperature Reactor
IMSBR	Indian Molten Salt Breeder Reactor
ISI	In-Service Inspection
LBE	Lead-Bismuth Eutectic
LEU	Low-Enriched Uranium
LHR	Linear Heat Rating
LOCA	Loss Of Coolant Accident
LSBO	Long Station BlackOut
MHT	Main Heat Transport
MINA	MINI Sodium Fire Facility
MSBRDF	Molten Salt Breeder Reactor Development Facility
MW_e	MegaWatt electrical
MW_{th}	MegaWatt thermal
OGDHR	Operating-Grade Decay Heat Removal

PARCs	Passive Autocatalytic ReCombiners
PARTH	Proving Advanced Reactor Thermal Hydraulics
PATH	PostAccident Thermal Hydraulics facility
PEC	Practically Eliminated Condition
PPIS	Passive Poison Injection System
RY	Reactor per Year
SA	SubAssemblies
SDS	Shut-Down System
SFEF	Sodium Fire Experimental Facility
SG	Steam Generator
SOCA	SODium CAble interaction facility
SOFI	SODium-Fuel Interaction facility
SSDHR	Secondary Sodium Decay Heat Removal
TG	TurboGenerator
USD	Ultimate Shut-Down

15.1 Introduction

India is planning to enhance its electrical power generation capacity to 80,000 MW_e by 2031–32 so as to significantly increase its per capita electrical consumption with a goal to reach the world average (~2700 kWh). To achieve this target, nuclear energy would have to make a significant contribution. As per the government data published before the Fukushima accident ([Integrated Energy Policy, 2006](#)), the nuclear share is expected to be increased from the current level of ~6800 MWe (18 PHWRs and 4 LWRs in operation and as on Jan 2022), by addition of several domestic and imported water cooled reactors. Eight water-cooled reactors with a total capacity of 6200 MW_e and a 500-MW_e Prototype Fast Breeder Reactor (PFBR) are currently at various stages of construction and commissioning. The balance increase in capacity would be achieved by imported light water reactors under the International Atomic Energy Agency safeguard, future Fast Breeder Reactors (FBRs), and domestic water-cooled reactors. India follows the Three-Stage Nuclear Power Program formulated by Dr. Homi Jahangir Bhabha, the designer and architect cum founder of the Indian nuclear power program, to achieve energy security with the modest indigenous natural uranium and vast thorium resources available in the country. This program has water-cooled reactors in the first stage, fast reactors in the second stage, and thorium-fueled reactors in the third stage. The first stage, with 18 Pressurized Heavy Water Reactors (PHWRs) in operation and many under construction and in the planning stages, has reached a state of commercial maturity. The second stage starts with the commissioning of PFBR by this year. Late in the second stage the program would have thorium as the fertile material along with plutonium so as to produce ²³³U for the third stage. India has one of the largest reserves of thorium in the world. The Atomic Minerals Directorate for Exploration and Research, a constituent unit of the Indian Department of Atomic Energy (DAE), has thus far established 11.93 million tons of monazite (thorium-bearing mineral) in India, which contains approximately 1.07 million tons of thorium oxide. In view of this, the third stage of the Indian nuclear power program is based on extensive use of ²³³U-fueled reactors with thorium as the fertile material. The reactors for the third stage are proposed to be breeder reactors and operating entirely on a ²³³U-Th fuel cycle. The Molten Salt Breeder Reactor (MSBR) is being considered as an attractive option for large-scale deployment during the third stage, in addition to Sodium Fast Reactors (SFRs). India has a very ambitious long-term plan of deployment of many FBRs and thorium-based reactors to achieve energy security. In addition, High-Temperature Reactors (HTRs) are being developed to produce hydrogen as an alternative to oil-based transport fuel. Thus India has several thermal and fast spectrum reactors on the long-term horizon. The reactors

currently under design at two reactor research centers (the Bhabha Atomic Research Center (BARC) and Indira Gandhi Center for Atomic Research (IGCAR) in DAE) have design goals similar to those of Generation-IV (Gen-IV) concepts. These include enhanced safety, economic attractiveness, and sustainability.

In this chapter the reactor concepts that are presented include three thermal spectrum reactors (i.e., the Advanced Heavy Water Reactor (AHWR), the Compact High-Temperature Reactor (CHTR), and the Innovative High-Temperature Reactor (IHTR)) and two fast spectrum reactors (i.e., SFRs and the Indian Molten Salt Breeder Reactor (IMSBR)). AHWR, CHTR, IHTR, and IMSBR are being designed at BARC, and SFR is designed at IGCAR. The salient conceptual design and safety features and an overview of the current status and Research and Development (R&D) activities in progress/planned for these reactors are highlighted.

15.2 Advanced Heavy Water Reactors (AHWRs)

The AHWR is designed and developed to achieve large-scale use of thorium for the generation of commercial nuclear power. This reactor will produce most of its power from thorium, with no external input of ^{233}U in the equilibrium cycle. The reactor incorporates several passive safety features and is associated with a closed fuel cycle having reduced environmental impact. At the same time, the reactor possesses several features that are likely to reduce its capital and operating costs. Many of these features that are part of the basic goals to be achieved by Gen-IV reactors also make AHWR a demonstration reactor for Gen-IV features on the near-term time horizon. Inherent and passive safety features are used extensively to achieve enhanced safety. A prototype AHWR is being developed currently at BARC. It is a 300-MW_e, vertical, pressure-tube-type, natural-circulation-based, boiling light water-cooled, and heavy water-moderated reactor (AHWR-300). AHWR-300 is a land-based nuclear power station. The reactor is designed to produce 920 MW of thermal power, generating 300 MW_e (gross) and 2400 m³/day of desalinated water. The plant can be configured to deliver higher desalination capacities with some reduction in electricity generation. An AHWR-based plant can be operated in base load as well as load-following modes.

15.2.1 Design features of AHWR-300

The schematic of an AHWR and major systems are shown in [Figure 15.1](#). The reactor fuel cluster is shown in [Figure 15.2](#). AHWR has average burn-up of 38,000 MWd/t. The flexibility to adopt different fuel cycles to enhance the utilization of fuel resources: AHWR can be used for diverse fuel cycle options including once-through and closed fuel cycles. AHWRs are also optimized to achieve high burn-up with Low-Enriched Uranium (LEU)-thorium-based fuel in AHWR300-LEU. The design provides for inherent safety characteristics through achievement of the required reactivity coefficients. In the closed fuel cycle conceived, thorium, ^{233}U , and plutonium will be recovered from the spent fuel. The recovered thorium and ^{233}U will be recycled back as Th- ^{233}U Mixed OXide (MOX) fuel, and reprocessed plutonium will be stored and will later be used as fuel for an FBR. The plutonium requirement for the reactor will be met by reprocessing of the spent fuel of PHWRs. A schematic of the fuel cycle for an AHWR is given in [Figure 15.3](#). The fuel cycle facilities (fabrication and reprocessing) for AHWR will be colocated with the reactor at the same site. The design life is 100 years. The major design parameters of AHWRs are shown in [Table 15.1](#).

15.2.2 Enhanced safety features

The emphasis in design has been to incorporate inherent and passive safety features to the maximum extent as a part of the defense-in-depth strategy. AHWR design provides a grace period of 7 days for the absence of any operator or powered actions in the event of an accident. The main objective has been to establish a case

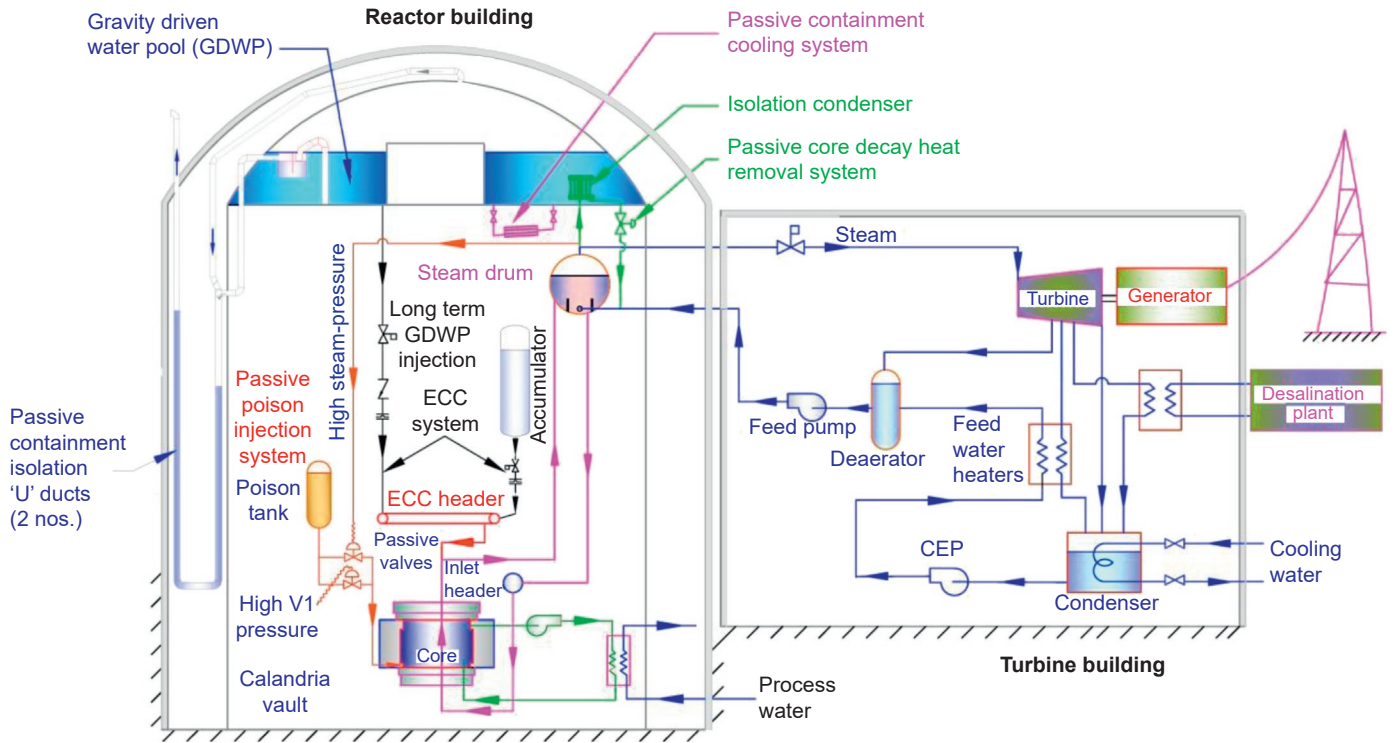


Figure 15.1. Schematic of Advanced Heavy Water Reactor (AHWR) and major systems

Figure 15.2. Advanced heavy water reactor fuel cluster. *MOX*, Mixed OXide

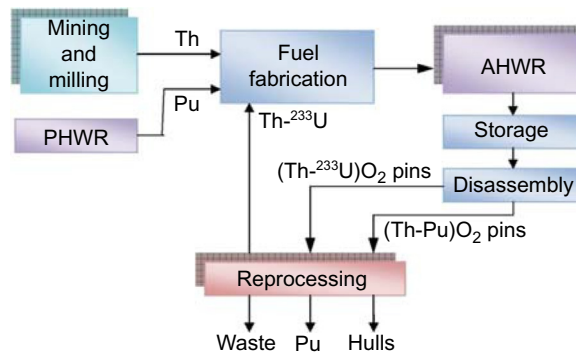
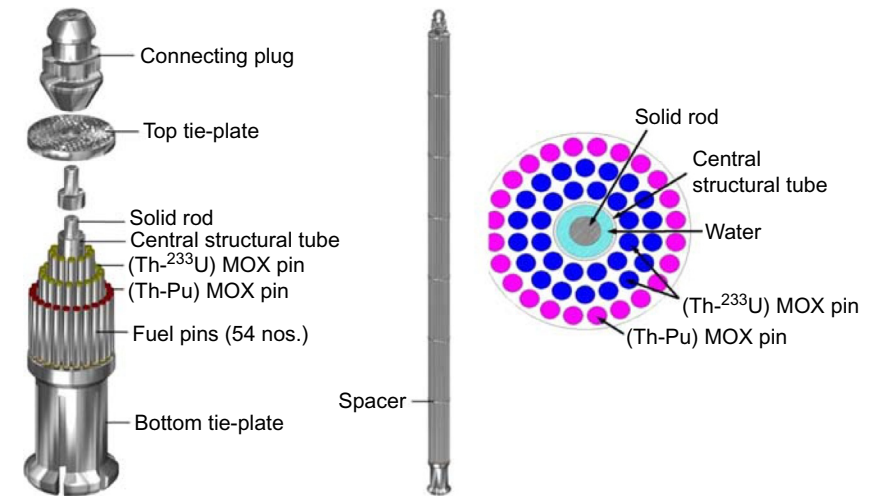


Figure 15.3. A schematic of the fuel cycle for an Advanced Heavy Water Reactor (AHWR). *PHWR*, Pressurized Heavy Water Reactor

Table 15.1. Advanced Heavy Water Reactors (AHWRs): proposed design and operating parameters

Attributes	Design parameters
Reactor power	920 MW _{th} (300 MW _e)
Fuel cluster	30 pins of (Th-Pu)O ₂ , 24 pins of (Th- ²³³ U)O ₂
Fuel discharge burn-up	40 GWd/Te (average, reference case)
Design life	100 years
Moderator	Heavy water
Coolant	Boiling light water
Core orientation	Vertical
Number of channels	452
Lattice pitch (square)	225 mm
Total core flow	2143 kg/s
Nominal operating pressure	7.0 MPa
Average core exit quality	19.1%
Total steam flow going out	408 kg/s
Feed-water temperature	403.0 K (130°C)
Coolant inlet temperature	531.4 K (258.25°C)

for elimination of the need for planning for evacuation in the case of an accident scenario in the plant. This is achieved through various passive and active safety systems designed to mitigate the consequences of Design-Basis Accidents (DBAs) and features to avoid escalation of a DBA to a severe accident. An increased reliability of the control system is achieved with the use of high-reliability digital control using advanced information technology, and increased operator reliability is achieved with the use of advanced displays and diagnostics using artificial intelligence and expert systems. The main features in these categories are listed in the following subsections.

15.2.2.1 Inherent safety features

- Negative void coefficient of reactivity, low core power density, negative fuel temperature coefficient of reactivity, and low excess reactivity
- Natural-circulation-driven heat removal during normal operation and hot shutdown
- Double containment system, use of moderator as a heat sink, presence of water in the calandria vault, and large main heat transport inventory
- Four independent Emergency Core Cooling System (ECCS) trains
- Direct injection of ECCS water into the fuel cluster
- Flooding of reactor cavity after a Loss Of Coolant Accident (LOCA)

15.2.2.2 *Passive safety systems*

- Passive injection of high-pressure and low-pressure emergency core coolant through the use of one-way rupture disks and non-return valves
- Shut-down cooling through isolation condensers in gravity-driven water pool by opening passive valve
- Passive containment isolation, after a large-break LOCA, with a water seal
- Passive shutdown by injection of poison in the moderator by use of system steam pressure in the case of failure of wired systems of Shut-Down System (SDS)-1 and SDS-2
- Passive containment cooling system
- Passive automatic depressurization system
- Core submergence after LOCA

15.2.2.3 *Features to deal with severe accidents and Fukushima types of scenarios*

- Core catcher with bottom flooding.
- Passive autocatalytic recombiners.
- Filtered hard vent system.
- Hook-up system for critical systems.
- Passive moderator and end-shield cooling systems.
- Passive union between V1 and V2 volume.
- AHWR design is found to be robust for Long Station BlackOut (LSBO) as well as LSBO with partial loss of heat sink based on analysis of postulating several scenarios relevant to the Fukushima event.

15.2.3 Safety goals

For AHWRs the goal for the frequency of severe core damage can be set at least 1 order of magnitude lower compared with the goal for new reactors of the present generation. Because the reactor uses passive heat removal systems, this goal appears to be reasonable and achievable. A peak cladding temperature value greater than or equal to 1200°C is considered to lead to core damage in a Level 1 PSA study that is performed for AHWRs. Likewise, a value of 10^{-7} per Reactor per Year (RY) can be set as a goal for large early release frequency. The point value for the Core Damage Frequency (CDF) is predicted by BARC to be less than 10^{-7} per RY. This value is approximately 2 orders of magnitude lower than the value specified for the current-generation reactors. Reliability analyses of various process systems and safety systems have been performed. The CDF was found to be approximately 5.46×10^{-8} per RY. Uncertainty analysis has also been performed taking into consideration the variability in component failure parameters. The 95% confidence value for CDF was found to be 8.13×10^{-7} per RY and the 99% confidence value was found to be 1.05×10^{-6} per RY.

15.2.4 Proliferation resistance

The technical features are incorporated to reduce attractiveness of its spent nuclear fuel material for use in any clandestine nuclear weapons program. The content of fissile plutonium in discharged fuel is very low. The radiation field from ^{233}U is very high because of the presence of ^{232}U . In the equilibrium condition, a high fraction of ^{234}U (up to 10%) will exist along with ^{233}U in the fuel. The reactor operates with low excess reactivity. Provision for nuclear material accounting is an inherent part of the AHWR-based nuclear fuel cycle, as has been the practice followed in the entire Indian nuclear program. High gamma activity in the fresh and reprocessed AHWR fuel is expected to facilitate its verification with high efficiency and reliability.

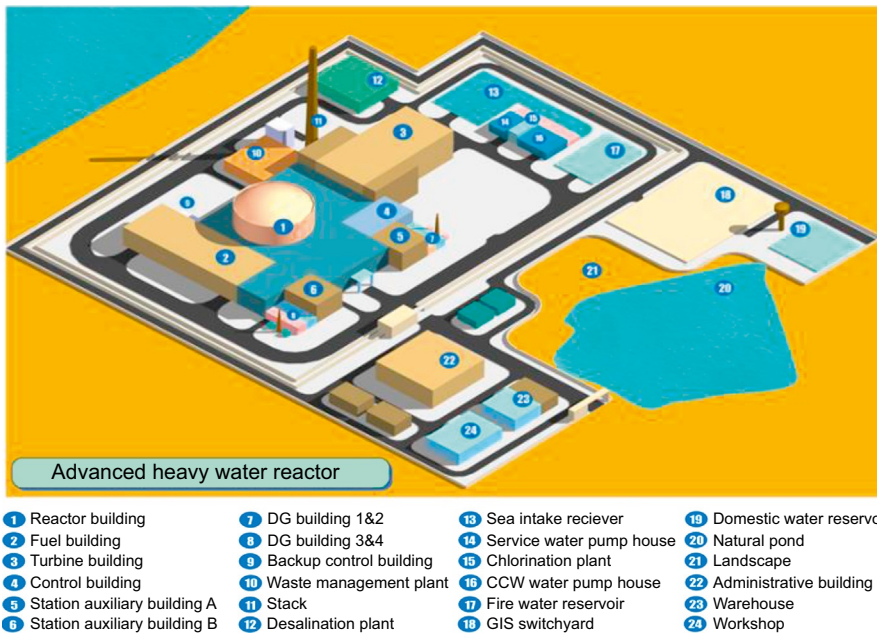


Figure 15.4. Advanced Heavy Water Reactor (AHWR) plant layout

15.2.5 Physical protection

The physical protection system is an integral part of the plant layout of AHWR. The plant is divided into a nuclear island and an administrative island. The plant layout is designed with a dual-layered security arrangement to provide enhanced physical protection to the nuclear island. The nuclear island is isolated from the administrative facilities by double-wire fencing with an additional security arrangement. The double fencing also provides for electronic surveillance. Independent roads for patrolling by security personnel are also provided. The plant layout is shown in Figure 15.4.

The Passive Poison Injection System (PPIS) is an additional system in AHWRs to fulfill the shut-down function during a low-probability event of failure of wired SDSs (i.e., anticipated transient without scram in the case of the SDS-1 and SDS-2 failure condition). PPIS passively injects the liquid poison into the moderator by system fluid pressure during such transients to shut down the reactor. This situation may arise because of human-induced malevolent action caused by insider threat or compromise of functioning of both SDSs.

15.2.6 Improved economics

Smaller capital investment and a shorter construction period will yield lesser risk and easier funding. There are several features that lower the capital cost of AHWRs, such as simpler and compact structures and components, elimination of the main circulation pump for the primary loop, use of light water coolant, etc. Other features such as higher burn-up of fuel, extensive use of passive features, 100 years of design life, and a higher capacity factor will help achieve reduced operating costs. Preliminary assessment shows that the unit energy cost, which is the measure of the economic competitiveness, is found to be comparable to conventional energy sources.

15.2.7 Research and development activities

The development of AHWRs is being supported by R&D in various aspects of reactor technology. Many experimental facilities have been built to validate AHWR design. A critical facility, a low-power research

reactor built for conducting physics experiments for validation of physics design parameters of AHWRs, was made critical in 2008 and is presently in operation. The integral test loop, which simulates the Main Heat Transport System (MHTS) and the safety systems of AHWR, is utilized to generate steady-state and stability data, start-up procedure validation, and to study parallel channel behavior. It is also used for performance validation of isolation condensers and ECCS through LOCA tests. Other facilities include the high-pressure natural circulation loop, the 3-MW_e boiling water loop, the parallel channel instability loop, and the Calandria model test facility. A facility for proving advanced reactor thermal hydraulics, a scaled facility simulating the MHTS, is built to establish safety margins and for performance testing of the prototype fueling machine. Various facilities to validate the performance of the containment system and passive system and components are being designed. Performance validation of additional safety systems incorporated to deal with post-Fukushima safety issues such as passive autocatalytic recombiners and a hardened vent system is also being studied.

15.3 High-Temperature Reactors (HTRs)

Nuclear hydrogen production by splitting water is the main goal for the Indian HTR program. Although development of relatively lower temperature hydrogen production processes (e.g., the copper-chlorine process) as well as high-temperature processes (e.g., sulfur-iodine process and high-temperature steam electrolysis) are being performed in India, a decision for more a challenging goal of development of technologies for reactor systems capable of producing process heat at 1000°C was taken. Therefore, under the Indian HTR program, technology development for a small-power CHTR, and a 600 MW_{th} IHTR, both capable of producing process heat at 1000°C, are being performed. For demonstration of IHTR technologies, a small-power (20 MW_{th}) version would be initially set up before deployment of large-power reactors. In this chapter, design and safety features of CHTR and a brief overview of IHTR are presented.

15.3.1 General description of compact High-Temperature Reactors (HTRs)

The CHTR is being developed as a prototype reactor for the development and demonstration of technologies associated with HTRs. The reactor is being designed to be compact in weight and size for ease in its deployment in remote locations for its use as a compact power pack. CHTR has a prismatic core. The reactor core consists of 19 hexagonal-shaped BeO moderator blocks. Each of these blocks contains a centrally located graphite fuel tube. Each fuel tube carries fuel inside of bores located on its wall. The fuel tube also serves as a coolant channel. Molten Lead-Bismuth Eutectic (LBE) has been chosen as the coolant to enable natural-circulation-based passive cooling. Reactor physics designs for ²³³U-Th as well as enriched ²³⁵U-based fuel has been established. A design based on enriched ²³⁵U-based fuel is currently being pursued. Fuel compacts are made up of TRISO (TRi-ISOtropic)-coated particle fuel, facilitating high burn-up and high-temperature applications. Eighteen blocks of BeO reflector surround the moderator blocks. Graphite reflector blocks surround these BeO reflector blocks. The reactor vessel is made of Nb–1%Zr–0.1%C alloy. A cross section of the core is shown in [Figure 15.5](#). Coolant plenums are provided above and below the reactor shell. Nuclear heat from the core is passively removed by natural-circulation-based flow of coolant between the two plenums, upward through the fuel tubes, and returning through the down comer tubes. Heat utilization vessels, set up above the upper plenum, act as an interface to systems for high-temperature process heat applications. A set of sodium heat pipes passively transfers heat from the upper plenum to these vessels. Another set of heat pipes transfers heat to the atmosphere in case of a postulated accident. A CHTR component layout is shown in [Figure 15.6](#). The major design parameters for CHTRs are shown in [Table 15.2](#).

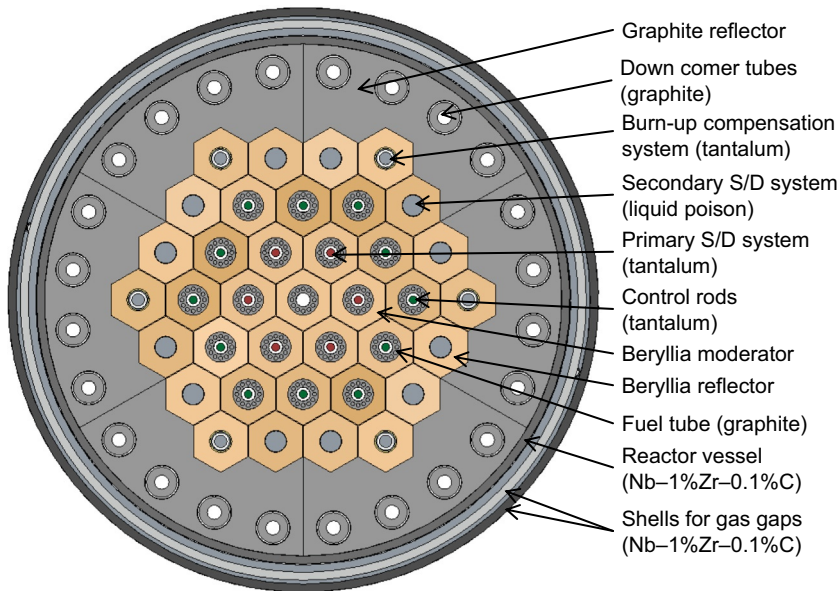


Figure 15.5. High-Temperature Reactor (HTR) core cross section. *S/D*, Shut-Down

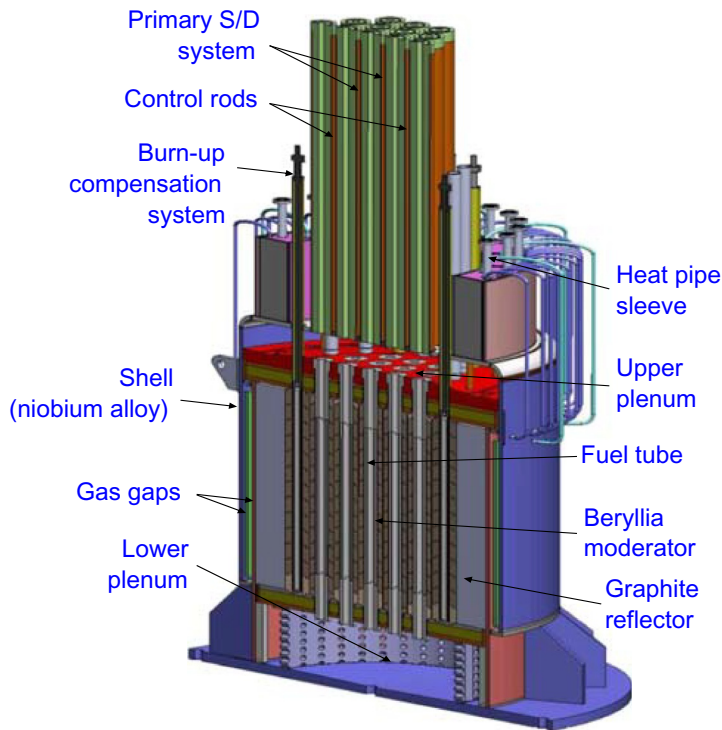


Figure 15.6. High-Temperature Reactor (HTR) component layout. *S/D*, Shut-Down

Table 15.2. Compact High-Temperature Reactors (HTRs): proposed design and operating parameters

Attributes	Design parameters
Reactor power	100 kW _{th}
Core configuration	Vertical, prismatic block type
Fuel	Enriched ²³⁵ U-based TRi-ISOtropic-coated fuel particles shaped into fuel compacts with graphite matrix

Continued

Table 15.2 Compact High-Temperature Reactors (HTRs): proposed design and operating parameter—cont'd

Attributes	Design parameters
Fuel pellet size	35 mm length and 10 mm diameter
Refueling interval	15 effective full-power years
Fuel burn-up	~68,000 MWd/t of heavy metal
Fuel tube material	High-density isotropic graphite (nuclear grade)
Moderator	BeO
Reflector	Partly BeO and partly high-density isotropic graphite
Coolant	Molten Pb-Bi eutectic alloy (44.5% Pb and 55.5% Bi)
Mode of core heat removal	Natural circulation of coolant
Coolant flow rate through core	6.7 kg/s
Coolant inlet temperature	1173°C
Coolant outlet temperature	1273°C
Loop height	1.4 m (actual length of the fuel tube)
Core diameter	1.27 m
Core height	1.0 m (height of the fueled part and axial reflectors)
Primary shut-down system	Mechanical shut-off rods made of Ta alloy and filled with tungsten pellets, located in six channels of the first ring of the reactor core
Secondary shut-down system	Liquid poison injection in carbon-carbon composite tubes provided in 12 BeO reflector blocks
Control system	Made of Ta alloy and filled with tungsten pellets, located in 12 channels of second ring of the reactor core
Burn-up compensation rods	Made of Ta alloy, filled with tungsten pellets, and located in six BeO reflectors

15.3.2 Reactor physics design

The reactor physics design of the CHTR has been performed with the main objectives of achieving high burn-up and a long refueling interval. The reactor fuel consists of 8 kg of enriched ^{235}U . Variation of k_{eff} with respect to burn-up is shown in [Figure 15.7](#). Fertile material and the burnable poisons make the fuel temperature coefficient negative, thus making the reactor inherently safe. The primary SDS consists of a set of six tantalum alloy shut-off rods, which fall by gravity in the six coolant channels in the first ring. Twelve control rods, made of tantalum alloy, are located in the next ring. The secondary SDS is in the form of a liquid poison injection system located in the BeO reflector region. The remaining six BeO reflectors house burn-up compensation rods, which are fully inserted in the beginning and periodically moved out.

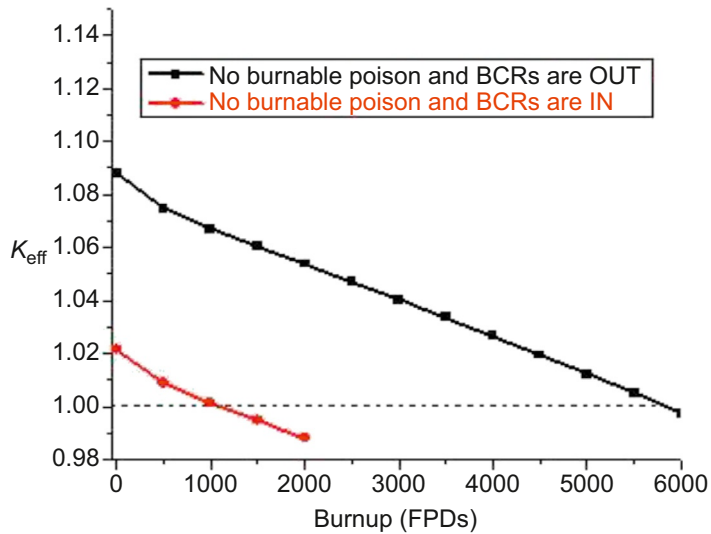


Figure 15.7. Variation of k_{eff} with respect to burn-up. *BCR*, Burn-up Compensation Rods

15.3.3 Thermal hydraulics design

As mentioned earlier, the reactor heat is removed by passive natural circulation of coolant. In addition to analytical studies and the development of computer codes, two experimental LBE loops for natural-circulation studies were set up. The first one with operating temperature of 500°C has been in operation since 2009. The second loop (Figure 15.8) with an operating temperature of 1000°C has been in operation for almost the last 1 year. In addition to these studies related to the freezing and defreezing of LBE as well as the development of oxygen sensors for LBE, level measurement probe, etc. were also carried out.

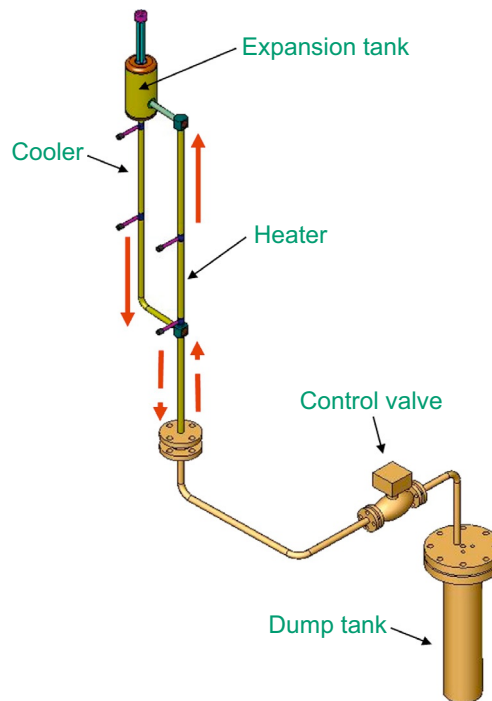


Figure 15.8. Schematic of Lead-Bismuth Eutectic (LBE) natural circulation loop (operating at 1000°C)

15.3.4 Fuel development

A typical CHTR fuel bed consists of a prismatic BeO moderator block with a centrally located graphite fuel tube carrying fuel compacts. Fuel compacts are made of TRISO-coated particle fuel with enriched ^{235}U -based fuel. A schematic of a single fuel bed is shown in Figure 15.9. The technology for fuel kernel manufacture has been long established at BARC by the sol-gel technique. A facility for coating TRISO-coated particle fuel and the radiography of a typical particle is shown in Figure 15.10. Fuel compacts with high packing density are shown in Figure 15.11. After developing the coating technology, coatings were successfully performed on natural UO_2 . Some of the coated particles have been irradiated in a Fast Breeder Test Reactor (FBTR) at IGCAR, Kalpakkam, India. In parallel, technology development for fuel compact manufacture has also been initiated. Compacts with high packing density ($\sim 45\%$) of particles with uniform distribution could be successfully made. Further development is mainly for characterization.

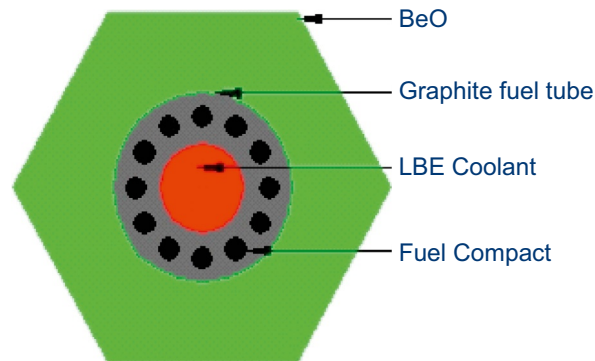


Figure 15.9. Schematic of single fuel bed for compact high-temperature reactor. *LBE*, Lead-Bismuth Eutectic

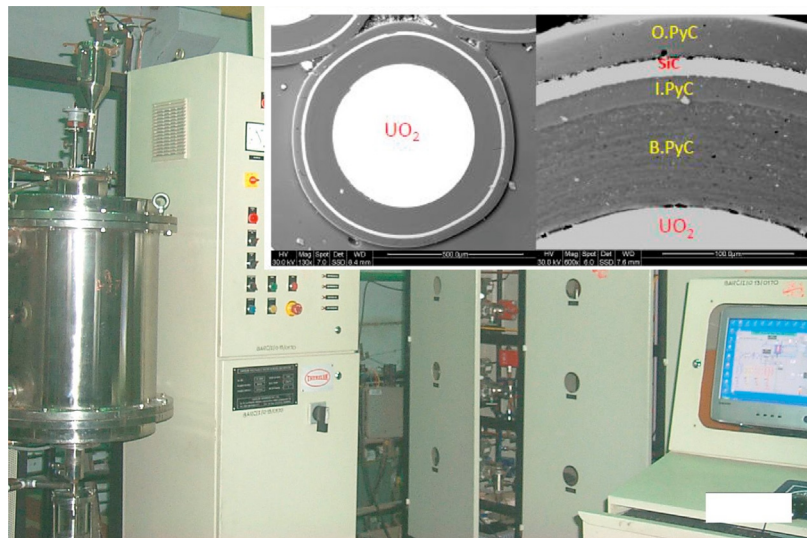


Figure 15.10. Facility for coating TRISO-coated particle fuel

15.3.5 Materials development

CHTR core materials comprise nuclear-grade high-purity materials. These are high-density isotropic BeO for moderator and reflector blocks (Figure 15.12), high-density isotropic graphite for fuel and down comer tubes, and reflector blocks (Figure 15.12). Other metallic structural materials are based on refractory metal alloys such as Nb-1%Zr-trace carbon (Figure 15.12) for reactor shell and coolant plenums and

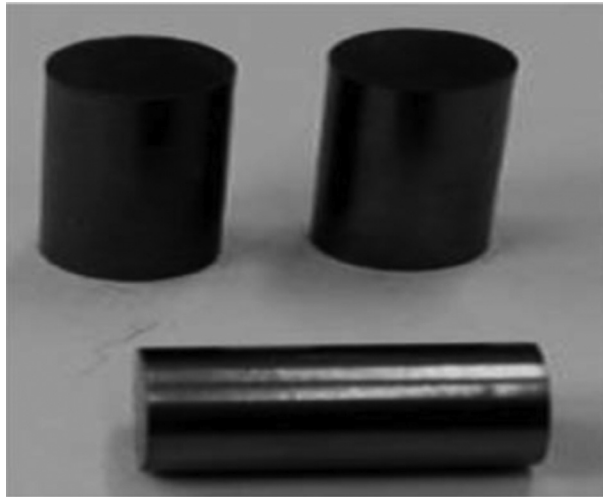


Figure 15.11. Fuel compacts for compact High-Temperature Reactor (HTR)

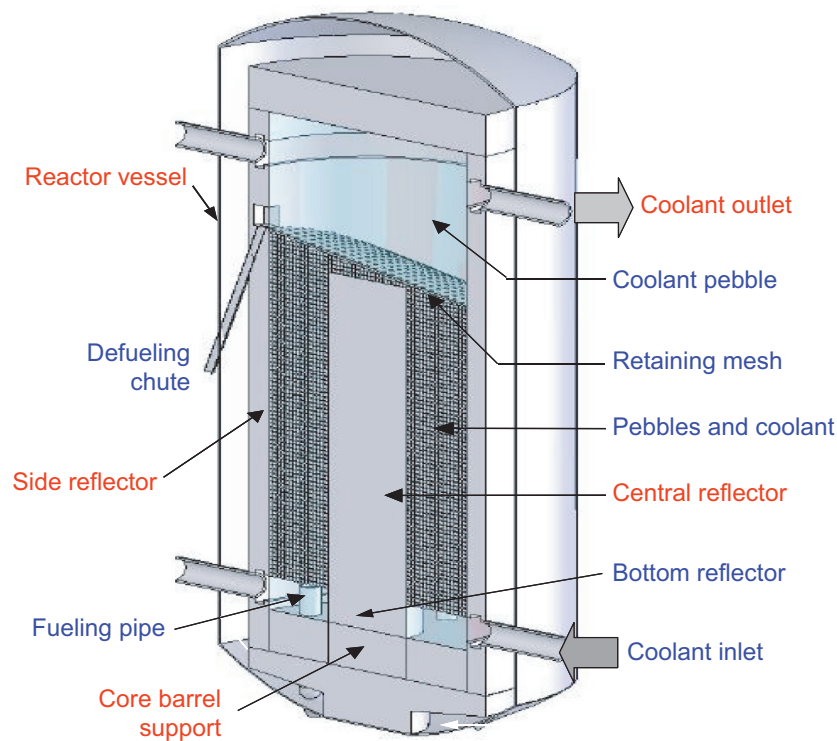


Figure 15.12. Schematic of Innovative High-Temperature Reactor (IHTR)

tantalum-tungsten-based alloy for safety and control rods. Graphite and these alloys are coated with oxidation-resistant coatings. These technologies have been successfully developed within DAE.

15.3.6 Inherent safety features and passive heat removal systems

CHTRs are being designed to have many features that make them inherently safe. Some of these features are a strong negative Doppler coefficient of the fuel, high thermal inertia of the all-ceramic core, low core power density, a very large thermal margin between the operating temperature and boiling point of the LBE, the chemical inertness and negative reactivity effects of LBE, low-pressure natural circulation of coolant, etc.

In addition, passive systems for reactor heat removal under normal and postulated accident conditions have been incorporated. This includes natural circulation of LBE for reactor heat removal, passive heat transfer to the secondary side using high-temperature sodium heat pipes, passive SDSs, passive dissipation of heat under a postulated accident scenario, etc.

15.3.7 Research and development activities

The major challenges to be addressed include coatings on TRISO-coated particle fuel and their characterization, production of high-density nuclear-grade BeO of intricate shapes, production of nuclear-grade high-density isotropic carbon-based materials and component manufacture, development of LBE-resistant structural material for high-temperature applications, oxidation-resistant coatings and their characterization, development of components and instrumentation for service in intimate contact with LBE coolant at high temperatures, LBE coolant technologies, and development of sodium-based high-temperature heat pipes. Most of the challenges have already been overcome, and R&D activities are in progress.

Major developmental activities planned for the future include studies related to design validation of a CHTR critical facility in the areas of high-temperature materials, thermal hydraulics, safety, and corrosion of structural materials; demonstration and testing of reactor control and SDSs; seismic qualification; qualification of passive heat removal systems under postulated conditions; development and demonstration of energy conversion technologies for utilizing high-temperature process heat; experimental facilities to demonstrate auxiliary systems such as coolant chemistry control/purification systems; and studying the irradiation behavior of new types of fuel, materials, and coatings. Subsequent to all developments, a critical facility for a CHTR would be set up.

15.3.8 Innovative High-Temperature Reactor (IHTR)

An IHTR is a pebble-bed molten salt-cooled reactor. Pebbles consist of TRISO-coated particle fuel, and the coolant is driven through natural circulation. The reactor core is a long right circular cylinder with an annular core that consists of fuel pebbles and molten salt coolant. [Figure 15.13](#) shows a schematic of a

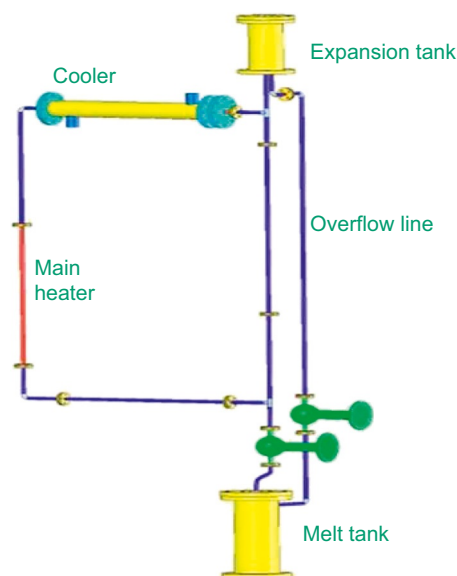


Figure 15.13. Molten salt natural-circulation loop

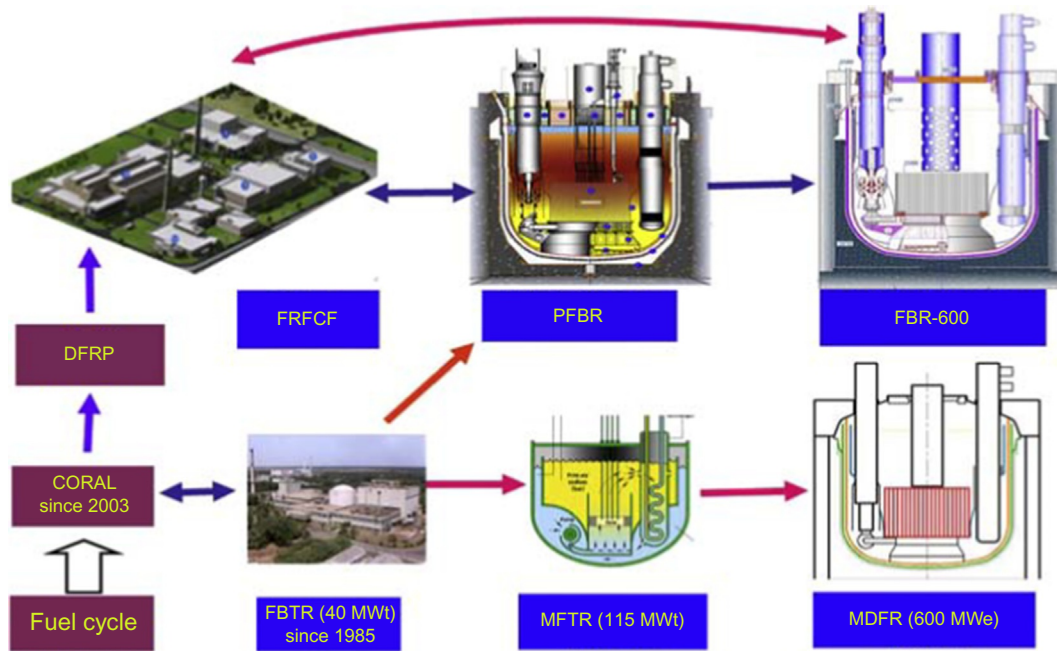


Figure 15.14. Fast Breeder Reactor (FBR) and associated fuel cycle program up to 2030

600-MW_{th} IHTR. There are graphite neutron reflectors in the center and on the top, bottom, and outside of this fuel annulus. Vertical bores in the central and outer reflectors are provided for the reactivity control elements. R&D activities being pursued include a molten salt natural circulation loop, as shown in Figure 15.14, which has been set up to perform thermal hydraulic studies of molten salts. In addition, an experimental facility to study the corrosion behavior of molten salt on the structural materials has also been set up. Experiments on various materials have been initiated. Future R&D activities include the manufacture of pebble-based fuel, a pebble feeding and removal mechanism, thermal hydraulic studies for molten salts in pebble-bed geometry, development of large-size graphite components, a high-efficiency power conversion system, and instrumentation and other components for the molten salt environment. The major design parameters of an IHTR are shown in Table 15.3.

Table 15.3. Innovative High-Temperature Reactor (IHTR): proposed design and operating parameters

Attributes	Design parameters
Reactor power	600 MW _{th} for the following deliverables <ul style="list-style-type: none"> –Hydrogen: 80,000 Nm³/h –Electricity: 18 MW_e –Drinking water: 375 m³/h } Optimized for hydrogen production
Coolant outlet/inlet temperature	1273/873°C
Moderator	Graphite
Coolant	Molten salt
Reflector	Graphite

Continued

Table 15.3 Innovative High-Temperature Reactor (IHTR): proposed design and operating parameter—cont'd

Attributes	Design parameters
Mode of cooling	Natural circulation of coolant
Fuel	$^{233}\text{UO}_2$ and ThO_2 -based high burn-up TRISO-coated particle fuel
Number of pebbles in the core	$\sim 150,000$
Packing fraction of pebbles	$\sim 60\%$
Packing fraction of TRISO particles	$\sim 8.6\%$
^{233}U requirement	$\sim 7.3\%$
Control	Passive power regulation and reactor shut-down systems
Energy transfer systems	Intermediate heat exchangers for heat transfer to system for hydrogen production + high-efficiency turbomachinery for electricity generation + desalination system for potable water
H_2 production	High efficiency thermochemical processes

TRISO, TRi-ISOtropic.

15.4 Fast Breeder Reactor (FBR)

15.4.1 Fast reactor program in India

The FBR program was started by constructing a loop-type FBTR, which has been in operation since 1985. With the PHWR program well on its growth path and having established comprehensive expertise in SFR technology through successful operation of FBTR for 30 years, India is now on a robust pathway for development of the SFR-based second stage of the program with a PFBR launched in October 2003. The PFBR is undergoing stage commissioning tests in a systematic manner. It is envisaged that six more FBRs introducing innovations for enhancing safety and improving economy compared to PFBR based on learning experience will be constructed beyond PFBR. Subsequently, 1000-MW_e SFRs using a metallic core (has high breeding potential) will be constructed to rapidly realize the nuclear power growth. However, complete realization of SFR technology involves many challenges in science, design, safety, and technology, especially in fuels and core structural materials and instrumentation aspects.

15.4.2 Fast breeder test reactors and their current status

The FBTR is a sodium-cooled, loop-type fast reactor fueled with a unique high Pu-mixed carbide fuel. It has two primary and two secondary sodium loops. Each secondary loop has two once-through, serpentine-type Steam Generators (SGs). All of the four SG modules are connected to a common steam-water circuit having a TurboGenerator (TG) and a 100% steam dump condenser. The first criticality was achieved in October 1985 with a small core of 22 fuel SubAssemblies (SAs) of MK-I composition (70% PuC + 30% UC), with a design power of 10.6 MW_{th} and peak Linear Heat Rating (LHR) of 250 W/cm. The core was progressively expanded by adding SAs at peripheral locations. Carbide fuel of MK-II composition (55%

PuC + 45% UC) was inducted in the peripheral locations in 1996. The TG was synchronized to the grid for the first time in July 1997. The LHR of MK-I fuel was increased to 400 W/cm in 2002. Eight high-Pu MOX fuel SAs (44% PuO₂) were loaded in the core periphery in 2006. The indigenously developed unique Pu-rich mixed carbide fuel has performed extremely well, crossing a burn-up of 165,000 MWd/t. One of the important achievements is closing of the fuel cycle of the FBTR. The FBTR fuel discharged at 155,000 MWd/t has been successfully reprocessed and refabricated. This is the first time that the Pu-rich carbide fuel has been reprocessed anywhere in the world.

The FBTR is being effectively used for the PFBR subassembly irradiation of MOX fuel up to a peak burn-up of 112 MWd/kg. Furthermore, the reactor is used for generating structural material data for cladding and wrappers, calibration of sensors, neutron detectors, and some special isotope productions. Furthermore, toward designing and building future metallic fueled test reactors, the irradiation of metallic fuel pins is in progress.

The reactor has so far been operated up to a power level of 20 MW_{th}. Furthermore, the reactor life is to be extended by 20 years to serve as an irradiation facility for future development. Apart from these, the FBTR has given high confidence for the successful construction, commissioning, and operation of SFRs.

15.4.3 The Prototype Fast Breeder Reactor (PFBR) and its current status

The PFBR is a 500-MW_e capacity pool-type reactor with two primary and two secondary loops with four SGs per loop. Pool- and loop-type concepts were studied comprehensively considering the associated merits and demerits specific to medium-size reactors such as the PFBR, and it was concluded that the pool type shall be the choice. The governing parameters meriting the choice are large thermal inertia that permits high thermal shock, higher structural reliability due to fewer associated critical welds, and the compact layout of the primary circuit components. It is also our perception that the complexities that are associated with the pool type of reactor such as thermal hydraulics, manufacturing, and handling of overdimensioned thin vessels with stringent tolerances can be successfully met by the designers and our industry. Subsequently, this has been confirmed from detailed analysis backed up with experimental validation and extensive 1:1 technology development exercise.

The overall flow diagram comprising a primary circuit housed in a reactor assembly, a secondary sodium circuit, and the balance of the plant is shown in [Figure 15.15](#), and the essential operating parameters of the plant are shown in [Table 15.4](#). The nuclear heat generated in the core is removed by circulating sodium from the cold pool at 397°C to the hot pool at 547°C. The sodium from the hot pool, after transporting its heat to four Intermediate Heat eXchangers (IHXs), mixes with the cold pool. The circulation of sodium from the cold pool to the hot pool is maintained by two primary sodium pumps, and the flow of sodium through the IHX is driven by a level difference (1.5 m of sodium) between the hot and cold pools. The heat from the IHX is in turn transported to eight SGs by sodium flowing in the secondary circuit. Steam produced in the SG is supplied to the TG. In the reactor assembly, the main vessel houses the entire primary sodium circuit including the core. The inner vessel separates the hot and cold sodium pools. The reactor core consists of approximately 1757 SAs including 181 fuel SAs. The control plug, positioned just above the core, mainly houses 12 absorber rod drive mechanisms. The top shield supports the primary sodium pumps, the IHX, the control plug, and the fuel handling systems. The PFBR uses MOX fuel with depleted and natural uranium and approximately 25% Pu oxide. For the core components, 20% cold worked D9 material (15% Cr–15% Ni with Ti and Mo) is used to have better irradiation resistance. Austenitic stainless steel type 316 LN is the main structural material for the out-of-core components and modified 9Cr-1Mo (Grade 91) is chosen for the SG. The reactor is designed for a plant life of 40 years with a load factor of 75%.

The design of the PFBR calls for complete understanding of unique fuel and structural material behavior under high-temperature, sodium, and irradiation environments as well as the science and technology aspects

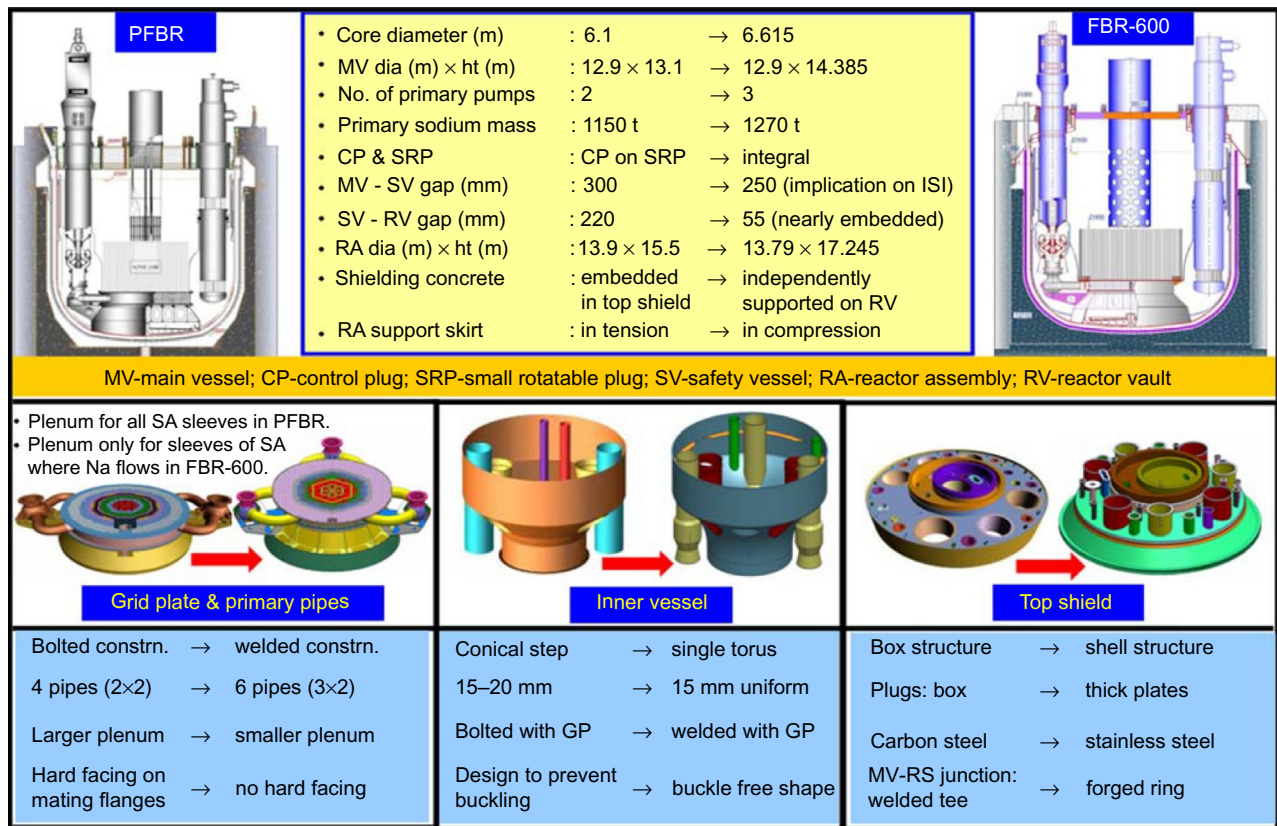


Figure 15.15. Design improvements of reactor assembly for FBR-600. *dia*, diameter; *ht*, height; *constrn.*, construction; *SA*, SubAssembly; *PFBR*, Prototype Fast Breeder Reactor

Table 15.4. Prototype Fast Breeder Reactor (PFBR): operating parameters

Attributes	Design parameters
Reactor thermal power	1250 MW _{th}
Electrical output	500 MW _e (gross)/470 MW _e (net)
Fuel	PuO ₂ + UO ₂
Number of fuel locations	181 (inner zone = 85; outer zone = 96)
Pu enrichment	Inner zone = 20.7% (w); outer zone = 27.7% (w)
Maximum fuel burn-up	100 GWd/t
Blanket material	Depleted UO ₂
Number of blanket locations	120
Type of core	Homogenous
Core orientation	Vertical
Lattice pitch (triangular)	135 mm

Continued

Table 15.4 Prototype Fast Breeder Reactor (PFBR): operating parameter—cont'd

Attributes	Design parameters
Concept of primary sodium circuit	Pool type
Coolant	Liquid sodium
Total core flow	6.8 t/s
Coolant inlet temperature	397°C
Coolant outlet temperature	547°C
Total steam flow	560 kg/s
Feed-water inlet temperature	235°C
Steam temperature at HP turbine inlet	490°C
Steam pressure at HP turbine inlet	16.7 MPa
Absorber material	B ₄ C enriched in B-10
Breeding ratio	1.04
Design life	40 years

in the domains of sodium chemistry, aerosol behavior, sodium fire and sodium water reactions, special sensors for sodium applications (detection of water leaks in the SG, sodium leaks, purity measurements, level detectors), thermal hydraulics, and structural mechanics (turbulences, instabilities, gas entrainments, thermal striping, stratifications, ricketing, etc.). Various failure modes are identified comprehensively and analyzed in detail using validated analytical, numerical, and experimental techniques.

The construction of PFBR has been completed, and commissioning is in the advanced stage. The commissioning of the primary system is currently performed with dummy core SAs having all of the mechanical and hydraulic features with steel pellets in the place of fuel. Before replacing the dummy assemblies with actual fuel assemblies, several tests are planned. In situ performance of primary and secondary pumps; electromagnetic pumps; in-vessel and ex-vessel fuel handling machines; and various mechanisms such as absorber rod drive mechanisms, under sodium scanners, eddy current flow meters, periscope, etc., are being qualified before and after filling sodium at various temperatures. These apart, vibrations of pumps and dummy core assemblies are checked. The first criticality is planned in the last quarter of 2015, and commercial power generation subsequently begins.

15.4.4 Motivation for improvements for future fast breeder reactors beyond the prototype Fast Breeder Reactor (FBR-600)

The design, R&D, safety review, construction, and commissioning experience derived from PFBR have motivated the commercial exploitation of MOX-fueled SFRs with a closed fuel cycle. Accordingly, in the roadmap prepared for the FBR development beyond PFBR, six more FBRs, each of 600 MWe (FBR-600) are planned in the first phase. The FBR-600 need to be improved with respect to the PFBR on economy (target: 20%–25% material reduction and reduction of construction time by at least 2 years) and safety (target: to have features in line with emerging safety criteria, broadly Gen-IV criteria evolved

after the Fukushima event). Among several measures taken to meet the requirements, an important one is that the sodium void reactivity should be kept lower than \$1. This value is \$2.7 for the PFBR, which is the lowest among the values reported for other international reactors designed before the Fukushima accident. On the basis of detailed optimization studies, it is concluded that a heterogeneous core is the most preferred solution with reference core size, fuel inventory, available knowledge, matured analysis capability, and international trend. Among a few potential options, introducing depleted uranium within the pins of a few SAs occupying the core central zone and/or introducing radial blankets in the central zones provide attractive solutions to derive a higher breeding ratio while restricting the sodium void reactivity. The heterogeneous core with only radial heterogeneity (Mark-I) has indicated that the breeding ratio of approximately 1.2 with the sodium void reactivity not exceeding \$1 is possible. Because the radial heterogeneous core occupies a little larger radial space, it has been chosen to have a flexibility to choose any heterogeneous core, which demands lesser diameter. This strategy has been adopted in a calibrated manner so that the reactor assembly dimensions do not change in the process of iterating and finally adopting the most optimized core with thorough validation including the associated core safety aspects. Accordingly, the Mark-I core with 3.4-m diameter has been chosen for the design finalization. In the subsequent design optimization studies, the reactor power has been raised to 600 from 500 MW_e for each unit. Furthermore, the main vessel diameter has been restricted not to exceed the PFBR main vessel diameter. The six FBRs will be built adapting twin units concepts (i.e., three twin units sharing several non-safety-related facilities). Conceptual design documents for FBR-600 have been prepared and reviewed independently by relevant experts.

The initial FBR would employ MOX fuel due to its proven experience. However, in order to achieve rapid growth rate in U-PU cycle in the second phase, FBRs with metal fuels, having high breeding ratio and low doubling time are essential. This motivates deployment of metal fueled fast reactors at the earliest. It is worth mentioning that the same may not be applicable to FBR to Th bearing fuel, since the change in breeding ratio from ceramic to metal fuel is minimal.

15.4.5 Conceptual design features of FBR-600

The sodium void coefficient of the MOX core will be less than 0.9, depending upon the kind of heterogeneity that will be finalized based on the further optimization study (in progress). The two-loop concept would be retained. A twin-unit concept, optimum shielding, use of 2/1/4 Cr-1 Mo in place of 304 LN for cold pool components and piping, three SG modules per loop with increased tube length of 30 m (PFBR has four modules per loop with 23 m length), 85% load factor, 60-year design life, reduced construction time (6 years), and enhanced burn-up (up to 200 GWd/t to be achieved in stages) are being considered. Furthermore, significant improvements have been introduced in the reactor assembly design (Figure 15.16), including (1) a welded grid plate with a smaller plenum to accommodate only those sleeves that support core SAs through which sodium flows, (2) an inner vessel having a single curved redan with uniform thickness, (3) thick-plate rotatable plugs, (4) a control plug integrated with a small rotatable plug, (5) torus-shaped thick-plate roof slab, (6) a support skirt for the reactor assembly kept under compression, (7) a safety vessel made of carbon steel embedded with the reactor vault, and (8) simplified fuel handling scheme with elimination of an inclined fuel transfer machine (Figure 15.17). These apart, major modifications introduced in the SG are consolidated in Figure 15.18.

These revisions call for three relatively smaller capacity primary sodium pumps instead of two larger capacity pumps. The revised parameters resulted from optimization study also include a marginal increase of operating temperatures (the mixed mean temperature of sodium outlet from the core increased by 10°C), a steam temperature of 510°C (490°C for PFBR), and an increase in load factor by 10%. The improved design concepts

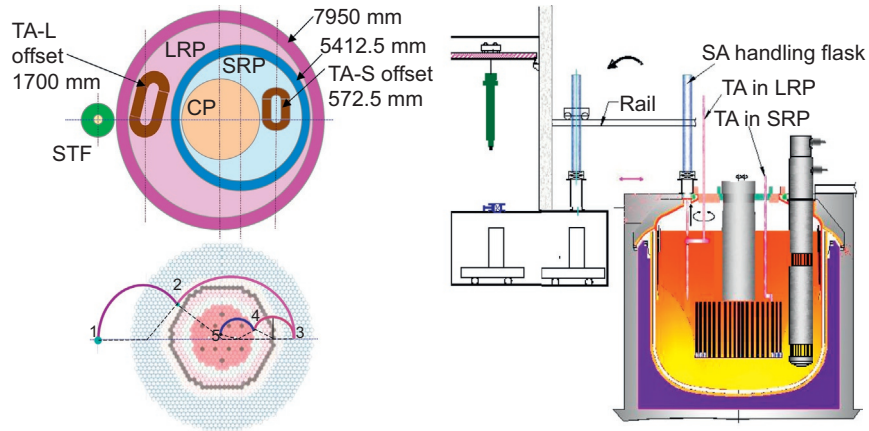


Figure 15.16. Simplified fuel handling scheme for FBR-600

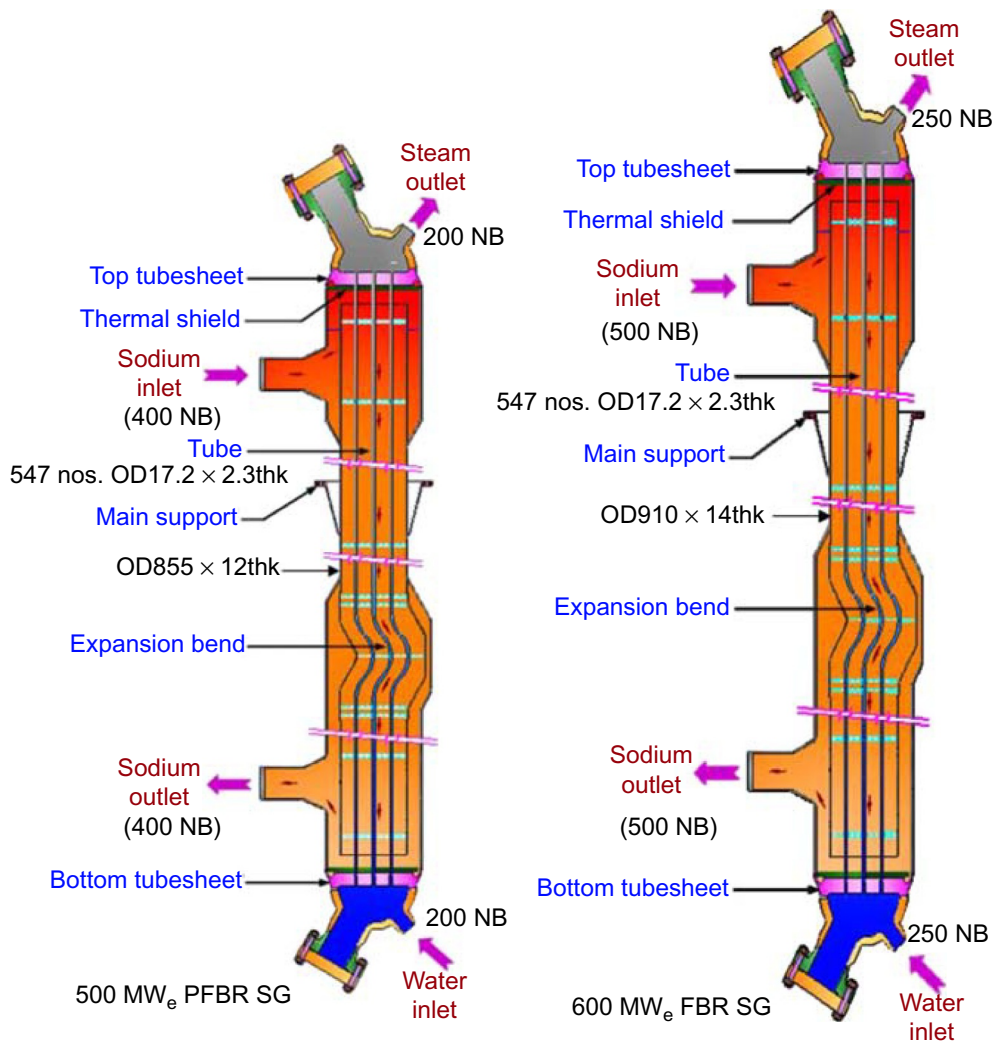


Figure 15.17. Comparison of 30-m long tube Steam Generator (SG) of 600-MW_e Fast Breeder Reactor (FBR) with the Prototype Fast Breeder Reactor (PFBR) SG. *OD*, Outer Diameter

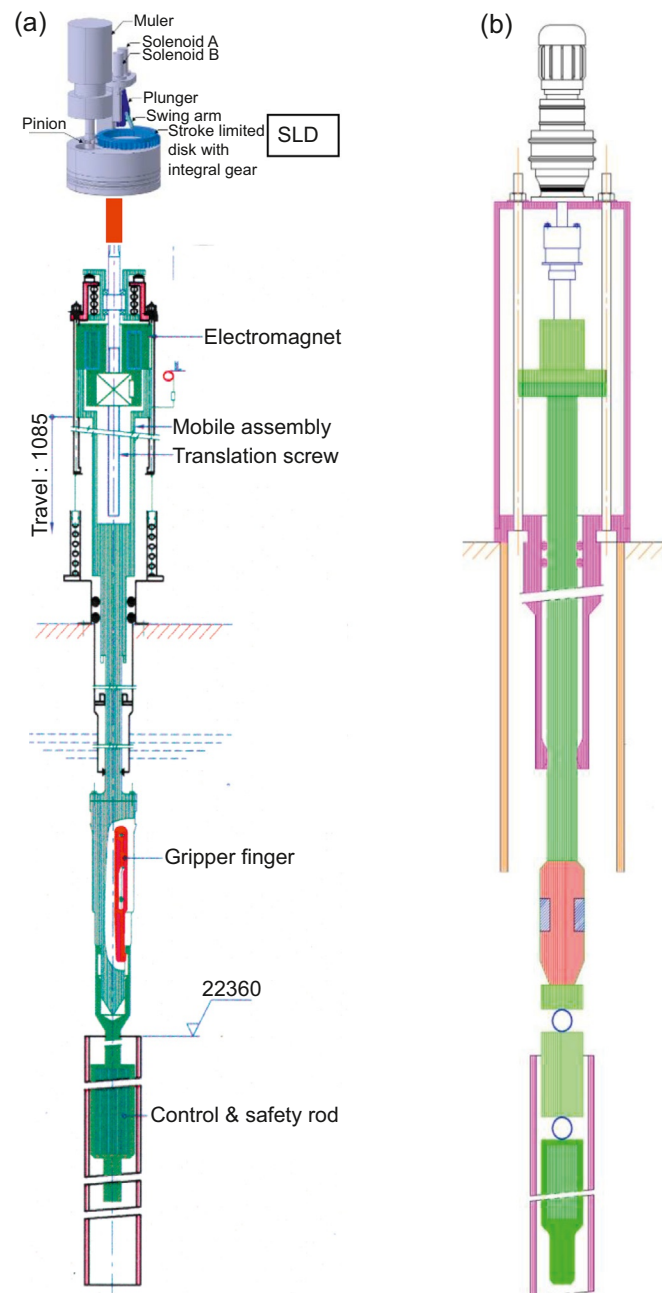


Figure 15.18. (a) Control and safety rod drive mechanism and (b) diverse shut-down rod drive mechanism with passive safety features proposed for FBR-600.

have indicated significant economic advantages, including a material inventory reduction by approximately 25%, a simplified fuel handling scheme, and reduced manufacture time. The new concepts introduced will be validated through executing systematic R&D, technology development exercise, testing and evaluation, etc.

15.4.6 Enhanced safety features

The safety features are introduced to meet the international safety criteria particularly evolved after the Fukushima accident. The major implication is need of detailed investigation of all beyond Design-Basis Events (DBEs), including prolonged station blackout conditions resulting in severe core damage and large

radioactivity release to the public as well as practical elimination of severe accident scenarios. The DBEs have been split into three subcategories: (1) Design Extension Condition-1 (DEC-1) without core melting, (2) Design Extension Condition-2 (DEC-2; which involves core meltdown), and (3) Practically Eliminated Condition (PEC). The aim of such categorization is to ensure that even in the worst-case accident scenario no early or long-term protective measures would be needed in the public domain. For both DEC-1 and DEC-2, the radioactivity release limit is 20 mSv. DEC-1 events are those events for which the site boundary dose is only limited (20 mSv). For those coming under DEC-2, the design measures should limit the event consequences within the specified time and distance. The accepted values of time and distance are yet to be internationally evolved. Events involving overheating of fuel pins (inadequate cooling of core under prolonged station blackout condition) and subsequent release of a large quantity of fission gas and fuel particles into the cover gas space are typical examples for DEC-2. Those events causing severe core damage resulting in large radioactivity release to the public come under PEC. Typical events coming under this category are (1) failure of structures lying along the core support path (roof slab, main vessel, core support structure, and grid plate), (2) simultaneous failure of the main vessel and safety vessel, (3) a Core Disruptive Accident (CDA), and (4) recriticality.

In the design of a SDS, the major improvements considered are (1) enhancing the reliability of SDSs (as in PFBR) with the introduction of passive safety features and (2) adequately addressing the recriticality issue. Toward further improving reliability of SDSs (at least by one order with reference to the PFBR), active/passive safety features are introduced, including a stroke limiting device to limit the uncontrolled withdrawal of control and safety rods in their drive mechanisms (Figure 15.19) and temperature-sensitive magnet/magnetic switch

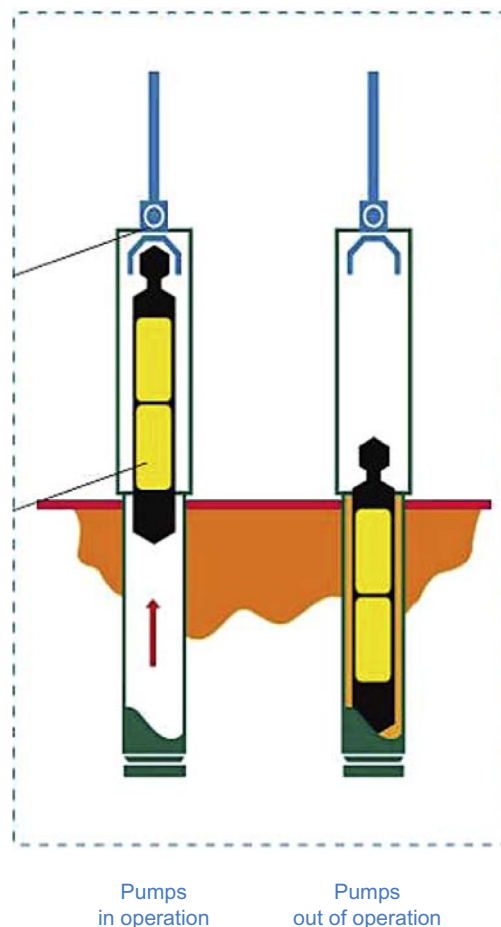


Figure 15.19. One hydraulically suspended absorber rod

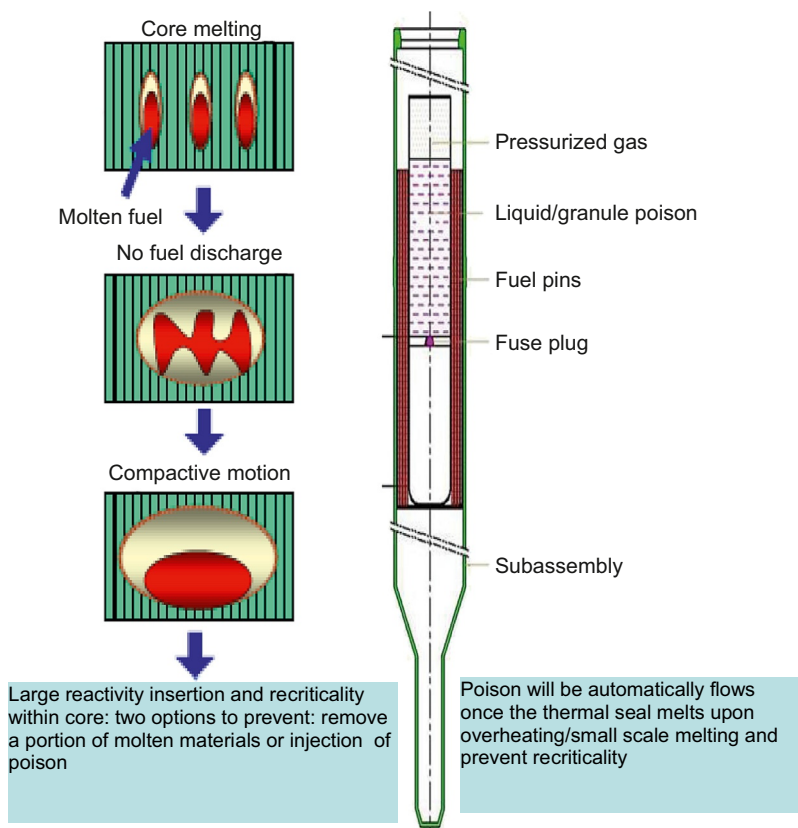


Figure 15.20. Concept of ultimate shut-down system for taking care of recriticality

(Curie point magnet) in the diverse shut-down rod drive mechanisms (Figure 15.19). These apart, introduction of hydraulically suspended absorber rods that would be dropped immediately once the primary sodium flow is reduced with the initiating events such as rupture of more than one primary pipe, seizure of all primary pumps, and total instantaneous blockage in fuel SAs is under consideration (Figure 15.20). To avoid recriticality, an adequate number of Ultimate Shut-Down (USD) systems that work on Liquid (Li-6) or granules (enriched B₄C powder) will be introduced. The recriticality issue and concept of the USD system are explained schematically in Figure 15.21. The scheme of the SDSs (type, number, and location) will be finally decided based on a deterministic approach with due considerations on the probabilistic approach. However, R&D activities on the systems previously mentioned that are in progress will be continued and adequate knowledge and data will be accumulated. R&D involves introduction of such systems in the FBTR itself to increase their confidence under an actual environment (sodium, irradiation, and high temperature).

Various Decay Heat Removal (DHR) systems are provided with high reliability to cater the needs under five situations: (1) fuel handling, (2) in-service inspection, (3) DBE, (4) DEC, and (5) postaccident conditions (Figure 15.22). High emphasis is given to address the prolonged station blackout condition. For meeting the DHR requirements for the first three situations, dedicated DHR systems ($4 \times 10 \text{ MW}_{\text{th}}$) in all of the four Secondary Sodium circuits (SSDHRs), an Operating-Grade Decay Heat Removal (OGDHR) system in the steam-water system in the PFBR, or a combination of SSDHRs and OGDHRs are being studied. This decision is yet to be taken after detailed assessment of design, operational simplicity, availability, reliability, economics, and experience. A marginal cost increase of the SSDHR systems compared with OGDHR systems of the same capacity is to be absorbed. For taking care of DHR during DEC (situation 4), the Safety-Grade Decay Heat Removal (SGDHR) system introduced in PFBR will be retained. SGDHR can be made operational by appropriate opening of the dampers in the case of any DBEs resulting in loss of power to the secondary sodium pumps. However,

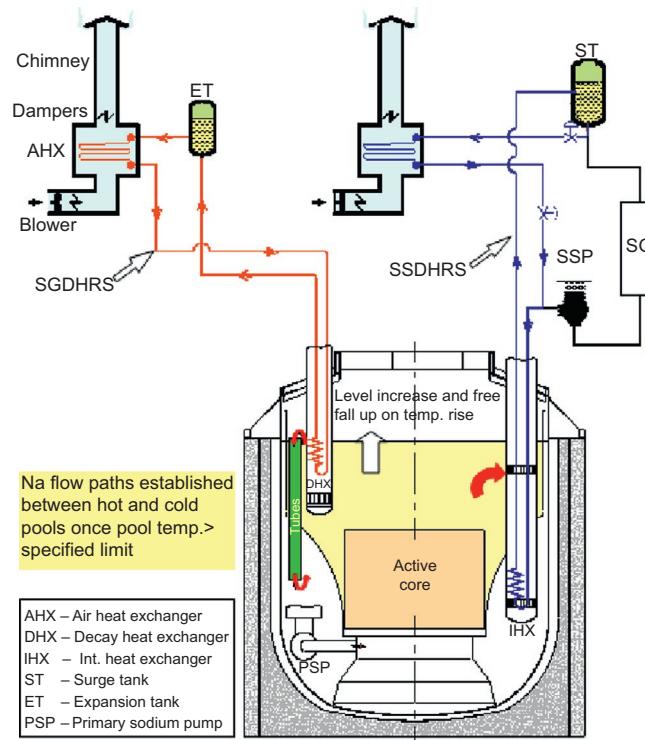


Figure 15.21. Decay heat removal systems conceived for a fast breeder reactor. *SGDHRS*, Secondary Sodium Decay Heat Removal System; *SG*, Steam Generator; *SSP*, Secondary Sodium Pump; *temp.*, temperature



Figure 15.22. Sodium-Fuel Interaction Facility (SOFI): facility for molten fuel interaction studies

design studies are in progress to make the SSDHR operational even during the loss of power to the pump to ensure high reliability of the DHR requirement. Finally, to meet the DHR requirement during postaccident situations, the current features incorporated in the PFBR will be retained (i.e., ensuring heat removal capacity of the SGDHR after a CDA and a core catcher to support the core debris resulting from the CDA). Further improvements required are ensuring the heat removal capacity features in the case of core debris resulting in whole core melt-down. Although it has been shown by computational fluid dynamics analysis that a large perforation created by the molten fuel while melting through the grid plate and core support structure facilitate adequate natural circulation of sodium to remove the heat from debris settled on the core catcher and to transport to the SGDHR inlet windows through the natural-convection mode, considerations are being given to incorporate a few pipes penetrating through the inner vessel for providing alternative/additional passages for the sodium flow once the mean temperature exceeds a certain value.

To maintain the concrete temperature less than the applicable allowable value in the case of simultaneous leakages in the main vessel and the safety vessel, design features have been introduced to provide oil cooling coils in the intervessel spaces.

15.4.7 Research and development status

Apart from R&D on material, structural mechanics, and thermal hydraulics testing and evaluation, R&D activities are in progress for the validation of passive shutdown systems based on Curie point magnet, liquid poison injection systems, passive DHR systems, and demonstration of a postaccident heat removal system. Toward this, a few unique facilities have been built at IGCAR, including the Sodium-Fuel Interaction Facility (SOFI) for the molten fuel coolant interaction studies (Figure 15.23), the Postaccident Thermal Hydraulics Facility (PATH) for postaccident heat removal studies (Figure 15.24), the MINI Sodium Fire Facility (MINA) for small-scale sodium fire studies (Figure 15.25),

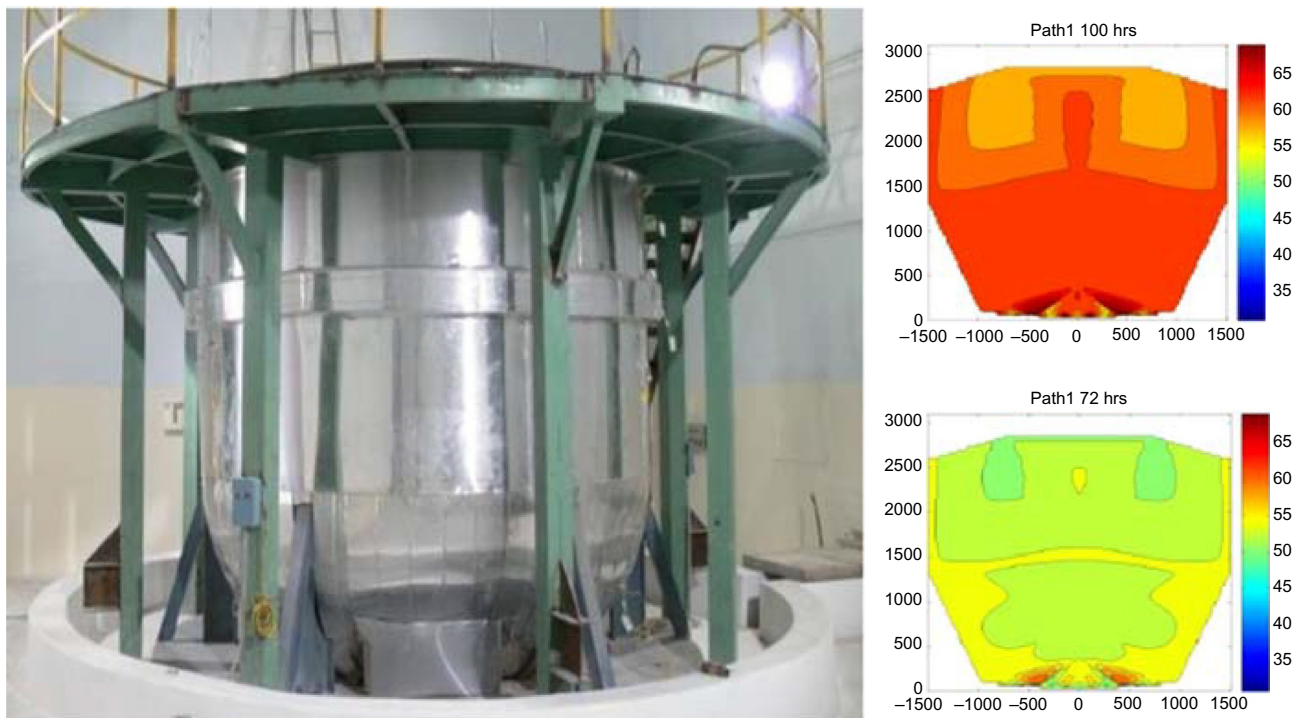


Figure 15.23. Postaccident Thermal Hydraulics Facility (PATH) for postaccident heat removal studies

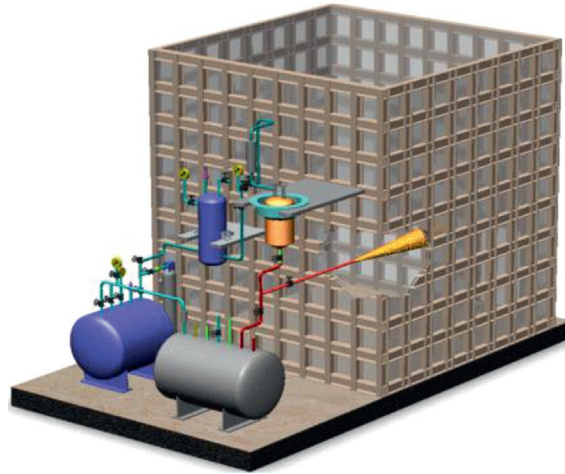


Figure 15.24. MINI Sodium Fire Facility (MINA): facility for the sodium fire studies

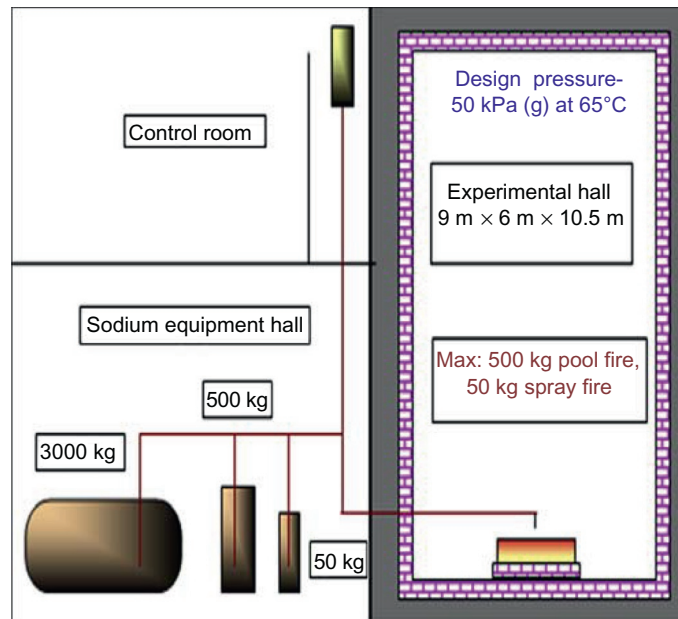
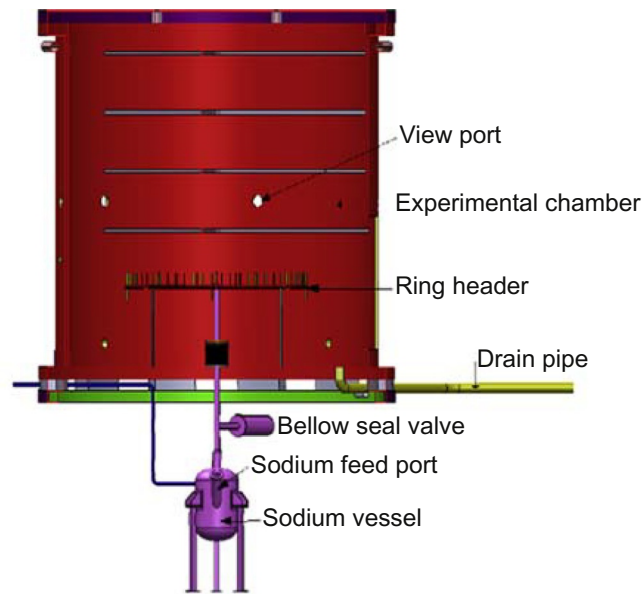


Figure 15.25. Sodium Fire Experimental Facility (SFEF): facility for large-scale sodium fire studies

the Sodium Fire Experimental Facility (SFEF) for large-scale sodium fire studies (Figure 15.26), and the Sodium Cable Interaction Facility (SOCA) for simulating sodium fire scenarios on the top shield platform (Figure 15.27). Some innovative SDSs could be introduced in the PFBR itself after thorough validations.

15.5 Molten Salt Reactors (MSRs)

India is developing two concepts of molten salt reactors. One of the concepts has a pebble-bed configuration with molten salt being used as the coolant. The pebbles are made of TRISO-coated particle fuel. This is explained in Section 13.3.8. The other configuration is the fluid-fueled MSBR. This portion of the chapter will describe Indian R&D efforts for the development of the IMSBR.



Internal details of test vessel

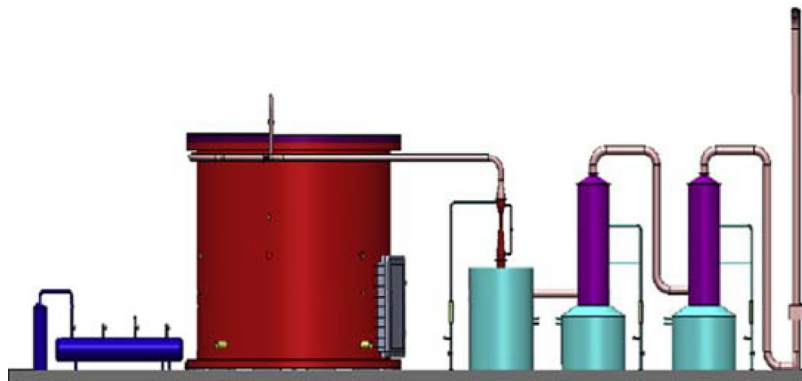


Figure 15.26. Sodium Cable Interaction Facility (SOCA): facility for simulating sodium fire scenario at the top shield

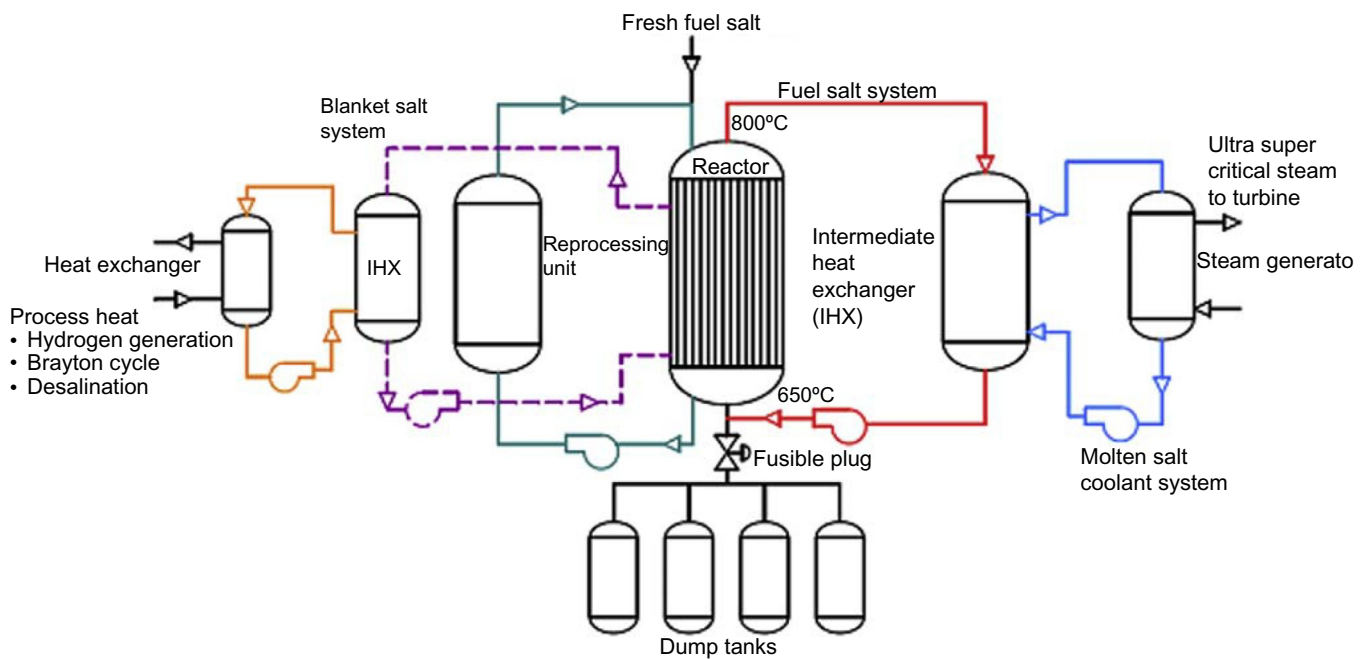


Figure 15.27. Schematic of Indian Molten Salt Breeder Reactor (IMSBR)

15.5.1 Conceptual designs of IMSBR

To arrive at the conceptual design, some of the design guidelines that are being followed include self-sustainability in the ^{233}U -Th cycle, enhanced and inherently safe designs, no use of beryllium and beryllium-based salts to avoid chemical toxicity, minimal waste generation and hence avoidance of the use of graphite, and the ability to replace in-core components. The IMSBR has a fuel salt and a blanket salt in the fluid form. These are made to flow through heat exchangers for ultimately transferring the high-temperature heat to the supercritical CO_2 -based Brayton cycle for power generation, which can produce electricity at an efficiency of approximately 45%. Currently two concepts (one loop type and another pool type) of 850MW_e IMSBR are being established. In parallel, the design of a small-power (5MW_{th}) technology demonstrator reactor is also being established. A schematic of the reactor is shown in Figure 15.28, and the component layout for the pool-type concept-based reactor is shown in Figure 15.29. The use of fluid fuel allows for removal of neutron-absorbing products almost as soon as they are formed, allowing for

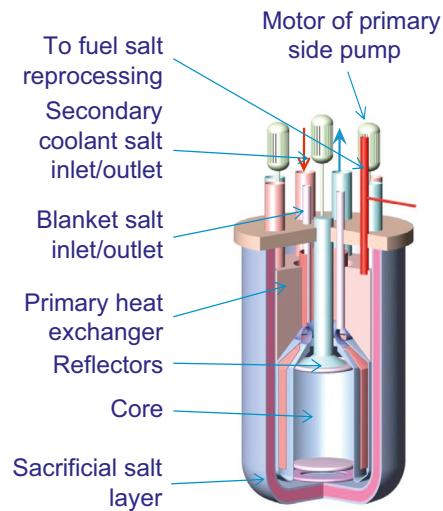


Figure 15.28. Pool-type Indian Molten Salt Breeder Reactor (IMSBR)

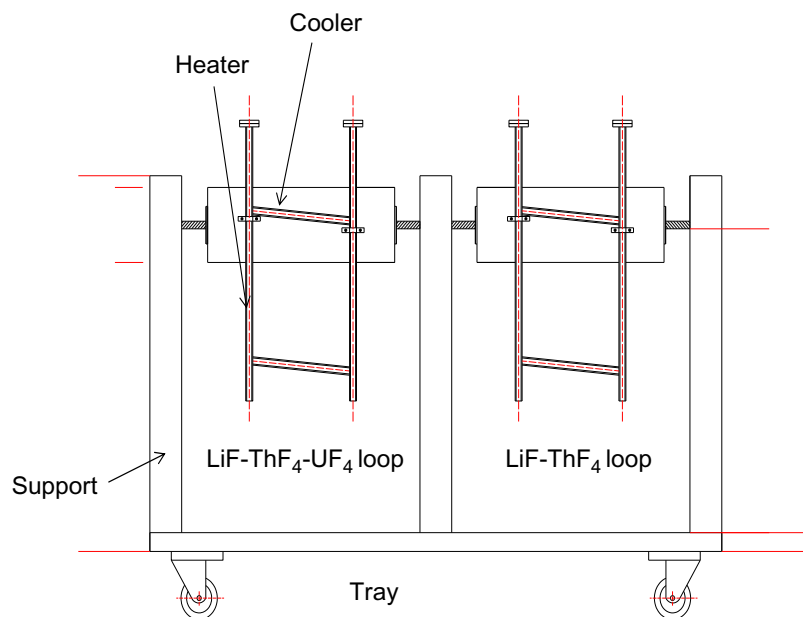


Figure 15.29. Schematic of the test facilities for a Molten Salt Reactor (MSR)

Table 15.5. Indian Molten Salt Breeder Reactor (IMSBR): proposed design and operating parameters

Attributes	Design parameters
Power	850 MW _e
Thermal efficiency	45%
Active core diameter/height	2/2.05 m
Core inlet/outlet	700/800°C
Fuel salt	LiF-ThF ₄ -UF ₄
Blanket salt	LiF-ThF ₄
Secondary salt	LiF-KF-AlF ₃
Flow rate (primary)	10.9 t/s
Flow rate (secondary)	6.3 t/s
Velocity (core)	0.85 m/s
Fuel salt inventory (total)	41.1 t (2.7 t of ²³³ U)
Pumping power	5.4 MW (at 90% efficiency)
Power production system	Based on supercritical CO ₂ Brayton cycle

efficient utilization of nuclear materials. The ²³³Pa removed is allowed to decay to ²³³U and is reintroduced into the reactor. The major design parameters of the IMSBR are shown in Table 15.5.

15.5.2 Design challenges

Some of the major challenges in which R&D has been initiated include

1. Modification of existing codes for reactor physics analysis with the capability to couple neutronics and thermal hydraulics and account for the online reprocessing system;
2. Thermal hydraulic and material compatibility studies for molten salts;
3. Large-scale salt preparation, purification, and characterization;
4. Development of structural materials and qualification to meet codes and design rules;
5. Online and batch-mode offline reprocessing, without cooling of fuel salt;
6. Instrumentation for operation at high-temperature, active molten salt environment;
7. Online chemistry control techniques for salts as well as tritium capture; and
8. Development of components for high-efficiency supercritical CO₂-based power cycle.

Currently, in addition to performing fundamental studies on various salts, facilities for natural-circulation-based thermal hydraulic studies and corrosion studies under an active molten salt (using ThF₄ and natural UF₄) environment are being commissioned. A schematic of the same is shown in Figure 15.29.

15.5.3 Research and development activities

For the IMSBR development, all technologies have been either initiated or are being initiated. In parallel, a conceptual design of a 5-MW_{th} IMSBR is being worked out. To perform technology development for various

technologies related to salts, materials, components, and power conversion systems, a Molten Salt Breeder Reactor Development Facility (MSBRDF) has been planned at the new BARC campus in the southern Indian city of Visakhapatnam.

15.6 Conclusions

Nuclear power is essential for India to meet its ambitious energy targets on the near- and long-term horizons. Introduction of innovative reactors involving thermal and fast neutron spectrums and various coolants such as water, gas, sodium, lead, and lead bismuth alloys as well as completion of R&D is the current focus of the DAE. The excellent operating experience of water reactors in the commercial domains and the FBTR, the commissioning of the PFBR, the robust roadmap for the rapid introduction of FBRs with metallic fuel, and the introduction of AHWRs and MSRs at the appropriate time to effectively utilize the vast thorium resources provide motivation and confidence to realize the targets. The reactor types developed would have several features to demonstrate economic competitiveness and enhanced safety acceptable to designers, regulators, and the public.

Development of energy systems will be largely governed by economic and environmental considerations. Relevant scientific breakthroughs and deployment of innovative technologies for meeting the challenges of long-term energy sustainability has to be the mantra for success.

Reference

Integrated Energy Policy, 2006. Planning Commission. Government of India.

Bibliography

AHWR

- Anantharaman, K., Ramanujam, A., Kamath, H.S., Majumdar, S., Vaidya, V.N., 2000. Thorium based fuel reprocessing & re-fabrication technologies and strategies, INSAC-2000. In: Annual Conference of the Indian Nuclear Society (Proc. of Annual Conf., Mumbai).
- Anantharaman, K., Shivakumar, V., Saha, D., 2008. Utilisation of thorium in reactors. *J. Nucl. Mater.* 383 (1–2), 119–121.
- Hari Prasad, M., Gera, B., Thangamani, I., Rastogi, R., Gopika, V., Verma, V., Mukhopadhyay, D., Bhasin, V., Chatterjee, B., Sanyasi Rao, V.V.S., Lele, H.G., Ghosh, A.K., 2011. Level-1, -2 and -3 PSA for AHWR. *Nucl. Eng. Des.* 241 (8), 3256–3269.
- IAEA-TECDOC-1485, 2005. Status of Innovative Small and Medium Sized Reactor Designs. pp. 357–378.
- Jain, V., Nayak, A.K., Dhiman, M., Kulkarni, P.P., Vijayan, P.K., Vaze, K.K., 2013. Role of passive safety features in prevention and mitigation of severe plant conditions in Indian advanced heavy water reactor. *Nucl. Eng. Technol.* 45 (5), 625–636.
- Sapra, M.K., Kundu, S., Pal, A.K., Vijayan, P.K., Vaze, K.K., Sinha, R.K., 2015. Design and development of innovative passive valves for Nuclear Power Plant applications. *Nucl. Eng. Des.* 286, 195–204.
- Sinha, R.K., Kakodkar, A., 2006. Design and development of the AHWR—the Indian thorium fuelled innovative nuclear reactor. *Nucl. Eng. Des.* 236 (7–8), 683–700.
- Sinha, R.K., 2011. Advanced nuclear reactor systems—an Indian perspective. *Energy Procedia* 7, 34–50.

HTRs

- Basak, A., Dulera, I.V., Vijayan, P.K., 2011. Design of high temperature heat pipes and thermosiphons for compact high temperature reactor (CHTR). In: Proceedings of the 21st National & 10th ISHMT-ASME Heat and Mass Transfer Conference, December 27–30, IIT Madras, India.
- Basak, A., Dulera, I.V., Vijayan, P.K., 2012. An approach for graphite component design for nuclear reactors. In: National Conference on Carbon Materials 2012, Mumbai.

- Borgohain, A., Maheshwari, N.K., Vijayan, P.K., Sinha, R.K., 2008. Heat transfer studies on lead-bismuth eutectic flows in circular tubes. In: Proceedings of 16th International Conference on Nuclear Engineering (ICONE), Orlando, Florida, pp. 11–15.
- Dulera, I.V., Sinha, R.K., 2008. High temperature reactors. *J. Nucl. Mater.* 383, 183–188.
- Kanse, D., Khan, I.A., Bhasin, V., Vaze, K.K., 2012. In: Micro-mechanical studies on graphite strength prediction models. National Conference on Carbon Materials 2012, Mumbai.
- Mollick, P.K., Venugopalan, R., Roy, M., Rao, P.T., Sathiyamoorthy, D., 2012. Characterisation of buffer pyrolytic carbon of TRISO coated particle developed in hot spouted bed. In: National Conference on Carbon Materials 2012, November 2012, Mumbai.
- Sinha, R.K., Dulera, I.V., 2010. Carbon based materials—applications. In: High Temperature Nuclear Reactors, First Asian Carbon Conference (FACC 2009). 25th–27th November 2009, Indian Habitat Center, New Delhi, India. *Indian J. Eng. Mater. Sci.* 17, 321–326.
- Tewari, R., Vishwanadh, B., Srivastava, D., Dey, G.K., Vaibhav, K., Jha, S.K., Mirji, K.V., Prakash, B., Saibaba, N., 2011. Development of Nb–1% Zr–0.1%C Alloy as Structural Components for CHTR. BARC. Report-BARC/2011/E/020.

FBRs

- Chellapandi, P., Kumar, P., 2014. Implementation of practical elimination, DEC and sodium voiding effects for the future SFRs: Indian approach. In: 4th Joint IAEA-GIF Technical Meeting/Workshop on Safety of Sodium-Cooled Fast Reactors.
- Chellapandi, P., Puthiyavinayagam, P., Balasubramanian, V., Ragupathy, S., Rajan Babu, V., Chetal, S.C., Raj, B., 2010. Design concepts for reactor assembly components of 500MW_e future SFRs. *Nucl. Eng. Int.* 240, 2948–2956.
- Chellapandi, P., 2014. Assessment of safety criteria of Indian SFR with respect to international scenarios. In: 4th Joint IAEA-GIF Technical Meeting/Workshop on Safety of Sodium-Cooled Fast Reactors.
- Chellapandi, P., 2015. Enhanced safety features of FBR 1 & 2 with respect to PFBR and Gen-IV reactors. In: Fifth Joint IAEA-GIF Technical Meeting/Workshop on Safety of Sodium-Cooled Fast Reactors. IAEA HQ, Vienna.
- Chetal, S.C., Chellapandi, P., Puthiyavinayagam, P., Raghupathy, S., Balasubramanian, V., Selvaraj, P., Mohanakrishnan, P., Raj, B., 2009. In: A perspective on development of future FBRs in India. Int. Conference on Fast Reactors and Related Fuel Cycles: Challenges and Opportunities (FR09), Kyoto, Japan.

MSBR

- Dulera, I.V., Vijayan, P.K., Sinha, R.K., 2013. Indian programme on Molten salt cooled nuclear reactor. In: Conference on Molten Salts in Nuclear Technology. Bhabha Atomic Research Centre, Mumbai.
- Vijayan, P.K., Basak, A., Dulera, I.V., Vaze, K.K., Basu, S., Sinha, R.K., 2015. Conceptual design of indian molten salt breeder reactor. *Pramana—J. Phys. Indian Acad. Sci.*

16

The safety and risk assessment of Advanced Reactors (ARs)

Romney B. Duffey^a and Dan Hughes^b

^aIdaho Falls, ID, United States

^bHughes and Associates, Perth, NY, United States

“Safeguards must be provided to prevent the use of technology from doing injury to the public health and well-being”

Admiral Hyman G Rickover, Hearings before the Joint Committee on Atomic Energy, 91st Congress, 2nd Session, March 19-20, 1970, p. 101, Washington, DC (Rickover,1970).

Nomenclature Abbreviations and acronyms

AC	Alternating Current
ACE	Army Corps of Engineers (USA)
ALARA	As-Low-As-Reasonably-Achievable
AOOs	Anticipated Operational Occurrences
AR	Advanced Reactor
ASME	American Society of Mechanical Engineers
ASTRID	Advanced Sodium Technological Reactor for Industrial Demonstration
ATWS	Anticipated Transient Without Scram
BC	Boundary Condition
BDBA	Beyond-Design-Basis Accident
BDEE	Beyond-Design Extreme Event
BEPU	Best Estimate Plus Uncertainty
BHWR	Boiling Heavy Water Reactor
BORAX	BOiling water ReActor eXperiment
BP	British Petroleum (UK)
BWR	Boiling Water Reactor
CAD	Computer-Aided Design
CAE	Computer-Aided Engineering
CCF	Common mode or Cause Failures
CDF	Cumulative Damage Function or Core Damage Frequency
CFD	Computational Fluid Dynamics
CFR	Code of Federal Regulations (USA)
CHF	Critical Heat Flux
CISE	Centro Informazioni Studi Esperienze
CNSC	Canadian Nuclear Safety Commission
COL	Combined Operating License
CSNI	Committee on the Safety of Nuclear Installations
CSAU	Code Scaling Applicability and Uncertainty

DA	Deterministic Analysis
DBAs	Design Basis Assessments
DBTs	Design Basis Transients
DC	Direct Current
DCD	Design Control Document
DHR	Decay Heat Removal
DHS	Department of Homeland Security (USA)
DiD	Defense-in-Depth
D&L	Design and Licensing
DNB	Departure from Nucleate Boiling
DWO	Density Wave Oscillations
EBWR	Experimental BWR
ELAP	Extended Loss of All Power
EPRI	Electric Power Research Institute (USA)
EPS	Emergency Power and cooling back-up Systems or Emergency Power Systems
EQ	Earthquake
ESBWR	Economic Simplified Boiling Water Reactor
et seq.	and what follows
EU	European Union
FBR	Fast Breeder Reactor
FEMA	Federal Emergency Management Agency (USA)
FLEX	diverse and FLEXible coping strategies
FSAR	Final Safety Analysis Report
GDC	General Design Criteria (US NRC)
GE	General Electric (USA)
Gen-IV	Generation-IV (four) reactor systems
GES	GEySering
GFR	Gas-cooled Fast Reactor
GIF	Generation IV International Forum
HEP	Human-Error Probability
HEX	Heat EXchanger
HPLWR	High Performance Light Water Reactor
HRA	Human Reliability Analysis
HSE	Health and Safety Executive (UK)
HTR	High Temperature Reactor
HTTR	High Temperature Test Reactor
IAEA	International Atomic Energy Agency
I&C	Instrumentation and Control
INES	International Nuclear and radiological Event Scale
INL	Idaho National Laboratory
ISAM	Integrated Safety Analysis Methodology
LB-LOCA	Large Break Loss Of Coolant Accident
LFR	Lead-cooled Fast Reactor (also, lead-bismuth-cooled)
LOCA	Loss Of Cooling Accident
LODC	Loss Of DC power
LOFW	Loss Of Feed Water
LOOP	Loss of Offsite/Onsite Power
LOPC	Loss Of Power and Cooling
LOPP	Loss Of Preferred Power
LOPS	Loss Of Power and/or cooling
LRF	Large Release Frequency
LUHS	Loss of Ultimate Heat Sink
LWR	Light Water Reactor
MSR	Molten Salt Reactor
NASA	National Aeronautics and Space Administration (USA)

NBO	Natural Boiling Oscillations
NC	Natural Circulation
NCL	Natural Circulation Loop
NEI	Nuclear Energy Institute (USA)
NPP	Nuclear Power Plant
NRC	Nuclear Regulatory Commission (USA)
NRVs	Non-Return Valves
OECD	Organization for Economic Co-operation and Development
OFI	Onset of Flow Instability
PDO	Pressure Drop Oscillations
PHWR	Pressurized Heavy Water Reactor
PIRT	Phenomena Identification and Ranking Table
PRA	Probabilistic Risk Analysis
PSA	Probabilistic Safety Assessment
PRHRS	Passive Residual Heat-Removal System
PT	Pressure Tube
PWR	Pressurized Water Reactor
QA	Quality Assurance
QRA	Quantitative Risk Assessment
REE	Rare or Extreme Event
R&D	Research and Development
RIDM	Risk-Informed Decision-Making
ROI	Return On Investment
RPV	Reactor Pressure Vessel
SA	Severe Accident
SBLOCA	Small-Break Loss Of Coolant Accident
SBO	Station Black Out
SAMGs	Severe Accident Management Guidelines
SARs	Safety Analysis Reports
SC CO₂	SuperCritical CO ₂
SCWR	SuperCritical Water-cooled Reactor
SDC	Safety Design Criteria
SFR	Sodium-cooled Fast Reactor
SG	Steam Generator
SMR	Small Medium and/or Modular Reactor
SO	Safety Objective
SPERT-I	Special Power Excursion Reactor Test
SRF	Small Release Frequency
SSCs	Structures, Systems and Components
SRVs	Safety, emergency and Relief Valves
TAO	Thermo-Acoustic Oscillations
TEPCO	Tokyo Electric Power Company (Japan)
TMI	Three Mile Island NPP (USA)
TRISO	TRi-structural ISOTropic (nuclear fuel)
UHS	Ultimate Heat Sink
UPS	Uninterruptible Power Supply
US/USA	United States of America
VHTR	Very High Temperature Reactor
VVER	Water Water Energy Reactor (Russia)
WENRA	Western European Nuclear Regulators Association

Subscripts

el electrical
th thermal

16.1 Basic safety principles

In this chapter, we review and describe the safety of new reactors and concepts, including the state of the art in assessment methods and challenges in analysis and testing. We organize the present analysis and critique based on published work by the GIF, prior reviews of AR concepts, recently submitted formal Safety Analysis Reports (SARs), the results of modern PRAs, suggestions related to AR regulation and licensing using risk-informed decision-making, and the large body of thermal–hydraulic work related to passive and natural circulation cooling.

Given there is no such thing as “absolute safety” or “zero risk,” the overall safety objective is to ensure employee and corporate safety, to assure environmental preservation, and to attain public trust and political acceptance. These goals are internationally variously interpreted and emphasized, but it is important to note that it is the operator/owner/investor, who carries the safety responsibility not the regulator or licensing body with their own myriad of rules and “guidance” that set minimum requirements (see Chapter 22 of this Handbook). As noted before (D’Auria et al., 2019), consideration suggests overlapping defense-in-depth requirements (not “barriers”) so that we follow the principles of process safety and what we have learned from prior events:

- (1) Elimination of unacceptable system statuses in and by design and by the margins to failure (e.g., no melt, no radioactivity release...).
- (2) Elimination of unacceptable system statuses by control (e.g., safe limits never exceeded, redundancy/diversity of indefinite cooling and of power ...).
- (3) Elimination of unacceptable system statuses by relentless focus on safety by the humans involved (e.g., in management, maintenance, and operation...).
- (4) Elimination of unacceptable financial risk so the focus remains on safety not on profit and price (e.g., investment incentives, guaranteed Return On Investment (ROI), large market place penetration...).

They are not the layered combined probabilistic-deterministic “protective strategies” defined by the US Nuclear Regulatory Commission (NRC) (US NRC, 2007), since that includes “the uncertainty associated with the parameter values and models” used in the PRA to “verify that the quantifiable margins... are acceptable.” From actual events and Fukushima, we already know these layers combine to provide potentially misleading and unverifiable estimates of the core damage frequency and do not fully or adequately include the human element in severe event prediction, causation, and remediation.

In this chapter, the terms ARs and Generation-IV systems include any that are different in design or concept from those currently licensed and commercially available. For technologically innovative and socially desirable reasons, it is generally agreed that new reactors, whatever their generation of design or operating principles, should be safer than any currently deployed. This has been particularly emphasized by the Fukushima reactor meltdowns, which were unexpected and caused significant social concern and political disruption in Japan and worldwide.

This core meltdown is, and was caused by, a rare event; a seismically induced tsunami of immense proportions that caused loss of almost all power and control. Thus, the initiating event lay outside the safety analysis envelope of what had been considered at the design stage, beyond the “design basis” of what had been considered for safety margin, and system and structural design, and was more severe than considered in risk assessments for natural hazards.

16.2 Safety and reliability goals

The top-level safety requirements for new reactor concepts have been stated and internationally agreed upon by the GIF (Kelly, 2014). These requirements are essentially applicable to all ARs, and are given as:

- (1) Excel in safety and reliability.

- (2) Have a very low likelihood and degree of reactor core damage.
- (3) Eliminate the need for offsite emergency response.

While these aims are splendid and desirable, the safety of any new system is still subject to interesting and known questions:

- What are the actual detailed safety requirements?
- How is safety to be analyzed?
- What scenarios or accidents are to be included?
- What is a “low likelihood or degree”?
- What are the uncertainties?
- How is new technology to be licensed?
- How to respond to accidents if no response is needed?
- What is or is not an acceptable risk?

New concepts for ARs come in many different forms and are called many different names by their proponents and developers. Some basic designs, like the many liquid–metal-cooled “fast reactors,” water-cooled “supercritical” systems, and helium-cooled “high-temperature” reactors, even date back 60 or more years. Many prototypes and demonstration plants were both built and operated, sometimes as part of military-related activities for nuclear propulsion and weapons material production. This plethora of acronyms and naming now includes the GIF systems, Small Medium and/or Modular Reactors (SMRs), and many types and variants of ARs. The historical nomenclature has come about largely for programmatic, funding, and commercial development reasons, with varying degrees and claims for improved, passive, enhanced, inherent, and/or super safety. Fortunately, from a purely nuclear safety perspective, the issues are entirely generic, and depend on establishing the chance of:

- Uncontrolled events that challenge the design;
- Extensive economic and/or social damage; and/or
- Potential or actual release of radionuclides.

The basic overarching and most important Safety Objective (SO) is to keep the reactor core cooled and controlled at all times (ASME, 2012, p. 32; Howlett, 1995, p. 5) and, if not, to be able to limit and/or manage the consequences without causing undue or unacceptable risk to the public. After all, if the reactor is not controlled and cooled, the core could melt and/or release radioactivity, which is undesirable physically and financially wrecking both the plant and the investment. The plethora of subsidiary goals, rules, criteria, assessments, regulations, and analyses are all aimed at demonstrating or supporting the achievement of this fundamental SO by a combination of design, back-up and system systems, and emergency measures and procedures, coupled with extensive safety, risk, and structural analysis.

Licensing procedures and processes to establish the public risk also vary by country and jurisdiction, but are simply a formal means to establish the degree of belief and justification for the above chance, using safety analysis reports, methods, assessments, reviews, or claims. The degree of detail and the exact approach adopted or expected by regulatory authorities vary widely, and today are often country and site specific.

16.2.1 Subsidiary safety requirements and licensing review

The subsidiary safety requirements flowing from this fundamental objective have been promulgated as legally enforceable safety and design criteria (see also Chapter 22 of this Handbook). For example, the licensing process for new reactors in the USA is regulated under the Code of Federal Regulations ([US NRC, 2004a,b](#)). These rules provide a process for establishing a standard or “certified” design basis, and require a “safety analysis report (that) describes the plant’s final design, safety evaluation, operational limits,

anticipated response of the plant to postulated accidents, and plans for coping with emergencies,” which is used for the purposes of formal safety analysis and review.

In such design and licensing review cases, all means available and possible as sources of water and cooling are invoked for cooling purposes, including safety, non-safety, backup, and emergency systems. Events that are “beyond” or challenge the design basis or were previously labeled “incredible” or “hypothetical” are now called “severe accidents” or “extended conditions.” The design and operation may also be subject to “stress tests,” additional measures, layered safety systems, and extensive emergency responses.

The most relevant, current, and publicly available set of subsidiary safety requirements for evaluating an AR are those used for the recent review of the Economic Simplified Boiling Water Reactor (ESBWR), the largest passively cooled reactor that has undergone the full licensing process. The ESBWR is over 1200 MW_{e1} and uses natural circulation of water for cooling. The NRC Safety Evaluation Report (US NRC, 2014) gives the criteria for risk assessment based on core damage frequency and the timescales for the use of safety and non-safety systems, as derived from a full-scope PRA analysis (Bhatt and Wachowiak, 2006). This NRC approach states the safety guidelines as follows:

- “First, the focused PRA maintains the same scope of initiating events and their frequencies as that identified in the baseline ESBWR PRA. As a result, non-safety-related Structures, Systems, and Components (SSCs) used to prevent the occurrence of initiating events will be subject to regulatory oversight commensurate with their risk.
- Second, following an initiating event, the event tree logic of the comprehensive, Level 3-focused PRA will not include the effects of non-safety-related standby SSCs. This will allow the Combined Operating License (COL) applicant to determine whether the passive safety systems, when challenged, can provide sufficient capability (without non-safety-related backup) to meet the NRC safety goal guidelines for a Cumulative Damage Function (CDF) of less than 1×10^{-4} per reactor year and for a Large Release Frequency (LRF) of less than 1×10^{-6} per reactor year.

The design certification applicant will also evaluate the containment performance, including bypass, during a severe accident. If the design certification applicant determines that non-safety-related SSCs must be added to the focused PRA model to meet the safety goals, these SSCs will be subject to regulatory oversight based on their risk significance.”

In addition, since there is a criterion that:

“SSC functions (are) relied upon to ensure long-term safety (beyond 72 hours) and to address seismic events....” and it is also required that:

“...the design certification applicant will use PRA insights, sensitivity studies, and deterministic methods to establish the ability of the design to maintain core cooling and containment integrity beyond 72 h. Non-safety-related SSCs that are required to meet deterministic regulatory requirements, resolve the long-term safety and seismic issues, and prevent significant adverse systems interactions are subject to regulatory oversight.

The staff expects regulatory oversight for all non-safety-related SSCs needed to meet NRC requirements, safety goal guidelines, and containment performance goals, as identified in the focused ESBWR PRA model.”

The requirements for the PRA are then stated as:

“This PRA includes all appropriate internal and external events for both power and shut-down operations. The process also includes adequate treatment of risk assessment uncertainties, long-term safety operation, and containment performance. A margins approach is used to evaluate seismic events. In addressing containment performance, the PRA considers the sensitivities and uncertainties in accident progression, as well as the inclusion of severe accident phenomena, including the explicit treatment of containment bypass. The PRA uses mean values to determine the availability of passive systems and the frequencies of core damage and large releases. The process estimates the magnitude of potential variations in these

parameters and identifies significant contributors to these variations using appropriate uncertainty and sensitivity analyses.”

Similar quantified goals exist in other nations for new builds and some have been promulgated as nominally “technology neutral,” i.e., the requirements do not depend on the type of reactor. The safety submission must show that the proposed design is meeting certain overall quantified criteria (CNSC, 2008):

“Core Damage Frequency (CDF)

The sum of frequencies of all event sequences that can lead to significant core degradation is less than 10^{-5} per reactor year.

Small Release Frequency (SRF)

The sum of frequencies of all event sequences that can lead to a release to the environment of more than 10^{15} Becquerel of Iodine-131 is less than 10^{-5} per reactor year. A greater release may require temporary evacuation of the local population.

Large Release Frequency (LRF)

The sum of frequencies of all event sequences that can lead to a release to the environment of more than 10^{14} Becquerel of Cesium-137 is less than 10^{-6} per reactor year. A greater release may require long-term relocation of the local population.”

Despite its apparent simplicity and attractiveness, there are two simple issues with this type of methodology as follows.

First, the original focus of formal safety case reviews used for all existing designs was on analyzing design basis transients and accidents, and conducting formalized PRAs that include external events, with the aim of demonstrating a low probability and managing the risk of core damage. The reactor accidents at the Fukushima Daiichi NPP demonstrated that the previous safety analyses and estimates were incomplete and overly optimistic; and did not adequately include extreme severe events; or even address the social consequences and public reaction to such accidents even when little radiation is released and no fatalities are directly attributable (Dudour and Carlucci, 2011; ASME, 2012; Suzuki, 2014).

Second, as actual events to date have demonstrated, the nominal 72-h requirement or any such similar interval partly based on subjectively assessing the timescales available for potential emergency response and recovery actions as well as the viability and feasibility of providing back-up power and cooling is likely too short and somewhat arbitrary. Even if emergency measures are “credited” after this time, or require deployment of qualified equipment, there is still a significant and finite probability of not fully restoring needed power for cooling (Duffey and Ha, 2013).

16.2.2 The safety focus for advanced concepts

Current data for reactor accidents illustrate that the actual CDF is higher than predicted, primarily due to the inadequate prevention and control of extreme and unexpected events. Hence, the focus for ARs concepts has moved to examining Severe Accidents (SAs) which include core damage, being Beyond-Design-Basis Accidents (BDBA), and/or Beyond-Design Extreme Events (BDEE) which challenge the safe “operating envelope” and safety systems and barriers, and also including Rare or Extreme Events (REE), which render multiple systems in-operable and require core cooling and/or emergency response actions over long timescales.

Hence, the modern safety analysis hierarchy has emerged as follows for the various classes and continuum of potential events.

Design Basis Assessments (DBAs) and Design Basis Transients (DBTs): A formal definition of what constitutes the expected structural, seismic, accident, and transient loads and systems that must be “designed into” the system. Demonstrate defense-in-depth and operational control by formal attention to structural integrity, engineering design, safety system operation, core physics, and physical barrier performance, adopting relevant codes, best practices, and engineering standards.

BDBAs, BDEEs, and SAs: An “extension” of the events that must be formally considered, in safety analysis that take the design well beyond its normal or limiting operational envelope, and contains degradation of systems, components, and structures. Analyze and address weaknesses and inform risk-dominant accidents using probabilistic safety analyses and develop emergency measures and procedures to manage the safety performance, using state-of-the-art computer codes and applicable data.

REEs: A “stress test” of what extreme might evolve that challenge the integrity, coolability, operability, and controllability of the reactor, including consequence mitigation and social impacts. Develop emergency response and equipment measures for responding to, and managing and coping with major challenges and damage to entire systems, to minimize the impact and health effects of radioactive releases and avoid or reduce social disruption and supporting strategic decision-making.

All Risk: Provide independent review and technical assessment of all aspects of analysis, design, construction, operation, licensing, maintenance, and management that impact process safety, and challenge and require verification of all claims, decisions, and regulations.

This hierarchy of severity corresponds and aligns closely to adopting the proposed “All Risk” philosophy for reactor safety to “prevent large radioactive releases that could cause major disruption of society” (ASME, 2012, p. 53), and agrees with the original and fundamental Rickover Safeguards Model.

16.2.3 Emerging and new safety design criteria

To formalize these needs and hierarchy for supporting AR design and concept development, a listing of some 83 Safety Design Criteria (SDC) has already been developed by the GIF. This list has evolved from specific considerations derived for the sodium-cooled fast reactor but is quite generically applicable to ARs.

These SDCs are quite extensive. The full listing and explanation have not been openly published, but the scope and importance can be seen from the information given in a series of International Workshops hosted by the IAEA and are shown below (note: some of the key ones are highlighted in italics for later reference, and the currently publicly unavailable criteria are left as deliberately unnumbered gaps).

Safety design criteria: partial listing with edited NRC review comments (Sofu, 2014; Nakai, 2013; information courtesy of the IAEA, Vienna)

- Criterion 1: Responsibilities in the management of plant design: applicant shall be responsible for ensuring that the design meets all applicable safety and security requirements.
- Criterion 2: Management system for the plant design: Quality Assurance (QA) requirements should extend beyond “design” considerations to address training of personnel, include a corrective action program, and address an inspection and test control program.
- Criterion 3: Safety of the plant design throughout the lifetime of the plant: applicant should retain QA responsibility for tasks that are assigned to external organizations for design of specific parts.
- Criterion 4: Fundamental safety functions: topic of “toxic chemicals” should be tied to nuclear safety (and coolant inventory control should be a safety function).
- Criterion 5: Radiation protection: use of As-Low-As-Reasonably-Achievable (ALARA) principle and acceptable dose limits for operational states and accident conditions.
- Criterion 6: Design for a nuclear power plant: should minimize contamination of the facility. Reliance on passive systems or inherent features to perform fundamental safety functions should be emphasized. DBTs should be included in the scope.
- Criterion 7: Application of defense-in-depth: definition of events outside of established safety envelope should include DBTs. Defense-in-Depth (DiD) (per IAEA definition) is a key element of safety philosophy but not a regulatory requirement in the United States.
- Criterion 8: Interfaces of safety with security and safeguards.

- Criterion 9: Proven engineering practices: scope to address materials selection, fabrication, installation, examination, and testing.
- Criterion 10: Safety assessment: definition of events outside of established safety envelope should include DBTs (and) include a QA provision for safety assessments and extended to include operational phase (not just design phase) to cover the changes in design.
- Criterion 11: Provision for construction: “Design” definition to include manufacturing, construction, assembly, and installation.
- Criterion 12: Features to facilitate waste management and decommissioning: rad-waste minimization provision should be included.
- Criterion 14: Design basis for items important to safety: definition of events outside of established safety envelope should include DBTs.
- Criterion 16: Postulated initiating events: reliance on manual initiation of systems instead of automatic action to mitigate the response to an initiating event is allowed only in a limited circumstances (e.g., fire protection), and definition of events outside of established safety envelope should include DBTs.
- Criterion 19: Design basis accidents: no guidance in the United States on evaluation of DBAs using best-estimate methods including uncertainty; new criteria may be needed to delineate the design basis sodium accidents for SFRs.
- Criterion 20: Design extension conditions: limited set of events more severe than DBAs (SB, ATWS, aircraft impact etc.) for “design extension” requirements. *The design shall be such that design extension conditions that could lead to significant radioactive releases are practically eliminated.*
- Criterion 21: Physical separation and independence of safety systems: separation and independence should apply in providing defense-in-depth for the design of a physical protection system.
- Criterion 23: Reliability of items important to safety: include the design of a physical protection system.
- Criterion 25: Single failure criterion: design of a physical protection system should prevent single failure that will render the security function ineffective or unavailable.
- Criterion 29: Calibration, testing, maintenance, repair, replacement, inspection, and monitoring of items important to safety: include physical security systems; worker exposures should be ALARA (not just below specified limits).
- Criterion 31: Aging management: provision should be made for providing adequate space in the facility to facilitate removal and repair/replacement of aging mechanisms/components.
- Criterion 32: Design for optimal operator performance: include design of a physical protection system; qualification of personnel and considerations essential to assure that operators can perform the functions associated with safe plant control (training, and human performance trending) should be addressed.
- Criterion 33: Sharing of safety systems between multiple units of a nuclear power plant: shall not be shared between multiple units unless this contributes to enhanced safety it can be shown that such sharing will not significantly impair their ability to perform their safety functions, including, in the event of an accident in one unit, an orderly shutdown and cool down of the remaining units.
- Criterion 34: Systems containing fissile material or radioactive material: should extend to facilitate physical protection of systems, including cyber security, to protect against radiological sabotage and the safeguards of special nuclear material from theft and diversion.
- Criterion 37: Communication systems at the plant: reliability of communication should be required for use following all postulated initiating events and in accident conditions, including applicable DBT.
- Criterion 38: Control of access to the plant: specific physical access control measures should include those necessary for detecting, assessing, and delaying insider threats for systems and equipment designated as vital.
- Criterion 42: Safety analysis of the plant design: both Anticipated Operational Occurrences (AOOs) and DBAs are evaluated in the safety analysis and include design of a physical protection system to protect against malevolent acts.

- Criterion 43: Performance of fuel elements and assemblies: specified acceptable fuel design limits should not be violated for AOOs.
- Criterion 44: Structural capability of the reactor core: addresses only internal events. Fuel assemblies are considered important to safety and therefore must accomplish their safety functions, allowing reactor shutdown and maintaining a coolable geometry, under internal and external DBA events.
- Criterion 45: *Control of the reactor core: the reactor core should have prompt inherent nuclear feedback characteristics to compensate for rapid reactivity insertions.*
- Criterion 46: Reactor shutdown: implies the specified design limits for the fuel are not exceeded for AOOs.
- Criterion 50: Cleanup of reactor coolant: introduction of chemicals should be addressed in a manner tied to nuclear safety and radiological risk and should address chemical protection.
- Criterion 54: Containment system for the reactor: should specifically include “internal events” and address the question of “confinement” vs traditional use of “containment.”
- Criterion 55: Control of radioactive releases from the containment: require that leak rate testing be performed at design basis pressures.
- Criterion 56: Isolation of the containment: inconsistent with GDC 56, which states that check valves cannot be used as the automatic isolation valve outside of containment.
- Criterion 58: *Control of containment conditions: containment is designed to withstand the worst DBA and/or severe accident conditions.*
- Criterion 61: Protection system: protection system independence should consist of independent trains such that a single failure would not prevent the protective action.
- Criterion 66: Supplementary control room: requirements for the control room should also apply to the supplementary control room.
- Criterion 71: Process sampling systems and postaccident sampling systems: process sampling systems and postaccident sampling systems shall be designed so that the dose to an operator taking samples from these systems is ALARA.
- Criterion 75: Lighting systems: redundant or extended service lamps should be used in high-radiation areas to maintain personnel exposures ALARA by reducing the frequency of lighting replacement. Design features should be provided to permit the servicing of lighting from lower radiation areas.
- Criterion 80: Fuel handling and storage systems: fuel handling and storage systems for irradiated and non-irradiated fuel shall be designed to maintain doses to operators ALARA.
- Criterion 81: Design for radiation protection: the plant layout should be designed to minimize exposures and contamination of operating personnel by controlling access to areas with radiation hazards and areas of possible contamination. Ventilation systems shall be designed to minimize personnel exposures and control the spread of contamination.
- Criterion 82: Means of radiation monitoring: facilities should be provided near the monitors for decontamination of contaminated personnel or equipment.

16.2.4 The safety goal and objective of “practical elimination”

A key point emerges. It is impossible for any design to survive extreme events like a meteor impact, or a major military attack, or the disintegration of society due to events like political upheavals, “regime change,” or massive super-volcanic eruptions, among others.

So, within the confines of what is considered by reasoning and logic as feasible and necessary, any inherent issues in the design can be addressed so that the effects and consequences are minimized and controlled. In addition, it is well known that claiming or deriving small Core Damage Frequencies (CDF) or activity release (LRF), using current PSA/PRA methods, leads to unreasonably low and basically unprovable numbers. It also leads to a subjective decision on what is or may be a lower bound or cutoff for event sequence frequency and claims of calculating even a CDF of $\sim 10^{-8}$ or less have been made, despite lack of data and the large uncertainty.

In part, these somewhat misleading low frequencies with large uncertainties have arisen because the initiating event frequencies and subsequent actions themselves are highly uncertain. These uncertainties are particularly important for the safety of ARs, for example, in potentially large seismic events (US NRC, 1997; EPRI, US DOE and US NRC, 2012; TEPCO, 2012, p. 437 et seq.), but also because of the overwhelming role of human error and of improper organizational decision-making in all known accidents (Reason, 1997; Duffey and Saull, 2008), which contribution is also poorly represented, inadequately modeled, and often underestimated.

These difficulties, and the potentially large consequences and design implications, have led to the concept of “practical elimination”, as italicized for emphasis in Criterion 20, and featuring in Criterion 45.

The stated goal and concept of “practical elimination” (Dufour and Carlucci, 2011; with italic emphasis added).

“Mitigation of the consequences of some accident situation must be excluded by design:

- Either because implementation of mitigation devices is not reasonably feasible,
- Or, because the R&D to be developed for demonstrating their efficiency is not reasonably feasible.
- *The first design objective is to make such situations physically impossible.*
- In compliance with DiD, “practical elimination” is acceptable only for a limited number of very well-identified situations.

The “practical elimination” of some accident situation requires implementation of independent reliable design features and a robust demonstration of their efficiency, e.g.:

- Combination of active and passive systems.
- Inherent characteristics.
- Operating procedures for verifying efficiency of protection devices (e.g., needs in-service inspection).

For implementing such an objective, principles for setting up a demonstration of practical elimination have been expounded (Okano, 2014) as follows which are consistent with the coupled deterministic and probabilistic safety approaches given above:

- “Demonstration is made on a case-by-case approach.
- Deterministic basis, supplemented by probabilistic studies.
- General principles for deterministic demonstration.
- Look for complete list of practical elimination situations.
- Introduce provisions to mitigate the consequences of initiating event.
 - Emphasis should be placed on:
 - Prevention of situations leading to “cliff edge effects.”
 - Efficiency and reliability of mitigating provisions cover a wider domain. And
 - Less sensitive to common mode failure.
- Probabilistic studies to ensure completeness and to establish expected frequency.”

Whether and how such approaches, concepts of which there are many candidates and proposals, are possible is the subject of current development, and is specific to each AR.

16.3 Safety objectives and the classification of advanced reactor types

There is no global or international consensus on the details of nomenclature, safety criteria, or licensing methods for new concepts and designs. Given that it is not possible to cover or foresee all future possibilities or variations in design and principles, the task is how to ensure some uniformity of approach toward meeting some agreed high-level safety goals. The important GIF effort has provided a common forum for such discussions, as has also the efforts of some nuclear regulators to “harmonize” their differing approaches without

relinquishing their statutory national regulatory authority. These efforts have resulted in so-called Safety Reference Levels (SRLs), which for existing reactors are summarized elsewhere (WENRA, 2014). For the new or advanced reactors of interest here, there are seven high-level Safety Objectives (SOs) promulgated and listed as follows (WENRA, 2009), with “SOs” and italics added for clarity:

“SO1. *Normal operation, abnormal events and prevention of accidents*

- reducing the frequencies of abnormal events by enhancing plant capability to stay within normal operation.
- reducing the potential for escalation to accident situations by enhancing plant capability to control abnormal events.

SO2. *Accidents without core melt*

- ensuring that accidents without core melt induce no off-site radiological impact or only minor radiological impact (in particular, no necessity of iodine prophylaxis, sheltering nor evacuation).
- reducing, as far as reasonably achievable: the core damage frequency taking into account all types of hazards and failures and combinations of events; the releases of radioactive material from all sources; providing due consideration to siting and design to reduce the impact of all external hazards and malevolent acts.

SO3. *Accidents with core melt*

- reducing potential radioactive releases to the environment from accidents with core melt, also in the long term, by following the qualitative criteria:
- accidents with core melt which would lead to early or large releases have to be practically eliminated; for accidents with core melt that have not been practically eliminated, design provisions have to be taken so that only limited protective measures in area and time are needed for the public (no permanent relocation, no need for emergency evacuation outside the immediate vicinity of the plant, limited sheltering, no long-term restrictions in food consumption) and that sufficient time is available to implement these measures.

SO4. *Independence between all levels of defense-in-depth*

- enhancing the effectiveness of the independence between all levels of defense-in-depth, in particular through diversity provisions (in addition to the strengthening of each of these levels separately as addressed in the previous three objectives) to provide, as far as reasonably achievable, an overall reinforcement of defense-in-depth.

SO5. *Safety and security interfaces*

- ensuring that safety measures and security measures are designed and implemented in an integrated manner. Synergies between safety and security enhancements should be sought.

SO6. *Radiation protection and waste management*

- reducing as far as reasonably achievable by design provisions, for all operating states, decommissioning and dismantling activities: individual and collective doses for workers; radioactive and non-radioactive discharges to the environment; quantity and activity of radioactive waste.

SO7. *Management of safety*

- ensuring effective management of safety from the design stage. This implies that the licensee: establishes effective leadership and management of safety over the entire new plant project and has sufficient in house technical and financial resources to fulfill its prime responsibility in safety; ensures that all other organizations involved in siting, design, construction, commissioning, operation, and decommissioning of new reactors demonstrate awareness among the staff of the nuclear safety issues associated with their work and their role in ensuring safety.”

We can all agree to these ideals. These are all fine words and with noble intent, but still mask the complexities of reality, and also do not reflect that safety is actually and in practice (as amply demonstrated by Fukushima

and most industrial accidents) the responsibility of the operator/owner of the plant, *not* the regulator. The regulatory process, whatever it is and wherever it occurs, simply ultimately grants a license that sets minimum standards or expectations for compliance by the owner and operator, as all such rules and regulations are intended to do. Requiring and undertaking periodic safety reviews, audits, and inspections of operations, desirable and necessary as they may be, cannot and must not be a substitute for the designer and operator to relentlessly improve safety experience, knowledge, skill, awareness, training, and commitment.

Setting aside for the moment the inevitable variability in design detail and in implementation, we can conveniently group the various Gen-IV, SMR, and AR concepts simply according to the medium utilized and needed for cooling the primary reactor. These three media are water, gas, or liquid (metal or salt) that also conveniently characterizes the safety analysis methods and claims relative to meeting the SO.

From reviews and compendiums of the current concepts and design variants which we need not repeat here (see [Pioro et al., 2020](#), and the references therein), globally there exists over 100 notionally different SMR, AR, and Gen-IV types, acronyms and concepts vying for financial, political, and marketplace endorsement. They are in all possible varying stages of design and deployment readiness, and for convenience and simplification we may classify and group by coolant Class, being 31W (water), 39L (liquid), 18G (gas), plus additional marine-based and micropower concepts. Despite the numerical and alphabetical plethora, all are subject to the same overall safety objective of maintaining cooling, but by using differing means.

The basic configurations of the ARs are similar also. All have a primary loop for extracting heat from the reactor core, inside some kind of pressure-retaining vessel, channel or container, with a heat exchanger or direct cycle to a turbine. The cycle efficiencies and physical layouts are all adequately described elsewhere (in Appendix A1 of this book, and the references given to [Table 16.1](#)), and need not be repeated here. However, the safety details between designs within a given Class are different, because of the inherent differences in operating temperatures and pressures, coolant heat capacity, natural circulation flows, reactor reactivity coefficients, and physical power limits, which all give rise to differing accident possibilities and event progression. Any and all proponents will and do formally claim to meet the safety objectives as a necessary condition for acceptance.

So, are these concepts safe?

Are some “safer” than others?

And how do we know?

We cannot simply turn to results or deliberations in the licensing process here, as these are not only still emerging, but also deliberately avoid analyzing comparative safety, as is also the case with commercial

Table 16.1. Probabilistic (PRA/PSA) and Deterministic Analysis (DA) comparison

SA safety aspect	PRA/PSA approach	DA approach	Note
Method	Fault and event trees, plus scoping	Complex safety codes	Wide scope vs narrow focus
Initiating events	Frequency of occurrence	Selected major	Cover “what if” scenarios
Failures	Probabilistic	Single and/or worst	Judgment involved
Initial conditions	Nominal operating or “best estimate”	Limiting or “conservative”	Judgment involved
Number of sequences	Limited by cutoff and importance	Limited by edict and selection	Judgment involved

Continued

Table 16.1 Probabilistic (PRA/PSA) and Deterministic Analysis (DA) comparison—cont'd

SA safety aspect	PRA/PSA approach	DA approach	Note
External events	Fire, flood, seismic, tornado, threats	Boundary condition	Large uncertainty for “rare” events
Treatment of Uncertainties	Included using distributions	Varying inputs and sampling outputs	Missing data and systematic errors
Safety measure	Core damage frequency	Safety limit margin	Both are failure to cool or control core
Consequences and offsite effects	Included and linked	Excluded	Supports Emergency Response measures
Safety systems operation	Reliability analysis	Defined functioning	Strong link to design
Human actions	Included and/or dynamic	Excluded and/or static	Large uncertainty
Passive safety systems	Included	In design basis	Claims vs reality
Management culture	Included via HRA	Excluded	Not measurable
Equipment maintenance and operation	Included via reliability assessment	Unknown	Limited data
Results	Relative ranking of risk	Absolute margin	Used for design and licensing decisions
Limitations	Too small numbers and limited treatment of humans	Only arbitrary and stylized sequences	Potential for undue reliance on paper vs “real” safety
Licensing use	Risk informing and screening	Margin confirmation in design	Regulatory inflexibility

aircraft. Technological innovation also generally leads regulation and licensing, not the other way round, as clearly shown by the evolution of computers, automobiles, and modern medicines. The present approaches and origins to reactor safety and licensing are based on water reactor traditions and are *not* directly applicable to a multitude of different concepts. In the USA, word changes to NRC licensing and regulations have been suggested to address this issue, including the vague term “concept neutral,” and to expand the applicability of existing methods and safety criteria to include selected others from Classes G and L than just Class W (US NRC, 2007; INL, 2014; CNSC, 2008).

Independent of reactor Class, existing modern safety analyses are based on the twin directions of: (1) assessing potential event initiators and quantifying estimates of the sequence evolution and responses using Probabilistic Risk/Safety Assessment (PRA/PSA); and (2) Deterministic Analyses (DA) where postulated events are analyzed largely independent of their likelihood. Combinations of many events, transients, and failures are considered, from simple upsets to loss of power, earthquakes, fires, and floods.

These two methods are consistent with the five stages of the generic “Integrated Safety Analysis Methodology” (ISAM) propounded by the GIF Risk and Safety Working Group (GIF, 2014b, p. 59). The overall methodology is openly published (GIF, 2011) and includes specific guidance for use (GIF, 2014a). The ISAM tools/stages are stated in the Roadmap Update as the following:

- qualitative safety requirements/characteristic review;
- Phenomena Identification and Ranking Table (PIRT);
- objective provision tree;
- deterministic and phenomenological analyses; and
- Probabilistic Safety Assessments (PSA).

Since neither deterministic nor probabilistic methods are perfect for establishing safety margins, damage, or activity release probabilities, or allow inclusion of all possible scenarios, the obvious intent is that one should complement the other.

The contrasts and complementary aspects between the approaches were summarized at the top level in (ASME, 2012) and are shown in more detail in Table 16.1. PRA/PSA is nominally more inclusive, realistic, and general, and DA is much more stylized and arbitrary. As can be seen, both have limitations but provide excellent support to, but are not a substitute for safety judgment.

To address and improve safety analysis, and address the key uncertainties in addressing extreme accidents, the key development approach therefore means radically enhancing and simplifying both Design and Licensing (D&L) by:

- Improving and simplifying the safety analysis;
- Making all safety and operating systems more robust;
- Assuring more “inherent” safety;
- Eliminating many possible initiating events;
- Requiring less active systems valves, pumps, and actuators;
- Reducing the need for human intervention and/or operator actions;
- Providing indefinite cooling and/or heat rejection;
- Eliminating or reducing the likelihood of core damage;
- Enhancing emergency response effectiveness;
- Reducing the potential for offsite releases;
- Having more “standardized” or “modular” structures; and
- Undertaking objective independent safety “stress testing.”

At the same time, the approach to reducing capital costs and risks often implies series building of multiple, perhaps smaller, units, sometimes utilizing common services and sites and reduced staffing, which all impact the potential for unexpected safety interactions. In addition, some options suggest using remote sites and alternate configurations, such as confinement buildings or underground silos, which also affect both the geological and topological risk as well as logistical and emergency response aspects.

16.4 Generic safety objectives and safety barriers

Physically, meeting the SO means providing and maintaining control at all times, plus Ultimate and indefinitely lasting Heat Sinks (UHSs). In essence, we can simplify these by representing levels of process safety “barriers” (see, e.g., Bea and Gale, 2011, pp. 5-11), corresponding to deeply layered defense-in-depth. In that reference, the “barriers” are classified as proactive, reactive, and interactive, and can be physical, procedural, and managerial. Hence, considering the failure or bypassing of one or multiple layers is necessary for setting

the safety design philosophy, where data and predictive uncertainties grow with the failure, bypass, or breaching of each layer.

The safety design objectives for barriers in all new technology systems are therefore to:

(1) Reduce the likelihood of initiating events

The chance of incidents and events is minimized by ensuring high reliability of active systems, effective actuation of passive systems, and imposing sufficient operating margins. In addition to robust design and construction of the primary system, buildings, components, pipes, and systems, additional margins are included in core thermal limits and redundancy and diversity in shut down and safety system deployment, and in safety and control equipment. This requires attention to the core physics and fuel design to provide void, temperature, and power reactivity coefficients having adequate margin which ensure automatically reducing and/or limiting the reactor power for all conceivable and postulated transients (e.g., an anticipated transient without scram, or a Loss Of Cooling Accident (LOCA) coincident with loss of offsite power). Multiple safety systems and instrumentation provide monitoring and control capability for all normal and upset conditions.

Almost all “routine” transients are expected to have benign results, without causing core damage. Therefore, challenges only arise from consequential major structural or system damage, primary system breaches, and/or severe extended Loss Of Power and/or Cooling (LOPC).

The methods used include operating experience and event data, including geo-tectonic historical records, analysis of sequences with coupled neutronic-thermal-hydraulic transient performance analysis codes, CAD-CAE systems, structural finite element methods, materials stress analysis, Human Reliability Analysis (HRA), risk assessments, and most importantly PRAs for providing input to RIDM as discussed further in [Section 16.9](#).

(2) Ensure long-term cooling

Despite meeting objective (1) stable long-term natural circulation and/or thermal radiation heat removal from the core must be provided. This means assuring removal of decay heat at all times to an UHS such as the atmosphere, including situations, where all power (from outside grid cables and from inside generators and batteries) has been lost for extended times. The other intent is to minimize or obviate the need for human actions, since these are themselves the cause of errors and accidents.

Some of the approaches that have been investigated for AR systems are based on current knowledge and available systems and include the following (for a comprehensive review, see [Boucau, 2022](#)):

- Provide natural circulation loops for systems with inherently large heat capacity coolants or moderators.
- Design for rapid depressurization to allow water injection to be assisted by the use of relief or “squib” valves and multiple loops. And
- Incorporate high hydrostatic heads, non-return valves, heat exchangers, and steam condensers to assist natural circulation, and water pools, without requiring operator actions for some extended time.

Therefore, the only challenges are in ensuring adequate heat removal, sufficient cooling, and power supply for the timescales and also ensuring the UHS and system integrity is maintained. This aspect is discussed in extensive detail in [Section 16.9](#). The methods used include validated thermal-hydraulic codes (see [Section 16.10](#)), system and component reliability analysis, and PRAs.

(3) Ensure effective elimination of emergency response

One GIF safety goal is to essentially eliminate the need for emergency response, thus avoiding evacuation requirements for surrounding people and any land contamination. Providing objectives (1) and (2) are met, but still assuming barrier failure, this goal requires essentially avoiding core damage, maintaining containment or confinement integrity, and providing completely robust seismic, terrorist, and tornado proof systems and structures. Additional options also include underground reactor buildings to reduce the “target,” and filtered venting to control potential overpressures and any potential for radioactivity release.

The challenges that remain are in actually proving that releases absolutely cannot occur (given it is hard to prove a negative and such data are scarce), and that all potential core damage states are either avoided and/or adequately cooled.

The methods used include severe accident analysis codes, structural failure mode analysis, radionuclide transport in buildings and the environment, historical geo-technical, hydraulic and seismic response analysis, and PRAs.

(4) Manage rare and extreme events

Despite meeting objective (3), REEs or BDEEs must be considered that address natural events in association with, or causing, failure of infrastructure (both on and off site), and intense social disruption. These “external events” may include extreme or tsunami-induced uncontrolled flooding, major ice storms, aircraft impact, fires, seismic, and terrorist threats, in conjunction or associated with major failures in power, control, and systems.

In so-called “stress tests,” such extreme scenarios are considered to test the ability to respond and maintain control, ensuring graceful degradation, and avoiding non-coolable molten core configurations (by providing “core catchers” or concrete building base mat protectors) and explosions due to uncontrolled hydrogen production (as occurred at Fukushima), including in more fragile structures. Therefore, challenges are in determining the bounds of the scenarios to be considered, and in predicting the course of such events, and in the deployment of emergency equipment in a timely manner, e.g., as in the FLEX “coping strategies” (NEI, 2012), to help to ensure a managed response that avoids panic and dismay. The methods used include risk assessment, PRAs, gaseous mixing and explosion analysis, and severe accident and consequence codes.

(5) Ensure rickover safeguards for public well-being

Despite meeting objectives (1)–(4), which are essential physical barriers, there are the other key aspects of corporate, management, and regulatory safety that require attention. All major events include a failure of safety performance at senior management levels as well as at the operational level, plus an inadvertent emphasis on process production over process safety.

These human performance barriers are not just the last line of defense; they are indeed the glue that holds the entire safety edifice together. It is well known that having the correct attitudes, training, emphasis, rewards structure, working environment, and philosophy, which all support safety, are key to effective implementation and to effective safety and process management. This actual human performance goes well beyond traditional human reliability analysis on task performance to consider and represent the difference between the claims and reality about safety “culture” and risk adverse behaviors. It is a necessary but not sufficient condition that the licensed owner–operator and the design authority, meet all regulations and requirements, but must still solely bear the safety burden and the risk. The regulator sets the standards, while management sets the expectations and meets the goals.

Therefore, challenges remain not only in ensuring the highest standards of safety performance, personal accountability, and attitudes, but in measuring and continuously improving that same performance. Social and public acceptance must be won, not by slogans but by example, and retained by unending emphasis on safety. This is particularly true and needed for any new technology (viz. the commercial aviation industry).

The methods used include providing a learning environment and effective informal issue communication, independent analysis, Red Teams (critical independent reviewers), management benchmarking, inspections, safety performance audits, on-site presence, intensive “bottom up” reporting, and most of all assuring personal responsibility and accountability.

The logical hierarchy invoked by ISAM is (GIF, 2014a, Figure 3).

Safety goals and objectives

- Fundamental safety functions;
- Probabilistic success criteria;
- Deterministic success criteria;

Defense-in-Depth (DiD) levels:

- 1st—Prevention;
- 2nd—Surveillance and control;
- 3rd—Accident management;
- 4th—Control of severe conditions and mitigation; and
- 5th—Mitigation of radiological consequences.

Accident investigation terminology (derived from: [US Department of Energy, April 2015](#)).

Accident investigation terminology

A **causal factor** is an event or condition in the accident sequence that contributes to the unwanted result. There are three types of causal factors: direct cause(s), which is the immediate event(s) or condition(s) that caused the accident; root cause(s), which is the causal factor that, if corrected, would prevent recurrence of the accident; and the contributing causal factors, which are the causal factors that collectively with the other causes increase the likelihood of an accident, but which did not cause the accident.

The **direct cause** of an accident is the immediate event(s) or condition(s) that caused the accident.

Root causes are the causal factors that, if corrected, would prevent recurrence of the same or similar accidents. Root causes may be derived from or encompass several contributing causes. They are higher-order, fundamental causal factors that address classes of deficiencies, rather than single problems or faults.

Systemic root causes involve a deficiency in a management system that, if corrected, would prevent the occurrence of a class of accidents.

Local root causes involve a specific deficiency that, if corrected, would prevent recurrence of the same accident.

Contributing causes are events or conditions that collectively with other causes increased the likelihood of an accident but that individually did not cause the accident. Contributing causes may be longstanding conditions or a series of prior events that, alone, were not sufficient to cause the accident, but were necessary for it to occur. Contributing causes are the events and conditions that “set the stage” for the event and, if allowed to persist or recur, increase the probability of future events or accidents.

Event and causal factors analysis includes charting, which depicts the logical sequence of events and conditions (causal factors that allowed the accident to occur), and the use of deductive reasoning to determine the events or conditions that contributed to the accident.

Barrier analysis reviews the hazards, the targets (people or objects) of the hazards, and the controls or barriers that management systems put in place to separate the hazards from the targets. Barriers may be physical or administrative.

Change analysis is a systematic approach that examines planned or unplanned changes in a system that caused the undesirable results related to the accident.

Error precursor analysis identifies the specific error precursors that were in existence at the time of or prior to the accident. Error precursors are unfavorable factors or conditions embedded in the job environment that increase the chances of error during the performance of a specific task by a particular individual, or group of individuals. Error precursors create an error-likely situation that typically exists when the demands of the task exceed the capabilities of the individual or when work conditions aggravate the limitations of human nature.

16.5 Risk informing safety requirements by learning from prior events

It is important to learn from actual prior outcomes and events and from major technological system disasters (Duffey and Saull, 2008), and ARs are no exception. Even with the massive rare events, there are many opportunities for learning from more frequent occurrences. For examining and learning from known events, precursors and accidents, a certain procedural formality has emerged which is relevant to improving operational and “real” rather than hypothetical safety. Typical terminology that is used for event investigations, barrier failure allocation, “root cause analysis,” and formal incident reviews is shown below.

Note that “barrier analysis” is a key step, as it fundamentally includes DiD, such as the those invoked against radioactivity release (fuel/primary system/containment), and is an adaptation of the “bow-tie” methodology that was commonly utilized in and by the oil and gas industry. However, it is now known that such physical, procedural, administrative, and managerial layers may be breached, bypassed or made ineffective or aggravated by human actions and subsequent loss of control, as exemplified by multiple severe accidents, such as the TMI loss of coolant, Davis–Besse head corrosion, Fukushima core melts and explosions, the Concorde and Air France AF447 aircraft crash, and the Deepwater Horizon offshore oil spill events (Duffey, 2012, 2015).

A notional example of a “barrier tree” for a loss-of-power LOPC BDEE-type event is given below in Figure 16.1, which has some 10 levels of physical, procedural, operational, and managerial barriers. Data and analysis of major events indicate that such barriers are penetrated and bypassed by human actions, decisions, and behaviors with an overall probability which is greater than $O(10^{-3})$, consistent with human learning and decision-making errors (Duffey, 2015).

16.6 Major technical safety issues

We may further classify the major generic technical safety issues for each of the three Classes, W, G, and L, using information derived from both experience and the published literature as given in the following discussions based on material from the GIF (GIF, 2014b; Kelly, 2014, by permission).

Safety design approaches to achieving GIF goals (adapted from Kelly, 2014)

- VHTR Safety (Class G): Restricted to 600 MW_{th}; huge thermal inertia of graphite structure and matrix; fuel not damaged below 1600 °C, single-phase inert coolant;
- SFR Safety (Class L): Inherent features such as natural circulation cooling and fuel expansion; single-phase coolant with high margin to boiling;
- SCWR Safety (Class L): single-phase coolant; passive safety systems;
- GFR Safety (Class G): Very-high-temperature fuel; complex engineered safety systems;
- LFR Safety (Class L): Single-phase, high-enthalpy coolant; large margin to boiling; amenable to natural circulation cooling;
- MSR Safety (Class L): No possibility of fuel melt; low fissile inventory; relatively low fission product inventory.

These top-level goals have been extended in more detail as follows, where we have made the GIF discussion generic to all systems for the appropriate AR Class.

Class W (GIF, 2014b, p. 44):

“The SCWR will be licensed only if it fulfills at least these stringent requirements. More specifically, the Fukushima Daiichi accident demonstrated the need for passive residual heat removal over long periods and the SCWR should be designed accordingly.”

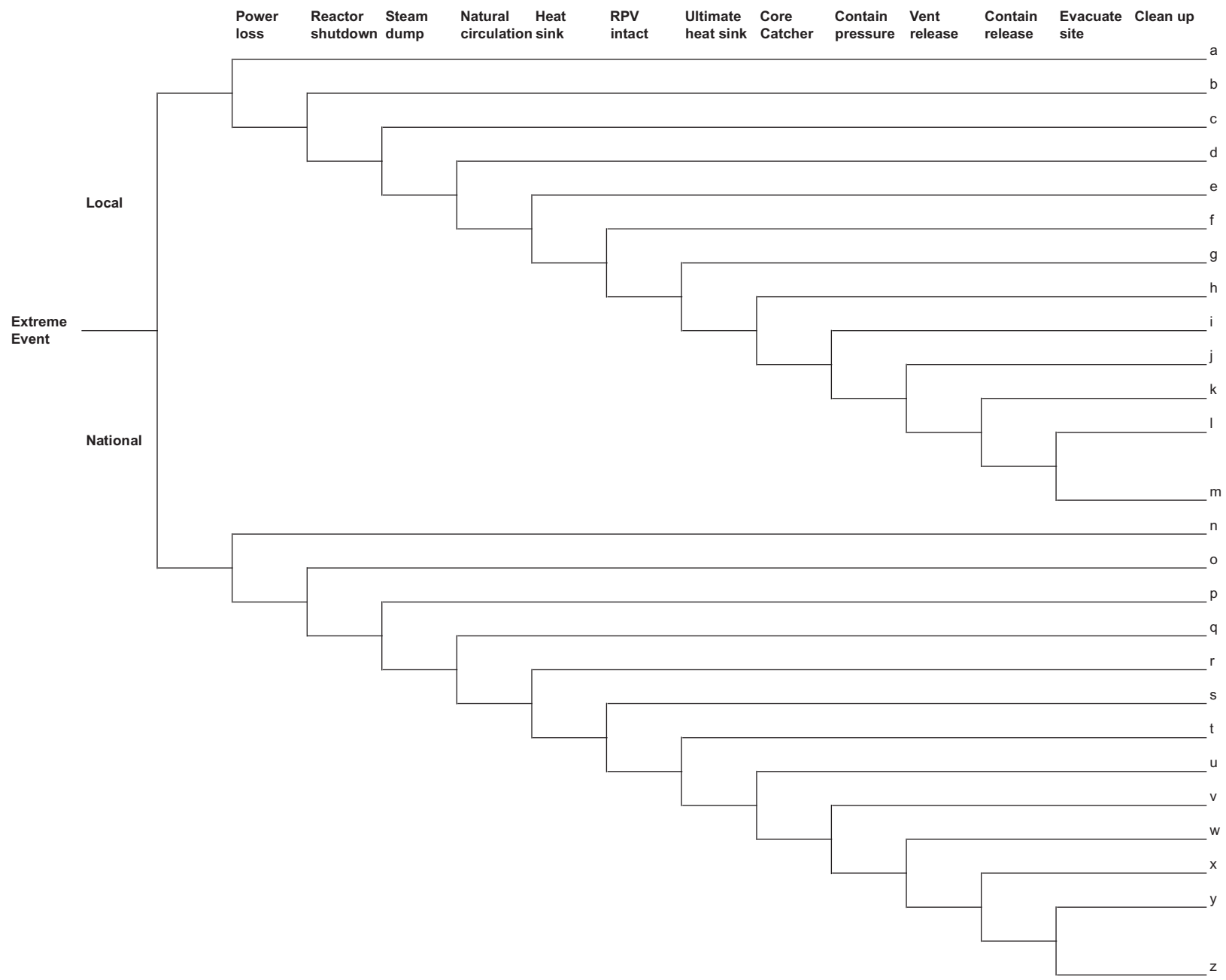


Figure 16.1. Notional Barrier or PRA/PSA event sequence tree for nuclear plant.

For the SCWR, with a very-high-pressure, high-temperature system (25 MPa), the depressurization rates and forces are potentially larger than in current LWRs. For the two concepts, both need to show that a simple LOCA or Reactor Pressure Vessel (RPV) or Pressure Tube (PT) failure, by cracking or damage does not lead to core damage.

In the basic concept of the RPV version (Oka and Mori, 2014), classic LWR transient analysis is used: whereas for the PT version, total loss of flow and cooling is addressed as in the Class G systems, using radiation cooling to an UHS. In both cases, the safety goal and requirement are to provide cooling and, hence, to avoid fuel melting and/or core damage for indefinite timescales, even for BDBAs, BDEEs, and REEs (Yetisir et al., 2012).

For such W-class systems, the major heat removal mechanism invoked is natural circulation (often called “passive”), not only in the primary system, but in back-up cooling, and in the eventual heat rejection to an Ultimate Heat Sink (UHS) which is usually the atmosphere or the earth.

The decision to provide that there be no core melt for any and all loss-of-cooling events has led to the SCWR PT-concept having thermal radiation only cooling mechanism that ensures that clad and fuel melting is not possible (Yetisir et al., 2015). In the NuScale (2020) AR concept, for example, the requirement to maintain cooling indefinitely has led to a series of natural circulation paths.

Class G (GIF, 2014b, p. 21):

For GFRs, “the need (is) to ensure robust Decay Heat Removal (DHR) without external power input, even in depressurized conditions, is now regarded as a requirement. Previous concepts used electrical (battery) driven blowers to handle depressurized DHR. Although the DRH system has no diesel power units that would need protection from potential flooding, integrity of the electrical infrastructure following an extreme event is still required.

Work is required on two fronts; first to reduce the likelihood of full depressurization and second, to increase the autonomy of the DHR system through the use of self-powered systems. While these self-powered systems cannot be considered passive, they do not require any external power input. Finally, the strategy to deal with severe accidents is to be established.”

The GFR also has a rapid heat up on loss of cooling, which as noted above cannot be maintained unless power to gas circulators (pumps) is available, which then means high-temperature-resistant fuel is needed. This has led to the adoption of so-called particle or pebble fuel. In addition, RPV or primary system failure is difficult, and so attention has even been given in the past to Class G using prestressed concrete vessels.

The need to initiate and maintain some natural circulation cooling is extremely demanding for such a high power–density concept, resulting in multiple layers of back-up gas circulators and power supplies.

Class G (GIF, 2014b, p. 51):

For VHTR, “passive Decay Heat Removal (DHR) systems have been designed to facilitate operation of the VHTR, with a final goal of simple operation and transparent safety concepts. Demonstration tests are planned to verify the system’s passive characteristics and to show that its safety margins are sufficient. Design-basis and beyond-design-basis accident analyses for the VHTR will need to include phenomena such as chemical attack of graphitic core materials, typically by either air or water ingress. Adequacy of existing models will need to be assessed, and new models may need to be developed and validated.”

Further demonstrations of the safety performance for both the prismatic and pebble bed concepts, at HTTR and HTR-10, emphasize the benefit of the strong negative temperature coefficient of reactivity, the high heat capacity of the graphite core, the large temperature increase margin, and the robustness of TRISO fuel in producing a reactor concept that does not need off-site power to survive multiple failures or severe natural events as occurred at the Fukushima Daiichi nuclear station.

Because of the need to limit ingress of a moderator or water that can produce potentially explosive hydrogen on interaction with hot graphite (e.g., $C + 2H_2O = CO_2 + 2H_2$), has led to consideration of adopting inert gas heat exchangers (e.g., using supercritical CO_2).

Class L (GIF, 2014b, p. 34):

For the sodium-cooled system (SFR), "... efforts will be concentrated on safety and operation (improving core inherent safety and I&C), prevention and mitigation of sodium fires, prevention and mitigation of severe accidents with large energy releases, and ultimate heat sink."

In addition, specifically for the SFR, there is a "Designer's choice" as a result of safety (Anzieu et al., 2014) (subtitled Applied Gen-IV Criteria to ASTRID), which partly states that:

"12. Prompt criticality shall not be reached either by core compaction or other core motion, or by a gas flow, or by collapse of the core support.

13. Loss of the decay heat removal function that could lead to a possible collapse of the primary circuit structures shall be practically eliminated.

14. Core sodium de-flooding shall be practically eliminated.

Comment: this criterion obviously includes leak of the two reactor vessels.

15. Core melting during handling shall be practically eliminated, for instance thanks to appropriate prevention means and handling error detection system"

None of these issues are new, since the sodium reacts exothermically with water, and the core is not in its most reactive configuration. Hence, major core transients and prompt criticality is possible from reconfiguration or inadvertently adding moderator, or by voiding the central part of the core by boiling. In fact, leakage of sodium through small holes in the HEX has been a major inconvenience and difficulty.

Class L (GIF, 2014b, p. 29):

"MSFR systems have been recognized to have favorable features making them a potential long-term alternative to solid-fueled fast-neutron systems. However, mastering the technically challenging technology will require concerted, long-term international R&D efforts, namely:

- system design: development of advanced neutronic and thermal–hydraulic coupling models;
- analysis of salt interactions with air or water in case of a severe accident;
- analysis of the accident scenarios (e.g., heat exchanger loss); and
- fluorides may offer large-scale power generation while maintaining full passive safety."

These issues are also well known, since on loss of power or flow, the reactor becomes subcritical as the core drains, and prototypes have been run to demonstrate feasibility.

16.7 Multiple modules and plant risk

Many of the ARs and Gen-IV systems are designated as "modular" in design, meaning that multiple units can be mass-produced with a common licensing basis, and having shared siting. Such approaches are already successfully used in the design and construction of industrial equipment and facilities, and in reducing the construction time of large nuclear plants. The AR/SMR intent is to use more but smaller units to enable:

- a. assembly-line processes with just-in-time delivery and less field work;
- b. lower the initial capital investment and produce an earlier ROI;
- c. shorter engineering and construction times;
- d. adding increments of power as demand requires and cash flow allows;
- e. reduced unit costs by series build rather than "on-off" or custom designs;
- f. up-front one-step review and licensing ("certification") of the duplicated design;
- g. sharing of common facilities and site infrastructure;
- h. reduction of staffing duplication for security and operations;
- i. reduced costs of unit downtime and flexible/standardized maintenance; and
- j. improved safety by system diversity and less activity release potential.

These are fine and desirable goals, but do contain increased specific costs, at least for the first few units that have to bear the development, licensing, module “factory,” and production-line set up. In addition, the issue has been discussed of the *relative* safety for multiple units that are colocated and may share interactions between systems and shared facilities. To date, most licensing and builds had been on the basis of one unit at a time, despite the presence or colocation of other facilities. This was also highlighted by Fukushima, because of the presence of spent fuel pools at the site, with the potential for additional activity release.

So, the apparently simple safety question for ARs is whether multiple, say, 10 small units have the same or more risk than one unit with some multiple of the power output, say, 10 times, and greater radioactive and spent fuel inventory per unit at the same site?

The considerations for multiple plant risk have already been addressed for the implications for PSA/PRA purposes (CNSC/OECD, 2014). The revisions needed to safety methods, assessments, rules and regulations have been considered, and a practical approach has been suggested as to how to include multiple units (Vecchiarelli et al., 2014). The overall objective is simply to provide protection to the public and “practically eliminate the potential for extensive social disruption,” in line with the ASME approach (ASME, 2012), and to aggregate (add) the individual CDFs to stay below some agreed overall site limit, while excluding some low-frequency events.

It should be noted that the units sharing or on adjacent sites are partially independent, and that unexpected interactions can exist, as has been demonstrated by Fukushima. This multitude of potential interactions has also been examined (Modarres, 2015). By examining the differing possible types of interactions, from an initial scoping study, it was concluded that Common Cause Failures (CCF) dominated due to systems, events, and human errors. In fact, considering the differing learning stages and operational experience levels, it has been shown that multiple facilities at multiple sites do indeed have higher risks (Duffey and Saull, 2008, Appendix F, p. 481). These results are not surprising by themselves, as events or damage that affect multiple units simultaneously, or even propagate from unit to unit, or hinder the operation of shared systems, or are common to the design, must now be included in the safety assessment, rather than using a single unit case as applicable to all other units.

16.8 The role of Safety R&D for ARs

R&D has a vital role in providing the methods, data, and sound judgments needed for developing and evaluating new technology. Adequate and exhaustive testing is essential, be it hardware, software, or firm-ware, for proving any new innovation or product, to establish or refute the safety claims, and to underpin system performance requirements.

Clearly all is not resolved for the formalization of the safety of ARs, and additional data, analyses, and thinking are all underway at the time of preparation this article. A useful summary is given by the GIF “Roadmap Update” (GIF, 2014b, p. 37) for the systems that they are pursuing:

“Additional R&D on safety issues highlighted by the Fukushima Daiichi accident is foreseen.... A primary focus on the following issues is anticipated:

- robust and highly reliable systems for adequate cooling of safety-relevant components and structures;
- geometric stability of the SFR core in case of a strong earthquake and assurance of reliable performance of the control rods;
- seismic-resistant design of the spent fuel pools and fuel-handling devices;
- integrity of the primary circuit and its cooling;
- design features aimed at excluding the risk of flooding of the reactor building; and
- effective options for dealing with severe accidents.”

16.9 Risk informing advanced reactor safety: Quantifying the probability and uncertainty of core damage due to loss of power and cooling

...it is very certain that, when it is not in our power to determine what is true, we ought to act according to what is most probable.

Rene Descartes, 1596-1650.

To determine what is most probable, we now address and quantify how AR and Gen-IV designs and concepts aspire to meeting the simple and necessary safety objectives given in [Section 16.4](#) to ensure cooling the core. Restated here, the only challenges are in ensuring adequate heat removal, sufficient cooling, and power supply for the timescales needed to prevent core damage (not activity release) and also ensuring the UHS and system integrity is maintained. The following sections reflect the discussion given in a detailed forthcoming paper ([Duffey and Zio, 2022](#)), and are included in order to provide a complete and full updating for this present second edition.

16.9.1 Introduction to RIDM

First, examine the modern idea of Risk-Informed Decision-Making (RIDM) as proposed and used in conjunction with PSA/PRA for all existing, advanced and Generation-IV systems when assessing for the probability of core damage due to severe and rare events causing extended loss of power and cooling ([US NRC, 2004a,b, 2007, 2020](#); [CNSC, 2008](#); [Apostolakis et al., 2012](#)).

As we have stated before ([Duffey, 2012](#)): “Certainly, the risk from energy systems, energy production, and energy use is low. But societies do not have a unified and universal measure of what constitutes acceptable risk. The attitude to risk varies with the activity, history, technology, and the regulatory or legal framework. This is already well known and documented in the study of risk analysis and is unlikely to change towards some more rational basis. The risk from nuclear energy use poses special questions, as its potential radiation threat is unseen and not very well understood by the public.”

Traditionally, radiation release causing some level of public harm is the governing paradigm used by nuclear plant regulators for quantifying or assessing risk consequence. The other consequences of core damage that must be considered are financial losses, societal disruption, and political risks, and constitutes the overall safety objective not being solely evaluating potential exceedance of radiation release or exposure limits for the affected public. Such a comprehensive consequence approach is available already for estimating the total societal costs of damage and numbers of casualties for earthquakes, floods, and hurricanes ([US FEMA, 2011, 2019](#)) and for restoring damaged civil/social infrastructure after such extreme events ([Loggins et al., 2019](#)). For nuclear systems, the multitude of possible or potentially different initiating events can be addressed whatever the initiating event or hazard by forming the BDBA/BDEE set {flood, fire, hurricane, ice storm, typhoon, earthquake, cyberattack, ...}, since, as shown in the preceding sections, the fundamental concern is the consequent non-restoration of Loss Of Power and Cooling (LOPC) and the capability to cool the core. Quantitative evaluation must include the reliability of “active” and “passive” emergency back-up systems using applicable and “exchangeable” data for nuclear *and* non-nuclear systems, including cyber system vulnerabilities ([US DHS \(2018\)](#)). For a wide range of known catastrophic events that cause widespread damage and societal disruption, the power outage duration can last for several hundred hours due to the degree of restoration difficulty. A major reconsideration and updating of modern risk-informed approaches is suggested for nuclear plant regulation, evaluating commercial risk exposure and undertaking rigorous design evaluations for all ARs and Generation-IV systems.

As shown by real events ([Duffey, 2015](#)), the consequences of core damage are far beyond the regulator: for any investor, operator or owner, the fundamental question is the uncertainty in present probabilistic estimates

and whether the risks are being correctly estimated. Therefore, core damage in and by itself is not then an acceptable risk even if activity releases and public radiation exposure remain within formal or legislated limits, an important issue for any proposed extended deployment of advanced and Gen-IV concepts. The top-down analysis which follows is truly also “concept neutral,” and valid for and independent of all the myriad of types of designs, coolants, nomenclatures, and plant sizes proposed for, say, any AR Class (W, L, G, advanced, passive, active, and Gen-IV systems), where extended loss of cooling can potentially lead to core damage or presaging potential activity release. This is particularly important for any future world energy scenario envisaging adding more reactors including any and all concepts, sizes or designs beyond the present 400 or so now operating in various parts of the world.

Presently, quantitative estimates of the probability of reactor Core Damage, P (CD), are universally derived from bottom-up Probabilistic Risk and Safety Analyses (PRAs and PSAs), where restoring power and hence cooling involves postulating sequences with multiple (dependent) steps, actions, and/or independent failures, including both “active” and “passive” safety systems. The most recent probabilistic status includes making a distinction between “classical” time-independent event trees and “dynamic” sampling to approximate the event evolution by updating the failure probabilities during a simulated DBEE (Mandelli et al., 2020). As stated in the reference, the latter idea “strongly simplifies the intrinsic complexity of modern system simulators¹ that solve a set of partial differential equations (mass, momentum, energy-conservation laws) and constituent laws over a mesh.” But, by clearly violating and neglecting the basic conservation laws of physics, these well-meaning PSA/PRA approximations are self-evidently incorrect and have unknown uncertainties, a topic we address and correct in Sections 16.9 and 16.10.

In severe or beyond-design-basis extreme events (grouped and variously abbreviated BDBA or BDEE), ultimately the fuel will eventually overheat, and the core or system actually be damaged (fuel failure, melting, circuit leakage, etc.), if power and cooling is not restored, depending on the decay heat, circulation cooling capacity, back-up battery lifetimes, and UHS capability (NEA/CSNI, 2015). So, in reality, the probabilities (or frequencies) of core damage and any subsequent release for differing designs are actually all (directly or indirectly) dominated by the chance and risk of extended Loss Of Power and Cooling (LOPC) and/or of the Ultimate Heat Sink (LUHS), also, including Extended Loss of All Power² (ELAP). Irrespective of the details of the system design or Class W, L, G, the simple quantification of the “concept neutral” core damage risk is, for any member of the set $\{BDEE\}$,

Probability of initiating event(s) causing extended loss of power and cooling to the core, times.

Probability of not restoring power and cooling before core or system damage occurs.

The overall probability or annual core or system damage frequency per annum, F (CD), for any reactor Class is represented by the sum of the individual sequences (US NRC, 2020), which codifies the use of a “base” PRA as part of formal RIDM licensing to try to provide some uniformity and discipline in the analysis and use of the results. The NRC safety goal guidelines are for a Cumulative Damage Function (CDF) or summed core damage frequency over all sequences of less than 1×10^{-4} per reactor year, so, for an assumed 60-year AR life, the probability of core damage for an individual reactor should be less than 6×10^{-3} , somewhat higher but comparable to other regulators (CNCS, 2008).

The BDEE initiating events set or “hazard group” are usually chosen in PRA/PSA to specifically challenge the capability of emergency response and safety design features to cool the core. Hence, the presently arbitrarily assumed timescale for complete Station Black Out (SBO) is 24 h but exclude operator actions or any external power restoration. Other postulated scenarios assume both LOOP/LOSP for at least 72 h, but “allow” the best efforts in deployment of Emergency Power and cooling back-up Systems (EPS), including

¹ These simulators are the established thermal hydraulic “nodal” or volume-averaged computer codes used globally in some form or variant by all reactor designers, regulators and operators to establish safety margins, uncertainty ranges (CSAU/BEPU) transient performance and system setpoints.

² The acronym has sometimes been restricted to only just Extended Loss of AC Power.

using informal Severe Accident Management Guidelines (SAMGs) and emergency equipment deployment (e.g., NEI, 2012; US CFR, 2017). These stylized 24- and 72-h “coping,” “success,” or “mission” times for use/deployment of EPS—whatever they are—ab initio are assumed sufficient for preventing core damage (NuScale, 2020, Section 19.1.4.1.1.3 p. 19.1–11). Only for external floods, based on undefined “engineering judgment” external power restoration is not assumed to occur within 72h, so cooling relies entirely on internal Emergency Power Systems (EPSs).

For power and cooling restoration, up to now, existing PRA/PSA methods (also, promulgated in professional society ASME and ANS “standards”) have not used real dynamic *system* severe event information *directly*, but proscribe and postulate failure–success path sequences for separately classified BDEE, or a “hazard group” that initiate failures (floods, fires, hurricanes (or wind), ice storms, earthquakes etc. (as also addressed in US FEMA (2011) and Loggins et al., 2019) leading to, arising from or including Loss Of Offsite and/or onSite Power (LOOP/LOSP) and subsequent core damage (e.g., see Westinghouse, 2004; NuScale, 2020, NEI, 2012; US NRC, 2020). The methods and results are included in formal safety submissions for any and all concepts, designs, coolants, and sites, specifically often in Chapter 19 of the US NRC Safety Analysis Report (SAR) or Design Control Document (DCD) submission.

Because of a paucity of data for such *hypothetical* severe events, and of course lack of new design experience, safety assessments of existing and new designs have recently relied heavily on qualitative judgments or semi-formal “Risk-Informed Decision-Making” (RIDM) (US NRC, 2007, 2020) using frequency-consequence curves not on just numerical F (CD) occurrence estimates. As stated in Chapter 22 of this Handbook, “The NEI 18-04 lays down a foundation for establishing licensing technical requirements to facilitate risk-informed and performance-based design and licensing of advanced non-light water reactors.”

In general, the equally hypothetical $F-C$ or $F-N$ boundary is given by, where n and m are some chosen exponents:

$$F \times C^n = F \times N^m = \text{defined constant or varying acceptable limit, } L(C, N).$$

However, it is defined, the implication of this acceptable boundary “limit” is that a small or incremental changes in frequency, ΔF , with an allowable large consequence or deaths, C or N , respectively, has the same relative safety improvement, risk importance or offsetting “value” as a small or incremental change in consequence, ΔC or ΔN at some high allowable frequency, F .

Socially, in terms of deaths, it is like saying that many car crashes with few fatalities in each is the same risk and as acceptable as one major train wreck or a plane crash with many passenger deaths.

The specific NRC “guidance” (US NRC, 2020) flexibly uses quantitative analyses only to inform qualitatively “acceptable” risk judgments:

“The base PRA provides a quantitative assessment of the identified risk of the as-built and as-operated plant in terms of scenarios that result in undesired consequences (e.g., core damage or a large early release) and their frequencies and is comprised of specific technical elements in performing the quantification”; and,

“That is, decisions are expected to be reached in an integrated fashion, considering traditional engineering and risk information, and may be based on qualitative factors as well as quantitative analyses and information” (US NRC, 2020).

But, as we have stated before: “Risk decision-making... is based on a balanced judgment between what we know vs what we do not know” (Duffey, 2020a, p. 218). In principle, the RIDM concept allows assessments to nominally encompass uncertainties using some formulation of expert judgment that must be informed by relevant data. Hence: “Judgment and expert opinions are required, because safety assessments must deal with rare events. The issue, therefore, is how to process this judgment and how to combine it with observations and frequencies. To achieve this, one applies the rules of the subjectivist theory of probability; that is, one must be coherent, which is synonymous with being objective. These methods are not a panacea” (Apostolakis, 1990).

Hence, the RIDM tautological statement of belief or ideology is that prior events can *only* provide guidance for “risk informed” posterior judgments, because: “It is the qualitative insights from operational experience that are useful in regulatory decision making, not the frequencies of core damage and release derived from this experience” (Apostolakis, 2016). By this definition, safety regulation and RIDM are subjective and qualitative, while not using the formal legal “balance of probabilities” for judgment and without any numerically or objective scientifically defined uncertainty. The fundamental paradox is that, by definition, all the elements in the bottom-up PSA/PRA (assumed initiating events, fault trees, sequence frequencies, and failure rates) contain, include and are actually derived from selected prior data on known, generic or estimated *component* and *system* failure rates and reliability estimates for a mix of similar or related systems, equipment and components (see Eide et al., 2007). For new designs and/or a lack of experience-based data, a recent article has even stated: “Here, your failure probabilities would be dominated by the subjective understanding of the system” (Denham, 2021), whatever that means given the absence of real knowledge.

As cautioned by Ellenberg (2014, p. 335) “There is real danger that, by strengthening our abilities to analyze some questions mathematically, we acquire a general confidence in our beliefs, which extends unjustifiably to those things we’re still wrong about,” so we need a common-sense check.

To reconcile the classical *bottom-up* summation of hypothetical separate core damage probabilities or frequencies, $\sum_{\text{BDEE}} F(CD)$, from event trees as proposed or required by conventional PSA/PRA methods in (US NRC, 2020), with real *top-down* accident probabilities we group together all such hazards and events that have been observed or likely to cause extended LOPC. We risk inform an overall top-down integrated probability, $P(CD)$, of ELAP leading to core and/or system damage for any reactor design, Class or concept that needs some form of cooling whatever the member of the whole initiating BDEE hazard set {flood, fire, hurricane, earthquake, ice storm, typhoon, terrorism, cyberattack, ...} of external and internal causes, using and updating existing experience (as in Kimura and Budnitz, 1987). For all these disparate natural or man-made initiating events, in order to “make definite predictions that can be tested,” the data-driven top-down analysis also supersedes and comprehensively discards using any arbitrary “mission” time constraint, and fully includes all relevant dynamic human decisions, actions, and responses needed to inform the emergency decision-making.

16.9.2 Addressing limitations of RIDM methodology and safety-related societal judgments

The “hand waving” argument is that bottom-up PRA/PSA only provides guidance on informing relative risk significance or acceptability arises from the acknowledged RIDM subjectivity and lack of absolute PSA/PRA verification.

The theoretical PSA/PRA $F(CD)$ values for a given consequence supposedly should demonstrate being within or below some such safety goal, regulatory limit line, public radiation exposure, and/or of lower comparative risk “significance” (see, e.g., NEI, 2018, 18–04, Figure 3.1). The original RIDM proposal was only made for hypothetical non-LWR AR and Gen-IV systems, presumably to “grandfather” (avoid revisiting) the safety submissions for the 400 or so existing operating plants and designs. But for investors, owners and operators of existing as well as advanced or Gen-IV systems, risk avoidance, and minimizing risk exposure is also key to assuring returns/profits in addition to just attaining any necessary formal licensing acceptance or design certification. This is the arena in which RIDM is potentially most useful, as in principle it can include reputational, commercial, and societal issues while just by having core damage could be an unacceptable and intolerable risk all by itself.

Other technologies and disciplines use variants of the RIDM ideology clothed with differing emphasis, terminology, and acronyms, and that technical information cannot be the sole basis for decision-making (NASA, 2010). In oil and gas extraction: “A major accident risk assessment, known as MAR, is a disciplined,

validated method to assess risks, likelihoods and consequences associated with major system accidents” (United States District Court Eastern District of Louisiana, 2010; BP, 2010), and develops a $F-N$ curve also referred to as a type of Quantitative Risk Assessment (QRA). In dam safety risk analyses, an acceptable frequency vs consequential deaths (or $F-N$) risk curve or “allowable” boundary is invoked, derived from public safety considerations for 1000’s of different dam types and ages (US FEMA, 2019; McCann and Lundquist, 2017). In the world of business and finance: “Enterprise Risk Management (ERM) promotes risk-informed decision making that allows resources to be prioritized and allocated based and encourages agencies to target their limited resources to activities likely to produce the greatest improvement in program performance” (US Department of Treasury, 2021). None of these elaborate and detailed risk evaluation concepts would prevent, foresee, predict, or quantify the probability of the TEPCO Fukushima nuclear plant flooding and meltdowns, the NASA Challenger shuttle loss, the BP Deepwater Horizon explosion and oil spill, and the US and global Great Financial Crisis, respectively. A major limitation and paradox is that all these were regarded as “acceptable risks until they actually happened” (Duffey and Saull, 2008, p. 268, Figure 7.2; Duffey, 2020a) and simply focusing on hypothetical consequences ignores the real massive industrial, financial, cultural, economic, and social impacts.

Justified and motivated by these very public predictive failures of “paper-based” RIDM and probabilistic assessments, and lack of inclusion of the massive indirect societal and economic impacts, a new practical RIDM approach too is needed. Data already exist for a wide range of natural or man-made severe events and hazards (floods, fires hurricanes, ice storms, earthquakes, etc.) needed for populating the set {BDEE}. Modern grid and supply system experience for BDEE set initiators show resulting loss of power and restoration efforts can last for many hundreds of hours or even months in regions with fragile grids (Romain et al., 2019; Duffey, 2019a, b). These major disasters also provide the timescale and reliability for deploying and actuating emergency power and cooling back-up systems (generators, batteries, “black start” plants, plus delivering pumps, and cooling equipment), including any concomitant widespread social disruption and access issues. Consequently, the known “non-nuclear specific” data also fully include all the decision-making, procedural techniques, operational and performance errors, emergency management responses, and human (un)reliability, which happen in any real not hypothetical disasters.

The numerous PRA “success paths” mean sequential failure probabilities of multiple systems, barriers, and components are unlikely unless there are common mode or Common Cause Failures (CCF), and usually also assume an invariant Human-Error Probability ($HEP \sim O(10^{-2})$). Therefore, claimed PRA/PSA-predicted annual frequencies for individual AR core damage sequences are tiny, from perhaps one in a few billion (10^9) to less than a trillion (10^{12}) years (e.g., NuScale, 2020), with total core damage risk assumed to be the summation of the probability/frequency for all the individual BDEE hazard group sequence outcomes. Clearly the small $F(CD)$ numbers for any sequence or differing “hazard group” summation or set {BDEE} are clearly unverifiable, being well outside the total span of human technological experience ($\sim 10^4$ years). The very-low-frequency results can be viewed as an artifact of the adopted methodology, especially given that severe core damage events have already occurred more frequently (Engler, 2020; Rose and Sweeting, 2016), a factor of 10 larger than any published PRA/PSA estimates for existing US plants (see, e.g., Barr et al., 2018, table 2.6).

The PRA/PSA results have been used for assessing “relative,” if not absolute numerical risks via incremental changes in $F(CD)$. But PSA/PRA event tree analysis is formally a theoretical framework, with the scientific requirement that all theories should be quantitatively “falsifiable,” and that: “A good theory will describe a large range of phenomena on the basis of a few simple postulates and will make definite predictions that can be tested” (Hawking, 2014).

Hence, to address this conundrum, we adopt the fundamental scientific view that the *prior* actual events—not hypothetical PRA/PSA ones—constitute the observations needed to substantiate and test any *present* theory, which then provide the objective and validated support needed to underpin subjective RIDM judgments made for all present, AR and Gen-IV systems.

The new general cumulative probability expressions for $P(\text{CD})$ for the set $\{\text{BDEE}\}$, provide the simplest results for RIDM without needing the details describing the detailed phenomenology of the core damage sequence itself (e.g., as exemplified by the OECD/ NEA/CSNI, 2015) benchmark). The realistic result is some 2–200 times greater than that derived by or in some modern PRA/PSA analyses and licensing submissions for modern system designs. We explain the possible reasons for this important under prediction, and hence, as espoused elsewhere (D’Auria et al., 2019), support requiring a modern, comprehensive and different approach to “risk informing” both licensing *and* design for both current and ARs which encompasses our *present* knowledge of the real not hypothetical uncertainties and potentially reduce risk and RIDM uncertainties by many orders of magnitude.

16.9.3 Using prior data to inform RIDM: Applicability and exchangeability

How can extreme event prior data and non-nuclear specific information be used in a “concept neutral” regulatory and safety system design process? The key is that the prior “failure” rate data from actual prior events are applicable for predicting the posterior probability of future events, informing and defining the uncertainty in the theoretical RIDM/PRA/PSA predictions. To illustrate this controversial idea, it is possible to conduct risk and safety analysis by providing more realistic safety analysis for modern designs, future AR, and Generation-IV-system design.

Note Extended Loss Of Power and Cooling (ELAP/LOPC) sequences are usually stylized, because: “In safety assessments, however, we are typically dealing with rare events, and the laws of large numbers are not of any particular usefulness” (Apostolakis, 1990).

There are in fact millions of directly *applicable and transferable* BDEE data for loss of power for all types of hazards that have not been fully utilized or formally incorporated to date by the global nuclear industry in RIDM, including extended power outages due to floods and hurricanes (Katrina in New Orleans and Maria in Puerto Rico), massive wildfires (in California), severe ice storms (in the United States and Canada), and actual reactor accidents (the Fukushima tsunami events). These societally disastrous events provide detailed timelines and failure rates not only for the power and cooling systems but also include the real human decision-making and emergency actions occurring during actual crises and valiant restoration efforts, so should somehow be applicable.

The use of data from similar *prior* core damage and other BDEE-like events has been previously dismissed as not usable or “exchangeable” system-to-system due to concomitant changes in knowledge, continuous learning and design changes (Apostolakis, 2016).

Lacking basic direct comparisons to data and validation, bottom-up PRA/PSA results are consequently claimed to actually be *not* predictive or quantitative but solely qualitative advice which “informs the decision makers’ current state of knowledge,” and any past event data are not “exchangeable” or directly usable for evaluating different, new or improved systems (Apostolakis, 2014, 2016). But since relevant prior experience exists, this allows and requires examination in order to quantify and inform the uncertainty or safety “margin” inherent in the subjective belief.

There are at least two definitions and many implications of something being “exchangeable,” beyond the common grammatical usage of substituting an item for another of “equivalent value.” Mathematically, exchangeable is defined in formal statistical probabilistic sequences as when “A sequence of random variables is invariant under variable permutations” (e.g., Niepert and Domingos, 2014), while also allowing finite or partial exchangeability. The NRC has independently added a third definition, where exchangeable events are *only* “independent events generated from a population of nominally identical reactors” (Siu et al., 2016). Any reactor suffering an event may be similar in concept to others in the world (e.g., W, L, or G Class), but will not be identical in detailed system design or core physics, so this definition justified NRC and others basing PRA/PSA input for RIDM solely on hypothetical event sequences not prior core-damage events and probabilities.

Data-based RIDM can remove this artificial restraint, being indifferent to and remaining unchanged from prior event-to-event or dynamic sequence order (see below). So, we may use partial exchangeability, where “Two events ... are said to be exchangeable, if ... there is indifference with respect to the order, because both intersections describe the occurrence of exactly one of the two events” (Cordnai and Wechsler, 2006).

When properly collected and analyzed the existing or prior severe or BDEE data are *logically applicable, formally exchangeable and generically transferable* to different systems.

16.9.4 Active and passive safety, power, and cooling systems

To minimize the dependence or reliance on human actions, engineered safeguards and mechanical failures, reactors include “passive” as well as “active” safety systems that in principle can provide, maintain, or restore power and cooling. As noted, to some degree, this is embedded in design and safety layout of all modern Class W, L, and G systems (e.g., PWR, BWR, SMR, HTR, VVER, MSR, LMR, SCWR, FBR, and PHWR), usually, based on maintaining natural circulation to some UHS, where the elevations of core and heat exchangers, piping connections, and possible leaks are designed to ensure (at least) removal of decay heat when active systems—notably, centrifugal pumps or emergency coolant injection—are not available. Thus, passive systems are (D’Auria et al., 2019):

- already an integral part of nuclear technology; and
- seen as inherently protective systems for whatever complexity or whatever unexpected situation in nuclear reactors.

Modern, “advanced “or “modular” reactor-system designs also utilize hybrid (active and passive) back-up Emergency Power Systems (EPS), sometimes in addition to diesel or turbine-driven generators by installing dedicated DC battery capacity for 24 and/or 72 h, so the standard SBO duration usually has negligible F (CD) following any uncomplicated major loss of power. By using battery-powered back-up systems, it is even argued that restoring Alternating Current (AC) power is not necessary since: “AC power is not needed for maintaining a safe shutdown state following SBO” (Section A-44 Station blackout in Westinghouse, 2004). Back up and dedicated battery bank lifetimes of 72 h can also be chosen to match the timing proposed and planned for FLEX EPS deployment. For example, in for the AP1000 safety design basis: “The Class 1E DC and UPS system has sufficient capacity to achieve and maintain safe shutdown of the plant for 72 hours following a complete loss of all AC power sources without load shedding for the first 24 hours,” with separate battery bank divisions dedicated to covering 24 and 72 h loads and supplies. A similar argument has been made for “passive plants,” where the “design is capable of performing safety related functions for 72 h” (NRC, 2007, 2016). In particular: “The ESBWR employs advanced, true passive safety systems and a simplified design utilizing natural circulation. These attributes result in the ability of the reactor to cool itself for more than seven days without operator intervention or AC power on or off site. Based on core damage frequency, the industry standard measure of safety, the ESBWR is the world’s safest approved nuclear reactor design” (GE, 2014).

In reality, the ELAP/LOPC issue remains as arbitrary 72–170 h durations are still not sufficient time, because a finite probability of LOOP lasts in excess of several hundred hours, and even longer in fragile grids such as Puerto Rico (Romain et al., 2019; Duffey, 2019a, b). At best, totally reliable or zero-failure rate on-site or in situ battery capacity extend the time available before ELAP so the probability of core damage can be adjusted by adding/allowing this time delay.

Other non-nuclear and cyber issues are also applicable, exchangeable, and transferable. The US DHS (2018) makes the not unreasonable assumption that restoration for power outages or “virtual” damage due to cyberattacks is similar to that for known severe events, like hurricanes and ice storms. The publicly available data shows cyberattack causes outages by disconnecting networks and operator control

before being restored after “several hours” (e.g., Lee et al., 2016). There was no concomitant access, physical damage, or societal disruption delaying recovery of the cyber infrastructure and associated computing/communication networks so, by analogy, cyberattacks can be included as a natural member of the set {BDEE} with varying degree of difficulty for regaining access and control.

The data-based method now described for RIDM input utilizes the top-down sequences for severe power outages and extreme events of national importance and impact.

16.9.5 Risk informing the probability of extended power loss and core damage

To establish a system-level emergent RIDM approach requires several basic premises consistent with the available statistical physics, human knowledge, and societal experience.

- As shown by data, power losses, outages, and restorations are indeed random whatever the cause, with recovery systematically depending on human actions including emergency management decisions.
- Because humans learn and think, and also as shown by the data, larger and longer outage events have lower probability, with restorations being iid (*independent and identically distributed*) events.
- For any and all initiating (hazard group or BDEE set) events in any and all reactors of any and all concepts, (L, W, G) core damage and hence investment loss occurs if power and cooling is not restored in time, h_{CD} .
- All members of the initiating BDEE hazard set {flood, fire, hurricane, earthquake, ice storm, typhoon, terrorism, cyberattack} are included and reflected in the prior grid system reliability, power outage, and emergency restoration human experience and power system databases.
- The available outage restoration datasets include a massive and sufficient number of sequences where all possible permutations and order of the invisible, unrecorded and unknown *internal* events and emergency and human actions are implicitly encompassed.

The dynamic probability of *Loss Of Power for Cooling* (LOPC) causing damage to the core, $P(CD)_{NR}$, in the time available before restoration of the power needed for cooling following any MW-loss outage size for the entire BDEE hazard set {flood, fire, hurricane, earthquake, ice storm, typhoon, terrorism, cyberattack}, is then simply given by the key probabilities.

$P(CD)_{NR \text{ set}\{BDEE\}} = \text{Probability of initial loss, } P(MW\text{-loss})_i \times \text{Probability of non-restoration of power for cooling, } P(NR)_h$, allowing time for damage.

We note that this sequence is statistically exchangeable. With deployment or use of any and all EPS (both active and passive systems), we must combine the above ongoing non-restoration probability, $P(NR)_h$, with the probability of failure to maintain, deploy or actuate any or all back-up emergency power and/or cooling systems (Westinghouse, 2004; Barr et al., 2018; Bhatt et al., 2006; GE, 2014; Duffey, 2019b; NuScale, 2020), including FLEX equipment, pumps, batteries, generators, and any and all improvisation (NEI, 2012). The dynamic probability of the onset of core damage to occur before the non-restoration of power needed for cooling for all members of the BDEE set {flood, fire, hurricane, earthquake, ice storm, typhoon, terrorism, cyberattack} now includes the *dependent* probability, $P(ELAP)_h$, of extended loss of *all* external, internal, EPS, FLEX-type equipment and sources used to avoid LUHS, with some known failure rate, λ_{EPS} .

$\Sigma P(CD)_{NR \text{ set}\{BDEE\}} (ELAP) = \text{Probability of initial loss, } P(MW\text{-loss})_i \times \text{Probability of extended non-restoration of power for cooling including back-up emergency systems(EPS), } P(ELAP)_h$, in time to prevent or avoid core damage.

This equation is quite general and applicable to any and all AR and Gen-IV nuclear systems, where LOPC/ELAP may occur. Since the probability of the initial loss for the set {BDEE} is derivable from past data for outages, so the initiating events are also formally exchangeable as the order of their prior occurrence is immaterial. In addition, despite the logical fact that physically loss must precede restoration, statistically this simple two-item sequence is exchangeable in order without altering the outcome probability magnitude. There

must be an outage for LOPC to occur; and the order of EPS back-up recovery/restoration is itself immaterial as only the overall EPS failure rate dominates.

In principle, data to evaluate the overall EPS failure rate, λ_{EPS} , are also available from prior events included in the entire BDEE set {flood, fire, hurricane, earthquake, ice storm, typhoon, terrorism, cyberattack} for any and all active or “passive” designs (Duffey, 2019b).

The distinct probabilities to be evaluated using applicable, exchangeable, and transferable public data are not presently included in present PRA/PSA or associated RIDM ideology, including any frequency-consequence bounds which do not include societal and economic impacts.

16.9.6 RIDM: Specific worked dynamic example and core damage uncertainty estimate

To provide a transparent worked example for dynamic nuclear RIDM, we can derive top-down probabilities that are predictable, transferable, and exchangeable and define uncertainties by utilizing the latest existing data from restoring power and cooling for multiple prior BDEE types affecting modern power systems. These include:

- (1) initial event outage probability, $P(MW-loss)_i$, based on data for *all* power losses and generating system failures in local regions and entire national grid systems (e.g., Murphy et al., 2017) including BDEEs causing widespread damage in an integrated power system that includes a fraction, $f(Q_N)$ of operating nuclear plants;
- (2) subsequent probability of non-restoration of power, $P(NR)_h$, with failure rate, β , providing the potential timescale for core damage, h_{CD} , using *all* human efforts, including BDEEs with major societal disruption that can inhibit and delay restoration efforts and perhaps lasting many hundreds of hours in systems that also now or in the future include nuclear plants (e.g., Duffey, 2019a,b; Romain et al., 2019); and.
- (3) failing to successfully restore, deploy, provide, or maintain emergency power and/or cooling, in time to avoid core damage using *all* emergency backup, battery, pumping, FLEX deployment, or “black start” systems, whether “active” or “passive,” with overall failure rate, λ_{EPS} , as already observed in prolonged major disasters including power systems with nuclear plants (US ACE, 2006; TEPCO, 2012; Duffey, 2019b, 2020b, 2021).

These data automatically and implicitly include all the essential human/operator actions, system reliability experience, emergency management procedures, multiple redundant or diverse “active” and “passive” power and cooling system configurations, plus the impact of infrastructure damage and access difficulty on restoration and outage duration. Being derived from the extensive power loss and restoration data existing for actual severe events therefore validates the predictive theoretical relations.

Including *all* restoration actions, access difficulty, infrastructure damage, FLEX actions, and emergency system deployment, for the entire set {BDEE}, the summed core damage probability, $\Sigma P(\text{CD})$, due to extended Loss Of system Power and Cooling loss (LOPC) for any AR is simply the fundamental physical formula derived elsewhere (Duffey, 2020b; Duffey and Zio, 2022).

$$\begin{aligned} \Sigma P(\text{CD})_{NR \text{ set}\{BDEE\}} (ELAP) &= P(MW - loss)_i \times P(ELAP)_h, \\ &= f(Q_N) \left[1 - e^{-\frac{\bar{Q}}{kQ}} \left\{ 1 - e^{-\frac{kQ}{Q}} \right\} \right] \left(\frac{\lambda_{\text{EPS}}}{\beta + \lambda_{\text{EPS}}} \right) \left[1 - e^{-(\beta + \lambda_{\text{EPS}})h_{\text{CD}}} \right] \end{aligned}$$

With the equivalent term-by-term description:

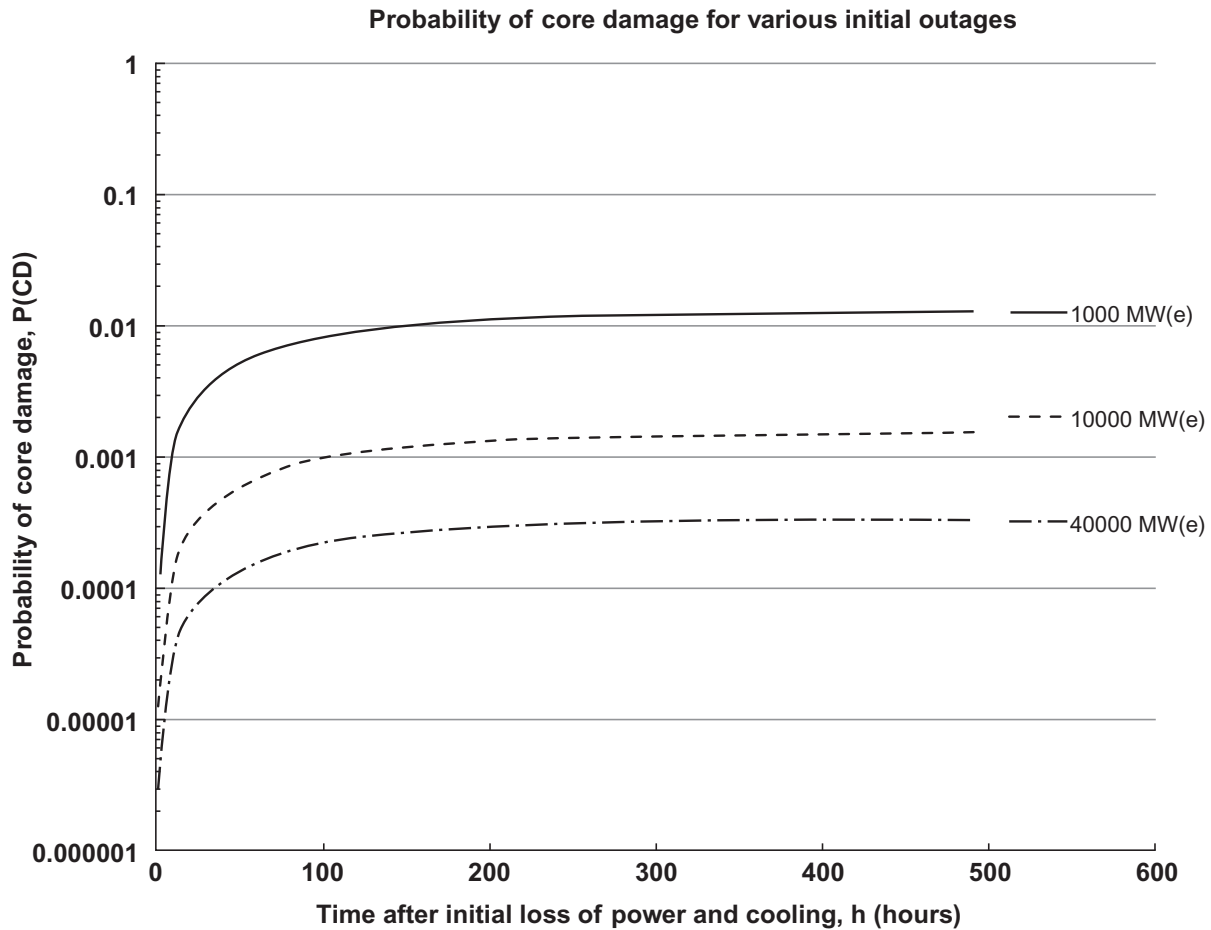


Figure 16.2. Illustrative predicted dynamic probability, $P(CD)$ of core damage due to extended Loss Of Power and Cooling (LOPC) for a range of initial outages in a totally nuclear-powered generating system, $f(Q_N) = 1$.

Summed probability of core damage due to extended LOPC/ELAP =

(Fraction of nuclear generation in entire power system)

× [Probability of power outage/LOOP of fractional MW size].

× (Ratio of overall power non-restoration, β , and emergency/passive/back-up systems, λ_{EPS} , failure rates).

× [Dynamic variation of power and cooling non-restoration before core damage time, h_{CD}].

The example dynamic prediction calculations illustrated in Figure 16.2 are for large-scale loss of power and cooling provisionally and initially assuming a fully nuclear-powered grid, using any AR Class W, G, L so $f(Q_N) = 1$, adopting $k = 2$, $\beta = 0.01$, and $\lambda = 0.003$ as derived from the correlation of multiple prior power outage and severe event data (Duffey, 2019a,b, 2020a,b). A 1000-MW_{el} outage is equivalent to extended LOPC at a single large 1000-MW_{el} unit with $f(Q)_N = 1$, predicting the largest $\Sigma P(CD) \sim 0.01$, almost exactly the prior Fukushima and Chernobyl values (Engler, 2020); or a cumulative frequency, CDF, of 0.00017 (1.7×10^{-4}) per annum for an assumed 60-year operating life of the plant. For a massive or unprecedented system-wide outage of >40,000 MW_{el} assuming only a 10% nuclear share of the total interrupted generating capacity or $f(Q_N) \sim 0.1$, predicts the lowest $\Sigma P(CD) \sim 0.00003$; or a frequency, CDF, of 0.0000005 (5×10^{-7}) per annum for an assumed single unit lifetime risk exposure of 60 operating years. In other words, the risk of core damage is highest for more frequent individual or local plant outages and resulting core damage, than for rare system-wide events, as already observed. This individual plant to system-wide outage

uncertainty is apparently about a factor of 100 and also obviously depends on the actual, anticipated or planned nuclear market “share” or fraction of the future overall generating capacity.

Irrespective of initial outage scale, after some 200 h all core damage $P(CD)_{NR}$ probabilities tend to the long timescale asymptote value for the entire set {BDEE}. By definition, these probabilities already include all restoration efforts taken to avoid core damage, whether procedural guidance, specialized emergency response, FLEX actions and equipment, back-up power and cooling, ad hoc repairs, “black start,” and management decisions throughout the extended LOPC duration.

16.9.7 Comparing and defining quantitative estimates of RIDM uncertainty

It is reasonable to ask how these dynamic and other top-down RIDM estimates (e.g., [Rose and Sweeting, 2016](#); [Engler, 2020](#)) differ from those derived using classic bottom-up PRA/PSA event tree sequences. Deriving a comparable bottom-up summation $\Sigma P(CD)$ is complicated, because of selecting LOPC-causes of core damage from among the hundreds of PRA/PSA hypothetical sequences in the safety submissions, each with differing acronyms and conventionally subdivided into multiple initiating event categories (i.e., for separate seismic, fire, flood, etc. BDEE scenarios). A limit comparison can however be made to the PRA sequence totals leading to core damage for five typical and recent openly published examples:

- (a) Passive system major contributions to $\Sigma P(CD)$ summed for Loss Of Preferred Power (LOPP) and Loss Of FeedWater (LOFW) analyzed for certification in the ESBWR PRA, (Bhatt et al., 2006, tables 7.2.2, 7.2.6, 7.2.7, 7.2.8, and 7.2.9).
- (b) Hybrid EPS PWR events contributing to the total PRA CDF, $\Sigma F(CD)$, summed for all listed loss-of-coolant and every internal-system initiators analyzed for large PWR ([Westinghouse, 2004](#), table 19-59-1, Items 1 to 26, inclusive and also, [UK HSE, 2008](#)).
- (c) Passive EPS summed CDFs, $\Sigma F(CD)$, for listed mean value PRA contributions for BDEE fire, flood, and hurricane hazards, plus LOOP and Loss Of DC power (LODC) for SMR module (listed in [NuScale, 2020](#), FSAR Chapter 19, table 19.1–80, p. 279).
- (d) Active EPS, summed for the listed PRA calculated average frequencies, $\Sigma P(CD)$, of ELAP and core damage for 12 existing licensed US BWR units (listed in [Barr et al., 2018](#), table 2.6); and.
- (e) Prior events (Fukushima and Chernobyl) proposed as providing top-down directly “exchangeable” Bayesian-probability estimates, $\Sigma P(CD)$, assuming a binomial distribution at 95% confidence (as tabulated by [Engler, 2020](#)).

For a nominal 60-year plant-life risk exposure (typical for current, ARs, and Gen-IV systems), [Table 16.2](#) shows the present RIDM theory estimates can range from 2 to over 200 times larger than those derived and given from and by published and submitted traditional PRA/PSA methods. Even subsuming all the BDEE CDFs sequences for both “active” and “passive” plants, as might have been anticipated, the predicted probability for a single 1000-MW_{el} unit is comparable to that for prior LOPC events, but derived in a completely different manner. As stated before, the NRC safety goal guidelines is for the Cumulative Damage Function (CDF) to be less than 6×10^{-3} per reactor for a 60-year lifetime risk exposure, which can be compared directly to the $\Sigma P(CD)$ BDEE estimates given above in [Table 16.2](#).

We can speculate on the underlying causes of, and major contributors to the uncertainty arising from the much lower apparent bottom-up PRA/PSA core damage predictions compared to those derived from top-down informing RIDM using exchangeable dynamic prior data.

First, the key practical issue is the extent of damage, social disruption or access difficulty is reflected in and by the much longer times (a smaller characteristic or e-folding “degree of difficulty”) in restoring power, including onsite, offsite (FLEX) and EPS means, which is not included in PRA/PSA as used today.

Second, some PRA bottom-up analyses adopt HEP in BDEE that continually decline with increasing time, or are invariant with very low probabilities of order 0.004 for the first or initiating human failures using

Table 16.2. Scoping lower limit RIDM comparisons for total core damage probabilities due to extended Loss Of Power and Cooling (LOPC)

Source/type	P(CD) BDEE	CDF/ annum
Sec. 16.9.6 AR: outage 40,000 MW _{el}	3×10^{-5}	5×10^{-7}
Sec. 9.9.6 AR: outage 1000 MW _{el}	10^{-2}	1.7×10^{-4}
(c) SMR 300 MW _{el}	1.5×10^{-7}	2.6×10^{-9}
(b) PWR 1200 W _{el}	1.4×10^{-5}	2.4×10^{-7}
(d) BWR 12-unit ELAP	1.2×10^{-3}	2×10^{-5}
(d) BWR 12-unit CDF	5.3×10^{-4}	8.9×10^{-6}
(e) Prior events (95%)	1.6×10^{-2}	2×10^{-4}
(a) ESBWR Table 7.2.2 et seq.	1.8×10^{-6}	3×10^{-8}
(a) ESBWR LOFW/LOPP/LOOP	3×10^{-8}	5×10^{-9}

classic task-by-task or action-by-action error rates (see, e.g., [NuScale 2020](#); [Swain and Guttman, 1983](#), [Figure 12.3](#)). However, from learning theory, the HEP during dynamic-system events with integrated human decisions is known to be 50:50 at early times falling to a defined lowest attainable minimum of order 0.01 later (as reviewed in [Duffey and Ha, 2013](#); [Duffey, 2020a](#)), a difference or uncertainty of some 2–100 times larger and not coincidentally covering the discrepancy range apparent in [Table 16.2](#).

Just from these two PRA/PSA bottom-up assumptions and models, a difference in core damage probability $\Sigma P(CD)$ of many orders of magnitude is possible, implying a quantifiable RIDM uncertainty of the same order. In a reverse argument, this justifies not using the unverified PRA BDEE results for RIDM simply because the uncertainties are so large.

We now turn to the resulting salient and key safety issue that is also the subject of extensive research. How can natural circulation and inherent and indefinite cooling be demonstrated for these seemingly many and varied AR and Gen-IV systems?

We proceed by fully examining the state of the art for the analysis and modeling of natural circulation flows and heat removal, which are so important to the effective long-term removal of heat to a UHS in all AR and Gen-IV concepts. We specifically avoid the analysis of heat removal for degraded cores, and the role of “core catchers,” which are added sacrificial and/or cooled and reinforced layers beneath the RPV. Instead, we rely simply on the empirical evidence from major and severe accidents to date (e.g., Three Mile Island, Chernobyl, and Fukushima) that demonstrate that highly degraded and complex core configurations are ultimately coolable; and that the primary safety goal or aim for ARs, *not* for existing reactor designs, is really to ensure adequate cooling prior to the onset of limited core damage, core melt, and public panic.

16.10 Natural circulation loop and parallel channel thermal-hydraulics

Our focus is on examining the inherent predictions using the basic conservation laws governing two-phase flows, and to reveal any impact of any adopted approximations from the extent and results of their

validation. The multiphase conservation equations for mass, momentum and energy have been derived in many varied ways, essentially averaging the Navier–Stokes relations over some multidimensional time and/or space to include components, flow regimes, loops, and phase change (Wulff, 1998). For the present purposes, we do not repeat these fundamental derivations or question their validity for application to natural circulation in W, L, and G Class systems, and indeed a whole separate literature has arisen (for details, see, e.g., D’Auria, 2017). Because of the interphase transfers (evaporation, condensation, drag, and turbulent dissipation), relevant phenomena also have to be represented by so-called “constitutive relations” or “balance conditions.” These relations are themselves derived from other extensive fields of study or application (e.g., drag on bubbles, flow in a pipe, boiling, unstable flow, critical flow, condensation, subchannel mixing...).

These basic conservation equations have been variously adopted, discretized, and adapted into computer codes for modeling transients in complex nuclear, boiler, and oil and gas systems, with the validation being by comparison against relevant data or tests. In nuclear safety analysis since c1965, these have included numerous named software “nodal codes,” using volume-averaging in usually a one-dimensional approximation with flow regime dependency (i.e., acronyms include TREACLE TOFFEE, TRAC, RELAP, RETRAN, CATHARE, CATHENA, SATAN, BLWDN, TRACE, ...), with continuing multiple numbered evolutionary versions often labeled updates or “releases” each with subtly different approximation, correlations, and/or coding. These system codes approximations and correlations introduce uncertainties due to averaging and the interphase constitutive transfer relations, and have also been supplemented by subchannel codes and CFD methods for examining more local multidimensional flows and turbulence phenomena.

Natural circulation is a huge technical field, both single and two-phase flow, including fossil and solar heaters and boilers, as well as for all Classes of nuclear reactors (see, e.g., Basu et al., 2014). There are also the uncertainties inherent in the use of “passive” and largely gravity-driven cooling primary system and EPS, as highlighted in recent and extensive work mainly in the EU (Aksan et al., 2018; D’Auria, 2017, 2018).

16.10.1 Introduction

Natural Circulation Loop (NCL) thermal–hydraulics is an essential aspect in the design, operation, and safety of all Generation-IV and AR concepts that claim some degree of “passive” safety. Some concepts rely on natural circulation for both normal operating conditions and off-normal safety conditions; while others depend on natural circulation only for passive off-normal safety conditions. The objective of natural-circulation passive safety systems is to maintain the system in safe shut down and adequately cooled states, for long periods of time, without the necessity of operator intervention or availability of electric power. The cores and heat exchangers of advanced water-, liquid-, and gas-cooled nuclear reactors are examples of components in a “passive” natural circulation loop in which flows in parallel channels occur to provide convective heat removal to mitigate, obviate or delay possible core damage due to extended LOPC.

Passive-safety systems based on natural circulation are intended to provide the UHS in cases of failure of the normal operation of the reactor cooling system. Due to its critical importance, fundamental understanding of the properties and characteristics of natural circulation hydrodynamics, thermal responses, and thermodynamics in the complex engineering equipment of nuclear reactor power systems is essential. For the AR and Gen-IV systems that are based on natural circulation at normal operating states, the properties and characteristics under steady-state conditions must also be well understood.

Generally, the natural circulation flows encountered in nuclear power plants will be associated with closed loops composed of piping, flow channels of various shapes, and several equipment components. The loops are generally closed but a failure in the piping that makes up the loop can disrupt the natural circulation and

make the system useless for its intended purpose. The secondary side of steam generators, for plants using natural circulation for normal operations, is characterized as a NCL with through-put; feedwater input from the condenser and steam extraction at the steam generator exit to feed the turbines. All these systems will have regions within which the flow is in parallel channels, such as fuel rods, and fuel-rod bundles, in the core, and tubing in steam generators and heat exchangers.

Natural circulation flows around loops and flows in parallel channels are both susceptible to departures from steady operation and excursions into oscillatory and, potentially, unstable states. Generation-IV nuclear-reactor power systems thus combine the type of fluid flow and geometries that are known to potentially lead to undesirable states. In particular, undesirable oscillatory states under steady-state operation should be avoided. The complete system and associated operational envelope are designed to avoid unstable states.

For both simplicity and fundamental understanding, the discussions in the following sections will focus on the thermal-hydraulic properties and characteristics of flows in parallel channels and natural circulation loops. The literature on general aspects of the analytical, experimental, mathematical modeling, numerical solution methods, and computational aspects of these flows will be briefly reviewed. These aspects when associated with specific AR and Gen-IV systems will also be discussed.

16.10.2 Natural circulation flows

The driving potential for natural circulation flows is created by buoyancy within the fluid itself. This is in contrast to forced circulation flows that are driven by power external to, and supplied into, the fluid, generally by means of a pump or other mechanisms. The driving potential for natural circulation flows is small relative to that which can be supplied from external power sources. At steady state, the induced buoyancy forces are balanced by the pressure losses around the loop, and this determines the steady-state mass flow rate in the NCL.

Thus, quasi-steady state NC flows are relatively easily analyzed and have been demonstrated as effective for heat removal in both Class W and Class L reactor systems (Zvirin, 1982; Singer et al., 1980; Gillette et al., 1980; Planchon et al., 1985; Kwi-Seok et al., 2010). At full reactor scale, these transient tests and analyses demonstrate the inherent capability of the overall single-phase (water or liquid sodium cooled) system to transition to natural circulation following loss of pumped flow, and even without a reactor trip providing the power and temperature coefficients of reactivity were sufficiently negative.

The small, internally induced driving potentials make natural circulation flows more susceptible to the onset of instability, because perturbations in the flow rate or power source feed directly to changes in the driving potential (D'Auria, 2018). Any equipment part, or region of the complete system, and the physical phenomena and processes associated with the part or region, has a potential to introduce perturbations. Start-ups of nuclear-powered natural-circulation systems, or changes in the steady operating state, for examples, are perturbations that will occur during the lifetime of the system.

A rough working definition of instability might be stated as a departure from an intended course of operation of a thermal-hydrodynamic system. Observed departures include sustained periodic oscillations, damped oscillations that return to smooth operation, growing oscillations in systems that can inject power into the fluid, and aperiodic, chaotic, oscillations. Nayak and Vijayan (2008) indicate that even at steady state conditions, oscillations in NC systems, including boiling two-phase systems, are generally present. Amplitudes greater than plus-or-minus 10% of the mean state are sometimes classified as instabilities. Others consider that amplitudes greater plus-or-minus 30% indicate instability. In complex engineered-equipment systems, the effects of interactions between the physical phenomena and processes that occur in the various components can be difficult to quantify. The chaotic response of deterministic mathematical models as

discovered by [Lorenz \(1963\)](#) is closely related to idealized models of fluid flow and heat transfer in natural circulation systems.

[Ruspini \(2012, 2013\)](#) has given detailed descriptions of the physical phenomena and processes associated with each of the several types of instability. The following is taken, by permission, from the Table of Contents of his PhD dissertation ([Ruspini, 2013](#)): “Two-phase-flow instability mechanisms”:

Characteristic pressure drop vs flow-rate instabilities

- Ledinegg instability;
- Flow-distribution instability;
- Flow-pattern transition;
- Pressure Drop Oscillations (PDO);
- Density Wave Oscillations (DWO)
 - Type I: Due to gravity, DWOI;
 - Type II: Due to friction, DWOII;
 - Type III: Due to momentum, DWOIII.

Compound density wave phenomena:

- Density wave oscillation in parallel channels.

Coupled neutronic thermo-hydraulic instabilities:

- Flashing instability (FSH);
- Thermal Oscillations (ThO);
- GEySering (GES);
- Natural Boiling Oscillations (NBO);
- Thermo-Acoustic Oscillations (TAO);

Instabilities in condensing flows:

- Self-sustained oscillations;
- Characteristic pressure drop vs flow-rate curve for condensing systems;
- Oscillations in parallel condensing channels;

Water-hammer phenomena

Flow-induced instabilities

This long list is an indication of the potential complexities that need to be considered for natural circulation systems. Extensive discussions, including experimental observations, for each of these are covered in his text and associated papers by [Ruspini et al. \(2010, 2011a, 2011b, 2012, 2014\)](#). [Manavela Chiapero et al. \(2012, 2013a, 2013b\)](#) have reported extensive investigations into pressure-drop oscillations.

Numerous factors have been determined to influence the performance, and, especially, the stability of NCLs. Many of these were enumerated in the earliest investigations of flow and heat transfer in NCLs. Others have been encountered as the original idealizations, both analytical and experimental, have been generalized to include additional and realistic aspects of the physical domain. Some of these factors include, among others:

- (1) Degree of subcooling of the fluid at the channel entrance;
- (2) The pressure gradient in the subcooled-liquid portion of a boiling channel;
- (3) Distribution of the pressure losses around the flow channel;
- (4) The operating pressure level;
- (5) The heat flux/channel power supplied to the fluid;
- (6) The void fraction/quality and its distribution, and the two-phase flow regime;
- (7) The mass flow rate of the fluid;
- (8) Geometric properties of the flow channels in the system;
- (9) The operating pressure level with larger regions of stability at increased pressure; and
- (10) The thermodynamic state of the coolant; single- or two-phase and its distribution.

Note that this list describes what can be characterized as a more or less pure thermally driven hydrodynamic NCL in that the effects of engineered equipment and the associated physical phenomena and processes are not listed. Some of these factors include power generation in nuclear fuel rods, heat conduction in all the solid-material boundaries the fluid, changes in flow-channel geometry around the loop, system-state-change perturbations introduced during normal operations, changes in boundary conditions, and operations of equipment that is coupled to the fluid. The list also does not address the known issues relative to numerical solution methods applied to mathematical models of NCLs, both simple and realistic, and the Onset of Flow Instability (OFI) in single and parallel channels.

While single-phase flow systems have been one focus of investigations of OFI, especially, under natural circulation conditions, two-phase flow systems, being inherently complex, have received more attention (Whittle and Forgan, 1967; Yadigaroglu and Bergles, 1969). Interest in boiling two-phase natural circulation systems for nuclear power applications was present at the early stages of research and development of the systems. Generally, these early developments were driven by the perceived advantages of natural circulation systems for nuclear submarines. Boure et al. (1973), Ruspini (2013), and Ruspini et al. (2014) have given detailed descriptions in the physical domain of the kinds of instabilities that have been observed, and the review by Ruspini et al. (2014) and his Doctoral Thesis (Ruspini, 2013) are especially comprehensive.

Pressure-loss distributions around the loop are known to be first-order affects relative to stability properties and characteristics under natural-circulation conditions. The locations of singular, reversible and irreversible, pressure changes, and losses, respectively, associated with geometry changes have been determined to be important. Local losses at the entrance and exits of energy supply or exchange components have been shown to be especially important. Pressure losses at the entrance are critically important relative to promoting stability and those at an exit to a lesser degree. Large losses at an exit can induce instability. The reversible pressure changes associated with continuous or abrupt changes in flow-channel geometry, such as nozzles and chimneys and abrupt expansions or contractions are also important. Wall-to-fluid friction, a distributed resistance to fluid motion, and its distribution along the flow channel, is also important.

Physical instabilities arise whenever discontinuities and/or adverse gradients, are present in a flow field. Classical situations that have been thoroughly investigated include discontinuities in velocity, temperature, pressure, and density, or combinations of these. In the case of mathematical modeling of NCLs, discontinuities introduced into algebraic representations of model-closures for wall, and interphase, friction, heat, and mass transfer, and the equation of state can also introduce instabilities. These are purely artifacts of mathematical constructs and are not encountered in the physical domain. The stopping criterion for numerical iterative methods must also be checked that the calculated results are independent of its value.

Representation of the wall-friction factor correlation in the transition between laminar and turbulent friction, for example, has been shown to have the potential to introduce artificial instability (Ambrosini et al., 2004, for an example). At the same time, in the physical domain, transition between laminar and turbulent flow due to variations in the fluid thermodynamic states around a loop can introduce instability. Such changes can be due to the dependency of the fluid viscosity on temperature, for example, or for changes in the flow area around the loop. Boiling and condensing two-phase flows are especially important examples of significant changes in the thermodynamic state. Likewise, fluids operating at supercritical thermodynamic states, receiving renewed interest for nuclear reactor designs, experience significant state changes around a NCL.

16.10.3 Literature review

In the following paragraphs, a brief summary of some of the literature associated with thermal-hydraulic properties and characteristics and performance, including onset of instability, in NCLs and parallel channels

is given. Generally, the literature on natural circulation loops and associated physical phenomena and processes is far too enormous to be reviewed in detail here. Instead many of the reviews recently available will be first summarized along with some of the earlier literature associated with nuclear power systems.

Many aspects of single- and two-phase flows, including flows in natural circulation loops and parallel channels have been discussed in the literature and texts (see, e.g., [Todreas and Kazimi, 1990](#); [Muñoz-Cobo et al., 2002](#); [D'Auria, 1997](#)). As noted above, [Ruspini et al. \(2014\)](#), based on Ruspini's doctoral thesis ([Ruspini, 2013](#)), have given an exhaustive review, citing over 200 literature sources, and additionally investigated mathematical modeling, numerical solution methods, including error estimates, for application to various experimental and analytical data. Related investigations developed during the course of this research are reported in [Ruspini \(2012\)](#) and [Ruspini et al. \(2010, 2011a,b, 2012\)](#).

[Basu et al. \(2014\)](#) have reviewed applications of single-phase NCLs for nuclear power applications, and [Misale \(2014\)](#) presented a summary of the status of single-phase NCLs. [Sarkar et al. \(2014\)](#) present a review of supercritical NCLs. Previous reviews that supplement these include [Prasad et al. \(2007\)](#), [Nayak and Vijayan \(2002\)](#), and [Vijayan and Nayak \(2010\)](#), who reviewed instabilities for boiling two-phase NCLs, including natural circulation BWRs. The latter reference has a list of instability events that have occurred in operating machines.

[Manavela Chiapero et al. \(2012, 2013a,b\)](#) have reviewed pressure drop oscillations in boiling systems. The exhaustive nature of the research at the Norwegian University of Science and Technology cannot be over-emphasized. Reviews of instabilities in the case of single and parallel channels include [Ozawa et al. \(1989\)](#), [Tadrist \(2007\)](#), and [Kakaç and Bon \(2007\)](#). The latter is especially complete.

[March-Leuba and Rey \(1993\)](#) presented a state-of-the-art review for the case of coupled thermo-hydraulic-neutronic instabilities in boiling water reactors.

The IAEA have provided compilation reports on both the general concepts and some focused aspects of Gen-IV nuclear reactors ([IAEA, 2001, 2002, 2004, 2005, 2009, 2012, 2014](#)). [Saha et al. \(2013\)](#) provide a summary of the general concepts of Generation-IV machines and the thermal-hydraulics research and development that will be required to develop and validate multiphase, multiscale, multiphysics advanced computational models and methods. [Rowinski et al. \(2015\)](#) provided a review of the various implementations of Small- and Medium-sized Reactors (SMRs) concepts.

Additional literature reviews, that generally predate those above, will be noted in the following discussions. We will focus more on nuclear reactor applications instead of the general case of parallel channels and NCLs, noting both situations, however, arise in nuclear power applications.

16.10.4 The early investigations

The concept of using natural circulation in nuclear-powered energy production systems dates from the earliest days, the early-1950s, of nuclear energy applications, first examining the question of the hydrodynamic stability of NCLs representative publications include [Chilton \(1957\)](#), [Wissler et al. \(1955, 1956\)](#), [Hamilton et al. \(1954\)](#), [Garlid et al. \(1961\)](#), [Anderson et al. \(1962\)](#), and [Lottes et al. \(1963\)](#) among others. An electronic literature search produces many citations to early publications from the 1950s that are difficult to obtain, especially in the United States where research was underway in a few National Laboratories, Universities, and private organizations. The latter were generally supported by government contracts with some of the work directed toward applications to nuclear powered naval vessels and aerospace applications, while [Lowdermilk et al. \(1958\)](#), [Jain \(1965\)](#), [Jeglic and Grace \(1965\)](#), [Creveling and Schoenhals \(1966\)](#), [Keller \(1967\)](#), and [Welander \(1967\)](#) carried out fundamental work on highly idealized systems. These papers are considered landmark initial studies and continue to be cited to this day, noting that experimental and analytical research had been underway for over a decade when the papers were published. The report by [Garlid et al. \(1961\)](#) has extensive citations to the very early literature including both

analytical and experimental investigations, and contains an analog computer program for the model equations. Alstad et al. (1956) investigated single-phase NCLs and Wissler et al. (1955, 1956) two-phase loops. The concept of a SCWR based on natural circulation was also investigated in the 1960s (see Harden, 1963; Cornelius, 1965a or 1965b, for examples). The renewed interest in SCWRs has recently driven significant additional research (as summarized in Piro and Duffey, 2005, 2007).

Early work in the United States was directed toward the various models of BWRs then under experimental and analytical investigations, which operating machines included the Experimental BWR (EBWR), SPERT-I, and the BORAX-I through BORAX-V facilities (Lottes et al., 1963). Fundamental analytical and experimental work continued throughout the 1950s into the 1970s, with various issues associated with BWRs, including stability and the onset of instability and effects of neutrons and power feedback, were primary areas of focus (Berenson, 1964; Levy and Beckjord, 1960). Stability of boiling two-phase flow and heat transfer, or Onset of Flow Instability (OFI), and Critical Heat Flux (CHF) or Departure from Nucleate Boiling (DNB) were all investigated. Berenson (1964) has a summary of the experimental results up to that time, and in general, the stability of BWRs during various phases of operation continues to be an active area of research (Rohde et al., 2010). All findings to date indicate that startup and operation of nuclear-powered natural circulation systems is readily achieved.

Experimental and analytical work was also underway in Europe at AB Atomenergi associated with the Marviken and Halden Boiling Heavy Water Reactor (BHWR) machines (Becker et al., 1963, 1964) and in Italy at CISE. The AB Atomenergi work included both extensive experimental facilities and mathematical modeling. In some regards, these efforts confirmed, and significantly supplemented the findings of the earlier work of the 1950s noted above.

The majority of the early research involved coupled experimental and analytical efforts, and that coupling continues to the present time. Analytical approaches were somewhat straight-forward because the mathematics leads to tractable problem statements. Findings from the early analytical investigations indicated that careful attention must be given to discretization and numerical solution of model equations when applied to investigations of the onset of instability. At the present time early in the 21st century, applications of multi-dimensional Computational Fluid Dynamics (CFD) are proving to be helpful in gaining deeper understanding of the physical phenomena and processes that can lead to the onset of instability. CFD is also proving useful for identifying deficiencies in the classical 0- and 1-dimensional analytical modeling of NCLs.

The early experimental data and associated analyses indicated that oscillatory behavior, while present, did not always lead to divergent growth, with closed regions or ellipsoidal areas of instability, bounded by both lower and higher power additions observed and theoretically predicted (Mertol et al., 1981; Duffey and Hughes, 1991; Rohatgi and Duffey, 1998). The boundaries and range of the closed regions varied with the operating pressure level and the thermodynamic state of the fluid, plus the diameter and length of the piping in the simple experimental systems, and other geometric details, were found to affect the stability properties of the systems as well.

The onset of instability in NCLs closely correlated with significant differences between the gradients in driving potential and the flow resistance around the loop. In this respect, the onset is exactly analogous to the onset of instabilities in the case of flows in single and parallel channels. The significant effects of the magnitudes of the flow resistances at the incoming and out-going legs of the loops at the energy supply were also noted. Increases in resistance on the incoming side increased the size of the region of stability, while the converse was found for the out-going side, so increasing the local flow resistance at the inlet side (using variable area orifices, venturi, or throttling) compared to the outlet continues to be a common method to avoid onset of instability, while at the same time, the effects of the resistance on the power capacity of the system must be considered.

The majority of the original and early experimental and analytical investigations were based on simple idealized experimental loops and one-dimensional formulations of the model equations, with some

involving model tube bundles ([Gruszynski and Viskanta, 1983](#)) or boilers ([Grace and Krejsa, 1967](#)). Even at this early phase of investigations, all the citations listed above utilized mathematical models as a means to gain deeper understanding, so one-dimensional, area-averaged mathematical models of the governing equations generally coincided with the level of measurements in experimental facilities. Additionally, the earliest investigations more or less omitted considerations of almost all aspects of loops in the physical domain; non-uniform flow-channel geometry, latencies associated with energy-transfer and transport processes such as conduction in all the solid material surrounding the fluid, changes in the state of boundary conditions that arise in heat exchangers, among others. The effect of energy production, void-power coupling, and pressure in the core of nuclear reactors was a focus (e.g., [Lee and Pan, 2005](#); [Walter and Linzer, 2006](#); [T'Joen and Rohde, 2012](#)).

Analytical investigations in the frequency domain, based on linearization of the model equations, are only useful for idealized systems. Generally, as the model equation system grows to account for additional physical phenomena and processes, and greater detail in engineered-equipment systems, the linear system gets too complex for carrying to completion. At this point, the linear systems and numerical solution, including numerical inversion of Laplace transformed systems, are incorporated into computer software. Frequency domain models and codes continue to be used for real-world systems. However, the ultimate investigations and quantifications are generally based on simulations in the time domain. Much of the available experimental data have been used to validate time-domain models and methods and gain approval for applications of these to safety issues.

Boundary conditions in the earlier mathematical models relied on: (1) specifications of the energy supply into the system, and equality of the energy rejection; or (2) specification of the temperature at the energy source and sink. This approach neglects the temporal response of the energy transfer processes from the boundary conditions of an ultimate source and to the boundary conditions of the ultimate sink. For applications to AR and Gen-IV nuclear-power production the engineered equipment that makes up the source and sink, and the processes occurring within that equipment, is required to be included in an analysis, and prototypical experimental facilities.

[Rao et al. \(2005a-d ; 2008\)](#) have generalized the mathematical models to include more nearly realistic boundary conditions by considering Heat EXchangers (HEXs) for the energy source and sink. Additional generalization can be obtained by use of more detailed modeling of the physical phenomena and processes that occur within the HEXs and the fluid states at the entrances to these; flow rate and thermodynamic state perturbations, for examples.

At this time, it had been established that: (1) as the pressure increases, the power at the onset of instability increases, and the frequency of oscillations increase; (2) the onset of instability decreases as the inlet sub-cooling increases, so that lower values are preferred relative to ensuring stable states; (3) as the local pressure loss at the inlet to the energy-supply is increased, the region of stable operation is increased; and (4) as the local pressure loss at the outlet is increased, the region of stable operation decreases. In the latter case, the loop flow is less stable.

Review of the literature was given by [Boure et al. \(1973\)](#) in which the physical mechanisms, and mathematical models in use up to that time, are discussed. The report has a summary of the computer codes that had been applied to the problem, in both the frequency and time domains. [Lahey and Drew \(1980\)](#) discussed instability issues associated with light water reactors.

16.10.5 Three Mile Island issues

Following the incident at the Three Mile Island nuclear plant in 1979, the nuclear industry as a whole around the world intensified experimental and analytical investigations into all aspects of natural circulation thermal-hydraulics. The Small-Break Loss Of Coolant Accident (SBLOCA) nature of the incident revealed

the critical importance of natural circulation to understanding the response of such systems under these conditions. The industry worked to ensure that understanding of all aspects SBLOCAs, for both existing and future systems, was correct and complete.

Major experimental programs were devised, developed, constructed, and successfully completed for water reactors, with the acronyms LOBI-MOD2, SPES, ROSA-III, ROSA-IV LSTF, BETHSY, MIST, and FIST. Experimental facilities originally built for LBLOCA investigations (Semi-scale and LOFT, for examples) were modified to look into the SBLOCA case. Data from these facilities continue to be used as validation exercises for mathematical models and computer codes. [Aksan et al. \(2018\)](#) have given a lengthy summary of experimental activities and phenomenological testing associated with the extensive validation of major system-analysis codes such as: TRACE, TRAC-P, TRAC-B, RELAP5, CATHARE, and ATHLET. Interest in Gen-IV machines has driven development of other models and codes.

[Zvirin \(1982\)](#) reviewed experimental data and analytical approaches appropriate for natural circulation and SBLOCA, with a focus on PWRs. Results of other investigations on single- and two-phase flow led by the Electric Power Research Institute (EPRI) include [Zvirin \(1979, 1982, 1985\)](#), [Zvirin et al. \(1981\)](#), [Duffey and Sursock \(1987\)](#), [Greif et al. \(1979\)](#), and [Mertol \(1980\)](#) among others. [Greif \(1988\)](#) presented a literature survey and summary to that time.

The 1980s, and continuing, saw an ever-increasing number of publications addressing experimental, analytical, numerical, and system-code applications to natural circulation loops. The extensive citations in the recent reviews listed above can be used to follow up on any aspects of both NCLs and parallel channels. The most recent activities have been driven by the proposed applications to Gen-IV, and beyond, nuclear-power reactors.

16.10.6 BWR stability in the time and frequency domains

Renewed focus was on instabilities in operating BWR systems, especially the effects of neutronics and power feedback and patterns of oscillatory flow in parallel channels, which are enclosed fuel rod arrays in these systems ([D'Auria, 1997](#)). Extensive effort was applied to models and analyses in the frequency domain and several computer codes were devised, developed, and applied ([Peng et al., 1984, 1986](#); [Lahey et al., 1990](#); [March-Leuba, 1984](#); and [March-Leuba and Rey, 1993](#)). A variety of frequency-domain analysis methods have also been developed including LAPUR ([Escrivá et al., 2008](#)) and NUFREQ-NP ([Peng et al., 1984](#)), among others.

The mathematical models and numerical solution methods used in the major systems-analysis computer codes employed in the industry were the subjects of research relative to applications to SBLOCA and natural circulation. During this period of intensive research, the critical importance of the discretization of the continuous equations and the associated numerical solution methods used in systems-analysis computer codes for non-linear analyses in the time domain was one area of primary focus.

The thermal-hydraulic codes for systems analysis and validation used included updated versions of RETRAN ([Computer Simulation & Analysis, 1998](#)), RELAP5 ([Information Systems Laboratories, 2001](#)), TRAC-BWR ([Spore et al., 1981](#)), TRACG ([General Electric, 1999](#)), CATHENA ([Richards et al., 1985](#)), CATHARE ([Bazin and Pelissier, 2006](#)), ATHLET ([Austregesilo et al., 2006](#)), TRACE/PARCS ([Xu et al., 2009](#); [Hu and Kazimi, 2012](#)), and RAMONA ([Rohatgi et al., 1998](#)) along with variations of these as they are developed for new applications. In addition to constant updating of these major codes to gain applicability to new analyses, models, methods, and code development continue around the world. Korea developed the TASS/SMR code ([Hwang et al., 2005, 2006](#)), for example, among others. In addition to these major codes, other time- and frequency-domain models and methods have been developed for local, special-purpose analyses of both experimental data and numerical solution methods. These special-purpose models and methods are generally not freely available.

Low flow stability tests conducted at the Peach Bottom nuclear plant in the USA (Woffinden and Niemi, 1981) have been used as a benchmark for validation of system-analysis models, codes and application procedures. Costa et al. (2008) applied the coupled RELAP5/MOD3.3 thermal-hydraulic code and PARCS-2.4 3D neutronics code to simulate these tests. Mori (1998) used the RETRAN-3D code, and Wulff et al. (1992) and Rohatgi et al. (1994) applied the Brookhaven National Laboratory Engineering Plant Analyzer approach. Costa et al. (2008) have summarized other events that have occurred in operating plants. These data, too, are used for validation.

Investigations into various aspects of stability issues in BWRs, especially natural circulation BWRs, continue to the present time (e.g., Hu, 2010; Hu and Kazimi, 2011). Faculty and staff at the Delft University of Technology, very likely due to the presence of the operating Dodewaard machine, have researched several aspects of BWR stability (Furuya, 2006; Marcel, 2007; Stekelenburg, 1994; van Bragt, 1998), while Van der Hagen et al. (2000) have reviewed information on BWR stability experiments.

16.10.7 Numerical methods and artifacts

Multinode or discretized volumes representations of NCLs and associated HEXs require solution of the coupled time-dependent and finite-differenced conservation equations. This is achieved using iterative calculational schemes coupled to two-phase flow regime maps, and is itself an over 50-year specialized field of mathematical, computational and algorithmic endeavor (see, e.g., Hancox and Banerjee, 1977; Hughes et al., 1981; Hughes and Katsma, 2015; Nourgaliev and Christon, 2012; Bestion and Serre, 2012; Chetty et al., 2021; and the many references therein). Almost all numerical methods implicitly introduce artifacts into the numerical solution techniques applied to the discrete approximations of the continuous model equations, introducing artificial diffusion, iteration or accuracy constraints, numerical instabilities, and sensitivity to discrete finite-differencing or nodalization choice. These artifacts significantly affect the dispersion and dissipation of the calculated response thus introducing errors into calculated propagation properties and decay rates. Because investigation of the stability of natural circulation flows is a primary objective of the analyses, it must be demonstrated that the numerical method itself does not introduce misleading or unphysical artificial instability or conversely stability. Implicit numerical solution methods, developed so that larger values of the discrete time step can be used, especially, introduce artificial stability into calculations. Thus, numerical solutions must be determined to be true instability or stability and not instability or stability introduced by the numerical methods themselves. Numerical methods can result in both false positives and false negatives; it must be determined that no artifacts are introduced into calculations by the numerical solution methods themselves.

The numerous complexities of the physical domain represented by all the components and associated detailed aspects of a system that affect the stability of the system must be: (1) realistically included into the mathematical models; (2) accurately resolved by the numerical solution methods; and (3) shown to not have introduced artifacts into the calculations. The numerically enhanced mathematical stability of implicit methods, the potential numerical instability of explicit methods, and the dissipative and dispersive characteristics of both implicit and explicit methods require careful investigations. Jensen (1992) has given examples of some of these effects. Both false-positive and false-negative results must be eliminated.

Ambrosini and Ferreri (1997a,b, 1998, 2000, 2003), Ambrosini et al. (2001), Ambrosini (2001 ; 2008), Ferreri (1999), and Ferreri et al. (1995) in a collaborative effort over a period of about 10 years, and with others, have presented an exhaustive investigation of the effects of numerical approximations to the continuous model equations, and the numerical solution method for these, on calculations of the onset of instability for both natural circulation and parallel-channel flows. The investigations have used special-purpose computer codes in both the frequency and time domains, and the RELAP5 system-analysis code.

16.10.8 AR and Gen-IV passive residual heat-removal systems

Most of the analytical and experimental investigations into natural circulation loops have been based on a single isolated loop. In contrast, passive cooling of nuclear power plants based on natural circulation operation requires coupled loops as follows. For the safe-shutdown condition for natural circulation Gen-IV machines, the Passive Residual Heat-Removal System (PRHRS) is made up of two coupled natural circulation systems; one that transports the energy from the RPV and the second that deposits the energy into the UHS, usually via HEXs. The latter process is the second natural circulation loop and the coupling to the primary loop is through an intermediate heat exchanger. That heat exchanger is often generally the same as that used during normal operation of the machine, i.e., the Steam Generator (SG). The energy is deposited into the ultimate heat sink, generally a large pool of water or the atmosphere, by means of a second heat exchanger.

The source of the energy in the primary NCL from the fuel rods in the reactor core, and the associated single- and two-phase thermal–hydraulic phenomena and processes must be accounted for in the mathematical and physical models developed for the system.

The fluid flow through the core, though the steam generator and the PRHRS heat exchanger, is characterized by flow through parallel channels. The channels in the core formed by the fuel rods and those in the SG and PRHRS by closed flow-tube channels. Such flow configurations, parallel flow channels, are susceptible to instabilities for both single- and two-phase flows. Under long-term safe-shutdown conditions, the PRHRS is expected to be a two-phase flow system.

Generally, the existing major system-analysis codes (as listed above) are equipped to model all the equipment components and associated physical phenomena and processes that are expected to occur (see, e.g., [D’Auria, 2017](#)). The codes and modeled natural circulation and parallel channel flows for the coupled NCLs case require validation by comparisons of predictions with experimental data and for any novel features, like helical SGs and condensing HEXs, or various coolants (e.g., [Guo et al., 2001](#); [Kumar and Gopal, 2016](#); [Mangal et al., 2012](#); [Colombo, 2013](#); [Papini et al., 2014](#); [Zhouhang et al., 2016](#)). The major systems codes, and the several locally developed special-purpose models and codes, and application procedures have been validated by use of many of the simple pure thermal-hydro experiments and analytical results for NCLs and parallel-channel flows ([Kozmenkov et al., 2012](#); [Mangal et al., 2012](#)). Generally, however, the general-purpose major codes must be validated for applications to complete coupled-loops systems for design, development of deep understanding, and safety-grade analyses.

16.10.9 Coupled natural circulation loops

The few investigations into the properties and characteristics of coupled natural circulation loops include [Salazar et al. \(1988\)](#) for idealized coupled loops with specified energy input and extraction over the primary and secondary loops, respectively. [Wu \(2011\)](#) has analyzed the case of a general number of coupled loops following the idealized approach of [Welander \(1967\)](#).

The major experimental loop for investigations of PRHRS coupled loops, and individual components, seems to be in Korea ([Park et al., 2014](#)). This facility, named Verification by Integral Simulation of Transients and Accident – Integral Test Loop (VISTA-ITL), has been developed to allow experiments involving coupled NCLs. The experimental data have been used for validation of the TASS/AMR-S ([Yang et al., 2008](#)) and MARS-KS thermal–hydraulic models and codes ([Park et al., 2008, 2014](#)). The data also can be used by other organizations for validation analyses. The Oregon State University – Multi-Application Small Water Reactor (OSU-MASLWR) loop in the United States is a scaled model of the complete NuScale natural circulation machine ([Mascari et al., 2012, 2019](#)). The VISTA-ITL facility is also used for experiments on the components that make up the complete system ([Kim et al., 2013](#)). A small-scale NCL, the Purdue University Multi-dimensional integral test Assembly (PUMA), has been constructed at Purdue University ([Ishii et al., 1996](#)).

Men et al. (2014) have conducted experiments on the natural convection heat transfer for a PRHRS heat exchanger in an In-containment Refueling Water Storage Tank (IRWST). Several empirical correlations for the forced convection flow internal to the HEX tube and the natural convection heat transfer outside the tube in the tank, for both the vertical and horizontal portion of the tube, were compared with experimental data. The Dittus–Boelter forced convection correlation and the McAdams correlations for natural convection proved to give the better model of the data. Wenbin et al. (2014) have conducted experiments for the secondary loop of the Chinese Advance Pressurized Water Reactor (CAPWR) for validation of the MISAP20 models and code. These and other papers are in a special issue of the *Science and Technology of Nuclear Installations* journal published in 2014 as indicated by the cited references.

16.10.10 Supercritical fluid states and NCLs

The historical investigations in the 1960s into supercritical fluids for natural circulation loops and nuclear-powered machines were mentioned above (Cornelius, 1965a,b). Chatoorgoon (1986, 2001) and Chatoorgoon et al. (2005a,b) have presented additional early sources in addition to making new contributions. The renewed interest in supercritical fluid states for nuclear power applications has resulted in many new experimental, analytical, and numerical investigations in many countries (see Piro and Duffey, 2003, 2005, 2007; Duffey and Piro, 2005; Oka and Mori, 2014; Bae and Kim, 2009; and the references therein).

The IAEA (2014) has produced a detailed summary of many aspects of supercritical natural circulation thermal–hydraulics and heat transfer for water reactors. The IAEA has identified SCWR concepts in Canada, China, Japan, Korea, Russia, and the EURATOM organization. A report on the 7th International Symposium on SCWRs has recently been released (Penttila, 2015). Supercritical-Carbon dioxide (CO₂) has also been proposed as the working fluid. Sarkar et al. (2014) gave a state-of-the-art review for supercritical water and Vijayan et al. (2013) have investigated the steady state and stability properties of supercritical CO₂ natural circulation loops. Ampomah-Amoako and Ambrosini (2013) have applied CFD for analyses of stability of flows of supercritical flows.

The significant rapid changes in thermodynamic state, transport, and thermophysical properties encountered, when dealing with fluids under supercritical conditions, open a potential for instabilities. Accounting for these variations, and the associated effects on fluid flow and heat transfer, also makes development of heat transfer and friction factor engineering models and correlations difficult. The significant changes act directly in the fluid and so directly affect the flow under natural circulation conditions.

The heat transfer and friction factor correlations for supercritical fluid states, and the stability of the flows used in the experiments, have been the subjects of many studies over the years. Piro and Duffey (2003), Piro et al. (2004), and Piro and Duffey (2007) completed an exhaustive and comprehensive review of the literature to that time, compiling massive amounts of literature, and reviewing friction factor and heat transfer coefficient correlations, and stability, among other issues. Cheng and Schulenberg (2001) reviewed the literature for applications to the High Performance Light Water Reactor (HPLWR). Recent investigations that supplement that information include Zhang et al. (2010), Bae and Kim (2009), Bae (2011), Chen et al. (2014), and Tilak and Basu (2015). The IAEA report (2014) and the conference proceedings by Penttila (2015) summarize the most recent information.

Swapnalee et al. (2011) and Chatoorgoon (2013) have validated the dimensionless numbers developed by Ambrosini and Sharabi (2008), Sharabi et al. (2008a, b), and Debrah et al. (2013) for supercritical fluid data. Zhang et al. (2010) have given a three-dimensional model and numerical solution method for the case of a supercritical CO₂ rectangular NCL.

Jain and Corradini (2006) reported a difference between model predictions and experimental data with a time-domain model indicating instability and SuperCritical CO₂ (SC CO₂) NCL data indicating stability. For supercritical water, a change to a more nearly accurate Equation of State (EoS) in the frequency domain

indicated stability. The frequency domain studies continued to indicate instability for the SC CO₂ system and thus still not in agreement with experimental data. The frequency domain analyses for both supercritical water and CO₂ did not always agree with the time domain results.

Jain and Rizwan-uddin (2008) report that the significant deviations from the results reported by Chatoorgoon et al. (2005b) of the numerical predictions with the FIASCO model and code are likely due to the larger time step sizes used in previous studies. A larger time-step size increases numerical dissipation and dispersion and thus indicates stable states that are due to numerical artifacts and not physical reality. Chatoorgoon et al. (2007) reported that a time-step size refinement study leads to results that are in agreement with Jain and Rizwan-uddin (2008). Increase in the pressure level with supercritical CO₂ shows a stabilizing effect similar to that observed in boiling two-phase NCLs. At a fixed power, an increase in pressure leads to reduced void fraction, which in turn leads to a **decrease** in wall friction and momentum flux pressure gradients, a stabilizing effect. The threshold power for OFI does not correspond to the maximum in the flow vs power curve.

16.10.11 Computational Fluid Dynamics (CFD)

Considerations of distributions across the flow channel, transverse to the primary flow direction, were first included in basically one-dimensional models by approximating the temperature distribution in the fluid parallel to the flow direction. Recently, there is an increasing application of CFD to a variety of single- and two-phase thermal-hydraulic analyses, including NCLs and supercritical fluid states, in nuclear power systems. These approaches also allow for resolution of the thermal stratification in horizontal, and vertical, sections of the loop, and resolution of gradients normal to the primary flow direction, and the consequent effects on calculated stability. Fully three-dimensional analyses are becoming the norm, but only for simple idealized single-phase cases.

Burroughs (2003) and Burroughs et al. (2005) applied analytical and numerical methods to laminar flow in the standard NCL geometry and observed behavior of stable response at Prandtl numbers less than those observed in the usual Lorenz (1963) ordinary differential equation model.

Pilkhwal et al. (2007) observed that CFD results demonstrated the onset of instabilities that could not have been observed with standard one-dimensional analyses. Angelo et al. (2012) have applied CFD to steady state analysis of an operating NCL.

Yadav et al. (2012a,b) used CFD modeling to determine heat transfer and friction factor correlations for CO₂ flows in NCLs, and investigated performance and stability of supercritical CO₂ NCLs having heat exchanger Boundary Conditions (BCs). He et al. (2004 ; 2008) applied CFD and turbulence modeling to heat transfer analysis of supercritical states, while Jingjing et al. (2015) examined instability of supercritical water flow in parallel channels. Jackson (2013), one of the pioneers in the mixed-convection heat transfer area, has presented a summary of many aspects. Ampomah-Amoako and Ambrosini (2013), Desrayaud et al. (2013), and Sharabi et al. (2008a, b) also investigated supercritical NCLs for stability by a CFD approach. Misale et al. (2000) introduced the effects of two-dimensional heat-conduction into NCL stability analyses.

16.10.12 Nanofluids

Natural circulation loops based on working fluids containing nanoparticles have been investigated (Misale et al., 2012, for example). Yu et al. (2015) have experimentally investigated the effects of nanoparticles on the Onset of Nucleate Boiling (ONB) and OFI. Both of these subjects are in the initial stages of investigations. Interaction of the nanoparticles with the microscopic structure of a boiling surface is indicated.

16.10.13 Sodium and liquid metal reactors

Aoto et al. (2014) and Okano (2014) have presented a summary of recent sodium-cooled fast reactor developments, and stability analyses have been examined by Sabharwall et al. (2012).

16.10.14 Parallel channels

The core of nuclear reactors is an example of a component in a natural circulation loop in which flows in parallel channels occurs (Vyas et al., 2010; Zvirin et al., 1981; Zvirin, 1982, 1985; Gartia et al., 2007). The stability of the parallel-channel flow through the core must and continues to be investigated (Hamidouche and Bousdia-salah, 2006; Colombo et al., 2012) and include effects of conjugate heat conduction and energy production by fission. Single- and two-phase flows under steady-state and transient conditions are important considerations relative to safety analyses of Gen-IV machines.

As in the case of the previous sections, there is an enormous literature on stability of fluid flow in single and multiparallel channels. The review by Kakaç and Bon (2008) is especially complete to that time, and Ruspini (2013) and Ruspini et al. (2014) include this situation in their review. Recent activity has focused on supercritical thermodynamic states with Xiong et al. (2012, 2013), Gu et al. (2015), and Zhao et al. (2014), as examples.

16.11 Conclusions

There is no global or international consensus on the details of nomenclature, safety criteria, or licensing methods for new concepts and designs. Given that it is not possible to cover or foresee all future possibilities or variations in design and principles, the task is how to ensure some uniformity of approach toward meeting some agreed high-level safety goals and the uncertainties when introducing new designs and safety systems.

The important GIF effort has provided a common forum for such discussions, as has also the efforts of some nuclear regulators to “harmonize” their differing approaches without relinquishing their statutory national regulatory authority. These efforts have resulted in so-called Safety Reference Levels (SRLs) for existing reactors, and high-level Safety Objectives (SOs) for the new or advanced reactors of interest here.

The modern idea of using RIDM must be critically examined for all existing, advanced and Generation-IV systems, motivated by the very public predictive failures in recent accidents of risk informed and Probabilistic Risk and Safety Assessment (PRA/PSA). From existing experience from the consequences of major accidents and US FEMA practice, the risk consequences that must be considered for the entire BDEE hazard set {fire, flood, hurricanes, ice storms, earthquakes, cyberattacks, ...} are financial losses, societal disruption, and infrastructure risks just due to core damage, and *not* solely evaluated or limited by the potential exceedance of solely regulatory radiation release or public exposure limits. This approach is reinforced by the fact that extended Loss Of Power and Cooling (LOPC) without restoration in time will inevitably lead to core damage and total plant/investment loss independent of any external radiation release however small, as exemplified by the consequences of the prior Three Mile Island and Fukushima events. The safety goal guidelines of NRC and others for the Cumulative Damage Function (CDF) to be less than some limit, say 6×10^{-3} per reactor for a 60-year lifetime risk exposure, and can be compared directly to the much overall greater summed probability of core damage, $\Sigma P(CD)$ BDEE, estimates from modern RIDM methods using applicable, transferable, and exchangeable prior data.

For extended LOPC, the summed probability of core damage, $\Sigma P(CD)$, comparing the estimates from traditional bottom-up PRA/PSA to top-down RIDM for a nominal 60-year plant life risk exposure (typical for future advanced reactor and Gen-IV concepts), the dynamic RIDM data analysis uncertainty

estimates can range from 2 to over 200 times larger, even subsuming all the BDEE CDFs sequences for both “active” and “passive” concepts. Using existing natural hazard and extreme event data, as might have been anticipated, the predicted probability for a single 1000-MW_{e1} unit is comparable to that known for prior LOPC events (e.g., Fukushima), but derived by dynamic data-driven RIDM in a completely different manner.

The implication is that the uncertainty is not fully included in PRA/PSA/RIDM as adopted today; and excludes the key practical issues of the extent of damage, social disruption, or physical access difficulty, especially for extremely severe outage events. Also, not fully reflected is the potential for much longer power and cooling restoration times, even deploying onsite, offsite (FLEX), active, passive, backup, and Emergency Power System (EPS) means. In addition, PRA/PSA bottom-up sequence analyses usually adopt a Human-Error Probabilities (HEP) in set {BDEE} that continually decline or are invariant with very low probabilities from using classic task-by-task or action-by-action error rates, even for the failure rates of so-called “passive” systems.

The cores and heat exchangers of advanced water-, liquid-, and gas-cooled nuclear reactors are examples of a component in a “passive” natural circulation loop in which flows in parallel channels occur to provide convective heat removal to mitigate, obviate, or delay possible core damage due to extended LOPC. The stability limits of the parallel-channel flow must be investigated, and these investigations include effects of conjugate heat conduction and energy production by fission in the material adjacent to the fluid. Single- and two-phase flows under steady-state and transient conditions are important considerations relative to safety analyses of Gen-IV machines. The present literature review indicates that experimental data from both simple idealized flows and more realistic complex systems are being used to validate models and codes that will be applied to analyses of AR and Gen-IV power plants. Experimental facilities for investigating long-term passive cooling are becoming available, and models and codes are becoming validated using the data in order to further quantify and refine the uncertainties.

References

- Aksan, N., D’Auria, F., Glaeser, H., 2018. Thermal-hydraulic phenomena for water cooled nuclear reactors. *Nucl. Eng. Des.* 330, 166–186.
- Alstad, C.D., Isbin, H.S., Amundson, N.R., 1956. The Transient Behavior of Single-Phase Natural Circulation Water Loop Systems. Argonne National Laboratory Report, ANL-5409.
- Ambrosini, W., Ferreri, J.C., 1997a. Numerical analysis of single-phase, natural circulation in a simple closed loop. In: Proceedings of 11th Meeting on Reactor Physics and Thermal Hydraulics, Pocos de Caldas, MG, Brazil, August 18-22, pp. 676–681.
- Ambrosini, W., Ferreri, J.C., 1997b. Stability analysis of single-phase thermo-syphon loops by finite-difference numerical methods. In: Proceedings of Post SMIRT 14 Seminar 18 on ‘Passive Safety Features in Nuclear Installations’, Pisa, August 25-27, E21-E210.
- Ambrosini, W., Ferreri, J.C., 1998. The effect of truncation error on the numerical prediction of linear stability boundaries in a natural circulation single-phase loop. *Nucl. Eng. Des.* 183, 53–76.
- Ambrosini, W., Ferreri, J.C., 2000. Stability analysis of single-phase thermosyphon loops by finite-difference numerical methods. *Nucl. Eng. Des.* 201, 11–23.
- Ambrosini, W., Ferreri, J.C., 2003. Prediction of stability of one-dimensional natural circulation with a low diffusion numerical scheme. *Ann. Nucl. Energy* 30, 1505–1537.
- Ambrosini, W., Sharabi, M.B., 2008. Dimensionless parameters in stability analysis of heated channels at supercritical pressures. *Nucl. Eng. Des.* 238, 1971.
- Ambrosini, W., D’Auria, F., Pennati, A., Ferreri, J.C., 2001. Numerical effects in the prediction of single-phase natural circulation stability. In: National Heat Transfer Conference of UIT, Modena, Italy, June 25-27.
- Ambrosini, W., Forgione, N., Ferreri, J.C., Bucci, M., 2004. The effect of wall friction in single-phase natural circulation stability at the transition between laminar and turbulent flow. *Ann. Nucl. Energy* 31, 1833–1865.
- Ampomah-Amoako, E., Ambrosini, W., 2013. Developing a CFD methodology for the analysis of flow stability in heated channels with fluids at supercritical pressures. *Ann. Nucl. Energy* 54, 251–262.

- Anderson, R.P., Bryant, L.T., Carter, J.C., Marchaterre, J.F., 1962. Transient Analysis of Two-Phase Natural-Circulation Systems. Argonne National Laboratory Report, ANL-6653.
- Angelo, G., Andrade, D.A., Angelo, E., Torres, W.M., Sabundjian, G., Macedo, L.A., Silva, A.F., 2012. A numerical and three-dimensional analysis of steady state rectangular natural circulation loop. *Nucl. Eng. Des.* 244, 61–72.
- Anzieu, P., Guidez, J., Sauvage, J.-F., Carlucci, B., 2014. France Proposal of Applied Generation IV SFR SDC, Joint IAEA-GIF SFR Safety Workshop. June.
- Aoto, K., Dufour, P., Hingyi, Y., Glatz, J.P., Kim, T.-I., Ashurko, Y., Hill, R., Uto, N., 2014. A summary of sodium-cooled fast reactor development'. *Prog. Nucl. Energy* 77, 247–265.
- Apostolakis, G., 1990. The Concept of Probability in Safety Assessments of Technological Systems. *Science* 250 (4896), 1359–1364.
- Apostolakis, G., 2014. Global statistics vs PRA results: which should we use? In: ANS presentation, Eastern Carolina, March 27.
- Apostolakis, G., 2016. A perspective on the use of risk information. In: Proceedings PSAM, Seoul, Korea, October, ANS.
- Apostolakis, G., Lui, C., Cunningham, M., Pangburn, G., Reckely, W., Adams, J., Call, M., Damon, D., Easton, E., McCartin, T., Mizuno, G., Piper, J., 2012. A Proposed Risk Management Regulatory Framework. NRC Risk Management Task Force report, April, 318 pages, NRC access # ML 12109A277, Washington, DC, USA.
- ASME, American Society of Mechanical Engineers, 2012. Forging a New Nuclear Safety Construct, Presidential Task Force on Response to Japan Nuclear Power Plant Events. ASME, New York, ISBN: 978-0-7918-3435-0.
- Austregesilo, H., Bals, C., Lerchl, G., Romstedt, P., 2006. ATHLET Mod 2.1 Cycle A Models and Methods, Gesellschaft für Anlagen und Reaktorsicherheit (GRS). GmbH Report GRS-P-1/Vol. 4.
- Bae, Y.-Y., 2011. Mixed convection heat transfer to carbon dioxide flowing upward and downward in a vertical tube and an annular channel. *Nucl. Eng. Des.* 241, 3164–3177.
- Bae, Y.-Y., Kim, H.-Y., 2009. Convective heat transfer to CO₂ at supercritical pressure flowing vertically upward in vertical tubes and an annular channel. *Exp. Thermal Fluid Sci.* 33, 329–339.
- Barr, J., Basu, S., Esmaili, H., Stutzke, M., 2018. Technical Basis for Containment Protection and Release Reduction Rulemaking for BWRs, NUREG-2206. US NRC, ONRR, Washington, D.C., USA.
- Basu, D.N., Bhattacharyya, S., Das, P.K., 2014. A review of modern advances in analyses and applications of single-phase natural circulation loop in nuclear thermal hydraulics. *Nucl. Eng. Des.* 280, 326–348.
- Bazin, P., Pelissier, M., 2006. CATHARE 2 V25_1: Description of the Base Revision 6.1 Physical Laws Used in the 1D, 0D and 3D Modules. CEA Report CEA/DER/SSTH/LDAS/EM/2005-038.
- Bea, R.G., Gale, W.E., 2011. Rule 26 Report on BP's Deepwater Horizon Macondo blowout, US District Court, Eastern District of Louisiana, 'Oil spill by the oil rig Deepwater Horizon in the Gulf of Mexico on April 20', 2:10-cv-4536, United States of America vs BP Exploration & Production, Inc., et al, TREX-2001.
- Becker, K.M., Jahnberg, S., Haga, I., Hansson, P.T., Mathisen, R.P., 1963. Hydrodynamic Instability and Dynamic Burnout in Natural Circulation Two-Phase Flow an Experimental and Theoretical Study. AB Atomenergi Report AE-156.
- Becker, K.M., Mathisen, R.P., Eklind, O., Norman, B., 1964. Measurements of Hydrodynamic Instabilities, Flow Oscillations and Burnout in a Natural Circulation Loop. AB Atomenergi Report AE-131.
- Berenson, P.J., 1964. Flow Stability in Multi-Tube Forced-Convection Vaporizers. Air Force Aero Propulsion Laboratory Report APL TDR 64-117.
- Bestion, D., Serre, G., 2012. On the modelling of two-phase flow in horizontal legs of a PWR. *Nucl. Eng. Technol.* 44 (8), 1–18. <https://doi.org/10.5516/NET.02.2012.719>.
- Bhatt, S.C., Wachowiak, R.M., 2006. ESBWR Certification Probabilistic Risk Assessment. General Electric Energy Nuclear, Wilmington, NC. Report No. NEDO 33201, rev. 1 (also, GE-Hitachi), ESBWR Certification Probabilistic Risk Assessment, Report.
- Boucau, J.B. (Ed.), 2022. Fundamental issues critical to the success of nuclear projects, Elsevier – Woodhead Publishing (WP). Duxford, UK, ISBN: 978-0-08-102472-0, p. 392.
- Boure, J.A., Bergles, A.E., Tong, L.S., 1973. Review of two-phase flow instability. *Nucl. Eng. Des.* 25, 165–192.
- BP, British Petroleum, 2010. Major accident risk (MAR) process, Report GP-48-50, United States District Court Eastern District of Louisiana, 2010, Oil spill by the oil rig Deepwater Horizon in the Gulf of Mexico on April 20, 2:10-cv-4536, United States of America vs BP Exploration & Production, Inc. et al., Exhibit TREX-01734.
- Burroughs, E., 2003. Convection in a thermosyphon, bifurcation and stability analysis (PhD Dissertation). The University of New Mexico, Albuquerque, New Mexico, USA.
- Burroughs, E.A., Coutsias, E.A., Romero, L.A., 2005. A reduced-order partial differential equation model for the flow in a thermosyphon. *J. Fluid Mech.* 543, 203–237.
- Chatoorgoon, V., 1986. A simple thermalhydraulic stability code. *Nucl. Eng. Des.* 93, 51–67.

- Chatoorgoon, V., 2001. Stability of supercritical fluid flow in a single channel natural-convection loop. *Int. J. Heat Mass Transf.* 44, 1963–1972.
- Chatoorgoon, V., 2013. Non-dimensional parameters for static instability in supercritical heated channels. *Int. J. Heat Mass Transf.* 64, 145–154.
- Chatoorgoon, V., Voodi, A., Fraser, D., 2005a. The stability boundary for supercritical flow in natural circulation loops Part I, H₂O studies. *Nucl. Eng. Des.* 235, 2570–2580.
- Chatoorgoon, V., Voodi, A., Upadhye, P., 2005b. The stability boundary for supercritical flow in natural circulation loops Part II, CO₂ and H₂. *Nucl. Eng. Des.* 235, 2581–2593.
- Chatoorgoon, V., Shah, M., Duffey, R., 2007. Linear predictions of supercritical flow instability in parallel channels. In: *Proceedings of 3rd International Symposium on SCWR-Design and Technology*, Shanghai, China, March 12-15, Paper SCR2007-P009.
- Chen, Y., Yang, C., Zhao, M., Bi, K., Du, K., 2014. Forced convective heat transfer experiment of supercritical water in different diameter of tubes. *J. Energy Power Eng.* 8, 1495–1504.
- Cheng, X., Schulenberg, T., 2001. *Heat Transfer at Supercritical Pressure – Literature Review and Application to an HPLWR*, Scientific Rept. FZKA6609. Forschungszentrum Karlsruhe, Germany.
- Chetty, K., Sharma, S., Buchanan, J., Lopez-de Bertodano, M., 2021. Density wave instability verification of 1-D computational two-fluid model. *Nucl. Sci. Eng.* <https://doi.org/10.1080/00295639.2021.1898920>.
- Chilton, H., 1957. A theoretical study of stability in water flow through heated passages. *J. Nucl. Eng.* 5, 273–284.
- CNSC, 2008. *Design of New Nuclear Power Plants*, Report RD-337. Canadian Nuclear Safety Commission, Ottawa, ISBN: 978-1-100-10645-8.
- CNSC/OECD, Canadian Nuclear Safety Commission, 2014. *International Workshop on Multi-unit Probabilistic Safety Assessment (PSA)*, Ottawa, Canada, November 17-20.
- Colombo, M., 2013. *Experimental investigation and numerical simulation of the two-phase flow in the helical coil steam generator*. (Doctoral Thesis), Politecnico di Milano, Italy.
- Colombo, M., Cammi, A., Papini, D., Ricotti, M.E., 2012. RELAP5/MOD3.3 study on density wave instabilities in single channel and two parallel channels. *Prog. Nucl. Energy* 56, 15–23.
- Computer Simulation & Analysis, Inc, 1998. *RETRAN-3D-A Program for Transient Thermal-Hydraulic Analysis of Complex Fluid Flow Systems*. Volume 1, Theory and Numeric. Electric Power Research Institute Report, NP-7405, Volume 1, Revision 3.
- Cordnai, L.K., Wechsler, S., 2006. Teaching Independence and Exchangability, ICOTS-7. https://iase-web.org/documents/papers/icots7/3I1_CORD.
- Cornelius, A., 1965a. *An Investigation of Instabilities Encountered During Heat Transfer to a Supercritical Fluid* (Ph. D. Thesis). Oklahoma State University, USA.
- Cornelius, A.J., 1965b. *An Investigation of Instabilities Encountered During Heat Transfer to a Supercritical Fluid*. Argonne National Laboratory Report, ANL-7032.
- Costa, A.L., Petrucci, A., D’Auria, F., Ambrosini, W., 2008. Analyses of instability events in the Peach Bottom-2 BWR using thermal-hydraulic and 3D neutron kinetic coupled codes technique. *Sci. Technol. Nucl. Install.* 2008, 423175. 17 pp. <https://doi.org/10.1155/2008/423175>.
- Creveling, H.F., Schoenhals, R.J., 1966. *Steady Flow Characteristics of a Single-Phase Natural Circulation Loop*. Technical Report No 15, Purdue Research Foundation, COO-1177-15.
- D’Auria, F. (Ed.), 1997. *State-of-the-Art Report on Boiling Water Reactor Stability*. OECD Report NEA/CSNI/R(96)21, OECD/GD(97)13.
- D’Auria, F. (Ed.), 2017. *Thermal Hydraulics in Water-Cooled Nuclear Reactors*. Woodhead Publishing Series in Energy, Elsevier, UK, ISBN: 978-0-08-100662-7.
- D’Auria, F., 2018. Status report on thermal-hydraulic passive systems design and safety assessment. In: *Invited at Focus Session “Safety of Advanced Nuclear Power Plants, (coordinators A. Schaffrath and T. Mull) of Annual Meeting on Nuclear Technology (AMNT)*, Berlin, May 29-30. <http://www.kernenergie.de/>. <http://www.nucleartech-meet.com/>.
- D’Auria, F., Debrecin, N., Glaeser, H., 2019. The technological challenge for current generation nuclear reactors. *Nucl. Energy Technol.* 5 (3), 183–199. <https://doi.org/10.3897/nucet.5.38117>.
- Debrah, S.K., Ambrosini, W., Chen, Y., 2013. Discussion on the stability of natural circulation loops with supercritical pressure fluids. *Ann. Nucl. Energy* 54, 47–57.
- Denham, M., 2021. On probabilistic risk assessment. *ANS Nucl. News* 64 (10), 55–59.
- Desrayaud, G., Fichera, A., Lauriat, G., 2013. Two-dimensional numerical analysis of a rectangular closed-loop thermosiphon. *Appl. Therm. Eng.* 50, 187–196.
- Dudour, P., Carlucci, B., 2011. Safety implication in the light of the Fukushima NPP accident. In: *GIF-INPRO Workshop*, November 30 – December 1, IAEA, Vienna.

- Duffey, R.B., 2012. A future at risk, mechanical engineering. ASME 134 (7).
- Duffey, R.B., 2015. Extreme events: causes and predictions. In: Proceeding of the Probabilistic Safety Analysis Conference PSA 2015, Sun Valley, Idaho, American Nuclear Society, Paper 12222.
- Duffey, R.B., 2019a. Power restoration prediction following extreme events and disasters. *Int. J. Disaster Risk Sci.* 10 (1), 134–148. <https://doi.org/10.1007/s13753-018-0189-2>.
- Duffey, R.B., 2019b. The risk of extended power loss and the probability of emergency restoration for severe events and nuclear accidents. *J. Nucl. Eng. Radiat. Sci.* <https://doi.org/10.1115/1.4042970>. ASME NERS-18-1122.
- Duffey, R.B., 2020a. *Learning about Risk: Life, Death ... and Money*. ISBN-13:9798630671134, Independent, USA.
- Duffey, R.B., 2020b. Predicting power system reliability and outage duration including emergency response. *Dependability* 20 (3), 3–14. <https://doi.org/10.21683/1729-2646-2020-3-3-14>.
- Duffey, R.B., Ha, T., 2013. The probability and timing of power system restoration. *IEEE Trans. Power Syst.* 28, 3–9.
- Duffey, R.B., Hughes, E.D., 1991. Static flow instability onset in tubes, channels, annuli, and rod bundles. *Int. J. Heat Mass Transf.* 34, 2483–2496.
- Duffey, R.B., Piro, I.L., 2005. Experimental heat transfer in supercritical carbon dioxide flowing inside channels (survey). *Nucl. Eng. Des.* 235, 913–924.
- Duffey, R.B., Saull, J.W., 2008. *Managing Risk: The Human Element*. John Wiley and Sons, Chichester, United Kingdom.
- Duffey, R.B., Sursock, J.P., 1987. Natural circulation phenomena relevant to small breaks and transients. *Nucl. Eng. Des.* 102, 115–128.
- Duffey, R.B., Zio, E., 2022. *Risk Informing Nuclear Reactor Safety: The Prediction of the Probability and Uncertainty of Core Damage Due to Loss of Power and Cooling*. MS to be published.
- Ellenberg, J., 2014. *How Not To Be Wrong: The Power of Mathematical Thinking*. Penguin Press, New York, NY, USA, ISBN: 978-1-59420-522-4.
- Engler, J.-O., 2020. Global and regional probabilities of major nuclear reactor accidents. *J. Environ. Manag.* 269. <https://doi.org/10.1016/j.jenvman.2020.110780>.
- EPRI, US DOE and US NRC, 2012. Technical Report: Central and Eastern United States Seismic Source Characterization for Nuclear Facilities. EPRI 1021097, DOE/NE-0140, NUREG-2115.
- Escrivá, A., Cobo, J.L., San Roman, J.M., Darriba, M.A., March-Leuba, J., 2008. LAPUR 60 manual, Oak Ridge National Laboratory, Report NUREG/CR-6958.
- Ferreri, J.C., 1999. Single-phase natural circulation in simple circuits - reflections on its numerical simulation. In: Invited Lecture at the Eurotherm Seminar No 63 on Single and Two-Phase Natural Circulation, September 6-8, Genoa, Italy.
- Ferreri, J.C., Ambrosini, W., D'Auria, F., 1995. On the convergence of RELAP5 calculations in a single-phase, natural circulation test problem. In: Proceedings of X-ENFIR, August 7-11, as de Lindoia, SP, Brazil, pp. 303–307.
- Furuya, M., 2006. *Experimental and Analytical Modeling of Natural Circulation and Forced Circulation BWR – Thermal-Hydraulic, Core-Wide, and Regional Stability Phenomena (Doctoral Thesis)*. Delft University of Technology, Netherlands.
- Garlid, K., Amundson, N.R., Isbin, H.S., 1961. A Theoretical Study of the Transient Operation and Stability of Two-Phase Natural Circulation Loops. Argonne National Laboratory Report, ANL-6381.
- Gartia, M.R., Pilkhwal, D.S., Vijayan, P.K., Saha, D., 2007. Analysis of metastable regimes in a parallel channel single phase natural circulation system with RELAP5/MOD3.2. *Int. J. Therm. Sci.* 46, 1064–1074.
- GE, General Electric Company, 2014. Certification of the World's Safest Reactor Paves way for Commercial Deployment in the U.S. and Worldwide, Wilmington, NC, USA, <https://www.ge.com/news/press-releases/ge-hitachis-esbwr-receives-nrc-design-certification-approval>, September, 2016, (Accessed 4 December 2021).
- General Electric Co, 1999. TRACG Model Description. Report NEDE-32176P.
- GIF, Generation IV International Forum, 2011. An Integrated Safety Assessment Methodology (ISAM) for Generation IV Nuclear Systems. GIF/RSWG/2010/002/rev1, Version 1.1.
- GIF, Generation IV International Forum, 2014a. Guidance document for integrated safety assessment methodology (ISAM) – (GDI). European Commission Joint Research Centre Report for GIF Risk and Safety Working Group, GIF/RSWG/2014/001, Version 1.0.
- GIF, Generation IV International Forum, 2014b. Technology roadmap update for generation IV nuclear energy systems, Nuclear Energy Agency Organization for Economic Co-operation and Development (NEA/OECD).
- Gillette, J.L., Singer, R.M., Tokar, J.V., Sullivan, J.E., 1980. Experimental study of the transition from forced to natural circulation in EBR-II at low power and flow. *J. Heat Transf.* 102 (3), 525–530. <https://doi.org/10.1115/1.3244335>.
- Grace, T.M., Krejsa, E.A., 1967. Analytical and Experimental Study of Boiler Instabilities Due to Feed-System - Subcooled Region Coupling. National Aeronautics and Space Administration Report NASA TN D-3961.
- Greif, R., 1988. Natural circulation loops. *J. Heat Transf.* 110, 1243–1258.
- Greif, R., Zvirin, Y., Mertol, A., 1979. The transient and stability behavior of a natural convection loop. *J. Heat Transf.* 101, 684–688.

- Gruszynski, M.J., Viskanta, R., 1983. Heat Transfer to Water from a Vertical Tube Bundle Under Natural-Circulation Conditions. Argonne National Laboratory Illinois, Report NUREG/CR-3167, ANL-83-7.
- Gu, H.Y., Zhao, M., Cheng, X., 2015. Experimental studies on heat transfer to supercritical water in circular tubes at high heat fluxes. *Exp. Thermal Fluid Sci.* 65, 22–32.
- Guo, L.-J., Feng, Z.P., Chen, X.-J., 2001. Pressure drop oscillation of steam-water two-phase flow in a helically coiled tube. *Int. J. Heat Mass Transf.* 44, 1555–1564.
- Hamidouche, T., Bousbia-salah, A., 2006. RELAP5/3.2 assessment against low pressure onset of flow instability in parallel heated cannels. *Ann. Nucl. Energy* 33, 510–520.
- Hamilton, D.C., Lynch, F.E., Palmer, L.D., 1954. The Nature of Flow of Ordinary Fluids in a Thermal Convection Harp, ORNL-1624. Oak Ridge Laboratory, Tennessee, USA.
- Hancox, W.T., Banerjee, S., 1977. Numerical standards for flow-boiling analysis. *Nucl. Sci. Eng.* 64, 106–123.
- Harden, D.G., 1963. Transient Behavior of a Natural-Circulation Loop Operating Near the Thermodynamic Critical Point. Argonne National Laboratory Report, ANL-6710.
- Hawking, S., 2014. The Universe in a Nutshell - Chapter 2. Bantam Books, NY, USA, ISBN: 9780385365413.
- He, S., Kim, W.S., Jiang, P.X., Jackson, J.D., 2004. Simulation of mixed convective heat transfer to carbon dioxide at supercritical pressure. *Int. J. Mech. Eng. Sci.* 218, 1281–1296.
- Howlett, R.C., 1995. The Industrial Operator's Handbook. Techstar Inc, Pocatello, Idaho, USA.
- Hu, R., 2010. Stability analysis of the boiling water reactor: Methods and advanced designs (PhD Dissertation). Massachusetts Institute of Technology, USA.
- Hu, R., Kazimi, M.S., 2011. Flashing-induced instability analysis and the start-up of natural circulation boiling reactors. *Nucl. Technol.* 176, 57–71.
- Hu, R., Kazimi, M.S., 2012. Boiling water reactor stability analysis by TRACE/PARCS: modeling effects and case study of time vs frequency domain approach. *Nucl. Technol.* 177, 8–28.
- Hughes, E.D., Paulsen, M.P., Agee, L.J., 1981. A drift-flux model of two-phase flow for RETRAN. *Nucl. Technol.* 54, 410–421.
- Hwang, Y.D., Yang, S.H., Kim, S.H., Lee, S.W., Kim, H.K., Yoon, H.Y., Lee, G.H., Bae, K.H., Chung, Y.J., 2005. Model Description of TASS/SMR Code. Korea Atomic Energy Research Institute. KAERI/TR-3082/2005.
- Hwang, Y.D., Lee, G.H., Chung, Y.J., Kim, H.C., Chang, D.J., 2006. Assessment of the TASS/SMR Code Using Basic Test Problems. Korea Atomic Energy Research Institute. KAERI/TR-3156/2006.
- IAEA, 2001. Thermohydraulic Relationships for Advanced Water Cooled Reactors, IAEA-TECDOC-1203, Vienna, Austria. <https://www.iaea.org/publications/6088/thermohydraulic-relationships-for-advanced-water-cooled-reactors>.
- IAEA, 2002. Natural Circulation Data and Methods for Advanced Water Cooled Nuclear Power Plant Designs, IAEA-TECDOC-1281, Vienna, Austria. https://www-pub.iaea.org/MTCD/Publications/PDF/te_1281_prn.pdf.
- IAEA, 2004. Status of Advanced Light Water Reactor Designs, IAEA-TECDOC-1391, Vienna, Austria. <https://www.iaea.org/publications/7123/status-of-advanced-light-water-reactor-designs-2004>.
- IAEA, 2005. Natural circulation in water cooled nuclear power Plants, Phenomena, models, and methodology for system reliability assessments, IAEA-TECDOC-1474. IAEA, Vienna. <https://www.iaea.org/publications/7376/natural-circulation-in-water-cooled-nuclear-power-plant>.
- IAEA, 2009. Passive Safety Systems and Natural Circulation in Water Cooled Nuclear Power Plants, IAEA-TECDOC-1624. IAEA, Vienna, Austria. <https://www.iaea.org/publications/8192/passive-safety-systems-and-natural-circulation-in-water-cooled-nuclear-power-plants>.
- IAEA, 2012. Natural Circulation Phenomena and Modelling for Advanced Water Cooled Reactors, IAEA-TECDOC-1677, Vienna, Austria. <https://www.iaea.org/publications/8638/natural-circulation-phenomena-and-modelling-for-advanced-water-cooled-reactors>.
- IAEA, 2014. Heat Transfer Behaviour and Thermohydraulics Code Testing for Supercritical Water Cooled Reactors (SCWRs), IAEA-TECDOC-1746, Vienna, Austria. <https://www.iaea.org/publications/10731/heat-transfer-behaviour-and-thermohydraulics-code-testing-for-supercritical-water-cooled-reactors-scwrs>.
- Information Systems Laboratories, Inc, 2001. RELAP5/MOD33 Code Manual Volume I, Code Structure, System Models, and Solution Methods. United States Nuclear Regulatory Commission Report, NUREG/CR-5535/Rev 1, Volume I.
- INL, Idaho National Laboratory, 2014. Guidance for Developing Principal Design Criteria for Advanced (Non-Light Water) Reactors. Idaho National Laboratory Report INL/EXT-14-31179 Rev. 1.
- Ishii, M., Revankar, S.T., Dowlati, R., Bertodano, M.L., Babelli, I., Wang, W., Pokharna, H., Ransom, V.H., Viskanta, R., Wilmarth, T., Han, J.T., 1996. Scientific design of Purdue University Multi-Dimensional Integral Test Assembly (PUMA) for GE SBWR. U.S. Nuclear Regulatory Commission Report NUREG/CR-6309.
- Jackson, J.D., 2013. Fluid flow and convective heat transfer to fluids at supercritical pressure. *Nucl. Eng. Des.* 264, 24–40.
- Jain, K.C., 1965. Self-Sustained Hydrodynamic Oscillations in a Natural-Circulation Two-Phase-Flow Boiling Loop. Argonne National Laboratory Report ANL-7073.

- Jain, R., Corradini, M.L., 2006. A linear stability analysis for natural-circulation loops under supercritical conditions. *Nucl. Technol.* 155, 312–323.
- Jain, P.K., Rizwan-uddin, 2008. Numerical analysis of supercritical flow instabilities in a natural circulation loop. *Nucl. Eng. Des.* 238, 1947–1957.
- Jeglic, F.A., Grace, T.M., 1965. Onset of Flow Oscillations in Forced-Flow Subcooled Boiling. National Aeronautics and Space Administration Report NASA TN D-2821.
- Jensen, P., 1992. BWR Stability Analysis Methods and Sensitivities. Nuclear Safety Analysis Center Report NSAC-172.
- Jingjing, L., Tao, Z., Mingqiang, S., Qijun, H., Yanping, H., Zejun, A., 2015. CFD analysis of supercritical water flow instability in parallel channels. *Int. J. Heat Mass Transf.* 86, 923–929.
- Kakaç, S., Bon, B., 2008. A review of two-phase flow dynamic instabilities in tube boiling systems. *Int. J. Heat Mass Transf.* 51, 399–433.
- Keller, J.B., 1967. Periodic oscillations in a model of thermal convection. *Journal of Fluid Mechanics* 26 (Part 3), 599–606.
- Kelly, J.E., 2014. Generation IV international forum: a decade of progress through international cooperation. *Prog. Nucl. Energy* 77, 240–246.
- Kim, S., Bae, B.-U., Cho, Y.-J., Park, Y.-S., Kang, K.-H., Yun, B.-J., 2013. An experimental study on the validation of cooling capability for the Passive Auxiliary Feedwater System (PAFS) condensation heat exchanger. *Nucl. Eng. Des.* 260, 54–63.
- Kimura, C.Y., Budnitz, R.J., 1987. Evaluation of External Hazards to Nuclear Power Plants in the United States. NRC NUREG/CR-5042, NRC, Washington, DC, NRC access # ML 14196A083.
- Kozmenkov, Y., Rohde, U., Manera, A., 2012. Validation of the RELAP5 code for the modeling of flashing-induced instabilities under natural-circulation conditions using experimental data from the CIRUS test facility. *Nucl. Eng. Des.* 243, 168–175.
- Kwi-Seok, H., Jeong, H.-Y., Cho, C., Kwon, Y.-M., Lee, Y.-B., Hahn, D., 2010. Simulation of the EBR-II loss-of-flow tests using the MARS code. *Nucl. Technol.* 169 (2), 134–142.
- Lahey Jr., R.T., Drew, D., 1980. An Assessment of the Literature Related to LWR Instability Modes. U.S. Nuclear Regulatory Commission Report NUREG/CR-1414.
- Lahey Jr., R.T., Podowski, M.Z., Clausse, A., DeSanctis, N., 1990. A linear analysis of channel-to-channel instability modes. *Chem. Eng. Commun.* 93, 75–81.
- Lee, J.D., Pan, C., 2005. Nonlinear analysis for a double-channel two-phase natural circulation loop under low-pressure conditions. *Ann. Nucl. Energy* 32, 299–329.
- Lee, R.M., Assante, M.J., Conway, T., 2016. Analysis of the cyber attack on the ukrainian power grid: Defense use case, E-ISAC Report. In: Electricity Information Sharing and Analysis Center. Industrial Control Systems, Washington, DC, USA (accessed at ics.sans.org/media/E-ISAC_SANS_Ukraine_DUC_5.pdf).
- Levy, S., Beckjord, E.S., 1960. Hydraulic instability in a natural circulation loop with net steam generation at 1000 psia. In: American Society of Mechanical Engineers, Heat Transfer Conference, Paper No 60-HT-27, Buffalo, New York, USA.
- Loggins, R., Little, R.G., Mitchell, J., Sharkey, T., Wallace, W.A., 2019. CRISIS: modeling the restoration of interdependent civil and social infrastructure systems following an extreme event. *Nat. Hazard. Rev.* 20 (3). [https://doi.org/10.1061/\(ASCE\)NH.1527-6996.0000326](https://doi.org/10.1061/(ASCE)NH.1527-6996.0000326). ASCE, ISSN 1527-6988.
- Lorenz, E.N., 1963. Deterministic non-periodic flow. *J. Atmos. Sci.* 20, 130–141.
- Lottes, P.A., Anderson, R.P., Hoflund, B.M., Marchaterre, J.F., Petrick, F.M., Popper, G.F., Weatherhead, R.J., 1963. Boiling Water Reactor Technology Status of the art Report. Argonne National Laboratory Report, ANL-6561.
- Lowdermilk, W.H., Lanzo, C.D., Siegel, B.L., 1958. Investigation of Boiling Burnout and Flow Instability for Water Flowing in Tubes. National Advisory Committee for Aeronautics Report NACA TN 4382.
- Manavela Chiapero, M., Fernandino, M., Dorao, C.A., 2012. Review on pressure drop oscillations in boiling systems. *Nucl. Eng. Des.* 250, 436–447.
- Manavela Chiapero, M., Fernandino, M., Dorao, C.A., 2013a. On the influence of heat flux updating during pressure drop oscillation - a numerical analysis. *Int. J. Heat Mass Transf.* 63, 31–40.
- Manavela Chiapero, E., Fernandino, M., Dorao, C.A., 2013b. Numerical analysis of pressure drop oscillations in parallel channels. *Int. J. Multiphase Flow* 56, 15–24.
- Mandelli, D., Alfonsi, A., Wang, C., Zhegang, M., Parisi, C., Aldemir, T., Smith, C., Youngblood, R., 2020. Mutual integration of classical and dynamic PRA. *Nucl. Technol., ANS*, 1–13. <https://doi.org/10.1080/00295450.2020.177603>. Paper 177603.
- Mangal, A., Jain, V., Nayak, A.K., 2012. Capability of the RELAP5 code to simulate natural circulation behavior in test facilities. *Prog. Nucl. Energy* 61, 1–16.
- Marcel, C.P., 2007. Experimental and numerical stability investigations on natural circulation boiling water reactors (Doctoral Thesis). Delft University of Technology, Netherlands.
- March-Leuba, J., 1984. Dynamic Behavior of Boiling Water Reactors (Doctoral Dissertation). University of Tennessee, Knoxville, USA.

- March-Leuba, J., Rey, J., 1993. Coupled thermo-hydraulic-neutronic instabilities in boiling water nuclear reactors: a review of the state of the art. *Nucl. Eng. Des.* 145, 97–111.
- Mascari, E., Vella, G., Woods, B.G., D’Auria, F., 2012. Analyses of the OSU-MASLWR experimental test facility. *Sci. Technol. Nucl. Install.* 2012, 528241. <https://doi.org/10.1155/2012/528241>.
- Mascari, E., Woods, B.G., Welter, K., D’Auria, F., 2019. Validation of the TRACE code against small modular integral reactor natural circulation phenomena, ANS. In: *Proceedings NURETH-18, Portland, Oregon, USA, August 18*, pp. 6701–6714.
- McCann, M.W., Lundquist, B.A., 2017. Development of F-N Curves for Public Safety Risks Associated With Dam Failures in the U.S. Association of State Dam Safety Officials, Inc, Lexington, KY, USA.
- Men, Q., Wang, X., Zhou, X., Meng, X., 2014. Heat transfer analysis of passive heat removal heat exchanger under natural convection condition on tank. *Sci. Technol. Nucl. Install.* 2014, 279791. 8 pp.
- Mertol, A., 1980. Heat transfer and fluid flow in thermosyphons (Ph D Dissertation). University of California at Berkeley, USA.
- Mertol, A., Grief, R., Zvirni, N.Y., 1981. The transient, steady state and stability behavior of a natural convection loop with a throughflow. *Int. J. Heat Mass Transf.* 24, 621–633.
- Misale, M., 2014. Overview on single-phase natural circulation loops. In: *Proceedings of the International Conference on Advances in Mechanical and Automation Engineering – MAE 2014*, DOI: 1015224/978-1-63248-022-4-101.
- Misale, M., Ruffino, P., Frogheri, M., 2000. The influence of the wall thermal capacity and axial conduction over a single-phase natural circulation loop, 2-D numerical study. *Int. J. Heat Mass Transf.* 36, 533–539.
- Misale, M., Devia, F., Garibaldi, P., 2012. Experiments with Al₂O₃ nanofluid in a single-phase natural circulation mini-loop: preliminary results. *Appl. Therm. Eng.* 40, 64–70.
- Modarres, M., 2015. Multi-unit nuclear plant risks and implications of the quantitative health objectives. In: *Proceedings of the American Nuclear Society Probabilistic Safety Analysis Conference (PSA2015)*, Sun Valley, Idaho, USA, April 26–30.
- Mori, M., 1998. Benchmarking and qualification of RETRAN-03 for BWR stability analysis by comparison with frequency-domain stability analysis code. *Nucl. Technol.* 121, 260–274.
- Muñoz-Cobo, J.L., Podowski, M.Z., Chiva, S., 2002. Parallel channel instabilities in boiling water reactor systems: boundary conditions for out of phase oscillations. *Ann. Nucl. Energy* 29, 1891–1917.
- Murphy, S., Apt, J., Moura, J., Sowell, F., 2017. Resource adequacy risks to the bulk power system of North America. *Appl. Energy* 212, 1360–1376. <https://doi.org/10.1016/j.apenergy.2017.12.097>.
- Nakai, R., 2013. Safety implication for Gen-IV SFR based on the lesson learned from the Fukushima Dai-ichi NPPs Accident, T4. In: *3rd Joint GIF-IAEA Workshop on SDC for SFRs*, February 26–27, Vienna, Austria.
- NASA, 2010. Risk-Informed Decision Making Handbook, NASA/SP-2010-576, Version 1.0 April. Office of Safety and Mission Assurance, NASA Headquarters, USA.
- Nayak, A.K., Vijayan, P.K., 2008. Flow Instabilities in boiling two-phase natural circulation systems, a review. *Sci. Technol. Nucl. Install.* 2008, 573192. 15 pp <https://doi.org/10.1155/2008/573192>.
- NEA/CSNI, 2015. Benchmark Study of the Accident at the Fukushima Daiichi Nuclear Power Plant (BSAF Project). Phase I Summary Report, R(2015) 18, February 2016 www.oecd-nea.org.
- NEI, 2012. Diverse and Flexible Coping Strategies (FLEX) Implementation Guide, Nuclear Energy Institute. Report NEI 12-06 [Draft Rev. 0], Washington, D.C., USA (US NRC Access number ML122221A205).
- NEI, 2018. Risk-Informed Performance-Based Guidance for Non-Light Water Reactor Licensing Basis Development. Technical Report 18-04, Washington, DC, USA, NRC access # ML 18271A172.
- Niepert, M., Domingos, P., 2014. Exchangeable variable models. In: *Proceedings 31st Conference on Machine Learning*, Beijing, China, arXiv: 1405.0501v1, 2 May, *JMLR: W&CP Vol. 32*.
- Nourgaliev, R., Christon, M., 2012. Solution Algorithms for Multi-Fluid-Flow Averaged Equations, INL/EXT-12-27187. Idaho National Lab, USA. September.
- NuScale, 2020. Standard Plant Design Certification Application. Part 2 Tier 2, Rev. 5, Chapter 19, NRC on-line access # ML20224A508.
- Oka, Y., Mori, H. (Eds.), 2014. *Supercritical-Pressure Light Water Cooled Reactors*. Springer, Tokyo, ISBN: 978-4-431-55024-2.
- Okano, T., 2014. SDC discussions related to practical elimination: of accident situations. In: *IAEA-GIF Workshop on Safety of SFR*, IAEA, Vienna, Austria, June 10–11.
- Ozawa, M., Akagawa, K., Sakaguchi, T., 1989. Flow instabilities in parallel-channel flow systems of gas–liquid two-phase mixtures. *Int. J. Multiphase Flow* 5, 639–657.
- Papini, D., Colombo, M., Cammi, A., Rocotti, M.E., 2014. Experimental and theoretical studies on density wave instabilities in helically coiled tubes. *Int. J. Heat Mass Transf.* 68, 343–356.
- Park, H.-S., Choi, K.-Y., Cho, S., Yi, S.-Y., Park, C.-K., Chung, M.-K., 2008. Experimental study on the natural circulation of a passive residual heat removal system for an integral reactor following a safety related event. *Ann. Nucl. Energy* 35, 2249–2258.

- Park, H.-S., Min, B.-Y., Jung, Y.-G., Shin, Y.-C., Ko, Y.-J., Yi, S.-J., 2014. Design of the VISTA-ITL test facility for an integral type reactor of SMART and a post-test simulation of a SBLOCA test. *Sci. Technol. Nucl. Install.* 2014, 840109. 14 pp.
- Peng, S.J., Podowski, M.Z., Lahey Jr., R.T., Becker, M., 1984. NUFREQ-NP, a computer code for the stability analysis of boiling water nuclear reactors. *Nucl. Sci. Eng.* 88, 404–411.
- Peng, S.J., Podowski, M.Z., Lahey Jr., R.T., 1986. BWR linear stability analysis. *Nucl. Eng. Des.* 93, 25–37.
- Penttila, S., 2015. Proceedings of the 7th International Symposium on Supercritical Water-cooled Reactors, ISSCWR-7, March 15-18, Helsinki, Finland, VTT Technology Report VTT 216.
- Pilkhwal, D.S., Ambrosini, W., Forgione, N., Vijayan, P.K., Saha, D., Ferreri, J.C., 2007. Analysis of the unstable behavior of a single-phase natural circulation loop with one-dimensional and computational fluid-dynamic models. *Ann. Nucl. Energy* 34, 339–355.
- Pioro, I.L., Duffey, R.B., 2003. Literature Survey of Heat Transfer and Hydraulic Resistance of Water, Carbon Dioxide, Helium and Other Fluids at Supercritical and Near-Critical Pressures. Atomic Energy of Canada Report AECL-12137, FFC-FCT-409.
- Pioro, I.L., Duffey, R.B., 2005. Experimental heat transfer in supercritical water flowing inside channels (survey). *Nucl. Eng. Des.* 235, 2407–2430.
- Pioro, I.L., Duffey, R.B., 2007. Heat Transfer And Hydraulic Resistance At Supercritical Pressures In Power Engineering Applications. ASME Press, New York, NY, USA, ISBN: 0-7918-0252-3.
- Pioro, I.L., Khartabil, H.F., Duffey, R.B., 2004. Heat transfer to supercritical fluids flowing in channels – empirical correlations (survey). *Nucl. Eng. Des.* 230, 69–91.
- Pioro, I., Duffey, R.B., Kirillov, P.L., Dort-Goltz, N., 2020. Current Status of Reactors Deployment and Small Modular Reactors Development in the World, *ASME Journal of Nuclear Engineering and Radiation. Science* 6 (4), 24. pages. Free download from: <https://asmedigitalcollection.asme.org/nuclearengineering/article/6/4/044001/1085654/Current-Status-of-Reactors-Deployment-and-Small>.
- Planchon, H.P., Singer, R.M., Mohr, D., Feldman, E.E., Chang, L.K., Betten, P.R., 1985. The EBR-II inherent shutdown and heat removal tests - A survey of test results. In: Paper CONF-850410-6, Presented at the International Topical Meeting on Fast Reactor Safety, April 21-15, U.S. Government contract No. W-3M09-ENG-38, Argonne National Laboratory Argonne, Illinois, USA.
- Prasad, G.V.D., Pandey, M., Kalra, M.S., 2007. Review of research on flow instabilities in natural circulation boiling systems. *Prog. Nucl. Energy* 49 (6), 429–451.
- Rao, N.M., Maiti, B., Das, P.K., 2005a. Comparison of dynamic performance for direct and fluid coupled indirect heat exchange systems. *Int. J. Heat Mass Transf.* 48, 3244–3252.
- Reason, J., 1997. *Managing the Risks of Organizational Accidents*. Ashgate Publishing, Aldershot, United Kingdom.
- Richards, D.J., Hanna, B.N., Hobson, N., Ardron, K.H., 1985. ATHENA, a two-fluid code for CANDU LOCA analysis. In: Third International Topical Meeting on Reactor Thermal Hydraulics, Newport, Rhode Island, USA, Oct 15-18, 7E-1 - 7E-14 (CATHENA formerly named ATHENA).
- Rohatgi, U.S., Duffey, R.B., 1998. Stability, DNB, and CHF in natural circulation two-phase flow. *Int. Commun. Heat Mass Transfer* 25, 161–174.
- Rohatgi, U.S., Mallen, A.N., Cheng, H.S., Wulff, W., 1994. Validation of the engineering plant analyzer methodology with peach bottom 2 stability tests. *Nucl. Eng. Des.* 151, 145–156.
- Rohatgi, U.S., Cheng, H.S., Khan, H.J., Mallen, A.N., Neymotin, L.Y., 1998. RAMONA-4B a Computer Code with Three-Dimensional Neutron Kinetics for BWR and SBWR System Transient – Models and Correlations. Brookhaven National Laboratory Report BNL-NUREG-52471-1.
- Rohde, M., Marcel, C.P., Manera, A., Van der Hagen, T.H.J., Shiralkar, J., 2010. Investigating the ESBWR stability with experimental and numerical tools: a comparative study. *Nucl. Eng. Des.* 240, 375–384.
- Romain, M.O., Stokes, E.C., Shrestha, R., Zhuosen, W., Schultz, L., Sepulveda Carlo, E.A., Qingsong, S., Bell, J., Molthan, A., Kal, V., Chuanyi, J., Seto, K.C., McClain, S.N., Enenkel, M., 2019. Satellite-based assessment of electricity restoration efforts in Puerto Rico after Hurricane Maria. *PLoS ONE* 14 (6), e0218883. <https://doi.org/10.1371/journal.pone.0211883>. 22 pp.
- Rose, T., Sweeting, T., 2016. How safe is nuclear power? A statistical study suggests less than expected. *Bull. At. Sci.* 72 (2), 112–115. <https://doi.org/10.1080/00963402.2016.1145910>.
- Rowinski, M.K., White, T.J., Zhao, J., 2015. Small and medium sized reactors (SMR), a review of technology. *Renew. Sust. Energ. Rev.* 44, 643–656.
- Ruspini, L.C., 2013. Experimental and numerical investigation on two-phase flow instabilities (Doctoral Thesis). Norwegian University of Science and Technology.
- Ruspini, L.C., Dorao, C.A., Fernandino, M., 2010. Dynamic simulations of Ledinegg instability. *J. Nat. Gas Sci. Eng.* 2, 211–216.
- Ruspini, L.C., Dorao, C.A., Fernandino, M., 2011a. Simulation of a natural circulation loop using a least squares hp-adaptive solver. *Math. Comput. Simul.* 81, 2517–2528.

- Ruspini, L.C., Dorao, C.A., Fernandino, M., 2011b. Modeling of dynamic instabilities in boiling systems. In: Proceedings of the 19th International Conference On Nuclear Engineering (ICONE-19), Makuhari, Japan, May 16-19.
- Ruspini, L.C., Dorao, C.A., Fernandino, M., 2012. Two-phase flow instabilities in boiling and condensing systems. *J. Power Energy Syst* 6 (2), 302–313.
- Ruspini, L.C., Marcel, C.P., Clausse, A., 2014. Two-phase flow instabilities: a review. *Int. J. Heat Mass Transf.* 71, 521–548.
- Sabharwall, P., Yoo, Y.J., Wu, Q., Sienicki, J.J., 2012. Natural circulation and linear stability analysis for liquid metal reactors with the effect of fluid axial conduction. *Nucl. Technol.* 178, 298.
- Saha, P., Aksan, N., Anderson, J., Yan, J., Simoneau, J.P., Leung, L., Bertrand, F., Aoto, K., Kamide, H., 2013. Issues and future direction of thermal-hydraulics research and development in nuclear power reactors. *Nucl. Eng. Des.* 264, 3–23.
- Salazar, O., Mihir, S., Ramos, E., 1988. Flow in conjugate natural circulation loops. *AIAA J. Thermophys.* 2, 180–183.
- Sarkar, M.K.S., Tilak, A.K., Basu, D.N., 2014. A state-of-the-art review of recent advances in supercritical natural circulation loops for nuclear applications. *Ann. Nucl. Energy* 73, 250–263.
- Sharabi, M.B., Ambrosini, W., He, S., 2008a. Prediction of unstable behaviour in a heated channel with water at supercritical pressure by CFD models. *Ann. Nucl. Energy* 35, 767–782.
- Sharabi, M., Ambrosini, W., He, S., Jackson, J.D., 2008b. Prediction of turbulent convective heat transfer to a fluid at supercritical pressure in square and triangular channels. *Ann. Nucl. Energy* 35, 993–1005.
- Singer, R.M., Gillette, J.L., Mohr, D., Tokar, J.V., Sullivan, J.E., Dean, E.M., 1980. Response of EBR-II to a complete loss of primary forced flow during power operation. In: Specialists' Meeting on Decay Heat Removal and Natural Convection in FBR's, Brookhaven National Laboratory Upton, Long Island, New York, February 28-29, Argonne National Laboratory, Argonne, Illinois, US DOE Contract W-31-109-Eng-38 for the U.S. DOE.
- Siu, N., Stutzke, M., Dennis, S., Harrison, D., 2016. Probabilistic Risk Assessment and Regulatory Decisionmaking: Some Frequently Asked Questions. US NRC, NUREG-2201, ONR, Washington, DC, NRC access # ML 16245A032.
- Sofu, T., 2014. Summary of US NRC comments on GIF SFR safety design criteria. In: 4th IAEA-GIF Technical Meeting/Workshop on Safety of SFRs, June 10-11, Vienna, Austria.
- Spore, J.W., Giles, M.W., Singer, G.L., Shumway, R.W., 1981. TRAC-BD1/MOD1, an Advanced Best Estimate Computer Program for Boiling Water Reactor Transient Analysis Volume 1 Model Description. Idaho National Engineering Laboratory Report, NUREG/CR-2178, EGG-2109.
- Stekelenburg, A.J.C., 1994. Statics and Dynamics of a Natural Circulation Cooled Boiling Water Reactor (Doctoral Thesis). Delft University of Technology, Netherlands.
- Suzuki, A., 2014. Managing the Fukushima challenge. *Risk Anal.* 34, 1–17.
- Swain, A.D., Guttman, H.E., 1983. Handbook of Human Reliability Analysis with Emphasis on Nuclear Power Plant Applications. NUREG/CR-1278, US NRC Washington, DC (SAND80-0200), NRC access #ML071210299.
- T'Joene, C., Rohde, M., 2012. Experimental study of the coupled thermo-hydraulic-neutronic stability of a natural circulation HPLWR. *Nucl. Eng. Des.* 242, 221–232.
- Tadrist, L., 2007. Review on two-phase flow instabilities in narrow spaces. *Int. J. Heat Fluid Flow* 28 (1), 54–62.
- TEPCO, 2012. Fukushima nuclear accident analysis report. In: Tokyo Electric Power Company Inc., and Japanese Government Report to IAEA Ministerial Conference on Nuclear Safety, Vienna, Austria.
- Tilak, A.K., Basu, D.N., 2015. Computational investigation of the dynamic response of a supercritical natural circulation loop to aperiodic and periodic excitations. *Nucl. Eng. Des.* 284, 251–263.
- Todreas, N.E., Kazimi, M.S., 1990. Nuclear Systems II: Elements of Thermal Hydraulic Design. Hemisphere Publishing Corporation, New York, NY, USA.
- UK HSE, 2008. New Reactor Build: Westinghouse AP 1000 Step 2 PSA Assessment, Health and Safety Executive, Nuclear Directorate, Nuclear Installations Inspectorate, Bootle, England.
- United States District Court Eastern District of Louisiana, 2010. Oil spill by the oil rig Deepwater Horizon in the Gulf of Mexico on April 20, 2:10-cv-4536, United States of America v. BP Exploration & Production, Inc., et al., Testimony of Dr. Robert Bea, February 26, 2013, Transcript p. 310.
- US ACE, US Army Corps of Engineers, 2006. Performance evaluation of the New Orleans and Southeast Louisiana hurricane protection system. In: Volumes I to VIII, Engineering and Operational Risk and Reliability Analysis, Interagency Performance Evaluation Task Force (all volumes available at US ACE Digital Library usace.contentdm.oclc.org/digital/collection/p266001coll1/id/2844/).
- US CFR, U.S. Code of Federal Regulations, 2017. Conditions of Licenses, U.S. Nuclear Regulatory Commission, Washington, DC, 10 CFR50.54 (**hh**), <https://www.nrc.gov/reading-rm/pdr.html>. Accessed 13 March 2019.
- US Department of Energy, April 2015. Accident Investigation Report, Phase 2: Radiological Release Event at the Waste Isolation Pilot Plant. February 14, 2014, Figure 1-9.
- US Department of Treasury, 2021. Financial Report of the United States Government. Department of the Treasury, Washington, DC. March.

- US DHS, U.S. Department of Homeland Security, 2018. Strengthening the Cyber Security of Federal Networks and Critical Infrastructure, Section 2(e): Assessment of Electricity Disruption Incident Response Capabilities. August 9 accessed at: www.dhs.gov/sites/default/files/publications/EO13800-electricity-subsectorreport.
- US Federal Emergency Management Agency (FEMA), 2019. Guidance for Flood Risk Analysis and Mapping: Dams/Reservoirs and Non-dam Features, U.S. Department of Homeland Security, Document 101, November.
- US FEMA Federal Emergency Management Agency, 2011. Multi-hazard Loss Estimation methodology (HAZUS-MH), Federal Emergency Management Agency, Technical Manual, Department of Homeland Security, Mitigation Division, Washington, DC, fema.gov/plan/prevent/hazus.
- US NRC, 2007. Feasibility Study for a Risk-Informed and Performance-Based Regulatory Structure for Future Plant Licensing. Main Report, NUREG 1860, Vols. 1 and 2.
- US NRC, 2014. Final Safety Evaluation Report, General Electric - Hitachi ESBWR, Office of New Reactors, NUREG 1966, Access # ML14099A519.
- US NRC, 2020. Acceptability of Probabilistic Risk Assessment Results for Risk-Informed Activities. , Draft Regulatory Guide 1.200 rev. 3, June, US NRC, Washington, DC, access # ML19308B636.
- US NRC, United States Nuclear Regulatory Commission, 1997. Recommendations for Probabilistic Seismic Hazard Analysis: Guidance on Uncertainty and use of Experts, CR-6372 UCRL-ID-122160, Vols. 1 and 2.
- US NRC, United States Nuclear Regulatory Commission, 2004a. Nuclear Power Plant Licensing Process. NUREG/BR-0298, Rev. 2.
- US NRC, United States Nuclear Regulatory Commission, 2004b. Final Safety Evaluation Report Related to the Certification of the Economic Simplified Boiling-Water Reactor Standard Design. NUREG-1966, ADAMS Accession number ML14100A187.
- van Bragt, D.D.B., 1998. Analytical Modeling of Boiling Water Reactor Dynamics (Doctoral Thesis). Delft University of Technology, Netherlands.
- Vecchiarelli, J., Dinnie, K., Luxat, J., 2014. Development of a Whole-site PSA Methodology. CANDU Owners Group. COG-13-9034, rev. 0.
- Vijayan, P.K., Nayak, A.K., 2010. Introduction to instabilities in natural circulation systems. In: IAEA Training Course on Natural Circulation Phenomena and Passive Safety Systems in Advanced Water-Cooled Reactors, ICTP, Trieste, Italy, May 17-21.
- Vijayan, P.K., Sharma, M., Pilkhwal, D.S., 2013. Steady State and Stability Characteristics of a Supercritical Pressure Natural Circulation Loop (SPNCL) with CO₂. Bhabha Atomic Research Centre Report BARC/2013/003.
- Vyas, H.P., Venkat, R.V., Nayak, A.K., 2010. Experimental investigations on steady state natural circulation behavior of multiple parallel boiling channel system. Nucl. Eng. Des. 240, 3862–3867.
- Walter, H., Linzer, W., 2006. The influence of the operating pressure on the stability of natural circulation systems. Appl. Therm. Eng. 26, 892–897.
- Welander, P., 1967. On the oscillatory instability of a differentially heated fluid loop. J. Fluid Mech. 29, 17–30.
- Wenbin, Z., Yanping, H., Zejun, X., Chuanxin, P., Sansan, L., 2014. Experimental research on passive residual heat removal system of Chinese advanced PWR. Sci. Technol. Nucl. Install. 2014, 325356. 8 pp.
- WENRA, Western European Nuclear Regulators Association, 2009. Safety Objectives for New Power Reactors, Study by WENRA Reactor Harmonization Working Group. pp. 9–10.
- WENRA, Western European Nuclear Regulators Association, 2014. Safety Reference Level for Existing Reactors. available at <http://www.wenra.org/harmonisation/reactor-harmonisation-working-group>.
- Westinghouse Electric Corporation, 2004. Design Reference AP1000 Design Control Document (DCD), Westinghouse Electric Corporation, Pittsburgh, PA, Report No. APP-GW-GL-700 (also “AP1000: Passive Safety Systems and Timeline for Station Blackout”) [http://www.westinghousenuclear.com/Portals/0/NewPlants/AP1000/AP1000Station Blackout.pdf](http://www.westinghousenuclear.com/Portals/0/NewPlants/AP1000/AP1000Station%20Blackout.pdf), timestamp 1404842353431, Accessed 8 July 2014).
- Whittle, R.H., Forgan, R., 1967. A correlation for the minima in the pressure drop vs flow-rate curves for sub-cooled water flowing in narrow heated channels. Nucl. Eng. Des. 6, 89–99.
- Wissler, E.H., Isbin, H.S., Amundson, N.R., 1955. The oscillatory behavior of a two-phase natural circulation loop. In: Presented at the Nuclear Engineering and Science Congress, Cleveland, Ohio, AIChE Preprint 59, 1955. (see also American Institute of Chemical Engineers Journal, Vol. 2, pp. 157-162).
- Wissler, E.H., Isbin, H.S., Amundson, N.R., 1956. Oscillatory Behavior of a Two-phase Natural Circulation Loop. AIChE J. 2, 157–162.
- Woffinden, F.B., Niemi, R.O., 1981. Low-Flow Stability Tests at Peach Bottom Atomic Power Station Unit 2 During Cycle 3. Electric Power Research Institute Report NP-972.
- Wu, Y., 2011. On the modeling and control of coupled multi-loop thermosyphons. In: Applications of Mathematics and Computer Engineering, 2011 American Conference on Applied Mathematics, pp. 105–110.
- Wulff, W., 1998. Integral methods for two-phase flow in hydraulic systems. Adv. Heat Tran. 31, 1–57.

- Wulff, W., Cheng, H.S., Mallen, A.N., Rohatgi, U.S., 1992. BWR Stability Analysis with the BNL Engineering Plant Analyzer. Brookhaven National Laboratory Report NUREG/CR-5816; BNL-NUREG-52312.
- Xiong, T., Yan, X., Xiao, Z.J., Li, Y.L., Huang, Y.P., Yu, J.C., 2012. Experimental study on flow instability in parallel channels with supercritical water. *Ann. Nucl. Energy* 48, 60–67.
- Xiong, T., Yan, X., Huang, S., Yu, J., Huang, Y., 2013. Modeling and analysis of supercritical flow instability in parallel channels. *Int. J. Heat Mass Transf.* 57, 549–557.
- Xu, Y., Downer, T., Walls, R., Ivanov, K., Staudenmeier, J., March-Lueba, J., 2009. Application of TRACE/PARCS to BWR stability analysis. *Ann. Nucl. Energy* 36, 317–323.
- Yadav, A.K., Gopal, M.R., Bhattacharyya, S., 2012a. CFD analysis of a CO₂ based natural circulation loop with end heat exchangers. *Appl. Therm. Eng.* 36, 288–295.
- Yadav, A.K., Gopal, M.R., Bhattacharyya, S., 2012b. CO₂ based natural circulation loops, new correlations for friction and heat transfer. *Int. J. Heat Mass Transf.* 55, 4621–4630.
- Yadigaroglu, G., Bergles, A.E., 1969. An Experimental and Theoretical Study of Density-Wave Oscillation in Two-Phase Flow. Massachusetts Institute Report DSR 74629-3.
- Yang, S.H., Chung, Y.-J., Kim, K.-K., 2008. Experimental validation of the TASS/SMR code for an integral type pressurized water reactor. *Ann. Nucl. Energy* 35, 1903–1911.
- Yetisir, M., Gaudet, M., Duffey, R., 2015. SuperSafe Reactor® (SSR): A supercritical water-cooled small reactor. In: Proceedings of the 22nd International Technical Meeting on Small Modular reactors, Canadian Nuclear Society, Ottawa, Canada, November 7-9.
- Yu, L., Sur, A., Liu, D., 2015. Flow boiling heat and two-phase flow instability of nanofluids in a minichannel. *J. Heat Transf.* 137. <https://doi.org/10.1115/1.4029647>. Paper No: HT-14-1408.
- Zhang, X.-R., Chen, L., Yamaguchi, H., 2010. Natural convective flow and heat transfer of supercritical CO₂ in a rectangular natural circulation loop. *Int. J. Heat Mass Transf.* 53, 4112–4122.
- Zhao, M., Gu, H.Y., Cheng, X., 2014. Experimental study on heat transfer of supercritical water flowing downward in circular tubes. *Ann. Nucl. Energy* 63, 339–349.
- Zhouhang, L., Yuling, Z., Kongzhai, L., Junfu, L., 2016. A quantitative study on the interaction between curvature and buoyancy effects in helically coiled heat exchangers of supercritical CO₂ Rankine cycles. *Energy* 116. <https://doi.org/10.1016/j.energy.2016.10.005>.
- Zvirin, Y., 1979. The effect of dissipation on free convection loops. *Int. J. Heat Mass Transf.* 22, 1539–1545.
- Zvirin, Y., 1982. A review of natural circulation loops in pressurized water reactors and other systems. *Nucl. Eng. Des.* 67, 203–225.
- Zvirin, Y., 1985. The instability associated with the onset of motion in a thermosyphon. *Int. J. Heat Mass Transf.* 28, 2105–2111.
- Zvirin, Y., Jeuck III, P.R., Sullivan, C.W., Duffey, R.B., 1981. Experimental and analytical investigations of a natural circulation system with parallel loops. *J. Heat Transf.* 103, 645–652.

Further reading

- IN, 2008. International standard problems and small break loss-of-coolant accident (SBLOCA). In: Presented at THICKET-2008 OECD-NEA/UNIPI Seminar of the Transfer of Competence, Knowledge and Experience Gained through CSNI Activities in the Field of Thermal-Hydraulics, University of Pisa (UNIPI), May 5-9.
- Ambrosini, W., 2001. On some physical and numerical aspects in computational modelling of one-dimensional flow dynamics. In: 7th International Seminar on Recent Advances in Fluid Mechanics, Physics of Fluids and Associated Complex Systems (Fluidos 2001), Buenos Aires, Argentina, October 17-19.
- Ambrosini, W., 2007. On the analogies in the dynamic behaviour of heated channels with boiling and supercritical fluids. *Nucl. Eng. Des.* 237, 1164–1174.
- Ambrosini, W., 2008. Lesson learned from the adoption of numerical techniques in the analysis of nuclear reactor thermal-hydraulic phenomena. *Prog. Nucl. Energy* 50, 866–876.
- Ambrosini, W., Ferreri, J.C., 2006. Analysis of basic phenomena in boiling channel instabilities with different flow models and numerical schemes. In: Proceedings of On Density Wave Instability Phenomena – Modelling and Experimental Investigation, 14th International Conference on Nuclear Engineering (ICONE 14), Miami, Florida, USA, July 17 20.
- Ambrosini, W., Di Marco, P., Ferreri, J.C., 2000. Linear and nonlinear analysis of density wave instability phenomena. *Int. J. Heat Technol.* 18, 27–36.
- CNSC, Canadian Nuclear Safety Commission, 2008. Design of New Nuclear Power Plants. CNSC Report RD-337.
- Colombo, M., Cammi, A., Papini, D., Ricotti, M.E., 2010. Numerical investigation on boiling channel instabilities by imposing constant pressure drop boundary conditions via a large bypass. In: Proceedings of the International Conference Nuclear Energy for New Europe 2010, Portoroz, Slovenia, September 6-9, Paper Number 413.

- Ferreri, J.C., Ambrosini, W., 1999. Verification of RELAP5/MOD31 With Theoretical Stability Results, United State Nuclear Regulatory Commission Report NUREG-IA-0151.
- Ferreri, J.C., Ambrosini, W., 2002. On the analysis of thermal-fluid-dynamics instabilities via numerical discretization of conservation equations. *Nucl. Eng. Des.* 215, 153–170.
- He, S., Kim, W.S., Jackson, J.D., 2008. A computational study of convective heat transfer to carbon dioxide at a pressure just above the critical value. *Appl. Therm. Eng.* 28, 1662–1675.
- Hughes, E.D., Katsma, K.R., 1983. Numerical solution method improvements for RETRAN. *Nucl. Technol.* 61, 167–180.
- Ishii, M., 1976. Study on flow instabilities in two-phase flow mixtures. Argonne National Laboratory Report ANL-76-23.
- Kumar, K.K., Gopal, M.R., 2009. Steady-state analysis of CO₂ based natural circulation loops with end heat exchangers. *Appl. Therm. Eng.* 29 (10), 1893–1903.
- Lakshmanan, S.P., Pandey, M., 2009. Analysis of startup oscillations in natural circulation boiling systems. *Nucl. Eng. Des.* 239, 2391–2398.
- Rao, N.M., Maiti, B., Das, P.K., 2005b. Dynamic performance of a natural circulation loop with end heat exchangers under different excitations. *Int. J. Heat Mass Transf.* 48, 3185–3196.
- Rao, N.M., Maiti, B., Das, P.K., 2005c. Pressure variation in a natural circulation loop with end heat exchangers. *Int. J. Heat Mass Transf.* 48, 1403–1412.
- Rao, N.M., Maiti, B., Das, P.K., 2005d. Stability behavior of a natural circulation loop with end heat exchangers. *J. Heat Transf.* 127, 749–756.
- Rao, N.M., Maiti, B., Das, P.K., 2008. Steady state performance of a single phase natural circulation loop with end heat exchangers. *J. Heat Transf.* 130 (8), 084506.
- Rickover, H.G., 1970. Testimony, Hearing Before the Joint Committee on Atomic Energy, 91st Congress, 2nd Session, March 19-20.
- Ruspini, L.C., 2012. Inertia and compressibility effects on density waves and Ledinegg phenomena in two-phase flow systems. *Nucl. Eng. Des.* 250, 60–67.
- Swapnalee, B.T., Vijayan, P.K., 2011. A generalized flow equation for single phase natural circulation loops obeying multiple friction laws. *Int. J. Heat Mass Transf.* 54, 2618–2629.
- USA NRC, 2012. USA National Report for the 2012 Convention on Nuclear Safety Extraordinary Meeting. NUREG 1750 rev4, Office of Nuclear Regulation, Access #ML12221A013.
- van der Hagen, T.H.J., Stekelenburg, A.J.C., van Bragt, D.D.B., 2000. Reactor experiments on type-I and type-II BWR stability. *Nucl. Eng. Des.* 200, 177–185.
- Vijayan, P.K., 2002. Experimental observations on the general trends of the steady state and stability behaviour of single-phase natural circulation loops. *Nucl. Eng. Des.* 215, 139–152.
- Eide, S.A., Wierman, T.E., Gentillon, C.D., Rasmuson, D.M., Atwood, C.L., 2007. Industry-Average Performance for Components and Initiating Events at U.S. Commercial Nuclear Power Plants, NRC NUREG/CR-6928, NRC Nuclear Regulatory Research, Washington, DC, access # ML 070650650.

Non-proliferation for Advanced Reactors (ARs): Political and Social aspects

Gerald Clark^a and Romney B. Duffey^b

^aUnited Kingdom ^bIdaho Falls, ID, United States

List of acronym

NPT Non-Proliferation Treaty

17.1 Introduction

Two fundamental goals of advanced reactors and new Generation-IV technologies rely on nuclear fuels and their use for providing globally sustainable energy supply while reducing the potential for abuse for nuclear weapons development and threats (Kelly, 2014), as follows:

“Sustainability: Generation IV nuclear-energy systems will provide sustainable energy generation that meets clean air objectives and promotes long-term availability of systems and effective fuel. They will minimize and manage their nuclear waste and notably reduce the long-term stewardship burden in the future, thereby improving protection for the public health and the environment.

Proliferation Resistance and Physical Protection: Generation IV nuclear-energy systems will increase the assurance that they are a very unattractive and the least desirable route for diversion or theft of weapons-usable materials, and provide increased physical protection against acts of terrorism.”

The underlying and existing technology of nuclear fuel is well described in standard textbooks, reference books and handbooks (Murray and Holbert, 2015; Nuclear Energy Encyclopedia, 2011; Handbook of Nuclear Engineering, 2010; Nuclear Engineering Handbook, 2009; Lamarsh and Baratta, 2001; Hewitt and Collier, 2000; Glasstone and Sesonske, 1994) and in Chapter 18 of this handbook.

Fundamentally, nuclear fission is a reaction in which the nucleus of a heavy nuclide splits into smaller nuclides; a few new neutrons are created; gamma rays are emitted and a significant amount of energy is released. Since then nuclear fission has been used as the basis for production of heat in all the current nuclear reactors. Even though these reactors can be categorized based on their cooling medium, pressure boundary, type of nuclear fuel, or neutron spectrum, they all have one common feature, which is the production of heat via a fission chain reaction in the nuclear fuel.

An important part of every reactor design involves the selection of a nuclear fuel and design of the fuel assemblies. As general requirements, a nuclear fuel should have a high melting point, acceptable thermal conductivity, sufficient mechanical stability, good dimensional and irradiation stability as well as chemical compatibility with the cladding and the coolant. Another important parameter that influences the design and

selection of a nuclear fuel is the dominant neutron spectrum of the reactor. Thus, in the past, the emphasis has been on Uranium-based fuels in commercial water-cooled reactors (PWRs, BWRs, and HWRs), and its ceramic oxide, UO_2 , and U_3O_8 , with only limited enrichment of the fissile ^{235}U isotope (<20%) as derived from gaseous diffusion and centrifuge separation technology (see e.g., the latest proposed Iran/US/IAEA/EU/UN Agreement [Joint Comprehensive Plan of Action \(JCPOA\) \(2015\)](#)). To meet the demanding Generation-IV Goals, many future concepts and designs for Advanced Reactors (ARs) focus on one or more of the following ideas, selection depending on the design details and preferred fuel cycle:

- extending the sustainability of the uranium and other fuel resources, by enhancing the burn-up, or fraction of fissionable atoms used per unit energy produced;
- using “breeding” fuel cycles and core designs that provide more fuel than is consumed, producing fissile Plutonium (^{239}Pu) and Uranium (^{233}U) isotopes from non-fissile material (^{238}U and ^{232}Th , respectively);
- adopting recycling strategies, by separating unusable fission products from “gently-used” fuel, and/or blending with virgin fuel for reuse, sometimes with an on-site facility to avoid transport and external facilities;
- providing fuel and core designs that are more “accident resistant,” using materials that are capable of withstanding higher temperatures before melting and/or damage occurs to the clad or fuel, or eliminating the possibility of core melt altogether, and avoiding the potential for hydrogen production and explosions;
- reducing high-level-waste streams, in both amounts and toxicity, especially, for very long-lived radionuclides, by recycling, isotopic conversion, and actinide burning;
- avoiding and limiting diversion opportunities by having “sealed” cores that can be removed and replaced infrequently only under outside or independent supervision, or having a so-called “closed” fuel cycle.

17.1.1 Non-proliferation: Past influence and future directions

The whole issue of non-proliferation is fraught with the politics of power and influence. The starting point the aims of nuclear Non-Proliferation Treaty (NPT) of 1968 and the parallel development of the role of the International Atomic Energy Agency established in Vienna in 1957, tasked with (among other things) the policing of a safeguards regime, whose aim was to make certain that civil nuclear materials were not diverted to military purposes. Originally, this safeguards regime only applied to “declared” facilities, but following the first Iraq War in 1991 it has aimed to be more all-embracing. The most recent amendments are supposed to allow surprise inspections, of anything, anywhere, at any time. The NPT has been surprisingly successful despite the weapons states not relinquishing their own weapons. In place of pessimistic predictions that by the year 2000 there would be 30–35 nuclear-armed states, there are still less than 10. But as the Treaty contains no provision for amendment or for sanctions against member states that flout their obligations, the system of which it is the foundation is beginning to look somewhat frayed. The system has learnt from its failures, but is finding it difficult to deal with a small minority of member states who have concluded that the possession of nuclear weapons is a greater prize than continued membership of a non-proliferation club dominated by the Weapons States. While the Indian and Pakistani weapons tests of May 1998 pose an insoluble formal difficulty, the substance looks set to be solved by pragmatic agreements in each case, aimed at bringing them into compliance. The motives for this small number of countries developing a weapons capability derive from their perception of their national needs, independence, defense, and pride, just as was the case earlier for the weapons states.

There are other shortcomings:

- Israel (although not a member of the Treaty) is known to have a clandestine weapons capacity, but this is passed over in silence by the United States;
- Iraq was revealed after the first Gulf War as having pursued a clandestine weapons program throughout the 1980s while appearing to be a model member of the Treaty. Following the Iraq revelations an Additional

Protocol was negotiated that allows the IAEA to be much more proactive in policing the system of which it is the guardian;

- Others—Iran, Libya, and North Korea—have also flouted their obligations as Treaty members. External political pressure brought Libya back into compliance. It remains to be seen whether the agreement reached in 2015 with Iran on nuclear-fuel limitation will have the declared effect of limiting Iran’s capacity to develop nuclear weapons. North Korea has demonstrated its ability to make a modest nuclear-weapon-type explosion, and remains defiant in the face of pressure to abandon its nuclear-weapons ambitions. This still leaves India, Pakistan, Israel, and others unresolved;
- Isolation as a policy of containment and retribution manifestly does not work—see the cases of Israel, India, Pakistan, Iran, and North Korea. The NPT has in consequence become inconsistent in application, ineffective in adoption and inequitable in practice.

As also noted in a fairly recent Massachusetts Institute of Technology (MIT) report ([The Future of Nuclear Power, 2003](#)):

“The current international safeguards regime is inadequate to meet the security challenges of the expanded nuclear deployment contemplated in the global growth scenario. The reprocessing system now used in Europe, Japan, and Russia that involves separation and recycling of plutonium presents unwarranted proliferation risk.”

Specifically, this inadequacy placed MIT in the difficult position of proposing that “... over at least the next 50 years, the best choice to meet these challenges is the open, once-through fuel cycle. We judge that there are adequate uranium resources available at reasonable cost to support this choice under a global growth scenario.”

We return to this key issue of global sustainability of nuclear fuels beyond the next decades later, simply noting that this statement is rather myopic or US-centric. It implies these significant weaknesses, in their view, would not allow the full use of the nuclear-fuel energy source. This is only reasonable if many other sustainable fuels exist, domestically and globally, and is at the heart of the NPT debate and the need for revision.

In the discussion of fuel-cycle issues the United States particularly, but the other weapons states also, have tended to adopt a hypocritical position, arguing for keeping the existing distribution of skills and services as they are. At the beginning of the first Preparatory Committee in April 2007 for the review conference of the NPT in 2010 the US delegate delivered a long speech full of self-praise about the great efforts the United States had undertaken to promote the civilian uses of nuclear energy, concentrating on power generation and the peripheral uses—medical isotopes, the use of nuclear techniques in agriculture and industrial measurement and so on—but skating over the tough efforts it has made over the years, decades even, to keep enrichment and reprocessing out of the hands of the non-weapons states. Originally, these efforts were directed to keeping a US monopoly of enrichment, and insisting that US-tagged material had eventually to be returned to the United States. Arguing from the general to the particular, the purpose of this speech was to attempt to demonstrate that Iran had no right under Article 4 of the NPT to assistance in the development of a native fuel cycle, which could incidentally be used for weapons production, whatever Iran’s declared intentions, and arguing that its civil needs could be met by an internationally backed guaranteed supply of fuel for its planned reactor if commercial channels failed to deliver.

Despite all these difficulties the international safeguards system does have real value. The key to it lies in the scientific detail, which forces the exploiters of nuclear energy to discriminate between deploying it in weaponry and using it as a source of energy for the generation of electricity. While the two branches have much in common, from the earliest days military programs have been developed quite separately from all the civil uses of nuclear energy.

An issue which has come to the fore recently, but it was always there, even in the early years, is the exploitation by the weapons states of a de facto monopoly on (closely held) enrichment technology for commercial advantage in international trade and nuclear-energy deployment, to the disadvantage of the rest. Thus

commercial gains became entwined with policy games. One way to strengthen the international safeguards system as a generally effective defense against proliferation is by:

- deploying licensed enrichment technology; and
- switching to more sustainable non-plutonium fuel cycles.

This would make it possible for civil nuclear power to spread to areas of the world that it has not yet reached, but needs to do.

We discuss the shortcomings of the Treaty, the measures, which have been taken to improve matters, and to discuss the actions of rogues states, the easier implications for resistance to global terrorism, and the points of weakness or danger for the future. *These lie in the nuclear fuel cycle rather than in the spread of nuclear power reactors.* Just as the Treaty at its inception reflected the political balance between the superpowers in the Cold War, the world's defenses against nuclear proliferation are likely to be more assisted by the continuing political commitment of its leading member states, especially, the United States, than by formal attempts to amend the Treaty to take account of exceptions which have arisen in its 40-year history. It thus points out how unhelpful the recent selectivity, persecution and bullying tactics of the United States have been. Finally, the paper reaffirms the continuing support of the civil nuclear industry, in whose interest it was created, to the international safeguards system (Table 17.1).

17.1.2 Past dreams and present realities of the politics of power

President Obama's 2009 initiative aimed at negotiating once again a reduction in the number of nuclear weapons in the world. He declared in Prague on 5 April 2009 that he wanted "a new treaty to end the production of fissile materials and—although this was probably not feasible in his lifetime—a world free of such weapons altogether" "A desirable, almost altruistic goal, such a reduction was intended to be approached step by step under the US-Russia bilateral Strategic Arms Reduction Treaty (START) talks, which foundered on

Table 17.1. Typical military nuclear stockpiles^a

Country	Stockpile(est)	Comment ^b
China	125	M, A
France	300	S, M
India	50	M
Israel	80	Undeclared
North Korea	~ 10	M
Pakistan	60	M
Russia	14,000	S, M, A, W
UK	160	S, M, A
USA	10,000	S, M, A, W

^a Although precise numbers are cited here, they are in fact approximations. Even if exact numbers were available for one specific moment in time, continuing stockpile changes as a result of deployment shifts and inspection and maintenance actions cause actual numbers to fluctuate.

^b S = Submarine, M = Missile, A = Aircraft, W = Shell delivery systems.
Source: The Independent, April 2009.

the principles of the need to “trust but verify” and the inability to achieve “zero.” The magnitude of the nuclear disarmament task is easily seen from the present declared or known weapons stockpiles that have their origins in regional and global conflicts.

There is some “surplus” weapons material (some in warhead form) that is just being stored or has been down-blended for making commercial fuel under the Gore-Chernomyrdin Agreement. There is clearly a small quantity in North Korea, and perhaps also some already in Israel and Iran.

For the past few years Iran’s construction of a working uranium enrichment plant, avowedly for peaceful purposes, has dominated the headlines, along with North Korea’s avowed pursuit of nuclear and rocket technology. The United States and the European Union (rather less confrontationally) have expressed determination to prevent Iran from going ahead. What is it all about? Why the apoplexy in Washington? Why do even the Russians and the Chinese pay lip service to the objective of preventing the Iranian enrichment plant, or the North Korea nuclear missile program, even if they do not show much solidarity with the Western Powers in taking measures in the Security Council to deter the Iranians?

Iran has asserted its rights under Article IV to develop enrichment technology for peaceful purposes, a position not palatable to those weapons states (notably the United States) that see the potential for weapons production. Iran’s^a position depends on its persuading people that it is fulfilling its obligations under Article II—it has not been entirely successful on this front largely because of its evasive accounts of earlier history. Meanwhile, North Korea alternates positions over peaceful versus military use, and between multilateral negotiations and unilateral withdrawal.

The essence is political—Revolutionary Iran, ever since the fall of the Shah in 1979, has been adamantly opposed to the United States, excoriated by Iran as the great Satan. The United States, which was humiliated in a number of incidents during the revolution and by the fiasco of its claim of Weapon of Mass Destruction (WMD) in Iraq, is unwilling to take an objective view of the situation. Although it routinely denounces Iran as a supporter of terrorism and finds it difficult to conceive that the Iranians could have neutral or benign objectives in developing a technology ostensibly for civilian use, but has tried to strike a compromise. The enrichment of uranium to the degree necessary to enable them to produce nuclear weapons in the relatively near future is a short step beyond using it to produce nuclear fuel. Therefore, to the chagrin of Israel, recent Agreements between the United States, EU, UN, and Iran aim to set thresholds on amounts, centrifuge counts and enrichment levels that hopefully delay the potential for weapons manufacture or deployment. Iran meanwhile continues to test missiles with the potential capability for weapons delivery.

For their part the Iranians claim that their intention is the peaceful development of nuclear energy, as is their right under the NPT. They assert that in an uncertain and generally hostile world it is a prime national interest of theirs to develop a complete nuclear fuel cycle rather than having to rely on outside supply for crucial parts of it. They are made more intransigent, just like anyone else, by being threatened, bullied and pilloried. They are not the first country to have thought or reacted in this way, as India had already demonstrated in the face of US objections and international boycotts and embargoes. However, many of the states which have a viable civil nuclear program have found it acceptable to import some of its key constituent parts, including enriched uranium fabricated into fuel for civil reactors. There are in fact good economic arguments for so doing, especially, if a country possesses only a small number of reactors. Russia, seeing an export opportunity, has made the Iranians an offer of guaranteed supplies of reactor fuel, which takes at face value the latter’s claim that they are only seeking to guarantee their supplies of fuel for their planned civilian reactors, the first of which has been completed with Russian assistance and Russian fueling.

Similarly, Communist North Korea warred against US and UN armies, withstood them, and backed militarily by China established the armistice line at the end of the War in 1953 close to the famous 38th parallel as

^a For an extensive discussion of the Article IV problem see Christopher Ford’s recent paper: “Nuclear Technology Rights and Wrongs: The NPT, Article IV, and Non-proliferation,” which can be found on the NPEC website.

the dividing line. It has held it ever since. As a result, the United States invested heavily in South Korea's economy, trade and technology, even supplying whole factories and designs for deploying commercial nuclear power plants, while trying to isolate North Korea, or offering similar technology and energy supplies as a quid pro quo for stopping nuclear weapons development. Thus was born the "Axis of Evil" of President George Bush, portrayed as arrayed against the forces of good.

To set this in context so as to make sensible recommendations for the future we shall also look at the history and present needs for energy independence, not allowing foreign policies to be dictated by the weapons states (like the United States, Russia, and France), and at national pride in self-reliance in the newly emerging economic power houses of the world (China and India), and the supply stranglehold of the major oil and gas producers (Russia and OPEC) on the US and EU users. Couple that with the needs of nations to grow, both economically and politically, and we have the elements of a world scene that must be and is changing. In fact, we may summarize the interests of many nations and their aspirations given recent statements and trends diagrammatically in the table which follows below.

The aim of the table is to show how widespread interest in the development of the fuel cycle is, both actually and potentially. *It also shows how "containing" or restricting enrichment and commercial nuclear technology to a few countries (weapons states) is unrealizable and unreasonable.* What everyone really wants is cheap, assured, sustainable and secure energy supply, using proven and economic designs.

This non-proliferation story has all the makings of a saga, which is a long way from resolution, with a long back history. The aim of this Chapter is to clarify the issues, which have led to the present position and to propose some new solutions and attitudes, not the least from the existing weapons states that recognize today's realities and needs (Table 17.2).

Table 17.2. Typical national fuel cycle capabilities and reactor types (disclosed, past, present, real, or proposed)

Country	Supply	Reprocess	Enrich	Fast	Thermal	Open	Closable
S. Africa	✓	✓	✓		✓	✓	
Argentina		✓	✓		✓	✓	✓
Australia	✓		✓		✓		
Belgium					✓	✓	
Brazil	✓	✓	✓		✓	✓	✓
Canada	✓		✓		✓	✓	
China		✓	✓	✓	✓	✓	✓
Egypt					✓	✓	
Finland					✓	✓	✓
France	✓	✓	✓	✓	✓	✓	✓
Germany					✓	✓	
India		✓	✓	✓	✓	✓	✓
Iran		✓	✓		✓	✓	
Israel		✓	✓		✓		✓

Continued

Table 17.2 Typical national fuel cycle capabilities and reactor types (disclosed, past, present, real, or proposed)—cont'd

Country	Supply	Reprocess	Enrich	Fast	Thermal	Open	Closable
Italy					✓	✓	
Japan		✓		✓	✓	✓	✓
N. Korea		✓	✓		✓	✓	
S. Korea					✓	✓	✓
Lithuania					✓	✓	✓
Norway	✓				✓	✓	✓
Mexico					✓	✓	✓
Philippines					✓	✓	
Poland					✓	✓	
Romania					✓	✓	
Saudi Arabia					✓	✓	
Spain					✓	✓	
Sweden	✓		✓		✓	✓	
Taiwan					✓	✓	
Turkey					✓	✓	
Mexico					✓	✓	
Norway	✓						
UAE					✓	✓	
Ukraine					✓	✓	
USA	✓	✓	✓	✓	✓	✓	
UK		✓	✓	✓	✓	✓	✓

One major new subplot is the widespread realization that to make a real difference a *massive* global deployment of nuclear energy (some 10 times the present) will be needed, if nuclear energy is to be used to resolve future energy sustainability and climate-change-driven reduced emissions targets and requirements. Existing regimes, paradigms and mechanisms are plainly inadequate faced with such a new era. The weapons states' offering of special "proliferation resistant" reactors and "assured fuel supply" is little better than applying a band-aid to a broken leg, and likely to be counterproductive.

17.1.3 The genesis of the Non-Proliferation Treaty (NPT) and its bargain

The foundation of the current international regime for containing the spread of nuclear weapons is the nuclear NPT. It was a product, following the ugly Cold War race to Mutually Assured Destruction (MAD), of a realization that WMD were potentially highly unstable as a national policy tool. It was opened

for signature in 1968 and came into force in the spring of 1970 when sufficient (40) ratifications of the treaty had been collected by the three depository powers (the United States, Britain, and the Soviet Union).

The NPT itself was the culmination of a lengthy process set in motion by President Eisenhower's Speech to the General Assembly of the United Nations in December 1953, known ever since as his "Atoms for Peace Speech." The speech also proposed the establishment of an International Atomic Energy Agency under the aegis of the United Nations, which would promote the benefits of the peaceful uses of nuclear energy at the same time as facilitating practical measures of military nuclear disarmament. One of its prime objectives was to develop a system whereby the proliferation of military technologies could be controlled by the application of "safeguards" on all nuclear establishments. What this meant was measuring, tracking, and labeling every atom of fissionable material in circulation or use, in a safeguards regime which had two main variants: installation-specific safeguards, as set out in INFCIRC 66, and "full-scope safeguards," set out in INFCIRC 153,^b in which all a member state's nuclear installations became subject to international safeguards policed by the inspectors of the IAEA.

The purpose of an inspection is to demonstrate the truth of a member state's claim that there has been no diversion of material, based on a voluntary declaration of the usage and facilities to be "under safeguards." If the inspector should find otherwise, he would have to report in the first instance through the Director General to the Board of Governors of the IAEA, who in turn decide whether to appeal to the Security Council for action to deal with the breach. The fallout from the fallacy of voluntary disclosure was yet to emerge.

The creation of this system was strongly influenced by the more or less simultaneous creation of EURATOM and its system of safeguards in 1957 by the six founder member countries of the European Community (Annex 1 on EURATOM).

While the establishment of the IAEA was a deal between the United States and its allies on one side and the Soviet Union and its cohorts on the other, tension between the two camps rose over the next 5 years culminating in the Cuban missile crisis of October 1962. The diffusion of the crisis without, fortunately, any of the threatened exchanges of nuclear missiles led to the negotiation of a number of international agreements aimed at reducing the risk of a repetition of this blood-curdling crisis in which disaster was avoided by a whisker. The nuclear NPT was one of these. By this time two more states had joined the ranks of those who possessed nuclear weapons, France in 1961, and the People's Republic of China in 1964, both doing so without any declarations, prior permissions or global agreements—they did so in pursuit of their own national and political self-interests, under President de Gaulle and Chairman Mao, thus setting a precedent. *They did so well before the Treaty was presented for signature, so they were not (and rejected being) bound by its later aims.*

The Treaty bargain (see Annex 2 for the full text) recognized straightforwardly that there were five nuclear weapons states at the time of signature, and its prime aim was to devise a way forward which would limit the total number of weapons states to those who already had them. It did this by enjoining on the weapons states not to pass on the technology of nuclear weapons to any non-weapon states (Article I), and by rewarding the self-denial of the non-weapon states (Article II) with promises of *equal access* for all "states parties" to the development of civilian nuclear power and other civilian technologies (Article IV).

These included what now seems bizarre—any civil spin off from "peaceful nuclear explosions" (Article V). (In the 1960s, there were both in the Soviet Union and in the United States enthusiastic supporters of using specially designed nuclear explosions to simplify mega civil works projects such as the diversion of the river Yenesei or the excavation of a second Panama Canal! Fortunately, wiser heads prevailed on both sides of the Iron Curtain before anything was done to implement these projects!)

Non-weapon states were enjoined to negotiate with the IAEA a full-scope safeguards agreement, together with specific "facilities attachment agreements" covering all their nuclear installations within 180 days of joining the Treaty (Article III). Some did, but many did not, or at least not for a number of years. The number

^b Easily found on the IAEA's website: www.iaea.org.

of inspections under “full scope safeguards” is supposedly proportionate to the amount of civilian-use nuclear material, and their frequency depends in part on the ease with which the material could theoretically be diverted from civilian to military use and the length of time that this would take.

Further, the Weapons States committed themselves to begin negotiations in good faith to end the nuclear arms race at an early date, and to work toward *complete* nuclear disarmament (Article VI). The insertion of Article VI was not entirely cynical. The Cuban Crisis of 1962 had brought home even to the super powers that their rivalry could lead to universal nuclear annihilation if not carefully regulated. The aspiration toward nuclear disarmament remained little more than an aspiration for the first 20 years of the Treaty’s life. As a result, this key part of the bargain has not yet been fulfilled, which has lent support to accusations that the Treaty remains discriminatory and inequitable.

In essence the case for reform can be summed up as follows:

“Non-proliferation is a set of bargains whose fairness must be self-evident if the majority of countries is to support their enforcement. The only way to achieve this is to enforce compliance universally, not selectively, including the obligations the nuclear states have taken on themselves.”

Non-Nuclear Weapons States (NNWS) such as Australia, Argentina, Brazil, Canada, and South Africa do not want to get shut out of an enrichment market that will grow if nuclear energy enjoys a renaissance. Other states resent being denied access to additional nuclear technologies when they feel that they have not benefited from nuclear cooperation as it is, and the nuclear weapons states have not delivered on the original disarmament bargain.”^c

The IAEA was formally given the responsibility of policing the Treaty. This resulted in a significant extension of its international safeguards system.

The Treaty originally was limited to 25 years duration, with provision for 5-yearly reviews, and consideration after 25 years of possible further extension. These provisions reflected the uncertainty among its sponsors when it was introduced. The very notion of international inspection of installations, which went close to the heart of what individual countries would regard as their most important security interests, was in the circumstances of the time (late 1960s) an amazing innovation. A number of countries held back from joining for a variety of reasons: because they still had ambitions to become nuclear weapons states (Argentina, Brazil, South Africa), or wanted to retain the freedom to help their allies or clients (France, China^d), or because they disliked the discriminatory nature of the Treaty (India) or because they did not want to fall in with the dictates of the super-powers (France) or because of regional political rivalries (Pakistan).

Some 185 countries have now signed up; the only exceptions being India, Pakistan, Israel, who have never joined, and North Korea (the DPRK), who withdrew from the Treaty in 2003. South Africa and Libya, gave up their weapons programs for different reasons: South Africa as it underwent internal political changes; Libya because the exposure of its involvement in the A.Q. Khan’s network made it realize that compliance with its NPT obligations was a more advantageous policy than proliferation.

17.1.4 Effects of the treaty

The NPT is an interstate treaty aimed at creating trust between states, and therefore, hopefully, at diminishing the desire of states to possess nuclear weapons. The international Safeguards System administered by the IAEA was designed in the first place to demonstrate that member states were doing what they declared they were doing, and thus to provide reassurance to other states. It was up to the states themselves to ensure that their employees were carrying out their instructions.

^c Carnegie Foundation’s 2007 Score Card.

^d At the opening for signature of the NPT China had still not replaced Taiwan as a member of the United Nations and the Security Council.

From some points of view the NPT has been the most successful arms control treaty ever. Certainly at the time of its inception it was generally believed that by the end of the 20th century there would be 30–35 nuclear weapons states. In practice there are still less than 10: with only eight clearly acknowledged nuclear-armed states. Pakistan and India broke cover in May 1998 and carried out a series of underground tests. Israel is widely assumed to have weapons capability, and has even on occasion admitted it, but has never carried out an observed weapons test. North Korea claimed that it carried out a nuclear test in October 2006, and a further test on a larger scale in April 2009. It has been suggested that although North Korea has been openly threatened by the United States, it did not fear them as it had already defeated them in battle in the Korean War; and China has until recently shown reluctance to bully or enrage a neighboring Communist state which was its ally in that same war.

Shortly before it handed over power to the ANC the apartheid regime in South Africa confessed to having developed nuclear weapons, but announced that it had decided to dismantle them. It surrendered its accumulated stockpile of fissionable material to the depository powers of the Treaty, allowed the IAEA to inspect its installations and their dismantlement in 1991, and joined the Treaty as a non-weapons state. The buildings and facilities stand as empty shells and monuments.

To put all this history another way, in the past 50 years a universalistic system of control of fissionable material has been established under the detailed supervision of the IAEA in Vienna. The NPT is its key document. The system has worked to the extent that the weapons states established by 1965 still dominate the division of the world into weapons and non-weapons states. This is what the system was designed to achieve, but it is fraying at the edges. It has NOT worked for example when disclosure was not complete, and undisclosed facilities have concealed weapons work. Further, two important states have demonstrably mastered the production of nuclear weapons, two others have probably done so, and several more have flirted with it, and have only been prevented by strong-arm tactics which have little to do with the formal system, and much to do with the projection of the military power of the United States. Despite four quinquennial review conferences of the Treaty since India and Pakistan drove a coach and horses through the formal system in 1998 the Governments of the acknowledged Weapons States for 10 years made no move to amend the Treaty, or even to engage in serious multilateral discussion of what might be done. (The British Foreign Office, however, issued a discussion paper on 4 February 2009 in preparation for the 2010 Review Conference[°]).

One reason for this inaction is that the IAEA/NPT system, which some say has served reasonably well for the past 50 years, is a product of the wider political shape of the world.

It is worth stressing at this point that the strategic aims of the Superpowers were little affected by the NPT. Until the late 1980s, the development of nuclear weapons by both the United States and the Soviet Union paid no attention to the aims of Article VI of the Treaty, but reflected the evolving strategies of both sides in their respective bids for supremacy. Even though they were sponsors of the Treaty the pieties of Article VI in no way hindered their arms race. The virtue of the Treaty as perceived in Moscow and in Washington was that it was a device, in practice quite an effective device, through which they were able to repress the complications which the entry of numerous other powers into the nuclear contest could have caused.

The Treaty was never perfect even as a system of super-power control, but has been used as a rationale for “regime change meaning invasions related to stopping “weapons of mass destruction,” and the imposition of “economic sanctions.”

China had been disappointed in the late 50s in its expectations of nuclear assistance from Moscow. By the time it acquired its own nuclear weapons in 1964. It was already engaged in a bitter ideological struggle with the Soviet Union. India, smarting from its defeat in the Himalayan confrontation with China in 1962 and from lack of Soviet support, clearly decided to bolster non-alignment and self-reliance with its own nuclear arsenal. The proliferation path opened: even though Pakistan was in theory covered by the US nuclear shield

[°] “Lifting the nuclear shadow: creating the conditions for abolishing nuclear weapons” an FCO Information Paper.

non-aligned India was much nearer and militarily much more powerful than Pakistan, a fact demonstrated forcibly by its support for the transformation of East Pakistan into independent Bangladesh, Pakistan sought assistance from China in order to match Indian developments. In South America, the rivalry of Argentina and Brazil for leadership prevented them for many years from accepting the protection of the IAEA's non-proliferation regime before finally signing a mutual pact of inspection and cessation. Israel had to develop a deterrent, having been invaded in 1948, and having fought bloody wars in 1967 and 1973 against Egypt in Sinai and Syria in the Golan Heights.

The world today is more fragmented, threatened and volatile than for 50 years, despite the peace, and the balance of global and political power is shifting to those who control regional energy resources, away from those who control weapons. The new emergence of the government control of global oil supply by the "Seven Stars" (Russia, Iran, Saudi Arabia, Venezuela, the United Arab Emirates, China, and Brazil) has changed the balance of global influence, where the producer states now own and control the world's major natural resources of oil and gas, in place of yesterday's "Seven Sisters" of the US and other global oil corporations (Mobil, Exxon, BP, Chevron, Shell, etc.). The reemergence of the United States as an oil (and gas) exporter has also led to quasi-instability in traditional energy pricing in the never-ending struggle for global market share, economic growth, international political power, and national and business revenue.

Paradoxically, in uranium resources where many of the major resources are in local ownership in Canada, Kazakhstan, Australia, we see an opposite trend, with the weapons states' fuel cycle companies seeking to expand their positions in resource control, because they either never had, or now do not have, large domestic uranium resources. The globalization of the nuclear fuel market will inevitably complicate proliferation control.

17.1.5 Shortcomings of the treaty

Its successes are clearly impressive, but all is not well with the system. The first Gulf War of 1991 revealed that the assumption that members of the Non-Proliferation Club (NPTC) would play by the rules (as it was so clearly in their interests to do so) was unduly complacent. Iraq had previously for a number of years been attempting to develop a nuclear weapon in defiance of the objectives of the Treaty of which Iraq was a founder member, even though the threat was greater than the reality.

The IAEA came in for much criticism from the United States for its failure to detect, still less to prevent, this gross breach of its rules. In its defense it would say that those rules were not sufficiently stringent, as disclosure was voluntary. But more stringent rules would have been unacceptable to the member states in the mid-60s when the Treaty and its rules were negotiated. Furthermore, there was an unspoken but nevertheless real bargain at the Agency that the superpowers would keep their own clients in order, and not interfere with the activities of the clients of the other.

Iraq was not the only player who hoped to avoid detection in clandestine disregard of their NPT obligations. Libya, Iran, and North Korea were all engaged in undeclared attempts to develop enrichment technology, weapons materials and missile delivery systems. NB^f: *Israel was not and is not a member of the Treaty. While the role of Israel is a sensitive issue for the US and Europe who supported its founding as a nation-state, the final report of the WMD Commission deals with Israel dispassionately and comprehensively.*^g

A safeguards system is only as good as the member states' ability, not to say willingness, to police it. This is exemplified in Iran's moves to develop a civilian nuclear power program as its right, and the NPT and others countries desire to ensure there is not a clandestine weapons development effort at the same time.

^f NB is the standard abbreviation for "Note Bene," the Latin for "note well."

^g Weapons of Mass Destruction Commission, final report, "Weapons of Terror: Freeing the World of Nuclear, Biological, and Chemical Arms," Stockholm, Sweden, 1 June 2006.

The NPT-based idea is to place limits on the level of U^{235} fuel enrichment (20% or less to avoid an efficient bomb), reduce the amounts produced by centrifuges and reactors (to be less than that required for easily making a bomb), and the avoidance of U^{238} fueled Pu-production reactors (to minimize a Pu^{239} threat). But the Agreement is limited in its scope, inspection regime and timescale, reflecting the low level of trust between the parties.

Even when the NPT was not as universal as it now is informal meetings of possible supplier states played a significant role in supporting the safeguards system. There were two main groupings: the so-called, Zangger Committee (named after its first Chairman) and the Nuclear Suppliers Group (NSG), who developed voluminous lists of so-called “sensitive” materials to be interdicted and/or not delivered without agreement or license. This was foreign policy hard at work, trying to be effective. Discussion of “diversion” tends to be in terms of diversion of fissionable material, but the development of viable military nuclear facilities also depends on the acquisition of the appropriate technologies. Many of the technologies which are useable in weapons production of course have other, civilian uses. Drawing up codes of conduct that took account of these complications, and sought to deny would-be proliferators the means to do so, was (and is) a complex and frustrating business in which a state’s national export interests are often in conflict with its NPT obligations. Lists include various types of steel or zirconium tubing, uranium ore, or explosives and propellants, and even certain radioisotopes. (While uranium ore itself is not subject to safeguards, countries which export are expected to report their exports to the IAEA.) All too often the export interests of specialized manufacturers prevailed over the wishes of bureaucrats in government ministries. Meetings of the Zangger Committee and the Nuclear Suppliers Group endeavored to square this circle. Whatever modest success they may have had to begin with, it was in practice undermined by the advent of globalization of international trade in the 80s and 90s, as has been very clearly shown in the IISS’s chilling account of the successes of the A.Q. Khan’s network.^h Here, and apparently with the connivance or at least the acquiescence of his government, the leading weapons designer from Pakistan sold, smuggled and supplied design details, materials and drawings, getting rich in the process.

A reassuring aspect of this, from one point of view, is the fact that the customers of A.Q. Khan’s designs and materials continued to be would-be proliferating states—Libya or North Korea or Iran. No-one has as yet uncovered any conclusive signs that individuals whether oligarchs or tribal chieftains have developed coherent plans to be the possessors of nuclear weapons, but the design details are out of the genie’s bottle too.

17.1.6 Attempts to improve the treaty system

A key discovery in 1991 was that Iraq had cynically been cheating for at least a decade and probably longer. This revelation gave a much needed impetus to the search for improvements in the system, and although the IAEA was attacked for its earlier complacency there seemed in practice little alternative to strengthening its rules and to encouraging it to be much more proactive in pursuit of breaches of those rules. An “Additional Protocol” was negotiated, which authorized the Agency to take the initiative in bringing to international attention any breaches or apparent breaches in the system and increased its powers of intervention. Twenty years later this Protocol is far from being ratified universallyⁱ: China ratified in 2002, while EURATOM and its member states all ratified on 30 April 2004. The United States finally ratified the Protocol and brought it into force on 6 January 2009. Iran signed it in December 2003, but following its dispute with the Agency over its enrichment program has not brought it into force.

^h “Nuclear Black Markets: Pakistan, A.Q. Khan and the rise of proliferation networks” an IISS strategic dossier, 2007.

ⁱ The IAEA’s latest status report listing those States who have signed or ratified the Additional Protocol can be found on its website at www.iaea.org/OurWork/SV/Safeguards/sg_protocol.html.

But the remaining issue is that the NPT is in a key respect de facto discredited. From the start, India openly defied the pressure to join, developed and tested weapons, possessing and developing enrichment technology and plutonium producing facilities (some diverted from peaceful research purposes after being supplied by the United States and Canada). A cynic would argue that because of its recent economic performance, global role, and trade growth, it is now “forgiven” in the sense that new Agreements are being written to allow the export of nuclear reactors and fuel to India to supply its industries and grid. The side agreements are not yet finalized, but aim to separate the weapons and civilian uses and facilities—but the truth is that India has won by ignoring everyone and the NPT. The example or model has been set—go your own way, ignore the NPT, become successful, be a key global commercial player, and be forgiven. The reason is simple: the non-proliferation club members can make money by selling nuclear reactors, natural uranium and enriched fuel to India, so the Club’s commercial interests prevail while at the same time the Club is pretending to control Indian access to nuclear materials. The cobbled up agreement is therefore a sham. The Indians argue that they were forced to proliferate by the challenges and threats they were subjected to by China and Pakistan. (This argument is not quite consistent with the normal Indian position that they are in principle opposed to the discriminatory nature of the Treaty. Nor is it entirely propaganda.) A careful reading of the Indian program shows them stalling development for a long time, until the threats from China and Pakistan tipped the balance, with the United States refusing to back or protect them against these two, while at the same time funding the Pakistan program (Moreover Pakistan is strictly speaking not a weapons state, as defined by Article I of the Treaty, as it is not a member of the Treaty!)

This is the nub of the problem- we have “declared” and “undeclared” weapons states, and different “rights” claimed as a result.

We also have the Christian Bomb (United States, France, and United Kingdom), the Communist Bomb (Russia, North Korea, and China), the Jewish Bomb (Israel), and the Hindi Bomb (India). It is not surprising that there has been persistent pressure for a Muslim Bomb.

This “cynical” view is not new or even eccentric. Throughout its history there has been a persistent conventional consensus that the NPT has failed, or that it is on the verge of failure, or that an inevitable cascade of proliferation following the diffusion of technical know-how will cause it to fail. But the real world has presented very little evidence in support of this consensus. For example the rate of proliferation peaked in the 1960s before the entry into force of the Treaty, and then declined over the next 30 years. The percentage of countries which acquired nuclear weapons is only about 25% of those who could have because they considered, inherited or acquired a nuclear option, but decided in the end to remain non-weapons states. Fewer countries are today seeking nuclear status than at any point since the end of WWII. The international safeguards system is not perfect, but it has achieved much since it was first introduced. It evolves in a positive direction with ever increasing support.^j

Meanwhile global stability and non-governmental threats exist, in the form of Islamist pressure spearheaded by the Taliban in the North West Frontier Province and numerous groups elsewhere (notably ISIS/ISIL, Al Qaeda, etc.).

17.2 Nuclear history and basic science

So far we have concentrated on the political issues presented by the division (in Articles 1 and 2 of the NPT) of the world into states which have and those which do not have nuclear weapons, and hence enrichment capacity for nuclear fuel production and sales. It is worth setting out why this is not simply a matter of political choice.

^j For a sophisticated account of the effects on policy of NPT membership see “Learning from Past Success: the NPT and the future of Non-proliferation”: Jim Walsh, for the Weapons of Mass Destruction Commission, 2005. See also Etel Solingen: “Nuclear Logics.”

The so-called “critical mass” for a bomb is reached when the chain reaction of fissions is so self-sustaining it becomes explosive from producing so much energy from fission so quickly as to vaporize the materials. Nuclear reactors are not designed to explode, and although they contain enough material for criticality (a self-perpetuating chain reaction) the rate of increase in neutron number (and hence, power) is controlled by poison rods that absorb neutrons, and by over-power trips and shutdown devices. The “reactivity margin” for the fuel is has design limits on the core configuration and the enrichment.

While the Second World War was under way, making the atom bomb first was a target for both the Allies and the Axis powers. It was perceived as a matter of survival. A huge effort was therefore put into the Manhattan Project, launched in March 1942 by the United States and its allies, which demonstrates a key facet of the problem. The Atom Bomb came first; civil nuclear power came later. All subsequent efforts to develop nuclear weapons have done so through dedicated weapons programs, quite separate from attempts to achieve electricity generation (see below).

Anyone seeking to produce nuclear weapons today has to follow one or both of the Manhattan routes, and the technologies have of course been refined and improved. Gas-centrifuge based separation of the uranium isotopes is a far more efficient technique than the electro-magnetic induction and gaseous diffusion based separation used in the Manhattan project. To manufacture reliable centrifuges is not easy. They have to be engineered to the precise tolerances necessary, require spinning at very high speed, use special tube materials, and are connected in what are called cascades of many thousands of centrifuges. This is the technology of choice today, and three more plants are now being built (in Europe, United States, and Japan) to produce nuclear fuel.

These details are fundamental. They have a major bearing on the nature of the threat of nuclear proliferation and on the measures taken to prevent it. An efficient (i.e., small) uranium bomb has in practice to contain around 93% U^{235} . Likewise, the plutonium weapons in the arsenals of the weapons states are over 90% Pu^{239} . The cleverest weapons designers employed at Los Alamos claim (controversially) that it is possible to create a weapon of some sort from any isotopic composition of Plutonium, and an inefficient bomb from uranium above around 20% enrichment. As they also admit this would certainly be inferior to using virtually pure Pu^{239} , and advance calculation of its effects would be much more difficult, the weapons states have in practice stuck to the latter.

To manufacture weapons grade material in sufficient quantities for an “efficient” (read high explosive) yield is a major industrial operation. It requires the level of technical attainment and the resources of a nation state. In the face of modern satellite observational technologies it is not so easy to hide the fabrication plants, though underground siting is obviously preferred and is known to occur.

It was not entirely a coincidence that the first Five Weapons States were the five permanent members of the Security Council!!!

17.2.1 Commercial nuclear power

The proliferation problem arises from the fact that power reactors, research reactors and nuclear weapons programs make use of the same applications of nuclear fission, and require the same skills. But in very different degrees, as well as to very different ends. The problem is becoming more acute, as after 30 years of hesitation and stagnation the civil nuclear power industry is on the threshold of a worldwide revival, with many “new” countries examining adopting nuclear energy (e.g., UAE, Jordan, Egypt, Malaysia, Saudi Arabia, Chile, Turkey, South Africa, ...) and others expanding (e.g., China, Russia, India, ...), while some even contract (e.g., Germany, France, Japan, and United Kingdom). This prospect has understandably fuelled renewed concerns about an increased danger of nuclear proliferation. However, we shall show below that proliferation does not arise from commercial power plants.

In contrast to the very high levels of uranium enrichment required by weapons programs, power reactors use either natural (un-enriched) uranium as the basis of their fuel, or relatively low levels of enrichment—up

to about 4%. Similarly with plutonium the isolation of pure Pu²³⁹ required for successful weapons design is not a priority for plutonium use in breeder reactors or for its recycling as Mixed OXide fuel (MOX) for use in current thermal reactors. The resultant fuels are not bomb material, and cannot be used directly for weapons production. However, the processes which are essential for the enrichment of uranium, or for the separation of plutonium from irradiated fuel are essentially the same in both civil and military applications.

The main differences lie in the length of time the processes continue: enrichment to weapons grade takes much longer; in contrast, the extraction of pure Pu²³⁹ has to take place very soon after irradiation with neutrons begins. In both cases “criticality” issues have to be taken into account: in other words precautions have to be taken to avoid the accumulation in a single vessel of a sufficient quantity of the fissile material that would permit a chain reaction (and therefore a burst of neutron discharge or even a spontaneous explosion) to occur.

In the 50 odd years of nuclear power generation since the opening of Calder Hall in 1956 *there has not been a single instance among the NPT's member states of diversion of nuclear material from the power sector to potential military ends.* The main reason is obvious. Light Water Reactors (LWRs) are some 80% of those in operation, are designed only to be fuelled when they are off-line—i.e., not generating electricity, and have been mainly located in countries with weapons stocks and enrichment technology (e.g., United States, Russia, India, France, and China) or have disavowed its use (e.g., Japan and Canada).

The cases which have given rise to so much anxiety in recent years—Iraq, Libya, North Korea, now Syria and Iran—are all countries, **which originally do not have nuclear power in operation**, though Iraq and Iran have both set out down the road of building civil nuclear power station systems. In practice all of them had and have research reactors in nuclear research establishments, which have been subject to safeguards. It has been an objective in all these cases to present a compliant front, and only when the façade could no longer be maintained has a public international row developed about those countries' observance (or lack of it) of their safeguards obligations.

India and Pakistan are awkward exceptions to this on the whole favorable narrative. But neither is a member of the NPT, and both have maintained consistent opposition to it from the outset, on the true grounds that it is *discriminatory*. India has recently signed on to a Nuclear Cooperation Agreements (NCAs) covering their civilian program, and this is directly related to the fuel cycle. Without indigenous uranium supplies, that must rely on imported fuel (and also LWRs) until their own thorium cycle is established. Both India and Pakistan made use of installations that were originally presented as civilian power stations to develop nuclear weapons. India has however (as explained above) now negotiated an accommodation with the international system in order to overcome bottlenecks caused by its isolation, and Pakistan, under US pressure, has abandoned the proliferating practices of Dr. A.Q. Khan, primarily for political reasons, which have little to do with nuclear policy.

17.2.2 Present situation and issues on research and sustainability

The Indian and Pakistani tests in May 1998, created a great formal problem for the non-proliferation regime. Paradoxically, they cannot now join the NPT, unless they abandon their weapons, of which there is no sign, either as weapons states or as non-weapons states. It remains to be seen whether the deal that India has struck with the Nuclear Suppliers Group led by the United States will cause the NPT bargain of 1968 to unravel. After all the integration of India, a nuclear-armed state, into the system in this way reduces the value of the benefits supposed to be received (under Article II–IV of the Treaty) by the NNWS as a result of their abandonment of the weapons option. The alleged development of “weapons of mass destruction,” meaning primarily nuclear weapons, was one of the principal overt excuses for the invasion of Iraq in the spring of 2003. Others have also been accused (by the United States) of harboring such designs: Libya, North

Korea, most recently Syria, and above all Iran. It is notable that none of these has a working power reactor until the Russians completed one reactor at Bushehr in Iran and brought it on line, just 37 years after the Deposed Shah gave the project the go-ahead. The new US/EU/UN/Iran Joint Agreement leaves Russia poised to supply and complete more units sometime after 2015, and may even have been approved with different terms by Iran, who-like North Korea- also persist in pursuing “peaceful” rocket launch development.

But there are some obvious points of weakness and even danger in the system.

17.2.2.1 Research for advanced reactors

Research reactors have been mentioned several times already as sources of weakness and known proliferation in the system, and of course are used to develop Generation-IV and AR concepts, materials and fuels. They are of course included in a member state’s full scope safeguards declaration to the IAEA, and therefore subject to inspection. How frequently depends on the nature of the material they contain. Unlike power reactors, which are large-scale well-protected industrial installations, research reactors are usually situated in academic institutions as one part of their scientific installations. They are much softer (easier) targets for theft of nuclear materials than power stations. Security is often lax, and if for example (as it often is) the research reactor is an open pool reactor physical protection is minimal compared with a massive pressurized power reactor. In the early days of the atomic age the enrichment of the research reactor fuel was high, comparable with bomb material. In the past 20 years however, the United States, backed by Russia and Britain, has campaigned with some success for the modification of these research reactors so that they use uranium enriched to less than 20%. However, there are still about 120 fuelled with so-called “weapons grade” HEU, as the United States pursued a policy of repatriating as much fuel as possible, by paying for it and its replacement.

But it is clear that in a world where we may expect more, not fewer, research reactors, and medical isotopes, and fuel production, a new attitude is needed.

Nuclear reactor development and deployment entails expansion also of the fuel cycle: after all that is the driver and enables energy security and independence, without greenhouse gas emissions. World nuclear use will grow as energy demand, economic needs, environment issues and supply security concerns grow. So the race is on to secure nuclear fuel supplies, particularly uranium for short term, hence large price increases (good news, up to a point, for those with resources.).

17.2.2.2 Commercial fuel supply

There is a major unspoken issue: supplies of uranium ore at reasonable economic prices are finite. This tends to be denied by uranium suppliers, who—just like the oil and gas producers—rightly assert that there is no shortage of supply today for the present, but omit to mention the price it will cost and what will happen if demand grows by a factor of 10, as it could. Drivers for increased demand are increasing need for energy security, and price changes in competitor fuels, coupled with climate change needs and concerns. With over 400 reactors operating today, present world demand is $\sim 70,000$ tU/a. A tenfold increase would give an upper bound estimate of demand for 4000 reactors needing $\sim 700,000$ tU/a by 2050. The present 400 reactors could be kept going for another 150 years, but that would leave a shortfall of over 3000 reactors (or some three-fourth of the postulated need) in the near foreseeable future.

Today’s estimates of identified reserves are about 5 MtU recoverable at a cost of $< \$130/\text{kg}$. Even allowing a doubling or tripling of this estimate to, say, 10 MtU, just 1000 reactors operating for 60 years will consume all the world’s cheapest uranium (in about 60,000 reactor operating-years) with present fuel cycles technology. So, as uranium producers say, there is no present shortage, but there is a long-term point of danger.

There is an unofficial “Nuclear Fuel Cycle Club” (United States, France, Japan, Russia, EU, and United Kingdom) who currently possess enrichment technology (and most of them nuclear weapons too). Under the banner of “non-proliferation” these same present uranium enrichment technology owners would restrict

others' access to enrichment technology. (See the most recent agreement between the United States and Abu Dhabi.^k) After first using all of today's cheap(er) uranium, these same nations (Japan, United States, France, and Russia) openly say they would deploy plutonium-fuelled, hopefully self-sustaining, "fast" reactors, whose design, technology and commercial exploitation they would also control. Those countries, such as those in the Club with large fuel reserves, favor "Regional Fuel Centres" which carve out the world, and which de facto they wish to control.

17.2.2.3 Alternate fuel cycles for advanced reactors

Those without large uranium reserves favor alternate Thorium cycles (India, China, Turkey). Moves to restrict acquisition of enrichment and recycling technology have recently included efforts by the United States to define "Fuel Cycle Nations," and form a Global Nuclear Energy Partnership (GNEP) (US DOE, 2007). So attempts to form energy policy, to influence global and national alliances, and simple economic and commercial pragmatism are now all intertwined with the NPT.

Unfortunately, not only are the present efforts and aims misdirected, there is a major issue of unintended consequences. The past inconsistent and selective use of the non-proliferation banner to further foreign policy and security aims has both been ineffective and given the admirable aim of non-proliferation of nuclear arms a bad reputation as a cloak for cynical political interference in other nations' internal affairs.

There are some other main points of danger.

The possibility that hitherto non-nuclear countries may soon acquire nuclear power stations is a neuralgic issue for the Greens. However, the further construction of power stations is not the real issue. The US Government may have pressurized Siemens not to proceed with the construction of the power station at Bushehr after the fall of the Shah in 1979, but now all the major players with the encouragement of their governments are seeking to gain contracts for the construction of power reactors round the globe. As the controversies over Iran (and to a lesser extent North Korea) and the proposed Agreements decisively show, the real proliferation fear is the fuel cycle.

Firstly it is more difficult to police than power stations, and more difficult to separate in the public mind as the processes for fuel production and for bomb material have elements in common. Secondly, as the history of the Dr. A.Q. Khan's network shows, would-be proliferators have so far aimed at procuring their essential materials and equipment afresh. In other words they have attempted to exploit the weaknesses of the export control regimes of potential supplier states rather than to steal existing machinery and material.

The two most obvious points in the fuel cycle at which proliferation could take place are enrichment of uranium and reprocessing of spent fuel. To do either on an industrial as opposed to laboratory scale requires huge and expensive establishments. The earliest such establishments grew out of the needs of the weapons programs of the weapons states, but when the civil power programs of the developed world required greater supplies of enriched uranium fuel expansion programs got under way. The United States has persistently argued that such production facilities should be in the hands of existing weapons states, and has over the years fought a rearguard battle against the establishment of enrichment facilities in other countries such as Brazil and Japan. Iran is just the latest example.

17.2.2.4 Enrichment

Enrichment is just one, albeit the most sensitive, stage in the transformation of the refined ore (i.e., yellowcake for uranium) into fresh fuel. The enriched uranium oxide has to be fabricated into fuel to fit the reactor design for which it has been ordered. In many discussions of the problem of proliferation control the fact that nuclear fuel is like a bespoke suit tends to be overlooked. The fuel fabricator has to take account of the precise degree of enrichment specified by the reactor operator and to set the fuel in assemblies that will deliver the

^k Signed 17 January 2009.

most efficient neutron flux for the reactor management's needs. One should not of course exaggerate the difficulties that this causes, but it is a weakness of calls (such as Senator Nunn's and others') for international fuel banks that they ignore it. Commercial interests of course dominate—the fuel cycle is where money can be made. So Russia offers an “international” fuel bank, using of course Russian fuel.

It is clear that providing “black box” or “sealed” enrichment technology will be possible, provided the supplier retains all the technology rights and the plant is inspectable. This does not seem to be the preferred approach of the present centrifuge owners, who wish to maintain their monopoly for commercial reasons and to own and operate their own plants and not to license the technology. This approach can actually encourage proliferation. If a nation wishes to achieve energy independence and policy freedom, then they *cannot* allow other nations to control their energy supply. And use this as a political lever. The client-customer basis has to take into account the market place realities, not just the political-commercial interests and overtones. If not, the nation will decide to “do it themselves,” whatever the cost (as the Iran, India, Pakistan, North Korea and other cases demonstrate).

17.2.2.5 Reprocessing and recycling

An alternative fuel cycle is to reprocess irradiated fuel with the aim of separating the plutonium 239 or Thorium 233 it has created from the rest of the material. Again this is a technique that has been in use since the beginning of the nuclear age, and one embarrassing consequence of this was the creation of large stockpiles of separated plutonium. The present practice of combining plutonium oxide with uranium oxide to make MOX is a relatively recent development. In a period of cheap and plentiful uranium there has been little or no economic incentive to use MOX, as it is more expensive. Even with much more expensive raw uranium there is still little incentive, as handling MOX in a reactor is more complicated than straight-forward fuel made of freshly enriched uranium.

If a “nuclear renaissance” does take place these proliferation points of anxiety in the fuel cycle will increase. Countries outside the present limits of the nuclear power world will enter it, perhaps at a much slower rate than current hype suggests. But the struggle of the Iranians to realize an ambition that goes back to the Shah in the 1970s will have its imitators in many other countries in the developing world. The issues are not simply technical. They are also political and commercial. It is clear that on a technical level an entrant county is not well placed to develop all stages of the fuel cycle at the same time. Nor is there any commercial incentive to do so. Autarky is a very expensive policy, even when it seems to be the only answer to political pressures. Iran might do well to take note of recent statements by USEC, the world's largest enrichment company with the widest customer base complaining of the difficulties of financing the centrifuge enrichment plant it is currently building, and its reported difficulties in obtaining Department of Energy financial support.!

It is a given, as mentioned above, that within each state the state has the duty of making sure that none of its citizens is breaking the law, and indulging in proliferating activity or actions that can be construed as likely to support proliferation. For the first few decades of the Treaty's existence this was a reasonable assumption, but the world has changed. Terrorists bring a new aspect to the whole story.

Terrorists are not the subjects of the NPT. They are not “states parties” but renegades who do not follow the “rules,” the niceties or words of a Treaty. They represent a threat to what is called “physical protection” aspects of non-proliferation, the “guns, guards and gates” mentality of the military, security and sanity. This aspect is dealt with by spending vast sums on clearances, background checks, identity tags, detection equipment, controls, procedures, scanners, and such, of the type so familiar in airports. But terrorists are really interested in attacking and dislocating high profile and payoff “soft” targets, not defended ones. The aim is, as in the military war, the supplies, infrastructure, communication and soft underbelly of the opponent. Nuclear systems and sites are already “hardened,” resistant to terrorists, unless a real whole scale nation-to-nation war breaks out.

The mechanisms of the Treaty are not well adapted to limiting the opportunities of opposition or terrorist groupings. By definition the first line of defense against them must be the member state whose installations are targets for the postulated subversive activity.

17.2.2.6 Future policy implications of nuclear fuel cycles

Major anomalies exist at present, being two declared nuclear-armed states not listed in Article I: India and Pakistan. Israel keeps its own counsel generally, but is universally regarded as a nuclear-armed state, and the fact that it is provokes tension throughout the Middle East. Iran is widely suspected of pursuing nuclear weapons under cover of developing civil nuclear power, and North Korea pursues a strange weaving path, which has included two underground nuclear test explosions, the first of which was probably a failure.

The Treaty has no real means of dealing with any of these anomalies. It makes the benign assumption that its member states will obey its rules; there are no provisions for punishment if they do not do so, or if any of them decide to leave the Treaty. Such sanctions have to be sought elsewhere, for example at the UN Security Council. Or through the determination of one or other of the superpowers, in practice the United States.

US policy toward India, North Korea, and Iran has been violently inconsistent as it is not governed by any obvious principle apart from expediency, and a desire to maintain US supremacy by whatever deal seems locally appropriate. The latest deal with India is a good example of the pragmatism of US policy. The nuclear isolation of India following the 1974 nuclear test had outlasted its usefulness. After the 1998 tests some means had to be found of bringing India into the international non-proliferation system. The deal that has been struck separates the civil from the military sector in a way not dissimilar to what prevails in the acknowledged weapons states; it also provides the United States (and other keen nuclear exporters such as France) with an entrée into the rapidly expanding Indian civil nuclear construction scene. While there is a now significant constraint that did not previously exist on India's freedom of action—the cause of much political difficulty in India—the benefit to India is access to the international fuel market and to the international construction market denied her for over 30 years. As isolated India's nuclear progress was much hampered by shortages of indigenous uranium and other bottlenecks the price seemed worth paying. In 2005 the Indian Government tacitly recognized the great disadvantages of this isolation by seeking an agreement first with the United States and then with other prominent members of the nuclear suppliers group, which would put an end to it.

As to North Korea, two whole nuclear reactors now lie in store rooms in South Korea, the United States having abandoned of building of them in North Korea by US contractors as failed “compensation” for giving up on their weapons program.

Taking the long view, it is possible to argue that in some respects the pragmatism of US policy has been more successful in restraining the rebels than adherence to the orthodoxies of the international non-proliferation system.

US policy toward Iran has been the exact opposite of its policy toward North Korea—initially refusing to build the sort of reactors which have been promised to the North Koreans as compensation for dropping their ambitions to have a nuclear weapon. This inconsistency may have contributed to Iranian intransigence. It also gave the Russians more than one unexpected export opportunity. Iran's intransigence has been intensified by the US use of sanctions (just as Saddam Hussein's defiance was in the 1990s), and has not been eased by the EU's attempt to mediate. Whereas North Korea was a comparatively isolated problem, Iran is embroiled in the Middle East crisis generally, the Arab—Israeli dispute, the continuing travail in Iraq and Afghanistan, and more important than any of these, Iran is an oil rich nation which is much less subject to economic pressure than the comparatively poverty stricken North Koreans.

Israel cannot be ignored altogether, although many discussions do just that. But whether or not Israel has the nuclear weapons usually accredited to her, she is unlikely to be a proliferator. She acquired the necessary materials and skills for her weapons program well before the NPT became the cynosure of arms control treaties that it is today. Her existence as a presumed weapons state is a serious lump of grit in an otherwise smooth system. It causes not only oceans of rhetoric, but also misplaced ambitions by other Middle Eastern states to match this presumed status, and is thus a weakness in the NPT system. Whether it is a direct threat to it is less clear.

17.3 A look at the future

This previous review of the present situation explains how we got to where we are, and points out areas of difficulty and weakness, even danger, in the present situation. But apart from the current usual global crises there are at least three explosive issues which will challenge the comfortable assumptions of the supporters of the NPT and affect the deployment of Advanced and Gen-IV Reactors on a global scale.

These are, firstly, the increasing recognition of the value of civil nuclear power as a possible means, perhaps the only effective possible means, of replacing hydrocarbons as our prime energy source, if we are to make inroads into combating the threat of global warming. For this to work the deployment of nuclear energy has not only to be at least 10 times its present deployment. It has also to penetrate the world outside the OECD countries on the same massive scale.

If the threat of Global warming seems too far off to warrant such a spectacular shift, secondly, security of energy supply has at last been recognized as a major desideratum. Those countries with indigenous energy resources have an economic advantage over those without, but the majority of the world's population resides in areas of relative energy poverty. They must rely on imported supplies of coal, oil, gas and nuclear fuel for now, but obviously will be looking at alternate fuel cycles and recycling as necessary means of supporting economic, national and political survival.

Thirdly, two thirds of the projected rise in energy demand over the next 50 years will be in this developing world and their huge populations. Faced with declining (and ever more expensive) oil and gas supplies developing countries will not wish to be excluded from the possibility of acquiring large scale installations of nuclear energy, as one can see from the rash of announced plans to build nuclear reactors in many countries which so far have never had them. Even oil rich countries such as Abu Dhabi and Iran are in the forefront of such schemes.

To satisfy this demand in the medium and long term is impossible if the world remains restricted to the once through cycle.

A transition through Generation-IV designs to a wholesale adoption of breeder reactors is thus inevitable.

17.3.1 Alternate fuel cycles

For those without access to large uranium reserves, or needing energy supply surety, a new Alternate Cycle (AC) is needed that will ensure sustainable supply and smaller waste streams. There should be a more intrinsically proliferation-resistant cycle, with no significant Pu generation, thus not requiring all of today's policing and international stress. It also must not require introducing a new reactor technology, and acknowledge the ownership and deployment of U-enrichment technology as a proliferation concern while still allowing vastly expanded reactor builds.

Such a fuel cycle is available now, using Thorium, which is more globally plentiful (perhaps 3 times more) than Uranium, and so could meet the medium-term future need. With careful fuel design and recycling, a thorium reactor would give a near breeding cycle, and so is more sustainable with much lower (up to 10 times

less) waste amounts and storage needs. This Thorium-switch would enable more reactor deployment using today's reactor technologies and help stabilize fuel cost and supply, and avoids having to introduce many fast reactors.

Such an AC path is already being explored (e.g., notably by India, Norway, China, Canada, and others), with the transition to a near self-sustaining predominantly thorium-fuelled cycle being initiated by burning Pu as the start-up fuel. The cycle thus reduces Pu inventories/stocks during transition to a primarily Thorium near-breeder cycle using separated U^{233} .

This transition is real and could totally alter the global fuel cycle and reactor deployment opportunities. In fact, some of India has already chosen to develop this AC route as a national priority. Such AC concepts are in fact not new; what is new is the concept that an alternate sustainable and closable fuel cycle may enable greater benefits to be gained from nuclear energy deployment worldwide.

Because of inherent technical characteristics, of D_2O moderation and distributed channels with flexible fuelling, HWRs have a great deal of fuel cycle flexibility and this has been the subject of significant R&D by AECL, and others. The combination of relatively high neutron efficiency (provided by heavy water moderation and careful selection of core materials), on-line fuelling capability and simple fuel bundle design mean that HWR reactors can use not only natural and enriched uranium, but also a wide variety of other fuels. These include:

- (a) recycled uranium;
- (b) thorium-based fuels with U^{233} recycle (see above);
- (c) minor actinides "intermediate burner";
- (d) MOX fuels; and
- (e) recycled LWR fuels.

17.3.2 Advanced reactors and the NPT

In the future, beyond say 2030, the aim will be to provide highly efficient AR concepts, such as the use of Gen-IV systems, which can couple thermal efficiencies of some 50% using a proliferation resistant thorium cycle with a near-breeder cycle. In addition, this advanced concept lends itself to indirect and direct hydrogen production, which can be coupled with a power grid, which then allows a greater usage of wind power. This in turn leads to wider deployment of nuclear energy. The development of criteria for assessing the proliferation resistance of AR systems has been proposed (GIF, 2011, 2014).

Against this projection of demand and the likely ways of satisfying it, the worldview of the NPT seems hopelessly restrictive. It is questionable that what made good sense when nuclear technology was confined to a few countries (primarily the weapons states, but also including a raft of allied or client states who were content to let the weapons states take the lead, in most of whom it was still very much a minority supplier of energy) could be extended without modification to a scene in which civil nuclear power is the energy of choice of most countries, because the obvious alternatives (coal, oil, gas) are becoming unavailable, or impossibly expensive, or unacceptably polluting. For example, the air in Beijing has become so bad that all industry in the region had to be closed for 2 months so as to purify the air which the¹ competing athletes were going to breathe during the 2008 Olympic Games!

As mentioned earlier economic and commercial factors lie behind the unwillingness of the have-powers to spread the rewards of the fuel cycle more thinly. It has been convenient commercially for the weapon states to argue that the possession of enrichment or reprocessing plants should be confined to the existing weapon states. But the practice has never been pure. Germany and the Netherlands (both NNWS) have enrichment plants tied by the treaty of Almelo to the United Kingdom (a Weapons State). The United States has had to

¹ Sharon Sassquoni: Looking Back: the 1978 Nuclear Non-proliferation Act; Arms Control Association December 2008.

accept that Japan and Brazil should now operate commercial enrichment plants. The US rearguard action to defend its fraying monopoly was undermined originally by its inability to supply what it had contracted to its customers during the first great expansion of nuclear power in the 1970s, and by the great superiority of the URENCO centrifuge technology over their old gaseous diffusion plants at Piketon and Paducah. But commercial centrifuge plants are very expensive—even USEC still the largest enricher in the world has run into financing difficulties arising from the huge cost of building its new centrifuge plant—and make little sense in economic terms until a country can provide sufficient customers for their output.

The same is true of reprocessing plants, which are even rarer in a world that is still wedded to the once through cycle. Originally the aim of reprocessing was to provide Pu suitable for weapons use (see above). It then became a possible way of reducing the volume of spent fuel a.k.a. high-level waste. More recently a number of technologies have been developed to enable reuse of the energy-rich components of spent fuel. The most obvious of these is Mixed Oxide Fuel (described above), which also has the advantage of being a way of reabsorbing the separated plutonium that had already accumulated in some countries. Other processes have been tested in the laboratory, but not yet on a commercial scale, whereby the plutonium is not released on its own, but only in conjunction with other fission products. These would make it unusable as a source of weapons material.

Underlying all the above discussion is the assumption that it is not in our interest generally, and not in the interests of the civil nuclear supplier companies (see next section) regardless of whatever point of the nuclear fuel cycle they operate at, that there should be an increase in the number of weapons states. Ideally there should be fewer. This was the main motive for introducing the NPT in the first place, and it remains the obvious driving force to continuing with the international safeguards system, improving it where possible. The fact that there has not been any practical use of a nuclear weapon since the Treaty came into force should not make us complacent. It is difficult and invidious to argue that some countries are more “responsible” in nuclear matters than others. The factors which have made the present weapons states “responsible” have little to do with the NPT, though peer group pressure has played a role, as it is clearly in no-one’s interest that a country should run amok brandishing nuclear weapons.

The civil nuclear industry which wishes to profit from the so-called nuclear renaissance, and those who would promote the substitution of nuclear power for the declining attractions of the hydrocarbon-based economy have a duty to ensure that the separation of the benefits to civil society of civil nuclear power from the temptations of nuclear arms are maintained. Systems of control are not impossible to devise and are significantly easier to monitor than reductions in CO₂ emissions through so called carbon trading, which has become the fashionable nostrum in the face of public fears of global warming. A more certain route to this end is to substitute fission for combustion as the principal form of energy production.

It will be easier to achieve acceptance of this if more progress is made to bring the original bargain of the NPT to fruition. In this regard the initiative of the British Foreign Secretary in February 2009, a move clearly coordinated with Washington, in launching a campaign to make progress on Article VI before the next review conference of the Treaty in 2010 is commendable. It goes some way toward providing a way to retreat from the less defensible decision of the last British Prime Minister, just before he left office, to launch renewal of Trident, the British submarine based nuclear deterrent.

17.4 The wider context

In conclusion, it is worth reminding ourselves that nuclear power does not exist in a vacuum. It is one of many ways of generating electricity. Compared with its competitors it has a number of characteristics, which add up, in the eyes of its supporters, to a compelling advantage over those competitors:

- It is a large-scale base-load generator. After half a century’s experience it is a reliable mature technology;
- The fuel is amazingly energy-dense. 1 kg of uranium has the energy equivalent of 17,000 tons of coal. Stockpiling the fuel or the raw material from which it is made is easy and takes up minimum space;

- Uranium ore bodies are mostly in stable countries (Australia, Canada, etc.);
- Transporting yellow cake or fabricated fuel is low cost, small scale compared with coal or oil—a year’s worth of fuel for Sizewell B barely fills the equivalent of one floor of a double-decker bus;
- Its “carbon footprint” is minuscule compared with most of its competitors, including wind;
- Existing known reserves are sufficient for the next half century’s projected use. More will undoubtedly be discovered as the element is omni-present in the earth’s crust (2–3 ppm) and existing known ore-bodies are the fruit of the last great expansion of nuclear power in the 1970–80s. In practice they were far more than sufficient to fuel what was actually built, leading to a slump in U prices which lasted until 2002. The recent spike in U spot prices has led, as one would expect to a revival of exploration and the first steps in the development of new mines;
- But even without dramatic new discoveries of ore bodies, the generating technology is poised (and has done the groundwork for) a number of great leaps in the efficiency of fuel exploitation. The first is straightforward recycling of spent fuel in thermal reactors, using MOX or DUPIC. The second is Generation-IV designs. The third is a return to the fast breeder, which in principle can extract all the latent energy in uranium, 97% of which remains in spent fuel from the once-through cycle used today. These advances in energy efficiency (a great clarion call of the antinuclear Greens) will be comparable to the improvements between James Watt’s first steam engine (1% efficient) and modern generating turbines, some 35%–40% efficient even before the introduction of Combined heat and Power techniques.

So why is it not an open and shut case? Basically public hostility, because of:

1. Fear of nuclear weapons—though one of the aims of this Chapter has been to show that these are two separate technologies which the international nuclear non-proliferation system has been spectacularly successful in keeping apart;
2. Fears about the safety of the technology especially after Chernobyl—the industry (coming from a very secretive, even hermetic culture) has been very incompetent in rebutting the wilder fears, or in developing reassurance^m; and
3. In a world of plentiful cheap fuels nuclear seemed (and was) expensive and inflexible;

But in a world facing an impending energy crisis because of surging demand exceeding supply, and awareness of the ill effects of carbon emissions from hydro-carbon based fuels the balance of advantage for nuclear power looks quite different.

It is therefore vital for the future of nuclear generation, as a means both of combating “global warming” and as a part of the answer to the cycles of “peak oil” and “cheap gas” (which should be the subject of another full paper), that the international safeguards system should be maintained and improved. The improved version should command public confidence. Extending it without those improvements, and without solving the problems posed by Iran or North Korea described above, may not command the public support necessary for it to function effectively.

It will also be vital for the preservation of the advanced technological civilization that we all enjoy, and even aspire to, that nuclear power (despite the misgivings of some) does expand into the vacuum left by the forthcoming retreat of oil. The eagerness with which oil-rich states like Iran and Abu Dhabi are striving to establish nuclear power in their territories is not based primarily on a covert desire to become weapons states, though they may flirt with that idea too, but on their need to survive the demise of oil.

As part of the bargain with the NNWS the weapons states committed themselves in Article VI of the Treaty to work toward divesting themselves of nuclear weapons, and toward complete and universal disarmament.

^m The two totemic disasters of Chernobyl and Three Mile Island were the result of incompetent practice in two experienced nuclear countries: to spread the technology to new countries inevitably gives rise to nervousness. But consider the record of South Korea over the last 40 years.

As adumbrated earlier, for the first 20 years of the Treaty this was little more than a pious ambition. The Treaty reflected the reality of superpower relationships, and was not itself the motive force behind their development. Both the superpowers piled up colossal quantities of nuclear weapons in what was eventually admitted to be a futile attempt to intimidate each other.

With the change of regime in Washington this has been recognized there. One of President Obama's first foreign policy initiatives has been to call on the Russian Government to revisit the START Agreements and take them further, suggesting that neither superpower required more than 1000 warheads, a reduction to about a third of what they at present deploy, and that it should be a priority task to come to an agreement of the modalities of making such a reduction.

The minor weapons states (Britain, France and China) have shunned the limelight and have usually said little about their levels of nuclear armaments, but these are measured in hundreds rather than thousands.

Discussion of the politics of the weapons states tends to concentrate on the United States and to some degree on Russia. China maintains a very low profile, often siding with the Russians, e.g., over discussion of possible sanctions against Iran, provoked by Security Council discussion to state a position. The British and French keep very quiet about their own nuclear armaments, but both, especially, the British tend to echo US positions on avoidance of proliferation. The position of all three is influenced by extraneous factors and their perception of their own fundamental national interests: the Chinese have strong oil import links with Iran; the French were certainly influenced by the contracts they had established with Saddam's regime in Iraq in opposing US/UK plans for invading Iraq in the Spring of 2003. There is nothing surprising in this: the NPT was created after all as a means of codifying the national interests of the nuclear powers that supported it.

The NPT remains the main instrument for achieving a framework that would and should allow peaceful deployment of ARs, but as we have noted the Treaty has some major shortcomings that need to be remedied if it is to remain useful and effective in the longer term.

Finally, the dangers of Global Warming and climate change have done much to change the public perception of nuclear power and the use of Plutonium and other fuel cycles. The civil nuclear industry believes with good reason that it has much to offer by way of mitigation of climate change. If it is to take its rightful place as one of the principal means of our reducing man-made greenhouse gas emissions it will be vital to reinforce the message to the public that the spread of civil nuclear power to regions which up to now have not had it and the deployment in the medium term of large numbers of breeder reactors can be done without increasing the dangers of nuclear weapons proliferation. The civil nuclear industry knows that a necessary condition for carrying the public with it is the continued existence of a respected and effective international safeguards regime.

Any great expansion in nuclear power stations will lead inexorably to the implementation of advanced fuel cycles, including thorium and the breeder economy. The IAEA supported by the industry will have to devise systems of safeguarding that give similar security in that context as they have achieved for the once-through cycle. It will be obliged to do so because of global warming and peak oil, because no-one will wish either to lead to nuclear war. To achieve this, the Agency will need vastly more resources and trained personnel. Strengthening the IAEA would also reduce the tendency of powerful players to use their weight to bully mavericks or to exert illegitimate commercial pressure.

17.5 Fuel cycles: Sustainable recycling of used fuel compared to retrievable storage

17.5.1 Introduction: The cost of not burying the past

Using fuel just once, irradiating for a few years in a thermal reactor to say 30,000 to 50,000 MWD/t, leaves about 99% of the fertile material (U^{238}) unused, and some equivalent 30% or more of the original fissile material (U^{235}) still available. So it is widely known that reuse of the fuel to extract more energy and reduce waste makes technical sense. The fuel goes in at a few % U^{235} , and comes out as "spent" while still containing

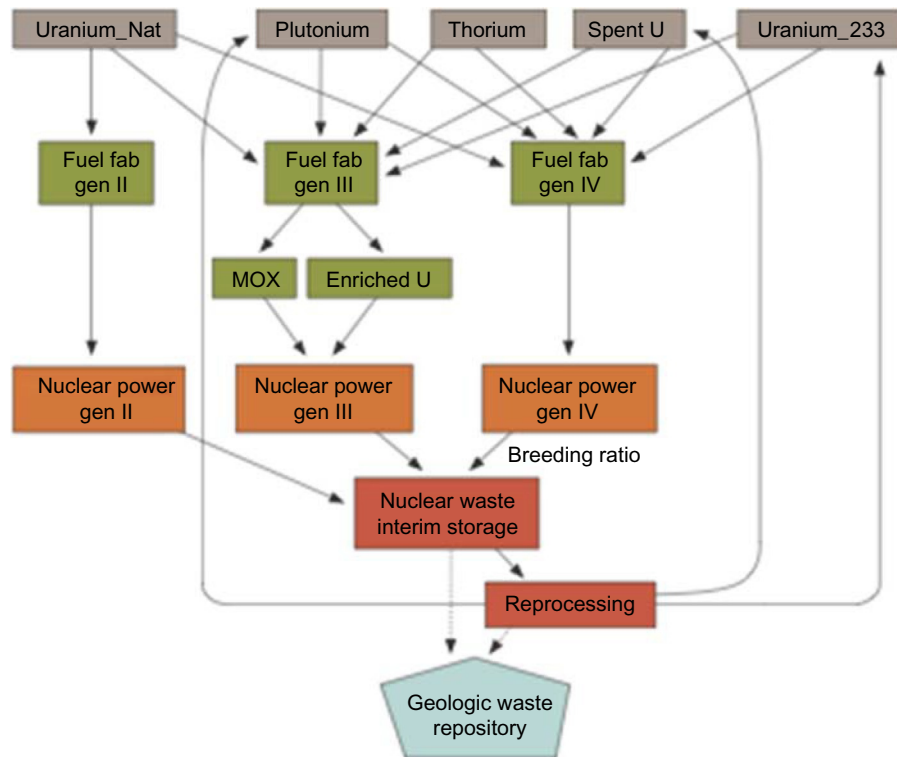


Figure 17.1. The various global nuclear fuel cycles (Edmonds et al., 2007)

about 0.3% Pu^{239} , and still capable of making more energy but is presently labeled as “waste.” This fissile material and the U^{238} fertile component could make more energy if converted (= upgraded) by breeding in a different reactor. There are many potential fuel cycles using different fissile fuels as their starting point and reprocessing and final radioactive waste storage (see Figure 17.1).

However, in both the United States and Canada, there is no recycling of used fuel allowed by political edict, which is not the case in, say India, Russia, and France. This ban is a legacy again of Cold War thinking, and public antipathy to the use of nuclear energy.

Instead, once used fuel is stored and allowed to cool (decay) on site at operating LWRs and HWRs, with the intent it be sent to an ultimate (underground storage facility. After over 20 years of study and debate, that was the purpose of the ill-fated Yucca Mountain site, where about \$10B has been spent to date without completing the facility due to deliberate political dallying and delay. In Canada, the idea is to use “retrievable storage,” presuming some use might be found for the fuel in the future.

The rationale for not recycling used fuel is largely socio-technological ones. Perhaps it is too deadly or toxic to be kept in “interim storage,” and requires expensive facilities for millennia to avoid leaking into ground water. If recycling is “allowed” some Plutonium or other fissile material might be diverted for some evil purpose (e.g., for atomic or radioactive bombs), Today, once-used fuel in the United States is stored on site in flask, or as in the Zwileg facility in Switzerland. Indeed, the NRC 1310-page Generic Environmental Impact Statement (GEIS) for continued and generally unplanned on-site storage found the environmental impacts for almost everything to be “small” (i.e., negligible risk), while assuming some long term repository is available in about 60 years (NRC, 2014). It has been reported that as of January 11, 2013, following yet another special Commission report (Blue Ribbon Commission on America’s Nuclear Future, 2012), that the Obama administration will ask Congress to approve a plan by building a pilot interim storage facility for nuclear storage by 2021 and a larger facility by 2025 “based on consent” of the host state.

The DOE reportedly has said: “the administration has now decided to pursue the siting and licensing of two interim storage facilities by 2025. The first initially would focus on accepting used nuclear fuel from reactor sites that have been shut down. The second site, to be available by 2025, would accept enough fuel to reduce expected government liabilities.” Another goal is to “make demonstrable progress,” meaning the legal costs and fines incurred by not accepting fuel as had been promised, including “the siting of permanent repository sites that could start accepting waste by 2048.”

This idea is similar in scope and timing to the on-going activity by the Nuclear Waste Management Organization (NWMO) in Canada, that has been focused on achieving consensus, and social acceptance and funding volunteer sites (NWMO, 2005). In that report, Table 8–1, the cost of an “Adaptive Phased Management” (APM) approach to a geologic facility is about \$20B over 350 years to be largely funded by the electric utilities (i.e., by the customers via a surcharge).¹¹ To ensure funding surety, “waste” fuel owners are required to deposit \$550M immediately, and then \$110M a year into a trust, depending on how much once-used fuel they have or expect. This is in addition to the some \$8.5B that was already set-aside in guarantees. There are no incentives in the NWMO report, or in their official mandate, for the NWMO to reduce the amounts of fuel stored, the timescales or the expected costs.

Apparently, US nuclear utilities pay about \$750 million into the Nuclear Waste Fund every year, plus several \$100M on dry storage casks and their secure storage on-site. For 60 years, as in the NRC scenario, this would be about \$45B collected from customers via a surcharge, plus any other interim storage costs.

Now future ARs would be expected to have a more sophisticated energy and resource efficient fuel cycle, and satisfy some sustainability argument. This concept of fuel reuse is often called “closing the fuel cycle,” and involves treatment, separation and new fuels. Indeed, the NRC defines this possibility as follows:

“Fuel reprocessing (recycling): *The processing of reactor fuel to separate the unused fissionable material from waste material. Reprocessing extracts isotopes from spent fuel so they can be used again as reactor fuel.*”

Generally, present fuel cycle policy in states with ample uranium and plutonium resources (e.g., United Kingdom, United States, and Canada) favors long-term geologic storage of once used fuel, with or without retrievable options, independent of the cost and recycling technology. In fact, reuse of CANDU fuel is only possible at present in China.

Many options, studies and tests have already been performed for existing reactor designs (IAEA-TECDOC-1122, 1999). There appears to be no “in principle” technical problems for recycling, particularly as additional irradiation reduces the long lived actinides and radio-toxicity, and hence can reduce storage times needed before decaying to safe or background levels.

Paradoxically and ironically, recycling has already occurred by “disposing” of excess weapons material, e.g., Pu²³⁹ and Th²³³ originally produced by military “production” reactors for use in now retired nuclear bombs. The United States has down-blended and used material from Russia as fuel for commercial reactors, and the United Kingdom is looking at some similar approaches to reduce its Pu “inventory.”

Since used fuel is radioactive and contains fission products, it must be placed in heavy containers and shielding, well-sealed against leakage, and any potential underground dissolution and migration into groundwater minimized. This APM is based on the concept of being able to retrieve the fuel at some unspecified point in the future if desired, for whatever reason. But all the costing and planning is based on essentially indefinite (or “passive APM”) safe storage below ground in a Deep Geologic Repository (DGR) consisting of underground tunnels, canisters, vaults and removable sealing. The timescales for storage

¹¹ Accounting techniques can estimate the “net present value,” by assuming the funds are all invested up front in some hypothetical fund; this technique is used to lower the apparent cost of future expenditures, but does not reduce the real \$ amounts of money actually spent both now and in the future.

are truly glacial, being envisaged as up to millions of years until the radiation decays to its premixed or background levels, so the DGR would have assured storage and disposal facilities for many thousands if not millions of years.

The siting process for the DGR/APM facility has itself been glacial, and is taking many years due to lengthy dialog and legalistic processes designed to be consensual, consultative, normative, sociologically acceptable, and fully transparent. After much such consultation with “stakeholders,” the NWMO has unsurprisingly selected DGR/APM as the “preferred” technical and social option. Costing for such a DGR using APM has been estimated by the NWMO at about \$12–24 billion in present worth moneys, for storing all the 4–8 million once-used fuel bundles produced to date. This DGR cost then represents an average upper limit storage and disposal cost per bundle of about $\$20,000,000,000/4,000,000 \sim \$5000/\text{bundle}$. Since each bundle weighs about 20 kgHM, this represents a cost of the “waste” disposal of $\sim \$250/\text{kgHM}$, which is even somewhat higher than so-called “natural” or non-enriched uranium presently sells for as fuel in the open market (a range depending on demand and speculation of, say, about \$60–130/kg HM).

This immediately raises an interesting question: why not resell, recycle or reuse this asset? This idea has not escaped the notice of the public, the media or the technical community who have variously stated in debate, comment and input sessions:

“There is no such thing as nuclear wasteit gives us the chance to follow France’s lead in developing complete reprocessing for nuclear material” (Tucker, 2009).

17.5.2 Economic and social aspects of recycling

Instead of burying used nuclear fuel, for ARs one can consider the sustainable option of actively recycling and reusing as being socially, economically, environmentally and technically more attractive and sensible. Reusing this fuel would help provide an assured future energy supply, reduce storage times by factors of 1000s, provide value by turning what is presently designated as “waste” into “energy,” and reduce ultimate storage liabilities, include the social and political costs. The goal is in fact “zero waste,” thus avoiding the embarrassment and social stigma if not being reused.

Such “advanced fuel cycles” have been examined in detail already (e.g., see Figure 17.2).

Extensive analyses have also been made of the economics of recycling, albeit commissioned on behalf of a fuel manufacturer (The Boston Consulting Group, 2006), which concludes:

“In addition, recycling, as part of a portfolio strategy, presents a number of benefits:

- Eliminates the need for additional repository capacity, beyond the initial 83,800 ton capacity at Yucca Mountain, until 2070.
- Contributes to early reduction of used fuel inventories at reactor sites—in particular, removing newer, hotter fuel for recycling within 3 years of discharge and eliminating the need for additional investments in interim storage capacity.
- Relies on existing technology—with appropriate modifications—and can provide an operational transition to future technology developments such as Advanced Fuel Cycles and fast reactors.
- Shows cash flow requirements that could fit until 2030 within the current financing resources available for the once-through strategy, or even until 2050⁺ if acceptance of used fuel at Yucca Mountain begins only after the first years of operation of the recycling plant.
- Offers a tool for nuclear power sector to protect against potential rises in uranium prices, by providing MOX and recycled UOX fuel, whose production cost is independent of uranium prices and enrichment costs.”

realizations place new pressures and obligations on the custodians of one of the world's major energy resources, to respond and position globally to the needs for a sustainable future, where by the classic definition, present practices do not endanger or restrict the options of future generations.

In fact, it is well known that modern processing and fuel cycle technology allows for a sustainable, and perhaps even a perpetually renewable future energy scenario using nuclear energy. Future ARs will breed and recycle fuel. Therefore, “waste” streams will be drastically reduced, separation and “burning” of long-lived actinides will occur, and repositories will only be needed just for less than a thousand not for the unnecessary million years (US DOE, 2006, 2007).

In today's modern world, inaction is unacceptable both technically and morally.

17.5.3 The cost savings of the future

A review of LWR reprocessing costs has been given (Rothwell, 2009), which established an estimate reprocessing cost range for a facility of between \$500 and \$4000/kg HM.

There is indeed a price for recycling, just like the blue box we use today for disposing and reusing household goods. But does “waste to energy” have to be cheaper than whatever we use or do today? Or does it just need to be cheaper than the alternates like DGR/APM?

There was and is no recycling of anything in the original Once Through Cycle (OTC), as this meant separations and enrichment of PU and other isotopes (see the above sections on non-proliferation implications). The OTC was born in the days after WWII, when nuclear energy was in its infancy, and the concept of finite energy resources seemed quite irrelevant when compared to the impacts of atomic energy, oil cartels and hydrogen bombs. However, this attitude was and is not true for those countries without large uranium reserves, notably France, Japan, Russia, India, China and Korea, where a longer-term view is taken since “raw” fuel ores must be bought abroad. For these uranium resource-poor countries, recycling and breeding are seen as the ultimate answer to sustainable nuclear energy supply using thorium, plutonium and enrichment based cycles, while also endowing the countries with energy independence.

The OTC is not sustainable, a fact not overlooked by nuclear energy opponents, and is actually a relic of the past decisions and norms. The global uranium resources of about 5 MMT U^{235} were regarded as large, at least compared to oil and gas, and the world did not envisage thousands of reactors with a global energy demand 5–10 times that of today. There has always been enough uranium to supply today's several hundred units and the uranium suppliers, like oil producers, always assure the markets that there is no shortage and ample present supply. A quick calculation shows that with over 400 reactors operating today, present world uranium (U^{235}) demand is $\sim 70,000$ t/a (tons per annum) U^{235} , or low enough for another 100–150 years or so based on present so-called recoverable reserves.

But we can provide an upper bound estimate of the demand for 4000 reactors needing $\sim 700,000$ t/a U^{235} by 2050. Today's estimates of identified reserves are about 5 MMtU U^{235} at a cost of $< \$130$ /kg (Duffey, 2008). Even allowing a doubling or tripling of this resource estimate to, say, 10 MMtU of U^{235} , just 1000 reactors operating for 60 years, which is their stated life, will use all the world's cheapest uranium (or by about 60,000 reactor operating-years) with present mainly OTC technology.

Another way to state it is that although the present 400 reactors could be kept going for another 150 years, this leaves a shortfall of about 3000 reactors (or some three-fourth of the need) in the near or not too distant future. Some 1000 reactors are easily envisaged by 2040 or so (i.e., after the era of “cheap gas”), not coincidentally just using up the cheapest uranium. This is not a cause for alarm—there is plenty of uranium, and more uranium reserves will be found but of course at steadily higher prices (cf. oil, gas and other commodity markets). Aggressively adopting recycling and increased fuel utilization might even allow up to 1500 reactors, but at increased cost of those processes and facilities, which are all known and/or existing technology.

This consideration of uranium cost leads to an analysis of the price natural uranium fuel would have to be at to make recycling attractive price-wise. The answer is a price that is two to three times today's, or about \$240–360/kgHM, almost exactly the same range (at least within the accuracy of these estimates) as the present cost of the DGR/APM storage at about \$300/kgHM.

So the order of magnitude of the costs are clear- and supports recycling as being about equal to the cost of using a DGR for disposal if the future includes about $10 \times$ more reactors. But there are also some other technical advantages and economic business opportunities for mining nations and the fuel (“waste”) owners, as well as massive social benefits.

17.5.4 Waste to energy: Burning the benefits

It would seem a no-brainer: recycling is good. But there are other considerations, like owners' liabilities, obligations and choices: “waste disposal” funds of many \$Bs already exist. As a simple worked example, consider that used fuel from CANDU reactors which is being produced at the rate of about 100,000 bundles per year, or about 2000 MMT HM/y of which 0.3% is useful fissile material (Pu²³⁹ and related isotopes) that can be separated and used again. This means CANDU's are producing about:

$$1000,000 \text{ bundles} \times 20 \text{ kg/bundle} \times 0.3\% = 6000 \text{ kg Pu/y} = 6 \text{ Mt Pu/year}$$

From a proliferation and security perspective, it would be preferable to destroy or use this plutonium, rather than entomb it, presuming no access (“intrusion”) or use is allowed or possible for a historic timescale of a million or so years. Interestingly, LWR “spent” fuel is at about 0.9% fissile, which is why France can and does recycle today, and why this used recycled fuel could also be recycled again directly again in CANDU (in the so-called, DUPIC cycle).

Assuming this once used fuel can be safely processed (see below), the 6 Mt Pu/year would be processed into $\sim 5\%$ enriched Pu-Th fuel to kick start the Pu²³⁹-Th²³²-U²³³ cycle, which can be reused as fuel and burnt to about 40,000 MW(t) d/t using present fuel technology.

The U²³³ so produced would then be separated and reused in an endless chain, replacing the Pu as the starter fuel. Assuming just 35% for the nominal thermal to electricity conversion efficiency, which is a low present design estimate as future reactor designs intend to reach 50%, then the electricity produced from just this recycled fuel is:

$$6 \text{ Mt/y at } 40 \text{ MWd/kg at } 35\% = 40,320,000,000 \text{ kWh/y} = 40 \text{ TWh/year}$$

or about the equivalent of the full electrical output from 6 or more small reactors. At the assumed equilibrium use rate of 6 MT/y, the lower life estimate of the existing Pu²³⁹ resource in Canadian used fuel alone is:

$$20 \text{ kg/bundle} \times 4 \text{ million bundles} \times 0.3\% / 6 \text{ Mt/year} = 2400 / 6 = 40 \text{ years}$$

This timescale is fully sufficient to start, transition to and implement a full Pu-Th²³²-U²³³ fuel cycle facility not just in Canada, but globally with India and China who both possess ample Thorium reserves, including fuel manufacturing, plutonium destruction and actinide separations.

The key is also a global transition to a parallel full thorium-based fuel cycle, as envisaged by India and China based on their small U resources, but large nuclear, energy and thorium resources. A full near-breeding Th fuel cycle is envisaged in an optimized reactor concept, with the Th cost being at about current market spot price of \sim \$120/kg, or again not coincidentally about the Natural U price.

Also key is the actinide separation as a technology step. By separating out from the “residual” waste streams the long-lived transuranics or actinides, namely Americium (Am) and Curium (Cm), removes over 90% of the DGR waste heat load and radio-activity, but only $<0.1\%$ of the used fuel mass. Removal and “burning” these actinides in thermal reactors is then feasible, since the actinide

destruction is about 90% or more. This is also desirable as it allows for lower decay heats, and smaller timescales of about 1000 years for the DGR. These timeframes are at least comparable to human experience with large structures and geologic knowledge (cf. the pyramids, Greco-Roman buildings, and natural caverns).

So the benefits are indeed burnt. Moreover, there is a positive income stream assuming that the electricity produced is sold in or to the open market at ~ 5 c/kWh using existing reactors, or even new special purpose ones. The income is then of order:

$$40 \text{ TWh/year} \times \$0.05/\text{kWh} = \$2 \text{ B/year}$$

For a 40 years reactor life this is about \$80B income. This income must offset and pay for the cost of processing and fuel manufacture, which over the same 40 years is $\sim \$10\text{--}20$ B for the fuel and reprocessing plants and $6 \text{ Mt/year} \times \text{range of } (\$500\text{--}\$4000/\text{kgHM}) = \$3\text{--}\$24 \text{ M/year}$, or an upper limit of about \$1 B, plus any other operating costs (say about \$200 M/year) to give a total lifetime expense of about \$30B.

Such a waste to energy facility has a Return On Equity (ROE) of about three times, and the lower estimate of the business benefit to cost ratio is then of order 1.5, assuming a 10% IR. This estimate is made without counting any of the “softer” societal benefits, increased jobs, future investment, spin offs, sustainability returns, carbon credits and global market share etc. that any such business case would have to be made.

This type of “storage cost recycling versus benefit” analysis can be generalized for any in-principle fuel cycle. But the fact that the costs (outlays) and the benefits (returns) are even remotely similar is quite amazing—and clearly represents a business and market opportunity in addition to the purely social job and technology advantages.

17.5.5 Overcoming the ostrich syndrome

- If it cannot be seen perhaps we can pretend that it does not exist. So it is with once used nuclear fuel. Originally seen by antinuclear activists as the Achilles Heel of nuclear energy, if used fuel cannot be stored then it is not a closable or viable system, but remains an open running sore. Sociology reigned, and desperate for a solution, the response was to bury it, “out of sight, out of mind,” and to undertake endless study and consultation with stakeholders and the “public.” The problem then was to find a socially and politically acceptable, even low profile approach, with the soluble technology considerations of mining, geology, tectonics, and chemical effects, not the insoluble NIMBY ones. This has led to the Yucca Mountain fiasco, where after spending perhaps \$10B or so and after 20 years of study, politics and sociology have finally said that NIMBY prevails and the used fuel cannot be buried after all. The only option is to literally “burn” it as a useful resource.

Annex 1: EURATOM

Around the same time as the foundation of the IAEA, the original six member states of the European Coal and Steel Community negotiated the establishment of two further Communities, the European Common Market and the European Atomic Energy Community (EURATOM), enshrined in the Treaty of Rome. At this time none of the Six had nuclear weapons, nor indeed had developed civilian nuclear power. The EURATOM Treaty reflects the issues that were paramount at the time (which included French and others’ fears of a revived Germany), and among its objectives as with the IAEA was **to make certain that civil nuclear materials are not diverted to other (particularly military) purposes.**

The Treaty introduced an extremely comprehensive and strict system of safeguards to ensure that civil nuclear materials were not diverted from the civil use declared by the Member States. The EU has exclusive powers in this domain, which it exercises through of a team of 300 inspectors who enforce the EURATOM safeguards throughout the EU.

These EURATOM safeguards are now applied in conjunction with those of the IAEA under tripartite agreements concluded between the Member States, the Community and the IAEA, and even though they are to some degree more stringent are best regarded as a subclass of the Agency's international safeguards. (This regional arrangement has of course been extended with the expansion of the European Communities' original six members over the past 50 years into the 27 current members of the Union.)

Annex 2: The 1997 IAEA additional protocol at a glance

In the 1980s, Iraq, an NPT state-party, had successfully circumvented IAEA safeguards by exploiting the Agency's original system of confining its inspection and monitoring activities to facilities or materials explicitly declared by each state in its safeguards agreement with the agency. To close the "undeclared facilities" loophole, the IAEA initiated a safeguards improvement plan known as "Program 93+2." The plan's name reflected the fact that it was drafted in 1993 with the intention of being implemented in 2 years.

Putting "Program 93+2" into effect, however, took more time than expected, and the program has in practice been implemented in two parts. The IAEA, within its existing authority, initiated the first part in January 1996. This first step added new monitoring measures, such as environmental sampling, no-notice inspections at key measurement points within declared facilities, and remote monitoring and analysis. The second part of "Program 93+2" required a formal expansion of the agency's legal mandate in the form of an additional protocol to be adopted by each NPT member to supplement its existing IAEA safeguards agreement. The IAEA adopted a Model Additional Protocol on May 15, 1997, which it encouraged its members to follow.

The additional protocol

Its essence was to reshape the IAEA's safeguards regime from a quantitative system focused on accounting for known quantities of materials and monitoring declared activities to a qualitative system aimed at gathering a comprehensive picture of a state's nuclear and nuclear-related activities, including all nuclear-related imports and exports. The Additional Protocol also substantially expands the IAEA's ability to check for clandestine nuclear facilities by providing the agency with authority to visit any facility, declared or not, to investigate questions about or inconsistencies in a state's nuclear declarations. NPT states-parties are not required to adopt an additional protocol, although the IAEA is urging all to do so.

The model protocol outlined four key changes that must be incorporated into each NPT state-party's additional protocol.

First, the amount and type of information that states will have to provide to the IAEA is greatly expanded. In addition to the former requirement for data about nuclear fuel and fuel-cycle activities, states will now have to provide an "expanded declaration" on a broad array of nuclear-related activities, such as "nuclear fuel cycle-related research and development activities—not involving nuclear materials" and "the location, operational status and the estimated annual production" of uranium mines and thorium concentration plants. (Thorium can be processed to produce fissile material, the key ingredient for nuclear weapons.) All trade in items on the Nuclear Suppliers Group (NSG) trigger list will have to be reported to the IAEA as well.

Second, the number and types of facilities that the IAEA will be able to inspect and monitor is substantially increased beyond the previous level. In order to resolve questions about the information, a state has provided on its nuclear activities, the new inspection regime provides the IAEA with "complementary," or

preapproved, access to “any location specified by the Agency,” as well as all of the facilities specified in the “expanded declaration.” By negotiating an additional protocol, states will, in effect, guarantee the IAEA access on short notice to all of their declared and, if necessary, undeclared facilities in order “to assure the absence of undeclared nuclear material and activities.”

- Third, the agency’s ability to conduct short notice inspections is augmented by streamlining the visa process for inspectors, who are guaranteed to receive within 1 month’s notice “appropriate multiple entry/exit” visas that are valid for at least a year.

Fourth, the Additional Protocol provides for the IAEA’s right to use environmental sampling during inspections at both declared and undeclared sites. It further permits the use of environmental sampling over a wide area rather than being confined to specific facilities.

References

- Blue Ribbon Commission on America’s Nuclear Future, 2012. Report to the Secretary of Energy. January, NRC Accession No. ML120970375DOE, Washington, DC, USA, 180 pp.
- Duffey, R.B., 2008. Future fuel cycles: a global perspective. In: Proceedings of the 16th International Conference on Nuclear Engineering (ICONE-16), May 11–15, Orlando, FL, USA.
- Edmonds, J.A., Wise, M.A., Dooley, J.J., Kim, S.H., Smith, S.J., Runci, P.J., Clarke, L.E., Malone, E.L., Stokes, G.M., 2007. Global Energy Technology Strategy: Addressing Climate Change Phase 2 Findings. Pacific Northwest National Laboratory, Joint Global Change Research Institute, College Park, MD, USA, p. 75 (Chapter 6 “Nuclear Energy”).
- Glasstone, S., Sesonske, A., 1994. Nuclear Reactor Engineering. Reactor Systems Engineering, fourth ed. vol. 2 Chapman & Hall, New York, NY, USA. 867 pp.
- Generation IV International Forum (GIF), 2011. Proliferation resistance and physical protection working group. In: Evaluation Methodology for Proliferation Resistance and Physical protection of Generation IV Energy Systems. Report GIF/PRPPWG/2011/003 Rev. 6, and IAEA CN_220 289.
- Generation IV International Forum (GIF), 2014. Annual Report, Section 4.2. pp. 105–106. Accessed at: www.gen-4.org/gif/upload/docs/application/pdf/gif_2014_annual_report_final.pdf.
- Cacuci, D.G. (Ed.), 2010. Handbook of Nuclear Engineering. vol. 5. Springer, New York, NY, USA.
- Hewitt, G.F., Collier, J.G., 2000. Introduction to Nuclear Power, second ed. Taylor & Francis, New York, NY, USA. 304 pp.
- IAEA-TECDOC-1122, 1999. Fuel Cycle Options for LWRS and HWRs. IAEA, Vienna.
- Joint Comprehensive Plan Of Action (JCPOA), 2015, Vienna, 14 July, Full Text, www.state.gov/documents/245317.pdf, 18 Pages Plus Annexes 1–5 (see also: www.whitehouse.gov/sites/default/files/docs/jcpoa_what_you_need_to_know.pdf, accessed January, 2016, and the Iran commentary at www.beibert.com of October, 2015).
- Kelly, J.E., 2014. Generation IV international forum: a decade of progress through international cooperation. Prog. Nucl. Energy 77, 240–246.
- Lamarsh, J.R., Baratta, A.J., 2001. Introduction to Nuclear Engineering, third ed. Prentice Hall, Upper Saddle River, NJ, USA. 783 pp.
- Murray, R.L., Holbert, K.E., 2015. Nuclear Energy, seventh ed. Elsevier, Waltham, MA, USA. 550 pp.
- NRC, 2014. Generic Environmental Impact Statement for Continued Storage of Spent Nuclear Fuel: Final Report, Volume 1 (NUREG-2157). September, Washington, DC, USA, 687 pp.
- Krivit, S.B., Lehr, J.H., Kingery, T.B. (Eds.), 2011. Nuclear Energy Encyclopedia: Science, Technology, and Applications. John Wiley & Sons, Hoboken, NJ, USA. 595 pp.
- Kok, K.D. (Ed.), 2009. Nuclear Engineering Handbook. CRC Press, Boca Raton, FL, USA. 768 pp.
- Nuclear Waste Management Organization (NWMO), 2005. Choosing a Way Forward, Final Study. November, Toronto, ON, Canada, 454 pp.
- Rothwell, G., 2009. Forecasting light water reactor fuel reprocessing costs. In: Proceedings of the Global Conference, Paris, France, September 6–11, Paper No. 9228, pp. 2959–2964.
- Shropshire, D.E., Williams, K.A., Boore, W.B., et al., 2008. Advanced Fuel Cycle Cost Basis, INL/EXT-07-12107. March, 613 pp.
- Anon., 2006. Economic Assessment of Used Nuclear Fuel Management in the United States, Report. The Boston Consulting Group. July, Boston MA, USA, 96 pp.
- The Future of Nuclear Power, 2003. An Interdisciplinary MIT Study. Massachusetts Institute of Technology (MIT), Cambridge, MA, USA. ISBN 0-615-12420-8, 26 pp.

Tucker, W., 2009. There is no such thing as nuclear waste. Wall Street J. March 13.

U.S. Department of Energy (DOE), 2007. Office of Nuclear Energy, Office of Fuel Cycle Management, "Global Nuclear Energy Partnership Strategic Plan". GNEP-167312, Rev 0, 2007 January.

U.S Department of Energy (DOE), 2006. Advanced Fuel Cycle Initiative (AFCI), Office of Nuclear Energy, Science and Technology. U.S. Department of Energy. January, 2 pp.

Thermal aspects of conventional and alternative nuclear fuels

Wargha Peiman^a, Igor L. Pioro^a, Kamiel S. Gabriel^b,
and Mohammad Hosseiny^a

^aFaculty of Energy Systems and Nuclear Science, University of Ontario Institute of Technology,
Oshawa, ON, Canada ^bFaculty of Engineering and Applied Science, Ontario Tech University,
Oshawa, ON, Canada

Nomenclature

B	Burnup, MW day/Mg(U)
c_p	Specific heat at constant pressure, J/kg K
\bar{c}_p	Average cross-sectional specific heat, $(\frac{h_w - h_b}{T_w - T_b})$, J/kg K
D_{hy}	Hydraulic-equivalent diameter, m
E	Young's modulus
f	Friction factor
G	Mass flux, $(m/A_{\bar{n}})$, kg/m ² s
G_b	Gibb's free energy, J/kg
G_f	Fission energy released per fission and absorbed by nuclear fuel, J
G_{sm}	Shear modulus, MPa
HD	Meyer hardness, MPa
H	Enthalpy, J
h	Specific enthalpy, J/kg
k	Thermal conductivity, W/mK
m	Mass flow rate, kg/s
P	Pressure, Pa
P_p	Porosity, %
Q	Heat transfer rate, W
Q_{gen}	Volumetric heat generation, W/m ³
q	Heat flux, W/m ²
R	Gas constant, cal/K mol
R'	Thermal-shock resistance, W/m
R_D	Percent diameter increase per atom percent burnup
s	Specific entropy, J/kg K
T	Temperature, K
t	Temperature, °C
V	Volume, m ³
V_i	Volume fraction of phase i

Greek symbols

α	Thermal diffusivity, $(\frac{k}{\rho c_p})$, m ² /s
α_{cf}	Ratio of capture to fission cross-sections
β	Volumetric thermal-expansion coefficient, 1/K
ϵ_{sm}	Spectral emissivity
$\dot{\epsilon}$	Creep rate, 1/h
$\dot{\epsilon}$	Steady-state creep rate, 1/h
η	Average number of neutrons emitted per neutron absorbed
θ	Einstein temperature, degree
μ	Dynamic viscosity, Pa s
ν_p	Poisson's ratio
ρ	Density, kg/m ³
Σ	Macroscopic cross-section, cm ⁻¹
$\Sigma_{R,g}(r)$	Neutron removal cross-section of energy group g , cm ⁻¹
$\Sigma_{f,g}(r)$	Macroscopic fission cross-section of neutrons in energy group g , cm ⁻¹
σ	Microscopic cross-section, cm ²
σ_s	Stress, Pa
$\phi_g(r)$	Neutron-flux density of energy group g (cm ² s) ⁻¹
ϕ_i	Neutron-flux associated with neutrons in energy group i (cm ² s) ⁻¹

Subscripts

amu	Atomic mass unit
avg.	Average
c	Capture
eff	Effective
g	Energy group
gen	Volumetric heat generation
hy	Hydraulic equivalent
i	Phase i
in	Inlet
m	Melting
out	Outlet
vol	Volume
wt	Weight
x	Element to element ratio

Abbreviations

ABWR	Advanced Boiling Water Reactor
AGR	Advanced Gas-cooled Reactor
ANSYS	ANalysis SYStem
BCT	Body-Centered Tetragonal
BN	Fast Sodium (reactor) (Быстрый Натриевый (in Russian abbreviations))
BR-10	Fast Reactor-10 MW _{th} (БР-10—Быстрый Реактор (in Russian abbreviations))
BWR	Boiling Water Reactor
BeO	Beryllium Oxide
CANDU [®]	CANada Deuterium Uranium (reactor) (Registered Trademark of AECL, used under license by Candu Energy Inc., Member of SNC-Lavalin Nuclear Group)
CLT	Center Line Temperature
EBR	Experimental Breeder Reactor
EC6	Enhanced CANDU-6
ETC	Effective Thermal Conductivity
FBR	Fast-Breeder Reactor
FBTR	Fast Breeder Test Reactor (India)
FCC	Face-Centered Cubic

FRWG	Fast Reactor Working Group
GE	General Electric (USA)
GFR	Gas-cooled Fast Reactor
GG	Green Granule
GIF	Generation IV International Forum
HEC	High-Efficiency fuel Channel
HERC	High-Efficiency Reentrant Channel
HTC	Heat Transfer Coefficient
HTR	High-Temperature Reactor
HWR	Heavy Water Reactor
IAEA	International Atomic Energy Agency
ID	Inner Diameter
LFR	Lead-cooled Fast Reactor
LGR	Light-water-cooled Graphite-moderated Reactor
LMFBR	Liquid-Metal Fast Breeder Reactor
LWR	Light Water Reactor
MOX	Mixed OXide
MSR	Molten Salt Reactor
NEA	Nuclear Energy Agency
NRX	National Research eXperimental
OD	Outer Diameter
OECD	Organization for Economic Co-operation and Development
ORNL	Oak Ridge National Laboratory
PBMR	Pebble Bed Modular Reactor
PCh	Pressure Channel
PFR	Prototype Fast Reactor (UK)
PHWR	Pressurized Heavy Water Reactor
PuO₂	Plutonium diOxide
PWR	Pressurized Water Reactor
RBMK	Reactor of Large Capacity Channel type (Реактор Большой Мощности Канальный (in Russian abbreviations))
SB	Slug Bisque
SCW	SuperCritical Water
SCWR	SuperCritical Water-cooled Reactor
SFR	Sodium-cooled Fast Reactor
SiC	Silicon Carbide
SMR	Small Modular Reactor
TD	Theoretical Density
TECDOC	TECnical DOCument (IAEA)
ThO₂	Thorium diOxide
TRISO	TRistructural ISOtopic
UC	Uranium Carbide
UC₂	Uranium diCarbide
U₂C₃	Uranium sesquiCarbide
UN	Uranium Nitride
UN₂	Uranium diNitride
U₂N₃	Uranium sesquiNitride
UO₂	Uranium diOxide
UO₂-BeO	Uranium diOxide composed of Beryllium Oxide
UO₂-C	Uranium diOxide composed of graphite fibers
UO₂-SiC	Uranium diOxide composed of Silicon Carbide
VHTR	Very-High-Temperature Reactor
VVER	Water-water power reactor (ВВЭР—Водо-Водяной Энергетический Реактор (in Russian abbreviations)) (Russia)
WNA	World Nuclear Association

18.1 Introduction

The genesis of nuclear power, similar to many advanced technologies, which are available to humanity today, is considered to be esteemed in the 19th century. A series of unprecedented scientific discoveries opened a new vista for releasing an enormous amount of energy from the atom. Through these discoveries, nuclear science and nuclear fission were developed. Nuclear fission is a reaction in which the nucleus of a heavy nuclide splits into smaller nuclides; a few new neutrons are created; gamma rays are emitted, and a significant amount of energy is released. Since then, nuclear fission has been used as a basis for production of heat in all the current nuclear reactors. Even though these reactors can be categorized based on their cooling medium, pressure boundary, type of nuclear fuel, or neutron spectrum, they all have one common feature, which is the production of heat via a fission chain reaction in the nuclear fuel.

An important aspect of every reactor design involves the selection of a nuclear fuel and design of fuel assemblies. As general requirements, a nuclear fuel should have a high melting point, acceptable thermal conductivity, sufficient mechanical stability, good dimensional and irradiation stability as well as chemical compatibility with the cladding and the coolant. Another important parameter that influences the design and selection of a nuclear fuel is the dominant neutron spectrum of a reactor. In this context, nuclear reactors can be categorized as fast-neutron-spectrum, epithermal-neutron-spectrum and thermal-neutron-spectrum. This classification is based on the energy group of neutrons that maintain the fission chain reaction. In a fast-neutron-spectrum reactor, the chain reaction is sustained mainly by fission of fast (e.g., high-energy) neutrons, while in an epithermal or thermal reactor, fission of epithermal (intermediate-energy), or thermal (low-energy) neutrons, respectively, maintain the chain reaction.

The neutron spectrum has an influence on the reactor design, selection of materials for the reactor core, the type of nuclear fuel and the associated fuel cycle. Unlike fast-neutron-spectrum reactors, thermal-neutron-spectrum reactors utilize a moderator such as water, heavy water or graphite in order to thermalize (reduce the energy of) high energy neutrons. Coolant is also different in these two types of reactors. Thermal-neutron-spectrum reactors utilize coolants such as water or CO₂, which are composed of light elements, especially, those having high scattering cross-sections, compared to liquid-metal coolants, such as sodium or lead, which are used in some fast-neutron-spectrum reactors (Alexander, 1964). However, it should be mentioned that gas-cooled fast-neutron-spectrum reactors are also considered (Waltar et al., 2012). The neutron spectrum also affects the isotopic concentration of fissile and fertile nuclides in the fuel. As shown in Table 18.1, fast-neutron-spectrum reactors require a higher percentage of fissile nuclides compared to thermal-neutron-spectrum reactors. The majority of the current commercial nuclear reactors have been designed as thermal-neutron-spectrum reactors. With recent interest in Small Modular Reactors (SMRs) as a viable energy solution, there has been significant progress in the deployment of SMR designs. HTR-MP is an example of a high-temperature helium-cooled SMR. HTR-PM consists of two SMRs with a total thermal power of 500 MW and an electrical power of 210 MW (IAEA, 2022). The first and second HTR-MP units reached their first criticality in September and November 2021, respectively. The dual-reactor unit was connected to grid in December 2021 (WNN, 2021). Table 18.1 lists a summary of these reactors (WNA, 2021a).

In a nuclear fuel, the fission chain reaction is maintained by fission of fissile elements, which are capable of sustaining the fission reaction with neutrons of all energies. As such, fissile nuclides are used in the fuel of both thermal-neutron-spectrum and fast-neutron-spectrum reactors. The fissile nuclides of importance for nuclear reactors are ²³³U, ²³⁵U, ²³⁹Pu, and ²⁴¹Pu. Among these fissile nuclides, only ²³⁵U is a naturally occurring nuclide while others are produced by neutron capture of other nuclides during operation of a nuclear reactor. For instance, ²³⁹Pu is bred by neutron capture of ²³⁸U; ²⁴¹Pu is bred by neutron capture of ²⁴⁰Pu; and ²³³U is bred by neutron capture of ²³²Th. Hence, the current nuclear reactors rely on ²³⁵U as the primary fissile element. In terms of the fuel composition, the nuclear fuel of the most nuclear reactors consists

Table 18.1. Fuels, coolants/moderators, and neutron spectrums of various types of operating nuclear-power reactors (WNA, 2021a)

Reactor type	Main Countries	Number	GW _{el} ^a	Fuel	²³⁵ U enrichment, wt%	Coolant/Moderator	Neutron spectrum
PWR	USA, France, China, Russia, S. Korea, Japan	303	289	Enriched UO ₂	2.1–3.1 ^b 4.5–5.5 ^c	Water/water	Thermal
BWR and ABWR	USA, Japan, Sweden	62	64	Enriched UO ₂	2.6–3.05 ^d	Water/water	Thermal
CANDU or PHWR	Canada, India	49	24	Natural UO ₂	0.71 ^e	Heavy water/heavy water	Thermal
AGR	UK	14	8	Enriched UO ₂	2.3	CO ₂ /graphite	Thermal
LGR (RBMK)	Russia	12	8	Enriched UO ₂	2.4 ^f	Water/graphite	Thermal
SFR (BN-600 & 800)	Russia	2	1.4	UO ₂ and PuO ₂	17, 21, and 26 ^g	Liquid sodium/none	Fast
HTR-PM	China	2	0.21	Enriched UO ₂	8.5	Helium/graphite	Thermal

^a GW_{el} = capacity in thousands of megawatts (gross).

^b Westinghouse design (Westinghouse Electric Corporation, 1984).

^c VVER design (Muraviev, 2014).

^d General Electric design (GE Nuclear Energy, 1972), initial enrichment is 1.7–2.0 wt% ²³⁵U.

^e EC6 design (Candu Energy, 2012).

^f RBMK design (Muraviev, 2014).

^g BN-600 design (WNA, 2021b).

primarily of ²³⁸U, which is a fissionable element that undergoes fission only with high-energy neutrons, with a smaller fraction of ²³⁵U. As shown in Table 18.1, fast-neutron-spectrum reactors require a higher percentage of fissile elements than thermal-neutron-spectrum reactors as the probability of fission reaction of fissile elements such as ²³⁵U and ²³⁹Pu with fast neutrons is lower.

Even though the majority of the commercial nuclear reactors are thermal-neutron-spectrum reactors, there has been a continuous scientific effort for design and operation of fast-neutron-spectrum reactors since the inception of the nuclear technology. First experimental fast-neutron-spectrum reactors (or fast reactors) such as Clementine, EBR-I, BR-10 and FBTR reached their first criticality, respectively, in 1946, 1951, 1958, and 1985. Later in the 1970s through 1990s, first prototype fast reactors Phenix, PFR, BN-600, and Monju SFR commenced their operation (Waltar et al., 2012). There is a renewed interest in fast-neutron-spectrum reactors to be included as part of the overall nuclear-fuel cycle, because of the advantages that these reactors offer. Currently, an international collaboration has focused on the development of six (6) concepts of the Generation-IV nuclear reactors. There are several fast-neutron-spectrum reactors among the selected designs. Table 18.2 provides a summary of the Generation-IV nuclear-reactor concepts (WNA, 2020a).

Table 18.2. Neutron spectrum, coolant, temperature/pressure, and fuel of Generation-IV nuclear-reactor concepts (WNA, 2020a)

Reactor	Neutron spectrum	Coolant	Temperature (°C)	Pressure ^a	Fuel	Fuel cycle	Uses
GFR	Fast	Helium	850	High	²³⁸ U + ^b	Closed, on site	Electricity & hydrogen
LFR	Fast	Lead or Pb-Bi	480–570	Low	²³⁸ U +	Closed, regional	Electricity & hydrogen
MSR	Fast	Fluoride salts	700–800	Low	UF in salt	Closed	Electricity & hydrogen
MSR—advanced high-temperature reactor	Thermal	Fluoride salts	750–1000	–	UO ₂ particles in prism	Open	Hydrogen
SFR	Fast	Sodium	500–550	Low	²³⁸ U & MOX	Closed	Electricity
SCWR	Thermal or fast	Water	510–625	Very high	UO ₂	Open (thermal) closed (fast)	Electricity
VHTR	Thermal	Helium	900–1000	High	UO ₂ prism or pebbles	Open	Hydrogen & electricity

^a High = 7–15 MPa and very high = ~25 MPa.

^b + = with some ²³⁵U or ²³⁹Pu.

Nuclear reactors can be designed on a basis of their fuel cycle, such that they breed more fissile nuclides than what they use. Breeder reactors can utilize uranium, thorium, and plutonium resources more efficiently. There are two types of breeder reactors: (1) fast-neutron-spectrum-breeder and (2) thermal-neutron-spectrum-breeder reactors, which are designed based on ²³⁸U (99.2% natural abundance) and ²³²Th (100% natural abundance), respectively. Fertile nuclides ²³⁸U and ²³²Th capture neutrons and transform, respectively, to fissile nuclides ²³⁹Pu and ²³³U. Through this process, which is known as breeding, the reactor produces more fissile nuclides than what it consumes. Fast-Breeder Reactors (FBRs) can also be used in order to transmute the long-lived minor actinides in the spent fuel to radionuclides with shorter half-lives. Thermal breeder reactors, on the other hand, produce less minor actinides in the spent fuel. ²³²Th-²³³U breeding cycle can be utilized in both fast and thermal reactors (Waltar et al., 2012). Even though both fast and thermal breeder reactors have been designed, FBRs are more efficient breeders. It is also notable that FBRs utilize the same fuel, UO₂-PuO₂, which has been used in some of the existing commercial nuclear reactors.

The ²³²Th-²³³U cycle is of interest because the abundance of thorium in the earth's crust is between three to five times that of uranium (OECD/NEA and IAEA, 2022; WNA, 2020b). In addition, there are large thorium deposits in some countries such as India, Brazil, Australia, and USA (WNA, 2020b). The ²³⁸U-²³⁹Pu cycle is most effective with fast neutrons. For ²³⁹Pu, the number of emitted neutrons in a fission reaction per absorbed neutrons is greater, when fission is induced by fast neutrons rather than thermal neutrons. The additionally emitted neutrons can be utilized for transforming more ²³⁸U nuclides to ²³⁹Pu. Hence, the FBRs are based on

^{238}U - ^{239}Pu in which ^{239}Pu and ^{238}U in the core undergo fission. In a two-region reactor, ^{238}U nuclides, in the core and in the blanket,^a are transmuted to ^{239}Pu (Alexander, 1964; Waltar et al., 2012).

Regardless of the nuclear fuel type and cycle, the fuel is designed in various geometrical configurations and chemical forms. In terms of geometrical configuration, nuclear fuels have been designed in the forms of cylindrical pellets, annular pellets, pebbles, plates, and TRistructural ISOtopic (TRISO) pellets. Cylindrical pellets are used in PWRs, BWRs, CANDU reactors; annular pellets are used in VVER and RBMK designs (IAEA, 2007); pebbles are used in PBMR (Kadak, 2005); TRISO pellets are used in VHTR (IAEA, 2010); plates are used in some research reactors such as Advanced Test Reactor (Stanley and Marshall, 2008). In addition to these geometrical configurations, nuclear fuels can also be classified into four categories based on their chemical makeup and atomic structure: (1) metallic fuels, (2) ceramic fuels, (3) hydride fuels, and (4) composite fuels. The following subsections provide an overview of these nuclear fuels.

18.2 Metallic fuels

Uranium, plutonium, and thorium are the most common metallic fuels (Kirillov et al., 2007). These metallic fuels have high thermal conductivity, high fissile atom density, good neutron economy and good fabrication characteristics (Ma, 1983) which have made them as fuels of choice for a number of reactors. For instance, the uranium metal fuel was used in NRX (Larson, 1961). However, the maximum fuel temperature was limited to about 668°C to prevent change from the α -phase to β -phase. A phase transformation results in a volume change in the fuel. For instance, α -phase of uranium metal is stable up to 670°C, the β -phase exists between 670°C and 776°C, and the γ -phase exists from 776°C up to the melting point of $\sim 1135^\circ\text{C}$ (Kirillov et al., 2007). To avoid volume changes during phase transformations, the use of metallic uranium fuel is limited to temperatures below 660°C (ORNL, 1965).

The α -phase uranium is characterized with a high anisotropic thermal expansion and shows poor dimensional stability during irradiation. The dimensional changes in the α -phase uranium are due to irradiation growth, irradiation creep, and irradiation swelling (Roy and Sah, 1985). Irradiation swelling which results in a volume increase caused by solid or gaseous fission products. The irradiation swelling is mainly due to formation of bubbles by gaseous fission products such as krypton and xenon. The bubble migration and hence the fuel swelling mainly depends on the temperature gradient between the outer surface temperature and the center temperature of the fuel. The temperature gradient itself depends on the thermal conductivity of the fuel which is relatively high for metallic fuels such as metallic uranium. Despite the small bubble migration (Roy and Sah, 1985) and the negative effects of radiation on the thermal conductivity (Kirillov et al., 2007), the performance of the metallic fuels is impacted by the swelling and release of gaseous fission products (Sundaram and Mannan, 1989).

Although the most desired property of metallic fuels is their high thermal conductivity, which results in small temperature gradients across the fuel leading to low temperatures at the center of the fuel elements, metallic fuels are susceptible to corrosion especially at high temperatures when exposed to air or water. Due to an inferior compatibility of the metallic fuels with light-water, metallic fuels have not gained interest in commercial light-water or heavy-water reactors. On the other hand, metallic fuels such as uranium and plutonium fuels were used in the first generation of FBRs (Hafele et al., 1970).

To further improve radiation stability and metallurgical properties of metallic fuels, the metallic fuels are alloyed with other metals such as zirconium, chromium, or molybdenum. Metallic fuels such as U-Fs, U-Zr, and U-Pu-Zr were used in Experimental Breeder Reactor II (EBR-II) for about 30 years (FRWG, 2018) and, also, in other fast-neutron-spectrum reactors. Fissionium (Fs) is a mixture consisting of natural stable forms of several fission products of atomic number 40–46 (Zr, Nb, Mo, Tc, Ru, Rh, and Pd) (Evans et al., 1960).

^a The blanket, which surrounds the reactor core, is the region containing the fertile nuclides.

A typical composition of U-Fs is as follows: 95.1 wt% uranium, 2.5 wt% molybdenum, 0.1 wt% zirconium, 1.5 wt% ruthenium, 0.3 wt% rhodium, and 0.5 wt% palladium (Sailer et al., 1956).

Metallic fuels have also been used in some power reactors and research reactors with relatively low operating temperatures. For instance, a uranium alloy has been used in Magnox reactors (Simnad, 2003). Magnox reactors are subject to two design temperature limits at steady-state conditions. First, the fuel temperature should be below 660°C. Second, the cladding temperature should be below 420°C (Zakova, 2012).

For use in high-temperature applications, a potential fuel must have a high melting point, high thermal conductivity, and good irradiation and mechanical stability (Ma, 1983). These requirements eliminate the use of metallic fuels mainly due to their low melting points and high irradiation creep and swelling rates (Ma, 1983). On the other hand, ceramic fuels have promising properties, which has made these fuels as the fuels of choice for the current commercial nuclear reactors and suitable candidates for high-temperature applications. Next section provides more information on ceramic fuels.

18.3 Ceramic fuels

Ceramic fuels have high melting points, good dimensional and radiation stability and are chemically compatible with most coolants and sheath materials. In addition to the melting point, the thermal conductivity of a fuel is a critical property that affects the operating temperature of the fuel (the highest temperature in a reactor is the fuel centerline temperature, for hollow pellets it will be the internal wall temperature). UO_2 has been used as the fuel of choice in BWRs, PWRs, and CANDU reactors. The thermal conductivity of UO_2 is approximately between 2 and 4 W/mK within the operating temperature range of 1000 and 2800°C. On the other hand, fuels such as UC_2 , UC, and UN have significantly higher thermal conductivities compared to that of UO_2 and other oxide fuels as shown in Figure 18.1. The high thermal conductivities of these fuels result in lower fuel temperatures compared to those of UO_2 under the same operating conditions (Peiman et al., 2015; Miletic et al., 2015; Abdalla et al., 2012; Grande et al., 2011).

Considering the chemical composition of ceramic fuels, these fuels can be categorized as oxide fuels, carbide fuels and nitride fuels. Oxide fuels such as UO_2 and ThO_2 have lower thermal conductivities compared to carbide and nitride fuels. Hence, from the heat-transfer point of view, oxide fuels can also be classified as low thermal-conductivity fuels. On the other hand, carbide (e.g., UC and UC_2) and nitride (e.g., UN) fuels are classified as high thermal-conductivity fuels. Table 18.3 lists basic properties of these fuels at 0.1 MPa and 25°C.

18.3.1 Oxide fuels

Oxides of uranium, thorium and plutonium have been used as nuclear fuels (i.e., UO_2 , ThO_2 , and PuO_2). These fuels have good corrosion resistance to water, high melting point, and excellent mechanical and irradiation stability. As such, UO_2 and PuO_2 have been used as fuel in commercial nuclear reactors such as PWRs, BWRs, CANDU reactors, etc. In addition, oxide fuels are chemically compatible with the cladding materials and water, which is used as the coolant in these reactors. On the other hand, the disadvantages of oxide fuels include low uranium atom density, low thermal conductivity and poor thermal shock resistance (Simnad, 2003). With a focus on thermo-physical properties, the following subsections provide a review of the properties of UO_2 and ThO_2 .

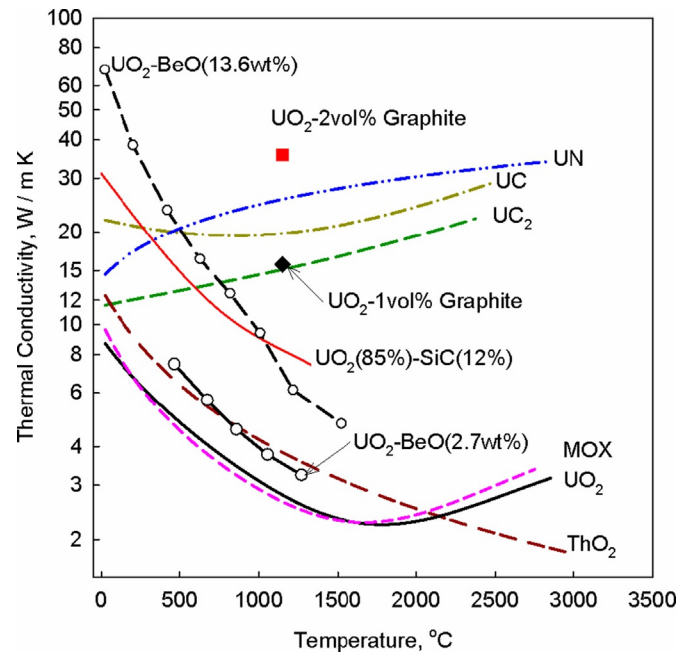


Figure 18.1. Thermal conductivity of several nuclear fuels (Cox and Cronenberg, 1977; Frost, 1963; IAEA, 2008; Ishimoto et al., 1996; Leitnaker and Godfrey, 1967; Khan et al., 2010, Kirillov et al., 2007; Lundberg and Hobbins, 1992; Solomon et al., 2005)

18.3.1.1 UO_2

As a ceramic fuel, Uranium diOxide (UO_2) is a hard and brittle material due to its ionic or covalent interatomic bonding. In spite of that, UO_2 is currently used in PWRs, BWRs, CANDU reactors, and other nuclear reactors due to its favorable properties. Oxygen has a very low thermal-neutron absorption cross-section, which does not result in a serious loss of neutrons. UO_2 is chemically stable and does not react with water within the operating temperatures of these reactors. UO_2 is structurally very stable such that the crystal structure of the UO_2 fuel retains most of the fission products even at high burn-ups (Cochran and Tsoulfanidis, 1999).

The thermal conductivity of the fuel is an important thermophysical property in the computation of the fuel temperature. The thermal conductivity of 95% theoretical density UO_2 can be calculated using the Frank correlation, shown as Eq. (18.1) (Carbajo et al., 2001). In Eq. (18.1), T is the temperature in K. This correlation is valid for temperatures in the range of 25–2847°C. Even though UO_2 has a high melting point, its thermal conductivity is very low compared to those of high thermal-conductivity or composite fuels. The properties of other fuels are discussed in the following sections.

$$k_{UO_2}(T) = \frac{100}{7.5408 + 17.692 \times (10^{-3}T) + 3.6142 \times (10^{-3}T)^2} + \frac{6400}{(10^{-3}T)^{5/2}} \exp^{-16.35/(10^{-3}T)} \quad (18.1)$$

The thermal conductivity of the fuel varies with temperature and is affected by manufacturing methods, the percentage of the porosity of the fuel, burn-up, fission gas release and deviation from stoichiometry. As such, there are uncertainties in the reported thermal conductivities. For UO_2 , the uncertainty is about 10% for temperatures below 1727°C (2000 K), while the uncertainty increases up to 20% for temperatures between 1727°C (2000 K) and 2847°C (3120 K) (IAEA, 2006). Figure 18.2 shows the thermal-conductivity profiles

Table 18.3. Basic properties of selected fuels at 0.1 MPa and 25°C (Chirkin, 1968; IAEA, 2008; Frost, 1963; Cox and Cronenberg, 1977; Leitnaker and Godfrey, 1967; Lundberg and Hobbins, 1992)

Property	Unit	UO ₂	MOX ^a	ThO ₂	UC	UC ₂	UN
Molecular mass	amu	270.3	271.2	264	250.04	262.05	252.03
Theoretical Density (TD)	kg/m ³	10,960	11,074	10,000	13,630 ^b	11,680	14,420
Melting point	°C	2847 ± 30	2750 ± 50 ^c	3378 ± 17 ^d	2507 ^e 2520 2532 ^f	2375 2562	2850 ± 30 ^g
Heat capacity	J/kgK	235	240	235	203 ^h	233	190
Heat of vaporization	kJ/kg	1530	1498	-	2120	1975 ± 20 ³	1144 ⁱ 3325 ^j
Thermal conductivity	W/mK	8.7	7.8 ^k	9.7	21.2	11.57	14.6
Linear expansion coefficient, × 10 ⁻⁶	1/K	9.75	9.43	8.9 ^l	10.1	18.1 ^m	7.52
Electric resistivity, × 10 ⁻⁸	Ωm	7.32	-	-	250	120	146
Crystal structure	-	FCC ⁿ	FCC	FCC	FCC	BCT ^o , <i>t</i> < 1820°C FCC, <i>t</i> > 1820°C	FCC

^a MOX—Mixed OXides (U_{0.8}Pu_{0.2})O₂, where 0.8 and 0.2 are the molar parts of UO₂ and PuO₂.

^b Frost (1963).

^c Popov et al. (2000).

^d IAEA (2006).

^e Cox and Cronenberg (1977).

^f Lundberg and Hobbins (1992).

^g At nitrogen pressure ≥ 0.25 MPa.

^h Leitnaker and Godfrey (1967).

ⁱ UN(s) = U(l) + 0.5N₂(g), Gingerich (1969).

^j UN(s) = U(g) + 0.5N₂(g), Gingerich (1969).

^k At 95% density.

^l At 1000°C, Bowman et al. (1966).

^m At 1000°C, Bowman et al. (1966).

ⁿ FCC—Faced-Centered Cubic.

^o BCT—Body-Centered Tetragonal.

of UO₂ as a function of fuel temperature for various percentages of theoretical fuel density, manufacturing, stoichiometry and irradiation. Figure 18.3 shows the impact of porosity and irradiation on thermal conductivity of UO₂. Thermal conductivity is shown for un-irradiated UO₂ and irradiated UO₂ with a neutron flux of 1.16×10^{19} neutrons/cm² at 527°C (800 K) before testing. In addition, Figure 18.4 shows the uncertainty

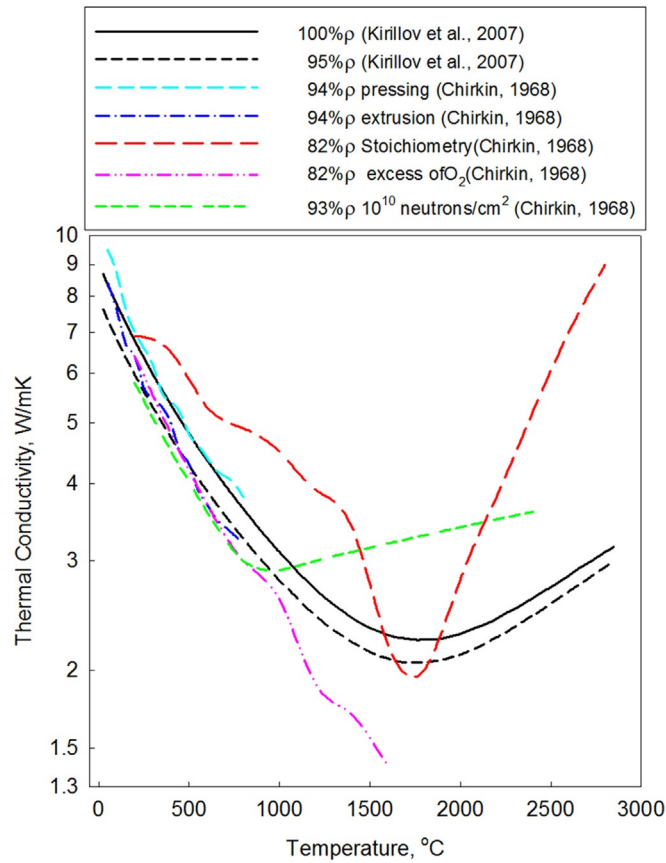


Figure 18.2. Thermal conductivity of UO_2 as a function of percentage of theoretical density, manufacturing, stoichiometry and irradiation

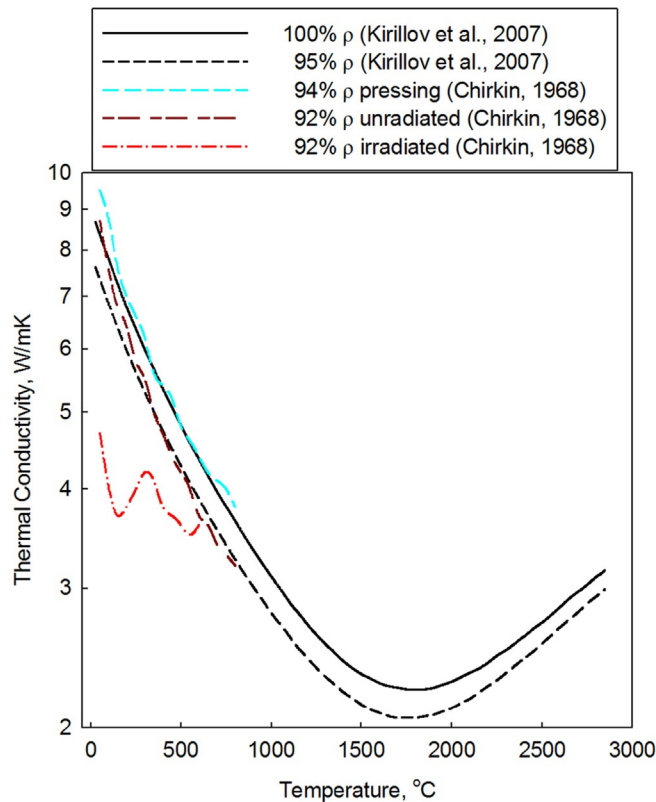


Figure 18.3. Impact of porosity and irradiation of thermal conductivity of UO_2

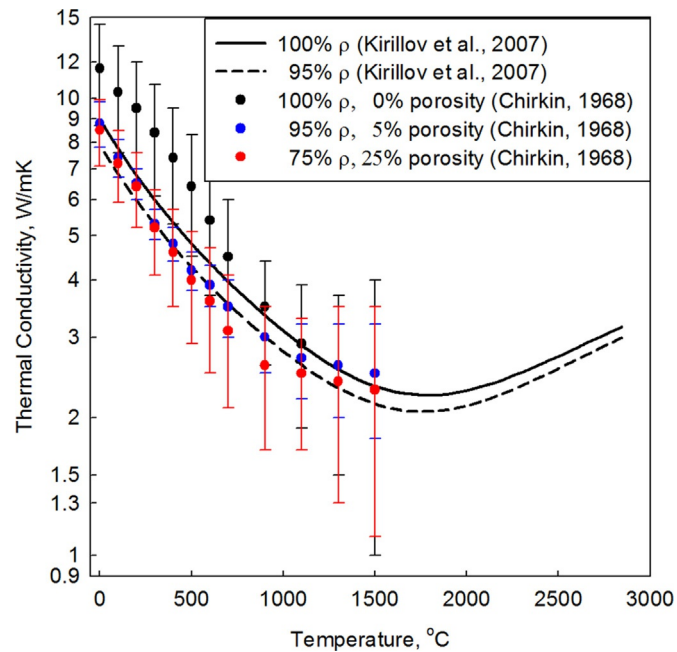


Figure 18.4. Uncertainty in thermal conductivity of UO_2

associated with the thermal conductivity of UO_2 for various percentages of fuel porosity. In these figures, the theoretical density of UO_2 is considered to be $10,960 \text{ kg/m}^3$.

18.3.1.2 ThO_2

Thorium is widely distributed in nature and is approximately three times as abundant as uranium. In addition to its abundance, thorium reduces the need for enrichment, provides a high conversion ratio in thermal-neutron-spectrum reactors, and has favorable neutron and thermophysical properties which have resulted in renewed interest in using thorium-based fuels in nuclear reactors.

Since ThO_2 does not have any fissile elements to fission with thermal neutrons, ThO_2 must be used in combination with a “driver” fuel (e.g., UO_2 , UC , or PuO_2), which has ^{235}U as its initial fissile elements. The presence of a “driver” fuel such as UO_2 in a nuclear-reactor core results in the production of enough neutrons, which in turn start the thorium cycle. In this cycle, ^{232}Th is converted into ^{233}Th , which decays to ^{233}Pa . Eventually, ^{233}U , which is a fissile element, is formed by the β -decay of ^{233}Pa (Cochran and Tsoulfanidis, 1999).

With a focus on the thermophysical properties of the thorium-based fuels, Jain et al. (2006) conducted experiments on thorium and the solid solutions of Thorium diOxide (ThO_2) and Lanthanum Oxide ($\text{LaO}_{1.5}$). As a result of their experiments, Jain et al. (2006) determined the density, thermal diffusivity, and specific heat for several compositions of ThO_2 and $\text{LaO}_{1.5}$ ranging from pure thorium to 10 mole percent $\text{LaO}_{1.5}$. These properties were measured for temperatures between 100°C and 1500°C (Jain et al., 2006).

In their analysis, the thermal conductivity values were calculated based on Eq. (18.2), which requires the measured values of the thermal diffusivity, specific heat, and density of these solid solutions. The correlation developed by Jain et al. (2006), which is shown as Eq. (18.3), has been used in order to calculate the thermal conductivity of ThO_2 fuel for the purpose of computing the fuel temperature. In Eq. (18.3), T is the temperature in K.

$$k = \alpha \rho c_p \quad (18.2)$$

$$k_{\text{ThO}_2} = \frac{1}{0.0327 + 1.603 \cdot 10^{-4} T} \quad (18.3)$$

Bakker et al. (1977) proposed a correlation, which is shown as Eq. (18.4), for the calculation of the thermal conductivity of ThO₂ with 95% theoretical density. This correlation is valid for the temperature range between 27°C (300 K) and 1727°C (2000 K) (Das and Bharadwaj, 2013). In Eq. (18.4), T is the temperature in K.

$$k_{\text{ThO}_2} = \frac{1}{4.20 \times 10^{-4} + 2.25 \times 10^{-4} T} \quad (18.4)$$

Belle and Berman (1984) also developed a correlation for the calculation of the thermal conductivity of ThO₂. This correlation is shown as Eq. (18.5), which is valid for ThO₂ with 100% theoretical density and in the temperature range between 25°C (298 K) and 2677°C (2950 K). In Eq. (18.5), T is the temperature in K.

$$k_{\text{ThO}_2} = \frac{1}{0.0213 + 1.597 \times 10^{-4} T} \quad (18.5)$$

Even though the above equations capture the variation in thermal conductivity of ThO₂ as a function of temperature, the thermal conductivity of ThO₂ also changes due to manufacturing methods, the percentage of the porosity of the fuel, burn-up, fission gas release and deviation from stoichiometry. Figure 18.5 shows the variation in thermal conductivity of ThO₂ for various porosities and densities as a function of temperature.

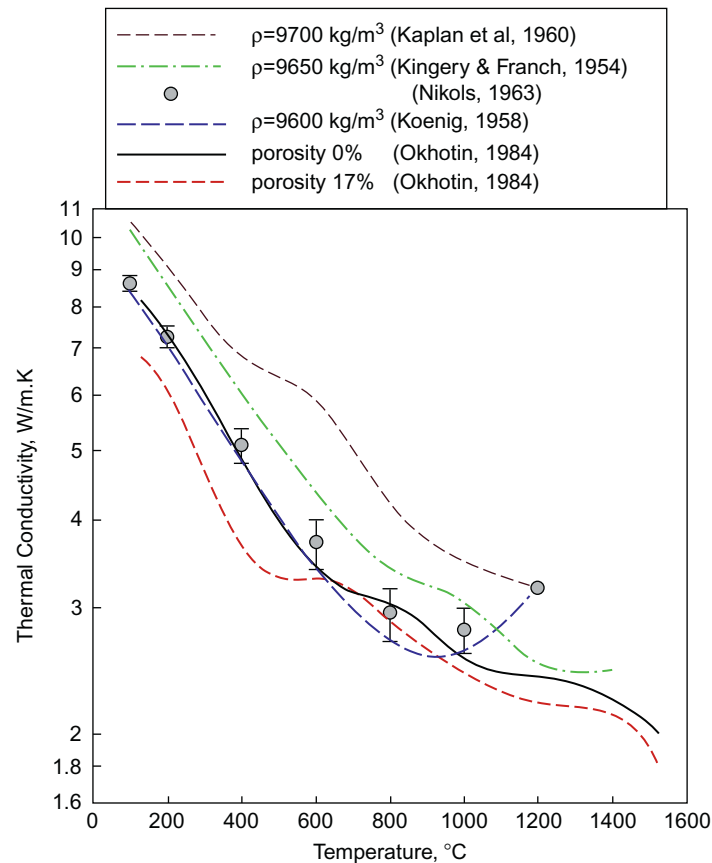


Figure 18.5. Thermal conductivities of thorium dioxide for various porosities and densities

18.3.2 Mixed oxide fuels

18.3.2.1 UO_2+PuO_2

Mixed oxide fuel refers to nuclear fuels consisting of more than one oxide. The most common mixed oxide fuel consists of UO_2 and Plutonium diOxide (PuO_2). The fuel was initially designed for use in Liquid-Metal Fast Breeder Reactors (LMFBRs) and in Light Water Reactors (LWRs), when reprocessing and recycling of the used fuel is adopted (Cochran and Tsoulfanidis, 1999). The uranium dioxide content of the mixed oxide fuel may consist of natural, enriched, or depleted uranium, depending on the application of the fuel. In general, the fuel contains between 3% and 5% PuO_2 blended with 95%–97% natural or depleted uranium dioxide (Carbajo et al., 2001). The small fraction of PuO_2 slightly changes the thermophysical properties of the fuel compared with those of the UO_2 fuel.

Most thermophysical properties of UO_2 and UO_2+PuO_2 (3%–5% PuO_2) fuels have similar trends. For instance, thermal conductivities of UO_2 and UO_2+PuO_2 fuels decrease as the temperature increases up to 1700°C (see Figure 18.1). Despite similar trends in thermal conductivity, UO_2 and UO_2+PuO_2 fuels have different densities and melting points. The density of the UO_2+PuO_2 fuel is slightly higher than that of the UO_2 fuel. The mixed oxide fuel has a lower melting temperature, lower heat of fusion, and lower thermal conductivity than UO_2 . For the same power, UO_2+PuO_2 has a higher stored energy, which results in a higher fuel centerline temperature compared with the UO_2 fuel. The fission-gas release rate from the mixed oxide fuel is higher compared to UO_2 , because of the lower thermal conductivity of UO_2+PuO_2 up to temperatures around 1500°C, which results in higher fuel temperatures. The most significant differences between these two fuels have been summarized in Table 18.3.

The thermal conductivities of UO_2+PuO_2 and UO_2 decrease as functions of temperature up to temperatures around 1527°C and 1727°C, respectively, and then they increase as the temperature increases (see Figure 18.1). In general, the thermal conductivity of MOX fuel is slightly lower than that of UO_2 . In other words, the addition of small amounts of PuO_2 decreases the thermal conductivity of the mixed fuel. However, the thermal conductivity of UO_2+PuO_2 does not decrease significantly, when the PuO_2 content of the fuel is between 3% and 15%. The thermal conductivity of UO_2+PuO_2 decreases as the concentration of PuO_2 increases beyond 15%. As a result, the concentration of PuO_2 in commercial mixed oxide fuels is kept below 5% (Carbajo et al., 2001; Popov et al., 2000). Carbajo et al. (2001) recommend the following correlation shown as Eq. (18.6) for the calculation of the thermal conductivity of the UO_2+PuO_2 fuel with 95% theoretical density. This correlation is valid for temperatures between 427°C and 2827°C, x less than 0.05, and PuO_2 concentrations between 3% and 15%. In Eq. (18.6), T is the temperature in K. The uncertainty associated with Eq. (18.6) is 7% for temperatures between 427°C (700 K) and 1527°C (1800 K). For temperatures above 2827°C (3100 K), the uncertainty increases to 20%.

$$k(T, x) = \frac{1}{A + C(10^{-3}T)} + \frac{6400}{(10^{-3}T)^{5/2}} \exp^{-16.35/(10^{-3}T)} \quad (18.6)$$

where x is a function of oxygen to heavy metal ratio ($x = 2 - O/M$) and $A(x) = 2.58x + 0.035$ (mK/W), $C(x) = (-0.715x + 0.286)$ (m/W).

18.3.2.2 ThO_2+UO_2 and ThO_2+PuO_2

ThO_2-UO_2 and ThO_2-PuO_2 are two thorium-based mixed oxide fuels. Figure 18.6 shows the thermal conductivities of ThO_2 , ThO_2-UO_2 , and ThO_2-PuO_2 as a function of temperature. The thermal conductivity of $(Th_{1-y}Pu_y)O_2$ is calculated based on Eq. (18.7), which is valid for the temperature range between 873 and

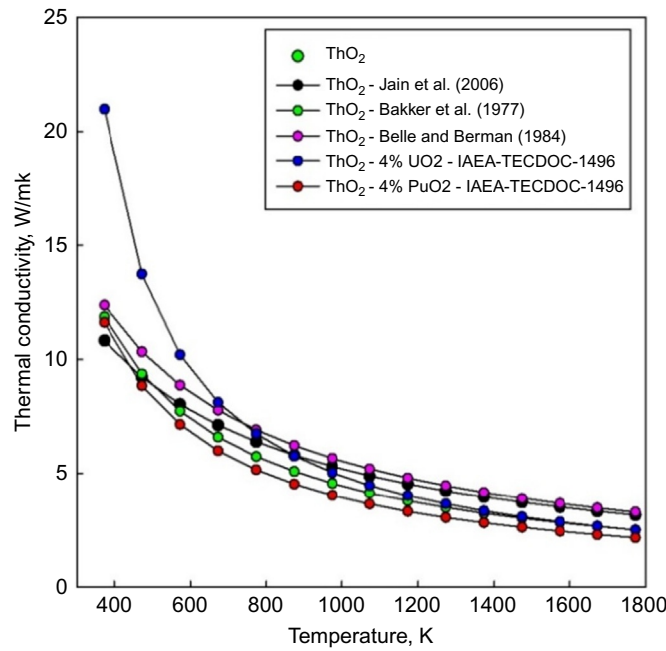


Figure 18.6. Thermal conductivity of ThO_2 , $\text{ThO}_2\text{-UO}_2$, and $\text{ThO}_2\text{-PuO}_2$ (Peiman et al., 2015).

1873 K (IAEA, 2006). In Eq. (18.7), k is the thermal conductivity in W/mK, T is the temperature in K, and y is the weight percent of PuO_2 . Das and Bharadwaj (2013), IAEA (2006) and Belle and Berman (1984) provide detail information about thorium-based fuels.

$$k_{(\text{Th}_{1-y}\text{Pu}_y)\text{O}_2} = \frac{1}{-0.08388 + 1.7378y + (2.62524 \times 10^{-4} + 1.7405 \times 10^{-4}y)T} \quad (18.7)$$

IAEA (2006) recommends Eq. (18.8) for the calculation of the thermal conductivity of $(\text{Th}_{1-y}\text{U}_y)\text{O}_2$ with 95% theoretical density for the temperature range between 600°C (873 K) and 1600°C (1873 K). In this equation, T is the temperature in Kelvin and y is the weight percent of UO_2 .

$$k_{(\text{Th}_{1-y}\text{U}_y)\text{O}_2} = \frac{1}{-0.0464 + 0.0034y + (2.5185 \times 10^{-4} + 1.0733 \times 10^{-7}y)T} \quad (18.8)$$

18.3.3 Carbide fuels

Carbides of uranium and thorium have been considered as nuclear fuels (Simnad, 2003). The use of carbides of plutonium has also been investigated as mixed carbides such as UC-PuC (Ogard and Leary, 1970). Compared to MOX fuel, mixed carbide fuel has a higher thermal conductivity, higher heavy-metal density and better neutron economy. Carbides of thorium, ThC and ThC_2 , are the most stable compounds of thorium after thorium dioxide. ThC is stable up to temperatures close to its melting point. Carbides of uranium have desirable properties such as high thermal conductivities and high melting points. Uranium Carbide (UC) and Uranium diCarbide (UC_2) are two carbides of uranium, which can be used as nuclear fuels. Uranium sesquiCarbide (U_2C_3) is another carbide of uranium. U_2C_3 cannot be manufactured through casting or compaction of a powder. But, UC_2 may transform to U_2C_3 at high temperatures and under stress (Frost, 1963). The following two subsections provide an overview of the thermophysical, mechanical and irradiation properties of UC and UC_2 .

18.3.3.1 UC

UC, which has a Face-Centered Cubic (FCC) crystal structure similar to those of UN and NaCl, has a high melting point approximately 2507°C and a high thermal conductivity, above 19 W/mK at all temperatures up to the melting point. UC has a density of 13,630 kg/m³, which is lower than that of UN, but higher than those of UO₂ and UC₂. It should be noted that the density of hypo-stoichiometric UC is slightly higher than that of stoichiometric UC, which is listed in Table 18.3. Coninck et al. (1975) reported densities between 13,730 and 13,820 kg/m³ at 25°C for hypo-stoichiometric UC. Moreover, Uranium atom density of UC is higher than that of UO₂ but lower than that of UN. The uranium atom densities of UC and UN are 1.34 and 1.4 times that of UO₂.

Many researchers have studied thermophysical properties of UC. Coninck et al. (1975) conducted experiments on hypo-stoichiometric and stoichiometric UC and determined the thermal diffusivity, thermal conductivity, and spectral emissivity of UC. For hypo-stoichiometric UC, the thermal diffusivity α , in m²/s, and thermal conductivity k , in W/mK, correlations are valid for a temperature range of 570°C and 2000°C. In Eqs. (18.9), (18.10), T is the temperature in K (Coninck et al., 1975).

$$\alpha = 10^{-4} \cdot [5.75 \cdot 10^{-2} + 1.25 \cdot 10^{-6}(T - 273.15)] \quad (18.9)$$

$$k = 100 \cdot [2.04 \cdot 10^{-1} + 2.836 \cdot 10^{-8}(T - 843.15)^2] \quad (18.10)$$

Coninck et al. (1975) provided two correlations for the calculation of the spectral emissivity of hypo-stoichiometric UC. Eq. (18.11) has been suggested for pure UC when temperature varies between 1100°C and 2000°C. Moreover, Eq. (18.12) can be used in order to determine the spectral emissivity of oxidized samples for temperatures between 1100°C and 1600°C. In Eqs. (18.11), (18.12), T is the temperature in K.

$$\varepsilon_{sm} = 5.5 \cdot 10^{-1} - 8.5 \cdot 10^{-5}(T - 273.15) \quad (18.11)$$

$$\begin{aligned} \varepsilon_{sm} = & -4.666 \cdot 10^{-1} + 1.050 \cdot 10^{-1}(T - 273.15) - 7.627 \cdot 10^{-5}(T - 273.15)^2 \\ & + 1.813 \cdot 10^{-8}(T - 273.15)^3 \end{aligned} \quad (18.12)$$

Coninck et al. (1975) provided two correlations, shown as Eqs. (18.13), (18.14), which can be used to determine the mean values of the thermal diffusivity and thermal conductivity of stoichiometric UC for a temperature range between 850°C and 2250°C, in m²/s and W/mK, respectively. In addition, Eq. (18.15) can be used to calculate the spectral emissivity of stoichiometric UC for temperatures between 1100°C and 2250°C (Coninck et al., 1975). In Eqs. (18.13)–(18.15), T is the temperature in K.

$$\alpha = 10^{-4} \cdot [5.7 \cdot 10^{-2} + 1.82 \cdot 10^{-12}(T - 1123.15)^3] \quad (18.13)$$

$$k = 100 \cdot [1.95 \cdot 10^{-1} + 3.57 \cdot 10^{-8}(T - 1123.15)^2] \quad (18.14)$$

$$\varepsilon_{sm} = 5.65 \cdot 10^{-1} - 5 \cdot 10^{-5}(T - 273.15) \quad (18.15)$$

In addition to Eqs. (18.10), (18.14), Kirillov et al. (2007) recommended another correlation, shown as Eqs. (18.16), (18.17), for the calculation of the thermal conductivity of UC, in W/mK, for temperatures up to 700°C and 2300°C, respectively. Figure 18.7 shows the thermal conductivity of UC calculated using Eqs. (18.10), (18.14), (18.16), (18.17) as a function of temperature. It is recommended to use Eq. (18.14) for the calculation of the thermal conductivity of UC fuel because this equation provides the lowest thermal conductivity values for a wide temperature range, leading to a conservative calculation of the fuel temperature profile. In Eqs. (18.16), (18.17), T is the temperature in K.

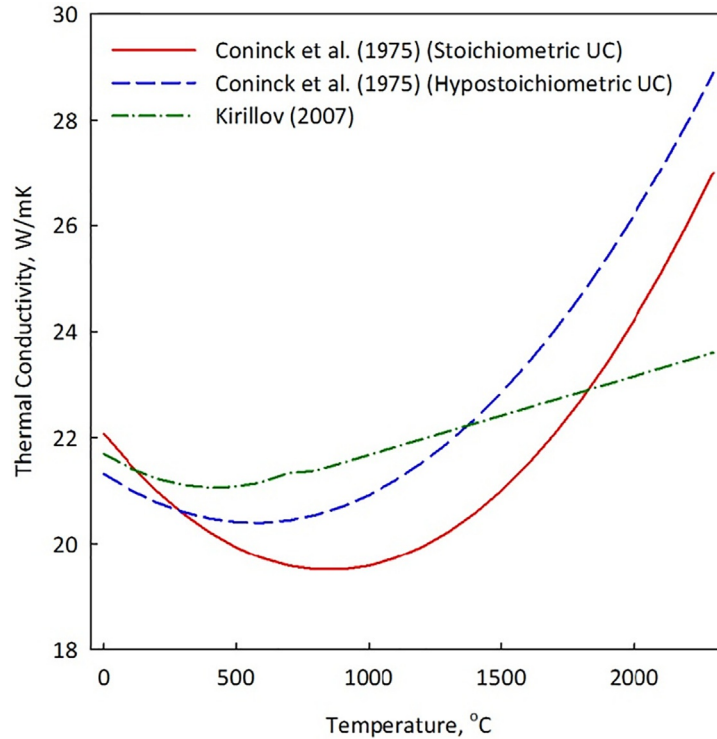


Figure 18.7. Thermal conductivity of UC resulted from various correlations.

$$k = 21.7 - 3.04 \cdot 10^{-3}(T - 273.15) + 3.61 \cdot 10^{-6}(T - 273.15)^2, 323 < T < 973 \text{ K} \quad (18.16)$$

$$k = 20.2 + 1.48 \cdot 10^{-3}(T - 273.15), 973 < T < 2573 \text{ K} \quad (18.17)$$

Leitnaker and Godfrey (1967) conducted experiments on UC in a temperature range between 298.15 and 2800 K. As a result, they provided Eqs. (18.18), (18.19), which can be used in order to calculate the specific heat and the enthalpy of UC based on the results of Leitnaker and Godfrey (1967), where T is the temperature in K and the specific heat and enthalpy are in J/kgK and J/kg, respectively. The average percent error associated with Eq. (18.19) is $\pm 0.84\%$.

$$c_p = 6 \cdot 10^{-15}T^5 - 6 \cdot 10^{-11}T^4 + 2 \cdot 10^{-7}T^3 - 3 \cdot 10^{-4}T^2 + 0.2655 T + 147.34 \quad (18.18)$$

$$H(T) - H(298 \text{ K}) = \frac{4184}{250.04} \left[14.430 T - 1.074 \cdot 10^{-3}T^2 + 1.890 \cdot 10^5 T^{-1} + 3.473 \cdot 10^{-5}T^{5/2} - 4.894 \cdot 10^3 \right] \quad (18.19)$$

The linear thermal expansion of UC, in 1/K, for a temperature range of 0–2000°C can be calculated using a correlation shown as Eq. (18.20) (IAEA, 2008) with an uncertainty of $\pm 15\%$. In Eq. (18.20), T is the temperature in K. Figure 18.8 shows the variations in the specific heat, enthalpy, and linear thermal expansion of UC as functions of temperature.

$$\alpha = 1.007 \cdot 10^{-5} + 1.17 \cdot 10^{-9}(T - 273.15) \quad (18.20)$$

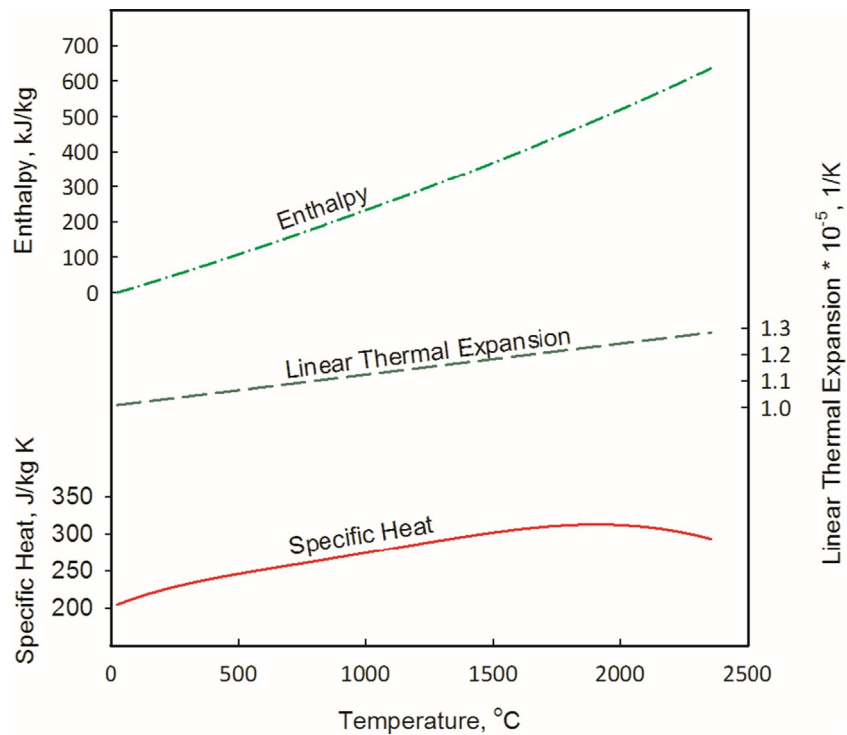


Figure 18.8. Thermodynamic properties of UC as function of temperature (IAEA, 2008; Leitnaker and Godfrey, 1967).

Frost (1963) developed a correlation shown as Eq. (18.21), which can be used to determine the diametric increase of UC fuel as a function of time-averaged fuel centerline temperature. According to Eq. (18.21), UC fuel undergoes significant swelling at temperatures above 1000°C. In Eq. (18.21), R_D and T are percent diametric increase per atom percent burn-up and time-averaged fuel centerline temperature in K, respectively. In addition, Harrison (1969) provided the volumetric swelling of UC as a function of burn-up for various temperatures. Figure 18.9 shows the result of the analysis conducted by Harrison (1969) on the volumetric swelling of UC.

$$R_D = 0.6 + 0.77 (9 T/5000 - 1) \quad (18.21)$$

Stellrecht et al. (1968) developed a correlation, shown as Eq. (18.22), which can be used to determine the compressive creep rate of UC in 1/h for temperatures between 1200°C and 1600°C and stress values between 20.68 and 68.95 MPa. This correlation was developed specifically based on data obtained on hyper-stoichiometric UC (e.g., UC_{1.08}). Seltzer et al. (1975) studied the effects of deviation from stoichiometry on the creep rate of UC and found that the creep rate decreases by increasing the C/U atomic ratio due to precipitation strengthening. Tokar et al. (1970) also demonstrated that the creep rate is higher for hypo-stoichiometric UC than hyper-stoichiometric UC due to the existence of free uranium in the microstructure of hypo-stoichiometric UC. However, this reduction in the creep rate depends on temperature and only exhibits at temperatures up to 1700°C. Figure 18.10 shows the creep rate of UC as a function of temperature for several selected stress values. In Eq. (18.22), σ_s is the stress in Pa; R is the gas constant in cal/K mole; and T is the temperature in K. As shown in Figure 18.10, the creep rate increases as the temperature increases; this indicates that the creep rate proportionally depends on temperature. In addition, the increase in temperature changes the creep mechanism from vacancy migration to dislocation motion (Tokar et al., 1970).

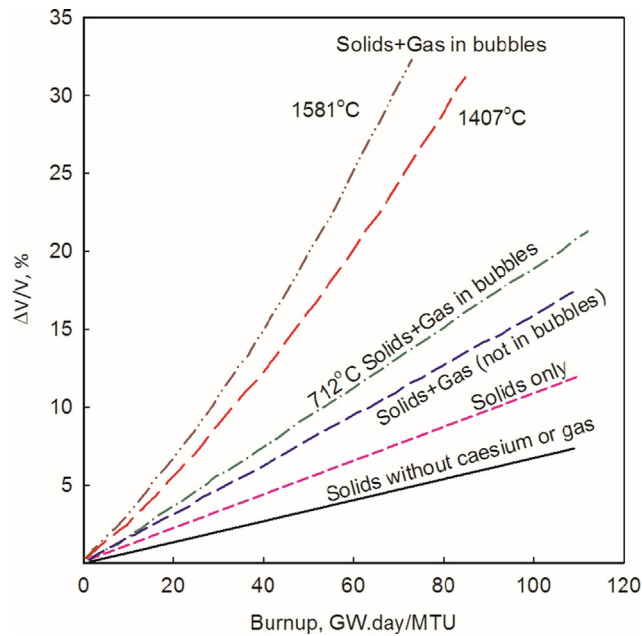


Figure 18.9. Volumetric swelling of UC as function of temperature and burn-up. *Based on Harrison (1969).*

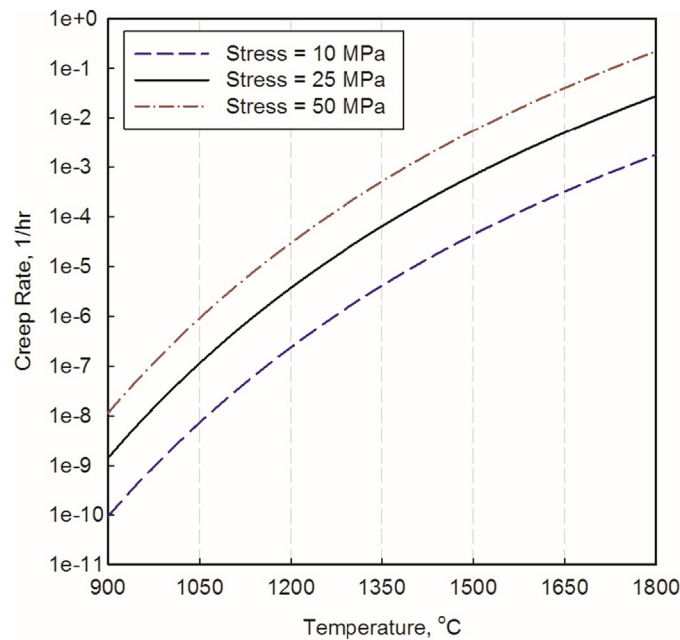


Figure 18.10. Creep rate of UC as function of temperature (Stellrecht et al., 1968).

$$\dot{\epsilon} = 1.8 \cdot 10^{-3} (\sigma_s / 6894.76)^3 e^{-\left(\frac{90,000}{RT}\right)} \quad (18.22)$$

18.3.3.2 UC₂

Uranium diCarbide (UC₂) is a carbide of uranium, which has a high melting point and a high thermal conductivity. UC₂ has a Body-Centered Tetragonal (BCT) crystal structure up to the transformation temperature of $1820 \pm 20^\circ\text{C}$, where it transforms to a FCC structure, similar to that of UO₂ (Frost, 1963). Frost (1963)

indicated that UC_2 has always been found in hypo-stoichiometric forms such as $\text{UC}_{1.75-1.90}$. The most common and probable composition of uranium dicarbide is $\text{UC}_{1.8}$, which is often written as UC_2 (Frost, 1963). In a VHTR design, UO_2 and UC_2 have been considered as the fuel with a ratio of 3:1 (Olander, 2009). The function of UC_2 is to reduce the UO_2 fuel back to UO_2 when oxygen is released from the UO_2 fuel.

The thermodynamic properties of UC_2 have been studied by several scientists. Coninck et al. (1976) conducted experiments on UC_2 and provided correlations for the calculation of the thermal diffusivity, thermal conductivity, and emissivity of UC_2 as functions of temperature. Coninck et al. (1976) used the modulated electron beam technique in order to determine the thermal diffusivity of UC_2 samples. In this technique, an electron gun is used to bombard a material in the form of a thin solid plate from one face. The electron gun is modulated to vary sinusoidally as a function of time. The phase difference between the temperature fluctuations of the two faces of the plate is measured, which is used to determine the thermal diffusivity of the material (Wheeler, 1965). Then, thermal conductivity is calculated as the multiplication of thermal diffusivity, density and specific heat as shown in Eq. (18.2).

Coninck et al. (1976) developed two correlations shown as Eqs. (18.23)–(18.26) for the calculation of the thermal diffusivity, in m^2/s , and thermal conductivity, in W/mK , of the nearly stoichiometric UC_2 . The correlations for slightly hypo-stoichiometric UC_2 and hypo-stoichiometric UC_2 are shown as Eqs. (18.27)–(18.32). In Eqs. (18.23)–(18.32), T is the temperature in K.

$$\alpha = 10^{-4} \cdot \left[0.0398 - 1.775 \cdot 10^{-6}(T - 273.15) - 8.65 \cdot 10^{-10}(T - 273.15)^2 \right], 873 < T < 2013 \text{ K} \quad (18.23)$$

$$\alpha = 0.0375 \cdot 10^{-4}, 2103 < T < 2333 \text{ K} \quad (18.24)$$

$$k = 100 \cdot \left[0.115 + 2.7 \cdot 10^{-5}(T - 273.15) + 2.8 \cdot 10^{-10}(T - 273.15)^2 + 3.035 \cdot 10^{-12}(T - 273.15)^3 \right], 873 < T < 2013 \text{ K} \quad (18.25)$$

$$k = 100 \cdot \left[0.082 + 5.64 \cdot 10^{-5}(T - 273.15) \right], 2103 < T < 2333 \text{ K} \quad (18.26)$$

Slightly hypo-stoichiometric:

$$\alpha = 10^{-4} \cdot \left[0.0454 - 4.73 \cdot 10^{-6}(T - 273.15) - 5.8 \cdot 10^{-10}T^2 \right], 873 < T < 1993 \text{ K} \quad (18.27)$$

$$\alpha = 0.045 \cdot 10^{-4}, 2093 < T < 2343 \text{ K} \quad (18.28)$$

$$k = 100 \cdot \left[0.1182 + 2.895 \cdot 10^{-5}(T - 273.15) + 3.8 \cdot 10^{-9}(T - 273.15)^2 + 1.9 \cdot 10^{-12}(T - 273.15)^3 \right], 873 < T < 1993 \text{ K} \quad (18.29)$$

$$k = 100 \cdot \left[0.102 + 4.88 \cdot 10^{-5}(T - 273.15) \right], 2093 < T < 2343 \text{ K} \quad (18.30)$$

Hypo-stoichiometric UC_2 :

$$\alpha = 10^{-4} \cdot \left[0.043 - 1.9 \cdot 10^{-6}(T - 273.15) - 1.2 \cdot 10^{-9}(T - 273.15)^2 - 4.11 \cdot 10^{-13}(T - 273.15)^3 \right], 873 < T < 1973 \text{ K} \quad (18.31)$$

$$k = 100 \cdot \left[0.132 + 1.9 \cdot 10^{-5}(T - 273.15) + 4.3 \cdot 10^{-9}(T - 273.15)^2 \right], 873 < T < 1973 \text{ K} \quad (18.32)$$

Figures 18.11 and 18.12 show the thermal conductivity and thermal diffusivity for stoichiometric, slightly hypo-stoichiometric, and hypo-stoichiometric UC_2 as functions of temperature. As shown in Figure 18.11,

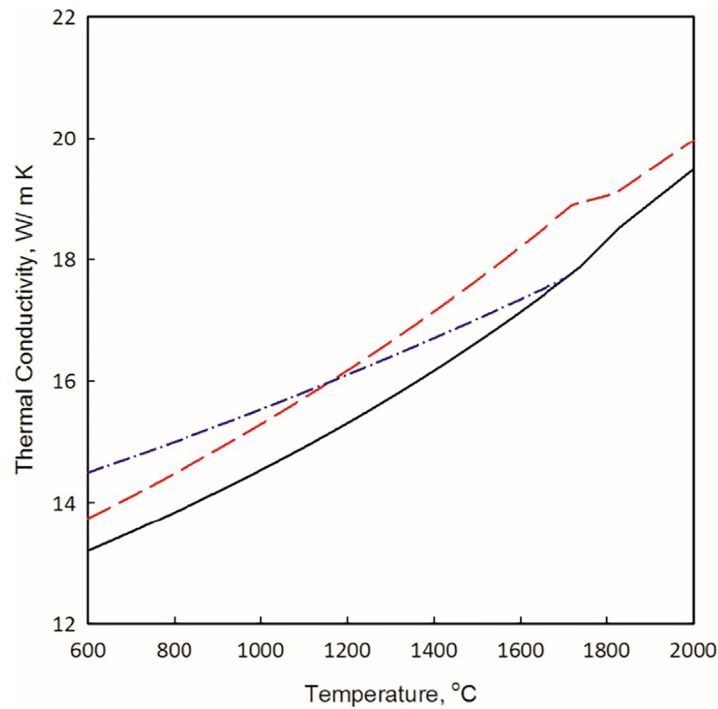


Figure 18.11. Thermal conductivity for stoichiometric, slightly hypo-stoichiometric, and hypo-stoichiometric UC_2 as function of temperature (Coninck et al., 1976).

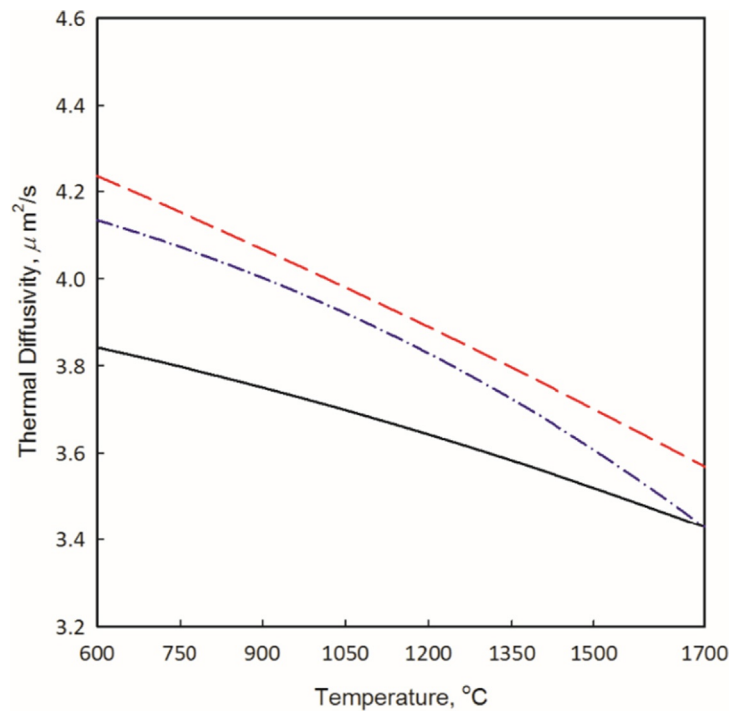


Figure 18.12. Thermal diffusivity for stoichiometric, slightly hypo-stoichiometric, and hypo-stoichiometric UC_2 as function of temperature (Coninck et al., 1976).

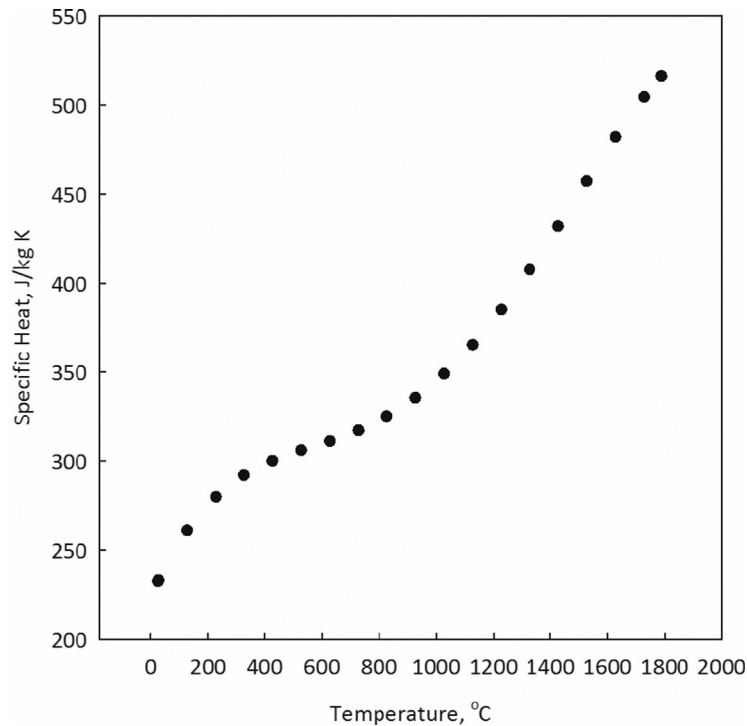


Figure 18.13. Specific heat of UC_2 as a function of temperature (Leitnaker and Godfrey, 1967).

the deviation from stoichiometry does not significantly change the thermal conductivity of UC_2 . For all cases, the thermal conductivity increases, and the thermal diffusivity (see Figure 18.12) decreases as temperature rises.

Leitnaker and Godfrey (1967) conducted experiments on a mixture consisting of 5.5% UC, 94.5% $\text{UC}_{1.91}$, and 7% carbon in a temperature range between 25°C and 2727°C. They provided the values of the specific heat of the mixture as shown in Figure 18.13. Eq. (18.33) can be used in order to calculate the specific heat of the mixture, in J/kg K, for a temperature range between 25°C and 1787°C. Moreover, Leitnaker and Godfrey (1967) provided Eqs. (18.34), (18.35), which can be used for the calculation of enthalpy in J/kg. Eqs. (18.34), (18.35) are valid for temperature ranges between 25°C and 1787°C and 1787–2308°C, respectively. The average percent errors associated with Eqs. (18.34), (18.35) are $\pm 0.25\%$ and $\pm 0.30\%$, respectively (Leitnaker and Godfrey, 1967). In Eq. (18.33)–Eq. (18.35), T is the temperature in K.

$$c_p = -1 \cdot 10^{-10} T^4 + 7 \cdot 10^{-7} T^3 - 11 \cdot 10^{-4} T^2 + 0.8401 T + 65.088 \quad (18.33)$$

$$H(T) - H(298 \text{ K}) = \frac{4184}{262.05} \cdot [4.076 T + 2.631 \cdot 10^{-2} T^2 - 2.332 \cdot 10^{-5} T^3 + 1.025 \cdot 10^{-8} T^4 - 1.573 \cdot 10^{-12} T^5 - 3.013 \cdot 10^3], 298.15 < T < 2060 \text{ K} \quad (18.34)$$

$$H(T) - H(298 \text{ K}) = \frac{4184}{262.05} \cdot [-2.512 T + 6.894 \cdot 10^{-3} T^2 + 1.806 \cdot 10^4], 2060 < T < 2581 \text{ K} \quad (18.35)$$

18.3.4 Nitride fuels

There are three compounds of uranium nitride system, namely, Uranium monoNitride (UN), Uranium diNitride (UN_2), and Uranium sesquiNitride (U_2N_3). Among these compounds, UN has been considered for use

in space nuclear reactors and sodium cooled fast breeder reactors (Matthews et al., 1988) because of its superior properties such as high thermal conductivity, high melting point and high uranium atom density. Further, the fuel residence time in the reactor core can be increased when UN is utilized (Zakova, 2012). The following section provides a literature survey on properties of UN.

18.3.4.1 UN

Uranium monoNitride or Uranium Nitride (UN) can be produced by several methods including (1) hot pressing, (2) cold pressing and sintering, and (3) carbothermic reduction of uranium dioxide plus carbon in nitrogen (Simnad, 2003; Shoup and Grace, 1977). The latter process produces UN with densities in the range of 65%–90% of theoretical density (Shoup and Grace, 1977). UN has a high melting point, high thermal conductivity, and high radiation stability. These properties enhance the safety of operation and allow the fuel to achieve high burn-ups (IAEA, 2008). In addition, UN has the highest fissile atom density, which is approximately 1.4 times that of UO_2 and greater than those of other fuels such as UC. In other words, when UN is used as a fuel, a smaller volume of fuel is required, which leads to a smaller core size. Even though UN is more stable in air than UC (Simnad, 2003), one disadvantage of the UN fuel is that under some conditions it decomposes to liquid uranium and gaseous nitrogen (IAEA, 2008), which in turn results in the formation of cracks in the fuel. The formation of cracks increases the possibility of the release of gaseous fission products and has adverse effects on the mechanical and thermophysical properties of the fuel.

It is significantly important to establish a temperature–pressure relationship for the melting point of the UN fuel in order to establish temperature limits for the UN fuel elements. UN melts congruently at high nitrogen pressures. In contrast, at high nitrogen pressures, UN melts incongruently, which means UN decomposes to liquid uranium and releases nitrogen gas. Therefore, it is expected to measure low UN vapor pressure over UN fuel due to its tendency to decompose. In comparison with the UO_2 fuel, the vapor pressure of UN over the UN fuel is four orders of magnitude less than the vapor pressure of UO_2 over the UO_2 fuel. The UN fuel melts congruently at high partial pressures of nitrogen; however, the decomposition of UN occurs at low nitrogen partial pressures. Therefore, the partial pressure of UN fuel is an indication of melting or decomposition of the fuel, which in turn can be used to establish engineering limits for the UN fuel (Hayes et al., 1990c).

Hayes et al. (1990c) developed an empirical correlation shown as Eq. (18.36), which can be used to calculate the melting point of UN, in K, as a function of partial pressure of nitrogen that depends on temperature. Eq. (18.36) is valid when the partial pressure of nitrogen is between 10^{-8} and 10^5 Pa. The partial pressure of nitrogen can be calculated using Eq. (18.37). In addition, Eq. (18.38) can be used to calculate the vapor pressure of uranium over UN in Pascal (Hayes et al., 1990c). The total vapor pressure over UN is the sum of the partial pressures of N_2 and U. Figures 18.14–18.16 show the partial pressures of nitrogen and uranium over UN as functions of temperature, and the melting point of UN as a function of partial pressure of nitrogen over UN, respectively. In Eqs. (18.37), (18.38), T is the temperature in K.

$$T_m = 3035.0 (P_{N_2}/1.01 \cdot 10^5)^{0.02832} \quad (18.36)$$

$$\log_{10}(P_{N_2}) = 1.01 \cdot 10^5 (1.8216 + 1.882 \cdot 10^{-3}T - 23543.4/T), 1400 < T < 3170 \text{ K} \quad (18.37)$$

$$\log_{10}(P_U) = 1.01 \cdot 10^5 (6.9654 - 5.137 \cdot 10^{-4}T - 26616.1/T), 1400 < T < 2400 \text{ K} \quad (18.38)$$

Ross et al. (1988) developed a correlation, shown as Eq. (18.39), for the calculation of the thermal conductivity of UN, in W/mK. In Eq. (18.39), T is the temperature in K. This correlation, which has an uncertainty within $\pm 10\%$, calculates the thermal conductivity of UN fuel with 100% theoretical density. In general, nuclear fuels are manufactured with porosity to accommodate for the gaseous fission products. Therefore, it is necessary to determine the thermal conductivity of a fuel based

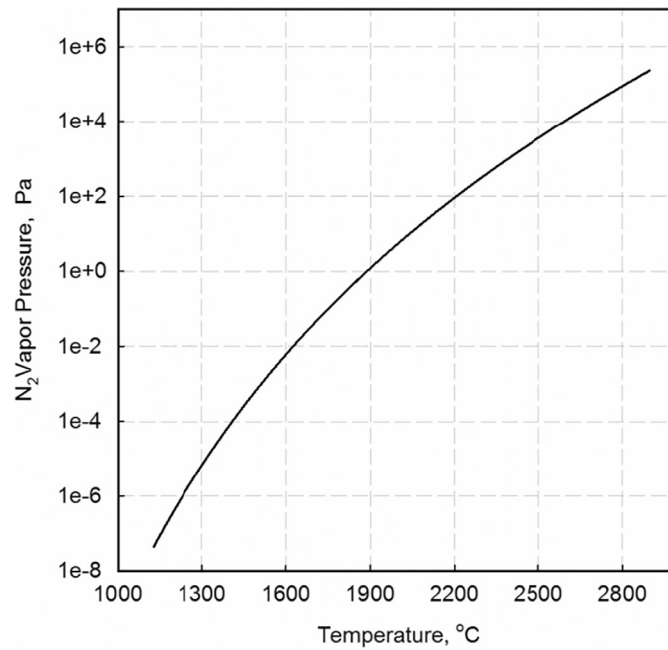


Figure 18.14. Vapor pressure of nitrogen as function of temperature.

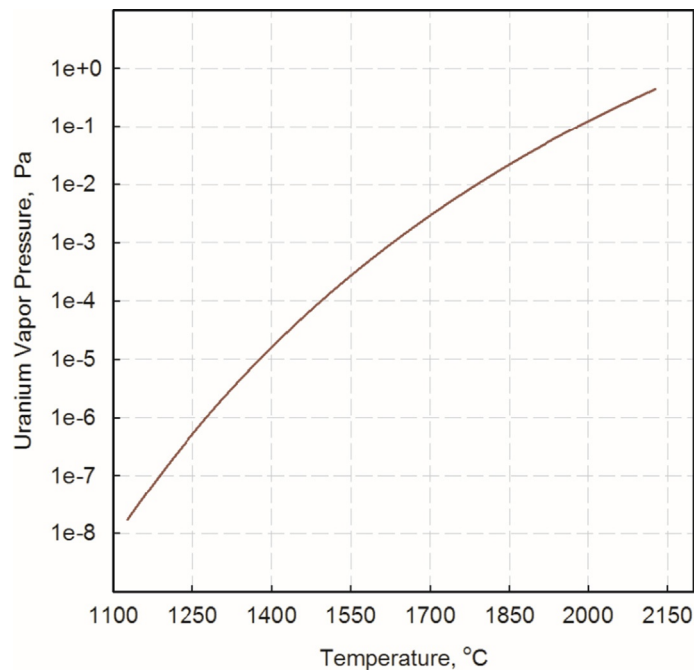


Figure 18.15. Vapor pressure of uranium as function of temperature.

on percent porosity. [Kikuchi et al. \(1972\)](#) developed a correlation, shown as Eq. (18.40), which can be used to calculate the Effective Thermal Conductivity (ETC) of porous UN fuel as a function of percent porosity. In Eq. (18.40), the coefficient β is independent of temperature and has a value of 1.79 ± 0.05 for porosities below 10%. The coefficient β becomes temperature dependent when porosity increases beyond 12%. The value of β varies from 1.38 ± 0.12 at 300°C to 0.09 ± 0.05 at 1300°C ([Kikuchi et al., 1972](#)).

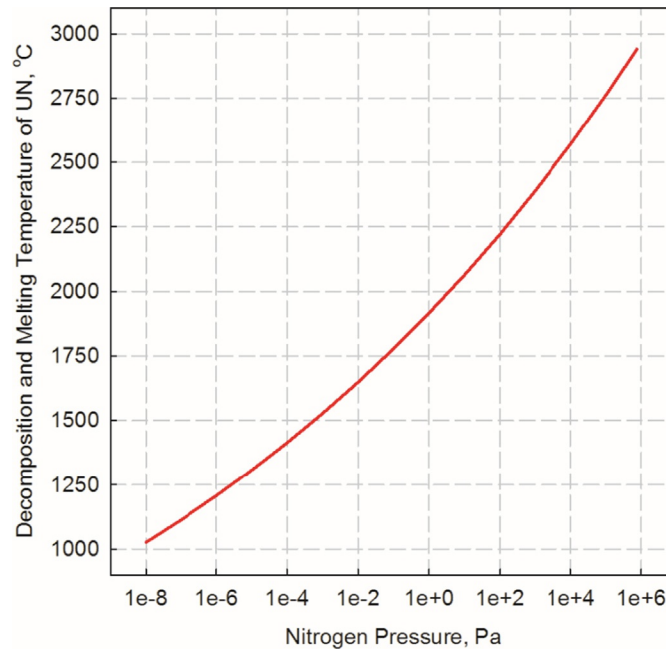


Figure 18.16. Melting point of UN as function of partial pressure of nitrogen.

$$k_{100\%TD} = 1.37 T^{0.41} \quad (18.39)$$

$$k_p = k_{100\%TD} \left(\frac{1 - P}{1 + \beta P} \right) \quad (18.40)$$

In addition to the Ross et al. correlation, Hayes et al. (1990a) developed another correlation shown as Eq. (18.41), which calculates the thermal conductivity of UN, in W/mK. This correlation, which is a function of both temperature and percent porosity, can be applied when porosity changes between 0% and 20% for temperatures in the range of 25°C and 1650°C (Hayes et al., 1990a). Figure 18.17 shows the thermal conductivity of UN with 5% porosity as a function of temperature, calculated based on these two correlations. As shown in Figure 18.17, the Hayes et al. correlation results in lower thermal conductivity values for temperatures approximately above 700°C. In other words, the Hayes et al. correlation is more conservative than the Ross et al. correlation in the prediction of the thermal conductivity of UN at temperatures above 700°C. In addition, the standard deviation of the Hayes et al. correlation is $\pm 2.3\%$ compared to $\pm 3.2\%$ for the Ross et al. correlation. Therefore, as a conservative approach, the Hayes et al. correlation may be used for the calculation of the thermal conductivity of UN fuel. In Eq. (18.41), T is the temperature in K.

$$k = 1.864e^{-2.14P} T^{0.361} \quad (18.41)$$

Hayes et al. (1990c) developed correlations for the calculation of the thermodynamic properties of UN including specific heat, enthalpy, entropy, and Gibbs free energy as functions of temperature; these correlations are shown as Eqs. (18.42)–(18.45), respectively. The specific heat and the entropy are in J/kg K. The enthalpy and the Gibbs free energy are in J/kg. In Eqs. (18.42)–(18.45), T is the temperature in K.

$$c_p = \frac{1000}{252.04} \cdot \left[51.14(\Theta/T) \frac{\exp(\Theta/T)}{[\exp(\Theta/T) - 1]^2} + 9.491 \cdot 10^{-3} T + \frac{2.642 \times 10^{11}}{T^2} \exp(-18081/T) \right] \quad (18.42)$$

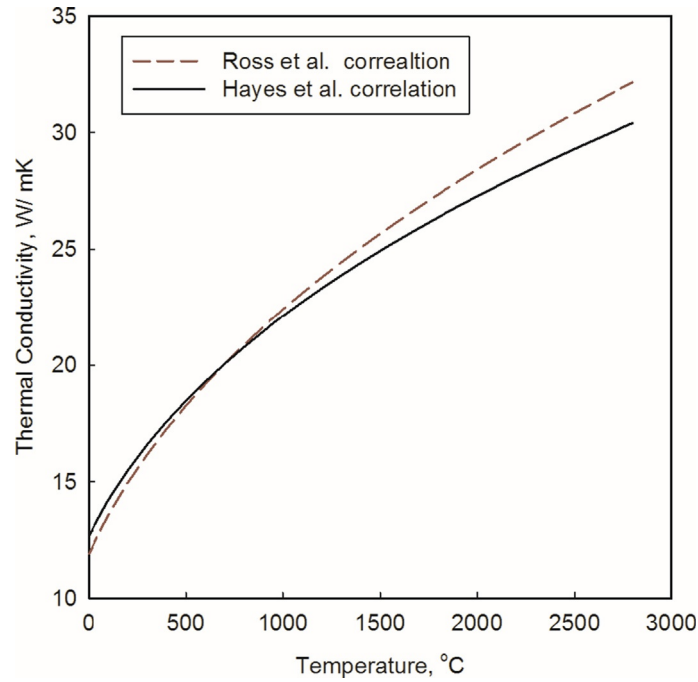


Figure 18.17. Thermal conductivity of 95%TD UN fuel. Based on the Ross et al. (1988) and Hayes et al. (1990a) correlations.

$$H(T) - H(298 \text{ K}) = \frac{1000}{252.04} \cdot \left[\frac{51.14\Theta}{\exp(\Theta/T) - 1} + 4.746 \cdot 10^{-3} T^2 - 8148.34 + 1.461 \cdot 10^7 \exp(-18081/T) \right] \quad (18.43)$$

$$S = \frac{1000}{252.04} \cdot \left[\frac{51.14(\Theta/T)}{\exp(\Theta/T) - 1} - 51.14 \ln \{1 - \exp(-\Theta/T)\} + 9.491 \cdot 10^{-3} T + 16.31 \right] \quad (18.44)$$

$$G = \frac{1000}{252.04} \cdot \left[51.14 T \ln \{1 - \exp(-\Theta/T)\} - 4.746 \cdot 10^{-3} T^2 - 16.31 + 1.461 \cdot 10^7 \exp(-18081/T) \right] \quad (18.45)$$

The specific heat correlation is valid for temperatures between 25 and 2355°C, where T is the temperature in K and Θ is the empirically determined Einstein temperature, which is 92.55°C (365.7K) for UN. Figure 18.18 shows the selected thermodynamic properties of UN.

It is essential for a fuel to maintain its structural integrity under the conditions of a nuclear reactor. In other words, the fuel must have an adequate mechanical stability and withstand stresses under operating conditions. The mechanical stability of a fuel is related to its mechanical properties. Thus, the study of mechanical properties of the fuel is an inseparable part of a design.

Mechanical properties of UN such as modulus of elasticity, shear modulus, and Poisson's ratio can be determined using Eqs. (18.46)–(18.48), where E , G_{sm} , ν_p , and TD are the Young's modulus, Shear modulus, Poisson's ratio, and theoretical density (e.g., $TD = 95$ for a fuel with a 95% theoretical density), respectively (Hayes et al., 1990b). Figure 18.19 shows the Young's modulus and shear modulus of UN, both in MPa, as functions of temperature for 95% TD UN. Eqs. (18.46)–(18.48) were developed based on percent theoretical densities between 70% and 100%; however, they can be used for fuels with higher porosities. In addition,

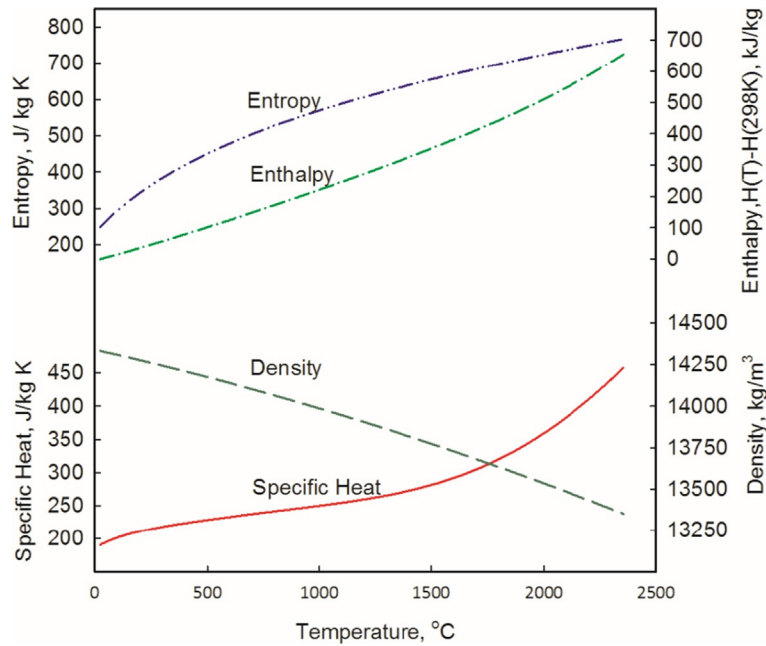


Figure 18.18. Thermodynamic properties of UN as function of temperature.

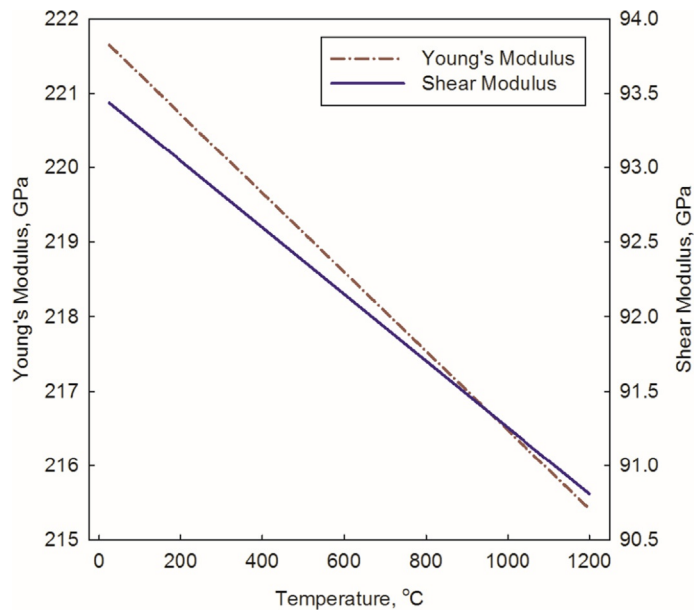


Figure 18.19. Young's and Shear moduli of UN with 95% TD as function of temperature.

Hayes et al. (1990b) provided a correlation, shown as Eq. (18.49), for the calculation of the hardness of UN in MPa. The latter correlation is valid for temperatures in the range of 25°C and 1400°C, and porosities between 0.0 and 0.26. Moreover, the density and linear expansion coefficient of UN, in kg/m^3 and $1/\text{K}$, can be calculated using Eqs. (18.50), (18.51), respectively, which are valid for temperatures between 25°C and 2250°C (IAEA, 2008). Figure 18.20 shows the linear thermal expansion of UN as a function of temperature. In Eqs. (18.42)–(18.51), T is the temperature in K.

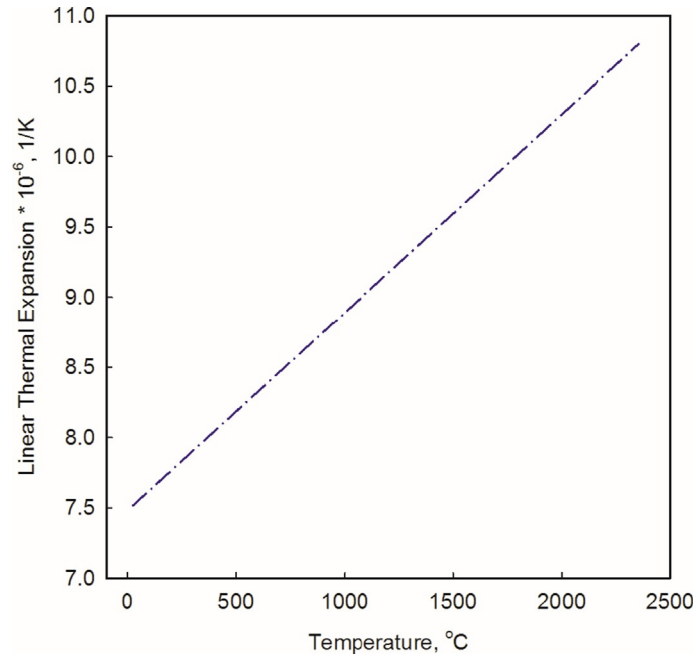


Figure 18.20. Linear thermal expansion of UN as function of temperature. Based on IAEA (2008).

$$E = 0.258 TD^{3.002} [1 - 2.375 \cdot 10^{-5} T], 298 \text{ K} < T < 1473 \text{ K} \quad (18.46)$$

$$G_{sm} = 1.44 \cdot 10^{-2} TD^{3.446} [1 - 2.375 \cdot 10^{-5} T], 298 \text{ K} < T < 1473 \text{ K} \quad (18.47)$$

$$v_p = 1.26 \cdot 10^{-3} TD^{1.174}, 298 \text{ K} < T < 1473 \text{ K} \quad (18.48)$$

$$HD = 9.807 \cdot [951.8 \{1 - 2.1P\} \exp(-1.882 \cdot 10^{-3} T)] \quad (18.49)$$

$$\alpha = 7.096 \cdot 10^{-6} + 1.409 \cdot 10^{-9} T \quad (18.50)$$

$$\rho = 14420 - 0.2779 T - 4.897 \cdot 10^{-5} T^2 \quad (18.51)$$

Irradiation swelling, growth, and creep are the primary effects of irradiation on the fuel. Irradiation swelling results in volumetric instability of the fuel at high temperatures while irradiation growth causes dimensional instability of the fuel at temperatures lower than 2/3 of the melting point of the fuel (Ma, 1983). In addition to dimensional and volumetric instability, a continuous and plastic deformation of the fuel due to creep may adversely affect its mechanical properties. Thus, it is required to study the behavior of the fuel under irradiation specifically the irradiation-induced swelling, irradiation-induced growth, and irradiation-induced creep of the fuel.

Ross et al. (1990) developed a correlation for the calculation of the percent volumetric swelling of UN fuel. This correlation is shown as Eq. (18.52), where T_{avg} is the volume average fuel temperature in K, B is the fuel burn-up in MW day/Mg(U), and $\rho_{\%TD}$ is the percent theoretical density of the fuel (e.g., $\rho_{\%TD}$ equals to 0.95 for a fuel with 5% porosity). In addition to this correlation, the volumetric swelling of UN can be calculated based on the fuel centerline temperature using Eq. (18.53) (Ross et al., 1990) where T is the temperature in K. The uncertainty of the volumetric swelling correlation, Eq. (18.53), is $\pm 25\%$ for burn-ups above 10,000 MW day/Mg (U). The uncertainty associated with this correlation increases to $\pm 60\%$ at lower

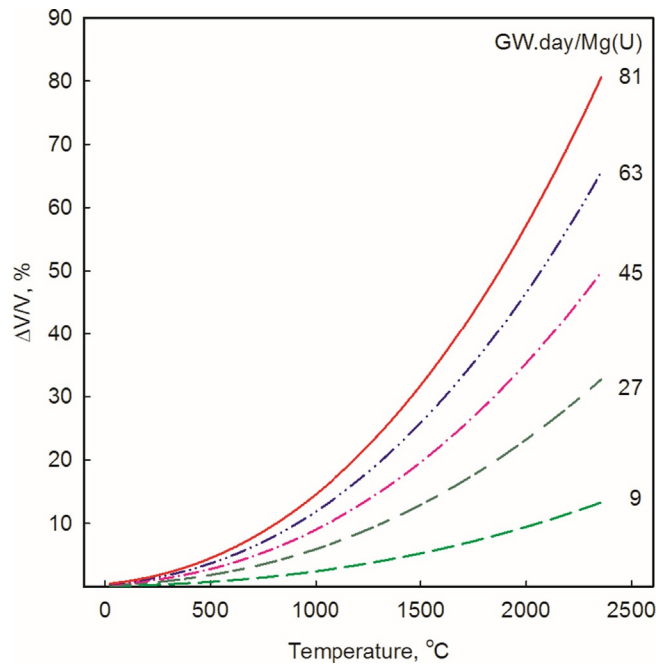


Figure 18.21. Percent volumetric swelling of UN as function of burn-up and temperature. *Based on Ross et al. (1990).*

burn-ups (Ross et al., 1990). Figure 18.21 shows the volume expansion of UN as a function of temperature for selected burn-up values.

$$\Delta V/V(\%) = 4.7 \cdot 10^{-11} T_{\text{avg}}^{3.12} \left(\frac{B}{9008.1} \right)^{0.83} \rho_{\%TD}^{0.5} \quad (18.52)$$

$$\Delta V/V(\%) = 1.16 \cdot 10^{-8} T_{\text{CLT}}^{2.36} \left(\frac{B}{9008.1} \right)^{0.82} \rho_{\%TD}^{0.5} \quad (18.53)$$

In addition, Hayes et al. (1990b) developed a correlation shown as Eq. (18.54) which gives the steady-state creep rate of dense UN with 100% TD, in 1/h. In Eq. (18.54), T is the temperature in K. This correlation is valid for temperatures between 1497°C and 1810°C and stresses, σ , in the range of 20–34 MPa. To account for the porosity of the fuel, Eq. (18.55) should be multiplied by the creep porosity correlation factor shown as Eq. (18.55) (Hayes et al., 1990b). In Eq. (18.55), P_p is the porosity in volume fraction. Figure 18.22 shows the creep rate of UN with 100% TD and 95% TD as a function of temperature for a stress value of 25 MPa. Figure 18.22 also indicates that the creep rate increases by increasing the porosity.

$$\dot{\epsilon} = 3600 \cdot 2.054 \cdot 10^{-3} \sigma^{4.5} \exp(-39369.5/T) \quad (18.54)$$

$$f(P_p) = \frac{0.987}{(1 - P)^{27.6}} \exp(-8.65 P_p) \quad (18.55)$$

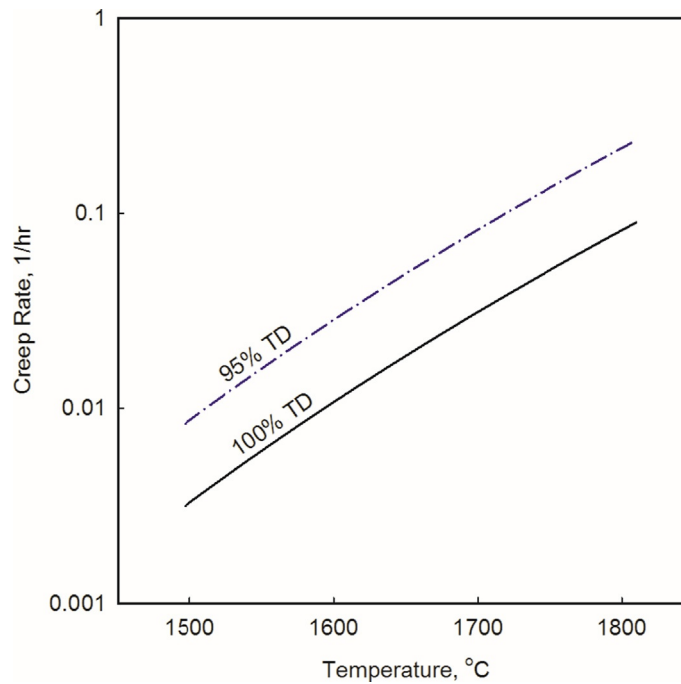


Figure 18.22. Steady-state creep rate of UN at 25 MPa stress as function of temperature. Based on Hayes et al. (1990b).

18.4 Hydride fuels

18.4.1 U-ZrH_{1.6}

A promising fuel for use in light-water reactors is the uranium-zirconium hydride fuel which has been used in TRIGA reactors. The density of the hydride fuel is 8.256 g/cm³. The atom density of uranium in the uranium-zirconium hydride fuel is less than that of the oxide fuels (i.e., UO₂). Hence, a higher enrichment of uranium is required in order to achieve the same burn-up with the same power density (Galahom et al., 2014). In the uranium-zirconium hydride fuel, U-ZrH_{1.6}, uranium metal phase is dispersed in the continuous ZrH_{1.6} phase, which allows the thermal conductivity of the uranium-zirconium hydride fuel to become significantly higher than that of oxide fuels such as UO₂. High thermal conductivity reduces the temperature gradient across the fuel which in turn decreases the release of gaseous fission products (Olander et al., 2009). Simnad (1980) recommended a thermal conductivity of 17.6 ± 0.8 W/m K for design purposes. Simnad's investigation showed that for U-ZrH_{1.6} with a hydrogen to zirconium ratio of 1.6 the thermal conductivity is insensitive to temperature and weight fraction of uranium (Simnad, 1980).

Tsuchiya et al. (2001) calculated the thermal conductivity of U-ZrH_x for hydrogen to zirconium ratios between 1.6 and 2.0 (1.6 ≤ x ≤ 2.0). Tsuchiya et al. (2001) experimentally measured the thermal diffusivity of ZrH_x and calculated the thermal conductivity based on the relationship among the thermal diffusivity, density, and specific heat. Further, they calculated the thermal conductivity of U-ZrH_x using the rule of mixture as expressed in Eq. (18.56). In Eq. (18.56), V_i and k_i are the volume fraction and thermal conductivity of the constituent phase i. Figure 18.23 shows the thermal conductivity of U-ZrH_x based on Simnad (1980) and Tsuchiya et al. (2001).

$$k_{\text{U-ZrH}_x} = V_U k_U + V_{\text{ZrH}_x} k_{\text{ZrH}_x} \quad (18.56)$$

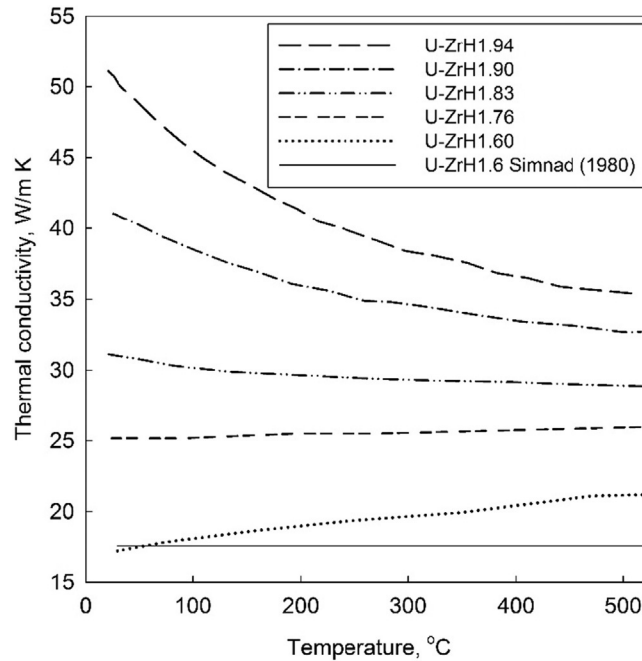


Figure 18.23. Thermal conductivity of U-ZrH_x (Simnad 1980; Tsuchiya et al., 2001).

In addition to its relatively high thermal conductivity, another advantage of U-ZrH_{1.6} fuel is that it has a large prompt negative temperature coefficient of reactivity (Zakova, 2012), which is caused by higher fuel temperatures due to an increase in reactor power. The reduction in reactivity, in turn, reduces the reactor power and hence the fuel temperature. On the other hand, U-ZrH_{1.6} has a large fission-product swelling, which is approximately three times that of oxide fuels. Due to large early swelling rates of the fuel, the maximum design temperature limit of the fuel is around 750°C for steady-state conditions and 1050°C during transients (Olander et al., 2009). Figure 18.24 shows the swelling of U-ZrH_{1.6} as a function of burn-up (Huang et al., 2001).

U-ZrH_{1.6} has chemical compatibility with water. Zirconium hydride has low reactivity rates when exposed to water, steam, or air up to temperatures around 600°C. The corrosion rate of the fuel is very low. The results of water quench tests, for the purpose of investigating the corrosion resistance and thermal shock resistance of the fuel, have shown no damaging effects on the fuel heated to 800°C. A surface discoloration was observed when fuel samples, which were heated up to 900°C, were quenched in water. Further experiments with fuel rods heated up to 1200°C showed cracks on the fuel pellets after being quenched in water. Nevertheless, no safety concern was caused, and the pellets were in good condition (Simnad, 1980).

18.4.2 UTh₄Zr₁₀H_x

Uranium-thorium-zirconium fuels are also of interest due to a significant amount of thorium resources and utilization of the fuels in breeder reactors. In UTh₄Zr₁₀H_x, metallic uranium is dispersed in ThZr₂H_{7-x} and ZrH_{2-x} hydrides. Similar to U-ZrH_{1.6}, UTh₄Zr₁₀H_x ($x=20, 24,$ and 27) fuels have higher thermal conductivities compared to those of oxide fuels such as UO₂ and ThO₂. Tsuchiya et al. (2000) provided the thermal conductivity of three UTh₄Zr₁₀H_x ($x=20, 24,$ and 27) fuels. The thermal conductivities are shown in Figure 18.25 as a function of temperature.

The density of UTh₄Zr₁₀H_x fuels is calculated using Eq. (18.57) as a function of the ratio of hydrogen to UTh₄Zr₁₀ at a temperature of 296 K. In comparison with UO₂, which has a density of 10,960 kg/cm³, the

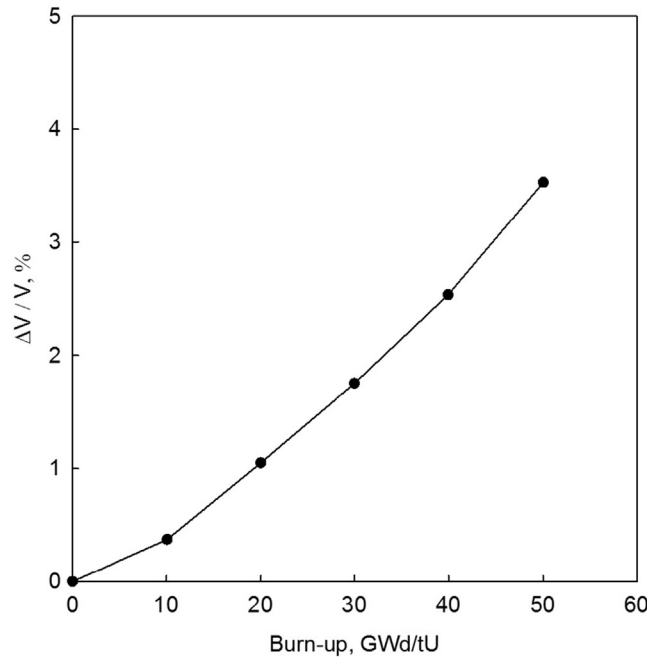


Figure 18.24. Calculated solid swelling of U-ZrH_{1.6} with 45 wt% uranium as a function of burn-up at 600°C (873 K) (Huang et al., 2001).

densities of uranium-thorium hydride fuels are less. For instance, the density of UTh₄Zr₁₀H₂₀ is estimated to be 7.8 g/cm³ at 25°C (298 K) based on Eq. (18.57). In Eq. (18.57), ρ is the density in g/cm³.

$$\rho = 8.40 - 2.99 \times 10^{-2}x \quad (18.57)$$

The specific heat of UTh₄Zr₁₀H_x ($x=20, 24,$ and 27) can be calculated using Eq. (18.58). Figure 18.26 shows the specific heat of UTh₄Zr₁₀H₂₀, UTh₄Zr₁₀H₂₄, and UTh₄Zr₁₀H₂₇ fuels as a function of temperature based on Eq. (18.58) (Tsuchiya et al., 2000). The calculated specific heat values based on Eq. (18.58) are in kJ/kg K and the temperature is in K.

$$c_p = -0.110 + 6.87 \times 10^{-4}T + 6.36 \times 10^{-3}x \quad (18.58)$$

18.5 Composite fuels

Currently, there is a great interest in developing high thermal-conductivity fuels and/or improving the thermal conductivity of low thermal-conductivity fuels such as UO₂. High thermal conductivities result in lower fuel centerline temperatures and limit the release of gaseous fission products (Hollenbach and Ott, 2010). As shown previously, UO₂ has a very low thermal conductivity especially at high temperatures compared to other fuels such as UC, UC₂, and UN. However, research has shown that the thermal conductivity of oxide fuels such as UO₂ can be increased by either adding a continuous solid phase or long, thin fibers of a high thermal-conductivity material (Hollenbach and Ott, 2010; Solomon et al., 2005).

A high thermal-conductivity material must have a low neutron absorption cross-section depending on the reactor (Hollenbach and Ott, 2010). In addition, it must have a high melting point and be chemically compatible with the fuel, the cladding, and the coolant. The need to meet these requirements narrows the potential materials to Silicon Carbide (SiC), Beryllium Oxide (BeO), and graphite (C). The following subsections provide information about the UO₂ fuels composed of SiC, graphite and BeO.

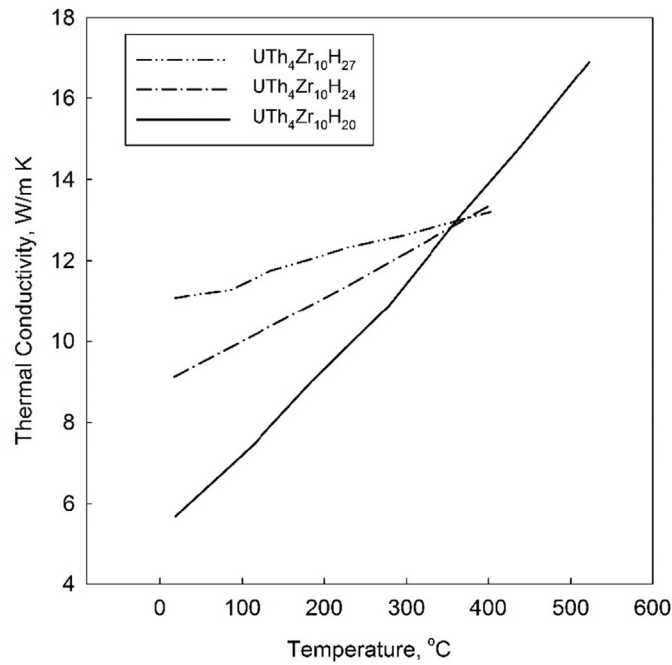


Figure 18.25. Thermal conductivity of $UTh_4Zr_{10}H_x$ as a function of temperature (Tsuchiya et al., 2000).

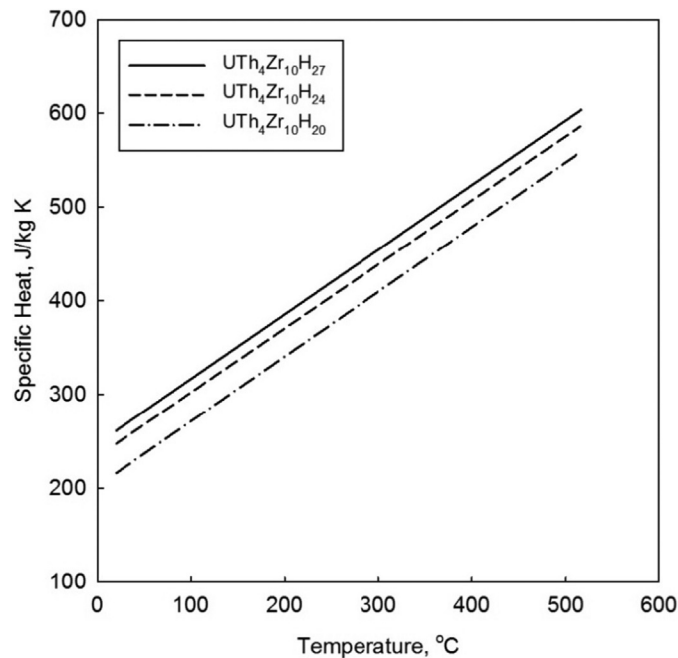


Figure 18.26. Calculated specific heats of $UTh_4Zr_{10}H_{20}$, $UTh_4Zr_{10}H_{24}$, and $UTh_4Zr_{10}H_{27}$ (Tsuchiya et al., 2000).

18.5.1 UO_2 -SiC

The thermal conductivity of the UO_2 fuel can be improved by incorporating Silicon Carbide (SiC) into the matrix of the fuel. SiC has a high melting point approximately at 2800°C , high thermal conductivity (78 W/mK at 727°C), high corrosion resistance even at high temperatures, low thermal neutron absorption,

and dimensional stability (Khan et al., 2010). Therefore, when used with UO_2 , SiC can address the problem of the poor thermal conductivity of the UO_2 fuel.

Calculation of the thermal conductivity of UO_2 plus SiC fuel falls under the theories of composites. Generally, theories contemplating the thermal conductivity of composites are classified into two categories. One category assumes that inclusions are randomly distributed in a homogeneous mixture. The ETCs of the composites, based on the aforementioned principle, are formulated by Maxwell. The other category, which is based on the work performed by Rayleigh, assumes that particles are distributed in a regular manner within the matrix.

Khan et al. (2010) provided the thermal conductivity of UO_2 -SiC fuel as a function of temperature and weight percent of SiC. Khan et al. (2010) assumed that a thin coat of SiC covered UO_2 particles and determined the thermal conductivity of the composite fuel for three cases. These cases, which are described in the following paragraph, were solved based on the Rayleigh equation shown as Eq. (18.59) (Khan et al., 2010).

$$k_{\text{eff}R(\psi)} = k_{\text{SiC}} \cdot \left[1 + 3 \frac{\psi}{\left[\frac{k_{\text{UO}_2} + 2 \cdot k_{\text{SiC}}}{3k_{\text{UO}_2} - k_{\text{SiC}}} \right] - \psi + 1.569 \left[\frac{k_{\text{UO}_2} - k_{\text{SiC}}}{3k_{\text{UO}_2} - 4k_{\text{SiC}}} \right] \cdot \psi^{10/3}} \right] \quad (18.59)$$

In Case I, it was assumed that all UO_2 particles are completely covered within a layer of SiC. In Case II, the coating on UO_2 particles is not complete. In other words, it was assumed that there were blocks of UO_2 covered with SiC along the radial direction of the fuel. Finally, in Case III, it was assumed that there were blocks of UO_2 coated with SiC. The SiC coating in the latter case was discontinued such that SiC covered only two opposite sides of each UO_2 block.

For all three examined cases, the thermal conductivities were calculated for 97% TD and when the weight percent of SiC was 12% and 8%. The results indicate a small difference between the ETC of Case I and Case II. This small difference was due to the continuity of SiC layer in Case I and II. However, in Case III, the discontinuity of SiC resulted in little improvement in the ETC of the fuel. Therefore, the addition of a continuous solid phase of SiC to UO_2 fuel increases the ETC of the fuel. In the present study, UO_2 -SiC fuel with 12 wt% SiC has been examined and its thermal conductivity has been calculated using Eq. (18.60). Eq. (18.60) has been developed based on the analysis conducted for Case I. In Eq. (18.60), T is the temperature in K.

$$k_{\text{eff}} = -9.59 \times 10^{-9} T^3 + 4.29 \times 10^{-5} T^2 - 6.87 \times 10^{-2} T + 4.68 \times 10^{+1} \quad (18.60)$$

18.5.2 UO_2 -C

Hollenbach and Ott (2010) studied the effects of the addition of graphite fibbers on thermal conductivity of UO_2 fuel. Theoretically, the thermal conductivity of graphite varies along different crystallographic planes. For instance, the thermal conductivity of perfect graphite along basal planes is more than 2000 W/mK (Hollenbach and Ott, 2010). On the other hand, it is less than 10 W/mK in the direction perpendicular to the basal planes. Hollenbach and Ott (2010) performed computer analyses in order to determine the effectiveness of adding long, thin fibbers of high thermal-conductivity materials to low thermal-conductivity materials to determine the ETC. In their studies, the high thermal-conductivity material had a thermal conductivity of 2000 W/mK along the axis, and a thermal conductivity of 10 W/mK radially, similar to perfect graphite. The low thermal-conductivity material had properties similar to UO_2 (e.g., with 95% TD at $\sim 1100^\circ\text{C}$) with a thermal conductivity of 3 W/mK.

Hollenbach and Ott (2010) examined the ETC of the composite for various volume percentages of the high thermal-conductivity material, varying from 0% to 3%. Figure 18.27 shows that the addition of just one volume percent of high thermal-conductivity material increases the ETC of the composite approximately by a

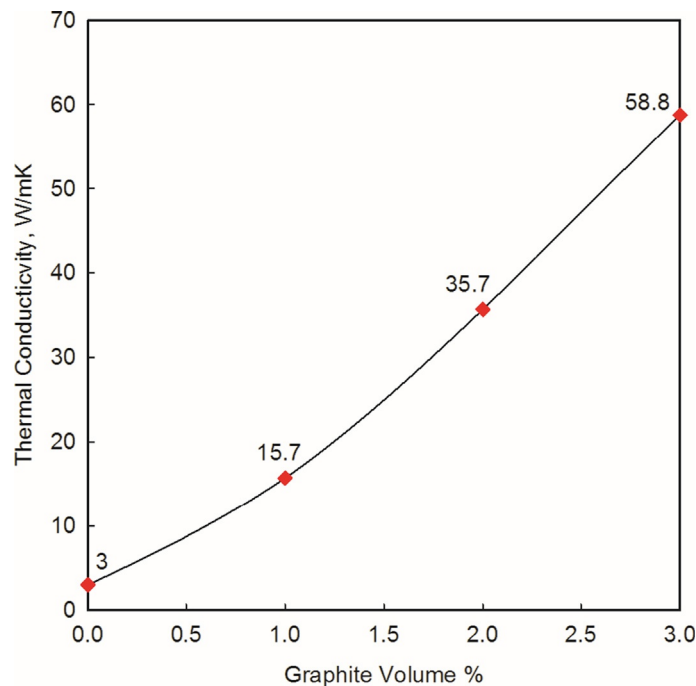


Figure 18.27. Thermal conductivity of UO_2 as function of graphite fiber volume percent (Hollenbach and Ott, 2010).

factor of 5. Moreover, if the amount of the high thermal-conductivity material increases to 2% by volume, the ETC of the composite reaches the range of high thermal-conductivity fuels, such as UN and UC.

18.5.3 UO_2 -BeO

BeO is a metallic oxide with a very high thermal conductivity. BeO is chemically compatible with UO_2 , most sheath materials including zirconium alloys, and water. In addition to its chemical compatibility, BeO is insoluble with UO_2 at temperatures up to 2160°C . As a result, BeO remains as a continuous second solid phase in the UO_2 fuel matrix while being in good contact with UO_2 molecules at the grain boundaries. BeO has desirable thermochemical and neutronic properties, which have resulted in the use of BeO in aerospace, electrical and nuclear applications. For example, BeO has been used as the moderator and the reflector in some nuclear reactors. However, the major concern with beryllium is its toxicity. But the requirements for safe handling of BeO are similar to those of UO_2 . Therefore, the toxicity of BeO is not a limiting factor in the use of this material with UO_2 (Solomon et al., 2005).

Similar to other enhanced thermal-conductivity fuels, the thermal conductivity of UO_2 can be increased by introducing a continuous phase of BeO at the grain boundaries. The effects of the presence of such second solid phase on the thermal conductivity of UO_2 is significant such that only 10% by volume of BeO would improve the thermal conductivity of the composite fuel by 50% compared to that of UO_2 with 95% TD. Figure 18.28 shows the thermal conductivity of UO_2 -BeO as a function of temperature for 0.9wt%, 2.7wt%, 10.2wt%, and 20.4wt% of BeO (Ishimoto et al., 1996; Latta et al., 2008; McDeavitt, 2009; Solomon et al., 2005).

Zhou et al. (2015) used the finite element modeling method in ANSYS to determine the thermal conductivity of UO_2 -BeO. In their analysis, Zhou et al. (2015) investigated the thermal conductivity of UO_2 -BeO based on the characteristics of the two available manufacturing methods, namely, Slug Bisque (SB) and Green Granule (GG) (Solomon et al., 2005). They found the UO_2 -BeO manufacturing based on the GG

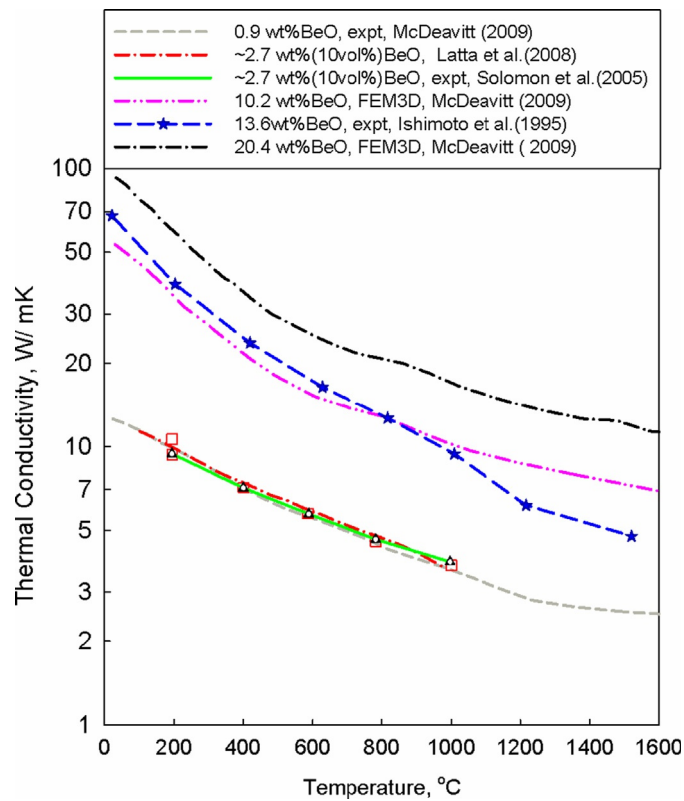


Figure 18.28. Thermal conductivity of $\text{UO}_2\text{-BeO}$ as function of temperature (Ishimoto et al., 1996; Latta et al., 2008; McDevitt, 2009; Solomon et al., 2005).

method possesses a higher thermal conductivity compared to those manufactured using the SS method. Zhou et al. (2015) provided correlations for the calculation of the thermal conductivity of the $\text{UO}_2\text{-BeO}$ for a wide range of volume percent of BeO varying from 0 to 10. Zhou et al. (2015) provided Eqs. (18.61), (18.62) for the calculation of the thermal conductivity of $\text{UO}_2\text{-BeO}$ with 10% volume percentage of BeO, respectively, for the SB and GG manufacturing methods. In these correlations, which are valid for a temperature range between -173°C (100 K) and 1800°C (2073 K), the temperature is in K.

$$k_{\text{eff}}(T) = 497.6 T^{-0.679} \quad (18.61)$$

$$k_{\text{eff}}(T) = 3348.5 T^{-0.928} \quad (18.62)$$

18.6 Analysis results

With an objective to illustrate the differences in the fuel temperatures of various categories of nuclear fuels, a thermal-power distribution inside a reactor core was calculated based on the neutronic properties of a fresh and symmetric core of a Pressure Channel SuperCritical Water-cooled Reactor (PCh-SCWR). The analyzed reactor core consists of 336 fuel channels with a total thermal power of 2540 MW. The coolant is light water with an inlet temperature of 350°C at a pressure of 25 MPa and an outlet temperature of about 625°C . Heavy water is chosen as the moderator. The temperature of the moderator is kept at 80°C at a low pressure. Table 18.4 provides a summary of the design specifications of the examined PCh-SCWR.

For the examined PCh-SCWR, the High Efficiency Reentrant Channel (HERC) was chosen as the reference fuel channel. The fuel assembly consists of 64 fuel elements located in two rings. There are 32 fuel

Table 18.4. Operating parameters of PCh-SCWR (Peiman, 2017)

PCh-SCWR specifications	Value
Total thermal power, MW _{th}	2540
Thermal efficiency	45%–48%
Total electric power, MW _{el}	1143–1219
Coolant/moderator	H ₂ O/D ₂ O
Average coolant mass flow rate, kg/s	4.45
Coolant inlet temperature, °C	350
Coolant outlet temperature, °C	625
Coolant outlet pressure, MPa	25
Fuel bundle design	64-element
Hydraulic diameter, mm	6.8
Heated length, m	5.0
Number of fuel channels	336
Core radius (including radial reflector region), m	2.55
Core height (including axial D ₂ O reflector regions), m	6.5

elements in each ring. The fuel assemblies are placed inside pressurized fuel channels. The lattice pitch is a square of 25 cm × 25 cm. Table 18.5 provides a summary of the specifications of the fuel assembly (Peiman, 2017).

A one-dimensional thermalhydraulic code was developed. The code accounts for the pressure drop of the coolant and includes a model for considering the impact of the gap conductance on the fuel temperature. In regard to the heat loss from the coolant to the moderator the developed thermalhydraulic code calculates the heat loss from the coolant to the moderator. The code also accounts for the volumetric heat generation rate inside the fuel. For this purpose, a thermalhydraulic/neutronic coupling was performed using data transfer between the neutronic and thermalhydraulic calculations.

As suggested by Eq. (18.63), the heat generation in a nuclear fuel varies in the radial direction of the fuel pellet. Considering a cylindrical fuel pellet in a reactor core, as illustrated in Figure 18.29, the heat generation in the fuel is affected with the neutron flux. In Figure 18.29, the fast-neutron flux is the maximum on the centerline of the nuclear fuel, and it decreases as the flux approaches the periphery of the fuel pellet. On the other hand, the thermal-neutron flux has its minimum on the centerline of the fuel, and its magnitude increases as the distance increases from the centerline of the fuel. A combination effect of the fission rate and neutron flux results in smaller heat-generation rate on the centerline of a nuclear fuel, and larger values as the radial distance increases from the centerline of the fuel for a thermal-spectrum reactor.

$$q_{\text{gen}}(r) = G_f \sum_{g=1}^{N_G} \sum_f(r) \phi(r) \quad (18.63)$$

Table 18.5. Specifications of 64-element fuel bundle

Inner ring outer ring	Inner ring	Outer ring
Number of rods	32	32
Pitch circle radius, cm	5.4	6.575
Radius of fuel pins, cm	0.435	0.460
Thickness of fuel cladding, cm	0.06	0.06
Materials of fuel pins	15 wt% PuO ₂ /ThO ₂ (i.e., Pu: 13.23; Th: 74.70; O: 12.07; density 9.91 g/cm ³)	12 wt% PuO ₂ /ThO ₂ (i.e., Pu: 10.59; Th: 77.34; O: 12.08; density 9.87 g/cm ³)
Material of cladding	Zr-modified 310 Stainless Steel	Zr-modified 310 Stainless Steel
Cladding material density, g/cm ³	7.90	7.90

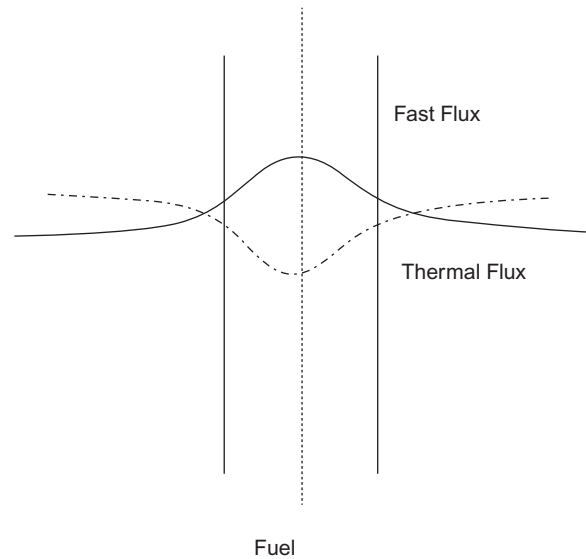


Figure 18.29. Schematic variation of fast and thermal fluxes inside cylindrical fuel element.

In Eq. (18.63), $q_{\text{gen}}(r)$ is the volumetric heat-generation rate, G_f is the fission energy released per fission an absorbed by the nuclear fuel, $\Sigma_{f, g}$ is the macroscopic fission cross-section of neutrons in energy group g in cm^{-1} , $\phi_g(r)$ is the neutron-flux density of energy group g in $(\text{cm}^2 \text{ s})^{-1}$.

In the developed code, the variation of the heat-generation rate has been taken into account by considering the variation of the flux profiles from the ring to ring and within each fuel element. As a result, the heat-generation rate is different for the fuel elements in the inner ring and the outer ring considering the fuel-bundle design of the subject PCh-SCWR. In addition, for each ring, the heat-generation rate varies in the

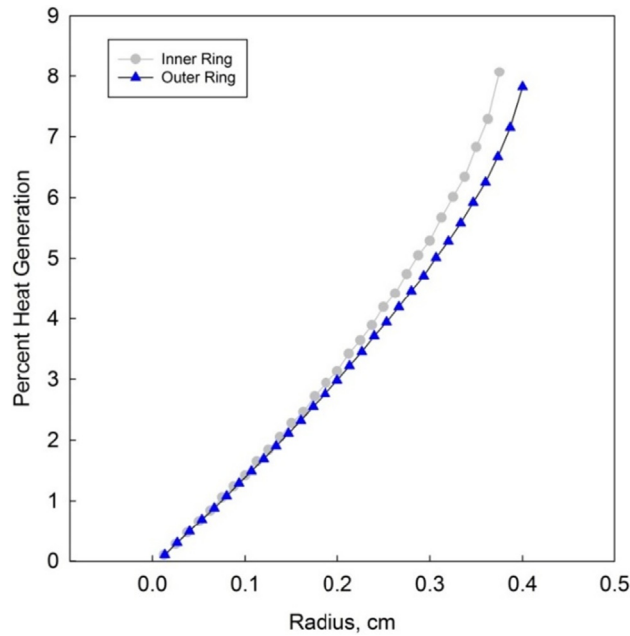


Figure 18.30. Percentage of heat generation along radial direction of fuel.

radial direction. To account for the spatial effect of heat generation, the transport calculations were conducted such that the fuel geometry was divided into 30 radial segments, and for each segment the integrated flux and fission rate were calculated, and the results were merged into nine energy groups. Then, the product of the fission rate and neutron flux was calculated for each energy group.

The heat generated from the fuel elements in the inner ring contributes 48.6% of the heat generated from the fuel bundle while 51.4% of the heat is released from the fuel elements in the outer ring of the fuel bundle. Figure 18.30 shows the percentage of the heat generation in the radial direction of the fuel elements for each of the 30 meshes along the radial direction of the fuel elements in the inner and the outer rings.

This analysis investigated the impact of the variation of the axial and radial heat-flux profiles of a fuel assembly as well as a non-uniform heat generation inside the fuel pellets on the fuel-centerline temperature. The results of this analysis show that the fuel-centerline temperature is more sensitive to the axial heat flux associated with various rings or fuel elements of a fuel bundle/assembly rather than to a non-uniform volumetric heat generation inside the fuel pellets. Thus, it is highly recommended to account for the variation of the axial heat flux for each ring of the fuel bundle. Further, the impact of a non-uniform volumetric heat generation on the fuel-centerline temperature is negligible. The results of this study further imply that the inclusion of a non-uniform heat generation in the calculation of the temperature distribution inside the fuel pellets should be commensurate with the scope and objectives of a study (Peiman, 2017).

As a conservative approach, the thermal power corresponding to a fuel channel with the maximum thermal power was utilized in order to calculate the heat flux and eventually the temperature profiles of the fuel elements. Figure 18.31 shows the axial heat-flux profiles associated with a channel with the maximum thermal power. For a number of nuclear fuels, the axial-temperature profiles of the fuel elements and their radial-temperature profiles at the location of the maximum temperature were computed for the inner and the outer rings. $\text{PuO}_2\text{-ThO}_2$ was selected as a representative of the low thermal-conductivity fuels. Figure 18.32 shows the variation of the fuel temperature at the location of the maximum temperature in the radial direction for the fuel elements in the inner ring and the outer ring. The maximum fuel-centerline temperature reaches 1811°C and 2074°C for the fuel elements in the inner ring and the outer ring, respectively.

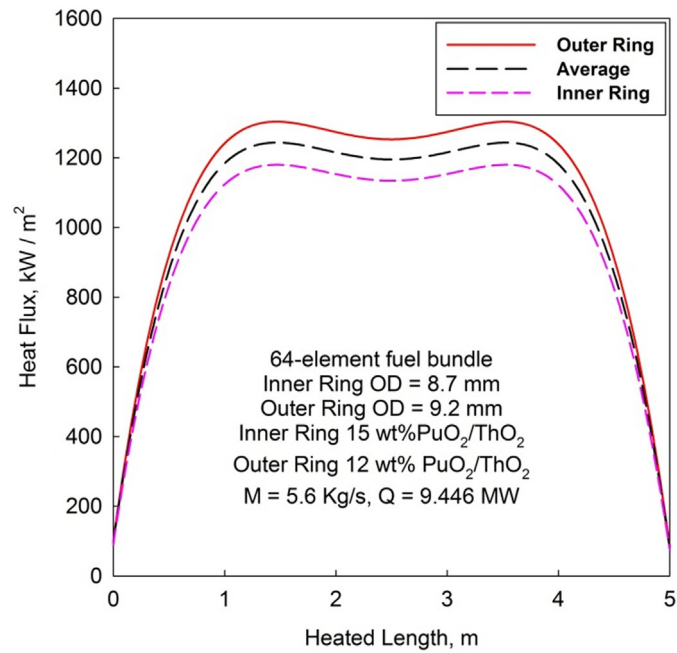


Figure 18.31. Cosine-shape axial heat-flux profile for channel with maximum thermal power.

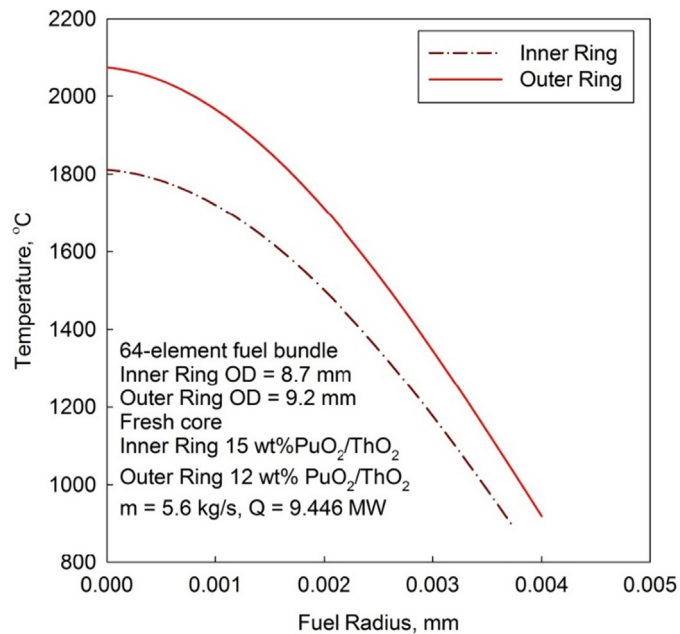


Figure 18.32. Temperature variation across $\text{ThO}_2\text{-PuO}_2$ fuel element at location of maximum temperature.

The variation of the fuel-centerline temperature along the heated length of the fuel channel is shown in [Figure 18.33](#).

As another low thermal-conductivity fuel, the fuel-temperature profiles were calculated for UO_2 under similar conditions, but with different fuel-bundle and fuel-channel designs. A 73-element fuel bundle and a reentrant fuel channel were chosen, respectively, as the reference fuel bundle and fuel channel. The specifications of the fuel bundle are identified in [Table 18.6](#). [Figure 18.34](#) shows an image of the fuel channel

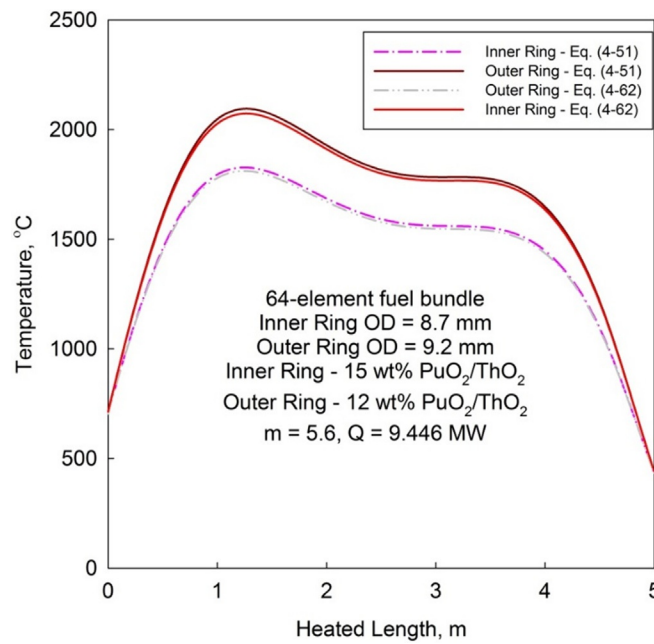


Figure 18.33. $\text{ThO}_2\text{-PuO}_2$ fuel centerline temperature along heated length of fuel channel.

Table 18.6. Specifications of 73-element fuel bundle (Peiman et al., 2015)

Parameter	Value
Total # of fuel elements	73
# of elements on ring 1, 2, 3, 4	9, 15, 21, 27
OD of central element, mm	18
OD elements on rings 1, 2, 3, 4, mm	9
Radius of ring 1, cm	1.0
Radius of ring 2, cm	2.0
Radius of ring 3, cm	3.0
Radius of ring 4, cm	4.1

(Peiman et al., 2015).^b The thermal-power distribution inside the reactor core was calculated based on the neutronic properties of a fresh and symmetric core. As a conservative approach, the thermal power corresponding to a fuel channel with a maximum thermal power of 9.5 MW was used in order to calculate the fuel-centerline and sheath temperatures with the use of a one-dimensional thermohydraulic code. The flow rate of the coolant was adjusted based on the thermal power of the examined fuel channel to obtain a coolant-outlet temperature of 625°C.

^b The operating conditions specified in this paragraph, the specification listed in Table 18.6, and the fuel channel shown in Figure 18.34 are used only for the calculation of the UO_2 fuel-temperature profiles. More detail information about the analysis is available in Peiman et al. (2015).

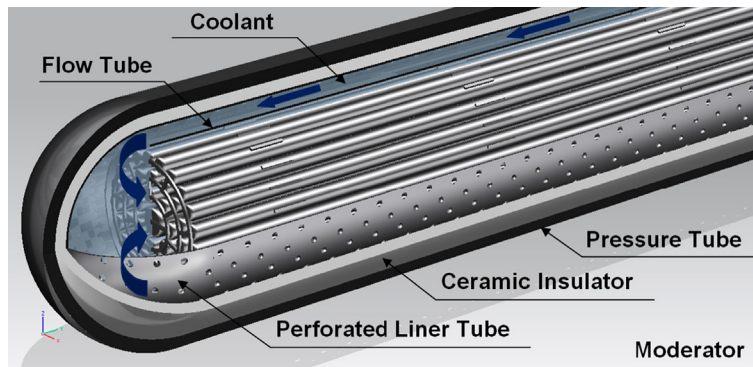


Figure 18.34. 3 reentrant fuel channel with ceramic insulator (Peiman et al., 2015).

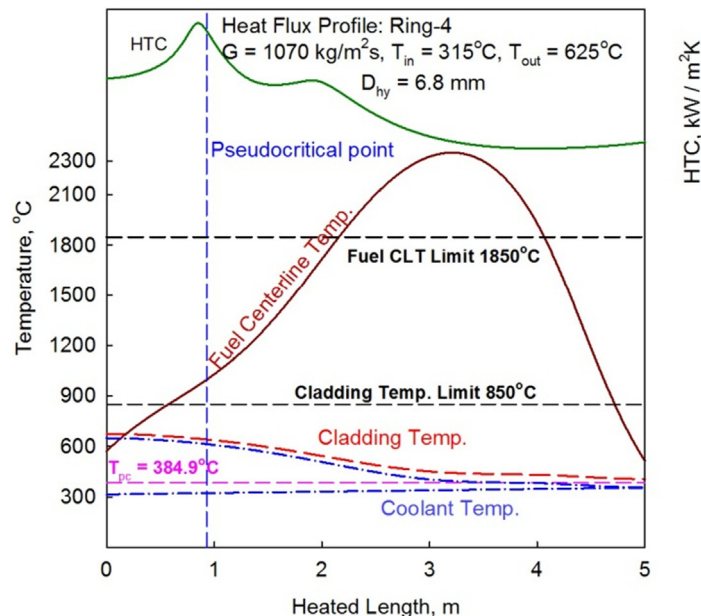


Figure 18.35. Coolant, sheath, and fuel-centerline temperature profiles for UO_2 fuel.

Fuel-centerline and sheath-temperature profiles are shown in Figure 18.35. These temperature profiles are calculated based on the heat flux associated with the outer ring of the fuel bundles, which has the maximum heat flux in the bundles. Figure 18.36 shows the axial heat-flux profile associated with the fuel elements on ring 1–4 of the fuel bundle as well as the average heat flux. As shown in Figure 18.35, the maximum fuel-centerline temperature of the UO_2 fuel reaches 2350°C . Figure 18.37 shows the temperature variation in the radial direction of a fuel element at a location with the maximum temperature based on the heat flux of ring 4.

Under the same conditions as described at the beginning of this Section, the temperature profiles were calculated for a composite fuel. For UO_2 with 89% SiC, the maximum fuel-centerline temperature reaches 1403°C and 1611°C , respectively, for the fuel elements in the inner ring and the outer ring. The variation of the fuel temperature in the radial direction at the location of the maximum fuel temperature for UO_2 -SiC is shown in Figure 18.38.

Similarly, for a high thermal-conductivity fuel, UC, the results show a further reduction in the fuel-centerline temperature. The maximum fuel-centerline temperature reaches 1041°C and 1105°C , respectively,

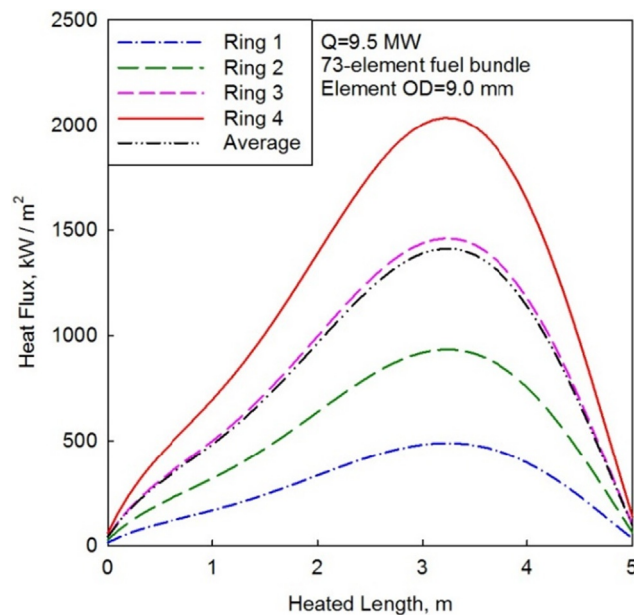


Figure 18.36. Heat-flux profiles associated with UO_2 fuel elements on ring 1–ring 4 of fuel bundle as well as average heat flux for fuel channel with maximum thermal power of 9.5 MW.

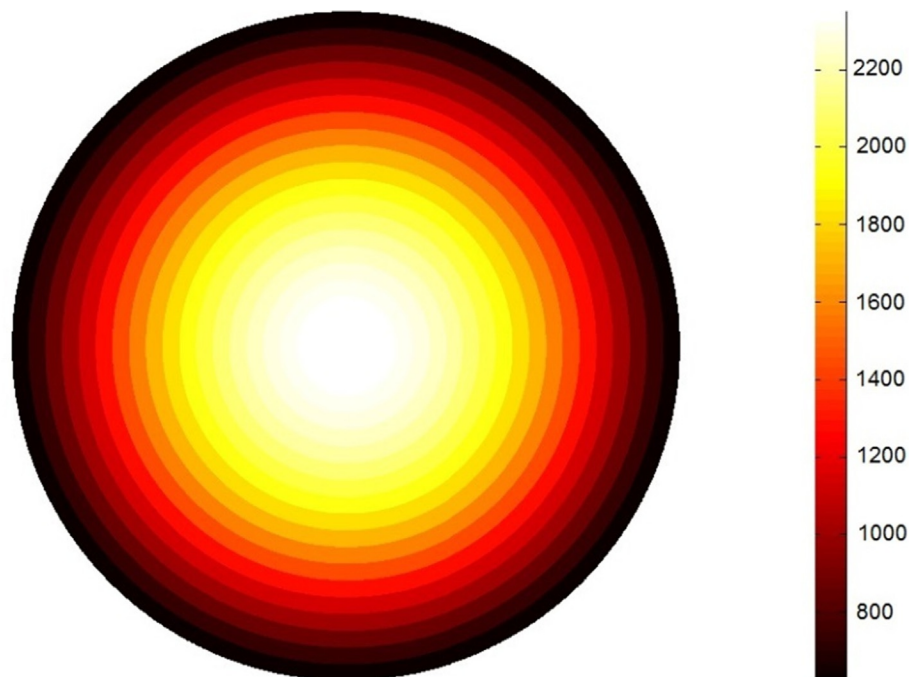


Figure 18.37. Temperature variation across UO_2 fuel element at location with maximum temperature.

for the fuel elements in the inner ring and the outer ring. Figure 18.39 shows the variation of the fuel temperature in the radial direction at the location of the maximum fuel temperature of 1105°C associated with the outer ring of the fuel bundle. The results of additional analyses on the fuel-temperature profiles of a number of nuclear fuels under different thermalhydraulic/neutronic conditions can be found in Miletic et al. (2015), Peiman et al. (2012a, b, 2013), and Grande et al. (2011).

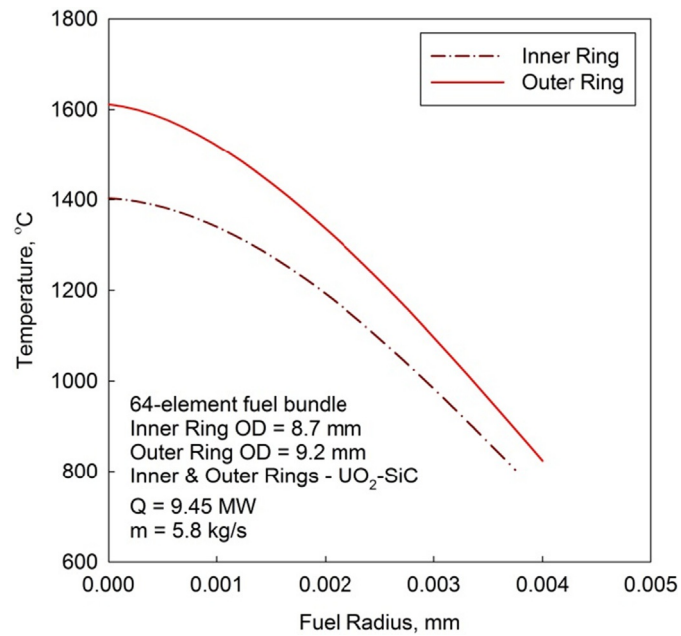


Figure 18.38. Temperature profiles across $\text{UO}_2\text{-SiC}$ fuel element at location with maximum temperature.

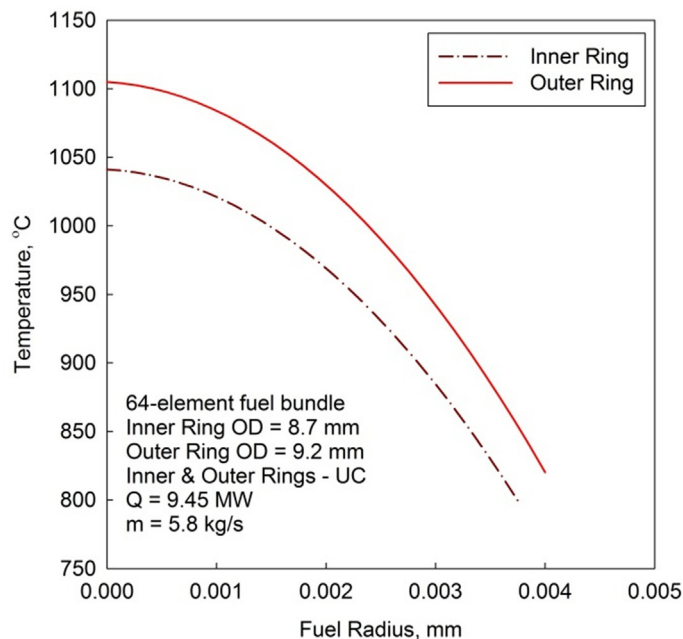


Figure 18.39. Temperature profiles across UC fuel element at location with maximum temperature.

18.7 Discussions

The most important factors associated with nuclear fuels for high-temperature applications include melting point, phase change, evaporation, high-temperature chemical stability, release of fission products, radiation-induced swelling, thermal-shock resistance, density, high-temperature creep, and mass of fissile elements (Lundberg and Hobbins, 1992). High thermal-conductivity fuels (e.g., UN and UC) have high melting points

and high thermal conductivities, which lead to lower fuel-centerline temperatures compared to low thermal-conductivity fuels (e.g., UO_2 , MOX, or ThO_2) for a given thermal power. Thus, other factors should be considered in order to determine the best fuel option(s).

One of these factors is the phase change. Among high thermal-conductivity fuels, UC_2 undergoes a phase change at temperatures within the range of 1765°C (Bowman et al., 1966) and 1820°C (Frost, 1963). This phase change results in an increase in the volume of the fuel, which in turn may jeopardize the mechanical integrity of the fuel and the sheath. This phase change significantly reduces the possibility of using UC_2 as a nuclear fuel in high-temperature applications. As a result, a comparison of the other factors has been drawn mainly among UN, UC, and UO_2 . The latter fuel has been taken into consideration, because UO_2 is widely used in nuclear reactors.

The atom density of uranium is another important factor, especially, in fast-neutron-spectrum reactors, because fission probability is significantly lower for fast neutrons compared to those of thermal neutrons. Both UN and UC have high uranium atom density, approximately 1.40 and 1.34 times that of UO_2 . Hence, use of UC or UN leads to smaller core sizes compared to that of the UO_2 fuel.

Stellrecht et al. (1968), Routbort (1972), Routbort and Singh (1975), and Hayes et al. (1990b) studied the steady-state creep strength and irradiation-induced creep of UN and UC and provided several correlations for the calculation of the steady-state and irradiation-induced creep rates of these nuclear fuels. These correlations can be used in order to predict the mechanical behavior of these fuels (e.g., dimensional stability and integrity) under operating conditions. Further studies have calculated the creep rates of fully dense UN and UC for a stress of 25 MPa (see Figures 18.22 and 18.10). In terms of irradiation-induced creep, both UN and UC have significantly lower irradiation-induced creep rates compared to UO_2 (Routbort and Singh, 1975). The results demonstrate that, when UC and UN fuels are compared, the irradiation-induced creep rate of UC was lower than that of UN at 1500°C . In other words, UC has a better creep strength and resistance to deformation than UN.

With the UC fuel, it is recommended to use hyper-stoichiometric UC (Routbort, 1972), because it has a lower steady-state creep rate compared to hypo-stoichiometric UC. In addition, hyper-stoichiometric UC has a higher mechanical strength than hypo-stoichiometric UC due to higher values of long-range stress (Routbort, 1972), which result in higher proportional limit values. As a result, hyper-stoichiometric UC has better mechanical behavior at high temperatures than hypo-stoichiometric UC and UN.

In addition to creep resistance, hardness is another mechanical property, which is an indication of the resistance of a material to deformation. Routbort and Singh (1975) identified the grain size, porosity, impurity contents, C/U or N/U ratios, and temperature as the most important factors affecting the hardness. They also have provided the hardness values at room temperature and 1000°C for UC and UN. For both UN and UC, the hardness decreases as the temperature increases. According to Routbort and Singh (1975), the hardness values, in kg/mm^2 , are 100, 120, and 50 for $\text{UC}_{1.05}$, $\text{UC}_{0.98}$, and UN respectively. The result of their investigation shows that UC has a higher hardness compared to UN; therefore, UC has a higher resistance against deformation, which in turn increases the mechanical integrity of the fuel under operating conditions of high-temperature nuclear applications.

The fission reaction, in a nuclear fuel, results in the production of gaseous fission products. These fission products are either contained in the fuel or released, which in turn exert stress on the sheath. In addition, the containment of the fission products in the fuel results in the swelling (e.g., a reduction in density due to a volume increase) of the fuel. Thus, it is essential to study the swelling rate of a nuclear fuel to ensure that the fuel and the cladding will withstand the stresses exerted on them and maintain their mechanical integrity under the operating conditions of a nuclear reactor, especially, when high burn-ups are required.

A comparison between the volumetric swelling of the UN and UC fuels shows that the percent volumetric swelling of UN is higher than that of UC (see Figures 18.21 and 18.9). For instance, the percent volumetric swelling of UN is approximately 17% and that of UC 12%, approximately at 1400°C and a burn-up of 40 GW day/Mg(U). It should be noted that the temperature of 1400°C has been chosen, because of the available

experimental data related to the swelling of UC. In addition, it should be noted that the swelling of both fuels can be reduced by increasing the porosity of the fuel (Frost, 1963). In contrast, Ma (1983) demonstrated that the fission-gas release is higher for porous fuels compared with dense fuels, which have less porosity. Nevertheless, UC has a lower percent volumetric swelling compared to UN.

The thermal-shock resistance of a nuclear fuel is an indication of the degree to which the fuel withstands sudden changes in temperature. A low thermal-shock resistance may result in the formation of cracks in the fuel, which in turn reduces the mechanical integrity of the fuel and increases the fission product release rate. As indicated by Eq. (18.64) (Kutz, 2005), the thermal-shock resistance of a fuel depends on its thermal conductivity, compressive strength, Poisson's ratio, the coefficient of thermal expansion, and Young's modulus of elasticity. The thermal-shock resistances of UC, UN, and UO₂ have been calculated based on Eq. (18.64) for a temperature range between 800°C and 1800°C. In Eq. (18.64), R' is the thermal-shock resistance in W/m, k is the thermal conductivity in W/mK, σ is the compressive strength in MPa, ν is the Poisson's ratio, α is the coefficient of thermal expansion in cm/cmK and E is the Young's modulus of elasticity in MPa. All required properties were determined for fuels with 95% theoretical density except the linear thermal-expansion coefficient, which was based on 100% theoretical density. The result shows that the thermal-shock resistances of both UN and UC are 5–15 times higher than those of UO₂ within the examined temperature range. The low thermal-shock resistance of UO₂ is mostly due to its low thermal conductivity, which makes this fuel vulnerable to sudden temperature changes at high operating temperatures. Thus, UN and UC have significantly higher thermal-shock resistances compared to UO₂ and are more suitable for high-temperature applications.

$$R' = \frac{k \cdot \sigma(1 - \nu)}{\alpha \cdot E} \quad (18.64)$$

The chemical compatibility of a nuclear fuel with coolant, which is an essential factor that affects the integrity of the fuel, can be studied in terms of the oxidation behavior of the fuel, when exposed to the coolant. Within the context of water-cooled reactors, UO₂ fuel is stable in water and has a high oxidation resistance in light water and heavy water at the LWR and Heavy Water Reactor (HWR) conditions (e.g., up to 320°C). However, UO₂ oxidizes at temperatures above 320°C, if it comes in direct contact with air or water in the case of a sheath breach (Ma, 1983). Similarly, UC has a poor oxidization resistance, when it comes in contact with water even at temperatures as low as 55°C (Ma, 1983). Likewise, UN oxidizes in water at temperatures above 100°C due to the deformation of the protective layer, which is formed on the surface of UN. The protective layer on the surface of UN is eventually lost at high temperatures, and cracks are formed. In addition, the oxidization resistance of UN is highly dependent on deviation from stoichiometry (Ma, 1983). In other words, the presence of free uranium or U₂N₃ significantly increases the oxidization rate. On the other hand, Kirillov et al. (2007) implied that UC and UN have better compatibility with coolant and cladding compared to UO₂. Therefore, further study is required on the chemical compatibility of UC and UN with water due to the discrepancy between the two available sources.

In terms of high-temperature stability, a great number of studies have been conducted on hypo-stoichiometric and hyper-stoichiometric UN. The results of these studies indicate that hyper-stoichiometric UN coexists with Uranium sesquiNitride (U₂N₃) in the temperature range of 1075°C and 1375°C for hyper-stoichiometric UN with N/U atomic ratios approximately between 1.2 and 1.5 (Matthews et al., 1988). According to the phase diagram provided by Matthews et al. (1988), U₂N₃ decomposes to UN and nitrogen at temperatures approximately above 1375°C. The release of nitrogen gas results in severe cracking of the fuel. This problem can be solved by using hypo-stoichiometric UN. However, it should be noted that Matthews et al. (1988) demonstrated that the fission-gas release rate is higher for hypo-stoichiometric UN than hyper-stoichiometric UN. If UN is chosen as a nuclear fuel, hypo-stoichiometric UN with adequate porosity should be utilized in order to minimize the negative impacts of the decomposition of U₂N₃ and accommodate for the fission products.

Another issue related to the UN fuel is that hypo-stoichiometric UN decomposes to uranium and nitrogen gas, which leads to cracking of the fuel due to the release of nitrogen. The results of several studies have shown that the incongruent vaporization of hypo-stoichiometric UN leads to the release of nitrogen and the formation of free uranium (Balankin et al., 1978). Balankin et al. (1978) reported of the appearance of free uranium in the temperature range between 1500°C and 1800°C. Moreover, Gingerich (1969) indicated that the incongruent vaporization of hypo-stoichiometric UN occurs in the temperature range between 1130 and 1800°C for N/U atomic ratios of 1.0 and 0.92, respectively. Gingerich (1969) also provided the results of experiments, which were conducted by Covert and Bonham, Vozzella and DeCrescente, and Inouye and Leitnaker on the decomposition of UN. Their experimental results, which are in agreement with Gingerich's results, indicate that incongruent decomposition of UN occurs at temperature ranges of 1600°C and 2000°C (based on Covert and Bonham), 1645°C and 1992°C (based on Vozzella and DeCrescente), and 1300°C (based on Inouye and Leitnaker). In addition, Oggianu et al. (2003) indicated that UN dissociates at temperatures higher than 1600°C, which is in agreement with other values published in the literature. Therefore, the release of nitrogen gas and formation of cracks in the fuel should be studied thoroughly, if UN is chosen as the fuel of choice for high-temperature applications, but it should be mentioned that this effect might not be significant, when the maximum fuel temperature of UN fuel is below 1300°C under normal operating conditions.

The study of neutronic properties of a nuclear fuel is as essential as analyzing its thermodynamic and mechanical properties. Oggianu et al. (2003) drew a comparison between neutronic properties of UO₂, UC, and UN, which have been summarized in Table 18.7. According to Oggianu et al. (2003), UN has higher fission and absorption cross-sections for the thermal neutrons than UC. These two parameters can be used to calculate the fission-to-capture ratio, which indicates that 43.7% of absorbed neutrons results in fission in UN fuel compared to 54.3% in UC. This shows that a higher neutron economy is achieved, when UC fuel is used. It should be noted that the fission-to-capture ratio for UO₂ is higher than that of UC. On the other hand, UO₂ has a smaller uranium-atom density compared to those of UN and UC. A high uranium-atom density indicates a smaller core size, which in turn reduces the costs. Thus, both UN and UC result in smaller core sizes.

It is beneficial to demonstrate an economic assessment among UO₂, UC, and UN fuels in order to provide a comparison between the fuel-cycle costs of these fuels. The result of the study conducted by Oggianu et al. (2003) shows that the cost of fuel is lower for UC compared to UN (Oggianu et al., 2003). This higher fuel cost for UN might be due to the necessity to enrich nitrogen to ¹⁵N to avoid the formation of ¹⁴C. Oggianu et al. (2003) calculated the cost of the fuel cycle plus the cost of forced outages, which indicates that still the overall cost is lower for the UC fuel. Thus, the UC fuel is economically more attractive than the UN fuel.

As noted, each fuel exhibits both desirable and detrimental properties all of which should be considered to ensure that the integrity and longevity of the fuel in the reactor is maintained. The study of the deleterious behavior of these fuels provides the means to select the most suitable fuel for the use in advanced reactors. Table 18.8 provides a summary of the properties of the UO₂, UN, and UC fuels.

Table 18.7. Neutronic properties of UO₂, UC, and UN (Oggianu et al., 2003)

Parameter	UO ₂	UC	UN
Fission cross section for natural uranium (at 0.025 eV), cm ⁻¹	0.102	0.137	0.143
Absorption cross-section for natural uranium (at 0.025 eV), cm ⁻¹	0.185	0.252	0.327
$\alpha_{cf} = \Sigma_c / \Sigma_f$ (capture to fission ratio)	0.831	0.839	1.286
η (average number of neutrons emitted per neutron absorbed)	1.34	1.34	1.08
Uranium atom density based on 100% TD , g/cm ³	9.67	12.97	13.52

Table 18.8. Properties of UO₂, UN, and UC fuels

Fuel	Property	Reference
UO ₂	Low thermal conductivity and high linear thermal expansion coefficient at high temperatures	
	low thermal-shock resistance at high operating temperatures (e.g., above 1100°C)	—
	Higher irradiation-induced creep than UN and UC	Routbort and Singh (1975)
	High fission product at $t > 1725^\circ\text{C}$	Lundberg and Hobbins (1992)
	High evaporation rate	Lundberg and Hobbins (1992)
	Lower uranium density compared to UC and UN	Ma (1983)
	Lower fuel density compared to UC and UN	Ma (1983)
	UN dissociates at	
	$t > 1130^\circ\text{C}$	Gingerich (1969)
	$t > 1500^\circ\text{C}$	Balankin et al. (1978)
	$t > 1600^\circ\text{C}$	Oggianu et al. (2003)
	Hyper-stoichiometric UN coexists with U ₂ N ₃ , which decomposes to UN and nitrogen at temperatures approximately above 1375°C	Matthews et al. (1988)
	Higher irradiation-induced creep compared with UC	Routbort and Singh (1975)
	Oxidation reaction with water	Oggianu et al. (2003)
	Relatively higher volumetric swelling compared to UO ₂	Ross et al. (1990)
	The necessity to enrich in ¹⁵ N to minimize the ¹⁴ C production	Oggianu et al. (2003)
	Lower hardness compared with UC	Routbort and Singh (1975)
	Relatively high gaseous fission products release from hypo-stoichiometric UN	Matthews et al. (1988)
UC	Speculative chemical compatibility with water (e.g., reacts with water)	Ma (1983); Kirillov et al. (2007)
	Relatively higher volumetric swelling compared to UO ₂	Frost (1963)
	Lower melting point (~12%) compared to UO ₂ and UN	Cox and Cronenberg (1977) Lundberg and Hobbins (1992)

References

- Abdalla, A., Peiman, W., Pioro, I., Gabriel, K., 2012. Sensitivity analysis of fuel centerline temperature in SCWRs. In: Proceedings of the 20th International Conference on Nuclear Engineering (ICONE-20)—ASME 2012 POWER Conference, July 30—August 3, Anaheim, California, USA. Paper #54530, 9 pp.
- Alexander, L.G., 1964. Breeder reactors. *Annu. Rev. Nucl. Sci.* 14, 287–322.
- Bakker, K., Cordfunke, E.H.P., Konings, R.J.M., Schram, R.P.C., 1977. Critical evaluation of the thermal properties of ThO₂ and (Th_{1-y}U_y)O₂ and a survey of the literature data on (Th_{1-y}Pu_y)O₂. *J. Nucl. Mater.* 250 (1), 1–12.

- Balankin, S.A., Loshmanov, L.P., Skorov, D.M., Skolov, V.S., 1978. Thermodynamic stability of uranium nitride. *J. Atomic Energy* 44 (4), 327–329.
- Belle, J., Berman, R.M., 1984. Thorium Dioxide: Properties and Nuclear Applications. Naval Reactors Office, United State Department of Energy, Government Printing Office, Washington, DC, USA.
- Bowman, A.L., Arnold, G.P., Witteman, W.G., Wallace, T.C., 1966. Thermal expansion of uranium dicarbide and uranium sesquicarbide. *J. Nucl. Mater.* 19, 111–112.
- Candu Energy, 2012. Enhanced CANDU 6 Technical Summary. http://www.candu.com/site/media/Parent/EC6%20Technical%20Summary_2012-04.pdf.
- Carbajo, J.J., Yoder, G.L., Popov, S.G., Ivanov, V.K., 2001. A review of the thermophysical properties of MOX and UO₂ fuels. *J. Nucl. Mater.* 299, 181–198.
- Chirkin, V., 1968. Thermophysical Properties of Materials for Nuclear Engineering. Atomizdat Publ. House, Moscow, Russia (in Russian).
- Cochran, R.G., Tsoufanidis, N., 1999. The Nuclear Fuel Cycle: Analysis and Management, second ed. American Nuclear Society, Illinois, USA.
- Coninck, R.D., Lierde, W.V., Gijs, A., 1975. Uranium carbide: thermal diffusivity, thermal conductivity spectral emissivity at high temperature. *J. Nucl. Mater.* 57, 69–76.
- Coninck, R.D., Batist, R.D., Gijs, A., 1976. Thermal diffusivity, thermal conductivity and spectral emissivity of uranium dicarbide at high temperatures. *J. Nucl. Mater.* 8, 167–176.
- Cox, D., Cronenberg, A., 1977. A theoretical prediction of the thermal conductivity of uranium carbide vapor. *J. Nucl. Mater.* 67, 326–331.
- Das, D., Bharadwaj, S.R., 2013. Thoria-Based Nuclear Fuels. Springer, London, UK. 405 pp.
- Evans, H.B., Hrobar, A.M., Patterson, J.H., 1960. Determination of zirconium in uranium fissium alloys. *Anal. Chem.* 32 (4), 481–483.
- Fast Reactor Working Group (FRWG), 2018. Nuclear Metal Fuel: Characteristics, Design, Manufacturing, Testing, and Operating History. Retrieved May 08, 2021, from, U.S. Nuclear Regulatory Commission. <https://www.nrc.gov/docs/ML1816/ML18165A249.pdf>.
- Frost, B.R., 1963. The carbides of uranium. *J. Nucl. Mater.* 10, 265–300.
- Galahom, A., Bashter, I.I., Aziz, M., 2014. Study the neutronic analysis and burnup for BWR fueled with hydride fuel using MCNPX code. *Prog. Nucl. Energy* 77, 65–71.
- GE Nuclear Energy, 1972. BWR/6 General Description of a Boiler Water Reactor. Retrieved from: NC State University. <http://www4.ncsu.edu/~doster/NE405/Manuals/BWR6GeneralDescription.pdf>.
- Gingerich, K.A., 1969. Vaporization of uranium mononitride and heat of sublimation of uranium. *J. Chem. Phys.* 51 (10), 4433–4439.
- Grande, L., Villamere, B., Allison, L., Mikhael, S., Rodriguez-Prado, A., Pioro, I., 2011. Thermal aspects of uranium carbide and uranium di-carbide fuels in supercritical water-cooled nuclear reactors. *J. Eng. Gas Turbines Power* 133 (2). February, 7 pages.
- Hafele, W., Faude, D., Fischer, E.A., Laue, H.J., 1970. Fast breeder reactors, annual review nuclear. *Science* 20, 393–434.
- Harrison, J.W., 1969. The irradiation-induced swelling of uranium carbide. *J. Nucl. Mater.* 30, 319–323.
- Hayes, S., Thomas, J., Peddicord, K., 1990a. Material properties of uranium mononitride-III transport properties. *J. Nucl. Mater.* 171, 289–299.
- Hayes, S., Thomas, J., Peddicord, K., 1990b. Material property correlations for uranium mononitride-II mechanical properties. *J. Nucl. Mater.* 171, 271–288.
- Hayes, S., Thomas, J., Peddicord, K., 1990c. Material property correlations for uranium mononitride-IV thermodynamic properties. *J. Nucl. Mater.* 171, 300–318.
- Hollenbach, D.F., Ott, L.J., 2010. Improving the thermal conductivity of UO₂ fuel with the addition of graphite fibers. In: Transactions of the American Nuclear Society and Embedded Topical Meeting “Nuclear Fuels and Structural Materials for the Next Generation Nuclear Reactors”, June 13–17, San Diego, CA, USA, pp. 485–487.
- Huang, J., Tsuchiya, B., Konashi, K., Yamawaki, M., 2001. Thermodynamic analysis of chemical states of fission products in uranium-zirconium hydride fuel. *J. Nucl. Mater.* 294, 154–159.
- IAEA, 2006. Thermophysical Properties Database of Materials for Light Water Reactors and Heavy Water Reactors, TECDOC-1496. Vienna, Austria https://www-pub.iaea.org/MTCD/publications/PDF/te_1496_web.pdf.
- IAEA, 2007. Computational Analysis of the Behaviour of Nuclear Fuel under Steady State, Transient and Accident Conditions, TECDOC-1578. Vienna, Austria https://www-pub.iaea.org/MTCD/publications/PDF/TE_1578_web.pdf.
- IAEA, 2008. Thermophysical Properties of Materials for Nuclear Engineering: A Tutorial and Collection of Data. Vienna, Austria <https://www.iaea.org/publications/7965/thermophysical-properties-of-materials-for-nuclear-engineering-a-tutorial-and-collection-of-data>.

- IAEA, 2010. High Temperature Gas Cooled Reactor Fuels and Materials, TECDOC-1645. Vienna, Austria https://www-pub.iaea.org/MTCD/Publications/PDF/TE_1645_CD/PDF/TECDOC_1645.pdf.
- IAEA, 2022. Advances in Small Modular Reactor Technology Developments. Vienna, Austria. https://aris.iaea.org/Publications/SMR_Booklet_2022.pdf.
- Ishimoto, S., Hirai, M., Ito, K., Korei, Y., 1996. Thermal conductivity of UO₂-BeO pellet. *J. Nucl. Sci. Technol.* 33 (2), 134–140.
- Jain, D., Pillai, C., Rao, B.K., Sahoo, K., 2006. Thermal diffusivity and thermal conductivity of thorium-lanthana solid solutions up to 10 mol.% LaO (1.5). *J. Nucl. Mater.* 353, 35–41.
- Kadak, A.C., 2005. A future for nuclear energy: pebble bed reactors. *Int. J. Crit. Infrastruct.* 1 (4), 330–345. http://web.mit.edu/pebble-bed/papers1_files/Future%20for%20Nuclear%20Energy.pdf.
- Khan, J.A., Knight, T.W., Pakala, S.B., Jiang, W., Fang, R., 2010. Enhanced thermal conductivity for LWR fuel. *J. Nucl. Technol.* 169, 61–72.
- Kikuchi, T., Takahashi, T., Nasu, S., 1972. Porosity dependence of thermal conductivity of uranium mononitride. *J. Nucl. Mater.* 45, 284–292.
- Kirilov, P.L., Terent'eva, M.I., Deniskina, N.B., 2007. *Thermophysical Properties of Nuclear Engineering Materials*, third ed. Izdat Publ. House, Moscow, Russia. revised and augmented. 194 pp.
- Kutz, M., 2005. *Mechanical Engineers' Handbook, Materials and Mechanical Design*, third ed. John Wiley and Sons.
- Larson, E.A.G., 1961. A General Description of the NRX Reactor, AECL-1377. retrieved May 06, 2021 https://inis.iaea.org/collection/NCLCollectionStore/_Public/41/057/41057258.pdf?r=1.
- Latta, R., Revankar, S.T., Solomon, A.A., 2008. Modeling and measurement of thermal properties of ceramic composite fuel for light water reactors. *Heat Transfer Eng.* 29 (4), 357–365.
- Leitnaker, J.M., Godfrey, T.G., 1967. Thermodynamic properties of uranium carbide. *J. Nucl. Mater.* 21, 175–189.
- Lundberg, L.B., Hobbins, R.R., 1992. Nuclear fuels for very high temperature applications. In: *Intersociety Energy Conversion Engineering Conf.*, San Diego, CA, USA. 9 pp.
- Ma, B.M., 1983. *Nuclear Reactor Materials and Applications*. Van Nostrand Reinhold Company Inc., New York, NY, USA.
- Matthews, R.B., Chidester, K.M., Hoth, C.W., Mason, R.E., Petty, R.L., 1988. Fabrication and testing of uranium nitride fuel for space power reactors. *J. Nucl. Mater.* 151, 334–344.
- McDeavitt, S.M., 2009. High Conductivity Fuel Concept UO₂-BeO Composite (Zr Cermet). Retrieved from. <http://tamu.edu/>.
- Miletic, M., Peiman, W., Farah, F., Samuel, J., Dragunov, A., Pioro, I., 2015. Study on neutronics and thermalhydraulics characteristics of 1200-MW_e pressure-channel SuperCritical water-cooled reactor (SCWR). *ASME J. Nucl. Eng. Radiat. Sci.* 1 (1). 10 pages.
- Muraviev, E.V., 2014. Fuel supply of nuclear power industry with the introduction of fast reactors. *Therm. Eng.* 61 (14), 1030–1039.
- OECD/NEA, IAEA, 2020. Uranium 2020: Resources, Production and Demand. https://www.oecd-nea.org/jcms/pl_52718/uranium-2020-resources-production-and-demand.
- Ogard, A.E., Leary, J.A., 1970 August. Plutonium Carbides. Retrieved June 15, 2015, from: US Department of Energy. <http://www.osti.gov/scitech/servlets/purl/4102301/>.
- Oggianu, S.M., No, H.C., Kazimi, M., 2003. Analysis of burnup and economic potential of alternative fuel materials in thermal reactors. *J. Nucl. Technol.* 143, 256–269.
- Olander, D., 2009. Nuclear fuels—present and future. *J. Nucl. Mater.* 389, 1–22.
- Olander, D., Greenspan, E., Garkisch, H.D., Petrovic, B., 2009. Uranium–zirconium hydride fuel properties. *J. Nucl. Eng. Des.* 239, 1406–1424.
- ORNL, 1965. Properties of Thorium, Its Alloys, and Its Compounds. Retrieved from: Oak Ridge National Laboratory. <http://web.ornl.gov/info/reports/1965/3445601336962.pdf>.
- Peiman, W., 2017. Study on Specifics of Thermalhydraulics and Neutronics of Pressure-Channel SuperCritical Water-cooled Reactors (SCWRs). Doctoral Thesis, Oshawa, Canada.
- Peiman, W., Pioro, I., Gabriel, K., 2012a. Thermal aspects of conventional and alternative fuels in SuperCritical water-cooled reactor (SCWR) applications. Chapter in book, In: Mesquita, A.Z. (Ed.), *Nuclear Reactors*. INTECH, Rijeka, Croatia, pp. 123–156. Free download from: <http://www.intechopen.com/books/nuclear-reactors/-thermal-aspects-of-conventional-and-alternative-fuels-in-supercritical-water-cooled-reactor-scwr-ap>.
- Peiman, W., Pioro, I., Gabriel, K., 2013. Thermal design aspects of high-efficiency channel for SuperCritical water-cooled reactors (SCWRs). *Nucl. Eng. Des.* 264, 238–245.
- Peiman, W., Pioro, I., Gabriel, K., 2015. Thermal-hydraulic and neutronic analysis of a re-entrant fuel channel design for pressure-channel supercritical water-cooled reactors. *ASME J. Nucl. Eng. Radiat. Sci.* 1 (2). 10 pp.

- Peiman, W., Saltanov, E., Grande, L., Pioro, I., Rouben, B., Gabriel, K., 2012b. Power distribution and fuel centerline temperature in a pressure-tube supercritical water-cooled reactor (PT SCWR). In: Proceedings of the 20th International Conference On Nuclear Engineering (ICONE-20)—ASME 2012 POWER Conference, July 30–August 3, Anaheim, California, USA. Paper #54596, 12 pp.
- Popov, S.G., Carbajo, J.J., Ivanov, V.K., Yoder, G.L., 2000. Thermophysical Properties of MOX and UO₂ Fuels Including the Effects of Irradiation. Retrieved July 12, 2015, from: Oak Ridge National Lab. <http://web.ornl.gov/~webworks/cpr/v823/rpt/109264.pdf>.
- Ross, S.B., El-Genk, M.S., Matthews, R.B., 1988. Thermal conductivity correlation for uranium nitride fuel. *J. Nucl. Mater.* 151, 313–317.
- Ross, S.B., El-Genk, M.S., Matthews, R.B., 1990. Uranium nitride fuel swelling correlation. *J. Nucl. Mater.* 170, 169–177.
- Routbort, J.L., 1972. High-temperature deformation of polycrystalline uranium carbide. *J. Nucl. Mater.* 44, 24–30.
- Routbort, J.L., Singh, R.N., 1975. Elastic, diffusional, and mechanical properties of carbide and nitride nuclear fuels — a review. *J. Nucl. Mater.* 58 (1), 78–114.
- Roy, P.R., Sah, D.N., 1985. Irradiation behaviour of nuclear fuels. *Pramana* 24, 397–421. <https://www.ias.ac.in/public/Volumes/pram/024/01-02/0397-0421.pdf>.
- Sailer, H.A., Dickerson, R.F., Bauer, A.A., Daniel, N.E., 1956. Properties of a Fissium-Type Alloy. Retrieved May 08, 2021, from: U.S. Department of Energy. <https://www.osti.gov/servlets/purl/4347233>.
- Seltzer, M.S., Wright, T.R., Moak, D.P., 1975. Creep behavior of uranium carbide-based alloys. *J. Am. Ceram. Soc.* 58, 138–142.
- Shoup, R.D., Grace, W.R., 1977. Process variables in the preparation of UN microspheres. *J. Am. Ceram. Soc.* 60 (7–8), 332–335.
- Sinnad, M.T., 1980. The U-ZrHx alloy: its properties and use in TRIGA fuel. *Nucl. Eng. Des.* 64, 403–422. Also General Atomic Report GA-A16029, 1980.
- Sinnad, M.T., 2003. Nuclear Reactor Materials and Fuels. <https://www.sciencedirect.com/science/article/pii/B0122274105004981?via%3Dihub>.
- Solomon, A.A., Revankar, S., McCoy, J.K., 2005. Enhanced Thermal Conductivity Oxide Fuels. Retrieved from: OSTI. <http://www.osti.gov/scitech/servlets/purl/862369-iDA0bl/>.
- Stanley, C.J., Marshall, F.M., 2008. Advanced test reactor—a national scientific user facility. In: Proceedings of the 16th International Conference on Nuclear Engineering (ICONE-16), May 11–15, Orlando, FL, USA.
- Stellrecht, D.E., Farkas, M.S., Moak, D.P., 1968. Compressive creep of uranium carbide. *J. Am. Ceram. Soc.* 51 (8), 455–458.
- Sundaram, C.V., Mannan, S.L., 1989. Nuclear fuels and development of nuclear fuel elements. *Sadhana* 14 (Part 1), 21–57. <https://www.ias.ac.in/article/fulltext/sadh/014/01/0021-0057>.
- Tokar, M., Nutt, A.W., Leary, J.A., 1970. Mechanical properties of carbide and nitride reactor fuels. *J. Reactor Technol.* <http://www.osti.gov/bridge/purl.cover.jsp?purl=/4100394-tE8dXk/>.
- Tsuchiya, B., Huang, J., Konashi, K., Saiki, W., Onoue, T., Yamawaki, M., 2000. Thermal diffusivity measurement of uranium-thorium-zirconium hydride. *J. Alloys Compd.* 312, 104–110.
- Tsuchiya, B., Huang, J., Konashi, K., Teshigawara, M., Yamawaki, M., 2001. Thermophysical properties of zirconium hydride and uranium-zirconium hydride. *J. Nucl. Mater.* 289, 329–333.
- Waltar, A.E., Todd, D.R., Tsvetkov, P.V. (Eds.), 2012. *Fast Spectrum Reactors*. Springer, New York, NY, USA. 532 pp.
- Westinghouse Electric Corporation, 1984. The Westinghouse Pressurized Water Reactor Nuclear Power Plant. http://www4.ncsu.edu/~doster/NE405/Manuals/PWR_Manual.pdf.
- Wheeler, M.J., 1965. Thermal diffusivity at incandescent temperatures by a modulated electron beam technique. *Br. J. Appl. Phys.* 16, 365–376.
- WNA, 2020a. Generation IV Nuclear Reactors. Retrieved May 05, 2021, from: World Nuclear Association. <http://www.world-nuclear.org/info/nuclear-fuel-cycle/power-reactors/generation-iv-nuclear-reactors/>.
- WNA, 2020b. Thorium. Retrieved May 05, 2021, from: World Nuclear Association. <http://www.world-nuclear.org/info/Current-and-Future-Generation/Thorium/>.
- WNA, 2021a. Nuclear Power Reactors. Retrieved May 05, 2021, from: World Nuclear Association. <http://www.world-nuclear.org/info/Nuclear-Fuel-Cycle/Power-Reactors/Nuclear-Power-Reactors/>.
- WNA, 2021b. Fast Neutron Reactors. Retrieved May 05, 2021, from: World Nuclear Association. <http://www.world-nuclear.org/info/Current-and-Future-Generation/Fast-Neutron-Reactors/>.
- WNN, 2021, December. Demonstration HTR-PM connected to grid. *World Nuclear News*. Retrieved from: <https://www.world-nuclear-news.org/Articles/Demonstration-HTR-PM-connected-to-grid> (Retrieved 23 July 2022).
- Zakova, J., 2012. *Advanced Fuels for Thermal Spectrum Reactors*. Doctoral Thesis, Stockholm, Sweden.
- Zhou, W., Liu, R., Revankar, S.T., 2015. Fabrication methods and thermal hydraulics analysis of enhanced thermal conductivity UO₂-BeO fuel in light water reactors. *Ann. Nucl. Energy* 81, 240–248.

Hydrogen production pathways for Generation-IV reactors

Rami S. El-Emam^a, Calin Zamfirescu^b, and Kamiel S. Gabriel^a

^aFaculty of Engineering and Applied Science, Ontario Tech University, Oshawa, ON, Canada

^bDurham College, Oshawa, ON, Canada

Nomenclature

AECL	Atomic Energy of Canada Limited
Ca-Br	Calcium-Bromium hybrid thermochemical cycle
CNL	Canadian Nuclear Laboratories
Cu-Cl	Copper-Chlorine hybrid thermochemical cycle
GA	General Atomics
GFR	Gas-cooled Fast Reactor
GIF	Generation IV International Forum
GTHTTR	Gas Turbine High-Temperature Reactor
HHV	High Heating Value
HTGR	High Temperature Gas-cooled Reactor
HTSE	High Temperature Steam Electrolysis
HTTR	High-Temperature Test Reactor
HyS	Hybrid Sulfur thermochemical cycle
IHX	Intermediate Heat eXchanger
JAEA	Japan Atomic Energy Agency
JAERI	Japan Atomic Energy Research Institute
LFTR	Lead-alloy Fast Reactor
LSM	Lanthanum Strontium Manganite
LWR	Light Water Reactor
Mg-Cl	Magnesium-Chloride hybrid thermochemical cycle
MHR	Modular Helium Reactor
MSR	Molten Salt Reactor
Na-O-H	Sodium-Oxygen-Hydrogen thermochemical cycle
OER	Oxygen Evolution Reaction
PBMR	Pebble Bed Modular Reactor
PEM	Polymer Electrolyte Membrane
S-I	Sulfur-Iodine cycle
SCWR	SuperCritical Water-cooled Reactor
SFR	Sodium-cooled Fast Reactor
SOEC	Solid Oxide Electrolysis Cell
SOE(O)	Solid Oxide Electrolyzer with Oxygen ion conduction
SOE(P)	Solid Oxide Electrolyzer with Proton ion conduction
U-Eu-Br	Uranium-Europium-Bromium thermochemical cycle
VHTR	Very High Temperature Reactor
YSZ	Yttria-Stabilized Zirconia

19.1 Introduction

The use of nuclear energy for hydrogen production using Generation-IV nuclear reactors could be a prospective for the expanding green economy. Nuclear hydrogen production technologies offer increase in efficiency and significant reductions in pollution. In addition, nuclear-based hydrogen production enhances global energy mix and represents a reliable, safe and economic pathway for sustainable, large-scale-hydrogen production. Generation-IV power plants for cogeneration of hydrogen and electricity represents an energy system that is characterized by economic stability, enhanced security from international volatility, and the elimination of massive balance-of-payment deficits.

Nuclear hydrogen production using low- and intermediate-temperature electrolysis technologies (i.e., conventional electrolysis) has been utilized for decades. Today, several projects around the world are considering conventional electrolysis to enable efficient load-following operation of current fleet of nuclear power plants. This is also believed to affect the profitability of operating nuclear power plants positively in some parts of the world. Some reactors of Generation-IV designs operate at high temperature that enables operating the power plant at high thermal efficiency. These reactors are feasible to provide the required source of energy to drive a thermochemical process for hydrogen production. [Figure 19.1](#) illustrates some of the possible routes of coupling hydrogen technologies to nuclear energy for large-scale hydrogen production.

19.2 Coupling hydrogen and Generation-IV reactor technologies

Two of the main selection criteria of suitable hydrogen technology to be coupled with a specific nuclear reactor are: (1) operating temperature and (2) electrical energy demand. [Figure 19.2](#) presents a comparative assessment of both factors for some of the promising technologies developed or under development for sustainable large-scale hydrogen production. However, the maximum temperature values and electrical energy consumption are not the only factors to determine the feasibility of linking hydrogen technology to a specific reactor technology. For instance, the pure thermochemical Sodium-Oxygen-Hydrogen (Na-O-H) process does not demand high temperature for operation, yet the rate of reaction could render it a non-feasible option. Also, pure thermochemical Uranium-Europium-Bromium (U-Eu-Br) process involves radioactive components. In addition, kinetics study is inevitable for every individual reaction of the cycle. The hybrid thermochemical cycles: Hybrid Sulfur (HyS), Copper-Chlorine (Cu-Cl), Calcium-Bromium (Ca-Br), and Magnesium-Chloride (Mg-Cl) fall on either side of the diagonal line in [Figure 19.2](#), where they may be noted to be more realistic options. This diagonal line connects the two extreme cases depicting thermal-only and electric-energy-only hydrogen production represented by the intersections with the x - and y -axis of the diagram, respectively. One may comment on this representation as follows: cycles at the lower side of the diagonal line may encounter chemistry and reaction rate problems while the ones at the upper side may be seen as economically unfeasible.

Based on their operating temperature range, [Table 19.1](#) presents the possible coupling based on the match of temperature and quality of thermal heat between different hydrogen production technologies and Generation-IV designs: the SuperCritical Water-cooled Reactor (SCWR), Gas-cooled Fast Reactor (GFR), Lead-alloy Fast Reactor (LFR), Very-High-Temperature Reactor (VHTR), Molten Salt Reactor (MSR), and Sodium-cooled Fast Reactor (SFR). [Figure 19.3](#) shows the temperature profiles for some of the proposed designs of Generation-IV reactors. The coolant temperature is plotted against the specific enthalpy. For LFR, the profile depicts the Euratom ELSY. Regarding the VHTR, the span of coolant temperature is indicated in the diagram represents the case when an intermediate-heat exchanger is not used but rather the coolant is used directly for the downstream process. In the case of VHTR systems operating with intermediate-heat exchangers, the temperature level of the coolant is lower.

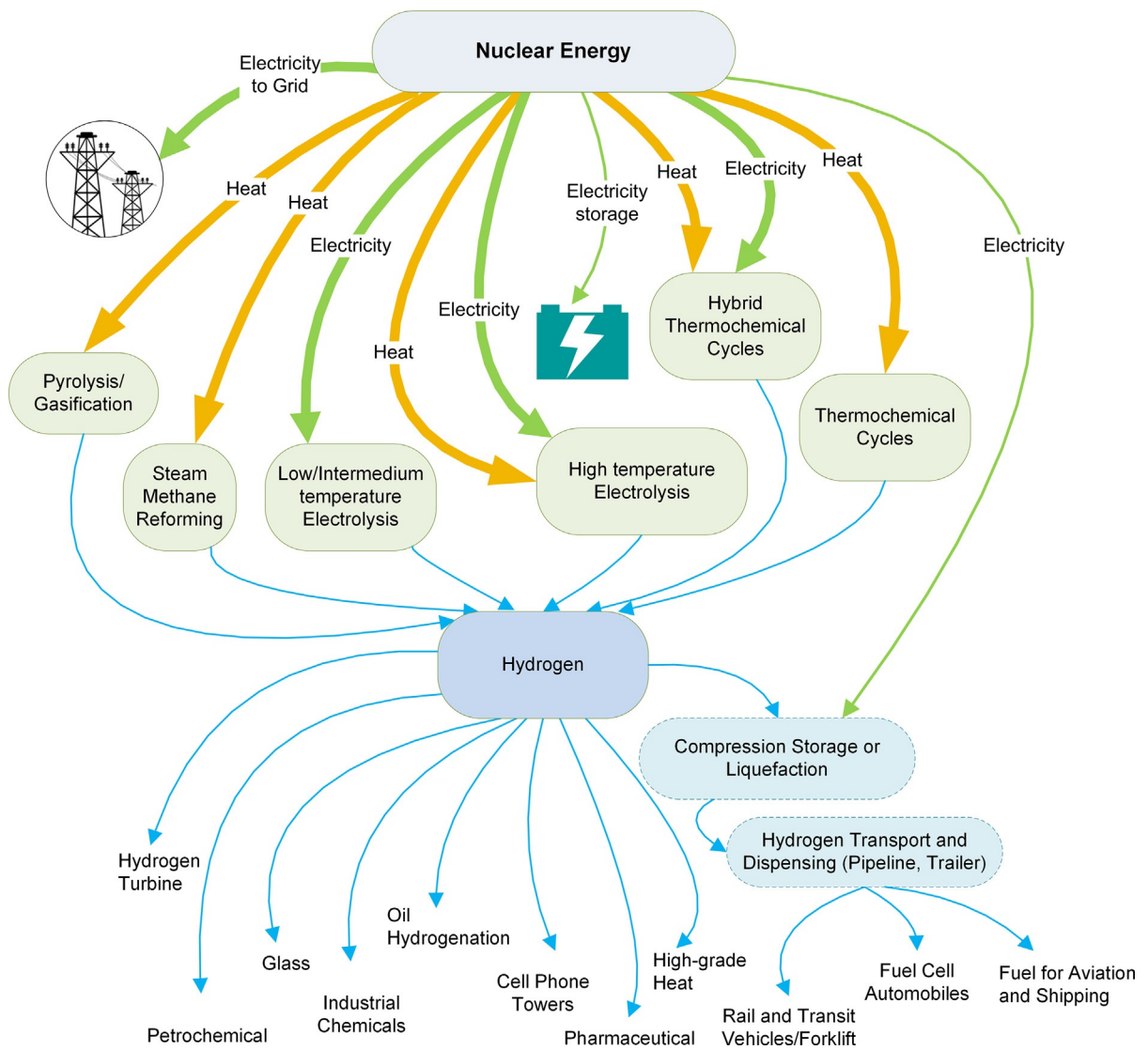


Figure 19.1. Alternative possible routes for nuclear cogeneration plants for large-scale hydrogen production

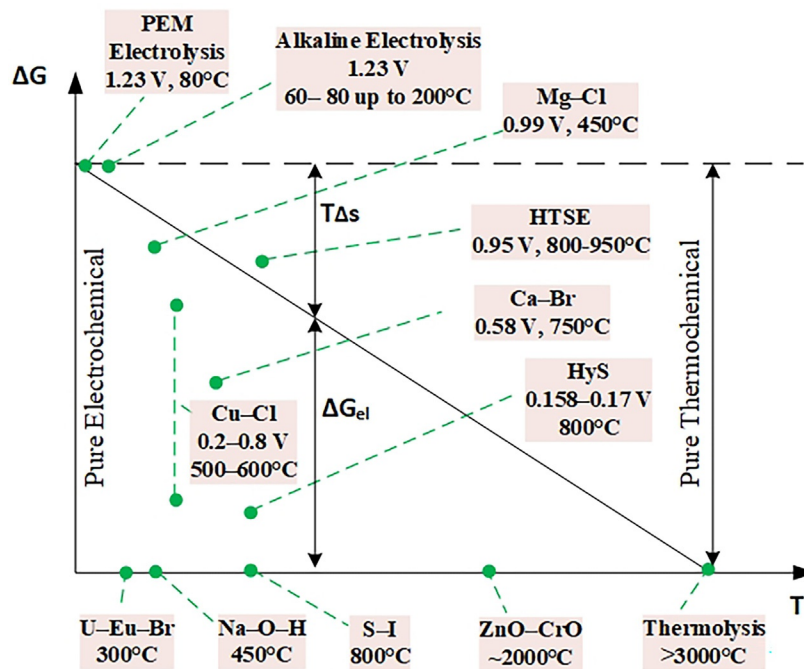
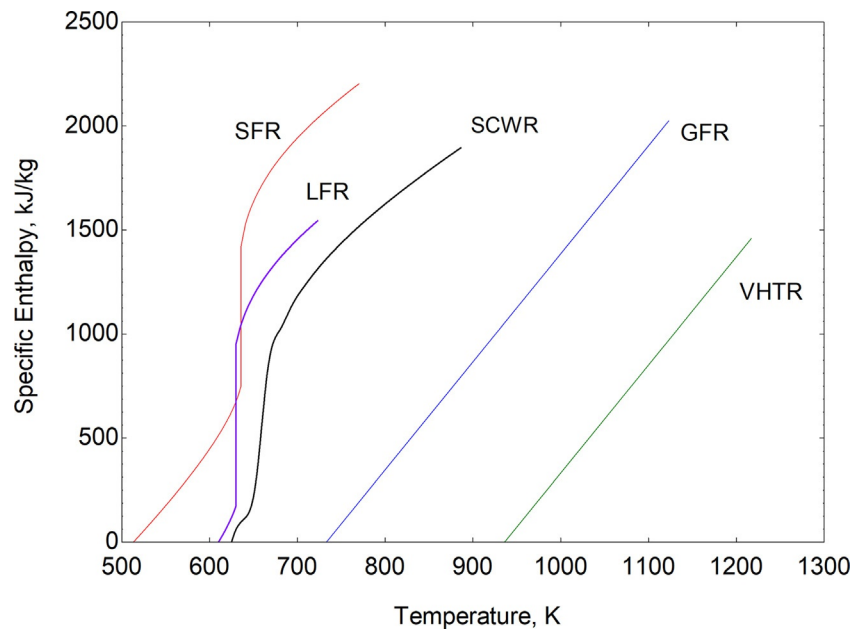


Figure 19.2. Maximum temperatures and theoretical electrical energy requirements of selected hydrogen production methods (El-Emam et al., 2020)

Table 19.1. Possible coupling between hydrogen technologies and Generation-IV designs for large-scale hydrogen production

	Electrolysis			Carbon-free Thermochemical cycles			Fossil & Biomass thermochemical processes		
	PEM <100°C	Alkaline ~200°C	High temp >800°C	S-I >800°C	HyS ~800°C	Cu-Cl >600°C	Steam methane reforming >700°C	Gasification >900°C	Pyrolysis >1000°C
SFR	✓	✓							
LFR	✓	✓	✓			✓			
SCWR	✓	✓				✓			
MSR	✓	✓	✓			✓	✓		
GFR	✓	✓	✓	✓	✓	✓	✓	✓	✓
VHTR	✓	✓	✓	✓	✓	✓	✓	✓	✓

Modified from El-Emam et al. (2020).

**Figure 19.3.** Temperature profiles for the coolants of some Generation-IV concepts

From the data provided in [Table 19.1](#), along with the information extracted from [Figures 19.2 and 19.3](#), a good understanding of the possible coupling between the different hydrogen technologies with nuclear reactors can be drawn. However, safety of coupling, process sustainability, and economic feasibility among other parameters are to be considered by decision makers. Alkaline water electrolysis at elevated temperature of ~200°C, High-Temperature Steam Electrolysis (HTSE), thermochemical water splitting via Sulfur-Iodine (S-I), HyS, or Cu-Cl cycles, nuclear assisted natural gas reforming and coal gasification are some of the technologies that can be envisaged for large-scale production of hydrogen with nuclear energy for near- and medium-term consideration. Steam water electrolysis can be coupled with most of high and very-high-temperature nuclear reactor designs such as MSR, GFR or VHTR. S-I and HyS are compatible with

GFR and VHTR designs. Cu-Cl cycle is compatible with roughly 70% of the proposed Generation-IV reactor designs: SCWR, MSR, GFR, and VHTR. Natural gas reforming and coal gasification processes are compatible with MSR, GFR, and VHTR.

Among the technologies listed in [Table 19.1](#) to produce large-scale hydrogen production, steam methane reforming is the most dominant in producing hydrogen today covering close to half of worldwide demand of hydrogen. Electrolysis shares in covering less than 5% of the global demand. The rest is provided through fossil-based technologies such as coal gasification and liquid hydrocarbons.

As hydrogen is an energy carrier and not a source of energy, it is only as clean as the energy source driving its production process. The use of nuclear thermal energy to provide the necessary high-quality heat to the steam methane reforming and gasification processes would result in tremendous reduction in greenhouse gas emissions produced if fossil fuel is burned for that purpose. To achieve the production of cleaner hydrogen, electric, thermal, electrochemical and hybrid water splitting technologies driven by nuclear energy is the pathway to take. In the following, the main routes for sustainable production of large-scale hydrogen that are considered for coupling to nuclear energy source (i.e., nuclear reactor) are discussed.

19.3 Biomass and fossil-based technologies

19.3.1 Steam methane reforming

Natural gas reforming involves an endothermic reaction of methane and steam at high temperatures according to the following overall process:



The process temperature has to be at least 700°C and up to 1000°C or above to generate a satisfactory yield of hydrogen. Almost 25% of supplied methane is burned to provide heat at the required temperature. This is achieved through two stages. In the first stage, around 12% of supplied gas is combusted to provide high-pressure steam at around 500°C (at ~30 bar) which mixes with methane in preparation to be fed to the reformer which is kept at over 700–850 °C. In the reformer, hydrogen separation is achieved by the separation membrane and provided catalysts in the reformer. Another 12%–13% of supplied methane is combusted to sustain the operation temperature of the reformer. In addition, a detailed description of past research and development experience in nuclear-based natural gas reforming in Germany was reported by [Verfondern \(2007\)](#). In that study, it was found by experiment that at least 30% more hydrogen can be generated for the same amount of emitted CO₂ if heat is derived from a nuclear reactor instead of combustion of an additional quantity of natural gas in an autothermal reforming process.

The Russian sodium cooled fast reactor (BN-600), providing steam at a little over 500°C and over 130 bar, was considered for powering the first stage of a steam methane reforming process for hydrogen production ([Khorasanov et al., 2015](#)). It was found to provide around 0.1% of global annual hydrogen production at that year. This is equivalent to a cut of over 130 thousand tons of CO₂ per year. Other VHTR designs of over 850° C can cover the demand of heat for both stages of the process.

19.3.2 Gasification

Hydrogen generation through gasification of coal, biomass, or heavy residual can be achieved through partial oxidation of hydrocarbons. In this process, the hydrocarbon fuel reacts with oxygen at very high temperature yielding a mixture of carbon monoxide and hydrogen. Hydrogen generation via coal gasification is shown in overall endothermic reaction described in the following equation:



The resulted syngas is further treated with steam to increase the hydrogen yield, and later cleaned from any impurities such as sulfur compounds. Water gas shift reaction is the process for upgrading the syngas to hydrogen. Pressure swing adsorption is used to bring hydrogen purity up to 99.8%. Gasification process requires high-quality heat. Biomass fluidized bed gasifiers have temperature of 800–900°C, exceeding 900°C in some designs (e.g., entrained-flow gasifier has peak gasification temperature of 1400–1700°C) while coal gasification operates at temperature of minimum 900°C. For the process to be economically competitive, temperature should reach around 1600°C and in some designs 1900°C. Due to the fact that hydrogen to carbon molar fraction is reduced in coal, the gasification process emits more CO₂ compared to other fossil-fuels reforming process. This can be reduced by blending coal with quantities of biomass. With the use of nuclear thermal energy of Generation-IV VHTR or GFR to drive the process, a substantial reduction of pollution can be obtained.

A pioneering study of coal gasification coupled to a nuclear reactor was published by [Schrader \(1975\)](#) followed by other studies such as [Rastoin et al. \(1979\)](#). Five years later, [Kirchhoff et al. \(1984\)](#) provided a description of a pilot plant for hydrogen generation with coal gasification and nuclear energy. More than a hundred large-scale coal gasification facilities are operating today, few of them integrate carbon capture process in the production line. Several technologies are being employed in operating biomass gasification plants around the globe including steam gasification, heat pipe reformers, and sorption enhanced reforming technologies. Biomass gasification requires water gas shift and pressure swing adsorption as well as other syngas cleaning processes to produce hydrogen ([El-Emam et al., 2014, 2015](#); [El-Emam and Dincer, 2014](#)). With the governmental incentives in many countries in response to mitigating climate change, biomass gasification will become more competitive as a clean route for hydrogen production.

19.3.3 Pyrolysis

Pyrolysis is a thermochemical decomposition process which is being investigated and used for several decades applied on biomass fuel and methane, with natural gas pyrolysis being utilized during the first quarter of the past century for the production of high-quality carbon black products. Methane pyrolysis is the decomposition of methane into hydrogen and carbon through thermal, plasma, and/or catalytic decomposition processes. Decomposition of methane may start at 700°C but temperature of 1000 to 1200°C is required to use the process for sustainable hydrogen production. Temperature requirements can be reduced with the utilization of catalysts to increase the hydrogen yield at relatively lower temperature. If the thermal energy to drive this process is delivered from a high-temperature nuclear reactor, methane pyrolysis becomes a clean hydrogen production technology.

19.4 Electrolysis

Electrolyzers can be classified into five different types depending on the nature of electrolyte: Polymer Electrolyte Membrane (PEM) electrolyzer, alkaline electrolyzer, Solid Oxide Electrolyzer with Oxygen ion conduction (SOE(O)), Solid Oxide Electrolyzer with Proton ion conduction (SOE(P)), and hybrid systems. In the following sections, an overview of the three most widely used proven electrolysis technologies for near-term large-scale hydrogen production: PEM, alkaline, and SOE(O), are introduced. In addition, [Table 19.2](#) shows some of the main characteristics and specifications of the three technologies. A simplified schematics of the three electrolysis principles are shown in [Figures 19.4–19.6](#).

Table 19.2. Characteristics and specifications of promising electrolysis technologies (El-Emam and Ozcan, 2019)

	PEM	Alkaline	SOE(O)
Electrolyte	Polymer (solid)	NaOH/KOH (liquid)	Ceramic (solid)
Charge carrier	H^+	OH^-	O^{2-}
Anode	Pt, Ir, Ru	Ni	LSMYSZ, $CaTiO_3$
Cathode	Pt, Pt/C	Ni alloys	Nicermets
Anode reaction	$2H_2O \rightarrow O_2 + 2H^+ + 2e^-$	$2OH^- \rightarrow H_2O + 0.5O_2 + 2e^-$	$O^{2-} \rightarrow 0.5O_2 + 2e^-$
Cathode reaction	$2H^+ + 2e^- \rightarrow H_2$	$2H_2O + 2e^- \rightarrow H_2 + 2OH^-$	$H_2O + 2e^- \rightarrow H_2 + O^{2-}$
Operating pressure/ temperature	15–45 bar 50–90°C	2–10 bar 60–90°C (up to 200)	1 and up to 30 bar 600–1000°C
Cell voltage	1.8–2.2 V	1.8–2.4 V	0.95–1.3 V
Current density	1–2 A/cm ²	0.2–0.5 mA/cm ²	0.3–1 mA/cm ²
Stack lifetime	<90,000 h	<90,000 h	<40,000 h
System lifetime	10–20 years	20–30 years	–
Efficiency (HHV)	67%–84%	62%–82%	~90%
Cold startup	<10 min	>15 min	> 60 min
Annual degradation	2%–4%	2%–4%	17% (testing)

HHV, High Heating Value; LSM, Lanthanum Strontium Manganite; YSZ, Ytria-Stabilized Zirconia; kW_{ch} , chemical energy of hydrogen (HHV).

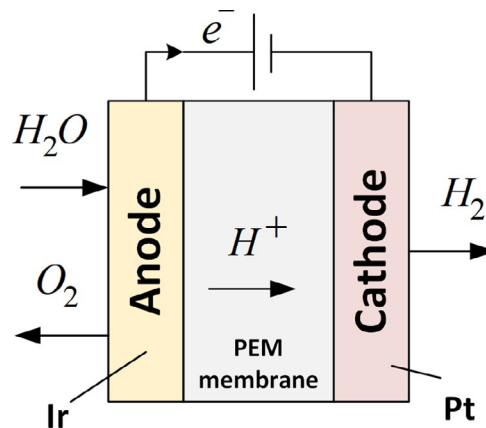


Figure 19.4. Schematic of PEM electrolysis process

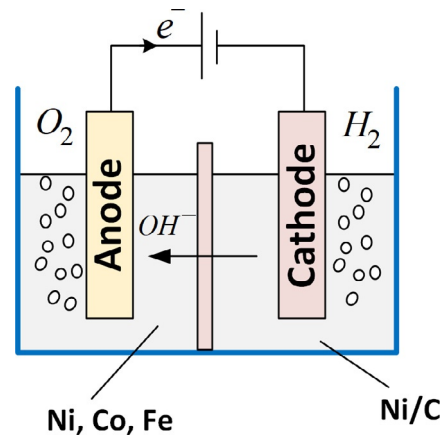


Figure 19.5. Schematic of alkaline electrolysis process

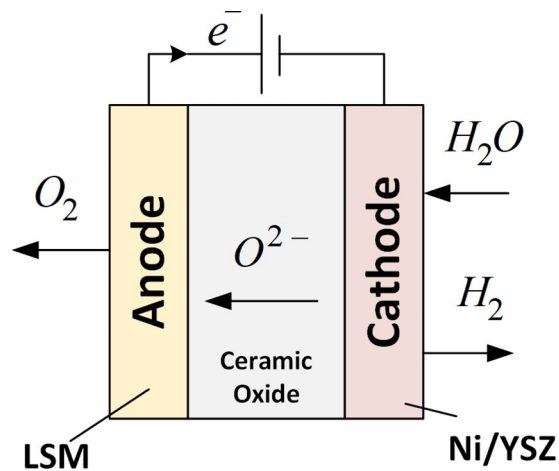


Figure 19.6. Schematic of SOE(O) HTSE

19.4.1 PEM electrolysis

PEM electrolysis splits water using an acidic non-liquid electrolyte and directly produces hydrogen at purity of 99.99 vol% and up to 99.999 vol%. This technology has higher partial load range and rapid response to system changes. The solid membrane of PEM electrolyzers enables compact design of the system and provides faster response to load variation and dynamic operation. This technology is mature and proven for early commercial small-scale hydrogen production. Yet, due to the high cost of polymeric membrane, noble metal catalysts, and materials for the bipolar plates, it is facing some challenges for commercialization at large scale in the near future. Several studies have been conducted considering first row transition materials based on iron, nickel, zinc, copper, and cobalt. Due to its abundance, high activity, and relatively low cost; cobalt-based catalysts are considered as a promising alternative for Oxygen Evolution Reaction (OER).

19.4.2 Alkaline electrolysis

Alkaline electrolyzer technology is mature, reliable, and safe, however, along with those listed in [Table 19.2](#), this technology has low partial load range. The produced hydrogen from this technology can

reach purity of 99.9 vol%, which can be improved by utilizing catalytic convertors and adsorptive dryers. It is used worldwide in commercial scale, with capital investment cost of \$1000–\$5000/kW. Further research for the development of an active stable catalyst for the OER is needed. Like PEM electrolyzers, Alkaline electrolyzers operate at low-temperature range with water flowing at liquid state, and it is operating at low pressure, yet some advanced alkaline electrolysis technologies can operate at high pressure and temperature up to 200°C.

19.4.3 High-temperature electrolysis

Solid oxide high-temperature electrolyzers typically operate with heat and electric power supplied simultaneously by advanced nuclear reactors. HTSE can be coupled to currently operating power plants when using electric heating to bring the cell to its operating temperature. In some operating condition, the heat necessary for operation is generated through the Ohmic losses in the cell, however, this is not the desirable operation mode for efficient performance. The heat provided to the input stream to the electrolyzer is reduced by recovering the heat from streams exiting the electrolyzer.

Electricity to heat ratio required to run the plant when coupled to a nuclear power plant is around 4.5 (considering operating temperature 800°C). This utilized heat is the thermal energy provided to generate steam at up to 300°C (considering water-cooled reactor designs). More thermal energy is required to bring the cell to the operating temperature. This can be covered when nuclear-produced electricity is used for electric heating to maintain the cell at its high operating temperature. In case of high-temperature reactors, this ratio changes as more thermal heat from the reactor is delivered for producing steam at higher temperature.

HTSE is a very promising method for large-scale hydrogen production in the future. It has the highest potential for successful deployment and demonstration coupled to high-temperature designs for Generation-IV reactors as it has less complex design with no intermediate chemical recycling. The hydrogen production efficiency of this technology is less sensitive to the level of operating temperature in the range of 650–950°C. Furthermore, high operation temperature lowers the electric power demand for the electrolysis process.

Planar Solid Oxide Electrolysis Cell (SOEC) is the most utilized technology, and it operates at high efficiency due to minimized voltage and current losses. In generation, an overall thermal conversion efficiency of HTSE powered by dedicated High-Temperature Gas-cooled Reactor (HTGR) is estimated as 48%–59%. This is considering hydrogen production efficiency as the heating value of produced hydrogen divided by the total thermal energy of the feed streams, thermal equivalent of the electricity utilized, and any extra process heat for process operation.

In 2005, an integrated conceptual plant was characterized and proposed by General Atomics (GA) in a meeting at the Japan Atomic Energy Agency (JAEA). This system considered a VHTR operating at 950°C to provide 292 MW of electric power and 68 MW of thermal energy to a coupled HTSE operating at 826°C. The system estimated to operate at 46% efficiency considering the lower heating value of hydrogen (Richards et al., 2005). In 2009, It was announced that HTSE with the VHTR Modular Helium Reactor (MHR) by GA is under development with production capacity of 720 million tons of hydrogen per year at delivery pressure of 5 MPa. The HTSE plant consists of modules of 0.5 MW (of equivalent electric power consumption) and each module comprises 500 planar cells (Elder and Allen, 2009). In 2019, another report from Idaho National Laboratory shows electricity to heat ratio as high as 9.8 considering steam delivered to the HTSE is provided from a Light Water Reactor (LWR) at 285°C (Frick et al., 2019). In this case, electric heating of around 26 MW was provided from the nuclear power plant. This is in addition to 1065 MW electricity and 108.7 MW of thermal energy both transferred to drive the HTSE. The hydrogen production efficiency based on high heating value was estimated as 33%.

19.5 Pure and hybrid thermochemical cycles

Thermochemical-based hydrogen production processes can bring a reduction of the high cost associated with the direct electrolysis of water (i.e., electricity-driven process). For instance, pure thermochemical processes are requiring thermal energy eliminated the huge loss associated with converting heat to electricity. However, these require very high-quality heat (i.e., heat at very high temperature). The operating temperature of some of these cycles could easily jeopardize the safety of operation due to their high values and add other challenges in the development of the process. A solution to lower the temperature requirement for thermochemical cycles, electric energy is utilized to drive an electrolysis process that comes as a part of the thermochemical cycle. Such processes (i.e., hybrid thermochemical cycles) can operate at relatively lower temperature compared to pure thermochemical cycles as it can be demonstrated in [Figure 19.2](#). In the following, three examples of promising thermochemical cycles (as previously introduced in [Table 19.1](#)) are discussed with their considered coupling to Generation-IV nuclear reactors.

19.5.1 Sulfur-Iodine (S-I) pure thermochemical cycle

The S-I cycle is the most investigated thermochemical process. This cycle is being studied and developed by JAEA for more than two decades. In 2019, they achieved continuous operation of the cycle for 150 h with production rate of 30 L of hydrogen per hour ([Kubo et al., 2019](#)). To reach sustainable long-term operation using industrial materials and to achieve successful coupling with the VHTR design of Japan, the prismatic block core High-Temperature Test Reactor (HTTR) is utilized in Ōarai, Ibaraki, Japan ([JAEA Press Release, 2019](#); [Kubo et al., 2019](#)). It worth mentioning that the focus on VHTR designs has moved toward relatively lower HTGRs in the countries considering VHTRs, including Japan, China and the US, to reduce the risk associated with the very high outlet temperature values of earlier VHTR designs. The HTTR is a HTGR design.

The proposed systems of integration between Generation-IV design of Japan and the S-I cycle considers coupling the S-I plants with the 300 MW_e Gas Turbine High-Temperature Reactor (GTHTR-300) reactor via an Intermediate-Heat Exchanger (IHX) with a helium circulator. The GTHTR is developed based on the HTTR of Japan Atomic Energy Research Institute (JAERI). The reactor has a secondary cooling loop at a lower temperature with helium. According to [Sakaba et al. \(2007\)](#), helium temperature at hottest side is 950°C and at the return is at around 490°C. The hot helium from the primary circuit passes first to the IHX where its temperature drops to 850°C; thereafter, expanded in the turbine where the temperature drops to about 590–600°C before it is further cooled and compressed to continue its cycle to the reactor inlet. In the secondary helium loop, helium exists the IHX at a little over 900°C and is supplied to the integrated thermochemical cycle (see [Figure 19.7](#)).

China is also conducting national project for the development of the S-I cycle which has progressed well since started with fundamental studies in 2005. They achieved continuous stable operation of the system for over 80 h with 60 h of hydrogen production at rate of 60 L/h in 2014 as reported by [Zhang et al. \(2018\)](#). This was followed by continuous work toward up-scaling of the process and coupling it to the HTGR design of pebble-bed core HTR-PM600 and HTR-10 ([Zhang et al., 2019](#)). Several other countries are developing the S-I cycle such as south Korea and the US.

19.5.2 Hybrid Sulfur (HyS) thermochemical cycle

was proposed and investigated in mid 1970s by Westinghouse as a hybrid variation of the S-I cycle, and the concept was also progressing in European research institutions including the European Joint Research Centre and the German Nuclear Research Centre in Jülich. Both cycles have the same range of operating temperatures. However, the chemistry complexity of the S-I cycle is reduced in the HyS cycle at the cost of electrical energy consumption.

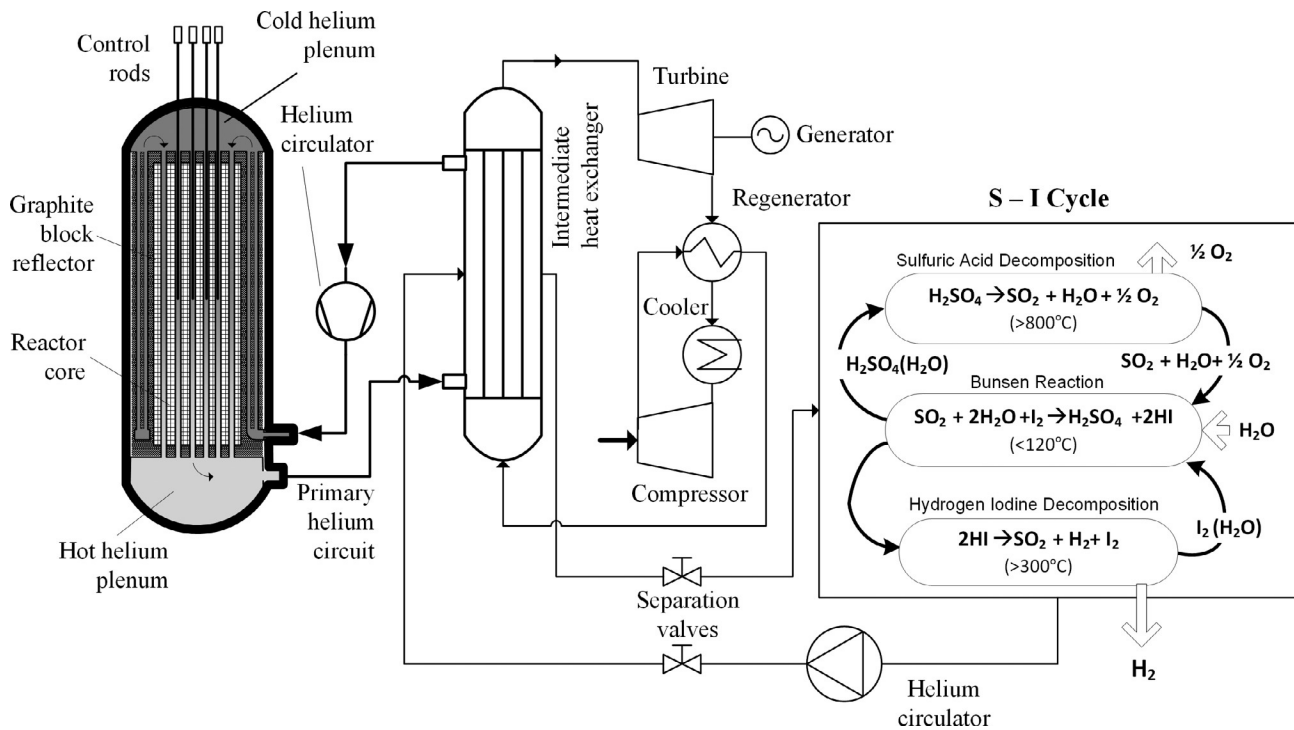


Figure 19.7. Integrated nuclear reactor S-I plant developed at JAERI of Japan

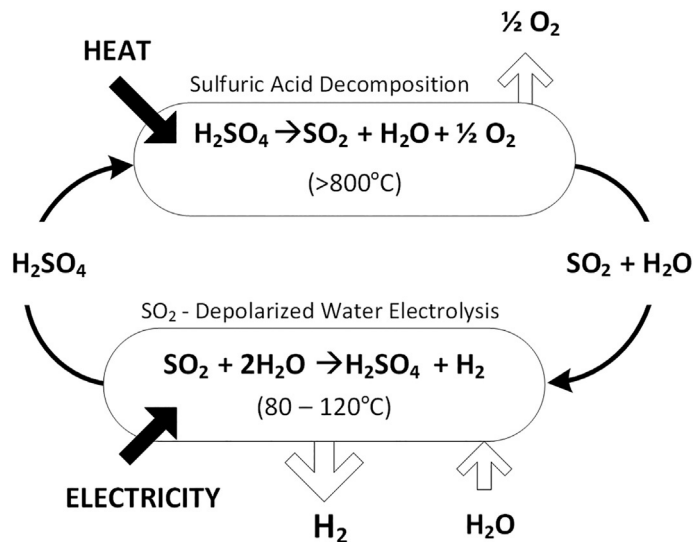
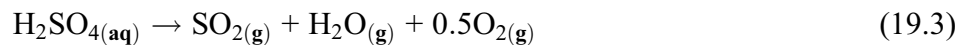
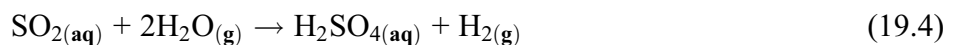


Figure 19.8. Schematic of the HyS process for hybrid thermochemical hydrogen production cycle

A simplified schematic of the two processes of the cycle is shown in Figure 19.8. The first step is the endothermic sulfuric acid decomposition reaction occurring at around 800°C:



Then comes the hydrogen production reaction; the thermochemical sulfur dioxide depolarized electrolysis of water which occurs at about 100°C and consumes only one third of conventional direct electrolysis process.



A consortium involving the Shaw Group and Westinghouse developed a conceptual design more than 10 years ago for integrated plant coupling HyS cycle for hydrogen production to the Pebble Bed Modular Reactor (PBMR), a VHTR. Two of the main challenges in the development of the cycle are cell potential of sulfur dioxide depolarized water electrolysis and the crossover during this process. Several research laboratories are investigating the cycle in many countries.

19.5.3 Copper-Chlorine (Cu-Cl) hybrid thermochemical cycle

Among the most studied thermochemical hydrogen production cycles is Cu-Cl of the Chlorine thermochemical hydrogen production series. An early investigation of the cycle was reported in 1974 on physicochemical disproportionation of cuprous chloride (Wentorf and Hanneman, 1974). In 2007, a consortium involving the Argonne National Laboratory, USA; Atomic Energy of Canada Limited (AECL) and the University of Ontario Institute of Technology (OntarioTech) in Canada; along with other institutes in the framework of Generation IV International Forum (GIF) was launched to investigate the cycle. Theoretical and experimental investigation on the reactions, thermodynamic assessments, and process performance of different configuration of the cycle is being conducted at Ontario Tech University in collaboration with Canadian Nuclear Laboratories (CNL) toward upscaling the cycle (Gabriel et al., 2021). Other projects investigating the cycle are progressing in China and India among others.

Integration of heat pump with nuclear reactors for heat upgrade to higher temperature proposed and studied by several researchers. For instance, Zamfirescu et al. (2010) proposed using bottoming cycle of cyclohexane chemical heat pump and topping supercritical cycle of biphenyl chemical heat pump to upgrade the heat available from CANDU6 moderator at 80°C and from the reactor at 250°C to over 400°C and up to 600°C using heat recovered from Cu-Cl cycle. In another study, Zamfirescu et al. (2011) discussed the potential of internal heat recovery from thermochemical cycles integrated with nuclear power plant. Figure 19.9 shows a conceptual integration of Generation-IV SCWR CANDU design to the Cu-Cl cycle. A heat pump proposed by El-Emam et al. (2019) is considered in this integration to elevate the temperature of reactor, which is slightly lower than the operating temperature of the Cu-Cl cycle to over 600°C after first expansion.

19.6 Nuclear hydrogen production toward climate change mitigation

We will begin with a general look on the potential of cogeneration using nuclear energy to achieve the climate mitigation goals. If we consider the currently operating nuclear power plants, there are at least two significant benefits to adopting cogeneration of Hydrogen and electricity. First, the recovery and reuse of heat rejected from the power plant condenser, with the possibility of upgrading the heat to higher temperature levels, and secondly, utilization of nuclear energy for hydrogen production which serves a wide range of industries as well as providing an energy storage when the demand fluctuates (El-Emam and Bhattacharyya, 2021).

Considering the recovery of 25% of the thermal heat rejected from currently operating nuclear power plants at reasonable quality (i.e., temperature) to be used for district heating, it can result in an annual reduction of at least 400 million tons of CO₂ and up to 800 million tons of CO₂ depending on the fossil-fuel used to produce the same amount of heat. Even considering the minimum carbon dioxide saving, this is equivalent to taking 90 million cars off the road per year, and would result in saving over 17 billion dollars of social cost of carbon per year. Currently, 4% of the 70 million tons of hydrogen worldwide-demand is covered by electricity-driven conventional electrolysis. If driven by nuclear-generated electricity, this would lead to avoiding almost 59 million tons of CO₂ per year: equivalent to taking 13 million cars off the road per year. The saved social cost of carbon is over 2 billion dollars per year. Furthermore, if the rest of current hydrogen

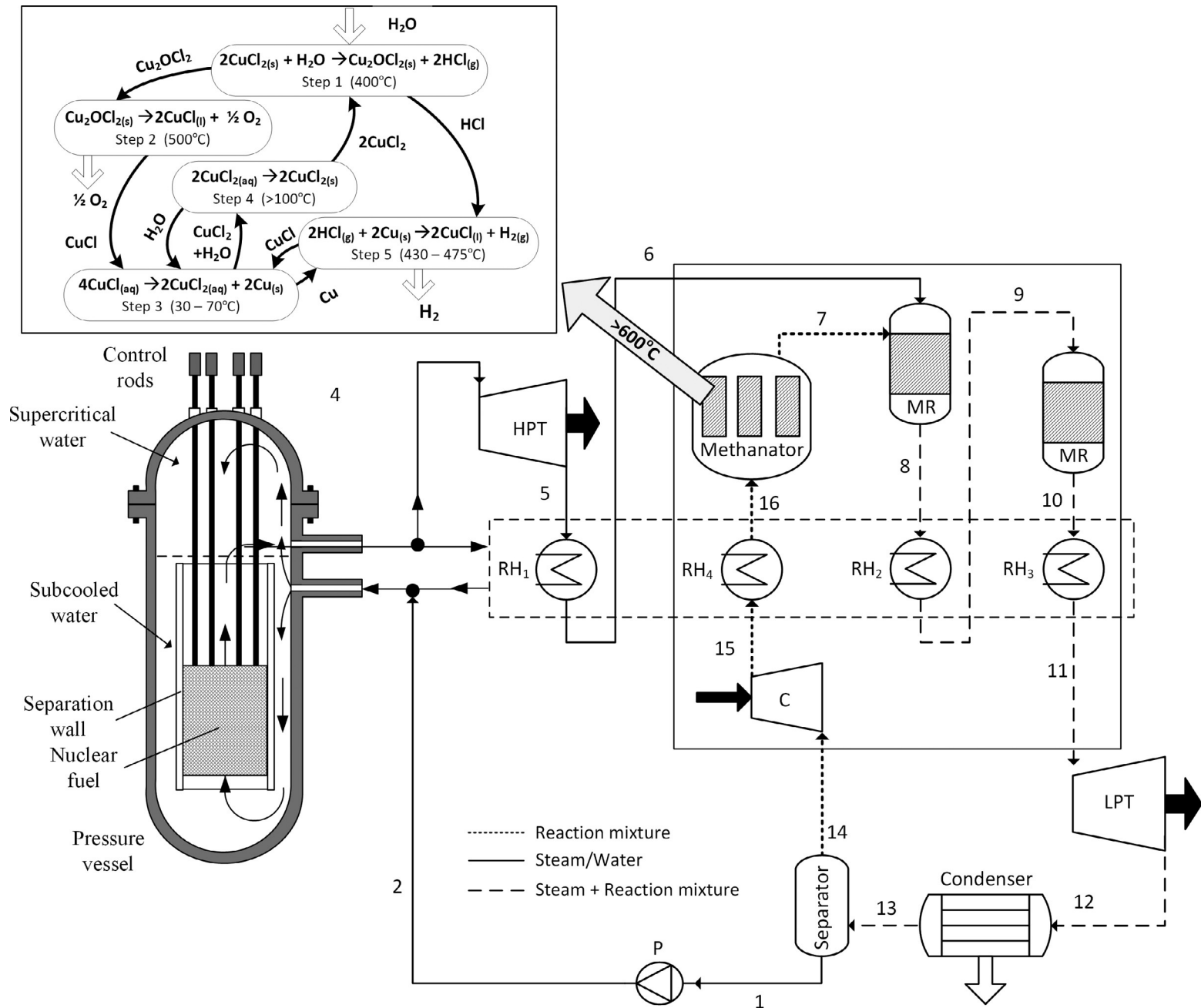


Figure 19.9. Schematic of Cu-Cl hybrid thermochemical process coupled to CANDU SCWR with heat upgrade

Table 19.3. Scenarios for understanding of the potential role of nuclear hydrogen production in combating climate change

	Carbon dioxide emissions (Mton CO₂/year)	Equ. cars taken off road in a year (million cars)	Social cost of carbon saving (Billion\$/year)
Savings if recovery of rejected-heat is used:			
Recovery of 25%	427*	93	17
*Considering methane as the fossil-fuel used to provide the same amount of heat			
Savings when using Nuclear for H ₂ today to cover:			
The 4% share from electrolysis:	58.9	12.8	2.35
Fossil-based production share:	508	110	20

demand (mainly generated from fossil-based steam methane reforming) is converted to nuclear hydrogen, this would result in avoiding over 500 million tons of CO₂, equivalent to taking 110 million cars off the roads in a year. This would also result in saving of around 20 billion dollars of the associated social cost of carbon per year. These results are summarized in [Table 19.3](#) below with the parameters and associated assumptions in these estimations listed in [Table 19.4](#).

Table 19.4. Assumptions and parameters considered for the estimations in [Table 19.3](#)

Nuclear power plant:	
Current nuclear capacity	399,370 MW _e (IAEA PRIS, 2019)
Average NPP operating efficiency	34%*
Plant capacity factor	90%*
*Assumed values are based on the literature	
Hydrogen production:	
Annual hydrogen demand	74 Mton/year (IEA, 2019)
Hydrogen from electrolysis	4%
Hydrogen from fossil-fuel-based methods	95%
CO₂ emissions:	
Power grid CO ₂ intensity	491 gCO ₂ /kWh (IEA, 2019)
From burning fossil fuel	280 gCO ₂ /kWh “average value” (EIA, 2019)
H ₂ from steam reforming	25 tonCO ₂ /MMscf of H ₂ (Praxair, 2010)
Car annual CO ₂ emissions	4.6 tonCO ₂ (EPA, 2019)
Social cost of carbon	\$40/tonCO ₂ (EDF, 2019)

19.7 Conclusion

Generation-IV nuclear reactors could be used for near and mid-term hydrogen production through various approaches. Low-temperature water electrolysis is an established technology but needs further improvements. The development and deployment of high efficiency HTSE and thermochemical processes are foreseen to play an important role in the long-term plans for large scale hydrogen production. HTSE is seen as a good option to be coupled with high-temperature nuclear reactors giving it the potential for successful deployment and demonstration with some of the Generation-IV reactors. Several countries are considering HTSE as a promising option for a sustainable large-scale hydrogen production based on nuclear energy to provide steam and electricity. Research is concentrating on the development and optimization of planar and tubular electrolysis cells, stack design, selection of appropriate materials, and finally the coupling to the nuclear heat source. Hydrogen production from low-temperature electrolysis and HTSE will not be competitive with steam methane reforming unless taxes on discharging of carbon dioxide into the atmosphere is enforced widely. Hydrogen production using electrolysis can be competitive if used at off-peak times with low electricity prices. This also solves the intermittency problem with solar and wind. Such operation mode fits well with the base-load operation of nuclear power plants.

For more than 40 years, several nations investigated the potential of many thermochemical cycles for efficient and sustainable hydrogen production. These processes require high-quality heat delivered at high temperatures (i.e., pure thermochemical cycles), or in a hybrid mode with electricity generation; both of which can be provided by nuclear energy. Thermochemical processes—both pure and hybrid—are among the most promising technologies considered for nuclear hydrogen production. Furthermore, the use of a high-temperature Generation-IV designs to provide thermal energy for driving coal gasifier or a methane reforming process represents a possible strategy to significantly reduce pollution of the environment by carbon dioxide emissions characteristic of fossil fuel processes.

References

- EDF, 2019. <https://www.edf.org/true-cost-carbon-pollution>.
- EIA, 2019. <https://www.eia.gov/tools/faqs/faq.php?id=73&t=11>.
- Elder, R., Allen, R., 2009. Nuclear hydrogen production: coupling a very high/high temperature reactor to a hydrogen production plant. *Prog. Nucl. Energy* 51, 500–525.
- El-Emam, R.S., Bhattacharyya, R., 2021. Toward the deployment of nuclear cogeneration projects—issues and considerations. *Energy Sources A: Recovery Util. Environ. Eff.* 43 (23), 3137–3150. <https://doi.org/10.1080/15567036.2021.1931569>.
- El-Emam, R.S., Dincer, I., 2014. Thermal modelling of fluidized bed gasification of rice straw. In: *Proceeding of The International Conference on Clean Energy (ICCE)*, Istanbul, Turkey.
- El-Emam, R.S., Dincer, I., El-Emam, S.H., 2014. Efficiency and environmental assessment of biomass gasification for hydrogen and power production. In: *Proceeding of Global Conference on Global Warming (GCGW-14)*, Beijing, China.
- El-Emam, R.S., Dincer, I., El-Emam, S.H., 2015. Gasification of biomass for hydrogen and power production: efficiency and environmental assessment. In: Dincer, I., Colpan, C., Kizilkan, O., Ezan, M. (Eds.), *Progress in Clean Energy*. Springer, Cham, https://doi.org/10.1007/978-3-319-17031-2_12.
- El-Emam, R.S., Dincer, I., Zamfirescu, C., 2019. Enhanced CANDU reactor with heat upgrade for combined power and hydrogen production. *Int. J. Hydrogen Energy* 44 (42), 23580–23588.
- El-Emam, R.S., Ozcan, H., 2019. Comprehensive review on the techno-economics of sustainable large-scale clean hydrogen production. *J. Clean. Prod.* 220 (31). <https://doi.org/10.1016/j.jclepro.2019.01.309>.
- El-Emam, R.S., Ozcan, H., Zamfirescu, C., 2020. Updates on promising thermochemical cycles for clean hydrogen production using nuclear energy. *J. Clean. Prod.* 262. <https://doi.org/10.1016/j.jclepro.2020.121424>.
- EPA, 2019. <https://www.epa.gov/greenvehicles/greenhouse-gas-emissions-typical-passenger-vehicle>.
- Frick, K., Talbot, P., Wendt, D., Boardman, R., Rabiti, C., Bragg-sitton, S., Levie, D., Frew, B., Ruth, M., Elgowainy, A., Hawkins, T., September 2019. Evaluation of Hydrogen Production Feasibility for a Light Water Reactor in the Midwest. Idaho National Laboratory, DoE, US.
- IAEA PRIS Databases, 2019.

- Gabriel, K.S., El-Emam, R.S., Zamfirescu, C., 2021. Technoeconomics of large-scale clean hydrogen production – a review. *Int. J. Hydrog. Energy*. <https://doi.org/10.1016/j.ijhydene.2021.10.081>. In press.
- IEA, 2019. <https://www.iea.org/tcep/power/>.
- JAEA Press Release, 2019. <https://www.jaea.go.jp/02/press2018/p19012502/>.
- Khorasanov, G.L., Kolesov, V.V., Korobeynikov, V.V., 2015. Concerning hydrogen production based on nuclear technologies. *Nucl. Eng. Technol.* 1 (2), 126–129.
- Kirchhoff, R., Van Heek, K.H., Jüntgen, H., Peters, W., 1984. Operation of a technical pilot plant for nuclear aided steam gasification of coal. *Nucl. Eng. Des.* 78, 233–239.
- Kubo, S., Takegami, H., Tanaka, N., Noguchi, H., Kamiji, Y., Iwatsuki, J., Myagmarjav, O., Inagaki, Y., 2019. Massive and efficient H₂ production technology on thermochemical water-splitting iodine-sulfur process. In: Presented at the World Hydrogen Technology Conference, Tokyo, Japan.
- Praxair Report, 2010. Analysis of CO₂ Emissions, Reductions, and Capture for Large-Scale Hydrogen Production Plants.
- Rastoin, J., Malherbe, J., Pottier, J., Lecoanet, A., 1979. Nuclear methane reforming for coal gasification. *Int. J. Hydrogen Energy* 4, 535–540.
- Richards, M., Shenoy, A., Schultz, K., Brown, L., Harvego, E., McKellar, M., Coupey, J.-P., Reza, S.M.M., 2005. H₂-MHR conceptual designs based on SI process and HTE. In: Nuclear Production of Hydrogen, Third Informational Exchange Meeting, Oarai, Japan, October 5–7.
- Sakaba, N., Kasahara, S., Onuki, K., Kunitomi, K., 2007. Conceptual design of hydrogen production system with thermochemical water-splitting sulfur-iodine process utilizing heat from the high-temperature gas-cooled reactor HTTR. *Int. J. Hydrogen Energy* 32, 4160–4169.
- Schrader, L., Strauss, W., Teggers, H., 1975. The application of nuclear process heat for hydro gasification of coal. *Nucl. Eng. Des.* 34, 51–57.
- Verfondern, K., 2007. Nuclear Energy for Hydrogen Production. vol. 58 Research Center Jülich.
- Wentorf, R.H., Hanneman, R.E., 1974. Thermochemical hydrogen generation. *Science* 185, 311–319.
- Zamfirescu, C., Naterer, G.F., Dincer, I., 2010. Upgrading of waste heat for combined power and hydrogen production with nuclear reactors. *J. Eng. Gas Turbines Power* 132 (10). <https://doi.org/10.1115/1.4000803>.
- Zamfirescu, C., Naterer, G.F., Dincer, I., 2011. Vapor compression CuCl heat pump integrated with a thermochemical water splitting cycle. *Thermochim. Acta* 512 (1–2). <https://doi.org/10.1016/j.tca.2010.08.020>.
- Zhang, P., Chen, S., Wang, L., Xu, J., 2019. R&D progress of nuclear hydrogen production in China. In: Presented at the World Hydrogen Technology Conference, Tokyo, Japan.
- Zhang, P., Wang, L., Chen, S., Xu, J., 2018. Progress of nuclear hydrogen production through the iodine-sulfur process in China. *Renew. Sustain. Energy Rev.* 81, 1802–1812.

20

Systems of Advanced Small Modular Reactors (ASMRs)

Fatih Aydogan

Jacksonville University, Jacksonville, FL, United States

20.1

Introduction

Abbreviations

4S	Super-Safe, Small and Simple
ABV	Nuclear, Modular, Water in Russian
ACS	Auxiliary Cooling System
ADS	Automatic Depressurization System
ADV	Advanced
Antares	AREVA New Technology Advanced Reactor Energy System
AP1000	ADvanced Passive 1000
ATWS	Anticipated Transient Without Scram
AUX BLDG	AUXiliary BulLDinG
BL	Base Load
BOO	Build-Own-Operate
CAP100/ACP100	Chinese Advanced Passive 100/Advanced China Power 100
CAREM-25	Central ARgentina de Elementos Modulares-25
CCR	Compact Containment water Reactor
CMT	Core Makeup Tank
CoGen	Co-Generation
CRDM	Control Rod Drive Mechanism
CS	Containment Spray
CVCS	Chemical and Volume Control System
DHR	Decay Heat Removal
DHRHX	Decay Heat Removal Heat eXchanger
DHRIV	Decay Heat Removal Isolation Valve
DMS	Double Modular Simplified and Medium Small reactor
DOE	Department Of Energy

DVI	Direct Vessel Injection
ECCS	Emergency Core Coolant System
ECT	Emergency Cooldown Tank
EDF	Electricité De France
EHRS	Emergency Heat Removal System
EMF	ElectroMagnetic Field
EMP	ElectroMagnetic Pump
FO	Fail Open valve
FWP	FeedWater Pump
Gen4	Generation 4
Gen-III+	Generation 3+
GTHT300	Gas Turbine High-Temperature Reactor 300 MWe
GT-MHR	Gas Turbine Modular Helium Reactor
HES	Hybrid Energy Systems
HR200	nuclear Heating Reactor with 200 MW of thermal power
HSBWR	Hitachi Small Boiling Water Reactor
HTR-PM	High-Temperature Reactor-Pebble bed Module
HWR	Heavy Water Reactor
IAEA	International Atomic Energy Agency
ICR WST	In-Containment Refueling Water Storage Tank
IMR	Integrated Modular water Reactor
IRACS	Intermediate Reactor Auxiliary Cooling System
IRC	Inside Reactor Containment
IRIS	International Reactor Innovative and Secure
KAERI	The Korea Atomic Energy Research Institute
LB	Large Break
LF	Load Following
LOCA	Loss Of Coolant Accident
LW	Light Water
MDBs	Multilateral Development Banks
MFIV	Main Feedwater Isolation Valve
MHGTR	Modular High-Temperature Gas-cooled Reactor
MHR	Modular Helium Reactor
MHTR	Modular High-Temperature Reactor
MSIV	Main Steam Isolation Valve
NEI	Nuclear Energy Institute
NHP	Nuclear Hydrogen Production
Non-LW	Non-Light Water
NPP	Nuclear Power Plant
OCC	Overnight Capital Cost
OKBM	OKB Mechanical engineering
OSU	Oregon State University
PCT	Peak Clad Temperature
PHWR220	Pressurized Heavy Water Reactor
PIUS	Process Inherent Ultimate Safety
PORV	Power-Operated Relief Valve
PRHRS	Passive Residual Heat Removal System
PRISM	Power Reactor Innovative Small Module
PRZ	PRessuriZer
PSV	Pressurizer Safety Valve
PTC	Production Tax Credit
RCP	Reactor Circulation Pump
RCS	Reactor Coolant System
RDT	Reactor Drain Tank
RHR	Residual Heat Removal

RV	Reactor Vessel
RVACS	Reactor Vessel Auxiliary Cooling System
RX	Reactor
SAFR	Sodium Advanced Fast Reactor
SB	Small Break
SCS	Shutdown Cooling System
SG	Steam Generator
SIR	Small Innovative Reactor
SIS	Safety Injection System
SMART	System-integrated Modular Advanced Reactor
SMR	Small Modular Reactor
SPWR	Simplified Pressurized Water Reactor
SVBR	Svintsovo-Vismutovyi Bystryi Reactor (or in English “lead-bismuth fast reactor”)
Triga	Training, research, isotopes, general atomic
TVO	Teollisuuden Voima Oyj
UHS	Ultimate Heat Sink
UN	Uranium Nitride
UP	Upper Plenum
US	United States
U-TRU-Zr	Uranium-TRansUranic-Zirconium alloy
VBER-150/300	Vodyanoi Blochnyi Energetichesky 150/300
VHTR	Very-High-Temperature Reactor
W_e	Watt electric
W-SMR	Westinghouse Small Modular Reactor
W_{th}	Mega Watt thermal
ZIRLO	ZIRconium Low Oxidation

Subscripts

e electric
th thermal

20.1.1 Introduction

The key words of “small” and “modular” make the Small Modular Reactors (SMRs) different than other reactors. “Small” denotes the reactor’s decreased power size. “Modular” denotes (1) the primary coolant system (such as the Reactor (RX) component in a light water SMR) enveloped by a pressure boundary; and (2) modular construction of components. Modular design requires compact architecture that is built in facility. For instance, the term of “modular” for a Light Water-SMR (LW-SMR) is used for the RX, since it covers the reactor core and primary coolant system so that the overall power of a power plant can easily be increased by increasing the modular units.

There is no concrete definition for the upper limit of SMRs’ power rating, but 300 MWe is usually used for a rough upper limit of SMRs. In addition to the reduced power level, most of the SMRs offer reduced spatial footprints and modularized compact designs fabricated in factories and transported to the intended sites, as well as improved safety features (such as passive safety, inherent or intrinsic safety, and safety-by-design). LW-SMRs employ a significantly less number of components in order to decrease costs and increase simplicity of design. However, new physical challenges have appeared with these changes. At the same time, ADVanced (ADV) SMR designs (such as Pebble Bed Modular Reactor, MHR Antares, Prism, 4S, Hyperion, etc.) are being developed that have improved passive safety and other features. Among the new SMRs, the US Department Of Energy (DOE) has begun to support SMR activities in the United States since 2012 years by issuing solicitations, such as “Financial

Assistance Funding Opportunity Announcement – Cost-Shared Development of Innovative Small Modular Reactor Designs.” DOE supports SMRs because of safety and economical benefits (Lyons, 2016):

- (1) Passive/inherent/safety-by-design safety systems, which do not require an operator or control system action;
- (2) Reduced source term inventory;
- (3) Elimination of postulated accidents by simplified design;
- (4) Reduction in Emergency Planning Zone;
- (5) Below-grade construction of the RX;
- (6) Flexibility to add reactor units;
- (7) Decreased financial risk and initial investment;
- (8) Potential replacement of old coal plants;
- (9) Usage of domestic resources, such as forgings and manufacturing;
- (10) Flexible power range with multiple units for various power grid needs and regional load growth;
- (11) Transportable modular components from factory to the site; and
- (12) Below-grade design of the RX and spent fuel storage pool for greater safety and security performance against external attacks and seismic events.

This support in the United States motivates US-based SMR vendors to compete with international (non-US) SMR companies. Some of the international SMR designs are given as

Russian designs:	KLT-40S (OKBM, 2015), VBER-150/300 (OKBM, 2015), VK-300 (Kuznetsov et al., 1999), ABV (OKBM, 2015), SVBR-100 (AKME, 2015),
Korean designs:	SMART (Park, 2011), VHTR
Chinese designs:	CAP100/ACP100 (Mingguang, 2013), HTR-PM (Li, 2014),
Argentinean design:	CAREM-25 (Magan et al., 2014),
Japanese designs:	IMR, CCR, DMS, GTHTR300, 4S.

Several SMRs have been discussed by categorizing SMRs in different ways. For instance, the International Atomic Energy Agency (IAEA) categorizes the small and midsize reactors based on primary coolant types (IAEA, 2012). For the current chapter, IAEA’s lists are updated by removing the midsize reactors (which produce more than 300 MWe/reactor unit) and adding the recent SMRs, as shown in Figure 20.1.1.

SMRs are classified into two groups in the scope of this study (Figure 20.1.1):

(1) LW-SMR:

LW-SMRs can be considered in the category of Generation III+ (Gen-III+). Some of the LW-SMRs, such as Westinghouse Small Modular Reactor (W-SMR), have inherited some safety features of licensed Gen-III+ reactors, such as the AP1000, which is the licensed commercial design. LW-SMRs generally use integrated RXs, which envelop the core, Steam Generator (SG), the pump, and the PRessuriZer (PRZ).

(2) Non-LW-SMRs:

Non-LW-SMRs can be considered in the category of Generation-IV (Gen-IV) reactors in that they are highly economical with improved passive safety and reduced levels of radioactive waste.

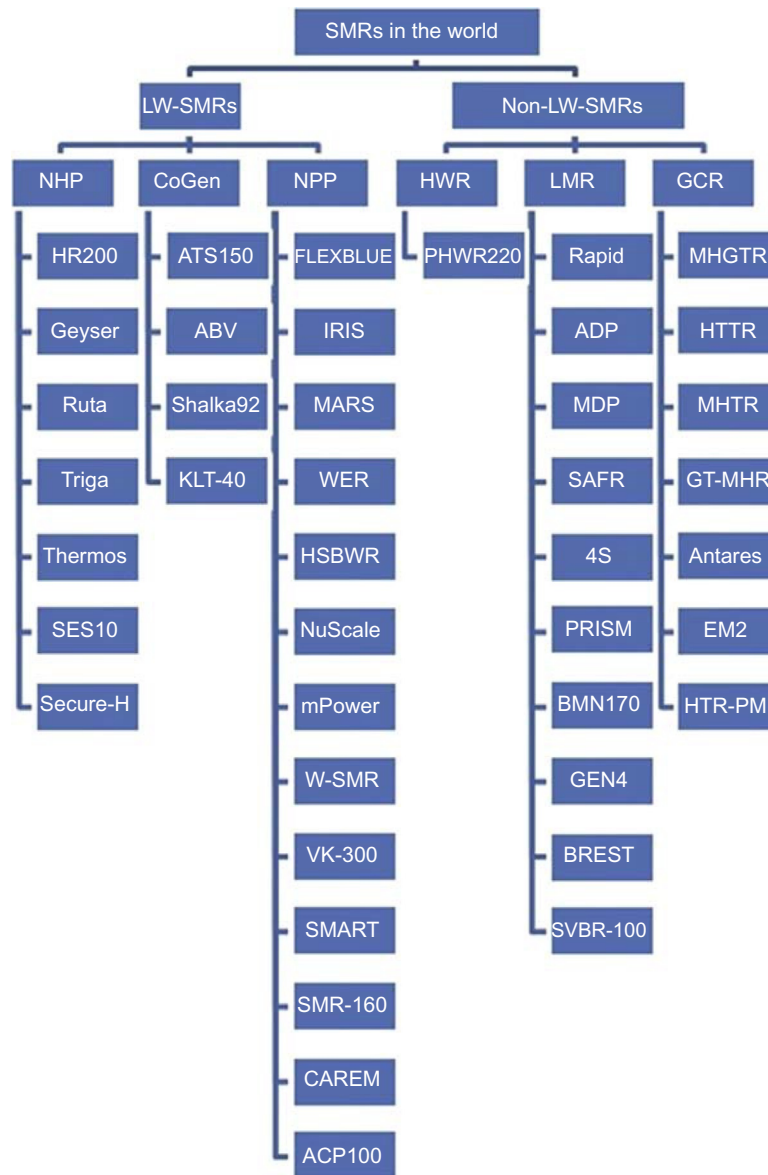


Figure 20.1.1. SMRs categorized based on coolant type (IAEA, 2001, 2012)

However, most of the non-LW-SMRs are in the early phase of development and are therefore unable to easily inherit significant licensed features of other commercial Gen-IV reactors because even these reactors are still in the development phase. Even though LW-SMRs are relatively similar to each other, Gen-IV designs include a wide range of design varieties, such as coolant types, control systems, fuels, etc.

This chapter firstly discusses the early designs of SMRs. Then it selects and compares some of the SMR designs between LW and ADV SMRs. The selection has been performed to include variety of SMRs based on nuclear reactors, Reactor Coolant Systems (RCSs), containment designs, and emergency core coolant system. Selected designs are NuScale (IAEA, 2011a), SMART (System-integrated Modular Advanced Reactor) (Matzie, 2015; Park, 2011), W-SMR (W, 2013), mPower (Babcock, 2013; IAEA, 2011b), International Reactor Innovative and Secure (IRIS) (Carelli et al., 2004) from LW-SMRs, and Power Reactor Innovative Small Module (PRISM) (PRISM, 1994), Super Safe, Small and Simple reactor (4S) (NRC, 2013), and Hyperion (Gen4energy, 2013) from ADV SMRs. Selected SMRs are compared based on: (1) nuclear reactors; (2) RCS components; (3) fuels; (4) containment; (5) Emergency Core Cooling System (ECCS); (6) cost evaluation; (7) security evaluation; and (8) flexibility of SMRs.

20.1.2 Early designs of small modular reactors

The first small size reactors have been designed in the 1960s for commercial and military applications. Some of these reactors are Shippingport in 1958, Yankee Rowe in 1960, Indian Point One in 1962, Dresden in 1960, TES-3 in 1961, US Savannah in 1962, OK-150 in 1957, and Otto Hahn in 1968. Even though there were several small size reactors designed in the 1960s, only a few of them inspired the current SMRs. Since most of the SMRs use integral/integrated design for RX, the following section will start to discuss the early integrated designs for naval and terrestrial applications.

Early integrated designs in which SGs and pumps are within the RX inspired the current SMR designs. One of the early designs is the Safe Integral Reactor (SIR) (Figure 20.1.2) that introduces a tall riser to enhance natural circulation just above the core (Forsberg and Reich, 1991). Sealed circulation pumps are located just below the PRZ. SGs are placed around the periphery of the vessel. A passive PRZ is at the top of the pressure vessel because of the presence of vapor. This design makes an LB Loss Of Coolant Accident (LB-LOCA) impossible because there is no primary coolant pump.

Hannerz (Forsberg, 1983) proposed a new concept that is a combination of an updated integrated design and a pool type reactor design. This concept is called the Process Inherent Ultimate Safety (PIUS) (Figure 20.1.3) design (Forsberg, 1983). The core is located at the bottom of riser. The hot flow at the exit of the riser conducts to the entrance of circulating flow pipes. These pipes connect the vessel and both SG and circulation pumps. The pump is attached to the exit of SG to decrease the pressured head required for circulation flow. The water is returned to the vessel from the pump and flows through a downcomer to the core. There is a connection gap between standpipe and pool at the lower end of standpipe. In the case of the LB-LOCA design, even though the pump head keeps the water flow through the downcomer to the reactor core at operating conditions, borated water in the pool starts to enter through a lower density lock so that

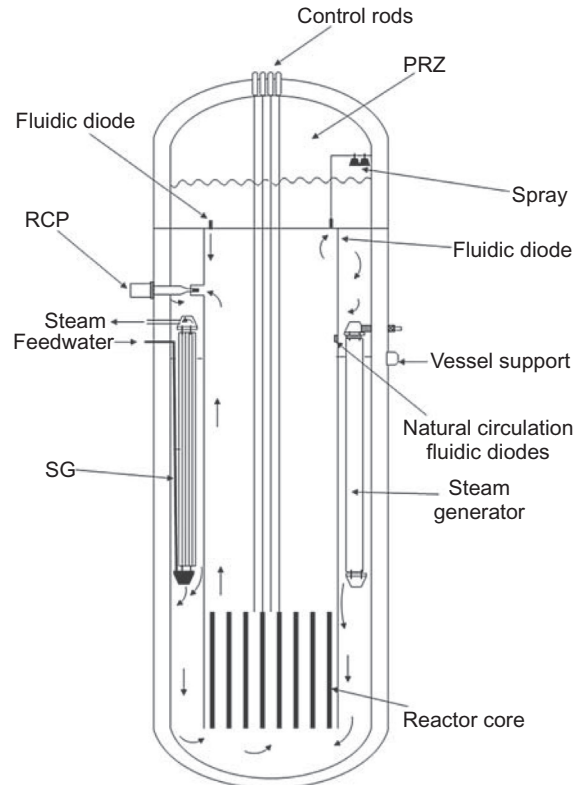


Figure 20.1.2. Configuration of SIR (Forsberg and Reich, 1991; Forsberg, 1983). PRZ, PResurizer; RCP, Reactor Circulation Pump; SG, Steam Generator

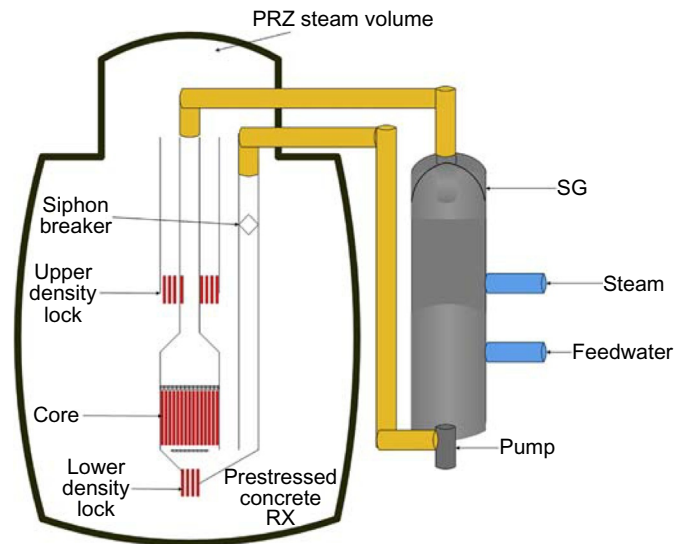


Figure 20.1.3. Configuration of PIUS (Forsberg and Reich, 1991; Forsberg, 1983). PRZ, PReSSuriZer; SG, Steam Generator

natural circulation starts between the lower and upper density lock connections. In other words, the pool water is not used in operating conditions. Even though there are circulation pipes connecting RX and SG, the vessel is located in a pool consisting of a large water inventory. Even though there might be an LB-LOCA on circulation pipes, the PIUS design is designed to handle even LB-LOCA with its large water inventory in the pool. The pool water inventory is cooled with the air to keep the pool temperature in a desired range in both accident and operating conditions. The water pool, the PRZ, and the core are enveloped with a prestressed concrete pressure vessel. The leakage from vessel is barred with a double stainless steel liner and concrete wall. PIUS's PRZ, similar to SIR, is at the top of the vessel.

Another design similar to SIR is the integrated reactor of Otto Hahn (Figure 20.1.4). This reactor was designed for a commercial ship in 1960s.

20.1.3 Nuclear reactors

Most of LW-SMR vessels are compact and integrated designs, which contain all the major RCSs along with SGs and an integral PRZ. Typical outlet temperatures are at around 300°C in LW-SMRs, which are much lower compared to ADV SMRs (non-LW-SMRs) as shown in Table 20.1.1. Outlet temperature could range from about 500°C to 1000°C.

Among the LW-SMRs, the IRIS vessel diameter is larger than other LW-SMRs because IRIS designers have increased the RCS inventory, and the IRIS power output is higher than other LW-SMRs. Obviously, increased RCS inventory increases the ratio of RCS inventory to produced power. In other words, there is more coolant inventory in the RCS to cool down the decay heat in accident conditions. This yields to flexibility for the safety margins, especially using US Nuclear Regulatory Commission (NRC)'s accident regulations for LWRs, defined in 10.CFR.50-46 regulations of NRC, for Loss Of Coolant Accident (LOCA). For instance, increased RCS coolant inventory provides better cooling in RX so that peak clad temperature is decreased.

Only W-SMR and mPower use internal Control Rod Drive Mechanism (CRDM) among LW-SMRs. This new design of CRDM eliminates the CRDM penetrations from the top of the RV to the core region. In addition, this new design provides free volume in the PRZ, Upper Plenum (UP), and in the riser of the RX. In addition, it not only simplifies the internal design of the reactor, but also decreases the pressure drop of the coolant and eliminates the maintenance of the penetrations including slaves, forging, etc.

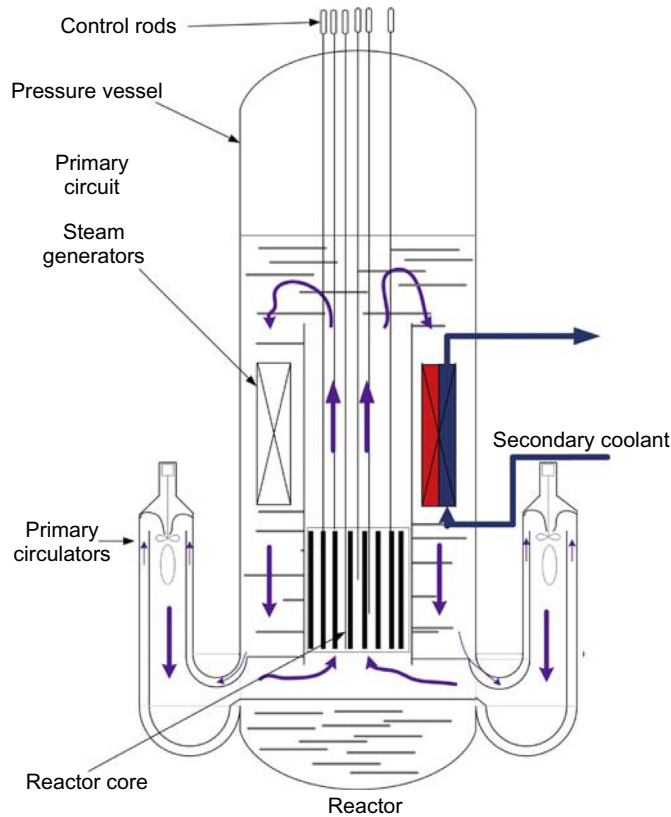


Figure 20.1.4. RX of Otto Hahn (Von Deobschuetz, 2005)

Table 20.1.1. Comparison of nuclear reactors

	Light water small modular reactor				
	NuScale (IAEA, 2011a, 2013; NuScale, 2013a,b; Reyes, 2012)	W-SMR (Matzie, 2015; NRC, 2014a; W, 2013)	IRIS (Carelli et al., 2003a,b,c, 2004)	SMART (Park, 2011; Kim et al., 2014)	mPower (Babcock, 2013; IAEA, 2011b; State of New Jersey, 2014; ANSI, 2012; Ghosh et al., 2014)
Vessel diameter (m)	~2.7	3.5	6.21	5.99	3.924
Vessel height (m)	~14	~27	22	~16.1	25.2984
Vessel penetration	SSP	SSP	SSP	SSP	NPBTC
Control rod drive mechanism	External	Internal	External	External	Internal

Continued

Table 20.1.1. Comparison of nuclear reactor—cont'd

Light water small modular reactor					
	NuScale (IAEA, 2011a, 2013; NuScale, 2013a,b; Reyes, 2012)	W-SMR (Matzie, 2015; NRC, 2014a; W, 2013)	IRIS (Carelli et al., 2003a,b,c, 2004)	SMART (Park, 2011; Kim et al., 2014)	mPower (Babcock, 2013; IAEA, 2011b; State of New Jersey, 2014; ANSI, 2012; Ghosh et al., 2014)
Thermal power (MW _{th})	160	~800	1000	330	530
Electricity power (MW _e)	45	~225	335	100	155 (for air-cooled condenser) 180 (for water-cooled condenser)
Capacity factor (%)	>95	–	>95	–	>95
Designer	NuScale	Westinghouse	IRIS Consortium	KAERI	Babcock & Wilcox
Mode of operation	BL	BL and LF	BL	BL and LF	BL and LF
Non-LW-SMR					
	PRISM (Power Reactor Innovative Small Module) (PRISM, 1994; GE Hitachi, 2015; Van Tuyle et al., 1989)		4S (Super Safe, Small and Simple reactor) (NRC, 2013; Toshiba CREIPI, 2013)		Hyperion (GEN4) (Gen4energy, 2013)
Reactor vessel dimensions (m × m)	5.74 × 16.9		2.5 × 23		1.5 × 2
Thermal power (MW _{th})	840		30–135		70
Electricity power (MW _e)	311		10–50		25
Moderator	No Mod.		No Mod.		No Mod.
Designer	GE		Toshiba		GEN4
Mode of operation	BL and LF		BL and LF		BL

SSP, Secondary Side Penetrations; BL, Base Load; LF, Load Following.

Some of the non-LW-SMRs offer load following capability even though most of the LW-SMRs work with base load. The following needs can be met with load following capability of some SMRs (IAEA, 2012; NRC, 2014a; Kumar et al., 2012):

- (1) Replace fossil fuel burning power plants with SMRs because both of them have the same range or power level;
- (2) Use SMRs in rural places where there are limited power grids; and
- (3) Integrate SMRs in hybrid energy systems.

Even though load following capability gives flexibility to SMRs to change power in response to changing demands, the power change rate should never exceed 5% per min to prevent the pellet clad interaction resulting in clad rupture (Bruynooghe et al., 2010). Therefore, SMRs employing load following capability, such as W-SMR, limit linear power rate increase with the value of 5% power change per min (NRC, 2014a). Mortensen et al. (1998) identifies the typical power change of various power plants during load following: %8/min power change is a typical power change for oil, even though this change is %4/min for gas and coal-fired units. Mortensen's power change values show that SMRs' power change is in the range of other thermal gas and coal fired units.

Reactor designs of LW and non-LW-SMRs are given in Figures 20.1.5–20.1.11.

20.1.4 Reactor coolant system components

The RCS is used to cool down the reactor core under operating conditions. Losing RCS coolant inventory will lead to core heat-up. In addition, the RCS coolant is enveloped generally within the pressure boundary, which is generally provided by the RV. Therefore, the penetrations on RV are eliminated to avoid Large Break (LB) or small break LOCA. Therefore, most of the integrated designs envelop RCS components in the pressure boundary.

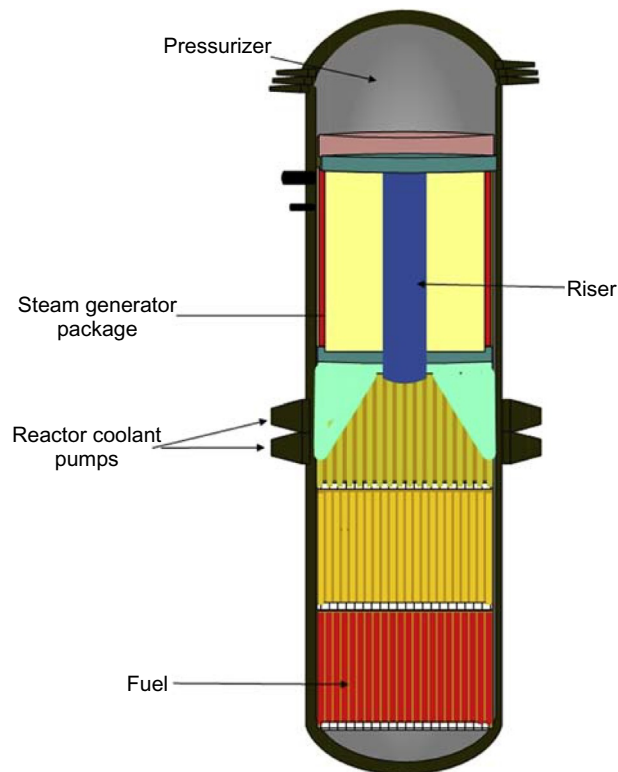


Figure 20.1.5. RX of W-SMR (Wheeler, 2012)

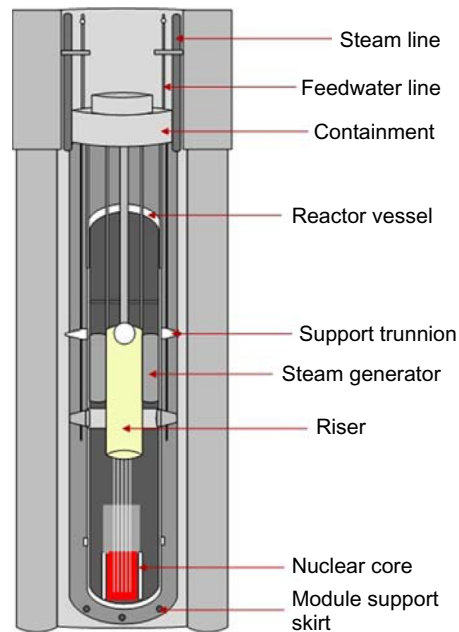


Figure 20.1.6. RX of NuScale (NRC, 2014b)

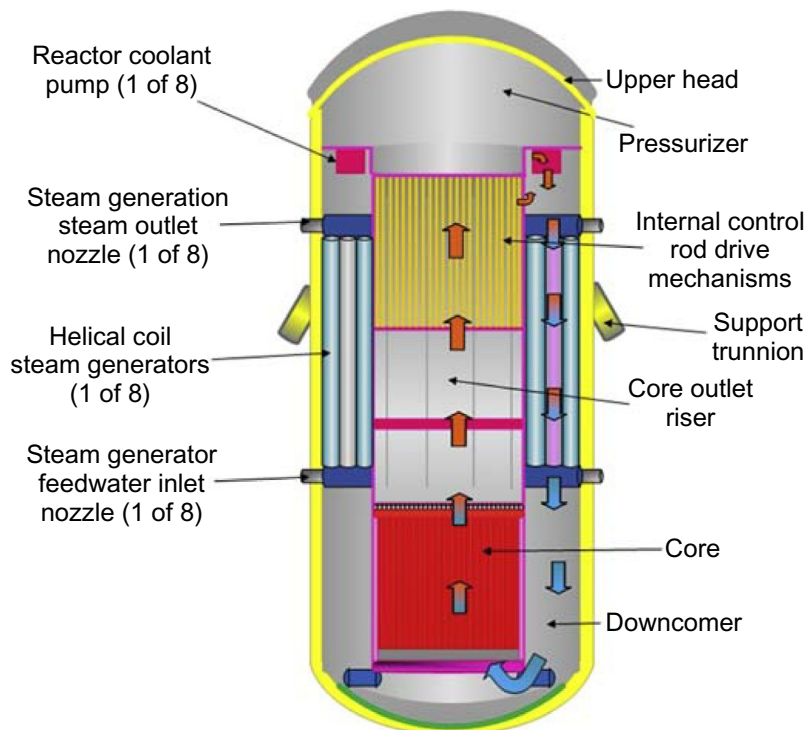


Figure 20.1.7. RX of IRIS (Carelli et al., 2003b)

Similar layouts (employing PRZ, SG, pump, etc.) are seen in most of the LW-SMRs, as shown in Figures 20.1.1–20.1.3 and 20.1.5–20.1.8. PRZ is located at the top of the RV since PRZ employs 2-phase flow. Even though long and thin PRZs are desired to decrease the water level uncertainty, PRZs of LW-SMRs are short. Even though PRZ designs in LW-SMRs are similar to each, IRIS PRZ is slightly different than other PRZs. The IRIS PRZ uses only PRZ heaters instead of heaters and sprays. Increasing PRZ volume allows IRIS to eliminate sprays.

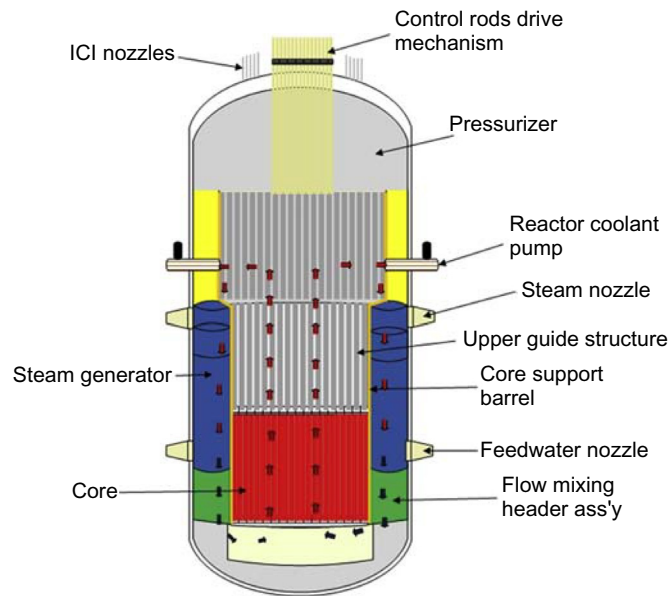


Figure 20.1.8. RX of SMART (IAEA, 2011a; Park, 2011). *ICI*, In-Core Instruments; *Ass'y*, Assembly

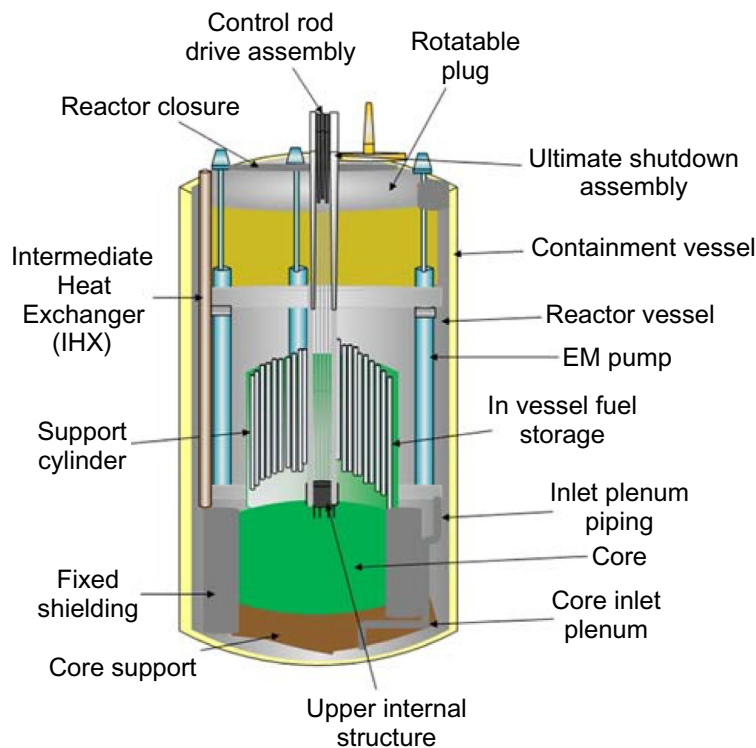


Figure 20.1.9. RX of PRISM (Nathan, 2013). *EM*, Electromagnetic Pump

Another challenge for LW-SMRs is the limited room in the RV. Therefore, sizing of each RCS component is challenging. For instance, W-SMR solves the sizing issue about SG by using two components (a low quality SG and a steam dome) instead of one typical commercial SG component (Figure 20.1.12) to produce high-quality vapor for turbines. The first component produces steam, which has small vapor fraction percentage that is not suitable for steam turbines. The second component separates the steam from liquid in the steam dome. This simple and effective approach is very common in early designs of navy reactors. By using this design, only secondary coolant is moved outside of the RV and enables a decrease in the size of RV.

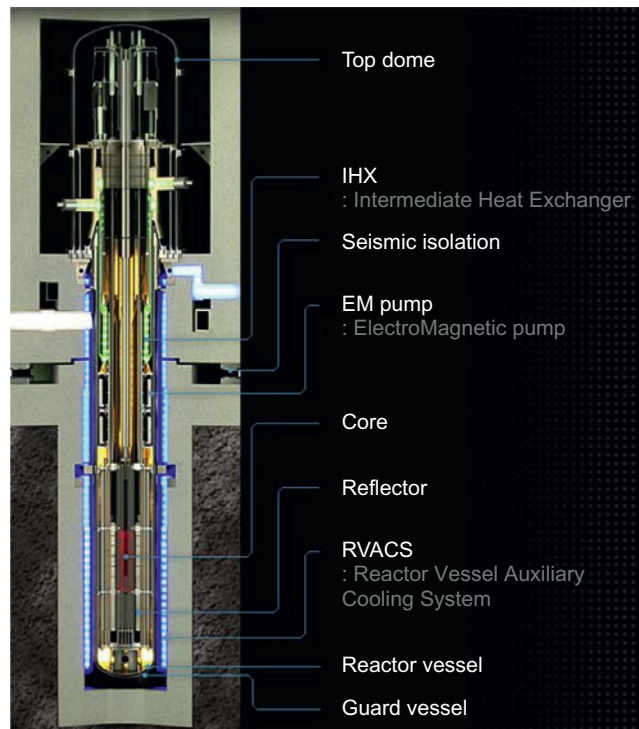


Figure 20.1.10. RX of 4S (Toshiba, 2015). Courtesy of Toshiba Corporation

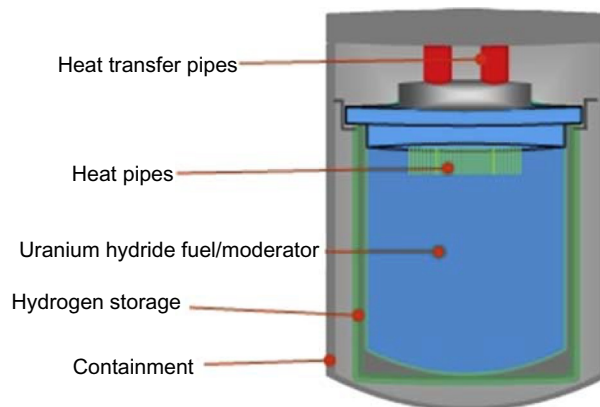


Figure 20.1.11. RX of Hyperion (Ganino, 2014)

NuScale is the only LW-SMR that uses natural circulation in operating conditions, as shown in Table 20.1.2. This feature decreases the number of RCS components. Since natural circulation is a challenging issue to get licensed in the United States, NuScale (like the AP1000) uses the scaled integrated experimental facility in Oregon State University for design of NuScale SMR and validation of code predictions.

High core outlet temperature of coolant can only be provided by the non-LW-SMRs. Therefore, N = non-LW-SMRs can be used to produce high-temperature steam for facilities/factories and to generate electricity with high efficiency.

The RCS comparison of SMRs is given in Table 20.1.2.

20.1.5 Fuels

Fuels used in SMRs are generally selected from the existing fuel designs. For instance, most of the LW-SMRs employ a 17×17 bundle design by decreasing its length. Using existing fuel designs decreases

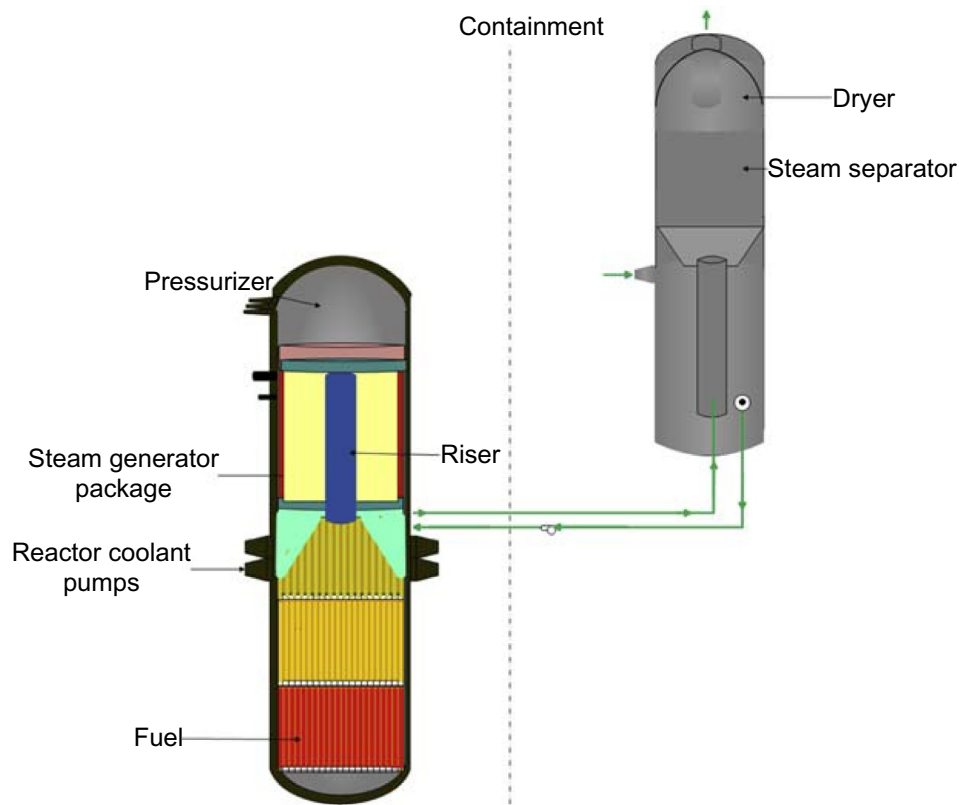


Figure 20.1.12. Split SG of W-SMR (Carelli et al., 2004; NRC, 2014a)

Table 20.1.2. Comparison of RCS components

Light water small modular reactors					
	NuScale (IAEA, 2011b, 2013; Babcock, 2013; NuScale, 2013a, b; Reyes, 2012)	W-SMR (Carelli et al., 2004; NRC, 2014a)	IRIS (Gen4energy, 2013; Carelli et al., 2003a,b, c)	SMART (Park, 2011; Kim et al., 2014)	mPower (PRISM, 1994; NRC, 2013; State of New Jersey, 2014; ANSI, 2012; Ghosh et al., 2014)
Outlet condition (°C)	~300°C (at 1500 psig/ 10.3421 MPa)	343°C (at 2500 psig/ 17.2368 MPa)	330°C	323°C	320°C (at 2050 psi/14.1342 MPa)
Steam generator type	Helical	Straight tube	Helical	Helical	Helical
Pressurizer in reactor vessel	Yes	Yes	Yes	Yes	Yes
Pressurizer active components	Heaters and sprays	Heaters and sprays	Heaters, no spray	–	Integral electric heaters
Circulation type	Natural	Forced	Forced	Forced	Forced

Non-LW-SMR

	PRISM (PRISM, 1994; GE Hitachi, 2015; Van Tuyle et al., 1989)	4S (NRC, 2013; Toshiba CREIPI, 2013)	Hyperion (Gen4energy, 2013)
Outlet condition (°C)	~500	510	500
Operating pressure (MPa)	Low pres.	0.3	Ambient pressure
Steam generator type	Helical	Straight tube	Helical
Circulation type	Natural	Forced (two electromagnetic pumps in series)	Forced
Coolant type	Sodium	Sodium	Lead-bismuth eutectic

LW-SMRs generally employ 5% fuel enrichment, and non-LW-SMRs can have much higher fuel enrichment value (Table 20.1.3). For example, Hyperion uses about 20% enriched U-235 and U-238.

number of experiments required for validation, thereby reducing development costs for LW-SMRs. However, non-LW-SMRs use relatively new fuel designs so that all these new fuel designs must be validated against experimental results, especially using radiation conditions. These kinds of uncompleted tasks for the licensing of the non-LW-SMRs may cause design changes in the future.

Typical 17×17 fuel assemblies are used in LW-SMRs (Table 20.1.3). The differences between fuels assemblies used in LW-SMRs and commercial LWRs (such as AP1000) are the height and fuel cycle length of the fuel. Most of the non-LW-SMRs utilize unique fuel designs, as shown in Table 20.1.3.

LW-SMRs control the reactivity by using very commonly used techniques, such as soluble boron, burnable absorbers, and control rods. However, non-LW-SMRs use innovative techniques to control reactivity. For instance, 4S uses movable reflectors to control the reactivity. Using movable reflectors instead of

Table 20.1.3. Comparison of fuel components

Light water small modular reactors					
	NuScale (IAEA, 2011a, 2013; NuScale, 2013a, b; Reyes, 2012)	W-SMR (Matzie, 2015; NRC, 2014a; W, 2013)	IRIS (Carelli et al., 2003a,b,c, 2004)	SMART (Park, 2011; Kim et al., 2014)	mPower (Babcock, 2013; IAEA, 2011b; State of New Jersey, 2014; ANSI, 2012; Ghosh et al., 2014)
Bundle type	17×17	17×17	17×17	17×17	17×17
Fuel length (m)	1.8288	2.4384	4.2672	2.01168	2.4130
Maximum fuel enrichment (w%)	4.95	<5	<5	<5	<5
Refueling frequency (years)	2–2.5	2	3.5	>3	4+

Continued

Table 20.1.3. Comparison of fuel component—cont'd

Light water small modular reactors					
	NuScale (IAEA, 2011a, 2013; NuScale, 2013a, b; Reyes, 2012)	W-SMR (Matzie, 2015; NRC, 2014a; W, 2013)	IRIS (Carelli et al., 2003a,b,c, 2004)	SMART (Park, 2011; Kim et al., 2014)	mPower (Babcock, 2013; IAEA, 2011b; State of New Jersey, 2014; ANSI, 2012; Ghosh et al., 2014)
Control rod drive mechanisms	External	Internal	External	External	Internal
Fuel type	UO ₂ pin	UO ₂ pin	UO ₂ pin	UO ₂ pin	UO ₂ pin
Active core height (m)	2	~2.4	~4.3	2	N/A
Cladding material	Zr-4 or advanced cladding	ZIRLO	Zr Alloy	Zr-4	Stainless steel
Lattice geometry	Square	Square	Square	Square	Square
Mode of reactivity control	Control rods, boric acid	Control rods, boric acid	Control rods, boric acid	Control rods, integrated B/A	Control rods, burnable poison
Mode of reactor shutdown	Control rods	Control rods	Control rods	Control rods, soluble boron	Control rods
Non-LW-SMR					
		PRISM (PRISM, 1994; GE Hitachi, 2015; Van Tuyle et al., 1989)	4S (NRC, 2013; Toshiba CREIPI, 2013)	Hyperion (Gen4energy, 2013)	
Bundle type		–	Hexagonal	–	
Fuel length (m)		–	2.5	–	
Maximum fuel enrichment (%)		26	18–19	<5	
Refueling frequency (years)		2	30	7–10	
Reactivity control system		Control rods + B4C Spheres	Axially movable reflectors	Hydrogen gas	
Fuel type		U-TRU-Zr (uranium-transuranic-zirconium alloy-metal fuel)	U-Zr (metal fuel)	UN	

B/A, Burnable Absorber.

chemical shim in the RCS eliminates the chemical control of chemical shim and chemical interaction between chemical shim and internal components of RCS. In addition, using a reflector around the reactor core is used as a passive (and/or an inherent) safety system to make the reactor subcritical in an accident condition. Economically, there is tradeoff between using a mechanical component to move the reflector and neglecting chemical control system for chemical shim. Another interesting example is Hyperion to control the reactivity since it uses hydrogen gases for reactivity control. The economical challenge for using hydrogen is its high production cost.

20.1.6 Containment

Containment is the last barrier in the defense in-depth strategy. Therefore, the containment vessel has to cover the components that may leak radioactive materials. In case of an accident, the containment wall has to be strong enough to handle high containment pressure. Ideally, a spherical containment shape is ideal for mechanical challenges. However, this design increases the capital cost of an SMR. Therefore, all the SMRs except IRIS use cylinder geometry (Table 20.1.4).

Containment designs are shown in Figures 20.1.13–20.1.17. NuScale’s containment design is the simplest containment design among SMRs. The reason is NuScale’s ECCS system, Triple Crown (NuScale, 2013a,b), does not need several emergency tanks. This design simplifies the ECCS as well as decreases ECCS components significantly. Triple Crown system is discussed in the ECCS section of this article in detail.

Table 20.1.4. Comparison of containments

Light water small modular reactor					
	NuScale (IAEA, 2011a, 2013; NuScale, 2013a,b; Reyes, 2012)	W-SMR (Matzie, 2015; NRC, 2014a; W, 2013)	IRIS (Carelli et al., 2003a,b,c, 2004)	SMART (Park, 2011; Kim et al., 2014)	mPower (Babcock, 2013; IAEA, 2011b; State of New Jersey, 2014; ANSI, 2012; Ghosh et al., 2014)
Containment shape	Cyl.	Cyl.	Sph.	Cyl.	Cyl
Containment size (ft × ft)	80 × 15 (24.384 × 4.572 m)	~89 × 32 (26.2128 × 9.7536 m)	82 (24.9936 m)	~144 (43.8912 m)	N/A
Non-LW-SMR					
	PRISM (PRISM, 1994; GE Hitachi, 2015; Van Tuyle et al., 1989)	4S (NRC, 2013; Toshiba CREIPI, 2013)	Hyperion		
Containment geometry	Cylinder (cont. vessel and dome)	Cyl./cph. geometry (guard vessel and top dome)	N/A		
Containment size (m × m)	6.04 m diameter	3.65 × 8	N/A		

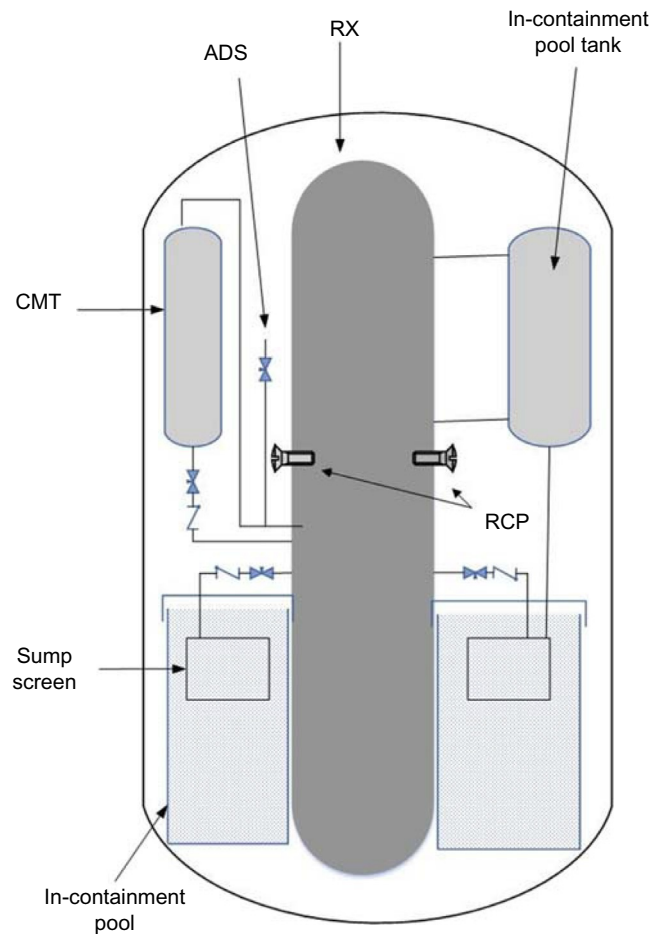


Figure 20.1.13. Containment of W-SMR (Carelli et al., 2004; NRC, 2014a). *ADS*, Automatic Depressurization System; *CMT*, Core Makeup Tank; *RX*, Reactor

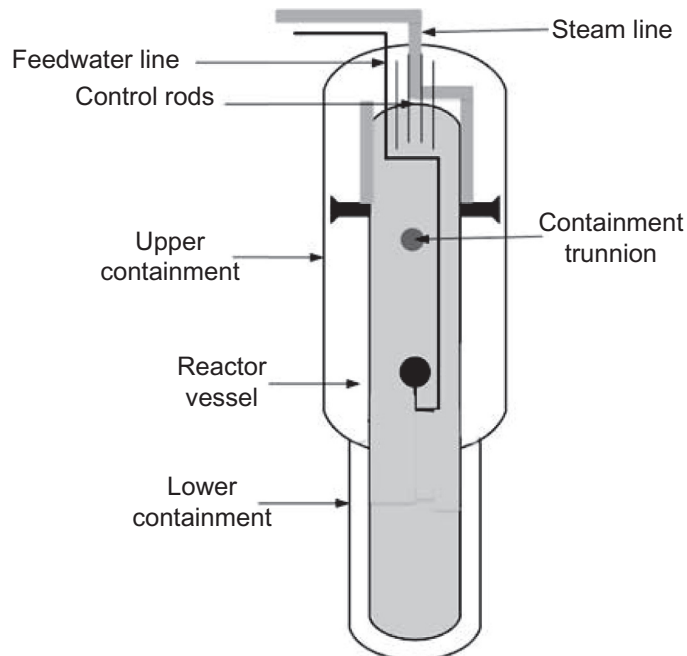


Figure 20.1.14. Containment of NuScale (NuScale, 2014)

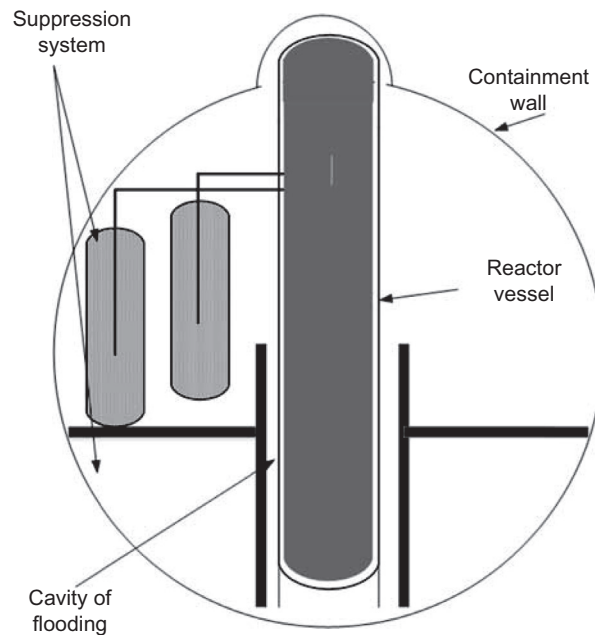


Figure 20.1.15. Containment of IRIS (Carelli et al., 2003b, 2004)

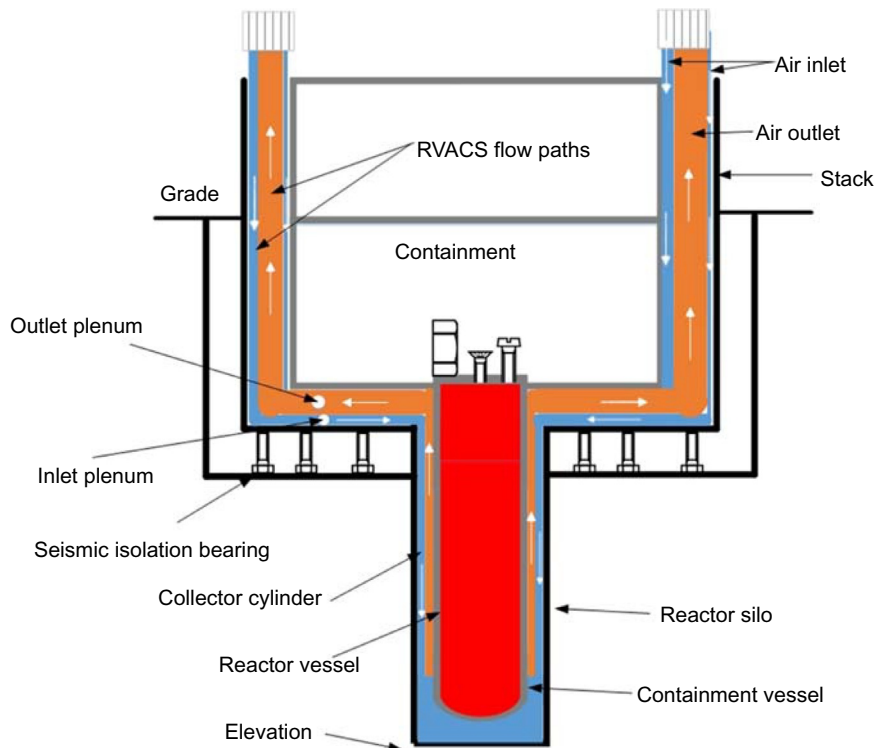


Figure 20.1.16. Containment of PRISM (GE Hitachi, 2015). RVACS, Reactor Vessel Auxiliary Cooling system

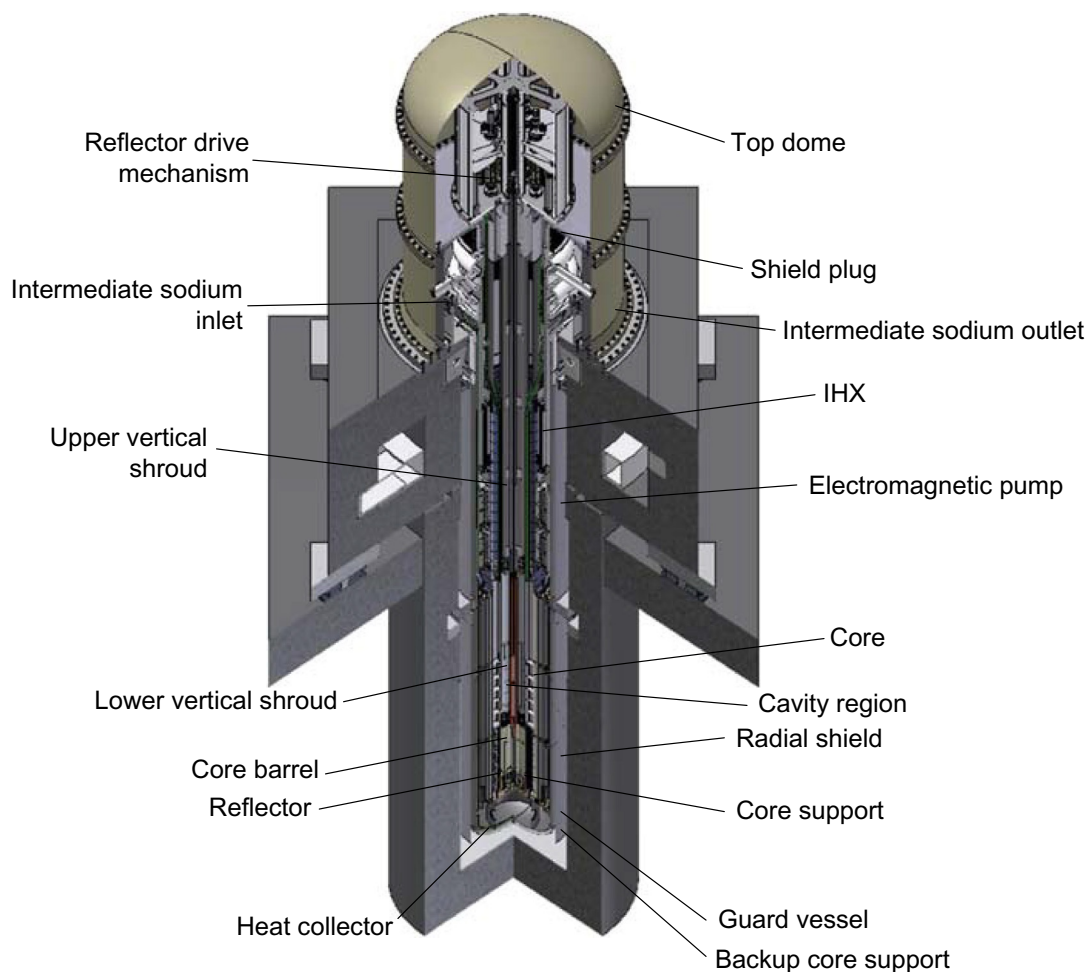


Figure 20.1.17. Containment of 4S (Toshiba, 2015). *IHX*, Intermediate Heat eXchanger. *Courtesy of Toshiba Corporation*

20.1.7 Emergency core cooling system

ECCS removes the decay heat during accident conditions. Because the DOE tends to fund passive safety systems, almost all the SMR designs employ passive safety systems. However, some of them can remove the decay heat for a limited time without operator and/or active component action.

NuScale's ECCS, Triple Crown (NuScale, 2013a,b), employing ECCS, can remove the decay heat indefinitely without an external power source such as a battery, operator action, and additional coolant (Figure 20.1.18). Safety valves in the NuScale design are opened without using an external power source just after an accident has been recognized. Then, the Triple Crown system removes the decay heat by using natural circulation (Figure 20.1.18). At the first step, water has been circulated between the RV and the coolant inventory in the containment. Then, latent heat removes the heat in the second stage. Finally, air cools the RV wall at the decreased level of decay heat, which is in the long-term cooling stage.

W-SMR employs several safety tanks to remove the decay heat at least 7 days, as summarized in Table 20.1.5 and shown in Figure 20.1.19.

IRIS's ECCS system is similar to W-SMR, as shown in Figure 20.1.20.

The safety system (Figure 20.1.21) of SMART includes a shutdown cooling system, residual heat removal system, safety injection system, reactor overpressure protection system, and emergency boron injection tank. Each of the four independent passive residual heat removal systems with 50% capacity can remove the core

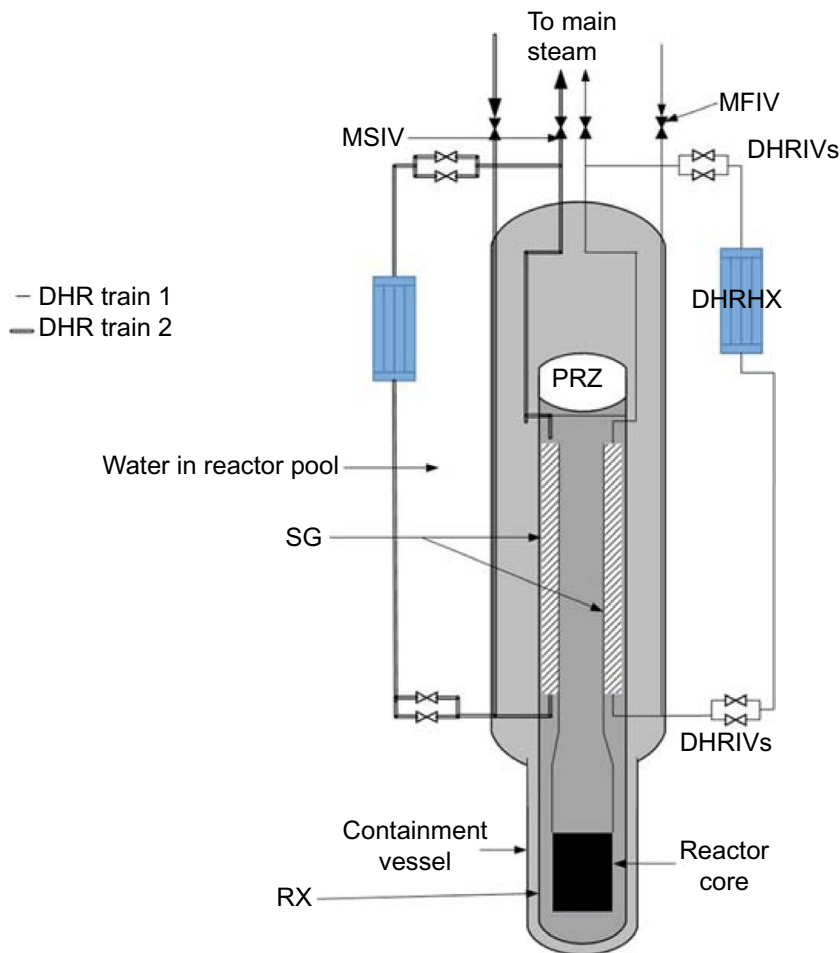


Figure 20.1.18. ECCS of NuScale (Reyes, 2012). *DHRIV*, Decay Heat Removal Isolation Valve; *MSIV*, Main Steam Isolation Valve; *RX*, Reactor; *MFIV*, Main Feedwater Isolation Valve; *DHRHX*, Decay Heat Removal Heat eXchanger; *DHRIV*, Decay Heat Removal Isolation Valve

Table 20.1.5. W-SMR nuclear safety components

Nuclear safety related actions	Which component is used for the nuclear safety action?
Short-term reactivity controls	Control rods
Long-term reactivity controls	Core makeup tanks
Decay heat removal	Passive residue heat removal heat exchanger/ultimate heat sink tank(s)
Long-term makeup water supply	In-containment pool tanks/sump
Ultimate heat sink	Ultimate heat sink tank (7 days)
Severe accident management	In-vessel retention

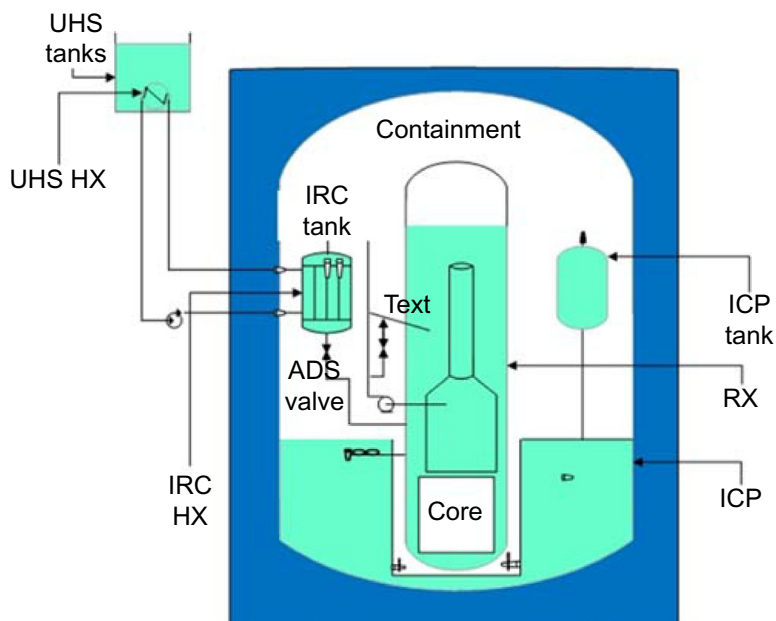


Figure 20.1.19. ECCS of W-SMR (Matzie, 2015; NRC, 2014a). IRC, Inside Reactor Containment; UHS, Ultimate Heat Sink; HX, Heat eXchanger; RX, Reactor; ADS, Automatic Depressurization System

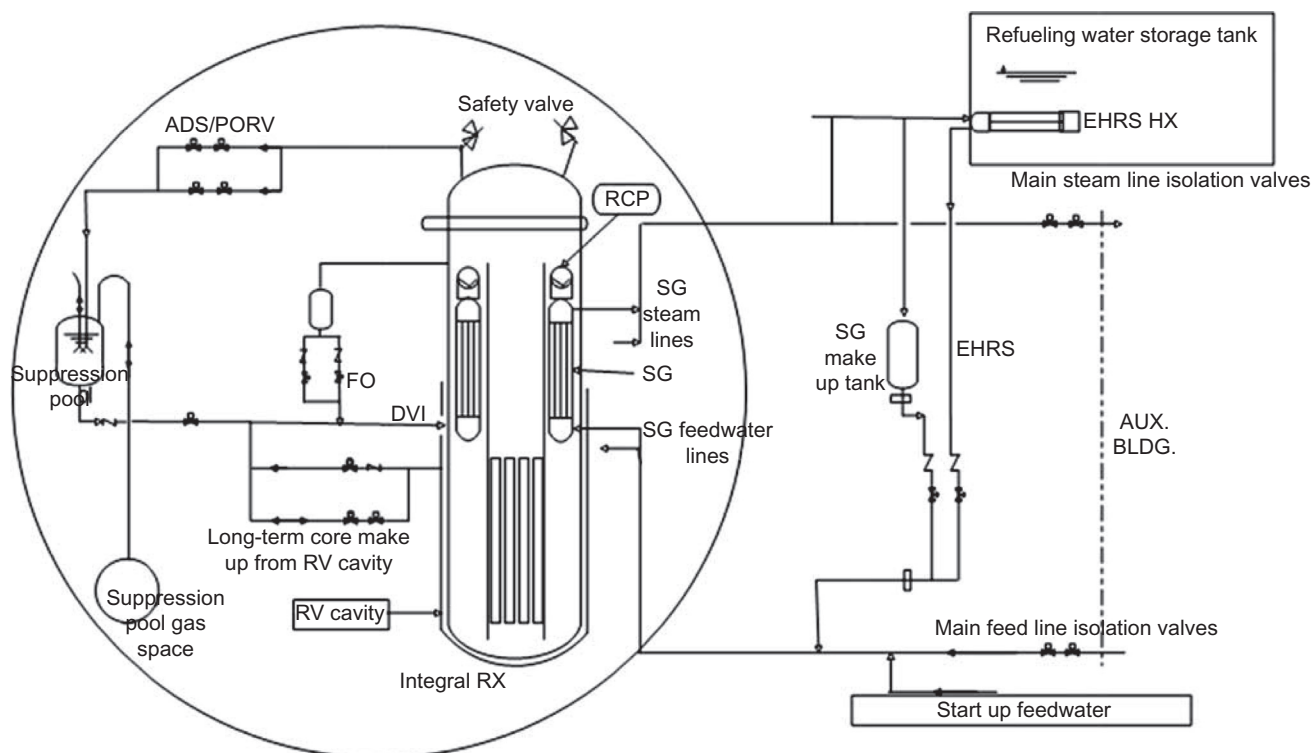


Figure 20.1.20. IRIS ECCS system (Carelli et al., 2003b,c). PORV, Power-Operated Relief Valve; SG, Steam Generator; RCP, Reactor Circulation Pump; EHRS, Emergency Heat Removal System; ADS, Automatic Depressurization System; RV, Reactor Vessel; FO, Fail Open valve; DVI, Direct Vessel Injection

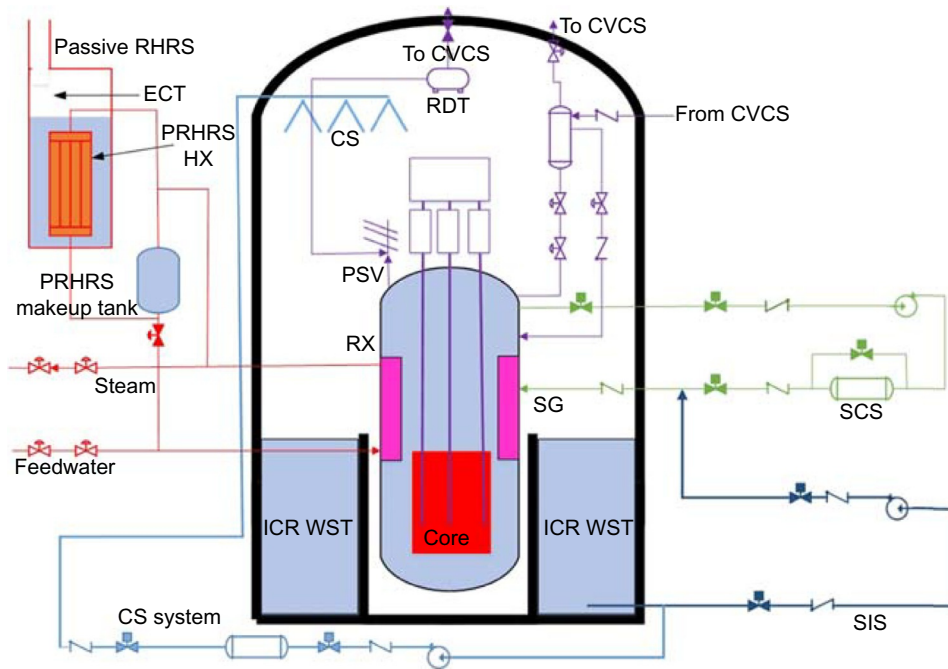


Figure 20.1.21. SMART ECCS system (Park, 2011). *PRHRS*, Passive Residual Heat Removal System; *RHRS*, Residual Heat Removal System; *CVCS*, Chemical and Volume Control System; *ICRWST*, In-Containment Refueling Water Storage Tank; *SG*, Steam Generator; *RDT*, Reactor Drain Tank; *SIS*, Safety Injection System; *ECT*, Emergency Cooldown Tank; *HX*, Heat Exchanger; *RX*, Reactor; *CS*, Containment System

decay heat through natural circulation at any design basis events. This feature can keep the core undamaged for 72 h without any corrective action by operators in a design basis accident (Kim et al., 2014).

ECCS of PRISM has varied shutdown features (IAEA, 2003). The passive safety system of PRISM has been supported by inherent safety features, such as Doppler effect, multidimensional fuel expansion, sodium density decrease, and also RV expansion. In addition, the passive Reactor Vessel Auxiliary Cooling System (RVACS) is the primary heat removal during not only anticipated transients without scram, but also all design basis accident conditions. Like NuScale's ECCS, PRISM's safety system can remove the decay heat in infinite time by using passive safety features. Similar to high-temperature gas reactors' reactor core cavity system, the decay heat is transferred from the RV to the containment vessel via thermal radiation. Containment is cooled by natural convection of air outside of containment. On top of typical passive safety systems in PRISM, auxiliary cooling system can also be used to remove decay heat by utilizing natural circulation of air past the SG.

4S (Super-Safe, Small and Simple) power plant has several safety systems: active, passive, and inherent (IAEA, 2003) (see Figure 20.1.22). Active shutdown systems are: (1) inserting reflectors by using gravitational force; and (2) inserting black control rods. The passive safety system of 4S uses natural circulation in RVACS and Intermediate Reactor Auxiliary Cooling System (IRACS). In addition, inherent safety system uses Doppler effect via metallic fuel and large inventory of coolant.

Gen4 or HYPERION's safety system can remove the decay heat in two ways: (1) dumping the steam to the condenser; and (2) if first decay heat removal way is not sufficient, back up decay heat removal system is used. This system utilizes natural circulation of primary coolant through bypass path in the core. The surface of Gen-IV module is cooled with latent of heat via water sprays provided by emergency cooling tank. The water inventory in this tank can be injected due to gravitational force to remove the decay heat for 2 weeks. The second system works as a passive safety system.

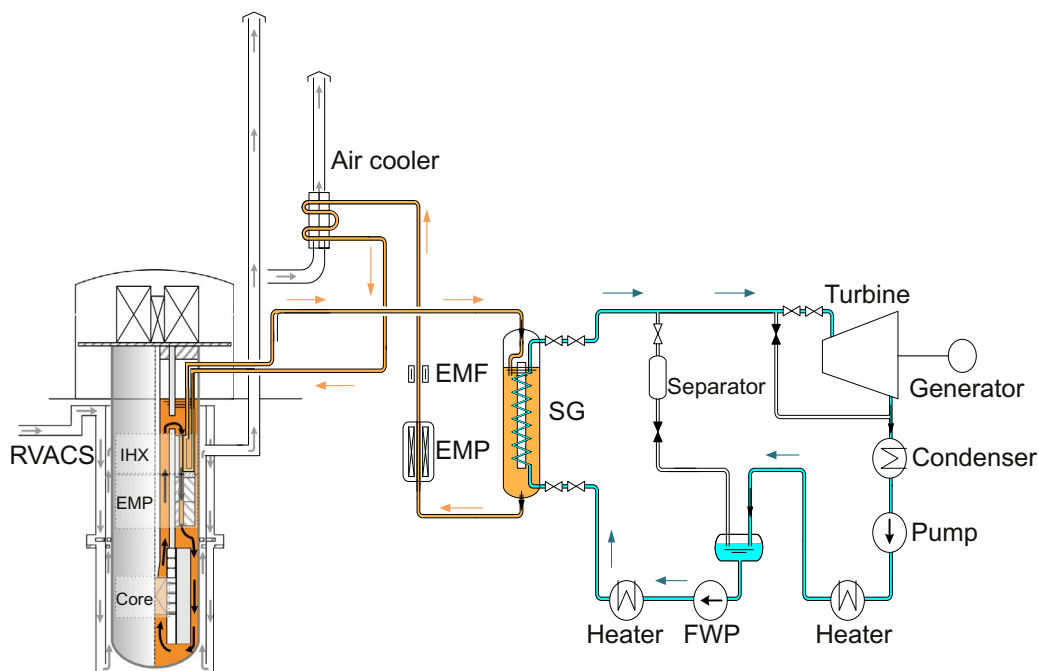


Figure 20.1.22. ECCS system of 4S (Prasad, 2012). *EMP*, ElectroMagnetic Pump; *EMF*, ElectroMagnetic Field; *SG*, Steam Generator; *IHX*, Intermediate Heat Exchanger; *FWP*, FeedWater Pump

20.1.8 Economic and financing evaluation

Given the early stage of SMR development, there is no directly applicable historical cost information available, nor is there any publicly available detailed vendor cost information. It is clear, however, that in line with the preceding review of SMR designs, there are several design features that not only make SMRs significantly different from typical large Nuclear Power Plants (NPPs), but also impact their projected costs. Most apparent is that their smaller reactor size and power output are substantially different from traditional NPPs. Some earlier studies attribute significant economies of scale to the construction of large nuclear plants (Christiensen and Greene, 1976; Krautmann and Solow, 1988). Under this assumption, the relationship between the overnight capital costs and the size of reactors of similar design and characteristics can be expressed as:

$$OCC_{\text{SMALL}} = OCC_{\text{LARGE}} \times (\text{Size}_{\text{SMALL}}/\text{Size}_{\text{LARGE}})^n$$

where OCC_{SMALL} and OCC_{LARGE} are the overnight capital costs of small and large NPPs, respectively, and $\text{SIZE}_{\text{SMALL}}$ and $\text{SIZE}_{\text{LARGE}}$ are respective reactor sizes, in MWe, and n is the scaling factor, often taken to be in the range of 0.4 to 0.7 (Phung, 1987).

Based on this view, scaling down from gigawatt-sized NPPs to smaller SMRs would result in a significant loss of scale economies with a resulting increase in overnight capital costs.

There are, however, several factors that contrast with this view. The first stems from the failure of anticipated declines in unit costs to be realized with the dramatic increase in the size of NPPs during the 1970s–1980s. This has led many to maintain that scale economies in NPPs are likely very modest and may, in fact, be negative (see, for example, Kessides, 2012; Grubler, 2010). Second, the relationship between reactor size and costs, as stated above, is estimated for reactors of similar design and characteristics. The comparisons of different SMR designs in the present study demonstrate that SMRs have several features that are significantly different from conventional large nuclear plant designs that are likely to offset any loss scale economies that may exist.

The simplified SMR design features described earlier result in a reduction in the number of components along with a reduction in overnight costs. In addition, the safety characteristics of SMR designs are enhanced due not only to smaller reactor sizes, but also to the use of passive cooling systems. Further, the modularity of SMR designs enables the fabrication of the major components of the power unit, including the RV, steam supply, and cooling system in centralized manufacturing facilities and shipped in component parts via rail, truck, or ship for on-site installation (Carelli et al., 2010). Modularity has several advantages, including standardization of both components and design and resulting significant economies of mass production.

Further, “economies of mass manufacturing” are achieved when the SMR modules are manufactured in centralized, large-scale manufacturing facilities rather than on-site for a large NPP. These economies of mass manufacturing have been shown to account for significant reductions in per unit manufacturing costs (Rosner et al., 2011; Boarin et al., 2012). The scale economies gained from modularization and mass manufacturing are enhanced from lessons learned during the manufacturing process. These result in productivity and efficiency gains with increases in the number of successive modules over the deployment schedule, and further reduce per unit overnight costs. Modularity also results in lower capital costs and reduced construction and installation times as compared to large nuclear or fossil fuel power plants. These, thereby, further reduce both financing costs and risk levels.

These cost advantages of SMRs suggest that SMRs can be economically competitive with large NPPs as well as energy production from fossil fuel and renewable energy facilities. Cost estimates include \$50,000/kWh for the SMART design (Vujic et al., 2012), \$4000/kWh for the NuScale design, and \$5000/kWh for the IRIS design (World Nuclear Association, 2008). These estimates imply that the levelized cost of electricity from SMRs will be cost competitive with renewables and coal facilities and with natural gas facilities outside of North America (World Nuclear Association, 2008). Further, the cost advantages of SMRs extend beyond the initial capital costs in that SMRs are subject to much lower fuel price sensitivity risk than large coal or natural gas facilities because fuel costs comprise a much lower share of operating costs than is the case for fossil fuel plants (Pratson et al., 2013). This is apparent in the relative stability of nuclear energy production operating costs over time, as shown in Figure 20.1.23 (NEI, 2014).

Besides overnight capital costs and all-in costs that include financing and construction, there are costs relating to development, design certification, and licensing. SMRs present new challenges for the industry and the NRC. With industry stakeholder input, the NRC has slowly but methodically been addressing issues for both Light Water (LW) and non-LW reactors relating to insurance requirements (US Nuclear Regulatory Commission, 2011a), the security regulatory framework (US Nuclear Regulatory Commission, 2011b), and

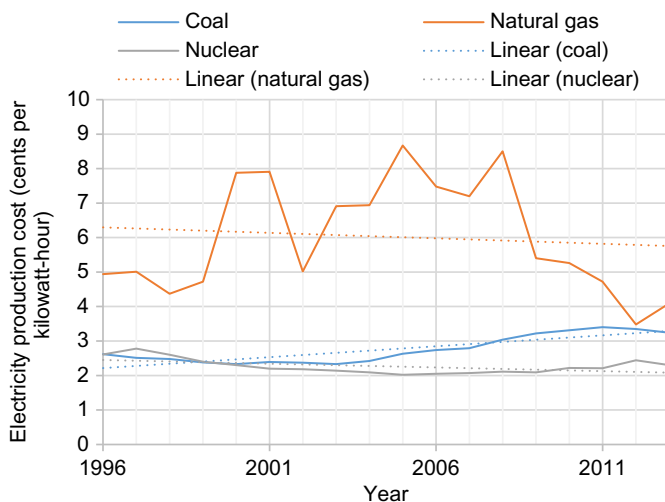


Figure 20.1.23. US electricity production costs (NEI, 2014). Where production costs = operations and maintenance costs + fuel costs. Production costs do not include indirect costs and are based on Federal Energy Regulatory Commission (FERC) Form 1 filings submitted by regulated utilities. Production costs are modeled for utilities that are not regulated. Ventyx Velocity Suite (NEI, 2014) (<http://www.nei.org/Knowledge-Center/Nuclear-Statistics/Costs-Fuel,-Operation,-Waste-Disposal-Life-Cycle/US-Electricity-Production-Costs-and-Components>)

mechanistic source term (US Nuclear Regulatory Commission, 2013), among others. The NRC is focusing primarily on the LW designs that have Department of Energy licensing support: mPower and NuScale. NRC policy papers, memoranda, and a 2012 report to Congress (US Nuclear Regulatory Commission, 2012) express the need for more research resources and international cooperation to fully address the human resource requirements to certify and license advanced designs. Advanced reactor high-temperature and liquid metal design and development costs would be negatively impacted if the NRC does not keep pace with development and research advances more quickly than anticipated.

The United States also provides incentives for SMRs that will assist with bringing all-in costs down for the first orders, assuming SMR development continues to advance. Eligibility for US incentives is predicated on domestic manufacturing and/or domestic installation and power production, depending on the particular incentive. The United States issued a draft federal loan guarantee solicitation announcement for advanced nuclear energy projects, of which \$10.6 billion is available for nuclear power facilities, including SMRs (US Department of Energy Loan Programs Office, 2014). The United States currently provides a Production Tax Credit (PTC) for a limited amount of nuclear capacity (Solan et al., 2010); it is possible that power for SMRs in the future may be eligible for remaining capacity under the PTC or a new set-aside for an SMR-specific PTC.

While the United States has taken some steps to incentivize nuclear power projects, including SMRs, one of the major hindrances to the building of new large nuclear projects at the global level is the lack of financing. Commercial banks, Multilateral Development Banks (MDBs), and export/import credit agencies provided funding in the past, but have not been willing to provide funds for nuclear projects. For commercial banks, high initial capital costs and extended construction periods, during which costs escalate have combined to increase the financing risk for nuclear builds. These projects also have significant delays in financing returns on investment, especially in liberalized electricity markets.

The decrease in funding from commercial banks has been accompanied by a commensurate decrease in lending on the part of MDBs over the same period. Indeed, some MDBs have placed moratoria on funding nuclear power projects. Major examples include the World Bank, which, while acknowledging that nuclear power can contribute to climate change goals, has not yet altered its policies against lending for nuclear projects, and the Asian Development Bank, which recently reaffirmed its policy of not funding nuclear power facilities (Findlay, 2012). The reluctance on the part of MDBs to invest in large nuclear power projects stems largely from the high up-front capital costs, the widespread underestimation of true final costs, and the inflexibility of NPPs as electricity generators, particularly for emerging economies (World Bank Technical Paper #154, 1994). These issues are mitigated by the features of SMRs, including reduced cost and financing risks, the ability to be integrated with other sustainable energy sources, and non-electric applications. In addition, increasing energy demands can be met incrementally without tying up large amounts of money for long periods of time.

Since the financial crisis, there has been a dramatic increase in funding for low-carbon energy projects on the part of MDBs (Bloomberg New Energy Finance Report, 2010). For example, The Asian Development Bank, Inter-American Development Bank, and the European Investment Bank all list low-carbon energy projects among their top priorities, with the latter listing renewable energy, energy efficiency, and nuclear projects as part of its corporate investment plan (Fu-Bertaux, 2011). The World Bank has significantly increased funding for low-carbon projects as well as district heating and displacement of carbon-intensive fuels as part of its energy strategy. The features of SMRs can further the achievement of these goals, and funding from MDBs for SMR deployment will increase. In addition, both SMR vendor countries and importing nations can use export/import credit agencies to assist with financing SMRs. Canada, for example, has used this route to promote its Canadian Deuterium Uranium reactor to developing countries (Bratt, 2006).

SMR development is also likely to take advantage of some of the new financing arrangements that have been established to compensate for the decrease in traditional funding options for nuclear builds. With the

escalation of costs and changing revenue streams in liberalized energy markets, vendors have taken on more of the risk from operators for both large nuclear and other large power facilities such as coal and hydro projects. Three possible avenues are fixed construction price contracts, fixed power price contracts, and Build-Own-Operate (BOO) contracts between vendors and operators. In fixed-price construction contracts, vendors agree to build the facility for an agreed upon price, effectively isolating operators from cost overruns. Such an agreement was used in the construction of the Olkiluoto 3 plant in Finland between AREVA (a French multinational group headquartered in Paris, France) and Finland's Teollisuuden Voima Oyj. In guaranteed price contracts, the operator's selling price for power is guaranteed when the investment decision is made, thereby reducing operator risk on the revenue side. This was the agreement between Electricité de France and AREVA for the United Kingdom's \$26 billion Hinkley Point C nuclear plant (Kidd, 2014; Reuters International, 2014), which has received approval from the European Commission. In BOO agreements, the vendor agrees to build and operate the plant and in return for selling power at fixed prices to domestic power companies. Since domestic economies do not have to finance such projects or bear the financial risk associated with them, BOO agreements are currently underway or being developed for nuclear projects in Turkey, Vietnam, Bangladesh, and other developing economies, and are a viable option for increasing the use of SMRs going forward.

20.1.9 Security of small modular reactors

The realm of nuclear security is centered upon the “intentional misuse of nuclear or radioactive materials” for the purpose of causing harm (Safety of Nuclear Power Reactors, 2015). The security of the SMRs for proliferation resistance and physical protection is increased for every SMR. Proliferation resistance is feature of an SMR that controls the fissile materials that can be used for weapons. In addition, a key emphasis is placed on potential threats to structural facilities, such as an RX, containment building, or a nuclear materials facility.

SMR designs claim that they have made improvements to nuclear security concerns. Most of the SMRs enhance the nuclear security by:

- (1) Housing the reactor underground: This feature protects the RX from an external threat, such as an airplane crash. In addition, this provides a physical barrier of ground for radiation leakage.
- (2) Limiting the access to the reactor building and control room. Since the most of the components (RX, control room, reactor circulation pump, SG, and other primary components) are underground, the access to this components are limited to protect for NPP for threats.
- (3) Decreasing the number of components in SMRs. Number of components of SMRs are reduced significantly. The security of the SMRs can be focused on the significantly decreased number of components that are potential for threats.
- (4) Improved safety systems by using passive, inherent safety or safety-by-design features eradicate the (un) intentional misuse of nuclear components.

20.1.10 Flexibility of small modular reactors

The power level of SMRs varies from 10 to 300 MW_e. Retired gas and coal power plants can easily be replaced with SMRs since SMRs' power and physical size are decreased significantly. In addition, the SMRs can be used for Hybrid Energy Systems (HES) (Figure 20.1.24).

The overall power can easily be managed in the power grids by using the SMRs in an HES. When the power demand decreases, the SMR power is used either in a heating system or a desalination system or

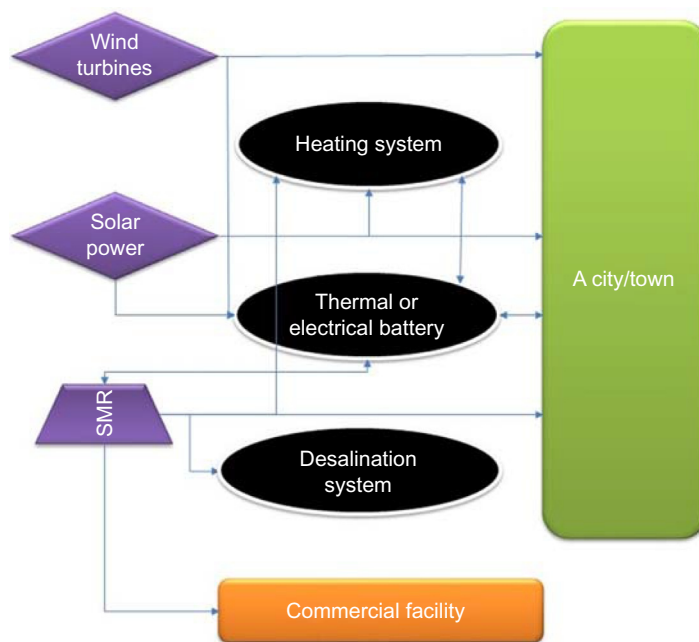


Figure 20.1.24. HES utilizing SMRs

a battery. If the energy is stored in a battery, the stored energy can be used when the electrical demand of a city or town increases. In the HES, solar power plants, wind turbines are cardinally is employed with SMRs-based variation of power generation and consumptions. Since the generation of power from solar power plants and wind turbines are not constant, the load following feature of SMRs are used to provide the necessary power when power demand is higher than power generation from power plants of solar and wind. Thermal and electrical batteries are the power buffer for this power network (Figure 20.1.24).

20.1.11 Conclusions and future trends

The historical development of SMRs started with integrated reactor designs, such as SIR and PIUS. The integrated design's major advantage is envelopment of majority (or all) RCS components. In addition, integrated design eliminates the pipe connections between the RCS components. For instance, there are hot leg, cold leg, surge line, and other pipes in integrated SMRs. Most of the integrated RVs are slim and tall to take advantage of chimney effect—movement of the coolant in the riser component, resulting from coolant buoyancy—in especially accident conditions.

This chapter compares selected LW and non-LW-SMRs in respect to nuclear reactors, fuels, containment, and ECCS. Even though there is no clear winner in this comparison, the following conclusions are highlighted:

- All SMR designs motivate US-based organizations to compete with their international peers. DOE financially supports two SMR projects, NuScale and mPower, to accelerate the development of LW-SMRs.
- Internal CRDM designs of NuScale and W-SMR eliminate the CRDM penetrations from top of the vessel (RV) to the core region. It also provides free volume in PRZ, UP, and in the riser of the RV. Since internal CRDM does not occupy space in the UP and PRZ in integrated RX, pressure drop due to friction on corresponding internals for CRDM decreases. This will yield to improve the flow distribution in RX.
- Some of the LW and non-LW-SMRs offer load following capability. Even though the power of these SMRs cannot be changed as quickly as coal or natural gas power plants, load following capability gives flexibility to the utilities to change the power based on electricity demand in the power grids.

- IRIS's PRZ design is slightly different than other LW-SMRs, since it eliminates the sprays in PRZ. This elimination requires bigger PRZ volume than other LW-SMRs' PRZ volumes.
- W-SMR's SG consists of two parts. This design decreases the size of the SG, which is in RV.
- IRIS's containment size is the largest among LW-SMRs to provide a large volume for safety. In addition, IRIS's containment is in a spherical shape to avoid edges and sides, which decreases the resistance of containment against a high pressure, different between the containment and air in the accident conditions.
- NuScale's safety system can remove the decay heat indefinitely, even though other LW-SMRs can remove for a limited period (generally 7 days).
- 4S's safety system has several active, passive, and inherent safety features. Especially advanced inherent safety feature and 30 years refueling frequency makes 4S different than other non-LW-SMRs.

SMRs have the potential to offset the traditionally perceived economies of scale for large NPPs with cost reductions from several types of economies, including cost savings due to modularization, mass manufacturing, reduced components from design simplicity, and passive safety systems. In addition to reducing the cost of manufacturing and installing SMR units, there are also associated reductions in operating costs. The financing community needs to be assured that the costs of building and operating SMRs are reasonable. Further, this technology needs to demonstrate a high capacity to contribute to carbon reduction goals while providing a viable route to meeting future energy demands. Ultimately, in addition to reducing uncertainty about the costs, sustained government support for SMR development is critical for the designs to be licensed for commercial operation. SMRs in HES will likely be employed because of flexible features of SMRs.

Acknowledgment

The images of 4S reactor has been used by using "Courtesy of Toshiba Corporation." The author thanks Toshiba Corporation.

References

- AKME, 2015. <http://www.akmeengineering.com/svbr100.html>.
- ANSI, 2012. <http://publicaa.ansi.org/sites/apdl/NESCCDocs/NSECC%2012-036%20-%20BM%20mPower%20Reactor%20Design%20Overview.pdf>.
- Babcock, 2013. <http://www.babcock.com/library/Documents/SP201-100.pdf>.
- Bloomberg New Energy Finance Report, November 2010. *Weathering the Storm: Public Funding for Low-Carbon Energy in the Post Financial Crisis Era*. United Nations Environment Programme and SEF Alliance.
- Boarin, S., Locatelli, G., Mancini, M., Ricotti, M., 2012. Financial case studies on small- and medium-size modular reactors. *Nucl. Technol.* 178 (2), 218–232.
- Bratt, D., 2006. *The Politics of CANDU Exports*. University of Toronto Press.
- Bruynooghe, C., Eriksson, A., Fulli, G., 2010. Load-Following Operating Mode at Nuclear Power Plants (NPPs) and Incidence on Operation and Maintenance (O&M) Costs. JRC Scientific and Technical Reports, EUR 24583EN.
- Carelli, M.D., Conway, L.E., Oriani, L., 2003a. Safety features of the IRIS reactor. In: *Nuclear Mathematical and Computational Sciences: A Century in Review, A Century Anew*, Gatlinburg, Tennessee, 6-11 April 2003, Conference Proceedings. ANS, LaGrange Park, Illinois. Paper 126.
- Carelli, M.D., Conway, L.E., Oriani, L., 2003b. The design and safety features of the IRIS reactor. In: *ICONE11-36564*, 11th International Conference on Nuclear Engineering, Tokyo, Japan. <https://www.nrc.gov/docs/ML0336/ML033600094.pdf>.
- Carelli, M.D., Conway, L.E., Collado, J., Cinotti, L., Moraes, M., Lombardi, C., Kujawski, J., 2003c. Integral layout of the IRIS reactor. In: *Proceedings of ICAPP'03*, May 4–7, Cordoba, Spain. <https://www.tib.eu/en/search/id/BLCP:CN057151314/Integral-Layout-of-the-IRIS-Reactor?cHash=89faadf729be0b435bd21d16fb66e419>.
- Carelli, M.D., Conway, L.E., Oriani, L., Petrović, B., Lombardi, C.V., Ricotti, M.E., Barroso, A.C.O., Collado, J.M., Cinotti, L., Todreas, N.E., Grgić, D., Moraes, M.M., Boroughs, R.D., Ninokata, H., Ingersoll, D.T., Oriolo, F., 2004. The design and safety features of the IRIS reactor. *Nucl. Eng. Des.* 230 (1–3), 151–167.
- Carelli, M., Garrone, P., Locatelli, G., Mancini, M., Mycoff, C., Trucco, P., 2010. Economic features of integral, modular, small-to-medium size reactors. *Prog. Nucl. Energy* 52 (4), 403–414.

- Christiansen, L., Greene, W., 1976. Economies of scale in U.S. electric power generation. *J. Polit. Econ.* 84 (1), 655–676.
- Findlay, T., 2012. *Nuclear Energy and Global Governance: Ensuring Safety, Security and Non-proliferation*. Routledge, London, p. 85. <https://www.routledge.com/Nuclear-Energy-and-Global-Governance-Ensuring-Safety-Security-and-Non-proliferation/Findlay/p/book/9780415532488>.
- Forsberg, C.W., 1983. A Process-Inherent, Ultimate-Safety (PIUS), Boiling Water Reactor. CONF-850610–34 <https://www.osti.gov/servlets/purl/5148883>.
- Forsberg, C.W., Reich, W.J., 1991. *Worldwide Nuclear Power Reactors with Passive and Inherent Safety*. Oak Ridge National Lab, Oak Ridge, TN. Report, ORNL/TM-11907 <https://www.osti.gov/biblio/6365276>.
- Fu-Bertaux, X., May 2011. *Financing the Sustainable Energy Transition: Rising Support from Multilateral Development Banks*. Worldwatch Institute.
- Ganino, 2014. http://www.ganino.com/hyperion_power_generation_accumulators.
- GE Hitachi, 2015. <http://gehitachiprism.com/what-is-prism/how-prism-works/>.
- Gen4energy, 2013. <http://www.gen4energy.com/>.
- Ghosh, A., Das, K., Basu, D., Miller, L., 2014. Soil structure and fluid interaction assessment of new modular reactor: Part-2-numerical study of soil reactor structure interaction. In: *Proceedings of the ASME 2014 Small Modular Reactors Symposium*, April 15–17, Washington DC., <https://doi.org/10.1115/SMR2014-3318>. SMR2014-3318, V001T02A003; 9 pages <https://asmedigitalcollection.asme.org/SMR/proceedings-abstract/SMR2014/45363/V001T02A003/286000>.
- Grubler, A., 2010. The costs of the French nuclear scale-up: a case of negative learning by doing. *Energy Policy* 38, 5174–5188.
- IAEA, 2001. *Small and medium sized reactors: Status and prospects*. In: *International Seminar, Egypt*. ISBN 92-0-114802-X https://www-pub.iaea.org/MTCD/Publications/PDF/CSPS-14-P/CSP-14_part1.pdf.
- IAEA, 2003. <http://www.iaea.org/NuclearPower/Downloadable/FR/booklet-fr-2013.pdf>.
- IAEA, 2011a. *Status of Small Medium Sized Reactor Designs*. IAEA.
- IAEA, 2011b. http://www.iaea.org/NuclearPower/Downloads/Technology/meetings/2011-Jul-4-8-ANRT-WS/3_USA_mPOWER_BABCOCK_DELee.pdf.
- IAEA, 2012. <https://aris.iaea.org/Publications/smr-status-sep-2012.pdf>.
- IAEA, 2013. <https://aris.iaea.org/sites/.%5CPDF%5CNuScale.pdf>.
- Kessides, I., 2012. In: *The Future of the Nuclear Industry Reconsidered: Risks, Uncertainties, and Continued Potential*. World Bank Policy Research Working Paper 6112. <https://openknowledge.worldbank.org/handle/10986/19935?locale-attribute=en>.
- Kidd, S., 2014. Financing nuclear projects—new options? *Nucl. Eng. Int.* <https://www.neimagazine.com/opinion/opinionfinancing-nuclear-projects-new-options-4194341/>.
- Kim, K.K., Lee, W.J., Choi, S., Kim, H.R., Ha, J.J., 2014. SMART: the first licensed advanced integral reactor. *J. Energy Power Eng.* 8, 94–102.
- Krautmann, A., Solow, J., 1988. Economies of scale in nuclear power generation. *South. Econ. J.* 55 (1), 70–85.
- Kumar, N., Besuner, P.M., Lefton, S.A., Agan, D.D., Douglas, D.H., 2012. *Power Plant Cycling Costs*. AES 12047831–2-1 Apter-tek Aptech, National Renewable Energy Laboratory. <http://wind.nrel.gov/public/WWIS/APTECHfinalv2.pdf>.
- Kuznetsov, Y.N., Lisitsa, F.D., Romenkov, A.A., Tokarev, Y.I., 1999. Nuclear plant with VK-300 boiling water reactors for power and district heating grids. In: *ICONE-7335, ICONE-ASME Conference, Japan*. <https://inis.iaea.org/search/searchsingle.asp?recordsFor=SingleRecord&RN=31010887>.
- Li, F., 2014. http://www.iaea.org/NuclearPower/Downloadable/Meetings/2014/2014-04-08-04-11-TM-NPTDS/2_Li01.pdf.
- Lyons, P., 2016. *Challenges: Nuclear Power Today and Megawatt Size Reactors*. In: *Workshop on Safe & Secure Megawatt–Size Nuclear Power WASHINGTON, DC MARCH 2016, Presentation, 3/16/2016*. https://arpa-e.energy.gov/sites/default/files/Weds_Lyons_Landscape.pdf.
- Magan, H.B., et al., 2014. *CAREM Prototype Construction and Licensing Status*. IAEA-CN-164–5S01, IAEA. https://www-pub.iaea.org/MTCD/Publications/PDF/P1500_CD_Web/htm/pdf/topic5/5S01_D.%20Delmastro.pdf.
- Matzie, R., 2015. *Small Modular Reactors: A Call for Action*. http://www.hoover.org/sites/default/files/pages/docs/matzie_smr_diagram_presentation_2015_0.pdf.
- Mingguang, Z., 2013. <https://www.iaea.org/NuclearPower/Downloadable/Meetings/2013/2013-06-18-06-20-TWG-NPTD/36-snerdichina-smr.pdf>.
- Mortensen, J.H., Moelbak, T., Andersen, P., Pedersen, T.S., 1998. Optimization of boiler control to improve the load-following capability of power-plant units. *Control. Eng. Pract.* 6 (12), 1531–1539. ISSN.
- Nathan, S., May 13, 2013. *Prism Project: A Proposal for the UK’s Problem Plutonium*. *The Engineer*. <https://www.theengineer.co.uk/prism-project-a-proposal-for-the-uks-problem-plutonium/>.
- NEI, 2014. <http://www.nei.org/Knowledge-Center/Nuclear-Statistics/Costs-Fuel,-Operation,-Waste-Disposal-Life-Cycle/US-Electricity-Production-Costs-and-Components>.

- NRC, 2013. <http://www.nrc.gov/reactors/advanced/4s.html>.
- NRC, 2014a. <http://www.nrc.gov/reactors/advanced/advanced-files/smr.jpg>.
- NRC, 2014b. <http://www.nrc.gov/reactors/advanced/nuscale.html>.
- NuScale, 2013a. NuScale Announces Major Technology Breakthrough—Safe Cooldown Over Indefinite Timeframe Achievable with No Operator Action, No Power, No Additional Water. <https://www.businesswire.com/news/home/20130416005128/en/NuScale-Announces-Major-Technology-Breakthrough-%E2%80%93-Safe-Cooldown-Over-Indefinite-Timeframe-Achievable-with-No-Operator-Action-No-Power-No-Additional-Water>. April 16.
- NuScale, 2013b. <http://www.nuscalepower.com/triplecrown.aspx>.
- NuScale, October 22, 2014. Retrieved February 3, 2015, from: <http://www.nrc.gov/reactors/advanced/nuscale.html>.
- OKBM, 2015. <http://www.okbm.nnov.ru/npp#regional>.
- Park, K.B., 2011. <https://nucleus.iaea.org/sites/INPRO/df3/Session%201/08.Park.pdf>.
- Phung, D., 1987. Theory and Evidence for Using the Economy-of-Scale Law in Power Plant Economics. Oak Ridge National Laboratory. Report ORNL/TM-10195 <https://www.osti.gov/biblio/6304295-theory-evidence-using-economy-scale-law-power-plant-economics>.
- Prasad, S., 2012. http://www.andrew.cmu.edu/user/ayabdull/Prasad_SMRDesc.pdf.
- Pratson, L., Haerer, D., Patino-Echeverri, D., 2013. Fuel prices, emission standards, and generation costs for coal vs natural gas power plants. *Environ. Sci. Technol.* 47 (9), 426–433.
- PRISM, 1994. NUREG-1368. <https://www.nrc.gov/docs/ML0634/ML063410561.pdf>.
- Reuters International, October 08, 2014. Update 5—First New British Nuclear Plant in Decades Wins EU Funding Fight.
- Reyes, J.N., 2012. NuScale plant safety in response to extreme events. NT 5-11-56, *Nucl. Technol.* 178. http://www.nuscalepower.com/images/our_technology/NuScale-Safety-Nucl-Tech-May12-pre.pdf.
- Rosner, R., Goldberg, S., Hezir, J., 2011. Small Modular Reactors—Key to Future Nuclear Power Generation in the U.S. Energy Policy Institute of Chicago (EPIC). <https://www.energy.gov/sites/prod/files/2015/12/f27/ECON-SMRKeytoNuclearPowerDec2011.pdf>.
- Safety of Nuclear Power Reactors, February 2015. Retrieved February 15, 2015, from: <http://world-nuclear.org/infor/Safety-and-Security/Safety-of-Plants/Safety-of-Nuclear-Power-Reactors/>.
- Solan, D., Black, G., Louis, M., Peterson, S., Carter, L., Peterson, S., Bills, R., Morton, B., Arthur, E., June 2010. Economic and Employment Impacts of Small Modular Nuclear Reactors. Center for Advanced Energy Studies' Energy Policy Institute. <http://epi.boisestate.edu/download.aspx?File=/3494/economic%20and%20employment%20impacts%20of%20smrs.pdf>.
- State of New Jersey, 2014. http://www.state.nj.us/dep/cleanair/hearings/.../09_mpower.ppt.
- Toshiba, 2015. <http://www.toshiba.co.jp/nuclearenergy/english/business/4s/features.htm>.
- Toshiba CREIPI, June 03, 2013. Super-Safe, Small and Simple Reactor (4S, Toshiba Design). Retrieved February 03, 2015, from: <https://aris.iaea.org/sites/..%5CPDF%5C4S.pdf>.
- US Department of Energy Loan Programs Office, October 2014. Federal Loan Guarantees for Advanced Nuclear Projects. OMB Control Number: 1910-5134.
- US Nuclear Regulatory Commission, 2011a. Policy Issue Information: Insurance and Liability Regulatory Requirements for Small Modular Reactor Facilities. <http://pbadupws.nrc.gov/docs/ML1133/ML113340133.pdf>.
- US Nuclear Regulatory Commission, 2011b. Policy Issue Information: Security Regulatory Framework for Certifying, Approving, and Licensing Small Modular Nuclear Reactors (M110329). <http://pbadupws.nrc.gov/docs/ML1129/ML112991113.pdf>.
- US Nuclear Regulatory Commission, August 2012. Report to Congress: Advanced Reactor Licensing. <http://pbadupws.nrc.gov/docs/ML1215/ML12153A014.pdf>.
- US Nuclear Regulatory Commission, May 30, 2013. Memorandum to Commissioners: Current Status of the Source Term and Emergency Preparedness Policy Issues for Small Modular Reactors. <http://pbadupws.nrc.gov/docs/ML1310/ML13107A052.pdf>.
- Van Tuyle, G.J., et al., 1989. Examining the inherent safety of PRISM, SAFR, and the MHTGR. *Nucl. Saf.* 91, 185–202.
- Von Deobschuetz, P., 2005. https://www.iaea.org/OurWork/ST/NE/NEFW/CEG/documents/ws052005_6E.pdf.
- Vujic, J., Bergmann, R., Skoda, R., Miletic, M., 2012. Small modular reactors: simpler, safer, cheaper? *Energy* 45, 288–295.
- W, 2013. <http://www.westinghousenuclear.com/SMR/index.htm>.
- Wheeler, B., April 01, 2012. Developing small modular reactor designs in the U.S. *Power Eng.* <http://www.power-eng.com/articles/npi/print/volume-5/issue-2/nucleus/developing-small-modular-reactor-designs-in-the-us.html>.
- World Bank Technical Paper #154, April 1994. Environmental Assessment Sourcebook Volume III: Guidelines for Environmental Assessment of Energy and Industry Projects by the World Bank Environment Department. pp. 83–89.
- World Nuclear Association, 2008. The Economics of Nuclear Power. <http://www.world-nuclear.org/uploadedfiles/org/info/pdf/economicsnp.pdf>.

20.2

Current status of SMRs and S&MRs development in the world

Igor L. Pioro^a, Romney B. Duffey^b, Pavel L. Kirillov^{c,*},
Georgy V. Tikhomirov^d, Nikita Dort-Goltz^a, and Anton D. Smirnov^d

^aFaculty of Energy Systems and Nuclear Science, University of Ontario Institute of Technology, Oshawa, ON, Canada ^bIdaho Falls, ID, United States ^cState Scientific Centre of the Russian Federation—Institute of Physics and Power Engineering (IPPE) named after A.I. Leipunsky, Obninsk, Russia ^dNational Research Nuclear University MEPhI (Moscow Engineering Physics Institute), Moscow, Russia

Nomenclature

P Pressure, MPa
s Specific entropy, J/kg K
T Temperature, °C

Subscripts

cr critical
el electrical
in inlet
out outlet
sat saturated or saturation
th thermal

Abbreviations

4S Super Safe Small and Simple (Japan)
ABV-6E Nuclear Modular Water-cooled reactor 6-MW_{el} (ABV-6E—Атомный Блочный Водяной (in Russian abbreviations) (Russia))
ACP Advanced Chinese Pressurized-water reactor
ACPR Advanced Chinese Pressurized-water Reactor
AECL Atomic Energy of Canada Limited
AFR Advanced sodium-cooled Fast Reactor (USA)
AGR Advanced Gas-cooled Reactor
A-HTR-100 Advance High-Temperature Reactor 100 MW_{th} (South Africa)
AHWR Advanced Heavy Water Reactor
ALFRED Advanced Lead Fast Reactor European Demonstrator (Italy)
ANL Argonne National Laboratory
ANTARES Areva's New Technology and Advanced gas-cooled Reactor for Energy Supply (France)
AO Joint Stock Company
ARC Advanced Reactor Concept (USA)
ARIS Advanced Reactors Information System (IAEA)
ASME American Society of Mechanical Engineers

* Professor P.L. Kirillov has participated in preparation of this Chapter, unfortunately, he has passed away on October 10, 2021 (for details, see <https://asmedigitalcollection.asme.org/nuclearengineering/issue/8/2>).

ASTRID	Advanced Sodium Technological Reactor for Industrial Demonstration (France)
Ave.	Average
BARC	Bhabha Atomic Research Centre (India)
BN	Fast Sodium (reactor) (БН—Быстрый Натриевый (in Russian abbreviations) (Russia))
BOP	Balance Of Plant
BREST-OD	Fast Reactor with Inherent safety Lead Coolant—Experimental Demonstration (БРЕСТ-ОД—Быстрый Реактор Естественной безопасности со Свинцовым Теплоносителем—Опытной Демонстрационный or Быстрый Реактор Естественной безопасности—Опытной Демонстрационный (in Russian abbreviations) (Russia))
BWR	Boiling Water Reactor
CA	Copenhagen Atomics (Denmark)
CAD	Computer-Aided Design
CAE	Computer-Aided Engineering
CANDU®	CANada Deuterium Uranium (reactor)
CAP	China Advanced Passive
CAREM	Central ARgentina de Elementos Modulares (Argentina)
CAS	Chinese Academy of Sciences
CCGT	Combined-Cycle Gas-Turbine
CCR	Compact Containment boiling-water Reactor (Japan)
CDF	Core Damage Frequency
CEA	Atomic Energy Commission (France)
CFR	China Fast Reactor
CGNPC	China General Nuclear Power Group
CIAE	China Institute of Atomic Energy
CIIRC	Czech Institute of Informatics, Robotics and Cybernetics
CMSR	Compact Molten Salt Reactor (Denmark)
CNEA	National Atomic Energy Commission (Argentina)
CNNC	China National Nuclear Corporation
CNP	China Nuclear Power
CPF	Coated-Particle Fuel
Cont.	Continuous
Corp.	Corporation
CRIEPI	Central Research Institute of Electric Power Industry (Japan)
CTU	Czech Technical University
DCNS	Direction des Constructions Navales (France)
DHR	District Heating Reactor (China)
DMS	Double MS (Modular Simplified and Medium Small) (Japan)
EDF	Électricité De France
Eff.	Efficiency
EFPD	Effective Full Power Day
EL	Element(s)
ELFR	European Lead-cooled Fast Reactor (Italy/EU)
EM²	Energy Multiplier Module (USA)
Eng.	Engineering
ENHS	Encapsulated Nuclear Heat Source (USA)
Enrich.	Enrichment
EPR	European Pressurized-water Reactor (Areva, France)
EU	European Union
FBNR	Fixed Bed Nuclear Reactor (Brazil)
FCM	Fully Ceramic Micro-encapsulated (fuel)
Fed.	Federal
FNPDS	Floating Nuclear Power & Desalination System
FNTThPP	Floating Nuclear Thermal-Power Plant
FOAK	First-Of-A-Kind

G4M	Gen4 Module (USA)
GE	General Electric (USA)
GEH	GE-Hitachi Nuclear Energy
GMFR	General Atomics Modular Fast Reactor (USA)
Gr.	Group
GT-MHR	Gas Turbine-Modular Helium Reactor (Russia/USA)
GTHTR300	Gas Turbine High-Temperature Reactor 300 MW _{el} (Japan)
HALEU	High-Assay Low-Enriched Uranium
HAPPY200	Heating-reactor of Advanced low-Pressurized and Passive safety system 200-MW _{th}
HEU	Highly Enriched Uranium
HM	Heavy Metal
HTGR	High-Temperature Gas-cooled Reactor
HTMR-100	High-Temperature Modular Reactor 100-MW _{th} (S. Africa)
HTR-PM	High-Temperature Reactor Pebble-bed Modular (China)
HTTR	High-Temperature Test Reactor
HWR	Heavy Water Reactor (can be PHWR or Light-water-cooled Heavy-water-moderated Reactor)
IAEA	International Atomic Energy Agency
IMR	Integrated Modular water Reactor (Japan)
IMSR	Integral Molten Salt Reactor (Canada)
Inc.	Incorporated
INET	Institute of Nuclear Energy and Technology (China)
Int.	International
IRIS	International Reactor Innovative and Secure
JAEA	Japan Atomic Energy Agency
JAERI	Japan Atomic Energy Institute
JSC	Joint Stock Company
KAERI	Korean Atomic Research Institute (S. Korea)
KALIMER	Korea Advanced LIquid MEtal Reactor (S. Korea)
KARAT	Boiling Nuclear Reactor of Autonomous Heat Supply (КАРАТ—Кипящий Атомный Реактор для Автономного Теплоснабжения (in Russian abbreviations) (Russia))
KLT	Container-carrier cargo-Lighter Transport (reactor) (КЛТ—Контейнеровоз Лихтеровоз Транспортный (реактор) (in Russian abbreviations) (Russia))
KP-FHR	Kairos Power Fluoride-salted-cooled High-temperature Reactor (USA)
Lab.	Laboratory/Laboratories
LBE	Lead-Bismuth-Eutectic
LEADIR-PS100	LEAD-cooled Integral Reactor-Passively Safe 100-MW _{th}
LEU	Low Enriched Uranium
LFR	Lead-cooled Fast Reactor
LFR-AS/TL-200/X	Lead-cooled Fast Reactor-Amphora-Shaped/Transportable Long-lived-200-MW _{el} (Luxembourg)
LFTR	Liquid-Fluoride Thorium Reactor (USA)
LHR	Light-water-cooled Heavy-water-moderated Reactor
LLC	Limited Liability Company
LMFR	Liquid-Metal-cooled Fast Reactor
LMR	Liquid-Metal-cooled Reactor
LSPR	LBE-Cooled Long-Life Safe Simple Small Portable Proliferation-Resistant Reactor (Japan)
Ltd.	Limited
LWR	Light Water Reactor
MCFR	Molten Chloride Fast Reactor (USA)
MCSFR	Molten Chloride Salt, Fast Reactor (Canada/USA)
MF	Metallic Fuel
MHI	Mitsubishi Heavy Industries (Japan)
MHR	Modular Heat Reactor (MHR—Модульный Тепловой Реактор (in Russian abbreviations) (Russia))

MHR-T	Modular Helium Reactor-high Temperature (Russia)
Mk1 PB-FHR	Mark 1 Pebble-Bed Fluoride-salt-cooled High-temperature Reactor (USA)
MMR	Micro Modular Reactor (USA)
MoveluX	Mobile-very-small reactor for local utility in X-mark (Japan)
MOX	Mixed OXide (fuel)
MRX	Marine Reactor (Japan)
MSF	Molten-Salt Fuel
MSK	Medvedev-Sponheuer-Karnik scale
MSR	Molten Salt Reactor
MSTW	Molten Salt Thermal Wasteburner reactor (Denmark)
Nat.	National
N/A	Not Available/Not Applicable
NHR	Nuclear Heating Reactor (China)
NIKIET	Научно-Исследовательский и Конструкторский Институт ЭнергоТехники (in Russian abbreviations) (N.A. Dollezhal Research and Development Institute of Power Engineering (RDIPE)) (Russia)
NPCI	Nuclear Power Corporation of India
NPP	Nuclear Power Plant
NUWARD	NUclear for WARD (France)
OKBM	Experimental Design Bureau of Mechanical-engineering (ОКБМ—Опытно-Конструкторское Бюро Машиностроения (in Russian abbreviations) (Russia))
PB-FHR	Pebble-Bed Fluoride-salt High-temperature Reactor
PBMR	Pebble-Bed Modular Reactor
PBWFR	Pb-Bi-cooled direct contact Boiling Water Fast Reactor (Japan)
PEACER	Proliferation-resistant Environment-friendly Accident-tolerant Continuable and Economical Reactor (S. Korea)
PeLUI	Pembangkit Listrik & Uap panas Industri (Electric Power and Industrial Hot Steam Plant) (Indonesia)
PGSFR	Prototype Gen-IV Sodium-cooled Fast Reactor
PHWR	Pressurized Heavy-Water Reactor
PP	Power Plant
PRISM	Power Reactor Innovative Small Module
PWR	Pressurized Water Reactor
QA	Quality Assurance
QC	Quality Control
RAPID-L	Refueling by All Pins Integrated Design-Lunar-base (Japan)
R&D	Research and Development
RDE	Reactor Daya Eksperimen (Experimental Power Reactor) (Indonesia)
RDIPE	Research and Development Institute of Power Engineering (Russia)
RITM-200M	Reactor Integral Type Modular 200-MW _{el} Modernized (РИТМ-200М—Реактор Интегрального Типа Модульный мощностью 200 МВт Модернизационный (in Russian abbreviations) (Russia))
RPV	Reactor Pressure Vessel
RUTA	Reactor Plant for Heat Supply with Atmospheric pressure in the first circuit (РУТА—Реакторная Установка для Теплоснабжения с Атмосферным давлением в первом контуре (in Russian abbreviations) (Russia))
S.	South
SC-HTGR	Steam Cycle High-Temperature Gas-cooled Reactor (USA)
SCWR	SuperCritical Water-cooled Reactor
SEALER	Swedish Advanced Lead Reactor
SFR	Sodium Fast Reactor
SG	Steam Generator
SINAP	Shanghai Institute of Applied Physics (China)
SmAHTR	Small modular Advanced High-Temperature Reactor (USA)
SMART	System-integrated Modular Advanced Reactor (S. Korea)
SMR	Small Modular Reactor, also, Small and Medium size Reactor
S&MRs	Small- and Medium-size Reactors

SNERDI	Shanghai Nuclear Engineering and Design Institute (China)
SNF	Spent Nuclear Fuel
SNP	State Nuclear Power (China)
SNUPPS	Standardized Nuclear Unit Power Plant System
SPIC	State Power Investment Corporation (China)
SSR	SuperSafe Reactor (Canada)
SUPERSTAR	Sustainable Proliferation-resistance Enhanced Refined Secure Transportable Autonomous Reactor (USA)
SVBR	Lead-Bismuth Fast Reactor (SVBR—Свинцово-Висмутный Быстрый Реактор (in Russian abbreviations) (Russia))
Techn.	Technologies
Th.	Thermal
TMSR-LF	Thorium Molten Salt Reactor-Liquid Fuel (China)
Tokyo Tech.	Tokyo Institute of Technology (Japan)
TRISO	TRi-structural ISOtropic
TRU	Transuranic
TWR-P	Traveling Wave Reactor-Prototype (USA)
UC	University of California
UCO	Uranium OxyCarbide (fuel)
UK	United Kingdom
UNITHERM	UNIversal THERMal reactor (Russia)
Univ.	University
UOIT	University of Ontario Institute of Technology
USA	United States of America
USNC	Ultra Safe Nuclear Corporation (USA)
UWB	University of West Bohemia (Czech Republic)
VBER	Water Safe Power Reactor (ВБЭР—Водяной Безопасный Энергетический Реактор (in Russian abbreviations) (Russia))
VHTR	Very High Temperature Reactor
VK	Water-cooled Boiling (BK—Водоохлаждаемый Кипящий (in Russian abbreviations) (Russia))
VVER	Water-Water Power Reactor (ВВЭР—Водо-Водяной Энергетический Реактор (in Russian abbreviations) (Russia))
W-SMR	Westinghouse Small Modular Reactor (USA)
WLFR	Westinghouse Lead-cooled Fast Reactor
WPu	Weapons-grade Plutonium

20.2.1 Small Modular and Small- & Medium-size Reactors (SMRs and S&MRs)

This Chapter is in addition to Chapter 20.1 in which more details are provided on selected SMRs concepts/designs. Also, this Chapter is mainly based on our previous publications [Pioro et al. \(2020a,b\)](#). Additional sources with more details on various SMRs are [ARIS IAEA \(2020a\)](#), which is updated once in 2 years, i.e., should be published in 2022, and [Handbook of Small Modular Nuclear Reactors \(2021\)](#).

Before a general discussion on Small Modular and Small- and Medium-size Reactors, which currently go under a single acronym SMRs, we have to separate these two groups of reactors, because they are not the same. Therefore, new acronym(s) should be introduced:

- (1) Small Modular Reactors (SMRs), i.e., modular-type reactors with installed capacities $\leq 300 \text{ MW}_{\text{el}}$, with claimed features of “modularity” in design, production, and/or construction. Currently, only four SMRs: Two Russian Pressurized Water Reactors (PWRs)—KLT-40S are in operation as a floating Nuclear Power Plant (NPP) (from December of 2019) and two Chinese High Temperature Reactors (HTRs) Pebble-bed Module (PM) (helium cooled, VHTR concept) are in operation from March of 2022. Also, a new acronym started to be used Advanced Modular Reactors (AMRs), i.e., reactors based on

some new or so far not deployed technology or concept, but having similar claimed features of “modularity” in design, production, and/or construction as SMRs.

- (2) S&MRs, which have installed capacities $\leq 300 \text{ MW}_{\text{el}}$ (Small) (in total 27 reactors in the world and $>300\text{--}700 \text{ MW}_{\text{el}}$ (Medium-size) (in total 85 reactors), respectively, many with claimed features of “modularity” in design, production, and/or construction.

In this case, we must also define what is meant or implied by the widespread use of the terms “module,” “modular design,” and “modular construction.” As adopted in building, modular design and construction usually refers simply to the use of off-site prefabricated construction and the on-site assembly of multiple (identical or duplicate module) sections (or part sub-modules) including for different functions and uses. Since there is no restraint on the definition, degree, extent or type of what constitutes a modular “module” (it could be the entire reactor core, the entire reactor, or the entire unit, or any such sub-units), we have *not* distinguished between the differing SMR nomenclatures or claims. Therefore, to avoid any misunderstanding and ambiguity, it is proposed to use the following acronym—S&MRs, i.e., small- and medium-size reactors. Currently, we have a relatively large number of S&MRs in operation in the world (in total 112). Also, it should be noted that actual SMRs can be included into S&MRs, but many S&MRs are not actual modular reactors.

The overarching requirements and objectives for any and all new nuclear reactors of any and all sizes are as the following (ARIS IAEA, 2020a):

- Safer than previous “generations”;
- Low financial risk exposure and capital cost;
- Ease and speed of build;
- Readily licensable—anywhere, anytime;
- Simple to operate and secure;
- Assured fuel supply and sustainability;
- Providing social value and acceptance, and, of course;
- Still be competitive.

We have examined the status of SMRs/S&MRs, which are today’s a very “hot” topic in nuclear engineering worldwide (Pioro et al., 2019; Handbook, 2016, 2021; ARIS IAEA, 2020a, b) and many variants exist in a plethora of potential design concepts using a wide variety of coolants, fuels, and core physics. According to the IAEA ARIS (Advanced Reactors Information System) data (ARIS IAEA, 2020a, b; Handbook, 2021), there are about 72 reactor designs/concepts, which can be classified as: (1) Water-cooled reactors (land based)—24 (see Table 20.2.1); (2) Water-cooled reactors (marine based)—6 (see Table 20.2.2); (3) High-temperature gas-cooled reactors—12 (see Table 20.2.3); (4) Fast-neutron-spectrum reactors—17 (see Table 20.2.4); (5) Molten-salt reactors—11 (see Table 20.2.5); and (6) Other reactors—2 (see Table 20.2.6). However, an additional number of SMRs/S&MRs (in total 27) was added into Tables 20.2.1–20.2.6 from other sources. Below Table 20.2.6 SMRs and S&MRs are listed just by numbers per each country, which develops these reactors.

Much design data is considered or labeled “proprietary” and, hence, not in the public domain. For the all-important status of the designs, we must rely here on published statements and claims, which are subject to some interpretation. We classify according to the typical phases in the normal design and development evolution process, which assists in characterizing the relative “maturity” or potential technical “feasibility,” recognizing that some may have had prior development, some may have a pause or hiatus between phases, and not all aspects in a phase may be at the same stage at the same time. We do not pass judgment regarding the viability, development potential, and probability of demonstration success of these alternatives, which will be ultimately determined in and by the evolving national and international marketplaces and any related enabling governmental policies.

Also, the phases may not be totally distinct in that they continually merge, transition and may overlap as the design progresses. A priori we don't know if all developers even use the same terminology, so here we, at least, attempt to standardize and define the status as far as possible to allow or enable intercomparison.

In addition, the degree and extent of independent reviews, safety and risk-analysis requirements, and the national licensing process will vary. The terminology and status may vary according to whether the design is in the commercial or governmental domain, or directly or indirectly subsidized, and whether the schedule and/or demonstration cost is known or even revealed.

The actual timing of the phases may also vary according to the market conditions, funding revenue, budget and incurred expenses, and R&D and licensing schedules.

20.2.1.1 Preconceptual

- Basic ideas, sketches, preliminary or scoping calculations, and possible parameter ranges, free-wheeling options in performance and costs, continual changes, objective evolution, evaluation of acceptable items or targets, competitive analyses, and concept scrubbing.

20.2.1.2 Conceptual

- Firm outline, optional layouts, R&D needs, design “cartoons”, range limits, performance goals and design targets set, initial physics and safety feasibility, economic and size requirements established, “show stoppers” identified, outline costing, project scope defined.

20.2.1.3 Basic

- Main layout, thermal limits and fuel requirements, commercial risk assessment, safety argument defined, R&D program initiated, initial CAD/CAE diagrams, system requirements specified, plant performance, and safety-analysis models, initial investment secured, documentation underway, initial independent reviews undertaken, preliminary business case made.

20.2.1.4 Developmental

- Design and layout in computer or CAD/CAE format, physics and core design semicomplete, engineering analyses underway, scoping costing, potential project schedule, safety analysis underway, confirmatory R&D in progress, performance and safety margins defined, fuel cycle and components definition, and refining of design optimization(s), commitments to proceed, and milestones established.

20.2.1.5 Preliminary

- Transition to formal project management, design review, uncertainties defined, layout fixed, formal change control initiated, reference parameters established, costing re-evaluated, fuel cycle, physics and thermal performance optimized, design changes subject to controls, R&D results incorporated, BOP and systems layout fixed, modules and manufacturing defined, supply chain established, bid estimate uncertainties defined, formal licensing basis established, desired build schedule established, project management structure and business controls, external independent review(s).

20.2.1.6 Final/Certified

- “Frozen” design, final safety analyses completed, R&D finished, engineering work nearly complete, final documentation of design, licensing basis, and/or “certification” review underway, commercial contracts

and suppliers in place, systems for QA/QC/change controls, all major construction tasks and sequence established and proven, advanced or long-lead components and manufacturing, interface agreements and integrated customer schedule in place, business model and financing established.

20.2.1.7 Construction

- Authorization to proceed, site preparation completed, project management assures product delivery, overall schedule and costs known, final work breakdown schedule, on-site work underway, prototype, FOAK or “demonstration” unit, manufacturing and component delivery in progress, interface agreements refined, building and system installation, staff training and assignments, licensing finalized or only subject to final review/verification, customer acceptance criteria, commissioning and operation planned, contingency refined.

20.2.2 SMRs and S&MRs by type

The following [Tables 20.2.1–20.2.6](#) list SMRs and S&MRs concepts by type (data were taken from [Pioro et al., 2020b; Handbook, 2016, 2021; ARIS IAEA, 2020a](#)). There are six types of SMRs and S&MRs concepts known so far: (1) Land-based Water-cooled (33 in total) (see [Table 20.2.1](#)); (2) Marine-based Water-cooled (7 in total) (see [Table 20.2.2](#)); (3) High-Temperature Gas-cooled (helium-cooled) (21 in total) (see [Table 20.2.3](#)); (4) Fast-Neutron-Spectrum (mainly sodium- and lead-cooled, but also, lead-bismuth-cooled and helium-cooled) (26 in total) (see [Table 20.2.4](#)); (5) Molten-Salt-cooled (17 in total) (see [Table 20.2.5](#)); and (6) Other Types (lead-cooled and based on heat pipes) (4 SMRs) (see [Table 20.2.6](#)).

20.2.3 SMRs and S&MRs by countries

The following [Tables 20.2.7–20.2.24](#) list SMRs and S&MRs concepts by countries according to decreasing numbers of reactors (data were taken from [Pioro et al., 2020a; Handbook, 2016, 2021; ARIS IAEA, 2020a](#)). Countries, which develop SMRs and S&MRs, are: (1) USA (27 in total) (see [Table 20.2.7](#)); (2) Russia (15 in total) (see [Table 20.2.8](#)); (3) China (13 in total) (see [Table 20.2.9](#)); (4) Japan (12 in total) (see [Table 20.2.10](#)); (5) Canada (6 in total) (see [Table 20.2.11](#)); (6) France (5 in total) (see [Table 20.2.12](#)); (7) South Korea (5 in total) (see [Table 20.2.13](#)); (8) South Africa (4 in total) (see [Table 20.2.14](#)); (9) UK (4 in total) (see [Table 20.2.15](#)); (10) Denmark (3 in total) (see [Table 20.2.16](#)); (11) Czech Republic (2 in total) (see [Table 20.2.17](#)); (12) India (2 in total) (see [Table 20.2.15](#)); (13) Italy (2 in total) (see [Table 20.2.19](#)); (14) Luxembourg (2 in total) (see [Table 20.2.20](#)); (15) Argentina (4 in total) (see [Table 20.2.21](#)); (16) Brazil (1 in total) (see [Table 20.2.22](#)); (17) Indonesia (1 in total) (see [Table 20.2.23](#)); and (18) Sweden (1 in total) (see [Table 20.2.24](#)).

Total number of SMRs and S&MRs by countries in the alphabetical order:

S. Africa—4 HTGRs.

Argentina—1 PWR.

Canada—6 (1 SCWR +1 PHWR; 1 HTGR; 2 MSRs; 1 Other).

China—13 (7 PWRs land-base; 1 PWR marine-based; 2 HTGR; 1 Fast Reactor; and 2 MSR).

Czech Republic—2 (1 HWR; and 1 MSR).

Denmark—3 MSRs.

France—5 (2 PWRs; 2 HTGRs; and 1 SFR).

India—2 PHWRs.

Indonesia—1 HTGR.

Italy—2 LFRs.

Japan—12 (4 PWRs land-base; 2 HTGR; 4 Fast Reactors; 1 MSR; and 1 other type reactor).

Luxemburg—2 (2 LFRs).

S. Korea—5 (1 PWR and 4 Fast Reactors).

Russia—15 (5 PWRs land-base; 5 PWRs marine-based; 3 HTGRs; and 2 Fast Reactors).

Sweden—1 LFR.

UK—4 (PWR; HTGR; and 2 MSRs).

USA—27 (5 PWRs land-base; 5 HTGRs; 9 Fast Reactors; 6 MSRs; and 2 other type reactors).

For SMRs developed in Canada (see [Table 20.2.11](#)) the following information in terms of their readiness for implementation is provided by the Canadian Nuclear Safety Commission (CNSC) (Oct. 30, 2021): <https://www.cnsccsn.gc.ca/eng/reactors/power-plants/pre-licensing-vendor-design-review/index.cfm#R3>:

1. **Completed prelicensing Vendor Design Reviews (VDR)** (Note: Due to the commercially sensitive and proprietary information in the full report, the CNSC is only able to post the Executive Summaries. For any detailed information concerning the results of a VDR, please contact the associated vendor).
 - **Moltex Energy—SSR-W300** (Stable Salt Reactor-Wasteburner, 300MW_{el}), UK: Phase 1 Pre-Licensing Vendor Design Review Executive Summary: Moltex Energy (May 2021).
 - **SMR, LLC.—SMR-160**, USA, Holtec Int.: Phase 1 Pre-Licensing Vendor Design Review Executive Summary: SMR, LLC. (Aug. 2020).
 - **ARC Nuclear Canada Inc.—ARC-100** (Advanced Reactor Concept—100-MW_{el} integrated sodium-cooled fast reactor with a metallic uranium alloy core): Phase 1 Pre-Licensing Vendor Design Review Executive Summary: ARC Nuclear Canada Inc. (Oct. 2019).
 - **Ultra Safe Nuclear Corporation (USNC)—MMR** (Micro Modular Reactor, He-cooled), USA: Phase 1 Pre-Licensing Vendor Design Review Executive Summary: Ultra Safe Nuclear Corporation (USNC) (Feb. 2019) Phase 2: Assessment in progress (June 2021).
 - **Terrestrial Energy Inc.—IMSR 400** (Integral MSR, 190MW_{el}), Canada: Phase 1 Executive Summary: Pre-Project Review of Terrestrial Energy's 400-MW_{th} Integral Molten Salt Reactor (IMSR400) (PDF, Nov. 2017).
 - Phase 2: Assessment in progress (Dec. 2018).
2. **Vendor design review service agreements in force between vendors and CNSC.**
 - **NuScale Power, LLC—NUScale PWR** (60MW_{el}), USA: Phase 2 Assessment in progress (Jan. 2020).
 - **U-Battery Canada Ltd.—U-Battery HTGas (He)** (4MW_{el}), UK: Phase 1 Pending.
 - **GE-Hitachi Nuclear Energy—BWRX-300**: Phase 2 Assessment in progress.
 - **X Energy, LLC—Xe-100 HTGas (He)** (80 MW_{el}), USA: Phase 2 Assessment in progress.
 - **LeadCold Nuclear Inc.—SEALER** (Molten Lead, 3MW_{el}), Sweden: Phase 1 On hold at vendor's request (Jan. 2021).
3. **Vendor design review service agreement between vendors and CNSC under development.**
 - **Westinghouse Electric Company, LLC,—eVinci Micro Reactor** (solid core and HPs) (up to 25MW_{el}), USA: Phase 2 Applied for (Feb. 2018).
 - **StarCore Nuclear—StarCore Module HTGas (He)** (10MW_{el}): Phase 1 & 2 Pending.

Table 20.2.1. Land-based Water-cooled SMRs and S&MRs (33 in total)

Country	Design	Output MW _{el/th} = Th.Eff., %	Type	Designers	Phase	Fuel enrichment/ cycle, years	Fuel type
Argentina	CAREM	30/100 = 30	PWR	CNEA	Construction	3.1%/1.2	UO ₂
Brazil	FBNR	70/134 = 52.2	PWR	Fed. University of Rio Grande do Sul	Conceptual	N/A/N/A	TRISO
Canada (1)	CANDU SMR	300/960 = 31.25	PHWR	Candu Energy Inc.	Conceptual	–/On-line	UO ₂
Canada (2)	SSR	300/667 = 45	SCWR ^a	AECL	Conceptual	Enriched	U or Th
China (1)	ACP100	125/385 = 33	PWR	CNNC	Basic	<5%/2	UO ₂
China (2)	DHR400	–/400 = N/A	LWR	CNNC	Basic	<5.0%/0.8	UO ₂
China (3)	CAP200	>200/600 ≥30	PWR	CGNPC	Conceptual	4.2%/2	UO ₂
China (4)	CNP-300	300–340/1000 =30–34	PWR	CNNC	Operational in China/Pakistan	<5%/1.25	UO ₂
China (5)	SNP350	350/1035 = 33.8	PWR	SNERDI	Conceptual	<5%/N/A	UO ₂
China (6)	NHR-200II	–/200 = N/A	PWR	INET	Final	<5%/N/A	UO ₂
China (7)	HAPPY200	–/200 = N/A	PWR	SPIC	Final	N/A/N/A	N/A
Czech Republic	TEPLATOR	–/50 = N/A	HWR	UWB Pilsen & CIIRC CTU	Conceptual	<1.2%/0.83	Spent VVER- 400 fuel
Several countries	IRIS	335/1000 = 34	PWR	IRIS Consortium	Conceptual	5%/4	UO ₂ /MOX
France	NUWARD	300–400/– = N/A	PWR	CEA, EDF, Naval Gr., TechnicAtome	Preliminary	N/A/N/A	N/A
India (1)	AHWR-300- LEU	304/920 = 33	LHR (HWR)	BARC	Conceptual	<5% (MOX)/Cont.	Th-U or Th-Pu, MOX

Table 20.2.1. Land-based Water-cooled SMRs and S&MRs (33 in total)—cont'd

Country	Design	Output MW _{el} /th = Th.Eff., %	Type	Designers	Phase	Fuel enrichment/ cycle, years	Fuel type
India (2)	PHWR-220	235/755 = 31.2	PHWR	NPCI Ltd.	16 Units Operational	<5%/Cont.	UO ₂
Japan (1)	DMS	300/840 = 36	BWR	Hitachi-GE	Basic	<5%/2	UO ₂
Japan (2)	IMR	350/1000 = 35	PWR	MHI	Conceptual	4.8%/2.2	UO ₂
Japan (3)	CCR	423/1268 = 33.4	BWR	Toshiba Corp.	Conceptual	N/A/2	N/A
Japan (4)	MRX	33.3/100 = 33.3	PWR	JAERI	Final	4.3%/3.5	UO ₂
Korea S.	SMART	100/330 = 30	PWR	KAERI	Certified	<5%/3	UO ₂
Russia (1)	ELENA	0.068/3.3 = 2	PWR	Kurchatov Institute	Conceptual	15.2%/25	UO ₂ (MOX)
Russia (2)	UNITHERM	6.6/30 = 22	PWR	NIKIET	Conceptual	19.8%/16.7	UO ₂
Russia (3)	RUTA-70	—/70 = N/A	PWR	NIKIET	Conceptual	3%/3	Cermet
Russia (4)	KARAT-45	45–50/180 = 25–28	BWR	NIKIET	Conceptual	4.5%/7	UO ₂
Russia (4)	KARAT-100	100/360 = 28	BWR	NIKIET	Conceptual	4%/7.5	UO ₂
Russia (5)	VK-300	250/750 = 33	BWR	NIKIET	Final	4%/6	UO ₂
UK	UK-SMR	443/1276 = 26	PWR	Rolls-Royce	Final	<5%/1.5–2	UO ₂
USA (1)	NuScale	50/160 = 31	PWR	NuScale Power	Preliminary	<5%/2	UO ₂
USA (2)	SMR-160	160/525 = 31	PWR	Holtec Int.	Preliminary	5%/1.5–2	UO ₂
USA (3)	mPower	195/575 = 34	PWR	BWX Techn.	Developmental	<5%/2	UO ₂
USA (4)	W-SMR	>225/800 ≥28	PWR	Westinghouse	Conceptual	<5%/2	UO ₂
USA (5)	BWRX-300	300/— = N/A	BWR	GE-Hitachi	Final	3.4–4.95%/N/A	UO ₂

^a Generation-IV concept.

Table 20.2.2. Marine-based water-cooled SMRs and S&MRs (7 in total)

Country	Design	Output MW _{el/th} = Th.Eff., %	Type	Designers	Phase	Fuel enrichment/ cycle, years	Fuel type
China	ACPR50S	50/200 = 25	PWR	CGNPC	Preliminary	<5%/2.5	UO ₂
France	Flexblue	160/600 = 26.7	PWR	DCNS	Preliminary	<5%/3	UO ₂
Russia (1)	SHELF	6.6/28.4 = 23	Immersed NPP	NIKIET	Preliminary	19.7%/6	UO ₂
Russia (2)	ABV-6E	6–9/38 = 16–24	Floating PWR	OKBM Afrikantov	Final	<20%/10–12	UO ₂
Russia (3)	KLT-40S	35/150 = 23	Floating PWR	OKBM Afrikantov	Operating	18.6%/2.5–3	UO ₂
Russia (4)	RITM-200M	50/175 = 29	Floating PWR	OKBM Afrikantov	Manufactured	<20%/10	UO ₂
Russia (5)	VBER-300	325/917 = 35	Floating NPP	OKBM Afrikantov	Licensing	4.95%/6	UO ₂

Table 20.2.3. High-temperature gas-cooled SMRs and S&MRs (21 in total) (Generation-IV concepts)

Country	Design	Output MW _{el/th} =Th.Eff., %	Designers	Phase	Fuel enrichment/ cycle, years	Fuel type
Africa S. (1)	HTMR-100	35/100 = 35	Steenkampskraal Thorium Ltd.	Conceptual	10%–93%/Online refueling	LEU, Th/LEU, Th/HEU, Th/Pu
Africa S. (2)	A-HTR-100	50/100 = 50	Eskom Holdings SOC Ltd.	Conceptual	LEU or WPu/N/A	CPF
Africa S. (3)	PBMR-400	165/400 = 41.3	PBMR SOC Ltd.	Preliminary	9.6% LEU or WPu/N/A	CPF
Africa S. (4)	PBMR-100	100/250 = 40	PBMR SOC Ltd.	Preliminary	N/A/Online	TRISO-coated UP ₂
Canada	Starcore SMR	20/36 = 55.6	Starcore	Preliminary	N/A/5	TRISO
China (1)	HTR-10	2.5/10 = 25	Tsinghua University/ INET	Operational	17%/On-line	Spherical El. with TRISO particles fuel
China (2)	HTR-PM	210/2 × 250 = 42	INET, Tsinghua University	Construction	8.5%/On-line refueling	Spherical El. with CPF
France (1)	Allegro	–/50–100 = N/A	CEA	Conceptual	N/A/N/A	MOX
France (2)	ANTARES	–/≥600 = N/A	AREVA	Conceptual	N/A/N/A	N/A
Indonesia	RDE/ Micro- PeLUIt	3/10 = 30	BATAN	Preliminary	17%/On-line	Spherical El. with coated particle fuel
Japan (1)	GTHTR300	100–300/<600 ≥17–50	JAEA	Basic	14%/4	UO ₂
Japan (2)	HTTR	–/30 = N/A	JAEA	Operational	3–10 (6 avg)%/ 660 EFPD	UO ₂ TRISO ceramic coated particle
Russia (1)	MHR-100	25–87/215 =12–41	OKBM Afrikantov	Conceptual	LEU < 20%/N/A	CPF

Continued

Table 20.2.3. High-temperature gas-cooled SMRs and S&MRs (21 in total) (Generation-IV concepts)—cont'd

Country	Design	Output MW _{el/th} =Th.Eff., %	Designers	Phase	Fuel enrichment/ cycle, years	Fuel type
Russia (2)	GT-MHR	288/600 = 48	OKBM Afrikantov	Preliminary	LEU or WPu/2.08	CPF
Russia (3)	MHR-T	4 × 206/4 × 600 = 34	OKBM Afrikantov	Conceptual	20%/2.5	CPF
UK (1)	U-Battery	4/10 = 40	URENCO	Preliminary	17%–20%/5	TRISO
USA (1)	Xe-100	75/200 = 37.5	X-energy LLC	Conceptual	15.5%/Online refueling	UCO TRISO
USA (2)	SC-HTGR	272/625 = 43.5	FRAMATOME Inc.	Conceptual	<20%/½ core replaced every 1.5 years	UCO TRISO particle fuel
USA (3)	Prismatic HTR	150/350 = 42.8	General Atomics	Developmental	15.5%/1.5	TRISO-coated UCO
USA (4)	MMR	5/15 = 33.3	USNC	Preliminary	N/A/Never	FCM
USA (5)	HOLOS	3–13/22 = 13.6–59.0	HolosGen	Preliminary	15%/3.5–8	TRISO

Table 20.2.4. Fast-neutron-spectrum SMRs and S&MRs (26 in total) (Generation-IV concepts)

Country	Design	Output $MW_{el/th}$ =Th.Eff., %	Type	Designers	Phase	Fuel enrichment/ cycle, years	Fuel type
China	CFR-600	600/1500 = 40	SFR	CIAE	Construction	N/A/N/A	UO ₂ /MOX
France	ASTRID	600/1500 = 40	SFR	CEA	Preliminary	N/A/N/A	MOX
Italy (1)	ALFRED	125/300 = 41.7	LFR	Ansaldo	Preliminary	N/A/5	MOX
Italy/EU (2)	ELFR	630/1500 = 42	LFR	Ansaldo	Conceptual	N/A/2.5	MOX
Japan (1)	4S	10/30 = 33	LMFR	Toshiba Corp.	Developmental	<20%/N/A	MF (U-Zr)
Japan (2)	LSPR	53/150 = 35.3	SFR	Tokyo Tech.	Developmental	10%–12.5%/12	U-Pu-N/U-Pu-Zr
Japan (3)	PBWFR-150	150/450 = 33.3	LMFR	Tokyo Tech.	Developmental	N/A/10	U-Pu nitride
Japan (4)	RAPID-L	0.2/5 = 4	LMFR	CRIEPI	Operating	40%/10	UN
Korea S. (1)	KALIMER-600	600/1523.4 = 39.4	LMFR	KAERI	Preliminary	N/A/1	U-TRU-Zr
Korea S. (2)	PGSFR	150/400 = 37.5	SFR	KAERI	Preliminary	N/A/~1	U-TRU-Zr
Korea S. (3)	PEACER	300/850 = 35	LMFR	Seoul Nat. University	Conceptual	N/A/1	U-TRU-Zr
Korea S. (4)	MicroURANUS	20/60 = 33.3	LMFR	UNIST	Preconceptual	8%, 10%, 12%/N/A	UO ₂
Luxembourg (1)	LFR-TL-X	5/15 = 33 10/30 = 33 20/60 = 33	LFR	Hydromine Nuclear Energy	Conceptual	19.8%/≥8.33	LEU
Luxembourg (2)	LFR-AS-200	200/480 = 42	LFR	Hydromine Nuclear Energy	Preliminary	14.6%–20.4%–23.2% in Pu/6.7 years for 5 batches	MOX
Russia (1)	SVBR-100	100/280 = 37	LFR	JSC AKME Engineering	Final	<19.3%/0.58–0.67	UO ₂
Russia (2)	BREST-OD-300	300/700 = 43	LFR	NIKIET (RDIPE)	Final	13.5%/2.46–4.1	Mixed U-Pu-N

Continued

Table 20.2.4. Fast-neutron-spectrum SMRs and S&MRs (26 in total) (Generation-IV concepts)—cont'd

Country	Design	Output MW _{el/th} =Th.Eff., %	Type	Designers	Phase	Fuel enrichment/ cycle, years	Fuel type
Sweden	SEALER	3/8 = 38	Lead Cooled	LeadCold	Conceptual	19.75%/27 full power years	UO ₂
USA (1)	SUPERSTAR	120/300 = 40	LMFR	Argonne National Lab.	Conceptual	<12%/15	Particulate- based U-Pu-Zr MF with weapons Pu
USA (2)	EM ²	265/500 = 53	GMFR	General Atomics	Conceptual	14.5% LEU/30	UC
USA (3)	WLFR	>450(Net)/950 ≥47	LFR	Westinghouse	Conceptual	≤19.75%/≥2	Oxide
USA (4)	AFR-100	100/250 = 40	LMFR	Argonne National Lab.	Conceptual	13.5%/N/A	U-Zr
USA (5)	ARC-100	100/260 = 38.5	LMFR	ARC	Final	N/A/20	LEU
USA (6)	G4M (HYPERION)	25/70 = 35.7	LMFR	Gen4 Energy Inc.	Conceptual	19.75%/10	UN
USA (7)	PRISM	311/500 = 62	LMFR	GE-Hitachi	Preliminary	N/A/1.33	U-Pu-Zr metal
USA (8)	ENHS	50/125 = 40	LFR	UC Berkeley	Conceptual	13% (U-Zr)/N/A	Pu-U/U-Zr
USA (9)	TWR-P	600/1475 = 41%	SFR	TerraPower	Conceptual	N/A/1.5–2	U-Zr10% MF

Table 20.2.5. Molten salt SMRs and S&MRs (17 in total) (Generation-IV concepts)

Country	Design	Output MW _{el/th} = Th.Eff., %	Designers	Phase	Fuel enrichment/ cycle, years	Fuel type
Canada (1)	IMSR	190/400 = 48	Terrestrial Energy	Basic	<5%/7 years before core-unit replacement	MSF
China (1)	smTMSR-400	168/400 = 42	SINAP, CAS	Preconceptual	19.75%/10 years	LiF-BeF ₂ -UF ₄ -ThF ₄ fuel salt
China (2)	TMSR-LF	168/373 = 45	SINAP	Conceptual	19.75%/Online	LiF-BeF ₂ -UF ₄ -ThF ₄ , LiF-BeF ₂ -PuF ₃ -ThF ₄
Czech Republic	Energy Well	8/20 = 40	Centrum vyzkumu Rez	Preconceptual	<20%/7	TRISO
Denmark (1)	CA Waste Burner	20/50 = 40	Copenhagen Atomics	Conceptual	N/A/N/A	LiF-ThF ₄
Denmark (2)	CA Waste Burner 0.2.5	-/100 = N/A	Copenhagen Atomics	Conceptual	N/A/Continuous	LiF-ThF ₄
Denmark (3)	CMSR (MSTW)	100–115/250 = 40–46 115/270 = 42.6	Seaborg Technologies	Conceptual	Preprocessed SNF (U 1.1% fissile, Pu 69% fissile)/6	Na-actinide fluoride (93% Th, 3.5% U, 3.5% Pu)
Int. Consortium	ThorCon	250 (per module)/557 = 45	Martingale	Basic	19.7%/8	12% HM in NaBe salt
Japan	FUJI	200/450 = 44	Int. Thorium Molten-Salt Forum	Pre conceptual	2.0% Pu or LEU (continuous operation is possible)	MSF with Th & U
UK (1)	Stable Salt Reactor-Wasteburner	300 (continuous as baseload)/750 = 40	Moltex Energy	Conceptual	Reactor grade Pu/12.5	MSF
UK (2)	Stable Salt Reactor—Th. Spectrum	300 (baseload)/750 = 40	Moltex Energy	Preconceptual	5%/2	MSF

Continued

Table 20.2.5. Molten salt SMRs and S&MRs (17 in total) (Generation-IV concepts)—cont'd

Country	Design	Output MW _{el/th} = Th.Eff., %	Designers	Phase	Fuel enrichment/ cycle, years	Fuel type
USA (1) & Canada (2)	MCSFR	50/100 = 50	Elysium Industries	Conceptual	10%–20%/online refueling	MSF
USA (2)	Mk1 PB-FHR	100/236 = 42	University of CA, Berkeley	Preconceptual	19.9%/2.1 months for fuel core residence time	TRISO particles
USA (3)	LFTR	250/600 = 42	Flibe Energy	Conceptual	N/A /continuous refueling	LiF-BeF ₂ -UF ₄
USA (4)	KP-FHR	140/311 = 45	Kairos Power	Prelicensing	19.75%/Online	TRISO particles
USA (5)	MCFR	N/A/N/A = N/A	TerraPower	Prelicensing	N/A/Online	N/A
USA (6)	SmAHTR	50/125 = 40	Oak Ridge National Lab.	Conceptual	19.75%/N/A	TRISO particles

Table 20.2.6. Other Types SMR (4 SMRs)

Country	Design	Output MW _{el/th} =Th.Eff., %	Type	Designers	Phase	Fuel enrichment/ cycle, years	Fuel type
Canada	Leadir-PS100	36/100 = 36	LMR	Northern Nuclear Industries	Conceptual	N/A/N/A	TRISO
Japan	MoveluX	N/A/10 = N/A	Heat Pipes	Toshiba	Preliminary	4.99/N/A	LEU
USA (1)	Aurora	1.5/N/A = N/A	Heat Pipes	Oklo	Preliminary	<20%/N/A	HALEU-U-Zr
USA (2)	eVinci	0.2–15/0.6–40 = 33.3–37.5	Heat Pipes	Westinghouse	Developmental	19.5%/10	UO ₂ or UN

Table 20.2.7. SMRs and S&MRs from USA (in total 27)

Design	Output MW _{el} /th =Th.Eff., %	Type	Designers	Status	Fuel enrichment/ cycle, years	Fuel type
Land-based water-cooled reactors (in total 5)						
NuScale	50/160 = 31	PWR	NuScale Power	Preliminary	<4.95%/2	UO ₂
SMR-160	160/525 = 31	PWR	Holtec Int.	Preliminary	4.95%/1.5–2	UO ₂
mPower	195/575 = 34	PWR	BWX Technology	Developmental	<5%/2	UO ₂
W-SMR	>225/800 ≥ 28	PWR	Westinghouse	Conceptual	<5%/2	UO ₂
BWRX-300	300/– = N/A	BWR	GEH	Final	N/A/N/A	N/A
High-Temperature Gas-cooled Reactors (HTGRs) (in total 5) (Generation-IV concept)						
Xe-100	75/200 = 38	HTGR	X-energy LLC	Conceptual	15.5%/ Online refueling	UCO TRISO
SC-HTGR	272/625 = 44	HTGR	Framatome Inc.	Conceptual	<20%/½ core replaced/ 1.5 years	UCO TRISO particle fuel
Prismatic HTR	150/350 = 42.8	HTGR	General Atomics	Developmental	15.5%/1.5	TRISO-coated UCO
MMR	5/15 = 33.3	HTGR	USNC	Preliminary	N/A/Never	FCM
HOLOS	3–13/ 22 = 13.6–59.0	HTGR	HolosGen	Preliminary	15%/3.5–8	TRISO
Fast-neutron-spectrum reactors (in total 9) (Generation-IV concept)						
SUPERSTAR	120/300 = 40	LMFR	ANL	Conceptual	<12%/15	Particle fuel U-Pu-Zr
EM ²	265/500 = 53	GMFR	General Atomics	Conceptual	14.5% LEU/ 30	UC
WLFR	>450(Net)/950 ≥ 47	LFR	Westinghouse	Conceptual	≤19.75%/≥2	Oxide

Continued

Table 20.2.7. SMRs and S&MRs from USA (in total 27)—cont'd

Design	Output MW_{el}/th =Th.Eff., %	Type	Designers	Status	Fuel enrichment/ cycle, years	Fuel type
AFR-100	100/250 = 40	SFR	ANL	Conceptual	13.5%/N/A	U-Zr
ARC-100	100/260 = 38.5	SFR	ARC	Final	N/A/20	LEU
Gen4 Module	25/70 = 35.7	LMFR	Gen4 Energy Inc.	Conceptual	19.75%/10	UN
PRISM	311/500 = 62	SFR	GE-Hitachi	Preliminary	N/A/1.33	U-Pu_Zr metal
ENHS	50/125 = 40	LMFR	UC Berkeley	Conceptual	13% (U-Zr)/ N/A	Pu-U/ U-Zr
TWR-P	600/1475 = 41	SFR	TerraPower	Conceptual	N/A/1.5–2	U-Zr10% MF
Molten Salt Reactors (in total 6) (Generation-IV concept)						
MCSFR	50/100 = 50	MSR	Elysium Industries	Conceptual	10%–20%/ online refuel.	Molten salt fuel
Mk1 PB-FHR	100/236 = 42	MSR	University of CA, Berkeley	Preconceptual	19.9%/ 2.1 months for fuel core residence time	TRISO particles
LFTR	250/600 = 42	MSR	Flibe Energy	Conceptual	N/A/cont. Refueling	LiF- BeF ₂ -UF ₄
KP-FHR	140/311 = 45	MSR	Kairos Power	Prelicensing	19.75%/ Online	TRISO particles
MCFR	N/A/N/A = N/A	MSR	TerraPower	Prelicensing	N/A/Online	N/A
SmAHTR	50/125 = 40	MSR	ORNL	Conceptual	19.75%/N/A	TRISO particles
Heat Pipes (HPs) reactors (in total 2)						
Aurora	1.5/N/A = N/A	HPs	Oklo	Preliminary	<20%/N/A	HALEU- U-Zr
eVinci	0.2–15/ 0.6–40 = 33–38	HPs	Westinghouse	Developmental	19.5%/10	UO ₂ or UN

Table 20.2.8. SMRs and S&MRs from Russia (in total 15)

Design	Output MW _{el} /th =Th.Eff., %	Type	Designers	Status	Fuel enrichment/ cycle, years	Fuel type
Land-based water-cooled reactors (in total 5)						
ELENA	0.068/3.3 = 2	PWR	Kurchatov Institute	Conceptual	15.2%/25	UO ₂ (MOX)
UNITHERM	6.6/30 = 22	PWR	NIKIET	Conceptual	19.75%/16.7	UO ₂
RUTA-70	-/70 = N/A	PWR	NIKIET	Conceptual	3%/3	Cermet
KARAT-45	45–50/ 180 = 25–28	BWR	NIKIET	Conceptual	4.5%/7	UO ₂
KARAT-100	100/360 = 28	BWR	NIKIET	Conceptual	4%/7.5	UO ₂
VK-300	250/750 = 33	BWR	NIKIET	Final	4%/6	UO ₂
Marine-based water-cooled reactors (in total 5)						
SHELF	6.6/28.4 = 23	Immersed NPP	NIKIET	Preliminary	19.7%/6	UO ₂
ABV-6E	6–9/38 = 16–24	Floating PWR	OKBM Afrikantov	Final	<20%/10–12	UO ₂
KLT-40S	35/150 = 23	Floating PWR	OKBM Afrikantov	Operating	18.6%/2.5–3	UO ₂
RITM-200M	50/175 = 29	Floating PWR	OKBM Afrikantov	Manufactured	<20%/10	UO ₂
VBER-300	325/917 = 35	Floating NPP	OKBM Afrikantov	Licensing	4.95%/6	UO ₂
High-Temperature Gas-cooled Reactors (HTGRs) (in total 3) (Generation-IV concept)						
MHR-100	25–87/ 215 = 12–41	HTGR	OKBM Afrikantov	Conceptual	LEU <20%/N/A	Coated particle fuel
MHR-T	4 × 205.5/ 4 × 600 = 34	HTGR	OKBM Afrikantov	Conceptual	20%/2.5	Coated particle fuel
GT-MHR	288/600 = 48	HTGR	OKBM Afrikantov	Preliminary	LEU or WPu/2.1	Coated particle fuel
Fast-neutron-spectrum reactors (in total 2) (Generation-IV concept)						
SVBR-100	100/280 = 36	LMFR	JSC AKME Eng.	Final	<19.3%/ 0.58–0.67	UO ₂
BREST-OD-300	300/700 = 43	LMFR	NIKIET	Final	13.5%/2.46–4.1	U-Pu-N

Table 20.2.9. SMRs and S&MRs from China (in total 13)

Design	Output $MW_{el/th}$ =Th.Eff., %	Type	Designers	Status	Fuel enrichment/ cycle, years	Fuel type
Land-based water-cooled reactors (in total 7)						
ACP100	125/385 = 33	PWR	CNNC	Basic	<4.95%/2	UO ₂
DHR400	-/400 = N/A	LWR	CNNC	Basic	<5.0%/0.8	UO ₂
CAP200	>200/600 ≥ 30.3	PWR	CGNPC	Conceptual	4.2%/2	UO ₂
CNP-300	300–340/ 1000 = 30–34	PWR	CNNC	Conceptual	<5%/N/A	UO ₂
SNP350	350/ 1035 = 33.8	PWR	SNERDI	Preliminary	N/A/N/A	N/A
NHR-200II	-/200 = N/A	PWR	INET	Final	<5%/N/A	UO ₂
HAPPY200	-/200 = N/A	PWR	SPIC	Final	N/A/N/A	N/A
Marine-based water-cooled reactor (in total 1)						
ACPR50S	50/200 = 25	PWR	CGNPC	Preliminary	<5%/2.5	UO ₂
High-Temperature Gas-cooled Reactors (HTGRs) (in total 2) (Generation-IV concept)						
HTR-10	2.5/10 = 25	HTGR	Tsinghua University/INET	Operational	17%/On-line	Spherical El. with TRISO particles fuel
HTR-PM	210/ 2 × 250 = 42	HTGR	INET, Tsinghua University	Construction	8.5%/On-line refuel.	Spherical El. with coated particle fuel
Fast-neutron-spectrum reactor (in total 1) (Generation-IV concept)						
CFR-600	600/ 1500 = 40	LMFR	CNNC	Construction	N/A/N/A	UO ₂ /MOX
Molten Salt Reactors (In total 2) (Generation-IV concept)						
smTMSR-400	168/400 = 42	MSR	SINAP, CAS	Preconceptual	19.75%/ 10 years	LiF-BeF ₂ -UF ₄ -ThF ₄ fuel salt
TMSR-LF	168/373 = 45	MSR	SINAP	Conceptual	19.75%/ Online	LiF-BeF ₂ -UF ₄ -ThF ₄ , LiF-BeF ₂ -PuF ₃ -ThF ₄

Table 20.2.10. SMRs and S&MRs from Japan (in total 12)

Design	Output MW _{el} /th = Th.Eff., %	Type	Designers	Status	Fuel enrichment/ cycle, years	Fuel type
Land-based water-cooled reactors (in total 4)						
DMS	300/840 = 36	BWR	Hitachi- GE	Basic	<5%/2	UO ₂
IMR	350/1000 = 35	PWR	MHI	Conceptual	4.8%/2.2	UO ₂
CCR	423/1268 = 33.4	BWR	Toshiba Corp.	Conceptual	N/A/2	N/A
MRX	33.3/100 = 33.3	PWR	JAERI	Final	4.3%/3.5	UO ₂
High-Temperature Gas-cooled Reactors (HTGRs) (in total 2) (Generation-IV concept)						
GTHTR300	100–300/<600 = 17–50	HTGR	JAEA	Basic	14%/4	UO ₂
HTTR	–/30 = N/A	HTGR	JAEA	Operational	3–10 (6 avg.)%/ 660 EFPD	UO ₂ TRISO ceramic coated particle
Fast-neutron-spectrum reactors (in total 4) (Generation-IV concept)						
4S	10/30 = 33	SFR	Toshiba Corp.	Developmental	<20%/N/A	Metal fuel (U-Zr)
LSPR	53/150 = 35.3	LMFR	Tokyo Tech.	Developmental	10%–12.5%/12	U-Pu-N/U- Pu-Zr
PBWFR- 150	150/450 = 33.3	LMFR	Tokyo Tech.	Developmental	N/A/10	U-Pu Nitride
Rapid-L	0.2/5 = 4	LMFR	CRIEPI	Operating	40%/10	UN
Molten Salt Reactor (in total 1) (Generation-IV concept)						
FUJI	200/450 = 44	MSR	Int. Th Molten- Salt Forum	Preconceptual	2.0% Pu LEU/N/A	Molten salt with Th & U
Heat-pipe reactor (in total 1)						
MoveluX	N/A/10 = N/A	Heat Pipes	Toshiba	Preliminary	4.99%/N/A	LEU

Table 20.2.11. SMRs and S&MRs from Canada (in total, 6)

Design	Output MW _{el/th} = Th.Eff., %	Type	Designers	Status	Fuel enrichment/ cycle, years	Fuel type
Land-based water-cooled reactors (in total 2) (Generation-IV concept)						
CANDU SMR	300/960 = 31.25	PHWR	Candu Energy Inc.	Conceptual	-/On-line	UO ₂
SSR	300/667 = 45	SCWR	AECL	Conceptual	Enriched /N/A	U or Th
High-Temperature Gas-cooled Reactor (HTGR) (in total 1) (Generation-IV concept)						
Starcore SMR	20/36 = 55.6	HTGR	Starcore	Preliminary	N/A/5	TRISO
Molten Salt Reactors (in total 2) (Generation-IV concept)						
IMSR	190/400 = 48	MSR	Terrestrial Energy	Basic	<5%/7 years	MSF
MCSFR	50/100 = 50	MSR	Elysium Industries	Conceptual	10%–20% /online refueling	MSF
Other reactors (in total 1)						
Leadir-PS100	36/100 = 36	LMR	Northern Nuclear Industries	Conceptual	N/A/N/A	TRISO

Table 20.2.12. SMRs and S&MRs from France (in total 5)

Design	Output MW _{el/th} = Th.Eff., %	Type	Designers	Status	Fuel enrichment/ cycle, years	Fuel type
Land-based water-cooled reactor (in total 1)						
Nuward	300–400/– = N/A	PWR	CEA, EDF, Naval Group, TechnicAtome	Preliminary	N/A/N/A	N/A
Marine-based water-cooled reactor (in total 1)						
Flexblue	160/600 = 26.7	PWR	DCNS	Preliminary	<5%/3	UO ₂
High-Temperature Gas-cooled Reactors (HTGRs) (in total 2) (Generation-IV concept)						
Allegro	-/50–100 = N/A	HTGR	CEA	Conceptual	N/A/N/A	MOX
ANTARES	-/≥600 = N/A	HTGR	Framatome	Conceptual	N/A/N/A	N/A
Fast-neutron-spectrum reactor (in total 1) (Generation-IV concept)						
ASTRID	600/1500 = 40	SFR	CEA	Preliminary	N/A/N/A	MOX

Table 20.2.13. SMRs and S&MRs from South Korea (in total 5)

Design	Output MW _{el/th} = Th.Eff., %	Type	Designers	Status	Fuel enrichment/ cycle, years	Fuel type
Land-based water-cooled reactor (in total 1)						
SMART	100/330 = 30	PWR	KAERI	Certified	<5%/3	UO ₂
Fast-neutron-spectrum reactors (in total 4) (Generation-IV concept)						
KALIMER-600	600/ 1523.4 = 39.4	SFR	KAERI	Preliminary	N/A/1	U-TRU-Zr
PGSFR	150/400 = 37.5	SFR	KAERI	Preliminary	N/A/~1	U-TRU-Zr
PEACER	300/850 = 35	LMFR	Seoul National University	Conceptual	N/A/1	U-TRU-Zr
MicroURANUS	20/60 = 33.3	LMFR	UNIST	Preconceptual	8%, 10%, 12%/N/A	UO ₂

Table 20.2.14. SMRs and S&MRs from South Africa (in total 4)

Design	Output MW _{el/th} = Th.Eff., %	Type	Designers	Status	Fuel enrichment/ cycle, years	Fuel type
High-Temperature Gas-cooled Reactors (HTGRs) (in total 4) (Generation-IV concept)						
HTMR-100	35/100 = 35	HTGR	Steenkampskraal Th Ltd.	Conceptual	10%–93%/ Online refuel.	LEU, Th/LEU, Th/HEU, Th/Pu
A-HTR- 100	50/100 = 50	HTGR	Eskom Holdings SOC Ltd.	Conceptual	LEU or WPu/ N/A	Coated particle fuel
PBMR-400	165/400 = 41.3	HTGR	PBMR SOC Ltd.	Preliminary	9.6% LEU or WPu/N/A	Coated particle fuel
PBMR-100	100/250 = 40	HTGR	PBMR SOC Ltd.	Preliminary	N/A/Online	TRISO-coated UP ₂

Table 20.2.15. SMRs and S&MRs from UK (in total 4)

Design	Output MW _{el/th} = Th.Eff., %	Type	Designers	Status	Fuel enrichment/ cycle, years	Fuel type
Land-based water-cooled reactor (in total 1)						
UK-SMR	443/1276 = 26	PWR	Rolls- Royce	Final	<5%/1.5–2	UO ₂
High-Temperature Gas-cooled Reactor (HTGR) (in total 1) (Generation-IV concept)						
U-Battery	4/10 = 40	HTGR	URENCO	Preliminary	17%–20%/5	TRISO
Molten Salt Reactors (in total 2) (Generation-IV concept)						
Stable Salt Reactor- Wasteburner	300/750 = 40	MSR	Moltex Energy	Conceptual	Reactor grade Pu/12.5	MSF
Stable Salt Reactor, Th. Spectrum	300 (baseload)/750 = 40	MSR	Moltex Energy	Preconceptual	5%/2	MSF

Table 20.2.16. SMRs and S&MRs from Denmark (in total 3)

Design	Output MW _{el/th} = Th.Eff., %	Type	Designers	Status	Fuel enrichment/ cycle, years	Fuel type
Molten Salt Reactors (in total 2) (Generation-IV concept)						
CA waste burner	20/50 = 40	MSR	Copenhagen Atomics	Conceptual	N/A/N/A	LiF-ThF ₄
CA waste burner	–/100 = N/A	MSR	Copenhagen Atomics	Conceptual	N/A/Continuous	LiF-ThF ₄
CMSR	100–115/250 = 40–46	MSR	Seaborg Technologies	Conceptual	Preprocessed SNF (U 1.1% fissile, Pu 69% fissile)/60	Na-actinide fluoride (93% Th, 3.5% U, 3.5% Pu)

Table 20.2.17. SMRs and S&MRs from Czech Republic (in total 2)

Design	Output MW _{el/th} = Th.Eff., %	Type	Designers	Status	Fuel enrichment/ cycle, years	Fuel type
Land-based water-cooled reactor (in total 1)						
TEPLATOR	-/50 = N/A	HWR	UWB Pilsen & CIIRC CTU	Conceptual	<1.2%/0.83	Spent VVER-400 fuel
Molten Salt Reactor (in total 1) (Generation-IV concept)						
Energy Well	8/20 = 40	MSR	Centrum vyzkumu Rez	Preconceptual	<20%/7	TRISO

Table 20.2.18. SMRs and S&MRs from India (in total 2)

Design	Output MW _{el/th} = Th.Eff., %	Type	Designers	Status	Fuel enrichment/ cycle, years	Fuel type
Land-based water-cooled reactors (in total 2)						
AHWR-300-LEU	304/920 = 33	PHWR	BARC	Conceptual	<5% (MOX)/ Continuous	Th-U or Th-Pu, MOX
PHWR-220	235/755 = 31.2	PHWR	NPCI Ltd.	16 Operational Units	<5%/Continuous	UO ₂

Table 20.2.19. SMRs and S&MRs from Italy (in total 2)

Design	Output MW _{el/th} = Th.Eff., %	Type	Designers	Status	Fuel enrichment/cycle, years	Fuel type
Fast-neutron-spectrum reactors (in total 2) (Generation-IV concept)						
ALFRED	125/300 = 41.7	LFR	Ansaldo	Preliminary	N/A/5	MOX
ELFR	630/1500 = 42	LFR	Ansaldo	Conceptual	N/A/2.5	MOX

Table 20.2.20. SMRs and S&MRs from Luxembourg (in total 2)

Design	Output MW _{el/th} = Th.Eff., %	Type	Designers	Status	Fuel enrichment/ cycle, years	Fuel type
Fast-neutron-spectrum reactors (in total 2) (Generation-IV concept)						
LFR-TL-X	5/15 = 33 10/30 = 33 20/60 = 33	LFR	Hydromine Nuclear Energy	Conceptual	19.8%/≥8.33	LEU
LFR-AS-200	200/480 = 42	LFR		Preliminary	14.6%–20.4%–23.2% in Pu/6.7 years for 5 batches	MOX

Table 20.2.21. SMRs and S&MRs from Argentina (in total 1)

Design	Output MW _{el/th} =Th.Eff., %	Type	Designers	Status	Fuel enrichment/ cycle, years	Fuel type
Land-based water-cooled reactor (in total 1)						
CAREM	30/100=30	PWR	CNEA	Construction	3.1%/1.2	UO ₂

Table 20.2.22. SMRs and S&MRs from Brazil (in total 1)

Design	Output MW _{el/th} =Th.Eff., %	Type	Designers	Status	Fuel enrichment/ cycle, years	Fuel type
Land-based water-cooled reactor (in total 1)						
FBNR	70/134=52.2	PWR	Federal University of Rio Grande do Sul	Conceptual	N/A/N/A	TRISO

Table 20.2.23. SMRs and S&MRs from Indonesia (in total 1)

Design	Output MW _{el/th} = Th.Eff., %	Type	Designers	Status	Fuel enrichment/ cycle, years	Fuel type
High-Temperature Gas-cooled Reactor (HTGR) (in total 1) (Generation-IV concept)						
RDE/Micro-PeLUIt	3/10=30	HTGR	BATAN	Preliminary	17%/On-line	Coated particle fuel

Table 20.2.24. SMRs and S&MRs from Sweden (in total 1)

Design	Output MW _{el/th} =Th.Eff., %	Type	Designers	Status	Fuel enrichment/ cycle, years	Fuel type
Fast-neutron-spectrum reactor (in total 1) (Generation-IV concept)						
SEALER	3/8=38	Lead Cooled	LeadCold	Conceptual	19.75%/27 full power years	UO ₂

It is evident from this still evolving listings that there are not only too many SMRs/S&MRs under development, but there are no accepted “acceptance criteria.” Many of them are in the early stages, and there is a general lack of public data about many of the actual details of even the “final” designs. Therefore, sometimes it is not easy to separate SMRs from S&MRs, because at the final stages SMRs can be considered as S&MRs and vice versa. In reviewing the literature, the overall goals of safety, sustainability, competitiveness, and social acceptance are widely claimed, but not demonstrated. While there are many small 10–300 MW_{el} units

and power plants already in operation, there are just three new demonstration SMR units planned or actually underway ([Nuclear News, 2022](#)):

- (a) Carem, Argentina;
- (b) HTR-PM, China; and
- (c) CFR-600, China.

Modular-construction technology, per se, is not new, being widely used in oil rigs, military equipment, buildings, data centers, computers, and CCGT unit installations. For NPPs specifically, some of the many stated advantages of SMRs are that they offer the vision of:

- (a) lowering total investment amounts and, hence, reduced project risks;
- (b) providing the opportunity for mass-production in module “factories,” thus reducing on-site costs and embody the “latest” manufacturing technology;
- (c) potentially reduced construction times due to simpler or less design complexity;
- (d) sharing expertise, facilities, and equipment at a multiple module site (e.g., staff, security, switchyard, operation and maintenance, etc.);
- (e) adding power/units in stages as demand and market allow;
- (f) “generic” licensing of some standard design; and
- (g) applicability in smaller markets and remote deployment.

Building and operating smaller units is, of course, how the nuclear industry actually began and is not itself a novelty, and prior examples of standardization include the Standardized Nuclear Unit Power Plant System (SNUPPS) series of PWRs. In general, as of today, a number of small nuclear power reactors with installed capacities (10–300 MW_{el}) operate around the world ([Nuclear News, 2022](#)). Moreover, some of them operate successfully for about 50 years, but, however, they cannot be named as SMRs. Also, France, Russia, UK, United States, and other countries have great experience in successful development, manufacturing, and operation of submarines, icebreakers, and ship’s propulsion reactors. Therefore, many modern designs/concepts of SMRs are based on these achievements (see [Table 20.2.2](#)). Also, it should be mentioned that a number of SMRs concepts are based on the six Generation-IV nuclear-power-reactor concepts (see [Table 20.2.1](#) for SCWR-SSR by Canada, [Table 20.2.3](#) for helium-cooled reactors, [Table 20.2.4](#) for liquid metal fast reactors, and [Table 20.2.5](#) for molten salt reactors).

Analysis of the data in [Tables 20.2.1–20.2.6](#) shows that many SMRs usually require a higher level of fuel enrichment up to <20% (the maximum level for LEU limited by the IAEA) to operate with smaller amount of fuel and to have longer terms between refueling and, usually, lower NPP thermal efficiencies compared to those of large nuclear-power reactors NPPs of the same type (see [Table 20.2.26](#) for RITM-200M and KLT-40S thermal efficiencies).

20.2.4 Russian KLT-40S and RITM-200M SMRs

Russia is the first country in the world, which developed, designed, and put into operation two SMRs. And this success is not an accidental one, because Russia has adjusted their proven marine reactor—KLT-40S for operation as an SMR for electricity generation and heat supply (also, a desalination of water is possible). The barge with two KLT-40S SMRs was towed to port of Pevek, Russia’s northernmost city in 2019, where it will gradually replace the Bilibino NPP and the Chaunskaya combined heat and power plant, which are being retired. These two SMRs were connected to grid in December of 2019 ([Nuclear News, 2022](#)).

However, it should be mentioned that the idea of using a nuclear reactor as a floating NPP belongs to the United States (<https://en.wikipedia.org/wiki/MH-1A>; accessed Feb. 19, 2022). The first in the world floating

NPP was the 10-MW_{el} MH-1A (Mobile High power) reactor (built in 1961) installed on the ship named “Sturgis” (built in 1945), which was towed to Panama Canal. The reactor has reached first criticality in 1967, and electricity was supplied from 1968 till 1975. The reactor has used LEU with enrichment from 4% to 7%. Containment vessel has weighted 350 tons. Also, similar projects have been developed in Germany and UK.

According to the JSC “Afrikantov OKBM” (Nizhny Novgorod, Russia: <http://www.okbm.nnov.ru/en/>)” The economic effect from the application of the Floating Nuclear-Thermal-Power Plant (FNThPP) on remote territories is conditioned primarily by the replacement of costly fossil fuel brought from afar, reduced need in vehicles and human resources that enable the fossil fuel delivery and storage chain. It may be noted that one built FNThPP with the KLT-40S reactor plant (with 150 Gcal/h of heat extracted for district heating) will make it possible to save around 350,000 tons of conditional fuel yearly. Competitive advantages of FNThPP: manufactured on a turnkey basis; existing cooperation scheme; autonomous, reliable, safe, compact; full after-sale services and repairs in existing specialized facilities; reduced fabrication time for the reactor-plant equipment; serial production; possible to change the operating site; disposed of in a specialized facility; the green-lawn principle implemented; and can be equipped with a desalination installation,” so-called, Floating Nuclear Power & Desalination System (FNPDS) with KLT-40S reactor(s).

Figure 20.2.2 shows a schematic of KLT-40S reactor and its systems; Figure 20.2.3—3-D image of the reactor KLT-40S with four steam generators and four reactor-coolant circulation pumps; Figure 20.2.4—KLT-40S reactor plant configuration; Figure 20.2.5—KLT-40S reactor-core cross section; Figure 20.2.6—general view of a fuel assembly; Figure 20.2.7—general view of the reactor compartment in the KLT-40S Reactor Plant; Figure 20.2.8a–c—(a) photo of the FNThPP with two KLT-40S reactors; (b) FNThPP layout; and (c) FNPDS with KLT-40S reactor(s) (artist image); and Table 20.2.25—main parameters of KLT-40S.

It should be stated that Figures 20.2.1–20.2.7, 20.2.8b, c, and 20.2.9 shown here are courtesy of the JSC “Afrikantov OKBM” and were taken from their booklets on KLT-40S and RITM-200M with the OKBM permission (<http://www.okbm.nnov.ru/en/media-center/booklets/>; accessed Feb. 19, 2022).

According to the JSC “Afrikantov OKBM”: “The reactor is a high-pressure vessel that consists of a body and a head (Figures 20.2.3, 20.2.4, and 20.2.7). The body incorporates an in-vessel core barrel and an upper core support structure. On the Reactor Pressure Vessel (RPV) head, there are 8 Compensating Group Drive Mechanisms (CGDM), 3 Safety Rod Drive Mechanisms (SRDM), and primary coolant-temperature measurement equipment. The reactor is connected to the equipment and auxiliary systems via 8 main nozzles and 5 small nozzles, which have the following purpose: 4 main nozzles to connect to steam generator pressure vessel; 4 main nozzles to connect to hydro-chambers in the pumps; and 5 small nozzles to connect to auxiliary systems. The RPV is a forged and welded structure. The RPV and the RPV head are made of heat-resistant, high-strength, pearlitic steel with anticorrosive hard-facing. The reactor core is designed to be used in the reactor as a source of heat energy (Figure 20.2.5). The reactor-core type is heterogeneous with a hard spectrum of thermal neutrons. The reactor core is based upon an array structure with fuel assemblies for various purposes and fuel with a high uranium content (Figures 20.2.6 and 20.2.7). The steam generator is a once-through, coiled-tube heat exchanger, where steam is generated on the tube side (Figures 20.2.3, 20.2.4, and 20.2.7). The steam-generator tubing system is made of a titanium alloy as cylindrical helical-coil tubes. The steam-generator pressure vessel is made of low-alloyed steel with anticorrosive hard-facing.

ElectroMechanical Reactor Scram System (EMRSS) (Figures 20.2.3, 20.2.4, and 20.2.7): The system is designed to scram (shutdown) the reactor and to keep the reactor subcritical in any modes, including design-basis and beyond-design-basis accidents. The system incorporates drive mechanisms of the reactor control and protection system. The drive mechanisms are divided into two banks:

- (1) SRDM—designed to scram the reactor and keep it subcritical in an emergency. The SRDM bank consists of three SRDMs. Each SRDM incorporates: (a) two safety rods; and (b) connecting elements and a drive.

Table 20.2.25. Main parameters of Russian SMRs: KLT-40S and RITM-200M (OKBM, 2020) (for thermal efficiencies—see Table 20.2.26, and for simplified T - s diagrams—see Figures 20.2.10 and 20.2.11, respectively)

Parameters	KLT-40S	RITM-200M
Reactor type	PWR	Integral PWR
Generation of SMRs	III	III ⁺
Reactor coolant/moderator		Light water
Thermal power, MW _{th}	150	175
Electric power, gross/net, MW _{el}	38.5/35	55/50
Thermal efficiency, %	~26	~31
Expected capacity factor, %	60–70	65
Maximum output thermal power, GJ/h (Gcal/h); MW	305.6 (73); 84.9	–
Production of desalinated water, m ³ /day	40,000–100,000 ^a	–
Operating range of power, %	10–100	–
Normal-mode power variation, %/s	0.1	–
Primary circuit pressure, MPa	12.7	15.7
Primary circuit T_{in}/T_{out} , °C	280/316	277/313
Reactor coolant mass-flow rate, t/h	680	3250
Primary circuit circulation mode		Forced
Power cycle		Indirect Rankine cycle
P_{steam} at steam-generator outlet, MPa	3.72	3.82
T_{sat} at P_{steam} , °C	246.1	247.4
Overheated T_{steam} at steam-generator outlet, °C	290	295
Steam mass-flow rate, t/h	240	261 (280)
T feedwater in-out, °C	70–130 (170)	–
RPV height/diameter, m	4.8/2.0	9.2/3.5
Maximum mass of reactor pressure vessel, t	46.5	–
Fuel type/Assembly array	UO ₂ pellets in silumin matrix	UO ₂ pellet/ hexagonal
Fuel assembly active length, m	1.2	2.0
Number of fuel assemblies	121	241
Core service life, h	21,000	75,000
Refueling interval, years	~3 ^b	Up to 10

Continued

Table 20.2.25. Main parameters of Russian SMRs: KLT-40S and RITM-200M (OKBM, 2020) (for thermal efficiencies—see Table 20.2.26, and for simplified T - s diagrams—see Figures 20.2.10 and 20.2.11, respectively)—cont'd

Parameters	KLT-40S	RITM-200M
Refueling outage, days	30—36	—
Fuel enrichment, %	18.6	Up to 20
Fuel burnup, GWd/t	45.4	—
Predicted core-damage frequency, event/reactor year	0.5×10^{-7}	—
Seismic design	9 point on MSK scale	0.3 g

^a In case of Floating Nuclear Power-DeSalination Complex (FNPDS);

^b The Floating Nuclear Thermal Power Plant (FNThPP) will save up to 200,000 metric tons of coal and 100,000 tons of fuel oil per year. Every 12 years, the FNThPP will be towed back to the manufacturing plant and overhauled there.

Explanations to Table 20.2.25:

Table 20.2.26. Typical ranges of thermal efficiencies (gross) of modern thermal and nuclear power plants

No.	Power plant	Gross Th. Eff.
1	Carbon-dioxide-cooled reactor (Advanced Gas-cooled Reactor (AGR)) NPP (Generation-III) (reactor coolant: $P=4$ MPa, $T=290$ – 650°C ; and steam: $P_{\text{in}}=17$ MPa ($T_{\text{sat}}=352.3^\circ\text{C}$) & $T_{\text{in}}=560^\circ\text{C}$ ($T_{\text{cr}}=374^\circ\text{C}$); and $P_{\text{reheat}}\approx 4$ MPa ($T_{\text{sat}}=250.4^\circ\text{C}$), $T_{\text{reheat}}=560^\circ\text{C}$)	Up to 42%
2	Sodium-cooled Fast Reactor (SFR) (BN-600 & BN-800) NPP (steam: $P_{\text{in}}=14.2$ MPa ($T_{\text{sat}}=337.8^\circ\text{C}$), $T_{\text{in}}=505^\circ\text{C}$ ($T_{\text{cr}}=374^\circ\text{C}$); and $P_{\text{reheat}}\approx 2.5$ MPa ($T_{\text{sat}}=224^\circ\text{C}$), $T_{\text{reheat}}=505^\circ\text{C}$)	Up to 40%
3	Pressurized-Water-Reactor (PWR) NPP (Generation-III ⁺) (reactor coolant: $P=15.5$ MPa ($T_{\text{sat}}=344.8^\circ\text{C}$), $T_{\text{out}}=327^\circ\text{C}$; steam: $P_{\text{in}}=7.8$ MPa, $T_{\text{in}}=T_{\text{sat}}=293.3^\circ\text{C}$; and $P_{\text{reheat}}\approx 2$ MPa ($T_{\text{sat}}=212.4^\circ\text{C}$), $T_{\text{reheat}}\approx 265^\circ\text{C}$)	Up to 36%–38%
4	Pressurized-Water-Reactor (PWR) NPP (Generation-III, current fleet) (reactor coolant: $P=15.5$ MPa ($T_{\text{sat}}=344.8^\circ\text{C}$), $T=292$ – 329°C ; steam: $P_{\text{in}}=6.9$ MPa, $T_{\text{in}}=T_{\text{sat}}=284.9^\circ\text{C}$; and $P_{\text{reheat}}\approx 1.5$ MPa ($T_{\text{sat}}=198.3^\circ\text{C}$), $T_{\text{reheat}}\approx 255^\circ\text{C}$)	Up to 34%–36%
5	Boiling-Water-Reactor (BWR) NPP (Generation-III, current fleet) (reactor coolant: $P=7.2$ MPa, $T_{\text{out}}=T_{\text{sat}}=287.7^\circ\text{C}$; steam: $P=7.2$ MPa, $T_{\text{in}}=T_{\text{sat}}=287.7^\circ\text{C}$ and $P_{\text{reheat}}\approx 1.7$ MPa ($T_{\text{sat}}=204.3^\circ\text{C}$), $T_{\text{reheat}}\approx 258^\circ\text{C}$)	Up to 34%
6	Pressurized Heavy Water Reactor (PHWR) NPP (Generation-III, current fleet) (reactor coolant: $P_{\text{in}}=11$ MPa/ $P_{\text{out}}=9.9$ MPa ($T_{\text{sat}}=310.3^\circ\text{C}$) & $T=260$ – 310°C ; steam: $P_{\text{in}}=4.7$ MPa, $T_{\text{in}}=T_{\text{sat}}=260.1^\circ\text{C}$; and $P_{\text{reheat}}\approx 1.2$ MPa ($T_{\text{sat}}=188^\circ\text{C}$), $T_{\text{reheat}}\approx 240^\circ\text{C}$)	Up to 32%

Continued

Table 20.2.26. Typical ranges of thermal efficiencies (gross) of modern thermal and nuclear power plant)—cont'd

No.	Power plant	Gross Th. Eff.
7	PWR SMR NPP (RITM-200M, Russia) (Generation-III ⁺) (not yet in operation as an SMR NPP) (reactor coolant: $P=15.7$ MPa ($T_{\text{sat}}=345.8^{\circ}\text{C}$), $T=277\text{--}313^{\circ}\text{C}$; steam: $P_{\text{in}}=3.82$ MPa ($T_{\text{sat}}=247.6^{\circ}\text{C}$), $T_{\text{in}}=295^{\circ}\text{C}$; no secondary steam reheat), for T - s diagram, see Figure 20.2.11	Up to $\sim 31\%$
8	PWR SMR NPP (KLT-40S, Russia) (Generation-III, current fleet) (reactor coolant: $P=12.7$ MPa ($T_{\text{sat}}=329^{\circ}\text{C}$), $T=280\text{--}316^{\circ}\text{C}$; steam: $P_{\text{in}}=3.72$ MPa ($T_{\text{sat}}=246.1^{\circ}\text{C}$), $T_{\text{in}}=290^{\circ}\text{C}$; no secondary steam reheat), for T - s diagram, see Figure 20.2.10	Up to $\sim 26\%$

The safety rod drive is electro-mechanical, of a rack-and-pinion type. The rod drop time is below 0.5 s. The rod withdrawal time is at least 20 s. The rods are dropped by a spring action after the holding electric magnets are de-energized.

- (2) CGDM—designed to compensate for the excess reactivity in the reactor startup mode, the power operation mode, and the shutdown mode. The CGDM bank consists of: (a) four peripheral CGDMs; (b) three middle CGDMs; and (c) one central CGDM. Each CGDM incorporates: (a) working member (compensating group); (b) connecting elements; and (c) drive. The drive of a compensating group consists of a reduction gear screw mechanism, a step-motor, a motion sensor, and a checkpoint sensor. After the motor is de-energized, the compensating-group screw comes down from any position to the mechanical stop. Elements of the compensating-group drive are made of wear-resistant stainless steel.”

“The FNThPP based on the KLT-40S reactors implements an integrated approach to safety, which is based upon three mutually superimposed protection levels: resistance to abnormalities, emergencies, and accidents; preventing fuel damage in emergencies and accidents (limiting emergency/accident development, postaccident stabilization of the plant in a safe state); limiting radiation consequences of an accident. The major safety assurance tools are: simple, reliable and proven designs and systems; natural water circulation in the reactor and in the cooling circuits; large design-basis margins for characteristics assuring reliability and safety, including strength; the use of self-actuated devices to start safety systems; and passive-safety systems.

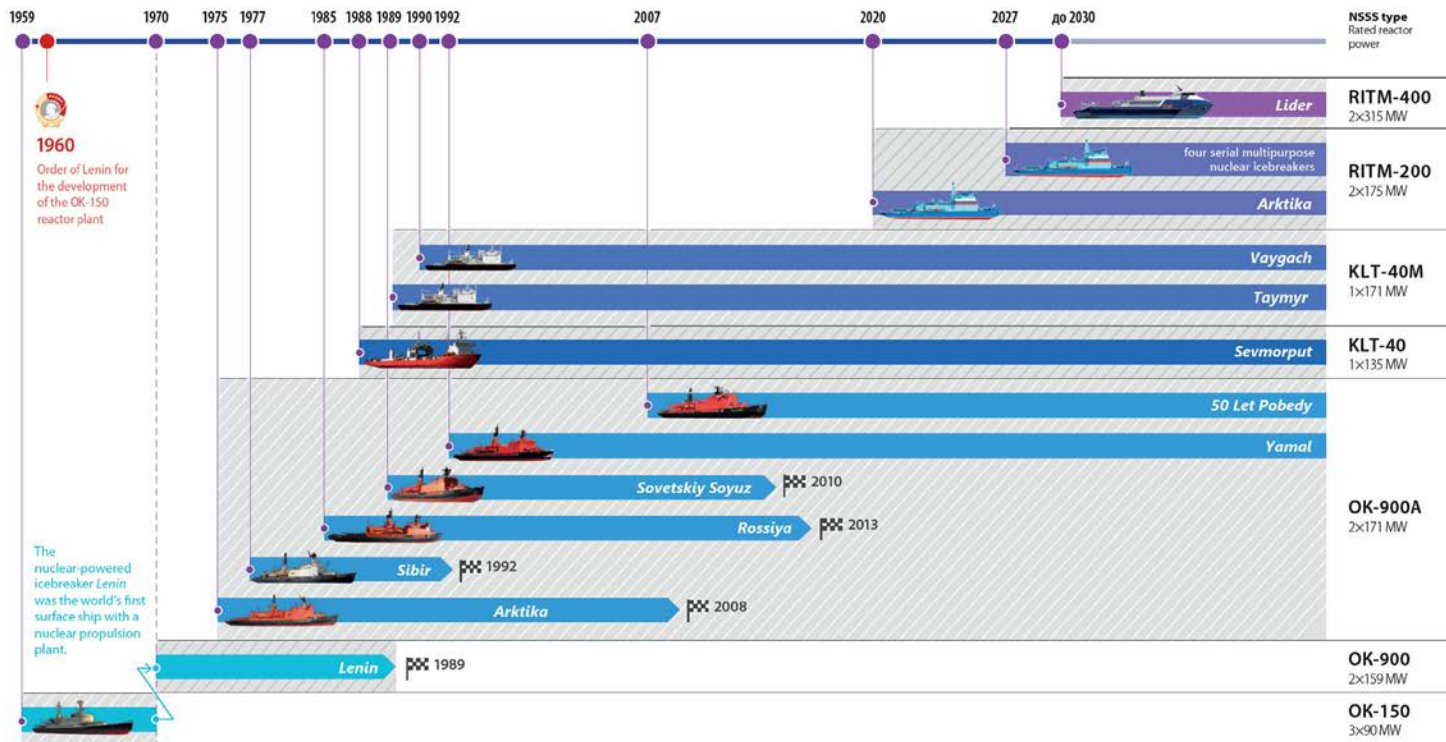
The safety basis for the FNThPP with the KLT-40S reactors is the plant’s inherent safety that is combined with the defense-in-depth functional and physical protection based upon the rational combination of active- and passive-safety systems (Figure 20.2.2). Physical properties of the reactor core (negative coefficients of power, fuel temperature and water temperature) enable self-adjustment of the reactor power as a function of the heat-removal capacity without any action of the reactivity-control elements, as well as a self-shutdown or reactor power self-limitation even without using the reactor-scrum system. Because of the strong negative “power-boiling” association, as soon as the power or the temperature grow, or steam appears in the KLT-40S reactor, the reaction rate reduces, the reactor decelerates, and the process slows down. There are no physical grounds for “unauthorized” growth of the reactor power and for the explosion-like processes.”

“Owing to the hydraulic characteristics and the selected reactor-module layout, the core cooling does not stop under any circumstances, because natural circulation of the primary coolant is ensured—the passive heat removal in emergency modes. The KLT-40S reactor has reiteratively redundant active- and passive-protection systems, which are built upon the variety principle used for the designs and action mechanisms. The passive-safety systems function with the use of the natural laws (gravitation, condensation, and

NSSS FOR THE NUCLEAR ICEBREAKER FLEET

JSC "Afrikantov OKBM" is a chief designer of reactor plants for the nuclear icebreaker fleet.

JSC "Afrikantov OKBM" has been developing reactor plant designs for nuclear-powered ships since 1954.



Twenty six nuclear reactors designed by JSC "Afrikantov OKBM" for 13 ships were manufactured totally (including 2 currently under construction). Moreover, a part of the reactor plant equipment was manufactured at the JSC "Afrikantov OKBM" production facilities.

The nuclear-powered icebreaker Lenin was the world's first surface ship with a nuclear propulsion plant.

Figure 20.2.1. History of development of small marine-propulsion reactors by the OKBM by the name of I.I. Afrikantov. Courtesy of JSC "Afrikantov OKBM": <http://www.okbm.nnov.ru/upload/iblock/7c6/fc8drypg4s59sma16g1pajwe86j2tay1.pdf>; accessed Feb. 19, 2022

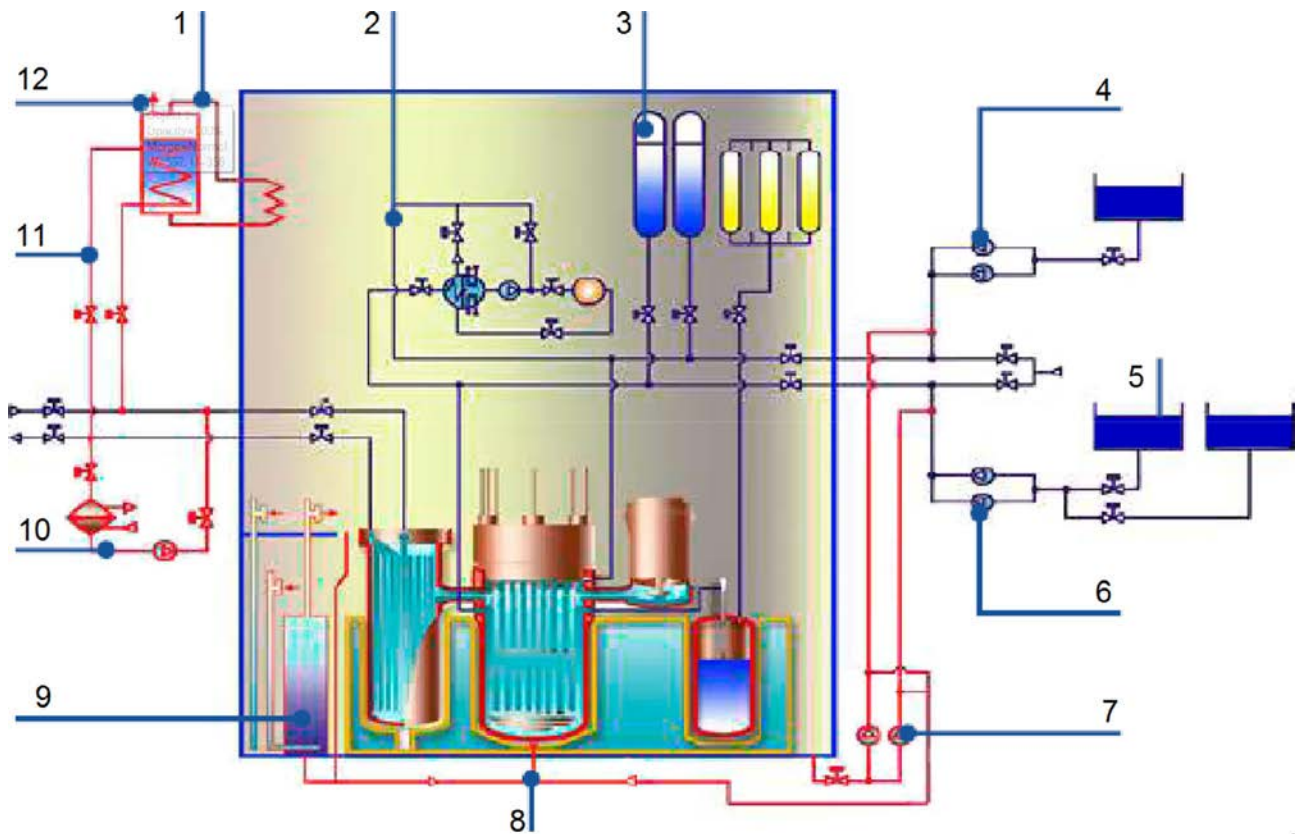


Figure 20.2.2. Schematic of KLT-40S reactor and its systems (in red—newly introduced safety systems): 1—Passive system of containment emergency pressure decrease (condensing system); 2—Active emergency-cooling system through heat exchangers of loops I–III; 3—Passive emergency core-cooling system (hydraulic accumulators); 4—Active emergency core-cooling system from feedwater pumps; 5—Active system for injecting liquid absorber; 6—Active emergency core-cooling system from feedwater pumps; 7—Active emergency core-cooling system through recirculation pumps; 8—System of reactor-caisson filling with water; 9—Containment passive-emergency pressure decrease system (bubbling); 10—Active emergency shutdown-cooling system (through process condensers); 11—Passive emergency shutdown-cooling system; and 12—To atmosphere. Based on <http://www.okbm.nov.ru/upload/iblock/69e/40i3dob8nyiig-sa0e5tlunlij2qr2mh9.pdf>; accessed Feb. 19, 2022

convection) without any consumption of energy or water, or actions by personnel. To enhance the efficiency of the safety systems and of the plant protection against personnel errors and functional failures of control elements, the KLT-40S reactor widely uses non-isolatable self-actuated devices to start protective systems while bypassing the traditional automation and protection circuits through directly employing the source parameter—the reactor pressure and the reactor-plant compartment pressure.”

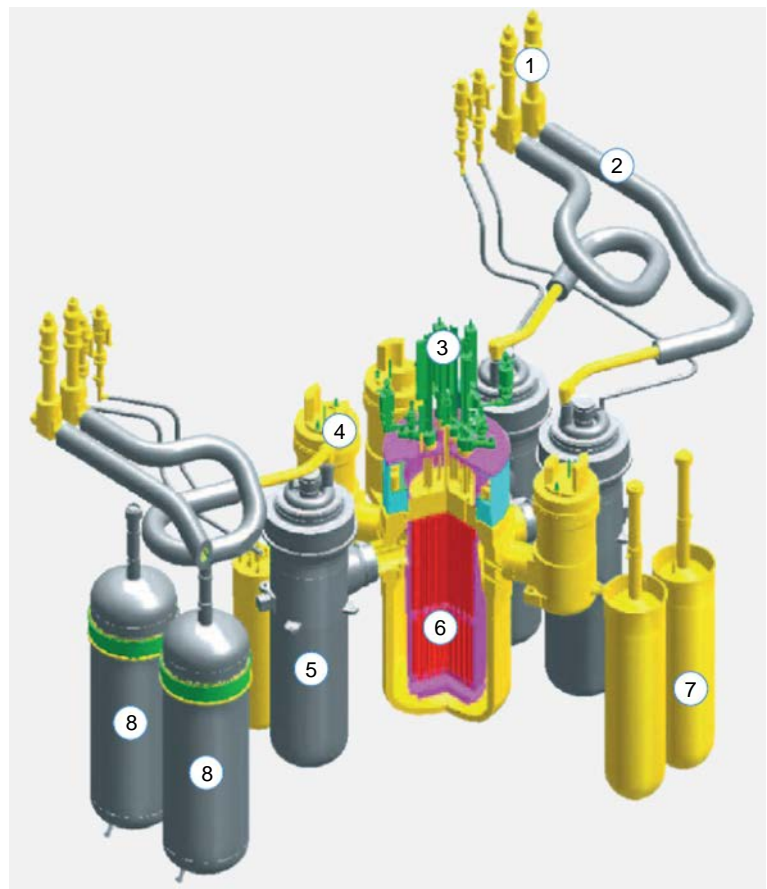
“Design Safety Features: (1) reactivity control features; (2) emergency shutdown-cooling system; (3) emergency core-cooling systems; (4) reactor-caisson water filling system; (5) emergency containment pressure-relief systems; (6) containment-flooding system; (7) containment; (8) protective enclosure; (9) isolation valves; and (10) liquid-absorber injection system” (Figure 20.2.2).

Also, Russia has developed and tested more advanced SMR—RITM-200M (see Figure 20.2.9 and Table 20.2.25), which is an integral PWR of Generation-III⁺ (booklet on RITM-200M by the JSC “Afrikantov OKBM”). Currently, Rosatom has decided to build an in-land NPP with RITM-200M SMRs in Yakutia.



Figure 20.2.3. Reactor KLT-40S (КЛТ-40С in Russian abbreviations) (in center) with four steam generators (larger cylinders) and four reactor-coolant circulation pumps (smaller cylinders). KLT—Container-carrier cargo-Lighter Transport (reactor) (Контейнеровоз Лихтеровоз Транспортный (реактор) (in Russia abbreviations). *Courtesy of JSC “Afrikantov OKBM”*: <http://www.okbm.nnov.ru/upload/iblock/93f/lz0fnvoyk1v5bvm81os1yljisjv1zr13.pdf>; accessed Feb. 19, 2022

Figure 20.2.4. KLT-40S Reactor-plant configuration: 1—Isolation valves; 2—Steam pipelines; 3—CRDMs (Control Rod Drive Mechanism); 4—Primary Circuit Circulation Pump (PCCP); 5—Steam generator; 6—Reactor; 7—Pressurizer; and 8—Hydro-accumulator. *Courtesy of JSC “Afrikantov OKBM”*: <http://www.okbm.nnov.ru/upload/iblock/69e/40i3dob8nyiigsa0e5tlunlij2qr2mh9.pdf>; accessed Feb. 19, 2022



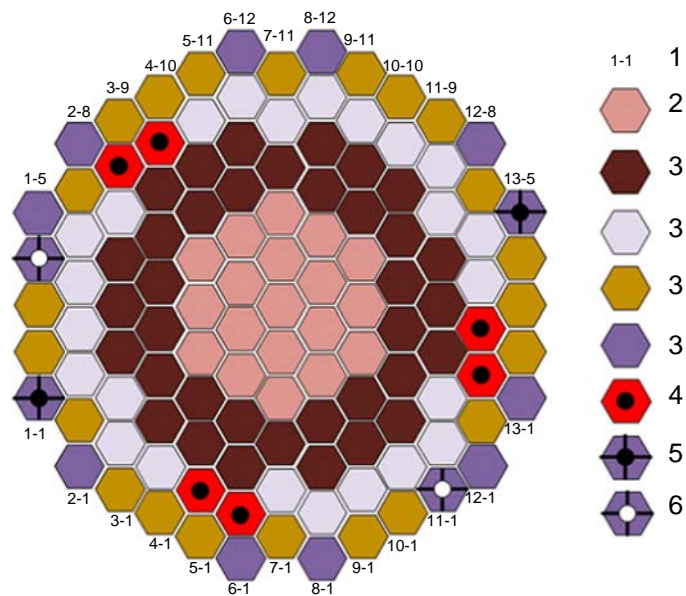


Figure 20.2.5. KLT-40S reactor-core cross section (Prepared by UOIT student A. Khan; based on original figure by JSC “Afrikantov OKBM”): 1—cell number; 2—main assembly in central zone; 3—main assemblies; 4—assembly with emergency shut-down rod; 5—assembly for neutron-absorber location; and 6—assembly peripheral zone for location of extra sensors for neutron-flux control. The reactor-core type is heterogeneous with a hard spectrum of thermal neutrons. The reactor core is based upon an array structure with fuel assemblies for various purposes and fuel with a high uranium content

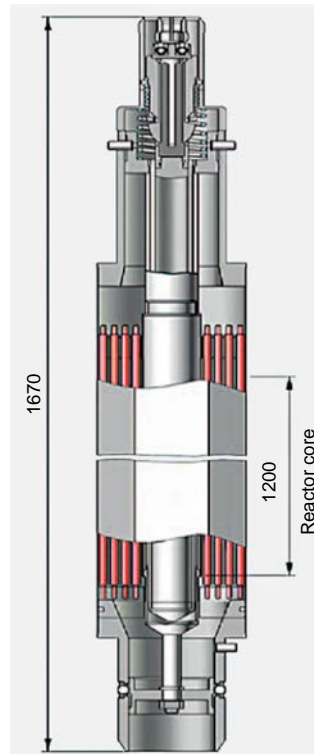


Figure 20.2.6. General view of a fuel assembly. Courtesy of JSC “Afrikantov OKBM”: <http://www.okbm.nnov.ru/upload/iblock/69e/40i3dob8nyiigsa0e5tlunlij2qr2mh9.pdf>; accessed Feb. 19, 2022

Figure 20.2.7. General view of the reactor compartment in the KLT-40S Reactor Plant: 1—Reactor Pressure Vessel (RPV) head; 2—Control Rod Drive Mechanisms (CRDM); 3—Reactor; 4—Primary Circuit Circulation Pump (PCCP); and 5—Steam generator. *Courtesy of JSC “Afrikantov OKBM”*: <http://www.okbm.nnov.ru/upload/iblock/69e/40i3dob8nyiiigsa0e5tlunlij2qr2mh9.pdf>; accessed Feb. 19, 2022

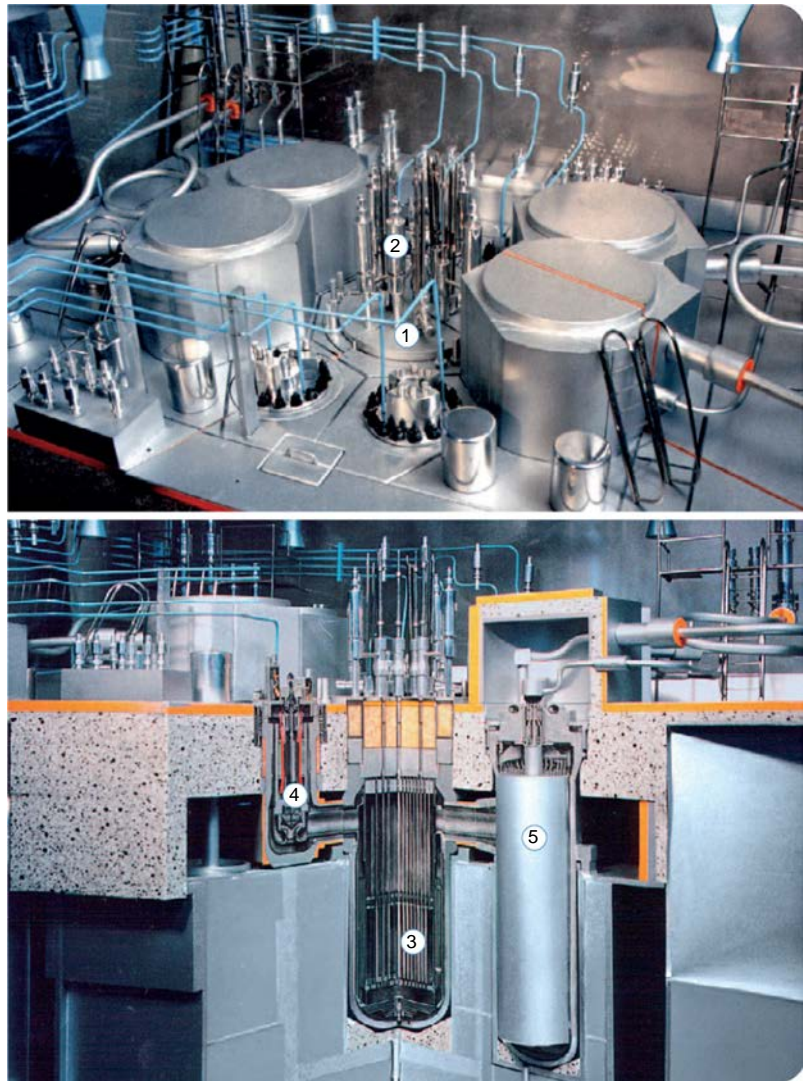


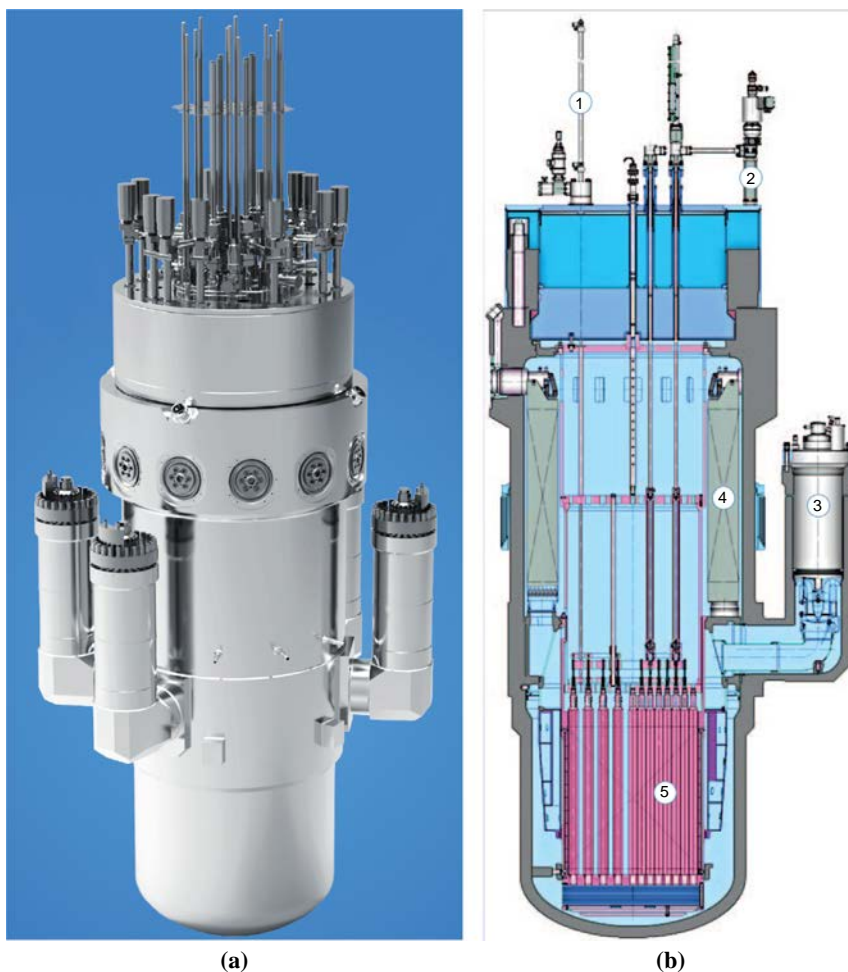
Figure 20.2.8. (a) Photo of Floating Nuclear Thermal-Power Plant (FNTThPP) (Плавающая Атомная Тепловая ЭлектроСтанция (ПАТЭС) (in Russian abbreviations)) on barge with two KLT-40S reactors on its way to port Pevek (<https://www.flickr.com/photos/rosatom/albums/72157692330711570>; accessed Feb. 19, 2022). Barge: Length—140 m; width—30 m; height of board—10 m; draught—5.6 m; displacement—~21,000 t; underwater foundation pit in m—175 (L) × 45 (W) × 9 (D); operating term of FNTThPP—40 years; number of servicing personal—~70; and construction term—4 years.

(Continued)



Figure 20.2.8, Cont'd (b) FNThPP layout with two KLT-40S reactors: 1—Reactors; 2—Steam-turbine power hall; 3—Underwater trench; 4—Waterside structures; 5—Heat point; 6—Hot-water tanks; 7—Switchgear and devices for electricity distribution and transmission to consumers. (c) Floating Nuclear Power & Desalination System (FNPDS) with KLT-40S Reactor(s) (artist image): 1—Coastal infrastructure; 2—Waterside structures; 3—Floating Power Unit (FPU); and 4—Floating Desalination Unit (FDU). (a) Courtesy of ROSATOM, photo by A. Bashkirov. (b) Courtesy of JSC “Afrikantov OKBM”: <http://www.okbm.nnov.ru/upload/iblock/7c6/fc8drypg4s59sma16g1pajwe86j2tay1.pdf>; accessed Feb. 19, 2022. (c) Courtesy of JSC “Afrikantov OKBM”: <http://www.okbm.nnov.ru/upload/iblock/7c6/fc8drypg4s59sma16g1pajwe86j2tay1.pdf>; accessed Feb. 19, 2022

Figure 20.2.9. (a) Generation III⁺ SMR—RITM-200M with 4 steam generators integrated inside pressure vessel; small cylinders—circulation pumps. (b) 1—Control Rod Drive Mechanism (CRDM) (6 in total); 2—Control Group Drive Mechanism (CGDM) (12 in total); 3—Primary Circuit Circulation Pump (PCCP) (4 in total); and 5—reactor core. *Courtesy of JSC “Afrikantov OKBM”*: <http://www.okbm.nnov.ru/upload/iblock/7c6/fc8drypg4s59sma16g1pajwe86j2tay1.pdf>; accessed Feb. 19, 2022)



Analysis of the data in Table 20.2.25 shows that KLT-40S and RITM-200M require LEU with enrichments of 18.6% and <20%, respectively, which are significantly higher than those in any modern light- or heavy-water nuclear power reactors. However, thermal efficiencies of these SMRs NPPs are lower than those of modern NPPs equipped with other types of reactors (see Table 20.2.26). Also, interesting fact is that both these SMRs NPPs have overheated steam at the outlet of steam generators compared to saturated steam at light- and heavy-water-cooled reactors NPPs (Figures 20.2.10–20.2.12). Also, based on the data from open literature the Rankine power cycle does not have a reheat option, which is common for any other NPPs. In addition, it should be noted that development of these two SMRs took significantly longer time (13 years) than it was expected from the beginning and original budget was overspent.

Extra things, which should be known, are (based on KLT-40S reactor and plant): “The reactor-plant equipment (cargo within the loading gage) is transported from the manufacturing companies to the builder-company by truck or by rail. The maximum mass of the transported equipment (RPV) is 46.5 t. The installation work on the power-plant equipment is performed on assemblies up to 300 t in mass, which are factory-assembled in specialized sectors. Other equipment is brought for installation as part of assemblies or separately. These assemblies are installed on the FNThPP with a 350-t crane. To bring other equipment and assemblies to the NPP, a 20-30-ton crane is sufficient.” Such method of construction guarantees high quality and shorten time.

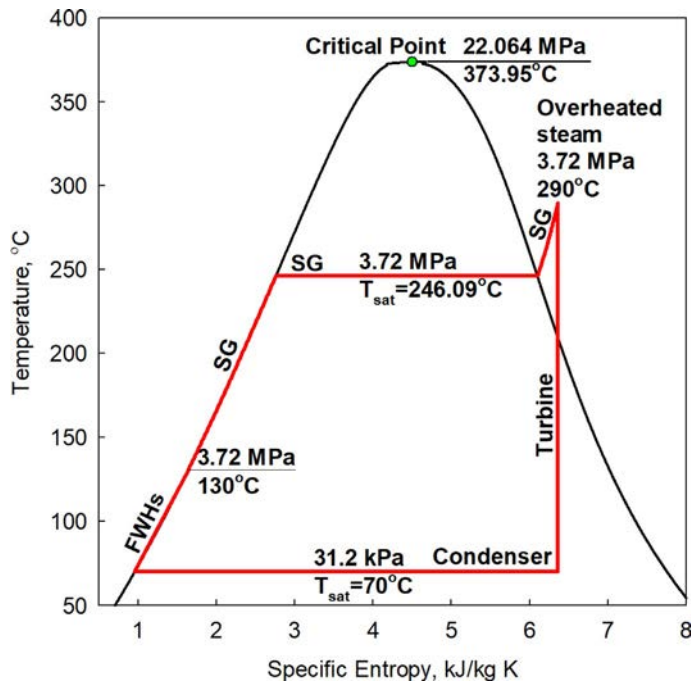


Figure 20.2.10. Simplified T - s diagram of 35-MW_{el} SMR KLT-40S (Akademik Lomonosov floating NPP, Chukotka, Russia) Rankine cycle (Pioro et al., 2020b). The diagram was prepared based on data available in the open literature. FWHs, FeedWater Heaters; SG, Steam Generator

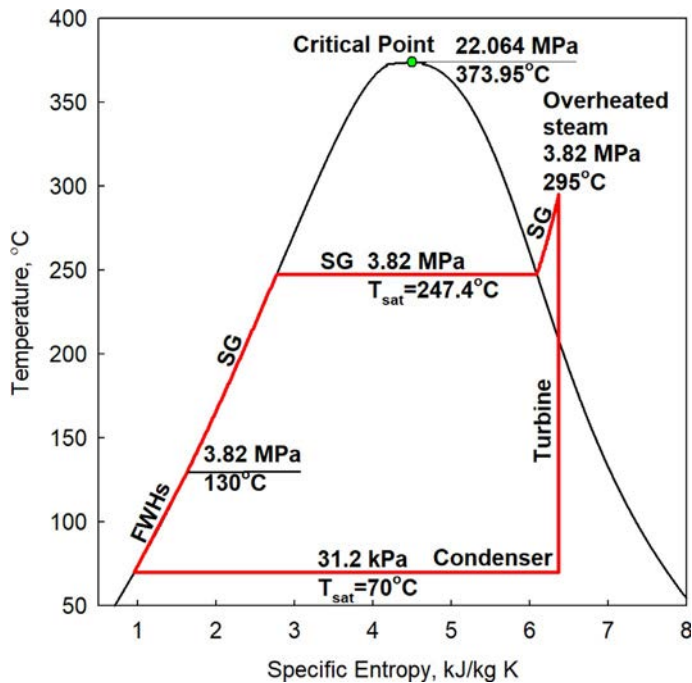
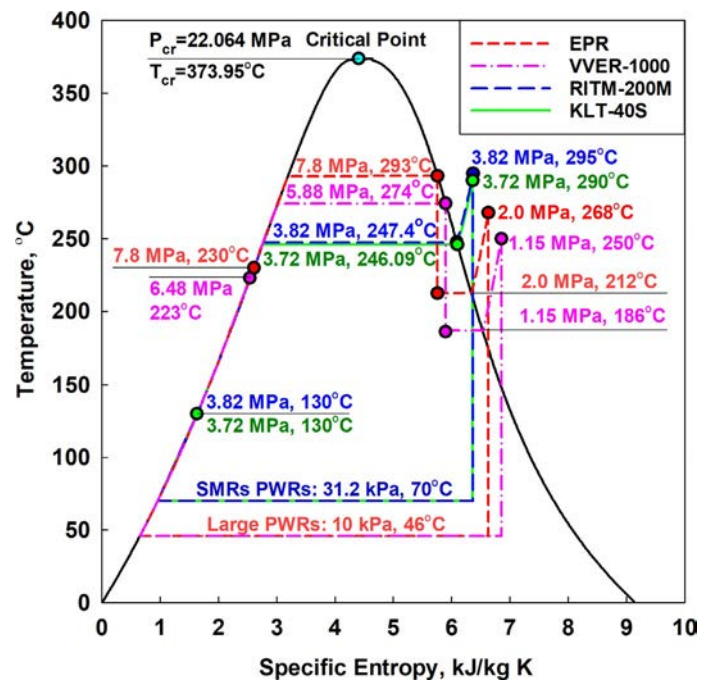


Figure 20.2.11. Simplified T - s diagram of 50-MW_{el} SMR RITM-200M (Generation-III⁺ SMR, Russia) Rankine cycle (Pioro et al., 2020b). Feedwater inlet and outlet temperatures were assumed to be the same as those in KLT-40S NPP. The diagram was prepared based on data available in the open literature. FWHs, FeedWater Heaters; SG, Steam Generator

Figure 20.2.12. Comparison of four simplified T - s diagrams for PWRs: (1) EPR; (2) VVER-1000; and Russian SMRs: (3) RITM-200M; and (4) KLT-40S. Areas inside T - s diagrams for SMRs RITM-200M and KLT-40S are smaller compared to those of large PWRs (EPR and VVER), due to that thermal efficiencies of NPPs with these SMRs are significantly lower, i.e., actually the lowest ones in nuclear power industry (for exact data, see Table 20.2.11).



20.2.5 Special considerations on SMRs and future development and implementation

20.2.5.1 Safety and licensing requirements

The basic overarching and most important Safety Objective (SO) is to keep the reactor core cooled and the system controlled at all times (ASME, 2012; Howlett, 2003). Often confused, it is important to distinguish between:

- (a) Improved safety and reduced risk in the sense of assuring event-free operation, “resilience” to unexpected happenings and challenges, market return on investment, reduced accident chances, and improved societal acceptance; For new builds, designs and concepts, it has been pointed out elsewhere that past safety-analysis practice and systems design really require updating and enhancement based on exploiting modern technological advances (D’Auria et al., 2019) and
- (b) Traditional formal licensing processes and regulatory requirements, which are based on providing and issuing siting and operation permits, and focus on ensuring public safety based on accident frequency, activity release and core damage estimates. The need to streamline or at least “harmonize” such past nationally different and cumbersome licensing processes is also being recognized, using a “risk-informed, performance-based, and technology-inclusive approach” (<https://dailyenergyinsider.com/news/23528-nrc-proposes-new-rule-for-emergency-preparedness-for-reactors/>).

In particular, it is not the responsibility of a regulator in any nation for actual plant operation, overall capacity factor, thermal efficiency, fuel-cycle sustainability, economic viability, project management or energy market share. Obviously safe operation is vital, so is linked to safety “culture,” reduced economic risks, and public acceptance. Current data for actual severe reactor accidents (Three Mile Island, Chernobyl, and Fukushima) illustrate that the actual Core Damage Frequency (CDF) is higher than predicted by state-of-the-art probabilistic assessments, primarily due to the inadequate prevention against and control of extreme and unexpected events.

With multiple new concepts and many innovative designs, especially, those that claim long-term cooling due to natural circulation or almost complete avoidance of core damage, the safety focus is shifted from

activity release consequences to verifying risk and safety margins with potentially limited experimental verification. In addition, initial studies by the SMR Regulators Forum have focused making the distinction between examining multiple reactor units and the safety of multiple modules potentially sharing common facilities, safety systems and sites (ARIS IAEA, 2020a, b). The Forum notes that multiunit SMR plants “may impact among others, the selection of initiating events, internal and external hazards, the approach to shared systems, defense in depth, human factors engineering and risk assessment.”

Furthermore, the Forum has stated that the existing arrangements for regulating large NPPs are also suitable for regulating activities involving SMRs, implying the same lengthy and onerous level of paperwork, inspection and review requirements *independent of the actual SMR concept or design*.

20.2.5.2 Pathways to success

Development and design of any nuclear reactor require not only excellent ideas, but also excellence and special experience, qualifications, and dedication of the nuclear engineering company and plant operating employees. Also, it should be a sort of a “critical mass” of a number of employees inside company to be able to deliver a complete design of a reactor. Of course, as additional factors, sophisticated test facilities, research reactor(s) for thermalhydraulics, fuels, and materials testing, and adequate funding are required for the success.

Other important considerations include:

- (1) SMRs and SMR NPPs will be expensive during construction and operation (based on the example of KLT-40S).
- (2) Operation of small NPPs will be more expensive per kW of installed capacity compared to that of large modern NPPs.

The only way to avoid these deficiencies is to build tens or even hundreds of SMRs. However, it will lead to the following problems:

- (1) How to keep high level of safety and reliability?
- (2) How to provide a proper operation of all these SMRs, continuous training and high qualification of thousands of employees spread over a country?
- (3) How to organize repairing services for a large number of SMRs scattering across a country including remote locations? and
- (4) Location of many “dangerous” objects as SMRs across a country will lead to more scare and opposition not only from a population, but, also, from a government, because it will be more difficult to secure and supervise all these small NPPs!

The nuclear power industry history shows that even large and well-known world companies with tens of thousands of experienced, highly qualified and dedicated employees, sophisticated test facilities, research reactors, and adequate funding had failed to deliver their nuclear reactors on time and on budget. Due to that they went through quite difficult times or even were split in parts and sold to other vendors and investors.

To the best of our belief, the SMR concepts will never directly replace or displace the role of large nuclear power reactors, and very few of the listed SMRs/S&MRs in Tables 20.2.1–20.2.24 will reach the final design stage despite significant “enthusiasm.” This includes worldwide efforts to develop various types of SMRs by well-known world nuclear vendors such as Areva, BARC, CEA/EDF, CNNC, General Atomics, Hitachi-GE, MHI, OKBM Afrikantov, Rosatom, Toshiba, Westinghouse, and others, as well as by multiple start-up companies, research organizations, venture capitalists, entrepreneurs, universities, etc. This statement is partly based on the latest experience by the Rosatom with the KLT-40S floating NPP (see Section 20.2.3), and the additional issues raised by A. Lankevich in “The main non-proliferation and safeguards challenges facing

the SMRs” (<http://atominfo.ru/en/news4/d0530.htm>). These include requiring: Legal frameworks for widespread enriched-fuel utilization and its interstate transportation; elimination of potential for plutonium production; sabotage and terrorist-attacks prevention; accounting and remote monitoring of nuclear materials; assured cooling of Spent Nuclear Fuel (SNF) during transportation; and equipment operating without maintenance for a time commensurate with core lifetime.

However, SMRs will undoubtedly have their unique “niche” applications of being implemented in remote areas, small electrical grids, military facilities, and as floating NPPs.

20.2.6 Conclusions

1. SMRs are today’s a very “hot” topic in nuclear engineering worldwide. According to the IAEA, there are more than 55 SMRs designs/concepts proposed in the world (in this Chapter about 108 SMRs/S&MRs are listed). Russia is the first country in the world, which put into operation two SMRs—KLT-40S reactors barge-based as a floating NPP for the Northern regions. These first PWR-SMRs require LEU with enrichments of 18.6%, which are significantly higher than those in any modern light- or heavy-water reactors. However, thermal efficiency of this floating NPP is lower than those of modern NPPs equipped with various types of reactors. In addition, it should be noted that development of these two KLT-40S SMRs took significantly longer time (13 years) than it was expected.
2. Development and design of any nuclear reactor require not only excellent ideas, but also excellence and special experience, qualifications, and dedication of the nuclear-engineering company and plant operating employees. Also, it should be a sort of a “critical mass” of a number of employees inside company to be able to deliver a complete design of a reactor. Of course, as additional factors, sophisticated test facilities, research reactor(s) for thermalhydraulics, fuels, and materials testing, and adequate funding are required for the success.
3. To the best of our belief, the SMR concepts will never directly replace or displace the role of large nuclear power reactors, and very few of the developed SMRs/S&MRs in the world will reach the final design stage despite significant “enthusiasm.” This includes worldwide efforts to develop various types of SMRs by well-known world nuclear vendors as well as by multiple start-up companies, research organizations, venture capitalists, entrepreneurs, universities, etc.
4. Some issues, which have to be resolved before a widespread implementation of SMRs, include: Legal frameworks for widespread enriched-fuel utilization and its interstate transportation; elimination of potential for plutonium production; sabotage and terrorist-attacks prevention; accounting and remote monitoring of nuclear materials; assured cooling of SNF during transportation; and equipment operating without maintenance for a time commensurate with core lifetime. However, in spite of all these difficulties in SMR development, they will undoubtedly have their unique “niche” applications of being implemented in remote areas, small electrical grids, military facilities, and as floating NPPs.

References

- ARIS IAEA, 2020a. Advances in Small Modular Reactor Technology Developments. A Supplement to: IAEA Advanced Reactors Information System (ARIS), p. 354. Free download from: https://aris.iaea.org/Publications/SMR_Book_2020.pdf.
- ARIS IAEA, 2020b. <https://aris.iaea.org/sites/overview.html>. (Accessed 15 July 2020).
- ASME (American Society of Mechanical Engineers), 2012. Forging a New Nuclear Safety Construct, Presidential Task Force on Response to Japan Nuclear Power Plant Events. ASME, New York, NY, USA. ISBN 978-0-7918-3435-0. Free download from: <https://files.asme.org/Events/NuclearSafetyConstructWorkshop/34231.pdf>.
- D’Auria, F., Debrecin, N., Glaeser, H., 2019. The technological challenge for current generation nuclear reactors. *Nuclear Energy Technol.* 5 (3), 183–199.

- Handbook, 2016. In: Pioro, I.L. (Ed.), Handbook of Generation IV Nuclear Reactors. Elsevier–Woodhead Publishing (WP), Duxford, UK, p. 940. Handbook content is available on: https://www.gen-4.org/gif/jcms/c_9373/publications.
- Handbook, 2021. In: Ingersoll, D.T., Carelli, M.D. (Eds.), Handbook of Small Modular Nuclear Reactors, second ed. Elsevier–Woodhead Publishing (WP), Duxford, UK. 609 pp.
- Howlett II, H.C., 2003. The Industrial Operator’s Handbook. Techstar Inc., Pocatello, ID, USA. 316 pp.
- Nuclear News, 2022. 24th Annual Nuclear News Reference Section, March. Publication of American Nuclear Society (ANS), March, pp. 64–69.
- OKBM, 2020. <http://www.okbm.nnov.ru/>.
- Pioro, I., Dort-Goltz, N., McKellar, J., 2020a. Current Status of Nuclear Power in the World Including Latest Developments on SMRs, Proceedings of the 29th International Conference Nuclear Energy for New Europe (NENE-2020). Portorož, Slovenia, September 7-10, Paper 409. 10 pp. Free download from: http://www.rcp.ijs.si/bojan/NENE2020USB/pdf/NENE2020_0409.pdf.
- Pioro, I., Duffey, R.B., Kirillov, P.L., Dort-Goltz, N., 2020b. Current status of reactors deployment and small modular reactors development in the world. ASME J. Nuclear Eng. Radiat. Sci. 6 (4). 24 pp. Free download from: <https://asmedigitalcollection.asme.org/nuclearengineering/article/6/4/044001/1085654/Current-Status-of-Reactors-Deployment-and-Small>.
- Pioro, I., Duffey, R.B., Kirillov, P.L., Pioro, R., Zvorykin, A., Machrafi, R., 2019. Current status and future developments in nuclear-power industry of the world. ASME J. Nuclear Eng. Radiat. Sci. 5 (1). 27 pp. Free download from: <https://asmedigitalcollection.asme.org/nuclearengineering/article/doi/10.1115/1.4042194/725884/Current-Status-and-Future-Developments-in-Nuclear>.

21

Alternative power cycles for
Generation-IV reactors

21.1

Alternative power cycles for selected Generation-IV reactors[☆]Igor L. Pioro^a, Romney B. Duffey^b, Mohammed Mahdi^a, and Roman Popov^a^aFaculty of Energy Systems and Nuclear Science, University of Ontario Institute of Technology,
Oshawa, ON, Canada ^bIdaho Falls, ID, United States

Nomenclature

- c_p Specific heat at constant pressure, J/kg K
 D Diameter, m
 G Mass flux, kg/m²s
 h Heat transfer coefficient, W/m²K
 k Thermal conductivity, W/mK
 L Length, m
 P Pressure, MPa
 T Temperature, °C

Greek symbols

- α Thermal diffusivity, m²/s; $\left(\frac{k}{c_p \cdot \rho}\right)$
 μ Dynamic viscosity, Pas
 η Efficiency, %
 ρ Density, kg/m³
 ν Kinematic viscosity, m²/s; $\left(\frac{\mu}{\rho}\right)$

Non-dimensional numbers

- Nu** Nusselt number; $\left(\frac{h \cdot D}{k}\right)$

[☆] This chapter is mainly based on our previous publications: Pioro et al. (2021), Pioro et al. (2017a,b, 2018), Pioro (2021), Mahdi et al. (2017, 2018), and Popov et al. (2017).

Pr Prandtl number; $\left(\frac{\mu \cdot c_p}{k}\right) = \left(\frac{\nu}{\alpha}\right)$

Re Reynolds number; $\left(\frac{G \cdot D}{\mu}\right)$

Acronyms/abbreviations

BN	Fast Sodium (reactor) (БН—Быстрый Натриевый (in Russian abbreviations) (Russia))
BREST-OD	Fast Reactor with Inherent Safety Lead Coolant—Experimental Demonstration (БРЕСТ-ОД—Быстрый Реактор Естественной безопасности со Свинцовым Теплоносителем—Опытно-Демонстрационный or Быстрый Реактор Естественной безопасности—Опытно-Демонстрационный (in Russian abbreviations) (Russia))
Comp.	Compressor
GFR	Gas-cooled Fast Reactor
GIF	Generation-IV International Forum
GT-MHR	Gas-Turbine Modular Helium-cooled Reactor
HPT	High-Pressure Turbine
HT	High Temperature
HTC	Heat Transfer Coefficient
HTGR	High-Temperature Gas-cooled Reactor
HTR	High-Temperature Recuperator
HX	Heat eXchanger
IHX	Intermediate Heat eXchanger
JSC	Joint Stock Company
K	Compressor
LFR	Lead-cooled Fast Reactor
LPT	Low-Pressure Turbine
LTR	Low-Temperature Recuperator
MSR	Molten Salt Reactor
NPP	Nuclear Power Plant
NRC “KI”	National Research Center “Kurchatov Institute”
OKBM	Experimental Design Bureau of Mechanical-engineering (ОКБМ—Опытно-Конструкторское Бюро Машиностроения (in Russian abbreviations) (Russia))
RF	Russian Federation
S	Supercritical
SC	SuperCritical
SCP	SuperCritical Pressure
SCWR	SuperCritical Water-cooled Reactor
SFR	Sodium-cooled Fast Reactor
SG	Steam Generator
T	Turbine
USA	United States of America
VG	High-temperature Gas-cooled (reactor) (Высокотемпературный Газовый (in Russian abbreviations) (Russia))
VGM	High-temperature Gas-cooled Modular (reactor) (Высокотемпературный Газовый Модульный (in Russian abbreviations) (Russia))
VHTR	Very-High-Temperature Reactor

Chapter 2 of this Handbook is dedicated to Generation-IV International Forum (GIF) original concepts of six advanced reactors: (1) Very-High-Temperature Reactor (VHTR) (Figure 2.5); (2) Gas-cooled Fast Reactor (GFR) (Figure 2.6); (3) Sodium-cooled Fast Reactor (SFR) (Figure 2.7); (4) Lead-cooled Fast Reactor (LFR) (Figure 2.8); (5) Molten Salt Reactor (MSR) (Figure 2.9); and (6) SuperCritical Water-cooled Reactor (SCWR) (Figure 2.11).

21.1.1 Basic-cycle options

These original GIF concepts represent technology developments dating or originating from about year 2000 or even earlier, as part of GIF cooperative R&D under formal bilateral or multilateral collaborative agreements. Hence:

- (1) VHTR is shown as a reactor connected with the hydrogen-production plant using thermochemical sulfur-iodine cycle (Figure 2.5). However, high-temperature reactor coolant He with T up to 1000°C can be used for generation of electricity with high thermal efficiency and process heat (see Figure 21.1.1 and Table 21.1.1). Therefore, VHTR has to be linked with a power cycle for electricity generation.
- (2) GFR is shown with the direct Brayton helium-turbine power cycle (Figure 2.6).
- (3) SFR was originally connected to the Rankine steam-turbine power cycle (Figure 2.7), which actually is the current option for two Russian SFRs—BN-600 and BN-800 reactors, and one small Chinese sodium-cooled reactor (20MW_{el})—China Experimental Fast Reactor (CEFR) connected to the subcritical-pressure Rankine superheated-steam-turbine power cycle.

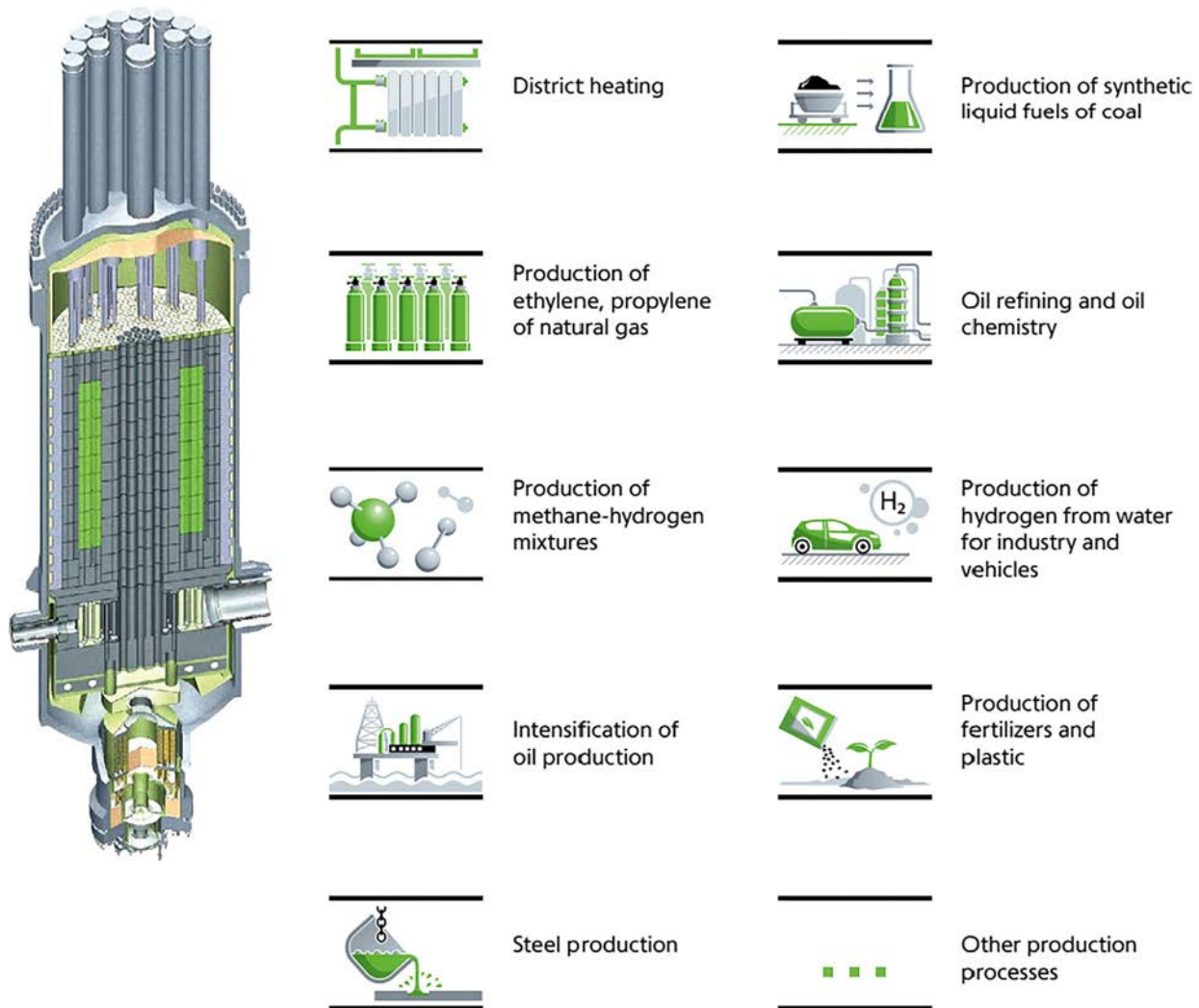


Figure 21.1.1. HTGR application options. *Courtesy of OKBM Afrikantov*

Table 21.1.1. Experience of HTGRs development in Russia

Specifications	State program in nuclear and hydrogen power		OKBM, NRC “KI,” VNIPIneft	Rosenergoatom	Agreement 2000 RF/USA
	–		Modular type		
Projects	VG-400	VGM	VGM-P	MHR-T	GT-MHR
Purpose	Heat and electricity generation for industrial processes		Heat generation for oil refinery	Hydrogen and electricity generation	Generation of electricity and heat for district heating
Thermal power, MW	1060	200	215	600	600
Coolant	Helium				–
Helium T at core outlet, °C	950	950	750	950	850
Status	Basic design		Technical proposal		Preliminary design Development of key technologies
	1987	1989	1991	2004	2002 2003–2014

Based on data by OKBM Afrikantov.

- (4) LFR and
 (5) MSR are shown with the indirect Brayton gas-turbine power cycle (Figures 2.8 and 2.9, respectively).
 And, finally,
 (6) SCWR is shown with the direct supercritical-pressure Rankine “steam”-turbine power cycle (Figure 2.11).

From all these power cycles, only three are well-known and proven in thermal power industry for tens of years:

- (1) Open Brayton gas-turbine cycle with combustion products (inlet temperature up to 1650°C) (combined-cycle of gas-fired power plants);
- (2) Subcritical-pressure Rankine superheated-steam-turbine power cycle (older coal-fired power plants); and
- (3) SuperCritical-Pressure (SCP) Rankine “steam”-turbine power cycle (advanced coal-fired power plants).

Also, it is well-known and proven from the thermal power industry that only combined cycle, i.e., high-temperature Brayton gas-turbine cycle with the subcritical-pressure Rankine superheated-steam-turbine power cycle, can achieve the highest thermal efficiencies up to 62% (Brayton cycle—30%; and Rankine cycle—40%) (see Table 1.1.7 and see also, Appendix A1.1.1). SCP Rankine “steam”-turbine power cycle is also quite efficient, but still its thermal efficiency is by 7% lower than that of the combined cycle.

Therefore, the major conclusion, based on proven experiences in thermal power industry, is that high-temperature Generation-IV nuclear-power reactors such as VHTRs and GFRs helium-cooled with the maximum outlet temperatures up to 1000°C and 850°C, respectively, should be connected to combined power cycles. Also, another problem, which limiting operational term of direct Brayton helium-turbine power cycle is ingress of helium into bearings of gas turbines (for more details on helium turbines and corresponding Brayton cycles, see next [Chapter 21.2](#)), thus rendering any direct helium cycle unusable with present materials and engineering technology.

To address the abovementioned issues and challenges with high-temperature-reactors power cycles new indirect combined cycles must be proposed and are currently under development in a number of countries. For other Generation-IV reactor concepts, e.g., SFRs—accounting that the boiling point of sodium is 883°C, and the current level of maximum temperature inside Russian BN-600 and BN-800 reactors is about 550°C, there is not much room to increase it. Therefore, Generation-IV SFRs will be possibly connected to the same indirect subcritical-pressure Rankine superheated-steam-turbine power cycle with thermal efficiency of 40% (max 42%), which is proven in the Russian nuclear-power industry for about 50 years (starting with BN-350 reactor—commercial operation from 1973 and till 1999). Also, it should be mentioned that some countries, e.g., USA, consider connecting SFRs with indirect SCP carbon-dioxide power cycle to avoid a possibility for any contact between sodium and water during a leak in a steam generator, but such power cycle(s) is only under development and has not been proven in industry yet.

For LFRs, Russia has a completed design of the BREST-OD-300 reactor with two options for the indirect power cycle: (1) subcritical-pressure Rankine superheated-steam-turbine power cycle with thermal efficiency up to 43%; and (2) SCP Rankine “steam”-turbine power cycle, which will have slightly higher efficiency. Moreover, the nationally-owned company Rosatom has started to build the first NPP with BREST-OD-300 reactor with the indirect power cycle (Option 1, see above) at the site of the Siberian Chemical Combine, a subsidiary of Rosatom’s TVEL Fuel Company, in Seversk, Russia’s Tomsk region (start of operation planned for 2026) (<https://rosatom.ru/en/search/?q=brest-OD-300&how=r>).

Of course, boiling point of lead is significantly higher than that for sodium, i.e., 1750°C compared to 883°C, however, current maximum temperature in the BREST-OD-300 reactor is planned about 540°C (parameters of the subcritical-pressure Rankine superheated-steam power cycle: steam generator: inlet— $P=17$ MPa and $T=340$ °C and outlet— $T=505$ °C). This is due to some other technical problems, which don’t allow to operate this reactor at higher lead temperatures for now. Also, the same as for SFRs indirect SCP carbon-dioxide power cycle is possible, but might be not necessary, because lead is quite inert liquid metal compared to very chemically active sodium as a representative of alkali metals. However, molten lead explodes violently on contact with water, so SC CO₂ is preferable from a safety perspective.

In terms of MSR, non-water-based power cycles are considered, the indirect Brayton gas-turbine power cycle and/or indirect combined cycles.

21.1.2 Cycles for gas-cooled reactors (VHTRs and GFRs) and SFR

Therefore, the following cycles have been originally proposed for helium-cooled reactors, i.e., VHTRs and GFRs, for which they are more suitable due to the highest reactor coolant (helium) outlet temperatures (up to 1000°C for VHTRs and up to 850°C to GFRs) compared to other Generation-IV reactors, but there is a possibility that they might be used and for other Generation-IV concepts with the exception of SCWRs, which intended to use direct or indirect SCP Rankine “steam”-turbine power cycle.

[Figure 21.1.2](#) shows a simplified layout of a VHTR NPP with the indirect combined cycle: Primary—Brayton gas-turbine cycle (working fluid—mixture of nitrogen and helium) and Secondary—subcritical-pressure Rankine steam-turbine cycle; and hydrogen cogeneration.

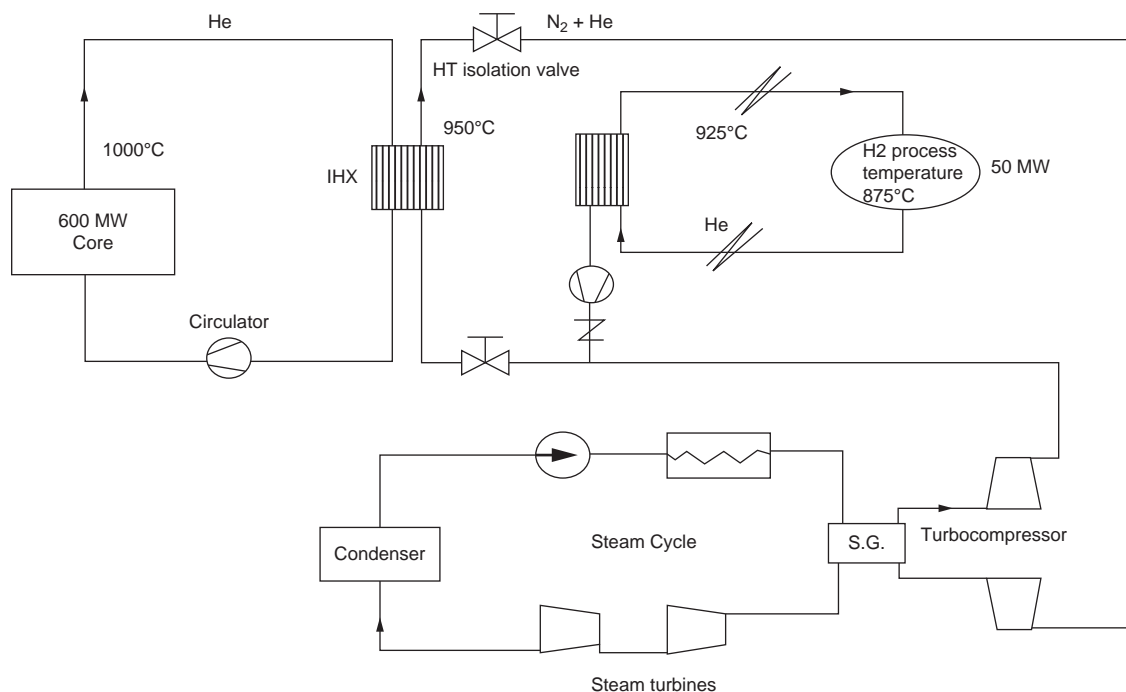


Figure 21.1.2. Simplified layout of VHTR NPP (reactor coolant—helium at 5 MPa) with indirect combined cycle (primary—Brayton gas-turbine cycle (working fluid—mixture of nitrogen and helium at 5 MPa) and secondary—Rankine steam-turbine cycle) and hydrogen cogeneration. *Based on Gauthier et al. (2004)*

Figure 21.1.3 shows a simplified layout of a VHTR NPP with the indirect combined cycle: primary—SCP Brayton gas-turbine cycle (working fluid—SC carbon dioxide at ~ 20 MPa) and secondary—SCP Rankine cycle (working fluid—SC carbon dioxide at ~ 21 MPa); power-plant layout—(a) and the corresponding T - s diagram—(b).

Figure 21.1.4 shows a simplified layout of a GFR with the indirect combined cycle: primary—SCP Brayton gas-turbine cycle (working fluid—mixture of nitrogen and helium at 6.5 MPa) and secondary—Rankine steam-turbine cycle (at 15 MPa); power-plant layout—(a) and the corresponding T - s diagram—(b).

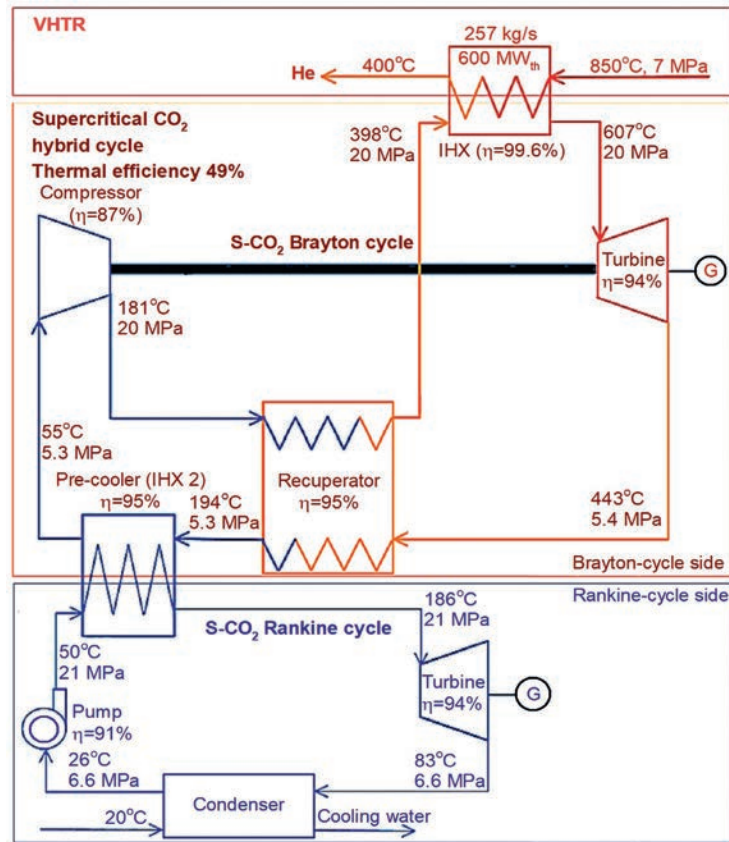
Figure 21.1.5 shows a simplified layout of a GFR with the indirect combined cycle: primary—SCP Brayton gas-turbine cycle (working fluid—nitrogen) and secondary—SCP Brayton cycle (working fluid—carbon dioxide); and with hydrogen cogeneration.

Figure 21.1.6. shows a simplified layout of an indirect SC CO₂ Brayton power cycle for a 600-MW_{th} GFR concept.

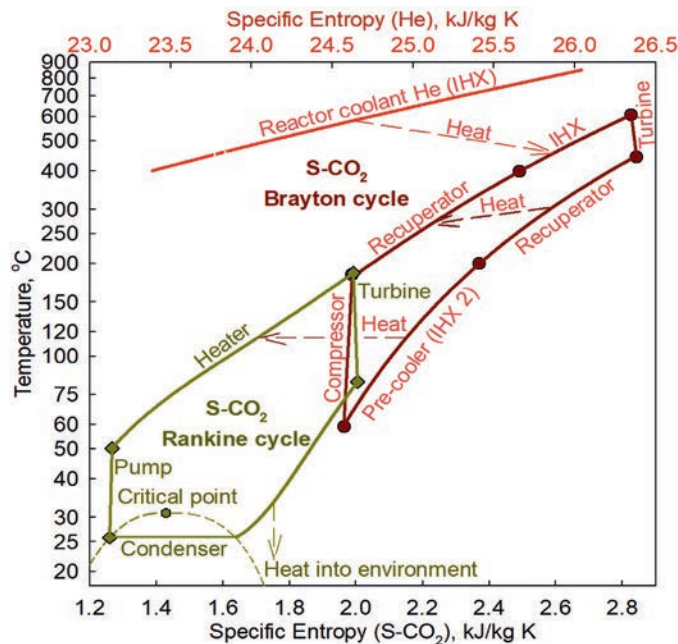
Figure 21.1.7 shows a simplified layout of an SFR NPP with the intermediate loop (heat-transfer fluid—sodium) and the indirect SCP Brayton gas-turbine cycle (working fluid—SC carbon dioxide): power-plant layout—(a) and the corresponding T - s diagram—(b).

Figure 21.1.8 shows effect of temperature on cycles thermal efficiencies.

Figure 21.1.9a–f shows profiles of thermophysical properties: (a) density; (b) thermal conductivity; (c) specific heat; (d) specific enthalpy; (e) dynamic viscosity; and (f) Prandtl number; vs temperature for water at 15.5 MPa (PWR conditions) and selected SuperCritical Fluids (SCFs) (carbon dioxide, helium;



(a) Power-plant layout



(b) T-s diagram

Figure 21.1.3. Simplified layout of VHTR NPP (reactor coolant—helium at 7 MPa) with indirect combined cycle: primary—SCP Brayton gas-turbine cycle (working fluid—SC carbon dioxide at ~20 MPa) and secondary—SCP Rankine cycle (working fluid—SC carbon dioxide at ~21 MPa)—(a) and the corresponding T-s diagram—(b). Based on Bae et al. (2014)

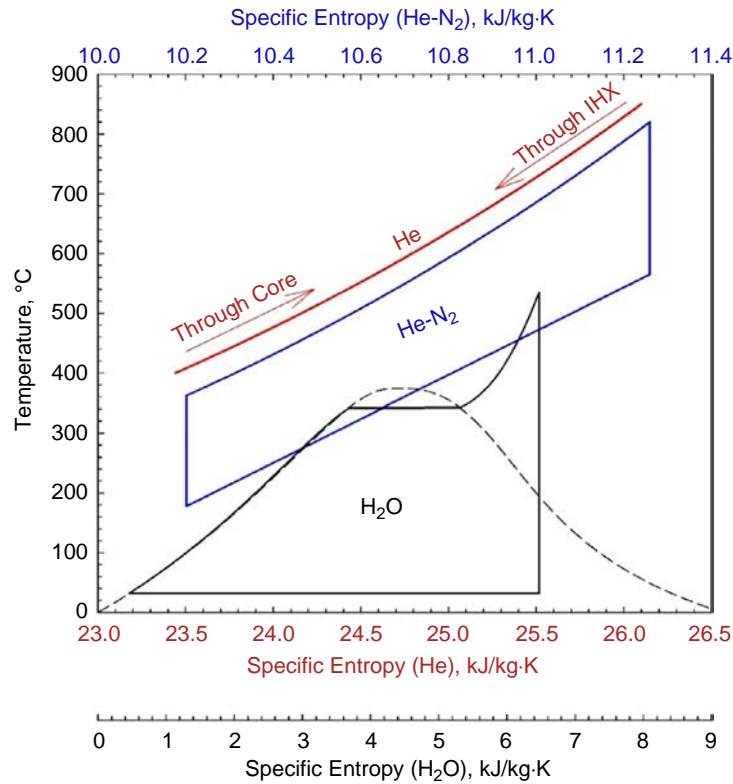
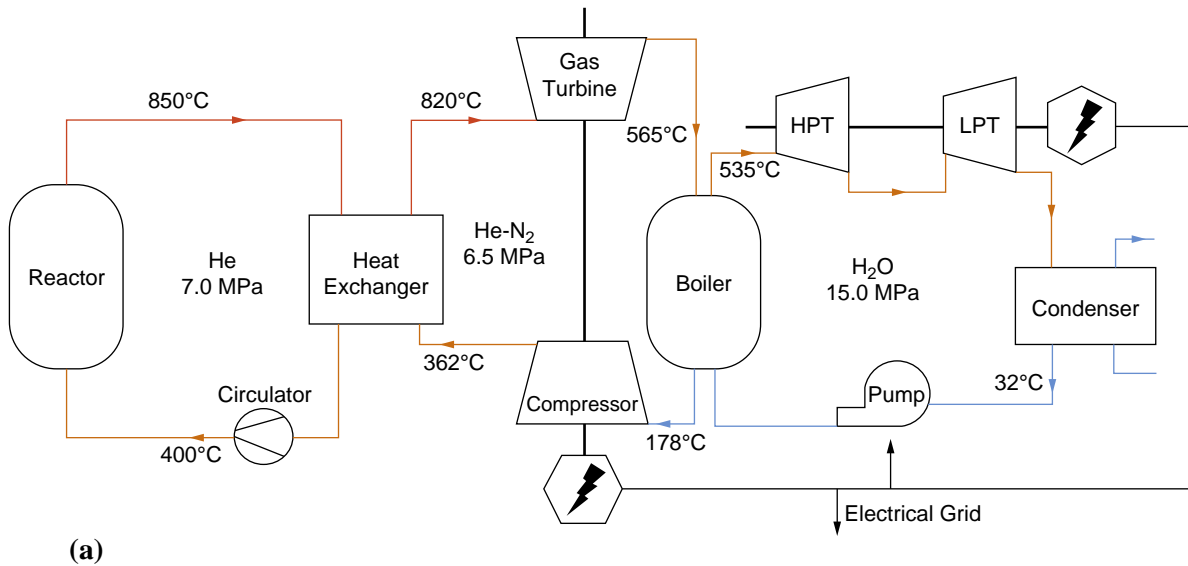


Figure 21.1.4. Simplified layout of GFR (reactor coolant—helium at 7 MPa) with indirect combined cycle: primary—SCP Brayton gas-turbine cycle (working fluid—mixture of nitrogen and helium at 6.5 MPa) and secondary—Rankine steam-turbine cycle (at 15 MPa): (a) power-plant layout and (b) T - s diagram. Based on Anzieu (2010)

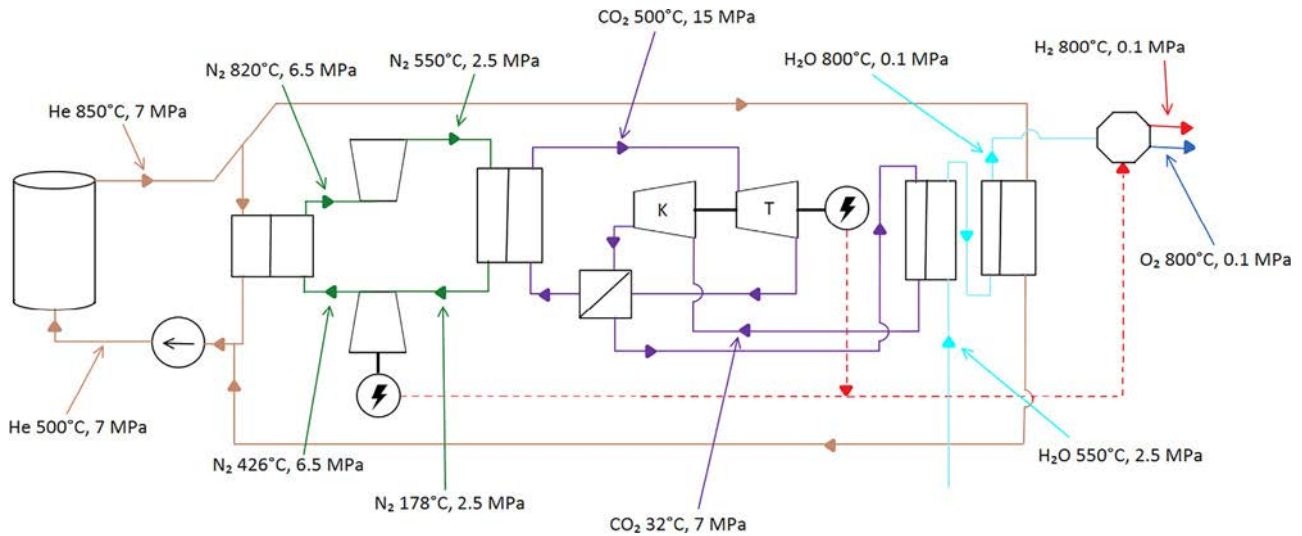


Figure 21.1.5. Simplified layout of GFR (reactor coolant helium at 7 MPa) with indirect Brayton cycles: primary—SCP Brayton gas-turbine cycle (working fluid—nitrogen at 6.5 MPa) and secondary—SCP Brayton cycle (working fluid—carbon dioxide at 15 MPa); and hydrogen cogeneration. *Based on Hajek and Doucek (2014)*

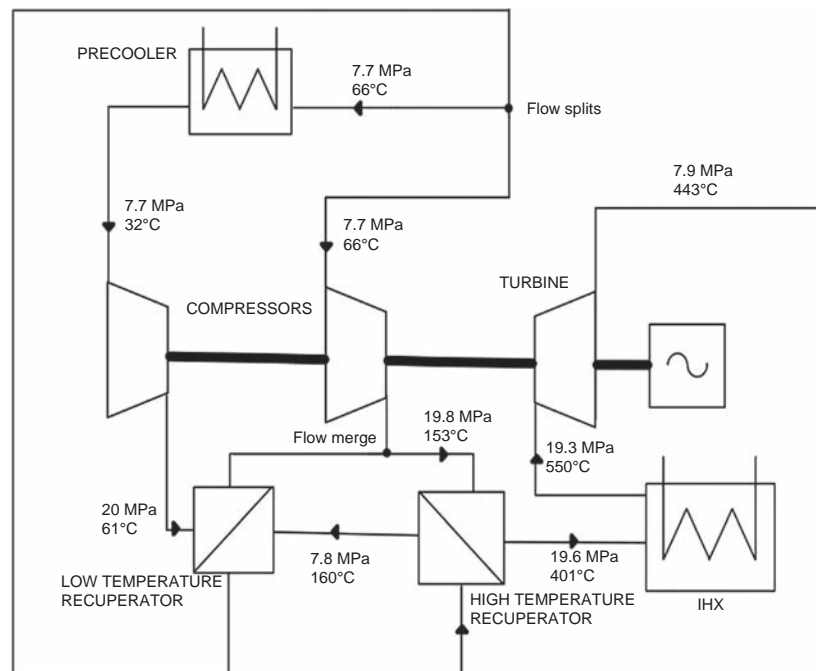


Figure 21.1.6. Simplified layout of indirect SC CO₂ Brayton power cycle for 600-MW_{th} GFR concept: IHX—Intermediate Heat eXchanger. *Based on Hejzlar et al. (2005)*

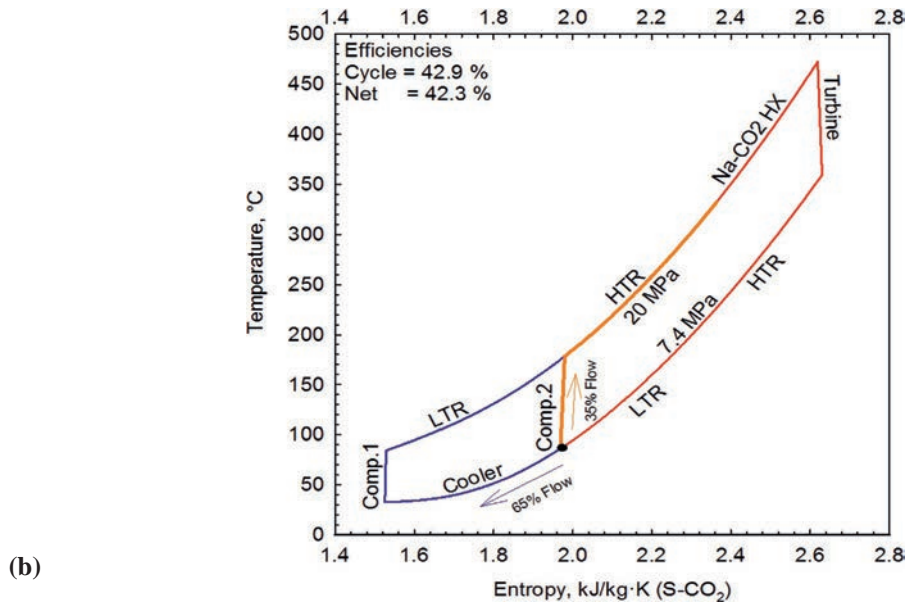
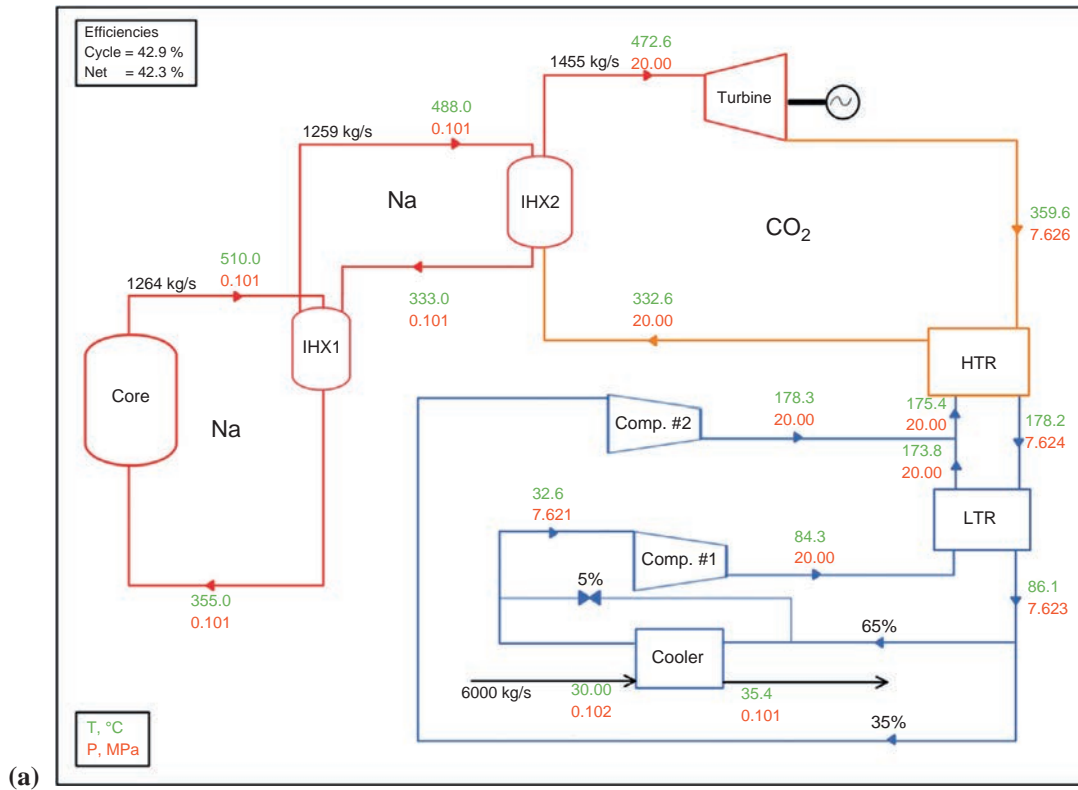


Figure 21.1.7. Simplified layout of SFR (reactor coolant—sodium at ~0.1 MPa) with intermediate loop (heat-transfer fluid—sodium at ~0.1 MPa) and indirect SCP Brayton gas-turbine cycle (working fluid—SC carbon dioxide at 20 MPa) (a) power-plant layout (*Comp.*—Compressor; *HTR*—High-Temperature Recuperator; *IHX*—Intermediate Heat eXchanger; and *LTR*—Low-Temperature Recuperator) and (b) *T-s* diagram. Based on Moiseyev and Siemicki (2009)

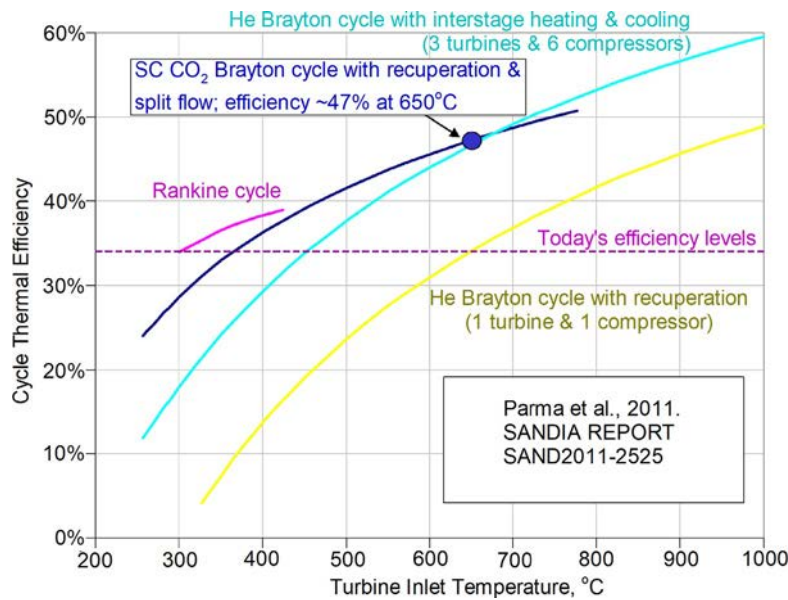


Figure 21.1.8. Effect of temperature on cycles thermal efficiency. Based on Parma et al. (2011). Free download from <https://vdocuments.mx/supercritical-co-direct-cycle-gas-fast-reactor-sc-gfr-concept-combined-turbinecompressorgenerator.html>

mixture of helium (20%) and nitrogen (80%); nitrogen; and water) at pressures corresponding to those of reactors outlets or inlets to power cycles.

In general, Figures 21.1.2–21.1.5 show a variety of different alternative combined power cycles, which might be used for VHTR and GFR helium-cooled high-temperature reactors. It is expected that combined power cycles will have higher thermal efficiencies compared to those of single cycles (e.g., see Figures 21.1.6 and 21.1.7) at the same level of inlet-turbine parameters (i.e., temperature and pressure) and lower-level cooling-medium parameters. However, the major setback for all these alternative cycles is that they have never been operated in nuclear-power industry.

In terms of the alternative SC CO₂ Brayton cycle for an SFR (Figure 21.1.7): Definitely the safety of a power plant will be enhanced due to elimination of water as working fluid in the Rankine power cycle, but the same setback as for VHTR and GFR alternative power cycles will apply. In general, similar cycle might be used for an MSR.

21.1.3 Cycles comparison

Comparison of several cycles in terms of thermal efficiency (see Figure 21.1.8) showed that at lower inlet-turbine temperatures (below 425°C) the Rankine cycle has some advantages, i.e., shows slightly higher thermal efficiencies. Within the range of temperature from 425°C and up to 650°C SC CO₂ Brayton cycle will have slightly higher thermal efficiencies compared to that of advanced helium Brayton cycle, which consists of three turbines and six compressors with interstage heating and cooling. However, for high-temperature applications this advanced helium Brayton cycle shows quite high thermal efficiencies compared to those of SCP Rankine cycle (~55%) and combined cycle of gas-fired power plants (about 62%). However, the ingress of helium into gas-turbine bearings has to be addressed.

Analysis of Figure 21.1.9a–f shows that helium has outstanding heat-transfer properties, i.e., the highest thermal conductivity and specific heat even in the case of SC water as the gas-like fluid (Figure 21.1.9b) and specific enthalpy, which is the highest one compared to that of all considered working fluids including subcritical and SCP water. Dynamic viscosity is also playing a role (see Eq. (21.1.2)), but for all considered working fluids and SC water as the gas-like fluid (Figure 21.1.9e) differences in its values are not so significant.

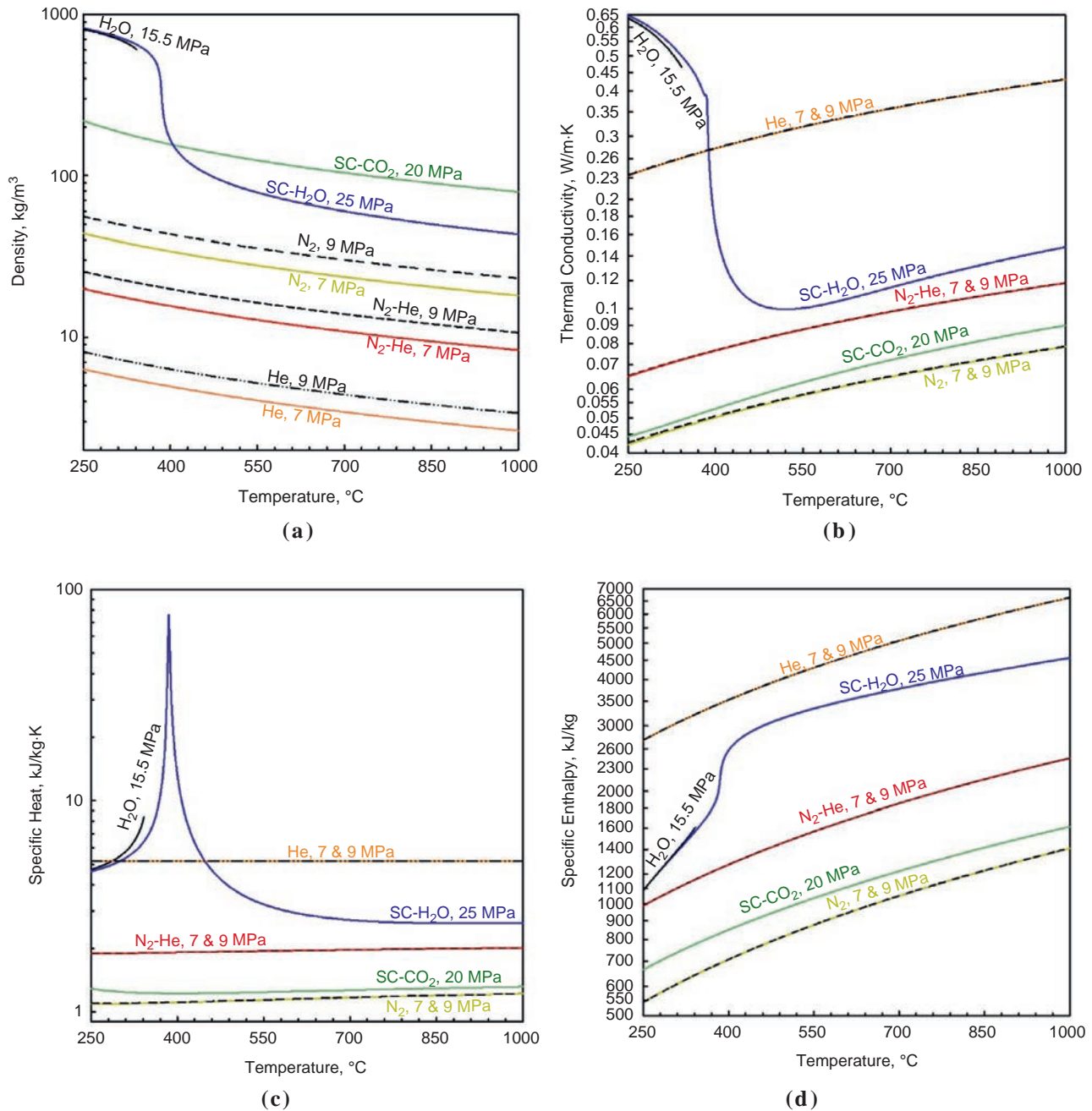


Figure 21.1.9. Profiles of thermophysical properties vs temperature for water at 15.5 MPa (PWR conditions) and selected SuperCritical Fluids (SCFs) at pressures corresponding to those of reactors outlets or inlets to power cycles: (a) density; (b) thermal conductivity; (c) specific heat; (d) specific enthalpy;

(Continued)

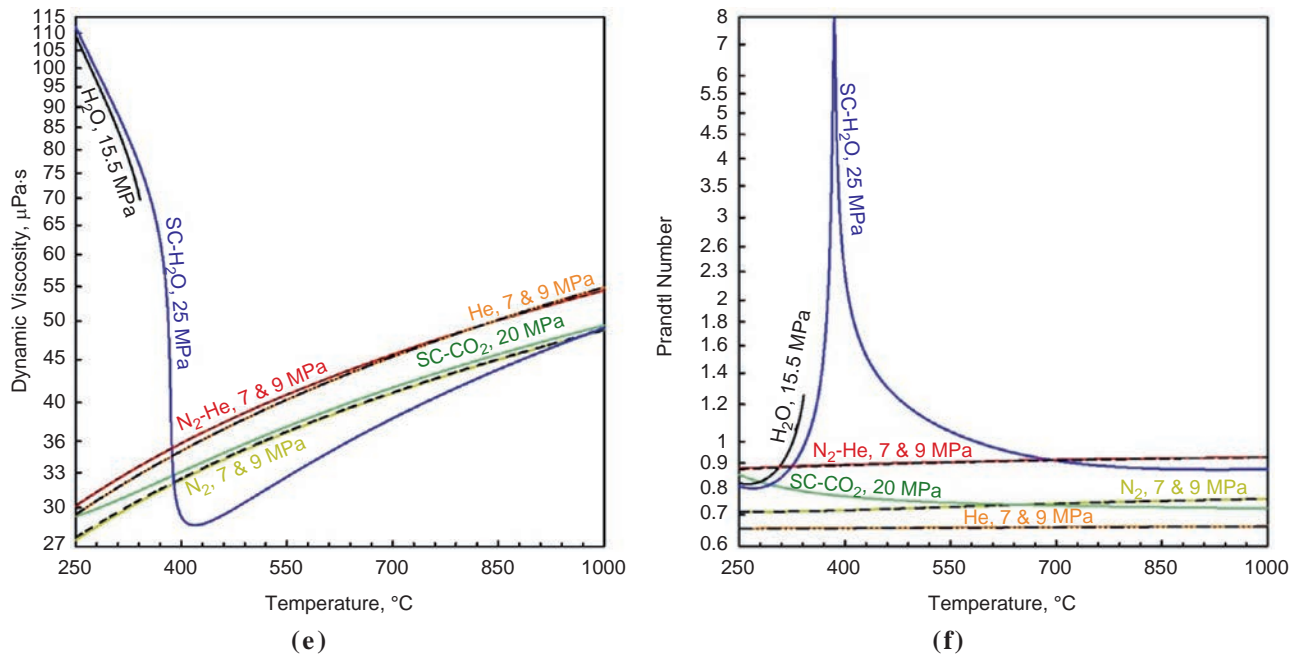


Figure 21.1.9, cont'd (e) dynamic viscosity; and (f) Prandtl number. All thermophysical-properties profiles are based on NIST (2018)

This statement is based on the following: Usually, forced convection of gases and liquids outside critical/pseudocritical region can be estimated according to the Dittus and Boelter correlation (1930) as introduced by McAdams (1942) (for details, see Winterton (1998)):

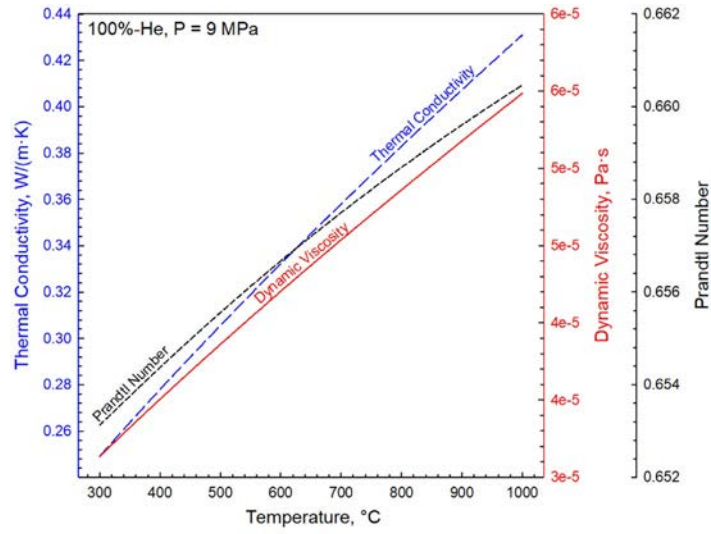
$$\text{Nu} = 0.023 \text{Re}^{0.8} \text{Pr}^{0.4} \quad (\text{for heating}) \quad (21.1.1)$$

This correlation is valid within the following ranges: $\text{Re} \geq 10,000$; $\text{Pr} \leq 160$; $L/D \geq 10$; and all thermophysical properties are based on the bulk-fluid temperature. Therefore, the following expression can be deduced:

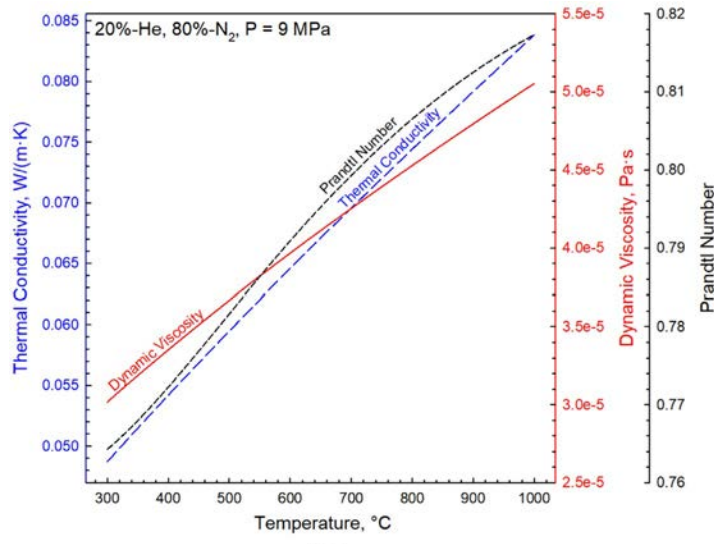
$$\text{HTC} \propto \frac{k^{0.6} c_p^{0.4}}{\mu^{0.4}} \quad (21.1.2)$$

Figure 21.1.10a–c shows thermophysical properties (thermal conductivity and dynamic viscosity) and Prandtl number vs temperature for helium (a), mixture of helium (20%) and nitrogen (80%) (b), and 100% nitrogen (c); and Figure 21.1.11a–c—Heat Transfer Coefficients (HTCs) calculated according to the Dittus and Boelter correlation (see Eq. (21.1.1)) for the same working fluids at pressure of 9 MPa, which corresponds to that of GFR, two mass-flux values of 1000 and 2500 $\text{kg}/\text{m}^2\text{s}$, and hydraulic-equivalent diameter of 10 mm. Analysis of these Figure 21.1.11a–c shows that HTCs for helium are ~ 4.6 –5 times higher than those for mixture of helium (20%) and nitrogen (80%), and for 100% nitrogen, respectively, at the same mass-flux value.

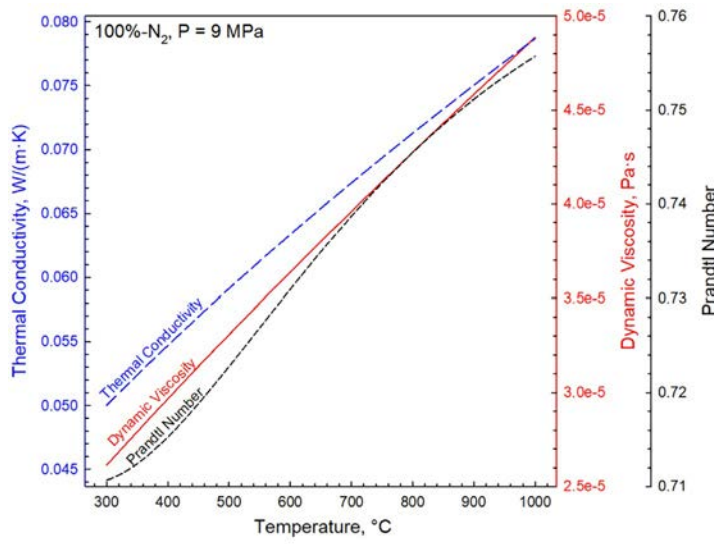
Also, for working fluid in a power cycle it is important to have higher specific-heat and specific-enthalpy values, simply because more internal energy is available for mechanical and electrical conversion within a certain temperature range.



(a)

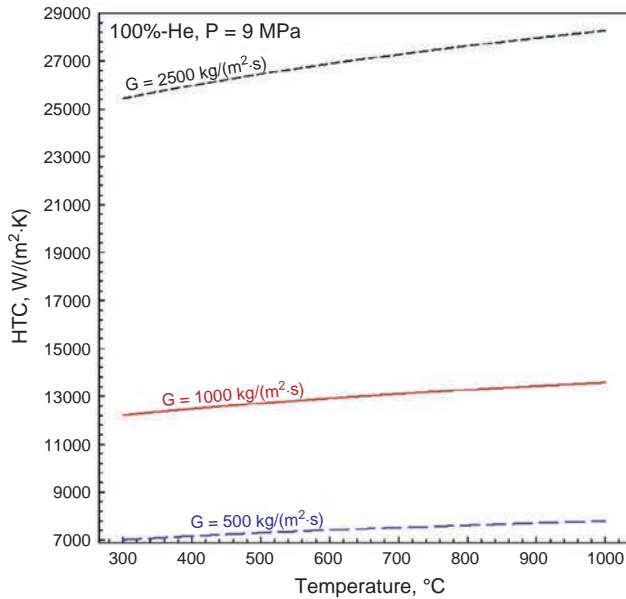


(b)

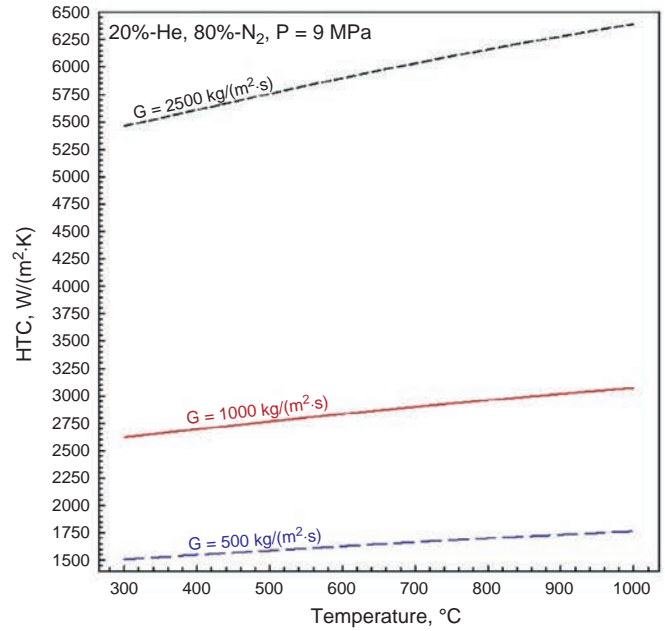


(c)

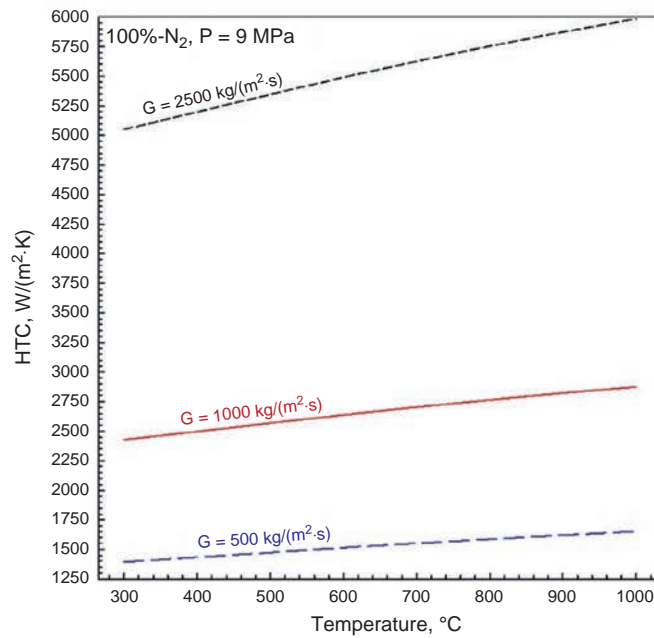
Figure 21.1.10. Comparison of basic thermophysical properties of: (a) helium; (b) mixture of helium (20%) and nitrogen (80%); and (c) nitrogen. All thermophysical-properties profiles are based on [NIST \(2018\)](#)



(a) Helium



(b) Helium (20%) / Nitrogen (80%)



(c)

Figure 21.1.11. Comparison of Heat Transfer Coefficients (HTCs) for forced convection of: (a) helium; (b) mixture of nitrogen (80%) and helium (20%); and (c) nitrogen; at following operation conditions—variable mass flux ($G=500$; 1000 ; and $2500 \text{ kg}/m^2 \cdot s$) and temperature (300 – $1000^{\circ}C$); and pressure 9 MPa ; inside tube diameter of 10 mm . Dittus and Boelter correlation was used: $Nu = 0.023 Re^{0.8} Pr^{0.4}$. All thermophysical properties are based on [NIST \(2018\)](#)

21.1.4 Conclusions

- (1) For the original GIF concepts only three power cycles were considered. As such, VHTR is shown as a reactor connected with the hydrogen-production plant using thermochemical sulfur-iodine cycle, GFR—with the direct Brayton helium-turbine power cycle; SFR—was originally connected to the Rankine steam-turbine power cycle, LFR and MSR were shown with the indirect Brayton gas-turbine power cycle.
- (2) From all these abovementioned power cycles only: (1) open Brayton gas-turbine cycle with combustion products (inlet temperature up to 1650°C) (combined-cycle of gas-fired power plants); (2) subcritical-pressure Rankine superheated-steam-turbine power cycle (older coal-fired power plants); and (3) SuperCritical-Pressure (SCP) Rankine “steam”-turbine power cycle (advanced coal-fired power plants); are well-known and proven in thermal power industry for tens of years. Also, it is well-known and proven from the thermal power industry that only combined cycle, i.e., high-temperature Brayton gas-turbine cycle with the subcritical-pressure Rankine superheated-steam-turbine power cycle, can achieve the highest thermal efficiencies up to 62%. SCP Rankine “steam”-turbine power cycle is also quite efficient, but still its thermal efficiency is by 7% lower than that of the combined cycle.
- (3) Therefore, the major conclusion based on proven experiences in thermal power industry is that high-temperature Generation-IV nuclear power reactors such as VHTRs and GFRs helium-cooled with the maximum outlet temperatures up to 1000°C and 850°C, respectively, should be connected to combined power cycles. However, it was found that the ingress of helium into bearings of gas turbines can limit operational term of direct Brayton helium-turbine power cycle.
- (4) To address the abovementioned issues and challenges with high-temperature-reactors power cycles new indirect combined cycles are proposed and, currently, under development in a number of countries. These cycles include: (1) combined cycle: primary—Brayton gas-turbine cycle (working fluid—mixture of nitrogen and helium) and secondary—subcritical-pressure Rankine steam-turbine cycle; (2) combined cycle: primary—SCP Brayton gas-turbine cycle (working fluid—nitrogen) and secondary—SCP Brayton cycle (working fluid—carbon dioxide); (3) combined cycle: primary—SCP Brayton gas-turbine cycle (working fluid—SC carbon dioxide) and secondary—SCP Rankine cycle (working fluid—SC carbon dioxide). Also, indirect single power cycles also are considered—SC CO₂ Brayton power cycle.
- (5) Comparison of several cycles in terms of thermal efficiency showed that at lower inlet-turbine temperatures (below 425°C) the Rankine cycle has some advantages, i.e., shows slightly higher thermal efficiencies. Within the range of temperature from 425°C and up to 650°C SC CO₂ Brayton cycle will have slightly higher thermal efficiencies compared to that of advanced helium Brayton cycle, which consists of three turbines and six compressors with interstage heating and cooling. However, for high-temperature applications this advanced helium Brayton cycle shows quite high thermal efficiencies compared to those of SCP Rankine cycle (~55%) and combined cycle of gas-fired power plants (about 62%). However, the ingress of helium into gas-turbine bearings has to be addressed.
- (6) Analysis of thermophysical-properties profiles shows that helium has outstanding heat-transfer properties, i.e., the highest thermal conductivity and specific heat; and specific enthalpy, which is the highest one compared to that of all considered working fluids (nitrogen, and SC CO₂) including subcritical and SCP water. Therefore, HTC_s for helium are ~4.6–5 times higher than those for mixture of helium (20%) and nitrogen (80%), and for nitrogen, respectively, at the same mass-flux value. Also, for working fluid in a power cycle it is important to have higher specific-heat and specific-enthalpy values, because in this case, more internal energy can be converted into mechanical and electrical ones within a certain temperature range.

References

- Anzieu, P., 2010. Gas-cooled Gen-IV systems VHTR & GFR. In: Presentation for CEA Meeting, February, Demanova, Slovakia, 34 slides. Free download from https://inis.iaea.org/collection/NCLCollectionStore/_Public/44/078/44078353.pdf?r/41.
- Bae, S.J., Ahn, Y., Lee, J.I., 2014. Preliminary study of the supercritical CO₂ hybrid cycle for the HTGR application. In: Transactions of the Korean Nuclear Society Spring Meeting, Jeju, Korea, May 29–30 (3 p.).
- Dittus, F.W., Boelter, L.M.K., 1930. Heat Transfer in Automobile Radiators of the Tubular Type. 2 University of California, Berkeley, Publications on Engineering, pp. 443–461. No. 13.
- Gauthier, J., Brinkmann, G., Copsey, B., Lecomte, M., 2004. ANTARES: the HTR/VHTR project at framatome ANP. In: Proceedings of the 2nd International Topical Meeting on High Temperature Reactor Technology (HTR 2004), Beijing, China, Sep. 22–24 (paper #A10, 13 p.).
- Hajek, P., Doucek, A., 2014. The effect of supercritical power cycles at hydrogen production plants. In: Proceedings of the 4th International Symposium on Supercritical CO₂ Power Cycles. Pittsburgh, PA, USA, Sep. 9–10 (6 p.).
- Hejzlar, P., Dostal, V., Driscoll, M., 2005. Assessment of gas cooled fast reactor with indirect supercritical CO₂ cycle. In: Proceeding of the International Congress in Advances of Nuclear Power Plants 2005 (ICAPP'05), Seoul, Korea. May 15–19 (11 p.).
- Mahdi, M., Popov, R., Pioro, I., 2017. Thermal efficiencies of various power cycles for VHTRs. In: Proceedings of the 37th Annual Canadian Nuclear Society (CNS) Conference and 41th CNS/CNA Student Conference, Niagara Falls, ON, Canada, June 4–7. 5 p.
- Mahdi, M., Popov, R., Pioro, I., 2018. Research on thermal efficiencies of various power cycles for GFRs and VHTRs. In: Proceedings of the 26th International Conference On Nuclear Engineering (ICONE-26), July 22–26, London, England. Paper #81618, 12 p.
- McAdams, W.H., 1942. Heat Transmission, second ed. McGraw-Hill, New York, NY, USA. 459 p.
- Moisseytsev, A., Sienicki, J., 2009. Investigation of alternative layouts for the supercritical carbon dioxide Brayton cycle for a sodium-cooled fast reactor. In: Proceedings of the Supercritical CO₂ Power Cycle Symposium, Rensselaer Polytechnic Institute. Troy, NY, USA. April 29–30.
- NIST REFPROP, 2018. In: Lemmon, E.W., Bell, I.H., Huber, M.L., McLinden, M.O. (Eds.), Reference Fluid Thermodynamic and Transport Properties, NIST Standard Reference Database 23, Ver. 10.0. National Institute of Standards and Technology, USA.
- OKBM Afrikantov, n.d. JSC “Afrikantov OKBM,” Nizhny Novgorod, Russia. <http://www.okbm.nnov.ru/upload/iblock/6b0/pxls42x9x5v9pvlqdn86qy4cbhwvx9cq.pdf> (Accessed 19 February 2022).
- Parma, E.J., Wright, S.A., Vernon, M.E., Fleming, D.D., Rochau, G.E., Suo-Anttila, A.J., Al Rashdan, A., Tsvetkov, P.V., 2011. Supercritical CO₂ Direct Cycle Gas Fast Reactor (SC-GFR) Concept, SANDIA REPORT, SAND2011-2525, May. Sandia National Laboratories, Albuquerque, NM and Livermore, CA, USA (55 p.).
- Pioro, I., 2021. Application of supercritical fluids in thermal- and nuclear-power engineering. In: Chen, L. (Ed.), Handbook of Research on Advancements in Supercritical Fluids Applications for Sustainable Energy Systems. IGI Global, Hershey, PA, USA, pp. 601–658. Chapter 17, 821 p. Available from <https://www.igi-global.com/book/handbook-research-advancements-supercritical-fluids/253256>.
- Pioro, I., Mahdi, M., Popov, R., 2017a. Application of supercritical pressures in power engineering. In: Chen, L., Iwamoto, Y. (Eds.), Advanced Applications of Supercritical Fluids in Energy Systems. IGI Global, Hershey, PA, USA, pp. 404–457. Chapter 13, 704 p.
- Pioro, I.L., Popov, R., Mahdi, M., 2017b. Latest research & development in thermodynamic cycles and heat transfer in nuclear and thermal power industries. In: Proceedings of the International Conference on Heat Transfer, Fluid Mechanics and Thermodynamics (HEFAT), Portoroz, Slovenia, July 17–19. 18 p.
- Pioro, I., Mahdi, M., Popov, R., 2018. Heat transfer media and their properties. In: Kulacki, F.A. (Ed.), Handbook of Thermal Science and Engineering. Springer, Cham, Switzerland, pp. 1353–1446. editor-in-chief. Chapter 33.
- Pioro, I., Duffey, R.B., Kirillov, P.L., Pioro, R., 2021. Pros and cons of commercial reactor designs, section 2: chapter. Part 1. Current status of electricity generation in the world and selected countries. In: Greenspan, E. (Ed.), Encyclopedia of Nuclear Energy, first ed. Elsevier, UK, pp. 263–287. 3656 p.
- Popov, R., Mahdi, M., Pioro, I., 2017. Thermal efficiencies of various power cycles for GFRs. In: Proceedings of the 37th Annual Canadian Nuclear Society (CNS) Conference and 41th CNS/CNA Student Conference, Niagara Falls, ON, Canada, June 4–7. 5 p.
- Winterton, R.H.S., 1998. Where did the Dittus and Boelter equation come from? Int. J. Heat Mass Transf. 41 (4–5), 809–810.

21.2

Closed Brayton-cycle configurations for Gas-cooled Fast Reactors (GFRs) and Very-High-Temperature Reactors (VHTRs)

Arnold A. Gad-Briggs^a, Emmanuel O. Osigwe^a, Filip Grochowina^a,
Pericles Pilidis^b, Theoklis Nikolaidis^b, Suresh Sampath^b,
and Joao Amaral Teixeira^b

^aEGB Engineering UK LTD, Southwell, United Kingdom ^bGas Turbine Engineering Group, Cranfield University, Cranfield, United Kingdom

Nomenclature

Symbols

A	Area (m ²)
C_p	Specific heat of gas at constant pressure (J/kgK)
CW	Compressor Work (W)
m or \dot{m}	Mass flow rate (kg/s)
M	Molar mass (g/mol)
N	Shaft rotational speed (rpm)
P	Pressure (Pa)
R	Gas constant (J/kg K)
PR	Pressure Ratio
q	Heat flux (W/m ²)
Q	Reactor thermal heat input (W) or heat quantity in the reversible heat transfer
S	Entropy (J/K)
SW/SP	Specific Work or Power/capacity (W/kg s)
T	Temperature (K)
T_{ref}	Reference atmospheric temperature (K)
TR	Temperature Ratio (T_4/T_1 ; expressed in K)
TW	Turbine Work (W)
u	Velocity (m/s)
UW	Useful Work (W)
V	Absolute Velocity (m/s)
W	Work (W)

Greek symbols

β	Beta decay
γ	Ratio of specific heats
Δ	Delta, difference
ϵ	Effectiveness (heat exchanger)
k	Thermal conductivity (W/mK)
η	Thermal efficiency (%)
η_{th}	Cycle thermal efficiency (%)
μ	Dynamic viscosity (Pas)
ρ	Density (kg/m ³)

- ν Kinematic viscosity (m^2/s) or volume (m^3)
 θ Temperature ratio

Subscripts

- c Compressor
 c_{in} Compressor inlet
 c_{out} Compressor outlet
 el Power for electrical conversion
 f Fluid (working fluid at the intercooled part of the GT)
 he Helium
 he_{min} Helium with minimum gas conditions
 ic Intercooled cycle; intercooled coefficient
 is_c Isentropic (compressor)
 is_t Isentropic (turbine)
 MHR Reactor (heat source)
 MHR_{in} Reactor (heat source) inlet
 MHR_{loss} Reactor (heat source) pressure losses
 MHR_{out} Reactor (heat source) outlet
 pc_{in} Precooler inlet (also applicable to intercooler)
 pc_{loss} Precooler pressure losses (same as above)
 pc_{out} Precooler outlet (same as above)
 $poly_c$ Polytropic (compressor)
 $poly_t$ Polytropic (turbine)
 re Recuperator
 re_{cold} Recuperator cold side
 re_{hot} Recuperator hot side
 re_{HPloss} Recuperator high-pressure losses
 re_{LPloss} Recuperator low-pressure losses
 re_{real} Recuperator real (specific heat transfer)
 re_{max} Recuperator max (specific heat transfer)
 rev Reversibility of heat quantity
 th Thermal power
 t Turbine
 t_{in} Turbine inlet temperature
 t_{out} Turbine outlet temperature
 w Whirl component (turbomachinery design)

Superscripts

- ' Recuperator inlet conditions

Abbreviations/acronyms

- Air_IC** Air InterCooled cycle
Air_ICR Air InterCooled Recuperated cycle
Air_R Air Recuperated cycle
Air_S Air Simple cycle
BCS Bypass Control System
C Compressor
CH Precooler
CO₂ Carbon dioxide
CO₂_IC Carbon dioxide InterCooled cycle
CO₂_ICR Carbon dioxide InterCooled Recuperated cycle
CO₂_R Carbon dioxide Recuperated cycle
CO₂_S Carbon dioxide Simple cycle
COT Core Outlet Temperature

DP	Design Point
EVO	EnergieVersorgung Oberhausen AG
FOAK	First Of A Kind
Gen-IV	Generation IV
GFR	Gas-cooled Fast Reactor
GH	Reactor/Gas Heater
GIF	Generation-IV International Forum
GT	Gas Turbine
GTHTTR	Gas Turbine High-Temperature Reactor
HE	Heat Exchanger (recuperator)
He	Helium
He_IC	Helium InterCooled cycle
He_ICR	Helium InterCooled Recuperated cycle
He_R	Helium Recuperated cycle
He_S	Helium Simple cycle
He-Ar	Helium-Argon mixture
He-CO₂	Helium-Carbon dioxide mixture
He-N₂	Helium-Nitrogen mixture
He-Xe	Helium-Xeon mixture
HHV	Hochtemperatur Helium Versuchsanlage
HP	High Pressure
HPC	High-Pressure Compressor
HST	Reactor Heat Source Temperature
HTR	High-Temperature Reactor
HTR	High-Temperature Recuperator
IC	Intercooled Cycle
IC	InterCooler
ICHX	InterCooler Heat eXchanger
ICR	Intercooled Cycle Recuperated
ICS	Inventory Control System
ICT	Inventory Control Tank
ICV	Inventory Control Valve
IPC	Inventory Pressure Control
LP	Low Pressure
LPC	Low-Pressure Compressor
LTR	Low-Temperature Recuperator
LWR	Light Water Reactor
N₂	Nitrogen
N₂_IC	Nitrogen InterCooled cycle
N₂_ICR	Nitrogen InterCooled Recuperated cycle
N₂_R	Nitrogen Recuperated cycle
N₂_S	Nitrogen Simple cycle
NASA	National Aeronautics and Space Administration (USA)
NGV	Nozzle Guide Vane
NOAK	N th Of A Kind
NPP	Nuclear Power Plant
NTU	Nnumber of Transfer Units
OD	Off-Design
ODP	Off-Design Point
OGV	Outlet Guide Vane
OoB	Out of Balance
OPR	Overall Pressure Ratio
PC	PreCooler
PCS	Power Conversion System
PR	Pressure Ratio

PWR	Pressure Water Reactor
R	Reactor
RC	Recuperated Cycle
RecupHP	Recuperator High-Pressure side
RecupLP	Recuperator Low-Pressure side
ReX	Recuperator
RH	ReHeat cycle
Rpm	Revolutions per minute
RPV	Reactor Pressure Vessel
RSCO₂	Recompressed Supercritical Carbon dioxide cycle
RX	Recuperator
SC	Simple Cycle
SCO₂	Supercritical Carbon dioxide cycle
SCR	Simple Cycle Recuperated
SFR	Sodium-cooled Fast Reactor
T	Turbine
TET	Turbine Entry Temperature
TR	Temperature Ratio
TRL	Technology Readiness Level
TUR	Turbine
VHTR	Very-High-Temperature Reactor
VIGV	Variable Inlet Guide Vane

21.2.1 Introduction

This chapter focuses on the design of closed Brayton-cycle configurations for Gas-cooled Fast Reactors (GFRs) and Very-High-Temperature Reactors (VHTRs), because these concepts make use of a reactor coolant such as helium. Also, helium will be used in a direct cycle. However, a mixture of helium and nitrogen, nitrogen, and/or carbon dioxide as working fluids will be used in indirect power-conversion cycles, which can be the Brayton gas-turbine cycle or a combination of the Brayton and Rankine cycles.

The gas turbine is very integral to the technology of these concepts, because the unit power provision for its size is by far superior to the current technology. The power delivery is complemented by the high efficiency of the process while offering the main benefit of a direct cycle through the reduction of the plant size. The use of coolants such as helium eliminates the issue associated with reactivity of the coolant during the fission process.

Based on these factors and the difficulties, which may arise during the conceptual-design process, this chapter provides a descriptive account of the technological considerations for designing helium cycles for GFRs and VHTRs, particularly, the impact of different cycle configurations on the plant efficiency during normal Design-Point (DP) and Off-Design-Point (ODP) operations. In addition, it focuses on design considerations for different working fluids such as carbon dioxide and nitrogen for the power cycles, with comparisons made focusing on performance, costs and technology readiness.

21.2.2 Gas turbine as a power-conversion machine

The gas turbine was first patented in 1791 by J. Barber. Since then, it has become one of the most significant inventions through the advancements that occurred in the 20th century and the way it has changed our everyday lives ([Saravanamuttoo et al., 2009](#)). Its development began prior to the Second World War with the initial application intent being for electrical power, but the technology proved to be uneconomical in comparison to the diesel engines and steam turbines. However, it gained importance at the end of the Second

World War in the development of military engines. Today, gas turbines provide the propulsive jet power for high bypass ratio civil jet engines such as the Rolls-Royce Trent XWB and shaft power for the GE Marine LM2500.

With reference to power generation, the first gas turbine was introduced by Brown Boveri of Switzerland in 1937. It offered a modest thermal efficiency of 17% at that time (Walsh and Fletcher, 2004) and opened the way for the development of other areas including nuclear power generation.

Gas turbines, which are used for industrial applications, are typically classed as open or closed cycles. Applications, which require the constant flow of air, are considered to be open. For closed direct- or indirect-cycle applications as required for nuclear, the working fluid can be nitrogen, air, water or gases that are chemically inert such as argon or helium (Gad-Briggs, 2017). The fluid is processed through the components of the cycle, with the heat provided by a heat source such as a nuclear reactor, which turns the coolant into a hot fluid/gas. The fluid is cycled through the components and returned back into the cycle, which includes exchanging of the waste heat to raise the temperature of the coolant before it reenters the heat source, i.e., so-called, regeneration. As this chapter will demonstrate that the benefits of transferring the waste heat back into the cycle include increased cycle efficiency and reduced turbomachinery size.

Commercially, the continuing interest in utilizing gas turbines as prime movers for closed-cycle applications has always been known, but for nuclear applications, an indirect cycle has always been proposed due to earlier problems of the direct cycle. Some of the earlier operational experiences are briefly discussed in the next subsection.

21.2.3 Operational experience of helium gas turbines

Admittedly, the use of gas turbines for power conversion in the nuclear industry has never reached the scale required for high-temperature reactors, when compared to steam turbines. This is due to the high temperature that is demanded by the Brayton cycle; thus historically, there has always been a limit on material choices. The operational experiences of known helium-gas-turbine projects are briefly discussed below.

21.2.3.1 Oberhausen II EVO helium turbine (1974)

The 50-MW helium turbine was a development project that aimed to improve the design of the helium turbomachinery for the Oberhausen project. The maximum hot-gas temperature was 750°C with the heating source provided by a combustor fueled by coke-oven gas. The operating test pressure was 1 MPa (Gad-Briggs, 2017). The project was run on two R&D test facilities; the first was Oberhausen II, which was operated between 1974 and 1988 by EVO (Energieversorgung Oberhausen AG), a German utility company and the second was the high-temperature test plant or Hochttemperatur Helium Versuchsanlage (HHV) in 1981. The original design intent of the project developers (Escher Wyss), who were initially responsible for the turbomachinery, was to deliver a 50-MW output at the generator. However, the turbomachinery suffered from unfavorable hub to tip ratio for the compressor and turbine due to lower rotational speeds. The efficiencies of the turbomachinery set were low, and the plant was prone to excessive cycle pressure losses (by a factor of 4). The combined effect of the pressure losses and the poor cooling and sealing flows resulted in a 33.3% cycle efficiency drop from a design intent of 34.5% (Fruttschi, 2005).

The EVO facility helped to resolve some of the issues by improving high-temperature blades and disks, the rotor dynamic problems and the use of magnetic bearings. The HHV facility had combined compressor power provided by the motor and the turbine (90 MW combined), and a mass flow rate of 200 kg/s. The initial problems of oil ingress and excessive helium leakage were resolved. This had a positive impact on cycle efficiency with the plant performance exceeded the design intent values. However, the turbine suffered from creep and fatigue crack growth at high temperatures.

21.2.3.2 Historical problems with helium gas turbines

With the design, fabrication, operational and maintenance experience gained from operating closed cycles, the benefits for a gas turbine to be coupled to a high-temperature reactor provided some promise. But with lacking substantial operational and development experience of helium turbomachinery, the technology was never scaled up due to the complexities of which the pertinent issues are discussed in some detail by [Gad-Briggs \(2017\)](#) and [Pradeepkumar \(2002\)](#):

- (1) The helium leakage through seals and gaps were hard to control. This was due to the small molecular size of helium, when compared to other gases. Seals were traditionally developed using air. This resulted in flaws in the seals' design and proved ineffective.
- (2) Tip leakages were also apparent as a result of leakages in turbomachinery. This resulted in heavy losses with the fluid escaping from the circuit. The outcomes were the poor component and cycle efficiencies, which led to the question of the viability of the technology.
- (3) The turbine was also expensive, because cooling technologies as currently adopted in jet engines had not been developed. The high flow rate of helium did not match the design configuration of early cooled turbines in terms of limiting thermal stresses. This meant that the turbine life was significantly reduced, if typical percentages of mass flow rate as utilized for air were used. Consequently, more helium than the design specification amount was debited, which impacted the performance of the plants.
- (4) Problems with welding of components were experienced during operation. This stopped the functioning of components such as the turbomachinery guide vanes, mechanical bearings (due to helium ingress) and control valves. In some cases, it damaged the components, which had to be replaced. This was caused by material transfer at high temperatures, when helium passed over two moving metallic surfaces.
- (5) Excessive rotor vibrations regularly occurred during development. This was attributed to the slim single rotors and the gearbox assembly that were used at the generator side of the power-conversion process.
- (6) Oil ingress due to mechanical defects in the seals was also known to occur. This was the case in the high-temperature fossil-fired helium plant in Germany.

21.2.4 Recent helium gas turbine tests

The GTHTR300 reactor design and development started in 2003 and initially included compressor aerodynamic-performance tests, magnetic-bearing tests and gas-turbine operational control tests ([No et al., 2007](#)). The compressor tests were performed on a 4-stage configuration, which was run at $\sim 11,000$ revolutions per minute (rpm), with helium introduced at 1 MPa. The scaled-down compressor with the high rpm replicated the circumferential speeds and Mach number of the flow; the rotor was balanced on a set of magnetic bearings. This also allowed the critical speeds and resonances to be assessed for high Out of Balance (OoB).

The robust development experience from the GTHTR300 program improved the understanding of the issues, which have been designed out and paved the way for high efficient turbomachinery components and a high efficient simple recuperated cycle ([Sato et al., 2014](#)). As of 2016, the GTHTR300 plant had improved the turbomachinery to achieve maximum efficiency; part of the improvements included efficient aerodynamic profiling of the aerofoils. The turbine assembly was modified to allow for very high temperatures in excess of 950°C ; the recuperator effectiveness had been increased by 1%. The combination of these improvements resulted in a cycle efficiency in excess of 50%. [Figure 21.2.1](#) illustrates the physical layout of the GTHTR300 Nuclear Power Plant (NPP).

Other closed gas turbine NPPs include the HTR-10GT, which is a Chinese high-temperature gas-cooled reactor test module (HTM-10) demonstrator, and pebble bed GFR that comprises a direct intercooled

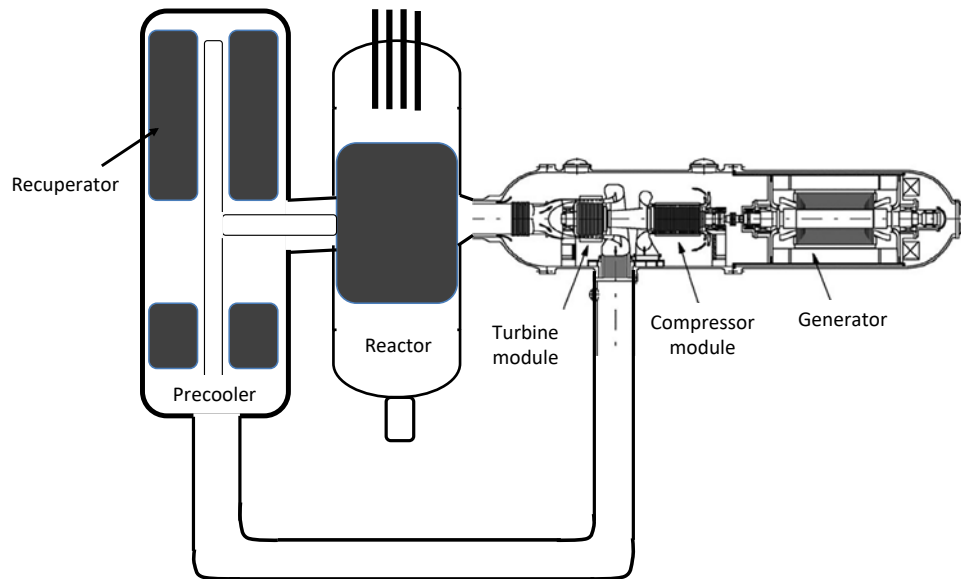


Figure 21.2.1. GT-HTR300 plant arrangement.

recuperated Brayton helium cycle. The HTR-10GT denotes the combination of the reactor and the Power Conversion System (PCS), which utilizes a gas turbine. The principle of the HTR-10GT is to avoid any intermediate circuits, thus minimizing the temperature drop and resulting complexities associated with such arrangements. The HTR-10 underwent several development tests as a steam-raising reactor with a helium circulator before the HTR-10GT introduced the gas-turbine system for direct helium coupling with the reactor (Huang et al., 2004).

21.2.5 Nuclear power plant closed cycles

Typically, NPP closed cycles can be classed as either Rankine (steam) cycle or Brayton cycle. All current NPPs in the world are based on the Rankine cycle, which is discussed in Appendix A1 and includes the various options of Rankine cycles for NPPs and their efficiencies. As such, the next set of sections describes the fundamental principles and key mathematical expressions that pertain to Brayton cycles.

21.2.5.1 Brayton cycles

A key benefit of a gas turbine is the ability for the machine to handle very high mass flow rates with very modest to high operating efficiencies (Decher, 1989).

With reference to Figure 21.2.2, the Brayton cycle involves four stages—the compression stage denoted as 1 to 2 or 2', the heating stage denoted as 2 or 2' to 3 or 3', the expansion stage denoted as 3 or 3' to 4 or 4'. The notation (') in the stages indicate the real cycle in order to differentiate from the ideal cycle.

Compression is achieved by providing work from the turbine to drive the compressor. The net work available is then used to drive a load. However, the compression and expansion phases are not ideal due to component efficiencies. The temperature rise within the cycle has a positive correlation to the flow of heat. If this heat quantity does not experience any changes, when there is a change in state, for instance, from a figuratively point A to point B and back to point A, then the heat quantity is shown to have values dependent on the

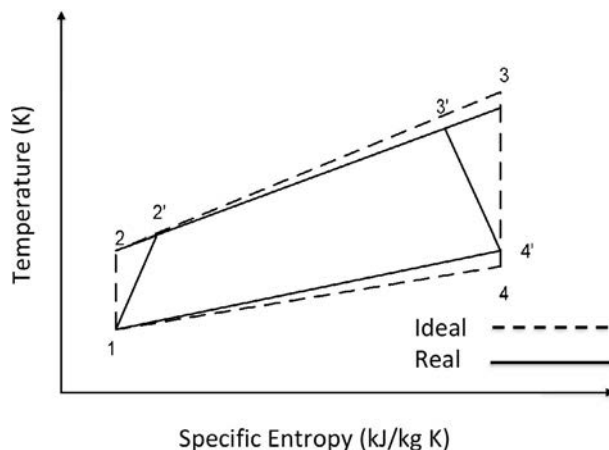


Figure 21.2.2. T-s diagram of the real and ideal Brayton cycle.

state variables (Decher, 1994). This property state defined through the reversible entropy heat transfer process is:

$$dS \equiv \frac{dQ_{\text{rev}}}{T} \quad (21.2.1)$$

with S is the entropy, Q_{rev} is the reversible heat quantity, and T (in K) is temperature. For a process with end states, the change in entropy can be expressed as:

$$\int_1^2 dS = \int_1^2 \frac{dQ_{\text{rev}}}{T} = S_2 - S_1 \quad (21.2.2)$$

The presence of entropy in the closed system is ideal in quantifying reversibility within the Brayton cycle, which for an ideal gas $S_2 - S_1$ is

$$S_2 - S_1 = Cp \cdot \ln \left(\frac{T_2}{T_1} \right) - R \cdot \ln \left(\frac{P_2}{P_1} \right) \quad (21.2.3)$$

Helium, as a real gas, acts as an ideal gas in most cases and respects the entropy relationship in Eq. (21.2.3), especially, when considering high temperatures under which the Brayton cycle would need to operate in order to gain maximum efficiency. However, the benefits of helium to enable high efficiency Gen-IV cycles cannot be explored without discussing helium in details.

21.2.6 Helium as a coolant

Thring (1960) stated that the desirable properties of a selected gas for nuclear power include non-adverse reaction with materials within the reactor, power conversion turbomachinery set, and peripheral units. In addition, Thring stated that such a gas should have low radioactivity being induced. The heat transport capabilities have to be very good. Furthermore, the thermodynamic properties should complement a simple turbomachinery design. Table 21.2.1 summarizes typical power-conversion coolant gases and properties.

Decher (1994) provided comparisons to understand the effects of reverting from air to helium.

A gas that is considered suitable for the turbomachinery is determined largely by the specific heat of the gas at constant pressure (C_p), as opposed to the ratio of specific heats (γ). The C_p value is directly proportional to the number of stages required for the compressor and turbine machines. Thus, the required pressure rise and the harnessing of the thermal power to drive the generator and the compressor is significantly

Table 21.2.1. Power-conversion gases and cycles (Decher, 1994)

Gas	Chemical compatibility with reactor and engine materials	Induced radioactivity and dissociation	C_p kJ/kg K, γ , M	General remarks
He	Very good	None	5.2 1.66 4.006	Good heat transport properties, but expensive
CO ₂	Satisfactory	Negligible radioactivity. Some dissociation at high temperatures	1.09 1.21 44.07	Good heat transport properties. May preclude use of graphite as moderator material at high temperatures (unless both moderator and fuel elements are canned)
N ₂	Probably satisfactory	Some induced radioactivity, not of significant level or type	1.09 1.4 28.02	Moderate heat transport properties
Air	Poor, due to oxidation of metals at high temperature	Some induced radioactivity in argon and nitrogen	1.006 1.4 28.9	Moderate heat transport properties
Ne	Good	None	1.048 1.64 20.18	Poor heat transport properties

dependent on this. Other gases such as dissociating gaseous mixtures, nitrogen, and carbon dioxide have been investigated in other studies and are summarized by Gad-Briggs (2017). Performance comparisons are also made in the latter part of this chapter, with this part of the chapter focusing on helium.

Helium is a chemically inert gas and is passive in a neutronic state. It also has two important characteristics—it does not contribute to corrosion and has favorable thermal properties that make it ideal for a high-temperature reactor.

Comparisons were made between helium and air in a study by Decher (1994). The study looked at the gases at 300 K and 1000 K for pressures of 0.1 MPa and 3 MPa, respectively. The values for C_p , γ , kinematic viscosity and thermal conductivity (ν and k) are shown in Table 21.2.2. The results in Table 21.2.2 reveal that

Table 21.2.2. Characteristics of helium and air at varying temperatures and pressures (Decher, 1994)

Property	P (MPa)	T (K)	Air	Helium
M (g/mol)			28.9	4
γ	0.1	300	1.4	1.67
	3	1000	1.36	1.67
C_p (kJ/kg K)	0.1	300	1.005	5.20
	3	1000	1.142	5.20
k (W/m K)	0.1	300	0.028	0.15
	3	1000	0.068	0.36
ν (m ² /s)	0.1	300	16	120×10^{-6}
	3	1000	3.4	28

Table 21.2.3. Compression characteristics of helium and air (1.5 temperature ratio) (Decher, 1994)

	Air	Helium
Pressure ratio (P_2/P_1)	4.4	2.66
Volume ratio (v_2/v_1)	0.36	0.55
Stage pressure ratio	1.2	1.03
Number of compressor stages	8	33
Flow velocity (m/s)	1	2.3
Flow area (high-pressure side) (m ²)	1	0.62
Flow area (low-pressure side) (m ²)	1	0.37

for both gases, ν and k change with temperature. The effects due to temperature and the impact of these effects on pertinent parameters are quantified in Table 21.2.3. Using a cascade flow, Jiang et al. (2015) studied the characteristics of a highly loaded compressor using helium and air. It was concluded that the effects at low Mach numbers were negligible, whereby the characteristics for both helium and air could not be distinguished on a compressor map. However, these differences were more apparent at high Mach numbers, whereby the increased loading of the cascade revealed that the Reynolds number affects the aerodynamic performance.

Such differences impact the turbomachinery design. For the volumetric ratio, helium turbomachinery designs derive smaller volumetric ratios for the compressor and turbine geometry. The volumetric ratio is:

$$\frac{V_2}{V_1} = \left(\frac{T_2}{T_1}\right)^{\frac{1}{\gamma-1}} \quad (21.2.4)$$

with T as the temperature in K. The pressure ratio of the turbomachinery is also impacted. For the compressor, the pressure ratio due to the pressure increase is:

$$\frac{P_2}{P_1} = \left(\frac{T_2}{T_1}\right)^{\frac{\gamma}{\gamma-1}} \quad (21.2.5)$$

When the exponential values of air (3.5) and helium (2.5) are considered in Eq. (21.2.5), a lower pressure ratio is expected for helium. This means that the compression is easier in comparison to air, as also denoted in Table 21.2.3.

When considering the primary circuit of an NPP, it is important to consider the pressure drops in the pipe work and ducts. This is because they affect the flow velocity, which impacts overall system design and compactness. For pressure losses and its effect, the allowable ratio of velocities relating to helium is:

$$\frac{u_{\text{He}}}{u_{\text{air}}} = \sqrt{\frac{\left(\frac{\gamma-1}{\gamma} \text{ mol}\right)_{\text{air}}}{\left(\frac{\gamma-1}{\gamma} \text{ mol}\right)_{\text{He}}}} = 2.27 \quad (21.2.6)$$

Velocities of 100 m/s are usually considered, when estimating typical losses (Gad-Briggs, 2017).

An important parameter for comparison is the specific heat. With helium having five times the specific heat in comparison to air, other parameters such as the flow cross-sectional area provide significant benefits in

combination with the specific heat. Helium superior specific heat means it carries five times more power per unit mass. The cross-sectional flow area expressed by the steady flow continuity equation is:

$$A = \frac{\dot{m}}{\rho u} \quad (21.2.7)$$

and the density is given by the equation of state, and the mass flow rate is given by an enthalpy flux:

$$\dot{m} \sim \frac{\text{power}}{C_p T} \quad (21.2.8)$$

with T as the temperature in K. The velocity is provided by determining the pressure loss effect relationship in Eq. (21.2.6), and the pressures on the high-pressure side equaled. When considering Eq. (21.2.8), the power for a helium turbomachinery is increased for the same temperature and a superior C_p value, but the mass flow rate can also be reduced in comparison to an air turbomachinery to maintain that power. This leads to a compact flow within turbomachinery in comparison to air.

The pressure level of helium on the turbomachinery has less of an effect on the efficiency. The pressure ratio and the temperature ratio have more of an impact on the efficiency. The pressure only becomes a dominant effect when flows through ducts in the cycle are considered. This effect is dependent on the density of the flow regime, which is defined by the static pressure and temperature. The plant's power output is affected by choice of pressure. Components that would also need to be considered in addition to ducts and flow pipes are heat exchanger components. The design criteria for heat exchangers are covered later in this chapter, and by Decher (1994).

21.2.7 Generation-IV closed-cycle configurations for GFRs and VHTRs

This part of the chapter focuses on two closed Brayton-cycle configurations that are proposed for electricity generation using GFRs and VHTRs. They are known as the Simple Cycle Recuperated (SCR) and Intercooled Cycle Recuperated (ICR).

The SCR makes use of one compressor module for the overall compression process and a turbine module for the expansion process of the turbomachinery. The compressor has to generate a pressure rise, which requires power to do so. This compressor power is provided by the turbine, which also generates enough power to drive the generator load. The compression and expansion phases are not isentropic processes meaning thermodynamically, the process is not adiabatic and reversible due to component inefficiencies. The effect of this is the cycle experiences losses, because heating and cooling within the turbomachinery modules are not achieved at constant pressure. The losses mean that the compression process will require more work. For the turbine, the heat added into the turbine is isobaric, meaning the pressure generated from the heat going into the turbine is not constant. This affects the power extraction by reducing the total power extracted as a result of the gas-exit pressure, and reduced the component efficiency of the turbine. What would be experienced as a result of the inefficiencies is a hotter than ideal inlet temperature.

The gas turbine in a closed Brayton cycle will not deliver the efficiencies and power output due to the higher inlet temperature and component losses. The inclusion of a precooler fore of the compressor, guarantees that the helium can be cooled to the required compressor inlet temperature, using a cooling medium such as seawater. This reduces the compressor power required to create the pressure rise as the helium gas has been cooled down. However, the low compressor power means that the compressor temperature rise at the exit is lower than required prior to entering the reactor. The main benefit of the recuperated cycle is to transfer the turbine exhaust heat back into the cycle. The heat from the helium gas at the low-pressure side of the recuperator (aft the turbine) is transferred onto the helium coolant at the high-pressure side of the recuperator

(aft of the compressor) before it enters the reactor. This raises the temperature, reduces the reactor thermal power, and improves the efficiency of the cycle. The effect of the recuperator on the SCR is an additional 6% improvement on the cycle efficiency.

To improve the specific power and useful power beyond the threshold of the SCR, the compression power needs to be reduced by decreasing the temperature. This is achieved by introducing an intercooler thus, the cycle becomes an Intercooled Cycle Recuperated (ICR). The ICR includes all the components, which are applicable to the SCR. However, as stated, it also includes a second compressor and an intercooler, which is positioned between both compressors. The intercooler reduces the temperature of the helium going into the second compressor with some pressure loss. The reduced compressor power means the ICR improves the cycle efficiency by a further 2% to 3%. Figures 21.2.3 and 21.2.4 show the schematics of both cycles' configurations.

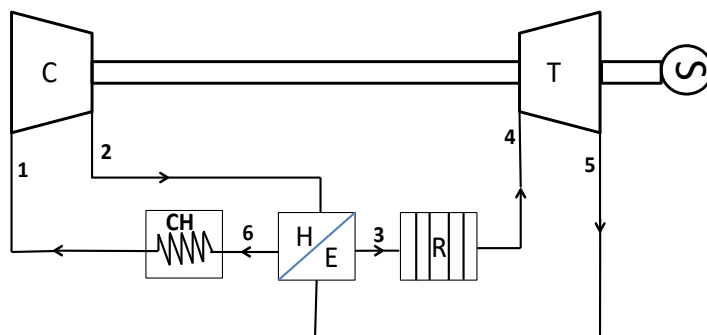


Figure 21.2.3. Simple cycle recuperated (Gad-Briggs et al., 2017a).

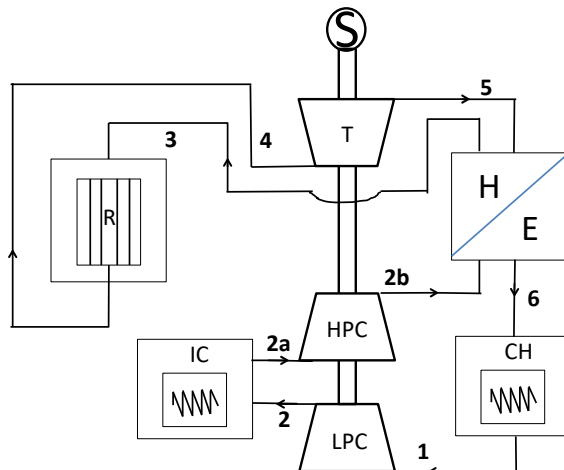


Figure 21.2.4. Intercooled cycle recuperated (Gad-Briggs et al., 2017a).

21.2.8 Component definition for design point performance

This section outlines the theoretical design considerations for components that are pertinent to Design Point (DP) performance of a Gen-IV (NPP), which utilizes any of the closed Brayton helium gas-turbine cycles discussed in the previous section.

21.2.8.1 Axial compressor

The compressor increases the total pressure of the helium in the gas stream using shaft power provided by the turbine. It comprises a row of rotor blades followed by a row of vanes called stators per compression

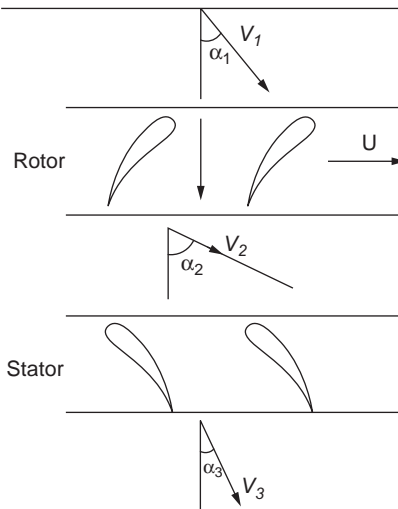


Figure 21.2.5. Row of rotor and stators for a single compression stage.

stage. Variable Inlet Guide Vanes (VIGVs) at the inlet to the compressor and Outlet Guide Vanes (OGVs) can be used to stabilize the flow by effecting the helium flow direction. The rows of rotor blades turn the shaft power into positive increases in absolute velocity, total temperature and static temperature, thereby generating enthalpy. The row of stators, on the other hand, do not produce work or transfer heat, but allow the flow to be diffused with velocity exchanges, which increases static pressure, with some fictional and turbulent losses observed as a result. The rotor blades and stator vanes contribute to the overall rise in pressure with limitation on the pressure rise per stage to reduce flow separation at the exit. Figure 21.2.5 depicts the row of rotor blades and stators in a cascade to show the velocity flow triangles, which define the aerodynamic flow per stage.

Table 21.2.4, which is based on the work of Walsh and Fletcher (2004), describes the thermodynamic process within the compressor for working fluids with similar behavior to air.

The pertinent parameters required for DP performance assessment of the compressor include the inlet mass flow rate, temperature and pressure of the helium gas, compressor pressure ratio, compressor efficiency (polytropic and isentropic), and the helium gas properties. These provide the governing expressions below, and are taken from Gad-Briggs and Pilidis (2017).

Table 21.2.4. Thermodynamic processes during the compression phase

Parameter	Rotor	Stator
Static pressure	Increase	Increase
Total pressure	Increase	Small decrease
Static temperature	Increase	Increase
Total temperature	Increase	Constant
Relative velocity	Decrease	Decrease
Absolute velocity	Increase	Decrease
Enthalpy	Increase	Constant
Density	Increase	Increase

The compressor outlet pressure (Pa) is:

$$P_{c_{out}} = P_{c_{in}} \cdot PR_c \quad (21.2.9)$$

The isentropic efficiency of the compressor is $\frac{T_{rise_{ideal}}}{T_{rise_{actual}}}$ and is also indicative of the work input or total temperature increase. Thus, the temperature (K) at the exit can be derived from the inlet temperature, pressure ratio, isentropic efficiency, and ratio of specific heats:

$$T_{c_{out}} = T_{c_{in}} \cdot \left[1 + \frac{\left(\frac{P_{c_{out}}}{P_{c_{in}}} \right)^{\frac{\gamma-1}{\gamma}} - 1}{\eta_{is_c}} \right] \quad (21.2.10)$$

It is important to account for the polytropic efficiency, when comparing compressors of varying pressure ratios. This is because compressors of the same level of technology and comparable geometry (i.e., the freedoms of the design such as the frontal area), will share the same polytropic efficiency regardless of the pressure ratio (Walsh and Fletcher, 2004). The polytropic efficiency can be derived from the following expression:

$$\eta_{poly_c} = \frac{\ln \left(\frac{P_{c_{out}}}{P_{c_{in}}} \right)^{\frac{(\gamma-1)}{\gamma}}}{\ln \left(\frac{T_{c_{out}}}{T_{c_{in}}} \right)} \quad (21.2.11)$$

which defines the polytropic efficiency as the isentropic efficiency of each infinitesimally small stage of the compression process. Hence, for a polytropic efficiency in a compressor, the relationship is expressed as:

$$\frac{P_{c_{out}}}{P_{c_{in}}} = \left(\frac{T_{c_{out}}}{T_{c_{in}}} \right)^{\eta_{poly_c} \frac{\gamma}{\gamma-1}} \quad (21.2.12)$$

thus, the temperature at the outlet can be derived from:

$$T_{c_{out}} = T_{c_{in}} \cdot \left(\frac{P_{c_{out}}}{P_{c_{in}}} \right)^{\frac{(\gamma-1)}{\gamma \eta_{poly_c}}} \quad (21.2.13)$$

The mass flow rate (kg/s) at the inlet is equal to the mass flow rate (kg/s) at the outlet as there are no compositional changes:

$$m_{c_{out}} = m_{c_{in}} \quad (21.2.14)$$

The compressor work (W) is the product of the mass flow rate, specific heat at constant pressure and the temperature delta:

$$CW = m_c \cdot Cp_{he} \cdot (\Delta T_c) \quad (21.2.15)$$

whereby

$$\Delta T_c = T_{c_{out}} - T_{c_{in}} \quad (21.2.16)$$

With regard to determining the outlet temperature for the compressor, Eq. (21.2.10) or (21.2.13) are applicable, and either equation can be used for convenience.

21.2.8.2 Axial turbine

The turbine extracts the power from the hot helium-gas stream using its rotor, which in turn drives the compressor and provides a mechanical drive for the generator. The hot gas enters the first row of Nozzle Guide Vanes (NGVs), whereby the flow is directed through the throat of the NGVs onto the row of rotor blades at an increased velocity. The power extraction by the rotor blades is because of the change of the tangential component of the absolute velocity (V) known as the whirl velocity (V_w), as depicted in Figure 21.2.6. Losses are encountered during this process, whereby the drop in total pressure is due to the frictional and turbulent flow of the hot gas velocity. Figure 21.2.6 shows an example of the turbine-stage arrangement, whereby the aerodynamic velocity triangles were calculated in a preliminary scoping study conducted by Gad-Briggs (2011). Table 21.2.5 describes the thermodynamic process in the turbine for working fluids with similar behavior to air, and is based on the work by Walsh and Fletcher (2004).

The pertinent parameters required for DP performance assessment of the turbine include the inlet mass flow rate, temperature and pressure of the hot helium gas, the outlet pressure, turbine efficiency (polytropic and isentropic), and the helium gas properties. These provide the governing expressions that are given below, and are taken from Gad-Briggs and Pilidis (2017).

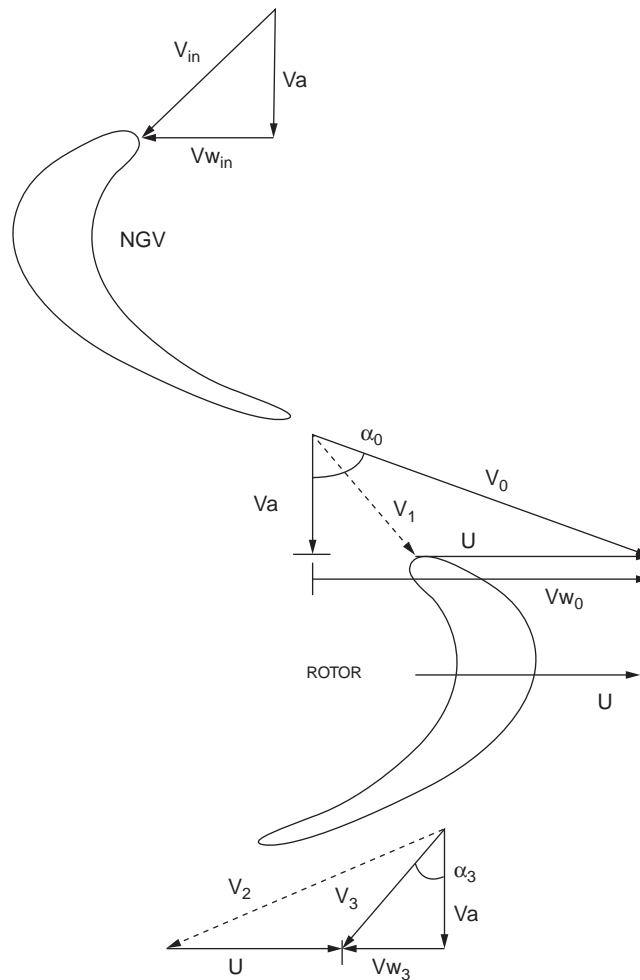


Figure 21.2.6. Turbine cascade showing NGV and rotor and typical reaction.

Table 21.2.5. Thermodynamic processes during the expansion phase (uncooled turbine)

Parameters	NGV	Rotor
Static pressure	Decrease	Decrease
Total pressure	Small decrease	Decrease
Static temperature	Decrease	Decrease
Total temperature	Constant	Decrease
Relative velocity	Increase	Increase
Absolute velocity	Increase	Decrease
Enthalpy	Constant	Decrease
Density	Decrease	Decrease

The temperature at the outlet is derived from the following expression, when considering the isentropic efficiency:

$$T_{t_{out}} = T_{t_{in}} \cdot \left\{ 1 - \eta_{is_t} \left[1 - \left(\frac{P_{t_{out}}}{P_{t_{in}}} \right)^{\frac{\gamma-1}{\gamma}} \right] \right\} \quad (21.2.17)$$

Just like the compressor, it is also appropriate to consider the polytropic efficiency for the same reasons regardless of the expansion ratio. The polytropic efficiency can be derived from:

$$\eta_{poly_t} = \frac{\ln \left(\frac{T_{t_{in}}}{T_{t_{out}}} \right)}{\ln \left(\frac{P_{t_{in}}}{P_{t_{out}}} \right)^{\frac{\gamma-1}{\gamma}}} \quad (21.2.18)$$

and it defines the polytropic efficiency to be the isentropic efficiency of each infinitesimally small stage of the turbine expansion process. As a result, the polytropic efficiency in a turbine is defined by this relationship:

$$\frac{P_{t_{in}}}{P_{t_{out}}} = \left(\frac{T_{t_{in}}}{T_{t_{out}}} \right)^{\frac{\gamma}{(\gamma-1)\eta_{poly_t}}} \quad (21.2.19)$$

and the temperature at the outlet can be derived from:

$$T_{t_{out}} = T_{t_{in}} \cdot \left(\frac{P_{t_{out}}}{P_{t_{in}}} \right)^{\frac{\gamma-1}{\gamma} \eta_{poly_t}} \quad (21.2.20)$$

As with the compressor, Eqs. (21.2.14) and (21.2.15) also apply to the turbine for mass flow rate conditions and turbine work but:

$$\Delta T_t = T_{t_{in}} - T_{t_{out}} \quad (21.2.21)$$

Like in the case of the compressor, Eq. (21.2.17) or (21.2.20) are applicable for determining the exit temperature of the turbine, and either equation can be used for convenience.

For performance purposes, Eqs. (21.2.9)–(21.2.21) provide the key parameters for temperature, pressure, mass flow rate (considering any bleed-off takes for cooling) and components' power of the turbomachinery

set. It allows a first-order, but accurate performance assessment to be made of the turbomachinery. The flow conditions established by the compressor are also critical to other components such as the heat exchangers and reactor.

21.2.8.3 Recuperator

The recuperator is responsible for transferring the exhaust heat back into the cycle downstream of the compression phase, with the purpose of raising the temperature of the helium going into the reactor. The heat transfer happens through the passage wall from the low-pressure side to the high-pressure side of the cycle.

The pertinent parameters for DP performance of the recuperator are the recuperator effectiveness, the conditions for the hot and cold legs with regards to temperature and pressure, and the pressure losses experienced in the low-pressure side and the high-pressure side. For a suitable design method, the Number of Transfer Units (NTU) method can be utilized to determine the performance of the recuperator. The NTU method has been documented by [Pitts and Sissom \(1997\)](#); its application in the design of a complex cross-flow heat exchanger is discussed in the work by [Navarro and Cabezas-Gomez \(2007\)](#). The recuperator design philosophy applied in this chapter, as expressed below, is taken from work by [Gad-Briggs and Pilidis \(2017\)](#).

The heat-exchanger effectiveness is defined when the maximum possible and actual heat transfer for a counter-flow geometry is understood. This is determined by the temperature differences between the hot inlets, and the cold inlets in each case. In addition, the heat capacity rates for the helium hot gas and helium cold fluid need to be defined. This is the product of the mass flow rate and the specific heat at constant pressure for the fluid in the cold leg and hot leg. Starting with fundamental basics, the effectiveness is:

$$\varepsilon_{\text{re}} = \frac{q_{\text{re,real}}}{q_{\text{re,max}}} \quad (21.2.22)$$

The maximum amount of heat flux (W/m^2) of the recuperator $q_{\text{re,max}}$ considers the hot and cold inlet conditions and the minimum specific heat. The idea is to ensure the fluid with the lowest heat capacity experiences the maximum change in temperature. This is expressed as:

$$q_{\text{re,max}} = \frac{Cp_{\text{he,min}} \cdot (T'_{\text{re,hot}} - T'_{\text{re,cold}})}{A} \quad (21.2.23)$$

and the real heat flux (W/m^2) is:

$$q_{\text{re,real}} = \frac{Cp_{\text{he,hot}} \cdot (T'_{\text{re,hot}} - T_{\text{re,hot}})}{A} = \frac{Cp_{\text{he,cold}} \cdot (T_{\text{re,cold}} - T'_{\text{re,cold}})}{A} \quad (21.2.24)$$

With helium as the working fluid, Cp is constant, meaning $Cp_{\text{he,min}} = Cp_{\text{he,cold}} = Cp_{\text{he,hot}}$ in the energy balance equation. The temperatures at the hot and cold legs can be obtained, when considering Eq. (21.2.24) (either hot or cold sides), and considering an arbitrary effectiveness. The temperatures for both ends are expressed as follows:

$$T_{\text{re,cold}} = T'_{\text{re,cold}} + \left[\varepsilon_{\text{re}} \cdot (T'_{\text{re,hot}} - T'_{\text{re,cold}}) \right] \quad (21.2.25)$$

With $Cp_{\text{he,min}} = Cp_{\text{he,cold}} = Cp_{\text{he,hot}}$, the energy balance is:

$$\left[m_{\text{re,cold}} \cdot (T_{\text{re,cold}} - T'_{\text{re,cold}}) \right] = \left[m_{\text{re,hot}} \cdot (T'_{\text{re,hot}} - T_{\text{re,hot}}) \right] \quad (21.2.26)$$

?thus, the hot outlet is:

$$T_{rehot} = T'_{rehot} - \left[\frac{m_{recold} \cdot (T_{recold} - T'_{recold})}{m_{rehot}} \right] \quad (21.2.27)$$

The pressures at the exit conditions can be calculated if the pressure drops (%) across the hot and cold sides are known:

$$P_{recold} = P'_{recold} \cdot (1 - \Delta P_{reHPloss}) \quad (21.2.28)$$

$$P_{rehot} = P'_{rehot} \cdot (1 - \Delta P_{reLPloss}) \quad (21.2.29)$$

Due to no compositional changes, mass flow rate (kg/s) conditions are:

$$m_{rehot} = m'_{rehot} \quad (21.2.30)$$

$$m_{recold} = m'_{recold} \quad (21.2.31)$$

21.2.8.4 Precooler and intercooler

The precooler and intercooler remove the heat from the helium gas using a cooling medium cold sink such as seawater.

For DP performance, the parameters that are of importance are the inlet temperature for the compressors, the pressure conditions, and the pressure losses. The expressions below are from [Gad-Briggs and Pilidis \(2017\)](#):

$$T_{pcout} = T_{cin} \quad (21.2.32)$$

$$P_{pcin} = P_{pcout} \cdot (1 + \Delta P_{pcloss}) \quad (21.2.33)$$

$$W_{pcout} = W_{pcin} \quad (21.2.34)$$

With regards to the intercooler, Eqs. (21.2.32)–(21.2.34) also apply. The addition of a second compressor for the intercooled cycle means that the pressure ratio for both compressors is determined as:

$$PR_{ic} = \sqrt[ic]{PR} \quad (21.2.35)$$

whereby the *ic* coefficient denotes the number of intercoolers in the cycle +1, leading to a reduction in the pressure ratio per compressor.

The precooler design (including the intercooler) has the capability of influencing the cycle inlet temperature. This is discussed later in this chapter.

21.2.8.5 Reactor

To simplify the DP performance, the reactor is considered as a heat source with constant reactor thermal power. The pertinent parameters for DP performance are the pressure losses and the thermal heat generated from the fission process, which is attributed to the Core Outlet Temperature (COT). The expressions below are from [Gad-Briggs and Pilidis \(2017\)](#).

Helium does not introduce any compositional changes in the reactor; thus mass flow rate (kg/s) is:

$$W_{MHR_{out}} = W_{MHR_{in}} \quad (21.2.36)$$

Pressure (Pa), taking into account losses (%):

$$P_{MHR_{out}} = P_{MHR_{in}} \cdot (1 - \Delta P_{MHR_{loss}}) \quad (21.2.37)$$

and the thermal heat input (W_{th}):

$$Q_{MHR} = W_{MHR_{in}} \cdot C_{p_{he}} \cdot (\Delta T_{MHR}) \quad (21.2.38)$$

whereby:

$$\Delta T_{MHR} = T_{MHR_{out}} - T_{MHR_{in}} \quad (21.2.39)$$

21.2.8.6 Cycle performance

The useful and specific work or power, and the cycle thermal efficiency are output conditions that determine the power generated by the cycle, including the capacity, and how efficient it generates the power for its given capacity.

The Useful Work (UW) is Watts electric (W_{el}), and the work available for driving the load:

$$UW = TW - CW \quad (21.2.40)$$

whereby Eq. (21.2.40) is also applicable to ICR, but Compressor Work (CW) is the summation of both compressors' work requirement to be delivered by the turbine. The Specific Work (SW) or capacity of the plant (W/kgs) is:

$$SW = UW/W \quad (21.2.41)$$

and the thermal efficiency (%) of the cycle is:

$$\eta_{th} = UW/Q_{MHR} \quad (21.2.42)$$

The outlined mathematical expressions in this section enable the basic conditions of the cycle to be determined in terms of the station parameters in Figures 21.2.3 and 21.2.4, and the cycle conditions. The next section discusses considerations for cycle design using the SCR and ICR as bases for comparison.

21.2.9 Cycle performance design considerations

The SCR and ICR are two main proposed cycle configurations for power conversion of gas-cooled and high-temperature reactors. As such, this section compares the key aspects that impact the choice of cycle and design.

21.2.9.1 DP performance comparison

Typically, the ICR benefits from lower compressor exit temperatures because of the intercooler. For similar inlet conditions, the SCR is expected to register a 70% to 75% increase in compressor exit temperatures. This means that for a similar compressor pressure ratio, the SCR would have a higher Compressor Work (CW) of 7% to 10%, meaning that the ICR would also have a higher cycle power output of between 4% and 6%. This superiority in power output and plant capacity for similar inlet pressures, temperatures and compressor pressure ratio, results in a more efficiency ICR by about 2% to 3%. A significant disadvantage of the ICR is the size of the plant due to the additional intercooler and second compressor. This impacts the complexity of the cycle. However, the specific overnight cost (\$/kW_{el}) increase for an ICR Nth Of A Kind (NOAK) NPP is

Table 21.2.6. SCR and ICR station output values

No	<i>m</i>			<i>P</i>			<i>T</i>		
	kg/s			MPa			°C		
	SCR	ICR	Δ , %	SCR	ICR	Δ , %	SCR	ICR	Δ , %
1	410	410	0.0	3.2	3.2	0.0	28	28	0.0
2	405	406	-0.3	6.4	4.5	41.0	135	78	73.0
2a	-	406	-	-	4.5	-	-	28	-
2b	-	406	-	-	6.4	-	-	78	-
3	405	405	0.0	6.4	6.4	0.0	678	677	0.1
4	406	406	0.0	6.2	6.2	0.0	950	950	0.0
5	410	410	0.0	3.5	3.5	0.0	701	702	-0.1
6	410.4	410	0.0	3.3	3.3	0.0	164	110	49.1

Table 21.2.7. SCR and ICR cycle output results

<i>CW</i>			<i>TW</i>			<i>UW</i>			η		
[MW]			[MW]			[MW]			%		
SCR	ICR	Δ (%)	SCR	ICR	Δ (%)	SCR	ICR	Δ (%)	SCR	ICR	Δ (%)
227	211	8.0	513	511	0.5	286	300	-4.7	49.7	51.8	-2.1

estimated to be $\sim 1\%$ more than the SCR for the construction capital costs under guidelines applicable to Gen-IV concepts. This estimation excludes the annual operating costs, fuel cycle costs, capital recovery, decontamination and decommissioning, research and development costs for First Of A Kind (FOAK) plants. [Tables 21.2.6 and 21.2.7](#) quantify the DP differences for both cycles, with reference to a 950°C Reactor COT.

21.2.9.2 Impact of temperature and pressure ratio on cycle efficiency and plant capacity

For the helium gas turbine Brayton cycles, an increase in COT has a positive effect on cycle thermal efficiency. At optimum pressure ratios, the cycle efficiency of the SCR and ICR is expected to have an increase of 20% to 22% at COTs between 500°C and 950°C , which is the key range for Gen-IV reactor designs. At high temperatures, the ICR will experience less deterioration in efficiency increase, when the pressure ratio is increased. The reason is the SCR does not offer a significant gain at the maximum pressure ratio achievable when it comes to the cycle efficiency, due to the significant increase in compressor work for the SCR. This is regardless of the general expectation, which is helium compressors operate at lower pressure ratios. Whereby the ICR has a higher rate of increase in efficiency, the SCR has a higher rate of increase in capacity. This means that for the closed Brayton helium gas turbine cycles, a maximum cycle efficiency does not correspond to maximum plant capacity. Typically, cycle economics do not prioritize the amount of power a plant can deliver over the level of efficiency achievable. This is a key reason for including the recuperator to significantly improve the cycles. [Figures 21.2.7 and 21.2.8](#) show the impact of Temperature and Pressure Ratios (TR and PR) on the efficiencies. [Figures 21.2.9 and 21.2.10](#) show the impact of TR and PR on the plant capacity (specific work).

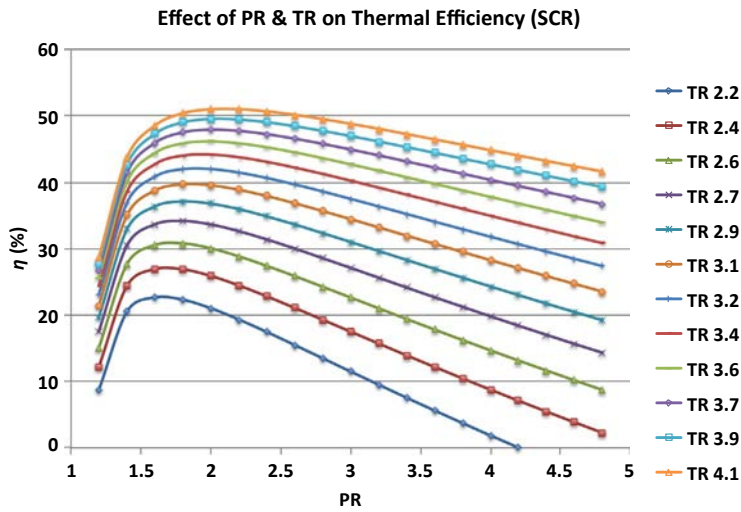


Figure 21.2.7. Pressure Ratios (PR) vs efficiency for given Temperature Ratio (TR) (SCR, helium).

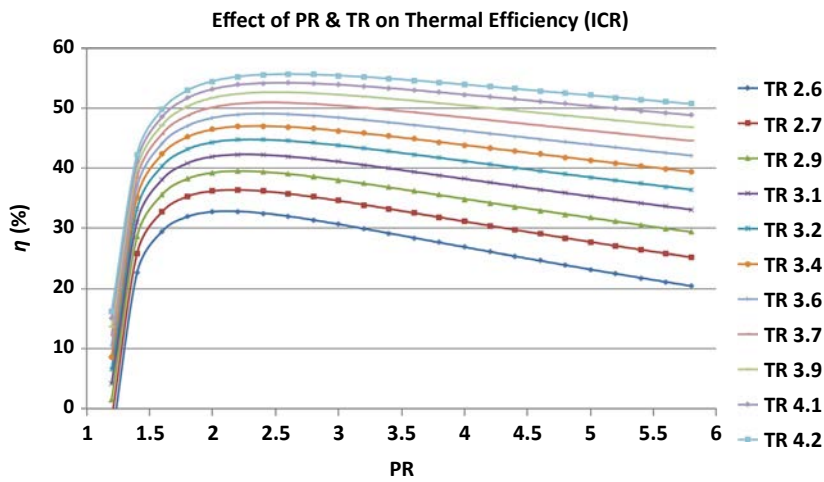


Figure 21.2.8. Pressure Ratio (PR) vs efficiency for given Temperature Ratio (TR) (ICR, helium).

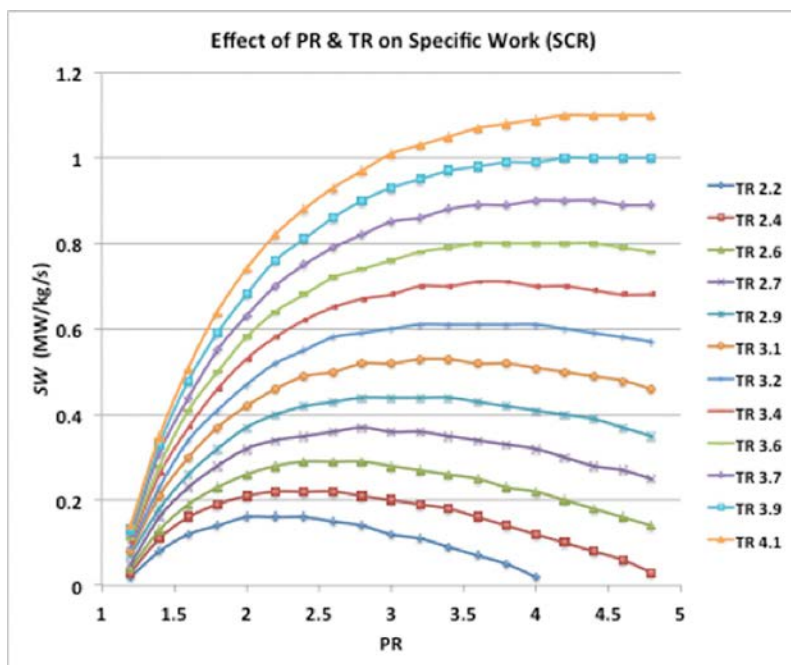
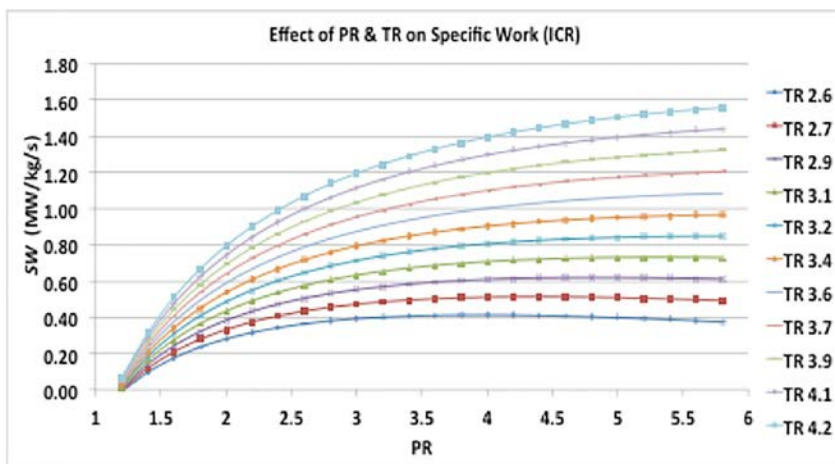


Figure 21.2.9. Pressure Ratio (PR) vs specific work for given Temperature Ratio (TR) (SCR, helium).

Figure 21.2.10. Pressure Ratio (PR) vs specific work for given Temperature Ratio (TR) (ICR, helium).



21.2.9.3 Component efficiencies

Component efficiencies are critical to maintaining or meeting requirements for increasing cycle efficiencies. For the SCR and ICR, the components that are key to the performance of the cycle are the compressor, turbine and recuperator. A low to medium technological level is between 80% and 85% efficiency; medium to high is 86% to 90%, and beyond high is $\geq 91\%$. The GTHTR300 NPP is an example of a plant with components beyond the high technology level. The compressor and turbine have isentropic efficiencies of 90% and 94%, respectively, while the recuperator has an effectiveness (efficiency) of 96%. This contrasts with the HTR-10GT NPP as at the time of compiling this chapter. As expected, the component efficiencies depict low technology components at the early stages of development.

Typically for the low technology range, the impact of the compressor on the cycle efficiency is between just over 1% for the SCR and $< 1\%$ for the ICR. For the SCR, improving the compressor with an efficiency of $\sim < 89\%$ offers more gains in cycle efficiency than the ICR. This is based on an analysis of the gains for every 1% improvement of the compressor. On the other hand, it can be argued that the ICR cycle efficiency is less sensitive to the compressor efficiency, when the compressor efficiency is $> 85\%$. In view of these gains, it is not cost-effective to develop the compressors beyond the mid to high technology level. The cost of developing such a compressor will have to consider the challenges of helium as a working fluid, including minimizing flow separation without compromising compressor stability and operating margins.

With regard to the turbine, the ICR is more sensitive to its efficiency when assessing the effect of turbine deterioration from the highest level to the low-level range. Typically, it is expected that the effect on the cycle efficiency is between 1% and 1.5% for the ICR and just over 1% for the SCR. Unlike the compressor, there are gains from developing the turbine beyond the high technology level.

The recuperator has the greatest effect on the cycle efficiency. Typical values are 1.5% to 2% in efficiency drop for the SCR and 1.75% to over 2% efficiency drop for the ICR. In fact, analysis from studies conducted by EGB Engineering (UK) and Cranfield University (UK) has shown that the rate of cycle efficiency increase per 1% improvement of recuperator effectiveness has a greater impact on the cycle beyond 95%. The recuperator from the GTHTR300 NPP was improved by 1% from 95%. This, combined with other improvements, contributed to an increase of $> 3\%$ in the cycle efficiency.

The turbine has the greatest impact on the plant capacity because it has to extract the power. A loss of 1% in efficiency amounts to 1.5% to 3% loss in plant capacity. The compressor has the least impact on the plant capacity, and the recuperator has no effect. The potential average combined effect of component degradation during plant operation can increase the cost of the plant by up to 9%. For this reason, the design of the plant must balance the technology level in accordance with the operational envelop of the plant, and ensure that maintenance periods are defined, and executed at the right intervals. Figures 21.2.11–21.2.14 illustrate the effects of component efficiencies on the cycle efficiencies and the plant capacity (specific work).

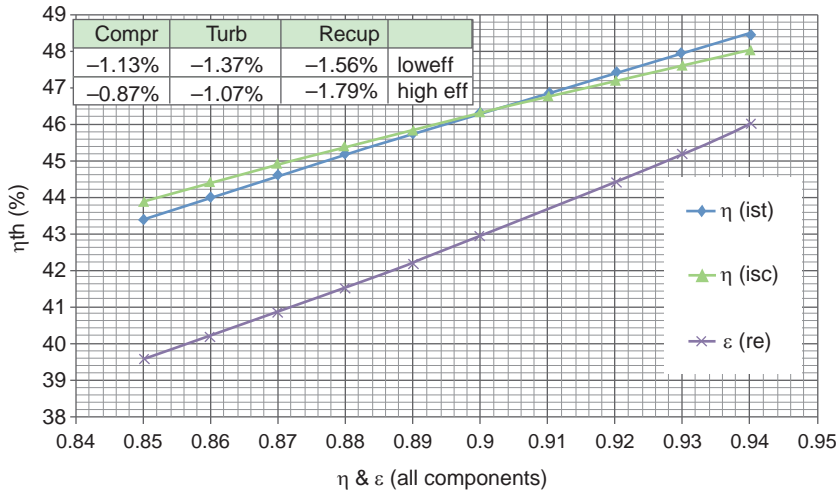


Figure 21.2.11. Sensitivity analysis—effect of component efficiencies on cycle efficiency (SCR, helium).

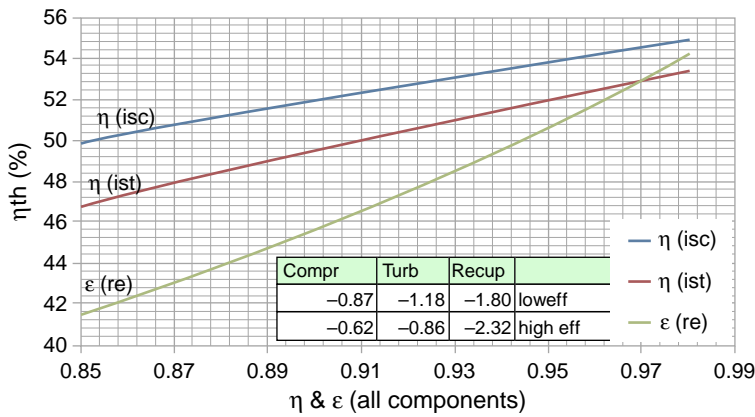


Figure 21.2.12. Sensitivity analysis—effect of component efficiencies on cycle efficiency (ICR, helium).

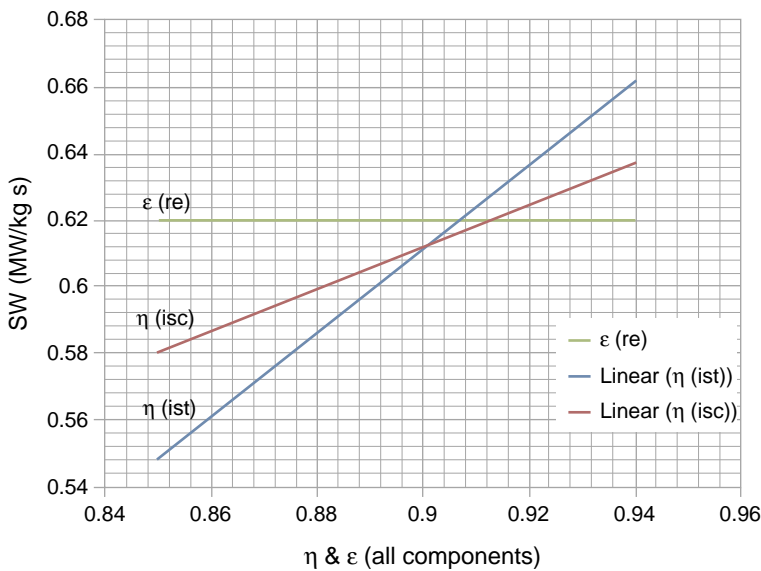
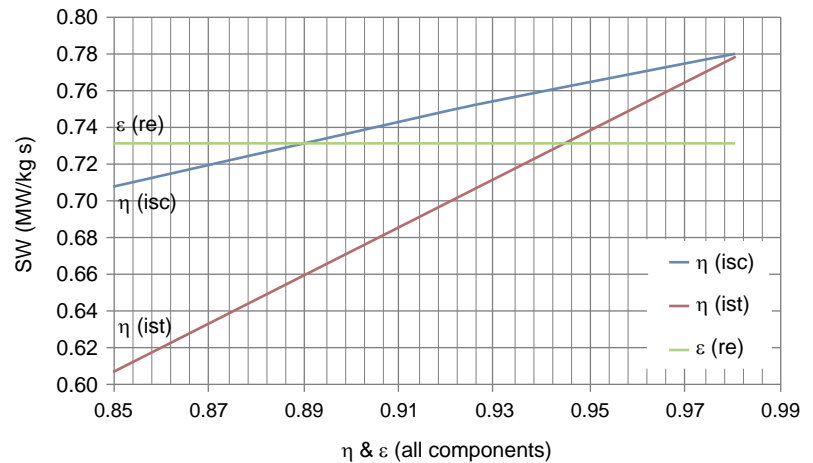


Figure 21.2.13. Sensitivity analysis—effect of component efficiencies on specific work (SCR, helium).

Figure 21.2.14. Sensitivity analysis—effect of component efficiencies on specific work (ICR, helium).



21.2.9.4 Compressor inlet temperature

The inlet temperature to the cycle can affect the compressor power. NPPs that operate in hot countries are expected to experience increased compressor work, which will require more power to compress the gas. The other possibility is the compression process will demand less power in colder countries. This effect is created by the ambient conditions under which the helium gas exchanges the heat from the recuperator low-pressure side exit. The precooler provides sea water at a given temperature, which acts as a heat sink. An increase in compressor power will limit the amount of power available to drive the generator, resulting in efficiency penalties. For every 1°C rise in temperature, the increase in compressor work is $\sim 0.3\%$. This translates to a drop in cycle efficiency of $\sim 1.3\%$ for every 5°C rise, with the increase in compressor power resulting in a $\sim 4 \text{ MW}_{\text{el}}$ decrease in plant capacity. As noted earlier, the design of the precooler and intercooler are important in maintaining adequate ambient conditions, and regulating the inlet temperature of the cycle. In addition, the quantified effects of the compressor inlet temperature on efficiency and plant capacity can be limited. In the case of the precooler design, a cocurrent or counter-current type of precooler will have to be assessed for the design conditions, including the intended location of the plant. This would also apply to the intercooler. Where ambient temperature changes are a concern for plant performance, the conditions can be minimized if load-following operations and Off-Design Point (ODP) performance operations are incorporated into the plant designs. These are covered in studies by (Gad-Briggs et al., 2017b, 2017e). Figure 21.2.15 illustrates the effects of compressor inlet temperature on cycle efficiencies.

21.2.9.5 Pressure losses

The combined pressure losses are expected to be greater for the ICR in comparison to the SCR by about 15% to 20%. The recuperator high-pressure side is expected to have the highest-pressure losses and the greatest effect on efficiency, followed by the reactor. The precooler and the recuperator low-pressure side follow that order in terms of the effect on efficiency. The effect on the capacity is similar to the effect on efficiency. This potential combined effect of losses (worse case average of 5% per component) can increase the cost of the plant by 4% to 6%. As such, it is important for the plant design to be modularized and compact in order to reduce pressure losses. This will require shorter pipe assemblies and ducts to reduce this effect. Figure 21.2.16 and Table 21.2.8 illustrate the effect of pressure losses on the efficiencies of the cycles.

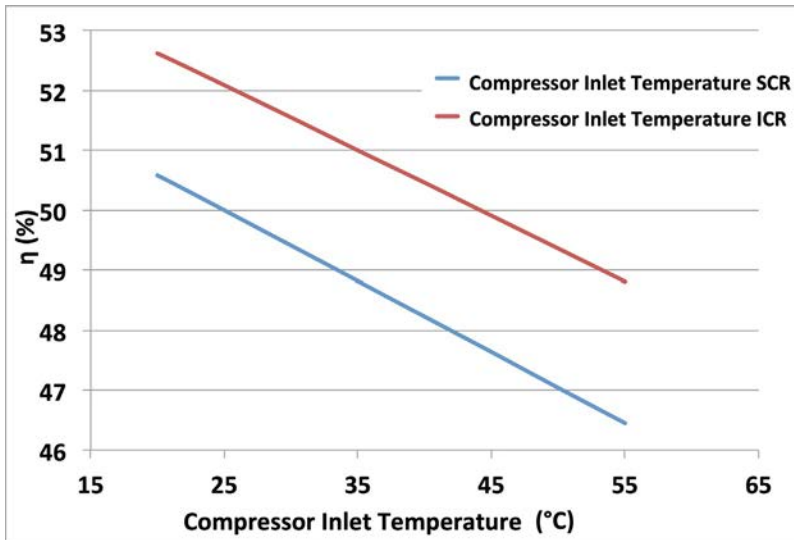


Figure 21.2.15. Sensitivity analysis—effect of compressor inlet temperature on cycle efficiency (helium).

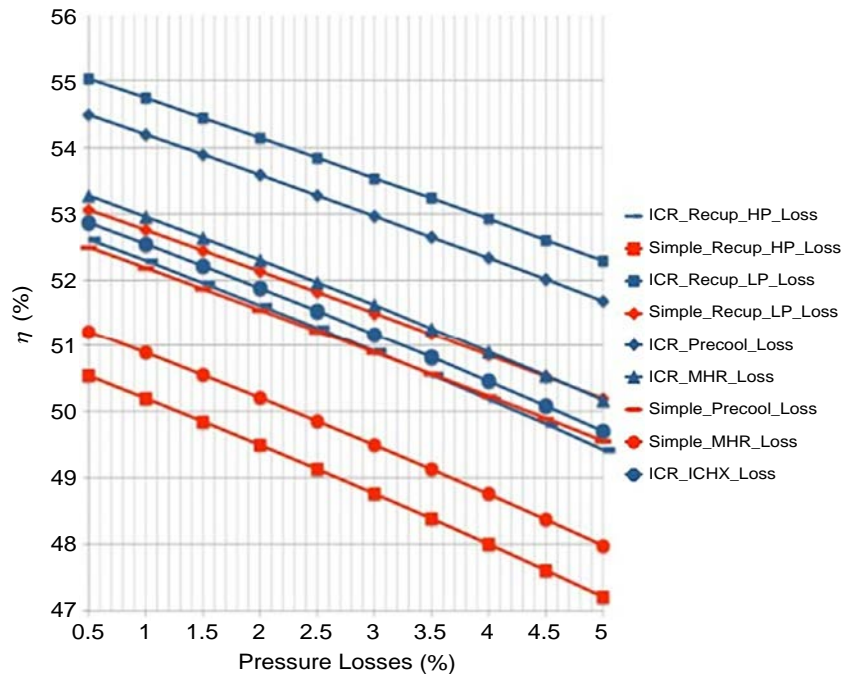


Figure 21.2.16. Sensitivity analysis—pressure losses (helium)

Table 21.2.8. Pressure losses effect on cycle efficiency (helium)

950°C						
ICR						
	RecupHP	Precooler	RecupLP	Reactor	ICHX	Total
Average (%)	1.43	1.21	1.16	1.37	1.41	6.59
Lower range (%)	1.27	1.11	1.08	1.22	1.24	5.93
Higher range (%)	1.54	1.26	1.20	1.46	1.51	6.96
Δ (%)	0.27	0.14	0.12	0.24	0.26	

Continued

Table 21.2.8. Pressure losses effect on cycle efficiency (helium)—cont'd

950°C					
SCR					
	RecupHP	Precooler	RecupLP	Reactor	Total
Average (%)	1.57	1.32	1.27	1.50	5.65
Lower range (%)	1.38	1.22	1.18	1.33	5.10
Higher range (%)	1.68	1.36	1.31	1.61	5.95
Δ (%)	0.30	0.14	0.13	0.28	

21.2.10 Working fluid for NPP cycle performance, and operation

Previous subsections of this chapter focused on helium as the working fluid. This section and subsequent sections focus on a variety of working fluids including helium for comparison of performance and costs.

In the last two decades, there have been various pilot cycle configurations, component designs, performance testing, and feasibility demonstration with different working fluids (Frutschi, 2005; Osigwe et al., 2019a,2020b). Interestingly, one factor that could influence the design and operational experience of the closed-cycle gas turbine, which is yet to be explored extensively, is the choice of the working fluid (Osigwe et al., 2019a).

This and subsequent sections, provide a robust understanding of coolants and working fluid options for the NPP with a major focus on the closed-cycle gas turbine. The purpose of assessing the selected working fluids is to identify and compare the candidate fluids suitable for investment decisions from a component design perspective, overall system performance and plant operations, and as well as potential risk considerations for each fluid.

As mentioned in previous sections, due to the self-containing nature of the nuclear powered closed-cycle gas turbine system, almost all permanently gaseous working fluid can be utilized, since the fluid will be operated in the gaseous region beyond its critical temperature throughout the cycle (Lee et al., 1981; Osigwe et al., 2019a). However, selecting an appropriate working fluid for the NPP system would depend on meeting several criteria, some of which are dictated by the fluid properties at varying conditions, special requirements of the existing conversion module, and techno-economic considerations. Also, any selected fluid should have an acceptable thermal stability level at the maximum cycle temperature, which is dictated by the reactor delivery temperature. It should not be corrosive to the materials of the machinery and should be readily available at a modest cost. Other factors to consider include flammability and toxicity in terms of the fluid management system. In the risk assessment section, some of these criteria will be comprehensively addressed.

21.2.10.1 Advances in working fluid studies

The freedom to choose which working fluid essentially suits a given design, makes the closed-cycle gas turbine a desirable energy conversion system for the NPP (Decher, 1994; Osigwe et al., 2019d). This is because it gives the designer the freedom to select a fluid that enables compact, affordable, and efficient design in terms of cycle performance, operation, and investment risk. The fluids commonly employed as coolants and working fluid for the NPP system include the monoatomic inert gases and

mixtures thereof, and air, nitrogen, and carbon dioxide (Invernizzi, 2017; Osigwe et al., 2019a,2020b,c; Wang and Gu, 2005).

To this end, many studies explored the design and performance potentials of the numerous gaseous working fluids mentioned, using different cycle arrangements as documented in references (Invernizzi, 2017; Lee et al., 1981; Osigwe et al., 2020c; Wang and Gu, 2005; Yousef and Zaamout, 1992). For example, El-Genk and Tournier (2009a,b) analyzed the cycle thermodynamic performance and turbomachinery design of helium and its binary mixtures such as helium-xenon and helium-nitrogen, for a very-high-temperature gas reactor plant coupled with the closed-cycle gas turbine. The study showed that a cycle with pure helium has better cycle performance when compared with other noble gases. However, the use of binary mixtures significantly impacts the turbomachinery design in terms number of stages and length of the shaft. In another analysis, El-Genk and Tournier (2009a,b) investigated the effect of helium and its mixtures on the turbomachinery shaft speed and size. In the work of Grochowina (2011), cycle performance was compared for helium and supercritical carbon dioxide using different cycle configuration for a Generation-IV nuclear power plant.

Similarly, Wang and Gu (2005) presented a comparative study of helium, nitrogen, and air for a direct and indirectly coupled high-temperature gas reactor. The results showed variation in cycle performance for the different fluid, with helium having a more favorable outcome. Lee et al. (1981) analyzed the effects of thermodynamic and transport properties of different gases at fixed pressure ratio factors for optimum selection of a coal-fired closed-cycle gas turbine design.

For a fluid such as carbon dioxide, Kato et al. (2004) presented a performance and design analysis for a medium temperature carbon dioxide gas turbine reactor, comparing the influence of intercoolers on the cycle performance for a nuclear reactor. Olumayegun et al. (2017) presented a preliminary study of nitrogen cycle performance and component design for a Sodium-cooled Fast Reactor (SFR), comparing the single and dual shaft arrangements. Ulizar and Pilidis (2000), described the possibility of handling a semiclosed-cycle gas turbine with carbon dioxide and argon. Additionally, Alpy et al. (2011) compared gas testing for nitrogen and carbon dioxide in a closed-cycle gas turbine component design prototype. Other research works that have explored numerous working fluid options for closed-cycle gas turbine technology are documented in Invernizzi (2017), Lee et al. (1981), Osigwe et al. (2019c), Wang and Gu (2005), and Yousef and Zaamout (1992).

21.2.10.2 Working fluid cycle configuration and performance

As previously mentioned, the design choice for the operating cycles based on the physical layout or configuration of the closed-cycle gas turbine power plant, is driven by the thermoeconomic analysis of the system, in order to get the right balance between thermal efficiency and capital cost (Osigwe et al., 2019a,c).

This section aims to provide an analysis of how the choice of working fluid, could potentially influence the decision on the type of cycle configuration that could be implemented for a nuclear power plant. The closed-cycle gas turbine consists of different assembled components, each accomplishing a specific thermodynamic process. The physical arrangement of these components to facilitate the successful conversion of the heat supplied from the nuclear reactor is called the cycle configuration. Consequently, the gas turbine has several possible arrangements to meet a given performance requirement, such as a simple cycle, recuperated, inter-cooled, reheat, and intercooled-recuperated.

The SCR arrangements usually consist of the cooling heat exchanger and the turbomachinery set, which have been employed in several nuclear power plants. To improve the cycle performance in terms of output power or thermal efficiency, the SCR could be modified with additional components such as recuperation, intercooler, reheating, recompressing, and other unique configurations. Ishiyama et al. (2008) and Noblis (2014) presented an analysis that describes the optimal number intercooling that could give an optimal cycle performance, and the trade-offs between the cycle performance and the capital costs of the overall system. On

Table 21.2.9. Major characteristics of cycle selection for closed-cycle gas turbine

Comparison	Simple cycle	Recuperated cycle	Intercooled recuperated cycle	Intercooled cycle	Reheat cycle
High-efficiency potential	Acceptable	Good	Good	Not economical	Not economical
Plant layout	Simple	Acceptable	Acceptable	Acceptable	Acceptable
Technology maturity	Proven	Proven	Proven	Not proven	Not proven
Component size	Proven	Acceptable	Acceptable	Acceptable	Acceptable
Future prospect	Acceptable	Good	Good	–	–
Potential heat sink usage	Very good	Good	Acceptable	Good	Very good

the other hand, reheating the cycle increases the cycle efficiency and output power by increasing the average temperature of heat addition.

Apart from the choice of the working fluid, other factors that could also affect the design choice of the cycle arrangement include environmental concerns and Technology Readiness Level (TRL) for the closed-cycle gas turbine components as it relates to each working fluid, and cost implications. It is important to emphasize that the added complexity to the simple plant design to improve the cycle performance marginally may not be warranted in terms of capital costs, but the long-term operations would recoup the initial investment capital costs.

Table 21.2.9 provides investors with an overview of the criteria to consider when attempting to select the cycle configuration that would meet their needs, based on major characteristics of the closed-cycle gas turbine. The narrative presented in Table 21.2.9 shows that investment choice for any cycle configuration would entail considering the high-efficiency potential, the complexity of the physical layout, technology maturity level, the component size, and potential heat sink usage. All these criteria could be influenced by the choice of the working fluid. For example, the simple cycle configuration has a simple layout and has been considered in several nuclear power plant designs. Hence, it is a technology and can be easily implemented for any working fluid. However, its efficiency potential, good heat sink usage, component TRL in relation to each working fluid, could also be considered before making a decision.

21.2.10.3 Case studies on working fluid cycle configuration and performance

In this section, an analysis is presented to show a comparison of the working fluid cycle configuration and performance. This analysis was carried out using an in-house model developed by the authors for closed-cycle gas turbine performance and preliminary design simulation (Osigwe et al., 2019d). Four working fluids were selected in this analysis which includes air, carbon dioxide, nitrogen, and helium.

An analytical evaluation of the numerous power plant cycle configuration was carried out, with baseline conditions as shown in Table 21.2.10. The different configurations were compared for the different working fluids (helium, air, carbon dioxide, and nitrogen). The analysis assumed that the nuclear reactor transfers a fixed heat rate to the working fluids at some specified temperature. The Gen-IV systems applicable to this analysis are the VHTRs and GFRs. Both reactors are high-temperature, with core outlet temperatures between 750°C (1023 K) and 950°C (1223 K). The GFRs uses a fast-spectrum core, while the VHTRs utilizes graphite moderation in the solid-state. Details on the assumptions made for this assessment can be found in Osigwe et al. (2019d).

Table 21.2.10. Baseline parameter for parametric study

Parameters	Values
Compressor mass flow rate (kg/s)	441
Compressor inlet temperature (K)	301
Compressor inlet pressure (MPa)	2.5
Compressor isentropic efficiency (%)	85
Turbine entry temperature (K)	1023
Turbine exit pressure (MPa)	2.55
Turbine isentropic efficiency (%)	85
ReX, IC and PC effectiveness (%)	85
GH effectiveness (%)	88

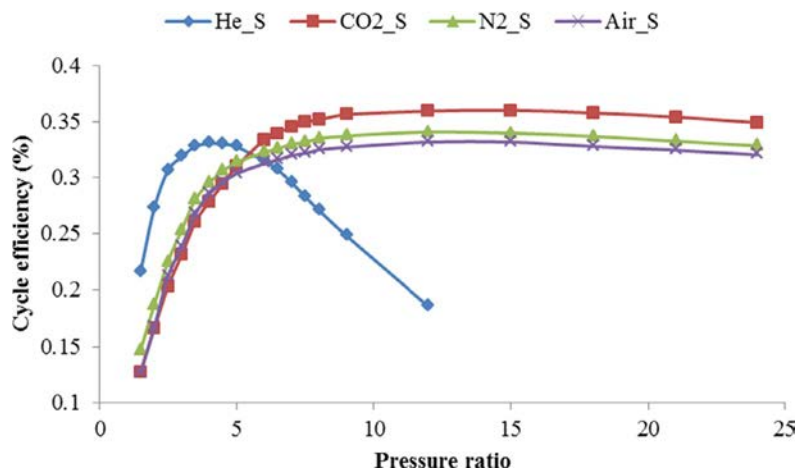


Figure 21.2.17. Simple cycle configuration efficiency for selected working fluids.

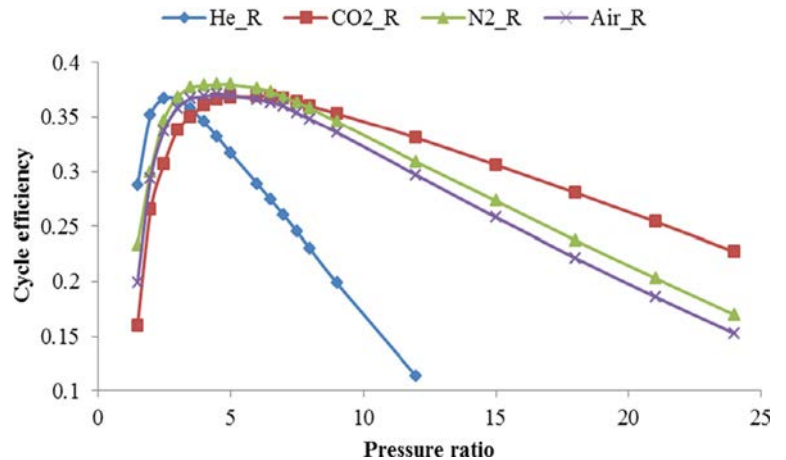
Figure 21.2.17 shows the effect of the selected cycle configuration on the overall cycle efficiency, at different pressure ratios, and for selected working fluids. The simple cycle is the most common form of closed-cycle configuration and offers the least efficiency at low-pressure ratios for most non-inert gases. For this cycle, the efficiency increases as the pressure ratio increases, until it reaches a maximum for a fixed TET.

The simple cycle efficiencies for the different working fluids peaked at 36% for carbon dioxide at a pressure ratio of 15:1, 34% for nitrogen at a pressure ratio of 12:1, 33.5% for air at a pressure ratio of 12:1, and 33.2% for helium at a pressure ratio of 4:1. Achieving the above optimum efficiencies at the specified optimum pressure ratios for a simple cycle, will result in a high number of compressor and turbine stages.

A pressure ratio of 4 for helium fluid could seem a bit high due to the complex nature of its turbomachinery design. However, due to the simple layout of this cycle configuration and its usage in several applications, adapting it for helium could be easily achieved when compared with other cycle configurations. It could be said that this configuration can also be applicable to other fluids like carbon dioxide. On the contrary, the optimum pressure ratio for carbon dioxide is 15; hence, this could have design and cost implications.

Introducing a recuperator offered a better cycle efficiency at lower pressure ratios for all working fluids. This is because of the utilization of the waste heat extracted from the turbine exhaust to preheat the working fluid prior to entering the reactor, thus allowing more working fluid to pass through, and increasing the

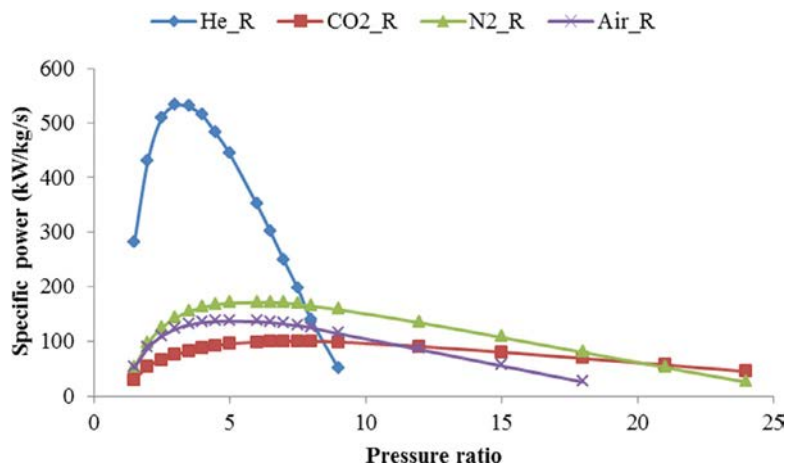
Figure 21.2.18. Recuperated cycle configuration efficiency for selected working fluids.



overall efficiency at every pressure ratio for which recuperation is possible. The recuperated cycle shows a maximum in cycle efficiency that occurred at a much lower pressure ratio than the simple cycle. The low-pressure ratio can be of benefit in the reducing the turbomachinery sizes, which means a great reduction in the overall cost of turbomachinery, especially for helium. Unlike the simple cycle, as the pressure ratio increases beyond its maximum efficiency, the need for recuperation becomes irrelevant. This is due to the temperature difference between the turbine exit, and compressor discharge as it approaches zero. The simulated results of the recuperated cycle in Figures 21.2.18 and 21.2.19 show a maximum cycle efficiency of 38.2% for carbon dioxide at a pressure ratio of 6.5:1, 37.9% for nitrogen at a pressure ratio of 4.5:1, 37% for air at a pressure ratio of 4.5:1, and 36.7% for helium at a pressure ratio of 2.5:1. The specific power for the recuperated cycle will be slightly lower than that of the simple cycle. This is due to a slight increase in the turbine discharge temperature, which reduces the turbine work. Similarly, for the recuperated cycle, the specific power peaked at pressure ratios of 9 for carbon dioxide at 101.6 kW/kg_s, 7:1 for nitrogen at 171.2 kW/kg_s, 7:1 for air at 137 kW/kg_s, and 4:1 for helium at 531.5 kW/kg_s. It is important to mention that the benefit of using recuperation will be at an additional initial cost incurred for the heat exchanger. However, this additional capital cost would be offset during the plant's long-term operation.

One advantage of the recuperated cycle configurations is that it has also been used in several nuclear plant design; hence, this technology could easily be adapted for each working fluid used in this study. For helium, the recuperated cycle could be seen as one of the most suitable configurations since the goal of a reduced pressure ratio at improved cycle efficiency could be easily achieved.

Figure 21.2.19. Recuperated cycle configuration specific power for selected working fluids.



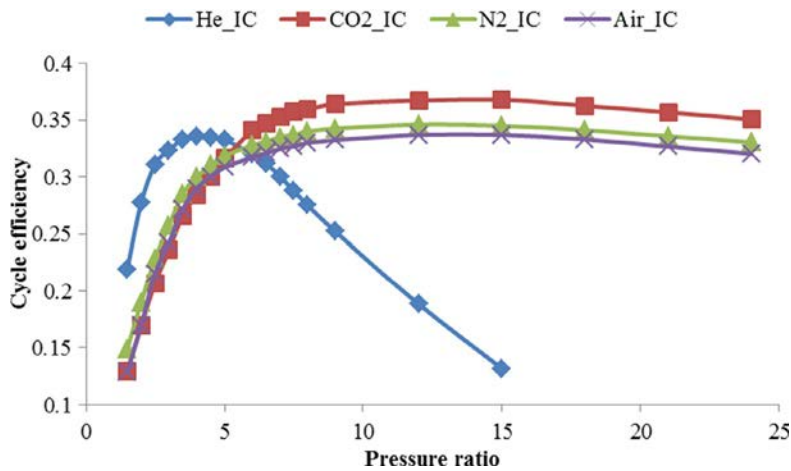


Figure 21.2.20. Intercooled cycle configuration efficiency for selected working fluids.

The decision of whether to incorporate an intercooler into the simple cycle is important to the thermodynamic cycle since it affects both the plant layout and heat rejection characteristics. Thus, introducing an intercooler reduces the total compressor work and improves the net output work. To evaluate the Intercooled Cycle (IC), the component efficiencies and pressure ratios in both compressors were assumed to be the same and equal to the square root of the pressure ratio. The cycle produces between 15% and 25% increase in output power, which is reflected in the specific power, as shown in Figure 21.2.20. Intercooling offers a slight advantage in cycle efficiency as aforementioned, compared with the simple cycle configuration. This is because it gives a lower compressor discharge temperature for the same pressure ratio as the simple cycle. Hence, the pressure ratio at which the compressor discharge temperature will become equal to the turbine discharge temperature is higher than that of a simple cycle arrangement, which increases the cycle peak pressure ratio (the point where maximum efficiency is obtained). However, this efficiency gain must be weighed against power plant complexities and differing heat rejection temperatures, based on the working fluid utilized.

Nonetheless, from the results shown, the maximum efficiency for each working fluid used in this study is as follows: 33.9% for helium, 36.4% for carbon dioxide, 34.5% for nitrogen, and 33.8% for air. The results also show that the major benefit of intercooling is the increased output power, which could be beneficial for working fluids such as carbon dioxide, nitrogen, and air with low heat capacity, when compared to helium.

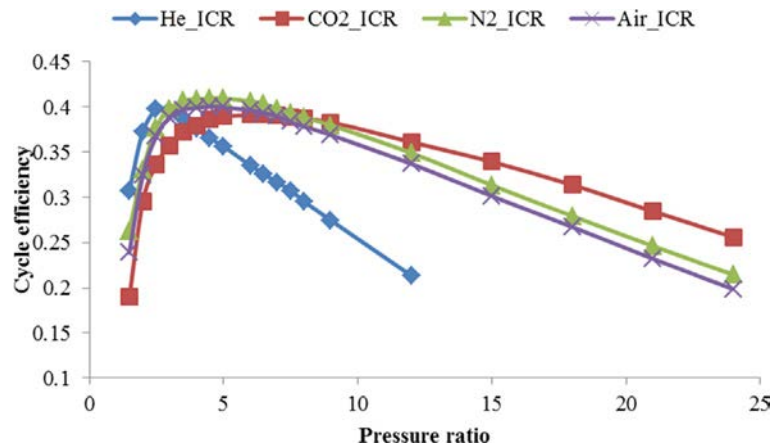
An intercooled cycle is well suited for district heating (Fruttschi, 2005; Osigwe, 2018). When considering the benefit of district heat, one could arguably suggest that using helium as a working fluid could be more beneficial in terms of compact heat exchangers, in comparison to other fluids. Helium could be the appropriate working fluid in this circumstance, but there must be a reasonable compromise in terms of the operational costs, since helium is an expensive working fluid. One of the constraints to using the intercooled cycle configuration could be associated with the gas turbine component TRLs. For fluids such as air and nitrogen, this may not be a problem, but for helium and carbon dioxide, the TRLs may signify early development.

A combination of intercooling and recuperation offers an optimal cycle performance. This is because each new component added, improves key cycle performance indicators. In this case, the intercooler increases the output power, while the recuperation provides an increase in the cycle efficiency, as indicated in Figure 21.2.21.

This also implies that the maximum cycle efficiency occurs at lower pressure ratios, compared with the simple cycle. The InterCooled-Recuperated cycle (ICR) improves the cycle efficiency between 10% and 15%. However, this extra benefit comes with an extra capital cost for the additional components.

Like the intercooled cycle configuration, the ICR is an emerging cycle configuration for NPPs. In the last decade, there has been growing research and development on the use of ICR. This is suitable for any fluid of choice, especially for carbon dioxide and helium, which have lower component design TRLs, compared to

Figure 21.2.21. Intercooled recuperated cycle configuration efficiency for selected working fluids.



air and nitrogen. From the design point of view, the implication of the cycle configuration analysis on the cycle efficiency, and specific power, set a reasonable compromise in terms of plant size, cost (capital and operational cost), turbomachinery, and heat exchanger design challenges for the ICR closed-cycle gas turbine.

21.2.10.4 CO₂ versus supercritical CO₂ as working fluid

Although carbon dioxide as a working fluid for NPPs has been discussed in the previous section, this section seeks to highlight the growing interest in utilizing carbon dioxide at supercritical compressor inlet conditions. This section also discussed other potential improvements due to the introduction of recompression in the supercritical carbon dioxide cycle.

Carbon dioxide as a working fluid is non-toxic and relatively stable. The fluid, when used in a conventional gas-turbine cycle, mostly behaves as an ideal compressible fluid as this operates in regions below the critical condition of CO₂. However, when CO₂ is operated near its critical condition of 7.38 MPa and 32°C, the fluid behaves more like an incompressible fluid resulting in low compression work. Supercritical carbon dioxide refers to operating conditions beyond the critical pressure, and temperature of CO₂.

The supercritical carbon-dioxide cycle has attracted lots of growing interest around the globe, when it was proposed in the late 1960s by [Feher \(1968\)](#) and [Angelino \(1968\)](#). Since then, different applications and cycle configurations have been proposed in many publications ([Dostal, 2004](#); [Dyreby, 2014](#)), including simple cycle, precompression, recompression with and without partial cooling, and many more possible arrangements. The supercritical carbon-dioxide cycle could take advantage of the high density and low viscosity of the fluid for a reduced compressor work, thereby achieving a high cycle thermal efficiency. This could also benefit from component compactness due to high system pressures.

In this section, the cycle performance for conventional CO₂ (ideal compressible gas) has been compared with the supercritical carbon dioxide cycle, and recompressed supercritical carbon dioxide cycle. In this analysis, a simple closed Brayton cycle was used for the conventional and supercritical carbon dioxide, while for the recompression cycle, high and low-temperature recuperators were introduced as well as a second compressor for the recompression process, as shown schematically in [Figure 21.2.22](#). The recompressed cycle has a bypass that diverts a fraction of the working fluid to a secondary compressor before the remainder of the flow stream enters the precooler. The bypassed working fluid is compressed by the recompressing compressor and reintroduced at a point between the low and high-temperature recuperator, as schematically shown in [Figure 21.2.22](#). For this analysis, the pressure-drop and mass-flow leakage were neglected. As the amount of

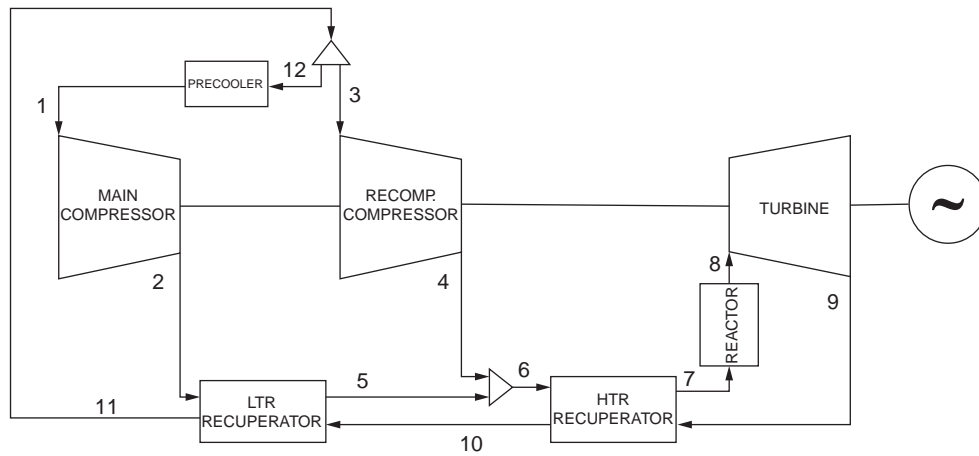


Figure 21.2.22. Schematic representation of recompression Brayton cycle (Grochowina, 2011).

Table 21.2.11. Cycle parameter specifications for the carbon dioxide cycles

Component parameter	CO ₂	SCO ₂	RSCO ₂
Mass flow rate	1 kg/s	1 kg/s	1 kg/s
Compressor inlet pressure	3 MPa	7.38 MPa	7.38 MPa
Compressor inlet temperature	27°C	32°C	32°C
Compressor isentropic efficiency	85%	85%	85%
Turbine isentropic efficiency	90%	90%	90%
Turbine entry temperature	850°C	850°C	850°C

bypassed working fluid increases, the temperature of the low-temperature recuperator stream increases. The maximum amount of working fluid split occurs, when the minimum temperature approach is reached.

Table 21.2.11 shows the cycle specifications and conditions for which the analysis and comparison were made. In all cases, pressure losses were neglected, and the cycle was simulated at different pressure ratios and TET of 850°C. The component efficiencies are as specified in the table below. The recuperator effectiveness of the recompression cycle was assumed as 86%. In Table 21.2.11 and other parts of this chapter, CO₂, SCO₂, and RSCO₂ refer to Carbon dioxide (CO₂), supercritical carbon dioxide and recompressed supercritical carbon dioxide cycle, respectively.

In Figure 21.2.23, the conventional CO₂ cycle efficiency is the lowest because of the higher compressor work requirement. As the compressor inlet condition is set at the supercritical region, the compressor work of the simple cycle is reduced, compared with the previous case. Thus, the cycle efficiency of the supercritical CO₂ simple cycle is higher than the cycle efficiency of the CO₂. A reduced compressor work would imply an increase in the net output power hence, the reason for an increase in cycle efficiency. For the recompressed SCO₂, the cycle efficiency increases due to the recuperator and the introduction of the recompression compressor. While the recuperator reduced the heat input, the recompression compressor reduces the overall compressor work. At a pressure ratio above 5.2, the cycle efficiency of the recompressed carbon dioxide cycle begins to decrease. Similarly, Figure 21.2.24 compares the output power for CO₂, SCO₂ and RSCO₂, respectively. The changes in output power are due to a reduced compressor work at the supercritical region.

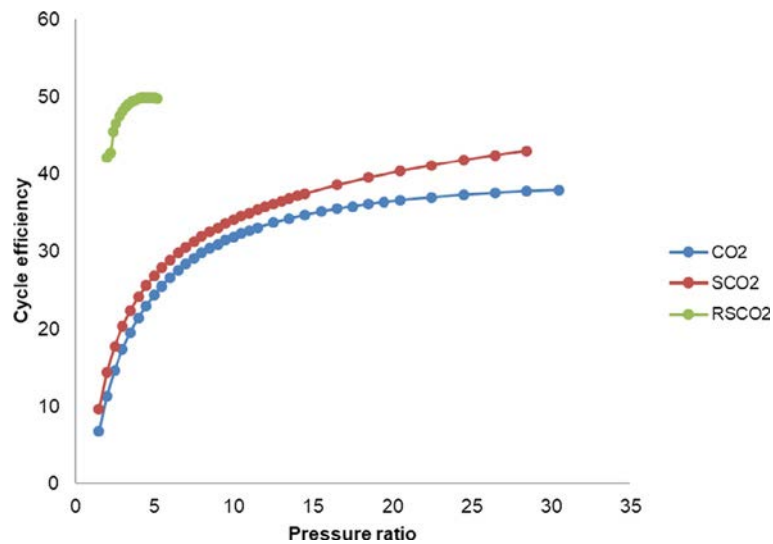


Figure 21.2.23. Cycle efficiency of CO_2 , SCO_2 and RSCO_2

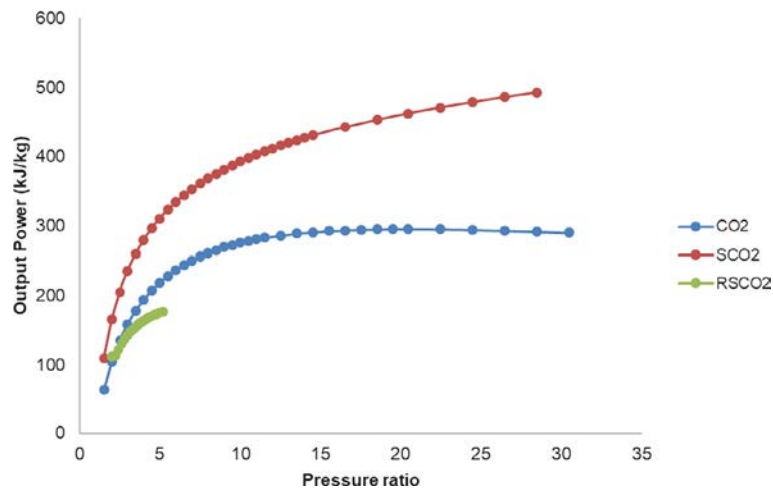


Figure 21.2.24. Cycle output power of CO_2 , SCO_2 and RSCO_2 .

Although the SCO_2 and the recompressed SCO_2 showed a better cycle efficiency, other factors must be considered when deciding on this fluid selection for NPPs. Among these factors are the design and operational constraints, especially for the compressor. As the CO_2 approaches its critical condition, its thermophysical properties vary significantly with small changes in temperature or pressure. These changes could lead to the compressor operating out of range, which could potentially damage the compressor. This poses a significant challenge because the TRL is below 5 for the turbomachinery design. Thus, development activities are required to optimize the design, and mitigate the issues raised.

21.2.10.5 Helium-nitrogen binary mixture as working fluid

Due to the self-containing nature of the closed-cycle gas turbine, noble gases such as helium, argon, neon, xenon, and other permanent gases such as carbon dioxide, nitrogen and air are considered viable working fluids for the NPPs. However, as mentioned in previous sections, selecting a suitable working fluid for an

NPP is driven by several factors such as the neutronic activity, cycle performance, system design, component material compatibility with fluid properties, availability, and thermoeconomic considerations (Osigwe et al., 2019a). The differing thermophysical properties of these gases would also affect the plant circuit layout. For example, selecting helium with low molecular weight and high thermal properties would increase the aerodynamic loading of the turbomachinery. Ideal and high thermal properties are advantageous because they support use as reactor coolants, with non-neutronic reactions, and enables compact heat-exchanger design. The disadvantage is the turbomachinery requires a significant number of stages if the traditional design method is utilized. For carbon dioxide, nitrogen and other heavier noble gases with less favorable thermal properties, and higher molecular weight, the condition is reversed compared to helium. These include decrease in aerodynamic loading, which reduces the number of turbomachinery stages, larger heat-exchanging surfaces.

To this end, a reasonable compromise would be to consider a binary or multiple mixtures that could balance the fluid property requirements for the NPP, such as a mixture of Helium with Xenon (He-Xe), Helium with Nitrogen (He-N₂), Helium with Argon (He-Ar), Helium with Carbon dioxide (He-CO₂) and many more. The thermophysical properties of these mixtures would be superior to those of the pure gases, and could compensate for optimal selection criteria. Some of these mixtures have been investigated in studies by Tournier and El-Genk (2008a,b). In their work, they compared the impact of the transport properties of He-Xe binary mixture with a molecular weight of 40 g/mole to He-N₂ binary mixture with a molecular weight of 15 g/mole, with respect to pressure losses, heat transfer coefficient and the aerodynamic loading of the blades in the turbomachinery. Their results show that the binary mixture of He-N₂ (45.8% mole nitrogen and 54.2% mole helium), has a transfer coefficient that is 4.4% higher than pure helium, and an induced turbomachinery aerofoil aerodynamic loading that is 26% more than pure helium, and almost three times that of He-Xe.

In this work, the cycle efficiency and output power of different mole fraction for the He-N₂ binary mixture have been studied. The reasons for selecting nitrogen are that the NPP can benefit from existing experience, and high TRL of nitrogen, which is similar to the behavior of air. In addition, the cost of acquiring nitrogen is lower, when compared to other noble gases. The downside of nitrogen is the nitriding effect at high temperatures and pressures. The other more critical disadvantage of using nitrogen as a full or part-coolant for reactors is that including it in the reactor produces the carbon-14 isotope. This is due to reactions in the fuel, the core structure material, and the moderator. The production rate depends on the spectrum and neutron flux, including the cross-section and concentrations of uranium, plutonium, oxygen, and nitrogen. Although it is a low emissive β , it is critical to keep the levels low. This study considers that the He-N₂ mix is part of a secondary loop, as opposed to a primary loop. It is also important to consider other potential effects, such as thermoeconomic considerations. A simple recuperated gas turbine cycle has been utilized in this analysis and is schematically represented in Figure 21.2.3. R represents a VHTR, with a reactor COT of 850°C. The recuperator (H/E), utilizes heat from the turbine exhaust to heat the working fluid before entering the reactor. The C and T represent the compressor and turbine turbosets, respectively, which are used to achieve compression and expansion of the working fluid. The CH is the precooler that returns the working fluid to the design compressor inlet conditions. Table 21.2.12 shows the cycle specifications using pure helium (100% helium). In this analysis, the mole concentration of helium was varied from 100% to 10%. Hence, the mole concentration of nitrogen in the binary mixture is given as:

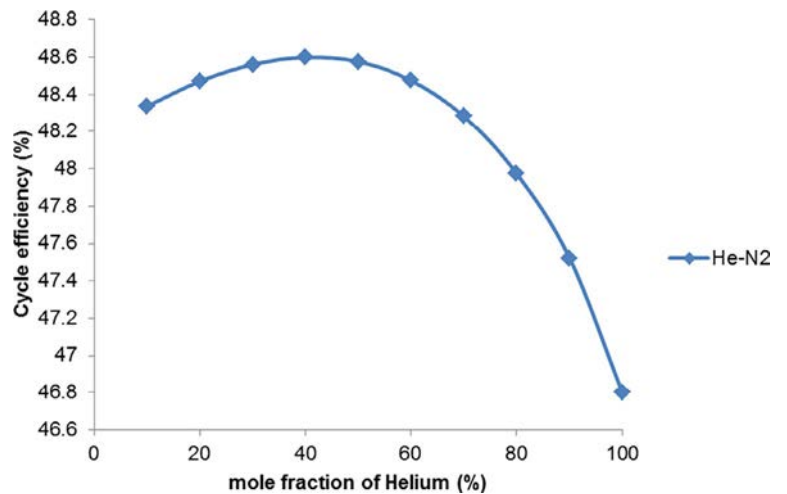
$$\% \text{mole of nitrogen} = 100\% - \% \text{mole of helium} \quad (21.2.43)$$

In Table 21.2.12, all values marked with asterisk were kept the same as the binary mixture concentrations were varied. The cycle efficiency and power output corresponding to binary mixture concentrations are compared against the pure helium (100% helium) cycle performance. The properties of the binary mixtures were obtained using mixture models of Thermo (Bell, 2016) and Cool Prop (Bell et al., 2014).

Table 21.2.12. Cycle parameter specifications for the reference plant design point for pure helium

Description	Reference plant DP for pure helium
Turbine entry temperature (°C)	850
Shaft speed (rpm)	3600
Compressor pressure ratio	2.0
Compressor inlet pressure (MPa.)	3.5
Compressor inlet temp. (°C)	28
Compressor polytropic efficiency (%)	90.5
Reactor power (MW)	600
Turbine polytropic efficiency (%)	93
Turbine pressure ratio	1.88
Turbine EGT (°C)	611
Flow rate at compressor (kg/s)	441.8
Turbine cooling (%)	1
Vessel cooling bypass (%)	0.5
Plant thermal efficiency (%)	46.8
PC effectiveness (%)	95
ReX effectiveness (%)	95
PC pressure loss (%)	2.5
ReX total pressure loss (%)	6
Rated power (MW)	280

Figure 21.2.25. Cycle efficiency as a function of mole fraction.



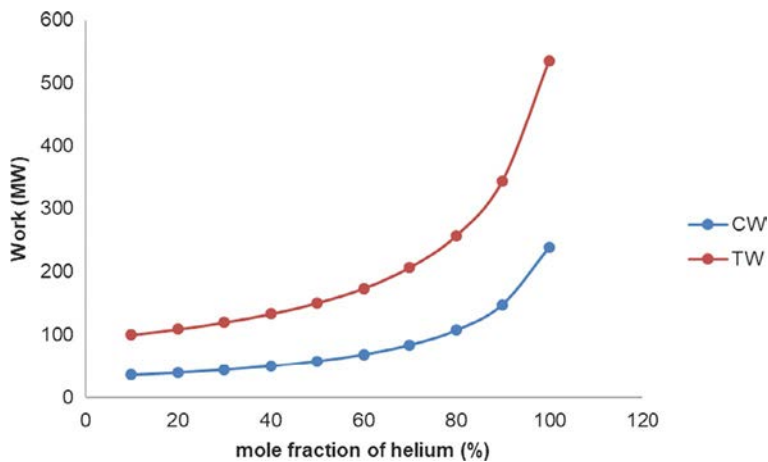


Figure 21.2.26. Compressor and turbine work as a function of mole fraction.

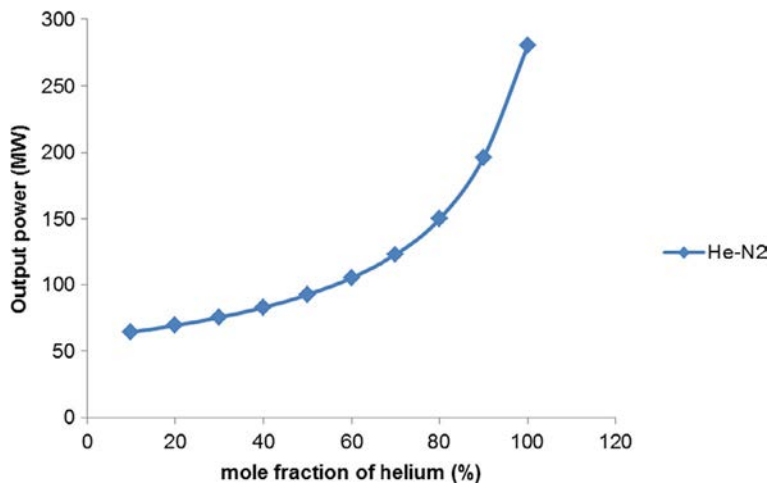


Figure 21.2.27. Cycle output power as a function of mole fraction.

Figure 21.2.25 shows the cycle efficiencies as the mole fraction of helium is varied from 100% to 10%. The positive deviation of cycle efficiency as the mole fraction of helium decreases from 100% to 10% is due to the behavior of helium as it deviates from an ideal gas, as the concentration decreases. Hence, the properties of the binary mixture become influenced by changes in pressure and temperature. In addition, there is a decrease in the isentropic exponent as the mole fraction of helium decreases.

The isentropic exponent is greatly affected by changes in pressure and temperature; hence, this will reflect or correspond with changes in the compressor and turbine work, as shown in Figure 21.2.26. In Figure 21.2.27, decreases in the cycle output power are observed, as the mole fraction decreases. This is because the heat capacity of the binary mixture is reduced as the helium fraction decreases. Hence, the shaft output power drops as the mole fraction of helium decreases in the binary mixture.

21.2.10.6 Thermophysical properties of reactor coolants and working fluids of power cycles

Thermal efficiencies have always been the driving force in the thermal power industry (Mahdi et al., 2018). However, the NPP overall cycle performance is greatly influenced by the thermophysical behavior

of the working fluids, as highlighted in previous sections. To understand how the thermophysical properties affect the cycle performance, [Mahdi et al. \(2018\)](#) provided a comparison on the thermophysical properties of nitrogen, helium-nitrogen mixture, supercritical carbon dioxide, pure helium, and water for a proposed NPP. The assessment shows that helium has the most stable thermophysical and nuclear properties of all the gases, as it behaves close to an ideal gas. Helium has high thermal conductivity and specific heat, compared with other gases in this study. Due to the stable thermophysical properties of helium, it is seemly suitable for VHTR and GFR NPPs ([Pioro et al., 2018](#); [Mahdi et al., 2018](#)). NPPs need to run at temperature to compete with current advanced thermal power plants. However, the issue of ingress into the bearing of gas turbines, and the cost of helium are major drawbacks in its use. In general, the information on thermophysical properties of various working fluids can be found in [Pioro et al. \(2017\)](#) and [Pioro \(2016\)](#).

21.2.11 Nuclear power plant controls and operations

Interestingly, the closed-cycle gas turbine offers a viable prospect for the stable conversion of the energy from the nuclear reactor into mechanical, and further forms of energy. This is due to (a) its easy adaptability (b) flexibility to changes in working fluid (c) high efficiency of electricity generation at part load, and (d) high levels of availability and low maintenance cost ([Osigwe et al., 2020a](#)). More so, it could offer potential savings in operating costs due to its ability to relatively maintain high overall performance under varying operating conditions ([Frutschi, 2005](#); [Pradeepkumar, 2002](#)). However, this potential advantage can be achieved by implementing an appropriate control strategy during operation of the NPP. Hence, the need for this section to provide a complete understanding of some of the closed-cycle gas turbine controls strategies ([Osigwe et al., 2021](#)).

The different control strategies that are applicable to the successful operation of the closed-cycle gas turbine NPP, have been discussed in [Bammert et al. \(1974\)](#), [Botha and Rousseau \(2007\)](#), [Covert et al. \(1974\)](#), [Gad-Briggs et al. \(2017c\)](#), [Openshaw et al. \(1976\)](#), and [Osigwe \(2018\)](#). In this section, only the inventory, bypass and reactor delivery temperature controls are considered. These control strategies, when implemented in the NPP system, would enable (a) the power plant to quickly adjust to a wide range of fluctuating load variations without significantly affecting the cycle thermal efficiency, (b) for prevention of thermal shocks on plant components during critical transients, (c) for providing automatic control maneuvers during plant start-ups and shut downs, and (d) for operational stability of the plant to avoid sudden eventualities.

21.2.11.1 Inventory Control Strategy (ICS)

The operating concept of this control option, is for the NPP to be able to store or save energy during off-peak periods and replenish this energy during peak load demand using the Inventory Control System (ICS). This would mean that the working fluid is either extracted or injected into the closed-cycle gas turbine, resulting in a relative change in the system pressure, density, mass flow rate, and corresponding change in output power levels.

During the NPP operations, the daily fluctuations in power demand as a result of varying operating conditions, are adjusted through the ICS. The ICS comprises the Inventory Control Tank (ICT) and Inventory Control Valves (ICV), as shown in [Figure 21.2.28](#). When there is a decrease in load demand from the grid, a reduction of shaft power is initiated by opening of ICV1, so that the working fluid flows from the High-Pressure Compressor (HPC) into the ICT. Similarly, if the load demand from the grid increases, the working fluid stored in the ICT(s) can be injected back into the closed-cycle gas turbine circuit by the opening of ICV3 and ICV6.

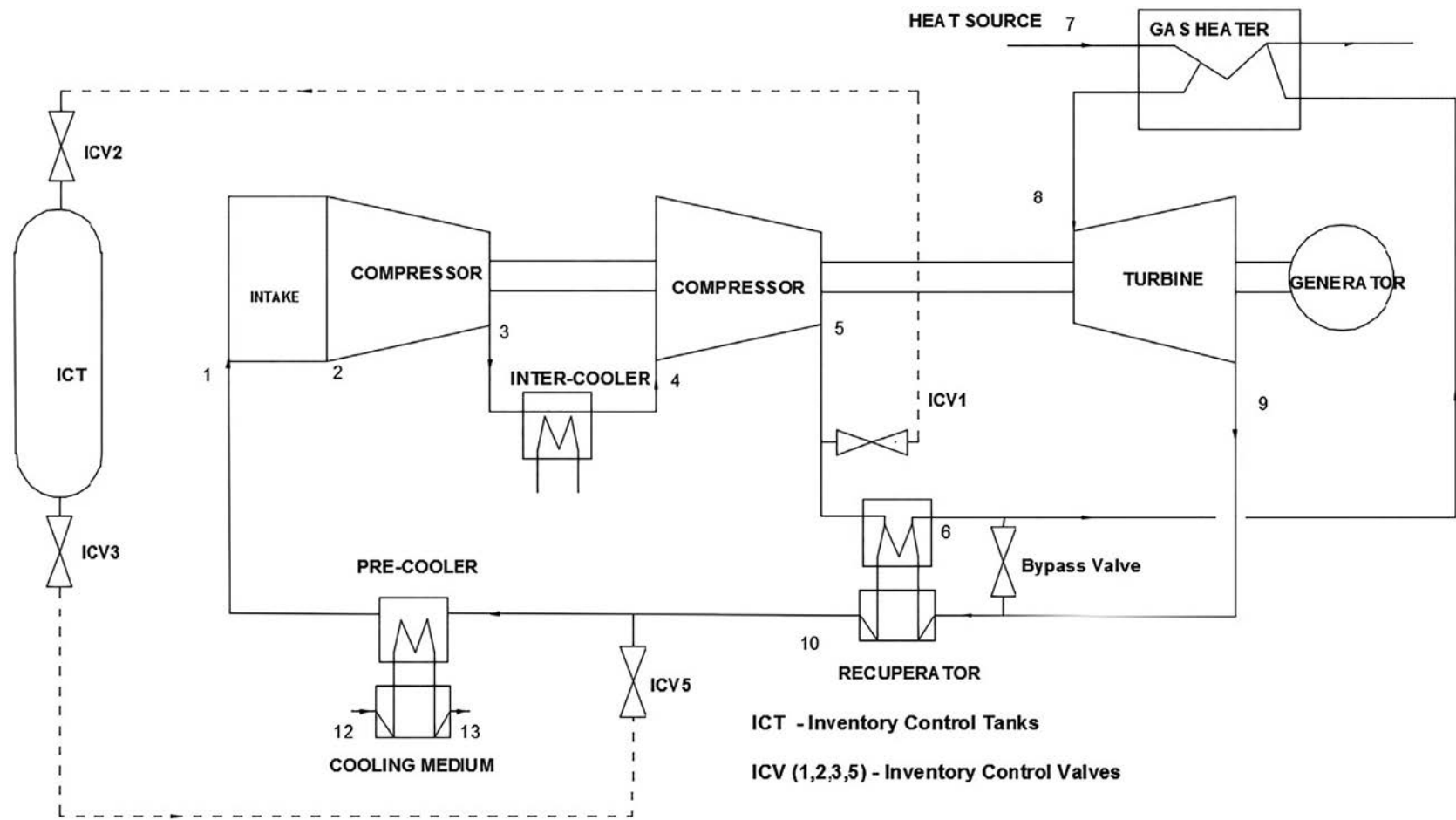


Figure 21.2.28. Scheme of reference plant circuit with different control options.

The ICS is regulated based on the pressure variation between the gas turbine cycle and the inventory tank. This variation determines the power limit, and ensures that high part-load efficiencies can be achieved. However, there are restrictions to the extent the ICS can maintain a high part-load efficiency. The restrictions are due to: (a) size and pressure of the inventory storage tank, (b) shaft rotational speed effect on blade tips, (c) location of inventory valves in the cycle loop, (d) availability of inventory transfer compressor, and (e) cost of implementing any of the options listed (Osigwe et al., 2019b, 2020a).

21.2.11.2 Bypass Control Strategy (BCS)

In this case, the power level is controlled by regulating the bypass valve, as shown in Figure 21.2.28. The high-pressured working fluid is bled off to short-circuit the reactor (GH) and the turbine to the low-pressure side of the recuperator. This results in observed drops in the mass flow rate, pressure ratio and efficiency of the turbine, thereby causing the output power to decrease. The redirected flow is recirculated into the compressor at an unchanged gas inventory, increasing the pressure level and compressor work. The Low-Pressure Compressor (LPC) decreases in pressure as the bypass valve opens. This decreases the turbine pressure ratio and the reduction of the turbine power. The same effect takes place in the HPC. The cycle gas path temperatures would remain relatively stable, with just the thermal power input from the reactor matching the deficits required to maintain the cycle temperatures at reduced mass flow rate.

The advantage of the BCS is that it can be initiated quickly during rapid power changes, or emergency stops to match the NPP requirement. Thus, this control option is usually implemented in closed-cycle gas turbines to achieve faster than normal control responses, and to prevent the shaft from overspeeding (Staudt, 1987; Yan, 1990). The cycle output analysis would consider the difference in the full mass flow rate observed within the compressor, when the mass flow rate in the reactor and turbine are discounted. An ideal cycle analysis would be expressed as (Osigwe et al., 2020a):

$$\text{Cycle thermal efficiency } \eta_{th}(\%) = \left[1 + \frac{SP}{SP_{max}} \left(\frac{\theta_8}{\theta_2} - 1 \right) \right]^{-1} \quad (21.2.44)$$

where

$$SP_{max} = \left(\frac{\theta_8}{\theta_2} - 1 \right) (\theta_2 - 1), \theta_8 = \frac{T_8}{T_{ref}}, \theta_2 = \frac{T_2}{T_{ref}} \quad (21.2.45)$$

21.2.11.3 Reactor delivery temperature control (HST)

The heat source temperature refers to the delivery temperature of the reactor to the gas turbine. Thus, the power level is altered by changing the working fluid's temperature at the reactor (GH) when there are changes in the reactor delivery temperature. In this case, the fluid circulating inventory remains constant, and a drop in TET, causes a decrease in the component cycle temperature and pressure distribution. These changes affect the overall performance of the NPP. The HST control is an effective control for the varying operating conditions. However, in reality, this control usually works together with the bypass control system to manage shaft overspeed events.

21.2.11.4 Combined control strategy

The combined control strategy utilizes integrated control actions of the control strategies mentioned above to regulate the plant behavior, in order to avoid limitations in shaft speed or low cycle efficiencies. This approach consists of controllers, which issue commanding signals to the control options subsystems, in order

to perform integrated control functions. The load demand acts as the primary input, which determines the appropriate control subsystem to be initiated. In real-time, operation of the NPP using all or part of these control methods discussed, is simultaneously enhances a diverse control requirement. Hence, a combined control system is usually integrated with several subsystems to allow the interactive control action as required. For example, a combined control mode can be designed to have an inventory control for slow load moderation; a bypass control for rapid load response, shaft speed control and emergency shut-down capability; and a reactor delivery temperature control to regulate the reactor heat input as may be required by the system. During this operation, a certain percentage of power-level change triggers the control response for load-following or load-rejection.

Generally, the primary goal of the control systems during operation would be to maintain high efficiencies, while keeping all components within their operating range. Theoretically, achieving this will mean that the overall temperature ratio and pressure ratio will be close to the steady-state limits. However, this may not be easily satisfied using a single control option, without compromising certain practical constraints, which were mentioned earlier in this chapter.

An example using an intercooled-recuperated closed-cycle gas turbine shown in [Figure 21.2.28](#) and plant characteristics in [Table 21.2.13](#) would describe the behavior of the NPP when the control options are implemented.

[Figures 21.2.29 and 21.2.30](#) provide the part-load performances of the reference plant, which were accomplished with the listed control strategies described in the preceding section. Each control option operates independently at the same power level. During the ICS operational mode, the mass of air is withdrawn from the power cycle as closely proportional to the power output to keep the TET constant, while all temperature across the cycle remained constant for the same LPC inlet conditions, which is controlled by the cooling medium. This withdrawal of mass flow reduces the density and pressures across the cycle. However, the pressure ratios of LPC and HPC remain constant because the operating point $\frac{N}{\sqrt{T}}$ and the non-dimensional mass flow do not change significantly. Hence, the cycle efficiency remains relatively constant, as shown in

Table 21.2.13. Summary of power plant description

Description	Unit
Heat source temp. (K)	1100
LPC pressure ratio	1.65
LPC inlet pressure (kPa)	830
LPC inlet temperature (K)	290
HPC pressure ratio	2.40
LPC and HPC efficiency (%)	86
Turbine efficiency (%)	90
Flow rate at LPC (kg/s)	230
Plant thermal efficiency (%)	41.2
IC effectiveness (%)	90
RX and GH effectiveness (%)	90
Rated power (MW)	40.8
Working fluid	Air

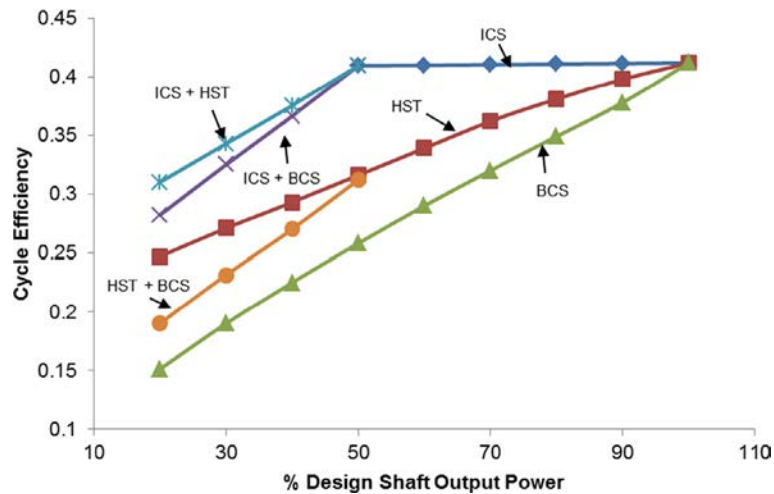


Figure 21.2.29. Cycle efficiency for different control strategy at part load.

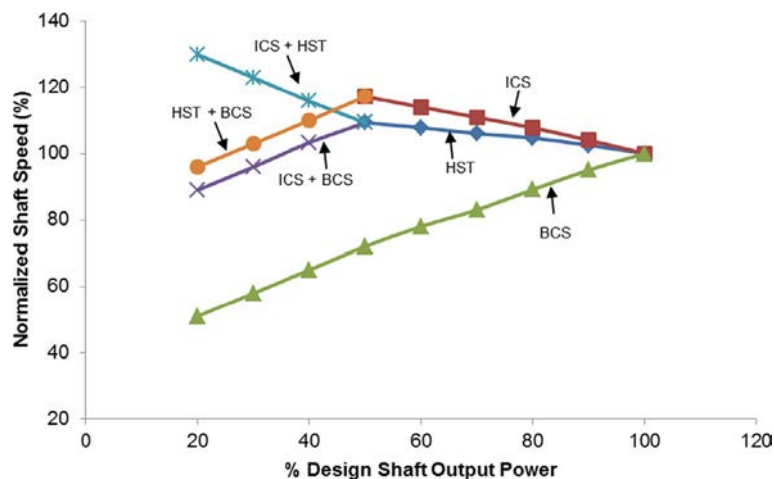


Figure 21.2.30. Shaft speed for different control strategy at part load.

Figure 21.2.29. At 50% output power, the cycle thermal efficiency is 40.1%. The slight drop in cycle efficiency is as a result of small changes in the working fluid properties. Nonetheless, the ICS control option brings about a rapid acceleration of the shaft as the load is reduced, which must be balanced.

With the ICS, it seems that the possibility to further operate at a lower part-load will still be economically beneficial, since the efficiency is still reasonably high. However, the possibility of maintaining high part-load efficiency to any desired limit using the inventory control, is restricted to the following: (a) the size and initial pressure of the tank, (b) centrifugal force on blade tip as a result of shaft rotational speed, (c) location of inventory valves in the cycle loop, (d) availability of inventory transfer compressor, and (e) cost of implementing any of the listed options.

Similarly, when the bypass mode was analyzed, ICS and HST were kept constant. The performance of the BCS is shown in Figures 21.2.29 and 21.2.30. As mass flow is bled off after the HPC to short-circuit the turbine, there is a relative mass flow rate difference between the compressor and turbine, which is translated into reducing the HPC and turbine pressure ratios and mass density. This reduction modifies the operating point to a new position (the new matching point between the compressor and turbine), and reduces the turbine

output power and cycle thermal efficiencies, as shown in [Figures 21.2.29 and 21.2.30](#). Both the LPC and HPC pressure ratios decrease with the dominant effect in the HPC. However, during this process, the LPC inlet pressure increases, and the discharge pressure remains relatively the same at a steady state when the fluid returns to the circuit, as shown in [Figure 21.2.28](#). Using BCS for a 50% output power drop, a cycle thermal efficiency of 25.8% is observed. This control option can be an effective means of part-load control from zero to full load rejection. However, its major drawback is the low efficiency obtained, when compared with other control options.

Another method part-load operation can be achieved by decreasing the cycle highest temperature, which is achieved via the reactor delivery temperature control (HST). With HST in active mode, both the ICS and BCS are assumed to remain constant. At part-load operation, $\frac{T_3}{T_2}$ decreases because of a reduction in HST. This results in a downward trajectory of the pressure ratios, thereby reducing the cycle thermal efficiency almost linearly from 41.2% to 31%, at 50% output power as shown in [Figure 21.2.29](#). During the process, as the TET decreases, the density of the fluid entering the turbine increases, thus decreasing the volumetric flow rate (for the same mass flow rate), which decreases the turbine pressure ratio. Alleviating this requires the fluid inventory to be increased. One drawback of this control option is that decreasing the system temperatures will require a slow rate of change to avoid thermal shock.

Assuming some of the limitations mentioned for each control option are neglected, [Figures 21.2.29 and 21.2.30](#) also show performance comparison at part load, in terms of overall cycle efficiency for each control option, and a combination of two control options (second control option follows after the first control option). Simulating inventory followed by temperature control may not be feasible in practice without other control mechanisms, since both strategies result in increases in shaft speed at part-load operations, which could lead to mechanical failure of components. Inventory control followed by bypass has been mostly used for many closed-cycle power plant operations. This has been the most convenient method to stop the engine, if required. Another realistic control measure is the temperature and bypass control.

21.2.12 Risk assessment

Unfortunately, technical risk and mitigation are often addressed late in the project development process, resulting in less optimal technology procurement decision-making, and higher risk mitigation costs. The incorporation of risk analysis from the outset of any project can assist in the early decision-making process. As previously mentioned, many factors could affect both the design and operating experience of a closed-cycle gas turbine system based on the choice of the working fluid. These factors range from items peculiar to the particular application, through to the fundamentals of mechanical component design. This section looks at qualitative risk assessment for the closed-cycle gas turbine technology, considering the effect of selected working fluids. The risk module provides an assessment of uncertainties and operational challenges of the closed-cycle gas turbine plant for helium, carbon dioxide, nitrogen, and air. Most significantly, the risk assessment provides discussions on reasonable trade-offs in the plant thermodynamic performance characteristics, and its impact on the closed-cycle gas turbine technology. [Figure 21.2.31](#) shows the scheme of the risk assessment discussed in this section.

The risk assessment presented, consists of two parts: financial and technological risk. The technological risk assesses the effect of the working fluid on material technology, the impact of operating a high TET for each working fluid, the working fluid management system, and the technology maturity level of the turbomachinery and heat exchangers for the selected working fluids. The financial risk aspect, assesses the influence of pressure ratio and mass flow rate on the capital cost for each working fluid, the sensitivities of the costs associated with the working fluid, and the impact of legislation on investment decision.

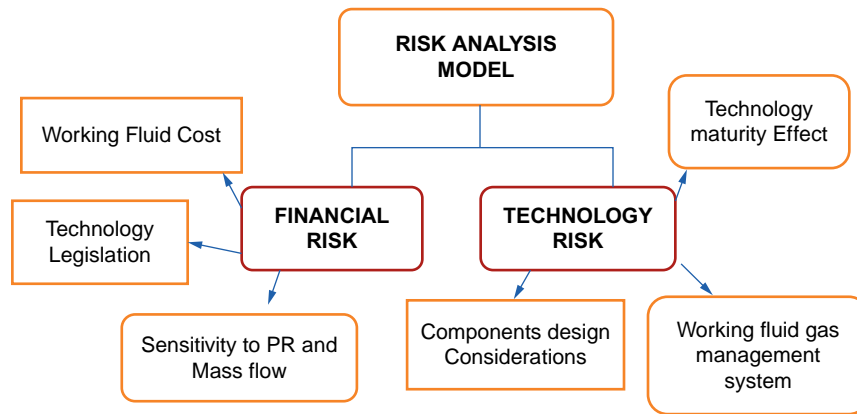


Figure 21.2.31. Scheme of risk assessment.

21.2.13 Technology risk

The success of the closed-cycle gas turbine is dependent on the technology level available for the design and production of its constituent parts. Thus, the technology maturity and operational challenges of the closed-cycle gas turbine components differ in terms of application for different working fluids considered. Some component technologies are very near state-of-the-art, whereas some are still in the development process. Hence, this can pose an investment risk, especially for technologies with TRLs below 4.

This section gives a holistic assessment of the technological risk associated with the working fluid capability for the closed-cycle components.

21.2.14 Material technology for high temperature and pressure

The key design drivers for the closed-cycle gas turbine are the level of cycle peak temperature into the turbine and the system pressure level that can be achieved, compared with current technology. As indicated in [Osigwe et al. \(2019b\)](#), an increase in cycle peak temperature to its maximum, would increase the cycle efficiency reasonably. However, this is limited by the material technology and the working fluid characteristics at this temperature. Currently, in a real application, the maximum cycle temperature for the closed-cycle gas turbine is at 1123 K for the VHTR and GFR. Similarly, designing for a high system pressure level would allow for compact component designs, reducing cost, and allowing for stability of the working fluid properties above their critical pressure and temperature. As the system pressure is increased, the sizes of the components for the closed-cycle gas turbine are reduced. This results in a reduction in cost, up to the point where the thickness of the component casings and shells becomes significantly high, and the thickness of heat exchanger tubes is sufficient, thereby any temperature drop through the tube wall becomes a major factor. In practice, a peak system pressure of 2 to 3 MPa is usually favored except for large fission or fusion reactor heat sources, in which case pressures of 3 to 5 MPa are commonly chosen ([Frutschi, 2005](#); [Osigwe, 2018](#)).

To this end, the critical components that will be at potential risk are the reactor, heat exchanger and turbine based on the current material technology levels, applicable to the closed-cycle gas turbine plant. The turbine section is usually made of nickel-based alloys, with varying amount of aluminum and titanium, while the heat exchangers and reactor are made of ferritic-martensitic steel, alloyed with chromium, aluminum and molybdenum. Raising the system peak pressures and temperatures to achieve competitive cycle performance, compared with other conventional energy conversion systems, will pose a possible risk to the material and working fluid characteristics, except new materials laced in ceramics for the heat exchanger and the reactor are considered, and adequate cooling technology is introduced for the turbine and the reactor vessel, which may lead to a significant decrease in cycle efficiency. Increased pressures and temperatures will increase the

stress level and mechanical integrity of the components, which could be a safety concern, and may require additional cost to mitigate some of the safety issues. Apart from the impact on mechanical integrity, the working fluids are also prone to system risks at high temperature and pressure. For helium, operating at a very high temperature could induce a welding effect as it passes through the components' metallic surfaces. This could have a hazardous effect on sensitive equipment such as the control valves, guide vanes, support bearings, and bushes. Shaft seal materials could also be affected, especially with helium at high temperature and pressure. For carbon dioxide, at temperatures above 1000 K, there can be small pickups of carbon which could lead to decarburization; thus, at this elevated temperature, the material used has to be coated to prevent decarburization. For air, the possibility for oxidation attack is increased; however, air will have a more favorable outcome than helium at high temperature if iron-chrome-nickel alloy materials are used. The behavior of nitrogen in terms of oxidation capability at high temperature is similar to air. Nitrogen also has great chances of nitriding and embrittlement of material at high temperature. All these will affect the life of the components, and the consequence of any component failure could lead to ingress, especially for the heat exchangers.

The implications of these are that considerations of the working fluid characteristics would have to be at high pressures and temperatures, including the detrimental effects on the component materials and system. With reference to the fluids considered in this discussion, helium seems to show reasonable stability, with less detrimental effects on the system at high pressures and temperatures, making it a good selection for the closed-cycle gas turbine NPP, compared to air, carbon dioxide and nitrogen. Thermal stability and fluid compatibility with materials and lubricants that may be in contact at high temperatures and pressures are critical to the desired life and cost-effectiveness of the NPP. Chemical decomposition of the working fluid not only reduces the plant cycle efficiency, and makes the replacement of the working fluid necessary, it could have corrosive effects on the materials of the system, especially for fluids such as carbon dioxide and nitrogen. Thermal stability here refers to the stability of the working fluid molecules at high temperatures and pressures. This implies that working fluid with high stability would have high resistance to decomposition at those extreme conditions.

21.2.15 Working fluid gas management

Handling the working fluids is another potential technological risk for the closed-cycle gas turbine NPP investment plan. This is important because the working fluid usually remains in the cycle until it is renewed, in most case annually. The decision to select a particular working fluid over others, would also be influenced by how the fluid can be effectively managed without causing system safety, or environmental concerns, when there is sudden leakage, or interaction with the component materials.

Air is a readily available fluid and is easy to manage because it does not have any detrimental effect when exposed to the environment, except on metal surfaces. With this in mind, it becomes easy to handle or store in the inventory tank over a long period. As previously mentioned, the only main concern for the use of air is the oxidation of the gas turbine components. Although helium is an inert gas, its use is limited because its supply is controlled by the US government (TNAP, 2000). Hence, storage concerns can be factored in as a possible risk for the selection of helium. Storage is particularly important for helium because of the nature of its supply thus, the issue of seal leakage associated with helium could limit its selection and operational use.

Chemical interaction between the reactor cooling medium and the system working fluid is controlled to prevent potential ingress into the system, or chemical reaction with the gas turbine component. Helium is chemically inert and neutrally transparent, which minimizes problems of system corrosion. Carbon dioxide and nitrogen, when exposed to the environment, would readily react with atmospheric oxygen to cause acid rain and contribute to global warming. As a result, both have to be managed in such a way that would minimize or eliminate possibilities of this risk.

Another factor to consider in fluid management is the influence of the working fluid molecular weight on the storage facility size. One may think that this would not have a great effect on risk assessment, but from its impact on the cost of building the storage facility, it is worth considering. For the same output power, helium

with the least molecular weight would enable the least storage facility size. This is not so for carbon dioxide or nitrogen.

The decision to use any selected working, has to incorporate appropriate working fluid management, especially in a nuclear-powered application where a high factor of safety is required. This assessment can only provide a reasonable argument for such considerations.

21.2.16 Technology maturity level for components based on selected working fluid

Technology maturity or readiness level is a disciplined independent programmatic figure of merit, that allows for effective assessment and communication regarding the maturity of new technologies (Di Lorenzo, 2010). Each technology project is evaluated against the parameters for each technology level, and is then assigned a TRL rating based on the progress of the project, as described by the National Aeronautics and Space Administration (NASA) (Hirshorn and Jefferies, 2016). This involves the progression of technologies from a scientific principle, and technological concept, to laboratory-scale, bench scale, full-scale prototypes, and finally, full deployment.

Considering the working fluids selected, the components designed for specific fluids are at various TRLs. While some are still theoretical, some have been proven and deployed in several applications. Thus, the TRLs of the closed-cycle gas turbine NPP and associated components are technological risky for any investment decision and needs to be incorporated into the costs directly or indirectly. In this assessment, the TRL was assigned according to the development and deployment of components (number of projects), that allowed the use of each selected working fluid in a closed-cycle gas turbine NPP application. Although a precise judgment on the projects is not certain, this assessment considers assessments from open literature for components that use the selected working fluid.

21.2.17 Working fluid TRL for turbomachinery components

The aerodynamic and mechanical design for turbo-components that use air as working fluid is widely proven, and its configuration for any application, whether axial, centrifugal or radial, can be easily implemented. This makes air as a working fluid for closed-cycle gas turbine design less risky because its TRL can be put at 9. This is because many designers or operators are very familiar with the design and operational challenges of turbomachinery utilizing air as the working fluid. Thus, further improvements to suit any design specification, or optimum decision indicators, can be easily implemented. Typical applications of the air turbomachinery for the NPPs are the Coventry (0.7MW) and Paris (12MW) NPPs built between the 1950s and 1960s (Frutschi, 2005).

Although the basic aerodynamic design principles used for air turbomachinery can be applied to helium, carbon dioxide, nitrogen, and any selected fluid, it is important to recognize that there are reasonable differences in the thermodynamic behavior of the working fluids. This is especially true helium and carbon dioxide, when compared to air, hence, these fluids would require unique design considerations and development activities to increase the TRLs.

For helium, its high specific heat capacity, and low molecular weight make its aerodynamic design a complex issue. Going with plants that operated with helium as documented in references (Frutschi, 2005), it becomes obvious that there is still limited design and operational experience in using helium turbomachinery for the closed-cycle gas turbine NPP. Although there have been a growing number of research and development activities in the last decade, the TRL is still below level 7. Thus, the technology risk for helium turbomachinery will be higher than that of air.

For carbon dioxide turbomachinery, there were no relevant projects before the 1990s when supercritical carbon dioxide power cycles started to gain relevance, except for the Feher module, which was experimental (Feher, 1968). Most carbon dioxide turbomachinery designs are still at the preliminary or laboratory test stage (Olumayegun et al., 2016). Thus, the risk level for carbon dioxide turbomachinery will be higher than helium or air due to its limited design and operational experience in closed-cycle gas turbine applications. This would have an additional effect on investment decisions for a closed-cycle gas turbine with carbon dioxide as a fluid choice. The TRL is considered to be below 6, which put it at a greater risk, when compared with other fluids discussed in this paper.

For nitrogen, its thermodynamic behavior at different temperatures and pressures is similar to that of air, making its aerodynamic and mechanical design easy to adapt and implement for the closed-cycle gas turbine NPP. In addition, some experimental and operational power plants utilize nitrogen turbomachinery, although this is not as popular as the use of air. From the authors' view, adapting the nitrogen turbomachinery for closed-cycle gas turbine applications may pose less of a risk than helium and carbon dioxide. This is because of its similarity with air; hence, the possibility of having comparable or familiar operational challenges. The TRL level of nitrogen turbomachinery would be between 7 and 9.

21.2.18 Working fluid TRL for heat exchangers

The heat exchanger is one of the main components of the closed-cycle gas turbine NPP that influences its performance; hence, the TRL plays a vital role in the success of power plant applications. The TRL level is assessed in terms of effectiveness, and ability to operate at high temperatures and pressures for different working fluids. Although material technology capabilities have been discussed in the previous section, this part will only focus on the TRL of heat exchangers for the different working fluids selected.

Heat exchangers are usually very complex, expensive, and large in size; hence, it represents a significant driver in the closed-cycle gas turbine plants' capital cost and technical viability. Thus, the development of highly reliable, highly compact heat exchanger, and fewer pressure losses, remains an active area of research, especially for high-temperature applications. The effect of the working fluid chemical interaction on the heat exchanger materials, thermal stress under extreme operating conditions, and thermal-hydraulic performance are still at the research and development stage. However, the TRL of the heat exchanger will be influenced by the working fluid in use.

Like the turbomachinery TRL discussed earlier, there are several projects and application of heat exchangers with air as the working fluid, which puts its TRL at high levels. However, the challenging decision will be in its robustness when being operated, when considering reliability, maintainability, corrosion, compactness, and cost. The use of air will give a larger heat exchanger compared with helium.

On the other hand, one advantage of helium heat exchanger is the compactness due to its thermodynamic properties. The considerations for a high performing heat exchanger can be easily achieved with helium for less of the cost than any other fluids considered in this chapter. However, the disadvantage of helium is its tendency to leakage at high temperature and pressure, which could pose as a risk factor. The TRL with reference to closed-cycle gas turbine NPP is low. This is because the technology is currently in development; this is also the case for carbon dioxide heat exchangers. A concern for carbon dioxide is its negative thermodynamic influence on the size, which requires plate finned complex geometries. The TRL for helium and carbon dioxide heat exchangers would be between 5/6.

Nitrogen has been highlighted in several sections as having similar behavior to air; hence, the technology could easily be replicated. This is the reason nitrogen is becoming of unique interest in nuclear power plant systems. For this reason, the TRL level for nitrogen will be a little below that of air (between 7 and 9).

21.2.19 Financial risk

The financial risk assessment is an essential component of risk analysis. The section provides an understanding of certain factors that could affect the initial capital investment and cash flow of the closed-cycle gas turbine NPP system. To this end, the influence of working fluid cost, pressure ratio, mass flow rate, and the effect of the legislation are considered.

21.2.20 Cost of working fluid

Although the working fluid initial cost may not significantly affect the capital cost, it will affect the operational cost of the power plant. The cost of helium is about five (5) times more than nitrogen, eight (8) times more than carbon dioxide, and twelve time more than air.

However, looking at each fluid in terms of cost, helium poses the most significant risk for any investment decision, due to the control the supply of helium. Thus, there is a limited supply to the market, which puts long-term operation at risk. The helium market is based on a comprehensive framework that includes geological uncertainty, depletability, and multistage processing (TNAP, 2000).

Helium is a non-renewable, finite resource that complicates its optimal allocation. Thus, scarcity and resource quality variation would mean that the future sources of helium will cost more to exploit (Gerrard, 2007).

Theoretically, in a perfectly competitive market, any working fluid cost value will appreciate overtime at the discount rate minus the cost escalation rate. However, due to the limited access to helium, its escalation rate may increase by 10% to 15% more than the other working fluids, if the demand for helium plants increases (TNAP, 2000). Also, as previously mentioned, storage is particularly important in the helium market because of the nature of its supply; As such, maintenance on storage facilities can significantly put additional costs on the storage and use of helium.

Nitrogen is another fluid that can be of potential financial risk due to the cost of processing nitrogen from ammonia. This could also influence its future use for the closed-cycle gas turbine NPP. For carbon dioxide, many western countries are putting tax incentives for carbon sequestration thus, the cost of carbon dioxide may remain relatively stable over longer periods. For air, it is understandable that this is nature's free product. However, the air would need to be processed to remove impurities, considering the closed-cycle system in which the working fluid operates. Thus, processing the removal of impurities has a cost implication. Comparing each working fluid operational cost would put air at an advantage. Nonetheless, other trade-offs will have to be considered.

21.2.21 Sensitivity to pressure ratio and mass flow rate

This section discusses the influence of compressor pressure ratio and mass flow rate on capital costs. The design choice for any closed-cycle gas turbine NPP depends on the maximum cycle efficiency obtained for a given pressure ratio. The choice of cycle pressure ratio determines the size of the turbomachinery in terms of the number of stages and length of the turbomachinery. Thus, this will directly affect the cost of the turbomachinery, based on the component cost analysis presented in Osigwe et al. (2019c). As the pressure ratio increases, the number of stages of the turbomachinery increases, and the system pressure is also increased. This increase may seem to favor the heat exchanger design in terms of size, but could also result in observed detrimental effects (especially mechanical integrity), due to system overpressurization.

How does this impact cost? The cost implication of helium is that its turbomachinery would increase in cost rapidly compared to other selected working fluids because of the effect of pressure ratio on the component size. Similarly, the mass flow rate affects the component surface area and the output power of the NPP. For fluids such as helium with its specific heat capacity, which is five times greater than air and nitrogen, it implies that its specific power will be five times greater than air or nitrogen fluid for a given mass flow rate. Consequentially, helium will be more compact with larger power output, at a reasonable cost. In terms of size, carbon dioxide will be the largest because of its thermodynamic properties (Osigwe et al., 2020).

A typical demonstration of the effect of working fluid on the turbomachinery is shown in Figures 21.2.32 and 21.2.33. In the analysis, a simple recuperated closed-cycle gas turbine NPP was utilized. For each working fluid, the same shaft output power (38.2 MW), and the overall temperature rise and drop for the compressor and turbine, were assumed (Osigwe et al., 2019c). Also, a constant mean speed was assumed in this analysis.

Designing for low-pressure ratios, would be one way to manage aerodynamic and mechanical design difficulties using helium as a working fluid. For carbon dioxide, its heat exchanger size would be the largest because of its transport properties. This will affect the cost of the heat exchanger. Both air and nitrogen have similar design characteristics because their fluid properties behave almost the same. This similarity could be a good advantage for operational reasons, as documented in Osigwe et al., 2020c.

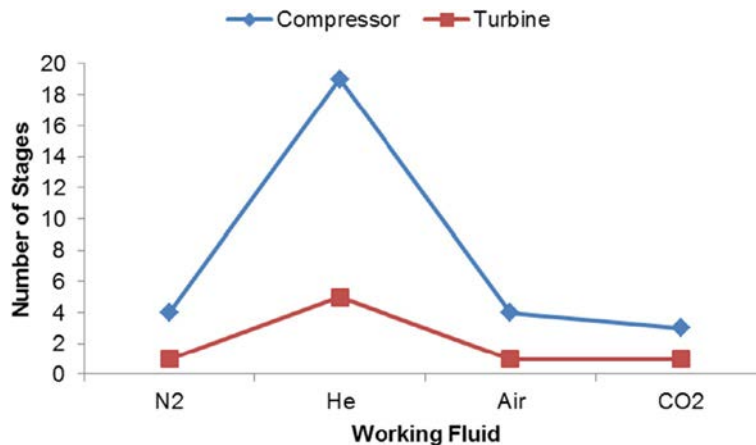


Figure 21.2.32. Turboset sizing for same output power and overall number of stages.

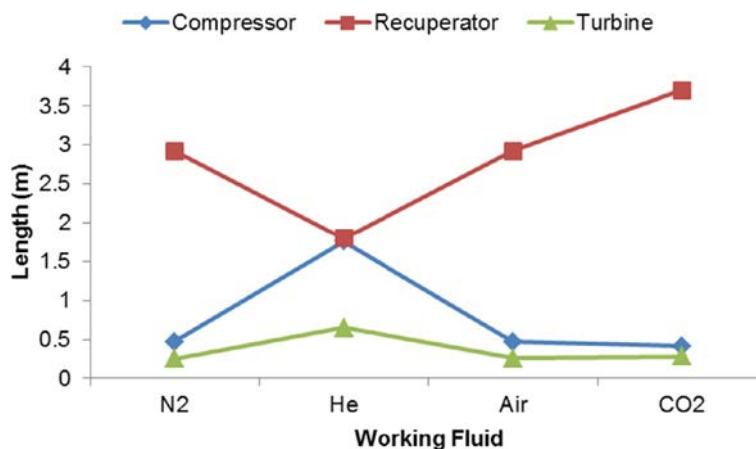


Figure 21.2.33. Turboset sizing for same output power and overall length.

21.2.22 Legislation

Legislation also plays a vital role in the potential financial risks of any investment into closed-cycle gas turbine NPPs, especially regarding reactor and working fluid options. The experiences of Chernobyl and Fukushima NPPs, coupled with waste management, have created a negative perception in society. This has justified the need for more legislation on NPP projects. This perception directly impacts the financial risk associated with such projects, especially nuclear-powered closed-cycle gas turbines.

From the working fluid perspective, and with consideration of helium, the supply and sales can be subject to political activities, or the lack of it especially when favorable policies are required. This could have cost implications on investment. Also, variation in the cost of carbon dioxide could differ in other territories, due to legislation on tax and incentivization. As such, any changes may affect the cost of the investment. This may also be the case for nitrogen since the demand for ammonia for other industrial and agricultural purposes, could affect demand and supply.

21.2.23 Other design considerations

Apart from the DP considerations, the ODP is key to the flexible operation of the NPP for peak load.

21.2.23.1 Long-term off-design point performance and operation

The NPP compressor inlet is influenced by ambient conditions in most cases, as highlighted by [Gad-Briggs et al. \(2021\)](#). A change of the DP temperature from 28°C, or the actual power output demand, results in an off-design condition for the NPP, which requires optimization for Off-Design (OD) operation. An OD operation that is not optimized will not be economically advantageous for the plant, especially for long periods. It has to run at designated ODPs, where the equilibrium of all component characteristics is guaranteed. Assessments in [Gad-Briggs and Pilidis \(2017\)](#) show that for an inlet temperature range of -35°C to 50°C, and at COTs between 750°C and 1000°C, ODP low-temperature inlet conditions of between 9°C and -9°C yielded cycle efficiencies that are 10% to 18% lower for the ICR. This is the case when compared to the DP cycle efficiency. Typically, the efficiency and power output are expected to increase with decreasing temperature, as the case is with the SCR. Additional studies also indicated that there were notable changes in the CW , regardless that the ICR aims to reduce the CW , which indicated some non-linearity. The non-linearity is dependent on the increased level of complexity (additional components) during OD matching calculations. For the ICR, the two additional components, especially the intercooler, are judged to have a greater influence on this phenomenon. This is further analyzed in [Gad-Briggs and Pilidis \(2017\)](#).

When the COT is varied to change the power, the results indicate some improvement for the ICR. The ICR has 12% more power output than the SCR, for the same COT of 750°C. However, this reduces to 3% at 900°C. The results when the COT is varied indicates that the ODP performance of an NPP at lower COT, is better suited with an ICR configuration is adopted. The noticeable difference between both cycles affects changes in the mass flow rate. The change at 750°C translates into an increase of 0.26% in mass flow rate for the ICR in comparison to the SCR (0.20%). At 1000°C, there is a reduction in mass flow rate, which is greater for the ICR than the SCR by a factor 3. The variation in mass flow rate impacts the control methods for the short-term operation of the power plant. It will also demand a sizeable working fluid inventory for the ICR in comparison to the SCR.

21.2.23.2 Short-term off-design point performance and operation

According to Gad-Briggs et al. (2021), the Inventory Pressure Control (IPC) or ICS method is critical in regulating the power to counteract sudden changes in ambient conditions or demands for immediate power adjustment. Figure 21.2.34 shows a typical IPC arrangement for the SCR, which can also be adapted for the ICR configuration. For comparison purposes, and with all conditions being the same, Figure 21.2.35 demonstrates the transient performances of the SCR and the ICR, based on studies conducted by Gad-Briggs et al. (2017c). The helium inventory was withdrawn using an average flow rate of 0.13 kg/s adopted for the studies, based on work conducted by Sato et al. (2012), with the aim of reducing the power output of the NPPs for both configurations to 50%. The results from the study show that the SCR took 9 min 27 s, while the ICR achieved 19 min 8 s. This indicates a sizeable volumetric inventory requirement for the ICR, which is 102% larger than the SCR. This size difference in inventory storage takes into account the complete removal of the inventory from the cycle in emergency situations. The percentage (%) reduction in CW and TW are matched for both cycles. A typical limitation for the use of the IPC method is expected to be no less than 50% of full-power operation.

For the load-following operations, both cycles can match the requirements to regulate power output in order to maintain the reactor thermal power. This is very useful in countering changes in ambient temperature. According to studies by Gad-Briggs et al. (2017b), the SCR can regulate the flow to within 2 s, while the ICR can regulate the flow to within 3 s. It was noted during the study that the SCR loses more power

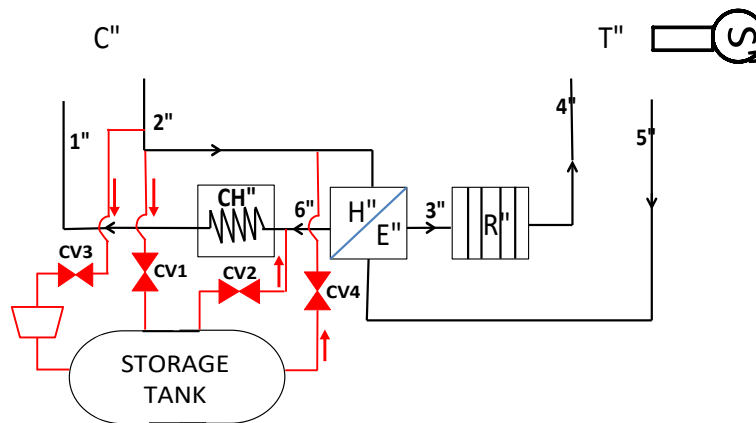


Figure 21.2.34. Simple Cycle with Recuperator (SCR) with inventory pressure control schematic for helium cycles.

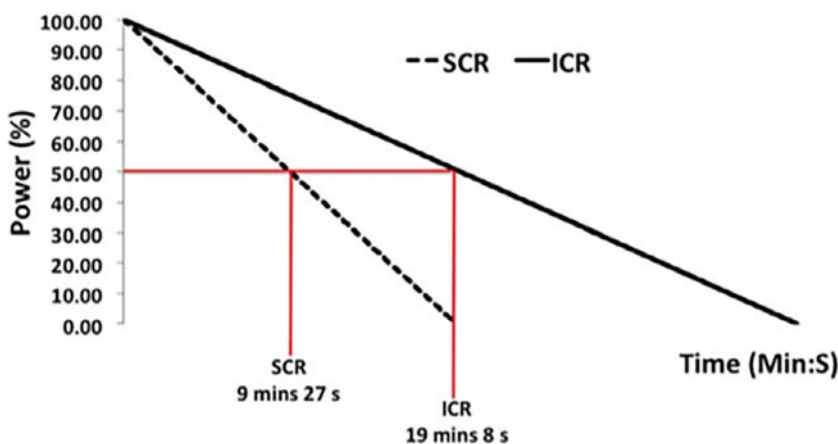


Figure 21.2.35. Transient part power performance for helium cycles (T_1 at DP).

output (between 3% and 5% drop in power output) than the ICR (1%–3% drop in power output) in order to maintain reactor thermal power at high inlet temperatures. At lower inlet temperatures, both cycles gain the same level of increase in power output at lower cycle inlet temperatures, which is typically an increase of ~3% per 10°C drops in cycle inlet temperature.

21.2.23.3 Reactor technology status

The development of the high-temperature gas-cooled reactors has greatly influenced the Gen-IV VHTR designs. The standard form of fuel—the TRISO tri-isotropic coated particle fuel—is based on the pedigree and technology from the last half a century of development from the first Dragon reactor. Today, the latest VHTR designs are pioneered by Asia, with the High-Temperature engineering Test Reactor (HTTR) in Japan, and the High-Temperature test Reactor (HTR-10) in China. Both reactors have different COTs, the HTR-10 (~700°C) and the HTTR (950°C), and both designs sharing the passive safe philosophies of the VHTR objective (Yan, 2016). The VHTR design is a near-term deployment and suitable for electricity generation, as well as hydrogen production and seawater desalination, due to the high-temperature COT. The typical core for the VHTR is of a prismatic cylindrical core (HTTR) or annular core (GTHTR300), or a pebble bed core. The prismatic core provides modularity advantages in design, with the benefit of being able to optimize the number of enrichments in the core. This will minimize the power peaking and peak fuel temperature throughout the core burnup period (Yan, 2016). The pebble bed core has fuel in the form of pebbles, which are stacked together. It can be controlled as proposed for the PMBR design, whereby the control rods will be inserted at proximity to the surrounding graphite reflector, with the control achieved by using neutral absorbers contained within the pebbles.

With regard to the GFRs, the technology's biggest potential, in addition to its high-temperature capability for process heat, is the high breeder capability of the reactor. This makes for shorter doubling times, higher power densities and burner capabilities to minimize waste. The economic advantage is to have the high power density capability, without intermediate loops, while minimizing spent fuel inventory, and uranium resources. However, safety concerns relating to high core neutronic leakage, leading to high fissile loading, challenges the proliferation resistance characteristics. Near term, deployment is still far away in comparison to the VHTR due to these design challenges. Nonetheless, the analysis is applicable to both technologies due to potential COTs (850–950°C), and the favorable benefits of using helium as a working fluid, with the working pressures within the circuit at up to 7 MPa, and the capacity to utilize IPC/ICS for both designs.

21.2.24 Future trends

21.2.24.1 Smaller high-pressure ratio cycle configuration

One future trend is to simplify the cycle and plant design. As a key requirement under the Gen-IV framework, simplification will ensure improved life cycle costs, and costs of energy production. The Intercooled Cycle (IC) has undergone technological advancements with gas turbines, prompting studies to explore the potential of this cycle for VHTRs and GFRs, as documented in Gad-Briggs et al. (2017d). Incorporating this cycle configuration without a recuperator before now has not been fully explored due to the perceived economics of a nuclear gas turbine cycle without a recuperator to capture the exhaust heat and transfer it back into cycle. Nonetheless, its performance potential was analyzed and reported in Gad-Briggs and Pilidis (2017) and Gad-Briggs et al. (2017d). Figure 21.2.36 illustrates the IC configuration.

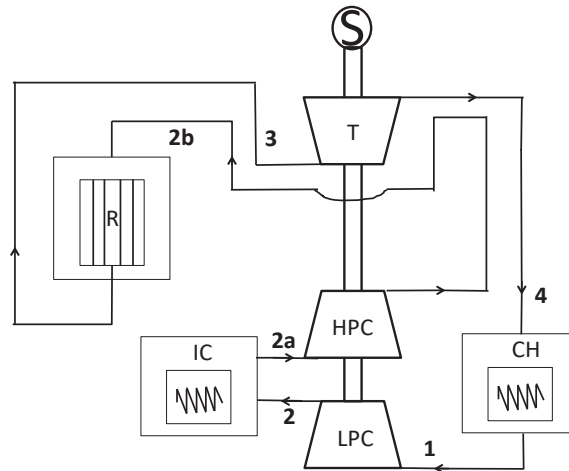


Figure 21.2.36. Typical intercooled cycle without recuperator (IC).

21.2.24.2 Higher core outlet temperature $>1000^{\circ}\text{C}$

Figure 21.2.37 shows the cycle efficiencies for SCR and ICR, including the IC and a Simple Cycle (SC). The SC is neither intercooled nor recuperated. A study by Gad-Briggs et al. (2017a) looked at two turbine blades with different maximum blade metal temperatures. Blade A had a lower metal temperature, which is 13% less than blade B. The study looked at understanding the amount of helium cooling demanded by the turbine, and to demonstrate the performance benefits of improved turbine blade materials. The study reviewed COTs/TETs in excess of 1200°C and considered the viability of such temperatures. The study concluded on immediate to near term goals, which limited the SCR and the ICR to 950°C , until improvements in high-temperature recuperators have been conceived, with the need for economic studies showing real benefit.

Current reactor development could explore temperatures in excess of 1200°C for Gen-IV applications, which will be beneficial for increasing the efficiency of the cycle. Judging by the advantage of the ICR and the SCR as illustrated in Figure 21.2.37, it is evident that cycle efficiency gains could offer competitive savings, but economic studies by Gad-Briggs et al. (2019) concluded that there was no real economic

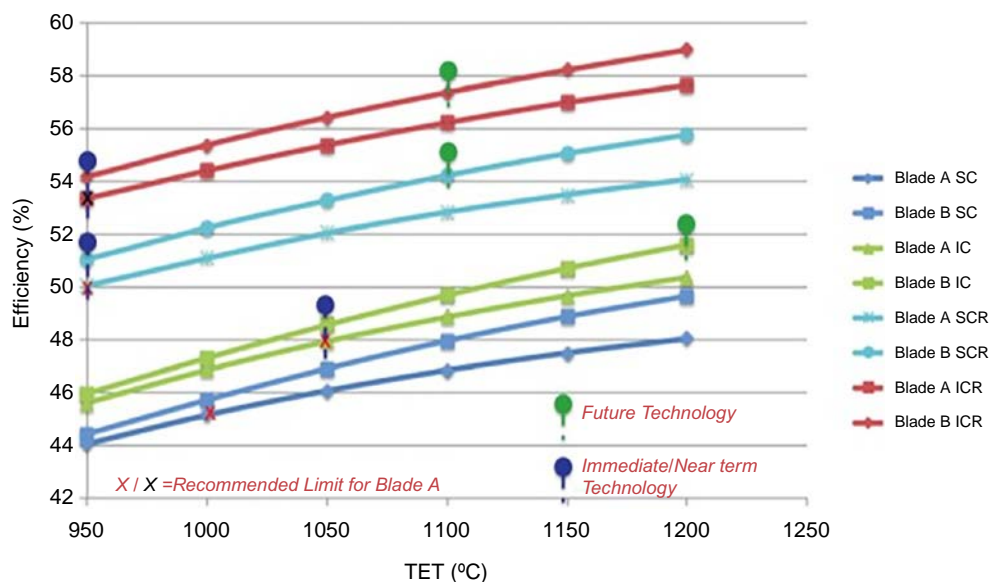


Figure 21.2.37. Technological assessment (helium cycles).

advantage of COTs in excess of 1000°C for electricity generation alone, but the benefits of considering other industries such iron and steel production and hydrogen as part of cogeneration will need to be explored. The SC is not recommended because it was included for comparative basis, which is to demonstrate the efficiency benefits of the recuperator to the SCR and the ICR configurations.

21.2.24.3 Improved helium compressors

Helium is very difficult to compress in comparison to air, due to its thermophysical properties. As such, helium requires more stages to achieve the level of compression required by the cycles. Helium compressor designs have followed the same approach adopted for traditional air compressor designs. However, the flow conditions of helium, such as higher speed of sound and lower Mach number in comparison to air, means a different and robust approach to helium compressor design needs to be investigated to understand how the design activities can reduce the number of stages, through increasing the stage loading, and an assessment of aerodynamic losses.

21.2.25 Conclusion

The merits of the closed Brayton gas turbine recuperated cycles for Gas-cooled Fast Reactors (GFRs), and Very-High-Temperature Reactors (VHTRs) have been discussed in the chapter. This chapter also discussed the operational experiences, which have led to revolutionary improvements in the design of helium cycles, particularly in the areas of minimizing leakage, and minimizing lubricant ingress by using magnetic bearings. The significant benefits to be realized is in the fact that the Brayton helium gas turbine cycles are more efficient than the incumbent Rankine cycles, which deliver power at relatively low efficiencies, when compared to efficiencies of approximately 50% for the Brayton gas turbine cycles.

Two recuperated cycles that are currently being considered in closed Brayton helium cycle configurations were reviewed. They are the simple cycle recuperated (ICR) and the Intercooled Cycle Recuperated (ICR). The cycle Design Point (DP) considerations included the component definition. The key aspects that impact the choice of cycle and design are summarized below.

- The ICR has an efficiency, which is 2% to 3% more than the SCR, which for similar inlet conditions results in a capacity increase of 4% to 5%.
- The recuperator effectiveness has the biggest effect on the efficiency of the plant, followed by the turbine. Furthermore, a 5°C rise in compressor inlet temperature results in a 1.3% drop in efficiency and a 4 MW_e decrease in plant capacity.
- The combined pressure loss will be less of the SCR than the ICR. The ICR pressure losses are estimated to be 15% to 20% greater than the SCR pressure losses for the same inlet conditions. For both cycles, the effect on plant cost can be as much as 4% to 6%, which means modularization and compact plant designs are important to minimize this effect.

Among the fluids discussed in this chapter, helium is commonly chosen in design studies as a working fluid for closed-cycle gas turbine systems. This is mainly because of its high thermal conductivity, coupled with its high specific heat, making it a better heat transfer fluid than any other gas used in this study. A major disadvantage of helium is its cost because of limited supply; hence, one has to make room for cost exigencies, if helium is selected as a working fluid design choice for the closed-cycle gas turbine NPP. Also, helium poses a requirement challenge for the exceptionally high degree of leak-tightness throughout the closed system, particularly with respect to the shaft seal. Carbon dioxide and nitrogen are also candidates, primarily because on the surface, they appear to reduce the oxidation and corrosion problems. However, it has been found that iron-chrome-nickel alloys owe their high-temperature oxidation resistance to the formation of a

dense, protective oxide film much like that of the oxide film on the anodized aluminum. For these iron-chrome-nickel alloys, strongly oxidizing conditions are required not only to form this film initially, but also to maintain it in the face of tendencies to form minute cracks with thermal strain cycling at temperatures above 600°C. Ordinarily, air is a more favorable environment for the iron-chrome-nickel alloys than is helium; hence there is really no incentive from the structural materials standpoint to use helium over than air.

The output of a closed-cycle gas turbine system is normally controlled by varying the system pressure. The most difficult control condition that must be met, is the abrupt loss of load as a consequence of a circuit breaker trip. For this condition, the control problem is greatly eased, if the working fluid can simply be vented to the atmosphere; a step that presents no problem with air, but would represent an important expense if helium, nitrogen, or carbon dioxide were employed.

Helium has the advantage of smaller turbine and compressor units, but the number of stages of these units increase, in comparison to other working fluids. No helium machines are in production, and hence there is a strong incentive to employ air as a working fluid so that existing gas turbomachinery can be employed without carrying out a substantial design and development effort. This is also the case for carbon dioxide. Nitrogen has recently been of great interest for NPPs because of its thermodynamic behavior, and some characteristics that could be traded off using air as a working fluid. Nitrogen is an inert gas and does not easily degrade seals. Hence, it is less prone to leaks and the issue of oxidation is avoided.

However, the question to answer would be, can the advantages of using these fluids out-weigh the potential risks? The answer to these lies from the view point of the investment decision, based on the opportunity cost, and research and development into possibilities of using a mixture of different working fluids. From the authors' perspective, there is no specific fluid in this study that is deemed the best choice, but the purpose of this discussion is to provide reasonable insight into the potential risks and compromise that would be expected for any investment decision.

Finally, the overarching discussion on the working fluid cycle configuration, operations and risk assessment for the closed-cycle gas turbine can be concluded as follow:

- The choice of working fluid to a reasonable extent, affects the design choice cycle configuration. It sets a reasonable compromise regarding plant size, cost (capital and operational cost), and turbomachinery design challenges. For working fluid such as carbon dioxide, its optimal performance is achieved above its critical points, which will mean pressurizing the system or operating at a very-high-pressure ratio for a simple cycle configuration. However, cycles with high-pressure ratios tend to pose extra challenges in terms of component design, especially when used for simple cycle layout or configurations that have not previously been proven. For this reason, a configuration with intercooling (IC or ICR), which allows for recompression of carbon dioxide, seems to be competitive in terms of achieving good performance by splitting the pressure ratio into two compressions. For fluids such as helium with low molecular weight and high gas properties (γ and C_p), the simple or recuperated cycle configuration may seem more realistic due to its thermodynamic and heat properties. Other factors that may influence the design choice selection of cycle configuration include proven component design and operation (technology readiness for each component related to the working fluid), reliability, maintainability, cooling medium of the nuclear reactor, overall nuclear plant layout, the potential for energy utilization and sustainability, working fluid management and costs. These factors could give a reasonable justification for a configuration that is deemed suitable for each working fluid.
- The potential cycle efficiency for each working fluid is greatest for a working fluid with a higher ratio of specific heat at a low-pressure ratio, in addition to ratio of specific heats at a higher-pressure ratio. Since the specific heat ratio of helium is larger than air, nitrogen and carbon dioxide, the optimum efficiency for helium occurs at the lowest pressure ratio compared with other fluids. However, the decision for suitable cycle configuration is not only hinged on the fluid cycle efficiency potential.

- To operate in an efficient, safe, secure, and reliable manner, each control mechanism is synchronized to maintain a symbiotic relationship with load demand or the electric grid, especially during instabilities, interruptions and emergency conditions. To avoid as much as possible the limitations on shaft speed, or low efficiencies at reduced power, would require a combined control mode to be adopted, such as the bypass control usually implemented for rapid load response and shaft speed control.
- The possible leaks in the valve could lead to performance losses; hence, appropriate seal materials and external insulation could be incorporated to minimize the losses.
- The risks to consider when selecting helium as a working fluid would be how to overcome the problem of shaft seal leak at high pressure and temperature. Helium diffuses through solids three times faster than air. Secondly, the high cost of helium due to it been regulated, could have an impact on the operations of the plant and the impact of its thermodynamic properties on the turbomachinery aerodynamic and mechanical design, since the technology readiness level is not as high as air.
- For nitrogen, the possibility of nitriding and embrittlement of material at high temperature and pressure could influence the life of the components, and the consequence of any component failure could lead to ingress, especially for the heat exchangers.
- For carbon dioxide, at elevated temperature, there could be small pickups of carbon, which could lead to decarburization. Also, the component sizing for carbon dioxide could affect the overall system costs, especially the heat exchangers.
- For air, the possibility of oxidation and corrosion attack could affect the life of the component.

Future trends for Gen-IV including the viability of Core Outlet Temperatures (COTs) in excess of 1000°C in order to further increase the efficiency of the plants and cycles without recuperation, to investigate the merits of cycles with higher pressure ratios that maximize plant capacity at reduce plant sizes, and the different design philosophy for helium turbomachinery design. These are all worthy merits that will ensure the cost-effectiveness of the technologies, in their respective operational capacities.

References

- Alpy, N., Cachon, L., Haubensack, D., Floyd, J., Simon, N., Gicquel, L., Rodriguez, G., Saez, M., Laffont, G., 2011. Gas Cycle testing opportunity with ASTRID, the French SFR prototype. In: Proceedings of Supercritical CO₂ Power Cycle Symposium. Boulder, Colorado, pp. 42–51.
- Angelino, G., 1968. Carbon dioxide condensation cycles for power production. *J. Eng. Gas Turbines Power* 90 (3), 287–295.
- Bammert, K., Krey, G., Krapp, R., 1974. Operation and control of the 50-mw closed-cycle helium turbine Oberhausen. In: ASME, (74-GT-13), pp. 1–8.
- Bell, C., 2016. Thermo: Chemical Properties Component of Chemical Engineering Design Library.
- Bell, I., Wronski, J., Quoilin, S., Lemort, V., 2014. Pure and Pseudo-pure fluid thermophysical property evaluation and open-source thermophysical property library CoolProp. *Ind. Eng. Chem. Res.* 53 (6), 2498–2508.
- Botha, B.W., Rousseau, P.G., 2007. Control options for load rejection in a three-shaft closed cycle gas turbine power plant. *Trans. ASME* 129, 806–813.
- Covert, R.E., Krase, G., Morse, D.C., 1974. Effect of various control modes on the steady-state full and part load performance of a direct-cycle nuclear gas turbine power plant. In: ASME, (74-WA/GT-7), pp. 1–9.
- Decher, R., 1989. Brayton cycles with reciprocated work components. In: 25th Joint Propulsion Conference. AIAA, Monterey, Canada.
- Decher, R., 1994. *Energy Conversion: Systems, Flow Physics and Engineering*. Oxford University Press, New York.
- Di Lorenzo, G., 2010. *Advanced Low-Carbon Power Plants: The T.E.R.A Approach*. Cranfield University.
- Dostal, V., 2004. *A Supercritical Carbon Dioxide Cycle for Next Generation Nuclear Reactors*. Massachusetts Institute of Technology.
- Dyreby, J.J., 2014. *Modelling the Supercritical Carbon Dioxide Brayton Cycle with Recompression* (PhD Thesis). University of Wisconsin-Madison, USA.
- El-Genk, M.S., Tournier, J., 2009a. Performance analyses of VHTR plants with direct and indirect closed Brayton cycles and different working fluids. *Prog. Nucl. Energy* 51, 556–572.

- El-Genk, M.S., Tournier, J., 2009b. Effects of working fluid and shaft rotation speed on the performance of HTR plants and the size of CBC Turbo-machine. *Nucl. Eng. Des.* 239, 1811–1827.
- Feher, E.G., 1968. The supercritical thermodynamic power cycle. *Energy Convers.* 8 (2), 85–90.
- Frutschi, H.U., 2005. *Closed-Cycle Gas Turbines: Operating Experience and Future Potential*, first ed. ASME, New York.
- Gad-Briggs, A., 2011. *Effect of Change in Role of an Aircraft on Engine Life* (M.Sc Thesis). Cranfield University.
- Gad-Briggs, A., 2017. *Addendum Report: Detailed Review of Nuclear Energy for Generation IV Nuclear Power Plants*, Cranfield, UK. Available at: <https://dspace.lib.cranfield.ac.uk/handle/1826/12674>.
- Gad-Briggs, A., Pilidis, P., 2017. Analyses of the off-design point performance of a high pressure ratio intercooled brayton helium gas turbine cycle for generation IV nuclear power plants. In: *Proceedings of the 2017 25th International Conference on Nuclear Engineering ICONE25*, 2017.
- Gad-Briggs, A., Pilidis, P., Nikolaidis, T., 2017a. A review of the turbine cooling fraction for very high turbine entry temperature helium gas turbine cycles for generation IV reactor power plants. *ASME J. Nucl. Eng. Radiat. Sci.* 3 (2).
- Gad-Briggs, A., Pilidis, P., Nikolaidis, T., 2017b. Analyses of the load following capabilities of Brayton helium gas turbine cycles for generation IV nuclear power plants. *J. Nucl. Eng. Radiat. Sci.* 3 (4).
- Gad-Briggs, A., Pilidis, P., Nikolaidis, T., 2017c. Analyses of the control system strategies and methodology for part power control of the simple and intercooled recuperated Brayton helium gas turbine cycles for generation IV nuclear power plants. *ASME J. Nucl. Eng. Radiat. Sci.* 3 (4).
- Gad-Briggs, A., Pilidis, P., Nikolaidis, T., 2017d. Analyses of a high pressure ratio intercooled direct Brayton helium gas turbine cycle for generation IV reactor power plants. *J. Nucl. Eng. Radiat. Sci.* 3 (1), 2017.
- Gad-Briggs, A., Nikolaidis, T., Pilidis, P., 2017e. Analyses of the effect of cycle inlet temperature on the precooler and plant efficiency of the simple and intercooled helium gas turbine cycles for generation IV nuclear power plants. *Appl. Sci.* 7 (4).
- Gad-Briggs, A., Osigwe, E., Pilidis, P., Nikolaidis, T., Sampath, S., Teixeira, J.A., 2021. Benefits, drawbacks, and future trends of Brayton helium gas turbine cycles for gas-cooled fast reactor and very-high temperature reactor generation IV nuclear power plants. *ASME J. Nucl. Eng. Radiat. Sci.* 7 (1).
- Gad-Briggs, A., Pilidis, P., Nikolaidis, T., 2019. Analyses of the costs associated with very high turbine entry temperatures in helium recuperated gas turbine cycles for generation IV nuclear power plants. *ASME J. Nucl. Eng. Radiat. Sci.* 5 (1).
- Gerrard, A.M., 2007. *Guide to Capital Cost Estimating*, Fourth ed. IChemE, Rugby.
- Grochowina, F., 2011. *Performance Evaluation of Gas Turbines for Nuclear Power Plants*. Cranfield University.
- Hirshorn, S., Jefferies, S., 2016. *Final Report of the NASA Technology Readiness Assessment (TRA) Study Team.*, NASA. Available at <https://ntrs.nasa.gov/archive/nasa/casi.ntrs.nasa.gov/20170005794.pdf>. (Accessed 27 March 2018).
- Invernizzi, C.M., 2017. Prospects of mixtures as working fluids in real-gas Brayton cycles. *Energies* 10, 1–15.
- Ishiyama, S., Muto, Y., Kato, Y., Nishio, S., Hayashi, T., Nomoto, Y., 2008. Study of steam, helium, and supercritical CO₂ turbine power generations in prototype fusion power reactor. *Nucl. Energy* 50, 325–332.
- Jiang, B., et al., 2015. Similarity and cascade flow characteristics of a highly loaded helium compressor. *Nucl. Eng. Des.* 286, 286–296. Available at: <https://doi.org/10.1016/j.nucengdes.2014.12.039>.
- Kato, Y., Nitawaki, T., Muto, Y., 2004. medium temperature carbon dioxide gas turbine reactor. *Nucl. Eng. Des.* 230, 195–207.
- Lee, J.C., Campbell, J., J. and Wright, D.E., 1981. Closed-cycle gas turbine working fluids. *Trans. ASME* 103, 220–228.
- Mahdi, M., Popov, R., Pioro, I., 2018. Research on thermal efficiencies of various power cycles for GFRs and VHTRs. In: *Proceedings of ICONE26*, July 22–26, London, England, Paper #82085, p. 14.
- Navarro, H.A., Cabezas-Gomez, L.C., 2007. Effectiveness-NTU computation with a mathematical model for cross-flow heat exchangers. *Braz. J. Chem. Eng.* 24 (4), 509–521.
- No, H.E.E.C., Kim, J.I.H., Kim, H.M.I.N., 2007. A review of helium gas turbine technology for high-temperature gas-cooled reactors. *J. Nucl. Eng. Technol.* 39 (1), 21–30.
- Noblis, C.W., 2014. *Analysis of Brayton Cycles Utilizing Supercritical Carbon Dioxide.*, <https://doi.org/10.2172/1490264>. New York.
- Olumayegun, O., Wang, M., Kelsall, G., 2016. Closed-cycle gas turbine for power generation: a state-of-the-art review. *Fuel* 180, 694–717.
- Olumayegun, O., Wang, M., Kelsall, G., 2017. Thermodynamic analysis and preliminary design of closed Brayton cycle using nitrogen as working fluid and coupled to small modular sodium-cooled fast reactor (SM-SFR). *Appl. Energy* 191, 436–453.
- Openshaw, F., Estrine, E., Croft, M., 1976. Control of a gas turbine HTGR. In: *ASME*, (76-GT-97), pp. 1–12.
- Osigwe, E.O., 2018. *Techno-Economic and Risk Analysis of Closed-Cycle Gas Turbine Systems for Sustainable Energy Conversion*. Cranfield University.
- Osigwe, E.O., Gad-Briggs, A., Igbong, D., Nikolaidis, T., Pilidis, P., 2020. Performance modelling and analysis of a single-shaft closed-cycle gas turbine using different operational control strategy. *ASME J. Nucl. Eng. Rad. Sci.* 6 (2), 021201.

- Osigwe, E.O., Gad-Briggs, A., Nikolaidis, T., Pilidis, P., Sampath, S., 2020b. Performance analyses and evaluation of CO₂ and N₂ as coolants in a recuperated brayton gas turbine cycle for a generation IV nuclear reactor power plant. *ASME J. Nucl. Rad. Sci.* 6 (2), 021102.
- Osigwe, E.O., Gad-Briggs, A., Nikolaidis, T., Pilidis, P., Sampath, S., 2020c. Performance simulation to understand the effects of multi-fluid scaling of gas turbine components for generation IV nuclear power plants. *ASME J. Nucl. Rad. Sci.* 6 (2).
- Osigwe, E.O., Gad-Briggs, A., Pilidis, P., Nikolaidis, T., Sampath, S., 2019a. effect of working fluid on selection of gas turbine cycle configuration for GEN-IV nuclear power plant system. In: *International Conference on Nuclear Engineering, Proceedings, ICONE, 2019-May*. Ibaraki.
- Osigwe, E.O., Gad-Briggs, A., Pilidis, P., Nikolaidis, T., Sampath, S., 2019b. Inventory control systems for nuclear powered closed-cycle gas turbine: Technical studies on the effect of working fluid options. In: *International Conference on Nuclear Engineering, Proceedings, ICONE*. Ibaraki.
- Osigwe, E.O., Pilidis, P., Nikolaidis, T., Igbong, D., 2019c. Risk assessment on working fluid selection for closed cycle gas turbine system. In: *Proceedings of the ASME 2019 26th Power Conference*. (Utah).
- Osigwe, E.O., Pilidis, P., Nikolaidis, T., Sampath, S., 2019d. Gas turbine Arekret-cycle simulation modelling for training and educational purposes. *ASME J. Nucl. Eng. Radiat. Sci.* 5 (4).
- Osigwe, E.O., Gad-Briggs, A., Obhuo, M., Pilidis, P., 2021. Techno-economic study on implementation of inventory control requirements for nuclear powered closed-cycle gas turbine power plant. *ASME J. Nucl. Rad. Sci.* 7 (3).
- Osigwe, E.O., Gad-Briggs, A., Tukur, N., Pilidis, P., 2020. Design and operational challenges of switching working fluid for a gen IV nuclear powered closed-cycle gas turbine: case studies of nitrogen and air, helium and argon. In: *Proceedings of the 2020 International Conference on Nuclear Engineering Collocated with the ASME 2020 Power Conference*. Virtual, Online.
- Pioro, I., 2016. *Handbook of Generation IV Nuclear Reactors*. Elsevier – Woodhead Publishing (WP), Duxford, UK, p. 940. Free download of content https://www.gen4.org/gif/jcms/c_9373/publications.
- Pioro, I., Mahdi, M., Popov, R., 2017. Heat-transfer media and their properties. In: Kulacki, F.A. (Ed.), *Handbook of Thermal Science and Engineering*. Springer, p. 100.
- Pioro, R., Zvorykin, A., Rachid, M., Pioro, I., 2018. Study on current status and future developments in nuclear-power industry of the world. In: *Proc. of ICONE26, July 22-26, London, England, Paper #82085*, p. 14.
- Pitts, D.R., Sissom, L.E., 1997. *Theory and Problems of Heat Transfer*, second ed. McGraw-Hill, New York.
- Pradeepkumar, K.N., 2002. *Analysis of a 115MW, 3- Shaft, Helium Brayton Cycle Using Nuclear Heat Source*. Cranfield University.
- Saravanamuttoo, H.I.H., et al., 2009. *Gas Turbine Theory*, sixth ed. Pearson Education Limited, England.
- Sato, H., Yan, H., Ohashi, H., Tachibana, Y., Kunitomi, K., 2012. Control Strategies for VHTR Gas-Turbine System with Dry Cooling. In: *Proceedings of the 2012 20th International Conference on Nuclear Engineering ICONE20-Power2012*.
- Sato, H., et al., 2014. GTHTR300—a nuclear power plant design with 50% generating efficiency. *Nucl. Eng. Des.* 275, 190–196. Available at: <http://linkinghub.elsevier.com/retrieve/pii/S002954931400274X>. (Accessed 15 August 2014).
- Staudt, J.E., 1987. *Design Study of an MGR Direct Brayton-Cycle Power Plant*. Massachusetts Institute of Technology.
- Thring, M.W., 1960. *Nuclear Propulsion*. Butterworth & Co, London, UK.
- TNAP, 2000. *The Impact of Selling the Federal Helium Reserve*. (Washington).
- Tournier, J., El-Genk, M.S., 2008a. Properties of helium, nitrogen, and He-N₂ binary gas mixtures. *J. Thermophys. Heat Transf.* 22 (3), 442–456.
- Tournier, J., El-Genk, M.S., 2008b. Transport properties of HeN₂ binary gas mixtures for CBC space applications. In: *American Institute of Physics Conference Series*. vol. 969, pp. 637–647.
- Ulizar, I., Pilidis, P., 2000. Handling of Semiclosed cycle gas turbine with a carbon dioxide-argon working fluid. *ASME* 122, 437–441.
- Walsh, P.P., Fletcher, P., 2004. *Gas Turbine Performance*, second ed. Blackwell Science, Oxford.
- Wang, J., Gu, Y., 2005. Parametric studies on different gas turbine cycles for a high-temperature gas-cooled reactor. *Nucl. Eng. Des.* 235, 1761–1772.
- Yan, X., 1990. *Dynamic Analysis and Control System Design for an Advanced Nuclear Gas Turbine Power Plant*. Massachusetts Institute of Technology.
- Yan, X.L., 2016. In: Pioro, I.L. (Ed.), *Very high-temperature reactor*, in *handbook of generation IV nuclear reactors*, first ed. Woodhead Publishing, Duxford, United Kingdom, pp. 55–90.
- Yousef, S.H., Zzaamout, M.S., 1992. Comparative performance of closed-cycle gas turbine engine with heat recovery using different gases. *Heat Recovery Syst. CHP* 12 (6).
- Z. Huang, J. Wang, and J. Li, 2004. Study on the thermodynamic cycle of HTR-10GT. In: *2nd International Topical Meeting on High Temperature Reactor Technology*.

Further reading

The below literature list, in addition to publications referenced in this Chapter, are recommended for further reading:

- Aungier, R.H., 2006. *Turbine Aerodynamics: Axial-Flow and Radial-Inflow Turbine Design and Analysis*. ASME, New York.
- Bammert, K., 1971. Design of a Fossil-Fired Helium Turbine Plant for Combined Power and Heat Production.Pdf. In: *The 8th World Energy Conference*. Bucharest, Romania: Atomkernenergie.
- Bammert, K., Deuster, G., 1974. Layout and present status of the closed- cycle helium turbine layout and present status of the closed- cycle helium turbine plant Oberhausen. *ASME Gas Turbines Power J.*, 0–8.
- Black and Veatch, 1996. In: Drbal, F.L., et al. (Eds.), *Power Plant Engineering*, first ed. Springer, NY.
- Fielding, L., 2000. Turbine Design; the Effect on Axial Flow Turbine Performance of Parameter Variation. ASME, New York.
- Gad-Briggs, A., Nikolaidis, T., Pilidis, P., 2017. Analyses of the effect of cycle inlet temperature on the precooler and plant efficiency of the simple and intercooled helium gas turbine cycles for generation IV nuclear power plants. *Appl. Sci. (Switz.)* 7 (4).
- Gad-Briggs, A., Pilidis, P., Nikolaidis, T., 2017. Analyses of the control system strategies and methodology for part power control of the simple and intercooled recuperated Brayton helium gas turbine cycles for generation IV nuclear power plants. *ASME J. Nucl. Eng. Radiat. Sci.* 3 (4).
- Jiang, B., et al., 2015. Similarity and cascade flow characteristics of a highly loaded helium compressor. *Nucl. Eng. Des.* 286, 286–296. Available at: <https://doi.org/10.1016/j.nucengdes.2014.12.039>.
- Wark, K., Richards, D., Richards, D.E., 1998. *Thermodynamics*, sixth ed. McGraw-hill.
- Gad-Briggs, A., Pilidis, P., 2016. Analyses of simple and intercooled recuperated direct Brayton helium gas turbine cycles for generation IV reactor power plants. *ASME J. Nucl. Eng. Radiat. Sci.* 3, 011017-1–011017-7.
- Massachusetts Institute of Technology, MIT Gas Turbine Laboratory, n.d. Early Gas Turbine History. Available at: http://web.mit.edu/aeroastro/labs/gtl/early_GT_history.html#stodola [Accessed 14 November 2017].
- Naidin M., et al., 2009. Super Critical Water-Cooled Nuclear Reactors (SCWRs) Thermodynamic Cycle Options and Thermal Aspects of Pressure-Channel Design.
- Zhang Z., Wu Z., Wang D., Xu Y., Sun Y., Li F., 2009. Current status and technical description of Chinese 2 × 250MWth HTR-PM demonstration plant. *Nucl. Eng. Des.* 239 (7): 1212-1219. Available at: <http://linkinghub.elsevier.com/retrieve/pii/S0029549309001332> (Accessed 24 August 2014).

Regulatory and licensing challenges with Generation-IV nuclear energy systems

Seyun Eom, Jovica Riznic, Thambiayah Nitheanandan, and Ken Kirkhope
Canadian Nuclear Safety Commission, Ottawa, ON, Canada

Acronyms

AEC	Atomic Energy Commission, US
AM	Aging Management
AMP	Aging Management Program
AOO	Anticipated Operational Occurrence
ASME	American Society of Mechanical Engineers
BDBA	Beyond-Design-Basis Accident
BWR	Boiling Water Reactors
CANDU[®]	CANada Deuterium Uranium (CANDU is a registered trademark of Atomic Energy of Canada Limited.)
CEU	Council of the European Union
CFR	Code of Federal Regulation, US
CNSC	Canadian Nuclear Safety Commission
CORDEL	CoOperation in Reactor Design Evaluation and Licensing
CSA	Canadian Standards Association
DBA	Design-Basis Accident
DBE	Design Basis Earthquake
DEC	Design Extension Condition
DFM	Deterministic Fracture Mechanics
DG	Draft regulatory Guide
DiD (or DID)	Defense-in-Depth
DMWs	Dissimilar Metal Welds
DOE	Department Of Energy, US
EAC	Environmentally Assisted Cracking
EAF	Environmentally Assisted Fatigue
EC	European Commission
ECCS	Emergency Core Cooling System
ECIS	Emergency Core Injection System
ENISS	European Nuclear Installations Safety Standards
EQ	Environmental Qualification
ERDA	European Reactor Design Approval group
EU	European Union
EUR	European Utility Requirements
FA	Focus Area
FAC	Flow Accelerated Corrosion
FFS	Fitness-For-Service

FMEA	Failure Modes and Effects Analysis
FORATOM	Trade association for the nuclear energy industry in Europe
GDC	General Design Criteria
GEN IV	Generation Four (4)
GIF	Generation-IV International Forum
HAZ	Heat Affected Zone
HEL	High Energy Line
HTGR	High-Temperature Gas-cooled Reactor
IAEA	International Atomic Energy Agency
IEA	International Energy Agency
INL	Idaho National Laboratory
ISI	In-Service Inspection
LBB	Leak Before Break
LMP	Licensing Modernization Project
LOCA	Loss Of Coolant Accident
LPM	Loose Parts Monitoring
LWR	Light Water Reactor
MDEP	Multinational Design Evaluation Program
MHTGR	Modular High-Temperature Gas-cooled Reactor
MW_e	Mega Watt electrical
MW_{th}	Mega Watt thermal
NEA	Nuclear Energy Agency
NPC	Negative Pressure Containment
NPP	Nuclear Power Plant
NRC	Nuclear Regulatory Commission
NSCA	Nuclear Safety and Control Act
OECD	Organization for Economic Co-operation and Development
OPEX	OPerating EXperience
PARTRIDGE	Probabilistic Analysis as a Regulatory Tool for Risk Informed Decision Guidance
PDC	Principal Design Criteria
PFM	Probabilistic Fracture Mechanics
PIE	Postulated Initiating Event
PRSC	Pressure Retaining Systems and Components
psig	pound per square inch (gauge)
PWR	Pressurized Water-cooled Reactor
R&D	Research and Development
REGDOC CNSC	REGulatory DOCument
RG	Regulatory Guide
RI-ISI	Risk-Informed In-Service Inspection
SCC	Stress Corrosion Cracking
SCT	Safety Critical Target
SDC	Shut Down Cooling
SDS	Shut Down System
SFR	Sodium-cooled Fast Reactor
SMR	Small Modular Reactor
SSCs	Structures Systems and Components
TLAA	Time Limited Aging Analysis
TSO	Technical Support Organizations
TWC	Through Wall Crack
UK	United Kingdom
UN	United Nations
US	United States of America
VDR	Vendor Design Review
WENRA	Western European Nuclear Regulator's Association
WNA	World Nuclear Association

22.1 Introduction

With almost 70 years of experience and 440 nuclear reactors in operation in 30 countries, nuclear energy provides 10% of the world's electricity and it is the world's second largest carbon-free power (29% of the total electricity generated in 2017). In addition, almost 50 countries are relying on about 220 research reactors to produce medical and industrial isotopes. Furthermore, approximately 200 nuclear reactors with over 13,000 reactor years of reliable and safe operating experience power more than 160 ships. We should note here that approximately 50 new Nuclear Power Plants (NPPs) are under construction to bring an additional 15% of electricity generation capacity to the existing fleet of operating reactors. The performance of NPPs has improved significantly over past years. For example, 62% of reactors achieved a capacity factor higher than 80% in 2018, compared to a poor 28% in 1978. More than 30% of operating NPPs reached between 90% and 100% of design capacity in 2018 (WNA, 2020), and continue with their strong performance.

There is a clear need for new generating capacity around the world, both to meet increased demand for electricity in many countries and to replace old fossil fuel units and transition to the use of low and carbon-free energy. Consider the fact that in 2017, fossil-fueled power plants generated approximately 65% of electricity worldwide. Despite the strong support for, and growth of intermittent renewable electricity sources in recent years, the fossil fuel contribution to power generation has remained virtually unchanged in the last 10 years or so (66.5% in 2005) (WNA, 2020). The OECD International Energy Agency (IEA) projects that "Sustainable Development" or "Decarbonization" scenario, consistent with the provision of clean and reliable energy and a reduction of air pollution, calls for electricity generation from nuclear to increase by almost 62% by 2040 to 4409 TWh, and capacity growth to 601 GW_e (IEA, 2019; WNA, 2020).

Therefore, nuclear technology has a great potential to play a key role in the distant future to continue providing the world with a safe, reliable, economically competitive, and secure proliferation-resistant source of energy. However, we must note that new nuclear reactors coming online have more or less been balanced by the retirement of old units in recent years. Between the period of 1998 and 2018, a total of 89 reactors were retired, while only 98 new nuclear reactors started operation. Based on this long-term vision and building on 70 years of practical experience, the US Department Of Energy's (DOE) Office of Nuclear Energy, Science and Technology convened a group of senior governmental representatives from the original nine countries in January 2000 to begin discussions on international collaboration in the development of advanced nuclear energy systems known as Generation IV. The Generation-IV International Forum (GIF) grew from nine to 14 countries with the aim to organize and coordinate international collaboration on research and development of the fourth generation of nuclear energy systems. Building on over 17,000 reactor-year operating experience with current fleet, the Generation-IV nuclear plants will be based on better technologies capable of offering superior solutions for future energy production and environment protection challenges. The nuclear industry learned a hard lesson that in order to get a favorable public perception and approval by a financial sector, the GEN IV systems must be economically competitive with other sources of energy, while satisfactorily addressing safety, waste management and proliferation-resistance concerns. Because of these stringent requirements, Generation IV is bringing in new innovative technological solutions which should be accommodated within a regulatory and licensing framework developed over years to suit current technologies. This represents a substantial challenge on its own.

22.2 The regulatory status

The purpose of regulation is to direct individual or organizational behavior toward making positive impacts on solving societal and economic problems. Regulations consist of rules and norms adopted by government and backed up by some threat of consequences. Regulations are derived from a number of

institutional sources ranging from parliaments, legislatures, ministries to industrial standards development organizations, and self-regulating professional associations. Given such a variety, regulations can be described using different terms like legislation, statutes, rules, directives, standards, and so forth. While nuclear regulations address broad issues, the safety of the public and protection of the environment are the paramount imposed on any activity involving nuclear material and technology. Consequently, nuclear licensing is a process that ensures that the nuclear activity conforms to safety and environmental requirements set by regulations.

The International Atomic Energy Agency (IAEA) defines nuclear safety as “*The achievement of proper operating conditions, prevention of accidents and mitigation of accident consequences, resulting in protection of workers, the public and the environment from undue radiation risks*” (IAEA, 2019). A national nuclear regulatory body or nuclear safety authority are established by government to protect the public interest through the administration of national and international regulations with particular nuclear activity. Authorization and oversight of operation of nuclear facilities through a process of licensing is within the mandate of a national nuclear regulatory body.

The regulator has a unique role in technology research, development and its deployment and it appears that this role is unique by the virtue of regulatory concept. In the case of nuclear regulator, [Bajorek \(2019\)](#) attributes the origins of this tradition to the Atomic Energy Act of 1946 in the United States, which transferred control of nuclear technology from military to civilian control. The Act established the US Atomic Energy Commission (AEC) with the mandate to foster and control the peacetime development of atomic science. The Act, which created the AEC, transferred a number of national nuclear laboratories that were instrumental in the initial understanding of nuclear science and safety, from military to civilian control. A similar process was followed in the United Kingdom and in Canada. The Parliament of Canada established legislative control and federal jurisdiction over the development and use of nuclear energy and nuclear substances in 1946, and created the Atomic Energy Control Board (AECB) as a national regulatory body. Going back to the case of the United States, the Atomic Energy Act actually put the AEC in a conflicting position of ensuring safety to the public and the environment and at the same time promoting further development and commercial deployment of nuclear power industry. This dual role was subject to increasing criticism particularly during the expansion of the nuclear industry in the 1960s, so the US Congress split the AEC into two distinct bodies, the Energy Research and Development Administration (ERDA) and the US Nuclear Regulatory Commission (NRC). A number of years later, in 1977, the ERDA merged with several other agencies to create the US Department Of Energy (DOE).

22.3 Regulatory requirements

There is no common approach to nuclear regulation and licensing even for the current fleet of NPPs. The regulation and licensing practices vary from one country to another and they are based on each country’s legislation and their established practices. In principle, regulatory regimes span between two distinct approaches; prescriptive vs. performance or goal based regulations. Traditionally, the US approach is credited for establishing a set of detailed, prescriptive regulatory requirements the licensee must satisfy in order to be licensed to operate its nuclear facility. On the other side of the spectrum, the United Kingdom and Canada adopted a more flexible approach based on setting high-level safety targets; the licensees are required to demonstrate that they achieve the set targets or performance criteria. Even though these two approaches may appear to be on opposite extremes, even performance-based regulations contain a certain level of prescriptive requirements. In addition to national legislature, the International Conventions are legally binding for signing countries, and industry must comply with these as well. Some of the well-

known International Conventions, which apply to both, current fleet and future generations of NPPs include:

- Nuclear Liability Conventions, 1964–2017
- Non-Proliferation Treaty (UN, 1968)
- Convention on Assistance in the Case of a Nuclear Accident or Radiological Emergency (IAEA, 1986)
- Convention on Nuclear Safety (IAEA, 1994a)¹
- Joint Convention on the Safety of Spent Fuel Management and on the Safety of Radioactive Waste Management (IAEA, 1997)

At the international level, the IAEA is the most important organization in the development of international nuclear regulations and standards. The IAEA is the world's central intergovernmental forum for scientific and technical cooperation in the nuclear field. It works for the safe, secure and peaceful uses of nuclear science and technology, contributing to international peace and security and the United Nations' Sustainable Development Goals. The IAEA was created in 1957 in response to the deep fears and expectations generated by the discoveries and diverse uses of nuclear technology. The Agency's genesis was US President Eisenhower's "*Atoms for Peace*" address to the General Assembly of the United Nations on December 8, 1953. The US Ratification of the Statute by President Eisenhower, July 29, 1957, marks the official birth of the IAEA (IAEA, 2020). The current membership of IAEA stands at 171 countries. Even though, IAEA standards are not mandatory, member states are expected to use IAEA standards as a benchmark in developing their own national standards and regulations.

The Organization for Economic Co-operation and Development (OECD) is a unique forum where the governments of 35 democracies work together to address the economic, social and environmental challenges of globalization. The OECD European Nuclear Energy Agency (ENEA) was established in 1958 with the mission to assist its member countries with a safe, environmentally friendly and economical use of nuclear energy for peaceful purposes. The agency's name changed in 1972 to the Nuclear Energy Agency (NEA) when the member countries grew beyond Europe's boundaries. The NEA's current membership consists of 31 countries in Europe, North America, Asia and the Pacific region. The NEA launched a Multinational Design Evaluation Program (MDEP) in 2006 between 10 national regulators. Under international regulatory groups such as MDEP, the regulators and Technical Support Organizations (TSO) have the ability to share their review results and insights on several reactor designs openly. There is no direct decision process proposed but there is a lot of exchanges and cooperation between regulators allowing that any finding in one country is quickly shared among the regulator community. In fact, there are many possibilities to organize an "international" collaboration and feedback on safety assessment: stress tests conducted across several countries after Fukushima are a good example. Up until now, the MDEP goal is to first issue widely shared safety principles and then to eventually adapt them within national regulatory frames.

The World Nuclear Association (WNA) is an international body with a mission to promote a wider understanding of nuclear energy among key international influencers by producing authoritative information, developing common industry positions, and contributing to the energy debate. The current WNA membership consists of 186 companies from 43 countries, covering all aspects of the global nuclear industry, including major reactor vendors, nuclear utility companies (responsible for 70% of the world's nuclear energy production), uranium mining, conversion, enrichment and fuel fabrication companies, nuclear engineering, construction and waste management companies, TSO and R&D organizations. In January

¹ Convention on Nuclear Safety (1994)—This international convention, which was developed under the auspices of the IAEA, aim to legally commit participating States' operating land-based nuclear power plants to maintain a high level of safety by setting international benchmarks to which States would subscribe. The obligations of the Parties cover for instance, siting, design, construction, operation, the availability of adequate financial and human resources, the assessment and verification of safety, quality assurance and emergency preparedness.

2007, the WNA established the CoOperation in Reactor Design Evaluation and Licensing (CORDEL) Working Group. The aim of the CORDEL is to stimulate a dialogue between the nuclear industry (including reactor vendors, operators, and utilities) and nuclear regulators (national and international organizations) on the benefits and means of achieving a worldwide convergence of reactor safety standards for reactor designs (WNA, 2015).

The European Commission (EC) plays an important role in issuing directives related to safety at nuclear facilities (CEU, 2009; CEU, 2014) and the use of nuclear fuel and radioactive waste (CEU, 2011). The European Commission directives set the scope of the use of nuclear energy in the member countries. The European Commission also encourages the development of a harmonized licensing process for nuclear facilities at the EU level. The European Nuclear Regulators Group (ENSERG) was established in 2007 as an independent nuclear regulators body within the EC. In an attempt to develop a harmonized licensing process for nuclear facilities within EC, the European Nuclear Energy Forum (ENEF) created the European Reactor Design Approval (ERDA) group (ERDA, 2011). An international regulatory framework within Europe is under responsibility of the Western European Nuclear Regulator's Association (WENRA). The main objectives of the WENRA are, *"to develop a common approach to nuclear safety, to provide an independent capability to examine nuclear safety in member countries and to be a network of chief nuclear safety regulators in Europe examining experience and discussing significant safety issues"* (WENRA, 2009). Currently, WENRA has 17 member states and 9 neighboring European countries as observers. In 2014, WENRA revised its Reference Levels (WENRA, 2014) as the basis for the harmonization of national safety requirements for operating NPPs. Safety Objectives (WENRA, 2009) define the basis for the harmonization of national safety requirements for all new NPPs to be built in EC. WENRA regulations are not strictly legally binding, however, member countries agreed to implement these regulatory requirements into their national nuclear regulations.

EC launched, "European Industrial Initiative on sustainable nuclear energy" in 2010 with the key objective to, *"...enable the commercial deployment of Generation-IV FNRs from 2040, while in the meantime maintaining at least a 30% share of EU electricity from currently available reactors with an expansion towards the cogeneration of process heat for industrial applications when such markets develop..."* One of the Indicative Key Performance Indicators (KPIs) was to achieve demonstration of the safety and security credentials of the fast neutron reactors by obtaining a license to enable operation of the prototype and demonstrator reactors to start in 2020 (EC, 2020).

Established in 2005, ENISS is the European Nuclear Installations Safety Standards Initiative. It represents nuclear installation license holders from 16 European countries with nuclear power units, fuel reprocessing plants or large waste storage facilities. ENISS provides the nuclear industry with a platform to exchange information on national and European regulatory activities, to express its views and provide expert input on all aspects related to international safety standards. ENISS is the common channel through which European nuclear license holders interact with WENRA (nuclear regulators), the European Institutions and the IAEA. Although ENISS is hosted by FORATOM, it enjoys full autonomy about its strategy, priorities and decisions, which are discussed, reviewed and approved by its own governance bodies. Key mission of the ENISS is to develop common views and positions on the evolutions of the nuclear safety standards (ENISS, 2020).

Several European Utilities launched the EUR (European Utility Requirements) effort in December 1991. The main objective of the EUR organization is to produce a common set of utility requirements, endorsed by major European utilities for the next generation of Light Water Reactor (LWR) NPPs. In 1997, an effort was undertaken by the EUR organization to develop a document, which would become "Volume 3" of the EUR. The objectives of Volume 3 were to develop a description of the standard nuclear island designs; an assessment of design compliance with the EUR Volume 1 and 2 against these designs; and to define the requirements for the specific nuclear island designs (Borbey and Ingemarsson, 2004). The EUR document is

structured into four volumes: Volume 1 (Main policies and objectives) defines the major design objectives and presents the main policies that are implemented throughout the EUR document. Volume 2 (Generic nuclear island requirements) contains all the generic requirements and preferences of the EUR utilities for the nuclear island. Volume 3 (Application of EUR to specific designs) is divided into a number of subsets. Each subset is dedicated to a specific design that is of interest to the participating utilities. A subset includes a description of the design and an analysis of compliance vs. the generic requirements of Volume 2. Volume 4 (Power generation plant requirements) contains the generic requirements related to the power generation plant.

WENRA on the regulatory side, the European Nuclear Installation Safety Standards and European Utility Requirements on the industry side, have been working on harmonization requirements on the European level (Soderholm, 2013). International standardization of licensing as well as harmonization of regulatory requirements has been a goal of several programs, including those of CORDEL, MDEP, and ERDA (European Reactor Design Approval). The success with the harmonization of nuclear regulations on international level is so important that CORDEL has even looked at international aviation licensing (WNA, 2013) as a model to derive good practices.

22.4 Regulatory challenges for advanced reactors

Effective regulatory and licensing system is one of the key pillars in ensuring reactor safety as well as successful development and deployment of any advanced nuclear energy systems including Generation IV and Small Modular Reactors (SMRs). Like technology, the field of licensing and regulation kept evolving from the early days of nuclear power generated electricity. Three major reactor accidents (1979 Three Mile Island Unit 2, 1986 Chernobyl Unit 4, and 2011 Fukushima Daiichi Units 1, 2, 3, and 4) suggest that the current regulatory framework has not been completely successful in ensuring safe operation and accident management. The majority of Generation-IV or SMR concepts have roots that have been tried in some forms, whether as a demonstration or pilot plants, from the early days of nuclear power. The first nuclear generated electricity came from a liquid metal-cooled reactor (US Experimental Breeder Reactor EBR-1), which began, albeit for a short period, producing electricity far back in 1951. Gas-cooled reactors are still in operation in the United Kingdom, while molten salt and supercritical water reactors were extensively tested at various scales in laboratories across the world. Arguably, water-reactor technology for nuclear submarines and its successful replication at Shippingport Atomic Power Station eventually led to widespread commercial deployment of light and heavy Water Cooled Reactors (WCRs). Other technologies remain the subject of research and deployment (Riznic and Duffey, 2017; Magwood and Paillere, 2018).

In the early days of development of large nuclear reactors, the US Atomic Energy Commission (AEC) established a range of rules and guidance for designing, sitting, constructing and operating the first commercial nuclear reactors. Even today, many of the US NRC's and OECD member countries' current nuclear regulations and licensing practices are based on those that the AEC developed in the early 1960s. Even though current fleet of NPPs is dominated by light and to the smaller extent heavy WCRs, the early development of commercial nuclear power included consideration of many technologies and designs. Early development of nuclear regulations in the United States, France, and the United Kingdom consider non-water cooled reactors to reflect the specific fuel forms, coolants and moderators as well as operating conditions associated with gas-cooled and liquid-metal cooled reactors. For example, a pressure-venting containment design was approved for the Fort St. Vrain High-Temperature Gas-cooled Reactor (HTGR). The Fort St. Vrain was licensed by the US Atomic Energy Commission and in operation from 1979 to 1989. The reactor was shut down for economic rather than safety concerns. On the other side, all water-cooled reactors were licensed on premise of use of pressure retaining and pressure-suppression containment design.

Building on the existing experience US Department of Energy, Office of Nuclear Energy, and the US Nuclear Regulatory Commission (NRC), Office of New Reactors in 2013 established a joint initiative to develop a licensing framework for advanced non-light water reactor technologies (Kelly, 2014). The key aspect of this initiative was to address the General Design Criteria (GDC) for licensing advanced reactor designs. In December 2014, the DOE national laboratories team issued the technical report “*Guidance for Developing Principal Design Criteria for Advanced (Non Light-Water) Reactors*” (INL, 2014). The report offers Advance Reactors Design Criteria applicable to most advanced concepts and technologies specific criteria for Sodium Fast Reactor and modular High-Temperature Gas Reactors for consideration by US NRC in developing regulatory guidance. In 2018, the US Nuclear Regulatory Commission issued a Regulatory Guide 1.232, Revision 0. This regulatory guide proposes guidance on how the General Design Criteria (GDC) in Appendix A, “*General Design Criteria for Nuclear Power Plants*” of Title 10 of the Code of Federal Regulations (10 CFR) Part 50, “*Domestic Licensing of Production and Utilization Facilities*” may be adapted for non-light-water reactor (non-LWR) designs. Reactor designers, applicants, and licensees are to develop Principal Design Criteria (PDC) for any non-LWR designs, as required by the applicable NRC regulations for NPPs, and may use this guidance. The RG also describes the NRC’s proposed guidance for modifying and supplementing the GDC to develop PDC that address two specific non-LWR design concepts: Sodium-cooled Fast Reactors (SFRs), and Modular High-Temperature Gas-cooled Reactors (MHTGRs) (USNRC, 2018).

In September 2018, the Nuclear Energy Institute submitted their Draft Revision N of guidance on proposed process for the efficient licensing of advanced non-light water reactors. The guidance came as a result of industry led and US DOE cost shared, a Licensing Modernization Project (LMP). Revision 1 of the guidance was issued later in 2019, as NEI Technical Report NEI 18-04 (NEI, 2019) to address feedback received from US NRC and lessons learned during the use of draft guidance on several pilot applications by reactor vendors and developers. The NEI 18-04 lays down a foundation for establishing licensing technical requirements to facilitate risk-informed and performance-based design and licensing of advanced non-light water reactors. The proposed licensing process builds on achievable safety enhancements with advanced designs innovations and current state of knowledge of nuclear technology, creating an opportunity for reduced regulatory complexity. Shortly after NEI proposed guidance, US NRC issued a draft regulatory guide DG-1353 with guidance for a technology-inclusive, risk-informed, and performance-based methodology to inform the licensing basis and content of applications for licensing, certifications, and approvals for non-light water reactors (NRC, 2019). This regulatory guide endorses NEI 18-04 as one acceptable method for non-light water reactor designers to use when applying for permits, licenses, certifications and regulatory approvals, under 10 CFR Part 50 (CFR, a, n.d.) and Part 52 (CFR, b, n.d.). The DG-1353 was issued as RG 1.233 in June 2020 (NRC, 2020) to provide guidance about the licensing basis and determining an appropriate level of information for parts of safety analysis reports for advanced non-light water reactors, including, but not limited to, molten salt reactors, HTGRs, and a variety of fast reactors at different thermal capacities.

Other countries were also proactive in preparation for the forthcoming requests by industry about nuclear regulations and licensing process to be applied for advance reactors. For example, the Canadian Nuclear Safety Commission (CNSC) issued a number of regulatory documents discussing advanced reactors. REGDOC-2.5.2, *Design of Reactor Facilities: Nuclear Power Plants* sets out the CNSC’s requirements and guidance for the design of new water-cooled NPPs. Regulatory document REGDOC-1.1.5, *Supplemental Information for Small Modular Reactor Proponents*, provides information in addition to three other CNSC Regulatory Documents (REGDOC-1.1.1, RD/GD 369, and REGDOC-1.1.3). REGDOC-1.1.5 is a new regulatory document and meant to be used in conjunction with these three other documents, which set out requirements and guidance for an applicant to consider prior to submitting a license application to the CNSC for a SMR. REGDOC-1.1.5 also identifies the CNSC’s considerations in assessing the adequacy of a license application (CNSC, 2011, 2012, 2014, 2018a, b).

22.5 Case study-Canadian perspectives on the design of Pressure Retaining Systems and Components (PRSCs) in small modular reactors

The IAEA defines “small” as a reactor under 300 MW electrical (MW_e) (IAEA, 2016b), and up to about 700 MW_e as “medium”—including many operational reactors from the 20th century.

Currently developed SMRs can be categorized according to the following types of cooling mediums (IAEA, 2016b):

- Water-cooled (e.g., using light water) SMRs;
- Gas-cooled (e.g., using helium) SMRs;
- Liquid metal (e.g., using sodium or lead) cooled SMRs; and
- Molten salt (e.g., using fluoride based salt) cooled SMRs.

In CNSC REGULATORY DOCUMENT, REGDOC-3.6 (CNSC, 2019), a small reactor facility is defined as a reactor facility containing a reactor with a power level of less than approximately 200 MW thermal (MW_{th}) that is used for research, isotope production, steam generation, electricity production, or other applications. The CNSC has been reviewing several different types of SMRs (e.g., water-cooled, gas-cooled, liquid metal, and molten salt SMRs) in accordance with the VDR process described in CNSC Regulatory Document, REGDOC-3.5.4, on Pre-Licensing Review of a Vendor’s Reactor Design (CNSC, 2018a, b).

The Vendor Design Review (VDR) is an optional service provided by the CNSC in order to identify and resolve potential regulatory or technical issues in the early stages of the design process. The objective of a prelicensing review is to increase regulatory certainty while ensuring public safety. However, this service does not certify a reactor design, and does not involve the issuance of a license under the Nuclear Safety and Control Act (NSCA).

CNSC Regulatory Document, REGDOC-3.5.4, provides three phases for the VDR process. The required details and the review scrutiny are incrementally intensified from one phase to the next as follows:

- Phase 1 Review—Compliance with regulatory requirements: CNSC staff assess the information submitted in support of the vendor’s design and determine if, at a general level, the design intent complies with CNSC design requirements (for new NPPs as specified in CNSC REGULATORY DOCUMENT, REGDOC-2.5.2 (CNSC, 2014a), and related regulatory requirements.
- Phase 2 Review—Prelicensing assessment: This phase goes into further detail, with a focus on identifying potential fundamental barriers to the licensing of the vendor’s design for a NPP or small reactor in Canada.
- Phase 3 Review—Preconstruction follow-up: In this phase, the vendor can choose to follow-up on one or more Focus Areas (FAs) covered in Phase 1 and 2 against CNSC requirements pertaining to a license to construct. For those areas, the vendors’ anticipated goal is to avoid a detailed revisit by CNSC during the review of the construction license application.

Phase 1 and 2 reviews have 19 review FAs, representing key areas of importance for a future construction license, while the Phase 3 review is tailored on a case-by-case basis. Nineteen FAs are reviewed during Phases 1 and 2 of a design review and include topics of significant safety importance; enabling the vendor early in the design process to address any identified issues. This section discusses a review framework for the following five FAs for the VDR of Pressure Retaining Systems and Components (PRSCs) in the SMRs:

- Focus Area (FA) #1—General Plant Description, Defense in Depth, Safety Goals and Objectives, Dose Acceptance Criteria: To determine, with reasonable confidence, whether the provisions made in the design are meeting CNSC expectations and regulatory requirements. This Defense in Depth (DiD) is one of the safety concepts that should be implemented in the design.

- Focus Area (FA) #2—Classification of Structures, Systems, and Components (SSCs): To determine, with reasonable confidence, whether the provisions made in the design, as it is evolving, are meeting the CNSC expectations and regulatory requirements as they pertain to safety classification of SSCs and requirements for other specific classifications [e.g., seismic and Environmental Qualification (EQ)].
- Focus Area (FA) #10—Safety Analysis: To confirm that the design, as it is evolving, is meeting CNSC expectations for Probabilistic Safety Assessment (PSA) and Deterministic Safety Analysis (DSA). This case study will focus on three aspects [i.e., Postulated Initiating Events (PIEs), plant states, and quantitative safety goals] that can be evaluated through PSA. Design input (e.g., temperature and pressure) at each service loading condition for PRSC in the SMRs will be determined based on these aspects.
- Focus Area (FA) #11—Pressure Boundary Design: To confirm that the vendor understands CNSC expectations and regulatory requirements as they pertain to the pressure boundary design. In Canada, the Canadian Standards Association (CSA) N285.0-12 (CSA, 2012) provides the design rules of the PRSC of a nuclear or non-nuclear system.
- Focus Area (FA) #16—Vendor Research and Development Program: To assess the vendor’s overall Research and Development (R&D) program in terms of, (1) *overall program scope and depth (particularly in areas of novel design)*; (2) *how well the program will support the design’s safety case, should it be selected for construction by a license applicant*; (3) *whether design gaps will be resolved in a timely manner, in order to meet regulatory requirements, should the design be selected for construction (e.g., clarify “gray” design areas, decrease uncertainties)*; and (4) *how continuing R&D efforts would support licensees, once the design is built and is being operated*. The R&D program should be updated by consideration of previous operating experience and inspection results.

22.5.1 Review framework for FA #1 on defense-in-depth

Sections 4.3 and 6.1 of REGDOC-2.5.2 (CNSC, 2014a) state that two safety concepts are required to be applied to the design: One is operational limits and conditions; the other is defense-in-depth.

22.5.1.1 Operational limits and conditions

The purpose of operational limits and conditions is to ensure that plants operate in accordance with design assumptions and intent (parameters and components), and include the limits within which the facility has been shown to be safe. Therefore, the operation history of SSCs must be recorded and tracked by monitoring systems (e.g., thermal/pressure transient monitoring system or vibration monitoring system, etc.) over the entire operating life of SSCs.

The purpose of the DiD is to ensure that the design is subject to overlapping provisions and demonstrate the provision of a series of physical barriers to confine radioactive material at a specific location. In order to do that, REGDOC-2.5.2 states that the design shall provide five levels of defense. For instance, implementation of a leak detection system is considered to satisfy Level 2 DiD for control of abnormal operation and detection of failures. In addition, the DiD Level 3 (CNSC, 2014a) is divided into the following sublevels 3a and 3b (IAEA, 2016a):

- Level 3a: The objective is to control the postulated accidents (Class 1 and Class 2) arising from single initiating events and their consequential effects in order to limit the releases of radioactive materials.
- Level 3b: The objective is to control Design Extension Conditions (DECs).

Therefore, a refined Level 3 approach (i.e., Level 3a and Level 3b) would effectively demonstrate the DiD under DECs.

22.5.1.2 *Defense-in-depth*

In accordance with Section 4.3 of REGDOC-2.5.2, the purpose of the defense-in-depth is to ensure that the design is subject to overlapping provisions and demonstrate the provision of a series of physical barriers to confine radioactive material at a specific location. In addition, the design requirements in Sections 6.1 and 7.7 of REGDOC-2.5.2 are provided to satisfy the intent of the DiD that the design of PRSCs should incorporate provisions to detect leaks at an early stage in order to minimize the release of radioactive cooling medium in a PRSC in accordance with Section 4.3 of REGDOC-2.5.2. In general, the following seven elements should be incorporated in the design of the PRSC to ensure a safe reactor shutdown in a timely manner and to mitigate the consequence of SSC failure in accordance with the design requirements in REGDOC-2.5.2:

- Element #1: Leak detection;
 - Capability, sensitivity, and reliability of leak detection systems;
 - Response time from initial leak to leak detection of each leak detection system to remedy the leakage in a timely manner; and
 - Test plan to verify the capacity and sensitivity of each leak detection system.
- Element #2: Aging Management Plan (AMP);
- Element #3: Materials;
- Element #4: Leak rate;
- Element #5: Loadings;
- Element #6: Engineering assessment (i.e., LBB assessment); and
- Element #7: Redundancy, diversity, and separation philosophy.

The six elements (i.e., Element #1 to Element #6) are key components used in a Leak Before Break (LBB) analysis. The application of LBB concept is used to ensure a safe reactor shutdown in a timely manner following leak detection and to minimize the consequence of PRSC failure (i.e., minimizing the release of radioactive material). Hence, LBB is considered to be Level 2/3 DiD approach. On the other hand, the application of redundancy, diversity, and separation philosophy into the layout of SSCs is used to mitigate the consequence of PRSC failure. Therefore, the Element #7 is considered as Level 3 DiD approach.

LBB concept was originally proposed and developed to eliminate a pipe whip support in the United States. The main driving force for applying the LBB concept in the design of PRSCs is to determine/verify operational leak rate and shutdown leak rate with some margins (GIF, 2016) because it is expected that there would be a certain level of background leak over an entire operating period in new Generation-IV reactors including SMRs. In general, the leak contains radioactive material, and it must be tightly controlled to meet the requirements associated with nuclear safety and health and safety.

22.5.1.3 *Element #1: Leak detection system*

The OPEX of several different types of reactors (e.g., CANDU, PWR, BWR, SFR, and MHTGRs) indicates that a certain level of background leak inside a reactor building is captured and monitored. The background leak level depends on the design features and the maintenance level of mechanical components. However, maintaining zero leaks over the entire operating conditions are extremely challenging. Therefore, the gradual/sharp increment of the background leak rate monitored over a certain operating period would lead to a leak search activity and a reactor shutdown. Hence, the implementation of a reliable leak detection system with sufficient capability to monitor the background leak and with sufficient sensitivity to capture the variation of the background is a fundamental design requirement to ensure a reactor shutdown in a timely manner following leak detection.

22.5.1.4 Element #2: Aging Management Plan (AMP)

The leak from a sealing device on PRSC and a Through Wall Crack (TWC) on PRSC would be the major sources of leak, and would further increase with operation time (i.e., increasing the background leak level with operation time). The failure of a sealing device and the development of TWC are driven by degradation mechanism and stress level at a leak location. For instance, in order to achieve very small leakage or no leakage over various reactor-operating conditions, a seal device on SSCs penetrating the reactor vessel and a containment boundary is a key component. Maintaining very small leakage at elevated temperature over the entire operating conditions may be practically very challenging. In particular, the failure of sealing bellows due to high cycle fatigue resulting from the flow through the valve could lead to consequential leakage even though the valve has operated only infrequently. This type of seal failure has been reported for some isolation valves installed in CANDU type reactors. In particular, an excessive leakage of some SMRs using liquid metals (e.g., sodium, lead) as a cooling medium could result in undesirable consequences (e.g., fire, explosion, and air contamination). Hence, actual leak tests or periodic pressure tests may be required to verify the integrity of the sealing devices. As a contingency plan for excessive leak due to failure of sealing device integrity, the following elements need to be discussed:

- Effect of excessive leakage to containment and environment on health and safety (e.g., fire, explosion, air contamination, reactor shutdown);
- Operating procedure to shut down a plant depending on a detected leak rate; and
- Capability, sensitivity, diversity, redundancy, and reliability of leak detection systems.

In particular, active/plausible degradation mechanisms and damage modes for SMRs operating at the elevated temperatures are quite different with those for conventional reactors operating below 370°C. For instance, thermal embrittlement and creep would accelerate the material degradation rate (e.g., reduce material ductility with operating time) for SSC operating at the elevated temperature. Therefore, the identification of active/plausible degradation mechanisms is an essential element to evaluate a leak rate and to determine the scope of Aging Management Program (AMP). The AMP is the set of engineering, operational, inspection and maintenance actions that control, within acceptable limits, the effects of physical aging and obsolescence of SSCs that occur over time or with use. Hence, the AMP for PRSC must be initiated at the design stage to determine a design life of PRSC and to evaluate the leak rate accordingly. The AMP must be updated based on OPEX and ISI results for the effectiveness of this program. Application of a Failure Modes and Effects Analysis (FMEA) is one way to identify and address the following aspects that must be included in the AMP: (1) typical/plausible degradation mechanisms; (2) failure location; (3) failure mode; (4) failure effect; (5) detection method; (6) mitigation task; and (7) governing parameters leading to a given degradation.

22.5.1.5 Element #3: Materials

Material properties (e.g., yield strength, ultimate strength, and fracture toughness) are used to determine: (1) leak rate; (2) crack growth rate, and (3) crack stability. In particular, material properties under the elevated temperature and high radiation change with operation time (i.e., time limited degradation mechanism). The effects material degradation on LBB concept is crucial to ensuring a reactor safe shutdown in a timely manner over the entire design intended life. In addition, the consideration of material degradation is an essential element to determine a design life of PRSC in SMRs.

22.5.1.6 Element #4: Leak rate

The leak rate is a function of: (1) material properties; (2) crack morphology; (3) a crack shape; and (4) magnitude of loads subjecting to a given crack together with, (5) coolant condition. A leak rate calculation, as the part of LBB concept, could predict the amount of coolant leak for a given crack size to appropriately

design safety systems (e.g., the size of rupture disc, the capacity of fire extinguishers, and fire wall) to mitigate the consequence of a coolant leak and ensure the capability and sensitivity of leak detection systems.

22.5.1.7 Element #5: Loadings

There is a very low possibility of a sudden pipe rupture in the primary coolant system and in the intermediate piping system for some SMRs operating with low operating pressure. However, a rupture or leak due to progressive crack growth cannot be completely ruled out because of the failure modes (e.g., creep rupture, creep-fatigue failure, buckling) at elevated temperatures. In addition, SSCs in SMRs may be more frequently subject to the non-design basis loading conditions, not considered in the design stage, due to the complex configuration of reactor internal structure and uncertainties in PIEs which are input for determining transient conditions at each service loading condition. In particular, it is important to set out load combination criteria and acceptance criteria for non-design basis loads with other loads in order to: (1) evaluate the structural integrity of the important to safety systems subjecting to non-design basis loading conditions; and (2) use combined loads to an analysis (e.g., design analysis, LBB assessment) for a) determining the design life of SSCs and evaluating time interval from leak detection to PRSC failure. In addition, the consideration of the non-design basis loading conditions would be a key to determine remaining operating life of PRSC in SMRs [i.e., Fitness-For-Service (FFS)]. Hence, the operational history important to safety systems must be recorded and tracked by monitoring systems (e.g., thermal/pressure transient monitoring system, vibration monitoring system, chemistry monitoring system in coolant, etc.) over the entire operating life. The operating history captured by the monitoring systems can be used to: (1) confirm that the important to safety systems operate within transient limits provided in design specification; and (2) evaluate the remaining operating life of systems important to safety when operating history indicates that they operate beyond design transient limits (e.g., operate at a non-design basis loading condition).

22.5.1.8 Element #6: Analysis

Three different types of failure modes could be used in the LBB analysis: First, one is a Linear Elastic Fracture Mechanics approach, second one is Elastic Plastic Fracture Mechanics approach, and the third one is plastic collapse approach. Several parameters (e.g., the detection limit of leak detection systems, material properties, a crack growth rate for a given degradation mechanism, initial crack size based on a detection limit of inspection tool, leak rate, loads) are used in the analysis. The purpose of LBB analysis is to demonstrate that there is a sufficient time interval from a postulated crack assumed in the analysis until it grows to a critical crack size that result in a sudden rupture of PRSC. Generally, a safety factor is applied to several input parameters (e.g., capability of leak detection system and loads) to accommodate uncertainties in the LBB assessment. However, deterministic LBB is not applicable for active/plausible degradation mechanisms without identified mitigation or preventive strategies. Furthermore, the LBB assessment could be used to determine the operational and shutdown leak rate limits for SMRs. However, the low operating pressure and the use of a liquid metal cooling medium whose freezing temperature is higher than the ambient temperature (e.g., 21°C) make it difficult for detecting a leak in a timely manner. Hence, capability and sensitivity of leak detection systems and a leak rate estimating software are essential parts of a LBB analysis in determining the operational and shutdown leak rate limits. Currently, international collaboration on the LBB is being pursued in the form of a benchmark study (e.g., OECD/NEA program). The objective of the benchmark is to compare the leak rate computation practices along the limitations of tools and software used. In this international collaboration, a benchmark on leak rate calculation will be conducted based on new experimental data relevant for the threshold of leak detection systems. The benchmark result could reveal the state of the art leak rate prediction based on a comparison of different approaches, and could be used to evaluate leak rate in a given SMR.

22.5.1.9 Element #7: Redundancy, diversity, and separation philosophy

Incorporation of this philosophy into the layout of the High Energy Lines (HELs) and Safety Critical Targets (SCTs) is essential to mitigate the consequential damage associated with the postulated failure. The SCTs consist of several systems that are required to reactor shutdown and fuel cooling. For instance, active systems (e.g., valve), Instrumentation and Control (I&C) equipment (e.g., instrument panel, conduit, cables) and instrument lines are considered as the SCTs. The purpose of the implementation of this philosophy into the layout/location is to ensure the safe shutdown of SMRs following the event of a failure (e.g., guillotine break). The possibility of cascading failures like a pipe whip under the low operating pressure can be ruled out, but a rupture or leak due to progressive crack growth cannot be completely ruled out because of the possible existence of several failure modes (e.g., creep rupture, creep buckling, high/low cycle fatigue in conjunction with creep fatigue) at the elevated temperature. Therefore, the following two elements need to be discussed:

- Definition of HELs: The applicability of current definition of the HELs originally developed for water-cooled reactor.
- Consequence of a pipe failure: The layout of SCTs should be determined to mitigate the consequential damage of the SCT failure due to a pipe failure. For instance, the partitioning or the housing of cable trays and building steel structure against fire would be a good design practice to minimize/mitigate the consequential damage.

For instance, in the CANDU 6 reactor, SCTs are considered to include any portion(s) of:

1. Four special safety systems, i.e., (a) Shut Down System (SDS) SDS1, (b) SDS2, (c) Negative Pressure Containment (NPC), and (d) Emergency Core Injection System (ECIS);
2. Two safety support systems (i.e., a) high-pressure service water system, and b) emergency water supply system);
3. Fueling machine equipment; or
4. EQ equipment located inside the reactor building.

Electrical systems (e.g., cable tray, conduit, and electric panel) and active components belonging to the aforementioned safety systems were included in the SCTs. However, operating conditions and safety systems proposed for most of SMRs are quite different from those for the CANDU type reactors. Furthermore, SCTs in SMRs would be located in a compact space such that the implementation of separation philosophy would be challenging. Hence, this section proposes to apply the following feedback design process and adequately implement a redundancy, diversity, and separation philosophy into the layout and location of PRSCs, important to safety systems, and SCTs at the early design stage:

- Step 1: Identify plausible degradation mechanisms that could lead to the SCT failure;
- Step 2: Identify all plausible failure locations (e.g., all weld points, valves) by the consideration of all plausible degradation mechanisms;
- Step 3: Categorize SCTs by the consideration of safety features that will be used for reactor shutdown and fuel cooling, and containment integrity;
- Step 4: Conduct assessments in order to identify the consequential damage (e.g., pipe break, fire, explosion, air contamination) at each plausible break location by the consideration of: (1) the layout of PRSCs and (2) the location of important to safety systems and SCTs. In addition, the effects of the consequential damage assessed in this step should be covered/enveloped by events in a safety analysis report;
- Step 5: Address methods to detect/prevent/mitigate/confine consequential damage (e.g., pipe whip restraint, extinguisher, physical barrier, leak detection systems, AMP);

- Step 6: Update the layout of the PRSCs and the location of important to safety systems and SCTs or update methods to detect/prevent/mitigate/confine consequential damage on the basis of Step 4 and Step 5; and
- Step 7: As DiD, a deterministic LBB or probabilistic LBB could be used to demonstrate the low failure probability of important to safety systems.

In summary, based on the OPEX of several different types of reactors (e.g., CANDU, PWR, BWR, SFR, MHTGRs), maintaining zero leaks over the entire operating conditions are extremely challenging for new Generation-IV reactors including SMRs. Therefore, it is expected that advanced reactors would be subject to the variation of background leak rate during an operating period due to several reasons (e.g., the degradation of sealing device, crack). The excessive release of radioactive material due to leaks would affect nuclear safety. Hence, the application of the following DiD approaches are reasonable design practices that need to be discussed at the early design stage of SMRs:

- LBB concept using Element #1 to Element #6 in order to ensure the reactor shutdown in a timely manner following leak detection for the purpose of minimizing the consequence of PRSC failure; and
- Redundancy, diversity, and separation philosophy (i.e., Element #7) into the layout of SSCs for the purpose of mitigate the consequence of PRSC failure.

In addition, Section 7.7 of CNSC REGDOC-2.5.2 states that, “*If a full inspection is not achievable, then it shall be augmented by indirect methods such as a program of surveillance of reference components. Leak detection is an acceptable method when the SSC is leak-before-break qualified.*” Therefore, the level of depth for the application of the aforementioned two DiD approaches needs to be determined by considering the following aspects:

- Effect of excessive leakage to containment and environment on health and safety (e.g., fire, explosion, air contamination);
- Operating conditions (e.g., operating temperature and pressure);
- Capability, sensitivity, and reliability of leak detection systems;
- A energy level of a broken pipe (i.e., whether a broken pipe has sufficient energy to damage the SCTs (i.e., the level of dynamic effect) that will be used for reactor shutdown, fuel cooling, and the integrity of containment structure;
- The lay-out of the SCTs and the PRSCs;
- Types of plausible/susceptible degradation mechanisms (i.e., whether a degradation mechanism is manageable);
- Accessibility for inspection; and
- Reparability.

22.5.2 Review framework for FA #2 on classification of systems, structures and components

22.5.2.1 Code classification requirements

Classification is a fundamental design basis for a system (process system or special safety system) and is dependent on the different levels of importance associated with the function (e.g., transporting heat from nuclear fuel, forming the containment boundary) or consequence of failure of pressure-retaining sections of a system as it relates to the safe operation of the NPP. Approval of the code classification for PRSC must be obtained from the CNSC. CSA N285.0-12 (CSA, 2012) provides general requirements to specify the code

classification of SSCs as Classes 1, 1C, 2, 2C, 3, 3C, 4, and 6. For example, the rules for the classification of process systems and their supports are based on the following parameters:

- Failure causes Loss Of Coolant Accident (LOCA),
- Containment boundary is penetrated,
- Concentration level of radionuclides in the process fluid or the dose consequence if the fluid were released; and
- Nominal Pipe Size (NPS).

However, these rules were developed based on the experience gained from existing CANDU reactor designs. As well, the rules for classification given in CSA N285.0-12 should not be considered relevant unless:

- The facility has a defined exclusion zone,
- Access to the facility is controlled, permitting entry only by authorized personnel; and
- The reactor is inside a containment structure that is capable of limiting releases to the environment in the event of the failure of a pressure-retaining component.

The American Society of Mechanical Engineers (ASME) Section III Division 5 (ASME, 2020) introduces new Code Classes A and B for high-temperature reactor components that are not considered in the present CSA N285.0-12. Therefore, since the existing rules for code classification in N285.0-12 may not be applicable for SMRs, further development of relevant CSA Standards and discussions with the CNSC are needed.

22.5.3 Review framework for FA #10 on safety analysis

22.5.3.1 Accident prevention and plant safety characteristics

As per Section 6.3 in REGDOC-2.5.2 (CNSC, 2014a), *The design shall apply the principles of defense in depth to minimize sensitivity to PIEs. Following a PIE, the plant is rendered safe by: 1. inherent safety features, 2. passive safety features, 3. specified procedural actions, 4. action of control systems, 5. action of safety systems, and 6. action of complementary design features.* In particular, passive safety systems are extensively used in most SMRs because of their advantages (e.g., simplicity and reliability). However, the following detractions of the passive safety systems should be discussed (IAEA, 1994b):

- Lack of data on important phenomena;
- Need to understand performance in a wide range of conditions; and
- Testability of passive safety system to verify its intended function.

22.5.3.2 Postulated Initiating Events (PIEs)

Assumptions and engineering judgment concerning the operating information (e.g., transient history of pressure and temperature, and type of load, etc.) in each state is essential for the design of PRSC. Thus, Section 7.4 in REGDOC-2.5.2 (CNSC, 2018a, b) states that, *“The design for the Nuclear Power Plant (NPP) shall apply a systematic approach to identifying a comprehensive set of postulated initiating events, such that all foreseeable events with the potential for serious consequences or with a significant frequency of occurrence are anticipated and considered.”* Engineering judgment, deterministic assessment (CNSC, 2014b) and probabilistic assessment (CNSC, 2014c) are used to cover all foreseeable events with the potential of serious consequences or with a significant frequency of occurrence. In general, the PIEs are determined by the consideration of several aspects such as all internal and external events, all normal operating configurations, various plant and site conditions, and failure in other plant systems (e.g., storage for irradiated fuel and tanks for radioactive substances).

The PIEs can lead to an Anticipated Operational Occurrence (AOO), a Design-Basis Accident (DBA), or a Beyond-Design-Basis Accident (BDBA), and include credible failures or malfunctions of SSCs, as well as operator errors, common-cause due to internal hazards, and external hazards. In addition, uncertainty in material behavior also poses a challenge for classification of initiating events.

22.5.3.3 Plant states

As per Sections 4 and 7 in REGDOC-2.5.2, *SSCs are designed / operated in a manner that will protect individuals, society and the environment during operation and or during an accident.* In order to do that, the safety analysis should examine the plant performance during different plant conditions (i.e., a comprehensive set of PIEs), namely (1) *normal operation*, (2) *AOOs include all events with frequencies of occurrence equal to or greater than 10^{-2} per reactor year*, (3) *DBAs include all events with frequencies of occurrence equal to or greater than 10^{-5} per reactor year but less than 10^{-2} per reactor year. This class of events also includes any events that are used as a design basis for a safety system, regardless of whether the estimated frequencies are less than 10^{-5} per reactor year*, and (4) *BDBAs include events with frequencies of occurrence less than 10^{-5} per reactor year* (CNSC, 2014a; CNSC, 2014b). In particular, DEC are a subset of *BDBAs*, and are considered in the design process of the facility. Thus, design requirements [e.g., ASME Section III Level D requirement or other requirements (ASME, 2020)] for structural integrity of SSC important to safety under the DEC should be discussed in order to keep releases of radioactive material within acceptable limits.

22.5.3.4 Quantitative application of the safety goals and PSA

As per Section 4.2.2 in REGDOC-2.5.2 (CNSC, 2014a), *quantitative safety goals have been established.* The three quantitative safety goals are: (1) core damage frequency, (2) small release frequency, and (3) large release frequency. However, certain types of SMR use liquid fuel. In these cases, definition of core melting, which has been used to define Core Damage in Probabilistic Safety Analysis (PSA), should be revisited.

In addition, failure probability of passive components is generally provided as an input for the PSA in a form of initiating event. Certain types of SMRs use a non-conventional form of fuel (e.g., molten salt fuel, thorium) along with elevated operating temperatures. The determination of failure rates of novel materials, SSCs exposed to high temperatures and neutron fluxes and passive components in some SMRs is challenging. These failure rates are inputs into PSAs.

22.5.4 Review framework for FA #11 on pressure boundary design

The purpose of FA#11 on pressure boundary design is to ensure the structural integrity of PRSC over their design intended operating life. This section proposes to consider the following areas: (i.e., (1) design rules and limitations; (2) pressure boundary program and CSA Standards; (3) non-design basis loading condition; (4) Helical Coil Steam Generator (HCSG); (5) PFM; (6) aging and wear; and (7) in-service testing, maintenance, repair, inspection and monitoring) at the early design stage of SMRs.

22.5.4.1 Design rules and limitations

As per Section 7.5 in REGDOC-2.5.2, the design authority shall specify the engineering design rules for all SSCs. These rules shall comply with appropriately accepted engineering practices. Development and application of design rules of metallic and non-metallic mechanical components operated at elevated temperatures under high radiation is challenging. Current codes and standards cover materials that will be used at elevated temperatures; however PRSC of SMRs that operate under very high temperatures are not fully accommodated by the current provisions of the ASME Code. Several types of metallic and non-metallic materials (e.g., low alloy steel, nickel basis alloy, graphite, ceramic, etc.) have been proposed for use in SMRs. In particular, the design of the PRSC is challenging, as there is insufficient OPEX of a SMR operating

under severe environments for the PRSC over its design life. Thus, determination of safety factors and acceptance criteria in the design code for metallic and non-metallic components is important to accommodate uncertainties (e.g., material imperfection, unknown degradation mechanisms, deterioration rate of PRSC due to degradation mechanisms, etc.). The current CSA N285.0-12 provides design rules of the PRSC of nuclear or non-nuclear systems based on technical requirements in ASME Section III Division 1 for water-cooled type of reactors, but not as per ASME Section III Division 5 for high-temperature reactors. Hence, the current version of CSA N285.0-12 Standard does not cover the design of the SMRs that will be operating at elevated temperatures (i.e., over 370°C). A high-level concern on the design of PRSC operated at elevated temperatures is ensuring design margins. The design margins in ASME Sec. III Div.1 have been established based on several tests and OPEX, but those in ASME Sec. III Div.5 have not been fully verified for long-term operation because of insufficient SMR OPEX and limited knowledge in material behavior at elevated operating temperatures combined with radiation conditions. Thus, a gap analysis is recommended to identify gaps between design requirements, which have been used for new design for conventional types of reactors as per the codes and standards, and design features of new SMRs. A transition plan needs to be submitted, approved, and implemented if gaps are identified.

22.5.4.2 Seismic classification, category, and qualification

As per Section 7.13 in REGDOC-2.5.2, *SSCs important to safety should be seismically classified and qualified accordingly*. Consistent with Canadian Seismic Standard, CSA N289.1-18 (Standards, 2019), SSC in a SMR shall be designed and constructed to ensure that the effects of an earthquake do not lead to unacceptable radiation exposure. Seismic classification is a necessary design activity for those SSCs that are required to cool the fuel and remove decay heat.

The following two seismic categories are used to identify the extent to which SSCs shall remain operational during and/or after an earthquake:

- Seismic Category A: SSCs shall maintain their structural integrity and shall retain their pressure boundary integrity during and/or following an earthquake; and
- Seismic Category B: SSCs shall maintain their structural integrity and detailed functional requirements during and/or following an earthquake. Category B SSCs shall also retain their pressure boundary integrity, where applicable.

The seismic qualification is a verification process through testing, analysis, or other methods, of the ability of a structure, system, or component to perform its intended function (i.e., reactor safe shutdown and fuel cooling) during and/or following the designated earthquake [e.g., Design Basis Earthquake (DBE)]. The seismic qualification of all PRSC shall meet the requirements of Canadian national or equivalent standards. The design should include instrumentation for monitoring seismic activity at the site for the life of the plant.

New technology (e.g., special feature of vibration isolator) was proposed for a certain SMR to reduce the level of seismic induced loadings to PRSC. The design of the seismic isolation device should be investigated as part of PRSC design. Most SMRs could be located underground and without a real containment, and a soil structure interaction analysis is required to estimate the seismic loads for the design of the PRSC.

22.5.4.3 Pressure boundary program and CSA standards

Under the current operating license condition for a power reactor, the licensee must satisfy the requirements under the “Pressure Boundary Program” license condition: *“The licensee shall implement and maintain a pressure boundary program and have in place a formal agreement with an Authorized Inspection Agency”*. Therefore, the pressure boundary program for the power reactor including SMRs must be developed and implemented by incorporating elements that must be included in the pressure boundary program. These elements are provided in Clause 15 of CSA Standard N285.0-12 stipulating general requirements for

PRSCs in CANDU NPPs. The pressure boundary program elements are discussed in licensee's pressure boundary documents showing how the requirements of CSA N285.0-12 are addressed by the licensee's processes and procedures for a nuclear facility. However, for instance, the following elements in the pressure boundary program provided in the CSA N285.0-12 may not be applicable or required for some SMRs whose operating conditions and design features are different with those for the CANDU type reactor:

- Elements on design rules for nuclear class PRSC in CSA N285.0-12 (e.g., ASME Section III Division 1) are not applicable for PRSCs in some SMRs operated at the elevated temperature; and
- Elements on (1) over pressure protection; and (2) overpressure protection devices program may not be required for some SMRs that will be operated at or near atmospheric pressure (i.e., 14.7 psig or 101.3 kPa).

The purpose of ISI is to provide assurance that the likelihood of a failure that could endanger the radiological health and safety of persons has not increased significantly since the plant was put into service. The ISI is one of the pressure boundary program elements. Clause 13 of the CSA N285.0-12 states that components covered by CSA N285.0-12 shall be subject to inspection in accordance with CSA N285.4-19 and N285.5-18. However, inspection requirements in the CSA N285.4-19 and N285.5-18 have been developed and updated by the consideration of dominant degradation mechanisms [e.g., fatigue, Flow Accelerated Corrosion (FAC)] identified by OPEX of CANDU type reactors. Hence, inspection requirements in the current relevant CSA standards for inspection [e.g., CSA N285.4-19, N285.5-18 (CSA and Standards, 2019)] need to be updated/revised in order to ensure the structural integrity of SSCs in SMRs with operating conditions, safety systems, and cooling mediums different than those for CANDU type reactors.

- Step 1: Identify Clauses and pressure boundary program elements that could be affected by: (1) new design features (e.g., seismic isolator, passive safety systems, cooling mediums); (2) the operating conditions (e.g., low operating pressure, high operating temperature) of SMRs; and (3) proposed rules for design and ISI program of SMRs (e.g., ISI rules in accordance with ASME Section XI, design rules in accordance with ASME Section III Division 5);
- Step 2: Identify CSA Standards that are referred in the Clauses and pressure boundary program elements identified at Step 1; and
- Step 3: Update/Modify CSA Standards identified in Step 2.

22.5.4.4 Non-design basis loading condition

The objective of design rules in ASME Boiler and Pressure Vessel (B&PV) is to afford reasonably protection of life and property and to provide a margin for deterioration in service to give a reasonably long, safe period of usefulness. Therefore, loading conditions established in the ASME design specification for each code component do not cover all plausible loading conditions that could occur during code specified loading conditions (i.e., Level A, B, C, and D conditions). For instance, some loading conditions (e.g., thermal mixing, thermal stratification, high cycle fatigue) are classified as non-design basis loading conditions because they were not taken into account at the design stage of important to safety SSC in conventional types of reactors. OPEX of the conventional power reactors indicates that many failures have resulted from non-design basis loads. However, plausible locations and effects of non-design basis loading conditions are usually verified by OPEX because several thermal hydraulic parameters together with configuration of system/component and condition of important to safety systems are involved in actual operating conditions. In particular, SSCs in SMRs may be more frequently subject to the non-design basis loading conditions due to the following reasons (Eom et al., 2019):

- Complex configuration of a reactors internal structure in a small size reactor vessel along with the properties of a cooling medium (e.g., high viscosity, high thermal conductivity) affecting a pressure/

- temperature profile and a flow pattern, pose specific challenges to properly determine transient limits at each service loading condition; and
- PIEs, which are input for determining transient conditions at each service loading condition, are under development for most of SMRs. The PIEs are determined by the consideration of several aspects such as all internal and external events, all normal operating configurations, various plant and site conditions, and failure in other plant systems (e.g., storage for irradiated fuel, and tanks for radioactive substances).

The operational history of importance to safety systems must be recorded and tracked by monitoring systems (e.g., thermal/pressure transient monitoring system, vibration-monitoring system, chemistry monitoring system in coolant, etc.) over the entire operating life of important safety systems. The operating history captured by the monitoring systems can be used: (1) to confirm that the important to safety systems operate within transient limits provided in design specification; and (2) to evaluate the remaining operating life of systems important to safety when operating history indicates that they operate beyond design transient limits (e.g., operate at a non-design basis loading condition). Hence, we propose to consider the following elements in order to evaluate the effects of the non-design loading conditions on the structural integrity of the important to safety systems accordingly:

- Identify plausible non-design basis loading conditions [e.g., Flow Induced Vibration (FIV), thermal stratification, thermal striping, and thermal mixing] and plausible locations for the non-design basis loading conditions. A FMEA is one way to identify types of non-design basis loading conditions and their plausible locations;
- Set out load combination criteria and acceptance criteria for non-design basis loads with other loads in order to evaluate the effects of non-design basis loading conditions on the structural integrity of the important to safety systems; and
- Install monitoring systems to detect governing parameters for operation (e.g., pressure/temperature transient profile, vibration level). Operating history captured by the monitoring systems can be used: (1) to ensure that the important to safety systems operate within transient limits and (2) to evaluate a remaining operating life of the important to safety systems.

22.5.4.5 Helical coil steam generator

Currently, the use of the HCSG is widely proposed in several SMR designs in order to improve thermal efficiency and compactness. OPEX of existing Steam Generators (SGs) indicates that SG tubes are often the weakest link in maintaining the structural integrity of SG over its design life. As well, the failure of SG tubes for some SMRs could affect the structural integrity of mechanical components in a primary side and could lead to the failure of Intermediate Heat eXchanger (IHX) (e.g., a pressure wave resulting from a chemical reaction between water and liquid sodium). However, OPEX for the HCSG are relatively insufficient while the U-type tube SG in PWR has been improved based on a large amount of OPEX. Hence, the following elements, which were discussed for the design improvements of the more conventional U-type tube SG, need to be taken into account for the design of the HCSG in SMRs:

- Material selection for SG tubes;
- Types of degradation mechanisms and failure modes on tube;
- Prevention of FIV on tube bundles;
- Fabrication method for the HCSG (e.g., tube-to-tube supports, tube-to-tubesheet);
- Accessibility for inspection and maintenance;
- Inspection method for curved tube;
- Number of SG tube failures for the transient;

- Types and locations of leak detection systems for tubes with the demonstration of capability, sensitivity, diversity, redundancy, and reliability of leak detection systems;
- Operation and shutdown leakage limit for tubes; and
- LBB application to tubes.

Application of a FMEA is one way to identify and address the aforementioned elements at a detailed design stage of the HCSG. A literature review on: (1) design rules; (2) ISI program; and (3) OPEX of SGs in various types of reactors [e.g., CANDU, PWR, Sodium-cooled Fast Reactor (SFR), and Fast Breed Reactor (FBR)] can be used as input for the FMEA (Eom et al., 2019).

22.5.4.6 Probabilistic fracture mechanics

Recently, US NRC released a technical letter report, TLR-RES/DE/CIB-2018-01, titled “*Important Aspects of Probabilistic Fracture Mechanics Analyses*” (Raynaud et al., 2018). This report defined the concept of a PFM analysis and outlined important concepts that should be considered when producing a high quality, high-confidence PFM analysis in conjunction with addressing the characteristics and the application of Deterministic Fracture Mechanics (DFM) and PFM as follows:

- DFM and PFM approaches are thus fundamentally similar: both are mathematical abstractions used to approximate reality. Moreover, both share the common goal of representing the uncertainties in a mathematical form that enables problem solution, although they achieve this by different means;
- Both DFM and PFM analyses are models used to represent reality. Although use of DFM has met its objectives, as reflected in various engineering support for different purposes throughout the nuclear industry, there is more room for using PFM as an alternative to better quantify implicit and explicit conservatism in nuclear components;
- Both DFM and PFM analyses treat uncertainties mathematically but in different ways. Furthermore, it may not be possible to properly account for every uncertainty; and
- Use of DFM or PFM methods does not represent an either-or choice. In many circumstances, DFM and PFM methods are complementary parts of a safety case.

Currently, PFM codes and databases of operating experience are widely used to assess potential risks associated with the operation of aging NPPs. CNSC staff has participated in the Probabilistic Analysis as a Regulatory Tool for Risk Informed Decision Guidance (PARTRIDGE) program. The PARTRIDGE program is an international, multiclient cooperative program to develop a probabilistic analysis tool for making risk informed regulatory decisions regarding PHT system piping LOCA. The following issues were mainly discussed in the PARTRIDGE program in order to update the PFM code, Pro-LOCA that predicts pipe rupture frequencies of reactor coolant system piping affected by on-going degradation mechanisms:

- Validation and Verification (V&V) of the Pro-LOCA;
- Sensitivity analyses to assess the drivers of the uncertainty;
- Develop/Enhance ways to obtain efficient “low probabilities”; and
- Direction to improve a PFM code in order to predict pipe rupture frequencies realistically.

In the future, there is potential to write a new standard and/or REGDOC regarding PFM in order to provide guidance to perform and evaluate PFM analyses. However, at this time, there is no firm technical basis for the treatment of uncertainties in PFM codes. Moreover, allowable failure probabilities have not been adequately defined. Recently, IAEA Coordinated Research Project (CRP), I31030, was initiated and implemented by the Division of Nuclear Power, Nuclear Power Technology Development Section (NPTDS). Nine organizations (5 research contracts and 4 research agreements) in eight countries participate in this project. The objective of this project is to develop new methodology in order to predict pipe failure rates in advanced WCRs for

improved safety design. The methodology established in this project could be utilized to determine the allowable failure probabilities for a given SMR having insufficient OPEX (Eom et al., 2019).

In addition, the selection of input distributions should be appropriately justified with a sufficient technical basis. Appropriate validation accompanied by uncertainty analysis should support the credibility of reported probabilistic estimates. Hence, PFM evaluations would be adequate to identify governing inputs that affect simulation results, and uncertainty estimates allowing for a more efficient direction of the resources into the subject matter of interest (Wasiluk et al., 2019). Therefore, low probability results for PRCS failure emanating from PFM codes can only support the deterministic analysis for: (1) the FFS of a degraded PRSC and (2) the design for the new reactor.

22.5.4.7 Aging and Wear

As per Section 7.17 of REGDOC-2.5.2 (CNSC, 2014a) and REGDOC-2.6.3 (CNSC, 2014d), “the design shall take due account of the effects of aging and wear on SSCs.” REGDOC-2.6.3 emphasizes the need for proactive consideration of aging of PRSC and Aging Management (AM) during each lifecycle phase of a reactor facility. A systematic approach at the design stage must be applied to ascertain the understanding of aging of PRSC, in order to evaluate effective approaches and design features for aging prevention, monitoring and mitigation, and to establish AMP for PRSC.

The qualification of new materials proposed for SMRs represents a major challenge; especially for those materials not listed as acceptable materials for nuclear applications in ASME Section II or ASME Section III Division 5 for high-temperature reactors. Furthermore, material degradation and corrosion/erosion are typical aging mechanisms for PRSC subjected to high operating temperature and radiation. Thus, a systematic approach and a well-designed research and development program are needed to address the knowledge gap in material behavior in the early design stage for SMRs.

The CNSC REGDOC-2.6.3 (CNSC, 2014d) requires that the AMP be developed to address the following nine attributes for an effective AM program:

- **Attribute #1:** Scope of the Aging Management Program based on understanding aging;
- **Attribute #2:** Preventive actions to minimize & control aging degradation;
- **Attribute #3:** Detection of aging effects;
- **Attribute #4:** Monitoring and trending of aging effects;
- **Attribute #5:** Mitigating aging effects;
- **Attribute #6:** Acceptance criteria;
- **Attribute #7:** Corrective actions;
- **Attribute #8:** OPEX feedback & feedback of R&D results; and
- **Attribute #9:** Quality management.

In particular, CNSC REGDOC-2.6.3 in Appendix A provides the following descriptions for attribute #1:

- *Systems, Structures and Components (SSCs) subject to Aging Management (structures include structural elements); and*
- *Understanding of aging phenomena (significant aging mechanisms, susceptible sites):*
 - *Design and licensing basis requirements relevant to aging;*
 - *SSC materials, service conditions, stressors, degradation sites, aging mechanisms and effects;*
 - *SSC condition indicators and acceptance criteria; and*
 - *Quantitative and qualitative predictive models of relevant aging phenomena.*

Application of a FMEA is one way to identify and address the following aspects: typical/plausible degradation mechanisms, failure location, failure mode, failure effect, detection method, mitigation task, and

governing parameters leading to a given degradation. The FMEA can be used to support ongoing confidence in the condition of a given system/component in a SMR. In addition, effects on structural integrity due to non-design basis cyclic loads (e.g., thermal stratification, thermal mixing, or vibration, etc.) must be assessed through the FMEA. The design operating life can be assumed based on evaluation results of the FMEA.

A main requirement associated with attribute #1 is to determine the scope of the AMP by taking into account all potential aging mechanisms and their effects on the structural integrity of a selected PRSC. The effectiveness of the AMP of a given PRSC should be determined by the condition of PRSC monitored, and through the review of condition indicators obtained from OPEX, inspections, and research after the start of commercial operation. The AMPs should be updated on a regular basis to incorporate OPEX, research findings (Eom et al., 2018).

22.5.4.8 In-service testing, maintenance, repair, inspection, and monitoring

Section 7.14 in REGDOC-2.5.2, the design should incorporate provisions recognizing the need for in-service testing, maintenance, repair, inspection, and monitoring for the purpose of maintaining the SSCs within the boundaries of the design. Thus, the development of strategies and programs to address in-service testing, maintenance, repair, inspection, and monitoring is a necessary aspect of the plant design stage. In particular, SSCs important to safety should be designed and located to make surveillance and maintenance simple, to permit timely access, and in the case of failure, to allow diagnosis and repair, and minimize risks to maintenance personnel.

Any SSCs important to safety could be subjected to an unexpected degradation mechanism that was not considered at the design stage due to a lack of knowledge and OPEX (i.e., epistemic uncertainty). Moreover, the primary coolant for some SMRs contains nuclear fuel such that inspection of reactor internal components and the SSC may be challenging due to access limitation and high radiation. Alternative ways of performing inspections to capture degradation mechanisms and trends of degradation mechanisms should be considered. The modularization of SMRs would be a good design practice or be considered an alternative way to repair or replace a degraded PRSC in a timely fashion. Therefore, the following monitoring systems/programs should be implemented to ensure the safe operation of SMRs:

- Implementation of a monitoring program to record and track the operation history of SSCs (e.g., thermal/pressure transient monitoring system or vibration monitoring system, etc.) over the entire life of the SSCs;
- Material surveillance program to capture any changes in material properties under a given operating condition (e.g., changes in material strength, strain hardening rate or fracture toughness with operation time);
- Implementation of a Loose Parts Monitoring (LPM) program to detect loose metallic parts in the PRSC at an early stage; and
- Implementation of more than one leak detection system to capture leakage from the reactor coolant system at an early stage to shut down the plant safely. The sensitivity of leak detection system should be demonstrated.

In addition, REGDOC-2.5.2 states that RI-ISI could be used when the methodology is clearly documented. However, the RI-ISI can be utilized with understanding of the types of plausible or potential degradation mechanisms and their degradation rates, which are established, based on deterministic ISI and OPEX. A failure probability of the PRSC, which is a key input for determining the interval and the scope of the RI-ISI, can be adequately determined by understanding the degradation mechanisms (Eom et al., 2018).

22.5.5 Review framework for FA #16 on vendor Research and Development program

As per Section 5.1 in REGDOC-2.5.2 and Attribute #1 in REGDOC-2.6.3, “*Research activities are important to establish 1) a knowledge base of relevant aspects of the plant design and 2) establish solutions to Aging Management problems in order to mitigate or prevent degradation.*”

Thus, research activities should be conducted to investigate matters such as:

- Types of degradation mechanisms and susceptible locations to degradation mechanisms;
- Any new feature in the design to which there is no adequate qualified data and OPEX;
- Any changes in material properties under a given operating condition (e.g., changes in material strength, strain hardening rate or fracture toughness with operation time);
- Effect of the degradation mechanisms on the design conditions (i.e., fabrication and construction conditions, and operating conditions associated with the SSC);
- Means of monitoring degradation mechanisms;
- Means of mitigating or preventing degradation mechanisms; and
- Modeling and simulation of degradation mechanisms to predict a trend of degradation mechanisms in order to proactively repair and replace a degraded SSC.

Therefore, systematic categorization of research areas is crucial to design SMRs against potential/plausible degradation mechanisms that could lead to a significant reduction of the operating life.

Time Limited Aging Analyses (TLAAs) were developed to evaluate the effect of aging during an extended operating life of Pressurized Water-cooled Reactor (PWR). TLAA categories have been determined based on several research results and OPEX of PWRs. Thus, the TLAA categories could cover types of degradation mechanisms that could happen during operating life of a SMR. Based on the review of US practices and the IAEA document for the TLAA (IAEA, 2015) together with several documents summarizing design features of SMRs (IAEA, 2016b), the following research categories for the design of PRSC for both metallic and non-metallic components (e.g., graphite, ceramic) could be applicable:

- Types of degradation mechanisms and susceptible locations to degradation mechanisms;
- Means of mitigating or preventing degradation mechanisms;
- Means of monitoring degradation mechanisms;
- Radiation induced material changes (e.g., segregation and phase transformation, swelling and creep, embrittlement);
- Effects of high temperatures on structures (e.g., creep, shrinkage, thermal embrittlement);
- Synergistic effects of both radiation and elevated temperature on material changes;
- Embrittlement due to hydrogen;
- Corrosion and erosion;
- Mechanical fatigue (e.g., low cycle fatigue and high cycle fatigue);
- Environmentally Assisted Cracking (EAC) [e.g., Stress Corrosion Cracking (SCC)];
- Cracking on Dissimilar Metal Welds (DMWs);
- Cracking on non-metallic component (e.g., graphite);
- The performance of weldments including both weld metal and the adjacent Heat Affected Zone (HAZ); and
- Environmental Qualification (EQ).

In general, most SMRs have not been commercially operated yet, and as such, there is limited feedback available for key elements (e.g., inspection, degradation mechanisms, and maintenance and repair) that are required for the operation of SMRs. Thus, a literature review should be conducted at an early stage of the design to identify current knowledge, practices and pending issues associated with design rules of metallic

and non-metallic mechanical components, types of plausible/potential degradation mechanisms, and material degradation in elevated temperatures coupled with high radiation fields (Awad et al., 2016).

In particular, understanding and characterization of governing parameters on the Environmentally Assisted Fatigue (EAF) is important because the composition, the dissolved components, and the operating conditions of the coolant would affect crack initiation/growth of the metallic component carrying it.

For instance, numerous laboratory tests have shown that the fatigue life of metallic components in the current operating Pressurized Water Reactors (PWRs) is significantly reduced by its exposure to a coolant environment (ANL, 2007). The influencing parameters include, but are not limited to strain rate, strain amplitude, effects of chemical contents in coolant, temperature, dissolved oxygen, water conductivity, sulfur content in steel, hold periods, surface flow rate, and neutron irradiation. For water-cooled SMRs with similar operating conditions to the current operating PWRs, Regulatory Guide 1.207 (NRC, 2007) is recommended for evaluating the fatigue analysis. For other types of SMR designs (e.g., gas-cooled, liquid metal-cooled), which are intended to be operated at higher temperatures (creep range), environmental effects on fatigue, creep and creep-fatigue interactions should be considered. Therefore, the fatigue design curves for each specific SMR operating condition should be derived from a statistically significant number of tests. In other words, the design curves should provide a high confidence that the fatigue and/or creep life of all the test data will be greater than that predicted by the design curves. Prototypical components tests are recommended for validating the conservatism in the design curves.

Research results should be used as input to the FMEA to appropriately estimate design life and establish/update the AMP for operation (Eom et al., 2018).

22.6 Conclusions

Based on lessons learned from operating experience with current fleet of NPPs and prospective solutions for future energy production and environment protection challenges, Generation-IV reactors have been developed to accommodate new innovative technological solutions to satisfy stringent regulatory and licensing requirements in terms of safety, waste and management. Hence, a recent surge of nuclear industry interest in the development of small, factory built, and inherently safe Generation-IV reactors including SMRs has been underway for the last few years.

Most of the proposed new Generation-IV and SMR designs use non-conventional cooling mediums and operate at high temperatures. Such combination will likely create many new challenges to the regulators and the designers. Furthermore, SMRs offer many features to meet the expectations of Generation-IV design features. These include better economy, improved operating safety features, and non-proliferation characteristics. Along with these potential advantages come new challenges that need to be addressed at the early stages of the developments of these reactors.

Many of the proposed SMR concepts operate at or near atmospheric pressure along with elevated operating temperatures. Therefore, it is expected that material degradations associated with high operating temperatures and environmentally assisted degradation mechanisms will govern the design rather than pressure loads. Therefore, it is crucial to understand material behavior and identify plausible degradation mechanisms and damage modes by the consideration of operating conditions in which SMRs are essential elements in order to ensure the structural integrity of PRSCs over their design life.

However, most SMRs have not been commercially operated yet, and as such, there is limited feedback available for key elements (e.g., inspection, degradation mechanisms, and maintenance and repair) that are required for operation of SMRs. Thus, an operating experience and literature review should be conducted at an early stage of the design to identify current knowledge, practices and pending issues associated with

design rules of metallic and non-metallic mechanical components, types of plausible/potential degradation mechanism, and material degradation in elevated temperatures coupled with high radiation fields. Hence, application of a FMEA is one way to identify and address the following aspects: typical/plausible degradation mechanisms, failure location, failure mode, failure effect, detection method, mitigation task, and governing parameters leading to a given degradation.

To summarize, the authors acknowledge that the emerging SMR technologies provide opportunities to fulfill the global energy needs at very low-carbon foot print and comparable prices. However, they also present regulatory challenges that require creative resolutions to expedite the review process without compromising the safety requirements. This work was an exercise to highlight the main issues that require focused attention with respect to PRSCs. These issues can be summarized as follows:

- Code classification;
- The qualification of new materials proposed for SMRs;
- Plausible degradation mechanisms and damage modes in the consideration of SMR operating conditions to quantify design margins under relatively high neutron fluxes and at elevated temperatures;
- A deterministic LBB and a probabilistic LBB [i.e., using Probabilistic Fracture Mechanics (PFMs) codes] application;
- Consideration of non-design basis loading conditions and monitoring systems; and
- ISI requirements.

Thus, further development of the relevant design Codes and Standards will be needed in order to cover the aforementioned issues in conjunction with a well-defined research program and a FMEA.

References

- ANL, 2007. Effect of LWR Coolant Environments on the Fatigue Life of Reactor Material. Argonne National Laboratory. NUREG/CR-6909, February 2007.
- Awad, R., Eom, S., Sadek, N., Xu, S., 2016. Key aspects for design and fitness for service of mechanical components in small modular reactors. In: CNS Paper, 4th International Technical Meeting on Small Reactors (ITMSR-4). Ottawa, November 2–4.
- ASME, 2020. ASME Boiler & Pressure Vessel Codes Section III. American Society of Mechanical Engineers (ASME), New York, NY.
- Bajorek, S., 2019. In: Martin, R., Frepoli, C. (Eds.), Regulatory Status, Chapter 1 in Design Basis Accident Analysis Methods for Light-Water Nuclear Power Plants. World Scientific Publishing Co.
- Berbey, P., Ingemarsson, K.-F., 2004. European utility requirements: common rules to design next LWR plants in an open electricity market. In: Paper 4191, Proceedings of ICAPP '04, Pittsburgh, PA USA. American Nuclear Society. June 13–17.
- CEU, 2009. Council Directive 2009/71/Euratom of 25 June 2009 establishing a Community framework for the nuclear safety of nuclear installations. Off. J. Eur. Union 172, 18–22.
- CEU, 2011. Council Directive 2011/70/Euratom of 19 July 2011 establishing a Community framework for the responsible and safe management of spent fuel and radioactive waste. Off. J. Eur. Union 199, 48–56.
- CEU, 2014. Council Directive 2014/87/Euratom of 8 July 2014 amending Directive 2009/71/Euratom establishing a Community framework for the nuclear safety of nuclear installations. Off. J. Eur. Union 219, 42–52.
- CFR, a, U.S. Code of Federal Regulations (CFR), n.d. Domestic Licensing of Production and Utilization Facilities, Part 50, Chapter 1, Title 10, “Energy”.
- CFR, b, U.S. Code of Federal Regulations (CFR), n.d. Licences, Certifications, and Approvals for Nuclear Power Plants, Part 52, Chapter 1, Title 10, “Energy”.
- CNSC, 2011. Design of Small Reactor Facilities, CNSC Document, RD-367. Canadian Nuclear Safety Commission, Ottawa. June 2011.
- CNSC, 2012. Pre-Licensing Review of a Vendor’s Reactor Design, CNSC Document, GD-385. Canadian Nuclear Safety Commission, Ottawa. May 2012.
- CNSC, 2014. Physical Design—Design of Reactor Facilities: Nuclear Power Plants, CNSC Document, REGDOC-2.5.2. Canadian Nuclear Safety Commission, Ottawa. May 2014.

- CNSC, 2018a. Licence Application Guide: Small Modular Reactor Facilities, CNSC Document REGDOC-1.1.5. Canadian Nuclear Safety Commission, Ottawa. July 2018.
- CNSC, 2014a. Physical Design—Design of Reactor Facilities: Nuclear Power Plants. Canadian Nuclear Safety Commission (CNSC) Document, REGDOC-2.5.2, May 2014.
- CNSC, 2014b. Deterministic Safety Analysis. Canadian Nuclear Safety Commission Document, REGDOC-2.4.1, May 2014.
- CNSC, 2014c. Probabilistic Safety Assessment (PSA) for Nuclear Power Plants. Canadian Nuclear Safety Commission (CNSC) Document, REGDOC-2.4.2, May 2014.
- CNSC, 2014d. Fitness for Service—Aging Management. Canadian Nuclear Safety Commission (CNSC) Document, REGDOC-2.6.3, March 2014.
- CNSC, 2018b. Pre-Licensing Review of a Vendor’s Reactor Design. Canadian Nuclear Safety Commission (CNSC) Document, REGDOC-3.5.4, November 2018.
- CNSC, 2019. Glossary of CNSC Terminology. Canadian Nuclear Safety Commission Document, REGDOC-3.6, December 2019.
- CSA, 2012. General Requirements for Pressure-Retaining Systems and Components in CANDU Nuclear Power Plants/Material Standards for Reactor Components for CANDU Nuclear Power Plants. Canadian Standards Association (CSA) Standard. N285.0–12, August.
- Eom, S., Sadek, N., Chaudhury, K., Cole, C., Awad, R., Duan, X., 2018. Proposed Review Framework for Design of Pressure Retaining Systems and Components (PRSC) in Small Modular Reactor (SMR). ASME Paper, PVP2018-85106, Prague, Czech Republic, July 15–20.
- Eom, S., Kirkhope, K., Sadek, N., Nitheanandan, T., Awad, R., 2019. Perspectives on the Design of Pressure Boundary Systems and Components in Small Modular Reactors. Transactions of SMiRT-25, Division X, Charlotte, NC, August 4–9.
- CSA, N285, Standards, CSA, 2019. CSA. Periodic Inspection of CANDU Nuclear Power Plant Components, CSA N285.5–18, Periodic Inspection of CANDU Nuclear Power Plant Containment Components, CSA N285.7–19, Periodic Inspection of CANDU Nuclear Power Plant Balance of Plant Systems and Components N285.4–19.
- EC, 2020. European Industrial Initiative on Sustainable Nuclear Energy. European Commission. <https://setis.ec.europa.eu/european-industrial-initiative-sustainable-nuclear-energy>. Available at (last updated April 24, 2020. Retrieved April 27, 2020).
- ENISS, 2020. ENISS—European Nuclear Installations Safety Standards. www.eniss.eu. Available at retrieved April 27, 2020.
- ERDA, 2011. Roadmap Towards European Licensing and Project Development of New Nuclear Plants. European Reactor Design Approval (ERDA). 2013.
- GIF, 2016. Safety Design Guidelines on Safety Approach and Design Conditions for Generation IV Sodium-cooled Fast Reactor Systems. GEN IV International Forum. SDC-TF/2016/01, March 04.
- IAEA, 1986. Convention on Assistance in the Case of a Nuclear Accident or Radiological Emergency, Date of Adoption: 26 September 1986/ Date of Entry into Force: 26 February 1987. International Atomic Energy Agency, Vienna.
- IAEA, 1994a. Convention on Nuclear Safety, Date of Adoption: 17 June 1994/ Date of Entry into Force: 24 October 1996, Last Updated 12 March 2013. International Atomic Energy Agency, Vienna.
- IAEA, 1994b. Technical Feasibility and Reliability of Passive Safety System for Nuclear Plants. , IAEA Document, TECDOC-920, November 1994.
- IAEA, 1997. Joint Convention on the Safety of Spent Fuel Management and on the Safety of Radioactive Waste Management, Date of Adoption: 5 September 1997, Date of Entry into Force: 18 June 2001. International Atomic Energy Agency, Vienna.
- IAEA, 2015. Ageing Management for Nuclear Power Plants: International Generic Ageing Lessons Learned (IGALL). IAEA Safety Reports Series No. 82, April.
- IAEA, 2016a. Considerations on the Application of the IAEA Safety Requirements for the Design of Nuclear Power Plants. IAEA Document, TECDOC-1791 May.
- IAEA, 2016b. Advances in Small Modular Reactor Technology Developments. IAEA (August 2016).
- IAEA, 2019. IAEA Safety Glossary—Terminology Used in Nuclear Safety and Radiation Protection, 2018 ed. International Atomic Energy Agency, Vienna.
- IAEA, 2020. History, International Atomic Energy Agency. <https://www.iaea.org/about/overview/history>. Available at: retrieved April 28, 2020.
- IEA, 2019. World Energy Outlook 2019. OECD International Energy Agency, Paris.
- INL, 2014. Guidance for Developing Principal Design Criteria for Advanced (Non-Light Water) Reactors. INL Report INL/EXT-14-31179, Rev.1, Idaho National Laboratory, December.
- Kelly, J., 2014. Joint Initiative Regarding U.S. Nuclear Regulatory Commission Licensing Strategy for Advanced (Non-Light Water) Reactor Technology. DOE Memorandum, December 8.
- Magwood IV, W.D., Paillere, H., 2018. Looking ahead at reactor development. Prog. Nucl. Energy 102, 58–67.
- NEI, 2019. Risk-Informed Performance-Based Technology Inclusive Guidance for Non-Light Water Reactor Licensing Basis Development. NEI Technical Report 18–04, Revision 1, Nuclear Energy Institute, Washington, DC, August.

- NRC, 2007. Guidelines for Evaluating Fatigue Analyses Incorporating the Life Reduction of Metal Components due to the Effects of the Light-Water Reactor Environment for New Reactors. US NRC Document, the Regulatory Guide 1.207, March.
- NRC, 2018. Guidance For Developing Principal Design Criteria For Non-Light-Water Reactors. Regulatory Guide 1.232, Revision 0, U.S. Nuclear Regulatory Commission, Washington, DC., April.
- NRC, 2019. Guidance for a Technology-Inclusive, Risk-Informed, and Performance-Based Methodology to Inform the Licensing Basis and Content of Applications for Licenses, Certifications, and Approvals for Non-Light-Water Reactors, Draft Regulatory Guide DG-1353. U.S. Nuclear Regulatory Commission. April.
- NRC, 2020. Guidance for a Technology-Inclusive, Risk-Informed, and Performance-Based Methodology to inform the Licensing Basis and Content of Applications for Licenses, Certifications, and Approvals for Non-Light-Water Reactors. Regulatory Guide 1.233, Revision 0, June 2020, ADAMs Accession Number ML20091L698.
- Raynaud, P., Kirk, M., Benson, M., Homiack, M., 2018. Important Aspects of Probabilistic Fracture Mechanics Analyses. Technical Letter Report: TLR-RES/DE/CIB-2018-01, U.S. NRC, September 14.
- Riznic, J., Duffey, R., 2017. 60 Years in motion: short history of nuclear engineering division. *J. Nuclear Eng. Radiat. Sci.* 3 (1). pp. 0108801-1-13, 2017.
- Soderholm, K., 2013. Licensing Model Development for Small Modular Reactors (SMRs)—Focusing on the Finnish Regulatory Framework. PhD Thesis, Lappeenranta University of Technology, Acta Universitatis Lappeenrantaensis 528, Lappeenranta, 27th of September.
- UN, 1968. Treaty on the Non-Proliferation of Nuclear Weapons (NPT). United Nations, New York, NY.
- Wasiluk, B., Carroll, B., Tsembeles, K., Jin, J., 2019. Application of Probabilistic Fracture Mechanics for Pressure Tubes. Transactions SMiRT-25 Division II, Charlotte, NC. August 4-9.
- WNA, 2013. Aviation Licensing and Lifetime Management—What Can Nuclear Learn? World Nuclear Association Report.
- WNA, 2015. Facilitating International Licensing of Small Modular Reactors, Prepared by the Cooperation in Reactor Design Evaluation and Licensing, (CORDEL) Working Group of the World Nuclear Association. Report No. 2015/004, World Nuclear Association, August.
- WNA, 2020. Nuclear Power in the World Today. World Nuclear Association. <https://www.world-nuclear.org/information-library/current-and-future-generation/nuclear-power-in-the-world-today.aspx>. Available at: retrieved April 28, 2020.
- CSA, N289. CSA Standards, CSA N289.1–18, 2019. General Requirements for Seismic Design and Qualification of CANDU Nuclear Power Plants, CSA N289.2, Ground Motion Determination for Seismic Qualification of Nuclear Power Plants, CSA N289.3-20, Design Procedures for Seismic Qualification of Nuclear Power Plants, CSA N289.4, Testing Procedures for Seismic Qualification of Nuclear Power Plant Structures, Systems, and Components, CSA N289.5, Seismic Instrumentation Requirements for Nuclear Power Plants and Nuclear Facilities..
- WENRA, 2009. *Safety Objectives for New Nuclear Power Reactors*, Study by WENRA Reactor Harmonization Working Group, Western European Nuclear Regulator's Association WENRA, December 2009.
- WENRA, 2014. *Safety Reference Levels for Existing Reactors*, Reactor Harmonization Working Group, Western European Nuclear Regulator's Association WENRA, 24 September 2014.

Further reading

- Hidayatullah, H., Susyadi, S., Hadid Subki, M., 2015. Design and technology development for small modular reactors—safety expectations, prospects and impediments. *Prog. Nucl. Energy* 79, 127–135. 2015.
- Holbrook, M.R., Kinsey, J.C., Moe, W.L., 2016. Licensing basis event selection framework for advanced reactors. In: 2016 International Mechanical Engineering Congress & Exposition—IMECE 2016, Paper IMECE2016-67520, Phoenix, AZ, November 11–17.
- IAEA, 2014. Safety Classification of Structures, Systems and Components in Nuclear Power Plants. IAEA Specific Safety Guide No. SSG-30, May.
- Walker, J.S., Wellock, R.R., 2010. A Short History of Nuclear Regulation, 1946–2009, NUREG/BR-0175, rev.2. U.S. Nuclear Regulatory Commission, Washington, DC.
- Wang, Q., Chen, X., 2012. Regulatory failures for nuclear safety- the bad example of Japan-implication for the rest of world. *Renew. Sustain. Energy Rev.* 16, 2610–2617.

ITER, the way to fusion energy[☆]

Michel Claessens

European Commission and Free University of Brussels, Brussels, Belgium

Nomenclature

Symbols

<i>C</i>	Light speed, m/s
<i>E</i>	Energy, J
<i>M</i>	Mass, kg
<i>n</i>	Density, kg/m ³
<i>P</i>	Power, W
<i>T</i>	Temperature, °C or K
τ_E	Confinement time, s

Subscripts

<i>el</i>	electric
<i>fusion</i>	power released by the fusion reaction
<i>heating</i>	heating power to bring the plasma at the temperature required for fusion
<i>th</i>	thermal

Acronyms/abbreviations

ADEME	Agence De l'Environnement et de la Maîtrise de l'Energie (France)
AERE	Atomic Energy Research Establishment (UK)
AIF	Agence ITER France
ASDEX	Axially Symmetric Divertor Experiment (Germany)
ASN	Autorité de Sûreté Nucléaire (France)
BNI	Basic Nuclear Installation
CAD	Computer-Aided Design
CATIA	Conception Assistée Tridimensionnelle Interactive Appliquée
CFR	Compact Fusion Reactor (USA)
CFS	Commonwealth Fusion Systems (USA)
CMA	Construction Manager-as-Agent
CANDU	CANada Deuterium Uranium (reactor)
CFC	Carbon Fiber Composite
CFETR	China Fusion Engineering Test Reactor (China)
CDA	Conceptual Design Activities
CEA	Commissariat à l'Énergie Atomique et aux énergies alternatives (France)
CERN	European Organization for Nuclear Research (Switzerland)

☆ This chapter is mainly based on the following book: [Claessens \(2020\)](#). The book provides a presentation of the ITER project in its many different dimensions—historical, scientific, technical, political, economic, human and even philosophical.

DA	Domestic Agency
DOE	Department Of Energy (USA)
EC	European Community
EDA	Engineering Design Activities
ELM	Edge-Localized Mode
EPFL	Ecole Polytechnique Fédérale de Lausanne (Switzerland)
ESRF	European Synchrotron Radiation Facility (France)
EU	European Union
EUR	Euros
Euratom	European Atomic Energy Community
F4E	Fusion for Energy (Europe)
H-mode	High-confinement mode
HEL	Highly Exceptional Load
IAEA	International Atomic Energy Agency
ICF	Inertial Confinement Fusion
IDEP	Institut D'Économie Publique de Marseille
IEA	International Energy Agency
IFMIF	ITER Fusion Material Irradiation Facility
INSEE	Institut National de la Statistique et des Études Économiques (France)
IO	ITER Organization
IRSN	Institute de la Radioprotection et de la Sûreté Nucléaire (France)
ITER	International Thermonuclear Experimental Reactor
IUA	ITER Unit of Account
JET	Joint European Torus (EU)
JT-60	JAERI Tokamak 60 (Japan)
LHC	Large Hadron Collider
LMJ	Laser MegaJoule (France)
LPPFusion	Lawrenceville Plasma Physics Fusion (USA)
MIT	Massachusetts Institute of Technology (USA)
NIF	National Ignition Facility (USA)
NREL	National Renewable Energy Laboratory (USA)
NSTX	National Spherical Torus eXperiment (USA)
PACA	Provence-Alpes-Côte d'Azur
PCR	Project Change Request
PF	Poloidal Field coil
RTE	Réseau de Transport d'Electricité (France)
SSC	Superconducting Super Collider (USA)
T-1	Tokamak-1, Kurchatov Institute (USSR)
TAE	TriAlpha Energy (USA)
TBM	Tritium Breeding Module
TF	Toroidal Field coil
TFR	Tokamak Fontenay-aux-Roses (France)
TFTR	Tokamak Fusion Test Reactor (USA)
Tokamak	Toroidal chamber with magnetic coils (in Russian “тороидальная камера с магнитными катушками”)
US	United States
USA	United States of America
USSR	Union of Soviet Socialist Republics
WEST	Tungsten (W) Environment in Steady-state Tokamak
WWII	World War II

ITER, currently one of the most ambitious scientific projects, is under construction in southern France. About 10 times larger than the largest machine of its kind ever built, ITER should demonstrate that hydrogen fusion, naturally occurring in the Sun and the stars, can be replicated on earth for several minutes and produce power equal to several hundreds of millions of watts. Thus, if ITER succeeds and if the technology turns out

be economically sustainable, fusion could become a new power source used on an industrial scale to produce electricity on earth in a safe and environmentally friendly way. This is the new nuclear: fusion uses a very abundant fuel (hydrogen) and produces little waste. ITER will produce a “green nuclear” energy, without any major drawbacks. The advantages are therefore high. The seven members of ITER, who committed to build the machine together, realized this quite a long time ago. By mobilizing considerable resources and several thousand people around the world, ITER is, in some respects, not so much different from WWII’s Manhattan project, albeit in the field of scientific research. It is possible that ITER will revolutionize nuclear power forever.

But we are not there yet. There are still, under the fusion star, areas of shadow and black spots. The project’s difficulties are in proportion to its challenges; delays are accumulating (the first experiments will take place in 2025 at the earliest) and the budget is quadruple its original size (according to the latest estimates, the construction only will cost more than EUR 40 billion). High-tech experts are used to put these problems in perspective as this is the most complex machine ever built by mankind. Some also compare ITER to the Apollo project due to its technological sophistication and its potential to modify irreversibly both the course of history and the future of our civilization. The seven ITER members actually represent 35 countries—more than half the global population—which have decided to work together to construct the project. ITER is among the world’s largest scientific and peaceful cooperation projects. Although this it is not often pointed out, ITER is a “generous” project: the countries participating in the experiment have decided to learn together and share all the knowledge that will be developed in the framework of this huge international cooperation. This is obviously not just about science and technology: the objective is also to develop a worldwide fusion industry. Furthermore, ITER is only the beginning of the story. All ITER members have already plans for the next steps. Euratom, the EU’s nuclear energy community, has a detailed road map to fusion energy.

The previous Director General of the ITER Organization (IO) liked to say (Bigot, 2019) that “only fusion can meet the energy challenge mankind is facing.” What is true is that the demand for energy continues to grow in virtually every country in the world, a “natural” consequence of demographic changes, boosted by the almost universal increase in quality of life and by the development of emerging economies. The world’s energy consumption has more than doubled since 1973; it could be further tripled by the end of the century. Though the planet’s main fossil fuels—oil, natural gas, and coal—are being depleted, they still provide about 80% of the energy consumed. But the need for fusion energy is somewhat controversial. Several studies carried out in various countries and political contexts seem to converge toward the idea that an energy supply based solely on renewable sources is possible by 2050, as supported for example by the work of the National Renewable Energy Laboratory (NREL), which aims at a “100% green” scenario for the United States (US).^a However, most experts do not envisage green energies completely supplanting all “unsustainable” sources before the end of this century. Energy, in the future, will be supplied through a “mix” of energy sources.

In this chapter, we take a look at the major milestones that accompanied the genesis of the ITER program and recall the principles of nuclear fusion. Then we will examine the machine currently under construction in Provence and address the key questions about ITER. Due to the recurring delays and the exponential increase of the budget, two of the seven ITER members, specifically the United States and India, have considered withdrawing from the project. If this happened, would it mean the delay or even the death of ITER? Some think, even within the scientific community, that fusion energy will always remain a mystical chimera. Recalling that fusion energy has been in development for over 30 years, the most skeptical state that it will forever be 30 years away... A view that seems to be confirmed every day by the slipping delays (Figure 23.1).

^a See also the work carried out in Europe, in particular by France’s Agence de l’Environnement et de la Maîtrise de l’Energie (ADEME) and the négaWatt association, who argue for the feasibility of a total conversion into renewable energies by 2050 as, on top of its advantages, it would lead to savings of hundreds of billions of euros and the creation of some 500,000 jobs in France: <https://www.negawatt.org/>.



Figure 23.1. Aerial view of the ITER worksite in Cadarache (close to Marseille) in February 2022. The site has a total area of 181 ha (1,810,000 m²). On the right side, the headquarters of the international organization (the bent building with a dark façade). The reactor will be located in the building surrounded by four cranes, which is next to the other tallest building on the platform (known as the “assembly hall”). Nearly 3000 people are currently working on the site. *Credit: ITER Organization*

23.1 Nuclear fusion

Nuclear fusion reactions are universal in the most fundamental sense; they occur all over the Universe, as it is fusion that allows the stars to ignite and produce energy. One hundred million years after the Big Bang, the very first fusion reactions occurred in the centers of immense gaseous spheres. As the temperature of the gas inside a sphere climbed, it would “ignite,” marking the birth of a new star. Brought to several million degrees, the gas that made up the stars would then become a “plasma”: a state of matter where the nuclei and electrons that make up atoms have been completely dissociated from each other. Billions of years after the Big Bang, this process is still going strong and, at the scale of the observable Universe, plasma is probably the most common state of matter. Our Sun, which accounts for 99.9% of the total mass of the solar system, is a huge ball of plasma composed mostly of hydrogen, and it has been over four billion years since the first fusion reactions ignited in its heart.

But scientists have known all this only since the beginning of the 20th century. In 1920, the British astrophysicist Arthur Eddington (1882–1944) was the first to suggest that the stars burn because of a nuclear reaction, namely the transmutation of hydrogen into helium.

However, it took almost 20 years—until 1939—for the German physicist Hans Bethe (1906–2005) to articulate the exact sequence of reactions involved. This is the famous “proton-proton chain,” which starts with four hydrogen nuclei, and ends with a helium-4 nucleus (alpha particle). This achievement, along with a broader explanation of the process of transmutation of matter within the stars, earned Bethe the Nobel Prize in physics in 1967.

In science, practice sometimes precedes theory, and in 1934, 5 years before Bethe worked out the process of fusion in stars, the physicist Ernest Rutherford (1871–1937), born in New Zealand, made history by achieving fusion in the laboratory for the first time. He managed to fuse deuterium into helium. Having noted

the considerable effect that this reaction produced, Rutherford paved the way to fusion research, of which ITER, more than 80 years later, is the culmination. Rutherford's assistant, the Australian Mark Oliphant (1901–2000), also played a key role in the development and observation of these early fusion experiments. In particular, he discovered other “fuels” for fusion: namely tritium, the second heavy isotope of hydrogen; and helium-3, a promising isotope, which might be used in the next generation of reactors.

To achieve fusion on Earth, one must create “astronomical” temperatures of tens or even hundreds of millions of Celsius. For example, the H-bomb (also known as hydrogen bomb or thermonuclear bomb), actually a double bomb, contains a primary fission A-bomb (made of uranium or plutonium) that explodes only to compress and heat the gas inside (tritium, deuterium or lithium deuteride) up to about one hundred million of Celsius. This triggers hydrogen fusion reactions, which constitute the thermonuclear explosion of the bomb.

In the 1950s, scientists quickly realized that fusion holds huge potential for peaceful applications and controlled (non-explosive) systems. As the American science journalist Daniel Clery wrote (Clery, 2013), “Fusion seems too good to be true and to the fusion pioneers in the late 1940s and early 1950s, although they wouldn't have known all of these details, it was clear that fusion would be a vastly superior energy source compared to fission.” But these visionary scientists clearly underestimated the difficulties and technical hurdles they would encounter on the road to fusion that complicated, if not prevented, the road to peaceful application of the technology.

To control fusion, physicists began by exploiting the phenomenon of “magnetic self-constriction,” which develops in gaseous plasmas when an electromagnetic field is applied. For example, in a plasma that is shaped symmetrically around one axis, the electric current flowing in the plasma column itself generates a magnetic field through electromagnetic induction. This magnetic field exerts a force that confines the gas and “pinches” the plasma, hence the names “pinch effect,” “Z-pinch,” or “zeta pinch” given to this phenomenon (Z/zeta representing the direction of the axis).

A large torus-shaped (broadly, doughnut-shaped) machine called Zeta was built in 1954. Zeta was located in the UK Atomic Energy Research Establishment, known as AERE or Harwell Laboratory, in Oxfordshire. This laboratory, not far from London, was the main center for atomic energy research and development from the 1940s to the 1990s. Zeta exploited the pinch effect to stabilize very hot plasmas. But the researchers encountered an early hurdle, as although the magnetic fields and electric currents nicely combined to constrain the particles, vertical drift led them to deviate and hit the walls of the vessel, losing their energy. The pinch effect, therefore, had to be augmented with other magnetic-field configurations to produce a sort of “magnetic bottle.” Thus, the Harwell team learnt that their machine had to be surrounded by powerful magnets in order to contain the charged particles and prevent them from touching the walls.

In fact, this principle of “magnetic confinement” had already been applied in the early 1950s on the other side of the “Iron Curtain” by Russian theoretical physicists Igor Tamm (1895–1971) and Andrei Sakharov (1921–1989), who had in fact designed a toric (torus-shaped) device with several magnets, which they called the “tokamak.” And at about the same time, in the United States, a more complex machine called the “stellarator”^b had been developed by the theoretical physicist and astronomer Lyman Spitzer (1914–1997). Magnetic confinement was therefore in vogue at that time (Figure 23.2).

In a tokamak, the geometric configuration of the machine makes the plasma's electrons and nuclei move in helical (spiral-shaped) paths. If the magnetic fields produced by the external magnets are correctly calibrated, these helical paths create magnetic surfaces that close in on themselves inside the vacuum chamber that contains the plasma. The tokamak generates an infinite number of such surfaces, nested one inside the other, in which the particles are virtually imprisoned (in the absence of collisions and magnetic turbulence) and faithfully follow the electromagnetic field lines as if they were invisible rails.

^b The name derives from the fact that its promoters hoped to achieve, with this configuration, temperatures comparable to stellar plasmas.

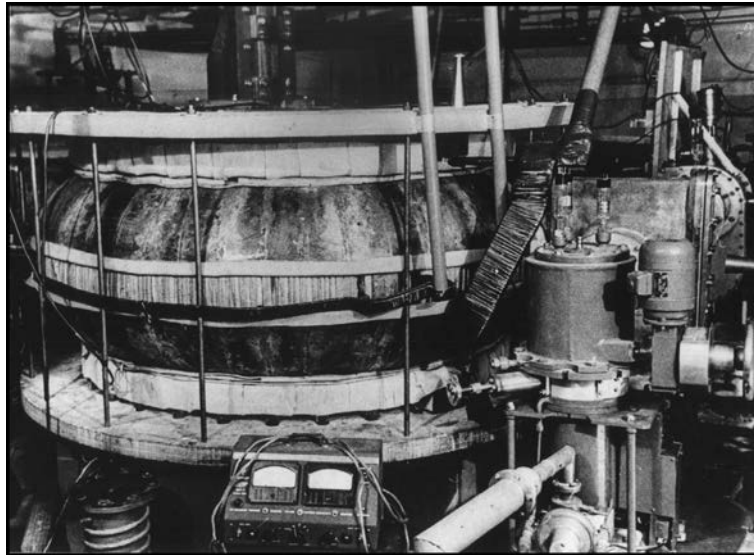


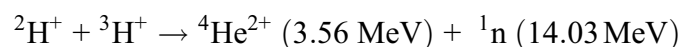
Figure 23.2. The Kurchatov Institute’s T-1 was the first tokamak in the world. With a radius of only 67 cm, it was a very small machine compared to JET, ITER and the like

The “poloidal field,”^c parallel to the central axis of the torus, is created mainly by a high-intensity induced current that circulates in the plasma and contributes to its confinement. Unfortunately, this magnetic field is maintained only if the intensity of the current is constantly increasing, which is not feasible over a long period. Furthermore, the impurities and instabilities of the plasma increase its resistance to the current, which eventually dies out, as well as the magnetic field associated with it. This is why a tokamak has to work in relatively short “plasma shots” rather than operating continuously. This way of working also implies—another disadvantage—that the tokamak goes through a succession of heating and cooling, which causes fatigue for the machine, particularly the parts that face the plasma.

The situation is quite different in a stellarator, where the magnetic fields are entirely produced by coils outside the plasma. The shape of the machine gives the magnetic field lines the appearance of a Moebius strip. No current flows in the plasma, which makes this type of reactor much more stable and longer-lasting. On the other hand, the complex three-dimensional geometry of the stellarator and the resulting costs create headaches for engineers and sleepless nights for fund-raisers...

At present, the most powerful machine of this type is located in northern Germany, in Greifswald, where the Wendelstein 7-X stellarator, built by the Max Planck Institute for Plasma Physics, was inaugurated and commissioned on February 3, 2016, in the presence of then Chancellor, Angela Merkel. W7-X, as physicists call it, is far from performing as ITER is expected to, and will not itself generate energy. However, it will test the feasibility of a future fusion reactor using stellarator technology and check the stability of the plasmas produced. This experiment may therefore provide good news in the future.

In order to produce energy from the fusion of light atoms, nature offers a dozen possible combinations. But with the current state-of-the-art technology, the deuterium-tritium fusion reaction is characterized by the largest cross-section, with a maximum at a relatively low energy—of the order of 100 keV. Finally, this reaction releases a large amount of energy, three quarters of which is carried away by the neutron produced by it:



The equation means that the fusion of one deuterium nucleus and one tritium nucleus produces one helium-4 nucleus (carrying 3.56 MeV of kinetic energy) and a neutron (with 14.03 MeV of kinetic energy, traveling at

^c The name “poloidal field” comes from an analogy with the Earth’s magnetic field, which has a poloidal component (parallel to the North-South axis) and a toroidal component (parallel to the lines of latitude).

roughly one sixth of the speed of light). This means that 1 g of D-T 50/50 mixture produces, through nuclear fusion, as much energy as the combustion of 8000 tons of oil. “Burning” fossil fuels releases chemical energy, whereas the energy that comes from fusion is released through reorganizing the bonds that form the helium nucleus. Through this reorganization, a small amount of mass is converted to energy, using none other than Einstein’s famous equation $E = mc^2$. In this chapter, we focus mainly on magnetic confinement (realized in tokamaks and stellarators) but we should note here that other technologies are being developed to generate fusion energy.

23.2 The history of the ITER project

Researchers in nuclear fusion quickly realized that international cooperation was the best way to go. Since the middle of the last century, plasma physicists have been facing up one fact: fusion is a very complex scientific specialty that requires a major research effort as well as very large and sophisticated instruments—in effect, very difficult to build and operate. Therefore, to produce fusion energy, the scientific community had no choice but to pool its innovative potential, its technological expertise and of course its financial resources. Remarkably enough scientists managed to convince their political authorities of this fact.

This international cooperation started over 60 years ago, in the midst of the Cold War. At that time, fusion research was still considered a classified defense activity. But cracks were beginning to show in the official secrecy surrounding fusion research. On December 8, 1953, in a speech to the United Nations General Assembly, US President Dwight D. Eisenhower announced his intention to launch a program to develop nuclear technologies that would have no military application and could therefore be used freely for the benefit of mankind. This program would become known as “Atoms for Peace,” after the title of the speech. The initiative was followed by the first international conference on the peaceful uses of nuclear energy in Geneva in 1955, which was attended by no less than 25,000 participants. For the first time since the Second World War, scientists in the West could talk publicly with their counterparts in the East, across the “Iron Curtain.”

The US and British governments then officially acknowledged supporting fusion research programs and began to exchange views on the subject. They were followed by other countries, including the Soviet Union. It is not widely known that a high-level meeting took place on April 25, 1956, in Harwell Laboratory, in the presence of a large contingent of British and Soviet scientists, to discuss the topic of nuclear fusion. Accompanying Nikolai Bulganin, the chairman of the Council of Ministers of the Soviet Union, and Nikita Khrushchev, secretary general of the Communist Party, a Soviet scientific delegation met some 300 physicists gathered in the sacred heart of British nuclear research. In a rare instance of transparency for that time, the director of the Soviet nuclear program, Igor Kurchatov, delivered a lecture entitled “The possibility of producing thermonuclear reactions in a gaseous discharge.”^d It was already very clear that only free and transparent international cooperation could overcome the huge difficulties, both theoretical and practical, that nuclear fusion posed (Figure 23.3).^e

Europe strongly encouraged the integration of this emerging scientific community. A decisive step was the ratification of the Treaty establishing the European Atomic Energy Community (Euratom), which was signed in Rome on March 25, 1957, the same day as the founding text of the European Community (EC, later renamed as EU—European Union).^f The six founding countries of the Community, Belgium, France, Germany, Italy, Luxembourg and the Netherlands, considered atomic energy, as it was called at that time, as a means to achieve independence in energy supply. An interesting detail: in the 176 pages of the Euratom

^d https://fire.pppl.gov/kurchatov_1956.pdf.

^e Actually, fusion was the first—and over the years, most intense—area of cooperation between US and Russian nuclear laboratories.

^f Euratom is legally distinct from the European Union (EU), but has the same members, and is governed by many of the EU’s institutions. Since 2014, Switzerland has also participated in Euratom programmes as an associated state.



Figure 23.3. On April 25, 1956, in Harwell Laboratory, a high-level Soviet delegation met a large contingent of British scientists, to discuss the topic of nuclear fusion: left to right Mr Selwyn Lloyd, QC Secretary of state for Foreign Affairs, Mr Nikita Khrushchev, leader of the Russian Communist party, Sir John Cockroft, Director of Harwell, Dr. Basil Schonland, Deputy Director of Harwell, Marshal Nikolai Bulganin, Soviet Prime Minister, and Sir Edwin Plowden, chairman of the UKAEA. *Credit: Nuclear Decommissioning Authority*

Treaty, only one line is dedicated to fusion—a surprising contrast to the huge development it will later undergo in Europe. And this reference appears only in the annex, which lists the areas of research that “the Commission shall be responsible for promoting and facilitating [...] in the Member States and for complementing it by carrying out a Community research and training programme” in subparagraph (e): “study of fusion, with particular reference to the behaviour of an ionized plasma under the action of electromagnetic forces and to the thermodynamics of extremely high temperatures.”^g

The 70s marked the beginning of a new age for fusion. The combination of several breakthroughs and the dynamism of the European Community helped boost national research programs, and not just those of the EC Member States. All major countries equipped themselves with quite powerful tokamaks. France had its TFR (Tokamak Fontenay-aux-Roses), Germany its ASDEX (Axially Symmetric Divertor EXperiment), the United States their TFTR (Tokamak Fusion Test Reactor), Japan its JT-60 (JAERI tokamak 60), etc. It was in the German machine that a spectacular unexpected phenomenon, the “H-mode” (“High”-mode), was discovered in 1982. The H-mode is a particular plasma configuration that improves its stability and offers the possibility of lengthening its confinement time—doubling it, or even more. Since then, physicists have been able to reproduce the H-mode in almost all the tokamaks in the world, even if they do not yet agree on the source of this interesting phenomenon.

At that time, Europe was firmly in the driving seat of the fusion research momentum that was developing worldwide. Riding on the wave of collective scientific excitement, in the early 70s European leaders conceived an even more ambitious project for the Euratom framework. It was to be a larger, more powerful machine for testing D-T plasmas (using a mix of deuterium and tritium as its fuel) to achieve “real” fusion

^g <https://eur-lex.europa.eu/legal-content/EN/TXT/PDF/?uri=CELEX:11957A/TXT&from=EN>.

and release large amounts of energy. The project eventually coalesced into the first plans for the Joint European Torus (JET). Paul-Henri Rebut was asked to lead the working group for its development.

Presented to the European Commission for approval in 1975, JET was officially accepted 3 years later. Funding was approved on April 1, 1978, for the “JET Joint Undertaking.” Construction started immediately on a former Royal Navy airfield at Culham, near Oxford, about 100 km northwest of London. In 1983, JET created its first plasma. This machine and its American counterpart TFTR were designed to work toward achieving *breakeven* conditions, which is achieved when the power released by the fusion reaction equals the power injected to heat it. From an industrial perspective, breakeven is the minimum requirement for a productive fusion reactor: in simple terms, the power “out” must exceed the power “in.”

Inaugurated on April 9, 1984, by Queen Elizabeth II and French President François Mitterrand, the European tokamak performed the world’s first D-T experiment on November 9, 1991. It produced nearly 2 MW_{th} of fusion power, a major achievement that led Paul-Henri Rebut to announce to the press (JET, 1991): “this is the first time that a significant amount of power has been obtained from controlled nuclear fusion reactions. It is clearly a major step forward in the development of fusion as a new source of energy.” But the specialists knew well that this first result was well below JET’s real capabilities as, for this first experiment, the senior management had opted for a modest set-up, using a fuel with low tritium content (representing only 10% of the gas mixture) so as not to irradiate the inner walls of the reactor too much (Figure 23.4).

At the end of the last century, thanks to JET and other similar machines, mankind entered the era of controlled thermonuclear fusion. These achievements lent scientific credibility to fusion energy and supported new proposals to move to the next stage: reaching or even exceeding breakeven.

A historic turning point came in 1985. Precisely, on the 19th and 20th of November, when the Secretary General of the Communist Party of the Soviet Union, Mikhail Gorbachev, met the then President of the United States, Ronald Reagan, for the first time. The two leaders met in Geneva to hold talks on international diplomatic relations and to find a way out of the Cold War that had lasted almost 40 years. As a priority, they addressed the looming arms race; both leaders wanted to reduce the number of nuclear weapons in the arsenals of the great powers of the planet. However, quite surprisingly, the final communiqué published at the end of this historic summit mentions fusion. The thirteenth point, carefully phrased and very diplomatic in style, stated that both countries emphasized “the potential importance of the work aimed at utilizing controlled thermonuclear fusion

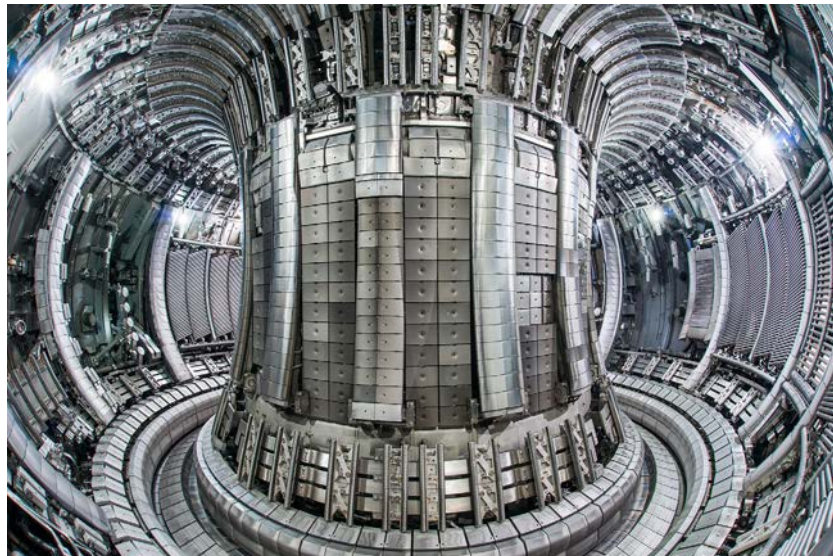


Figure 23.4. The UK government and the European Commission continue to fund the JET experiment, despite the fact that the country left the EU. JET is still the world’s most powerful tokamak machine. *Credit: EUROfusion*

for peaceful purposes and, in this connection, advocated the widest practicable development of international cooperation in obtaining this source of energy, which is essentially inexhaustible, for the benefit of all mankind.” These words were what the international fusion community had been waiting for.

The start of ITER was however quite laborious; it wasn’t until after another meeting between Reagan and Gorbachev in Reykjavik in 1986 that a first draft agreement was put on paper. Then, with the participation of the Soviet Union, the United States, Euratom and Japan, a committee had been set up in 1988 to work on the initial design of the machine. The Director General of the European Commission’s DG XII (Science, research and development), the Italian Paolo Fasella, gave the new project its name: *International Thermonuclear Experimental Reactor*—ITER.

A few months later, on April 21, 1988, the Official Journal of the European Communities announced (EC, 1988) a “Commission Decision [...] concerning the conclusion of an Agreement of participation in the International Thermonuclear Experimental Reactor (ITER) Conceptual Design Activities, by the European Atomic Energy Community, with Japan, the Union of Soviet Socialist Republics, and the United States of America, by the Commission for and on behalf of the Community.” This is how the four members decided to build ITER, the world’s largest fusion experimental reactor, under the authority of the IAEA.

The EC official publication gave a genuine legitimacy to the project, on the basis of which the partners could then work to launch the Conceptual Design Activities (CDA) and create a first conceptual design for the fusion reactor. The aim was first to determine and agree on the main characteristics of the machine, taking into account the technology available at the time and the various fusion programs that were running around the world. This work ended in December 1990. A few months later, the Parties entered into a series of consultations on how ITER should proceed further. In July 1992, a new agreement was formalized in order to initiate the technical design phase (Engineering Design Activities, EDA), which was intended to create the detailed plans of the machine. This was a decisive step, as the four members agreed to share the intellectual property produced through their work and to commit up \$1.2 billion to carry out these detailed studies and realize required full-scale prototypes before the end of the century.

However, the EDA took more time than expected and it appeared that the machine’s detailed plans would not be finalized before the end of the century. These delays were caused in part by profound differences of opinion between Paul-Henri Rebut and the ITER Council, the governing body of the consortium which takes the most important decisions regarding the management of the project and the resources to be allocated. In 1993, the project entered severe turmoil that almost killed it. The machine that had been conceived by the team was huge. With a plasma volume of a thousand cubic meters, almost 12 times as much as that of JET, it was designed to deliver an output thermal power estimated at 1.5 GW_{th}. The total cost was then estimated at \$11 billion (of that time).

In the mid-1990s, the general climate changed radically; major difficulties arose on the international stage, such as the collapse of the USSR and the abrupt fall in the cost of petroleum (which, in the eyes of certain politicians, reduced the urgency of research on new sources of energy). But the most dramatic change came from America and was nearly fatal to the project. Under the influence of the new Republican majority elected in 1994, the United States was drastically cutting public spending. For example, the budget devoted to magnetic fusion by the Department Of Energy (DOE) was reduced in 1996 to \$244 million, which was markedly insufficient to cover participation in ITER. In an article published in 1997 (Browne, 1997: “Money Shortage Jeopardies Fusion Reactor”), the *New York Times* lambasted the Republican decision to reduce the fusion research budget by 33%, which led to the closure of Princeton’s TFTR.^h The budget allocated to ITER, now fixed at EUR 50 million per year, was unrealistic.

^h TFTR was followed by the NSTX spherical tokamak, upgraded as NSTX-U at the end of 2015, but it broke down in July 2016, which caused the Director of Princeton Plasma Physics Laboratory, Stewart Prager, to resign after 8 years in the service of the project. This means that only one major fusion facility is currently operational in the United States: DIII-D, located in San Diego (California) and owned by General Atomics, a US defense partner.

In this context, and under strong pressure from Congress, the United States withdrew from the consortium in July 1998. However, the three remaining partners decided to finalize the design and engineering phase, and confirmed their commitment to bringing the project to completion. Nevertheless, taking into account the delays, the persistent economic crisis in Japan, and the reduction of ITER's total funding due to the US withdrawal, the members gave themselves an additional 3 years to continue and complete the work in progress.

The final detailed design of ITER was eventually completed in 2001. The final document outlined a modest machine with a vacuum chamber of eight hundred cubic meters, with a target output of 500 MW_{th} of fusion power. According to Robert Aymar, who succeeded to Paul-Henri Rebut as director of the ITER project (1993–2003), it was the appropriate size to realize a self-sustained plasma and achieve net energy production.

The “Aymar report,” which was several thousand pages long, was approved by the ITER Council in June 2001 and published the following month. Subsequently, a new round of negotiations started in November 2001 in order to draft the “Joint Implementation Agreement,” which would detail the construction, operation and dismantling of ITER, and also define the members' responsibilities for supplying the machine components. In order to provide data for the cost estimates on as realistic a basis as possible, the cost structure of ITER was broken down into 85 “procurement packages,” each about the size of a plausible procurement contract. Last but not least, the document included an estimate of the financial, organizational and human resources needed to implement the project, allowing the members to choose the best possible location for the tokamak.

ITER could have been built in any one of the 35 countries that are participating in the project. Overall, it took no less than 10 years of technical studies, political negotiations and diplomatic arrangements before Cadarache in France was finally chosen to host ITER.

Formally speaking, the discussions about the site started in spring 2001, when the report on ITER's detailed design was being finalized. The three project members (Europe, Japan, and Russia) started to consider fundamental practical questions. Where were they going to build ITER? How much would it cost? Who would pay for what? All these questions had major political, economic and technical implications, as the selected site (and its host country) would receive concrete benefits, while also defining myriad practical concerns such as transport, water and electricity supplies, etc.

Actually, only four countries proposed to host ITER: Canada, France, Japan and Spain. EU countries first decided to retain France as the European candidate. Then Canada withdrew from the discussions. In 2003, the ITER consortium gained three new members: China, Korea and the United States, which decided to return at the negotiation table. But over 3 years of technical and diplomatic discussions yet deemed necessary to reach a consensus. Intense negotiations lasted until June 28, 2005, when the ministers of the ITER Parties met in Moscow. After a few hours of discussion, a consensus was finally reached, with members unanimously accepting that the experimental fusion reactor that China, the European Union, Japan, Korea, Russia and the United States had decided to build together (India would join them at the end of the year) would eventually be installed in Cadarache, in the small commune of Saint-Paul-lez-Durance (980 inhabitants), approximately 80 km to the north of Marseille. Construction works began on-site at the end of 2007. The 181-ha site where ITER now stands is leased by CEA to the IO through a 99-year long-term lease.

The long-awaited decision was reported in a joint press release by the European Commissioner for Science and Research, Janez Potočnik and the Japanese Minister of Science and Technology, Nariaki Nakayama. The former declared (EC, 2005): “Today, a page has been written in the history of international scientific cooperation. Now that we have reached consensus on the site for ITER, we will make every effort to finalize the agreement on the project, so that construction can begin as soon as possible,” and the latter, very honorably but with some regrets (Associated Press, 2005): “I wish to say that today Japan is both sad and happy. However, this project is so important that we have decided to overcome our grief and transform it into joy.”

Behind the scenes, an agreement had been reached a few weeks before between the European Commission and Japan, on May 5, 2005, to establish a number of compensations, including the fact that the first Director General of the ITER Organization would be a Japanese citizen, or in diplomatic language: “The host member



Figure 23.5. Signing ceremony of the ITER International Fusion Energy Agreement in the Palais de l'Élysée, Paris, November 21, 2006. *Credit: Photographic service of the Presidency of the French Republic—L. Blevenec*

shall support for the position of Director General an appropriately qualified candidate of the non-host member.”

Chinese, Europeans, Japanese, Koreans, Russians and Americans had demonstrated their capacity to find a solution that was acceptable to all (India joined ITER at the end of 2015). The project had become a program (Figure 23.5).

23.3 A gigantic fusion machine

In principle, a tokamak is a relatively simple machine: it is a toroidal vacuum chamber surrounded by magnets that confine the plasma and keep charged particles from touching the walls. Hydrogen gas is injected into the chamber and heated, reaching temperatures of tens or even hundreds of millions of degrees. Energy is generated by the fusion of hydrogen nuclei, and comes out of the fusion reaction as the kinetic energy of the neutrons produced. As neutrons are not electrically charged, they are not affected by the magnets that are surrounding the chamber, so they hit the walls and their kinetic energy is absorbed as heat. As with conventional power generators, an operational fusion plant would use this heat to convert water into steam and produce electricity through turbines and alternators. Simple in principle but complex in practice, the ITER tokamak will be a perfectly formed jewel of technology.

Developed by Soviet physicists in the early 1950s, the tokamak concept has produced interesting results and undergone substantial improvements. This is the main reason why this type of reactor is today the dominant model for researchers working on magnetic confinement fusion, particularly those developing this technology to produce fusion energy (remember that ITER will remain an experimental machine, designed to explore the technical feasibility of fusion energy on earth, and will never produce any electricityⁱ).

ⁱ Most visitors of ITER are surprised when they are told that ITER will not exploit the energy produced by the fusion reactions (apart from producing steam).

The first tokamaks were small enough to sit on a laboratory bench. The technology and control systems were quite basic. However, using them, scientists managed to generate high-temperature plasmas and confine their energy for an amount of time (still relatively short: just a few milliseconds). These first experiments afforded a first glimpse at new physical phenomena such as anomalous transport, which is generated by turbulences and micro-instabilities that affect the behavior of the plasma. Similarly, physicists discovered scaling laws, which allowed them to predict that the plasma energy's confinement time could be much longer in a larger machine equipped with powerful magnets. In the tokamak family, size matters!

The second generation of tokamaks, which appeared in the years 1970–1980, was characterized by extensive use of external heating systems (i.e., heating being injected into the plasma from outside). Further improvements were made for this generation of machines, such as adding a “divertor,” a sort of giant ashtray at the bottom of the machine to collect non-hydrogen particles and the product of the fusion reaction (helium in the case of D-T fusion). These technological developments allowed designers and engineers to confine the plasma more securely, therefore reducing the neutron and heat loads on the internal walls of the machine. This was a significant improvement, as the extreme conditions within the vacuum chamber during the experiments are difficult for all but the toughest materials to withstand on the walls of the chamber and other plasma-facing components.

These new tokamaks, larger than those before them, such as JET in Europe, JT-60 in Japan, TFTR in the United States and T-15 in the Soviet Union, allowed scientists to study plasmas in conditions as close as possible to those of a fusion reactor. Integrating the latest developments in fusion science and technology, these machines have been regularly renovated and updated, in particular with superconducting magnets and remote handling tools. A few of them have become able to operate with deuterium-tritium mixtures. Overall, these second-generation devices have made it possible to make significant progress in fusion research and in plasma physics.

For example, on February 4, 1982, when operating the ASDEX machine in Garching, the German physicist Friedrich Wagner discovered a dramatic change in the plasma's behavior under certain conditions. Now called “high-confinement mode” or “H-mode,” the phenomenon was previously unknown but is now famous in the fusion community. It also triggered a lot of research in plasma physics, as it took scientists almost 40 years to understand the theory behind the effect.

Initially skeptical, Wagner took a full weekend to check and analyze his data, and eventually confirmed that the phenomenon was real. Arriving at his office on the following Monday, he announced victoriously that he had observed a transformation of the plasma during the experiences that he had performed a few days before. Having reproduced the phenomenon in a new series of experiments, Wagner concluded that a sudden and remarkable change in plasma characteristics can occur above a certain threshold of heating. This change suddenly improves the performance of the plasma with an increase not only in confinement time but also in energy production, as scientists were soon to observe in JET.

The H-mode can be reproduced in any tokamak and even any stellarator, provided that a threshold of thermal power is exceeded. The exact value of the threshold depends on parameters like magnetic field and plasma density, but also varies from device to device. After 1982, even greater modes of stability, known as VH (“very high”), were observed in certain machines. This result is just one of the most visible aspects of the amount of scientific knowledge and technical know-how that has been amassed over the decades thanks to these machines. Together with the many lessons learnt through the experiments themselves, this expertise has been incorporated in the design of ITER.

Thanks to these increasingly powerful machines, fusion research entered the era of “burning plasmas.” A burning plasma is one in which the heat from the fusion reaction is contained in sufficient quantities and for a sufficiently long time that the energy produced in the plasma is sufficient to maintain its temperature. The external heating can therefore be vastly reduced or even switched off altogether.

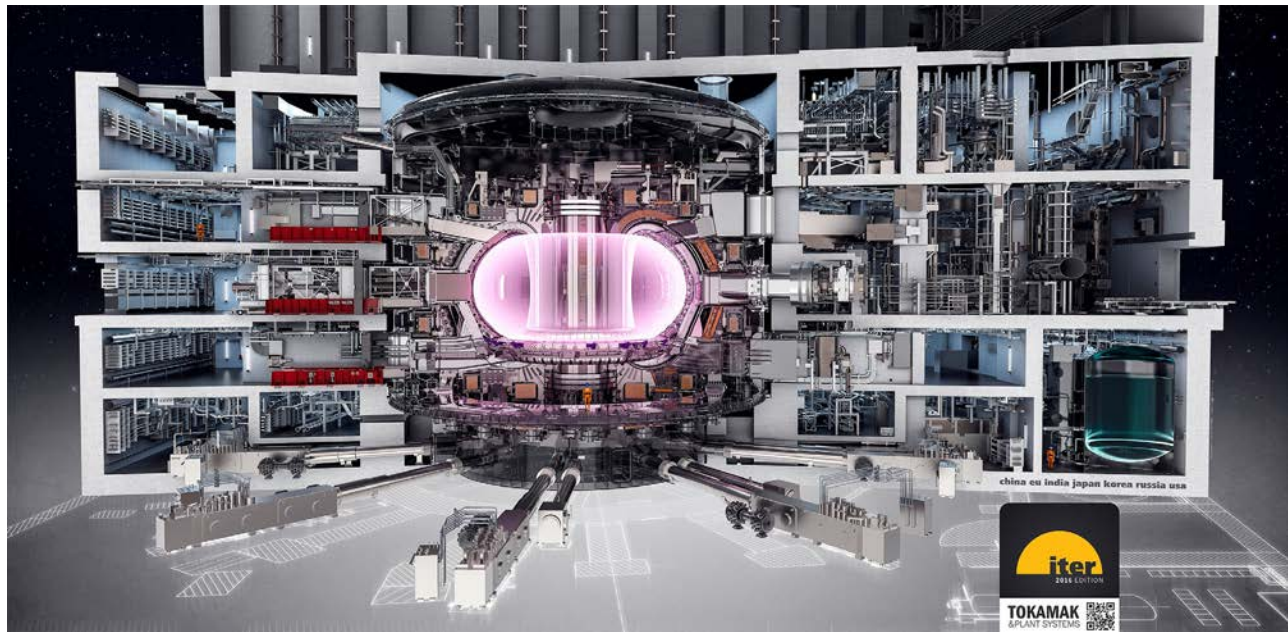


Figure 23.6. Computerized image of the ITER reactor. At the center is the vacuum chamber (pink) that will contain the plasma, and around it are the magnets and related technical systems. *Credit: ITER Organization*

The advantage of a burning plasma is not just that it allows the external heating to be reduced—it also allows fusion reactions to maintain themselves for longer periods of time. This is a crucial step forward if the aim is to exploit fusion energy commercially; a full-scale commercial reactor would have to be operated continuously for several minutes if not several hours. Investigating burning plasmas would therefore allow scientists and engineers to address this issue, as achieving plasma stabilization is crucial to ensuring the economic viability and the industrial feasibility of fusion energy. As ITER will study burning plasmas, operating ITER and executing its research program should in principle validate (or invalidate) the feasibility of fusion energy. In the next pages, we are going to review the ITER tokamak’s main components: the vacuum vessel, the magnets, the inner walls, the divertor, the cryostat, and the heating techniques (Figure 23.6).

When the ITER tokamak will be in operation (from 2025 onward if all goes very well but most likely around 2030), vacuum pumping will be required in the chamber prior to starting any fusion reaction. This is necessary to eliminate non-hydrogen molecules that would otherwise pollute the plasma. This elimination will be achieved by lowering the pressure in the chamber as much as possible before injecting the hydrogen gas. Mechanical and cryogenic pumps will be activated until the pressure inside has dropped to one millionth of normal atmospheric pressure. Given the volume of ITER, this operation will take 24–48h. ITER’s six cryogenic pumps will be among the most powerful in the world.

When the pressure in the vessel reaches its target, the magnetic system will be ready to confine and control the plasma. Then, the injection system will feed in the low-density gaseous fuel. In principle, this will be a D-T mixture, but in the first experiments the gas will be helium or regular hydrogen. A key component of the tokamak, the central solenoid will then induce a powerful current in the gas through electromagnetic induction. This current will be maintained during each plasma “pulse,” and it is this current that will ionize the gas and transform it into a plasma. ITER and other tokamaks essentially act as large transformers, where the central solenoid is the primary winding, and the plasma the secondary winding. But the role of the central solenoid doesn’t end there. As the high-intensity current circulates within the plasma, resistance will be created through collisions between energized particles. This will contribute to heating the plasma.

As the plasma heats up, the kinetic energy of the electrons and ions will gradually increase. However, as the plasma is not in thermodynamic equilibrium, the temperatures of the electrons and ions will not be the same. A number of additional heating technologies will then intervene to bring the ITER plasma to a high

enough temperature for fusion, i.e., 150 million °C. At this temperature, the nuclei will overtake the electrostatic repulsion and fuse, releasing huge amounts of energy.

A critical task will be to effectively control and confine the plasma using the electromagnetic coils that surround the vessel. Technicians in the future tokamak control room will have to play with the current in these coils, the external heating power, the density of the gas, and many other parameters to stabilize the plasma against turbulence and instability. It may take several months, if not years, to effectively master the machine and learn to control the plasma. Hopefully, a single fusion experiment can then last several minutes.

Thus, ITER will host the highest temperature gradient on Earth, and even beyond. Indeed, over a distance of just 3 m (between the heart of the plasma and the supercooled superconducting magnets), the temperature will fall abruptly from 150 million to -269°C .

ITER's chamber will be huge: 19 m high and 6 m in diameter, the empty vacuum vessel will weigh approximately 5200 tons (8500 tons once fully equipped) and will have a volume of 1400 m^3 , similar to a four-story building. It will be an unprecedented experimental tool, as the volume of ITER's plasma (840 m^3) will be 10 times larger than that of JET.

Inside the chamber, under the influence of the magnetic field created by the magnets and the plasma, charged particles will follow a helical (spiral-shaped) trajectory around the doughnut without touching the walls. The vacuum chamber will act as a first safety barrier against the radiation and the many neutrons produced by the fusion reaction. It will also hold some of the tokamak's internal components, such as the blanket and the divertor.

The vacuum chamber will have 44 "ports" (openings) to allow access for measurement, heating, injection and pumping equipment. These entrances will also be used by the robots that will perform maintenance work. Three windows are reserved for the neutral beam that will inject particles and heat the plasma; five windows will give access to the divertor for replacement and maintenance, while a further four windows will be reserved for the vacuum pumping systems. During operation, these openings will be closed with watertight doors to ensure the vessel is completely airtight.

The vacuum vessel is a huge challenge to manufacture. Principally because of its dimensions; ITER's chamber will be among the world's largest. Despite its complex geometry, it will need to be perfectly airtight. In addition, the openings and the fixing points must be positioned very precisely, with a margin of error of less than 1 mm; a gigantic task given the size of the chamber. And in 2001, the ITER members added yet another layer of complexity as they decided that the chamber would be partly built in Europe and partly in South Korea.

The vacuum chamber will be assembled from 9 sectors, each 11 m high and 7 m wide. Originally, two of these sectors were to be provided by South Korea, the other seven by Europe. But Europe experienced significant delay because of difficulties unrelated to ITER encountered by three companies involved in the manufacturing. Accordingly, the IO asked South Korea to manufacture two additional sectors. As of June 2022, South Korea delivered three sectors, Europe none. Unfortunately the three sectors arrived damaged on the site; they cannot be welded together as they should be and need to be repaired before.

In the tokamak, the vacuum vessel will not be directly exposed to the plasma. The inner walls of the vessel will be covered by 440 blanket modules (also called bricks), which will shield the steel vacuum vessel and the external machine components from the high-energy neutrons produced during the fusion reaction. This blanket, designed to support a thermal load of 700 MW, will absorb the neutrons, transforming their kinetic energy into heat, which will then be absorbed and carried away by water circulating behind the bricks. In future fusion power plants, this energy will be used to produce steam, and then electricity via turbines and alternators.

Each brick will be about 2 m tall and 1 m wide, and will weigh up to 5 tons. There will be no less than 100 different types of brick, determined by each brick's precise location in the vacuum chamber. The blanket will also include openings for measurement, robotics and plasma heating systems.

The blanket modules are one of the most important and economically sensitive components, as they are next to the hot plasma and therefore on the front line for the thermal loads and neutron fluxes. The bricks will

be coated by a thin layer of beryllium. With unique physical properties such as a very high evaporation point and a similarly high melting point (1287°C), this light metal will contaminate the plasma as little as possible, and absorb almost no hydrogen.

Once ITER has already been operational for a few years, from 2029 at the earliest, “Tritium Breeding Modules” (TBM) will be installed in the blanket. These special bricks will contain lithium, which will be converted into tritium when hit by a neutron. By installing and testing various prototypes, scientists hope to find a way to generate tritium inside the vacuum chamber itself to fuel the fusion reaction. While deuterium can be extracted from seawater in virtually boundless quantities, only minute amounts of tritium can be found in nature. The biggest sources of tritium today are the CANDU nuclear fission reactors, which are powered by natural (unenriched) uranium and cooled using heavy water (water that contains more deuterium than normal). Today, only a few countries operate CANDU reactors; in addition to Canada, the world largest producer, there is South Korea, Romania, and China.

In this way, ITER will be a unique opportunity to study TBM in a real fusion environment. Indeed, as ITER will probably consume all of the world’s inventory of tritium (around 40 kg), for any future fusion power plant a method of producing tritium is absolutely crucial. Initially, six different test modules were going to be used in the machine, which varied mainly in the form of lithium used (liquid or solid such as lithium lead, ceramic or metal). But the number of ports available for TBM experiments was recently reduced from three to two, allowing space for only four options in total.^j The ITER engineers will test four different technologies and select the best one. This aspect of the project is essential, as there will be no industrial development of fusion energy if self-sufficiency in tritium cannot be achieved.

Another major technological challenge is the magnetic confinement of the plasma. In the ITER tokamak, the confinement will be ensured by about 40 superconducting magnets, totaling over 10,000 tons in weight. This number breaks down as follows: 18 D-shaped toroidal magnets 17 m high, each weighing 310 tons; six circular poloidal magnets 6–24 m in diameter, the heaviest weighing 400 tons; a central solenoid 17 m tall, 4 m wide and 1000 tons; and 18 smaller correction coils. ITER’s magnet system will be the largest and most complex ever built. It will generate a magnetic field strength of 13 Tesla and will concentrate a total magnetic energy of over 50 billion joules. Distributed around the vacuum chamber, toroidal magnets will be placed vertically and poloidal magnets horizontally. Whereas the toroidal field is a static field, the poloidal field is variable; its main function consists in inducing an electrical current of several mega amperes in the plasma and controlling its mechanical equilibrium and shape. In addition, 31 non-superconducting coils will be fixed to the inner wall of the vessel to suppress or reduce certain types of plasma instabilities that occur on the edge of the plasma, the so-called Edge-Localized Modes (ELMs). If not properly controlled, these instabilities can lead to violent expulsion of heat and particles, which can damage the blanket and the rest of the machine (Figure 23.7).

ITER’s magnets are made of superconducting alloys—either Niobium-tin (Nb₃Sn) or Niobium-Titanium (Nb-Ti). When cooled down to –269°C (4 K), close to absolute zero, the alloys exhibit their superconducting qualities, meaning that electric current moves through them without any resistance.

The cables that form ITER’s superconducting magnets have a complex structure (see Figure 23.8). In the toroidal magnets, each cable is composed of about 1000 superconducting strands, each containing filaments no wider than a human hair, which are encased inside a stainless steel jacket 4 cm in diameter. The wires are then twisted together in a carefully designed pattern and fitted inside a stainless steel conduit or jacket. Alongside the filaments, there is space for liquid helium to flow, keeping the magnets at the very low temperatures needed to ensure they work as superconductors. The cables need to be wound with an accuracy of 0.05 mm/m and niobium-tin cables are heat-treated at 650°C in an inert atmosphere. This winding is

^j The decision was recently taken to reduce the number of vacuum vessel ports available for tritium breeding systems from three to two, which implies a reduction of the number of experiments from six to four. As the tritium experiments are “owned” by individual members, each member has therefore been invited to consider either canceling their experiment or cooperating with another one.

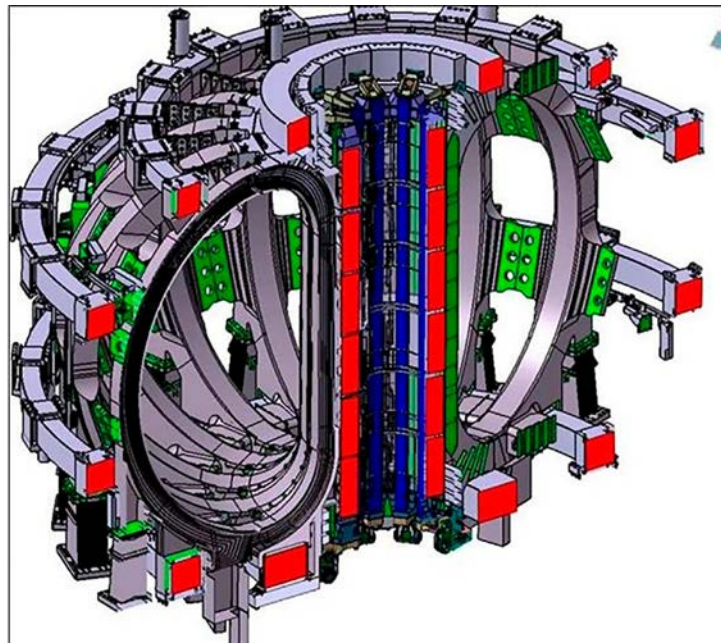


Figure 23.7. Computerized view of the ITER magnet system, showing the D-shaped toroidal field coils (18 in total), the 6 ring-shaped horizontal poloidal field coils and the central solenoid. *Credit: ITER Organization*



Figure 23.8. A section of a niobium-tin superconducting Cable-In-Conduit Conductor (CICC) used for the ITER toroidal magnets, showing the cable organization in strands and filaments. *Credit: ITER Organization*

extremely challenging because the conductors need to fit perfectly in the radial plate, a stainless steel D-shaped structure with grooves on both sides. This kind of cable, called “cable-in-conduit,” was invented in the United States in the 1970s (both the Massachusetts Institute of Technology (MIT) and the Oak Ridge National Laboratory stake a claim to it), and is used in all tokamaks. These cables are a key component of ITER’s magnet system, and are each 1 km long. This is the maximum technically feasible length while allowing a minimum number of joints between superconducting strands.

The superconducting niobium-tin alloy that will be used for the toroidal coils and the central solenoid can generate very high magnetic fields but has a few disadvantages. It is more expensive to produce and more difficult to process than the more “standard” niobium-titanium alloy. Indeed, unreacted, not-yet-

superconducting niobium-tin strands must first be assembled into cables and the cables then wound into a coil. Otherwise, the strands would be too brittle to withstand the cabling process and would lose their superconducting properties. Finally, the coil must be heat-treated at about 650°C for several days to make it superconducting through a complex chemical process.

The niobium-tin compound was discovered as a superconductor alloy in 1954, 8 years before the discovery of niobium-titanium. However, the latter was used for the construction of the European Organization for Nuclear Research (CERN)'s Large Hadron Collider, due to its greater availability, higher ductility and excellent electrical and mechanical properties. Even if it is more complicated to produce, there has been a renewed interest for niobium-tin in recent years since it can produce stronger magnetic fields. In total, nine suppliers in six countries have produced close to 500 tons of niobium-tin strands for ITER, representing a total length of almost 100,000 km. This has increased the world's annual production from 15 to 100 tons and enabled three new suppliers to enter the global market.

Toroidal and poloidal magnets will consist of several kilometers of cables-in-conduit, made rigid and insulated by an epoxy polymer resin and compacted into large "pancakes." Assembled two by two in double pancakes, they will be stacked to form winding packs, which will be encased in large stainless steel structures. ITER's magnets account for a quarter of the total weight of the machine.

The central solenoid is another key component of the machine, as it will act as the backbone of the tokamak. It will consist of six separate coils made of niobium-tin superconducting cables, and will be one of the most complex and powerful superconducting magnets ever built. The function of the central solenoid will be to induce a large electric current in the plasma, which will in turn create a powerful magnetic field that will contribute to confining the plasma. The current will also help with heating. If this thermal (ohmic) heating was the only source of heat, the plasma would reach a temperature of about 20 million °C. This is a lot, but insufficient to induce fusion reactions.

Examining the magnets gives a good idea of the kind of headaches that ITER's engineers have to face. Europe is manufacturing 10 of the toroidal coils and Japan is producing eight plus one spare; the poloidal coils will be supplied by Europe (four), Russia and China (one each); and the central solenoid is being produced by the United States. The companies involved have been given very detailed technical specifications to ensure that the magnets are compatible, if not identical. Interestingly, to ensure that the stainless steel is of the same chemical composition for all the magnets, irrespective of their origin, all of the manufacturers decided among themselves to use the same supplier, a company located in Le Creusot, France (Figure 23.9).

The teams involved in the manufacturing of the ITER superconducting magnets had to face difficulties which were as much as about management and logistics than about technology. With six of the seven ITER members producing cables, they had to make sure that each manufacturer used the same procedures and quality assurance. In particular, it was difficult to obtain the famous "CE marking," which certifies that a product conforms to health, safety, and environmental protection standards that apply in Europe (the European Economic Area). This leads to lengthy and cumbersome negotiations, and Project Change Requests (PCRs), which allow the agencies to recover part of the cost incurred by conforming to the regulations. There are also organizational difficulties, as 23 manufacturers are involved for the conductors alone, and about 150 intermediaries. No less than 1000 people are involved in the production of ITER's magnets worldwide. Another problem is storage; kilometers of conductors were produced well before the magnet manufacturers were ready to use them. As a result, hundreds of tons of cables are stored in several places all over the world.

Positioned at the bottom of the vacuum vessel, the divertor is yet another essential element of ITER. Its main task: to remove the helium produced by the fusion reaction and impurities in the chamber, mostly released by the inner walls, minimizing plasma contamination. The divertor will also extract part of the heat produced by the fusion reaction - up to 20 MW per square meter, a heat load 10 times higher than that on a spacecraft reentering the Earth's atmosphere.

As in the divertor parts of the plasma actually touch the wall, its surface will reach a temperature of almost 2000°C. In order to carry away the huge heat load and prevent the material from being melted or vaporized,

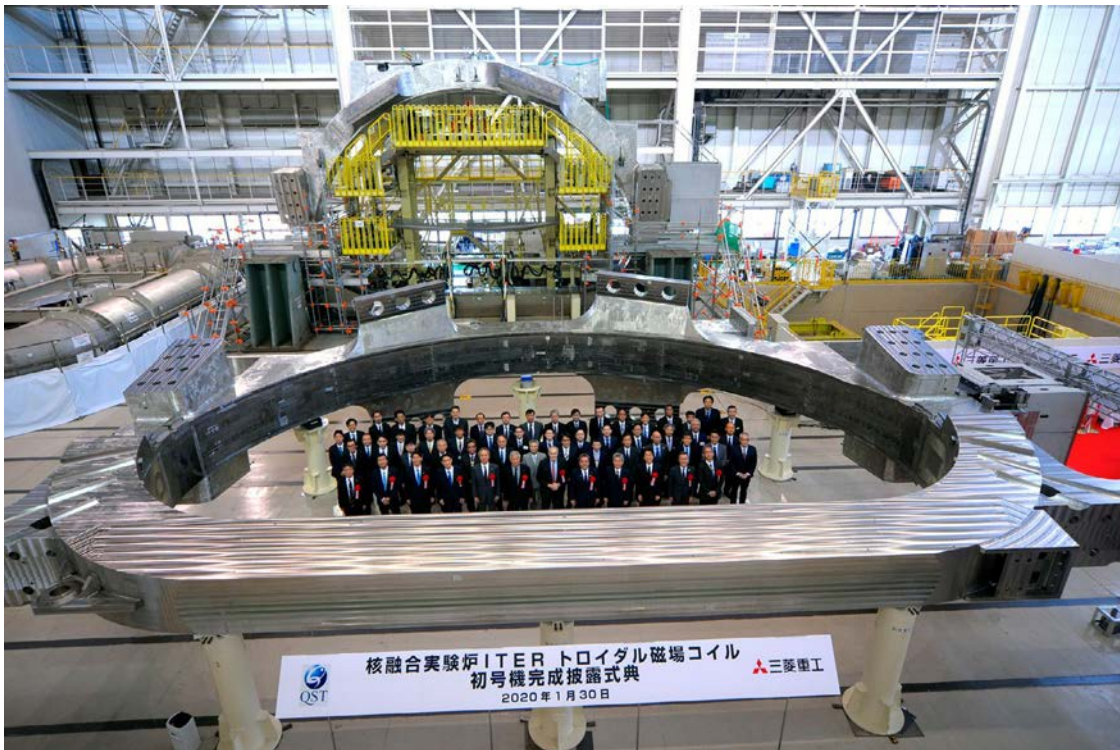


Figure 23.9. The ITER first toroidal magnet case produced in Japan by Mitsubishi Heavy Industries. This will be one of the world's largest magnets, with a height of 17 m. *Credit: ITER Organization*

pressurized water will flow just a few millimeters below the surface. The water will reach a temperature of about 200°C. This means a very steep temperature gradient that will result in significant expansion and mechanical stress on the components.

Composed of 54 “W”-shaped cassettes that slot together to form a circle, ITER’s divertor will act literally as a giant nuclear ashtray. Subject to intense flows of high-speed particles, it will be a real challenge for materials science and engineering.

The divertor will be placed in a position where the magnetic field strength is almost zero. As a result, particles will leave the plasma, flowing along the magnetic field lines, and then going through the cassettes to the outside of the reactor. The cassettes will also contain a number of measurement tools for plasma control and physics optimization.

Up to 2009, the IO was considering beginning plasma operations with Carbon Fiber Composite (CFC) covering the parts of the divertor that are expected to receive the highest heat loads. However, in 2011, as a result of budget restrictions, Osamu Motojima, the then Director General, wished to explore the possibility of using tungsten instead, which is known for its very high refractivity and is also cheaper than carbon fibers.

Carbon fibers present two major drawbacks as divertor armor material: they chemically react with tritium, and they trap the fuel like a sponge, leading to enhanced material erosion and unacceptable levels of tritium retention within the machine. Tungsten has the advantage of not absorbing tritium, but at the same time it doesn’t offer the same forgiving behavior as carbon in terms of compatibility with the plasma. However, it is more stable, tungsten having the highest melting point of all the elements (3422°C). As a consequence, instead of the divertor being replaced twice during the life-span of the tokamak, it would only need to be replaced once if it was made of tungsten, representing a substantial saving.

However, it was necessary to ensure that the tungsten divertor would resist the first test campaigns planned for ITER, which will use helium gas. After almost 2 years of design, research, testing and prototype development work carried out by several international expert groups, in 2013 the ITER Council gave the green

light for the production of a tungsten divertor. At the end of 2016, Tore Supra, the French tokamak (and ITER's neighbor) built by the Commissariat à l'Énergie Atomique et aux énergies alternatives (CEA), was equipped with a tungsten divertor to test the IO's conclusion in real conditions. These experiments confirmed that tungsten was the right choice. Incidentally, in doing so, CEA management offered a second life to Tore Supra, which has been renamed WEST, (Tungsten (W) Environment in Steady-state Tokamak) and whose objective is to test technologies that will be used in ITER.

All of this work will soon come to fruition in 54 tungsten-covered cassettes weighing 10 tons each, which will together make the world's largest ashtray. It is planned that each cassette will be replaced once during the operational phase, using remote handling tools specially designed for ITER.

The ITER tokamak will not sit alone in its building; it will be enclosed within a kind of giant thermos flask, a huge cylindrical cryostat, which will provide structural support to the tokamak, and ensure that the superconducting magnets are insulated by an ultra-cool and high-vacuum environment. ITER's cryostat will be among the world's largest stainless steel vacuum chambers, almost 30 m high and 30 m wide. The size of the cryostat directly reflects the size of the tokamak as it will encase the whole reactor, including all its magnets. The base section of the cryostat weighs 1250 tons; it is the heaviest single component of the machine (see [Figure 23.10](#)).

This giant structure will have 23 openings to allow access for maintenance, as well as over 200 other apertures—some as large as 4 m in size—that will provide access for cooling systems, magnet feeders, auxiliary heating, diagnostics, and the removal of blanket sections and parts of the divertor.

Large bellows situated between the cryostat and the vacuum vessel will allow for thermal contraction and expansion in the structures during operation—up to 5 cm. The ITER tokamak will be a structure overrun with movement, expansion and contraction under the influence of magnetic fields and temperature changes.



Figure 23.10. The base section of the ITER cryostat gives a good sense of the real size of the future reactor. The complete structure will be 30 m high. Weighing 1250 tons, it is the single heaviest component of the ITER machine. *Credit: ITER Organization*

In order to allow for the horizontal and rotational forces generated by the movement of the tokamak, 18 spherical bearings will support the cryostat. Weighing 5 tons each, the bearings will smoothly transfer all the tremendous forces that will be exerted on the machine to the ground, both during normal operation and in exceptional events such as an earthquake.

The cryostat has been manufactured in India and supplied in 54 segments, which were delivered one after another by boat and as wide loads on roads. Since September 2016, on-site welding has been taking place on the cryostat under the responsibility of the Indian Domestic Agency (DA).^k A leak inside the cryostat is now considered by the IO as the most serious risk for delaying the first experiments (besides delayed in-cash contribution by some ITER Members or delayed in-kind contribution due to budgetary or quality problems in some Members).

The cryostat will also host a number of supporting systems such as heating, diagnostic and fuelling systems. In addition to the central heating that will be induced by the central solenoid, the tokamak will use two other systems to bring the plasma up to the temperature needed for fusion: a neutral beam injector (consisting in high-energy neutral particles that will enter the magnetic confinement field and transfer most of their energy by collisions to the plasma particles), and two sources of high-frequency electromagnetic waves.

This quick overview of the ITER tokamak gives an idea of the technological challenges that the ITER designers and engineers have had to face—and are still facing. Some of these challenges are not completely new as they have already been tackled in other tokamaks. But at ITER, the size and complexity of the machine imposes constraints on the technology and challenges for industry. With approximately 1 million components, ITER will be one of the most complex machines ever built by mankind.

However, tokamak engineers are nowhere near the end of their troubles. ITER will be an important step toward commercial reactors, as it should break new ground and be able to test many technologies under the conditions of a real fusion plant. But ITER is not the end of the fusion energy story, it is just the beginning. The economic feasibility of tokamaks is yet to be demonstrated.

23.4 A pharaonic worksite

The year 2010 marked the real start of construction on the ITER site in Cadarache. That year, the IO signed one of its largest procurement packages (EUR 537 million) with the European DA, Fusion for Energy (F4E) for the construction of a dozen of buildings and site infrastructure. F4E is located in Barcelona with about 500 staff, and manages the EU contribution to ITER.

These massive excavation works, which lasted 8 months, created a pit 90×130 m wide (roughly the size of a football pitch) and 17 m deep. This represents about $210,000 \text{ m}^3$ of earth and stones that had to be moved to behind a hill on the south-east side of the site. The pit is now host to the “tokamak complex” composed of three buildings, which host the reactor, the tritium storage facility and the diagnostics facility.

Today’s visitors hold their breath when they see this huge worksite for the first time. This is quite understandable; ITER is currently one of the largest worksites in Europe in terms of the surface area and the volume (and cost) of the constructions.

Thus, from 2007 to 2010, France paid for and carried out major preparatory works in the Cadarache forest to allow the construction of 39 buildings. Agence ITER France (AIF), a department created within the CEA to manage France’s in-kind and financial contributions to ITER, led 2 years of preparatory works such as

^k Each ITER Member has created a DA to fulfill its procurement and manufacturing responsibilities to ITER. These agencies employ their own staff, have their own budget and contract directly with industry.

clearing, leveling, fencing and installing networks for water and electricity. They created a space of 42 ha, one of the largest areas ever leveled in Europe, to host all the buildings. Within this, there is also a “contractor area” with offices for a thousand employees and a complete selection of equipment and services such as meeting rooms, canteen, etc. These works were part of the commitments undertaken by France, as the host country, and Europe, as the host partner. They amounted to a total cost of EUR 150 million, 40% of which came from F4E and 60% of which came from AIF.

As the project owner for the preparatory works, the CEA was required by French law to compensate for the devastation of this wooded parcel of the Cadarache forest. Thus, the Agency took a series of measures, including the acquisition and preservation of 480 ha of forest; the ecological surveying and preserving of 1200 ha of grounds around the ITER site; and a program to raise awareness on biodiversity, particularly targeting schoolchildren. Today, experts in the field refer to this innovative environmental program as a model compensation initiative (Mercier and Brunengo-Basso, 2016).

Alongside F4E, France also financed the construction of the IO’s headquarters. It is probably the most photographed building of the site, as it is the only one that is wholly visible from the road. The building was designed by two architects native to Provence: Rudy Ricciotti and Laurent Bonhomme.

The electricity supply to operate the facility is another contribution that France arranged and paid for. In 2012, RTE (“Réseau de Transport d’Electricité”), the French electricity transmission system operator, installed a 3-km high voltage (400,000 V) line, and a switchyard to connect ITER to the grid (with nearly 105,000 km of lines, RTE’s grid is the largest in Europe). Electricity is channeled from a giant switchyard located to the west of Avignon in Tavel. From there, electricity travels 125 km to a large substation in the village of Boutre, which is some three kilometers southeast of the ITER platform. The 400 kV “Boutre-Tavel” is the only power line that supplies electricity to the vast Provence area including, since the late 1980s, CEA-Euratom’s Tore Supra. The main electricity consumers at ITER will be the tokamak cooling water system (which will use 40% of the 110 MW required by the plant), followed by the cryoplat (30%), the building services and the tritium plant (10% each). Thus, the ITER fusion reactor will be powered by nuclear fission reactors in the Rhône valley.

France also set up 36 km of hydraulic networks to connect ITER to the French sewerage system, as well as a huge storm basin and four cooling water basins. Part of this network will be used by the pressurized tokamak cooling water that circulates through the reactor. The aim is to remove the heat load from the vacuum vessel, its plasma-facing components, and plant systems such as heating and power systems. The water will circulate through a cascade of cooling loops to the heat rejection zone located on the northern edge of the site, where it will be cooled through evaporation in a cooling tower and test basins. The tower is currently under construction in India. After a while in the basins, the water will be tested for various parameters such as temperature (the water cannot be released until it has cooled to 30°C), its pH level, and the presence of hydrocarbons, chlorides, sulfates, and tritium. Only water that meets the stringent environmental release criteria established by local authorities can then be released into the nearby Durance River. The cooling water will be taken directly from the “Canal de Provence,” a man-made network of channels that passes just a few kilometers away and delivers drinking water to more than 2 million people in 110 villages and towns including Marseille, as well as 6000 farms and 500 factories large and small. Like other projects in Cadarache, ITER will draw water from the Canal—cooling the machine will require some 1.7 million cubic meters of water a year, two-thirds of which will evaporate and one-third of which will be returned to the Durance River. Altogether, ITER’s consumption will account for less than 0.25% of the 230 million cubic meters that flow through the Canal every year.

From the laying of the first foundation stone, F4E took over from AIF. So far, over a thousand contracts have been signed with EU companies to carry out the construction works, equipment for the buildings, and the manufacturing work assigned to Europe. This represents over 3 million working hours and a total investment (so far) of around EUR 5 billion.

Given the complexity of the work required and the risks associated with a big project such as ITER, participating companies, even those of large size, often prefer to respond to calls for tenders as a consortium or together with other partners in order to offer more flexibility, resources and know-how. It is also the most effective way to develop a long-term working relationship and implement the multicultural approach that is required to deal with the Tower of Babel that is the IO. This was particularly the case in the field of engineering, with the creation of a French-English-Spanish consortium called “Engage.”¹ Similarly, a French-English-Korean consortium won the contract to assemble the tokamak itself out of all the components arriving from the four corners of the globe.

Today, around 400 companies (80% of them French) and more than 3000 people work on the ITER site, one of Europe’s largest worksites. All the construction and installation works should be finished before 2025 in order to complete commissioning and achieve “First Plasma,” i.e., the first experiment which will demonstrate that the reactor is fully operational and that it all works as intended (at least with plasmas that do not produce neutrons as part of the reaction. Some buildings and installations will have to be finalized between 2025 and 2035 to allow the start of operation with D-T plasmas.

So, a genuine scientific and international village is being set up in Cadarache. Until the end of its experiments, scheduled for 2047, there should be a 1000 people working there on a permanent basis. Some 30 nationalities are already represented among the staff. Although there is no accommodation on the site, ITER still provides almost all the daily necessities such as a cafeteria, canteen, library, concierge, recreational space, and even a bank.

23.5 Organizing a huge logistics

ITER project’s founding fathers decided to divide the tokamak’s manufacture among the 35 participating countries. In total, 1 million components—about 10 million pieces—are converging to Cadarache in France. This is another logistics challenge: with thousands of annual deliveries and millions of coded products stored in facilities both on and off site, it couldn’t be done without a sophisticated materials management system.

The main purpose of ITER is indeed to enable the participating countries to learn and develop the most advanced fusion technologies together and, since the project is funded by public money, to share the experimental results and any intellectual property that will be generated by the project. But the aim is also for the members to support the development of their respective fusion industries. This is why the decision was taken in 2001 to decentralize the manufacturing of the machine.

At present, the entire ITER exists only in the form of an electronic “package” over 2 TB (terabytes) in size, containing the detailed plans of the machine and buildings. To avoid a catastrophic loss, these plans are saved every night on ITER’s computers and servers. It took almost 20 years for a hundred designers to finalize these detailed 3D models, which can be viewed through specialized software (CATIA, “Conception Assistée Tridimensionnelle Interactive Appliquée,” developed by Dassault Systems). The designers constantly improve and update the 3D models, working closely with the IO’s technical departments.

In the early 2000s, these models were sufficiently precise to allow the estimation of the “value” of the construction and manufacturing, and to establish each member’s contribution in 2001. With the exception of Europe, which provides 45.6% of the constructions and manufacturing, each ITER member contributes 9.1% of ITER’s total value.

After the project started in 2007, difficulties quickly appeared; some scientists and engineers proposed modifications to certain elements in order to improve ITER’s performance. However, in some cases, modifying a component or a system necessitated changes in other parts of the machine, sometimes even in other

¹ The architect engineer assists F4E during the entire construction process, from the elaboration of the detailed design to the final acceptance of the works, including the ITER buildings, the site infrastructures and the distribution of the power supplies.

buildings, which often lead to non-conformities and even physical incompatibilities. In some cases, the departments concerned refused the changes for technical reasons; in others the DAs in charge declined to bear the additional costs, refusing to take responsibility for these changes or corrections. As a consequence, the list of PCRs awaiting decision has been steadily growing since construction started in 2010. This explains a good part of the delays that have accumulated over the years—actually since the very beginning, as the very first schedule from 1993 anticipated that the machine would be ready in 2010.

The division of the procurements needed for ITER was decided in 2001 during the negotiations before the ITER Agreement was signed. Manufacturing of the ITER components and systems were allocated to each Member pro-rata their financial contribution to the project (45.6% for the EU and 9.1% for the other Members) and taking into account each Member's technical expectations and industrial capabilities. Therefore, through the ITER Council, the Members themselves distributed the work, but they pushed this logic to its extremes. For example, the manufacture of key systems is distributed across several members: Europe and Korea share the nine segments of the vacuum chamber; the central solenoid is procured by the United States and Japan; Europe, Russia and Japan are collaborating on the divertor; India and the United States share responsibility for the water cooling system; the manufacturing of the blanket modules is distributed among China, Europe, Korea, Russia, and the United States; and six of the seven Members have been involved in the production of superconducting cables and magnets.

The internal documents of the IO do not refer to the total cost of construction of the tokamak. The reason is that each Member contributes to the total value of the project. Most of the financial data refer to the value of the machine estimated in 2001, expressed in ITER units of account, so that each member can convert the figures in their own currency. The IO does not manage the real costs. Each Member is credited an amount of IUAs when a component or building is completed and accepted by the IO.

The IO, which is the design authority and coordinator of the whole program, has placed over a hundred procurement arrangements with the DAs, representing more than 90% of the total value of the machine and buildings. These agencies have in turn launched calls for tenders to their respective industries, resulting in over 3000 design and manufacturing contracts signed so far. In Europe, in Asia, on the American continent, thousands of factories are now working at full speed to build the world's largest *Meccano*, with more than 10 million parts. Since the first deliveries, which arrived onsite in the third quarter of 2013, the pace has intensified substantially with several trucks arriving onsite every day bearing the fruits of the factories' labor. There are also quite often deliveries that are highly unusual in size, weight or shape, delivering the largest parts of the tokamak and the technical systems. The IO's Director General announced on October 11, 2018 ([GCR staff, 2018](#)) that "All the main components of ITER will be on site in 2021."

The complexity of such an operation is obvious; all of these components, some strictly identical, some manufactured in different countries, have to arrive in France in full conformity with the technical specifications and compliance with the necessary standards and requirements, as well as matching the others perfectly. There is no room for error. For some components, tolerances are less than a millimeter. This has two consequences: firstly, that the technical specifications had to be drafted with the utmost accuracy, and secondly, that quality assurance and quality control are key elements of the project. A whole department of the IO is dedicated to these issues. The terms of reference are clearly specified in the procurement and tender specifications. The IO is also responsible for the evaluation and selection of the subcontractors and for the inspection and verification of the components produced under the responsibility of the DAs. Every week, several employees of the Organization leave Cadarache to visit companies in the seven members and verify that the product requirements are conformed to and that the quality procedures are fulfilled. The inspection may also include performance testing during manufacturing. If everything goes as planned, a conformity report is signed and will in general be followed by an interim payment being made to the manufacturer.

In most cases, ITER's components are high-tech objects with very precise specifications. The safety-critical components are subject to particularly strict controls. In addition to the company's own quality

control procedures, progress is regularly reviewed by representatives of the corresponding DA, the IO, and external experts. Inspectors from the “Autorité de Sûreté Nucléaire” (ASN), the French nuclear safety authority, may also visit abroad and check the manufacturing of the most sensitive elements.

Contributing to ITER imposes severe constraints on the companies involved, which their staff are keen to underline when they meet the project’s senior management. The first-of-a-kind nature of ITER and the risks posed by the tight schedule and the technological requirements create genuine challenges for the companies taking part as well as ITER’s management. The conditions of their contracts require them to take a significant technical and financial risk. Most contractors have to cope with unforeseen events and last-minute changes. Working in an international context adds additional complexity. However, in one-on-one meetings, the industrialists involved in ITER generally acknowledge that the benefit is considerable, probably less in terms of immediate profit than in terms of the company’s development. The program is clearly an investment in the future.

The assembly of the reactor itself has started in 2020. Quite surprisingly, this activity which is one of the most visible and important ones, has long been one of the most discreet and underestimated ones. But ITER is now in a critical phase. ITER’s engineers and hundreds of businesses are now building their gigantic jigsaw puzzle. In parallel, they will install plant systems such as radio frequency heating, fuel cycle, cooling water and high-voltage electrical systems. So, any mistake or missing item in the plant’s assembly planning will impact the overall project schedule. And everybody recalls the words of the last Director General: “One day of delay means an extra cost of one million euros” (Figures 23.11 and 23.12).

Much like rockets, interplanetary probes and medical imaging, ITER is based on state-of-the-art technology that is constantly evolving and improving. After all, magnetic confinement, cryogenic pumps,

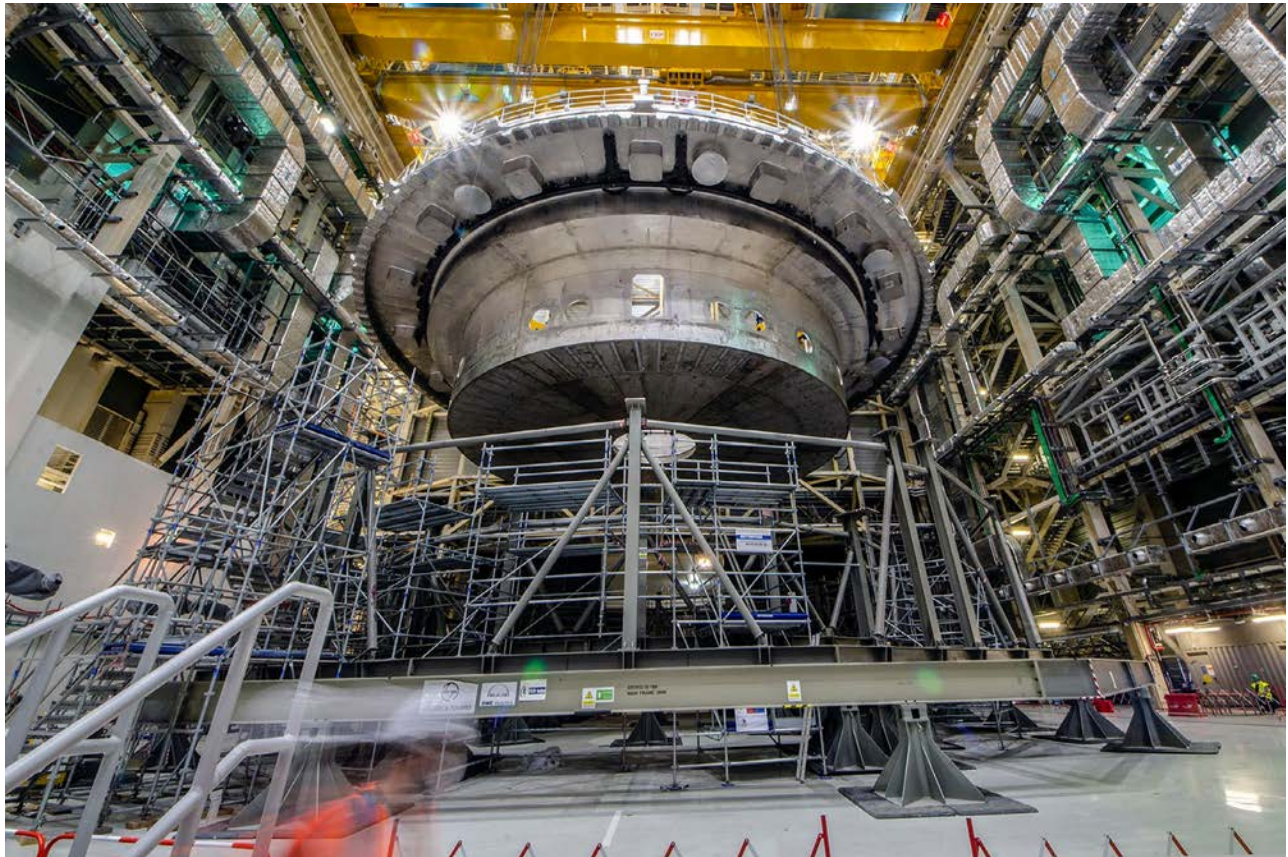


Figure 23.11. On May 26, 2020, the first major component of the Tokamak (cryostat base) is lifted to enter the reactor’s assembly pit. *Credit: ITER Organization*



Figure 23.12. On August 22, 2020, the cryostat lower cylinder (lightly wrapped to protect it from weather, moisture and dust), 30 m in diameter and 375 tons, enters the Assembly Hall as it is transported out of the workshop by self-propelled modular transporter. *Credit: ITER Organization*

superconducting coils and vacuum vessels are anything but new technology. But ITER pushes its technology to its limit. ITER innovates by its sheer size. The machine's complexity is unparalleled; made from about 10 million parts in total, produced in 35 countries. The precision required and the tiny tolerances are particularly demanding. And this is only one among ITER's many challenges.

Once delivered to the site—another logistical challenge as we will see—the components will be assembled in predetermined sequences. The accurate alignment of components is essential to the successful operation of the machine. For example, the 17-m high toroidal magnets will have to be positioned within a millimeter's tolerance. Assembly sequences have been planned with this in mind.

The first components arrived onsite in 2013, 6 years before the start of assembly. At the time of their arrival, they were inspected and assigned a location in one of ITER's five storage areas. This is another logistical challenge: with thousands of annual deliveries and millions of coded products stored in facilities both on- and off-site, a sophisticated materials management system is essential. In principle, components should arrive on site a minimum of 90 days before they will be needed to allow time for proper labeling and storage. The IO has developed a centralized system, which collects product information from the seven DAs and links to other databases.

The order and timing of the assembly from now to the start of operation in 2025 at the earliest are carefully planned as part of an assembly master plan, which—for the tokamak alone—is over 40,000 lines long and describes in detail, almost hour by hour, the sequence of operations to be carried out. These activities will require 1.5 million man hours over 5 years and approximately 1000 workers.

On June 27, 2016, the IO signed a major contract to provide assistance for the assembly of the tokamak and related systems. Under this contract, worth EUR 174 million, a consortium of three companies will oversee and coordinate, as the Construction Manager-as-Agent (CMA), the assembly activities, whether carried out by the IO or by subcontractors of the DAs of the ITER members. The consortium will work with the IO to plan, manage and supervise the works onsite—helping in particular to ensure that all the different work crews

are able to work most efficiently, having to hand the million components, drawings, documents and facilities to construct the ITER Tokamak and plant systems to a high quality, on time and within cost.

The principal assembly activities will be performed in the tokamak building, where ITER will be installed inside a partially underground, 3.2-m-thick concrete bioshield. During the assembly, the tokamak building will be operated as a “clean area” and maintained at a constant temperature to stop the largest components growing or shrinking. Preassembly activities will take place in the adjacent assembly hall, the atmosphere of which will be monitored in such a way as to maintain a uniform temperature of between 20°C and 25°C in the summer and a relative humidity of less than 70%. The heating, ventilation and air-conditioning system and the antidust coating on the floor will help guarantee the air quality required to assemble the components of the vacuum chamber. All in all, over a hundred different types of custom tools will be required to assemble, lift and finally maneuver ITER’s supersized components. These tools are currently being installed in the assembly hall.

Assembly proceeds in a “bottom-up” fashion. It begun with the base section of the cryostat, and is continuing with the lower cryostat components and magnets, the nine large preassembled sectors of the tokamak (each made up of a vacuum vessel sector, its surrounding thermal shields, and two toroidal field coils), and finally the components at the top of the machine, including two poloidal field coils and the roof of the cryostat.

For the tokamak to function optimally, the engineers will need to precisely align its critical elements, especially the magnets and the components of the vacuum vessel. For many of the machine’s largest components, the assembly tolerances are of the order of 1–3 mm. Optical metrology techniques will be used at each stage of the assembly process. These three-dimensional controls will play an essential role in ensuring that tolerances are respected. Engineers will also verify in real time, thanks to CAD (Computer-Aided Design) models, the tokamak’s compliance with the detailed drawings of the machine and buildings. This will allow them to correct any errors in alignment before fixing the components in place.

However, on 25 January 2022, ASN decided to put the assembly of the reactor on hold, for three reasons: dimensional non-conformities affecting three sectors of the vacuum chamber, the need to carry out an in-depth design review of the reactor and unsatisfactory control of the limitation of exposure to ionizing radiation.

Transport is yet another major challenge for ITER. When the members decided to build the fusion reactor in Cadarache in France—and not in Rokkasho-Mura in Japan—they knew that they would have to solve a major logistical problem: how to deliver the parts and components of the machine to the site? This is a real issue as it was clear from the outset that several non-European countries would have to deliver magnets and other equally huge components. The French and European managers of the ITER project therefore had to figure out what the most efficient and economical means to transport the large components to the ITER site would be, taking into account the fact that they would be shipped from factories all over the world. More concretely, how could they be transported from the harbor of Fos-sur-Mer on the Mediterranean Sea, where most of the boats are likely to dock, to Cadarache, some 80 km up north, with every guarantee of safety and security, both for the components and for the local residents? Together with French experts, the IO explored various solutions such as transport by rail and by airship.

It was finally decided to build a special “ITER itinerary,” a 104-km route connecting the small harbor of La Pointe de Berre (near Fos-sur-Mer) to Cadarache (see [Figure 23.13](#)) by road. This route has been operational since 2013, essentially using the existing road network, although it has been necessary to adapt and strengthen certain parts. Some roads were widened, bridges reinforced, villages bypassed, parking areas installed and roundabouts modified in order to make them compatible with the weight and size of the special convoys. France took responsibility for these large-scale public works, including the financial responsibility, as part of its commitments to ITER. From the first technical studies in 2006 until the completion of the major works in 2011, the total cost was estimated at EUR 110 million and was shared by the Departmental Council of Bouches-du-Rhône (the *département*—territorial region—of France that the route is in) and the French State (respectively at 66% and 34%).



Figure 23.13. A map of the 104 km “ITER itinerary.” Some 10,000 ITER transports will use it, including 200 very exceptional convoys. The first of these HELs arrived on the ITER site on January 14, 2015. *Credit: CEA-AIF*

The 104 km connecting the harbor of La Pointe de Berre, situated on the lake “L’Etang de Berre,” to Cadarache through the Durance Valley, form the “sacred avenue” of ITER. It is this route that, since 2014 and probably until 2040, the vast majority of ITER’s components take toward their final resting place.

This is the challenge within the challenge: up to 2023, about 200 “Highly Exceptional Loads” (HELs) are foreseen to deliver ITER’s large components, which means on average about 20 convoys per year. This looks quite easy to manage, but we have to take into account that these convoys are not allowed to drive during the weekends, in July and August (because of tourism), or during school holidays. Actually, up to 2023, these HELs will follow each other very frequently.

Some of these HELs will use a 352-wheeled platform with a second and rear double cabin and 88 multi-directional axles (Figure 23.14). By its dimensions (46 m long for 9 wide), the trailer is capable of carrying a payload of about 1000 tons and moving at a maximum speed of 5 km per hour. Unique in Europe (there is only one, which belongs to the German subsidiary of the French company Daher), it is used to bring the largest components of the tokamak, such as the stainless steel segments of the vacuum vessel (7.45 m from top and over 400 tons each) manufactured in Italy and Korea, the toroidal coils (17.30 m high and 530 tons each) that are sent by Japan and Italy, the cryostat segments coming from India and two poloidal coils that are provided by Russia and China. Once each component is delivered to the site, the platform is dismantled and all its elements are put in a normal lorry, which will drive back to the Daher site near Marseille. Interestingly, it is impossible for the platform to take the ITER route in the opposite direction. Therefore, a defective large component cannot be returned by road to its sender...

Following a well-established protocol, boats unload the components in Fos-sur-Mer (which boats from the Asian ITER members take an average of 45 days to reach). Then, their onward journey takes them along the “Canal de Caronte” and then across a large lake, “L’Etang de Berre,” using a 75-m-long barge, before the road transfer to Cadarache. Road convoys normally start in the evening (around 9:30 pm) and travel overnight (until 6 am at the latest) to minimize traffic congestion. Within this timeframe, the convoy progresses 5 km at a time; around it, the road is blocked off to create a kind of “security bubble” to move and protect the main actors—the components and the technical staff—and of course the local residents. The sections are reopened once the road signage had been reinstalled and clearance has been given by the local authorities.

In total, the IO and F4E will manage around 10 thousand transports in total (road, rail, inland waterways, maritime and air transport), even if, given the geographical locations of the DAs, maritime will be the main



Figure 23.14. A 352-wheel platform, unique in Europe, is used to transport ITER’s highly exceptional loads from the Mediterranean Sea to Cadarache. *Credit: ITER Organization*

means of transport. All DAs have a contractual obligation to work with Daher for their HELs. This allows the process to be harmonized and the upstream logistics to be simplified.

23.6 Delays and budget increases

Although few people are well-informed about the progress of fusion, everybody is aware of ITER's delays! The arrival of fusion energy has long been announced and hoped for. But as delays accumulate, fusion skeptics are keen to repeat the well-known joke: "Fusion energy is 30 years away, always has been and always will be."

The problem is anything but new. After the signature of the ITER agreement, the commissioning of the tokamak was first scheduled for 2016. In July 2010, the ITER Council postponed that date to November 2019. In 2015, after an in-depth analysis of the ongoing work, the date of First Plasma was rescheduled for December 2025, with D-T operations by the end of 2035. As of today (June 2021), the ITER Council is no longer unwavering in their conviction that they will meet the 2025 deadline. Quite rightly, politicians, media, students, and the general public are all asking the same question: why ITER is so late and when can we expect the first results?

Everybody is ready to accept that the unprecedented complexity of ITER and its first-of-a-kind nature may cause delays in the manufacturing and construction—let alone the financial and political context. It is obvious that difficulties of all kinds (technological, organizational, financial, geopolitical, etc.) may arise and create, as in any technological project, delays in delivery, costs overruns and even reduced safety margins in design and implementation. However, the key issue remains: why have there been so many delays in ITER's case? With more than a hundred tokamaks operating in the world, one can hardly say that ITER is "first-of-a-kind." So, does the problem lie in its management?

We have seen that technical, budgetary, political and other difficulties have slowed down the project since its beginning. It took no less than 15 years to get the foundations of the project right, 5 years to select the site for hosting ITER and five more years to transform the project into a genuine program. Then, institutional and organizational difficulties emerged. A management assessment report released in 2013 described ITER as a highly complex structure with a bureaucratic mode of operation, lacking efficiency, staff, and central authority.

In fact, ITER is exposed to all possible potential causes of delay that one can imagine: technological show-stoppers, design changes of the machine and buildings, late signature of contracts, manufacturing difficulties, late deliveries, quality problems, detection of non-conformities, plus underestimated risks and contingencies. Nobody could have predicted the earthquake and the tsunami that hit Japan on March 11, 2011. But this event alone delayed the Japanese contribution by a year, and hence the project as a whole. And the same happened in 2020-2021 with the Covid-19 pandemic.

You could argue that most of the big technological projects of recent years have accumulated operational delays and budget increases.^m But this attitude leads to a sort of technological fatalism, which is not acceptable when dealing with public money. A better approach would be to address the program-specific management issues and the risks at all stages of production. These are two areas where the IO lagged behind until 1 or 2 years ago.

In this section, we will review three specific examples of delays to ITER's construction. These are only "case studies" among many other delays. But these three will serve as concrete examples of delays that have impacted the program.

^m This was particularly true of the French EPR (European Pressurized Reactor) nuclear plant. Originally scheduled for 2012, the commissioning of the EPR was postponed to the end of 2019. Initially estimated at EUR 3.4 billion, the cost of the reactor has almost tripled as it was readjusted in 2008, 2010, 2011, 2012 and 2018 to be (currently) EUR 10.9 billion.



Figure 23.15. ITER’s ground support structure (photo taken on November 6, 2012). The 17-m deep, 1.5-m thick basemat, the retaining walls and the 493 separate columns constitute ITER’s seismic isolation pit. *Credit: ITER Organization*

The first case relates to the foundations of the tokamak complex, in particular to the completion of the level B2 basemat slab (B2 for the second level of the basement, or the second level below ground floor). Work started in December 2013. The concrete slab, with a surface area of over 9000 m² and one and a half meters thick, rests on 493 pillars topped with antiseismic bearings (see Figure 23.15). This structure serves as the “floor” of the tokamak complex, and sits on rock 17 m below ground level. Thanks to the seismic columns, the basemat has a capacity for lateral movement of up to 10 cm in any direction (there is a gap of approximately 1.5 m between the B2 slab and the surrounding retaining walls).

In summer 2013, the companies that were responsible for the construction of the tokamak complex started to install the formwork and steel reinforcement. However, during an inspection on October 24, 2013, ASN staff detected non-compliance in certain steel bars in the central reinforcement area. Some rods were a smaller diameter than expected and were therefore likely to weaken the whole basemat. A few days later, ASN wrote to the IO requesting a “corrective action” and imposed a “hold point” on the pouring of concrete in the central area.¹¹ This was not a trivial issue; the B2 slab must support the whole tokamak complex, i.e., three buildings plus the reactor itself—400,000 tons in total.

F4E scrutinized the central area of the tokamak pit, where the reinforced steel created a particularly tight and complex grid pattern. They recalculated the resistance of the steel and concluded that, as suggested by ASN, it needed to be strengthened in several places. Once these corrections were completed, the IO replied to ASN on January 20, 2014, asking for authorization to pour the concrete in this area. On July 10, 2014, this authorization was granted. Pouring started a few days later (14,000 m³ of concrete in total) and ended on August 27, 2014, at 6 am, with the pouring of the 15th and last segment of the slab. Beyond illustrating how a technical problem caused 6 months’ delay to the construction of the tokamak complex, this case also demonstrates ASN’s key role in regulating construction and manufacturing.

A second example of significant delay is in the production of the poloidal field magnets. In this case, the problems have nothing to do with technology or the manufacturing itself. Just remember that of the six

¹¹ Most of these emails and letters can be consulted on ASN’s website: [https://www.asn.fr/L-ASN/ASN-en-region/Division-de-Marseille/Activites-de-recherche/Site-de-Cadarache/Iter/\(rub\)/106342](https://www.asn.fr/L-ASN/ASN-en-region/Division-de-Marseille/Activites-de-recherche/Site-de-Cadarache/Iter/(rub)/106342).

circular magnets, one will be supplied by Russia (the smallest one, PF1, 6 m in diameter) and the five others by Europe (PF2 to PF6) as their huge dimensions (9–24 m in diameter) prevent them from being transported by road. These five magnets are therefore being wound and assembled in Cadarache. These are the only components of the tokamak that are manufactured onsite. F4E constructed a dedicated building 257 m long for the production of these five magnets—the longest building on the site.

At the beginning of 2012, F4E published a European call for tenders to select a company to manufacture the five European poloidal magnets. Within the time limit set, only one bid was received in Barcelona. However, the European experts who assessed the quality of the bid at the technical and financial level concluded that the prices proposed were very high. As a result, F4E canceled the call for tenders in the summer 2012, deciding to divide the work into five lots in order to reduce their size and the related risks. A few months later, the call for tenders was republished. By the end of 2013, the first contract was signed, covering the manufacturing of the magnets. It was followed by four others, covering the supply of machine tools, the site and infrastructure management, the manufacturing and the tests at low temperature. In the end, the production of the poloidal magnets started with over a year's delay, for reasons related to the rules of European public procurement and the contractual obligations of the selected companies.

Last but not least, a third example of a delay: the cooling towers. ITER will have two independent cooling water circuits. The first will extract the heat generated in the plasma during the deuterium-tritium reaction. The heat will then be transferred to the second system, which incorporates multiple closed heat transfer loops plus an open-loop heat rejection system. In operation, the tokamak and its auxiliary systems will produce an average of 500 MW_{th} of heat during a typical plasma pulse cycle, and all of this heat will need to be dissipated out into the environment. This will be accomplished through the water's evaporation as it passes through a 10-cell, 20-m-tall cooling tower building.

The towers have been constructed in India. However, at the end of 2015, managers at F4E realized from the first plans sent by their Indian counterparts that the tower would be larger than foreseen and could therefore not be installed in the building designed for that purpose. There were intensive discussions between the two organizations, but the Indians had the last word: they explained that they had scrupulously followed the technical specifications attached to the procurement arrangement which was signed. They rejected any liability in this case. The Europeans therefore had to urgently modify the building plans, as the construction was going to start very soon. The result: another 6 months delay, effectively because of miscommunication between two DAs.

Cultural issues (together with technical difficulties) can also slow down decisions. For example, this occurred in 2012, when difficulties arose in the production of the niobium-tin superconducting cables for the toroidal magnets and the central solenoid. The situation was complicated because as many as 10 companies located in six members were providing the strands and cables for ITER. The Japanese industry, which was still recovering from the 2011 tsunami, nevertheless wanted to take part in this enormous and unique task as they had previously worked on a prototype of the central solenoid. The challenge was immense; almost 200 km of superconducting cables had to be manufactured.

In 2010, the two Japanese companies selected for the production of conductors for the solenoid sent their first samples to a Swiss facility called SULTAN, which belongs to the Ecole Polytechnique Fédérale de Lausanne (EPFL). Capable of producing a strong magnetic field (up to 11 T), high current (up to 100,000 A) and high mass flow rate of helium for cooling, SULTAN is the only facility in the world capable of testing samples of ITER's magnets under operating conditions similar to those that they will be exposed to in ITER. These tests revealed that the quality of the Japanese conductors was particularly poor. While the solenoid has been designed to produce some 60,000 pulses of high magnetic field during the lifespan of the project, the Japanese conductors deteriorated after just 6000 cycles. The Japanese companies tried hard to improve the quality of the strands but without success.

On the other side of the Pacific Ocean, in Oak Ridge at the headquarters of US ITER, the US DA, which is responsible for the manufacturing of the central solenoid, the managers were becoming somewhat nervous. They had identified a US company to provide them with samples, which passed the tests in Switzerland successfully. However, the Japanese industry refused to give up, arguing that they would make every effort to achieve the required quality. And after over 2 years of discussions between Japan and Switzerland, between Japan and the United States, the conductors eventually met the required quality standards. Everyone in Cadarache, Tokyo and Oak Ridge breathed a sigh of relief. The problem should never have grown to such a size, but the teamwork and international collaboration deployed to solve it were remarkable.

The examples presented in this section show that a great many kinds of problems may delay the implementation of a project like ITER. This is quite common with cutting-edge technology projects, most of which are experiencing substantial delays and large budget increases. ITER is no exception.

Another fundamental difficulty is linked to the way that the project is organized and the work is divided. Most ITER components are manufactured on different continents. They have to be transported to several locations. The process can block in many places and at any time. However, regardless the place of manufacturing, the components must be identical. In short, ITER's complexity is "built-in." It is an integral part of the program's structure as decided by its founders. The possible late delivery of components would naturally lead to squeezing the schedule for assembly. For this kind of project, this is a risk one could anticipate, but only in 2018 was the IO asked to clarify how this would be handled.

Obviously, it can be expected that there will be more significant delays. Internal sources in the IO give now 2030 as the best estimate for First Plasma. But the ITER Council is now closely following the performance of the IO and the seven DAs through a series of well-defined milestones. The construction and manufacturing activities have been split into 18,000 individual tasks, which are listed in a database that makes up what is called the Master Schedule. The details of these tasks, including the date of finalization or delivery, are updated every month. Thus, any delay or cost increase can be quickly identified, as well as their possible consequences for other systems. Should this happen, the problem is carefully examined and mitigated as appropriate.

Obviously, these delays do not serve the ITER project well, as they lead to cost increases. But it is equally important that ITER's slow progress is not good for fusion in general either. The biggest skeptics are keen to exploit this situation to campaign to reduce fusion investment in favor of technologies that may provide a faster return. Furthermore, the influence of industry and the urgent need to fight climate change provide a strong incentive for developing fusion.

How much will ITER cost? This is the billion-dollar question, which is systematically raised in all visits, discussions, lectures, and interviews about ITER. This is understandable: ITER is financed by taxpayers' money, and everyone has heard about the seemingly never-ending delays and budget increases. But it is also a frustrating question, because no-one is satisfied with its answer. Regarding the cost of constructing the tokamak, it is not possible, and it will never be possible, to give a precise figure. In fact, we will never know the exact cost of ITER because close to 90% of the members' contributions to the program are made in-kind. In most cases, the contributors do not wish to disclose the cost of the parts they have produced.

Since each of the ITER members is responsible for providing in-kind components that have been manufactured on its own territory and paid for in its own currency, conversion of the estimated cost of construction into a single currency is not appropriate. The authors of the ITER Agreement understood this and, after a proposal made by Robert Aymar, created a single currency, a sort of "fusion euro": the "ITER Unit of Account" (IUA^o). This system takes into account the different exchange rates as well as changes in the cost of living, so as to distribute the value of each procurement arrangement between the members of the project in the fairest way possible.

^o 1 IUA is defined as the equivalent purchasing power of USD 1000 as per January 1989.

In 2010, the European Union valued its contribution to ITER as EUR 6.6 billion up to 2020 (of which EUR 6 billion is for construction and manufacturing and EUR 600 million is for management and administration, participation in the Broader Approach—the specific EU-Japan program on fusion research—etc.). On this basis, the total cost of constructing ITER over this period could be estimated at close to EUR 15 billion. The contribution of the other Parties is in principle set at 9% of the total value of the program, but in practice depends on the industrial costs specific to each country, which may be higher or lower. France's situation is somewhat unique. As the host country, France pays 20% of the European contribution to the construction of ITER, which is slightly more than EUR 1.1 billion, including EUR 220 million out of the EUR 467 million contribution provided by the local authorities and regional governments of the Provence-Alpes-Côte d'Azur (PACA) region.

However, at the ITER Council meeting in November 2016, the members adopted a new baseline that integrated new delivery dates for all components under a revised construction budget. The result was an additional 5 years of delay, meaning that the commissioning of the tokamak and the first experiments (“First Plasma”) are now officially scheduled for December 2025 at the earliest.^P For Europe, this means an additional budget of EUR 3.9 billion, making an estimated total cost of EUR 10.4 billion (2008 values) up to December 2025. But this is not the end, as adjustments to the machine will still be necessary before 2035 in order to start the real (D-T) fusion operations. Estimated additional cost: EUR 3.2 billion for Europe.

All in all, the total European contribution to the tokamak ITER in its final configuration (capable of delivering D-T fusion reactions) will therefore add to EUR 13.6 billion, which gives an estimated cost (to date) for the whole machine of EUR 30 million in 2008 values and about EUR 40 billion in current values. However, this assumes that all the manufacturing is carried out in Europe and paid for in euros, which is not how the project works. This figure is therefore most likely an overestimate. A better basis is the *value* of ITER, which was estimated in 2016 at 7800 IUA, i.e., about EUR 13.6 billion.^Q But this is an underestimate of the real cost as it does not take into account insurance, administration fees etc. So, what we can say is that the cost of ITER is today between 20 and 40 billion euros, and most probably closer to the upper limit. By way of comparison, the LHC particle accelerator in Geneva cost EUR 6 billion. ITER is likely to be the most expensive scientific facility on Earth.

In the current economic context, it is easy to see why the governments financing ITER do not appreciate cost increases or delays. In Europe, the Parliament and Council at first refused the new ITER budget in 2009 and 2010. At that time, discussions in the corridors of the IO were often about the possible termination of the project. There is a precedent: the US Superconducting Super Collider (SSC) project (nicknamed *Desertron*). It was supposed to be the world's largest and most energetic particle accelerator. Constructions started in 1987 in the vicinity of Waxahachie, Texas, but the project was canceled in 1993 due to budgetary issues.

Quite obviously, decision-makers, journalists but also the public at large want to know the reasons of these cost increases. As it turns out, there are many.

One is the late finalization of the design of the tokamak. The first estimates were based on a “generic” machine, designed in 2001, whose plans were still not detailed enough to make a robust cost estimate. Moreover, this theoretical machine had to be adapted to the situation in Cadarache, which caused certain buildings to increase in size. At that point, the buildings as a whole were considered as “standard components” without a detailed technical description of their structures and interfaces.

Moreover, the estimate of 2001 did not include changes in labor costs or inflation and did not include any margin for contingencies. It also underestimated the complexity of the installation and assembly operations

^P As of today (June 2022), the date for First Plasma is likely to be 2027-2030.

^Q In 2022, the conversion factor of the ITER Unit Account is 1 IUA = 1749.84 euros (as set by the ITER Organization). The conversion factor is updated every year and takes into account the evolution of the cost of living in the seven members.

and did not provide for on-site storage of components. More fundamentally, in 2008, when research in the field of fusion had made significant progress, modifications were made to the machine as part of detailed design reviews, such as the addition of some magnets for the control of instabilities. These changes substantially increased the overall cost of the project. At the same time, the number of ITER Members grew from four to seven, thereby increasing the number of interfaces in the machine's design. Moreover, construction costs have significantly increased since 2001—steel has doubled in price and concrete has tripled.

Finally, the disastrous accident of Fukushima Daiichi impacted ITER; certain safety and security measures had to be reviewed, with consequent budget increases and construction delays.

Unsurprisingly, politicians do not look favorably at these successive budget increases. This is particularly true for Europe, as the EU is the partner with the biggest share of the construction costs of the project. Furthermore, the EU's budgetary procedures are not suitable for major and regular revisions. The US Senate has also pushed for leaving the ITER project, and the administration has a backlog of 2 years in paying its cash contribution. The same is true of the Indian government.

23.7 The management challenge

There is no doubt that ITER is a huge project management challenge. And this challenge is multifaceted: technological, industrial, organizational, logistical, and also about people. How to manage decentralized manufacturing over 35 countries? How to respect a timetable, when industry generates, by its very nature, numerous risks and unforeseen events? How to keep budget increases to a minimum? How to stay in control of such a complex endeavor that involves several thousand people all over the world? And how to manage a unique and unprecedented program that has no reference point for its organization and management?

This section explains the management and the governance which has been put in place by the IO with the seven DAs under the supervision of the ITER Council. Many changes were brought in after the publication of a management assessment report in 2013, which was very negative. Although the full report has never been made public, the summary is crystal clear: "There has been a lack of strong project management culture inside the IO. The IO's culture appears to be more academic and research oriented, which has often led to protracted debates and impeded rapid progress. [...] As a result, many of the best ideas were never heard nor expressed and key decisions lacked ownership."

Scientists are not natural managers, as many of them will freely admit. The first Directors General knew this and decided that the management of the IO would be evaluated every 2 years. Each ITER member takes on the responsibility of evaluation on a rotating basis. So, since 2007, seven management assessment reports have been completed, although not made available to the public. Their conclusions have all been generally the same from one to the next, except for the report of 2013.

Even within the first few months of the project, delays and cost increases materialized. The IO's managers discovered that the detailed design of the tokamak was far from completion. As early as 2008, they understood that the original schedule was not viable, and that they would have to increase the budget for construction and manufacturing. At the end of 2009, the ITER Council approved the first schedule change, postponing the first experiments to 2018–2019 (instead of 2016) and the Deuterium-Tritium (D-T) experiments to 2026. The situation culminated in 2013, with the publication of the biannual management assessment report, this time drafted by three US experts.

Given the nature of the evaluation and the project's specific troubles, it is no surprise that the report presented management and organizational shortcomings as the source of the problems. But at which level? These issues are not uncommon for major technology projects, and experience shows that projects like this tend to cost around three times their initial estimate (sometimes called the "pi factor" as pi is roughly 3.14). So why blame management?

The management report was like an earthquake in the fusion world. The ITER Council decided to replace Osamu Motojima at the beginning of 2015, and invited the seven members to submit applications. The context was difficult because at the time the United States was considering leaving the project for the second time. Some even said that the report was meant to pave the way for a US withdrawal. Inside the IO, the staff knew very well that the change of Director General, although desirable for the continuation of the program, would not solve its problems. This is a fundamental point; some key decisions are not in the hands of top management.

In my opinion, the report failed to identify a crucial issue for the project: staff management and recruitment. Indeed, almost no two ITER employees benefit from the same conditions as there are so many different types of contract, grades, and geographical locations. Correctly, the report recommended using “human resources and tools as a strategic asset for performance improvement and change.” However, the report did not mention the fact that for several years the number of employees was capped to 600 per a decision by the ITER Council. Everyone knew that this was ridiculously low given the project’s complexity and challenges.

After his appointment in March 2015, Bernard Bigot, the “ITER Director General” as he likes to introduce himself (rather than the “IO’s Director General”), quickly took a number of good decisions. He convinced the ITER members to set up a “reserve fund,” a special budget line enabling him to approve and finance missing or changes of certain components compared to the baseline in order to not delay the whole project (before, some changes would lead to endless discussions between members about how to finance them). However, this fund is still somewhat controversial, as recent reports have given contradictory feedback about its exact impact on the project. Bigot also set up an “Executive project board” composed of ITER’s senior management and the heads of the DAs, which initially met once a month (now every 2 weeks), strengthened the operational management of the organization, and improved communication with industry as a key stakeholder. However, some decisions came quite late. The IO made the decision to handle risks and contingencies that could affect ITER’s construction together with the DAs only 3 years ago. Risks are everywhere in such a complex and sophisticated project: it can be a late delivery of a component, the detection of a non-conformity, a shortage of budget, the bankruptcy of a contractor—you name it. Managing ITER could be seen as essentially a giant risk management exercise. Therefore, it is odd that risk management was so decentralized for so much of the project.

These early difficulties also reflect the fact that ITER is a political project. Of course, the idea was launched by two political leaders, Ronald Reagan and Mikhail Gorbachev, when they jointly advocated “the widest practicable development of international cooperation in obtaining [controlled thermonuclear fusion] energy, which is essentially inexhaustible, for the benefit of all mankind.” But this proposal was actively supported, if not entirely conceived, by the scientific community.

ITER is a political project because it is managed by politicians. The ITER Council is composed of representatives of the governments of each member - either ministers or very high-level officials. It is indubitably a political body, and so this makes the ITER Council very different to the board of a company. The Council drives negotiations between governments, and yet the ITER Council has to endorse industrial contracts, manage a huge worksite and work out long lists of technological issues. These duties do not exactly fit the archetypal profile of a government envoy; however, there is no doubt that the members of the Council are committed to the project and are making every effort to ensure its success. First and foremost, to maximize its financial return. The investments already made and the project’s international reputation are part of the explanation. However, despite featuring what Robert Bell (1998) calls “political technology” (technology developed and showcased for political reasons), ITER is a real driving force for research and industry in fusion. But the ITER governance reflects the importance of the “technostructure.” As argued by John Kenneth Galbraith (1967), the stockholders are without real power and decisions are effectively taken by groups of experts.

The project’s history also demonstrates the advantages of its political dimension. In policymakers, the fusion community has an anchor to the real world. With all due respect, scientists are not necessarily best-placed to manage a program like ITER, given that so much of it is located in industry. Nevertheless, this proximity is sometimes perceived as a threat, as policy-makers may decide to close the subsidy tap.

As a final note, although magnetic confinement fusion can be considered as a “diplomatic technology,” it is important not to overestimate the political aspects of the project. In the Council meetings, the representatives around the table try to act in the most responsible way. They manage public money and act in the public interest. Everyone is aware of each other’s difficulties, and nobody wants to lose the face. There is undeniably a genuine sense of solidarity. Let us not forget here that science has always had and will always have a political dimension. The idea that science is pure and represents a neutral force, independent of the real world, has never been true, and is probably less so today than ever. Politics directly influences the development of scientific knowledge, and not just through decisions about funding. On 28 February 2022, the European Parliament organised an exceptional hearing on ITER. The aim of this event was to discuss project’s delays and budget, radioprotection and staff management, after a suicide and a suicide attempt that happened in 2021 respectively in F4E in Barcelona and in the IO in Cadarache. The EU is now openly expressing its dissatisfaction in the way the ITER project is managed.

23.8 Nuclear licensing

ITER is the first fusion device ever that has had to go through the licensing process as a “Basic Nuclear Installation” (BNI) under French law.^f This is mainly because ITER will have a significant inventory of tritium, a radioactive element, onsite—about 4 kg in total. Therefore, throughout construction, commissioning and operation, ITER’s safety processes have to comply with French regulations, as verified regularly by ASN through audits and inspections. Thus, since 2005, the ITER site has been the subject of very strict regulation; ASN carries out unannounced inspections on the Cadarache site once every 2 months on average. Some ITER members find it quite strange that an international project like ITER falls under the remit of French law. The answer lies in the ITER Agreement, and more specifically Article 14 thereof: “The IO shall observe applicable national laws and regulations of the Host State [France^g] in the fields of public and occupational health and safety, nuclear safety, radiation protection, licensing, nuclear substances, environmental protection and protection from acts of malevolence.” Therefore, before building ITER, the IO had to provide the French authorities with evidence that every effort was being made to limit and monitor the impact on the environment and public health and, in any event, to comply with the legislation in force.

The IO submitted a preliminary safety report in March 2010 to ASN with a view to obtaining the authorization to create the ITER BNI.^h The next step was the submission of the application to a public enquiry, as required by the 2006 French Act on nuclear transparency and safety. This investigation took place in the 13 municipalities closest to Cadarache between June 15 and July 20, 2011. However, taking account of the fact that some of the residents would be away at some point during the summer, the commission in charge of the public enquiry decided to prolong the consultation until August 4, 2011. For almost 2 months, the public had the opportunity to make comments on and ask questions about the ITER project, in particular its environmental impact and its safety aspects.

^f The order setting the general rules relative to basic nuclear installations, called the “BNI Order,” was published in the Official Journal of the French Republic on 8 February 2012. It incorporates into French law rules corresponding to the best international practices. As explained on the ASN web site, “The provisions of the BNI Order primarily address the organization and responsibilities of the BNI licensees, the demonstration of nuclear safety, the control of nuisance factors and their impact on health and the environment, waste management, and emergency situation preparedness and management.” See <http://www.french-nuclear-safety.fr/Information/News-releases/General-technical-regulations-applicable-to-nuclear-facilities>, accessed on 6 May 2019.

^g https://www.iter.org/doc/www/content/com/Lists/WebText_2014/Attachments/245/ITERAgreement.pdf.

^h Author note.

ⁱ This report is accessible online, in agreement with article 29 of the French Act 2006–686 of 13 June 2006 on nuclear transparency and safety: <http://www.iter.org/fr/dac>. However, the link doesn’t work on some computers.

The quality of the work carried out by the commission was underlined by the IO.^v The members really got into the details of the file and developed a good understanding of it, diving into technical documents for several months and having multiple contacts with the staff and management of the IO. They tried to understand the issues at stake, the principles of tokamak technology and the complexities of the project. They took into account all of the contributions that they received, even those that arrived well after the deadline. They received 10,606 documents in total, out of which only 90 were unique contributions. The other 10,516 were photocopies of an antinuclear petition. Therefore, the commissioners carried out not just a quantitative analysis but a genuine qualitative assessment. On the basis of these contributions, the public inquiry commission issued a “favourable advisory opinion” to the ITER program on September 9, 2011, with a few recommendations. This opinion was an essential step toward the establishment of the ITER facility.

A few weeks later, in September 2011, the Institute of Radioprotection and Nuclear Safety (IRSN), acting as the ASN’s technical expert, submitted a 300-page report—including 800 questions to the IO—to a group of 30 experts appointed by ASN, the *Groupe Permanent*. The *Groupe Permanent* issued a favorable report at the end of 2011. With this, nothing could prevent ITER being set up in France. On June 20, 2012, the Director General of the IO was officially informed by ASN that the in-depth technical analysis of the ITER design and the operational conditions of the reactor had been concluded, and produced a favorable outcome. Coincidentally, on this date the ITER Council was in the middle of its 10th meeting in Washington, and the members of the seven delegations warmly applauded this announcement. On November 10, 2012, the French Prime Minister Jean-Marc Ayrault signed an official decree authorizing the IO to create France’s 174th BNI under the name of “ITER” in the commune of Saint-Paul-lez-Durance (Bouches-du-Rhône). In parallel, the IO had to submit a nuclear safety “stress test” report to ASN in late 2012. This kind of report was requested from all nuclear power plants and research infrastructures in France following the Fukushima Daiichi accident in March 2011. ASN recommended that the IO study in particular the potential impact of extreme climatic conditions such as tornadoes, hailstorms, etc. However, the stress test report did not lead to any additional costs.

23.9 Safety and waste management

Is fusion a safe and clean technology? The fact that small amounts of fuel (maximum 2 g of D-T) will be in the chamber, when ITER will be in operation implies that a fusion reactor like ITER will never produce large quantities of waste. (Also remember that the “burned” fuel in a fusion reactor after the reaction is helium, an inert gas.)

Nevertheless, it is estimated that during its operation, ITER will generate about 100 tons of “hot materials” per year. Neutrons hitting parts of the device will produce waste that is classified as very low, low, or medium-activity waste. All waste materials (such as components removed by remote handling during operation) will be treated, packaged, and stored onsite. Because the half-life of most radioisotopes contained in this waste will be less than 10 years, in a 100 years the radioactivity will have diminished so much that the materials could be recycled for use in other fusion plants. This timetable of 100 years could possibly be reduced for future devices through the continued development of “low-activation” materials, which is an important part of fusion research programs today.

Unlike conventional nuclear (fission) reactors, fusion reactors will therefore not produce long-lived radioactive waste. High-energy neutrons, another product of the reactions (as well as helium), are not classified as “waste.” Nevertheless, neutrons will be responsible for the activation or contamination of some tokamak components, the vacuum vessel, the fuel circuit, the cooling system, and even buildings. They will produce

^v Presided over by André Grégoire, Honorary Senior Member of the Court of Auditors, and appointed by the Bouches-du-Rhône administrative court, the ITER commission had five members, all volunteers.

an estimated 30,000 tons of waste that will be removed from ITER after its decommissioning. Over the entire lifespan of the program, ITER is expected to produce around 40,000 tons of waste.

The most problematic waste in ITER is one of the fuels, tritium. The machine will operate in successive “pulses,” during which the fusion reactions will take place. With an expected duration of about 400 s, each pulse will use only a few milligrams of tritium. However, being one of the lightest gaseous elements at room temperature, the tritium will spread to almost every part of the tokamak: it will of course be mixed with the fusion reaction products, and it will also diffuse in some of the reactor’s structures, which researchers want to control and limit as much as possible (Causey, Karnesky and San Marchi, 2012). Unfortunately, the scientific literature shows that tritium behaves quite complexly, particularly in its interaction with other materials (Gastaldi, 2007). In a fusion experiment, the majority of tritium should be recovered, purified, recycled and reused whenever possible.

Finally, ITER will also produce non-radioactive waste, some of which is toxic. This includes beryllium dust, which will be released by the 440 “first wall” panels, each covered with a 1-cm layer of beryllium, totaling approximately 12 tons of metal overall. The quantity of beryllium that will be released is estimated to be less than 6 g per year during construction (mainly through suspended dust particles following installation and cutting work) and approximately 1 g per year during the D-T phase. Beryllium is considered carcinogenic in France. Thus, in this area too, the IO will observe the French legislation and regulations that apply to beryllium as regards health and safety at work.

Despite these problems, magnetic confinement fusion is undeniably a cleaner technology than nuclear fission, as it will produce no long-lived radioactive waste and less waste overall. This is a direct consequence of the very small quantities of fuel involved. With 1 g of tritium, we are very far from the hundreds of tons of fuel contained in a nuclear fission reactor. However, the tokamak technology cannot (yet) be described as a “green” energy source.

Simulations and studies carried out on ITER and tokamaks in general show that this technology poses no major risk to the environment or human health. The fundamental characteristics of fusion physics and technology make a fission-style nuclear meltdown impossible. A Fukushima or Chernobyl-type accident could not happen at ITER. In the event of a disturbance, or if the optimum operating conditions (temperature, magnetic field, etc.) are degraded by the failure of any of the systems, the reactor will be unable to sustain the high temperatures required and the reaction will stop automatically, leaving virtually no residual heat.

Hypothetically, if the cooling system stopped working, for example in the event of an earthquake, there would be no impact on other systems such as the containment barriers, the large heat evacuation system, and the vacuum vessel, which constitutes a very efficient insulator. The temperature of the walls of the vacuum chamber, the first barrier of confinement, will always remain below the melting point of the materials.

Although very little tritium will be used during operation, the confinement of this radioactive isotope within the fuel cycle is one of the project’s most important safety challenges. ITER will even be the first fusion reactor in the world to be controlled by a nuclear regulator, in this case ASN, since neither JET in the UK nor TFTR in the United States were considered “nuclear” installations despite also operating with tritium. Tritium has long been the bugbear of ecologists.^w They argue that ITER’s safety is currently purely theoretical, as it remains to be seen how the safety measures will be implemented and how effective they will be. They have a point there.

A multilayered barrier system has been created to protect against the spread or release of tritium into the environment. The walls of the vacuum chamber will be a first (passive) safety barrier. A second (active) confinement system will consist of the buildings and the advanced detritiation systems for the recovery of tritium from gas and

^w Like all radioactive substances, tritium is a carcinogen, a mutagen, and a teratogen. However, given its low energy (beta) emission, tritium poses a health risk only when ingested, inhaled or absorbed through the skin.

liquids. Where tritium is handled, an efficient static confinement barrier (air pressure cascading in the buildings) will inhibit the outward diffusion of tritium.

The ITER detritiation system will be a world first in terms of the quantity of material that it will treat. This will of course be crucial for the protection of the environment. In its favorable opinion issued on September 9, 2011, the French public inquiry commission included a recommendation “that the optimisation phase of the detritiation systems [and robotisation] [is] carried out before the start of the experiments.”^x The official reply came a few years later, when the ITER Director General publicly acknowledged that the IO is “obliged to manage tritiated waste but not to detritiate the waste.”^y

Here we should note in passing the somewhat strange nature of the situation. In 2011, while this consultation was in progress to authorize the establishment of ITER as a BNI, construction works were already well under way. This makes the citizens’ consultation seem like a formality, but internally, managers at the IO explained to staff that they had preempted the French government’s decision and taken the risk of the authorization being refused.

Of course, documents that are available on the safety of tokamaks are quite reassuring. The IO’s preliminary safety report concluded that, under normal operation, the radiological impact of the installation on the most exposed populations will be insignificant, as it will be about one thousandth of the “background” level of radiation from natural sources. ITER’s design is such that, even if the containment was accidentally breached, the radiation level outside the ITER site would still be very low. In “worst-case scenarios” such as an explosion of the tritium plant, evacuations or other countermeasures for the local populations would not be required.^z

As already mentioned, in 2011 ASN compelled the IO to carry out additional “stress tests” to verify the safety of the installation and the relevance of its emergency measures. These tests confirmed the robustness of the safety design, as ASN proposed only a few improvements.

23.10 Natural hazards

ITER’s safety management is based on relatively simple principles. All possible and conceivable risks are identified, including the most unlikely, from both natural and artificial origin. On this basis, specific countermeasures are proposed and, if they are accepted by the IO, they are integrated into the design of the tokamak, buildings and auxiliary systems.

The consequences of the earthquake and tsunami that occurred in Japan on March 11, 2011, created legitimate questions and concerns about ITER. The number of hits on the IO’s website increased substantially during the weeks that followed, as if the public had renewed its interest in (or its concerns about) the project. The IO also received many emails, almost all asking the same question: what would happen if a major earthquake, a freak flood or a tsunami hit Provence?

Cadarache is situated in a low-to-moderate-level seismic area at the edge of the Durance River Fault, which extends for a hundred kilometers from Sisteron to Aix-en-Provence. The fault is responsible for small surface movements of up to 0.1 mm per year that can cause slight tremors in the region. These movements are caused not by plate tectonics but by the collapse of the nearby Alps Mountains, which are slowly spreading horizontally “like a ripe camembert.”

Provence has painful memories of two earthquakes: one around Manosque in 1708, which led to the destruction of several hundred houses but no human casualties, and another more serious earthquake around

^x <https://www.iter.org/doc/www/content/com/Lists/Stories/Attachments/888/conclusionsiter.pdf>.

^y http://cli-cadarache.org/fileadmin/user_upload/Cadarache/PV_REUNIONS/REUNIONS_PUBLIQUES/CLI_CADARACHE_PUBLIQUE_29_09_2016_PV.pdf.

^z As indicated previously, this report is part of the request to obtain the authorisation to create the ITER BNI: <http://www.iter.org/fr/dac>.

Lambesc on June 11, 1909. With a calculated magnitude of 6.2 on the Richter scale, the latter is the largest earthquake ever recorded in metropolitan France. In total, 46 people died, another 250 were injured, and approximately 3000 buildings were damaged. There are also geological traces of a “paleo-earthquake” that occurred in the Middle Durance Valley some 9000 to 26,000 years ago. Experts analyzed all of these events to calculate the “maximum historically plausible” level of a seismic event in the region. Reinforced by a strong safety margin, experts used a hypothetical 7-magnitude earthquake on the Richter scale to determine the seismic resistance of ITER’s nuclear buildings. According to experts, a tsunami would be impossible in this region; the volume of the Mediterranean Sea, the size of the submarine fault lines and the speed of the plates are insufficient to produce waves as large as those that struck Japan in 2011.

On this basis, seismic risk has been taken into account in ITER’s design. The second (B2) basemat, which supports the three buildings of the tokamak complex, rests on 493 columns, each 1.7 m high and topped with antiseismic bearings (Figure 23.15). 90 cm wide and 20 cm thick, these bearings are made of 10 alternating layers of steel and synthetic rubber. With a capacity for lateral movement of 10 cm, they are capable of filtering and absorbing any motion linked to earthquake-induced ground movement. Together with the columns, the 493 bearings will support the 400,000 tons of the tokamak complex.

The risk of flooding has also been taken into account in ITER’s design. Although Provence is not vulnerable to a tsunami, a major flood is possible, and its potential origins have been taken into account in the site plans. ITER’s engineers calculated that a 100-year flood^{aa} of the Durance River would reach a maximum height of 265 m. Therefore, the basemat of the nuclear buildings, which is 298 m above sea level, is safe. The experts also took into account the possibility a spectacular elevation of the groundwater table. In this case, the water could reach a height of 305 m. To be prepared for such an event, the lower floors of the tokamak complex will be sealed up to 315 m to provide an additional safety margin of 10 m. The experts even simulated a catastrophic scenario—a 100-year flood of the Durance combined with a failure of the Serre-Ponçon dam, located 140 km north of the site—but they concluded that it would have no impact on the tokamak complex. Nevertheless, in order to increase the safety margins, the platform was still raised by 10 m so as to protect it against every conceivable risk of flooding. In the most extreme hypothetical situation—that of a cascade of dam failures in the region—over 30 m will remain between the maximum height of the water and the first basemat of the nuclear buildings.

In the event of a major natural hazard, the ITER installation would immediately be switched to safe mode, meaning that any ongoing experiments would be interrupted, as well as any injection of fuel gas into the vacuum vessel. The residual fuel left in the injection circuits of the vacuum chamber would then be extracted using several pumps powered by independent batteries, and then trapped by molecular sieves. In principle, a few minutes will be sufficient to carry out these operations. Elsewhere, the other systems involved in the fuel cycle (injection, processing, recovery, etc.) would also be isolated. The interruption of the cooling system would have no environmental or health impact and would not jeopardize the safety of the installation.

In short, ITER has been designed to withstand all possible and conceivable accidents. The fact that very little fuel will be needed in the device at any one time is of course very reassuring. Another strong argument in favor of ITER’s safety is that it is under the control of ASN, whose approach has been summarized by the previous IRSN Director, Jacques Repussard (Menessier, 2011): “We have to imagine the unimaginable.” However, the IO could improve its transparency and communication on these topics, which are considered a priority by the public.

On the other hand, IRSN considers that the fusion community will soon face new safety challenges because (IRSN, 2018) “the future demonstration reactors will be different from ITER, in particular by using tritium breeding technology and operating significantly longer hours. These differences will have a very significant impact on the design and, as a result, on safety.” The issues raised by IRSN include the removal of

^{aa} A 100-year flood is a flood event that has a 1% probability of occurring in any given year.

residual power (estimated to be between one and two orders of magnitude higher than in ITER), which will pose rather strict constraints on cooling systems, and the presence of more tritium, both in the vacuum chamber and in other reactor structures like bricks. This increased amount of tritium will also require the designers to reexamine the consequences of possible accidents and even consider other types of accidents.

Nevertheless, the ITER installation opens up interesting prospects for the industrial exploitation of fusion. Unlike nuclear fission plants, we may even envisage, within a few decades, fusion reactors for which the risk of a serious civil nuclear accident would be virtually zero.

23.11 The impact of ITER on the economy

Even if you're not familiar with the details, it is easy to guess that ITER provides an economic advantage and an opportunity to showcase expertise for its host country. Many French politicians shared this conviction before the start of negotiations over where to locate the project, even including the then-French President, Jacques Chirac. They were not alone; the Spanish and Japanese governments also believed that ITER would give a boost to its host's economy. They were not mistaken. But a large project such as ITER can generate an economic benefit and imprint a social dynamic only if the host territory is prepared to welcome it and make the effort to meet its specific needs.

In the mid-1990s, about 10 years after the Reagan and Gorbachev initiative, the prospect of ITER arriving in the region was already triggering much interest and many discussions in political and economic circles. Public debates took place in Marseille, Aix-en-Provence, Manosque and other big cities in the region. As a consequence, the decision was taken to build an international *lycée*^{ab} in Luynes, in the suburbs of Aix-en-Provence—the first initiative specifically designed for the future ITER employees that would arrive from abroad.

Commitment came from the highest level, as the French government decided to coordinate ITER-related services itself. This official support filtered down to the local level as the PACA regional authorities^{ac} got involved in the program and made a significant financial contribution, estimated today to total EUR 467 million.

The neighboring CEA research center was also a supporter of the ITER project. Through conducting studies of the site, it helped to get the local political actors involved in the application. The Centre also welcomed the first employees of the IO by providing land, temporary offices, electricity and water networks, and other essential services such as transport, canteens and nurseries (the very first ITER team, composed of six staff, set up in Cadarache at the end of 2005). In 2006, the CEA established AIF, which acts as an interface between ITER and its host country and implements France's commitments to the project. It welcomes newcomers to the IO by finding accommodation in the region and providing integration services such as French language courses. AIF also set up the "ITER Industrial Committee" which facilitates relations between the IO and the local and European industry, in particular through providing information on calls for tender in the construction and assembly phases. In addition, in order to promote scientific training in the field of fusion, 12 universities and schools of engineering have combined their resources to propose a master's degree in "Fusion Science."

The real estate bubble, however, collapsed relatively quickly, although the public authorities did not directly support any accommodation-related projects. This was due in part to the fact that ITER's staff arrived gradually. The only significant initiative was the construction of the International School in Manosque, led by the local Prefecture's "ITER Mission."

The available data confirm that ITER is indeed boosting its host region's economic development. On a map showing France's employment published by *Le Monde* on July 24, 2013 (Chastand and Baruch, 2013), the area around Manosque was the only one to be cultured green (indicating that more than 6% of

^{ab} In the French educational system, a *lycée* is a state-funded school for students from 15 to 18 years old.

^{ac} The Departmental Councils of the six departments closest to ITER (Bouches-du-Rhône, Alpes-de-Haute-Provence, Var, Vaucluse, Alpes-Maritimes and Hautes-Alpes), the Regional Council of PACA, and the "Communauté du Pays d'Aix."

jobs had been created between 2008 and 2012), in contrast to both the north of the country (almost all in red, indicating a loss of more than 6% of jobs) and the south (yellow or pale green, meaning that employment was stable or slightly increasing). Manosque was unique in mainland France, with a record growth of 6.8% in the number of jobs created during the same period. Of course, this rapid increase cannot be attributed wholly to ITER. But the impact of the program in terms of jobs, direct, indirect or induced, is undeniable and spectacular.^{ad} The French National Institute of Statistics and Economic Studies (INSEE) published a study on the “30-min” territory around ITER (the 36 municipalities that are within 30 min drive from ITER, home to 130,000 people) (Lassagne and Loose, 2017). The experts note that private employment was very dynamic in this area after 2008, the first year of the financial crisis, “whereas it was subject to a sudden slow-down everywhere else.” While in similar areas, such as Sofia-Antipolis close to Nice in the Alpes-Maritimes, private employment rose by only 0.8% per year between 2004 and 2014, the growth rate around Manosque was almost three times higher at 2.3% annually. This represents 4700 additional jobs in 10 years—an impact that the INSEE experts wrote was “partly due to the ITER worksite” (Adaoust and Belle, 2017).

This job growth parallels, at least in part, the activity onsite at ITER. Since 2007, the IO, F4E, and AIF have awarded contracts worth a total of over EUR 10 billion. Over half of this has been awarded to French companies (EUR 5.5 billion worth of contracts), of which 73% (worth EUR 4.0 billion) was awarded to companies based in Provence in the past 15 years.^{ae}

This is not really a surprise. It is a well-established fact that a major scientific installation like ITER creates jobs, directly and indirectly, and also stimulates employment in the local economic system. The examples of JET in Culham (UK), CERN in Geneva (Switzerland) and the ESRF (the European Synchrotron Radiation Facility) in Grenoble (France) have shown that constructing a very large facility has a positive and lasting impact on its surroundings. All of these projects have been found to stimulate local development and attract new talent to the area. In their immediate neighborhoods, they stimulate new social, industrial, economic, technological and cultural dynamics. They also create synergies and boost new initiatives and structures, such as high-tech start-ups, laboratories, and service providers.

In order to deliver the European contribution to the ITER project, F4E first looks for companies through a European call for tenders. The agency rigorously applies the European Directives on public procurement, which enshrine the principles of transparency, free competition and sound management to ensure that public money is used properly.

The calls for tenders for construction are then advertised in the 28 (27 after Brexit) Member States of the European Union, plus Switzerland. Therefore, the fact that France obtains over half the contracts is an excellent result for the country. This is of course due to the high level of the French industry’s know-how in the construction, civil engineering and nuclear sectors. Nevertheless, Director General Motojima avoided quoting these figures in his public presentations. He did not want to raise questions about France’s excellent performance in the construction of ITER. The figures could also be misused as evidence that one country in particular is receiving substantial benefits from the international project.

ITER’s impact is tangible and significant, and not just in terms of the monetary value of contracts. For example, the major TB03 and TB04 contracts^{af} related to construction enabled their beneficiaries to hire

^{ad} Here we should note that unemployment also grew in the region, by 2.6% between 2007 and 2012, and by 0.3% between 2012 and 2016. These increases are close to the national averages (+2.1% and +0.4% respectively over the same periods). It is well-known that regions with a high unemployment rate may also be economically healthy. Conversely, a low unemployment rate may reflect local young people moving to find better work conditions: http://www.lemonde.fr/emploi/video/2017/03/29/pourquoi-un-faible-taux-de-chomage-n-est-pas-toujours-bon-sign_5102550_1698637.html#7FSLcCZdwIaSLZa2.99.

^{ae} Communication of AIF, April 2019. The data is not public.

^{af} TB03 (“Tender Batch number 3”) covers civil engineering works for the tokamak complex and 11 other buildings plus some other structures such as bridges (contract valued at EUR 300 million at the time of its signature, and now at EUR 600 million following many amendments and technical modifications). TB04 (“Tender Batch number 4”) concerns the mechanical and electrical equipment of nearly all buildings on the site (for a value of EUR 530 million at the time of its signature).

almost a thousand workers. According to a study carried out by the European Commission in 2018 (EC, 2018), European investment in ITER has had a positive impact on employment and economic development. ITER activities generated around 34,000 job years in the European economy between 2008 and 2017. For the period 2018–2030, the economic model used for the study predicts that ITER will generate EUR 15.9 billion in Gross Value Added, to be compared to EUR 13.9 billion of spending. Over the same period, the study predicts that 72,400 job years will be created, mainly in the business services and industry sectors.

Companies state that working for ITER has helped them develop new state-of-the-art technologies, improve their production and other processes, access business opportunities outside fusion, and create synergies and new opportunities.

An interesting finding in this study is that “12% [of industrial participants] developed new cutting-edge technologies in areas other than fusion as a result of their contracts.” The reverse is also true. For example, Belleli Energy (Italy) is a company that operates predominantly in traditional sectors, manufacturing components for the oil and gas industry, but it got involved in the construction of ITER’s vacuum vessel. Its Chief Executive Officer, Paolo Fedeli, said at a conference in Brussels in 2017: “Thanks to ITER, the company staff grew from 300 in 2010 to 1000 today. This includes a growth in the number of high-skilled engineers from 15 to 100. Although the ITER business represents only 10% of the company’s turnover, the ITER business line is the one giving the company the most dynamic growth. Participating in ITER has enabled our company to expand its market share in other sectors but also in the oil and gas business which still accounts for 90% of our Group business.^{ag}”

The study also compares ITER with CERN—an apt comparison as both organizations share a large infrastructure and a high cost of construction. In CERN’s case, it has been shown that the profit margins of firms involved in the construction of the LHC develop favorably. This is especially true for high-tech suppliers, while the effect for low-tech suppliers does not exhibit statistical significance. This is called the “CERN effect,” and according to the study, given the larger size of the fusion industry, an “ITER effect” is entirely plausible.

According to the projections of F4E, “local workers,” i.e., employees who live in the municipalities close to ITER (the “employment basin” of Manosque) could account for as much as 50% of the French labor force on the worksite. Local recruitment is therefore far from negligible. In total, a maximum of 3000 people will be working on the ITER construction site until 2026. The construction workforce is now slowly declining, and an increasing number of workers and technicians are involved in the assembly of the machine, up to about a 1000 people.

Of course, the economic impact of ITER is larger than the jobs that are created on the worksite itself. As early as 2003, anticipating the arrival of ITER in the region, the Institut D’Économie Publique de Marseille (IDEP), estimated that 3000 “indirect” jobs were likely to be created during the construction phase and 2400 during the operational phase (Jacquinot and Marbach, 2004).

An evaluation of the economic impact of ITER must also take into account the effects induced by the presence of staff, contractors and their families in Aix-en-Provence, Manosque and other cities around ITER. To meet the needs of this new (and international) population, shops and services have been created or expanded. As noted by the INSEE, 68% of the jobs induced in the “30-min” territory around ITER are in the sectors of catering/hospitality and health/social welfare. The contribution of ITER employees to the local economy, in the form of their wages spent in the local area, represents several tens of millions of euros annually.

This economic dynamic has been observed around similar projects in the past. For example, in the county of Oxfordshire around the JET facility, over a 1000 indirect and induced jobs have been created, in addition to its 450 employees; in Geneva around CERN (2500 staff), more than 7000 indirect and induced jobs have

^{ag} https://ec.europa.eu/energy/sites/ener/files/key_messages_final.pdf.

been created on both sides of the border between France and Switzerland. So far, AIF estimates that 1700 indirect and induced jobs have been created by ITER in the PACA region. While ITER is still in the construction phase, the project is likely to confirm that one euro injected into research and technological development typically generates two or three in the form of indirect and induced benefits (Mairesse and Mulkay, 2004).

Even if little data is publicly available, similar dynamics can be observed in the other ITER Members. For example, the US's participation in ITER led to some 600 contracts with companies, universities and national laboratories in 44 states. According to the DOE, these activities generated more than 500 direct jobs and over 1100 indirect jobs. The Department also estimated that the impact of these products and that of these US expenditure benefits “at 80%” to the United States (Van Dam, 2017). These figures were published to show the US senators—known to be predominantly opposed to ITER—that participation in ITER brings in substantial benefits.

Who works for ITER? There are definitely many employers working for ITER—the IO, F4E, AIF and several hundred contractors working on the site—plus all the enterprises situated outside France working for ITER. The jobs on offer vary depending on the employer, both in the work itself and in the contractual conditions. In total, there are an estimated 3000 people working for ITER in Cadarache, and over 15,000 worldwide (for the seven DAs and the thousands of contractors).

Joining the IO is a good way to start an international career. The minimum requirement is to be a national of one of the ITER Members. Today, around 1000 people work directly for the IO. The contracts on offer are generally for 5 years (but renewable) and the salaries are typical of international organizations. But be aware: if your contract is not renewed or extended, you are not entitled to any unemployment allowance or indemnity since the IO's staff do not pay any French social security contributions. Job vacancies are published online.^{ah} At the time of publishing, about two-thirds of the IO's employees are of European nationality. The next most represented nationality is now Chinese (11% of staff), of whom there are now a hundred at the IO.

According to F4E's data, more than two-thirds of the workers on the site are of French nationality. This obviously reflects the fact that the majority of construction and civil engineering contracts have been awarded to French companies. The other nationalities that are most numerous on the site are Spanish, Portuguese and Romanian. Job profiles are typical of a large construction site: bricklayers, welders, plumbers, electricians, etc. The French recruitment agency “Pôle Emploi” has set up a regional recruiting team to help both companies (publication of vacancies, selection of candidates) and jobseekers.^{ai} Every June, an ITER employment forum is organized by the City Hall of Saint-Paul-lez-Durance, which attracts a 1000 people and allows companies working on the site to establish direct contact with jobseekers. The projections made by F4E show that, out of the estimated 3000 workers on the construction site, about 50% of them come from the “30-min” territory around ITER, 30% from other French regions, and 20% from other European countries.

23.12 Will fusion become commercial?

About a hundred tokamaks have been constructed so far all over the world. None has achieved a net power gain, i.e., produced more fusion power than the power injected to heat the plasma. The world record is held by Europe's JET, which produced 59 megajoules of heat energy fusion during a period of 5 s, as announced on 9 February 2022.

^{ah} <http://www.iter.org/jobs>.

^{ai} <http://www.pole-emploi.fr/region/provence-alpes-cote-d-azur/actualites/iter-@/region/provence-alpes-cote-d-azur/index.jsp?id=117379>.

The energy efficiency of a fusion experiment can be described by a gain factor called “ Q ,” which corresponds to the thermal power released by the fusion reaction divided by the heating power used to bring the plasma to 100 million °C or so:

$$Q = P_{\text{fusion}}/P_{\text{heating}}$$

In the case of JET’s recent experiment, Q was equal to 0.33 (11/33). This was lower than JET’s historic experiment of 1997, which achieved a Q of 0.67.^{aj} Achieving break-even means reaching a Q of one, as at that point the power released by the fusion reaction is equal to the required heating power. In a burning plasma, the fusion reaction releases so much energy that the plasma “self-heats.” But experts tend to agree that in a typical tokamak, self-heating will not match the energy required from external sources until at least $Q=5$. If self-heating becomes more efficient, then less energy is needed from external sources to keep the plasma at the right temperature. Eventually, self-heating will keep the plasma hot enough on its own and the external heating source can be switched off, which would lead to an infinite value of Q . This point is known as ignition—the goal (and the dream) of all fusion specialists.

In most published materials about ITER, you will read that it is expected to produce a 10-fold return on energy ($Q=10$), or 500 MW_{th} of thermal fusion power from 50 MW_{th} of input plasma heating power. ITER will not capture the energy it produces as electricity, but—as the first of all fusion experiments in history to produce net energy gain—it could open the door to industrial exploitation.^{ak} What does this mean exactly?

It is easy to perceive that the production of fusion reactions in a laboratory is not the same as the production of fusion energy. Here we are confronted by what engineers call “scaling-up”—the process of transforming a laboratory-scale process into an industrial operation. In the case of tokamaks, as we have seen, industrial exploitation of fusion energy would be possible only if break-even can be reached. So, what are the factors that influence Q , the gain factor?

Unlike a conventional nuclear reactor, a tokamak is not a generator but an amplifier of energy. It is necessary to heat the plasma (and therefore supply energy) continuously in order to start off and maintain the fusion reactions, and then produce energy. If insufficient energy is supplied, the energy density will decrease due to various types of energy loss (conduction, radiation, etc.). In order to be “sustainable,” the fusion reactions must therefore generate enough energy to compensate for at least the losses inherent in their production. In this case, Q will be greater than or equal to 1. This is called creating a “thermonuclear plasma,” i.e., a situation in which the energy produced by the fusion reactions overcomes the thermal energy of the gas during the energy confinement time.

Let us now introduce the three main factors that affect the amount of energy produced: nuclei density (n), temperature (T), and confinement time (τ_E). In the case of deuterium-tritium fusion, John Lawson, a British engineer and physicist, established in 1955 that the product of these three quantities must exceed a precise value in order for the energy produced to exceed the losses, as expressed by the following formula:

$$n \tau_E T \geq 1.5 \times 10^{21} \text{ m}^{-3} \text{ keV s}$$

The so-called Lawson criterion captures the fact that in order to achieve a net fusion energy gain you need to maintain and compress a gas with a sufficiently high density of atoms/nuclei, for a sufficiently long time, at a sufficient temperature. As we do not have much control over the first two parameters, this leads to the astronomical temperatures required in fusion devices.

^{aj} This is the record for a civil experiment. We do not have much information about experiments carried out during military operations or tests of nuclear weapons, which are discussed in the penultimate chapter. However, the hydrogen bomb is so far the only man-made device to achieve a gain factor of more than 1.

^{ak} This assumes that the order of magnitude of Q is confirmed and that the construction and operational costs of future tokamaks are compatible with the economic sustainability of the technology.

This formula also shows how two very different confinement technologies have been developed: inertial fusion, which is designed to compress and heat micro-spheres containing the gaseous fuel to reach very high temperatures for very short periods of time, and magnetic fusion, where a very low-density gas is contained for a much longer period of time. In both techniques, the fuel must be heated to a temperature of at least 100 million °C.

Lawson's criterion means that in a tokamak, a density of 10^{20} ions per m^3 should typically be maintained at a temperature 10 times that of the Sun's core (i.e., 15 million °C) for an energy confinement time of at least 3 s. Achieving these values should not be a problem for ITER. The plasma should be confined for a minimum of 400 s, and its temperature should reach 150 million °C. This should be enough to reach breakeven and possibly ignition, but it would probably still be insufficient from an industrial point of view. However, if everything goes well, ITER's technicians will push the machine to its limits, and try to sustain fusion reactions during several tens of minutes.

ITER is expected to produce $500 \text{ MW}_{\text{th}}$ of thermal fusion power, compared to about $50 \text{ MW}_{\text{th}}$ that will be injected for the purposes of heating the plasma. This means, in these circumstances, that Q will be equal to 10.

However, if we want to estimate the energy efficiency of a tokamak and its potential use as an energy source at industrial scale, we should consider not only the heating power injected into the plasma but the power that will be supplied to all of its equipment and systems during the experiment (which are all necessary to keep the plasma at a given temperature). The industrial viability of fusion energy will only be proven if the output power exceeds the power consumed by the complete installation. What would be the point, from an economic point of view, of the $500 \text{ MW}_{\text{th}}$ produced by ITER if it turns out that the average electricity consumption on the site is the same amount or more than that? These are deemed as the minimal conditions.

It is therefore worthwhile to define an “engineering” Q factor which, following a more industrial logic, measures the profitability of the experiment from the point of view of the overall energy balance. In the case of the 1997 JET experiment, the total electrical power required to run the tokamak was $700 \text{ MW}_{\text{el}}$, of which only $24 \text{ MW}_{\text{th}}$ were injected into the plasma. Therefore, in this case, the “fusion” Q factor was 0.67 and the “engineering” gain factor was $16/700$, i.e., a mere 0.02.^{al} D-T experiments carried out in 1994 in the US's TFTR gave similar values: $10 \text{ MW}_{\text{th}}$ of output power for $37 \text{ MW}_{\text{th}}$ of heating power and $500 \text{ MW}_{\text{el}}$ for the plant's electric consumption, which mean a fusion Q of 0.27 and an engineering Q of 0.007 (Bell, 2016).

During operations at ITER, the electrical consumption of the machine and facilities should be of the order of $110 \text{ MW}_{\text{el}}$ (Arnoux, 2016). Therefore, taking this value into account, the fusion Q would be 10 and the engineering factor would be $500/110$, i.e., 4.5. It should also be noted that the plant's electrical consumption will be up to $620 \text{ MW}_{\text{el}}$ for peak periods of 30 s during plasma operation. The power will be taken from the national electricity grid (it is provided to the ITER site through a 400-kV high-voltage line, which already supplies the nearby CEA Cadarache site—a one-kilometer extension now links ITER to the network). For these peaks to not pose any problem for the power supply of Provence (possibly excepting some very cold winters), the team running the experiments at ITER will have to follow a precise protocol; they will need to receive two successive green lights (respectively 3 days and 1 h before the experiment) from the regional control center in Marseille.

But if we pursue the industrial logic, we need again to take into account the fact that the $500 \text{ MW}_{\text{th}}$ produced by the fusion reactions is thermal power, while the $110 \text{ MW}_{\text{el}}$ injected is electrical power. To account for the difference, we need to divide the first figure by three. This means that ITER's power efficiency (measured by the engineering gain factor) will be of the order of 1.5 ($500/3/110$). We are far from a gain factor of 10.

Steven B. Krivit, editor of the New Energy Times site devoted to low-energy nuclear reactions, argues that several fusion organizations have misled the public by using the fusion Q values to allege that ITER's output

^{al} Actually, we should take into account the fact that the $16 \text{ MW}_{\text{th}}$ are thermal power while the $700 \text{ MW}_{\text{el}}$ are electric power. As the conversion factor between thermal and electric power is about 1/3, this means that the engineering gain factor was only 0.007.

power will be 10 times the power injected (Krivit, 2020). Following his articles, the IO corrected several pages of its web site.^{am} Krivit estimates the average total power consumption of ITER to be 300 MW_{el}.

My point here is that using the fusion gain factor to justify the industrial relevance of fusion energy is questionable. Furthermore, this discussion is irrelevant in the case of ITER as its purpose is not to produce as much energy as possible but to demonstrate the technological feasibility of fusion.^{am} If everything seems to indicate that ITER will produce net power, its exact value depends on the reference point. We need to wait for the actual experiments to know exactly how the tokamak will operate, and in particular what the exact output and input power levels will be. It is not impossible, on the basis of the above, that ITER will yield a modest or even a negative net energy balance. One thing is certain: these calculations show that ITER has a significant advantage over JET as it will use superconducting magnets, which significantly reduce electricity consumption. A tokamak with conventional resistive magnets will never be viable from an industrial point of view.

23.13 DEMO and the projects after ITER

In nuclear fusion, research programs are not sequential but overlap. Even when JET was still under construction at the end of the 1970s its successor was already being discussed (under the name of Intor), and correspondingly, the conceptual design of DEMO is currently being worked out even though ITER has not yet started off. It took over 20 years to translate the ITER idea into a real project. This may be also the time needed to make the European DEMO a reality.

The road to fusion energy is now in its third stage. In 1970–1980, the first reactors, such as the US’s TFTR, Europe’s JET and Japan’s JT-60, demonstrated the scientific feasibility of fusion, making it clear that the concepts developed by researchers were valid and functioning. Secondly, a large machine has to be built to demonstrate technological feasibility by producing large quantities of energy and testing certain technologies that are essential to building a fusion reactor. This is the milestone that ITER represents. Thirdly, DEMO should demonstrate the commercial viability of an industrial prototype and produce electricity.

DEMO is going to be the machine that addresses the technological challenge of bringing fusion energy to the electricity grid. The principal goals for the DEMO phase of fusion research are the exploration of continuous or near-continuous steady-state regimes, the investigation of efficient energy capture systems, the achievement of a power output with a fusion Q value in the range of 30–50 (as opposed to ITER’s 10), and the in-vessel production of tritium (called tritium breeding). With DEMO, fusion energy research will approach the conditions of future commercial reactors as closely as possible. It is too early to say whether DEMO will be an international collaboration like ITER, or a series of national projects. In any event, each ITER member has already defined the broad lines of what its own DEMO might be (although this is less true for the United States than the other members).

This approach derives from the very essence of ITER, which is as much an educational program as a technological one; thanks to ITER, all of the members acquire the experience and knowledge that enables them to move to the next step. In short, DEMO cannot exist without ITER.

^{am} However, the following sentence, which is still online, is misleading: “ITER is designed to produce a 10 times return on invested energy: 500 MW of fusion power from 50 MW of input heating power ($Q = 10$). It will be the first of all fusion experiments in history to produce net energy” <https://www.iter.org/sci/Goals>.

^{am} As explained in the final report on ITER’s technical design (ITER EDA Documentation Series n°21, AIEA, Vienna, 2001): “The overall programmatic objective of ITER is to demonstrate the scientific and technological feasibility of fusion power for peaceful purposes. ITER would accomplish this objective by demonstrating controlled ignition and extended burn of deuterium-tritium plasmas, with steady-state as an ultimate goal, by demonstrating technologies essential to a reactor in an integrated system, and by performing integrated testing of the high-heat-flux and nuclear components required to utilize fusion energy for practical purposes.”

At an international conference on ITER and fusion energy that took place in Monaco in 2016, all of the ITER members presented their plans for DEMO. While the schedules and technical specifications vary among the seven parties, the objective was always the same: to build the machine that will demonstrate that fusion can produce electricity on an industrial scale by 2050.

China also has an intermediate project planned. It plans to explore the physics and engineering challenges of the future DEMO in a test reactor called CFETR (China Fusion Engineering Test Reactor). Three cities have been preselected to host the reactor: Shanghai, Hefei and Chengdu. China also confirmed its intention to start the construction of a DEMO in the next decade. Construction of CFETR should start in 2030. The aim is to produce 1 GW of thermal fusion power (compared to ITER's 500 MW_{th}), with tritium self-sufficiency, and then to generate electric power (by 2040).

The United States is a special case; for reasons related to how research is organized in this country, the DOE did not officially commit itself to a DEMO project. But most US fusion physicists consider that they would need two “intermediate” machines, one to address technological issues and the other to carry out scientific research before launching a genuine DEMO program.

So, what will the different DEMOs look like? Most likely, they will be larger than ITER. The major radius, which determines the overall size of the machine, should be between 6 and 10 m—to be compared to the six meters of ITER and to the three of JET. Their powers will range from 300 to 500 MW_{el} (electric megawatts) for the European DEMO to 1500 MW_{el} for the Japanese one, which is similar to the power of the third-generation European Pressurized (water) Reactors (EPR). Their objectives are roughly the same with some small differences; some DEMOs will be “preindustrial demonstrators,” while others will be “quasi-prototypes” which would not require an additional step before moving on to an industrial scale. For non-specialized eyes, all these machines will probably look the same! (Figure 23.16).

In a recent article, one of my colleagues, Gunther Janeschitz, a German engineer who contributed to the design of ITER, argued that an economically viable fusion reactor should produce at least 2.5 GW_e given that it will most likely cost over EUR 15 billion (and even 30 billion for the first model). Taking into account the physics of the process, he argues that future tokamaks will always be large machines (Janeschitz, 2019). But Janeschitz missed one point here: research is moving forward and we see that improvements in high-temperature superconducting magnets are increasing the magnetic field strength that we can attain, enabling a corresponding down-scaling of tokamak dimensions, and potentially costs. This scaling underlies MIT's recent initiative, which we will discuss in the next section.

In the fusion world, one project is somewhat different from all the others: it is the Russian DEMO (or rather pre-DEMO), which would be a “hybrid” machine combining the principles of both fusion and fission. It is based on the fact that a fusion reaction produces very high-energy neutrons. In a tokamak like ITER, these neutrons will penetrate the inner walls of the machine and generate heat that can be extracted to produce electricity. Some physicists consider that these energetic neutrons should be better exploited. They are therefore considering breeding fission in otherwise non-fissile fuels such as natural uranium or using them to “burn” radioactive waste. So, Russia decided to put theory into practice; the T-15 tokamak is being upgraded into a machine called T-15MD which will operate as a nuclear fusion-fission hybrid reactor. Currently being finalized in the Kurchatov Institute, it is expected to be commissioned in a couple of months.

Of course, the conceptual designs of all these machines are not yet finalized, and in some cases not even decided. Whatever options are taken, experience from ITER will have a key influence on the specifications of all the DEMO machines. The ultimate key milestone in the fusion history will be the large-scale production of energy. But before fusion can become an industrial source of energy, solutions will be needed for at least two distinct problems. The first is to determine the magnetic configuration and the optimal technical conditions for reliable and steady-state energy production, which will become the reference point for future fusion plants. Ongoing works and the commissioning of ITER are expected to provide essential information on this issue. The second challenge is to identify the best economic conditions for the industrial exploitation of



Figure 23.16. This is HOW the European “DEMO” may look like. The building in blue is the main difference with the ITER site: this is where the thermal power generated by the tokamak will be converted to electrical power by way of turbines and alternators. *Credit: EUROfusion and Fusion for Energy*

fusion energy, which involves in particular finding new structural materials for the reactor’s internal walls that can withstand the high energy and neutron fluxes (without needing the bricks to be replaced too frequently). The problem is that we are still missing such materials.

Last but not least, the supply of some existing materials might be an issue in the industrial fusion age. Tritium is one example. It is estimated that every D-T reactor will require about 100–200 kg per year. This is far more than the entire world’s civil inventory of tritium. It may be possible to achieve “tritium self-sufficiency” by breeding tritium inside the reactor, if lithium is present in the walls of the vessel (when struck by a neutron, a nucleus of lithium-6 transforms itself into one nucleus of helium and one of tritium). But this technology has yet to be developed. It is regarded as one of the most important issues to be solved on the pathway to fusion energy as commercial tritium resources are too scarce to supply the fusion projects that will follow ITER (China’s CFETR, DEMO, etc.). Another concern is the supply of beryllium and lithium-6 for the vessel’s blanket.

Today, there is no device that can adequately replicate the conditions inside a future industrial fusion reactor in order to test the resistance of specific materials. This is why the construction of a specific source of high-flux neutrons has come to light as an indispensable complement to ITER. This is the main purpose of the

“Broader Approach^{ao}” activities implemented by Europe and Japan. They plan to build an accelerator to irradiate and test materials under near-industrial conditions. In doing so, the European and Japanese representatives have responded to the suggestion of David King, a former scientific adviser to the UK Prime minister, who proposed in 2001 launching this accelerator as soon as possible, known as the IFMIF (ITER Fusion Material Irradiation Facility), and not wait until the construction of ITER was complete as originally planned. A linear prototype of the IFMIF accelerator is currently being installed at Rokkasho-Mura in Japan.

Despite having more questions than answers, this section shows at least that ITER’s members are preparing for the future of fusion energy in a very active way and with a long-term strategy. You might say that this is the very minimum we could expect. In any case, we should acknowledge the constructive approach taken by the countries involved in this scientific adventure. The challenges are huge and the way to go is still long, but an impressive international research effort is supporting the technological developments needed to make fusion a reality (Pacchioni, 2019).

23.14 Alternative technologies

ITER holds the spotlight in the field of controlled fusion, but this success should not hide the fact that several different kinds of technology are being explored in the quest to achieve nuclear fusion on earth. Let us briefly describe here these “alternative” projects, such as the National Ignition Facility (NIF) in the United States and the Laser MegaJoule (LMJ) in France. In addition, up to 30 or so fusion-related start-ups supported by private money have recently emerged and are moving fast in this competitive field.

Within magnetic confinement specifically, the proven technology of tokamaks is by far the most advanced along the road to the potential production of fusion energy. Pragmatism therefore dictated that it was the right choice for ITER; however, stellarators remain in the running. Even though they are intrinsically more complex than tokamaks (optimizing the design was impossible before the advent of supercomputers), stellarators have the advantage of being more reliable and stable in operation. The Wendelstein 7-X stellarator in Germany, which achieved First Plasma at the end of 2015, is expected to gradually approach ignition conditions and to perform at a level close to tokamaks of a similar size. In a report on the first results from the initial experiments, an international team of researchers show that the stellarator could potentially operate for 30 min straight, which is very encouraging (Wolf et al., 2019). These results might influence the design of DEMO, the successor to ITER, even if tokamak technology has been the preferred option so far.

Magnetic confinement fusion is defined by the presence of magnetic fields that confine the plasma. However, another possible technology being developed by several research centers is Inertial Confinement Fusion (ICF). This concept is of a very different nature, since its purpose is to heat and compress a fuel target, typically a microsphere that contains a mixture of deuterium and tritium, by means of powerful radiation to achieve a temperature of several tens or hundreds of millions of degrees, thereby triggering fusion reactions.

Inertial confinement was first developed for military purposes, as it makes it possible to simulate thermonuclear explosions in a laboratory. The technology is therefore a substitute for atmospheric or underground tests, allowing scientists to test new weapons and study the behavior of materials under explosive conditions.

^{ao} Entered into force on 1 June 2007 for at least 10 years, the Broader Approach Agreement, concluded between the European Atomic Energy Community (Euratom) and Japan, consists of activities which aim to complement the ITER project and to accelerate the realization of fusion energy through R&D and advanced technologies for future demonstration fusion power reactors (DEMO). Both parties contribute equally financially. The Broader Approach covers three main projects being built in Japan: an International Fusion Energy Research Centre (IFERC) equipped with a supercomputer in Rokkasho-Mura for modeling and simulation studies; a prototype for IFMIF, a future facility for neutron production also located in Rokkasho-Mura; and a “satellite” reactor to optimize plasma operation in ITER and to investigate advanced operating modes for DEMO to be tested on ITER, located in Naka. The Broader Approach agreement should be extended for a further 10 years.

In the 1970s, research suggested that very powerful lasers could be used to create high-temperature hydrogen plasmas and even produce fusion energy. However, scientists were divided about the amount of energy that could be obtained through this technology. For some of them, it would not be enough to achieve ignition; for others inertial confinement could lead to the industrial exploitation of fusion energy.

In any case, the United States decided to test this concept in 1978. As this research is classified, not much public information is available, but it seems that underground experiments were carried out between 1984 and 1988 in the Nevada desert to measure the amount of energy produced by fusion reactions. In a top-secret operation codenamed “Halite-Centurion,” scientists were apparently authorized by the military authorities to use radiation generated by underground explosions to convert hydrogen contained in small spheres into plasma. According to a New York Times report published in 1988 (Broad, 1988), researchers were even able to achieve ignition in a plasma in the years 1985–1986. They claimed that spheres filled with D-T gas had been ignited using an intense beam of X-rays that output 20 million joules of energy. But according to other unofficial information sources, the tests were less conclusive.

It is worth noting that the New York Times article coincided with the official launch announcement of the ITER project in the EU’s Official Journal. Was this a manoeuvre directed by inertial confinement experts to secure their political support and funding from the authorities in Washington? Or was it aimed at creating an additional line in the Department of Energy’s budget and publicizing civil applications of military research? It is plausible. However, we should keep in mind that the primary purpose of this military research is *not* the production of fusion energy.

In any case, the “Halite-Centurion” experiments apparently provided enough scientific basis for the United States to envisage the creation of a facility dedicated to inertial confinement at the end of the last century (Lindl, 1995). At the same time as—or because of—the United States’ withdrawal from ITER, the construction of the NIF, located within the Lawrence Livermore National Laboratory in California, was approved in 1997. Today, the NIF is one of the two most important facilities for inertial confinement in the world.

Operational since 2010, the NIF uses 192 powerful laser beams, each following a trajectory about 1500 m long. Their destination is the center of a spherical chamber 10 m in diameter. The target is a tiny beryllium capsule only a few millimeters across that contains a few milligrams of deuterium and tritium as fuel for the fusion reaction. The laser beams rapidly heat the surface of the target, forming an envelope of plasma around it. The heated outer layer explodes outward, producing a reaction force against the heart of the target and compressing it. During the final part of the capsule’s implosion, the fuel core reaches 20 times the density of lead and is heated up to about 100 million °C. The system develops a single 500 TW peak flash (roughly 1000 times the power produced at any one time by the United States) for a period of only a few picoseconds. However, so far, the NIF has failed to create a self-sustained nuclear fusion reaction, with fusion performance well below ignition levels and differing considerably from predictions. Practical and theoretical studies are still ongoing, as the energy efficiency is roughly three times lower than expected. This should not hide the defense-related purpose of the NIF, which is, according to the DOE, “to investigate hydrodynamic and mix phenomena relevant to modern nuclear weapons.” The NIF has stated that the total cost of the facility was \$3.5 billion.^{ap} On August 8, 2021, NIF announced a “historic result” as scientists obtained a record production of 1.35 megajoules of fusion energy, i.e. 70% of the power used to heat the plasma, putting researchers at the threshold of fusion ignition.

Inaugurated in the late 2014, close to Bordeaux in south-west France, the CEA’s LMJ exploits the same technology as its American counterpart. Its objectives are also the same. LMJ uses 176 laser beams that converge on a target to produce fusion reactions from D-T mixtures contained in a microbead of less than 1 mm in diameter. To achieve this, the mixture has to be very quickly compressed to a density of the order of several hundred grams per cubic centimeter, and heated to 100 million °C—like in the NIF. LMJ intends to achieve a fusion gain factor Q of approximately 10 between the thermal energy produced by the thermonuclear reactions and the laser energy supplied to the target.

^{ap} https://lasers.llnl.gov/about/faqs#nif_cost.

Producing fusion energy is not the primary purpose of either the NIF or LMJ; it is therefore not surprising that ICF has not yet shown that it could offer a quicker or more efficient solution than magnetic confinement. In Europe, the Euratom programs do not fund research on ICF. However, the European Commission is closely following the development of this technology.

In the last years, several private businesses have invested in the field of nuclear fusion, mainly in North America and the United Kingdom. This is not a completely new phenomenon; in the 1960s, the US company Lockheed Martin built the “Z machine” in its Sandia National Laboratories, which they claimed was the “world’s most powerful and efficient laboratory radiation source.” It used magnetic constriction to produce high temperatures, high pressures, and powerful X-rays for research in high energy density science. Sandia thought that Z could also accelerate the development of fusion energy. However, despite encouraging initial experiments, the machine’s performance did not allow Sandia to envisage any commercial application. Nowadays, the company supports a new project, which it is very secretive about but is nevertheless regularly featured in the press. They aim to develop a Compact Fusion Reactor (CFR), which would be small enough to be mounted on a truck. Publicly available information is very scarce, apart from the fact that Lockheed Martin recently patented it.

Fusion has also attracted high-profile investors over the last few years. Several small companies and start-ups have entered the still-embryonic market of fusion reactors, such as TriAlpha Energy (recently renamed to TAE Technologies) in California, Helion Energy in Seattle, LPPFusion in New York, General Fusion in Canada, Tokamak Energy, First Light Fusion and Applied Fusion Systems in the UK, Commonwealth Fusion Systems (CFS), set up by MIT in Boston, and recently a start-up devoted to stellarators, Renaissance World.

TAE Technologies has benefited from funding from the late Paul Allen,^{aq} cofounder of the Microsoft Corporation with Bill Gates; Helion Energy from Peter Thiel, a close relative of US President Donald Trump; General Fusion from Jeff Bezos, the founder of Amazon, who invested nearly 20 million dollars in 2011; and Applied Fusion Systems from Britain’s Richard Dinan, famous from reality television and now an entrepreneur targeting commercial fusion power. No doubt that there are potential (and substantial) financial benefits at stake: “You cannot expect people to invest in something they do not understand. But bearing in mind that the energy markets generate an annual turnover of USD 7 trillion and that nuclear fusion will be 1 day’s dominant energy source, fusion deserves attention (Dinan, 2017)” (Figure 23.17).

In Canada, General Fusion is building a prototype (scheduled to be completed in 2023) that combines magnetic and inertial confinement. Their engineers are working on the concept of “magnetized target fusion,” which exploits advances in electronics, materials and plasma physics. It uses a patented technology called reverse field configuration to create an overheated environment suitable for plasmas. The system consists of a sphere of approximately three meters in diameter that contains molten lead and lithium. As the metal mixture is rotated, a vortex is created at the center of the sphere. A D-T gas is then injected into the sphere and heated to fusion conditions. Gas-driven pistons located outside the sphere then push the liquid metal inward and collapse the vortex, thus compressing the plasma. The compression increases the temperature of the plasma at the point where deuterium and tritium nuclei fuse, releasing energy in the form of fast neutrons. Convinced by the potential of this technology, Jeff Bezos and companies like Microsoft and Cenovus Energy have sunk more than 127 million US dollars into the company. It’s no wonder, then, that in 2018 the Canadian government also made a 49-million Canadian dollar investment in General Fusion.

TAE Technologies is working on a laboratory machine in which the fusion of hydrogen and boron produces helium and energy. The advantage is that this reaction is “aneutronic”: it does not produce any neutrons which, as we have seen, degrade the materials from the reactor’s internal walls and make certain components

^{aq} Paul Allen visited the ITER site at the end of June 2018 a few weeks before he passed away: “I was at the Cannes Film Festival, supporting the new Star Wars film. A visit to ITER was my chance to see preparations for the birth of a star on Earth,” <https://www.iter.org/newsline/-/3048>.



Figure 23.17. The machine built by General Fusion (Canada) is rather original; no vacuum vessel but a spherical tank filled with a liquid lead-lithium mixture; no superconducting magnets but an array of pistons to compress the plasma. *Credit: General Fusion*

radioactive. The big challenge is that you need to heat the plasma up to 1 million °C! However, the Californian company recently announced that it was getting close to “sufficiently hot and sufficiently long” confinement conditions for fusion, without going into much detail (Boyle, 2018). The company recently created a subsidiary to commercialize a neutron beam machine to irradiate tumors in the head and neck. TAE Technologies executives hope to market the technology in China, where these types of cancer are apparently more common than elsewhere.

Tokamak Energy is a spin-off of JET and the Culham Laboratory close to Oxford, in the United Kingdom. Established in 2009 at a premise in Milton Park, close to JET, the company has already built two small spherical tokamaks, of which the latest model, named ST 40, was commissioned in May 2017, reaching a temperature of 15 million °C. It is expected to reach about a 100 million °C and explore D-T fusion reactions in compact spherical tokamaks. Tokamak Energy is also working on a project to build a reactor that will produce electricity. According to the company’s CEO, Jonathan Carling, a former Rolls-Royce engineer, who has led the company since the end of 2017, they will be ready to inject fusion power into the national electricity grid by 2030 (Nathan, 2018). However, it should be kept in mind that all these private initiatives are competing projects that all have to reassure their shareholders and attract additional funding. Therefore, the effects produced by announcements are important. For David Kingham, the company’s executive vice chairman, there is no doubt that these private ventures will soon reach their objectives: “Fusion projects in government laboratories have become increasingly expensive and slow. For example, ITER is now planning to start full power operations in 2035 (World Nuclear News, 2017).” He is quite right.

Helion Energy, based outside Seattle in the United States, is also working on a fusion machine that combines the principles of magnetic and inertial confinement. The objective is to magnetically accelerate plasmas

and then compress them very quickly. The fuel will be helium-3, which the company hopes to generate in the reactor. The advantage to this reaction is that it is cleaner than the D-T one, as it does not produce any neutrons. Helion hopes to produce 50MW_{th} of power in modules the size of shipping containers.

First Light Fusion was founded in 2011 by Nick Hawker, a doctoral student at Oxford University at the time, and Yiannis Ventikos, his thesis adviser. It is one of the few private companies developing fusion research in Europe. Their experimental “Machine 3” aims to accelerate disc-shaped bullets toward a target of deuterium-tritium pellets, hoping that the collision will generate enough heat to start fusion reactions. This release of energy, scaled-up and repeated, would eventually power electricity-generating plants, according to Hawker, who has raised 50 million US dollars from investors (Reed, 2019). On April 5, 2022, First Light Fusion announced to have achieved D-D fusion reactions in their novel machine. Yields are modest but these are encouraging results.

Finally, a US start-up located near New York, LPPFusion (for Lawrenceville Plasma Physics Fusion), also carries out hydrogen-boron fusion in a reactor that its managers like to call “Focus Fusion” because they use high-density compressed plasmas. In the Focus Fusion reactor, the product of the reaction is a carbon nucleus, which is instantly transformed into three helium nuclei. The energy from the reaction is taken directly from the helium cores. On the other hand, this reaction requires temperatures that are 10 times higher than those that ITER will reach. LPPFusion aims to manufacture units that will be cheaper and smaller than tokamaks that could sit in a garage and supply several thousand homes. Recently, the company announced that they had reached a temperature of almost 2 billion degrees! LPPFusion’s founder and CEO is Eric Lerner, a plasma physicist and successful author of the controversial book “The Big Bang never happened” (Lerner, 1992).

Very recently, the MIT set up a company called CFS to build and develop tokamak technology. The company is funded in part by Breakthrough Energy Ventures, the fund led by Bill Gates, Jeff Bezos, Michael Bloomberg and other billionaires, and by the Italian company Eni. The team is using new high-temperature superconductors to build a high-field tokamak called “Sparc,” which will be a scaled-down (3.3 m in diameter), easy to commercialize, version of the most recent tokamaks. Their plan is to achieve a fusion gain greater than three and produce 100 MW of thermal power by 2025 (Chandler, 2018). This is a promising technology and the project has been very influential in a recent [US National Academies of Sciences report \(2018\)](#). And last but not least, a European start-up set up in 2019, Renaissance Fusion, aims at using stellarator technology to produce electricity and develop medical applications.

Fusion is now attracting scientifically minded entrepreneurs and investors willing to make a long bet. According to the Fusion Industry Association, an 18-member trade group of private companies working on the commercialization of fusion, the total investment made in these entrepreneurial fusion projects is estimated to be about \$1.5 billion. However, most fusion experts tend to agree that these young companies are still quite far from mastering fusion energy. They aim to develop new technologies and hopefully find spin-off applications in other sectors, as TAE Technologies successfully did. Fusion is more of an alibi...

In any case, these stories seem to support Bill Gates, who declared in February 2016: “We need a massive amount of research into thousands of new ideas—even ones that might sound a little crazy—if we want to get to zero emissions by the end of this century. What we need to get that probability [of a breakthrough] up to be very high is to take 12 or so paths to get there,” he said. “Like carbon capture and sequestration is a path. Nuclear fission is a path. Nuclear fusion is a path. Solar fuels are a path. For every one of those paths, you need about five very diverse groups of scientists who think the other four groups are wrong and crazy (Murray, 2016).”

The proliferation of these public and private initiatives can only be welcomed. The dynamism and opportunities in a scientific field are measured by the research effort that accompanies it, and by their related indicators such as the number of publications and patents (Tirone, 2018). From this point of view, fusion is a powerful driver of scientific research and technological development.

An irreversible dynamic has been initiated in the wake of the ITER program. In any case, the new developments are being taken seriously in the fusion world. This new kind of global research effort even led to the US authorities considering privatizing magnetic confinement research, which would allow the Department of Energy to allocate public funding to other research areas.

23.15 The fusion era

From a historic point of view, ITER pays a tribute to the modern technological evolution that ends in huge scientific installations. It falls under the umbrella of “Big Science,” which has in recent decades led to the construction of scientific equipment with exceptional dimensions and breath-taking performance.^{ar} It seems that scientific research cannot be conceived today without these gigantic instruments that can only be financed through international agreements; giant accelerators, huge space stations, supercomputers, and information highways. Always faster, bigger, more powerful—this summarizes the recent evolution of technology. Always more complex too. Today’s machines are of considerable sophistication, consisting of an impressive number of components and interdependent subsystems. In addition, technology is evolving more and more rapidly, techniques are increasingly interconnected between themselves, and a complex social organization is required to make them fully operational.

This evolution is both the result and the origin of considerable progress, in particular in medicine; technology has advanced to the extent that some robotic scalpels are able to work at the cellular or even molecular level. It is also pushing the frontier of human knowledge; humanity has never stopped building increasingly sophisticated instruments to try to understand and master the Universe.

Besides the amount of money that large endeavors require from public budgets, who could disagree with these developments? They lead to substantial scientific progress, generate industrial benefits and increase a country’s prestige on the international scene. Perhaps their biggest critics would be the researchers themselves, as larger machines have bigger budgets, making them harder to access to carry out experiments.

But this evolution also has more subtle consequences; it even goes as far as changing the nature of science and technology themselves, now less and less separable or distinguishable. So-called “technoscience” doesn’t only affect the world around us, it also influences itself. Common practice in scientific research and even its objectives themselves have been changed by the emergence of numerical simulation tools; everything is moving toward being more “technical.” And the idea is gradually emerging that recent technological developments, in particular their impact on the way research is carried out and structured, are impacting the fundamental principles of the scientific method and hence the very definition of what science is. ITER is therefore both a brilliant incarnation of Big Science and a genuine product of the scientific and technological evolution that marked the 20th century, which is illustrated by the successes of giant particle accelerators, advances in space exploration and the breakthroughs in astronomy made possible by large telescopes. But is fusion energy only accessible through building a gigantic machine like ITER? Does bigger necessarily mean better, or is there another way? We see in other areas that, despite the success of Big Science, small machines have also a bright future, such as microcomputers versus supercomputers and light rockets versus major space programs.

The ITER program displays some interesting similarities to the World War II Manhattan project.^{as} In both cases, the aim was to develop a specific new technology through research (the atomic bomb in the case of Manhattan, fusion energy in the case of ITER) by mobilizing considerable resources and extensive

^{ar} This evolution is not restricted to technoscience. Investments in megaprojects have increased in recent years and represent 8% of the world’s wealth (Flyvbjerg, 2014).

^{as} Manhattan is the code name of the research project led by the United States with the support of the United Kingdom and Canada that produced the first atomic bomb during World War II. Launched in 1939, the project mobilized up to one hundred thousand people and cost about USD two billion, or around 30 billion dollars in today’s values.

international cooperation. But there are also important differences between the two. ITER's goal is peaceful, while the Manhattan project was clearly intended to make the United States the first country to possess the atomic bomb and, in doing so, to win the race against the Third Reich. The Manhattan project was developed in secret; the ITER program is a public initiative. Manhattan was a project carried out mainly by the United States; ITER is supported by seven international members.

That being said, the decision to build ITER can also be seen as the result of the lessons that the western world learnt from the Manhattan project. It profoundly influenced scientific policy in developed countries and led to the paradigm of scientific research being the engine that drives the development of our economies and societies. In particular, Manhattan inspired President Franklin Roosevelt's scientific advisor, Vannevar Bush. He designed a "linear" model that assumed a direct link between scientific knowledge and socio-economic development, through the successive stages of research, invention and innovation. This model, which is also based on the idea that fundamental research must be stimulated through the availability of resources, still influences the scientific policy of industrialized countries. It also inspired the founding fathers of the ITER project.

"We would be crazy not to build ITER," declared Geneviève Fioraso, then the French Minister of Research and National Education, at the inauguration of the headquarters of the IO on January 17, 2013. Bolstered by the indisputable successes of CERN, Hubble and Big Science in general, there is a lot of confidence in ITER, even if the difficulties are many and real. This also explains why political and international support for the project has (almost) never been called into question. This sustained support is also due to these large projects' tendency to generate spin-offs beyond their own fields. Even for projects driven by strategic or political motivations, as was the case with the Apollo lunar program, their technological spin-offs significantly outweigh their scientific contributions.

At present, the tokamak still appears to be the most promising way to achieve ignition and produce fusion energy. And in tokamaks, a fundamental scaling law applies: energy is generated by the volume of the plasma, while losses are proportional to its surface area. Through the experience of building the first and second generation machines, scientists soon realized that the plasma would ignite only in machines that had been substantially scaled-up, with a radius at least 10 times bigger and a volume at least a thousand times bigger. This "iron law" of magnetic confinement fusion necessitated increasingly larger machines, up to the size of ITER. Experience so far seems to confirm the theory; the biggest machines hold the world records for power produced and confinement time. In nuclear fusion, big is (still) beautiful. Indeed, the progresses made so far by tokamaks are encouraging. They also show that the effort is global and shared by several teams. The Tore Supra/WEST tokamak in France holds the record for the longest plasma duration time of any tokamak: 6 min and 30 s. The Japanese JT-60 achieved the highest value of the Lawson triple product (density, temperature, confinement time) and the highest ion temperature (520 million °C) of any device to date. And the current record for energy release is held by JET, which generated 59 megajoules of fusion energy. Such achievements have led fusion science close to an exciting point: reaching the energy breakeven and producing net fusion energy.

Against this technoscientific background, some people point out that the decision to build ITER followed the first oil crisis of 1973, which was still very clear in the public's memory when Reagan and Gorbachev met in Geneva. This is really why the decision was more than necessary. If the decision were to be taken today, it is not sure that ITER would be built, at least not in the form of a large-scale international collaboration. China has decided to build alone a reactor of an equivalent size, and 17 private projects aim to operate CFRs.

It is impossible to say definitively that big tokamaks will ultimately be the most efficient way to exploit fusion energy in the future—although the Financial Times did recently include ITER in the technologies that will change the way we live (Murgia, 2017). As we have seen, several companies are currently developing and even building small fusion reactors.

Russian physicist Lev Artsimovitch once said that “fusion will be ready when society needs it.” Will ITER lead to the industrial development of fusion? It is still too early to give a positive answer to this question. But what the Royal Society wrote in 1999 still seems valid: “Will fusion energy work? There is now no serious doubt that a machine could be built which would provide net energy. The issue that is still highly controversial is whether the technological difficulties, including some very severe materials problems, can be overcome so that a machine producing energy at an economic rate could be anticipated. Since world research in this area is proceeding at a spend rate of about \$1B per annum, there is reason to be confident that an answer to this question will emerge in the next decade or two. However, it seems very unlikely that fusion power could make a significant contribution to the energy needs of the world before, at the earliest, the second half of this century ([The Royal Society and The Royal Academy of Engineering, 1999](#)).”

The message is clear: fusion is no longer “30 years away.” Commercial fusion will be achieved when the maturation of fusion science is combined with the emergence of 21st century enabling technologies. ITER will definitely contribute to scientific knowledge about burning (nuclear) plasmas. It is still the only credible fusion machine that will make it possible to study the impact of the alpha particles (helium nuclei) produced by the reaction on the behavior of the plasma; whether they create major instabilities and disruptions or not. However, it is not a given that ITER will open the way to the industrial production of fusion energy.

In my opinion, ITER’s most important innovation is not about technology. There are a hundred of tokamaks in the world and ITER is just one more—albeit the biggest yet. ITER would never have been possible without long-term international collaboration; what makes it unique is the very fact that 35 countries are working together to build a complicated and sophisticated project. If ITER had been just a construction program, it would certainly have been organized differently.

International collaboration is an essential and original feature of the program. It is perhaps the only big decision that its founders took. Of course, working with seven members and 35 countries, all of which having different experiences and levels in the field of fusion, has proven difficult to implement. There can be no doubt, however, that this collaboration is extremely fruitful. By pooling their resources and demonstrating that they are able to overcome the major obstacles on the way to fusion, the ITER members broadcast a highly peaceful and globally very positive message. Collaboration and coordination between the different entities of the program are constantly improving. Research on fusion is remarkable in the sense that it has been the fruit of an international collaborative approach for a very long time. Advances and discoveries made in a particular country of the world are immediately shared with other research programs. This is a daily reality in the ITER program, which benefits from the diversity of its members’ experience, including ongoing research on operational tokamaks in many countries around the world. As a political project, ITER has a strong image that enables it to leverage public (and now private) finance to ensure a continuous flow of improvements and innovations. Based on his experience as Undersecretary of State for Science in the DOE from 2006 to 2009, Raymond Orbach argues that the ITER project constitutes a fascinating paradigm at the intersection of science and diplomacy that could inspire the promoters of other large-scale international projects ([Harding, Khanna and Orbach, 2012](#)). Conclusion: ITER has a wealth of lessons for politicians, increasingly confronted with major global challenges.

ITER’s biggest advantage and main role is to catalyze a leap forward in knowledge and to be a project carried by both the political and scientific communities. Although ITER’s spin-offs could be seen as relatively limited considering its budget, if it succeeds (and there is little doubt that it will), participation in ITER will open the door to the next step: DEMO. China is considering skipping this step and will soon begin to build a reactor that will produce electricity. Other projects may be successful before that.

Orbach’s analysis is very pertinent, but in my opinion, ITER is an emblematic example of *technology diplomacy*, as well as what has proved to be a *diplomatic technology*. This is what ITER tells us: a specific technology, namely magnetic confinement fusion, can be used to promote international relations, help to

overcome political tensions during the Cold War, and restore links between the eastern and western blocs in more than just technology. From this point of view, ITER really is a valuable case study. It allowed Russia and the United States to sit down at the same table and work together on a peaceful project. And the program embodies two other features of this *diplomatic technology*. The first is that ITER has created and nurtured a community of diplomats and engineers from such a wide variety of countries that cooperate despite the many geopolitical tensions that exist on the international scene. Beyond that, ITER has also demonstrated that diplomacy can be a catalyst for technological development: technology *through* diplomacy. None of the ITER members will contest the fact that the project has promoted its engineers and companies abroad and facilitated cooperation with other countries while developing commercial performance.

A second feature of this *diplomatic technology* is that ITER has facilitated the creation of a high-level pool of international technological expertise that the members now have at their disposal to consult as they see fit. This expertise is essential for diplomats and policymakers in addressing many areas outside fusion such as climate, food security and energy issues.

In addition, ITER has certainly reinforced the fusion community, already very strong and very international. Whatever happens, ITER will have a place in the annals of fusion history due to its key role in the current landscape. This role is both direct and indirect; it has also stimulated genuine competition in this field, with several rival projects now being promoted by administrative officials and ministerial offices.

In any case, mankind has entered the fusion era. It is likely that, sooner or later, this new energy will be exploited on earth—although some people fear it is already too late. When Lockheed Martin launched its project to build modest-sized fusion reactors in 2014 (Shalal, 2014), international media quickly seized on the spectacular announcement. At ITER, my phone wouldn't stop ringing. I invited ITER's scientific managers in my office and asked them: what is our position on this? Their answer was almost unanimous. In essence, they expressed a strong interest in the project but remained cautious given the very little information available. All expressed the hope that any fusion technology would emerge quickly to meet the pressing needs of mankind and reduce the threats of irreversible climate change. In a way, it was like the euphoria that followed the announcements of "cold fusion" in 1989. For a moment, concerns about technical details and the politics of technology faded away, yielding to excitement and hope for a new initiative. It is time to move forward and go beyond technology diplomacy. We should welcome and encourage the many public and private initiatives to support and develop fusion science and technology. It is possible that ITER and fusion energy will change the course of civilization.

References

- Adaoust, S., Belle, R., 2017. Territoire à 30 minutes autour d'Iter—Les services aux entreprises, réacteur de l'emploi malgré la crise. INSEE Analyses Provence-Alpes-Côte d'Azur, n°45, 20 March. Available from: <https://www.insee.fr/fr/statistiques/2663096>.
- Arnoux, R., 2016. The Balance of Power. Newline. 28 November, Available from: <https://www.iter.org/newline/-/2589>.
- Associated Press, 2005. France chosen as site for Nuclear Reactor. USA Today. 28 June, Available from: http://usatoday30.usatoday.com/news/world/2005-06-28-french-reactor_x.htm.
- Bell, M.G., 2016. The Tokamak fusion test reactor. In: *Magnetic Fusion Energy. From Experiments to Power Plants*. Elsevier, The Netherlands, pp. 119–166.
- Bell, R., 1998. *Les Péchés capitaux de la haute technologie*. Seuil, France. 345 pp.
- Bigot, B., 2019. Only fusion can meet the energy challenge mankind is facing. *Actual. Chim.* 442, 11–14.
- Boyle, A., 2018. TAE Technologies Pushes Plasma Machine to a New High on the Nuclear Fusion Frontier. *Geekwire*. 10 February, Available from: <https://www.geekwire.com/2018/tae-technologies-pushes-plasma-machine-new-high-fusion-frontier/>.
- Broad, W.J., 1988. Secret Advance in Nuclear Fusion Spurs a Dispute Among Scientists. *The New York Times*. 21 March, Available from: <http://www.nytimes.com/1988/03/21/us/secret-advance-in-nuclear-fusion-spurs-a-dispute-among-scientists.html?pagewanted=all>.

- Browne, M.W., 1997. Money Shortage Jeopardizes Fusion Reactor. *The New York Times*, p. 8. 20 May, Available from: <http://www.nytimes.com/1997/05/20/science/money-shortage-jeopardizes-fusion-reactor.html>.
- Causey, R.A., Karnesky, R.A., San Marchi, C., 2012. Tritium barriers and tritium diffusion in fusion reactors. In: Konings, R. (Ed.), *Comprehensive Nuclear Materials*. Elsevier Science, Amsterdam, pp. 511–549. Available from: http://arc.nucapt.northwestern.edu/refbase/files/Causey-2009_10704.pdf.
- Chandler, D., 2018. MIT and Newly Formed Company Launch Novel Approach to Fusion Power. *MIT News*. 9 March, Available from: http://news.mit.edu/2018/mit-newly-formed-company-launch-novel-approach-fusion-power-0309?utm_source=&utm_medium=&utm_campaign=.
- Chastand, J.B., Baruch, J., 2013. La carte de France des pertes d'emplois, *Le Monde*. 24 July, Available from: https://www.lemonde.fr/emploi/article/2013/07/24/la-carte-de-france-des-pertes-d-emplois_3452799_1698637.html.
- Claessens, M., 2020. *ITER, The Giant Fusion Reactor*. Springer, Switzerland. 216 pp.
- Clery, D., 2013. *A Piece of the Sun—The Quest for Fusion Energy*. Duckworth, USA. 320 pp.
- Dinan, R., 2017. *The Fusion Age*. Applied Fusion Systems Ltd, United Kingdom. 104 pp.
- EC, 1988. Commission Decision of 26 February 1988 concerning the conclusion of an Agreement of participation in the International Thermonuclear Experimental Reactor (ITER) Conceptual Design Activities, by the European Atomic Energy Community, with Japan, the Union of Soviet Socialist Republics, and the United States of America, by the Commission for and on behalf of the Community. *Off. J. Eur. Communities* 102, 31–44. 21 April 1988, Available from: https://eur-lex.europa.eu/legal-content/EN/TXT/?uri=uriserv:OJ.L_.1988.102.01.0031.01.ENG&toc=OJ:L:1988:102:TOC.
- EC, 2005. Daily news: Déclaration du Commissaire européen à la Recherche Janez Potocnik sur ITER. 28 June (only in French), Available from: <http://europa.eu/rapid/midday-express-28-06-2005.htm?locale=EN>.
- EC, 2018. *Study on the Impact of the ITER Activities in the EU*. European Commission, Belgium. The study is not public.
- Flyvbjerg, B., 2014. What you should know about megaprojects and why: an overview. *Proj. Manag. J.* 45 (2), 6–19. April–May, Available from: <https://doi.org/10.1002/pmj.21409>.
- Galbraith, J.K., 1967. *The New Industrial State*. Houghton Mifflin, USA. 576 pp.
- Gastaldi, O., 2007. Problematics due to tritium in materials in the nuclear field—some examples. In: *INIS Repository*, 39 (43), Colloquium ‘Materials, Mechanics, Microstructure: Hydrogen in Materials’, Saclay (France). 18–19 June 2007, Available from: http://www.iaea.org/inis/collection/NCLCollectionStore/_Public/40/034/40034735.pdf.
- GCR, 2018. Energy of stars: €19bn fusion reactor “to be in place by 2021”. *Global Construction Staff Review*. Available from: <http://www.globalconstructionreview.com/innovation/energy-stars-19bn-fusion-reactor-be-place-2021/>.
- Harding, T.K., Khanna, M.J., Orbach, R.L., 2012. *Science & Diplomacy*. vol. 1. 3 September 2012, Available from: <http://www.sciencediplomacy.org/article/2012/international-fusion-energy-cooperation>.
- IRSN, 2018. Réacteurs nucléaires de fusion // Considérations sur les questions de sûreté et de radioprotection des réacteurs de démonstration après l’installation ITER. IRSN, France.
- Jacquinet, J., Marbach, G., 2004. L’enjeu d’une grande collaboration internationale, *Revue internationale et stratégique*, 2004/3, n° 55., p. 173.
- Janeschitz, G., 2019. An economical viable tokamak fusion reactor based on the ITER experience. *Philos. Trans. R. Soc. A Math. Phys. Eng. Sci.* <https://doi.org/10.1098/rsta.2017.0433>. A377:20170433, Available from:.
- Joint European Torus, 1991. Press Release: JET Achieves Fusion Power. 9 November, Available from: <https://www.iter.org/doc/www/content/com/Lists/Stories/Attachments/731/press%20release%20jet.jpg>.
- Krivit, S.B., 2020. *New Energy Times*. 10 October, Available from: <http://news.newenergytimes.net/2020/10/10/iter-the-zero-megawatt-nuclear-fusion-reactor/>.
- Lerner, E., 1992. *The Big Bang Never Happened: A Startling Refutation of the Dominant Theory of the Origin of the Universe*. Vintage, USA. 496 pp.
- Lindl, J., 1995. Development of the indirect-drive approach to inertial confinement fusion and the target physics basis for ignition and gain. *Phys. Plasmas* 2 (11), 3933–4024. November 1995, Available from: <https://aip.scitation.org/doi/pdf/10.1063/1.871025>.
- Mairesse, J., Mulkay, B., 2004. Une évaluation du crédit d’impôt recherche en France, 1980–1997, Document de Travail du CREST-INSEE, n° 2004-43.
- Menessier, M., 2011. Accident nucléaire: “Il faut imaginer l’inimaginable”. *Le Figaro*. 17 June, Available from: http://www.lefigaro.fr/sciences/2011/06/17/01008-20110617ARTFIG_00610-accident-nucleaireil-faut-imaginer-l-inimaginable.php.
- Mercier, V., Brunengo-Basso, S., 2016. *Compensation écologique—De l’expérience d’Iter à la recherche d’un modèle*. Presses Universitaires d’Aix-Marseille, France. 93 pp.
- Murgia, M., 2017. Five Technologies That Will Change How We Live. *Financial Times*. 16 February, Available from: <https://www.ft.com/content/1bf4cdc8-f251-11e6-95ee-f14e55513608>.

- Murray, J., 2016. Bill Gates: World will Deliver 'Clean Energy Breakthrough' within 15 Years. *The Guardian*. 24 February, Available from: <https://www.theguardian.com/environment/2016/feb/24/bill-gates-world-will-deliver-clean-energy-breakthrough-within-15-years>.
- Lassagne, T., Loose, C., 2017. Territoire à 30 minutes autour d'Iter—Un territoire attractif aux portes de la métropole Aix-Marseille-Provence. *INSEE Analyses Provence-Alpes-Côte d'Azur*, n°44, 20 March. Available from: <https://www.insee.fr/statistiques/2662410>.
- Nathan, S., 2018. Interview: Jonathan Carling, Tokamak Energy's new CEO. *The Engineer*. 22 February, Available from: <https://www.theengineer.co.uk/jonathan-carling-tokamak-energy/>.
- The National Academies of Sciences, Engineering, and Medicine, 2018. Final Report of the Committee on a Strategic Plan for US Burning Plasma Research. The National Academies Press, USA, <https://doi.org/10.17226/25331>. Available from: .
- Pacchioni, G., 2019. The Road to Fusion. *Nature Reviews Physics*, <https://doi.org/10.1038/s42254-019-0069-8>. 19 May, Available from: .
- Reed, S., 2019. The Fusion Reactor Next Door. *The New York Times*. 13 May, Available from: <https://www.nytimes.com/2019/05/13/business/fusion-energy-climate-change.html>.
- The Royal Society and The Royal Academy of Engineering, 1999. Nuclear Energy—The Future Climate. United Kingdom, Available from: https://royalsociety.org/~media/Royal_Society_Content/policy/publications/1999/10087.pdf.
- Shalal, A., 2014. We Made a Huge Breakthrough in Nuclear Fusion. *Business Insider*. 15 October, Available from: <https://www.businessinsider.fr/us/andrea-shalal-lockheed-nuclear-fusion-breakthrough-2014-10>.
- Tirone, J., 2018. Billionaires Chase 'SpaceX moment' for the Holy Grail of Energy. *Bloomberg*. 30 October, Available from: <https://www.bloomberg.com/news/articles/2018-10-30/nuclear-fusion-financed-by-billionaires-bill-gates-jeff-bezos?srnd=premium-europe>.
- Van Dam, J.W., 2017. Update on the fusion energy sciences program. In: Conference at the 59th Annual Meeting of the American Physical Society, 23 October 2017. http://www.firefusionpower.org/UFA_2017_APS-DPP_JVD_171020_rev.pdf.
- Wolf, R.C., et al., 2019. Performance of Wendelstein 7-X stellarator plasmas during the first divertor operation phase. *Phys. Plasmas* 26, 082504. Available from: <https://doi.org/10.1063/1.5098761>.
- World Nuclear News, 2017. Spherical tokamak 'to put fusion power in grid' by 2030. 30 January, Available from: <http://www.world-nuclear-news.org/NN-Spherical-tokamak-to-put-fusion-power-in-grid-by-2030-30011702.html>.

Further reading

Neilson, G.H. (Ed.), 2016. *Magnetic Fusion Energy. From Experiments to Power Plants*. Elsevier, The Netherlands. 632 pp.

Additional materials (layouts, T - s diagrams, basic parameters, photos, etc.) on thermal and nuclear power plants

Igor L. Pioro^a, Romney B. Duffey^b, Pavel L. Kirillov^{c,*},
Georgy V. Tikhomirov^d, and Anton D. Smirnov^d

^aFaculty of Energy Systems and Nuclear Science, University of Ontario Institute of Technology, Oshawa, ON, Canada ^bIdaho Falls, ID, United States ^cState Scientific Centre of the Russian Federation—Institute of Physics and Power Engineering (IPPE) named after A.I. Leipunsky, Obninsk, Russia ^dNational Research Nuclear University MEPhI (Moscow Engineering Physics Institute), Moscow, Russia

Nomenclature

D_{hy} hydraulic-equivalent diameter, m
 G mass flux, kg/m²s
 P, p pressure, MPa
 s specific entropy, J/kg K
 T, t temperature, °C
 x quality, %

Greek symbols

Δ difference

Subscripts

c, cr critical
Comp compressor
el electrical
fw feed water
h heated
in inlet
max maximum
out outlet
rc reactor coolant
s, sat saturated or saturation
th thermal
turb turbine

* Professor P.L. Kirillov has participated in preparation of this Chapter, unfortunately, he has passed away on October 10, 2021 (for details, see <https://asmedigitalcollection.asme.org/nuclearengineering/issue/8/2>).

Acronyms and abbreviations

A	Appendix
ABWR	Advanced Boiling Water Reactor
ACR	Advanced CANDU Reactor (Canada)
AECL	Atomic Energy of Canada Limited
AES	Atomic Energy Station (in Russian, means NPP)
AG	Aktiengesellschaft (in German, same as Ltd. in English)
AGR	Advanced Gas-cooled Reactor
AHWR	Advanced Heavy Water Reactor
ANS	American Nuclear Society
AP	Advanced Passive (plant) (USA)
APR	Advanced PWR (South Korea)
APWR	Advanced Pressurized Water Reactor
ASME	American Society of Mechanical Engineers
ave	average
BARC	Bhabha Atomic Research Centre
BN	Fast Sodium (reactor) (Быстрый Натриевый (in Russian abbreviations)) (Russia)
Btu	British thermal unit
BWR	Boiling Water Reactor
CAD	Computer Aided Design
CANDU	CANada Deuterium Uranium (reactor) (Canada)
CANFLEX	CANada FLEXible (fueling)
CCPP	Combined-Cycle Power Plant
CCS	Carbon-dioxide Capture and Storage
CHF	Critical Heat Flux
CHP	Combined Heat and Power
CNL	Canadian Nuclear Laboratories
DAE	Department of Atomic Energy (India)
DC	Direct Current
DiD	Defense-in-Depth
EDF	Électricité de France
Eff.	Efficiency
EGP	Power Heterogeneous Loop (reactor) (Энергетический Гетерогенный Петлевой (реактор с 6-ю петлями циркуляции теплоносителя) (in Russian abbreviations))
EPR	Evolutionary Power Reactor
EUR	Euro (European currency)
FA	Fuel Assembly
GCR	Gas-Cooled Reactor
GE	General Electric (USA)
GIF	Generation IV International Forum
gpm	gallons per minute
GT	Gas Turbine
HP	High Pressure
HPH	High Pressure Heater
HRSG	Heat-Recovery Steam-Generator
HTC	Heat Transfer Coefficient
HTR-PM	High Temperature Reactor – Pebble-bed Module
HWR	Heavy Water Reactor
IAEA	International Atomic Energy Agency (Vienna, Austria)
ICV	Interval Control Valve
ID	Internal Diameter
IGCC	Integrated Gasification Combined Cycle
Inc.	Incorporated
IP	Intermediate Pressure
IPHWR	Indian PHWR

IPT	Intermediate Pressure Turbine
J.	Journal
KHNP	Korea Hydro & Nuclear Power
KLT-40S	KLT Container-carrier cargo-Lighter Transport (reactor) (Контейнеровоз Лихтеровоз Транспортный (реактор) (in Russian abbreviations)) (Russia)
LGR	Light-water-cooled Graphite-moderated Reactor
LHV	Low Heating Value
LLC	Limited Liability Company
LMFBR	Liquid-Metal-cooled Fast Breeder Reactor
LNG	Liquified Natural Gas
LP	Low Pressure
LPH	Low Pressure Heater
LPT	Low Pressure Turbine
Ltd.	Limited
LWR	Light Water Reactor
MHI	Mitsubishi Heavy Industries (Japan)
MOX	Mixed Oxide (nuclear fuel, 80% UO ₂ and 20% PuO ₂)
MSK	Medvedev–Sponheuer–Karnik (scale)
MVA	Mega Volt Amperes
N/A	Not Applicable
NERS	Nuclear Engineering and Radiation Science
NPP	Nuclear Power Plant
NRC	Nuclear Regulatory Commission (USA)
OBE	Operating Basis Earthquake ground motion
OD	Outside Diameter
OKBM	Experimental Design Bureau of Mechanical-engineering (Опытно-Конструкторское Бюро Машиностроения (in Russian abbreviations))
PCV	Primary Containment Vessel
PHWR	Pressurized Heavy Water Reactor
PP	Power Plant
PT	Pressure Tube
PWR	Pressurized Water Reactor
R&D	Research and Development
RAPS	Rajasthan Atomic Power Station (India)
RBMK	Reactor of Large Capacity Channel type (Реактор Большой Мощности Канальный (in Russian abbreviations) (Russia)
RITM-200M	Reactor Integral Type Modular 200 MW _{el} Modernized (Реактор Интегрального Типа Модульный мощностью 200 МВт Модернизационный (in Russian abbreviations) (Russia)
rpm	rotations per minute
RPV	Reactor Pressure Vessel
RSV	Rotary Selector Valve
RU	Recovered or Recycled Uranium
S.	South
SCW	SuperCritical Water
SCWR	SuperCritical Water-cooled Reactor
Sep.	September
SEU	Slightly Enriched Uranium
SFR	Sodium-cooled Fast Reactor
SMR	Small Modular Reactor
SS	Stainless Steel
SSE	Safe Shutdown Earthquake
SSE	Safe-Shutdown Earthquake ground motion
Temp.	Temperature
TOI	Typical Optimized Informatized (reactor, Russia)

TVO	Teollisuuden Voima Oyj (Finland)
UAE	United Arab Emirates
UK	United Kingdom
US, USA	United States of America
USD	US Dollars
USSR	Union of Soviet Socialist Republics
VHTR	Very High Temperature Reactor
VVER	Water Water Power Reactor (Водо-Водяной Энергетический Реактор (in Russian abbreviations) (Russia)

A1.1 Introduction

This Appendix is partially based on our previous publications (Pioro et al., 2018, 2019, 2021a,b, 2022; Duffey et al., 2021; Pioro and Duffey, 2007, 2015, 2019a,b; Handbook of Generation IV Nuclear Reactors, 2016; Dragunov et al., 2015; Kirillov et al., 2013; Pioro and Kirillov, 2013a,b,c,d) and provides additional materials (layouts, T - s diagrams, basic parameters, photos, etc.) on advanced thermal (combined cycle and supercritical-pressure Rankine steam-turbine cycle) Power Plants (PPs) and Nuclear Power Plants (NPPs) with modern nuclear-power reactors, which are in operation, of the following types:

- (1) Pressurized Water-cooled Reactors (PWRs);
- (2) Boiling Water-cooled Reactors (BWRs);
- (3) Pressurized Heavy-Water-cooled Reactors (PHWRs);
- (4) Advanced Gas-cooled Reactors (AGRs) (carbon-dioxide-cooled);
- (5) Gas-Cooled Reactors (GCRs) (helium-cooled);
- (6) Light-water-cooled Graphite-moderated Reactors (LGRs); and
- (7) Liquid-Metal-cooled Fast Breeder Reactors (LMFBRs), in particularly, Sodium-cooled Fast Reactors (SFRs).

Statistics on all current nuclear-power reactors connected to electrical grids is provided in Chapter 1.2 (also, latest statistics can be found in Nuclear News (ANS), annually, March issue; and on the following websites: <https://pris.iaea.org/pris/> and wnn@world-nuclear-news.org). Thermo-physical properties and Heat Transfer Coefficients (HTCs) of reactor coolants - in Appendix A2; and Thermal aspects of conventional and alternative nuclear fuels – in Chapter 18. Also, advantages/challenges of thermal and nuclear power plants compared to those of other energy sources including renewable ones are presented in Chapter 1.1. In addition, Chapter 1.1 lists largest power plants of the world and sectors' diagrams with % of use of various energy sources for the electricity generation in the world and selected countries (mainly, largest by populations and/or by economies).

The purpose of Appendix A1 is to provide readers with useful, interesting, and the latest information/materials from leading nuclear vendors from around the world, much of which is not well known even to many experts within the areas of nuclear engineering and nuclear power. It can be read in conjunction with prior useful publications on modern and future nuclear-power reactors and plants including: Generation IV International Forum (<https://www.gen-4.org/gif/>); Greenspan (2021), Handbook of Nuclear Engineering (2010), Handbook of Small Modular Nuclear Reactors (2021), Pressurized Heavy Water Reactors: CANDU (2021), Fundamental Issues Critical to the Success of Nuclear Projects (2021), IAEA (2020), Nuclear Engineering Handbook (2017), Nuclear Energy (2018), Nuclear Energy Encyclopedia: Science, Technology, and Applications (2011), Lewis et al. (2017), Hewitt and Collier (2000), Tang et al. (1978), etc.

Thermal-power industry is ahead of nuclear-power industry by tens of years, therefore, many proven ideas in thermal-power industry in terms of power cycles are used in nuclear-power industry, in particular, subcritical-pressure Rankine cycles, and are considering to be used in next generation – Generation-IV nuclear-power reactors, in particular, combined cycles and supercritical-pressure Rankine cycles (see [Chapters 2](#) and [21.1](#)).

Thermal efficiency was and still is the major driving force for all advancements in thermal-power industry from its beginning. However, nuclear-power reactors from their beginning were intended more for military applications in terms of nuclear materials for powerful bombs/missiles, and due to that not much attention was paid to the thermal efficiency of NPPs. Nevertheless, nowadays, NPPs have to compete with other PPs including non-renewable- and renewable-energy sources. Therefore, thermal efficiency is also the driving force in nuclear-power industry. However, the safety of modern advanced nuclear-power reactors/plants and thermal PPs cannot be compromised, and, eventually, it is enhanced with new advanced PPs.

[Table A1.1](#) lists typical ranges of thermal efficiencies (gross) of modern thermal and nuclear power plants.

TABLE A1.1 Typical ranges of thermal efficiencies (gross) of modern thermal and nuclear power plants (Pioro et al., 2019, 2020; [Handbook of Generation IV Nuclear Reactors, 2016](#))

No	Power plant	Gross thermal efficiency
1	Combined-cycle power plant (combination of Brayton gas-turbine cycle (fuel - natural gas or LNG; combustion-products parameters at gas-turbine inlet: $P_{in} \approx 2.5$ MPa, $T_{in} \approx 1650^\circ\text{C}$) and subcritical-pressure Rankine steam-turbine cycle (steam parameters at turbine inlet: $P_{in} \approx 12.5$ MPa ($T_{sat} = 327.8^\circ\text{C}$), $T_{in} \approx 620^\circ\text{C}$ ($T_{cr} = 374^\circ\text{C}$)). (For details, see Figs. A1.1–A1.10).	Up to 62%
2	Supercritical-pressure coal-fired power plant (Rankine-cycle steam inlet turbine parameters: $P_{in} \approx 23.5\text{--}38$ MPa ($P_{cr} = 22.064$ MPa), $T_{in} \approx 540\text{--}625^\circ\text{C}$ ($T_{cr} = 374^\circ\text{C}$); and $P_{reheat}^a \approx 4\text{--}6$ MPa ($T_{sat} = 250.4\text{--}275.6^\circ\text{C}$), $T_{reheat} \approx 540\text{--}625^\circ\text{C}$). (For details, see Figs. A1.11–A1.20).	Up to 55%
3	Internal-combustion-engine generators (Diesel cycle and Otto cycle with natural gas as fuel).	Up to 50%
4	Subcritical-pressure coal-fired power plant (older plants; Rankine-cycle steam: $P_{in} = 17$ MPa ($T_{sat} = 352.3^\circ\text{C}$), $T_{in} = 540^\circ\text{C}$ ($T_{cr} = 374^\circ\text{C}$); and $P_{reheat}^a \approx 3\text{--}5$ MPa ($T_{sat} = 233.9\text{--}263.9^\circ\text{C}$), $T_{reheat} = 540^\circ\text{C}$). (For T - s diagram, see Fig. A1.87 (diagram is similar to that of AGR NPP)).	Up to 43%
5	Advanced Gas-cooled Reactor (AGR) NPP (Generation-III) (reactor coolant - carbon-dioxide: $P = 4$ MPa, $T = 290\text{--}650^\circ\text{C}$); (Rankine-cycle steam: $P_{in} = 17$ MPa ($T_{sat} = 352.3^\circ\text{C}$) & $T_{in} = 560^\circ\text{C}$ ($T_{cr} = 374^\circ\text{C}$); and $P_{reheat}^a \approx 4$ MPa ($T_{sat} = 250.4^\circ\text{C}$), $T_{reheat} = 560^\circ\text{C}$). (For details, see Figs. A1.85–A1.87).	Up to 42%

Continued

TABLE A1.1 Typical ranges of thermal efficiencies (gross) of modern thermal and nuclear power plants (Pioro et al., 2019, 2020; Handbook of Generation IV Nuclear Reactors, 2016)—cont'd

No	Power plant	Gross thermal efficiency
6	Gas-Cooled Reactor (GCR) (High Temperature Reactor – Pebble-bed Module (HTR-PM)) NPP (Generation-IV) (reactor coolant - helium: $P=7$ MPa, $T=250$ – 750°C ; and Rankine-cycle steam: $P_{\text{in}}=14.2$ MPa ($T_{\text{sat}}=337.8^{\circ}\text{C}$), $T_{\text{in}}=556^{\circ}\text{C}$ ($T_{\text{cr}}=374^{\circ}\text{C}$); and $P_{\text{reheat}}^a \approx 3.5$ MPa ($T_{\text{sat}}=242.6^{\circ}\text{C}$), $T_{\text{reheat}}=560^{\circ}\text{C}$). (For details, see Figs. A1.88–A1.91).	Up to 42%
7	Sodium-cooled Fast Reactor (SFR) (BN-600 & BN-800) NPP (reactor coolant: $P=0.1$ MPa, $T=377$ – 550°C , and Rankine-cycle steam: $P_{\text{in}}=14.2$ MPa ($T_{\text{sat}}=337.8^{\circ}\text{C}$), $T_{\text{in}}=505^{\circ}\text{C}$ ($T_{\text{cr}}=374^{\circ}\text{C}$); and $P_{\text{reheat}}^a \approx 2.5$ MPa ($T_{\text{sat}}=224^{\circ}\text{C}$), $T_{\text{reheat}}=505^{\circ}\text{C}$). (For details, see Figs. A1.100–A1.105).	Up to 40%
8	Pressurized-Water-Reactor (PWR) NPP (Generation-III ⁺) (reactor coolant: $P=15.5$ MPa ($T_{\text{sat}}=344.8^{\circ}\text{C}$), $T_{\text{out}}=327^{\circ}\text{C}$; steam: $P_{\text{in}}=7.8$ MPa, $T_{\text{in}}=T_{\text{sat}}=293.3^{\circ}\text{C}$; and $P_{\text{reheat}}^a \approx 2$ MPa ($T_{\text{sat}}=212.4^{\circ}\text{C}$), $T_{\text{reheat}} \approx 265^{\circ}\text{C}$). (For details, see Figs. A1.24–A1.32).	Up to 36-38%
9	Pressurized-Water-Reactor (PWR) NPP (Generation-III, current fleet) (reactor coolant: $P=15.5$ MPa ($T_{\text{sat}}=344.8^{\circ}\text{C}$), $T=292$ – 329°C ; steam: $P_{\text{in}}=6.9$ MPa, $T_{\text{in}}=T_{\text{sat}}=284.9^{\circ}\text{C}$; and $P_{\text{reheat}}^a \approx 1.5$ MPa ($T_{\text{sat}}=198.3^{\circ}\text{C}$), $T_{\text{reheat}} \approx 255^{\circ}\text{C}$). (For details, see Figs. A1.45–A1.47).	Up to 34-36%
10	Boiling-Water-Reactor (BWR) or Advanced BWR (ABWR) NPP (Generation-III or III ⁺ , current fleet) (reactor coolant: $P=7.2$ MPa, $T_{\text{out}}=T_{\text{sat}}=287.7^{\circ}\text{C}$; steam: $P=7.2$ MPa, $T_{\text{in}}=T_{\text{sat}}=287.7^{\circ}\text{C}$ and $P_{\text{reheat}}^a \approx 1.7$ MPa ($T_{\text{sat}}=204.3^{\circ}\text{C}$), $T_{\text{reheat}} \approx 258^{\circ}\text{C}$). (For details, see Figs. A1.67, and A1.69–A1.72).	Up to 34%
11	Light-water-cooled Graphite-moderated Reactor (LGR) (Russian RBMK-1000) NPP (Generation-III, current fleet) (reactor coolant: $P=6.4$ MPa, $T_{\text{out}}=T_{\text{sat}}=279.8^{\circ}\text{C}$; steam: $P=6.4$ MPa, $T_{\text{in}}=T_{\text{sat}}=279.8^{\circ}\text{C}$ and $P_{\text{reheat}}^a \approx 0.3$ MPa ($T_{\text{sat}}=133.5^{\circ}\text{C}$), $T_{\text{reheat}} \approx 263^{\circ}\text{C}$). (For details, see Figs. A1.92–A1.94).	Up to 34%
12	Pressurized Heavy Water Reactor (PHWR) NPP (Generation-III, CANDU [®] -6, current fleet) (reactor coolant: $P_{\text{in}}=11$ MPa/ $P_{\text{out}}=9.9$ MPa ($T_{\text{sat}}=310.3^{\circ}\text{C}$) & $T=260$ – 310°C ; steam: $P_{\text{in}}=4.7$ MPa, $T_{\text{in}}=T_{\text{sat}}=260.1^{\circ}\text{C}$; and $P_{\text{reheat}}^a \approx 1.2$ MPa ($T_{\text{sat}}=188^{\circ}\text{C}$), $T_{\text{reheat}} \approx 240^{\circ}\text{C}$). (For details, see Figs. A1.76–A1.82).	Up to 32% (34%)
13	PWR SMR NPP (RITM-200M, Russia) (Generation-III ⁺) (not yet in operation as SMR NPP ^b) (reactor coolant: $P=15.7$ MPa ($T_{\text{sat}}=345.8^{\circ}\text{C}$), $T=277$ – 313°C ; steam: $P_{\text{in}}=3.82$ MPa, $T_{\text{in}}=295^{\circ}\text{C}$ ($T_{\text{sat}}=247.6^{\circ}\text{C}$). (For details, see Figs. 20.2.9 and 20.2.11).	Up to ~31%

TABLE A1.1 Typical ranges of thermal efficiencies (gross) of modern thermal and nuclear power plants (Pioro et al., 2019, 2020; Handbook of Generation IV Nuclear Reactors, 2016)—cont'd

No	Power plant	Gross thermal efficiency
14	PWR SMR NPP (KLT-40S, Russia) (Generation-III, current fleet) (reactor coolant: $P = 12.7$ MPa ($T_{\text{sat}} = 329^\circ\text{C}$), $T = 280\text{--}316^\circ\text{C}$; steam: $P_{\text{in}} = 3.72$ MPa, $T_{\text{in}} = 290^\circ\text{C}$ ($T_{\text{sat}} = 246.1^\circ\text{C}$). (For details, see Figs. 20.2.2, 20.2.3 and 20.2.10).	Up to $\sim 26\%$

^aUsually, secondary-steam pressure is about $\frac{1}{4}$ of primary-steam pressure.

^bIn 2021, Rosatom has started work on a site of the future SMR NPP, which is planned to be built in Yakutia. The SMR will be RITM-200 ship-based reactor (<https://www.neimagazine.com/news/newsrosatom-to-being-work-on-land-based-smr-8436408>).

A1.2 Fossil-fuel thermal power plants

A1.2.1 Combined-Cycle Power Plants (CCPPs)

Natural gas is considered as a clean fossil fuel compared to coal and oil, but still due to combustion process emits carbon dioxide, when it used for electrical generation (for details, see Chapter 1.1). The most efficient modern thermal power plants with thermal efficiencies within the range of 50 – 60% (up to 62.5%) are, so-called, combined-cycle power plants (combination of Brayton gas-turbine and Rankine steam-turbine power cycles) (see Figs. A1.1–A1.10, and Tables A1.2 and A1.3), which use mainly natural gas^a as a fuel.

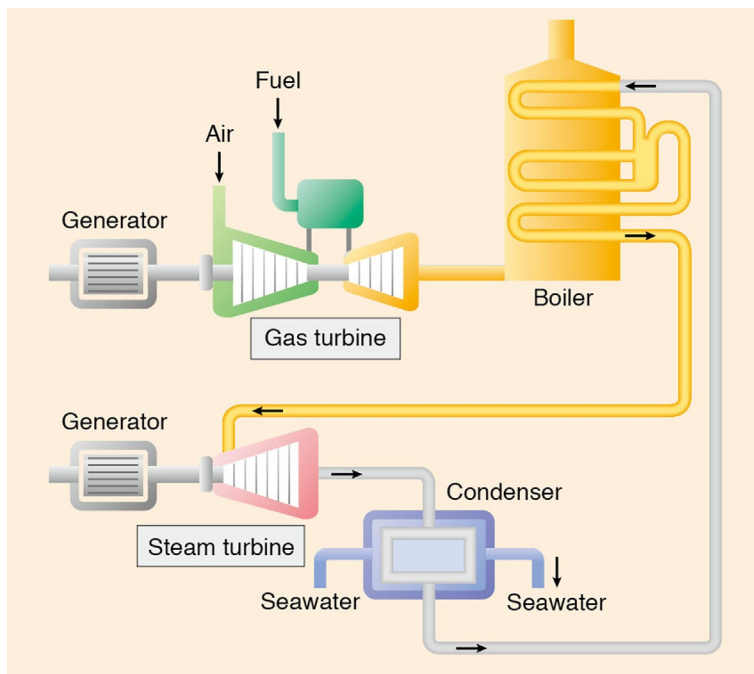


FIG. A1.1 Simplified layout of combined-cycle power plant. Thermal efficiencies are the highest in power industry – up to 62.5% (Brayton cycle – $\sim 30\%$ and Rankine cycle – $\sim 40\%$). Current level of inlet temperatures to gas turbine is about $1600\text{--}1650^\circ\text{C}$ and to steam turbine – $\sim 620^\circ\text{C}$. Courtesy and copyright of MHI

^aIn general, these plants can use any clean gaseous fuels, for example, Liquefied Natural Gas (LNG), blast-furnace gas,

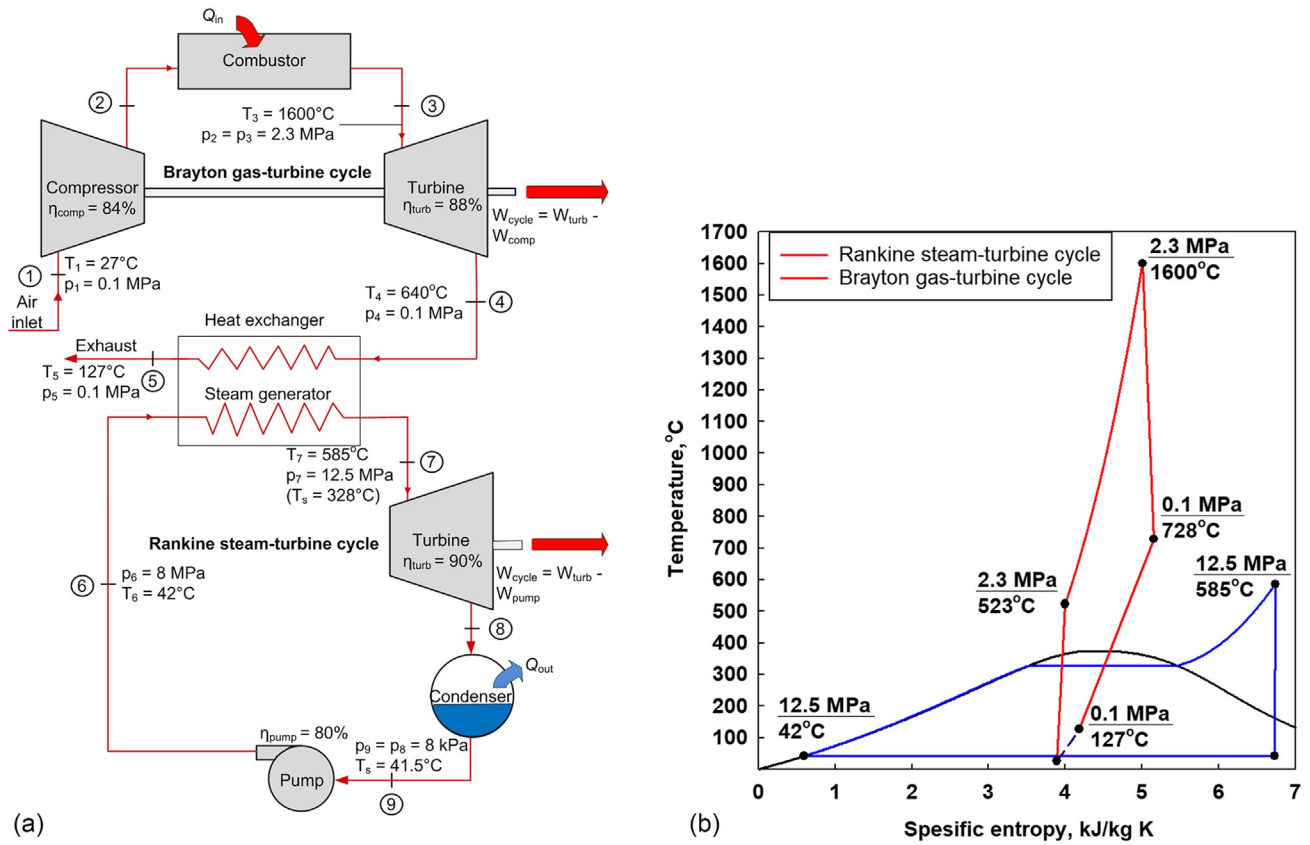


FIG. A1.2 Modern combined-cycle power plant simplified thermodynamic layout (a) and T-s diagram (b). *Partially based on data from MHI and Siemens*

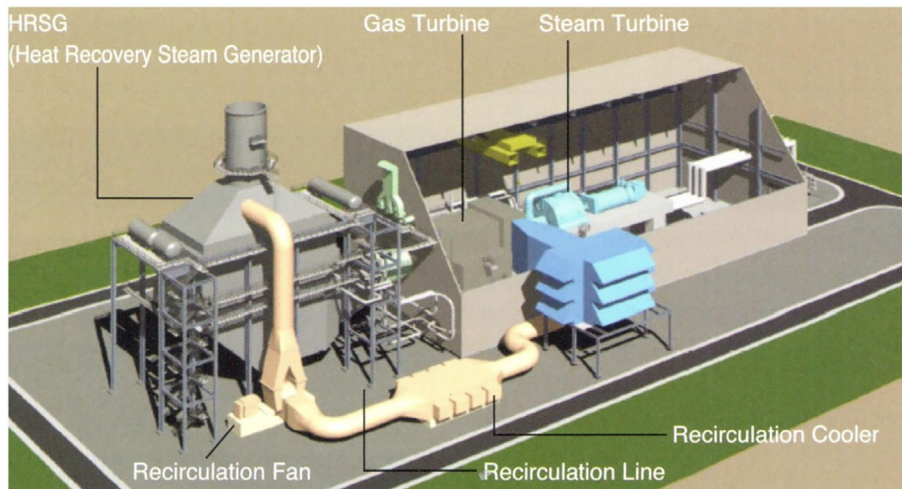


FIG. A1.3 General layout of near-future combined-cycle power plant with inlet gas-turbine temperatures of up to $1,700^\circ\text{C}$ and gross thermal efficiency of beyond 62% . *Courtesy and copyright of MHI*

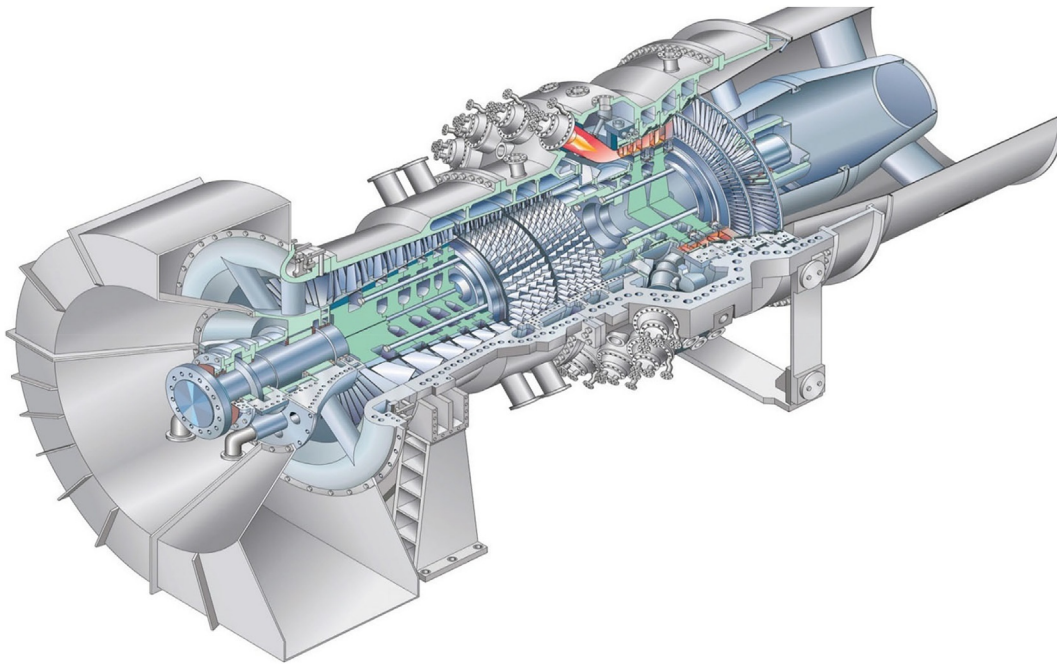


FIG. A1.4 3-D CAD image of SGT6-6000G gas turbine for power generation at 60-Hz-frequency output from electrical generator. Turbine consists of 16-stage axial-flow compressor, dry low- NO_x -emissions combustion system composed of 16 can-annular combustors, and 4-stage turbine. Turbine has steam-cooled combustion-system components for higher thermal efficiency of combined power cycle and advanced cooling technologies allowing higher flow-path gas temperatures, while keeping metal temperatures at level of previous engines. Turbine can be used for heat-recovery applications, including Integrated Gasification Combined Cycle (IGCC), combined-cycle co-generation, and re-powering.

IGCC technology uses a gasifier to turn coal and other carbon-based fuels into synthesis gas (known as syngas) and removes also impurities from syngas before it is combusted. Some of the potential pollutants, for example, sulfur, can be turned into re-usable by-products, resulting in lower emissions of SO_2 , particulates, and mercury. With additional process equipment, reacting the carbon in syngas with water (so-called, water-gas shift reaction) results in hydrogen and CO_2 , which can be compressed and permanently sequestered. Excess heat from primary combustion and syngas-fired generation is used in a steam Rankine cycle, similar to that of CCPP, which results in improved thermal efficiency compared to conventional pulverized-coal-fired power plants. *Siemens press figure; copyright Siemens AG, Munich/Berlin, Germany*

Currently, electricity generation from natural gas/LNG is about 23.5% in the world – the second largest “piece of pie” after coal-based generation (for details, see Fig. 1.1.3a)!

A1.2.2 Coal-fired thermal power plants

For thousands years, mankind used and still is using wood and coal for heating purposes. For about 100 years, coal is used for generating electrical energy at coal-fired thermal power plants worldwide (currently, electricity generation from coal is about 36.7% in the world – the largest “piece of pie” (for details, see Fig. 1.1.3a)). Usually, coal-fired power plants operate based on, so-called, steam Rankine cycle, which can be organized at two different levels of pressures: 1) older

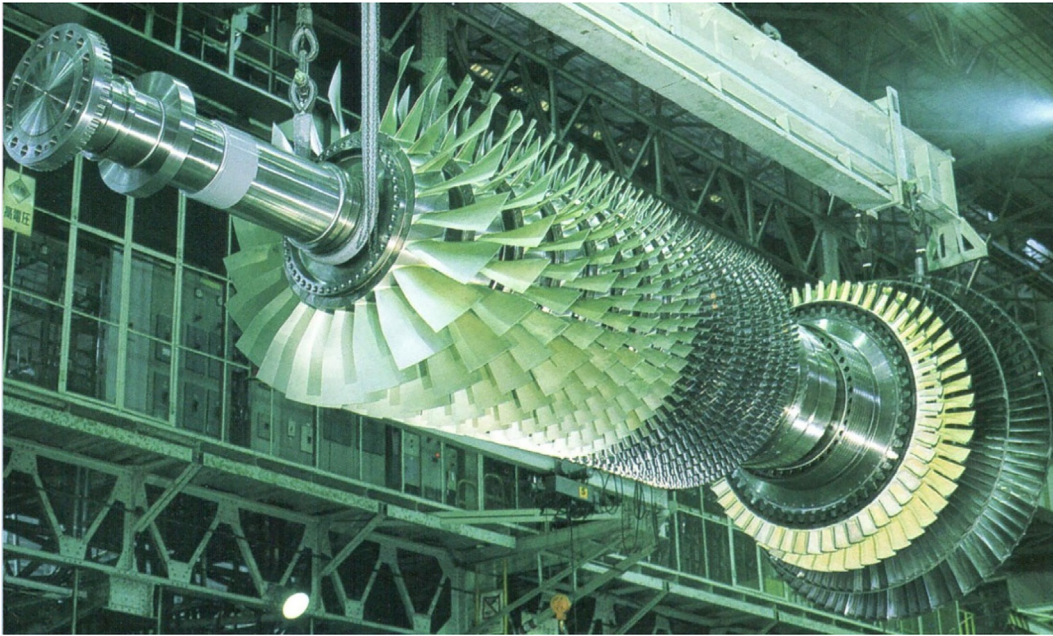


FIG. A1.5 Photo of combined-cycle power-plant gas-turbine rotor with compressor blades (at front) and turbine blades (at rear). *Courtesy and copyright of MHI*

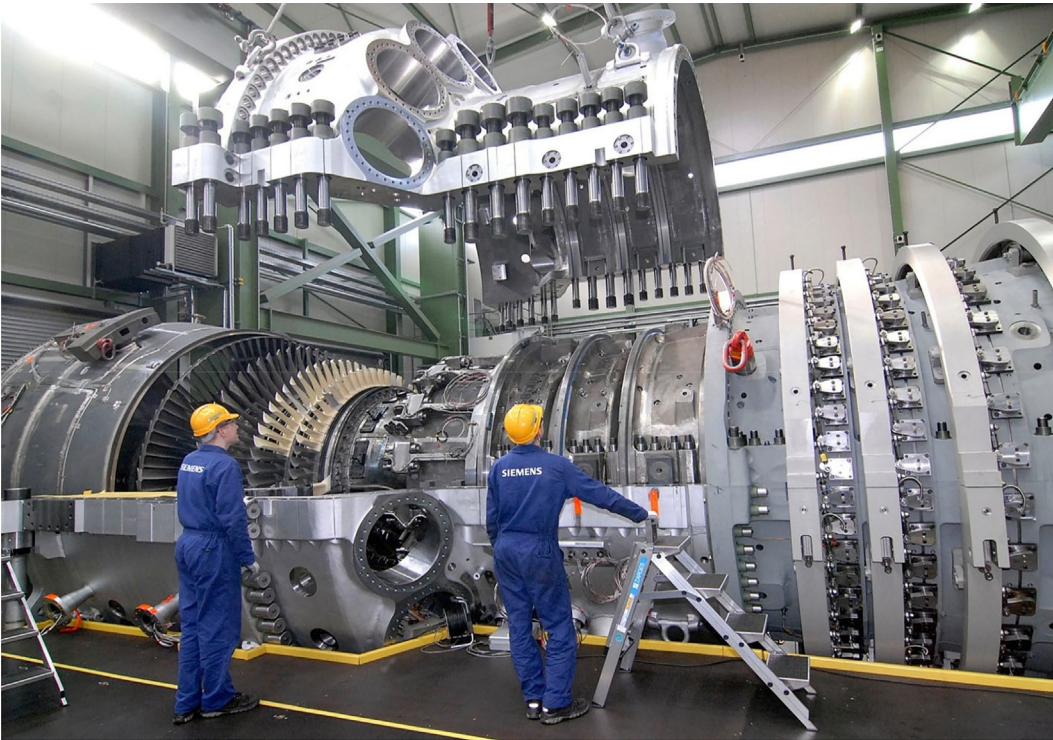


FIG. A1.6 Final assembly of 375-kW Gas Turbine (GT) SGT5-8000H for power plant in Irsching, Germany: Fuel – natural gas; GT output – 340 MW_{el}; 13-stage compressor; pressure ratio – 19.2: 1; high-temperature-can annular-combustion system air-cooled; 4-stage air-cooled turbine; exhaust mass-flow rate – 820 kg/s and temperature 625°C; air-cooled design; fast-start capability and high operation flexibility with lowest life-cycle costs; Heat-Recovery Steam-Generator (HRSG) (Benson boiler)/Water-Steam (WS) cycle – 600°C/17 MPa; steam turbine – two casing HP and LP cylinders (LP double-flow arrangement); single-shaft combined-cycle arrangement; water-cooled 50-Hz electrical generator; combined-cycle output (net) – 530 MW_{el} and thermal efficiency about 60%. As an interesting fact, the increase of thermal efficiency by 2% results in approximately 40,000 tons less CO₂ emissions per year. *Photo Westhafen, 2007; Siemens press photo; copyright Siemens AG, Munich/Berlin, Germany*

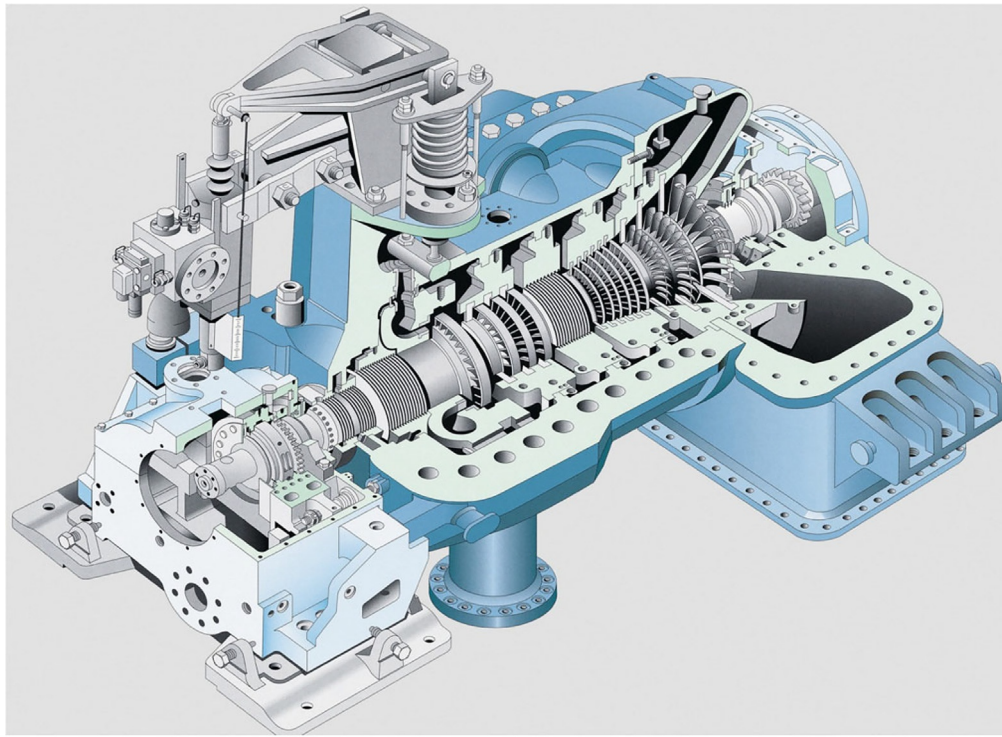


FIG. A1.7 3-D CAD image of SST-800 industrial steam turbine with a capacity up to 150 MW for power generation at 50- (3000 rpm) and 60- (3600 rpm) Hz-frequency output from electrical generator

The SST-800 is a single-casing direct-drive turbine with reverse-flow design for generator applications. Turbine parameters: Inlet pressure/temperature up to 16.5 MPa/565°C; double-controlled extraction up to 4.5 MPa; bleed up to 6 locations at various pressure levels; exhaust area 1.1–5.6 m²; typical dimensions - length 20 m; width 8.5 m; and height 6 m. Such steam turbines can be used for combined-cycle power plants; industrial power plants; industrial CHP (Combined Heat and Power), e.g., in chemical and food industries, pulp and paper mills; petrochemical industry, and in desalination plants. *Siemens press figure; copyright Siemens AG, Munich/Berlin, Germany*

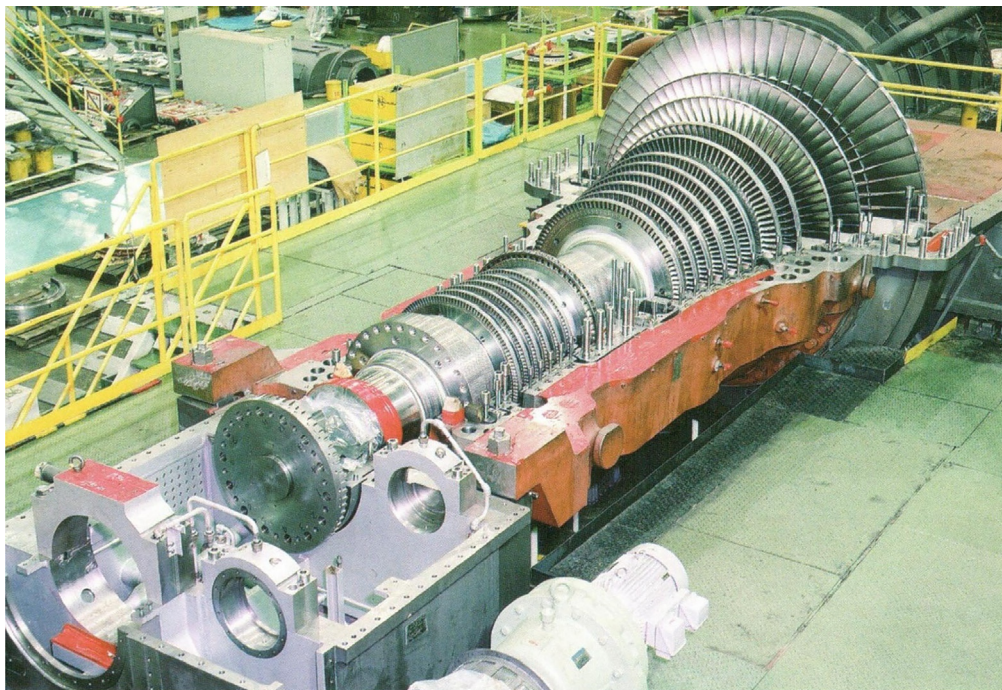


FIG. A1.8 Photo of combined-cycle power-plant steam-turbine with open cover. Single-cylinder reheat turbines are used. *Courtesy and copyright of MHI*



FIG. A1.9 Photo of 476-MW SST5-6000 steam turbine (barrel-type 1 HP, 1 double-flow IP and 1 double-flow LP cylinders) with hydrogen-cooled electrical generator (tandem arrangement) at cogeneration plant in Altbach, Germany. The plant can supply up to 280 MW_{th} of district heat. *Siemens press photo; copyright Siemens AG, Munich/Berlin, Germany*

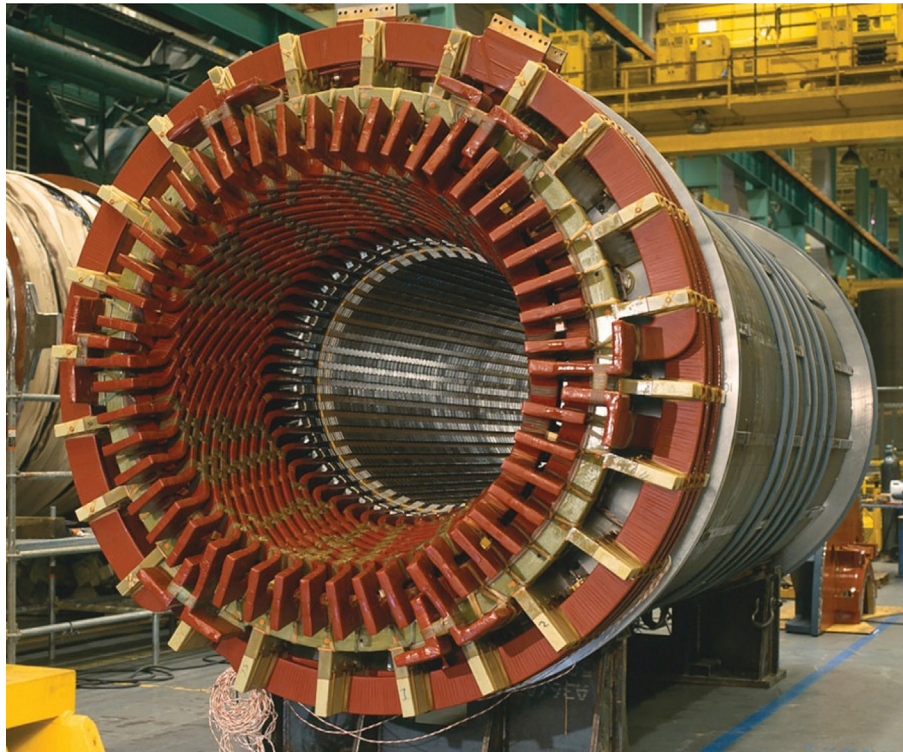


FIG. A1.10 Photo of air-cooled SGen5-1000A electrical generator (only stator shown with open covers) at Charlotte Combined-Cycle Power Plant (CCPP) in North Carolina, USA. Air-cooled electrical generators can be either Totally Enclosed Water-to-Air-Cooled (TEWAC) or Open Air-Cooled (OAC) systems. Due to their compact design these generators can be implemented in simple cycle, combined cycle (CCPP), cogeneration and steam power plants with ratings up to 350 MVA. *Siemens press photo; copyright Siemens AG, Munich/Berlin, Germany*

TABLE A1.2 Reference data on selected Combined-Cycle Power Plants (CCPPs) designed and manufactured by MHI

Model	Plant output kW	LHV heat rate			Plant efficiency %	Gas turbine power kW	Steam turbine power kW	No. of gas turbines
		kJ/kWh	kcal/kWh	Btu/kWh				
50 Hz								
M701DA	212,500	7,000	1,673	6,635	51.4	142,100	70,400	1
M701F4	477,900	6,000	1,433	5,687	60.0	319,900	158,000	1
	958,800	5,981	1,429	5,668	60.2	639,800	319,000	2
M701F5	525,000	5,902	1,410	5,594	61.0	354,000	171,000	1
	1,053,300	5,883	1,405	5,576	61.2	708,000	345,300	2
M701G2	498,000	6,071	1,450	5,755	59.3	325,700	172,300	1
	999,400	6,051	1,445	5,735	59.5	651,400	348,000	2
M701J	680,000	5,835	1,394	5,531	61.7	463,000	217,000	1
60 Hz								
M501DA	167,400	7,000	1,673	6,635	51.4	112,100	55,300	1
M501F3	285,100	6,305	1,506	5,976	57.1	182,700	102,400	1
	572,200	6,283	1,501	5,955	57.3	365,400	206,800	2
M501GAC	404,000	6,080	1,452	5,763	59.2	269,000	135,000	1
	810,700	6,060	1,447	5,744	59.4	538,000	272,700	2
	1,216,000	6,060	1,447	5,744	59.4	807,000	409,000	3
M501J	470,000	5,854	1,398	5,549	61.5	322,000	148,000	1
	942,900	5,835	1,394	5,531	61.7	644,000	298,900	2

Courtesy of MHI.

TABLE A1.3 Reference data on selected gas turbines for combined-cycle power plants designed and manufactured by MHI

Model	ISO-base rating* kW	LHV heat rate			P ratio -	Air flow kg/s	Turbine speed rpm	Exhaust temp. °C
		kJ/kWh	kcal/kWh	Btu/kWh				
50 Hz								
M701DA	144,090	10,350	2,473	9,810	14	441	3,000	542
M701F4	324,300	9,027	2,156	8,556	18	712	3,000	592

Continued

TABLE A1.3 Reference data on selected gas turbines for combined-cycle power plants designed and manufactured by MHI—cont'd

Model	ISO-base rating* kW	LHV heat rate			P ratio -	Air flow kg/s	Turbine speed rpm	Exhaust temp. °C
		kJ/kWh	kcal/kWh	Btu/kWh				
M701F5	359,000	9,000	2,150	8,530	21	712	3,000	611
M701G2	334,000	9,110	2,175	8,630	21	737	3,000	587
M701J	470,000	8,783	2,098	8,325	23	861	3,000	638
60 Hz								
M501DA	113,950	10,320	2,465	9,780	14	346	3,600	543
M501F3	185,400	9,740	2,325	9,230	16	458	3,600	613
M501GAC	272,000	9,074	2,167	8,600	20	598	3,600	614
M501J	327,000	8,783	2,098	8,325	23	598	3,600	636
MF-111	14,570	11,630	2,778	11,020	15	55	9,660	530
MF-221	30,000	11,260	2,688	10,670	15	108	7,200	533
MFT-8	26,780	9,310	2,223	8,820	21	86	5,000	464

Courtesy of MHI.

or smaller capacity power plants operate at steam pressures no higher than ~18 MPa (usually, 15–17 MPa) and 2) modern large capacity power plants (see [Figs. A1.11–A1.20](#)) operate at supercritical pressures from 23.5 MPa and up to 38 MPa (usually, 23.5–30 MPa). Supercritical pressures mean pressures above the critical pressure of water, which is 22.064 MPa. From thermodynamics it is well known that higher thermal efficiencies correspond to higher temperatures and pressures.

Therefore, usually subcritical-pressure plants have thermal efficiencies up to 43% and modern supercritical-pressure plants – up to 55%. Steam-generators outlet temperatures or steam-turbine inlet temperatures have reached level of about 625°C at pressures of 23.5–30 (up to 38) MPa. However, a common level is about 535–585°C at pressures of 23.5–26 MPa. [Fig. A1.21](#) shows possible solutions for Carbon-dioxide Capture and Storage (CCS) at thermal power plants.

In spite of advances in coal-fired power-plants design and operation worldwide they are still considered as not environmental-friendly due to producing a lot of carbon-dioxide emissions as a result of combustion process plus ash, slag and even acid rains (for details, see [Chapter 1.1](#) and [Pioro and Duffey \(2007\)](#)). However, it should be admitted that known resources of coal worldwide are the largest compared to those of other fossil fuels (natural gas and oil) (for details, see [Tables in Appendix A8.2](#)).

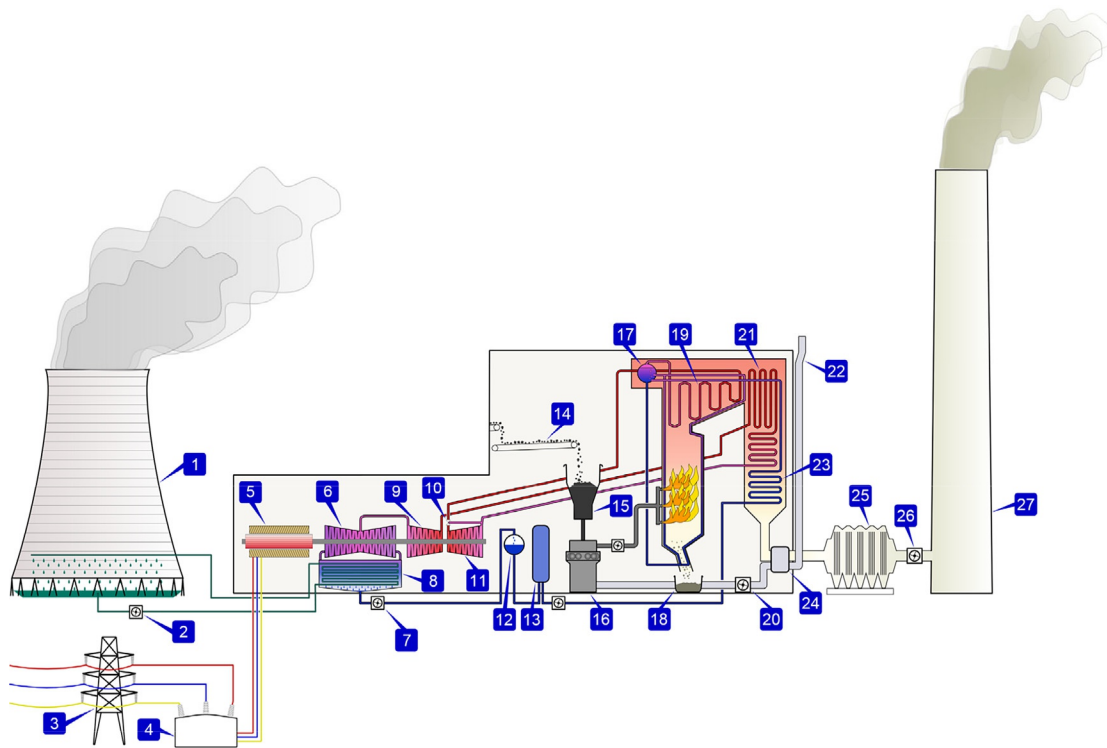


FIG. A1.11 Typical scheme of coal-fired thermal power plant (Author/User: BillC; <https://commons.wikimedia.org/wiki/File:PowerStation2.svg>, website approached January 26, 2016): 1) Cooling tower; 2) Cooling-water pump; 3) Transmission line (3-phase); 4) Step-up transformer (3-phase); 5) Electrical generator (3-phase); 6) Low-pressure steam turbine; 7) Condensate pump; 8) Surface condenser; 9) Intermediate-pressure steam turbine; 10) Steam control valve; 11) High-pressure steam turbine; 12) Deaerator; 13) Feedwater heater; 14) Coal conveyor; 15) Coal hopper; 16) Coal pulveriser; 17) Boiler steam drum; 18) Bottom-ash hopper; 19) Superheater; 20) Forced-draught (draft) fan; 21) Reheater; 22) Combustion-air intake; 23) Economiser; 24) Air preheater; 25) Precipitator; 26) Induced-draught fan; and 27) Flue-gas stack

The explanations for the gap in operating pressures between subcritical-pressure and supercritical-pressure Rankine cycles, i.e., from 17 (18) MPa and up to 23.5 MPa, are provided below and in Fig. A1.22. In general, we have two limitations or detrimental effects: 1) With saturation-pressure increase the saturation-temperature profile is leveled off, i.e., even significant increase in pressure above ~ 1.6 MPa ($T_{\text{sat}} = \sim 200^\circ\text{C}$) does not correspond to significant increase in saturation temperature (see Fig. A1.22a); and 2) Critical Heat Flux (CHF) or the maximum heat flux in flow boiling at which heated surface can be significantly overheated and ruptured (see Fig. A1.22b) is decreasing very fast with the saturation pressure approaching the critical one (for water – 22.064 MPa). In the critical point there are no differences in densities of liquid (water) and vapor (steam), i.e., we have single-phase fluid and due to that latent heat of evaporation is 0.

In any power system cooled with water there are usually some fluctuations of pressure, mass flux, heat flux, etc., i.e., operating parameters, and operating close to critical pressure from above can lead to dropping down to slightly subcritical pressure, where the CHF is close to 0.

Fig. A1.22c shows complexity of flow-boiling process/phenomena in a vertical bare tube.

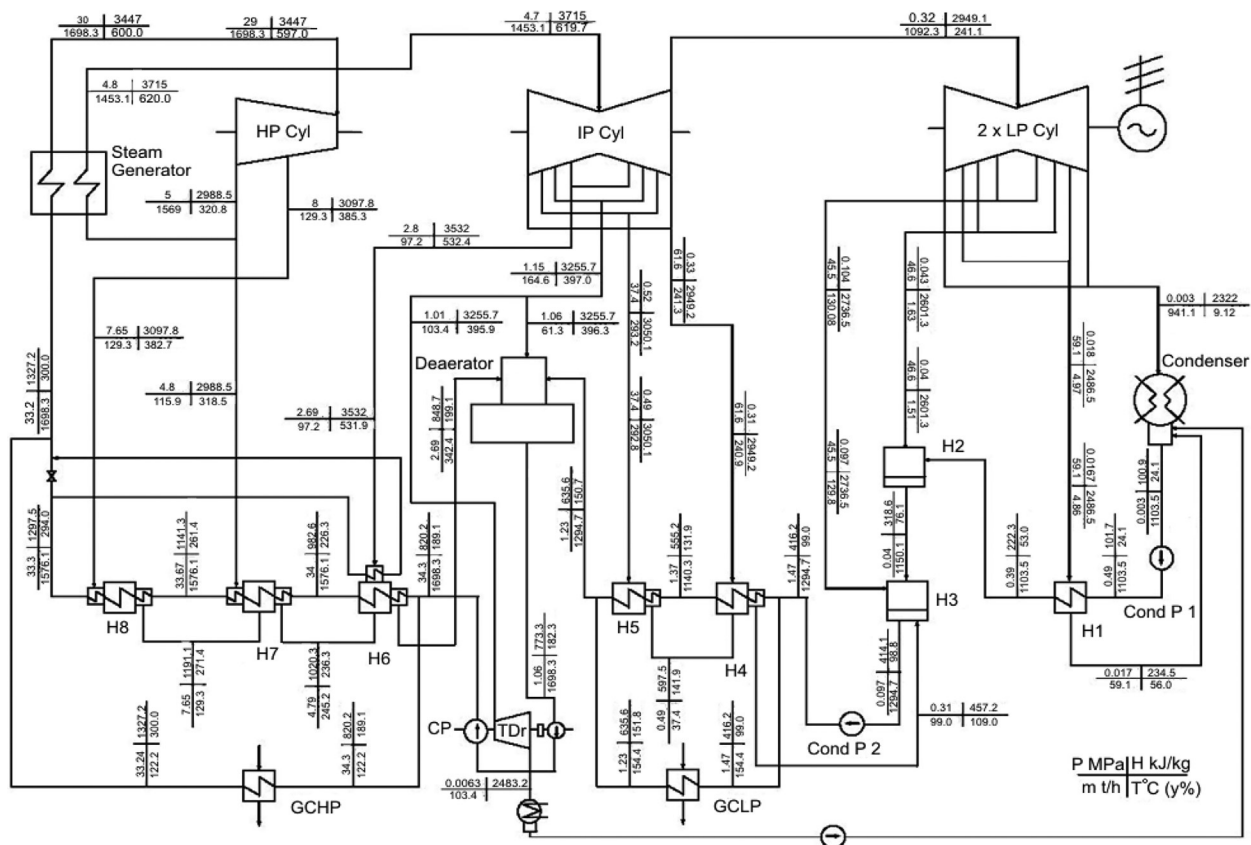


FIG. A1.12 Single-reheat-regenerative cycle 600-MW_{el} Tom'-Usinsk thermal power plant layout (Kruglikov et al., 2009; TsKTI, Russia): Cyl – Cylinder; H – Heat exchanger (feedwater heater); CP – Circulation Pump; TDr – Turbine Drive; Cond P – Condensate Pump; GCHP – Gas Cooler of High Pressure; and GCLP – Gas Cooler of Low Pressure

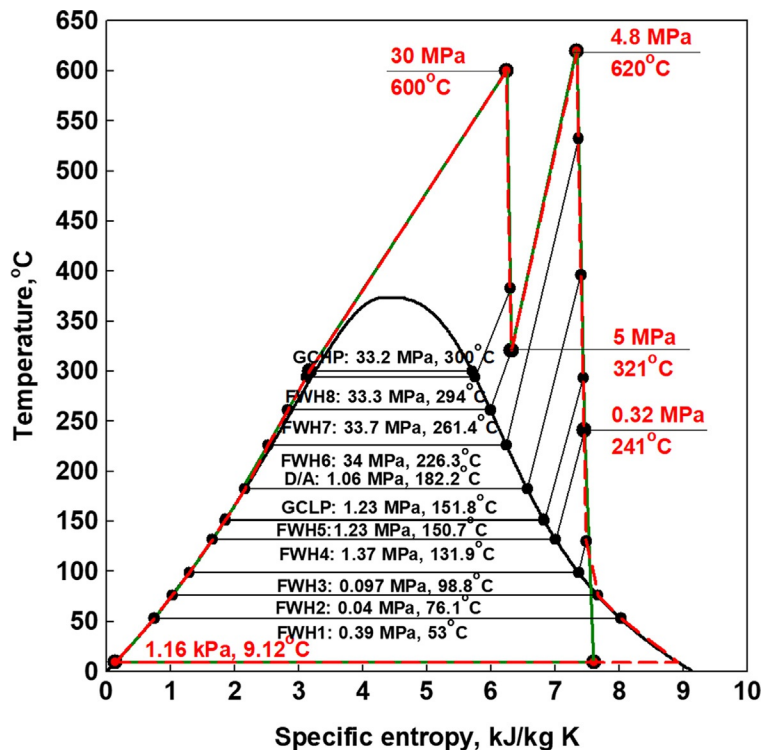


FIG. A1.13 Simplified $T-s$ diagram for Tom'-Usinsk coal-fired thermal-power-plant supercritical-pressure Rankine steam-turbine cycle



FIG. A1.14 Photo of Tomato-Atsuma (Japan) coal-fired-power-plant Unit No. 4 - supercritical-pressure steam turbine: 1 High-Pressure (HP), 1 Intermediate Pressure (IP) and 2 double-flow Low-Pressure (LP) cylinders: 700 MW_e, TC4F-43, 3000 rpm, steam parameters - 25.0 MPa pressure and 600/600°C (primary steam/reheat) temperature. *Courtesy and copyright by Hitachi, Ltd*

A1.3 Current nuclear-power reactors and NPPs

A1.3.1 Introduction

This Section is in addition to [Chapter 1.2](#) and provides details on modern nuclear-power reactors/NPPs including their layouts, *T-s* diagrams, basic parameters, and photos. Nuclear-power reactors and corresponding NPPs are listed in the decreasing numerical sequence for the number of particular types of reactors currently operating in the world (see Table 1.2.1 in [Chapter 1.2](#)):

- (1) PWRs/Advanced PWRs;
- (2) BWRs/ABWRs;
- (3) PHWRs;



FIG. A1.5 Photo of Low-Pressure (LP) double-flow steam-turbine rotor with blades for supercritical-pressure coal-fired power plant. *Siemens press photo; courtesy and copyright Siemens AG, Munich/Berlin, Germany*

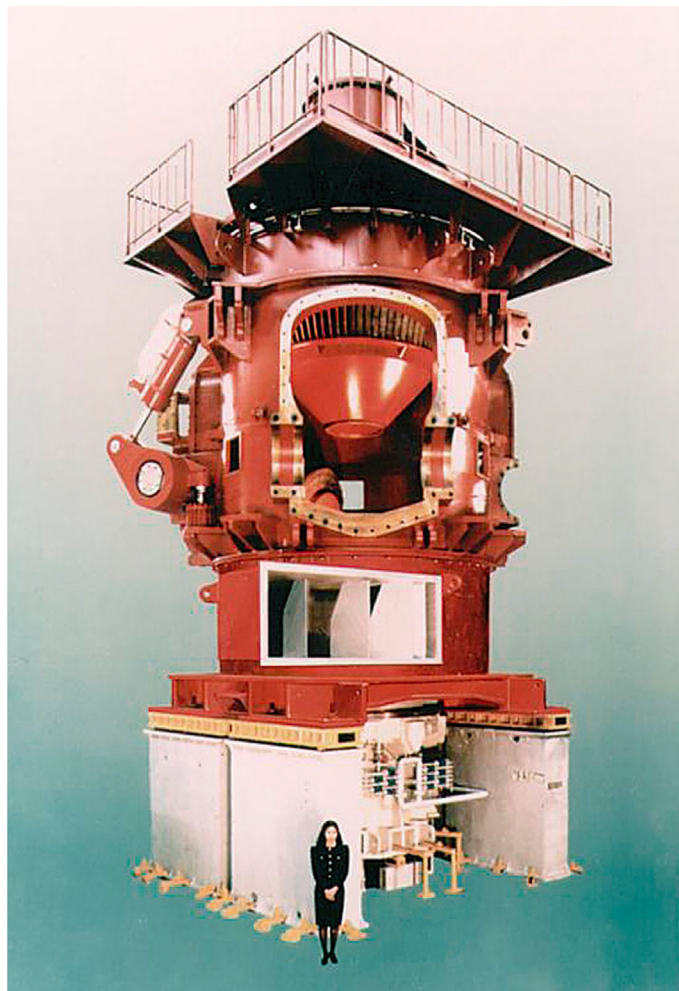


FIG. A1.16 Photo of coal-fired-power-plant Mitsubishi Rotary Separator (MRS) mill. *Courtesy and copyright of MHI*



FIG. A1.17 Photo of thermal-power-plant water-circulating pump. *Courtesy and copyright of MHI*



FIG. A1.18 Photo of thermal-power-plant-boiler feedwater pump. *Courtesy and copyright of MHI*

- (4) AGRs and GCRs;
- (5) LGRs (RBMKs and EGP); and
- (6) LMFBRs - SFRs (BN-600 and BN-800).

Number of nuclear-power reactors connected to electrical grids by types and by countries including forthcoming reactors are listed in Table 1.2.6 in [Chapter 1.2](#). It should be noted that numbers of Rankine-cycle nuclear-power reactors connected to electrical grids in the world and by countries include all reactors connected, but not all of them are currently in operation so these data



FIG. A1.19 Photo of thermal-power-plant-boiler feedwater booster pump. *Courtesy and copyright of MHI*

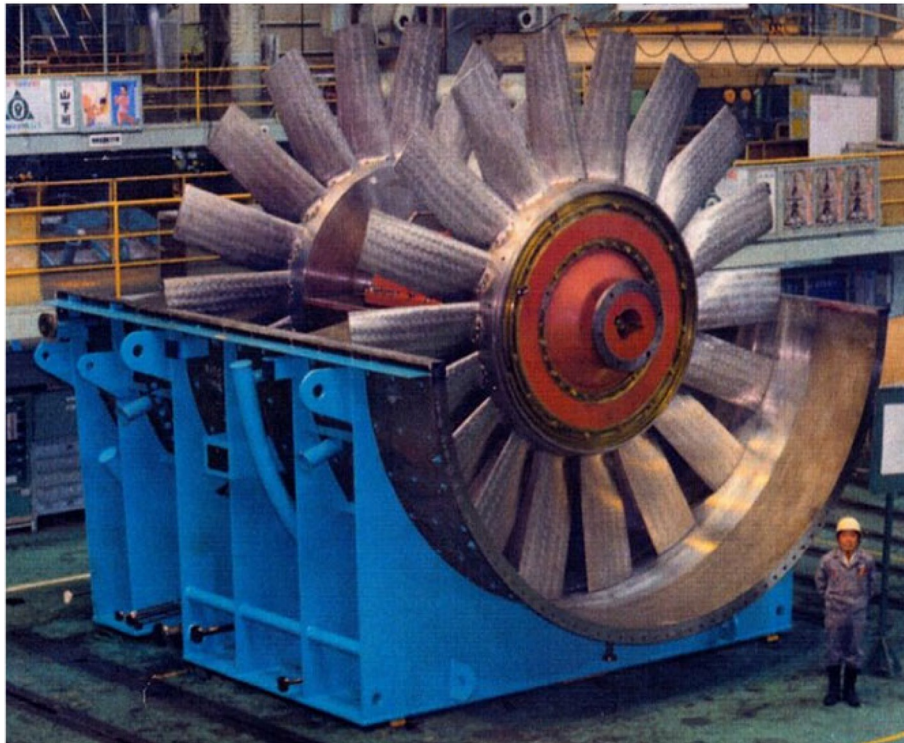


FIG. A1.20 Photo of thermal-power-plant fan. *Courtesy and copyright of MHI*

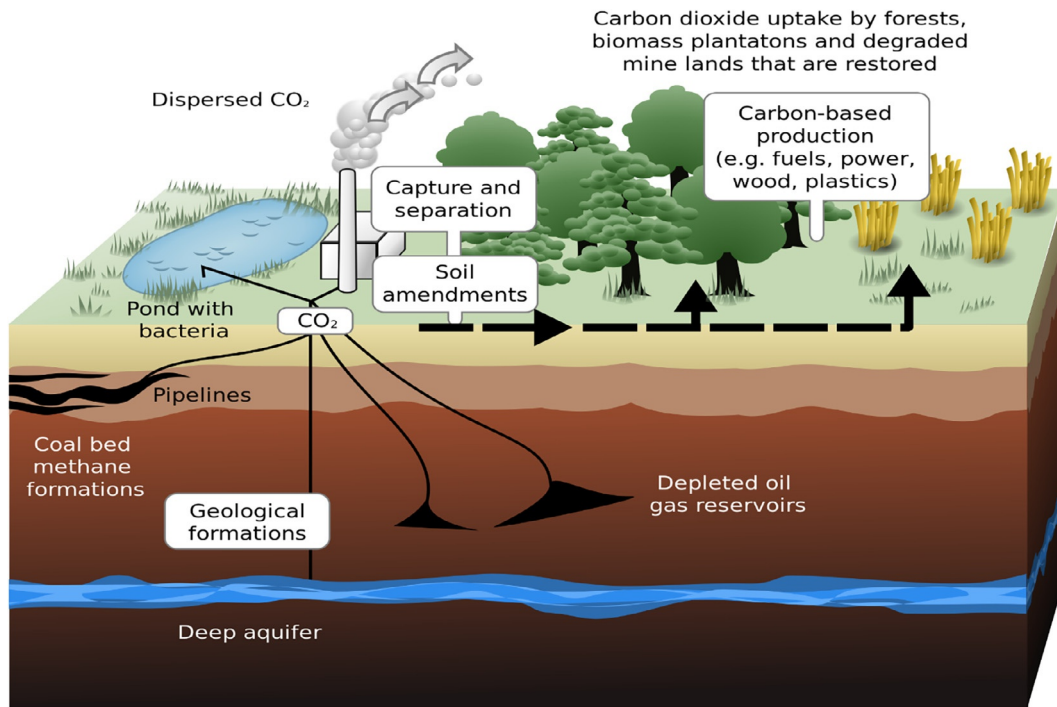


FIG. A1.21 Possible solutions are shown for Carbon-dioxide Capture and Storage (CCS) using terrestrial and geological sequestration of emissions from coal-fired power plants. Rendering by L. Hardin & J. Payne: http://www.ornl.gov/info/ornlreview/v33_2_00/research.htm; courtesy of the Oak Ridge National Laboratory, U.S. Department of Energy

are an upper estimate. Currently, electricity generation from NPPs is about 10.4% in the world – the fourth largest “piece of pie” after coal-, natural-gas-, and hydro-based generation (for details, see Fig. 1.1.3a).

Summary of basic parameters of all current reactors are listed in Table 1.2.3 in Chapter 1.2. All of the power-conversion cycles for current NPPs are based solely on the subcritical-pressure Rankine steam-turbine cycle of several configurations (see Table 1.2.4 in Chapter 1.2). Gross thermal efficiencies of current NPPs are listed in Table A1.1. Fig. A1.23 shows typical operating conditions of selected light- and heavy-water^b-cooled reactors on the Pressure-Temperature diagram, and Table A1.4 lists selected typical Heat-Transfer-Coefficient (HTC) ranges of various coolants.

We have quite substantial number of definitions of nuclear-power-reactors generations, which currently, consist of Generations I; II; III; III⁺; and IV. However, it does not matter which definition is used, all of them are quite vague in terms of years and description of generations. Therefore, some sort of combination from several definitions is presented below.

First success of using nuclear power for electrical generation was achieved in several countries within 50-s, and currently, Generations II; III; and III⁺ nuclear-power reactors are operating around the world.

In general, definitions of nuclear-reactors generations can follow their vintage of design and build timeframes:

- (1) Generation I (1950 – 1965) – prototypes of nuclear reactors and none currently in operation;

^b Including reactors with light- and heavy-water coolants.

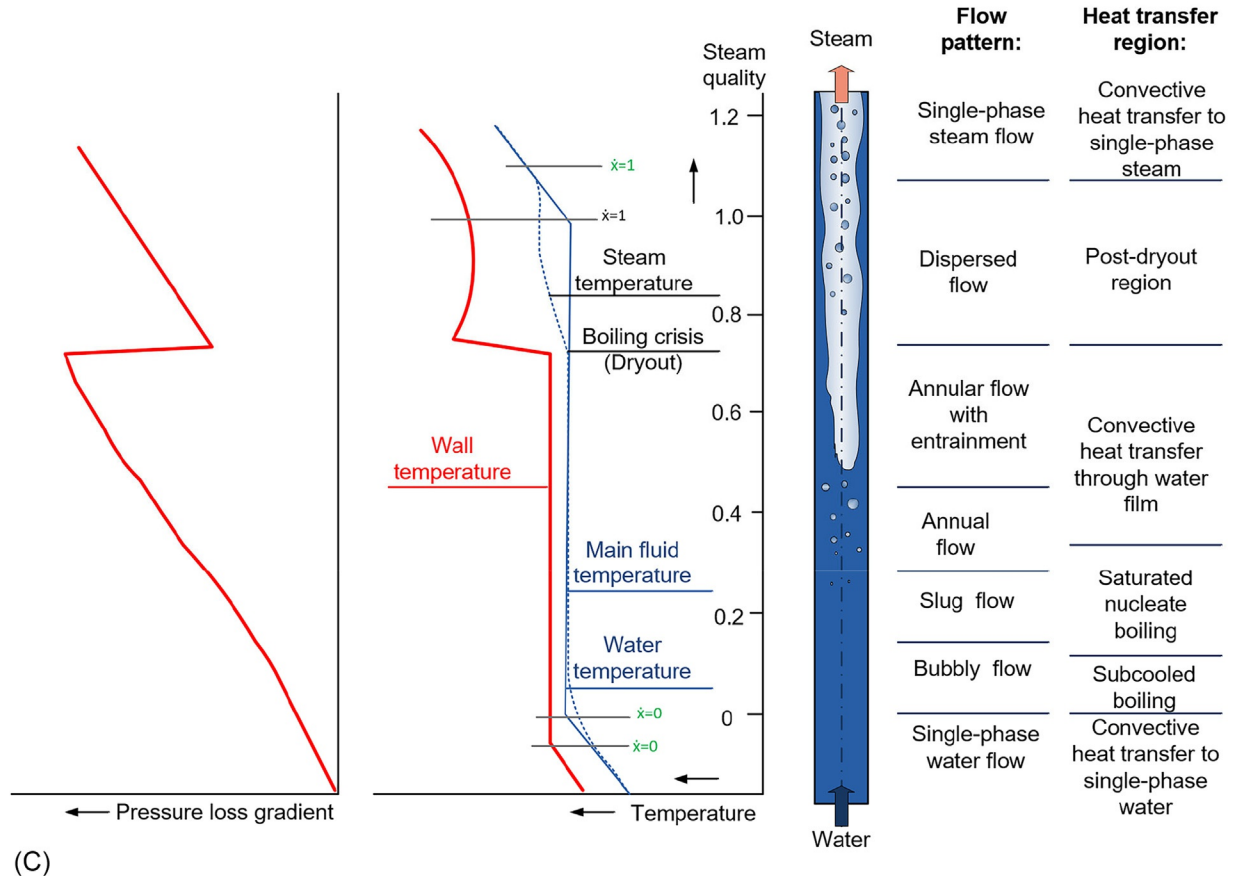
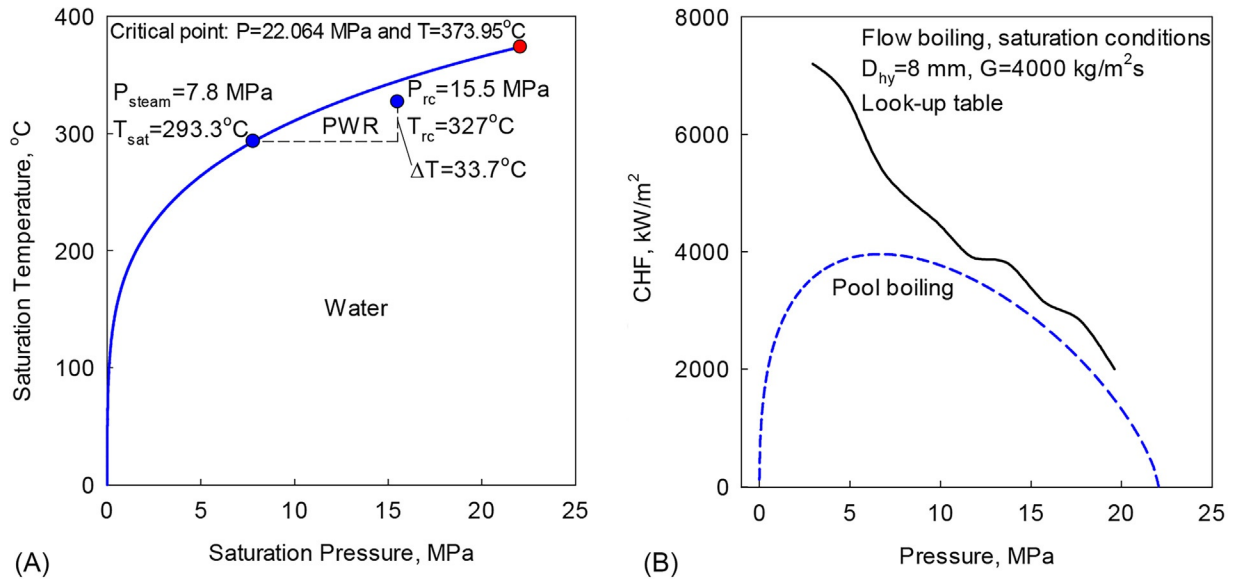


FIG. A1.22 Limitations on maximum heat flux at subcritical-pressure forced-convection close to critical point. (a) Saturation-Temperature Profile vs. Saturation Pressure: Water. (b) Critical-Heat-Flux (CHF) Profile vs. Pressure: Water, flow boiling, $G=4000 \text{ kg/m}^2\text{s}$, $D_{hy}=8 \text{ mm}$. (c) Wall- and Bulk-Fluid-Temperature and Pressure-Loss-Gradient Profiles in uniformly heated, vertical, bare tube at flow boiling. Based on Fig. 4 from Siemens: 25JahreBENSONbild_E.doc; accessed Feb. 22, 2022

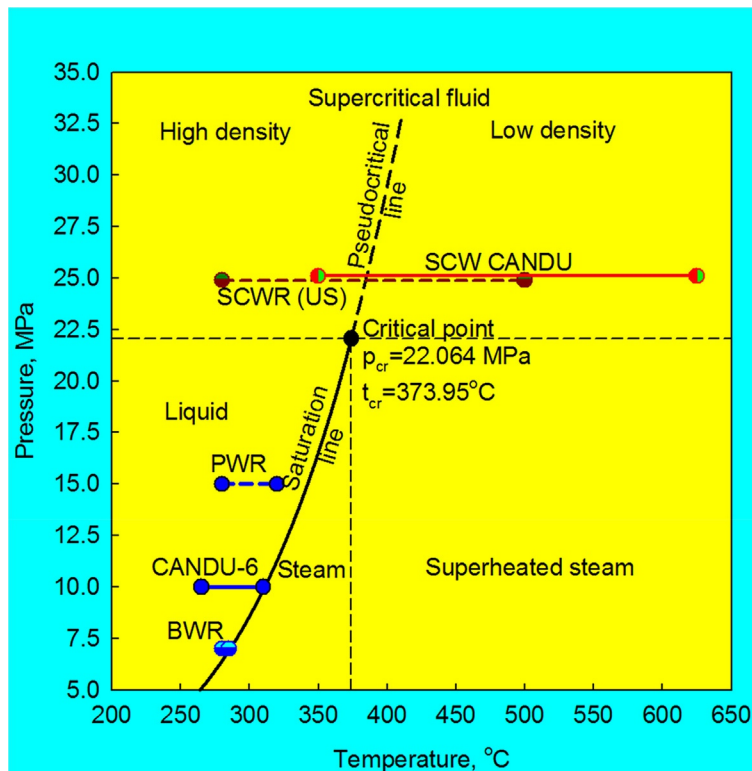


FIG. A1.23 Typical operating conditions (pressure drop is not accounted for) in P - T coordinates for BWRs, CANDU reactors, PWRs, and SCWRs (Generation-IV concept)

TABLE A1.4 Selected typical Heat-Transfer-Coefficient (HTC) ranges of various coolants (Hewitt and Collier, 2000)

No.	Coolant	Heat transfer coefficient, kW/m ² K
1	Na (forced convection)	55 – 85
2	Boiling water (flow boiling)	60
3	CANDU reactor	50
4	Pb (forced convection)	25 – 35
5	Water (single-phase forced convection)	30
6	Pb-Bi (forced convection)	20 – 30
7	SCW	10 – 25
8	He (rough surface)	10
9	CO ₂ (high pressure)	2 – 5

- (2) Generation II (1965 – 1995) - commercial power reactors, which are still in operation from 1969, therefore, “officially” based on these time frame some can be considered as Generation II. However, all of them have been upgraded with enhanced-safety systems, so might be considered as Generation III;

- (3.1) Generation III (1995 – 2010) – reactors including water-cooled with thermal efficiency within 30 – 36%; carbon-dioxide-cooled with thermal efficiency up to 42%; and liquid sodium-cooled thermal efficiency about 40%, including reactors that have been built after 2010 until now.
- (3.2) Generation III+ (2010 – 2025) – reactors with improved parameters and evolutionary-design changes, including passive-safety cooling systems, core catcher, etc. This generation of water-cooled-reactors has thermal efficiency up to 38% (for details, see below) and, also, various SMR concepts, which are not yet deployed or still in prototype development. However, in Japan reactors named “Advanced BWRs” (ABWRs) are considered early Generation-III+ being placed into operation in 1996, 1997, 2005 and 2006. And
- (4) Generation IV (2025 - ...) – reactors in principle with new parameters, improved safety and not yet commercially deployed, including higher-temperature coolants with thermal efficiencies of 40 – 50% and even higher for various systems.

Selected Generation-III⁺ reactors:

- ABWR – Toshiba-GE (Japan-USA) (1 unit, 1996); Hitachi-GE (Japan-USA) (1 unit, 1997); Toshiba (1 unit, 2005) and Hitachi (1 unit, 2006): Kashiwazaki-Kariwa NPP Units #6 & 7 are the 1st & 2nd ABWRs in the world (1996 & 1997); 3rd – Hamaoka #5 (2005); 4th – Shika #2 (2006) (Japan).
- Advanced CANDU Reactor (ACR-1000) - Candu Energy (former AECL) (Canada).
- Advanced Passive (plant) (AP-1000) – Westinghouse (USA) (4 in operation in China and 2 will be put into operation in 2023 in USA).
- Advanced PWR (APR-1400) – Doosan (South Korea) (2 in operation and 2 under construction in S. Korea and 3 in operation and 1 will be put into operation in 2024 in UAE).
- Advanced PWR (1500 MW_{el}) – MHI (Japan).
- AHWR (India).
- BREST-300-OD - Rosatom (Russia)
- SFR – BN-800 - Rosatom (Russia) (in operation from 2016).
- Evolutionary Power Reactor (EPR) - AREVA (France) (2 in operation in China and 1 in Finland, and 1 under construction in France and 2 in UK).
- SMR – PWR - RITM-200M - Rosatom (Russia).
- VVER (designs VVER-TOI and VVER-1200 with ~1100-1175 MW_{el}) – GIDROPRESS (Russia) (2 in operation and 5 under construction in Russia and 4 under construction in Turkey) (VVER or WWER - Water Water Energy (Power) and TOI - Typical Optimized Informatized Reactor in Russian abbreviations).

Based on the above mentioned, we can conclude that, currently, we have mostly operating reactors of Generation-III and relatively small number of operating reactors of Generation-III⁺, which are mainly built nowadays, and several operating concepts of Generation-IV reactors, i.e., two SFRs in Russia and one in China, and two VHTRs (HTR-PM helium-cooled) in China. However, possibly, it cannot be stated that these reactors are actually operating Generation-IV reactors, because some additional enhancements in their design/safety systems are required!

A1.3.2 Current status, advantages and challenges of nuclear-power reactors

Nuclear power without used-fuel reprocessing and recycling is incorrectly considered to be a non-renewable energy source like the mined fossil fuels, such as coal, oil, and gas. Although, the resources of *naturally* occurring fissile fuels (uranium and thorium) are limited in extent (see Tables in Appendix A8.3), and geographically concentrated in regions of relatively lower population, there is an opportunity to recycle and re-use fuel, and indeed to “breed” or produce more fuel, and to switch to alternate fuel cycles in the future. Thus, nuclear resources can be used for significantly longer time than some fossil fuels, and in some cases almost indefinitely, if recycling of

unused or low burn-up uranium fuel, thorium-fuel resources, and fast-neutron-spectrum reactors, i.e., fast-breeder reactors, that literally can “breed” plutonium are used.

The major advantages of nuclear power are:

- (1) Concentrated and reliable source of long-term or even infinite energy, which is almost independent of weather conditions and its cyclical variations.
- (2) High-capacity factors are achievable, often in excess of 90% with long operating cycles, making units suitable for continuous base-load operation (see Table 1.1.8 in [Chapter 1.1](#)).
- (3) Essentially negligible operating emissions of carbon dioxide and relatively small amounts of wastes generated compared to alternate fossil-fuel thermal power plants (see Table 1.1.9 and Fig. 1.1.6, and Table 1.1.12 in [Chapter 1.1](#)).
- (4) Relatively small amount of fuel required compared to that of fossil-fuel thermal power plants (see Table 1.1.11 in [Chapter 1.1](#)). And
- (5) NPPs can supply relatively cheap electricity for re-charging of electrical vehicles during night hours as they usually operate at full load (base load) capacity for 24/7 (see Figs. 1.1.49 and 1.1.51 in [Chapter 1.1](#)).

As a result, nuclear power is considered as the most viable source for electricity generation within next 50 – 100 years without re-cycling, and indefinitely with improved fuel cycles and breeding. However, nuclear power must operate and compete in energy markets based on relative costs and strategic advantages of the available fuels and energy types.

Specific unique issues, trends, and challenges for nuclear power now and in the future include:

- (1) Public fear of exposure to radiation from accidents, exacerbated by the events at the Chernobyl and Fukushima-Daiichi NPPs (see Figs. 1.2.2 and 1.2.3 in [Chapter 1.2](#)), that might result in radioactivity release to the environment due to damage or core melt.
- (2) Significant competitive disadvantage due to the capital investment and construction costs that are larger than those for other electricity sources.
- (3) Relatively long environmental planning and safety licensing times, which increase both uncertainty and investment return timescales.
- (4) Concerns over non-proliferation and the potential spread of nuclear know-how into undesirable “hands” that have led to international Treaties, Agreements, Supplier, and technology-transfer restrictions, for controls over fissile materials, supply assurances, reprocessing restrictions, and, hence, additional bureaucratic, legal, operational, and regulatory demands that are not required for other sources.
- (5) Limited manufacturing and supply chain capabilities, and long gestation times for necessary national manufacturing capabilities to be established, thus causing limited ability to replicate and mass-produce, when necessary multiple an Nth-Of-A-Kind (NOAK) units.
- (6) Despite Item 3 above, lack of actual financial incentives for lower atmospheric emissions, and little implementation or use of “carbon credits” as adopted for incentivizing renewables.
- (7) The absence of a national and international long-term strategies and actual facilities for interim and long-term storage of small amounts of once-used nuclear fuels and their associated waste streams; although siting reviews and “retrievable” technology studies have been underway for many years in a number of countries (Canada, Russia, Sweden, Switzerland, UK, US, etc.).
- (8) The general lack of global investment in Research and Development (R&D) and demonstrations of completely new technologies, except in China, where literally “one-of-every reactor type” is being built and tested. And
- (9) Lack of an agreed international licensing process or “certification” for essentially duplicate designs, as adopted in and by the airline industry leading to expensive, excessive, and likely unnecessary effort involving multi-layered reviews, and expensive delays, all producing non-standard designs, and schedule uncertainty.

A1.3.3 Technical considerations of various types of nuclear-power reactors and plants

From the beginning it should be stated here that there is no such term as “the best” reactor design by all features or parameters. Each reactor design has some pros and cons.

A1.3.3.1 Classifications of nuclear-power reactors and plants

Analysis of the basic parameters of current reactors (see Table 1.2.3 in [Chapter 1.2](#)) shows that various types of reactors have the following differences:

By neutron spectrum

- (1) Thermal spectrum - vast majority of reactors, i.e., 440 from 443 or 99.3%, which includes LWRs (PWRs (309 units) and BWRs (57)/ABWRs (4)), PHWRs (48), and LGRs (11); and gas-cooled reactors – AGRs (9) and GCRs (2). And
- (2) Fast spectrum – LMFBRs (3 units), i.e., SFRs - two Russian BN-600 and BN-800 reactors and small SFR in China. In general, fast reactors are considered to be the future of nuclear-power industry, because fast-neutron-spectrum reactors can “breed” plutonium and can reprocess radioactive wastes. However, fast reactors require higher enrichment of nuclear fuel compared to that of thermal-spectrum reactors, and, for now, light and heavy water are not considered as a reactor coolant in such reactors. Due to that, there are some limitations, which reactor coolant can be used in fast reactors (currently - sodium, in the nearest future - lead, and in the future - lead-bismuth, helium, and molten salt are considered). A number of nuclear-power advanced countries have tried to develop fast-reactors technologies, but, as of today, only Russia has two operating SFRs and China has one designed by Russia.

By reactor coolant and moderator

- (1) Reactor coolants: (a) the most widely used – light water (LWRs (370 units) and LGRs (11)); (b) heavy water (PHWRs) (48); (c) carbon dioxide (AGRs) (9); (d) liquid sodium (SFRs) (3); and helium (GCRs) (2).
- (2) Moderator: (a) light water used in LWRs (370 units), and there is no separation between reactor coolant and moderator; (b) heavy water in PHWRs (48), and here reactor coolant and moderator are separated through fuel channels, i.e., reactor coolant is inside fuel channels and moderator - outside; (c) graphite in LGRs (11), and here reactor coolant and moderator are separated through fuel channels; (d) graphite in AGRs (9) and here graphite is in contact with reactor coolant and in GCRs (2) – HTR-PM with pebble-bed spherical fuel covered with graphite and here graphite is in contact with reactor coolant; and (e) there is no moderator in fast reactors, i.e., in SFRs (3).

Properties of various reactor coolants and comparison of heat transfer coefficients in various reactors are shown in Appendix A2. Comparison of light- and heavy-water thermophysical properties is shown in [Petriw et al. \(2019\)](#) and [Sabir et al. \(2019\)](#).

By pressure-boundary design

- (1) Reactor Pressure Vessel (RPV) - vast majority of reactors, i.e., 370 LWRs (RPVs made of steel) and 9 AGRs (RPVs made of concrete) or in total 86% of all reactors. In general, RPV of LWRs have two levels of pressures: 1) PWRs – 15 – 16 MPa (older reactors, e.g., VVER-440, and modern PWR SMR KLT-40S have pressures within 12 – 13 MPa); and 2) BWRs – around 7 MPa. AGRs carbon-dioxide-cooled have pressure around 4 MPa GCRs helium-cooled have pressure of ~7 MPa.

- (2) Vessel reactors – two Russian SFRs and one in China (in total only 0.7%), because pressure above the pool of liquid sodium is close to the atmospheric one; and
- (3) Pressure-channel reactors – 48 PHWRs (pressure up to 11 MPa, e.g., in CANDU® reactors) and 11 LGRs (pressure about 6 – 7 MPa) or in total 13% of all reactors.

Which pros and cons we have for these different pressure-boundary designs:

Pressure vessel contains reactor core, i.e., bundle strings or fuel-elements (rods) assemblies, which oriented vertically. Pressure vessel has an upper cover and internal insert or flow tube to guide reactor-coolant flow downwards from the inlet through the gap between the reactor vessel and flow tube and after that upward through the reactor core to the outlet. Pressure-vessel wall thickness depends mainly on inside pressure and internal diameter of a pressure vessel, and can be for: 1) VVER-1000: Pressure around 16 MPa and ID=4.14 m - wall thickness ~19 cm; 2) US PWR: Pressure around 16 MPa and ID=3.96 m - wall thickness - ~22 cm; and 3) US BWR: Pressure around 7 MPa and ID=6.4 m - wall thickness - 15 cm. Therefore, a pressure vessel is a very important part in a reactor. Due to the three severe nuclear accidents a number of pressure-vessel manufacturing plants in the world were closed or transferred to another production affecting a maximum number of pressure vessels, which can be manufactured in the world. Also, some of these RPV manufacturing plants are oriented only to a certain nuclear vendor, e.g., Russian Atommas (“АТОММАШ”) for VVER RPVs.

Traditionally, PHWRs are pressure-channel or pressure-tube. In particularly, CANDU® reactors have horizontal orientation of fuel channels. Due to small OD/ID of fuel channels, many plants worldwide can manufacture them.

By power cycle

Currently, all nuclear-power reactors are connected to subcritical-pressure Rankine steam-turbine cycles. The vast majority of NPPs equipped with AGRs, GCRs, LMFBRs (SFRs), PHWRs and PWRs (371 reactors from 443 or 84%) have, so-called, an indirect Rankine cycle, which includes a double loop (AGR, PWR, and PHWR): 1) reactor-coolant circulation loop, which includes RPV with reactor core, circulation pumps, and steam generators (all these equipment are located inside a containment building), and Rankine-cycle loop; and 2) triple loop (LMFBRs – SFRs), which includes a primary loop - reactor vessel with fueled core, circulation pumps, and heat exchangers; intermediate loop with liquid sodium as the working fluid, circulation pump(s), and steam generator(s); and Rankine-cycle loop.

In general, the indirect cycle in which reactor coolant circulates only inside a containment building enhances reactor safety. However, this cycle requires steam generators or heat exchangers through which ~30 – 40°C of a temperature difference is usually lost (as such, for PWRs (double loop) - APR-1400: Reactor outlet $T=324^{\circ}\text{C}$, steam-generator saturated steam $T_{\text{out}}=285^{\circ}\text{C}$, and $\Delta T=\sim 40^{\circ}\text{C}$; for EPR - $\Delta T=\sim 35^{\circ}\text{C}$; in terms of SFR – BN-800 (triple loop): Inside reactor $T_{\text{max Na}}=547^{\circ}\text{C}$; inside intermediate loop $T_{\text{max Na}}=505^{\circ}\text{C}$; and superheated steam $T_{\text{max}}=490^{\circ}\text{C}$, and $\Delta T=\sim 57^{\circ}\text{C}$).

Therefore, in general, the direct cycle is considered to be more efficient from the thermodynamic point of view. Actually, Generation-III⁺ ABWRs have reached levels of pressures up to 7.2 MPa and saturated steam temperature of 287.7°C (NPP thermal efficiency of about 34%). However, Generation-III⁺ PWRs, in particular, the largest in the world 1660-MW_{el} EPRs, have reached saturation-steam pressures close to 7.8 MPa and corresponding to that $T_{\text{sat}}=293.3^{\circ}\text{C}$ in the Rankine cycle. Therefore, as of today, NPPs with advanced PWRs have reached thermal efficiency of 36%-37% (38%), which is the highest thermal efficiency among all NPPs equipped with light- and heavy-water reactors.

A1.3.3.2 Comparison of various nuclear-power reactors by major features

Based on the above mentioned and accounting that AGRs and LGRs will never be built again, these two reactors' types will not be considered in the following comparison. Also, SFRs will not be compared to PWRs/BWRs/PHWRs, because only three of them are in operation in Russia and China, and just a couple of them are planned to be built in China and India and might be in other countries in the future.

Therefore, first comparison is PWRs vs. BWRs (see [Table A1.5](#)).

The second comparison is PWRs vs. PHWRs (CANDU-type reactors) (see [Table A1.6](#)), and [Table A1.7](#) lists technical and deployment advantages and disadvantages of PHWR-type reactors.

TABLE A1.5 Major similarities and differences between PWRs vs. BWRs

No.	Major features	
	PWRs	BWRs
1	Reactor design – reactor pressure vessel	
	Pressures up to 15-16 MPa	Pressures up to 7.2 MPa
	BWR RPV diameter and height can be larger than those in PWRs, but wall thickness is smaller	
	Bundle strings (assemblies) quite similar with vertical orientation and a large number of fuel elements (rods)	
	Control and shut-down rods installed from the top of RPV;	Control and shut-down rods installed from the bottom of RPV;
	Control rods are moved with electrical motors; Shut-down rods are kept in the upper position with magnetic lock, dropped down by gravity force (initial acceleration is due to a compressed spring) (passive-safety system)	Control and shut-down rods are moved with electrical motors or/and hydraulic mechanism
	Batch refueling	
	Fuel enrichment of 3-5% (can be up to 20% for SMRs)	Fuel enrichment of 1.9-2%
2	Reactor coolant and moderator – light water, no separation between them	
	Non-boiling reactor coolant	Boiling reactor coolant
	Small changes of water density from inlet to outlet of RPV	Significant changes of water density from inlet to outlet of RPV
	At the RPV outlet – subcooled water with maximum temperatures up to $\sim 330^{\circ}\text{C}$ or $\sim 15\text{--}25^{\circ}\text{C}$ below saturation temperature	At the RPV outlet – saturated water-steam mixture with maximum temperatures up to 287.7°C
3	Wide range of installed capacities from 30 MW_{el} (SMRs) and up to 1660 MW_{el}	Smaller range of installed capacities from 150 MW_{el} and up to 1435 MW_{el}

TABLE A1.5 Major similarities and differences between PWRs vs. BWRs—cont'd

No.	Major features	
	PWRs	BWRs
4	Power cycle – subcritical-pressure Rankine steam-turbine cycle with primary saturated steam and secondary overheated steam (secondary steam is heated with primary steam)	
	Indirect (double loop)	Direct (single loop)
5	Thermal efficiency up to 37% (38%)	Thermal efficiency up to 34%

TABLE A1.6 Major differences and similarities between PWRs vs. PHWRs (CANDU-type reactors)

No.	Major features	
	PWRs	CANDU [®] -type reactors
1	Pressure vessel	Pressure channel or pressure tube
2	Vertical bundle strings	Horizontal fuel channels
3	Relatively long bundle strings (~4 m)	Short bundles (495.3 mm each, 12 bundles per channel)
4	Bundle-string cross section - square or hexagonal	Bundle cross section - circular
5	Large number of fuel elements (rods) in bundle string, e.g., 17 × 17	Relatively small number of fuel elements (rods) in bundle - usually, 37 el., proposed 43 el.
6	Reactor coolant/moderator – H ₂ O (light water), no separation between them	Reactor coolant – D ₂ O (heavy water), Moderator - D ₂ O (heavy water), reactor coolant - inside fuel channel, moderator - outside
7	Higher P_{out}/T_{out} inside reactor: 15.5 MPa/330°C	Lower P_{out}/T_{out} inside reactor: 9.9 MPa/310°C
8	Higher P_{in}/T_{in} to turbine inlet: 7.72 MPa/292°C (EPR)	Lower P_{in}/T_{in} to turbine inlet: 4.7 MPa/260°C (Enhanced CANDU-6 (EC6))
9	Higher thermal efficiency of NPP: up to 37% (38%)	Lower thermal efficiency of NPP: up to 32% (33%)
10	Batch refuelling	Refuelling on-line
11	Fuel enrichment 3-5%	Fuel – natural UO ₂ (enrichment ~0.7%)
12	Wide range of installed capacities from 30 MW _{el} (SMRs) and up to 1660 MW _{el}	Small- and medium-size reactors: 90-880 MW _{el}

One of the unique features of the CANDU[®]-reactor design is its ability to operate with alternative fuels such as a Recovered Uranium (RU) from the reprocessing of LWR spent fuel, MOX (80% UO₂ and 20% PuO₂), and thorium-based fuels, in addition to the conventional natural-uranium fuel.

TABLE A1.7 Technical and deployment advantages and challenges of PHWR-type reactors

No	Advantages
1	Ease of build as does not require large items that can be manufactured by very few heavy industrial plants in the world
2	Mass-flow rates and power shapes can be controlled in individual fuel channels
3	Reactor-coolant flow in pressure channels is interlaced (i.e., in neighboring channels flow has opposite directions), which allowing more uniform axial-density distribution/neutron flux
4	Flexible fuel cycles use natural-uranium plus spent fuel from PWRs and BWRs, and using thorium fuel allow optimum resource use
5	Refuelling on-line provides higher capacity factors compared to batch-refuelling reactors
6	Extra passive-safety system, as liquid-moderator heat sink, separated from reactor coolant
7	Channel and steam generator replacement/refurbishment allow long plant operation
8	Proven performance in fuel and major components have been demonstrated
9	Inherently modular-core design and SMR design
10	Extensive operating and build experience in multiple countries
Challenges	
1	Heavy-water reactor coolant and moderator more expensive than light water and require production facilities
2	Heavy water and natural uranium use gives slightly positive void and power coefficients, necessitating auto-control and two independent and diverse shut-down systems
3	Pressure tubes subjected to creep and sagging, which require their replacement in 20-30 years
4	About 5% of heat is generated in moderator with gamma-rays, which is waste heat at low temperature (taking out with outside cooling water)
5	Non-proliferation issues, because of on-line refuelling and potential plutonium diversion, with potential for mixing civilian with overt or covert military uses
6	Limited additional development potential demonstrated to date and no new prototypes with exception of Indian PHWRs
7	No known or existing long-term high-level-waste repository despite many years of study
8	Significant new build commitment in India, none in Canada
9	Focus on life extension with limited R&D investment in PHWRs
10	Move towards "fashionable" SMR developments has seemingly bypassed Advanced HWRs (AHWRs)

In summary, [Table A1.8](#) provides an overview of a possible “top ten” listing of the Pros (Advantages) and Cons (Disadvantages) for just the five principle general types of classes of reactors still actively involved or being considered in and for the power and energy markets. This [Table A1.8](#) simply contrasts and compares the possible claims and issues for the generic PWR, BWR, PHWR, SFR, and SMR types, but without any distinction or differentiation between the multitude of design details and engineering variations, which have been illustrated in this Chapter.

TABLE A1.8 Technical and deployment advantages and challenges of various types of reactors

No	Advantages	PWR	BWR	PHWR	SFR ^a	SMR ^b (PWR)
1	Known technology, licensing, and siting	✓	✓	✓	✓	✓
2	Low carbon-emissions and environmental footprint	✓	✓	✓	✓	✓
3	Passive-safety systems/features plus independent and diverse shut-down systems	✓	✓	✓	✓	✓
4	Flexible fuel cycles for optimum resource use			✓	✓	✓
5	High-capacity factors demonstrated	✓	✓	✓	✓	✓
6	Known operating and maintenance costs	✓	✓	✓	✓	✓
7	Components and steam-generator replacement/refurbishment allow long plant operation	✓	✓	✓	✓	N/A
8	Proven performance in fuel, systems, and major components demonstrated	✓	✓	✓		
9	Inherently modular-core design			✓		✓
10	Extensive operating and build experience in multiple countries	✓	✓	✓	✓	
Challenges						
1	Specialized production and major manufacturing facilities	✓	✓		✓	
2	High initial investment and build costs plus low efficiency	✓	✓	✓		
3	Circuit materials/components subjected to radiation and ageing, necessitating eventual replacement	✓	✓	✓	✓	✓
4	Non-proliferation issues, and potential fissile diversion, with mixing civilian with overt or covert military uses			✓	✓	✓
5	Limited additional development potential demonstrated to date and no new prototypes			✓		

Continued

TABLE A1.8 Technical and deployment advantages and challenges of various types of reactors—cont'd

No	Challenges	PWR	BWR	PHWR	SFR	SMR (PWR)
6	No known or existing long-term high-level waste repository despite many years of study	✓	✓	✓	✓	✓
7	Lack of significant new build commitment		✓	✓	✓	✓
8	Focus on life extension with limited R&D investment	✓	✓	✓		N/A
9	Move towards “fashionable” or unproven SMR developments	✓	✓	✓	✓	✓
10	Prior major core-melt accidents	✓	✓	-	✓	-

Note: A check mark (✓) indicates the possession of the numerically listed advantage or disadvantage by that reactor type.

^aSFR data are mainly based on limited Russian and some other countries (France, Japan, etc.) experiences.

^bSMR data are mainly based on limited Russian experience.

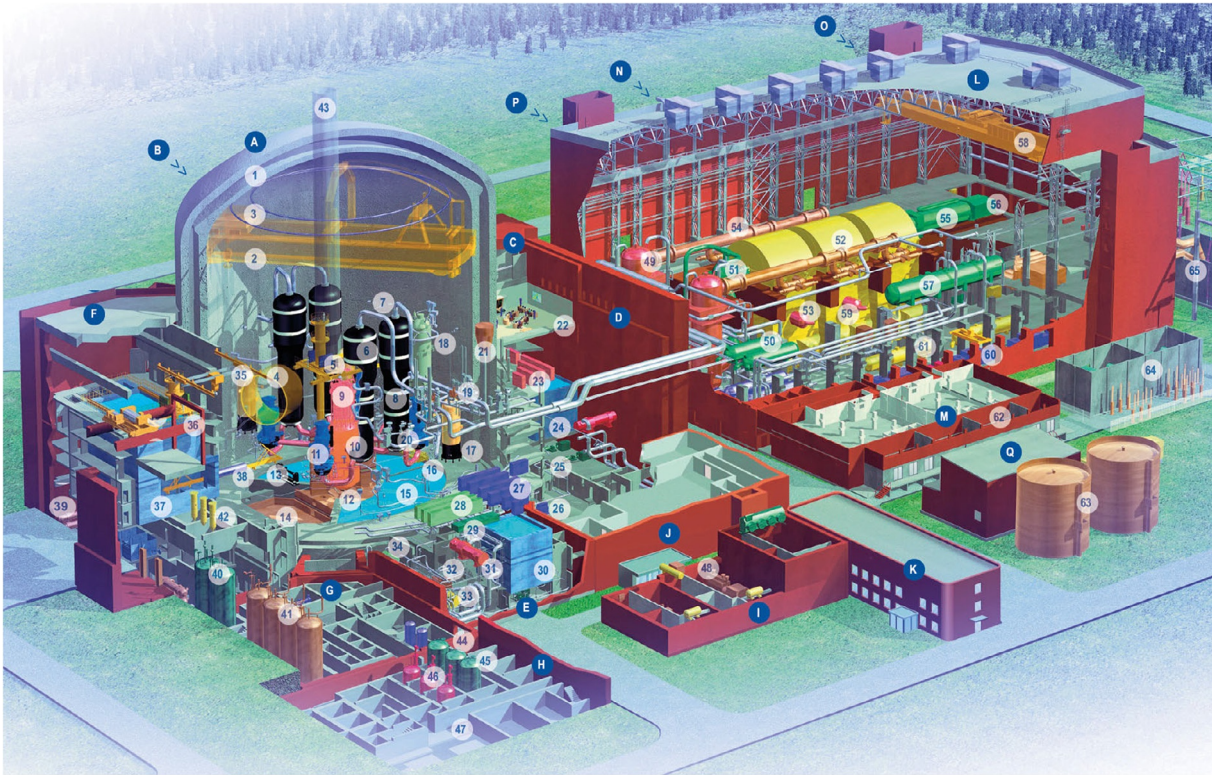
And, possibly, the final feature, which influences a decision for implementation of a type of reactor, is reactors/NPPs generation changing due to technological advances, accumulated operational knowledge, and design evolutions. Currently, we have nuclear-power reactors mainly of Generation-III. However, from 1990s, reactors of Generation-III⁺ have been built. The first ones were ABWRs built and put into operation in Japan. However, nowadays, advanced PWRs of Generation-III⁺ are being built around the world. Major differences between Generation-III⁺ and III are as the following:

- (1) In general, NPPs with Generation-III⁺ reactors have slightly higher thermal efficiencies (see [Table A1.1](#)) compared to those of the same type-reactor NPP of Generation-III.
- (2) Generation-III⁺ reactors are usually equipped with passive-safety systems (see [Figs. A1.38, A1.39, and A1.42](#)), which enhance safety and molten core (corium) catcher (see [Figs. A1.26, A1.55, and A1.56](#)).
- (3) Generation-III⁺ reactors are designed for operation of 60 years compared to 30-45 years of Generation-III reactors (however, currently, in USA and other countries some Generation-III reactors have received operational terms extensions up to 60 years and even up to 80 years!).

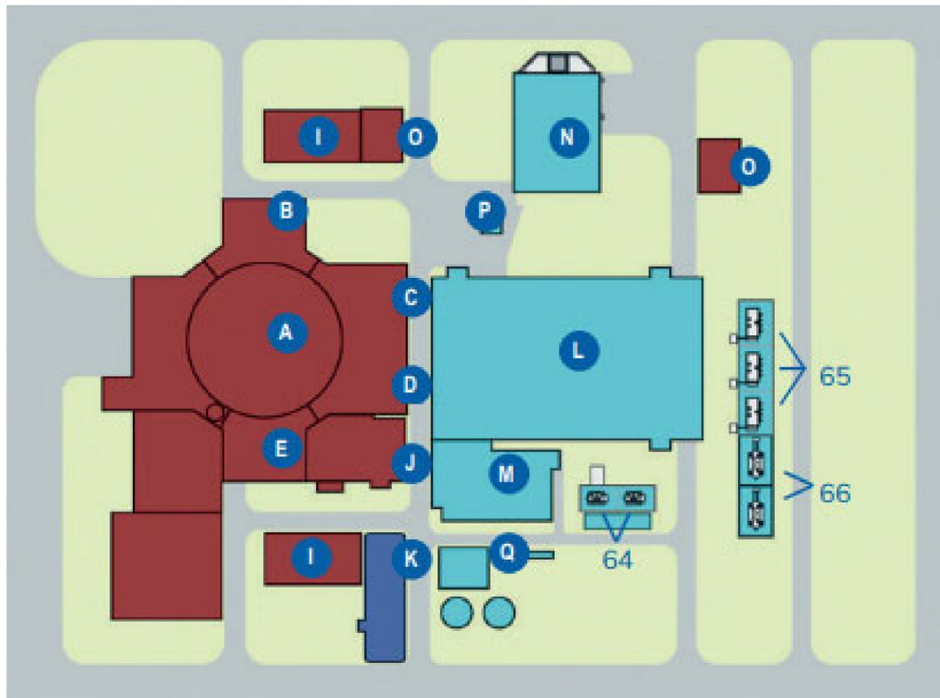
A1.3.3.3 Modern nuclear-power reactors and plants: Design features

Accounting on the available information in the open literature and figures provided by the U.S. NRC and major nuclear vendors/operators (AREVA/EDF (France), Doosan/KHNP (S. Korea), Mitsubishi Heavy Industries (MHI) (Japan); Sanmen Nuclear Power Company, Ltd. (China); Westinghouse Electric Company LLC (USA); Rosatom/Rosenergoatom (Russia), TVO (Finland)), it was decided to show the following reactors and NPPs below:

- EPR NPPs (Generation-III⁺) (France) in Finland and China (see [Figs. A1.24–A1.35](#) and [Tables A1.9 and A1.10](#));



(a)



(b)

FIG. A1.24 See figure legend on next page

FIG. A1.24 General layout of 1,600-MW_{el} Olkiluoto-NPP EPR, Unit 3, (https://www.tvo.fi/material/collections/20210119110706/7NTOAyMN7/OL3_juliste_500x700_FI_2019_ok_1.1.pdf):

(a) detailed general layout and (b) location of major buildings.

A - Reactor (containment) building: 1 - Inner and outer shell; 2 - Polar crane; 3 - Containment heat-removal system (sprinklers); 4 - Equipment hatch; 5 - Re-fueling machine; 6 - Steam generator; 7 - Main steam lines; 8 - Main feed-water lines; 9 - Reactor Control-Rod Mechanism (RCRM); 10 - Reactor Pressure Vessel (RPV); 11 - Primary-circuit main-circulation pump; 12 - Primary-circuit cooling piping; 13 - Primary Circuit Volume-Control System (CVCS) (heat exchangers); 14 - Corium (molten-core) spreading area; 15 - In-containment refuelling water-storage tank; 16 - Residual heat-removal system (heat exchanger); 17 - Reactor-emergency-cooling system (pressure accumulator); 18 - Primary-circuit pressurizer; 19 - Main-steam isolation valves; 20 - Supply-water valves; 21 - Safety of main steam-system outflow of pressure-relief valves; **B - Safety-system building 1;** **C - Safety-system building 2:** 22 - Main-control room; 23 - Computer room; 24 - Emergency-supply-water tank; **D - Safety-system building 3:** 25 - Emergency-feed-water pump; 26 - Medium-pressure safety-injection pump; **E - Safety-system building 4:** 27 - Electrical area; 28 - I & C cabinets; 29 - Battery rooms; 30 - Emergency-feed-water tank; 31 - Closed-Cooling-Water-System (CCWS) heat exchanger; 32 - Low-pressure emergency-injection pump; 33 - Containment-cooling system (heat exchanger (sea-water side)); 34 - Containment-heat-removal-system heat exchanger; **F - Fuel building:** 35 - Fuel-building crane; 36 - Fuel-transfer machine; 37 - Fuel tanks; 38 - Fuel-transfer tube; 39 - Fuel-tank cooling system (heat exchanger); **G - Nuclear auxiliary building:** 40 - and 41 - Primary-circuit cooling-water storage tanks; 42 - Exhaust-gas delay tank; 43 - Vent stack; **H - Radioactive-waste processing building:** 44 - Wastewater-collection tank; 45 - Control tanks; 46 - Concentration tanks; 47 - Waste-barrel storage; **I - Emergency-diesel-generator building:** 48 - Emergency-power diesels; **J - Entrance building;** **K - Office building;** **L - Turbine building:** 49 - Interconnector; 50 - High-pressure feedwater heaters; 51 - High-pressure turbine; 52 - Low-pressure turbines; 53 - Condensers; 54 - Overflow pipes for steam; 55 - Electrical generator; 56 - Magnetizer; 57 - Supply-water tank; 58 - Main crane of turbine building; 59 - Low-pressure water-heaters; 60 - Supply-water pumps; 61 - Low-pressure water-heaters; **M - Switching-plant building;** 62 - Transformers; **N - Seawater-pumping station;** **O - Certified marine-water-system pumping station;** **P - Pumps building;** **Q - Auxiliary steam-boiler building;** 63 - Full salt-extracted water-storage tanks; 64 - Backup-feed transformer; 65 - Main transformers; to the right beyond Figure: 66 - Transformers; 67 - Clutch field; and 68 - High-voltage lines. *Courtesy of TVO, Finland*

- APR-1400 NPPs (Generation-III⁺) in South Korea (see Figs. A1.36 and A1.37 and Table A1.11);
- AP1000 (Generation-III⁺) Westinghouse Electric Company LLC (USA) (see Figs. A1.38–A1.40 and Table A1.12);
- Typical US PWR NPP (Generation-III) (see Fig. A1.41 and Table A1.13);
- MHI (Japan) Advanced PWR NPP layout and typical PWR fuel assembly (see Figs. A1.42–A1.44);
- VVER NPPs (Generations-III and III⁺) in Russia (see Figs. A1.45–A1.66 and Tables A1.14 and A1.15);

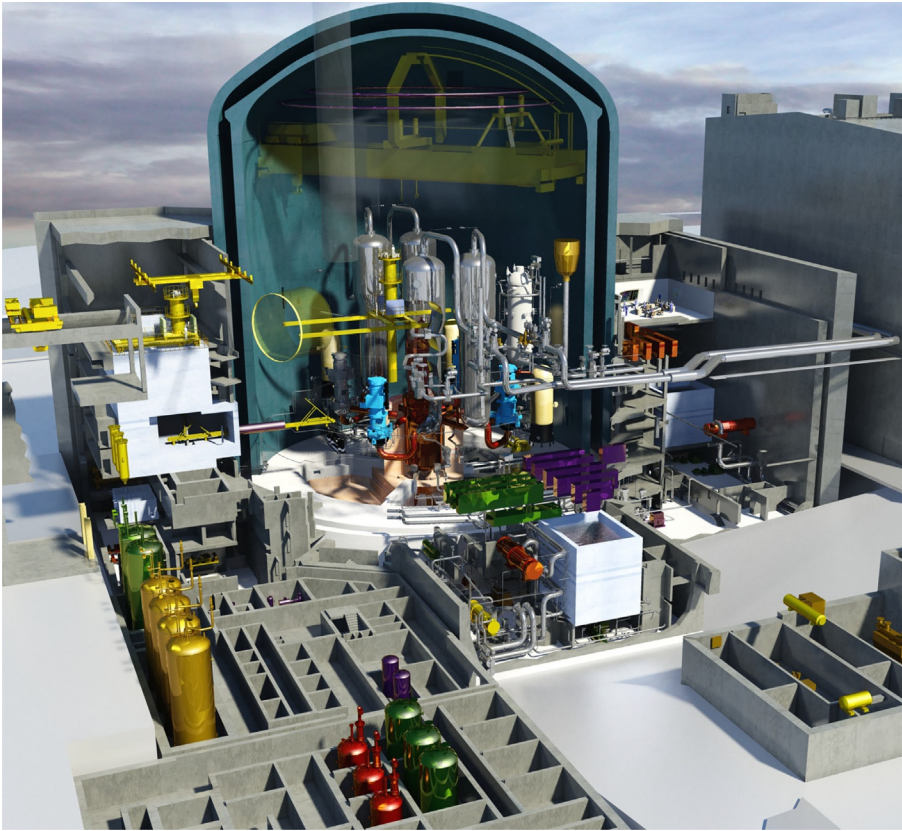


FIG. A1.25 General layout of EPR and its major components inside containment building and other buildings with NPP equipment nearby. *Courtesy and copyright of EDF Energy*

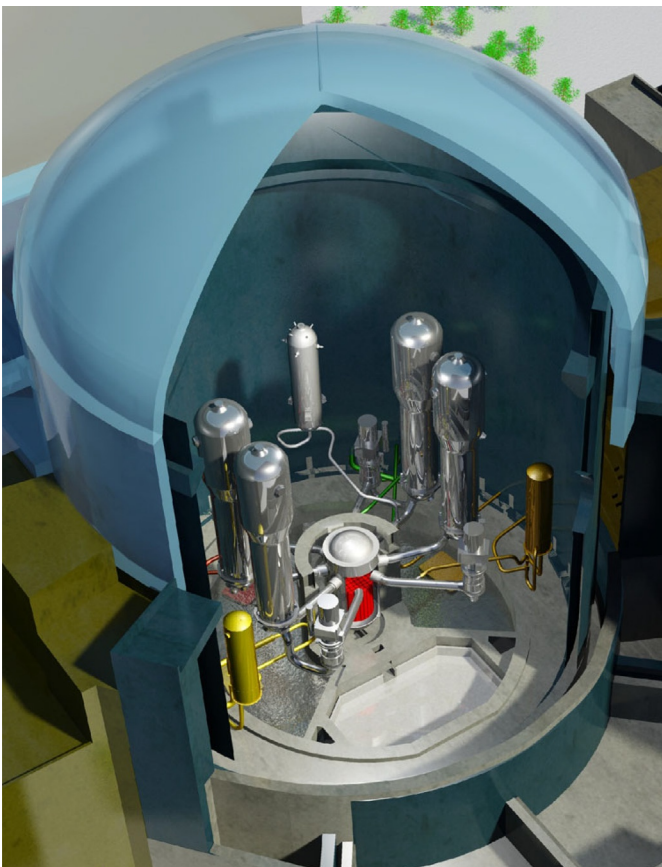


FIG. A1.26 General layout of EPR and its major components inside containment building: In front of reactor (in red color) - water-cooled pool for corium in case of severe accident (ultimate passive-safety feature). *Courtesy and copyright of EDF Energy*

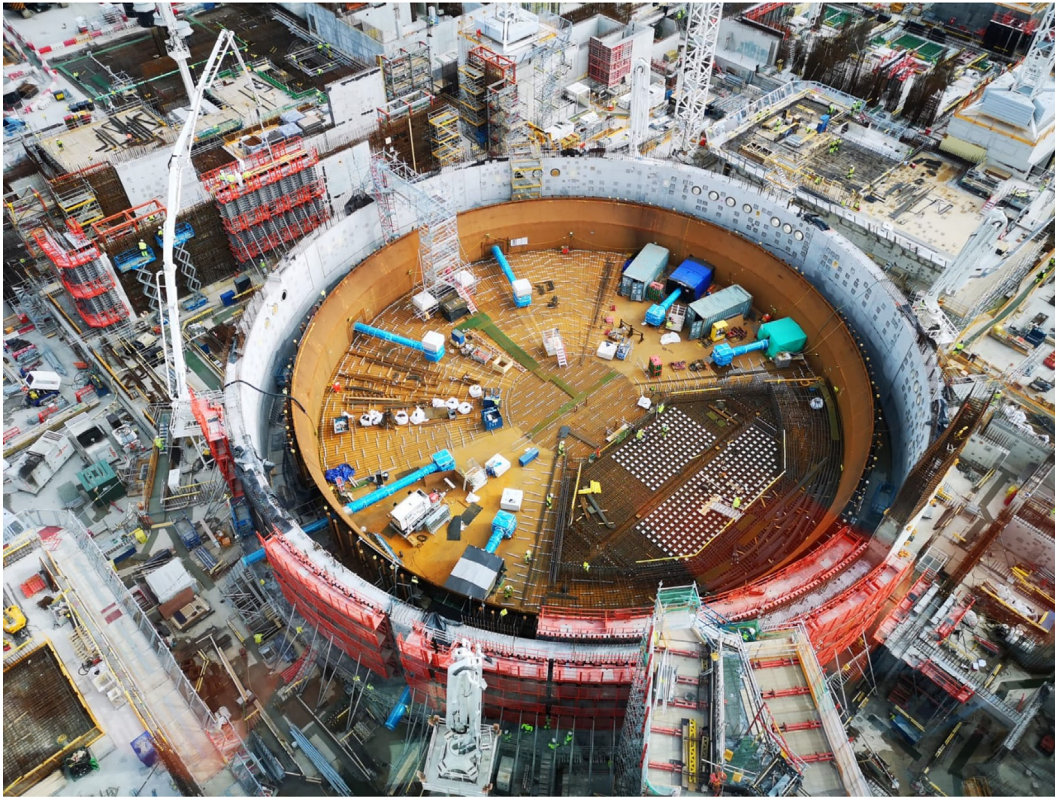


FIG. A1.27 Aerial view of containment building – beginning of construction (<https://www.edfenergy.com/media-centre/news-releases/new-engineering-design-centre-strengthens-britains-nuclear-expertise>). A number of years ago, it was found that construction time can be significantly decreased if containment building is constructed at the same time with all internals (i.e., reactor itself and its equipment) level (floor) by level with help of heavy cranes. *Courtesy and copyright of EDF Energy*

- Typical US BWR NPP (Generation-III) (see Fig. A1.67 and Table A1.16);
- ABWR NPPs (Generation-III⁺) Hitachi-GE Nuclear Energy Ltd. and Toshiba (Japan) (see Figs. A1.68–A1.73 and Table A1.17);
- PHWR NPPs (Generations-III and III⁺) AECL/Candu Energy (Canada) and Siemens (Germany/Argentina) (see Figs. A1.74–A1.84 and Tables A1.18–A1.20);
- AGR NPP (Generation-III) (UK) (see Figs. A1.85–A1.87);
- VHTR concept (HTR-PM SMR) (China) (see Figs. A1.88–A1.91, 3.6, 14.8 and Tables A1.21, 3.6, 14.1);
- LGR NPPs (Generations-III and II) (RBMK and EGP) (Russia) (see Figs. A1.92–A1.97 and Table A1.22); and
- SFR NPP (Generations-III and III⁺) OKBM by the name of Afrikantov/Rosatom (Russia) (see Figs. A1.98–A1.113 and Tables A1.23 and A1.24)

It should be noted that in all NPPs with PWRs, ABWRs, BWRs, PHWRs, and LGRs subcritical –pressure Rankine steam-turbine cycle is used (for details, see Table 1.2.4 in Chapter 1.2). Primary steam is a saturated steam at the corresponding pressure. For the reheat the primary saturated steam is used. Therefore, the reheat temperature is lower than the primary steam temperature.

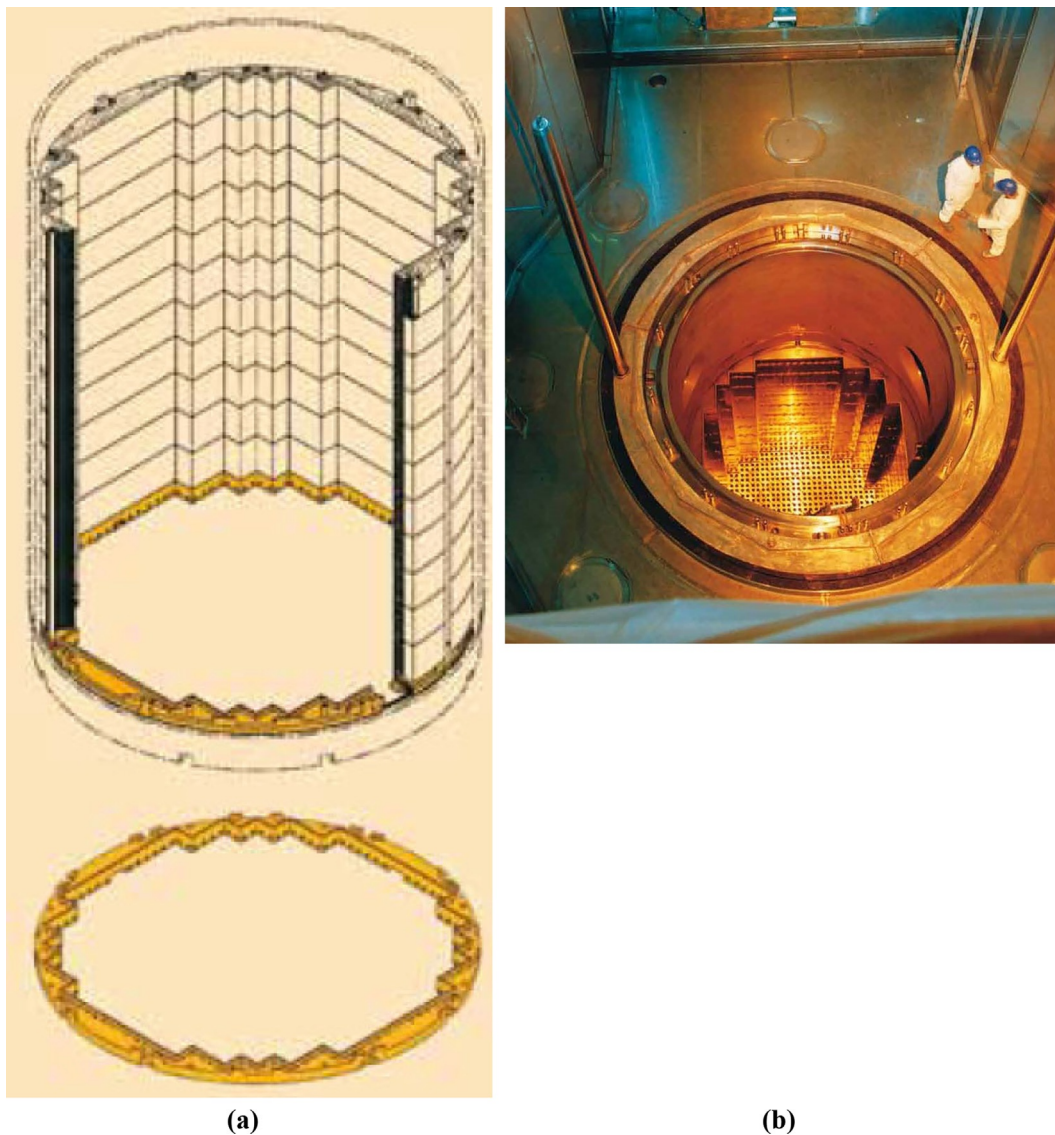


FIG. A1.28 Neutron reflector: (a) artist image and (b) photo of RPV internals with flow tube and neutron reflector (<http://www.ftj.agh.edu.pl/~cetnar/epr/EPR-broszura.pdf>). Neutron reflector is a stainless-steel structure, surrounding core, made of rings piled up one on top of the other. It is innovative feature that gives significant benefits: by reducing flux of neutrons escaping from core, reflector ensures that greater neutron fraction is available to take part in chain-reaction process. Result is improved fuel utilisation, making it possible to decrease the fuel-cycle cost by reducing flux of neutrons escaping from core, reflector protects Reactor Pressure Vessel (RPV) against aging and embrittlement induced by fast-neutron fluence, helping to ensure 60-year design life of EPR™ RPV. Also, for more details, see Fig. A1.50. *Courtesy and copyright by Areva (EDF)*

In general, the primary-steam and secondary-steam parameters at NPPs are significantly lower than those at thermal power plants. Due to this, thermal efficiencies of these NPPs equipped with water-cooled reactors are lower than those of NPPs equipped with AGRs and LMFBRs (SFRs), and significantly lower than those of modern advanced combine-cycle and supercritical-pressure thermal power plants.

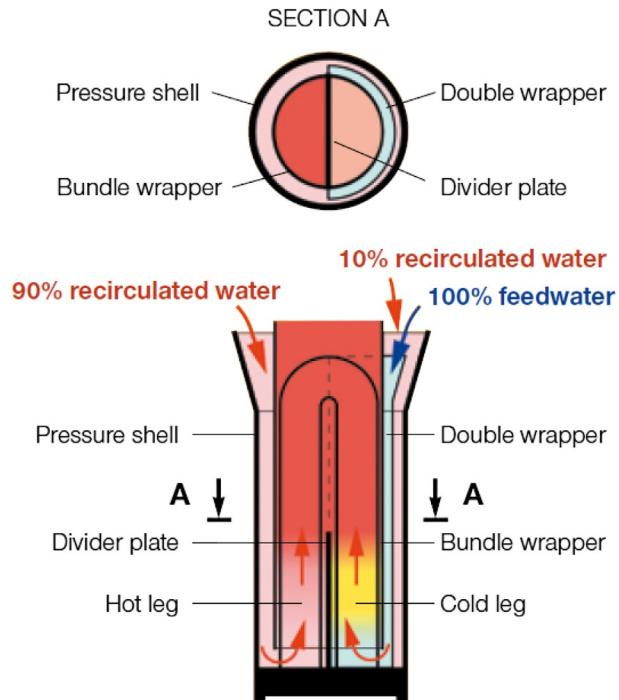


FIG. A1.29 Axial economizer (steam generator). To increase heat-transfer efficiency, axial economizer directs 100% of cold feedwater to cold leg of tube bundle, and about 90% of hot recirculated water to hot leg. This is done by adding wrapper to guide feedwater to cold leg of tube bundle and partition plate to separate cold leg from hot leg. This design improvement increases steam pressure by about 0.3 MPa compared to conventional steam generator. *Courtesy and copyright by AREVA (EDF)*

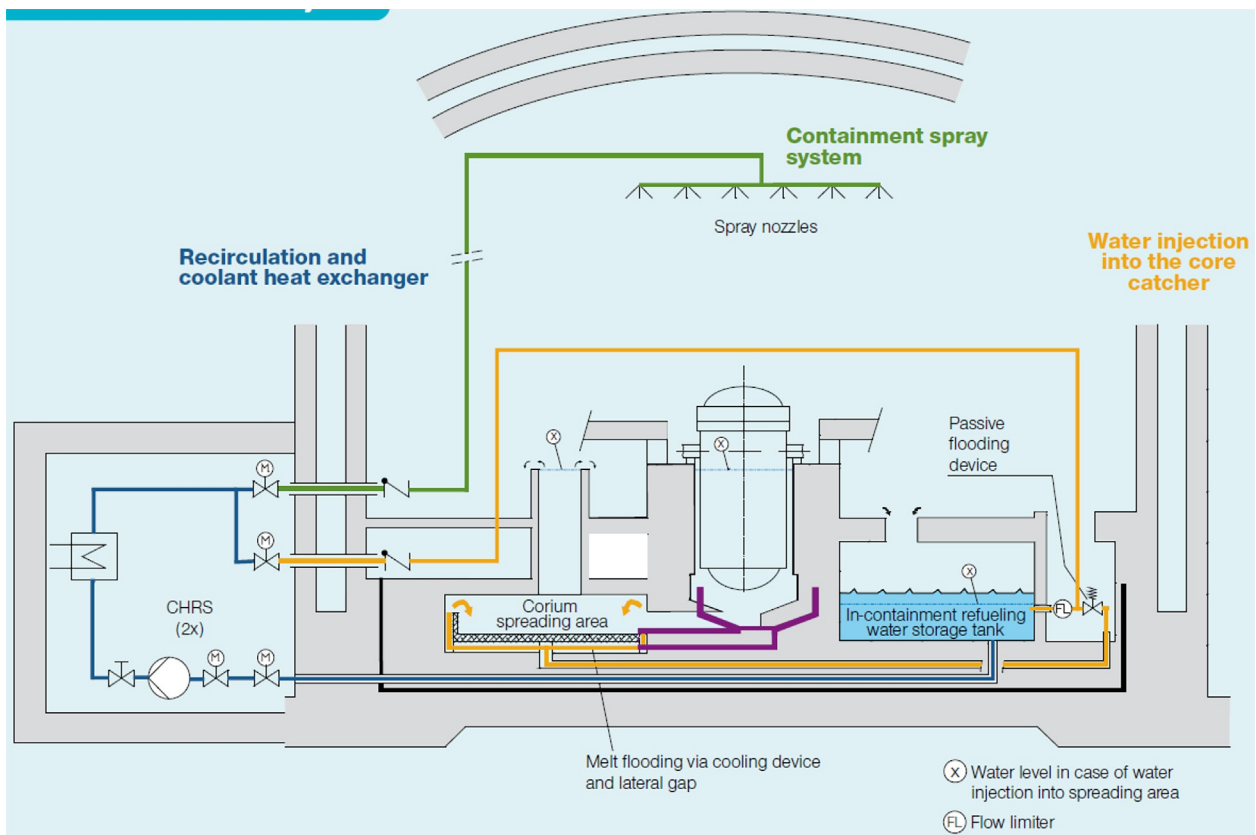


FIG. A1.30 Containment Heat-Removal System (CHRS). Two fully redundant trains with specific diversified heat sink. *Courtesy and copyright by AREVA (EDF)*



FIG. A1.31 Spent-fuel pool. HPC is currently moving through planning process to change interim-waste-storage method from wet store to dry store. *Courtesy and copyright by AREVA (EDF)*

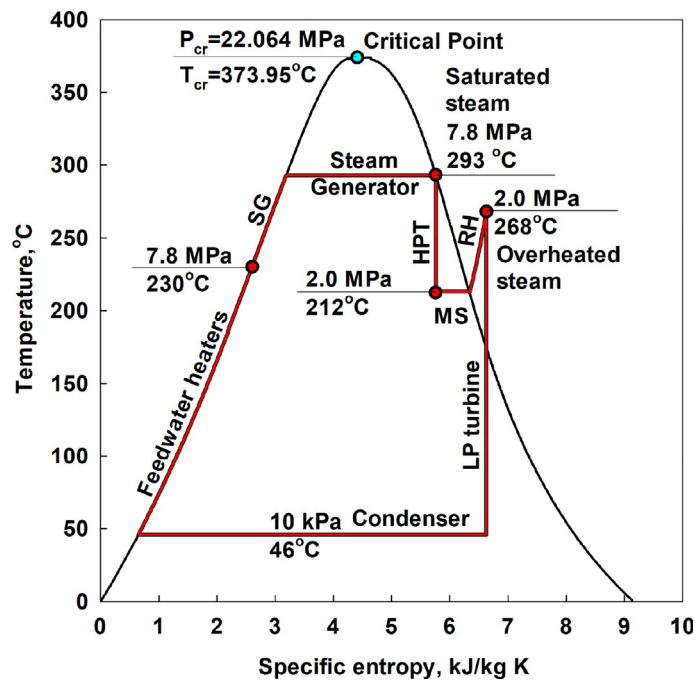


FIG. A1.32 Simplified Temperature (T) vs. Specific Entropy (s) diagram of EPR subcritical-pressure saturated-steam Rankine power cycle with secondary steam reheat: SG – Steam Generator; HPT – High-Pressure Turbine; MS – Moisture Separator; RH – ReHeater; and LP – Low Pressure

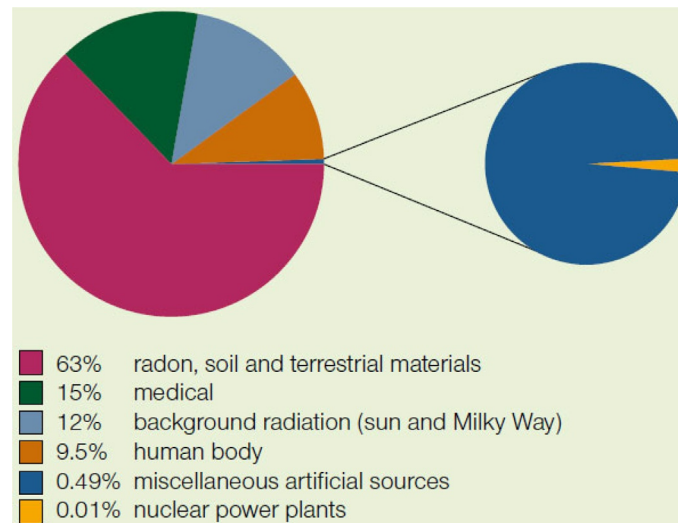


FIG. A1.33 Typical distribution of annual dose to population from all sources. *Courtesy and copyright by AREVA (EDF)*



FIG. A1.34 Taishan Nuclear Power Plant, Units 1 & 2, Guangdong, China (year 2020): (<https://www.edfenergy.com/media-centre/news-releases/chinas-second-epr-reactor-taishan-enters-commercial-operation>). Taishan Units 1 and 2 are largest in world nuclear-power reactors. These two reactors based on 1,750-MW_{el} EPR design (net installed capacity is 1,660 MW_{el}, i.e., 90 MW_{el} are used for internal needs (~5% of nominal capacity); NPP gross thermal efficiency – 38% and net – 36%), which were connected to grid in Dec. 2018 and Sept. 2020, respectively. They form part of EUR 8.0 billion (USD 9.7 billion) contract signed by Areva (France) and China General Nuclear Power Group (CGNPG) (China) in Nov. 2007. The EPR design adopted in Taishan was developed by Framatome (France). These EPRs are equipped with Arabelle generators, which are largest single-piece electric generators in world, each weighing 495 tonnes and built by Dongfang Electric. *Courtesy and copyright of EDF Energy. Based on: <https://www.world-nuclear-news.org/Articles/Chinese-EPR-experiences-performance-issue> and https://fr.xco.wiki/wiki/Taishan_Nuclear_Power_Plant*



FIG. A1.35 Shown part of control hall: 1,600-MW_{el} EPR, Olkiluoto NPP, Finland (connected to grid in March 2022). *Courtesy of TVO (Teollisuuden Voima Oyj), Finland*

TABLE A1.9 Technical data summarizing design parameters of Evolutionary Power Reactor (EPR) (see Figs. A1.24–A1.35.)

Number of EPRs in the world	
1,660-MW _{el net} 2 Units in operation from 2018 and 2019 (Taishan, China) and 1,600-MW _{el net} one Unit in operation from 2022 (Olkiluoto, Finland); 1,630-MW _{el net} one Unit planned to put into operation in 2024 (Flamanville, France) and 2 units - in 2026 and 2027 (Hinkley Point, UK)	
General-plant data	
Parameter	Value
Reactor thermal output	4,590 MW _{th}
Gross power-plant output	1,770 MW _{el}
Net power-plant output	1,660 MW _{el}
Gross/Net power-plant efficiency	38.6%/36.2%
Mode of operation	Baseload and Load follow
Plant-design life	60 years
Plant availability target	> 92%
Seismic design, SSE	0.25

Continued

TABLE A1.9 Technical data summarizing design parameters of Evolutionary Power Reactor (EPR) (see Figs. A1.24–A1.35.)—cont'd

Primary coolant/Moderator	Light water
Secondary coolant	Light water
Thermodynamic cycle	Rankine
Type of cycle	Indirect
Safety goals	
Core-damage frequency	$< 10^{-6}$ /Reactor-Year
Large early release frequency	$< 10^{-7}$ /Reactor-Year
Occupational radiation exposure	< 0.35 Person-Sv/R Y
Nuclear steam-supply system (NSSS)	
Steam flow rate at nominal conditions	2,604 kg/s
Steam pressure/saturation temperature (T_{sat})	7.72 MPa(a)/292.5°C
Feedwater flow rate at nominal conditions	2,630 kg/s
Feedwater temperature	230°C
Reactor-coolant system (RCS)	
Primary coolant flow rate	33,978 kg/s
Reactor operating pressure (saturation temperature, T_{sat})	15.5 MPa(a) (344.8°C)
Core-coolant inlet temperature	295.2°C
Core-coolant outlet temperature	330°C
Reactor core	
Active core height	4.2 m
Average linear heat rate	16.67 kW/m
Fuel	UO ₂ and MOX
Outer diameter of fuel rods	9.5 mm
Rod array of fuel assembly	17×17
Number of fuel assemblies	241
Total number of fuel rods	69,649
Enrichment of reload fuel at equilibrium core	4.95% _{weight}
Fuel-cycle length	24 months
No of RCCAs (Rod Cluster Control Assemblies)	89

TABLE A1.9 Technical data summarizing design parameters of Evolutionary Power Reactor (EPR) (see Figs. A1.24–A1.35.)—cont'd

Burnable absorber (strategy/material)	Gd ₂ O ₃
Control-rod absorber material	Hybrid (AIC/B ₄ C)
Soluble neutron absorber	H ₃ BO ₃
Reactor-pressure vessel (RPV)	
Cylindrical-shell ID	4,870 mm
Cylindrical-shell wall thickness	250 mm
Design pressure	17.6 MPa(a)
Design temperature	351°C
Base material	16MND5
Total height, inside	13.083 m
Transport weight	520 t
Steam generator/heat exchanger	
Type	U-tubes with axial economizer
Number	4
Total tube outside-surface area	7,960 m ²
Number of heat-exchanger tubes	5,980
Tube OD	19 mm
Tube material	Inconel 690
Transport weight	550 t
Reactor coolant pump (primary circulation system)	
Pump type	Shaft seals
Number of pumps/loops	4
Pump speed	1,500 rpm
Head at rated conditions	102.1 m
Volumetric flow at rated conditions	7.87 m ³ /s or 28,332 m ³ /h
Pressurizer	
Total volume	75 m ³
Steam volume (working-medium volume) at full power	35 m ³
Steam volume (working medium volume) at zero power	50 m ³
Heating power of heater rods	2,600 kW

Continued

TABLE A1.9 Technical data summarizing design parameters of Evolutionary Power Reactor (EPR) (see Figs. A1.24–A1.35.)—cont'd

Primary containment	
Overall shape (cylindrical/spherical)	Cylindrical
Diameter	46.8 m
Height	57.5 m
Design pressure	0.55 MPa
Design temperature	170°C
Design leakage rate	0.3% _{volume} /day
Residual heat-removal systems	
Active/Passive systems	Active
Safety-injection systems	
Active/Passive systems	Active and Passive
Turbine	
Turbine speed	1,500 rpm
Generator	
Voltage	24 kV
Frequency	50 Hz
Feedwater pumps	
Number	3

Based on data from: <https://aris.iaea.org/PDF/EPR.pdf>.

TABLE A1.10 Technical data of 1,600-MW_{el} EPR (early design option), Olkiluoto NPP, Finland (<https://www.tvo.fi/en/index/production/plantunits/ol3.html>)

Framatome ANP's 1600-MW_{el} EPR was selected as the preferred reactor based on operating cost, also, Siemens was selected to provide the turbines and generators. TVO signed a fixed-price EUR 3.2 billion turnkey contract with Areva NP and Siemens for the unit in Dec. 2003, and construction started in 2005. Commercial operation was originally scheduled for 2009, but the project has encountered various delays and setbacks (<https://www.world-nuclear-news.org/Articles/Europe-s-first-EPR-reaches-criticality>). Finally, it was put into operation in March of 2022.

Parameter	Value
Reactor thermal output	4,300 MW _{th}
Net power-plant output	1,600 MW _{el}
Net thermal efficiency of plant	37.2%

TABLE A1.10 Technical data of 1,600-MW_{el} EPR (early design option), Olkiluoto NPP, Finland (<https://www.tvo.fi/en/index/production/plantunits/ol3.html>)—cont'd

Annual electricity output approximately	13 TW h
Reactor operating pressure	15.5 MPa
Number of fuel assemblies	241
Fuel	Uranium dioxide (UO ₂)
Fuel consumption	32 t/year
Total fuel weight	128 t
Number of control elements	89
Containment-building height/diameter	63 m/57 m
Main steam temperature	290°C
Number of turbines	1 HP + 3 LP
Rated speed of the turbine	1,500 rpm for 50 Hz frequency
Sea water flow rate	57 m ³ /s

Basic parameters of all current reactors' types are listed in Table 1.2.3 (Chapter 1.2).

Advanced Pressurized Water Reactors (APWRs) and PWRs

The largest group of all nuclear-power reactors, i.e., 309 from 443 or 69% and the most built type of reactors as of today and in the nearest future (for details, see Chapter 1.2).

EPR (EDF, France) EPR - Evolutionary Pressurised-water Reactor; previously - European Pressurised-water Reactor or European Power Reactor. EPR is the Generation-III⁺ reactor or APWR developed by the French nuclear vendor Framatome, later on, by Areva, and, nowadays, nuclear-part of Areva belongs to EDF. The largest PWR in the world by the installed capacity: Two 1660-MW_{el net} EPRs are in operation in China, Taishan NPP (see Fig. A1.34) (commercial operation from Dec. 2018 and Sep. 2019); one 1600-MW_{el net} EPR is in operation in Finland, Olkiluoto NPP (see Figs. A1.24–A1.26 and A1.35) (commercial operation from March 2022); one 1630 MW_{el net} is under construction in France, Flamanville NPP, and two with the same installed capacity – in UK, Hinkley Point NPP. The closest competitors by the installed capacities are two 1500-MW_{el net} PWRs located at the Chooz NPP, France (commercial operation from 2000) and two 1495-MW_{el net} PWRs located at the Civaux NPP, France (commercial operation from 2002). Also, it should be mentioned that EPR NPP has the highest thermal efficiency of 36.2%/38.6% (net/gross) compared to any other light- and heavy-water-cooled reactors NPPs! This is mainly due to the highest inlet pressure (7.8 MPa) and corresponding to that the highest saturation temperature (~293°C) of the primary steam (see Tables A1.1 and A1.9 and Fig. A1.32). The following Figs. A1.24–A1.35 and Tables A1.9 and A1.10 provide a general overview of EPRs in operation in China and Finland.

EPR as the Generation-III⁺ design is equipped with the water-cooled pool for corium in front of a reactor in the case of severe accident (ultimate passive-safety feature; implementation of this feature into Generation-III⁺ reactors was triggered with the Chernobyl NPP the most severe accident during which it was a serious scare that a high-temperature corium can damage the concrete foundation of the RBMK reactor shaft and drop further down) and with Containment Heat-Removal

Advanced Power Reactor 1400

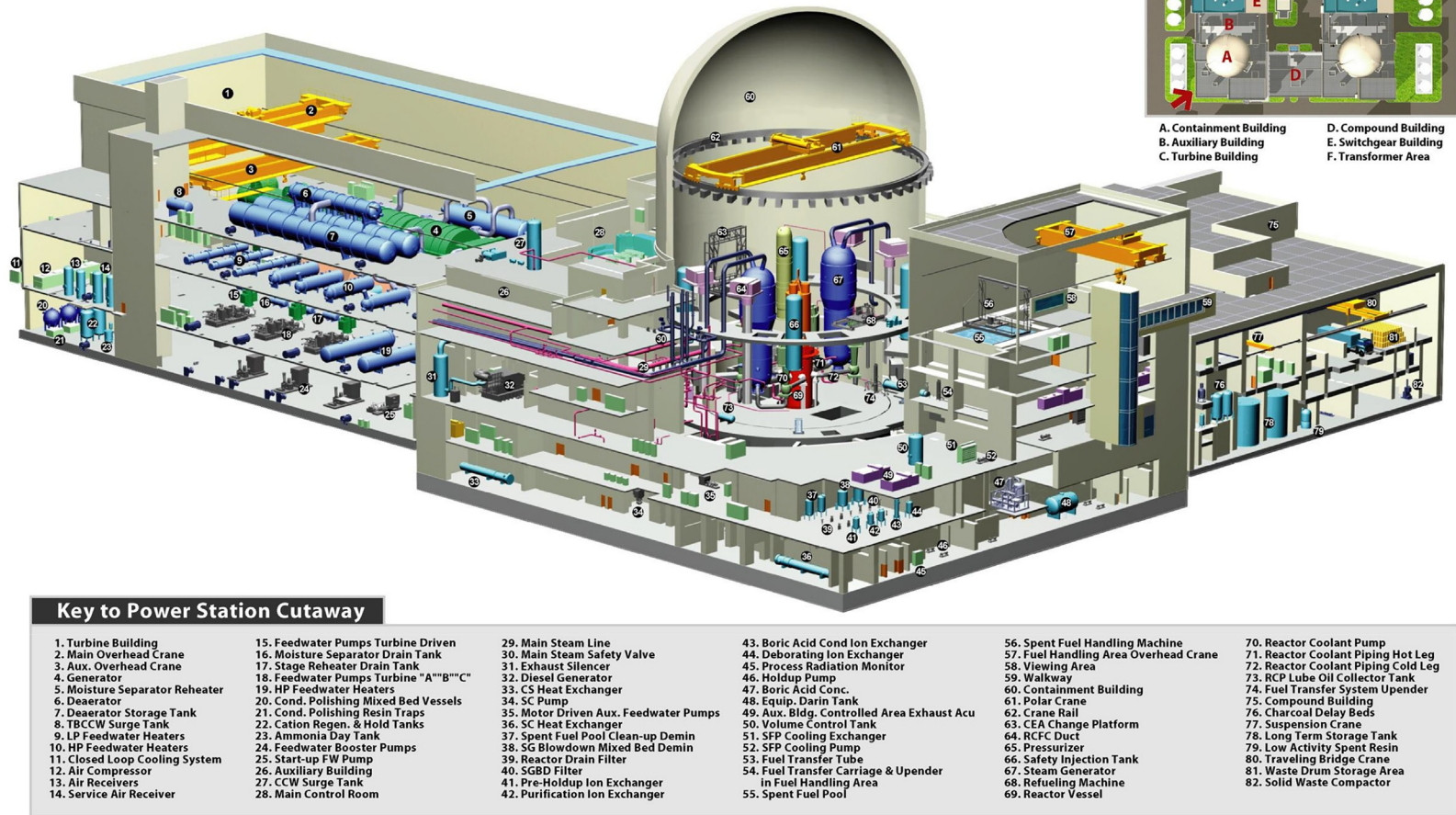


FIG. A1.36

Continued

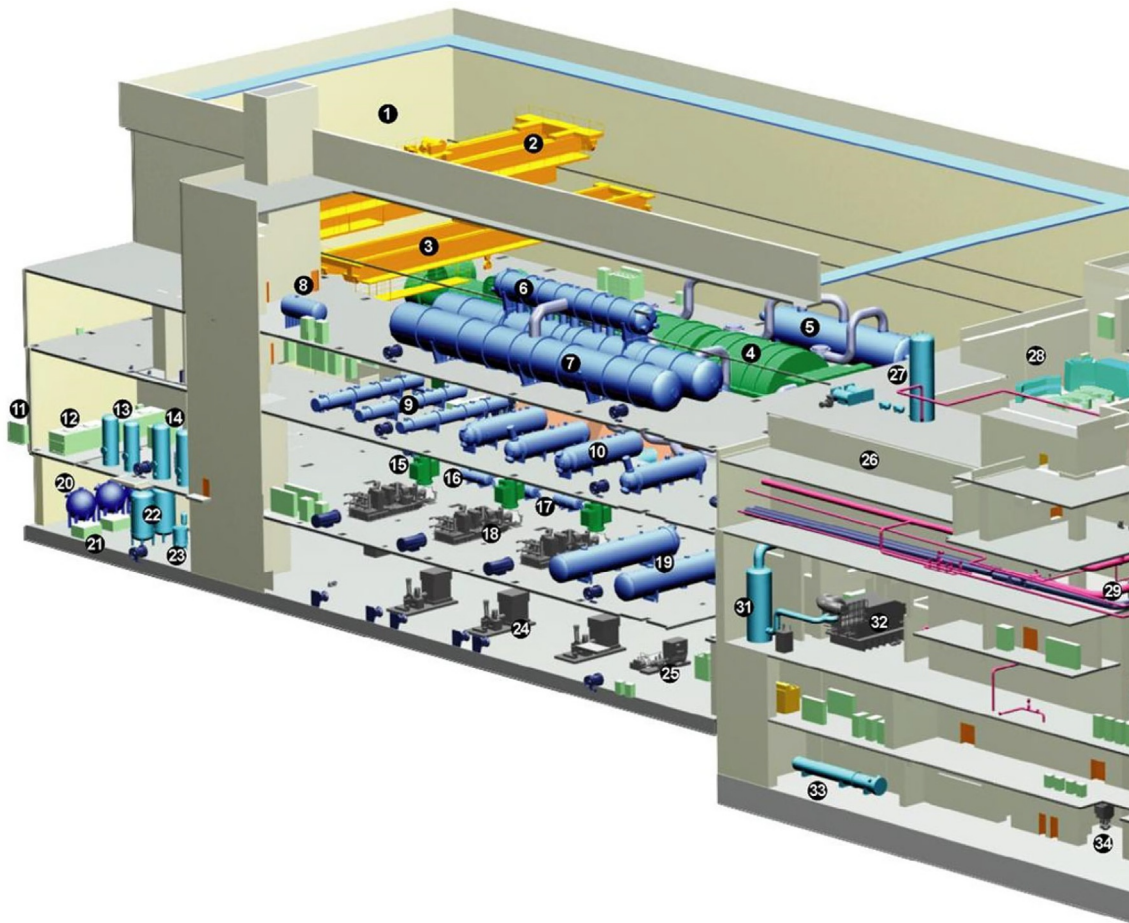


FIG. A1.36, CONT'D

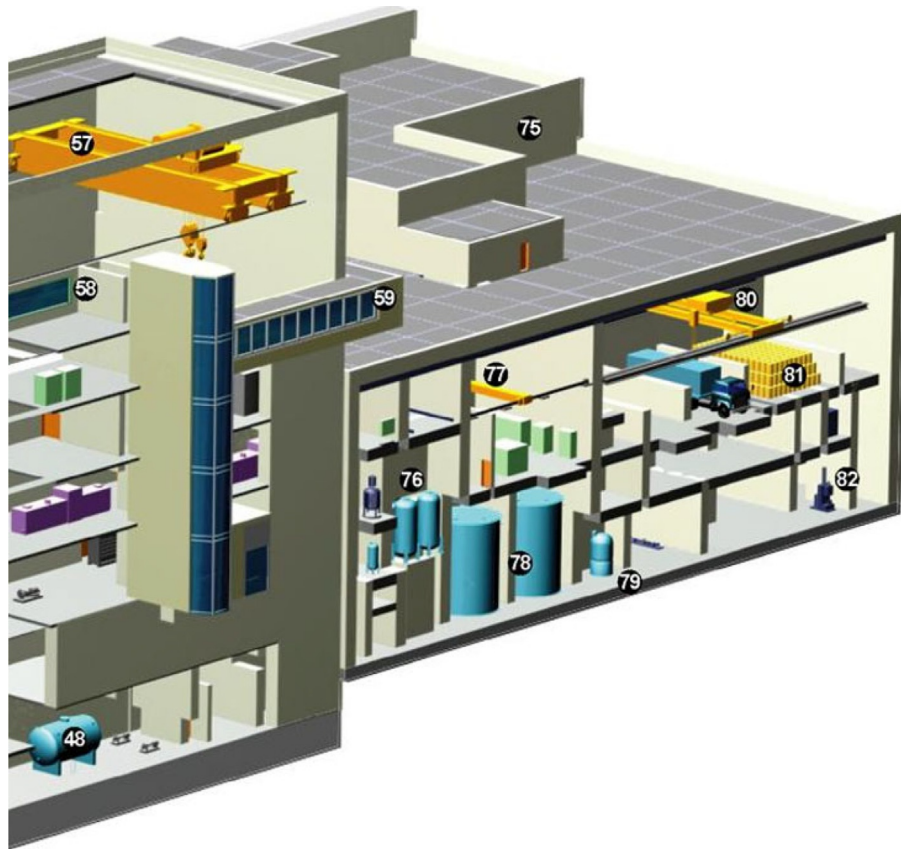


FIG. A1.36 See figure legend on next page

FIG. A1.36 General layout of 1,400-MW_{el} APR-1400 NPP: 1 – Turbine building; 2 – Main overhead crane; 3 – Axillary overhead crane; 4 – Generator; 5 – Moisture-separator and reheater; 6 – Deaerator; 7 – Deaerator-storage tank; 8 – Turbine-Building Closed-Cooling-Water (TBCCW) surge tank; 9 – LP-feedwater heaters; 10 – HP-feedwater heaters; 11 – Closed-loop cooling system; 12 – Air compressor; 13 – Air receivers; 14 – Service-air receiver; 15 – Feedwater pumps turbine-driven; 16 – Moisture-separator-drain tank; 17 – Stage-reheater-drain tank; 18 – Feedwater-pumps turbine A, B, and C; 19 – HP-feedwater heaters; 20 – Condenser polishing mixed-bed vessels; 21 – Condenser-polishing-rasin traps; 22 – Cation-regeneration & hold tank; 23 – Ammonia day tank; 24 – Feedwater (FW) booster pumps; 25 – Start-up FW pump; 26 – Auxiliary building; 27 – Component-Cooling-Water (CCW) surge tank; 28 – Main control room; 29 – Main steam line; 30 – Main-steam safety valve; 31 – Exhaust silencer; 32 – Diesel generator; 33 – Carbon-Steel (CS) heat exchanger; 34 – SC pump; 35 – Motor-driven auxiliary FW pumps; 36 – SC heat exchanger; 37 – Spent-fuel-pool clean-up demin; 38 – SG-blowdown mixed-bed demin; 39 – Reactor-drain filter; 40 – SGBT filter; 41 – Pre-holdup ion exchanger; and 42 – Purification ion exchanger. *Courtesy of KHNP, S. Korea and Dr. D. Hahn (IAEA)*



FIG. A1.37 Shin-Kori Nuclear Power Plant, Units 3 and 4, Ulju-gun, Ulsan, S. Korea. These Units are 1,416- and 1,418-MW_{el} APR-1400 Generation-III+ design put into operation in 2016 and 2019. In addition to these APRs three more will be connected to grid in next three years. Also, three APRs-1400 are currently in operation in UAE, and one more are planned to be connected to grid in next two years. *Courtesy of Korea Hydro & Nuclear Power (KHNP) Company*

System (CHRS) (see Figs. A1.26, A1.27 and A1.30, respectively). Also, it should be pointed out on the neutron reflector installed inside Reactor Pressure Vessel (RPV) internal flow tube or core barrel, which is the important and distinctive feature for all PV reactors, i.e., PWRs and BWRs (see Fig. A1.28). The neutron reflector protects internal flow tube and, especially, RPV from detrimental effects of high neutron flux, which allows to extend operational term of RPV for 60 (several PWRs in Japan, Mexico and some other countries) or 80 (a number of PWRs and BWRs in USA), and might be even, for 100 years (for other benefits of the neutron reflector, see the caption to Fig. A1.28).

TABLE A1.11 Basic parameters of 1345-1418-MW_{el net} APR-1400 (Advanced Power Reactor) (Generation III⁺) PWR (Reactor supplier Doosan, South Korea) ([Handbook of Nuclear Engineering, 2010](#))

Number of APRs in the world

1,415-MW_{el net} 2 Units in operation from 2016 and 2019 (Shin-Kori NPP, S. Korea); 1,340-MW_{el net} 2 Units in operation from 2022 (Shin-Hanul NPP, S. Korea); and 1,345-MW_{el net} 3 Units in operation from 2021 and 2022 (Barakah NPP, UAE); in addition, 1,340-MW_{el net} 2 Units are planned to put into operation in 2023 - 2024 (Shin-Kori NPP, S. Korea) and 1 unit - in 2023 (Barakah NPP, UAE).

Parameter	Value
Reactor core	
Thermal power	3,983 MW _{th}
Electric power	1,400 MW _{el}
Gross thermal efficiency	34–35%
Active fuel length	3.81 m
No of fuel assemblies	241
Fuel assembly array	16 × 16
No of fuels rods in fuel assembly	236
No of fuel rods	56,876
Fuel	UO ₂
Core equivalent diameter	3.65 m
Operation cycle length more than	18 months
Fuel rod outer diameter/sheath-wall thickness	9.5 mm/0.57 mm
Burnable absorber material	Gd ₂ O ₃ -UO ₂
Reactor coolant system	
No of pumps	4
Nominal flow	21,618 m ³ /h
Reactor inlet temperature	291°C
Reactor outlet temperature ($T_{\text{sat}} = 344.8^\circ\text{C}$ at 15.5 MPa)	324°C
Operating pressure	15.5 MPa
Power cycle	
Number of steam generators	4
Steam pressure at full power	6.89 MPa
Stem saturated temperature at full power	285°C

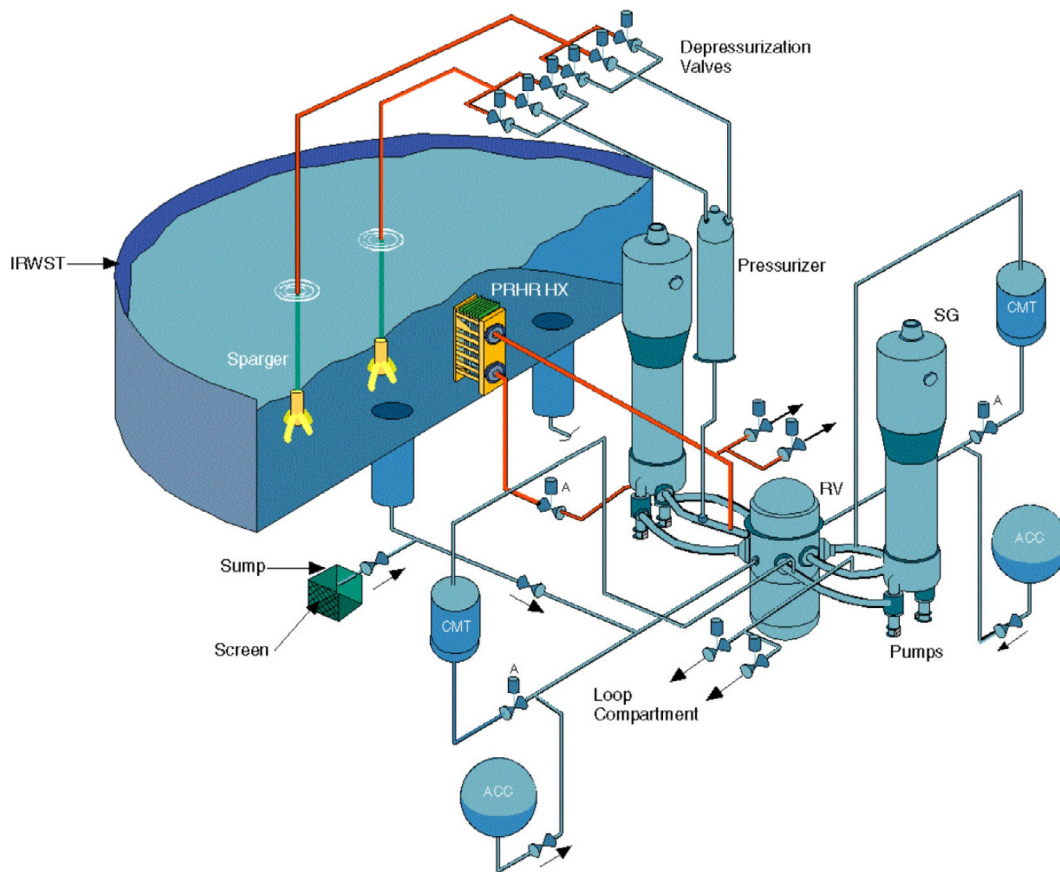


FIG. A1.38 AP1000 (Advanced Passive) Plant Passive-Core-Cooling System (PCCS): ACC – ACCumulator; AP – Advanced Plant; CMT – Core Makeup Tank; IRWST – In-containment Refueling Water Storage Tank; PRHR HX – Passive Residual Heat Removal Heat eXchanger; PCCS – Passive Core Cooling System; RV – Reactor Vessel; SG – Steam Generator (Friedman, 2019; ASME J. NERS). Courtesy of Westinghouse Electric Company LLC

APR-1400 (Doosan, South Korea) APR-1400 is the Advanced Power Reactor of Generation-III⁺ (APWR type) designed by the South Korean nuclear vendor Doosan (see Figs. A1.36 and A1.37, more information on this reactor is provide in the captions to these Figures) and has installed capacities within the range of 1345 – 1418 MW_{el net} (see Table A1.11).

AP-1000 (Westinghouse, USA) AP-1000 is the Advanced Passive plant with the Generation-III⁺ reactor (APWR type) designed by the Westinghouse Electric Company LLC - US nuclear vendor (see Figs. A1.38–A1.40, more information on this reactor is provided in the captions to these Figures) and has installed capacities within the range of 1345 – 1418 MW_{el net} (see Table A1.12).

PWR (USA) USA have 61 PWRs of Generation-III design in operation from the total of 92 reactors (the rest are BWRs). Typical simplified PWR NPP layout is shown in Fig. A1.41, and typical basic parameters in Table A1.13.

Advanced PWR (MHI, Japan) Layout of the 1500-MW_{el net} APWR of the Generation-III⁺ NPP by the MHI (Japan) is shown in Fig. A1.42 and corresponding to that thermodynamic layout of the

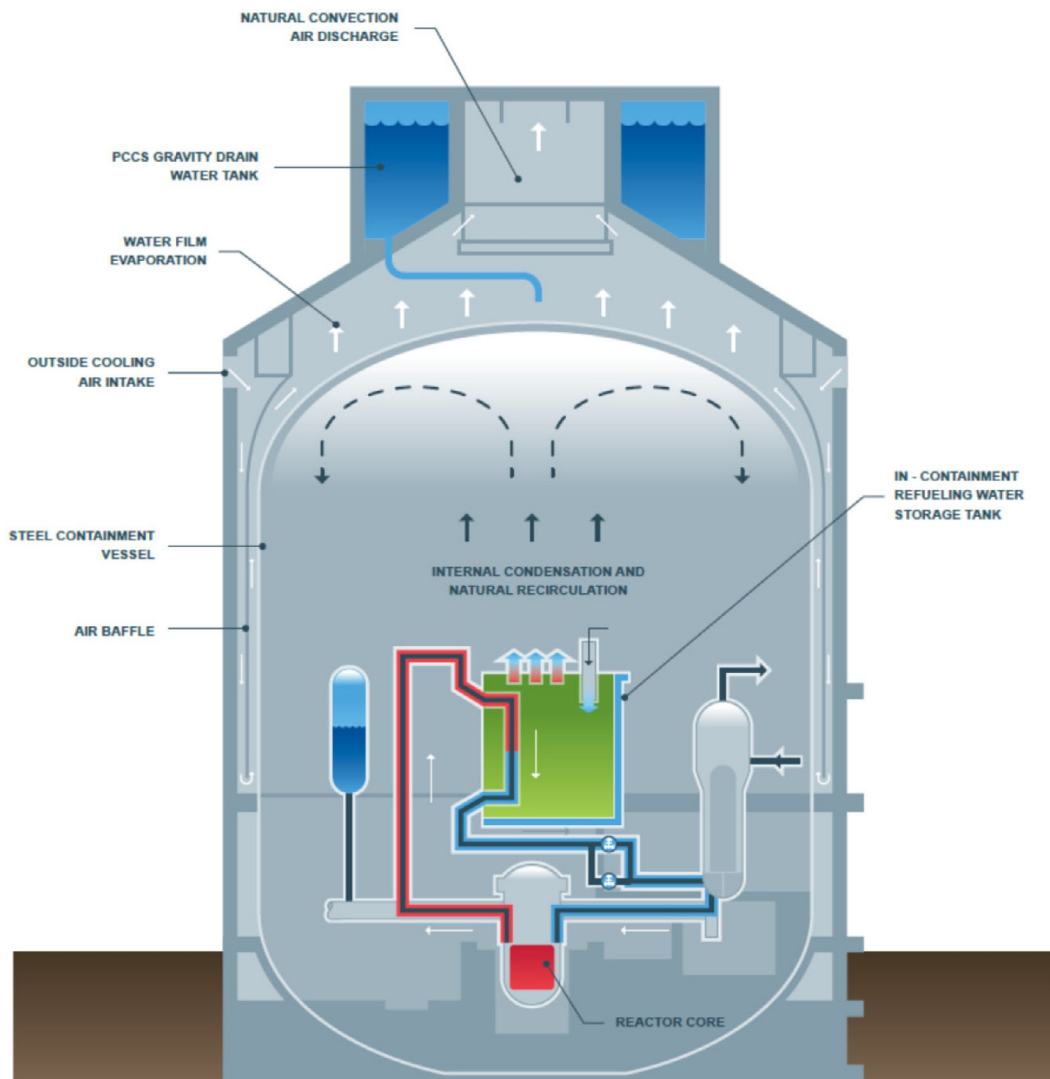


FIG. A1.39 AP1000 Plant Passive-Containment-Cooling System (PCCS) operation. Showcasing major design features and parameters of AP1000[®] Plant (Friedman, 2019; ASME J. NERS). *Courtesy of Westinghouse Electric Company LLC*



FIG. A1.40 Two 1157-MW_{e1} AP1000 reactors (Generation-III+) located in two cylindrical-shape containment buildings (commercial operation from 2018) at Sanmen Nuclear Power Plant (Friedman, 2019; ASME J. NERS). *Courtesy of Sanmen Nuclear Power Company, Ltd*

TABLE A1.12 Showcasing major design features and parameters of AP1000 Plant (Generation-III+)

Number of AP1000 reactors in the world

1,157-MW_{el net} 2 Units in operation from 2018 (Sanmen, China) and 1,170-MW_{el net} 2 Units in operation from 2018 and 2019 (Haiyang, China); 1,100-MW_{el net} 2 Units planned to put into operation in 2022 and 2023 (Vogtle NPP, USA) and one might be in Ukraine (year unknown)

Overall

Installed capacity:

MW_{el net}/MW_{th} - Thermal efficiency, % 1,157 – 1,160/3,400 - ~34%

Plant-design lifetime 60 years

Reactor-coolant system (RCS)

Number of loops 2

Number of Reactor-Coolant Pumps 4 (2 per loop)

RCS operating pressure ($T_{\text{sat}}=344.9^{\circ}\text{C}$) 15.52 MPa abs (2,250 psia)

RCS design pressure 17.24 MPa abs (2,500 psia)

Pressurizer size, total volume 59.5 m³ (2100 ft³)

Secondary side

Secondary side design pressure 8.276 MPa abs (1200 psia)

Core design

Number of Fuel Assemblies (FAs) 157

Type of FAs 17×17 XL

Active length 4.27 m (14 ft)

Average Linear Heat Rate (ALHR) or Linear Heat Flux (LHF) 18.72 kW/m

Number of control rods 69

Total flow rate 68,110 m³/h (299,880 gpm)

Vessel inlet/outlet temperatures 279.7°C (535.5°F)/322.1°C (611.7°F)

U-235 Fuel enrichment (max) 4.95%

Core control

Number and kind of control rods 53 Rod-Cluster Control Assemblies (RCCAs) 16 Gray rod-cluster assemblies

Control principle at rated power Mechanical shim

Continued

TABLE A1.12 Showcasing major design features and parameters of AP1000 Plant (Generation-III+)—cont'd

Primary components

Reactor Pressure Vessel

Material SA-508, SA-533

Size 4.04 m (159 in) Inside Diameter (ID)

Steam Generator

Heat-transfer surface 11,477 m² (123,538 ft²)

Number of tubes 10,025

Courtesy of Westinghouse Electric Company LLC, Cranberry Township, PA, USA (Friedman, 2019; ASME J. NERS).

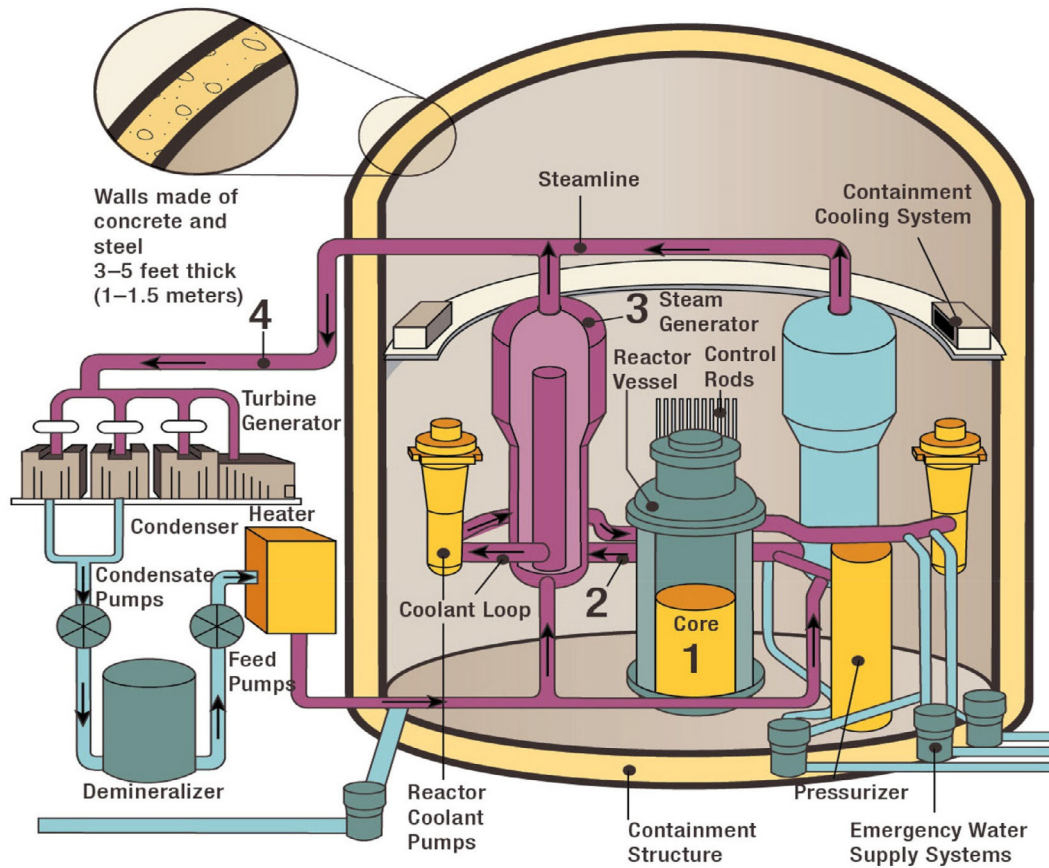


FIG. A1.41 Typical simplified Pressurized-Water-Reactor (PWR) NPP layout. Courtesy of US NRC

TABLE A1.13 Typical basic parameters of US PWR NPP (Generation-III) (tens of these reactors are in operation in the USA and world for tens of years) (Shultis and Faw, 2007)

Parameter	Value
Thermal power, MW _{th}	3800
Electrical power, MW _{el}	1300
Thermal efficiency, %	34
Specific power, kW/kg(U)	33
Power density, kW/Liter	102
Average linear heat flux, kW/m	17.5
Rod heat flux average/max, MW/m ²	0.584/1.46
Core	
Length, m	4.17
OD, m	3.37
Reactor coolant system	
Pressure, MPa	15.5
Inlet temperature, °C	292
Outlet temperature, °C	329
Mass flow rate (m), kg/s	531
Steam generators	
Total number	4
Outlet pressure, MPa	6.9
Outlet temperature, °C	284
Mass-flow rate, kg/s	528
Reactor pressure vessel (RPV)	
OD, m	4.4
Height, m	13.6
Wall thickness, m	0.22
Fuel	
Fuel pellets	UO ₂
Pellet OD, mm	8.19
Rod OD, mm	9.5

Continued

TABLE A1.13 Typical basic parameters of US PWR NPP (Generation-III) (tens of these reactors are in operation in the USA and world for tens of years) (Shultis and Faw, 2007)—cont'd

Parameter	Value
Zircaloy clad thickness, mm	0.57
Rods per bundle (17×17)	264
Bundles in core	193
Fuel loading, ton	115
Enrichment, %	3.2
Reactivity control	
No. of control assemblies	68
Shape	Rod clusters
Absorber rods per assembly	24
Neutron absorber	Ag-In-Cd and/or B ₄ C
Soluble-poison shim	Boric acid H ₃ BO ₃

plant – in Fig. A1.43. Typical fuel-bundle string or assembly of PWR (square cross section) is shown in Fig. A1.44. The MHI have designed and put into operation many Generation-III PWRs with the installed capacities from 550 and up to 1127 MW_{el net}.

PWRs (Russia) Russia has 24 PWRs of Generation-III (see Figs. A1.45–A1.47, A1.50, A1.52, A1.53, A1.60, A1.66a and Table A1.13) and III⁺ (see Figs. A1.48, A1.49, A1.51, A1.55–A1.59, A1.61–A1.65 and Table A1.15) with installed capacities from 32 (two first SMRs) and up to 1100 MW_{el net}. Also, Russia is very active with its PWRs on the international level (for details, see Table 1.2.10 in Chapter 1.2). Russian SMRs – PWRs – KLT-40S (Generation-III) and RITM-200M (Generation-III⁺) (see Fig. A1.66a,b) are described in Chapter 20.2: Figs. 20.2.2–20.2.8, 20.2.10, 20.2.12 and Figs. 20.2.9, 20.2.11, 20.2.12, respectively, and basic parameters for both SMRs are listed in Table 20.2.25.

Boiling Water Reactors (BWRs) and Advanced BWRs (ABWRs)

Accounting on the available information in the open literature and figures provided by major nuclear vendors (Hitachi and Toshiba) and U.S. NRC it was decided to show the following reactors and NPPs as typical representatives of Generation III and III+ BWR NPPs:

- Typical US BWR NPP layout (see Fig. A1.67) and its parameters (see Table A1.16);
- ABWR NPP (Hitachi-GE Nuclear Energy, Ltd., Japan) (see Figs. A1.68–A1.70, A1.73) and comparison of ABWR and BWR basic parameters (see Table A1.17); and
- ABWR NPP (see Figs. A1.71 and A1.72) (based on data from Toshiba company).

BWR (USA) USA have in operation 31 BWRs (installed capacities ranging from 620 and up to 1433 MW_{el net} and all of them are of Generation-III), which approximately twice less than the number of PWRs. All US BWRs were designed by the General Electric company. Also, unfortunately,

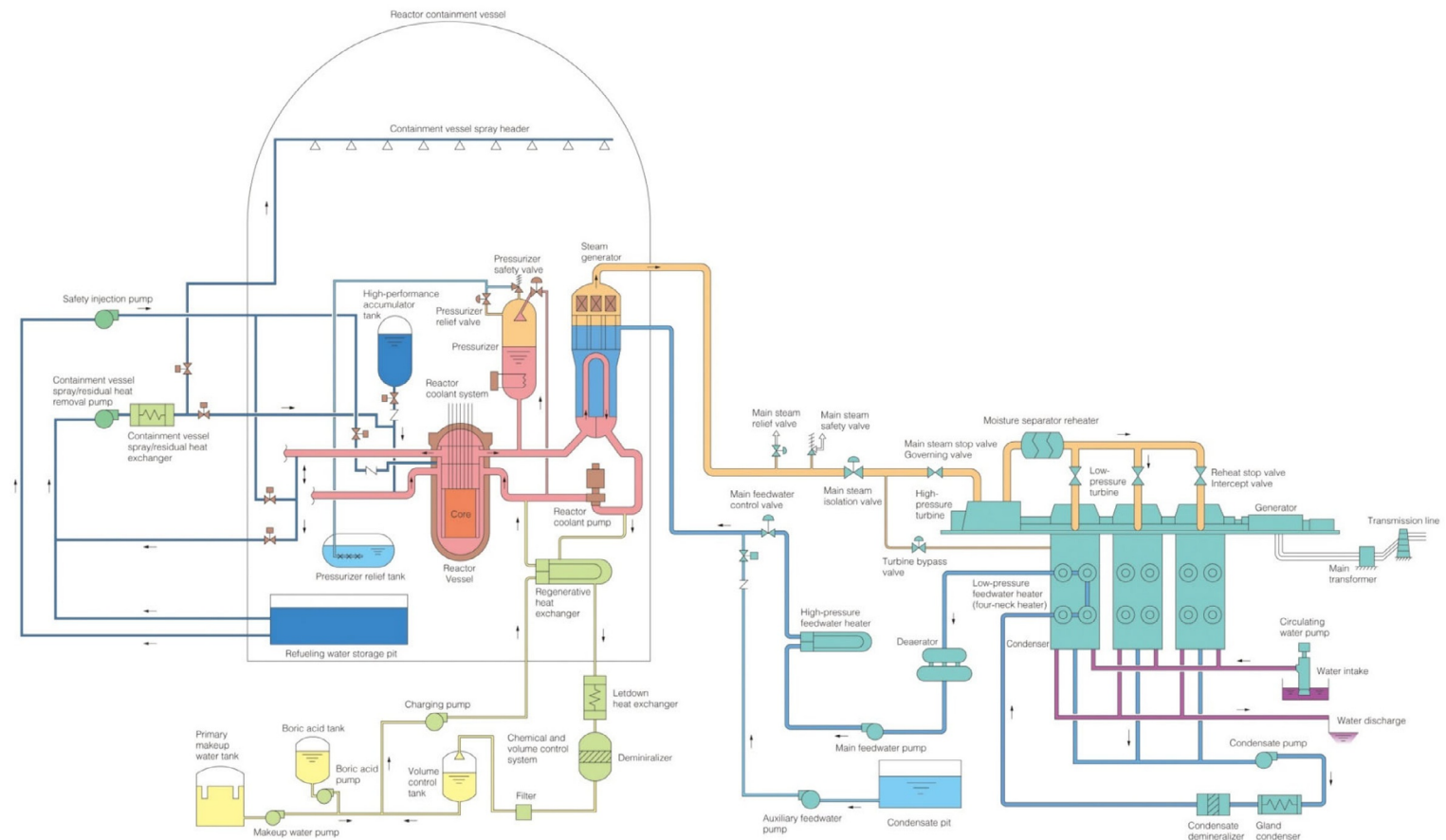


FIG. A1.42 Mitsubishi Heavy Industries (MHI) 1500-MW_{el} Advanced PWR (Generation-III+) NPP simplified layout (has not been built yet) (two-stage reheat cycle). *Courtesy and copyright of MHI*

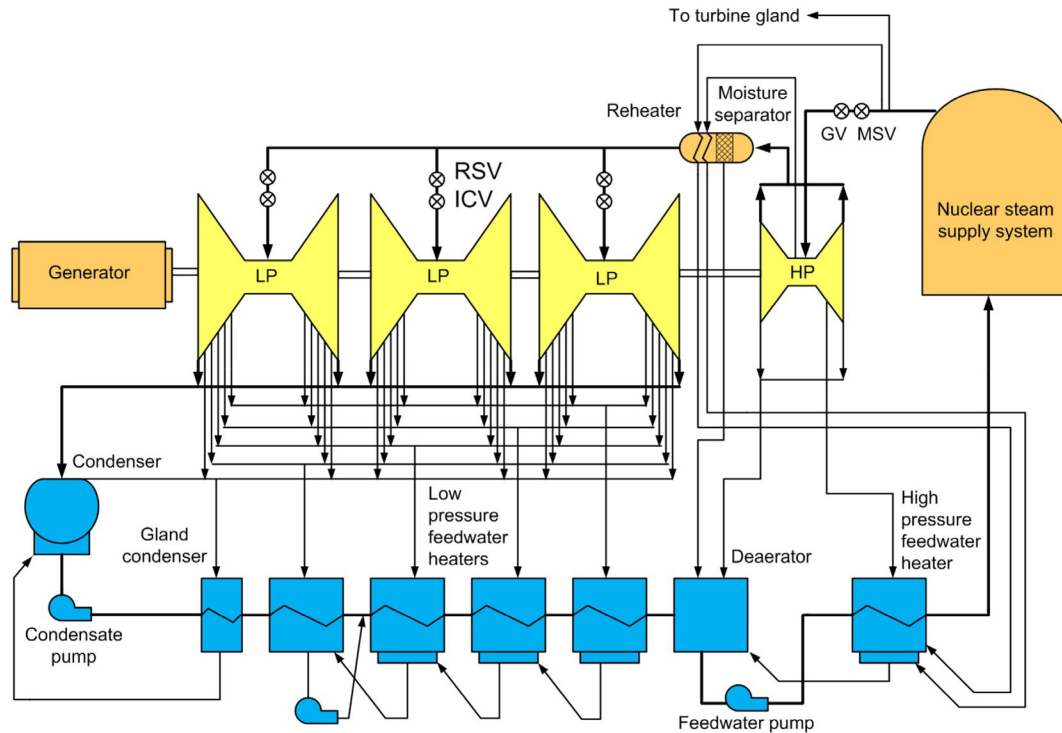


FIG. A1.43 MHI 1500-MW_{el} Advanced PWR (Generation-III+) NPP simplified thermodynamic layout based on subcritical-pressure saturated-steam Rankine power cycle with secondary two-stage steam reheat. *Courtesy and copyright of MHI*

there are no plans to build new BWRs or ABWRs in US. Fig. A1.67 shows simplified layout of a typical BWR NPP (courtesy of US NRC), and Table A1.16 - typical parameters of US BWR (Generation-III).

ABWRs (Japan) Toshiba's ABWR is a reactor that has been in operation since 1996 on the basis of proven technologies of BWRs around the world. In 1996, Unit 6 at the Kashiwazaki-Kariwa NPP was put into operation as the world's first ABWR plant (Generation-III⁺ design) (see Fig. A1.68). In 1997, Unit 7 was started its operation at the same plant. In addition, one ABWR has started operation as Unit 5 at the Hamaoka NPP^c in 2005, and another one as Unit 2 - at the Shika NPP in 2006. In general, Japan has 13 BWRs and 4 ABWRs plus 16 PWRs. However, no one BWR or ABWR was in operation after the Fukushima Daiichi NPP severe accident in March of 2011. As of today, i.e., November 17, 2022, only 6 PWRs are in operation and one is during adjustment operation (for everyday details, see: <https://www.genanshin.jp/db/fm/plantstatusN.php?x=d>).

Aerial view of the Kashiwazaki-Kariwa NPP Units 6 & 7 are shown in Fig. A1.68. Fig. A1.69 shows a simplified layout of an ABWR NPP by the Hitachi-GE Nuclear Energy, Ltd.; and Fig. A1.70 - a simplified layout of a typical ABWR with all internals. Simplified thermodynamic layout of an ABWR NPP (based on data from Toshiba) and the corresponding *T-s* diagram are shown in Figs. A1.71 and A1.72, respectively. Fig. A1.73 provides information on the classification of radioactive wastes and process flow by the Hitachi-GE Nuclear Energy, Ltd.

^c It should be noted that due to the earthquake and tsunami disaster in Japan in March of 2011, which resulted in the Fukushima NPP accident, all left after this accident Japanese 48 reactors have been shut down. Recently, i.e., January of 2016, just a couple of reactors have been restarted.

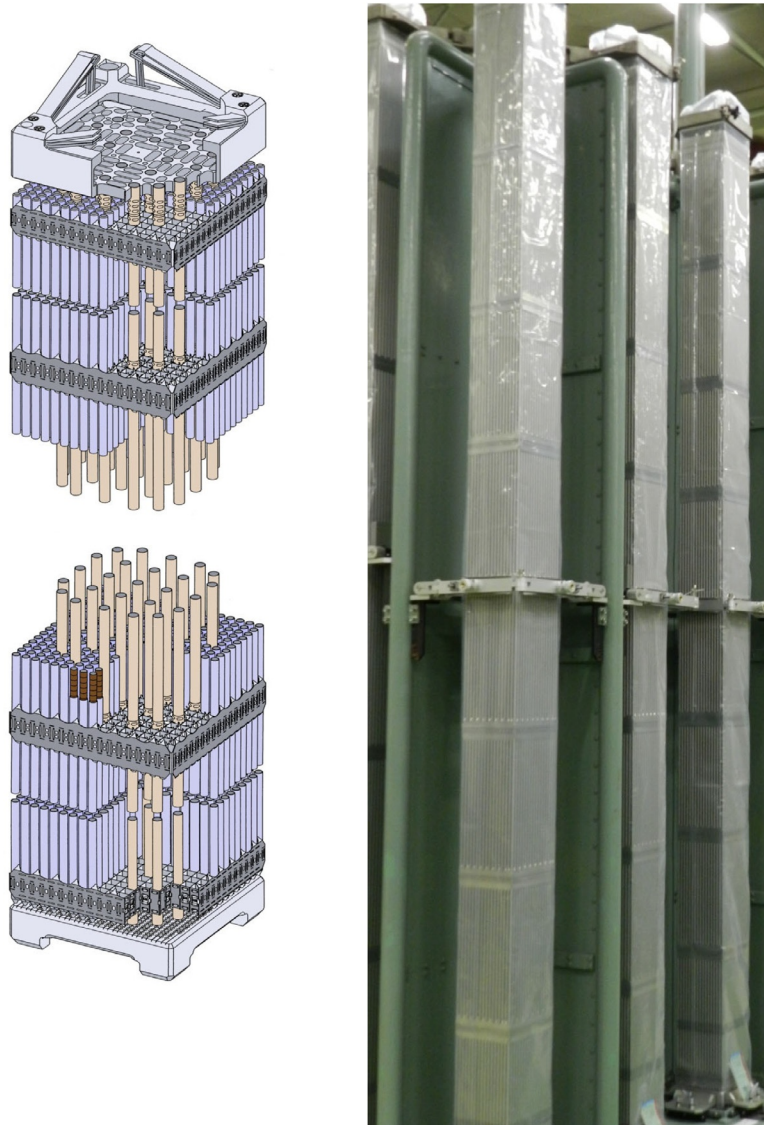


FIG. A1.44 Fuel-bundle string or assembly of PWR (square cross section). *Courtesy & copyright by MHI*

From the thermodynamic point of view, if you have high-temperature medium, i.e., a reactor coolant, then a direct power cycle (single loop) will have certain advantages compared to that of an indirect cycle with the double loop and a heat exchanger (steam generator) in between them in terms of thermal efficiency (there is a temperature drop through steam generator), space and costs of a steam generator. However, due to significantly higher pressures and temperatures inside PWRs compared to ABWRs/BWRs (see [Table A1.1](#) Items 8 and 10), PWR power cycle has higher saturation pressure and temperature compared to that of ABWR/BWR, due to that PWR NPP has slightly higher thermal efficiency. On another hand, the Fukushima Daiichi NPP severe accident, which had happened with older design of BWRs, showed that double loop, i.e., indirect cycle, has enhanced safety. Possibly due to this there are no plans to build new ABWRs/BWRs in the world with the exception of Japan (based on [Nuclear News \(2022\)](#)). However, even in Japan only two ABWRs were planned to be built, but currently, there is no definite dates for their commercial start, i.e., “Commercial start – Indefinite”.

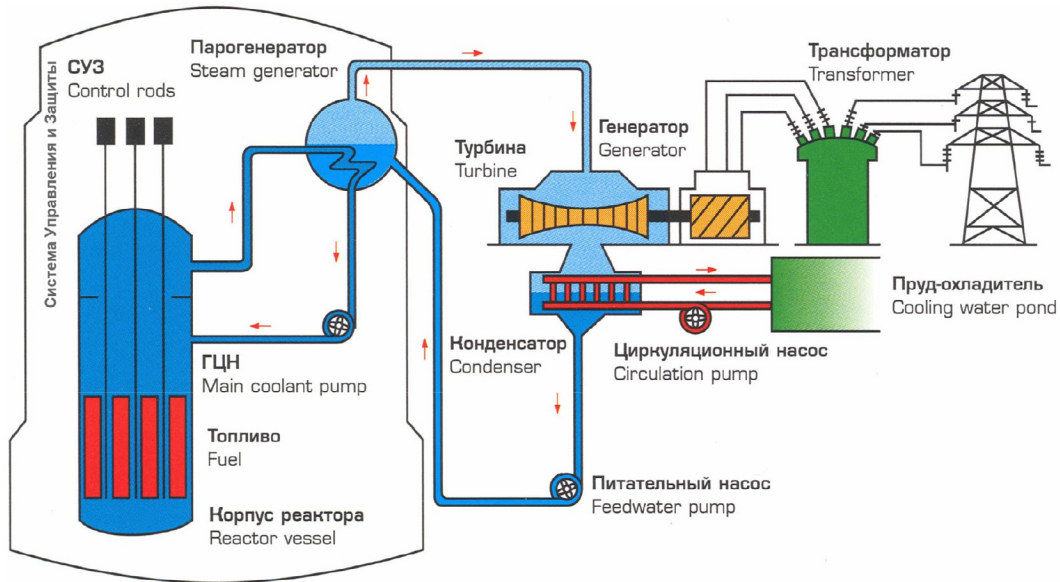


FIG. A1.45 Simplified scheme of typical Pressurized Water Reactor (PWR) (Russian 950-MW_{el} VVER-1000, Generation-III) NPP (Rosenergoatom, 2004): General basic features – 1) thermal neutron spectrum; 2) uranium-dioxide (UO₂) fuel; 3) fuel enrichment about 4%; 4) indirect cycle with steam generator(s) (also, a pressurizer required (not shown)), i.e., double flow circuit (double loop); 5) Reactor Pressure Vessel (RPV) with vertical fuel rods (elements) assembled in bundle strings cooled with upward flow of light water; 6) reactor coolant and moderator are the same fluid; 7) reactor-coolant outlet parameters: Pressure 15 – 16 MPa ($T_{sat} = 342 - 347^{\circ}\text{C}$) and temperatures inlet/outlet 290 – 325°C; and 8) power cycle - subcritical-pressure regenerative Rankine steam-turbine cycle with steam reheat (working fluid - light water, turbine steam-inlet parameters: Saturation pressure of 6 – 7 MPa and saturation temperature of 276 – 286°C). Courtesy of Rosenergoatom

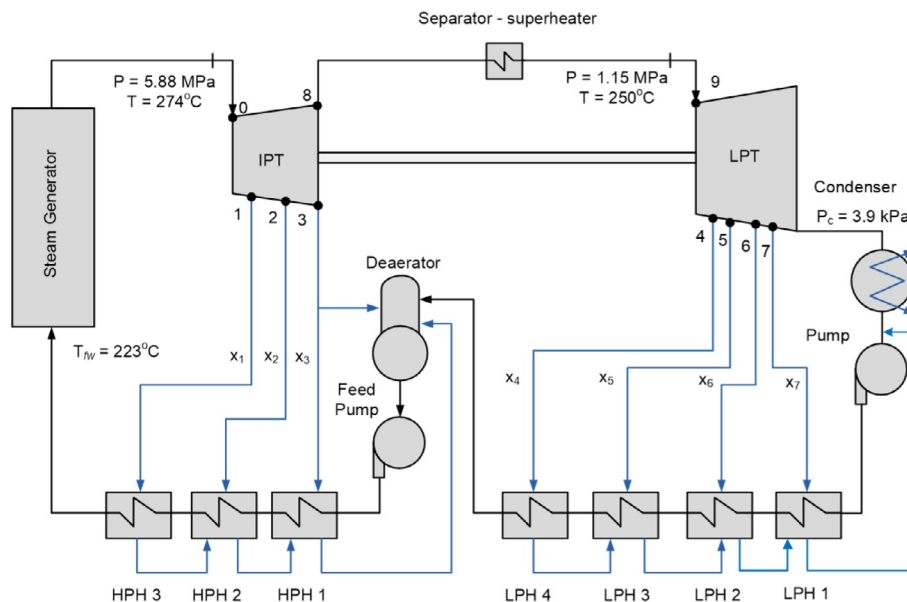


FIG. A1.46 Simplified thermodynamic layout of PWR (950-MW_{el} VVER-1000, Generation-III) NPP (winter operation). Based on Grigor'ev and Zorin, 1988; Margulova, 1995

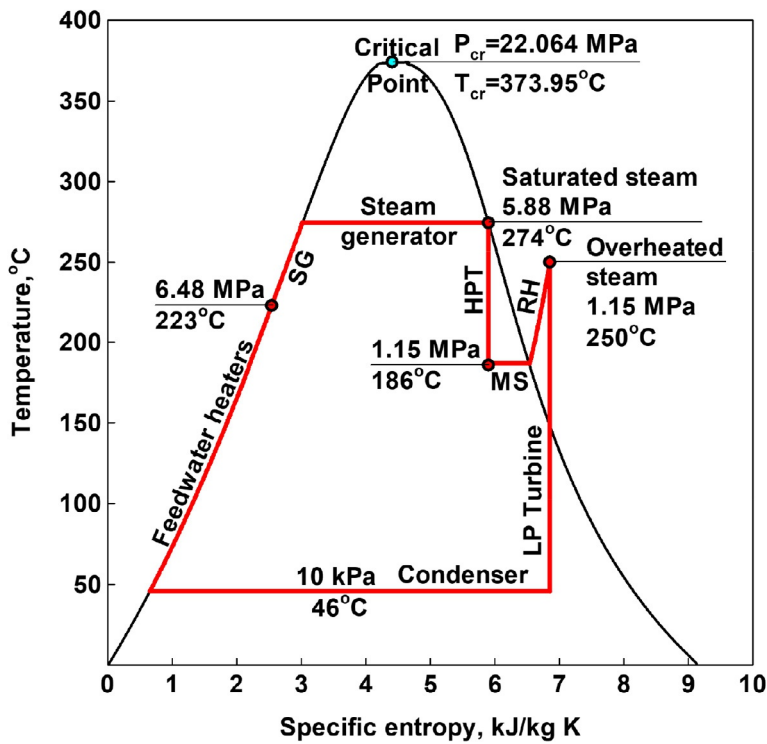


FIG. A1.47 Simplified T - s diagram of subcritical-pressure saturated-steam Rankine cycle with reheat option (secondary steam is reheated with primary steam in preheater) of PWR (950-MW_{el} VVER-1000, Generation-III) NPP (summer operation): HP – High Pressure; HPT – HP Turbine; LP – Low-Pressure; MS – Moisture Separator; RH – ReHeater; SG – Steam Generator



FIG. A1.48 Reactor hall without reactor, 1100-MW_{el} VVER-1200/AES-2006 (Unit 1), Novovoronezh NPP-2. Courtesy of Rosatom: <https://www.flickr.com/photos/rosatom/28691689604/in/album-72157672133127091/>; Photo by R. Pyshkin, 2016



FIG. A1.49 Loading Reactor Pressure Vessel (RPV), 1100-MW_{e1} Unit 1 (Generation-III+), Leningrad NPP-2, year 2014: <https://www.flickr.com/photos/rosatom/27143904732/in/album-72157668094181020/>. Large openings (850 mm ID) are for reactor-coolant flow in - lower level and out – upper level; smaller ID (300 mm) opening to the left upper level is for emergency cooling; and two pivots for crane for lifting RPV parts are shown: one to the left lower level and one to the right upper level with other two pivots 180° apart. *Courtesy of Rosatom*

In spite of all these problems, ABWRs/BWRs nuclear vendors all around the world significantly improved their reactor/plant designs. Therefore, below summary of these improvements in operation and safety are presented based on those from the Hitachi-GE Nuclear Energy, Ltd. in terms of their improvements introduced into ABWR/plant designs. In addition, some new features implemented into ABWRs are compared to those in BWR-5 (for details, see [Table A1.17](#)).

Advanced boiling water reactor (ABWR) (Hitachi-GE Nuclear Energy, Ltd.)

Application of “Evolutional Designs”:

- Large capacity, high efficiency plant systems
- Emergency Core-Cooling Systems with enhanced safety
- Highly economical reactor core
- Reactor recirculation system applying internal pumps
- Advanced Fine-Motion Control-Rod Drive System (CRDS)
- Advanced Main Control Room with Full Digital system and improved Human–Machine Interface & Automatic Operation
- Reinforced-Concrete Containment Vessel

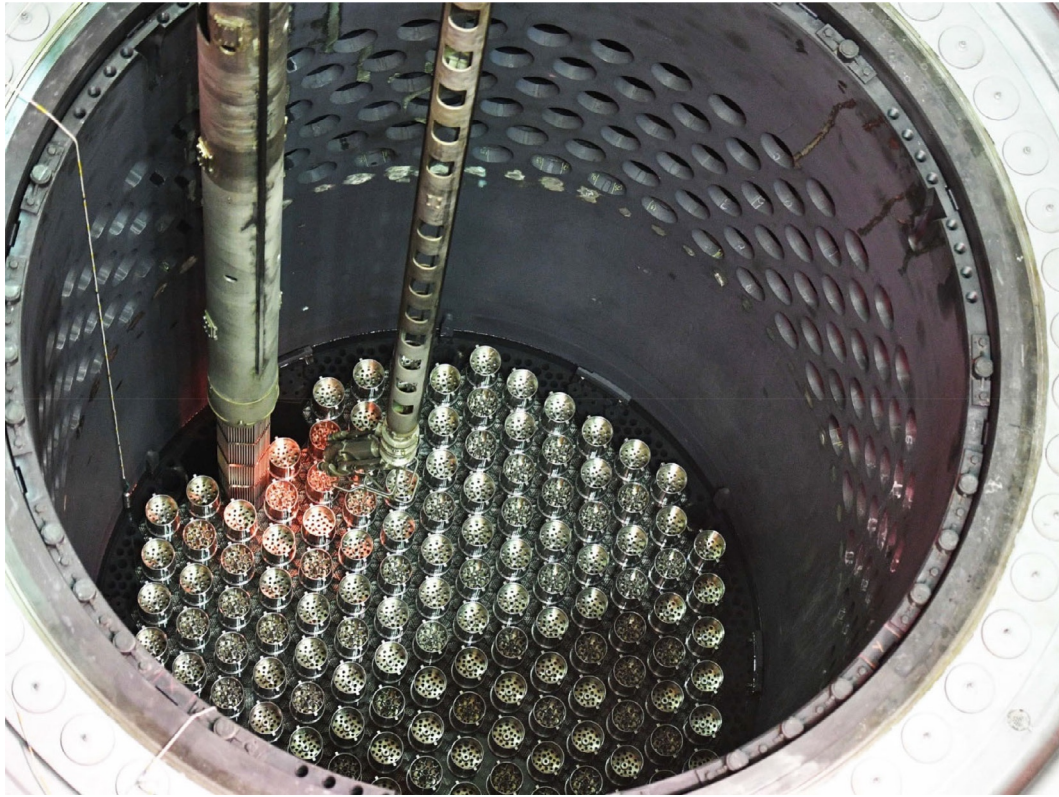


FIG. A1.50 Installing last fuel-bundle string or assembly into RPV core barrel (flow tube) of VVER-1000/V320 (Unit 4, Generation-III), Rostov NPP, year 2017: <https://www.flickr.com/photos/rosatom/25137456038/in/album-72157670840564464/>. Top of neutron reflector made of stainless steel is seen inside flow tube at level of fuel-bundle strings. *Courtesy of Rosatom*

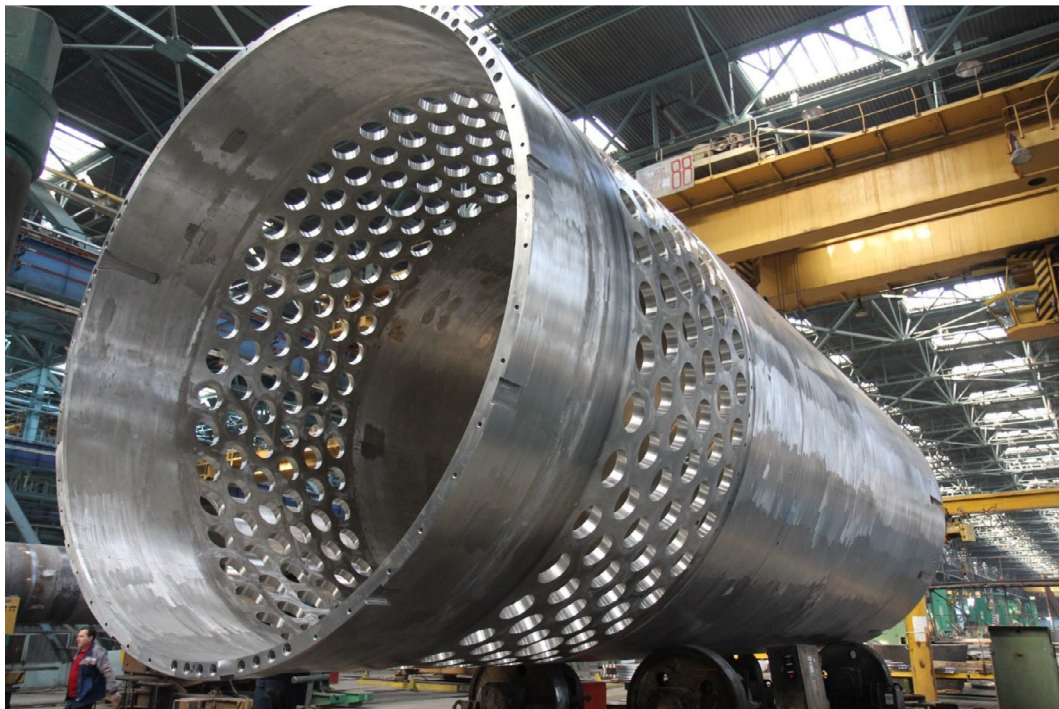


FIG. A1.51 Manufacturing of RPV core barrel (flow tube) for 1100-MW_{e1} VVER-1200 (Generation-III+) *Courtesy of Rosatom: <https://www.flickr.com/photos/rosatom/30463490342/in/album-72157675727427445/>; Photo by E. Lyadov, Atommash, 2015*

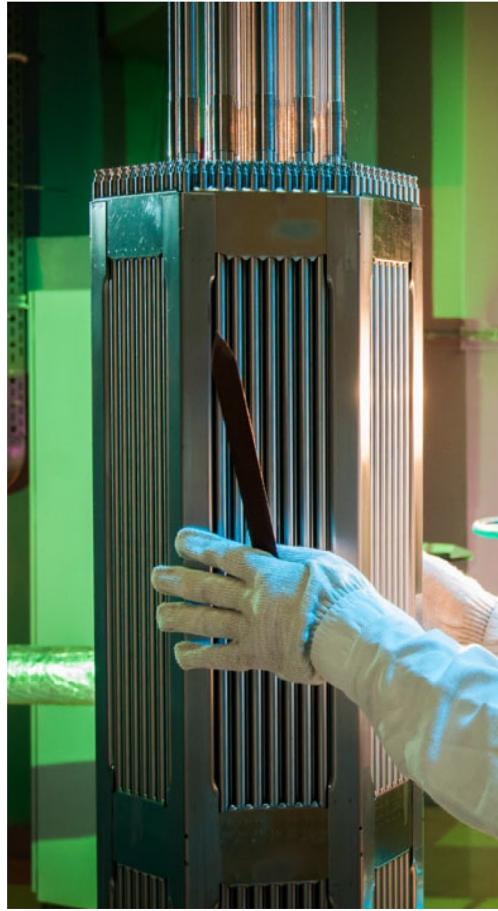


FIG. A1.52 Final check of fuel-bundle string or assembly of VVER-1000 (Generation-III) (hexahedron cross section) (shown upper part). *Courtesy of Rosatom: <https://www.flickr.com/photos/rosatom/25761756447/in/album-72157692396689951/>; Photo by A. Antonov, 2015*

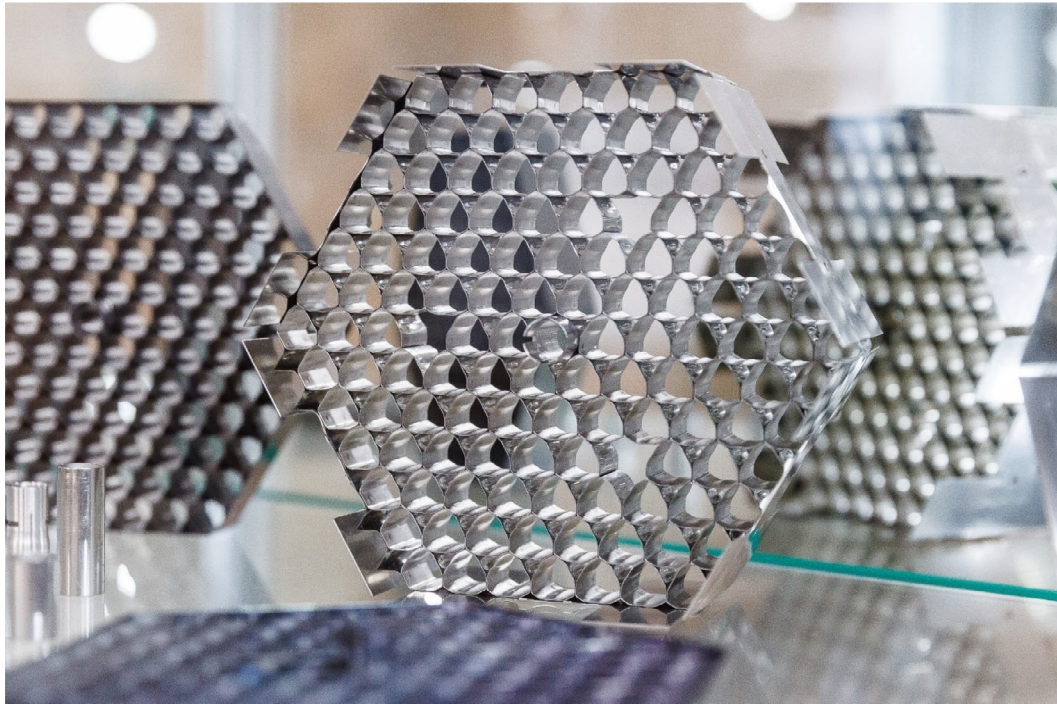


FIG. A1.53 VVER-440 (older PWR design) bundle grids or appendages to keep fuel rods in place. *Courtesy of Rosatom: <https://www.flickr.com/photos/rosatom/25761752627/in/album-72157692396689951/>; Photo by A. Bashkirov, 2016*



FIG. A1.54 Square-shape fuel bundle or assembly for PWRs (non-VVER type, also, see Fig. A1.44). Courtesy of Rosatom: <https://www.flickr.com/photos/rosatom/33012084356/in/album-72157677073459854/>; Photo by NZHK, 2009

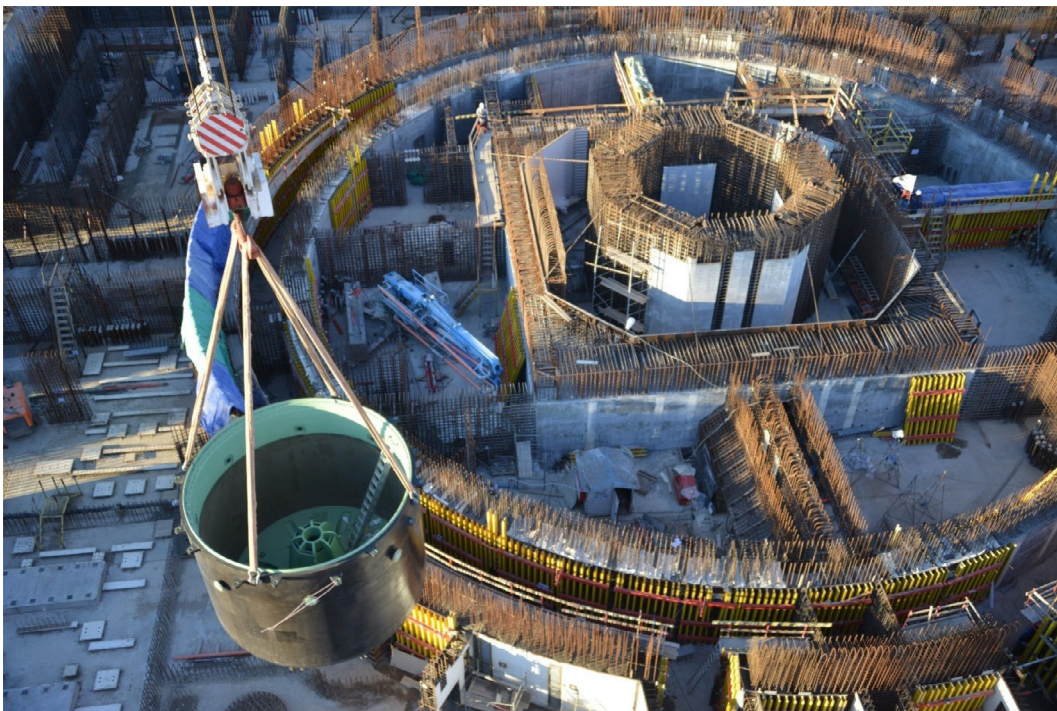


FIG. A1.55 Installation of molten-core (corium) catcher for 1175-MW_{el} VVER-TOI (Generation-III⁺) at Kursk-2 NPP inside reactor concrete shaft (Generation-III+ reactor's feature). Courtesy of Rosatom: <https://www.flickr.com/photos/rosatom/45774059035/in/album-72157672381108490/>; Photo by A. Duginov



FIG. A1.56 More detailed view of molten-core (corium) catcher for 1100-MW_{e1} VVER-1200 (Generation-III⁺) at Novovoronezh NPP (Generation-III+ reactor's feature): <https://www.flickr.com/photos/rosatom/29235111681/in/album-72157672133127091/>. Such catchers can be water cooled or without water cooling. *Courtesy of Rosatom*

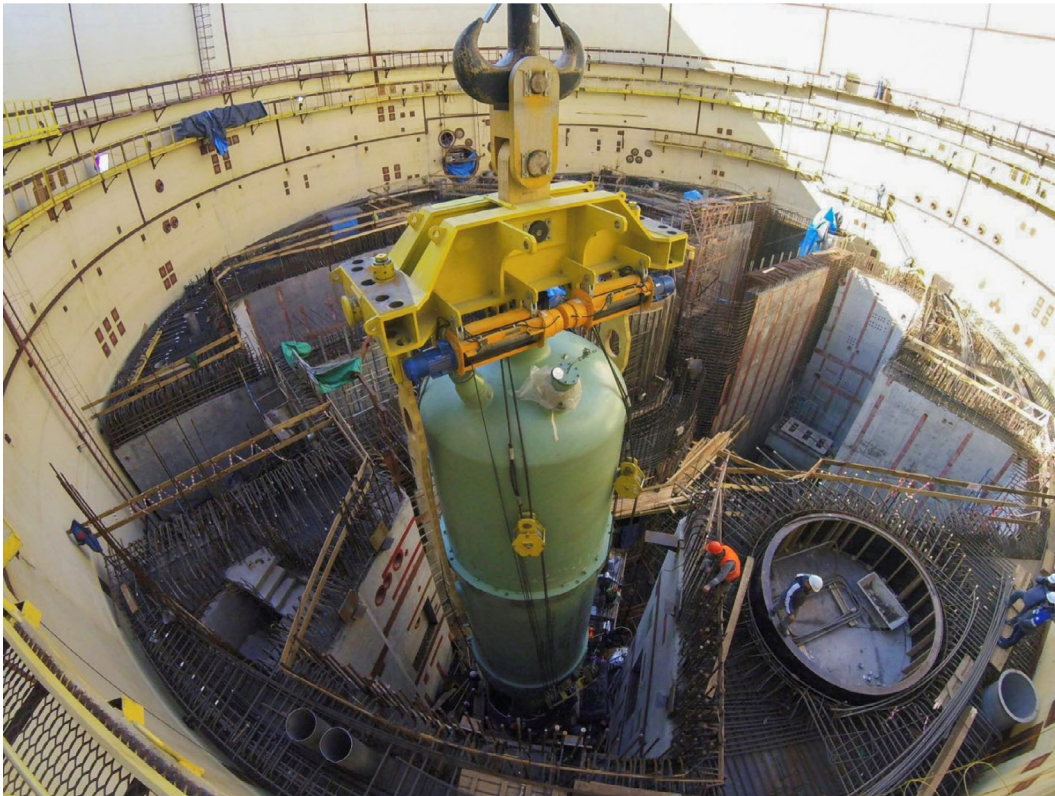


FIG. A1.57 Installation of pressurizer for 1066-MW_{e1} VVER-1200 (Generation-III+), Unit 2, Leningrad NPP-2, year 2017: <https://www.flickr.com/photos/rosatom/26539407989/in/album-72157668094181020/>. Modern construction method is to install reactor and all related equipment into containment building through the open top floor by floor and after that to build containment cover (also, see Figs. A1.27, A1.55, and A1.59). *Courtesy of Rosatom*



FIG. A1.58 Installation of electrical motor for main circulation pump for 1100-MW_{el} VVER-1200 (Generation-III+), Unit 1, Leningrad NPP (2 units in operation), year 2016: <https://www.flickr.com/photos/rosatom/37596923564/in/album-72157668094181020/>. Courtesy of Rosatom



FIG. A1.59 Upper part of reactor containment building under final stages of construction, 1066-MW_{el} VVER-1200 (Generation-III+), Unit 2, Leningrad NPP-2, year 2018. Containment building should withstand direct hit by airplane (intentional – terrorist attack or not intentional – air-accident): <https://www.flickr.com/photos/rosatom/44271493640/in/album-72157668094181020/>. Courtesy of Rosatom



FIG. A1.60 Turbine-generator hall of Kudankulam NPP, Unit 2, VVER AES-92 (Generation-III), 932 MW_{el}, year 2016. Courtesy of Rosatom: <https://www.flickr.com/photos/rosatom/27048124128/in/album-72157674579625065/>; Photo Press Service IK "ASE"



FIG. A1.61 Turbine assembling: From left to right – Shaft, double-flow high-pressure turbine and double-flow low-pressure turbine, VVER-1200 (Generation-III⁺), 1066 MW_{el}, Unit 2, Leningrad NPP. Courtesy of Rosatom: <https://www.flickr.com/photos/rosatom/32216583188/in/album-72157668094181020/>; Photo by S. Kashin/Titan-2, 2018



FIG. A1.62 Installation of double-flow low-pressure-turbine rotor with blades for VVER-1200 (Generation-III⁺), 1066 MW_{el}, Unit 2, Leningrad NPP, year 2018: <https://www.flickr.com/photos/rosatom/40900768181/in/album-72157668094181020/>. Courtesy of Rosatom



FIG. A1.63 Set of 4 steam generators (PIGB-1000) for VVER-1200 (Generation-III⁺), 1110 MW_{el}, Belarus' NPP (2 units in operation). Courtesy of Rosatom: <https://www.flickr.com/photos/rosatom/37621538806/in/album-72157675727427445/>; Photo by E. Lyadov, Atommash, 2017



FIG. A1.64 Heat-transfer tubes for steam generator (ПГБ-1000) for VVER-1200 (Generation-III⁺), 1110 MW_{el}, Unit 2, Belarus' NPP (2 units in operation). *Courtesy of Rosatom: <https://www.flickr.com/photos/rosatom/36999718643/in/album-72157675727427445/>; Photo by E. Lyadov, Atommash, 2016*



FIG. A1.65 Control hall, putting into operation Unit 1, 1100-MW_{el} VVER-1200 (Generation-III⁺), Leningrad NPP-2, year 2018: <https://www.flickr.com/photos/rosatom/40006970035/in/album-72157668094181020/>. *Courtesy of Rosatom*



FIG. A1.66 Photos of Russian SMRs – PWRs: (a) KLT-40S (Generation-III): large grey cylinders – 4 steam generators and small green cylinders – 4 circulation pumps. Two reactors installed on a barge and operate as floating NPP (Port Pevek). (b) Generation III⁺ SMR - RITM-200M with steam generators integrated into pressure vessel; small cylinders – circulation pumps. NPP with these reactors will be built in Yakutia. (c) Defense-in-depth arrangement schematics of floating NPP Courtesy of Rosatom. (a) Photo Baltzavod, 2013: <https://www.flickr.com/photos/rosatom/42425233062/in/album-72157692330711570/> and (b) Photo by N. Greidin, Baltzavod: <https://www.flickr.com/photos/rosatom/24835999197/in/album-72157671934046766/>; and (c) Courtesy of JSC “Afrikantov OKBM”, Nizhny Novgorod, Russia: <http://www.okbm.nnov.ru/upload/iblock/69e/40i3dob8nyjigsaoe5tlunlij2qr2mh9.pdf>; accessed Feb. 19, 2022

TABLE A1.14 Additional typical parameters of 950-MW_{el} VVER-1000 series 300 and 400 (for basic parameters, see Table A1.13)

Parameter	Value
Pressure vessel ID, m	4.14
RPV wall thickness, m	0.19
RPV height without cover, m	10.9
Core equivalent diameter, m	3.12
Core height, m	3.56
Volumetric heat flux, MW/m ³	110
Average volumetric flow rate in assembly, m ³ /h	515±55
No. of fuel assemblies	163
No of rods per assembly	317
Fuel mass, ton of UO ₂	80
Part of fuel reloaded during year	1/3
Fuel	UO ₂
Fuel enrichment, %	4

TABLE A1.15 Reference parameters of Generation III+ VVER (PWR)

Parameter	Value
Thermal power, MW _{th}	3200
Electric power, MW _{el}	1160
NPP thermal efficiency, %	36
Primary coolant pressure, MPa	16.2
Steam-generator pressure, MPa	7.0
Coolant temperature at reactor inlet, °C	298
Coolant temperature at reactor outlet, °C	329
Steam-generator pressure/temperature, MPa/°C	6.27/278
NPP service life, years	50
Main equipment service life, years	60
Replaced equipment service life, years, not less than	30
Capacity factor, %	up to 90

TABLE A1.15 Reference parameters of Generation III+ VVER (PWR)—
cont'd

Parameter	Value
Load factor, %	up to 92
Equipment availability factor	99
Length of fuel cycle, years	4 - 5
Frequency of re-fuelling, months	12 - 18
Fuel assembly maximum burn-up, MW day/kgU	up to 60 - 70
Inter-repair period length, years	4 - 8
Annual average length of scheduled shut-downs (for re-fuelling, scheduled maintenance work), days per year	16 - 40
Refueling length, days per year	≤16
Number of not scheduled reactor shutdowns per year	≤1
Frequency of severe core damage, 1/year	<10 ⁻⁶
Frequency of limiting emergency release, 1/year	<10 ⁻⁷
Efficient time of passive safety and emergency control system operation without operator's action and power supply, hour	≥24
OBE/SSE, magnitude of MSK-64 scale	6 and 7*
Compliance with EUR requirements, yes/no	Yes
RP main stationary equipment is designed for SSE of magnitude 8.	

Mainly based on data from [Ryzhov et al. \(2010\)](#).

ABWR Safety Features:

- Diversified water-injection methods
- Large capacity of heat sink (pool)
- Inactivated Primary-Containment Vessel (PCV)
- High seismic resistance
- No large-bore pipes lower than the top of fuel assemblies
- Core Damage Frequency (CDF): 1.6×10^{-7}

Additional features

- (1) Secure Power Source
 - Alternative DC Power Source
 - Diversity of Power Source (Water-cooled Diesel Generator (DG), Air-cooled DG)
 - Sealed building structure to secure components and power panels in case of flooding
- (2) Secure water-injection systems and ultimate heat sink
 - Diversity of alternate water-injection capabilities
 - Enhancement of mobility by applying portable pumps

Typical Boiling-Water Reactor

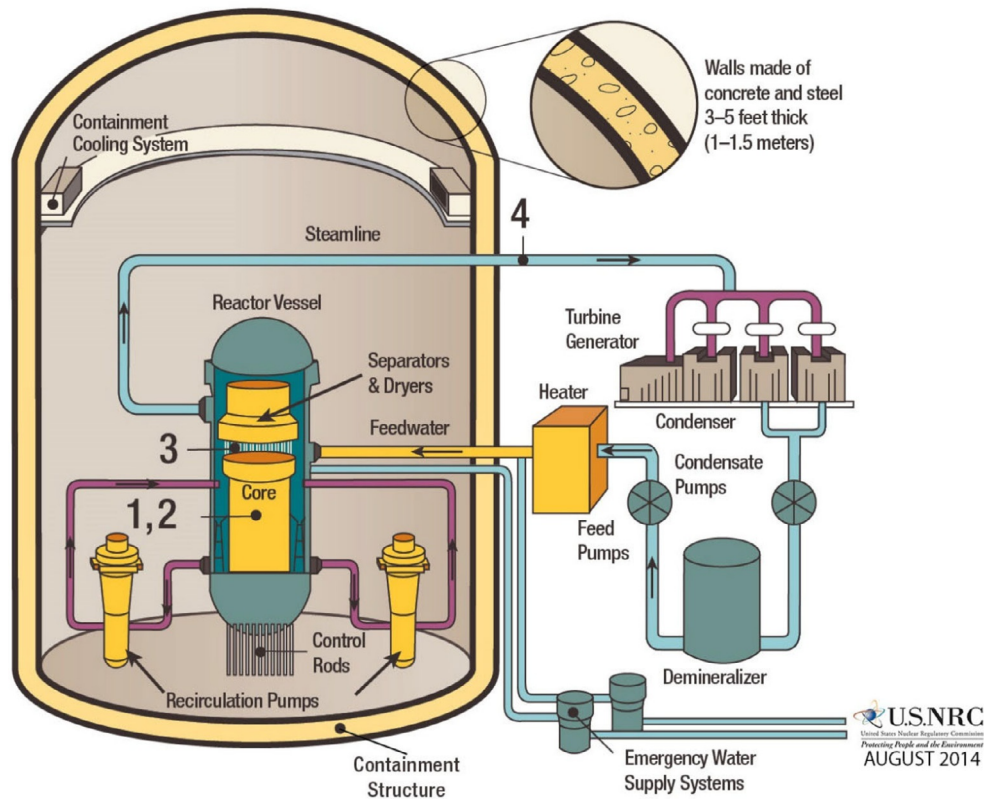


FIG. A1.67 Simplified layout of typical Boiling Water Reactor (BWR) NPP: General basic features – 1) thermal neutron spectrum; 2) uranium-dioxide (UO_2) fuel; 3) fuel enrichment about 3%; 4) direct cycle with steam separator (steam generator and pressurizer are eliminated), i.e., single-flow circuit (single loop); 5) RPV with vertical fuel rods (elements) assembled in bundle strings cooled with upward flow of light water (water and water-steam mixture); 6) reactor coolant, moderator and power-cycle working fluid are the same fluid; 7) reactor coolant outlet parameters: Pressure about 7 MPa and saturation temperature at this pressure is about 286°C; and 8) power cycle - subcritical-pressure regenerative Rankine steam-turbine cycle with steam reheat. *Courtesy of U.S. NRC*

- Diversity of heat sink through use of portable heat-removal system
- (3) Prevention of Primary Containment Vessel (PCV) damage
 - Prevention of PCV damage caused by elevated temperatures by enhancing the PCV-cooling system
- (4) Secure Spent Fuel-Pool Cooling function
 - Diversity of pool water-injection method
 - AM operability enhancement by applying external-water injection filler
 - Incorporation of additional Spent Fuel Pool (SFP) temperature- and water-level monitoring systems in case of severe accident.

ABWR counter-measures against Fukushima Daiichi NPP severe accident (based on information from Hitachi-GE Nuclear Energy) Further Enhanced Safety Features regarding Fukushima–Daiichi NPP severe accident:

TABLE A1.16 Typical parameters of US BWR (Generation-III)
(Shultis and Faw, 2007)

Parameter	Value
Thermal output, MW _{th}	3830
Electrical output, MW _{el}	1330
Thermal efficiency, %	34
Specific power, kW/kg(U)	26
Power density, kW/Liter	56
Average linear heat flux, kW/m	20.7
Rod heat flux ave/max, MW/m ²	0.51/1.12
Core	
Length, m	3.76
OD, m	4.8
Reactor-coolant system	
Pressure, MPa	7.17
Feed-water temperature, °C	216
Outlet steam temperature, °C	290
Outlet steam flow rate, kg/s	2083
Core flow rate, kg/s	14,167
Core void fraction ave/max	0.37/0.75
Reactor pressure vessel	
ID, m	6.4
Height, m	22.1
Wall thickness, m	0.15
Fuel	
Fuel pellets	UO ₂
Pellet OD, mm	10.6
Rod OD, mm	12.5
Zircaloy clad thickness, mm	0.86
Rods per bundle (8 × 8)	62
Bundles in core	760
Fuel loading, ton	168
Enrichment, %	1.9

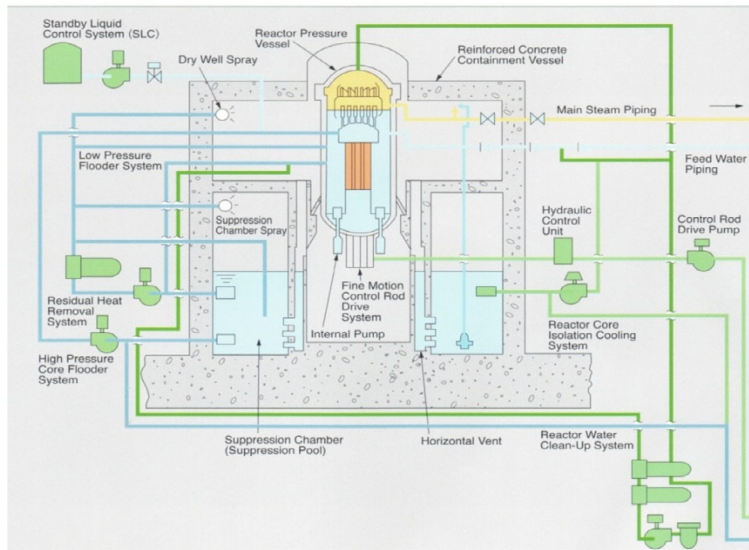
Continued

TABLE A1.16 Typical parameters of US BWR (Generation-III) (Shultis and Faw, 2007)—cont'd

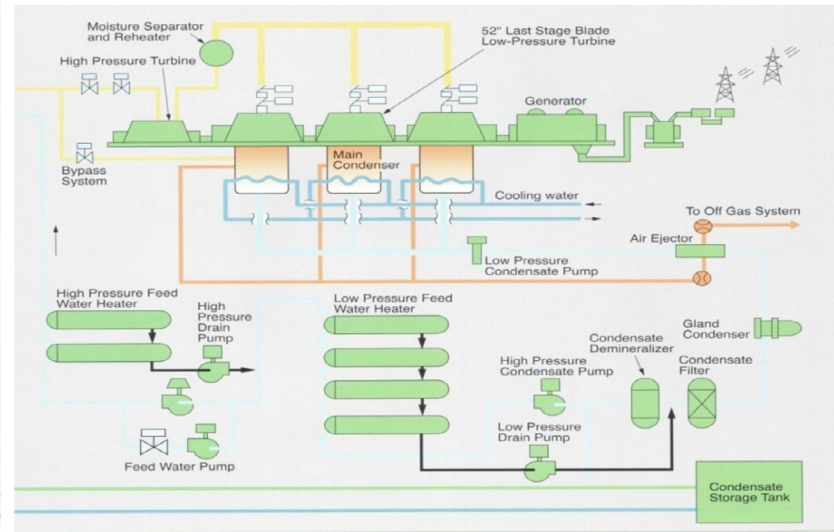
Parameter	Value
Reactivity control	
No. of control assemblies	193
Shape	Cruciform
Overall length, m	4.42
Length of poison section, m	3.66
Neutron absorber	Boron carbide
Soluble poison shim	Gadolinium



FIG. A1.68 Aerial view of Kashiwazaki-Kariwa NPP Units 6 & 7 – the 1st & 2nd ABWRs/first two Generation-III+ reactors in the world (1996 & 1997). *Courtesy and copyright by Hitachi-GE Nuclear Energy Ltd*



(a)



(b)

FIG. A1.69 Simplified layout of Advanced Boiling Water Reactor (ABWR) (Generation-III+) NPP: (a) reactor inside a reinforced concrete containment vessel, and (b) turbine-generator unit. *Courtesy and copyright by Hitachi-GE Nuclear Energy, Ltd*

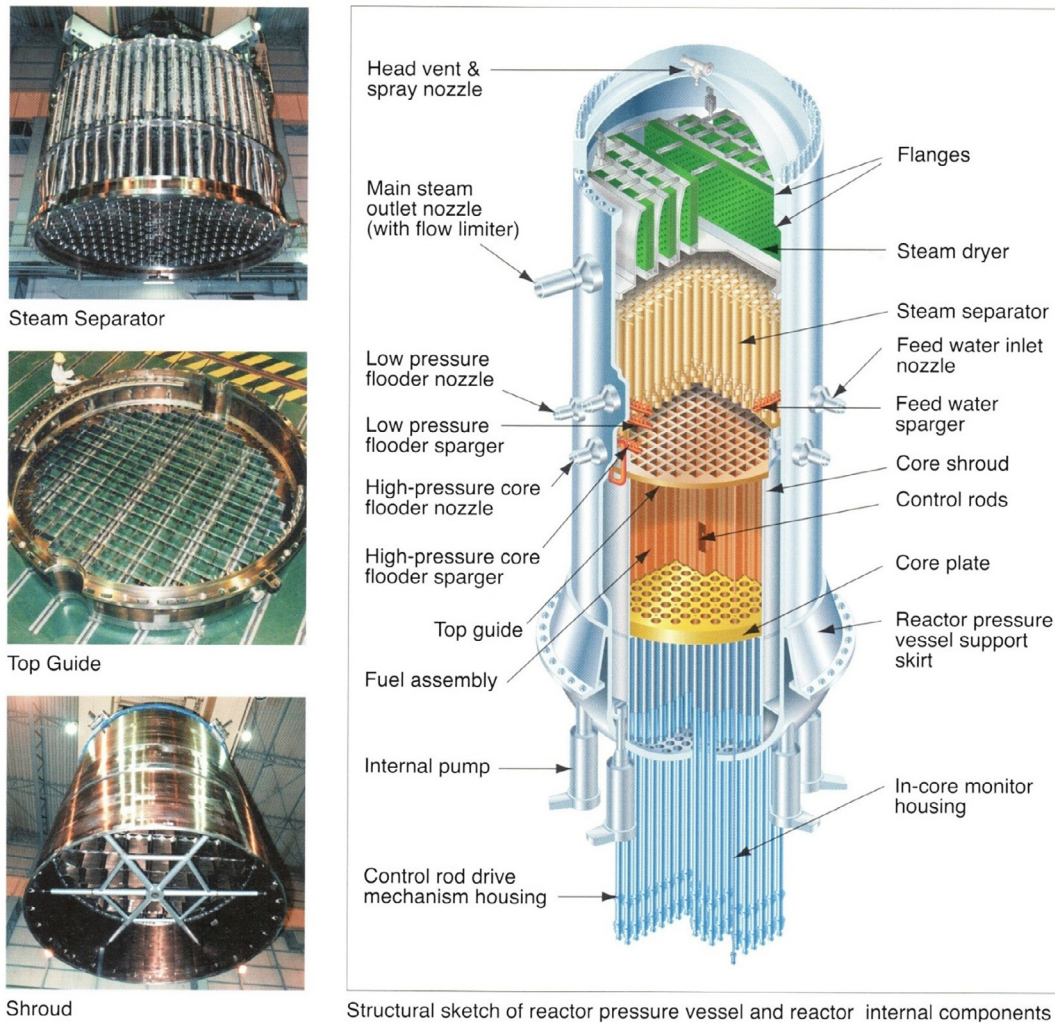


FIG. A1.70 Simplified layout of typical Advanced Boiling Water Reactor (ABWR) NPP. *Courtesy and copyright by Hitachi, Ltd*

- ABWR safety features are based on the Defense in Depth (DiD) concept wherein multiple layers of protection are provided with each layer designed to provide the safety function with no reliance on the other layers.
- ABWR design is compliant with the international criteria by well-designed Safety Systems to achieve a sufficiently low core damage frequency.
- Furthermore, to accomplish an enhanced level of nuclear safety, supplementary safety enhancements against severe conditions have been incorporated. These enhancements on further layer in DiD are designed to address the Fukushima–Daiichi NPP accident caused by the huge earthquake and subsequent tsunamis on March 11, 2011.
- The major enhancements are the further prevention of Station Black Out (SBO) and/or Loss of Ultimate Heat Sink (LUHS). Moreover, the enhanced functions ensure water supply into the reactor, PCV integrity, and SFP water level is maintained even in the event of SBO and/or LUHS.

These enhancements, based on lessons learned from the Fukushima Accident, provision and maintenance of the Severe Accident Management Guidelines, ensure that the integrity of inherent safety features of the ABWR is retained even in the event of a severe accident.

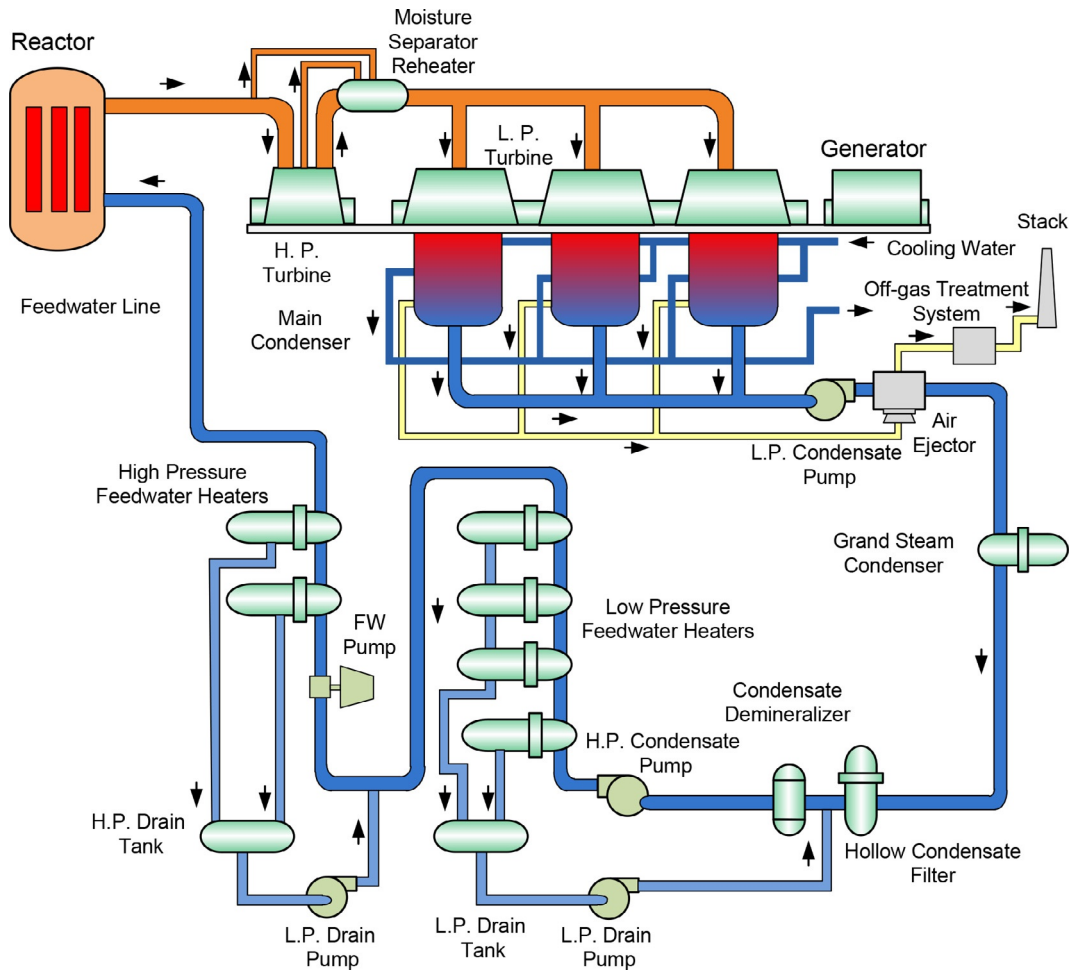


FIG. A1.71 Simplified layout of ABWR NPP. Based on data from Toshiba (2011)

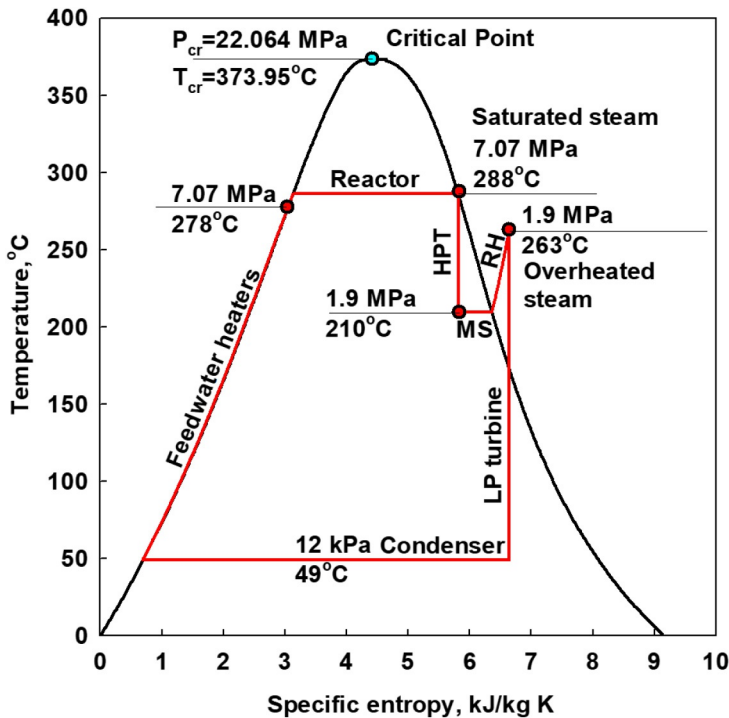


FIG. A1.72 Simplified T-s diagram of typical ABWR NPP turbine cycle (reheat pressure was assumed to be 1/4 of the main steam pressure)

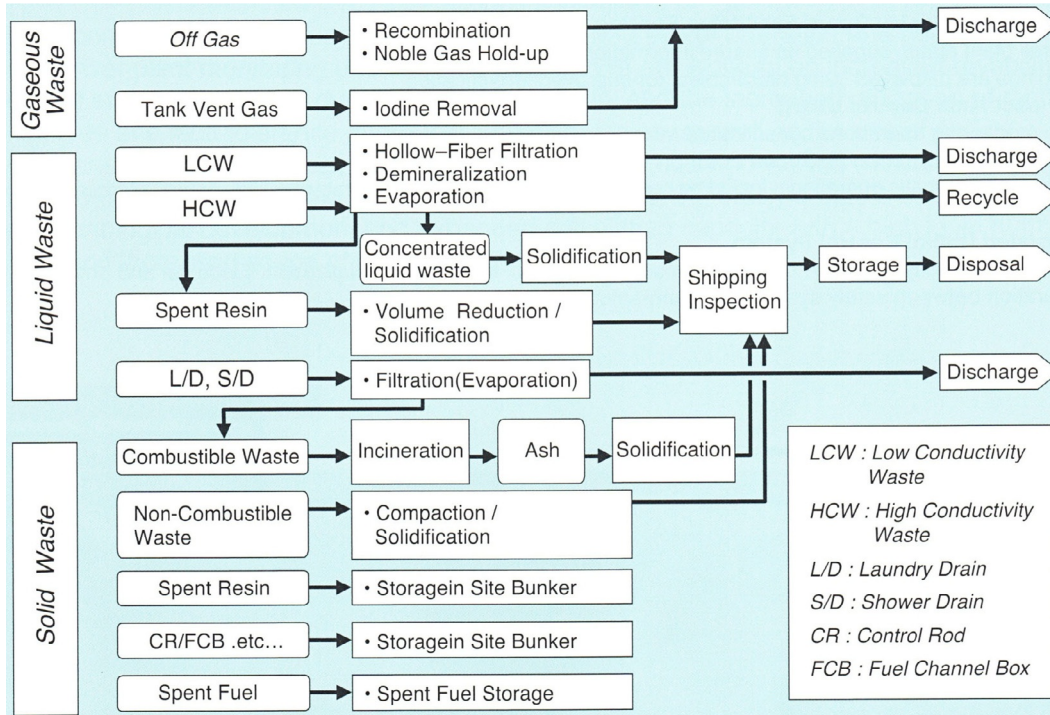


FIG. A1.73 Classification of radioactive wastes and process flow. Courtesy and copyright by Hitachi-GE Nuclear Energy, Ltd

TABLE A1.17 Key specifications of ABWR (Generation-III+) and BWR-5 (Generation-III)

Parameter	Item	ABWR	BWR-5
Power	Electrical	1,350 MW _{el}	1,100 MW _{el}
	Thermal	3,926 MW _{th}	3,293 MW _{th}
Thermal efficiency (gross), %		34	33.4
Reactor core	Fuel assemblies	872	764
	Control rods	205	185
Reactor equipment	Recirculation system	Internal pump method	External recirculation type
	Control rod drive	Hydraulic/electric motor drive methods	Hydraulic drive
Reactor containment vessel		Reinforced concrete with built-in liner	Free-standing vessel
Residual heat-removal system		3 systems	2 systems
Turbine Systems	Thermal cycle	Two-stage reheat	Non-reheat
	Turbine (blade length)	1.32 m (52")	1.09 m (43")
	Moisture-separation method	Reheat type	Non-reheat type
	Heater drain	Drain up type	Cascade type

Courtesy of Hitachi-GE Nuclear Energy, Ltd.

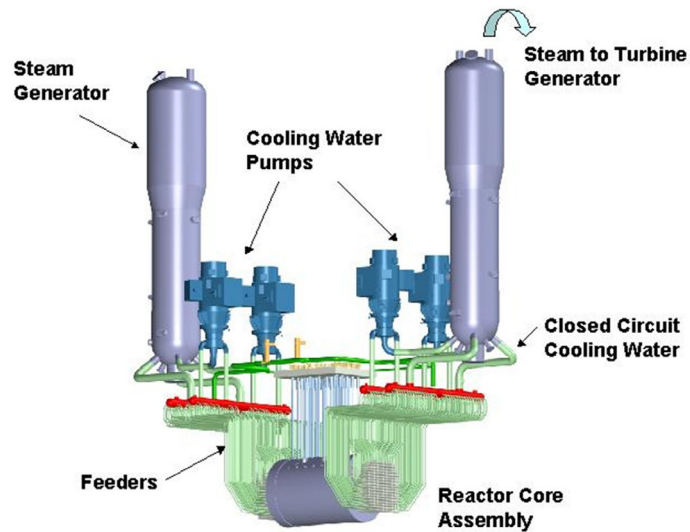


FIG. A1.74 Typical PHWR layout. *Courtesy of R.B. Duffey*

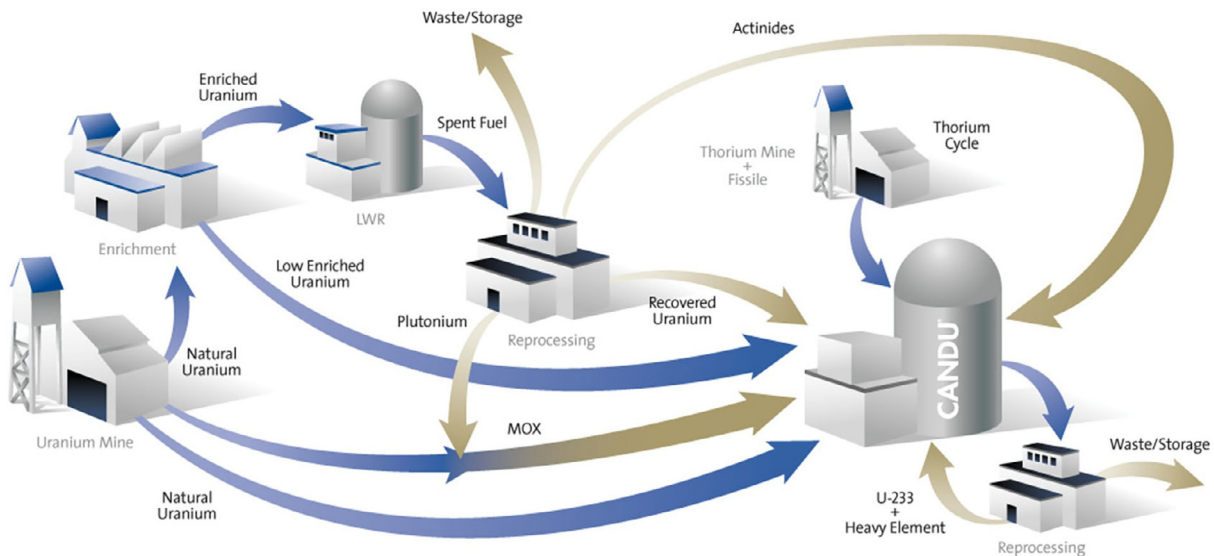


FIG. A1.75 PHWR alternative and advanced fuel cycles. *Courtesy of R.B. Duffey*

Pressurized Heavy Water Reactors (PHWRs)^d

History and global context of PHWRs It is clear from Table A.1.2.6 (Chapter 1.2) that the majority of PHWRs are located in two countries - Canada and India, with additional units in Argentina, China, S. Korea, and Romania. The reasons stem from global historical developments and the international political context, particularly related to nuclear weapons and non-proliferation issues, and the development of commercial PHWRs, which important background is recounted in details in publications by Goldschmidt (1982), Perkovich (2002), and Hurst (1997).

Briefly, as a result of post-WW2 Cold-War nuclear policies, the UK, Canada, France, and Russia were forced to develop their own nuclear-power programs based initially on the graphite and D₂O

^d This Section is mainly based on Duffey, R.B., Piro, I., and Piro, R., 2021. World Energy Production and the Contribution of PHWRs, Chapter 1. Introduction, pp. 1-44; in the book: Vol. 7. Pressurized Heavy Water Reactors: CANDU, Editor J. Riznic, Elsevier, UK, 546 pages.

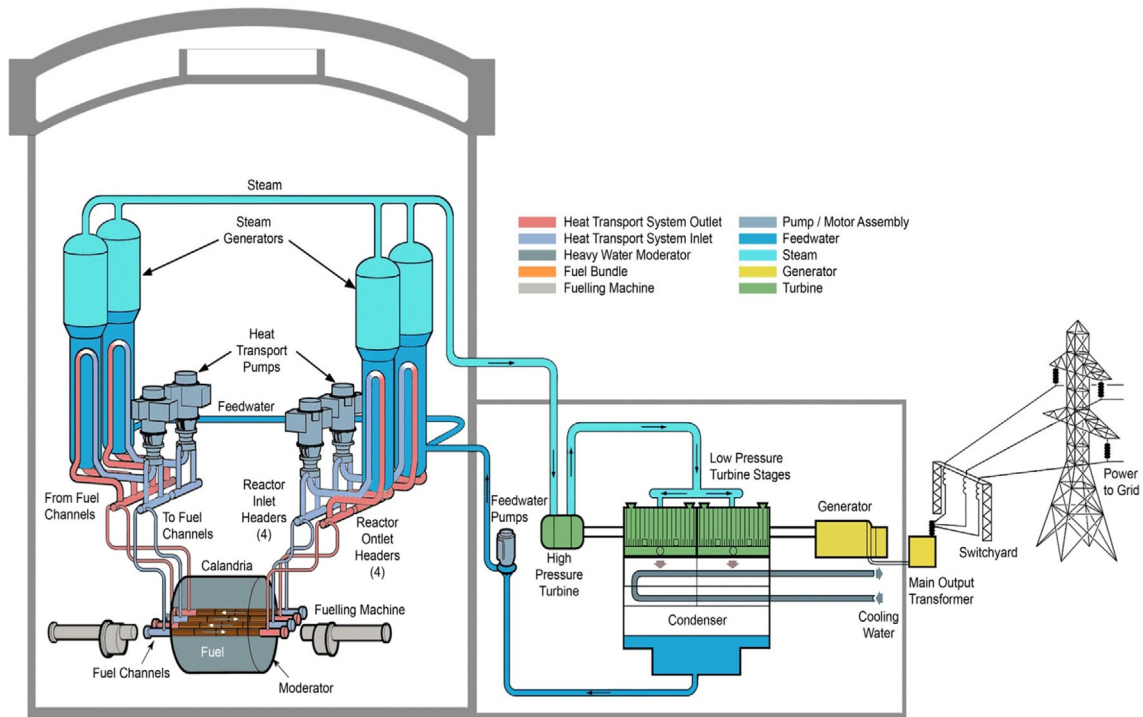


FIG. A1.76 Simplified CANDU-reactor NPP flow diagram: Moisture Separator and Reheater (MSR) are not shown. *Courtesy of SNC-Lavalin*

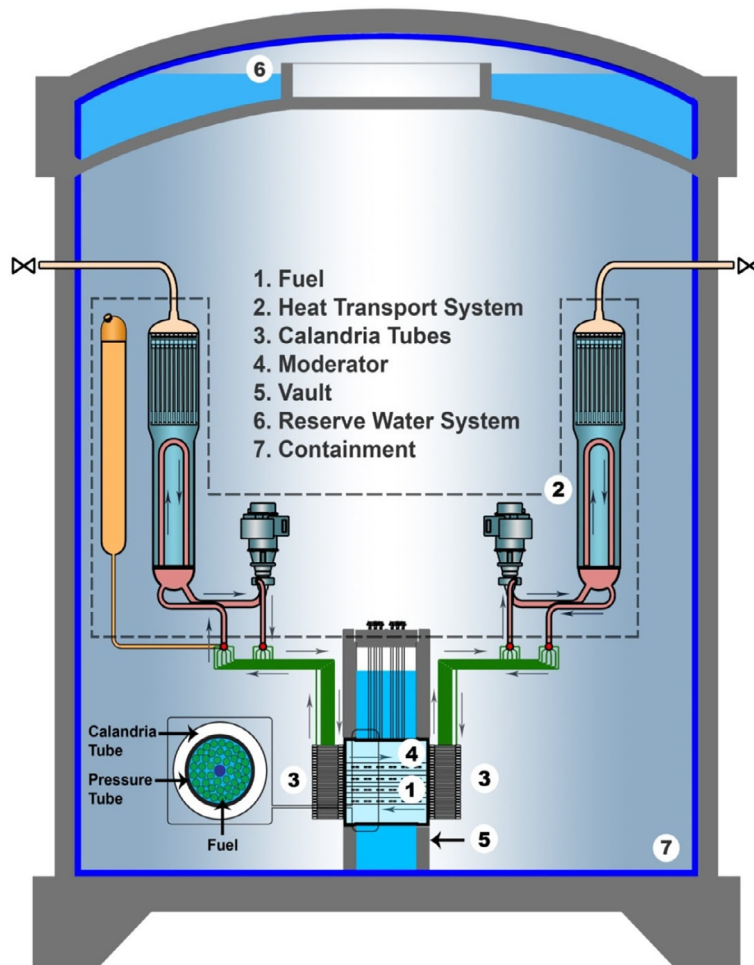


FIG. A1.77 Barriers for prevention of releases. *Courtesy of SNC-Lavalin*

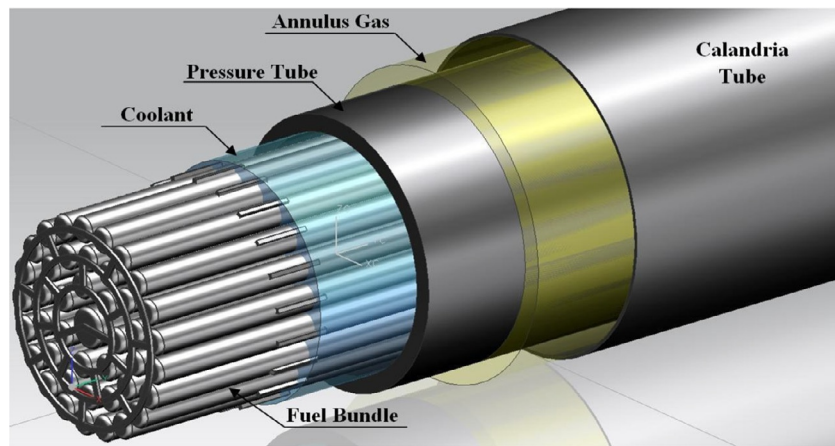


FIG. A1.78 3-D image of CANDU-reactor fuel channel with bundle. Based on data from AECL

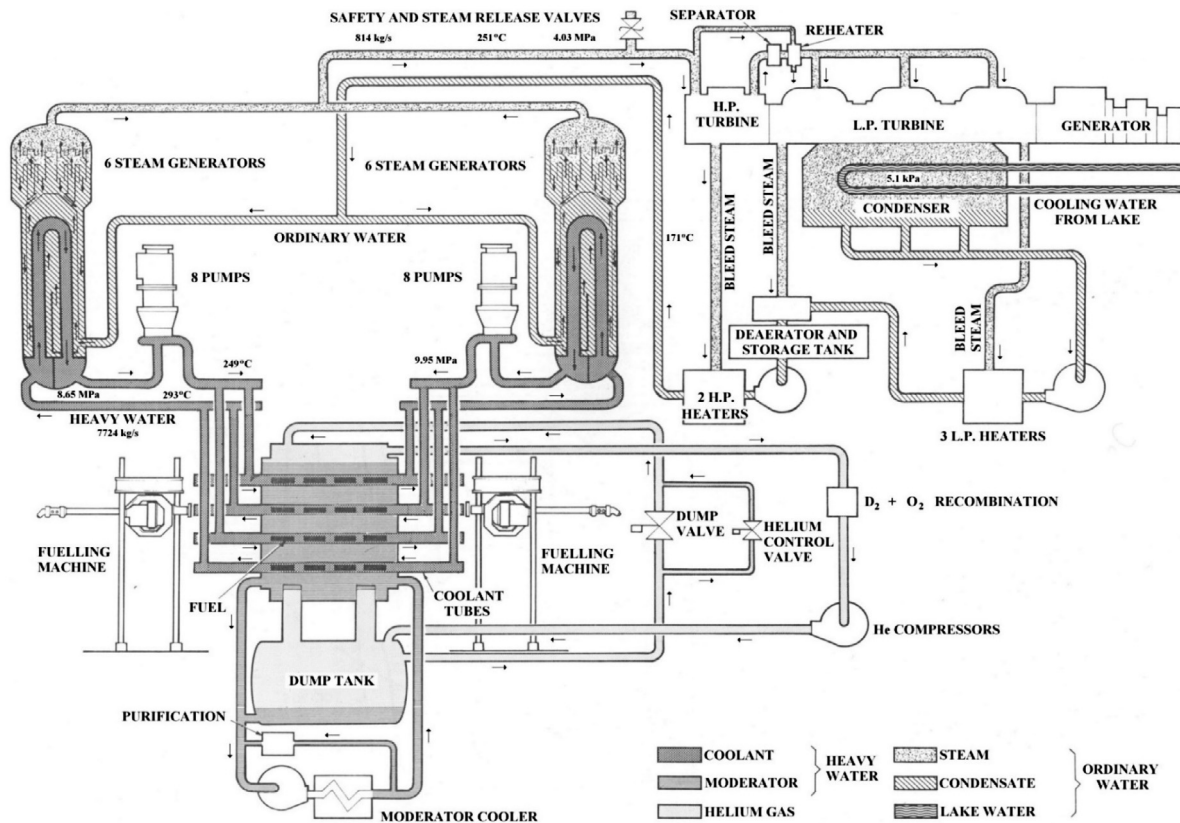


FIG. A1.79 Simplified flow diagram of 515-MW_e CANDU-reactor NPP (Pickering Power Plant, Ontario, Canada) (AECL Report, 1969): These 515-MW_e CANDU reactors are the smallest ones in Canada, and first two of them were put into operation in 1971. Note: Also, a pressurizer required (not shown)

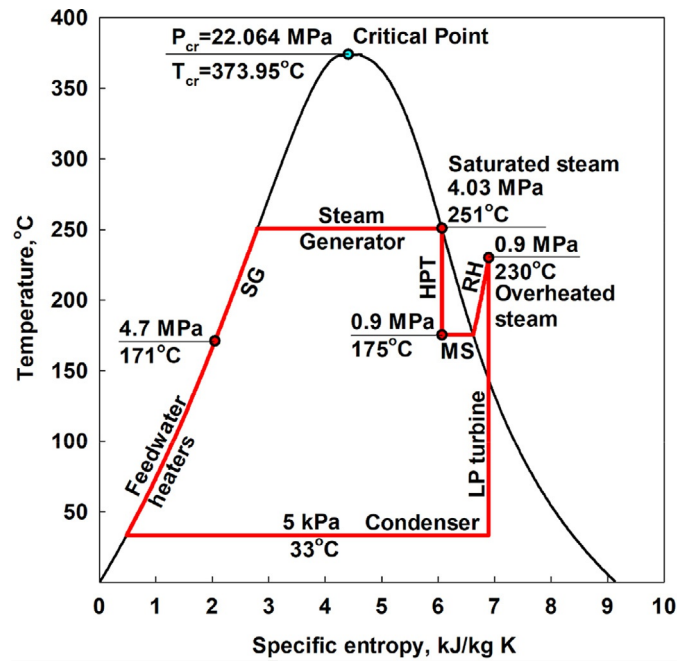


FIG. A1.80 T - s diagram for 515-MW_{el} CANDU-reactor Pickering NPP (Ontario, Canada) turbine cycle: HPT – High-Pressure Turbine; LP – Low-Pressure; MS – Moisture Separator; RH – ReHeater; and SG – Steam Generator

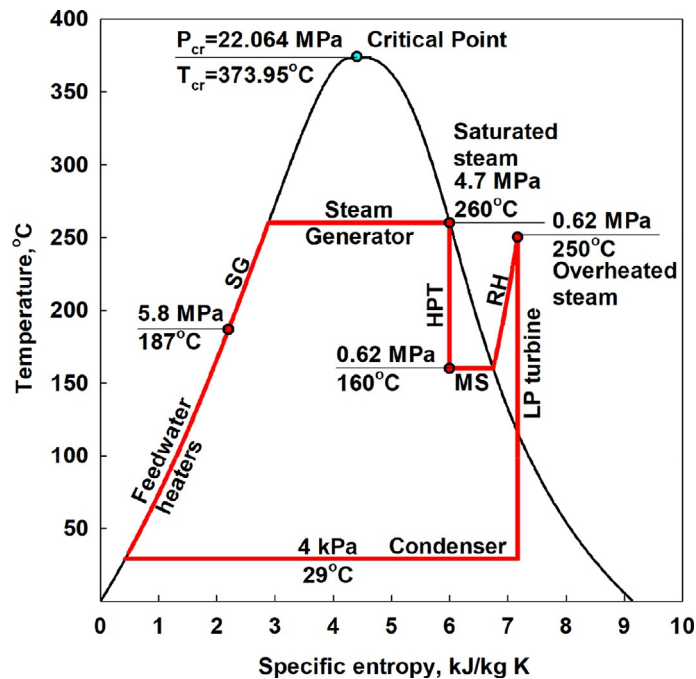


FIG. A1.81 Simplified T - s diagram of 730-MW_{el} CANDU-6 reactor NPP Rankine cycle (current design of CANDU reactors) (winter operation): HPT – High-Pressure Turbine; LP – Low-Pressure; MS – Moisture Separator; RH – ReHeater; and SG – Steam Generator

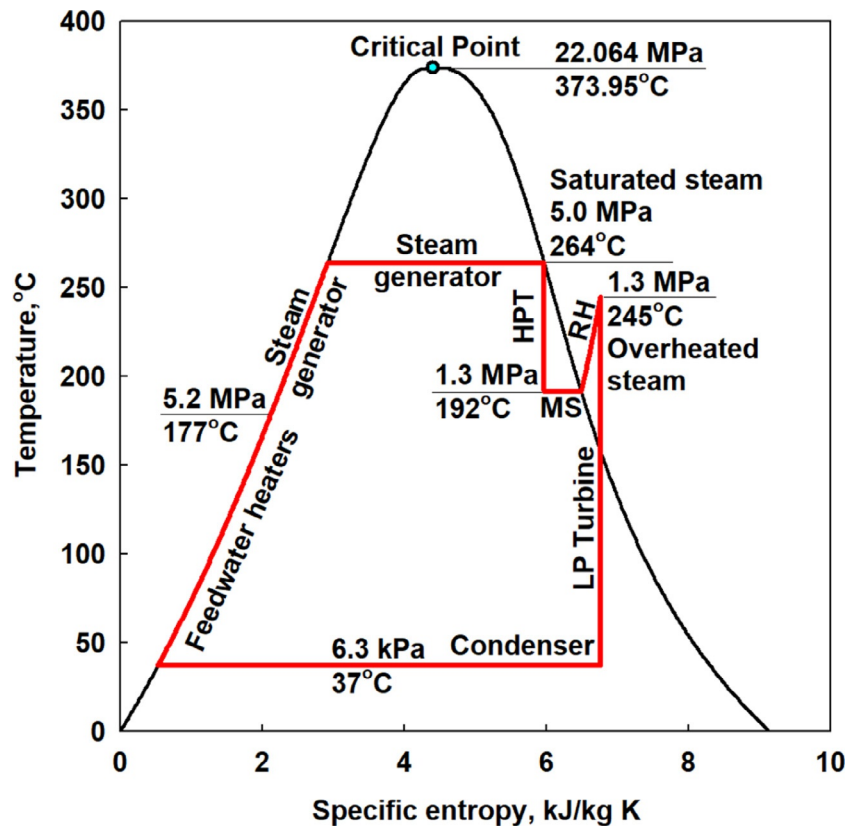


FIG. A1.82 T - s diagram of 878-MW_{e1} CANDU[®]-reactor Darlington NPP (Ontario, Canada) Rankine cycle (the largest CANDUs in the world with the most efficient CANDU Rankine cycle). Exact steam-reheat parameters (P and T) were not known and were estimated based on the following, i.e., secondary-steam (reheat) pressure is $\sim 1/4$ of primary-steam pressure and maximum T_{reheat} is $\sim 20^\circ\text{C}$ below primary-steam temperature. Cooling-water-temperature 25.5°C (summer operation): HPT – High-Pressure Turbine; LP – Low-Pressure; MS – Moisture Separator; RH – ReHeater; and SG – Steam Generator

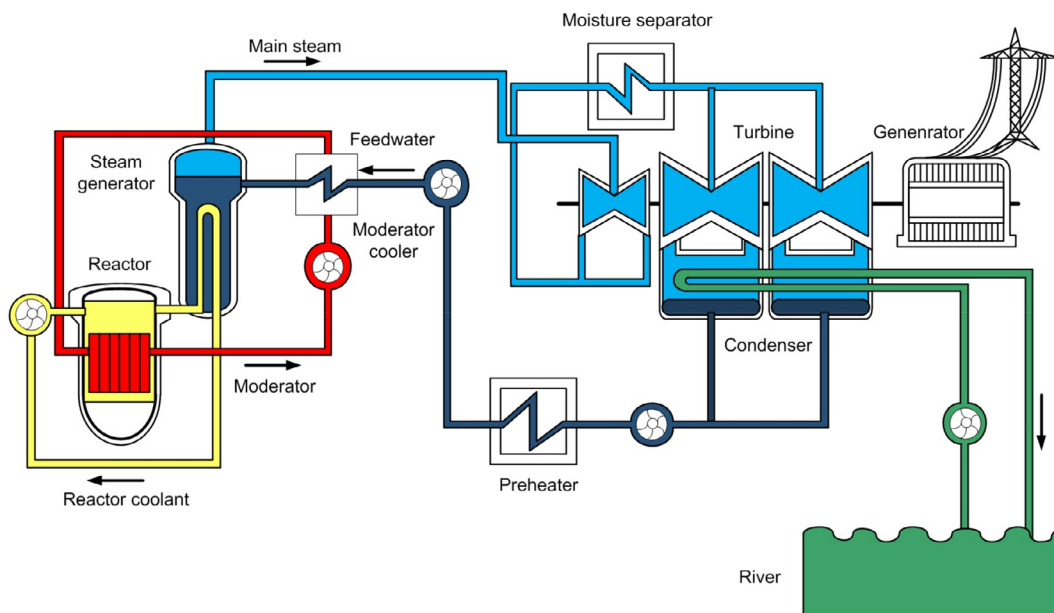


FIG. A1.83 Simplified PHWR NPP flow diagram (Siemens design) (Atucha, Argentina). Currently, both Unit 1 (335 MW_{e1}) and Unit 2 (692 MW_{e1}) are in operation. Based on *Nuclear Engineering International*, Sept. 1982, England

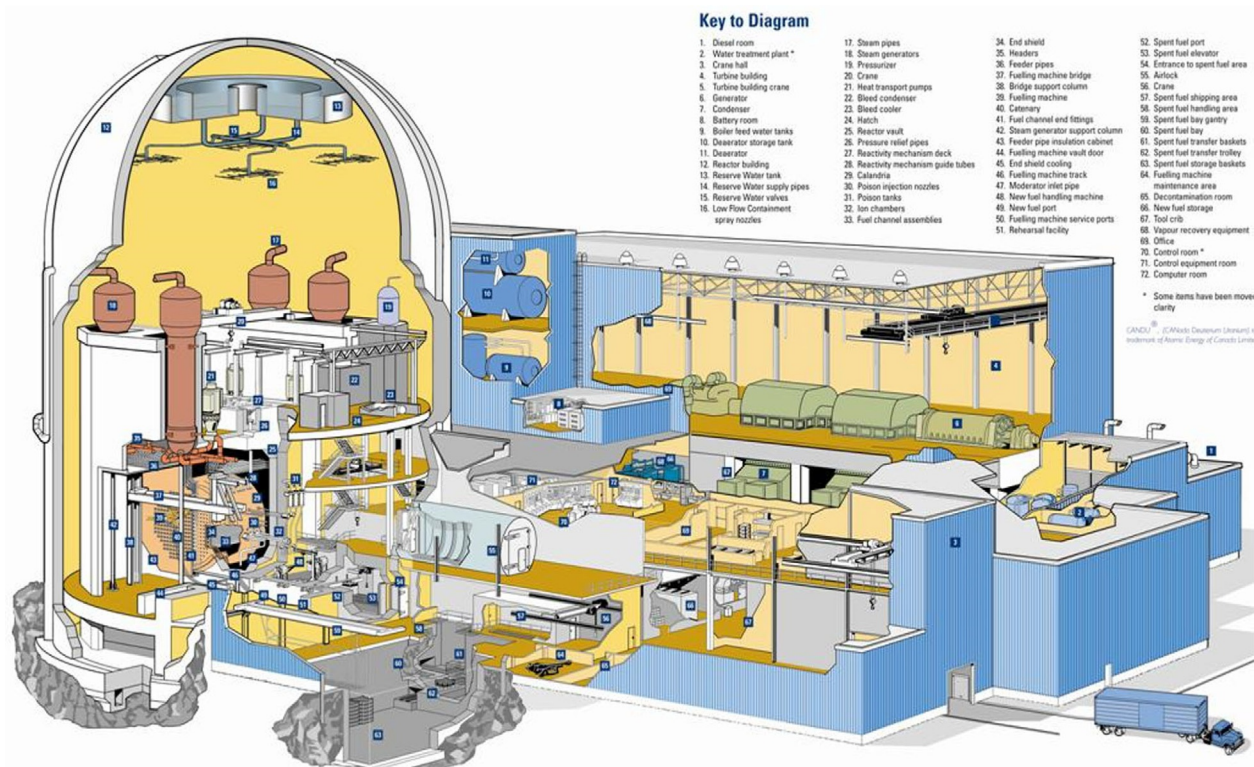
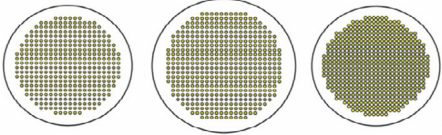

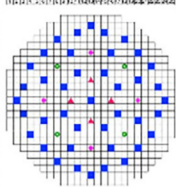


FIG. A1.84 Layout of generic PHWR NPP (artist image)

TABLE A1.18 Basic design parameters of PHWRs

Parameters	C-6	C-9	ACR-1000	IPHWR-700	AHWR
Outlet header: P , MPa	9.9	9.9	11.1	9.8	6.83
T , °C	310	310	319	310	285
Inlet header: P , MPa	11.2	11.3	12.5	10	7
T , °C	260	267	275	266	259.5
Single channel flow (max), kg/s	28	27.4	28	24	4.7
No. of SGs	4	4	4	4	None
Type of SG	Vertical U-tube/integral pre-heater			Ditto	Drum
Nominal tube OD, mm	15.9	15.9	15.9	19	-
Steam: T_{nominal} , °C	260	265	275.5	256.3	-
Steam void fraction	0.9975	0.9975	0.999	-	-
Steam: p , MPa (g)	4.6	5.0	5.9	4.5	-
Moderator system, t	265	312	250	282	-

TABLE A1.18 Basic design parameters of PHWRs—cont'd

Parameters	C-6	C-9	ACR-1000	IPHWR-700	AHWR
Heat-transport system, t	192	280	0	-	-
Total, t	457	592	250	-	-
Reactor output, MW _{th}	2064	2657	3187	2166	920
Pressurized coolant	D ₂ O	D ₂ O	H ₂ O	D ₂ O	H ₂ O
Moderator	D ₂ O	D ₂ O	D ₂ O	D ₂ O	D ₂ O
Calandria vessel OD, m	7.6	8.5	7.5	-	-
Fuel channel material	Horizontal Zr 2.5% _w Nb alloy PTs with modified SS403 end-fittings			Ditto	Vertical
No. of fuel channels	380	480	520	392	452
Lattice pitch, mm	286	286	240	-	225
PT wall thickness, mm	4	4	6.5	-	4
Core/Calandria section	cross				 
Steam-turbine type	Impulse-type tandem-compound	Ditto	Ditto	-	-
Steam-turbine composition	One double-flow cylinder	high-pressure			Ditto
Net to turbine, MW _{th}	2060	2650	3180	-	920
Gross/Net electrical output (nominal), MW _{el}	728/666	935/881	1165/1085	700	300/284
Thermal cycle efficiency, %	35.3	35.3	~36.6	29	30.9
Steam <i>T</i> at main stop valve, °C	258	263	273	256.3	285
Final feedwater: <i>T</i> , °C	187	177	217	180	130

Based on public domain data from AECL 2000-2011, DAE BARC, 2006-2011, IAEA, and [Torgerson et al., 2004](#).

TABLE A1.19 Basic parameters of PHWR fuel channels

Parameters/bundles	37- Element	CANFLEX	IPHWR- 700	AHWR
No. of elements (fuel rods)	37	43	37	54
Fuel	0.7% NU	0.7% NU	0.7% NU	3%+ThUO ₂ /PuO ₂
Bundle, pressure-tube and calandria-tube materials – zircaloy	-	-	-	-
Bundle rings	-	-	-	-
Centre ring (1 element)	13.08	13.5	13.1	11.2
Inner ring	13.08	13.5	13.1	-
Intermediate ring	13.08	11.5	13.08	-
Outer ring	13.08	11.5	-	-
Discharge burn up (MWd/t) av	-	-	7,000	38,000-64,000
Wall thickness (mm)	0.47	0.46/0.39	-	0.6
Heated/Total bundle length (mm)	481/495.3	-	495	3500
No. of bundles per channel	12	12	12	1
Heated/Total bundle-string length (m)	-	5.772/5.9436	-	-
Heated area (m ²)	8.76	9.26	-	-
ID Pressure Tube (PT) (mm)	103.45	103.45	103.4	120
Flow area (mm ²)	3,449	3,625	-	-
Hydraulic-equivalent diameter: D_{hy} (mm)	7.64	7.52	-	-
Heated-equivalent diameter: D_h (mm)	9.00	9.01	-	-
OD pressure tube (mm)	112	112	-	168
PT wall thickness (mm)	4.3	4.3	-	4
ID calandria tube (mm)	129	129	-	-
OD calandria tube (mm)	132	132	-	-
Wall thickness of calandria tube (mm)	1.4	1.4	-	-

Based on above mentioned public domain data from AECL 2000-2011; DAE BARC 2006-2011; IAEA; and [Sinha and Kakhodar, 2006](#).

TABLE A1.20 Advantages and Challenges of PHWRs (also, in addition, see [Table A1.7](#))

No	Advantages
1	Pressure-channel reactor does not require heavy-weight pressure vessel, so can be manufactured by many plants in the world
2	Mass-flow rates can be individually controlled in fuel channels, to optimise performance
3	Reactor-coolant flow in pressure channels is interlaced (i.e., opposite directions in neighboring channels), providing more uniform axial density distribution/neutron flux
4	Natural-uranium fuel, can operate using spent/recycled (RU/SEU) fuel from PWRs and BWRs, and, also, Th and Pu fuels
5	Refuelling on-line provides higher capacity factors compared to batch-refuelling reactors
6	Superior passive-safety system as liquid moderator separated from reactor coolant
Challenges	
1	Heavy-water reactor coolant and moderator more expensive than light water
2	Lower pressures/temperatures inside reactor and at steam turbine decrease thermal efficiency of NPP
3	Pressure tubes subjected to creep and sagging, which require replacement in 20-30 years
4	Positive power and void coefficients require auto controls and safety systems
5	On-line refuelling raises unnecessary Pu proliferation/diversion concern
6	Need to increase current small market share

moderators suitable for using Natural (NU) or Low-Enriched Uranium (LEU). Canada has developed and deployed PHWRs after they were excluded from nuclear cooperation with USA by the McMahon Act; and after building Douglas Point (Fig. 1.1.15 in [Chapter 1.1](#)), AECL directly helped India to build RAPS CANDU-type Units 1 and 2 in Rajasthan (see [Nuclear News, 2022](#)). The Pu produced and then discharged from PHWRs during the online refuelling necessary to maintain criticality with NU fuel was seen as potentially aiding India in developing its own needed nuclear-weapon capabilities.

Following the Non-Proliferation Treaty (NPT) ban on India in 1970 (because of their successful nuclear-weapons tests and deployment), cooperation on nuclear power between Canada and India then completely ceased, and India was essentially forced to “reverse engineering” and deploy their own PHWR designs. In that sense, necessity became a virtue, as the Indian nuclear program then went on to build new units to develop alternate fuel cycles due to uranium shortage, and only recently has the NPT ban been revisited for other reasons. Hence, India had developed their own PHWR technology, expertise, and national capability, as well as their own nuclear weapons ([Perkovich, 2002](#); [Ram, 1990](#)). As noted later, this also reinforced a program of coupling fast-spectrum sodium-cooled reactors with the breeding/production of Pu/Th fuels aimed at becoming energy self-sufficient and independent of external uranium supply, which is not an issue for Canada.

Additional development continued on HWR variants with light-water (H₂O) cooling the pressure-tube fuel channels, including the SGHWR in UK (100-MW_{el} prototype operating during

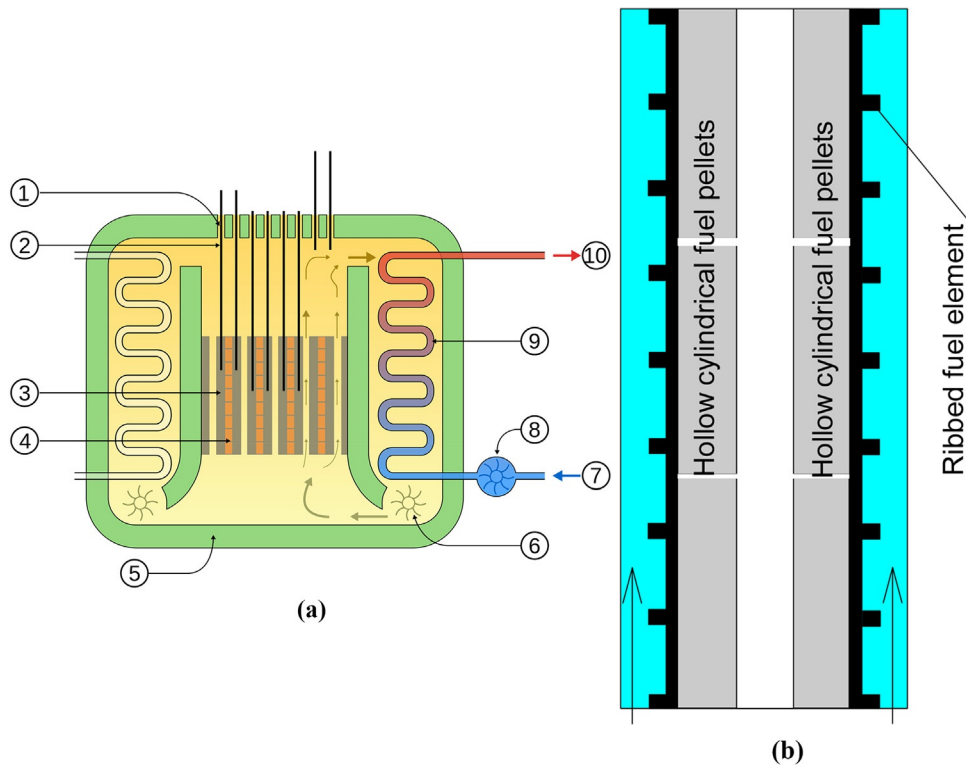


FIG. A1.85 (a) Simplified layout of Advanced Gas-cooled Reactor (AGR) (Author: [Messer Woland](https://commons.wikimedia.org/wiki/File:AGR_reactor_schematic.svg), https://commons.wikimedia.org/wiki/File:AGR_reactor_schematic.svg; website approached January 28, 2016): 1 - Charge tubes; 2 - Control rods; 3 - Graphite moderator; 4 - Fuel assemblies; 5 - Concrete pressure vessel and radiation shielding; 6 - Gas circulator; 7 - Water; 8 - Water circulator; 9 - Heat exchanger; and 10 - Steam. Heat exchanger is contained within steel-reinforced concrete combined pressure vessel and radiation shield; and (b) AGR ribbed fuel element with hollow fuel pellet ([Hewitt and Collier, 2000](#))

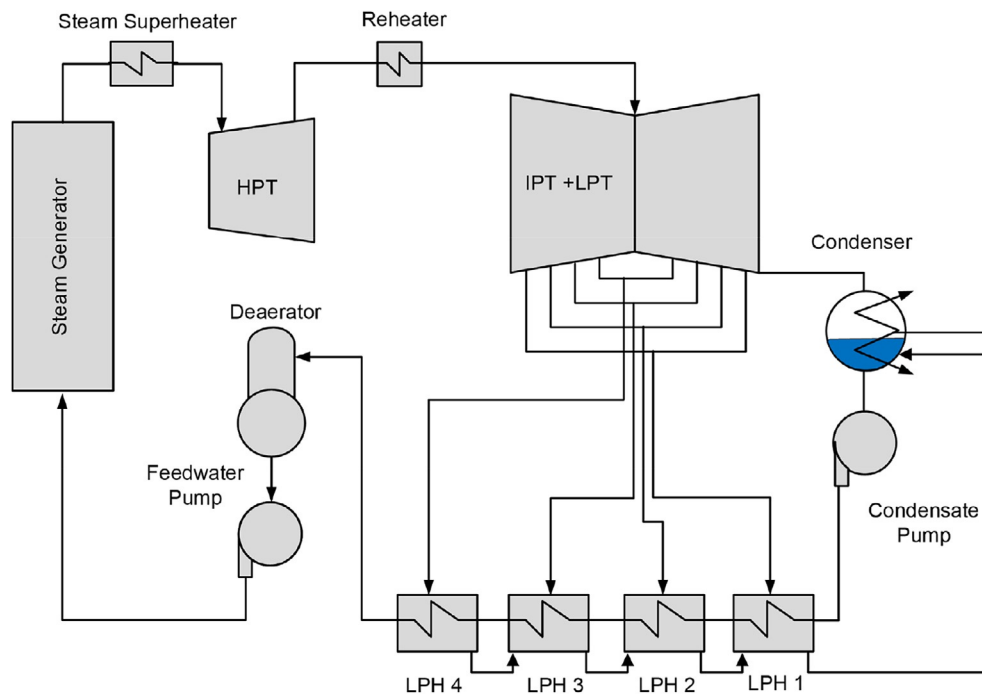


FIG. A1.86 Thermodynamic layout of AGR Torness NPP. Based on data from [Nonbøl \(1996\)](#)

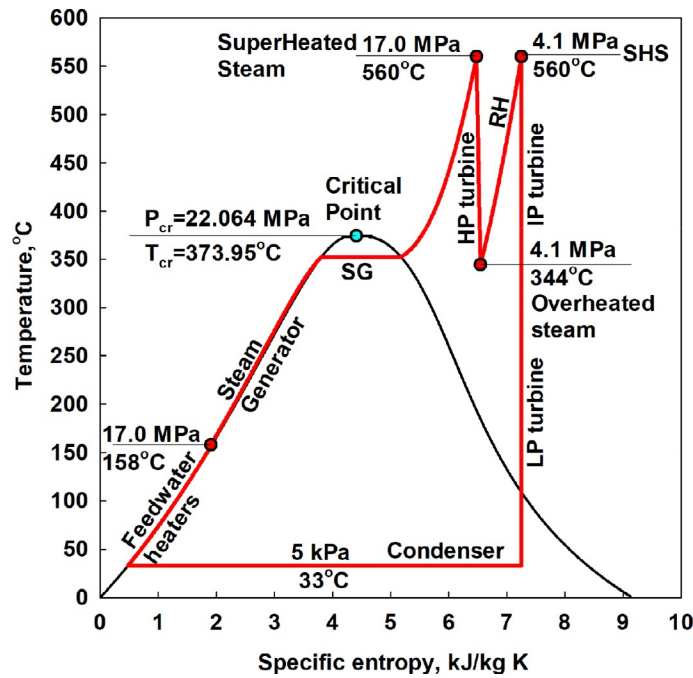


FIG. A1.87 Simplified $T-s$ diagram for AGR Torness NPP turbine cycle. By basic power-cycle parameters this $T-s$ diagram is more or less the same as that of older coal-fired power plants

1967-1990), Fugen reactor in Japan (a demonstration Advanced Thermal Reactor, heavy-water moderated, but with boiling light-water reactor coolant, operated from 1979 till 2003), and CIRENE in Italy (also, heavy-water moderated, but with boiling light-water reactor coolant, completed in 1988, but never put into operation), all now abandoned. The first PHWRs were small units in terms of power output, for reasons related to physics, channel- and core-design component size (calandria and steam generators) and D_2O availability. All these problems were solved with the subsequent excellent performance and development of sophisticated control and safety systems, advanced fuels and pressure-tube materials supported by in-depth R&D as detailed in the book on [Pressurized Heavy Water Reactors: CANDU \(2021\)](#).

According to the information in [Nuclear News \(March, 2022\)](#) the vast majority of PHWRs in the world are CANDU-type reactors designed by the Atomic Energy of Canada Limited (AECL). Currently, the CANDU-reactor technology in Canada is being developed by the Candu Energy Inc. (<http://www.candu.com/en/home/aboutcandu/default.aspx>), SNC-Lavalin Group (Mississauga, ON, Canada). Therefore, all information on CANDU reactors presented in this section is based on brochures obtained from the Candu Energy Inc. and figures on CANDU reactors/NPPs have been also provided by the Candu Energy Inc. and published here with their permission. For the latest data and developments in the CANDU-reactor technologies, please, refer to Candu Energy Inc. website (<https://www.snclavalin.com/en/markets-and-services/markets/nuclear>).

Therefore, basic information on PHWRs is provided based on CANDU-reactor designs (for details, see [Figs. A1.74–A1.82](#)). In addition, just for reference purposes a simplified layout of the PHWR NPP (Siemens design) (Atucha, Argentina) and more detailed layout of a generic PHWR NPP are also shown in [Figs. A1.83 and A1.84](#), respectively.

The latest Generation-III design of CANDU reactor is a 700-MW_e-class heavy-water moderated and heavy-water cooled pressure-tube (pressure-channel) EC6 reactor. Basic features and parameters of this reactor and corresponding NPP are as the following: 1) thermal-neutron spectrum; 2)

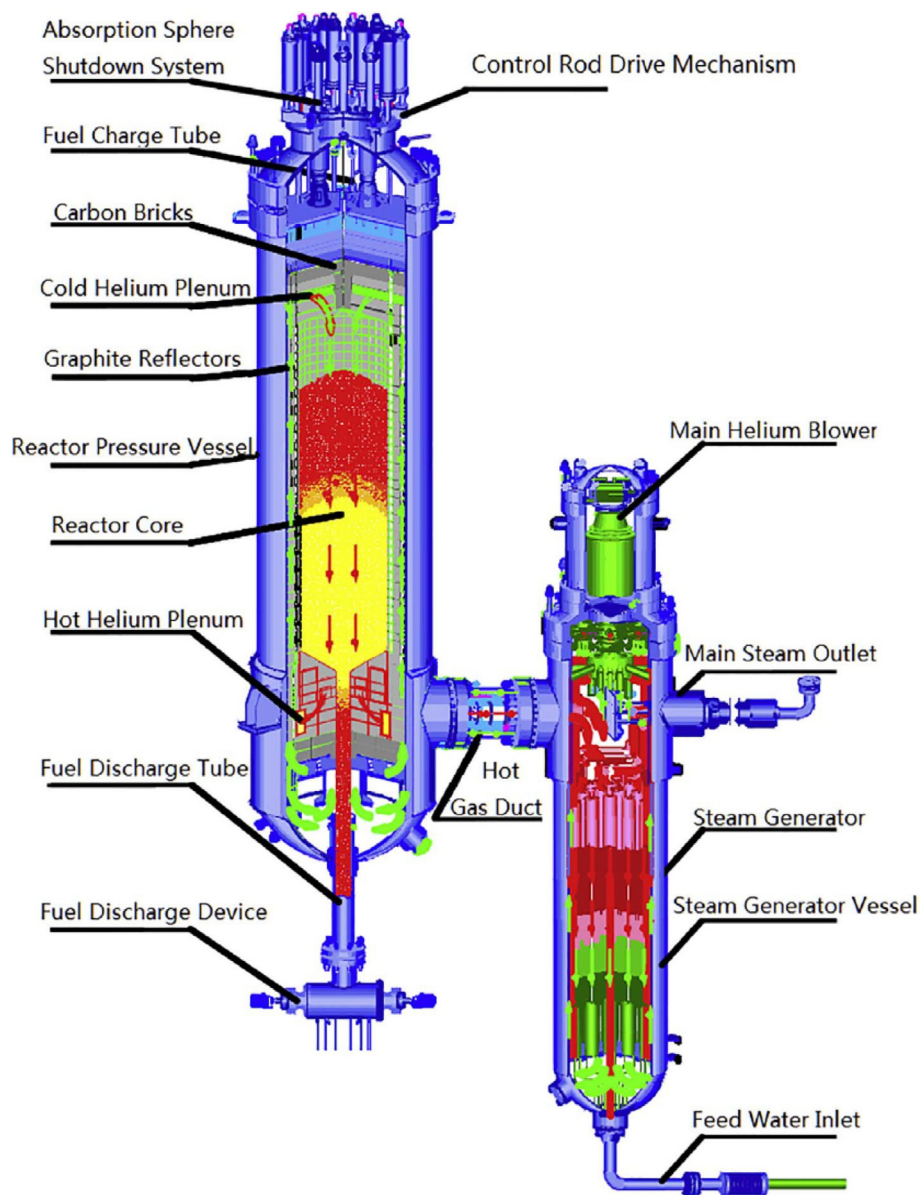


FIG. A1.88 Simplified layout of Gas-Cooled Reactor (GCR) - 100-MW_{el} helium-cooled High Temperature Reactor Pebble-bed Module (HTR PM) – SMR (Very High Temperature Reactor (VHTR) Generation-IV concept) (China) (Sun et al., 2018) (Copyright by Elsevier)

natural uranium-dioxide (UO₂) fuel; 3) fuel enrichment about 0.71wt%U²³⁵; 4) indirect cycle with steam generator, i.e., double-flow circuit (double loop); 5) pressure-channel design: Calandria vessel with horizontal fuel channels; 6) reactor coolant and moderator separated, but both are heavy water; 7) reactor-coolant parameters: (a) inlet-header operating pressure 11.05 MPa and temperature 265°C; (b) outlet-header operating pressure 9.89 MPa and temperature 310°C (close to saturation temperature); and (c) maximum single-channel mass-flow rate 28.5 kg/s; 8) on-line refuelling; and 9) power cycle - subcritical-pressure regenerative Rankine steam-turbine cycle with steam reheat (working fluid light water, turbine – one HP and two double-flow LP cylinders; net thermal output 2080 MW_{th}; gross/net electrical output (nominal) 740/690 MW_{el}; turbine steam-inlet parameters: Saturation pressure 4.69 MPa and temperature 260°C; condenser vacuum 4.9 kPa).

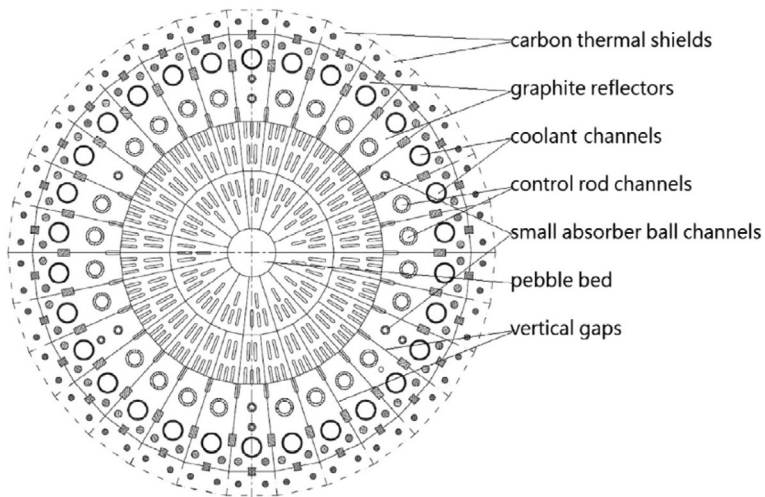


FIG. A1.89 Horizontal cross section of HTR-PM core (Sun et al., 2018) (Copyright by Elsevier)

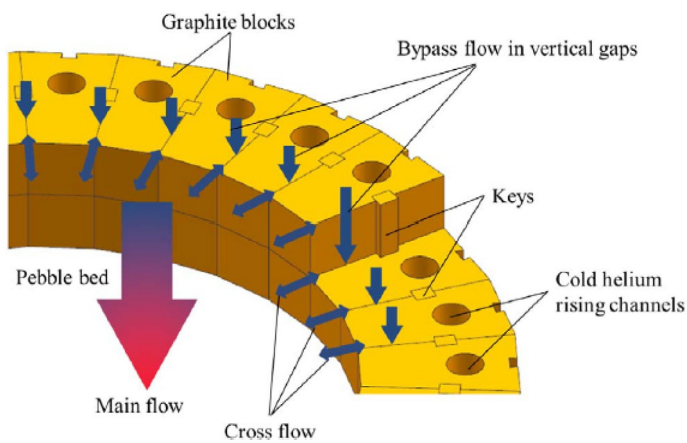


FIG. A1.90 Vertical gap and cross flow in HTR-PM core (Sun et al., 2018) (Copyright by Elsevier)

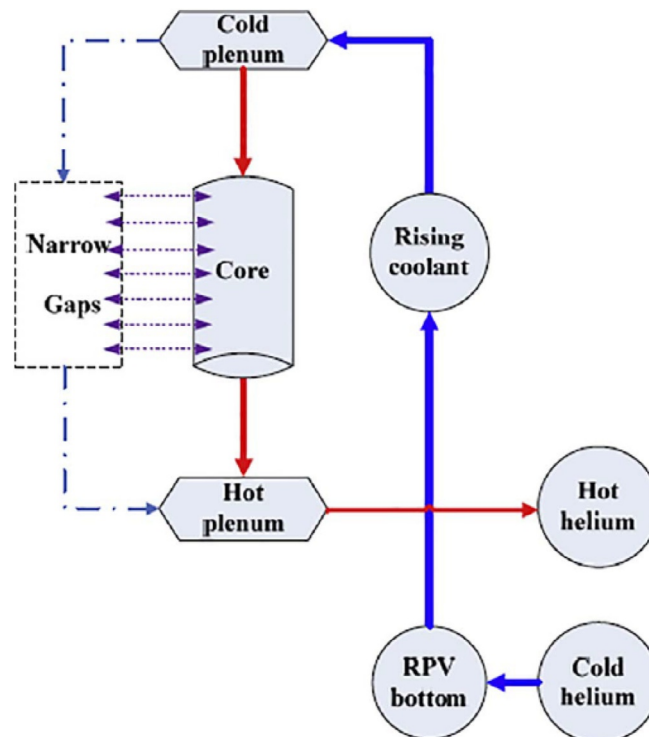


FIG. A1.91 Simplified layout of main and bypass flows (Sun et al., 2018) (Copyright by Elsevier)

TABLE A1.21 Main design parameters of HTR-PM (GCR) (Institute of Nuclear and New Energy Technology (INET), Tsinghua University, (China))

No.	Parameter	Value
1	Reactor type	Modular pebble-bed high temperature gas (He)-cooled reactor
2	No. of reactors	Two reactors per one power cycle
3	Installed capacity	$2 \times 250 \text{ MW}_{\text{th}}/210 \text{ MW}_{\text{el}}$
4	Thermal efficiency of NPP	42% (gross)
5	Coolant/Moderator	Helium/Graphite
6	Primary circulation	Forced with downward flow of He in reactor core
7	Pressure of reactor coolant	7 MPa
8	Temperature of reactor coolant	$T_{\text{out}}/T_{\text{in}} = 750^{\circ}\text{C}/250^{\circ}\text{C}$
9	Flow rate of reactor coolant	96 kg/s
10	RPV height/diameter (inner)	25 m/5.7 m
11	Active core diameter/height	3 m/11 m
12	Average core power density	$3.22 \text{ MW}/\text{m}^3$
13	RPV weight	800 ton
14	Rankine-cycle steam pressure/temperature: outlet/inlet	14.1 MPa/570°C/205°C
15	Main steam flow rate at the inlet of turbine	673 t/h
16	Fuel type	TRISO (UO ₂)
17	Fuel shape/assembly array	Spherical elements (60-mm OD) with coated particle fuel
18	Diameter of fuel zone	50 mm
19	Diameter of kernel	0.5 mm
20	Number of fuel assemblies in core	420,000
21	Fuel enrichment	8.5%
22	Core discharge burnup	90 GWd/ton
23	Average fuel power density	85.7 kW/kgU
24	Heavy-metal loading per fuel element	7 g
25	Fuel cycle	LEU, open cycle, spent fuel intermediate storage at plant
26	Refuelling	On-line

TABLE A1.21 Main design parameters of HTR-PM (GCR) (Institute of Nuclear and New Energy Technology (INET), Tsinghua University, (China)—cont'd

No.	Parameter	Value
27	Reactivity control mechanism	Control rod insertion
28	Safety systems	Combined active and passive
29	Special features	Inherent safety, no need for offsite emergency measures
30	Design life	40 years
31	Seismic design (SSE)	0.2 g

Based on: https://aris.iaea.org/Publications/SMR_Book_2020.pdf.

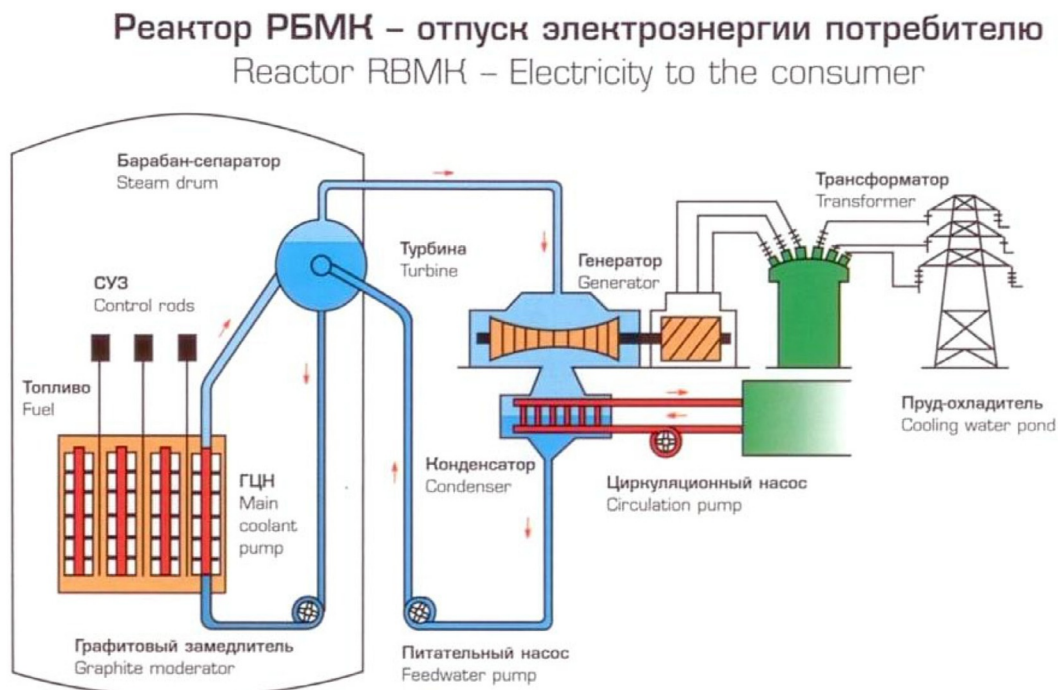


FIG. A1.92 Simplified layout of 1000-MW_{e1} Light-water-cooled Graphite-moderated Reactor (LGR) (Russian RBMK) NPP (Rosenergoatom, 2004). Courtesy of Rosenergoatom

Details on present and advanced PHWRs While current PHWRs have heavy-water reactor coolant and moderator, and may add enhanced safety and performance features, new proposed and advanced designs and Generation-IV reactor concepts use light water as a reactor coolant retaining heavy water as a moderator. These latter include Generation III⁺ concepts such as Advanced CANDU[®] Reactor (ACR[®]-1000) (AECL design, Canada), the Advanced HWR (AHWR) (BARC design, India), (see Chapter 15) and Generation-IV SuperCritical Water-cooled Reactor (SCWR) (AECL concept, Canada) and Canadian SCWR (CNL concept, Canada) (see Chapter 8). Importantly, the final development and commercial deployment of the new ACR-1000 was terminated (nominally “completed”) soon after the re-organization and sale of the commercial parts of

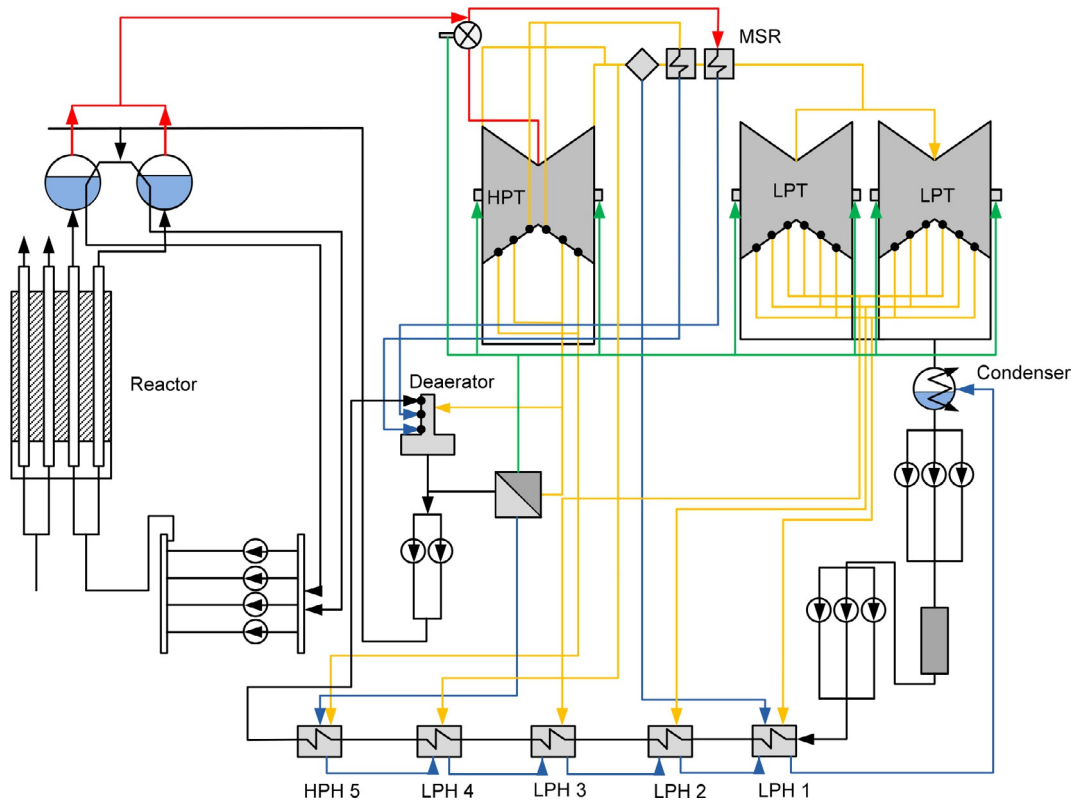


FIG. A1.93 Thermodynamic layout of RBMK-1000 NPP. Adapted and simplified from *Channel Nuclear Power Reactor (RBMK)* (2006)

AECL in 2012 (then a Crown Corporation), with the SCWR program then becoming purely governmental R&D as part of the GIF.

For reference purposes, a typical conceptual overall PHWR circuit layout is shown in Fig. A1.74. Specific design variants simply change the number of horizontal fuel (pressure tube) channels, core diameter, total steam generators, main pumps and entry (feeder) and exit (riser) pipework layout according to the plant output and limits on peak channel power; with the core fully immersed into a calandria or tank holding D_2O , with the entire primary system enclosed in a containment building.

A comparison of light- and heavy-water thermophysical properties at 10 – 11 MPa (i.e., PHWR-reactor operating range) shows that, in general, they are quite close (Sabir et al., 2019; Petriw et al., 2019). The most “significant” differences up to 11% are for densities of liquids, i.e., density of heavy water is higher than that of light water, and for liquid thermal conductivities, i.e., heavy-water thermal conductivity is lower up to 13% compared to that of light water.

In general, all thermalhydraulics experiments on heat transfer, Critical Heat Flux (CHF), Post-DryOut (PDO) heat transfer, emergency-cooling-system performance, etc. for PHWRs are conducted using light water, but results adopted for heavy-water conditions through physical scaling laws (Pioro et al., 2001). Also, it should be mentioned that, eventually, for a wider range of experiments, they are also performed in modelling fluids such as R-134a (previously, in R-12), and scaled into light- or heavy-water conditions (Guo et al., 2006; Leung et al., 2003; Pioro et al., 2000, 2001, 2002a,b).

The major statistics on PHWRs are shown in Chapter 1.2; basic design parameters of PHWRs – in Table A1.18; and basic parameters of PHWR fuel channels – Table A1.19.

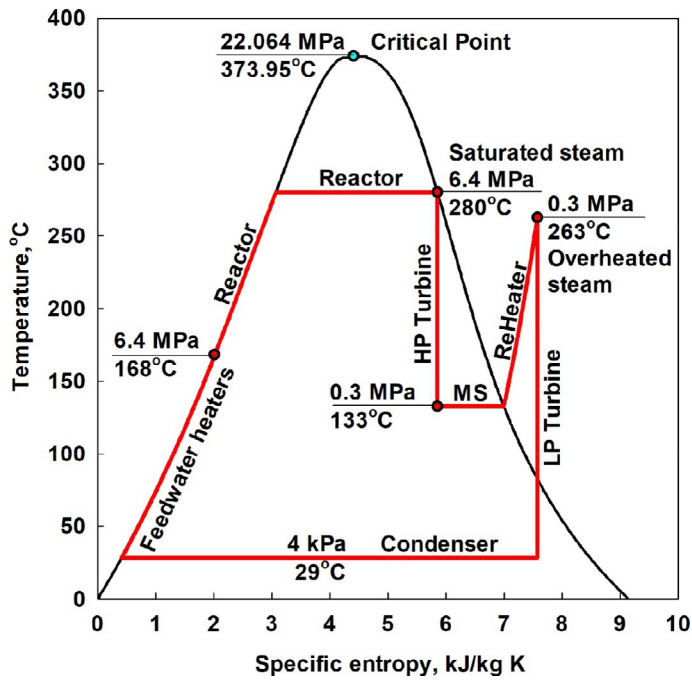


FIG. A1.94 Simplified T - s diagram for RBMK-1000 NPP turbine cycle

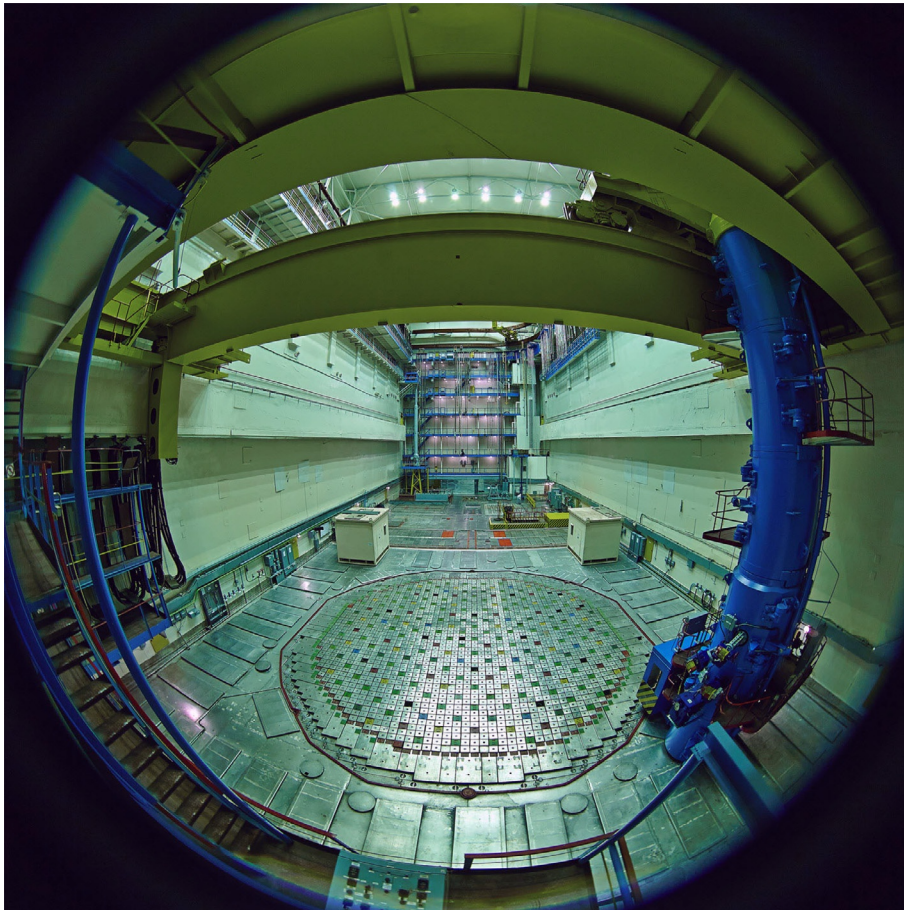


FIG. A1.95 RBMK reactor hall at Smolenskaya NPP: <https://www.flickr.com/photos/rosatom/29137381652/in/album-72157672990867205/>. In front and center – reactor; to the right - refueling machine with operator cabin near floor. *Courtesy of Rosatom*

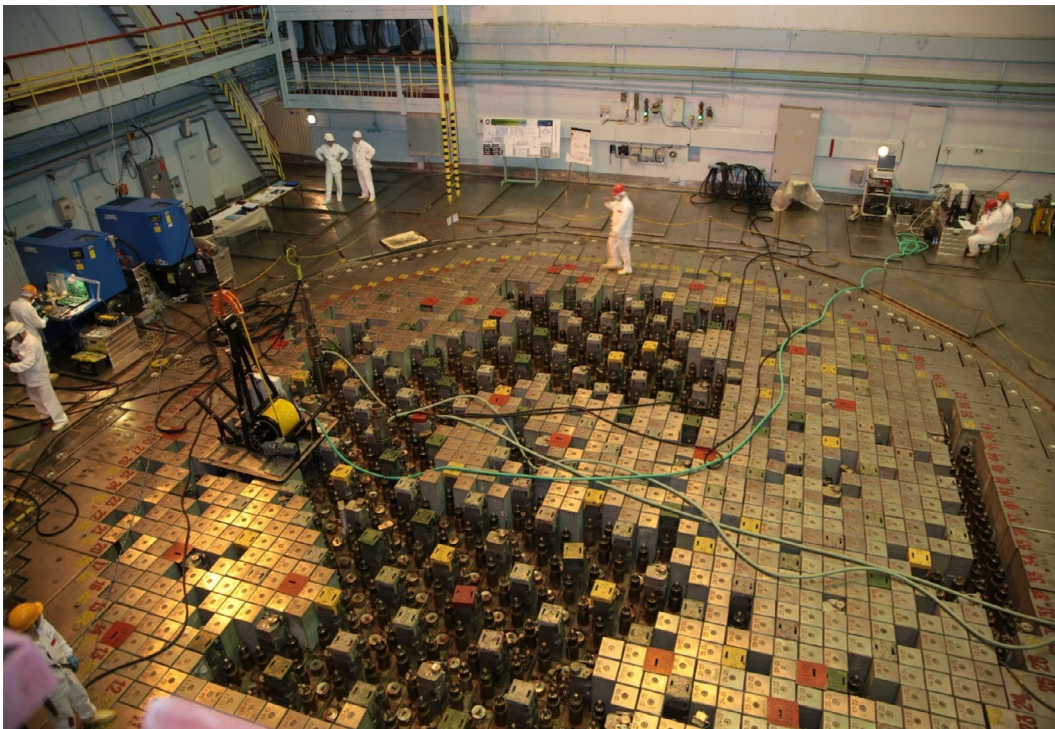


FIG. A1.96 Repairs of graphite-moderator blocks of RBMK reactor at Kursk NPP: <https://www.flickr.com/photos/rosatom/26246306197/in/album-72157672344243460/>. Courtesy of Rosatom

It is important to note that some of the principal objectives for these advances and proposed changes were in:

- (a) adopting alternative and more flexible fuel cycles and increased uranium/plutonium utilization via increased burn up, recycling and/or transition to a self-sustaining (U/Pu/Th fuel cycle);
- (b) decreasing the positive power and void coefficients inherent in the original NU/D₂O HWR by slight fuel enrichment and lattice-pitch reduction;
- (c) reducing the capital cost and the needed D₂O inventory in the primary circuit; and
- (d) continuing to compete in both the large- and small-reactor markets.

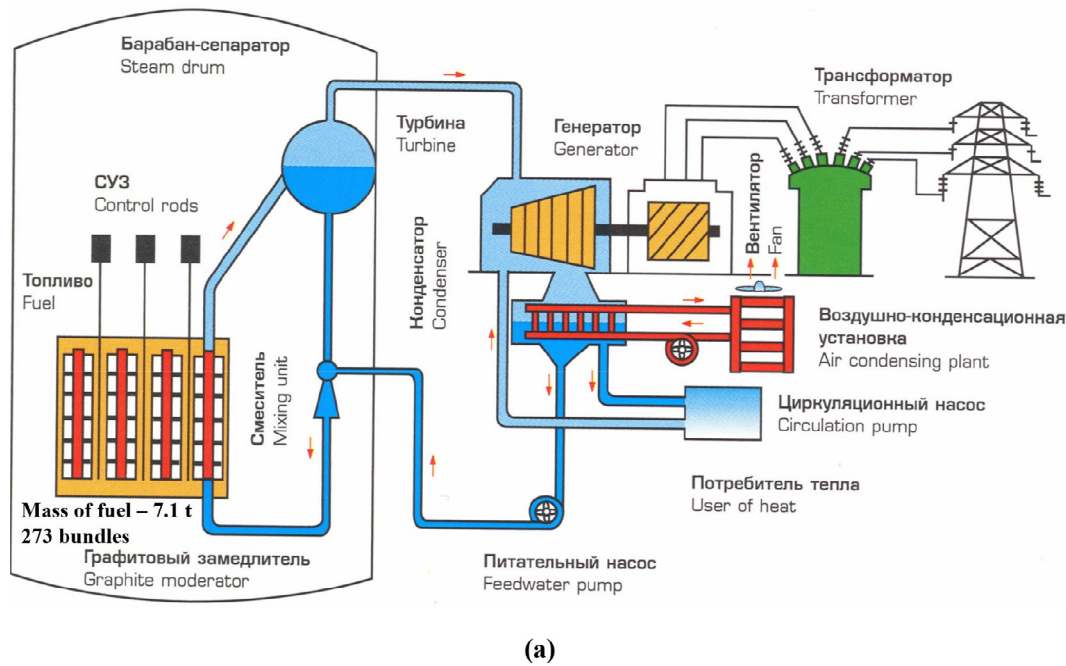
In addition to a large number of various publications on PHWRs, the official and the latest information can be obtained only from research establishments/companies/organizations, which involved in the R&D, design, construction, and operation of PHWRs (see list of literature sources at the end of Section).

Summary of PHWR status and issues going forward Having summarized the overall role, salient design and operating characteristics, and some potential development directions, we can now also summarize issues going forward as a balance between the Advantages and the Challenges.

Maximizing the Advantages and addressing the Challenges requires innovative thinking, and we briefly review the current situation.

Extending life of existing units Presently, the short-term Canadian approach is to delay or defer any new PHWR builds and to “refurbish” and life extend many of the existing units, as is

Реактор ЭГП-6 – отпуск электроэнергии потребителю
 Reactor EGP-6 – Electricity to the consumer



(a)



(b)



(c)

FIG. A1.97 Simplified layout of 11-MW_{el} EGP-6 (Power Heterogeneous Loop (in Russian abbreviations) reactor NPP – graphite-moderated, boiling light-water-cooled with natural circulation (also, Light-water-cooled, Graphite-moderated Reactor (LGR) by type), pressure-channel power reactor for production of electricity and heat, air-cooled condenser; prototype of RBMK (a); photo of reactor hall; and (c) photo: close look on reactor with open cover (Rosenergoatom, 2004). EGP-6 is smallest operating reactor by installed capacity, i.e., 11 MW_{el net}/65 MW_{th}. Also, it should be admitted that this reactor is the only one with natural circulation of reactor coolant (boiling light water in vertical channels) in the world as of today. Only three left at Bilibino NPP, Chukotka, Russia. However, all of them will be shut down forever within several years. Courtesy of Rosenergoatom

TABLE A1.22 Major parameters of USSR/Russian LGRs

Parameter	EGP-6	RBMK-1000	RBMK-1500 ^a
Star of operation	1975; 1976; 1977	1979; 1980; 1981; 1982; 1984; 1985; 1986; 1989	1983-2004; 1987-2009
Thermal power, MW _{th}	65	3200	4800
Electrical power, MW _{el}	12	1000	1500
Thermal efficiency, %	18.5	31.3	31.3
Coolant <i>P</i> , MPa	6.2	6.9	6.9
Coolant flow, t/h	600	32,000	48,000
Coolant <i>T</i> , °C	265	284	284
Steam flow rate, t/h	100	5600	8400
Steam pressure, MPa	6.5	6.6	6.6
Steam <i>T</i> , °C	280	280	280
Core: <i>D/H</i> m/m	4.2/3.0	11.8/7	11.8/7
Fuel enrichment, %	3.0; 3.6	2.0-2.4	2.0
No. fuel assemblies	273	1580	1661

Explanations to Table: EGPs and RBMKs are LGRs or vertical pressure-channel boiling reactors (outlet fuel-channel steam quality is ~14% (maximum 20%) (in BWRs - about 10%).

^aAll RBMK-1500 reactors, which were the largest reactors ever designed and built in the USSR, were shut-down. There were only 2 reactors at the Ignalina NPP (Lithuania).

also done for many LWRs in the USA. For PHWRs this has already been demonstrated and is achieved by being able to fully replace:

- (1) all pressure tubes and end fitting as they approach end of life in terms of allowable creep margins and irradiation;
- (2) feeder and riser pipework as needed, particularly, if and where there is any flow assisted corrosion or wall thinning, using advanced tubing materials; and
- (3) steam generators, where excessive corrosion and chemical attack, have caused leaking tubes (resulting in many being plugged), but now using longer – life tube advanced materials.

The refurbishment and outage cost is justified as it is lower than building an entirely new plant on a different site and can provide more than another 20 years of operation, while, R&D continues to examine life-limiting factors.

Two unique PHWRs (Siemens design) have been built and connected to grid in Argentina (see Fig. A1.83 and Nuclear News, 2022). The most recent completed in 2016 after many years of delay, has an installed capacity of 693 MW_{el}, (gross electrical power is 745 MW_{el} and gross thermal efficiency of ~34.3%. Unfortunately, as for now, there are no plans to build such reactors further. Therefore, the latest information on these PHWRs and the Atucha NPP can be found on the website of Nucleoeléctrica Argentina (NA-SA): <http://www.na-sa.com.ar/>.

Sodium-cooled fast reactors are the main reactor type for implementing the closed fuel cycle.

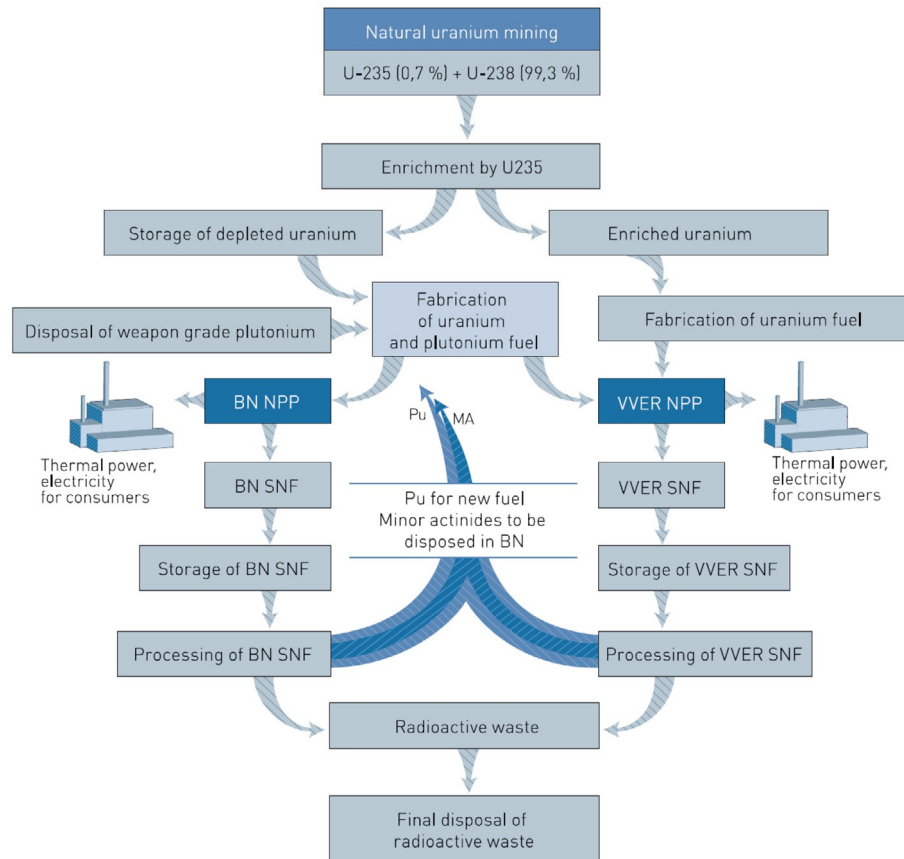


FIG. A1.98 Diagram of closed fuel cycle for VVER (PWR) and BN reactors. Courtesy of JSC “Afrikantov OKBM”. (Accessed Feb. 19, 2022): <http://www.okbm.nnov.ru/upload/iblock/340/hkrhdgf35afpjjuduvd7n2v0848fr0rye.pdf>

Upgrading existing designs To maintain a commercial market presence, the existing C-6 design has been upgraded or “Enhanced” by adding additional safety features and modernizing the plant equipment, and modular construction, while still retaining the same fundamental core, primary and safety systems, BOP performance, core-design features and fuel. The key design parameters largely remain as shown in Table A.1.18.

In India, the effectively standard design PHWR-700 has been developed, building on the 200 and 550 MW_{el} units experience (Table A1.18), a size that fits with the power grid, manufacturing capability, technology support and future energy needs of this rapidly developing nation (for details, see Sinha et al., 2016 and <https://aris.iaea.org/PDF/AHWR.pdf> (Accessed: June 21, 2020)).

Recently, the SNC-Lavalin Inc. announced a 300-MW_{el} SMR being a conceptual PHWR-300 built on previous Canadian small-reactor PHWR technology, namely, of course, the RAPS Units 1 & 2



FIG. A1.99 History and geography of USSR/Russian fast reactors. *Courtesy of JSC “Afrikantov OKBM”*: <http://www.okbm.nnov.ru/upload/iblock/340/hkrhdgf35afpjjudvwd7n2v0848fr0rye.pdf>; Accessed Feb. 19, 2022

built by AECL in India (https://www.snclavalin.com/~media/Files/S/SNC-Lavalin/download-centre/en/brochure/our-candu-smr_en.pdf; Accessed: June 21, 2020.) and a purely conceptual AECL “CANDU-3” design.

Advanced PHWR concepts and fuel cycles One of the unique features of the PHWR design is its ability to operate with alternative fuels such as a Recovered Uranium (RU) from the reprocessing of LWR spent fuel, MOX (80% UO_2 and 20% PuO_2), and thorium-based fuels, in addition to the conventional natural uranium fuel (see Fig. A1.75) (<https://www.snclavalin.com/~media/Files/S/SNC-Lavalin/documents/advanced-fuel-candu-reactor-en.pdf>; Accessed: June 21, 2020).

Since 2011, SNC-Lavalin with Chinese partners have been developing an Advanced Fuel CANDU Reactor (AFCR™), which technology is attractive for countries such as China, India,

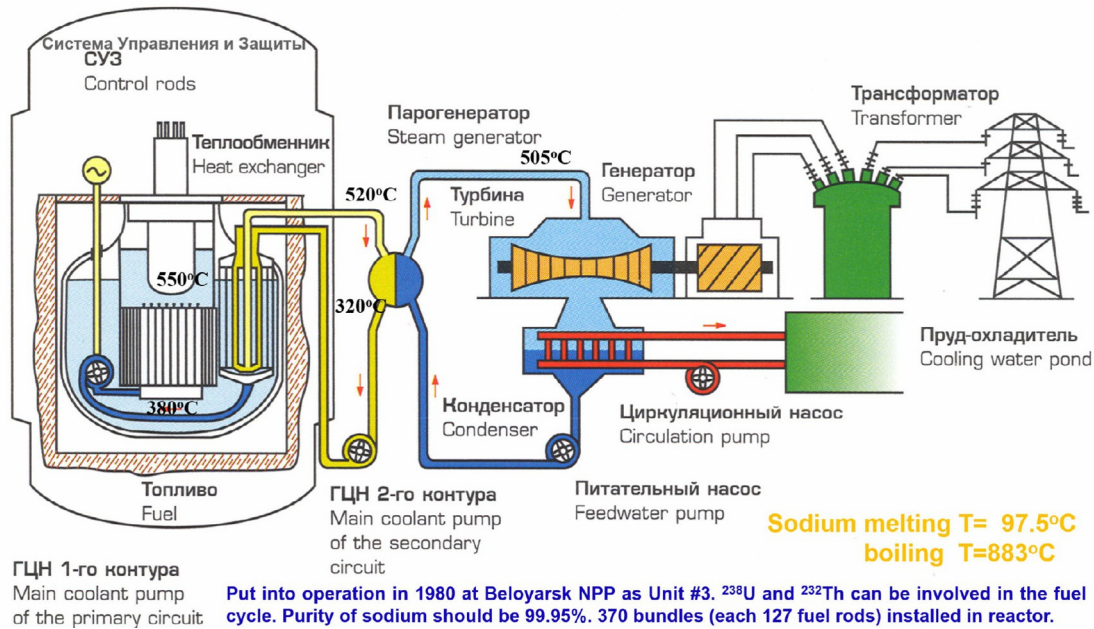


FIG. A1.100 Layout of Liquid-Metal Fast-Breeder Reactor (LMFBR) or SFR (Russian BN-600) NPP (Rosenergoatom, 2004). Sodium can cause serious or permanent injury. Can be ignited under almost all ambient temperature conditions (autoignition temperature in air of liquid Na: 120 – 470°C). Readily undergoes violent chemical changes at elevated temperatures and pressures. Reacts violently or explosively with water with hydrogen generation. *Courtesy of Rosenergoatom*

etc., which rely on foreign sources of uranium, but might have reserves of depleted uranium, a by-product of enrichment processes, used or 'spent' uranium from conventional LWRs as well as thorium fuel.

Some time ago, the AECL developed a Generation-III⁺ reactor design, i.e., 1200-MW_{el} Advanced CANDU[®] Reactor (ACR[®]-1000), which will use light water as a reactor coolant and heavy water as a moderator (ACR-1000[®] Technical Summary, 2010. AECL), but with negative void and power coefficients, which was also designed to be able to use alternative fuels, including Th and Pu.

Conclusions

- (1) Only two countries are front runners in using PHWRs: Canada with 19 reactors; and India with 19, and they have been the major developers of the PHWR technologies. Currently, the largest operating NPP in the world is the Canadian Bruce NPP, which is equipped with 8 PHWRs. Also, India is now planning to deploy seven (4 planned to put into operation within 2026 – 2028 and 5 – without exact dates) IPHWR-700 units.
- (2) All current PHWRs have heavy water as a reactor coolant and moderator. However, advanced reactors of Generation-III⁺ (ACR-1000 (Canada); APHWR-700 (India), and Generation-IV type (Canadian SCWR and SSR SMR)) will use light water as a reactor coolant, but still have heavy water as a moderator. Therefore, these reactors are Light-water-cooled Heavy-water-moderated Reactors or LHRs.
- (3) One of the unique features of the CANDU[®]-reactor design is its ability to operate with alternative fuels such as a Recovered Uranium (RU) from the reprocessing of LWR spent fuel, MOX (80% UO₂ and 20% PuO₂), and thorium-based fuels. In addition to the

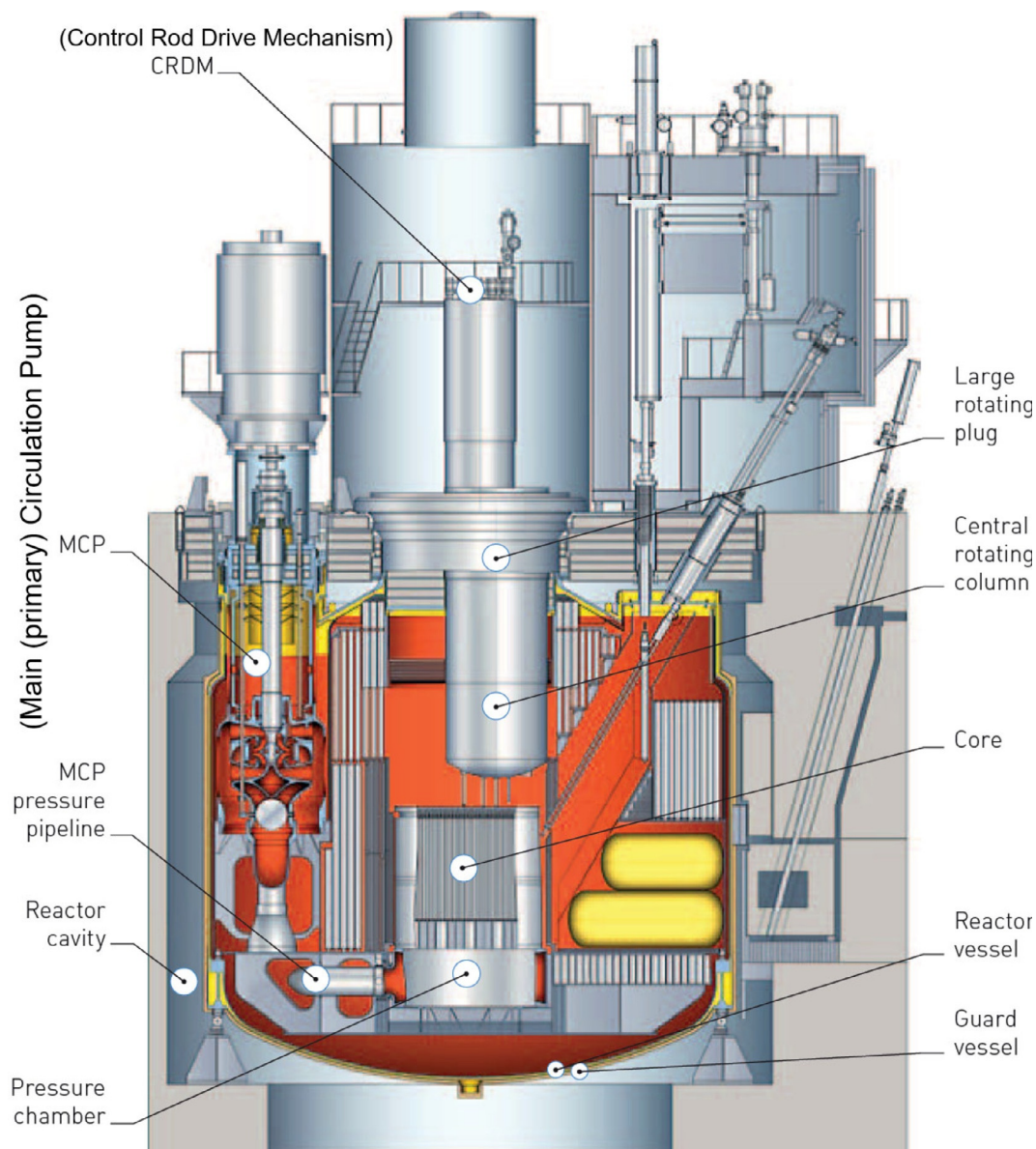


FIG. A1.101 Layout of BN-600 reactor. Courtesy of JSC "Afrikantov OKBM": <http://www.okbm.nnov.ru/upload/iblock/340/hkrhdgf35afpjuduud7n2v0848fr0rye.pdf>; Accessed Feb. 19, 2022

conventional natural-uranium fuel, which enables safe, sustainable and large-scale development of nuclear power, while improving uranium-resource-utilization rates and reducing fuel costs for utilities.

- (4) The major Challenges for PHWR identified include increasing the relatively small market share, enhanced competitiveness, while addressing proliferation issues and demonstrating advanced-reactor efficiency and fuel-cycle technologies.

Additional PHWR information sources

Canada

Design: Candu Energy Inc., a member of the SNC-Lavalin Nuclear Group (Mississauga, ON, Canada): <https://www.snclavalin.com/en/markets-and-services/markets/energy/nuclear>.

Research: Canadian Nuclear Laboratories (CNL): <https://www.cnl.ca/en/home/default.aspx>.

Safety: Canadian Nuclear Safety Commission (CNSC): <https://nuclearsafety.gc.ca/eng/>.

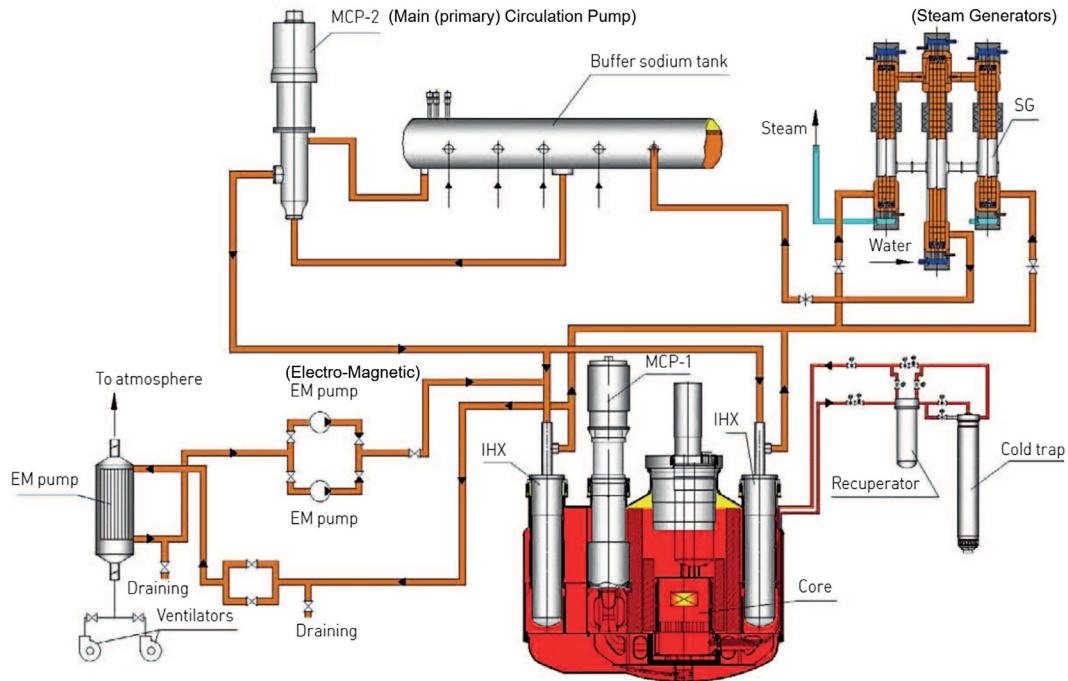


FIG. A1.102 Layout of BN-600 NPP. Courtesy of JSC "Afrikantov OKBM": <http://www.okbm.mnov.ru/upload/iblock/340/hkrhdgf35afpjduvd7n2v0848fr0rye.pdf>; Accessed Feb. 19, 2022

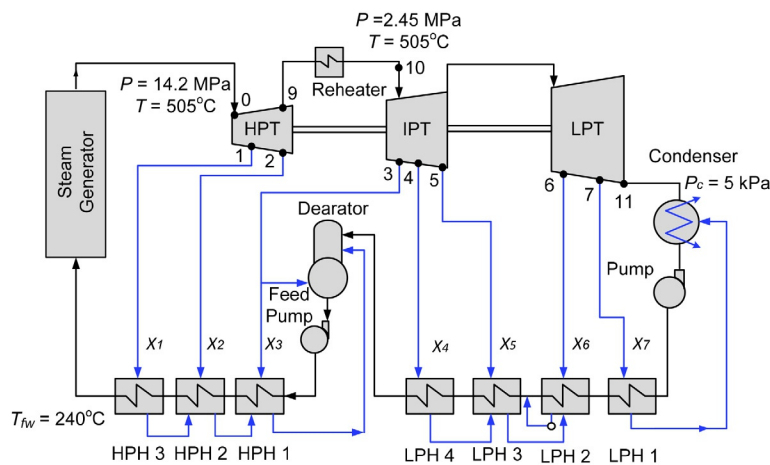


FIG. A1.103 Thermodynamic layout of 600-MW_{el} BN-600 SFR NPP. Based on data from Grigor'ev and Zorin (1988), Margulova (1995)

Operators:

Ontario Power Generation (OPG) (Darlington and Pickering NPPs): <https://www.opg.com/>;
 Bruce Power (BP) (Bruce NPP): <https://www.brucepower.com/>; and
 New Brunswick Power (NBP) (Point Lepreau Nuclear Generating Station - NPP): <https://www.nbpower.com/en/about-us/divisions/nuclear/>.

CANDU[®] Owners Group (COG): <http://www.candu.org/SitePages/Home.aspx>.

COG members are comprised of Canadian and international nuclear utilities.

Canadian members: 1) OPG; 2) NBP; and 3) CNL.

International members:

(1) Korea Hydro and Nuclear Power (KHNP): <https://npp.khnp.co.kr/index.khnp>;

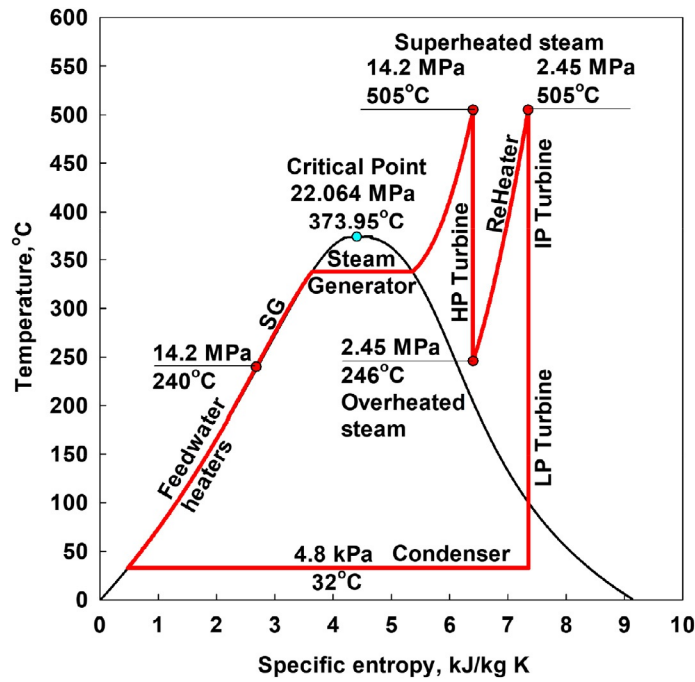


FIG. A1.104 Simplified T - s diagram for the 600-MW_{el} BN-600 SFR NPP turbine cycle

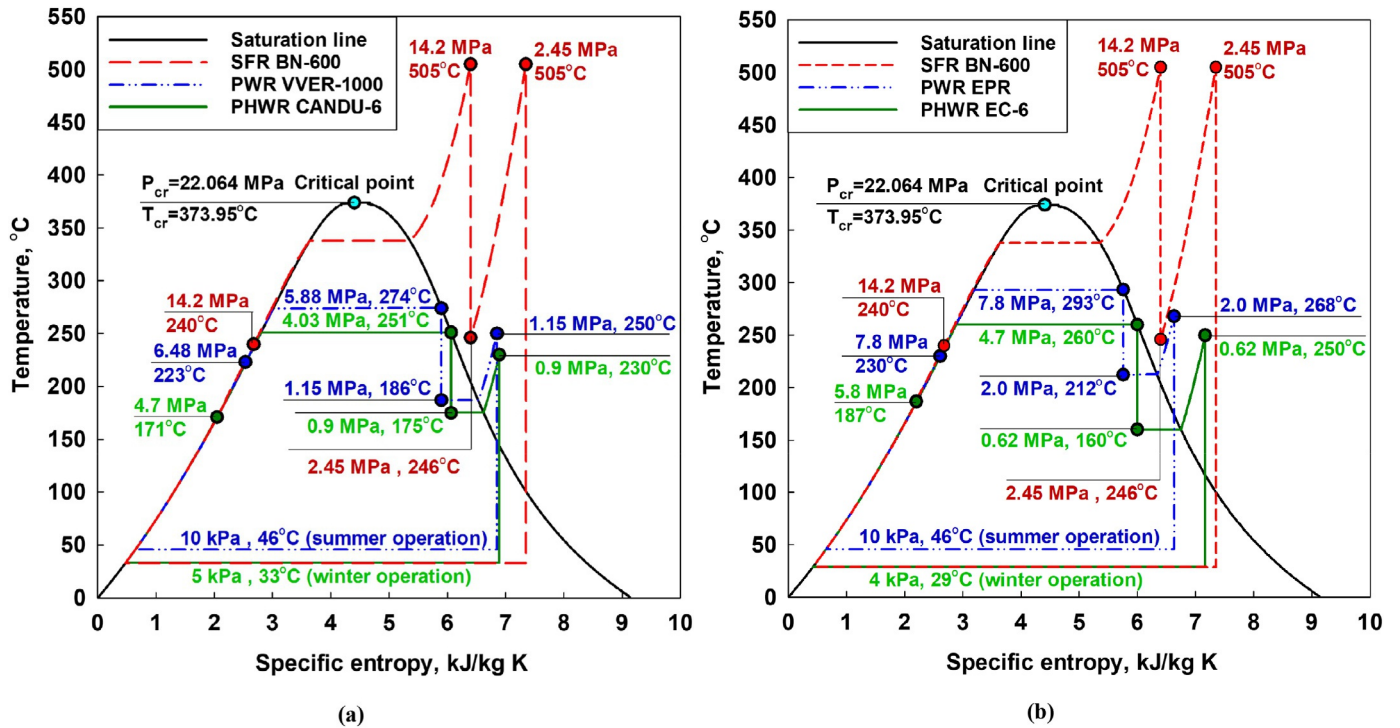


FIG. A1.105 Comparison of T - s diagrams for several nuclear-power-reactors: SFR BN-600 (Russia) with (a) PWR VVER-1000 (Russia); PHWR CANDU-6 (Pickering NPP) and (b) PWR EPR (France); PHWR EC-6

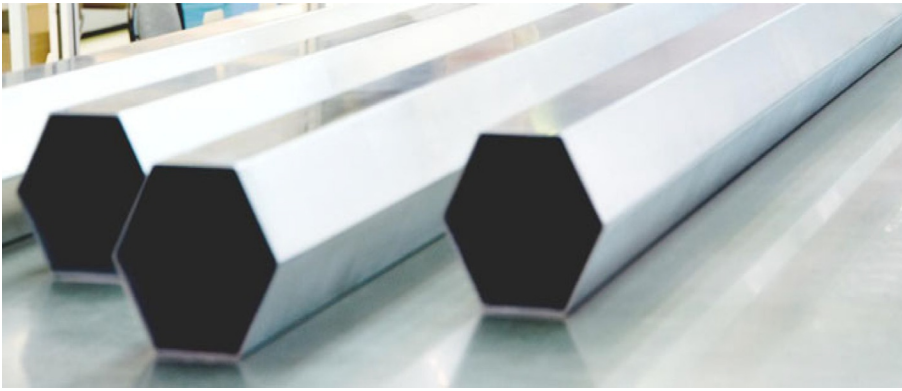


FIG. A1.106 Flow tubes (hexahedron cross section) for BN-600. Courtesy of Rosatom: <https://www.flickr.com/photos/rosatom/40632327951/in/album-72157692396689951/>; Photo by MSZ, 2014



(a)



(b)

FIG. A1.107 Sodium-cooled Fast Reactor (SFR) - BN-800, 820 MW_{el}, Beloyarsk NPP, year 2017: (a) reactor hall and (b) turbine-generator hall: <https://www.flickr.com/photos/rosatom/35647612034/in/album-72157671632599611/>. Courtesy of Rosatom

FIG. A1.108 Layout of BN-800 reactor. Courtesy of JSC "Afrikantov OKBM": <http://www.okbm.nnov.ru/upload/iblock/340/hkrhdgf35afpjudu vd7n2v0848fr0rye.pdf>; Accessed Feb. 19, 2022

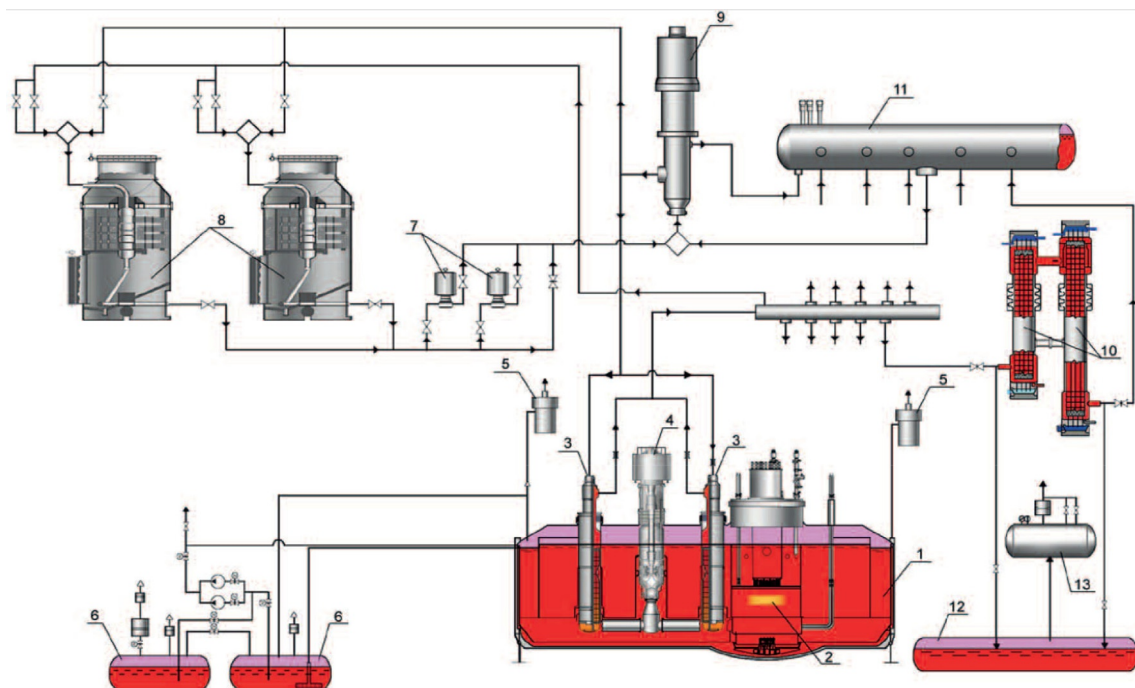
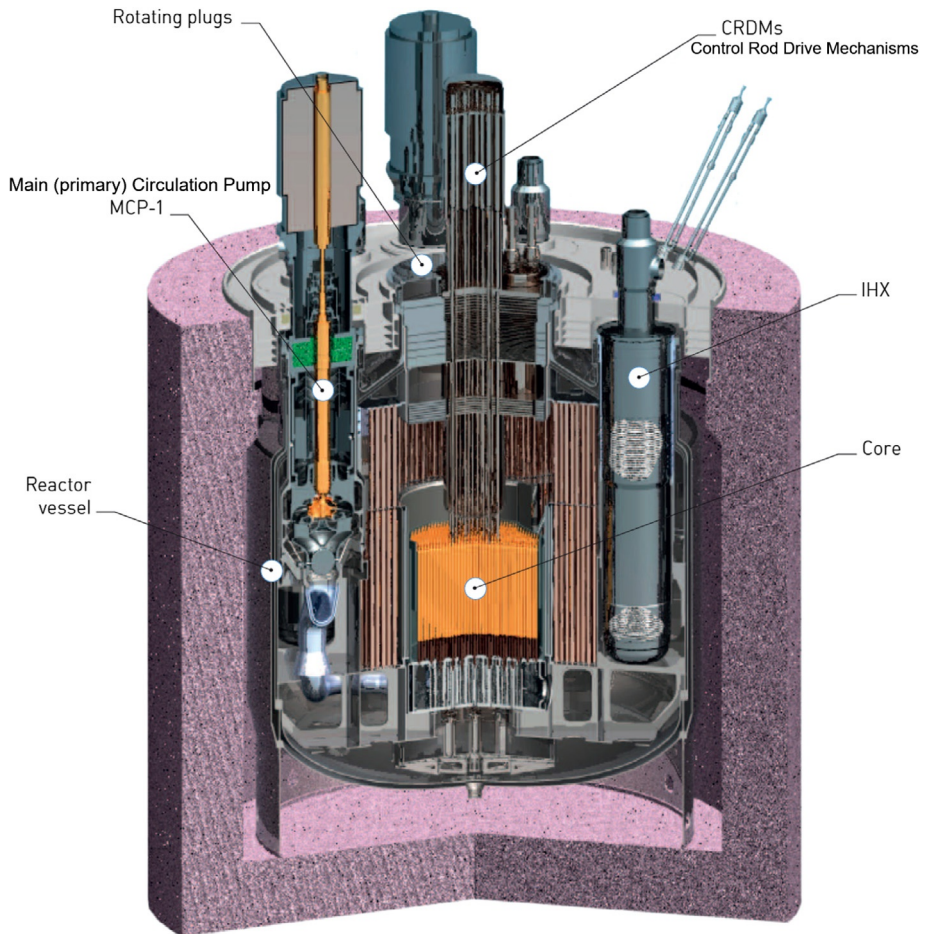


FIG. A1.109 Layout of BN-800 NPP. 1 – reactor; 2 – core; 3 – Intermediate Heat eXchanger (IHX); 4 – Main (primary) Circulation Pump (MCP-1); 5 – hydraulic lock; 6 – compensating tank; 7 – electromagnetic pump; 8 – air-heater exchanger; 9 – MCP-2; 10 – Steam Generator (SG); 11 – buffer tank; 12 – secondary draining tank; and 13 – emergency discharge tank. Courtesy of JSC "Afrikantov OKBM": <http://www.okbm.nnov.ru/upload/iblock/340/hkrhdgf35afpjudu vd7n2v0848fr0rye.pdf>; Accessed Feb. 19, 2022

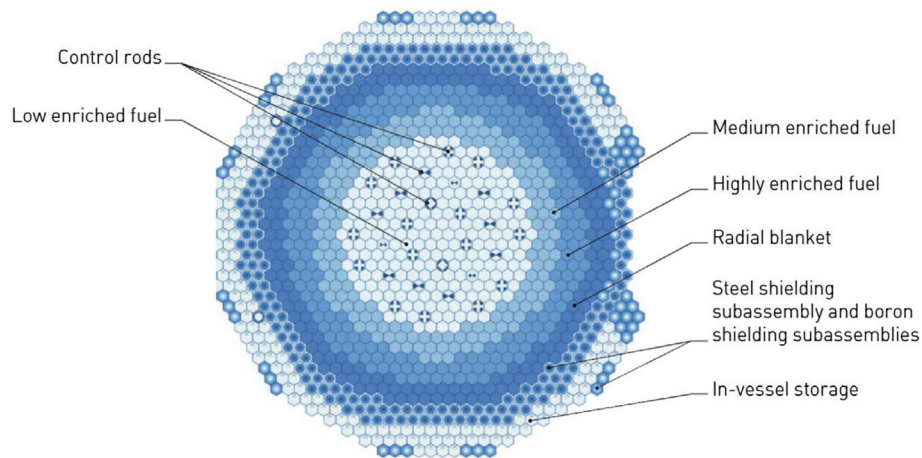


FIG. A1.110 BN-800 core map. Courtesy of JSC "Afrikantov OKBM": <http://www.okbm.nnov.ru/upload/iblock/340/hkrhdgf35afpjduvd7n2v0848fr0rye.pdf>; Accessed Feb. 19, 2022

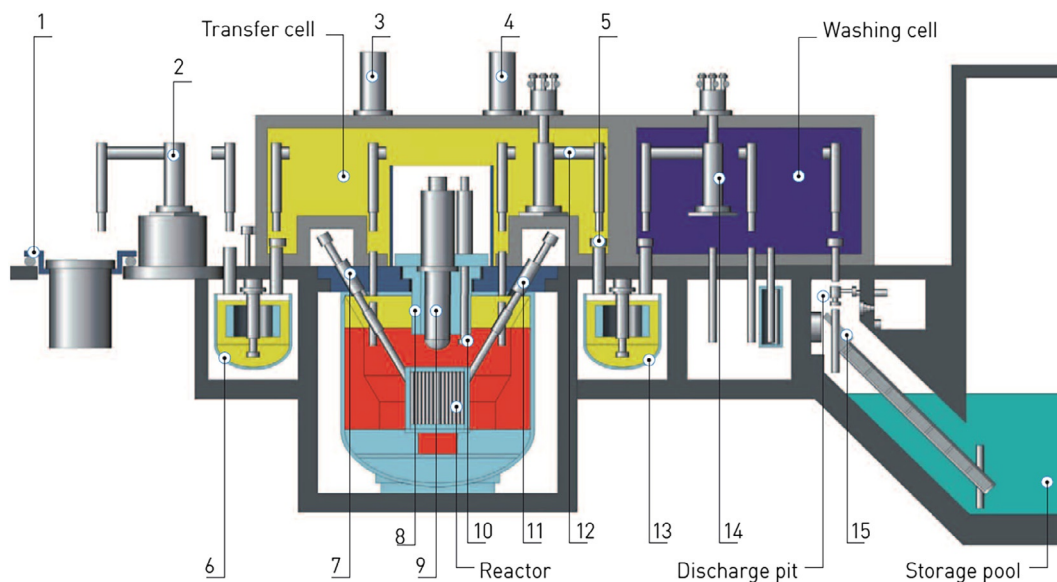


FIG. A1.111 BN-800 refueling scheme: 1 – rotating seat; 2 – fresh-subassembly-transfer mechanism; 3 – loading-elevator-plug-lifting mechanism; 4 – unloading-elevator-plug-lifting mechanism; 5 – gas-gate valve; 6 – fresh-subassembly drum; 7 – loading elevator; 8 – rotating plug; 9 – central-rotating plug; 10 – refueling mechanism; 11 – unloading elevator; 12 – fuel-transfer-cell mechanism; 13 – spent-fuel drum; 14 – fuel-washing-cell-transfer mechanism; and 15 – inclined elevator of fuel-discharge pit. Courtesy of JSC "Afrikantov OKBM": <http://www.okbm.nnov.ru/upload/iblock/340/hkrhdgf35afpjduvd7n2v0848fr0rye.pdf>; Accessed Feb. 19, 2022

- (2) Nucleoeléctrica Argentina, (NA-SA): <http://www.na-sa.com.ar/>;
- (3) Societatea Nationala Nuclearelectrica (SNN), Romania: <http://www.nuclearelectrica.ro/>;
- (4) CNNP Nuclear Power Operations Management, CNNO, China: <http://www.cnnp.com.cn/>;
and
- (5) Nuclear Power Corporation of India Ltd. (NPCIL): <https://www.npcil.nic.in/Content/Hindi/index.aspx>.

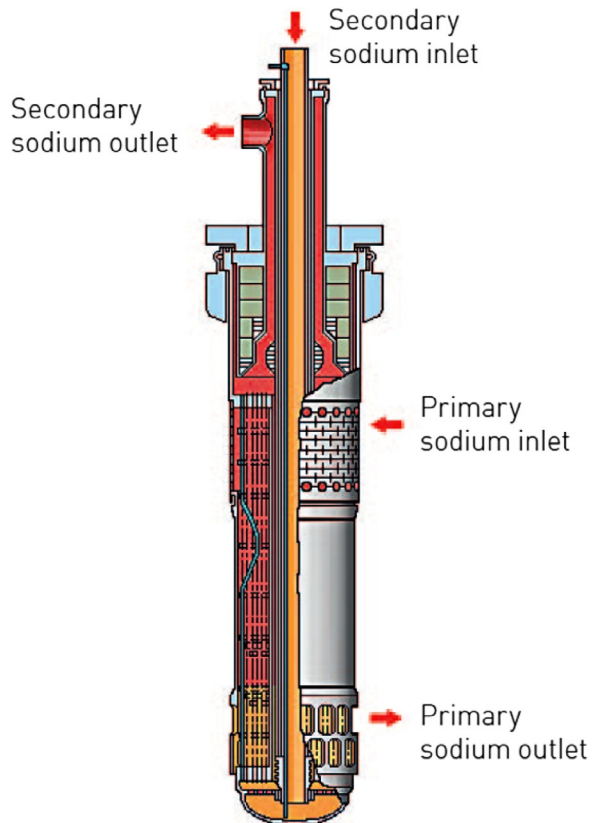


FIG. A1.112 BN-800 IHX. Courtesy of JSC "Afrikantov OKBM": <http://www.okbm.nnov.ru/upload/iblock/340/hkrhdgf35afpjuduud7n2v0848fr0rye.pdf>; Accessed Feb. 19, 2022

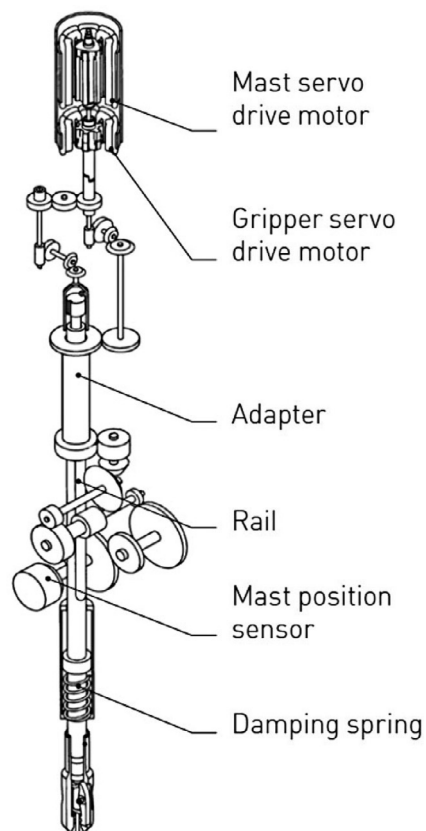


FIG. A1.113 BN-800 CRDM. Courtesy of JSC "Afrikantov OKBM": <http://www.okbm.nnov.ru/upload/iblock/340/hkrhdgf35afpjuduud7n2v0848fr0rye.pdf>; Accessed Feb. 19, 2022

TABLE A1.23 Key-design parameters of USSR/Russian SFRs – BN reactors (<http://www.okbm.nnov.ru/upload/iblock/340/hkrhdgf35afpjuduvd7n2v0848fr0rye.pdf>; accessed Feb. 19, 2022)

No.	Parameter	BN-350	BN-600 ^a	BN-800 ^a	BN-1200 ^b
1	Generation of reactor	II	III	III ⁺	IV
2	Thermal power, MW _{th}	750	1470	2100	2800
3	Electrical power, MW _{el}	150	600	880	1220
4	Thermal efficiency of NPP: gross/net	20/-	40.8/40.0	41.9/38.8	43.6/40.5
5	Basic components: No of turbines × type No of generators × type	-	3 × K-200-130 3 × TGB-200-M	1 × K-800-130 1 × T3B-800-2	1 × K-1200-160 1 × T3B-1200-2
6	Vessel Diameter, m Height, m Layout	- Loop	12.86 12.60 Integral	12.96 14.82 Integral	16.9 20.72 Integral
7	No of heat-transfer loops	-	3	3	4
8	Temperature of reactor coolant: sodium, primary loop – T_{in}/T_{out} °C	280/440	377/550	354/547	410/550
9	Temperature of intermediate coolant: sodium, secondary loop – T_{in}/T_{out} °C	270/420	328/518	309/505	355/527
10	Temperature of power-cycle working fluid: water/steam – T_{in}/T_{out} °C	160/410	240/505	210/490	275/510
11	Pressure at steam-generator outlet, MPa	4.9	14	14	17
12	Scheme of steam reheat with		Sodium	Steam	Steam
13	Basic unchangeable components service term, years		30	40	60
14	Fuel	UO ₂	UO ₂	MOX	MOX/ UpuN
15	Fuel enrichment, % (zones: internal/intermediate/external)	-	17/20/27	17/20/24	20
16	Breeding ratio	0.93 Pu factor	0.85 Pu factor	1.0	1.2-1.4
17	Basic unchangeable components service term, years	-	30 (41)	40	60

^aBN-600 and BN-800 are currently in operation at the Beloyarsk NPP; BN-600 commercial start – 1981 and BN-800 – 2016.

^bBN-1200 – design of Generation-IV Russian SFR.

TABLE A1.24 Evolution of technical solutions for safety enhancement of fast-reactor designs

No.		BN-600	BN-800	BN-1200
1	Solutions for sodium loops:			
	Sodium-sodium intermediate loop	+	+	+
	Jacketing of vessels with radioactive Na	+	+	+
	Jacketing of pipelines with radioactive Na	+	+	-
	Jacketing of secondary pipelines	partially	partially	+
2	Emergency protection			
	Active	+	+	+
	Passive based on hydraulically suspended rods	-	+	+
	Passive based on temperature	-	-	+
3	Emergency heat-removal system			
	Within the tertiary loop	+	+	+
	Air-cooled HXs connected to secondary loop	-	-	
	Air-cooled HXs connected to primary loop	-		
4	Core melt retaining system	-	+	+
5	Emergency discharge isolation system	-	-	+

India

R&D/Design: Bhabha Atomic Research Center (BARC): <http://www.barc.gov.in/randd/artnp.html>;

Department of Atomic Energy (DAE): <http://www.dae.gov.in/>.

Operator: Nuclear Power Corporation of India Ltd. (NPCIL): <https://www.npcil.nic.in/Content/Hindi/index.aspx>;

Argentina

Design: Siemens (Germany) <https://new.siemens.com/global/en.html>.

Operator: Nucleoeléctrica Argentina, (NA-SA): <http://www.na-sa.com.ar/>.

Education

The Essential CANDU. A Textbook on the CANDU Nuclear Power Plant Technology, 2014. Editor-in-Chief: W.J. Garland, 1614 pages. Free download from: www.unene.ca/education/candu-textbook.

Advanced Gas-cooled Reactors (AGRs) and Gas-Cooled Reactors (AGRs) and gas-cooled reactors^e (GCRs)

AGRs carbon-dioxide cooled Accounting on the available information in the open literature it was decided to show a simplified layout of an AGR and ribbed fuel element; thermodynamic layout and *T-s* diagram of the AGR Torness NPP (see Figs. A1.85–A1.87, respectively).

^e Originally, the vast majority of GCRs were carbon-dioxide-cooled reactors of Generations I and II (about 29 Magnox reactors in UK; 8 GCRs in France, and some other countries), i.e., predecessors of current AGRs. However, several GCRs were helium-cooled. Nevertheless, all these early GCRs of Generations I and II were shut-down (operated within 1956 - 2012).

Basic data of AGR are as the following: Reactor coolant - carbon dioxide; pressure - 4 MPa ($P_{cr}=7.37$ MPa); outlet/inlet temperature - 650/292°C ($T_{cr}=\sim 31$ °C); primary steam - 17 MPa and 560°C and secondary steam - 4.1 MPa and 560°C; fuel rods - stainless-steel sheath with ribs; hollow fuel pellets; enriched fuel 2.3%; thermal efficiency - 41.6% (one of the highest in nuclear-power industry as of today (see [Table A1.1](#))). However, in spite of all uniqueness and advantages of this reactor and NPP, all of them will be shut down and will not be built again. One of the major problems is relatively low heat transfer coefficients of forced convection in carbon dioxide. Due to this Generation-IV gas-cooled reactors will use helium as the reactor coolant. Therefore, there is no point to provide extended information on this reactor type/NPP. However, it should be admitted that there are some ideas on supercritical carbon-dioxide-cooled reactors of the future ([Kim et al., 2016](#); [Parma et al., 2011](#); [Handwerk, 2007](#); [Pope, 2004, 2006](#); [Kato et al., 2004](#); [Kemmish et al., 1982](#)).

GCRs helium-cooled High Temperature Reactor Pebble-bed Module (HTR-PM) is helium cooled ~ 100 MW_{el} SMR designed in China (see [Figs. A1.88–A1.91](#) and [Table A1.21](#)) (for more details, see Chapters 3 and 14). Two HTR-PM were put into operation in March of 2022. These reactors are connected to a subcritical-pressure Rankine power cycle with primary and secondary steam superheat at pressures of 14.1 MPa and ~ 3.5 (estimated by authors), respectively. This power cycle is quite similar to that of Russian SFR – BN-600 (see [Fig. A1.104](#)) just steam temperatures are slightly higher (570°C for HTR-PM NPP and 505°C for – BN-600 NPP and due to that its thermal efficiency is also slightly higher, i.e., 42% gross for HTR-PM NPP and 40% gross for – BN-600 NPP (see [Table A1.1](#) Items 6 and 7). It should be noted that [Table A1.21](#) lists design parameters (operating parameters have not been found/published yet). Also, there is no information on the secondary steam reheat and its parameters, but based on our knowledge of Rankine-cycle arrangements for NPPs, it is impossible to get such thermal efficiency without the secondary-steam reheat, and standard approach here, as it is proven for old coal-fired thermal power plants, AGR NPPs, and SFR NPPs, that the secondary-steam temperature is usually the same as that of the primary one, and the secondary-steam pressure is about $\frac{1}{4}$ of that of primary steam. The HTR-PM NPP together with AGR NPPs have the highest value of thermal efficiency ($\sim 42\%$ gross) compared to those of any other NPPs as of today.

Eventually, HTR-PM is the VHTR concept of Generation-IV reactors. Also, these reactors are the first SMRs developed and put into operation by China and the second ones after the Russian SMRs – PWRs – KLT-40S reactors put into operation in December of 2019. In general, helium-cooled reactors with pebble-bed fuel-type have been developed by a number of countries, but only China has succeeded in their industrial operation. Of course, it is very important to check how these reactors will perform within next 3 – 5 years to be sure that this type of reactors and this type of nuclear fuel have not any hidden problems during operation as nuclear-power reactors.

Light-water-cooled Graphite-moderated Reactors (LGRs): RBMKs and EGPs

Accounting on the available information in the open literature it was decided to show a simplified plant layout, thermodynamic layout, T - s diagram of a 1000-MW_{el} RBMK NPP (see [Figs. A1.92–A1.94](#), respectively) and two photos of the reactor hall (see [Fig. A1.95](#)) and RBMK with open channel covers (see [Fig. A1.96](#)). A simplified layout of an 11-MW_{el} EGP-6 NPP, photos of the reactor hall and reactor itself without cover are shown in [Fig. A1.97a,b,c](#), respectively. Basic data on USSR LGRs are listed in [Table A1.22](#).

However, in spite of all uniqueness of this reactor type and many reactor years of operation, all of them will be shut down (currently, 8 RBMKs and 3 EGPs are in operation) and will not be built again due to the most severe accident, which had happened at the Unit 4 of the Chernobyl NPP on April 26, 1986. Therefore, there is no point to provide extended information on these reactors type/NPPs.

It should be mentioned that RBMK-1000 ($\sim 1000 \text{ MW}_{\text{el}}$) and RBMK-1500 ($\sim 1500 \text{ MW}_{\text{el}}$) have the same size of reactor core. This became possible after long-term thermalhydraulics experiments, which help to increase significantly critical heat flux at flow boiling in the RBMK-1500 compared to that in the RBMK-1000.

Sodium-cooled Fast Reactor (SFR): BN-600 (Generation-III), BN-800 (Generation-III⁺), and BN-1200 (Generation-IV)

Currently, SFRs are the only nuclear-power reactors with the fast-neutron spectrum in the world. As of today, two SFRs – BN-600 ($560 \text{ MW}_{\text{el net}}$; commercial operation from 1981) and BN-800 ($820 \text{ MW}_{\text{el net}}$; commercial operation from 2016) are in operation in Russia (Beloyarsk NPP) and one $20 \text{ MW}_{\text{el net}}$ – in China. Eventually, a number of countries have been involved in the development of SFRs, e.g., France ($233\text{-MW}_{\text{el}}$ Phénix reactor, 1974-2009), Japan ($246\text{-MW}_{\text{el}}$ Monju reactor); UK ($250\text{-MW}_{\text{el}}$ Dounreay PFR); and USA (several LMFBRs), but all these early SFR prototypes have been shut-down quite long time ago. Of course, nowadays, some new developments on SFRs are in progress in a number of countries (e.g., China: Two SFRs – CFR-600 are planned, first unit is scheduled for 2023 start up; for the second unit the due date is unknown; the latest information on European Union (EU) activities on SFR development can be found in the ASME Journal of Nuclear Engineering and Radiation Science, 2022, January Special Issue, Vol. 8, No. 1: European SFR SMART Project: <https://asmedigitalcollection.asme.org/nuclearengineering/issue/8/1> (also, see Chapter 11); India: One $470\text{-MW}_{\text{el}}$ LMFBR is planned to be put into operation in 2022 – 2023 (Information on planned SFRs is taken from [Nuclear News, 2022](#)). Therefore, our information on SFRs will be based on long-term Russian experience (see [Fig. A1.99](#) and [Table A1.23](#)).

Basis for Fast Reactors (FRs) (Taken from the brochure by the JSC “Afrikantov OKBM” Fast Neutron Reactor Plants with their permission: From Experience to Prospects: <http://www.okbm.nnov.ru/upload/iblock/8df/uzfw9j3m1zd8vibr0v4gvhzwjnrvh61c.pdf>)

On the one side, objective processes of reduction in organic fuel resources, reduction in availability of organic fuel resources, an increase in the cost of these resources and, respectively, the cost of power produced, as well as the requirement for reducing the impact on the environment and population form the basis for predictions concerning an increase in nuclear power.

Currently, the basis for the world’s nuclear power is the thermal-reactor technology. In Russia, it is mainly the VVER (Russian PWR) technology that reached the high level of safety and commercialization. Thermal reactors use U^{235} as the fuel. This isotope in any unit mass of planetary uranium is 0.7% and the remaining 99.3% is U^{238} , which is not a nuclear fuel for thermal reactors as it is practically non-fissionable in the thermal-neutron spectrum.

In total, the entrails of the Earth contain 10–14 millions of tons of uranium, of which nearly 4 millions have already been developed.

According to the expert opinion, if only thermal reactors operate the stores of planetary U^{235} will be depleted by the end of this century. Therefore, nuclear power based on these reactors only has the same crucial disadvantage as the conventional organic-fuel power industry does. Nevertheless, there is a nuclear process that makes it possible to use the dominating portion of natural U^{238} ; at neutron capture, U^{238} transforms to Pu^{239} , which is also fissionable as U^{235} . At irradiation, Pu^{239} not only undergoes fission, but also captures neutrons; therefore, other isotopes such as Pu^{240} , Pu^{241} and Pu^{242} are generated. Such transformation most effectively takes place in fast reactors. Of principal importance is that during this process plutonium can be produced in the quantity that exceeds the needs of the reactor itself (breeder reactor). Due to this, plutonium is produced not only to support operating fast reactors, but also to gradually accumulate it for other reactors.

In this connection, it is obvious that introduction of Fast Breeder Reactors (FBRs) is a necessary condition for developing a large-scale nuclear power.

During operation of fast reactors, an important task of creating a closed nuclear-fuel cycle shall be solved (see Fig. A1.98). The closed nuclear-fuel cycle is characterized by repeated cycles of processing the spent nuclear fuel and manufacturing new fuel based on the produced plutonium. Solution of this task will make it possible to: arrange extended reproduction of uranium–plutonium fuel with utilization of plutonium accumulated in thermal reactors, as well as weapon-grade plutonium by increasing efficiency of using natural uranium by ~100 times; separate radioactive waste from thermal and fast reactors that generates in nuclear reactions; ensure in prospect burning of most hazardous radioactive waste, i.e., trans-uranium elements (isotopes of neptunium, americium, and curium with the long high-life).

Basic data on Russian SFRs – BN reactors are listed in Tables A1.23 and A1.24, and shown in Figs. A1.98–A1.114.

BN-600 Basic information on the BN-600 reactor (Generation-III) and plant are listed in Table A1.23 and A1.24, and shown in Figs. A1.98–A1.105. Many technical solutions implemented in the BN-600 design are successive to those, which were proven in the BN-350 reactor (see Table A1.23) (Courtesy of JSC “Afrikantov OKBM”): (<http://www.okbm.nnov.ru/upload/iblock/340/hkrhdgf35afpjuduvd7n2v0848fr0rye.pdf>; accessed Feb. 19, 2022).

The BN-600 reactor NPP has the following distinctive features:

- (1) Integral primary circuit with the reactor that houses not only the core, but also main circulation pumps and intermediate sodium-to-sodium heat exchanger.
- (2) Straight-tube section-module steam generator that provides power-unit operation at the nominal power without one or even two sections.
- (3) Larger power and better thermodynamic parameters as compared with the BN-350 reactor plant.
- (4) Better natural-circulation conditions for the primary and secondary coolant. And
- (5) Guard vessel of the same strength as the main one.

In the course of operation, BN-600 demonstrated high indicators and thus solved the assigned task aimed at validating the reliability and safety of SFRs as a whole and of sodium coolant in particular. BN-600 was recognized three times as the best power unit in Russia concerning reliability and safety indicators.

Safety of BN-600 is based on:

- (1) Inherent safety due to intrinsic physical properties;
- (2) Three-loop thermal arrangement that excludes a contact of primary radioactive sodium with the tertiary light water (Rankine power-cycle working fluid).
- (3) Liquid-metal sodium coolant of the high thermal inertia and large thermal margin in the primary and secondary loops.
- (4) Negative effect of reactivity in all operating modes.
- (5) Low-pressure reactor vessel with no water and water-steam.

In April of 2010, the reactor has completely worked out its design service life of 30 years as it was originally planned. The construction of the reactor plant retained sufficient operability that made it possible to obtain a license for extension of the operating life by 10 years. It is possible to additionally extend the BN-600 operating life (currently, it is operated for 41 years, i.e., from 1981!).

JSC “Afrikantov OKBM” supervises operation of BN-600 at Beloyarsk NPP, Unit 3, by solving together with Beloyarsk NPP specialists issues related to ensuring reliable and safe operation of this reactor through the entire service life.

Accounting on the available information in the open literature it was decided to show a simplified layouts and T - s diagram of a 560-MW_{el net} BN-600 NPP (see Figs. A1.100–A1.106).

BN-800 Basic information on the BN-800 reactor (Generation-III⁺) and plant are listed in Tables A1.23 and A1.24, and shown in Figs. A1.107–A1.113. Many technical solutions implemented in the BN-800 design are successive to those, which were proven in the BN-350 and BN-600 reactors (see Table A1.23) (Courtesy of JSC “Afrikantov OKBM”).

Reactor vessel The vessel accommodates internals, primary sodium (reactor coolant), and argon gas. It is a cylindrical vessel with cone head and elliptical bottom with the support ring. The main vessel is enclosed in the guard vessel, which shape repeats the same of the main vessel. The outer surfaces of both vessels are thermally insulated. Also, the main vessel accommodates the following: 1) skirt that supports all internals, and in-vessel equipment; 2) distributing header with core assemblies; and 3) in-vessel protection that ensures minimum activation of primary sodium.

Reactor core The reactor core is made up of fuel assemblies, radial blanket, absorber rods, steel shielding assemblies, boron shielding assemblies, and spent fuel assemblies in the in-vessel storage. Radially, the core has three fuel zones with different plutonium mass in the uranium and plutonium mixture. These zones are of relatively low, medium, and high enrichment. Fuel in the core is encircled by the radial blanket with the depleted uranium.

Refueling system A set of refueling mechanisms moves core sub-assemblies along the refueling path and includes as in-vessel and ex-vessel portions. All mechanisms and equipment of this system operate during refueling and are in a standby position in between.

In vessel refueling equipment performs the following:

Rotating plugs and central rotating column:

Accommodate refueling mechanisms and other equipment, guide the refueling mechanism towards the core cells and interface Control Rod Drive Mechanisms (CRDMs) with control rods;

Provide biological shielding and thermal protection for the operating personnel;

Seal the reactor primary circuit with respect to the environment in all operating modes of the plant;

Refueling mechanism

Withdraws, turns and installs subassemblies in the reactor core and elevator sleeves, as well as samples gas in the course of subassembly leak tests.

Elevator

Moves core subassemblies from the reactor core to the reactor fuel-handling cells and back.

The ex-vessel refueling system performs the following:

Takes fresh subassemblies to the fresh subassembly drum, heats them in this drum before loading to the reactor and loads them into the reactor;

Unloads spent-fuel assemblies from the reactor, places and temporarily keeps them in the spent-fuel-subassembly drum to remove residual heat;

Transfers spent-fuel assemblies from the fresh-fuel-assembly drum to the washing cells and transfers them after washing to the inclined elevator of the fuel-discharge pit;

Seals reactor fuel-handling ducts and ducts of the fresh-fuel drum and spent-fuel drum; and

Provides biological shielding for the operating personnel.

Spent fuel is transported along the external fuel-handling duct in isolated gas volume in the inert medium.

Intermediate Heat eXchangers (IHXs) transfer heat from the primary coolant, i.e., sodium reactor coolant, that circulates on the shell side to the secondary sodium coolant that circulates in tubes. Six IHXs are used. A vertical shell-and-tube counter-flow heat exchanger with co-axial supply and removal of the secondary coolant is used. It has a tube system, pressure chamber, drainage chamber, central tube, protection-tube unit, guard vessel, and fasteners.

Main characteristics:

Thermal power	350 MW
Heat-transfer surface	1657 m ²
IHX height	13.5 m
Mass	56 ton
Assigned operational term	45 years

Steam generator (SG) A once-through, high-pressure, section and modular SG is used. The SG in every loop has 10 sections, a buffer tank and connecting pipelines in the secondary and tertiary loops; each section has two modules. The module is a vertical shell-and-tube straight-tube heat exchanger. These modules are an evaporator and a superheater. The SG produces high-pressure superheated steam. Also, in all other operational modes of the plant, during which feed-water is supplied, the SG cools the reactor.

Main characteristics:

Thermal power	750 MW
Steam mass-flow rate	292 kg/s
Assigned operational term	45 years

Safety of the BN-800 reactor

The BN-800 design is based on progressive solutions to enhanced safety:

- Emergency-cooling-down system with the air-cooled heat exchanger connected to the secondary loop;

- Core with the sodium void-effect of reactivity close to zero;

- Passively hydraulically suspended control rods;

- Tray under pressure chamber to catch corium at core melting in case of severe accident.

With implemented safety improvements, the BN-800 design satisfies requirements set for Generation-III⁺ reactors.

Prospects of the fast-reactor technology—BN-1200 Development and implementation of the BN-350, BN-600, and BN-800 projects made it possible to set up an effective design, production and operation infrastructure as a basis for further development of the fast-reactor technology.

Objectives of BN-1200 development Make a reliable design of the next generation reactor and plant for the serial commercial power units equipped with the fast reactor intended to fulfill top-priority tasks of transition of the closed fuel cycle in nuclear power;

- Raise technical and economic indicators of the power unit equipped with the fast reactor to the those of the state-of-the-art VVER (PWR) of the same power; and

- Enhance safety to satisfy requirements set for Generation-IV reactors and plants.

The BN-1200 design has used the main technical solutions proved for the BN-600 and BN-800 designs (see [Tables A1.23 and A1.24](#), and [Fig. A1.114](#)).

To enhance safety and raise cost efficiency, several new loop and layout solutions have been used:

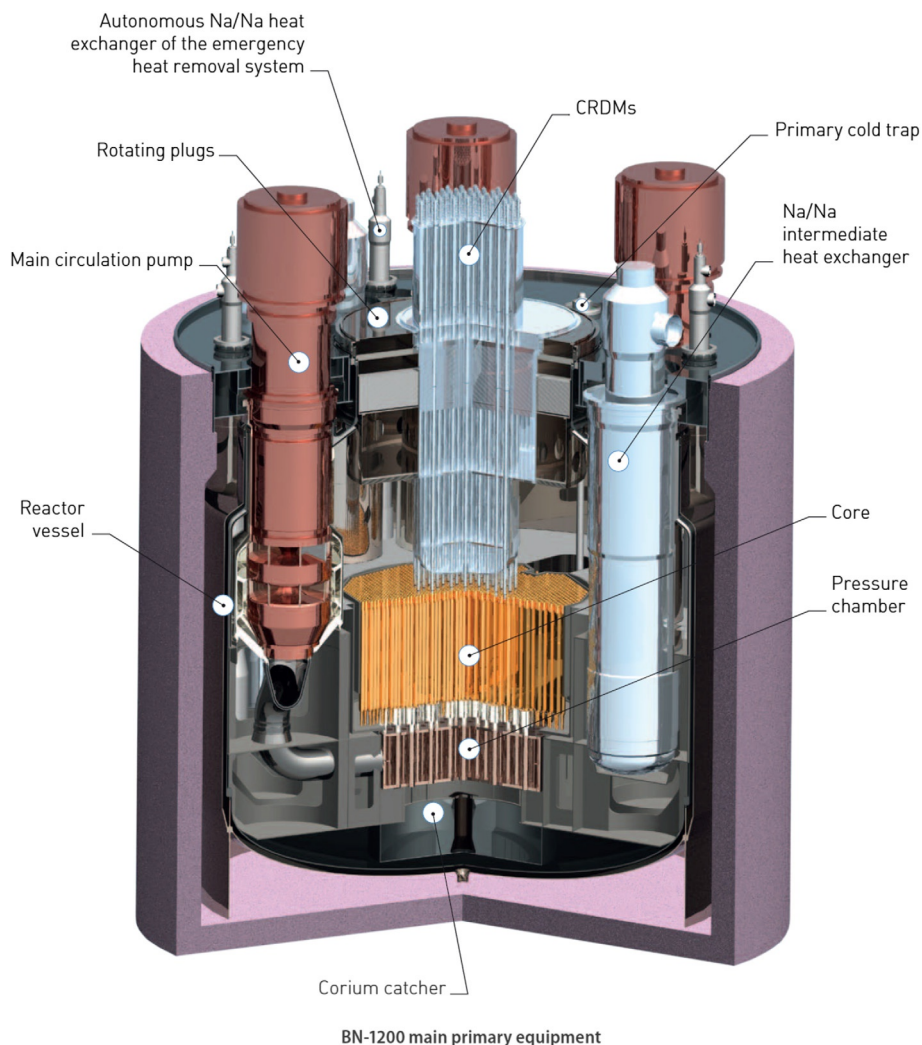


FIG. A1.114 Layout of BN-1200 reactor. Courtesy of JSC "Afrikantov OKBM": <http://www.okbm.nnov.ru/upload/iblock/340/hkrhdgf35afpjjuduud7n2v0848fr0rye.pdf>; Accessed Feb. 19, 2022

Integral primary loop with all sodium systems – including cold traps, neutronic- and chemical monitoring systems – in the reactor tank;
 Transfer from section modular SGs to integral generators based on a large capacity straight tube modules that significantly reduces material consumption;
 Long-term hold out of fuel assemblies in the in-vessel storage that made it possible to exclude the sodium drum in the refueling system; and
 Long fuel life due to enlarge fuel assemblies that will reduce costs for fuel.

Power of the serial power units has been selected based on the following requirements:

The same electric power as that of the latest Generation-III⁺ VVERs (VVER-1200; VVER-TOI), i.e., up to 1200 MW_{el}, to ensure coordinated selection of NPP sites and to unify the turbo-generator and other electric equipment of the electricity output system; and
 Portability of large-sized equipment by rail (reactor vessel and large rotating plug are assemblies at the site).

Safety of the BN-1200 reactor The BN-1200 reactor design uses several new technical solutions for enhancing safety:

Sodium systems and primary equipment are fully integrated in the reactor tank with the system for sodium purification from oxides also located in the reactor tank to exclude radioactive-sodium leaks and sodium interaction with air that is the severest design-basis accident in fast reactors.

The improved emergency heat-removal system is used with autonomous heat exchangers built in the reactor vessel that ensures natural sodium circulation immediately through the core fuel assemblies due to the passive check valve in the autonomous heat exchanger to increase the quantity of removed power at the admissible temperature state of the core.

In addition to the PAZ-G (Пассивно срабатывающих стержней Аварийной Защиты (ПАЗ)) passive-shutdown system based on hydraulically suspended rods, which was well proven in BN-800, the PAZ-T system of rods that respond to the change in the sodium temperature at the core outlet is implemented. These devices are sensitive to the increase in the coolant temperature in all accidents with the imbalance between power and flowrate and, therefore, they ensure additional enhancement of reactor safety.

A compartment above the reactor is leak-tight to isolate radioactive products in case of severe beyond-design basis accidents.

BN-1200 power unit is planned for the Beloyarsk NPP as Unit 5. The BN-1200 design implemented in the head power unit and next series of the power units will make it possible to retain the scientific and production potential and strengthen the leading position of Russia in the world with respect to the fast-sodium-reactor technology.

Solutions adopted for the design of reactors and plants use of passive safety systems and inherent safety properties of the sodium coolant make it possible to ensure the safety level that excludes necessity of population evacuation in case of any technically possible accidents.

A1.4 Conclusions

The BN-1200 design is based on a large positive experience in development and operation of sodium-cooled fast reactors and maximum possible use of achievements of this technology thus making it possible to develop in the nearest term a reliable head-power unit followed by a serial construction.

Technical and economic indicators of the BN-1200 power unit developed for serial construction are comparable with ones of next-generation PWRs.

Implementation of the fast-reactor technology will make it possible to:

Develop competitive NPPs with the high safety level;

Make the structure of the closed fuel cycle at the production scale to solve the issue of fuel supply for the nuclear power in the long prospect; And

Reduce the scope of radioactive waste by processing the VVER (PWR) spent nuclear fuel and by using plutonium and minor actinides extracted from it.

Acknowledgment

Authors would like to express their great appreciation to Mr. Sumio Fujii (Mitsubishi Heavy Industries (MHI)), Mr. Yuchiro Yoshimoto (Hitachi GE Nuclear Energy, Ltd.), Mr. Ala Alizadeh (CANDU Energy Inc., SNC-Lavalin Group), and to AECL (Canada), AREVA/EDF (France), Candu Energy (Canada), Hitachi (Japan), Hitachi GE Nuclear Energy (Japan – USA), JSC

“Afrikantov OKBM” (Russia), KHNP (S. Korea), MHI (Japan), Oak Ridge National Laboratory (U.S. DOE), Sanmen Nuclear Power Company (China), SNC-Lavalin (Canada), Rosenergoatom (Russia), Rosatom (Russia), Siemens AG (Germany), Toshiba (Japan), TVO (Finland), U.S. DOE, U.S. NRC, Westinghouse (USA), and authors of figures from the Wikimedia-Commons website for their materials used in this Appendix.

References

- AECL Report, 1969. Pickering Generation Station. Design Description, Report Prepared by Atomic Energy of Canada Limited. 229 pages.
- Cherkashov, Y.M. (Ed.), 2006. Channel Nuclear Power Reactor (RBMK) (Канальный Ядерный Энергетический Реактор РБМК). Publishing House GUP NIKIET, Moscow, Russia. 631 pages (In Russian).
- Dragunov, A., Saltanov, E., Pioro, I., Kirillov, P., Duffey, R., 2015. Power cycles of generation III and III⁺ nuclear power plants. *J. Nucl. Eng. Radiat. Sci.* 1 (2). 10 pages.
- Duffey, R.B., Pioro, I., Pioro, R., 2021. World energy production and the contribution of PHWRs, Chapter 1. Introduction. In: Riznic, J. (Ed.), *Pressurized Heavy Water Reactors: CANDU*. vol. 7. Elsevier, UK, pp. 1–44. 546 pages.
- Friedman, B.N., 2019. The AP1000 plant and the China project commissioning success. *J. Nucl. Eng. Radiat. Sci.* 5 (1). 3 pages.
- Boucau, J. (Ed.), 2021. *Fundamental Issues Critical to the Success of Nuclear Projects*. Elsevier—Woodhead Publishing (WP), Duxford, UK. 392 pages.
- Goldschmidt, B., 1982. *The Atomic Complex: A Worldwide Political History of Nuclear Energy*, first ed. American Nuclear Society (ANS), La Grange Park, IL, USA. 478 pages.
- Greenspan, E. (Ed.), 2021. *Encyclopedia of Nuclear Energy*, first ed. Elsevier, UK. 3656 pages.
- Grigor’ev, V.A., Zorin, V.M. (Eds.), 1988. *Thermal and nuclear power plants*. In: *Handbook*, second ed. Energoatomizdat Publishing House, Moscow, Russia. 625 pages, (In Russian).
- Guo, Y., Bullock, D.E., Pioro, I.L., Martin, J., 2006. Measurements of sheath temperature profiles in bruce LVRF bundles under post-dryout heat transfer conditions in Freon. In: *Proceedings of the 14th International Conference on Nuclear Engineering (ICONE-14)*, July 17–20, Miami, Florida, USA. Paper #89621, 9 pages.
- Pioro, I.L. (Ed.), 2016. *Handbook of Generation IV Nuclear Reactors*. Elsevier – Woodhead Publishing (WP), Duxford, UK. 940 pages. Free download of content: https://www.gen-4.org/gif/jcms/c_9373/publications.
- Cacuci, D.G. (Ed.), 2010. *Handbook of Nuclear Engineering*. Springer, New York, NY, USA. 5 Volumes.
- Ingersoll, D.T., Carelli, M.D. (Eds.), 2021. *Handbook of Small Modular Nuclear Reactors*, second ed. Elsevier – Woodhead Publishing (WP), Duxford, UK. 609 pages.
- Handwerk, C.S., 2007. *Optimized Core Design of a Supercritical Carbon Dioxide-cooled Fast Reactor* (Ph.D. dissertation). Department of Nuclear Science and Engineering, Massachusetts Institute of Technology, Boston, USA.
- Hewitt, G.F., Collier, J.G., 2000. *Introduction to Nuclear Power*, second ed. Taylor & Francis, New York, NY, USA. 304 pages.
- Hurst, D.G., 1997. *Canada Enters the Nuclear Age. A Technical History of Atomic Energy of Canada Limited as Seen from Its Research Laboratories*. McGill-Queen’s University Press, Montreal, QC, Canada. 448 pages.
- IAEA, 2020. *Advances in Small Modular Reactor Technology Developments. A Supplement to: IAEA Advanced Reactors Information System (ARIS)*. IAEA. 354 pages. Free download from: https://aris.iaea.org/Publications/SMR_Book_2020.pdf.
- Kato, Y., Nitawaki, T., Muto, Y., 2004. Medium temperature carbon dioxide gas turbine reactor. *Nucl. Eng. Des.* 230, 195–207.
- Kemmish, W.B., Quick, M.V., Hirst, I.L., 1982. The safety of CO₂ cooled breeder reactors based on existing gas cooled reactor technology. *Prog. Nucl. Energy* 10 (1), 1–17.
- Kim, Y., Hartanto, D., Yu, H., 2016. Neutronics optimization and characterization of a long life SCO₂-cooled micro modular reactor. *Int. J. Energy Res.* 41 (6), 976–984.
- Kirillov, P.L., Zhukov, A.V., Loginov, N.I., Makhin, V.M., Pioro, I.L., Yur’ev, Y.S., 2013. In: Kirillov, P.L. (Ed.), *Handbook on Thermalhydraulics Calculations in Nuclear Engineering: Vol. 2, Nuclear Reactors, Heat Exchangers, Steam Generators*. Izdat Publishing House, Moscow, Russia. (In Russian), 688 pages.
- Kruglikov, P.A., Smolkin, Y.V., Sokolov, K.V., 2009. Development of engineering solutions for thermal scheme of power unit of thermal power plant with supercritical parameters of steam. In: *Proc. Int. Workshop "Supercritical*

- Water and Steam in Nuclear Power Engineering: Problems and Solutions”, Moscow, Russia, October 22–23. (In Russian), 6 pages.
- Leung, L.K.H., Pioro, I.L., Bullock, D.E., 2003. Post-dryout surface-temperature distributions in a vertical freon-cooled 37-element bundle. In: Proceedings of the 10th International Topical Meeting on Nuclear Reactor Thermal Hydraulics (NURETH-10), Seoul, Korea, October 5-9. Paper #C00201, 13 pages.
- Lewis, B.J., Onder, E.N., Prudil, A.A., 2017. Fundamentals of Nuclear Engineering. Wiley and Sons, Ltd., Hoboken, NJ, USA. 960 pages.
- Margulova, T.C., 1995. Nuclear Power Plants. Izdat Publishing House, Moscow, Russia. (in Russian), 289 pages.
- Nonbøl, E., 1996. Description of the Advanced Gas Cooled Type of Reactor (AGR). Report NKS/RAK2(96)TR-C2, November, Risø National Laboratory, Roskilde, Denmark. 88 pages.
- Nuclear Energy, 2018. In: Meyers, R.A., Tsoufanidis, N. (Eds.), A Volume Ion Encyclopedia of Sustainability Science and Technology Series, second ed. Springer. 438 pages.
- Krivit, S.B., Lehr, J.H., Kingery, T.B. (Eds.), 2011. Nuclear Energy Encyclopedia: Science, Technology, and Applications. J. Wiley & Sons, Hoboken, NJ, USA. 624 pages.
- Kok, K.D. (Ed.), 2017. Nuclear Engineering Handbook, second ed. CRC Press, Boca Raton, FL, USA. 978 pages.
- Nuclear News, 2022. 24th Annual Nuclear News Reference Section, March. Publication of American Nuclear Society (ANS), pp. 41–69.
- Parma, E.J., Wright, S.A., Vernon, M.E., Fleming, D.D., Rochau, G.E., Suo-Anttila, A.J., Rashdan, A.A., Tsvetkov, P.V., 2011. Supercritical CO₂ direct cycle gas fast reactor (SC-GFR) concept, Sandia National Laboratories. Report No. SAND2011-2525.
- Perkovich, G., 2002. India’s Nuclear Bomb. The Impact on Global Proliferation, Updated Edition with a New Afterword. University of California Press, Berkeley, CA, USA. 654 pages.
- Petriw, L., Sabir, S.M., Chun, K., Pioro, I.L., 2019. Comparison of thermophysical properties of heavy and light water (NIST REFPROP VER. 10) at CANDU reactor operating conditions. In: Proceedings of the 39th Annual Conference of the Canadian Nuclear Society and 43rd Annual CNS/CNA Student Conference, Ottawa, ON, Canada, June 23–26. Paper #25, 7 pages.
- Pioro, I.L., Duffey, R.B., 2007. Heat Transfer and Hydraulic Resistance at Supercritical Pressures in Power Engineering Applications. ASME Press, New York, NY, USA. 334 pages.
- Pioro, I., Duffey, R., 2015. Nuclear power as a basis for future electricity generation. J. Nucl. Eng. Radiat. Sci. 1 (1). <http://nuclearengineering.asmedigitalcollection.asme.org/article.aspx?articleID=2085849>. 19 pages.
- Pioro, I., Duffey, R., 2019a. Current status of electricity generation in the world and future of nuclear-power industry. In: Letcher, T. (Ed.), Managing Global Warming, an Interface of Technology and Human Issues. Elsevier – Academic Press, London, UK, pp. 67–114. 804 pages, Chapter 3.
- Pioro, I., Duffey, R., 2019b. Current and future nuclear-power reactors and plants. In: Letcher, T. (Ed.), Managing Global Warming, an Interface of Technology and Human Issues. Elsevier – Academic Press, London, UK, pp. 117–197. 804 pages, Chapter 4.
- Pioro, I., Kirillov, P., 2013a. Current status of electricity generation in the world. In: Méndez-Vilas, A. (Ed.), Materials and Processes for Energy: Communicating Current Research and Technological Developments, Energy Book Series #1. Formatex Research Center, Spain, pp. 783–795. Free download from: <http://www.formatex.info/energymaterialsbook/book/783-795.pdf>.
- Pioro, I., Kirillov, P., 2013b. Current status of electricity generation at thermal power plants. In: Méndez-Vilas, A. (Ed.), Materials and Processes for Energy: Communicating Current Research and Technological Developments, Energy Book Series #1. Formatex Research Center, Spain, pp. 796–805. Free download from: <http://www.formatex.info/energymaterialsbook/book/796-805.pdf>.
- Pioro, I., Kirillov, P., 2013c. Current status of electricity generation at nuclear power plants. In: Méndez-Vilas, A. (Ed.), Materials and Processes for Energy: Communicating Current Research and Technological Developments, Energy Book Series #1. Formatex Research Center, Spain, pp. 806–817. Free download from: <http://www.formatex.info/energymaterialsbook/book/806-817.pdf>.
- Pioro, I., Kirillov, P., 2013d. Generation IV nuclear reactors as a basis for future electricity production in the world. In: Méndez-Vilas, A. (Ed.), Materials and Processes for Energy: Communicating Current Research and Technological Developments, Energy Book Series #1. Formatex Research Center, Spain, pp. 818–830. Free download from: <http://www.formatex.info/energymaterialsbook/book/818-830.pdf>.
- Pioro, I.L., Cheng, S.C., Vasić, A., Felisari, R., 2000. Some problems for bundle CHF prediction based on CHF measurements in simple flow geometries. Nucl. Eng. Des. 201 (2–3), 189–207.
- Pioro, I.L., Groeneveld, D.C., Cheng, S.C., Doerffer, S., Vasić, A., Antoshko, Y.V., 2001. Comparison of CHF measurements in R-134a cooled tubes and the water CHF look-up table. Int. J. Heat Mass Transf. 44 (1), 73–88.

- Pioro, I.L., Groeneveld, D.C., Doerffer, S.S., Guo, Y., Cheng, S.C., Vasic, A., 2002a. Effects of flow obstacles on the critical heat flux in a vertical tube cooled with upward flow of R-134a. *Int. J. Heat Mass Transf.* 45 (22), 4417–4433.
- Pioro, I.L., Groeneveld, D.C., Leung, L.K.H., Doerffer, S.S., Cheng, S.C., Antoshko, Y.V., Guo, Y., Vasić, A., 2002b. Comparison of CHF measurements in horizontal and vertical tubes cooled with R-134a. *Int. J. Heat Mass Transf.* 45 (22), 4435–4450.
- Pioro, I., Mahdi, M., Popov, R., 2018. Heat Transfer Media and Their Properties. In: Kulacki, F.A. (Ed.), *Handbook of Thermal Science and Engineering*. Springer, Cham, Switzerland, pp. 1353–1446 (Chapter 33).
- Pioro, I., Duffey, R.B., Kirillov, P.L., Pioro, R., Zvorykin, A., Machrafi, R., 2019. Current status and future developments in nuclear-power industry of the world. *J. Nucl. Eng. Radiat. Sci.* 5 (2). 27 pages, Free download from: <https://asmedigitalcollection.asme.org/nuclearengineering/article/doi/10.1115/1.4042194/725884/Current-Status-and-Future-Developments-in-Nuclear>.
- Pioro, I., Duffey, R.B., Kirillov, P.L., Dort-Goltz, N., 2020. Current status of reactors deployment and small modular reactors development in the world. *J. Nucl. Eng. Radiat. Sci.* 6 (4). 24 pages, Free download from: <https://asmedigitalcollection.asme.org/nuclearengineering/article/6/4/044001/1085654/Current-Status-of-Reactors-Deployment-and-Small>.
- Pioro, I., Duffey, R.B., Kirillov, P.L., Pioro, R., 2021a. Pros and cons of commercial reactor designs, Volume 1, Section 2: Chapter. Part 1. Current status of electricity generation in the world and selected countries. In: Greenspan, E. (Ed.), *Encyclopedia of Nuclear Energy*, first ed. Elsevier, UK, pp. 263–287. 3656 pages.
- Pioro, I., Duffey, R.B., Kirillov, P.L., Pioro, R., 2021b. Pros and cons of commercial reactor designs, Volume 1, Section 2: Chapter. Part 2. Current status and future trends in the world nuclear-power industry and technical considerations of nuclear-power reactors. In: Greenspan, E. (Ed.), *Encyclopedia of Nuclear Energy*, first ed. Elsevier, UK, pp. 288–303. 3656 pages.
- Pioro, I., Duffey, R.B., Pioro, R., 2022. Overview of current status of nuclear-power industry of the world. In: Boucau, J. (Ed.), *Fundamental Issues Critical to the Success of Nuclear Projects*. Elsevier – Woodhead Publishing (WP), Duxford, UK. 392 pages, Chapter 2.
- Pope, M.A., 2004. *Reactor Physics Design of Supercritical CO₂-Cooled Fast Reactors* (M.S dissertation). Department of Nuclear Science and Engineering, Massachusetts Institute of Technology, Boston, USA.
- Pope, M.A., 2006. *Thermal Hydraulic Design of a 2400 MW Direct Supercritical CO₂-Cooled Fast Reactor* (Ph.D. dissertation). Department of Nuclear Science and Engineering, Massachusetts Institute of Technology, Boston, USA.
- Riznic, J. (Ed.), 2021. *Pressurized Heavy Water Reactors: CANDU*. Elsevier, UK. 546 pages.
- Ram, K.S., 1990. *Basic Nuclear Engineering*. Wiley Eastern Ltd., New Delhi, India. 221 pages.
- Rosenergoatom, 2004. *Russian Nuclear Power Plants. 50 Years of Nuclear Power*, Moscow, Russia. 120 pages.
- Ryzhov, S.B., Mokhov, V.A., Nikitenko, M.P., et al., 2010. Advanced designs of VVER reactor plant. In: *Proceedings of the 8th International Topical Meeting on Nuclear Thermal-Hydraulics, Operation and Safety (NUTHOS-8)*, Shanghai, China, October 10–14.
- Sabir, S.M., Chun, K., Petriw, L., Saifullah, M., Vashi, A., Zvorykin, A., Clark, S., Pioro, I., 2019. Comparison of thermophysical properties (NIST REFPROP Ver. 10) and heat transfer to heavy and light water at subcritical pressures. In: *Proceedings of the 27th International Conference On Nuclear Engineering (ICONE-27)*, May 19-24, Tsukuba, Ibaraki, Japan. Paper #2017, 10 pages.
- Shultis, J.K., Faw, R.E., 2007. *Fundamentals of Nuclear Science and Engineering*, second ed. CRC Press, Boca Raton, FL, USA. 591 pages.
- Sinha, R.K., Kakhodar, A., 2006. Design and development of the AHWR—the Indian thorium fueled innovative nuclear reactor. *Nucl. Eng. Des.* 236, 683–700.
- Sinha, R.K., Chellapandi, P., Srinivasan, G., Dulera, I., Vijayan, P.K., Chande, S.K., 2016. Generation IV concepts: India. In: Pioro, I.L. (Ed.), *Handbook of Generation IV Nuclear Reactors*. Elsevier – Woodhead Publishing (WP), Duxford, UK, pp. 413–452 (Chapter 15).
- Sun, X.M., Chen, Z.P., Sun, J., Liu, Y., Zheng, Y.H., Li, F., Shi, L., 2018. CFD investigation of bypass flow in HTR-PM. *Nucl. Eng. Des.* 329, 147–155.
- Tang, Y.S., Coffield, R.D., Markley, R.A., 1978. *Thermal Analysis of Liquid Metal Fast Breeder Reactors*. ANS, La Grange Park, IL, USA, p. 395.
- Torgerson, D.F., Hedges, K.J., Duffey, R.B., 2004. *Evolutionary CANDU Reactor—Past, Present, and Future, Physics in Canada*. vol. 60, No. 6, pp. 341–354.
- Toshiba, 2011. *Leading Innovation. Advanced Boiling Water Reactor (ABWR)*, Booklet. Toshiba Corporation, Japan.

Comparison of thermophysical properties of reactor coolants^a

Igor L. Piro, Alexey Dragunov, Eugene Saltanov, and Brian Ikeda

Faculty of Energy Systems and Nuclear Science, University of Ontario Institute of Technology,
Oshawa, ON, Canada

Nomenclature

c_p	specific heat at constant pressure, J/kgK
D_{hy}	hydraulic-equivalent diameter, m
G	mass flux, kg/m ² s
h_{fg}	latent heat of evaporation, J/kg
k	thermal conductivity, W/mK
P	pressure, Pa
q	heat flux, W/m ²
T	temperature, °C
v	specific volume, m ³ /kg

Greek symbols

Δ	difference
μ	dynamic viscosity, Pa·s
ρ	density, kg/m ³

Non-Dimensional Numbers

Pr	Prandtl number $\left(\frac{\mu c_p}{k}\right)$
----	---

Subscripts

cr	critical
f	fluid
g	gas
hy	hydraulic-equivalent
in	inlet
max	maximum
out	outlet
pc	pseudocritical
sat	saturation
scw	supercritical water
v	vapor

^a This chapter is partially based on the paper by [Dragunov et al. \(2013\)](#).

Abbreviations/Acronyms

AGR	Advanced Gas-cooled Reactor
BN	Fast Sodium (reactor) (Быстрый Натриевый (in Russian abbreviations)) (Russia)
BREST-OD	Fast Reactor with Inherent safety Lead Coolant – Experimental Demonstration (БРЕСТ-ОД – Быстрый Реактор Естественной безопасности со Свинцовым Теплоносителем – Опытно-Демонстрационный or Быстрый Реактор Естественной безопасности – Опытно-Демонстрационный (in Russian abbreviations)) (Russia)
BWR	Boiling Water Reactor
CANDU	CANada Deuterium Uranium (reactor)
Eff.	Efficiency
GCR	Gas-Cooled Reactor
GFR	Gas-cooled Fast Reactor
HTGR	High-Temperature Gas Reactor
HTR	High-Temperature Reactor
HTR PM	High-Temperature Reactor Pebble-bed Module (helium-cooled, China)
IAEA	International Atomic Energy Agency
KLT-40S	Container-carrier cargo-Lighter Transport (reactor) (КЛТ – Контейнеровоз Лихтеровоз Транспортный (реактор) (in Russian abbreviations)) (Russia)
LBE	Lead-Bismuth Eutectic
LFR	Lead-cooled Fast Reactor
LGR	Light-water-cooled Graphite-moderated Reactor
LMR	Liquid Metal-cooled Reactor
LiNaK	LiF + NaF + KF salt
LMR	Liquid Metal-cooled Reactor
MSR	Molten Salt Reactor
MSFR	Molten Salt Fast Reactor
NEA	Nuclear Energy Agency
NIST	National Institute of Standards and Technology (USA)
NPP	Nuclear Power Plant
PCh	Pressure Channel
PHWR	Pressurized Heavy-Water Reactor
PT	Pressure Tube
PV	Pressure Vessel
PWR	Pressurized Water Reactor
RBMK	Reactor of Large Capacity Channel-type (Реактор Большой Мощности Канальный (in Russian abbreviations)) (Russia)
REFPROP	REFeRence PROPERTIES
RITM-200 M	Reactor Integral Type Modular 200 MW _{el} Modernized (РИТМ-200М – Реактор Интегрального Типа Модульный мощностью 200 МВт Модернизационный (in Russian abbreviations)) (Russia)
SC	SuperCritical
SCF	SuperCritical Fluid
SCP	SuperCritical Pressure
SCW	SuperCritical Water
SCWR	SuperCritical Water-cooled Reactor
SFR	Sodium-cooled Fast Reactor
SMR	Small Modular Reactor
SVBR	Lead-Bismuth Fast Reactor (Свинцово-Висмутовый Быстрый Реактор (in Russian abbreviations)) (Russia)
TECDOC	TECHnical DOcument
Th.	Thermal
V	Vessel
VHTR	Very High Temperature Reactor
VVER	Water Water Power Reactor (ВВЭР - Водо-Водяной Энергетический Реактор (in Russian abbreviations)) (Russia)

A2.A Introduction

A2.A.1 Generations II, III and III+ reactor coolants

The current fleet of nuclear-power reactors uses the following reactor coolants (see also [Table A2.1](#)):

- 1) Light water (H₂O) at subcritical pressures and temperatures^b – in PWRs (single-phase cooling, i.e., liquid cooling); BWRs (two-phase cooling, i.e., with flow boiling, outlet reactor steam quality is usually about 10%), and LGRs (two-phase cooling, i.e., with flow boiling, outlet fuel-channel steam quality is usually about 14% (maximum – 20%));

TABLE A2.1 Typical ranges of thermal efficiencies (gross^a) for selected modern nuclear-power plants (NPPs arranged by decreasing values of thermal efficiency) (based on [Pioro et al., 2021](#)). Also, for more details, see Appendix A1 on modern reactors and NPPs

No	Power Plant	Gross Th. Eff. (up to)
1	Combined-cycle power plant (combination of Brayton gas-turbine cycle (fuel - natural gas or Liquefied Natural Gas (LNG); combustion-products parameters at gas-turbine inlet: $P_{in} \approx 2.5$ MPa, $T_{in} \approx 1650$ °C) and subcritical-pressure Rankine steam-turbine cycle (steam parameters at turbine inlet: $P_{in} \approx 12.5$ MPa ($T_{sat} = 327.8$ °C), $T_{in} \approx 620$ °C ($T_{cr} = 374$ °C)).	62%
2	Supercritical-pressure coal-fired power plant (Rankine-cycle steam inlet turbine parameters: $P_{in} \approx 23.5$ -38 MPa ($P_{cr} = 22.064$ MPa), $T_{in} \approx 540$ -625 °C ($T_{cr} = 374$ °C); and $P_{reheat} \approx 4$ -6 MPa ($T_{sat} = 250.4$ -275.6 °C), $T_{reheat} \approx 540$ -625 °C).	55%
3	Carbon-dioxide-cooled-reactor (Advanced Gas-cooled Reactor (AGR)) NPP (Generation-III) (reactor coolant: $P = 4$ MPa, $T = 290$ –650 °C; and Rankine-cycle steam: $P_{in} = 17$ MPa ($T_{sat} = 352.3$ °C) and $T_{in} = 560$ °C ($T_{cr} = 374$ °C); and $P_{reheat} \approx 4$ MPa ($T_{sat} = 250.4$ °C), $T_{reheat} = 560$ °C).	42%
4	Gas-Cooled-Reactor (GCR) (High Temperature Reactor – Pebble-bed Module (HTR PM), helium cooled) NPP (reactor coolant: $P = 7$ MPa, $T = 250$ –750 °C; and Rankine-cycle steam: $P_{in} = 14.1$ MPa ($T_{sat} = 337.2$ °C), $T_{in} = 556$ °C ($T_{cr} = 374$ °C); and $P_{reheat} \approx 3.5$ MPa ($T_{sat} = 242.6$ °C), $T_{reheat} = 560$ °C).	42%
5	Sodium-cooled-Fast-Reactor (SFR) (BN-600 & BN-800) NPP (reactor coolant: $P = 0.1$ MPa, $T = 377$ –550 °C; and Rankine-cycle steam: $P_{in} = 14.2$ MPa ($T_{sat} = 337.8$ °C), $T_{in} = 505$ °C ($T_{cr} = 374$ °C); and $P_{reheat} \approx 2.5$ MPa ($T_{sat} = 224$ °C), $T_{reheat} = 505$ °C).	40%
6	Pressurized-Water-Reactor (PWR) NPP (Generation-III ⁺) (reactor coolant: $P = 15.5$ MPa ($T_{sat} = 344.8$ °C), $T_{out} = 327$ °C; steam: $P_{in} = 7.8$ MPa, $T_{in} = T_{sat} = 293.3$ °C; and $P_{reheat} \approx 2$ MPa ($T_{sat} = 212.4$ °C), $T_{reheat} \approx 265$ °C).	36-38%

Continued

^b Water: Critical pressure - 22.064 MPa and critical temperature – 373.946 °C (NIST REFPROP, 2018).

TABLE A2.1 Typical ranges of thermal efficiencies (gross) for selected modern nuclear-power plants (NPPs arranged by decreasing values of thermal efficiency) (based on [Pioro et al., 2021](#)). Also, for more details, see Appendix A1 on modern reactors and NPPs—cont'd

No	Power Plant	Gross Th. Eff. (up to)
7	Pressurized-Water-Reactor (PWR) NPP (Generation-III, current fleet) (reactor coolant: $P=15.5$ MPa ($T_{\text{sat}}=344.8$ °C), $T=292$ – 329 °C; steam: $P_{\text{in}}=6.9$ MPa, $T_{\text{in}}=T_{\text{sat}}=284.9$ °C; and $P_{\text{reheat}}\approx 1.5$ MPa ($T_{\text{sat}}=198.3$ °C), $T_{\text{reheat}}\approx 255$ °C).	34-36%
8	Boiling-Water-Reactor (BWR) / ABWR NPP (Generation-III, current fleet) (reactor coolant: $P=7.2$ MPa, $T_{\text{out}}=T_{\text{sat}}=287.7$ °C; steam: $P=7.2$ MPa, $T_{\text{in}}=T_{\text{sat}}=287.7$ °C and $P_{\text{reheat}}\approx 1.7$ MPa ($T_{\text{sat}}=204.3$ °C), $T_{\text{reheat}}\approx 258$ °C).	34%
9	Light-water-cooled Graphite-moderated Reactor (LGR) (Russian RBMK-1000) NPP (Generation-III, current fleet) (reactor coolant: $P=6.4$ MPa, $T_{\text{out}}=T_{\text{sat}}=279.8$ °C; steam: $P=6.4$ MPa, $T_{\text{in}}=T_{\text{sat}}=279.8$ °C and $P_{\text{reheat}}\approx 0.3$ MPa ($T_{\text{sat}}=133.5$ °C), $T_{\text{reheat}}\approx 263$ °C).	34%
10	Pressurized-Heavy-Water-Reactor (PHWR) NPP (Generation-III, current fleet) (reactor coolant: $P_{\text{in}}=11$ MPa / $P_{\text{out}}=10$ MPa ($T_{\text{sat}}=311$ °C) & $T=260$ – 310 °C; steam: $P_{\text{in}}=4.7$ MPa, $T_{\text{in}}=T_{\text{sat}}=260.1$ °C; and $P_{\text{reheat}}\approx 0.6$ MPa ($T_{\text{sat}}=158.8$ °C), $T_{\text{reheat}}\approx 250$ °C).	32%
11	PWR-SMR NPP (RITM-200 M, Russia) (Generation-III+) (not yet in operation as an SMR NPP) (reactor coolant: $P=15.7$ MPa ($T_{\text{sat}}=345.8$ °C), $T=277$ – 313 °C; steam: $P_{\text{in}}=3.82$ MPa, $T_{\text{in}}=295$ °C ($T_{\text{sat}}=247.6$ °C); no reheat).	31%
12	PWR-SMR NPP (KLT—40S, Russia) (Generation-III, current fleet) (reactor coolant: $P=12.7$ MPa ($T_{\text{sat}}=329$ °C), $T=280$ – 316 °C; steam: $P_{\text{in}}=3.72$ MPa, $T_{\text{in}}=290$ °C ($T_{\text{sat}}=246.1$ °C); no reheat).	26%

^aGross Thermal Efficiency (Gross Th. Eff.) of a unit during a given period of time is the ratio of the gross electrical energy generated by a unit to the thermal energy of a fuel consumed during the same period by the same unit. The difference between gross and net thermal efficiencies includes internal needs for electrical energy of a power plant, which might not be small (5% or more).

- 2) Heavy water (D₂O) at subcritical pressures and temperatures^c – in PHWRs (single-phase cooling; however, there is a possibility for boiling within some subchannels at the fuel-channel outlet, steam quality usually does not exceed 5%);
- 3) Carbon dioxide (CO₂) at subcritical pressure, but at supercritical temperatures^d – in AGRs; and
- 4) Liquid sodium (Na)^e – in SFRs (Generation-IV concept).
- 5) Helium (He)^f at supercritical pressure and temperatures – in HTR-PM (Generation-IV VHTR concept).

^c Heavy water: Critical pressure - 21.6618 MPa and critical temperature – 370.697 °C (NIST REFPROP, 2018).

^d Carbon dioxide: Critical pressure - 7.3773 MPa and critical temperature – 30.9782 °C (NIST REFPROP, 2018).

^e Sodium: Melting temperature – 97.7 °C and boiling temperature – 882.8 °C.

^f Helium: Critical pressure - 0.22832 MPa and critical temperature – -267.9547 °C (NIST REFPROP, 2018).

Power cycles of Generation III and III⁺ NPPs are shown in Appendix A1 and [Dragunov et al. \(2015\)](#).

A2.A.2 Generations-IV reactor coolants

Generation-IV nuclear-reactor concepts proposed have identified the use of the following reactor coolants (see also, [Table A2.2](#)):

- 1) Light water (H₂O) at supercritical pressures and temperatures³ - in SCWRs (single-phase cooling, because at supercritical pressures fluids are considered single-phase substances);

TABLE A2.2 Estimated ranges of thermal efficiencies (gross) of Generation-IV NPP concepts (NPP/reactor concepts shown according to the decreasing values of thermal efficiency) (based on [Pioro, 2020](#)). Also, for more details, see Chapter 2 on Generation-IV reactor concepts and Chapter 21.1 – on power cycles

No	Nuclear reactors	Gross eff., %
1	Very-High-Temperature-Reactor (VHTR) NPP (reactor coolant – helium (SCF): $P=7$ MPa and $T_{in}/T_{out}=640/1000$ °C; primary power cycle – direct SCP Brayton helium-gas-turbine cycle; possible back-up – indirect Brayton, Rankine or combined cycles).	≥ 55
2	Gas-cooled-Fast-Reactor (GFR) NPP (reactor coolant – helium (SCF): $P=9$ MPa and $T_{in}/T_{out}=490/850$ °C; primary power cycle – direct SCP Brayton helium-gas-turbine cycle; possible back-up – indirect SCP Brayton, Rankine or combined cycles).	≥ 50
3	SuperCritical-Water-cooled-Reactor (SCWR) NPP (one of the Canadian concepts; reactor coolant – SC light water: $P=25$ MPa and $T_{in}/T_{out}=350/625$ °C ($T_{cr}=374$ °C); direct or indirect cycle; SCP Rankine cycle with high-temperature secondary steam superheat: $T_{out}=625$ °C).	45–50
4	Molten-Salt-Reactor (MSR) NPP (reactor coolant – sodium-fluoride or chloride salts with dissolved uranium fuel: $T_{in}/T_{out}=700/800$ °C; primary power cycle – indirect SCP CO ₂ Brayton gas-turbine cycle; possible back-up – indirect Rankine steam-turbine cycle).	~ 50
5	Lead-cooled-Fast-Reactor (LFR) NPP (Russian design BREST-OD-300: reactor coolant – liquid lead: $P \approx 0.1$ MPa and $T_{in}/T_{out}=420/540$ °C; primary power cycle – indirect subcritical-pressure Rankine steam cycle: $P_{in} \approx 17$ MPa ($P_{cr}=22.064$ MPa) and $T_{in}/T_{out}=340/505$ °C ($T_{cr}=374$ °C); high-temperature secondary steam superheat); (in one of the previous designs of BREST-300 NPP primary power cycle was indirect SCP Rankine “steam”-turbine cycle: $P_{in} \approx 24.5$ MPa ($P_{cr}=22.064$ MPa) and $T_{in}/T_{out}=340/520$ °C ($T_{cr}=374$ °C); also, note that power-conversion cycle in a different LFR design than that of other countries is based on SCP CO ₂ Brayton gas-turbine cycle).	$\sim 41-43$
6	Sodium-cooled-Fast-Reactor (SFR) NPP (Russian design BN-600: reactor coolant – liquid sodium (primary circuit): $P \approx 0.1$ MPa and $T_{in}/T_{out}=380/550$ °C; liquid sodium (secondary circuit): $T_{in}/T_{out}=320/520$ °C; primary power cycle – indirect Rankine steam-turbine cycle: $P_{in} \approx 14.2$ MPa ($T_{sat} \approx 337$ °C) and $T_{in \max}=505$ °C ($T_{cr}=374$ °C); secondary-steam superheat: $P \approx 2.45$ MPa and $T_{in}/T_{out}=246/505$ °C; possible back-up in some other countries – indirect SCP CO ₂ Brayton gas-turbine cycle).	~ 40

- 2) Helium (He) at supercritical pressures and temperatures^g – in GFRs and VHTRs;
- 3) Liquid sodium (Na)⁶ – in SFRs;
- 4) Liquid lead (Pb)^h – in LFRs;
- 5) Liquid Lead-Bismuth Eutectic (LBE) (44.5% Pb and 55.5% Bi)ⁱ - in Liquid Metal-cooled Reactors (LMRs), for example, in Russian SVBR; and
- 6) Molten fluoride salts (for example, FLiNaK)^j– in MSR.

For a better understanding of the thermodynamic terms such as subcritical / supercritical pressures, supercritical fluid, superheated / saturated steam, etc., thermodynamic diagrams for light water, carbon dioxide, and helium are shown in Figs. A2.1–A2.3 (partially based on figures in Mann and Pioro (2015)).

A glossary of the terms used in Figs. A2.1–A2.3 and used elsewhere in the text is given below:

Compressed fluid is a fluid at a pressure above the critical pressure, but at a temperature below the critical temperature.

Critical point (also called a critical state) is a point at which the distinction between the liquid and gas (vapor) phases disappears, i.e., both phases have the same temperature, pressure, and specific volume or density. The critical point is characterized using the phase-state parameters T_{cr} , P_{cr} and v_{cr} (or ρ_{cr}), which have unique values for each pure substance.

Pseudocritical line is a line, which consists of pseudocritical points.

Pseudocritical point (characterized with P and T_{pc}) is a point at a pressure above the critical pressure, where the temperature ($T_{pc} > T_{cr}$) corresponds to the maximum value of the specific heat for this particular pressure.

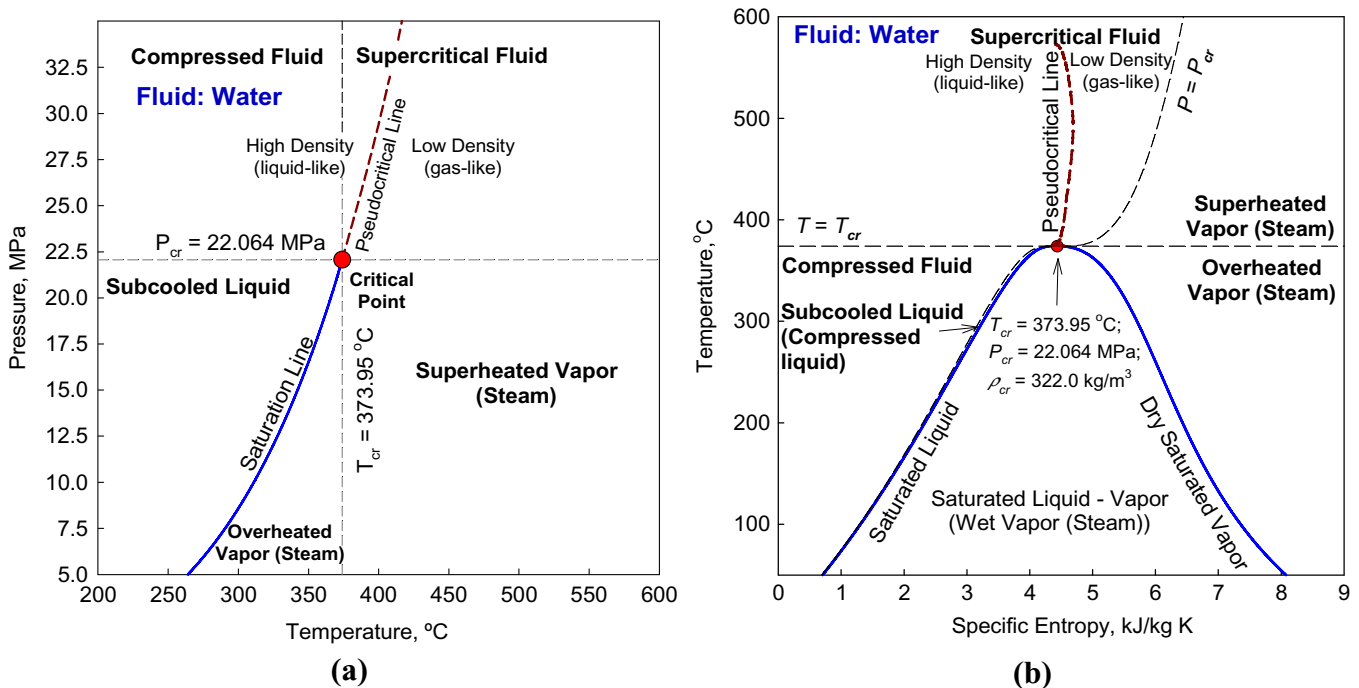


FIG. A2.1 Thermodynamic diagrams for light water: (a) Pressure–Temperature diagram; and (b) Temperature–Specific-Entropy diagram

^g Helium: Critical pressure - 0.2276 MPa and critical temperature – -267.95 °C (NIST REFPROP, 2018).

^h Lead: Melting temperature – 327.5 °C and boiling temperature – 1750 °C.

ⁱ LBE: Melting temperature – 123.5 °C and boiling temperature – 1670 °C.

^j FLiNaK (LiF-NaF-KF): Melting temperature – 454 °C and boiling temperature – 1570 °C.

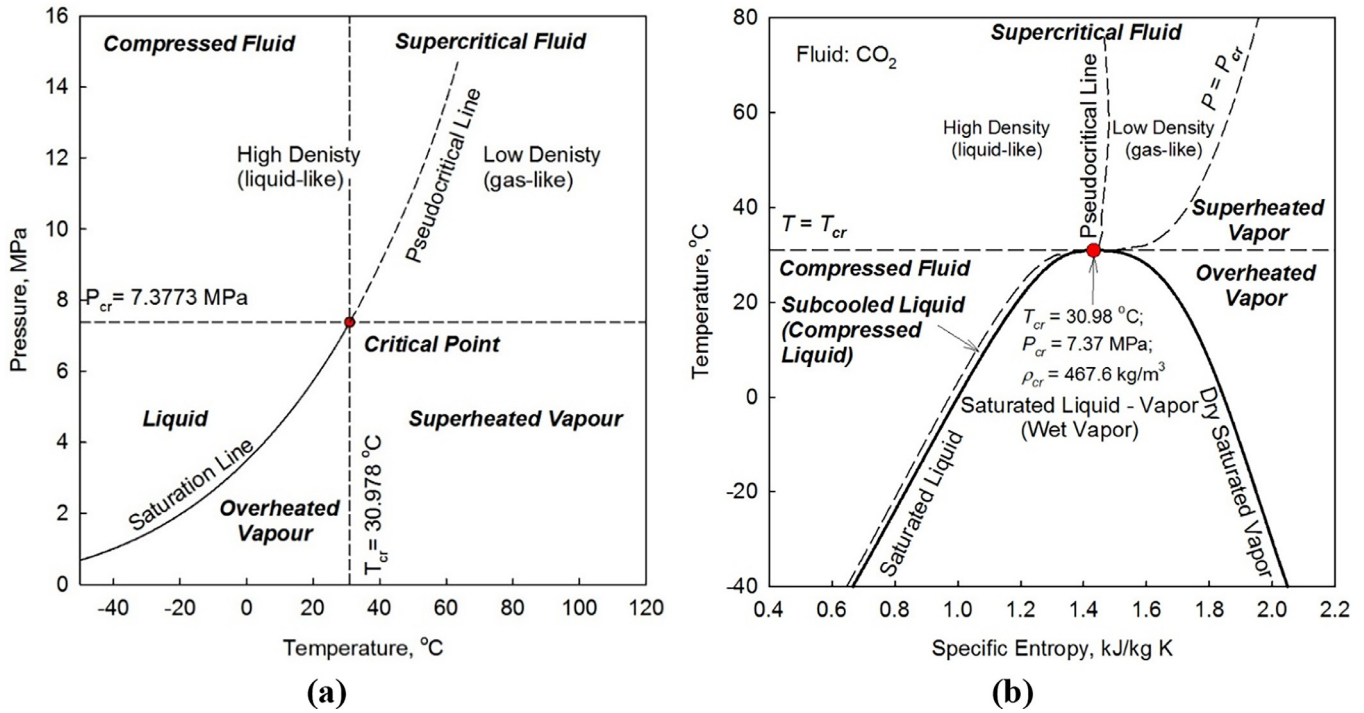


FIG. A2.2 Thermodynamic diagrams for carbon dioxide: (a) Pressure–Temperature diagram; and (b) Temperature–Specific-Entropy diagram

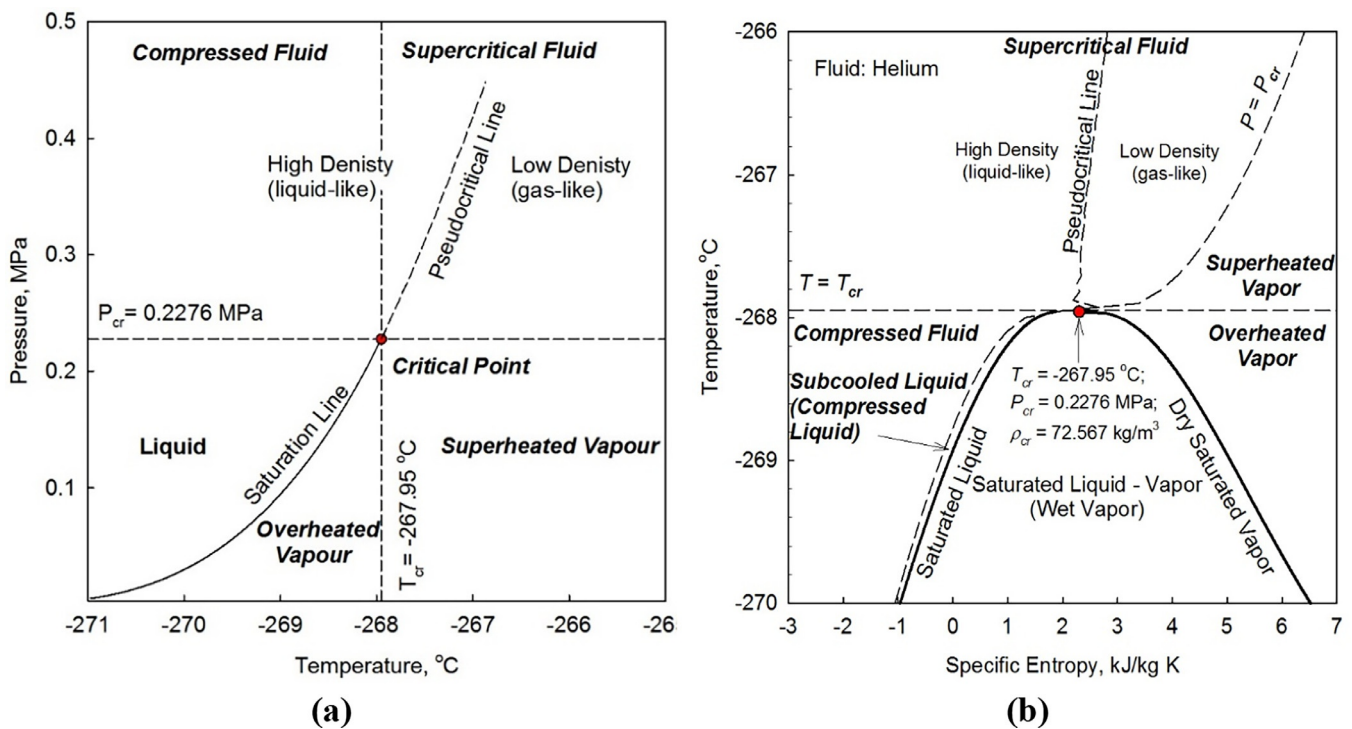


FIG. A2.3 Thermodynamic diagrams for helium: (a) Pressure–Temperature diagram; and (b) Temperature–Specific-Entropy diagram

Pseudocritical region is a narrow region around a pseudocritical point, where all thermophysical properties of a pure fluid exhibit rapid variations. For light water it is about $\pm 25^\circ\text{C}$ from the pseudocritical temperature.

Supercritical fluid is a fluid at pressures and temperatures that are higher than its critical pressure and critical temperature. However, quite often in various publications, a term - supercritical fluid includes both terms – supercritical fluid and compressed fluid.

Overheated vapor is a dry vapor at a pressure and temperature below the critical pressure and temperature, respectively, but above the corresponding parameters of dry saturated vapor.

Supercritical “steam” is actually supercritical water, because at supercritical pressures the fluid is considered as a single-phase substance. However, this term is widely (and incorrectly) used in the literature in relation to supercritical-“steam” generators and turbines.

Superheated vapor is a vapor at pressures below the critical pressure, but at temperatures above the critical temperature.

A2.B Reactor coolants by type

A2.B.1 Fluid coolants

Subcritical-pressure light water is very well-known and is the mostly used reactor coolant (for details, see Chapter 1.2). Due to that it will be used in the subsequent comparisons as a reference case. In general, heavy water has many thermophysical properties and behaviors that are quite close to those of light water (for details, see Table A2.3 and publications by Petriw et al. (2019) and Sabir et al. (2019)). However, heavy

TABLE A2.3 Comparison of selected thermophysical properties of heavy water and light water (data based on (NIST REFPROP, Ver. 10 (2018): <https://www.nist.gov/srd/refprop>))

Coolant	ρ kg/m ³	c_p J/kg K	k W/m K	μ μPa s	Pr -	
(a) at subcooled conditions: $P = 11$ MPa and $T = 260^\circ\text{C}$ (approximately CANDU-reactor fuel-channel inlet conditions)						
D ₂ O	875.4	4657.1	0.536	114.7	0.997	
H ₂ O	791.5	4887.5	0.618	103.7	0.820	
Δ , %	9.6	-5.0	-15.3	9.6	17.7	
Coolant	$\frac{\rho_f}{\rho_v}$ kg/m ³	$\frac{c_{pf}}{c_{pv}}$ J/kg K	$\frac{k_f}{k_v}$ W/m K	$\frac{\mu_f}{\mu_v}$ μPa s	$\frac{Pr_f}{Pr_v}$ -	h_{fg} kJ/kg
(b) at saturated conditions: $P = 10$ MPa and $T_{\text{sat}} = 310^\circ\text{C}$ for heavy water (approximately CANDU-reactor fuel-channel outlet conditions) and $T_{\text{sat}} = 311^\circ\text{C}$ ($\Delta = 0.3\%$) for light water						
D ₂ O	$\frac{760.0}{62.5}$	$\frac{5823.6}{6730.7}$	$\frac{457.7}{82.0}$	$\frac{89.2}{20.2}$	$\frac{1.13}{1.66}$	1178.8
H ₂ O	$\frac{688.4}{55.5}$	$\frac{6123.7}{7140.8}$	$\frac{526.8}{76.6}$	$\frac{81.7}{20.2}$	$\frac{0.95}{1.88}$	1317.4
Δ , %	$\frac{9.4}{11.2}$	$\frac{-5.2}{-6.1}$	$\frac{-15.1}{6.6}$	$\frac{8.4}{0}$	$\frac{16.3}{-13.5}$	-11.8

water has a significantly lower [neutron-capture](#) cross-section compared to that of light water, which allows for more thorough moderation. Therefore, only heat-transfer characteristics of subcritical-pressure heavy water will be compared with those of other coolants.

One of the advantages of light / heavy water is the high heat transfer coefficients at forced convection and at flow boiling. However, there is a limit for efficient heat transfer, called Critical Heat Flux (CHF), which usually cannot be exceeded during nuclear-reactor operation.

$$\Delta = \frac{\text{Property}_{D_2O} - \text{Property}_{H_2O}}{\text{Property}_{D_2O}} \times 100\%$$

SuperCritical Water (SCW) is a coolant in an SCWR concept with an operating pressure of about 25 MPa, and reactor inlet and outlet temperatures of about 350 °C and 625 °C (max), respectively. Specifics of SCW thermophysical properties and heat transfer are discussed in Appendices A3 and A4, respectively, and in the following publications: [Pioro \(2019, 2020, 2021\)](#); [IAEA-TECDOC-1900 \(2020\)](#); [Pioro \(2011\)](#); [Pioro and Mokry \(2011\)](#); and [Pioro and Duffey \(2007\)](#).

Main disadvantage of water as a reactor coolant is, that to reach higher thermal efficiencies of NPP higher temperatures are needed, which in turn requires high or even supercritical pressures.

A2.B.2 Gas coolants

For comparison purposes in this Appendix, it was decided to consider subcritical-pressure carbon dioxide. Carbon dioxide at subcritical pressures is currently being used in the most efficient nuclear-power reactors – AGRs. In general, carbon dioxide is not a strong absorber of thermal neutrons and does not become very radioactive. Another advantage of carbon dioxide is its chemical stability within the operating range of temperatures (292 °C - 650 °C). In addition, carbon dioxide does not react with either the moderator or fuel.

Using helium as a reactor coolant at high outlet temperatures (850 °C and 1000 °C in GFR and VHTR, respectively) makes it possible to achieve very high thermal efficiencies of the plant that are close to those of modern advanced thermal power plants. The major advantages of helium are: 1) a relatively high thermal conductivity compared to that of other gases (an exception is hydrogen), which is close to that of liquids; and 2) its behavior as a noble or inert gas.

In general, the advantages of gaseous reactor coolants compared to water are a possibility to achieve high, or even very high, temperatures at the reactor outlet using significantly lower pressures; and there is no critical-heat-flux phenomena at gas cooling, which limits heat transfer in fluid cooling. However, heat transfer coefficients at gas forced-convection cooling are usually significantly lower than those at water cooling.

A2.B.3 Liquid-metal coolants

Liquid sodium is currently used in the Russian BN-600 and BN-800 – the only ones medium / large capacity operating SFRs so far in the world – and is proposed to be used in Generation-IV SFRs. Sodium is a well-known low-melting-point (97.7 °C) alkali metal, which has the main advantages of high thermal conductivity and low neutron-absorption cross-section. Also, the relatively high boiling point (882.8 °C) of sodium allows a reactor to operate at pressures close to ~0.1 MPa. In addition, very high heat transfer coefficients can be achieved with sodium cooling.

However, sodium is very chemically-reactive substance, which requires special precautions to be taken, when it used as the reactor coolant. Therefore, for improved reactor safety a secondary sodium loop is utilized, which acts as a buffer between the radioactive sodium – reactor coolant in the primary loop and the water / steam in the third loop – a Rankine power cycle.

Lead is proposed for use in an LFR at pressures close to ~ 0.1 MPa. Lead has higher melting point (327.5°C) and significantly higher boiling point (1750°C) compared to that of sodium, which significantly impacts the manner of operating a reactor. Also, it is a more inert liquid metal than sodium. Due to that, the LFR has only two loops: 1) a primary loop with lead as a reactor coolant and 2) a secondary loop with water / steam as a Rankine power cycle.

LBE is an eutectic alloy of lead (44.5%) and bismuth (55.5%) being considered instead of lead as an option for the LFR. One of the main advantages of LBE is its melting point of 123.5°C , which is significantly lower than that of lead and quite close to that of sodium. Neither lead, nor LBE react readily with water or air, in contrast to sodium, which allows for the elimination of the intermediate-coolant loop used in SFRs. Moreover, LBE is not a new technology – it has been proven by years of reliable experience as a coolant in nuclear-powered submarines operated by the Soviet Union since the 1970's.

A major advantage of liquid-metal reactor coolants is low operating pressures inside a reactor (close to atmospheric one) with a possibility to achieve high temperatures. Also, all current liquid-metal reactors use a fast-neutron spectrum, which allows for more efficient fuel cycles.

More information on liquid-metal reactor coolants can be found in the following publications: [Beznosov et al. \(2007\)](#); [Todreas et al. \(2004\)](#); [Dementyev \(1990\)](#); [IAEA \(1985\)](#); and [Waltar and Reynolds \(1981\)](#).

A2.B.4 Molten-salt coolants

Molten salt fluorides, which are proposed as coolants for MSR, have promising thermophysical and thermal–hydraulic properties. [Molten salts](#), similar to liquid metals, have a low [vapor pressure](#) even at high temperatures, which is quite attractive compared to water and gaseous coolants. The salts are less chemically reactive than sodium. In addition, salts can provide moderation due to their light-element composition – like [F](#), [Li](#), and [Be](#) in FliBe.

In the next section, a comparison of the main thermophysical properties will be conducted for all the coolants mentioned above. The range of temperatures investigated covers the operating ranges of the corresponding reactors (see [Tables A2.1 and A2.2](#), and [Fig. A2.4](#)). Basic, averaged parameters for the coolants used in each of the reactors utilized are listed in [Table A2.4](#).

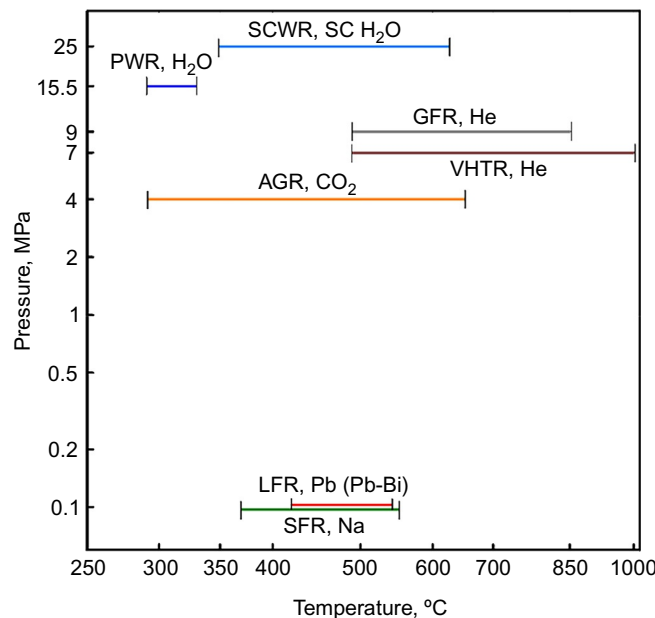


FIG. A2.4 Pressure–Temperature diagram showing operating ranges of coolants for PWR, AGR, SFR, and proposed Generation-IV reactor concepts (pressure drop is not considered)

TABLE A2.4 Basic reference parameters of selected Generations III, III⁺, and IV nuclear-power reactors/concepts

Reactor	Neutron spectrum	Core design		Reactor coolant	Moderator	Reactor cycle	No of circuits	<i>P</i> MPa	<i>T</i> °C
PWR	Thermal	Heterogeneous	PV	Water		Indirect	2	~15.5	292–329
AGR	Thermal	Heterogeneous	PV ^a	CO ₂	Graphite	Indirect	2	4	292–650
SFR	Fast	Heterogeneous	V	Sodium	–	Indirect	3	~0.1	370–550
GFR	Fast	Heterogeneous	PV	Helium	–	Direct	1	9	490–850
						Indirect	2		
VHTR	Thermal	Heterogeneous	PV	Helium	Graphite	Direct	1	7	490–1000
						Indirect	2		
LFR	Fast	Heterogeneous	V	Lead LBE	–	Indirect	2	~0.1	550–800 (420–540)
MSR	Epithermal	Homogeneous	V	Sodium fluoride with dissolved uranium	Graphite	Indirect	3	~0.1	<i>T_{out}</i> = 700–800
MSFR	Fast	Homogeneous	V	Sodium fluoride with dissolved uranium	–	Indirect	3	~0.1	<i>T_{out}</i> = 700–800
SCWR	Thermal	Heterogeneous	PV	Water	Water	Direct	1	~25	300–625
			PCh (PT)		Heavy water	Indirect	2		
	Fast	PV	Water	–	Direct	1	300–625		
				Indirect	2				

^aThough coolant flows through individual channels inside graphite moderator, the actual pressure boundary is the vessel surrounding the moderator.

A2.C Thermophysical properties of Generation III, III⁺, and IV reactor coolants

In this section a comparison of the main thermophysical properties of various coolants for Generation-III, III⁺, and IV reactor systems is presented. It is important to note that the basic properties are shown for a wide range of temperatures (from 250 °C to 1000 °C) that covers the operating ranges of current and Generation-IV reactors (see Fig. A2.4 and Tables A2.1 and A2.2).

Properties of subcritical and supercritical water, carbon dioxide, and helium were obtained from NIST REFPROP (Ver. 10 (2018): <https://www.nist.gov/srd/refprop>). Properties of sodium were taken from Kirillov et al. (2007). Properties of other coolants were calculated either using the original correlations listed in NEA (2007) or using correlations recommended by authors of this book.

Before comparing the thermophysical properties of the coolants, it is reasonable to have a general overview of the desired characteristics of a generic reactor coolant. Nuclear reactors have certain specific requirements for coolants, such as:

- high specific heat, thermal conductivity, and low viscosity;
- low corrosive and low erosive effects on all the reactor materials;
- high boiling point and low melting point (not related to gaseous coolants);
- high thermal resistance and radiation resistance;
- low neutron-absorption cross-section;
- explosion-proof, non-combustible, non-toxic;
- widely available (not rare); and
- low neutron activation.

Fig. A2.5 shows densities profiles of reactor coolants vs. temperature. As expected, molten lead and lead-bismuth alloy have the highest densities following by molten salt and sodium. Actually, at ~250 °C the densities of molten sodium, subcritical pressure water, and SCW are quite close. However, with temperature increase the densities of water and SCW steadily decline. Within the pseudocritical range, the SCW density

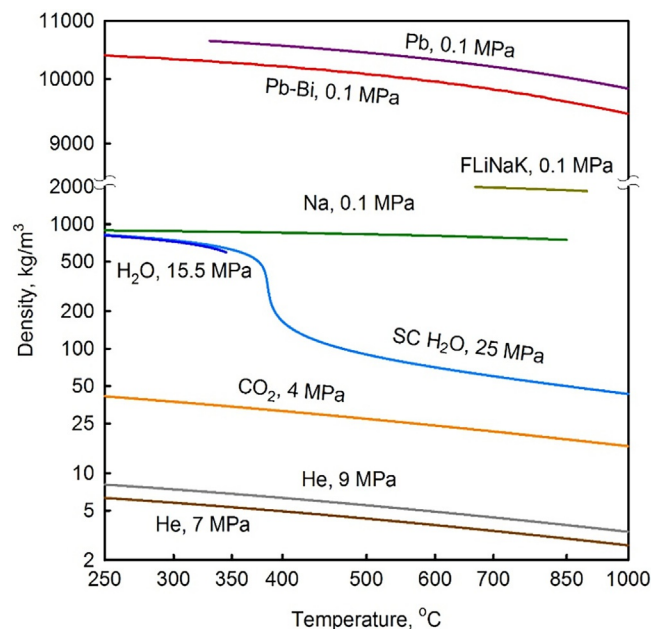


FIG. A2.5 Density of selected coolants vs. temperature

drops quite significantly due to the transition from a “liquid-like” fluid to a “gas-like” fluid. Gases, especially, helium, have the lowest densities. The density of carbon dioxide significantly higher than that of helium.

In general, densities of the reactor coolants (with exception of SCW) decline almost linearly with increasing temperature (see Fig. A2.5). The densities of gases (helium and carbon dioxide) decrease about 1.6 times, but the density change for liquid metals is insignificant. For SCW the density drops by almost 8 times within the pseudocritical region.

As one would expect, the thermal conductivity of liquid metals is significantly higher than that of gases (50–3000 times, see Fig. A2.6). The thermal conductivity of Na drops slightly, while that for Pb, LBE, He, and CO₂ increases linearly with the temperature. The thermal conductivity behavior of SCW is special. The thermal conductivity decreases linearly for temperature between 250 and 350 °C, then goes through a small peak in the pseudocritical point before decreasing smoothly from about 0.4 W/mK to 0.1 W/mK. As the temperature increases above 500 °C the thermal conductivity increases linearly to values higher than those of CO₂, but lower than those of He.

The majority of thermal properties^k of FLiNaK molten salt have intermediate values between those of liquid metals and fluids. However, the viscosity of FLiNaK appears to be significantly higher than that of the rest of the coolants. This also causes the Prandtl number to be very high.

The temperature dependence of the viscosity of liquid metals is quite the opposite behavior to that of gases (Fig. A2.7). The viscosity of Na and Pb drops linearly over the whole range of temperature, while the viscosity of Pb—Bi has a slower linear drop, up to 600 °C and then the viscosity increases for temperatures between 600 and 1000 °C. Near 1000 °C the viscosity returns to a value close to that measured at 250 °C. The viscosities of gases increase linearly with temperature, and the viscosity of SCW at temperatures beyond the pseudocritical range behave in a fashion similar to that of gases. In general, the shape of the viscosity-temperature curve for SCW is similar to that of its thermal conductivity. However, the viscosity does not exhibit a peak in the pseudocritical point.

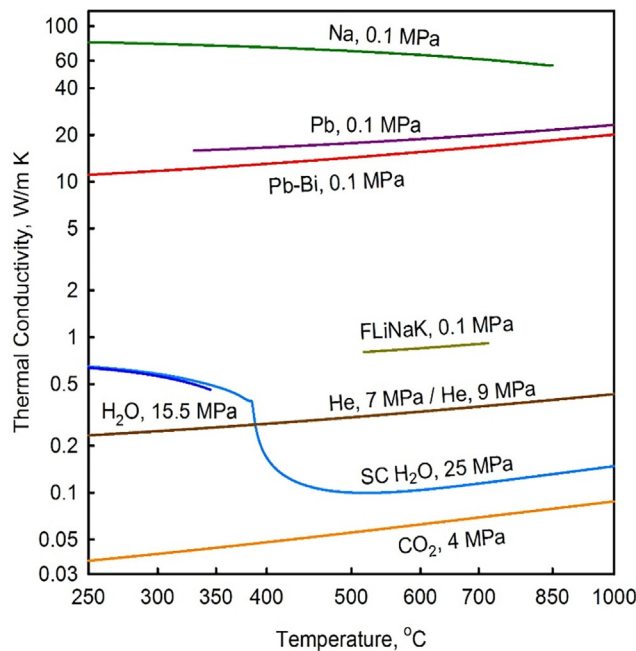


FIG. A2.6 Thermal conductivity of selected coolants vs. temperature

^k Thermal properties of FLiNaK were calculated based on Sohal et al. (2010); Khokhlov et al. (2009); Williams et al. (2006); and Cherenkova et al. (2003).

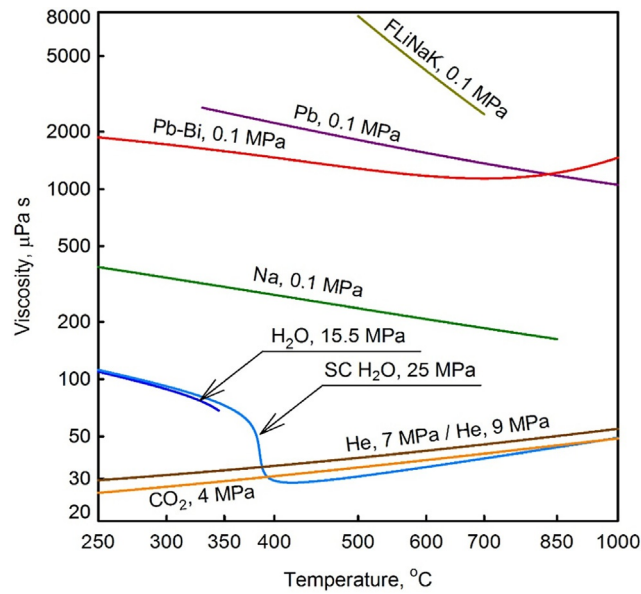


FIG. A2.7 Dynamic viscosity of selected coolants vs. temperature

The specific heat of He, Na, Pb, and Pb—Bi (Fig. A2.8) is nearly constant over the whole range of operational parameters. In the case of CO₂, the specific heat increases linearly and reaches the same value as that for Na at around 750 $^{\circ}\text{C}$. The specific heat of water goes through a peak (where its value increases almost 8 times) within the pseudocritical region. The specific heats of Pb and LBE are nearly identical and 10 times less than those of Na and CO₂, and almost 40 times less than that of He. At temperatures higher than 450 $^{\circ}\text{C}$ the specific heat of He is higher than that of SCW.

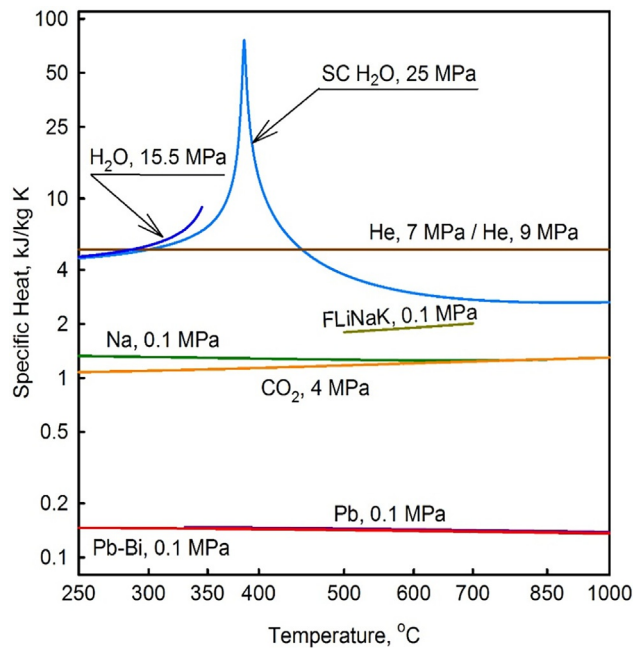


FIG. A2.8 Specific heat of selected coolants vs. temperature

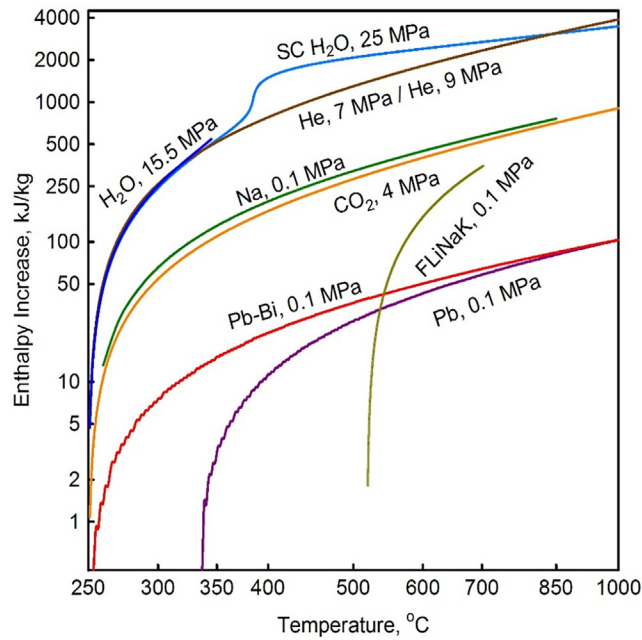


FIG. A2.9 Specific-enthalpy difference (value at T_{in} is taken 0 for all coolants) of selected coolants vs. temperature

Fig. A2.9 shows the enthalpy increase vs. temperature for all reactor coolants. The enthalpy increase is straight-forward and is related to the behavior of the specific heat. Therefore, the highest increase in enthalpy is in SCW, especially, within the pseudocritical range, where the specific heat has a peak. Eventually, SCW, water, and helium show quite close trends in enthalpy increase. The enthalpy increases for sodium and carbon dioxide and lie in the middle of the range. The lowest enthalpy increases are shown by the lead-bismuth alloy, and, especially, by lead itself. The enthalpy rise for the molten salt is very sharp starting from relatively low values (below that for lead and lead-bismuth alloy) and almost reaching values for carbon dioxide and sodium at higher temperatures.

The dependence of the Prandtl number (Pr) (which is defined as a ratio of product of viscosity and specific heat to thermal conductivity) on temperature for different coolants is shown in Fig. A2.10. As follows from the definition, the shape of Pr is governed by the more significantly changing property of the coolant. We have established that the specific heat is nearly constant for all of the Generation-IV reactors coolants except for SCW. Therefore, for most of the coolants the ratio of the viscosity to the thermal conductivity will affect the shape of the Pr /temperature curve.

As we see from Figs. A2.6 and A2.7, the changes in the thermal conductivity and viscosity of gases are such that they compensate each other, and the Pr of gases is virtually constant over most of the 750 °C temperature span. However, for the liquid metals the viscosity drops more significantly than the thermal conductivity increases. As a result, the Pr of liquid metals drops almost linearly with temperature. Due to an increase in viscosity of LBE at high temperatures, the corresponding value of Pr for Pb—Bi also increases. Since the specific heat of SCW goes through the most rapid changes compared with its other thermophysical properties, the Pr of SCW behaves similar to its specific heat. At high temperatures (>500 °C), the Pr of SCW behaves similar to that of the gases.

The volumetric expansivity of liquid metals is much smaller than that of the remaining coolants and stays almost constant (see Fig. A2.11). The volumetric expansivity of gases drops almost twice, in a linear fashion, from 250 to 1000 °C. Remarkably, the values of volumetric expansivity for SCW at temperatures below the

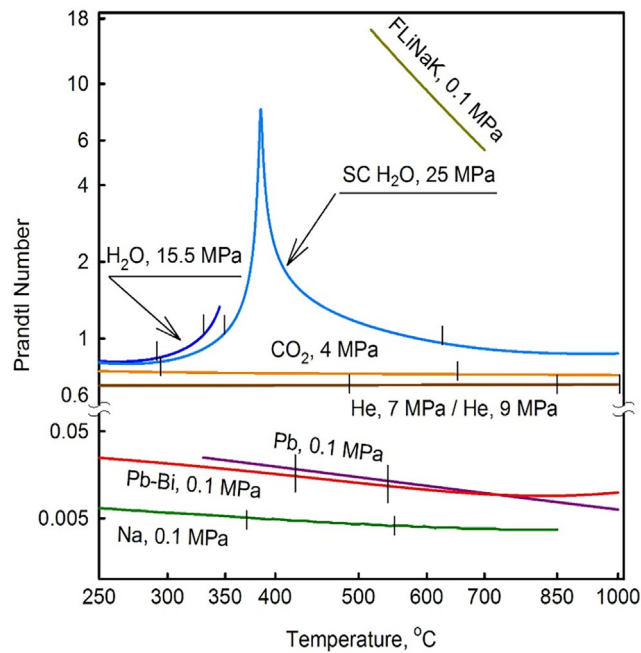


FIG. A2.10 Prandtl number of selected coolants vs. temperature

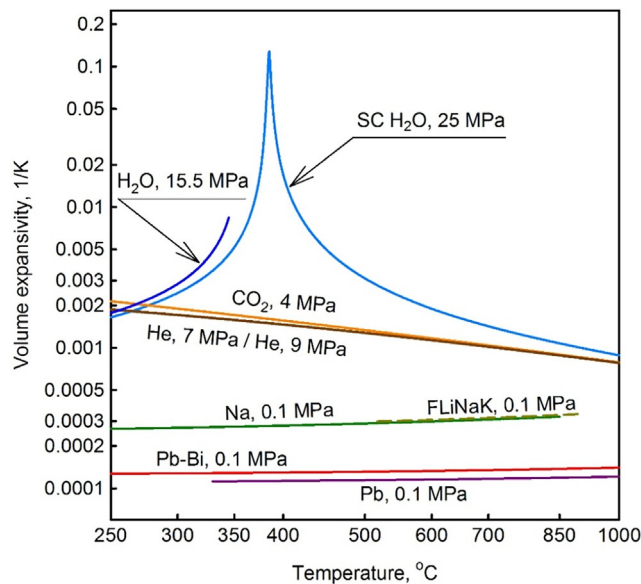


FIG. A2.11 Volume expansivity of selected coolants vs. temperature

pseudocritical point are close to those for gases. Near the pseudocritical point, the volumetric expansivity of SCW peaks. At higher temperatures, the volumetric expansivity of SCW gradually reaches values corresponding to those of gases.

To summarize the above, the thermophysical properties of liquid metals and gases experience only minor linear changes with increasing temperature. However, all the properties of water at pseudocritical conditions go through very rapid changes. The basic properties of helium, carbon dioxide, and water are summarized in [Table A2.5](#). Basic properties of lead, molten salt (FLiNaK), and sodium are summarized in [Table A2.6](#).

TABLE A2.5 Basic properties of helium, carbon dioxide, and water (based on NIST REFPROP, Ver. 10 (2018): <https://www.nist.gov/srd/refprop>)

No	Properties	Fluids		
		Helium	Carbon Dioxide	Water
1	Chemical formula	He	CO ₂	H ₂ O
2	Molar mass, kg/kmol	4.0026	44.01	18.015
3	Triple point, °C	-270.97	-56.558	0.01
4	Normal boiling-point temperature, °C	-268.93	-78.464	99.974
5	Critical point temperature, °C	-267.9547	30.9782	373.946
6	Critical point pressure, MPa	0.22832	7.3773	22.064
7	Critical point density, kg/m ³	72.567	467.6	322.0
8	Flammability	-	-	-
9	Explosion hazard	-	-	-
10	Chemical reactivity	Inert gas	Moderate	Moderate-high
11	Toxicity	-	-	-
12	Corrosiveness	Inert gas	Yes	Vary

TABLE A2.6 Basic properties of lead, lead-bismuth, molten salt, and sodium

No	Properties	Fluids			
		Lead	Lead-Bismuth	Fluoride Salt ^a	Sodium
1	Chemical formula	Pb	44.5 Pb-55.5 Bi	FliNaK	Na
2	Molar mass, kg/kmol	207.2	~208	41.3	23
3	Density at 20 °C, kg/m ³	11,340	10,500	–	968
4	Melting-point temperature, °C	327.5	123.5	454	97.8
5	Boiling-point temperature, °C	1749	1670	1570	883
6	Heat of fusion, kJ/mol (kJ/kg)	4.77 (23.0)	8.08 (38.8)	–	2.60 (113.0)
7	Heat of vaporization, kJ/mol (kJ/kg)	179.5 (866.3)	178.1 (856.3)	–	97.42 (4236)

Continued

TABLE A2.6 Basic properties of lead, lead-bismuth, molten salt, and sodium—cont'd

No	Properties	Fluids			
		Lead	Lead-Bismuth	Fluoride Salt	Sodium
8	Flammability	Highly purified lead fine powder can ignite in air	Fine powder can ignite in air	–	Spontaneously ignites when heated above 115 °C in air that has even modest moisture content; Generates flammable H ₂ and caustic sodium hydroxide upon contact with water
9	Explosion hazard	Fine powder can ignite in air	Fine powder can ignite in air	–	Sodium powder is highly explosive in water and may spontaneously explode in the presence of oxygen
10	Chemical reactivity	Reactive (oxidized in air)	Corrosive	–	Highly reactive
11	Toxicity	Poisonous	Poisonous	–	Can be poisonous
12	Corrosiveness	Yes Can embrittle metals	Yes	Yes	High

^aBased on paper by Williams et al. (2006). More details on molten salts are provided in Appendix A7.

A2.D Heat transfer coefficients in nuclear-power reactors

Typical heat-transfer-coefficient ranges for various reactor coolants are listed in Table A2.7. It shows that sodium has the highest heat transfer coefficient among all the proposed coolants, making it a more competitive fluid for power conversion.

Fig. A2.12 shows calculated heat transfer coefficients at conditions corresponding to those of the operating reactors. The calculated values fall very close to those presented in Table A2.7. Among the coolants considered, sodium, in conditions close to SFR, has the highest heat transfer coefficient of all the proposed coolants (70–80 kW/m²K). Conditions achieved in a generic CANDU reactor (added for comparison purposes) allow heat transfer coefficients above 60 kW/m²K. Calculations also showed that in a PWR, the heat transfer coefficients are about 45 kW/m²K. Lead, as expected, has heat transfer coefficients around 25 kW/m²K, which is lower than that of another liquid-metal – sodium. Heat transfer coefficients of SCW (5–15 kW/m²K) and CO₂ (1.8–2.5 kW/m²K) also lie within the typical ranges of values.

For calculations of subcritical H₂O, D₂O, CO₂, and He the value of heat flux was not taken into account, while for SCW, Pb, and Na the value of heat flux was assumed to be 970 kW/m². A hydraulic-equivalent diameter of 8 mm was used in the calculations for all coolants.

Fig. A2.13 shows heat transfer coefficients calculated for all coolants (including FLiNaK) for the generic conditions: $G = 1000 \text{ kg/m}^2\text{s}$, $q = 970 \text{ kW/m}^2$, $D_{hy} = 8 \text{ mm}$.

TABLE A2.7 Typical ranges of heat transfer coefficients, heat fluxes, and sheath temperatures for reactors' coolants; and capacities per reactor-core volume (based on Hewitt and Collier (2000) and data provided by P.L. Kirillov)

Typical ranges of heat transfer coefficients for reactors' coolants		
Coolant	Heat transfer coefficient, kW/m²K	
Na (forced convection) (~SFR conditions)	50–80	
Boiling water (flow boiling) (~BWR conditions)	~40	
CANDU-type reactor	~50	
Water (single-phase forced convection)	~30	
SCW (~SCWR conditions)	7-10	
Pb (forced convection) (~LFR conditions)	25–35	
Pb-Bi (forced convection) (~SVBR conditions)	20–30	
He (rough surface)	10	
CO ₂ (high pressure) (~AGR conditions)	2–5	
Typical ranges of heat fluxes for reactors' coolants		
Coolant	Heat Flux, kW/m ²	$T_{\text{sheath}} - T_{\text{coolant}}$, °C
Na (forced convection) SFR	2000 (1800-2400)	25-30
Water (single-phase forced convection)	1500	50
Boiling water (flow boiling) BWR	1000	15
CANDU reactor	625	15
Boiling water in a kettle	150	15
Reactor Type	Sheath Temperature, °C	
AGR	750	
SFR	700	
PWR	390	
BWR	300	
Typical ranges of average capacity (kW) per reactor-core volume (liter)		
Reactor Type	kW/l	
AGR, HTGR, VHTR	6–10	
RBMK	4–6	
BWR	40–50	
PWR, VVER	100–150	
SCWR, VVER-SKD ^a	100	
SFR, BN	400–550	

^aSKD –SuperCritical Pressure in Russian abbreviations.

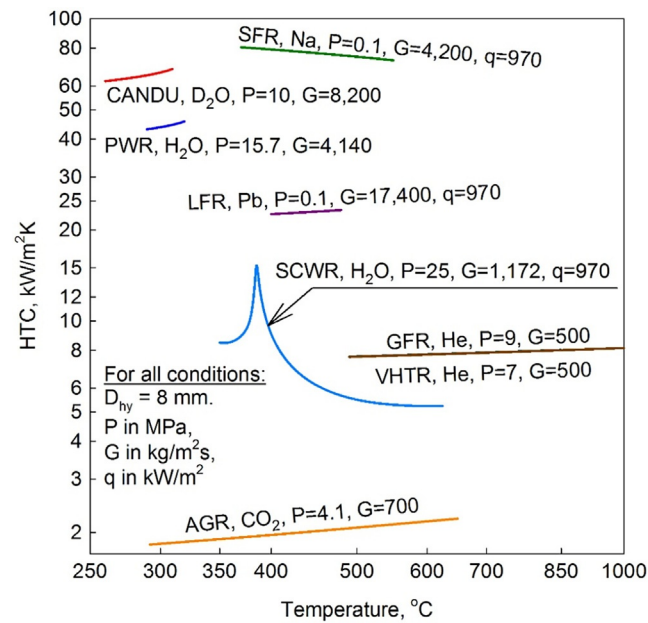


FIG. A2.12 Heat transfer coefficients calculated for flow of coolants in Generation-IV, AGR, and PWR reactors in a bare tube at nominal operating pressures and at mass fluxes close to actual mass fluxes for the respective reactor

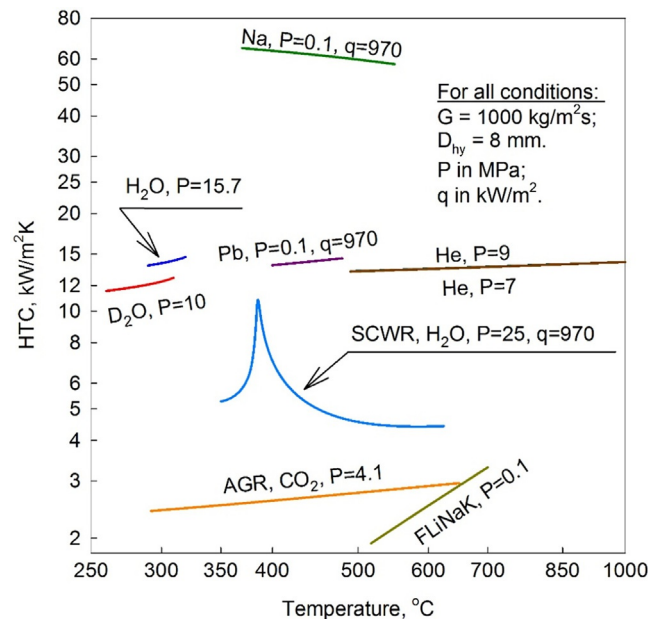


FIG. A2.13 Heat transfer coefficients calculated for flow of coolants in Generation-IV, AGR, and PWR reactors in a bare tube at generic operating conditions

It can be seen that at the chosen generic conditions, a sodium coolant has the highest heat transfer coefficients, ranging within 58–96 kW/m²K, while CO₂ and FLiNaK have the lowest heat transfer coefficients, ranging within 1–4 kW/m²K. The heat transfer coefficient of SCW starts at ~5 kW/m²K, then goes through a peak in the pseudocritical region, where its value increases by almost 2 times, and after that drops close to 4 kW/m²K at temperatures above 450 °C. The heat transfer coefficients of the gases, water, heavy water, and lead increase slightly with temperature. Heat transfer coefficients of the molten salt increase quite significantly with temperature. The heat transfer coefficient of sodium drops linearly with temperature increase.

A2.E Conclusions

Based on the above the following conclusions can be made.

- In general, liquid-metal coolants have high thermal stability, high boiling points, and very low saturated-vapor pressures, which distinguish them from other types of nuclear coolants.
- The specific heats of Pb and LBE are nearly identical and 10 times less than those of Na and CO₂, and are almost 40 times less than that of He. At temperatures higher than 450 °C, the specific heat of He is even higher than that of SCW.
- As one would expect, the thermal conductivity of liquid metals is significantly higher than that of gases (50–3000 times). The highest thermal conductivity is for sodium (60–70 W/mK).
- The volumetric expansivity of liquid metals is much lower than that of the other coolants examined, and stays almost constant.
- The thermophysical properties of liquid metals and gases show only small linear changes with temperature. However, all properties of SCW go through very rapid changes within the pseudocritical range.
- The thermophysical properties of LBE, except for the thermal conductivity, are close to the average values of those of lead and bismuth.
- At high temperatures (more than 500 °C) the Prandtl number of SCW behaves similar to gases.
- One of the least desirable properties of water is its high vapor pressure, which increases rapidly with temperature. Its relatively low critical temperature (~374 °C) limits the maximum temperature of the coolant and significantly limits the efficiency of the power-conversion cycle.
- The specific heat of He is higher than that of CO₂ and liquid metals. The thermal conductivity of He is 10 times greater than that of CO₂. This characteristic facilitates heat transfer and reduces the size of heat exchangers. He is far more inert than CO₂, does not absorb neutrons, and cannot become radioactive on its own.

References

- Beznosov, A.V., Dragunov, Y.G., Rachkov, V.I., 2007. Heavy-Liquid Metal Coolants in Nuclear Engineering. Izdat Publishing House, Moscow, Russia. 434 pp. (in Russian).
- Cherenkova, M., Danek, V., Vasiljev, R., Silny, A., Kremenetsky, V., Polyakov, E., 2003. Density and viscosity of the (LiF-NaF-K-F)_{eut}-KBF₄-B₂O₃ melts. *J. Mol. Liq.* 102 (1), 213–226.
- Demytyev, B.D., 1990. Nuclear Power Reactors. Energoatomizdat Publishing House, Moscow, Russia. 352 pp. (in Russian).
- Dragunov, A., Saltanov, E., Pioro, I., Ikeda, B., Miletic, M., Zvorykina, A., 2013. Investigation of thermophysical and nuclear properties of prospective coolants for Generation-IV nuclear reactors. In: Proceedings of the 21st International Conference on Nuclear Engineering (ICONE-21), July 29-August 2, Chengdu, China, Paper #16020. 11 pp.
- Dragunov, A., Saltanov, E., Pioro, I., Kirillov, P., Duffey, R., 2015. Power cycles of Generation III and III⁺ nuclear power plants. *ASME J. Nucl. Eng. Radiat. Sci.* 1 (2). 10 pp.
- Hewitt, G.F., Collier, J.G., 2000. Introduction to Nuclear Power, second ed. Taylor and Francis Publishing Office, USA. 304 pp.
- IAEA, 1985. Status of Liquid Metal Cooled Fast Reactors. Technical Report Series No. 246, IAEA, Vienna, Austria. Free download from: <https://www.iaea.org/publications/1348/status-of-liquid-metal-cooled-fast-breeder-reactors>.
- IAEA-TECDOC-1900, 2020. Understanding and Prediction of Thermohydraulic Phenomena Relevant to Supercritical Water Cooled Reactors (SCWRs). IAEA TECDOC Series, Vienna, Austria. 544 pp., Free download from: <https://www.iaea.org/publications/13636/understanding-and-prediction-of-thermohydraulic-phenomena-relevant-to-supercritical-water-cooled-reactors-scwrs>.
- Khokhlov, V., Ignatiev, V., Afonichkin, V., 2009. Evaluating physical properties of molten salt reactor fluoride mixtures. *J. Fluor. Chem.* 130, 30–37.
- Kirillov, P.L., Terentjeva, M.I., Deniskina, N.B., 2007. Thermophysical Properties of Materials for Nuclear Engineering, second ed. Izdat Publishing House, Moscow, Russia. 192 pp.

- Mann, D., Pioro, I., 2015. Study on specifics of thermophysical properties of supercritical fluids in power engineering applications. In: Proceedings of the 23rd International Conference on Nuclear Engineering (ICONE-23), May 17–21, Chiba, Japan, Paper #1730. 11 pp.
- National Institute of Standards and Technology, 2018. NIST Reference Fluid Thermodynamic and Transport Properties—REFPROP. NIST Standard Reference Database 23, Ver. 10. Department of Commerce, Boulder, CO, US.
- NEA No. 6195, 2007. Handbook on Lead-bismuth Eutectic Alloy and Lead Properties, Materials Compatibility, Thermal-hydraulics and Technologies. Nuclear Energy Agency (NEA) and Organisation for Economic Co-operation and Development (OECD), France. 693 pp. Free download from: <https://www.oecd-nea.org/science/reports/2007/pdf/lbe-handbook-complete.pdf>.
- Petriw, L., Sabir, S.M., Chun, K., Pioro, I.L., 2019. Comparison of thermophysical properties of heavy and light water (NIST REFPROP VER. 10) at CANDU reactor operating conditions. In: Proceedings of the 39th Annual Conference of the Canadian Nuclear Society and 43rd Annual CNS/CNA Student Conference, Ottawa, ON, Canada, June 23–26, Paper #25. 7 pp.
- Pioro, I., 2011. The potential use of supercritical water-cooling in nuclear reactors. In: Krivit, S.B., Lehr, J.H., Kingery, T.B. (Eds.), Chapter in Nuclear Energy Encyclopedia: Science, Technology, and Applications. J. Wiley & Sons, Hoboken, NJ, USA, pp. 309–347.
- Pioro, I., 2021. Application of supercritical fluids in thermal- and nuclear-power engineering. In: Chen, L. (Ed.), Chapter 17 in Book: Handbook of Research on Advancements in Supercritical Fluids Applications for Sustainable Energy Systems. IGI Global, Hershey, PA, USA, pp. 601–658. 821 pp. Website: <https://www.igi-global.com/book/handbook-research-advancements-supercritical-fluids/253256>.
- Pioro, I., Mokry, S., 2011. Thermophysical properties at critical and supercritical conditions. In: Belmiloudi, A. (Ed.), Chapter in Book “Heat Transfer. Theoretical Analysis, Experimental Investigations and Industrial Systems”. INTECH, Rijeka, Croatia, pp. 573–592. Free download from: <http://www.intechopen.com/books/heat-transfer-theoretical-analysis-experimental-investigations-and-industrial-systems/thermophysical-properties-at-critical-and-supercritical-pressures>.
- Pioro, I., Duffey, R.B., Kirillov, P.L., Pioro, R., 2021. Pros and cons of commercial reactor designs, volume 1, section 2: chapter. Part 1. Current status of electricity generation in the world and selected countries. Editor-in-Chief, In: Greenspan, E. (Ed.), Encyclopedia of Nuclear Energy, first ed. Elsevier, UK, pp. 263–287. 3656 pp.
- Pioro, I.L., 2019. Current status of research on heat transfer in forced convection of fluids at supercritical pressures. Nucl. Eng. Des. 354. 14 pp.
- Pioro, I.L., 2020. Supercritical-fluids thermophysical properties and heat transfer in power-engineering applications. In: Pioro, I. (Ed.), Chapter 1 in Book “Advanced Supercritical Fluids Technologies”. IntechOpen Ltd, London, UK, pp. 1–42. Free download from: <http://mts.intechopen.com/articles/show/title/supercritical-fluids-thermophysical-properties-and-heat-transfer-in-power-engineering-applications>.
- Pioro, I.L., Duffey, R.B., 2007. Heat Transfer and Hydraulic Resistance at Supercritical Pressures in Power Engineering Applications. ASME Press, New York, NY, USA. 334 pp.
- Sabir, S.M., Chun, K., Petriw, L., Saifullah, M., Vashi, A., Zvorykin, A., Clark, S., Pioro, I., 2019. Comparison of thermophysical properties (NIST REFPROP Ver. 10) and heat transfer to heavy and light water at subcritical pressures. In: Proceedings of the 27th International Conference On Nuclear Engineering (ICONE-27), May 19-24, Tsukuba, Ibaraki, Japan, Paper #2017. 10 pp.
- Sohal, M., Ebner, M., Sabharwall, P., Sharpe, P., 2010. Engineering Database of Liquid Salt Thermophysical and Thermochemical Properties. INL/EXT-10-18297 Report, 70 pp., Retrieved from: <http://www.inl.gov/technicalpublications/Documents/4502650.pdf>. on September 1, 2014.
- Todreas, N.E., MacDonald, P.E., Heizlar, P., Buongiorno, J., Loewen, E., 2004. Medium-power lead-alloy reactors: missions for this reactor technology. Nucl. Technol. 147 (3), 305.
- Waltar, A.E., Reynolds, A.B., 1981. Fast Breeder Reactors. Pergamon Press, USA. 853 pp.
- Williams, D.F., Toth, L.M., Clarno, K.T., 2006. ORNL-TM-12-2006. Assessment of Candidate Molten Salt Coolants for the Advanced High-Temperature Reactor (AHTR). ORNL/TM-2006/12 Report, 86 pp., Retrieved from: <http://web.ornl.gov/~webworks/cpp/y2006/rpt/124584.pdf>. on August 19, 2014.

Index

Note: Page numbers followed by *f* indicate figures, and *t* indicate tables.

- A**
ABRs. *See* Advanced burner reactors (ABRs)
Accelerator driven system (ADS), 241
Accident-tolerant fuel (ATF), 341–342
Additional Gen IV systems, 215–227
 advanced lead-cooled fast reactor
 European demonstrator (ALFRED), 215, 216*f*, 216*t*
 Chinese CLEAR-I reactor, 222, 222–223*t*, 223*f*
 LFR-TL-X, 219–220, 220*f*, 221*t*
 Newcleo LFR-AS-200, 218, 218*f*, 219*t*
 Pb-Bi cooled direct contact boiling water fast reactor (PBWFR), 223–224, 224*f*, 224*t*
 South Korean URANUS-40 system, 220–221, 221*t*, 222*f*
 SVBR-100, 225, 225*t*, 226*f*
 Swedish advanced lead reactor (SEALER), 226–227, 227*f*
 Westinghouse LFR, 215–217, 217*t*, 217*f*
Advanced boiling water reactor (ABWR), 88–89, 288
Advanced burner reactors (ABRs), 169, 296
Advanced gas-cooled reactors (AGRs), 88–89, 136
Advanced light water reactors (ALWRs), 288
Advanced Manufacturing and Material Engineering Task Force (AMME TF), 129
Advanced modular reactors (AMRs), 717
Advanced Reactors Information System (ARIS), 87
Advanced sodium technological reactor for industrial demonstration (ASTRID), 175–176
AEC. *See* Atomic Energy Commission (AEC)
AECL. *See* Atomic Energy of Canada Limited (AECL)
American Nuclear Society (ANS), 87
Atomic Energy Commission (AEC), 840
Atomic Energy Control Board (AECB), 840
Atomic Energy of Canada Limited (AECL), 676
Automatic depressurization systems (ADSs), 273–274
- B**
Basic-cycle options, electricity generation, 761–763, 761*f*, 762*t*
Basic design choices, 198–201
 lead coolant reactor design, 199–200, 200*t*
 lead *vs* LBE, 198–199, 198*t*
 primary system, evolution, challenges, 200–201
 development, 201, 202*f*
 sodium-cooled fast reactor concept, 200–201
Basic nuclear installation (BNI), 903
BELLA, 226
Boiling water reactors (BWRs), 88–89, 260, 288
Boron carbide (B₄C), 145
- C**
Canada Uranium Deuterium (CANDU), 271
Canadian Nuclear Laboratories (CNL), 676
Canadian Nuclear Safety Commission (CNSC), 721–740
Canadian perspectives, pressure retaining systems and components (PRSCs), 845–861
 review framework, FA1, 846–851
 aging management plan (AMP), 848
 analysis, 849
 defense-in-depth, 847
 leak detection system, 847
 leak rate, 848–849
 loadings, 849
 materials, 848
 operational limits, conditions, 846
 redundancy, diversity, separation philosophy, 850–851
 review framework, FA2, 851–852
 code classification requirements, 851–852
 review framework, FA10, 852–853
 accident prevention, plant safety characteristics, 852
 plant states, 853
 postulated initiating events (PIEs), 852–853
 quantitative application, safety goals, 853
 review framework, FA11, 853–859
 aging, wear, 858–859
 design rules, limitations, 853–854
 helical coil steam generator, 856–857
 in-service testing, maintenance, 859
 nondesign basis loading condition, 855–856
 pressure boundary program, CSA standards, 854–855
 probabilistic fracture mechanics, 857–858
 seismic classification, category, qualification, 854
 review framework, FA16, 860–861
Carbon fiber composite (CFC), 885
CCGT. *See* Combined cycle gas turbine (CCGT)
Ceramic fuels, 620–641, 621*f*, 622*t*
 carbide fuels, 627–634
 uranium carbide (UC), 628–631, 629–631*f*
 uranium dicarbide (UC₂), 631–634, 633–634*f*
 mixed oxide fuels, 626–627
 ThO₂+UO₂ and ThO₂+PuO₂, 626–627, 627*f*
 UO₂+PuO₂, 621*f*, 626
 nitride fuels, 634–641
 uranium nitride (UN), 635–641, 636–642*f*
 oxide fuels, 620–625
 thorium dioxide (ThO₂), 623–625*f*, 624–625
 uranium dioxide (UO₂), 621–624
China Fast Reactor 600 (CFR-600), 101–102, 175–176
China Nuclear Engineering Corporation (CNEC), 349
Chinese Experimental Fast Reactor (CEFR), 123
Clean burn, 143
Clinch River Breeder Reactor (CRBR), 181–182
Closed fuel cycle, 183
CNL. *See* Canadian Nuclear Laboratories (CNL)
CNSC. *See* Canadian Nuclear Safety Commission (CNSC)
Coeur 'a Faible Vidange (CFV), 179
Cogeneration, 666
Combined cycle gas turbine (CCGT), 31
Combined heat and power (CHP), 119–120
Compensating group drive mechanisms (CGDM), 742
Component definition, design point performance, 788–795
 axial compressor, 788–790, 789*f*, 789*t*
 axial turbine, 791–793, 791*f*, 792*t*
 cycle performance, 795
 precooler, intercooler, 794
 reactor, 794–795
 recuperator, 793–794
Composite fuels, 644–648, 645*f*
 UO₂-BeO, 647–648, 647–648*f*
 UO₂-C, 646–647
 UO₂-SiC, 645–646
Concentrated solar power plant (CSPP), 56–58
Conceptual design activities (CDA), 876
Containment, 695–696*t*, 697
Control rod drive mechanism (CRDM), 687

- Core damage frequency (CDF), 332, 754
 Core design, 259
 Core fuel element/fuel pin, 178
 Core outlet temperature (COT), 794
 Coupling hydrogen, generation-IV reactor technologies, 666–669, 667–668f, 668t
 CSPP. *See* Concentrated solar power plant (CSPP)
 Current Generation-III reactors, 98
 Current reactors, 98
 Cycle configurations, gas-cooled, high temperature reactors, 795–802
 component efficiencies, 798–799
 compressor inlet temperature, 799–801f, 800
 DP performance comparison, 795–796, 796t
 pressure loss, 800–802, 801–802t, 801f
 temperature, pressure ratio, 796–797, 797–798f
 Cycle, plant design, research needs, 828–830
 higher core outlet temperature, 829–830, 829f
 improved helium compressors, 830
 smaller high-pressure ratio cycle configuration, 828, 829f
 Cycles comparison, thermal efficiency, 769–771, 770–773f
 Cycles, gas-cooled reactors (VHTRs, GFRs), SFR, 763–769, 764–769f
- D**
 Department of Energy (DOE), 297, 840
 Design-point (DP), 780
 Design considerations, 826–828
 long-term off-design point performance, operation, 826
 reactor technology status, 828
 short-term off-design point performance, operation, 827–828, 827f
- E**
 Economic, financing evaluation, 704–707, 705f
 Economics Modelling Working Group (EMWG), 128
 Edge-localized modes (ELMs), 882
 Education and Training Working Group (ETWG), 128
 EED. *See* Electro-electrodialysis (EED)
 Effective thermal conductivity (ETC), 635–637
 Electrical energy consumption (EEC), 3–4
 Electricity generating sources
 advantages, disadvantages, 20f, 27–31, 27t, 28f, 29–32t, 33f
 industrial, 21t, 22–27, 23–25t
 Electricity generation, 3–19, 3–4t, 5–6f, 6t, 8–13f, 14t, 16f, 19t, 20f
 Electric Power Research Institute (EPRI), 115
 Electro-electrodialysis (EED), 155–157
 Electrolysis, 670–673, 671–672f, 671t
 alkaline, 672–673
 high-temperature, 673
 PEM, 672
 Emergency core cooling system, 697t, 698–703f, 700–703, 701t
 Energy Research and Development Administration (ERDA), 840
 ESRF. *See* European sodium fast reactor (ESFR)
- ESFR-SMART primary system
 description, 366–376, 367f
 characteristics, 366–370, 368–370t
 core, 371, 371f
 core catcher, 374–375
 core support structure, connection map, 374
 decay-heat removal concept, 376
 DHRS-3, 362f, 373
 inner vessel, 371–372
 intermediate heat exchanger, 375–376
 main vessel, 371
 polar table/dome, 376
 primary pump, 375
 primary sodium confinement, 374
 reactor bit, 372–373, 373f
 reactor roof, 372
 ESRF-SMART project, 356
 containment, 360–363
 in-vessel core catcher, 360–361, 362f
 massive metallic roof, sodium reactor coolant, 361
 reactor pit, 360, 361–362f
 roof penetrations, 362–363
 decay-heat removal, 363–364, 364–365f
 dosimetry, releases, 365–366
 examples, 359–366
 reactivity control, 359–360
 R&D needs, 390–392, 390–391f
 reactivity control
 eliminated situations, 360
 passive-control rods, 359
 reduced sodium void effect, 359
 ultra-sonic measurements, 359
 safety improvement, 358–359
 severe-accident mitigation, 365
 simplicity, human factor, reactor safety, 366
 sodium fire, 364
 sodium/water reaction, 364
- ESFR SMART secondary loops, 377–383
 description, 377–378, 377f
 DHRS-1 system, 379–381, 380–381f
 general layout, 385, 385–386f
 handling systems, 386–388
 components, 388
 fresh-fuel, 388
 spent-fuel, 386–388, 387f
 piping, 381–383, 383f
 safety analysis, 383–384, 384f
 safety improvements, 388–389, 390f
 secondary pump, 378, 378f
 steam generator, 379, 379t, 380f
- EU Energy Union (2015), EU Green Deal (2020), 304–310
 energy transition, climate neutrality, 309–310
 EU's ambition, world's 1st major economy, 306–308
 106 nuclear power reactors, EU, 304–306
 district heating, industrial heat applications world-wide, 305–306
 good health, well-being, 306
 EURATOM, 310–320
 brief history, IAEA, OECD/NEA, 310–313
- European Nuclear Education Network (ENEN), 319–320
 legal framework, 313–315
 science, technology, innovation, 316–318
 Euratom Fission Training Schemes (EFTS), 319
 Euratom leadership, nuclear fission R&D, 350–353
 Euratom research, training actions, innovative reactor systems, 338–344
 European sustainable nuclear fission industrial initiative (ESNII), nuclear cogeneration industrial initiative (NC2I), 342–344
 six GIF reactor systems, 338–342
 European Energy Research Alliance (EERA), 312
 European Investment Bank (EIB), 307
 European Lead-cooled SYstem (ELSY), 197–198
 European Nuclear Energy Agency (ENEA), 841
 European Nuclear Safety Regulators Group (ENSREG), 314–315
 European sodium fast reactor (ESFR), 344
 European Sustainable Nuclear Industrial Initiative (ESNII), 197–198
 European Technology and Innovation Platforms (ETIPs), 312
 Evaluation and Viability Of Liquid fuel fast reactor systems (EVOL), 234
 Experimental research reactors, EU, small modular reactors, 344–350
 SMR technology, 348–350
 training, materials testing, isotope production, 344–347
- F**
 Fast Flux Test Facility (FFTF), 174–175
 Fast-response power plants, 81
 Fast spectrum, 215
 Federation of Electric Power Companies (FEPC), 159
 Feed-water pumps (FP), 260–261
 Financial risk, 824
 Fissile fuels (uranium, thorium), 87
 Fission product(s) (FPs), 183, 197, 233
 Fitness-for-service (FFS), 849
 Floating nuclear power & desalination system (FNPDs), 742
 Floating nuclear thermal-power plant (FNThPP), 102
 Fluoride-salt-cooled high-temperature reactor (FHR), 125–126
 Fuel assembly concept, Canadian SCWR, 269–272, 270f, 271t, 272f
 fast reactor, 262f, 268, 269f
 high-performance light water reactor (HPLWR), 267–268, 267–268f
 Fuel assembly/fuel subassembly, 178
 Fuels, 693–697, 694–695t
 Fuel salt chemistry, material issues, 238–240
 processing schemes, 238–239, 239f
 salt composition impact, 240

- Functional failure mode and effects analysis (FMEA), 245–247
- Fusion power, 911–914
- G**
- Gas-cooled fast reactor(s) (GFR(s)), 121–122, 121*f*, 167, 291, 666, 780
 history, R&D bridge, 167–169
 small modular reactor, micro reactors, 171–172, 172*t*
 technology, 169–171, 170–171*t*
- Gas-cooled reactors (GCRs), 88–89
- Gasification, 669–670
- Gas turbine combined cycle (GTCC) power plant, 162
- Gas turbine high-temperature reactor (GTHTR), 674
- Gas turbine, power-conversion machine, 780–781
- General design criteria (GDC), 844
- Generation III pressurized water reactors (PWRs), 115
- Generation-III reactors, 98
- Generation-III⁺ reactors, 102
- Generation-III⁺ water-cooled reactors, 101–102
- Generation-IV closed-cycle configurations, 787–788, 788*f*
- Generation-IV GFRs, 171–172
- Generation-IV, India, 486–487
 fast breeder reactor, 500–511
 current status, 500–501
 FBR-600, 504–506
 improvements, 503–504, 505*f*
 program, 500
 prototype, 501–503, 502*f*, 502–503*t*
 R&D, 510–511
 safety features, 505–507*f*, 506–510, 509*f*
- heavy water reactors, 487–492
 AHWR-300, 487, 488*f*, 489*t*
 enhanced safety features, inherent, passive, Fukushima, 487–490
 improved economics, 491, 491*f*
 physical protection, 491
 proliferation resistance, 490
 R&D, 491–492
 safety goals, 490
- high-temperature reactors, 492–499
 description, 492–493
 fuel development, 496
 innovative, 498–499, 498–499*f*, 499–500*t*
 materials development, 496–497, 496–497*f*
 passive heat removal, inherent, 497–498
 R&D, 497*f*, 498
 reactor physics design, 493*f*, 493–494*t*, 494, 495*f*
 thermal hydraulics design, 495, 495–496*f*
- molten salt reactors, 510–511*f*, 511–515
 design challenges, 514, 514*t*
 IMSBR, 512–513*f*, 513–514
 R&D, 514–515
- Generation IV International Forum (GIF), 113, 113*f*, 176, 197, 291, 523, 839
 goals, 114–116, 115*t*
 methodology working groups, task forces
 cross-cutting items, 128–130
 nuclear-energy systems, 119–128, 119*f*, 121*f*, 123–127*f*
 origins, 114, 114*f*
 system, selection, 116–118, 116–117*f*, 118*t*
- Generation IV LFR, 208–227
 reference Gen IV systems, 208–214
 BREST-OD-300 reactor, 209–212, 212*t*, 213*f*
 European Lead-cooled fast reactor (ELFR), 208–209, 209*f*, 210–211*t*
 small secure transportable autonomous reactor (SSTAR), 212–214, 213–214*t*, 214*f*
- Generation-IV nuclear energy systems, eight
 high-level goals, 328–338
 economics, 334–336
 proliferation resistance, physical protection, 336–338
 safety, reliability, 330–333
 sustainability, 328–330
- Generation-IV, nuclear power China, 451–452, 451*f*
 advanced nuclear reactors, 452
 LFR research, development, 476–480, 477*f*
 clear-0, 477
 clear-I, 477–478, 478*f*, 479*t*
 clear-II, 479
 clear-III, 479
 LESMOR, 480, 480*t*, 480*f*
 research, development, 452–480
 CDFR, 455–457, 455–456*f*
 China SFR, CEFR, 453–457, 453–454*f*
 post-CDFR, 457
 SFR, CEFR construction, 452–457
- very-high-temperature reactor (VHTR), 457–461
 CSR1000 concept design, 465–467, 466*t*, 466–467*f*
 FuSTAR, 475–476, 476*f*
 HTGR program, 457–458
 HTR-PM project, 460–461, 462*f*
 HTR-10 test module project, 458–461, 459*f*
 material, salts research, 473–475, 474*f*
 molten salt test loops, 473
 MSR, thermal-hydraulic, 467–476, 468*f*, 469–470*t*, 471–472*f*
 neutronic modeling, 471–473
 SCWR, SCWR-M, 461–467, 463–464*t*, 464–465*f*
 thermo-hydraulics, neutronics coupling, 473, 474*f*
- Generation-IV, nuclear power, Korea, 420–421
 HELP, 420
 lead fast reactor, 438–442, 439–442*f*
 molten salt reactor (MSR), 443–444
 PEACER, 444
 reactors, 421–425
 sodium-cooled fast reactor, 421–422, 422*f*
 very-high-temperature gas-cooled reactor (VHTR), 422–425, 423–424*f*
 research, development, 425–444
 sodium-cooled fast reactor, 425–432
 core design, 425
 fluid system design, 428
 fuel design, 425–428, 426–427*t*, 427*f*
 mechanical structure design, 428, 429*f*
 150 MW_{el} prototype, 425–428
 research, development activities, 428–432
 very-high-temperature reactor, 432–438
 design, analysis codes, 432–434, 433*f*
 high-temperature materials, 436–437
 hydrogen production, 437–438, 437–439*f*
 TRISO fuel technology, 434–436, 434–435*f*
- Generation-IV nuclear-reactor concepts, 617, 618*t*
 United States, 288–289
- Generation-IV (Gen-IV) reactors, 238, 414, 684
 culture, 116
 deployment perspectives, schedule, 297–299
 electrical grid integration, 294–295
 industry, utilities interest, 295–296, 296*t*
 SFR prototype/demonstration reactors, 183
 small modular reactors, micro reactors, 296–297
- Generation-IV, sustainability, safety, performance (GIF, IAEA-INPRO), 320–327
 generation-IV International Forum (GIF), 320–324
 GIF technology roadmap, 324
 nuclear fission, Generation I to IV, 320–324
 GIF roadmaps 2002, 2013, 325
 IAEA programme INPRO, 325–326
 NRC (USA), IRSN (FR), MDEP (OECD/NEA), 326–327
 Senior Industrial Advisory Panel (SIAP), 326
- Geothermal plants, 66–68, 66–67*f*, 67–68*t*, 69–73*f*
- GFRs. *See* Gas-cooled fast reactors (GFRs)
- GIF Policy Group (PG), 114
- Gigantic fusion machine, 878–887, 880*f*, 883*f*, 885–886*f*
- H**
- HDI. *See* Human development index (HDI)
- Heat transfer coefficients (HTCs), 771
- Heavy liquid metal, 198
- Helium, coolant, 784–787, 785–786*t*
- Helium gas turbines, 781–782
 historical problems, 782
 Oberhausen II EVO helium turbine (1974), 781
- High efficiency Re-Entrant Channel (HERC), 614
- High energy lines (HELs), 850
- Higher heating value (HHV), 155–157
- High fuel burn-up and long operation cycle length, 177
- High-pressure compressor (HPC), 814
- High-pressure preheaters (HP-PH), 262–263
- High temperature engineering test reactor (HTTR), 134
- High temperature gas-cooled reactor (HTGR)/very-high temperature gas-cooled reactor (VHTR), 134, 673, 843
 cogeneration, 155–157
 desalinization, 157, 157*f*, 158*t*

- High temperature gas-cooled reactor (HTGR)/very-high temperature gas-cooled reactor (VHTR) (*Continued*)
hydrogen, 155–157, 156f
development, current status, 134–136, 135t
economics, 158–163
desalination cogeneration cost, 162–163, 162f
electricity generation cost, 158–161, 160–161f
hydrogen production cost, 161, 161f, 162f
fuel burnup, 140–144
plutonium, 143–144, 143–144t
uranium, 140–142, 142–143t
fuel design, 139–140, 139f, 141t
industrial application, 157–158, 159f
plant design, 149–150, 150f
plant operations, 150–154
dynamic simulation, 152–154, 153f
startup, rated operation, shutdown, 150–152, 151–152f
power generation, 154, 155t, 156f
reactor design, 145–148
pebble bed, 146–148, 148f
prismatic core, 145–146, 145–146f, 147t
safety approaches, 148–149, 149f
technology, 136–154
design features, 138–139, 139f
design types, 136–137, 137f
- High-temperature helium-cooled thermal reactors, 168
- High-temperature reactor pebble-bed module (HTR-PM), 88–89
- High temperature steam electrolysis (HTSE), 668–669
- High-temperature test reactor (HTTR), 674
- Hochtemperatur Helium Versuchsanlage (HHV), 781
- Homogeneous molten salt fast reactor (MSFR), 232–233
- Homogeneous reactor experiment (HRE), 233
- HTGR. *See* High temperature gas-cooled reactor (HTGR)
- HTR-PM. *See* High-temperature reactor pebble-bed module (HTR-PM)
- Human development index (HDI), 3–4
- Hydride fuels, 642–644
uranium-thorium-zirconium fuels, $UTh_4Zr_{10}H_x$, 643–644
uranium-zirconium hydride fuel, U-ZrH_{1.6}, 642–643, 643–644f
- Hydrogen iodide (HI), 155–157
- Hydrogen production, 666, 667f
- Hydro-power plants, 21t, 23t, 44–48, 44–45f, 48–49f
conventional, 20f, 21t, 25t, 27t, 28f, 29–30t, 32t, 33f, 44–45f, 46, 47f
pumped-storage hydro-electric power plant (PSHEPP), 48, 49f
run-of-the-river, 23t, 47, 48f
- I**
- IAEA. *See* International Atomic Energy Agency (IAEA)
- IEA. *See* International Energy Agency (IEA)
- India's prototype fast breeder reactor (PFBR), 123
- Inertial confinement fusion (ICF), 917
- Inherent reactivity feedback, 184–185
- Integrated Safety Assessment Methodology (ISAM), 245, 332–333
- Intercooled cycle recuperated (ICR), 787
- Intermediate heat exchanger (IHX), 151–152
- Intermediate reactor auxiliary cooling system (IRACS), 703
- International Atomic Energy Agency (IAEA), 87, 113, 840
- International Energy Agency (IEA), 839
- International Project on Innovative Nuclear Reactors and Fuel Cycles (INPRO), 113, 184
- International Reactor Innovative and Secure (IRIS), 685
- International Thermonuclear Experimental Reactor (ITER)
delays, budget increases, 896–901, 897f
DEMO, ITER, 914–917, 916f
economy, 908–911
huge logistics, 889–896, 891–892f, 894–895f
management challenge, 901–903
modern technological evolution, 922–925
project, 873–878, 874–875f, 878f
safety, waste management, 904–906
- Inventory control tank (ICT), 814
- Iodine-sulfur (IS) process, 155
- IRIS. *See* International Reactor Innovative and Secure (IRIS)
- Isolation condenser (IV), 209
- J**
- Japan Atomic Energy Agency (JAEA), 2, 673
- Joint European Torus (JET), 874–875
- Joint Research Centre (JRC), 310
- JSFR (Japan sodium-cooled fast reactor)
design, 398–412
features, 398–403, 399f, 400t, 401f
Fukushima Daiichi accident, 412–414, 413t
innovative technologies, 403–412
advanced seismic isolation, 412
compact reactor system, 406–407, 407f
high burn-up core, 403–404
integrated intermediate heat exchanger, 408–409
natural-circulation decay heat removal system, 409–410, 410f
reliable steam generator, 408f, 409, 410f
safety enhancement, 404–406, 404–405f
simplified fuel handling system, 410–411
steel plate-reinforced concrete, 411–412, 411f
two-loop cooling system, 407–408, 408f
- L**
- LB loss of coolant accident (LB-LOCA), 686
- Lead-alloy fast reactor (LFR), 666
- Lead-bismuth eutectic (LBE), 124, 198
- Lead-cooled fast reactor (LFR), 124, 124f, 196–198, 291, 298
advantages, 205–206
fuel technology, fuel cycles, 204–205, 205t
key challenges, 206–208
safety principles, 202–204
- Leak before break (LBB), 847
- Leak detection, 846
- Legislation, 826
- Levelized cost of energy (LCOE), 31
- Levelized Unit Energy Costs (LUEC), 334
- Light water-cooled reactors (LWRs), 89–90
- Light-water, graphite-moderated reactors (LGRs), 88–89
- Light-water reactors (LWRs), 143, 174, 241, 289, 626
- Lines of defense (LoD), 247–248
- Liquid fuel, 233
- Liquid-metal-cooled fast reactors (LMFRs), 169
- Liquid-metal fast breeder reactors (LMFBRs), 88–89, 626
- Long-term operation (LTO), 43
- Loss-of-coolant accident(s) (LOCA(s)), 206, 275, 289
- Low enriched uranium (LEU), 120, 266
- Low-pressure preheaters (LP-PH), 260–261
- LWRs. *See* Light water-cooled reactors (LWRs)
- M**
- Magnetic confinement, 871
- Master logical diagram (MLD), 245–247
- Material technology, high temperature, pressure, 820
- Metallic fuels, 619–620
- Minor actinide(s) (MA(s)), 183, 205, 241
- Minor actinides-bearing fuel, 183
- Minor actinides recycling in molten salt (MARS), 244
- Mixed oxide (MOX), 175–176, 266
- Moisture separator reheater (MSR), 263
- Molten salt breeder reactor (MSBR), 233
- Molten salt reactor (MSR), 125, 125–126f, 238–239, 291, 666
- Molten salt reactor experiment (MSRE), 233
- MSFR (molten salt fast reactor), 234–238
core, system description, 234–236, 234–235f, 235–236f
fuel cycle, 240–243, 241–243f
transient calculations, 236–238, 238f
viability, 251–253
demonstration steps, 252, 252f
identified limits, 251
other R&D activities, 253
- Multinational Design Evaluation Program (MDEP), 327, 841
- Multipurpose Hybrid Research Reactor for High-tech Applications (MYRRHA), 197–198
- Multistage flash (MSF) system, 157
- N**
- National Aeronautics and Space Administration (NASA), 331–332
- National Nuclear Security Administration (NNSA), 290

- National Renewable Energy Laboratory (NREL), 869
- Natural convection, 187–188
- Natural hazards, 906–908
- Near-Term Deployment Group (NTDG), 297
- New nuclear power plants (NPPs), 839
- Next Generation EU (NGEU), 309
- Next generation/generation-IV fast-spectrum reactors, 31
- Next-generation nuclear plant (NGNP), 136, 298
- Next-generation nuclear reactors, 113
- Nonelectrical Application of Nuclear Heat Task Force (NEaNH TF), 129
- Nonproliferation, 579–591
- cost savings, 607–608
 - economic, social aspects, recycling, 605–607, 606f
 - enrichment, 595–596
 - EURATOM, 609–610
 - fuel cycles, 595, 602–609, 603f
 - global crises, 598–600
 - advanced reactors, NPT, 599–600
 - alternate fuel cycles, 598–599
 - IAEA additional protocol, 610–611
 - international treaties, 590–591
 - nonproliferation treaty (NPT), 584–585t, 585–587
 - nuclear history, basic science, 591–598
 - commercial nuclear power, 592–593
 - research, sustainability, 593–598
 - ostrich syndrome, 609
 - past influence, future, 580–582
 - policy implications, nuclear fuel cycles, 597–598
 - politics power, 582–585, 582f
 - reprocessing, recycling, 596–597
 - shortcomings, treaty, 589–590
 - treaty, 587–589
 - waste to energy, 608–609
 - wider context, 600–602
- Nonrenewable-energy power plants, 32–43
- Nozzle guide vanes (NGVs), 791
- NREL. *See* National Renewable Energy Laboratory (NREL)
- Nuclear fuels
- analysis, 648–655, 649–650t, 650–653f, 653t
 - high-temperature applications, 654–656f, 656–659, 659–660t
- Nuclear fusion, 870–873, 870f, 872f
- alternative technologies, 917–922, 920f
- Nuclear hydrogen production, climate change mitigation, 676–678, 677f, 678t
- Nuclear licensing, 903–904
- Nuclear power industry evolution, 288–292, 290t, 292t
- Nuclear power plant (NPP), 20f, 21t, 23–25t, 27t, 28f, 32–33t, 33f, 37f, 42–43, 42f, 89–90, 260, 704, 782
- closed cycles, 783–784
 - Brayton cycles, 783–784, 784f
 - controls, operations, 814–819
 - bypass control strategy (BCS), 816
 - combined control strategy, 816–819, 817t, 818f
 - inventory control strategy (ICS), 814–816, 815f
 - reactor delivery temperature control (HST), 816
- Nuclear-power reactors, 87, 87–89t, 90–92f, 93–97t, 99–101t, 102–105f, 106t, 261, 687–690, 688–689t, 690–693f
- Nuclear reactor safety, risk assessment
- classification, 529–533, 531–532t
 - goals
 - emerging, criteria, 526–528
 - practical elimination, 528–529
 - safety focus, 525–526
 - subsidiary, 523–525
 - modules, plant risk, 540–541
 - natural circulation loop, parallel channel
 - thermal-hydraulic, 553–566
 - AR, Gen-IV passive residual heat-removal, 563
 - BWR stability, 561–562
 - computational fluid dynamics (CFD), 565
 - coupled natural circulation loops, 563–564
 - early investigations, 558–560
 - literature review, 557–558
 - nanofluids, 565
 - natural circulation flows, 555–557
 - numerical methods, artifacts, 562
 - parallel channels, 566
 - sodium, liquid metal reactors, 566
 - supercritical fluid states, 564–565
 - three mile Island, 560–561
 - principles, 522
 - quantifying probability, RIDM, 542–553
 - applicability, exchangeability, 547–548
 - core damage uncertainty estimate, 550–552, 551f
 - limitations, 545–547
 - modern idea risk-informed decision-making (RIDM), 542–545
 - power, cooling, 548–549
 - power loss, core damage, 549–550
 - quantitative estimates, 552–553, 553t
 - risk informing safety, 536t, 537, 538f
 - role, ARs, 541
 - safety barriers, 533–536
 - technical safety, 537–540
- Nuclear regulation, 839–840
- Nuclear Regulatory Commission (NRC), 290, 687, 840
- Nuclear safeguards, 581
- Nuclear steam supply system (NSSS), 150
- Number of transfer units (NTU), 793
- O**
- Oak Ridge National Laboratory (ORNL), 125, 233
- OECD. *See* Organization for Economic Co-Operation and Development (OECD)
- Off-design-point (ODP), 780
- Organization for Economic Co-Operation and Development (OECD), 841
- Organization for Economic Co-operation and Development/Nuclear Energy Agency (OECD/NEA), 182–183, 198
- Original equipment manufacturer (OEM), 162
- Outlet guide vanes (OGVs), 788–789
- Oxide dispersion strengthened (ODS) steel, 188
- Oxygen evolution reaction (OER), 672
- P**
- Paper reactors, 168
- Passive moderator cooling system (PMCS), 277
- Passive safety, 184, 683–684
- Passive shutdown mechanism, 184–185
- Pharaonic worksite, 887–889
- PHES. *See* Pumped hydro-electric energy storage (PHES)
- Plutonium uranium redox extraction (PUREX), 267
- Polonium, 199
- Postulated initiating events (PIEs), 245–247
- Power conversion system (PCS), 782–783
- Power grid, nonrenewable/renewable sources, 69–81, 77–80f
- Power Reactor Information System (PRIS), 87
- Power Reactor Innovative Small Module (PRISM), 175–176
- Pressure retaining systems and components (PRSCs), 845–846
- Pressurized heavy-water reactors (PHWRs), 88–89
- Pressurized water reactors (PWRs), 88–89, 717
- Process inherent ultimate safety (PIUS), 686–687
- Project change requests (PCRs), 884
- Proliferation Resistance and Physical Protection Working Group (PRPP WG), 128
- Prototype fast breeder reactor (PFBR), 175–176
- Provisional System Steering Committee (PSSC), 197
- PSH. *See* Pumped-storage hydro-electricity (PSH)
- PSHEPP. *See* Pumped-storage hydro-electric power plant (PSHEPP)
- Pumped hydro-electric energy storage (PHES), 48
- Pumped-storage hydro-electricity (PSH), 48
- Pure, hybrid thermochemical cycles, 674–676
- copper-chlorine (Cu-Cl) hybrid thermochemical cycle, 676
 - hybrid sulfur (HyS) thermochemical cycle, 674–676, 675f
 - sulfur-iodine (S-I) pure thermochemical cycle, 674, 675f
- R**
- Rankine steam-turbine power cycle, 33–34, 774
- R&D Infrastructure Task Force (RDITF), 129
- R&D Outlook for Generation IV Nuclear Energy Systems: 2018 Update*, 116–117
- Reactor coolant systems (RCSs), 685, 690–693, 694f
- Reactor physics, 237
- Reactor pressure vessel (RPV), 89–90, 136–137
- Reactor vessel air/auxiliary cooling system (RVACS), 203, 703
- Recent helium gas turbine tests, 782–783, 783f
- Recovered energy generation (REG) power plants, 41

- Regulatory concept
 challenges, advanced reactors, 843–844
 requirements, 840–843
 status, 839–840
- Release frequency, 525
- Renewable-energy power plants, 44–69
- Request for information (RFI), 298
- Risk and Safety Working Group (RSWG), 128, 332–333
- Risk assessment, 819, 820f
- Russian KLT-40S, RITM-200M SMRs, 741–753, 743–745t, 746–753f
- S**
- Safety Assessment of Molten salt Fast Reactor (SAMOFAR), 234
- Safety critical targets (SCTs), 850
- Safety Design Criteria (SDC), 176, 326, 397–398
- Safety Design Criteria Task Force (SDC-TF), 129
- Safety design guidelines (SDGs), 176
- Safety methodology, risk analysis, 244–251
 recommendations, 250–251
 LFR specificity, decay heat removal, 244–245, 244f
 safety approach, 245, 246f
 safety evaluation, 245–249, 247–249f
- Safety rod drive mechanisms (SRDM), 742
- Safety system concept, 272–277
 Canadian SCWR safety, 274–277, 275f
 atmospheric air heat exchangers, 277
 automatic depressurization system, 276
 containment pool, 275–276
 gravity-driven core flooding system, 276
 isolation condensers, 276–277
 passive moderator cooling system, 277
 reserve water pool, 277
 pressure vessel type SCWR, 273–274, 274f
- SC-HTGR (Steam cycle-HTGR), 136
- SEGS. *See* Solar energy generating systems (SEGS)
- Selected supercritical fluids (SCFs), 764–769
- Selective catalytic reduction (SCR), 35
- Senior Industrial Advisory Panel (SIAP), 130
- Sensitivity, pressure ratio, mass flow rate, 824–825, 825f
- Severe Accident MOdeling and Safety Assessment for Fluid-fuel Energy Reactors (SAMOSAFER), 234
- SFRs. *See* Sodium-cooled fast reactors (SFRs)
- Silicon carbide (SiC), 120–121
- Silicon-carbide fiber reinforced silicon carbide (SiCf/SiC), 122
- Simple cycle recuperated (SCR), 787
- Small modular reactors, (SMRs), 94, 113, 149, 683–685, 685f
 development, implementation, 754–756
 pathways, success, 755–756
 safety, licensing requirements, 754–755
 early designs, 686–687, 686–688f
 flexibility, 707–708, 708f
 security, 707
- Small modular, small-, medium-size reactors (SMRs and S&MRs), 717–720
- basic, 719
 conceptual, 719
 construction, 720
 developmental, 719
 final/certified, 719–720
 preconceptual, 719
 preliminary, 719
 type, 720, 722–730t
- Sodium-cooled fast reactors (SFRs), 88–89, 122, 123f, 174, 291, 666
 core configurations, 177–179, 178–179f
 design features, 176–177, 176t
 development history, 174–176
 fuel cycle technology, 182–183
 loop, pool type, 180f, 181–182, 182t
 plant system, 179–181, 180f
 research, development activities
 metal fuel, 430–431, 430–432f
 reactor physics experiment, 432
 safety, 183–186
 design, characteristics, 184–186
 design criteria, guidelines, 183–184
 system characteristics, 176–183
- Sodium fast reactors, 356–358, 356f
- Sodium Test Loop, Safety Simulation and Assessment (STELLA)-1, 420
- Solar energy generating systems (SEGS), 56–58
- Solar power plants, 53–66, 58f, 60–65f
 concentrated, sun-tracking heliostats, 24t, 54–58, 58f, 60–62f
 flat-panel, concentrated PV, 20f, 23–25t, 27t, 32t, 33f, 59–66, 63–65f
- Solid oxide electrolysis cell (SOEC), 673
- Sparc, 921
- Spent nuclear fuel (SNF), 755–756
- Spiral tube steam generator (STSG), 218
- Steam generator (SG), 200
- Steam generator tube rupture (SGTR), 203
- Steam methane reforming, 669
- Structures, system, and components (SSCs), 184, 846
- Supercritical-pressure (SCP), 762
- Supercritical water (SCW), 127–128
- Supercritical water-cooled reactors (SCWR), 126–127f, 127, 260, 291, 666
 advantages, disadvantages, 281–282
 concepts, main system parameters, 260–262, 261–262f
 pressure tube concept, 263–266, 264–266f
 pressure vessel concept, 262–263, 263f
 dynamics, control, 278–279, 278f
 fuel cycle technology, 266–267
 fuel qualification test, 282–283, 283f
 key challenges, 282
 stability analysis, 280–281
 start-up systems, 279–280
 pressure tube-type, 279–280, 280f
- Superphenix reactor, 356
- Sustainable Development Goals (SDGs), 306
- Sustainable Nuclear Energy Technology Platform (SNETP), 197–198, 312
- Swedish advanced lead reactor (SEALER), 344
- System-integrated Modular Advanced Reactor (SMART), 685
- System Steering Committee (SSC), 130, 233
- T**
- Technical review panel (TRP), 297
- Technical support organizations (TSOs), 326
- Technology maturity level, selected working fluid, 822
- Technology readiness level (TRL), 804
- A Technology Roadmap for Generation IV Nuclear Energy Systems*, 116–117
- Technology risk, 819
- Technology Roadmap Update (2014), 116
- Technoscience, 922
- Thermal-neutron-spectrum reactors, 616, 617t
- Thermal power plants, 8–13f, 32–42
 coal-fired, 33–36, 34–37f
 gas-fired, 20f, 21t, 24t, 28f, 33f, 35–37f, 36–38
 internal-combustion engines, 24t, 39–40, 40f, 41t
 mazut/heavy-oil-fired, 39
 oil-shale-fired, 23t, 38, 39f
 peat-fired, 38
- Thermochemical cycles, 666
- Three-stage program, 486–487
- Tidal plants, 68, 73–74f, 74–75t
- Tokamak, 871
- Transient fission matrix (TFM), 237
- Transient reactor test facility (TREAT), 186
- Transition phase, 186
- TRansUranium (TRU), 125, 138, 205, 233
- TRistructural ISOtropic (TRISO), 120–121, 134
- U**
- Ubiquitous, Robust, Accident-forgiving, Nonproliferating and Ultra-lasting Sustainer (URANUS), 220–221, 440–442
- Ultra Safe Nuclear Corporation (USNC), 721
- Uranium carbide (UCO), 136
- Uranium dioxide (UO₂), 138
- Uranium oxycarbide (UOC), 138
- Uranium-plutonium (U-Pu) fuel, 176–177
- US Department Of Energy (DOE), 136
- US energy markets, 292–294
- USNC. *See* Ultra Safe Nuclear Corporation (USNC)
- V**
- Variable inlet guide vanes (VIGVs), 788–789
- Very-high-temperature reactor(s) (VHTR(s)), 119, 119f, 293, 666, 780
- W**
- Wave power plants, 69, 75–76f, 77t
- Wind power plants, 48–53
 off-shore, 23t, 53, 55–56f, 57t
 on-shore, 20f, 21t, 23–25t, 28f, 32t, 33f, 48–52, 49–53f
- WNA. *See* World Nuclear Association (WNA)
- Working fluid
 cost, 824
 gas management, 821–822
 TRL, heat exchangers, 823
 TRL, turbomachinery components, 822–823

- Working fluid, NPP cycle performance,
802–814
case studies, 804–808, 805–808*f*, 805*t*
CO₂, supercritical CO₂, 808–810,
809–810*f*, 809*t*
helium-nitrogen binary mixture, 810–813,
812*t*, 812–813*f*
thermophysical properties,
813–814
working fluid cycle configuration, 803–804,
804*t*
working fluid studies, 802–803
- Working Group on Lead-Bismuth Eutectic
(WG-LBE), 227
- World Nuclear Association (WNA), 87,
841–842
World Nuclear News (WNN), 87
Wrapper tube, 178
- Z**
Zirconium carbide (ZrC), 140